


THE 19th INTERNATIONAL CONFERENCE ON MAGNETISM

July 8 - 13, 2012 Bexco, Busan, Korea
www.icm2012.org



Hosted by **KPS** The Korean Physical Society


 The Korean Magnetics Society

 International Union of Pure and Applied Physics



THE 19th INTERNATIONAL CONFERENCE ON MAGNETISM

CONTENTS

- Welcome Address • 3
 - Organizing Committee • 4
 - Int'l Advisory Committee • 5
 - Program Committee • 7
 - Editors & Speakers • 10
 - Program at-a-Glance • 11
 - Venue Layout • 18
 - Ceremony & Event Program • 20
 - General Information • 22
 - Exhibition • 25
 - Sponsor • 26
- 
- Oral Presentation • 27
 - Plenary Lecture • 28
 - Half-Plenary Lecture • 30
 - Invited & Contributed Presentation • 33
 - Poster Presentation • 115
 - July 9 (PA~PO) • 116
 - July 10 (QA~QP) • 182
 - July 12 (RA~RR) • 249
 - July 13 (SA~SO) • 316
 - Author Index • 373

Plenary Lecture	28
Half-Plenary Lecture	30
Invited & Contributed Presentation	33
July 9 (Mon)	33
AA: Multiferroics I - mainly manganites AD: Surface and interface effects I AG: Arrays of magnetic nanostructures I AJ: Crystalline, nanocrystalline and amorphous materials BC: Organic and molecular magnetism / Spin ladder BF: 3d transition metal oxides BI: STT MRAM and magnetic logic	AB: Non-fermi liquids and quantum phase transitions I AE: Electric field effect on magnetic systems AH: Magnetic transducers in biomedicine BA: Superconductivity I - cuprate and other superconductors BD: Exchange bias BG: Energy assisted magnetic recording BJ: Ferrites, garnets and other materials
	AC: Low-dimensional / Frustrated spin systems AF: Advanced methods of spin structure determination AI: Semiconductor spintronics I - group IV materials BB: Valence fluctuations I BE: Magnetic semiconductor BH: Interdisciplinary technology
July 10 (Tue)	48
CA: Superconductivity II - cuprate and other superconductors CD: Heavy fermions I CG: Semiconductor spintronics II - group III-V materials CJ: Magneto-dielectric materials or meta-materials DC: Spin-orbit / Spin-lattice / Spin-orbital physics DF: Chiral magnet and magnetic skyrmions DI: Spin caloritronics I EB: SCES theory I EE: Spin-orbit spin torque EH: Novel materials and devices I	CB: Magnetic nanoparticles I CE: Spin transfer oscillators CH: Heusler alloys etc DA: Superconductivity III - Fe-based superconductors DD: Diluted magnetic semiconductors and others DG: Magnetic nanowires DJ: Applications EC: Electronic structure / Spintronic materials EF: Intermetallic compounds EI: Perpendicular magnetic anisotropy materials
	CC: Spin liquid / Spin ice CF: Actinides and lanthanides CI: Multiferroics II - scattering DB: Kondo systems I DE: Magnetic memories and logics DH: Oxide EA: Non-Fermi liquids and quantum phase transitions II ED: Magnetic thin films and nanostructures I EG: Metal spintronics I EJ: Rare-earth hard magnetic materials
July 11 (Wed)	72
FA: Spin caloritronics II FD: Vortex dynamics I	FB: Heavy fermions II FE: SCES theory II
	FC: Ultrafast switching I
July 12 (Thu)	75
GA: Superconductivity IV - Fe-based superconductors GD: Ultrafast switching II GG: Arrays of magnetic nanostructures II GJ: Intermetallic and other hard magnets HC: Magnetism in s,p electron systems HF: Spin transfer torque switching HI: Topological insulators I IB: [Symposium] High performance soft magnetic materials and their applications II IE: Domain wall motion II IH: Surface and interface effects II	GB: Multiferroics III - nonreciprocal effect and electronic ferroelectricity GE: Domain wall motion I GH: Novel materials and devices II HA: Superconductivity V - Fe-based superconductors HD: Spin waves I HG: Magnetometry in nano-scale HJ: 4d and 5d compounds IC: Magnetic phase transition IF: Magnetic tunnel junctions II: Topological insulators II
	GC: Heavy fermions III GF: Spin glasses and diluted magnets GI: Organic spintronics and carbon-based spintronics HB: [Symposium] High performance soft magnetic materials and their applications I HE: Metal spintronics II HH: Magnetometry in macro-scale IA: Non-fermi liquids and quantum phase transitions III ID: Vortex dynamics II IG: Valence fluctuations II II: Ferrites and other materials
July 13 (Fri)	98
JA: Superconductivity VI - Fe-based and other superconductors JD: Magnetism theory / Simulation of quantum and classical systems JG: Spin waves II JI: Magnetocaloric effects / Magnetoelastic materials KC: Magnetic thin films and nanostructures II KF: Novel spintronic devices and materials KI: Theoretical calculation	JB: Multiferroics IV - noncollinear magnets JE: Domain wall motion III JH: Nanostructured and composite hard magnetic materials KA: Kondo systems II KD: Characterization of magnetic properties KG: SCES theory III KJ: New developments
	JC: Heavy fermions IV JF: Metal spintronics III JI: Strong magnetic anisotropy materials KB: Magnetic nanoparticles II KE: Domain walls and spin ice system KH: Coercivity mechanism
Poster Presentation	115
July 9 (Mon)	116
PA: Multiferroics I PD: Heavy fermions I PG: Magnetic materials and characterization methods PJ: Spin-dependent transport I PM: Soft magnetic materials I	PB: Superconductivity I PE: Kondo Impurity and kondo lattice systems PH: 3d transition metal oxides I PK: Perpendicular magnetic anisotropy and strong anisotropy PN: Dilutedmagnetic semiconductor/nano-composite I
	PC: Superconductivity V PF: Theory of strongly correlated matter I PI: 3d transition metal oxides II PL: Surface and interface effects including exchange bias PO: Interdisciplinary topics
July 10 (Tue)	182
QA: Multiferroics II QD: Valence fluctuations QG: Intermetallic compounds I QJ: Lanthanides II QM: Magnetic characterization QP: Magnetic recording and memories /	QB: Superconductivity II QE: Frustrated systems, kagome, triangular systems QH: Intermetallic compounds II QK: Spin-dependent transport II QN: Soft magnetic materials II
	QC: Heavy fermions II QF: 1D, low-dimensional systems QI: Lanthanides I QL: Diluted magnetic semiconductors and others QO: Novel magnetic materials and devices II
July 12 (Thu)	249
RA: Multiferroics III RD: Heavy fermions III RG: Theory of strongly correlated matter III RJ: Vortex dynamics RM: Theoretical calculation RP: Measuring techniques and instrumentation I	RB: Superconductivity III RE: Non-fermi liquids and quantum phase transitions I RH: Theory, spin, magnetic materials RK: Ultrafast dynamics RN: Magnetic nanoparticles RQ: Measuring techniques and Instrumentation II
	RC: Topological insulators I RF: Theory of strongly correlated matter II RI: Phase transition RL: Spin electronics I RO: Hard magnetic materials I RR: Industrial applications
July 13 (Fri)	316
SA: Multiferroics IV SD: Topological insulators II SG: New developments SJ: Modeling SM: Magnetic thin films and others	SB: Superconductivity IV SE: Heavy fermions IV SH: Domain and domain walls SK: Spin electronics II SN: Hard magnetic materials II
	SC: Superconductivity VI SF: Non-fermi liquids and quantum phase transitions II SI: Spin waves SL: Magnetic nanostructures and arrays SO: Novel magnetic materials and devices I

Dear Colleagues,

On behalf of the Organizing Committee, and all of those who were involved in preparing for the 19th International Conference on Magnetism (ICM2012), we wish to extend a warm-hearted welcome to all participants of ICM2012. It is our great honor and privilege to host the ICM2012 in Korea.

The major scientific societies in Korea, the Korean Physical Society (KPS) and the Korean Magnetism Society (KMS) are pleased to co-host the ICM2012, under the auspices of the International Union of Pure and Applied Physics (IUPAP). The ICM2012 incorporates the International Conference on Strongly Correlated Electron Systems (SCES) held annually.

As the most highly acclaimed conference, a considerable number of abstracts have been submitted from 52 countries around the world. In this conference, we expect over 1,700 participants around the world. For the scientific program, we have planned 7 plenary lectures including 3 Nobel laureates' lectures, 14 Half-plenary lectures, 509 oral presentations including 135 invited lectures, along with 1,502 poster presentations. In addition, 7 satellite symposia will be held before or after the ICM2012.

I wish to take this opportunity to thank all the sponsors for their generous support for the ICM2012. Also, I would like to convey my sincere gratitude to the international advisory members for their valuable advices and to the members of the ICM2012 organizing committee for their tremendous efforts in making this conference a success.

We wish you all a fruitful meeting and hope that you will benefit from the rich scientific programs, and your visit to wonderful Busan will last forever as a pleasant memory.



Prof. Sung-Chul Shin
Chairperson, ICM2012
President, DGIST

ORGANIZING COMMITTEE

Chairperson	Sung-Chul Shin	DGIST	Korea
Secretary General	Kungwon Rhie	Korea University	Korea
Program Committee			
Co-Chair	Yoon Hee Jeong	POSTECH	Korea
	Samuel Bader	Argonne National Lab.	USA
Executive Member	Hideo Ohno	Tohoku University	Japan
	Byung Il Min	POSTECH	Korea
	Sang Ho Lim	Korea University	Korea
	Tae Won Noh	Seoul National University	Korea
	Yong-Seung Kwon	DGIST	Korea
	Yunkyu Bang	Chonnam National University	Korea
	Tuson Park	Sungkyunkwan University	Korea
	Cathy Stampfl	Sydney University	Australia
	Sang-Koog Kim	Seoul National University	Korea
Publication Committee			
Chair	Jae Il Lee	Inha University	Korea
Member	Dong Ho Kim	Yeungnam University	Korea
	Soonchil Lee	KAIST	Korea
	Joo Yull Rhee	Sungkyunkwan University	Korea
Treasurers Committee			
Chair	Bo Wha Lee	Hankuk University of Foreign Studies	Korea
Member	Sug-Bong Choe	Seoul National University	Korea
Public Relation Committee			
Chair	Chun-Yeol You	Inha University	Korea
Member	Taejoon Kouh	Kookmin University	Korea
	Bongjin Simon Mun	Hanyang University	Korea
	Hae-In Yim	Sookmyung University	Korea
Industrial Support Committee			
Chair	Kyung-Ho Shin	Korea Institute of Science and Technology	Korea
Member	Derac Son	Hannam University	Korea
Exhibition Committee			
Chair	Chan Yong Hwang	Korea Reserch Institute of Standards and Science	Korea
Member	Jae-Hoon Park	Pohang University of Science and Technology	Korea
Local Committee			
Chair	Hae-Woong Kwon	Pukyung National University	Korea
Member	Sunglae Cho	University of Ulsan	Korea
	Myung Hwa Jung	Sogang University	Korea
	Gwan Soo Park	Pusan National University	Korea

INT'L ADVISORY COMMITTEE

Gabriel Aeppli	University College London	UK
Jun Akimitsu	Aoyama Gakuin University	Japan
Koji Ando	National Institute of Advanced Industrial Science and Technology (AIST)	Japan
David Awschalom	University of California	USA
Elisa Baggio-Saitovitch	Brazilian Center for Research in Physics - CBPF	Brazil
Mario Baibich	Ministry of Science and Technology of Brazil	Brazil
Ganapathy Baskaran	The Institute of Mathematical Sciences	India
Ernst Bauer	Vienna University of Technology	Austria
Robert Buhrman	Cornell University	USA
Ching-Ray Chang	National Taiwan University	Taiwan
John Chapman	University of Glasgow	UK
Sang-Wook Cheong	Rutgers University	USA
Lesley Cohen	Imperial College	UK
Alessandra Continenza	Universita' degli studi dell'Aquila	Italy
E. Dan Dahlberg	University of Minnesota	USA
Bernard Dieny	Commissariat à l'Energie Atomique	France
Tomasz Dietl	University of Warsaw	Poland
You-Wei Du	Nanjing University	China
Albert Fert	Universite Paris-Sud	France
Dino Fiorani	National Research Council	Italy
Peter Fischer	Lawrence Berkeley National Laboratory	USA
Zachary Fisk	University of California	USA
Catherine Foley	The Commonwealth Scientific and Industrial Research Organisation	Australia
Mark Freeman	University of Alberta	Canada
Hiroyasu Fujimori	Tohoku University	Japan
Peter Fulde	Asia Pacific Center for Theoretical Physics	Germany
Mohammad Ghafari	Karlsruhe Instiute of Technology	Germany
Amitabha Ghoshray	Saha Institute of Nuclear Physics	India
Laura Greene	University of Illinois at Urbana Champaign	USA
Peter A. Grünberg	Institute of Solid State Resaerch	Germany
Ott Hans Rudolf	Eidgenössische Technische Hochschule Zürich	Switzerland
Bret Heinrich	Simon Fraser University	Canada
Laura Heyderman	Paul Scherrer Institute	Switzerland
Burkard Hillebrands	TU Kaiserslautern	Germany
Axel Hoffman	Argonne National Laboratory	USA
Nguyen Huu Duc	Vietnam National University	Vietnam
Manuel Ricardo Ibarra	Zaragoza University	Spain
Flouquet Jacques	Commissariat à l'Energie Atomique	France
Sung-Ho Jin	UC San Diego	USA
Xiaofeng Jin	Fudan University	China
Borje Johansson	University of Uppsala	Sweden
Il Koo Kang	The Korean Magnetics Society	Korea
Bernhard Keimer	Max Planck Institute for Solid State Research	Germany
Zheong Gou Khim	Seoul National University	Korea
Chul Koo Kim	Yonsei University	Korea
Chul Sung Kim	Kookmin University	Korea
Jürgen Kirschner	Max Planck Institute of Microstructure Physics	Germany
Guangli Kuang	Chinese Academy of Sciences	China
Budhy Kurniawan	University of Indonesia	Indonesia

J. Raynien Kwo	National Tsing Hua University	Taiwan
Patrick Lee	MIT	USA
Liang Li	Huazhong University of Science and Technology	China
Peter Littlewood	Argonne National Laboratory	USA
Bo Liu	Data Storage Institute	Singapore
Hilbert Löhneysen	Karlsruhe Institute of Technology	Germany
Jan Cees Maan	Radboud University Nijmegen	Netherlands
Allan MacDonald	University of Texas at Austin	USA
Sadamichi Maekawa	The Japan Atomic Energy Agency	Japan
Yoshiteru Maeno	Kyoto University	Japan
Brian Maple	University of California, San Diego	USA
Andrew Millis	Columbia University	USA
Laurens W. Molenkamp	Wuerzburg University	Germany
John Mydosh	Leiden University	Netherlands
Kevin O'Grady	The University of York	UK
Yoshichika Onuki	Osaka Univeristy	Japan
Martha Pardavi-Horvath	The George Washington University	USA
Stuart Parkin	IBM Almaden Research Center	USA
Massimo Pasquale	L'Istituto Nazionale di Ricerca Metrologica	Italy
Danilo Pescia	Eidgenössische Technische Hochschule Zürich	Switzerland
Stefania Pizzini	Centre National de la Recherche Scientifique	France
Sergio Rezende	Universidade Federal de Pernambuco	Brazil
John Sarrao	Los Alamos National Laboratory	USA
Ivan Schuller	University of California-San Diego	USA
Zhi-Xun Shen	Stanford University	USA
Teruya Shinjo	International Institute for Advanced Studies	Japan
Qimiao Si	Rice University	USA
Manfred Sigrist	ETH Zürich	Switzerland
John Slonczewski	IBM Research Center	USA
Robert Stamps	University of Glasgow	UK
Frank Steglich	Max Planck Institute for Chemical Physics of Solids	Germany
Takao Suzuki	University of Alabama	USA
Henryk Szymczak	Polish Academy of Sciences	Poland
Toshiro Takabatake	Hiroshima University	Japan
Hidenori Takagi	University of Tokyo	Japan
Migaku Takahashi	Tohoku University	Japan
Koki Takanashi	Tohoku University	Japan
Yoshinori Tokura	University of Tokyo	Japan
Kazuo Ueda	University of Tokyo	Japan
Chandra Varma	University of California, Riverside	USA
Manuel Vazquez	Spanish National Council for Research	Spain
Hai-Hu Wen	Nanjing University	China
Yeong-Der Yao	Fu Jen University	Taiwan

Co-Chairs	Yoon Hee Jeong	POSTECH	Korea
	Samuel Bader	Argonne National Lab.	USA
Executive Member	Hideo Ohno	Tohoku University	Japan
	Byung Il Min	POSTECH	Korea
	Sang Ho Lim	Korea University	Korea
	Tae Won Noh	Seoul National University	Korea
	Yong-Seung Kwon	DGIST	Korea
	Yunkyu Bang	Chonnam National University	Korea
	Tuson Park	Sungkyunkwan University	Korea
	Cathy Stampfl	Sydney University	Australia
	Sang-Koog Kim	Seoul National University	Korea
1. Strongly Correlated Electron System (SCES) (including Superconductivity/ Multiferroics)			
1-1	Keehoon Kim	Seoul Natonal University	Korea
Multiferroics	Taka-hisa Arima	University of Tokyo	Japan
	M. Fiebig	ETH	Switzerland
	Tsuyoshi Kimura	Osaka University	Japan
	Tae Won Noh	Seoul Natonal University	Korea
	Je-Geun Park	Seoul Natonal University	Korea
	L. P. Regnault	ILL	France
1-2	T. Devereaux	Standford University	USA
Superconductivity	Yunkyu Bang	Co-chair / Chonnam National Universityty	Korea
	D. L. Feng	Fudan University	China
	Changyoung Kim	Yonsei University	Korea
	Matthias Vojta	Technische Universitaet Dresden	Germany
1-3	Hu-Jong Lee	POSTECH	Korea
Topological Insulators	Mahn-Soo Choi	Korea University	Korea
	Jun Sung Kim	Pohang University of Science and Technology	Korea
	Young-Woo Son	Korea Institute for Advanced Study	Korea
	Han Woong Yeom	Pohang University of Science and Technology	Korea
1-4	Joe D. Thompson	Co-chair / Los Alamos National Laboratory	USA
Heavy Fermion Systems	Meigan Aronson	Brookhaven National Laboratory	USA
	Piers Coleman	Rutgers University	UK
	Noriaki Sato	Nagoya University	Japan
1-5	Tuson Park	Sungkyunkwan University	Korea
Valence Fluctuations	Jeongsoo Kang	The Catholic University of Korea	Korea
	Kazumasa Miyake	Osaka University	Japan
	Huiqiu Yuan	Zhejiang University	China
1-6	Suchitra Sebastian	University of Cambridge	UK
Non-Fermi Liquids and	A. Huxley	University Edinburgh	UK
Quantum Phase	Yuji Matsuda	Kyoto University	Japan
Transitions	Toby Perring	ISIS	UK
1-7	Steffen Wirth	Max Planck Institute for Chemical Physics of Solids	Germany
Konndo Impurity and	Bernard Coqblin	University Paris	France
Kondo Lattice Systems	Jeongsoo Kang	The Catholic University of Korea	Korea
	Yongseung Kwon	DGIST	Korea
1-8	Takami Tohyama	Kyoto University	Japan
Theory of Strongly	T. Devereaux	Standford University	USA
Correlated Matter	Dirk Manske	Max Planck Institute for Solid State Research	Germany
	Jaejun Yu	Seoul National University	Korea

2. Quantum and Classical Spin Systems

Byungil Min	POSTECH	Korea
Giniyat Khaliullin	Max Planck Institute for Solid State Research	Germany
Mi Young Kim	Ajou University	Korea
Jae-Hoon Park	POSTECH	Korea
Myriam P. Sarachik	City College of New York-CUNY	USA

3. Magnetic Structures and Interactions

Kibong Lee	POSTECH	Korea
Des McMorrow	University College London	UK
Seung-Hun Lee	University of Virginia	USA
Je-Geun Park	Seoul National University	Korea
Kazuyoshi Yamada	KEK	Japan

4. Magnetization Dynamics and Micromagnetics

Sang-Koog Kim	Seoul National University	Korea
Kristen Buchanan	Colorado State University	USA
Sug-Bong Choe	Seoul National University	Korea
Oksana Chubykalo-Fesenko	Instituto de Ciencia de Materiales de Madrid, CSIC	Spain
Volodymyr Kruglyak	University of Exeter	UK
Guido Meier	University of Hamburg	Germany

5. Spin-Dependent Transport

Hyun-Woo Lee	POSTECH	Korea
Myung-Hwa Jung	Sogang University	Korea
Stephen Russek	NIST	USA
Henk Swagten	Eindhoven University of Technology	Netherlands
Suzuki Yoshishige	Osaka University	Japan

6. Spin Electronics

Byoung Chul Min	KIST	Korea
Ursula Ebels	SPINTEC	France
Xiufeng Han	State Key Laboratory of Magnetism	China
Kyung-Jin Lee	Korea University	Korea
Teruo Ono	Kyoto University	Japan
Joerg Wunderlich	Hitachi Cambridge Lab	UK

7. Magnetic Thin Films, Particles and Nanostructure

Sang Ho Lim	Korea University	Korea
Chan Yong Hwang	KRIS	Korea
Tae Hee Kim	Ewha Womans University	Korea
Seiji Mitani	NIMS	Japan
Zi Q. Qiu	UC-Berkeley	USA

8. Soft and Hard Magnetic Materials and their Applications

Hae-Woong Kwon	Pukyong National University	Korea
Hirotohi Fukunaga	Nagasaki University	Japan
Satoshi Sugimoto	Tohoku University	Japan
Seong-cho Yu	Chungbuk National University	Korea

9. Novel Materials and Device Applications

Sunglae Cho	University of Ulsan	Korea
Beongki Cho	Gwangju Institute of Science and Technology (GIST)	Korea
Alessandra Continenza	Universita' degli studi dell'Aquila	Italy
Gendo Oomi	Kurume Institute of Technology	Japan

10. Magnetic Recording and Memories

Eunsik Kim	Samsung Electronic Co.	Korea
Sung Woong Chung	Hynix	Korea
Katsuji Nakagawa	Nihon University	Japan
Shin Saito	Tohoku University	Japan

11. Measuring Techniques and Instrumentation

Derac Son	Hannam University	Korea
Michael Hall	National Physical Laboratory	UK
Massimo Pasquale	INRIM	Italy
Kwon Sang Yoo	KRIS	Korea

12. Industrial Applications

Kyung-Ho Shin	KIST	Korea
Sang Yun Cha	POSCO	Korea

13. Interdisciplinary Topics

Cheol Gi Kim	Chungnam National University	Korea
Hubert Brueckl	AIT Austrian Institute of Technology GmbH	Austria
Wooyoung Lee	Yonsei University	Korea
Jian-Ping Wang	University of Minnesota	USA

Editors

Chief	Jae Il Lee	Inha University	Korea
Member	Joonyeon Chang	KIST	Korea
	Soon Cheol Hong	University of Ulsan	Korea
	Namjung Hur	Inha University	Korea
	Young-Rok Jang	University of Inchoen	Korea
	Gun Sang Jeon	Ewha Womans University	Korea
	Kee Hoon Kim	Seoul National University	Korea
	Dong-Hyun Kim	Chungbuk National University	Korea
	Dong Ho Kim	Yeungnam University	Korea
	Tae Wan Kim	Sejong University	Korea
	Sang-Suk Lee	Sangji University	Korea
	Soonchil Lee	KAIST	Korea
	Joo Yull Rhee	Sungkyunkwan University	Korea
	Seok-Soo Yoon	Andong National University	Korea

Plenary Speakers

Albert Fert	CNRS/Thales and University Paris-Sud	France
<i>*Nobel laureate in Physics (2007)</i>		
Andre Geim	University of Manchester	UK
<i>*Nobel laureate in Physics (2010)</i>		
Klaus von Klitzing	Max Planck Institute for Solid State Research	Germany
<i>*Nobel laureate in Physics (1985)</i>		
Sang-Wook Cheong	Rutgers University	USA
Zachary Fisk	University of California, Irvine	USA
Sadamichi Maekawa	Japan Atomic Energy Agency	Japan
Roland Wiesendanger	University of Hamburg	Germany

Half-Plenary Speakers

Gabriel Aeppli	University College London	UK
Piers Coleman	Rutgers University	UK
Claudia Felser	Max Planck Institute for Chemical Physics of Solids	Germany
Laura Heyderman	Paul Scherrer Institute	Switzerland
Bernhard Keimer	Max Planck Institute for Solid State Research	Germany
Hyun-Woo Lee	POSTECH	Korea
Tae Won Noh	Seoul National University	Korea
Hideo Ohno	Tohoku University	Japan
Yoshichika Onuki	Osaka University	Japan
Stuart Parkin	IBM Almaden Research Center	USA
Caroline Ross	Massachusetts Institute of Technology	USA
Yoshinori Tokura	University of Tokyo	Japan
Shoucheng Zhang	Stanford University	USA
Xiaozhong Zhang	Tsinghua University	China

Time	July 8 (Sun)	July 9 (Mon)	July 10 (Tue)	July 11 (Wed)	July 12 (Thu)	July 13 (Fri)
08:30		Opening & Award		Plenary 4 PP04		
09:00		Plenary 1 PP01	Half-Plenary 1~6 HP11~HP32	Plenary 5 PP05	Half-Plenary 9~14 HP51~HP72	Invited & Contributed JA~JJ
10:00		Coffee Break				
11:00		Plenary 2 PP02	Coffee Break	Coffee Break	Coffee Break	Coffee Break
12:00		Plenary 3 PP02	Invited & Contributed CA~CJ	Invited & Contributed FA~FE	Half-Plenary 7-8 HP41~HP42	Invited & Contributed GA~GJ
13:00		Lunch	Lunch		Lunch	Lunch
14:00	Registration	Poster Presentation I PA~PO	Poster Presentation II QA~QP	Excursion	Poster Presentation III RA~RR	Poster Presentation IV SA~SO
15:00	KPS 60th Anniversary Nobel laureate in Physics Public Lecture	Invited & Contributed AA~KJ	Invited & Contributed DA~DJ		Invited & Contributed HA~HJ	Plenary 6 PP06
16:00		Break	Break		Break	Plenary 7 PP07
17:00	Welcome Reception	Invited & Contributed BA~BJ	Invited & Contributed EA~EJ		Invited & Contributed IA~IJ	Closing
18:00						
19:00					Banquet	
20:00						

PROGRAM AT A GLANCE

PROGRAM AT A GLANCE

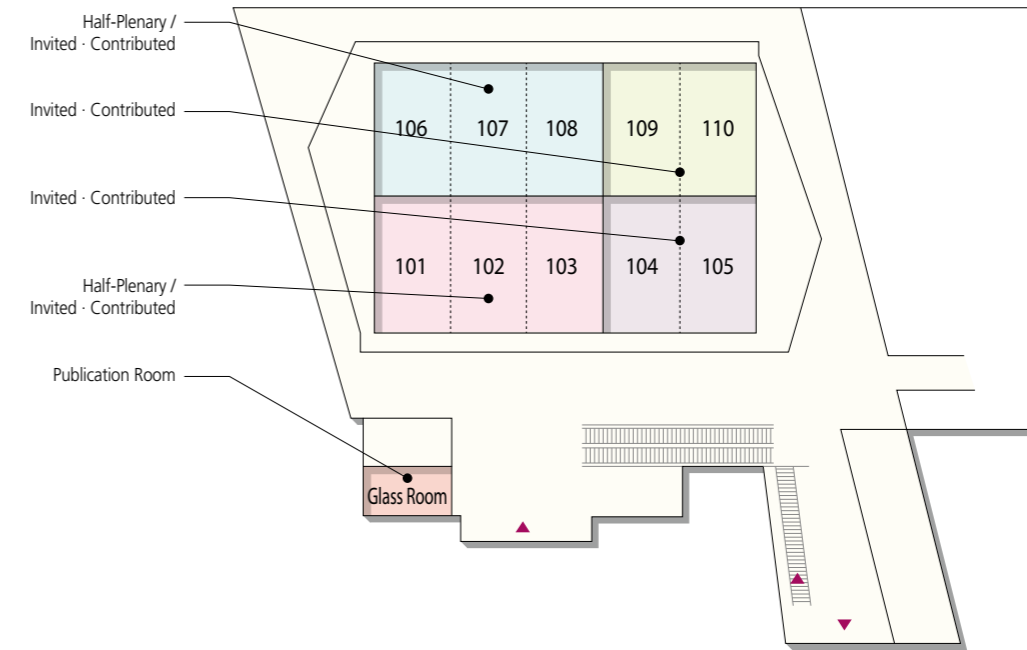
July 8 (Sun)												
Auditorium	1F			2F			3F			Exhibition		
	Room 101-3	Room 106-8	Room 104-5	Room 109-10	Room 201	Room 202	Room 203	Room 204	Room 205		Room 206	Room 301
08:00												
09:00												
10:00												
11:00												
12:00												
13:00												
14:00												
15:00												
16:00	KPS 60th Anniversary Nobel laureate in Physics Public Lecture 1) Albert Fert 2) Klaus von Klitzing											
17:00												
18:00					Welcome Reception (2F, Lobby)							
19:00												
20:00												

July 9 (Mon)												
Auditorium	1F			2F			3F			Exhibition		
	Room 101-3	Room 106-8	Room 104-5	Room 109-10	Room 201	Room 202	Room 203	Room 204	Room 205		Room 206	Room 301
08:00												
09:00	Opening & Award PP01 Plenary 1 Albert Fert											
10:00	Coffee Break PP02 Plenary 2 Sadamichi Maekawa											
11:00	PP03 Plenary 3 Zachary Fisk											
12:00	Lunch											
13:00	Lunch											
14:00												
15:00												
16:00	AA Multiferroics I - mainly manganites	AB Non-fermi liquids and quantum phase transitions I	AC Low-dimensional / Frustrated spin systems	AD Surface and interface effects I	AE Electric field effect on magnetic systems	AF Advanced methods of spin structure determination	AG Arrays of magnetic nanostructures I	AH Magnetic transducers in biomedicine	AI Semiconductor spintronics I - group IV materials	AJ Crystalline, nanocrystalline and amorphous materials		
17:00	BA Superconductivity I - cuprate and other superconductors	BB Valence fluctuations I	BC Organic and molecular magnetism / Spin ladder	BD Exchange bias	BE Magnetic semiconductor	BF 3d transition metal oxides	BG Energy assisted magnetic recording	BH Interdisciplinary technology	BI STT MRAM and magnetic logic	BJ Ferrites, garnets and other materials		
18:00												
19:00												
20:00												

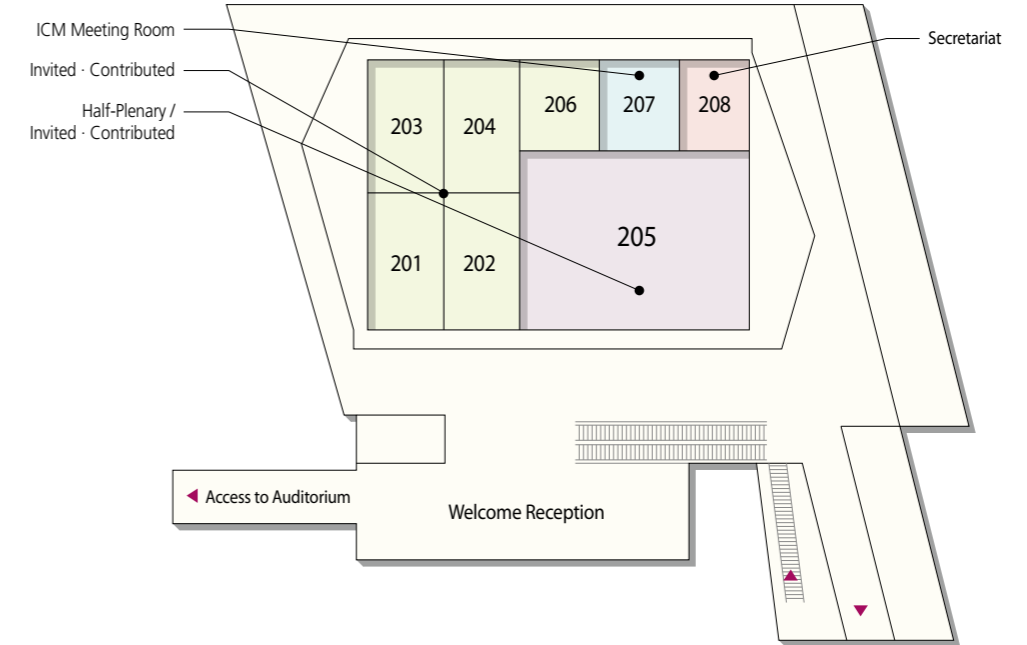
BEXCO



Convention Hall (1F)



Convention Hall (2F)



KPS 60th Anniversary Nobel Laureate Public Lectures in Physics

In celebration of the KPS's 60th anniversary, the Public Lecture of Nobel laureate in Physics will be a program allowing the general public to learn about the interesting aspects of Physics. This public lecture program will be an exciting and enjoyable experience. Please do not miss this change to take the lectures on free.

This public lecture program will be an exciting and enjoyable experience for Korean audience interested in Physics.

- Date & Time: July 8 (Sun), 15:00~17:00
- Venue: Auditorium
- Lecture: 1. Prof. Albert Fert - Spintronics and its impact on information and communication technologies
2. Prof. Klaus von Klitzing - New applications of my Nobel prize

Welcome Reception

You will experience a warm welcome from the host of ICM2012. All participants are highly welcome. Light refreshments and beer will be provided free of charge.

- Date & Time: July 8 (Sun), 17:00~19:00
- Venue: Lobby of Convention Hall, 2F

Opening Ceremony

ICM2012 will officially get started with a ceremony at Auditorium in Bexco. All registered participants are cordially invited to join us and celebrate the official opening.

- Date & Time: July 9 (Mon), 08:30~09:00
- Venue: Auditorium

ICM Award 2012

The IUPAP Magnetism Award and Néel Medal are presented every three years at the International Magnetism Conference to a scientist in recognition of an outstanding contribution to the field of magnetism. The award is sponsored by Elsevier Science B.V.. The IUPAP Young Scientist Medals in the field of magnetism are presented every three years at the International Magnetism Conference. The medals are sponsored by IUPAP.

- Date & Time: July 9 (Mon), 08:30~09:00
- Venue: Auditorium

Magnetism Award and Néel Medal 2012

- Sadamichi Maekawa (Japan Atomic Energy Agency, Japan)
Heat and spin
- Yoshinori Tokura (University of Tokyo, Japan)
Electrodynamics of skyrmions

Young Scientist Medals in the Field of Magnetism

- Suchitra E. Sebastian (University of Cambridge, UK)
Nodal pocket revealed by quantum oscillations in an underdoped cuprate superconductor

Banquet

Please join us to share an unforgettable evening. A delicious dinner with a traditional Korean music show, Samulnori (traditional percussion quartet) and 'B-boy', is combined to recreate the wonderful excitement performance.

- Date & Time: July 12 (Thu), 19:00~20:30
- Venue: Room 301 (3F), Convention Hall

Closing Ceremony

Have the opportunity to say farewell to friends and colleagues and to preview the next venue of ICM2015.

- Date & Time: July 13 (Fri), 17:30~18:00
- Venue: Auditorium

Industrial Tour

Participants those who applied for industrial tour of Samsung Heavy Industries Co., Ltd. should be gathered at 13:20 on July 11 (Wed) at the lobby. We will leave 13:30 on time. Application can be acceptable until 10:00 on July 9 at the information desk (Max. 100 people).

- Date & Time: July 11 (Wed), 13:30~18:00
- Destination: Samsung Heavy Industries Co., Ltd.

Scientific Program

ICM2012 program will consist of 7 plenary talks (1 hr), 14 half-plenary talks (45 min) and 135 invited talks (30 min). Over 2,000 contributed papers will be presented, 353 of them have been selected for oral presentation (15 min). In addition, poster presentations with ample time for discussion will be conducted. The official conference language is English. The program will focus on following topics;

1. Strongly Correlated Electron System (SCES)
2. Quantum and Classical Spin Systems
3. Magnetic Structures and Interactions
4. Magnetization Dynamics and Micromagnetics
5. Spin-Dependent Transport
6. Spin Electronics
7. Magnetic Thin Films, Particles and Nanostructures
8. Soft and Hard Magnetic Materials and Their Applications
9. Novel Materials and Device Applications
10. Magnetic Recording and Memories
11. Measuring Techniques and Instrumentation
12. Industrial Applications
13. Interdisciplinary Topics

Registration

All attendees will be required to wear the ICM2012 badge to access to all session.

- Venue: Lobby, Exhibition Hall 1
- Operation: July 8 (Sun) / 13:00~19:00
July 9 (Mon) ~ 12 (Thu) / 08:00~19:00
July 13 (Fri) / 08:00~13:00

Registration Fee

	Category	On-site Registration
Registration Fee	Regular Participant	KRW 750,000
	Student/Retired Participant	KRW 400,000
	Accompanying Person	KRW 250,000
Banquet Fee (July 12)	All Participants	KRW 60,000

* Participant's registration includes: Welcome reception, coffee breaks, admission to all scientific sessions, and a conference bag including abstract book
* Accompanying person's registration includes: Welcome reception, coffee breaks, banquet coupon and conference bag. Admission to scientific sessions is not included.

Certificate of Attendance

The certificate of attendance is provided at the information desk on request or available for download via the website after the conference (www.icm2012.org).

Internet Lounge

Internet access will be available during the conference at the Exhibition Hall where a PC computer pool will be provided.

Publication Room

Authors can check the status of their manuscripts in the Publication Room, located in the Glass Room on the first floor of convention hall. Office hour of the Publication Room for authors will be as follows.

- Operation Hours: July 9 (Mon), 15:00~17:00
July 10 (Tue), 12 (Thu), 10:00~12:00, 15:00~17:00
July 11 (Wed), 13 (Fri), 10:00~12:00

Oral Presentation Guideline

Authors are expected to bring their presentations on their own laptop computer, and to have it powered up and ready to connect to the projector. Only standard PC-style VGA connections to the LCD projector will be supplied, therefore you must supply any required adaptor to connect up your computer.

Poster Presentation Guideline

Posters are displayed in the Exhibition Hall 1 (1F). Poster should be posted by 08:30 and dismantled after 18:00 on the allotted date. The secretariat will not be held liable for any lost or damaged posters. All poster presenters are encouraged to be at their poster panels for discussion with participants during the time. All posters will be eligible for nomination for the best poster awards in each day.

- Venue: Exhibition Hall 1
- Operation: July 9, 10, 12, 13 (4days), 13:30~15:30
Affixation: 08:30~13:00 / Presentation: 13:30~15:30 / Removal: 18:00~19:00
- Affixation & Removal: All presenters are requested to affix their posters and remove them after their presentation according to the above schedule. The secretariat will not be held liable for any posters lost or damaged.
- Best Poster Award: There is a competition for the best poster. This award is given to recognize excellence in research and presentation. There will be two awards for each day. Each session chair is to nominate a single poster. The final review will be run by program executive members and the best awards are announced 30 minutes before the closing of the session.

Coffee Break

Enjoy your break with a cup of coffee or tea that will be prepared as below;

	July 9 (Mon)	July 10 (Tue)	July 11 (Wed)	July 12 (Thu)	July 13 (Fri)
Morning	10:00~10:20	10:30~11:00	10:30~11:00	10:30~11:00	10:30~11:00
	Lobby Auditorium	1F, 2F Lobby Conventional Hall	1F, 2F Lobby Conventional Hall	1F, 2F Lobby Conventional Hall	1F, 2F Lobby Conventional Hall
Afternoon	13:30~15:30	13:30~15:30	-	13:30~15:30	13:30~15:30
	Exhibition Hall	Exhibition Hall	-	Exhibition Hall	Exhibition Hall

Complimentary Shuttle Service

Shuttle bus will run between the conference venue and hotels. You may check the schedule and shuttle bus stop. The bus stop will be marked with banner stands at BEXCO.

Hotel	July 8 (Sun)		July 9 (Mon)		July 10 (Tue)		July 11 (Wed)		July 12 (Thu)		July 13 (Fri)	
	H → B	B → H	H → B	B → H	H → B	B → H	H → B	B → H	H → B	B → H	H → B	B → H
The Westin Chosun Busan	13:00 14:00	18:00 19:00	08:00 08:30	19:10 19:40	08:00 08:30	19:10 19:40	08:00 08:30	13:00 14:00	08:00 08:30	19:10 21:00	08:00 08:30	18:30 19:00
Paradise Hotel Busan Seacloud Hotel	13:00 14:00	18:00 19:00	08:00 08:30	19:10 19:40	08:00 08:30	19:10 19:40	08:00 08:30	13:00 14:00	08:00 08:30	19:10 21:00	08:00 08:30	18:30 19:00
Hotel Riviera Haeundae	13:00 14:00	18:00 19:00	08:00 08:30	19:10 19:40	08:00 08:30	19:10 19:40	08:00 08:30	13:00 14:00	08:00 08:30	19:10 21:00	08:00 08:30	18:30 19:00
Novotel Hotel Busan Ambassador	13:00 14:00	18:00 19:00	08:00 08:30	19:10 19:40	08:00 08:30	19:10 19:40	08:00 08:30	13:00 14:00	08:00 08:30	19:10 21:00	08:00 08:30	18:30 19:00
Lotte Hotel Busan	14:00	19:00	8:00	19:10	8:00	19:10	8:00	13:00	8:00	19:10	8:00	18:30
Hanwha Resort	13:00 14:00	18:00 19:00	08:00 08:30	19:10 19:40	08:00 08:30	19:10 19:40	08:00 08:30	13:00 14:00	08:00 08:30	19:10 21:00	08:00 08:30	18:30 19:00

H → B: From Hotel to Bexco, B → H: From Bexco to Hotel
* Shuttle Service won't be provided for Haeundae Centum Hotel and ARPINA Buasn Youth Hostel located in walking distance.
* Participant who is staying in Haeundae Grand Hotel, please take a shuttle bus at the Westin Chosun Busan.

Cloak Room

The cloakroom will be located in the exhibition hall so that you could keep your luggage during the conference.

Water Station

One or two bottles of water will be provided each day. The Water Coupons will be given to all participants when you register. It will be contributed at the cloak room.

Venue: BEXCO (Busan Exhibition Convention Center)

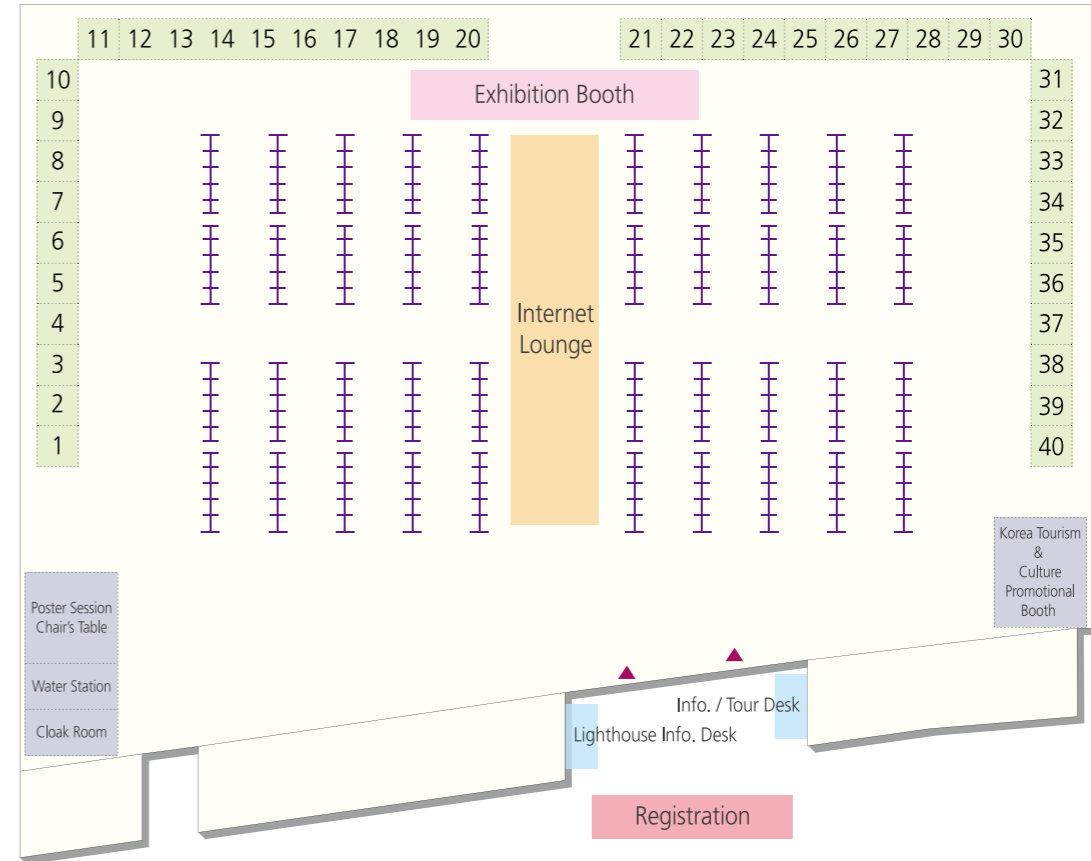
BEXCO, a landmark in the world-famous port city of Korea, has emerged as the most competitive exhibition and convention center in Northeast Asia.

- Address 43 APEC-ro, Haeundae-gu, Busan 612-740, Korea
- Tel +82-51-740-7300
- Fax +82-51-740-7320
- Website www.bexco.co.kr

ICM2012 Secretariat

- **Onsite Secretariat Office:** Room 208, Convention Hall, Tel: 051-740-3730
- **After the Conference:** 1f Haeoreum Bldg., 16, Yeoksamro 17 gil, Gangnam-gu, Seoul 135-925, Korea
Tel: +82-2-557-8422 Fax: +82-2-566-6087 Email: icm@icm2012.org
Website: www.icm2012.org

Exhibition Hall (1F)



Venue: Exhibition Hall 1

Exhibition Schedule

- Installation: Shell Scheme Booth: July 8 (Sun) 08:00~ Exhibits & Display: July 8 (Sun) 18:00~24:00
- Exhibition Hours: July 9 (Mon)~12 (Thu), 09:00~19:00
July 13 (Fri), 09:00~16:00
- Removal: July 13 (Fri), 16:00~20:00

Exhibitor	Booth No.	Exhibitor	Booth No.	Exhibitor	Booth No.
Aaron. Co., Ltd.	16	Hyundai Motor Company	21, 22, 23	Quantum Design	24, 25
Ask Co.	9	ICM2015-Barcelona	40	ReC-SDSW(Seoul National University)	7
Carl Zeiss	27	Korea I.T.S.	17, 18	Rigong International Inc.	13
ChangSung Co.	19, 20	Lake Shore Cryotronics	8	Semi-Ence Co., Ltd.	32
Coxem	31	Namotec	15	SmartTip BV	11
Cryogenic Ltd.	30	Nanomagnetics Instruments	10	Springer	36, 37
DGIST	1, 2	NT-MDT ANT Co.	26	Surface Systems Korea	12
Effucell	33	Oxford University Press	38	The Physical Society of Japan	39
ExaTech	29	PANalytical Korea	34	Top Techology Ltd.	14
HANARO @ KAERI	6	Park Systems Co.	35	UNIST	3
Hinds Instruments Inc.	28	Pohang Accelerator Laboratory	4, 5		

SPONSOR

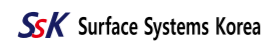
Gold



Silver



Bronze



ORAL PRESENTATION

Plenary Lecture • 28

Half-Plenary Lecture • 30

Invited & Contributed Presentation • 33

PP01

Recent developments and emerging directions in spintronics

Albert Fert

Unité Mixte de Physique CNRS/Thales, Palaiseau, and Université Paris-Sud, Orsay, France

Spintronics develops today in many promising directions. We focus on three topics. First: "Microwave generation by spin transfer", a field with fast recent advances anticipating short term applications. Second topic: "Spintronics with graphene or carbon nanotubes (CNT)", with fascinating long term prospects for "beyond CMOS". Finally: "Oxtronics", overview of results on devices associating magnetic, ferroelectric and multiferroic oxides. 1) Microwave generation by spin transfer. Microwave oscillations are obtained by using spin transfer to induce magnetization precessions or gyrations of magnetic vortices. Large powers (μW range) and narrow emission widths (≈ 0.1 MHz) can be today obtained at zero field by vortex gyration [1]. Synchronization is an additional way to increase the power and reduce the emission width [2]. 2) Spintronics with graphene and CNT: Several concepts of spintronics (logic gates, "spin only logic circuits", etc) are based on spin transport in lateral channels between magnetic contacts. Recent experiments show the outstanding potential of graphene and CNT for spin transport to long distance (above $100 \mu\text{m}$) in such devices [3]. 3) Oxtronics: We illustrate the potential of oxtronics by results on tunnel junctions with ferroelectric barriers: giant electro-resistance [4], interplay between ferroelectric and spin polarizations, prospects for ferroelectric memories and memristors.

[1] A. Dussaux, B. Georges, J. Grollier, V. Cros, A.V. Khvalkovskiy, A. Fukushima, M. Konoto, H. Kubota, K. Yakushiji, S. Yuasa, K. A. Zvezdi, K. Ando, A. Fert *Nature Communications* 1, 8, 2010. [2] A. Dussaux, A. V. Khvalkovskiy, J. Grollier, V. Cros, A. Fukushima, M. Konoto, H. Kubota, K. Yakushiji, S. Yuasa, K. Ando, and A. Fert. *Appl. Phys. Lett.* 98, 132506, 2011. [3] B. Dlubak, P. Senoor, A. Anane, M-B. Martin, C. Deranlot, B. Servet, S. Xavier, R. Mattana, M. Sprinkle, C. Berger, W. A. de Heer, F. Petroff, and A. Fert, *Nat. Phys.*, DOI: 10.1038. [4] V. Garcia, S. Fusil, K. Bouzehouane, S. Enouz-Vedrenne, N.D. Mathur, A. Barthélémy, M. Bibes, *Nature* 600, 81, 2009.

PP02

Heat and spin

Sadamichi Maekawa

Japan Atomic Energy Agency, Japan

When metals and semiconductors are placed in a temperature gradient, the electric voltage is generated. This mechanism to convert heat into electric energy, the so-called Seebeck effect, has attracted much attention as the mechanism for utilizing wasted heat energy. The Seebeck effect is due to the entropy carried by the electric current so that it may be enhanced by the internal degrees of freedom of electrons, i.e., spin and orbital [1]. Ferromagnetic insulators are good conductors of spin current, i.e., the flow of electron spins [2]. When they are placed in a temperature gradient, generated is the spin voltage [3], i.e., spin accumulation. Once the spin voltage is converted into the electric voltage by spin Hall effect in attached metal films such as Pt, the electric voltage is obtained from heat. This is called the spin Seebeck effect. Here, we discuss the Seebeck effect and spin Seebeck effect based on the fluctuation-dissipation theorem and introduce a variety of the devices.

[1] S. Maekawa et al, *Physics of Transition Metal Oxides* (Springer, 2004). [2] S. Maekawa: *Nature Materials* 8, 777 (2009). [3] *Concept in Spin Electronics*, eds. S. Maekawa (Oxford University Press, 2006).

PP03

Heavy electrons and superconductivity

Zachary Fisk*

University of California, Irvine, USA

Heavy electron materials are the only class of materials in which we know where to look for superconductivity. We discuss the relation between single ion and dense Kondo heavy electron physics, what sets the energy scale in these materials, and the ways in which their low temperature exotic superconductivity is a prototype for all highly correlated electron superconductivity.

PP04

Correlated electrons in quantum hall systems

Klaus V. Klitzing*

Max-Planck-Institut für Festkörperforschung, Heisenbergstr.1, D-70569 Stuttgart, Germany

The narrow energy bands of a two-dimensional electron system in strong magnetic fields lead to characteristic electron-electron interaction phenomena related to quantum Hall physics. The talk summarizes some of the most prominent correlation phenomena in quantum Hall devices including exciton condensation/superfluidity in bilayers and roton minima in the excitation spectrum of fractional quantum Hall states. * In cooperation with W.Dietsche, X. Huang, I. Kukushkin, and J.H. Smet

PP05

From single-atom magnetometry to tailored nanomagnets and atomic-scale spintronic devices

Roland Wiesendanger*

Institute of Applied Physics, University of Hamburg, Germany

The developments of novel magnetic materials as well as spin-based electronics are hot topics of current research in magnetism. Both research fields could profit tremendously from atomic-scale insight into magnetic properties and spin-dependent interactions at the atomic level. Based on the development of spin-polarized scanning tunneling microscopy (SP-STM) we have recently established the novel method of single-atom magnetometry which allows the measurement of magnetization curves and the determination of magnetic moments on an atom-by-atom basis. While the sensitivity level of single-atom magnetometry is below one Bohr magneton, it can easily be combined with the atomic-resolution imaging and manipulation capabilities of conventional STM, thereby offering a novel approach towards a rational material design based on the knowledge of the atomic-level properties and interactions within the solid state. Moreover, an atom-by-atom design and realization of all-spin logic devices has recently been demonstrated by our group based on the combined knowledge derived from surface physics, nanoscience, and magnetism. Alternatively, self-assembly of atomic magnetic chains on nanostructured substrates has been employed in order to create model-type systems for atomic-scale information transfer based on the concept of vector-spin chirality.

PP06

Multiferroic vortex network with $Z_2 \times Z_3$ symmetry

Sang-wook Cheong*

Rutgers University, USA

Hexagonal REMnO_3 (RE= rare earths) with RE=Ho-Lu, Y, and Sc, exhibit unique patterns of trimerization and ferroelectric domains, which meet in cloverleaf arrangements that cycle through all six-possible domain configurations. Occurring in pairs, the cloverleaves can be viewed as vortices and antivortices, in which the cycle of domain configurations is reversed. Vortices and antivortices are topological defects: even in a strong electric field they won't annihilate readily. These ferroelectric vortices/antivortices are also associated with a vortex configuration of magnetism. The seemingly irregular configurations of a zoo of multiferroic vortices and antivortices in h- REMnO_3 can be neatly analyzed in terms of graph theory and this graph theoretical analysis reflects the nature of self-organized criticality in complexity phenomena. These numerous multiferroic vortices/antivortices can be understood as an arrested Kosterlitz-Thouless phase. We have also discovered the emergence of $Z_2 \times Z_3$ symmetry in the seemingly-random network of numerous ferroelectric vortices, and electric poling or self-poling due to a surface charge boundary condition induces global topological condensation through breaking of the Z_2 part of the $Z_2 \times Z_3$ symmetry. The opposite process of restoring the Z_2 symmetry can be considered as topological evaporation.

PP07

Graphene's magnetism

Andre Geim

University of Manchester, United Kingdom

Graphene - a free-standing atomic plane of graphite - has turned out to be a wonder material. Like a magnet, it has attracted a large and still rapidly growing research community. After a short introduction describing reasons for this interest, I will focus on the main topics of this conference (namely, magnetism and correlations) and overview our recent work on magnetic properties of graphene, which are still poorly understood, and pronounced correlation effects observed in graphene double-layer heterostructures. As for magnetism, I will discuss the spin Hall effect [1] and (para) magnetism of pristine and defected graphene [2,3]. As for correlations, I plan to touch on renormalization of graphene's linear spectrum [4] and Coulomb drag between two Dirac-like systems in the limit of maximum interaction (unpublished but see [5]).

1. D. Abanin et al, *Science* 332, 328 (2011) 2. M. Sepioni et al, *PRL* 105, 207205 (2010) 3. R. Nair et al, *Nature Phys.* 8, 199 (2012) 4. D. Elias et al, *Nature Phys.* 7, 701 (2011) 5. L. Ponomarenko et al, *Nature Phys.* 7, 958 (2011)

HP11

Heavy fermions and unconventional superconductivity in high-Quality single crystals of rare earth and actinide compounds

Yoshichika Onuki¹, Rikio Settai¹, Tetsuya Takeuchi², Kiyohiro Sugiyama¹, Fuminori Honda¹, Yoshinori Haga³, Etsuji Yamamoto³, Tatsuma Daruma Matsuda³, Naoyuki Tateiwa³, Dai Aoki⁴, Ilya Sheikin⁵, Hisatomo Harima⁶ and Hiroshi Yamagami⁷

¹ Graduate School of Science, Osaka University, Japan

² Low temperature Center, Osaka University, Japan

³ Advanced Science Research Center, JAEA, Japan

⁴ IMR, Tohoku University, Japan

⁵ LNCMI-G, CNRS, France

⁶ Department of Physics, Kobe University, Japan

⁷ Department of Physics, Kyoto Sangyo University, Japan

The f electrons in rare earth and actinide compounds exhibit variety of characteristic properties including heavy fermions and unconventional superconductivity. Fermi surface properties in rare earth and actinide compounds such as CeSn3, USi3, NpGe3 and PuIn3 are clarified by the de Haas-van Alphen experiments on the basis of the results of energy band calculations. An abrupt nonlinear increase of magnetization, namely metamagnetic behavior is found in the heavy fermion compounds including YbT2Zn20 (T: Co, Rh, Ir). An effect of pressure on the electronic state of YbT2Zn20 and antiferromagnets CeRhIn5 and CeIrSi3 are also studied in magnetic fields. The electronic instability including unconventional superconductivity occurs at about 2.4 GPa in CeRhIn5 and 2.6 GPa in CeIrSi3.

HP12

Effects of spin-orbit-coupling in the electronic structures of 5d transition metal oxides

T. W. Noh

Physics and Astronomy, Seoul National University, Korea

In 5d transition metal oxides, the magnitude of spin-orbit (SO) coupling becomes comparable to those of other fundamental interactions, such as electron-phonon and on-site Coulomb interactions. Recent investigations of 5d transition metal oxides indeed reveal that the SO coupling can modify their electronic and magnetic structures significantly. Especially, it produces a novel quantum state that has never been observed in 3d and 4d transition metal oxides. Namely, the large SO coupling combined with the on-site Coulomb repulsion results in an unusual Jeff=1/2 Mott insulating state in Sr2IrO4. By changing the dimensionality in Ruddlesden-Popper series, the irridates change from insulator (n=1 and 2) to metal (n=∞). Further studies on double perovskite A2FeReO6 and perovskite (Ca,Sr)IrO3 thin films showed that their electronic structures are indeed determined by subtle interplay of the SO coupling, electron correlation, and lattice distortion. We will present the interesting role of SO coupling by combining the spectroscopic tools with first-principles band calculations. In addition, the layered honeycomb lattice Na2IrO3 and pyrochlore A2Ir2O7 were recently suggested as possible topological insulators, though topological insulators with transition metal d electrons have not been fully investigated. Spectroscopic result on these irridate systems will be also discussed.

HP21

Magnetization dynamics of rashba ferromagnet

Kyoung-whan Kim¹, Soo-man Seo², Jisu Ryu¹, Jung-hwan Moon², Kyung-jin Lee² and Hyun-woo Lee^{2*}

¹ Department of Physics, POSTECH, Korea

² Department of Materials Science and Engineering, Korea University, Korea

Rashba spin-orbit coupling (RSOC) arises generically when structural inversion symmetry is broken. Surface electronic structure of heavy atomic elements such as Bi/Ag alloy [1] is known to exhibit large RSOC with characteristic RSOC parameter of the order of 1 eV·Å. Topological insulator [2,3] is another class of material with large RSOC. Recently it was reported [4] that ultrathin magnetic layers may be subject to large RSOC when in contact with proper heavy metallic elements in strongly asymmetric environment. In this talk, we explore magnetization dynamics of such ultrathin magnetic layers with strong RSOC. It will be demonstrated that RSOC induces the deviation of conduction electron spin direction from local magnetization direction and thus modifies the spin torque [5,6] and current-driven magnetization dynamics properties considerably. We also discuss the phenomenon of the spin-dependent electric field induction [7,8,9] by magnetization dynamics. It will be illustrated that RSOC can strengthen the spin-dependent electric field more than one order of magnitude, so that the field can induce spin current sufficiently large enough to modify the magnetization dynamics itself. Thus ultrathin magnetic layers with strong RSOC are good systems to test various aspects of RSOC effects.

[1] C. R. Ast et al., Phys. Rev. Lett. 98, 186807 (2007). [2] K. Ishizaka et al., Nature Mater. 10, 521 (2011). [3] M. S. Bahramy, B.-J. Yang, R. Arita, and N. Nagaosa, arXiv:1110.6846. [4] I. M. Miron et al., Nature Mater. 9, 230 (2010). [5] J. C. Slonczewski, J. Magn. Mag. Mater. 159, L1 (1996). [6] L. Berger, Phys. Rev. B 54, 9353 (1996). [7] L. Berger, Phys. Rev. B 33, 1572 (1986). [8] G. E. Volovik, J. Phys. C 20, L83 (1987). [9] S. E. Barnes and S. Maekawa, Phys. Rev. Lett. 98, 246601 (2007).

HP22

Giant Ising anisotropy and hastaticorder in URu2Si2 (1,2)

Piers Coleman*

Dept of Physics and Astronomy, Rutgers University, United Kingdom

The hidden order that develops below 17.5K in the heavy fermion compound URu2Si2 has eluded identification for twenty five years. We show that the recent observation of Ising quasiparticles in URu2Si2 suggests a novel two-component order describing hybridization between electrons and the Ising 5f² states of the uranium atoms. This “hastatic order” is distinct from conventional magnetism, breaking both single and double time-reversal symmetry operations, mixing states of different Kramers parity. It accounts for the magnetic anomalies in torque magnetometry and the pseudo-Goldstone mode in neutron scattering. Hastatic order is predicted to induce a basal-plane magnetic moment of order \$0.01\mu_B\$, a gap to longitudinal spin fluctuations that vanishes continuously at the first-order antiferromagnetic transition, a giant Ising anisotropy in the non-linear susceptibility and a narrow resonant nematic feature in the scanning tunneling spectra.

(1) R. Flint, P. Chandra and P. Coleman to be published. (2) Work supported by the Simons Foundation and NSF grant 0907179. (3) M. M. Altarawneh et al., Phys. Rev. Lett. 108, 066407 (2012).

HP31

Electrodynamics of skyrmions

Yoshinori Tokura

Department of Applied Physics, University of Tokyo, Japan

Skyrmions are nanometric spin-swirling vortex-like objects in solids, typically observed in the helimagnets of B20 type (FeSi type) transition-metal silicides and germanides. Due to their topological nature, the spin chirality or skyrmion number can give rise to the fictitious magnetic field acting on conduction electrons; in the strong coupling limit one skyrmion works as a single flux quantum. There, the topological Hall effect of conduction electron is observed in proportion to skyrmion density, while as its counteraction the Hall motion of skyrmions is anticipated in addition to the current-driven sliding motion. Here, we overview the late progress in experimental observations of skyrmions and skyrmion lattices in bulk and thin film forms as well as their spectacular topological transport phenomena. The materials family is now being extended to some multiferroic oxides, in which electric-field drive of the skyrmion would be possible.

HP32

Spin and charge fluctuations in cuprate superconductors

Bernhard Keimer

Max Planck Institute for Solid State Research, Germany

I will present recent inelastic neutron scattering and resonant inelastic x-ray scattering (RIXS) data that throw new light on the role of low-energy spin and charge fluctuations in the mechanism of high-temperature superconductivity and its interplay with competing spin- and charge-density-wave order. I will also discuss parallels and contrasts with iron pnictide superconductors.

M. Le Tacon, G. Ghiringhelli, J. Chaloupka, M. Moretti Sala, V. Hinkov, M.W. Haverkort, M. Minola, M. Bakr, K. J. Zhou, S. Blanco-Canosa, C. Monney, Y. T. Song, G. L. Sun, C. T. Lin, G. M. De Luca, M. Salluzzo, G. Khalilullin, T. Schmitt, L. Braicovich and B. Keimer, Nature Physics 7, 725 (2011).

HP41

The spin on domain walls!

Stuart Parkin

IBM Almaden Research Center, USA

The formation and manipulation of magnetic domain walls (DWs) is of considerable interest both from a scientific as well as a technological perspective. A number of very interesting and potentially useful memory and logic devices based on the controlled manipulation of DWs in magnetic nano-elements have recently been proposed and are under intensive investigation. Using spin torque transfer from spin-polarized currents a series of domain walls can be moved in lock-step at high speed along magnetic nano-wires, enabling the Racetrack Memory [1]. We contrast the current induced motion of DWs in nano-wires with in-plane and out-of-plane magnetization and demonstrate an additional interface induced driving force in the latter case, which leads to very high domain wall velocities of up to almost 1 km/sec. Even higher efficiencies result from temperature gradient induced spin currents which we show are ~1,000 times more efficient in moving DWs than electrically generated spin polarized currents. Many of these devices depend critically on the detailed structure of the DW: we discuss methods by which the chirality and polarity of a vortex DW can be deterministically controlled and we use this to create a chirality based biplexer and ultra-stable domain wall topological bound states.

[1] S.S.P. Parkin, US Patent 6,834,005 (2004); S.S.P. Parkin et al., Science 320, 190 (2008); S.S.P. Parkin, Scientific American (June 2009); M. Hayashi, L. Thomas, R. Moriya, C. Rettner and S.S.P. Parkin, Science 320, 209 (2008); L. Thomas et al., Science 330, 1810 (2010); X. Jiang et al. Nat. Comm. 1:25 (2010) and Nano Lett. 11, 96 (2011); L. Thomas, M. Hayashi, R. Moriya, C. Rettner and S.S.P. Parkin, Nat. Commun. (accepted).

HP42

Orbitronics in silicon

Gabriel Aeppli

University College London, United Kingdom

We describe the control and observation of coherent superpositions of defect orbitals in silicon using both scanning tunneling microscopy and pulsed THz radiation generated by the Dutch-UK free electron laser FELIX. The results are contrasted with those for the microwave control of defect spins, and implications for future silicon-based information processing are discussed.

PNAS 105 10649-10653 (2008) Nature 465 1057-61 (2010) Nature Materials 9 725-9 (2010)

HP51

360 degree domain walls in magnetic nanowires

Caroline A Ross

Department of Materials Science and Engineering, Massachusetts Institute of Technology, USA

Domain walls are important in a wide range of magnetic memory and logic devices. Most work has focussed on isolated 180 degree domain walls in magnetic wires, but impingement of two 180 degree walls can create 360 degree walls which exhibit facinating behavior. 360, 540 and higher order walls are created by successive injection of 180 degree walls into a wire or during reversal of a thin film ring. Current-driven motion of 360 degree domain walls is qualitatively different from that of 180 degree walls. The velocity of a 360 degree wall scales with dc current but is independent of applied field along the stripe, and an annihilation process occurs at a field-dependent critical current density. 360 degree walls oscillate at a characteristic field-tunable frequency in the gigahertz range. The stray field from a 360 degree wall in one layer of a multilayer can affect the reversal of an adjacent soft magnetic layer, allowing the wall to be used as a gate for the reversal of the soft layer. 360 degree walls can be created, moved, annihilated to deliver spinwave energy, and detected, and could serve as a data token in a magnetoelectronic device.

HP52

Perpendicular CoFeB-MgO for spintronics devices

Hideo Ohno*

CSIS/RIEC, Tohoku University, Japan

bcc(100) CoFeB-(100) MgO is a preferred system for spintronics applications, because it offers a large tunnel magnetoresistance (TMR) of > 100% in magnetic tunnel junctions (MTJs) through symmetry filtering of wavefunctions, which is required for nonvolatile memory cells. Integration of high performance MTJs in the CMOS back-end not only enables non-volatile, high density, and fast stand-alone and embedded RAMs, but also makes it possible to realize nonvolatile logic-in-memory CMOS VLSIs [1]. To this end, we showed that a perpendicular interface anisotropy at the CoFeB-MgO interface [2, 3], strong enough (K_i = 1.3 mJ/m²) to overcome the demagnetization, can be used to realize 40 nm perpendicular MgO-CoFeB MTJs with high TMR (>100 %) and low switching current of 49 μA [3]. We further showed that “activation volume” of the system plays an important role in determining the thermal stability of the MTJs [4]. It was also shown that the CoFeB-MgO system withstands a high annealing temperature of 400 °C required for logic integrated circuit applications [5]. If time allows, I will touch upon current-induced domain wall motion and related phenomena in perpendicular CoFeB-MgO films [6, 7], where perpendicular anisotropy is required to reduce the critical current density for domain wall motion.

This work was supported by the FIRST program from JSPS. [1] S. Ikeda, et al. IEEE Trans. Electron Devices, 54, 991, 2007. [2] M. Endo, et al. Appl. Phys. Lett., 96, 212503, 2010. [3] S. Ikeda, et al. Nature Mat., 9, 721, 2010. [4] H. Sato, et al. Appl. Phys. Lett. 99, 042501, 2011. [5] H. D. Gan et al. Appl. Phys. Lett. 99, 252507, 2011. [6] S. Fukami et al. Appl. Phys. Lett. 98, 082504, 2011. [7] T. Suzuki et al. Appl. Phys. Lett. 98, 142505, 2011.

HP61

Geometric enhancement of low field magnetoresistance in silicon

Xiaozhong Zhang

Department of Materials Science and Engineering, Tsinghua University, China

The magnetic sensing industry are greatly dependent on the use of both GMR and TMR devices. Both of them are made of magnetic/rare earth materials. However, the rare earth materials are getting more and more difficult to obtain. Magnetoresistance (MR) reported in some non-magnetic semiconductors particularly silicon has triggered considerable interest owing to the large magnitude of the effect. Here we showed that MR in lightly doped n-Si can be significantly enhanced by introducing a p-n junction and proper design of the carrier path [1]. We designed an MR device whose room-temperature MR ratio reaching 30% at 0.065 T, 5000% at 0.4 T, and 20000% at 1.2T, respectively, approaching the performance of commercial MR devices. The combination of high sensitivity to low magnetic fields and large high-field response should make this device concept attractive to the magnetic field sensing industry. Moreover, because our device is based on a conventional silicon platform, it should be possible to integrate it with existing silicon devices and so aid the development of silicon-based magnetoelectronics. Also combining MR devices and semiconducting devices in a single Si chip may lead to some novel devices.

[1] Caihua Wan, Xiaozhong Zhang, et al., Nature, 477, 304 (2011).

HP62

Artificial spin ice systems: exploring frustration and emergent magnetic monopoles with nanomagnets

Laura Heyderman*

Paul Scherrer Institute, Switzerland

Artificial spin ice systems, consisting of two-dimensional arrangements of dipolar coupled single-domain nanomagnets, are in the focus of scientific interest since they allow the study of the effects of frustration. Our work has concentrated on artificial kagome spin ice, with elongated nanomagnets forming an array of hexagonal rings, using synchrotron x-ray photoemission electron microscopy to directly image the magnetic states. Focussing on finite building blocks comprising one, two and three hexagonal rings, allows the full characterization of the energy levels and indicated that an effective thermal anneal via demagnetisation does not lead to the ground state for the larger structures [1]. More recent observations demonstrate the existence of emergent magnetic monopoles in a quasi-infinite nanomagnet array [2]. In an applied magnetic field, monopole-antimonopole pairs nucleate and separate in an avalanche-type manner along one-dimensional Dirac strings consisting of overturned dipoles, and the behaviour is quantitatively explained by Monte Carlo simulations. This work opens the way to making use of the multiple states in coupled nanomagnet systems [3] and the controlled manipulation of magnetic charges that may lead to new spintronic devices.

[1] E. Mengotti, L.J. Heyderman, A. Fraile Rodriguez, A. Bisig, L. Le Guyader, F. Nolting, and H.B. Braun, Phys. Rev. B 78, 144402 (2008) [2] E. Mengotti, L.J. Heyderman, A. Fraile Rodriguez, F. Nolting, R.V. Hugli, H.B. Braun Nature Physics 7, 68 (2011) [3] L.J. Heyderman, T. Jung, E. Mengotti, A. Bisig, A. Fraile Rodriguez, F. Nolting, H.B. Braun, T. Schrefl United States Patent US 8,085,578 B2, 27.12.2011

HP71

Topological Insulators

Shoucheng Zhang
Physics, Stanford University, USA

In this talk I plan to give an overview of the recent progress on topological insulators. I will focus on the interplay between topological and magnetic orders in novel materials, and discuss the topological magneto-electric effect.

X. L. Qi, S. C. Zhang, Phys. Today 63, 33 (2010). X. L. Qi, S. C. Zhang, Rev. Mod. Phys. 83, 1057 (2011).

HP72

Heusler compounds: from semiconductors to spintronics

Claudia Felser*
Max Planck Institute for Chemical Physics of Solids, Germany

Heusler compounds are a remarkable class of intermetallic materials with 1:1:1 (often called Half-Heusler) or 2:1:1 composition comprising more than 1500 members [1]. New properties and potential fields of applications emerge constantly; the prediction of topological insulators is the most recent example [2]. Surprisingly, the properties of many Heusler compounds can easily be predicted by the valence electron count or within a rigid band approach. The subgroup of more than 250 semiconductors is of high relevance for the development of novel materials for energy technologies. Their band gaps can readily be tuned from zero to 4 eV by changing the chemical composition. Thus, great interest has been attracted in the fields of thermoelectrics and topological insulator research. Ternary materials based on multifunctional properties, i.e. the combination of two or more functions such as superconductivity and topological edge states will revolutionize technological applications. The wide range of the multifunctional properties of Heusler compounds is reflected in extraordinary magneto-optical, magneto-electronic, and magneto-caloric properties. Tetragonal Heusler compounds Mn₂YZ as potential materials for STT applications can be easily designed by positioning the Fermi energy at the van Hove singularity in one of the spin channels [3].

[1] Simple Rules for the Understanding of Heusler Compounds, Tanja Graf, Stuart S. P. Parkin, and Claudia Felser, Progress in Solid State Chemistry (2011), doi:10.1016/j.progsolidchem.2011.02.001, invited review [2] Tunable Multifunctional Topological Insulators in Ternary Heusler Compounds, S. Chadov, X.-L. Qi, J. Kubler, G. H. Fecher, C. Felser, S.-C. Zhang, Nature Mat. 9 (2010) 541, arXiv:1003.0193

AA01

Orbital and spin states of bi-layered manganites La_{2-2x}Sr_{1+2x}Mn₂O₇

Jae-Hoon Park
Pohang University of Science and Technology, Korea

The bi-layer manganites La_{2-2x}Sr_{1+2x}Mn₂O₇ display variety of ordering behaviors involving charge, spin, and orbital degrees of freedom and exhibits various intriguing physical properties. Here I will present soft x-ray scattering study results on the spin states of bi-layer manganites with x = 0.5 and x = 0.3. The x = 0.5 half-doped system exhibits two types of antiferromagnetic spin orders, A-type and CE-type, which both involves the CE-type charge and orbital orders. The results show coupling behaviors between the spin and orbital ordering and also between different spin ordered states. On the other hand, the x = 0.3 system, known as a colossal magnetoresistance manganite, shows a large magneto-elastic response. We found that the spin state is coupled with the orbital state and the magnetic field affects both states resulting in the large magneto-elastic response.

AA02

First-principles calculation of multiferroic bilayer manganite

Kunihiko Yamauchi^{1*} and Silvia Picozzi²
¹ ISIR-Sanken, Osaka University, Japan
² CNR-SPIN, L'Aquila, Italy

'Improper multiferroics', materials where ferroelectricity is driven by spin ordering, charge ordering or orbital ordering, constitute a playground for the physics of cross-correlation between the different long-range orderings [1]. Recently, a complex mechanism of ferroelectricity driven by spin- and charge-orderings has been proposed in hole-doped manganites, supported by theoretical studies [2]. In such system, it is considered that slightly charge-disproportionated two magnetic ions (i.e. Mn³⁺ and Mn⁴⁺) form dimers via double exchange interaction, resulting in sizable electric dipoles. In the particular case of bilayer-manganite Pr(Sr_{0.1}Ca_{0.9})₂Mn₂O₇, it has been experimentally suggested that the transition between two different CO phases is accompanied by the rotation of orbital stripes, in turn related to ferroelectricity [3]. In this paper, we provide insights into the cross-correlation phenomena and the ferroelectric instability in the bilayer manganite via first-principles approaches. Along this line, we also discuss the magnetic property and the stability of charge- and orbital-orderings.

[1] S. Picozzi, and C. Ederer, J. Phys.: Cond. Mat. 21, 303201 (2009). [2] D. V. Efremov, J. van den Brink, and D. Khomskii, Nature Mater. 12, 856 (2004). [3] Y. Tokunaga et al., Nature Mater. 5, 937 (2006).

AA03

Coupling between lattice and spin degrees of freedom in multiferroic h-RMnO₃

Xavier Fabreges^{1*}, Sylvain Petit² and Isabelle Mirebeau²
¹ LNCMI, Toulouse, CNRS, France
² Laboratoire Leon Brillouin, CEA Saclay, France

Hexagonal RMnO₃ forms a class of triangle-based multiferroic materials, which have been widely studied in the recent years [1]. Magnetic frustration combined with a striking magneto-elastic coupling seems to be at the origin of their properties, a cocktail that has a strong potential for novel physics. Here, we report on neutron scattering experiments carried out to study the structure and spin dynamics in this series of compounds. The spinwave spectra can be accounted for by numerical calculations, giving precious informations on exchange and anisotropy parameters [2-4]. Meanwhile, the 120° Neel order due to geometric frustration is accompanied by an isostructural transition [4,5]. This transition is a systematic feature in this series as shown by our high-resolution neutron diffraction and inelastic neutron scattering. In addition, we have established a correlation between the atomic positions, the type of magnetic structure, and the nature of the spin waves, depending on the compound and its magnetic structure. The key parameter is the Mn position within the triangular plane, which tunes the sign of the exchange interaction [4]. Our inelastic neutron scattering experiments also reveal a strong coupling of the Mn sublattice with the rare-earth magnetic moments. The cases of HoMnO₃ and YbMnO₃ are presented.

[1] Cheong S.W and Mostovoy M. Nature materials, 6, 13 (2007) and references therein, [2] S. Petit et al, PRL 99, 266604 (2007), [3] S. Pailhes et al, PRB 79, 134409 (2009), [4] X. Fabreges et al, PRL 103, 067204 (2009), [5] S. Lee et al. Nature 451,805 (2008)

AA04

Magnetoelectric coupling in hematite amplified by the collective transition

J. L. Musfeldt^{1*}, P. Chen¹, N. Lee², S. Mc Gill³ and S. W. Cheong²
¹ Department of Chemistry, University of Tennessee, USA
² Department of Physics, Rutgers University, USA
³ National High Magnetic Field Laboratory, USA

We investigated the magneto-optical properties of alpha-Fe₂O₃ in order to understand the interplay between charge and magnetism in a model transition metal oxide. We discovered that hematite appears more red in applied magnetic field than in zero field conditions, an effect that is amplified by the presence of the spin flop transition. Analysis of the exciton pattern on the edge of the d-d color band reveals C2/c monoclinic symmetry in the high field phase. These findings advance our understanding of magnetoelectric coupling away from the static limit and motivate spectroscopic work on other iron-based materials under extreme conditions.

AA05

Time dependence of multiferroic switching

Max Baum¹, Thomas Finger¹, Simon Holbein¹, Jonas Stein¹, Jeannis Leist², Gotz Eckold², Paul Steffens³, Arno Hiess³, Karin Schmalz³, Petra Becker⁴, Ladislav Bohaty⁴ and Markus Braden¹
¹ II. Physikalisches Institut, Universitat zu Koln, Germany
² Institut für Physikalische Chemie, Georg-August-Universität Göttingen, Germany
³ Institut Laue-Langevin (ILL), Grenoble, France
⁴ Institut für Kristallographie, Universitat zu Koln, Germany

Neutron scattering with spherical polarization analysis gives direct access to the chiral components of the magnetic structure which is directly linked to the electric polarization and thus may be controlled by an electric field. We applied stroboscopic techniques in order to investigate how fast the magnetic chirality adapts to an instantaneously switched electric field in MnWO₄ finding quite long relaxation times in the range of 10 milliseconds. We will discuss the dependence of the multiferroic relaxation on electric field strength, sample thickness and temperature. Furthermore we present the first results on controlling ferrotoroidal domains in LiFeSi₂O₆ by vertical magnetic and electric fields.

AB01

Quantum criticality, non-fermi liquid and unconventional superconductivity

Qimiao Si
Department of Physics and Astronomy, Rice University, USA

Competing orders frequently arise in strongly correlated electron systems, and the accompanying quantum criticality provides a route towards both non-Fermi liquid behavior and unconventional superconductivity. Among the many important questions is whether the theoretical description of quantum criticality conforms to, or goes beyond, the Landau framework of order-parameter fluctuations. Using heavy fermions as a concrete setting, I will summarize the theoretical aspects of local quantum criticality, which is based on the "beyond-Landau" physics of Kondo destruction, as well as the experimental evidence for this picture [1]; the latter includes anomalous dynamical scaling, multiple scales of collapsing energies, and Fermi surface jump. I will also discuss the theoretical reasoning for the emergence of novel magnetic phases and the corresponding global phase diagram [2,3], and attempt to place various quantum-critical heavy fermion compounds in this global phase diagram. Finally, I will outline some promising issues to explore in the future, including the interplay among electron localization (in the form of Kondo destruction in the present context), magnetism and unconventional superconductivity, both in connection with existing experiments [4,5] and as a general theoretical issue.

[1] Q. Si and F. Steglich, Science 329, 1161 (2010). [2] Q. Si, Physica B378, 23 (2006); Phys. Status Solidi B247, 476 (2010). [3] P. Goswami and Q. Si, Phys. Rev. Lett. 107, 126404 (2011). [4] T. Park et al., J. Phys.: Condens. Matter 23, 094218 (2011); H. Shishido et al., J. Phys. Soc. Jpn. 74, 1103 (2005). [5] O. Stockert et al., Nature Phys. 7, 119 (2011).

AB02

Ternary compounds with ZrFe₂Si₂ structure type: A new playground for ferromagnetic and antiferromagnetic quantum criticality

Christoph Geibel^{1*}, Cornelius Krellner¹, Nadang Mufli¹, Helge Rosner¹, Manuel Brando¹, Frank Steglich¹, Stefan Lausberg¹, Alexander Steppke¹, Luis Pedrero¹, Lucia Steinke¹, Robert Kuchler¹, Edith Lengyel¹, Michael Nicklas¹, Christoph Bergmann¹, Katharina Weber¹, Till Goltz², Johannes Spohling², Nicolas Yeché², Hans-henning Klauss², Theo Woike³, Hubertus Luetkens³, Kamil Sedlak⁴ and Christopher Baines⁴
¹ Max Planck Institute for Chemical Physics of Solids, Germany
² Institute for Solid State Physics, Technical University Dresden, Germany
³ Institute for structural Physics, Technical University Dresden, Germany
⁴ Laboratory for Muon-Spin-Spectroscopy, Paul-Scherrer-Institute, Switzerland

The ZrFe₂Si₂ structure type is promising for the search of quantum critical systems because both the Fe and the Zr sublattices present a quasi-one-dimensional character with geometrical frustration. In the last years we prepared several compounds crystallizing in this structure and found two very different kinds of systems close to a quantum critical point (QCP) separating a magnetic ordered ground state from a non-ordered one: in YbNi₃P₂ a strong Kondo interaction acting on the magnetic trivalent Yb-Ions (Ni atoms are non-magnetic) results in a strongly reduced ferromagnetic (FM) ordering temperature of only 170 mK, locating this system close to a FM QCP. In contrast in the AF₂X₂ family of compounds (A = Sc, Y, Lu, Zr, X = Si, Ge) it is the 3d metal Fe which is magnetic while the A-element is non-magnetic. Although the energy scale of magnetic interactions in these compounds is of the order of 200 K, their ground state can be tuned from a frustrated antiferromagnetic ground state with a rather low T_N of 32 K in LuFe₂Ge₂ to a ground state dominated by critical fluctuations in ZrFe₂Si₂. We studied these compounds using different kinds of techniques and shall present and discuss our results.

AB03

Anomalous thermoelectric effects in the heavy fermion superconductor Ce₂PdIn₈

Marcin Matusiak, Daniel Gnida and Dariusz Kaczorowski*
 Institute of Low Temperature and Structure Research, Polish Academy of Sciences, Poland

Ce₂PdIn₈ is a recently discovered [1,2] ambient-pressure heavy-fermion superconductor that in many aspects closely resembles the structurally related compound CeCoIn₅. In particular, the superconducting gap that opens at T_c = 0.7 K [3-5] exhibits a nodal character and a magnetic-field-induced quantum critical point (QCP) resides near the upper critical field H_{c2}(0) = 2.4 T [3,4]. Moreover, the necessary conditions for the formation of modulated FFLO phase are met in the superconducting state of Ce₂PdIn₈, and this unique phase possibly appears in the low-temperature-high-field corner of the H-T phase diagram [3]. The reported Nernst effect (ν) and thermoelectric power (S) studies were performed for Ce₂PdIn₈ with the main aim at probing QCP in the temperature region, in which distinct non-Fermi liquid features were previously revealed in the electrical resistivity and heat capacity data [1-5]. In a manner markedly similar to CeCoIn₅, the Nernst coefficient of Ce₂PdIn₈ becomes greatly enhanced and field-dependent in the coherent Kondo state. Both thermoelectric coefficients behave highly anomalously at low temperatures, namely the ratios S/T and ν/T diverge logarithmically towards T = 0. The observed behaviors strongly support a 2D antiferromagnetic spin-density-wave scenario of the quantum criticality in Ce₂PdIn₈, recently inferred from the thermodynamic data [4].

[1] D.Kaczorowski, A.Pikal, D.Gnida, and V.H.Tran, *Phys. Rev. Lett.* **103** (2009) 027003; *ibid* **104** (2010) 059702. [2] D.Kaczorowski, D.Gnida, A.Pikal, and V.H.Tran, *Solid State Commun.* **150** (2010) 411. [3] J.K.Dong, H.Zhang, X.Qiu, B.Y.Pan, Y.F.Dai, T.Y.Guan, S.Y.Zhou, D.Gnida, D.Kaczorowski, and S.Y.Li, *Phys. Rev. X* **1** (2011) 011010. [4] Y.Tokura, P.Gegenwart, D.Gnida, and D.Kaczorowski, *Phys. Rev. B* **84** (2011) 140507(R). [5] V.H.Tran, D.Kaczorowski, R.T.Khan, and E.Bauer, *Phys. Rev. B* **83** (2011) 064504.

AB04

Pressure driven quantum critical point in CeNiAsO

Yongkang Luo¹, Leonid Pourovskii², Stephen Rowley³, Yuke Li⁴, Chunmu Feng¹, Antoine Georges¹, N. P. Ong², Jianhui Dai¹, Guanghan Cao¹ and Zhuan Xu^{1*}
¹ Department of Physics, Zhejiang University, China
² Centre de Physique Théorique, Ecole Polytechnique, France
³ Department of Physics, Princeton University, USA
⁴ Department of Physics, Hangzhou Normal University, China

We perform a systematic investigation on the pressure effect on the antiferromagnetic dense Kondo lattice CeNiAsO [1]. Both hydrostatic pressure and chemical pressure (i.e. P-for-As doping) are successful in tuning the electronic state to get a pressure driven quantum critical point. We found that ST₁{N1} decreases slowly with initial pressure, but 'suddenly' disappears around 4 kbar. In contrary to the first-order-like quantum phase transition of ST₁{N1}, ST₁{N2} is continuously suppressed with increasing pressure. A QCP like phase transition is observed near 6.7 kbar, where ST₁{N2} is totally suppressed, and non-Fermi-liquid (non-FL) behavior is observed, accompanied with a 'divergent' density of state (DOS) and a sign change of Hall coefficient. In the highly pressurized condition, it exhibits as a typical Kondo lattice metal. In P doped CeNiAs_{1-x}P_x samples, the chemical pressure leads to similar phenomena, with the critical doping level x_c = 0.4. Magnetic susceptibility measurement points to the delocalization of Ce-4f electrons. Band structure and Fermi surface topology of CeNiAsO and CeNiPO were calculated by the method of LDA+DMFT. A new hole pocket contributed by Ce 4f band emerges in CeNiPO. The calculated Kondo scales for CeNiAsO and CeNiPO are T_K = 15 K and 527 K respectively, which qualitatively agrees with the experiment.

[1] Yongkang Luo, et al. CeNiAsO: an antiferromagnetic dense Kondo lattice. *J. Phys.: Condens. Matter* **23**, 175701 (2011). [2] Philipp Gegenwart, et al. Quantum criticality in heavy-fermion metals. *Nature Physics* **4**, 186-197 (2008).

AC01

HgTe as a topological insulator

Laurens Wigbolt Molenkamp
 Experimental Physics 3, University of Wuerzburg, Physics Institute, Germany

HgTe is a zincblende-type semiconductor with an inverted band structure. While the bulk material is a semimetal, lowering the crystalline symmetry opens up a gap, turning the compound into a topological insulator. The most straightforward way to do so is by growing a quantum well with (Hg,Cd)Te barriers. Such structures exhibit the quantum spin Hall effect, where a pair of spin polarized helical edge channels develops when the bulk of the material is insulating. Our transport data provide very direct evidence for the existence of this third quantum Hall effect, which now is seen as the prime manifestation of a 2-dimensional topological insulator. To turn the material into a 3-dimensional topological insulator, we utilize growth induced strain in relatively thick (ca. 100 nm) HgTe epitaxial layers. The high electronic quality of such layers allows a direct observation of the quantum Hall effect of the 2-dimensional topological surface states. Moreover, on contacting these structures with Nb electrodes, a supercurrent is induced in the surface states.

AC02

Spin liquid and spin glass states in frustrated magnets

Seung-hun Lee
 University of Virginia, USA

In frustrated magnets, the topology of the magnetic interactions between magnetic moments leads to macroscopic ground state degeneracy. The nature of the ground states that emerge in frustrated magnets is yet to be understood. In this talk, I will discuss a few examples that exhibit spin liquid and spin glass behaviors at low temperatures. I will present some simple and eloquent ways of thinking about the complex frustrated magnetic interactions that help us greatly to understand the nature of the ground states and their low energy excitations.

AC03

A novel magnetic order of ZnCr₂O₄ revealed by magneto-optical measurements in ultra-high magnetic fields of up to 600 T

Atsuhiko Miyata^{1*}, Shojiro Takeyama¹ and Hiroaki Ueda²
¹ Institute for Solid State Physics, University of Tokyo, Japan
² Department of Chemistry, Graduate School of Science, Kyoto University, Japan

Cr³⁺ ions in ACr₂O₄ (A = Zn, Cd, Hg) form a pyrochlore lattice and these compounds are regarded as geometrically frustrated magnets. CdCr₂O₄ and HgCr₂O₄ exhibit diverse magnetic phases including a 1/2 plateau phase under magnetic fields, which can be described by a theory taking account of a spin-lattice coupling by Penc et al.. On the other hand, ZnCr₂O₄ shows a quite-small spin-lattice coupling, and there are high possibilities that another novel magnetic phases exist in ZnCr₂O₄. We investigated magnetic phases of ZnCr₂O₄ by the Faraday rotation and magneto-optical absorption spectral measurements up to 600 T by the electro-magnetic flux compression method. A ferromagnetic phase transition was observed at 410 T and 4.6 K. Furthermore, an unambiguous anomaly was found in magneto-optical absorption spectra at lower magnetic field side of the ferromagnetic phase. This indicates existence of a novel magnetic phase which could only be explained by a theory beyond that by Penc et al.. A magnetic structure of the novel phase was inferred from analogical consideration with quantum phases in 4He, based upon similarity of a symmetry breaking. As a result, we concluded that the novel phase corresponds to a magnetic "superfluid" state with an umbrella-like magnetic structure.

[1] M. Przybylski, M. Dabrowski, U. Bauer, M. Cinal, M. Przybylski, J. Kirschner, *J. Appl. Phys.*, in print (2012). [2] U. Bauer, M. Dabrowski, M. Przybylski, J. Kirschner, *Phys. Rev. B* **84**, 144433 (2011). [3] J. Li, M. Przybylski, F. Yildiz, X.-D. Ma, Y. Wu, *Phys. Rev. Lett.* **102**, 207206 (2009).

AC04

Origin and signatures of magnetic chirality in the frustrated multiferroic Ba₃NbFe₃Si₂O₁₄

Andrej Zorko¹, Virginie Simonet² and Rafik Ballou²
¹ Jozef Stefan Institute, Slovenia
² Institut Neel, CNRS and Université Joseph Fourier, France

Geometrical frustration is the key promoter of exotic collective magnetic ground states in condensed matter, including spin liquids, spin ice and unconventional spin orders. On frustrated lattices, the dominant isotropic exchange interactions are often unable to raise the degeneracy of the ground state. Then, minute magnetic-anisotropy terms can become crucial for selecting the ground state. The acentric Fe-Langasite Ba₃NbFe₃Si₂O₁₄ features a frustrated arrangement of spin-5/2 Fe³⁺ ions on vertices of equilateral triangles arranged into 2D triangular lattice [1]. It has been drawing considerable attention due to its multiferroic properties and its unique magnetic ground state. The long-range magnetic order that develops simultaneously with the electric polarization below TN = 26 K is a unique double-chiral single-domain state, whose realization appears mysterious [1]. Recently, we have extended research of the chiral properties of Ba₃NbFe₃Si₂O₁₄. Our inelastic neutron scattering study has revealed that one of the two excitation branches is completely chiral over the whole energy spectrum, which is a unique dynamical fingerprint of the chiral ground state [2]. Moreover, our electron spin resonance investigation has unveiled the origin of the mysterious selection of the ground state [3]. We will highlight the crucial role of minute Dzyaloshinsky-Moriya magnetic anisotropy in this system.

[1] K. Marty, V. Simonet, E. Ressouche, R. Ballou, P. Lejay, and P. Bordet, *Phys. Rev. Lett.* **101**, 247201 (2008). [2] M. Loire, V. Simonet, S. Petit, K. Marty, P. Bordet, P. Lejay, J. Olivier, M. Enderle, P. Steffens, E. Ressouche, A. Zorko, and R. Ballou, *Phys. Rev. Lett.* **106**, 207201 (2011). [3] A. Zorko, M. Pregelj, A. Potocnik, J. van Tol, A. Ozarowski, V. Simonet, P. Lejay, S. Petit, and R. Ballou, *Phys. Rev. Lett.* **107**, 257203 (2011).

AD01

Investigating magnetic dipolar interactions between Co nano-islands with spin-polarized scanning tunneling microscopy

Chun-i Lu, Pin-jui Hsu, Szu-wei Chen, Yu-hsun Chu, Chuang-han Hsu, Wang-jung Hsueh and Minn-tsong Lin^{1,2*}
¹ Department of Physics, National Taiwan University, 10617 Taipei, Taiwan
² Institute of Atomic and Molecular Sciences, Academia Sinica, 10617 Taipei, Taiwan

In application of spin-polarized scanning tunneling microscopy (SP-STM), we investigated magnetic interaction in nanometer scale between triangular Co nano-islands formed in the sub-monolayer Co deposited on Cu(111) substrate. The SP-STM images the magnetization or the relative spin configuration of the Co islands. The results indicate a competition between exchange coupling and dipolar interaction in nanometer scale among the conjoint Co islands. The parallel magnetization of a set of conjoint Co nano-islands is anticipated due to the ferromagnetic exchange coupling. However, significant numbers of sets with anti-parallel ordering can still be observed. In order to explain the anti-parallel data, we calculate the dipolar interaction between conjoint Co islands to realize if it is comparable with the exchange coupling strength, which could be correlated to the length of contact region. As a result, the SP-STM images and the statistical data indicate a competition between the dipolar interaction and the exchange coupling in nanometer scale. The anti-parallel configuration, in which dipolar energy dominates, is shown to be limited by the contact length of two conjoint islands, which scales the strength of exchange coupling.

AD02

Temperature-driven oscillatory magnetic anisotropy in ultrathin ferromagnetic films

Maciej Dabrowski¹, Uwe Bauer¹, Marek Przybylski^{1*}, Marek Cinal², Emmanuelle Jal³, Jean-marc Tonnerre³ and Jurgen Kirschner¹
¹ Max-Planck-Institut für Mikrostrukturphysik, Halle, Germany
² Institute of Physical Chemistry of Polish Academy of Sciences, Warszawa, Poland
³ Institut Neel, CNRS & Université J. Fourier, Grenoble, France

A contribution of quantum well states (QWS) to magnetic anisotropy energy (MAE) can be expected if the spread of the Fermi function is much smaller than the energy difference between the two states of each QWS pair contributing to the MAE [1]. Such a temperature effect on MAE is shown and discussed e.g. for fcc-Co films on vicinal surfaces of Cu(001) [2] and for bcc-Fe films on vicinal surfaces of Ag(001) [3]. In particular, the role of QWS in the vicinity of a spin reorientation transition is analyzed in the context of a model describing the anisotropy of ferromagnetic (FM) films grown on vicinal surfaces. The model reproduces not only oscillatory behavior of the uniaxial step-induced anisotropy, but also of the oscillatory tilting angle of magnetization. Interestingly, a small amount of e.g. Au on top of an Fe film completely changes how the magnetic anisotropy evolves with varying thicknesses of an Fe film. More details on the depth profile of the FM magnetization due to QWS are obtained from soft x-ray resonant magnetic reflectivity (SXRMR). In particular, it is found that the magnetization is not homogeneous in all Fe atomic layers.

[1] M. Przybylski, M. Dabrowski, U. Bauer, M. Cinal, M. Przybylski, J. Kirschner, *J. Appl. Phys.*, in print (2012). [2] U. Bauer, M. Dabrowski, M. Przybylski, J. Kirschner, *Phys. Rev. B* **84**, 144433 (2011). [3] J. Li, M. Przybylski, F. Yildiz, X.-D. Ma, Y. Wu, *Phys. Rev. Lett.* **102**, 207206 (2009).

AD03

Magnetism of ultrathin Fe films on BaTiO₃(001)

Seolun Yang¹, Jae-sung Kim^{1*}, Xumin Chen², Axel Enders², Jan Honolka³, Violetta Sessi⁴, Tiffany Santos⁵ and Matthias Bode⁶
¹ SookMyung Women's University, Korea
² University of Nebraska, Lincoln, USA
³ Max Plank Institute for Solis state physics, Germany
⁴ European synchrotron research facility, France
⁵ Argon National Laboratory, USA
⁶ University of Wuerzburg, Germany

Pristine (< 1 monolayer (ML)) Fe films can be grown on BaTiO₃(001) template [1] around 10 K by thermal evaporation. X-ray magnetic circular dichroism revealed superparamagnetism of the Fe films due to their cluster formation. Their saturation magnetic moments increase with the increase of the coverage, reaching beyond that of bulk Fe for 0.7 ML, which indicates that the clusters coalesce to form extended film, while the thickness of the clusters are thicker than 1 ML as found in our scanning tunneling microscopy. Fe films show in-plane easy axis, in contrast to the prediction of perpendicular magnetic anisotropy for flat 1 ML film. Their in-plane easy axis may be attributed to magnetoelastic anisotropy of the strain, multilayer formation of the Fe films and also atoms at highly populated edge sites. Fe films are found to induce magnetic moments of Ti, but none of Ba ions as predicted by first principles calculations.[1]

[1]X. Chen, S. Yang, J.-H. Ki, H.-D. Kim, J.-S. Kim, G. Rojas, R. Skomski, H. Lu, A. Bhattacharya, T. Santos, N. Guisinger, M. Bode, A. Gruvermann, and A. Enders, submitted to *New J. Phys.* **13** 083037 (2011). [2]C.-C. Duan, S. S. Jaswal, and E. Y. Tsymlal, *Phys. Rev. Lett.* **97** 047201 (2006).

AD04

Thickness-dependent exchange splitting of EuO ultrathin films

Hidetoshi Miyazaki^{1*}, Tetsuya Hajiri², Masaharu Matsunami³, Takahiro Ito² and Shin-ichi Kimura³
¹ Center for Fostering Young and Innovative Researchers, Nagoya Institute of Technology, Japan
² Graduate School of Engineering, Nagoya University, Japan
³ UVSOR, The Graduate University for Advanced Studies, Japan

EuO is a ferromagnetic semiconductor with the Curie temperature (TC) of about 70 K [1]. In the electron doping case by the substitution of trivalent ions, such as La³⁺, TC increases to the temperature as high as 200 K [2]. To apply EuO to spintronics devices such as spin filter tunnel barriers, it is important to fabricate ultrathin films with a few atomic layers and to clarify the electronic structure including the exchange splitting energy as well as the TC. Recently, we succeeded to fabricate single-crystalline EuO ultrathin films by a molecular beam epitaxy method [3]. Using the three-dimensional angle-resolved photoemission spectroscopy, we observed the electronic structure of the EuO ultrathin films. Then we could determine the thickness-dependent exchange splitting energy and clarify the mechanism of the changing magnetic property with decreasing thickness. Both of TC and the exchange splitting energy gradually decrease with decreasing thickness. The decrease of the hybridization intensities between the Eu 4f and O 2p states and between the Eu 4f and Eu 5d states due to the decrease of the neighbor atom number are the origin of the change of the magnetic properties of EuO ultrathin films.

[1] A. Mauger et al., *J. Phys. (Paris)* **39**, 1125 (1978). [2] H. Miyazaki et al., *Appl. Phys. Lett.* **96**, 232503 (2010). [3] H. Miyazaki et al., *Submitted to J. Phys. Conf. Series*.

AE01

Magnetoelectric control of magnetic anisotropy in ultrathin Fe films using a charge-trap heterostructure

Uwe Bauer¹, Marek Przybylski², Jurgen Kirschner² and Geoffrey Beach^{1*}
¹ Materials Science and Engineering, MIT, USA
² Max-Planck-Institut für Mikrostrukturphysik, Germany

Magnetoelectric switching of the magnetization vector could enable new low-power logic devices and non-volatile memory cells. Magnetoelectric switching typically requires complex multiferroic oxides or strain coupled magnetostriictive/piezoelectric composites. However, recently it has been shown that surface magnetic anisotropy in ultrathin ferromagnetic metal films can be directly controlled by application of a gate voltage across an adjacent oxide layer [1]. Unfortunately, magnetoelectric effects in metals require a relatively large electric field and are inherently volatile. In this work [2], we examine magneto-electric switching in ultrathin epitaxial Fe films on Ag(001). We show that a charge-trapping layer integrated into the gate dielectric can provide the missing non-volatility to the magnetoelectric effect and enhances its efficiency by an order of magnitude. We report the largest voltage-induced change to surface magnetic anisotropy yet demonstrated for a metallic thin film, and directly correlate this change with the density of trapped charge in an adjacent charge storage layer. We also demonstrate a novel optical charge pumping mechanism, which offers the unique possibility of optical imprinting of the magnetic state in a continuous Fe film. Supported by the National Science Foundation through grant ECCS-1128439.

[1] T. Maruyama et al. *Nature Nanotechnology* **4**, 158 - 161 (2009) [2] U. Bauer, M. Przybylski, J. Kirschner, and G. S. D. Beach, *Nano Letters* ASAP DOI: 10.1021/nl204114t (2012).

AE02

The origin of electric-field effects on magnetic anisotropy in FePd ultrathin film

Shinya Haraguchi¹, Yuusaku Taguchi¹, Masahito Tsujikawa² and Tatsuki Oda^{3*}

¹ Graduate School of Natural Science and Technology, Kanazawa University, Japan

² CSIS, Tohoku University, Japan

³ Institute of Science and Engineering, Kanazawa University, Japan

The electric-field (EF) (assisted) magnetization reversal technique that has the advantage of low-power consumption has been suggested. The EF dependence measurement on the coercivity or the magnetic anisotropy in FePt[1] and FePd[1,2] thin films has been reported. We have performed theoretical analysis for EF effects on magnetic anisotropy energy (MAE) in Pt/Fe/Pt(001)[3] and Pd/Fe/Pd(001)[4] thin films and found that these systems show the inverse EF effect between the Pt and Pd systems. It was also found that this effect corresponds well to the experimental observations [1,2]. The microscopic origin for the inverse issue has not been discussed deeply, although the systems of Pt and Pd are similar to each other. The distinct property of Pd against Pt is magnetic polarization. In order to clarify origins for the inverse effect in Pd/Fe/Pd(001), by using the density functional calculation, we have further estimated MAE and its EF effect in the several sets of spin-orbit coupling choice for atoms. As a result, we found that the contribution from the Pd substrate is very important in the inverse issue. In the presentation, we will show results of MAE density map in real space and discuss comparison with the Pt system.

[1] M. Weisheit et al., *Science* 315, 349 (2007). [2] F. Bonell et al., *Appl. Phys. Lett.* 98, 232510 (2011). [3] M. Tsujikawa and T. Oda, *Phys. Rev. Lett.* 102, 247203 (2009). [4] S. Haraguchi et al., *J. Phys. D: Appl. Phys.* 44, 064005 (2011).

AE03

Ferroelectric control of spin polarization

Manuel Bibes^{1*}, Vincent Garcia¹, Sergio Valencia², Arnaud Crassous¹, Laura Bocher³, Alexandre Gloter³, Stephane Fusil¹, Karim Bouzehouane¹, Xavier Moya⁴, Neil D Mathur¹ and Agnes Barthelemy¹

¹ Unite Mixte de Physique CNRS/Thales, France

² HZB Berlin, Germany

³ Lab. Physique des Solides, Orsay, France

⁴ University of Cambridge, United Kingdom

A current drawback of spintronics is the large power required for magnetic writing. Aiming at a non-volatile low-power electrical control of spintronics properties we have combined two ferromagnetic electrodes (namely La_{0.7}Sr_{0.3}MnO₃ and Fe or Co) with a ferroelectric BaTiO₃ tunnel barrier. We have found that the TMR depends on the direction of the ferroelectric polarization in the barrier. This demonstrates a local, large, and nonvolatile control of spin polarization by electrically switching ferroelectric polarization. Interestingly, just as ferroelectricity in the BaTiO₃ influences the spin polarization of the adjacent Fe or Co magnetic electrodes, magnetism is induced by the electrodes in the ferroelectric. We have used soft X-ray resonant magnetic scattering to evidence that, in addition to being ferroelectric, the BaTiO₃ barrier possesses a hysteretic magnetization at room temperature. Ab initio calculations of realistic interface structures provide insight into the origin of the induced moments and perspectives towards new multifunctional interfaces for spintronics.

V. Garcia et al, *Science* 327, 1106 (2010) ; S. Valencia et al, *Nature Mater.* 10, 753 (2011) ; L. Bocher et al, *Nano Lett.* 12, 376 (2012) ; Financial support from ERC advanced grant no. 267579.

AE04

Voltage controlled spin transport channel

Hyuk-jae Jang^{1*}, Oleg A. Kirillov², Oana D. Jurchescu³ and Curt A. Richter²

¹ NIST & WFU, USA

² NIST, USA

³ Physics, Wake Forest University, USA

Two-terminal metal-oxide-based devices in which memory-resistive(memristive) switching occurs show great potential for use in next generation technologies such as non-volatile memories and neural networks[1,2]. It has been reported that TaO_x-based devices combined with Cu and Pt electrodes show memristive behavior utilizing metal precipitation to create conductive channel (tens of nanometers in diameter) inside of the oxide thin film when an electric voltage (only around 1V between two electrodes sandwiching the oxide layer) is applied[3]. This unique mechanism can deliver an opportunity to explore a new type of technological application, an electron spin transport channel controlled by an external voltage. We have explored this possibility by investigating devices with a TaO_x thin film sandwiched between two ferromagnetic metal electrodes. Three different sets of devices, Co/TaO_x/Cu/Py, Py/TaOx/Cu/Co, and Co/TaO_x/Py were prepared in cross-bar shape. Only devices with a Cu layer show memristive behavior having a typical OFF/ON resistance ratio of 10³. Magnetoresistance measurements performed by sweeping an external magnetic field display evidence of spin transport in the low-resistance ON-state at 77 K. No magnetoresistance was detected in the OFF-state indicating spin transport vanishes. Our study illustrates that we experimentally realized a continuous electron spin transport channel controlled by a low power voltage[4].

[1] J. J. Yang et al., *Appl. Phys. Lett.* 97, 232102 (2010). [2] S. H. Jo et al., *Nano Lett.* 10, 1297 (2010). [3] T. Sakamoto et al., *Appl. Phys. Lett.* 91, 092110 (2007). [4] H.-J. Jang et al., *Appl. Phys. Lett.* 100, 043510 (2012).

AE05

Zeeman-type spin splitting controlled by an electric field

Hongtao Yuan^{1*}, Mohammad Saeed Bahramy², Kazuhiro Morimoto¹, Kentaro Nomura³, Hidekazu Shimotani¹, Ryotaro Arita¹, Christian Kloc¹, Naoto Nagaosa¹ and Yoshihiro Iwasa¹

¹ Department of Applied Physics, University of Tokyo, Japan

² CREG, RIKEN, Japan

³ Department of Physics, Tohoku University, Japan

⁴ School of Materials Science and Engineering., Nanyang Technological University, Singapore

Electrically manipulating electron spins based on Rashba-type spin-orbit interaction (SOI) is a key path-way for applications of spintronics and spin-based quantum computing. Two-dimensional electronic system (2DES) is a particularly important SOI platform, where the in-plane spin polarization can be tuned with an electric field perpendicular to the 2DES (also spins). In contrast, electric manipulation of out-of-plane polarized spins remains elusive and a great challenge though it is known beneficial for longer spin lifetime. Here, we present a new concept, in which an out-of-plane spin polarization is realized and further controlled with the external perpendicular electric field (parallel to polarized spins), by combining the first-principle calculations and magnetotransport experiments in a field effect transistor made of the transition metal dichalcogenide WSe₂. Such an out-of-plane spin splitting is shown to take place at the corners of WSe₂ Brillouin Zone in a form of Zeeman-type spin polarization, due to the exposure of a large but hidden in-plane electric dipole of WSe₂ layers, thereby enabling new degrees of control for quantum confined spintronic devices.

AF01

Femtosecond magnetically induced lattice distortions in multiferroic TbMnO₃

Helen Walker^{1*}, Francois De Bergevin², Federica Fabrizio³, Luigi Paolasini², Andrew Boothroyd³, Dharmalingam Prabhakaran³ and Desmond Memmorrow⁴

¹ Resonant Scattering and Diffraction Beamline P09, PETRA III, HASYLAB at DESY, Germany

² European Synchrotron Radiation Facility, France

³ Department of Physics, University of Oxford, United Kingdom

⁴ London Centre for Nanotechnology, University College London, United Kingdom

The discovery of the canonical spin-cycloid multiferroic TbMnO₃ [1], in which the onset of a spontaneous ferroelectric polarization is concomitant with a magnetic phase transition, has generated considerable interest in the control of electric polarization by magnetic fields, and vice versa. Although comprehensive, microscopic descriptions of the magnetic structure have been obtained, our understanding of the ferroelectric state is still developing. Competing theoretical models proposed to explain the ferroelectricity are associated with either ionic displacements, arising due to antisymmetric exchange interactions [2], or charge transfer [3]. By exploiting the magneto-electric coupling in TbMnO₃, we used an electric field to produce a single magnetic domain state, and a magnetic field to induce ionic displacements. Under these conditions, interference charge-magnetic x-ray scattering arose, encoding the amplitude and phase of the displacements. When combined with a theoretical analysis, our data allow us to resolve ionic displacements at the femtosecond which contribute a significant fraction of the zero-field ferroelectric moment, and reveal that both symmetric and antisymmetric Dzyaloshinskii-Moriya interactions need to be included into the microscopic models [4]. Thus our results represent an important step forward towards the goal of realising the technological potential of these materials.

[1] T. Kimura et al., *Nature* 426 55 (2003) [2] I. A. Sergiyenko & E. Dagotto, *Phys. Rev. B* 73 094434 (2006) [3] H. Kasura, N. Nagosa, A. V. Balatsky, *Phys. Rev. Lett.* 95 057205 (2005) [4] H. C. Walker et al., *Science* 333, 1273 (2011)

AF02

Direct measurement of the interatomic distance dependence of the magnetic exchange interaction

Alexander Schwarz^{1*}, Rene Schmidt¹, Cesar Lazo², Stefan Heinze² and Roland Wiesendanger¹

¹ Institute of Applied Physics, University of Hamburg, Germany

² Christian-Albrecht University Kiel, Germany

Recently, we demonstrated the feasibility to utilize the short-ranged magnetic exchange interaction to map spin textures of surfaces with atomic resolution on insulators [1] as well as on metals [2] with magnetic exchange force microscopy. Even more promising is the spectroscopic mode, i.e., magnetic exchange force spectroscopy (MEXFS), which enabled us to directly probe the distance dependence of magnetic exchange interaction [3]. The experimental data were acquired with a magnetically coated tip on the antiferromagnetic Fe monolayer on W(110). First, the distance dependence of the total tip-sample interaction was measured on Fe surface atoms of oppositely oriented magnetic moments. Thereafter, the magnetic contribution was obtained by subtracting both curves from each other. This approach guarantees that all non-magnetic interactions, e.g., the short-ranged chemical interaction and the long-range van der Waals interaction, cancel out. The result, i.e., the magnetic exchange interaction, exhibits excellent agreement with ab-initio calculations based on density functional theory performed for the same tip-sample system.

[1] U. Kaiser, A. Schwarz and R. Wiesendanger, *Nature* 446, 522 (2007). [2] R. Schmidt et al., *Nano Lett.* 9, 200 (2009). [3] R. Schmidt et al., *Phys. Rev. Lett.* 106, 257202 (2011).

AF03

Magnetic nanodomains in manganites revealed by Lorentz TEM and small-angle electron scattering

Yoshihiko Togawa¹, Tsukasa Koyama², Ken Harada² and Shigeo Mori²

¹ Nanoscience and Nanotechnology Research Center, Osaka Prefecture University, Japan

² Department of Materials Science, Osaka Prefecture University, Japan

La_{1-x}Sr_xMnO₃ (LSMO) shows a complex variety of magnetic and electronic ground states, which depend on the Sr doping concentration (x). Here, we have thoroughly examined magnetic microstructures in single crystals of LSMO by using low-temperature Lorentz transmission electron microscopic (TEM) and small angle electron scattering experiments. The magnetic stripe domains with periodic separation of approximately 200 nm are formed in the orthorhombic structure of La_{1-x}Sr_xMnO₃ for x ~ 0.175 in the zero magnetic field. An in-situ Lorentz TEM observation revealed that, when the vertical magnetic field is applied by utilizing the magnetic field of object lens, the magnetic stripe domains change into a form of the magnetic vortex with the 100 nm size. These magnetic nanodomains with chiral spin configuration (magnetic vortex) are new kinds of magnetic ground states (spin textures) in manganites. In the presentation, we will explain detailed responses of magnetic vortices to external magnetic fields and discuss the nucleation and growth mechanism of magnetic vortices in the magnetic stripe domains.

[1] Y. Togawa, T. Koyama, M. Kobayashi, K. Takayanagi, K. Harada, and S. Mori, submitted.

AF04

Morin transition control of antiferromagnetic α-Fe₂O₃ films with epitaxial strains

Seonghun Park¹, Jae-hoon Park² and Jae-young Kim^{3*}

¹ department of physics, POSTECH, Korea

² department of physics, POSTECH, Korea

³ Pohang Accelerator Laboratory, Korea

It is well known that hematite(α-Fe₂O₃) undergoes a spin reorientation transition at around 263 K. It is Morin transition only found in hematite and some orthoferrites. J.O. Artman, J.C. Murphy, and S. Foner suggested that it is caused by the competition between the single ion anisotropy and the magnetic dipole anisotropy[1]. Their model has been confirmed with the fine particles and pressurized single crystal and it becomes clear that the lattice constants in c-plane are critical to determining the Morin temperature [2,3]. However, when Fe₂O₃ are grown in the form of epitaxial films, no one has observed the transition despite the expectation that the epitaxial strain can be controlled better in the form of films [4,5]. In this work, we have grown a series of epitaxial α-Fe₂O₃ films on Al₂O₃ substrates. The lattice constants of them are successfully controlled with the Cr₂O₃ buffer layer and the strain relaxation. We found that the Morin temperature changes consistently with the lattice constants and it reaches 360 K for thinnest film. The results are well in accordance with the theoretical model. This research was supported by NRF funded by MEST (2009-0088969, 2010-0018733).

J.O. Artman, J.C. Murphy, and S. Foner, *Phys. Rev.* 138, 912 (1965). 2. N. Yamamoto, *J. Phys. Soc. Jpn.* 24, 23 (1968) 3. R.C. Wynn and D.H. Anderson, *Phys. Rev.* 155, 496 (1967) 4. S. Gota, M. Gautier-Soyer, and M. Sacchi, *Phys. Rev. B*, 64, 22407 (2007) 5. A. Barbier, R. Bellhou, P. Ohresser, M. Gautier-Soyer, O. Bezenconet, M. Mulazzi, M.-J. Guinet, and J.-B. Moussy, *Phys. Rev. B*, 72, 245423 (2005)

AF05

Surface plasmons and magneto-optical activity in hexagonal Ni anti-dot arrays

Emil Melander*, Evangelos Papaioannou, Vassilios Kapaklis and Bjorgvin Hjorvarsson

Department of Physics and Astronomy, Division of Materials Physics, Uppsala University, Sweden

The interaction between the surface plasmon polaritons (SPPs) and a magnetic field in a pure magnetic metal is presented in this work. By utilizing nano patterned structures one can create plasmonic resonances on magnetic surfaces. We have investigated how hexagonal arrays of circular holes (250-275 nm) in a Ni matrix (anti-dot arrays) couple to plasmonic resonances and therefore how it changes the optical and magneto-optical spectra. We have performed angularly resolved scans of the reflectivity and transmission with and without application of magnetic field and compared them to theoretical calculations. We present signatures of SPPs as troughs in reflectivity and extraordinary transmission through the holes. In the plasmonic regimes a big enhancement of the magneto-optical response (polar moke) is observed. Application of a transverse magnetic field influences the excitation of SPPs as it can be seen by the big increase of magnetic contrast measured in the transverse Moke configuration. These effects pave the road for the development of new optical components and sensors with great application potential

E. T. Papaioannou, V. Kapaklis, E. Melander, B. Hjorvarsson, S. D. Pappas, P. Patoka, M. Giersig, P. Fumagalli, A. Garcia-Martin and G. Cistis, "Surface plasmons and magneto-optic activity in hexagonal Ni anti-dot arrays", *Opt. Express* 19, 23867 (2011)

AG01

Magnetic nanodots induced novel magnetic phenomena

Jian Shen

Department of Physics, Fudan University, China

Study of Magnetic nanodots is at central in the field of nanomagnetism. Besides the interesting properties caused by dimensionality effect, magnetic nanodots can induce many novel phenomena when forming heterostructures with other materials. In this work, I will use several examples to demonstrate their effect. These examples include collective ferromagnetism of nanodot arrays on 2-dimensional electron gas, colossal Coulomb blockade magnetoresistance in tri-layers, and dramatic enhancement of metal-insulator transition temperature in manganites. All these fascinating phenomena originate directly from the presence of magnetic nanodots. Their underlying mechanisms, while somewhat understood, need further theoretical studies.

1. T.Z. Ward, Z. Gai, X.Y. Xu, H.W.Guo, L.F. Yin, J. Shen, *Phys. Rev. Lett.* 106, 157207 (2011). 2. Dali Sun, Lifeng Yin, Chengjun Sun, Hangwen Guo, Zheng Gai, X.-G. Zhang, T. Z. Ward, Zhaohua Cheng, and Jian Shen, *Phys. Rev. Lett.* 104, 236602 (2010). 3. Lifeng Yin, Di Xiao, Zheng Gai, Thomas Z. Ward, Noppi Widjaja, G. Malcolm Stocks, Zhao-hua Cheng, E. Ward Plummer, Zhenyu Zhang, and Jian Shen, *Phys. Rev. Lett.* 104, 167202 (2010).

AG02

Magnetic properties of Fe-(Pt,Pd) thin films patterned by self-assembling of polystyrene nanospheres

Paola Tiberto¹, Luca Boarino¹, Gabriele Barrera¹, Federica Celegato¹, Marco Coisson¹, Natascia De Leo¹, Franco Vinai¹, Franca Albertini², Francesca Casoli² and P. Ranzieri²

¹ Electromagnetics, INRIM, Italy

² IMEM-CNR, Italy

Arrays of nanoparticles with high magnetic anisotropy are studied for magnetorecording. Nanolithography techniques are employed to prepare arrays of magnetic dots/holes. Polystyrene nanosphere (PN) lithography has been recently exploited for magnetic thin films nanostructuring, due to its low-cost and large covering area [1,2]. Dot arrays of Fe₃Pt₄ (MgO(100) substrate heated at 400 °C) were obtained by assembling PN monolayers on a continuous film (10 nm), followed by sputter etching with Ar⁺ ions (final dots diameter 80 ÷ 400 nm) [1]. Antidot arrays of Fe₃Pd₅₀ (50 nm, Si substrate, post deposition annealing at 550 °C) have been created by exploiting PN as diffraction masks in combination with a mercury lamp [2]. In this alternative lithography technique, the PN behave as optical lenses to generate regular diffraction patterns (holes, diameter = 300 nm) on a photoresist. In both cases, the annealing induces the order-disorder transformation towards the L10 tetragonal phase. Sample microstructure was studied with SEM and AFM microscopy. Parallel and perpendicular hysteresis loops were measured by AGFM, confirming the presence of the tetragonal phase. The complex multidomain magnetic pattern was studied in both compositions with MFM and related to dot/hole diameter and their mutual distance.

[1] P. Tiberto, L. Boarino, F. Celegato, M. Coisson, N. De Leo, F. Vinai, *J. Appl. Phys.* 107, 09B502 (2010) [2] P. Tiberto, L. Boarino, , F. Celegato, G. Barrera, M. Coisson, N. De Leo, F. Vinai, *P. Alita, MRS Proc.* (2012) in press

AG03

Position dependence of vortex core oscillation in polygonal nanomagnets

Satoshi Yakata¹, Masahiko Miyata², Kohei Kiseki³, Hirofumi Wada² and Takashi Kimura^{1*}

¹ INAMORI Frontier Research Center, Kyushu University, Japan

² Department of Physics, Kyushu University, Japan

³ Department of Electronics, Kyushu University, Japan

A magnetic vortex structure formed in a micron-scale ferromagnetic dot has been gathering attention because of its superior performance for a unit cell in spintronic devices[1] and intriguing magnetic responses such as bloch point reversal[2]. Control and further understanding of vortex properties are required for the practical application. Previously, we showed that the vortex chirality can be controlled simply by the application of the in-plane magnetic field in a regular polygonal-shape nanomagnet[3]. This enables us to control the core position precisely by applying the external magnetic field. Since the potential distribution for the core in the polygonal nanomagnet should be different from a simple harmonic potential formed in a circular magnetic dot, we expect that the resonant frequency depends on the core position. In the present work, we investigate the vortex core dynamics in a triangular nanomagnet under the external magnetic field using an electrical homodyne detection technique and the transmission impedance measurements using a vector network analyzer. The resonant frequency was found to increase with decreasing the distance between the core and the vertex.

[1] V. S. Pribiag, I. N. Krivorotov, G. D. Fuchs, P. M. Braganca, O. Oezatay, J. C. Sankey, D. C. Ralph, and R. a. Buhrman, *Nature Physics* 3, 498-503 (2007). [2] A. Thiaville, J. Garcia, R. Dittich, J. Millat, and T. Schrefl, *Physical Review B* 67, 1-12 (2003). [3] S. Yakata, M. Miyata, S. Nonoguchi, H. Wada, and T. Kimura, *Applied Physics Letters* 97, 222503 (2010)

AG04

Huge magnetic anisotropy and coercivity in Fe island and atomic wire on

Takeshi Nakagawa^{1*}, Toshihiko Yokoyama¹, Torsten Methfessel², Sandra Perker² and Hans-joachim Elmers²

¹ Institute for Molecular Science, Japan

² Mainz University, Germany

We have investigated huge magnetic anisotropy energy and coercivity of Fe nano islands and nano stripes on flat and stepped W(110) using x-ray circular dichroism (XMCD) and scanning tunneling microscope, which has not been directly decided so far due to its large anisotropy [1]. The anisotropy energy is 1 meV per Fe atom as determined from magnetization curve by XMCD at Fe L edge, almost constant both for the nano island and the nano stripe below one monolayer. This anisotropy energy corresponds to an anisotropy field of 17 T. The coercivity, Hc, for the nano islands at 0.25 ML is very large, ~5 T, but it rapidly decreases to 1 T at 0.6 ML, which follows Hc ~ 1/r (radius of island). On the other hand, the coercivity for the nano stripes is almost constant, Hc ~ 3 T below 0.5 ML. The obtained coercivity is much smaller than the anisotropy field, suggesting that the magnetization reversal process is via a domain wall creation, not a coherent rotation. This contrasted behavior is explained by the shape of deposited Fe on the stepped and flat W surfaces and the creation of domain wall.

[1] M. Prutzer, et al., Phys. Rev. Lett., 87, 127201(2001)

AG05

Oscillation of critical fields in highly dense arrays of magnetic nanodisks

Alexey Ognev*, Maxim Stebliy, Alexander Samardak and Ludmila Chebotkevich Far Eastern Federal University, Institute of Automation and Control Processes FEBRAS, Russia

Magnetostatic interaction between magnetic nanostructures composing a highly dense array influences on its magnetization reversal and micromagnetic configuration. In this paper we demonstrate the effect of nanodisk array dimension N on magnetic properties. The nanodisk patterns with 600 nm in diameter and distance between disk's centers d from 700 nm to 1um were fabricated by electron-beam lithography. The number of disks on a boundary N was varied from 2 to 20. After sputtering of Py films and lift-off process the nanodisks with thickness t =9, 22 and 30 nm were prepared. Using magnetic hysteresis curves we found out that with an increase of N the fields of magnetic vortex nucleation Hn and annihilation Ha decreased. At the first time we demonstrate the oscillations of function Hn = f(N) in arrays. The maximum amplitude of oscillations was observed in case of nanodisks with t=22 nm and d=800 nm. Magnetic force microscopy shown that at t=22 nm the magnetization reversal was occurred mainly via vortex core motion. We were carried out the calculation of critical fields Hn and Ha with in "rigid" vortex model for different N. The theoretical result is in a good qualitative agreement with the experimental data.

AH01

Magnetic tools for molecular diagnosis

Joerg Schotter*, Astrit Shoshi¹, Stefan Schrittwieser¹, Hubert Brueckl¹, Frank Ludwig², Katerina Soulantika³, Manfred Meindl⁴ and Christian Zilch⁵

¹ Health & Environment Department, AIT Austrian Institute of Technology, Austria

² Institute of Electrical Measurement and Fundamental Electrical Engineering, TU Braunschweig, Germany

³ LPCNO, Université de Toulouse: INSA, UPS, LPCNO, and CNRS, France

⁴ Danube Mobile Communications Engineering (DMCE), Austria

⁵ Magna Diagnostics GmbH, Germany

This talk shows examples for the application of magnetic transducers such as magnetoresistive sensors (→ 'Lab-on-a-chip') or multifunctional magnetic nanoparticles (→ 'Lab-on-a-bead') as tools for molecular diagnosis. Regarding Lab-on-a-chip systems, we demonstrate in-vitro studies of magnetic particle uptake (phagocytosis) by cell cultures (e.g. NHDF or DU145 cells). The method is based on distance changes of the magnetic particles to embedded magnetoresistive sensors during phagocytosis and allows analysis of factors that are relevant for applications like magnetofection or hypothermia. As a second Lab-on-a-chip application, we show the concept and progress of a CMOS-integrated tunneling magnetoresistance sensor chip currently under development for a point-of-care device for sepsis diagnosis. Our Lab-on-a-bead approach focuses on homogeneous immunodiagnosics based on manipulation and observation of multi-functional nanoparticles. This new biosensor concept is based on highly sensitive plasmon-optical detection of the rotational dynamics of anisotropic magnetic nanoparticles immersed in the sample solution, which changes on the binding of analyte molecules to the nanoparticles. We present model calculations of the optical, magnetic and hydrodynamic properties of both the required nanoparticles and measurement conditions. Experimentally, we show transmission measurements on plain ferromagnetic nanorod dispersions in rotating magnetic fields.

Schrittwieser S, Ludwig F, Dieckhoff J, Soulantika K, Van G, Lucrot L-M, Lentijo SM, Boubelri R, Maymaide J, Huettner A, Brueckl H, Schotter J. Modeling and Development of a Biosensor Based on Optical Relaxation Measurements of Hybrid Nanoparticles. ACS Nano, 2012;6:791

AH02

Control of the living cell machinery with nanomagnets

Vitalii Zablotskii*, Alexandr Dejneka¹, Oleg Lunov², Lubomir Jastrabik¹, Tatiana Syrovets² and Thomas Simmet²

¹ Applied Optics, Institute of Physics, Czech Republic

² Institute of Pharmacology of Natural Products & Clinical Pharmacology, Ulm University, Germany

We present proof-of-concept experiments on magnetically controlled cellular endocytosis of functionalized magnetic nanoparticles. The possibility of remote control of the cellular endocytosis and/or exocytosis rates by an externally applied magnetic field without using various types of inhibitors seems to be a very intriguing direction in nanomedicine [1]. By pharmacological and in vitro knockdown approaches, the principal cellular uptake mechanism for two types of magnetic nanoparticles was identified [2]. A model of the uptake process that allows determination of key parameters of endocytosis, including the rate of uptake, the number of nanoparticles per cell in saturation, the mean uptake time, and the correlation between the number of internalized nanoparticles and their extracellular concentration was developed. We also describe our recent progress in the applications of nanomagnets for magnetic hyperthermia treatments and targeted drug delivery [3]. In particular, we will propose a new mode of hyperthermia that we have analyzed. The obtained results have important implications for the fundamental knowledge on intracellular nanomechanics and open ways for magnetic controlling of the living cell machinery.

[1] V. Zablotskii, O. Lunov, A. Dejneka, L. Jastrabik, T. Poljakova, T. Syrovets, Th. Simmet, Appl. Phys. Lett. 99, 183701 (2011). [2] O. Lunov, V. Zablotskii, T. Syrovets, C. Rucker, K. Tron, G. U. Nienhaus, Th. Simmet, Biomaterials 32, 547 (2011). [3] O. Lunov, V. Zablotskii, M. P. Gutierrez, J. I. Perez-Landazabal, C. Gomez-Polo, T. Syrovets, Th. Simmet, American Institute of Physics, Conference Proceeding Series 1311, 288 (2010).

AH03

Bio-functionalized magnetic nanoparticles for in-vitro diagnosis of colorectal cancer

Charles Shieh-yueh Yang*, Herm-er Horng², Hong-chang Yang³, K.w. Huang⁴ and Chau-chung Wu⁵

¹ MagQu Co., Ltd., Taiwan

² Institute of Electro-optical Science and Technology, National Taiwan Normal University, Taiwan

³ Department of Physics, National Taiwan University, Taiwan

⁴ Department of Surgery & Hepatitis Research Center, National Taiwan University Hospital, Taiwan

⁵ Departments of Internal Medicine and Primary Care Medicine, National Taiwan University, Taiwan

Colorectal cancer (CRC) is the most popular cancer. Carcinoembryonic antigen (CEA) has been used as bio-markers for CRC. The signals for CEA solutions of various concentrations, or with interfering materials are detected via immunomagnetic reduction (IMR), the assay technology involves the utilities of bio-functionalized magnetic nanoparticles to label CEA. By using the bio-functionalized magnetic nanoparticles and the analyzer, the detection threshold and interference tests for assaying CEA are examined. Several serum samples from normal people and CRC patients are used for the detections of CEA concentration via IMR. The results of assaying CEA with IMR and enzyme-linked immunosorbent assay (ELISA) were compared. As compared to ELISA, the detection threshold for assaying CEA with IMR is lowered by at least two orders of magnitude. For the interfering materials noted commonly in serum such as hemoglobin, bilirubin, triglyceride, and vascular endothelial growth factor, there is no detectable interfering effect for assaying CEA with IMR. These results reveal the feasibilities of assaying CEA in the blood using IMR, as well as achieving a high-sensitive and high-specific assay for CEA.

J. C. Yang, S.Y. Yang, J.J. Chieh, H.E. Horng, C.Y. Hong, H.C. Yang, K.H. Chen, B.Y. Shih, T.F. Chen, and M.J. Chiu, ACS Chem. Neurosci. 2, 500 (2011). 2 K.W. Huang, S.Y. Yang, C.Y. Yu, J.J. Chieh, C.C. Yang, H.E. Horng, C.Y. Hong, H.C. Yang, and C.C. Wu, J. Biomed. Nanotechnol. 7, 535 (2011). 3 S.Y. Yang, J.J. Chieh, H.C. Yang, C.Y. Yu, N.S. Hung, H.E. Horng, C.Y. Hong, H.C. Yang, C.F. Chang, and H.Y. Lin, J. Magn. Magn. Mater. 323, 681 (2011).

AH04

Multiplexing capabilities of multi-frequency magnetic ratchets

Benjamin B. Yellen^{1,2}, Yuyu Ouyang¹, Lu Gao², Mukarram A. Tahir², Daniel J. Lichtenwalner³ and Lawrence. N. Virgin⁴

¹ University of Michigan – Shanghai Jiao Tong University Joint Institute, Shanghai Jiao Tong University, Shanghai, P.R.C.

² Duke University, Department of Mechanical Engineering and Materials Science, Center for Biologically Inspired Materials and Material Systems, Durham, NC 27708

³ North Carolina State University, Department of Materials Science and Engineering, Raleigh, NC 27606

Through a combination of theory, numerical simulation, and experiment, we investigate the motion of magnetic beads on the surface of a magnetic ratchet driven by multi-frequency fields. We demonstrate that in multifrequency driving fields, two different bead types experience differential motion by modulating the phase difference between the two driving frequencies. We use perturbation analysis to demonstrate that static forcing terms are the origin for why two different bead types can move in opposite directions on the same ratchet potential. Based on these theoretical results, we conduct experimental investigations that explore the effects of bead size and static forcing coefficient on the direction of bead motion, which confirm most of the expected trends. These results shed light both on past experimental work both by ourselves and others, as well as elucidate the more general multiplexing capabilities of ratchets.

AIO1

Quantum control of single spins in diamond and silicon carbide

David D. Awschalom*

Center for Spintronics and Quantum Computation, University of California, USA

A motivation behind modern research into quantum physics has been to identify robust quantum states that can be easily controlled for future use in advanced information technologies. Recently, a defect in diamond known as the nitrogen-vacancy (N-V) center has attracted interest because it possesses an atomic scale electronic spin state that can be used as an individually addressable, solid state quantum bit (qubit) even at room temperature. The N-V center's optical transitions become coherent, spin-dependent, and may be precisely controlled with gate voltages in micron-scale devices [1]. Moreover, engineered coupling of this electron spin with the proximal single nitrogen nuclear spin enables a scalable quantum memory [2]. These exceptional coherent properties have motivated theoretical efforts to predict similar defects in other semiconductors with expanded functionality [3]. We show that spin states in various polytypes of SiC can be optically addressed and coherently controlled at temperatures ranging from 20 to 300 K with coherence properties comparable to diamond N-V centers. These spins are optically active near telecom wavelengths within an industrial scale material having advanced microfabrication techniques. This makes them promising candidates for photonic, spintronic, and quantum information applications that merge quantum degrees of freedom with classical electronic and optical technologies [4].

[1] L.C. Bassett, F.J. Heremans, C.G. Yale, B.B. Buckley, & D.D. Awschalom, Phys. Rev. Lett. 107, 266403 (2011). [2] G. D. Fuchs, G. Burkard, P. V. Klimov, and D. D. Awschalom, Nature Physics 7, 789 (2011). [3] J. R. Weber, W. F. Koehl, J. B. Varley, A. Janotti, B. B. Buckley, C. G. Van de Walle, and D. D. Awschalom, Proc. Natl Acad. Sci. 107, 8513 (2010). [4] W. F. Koehl, B. B. Buckley, F. J. Heremans, G. Calusine, & D. D. Awschalom, Nature 479, 84 (2011).

AIO2

Dynamical spin injection into p-type Si using the spin pumping and spin transport at room temperature

Kazuki Kubo^{1*}, Eiji Shikoh¹, Kazuya Ando², Eiji Saitoh², Teruya Shinjo¹ and Masashi Shiraishi¹

¹ Graduate School of Eng. Sci., Osaka Univ., Japan

² Inst. for Materials Research, Tohoku Univ., Japan

For observation of spin-transport in p-type Si, ferromagnetic Ni₈₀Fe₂₀ and paramagnetic Pd were separately formed with various gap distances on a p-Si with doping concentration of 1×10¹⁹ cm⁻³. The sample was placed near the center of a microwave cavity in ESR system. In a ferromagnetic resonance condition of the Ni₈₀Fe₂₀, the steady magnetization precession was maintained by the absorption of the microwave and the angular momentum was transferred from the local spins to conduction electrons. Then conservation of spin angular momentum induced spin pumping into the p-Si, which generated pure spin current in the p-Si. The spin current propagated in the p-Si, and was absorbed into the Pd, where the spin current was converted to a charge current by the inverse spin-Hall effect (ISHE) in Pd. When the gap length was 490 nm, the output voltage of 1.4 μV due to the ISHE was obtained. Using the results, the spin diffusion length and spin coherence time in p-Si at room temperature were estimated to be at least 130 nm and 94 ps, respectively[1]. In the presentation, we will discuss the detail of the research.

[1] E. Shikoh, K. Kubo, et al., arXiv:1107.0376.

AIO3

Studying the optical spin orientation in Ge by exploiting the spin filtering in Fe/MgO/Ge photodiodes

Christian Rinaldi*, Matteo Cantoni, Daniela Petti and Riccardo Bertacco Department of Physics, CNISM and L NESS - Politecnico di Milano, Via Anzani 42, 22100, Italy

Spin-polarized carriers can be photo-excited in a semiconductor by monochromatic circularly polarized light. To date, several techniques have been introduced to detect the excited spin polarization. In this work, the spin filtering effect at the Fe/MgO interface has been employed to measure the degree of spin polarization of both electrons and holes in Ge. We have fabricated photodiodes by means of optical lithography, starting from fully epitaxial Fe/MgO/Ge(001) heterostructures [1,2]. Spin-detection experiments are performed by illuminating photodiodes with circularly polarized light in a magnetic field applied parallel to the light helicity. Photo-generated carriers in Ge are spin-filtered by the MgO barrier depending on the direction of the spin. The degree of spin polarization (DSP) is related to the variation of the photocurrent due to full reversal of the Fe magnetization. As predicted by Rioux and Sipe [3], the DSP is maximum when the photon energy is resonant with the direct energy gap of Ge and decreases with the photon energy for both holes and electrons. Moreover, as the DSP is different from zero in the frequency range from 1300 nm to 1550 nm, the device is suitable for integrated detection of light helicity at room temperature in novel spin-optoelectronics systems.

[1] M. Cantoni et al., Appl. Phys. Lett. 98 (2011) 032104. [2] D. Petti et al., J. Appl. Phys. 109 (2011) 084909. [3] J. Rioux and J. E. Sipe, Phys. Rev. B 81 (2010) 155215.

AIO4

Transition from spin injection into interface states to the channel in n-Ge

Abhinav Jain¹, Juan-carlos Rojas¹, Murat Cubukcu¹, Julian Peiro², Jean-christophe Le Breton², Eric Prestat¹, Celine Vergnaud¹, Lamis Louahadj¹, Celine Portemont¹, Clarisse Ducruet¹, Vincent Baltz², André Barski¹, Pascale Bayle-guillemaud¹, Laurent Vila¹, Jean-philippe Attane¹, Emmanuel Augendre⁴, Serge Gambarelli¹, Henri Jaffres², Jean-marie George² and Matthieu Jamet^{1*}

¹ INAC, Commissariat a l'Energie Atomique et aux Energies Alternatives, France

² Unite Mixte de Physique CNRS-Thales, CNRS, France

³ CROCUS Technology, France

⁴ LETI, Commissariat a l'Energie Atomique et aux Energies Alternatives, France

Spin injection into semiconductors is crucial for exploring spin physics and new spintronic devices. Unlike GaAs or Si, very few studies have dealt with spin injection in Ge [1,2,3,4]. This material is of great interest for high carrier mobility, long spin diffusion length and large spin-orbit coupling to perform electric field spin manipulation through Rashba interaction. However the exact role of interface states in spin injection mechanism in n-Ge has not been clarified yet and except in ref. [1] no clear evidence of spin accumulation in the channel has been given. In this paper, we show a clear transition from spin injection into interface states to the channel. For this purpose, we have grown CoFeB/MgO spin injector on Ge [2]. We observe spin signal amplification at low temperature due to spin accumulation into interface states. At 200 K, we observe a clear transition to spin injection in the channel up to room temperature: the spin signal is reduced to a value compatible with spin diffusion model and more interesting we could demonstrate spin signal modulation applying a back gate voltage and spin-pumping by the ferromagnetic resonance of the CoFeB layer which are clear manifestations of spin accumulated in the channel.

[1] Y. Zhou, W. Han, L.-T. Chang, F. Xu, et al., Phys. Rev. B 84, 125323 (2011). [2] A. Jain, L. Louahadj, J. Peiro, J. C. Le Breton, C. Vergnaud, A. Barski, C. Beigne, L. Noin, A. Marty, V. Balz, S. Jaffres, E. Augendre, H. Jaffres, J.-M. George, M. Jamet, Appl. Phys. Lett. 99, 162102 (2011). [3] H. Saito, S. Watanabe, Y. Mineno, S. Sharma, et al., Solid State Comm. 151, 1159 (2011). [4] K. R. Jeon, B.-C. Min, Y. H. Jo, H.-S. Lee, J. Shin, C.-Y. Park, S.-Y. Park, S.-C. Shin, Phys. Rev. B 84, 163515 (2011).

AIO5

Tunneling anisotropy in crystalline Si/MgO/Fe devices

Sandeep Sharma^{1*}, Aurelie Spiesser¹, Hidekazu Saito¹, Shinji Yuasa¹, Bart J. Van Wees² and Ron Jansen¹

¹ AIST Tsukuba, Japan

² Zernike Institute for Advanced Materials, Univ. of Groningen, Netherlands

Key advances in the electrical creation of spins in silicon at room temperature have recently been made, using ferromagnetic tunnel contacts to inject a spin accumulation, and to detect it [1,2]. This enables the systematic study of the various parameters that govern spin injection into silicon. Here we demonstrate that spin transport in ferromagnet/oxide/silicon tunnel devices is anisotropic, i.e., depends on the absolute orientation of the magnetization direction of the ferromagnetic electrode. In particular, we show that the magnitude of the spin accumulation induced in the Si is anisotropic and changes when the magnetization is rotated either in the in-plane or the out-of-plane direction. We present a systematic study of the anisotropic tunnel conductance of crystalline Si/MgO/Fe spin tunnel contacts at 300 K. We observe an in-plane anisotropy that reflects the crystal symmetry of the tunnel contact. The out-of-plane anisotropy shows a bias-dependent, non-trivial variation with magnetization angle that arises from a superposition of different contributions to the anisotropy, one of which is the anisotropy of the tunnel spin polarization. The results will be compared to anisotropy data on contacts with an amorphous Al₂O₃ tunnel barrier, n-type and p-type silicon, and Ni and Fe as the ferromagnet.

[1] S.P. Dash, S. Sharma, R.S. Patel, M.P. de Jong and R. Jansen, Nature 462, 491 (2009). [2] S.P. Dash, S. Sharma, J.C. Le Breton, H. Jaffres, J. Peiro, J.M. George, A. Lemaire and R. Jansen, PRB 84, 054410 (2011).

AJ01

Micromagnetic models in glass-coated microwires with circumferential anisotropy

Jacob Torrejon¹, Andre Thiaville^{1*}, Anne Lise Adenot Engelvin² and Manuel Vazquez³

¹ Laboratoire de Physique des Solides, Univ. Paris-Sud, CNRS, 91405 Orsay, France, France

² CEA, DAM, Le Ripault, 37260 Monts, France, France

³ Instituto de Ciencia de Materiales, CSIC, 28049 Madrid, Spain, Spain

The magnetic behaviour of amorphous glass-coated microwires, with ultrasoft magnetic behaviour, has been modelled by quasi-analytical 1D micromagnetics. Co-based alloys with negative magnetostriiction present a noticeable circumferential anisotropy where an axial core responds to the minimization of exchange energy. The theoretical approach is based on one-dimensional micromagnetic model where exchange, magnetoelastic and magnetostatic energies are considered. We assume that magnetization profile varies only along radial direction and magnetoelastic anisotropy does not depend to the radial coordinate. Solving firstly the variational problem that leads to Euler-Lagrange equation, we estimate the size of the core and the axial hysteresis loops as a function of radius, exchange coefficient A and anisotropy constant K [1]. The critical nucleus radius below which the magnetization is fully axial was analytically obtained. The model was extended to high frequency dynamics under axial ac field. The microwave permeability has been computed as a sum of eigenmodes. These modes are obtained as solution of a Schrodinger equation where the potential derives from static solution. Finally, comparison with experimental measurements shows the important role of the skin effect for thicker wires.

[1] J. Torrejon et al.; J. Magn. Magn. Mater., 323 (2011) 283.

AJ02

Manipulation of domain wall dynamics in microwires by transverse magnetic field

Juan Maria Blanco¹, Alexandr Chizhik², Valeria Rodionova³, Mihail Ipatov², Valentina Zhukova², Ahmed Talaat² and Arcady Zhukov^{4*}
¹Dpto. de Física Aplicada, Basque Country University, UPV/EHU, Spain
²Dpto. Física de Materiales, Fac. Químicas, Basque Country University, UPV/EHU, Spain
³Dpto. Física de Materiales, Fac. Químicas and Faculty of Physics, Basque Country University, Moscow State University and Immanuel Kant Baltic-Federal University, Spain
⁴Dpto. Física de Materiales, Fac. Químicas, Basque Country University, UPV/EHU, and Iberbasque, Basque Foundation for Science, Spain

Recently fast domain wall (DW) propagation of thin magnetic wires gained considerable interest owing to possibility of applications for data storage devices and extremely fast DW propagation in composite glass-coated amorphous microwires. A number of interesting effect, such as collisions between two DWs, trapping and injecting of DWs by local fields and DW dynamics manipulation through the magnetoelastic energy have been reported. In this paper we studied effect of transversal magnetic field on DW propagation in microwires. In order to activate DW propagation from the determined wire end in our experiment we placed one end of the sample outside the magnetization solenoid. Under certain transversal magnetic field, Ht, we were able to create additional DW on the opposite wire end. Changing the Ht we were able to tailor propagation field of this additional DW and observe DW collision in different parts of microwire. Previously we observed spontaneous DW nucleation on local defects limiting single DW dynamics regime in microwires. The collisions realized by us by application of transversal magnetic field can be used to release such additional DWs to achieve higher DW velocity extending single DW regime to higher external magnetic fields.

AJ03

Effect of process parameters on the microstructure and magnetic properties of electrodeposited FeCo thin films

Weï Lu^{1*}, Chenchong He², Zhe Chen² and Biao Yan²
¹School of Materials Science and Engineering, Tongji University, Shanghai, China
²Tongji University, China

FeCo alloys have been extensively studied as soft magnetic materials due to their superior properties relative to Fe-Ni alloys as write head core materials in hard-disk-drives. Electrodeposition represents a simple, cost-effective way of fabricating thin film recording heads, although stable plating baths are needed for commercial processing. It has been a challenge to fabricate FeCo films that have high saturation magnetizations (>2 T) with good soft magnetic properties (low coercivities Hc) by electrodeposition methods. In this study, the magnetic properties of FeCo thin films plated, under a number of different processing conditions, are investigated. The aim is to optimize the microstructure and magnetic properties such as saturation magnetic flux density and coercivity. The effect of current density (15-50 mA/cm²), cobalt/iron ions concentration and bath temperature (room temperature to 45oC) on the films microstructure and properties were studied. The microstructure of electrodeposited films was characterized by XRD, TEM and scanning probe microscope. The magnetic properties of electrodeposited films were investigated by VSM and show dependence on the deposition conditions. After optimization of process parameters, high saturation magnetization (~2.1T) and low coercivity (~10Oe) were obtained for electrodeposited FeCo thin film in present study.

AJ04

Structure and magnetic properties of FeCo alloy synthesized by a one-step polyol process

Prakash Karipoth, Arun Thirumurugan and Raphael Justin Joseyphus*
 Department of Physics, National Institute of Technology, Tiruchirappalli 620 015, India

Most of the chemical methods for the synthesis of FeCo employ complex experimental conditions, expensive chemicals and carbonyl precursors which are less preferable [1]. Moreover each chemical method results in FeCo of various composition, particle size, order-disorder behaviour and oxide fraction which subsequently affect its magnetic properties [2]. In this report, we present the synthesis of FeCo nanoparticles of varying composition by a unique one-step polyol process and report its magnetic properties. The synthesis of FeCo alloys were undertaken in ethylene glycol using hydrated FeCl₂ and Co(II)acetate and NaOH. The samples were prepared at various temperatures upto 190 oC. The samples are characterized using XRD, TEM-EDX and VSM. The variation of Curie temperature is determined using Thermo-Magnetic Analysis and is found to be in accordance with the composition of the FeCo alloy. The fcc to bcc phase transition temperatures is also evident from the Differential Thermal Analysis. The morphology of the particles is studied using TEM and it showed spherical or cubic nature depending on the hydrous precursors used in the synthesis. The present synthesis method can be employed for large scale synthesis of FeCo alloys with controlled structure and magnetic properties which shall be discussed in detail.

[1] D. Sudfeld et al., J. Appl. Phys. 93 (2003) 7328. [2] F. Dumestre et al., Science 303 (2004) 821

AJ05

Investigations of the magnetic and structural properties of a metalloid-free Co₉₀Zr₁₀V₁₀ amorphous alloy

Eric Fleury^{1*}, Christian Meny² and Shashank N. Kane³
¹Center for High Temperature Energy MAaterials, Korea Institute of Science and Technology, Seoul, Korea
²UMR 7504 CNRS-UDS, Institut de Physique et Chimie des Matériaux de Strasbourg, 67034 Strasbourg, France
³School of Physics, D. A. University, Khandwa road Campus, Indore 452001, India

Nanocrystalline ferromagnetic materials used in magnetic applications are obtained from Fe- and Co-based amorphous alloys containing metalloid elements. In these systems, the magnetic properties are optimized by adjusting the size of the nanocrystals forming from the metastable amorphous phase upon annealing. This study was undertaken to investigate the correlation between the variations in the magnetic properties upon annealing of a metalloid-free Co-based amorphous alloy. For that purpose the measurements of the magnetic properties have been complemented by a microstructural analysis by means of nuclear magnetic resonance. The hysteresis loops of as-cast and annealed samples were measured at 50 Hz (Hmax = 1 kA/m) to get information on the dependence of the coercive field (Hc) and saturation induction (BI000) with the annealing treatment. Zero field 59Co NMR spectra have been recorded with an automated broadband spectrometer. The lowest value of coercivity was found to be 5.8 A/m and highest saturation induction of 0.7 Tesla in the sample annealed at 425oC for 20 minutes. The NMR investigation suggested an important contribution of pure Co atoms. The dependency of the magnetic properties upon the annealing treatment will be discussed based on local atomic arrangement in the amorphous structure.

AJ06

Magnetocaloric effect in Fe-Ni-Zr alloys prepared by rapidly quenched method

Nguyen Huy Dan^{1*}, Nguyen Huu Duc¹, Tran Dang Thanh¹, Nguyen Hai Yen¹, Pham Thi Thanh¹, Ngac An Bang², Do Thi Kim Anh², Phan The Long² and Seong Cho Yu³
¹Institute of Materials Science, 18 Hoang Quoc Viet, Hanoi, Viet Nam
²Hanoi University of Science, 334 Nguyen Trai, Hanoi, Viet nam
³Department of Physics, Chungbuk National University, Cheongju 361 - 763, Korea

Fe_{90-x}Ni_xZr₁₀ (x = 0, 5, 10, 15, 20 and 25) ribbons with various thickness were prepared by melt-spinning technique. Curie temperature, T_C, of the alloys is dramatically decreased from ~960 K to room temperature region by high quenching rates. When the alloys are in amorphous structure, their TC strongly depends on the Ni-concentration. Maximum entropy change, |ΔS_m|_{max}, with ΔH = 12 kOe, of the alloys is around 1 J.kg⁻¹.K⁻¹ in room temperature region. On the other hand, the full width at haft the maximum peak of the entropy change is quite large, FWHM ~ 85 K, making it possible for application in magnetic refrigerators at room temperature.

PACS number: 75.30.Sg, 07.20.Mc, 75.50.Kj

Keywords: Magnetocaloric effect, Refrigeration, Amorphous magnetic materials

BA01

Nodal pocket revealed by quantum oscillations in an underdoped cuprate superconductor

Suchitra Sebastian¹, Gil Lonzarich¹, Neil Harrison², Moaz Altarawneh², Chuck Mielke², Ruixing Liang³, Doug Bonn³ and Walter Hardy³
¹Department of Physics, University of Cambridge, United Kingdom
²National High Magnetic Field Laboratory, Los Alamos National Laboratory, USA
³Department of Physics, University of British Columbia, Canada

Quantum oscillations have proved a vital tool in uncovering the electronic structure underlying the normal state of the underdoped cuprates. Our experiments have established that quasiparticles in this regime are governed by fermi dirac statistics, yet a comprehensive description of the fermi surface geometry remains elusive. We use an array of quantum oscillation measurements in the underdoped cuprate YBa₂Cu₃O_{6-x} in tandem with results from complementary experimental techniques to distinguish between alternative Fermi surface possibilities. We present evidence including quantum oscillations that persist down to low magnetic fields, a low doping quantum critical point that mirrors the nodal Fermi velocity collapse in photoemission, and oscillations of the chemical potential, all of which strongly point to a Fermi surface comprising solely nodal pockets. Possibilities for the origin of the antinodal gapping of density of states at the Fermi level are discussed.

S. E. Sebastian et al. Nature Communications 2, Article number: 471

BA02

Low-Dimensional Superconductivity in δ -Doped SrTiO₃

Harold Hwang*
 Stanford University & SLAC, USA

SrTiO₃ is the lowest density bulk superconductor, which when incorporated in heterostructures provides an opportunity for band-structure engineering this superconducting semiconductor. We take this opportunity by selectively doping a channel of finite thickness in an undoped matrix, which is analogous to δ -doping in semiconductors. By varying the thickness of a Nb doped channel, we have studied the crossover from 3D to 2D in the superconducting and normal state properties, as the thickness of the doped layer is decreased. A notable feature of these structures is that the mobility strongly increases in the 2D limit. This aspect suggests that a new regime of 2D superconducting phase transitions can be experimentally accessed approaching the clean limit. Prospects and progress in understanding the spin-orbit coupling and coupling bi-layer structures will be discussed.

BA03

Resonant x-ray scattering from YBCO family

Matthieu Le Tacon^{1*}, Giacomo Ghiringhelli², Jiri Chaloupka¹, Marco Moretti Sala³, Santiago Blanco-canaosa¹, Matteo Minola⁴, Giniyat Khalullin¹, Thorsten Schmitt⁵, Lucio Braicovich⁶ and Bernhard Keimer¹
¹Max Planck Institute For Solid State Research, Germany
²CNR-SPIN, Dipartimento di Fisica, Politecnico di Milano, I-20133 Milano, Italy
³European Synchrotron Research Facility, France
⁴CNR-SPIN, Dipartimento di Fisica, Politecnico di Milano, Italy
⁵Swiss Light Source, Switzerland
⁶CNR-SPIN, Dipartimento di Fisica, Politecnico di Milano, I-20133 Milano, Italy

Motivated by the search for the mechanism of high-temperature superconductivity, an intense research effort has been focused on the evolution of the spin excitation spectrum upon doping from the antiferromagnetic insulating to the superconducting states of the cuprates. Here we take advantage of the recent developments of high-resolution resonant inelastic x-ray scattering [1] to show that a large family of superconductors, encompassing the model compounds YBa₂Cu₄O₈ and YBa₂Cu₃O₇, exhibits damped spin excitations - or paramagnons - with dispersions and spectral weights closely similar to those of magnons in undoped, antiferromagnetically ordered cuprates over much of the Brillouin zone[2]. A numerical solution of the Eliashberg equations based on the experimental spin excitation spectrum of YBa₂Cu₃O₇ reproduces its superconducting transition temperature within a factor of two and strongly supports magnetic Cooper pairing models for the cuprates. Charge excitations are also investigated and reveal evidences for charge order in the pseudogap state of underdoped compounds [3].

[1] I. Braicovich, L. et al. Magnetic Excitations and Phase Separation in the Underdoped La_{2-x}Sr_xCuO₄ Superconductor Measured by Resonant Inelastic X-Ray Scattering, Phys. Rev. Lett. 104, 077002 (2010). [2] Le Tacon, M. et al. Intense paramagnon excitations in a large family of high-temperature superconductors. Nat Phys 7, 725-730 (2011). [3] Ghiringhelli, G. et al. in preparation.

BA04

Evolving electronic structures of high-tc cuprates studied by Compton scattering

Yoshiharu Sakurai^{1*}, Masayoshi Itou¹, Bernardo Barbiellini², Susmita Basak², Robert S. Markiewicz², Peter E. Mijnderens³, Shuichi Wakimoto⁴, Masaki Fujita⁵, Arun Bansil² and Kazuyoshi Yamada¹
¹Japan Synchrotron Radiation Research Institute, Japan
²Northeastern University, USA
³Delft University of Technology, Netherlands
⁴Japan Atomic Energy Agency, Japan
⁵Tohoku University, Japan

The evolution of electronic structures with carrier doping is essential to understanding the mechanism of high-temperature superconductivity. Several spectroscopies, such as photoemission [1], x-ray absorption [2] and Compton scattering [3] have succeeded in probing the evolving nature of high-Tc cuprates and provided information about the electronic dispersions, Fermi surfaces, and orbital characters of doped carriers. In this presentation, we provide a new piece of information on the evolving electronic structure of La_{0.8}Sr_{0.2}CuO (LSCO) by means of Compton scattering. Compton scattering is complementary to other spectroscopies and uniquely measures the ground-state electron momentum distribution, i.e. Compton profile, of all electrons in a compound. This is bulk-sensitive because of a high-energy photon-in and photon-out technique. We have performed Compton profiles measurements of LSCO with x=0, 0.08, 0.15 and 0.3, and obtained two-dimensional electron momentum density (EMD) and k-space electron occupation density (EOD) projected along the c-axis. The EMD and EOD show a doping x dependency and their evolution is discussed in the light of some scenarios.

[1] A. Damascelli et al., Rev. Mod. Phys. 75, 473 (2003) [2] D. C. Peets et al., Phys. Rev. Lett. 103, 087402 (2009) [3] Y. Sakurai et al., Science 332, 698 (2011)

BB01

Valence fluctuations and their possible role in stabilizing the correlated electron state in the system Ce_{1-x}Yb_xCoIn₃

M. Brian Maple*
 Physics, University of California, San Diego, USA

The extraordinary correlated electron phenomena found in compounds containing lanthanide ions with an unstable valence (Ce, Pr, Sm, Eu, Tm, Yb) can be traced to the hybridization of localized 4f and conduction electron states. The physics underlying the correlated electron phenomena is associated with the Kondo effect for moderate hybridization in which the valence (4f shell occupation) is nearly integral and “valence fluctuations” for strong hybridization where the valence is nonintegral. After a brief review of “valence fluctuation” phenomena, we describe recent experiments on the superconducting heavy fermion system Ce_{1-x}Yb_xCoIn₃ which reveal that the correlated electron state is stabilized throughout the range 0 ≤ x ≤ 0.8, apparently due to cooperative behavior of Ce and Yb ions involving their unstable valences [1]. Interestingly, the superconducting critical temperature decreases linearly with x from 2.3 K at x = 0 towards 0 K at x = 1. Non-Fermi liquid behavior is observed at low temperature, although there is no readily identifiable quantum critical point [2]. The intermediate valence of Yb in Ce_{1-x}Yb_xCoIn₃ has been verified by ARPES, EXAFS, and XANES measurements [3,4]. Research supported by U.S. DOE Grant No. DE-FG02-04ER46105 (crystal growth) and NSF Grant No. 0802478 (low temperature measurements).

[1] J. L. Shu, R. E. Baumbach, M. Janoschek, E. Gorzaltes, K. Huang, T. A. Sayles, J. Pagliano, J. O'Brien, D. A. Zocco, P.-C. Ho, C. A. McElroy, M. B. Maple, Phys. Rev. Lett. 106, 156403 (2011), [2] M. B. Maple, R. E. Baumbach, N. P. Butch, J. J. Hamlin, M. Janoschek, J. Low Temp. Phys. 161, 4 (2010), [3] C. H. Booth, T. Durakiewicz, C. Capan, D. Hurt, A. D. Bianchi, J. J. Joyce, Z. Fisk, Phys. Rev. B 83, 235117 (2011), [4] L. Dudy, J. D. Denlinger, L. Shu, M. Janoschek, J. W. Allen, M. B. Maple, in preparation.

BB02

Electronic structures of novel Ce-based systems via photoemission spectroscopy

J.-S. Kang*
 Department of Physics, The Catholic University of Korea, Korea

Ce-based intermetallic compounds exhibit novel physical properties due to the unique character of the localized Ce 4f electrons that have a large hybridization with the conduction-band electrons. In this talk we will describe the photoemission spectroscopy (PES) study of the electronic structures of the Ce compounds that show diverse physical properties, such as superconductivity, pseudo-gap formation, charge-density-wave (CDW) formation, and colossal magneto-resistance. We will discuss on CeNiSn, CeTe₂, CeRu₃, and La_{0.7}Ce_{0.3}MnO₃, for which the valence states of Ce ions vary from being trivalent (Ce³⁺) to being mixed-valent and tetravalent (Ce⁴⁺), depending on the strength of the hybridization. Our study shows the different roles of Ce 4f states in determining their ground states. In particular, we will report our recent angle-resolved PES (ARPES) study of the quasi-two dimensional CDW system CeTe₂ in comparison with the band-structure calculations [1,2]. Our ARPES study provides the information on the role of the Ce 4f states in the CDW formation, the carriers near the Fermi level, the effect of band-folding due to the interaction with Ce-Tc(2) layers on the Fermi surface, and the CDW modulation vector in CeTe₂. Keywords: ARPES, CDW, electronic structure, quasi-two dimensional system

[1] J. H. Shim, J.-S. Kang, and B. I. Min, Phys. Rev. Lett. 93, 156406 (2004). [2] J.-S. Kang, D. H. Kim, H. J. Lee, J. H. Hwang, H. K. Lee, H.-D. Kim, B. H. Min, K. E. Lee, Y. S. Kwon, J. W. Kim, Kyoo Kim, B. H. Kim, B. I. Min, Phys. Rev. B 85, 085104 (2012).

BB03

Valence state and spin state of Fe in SrFe_{1-x}(Sc,Sr)_xO₃ perovskites

Youssef Rizki¹, Jean-marie Le Breton^{1*}, Yohann Breard², Emeric Folcel¹ and Antoine Maignan²
¹Groupe de Physique des Matériaux - UMR 6634, CNRS - Université de Rouen, France
²CRISMAT, UMR 6508 CNRS, ENSICAEN - Université de Caen, France

The coexistence of Fe³⁺ and Fe⁴⁺ in SrFeO_{3-d} in relation with oxygen vacancies, influences the electronic conductivity and is at the origin of the giant negative magnetoresistance effect [1,2]. With the aim to investigate the influence of the valence state of Fe on the physical properties (magnetism, transport) in SrFe_{1-x}M_xO_{3-d} perovskites (M=Sc,Sr and 0≤x≤1) were prepared by solid state synthesis method and investigated by X-ray diffraction, 57Fe Mossbauer spectrometry and susceptibility measurements. Replacing Fe ions with ions with a fixed valence state (Sc³⁺ or Sn⁴⁺) modifies the Fe³⁺/Fe⁴⁺ ratio and the oxygen content. Introducing Sc³⁺ ions leads to a decrease of both Fe⁴⁺ and oxygen contents without affecting the crystal structure. However, the substitution is limited. In the SrFe_{0.5}Sc_{0.5}O_{2.5} limit compound, only Fe²⁺ ions are detected, in two different spin states. Introducing Sn⁴⁺ ions leads to a decrease of the Fe⁴⁺ content and to an increase of the oxygen content. The substitution is not limited, and Fe³⁺ and Fe²⁺ ions coexist in the whole composition range. The spin state of the Fe³⁺ and Fe⁴⁺ ions is discussed. This work was supported by the French Agence Nationale de la Recherche (project ANR-08-BLAN-0005-01).

[1] Y.M. Zhao, R. Mahendiran, N. Nguyen, B. Raveau and R.H. Yao, Phys. Rev. B 664 (2001) 024414 [2] A. Maignan, C. Martin, N. Nguyen and B. Raveau, Sol. State Sci. 3 (2001) 57

BE02

Experimental probing of the magnetic order in ultrathin (Ga,Mn)As

M. Sawicki¹, D. Chiba², O. Proselkov³, A. Korbecka⁴, Y. Nishitani⁵, F. Matsukura⁶, J. A. Majewski⁷, J. Sadowski⁸, T. Dietl⁹ and H. Ohno⁹

- ¹ Institute of Physics, Warsaw, Poland, and RIEC, Tohoku University, Sendai, Japan, Poland
- ² Institute for Chemical Research, Kyoto University, Uji, Kyoto, Japan
- ³ Institute of Physics, Polish Academy of Sciences, Warsaw, Poland
- ⁴ Institute of Theoretical Physics, University of Warsaw, Poland
- ⁵ Laboratory for Nanoelectronics and Spintronics, RIEC, Tohoku University, Sendai, Japan
- ⁶ Laboratory for Nanoelectronics and Spintronics, and CSIS, Tohoku University, Sendai, Japan
- ⁷ Institute of Physics, Warsaw, Poland, and MAX-Lab, Lund University, Lund, Sweden
- ⁸ Institute of Physics, Warsaw, and Institute of Theoretical Physics, University of Warsaw, Poland

Colossal negative magnetoresistance and the associated insulator-to-metal transition are arguably the most characteristic features of magnetic and dilute magnetic semiconductors. Particularly intriguing is the case of (Ga,Mn)As and related systems in which spin-spin coupling is mediated by holes. In order to find out how magnetism evolves when the carrier density is diminished, we have probed magnetization changes induced by: (i) electric field in metal/insulator/(Ga,Mn)As structures [1] and (ii) thinning of the channel by sequential chemical etching. Our findings show that both the channel depletion and thinning results in a monotonic decrease of Curie temperature and spontaneous magnetic moment, with no evidence for the maximum expected within the impurity-band models but explained theoretically in terms of the p-d Zener model, modified for the thin film case [1]. They also confirm the presence of the theoretically predicted spin reorientation transition. We have found that the transformation to a non-magnetic state proceeds via the emergence of a hitherto non-revealed superparamagnetic-like spin arrangement, driven by critical fluctuations in the local density of states, specific to the Anderson-Mott quantum transition. Within our model, these nanoscale fluctuations of magnetization give rise to critical scattering which vanishes when localized spins are ordered by an external magnetic field.

[1] M. Sawicki, D. Chiba, A. Korbecka, Y. Nishitani, J.A. Majewski, F. Matsukura, T. Dietl, H. Ohno, Nature Phys. 6, 22 (2010).

BE03

Origin of ferromagnetism in Ga_{1-x}Mn_xN

Thibaut Devillers^{1*}, Maciej Sawicki², Wiktor Stefanowicz², Sylwia Dobkowska², Bogdan Faina¹, Andrea Navarro-quezada¹, Tian Li¹, Andreas Grois¹, Mauro Rovezzi³, Tomasz Dietl² and Alberta Bonanni¹

- ¹ Institute for Semiconductor and Solid State Phys., Johannes Kepler University, Austria
- ² Institute of Physics, Polish Academy of Sciences, Warsaw, Poland
- ³ European Synchrotron Radiation Facility, Grenoble, France

Despite Ga_{1-x}Mn_xN is the model system for a broad class of dilute magnetic semiconductors and oxides, diverging opinions about its magnetic ground state have been reported: this material was found to be either spin glass, or an antiferromagnet or a ferromagnet with rather disperse values of the T_c, ranging from below 10 K up to over 300 K [1,2]. By employing a range of ion beam, diffraction, and spectroscopy methods we have demonstrated [3,4] that particular magnetic signatures can be linked to a specific distribution of the magnetic ions and to their charge state, both affected by growth conditions and by the presence of shallow impurities. By combining extensive epitaxy and nanocharacterization programs with high sensitivity mK-SQUID measurements, we demonstrate that Ga_{1-x}Mn_xN with randomly distributed Mn²⁺ ions is a ferromagnet with T_c below 5 K for x < 5%. To clarify the origin of ferromagnetism in this material with no band carriers, we examine To(x) ~ x^m and show that the value m = 2 is consistent with ferromagnetic superexchange. We discuss our results in the light of the available ab initio studies and compare our system to Cr chalcogenide and oxide spinels, where ferromagnetic and antiferromagnetic superexchange coexist.

[1] A. Bonanni and T. Dietl, Chem. Soc. Rev. 39, 528-539 (2010) [2] T. Dietl, Nature Mat. 9, 965-974 (2010) [3] W. Stefanowicz, D. Stenkiel, B. Faina, A. Grois, M. Rovezzi, T. Devillers, A. Navarro-Quezada, T. Li, R. Jakiela, M. Sawicki, T. Dietl, and A. Bonanni, Phys. Rev. B 81, 235210.1-14 (2010) [4] A. Bonanni, M. Sawicki, T. Devillers, W. Stefanowicz, B. Faina, Tian Li, T. E. Winkler, D. Stenkiel, A. Navarro-Quezada, M. Rovezzi, R. Jakiela, A. Grois, M. Wegscheider, W. Jantsch, J. Suffczyński, F. D'Acapito, A. Meingast, G. Kothleitner, and T. Dietl, Phys. Rev. B 84, 035206.1-11 (2011).

BE04

The effects of non-magnetic dopant on semiconductor materials

Caihong Zhang* and Dickon H. I. Ng
Physics Department, The Chinese University of HongKong, China



BE05

I-Mn-V room temperature antiferromagnetic semiconductors

Xavier Martí^{1*}, Peter Wädley², Helena Reichlova², Premysl Beran¹, Olya Steinhakovyč¹, Ineke Wijnheijmer³, Paul Koenraad⁴, Frantisek Maca⁵, Jan Masek⁶, Klara Uhlirova⁶, Vit Novak⁶ and Tomas Jungwirth⁷

- ¹ Condensed Matter Physics, Charles University in Prague, Czech Republic
- ² Institute of Physics ASCR, Czech Republic
- ³ Nuclear Physics Institute ASCR, Czech Republic
- ⁴ Charles University in Prague, Czech Republic
- ⁵ COBRA Inter-University Research Institute, Netherlands
- ⁶ COBRA, Inter-University Research Institute, Netherlands

Recent observation of a large magnetoresistance in an antiferromagnet (AFM) based spin-valve opens the prospect for utilizing AFMs in spintronics [1]. This motivates a search for new materials which may be suitable for spintronics and are room-temperature AFMs. The desired control of devices via electrical fields could be further exploited if the materials involved would be also semiconductors. We present our results [2] in the growth and characterization of a new family of room-temperature antiferromagnetic semiconductors and semimetals. We show X-ray diffraction, magnetization, transport, and differential thermal analysis measurements of chemically synthesized bulk CuMnAs and CuMnSb. Experiments are complemented by theory calculations of band structure and magnetic structure. The progress in bulk I-Mn-V materials encourages also the investigation of thin layers. We will show the epitaxial growth of LiMnAs [3] and CuMnAs on conventional GaAs. Scanning tunneling microscopy has shown that in the case of LiMnAs there is a bandgap [4].

[1] B. G. Park et al, Nature Materials 10, 347 (2011) [2] F. Maca et al, J. Magn. Magn. Mater. 324, 1606 (2012) [3] T. Jungwirth, et al, Phys. Rev. B 83, 035321 (2011) [4] I. Wijnheijmer, et al, submitted

BF01

The verway phase of magnetite - a long-running mystery in magnetism

J Paul Attfield
University of Edinburgh, United Kingdom

Magnetite (Fe₃O₄) undergoes a complex structural distortion and becomes electrically insulating below 125 K. Verwey proposed in 1939 that this transition is driven by a charge ordering of Fe²⁺ and Fe³⁺ ions, but the low temperature state has remained contentious as twinning of crystal domains hampers diffraction studies of the structure. A variety of ground state models has been proposed over seven decades of study. We have recently reported the full low temperature superstructure of magnetite, determined by high energy x-ray diffraction from a 40 μm grain, and we identify the emergent order. The acentric structure is described by a superposition of 168 frozen phonon modes all with amplitude <0.24 Å. Distortions of the FeO₄ octahedra show that Verwey's hypothesis is correct to a first approximation. However, anomalous shortening of some Fe-Fe distances shows that the localised electrons are distributed over linear three-Fe-site units that we describe as 'trimérons' - this description is supported by band structure calculations. The charge order and trimeron distortions induce substantial off-centre atomic displacements and couple the resulting large electrical polarisation to the magnetisation so that multiferroic behaviour is expected. Trimérons may be significant quasiparticles above the Verwey transition and in other transition metal oxides.

M.S. Senn, J.P. Wright and J.P. Attfield, Nature 481, 173 (2012). M.S. Senn, I. Loa, J.P. Wright and J.P. Attfield, Phys. Rev. B, in press (2012).

BF02

Possible link of a structurally driven spin flip transition and the insulator-metal transition in the perovskite La_{1-x}Ba_xCoO₃

Despina Louca and Peng Tong
Department of Physics, University of Virginia, USA

The intricate nature of the magnetic ground state near the insulator-metal transition (IMT) in La_{1-x}Ba_xCoO₃ was investigated via neutron scattering. For x less than the critical concentration, x_c ~ 0.22, a commensurate antiferromagnetic (AFM) phase initially appears. As x approaches x_c, the AFM component continuously weakens while ferromagnetic (FM) order sets in the rhombohedral lattice. The two magnetic phases appear to be growing in different domains and have different ordering temperatures, with the FM order parameter setting in first at higher temperatures while the AFM order parameter occurs at lower temperatures. At x_c, a spin flip to a new FM state occurs while the crystal transforms to an orthorhombic (Pnma) symmetry. The magnetic Pnma phase coincides with the minimum saturation reached in the resistivity. It is proposed that the orbital overlap in the Pnma phase is the most conducive to charge hopping. The structurally driven spin flip creates metallic FM droplets and the percolation of these droplets drives the system to become metallic. This, in turn, suggests that the FM domains in the rhombohedral phase are in fact insulating. This is fundamentally distinct from other magnetoresistive perovskites where only one FM transition is observed prior to the IMT.

BF03

Slow magnetic crossover in the frustrated magnet Ca₃Co₂O₆

Stefano Agrestini^{1*}, Martin R Lees², Catherine L Fleck², Oleg A Petrenko², Laurent C Chapon³, Claudio Mazzoli¹ and Alessandro Bombardi³

- ¹ Max-Planck Institut CPIS, Dresden, Germany
- ² Department of Physics, University of Warwick, Coventry, United Kingdom
- ³ ILL, Grenoble, France
- ⁴ Dipartimento di Fisica, Politecnico di Milano, Milano, Italy
- ⁵ Diamond Light Source, Didcot, United Kingdom

Time-dependent phenomena play a crucial role in the properties of many magnetic systems, including spin-glasses, single-molecule magnets and superparamagnets. However time-dependent magnetism is not expected to be observed in the presence of long-range magnetic order. Here we challenge this view by reporting the observation of a new time-dependent behavior where a transition from one long-range magnetically ordered state to another occurs in zero magnetic field over a time scale of several hours. We performed an extensive neutron diffraction study of the spin chain system Ca₃Co₂O₆ whose step-like magnetization versus magnetic field aroused great interest in the scientific community. Our data show that for T < 14K < TN = 25K the spin-density-wave order observed immediately below TN, becomes unstable and a commensurate antiferromagnetic phase appears via a very slow transformation process. As the temperature is reduced the characteristic time of the transition process increases rapidly and at low temperatures the magnetic states become frozen. The transition is also noteworthy because the two phases have different propagation vectors. Very rarely transitions between two magnetically ordered phases involve a change of translational symmetry. This discovery sheds new light on the peculiar dynamic properties of Ca₃Co₂O₆. S. Agrestini et al., Phys. Rev. Lett. 106, 197204 (2011).

BF04

Incommensurate magnetic states in itinerant systems

Marat Timirgazin and Anatoly Arzhnikov
Physical-Technical Institute of Ural Branch of Russian Academy of Sciences, Russia

We study the ground state of the Hubbard model within the Hartree-Fock approximation taking into account both the incommensurate magnetic phases (spiral and collinear spin-density waves) and their possible participation in the phase separation (PS). We construct magnetic phase diagrams for 2D and 3D lattices with different values of the parameter of the electron hopping between the next-nearest neighbors [1]. We show that the incommensurate magnetic state is the ground one in a wide range of the model parameters. There is a large region of the PS in the vicinity of half-filling. The data obtained agree well on a qualitative level with experimental data on the magnetic state of a superconducting compound La_{2-x}Sr_xCuO₄ [2]. We consider the metal-insulator transition (MIT) at half-filling taking into account incommensurate magnetic states. Calculations show that, for the square lattice, MIT coincides with the first-order magnetic transition from a spin-spiral to antiferromagnetic state. To our knowledge this result is the first example of MIT between two magnetically ordered states in the 2D lattice. Previously, the critical dimension for this transition was considered to be in a range from 2 to 3. Thus, our investigation proves this value to be below 2.

[1] Igoshev P. A., Timirgazin M.A., Katanin A.A., Arzhnikov A.K., and Irkhin V.Yu. Phys. Rev. B 81, 094407 (2010) [2] Fujita M. et al., Phys. Rev. B 65, 064505 (2002)

BF05

Canted spins of Mn₃O₄ investigated by 55Mn²⁺ and 55Mn³⁺ nuclear magnetic resonance in magnetic field

Changsoo Kim, Jeong Hyun Shim, Euna Jo, Byeongki Kang, Sangil Kwon and Soonchil Lee*
Department of Physics, KAIST, 291 Daehak-ro, Yuseong-gu, Daejeon 305-701, Korea

For a long time, huge magnetic anisotropy in Mn₃O₄ has attracted a lot of interest from researchers. The magnetization along the c-axis is smaller than that along the ab-plane even in 30 Tesla. It has been believed that this phenomena occurs due to a uniaxial anisotropy of Mn³⁺ along the c-axis. However, there has been no experiment to verify this theory. We measured 55Mn²⁺ and 55Mn³⁺ Nuclear Magnetic Resonance of a Mn₃O₄ single crystal in 7 Tesla external magnetic field. The angle between each magnetic moment and the field was calculated from the spectral shifts obtained for various magnetic field directions between the a, b and c-axes. From the fact that Mn²⁺ moments are tied to the ab-plane when the magnetic field is in the direction along the c-axis, we concluded that the Mn³⁺ moment has a large in-plane anisotropy contrary to the previous reports. In contrast, Mn²⁺ moments were tilted toward the field direction, implying that the Zeeman energy of a Mn²⁺ moment is competing with the energy of the exchange interaction between Mn²⁺ and Mn³⁺ moments and the magnetic anisotropy energy of Mn²⁺.

BG01

L10 ordered FePt based granular films for thermally assisted magnetic recording

Y K Takahashi*, B Varaprasad, C Min, L Zhang and K Hono
National Institute for Materials Science, Japan

L10 ordered FePt is considered to be one of the candidate for ultrahigh density perpendicular recording media beyond 1 Tb/in2 due to its high magnetocrystalline anisotropy. We recently reported well controlled microstructure of FePtAg-C granular film with an average particle size of about 6 nm and small size distribution of about 20 % [1]. Furthermore, we demonstrated areal density of 550 Gb/in2 by a static test using a head for thermally assisted magnetic recording [2]. Although we achieved a particle size of 6 nm with narrow size distribution, the FePt-C system has a weakness in attaining small surface roughness with a columnar structure due to the strong phase separation tendency between FePt and C in not only the lateral direction but also the growth direction. To attain columnar structure with smooth surface, we chose TiO₂ as a matrix. In this presentation, we will show FePt granular film with columnar structure and smooth roughness.

[1] L. Zhang, Y.K. Takahashi, A. Perumal and K. Hono, JMMM322,2658 (2010). [2] L. Zhang, Y.K. Takahashi, K. Hono, B. C. Stipe, J.-Y. Juang, and M. Grobis, IEEE Trans. Magn. 47, 4062 (2011).

BG02

Nanogranular FePt films for thermally assisted recording

Tiffany Santos, O. Mosendz, J. Reiner, S. Pisana, G. Parker and D. Weller
Hitachi GST, USA

In order to extend the data storage density in hard disk drives beyond 1 Tb/in2, using a high crystalline anisotropy (Ku) material as the magnetic media layer is required to reduce the grain size further while maintaining thermal stability. However, the magnetic field applied by a conventional write head is not strong enough to reverse the magnetization of the high-Ku media. A promising approach to recording using high-Ku materials is thermally-assisted recording (TAR), in which the media is locally heated near the Curie temperature by an optically-generated heat pulse in the presence of a magnetic field, both applied by a laser-integrated write head, in order to write a bit. Given its moderate T_c, high Ku, corrosion durability, and high dKu/dT near T_c, FePt alloy with L10 crystalline order is a potential candidate for TAR media. We deposit FePt nano-granular films by sputtering on glass substrates at elevated temperature. Underlayer materials are selected for heat-sinking and to obtain high, out-of-plane L10 order. Structural and magnetic characterization and transmission electron microscopy of the media show that we can achieve properties that are promising for TAR, such as isolated grains with an average grain size <7.5nm, a low size distribution and Ku>4.5x10⁷ erg/cm³.

BG03

Single crystalline isolated grains of L10-ordered FeCuPt prepared by combination of rapid thermal annealing with rapid cooling and additional annealing

Tatsuya Ubana¹, Arata Tsukamoto^{2*} and Akiyoshi Itoh²
¹ Graduate School of Science and Technology, Nihon university, Japan
² College of Science and Technology, Nihon university, Japan

We reported¹⁾²⁾, that the Rapid Thermal Annealing (RTA) of FeCuPt multilayered continuous films are effective to obtain perpendicularly magnetized small L10-FeCuPt grains on thermally oxidized Si substrate. In this report, we introduced a rapid cooling process (RCP) into RTA and compared with the natural cooling processes. FeCuPt grains were fabricated under the variety of heating up rate (TR) and the maximum temperature (Tm). Isolated grains are obtained at higher TR and Tm. With RCP, growing of grains are prevented, however new peaks in XRD (X-ray diffractometer) profile are appeared at slightly lower angle of (002) and it may be correspond to the disordered structure of FeCuPt. From electron diffraction patterns and dark field images by TEM, mostly L10-ordered polycrystalline structure was observed. Therefore, we preformed additional annealing for above isolated FeCuPt grains (600 degree C, 1 hour). Annealing condition was decided from an estimation of atomic diffusion length³⁾. After additional annealing, grains kept almost similar size and the new peak was banished in XRD profile. Furthermore, we observed single crystalline L10-ordered structure from electron diffraction pattern of a single grain. As a result, single crystalline L10-FeCuPt isolated grains are obtained by RTA with rapid cooling and additional annealing.

1) Y. Itoh, T. Aoyagi, A. Tsukamoto, K. Nakagawa, A. Itoh and T. Katsuyama: Jpn. J. Appl. Phys., 43, 12, 8040(2004). 2) A. Itoh, Y. Itoh, K. Namba, Y. Adachi, M. Motokashi, and A. Tsukamoto: J. Appl. Phys., 99, 08Q906(2006). 3) M. Remhof, B. Sepol, M. Stadelock, D. Konic, S. Stanok, G. Vogl, M. Koclovski, R. Koczinski, A. Vanrompaey, J. Meerschaert, R. Ruffer, and A. Gupta, Phys. Rev. B 74, 104301, (2006).

BG04

Oscillation characteristics of spin-torque oscillator calculated using integrated simulator with spt writer

Kazuetsu Yoshida¹, Souta Asaka², Takuya Hashimoto² and Yasushi Kana³

¹ Information and Communications Engineering, Kogakui University, Japan

² Graduate school of electrical engineering and electronics, Kogakui University, Japan

³ Information and Electronics Engineering, Niigata Institute of Technology, Japan

Microwave-assisted magnetic recording (MAMR) requires a spin-torque oscillator (STO) to induce magnetic resonance in the recording medium. The oscillation characteristics of an STO have previously been investigated using micromagnetic simulators based on spatially isolated models [1]-[3], which neglect the magnetostatic interactions between an STO and a Single-Pole-Type (SPT) writer. We have developed a new simulator that takes into account the magnetostatic interaction between an SPT writer and an STO, and we refer to this as an integrated MAMR simulator. This interaction was found to have considerable influences on the oscillation behaviors of an STO. Simulations were carried out for an STO with a lateral length of 30 nm and a thickness of 10 nm inserted in the gap between a main-pole and a floating-type trailing shield. The stray field in the gap increased by approximately 30% by inserting the STO and its oscillation frequency was 8 GHz. For comparison, the oscillation frequency calculated using a conventional isolated STO simulator was found to be 16 GHz. This decrease in frequency may be the result of an energy loss in the main-pole of an SPT writer that is excited by the high-frequency field from an STO.

[1] J.-G. Zhu, X. Zhu, and Y. Tang, "Microwave Assist Magnetic Recording," *IEEE Trans. Magn.*, 44, No. 1, 125-131(2008). [2] D. Houssemeldine, et al., "Spin-torque oscillator using a perpendicular polarizer and a planar free layer," *Nature Mater.*, 16, 447-453(2007). [3] K. Yoshida, M. Yokoe, Y. Ishikawa, and Y. Kana, "Spin-Torque Oscillator with Negative Magnetic Anisotropy," *IEEE Trans. Magn.*, 46, 2466-2469(2010).

BH01

Magnetic nanotechnology for cancer treatment

Thanos Mitrelas¹, Valerii Orel², Marina Tselepi³, Crispin Barnes², I Schepotin², A Romanov² and A Shevchenko²

¹ Cavendish Laboratory, University of Cambridge and Cavendish NanoTherapeutics Ltd, United Kingdom

² National Cancer Institute, Kiev, Ukraine

³ Cavendish Laboratory, University of Cambridge and Cavendish NanoTherapeutics, United Kingdom

⁴ Cavendish Laboratory, University of Cambridge, United Kingdom

⁵ Kurdyumov Institute for Metal Physics, Kiev, Ukraine

Often the conventional therapies needed to annihilate cancer cells have high systemic toxicity effects. We are developing systems which utilise magnetic nanoparticles loaded with therapeutic agents, directed and guided towards the tumour site and preferentially attached to the tumour to destroy it. The cancer cells are killed by the combined action of the drugs and a local temperature increase in the area around the tumour site using externally applied electromagnetic irradiation (hyperthermia). The aim is to avoid most side effects since the nanoparticles target specifically the tumour area and leave most of the surrounding tissues unaffected, therefore higher doses of the drug reach the target area even if lower overall doses are administered. Our preliminary clinical trials and pilot studies have demonstrated significant effects in the reduction of the tumour size and a 50% increase in the survival rates (on average) of patients with breast, lung, endometrial, colorectal, malignant melanoma, etc. For example, in patients with lung cancer IIIA stage we have demonstrated a tripling in the 5-year survival rates. The unique aspects of our platform technology are (i) synthesis of nanoparticles with high magnetization, (ii) less tendency to agglomerate, (iii) generation of spatially non-homogeneous electromagnetic fields.

BH02

The low magnetic field effect of sanals of primo vascular system

Sang-suk Lee¹, Kwang-sup Soh², Min-suk Rho³, Yeong-min Yoo⁴, Jong-gu Choi⁵, Sung-ah Shim¹, Young-il No¹, Jun-yeong Shin¹ and Ran-hyang Kim¹

¹ Oriental Biomedical Engineering, Sangji University, Korea

² Nano-Primo Research Center, Seoul National University, Korea

³ Sangji University, Korea

⁴ Biomedical Engineering, Yonsei University, Korea

⁵ Eastern-Western Biomedical Engineering, Sangji University, Korea

The motion features of sanals inside of the primo vascular system (PVS), that is so-called the Kyungrak system, are investigated under a low static magnetic field by using the anatomy technology and optical microscope. The sanals with a size of about 1 μm selected and separated from the primo vessel and node of the real PVS inside of the surface of the internal organs are observed from rabbits' abdominal wall and dipped with PBS liquid inside of petri dish. The sanal's moving velocity along the direction of magnetic field (x-direction) and perpendicular to the direction of magnetic field (y-direction) under the low magnetic field of 0 Oe, 20 Oe, 40 Oe, 60 Oe, and 80 Oe, respectively, is observed below a internal temperature of 38 oC. Ten sanals' moving velocities versus magnetic field are shown two differently dominant tendencies with an average velocity of 0.9 pixel/s and a random velocity according to the x-direction and y-direction, respectively. This experimental results imply that the rotating motion of sanal with nuclei DNA composed of many inorganic magnetic materials of Mn and Co is monotonically weakened by the increase of applied magnetic field.

[1] K. S. Soh, J. Kor. Phys. Soc. 45, 1196 (2004). [2] K. S. Soh, J. Acupunct. Meridian Stud. 2, 93 (2009). [3] B. C. Lee, K. W. Kim, and K. S. Soh, J. Acupunct. Meridian Stud. 2, 66 (2009). B. H. Kim, J. Jo Sun Med. 9, (Koreana) 5 (1962). [4] B. H. Kim, J. Jo Sun Med. 90, (Korean) 6 (1963). [5] B. H. Kim, J. Jo Sun Med. 108, (Korean) 1 (1965). [6] B. H. Kim, J. Jo Sun Med. 108, (Korean) 39 (1965). [7] B. H. Kim, J. Jo Sun Med. 108, (Korean) 1 (1965).

BH03

Magnetic targeting of mesenchymal stem cells in the spinal cord

Vaclav Vanecek¹, Jiri Ruzicka¹, Serhiy Forostiak¹, Michal Babic², Vit Herynek¹, Alexandr Dejneka⁴, Vitalii Zablotskii⁵, Sarka Kubinova¹, Pavla Jendelova³ and Eva Sykova¹

¹ Institute of Experimental Medicine, Czech Republic

² Institute of Macromolecular Chemistry, Czech Republic

³ MR-Unit, Institute for Clinical and Experimental Medicine, Czech Republic

⁴ Institute of Physics, Czech Republic

Mesenchymal stem cells (MSC) are currently under intensive study as a possible therapeutic agent in spinal cord injury [1]. MSCs labeled with superparamagnetic iron oxide nanoparticles (SPIO) can be manipulated by an externally applied magnetic field and successfully targeted to different organs. We transplanted SPIO-labeled MSC into rats with a magnetic implant or a non-magnetic substitution inserted above the spinal cord intrathecally via lumbar puncture one week after spinal cord injury. The fate of the grafted cells was monitored by means of magnetic resonance imaging (MRI) [2] and histologically. In our experiments, the transplanted cells were present mostly on the surface of the spinal cord (in the subarachnoid space) in both the magnetic and non-magnetic (control) groups. In the lesion area of the spinal cord, there was a significant difference in cell distribution between the magnetic and non-magnetic groups. The SPIO-loaded cells circulating in the subarachnoid space were gathered under the magnetic implant near the site of injury. Additionally, we suggest how magnetic cell targeting can be improved by using a magnet specially designed to produce spatially modulated multigradient stray fields [3]. The proposed magnetic delivery system might be attractive for clinical application development. Supported by P304/12/1370, AVOZ503905703.

1. E. Sykova, et al., *Cell Mol Neurobiol*, 26 (7-8) 1113 (2006). 2. E. Sykova and P. Jendelova, *Ann N Y Acad Sci.*, 1049, 146 (2005). 3. V. Zablotskii, et al., *American Institute of Physics, Conference Proceeding Series 1311*, 152 (2010).

BH04

Tilted bianchi type - I magnetised viscous fluid cosmological model

Subrata Kumar Sahu

Mathematics, Lingayas university, India

Tilted Bianchi type - I cosmological model for viscous fluid distribution embedded in a magnetic field is investigated. The role of the bulk viscosity and electromagnetic field in getting an inflationary phase and in establishing the tilted universe is discussed.

BH05

Growth of highly uniform graphene for spintronic applications

Shiro Entani, Yoshihiro Matsumoto, Manabu Ohtomo, Pavel V Avramov, Hiroshi Naramoto and Seiji Sakai

Advanced Science Research Center, Japan Atomic Energy Agency, Japan

Graphene has attracted wide attention for nanoelectronics and spintronics. In this study, in-situ analysis were performed on the graphene growth in ultrahigh vacuum chemical vapor deposition (UHV-CVD) by exposing the epitaxial Ni(111) thin film to benzene vapor at 873 K. It is shown that the uniform single- and bi-layer graphenes can be synthesized by the control of benzene exposure in the range of 10-105 langmuirs, reflecting a change in the graphene growth-rate by three orders of magnitude in between the first and second layer. It is also suggested that the chemical interaction between bi-layer graphene and Ni(111) is weak in comparison with that between single-layer graphene and Ni(111). Ex-situ micro-Raman analysis on the large area graphene film transformed on a SiO₂ substrate makes it clear that the structural and electrical uniformities can be improved remarkably under the specific exposure conditions at which the growth of the respective graphene layers are completed. The present results demonstrate that the UHV-CVD method enables the growth of highly uniform graphene which would be necessary for controlling the spin transport process as well as realizing a long spin-relaxation length in the graphene-based spintronic devices by optimizing the dosage of precursors and the growth temperature.

BH06

Depth-resolved XMCD spectroscopy on single-layer graphene / Ni structure

Yoshihiro Matsumoto¹*, Shiro Entani¹, Manabu Ohtomo¹, Pavel V Avramov¹, Hiroshi Naramoto¹, Kenta Amemiya² and Seiji Sakai¹

¹ Advanced Science Research Center, Japan Atomic Energy Agency, Japan

² Institute of Materials Structure Science, High Energy Accelerator Research Organization, Japan

The graphene-metal interaction is not only of fundamental interest but also of technological importance in view of spintronic applications. For example, a recent theoretical calculation predicts a spin filtering effect of graphene attached on the ferromagnetic metal surface under the current-perpendicular-to-the-plane configuration [1]. For the purpose of clarifying the electronic and magnetic states of the single layer graphene (SLG)/FM structure especially at the interface region, depth-resolved X-ray absorption and X-ray magnetic circular dichroism (XMCD) spectroscopy are performed on the SLG/Ni(111) structure grown by using the ultrahigh vacuum chemical vapor deposition and molecular beam epitaxy techniques. An intense XMCD signal is observed in the C K-edge XMCD spectrum taken under the surface sensitive condition. This indicates that there exists the Ni-induced spin polarization in the orbitals of SLG even at room temperature. It is also found that the XMCD intensity shows a dramatic change with the probing depth. The depth-resolved analysis of the Ni L-edge XMCD spectrum makes clear that the magnetization of Ni is decreased by 20-30% within a few atomic layers from the interface with SLG, possibly associated with the formation of C-Ni bonds.

[1] V. M. Karpan et al., *PRL* 99 (2007) 176602.

BIO1

Magnetoresistance and spin-transfer torque in magnetic tunnel junctions

Shinji Yuasa^{1,2*}, Kay Yakushiji¹, Akio Fukushima¹, Hitoshi Kubota¹, Takayuki Nozaki¹ and Koji Ando¹

¹ Spintronics Research Center, National Institute of Advanced Industrial Science and technology (AIST), Japan

² Distinguished Lecturer of IEEE Magnetic Society, Japan

A magnetic tunnel junction (MTJ) consisting of a tunnel barrier sandwiched between two ferromagnetic electrodes exhibits the tunnel magnetoresistance (TMR) effect due to spin-dependent electron tunneling. Since the discovery of room-temperature TMR in the mid-1990s, MTJs with an amorphous aluminum oxide (Al-O) tunnel barrier have been studied extensively. Such MTJs exhibit a magnetoresistance (MR) ratio of several tens of percent at room temperature (RT) and have been applied to magnetoresistive random access memory (MRAM) and the read heads of hard disk drives. MTJs with MR ratios substantially higher than 100%, however, are desired for next-generation spintronic devices. In 2001, first-principle theories predicted that the MR ratios of epitaxial Fe/MgO/Fe MTJs with a crystalline MgO(001) barrier would be over 1000% due to the coherent tunneling of specific Bloch states. In 2004, MR ratios of about 200% were obtained for MgO-based MTJs [1]. MTJs with a CoFeB/MgO/CoFeB structure were developed for practical application and found to have MR ratios of above 200% and other practical properties [1,2]. The talk focuses on the physics of magnetoresistance and spin-transfer torque in MTJs and the application of MTJs to various spintronic devices such as magnetic sensors and spin-transfer-torque MRAM especially with perpendicularly magnetized electrodes.

[1] S. Yuasa and D. D. Djayaprawira, *J. Phys. D: Appl. Phys.* 40, p.R337 (2007). [2] D. D. Djayaprawira, K. Tsunekawa, M. Nagai, H. Mochizuki, S. Yamagata, N. Watanabe, S. Yuasa, Y. Suzuki and K. Ando, *Appl. Phys. Lett.* 86, 092502 (2005).

BIO2

MTJ based non volatile logic for ultimate power management

Tetsuo Endoh, Takashi Ohsawa, Takahiro Hanyu and Hideo Ohno

Tohoku University, Japan

Recently, the achievement of the silicon-LSI's target performance is becoming difficult only by scaling technologies. First, the speed-gap between the operation speed of logic and each memory has expanded. Moreover, its power consumption increases rapidly, too. In this paper, we describe both MTJ based Non Volatile (NV-) Embedded SRAM and MTJ based NV-Logic circuit. Firstly, we show the proposed MTJ based SRAM that consists of 4 MOSFETs and 2 MTJs. This STT-SRAM achieves an excellent static noise margin that is larger than the resistive load SRAM counterpart by taking advantage of the MTJ's switching characteristics. The cell size becomes comparable with the conventional 6-transistor SRAM and even smaller as the MTJ size shrinks along with the MOSFET scaling. Next, from the viewpoint of super-low power consumption systems, MTJ based NV-Logic, that fuses the STTRAM with semiconductor CMOS logic, is discussed. Especially, we describe the proposed MTJ based NV-Latch circuit with high speed operation of 600MHz. It is shown that with using our novel MTJ based NV-Latch circuit, the NV-F/F type NV-Logic can be realized. Finally, we discuss the Logic-in-Memory type NV-Logic. From all, we show novel ultimate power management technique with both MTJ based Embedded NV-Memory and MTJ based NV-Logic.

[1] T. Endoh, *SEMI Technology Symposium in SEMICON Japan, 2007 (Invited Paper)* [2] S. Matsunaga et al. *APEX 1*, 091301, 2008. [3] D. Suzuki et al. *VLSI Circuit Symposium 2009* [4] H. Ohno et al. *IEDM 2010 (Invited Paper)* [5] T. Endoh, *2011 CMOS ET Workshop 2011 (Invited Paper)* [6] T. Endoh, *ITRS Emerging Research Memory Technologies Workshop 2010* [7] T. Endoh, *SEMICON Korea2010 (Invited Paper)* [8] T. Endoh, *Materials R research Society 2010 Spring Meeting, 2010 (Invited Paper)* [9] T. Endoh, *INCT, 2011* [10] T. Ohsawa et al., *SSDM*, pp. 959-960, 2011 [11] T. Endoh, et al., *IEDM 2011*

BIO3

Spin gating a transistor and spintronics with antiferromagnets

Tomas Jungwirth

Institute of Physics ASCR, v.v.i., Prague and University of Nottingham, Czech Republic

Spintronics is among leading technologies for reading, writing, and storing information. Spintronic sensors and memory bits rely on spin-dependent electron transport through the device and the same applies to the currently explored concepts for spintronic transistors. Here we demonstrate a new route for using spin in transistors by moving the spin functionality from the transport channel to the capacitively coupled gate. In our transistor, the spin state of the gate controls the charge transport through a conventional non-magnetic electron channel. We explain the phenomenon using the relativistic, spin-orbit coupling theory framework employed in recent studies of anisotropic magnetotransport in spintronic nanodevices. The relativistic magnetic anisotropy phenomena are an even function of the microscopic magnetic moment vector. This means that they can be equally strong in antiferromagnets as in ferromagnets which opens the possibility to realize spin dependent microdevices based on antiferromagnets. As a demonstration we present our experimental observation of >100% tunneling anisotropic magnetoresistance in a device with an antiferromagnetic tunnel electrode.

B. G. Park et al. *Nature Mater.* 10, 347 (2011) X. Marti et al. *Phys. Rev. Lett.* 108, 017201 (2011)

BJ01

Co2y-nicuzn ferrite composites with high permeability

Hsing-i Hsiang* and Po-wen Cheng

Resources Engineering, National Cheng Kung University, Taiwan

Hexagonal structure magnetoplumbite ferrites have revealed a higher dispersion frequency than that of nickel ferrites because of the magnetoplumbite's magnetic anisotropy. The magnetoplumbite ferrite densification temperature always exceeds 1000oC and the initial low temperature firing permeability of magnetoplumbite ferrites with added glass is too low (μi = 2-4). Therefore, it is desirable to develop a material that has a higher permeability at above 300 MHz and can be densified at temperatures below 900°C. The Bi₂O₃-B₂O₃-ZnO-SiO₂ (BBSZ) glass addition effects on the densification and magnetic properties of Co₂Y-NiCuZn ferrite composites with various Co₂Y/NiCuZn ferrite ratios were investigated. The densification of Co₂Y-NiCuZn ferrite composites was enhanced by the addition of glass at low sintering temperatures (<900oC) due to the liquid phase sintering. Co₂Y-NiCuZn ferrite composites with 4 wt% BBSZ glass sintered at 900°C show a relative density above 90%, a high-initial-permeability of 5-6, a quality factor of above 30 in the 200-300 MHz frequency and a resonance frequency above 1 GHz, which can be used in high frequency multilayer chip inductors.

BJ02

Investigation of Fe₂YZ (Y=Ni, Cu; Z=Sn, Ga): The Heusler compounds with tetragonal structure

Margarit Gjoka¹, Dimitris G Niarchos¹, Eamon Devlin¹ and George Hadjipanayis²

¹ Institute of Materials Science, NCSR DEMOKRITOS, Greece

² Physics and Astronomy, University of Delaware, USA

Heusler compounds, a remarkable class of intermetallic materials with 1:1:1 (often called Half-Heusler) or 2:1:1 composition, have attracted considerable interest since their discovery, mainly because of their versatile magnetic properties. Recently has been published a computational study on X₂YZ full Heusler alloys. According to this work, the predicted enthalpies of formation evidence 27 phases to be thermochemically stable against the elements and the regular X₂YZ type. A chemical-bonding study yields an inherent tendency for structural distortion in a majority of these alloys, so they predict the existence of the new tetragonal phase Fe₂CuGa (P42/nm; a = 5.072 Å, c = 7.634 Å; c/a ≈ 1.51) with a saturation moment of μ = 4.69 μB per formula unit. In this work is reported the attempt to synthesize experimentally this new phase. Fe₂MnNiSn and Fe₂CuGa (x = 0, 1, 2) alloys were prepared by arc-melting and annealed at different temperatures in the interval 800-1300K. The Curie temperature (TC) was determined from the high temperature magnetization measurements carried out in a field of 0.05 T using a vibrating sample magnetometer (VSM). The indexing of all XRD patterns of annealed samples and microstructure characterization are in progress and will be present in conference.

Supported by the project REFREPERMAG of the EU

BJ03

Crystallite growth kinetics and microwave properties of Fe-Ti substituted (La,Sr)MnO₃ prepared by mechanical alloying
 Nastiti Elwindari, Hinu Pramuji and Azwar Manaf*
Departement of Physics, Faculty of Natural Sciences Universitas Indonesia, Indonesia



BJ04

Electromagnetic characteristics of Cu substituted Co₂Z-type ferrites Ba₃Co_{2-x}Cu_xFe₂₄O₄₁
 Ji Yeon Song and Young Ho Han*
Materials Engineering, Sungkyunkwan University, Korea

Cu substituted Z-type hexaferrites (Ba₃Co_{2-x}Cu_xFe₂₄O₄₁ with x=0-1.0, Z-hex) were prepared by two step calcinations [1]. The stoichiometric mixture for M-type ferrite was precalcined at 900°C, and then single phase Z-type ferrite powders were synthesized at 1300°C by replacing CoO with various amounts of CuO. The frequency dependence of initial permeability of all samples was measured from 0.01 to 3GHz. The permeability varied with Cu contents, a maximum permeability of μ= 9.8 at 10MHz was observed for x=0.8. The permeability behavior was dependent on the content of Z-type ferrite phase and microstructure [2]. For x=0.8 the content of Z-type ferrite phase was estimated to be 89%, and the average grain size was around 2μm. The density of (Cu_{1-x}Co_{0.8x})Z-hex showed almost complete densification. However, the resonance frequency decreased to 700MHz as the permeability of Cu substituted Z-type hexaferrites (Ba₃Co_{2-x}Cu_xFe₂₄O₄₁) increased. Cu substituted Co₂Z hexagonal ferrites could be a candidate material for wireless device applications.

[1] J. Jeong, K.W. Cho, D.W. Hahn, B.C. Moon, Y.H. Han, *Mater. Lett.* 59 (2005) 3959-62 [2] M. Aoyama, J. Temuujin, M. Senna, T. Masuko, C. Ando, H. Kishi, *J. Electroceram* 17 (2006) 61-4

BJ05

Electrical and magnetic properties of nickel and magnesium co-substituted lithium ferrites

Ramesh M.¹, Rao G.s.n.², Parvatheswara Rao B.^{1*} and Samatha K.¹
¹ *Physics Department, Andhra University, India*
² *Physics Department, Dr. V.S. Krishna College, Visakhapatnam, India*

Lithium ferrites are widely used in electronics and telecommunication applications owing to their low dielectric loss, high resistivity coupled with good magnetic properties. There is a need to further improve their performance by incorporating different cationic substitutions for microwave device applications [1,2]. Most of the reports in the literature focused only on single ion substitutions for enhancement of one property at the cost of other. However, only a scanty research work has been reported so far on cationic co-substitutions in these ferrites. It is therefore interesting to study and find out the influence of co-substitution of nickel and magnesium in place of lithium and iron in lithium ferrites. For this purpose, Li_{0.5-x}Ni_xMg_xFe_{2.5-x}O₄ where x = 0.00 to 0.25 in steps of 0.05, are prepared by conventional ceramic method. Structural, magnetic, resistivity and dielectric measurements have been carried out on all the samples. Lattice parameter has been observed to increase with the concentration where as Curie temperature, grain size and initial permeability gradually decreased. High resistivity and low dielectric loss apart from reasonable magnetization and Curie temperature are obtained at concentrations. The results are explained on the basis of cation influences on the electromagnetnic properties at different crystallographic sites.

[1] X. Qi, J. Zhou, Z. Yue, Z. Gui, and L. Li, *Mater. Sci. Eng.*, B 99, 278, 2003. [2] K. U. Kang, S. W. Hyun, and C. S. Kim, *J. Appl. Phys.* 99, 08M917, 2006. *Authors & Affiliations:* M. Ramesh¹, G.S.N.Rao², B. Parvatheswara Rao¹ and K. Samatha¹ | *Department of Physics, Andhra University, Visakhapatnam-530003, India 2Dr. V.S. Krishna College, Visakhapatnam, India.*

BJ06

Resistivity and complex permeability dependence on isochronal recovery in polycrystalline yttrium iron garnet (Y₃Fe₅O₁₂)

Ismayadi Ismail¹, Mansor Hashim^{1*} and Nor Hapishah Abdullah²
¹ *Advanced Materials and Nanotechnology Laboratory, Universiti Putra Malaysia, Malaysia*
² *Physiscs Department, Faculty of Science, Universiti Putra Malaysia, Malaysia*

We propose to establish whether or not crystal atomic defects have any influence on the value of its complex permeability and electrical resistivity after undergoing heat treatments. A technique involving defects creation and their subsequent elimination within equal time-length durations was used: this is a technique for establishing isochronal recovery behavior of any atomic defects-dependent properties. YIG was prepared via mechanical alloying with a mixture of Y₂O₃ and Fe₂O₃ involving a 24 hours milling time. They were then sintered at different temperatures between 900°C to 1350°C and subsequently heated for 2 hours at 1000°C and quenched in cooking oil. Then, annealing of the samples at 1000°C for 2 hours was carried out. The magnetic and electrical properties before and after quenching and also after annealing were studied. The permeability and loss factor showed an isochronal recovery behaviour in which a parameter's value was decreased after quenching and increased back even higher after annealing suggesting that magnetic permeability and energy loss in YIG could significantly show an atomic defect-dependent behaviour. The resistivity value of the samples was observed to have an isochronal recovery behavior which the value dropped after quenching and increased almost gradually back even higher after isochronal annealing series.

CA01

Spin and charge excitations in cuprates and iron pnictides revealed by simulated resonant inelastic x-ray scattering

Takami Tohyama¹, Eiji Kaneshita² and Kenji Tsutsui³
¹ *Yukawa Institute for Theoretical Physics, Kyoto University, Japan*
² *Sendai National College of Technology, Japan*
³ *Synchrotron Radiation Research Center, Japan Atomic Energy Agency, Japan*

We first examine Cu L3-edge resonant inelastic x-ray scattering (RIXS) spectra for cuprates based on the exact diagonalization results of the t-t'-t''-J model. Both spin and charge excitations are included in the calculations on the same footing. The calculated results are compared with recent experimental data [1]. We next examine the orbital excitations coupled to the spin degree of freedom in the iron pnictides, based on the calculation in a five-band itinerant model [2]. The calculated Fe L3-edge RIXS spectra disclose the presence of spin-flip excitations involving several specific orbitals. Magnon excitations predominantly composed of a single orbital component can be seen in experiments, although its spectral weight is smaller than spin-flipped interorbital high-energy excitations. The detailed polarization and momentum dependence is also discussed.

[1] T. Tohyama and K. Tsutsui, *in preparation*. [2] E. Kaneshita, K. Tsutsui, and T. Tohyama, *Phys. Rev. B* 84, 020511(R) (2011).

CA02

Discovery of fermi surface near anti-node in pseudogap phase of the under-doped Bi-2212

Chung Koo Kim¹, Jinhwan Lee², Kazuhiro Fujita³, Hiroshi Eisaki⁴, Shinichi Uchida⁴, J. C. Seamus Davis⁵ and Jinho Lee^{6*}
¹ *BNL/Cornell, USA*
² *KAIST, Korea*
³ *Cornell, USA*
⁴ *AIST, Japan*
⁵ *Tokyo U., Japan*
⁶ *Cornell/BNL, USA*
⁷ *BNL/SNU, Korea*

Quasi-Particle Interference (QPI) measured by spectroscopic-imaging scanning tunneling microscope (SI-STM) became an extremely useful tool in the study of correlated electron systems (CES). Particle-hole (p-h) symmetric QPI observed in the superconducting cuprates revealed many interesting phenomena including the disappearance of the QPI signal around the reduced zone boundary [1]. Recently, the most dominating band of Sr₂Ru₂O₇ was identified [2] and p-h asymmetric QPI in the parent compound of the ferro-pnictide superconductor revealed a nematic like features [3]. On the other hand, identification of the exact Fermi surface (FS) topology in "pseudo-gap"(PG) phase of the cuprate superconductors is one of the central issues of the modern condensed matter physics. ARPES data indicates "Fermi arc" develops in PG phase while quantum oscillation (QO) results show evidence of the electron pockets. To resolve this PG mystery, we investigated deeply under-doped Bi₂Sr₂CaCu₂O_{8+δ} above and below T_c using SI-STM and found that there is a QPI showing continuous, p-h asymmetric dispersion through EF above T_c which originates from anti-nodal FS which is disconnected from the nodal FS. This observation implies existence of Fermi surface with very low quasiparticle(QP) weight Z_k in anti-node in PG phase. We also try to explain nodal anti-nodal dichotomy in terms of Z_k.

[1] T. Kohsaka et al., *Nature* 454, 1072 (2008) [2] Jinho Lee et al., *Nature Physics* 5, 800 (2009) [3] T.-M. Chuang et al., *Science* 327, 181 (2010)

CA03

Feedback effect on high-energy magnetic fluctuations in the model high-temperature superconductor HgBa₂CuO_{4+d}

Yuan Li^{1*}, Mathieu Le Tacon¹, Mohammed Bakr¹, Damien Terrade¹, Dirk Manske¹, Rudi Hackl², Lina Ji¹, Mun K. Chan³, Neven Barisic³, Xudong Zhao³, Martin Greven³ and Bernhard Keimer¹
¹ *Max Planck Institute for Solid State Research, Germany*
² *Walther Meissner Institute, Bavarian Academy of Sciences, Germany*
³ *University of Minnesota, USA*

It is widely accepted that magnetic excitations make important contribution to the Cooper-pairing mechanism in cuprate high-temperature superconductors. Contribution from excitations below ~60meV is manifested by a generic 'resonance' feature observed by neutrons, which signifies a feedback effect of pairing on the magnetic excitations. However, the insufficient spectral weight of the resonance is unable to explain the high superconducting temperature (T_c). Recent research has demonstrated that intense excitations above 100meV are available as a possible resource for pairing, but it remains largely unknown whether this resource is actually utilized. Here we present a systematic electronic Raman scattering study of the model single-layer cuprate superconductor HgBa₂CuO_{4+d}. In an overdoped sample, we observe a pronounced enhancement of a high-energy peak related to two-magnon excitations in insulating cuprates upon cooling below T_c. This is accompanied by the appearance of the superconducting gap and a pairing peak above the gap in the Raman spectrum, and it can be understood as a high-energy feedback effect which evinces a direct involvement of the high-energy excitations in the Cooper-pairing mechanism. All of these effects occur already above T_c in two underdoped samples, demonstrating a related feedback mechanism associated with the pseudogap.

[1] Y. Li et al., *arXiv:1112.2725*

CB01

Ferromagnetism of Au nanoparticle assemblies: Role of chemical and structural parameters in magnetic properties

Tae Hee Kim^{1*}, Eun Ju Her¹, Yu Jeong Bae¹, Seung Hyo Ko¹, Seung Ho Moon², Jung-tak Jang², Jinwoo Cheon² and Eisuke Ito³
¹ *Physics Department, Ewha Womans University, Korea*
² *Chemistry Department, Yonsei University, Korea*
³ *3Flucto-Order Functions Research Team, RIKEN Advanced Science Institute, Japan*

Ferromagnetism induced by the surface atoms and protective organic molecules in Au nanoparticles has been investigated for both fundamental and application interests of magnetism.[1] Possible explanations of the ferromagnetism could be attributed to 5d localized holes generated by the surface atoms and the high spin-orbit coupling of Au. Further understanding of this mechanism requires to study the magnetic properties of the particles related to their relative distance (change of the ligand length) and the nature of the ligand-particle binding. In this work, we explored the effect of these parameters for Au nanoparticles assemblies which were cast in the form of compact pellet made by cold-pressing technique. The magnetic behaviors in thiol and octylamine-capped Au nanoparticle assemblies were investigated by different spectrometers and magnetometers. The evidence of ferromagnetic behavior at 300K was seen clearly in ~ 6nm size dodecanethiolated Au nanoparticles: surprisingly, for the diameter much larger than 2nm, a typical ferromagnetic magnetization curve with the saturation value of 0.25emu/g observed, while superparamagnetism with a blocking temperature around 50K shown in octylamine-capped Au nanoparticles. The surface analyses by XPS, ESR and FTIR indicated that the magnetic properties could be tuned upon not only the particle size but also their surface environments.

[1] P. Crespo et al. *Phys. Rev. Lett.* 98, 087204 (2004)

CB02

Air-stable Fe@Au nanoparticles synthesized by the microemulsion's method

J. Rivas^{1*}, E. Iglesias-silva², J. M. Vilas-vilela¹, L. M. Leon¹ and M. A. Lopez-quintela⁴
¹ *INL-International Iberian Nanotechnology Laboratory; University of Santiago de Compostela, Spain*
² *University of Santiago de Compostela; University of the Basque Country, Spain*
³ *University of the Basque Country, Spain*
⁴ *University of Santiago de Compostela, Spain*

Magnetic particles covered by gold are very important in many biological applications. However, there are not simple methods to produce small (< 5-10nm) nanoparticles. One of the main reasons for that is the general use of iron oxides as magnetic cores, which have a large crystalline mismatch with gold. The use of Fe would be more appropriate, but its high tendency to oxidation has largely precluded it from being used as a core. Here, we will show that using a simple "one-pot" successive reaction method in microemulsions, can avoid such problems and is able to produce very stable core-shell Fe@Au nanoparticles. By this successive "one-pot" procedure, nanoparticles of ~ 6 nm with an Fe core of 1.5 nm can easily be obtained. These Fe@Au nanoparticles, with a saturation magnetization of 1.7 emu/g, are very stable even in air after magnetic separation from the solution, which shows the good covering of the Fe core by the Au shell. In this contribution we will report the key parameters, which have to be taken into account, to prepare such stable Fe@Au dispersions and analyze their optical and magnetic properties, as well as their possible applications as biosensors, targeted magnetic separation, etc.

1. J. Rivas, A. J. Garcia-Bastida, M. A. Lopez-Quintela and C. Ramos. "Magnetic properties of Co/Ag core/shell nanoparticles prepared by successive reactions in microemulsions". *J.Magn.Magn.Mat.* 2006, 300, 185-191. 2. J.Vidal Vidal, J. Rivas, M.A. Lopez-Quintela. "Synthesis of monodisperse maghemite nanoparticles by the microemulsion method". *Colloids and Surfaces A*, 2006, 288, 44-51.

CB03

Numerical study of the exchange bias effects in assemblies of core/shell nanoparticles

Kalliopi Trohidou*, Marianna Vasilakaki and George Margaris
Institute of Materials Science, National Center for Scientific Research 'Demokritos', Greece

The study of the magnetic behaviour of random assemblies of nanoparticles with core / shell structure is a relatively new field of experimental and theoretical interest. We study numerically using the Monte Carlo simulations technique with the implementation of the Metropolis algorithm the role of the magnetostatic and exchange interactions on the magnetic behaviour of composite nanoparticle assemblies. The aim of our work is to determine the factors that influence the exchange bias behaviour in the assemblies. We have developed a simplified model that describes the complex internal structure of the nanoparticles and also includes the interparticle interactions. We have calculated the hysteresis loops and the Zero Field Cooled magnetization curves of the assemblies for different sizes of the shell thickness for each nanoparticle and as a function of the particle concentration and the size of the dipolar and interparticle exchange strength in the assembly. Our simulations show that for small shell thickness and at high particle concentration the interparticle exchange interactions cause a big increase in the exchange bias field (Hex) and the coercive field (Hc). As the shell thickness increase the effect of the exchange interparticle interactions is Our results are compared with experimental findings [1,2].

1. J. Nogues, V. Skamryev, J. Sort, S. Stoyanov, D.Givord, *Phys. Rev. Lett.* 97 (2006) 157203 ; 2. N.Domingo, A. M. Testa, D. Fiorani, C. Binns, S. Baker, *J.Tejada J. M. M. M. 316 (2007) 155-158*

CB04

Exploring the effect of Co doping in the magnetic and magneto-optical properties of fine maghemite nanoparticles

Elvira Fantechi¹, Giulio Campo¹, Daniela Carta², Anna Corrias², Cesar De Julian Fernandez^{2*}, Claudia Innocenti¹, Francesco Pineider³, Francesco Rugi¹ and Claudio Sangregorio³
¹ *INSTM and University of Florence, Italy*
² *INSTM and Department of Chemical Sciences, Universita di Cagliari, Italy*
³ *CNR - ISTM Milano @ INSTM Udr Florence, Italy*
⁴ *CNR - ISTM Padova @ INSTM Udr Florence, Italy*

Nanosized spinel ferrites are the subject of increasing interest due to their remarkable magnetic, catalytic, electric and optical properties, which, in most cases, differ from bulk. Cobalt ferrite is the ferrite with larger magnetic anisotropy that can be directly controlled by varying the cobalt content. However other factors, like chemical state or inversion degree, determine the final magnetic properties. We present a study of the structural, magnetic and magneto-optical properties of a series of Co substituted ferrite nanoparticles prepared by thermal decomposition. The structural characterization, carried out by using several techniques (TEM, XRD, XAS) showed all the samples are high crystalline, 5-6 nm spherical NPs with the cubic spinel structure typical of ferrites. The evolution of lattice parameters with cobalt content suggests that the material is Co-substituted maghemite, also confirmed by XAS and Magneto optical spectroscopy. The investigation of the magnetic and magneto-optical properties displays peculiar trends with the cobalt content, the main features being the large increase of the saturation magnetization and the anomalous dependence of magnetic anisotropy which reaches its maximum values for intermediate compositions. The large tuneability of this material makes it possible to implement the performances of devices used in biomedical and sensing applications.

CB05

Novel technique for self assembly of magnetic nanoparticles by cluster beam deposition

Ozan Akdogan^{1*}, Wanfeng Li², George Hadjipanayis² and David Sellmyer³
¹ *University of Delaware, USA*
² *Physics and Astronomy, University of Delaware, USA*
³ *Physics and Astronomy, University of Nebraska, USA*

Mono-layer dispersion and self-assembly of nanoparticles are of a key importance in many fields of science and industry. In chemical synthesis [1] and recent high-energy ball milling studies [2] self assembled nanoparticles have been obtained by the aid of surfactants and wet processing. Another promising technique for nanoparticle production is cluster beam deposition which provides excellent material purity. However, it lacks the ability to form nanoparticles in the self-assembled array form. In recent studies, particles have been deposited onto poly(vinyl alcohol) [3] and phospholipid [4] coated substrates to form arrays. Nevertheless, these coatings either lack the continuous array formation or need time consuming coating steps and post deposition treatments. In this study, we have chosen Oleic Acid (OA) as a cost effective and easier alternative to the above mentioned coatings. SmCo₂ nanoparticles have been deposited for 10 sec. at 25 W sputtering power onto both bare and OA-coated single crystalline Si substrates for comparison. Mono dispersed particles with self-assembly formation have been observed on OA coated substrates while a non-uniform distribution has been observed on bare substrates. Such dispersion can reduce the exchange interactions between the nanoparticles which is expected to effect the coercivity of the nanoparticles.

[1] S. Sun, C.B. Murray, D. Weller, L. Folks and A. Moser, *Science* 287, 1989 (2000) [2] N. G. Akdogan, G. C. Hadjipanayis and D. J. Sellmyer, *Nanotechnology* 21, 293705 (2010). [3] J. Wang, J. Qiu, T. A. Taton and B. Kim, *IEEE Trans. Magn.* 42, 3042 (2006). [4] A. Terheiden, C. Mayer, K. Moh, B. Stahmecke, S. Stappert, M. Acet and B. Rellinghaus, *Appl. Phys. Lett.* 84, 3891(2004).

CC01

Magnetricity and magnetic monopoles in spin ice

Steven Bramwell
London Centre for Nanotechnology and Department of Physics and Astronomy, University College London, United Kingdom

The analogy between spin configurations in spin ice materials like Ho₂Ti₂O₇ and proton configurations in water ice, H₂O, has been appreciated for many years (see Ref. [1] for a review). However it is only in the last few years that this equivalence has been extended into the realm of electrodynamics [2]. In this talk I shall describe our recent experimental work that identifies emergent magnetic charges ('monopoles'), transient magnetic currents ('magnetricity') and the universal properties expected of an ideal magnetic Coulomb gas (magnetic electrolyte - 'magnetolyte'). These universal properties include the Onsager-Wien effect, 'corresponding states' behaviour, Debye-Huckel screening and Bjerrum pairing [4-6]. I will describe experimental results for both traditional spin ice materials (Ho₂Ti₂O₇, Dy₂Ti₂O₇) and a recently discovered system (Dy₂Ge₂O₇).

[1] Bramwell and Gingras, *Science*, 294 1495 2001 [2] Ryzhkin, *JETP* 101 481 (2005); Castelnuovo et al., *Nature* 451 42 (2008) [4] Bramwell et al. *Nature* 461 956 (2009) [5] Fennell et al., & Bramwell *Science* 326 415 (2009) [6] Giblin, Bramwell et al., *Nature Physics* 7 252 (2011) [7] Zhou, Bramwell et al., *Nat Comm.* 478, 1483 (2011)

CC02

Recent developments in quantum spin liquid candidates

Luis Balicas*
Condensed Matter Sciences, NHMFL, USA

We discuss a few geometrically frustrated magnetic systems exhibiting ground states characterized by correlated spin excitations. The first system, Pr₂Ir₂O₇ is a metallic pyrochlore, which does not exhibit a spin-ice ground state but a state which is claimed to be a chiral spin-liquid where the interaction between the Pr moments and the itinerant Ir carriers leads to an anomalous Hall-effect (AHE), which remains finite even in the absence of an external magnetic field and of long range magnetic order. We show that this spontaneous AHE is hysteretic and anisotropic depending strongly on the previous application of an external field along specific crystallographic directions. We will argue that our observations suggest the possibility that Dirac monopole and antimonopole pairs are deconfined acquiring a finite quantum-mechanical average in the zero-field state of Pr₂Ir₂O₇. Finally, we briefly discuss and compare two new triangular lattice systems 4,5, Ba₃CuSb₂O₈ and Ba₃NiSb₂O₈ having S=1/2 and S=1 moments respectively, which despite their insulating character, exhibit large electronic specific heat coefficients of 43.4 and 168 mJ/molK², respectively. This can be understood if the spin excitations behave as coherent fermionic (or charge-like) excitations which in these systems form a Fermi surface at low temperatures.

In collaboration with S. Nakatsuji (ISSP-Tokyo) and H. D. Zhou (NHMFL - Tallahassee) 1. Y. Machida et al., *Nature* 463, 210 (2010). 2. L. Balicas et al., *Phys. Rev. Lett.* 106, 217204 (2011). 3. H. D. Zhou, E. S. Choi, G. Li, L. Balicas, C. R. Wiebe, Y. Qiu, J. R. D. Copley, and J. S. Gardner *Phys. Rev. Lett.* 106, 147204 (2011). 4. J. G. Cheng, G. Li, L. Balicas, J. S. Zhou, J. B. Goodenough, Cenke Xu, and H. D. Zhou, *Phys. Rev. Lett.* 107, 197204 (2011).

CC03

Static and dynamic properties of a strong-leg spin ladder

David Jan Schmidiger¹, Pierre Bouillot², Sebastian Muhlbauer¹, Severian Gvasaliya¹, Georg Ehlers³, Corinna Kollath¹, Thierry Giamarchi⁴ and Andrey Zheludev^{1*}
¹ Neutron Scattering and Magnetism, Laboratory for Solid State Physics, ETH Zurich, Switzerland
² DPMC-MaNEP, University of Geneva, CH-1211, Geneva, Switzerland
³ Neutron Scattering Science Division, Oak Ridge National Laboratory, Oak Ridge, Tennessee 37831-6475, USA
⁴ DPT-MaNEP, University of Geneva, CH-1211, Geneva, Switzerland

Static and dynamic properties of the strong-leg S=1/2 Heisenberg spin ladder system (C₄H₉N)₂CuBr₂ are studied using inelastic neutron scattering and bulk magneto-thermodynamic measurements. The leg-odd excitation channel is dominated by long-lived single-magnon states in the entire Brillouin zone, which supports a symmetric ladder model with exchange constants J_{leg} = 1.42(6) meV and J_{rung} = 0.82(2) meV [1,2]. In the leg-even channel, a considerable fraction of the spectral weight is contained in a novel long-lived two-magnon bound state [2]. In applied magnetic fields we observe a Bose-Einstein condensation of magnons that manifests itself in 3D long-range antiferromagnetic ordering emerging beyond H_c = 2.8 T. The field-temperature phase diagram showing the spin liquid, Tomonaga-Luttinger spin liquid and BEC phase is mapped out by specific heat measurements. The experimental results are in spectacular agreement with state-of-the-art DMRG calculations [2]. The latter provide additional insight on certain spin ladder properties specific to the strong-leg regime. This work was partially supported by the Swiss National Fund and MANEP.

[1] D. Schmidiger, S. Muhlbauer, S. Gvasaliya, T. Yankova, A. Zheludev, *Phys. Rev. B* 84, 144421 (2011) [2] D. Schmidiger, P. Bouillot, S. Muhlbauer, S. Gvasaliya, C. Kollath, T. Giamarchi, A. Zheludev, arXiv:1112.4307 (2011)

CC04

Nonstationary processes in the spin-ice materials Dy₂Ti₂O₇ and Ho₂Ti₂O₇ investigated by ultrasound

S. Zherlitsyn^{1*}, S. Erfanifam¹, J. Wosnitza¹, R. Moessner², O. A. Petrenko³, G. Balakrishnan³ and A. A. Zvyagin⁴
¹ Hochfeld-Magnetlabor Dresden, Helmholtz-Zentrum Dresden-Rossendorf, Germany
² Max-Planck Institut fuer Physik komplexer Systeme, Germany
³ Department of Physics, University of Warwick, United Kingdom
⁴ B. I. Verkin Institute for Low Temperature Physics and Engineering, Ukraine

We report on a low-temperature comparative study of two spin-ice materials, Dy₂Ti₂O₇ and Ho₂Ti₂O₇, by use of longitudinal and transverse ultrasound waves. In both materials the sound velocity and the sound attenuation exhibit a number of anomalies versus applied magnetic field for temperatures below the freezing temperature. The anomalies show a broad hysteresis with a very clear signature of the transition to the saturated state for magnetic fields applied along the [111] direction. Additionally, in Dy₂Ti₂O₇ the sound velocity and the sound attenuation exhibit a number of well-defined spikes which are highly asymmetric due to the fundamentally distinct nonequilibrium mechanisms involved: the release of the Zeeman energy from the spins and the transfer of energy out of the sample [1]. In case of Ho₂Ti₂O₇, both acoustic characteristics demonstrate much smoother anomalies. We discuss some possible reasons for the observed differences in the ultrasound features of these spin-ice materials.

[1] S. Erfanifam, S. Zherlitsyn, J. Wosnitza, R. Moessner, O. A. Petrenko, G. Balakrishnan, and A. A. Zvyagin, *Phys. Rev. B* 84, 220404(R) (2011).

CC05

Study of low-temperature magnetism in a pr-based pyrochlore magnet

Kenta Kimura^{*}, Satoru Nakatsuji¹, Agung Nugroho², Yoshitomo Karaki³, Kazuyuki Matsuhira⁴, Yasuyuki Shimura¹ and Toshiro Sakakibara¹
¹ ISSP, Univ. of Tokyo, Japan
² Bandung Inst. Tech, Indonesia
³ Ryukyuu Univ., Japan
⁴ Kyusyu Inst. Tech., Japan

Pr-based pyrochlore magnets have been recognized as a fascinating venue to search unconventional magnetism as a result of frustration and quantum effects. For example, Pr₂Ir₂O₇ exhibits a novel spin liquid state, which has the “2-in, 2-out” short-range correlation, the same as a spin ice system, and simultaneously breaks time reversal symmetry [1, 2]. Here we report the detailed physical properties of single crystals of the related insulating compound Pr₂Zr₂O₇. Magnetic susceptibility fits to the Curie-Weiss law below 10 K, yielding the effective moment of 2.5μB and Weiss temperature of -0.4 K, consistent with the previous powder results [3]. Furthermore, magnetization measurement at very low temperature confirmed a magnetic anomaly signaling spin ice correlation. In the presentation, we will discuss the low temperature magnetism based on the results including specific heat and AC susceptibility measurements.

[1] S. Nakatsuji et al., *PRL*, 96, 087204 (2006). [2] Y. Machida et al., *Nature* 463, 210 (2010). [3] K. Matsuhira et al., *J. Phys.: Conference Series* 145 (2009) 012031

CD01

A materials-based global phase diagram for heavy-fermion quantum criticality

S. Paschen^{1*}, J. Custers¹, J. Larrea J.¹, K. - A. Lorenzer¹, M. Mueller¹, A. Prokofiev¹, A. Sidorenko¹, H. Winkler¹, A. M. Strydom², Y. Shimura³, T. Sakakibara⁴, R. Yu⁴ and Q. Si¹
¹ Institute of Solid State Physics, Vienna University of Technology, Austria
² Physics Department, University of Johannesburg, South Africa
³ Institute for Solid State Physics, University of Tokyo, Japan
⁴ Department of Physics and Astronomy, Rice University, USA

Heavy fermion compounds have in recent years emerged as prototypical quantum critical systems. Studies in the anisotropic heavy-fermion compound YbRh₂Si₂ have shown that different types of quantum critical points (QCPs) are induced by variations of the magnetic field, chemical or external pressure, raising the question of the extent to which heavy-fermion quantum criticality is universal. We have identified a cubic heavy-fermion material, CePd₉Si₆, as exhibiting a field-induced quantum phase transition as the lower of two consecutive phase transitions is suppressed to zero. Thus, here the QCP separates two different ordered phases. This transition is accompanied by an abrupt change of Fermi surface, reminiscent of what happens across the field-induced antiferromagnetic to paramagnetic transition in YbRh₂Si₂. From these results we have proposed a materials-based global phase diagram that points to the importance of dimensionality - and may serve as guide in the search for a unified theoretical description [1]. To weaken the lower phase transition temperature and possibly detach the Kondo destruction scale from the phase transition scale, we are now studying (Ce_{1-x}La_x)Pd₉Si₆ and CePd₉Si₆ under hydrostatic pressure. We acknowledge financial support from the European Research Council (ERC Advanced Grant No 227378).

[1] J. Custers, K.-A. Lorenzer, M. Muller, A. Prokofiev, A. Sidorenko, H. Winkler, A. M. Strydom, Y. Shimura, T. Sakakibara, R. Yu, Q. Si, and S. Paschen, *Nature Materials*, doi:10.1038/nmat3214.

CD02

Anomalous metals with strong valence / orbital fluctuations

Satoru Nakatsuji, Yosuke Matsumoto, Kentaro Kuga, Eoin T. C. O' Farrell and Akito Sakai
Institute for Solid State Physics, University of Tokyo, Japan

In strongly correlated electron systems, quantum criticality normally emerges on the border of magnetism accompanied by critical spin fluctuations. In particular for the 4f based heavy fermions, it has been discussed using Doniach type picture based on the Kondo lattice with integer valence. Here we discuss unconventional type of quantum criticality and anomalous metallic phases found with strong valence and orbital fluctuations. The first material is the Yb based heavy fermion superconductor β-YbAlB₃ [1]. Interestingly, this exhibits a zero field quantum criticality without tuning as the first example in a metal [2]. Doping and pressure effects indicate no magnetic phase in the immediate vicinity of the ambient pressure quantum criticality. The instability associated with electronic structure or valence may be the origin of the novel quantum criticality. Secondly, we discuss the anomalous metallic phase found in the Pr based cubic compounds PrTr₂Al₁₀ (Tr: transition metal) [3]. These allow us to study the competition between the strong hybridization effects and quadrupolar ordering. Orbital fluctuations under strong hybridization with conduction electrons suppresses orbital ordering and lead to prominent non-Fermi liquid behavior, suggesting the possibility of a nonmagnetic type of Kondo effect.

[1] S. Nakatsuji, K. Kuga, Y. Machida, T. Tayama, T. Sakakibara, Y. Karaki, H. Ishimoto, S. Yonezawa, Y. Maeno, E. Pearson, G. G. Lonzarich, L. Balicas, H. Lee, and Z. Fisk, *Nature Physics* 4, 603 (2008). [2] Y. Matsumoto, S. Nakatsuji, K. Kuga, Y. Karaki, N. Horie, Y. Shimura, T. Sakakibara, A. H. Nevidomskyy, and P. Coleman, *Science* 331, 316 (2011). [3] A. Sakai and S. Nakatsuji, *Journal of the Physical Society of Japan*, Letter 80, 063701 (2011). Editor's Choice

CD03

Ce-based iron-pnictides: Intermediate valence and heavy-fermion behavior versus magnetism and superconductivity

Matthias Holder¹, Denis V. Vyalkikh¹, Steffen Danzenbacher¹, Anton Jesche², Cornelius Krellner², Christoph Geibel², Pierre Lombardo³, Roland Hayn³, Rolf Follath⁴, Serguei L. Molodtsov⁵ and Clemens Laubschat^{1*}
¹ Institut für Festkörperphysik, Technische Universität Dresden, D-01062 Dresden, Germany
² Max-Planck-Institut für Chemische Physik fester Stoffe, D-01187 Dresden, Germany
³ Institut Materiaux, Microelectronique et Nanosciences de Provence, FR-13397 Marseille, France
⁴ Helmholtz-Zentrum Berlin, Elektronenspeicherring BESSY II, D-12489 Berlin, Germany
⁵ European XFEL GmbH, D-22671 Hamburg, Germany

In the last few years layered iron pnictides have attracted considerable interest due to their superconducting properties characterized by critical temperatures, TC, up to 55 K. In Ce-based compounds of these series superconductivity competes with heavy Fermion behavior, spin density wave formation and magnetic order. High-resolution angle-resolved photoemission allows for direct insight into the correlated electronic structure of these systems. We show that the dispersion of Fe-3d derived bands close to the Fermi energy is strongly modified by hybridization with localized Ce 4f states what affects possible participation of these bands in other many-body interactions. Spectral 4f signatures as probed by resonant photoemission consist on a weakly dispersive peak just at the Fermi energy (in addition to an ionization peak at about 2 eV binding energy) and admixtures to the valence bands. The spectroscopic data are discussed in the light of band-structure calculations and a novel approach to the periodic Anderson model.

CD04

Observation of the quantum critical point in CeRhSi₃ with the muon spin rotation technique

Nikola Egetenmeyer^{*}, Jorge L. Gavilano¹, Alexander Maisuradze², Alexander Maisuradze³, Simon Gerber¹, Michel Kenzelmann¹, Gabriel Seyfarth¹, Daniel Andreica⁴, Alexandre Desilets-benoit⁵, Andrea D. Bianchi¹, Christopher Baines⁶, Rustem Khasanov⁷ and Douglas E. Maclaughlin⁸
¹ Laboratory for Neutron Scattering, Paul Scherrer Institut, 5232 Villigen PSI, Switzerland
² Laboratory for Muon Spin Spectroscopy, Paul Scherrer Institut, 5232 Villigen PSI, Switzerland
³ Physik-Institut, Universität Zurich, 8057 Zurich, Switzerland
⁴ Laboratory for Developments and Methods, Paul Scherrer Institut, 5232 Villigen PSI, Switzerland
⁵ Departement de physique de la matiere condensée, Université de Geneve, 1211 Geneva, Switzerland
⁶ Faculty of Physics, Babes-Bolyai University, 400084 Cluj-Napoca, Romania
⁷ Departement de Physique, Université de Montreal, Montreal H3C 3J7, Canada
⁸ Department of Physics and Astronomy, University of California, Riverside, USA

The interplay of superconductivity and magnetism has been a central issue of research for many years. A variety of these systems have been found to display a so-called quantum critical point which marks the transition point between a nonmagnetic and a magnetic metal phase. The external tuning parameter can be doping, an external magnetic field or external pressure. We conducted a muon spin rotation study on the heavy fermion and noncentrosymmetric compound CeRhSi₃ which is an antiferromagnet at ambient pressure and displays superconductivity at high pressure. In this system, we were able to unravel the quantum critical point hidden inside of the pressure-induced superconducting phase of the pressure-temperature phase diagram. We directly observed the continuous suppression of the internal fields, and thus the magnetic moments at the critical pressure p* = 23.6 kbar. Simultaneously the Neel temperature goes to zero and we conjecture a spin density wave type quantum critical point.

CE01

Self-modulation in perpendicular anisotropy Co/Ni based spin-torque oscillators

Johan Akerman
Physics Department, University of Gothenburg, Sweden

Nano-contact spin-torque oscillators (NC-STO) are nanoscale microwave signal generators based on the transfer of spin angular momentum from a spin polarized current to the local magnetization of a thin magnetic layer. While standard, NiFe based, NC-STOs require large external fields of about 1 T for operation, we here present low-field operation of Co/Ni based NC-STOs comprising a 50-300 nm diameter nano-contact on top of a Co8nm(IP)/Cu8nm/Co0.3nm-[Ni0.8nm/Co0.4nm]x4(PMA) orthogonal spin valve. Frequencies above 12 GHz are observed for close to zero-field (0.02 T) operation, which further increase up to 24 GHz in moderate fields of 0.4 T [1]. When the applied is further increased, we find a discontinuity in STO frequency around 0.68 T. The STO frequency drops by almost 10 GHz and at the same time sidebands appear with the main STO signal. These sidebands indicate a self-modulation of the main high-frequency mode with a low-frequency (~1 to 2 GHz) oscillator mode. We interpret this transition as the formation of a magnetic bubble underneath the NC. The low-frequency magnetodynamics of the bubble then modulates the NC-STO precession frequency.

[1] High frequency operation of a spin-torque oscillator at low field, S. M. Mohseni, S. R. Sani, J. Persson, T. N. Anh Nguyen, S. Chung, Ye. Pogoryelov and Johan Akerman, *Phys. Status Solidi RRL*, 5, 432 (2011).

CE02

Magnetization tilt angles in [Pd/Co]/Cu/[Co/Pd]-NiFe pseudo spin valves

Anh T. N Nguyen¹, Sunjea Chung¹, S. M. Mohseni¹, R. K. Dumas² and Johan Akerman^{2*}
¹ Materials Physics, KTH, Royal Institute of Technology, Sweden
² Department of Physics, University of Gothenburg, 412 96 Gothenburg, Sweden

Future spintronic devices based on spin-transfer torque require a delicate engineering of the constituent magnetic layers. A fixed layer magnetization that is tilted out of the plane allows for zero-field operation, as well as increased output efficiency and quality, e.g. linewidth. We recently proposed a [Co/Pd]-NiFe exchange spring for use as a spin polarizing layer with a tilted magnetization for applications in spin torque oscillators (STOs) [1]. We have shown that it is possible to easily tune the spin configuration by engineering the effective exchange coupling between a NiFe layer with in-plane anisotropy and [Co/Pd] multilayer with perpendicular anisotropy. Here, we report on magnetization tilt angles in complete [Pd/Co]/Cu/[Co/Pd]-NiFe(t_{NiFe}) pseudo spin valves (PSVs) using angular dependent transport measurements. The tilt angle of the [Co/Pd]-NiFe is deduced from the angular dependence of the effective switching fields. As t_{NiFe} is increased, the tilt angle of the [Co/Pd]-NiFe increases. These results provide a first observation of the tilt angle in a PSVs structure, which are similarly used in real STOs. This work provides meaningful insights for the future realization and optimization of tilted STO devices.

[1] T. N. Anh Nguyen, , Y. Fang, V. Fallahi, N. Benatmane, S. M. Mohseni, R.K. Dumas, and Johan Akerman, *Appl. Phys. Lett.* 98, 172502 (2011)

CE03

Temperature dependence of microwave voltage emission associated to spin-transfer induced vortex oscillations in magnetic tunnel junctions

Paolo Bortolotti^{*}, A. Dussaux¹, J. Grollier¹, V. Cros¹, A. Fukushima², H. Kubota², K. Yakushiji², S. Yuasa², K. Ando² and A. Fert¹
¹ Unite Mixte de Physique CNRS/Thales, France
² National Institute of Advanced Industrial Science and Technology (AIST), Japan

The growing market of telecommunication applications demands reduction of energy consumptions and devices miniaturization. Spin transfer-torque nanoscriptors (STO) can fulfill such necessities and, given their rapidly improving characteristics, will might be able to replace conventional oscillators. In the past, their drawbacks were the low emitted power and large linewidth. We recently proved[1,2] that these issues can be overcome by considering a MgO-based magnetic tunnel junction[3,4] with a vortex free layer, i.e., spin transfer-torque vortex nano-oscillator (STVO). The obtained signal has large output power (>50 nW) and small linewidth (<1 MHz). In order to further optimize its characteristics, we have to understand the mechanisms underlying the linewidth generation. Thus, we consider the effect of temperature on such STVO by ranging T from 20 to 300 K. We first observe a linear decrease of the linewidth with decreasing temperature and a bottom limit of the linewidth (700 kHz) at lower temperature[5]. Thermal effects and spin torque non-linearities are not sufficient to explain such behaviour and one additional source of phase noise should be considered. To clarify the origin of such phase noise, frequency and time-domain measurements are compared. Support from ANR VOICE PNANO-09_P231-36, EU MASTER NMP-FP7-212257, CANON-ANELVA for MTJ film are acknowledged.

[1] A. Dussaux et al., *Nat. Comm.* 1 1 (2010) [2] A.V. Khvalkovskiy et al., *Phys. Rev. B* 80 140401(R) (2009) [3] A.M. Deac et al., *Nat. Phys.* 4 803 (2008) [4] D. Houssamedine et al., *Appl. Phys. Lett.* 93 022505 (2008) [5] P. Bortolotti et al., *Appl. Phys. Lett.* 100 042408 (2012)

CE04

Zero external-field microwave oscillations in MgO magnetic tunnel junctions

Jae Hyun Park¹, Seung-young Park², Byoung-chul Min^{1*}, Jung-hwan Moon³, Kyung-jin Lee³, Young-hun Jo² and Kyung-ho Shin¹

¹ Korea Institute of Science and Technology, Korea

² Korea Basic Science Institute, Korea

³ Korea University, Korea

We report a potential solution to overcome major challenges for the implementation of spin transfer nano-oscillators (STNOs) in real microwave applications, namely a weak output power and broad spectral linewidth of STNO microwave signals. In addition to the challenges, an external magnetic field is often required for the microwave generation from STNOs. We have observed high-power microwave oscillations having a narrow linewidth, even without applying external magnetic fields, from STNOs based on MgO magnetic tunnel junctions (MTJs). The MTJs consist of SiO₂ substrate/ buffer layer/ synthetic antiferromagnet/ Co₄₀Fe₂₀B₂₀ (5)/ MgO (1)/ Co₄₀Fe₂₀B₂₀ (2)/ capping layer (in nm). A typical STNO has a resistance of 45 Ohm in the parallel state and 75 Ohm in the antiparallel state, showing a tunnel magnetoresistance of 67%. The STNO exhibits an oscillation peak of 70 nV/Hz³ at 3 GHz at zero external magnetic field, and the full width at half maximum of the peak is less than 60 MHz. The microwave spectra as a function of bias current and in-plane external magnetic field (H_{ext}) will be discussed in detail.

CE05

NCMR based spin-torque microwave generator and detector with high signal purity

Yuuki Kozono^{1*}, Yoshihito Okutomi¹, Kohsaku Miyake¹, Susumu Hashimoto², Hitoshi Iwasaki² and Masashi Sahashi¹

¹ Department of Electronic Engineering, Tohoku University, Japan

² Corporate Research and Development Center, Toshiba Corporation, Japan

Nano-contacts magnetoresistive (NCMR) devices have many ferromagnetic ohmic nano-contacts (NCs) with the diameter of around 1nm, which connect the free and reference layer in the spacer layer called nano-oxide layer (NOL). In each NC, the domain wall is geometrically confined and produces the magnetoresistance by spin accumulation [1] and miss-tracking effect [2]. Furthermore, in injecting current, these NCs can increase the density of current and provide the high emission power with narrow linewidth. In this study, we systematically investigated the spin-transfer induced microwave oscillation [3], unique frequency modulation characteristics [4] and spin-torque ferromagnetic resonance (ST-FMR) [5] for the NCMR devices with thick free-layer with the thickness of ~15nm. In the microwave measurement, the high emission power (up to 100nW) with the narrow linewidth (down to 6.5MHz) was excited at the frequency of around 1GHz caused by auto-oscillation at multi-domain state, which is the intermediate state between parallel and antiparallel state. In the same magnetic state, ST-FMR signal also showed high sensitivity of ~250µV/100µW at almost same frequency as dc current induced microwave oscillation. As a result, we confirmed that NCMR device has the possibility to become the nano-sized microwave generator and detector.

[1] J. Sato, K. Matsushita, and H. Imamura, *J. Appl. Phys.* 105, 07D101(2009) [2] M. Takagishi, H. N. Fuke, S. Hashimoto, H. Iwasaki, S. Kawazaki, R. Shirasaki, and M. Sahashi, *J. App. Phys* 105 07B725(2009) [3] Y. Okutomi, Y. Kozono, K. Miyake, S. Hashimoto, H. Iwasaki, and M. Sahashi, *Appl. Phys. Letters*, submitted [4] M. A. Mahdavi, M. Doo, S. Hashimoto, H. N. Fuke, H. Iwasaki, and M. Sahashi, *IEEE Trans. Magn.* 47, 3380(2011), [5] A. A. Tulupovskay, V. Slezaki, A. Fakhoshina, H. Kubota, H. Hara, K. Tsunakawa, D. D. Djuyevskaya, N. Watanabe, and S. Yuasa, *Nature(London)*438, 339(2005)

CE06

Conditions for zero field spin transfer induced vortex oscillations with a perpendicular spin polarizer

E. Grimaldi^{1*}, A. Dussaux¹, B. Sallès², J. Grollier¹, A. Fukushima², H. Kubota², K. Yakushiji², S. Yuasa², V. Cros¹ and A. Fert¹

¹ Unite Mixte de Physique CNRS/Thales, 1 Av Fresnel, Campus de l'Ecole Polytechnique, 91767 Palaiseau, France

² National Institute of Advanced Industrial Science and Technology (AIST), 1-1-1 Umezono, Tsukuba, Japan

Despite the theoretical and experimental progress achieved, power, linewidth and zero-field emission remain critical issues for spin transfer nano-oscillators (STNOs) [1,2] in telecommunication applications. Here we investigate spin transfer induced vortex dynamics in specific STNOs [SAF / MgO / NiFe (vortex magnetization) / Cu / [Co/Ni] (perpendicular polarizer)]. Such a hybrid GMR/TMR system has been designed to obtain large amplitude spin torque induced magnetization oscillations at zero field owing to the perpendicular polarized spin current. In the best MTJ we measure large emitted power (600 nW) and narrow linewidth (590 kHz) at zero magnetic field, making these hybrid devices very promising for radiofrequency applications. In addition we investigate in detail the strong impact of vortex configuration (polarity, chirality) on the frequency and the linewidth of the signal [3]. These results are analysed in the frame of a nonlinear analytical model for the vortex dynamics [4]. We thank CANON ANELVA for preparing the MTJ films, the ANR VOICE grant and MASTER grant and E.G. acknowledge financial support from CNES and DGA.

[1] V.S. Pribiag et al., *Nat. Phys.* 3, 498 (2007) [2] A. Dussaux et al., *Nat. Comm.* 1, 8 (2010) [3] A. V. Khvalkovskiy et al., *Phys. Rev. B* 80, 140401 (R) (2009). [4] A. Dussaux et al., to be published

CF01

Spin-orbital short-range order on a honeycomb based lattice

C. Broholm^{1*}, S. Nakatsuji², H. Sawa³, M. Hagiwara⁴ and F. Bridges⁵

¹ Institute for Quantum Matter and Department of Physics and Astronomy, Johns Hopkins University, USA

² Institute for Solid State Physics, University of Tokyo, Japan

³ Department of Applied Physics, Graduate School of Engineering Nagoya University, Japan

⁴ KYOKUGEN, Osaka University, Japan

⁵ Physics Department, University of California, Santa Cruz, USA

Strong antiferromagnetic interactions indicated by ΘCW=47 K, fail to produce static spin correlations above T=0.1 K in Ba₂CuSb₂O₈. Magnetic neutron scattering at T=1.5 K is inelastic with a broad peak at 5.5 meV that shifts to higher energies upon warming and wave vector dependence indicating near neighbor singlet formation. While these features are difficult to reconcile with the previously inferred triangular lattice structure, short-range correlations of CuSbO₈ dumbbells resulting from structural frustration as revealed by synchrotron x-ray diffraction and EXAFS provides the essential lead. The resulting magnetic sub-lattice forms a nano-structured honeycomb lattice with nearest neighbor interactions. Based on the new structure we propose the unusual magnetic properties and the absence of a coherent, static Jahn-Teller transition indicate a two-dimensional random singlet phase or a spin-orbital quantum liquid.

* This work is partially supported by Grant-in-Aid for Scientific Research from JSPS (No. 20340089, 21684019) and from MEXT on Priority Areas (No. 19051010, 19052003), by Global COE Programs “the Physical Sciences Frontier” and “Core Research and Engineering of Advanced Materials” MEXT, Japan, by a Toray Science and Technology Grant and by the US-Japan Cooperative Program, ISSP. Work at IQM was supported by DoE, Office of Basic Energy Sciences, Division of Materials Sciences and Engineering under Award DE-FG02-08ER46544.

CF02

Quadrupolar waves in uranium dioxide

Paolo Santini
University of Parma, Italy

In solids with d- and f-electrons, under certain conditions the orbitals align to form an ordered pattern. Collective excitations breaking this arrangement can take the form of oscillations of electric quadrupoles, so-called quadrupolar waves. These represent a propagating pattern of charge densities implying a modulation of quadrupolar moments. We show that quadrupolar waves constitute a major component of the dynamics of uranium dioxide in its magneto-quadrupolar ordered phase [1,2]. The distinct roles of Jahn-Teller and superexchange mechanisms as sources of quadrupolar interactions are identified. The theory is fully consistent with earlier and recent [3] inelastic neutron scattering data.

[1] P. Santini et al., *Rev. Mod. Phys.* 81, 807 (2009) [2] S. Carretta, P. Santini, R. Caciuffo, G. Amoretti, *Phys. Rev. Lett.* 105, 167201 (2010) [3] R. Caciuffo, P. Santini, S. Carretta, G. Amoretti, A. Hiess, N. Magnani, L.-P. Regnault, G. H. Lander, *Phys. Rev. B* 84, 104409 (2011)

CF03

Magnon gap formation and charge density wave effect on thermoelectric properties in SmNiC₂ compound

Jin-hee Kim¹, Gyeong Im Min², Jong-soo Rhyee¹ and Yong Seung Kwon^{2*}

¹ Applied Physics, KyungHee University, Korea

² Physics, Sungkyunkwan University, Korea

We studied the magnetic, electrical, and thermal properties of polycrystalline compound of SmNiC₂. The electrical resistivity and magnetization measurement show the interplay between the charge density wave at T(CDW) = 157 K and the ferromagnetic ordering of T_c = 18 K. Below the ferromagnetic transition temperature, we observed the magnon gap formation of 4.3 ~ 4.4 meV by ρ(T) and Cp(T) measurements. The charge density wave is attributed to the increase of Seebeck coefficient resulting in the increase of power factor S^{2σ}. The thermal conductivity anomalously increases with increasing temperature as the whole measured temperature range which implies the weak attribution of Umklapp phonon scattering. The thermoelectric figure-of-merit ZT significantly increases due to the increase of power factor at T(CDW) = 157 K. Here we argue that the competing interaction between electron-phonon and electron-magnon couplings exhibits the unconventional behavior of electrical and thermal properties.

CF04

Effect of R ion size variance on spin and orbital order in RVO₃ (R=rare earth and Y)

S. Miyasaka^{1*}, R. Fukuta¹, K. Hemmi¹, N. Sasaki¹, S. Tajima¹, D. Kawana², K. Ikeuchi², Y. Yamasaki², A. Nakao², H. Nakao², R. Kumai², Y. Murakami² and K. Iwasa³

¹ Department of Physics, Osaka University, Japan

² KEK-PF/CMRC, Japan

³ Department of Physics, Tohoku University, Japan

Perovskite RVO₃ has orbital degrees of freedom between dyz and dxz orbitals in V³⁺ ions, and shows two types of spin/orbital order (SO/OO): C-type SO (C-SO)/G-type OO (G-OO), and G-SO/C-OO. In this system, the transition temperature of each SO/OO depends on the R-site ionic radius and structural randomness caused by the size mismatch of R ions². We have investigated the single crystals of Y_{1-x}(La_{0.195}Lu_{0.805})VO₃, Eu_{1-x}(La_{0.2542}Y_{0.7458})VO₃, Sm_{1-x}(La_{0.322}Y_{0.678})VO₃, and Nd_{1-x}(La_{0.491}Y_{0.509})VO₃ in order to clarify the effect of R ion size variance on SO/OO in RVO₃. In the present systems, the average ionic radius of R-site is constant, while the size variance of R ion is proportional to x. In R=Y_{1-x}(La_{0.195}Lu_{0.805})VO₃, Eu_{1-x}(La_{0.2542}Y_{0.7458})VO₃, and Sm_{1-x}(La_{0.322}Y_{0.678})VO₃ systems, the R ion size variance suppresses C-SO/G-OO, while it stabilizes the other SO/OO. By the neutron and resonant X-ray scattering measurements, other order is confirmed as G-SO/C-OO. In Nd_{1-x}(La_{0.491}Y_{0.509})VO₃ with larger R-site ions, however, C-SO/G-OO is so stable that the R ion size variance cannot induce the other SO/OO.

1 S. Miyasaka et al., *Phys. Rev. B* 68, 100406(R) (2003). 2 R. Fukuta et al., *Phys. Rev. B* 84, 140409(R) (2011).

CG01

Spin Hall effects in n-GaAs near the metal-insulator transition

Paul A Crowell
School of Physics and Astronomy, University of Minnesota, USA

We have measured the direct and inverse spin Hall effects in GaAs and InGa_{1-x}As in samples doped near the metal-insulator transition. The direct spin Hall effect is measured through the spin accumulation induced at the edges of the semiconductor channel in the presence of a charge current. The inverse spin Hall effect is measured as a Hall voltage induced by injection of a spin current. We find that the magnitude and temperature dependence of the direct spin Hall effect is consistent with simple models for spin-orbit scattering from ionized impurities. The inverse spin Hall effect shows both an anomalously large magnitude and an unusual magnetic field dependence, suggesting that hyperfine interactions play an important role. I will review this work with an emphasis on our attempts to understand spin transport in GaAs near the metal-insulator transition.

This work was carried out in collaboration with C. Geppert, K. Christie, E. Garlid, Q. Hu, S. Patel, and C. J. Palmstrom and was supported by the National Science Foundation and the Office of Naval Research.

CG02

The effect of an inhomogeneous interface on the transport properties across Fe/GaAs(001) films

Luke Fleet¹, K. Yoshida², H. Kobayashi², Y. Kaneko³, S. Matsuzaka³, Y. Ohno³, H. Ohno³, S. Honda⁴, J. Inoue² and A. Horihata^{1*}

¹ The University of York, United Kingdom

² Nagoya University, Japan

³ Tohoku University, Japan

⁴ University of Tsukuba, Japan

Efficient electrical spin-injection is the greatest challenges for semiconductor spintronics. Fe/GaAs remains one of the leading candidate systems for achieving this feat due to the small lattice mismatch. We report the first observation of different interface structures in Fe/GaAs(001) films. Both the ideal and mixed interfaces were observed leading to a distribution of Schottky barrier properties [1]. Regions with mixing have a lower barrier height creating pin-hole type areas where transport will be focused, leading to heating. This increases the contribution to the transport from thermionic emission, therefore reducing the spin injection efficiency. Using ab-initio calculations we show that resonance states form in the minority spin DOS for the mixed interface causing a polarization inversion. We show it is possible to create well behaved reproducible devices if an abrupt interface is created. Transport properties of 3-terminal devices which have a predominantly abrupt interface give spin lifetimes of over 30 ns at 5 K with a spin diffusion length of 16 µm at 10 K. Full details of the interface structures and transport properties of Fe/GaAs(001) films will be presented in the full paper.

[1] L. R. Fleet et al., *IEEE T Magn* 47, 2756 (2011).

CG03

Spin accumulation and decoherence mechanisms at ferromagnetic/tunnel barrier/semiconductor interfaces

Julian Peiro¹, Jean-christophe Lebreton¹, Cyrille Deranlot¹, Aristide Lemaître², Abhinav Jain¹, Celine Vergnaud¹, Matthieu Jamei¹, Henri Jaffres¹ and Jean-marie George^{1*}

¹ Unite Mixte de Physique CNRS/Thales, Campus Polytechnique, 1 av. Augustin Fresnel, 91767 Palaiseau., France

² CNRS-Laboratoire de Photonique et Nanostructures, route de Nozay, 91460 Marcoussis, France

³ INAC/SP2M, CEA-Université Joseph Fourier, 17 rue des Martyrs, 38054 Grenoble, France

The ability to inject spins into a semiconductor (SC) by electrical means and the possibility to convert a spin accumulation into an electrical signal is expected to bring new functionalities. However, it has been shown that the injection of spin-polarized carriers from a ferromagnetic transition metal (FM) into a SC requires the addition and the fine tuning of a spin-conserving resistance at the FM/SC interface. Following the work on Co/Al₂O₃/GaAs interface [1], we now carry out a systematic study on the enhancement of spin accumulation involving modification of the interfacial properties by probing several semiconductor materials involving GaAs, Ge and InP as well as MgO and Al₂O₃ barriers. Inverted Hanle effect measurements reveals the influence of a fluctuating magnetic field leading to decoherence of the spin accumulation at the FM/SC interface whose origin resides in stray magnetic field due interface roughness [2-3], or in hyperfine interaction in case of transport through localized states of GaAs. Both 3-terminal Hanle and Inverted Hanle measurements highlight effects of spin accumulation at the FM/SC interface, few orders of magnitude larger than the expected. The amplitude of the effects can be understood by a sequential injection mechanism through localized interfacial states at the barrier/SC interface.

[1] M. Tran, et al., *Enhancement of the Spin Accumulation at the Interface between a Spin-Polarized Tunnel Junction and a Semiconductor*, *Physical Review Letters* 102, 3-036601, 2009. [2] S.P. Dash, et al., *Spin precession and decoherence near an interface with a ferromagnet*, *Phys. Rev. B* 84, 054410 (2011) [3] A. Jain, et al., *Electrical spin injection and detection at Al2O3/n-type germanium interface using three terminal geometry* *Appl. Phys. Lett.* 99, 162102 (2011)

CG04

Electrical spin accumulation and detection in Fe₃O₄/MgO/GaAs systems

Shwetha G. Bhat^{*}, Cijy Mathai and Anil P. S. Kumar
Department of Physics, Indian Institute of Science, Bangalore, India

The Hanle effect is one of the effective and direct methods for studying the spin injection from a ferromagnet and it is useful for understanding the decay of these injected spins in the semiconductor [1,2]. We have chosen Fe₃O₄/MgO/GaAs (n-doped) system for our study, where the spin polarized electrons are injected from Fe₃O₄ (10nm) to GaAs through thin MgO layer (2nm). This is the first ever attempt in studying the spin injection and decay of spins in the above mentioned system. Fe₃O₄ is a room temperature ferrimagnet which is reported to have 100% spin polarization. The 3-terminal non local Hanle measurement [3,4] is usually carried out in these systems. From our studies, the I-V measurements on the structured junctions of size varying from 200x150µm² to 200x25µm² exhibit tunnel behavior with no considerable rectification. The 3-terminal non local measurements on these devices show a clear indication of the variation of non local voltage ΔV as a function of perpendicular magnetic field for the biasing current I≥1µA. Also, the Hanle plots show the dependency on the extraction and injection of the bias electrons to the above mentioned devices accordingly.

[1] M. Johnson et al., *PRL* 55, 1790 (1985), [2] M. Johnson et al., *PRB* 37, 5326 (1988) [3] M. Tran et al., *PRL* 102, 036601 (2009) [4] C. H. Li et al., *Nat. Commun.* 2, 245 (2011)

CG05

Spin relaxation in defect-free InGaN/GaN quantum wells

Animesh Banerjee^{1*}, Fatih Dogan², Aurelien Manchon² and Pallab Bhattacharya¹
¹ Department of Electrical Engineering and Computer Science, University of Michigan, Ann Arbor, MI 48109-2122, USA
² Division of Physical Science and Engineering, King Abdullah University of Science and Technology, Thuwal 23955, Saudi Arabia

Due to ferromagnetic (FM) properties it presents at room temperature in its n-doped state (with rare-earth metals), and combination of wide-gap and low spin-orbit coupling (SOC), GaN has been identified as a promising compound for spintronics applications. In this work [1], we present numerical analysis of spin relaxation time in defect-free two-dimensional In doped GaN quantum wells grown on GaN nanowires [2]. Data, of wurtzite crystalline structure, has been collected in a range of temperatures, from 100 K to room temperature and at different doping concentrations and energy levels using photoluminescence techniques. In the analysis, spin relaxation mechanisms considered are Elliot-Yafet (EY) and D'yakovov-Perel'(DP). Relative importance and relevance of EY vs. DP mechanism [3] has been investigated. It was found that EY mechanism is very ineffective while DP mechanism dominates as the source of spin relaxation. We have also calculated Rashba and Dresselhaus coefficients for each doping concentrations and shown that increase in doping also changes Rashba and Dresselhaus coefficients in accordance with accepted values for InN and GaN.

1. A. Banerjee, F. Dogan, A. Manchon, and P. K. Bhattacharya *Nano Lett.*, 11, 5396-5400 (2011) 2. W. Guo, M. Zhang, A. Banerjee, and P. Bhattacharya, *Nano Lett.* 10, 3355-3359 (2010) 3. N. J. Harmon, W. O. Patikha, and R. Joynt, *Appl. Phys. Lett.* 98, 073108 (2011)

CH01

Magnetic, magnetotransport and magnetocaloric properties of quaternary Ni-Mn-In-Z Heusler alloys

Alexander Kazakov¹, Valerii Prudnikov¹, Igor Rodionov¹, Denis Mettus¹, Nikolai Perov¹, Alexander Granovsky^{1*}, Arcady Zhukov², Julian Gonzalez², Igor Dubenko³, Arjun Kumar Pathak³, Tapas Samanta³, Shane Stadler⁴, Philip Adam⁴, Joseph Prestigiacomo⁴ and Naushad Ali³

¹ Lomonosov Moscow State University, Russia
² Universidad del Pais Vasco, Spain
³ Southern Illinois University, Carbondale, USA
⁴ Louisiana State University, USA

We present recent results on structural, magnetic, magnetotransport, and magnetocaloric properties of Ni₂Mn_{1-x}In_{1-x}Z_x (Z=In, Ge, Al, B, Si) and Ni₂Mn_{1-x}In_{1-x}Si_xB_x Heusler alloys in the austenitic and martensitic state focusing on behavior of magnetocaloric effect, ordinary and anomalous Hall effect (OHE and AHE) in the close vicinity of phase transitions. The adiabatic changes of temperature ΔT_{ad} at the phase transitions have been found by direct measurements using an adiabatic magnetocalorimeter as well as by indirect method using heat capacitance measurements and thermomagnetic curves M(H,T). Negative and positive values of T_{ad} of about -2K and +2K have been observed in the vicinity of the martensitic transition (MT) and Curie temperatures, respectively, for applied magnetic field ΔH=1.8T. To find OHE and AHE coefficients we used asymptotic values of the Hall resistance in weak and strong magnetic fields as well as thermomagnetic curves M(H,T) and magnetoresistance. It was shown that OHE and AHE coefficients near MT depend on magnetization. In spite of strong change of resistivity near MT the temperature dependence of AHE coefficient is weak. It clearly indicates that both Berry phase contribution and side-jump mechanism are not responsible for AHE in inhomogeneous alloys.

This work was partly supported by the Russian Foundation for Basic Research and by the Office of Basic Energy Sciences, Material Science Division of the U.S. Department of Energy (Grant No. DE-FG02-06ER46291).

CH02

Composition dependence of magnetic properties in tetragonal Heusler-like Mn-Ga alloy films with large perpendicular magnetic anisotropy

Shigemitsu Mizukami^{1*}, Takahide Kubota¹, Qinli Ma¹, Zhang Xianmin¹, Hiroshi Naganuma², Mikihiko Oogane², Akimasa Sakuma², Yasuo Ando² and Terunobu Miyazaki¹

¹ WPI-Advanced Institute for Materials Research, Tohoku University, Japan
² Department of Applied Physics, Graduate School of Engineering, Tohoku University, Japan

Magnetic films with perpendicular magnetic anisotropy (PMA) are advantageous to spin torque applications using magnetic tunnel junctions, such as magnetic random access memory, because PMA reduces switching current and increase thermal stability. It has been predicted that a tetragonal Heusler-like alloy Mn₃Ga exhibits large spin polarization as well as large uniaxial magnetic anisotropy [1]. We have obtained Mn₃Ga (x=0.5) epitaxial films and reported a large perpendicular magnetic anisotropy energy Ku ~ 12 Merg/cc and also low saturation magnetization Ms ~ 250 emu/cc, so far [2]. Furthermore, Gilbert damping for the alloys were relatively smaller than those in other PMA films [3]. We report here composition dependence of magnetic properties for Mn_{3-x}Ga alloy films. The Mn_{3-x}Ga films were fabricated using UHV magnetron sputtering on Cr buffered MgO substrates. X-ray diffraction showed all the films were of c-axis oriented epitaxial structures. Magnetization curves for the films show perpendicular magnetizations with squareness close to unity. The Ms for the films decreased linearly with increasing Mn content, whereas Ku show no remarkable decreases [4]. The results will be discussed with the ab-initio calculations [5]. This work was partially supported by the Strategic International Cooperative Program ASP/MATT (JST) and WPI program (MEXT) in Japan.

[1] B. Balke et al., *Appl. Phys. Lett.* 90, 152504 (2007). [2] F. Wu et al., *Appl. Phys. Lett.* 94, 122503 (2009). [3] S. Mizukami et al., *Phys. Rev. Lett.* 106, 117201 (2011). [4] S. Mizukami et al., *Phys. Rev. B* 85, 014416 (2012). [5] J. Winterlik et al. *Phys. Rev. B* 77, 054406 (2008).

CH03

Optical spectroscopy of half-metallic and thermoelectric Heusler compounds

Jaroslav Hamrle^{1*}, Dominik Legut¹, Kamil Postava¹, Jaromir Pistora¹, Enrique Vilanova², Mirko Emmel², Gerhard Jakob³, Siham Ouardi³, Gerhard H. Fecher⁴ and Claudia Felser³

¹ Department of Physics and Nanotechnology Centre, VSB - Technical University of Ostrava, Czech Republic
² Institute of Physics, Mainz University, Germany
³ Institute of Inorganic Chemistry and Analytical Chemistry, Mainz University, Germany

Heusler compounds are versatile material class allowing to design desired properties through various constituent atoms, i.e. properties intrinsically related to the modification of the atomic electronic structure. Among the studied classes are half-metallic and thermoelectric materials. Although Heusler compounds are thoroughly studied by number of techniques, optical spectroscopies are often omitted. However, they can provide information of phonon energies, gap size and its purity, shape of critical points, presence of quasi-particles such as exciton, conductivity estimation from IR absorption, etc. Knowledge of complex refraction index is important for mass production control check of thin films, to check e.g. their thickness and roughness. Also, half-metallic Heusler compounds are promising materials for magneto-optical applications, due to low photon absorption for energies below half-metallic gap. Within this contribution we present complex refractivity index, determined in wide spectral range from far-infrared to near-ultraviolet, of half-metallic Heusler compounds Co₂FeSi, Co₂FeAl_{0.5}Si_{0.5} and Co₂FeGa_{0.5}Ge_{0.5} and thermoelectric on CoTiSb and NiTiSn (later also doped with Sc and V) measured by ellipsometry and infrared reflectometry. The features of optical spectra are related with details of the electronic structure. The experimental optical properties are compared with ab-initio calculations.

CH04

Verification of band structure calculations for the Heusler compound Co₂MnGa

Michaela Kolbe¹, Stanislav Chadov², Elena Arbelo Jorge¹, Claudia Felser², Hans-joachim Elmers¹, Gerd Schonhense¹, Mathias Klau¹ and Martin Jourdan^{1*}

¹ Institute of Physics, University Mainz, Germany
² CA, Max-Planck-Institut für Chemische Physik fester Stoffe, Germany

Among ferromagnetic Heusler materials many compounds are predicted to be half metals, which makes them highly attractive for spintronics applications. However, direct experimental evidence for the validity of band structure calculations for this class of materials is scarce. Here, the electronic density of states is probed by spin averaged and spin resolved ultraviolet photoemission spectroscopy for the Heusler compound Co₂MnGa using a novel spin filter [Kol10]. The spectroscopy is performed in-situ on epitaxial thin films which show almost complete absence of oxidation after the measurement. This means a further reduction of sample degradation compared to our recent experiments [Hah10]. The experiments show several characteristic features such as a clear Fermi edge and two pronounced emission intensity maxima in the spin averaged data. In spin resolved photoemission a Heusler record polarization of 55% at the Fermi edge is followed by a sign change at E-E_F= -0.7eV. Calculations of the band structure accounting for the many-body effects and the related photoemission spectrum were performed using the LSDA+DMFT approach in the framework of a fully relativistic spin-polarized Korringa-Kohn-Rostoker (SPRKKR) formalism. Good agreement observed between the experimental data and the calculations demonstrates the feasibility to predict the electronic properties of Heusler compounds in general.

[Kol10] M. Kolbe, P. Lushchik, B. Peteret, H. J. Elmers, G. Schonhense, A. Oelsner, C. Tische, and J. Kirschner, *Phys. Rev. Lett.* 107, 207601 (2011). [Hah10] M. Hahn, G. Schonhense, E. Arbelo Jorge, and M. Jourdan, *Appl. Phys. Lett.* 98, 232503 (2011)

CH05

Field-driven domain-wall ratchet shift register

Jeroen Franken^{*}, Henk Swagten and Bert Koopmans
 Department of Applied Physics, Eindhoven University of Technology, Netherlands

Magnetic domain wall shift registers are considered for application in memory [1] and logic circuits [2]. However, to shift all domain walls in a nanowire in the same direction, one requires either impractically high current densities [1] or rotating magnetic fields [2]. Other issues include strict geometrical restrictions, and randomness in the domain wall displacement. We propose a new domain wall shift register suitable for magnetic materials with perpendicular anisotropy (PMA). Using focused ion beam irradiation [3], we engineer an energy landscape for the domain walls that is asymmetric along the propagation direction. This favors ratchet propagation of domain walls in one direction through a nanotrack. Whereas it is often believed that domain walls of opposite polarity cannot be shifted in the same direction since the magnetization will align with the magnetic field, we simply use an AC field to achieve a domain wall shift register. In a proof of principle experiment, indefinite propagation of two domain walls along a closed loop is shown.

[1] S. S. P. Parkin, M. Hayashi, and L. Thomas, *Science* 320, 190 (2008). [2] D. A. Allwood, G. Xiong, M. D. Cooke, C. C. Faulkner, D. Atkinson, N. Vernier, and R. P. Cowburn, *Science* 296, 2003 (2002). [3] J. H. Franken, M. Hoeijmakers, R. Lavrijsen, and H. J. M. Swagten, *J. Phys. Cond. Matter* 24, 024216 (2012).

CI01

Solitonic lattice and Yukawa forces in the rare earth orthoferrite TbFeO₃

Sergey Artyukhin¹, Maxim Mostovoy¹ and Dimitrios Argyriou^{2*}
¹ Zernike Institute for Advanced Materials, University of Groningen, Netherlands
² European Spallation Source ESS AB, Sweden

The control of domains in ferroic devices lies at the heart of their potential for technological applications. Multiferroic materials offer another level of complexity as domains can be either or both of a ferroelectric and magnetic nature. Here we report the discovery of a novel magnetic state in the orthoferrite TbFeO₃ using neutron diffraction under an applied magnetic field. This state has a very long incommensurate period of 340 Å at 3 K and exhibits an anomalously large number of higher-order harmonics, allowing us to identify it with the periodic array of sharp domain walls separated by many lattice constants. These domain walls are formed by Ising-like Tb spins. They interact by exchanging spin waves propagating through the Fe magnetic sublattice. The resulting force between the domain walls has a large but finite range that determines the period of the incommensurate state. It is analogous to the pion-mediated Yukawa interaction between protons and neutrons in nuclei.

CI02

Ferroelectricity from magnetic helicity in ferroaxial crystals

Laurent C Chapon
 Institut Laue-Langevin, France

Spin-driven ferroelectricity in most non-collinear magnets, such as TbMnO₃, is induced by the so-called inverse Dzyalonshinskii-Moriya mechanism and requires a cycloidal magnetic structure, an ordered magnetic state that is not truly chiral (or lacks helicity). Conversely, in a truly chiral magnetic state (proper helix), the pseudo-scalar helicity can not couple directly to the electric polarization, and therefore can't induce ferroelectric order. However, in systems of specific crystal symmetry, named here "ferroaxials," the presence of collective structural rotations mediates an indirect coupling between magnetic helicity and ferroelectricity. I will review our recent experimental results for new compounds of this class, obtained by magnetic X-ray and neutron diffraction techniques, including a clear demonstration that the magnetic helicity can be controlled by an electric field in RbFe(MoO₄)₂, and the existence of 'giant' improper ferroelectricity in CaMn₂O₁₂.

CI03

Chemical-doping control of magnetoelectric multiferroics

Jae-ho Chung^{1*}, Young-sang Song¹, Hak-bong Lee¹, Hun Chang¹ and Kee Hoon Kim²
¹ Dept. of Physics, Korea University, Korea
² Dept. of Physics & Astronomy, Seoul National University, Korea

In magnetoelectric multiferroics, electric polarizations can establish without ionic displacements via spin-orbit coupling that involves spin moments with noncollinear spatial arrangements. In this spin-current multiferroics the direction of electric polarization is determined by the spatial arrangement of interacting magnetic moments, for which inversion symmetry should be absent. In our most recent works, we have demonstrated the ability to control the magnetoelectricity in two different multiferroic materials via chemical doing, namely Mn_{1-x}Co_xWO₄ and Ba_{0.5}Sr_{1-x}Zn_{1+x}(Fe_{1-x}Al_x)₁₂O₂₂. It is found that the substitution of Co²⁺ ions on Mn²⁺ sites not only stabilizes the incommensurate spiral phase, but also changes the orientation of its easy plane. The direction of the ferroelectric polarization subsequently changes from the b to the a axis. In Ba_{0.5}Sr_{1-x}Zn_{20x}Sr_{1-x}Zn₂(Fe_{1-x}Al_x)₁₂O₂₂, on the other hand, the substitution of nonmagnetic Al³⁺ ions on Fe³⁺ sites induces the transition from planar proper screw to conical spin structures by additionally introducing commensurate axial components. This change in magnetic structure is ascribed to the reduction in planar magnetic anisotropy, which eventually leads to the reduction of low critical field for the field-induced magnetoelectric phase. These results indicate that it is possible to manipulate the magnetoelectricity of certain multiferroics materials by selective and precise control of chemical doping.

CI04

Magnetic x-ray scattering studies on multiferroic SmFe₃(BO₃)₄

Dinesh Kumar Shukla^{1*}, Joerg Stempfler¹, Arvid Skaugen¹, Sonia Francoual¹, Martin Von Zimmermann¹, Leonard N Bezmaternykh², Irina A Gudim² and Vladislav L Temerov²
¹ Deutsches Elektronen-Synchrotron DESY,22607 Hamburg, Germany
² L.V. Kirensky Institute of Physics, Krasnoyarsk 660036, Russia

In recent years rare-earth ferrobates, RFe₃(BO₃)₄, have been identified as potential multiferroic materials from both, application as well as fundamental physics point of view. Due to the presence of two magnetic sublattices these materials offer a platform for understanding several interesting physics problems related to structural and magnetic anisotropy. We here present resonant and non-resonant x-ray scattering measurements on single crystalline SmFe₃(BO₃)₄. This compound crystallizes in trigonal structure (s.g. R32) and preserves this structure at all temperatures. Below T_N, magnetic reflections are found at (h k l) ± (0 0 3/2). Resonant x-ray measurements are performed using photon energies close to the Sm L-edges and Fe K edge. Non-resonant measurements are performed using photon energies above and below the edges as well as at 100 keV photon energy. The temperature dependence of the magnetic peak at the Sm L₂ edge reveals the polarization of the Sm moments by the Fe moments in form of an accelerated ordering of the Sm moments upon decreasing temperature. Our measurements confirm the easy-plane magnetic anisotropy for the two magnetic sublattices of Sm and Fe. Non-resonant measurements performed at 100 keV photon energy, with and without magnetic field indicate spin rotations in the basal plane.

CJ01

Spin excitations and transformation of domain structure in nanocrystalline CoFeB-SiO₂ films with growth induced anisotropy

Alexander Grishin^{*}
 Department of Condensed Matter Physics, KTH Royal Institute of Technology, Sweden

We survey results on strong in-plane magnetic anisotropy of electrical transport and broad frequency band spin dynamics in (CoFeB)_x-(SiO₂)_{1-x} films. Samples with less metallic content show higher anisotropy of electric conductivity and isotropic giant magnetoresistance (GMR), while films with smaller x have less anisotropic resistivity and show a mixture of GMR and anisotropic magnetoresistance (AMR). Oppositely, field of magnetic anisotropy Hp increases with "metallization" reaching 535 Oe for the film with x = 0.235. "Soft" magnonic modes were observed in a whole range of oblique orientations of magnetic field perpendicular to the "easy" magnetic axis. FMR frequency nullifies at the line of "spindal decomposition". At descending branch of magnetization curve we found the sequence of domain structure transformations. Uniformly magnetized film breaks to stripe domains separated by low-angle Neel domain walls (DWs). Then, spontaneous nucleation of kinks of Bloch-type DWs occurs. DWs have different chirality and are separated by segments of Neel DW. When H → 0, they shrink converting to the vertical Bloch lines (VBL). After field reversal, Bloch DW loaded with VBLs becomes energetically unfavorable and transforms instantaneously into Neel DW which gradually disappears with film's saturation.

CJ02

GMI effect of amorphous microwires with enhanced magnetic softness

Arcady Zhukov¹, Mihail Ipatov², Ahmed Talaat² and Valentina Zhukova²
¹ Dpto. Fisica de Materiales, Fac. Quimicas, Basque Country University, UPV/EHU and Ikerbasque, Basque Foundation for Science, Spain
² Dpto. Fisica de Materiales, Fac. Quimicas, Basque Country University, UPV/EHU, Spain

Amorphous microwires exhibit outstanding magnetic properties such as magnetic bistability, fast domain wall propagation, magnetically soft properties and GMI effect. We studied hysteresis loops and GMI effect (GMI ratio, ΔZ/Z, impedance tensor components and pulsed GMI effect) at frequencies, f, till 4 GHz in amorphous microwires with different ratios, ρ, of metallic nucleus diameter, d, and total diameter, D. This allowed us to control the magnetoelastic anisotropy, since the strength of internal stresses is determined by the ρ-ratio. GMI effect and hysteresis loops exhibited strong sensitivity to the ρ-ratio. Hysteresis loops of Co-rich low-magnetostrictive microwires exhibit low coercivity (<10A/m). Magnetic anisotropy field increases when ρ decreases. Field dependence of the off-diagonal voltage response measured in pulsed scheme exhibits anti-symmetrical shape with monotonic growth within the certain field range. Annealing (under stress and/or magnetic field) significantly affects magnetic anisotropy and GMI effect of microwires. After stress annealing GMI effect of Fe-rich microwires (which did not exhibit detectable GMI effect in as-prepared state, ΔZ/Z<1% at f=10 MHz) can be considerable improved (ΔZ/Z=60% at f=10 MHz) as a result of stress-annealing induced magnetic anisotropy. Low field GMI hysteresis, related with helical magnetic anisotropy, can be suppressed by the circular bias magnetic field.

CJ03

Micro-fabricated silicon spiral spring based electromagnetic energy harvester

Jong C. Park, Dong H. Bang and Jae Y. Park^{*}
 Electronic Engineering, Kwangwoon University, Korea

In this study, a micro-fabricated electromagnetic energy harvester was newly designed, fabricated, and characterized to generate electrical energy from ultra-low ambient vibrations under 0.3g. The proposed energy harvester was comprised of a highly miniaturized Neodymium Iron Boron (NdFeB) magnet, silicon spiral spring, multi-tuned copper coil, and polydimethylsiloxane (PDMS) housing. When an external vibration directly moves the magnet mounted as a seismic mass at the center of the spiral spring, the mechanical energy of the moving mass is transformed into electrical energy through the 183 turns of the solenoid copper coils. The silicon spiral spring was used to generate a high electrical output power by maximizing the deflection of the movable mass in response to low level vibrations. The fabricated energy harvester exhibited a self resonant frequency of 36Hz and an optimal load resistance of 99Ω, respectively. It generated an output power of 29.02μW and load voltage of 107.3mV at a vibration acceleration of 0.3g. It also exhibited a power density and normalized power density of 48.37μW/cm³ and 537.41μW/cm³ g², respectively. The total volume of the fabricated energy harvesters was 1cm x 1cm x 0.6cm (height).

[1] S. Roundy, P. K. Wright, J. Rabaey, *A study of low level vibrations as a power source for wireless sensor nodes*, *Comput. Commun.* 26 (2003) 1131-1144. [2] D. P. Arnold, *Review of microscale magnetic power generation*, *IEEE Trans. Magn.* 43 (11) (2007) 3940-3951. [3] S. P. Beeby, M. J. Tudor, N. M. White, *Energy harvesting vibration sources for Microsystems applications*, *Meas. Sci. Technol.* 17 (2006) R175-R195. [4] N. S. Hudak, G. G. Amatacci, *Small-scale energy harvesting through thermoelectric, vibration, and radiofrequency power conversion*, *J. Appl. Phys.* 103 (2008) 010301.

CJ04

Magneto-optical study of magnetization reversal in sub-micrometric glass covered wires

Alexander Chizhik^{1*}, Arcady Zhukov² and Julian Gonzalez¹

¹ Universidad del Pais Vasco UPV/EHU, Spain

² Universidad del Pais Vasco UPV/EHU, IKERBASQUE, Basque Foundation for Science, Bilbao, Spain, Spain

With the purpose of the miniaturization of basic elements of magnetic sensors the magneto-optical Kerr effect (MOKE) [1] investigation of the magnetization reversal has been performed in Fe-rich sub-micrometric amorphous wires. The axial tensile stress and torsion stress have been applied during the experiments. The series of the microwires with different values of radius of metallic nucleus (400 nm, 700 nm, 1000 nm) has been studied. In the extremely thin sub-micrometric wires, the magnetic bistable behavior is observed. It confirms the existence of the Surface Large Barkhausen Jump in sub-micrometric glass covered wires like in glass covered wires of micro-scale. The highest value of the surface coercive field is observed for the smallest value of the radius. It has been attributed to the increasing of the strength of internal stresses as increasing the glass coating thickness. The performed analysis of the tensile and torsion stresses transformation of surface hysteresis loop demonstrates that about one order decrease of the wire scale does not abolish the basic effects observed earlier in thicker wires. It permits to reduce considerably the size of basic elements of magnetic sensors.

[1] J. Gonzalez et al., *Journ. of Physics: A*, 208 (2011) 502.

CJ05

The magnetic transition and large magnetoresistance effect in perovskite Nd_{1-x}Sr_xMnO₃ system

Khai Van Vu^{1*}, Thang Viet Do², Sinh Huy Nguyen³ and Anh Thi Kim Do³

¹ Construction Mechanical Faculty, National University of Civil Engineering, Viet Nam

² Faculty of Science, Haiphong University, Viet Nam

³ Faculty of Physics, University of Science, Vietnam National University, Hanoi, Viet Nam

The magnetic transition of Nd_{1-x}Sr_xMnO₃ (with x = 1/3, 0.40 and 0.50) has been investigated with zero field cooling (ZFC) and field cooling (FC) measurements in the temperature range of 77 K - 350 K. It is indicated that the temperature dependence of magnetization of all samples complied with Bloch's law in the area of T < TC. The magnetoresistance of Nd_{1-x}Sr_xMnO₃ system has been determined with magnetic field of 0.0-0.4T. It is found that the obtained magnetoresistance ratio (CMR%) decreased with increasing doped Sr concentrations. The maximum value of CMR(%) is out of the Curie temperature (TC) and metal-insulator transition temperature (Tp) regions. The magnetoresistance ratio nearly linearly increased by decreasing temperature at x = 0.50 compound. The dependence of CMR(%) on the doping Sr in this system has been fitted with hyperbol function.

DA01

Superconducting symmetry of Fe-based systems studied by impurity effects and neutron inelastic measurements

Masatoshi Sato^{1*}, Yoshiaki Kobayashi², Takayuki Kawamata³, Yukio Yasui², Kazunori Suzuki², Masayuki Itoh², Ryoichi Kajimoto¹, Kazuhiko Ikeuchi¹, Masatoshi Arai¹ and Philippe Bourges⁴

¹ Research Center for Neutron Science and Technology, Comprehensive Research Organization for Science and Society, Japan

² Department of Physics, Nagoya University, Japan

³ Department of Applied Physics, Tohoku University, Japan

⁴ Materials and Life Science Division, J-PARC Center, JAEA, Japan

⁵ Laboratoire Leon Brillouin, CEA/Saclay, France

We have focused on the superconducting symmetry of Fe-pnictides, because it is directly connected with the pairing mechanism. Effects of nonmagnetic-impurities on Tc, magnetic excitation spectra χ'' and NMR 1/T1-T curve, all of which are sensitive to the relative signs between the order parameters on their disconnected Fermi surfaces around Γ and M points, have been studied. If the signs are opposite (symmetry S_z) the magnetic mechanism is relevant, while the same signs (symmetry S₊₊) indicate a novel mechanism, because the ordinary phonon mechanism cannot realize Tc as high as ~55 K in Ln1111 (Ln=lanthanides). Results are as follows. (a)Very small rates of Tc-suppression by M impurities in LaFe_{1-x}M_xAs_{0.88}F_{0.11-x} (M=Ni, Co, Ru) can be explained only by S₊₊[1, 2]. (b) χ'' -data for Ba(Fe, Co)As₂ (Tc=23 K) and Ca-Fe-Pt-As crystals (Tc=33 K) can be well explained by S₊₊ rather than by S_z[3]. (c)The NMR data can be understood by S₊₊, too. They strongly support S₊₊ and the existence of a novel pairing mechanism. The symmetry is consistent with the observed elastic softening of C66[4]expected from the orbital-fluctuation (OF) mechanism. Anomalous behavior of phonons by neutron studies are also presented in relation to the OF.

[1] M. Sato et al. *J. Phys. Soc. Jpn.* 79 (2010) 014710. [2] T. Kawamata et al. *J. Phys. Soc. Jpn.* 80 (2011) 084720. [3] J. *Phys. Soc. Jpn.* 80 (2011) 093709. [4] T. Goto et al. *J. Phys. Soc. Jpn.* 80 (2011) 073702.

DA02

Carrier doping versus impurity effects in transition metal-substituted iron-based superconductors revealed by ARPES

Atsushi Fujimori

Department of Physics, University of Tokyo, Japan

In the electron-doped Fe pnictides, superconductivity is realized by substitution of transition-metal atoms for Fe. However, it has been controversial whether itinerant carriers are indeed doped into the system and how the impurity potential affects the electronic properties [1]. In order to address these issues, we have performed a systematic ARPES study of Ba(Fe,M)₂As₂, where M = Mn to Zn. For M = Co, Ni, and Cu, the substitution expands the electron Fermi surfaces and shrinks the hole Fermi surfaces, as expected. However, the number of doped electrons estimated from the Fermi surface volumes is generally smaller than the nominal value, indicating that part of the doped electrons do not become itinerant. Such a tendency becomes stronger in going from Co, Ni to Cu. Concomitantly, energy bands are distorted and M 3d-like states are split off below the Fe 3d bands. As for Mn and Zn, on the other hand, ARPES shows characteristic features of the antiferromagnetic state without any signature of carrier doping. This indicates that the half-filled and fully occupied 3d shells are stabilized in the divalent state of Mn and Zn, respectively.

[1] H. Wadati et al., *Phys. Rev. Lett.* 105, 157004 (2010).

DA03

Specific heat measurements on fepn in fields up to Hc2 - a probe of nodal structure

Greg Stewart*

Physics, Univ. Florida, USA

We report the specific heat gamma as a function of field up to 30 T in Co- and Ni-doped 122, as well as in LiFeAs. The overdoped Co-doped sample displays qualitatively different behavior than the underdoped. Preliminary gamma as a function of angle data will also be discussed.

DA04

NMR study on high temperature Fe-pnictide superconductor Ln-Fe-As-O with Tc=50 K

Hidekazu Mukuda^{1*}, Satoshi Furukawa¹, Mitsuharu Yashima¹, Yoshio Kitaoka¹, Parasharam M Shirage², Hiroshi Eisaki² and Akira Iyo²

¹ Osaka University, Japan

² National Institute of Advanced Industrial Science and Technology (AIST), Japan

Superconducting(SC) transition temperature (Tc) of Ln-FeAsO (1111)-based compounds (Ln: Rare earth) rises to 55 K when the Ln=Sm. In NMR investigation, however, the high-Tc Ln-1111 compounds are affected by the magnetism of rare earth ions, which prevents us from probing the intrinsic nuclear relaxation rate(1/T1) of the quasi-particles in the SC state. In order to reveal the mechanism of high Tc more than 50 K in Ln-1111 system, we have investigated the normal-state and SC characteristics of (La_{0.05}Y_{0.95})FeAsOy (La_{0.05}Y_{0.95}1111) with Tc=50 K by means of 57Fe/75As-NMR measurements. In the SC state, the measurements of 1/T1 have revealed in terms of a multiple fully-gapped s(+)-wave model that the SC gap becomes larger than that in optimally-doped LaFeAsOy (La111(OPT)) with Tc=28 K. In the normal state, the increase of 1/T1T upon cooling indicates that the antiferromagnetic(AFM) spin fluctuations develop toward Tc, which is more significant than in La111(OPT) and (La_{0.8}Y_{0.2}1111) (Tc=34K)[3]. However, these antiferromagnetic spin fluctuations were weaker than in Ba_{0.7}K_{0.4}Fe₂As₂ (Tc=38K) and (Ca₁Al_{1-x}O_x)(Fe₂As₂) (Tc=27K), which have lower Tc values than in La_{0.05}Y_{0.95}1111, suggesting that the AFM spin fluctuations are not an unique factor to increase the Tc in Fe-pnictide superconductors.

DB01

Ultrahigh-resolution and time-resolved laser photoemission study on kondo materials

Shik SHIN

University of Tokyo, Japan

Recently, photoemission spectroscopy has been developed very rapidly and found to be very powerful for the study of Kondo materials. For example, 1. The resolution of 150 μ eV at 1.8K is achieved by the development of laser photoemission. 2. High resolution hard X-ray photoemission becomes possible using high brilliant synchrotron radiation. 3. The angle resolved photoemission in soft X-ray region also shows beautiful results using high brilliant synchrotron radiation. 4. Time resolved photoemission becomes possible very recently using Femto-second laser. I would like to talk on these new experimental results on YbAlB₄ [1] and YbS and Yb metal [2] as well as several Ce, U, and Pr compounds using ultra-high resolution laser-photoemission and high resolution hard X-ray photoemission. I will also talk on the possibilities of time resolved photoemission spectroscopy on heavy electron systems.

[1] Okawa et. al., *Phys Rev. Lett.*, 104(2010) 247201. [2] Matsunami et. al., *PRB* 78(2008)195118.

DB02

Magnetic moment screening in the correlated Kondo lattice model

Peter Thalmeier¹, Mohammad Siahatgar¹, Burkhard Schmidt¹ and Gertrud Zwicknagel²

¹ Max Planck Institute for Chemical Physics of Solids, Germany

² Technical University Braunschweig, Germany

The magnetic correlations, local moments and susceptibility in the correlated 2D Kondo lattice model at half filling are investigated. We calculate their systematic dependence on the Kondo coupling J_K and Coulomb repulsion U. Exact diagonalisation (ED) approach for ground state properties as well as finite temperature Lanczos method (FTLM) for specific heat and the uniform susceptibility are employed for small tiles on the square lattice. The competition of on-site screening and induced inter-site correlations are monitored and a phase diagram is constructed. In particular it is shown that the screened local moment exhibits nonmonotonic behavior as function of U for weak Kondo coupling J_K. In the large U limit the model is equivalent to the 2D Kondo necklace model with two types of localized spins. In this limit the numerical results are compared to those of the analytical bond operator method in mean field treatment and excellent agreement for the total paramagnetic moment is found. The temperature dependence of the susceptibility allows to extract the dependence of the Kondo temperature scale on the correlation strength U. A monotonic increase for small U is found in agreement with earlier analytical impurity calculations.

DB03

Influence of magnetic anisotropy on the underscreened Kondo effect in the presence of ferromagnetism

Maciej Misiorny^{1,2*}, Ireneusz Weymann² and Jozef Barnas^{2,3}

¹ Peter Grünberg Institut (PGI-2), Forschungszentrum Jülich & JARA Jülich Aachen Research Alliance, 52425 Jülich, Germany

² Faculty of Physics, Adam Mickiewicz University, 61-614 Poznań, Poland

³ Institute of Molecular Physics, Polish Academy of Sciences, 60-179 Poznań, Poland

The prominent role of magnetic anisotropy (MA) in formation of the Kondo effect has recently been demonstrated experimentally [1,2]. In particular, it turned out that in systems of spin S>1/2, such as magnetic adatoms (i.e. Fe, Co or Mn) or magnetic molecules, the Kondo effect can be tuned by modifying the system's MA. Furthermore, theoretical studies also indicate that MA can be a key factor determining spin-polarized transport through a magnetic nanosystem [3]. Motivated by the recent experiment [2], in this communication we address how the MA affects the underscreened Kondo effect (i.e. partial compensation of the molecular spin by conduction electrons) in the case of an artificial molecule of spin S=1 coupled to a reservoir of spin-polarized conduction electrons [4]. The crucial ingredient of the model is the presence of uniaxial MA. The problem is analyzed by means of Wilson's numerical renormalization group (NRG) method, which allows for calculating the spectral function of the molecule. We show that the interplay of MA and ferromagnetism has a fundamental significance for occurring of the Kondo effect. Most importantly, despite the presence of the effective exchange field [5] the Kondo effect can be restored by adjusting the magnitude of MA.

1. A.F. One et al., *Nature Phys.* 4, 847 (2008). 2. J.J. Parks et al., *Science* 328, 1370 (2010). 3. M. Misiorny, I. Weymann and J. Barnas, *Phys. Rev. Lett.* 106, 126602 (2011); *Phys. Rev. B* 84, 035443 (2011). 4. A. I. Weymann and L. Borda, *Phys. Rev. B* 81, 115445 (2010). 5. J. Martinek et al., *Phys. Rev. Lett.* 91, 127203 (2003); *Phys. Rev. B* 72, 121302 (2005).

DB04

Quantum criticality out of equilibrium in the pseudogap Kondo model

Chung-hou Chung^{1*} and Yi-jie Zhang²

¹ Electrophysics Dept., National Chiao-Tung University, HsinChu, Taiwan, R.O.C., Taiwan

² Electrophysics Dept., National Chiao-Tung University, HsinChi, Taiwan, R.O.C., Taiwan



DB05

A spin-selective kondo-insulator - cooperation between ferromagnetism and kondo-effect

Robert Peters and Norio Kawakami

Kyoto University, Japan

The Kondolattice model has been intensively studied for the last thirty years as a fundamental model for heavy fermions, Kondo insulators, and transition metals, e.g. the manganites. Yet, the understanding is far from complete. Taking ferromagnetic heavy fermion compounds as motivation we analyze the mechanism stabilizing the ferromagnetic state in the antiferromagnetically coupled Kondo lattice model. We find that even for this ferromagnetic state Kondo screening plays an essential role in stabilizing the ferromagnetic state at zero temperature leading to very interesting properties: while the majority-spin electrons are metallic, the minority-spin electrons form an insulating state. We clarify that this state is due to partial Kondo screening, so that parts of the local moments are bound to the electrons, resulting in a dynamically-induced commensurability which is essential for producing the gap in the minority-spin electrons. We believe that the mechanism proposed here, the dynamically generated commensurability, is generic for the ferromagnetic phase in the antiferromagnetically coupled Kondo lattice model, thus providing new insights into the zero temperature physics for the Kondo lattice model.

DC01

Spin-orbit entangled ground states and excitations in iridium oxides

Giniyat Khaliullin

Max Planck Institute for Solid State Research, Germany

A relativistic spin-orbit coupling may drive unusual interactions and orderings in Mott insulators. This coupling entangles the spin and orbital subspaces leading to a rich variety of effective Hamiltonians and exotic phases depending on the lattice geometry and orbital structure. Particular examples to be discussed are: (i)Iridium perovskite Sr₂IrO₆ where the magnetic order and excitations closely resemble those of high-T_c cuprates [1,2]; (ii)The honeycomb lattice Li₂IrO₃ and Na₂IrO₃ where the celebrated Kitaev model with spin liquid ground state might be at work [1,3]; (iii)Vanadate Sr₂VO₄ which is predicted to exhibit a magnetically hidden octupolar order [4].

[1] G. Jackeli, G. Khaliullin, *Phys. Rev. Lett.* {102}, 017205 (2009). [2] J. Kim {vit et al.}, *arXiv:1110.0759*. [3] J. Chaloupka, G. Jackeli, G. Khaliullin, *Phys. Rev. Lett.* {105}, 027204 (2010). [4] G. Jackeli, G. Khaliullin, *Phys. Rev. Lett.* {103}, 067205 (2009).

DC02

Elementary magnetic excitations of iridates and cuprates probed by resonant inelastic X-ray scattering

Jeroen Van Den Brink*
IFW Dresden, Germany

Resonant Inelastic X-ray Scattering (RIXS) provides direct access to elementary charge, spin and orbital excitations in complex oxides. As a technique it has made tremendous progress with the advent high-brilliance synchrotron X-ray sources. From the theoretical perspective the fundamental question is to precisely which low-energy correlation functions RIXS is sensitive. Depending on the experimental RIXS setup, the measured charge dynamics can include charge-transfer, phonon, d-d and orbital excitations [1]. The focus of this talk will be on RIXS as a probe of spin dynamics, in particular magnon and bi-magnon dispersions [2,3]. Based on the experimental observations, the novelties that RIXS reveals on the spin dynamics of high-Tc cuprates [4,5] and strongly spin-orbit coupled iridium-oxides will be discussed [6].

[1] L. Ament, M. van Veenendaal, T. Devereaux, J.P. Hill and JvdB, Rev. Mod. Phys. 83, 705 (2011). [2] L. Braicovich et al., PRL 102, 167401 (2009). [3] L. Ament, G. Ghiringhelli, M. Moretti Sala, L. Braicovich and JvdB, PRL 103, 117003 (2009). [4] L. Braicovich et al., PRL 104, 077002 (2010). [5] M. Guarise et al., PRL 105, 157006 (2010). [6] L. Ament, G. Khalullin and JvdB, PRB 84, 020403 (2011).

DC03

Resonant Inelastic X-ray Scattering study of Na₂IrO₃

Hlynur Gretarsson¹, Heungsik Kim², Xuerong Liu³, John Hill³, Yogesh Singh⁴, P Gegenwart⁴, Jung-ho Kim⁵, Diego Casa⁶, Thomas Gog⁵, Mary Upton⁵, Jaejun Yu⁵ and Young-june Kim^{1*}
¹Department of Physics, University of Toronto, Canada
²Department of Physics, Seoul National University, Korea
³Brookhaven National Laboratory, USA
⁴Georg-August-Universität Göttingen, Germany
⁵Advanced Photon Source, Argonne National Laboratory, USA

Recently there are intensive research efforts to elucidate physics of materials with 5d electrons, for which spin orbit coupling (SOC) is comparable to other energy scale of the system, such as Coulomb repulsion and crystal field splitting [1-3]. The layered iridate Na₂IrO₃, with Ir⁴⁺ spins sitting on a distorted honeycomb lattice, is such an example [4-7]. Depending on the value of the Coulomb repulsion in such a lattice, the SOC can give rise to a topological insulator or a Kitaev-Heisenberg system for the possible spin-liquid phase [5]. The electronic structure of Na₂IrO₃ has been investigated using resonant inelastic x-ray scattering (RIXS) and density functional theory calculations. Crystal field split d-d excitations are resolved in the high-resolution RIXS spectra. We observe a large splitting between the two eg orbitals, which arises from the dimerization of Ir atoms due to the metal-metal bonding. The low energy d-d excitations exhibit small momentum dependence, which can be described as due to spin-orbital coupled excitation.

[1] Y. Okamoto et al. Phys. Rev. Lett. 99, 137207 (2007). [2] B. J. Kim et al., Phys. Rev. Lett. 101, 076402 (2008). [3] D. Pesin and L. Balents, Nat. Phys. 6, 376 (2010). [4] A. Shitade et al., Phys. Rev. Lett. 102, 256403 (2009). [5] G. Jackeli and G. Khalullin, Phys. Rev. Lett. 102,017205 (2009). [6] Y. Singh and P. Gegenwart, Phys. Rev. B 82, 064412 (2010). [7] X. Liu et al., Phys. Rev. B 83, 220403 (2011).

DC04

Magnetization plateaus in generalized Shastry-Sutherland models

Pinaki Sengupta^{1*}, Keola Wierschem¹, Takafumi Suzuki² and Naoki Kawashima³
¹Nanyang Technological University, Singapore
²Hyogo University, Japan
³University of Tokyo, Japan

The Shastry-Sutherland model is known to exhibit a novel sequence of magnetization plateaus in the presence of an applied field. It has been shown in the recent past that inclusion of anisotropic and/or additional interactions to the standard Shastry-Sutherland model can change the magnetization profile completely - resulting in different sequences of magnetization plateaus. In the present work, we use large scale numerical simulations to systematically study the effects of Ising-like exchange anisotropy and a 3rd nearest neighbor ferromagnetic interaction on the field induced magnetization behavior. In particular we follow the evolution of the m_z/m_s=1/3 and 1/2 plateaus as the strength of the additional terms are varied. The results are valuable in understanding the behavior of the rare-earth tetraboride family of quantum magnets whose magnetic properties are described by generalized Shastry-Sutherland models of the kind considered in this study.

DD01

Modulated spinodal decomposition and magnetotransport in (Ge,Mn) films grown on GaAs(001)

Ing-song Yu¹, Thibaut Devillers¹, Andre Barski¹, Pascale Bayle-guillemaud¹, Cyrille Beigne¹, Johan Rothman², Vincent Baltz¹, Joel Cibert³ and Matthieu Jamet^{1*}
¹INAC, Commissariat a l'Energie Atomique et aux Energies Alternatives, France
²LETI, Commissariat a l'Energie Atomique et aux Energies Alternatives, France
³Institute NEEL, CNRS, France

The field of ferromagnetic semiconductors evolves very fast nowadays for their potential use in spintronic devices. Up to now, efforts have mainly focused on Diluted Magnetic Semiconductors but Curie temperatures in these materials still remain modest. One possible route to increase at least locally transition temperatures is to use spinodal decomposition leading to transition metal-rich high-TC nanostructures. We focus here on (Ge,Mn) considered as a model system for spinodal decomposition and compatible with Si-based microelectronics. While the growth of (Ge,Mn) films on Ge substrates leads systematically to Mn-rich self-assembled nanocolumns exhibiting high-TC, we demonstrate the fine control of spinodal decomposition in (Ge,Mn) films grown on GaAs. Using different surface preparations, we clearly identify the role of surface morphology and impurity diffusion from the substrate (Ga or As) on the nanocolumns growth and the electrical properties (MR and AHE)[1]. In particular holes exhibit an anomalous Hall effect, and electrons exhibit a tunneling magnetoresistance, both with a clear dependence on the magnetization of the Mn-rich inclusions; holes exhibit orbital MR, and electrons show only the normal Hall effect, and an additional component of magnetoresistance due to weak localization, all three being independent of the magnetic state of the Mn-rich inclusions.

[1] I. S. Yu, M. Jamet, T. Devillers, A. Barski, P. Bayle-Guillemaud, C. Beigne, J. Rothman, V. Baltz, J. Cibert, Phys. Rev. B 82, 035308 (2010).

DD02

Homogenous and heterogeneous magnetism in (Zn,Co)O

Maciej Sawicki¹, Ela Guzewicz², Malgorzata I Lukaszewicz², Oleg Proselkov¹, Iwona Kowalik¹, W. Lisowski², Piotr Dłuzewski¹, Wojciech Paszkowicz², Rafal Jakiela¹, Bartłomiej S Witkowski¹, Lukasz Wachnicki¹, F.J. Luque³, D. Arvanitis⁴, W. Sobczak², M. Krawczyk², A. Jablonski², Wiktor Stefanowicz², Dariusz Szentkiewicz¹, Marek Godlewski¹ and Tomasz Dietl¹
¹Institute of Physics, Polish Academy of Sciences, Poland
²Institute of Physical Chemistry, Polish Academy of Sciences, Poland
³Depto. de Física de la Materia Condensada, Universidad Autónoma de Madrid, Spain
⁴Department of Physics and Astronomy, Uppsala University, Sweden

For more than a decade ZnO doped with Mn and Co has remained as one of the most prospected DMS for the room temperature (intrinsic) ferromagnetism resulting in numerous reports on room temperature ferromagnetism conflicted with those which deny existence of any coupling at all. In order to clarify this issue we investigate ZnCoO layers grown by ALD at low temperatures [1]. We employ and relay on wide range of extensive material characterisation which in combination with SQUID magnetometry allow us decisively exemplify the growth temperature Tg as the key factor discriminating between paramagnetic (obtained at Tg=160oC) and various forms of ferromagnetic responses (seen when Tg>200oC). When the ferromagnetism is found, our data indicate presence of nearly temperature independent and highly anisotropic response which we unambiguously associate with few nm thin metallic Co-mesh located at the (Zn,Co)O/substrate interface. It explains why the magnitude of the ferromagnetic-like signal is virtually independent of the film thickness as well as elucidates the origin of magnetic anisotropy, as observed by us and others [2]. Furthermore, it makes it possible to understand significant deviations from the standard superparamagnetic behavior visible in our samples as well as in many high-temperature DMSs and DMOs [3].

[1] M. Sawicki et al., cond-mat arXiv:1201.5268 [2] Venkatesan et al, Phys. Rev. Lett., 93, 177206 (2004). [3] J.M.D. Coey et al., New J. Phys., 12, 053025 (2010).

DD03

Magnetic and optical studies of hydrogenated Cu-doped ZnO film

Tong Li, Wen Xiao, Tun Seng Heng, Nina Bao and Jun Ding*
National University of Singapore, Singapore

ZnO doping with Cu has provoked broad interest recently.1,2 Some interesting findings, such as surface ferromagnetism (FM) in hydrogenated ZnO, and hydrogen enhanced green emission (GE) in ZnO film4 were reported previously. In this work, we focused on hydrogenated ZnO:Cu film. This study reported hydrogen enhanced FM and strong GE in ZnO:Cu (2 at%) film and possible mechanism. ZnO:Cu films (002) with different thickness were deposited on quartz (110) by PLD at 600 oC. Prior to H2 treatment, the areal saturation magnetization Msa (1×10-5 emu/cm²) was found to be insensitive to thickness, suggesting surface/interface magnetism5. After H2 treatment at up to 500 oC, Ms of ZnO:Cu (20 nm) reached 3.1×10-5 emu/cm² (15.4 emu/cm²), which was three times stronger than hydrogenated ZnO. Surprisingly, unlike hydrogenated ZnO, this hydrogen induced Msa drastically decreased with increasing thickness. It thus indicated that apart from surface FM resulting from OH attachment4, Cu dopants play a dominant role in FM enhancement in response to H2 treatment. Furthermore, although light emission of ZnO:Cu showed an obvious blue shift compared to ZnO, a similar strong GE was observed after 500 oC-H2 treatment. This GE is attributed to defect complexes and formation of porous structure that creates optical cavities.

1. Dietl, T., et al., Zener Model Description of Ferromagnetism in Zinc-Blende Magnetic Semiconductors. Science, 2000, 287(5455): p. 1019-1022. 2. Hergn, T.S., et al., Room-Temperature Ferromagnetism of Cu-Doped ZnO Films Probed by Soft X-Ray Magnetic Circular Dichroism. Physical Review Letters, 2010, 105(20). 3. Li, T., et al., Surface ferromagnetism in hydrogenated-ZnO film. Applied Physics Letters, 2011, 98(15). 4. Li, T., et al., Green random lasing in hydrogenated ZnO film. Journal of Physics D, under review. 5. Ong, C.S., et al., Strain-Induced ZnO Spinterfaces. The Journal of Physical Chemistry C, 2011, 116(1): p. 610-617.

DD04

Formation and investigation of structural and magnetic properties of Ni-Mn-In Heusler alloy thin films

Alexey Grunin*, Alexander Goikhman and Valeria Rodionova
Immanuel Kant Baltic Federal University, Russia

In this work we report on the different methods of formation of the Ni-Mn-In Heusler alloy thin films by pulsed laser deposition and the dramatic dependence of martensitic transition temperatures (Tm) and Curie temperatures (Tc) on the alloy composition. Using two-lasers co-deposition approach we have implemented various methods of the thin films formation with controlled stoichiometry: by ablation of one target (Ni₅₀Mn₂₅In₂₅), by simultaneous ablation of two targets (Ni₅₀Mn₂₅In₁₅ and In) or by simultaneous ablation in the appropriate ratio of three pure metals targets (Ni, Mn and In). The phase and chemical composition, structural and magnetic properties of as-grown Ni-Mn-In thin films have been probed by X-ray Diffraction (XRD), Raman scattering, Auger electron spectroscopy, Rutherford backscattering spectrometry and vibrating sample magnetometry. Temperature dependences of magnetic and structural properties are investigated by Physical properties measurement system (PPMS) and high-resolution XRD. It was shown that the films are not susceptible to degradation. We have observed that increasing of In concentration from 14 to 20% leads to Tc decreasing by 30K (from 330 to 300K). At the same time temperature hysteresis, corresponding to martensitic transitions changes from temperature range Tm=250-310K to Tm= 260-370K. The low-temperature phase transition has been found for all samples.

DD05

Magnetic excitations in rare earth based nanosystems

Karine Dumesnil^{1*}, Catherine Dufour¹, Sylvain Petit² and Alexandre Bataille²
¹Institut Jean Lamour - Lorraine University, France
²Laboratoire Leon Brillouin - CEA, France



DD06

Exchange coupled L10 FePt (hard)/ soft (A1 FePt or Co) nanocomposites

Thanassis Speliotis¹, George Giannopoulos¹, Dimitris G Niarchos¹, W F Li² and George Hadjipanayis³
¹Institute of Materials Science, NCSR DEMOKRITOS, Greece
²Department of Physics and Astronomy, U of Delaware, Newark, Delaware, USA
³Department of Physics and Astronomy, U of Delaware, Newark Delaware, USA

L10 ordered FePt is one of the most promising materials for ultra high density perpendicular magnetic recording, however its high coercivity greatly exceeds the writing field of available heads. Thus new media structures proposed in order to decrease the required writing field named as exchange coupled composites (ECC) or so-called exchange spring media. The ECC media consists of two or more exchange coupled sub-regions, in which the hard region stores the information and the soft region(s) promotes the magnetization reversal of the hard region, while keeping high thermal stability. In this work structural and magnetic properties of core-shell type hard/soft (L10 FePt / A1 FePt or Co) exchange coupled nanocomposites are presented. Semi spherical core-shell nanocomposites with L10 FePt core and A1 FePt (fcc) or Co shell were obtained by depositing A1-FePt or Co cap layers on type L10 FePt nanoparticles in order to understand the influence of the soft magnetic layer thickness on the magnetic properties of the system. Epitaxial growth is confirmed by x-ray diffraction and TEM, while the coercivity decreases dramatically for the L10/A1-FePt or Co system when the thickness of the A1-FePt or Co cap layers is increased.

Supported by the ARPA-E

DE01

Micromagnetic simulation of magnetic nanostructures

Thomas Schreffl*, Simon Bance, Lukas Exl, Johann Fischbacher, Harald Oezelt and Franz Reichel
St. Poelten University of Applied Sciences, Austria

Magnets are key elements of modern society. Examples of the wide spread use of magnets are magnetic data storage, permanent magnets for energy applications, wireless sensors, and biomedical systems. The design and development of magnetic devices heavily relies on simulations. Recent advances in hard- and software make it possible to bridge the length scales. In magnetic recording simulations the input and output are the write current and the read back voltage while magnetization dynamics is treated at the nano-scale. Nano-scale non-coherent magnetization reversal decouples the switching field and the thermal stability of magnetic recording media. In the talk we will show the potential of bit patterned magnetic recording systems for storage densities reaching 5 Tbit/in². In addition to the physics of magnetization reversal, we will review the methods and algorithms that are applied in numerical micromagnetics. Further examples of micromagnetic simulations will include low-rare earth containing permanent magnets and wireless magnetostriuctive sensors.

DE02

Multi-bit magnetic memory based on the extraordinary Hall effect.

Alexander Gerber and Amir Segal
School of Physics and Astronomy, Tel Aviv University, Israel

We propose a principle of multi-bit magnetic random access memory in which each memory cell is split among several multilevel dots exhibiting perpendicular anisotropy, and the extraordinary Hall effect (EHE) is used to extract the stored information. Four-, eight- and sixteen- memory state cells have been realized in the proof-of-concept study. In addition to multiplicity of states, probably the most important advantage of the split cell architecture is freedom in positioning dots of the same cell at separate locations and different levels, thus building an effective three-dimensional memory.

DE03

Epitaxial Fe/MgO/Fe tunnelling junctions on BaTiO₃ (001)

Greta Radaelli* and Riccardo Bertacco
LNESS center - Polo regionale di Como - Politecnico di Milano, via Anzani 42 (Como), Italy

Novel schemes for magnetic recording and reading are based on spintronic devices where a determinant role is played by materials or interfaces displaying magnetoelectric coupling. In this context the study of the Fe/BaTiO₃ (BTO) interface is particularly interesting in view of a possible magnetoelectric coupling at the interface as suggested by Duan et al [1] and Sahoo et al [2]. After an initial study of the magnetoelectric coupling at the interface between thin Fe films and BTO single crystal substrates [3] epitaxial Fe/BTO/Nb:SrTiO₃(001) and Fe/BTO/La_{0.7}Sr_{0.3}MnO₃/SrTiO₃(001) interfaces have been grown by combined use of molecular beam epitaxy and pulsed laser deposition. Finally, fully epitaxial Co/Fe/MgO/Fe/BTO heterostructures have been deposited and magnetic tunnelling junctions (MTJs) fabricated via optical lithography. I(V) curves clearly indicate that tunnelling is the dominant mechanism in our MgO junctions. Preliminary experiments testing the electric control of the TMR have been performed at different temperatures. A modulation of the TMR on the order of 10%, induced by application of an electric field across the BTO template, has been detected at 150 K. This result attests the great potential of this system for the electric control of magnetization of ferromagnetic electrodes in spintronic devices.

[1] C. Duan et al. Phys. Rev. Lett. 97 (2006) 047201 [2] S. Sahoo et al. Phys. Rev. B 76 (2007) 092108 [3] S. Brivio et al. Appl. Phys. Lett. 98 (2011) 092505

DE04

Experimentally performed periodic NOT/AND/OR magnetic quantum dots cellular automata gate

Hikaru Nomura*, Yukihiko Imanaga, Yusuke Hiratsuka and Ryoichi Nakatani
Division of Materials and Manufacturing Science, Osaka University, Japan

A magnetic quantum dots cellular automata (MQCA) [1, 2] can perform NAND/NOR logic operation [3] via magnetostatic interaction between the dots. The MQCA is composed of elliptical dots, and digital information of “0” and “1” are stored with a direction of dot magnetization. In general, the logic operations are executed by applying a uniform external magnetic field (clock field). However, in arrayed MQCA structures, it is difficult to control a data flow direction between the MQCA gates with the uniform clock field. Here we demonstrate a NOT/AND/OR logic operation in arrayed structure with a localized clock field from magnetic force microscopy (MFM) tip. As the NOT/AND/OR MQCA gate, four elliptical Ni-20at.%Fe dots with long/short axis of 110 nm/65 nm, thickness of 20 nm, were fabricated on a thermally oxidized Si(100) substrate with electron-beam lithography, ion beam sputtering, and lift-off technique. To write digital information to the dots, we use a magnetization manipulation method with MFM. With all possible initial states of the NOT/AND/OR MQCA gate, we confirm that the gate can perform expected logic operation at room temperature. With arrayed MLG structures, high functional circuits, such as adder circuit will be realized in the near future.

[1] R. P. Cowburn and M. E. Welland 2000 Science 287 1466 [2] A. Imre, G. Csaba, L. Ji, A. Orlov, G. H. Bernstein and W. Porod 2006 Science 311 205 [3] H. Nomura and R. Nakatani 2011 Appl. Phys. Express 4 013004

DE05

Energy-efficient control of vortex-core polarizations by tailored orthogonal pulse currents in cross-point architecture

Young-sang Yu¹, Ki-suk Lee², Hyunsung Jung¹, Youn-seok Choi¹, Dong-soo Han¹, Myoung-woo Yoo¹, Mi-young Im², Peter Fischer³ and Sang-koog Kim⁴*

¹ National Creative Research Initiative Center for Spin Dynamics & Spin-Wave Devices & Nanospices Lab, Research Institute of Adv. Materials, Dep. of Materials Sci. & Eng., Seoul Nat’l Univ., Seoul, Korea

² Center for X-ray Optics, Lawrence Berkeley National Laboratory, Berkeley CA 94720, USA

Magnetic vortices have been considered to be a potential candidate for information-storage applications due to their core binary states, as well as energetically stable configurations. Recent findings [1] of vortex-core switching with low-power consumption have stimulated further studies towards implementation of the magnetic vortices into actual nonvolatile random access memory [2]. In this presentation, we are going to report a low-power-consumption and reliable manipulation of vortex-core magnetizations in patterned magnetic disks. To achieve an alternative to switch the vortex-core magnetizations, we applied rotating fields that are generated by two orthogonal Gaussian-pulse currents. The threshold field strength required for vortex-core switching can be significantly reduced by optimizing the pulse widths and the time delay between the orthogonal pulses [3]. We also demonstrated a remarkable reduction in the threshold strength using a coherent train of rotating fields with their optimized time interval. For reliable memory-bit selection and information recording, we fabricated 2 × 2 vortex-state disks with crossed electrodes and demonstrated selective vortex-core switching at the intersection of the two crossed electrodes [4]. These results imply that the optimized pulse-type rotating fields in the basic cross-point-architecture are energy-efficient and reliable means of selective information recording based on magnetic vortex arrays.

*Corresponding author: sangkoog@smu.ac.kr [1] B. Van Waeyenberge et al., Nature 444, 461 (2006); M. Curcio et al., Phys. Rev. Lett. 101, 197204 (2008); K.-S. Lee et al., Phys. Rev. Lett. 101, 267206 (2008). [2] S.-K. Kim et al., Appl. Phys. Lett. 92, 022509 (2008). [3] Y.-S. Yu et al., Phys. Rev. B 83, 174429 (2011). [4] Y.-S. Yu et al., Appl. Phys. Lett. 98, 052507 (2011). [5] This research was supported by the Basic Science Research Program through the National Research Foundation of Korea (NRF) funded by the Ministry of Education, Science, and Technology (Grant No. 20110000441).

DF01

Skyrmion dynamics in metallic chiral ferromagnet

Jung Hoon Han¹, Jin-hong Park¹, Jiadong Zang², Naoto Nagaosa³ and Maxim Mostovoy⁴

¹ Physics, Sungkyunkwan University, Korea

² Physics, Fudan University, China

³ Applied Physics, The University of Tokyo, Japan

⁴ Zernike Institute for Advanced Materials, University of Groningen, Netherlands

Chiral ferromagnetic materials have recently been shown to be important platforms for the generation of novel topological spin texture called Skyrmions. Their easy generation by moderate magnetic field at relatively high temperature is beginning to open up the potential for device and memory applications. In this talk, I will review some history of its recent rapid development and present basic theory of thermodynamics and dynamics of Skyrmions. To conclude, a possible means of generating Skyrmions by purely electrical means, without relying on magnetic field, will be discussed.

[1] Dynamics of Skyrmion Crystals in Metallic Thin Films, Jiadong Zang, Maxim Mostovoy, Jung Hoon Han, and Naoto Nagaosa, Phys. Rev. Lett 107, 136804 (2011) [2] Skyrmion Lattice in Two-Dimensional Chiral Magnet, Jung Hoon Han, Jiadong Zang, Zhihua Yang, Jin-Hong Park and Naoto Nagaosa, Phys. Rev. B 82, 094429 (2010) [3] Real-space observation of a two-dimensional skyrmion crystal, X. Z. Yu, Y. Onose, N. Kanazawa, J. H. Park, J. H. Han, Y. Matsui, N. Nagaosa and Y. Tokura, Nature 465, 901 (2010)

DF02

Long-range crystalline nature of the skyrmion lattice in MnSi

Tim Adams¹, Sebastian Muhlbauer², Christian Pfleiderer³, Florian Jonietz², Andreas Bauer¹, Andreas Neubauer¹, Robert Georgii¹, Peter Boni¹, Uwe Keiderling⁴, Karin Everschor², Markus Garst⁵ and Achim Rosch⁶

¹ TU Munchen, E21, Germany

² Institut für Festkörperphysik, ETH Zurich, Zurich, Switzerland, Germany

³ Physik-Department E21, Technische Universität München, D-85748 Garching, Germany

⁴ Helmholtz Zentrum Berlin, BENS-C, D-14109 Berlin, Germany

⁵ Institute of Theoretical Physics, Universität zu Köln, D-50937 Köln, Germany

We report small angle neutron scattering of the Skyrmion lattice in MnSi using an experimental setup that minimizes the effects of demagnetizing fields and double scattering. Under these conditions, the Skyrmion lattice displays resolution-limited Gaussian rocking peaks that correspond to a magnetic correlation length in excess of several hundred micrometers. This is consistent with exceptionally well-defined long-range order. We further establish the existence of higher-order scattering, discriminating parasitic double scattering with Renninger scans. The field and temperature dependence of the higher-order scattering arises from an interference effect. It is characteristic for the long-range crystalline nature of the Skyrmion lattice as shown by simple mean-field calculations. A peculiar change of the pinning and a meandering around the direction parallel to the magnetic field suggests a symmetry breaking transition and a more complex interplay of the skyrmion lattice with the crystal structure.

T. Adams et al., Phys. Rev. Lett. 107, 217206 (2011) S. Muhlbauer et al., Science 323, 915 (2009) A. Neubauer et al., Phys. Rev. Lett. 102, 186602 (2009)

DF03

Magnetic textures and electron transport in chiral helimagnets

Jun-ichiro Kishine¹, Alexander Ovchinnikov², Igor Proskurin², Yoshihiko Togawa³, Yusuke Kousaka⁴ and Jun Akimitsu⁴

¹ Graduate School of Arts and Sciences, The Open University of Japan, Japan

² Department of Physics, Ural Federal University, Russia

³ N2RC, Osaka Prefecture University, Japan

⁴ Department of Physics, Aoyama Gakuin University, Japan

A coupling of free electrons with non-trivial spin textures has recently attracted a great attention because of an ability to manipulate magneto-transport properties through a control of the background spin subsystem. In this presentation, based on our recent two papers[1,2], I report magnetic texture formation and anomalous magneto-transport phenomena in magnetic crystals belonging to chiral space groups. In this class of magnets, the left- or right-handed helical spin texture along the crystallographic axis is stabilized by a competition between symmetric exchange and antisymmetric Dzyaloshinskii-Moriya (DM) exchange interactions. Then so-called chiral soliton lattice (CSL) is formed under weak magnetic field applied perpendicular to the helical axis. The CSL behaves as a magnetic superlattice potential and results in Bragg scattering of conduction electrons. Tuning of the weak magnetic field enables us to control a size of the superlattice Brillouin zone and gives rise to a series of resistivity anomalies originating from resonant Bragg scatterings. I will also mention CSL-related phenomena from theoretical viewpoints [3-5]. This talk is given from theoretical sides. A report from experimental sides will be given in the same session by Prof. Yoshihiko Togawa from Osaka Prefectural University.

[1] J. Kishine, I. Proskurin and A. S. Ovchinnikov, Phys. Rev. Lett. 107, 017205 (2011). [2] Y. Togawa, T. Koyama, K. Tokayanagi, S. Mori, Y. Kousaka, J. Akimitsu, S. Nishihara, K. Inoue, A. S. Ovchinnikov, and J. Kishine, to appear in Phys. Rev. Lett. [3] J. Kishine, A. S. Ovchinnikov, and I. Proskurin, Phys. Rev. B 82, 064407 (2010). [4] J. Kishine and A. S. Ovchinnikov, Phys. Rev. B 79, 220405(R) (2009). [5] I. Bostrom, J. Kishine and A. S. Ovchinnikov, Phys. Rev. B78, 064425(2008).

DF04

The hexagonal spin structure of A-phase in MnSi

Sergey Grigoriev^{1*}, Nadezhda M. Potapova¹, Evgeny V. Moskvin¹, Vadim A. Dyadkin¹, Charles Dewhurst² and Sergey V. Maleyev¹

¹ Condensed Matter Department, Petersburg Nuclear Physics Institute, Russia

² Institute Laue-Langevin, France

Inspired by recent work [1] we have revisited the cubic helimagnet MnSi to address the question of the origin of A-phase in the (H-T) phase diagram. In the present experiments we used the experimental geometry described in [1] when the magnetic field was applied along the neutron beam. We have mapped the A-phase boundaries in the field-temperature (H-T) phase diagram for three principal crystal-to-field orientations (H || [111], H || [110], H || [100]). The A-phase revealed itself on the neutron diffraction map as a hexagonal pattern of Bragg spots in a narrow range of the fields [0.12-0.20] T close to $T_{CS} = 29$ K. The orientational and translational orders (the directions and value of structure wavevectors k) are well preserved within the A-phase over the whole crystal of the size of 100 nm³. The small angle neutron scattering ascribed to the orientationally disordered hexagon spin structure was observed beyond the A-phase boundaries in the field range from H_D1 = 0.1 T to H_D2 = 0.25 T at temperatures down to 25 K. Contrary to the A-phase boundaries, the values of H_D1 and H_D2 are temperature independent for all the field-to-crystal orientations.

[1] S. Muhlbauer, B. Binz, F. Jonietz, C. Pfleiderer, A. Rosch, A. Neubauer, R. Georgii, P. Boni, Science 323 (2009) 915-919.

DG01

Preparation and analysis of ni nanowires on si gratings

Wolfgang Kreuzpaintner¹*, Boris P. Toperverg¹, Dieter Lott¹, Michael Stoermer², Volker Neu¹, Christina Bran¹, Stefan Mattauch¹, Andreas Schreyer³ and Peter Boeni¹

¹ Physik Department E21, Technische Universität München James-Frank-Strasse 1 85748 Garching, Germany

² Fakultät fuer Physik und Astronomie Ruhr-Universität Bochum 44780 Bochum, Germany

³ Helmholtz-Zentrum Geesthacht Max-Planck-Strasse 1 21502 Geesthacht, Germany

⁴ Magnetic Microstructures, IFW Dresden, Institute for Metallic Materials Helmholtzstrasse 20 01069 Dresden, Germany

⁵ JCMS Outstation at FRM II Forschungszentrum Juelich GmbH Lichtenbergstrasse 1 85747 Garching, Germany

Ni was e-beam evaporated onto a lithographically prepared Si grating under a shallow angle of incidence. By geometrical self-shading effects, Ni nanowires of 10nm x 10nm cross-section, a spacing of 750nm and a length of several cm, could be deposited homogeneously on a surface of approx. 4cm. 10nm of Al were sputter deposited as capping layer. The structural and magnetic properties of this sample will be presented: Initial structural analyses of the prepared Ni-nanowires were performed by SEM imaging. To confirm these results and to probe the magnetic character of the Ni nanowire sample, AFM and MFM micrographs were taken. The lateral periodicity over a macroscopic distance and the buried sample structures were probed by off-specular x-ray scattering and a Distorted-Wave Born Approximation based analysis was performed: first the specular reflectivity was extracted and a corresponding theoretical model was found by computer aided fitting. The obtained transverse layer structure with corresponding averaged scattering length densities was then modified by lateral variations and used to simulate the off-specular scattering behavior with excellent agreement between the measured and simulated intensities. These outstanding off-specular x-ray scattering results motivated polarized off-specular neutron scattering measurements which will also be presented.

DG02

Elaboration and characterization of Cu/Co multilayered nanowires

Julien Bran¹, Malick Jean¹, Rodrigue Larde¹, Jean-marie Le Breton^{1*} and Alain Pautrat²

¹ Groupe de Physique des Matériaux - UMR 6634, CNRS - Université de Rouen, France

² CRISMAT, UMR 6508 CNRS, ENSICAEN - Université de Caen, France

The Giant Magnetoresistance (GMR) effect discovered in 1988 [1] had inspired many researches on magnetoresistive materials. It has been predicted by the Valet-Fert model [2] that this effect is higher when the current is perpendicular to the layers (Current-Perpendicular-to-Plane CPP geometry). Over the past ten years, a lot of research works were focused on multilayered nanowires. Indeed, these structures, exhibiting a large aspect ratio (length/diameter), provide an ideal opportunity to investigate the CPP-GMR effect and represent good candidates for the development of new technologies in the high density storage domain. In our study, Cu/Co multilayered nanowires were elaborated by a low cost electrochemical process consisting of reducing alternatively the Cu²⁺ and Co²⁺ ions on a metallic substrate through a nanoporous template. Transmission Electron Microscopy (TEM) with Energy Dispersive Spectrometry was used to determine the roughness and the composition of each layer. Atom Probe Tomography (ATP) [3] was also used, additionally to conventional techniques, to characterize our samples. The (Cu20nm/Co20nm) nanowires exhibit a ferromagnetic behaviour, with a strong anisotropy. The magnetoresistance reaches 6% after a heat treatment at 450°C for 1 hour. The correlation between nanostructure and both magnetic and magnetoresistive properties of the nanowires will be discussed.

[1] M. N. Baibich, J. M. Broto, A. Fert, F. Nguyen Van Dau, F. Petroff, P. Etienne, G. Creuzet, A. Friederich, and J. Chazelas, Phys. Rev. Lett. 61(21) (1988) 2472-2475. [2] T. Valet and A. Fert, Phys. Rev. B. 48 (1993) 7099-7113. [3] D. Blavette, B. Deconihout, A. Bostel, J.M. Sarrau, A. Menard, Rev. Sci. Instrum., 64 (1993) 2911.

DG03

Microstructure and magnetic properties of as-deposited and annealed FeCo-based nanowires

Cristina Bran¹*, Javier Garcia², Victor Prida², Rafael Perez Del Real¹ and Manuel Vazquez²

¹ Institute of Materials Science of Madrid, CSIC. 28049 Madrid, Spain

² Dept. Física, Universidad de Oviedo. 33007 Oviedo, Spain

Ordered arrays of ferromagnetic nanowires are recently becoming the subject of intense research due to their potential as magnetic memory and sensor devices, as well as in spintronic and medical applications [1-2]. FeCo nanowires exhibit the necessary capability to be employed in novel generation of rare-earth free nanocomposite permanent magnets due to their high Curie temperature, large saturation magnetization, and relatively strong magnetocrystalline and inherent large shape anisotropies. Magnetic properties of FeCo alloys can be further tailored by adding other elements [3]. Anodic Aluminum Oxide membranes have been employed as templates to prepare highly ordered FeCo, FeCoCu alloy single nanowire and FeCoCu multilayer nanowire arrays with different diameters and alloy concentrations. As-deposited nanowire arrays were annealed in the temperature range up to 600°C, and their structure and magnetic properties analyzed. The angular and temperature dependence of magnetic behavior have been investigated revealing the role of the effective magnetic anisotropy in the coercivity mechanism. With increasing the annealing temperature both, the coercivity and squareness of hysteresis loop increase. Furthermore, the influence of applied magnetic field during the deposition is investigated to result in the improvement of the alignment of easy axis and induction of magnetic anisotropy.

[1] Zheng, H.; Wang, J.; Lofland, S. E.; Ma, Z.; Mohaddes-Ardabili, L.; Zhao, T.; Salamanca-Riba, L.; Shinde, S. R.; Ogale, S. B.; Bai, F.; Viehland, D.; Jia, Y.; Schlom, D. G.; Wuttig, M.; Royburd, A.; Ramesh, R. Science, 303, 661-663, 2004. [2] Skomski, R. J. Phys.: Condens. Matter, 15, R841-R896, 2003. [3] Ramazani, A., Kashi, M. A. Kabiri, S., Zanguri, M., J of Crystal Growth 327, 78-83, 2011.

DG04

FMR behavior of Co nanowire arrays

Massimo Pasquale*, Carlo Paolo Sasso, Elena Sonia Olivetti, Marco Coisson and Federica Celegato

Divisione Elettromagnetismo, INRIM, Italy

We characterize and analyze the microwave behavior of columnar arrays of Co nanowires (NW). The 50-60 nm diameter wires were electrochemically grown with different lengths from 5 to 50 microns within anodic alumina templates. The NW arrays present a high Ms, close to the Co bulk value and variable remanence states. Depending on the combination of shape, magnetocrystalline anisotropy and dipolar interactions, FMR frequencies from 7 to 25 GHz at 0 applied field were observed. The wire composition, structure and the morphology were determined by XRD and FESEM. The magnetic properties were measured using by AGFM, with field applied perpendicularly or parallel to the wire axis. The macroscopic magnetic behavior appears to be dominated by long-range magnetostatic interactions, but the magnetization state of each nanowire, as determined by the AFM/MFM at the membrane surface[1], is saturated in the up or down direction. A complete characterization and analysis of the field-and-frequency modulated microwave behavior of the arrays was performed using an electromagnet to sweep the magnetic field from -1.3 T to + 1.3 T along the wire axis, while measuring the absorption at single frequency values, from 1 to 40 GHz[2]. The results are interpreted with reference to measured magnetization curves.

[1] J. De La Torre Medina, et al., PRB 81, 144411 (2010) [2] B.K. Kuanr JMMM 286 (2005) 276-281

DG05

In situ magnetic field dependent Lorentz microscopy in Co nanowires grown by focused electron beam induced deposition

Luis Alfredo Rodriguez², Cesar Magen^{3*}, Luis Serrano-ramon¹, Etienne Snoeck⁴, Rosa Cordoba¹, Jose Maria De Teresa⁴ and Manuel Ricardo Ibarra¹

¹ LMA-INA, Universidad de Zaragoza, 50018, Zaragoza, Spain

² LMA-INA and ARAID, Universidad de Zaragoza, 50018, Zaragoza, Spain

³ ICMA, Universidad de Zaragoza-CSIC, 50009, Zaragoza, Spain

⁴ CEMES-CNRS 29, rue Jeanne Marvig B.P. 94347 F-31055, Toulouse Cedex, France

The accurate characterization and control of the magnetic configuration in nanostructures, namely domain walls (DWs) or vortex structures, by external parameters such as the magnetic field is essential for applications such as information storage, sensing or magnetic logic [1]. Transmission electron microscopy (TEM) allows the observation of the magnetic nanostructures with nanometer-range spatial resolution by Lorentz microscopy (LM). In this work, we performed in situ characterization and magnetic-field manipulation of DWs by LM in Co nanowires (NWs) in a FEI Titan Cube 60-300 TEM. These NWs were fabricated by focused electron beam induced deposition (FEIBID) with purity higher than 90% on Si₃N₄ membranes [2]. We determined the nucleation and propagation field of DWs by direct observation of the magnetic structure by LM of curved L-shape Co NW with varying width (w=125-1000 nm) and thickness (t=5-30 nm), demonstrating that for specific dimensions they are good DW propagators [3]. Focal series in LM were acquired in order to map the in-plane magnetic induction by solving the Transport-of-Intensity Equation. The nucleation process gives rise to transversal DW in the thinner NWs (t < 13 nm). Above this value, the crossover to complex structures was investigated, including multiple vortex walls on the thicker NWs.

[1] C. Chappert, A. Fert, F. N. Van Dau, Nature Materials., 6 813-823 (2007). [2] L. Serrano-Ramon et al., ACS Nano, 5 7781-7787 2011. [3] L. A. Rodriguez et al., in preparation.

DG06

Morphology and magnetic properties of GaAs/(Ga,Mn)As core-shell nanowires on Si (111) synthesized by self-catalyzed method

Xuezhe Yu, Hailong Wang and Jianhua Zhao*

State Key Laboratory of Superlattices and Microstructures, Institute of Semiconductors, Chinese Academy of Sciences, China

Diluted magnetic semiconductors, of which (Ga,Mn)As as a representative, and semiconductor nanowires (NWs) both have been hot issues of research in the past decade, due to their potential to enlarge and strengthen semiconductor based technology. Much work has been done on both systems respectively while few efforts are invested in their combined system until recently. It is of advantage to integrate such system on silicon, the most commonly used semiconductor, which our work features. Here, we present our work on GaAs/(Ga,Mn)As core-shell NWs synthesized on Si (111) substrate. Another characteristic of our work is self-catalyzed growth which utilizes no foreigner particles as seeds. We have attempted to incorporate different manganese content but it is found only a narrow growth window is permitted for successful fabrication. Magnetic properties of GaAs/(Ga,Mn)As core-shell are measured by SQUID. Magnetic hysteresis loops (M-H) along in-plane and out-of plane direction at 5 K show robust ferromagnetism and temperature dependence of remanent magnetization (M-T) reveals the Curie temperature of 20 K.

DH01

Novel functionality and devices via complex oxide heteroepitaxy

Yuri Suzuki^{1*}, Franklin Wong², Chunyong He², Brittany Nelson- Cheeseman² and Elke Arenholz³

¹ Applied Physics, Stanford University, USA

² Materials Science and Engineering, University of California, Berkeley, USA

³ Advanced Light Source, Lawrence Berkeley National Laboratory, USA

Interfaces of complex oxides materials provide a rich playground for the exploration of novel properties not found in the bulk constituents but also for the development of functional interfaces to be incorporated into technological applications. In this talk, I will present two recent examples of our work. We have demonstrated metallicity in epitaxial LaTiO₃ and LaVO₃ thin films under compressive epitaxial strain, although both are Mott insulators in the bulk; films under little to no epitaxial strain exhibit insulating behavior. The metallicity in LaTiO₃ can be understood in terms of a modification of the electronic structure due to anisotropic lattice distortions. The metallicity in LaVO₃ is an interface effect that may be attributed to electronic reconstruction. We have also developed a new class of spin filter devices composed entirely of magnetic layers. In these devices, spin polarized conduction is dominated by interface scattering or localized states depending on temperature. Through careful investigation of the magnetism at the interfaces, we have found that there is no magnetic coupling at one interface and strong interface coupling at the other. The nature of magnetism at these interfaces is essential in the realization of our all-ferromagnet junction device.

DH02

Quantum oscillations and subband properties of the LaAlO₃/SrTiO₃ heterointerface

Alix Mccollam^{1*}, Sander Wenderich², Michelle Kruize², Veerendra Guduru¹, Hajo Molegraaf², Mark Huijben², Gerjan Koster², Dave Blank², Guss Rijnders², Alexander Brinkman², Hans Hilgenkamp², Ulrich Zeitler² and Jan Kees Maan¹

¹ High Field Magnet Laboratory, Radboud University Nijmegen, Netherlands

² MESA+ Institute for Nanotechnology, University of Twente, Netherlands

Heterostructures of transition metal oxides offer myriad possibilities for multifunctional materials and device applications, as well as demonstrating new and complex fundamental properties [1-4]. Much of their potential stems from the possibility of interface properties that differ dramatically from those of the bulk components, and the discovery of a 2-dimensional electron gas at the interface between band insulators LaAlO₃ and SrTiO₃[1] is a striking realisation of this. Understanding and controlling this 2D electron gas is currently the central problem in the field. Here I will present the results of recent magnetotransport measurements of the LaAlO₃/SrTiO₃ interface, performed at millikelvin temperatures and in magnetic fields of up to 30 T. Quantum oscillations observed in the resistivity allow us to probe the bandstructure of the interface electron gas, and extract important information about the band energies and the properties of the mobile charge carriers. The strong dependence of the oscillations on magnetic field, temperature, and orientation with respect to the plane of the interface, reveals a complex 2D system of closely-spaced multiple electronic subbands with different carrier effective masses and mobilities. Measurements in tilted magnetic fields show evidence of inter-subband scattering and diamagnetic shift of the 2D confinement energies.

[1] A. Ohtomo et al., Nature 427, 423 (2004). [2] A. Brinkman et al., Nature Materials 6, 493 (2007). [3] N. Reyren et al., Science 317, 1196 (2007). [4] H.Y. Hwang et al., Nature Materials 11, 103 (2012).

DH03

Electronic ordering in sodium cobaltate

Daniel Graham Porter¹, Michel Roger², Andrew Boothroyd³, Carlo Vecchini⁴, Steve Collins⁵, S. Uthayakumar¹, D. Prabhakaran¹, Manoj Pandiyan¹ and Jon Goff⁶

¹ Department of Physics, Royal Holloway University of London, United Kingdom

² Service de Physique de l'Etat Condense, CEA Saclay, France

³ Clarendon Laboratory, University of Oxford, United Kingdom

⁴ Diamond Light Source, Harwell Science and Innovation Campus, United Kingdom

Sodium cobaltate (Na_xCoO₂) has emerged as a material of exceptional scientific interest due to the potential for thermoelectric applications, and because the strong interplay between the magnetic and superconducting properties has led to close comparisons with the physics of the superconducting copper oxides. The density x of the sodium in the intercalation layers can be altered electrochemically, directly changing the number of conduction electrons on the triangular Co layers. Previous measurements have determined the long range ordering of sodium superstructures for different values of x, and numerical calculations have found that this ordering has a profound effect on the charge carrying cobalt layer. Multiple valence states have been detected by NMR, but here we report new spatial measurements using Resonant X-ray Scattering on the Materials and Magnetism beamline I16 at Diamond. The sodium vacancies are found to condense into tri-vacancy clusters, and these order long range into stripes. We find resonant x-ray scattering with the same periodicity as the sodium superstructure, directly demonstrating that the electronic ordering in these cobalt layers is controlled by the sodium ordering. We are able to reproduce the energy, polarisation and azimuthal dependencies of the resonant x-ray scattering in calculations using the FDMNES code.

DH04

Electrical switching of the magnetic phase in semiconductor oxides

Antonio Ruotolo¹, Xiao Lei Wang¹, Chi Wah Leung² and Rolf Lortz³

¹ Department of Physics and Materials Science, City University of Hong Kong, Hong Kong

² Department of Applied Physics, Hong Kong Polytechnic University, Hong Kong

³ Department of Physics, Hong Kong University of Science and Technology, Hong Kong

The magnetic properties of thin-film ferromagnetic semiconductors can be altered by applying an electric field[1]. The effect is reversible but volatile. However, for technological applications, it would be desirable to have a film that retains the induced magnetic state until a reset command is given. We here demonstrate that the magnetic moment of a ferromagnetic oxide can be altered in a non-volatile and reversible manner. The studied system consists of Zn_{0.98}Mn_{0.02}O (ZMO) film sandwiched between a highly conductive Niobium Strontium Titanate (NSTO) substrates and a Platinum (Pt) top electrode. The current-voltage curves revealed that the electrical behavior was dominated by the Schottky interface between the NSTO and the ZMO. Reversible resistive switching[2,3] could be induced in the samples with high reliability and good retention time. By measuring the full magnetization loop, we found that a switching of the resistance corresponds to a switching of the magnetic phase. Remarkably, the threshold switching current was ~ 1 A/cm² in film devices, as well as in patterned devices. This is orders of magnitude smaller than that reported in similar, non-magnetic systems[2,3].

[1] Ohno, Nature 408, 944-946 (2000). [2] Yang, Nat. Nanotech. 3, 429 (2008). [3] Lee, Nat. Mater. 10, 625 (2011).

DH05

An approach to achieve layered spintronics material using Brownmillerite compound Ca_{2.5}Sr_{0.5}GaMn₂O₈

S. M. Yusuf* and A. K. Bera

Solid state physics division, bhabha atomic research centre, mumbai 400 085, India

Naturally occurring layered magnetic materials can play a significant role in shaping the next generation technology in the area of magnetic storage. We have, therefore, studied the magnetic and magnetotransport properties of the La-substituted compounds Ca_{2.5-x}La_xSr_{0.5}GaMn₂O₈ (x = 0, 0.05, 0.075, and 0.1). We have succeeded to introduce the double exchange (DE) interaction in the pure antiferromagnetic system Ca_{2.5}Sr_{0.5}GaMn₂O₈ by varying the ratio between Mn³⁺ and Mn⁴⁺ ions. The experimental results of dc magnetization, magnetotransport and neutron diffraction studies were interpreted on the basis of an electronic phase separation model, where a formation of ferromagnetic clusters (due to DE interaction) inside the layered antiferromagnetic matrix (due to superexchange interaction) in the La-substituted compounds is proposed. Significantly, the present study shows that the magnetic and electronic properties of the layered system Ca_{2.5}Sr_{0.5}GaMn₂O₈ can be tuned/optimized by appropriate chemical substitution to achieve a new spintronic material based on naturally occurring layered system for practical applications.

DI01

Magnon-drag thermopile

M. V. Costache¹, G. Bridoux¹, I. Neumann² and S. O. Valenzuela³

¹ Catalan Institute of Nanotechnology (ICN), Spain

² Catalan Institute of Nanotechnology (ICN) and Universitat Autònoma de Barcelona (UAB), Spain

³ ICREA, Catalan Institute of Nanotechnology (ICN) and Universitat Autònoma de Barcelona (UAB), Spain

Thermoelectric effects in spintronics are gathering increasing attention as a means of controlling spin information by using heat flow. Thermal magnons (spin-wave quanta) are expected to play a major role, however, the coupling between electrons and magnons in ferromagnetic metals remains poorly understood. We demonstrate a conceptually new device that enables us to gather information on magnon-electron scattering and magnon-drag effects[1]. The device resembles a thermopile formed by a large number of pairs of ferromagnetic wires placed between a hot and a cold source and connected thermally in parallel and electrically in series. By controlling the relative orientation of the magnetization in pairs of wires, the magnon drag can be studied independently of the electron and phonon drag thermoelectric effects. Measurements as a function of temperature reveal the effect on magnon drag following a variation of magnon and phonon populations. These results demonstrate the feasibility of directly converting magnon dynamics of nanomagnets into an electrical signal and could pave the way to novel thermoelectric devices for energy harvesting. This research was supported by the Spanish Ministry of Science (MICINN/MAT2010-18065) and by the European Community (FP7/NANOFUNCTION-257375).

[1] M.V. Costache, G.A. Bridoux, I. Neumann and S.O. Valenzuela, Nat. Mater. Advanced Online Publication (2011). <http://dx.doi.org/10.1038/NMAT3201>

DI02

Seebeck spin tunneling in silicon

Ron Jansen

National Institute of Advanced Industrial Science and Technology (AIST), Tsukuba, Ibaraki, Japan

The combination of thermoelectrics and spintronics offers unique possibilities. On the one hand, it provides a new, spin-based approach to thermoelectric power generation and cooling. On the other hand, it provides a thermal route to create and control the flow of spin in spintronic devices that make functional use of heat and temperature gradients. Here we describe and report the demonstration of Seebeck spin tunneling - a thermally driven spin flow, of purely interfacial nature - generated in a tunnel contact between electrodes of different temperatures. Seebeck spin tunneling arises from the spin dependence of the Seebeck coefficient of a tunnel junction and is thus the thermoelectric analog of spin-polarized tunneling. By exploiting this in ferromagnet-oxide-silicon tunnel junctions, we observe a thermal flow of spin angular momentum from the ferromagnet to the silicon without a charge tunnel current. The spin accumulation induced in the silicon scales linearly with heating power and changes sign when the temperature differential is reversed. This thermal spin current can be used by itself, or in combination with electrical spin injection. The results highlight the engineering of heat transport in spintronic devices and enable the (re-)use of heat to increase device efficiency and reduce energy consumption.

J.C. Le Breton, S. Sharma, H. Saito, S. Yuasa and R. Jansen, Nature 475, 82 (2011). R. Jansen, A.M. Deac, H. Saito and S. Yuasa, Preprint at <http://arxiv.org/abs/1112.3430> (2011).

DI03

Tunneling magneto Seebeck effect

Andy Thomas¹, Markus Munzenberg² and Christian Heiliger³

¹ Physics, Bielefeld University, Germany

² Physics, Göttingen University, Germany

³ Physics, Gießen University, Germany

Creating temperature gradients in magnetic nanostructures has resulted in a new research direction, that is, the combination of magneto- and thermoelectric effects. Here, we demonstrate the observation of one effect of this class: the tunneling magneto-Seebeck effect. It is observed when a magnetic configuration changes the charge-based Seebeck coefficient. In particular, the Seebeck coefficient changes during the transition from a parallel to an antiparallel magnetic configuration in a tunnel junction. In this respect, it is the analog of the tunnelling magnetoresistance. The Seebeck coefficients in parallel and antiparallel configurations are of the order of the voltages known from the charge Seebeck effect. The size and sign of the effect can be controlled by the composition of the electrodes' atomic layers adjacent to the barrier and the temperature. We realized up to 40% tunneling magneto-Seebeck effect and up to 330% TMR ratio in MgO based magnetic tunnel junctions. We show the temperature dependent investigations of this effect, supported by TEM studies of the microstructure, numeric simulations of the temperature profile in the junction and possible devices utilizing the tunneling magneto Seebeck effect.

[1] M. Walter et al., Seebeck effect in magnetic tunnel junctions, Nature Materials 10 (2011) 742

DJ01

Novel clathrate-based composite materials for energy-efficient magnetic refrigeration

Anurag Chaturvedi, Steve Stefanoski, George S. Nolas, Hariharan Srikanth and Manh-huong Phan*

Department of Physics, University of South Florida, USA

Magnetic refrigeration based on the magneto-caloric effect (MCE) is an area of exciting research. The grand challenge in this technology is to seek new material that exhibits large MCE over a wide temperature range, namely, the large refrigerant capacity (RC). In this talk, we will present our recent discoveries of the large MCE and RC in Eu₄Ga₁₆Ge₃₀ type-I and type-VIII clathrates and Eu₄Ga₁₆Ge₃₀ - EuO composite materials. We demonstrate that the tunneling of Eu²⁺ ions in the Eu₄Ga₁₆Ge₃₀ type I clathrate leads to the broadened MCE curve thus enhancing the RC in this material. This new finding may provide a route for improving the cooling efficiency in type-I clathrate materials for active magnetic refrigeration (AMR). The large table-like MCE and enhanced RC have been achieved in the Eu₄Ga₁₆Ge₃₀ type I - EuO composite materials, making them one of the best candidates for AMR in the liquid nitrogen temperature range.

DJ02

Magnetocaloric properties of doped La_{0.7}Sr_{0.3}MnO₃ bulk ceramic and thick films

Jong-woo Kim*, Jungho Ryu, Byung-dong Hahn, Jong-jin Choi, Woon-ha Yoon, Cheol-woo Ahn, Joon-hwan Choi and Dong-soo Park
Korea Institute of Materials Science (KIMS), Korea

The LaSmnO₃ manganite has attracted research interests due to its colossal magneto resistance effect, half-metallic behavior and magnetocaloric effect [1-3]. The magnetocaloric effect is the reversible temperature change of a magnetic material associated with external magnetic field change in an adiabatic process. These properties are strongly related with the interactions between the rare-earth and transition metal's charge states which can be varied by doping elements [4, 5]. In this study, the physical properties of magnetocaloric La_{0.7}Sr_{0.3}MnO₃ (LSMO) ceramic system, in both bulk and thick film, have been investigated according to various B-site elements doping. The substituted B-site elements were transition metal elements, i.e. Cr, Co, Ni, Cu with its contents of 0 ~ 3 %. The ceramic samples were prepared by conventional solid-state reaction process. The thick films were grown by Aerosol Deposition (AD) method [6, 7] on various substrates. The magnetocaloric properties measured by physical property measurement system (PPMS) in magnetic field up to 30 kOe and temperature range up to 400 K. In this presentation, the magnetocaloric properties of the entropy change, TC variation, Banerjee criterion [8] etc. according to the B-site doping and substrate effects will be discussed in detail.

[1] Physical Review Letters, 71 (1993) 2331-2333. [2] Reports on Progress in Physics, 68 (2005) 1479-1539. [3] J Magn Magn Mater, 308 (2007) 325-340. [4] Physical Review Letters, 74 (1995) 5144-5147. [5] Journal of Physics Condensed Matter, 20 (2008). [6] Sensor Actuat a-Phys, 153 (2009) 89-95. [7] Materials Letters, 65 (2011) 2762-2764. [8] Physics Letters, 12 (1964) 16-17.

DJ03

Structural ,magnetic and magnetocaloric properties of Ni₅₀Mn_{37.5}Sn_{12.5} ribbon Heusler alloys

Mst. Nazmunnahar*, Lorena Gonzalez², Juanjose Delval¹, Joanjosep Sunyo^{1,3}, Julianmaria Gonzalez¹ and Blanca Hernandez²

¹ Material Physics Department, University of Basque Country (UPV/EHU), Spain

² Material Physics Department, University of Oviedo, Spain

³ Material Physics Department, University of Girona, Spain

We present a detailed study of the magnetic and microstructural behavior of Ni₅₀Mn_{37.5}Sn_{12.5} Heusler ribbon alloy, which valence electron concentration per atom = 8.12. This ribbon, as flakes, around 1.5 - 2.0 mm width and 4 - 5 mm length, was obtained after quenching the master alloy by the melt-spinning technique in Ar atmosphere. Scanning Electron Microscopy (SEM, JEOL 6100) revealed a columnar structure of the Heusler-Based alloy. The averaged composition was determined by EDX (Inca Energy 200) from measurements taken at different points of the sample, obtaining Ni_{49.4}Mn_{36.7}Sn_{13.9}. Differential Scanning Calorimetry (DSC) and thermomagnetic curves confirm an austenite-martensite structural transformation below 400K. The start and finish temperatures of the martensitic phase transformation for the ribbon alloy were Ms = 279 K and Mf = 260 K, while the ones for austenite were As = 272 K and Af = 288 K, in agreement with previously reported values in similar compositions [1]. Moreover, it has been performed a study of magnetocaloric effect (MCE) by thermomagnetic measurements from which a direct and inverse magnetocaloric effects near Curie point and martensitic transformation temperature have been respectively observed.

[1] J.E. Muthu et al., J. Phys. D : Appl. Phys., 43 (2010) 425002

DJ04

Dependence of the magnetocaloric effect in ferromagnetic shape memory Heusler alloys on measurement protocol

Vladimir Khovaylo*, Konstantin Skokov², Hiroyuki Miki³ and Oliver Gutfleisch²

¹ National University of Science and Technology 'MISIS', Moscow 119049, Russia

² Institute for Metallic Materials, P.O. Box 270016, D-01171 Dresden, Germany

³ Institute of Fluid Science, Tohoku University, Sendai 980-8577, Japan

Results of direct measurements of the magnetocaloric effect in ferromagnetic shape memory alloys (FSMAs) Ni-Mn-X (X = Ga, In, Sn) showed that the adiabatic temperature change ΔTad is (i) small (typically smaller than in prototypical magnetocaloric material Gadolinium) and (ii) depends on thermal as well as on magnetic history of FSMAs samples. Here we discuss these features of ΔTad and show that the measurement protocol determines whether the adiabatic temperature change is reversible or irreversible. These characteristic of ΔTad are easy to understand considering thermodynamics of temperature- and magnetic field-induced thermoelastic martensitic transformations in the vicinity of the magnetostructural phase transition.

DJ05

Magnetocaloric effects in manganites with perovskite structure

Abdelwaheb Cheikhrouhou*, Wissem Cheikhrouhou-koubaa and Mohamed Koubaa
Materials Physics Laboratory, Faculty of Sciences of Sfax, Tunisia

Magnetocaloric refrigeration is a promising alternative technique to replace the conventional gas expansion-compression one based on the use of toxic gases. This novel technology presents several advantages, in fact besides the property of being environmentally friendly (it does not use coolants or emit greenhouse gases), it undergoes a higher efficiency and it is compact in size. Magnetocaloric materials, when subjected to a magnetic applied field at their phase transition temperature, undergo a magnetic transition which results in the entropy change of the magnetocaloric materials. This phenomenon is known as the magnetocaloric effect (MCE). The family of magnetic oxides with perovskite structure known as manganites have also shown interesting MCE, for a large temperature range around room temperature. In this work, we were interested in the study of the MCE in manganites with several compositions. Several compounds with general formula $La_{1-x}M_xMnO_3$ (M is a divalent alkali-earth or monovalent elements) have been elaborated and characterized. The entropy change versus temperature and versus magnetic applied field will be presented. Our results, compared to that observed in Gd or GdSiGe, show that the manganites exhibit a giant MCE around or above room temperature and are suitable for applications in the magnetic refrigeration area.

A. CHEIKHROUHOU1,2, W. CHEIKHROUHOU-KOUBAA1, M. KOUBAA1 1Laboratoire de Physique des Matériaux, Faculté des Sciences de Sfax, B. P. 1171, Sfax, Tunisia 2Institut Neel, CNRS, B. P. 166, 38042 Grenoble Cedex 9, France

EA01

Quantum phase transitions in heavy-fermion systems

Hilbert V. Lohneysen*
Karlsruher Institut für Technologie, Physikalisches Institut und Institut für Festkörperphysik, Germany

The canonical heavy-fermion system $CeCu_{6-x}Au_x$ exhibits a quantum phase transition (QPT) that can be accessed by varying the Au concentration x , hydrostatic pressure p , and magnetic field B . Its unusual features have prompted the suggestion of a novel type of QPT not envisaged by the extension of the Landau-Ginzburg-Wilson theory of (classical) phase transitions to $T = 0$ by Hertz, Millis and Moriya. We will review a range of new experiments on this system: (1) probing the Kondo resonance upon approaching the QPT by photoelectron spectroscopy, (2) establishing a link between the pressure and concentration dependence of the magnetic ordering vector as determined by elastic neutron scattering, (3) comparing the volume and magnetic Grüneisen parameters obtained from thermal expansion and magnetocaloric effect, respectively, and (4) determining the thermoelectric power close to the critical concentration x_c . $CePdAl$ is a heavy-fermion system with partial geometric frustration of one of the three Ce atoms in the unit cell. We will report on first experiments exploring the possible role of frustration on quantum criticality which can be accessed by Ni doping.

EA02

Lifshitz transitions and non-fermi liquid behavior in heavy-fermion metals

Matthias Vojta*
Institut fuer Theoretische Physik, Technische Universitaet Dresden, Germany

The field-driven non-Fermi liquid behavior in $YbRh_2Si_2$ has been proposed to arise from a reconstruction of the Fermi surface due to a breakdown of Kondo screening. Here we discuss an alternative scenario, namely a Zeeman-driven Lifshitz transition of a narrow heavy-fermion band, with Kondo screening remaining intact. Apparent non-Fermi liquid behavior emerges in a crossover regime above a small effective Fermi energy. As carrier doping provides a unique knob to tune the Lifshitz transition, we discuss the evolution of heavy-fermion bands with doping in a quantitative fashion and connect our results to recent data obtained on Fe-doped $YbRh_2Si_2$.

EA03

Sequential spin polarization of the fermi surface pockets in URu₂Si₂ and its implications for the hidden order

Neil Harrison¹, Moaz Altarawneh¹, Luis Balicas², P H Tobash¹, J D Thompson³, F Ronning³ and E D Bauer³
¹ National High Magnetic Field Laboratory, Los Alamos National Laboratory, USA
² National High Magnetic Field Laboratory, Tallahassee, USA
³ Los Alamos National Laboratory, USA

Using Shubnikov-de Haas oscillations measured in URu_2Si_2 over a broad range in a magnetic field of 11-45 T, we find a cascade of field-induced Fermi surface changes within the hidden order phase I and further signatures of oscillations within field-induced phases III and V. A comparison of kinetic and Zeeman energies indicates a pocket-by-pocket polarization of the Fermi surface leading up to the destruction of the hidden order phase I at ~35 T. The anisotropy of the Zeeman energy driving the transitions in URu_2Si_2 points to an itinerant hidden order parameter involving quasiparticles whose spin degrees of freedom depart significantly from those of free electrons.

Physical Review Letters 106 (14):146403 [2011]

EA04

Hydrostatic pressure study of the nematicity of Sr₃Ru₂O₇

Dan Sun¹, Wenlong Wu¹, Santiago Grigera², Robin Perry², Andrew Mackenzie² and Stephen Julian^{1*}
¹ The Department of Physics, University of Toronto, Canada
² Scottish Universities Physics Alliance, School of Physics and Astronomy, University of St. Andrews, United Kingdom
³ Centre for Science at Extreme Conditions, School of Physics, University of Edinburgh, United Kingdom

A 'electron-nematic phase' occurs in the bilayer ruthenate $Sr_3Ru_2O_7$, at very low temperature in the vicinity of a metamagnetic transition. It has been seen when the applied magnetic field, B , makes a large angle with the ab -plane [1,2,3]. The nematic phase is characterized by a spontaneously broken rotational symmetry for resistivity within the ab -plane. The underlying physics is not understood, but it is believed to be associated with a 'quantum critical endpoint' (QCEP) for the metamagnetic transition [2]. We show, using transport and magnetic susceptibility measurements on ultra-pure crystals, that this metamagnetic transition does not produce a nematic phase when the QCEP is reached by applying hydrostatic pressure [4] with the field applied in ab -plane. Moreover, a nearby region of nematicity is found to be robust against the application of pressure. Taken together our results suggest that proximity to a quantum critical point may not be the crucial ingredient for the nematicity.

[1] S. A. Grigera et al., Science 306, 1154 (2004). [2] R. A. Borzi, S. A. Grigera, J. Farrell, S. J. S. Lister, S. L. Lee, D. A. Tennant, Y. Maeno, and A. P. Mackenzie, Science 315, 214 (2007). [3] A.W. Rost, R. S. Perry, J. F. Mercure, A. P. Mackenzie, and S. A. Grigera, Science 325, 1360 (2009). [4] W. Wu et al., Rev. B 83, 045106 (2011).

EB01

Pump-probe response for correlated electron systems out of equilibrium

T. Devereaux*
Stanford University, USA

Pump-probe techniques have been used to extend equilibrium spectroscopic methods to the time-domain, revealing temporal dynamics associated with lattice degrees of freedom, collective modes of novel electronic phases and decay and recovery processes with typical time scales of several picoseconds. Recent advances have extended the temporal resolution of these techniques to femtosecond and attosecond time scales. In this talk I will present several severalKeldysh-based calculations and simulations for pump-probe spectroscopy across a metal-insulator transition, across a charge-density wave transition, and for electron-phonon coupled lattices. These results illuminate the intricate dynamics of how correlated materials return to equilibrium after photo-excitation.

EB02

Correlated electrons in strong electric fields

Philipp Werner¹, Martin Eckstein², Naoto Tsuji¹, Takashi Oka³ and Hideo Aoki³
¹ Department of Physics, University of Fribourg, Switzerland
² Max Planck Research Department for Structural Dynamics, University of Hamburg - CFEL, Germany
³ Department of Physics, University of Tokyo, Japan

We use the nonequilibrium extension of dynamical mean field theory to study the dynamics of the Hubbard model in the presence of external electric fields. Specifically, we discuss the transition from a Bloch oscillating to a direct current regime in weakly interacting systems subject to static electric fields [1], and the dielectric breakdown of the Mott insulator [2]. In periodically driven metallic systems, the electric field may lead to a dynamical band inversion and an associated conversion of the effective on-site interaction from repulsive to attractive [3].

[1] M. Eckstein and P. Werner, Phys. Rev. Lett. 107, 186406 (2011) [2] M. Eckstein, T. Oka, and P. Werner, Phys. Rev. Lett. 105, 146404 (2010) [3] N. Tsuji, T. Oka, P. Werner, and H. Aoki, Phys. Rev. Lett. 106, 236401 (2011)

EB03

Photoinduced charge order enhancement in one-dimensional extended hubbard model

Hantao Lu¹, Shigetoshi Sota¹, Hiroaki Matsueda², Janez Bonča^{3,4} and Takami Tohyama¹
¹ Yukawa Institute for Theoretical Physics, Kyoto University, Japan
² Sendai National College of Technology, Sendai, Japan
³ Faculty of Mathematics and Physics, University of Ljubljana, Slovenia
⁴ J. Stefan Institute, Slovenia

We present a compelling response of a low-dimensional strongly correlated system to an external optical perturbation[1]. By using time-dependent Lanczos method, the nonequilibrium evolution of one-dimensional Hubbard model at half-filling driven by transient laser pulse is investigated. When the system is close to the phase boundary, by tuning the laser frequency and strength, a sustainable charge order enhancement is found that is absent in the Mott insulating phase. We analyze the conditions and investigate possible mechanisms of emerging charge order enhancement. From the spectrum analysis on small size systems, it can be shown that with increasing the nearest-neighbor interactions, charge-order favorite eigenstates proliferate in the low energy regime, leaving themselves prone to be picked up by laser pulse. Feasible experimental realizations are proposed.

[1]Hantao Lu, S. Sota, H. Matsueda, Janez Bonča, and T. Tohyama, arXiv:1204.1107.

EB04

Electric-Field Effects on Complex Oxide Interfaces: Possible Two-Band Superconductivity

Jason T Haraldsen^{1*}, Alexander V Balatsky¹, Peter Woelfle² and Quanxi Jia³
¹ Theoretical Division and Center for Integrated Nanotechnologies, Los Alamos National Laboratory, USA
² Institute for Condensed Matter Theory and Institute for Nanotechnology, Karlsruhe Institute of Technology, Germany
³ Center for Integrated Nanotechnology, Los Alamos National Laboratory, USA

We examine the superconductivity produced at the complex oxide interface of $LaAlO_3$ and $SrTiO_3$ ($T_c = \sim 0.3$ K). Through a phenomenological and semi-classical approach, we investigate the effects of local and global electric fields on the superconducting order parameter, carrier density, and transition temperature for this system. We show that the general shape of the superconducting dome can be reproduced through basic electrostatics and a standard BCS formalism using the density of states. Given the similarity between the transition temperature for the interface and of bulk $SrTiO_3$, which is also superconducting at ~0.3 K upon optimal electron doping, we provide evidence that the interface superconductivity is intrinsic to $SrTiO_3$ and we infer that superconducting mechanism must also be similar. By examining bulk $SrTiO_3$, we show that the superconductivity may be described through weakly-coupled, two-band model. Finally, we predict that the superconductivity at the interface is most likely produced through a two-band coupling of the surface states of $SrTiO_3$ provided by an electron doping from a carrier source (in this case $LaAlO_3$).

EC01

Electronic structure and phonons in the high pressure phases of cerium

Borje Johansson^{1,2*} and D.Y. Kim³
¹ Department of Materials and Engineering, Royal Institute of Technology, Stockholm, Sweden
² Department of Physics, Uppsala University, Uppsala, Sweden
³ Geophysical Laboratory, Carnegie Institution of Washington, Washington, DC, USA

The isostructural γ - α transition in cerium under pressure has attracted a very extensive interest both experimentally and theoretically over the years. Since long it has also been known that at a pressure around 6.5 GPa cerium adopts the α -uranium crystal structure ($\alpha C4$). Recent developments have made it possible to use inelastic X-ray scattering to determine the phonon dispersions of elemental cerium in these high pressure structures1,2. This opened the possibility to compare the experimental data with theoretical calculations. When the 4f electrons in cerium are treated as itinerant a very good agreement was obtained. Very interestingly, also the observed pronounced phonon anomalies in Ce- $\alpha C4$ were well described by theory and points out a very close similarity between uranium and Ce- $\alpha C4$. At the low-pressure end of its stability range, theory suggests that Ce- $\alpha C4$ is on the verge of a lattice-dynamical instability and possibly a charge density wave. When this success of the itinerant picture for the 4f behavior in the high pressure phases of cerium is combined with the well-known knowledge that the 4f electron in γ -cerium is well described by a localized picture, one arrives at the conclusion that the γ - α transition in cerium is a Mott transition3.

1. M. Krisch, D. L. Farber, R. Xu, D. Antonangeli, C. M. Aracne, A. Beraud, T.-C. Chiang, J. Zarestky, D. Y. Kim, Eyyaz I. Isaev, R. Ahuja, and B. Johansson, Proceedings of the National Academy of Sciences of the United States of America (PNAS), 108, 9342 (2011) 2. I. Loa, Eyyaz I. Isaev, M. I. McMahon, D.Y. Kim, B. Johansson, A. Bosak and M. Krisch, Phys. Rev. Letters 108, 045502 (2012) 3. B. Johansson, Philos. Mag. 30, 469 (1974).

EC02

From SOC induced phenomena to non-collinear magnetism and electric field effects in magnetic systems

Arthur Freeman¹ and Kohji Nakamura²
¹ Northwestern University, USA
² Mie University, Japan

Quantum computational electronic structure theory, based on accurate density functional theory and structural modeling, has taken a leadership role in providing insight into the underlying physics of magnetism. Challenges currently lie in understanding non-collinear magnetism and magneto-transport properties in magnetic domain walls [1] and, more recently, externally driven electric-field magnetocrystalline anisotropy (MA) [2] in transition-metals that arise not only through the spin-orbit coupling (SOC): these phenomena provide new pathways for future magnetic devices at the nano-scale with the promise of ultra-low energy power consumption. This talk will present our recent first-principle predictions for magnetism and transport properties for i) magnetic domain walls (modeled by a spin-spiral) and ii) electric-field-driven MA in transition-metals, carried out using our non-collinear magnetism full-potential linearized augmented plane-wave (FLAPW) method in which the external electric field is directly incorporated and the conductivity tensor is obtained by applying the Kubo formula of linear response theory. *Supported at Northwestern by the U.S. D.O.E. and the Japan Society for the Promotion of Science.

[1] K. Nakamura, N. Mizuno, T. Akiyama, T. Ito, and A. J. Freeman, JAP 105, 07C304 (2009); JAP 101, 09G521 (2007); PRL 93, 057202 (2004). [2] K. Nakamura, R. Shimabukuro, Y. Fujiwara, T. Akiyama, T. Ito, A.J. Freeman, PRL 102, 1877201 (2009); K. Nakamura, T. Akiyama, T. Ito, M. Weinert, A.J. Freeman, PRB 81, 220409R (2010).

EC03

First-principles calculation of the A-site ordered perovskite CaCu₃Fe₆O₁₂

Takuya Ueda¹, Mitsuru Kodera¹, Kunihiko Yamauchi¹ and Tamio Oguchi^{2*}
¹ Osaka University, Japan
² Osaka University & JST-CREST, Japan

Oxides with anomalous-valence ion Fe^{4+} have been studied for many years and such systems have been recently found among the so-called A-site ordered perovskites $AA'B_3O_{12}$. In the $AA'B_3O_{12}$ perovskites, A and A' cations occupy the A-site of the original simple perovskite ABO_3 and the A' cations are coordinated by four O ions in a planar fashion instead of the original twelve coordination. The cation sites may consist of magnetic ions, leading to several possible magnetic interactions between them. $CaCu_3Fe_6O_{12}$ reveals charge disproportionation $2Fe^{4+} \rightarrow Fe^{3+} + Fe^{5+}$ at 210K with a transition from paramagnetic to ferrimagnetic state. Quite recently, the magnetic couplings between cations in $CaCu_3Fe_6O_{12}$ are experimentally determined by x-ray magnetic circular dichroism (XMCD) measurements [1]. In this paper, the electronic structure of the A-site ordered perovskite $CaCu_3Fe_6O_{12}$ is studied by means of first-principles calculations. X-ray absorption spectroscopy and XMCD spectra at the Fe and Cu L2,3 edges and O K edge are calculated and compared with experiments to discuss the magnetic order and coupling.

[1] M. Mizumaki et al., Phys. Rev. B 84, 094418 (2011).

EC04

Pr partial electron donation and Co spin state changes at the metal-insulator transition in $(Pr_{1-x}Y_x)_{1-x}Ca_xCoO_3$ as seen by x-ray absorption and emission

Javier Herrero-martin^{*†}, Jose Luis Garcia-munoz[‡], Carlos Frontera[‡], Aura Janeth Baron-gonzalez[‡], Jessica Padilla[‡], Sergio Valencia[‡], RalfFeyerherm[‡], Esther Dudzik[‡], Florin Radu[‡], Radu Abrudan[‡], Gloria Subias[‡] and Javier Blasco[‡]

[†]Institute of Materials Science of Barcelona - CSIC, Spain

[‡]Helmholtz-Zentrum Berlin, BESSY, Germany

[‡]Institut für Experimentalphysik/Festkörperphysik, Ruhr-Universität Bochum, Germany

[‡]Instituto de Ciencia de Materiales de Aragon, CSIC-Univ. Zaragoza, Spain

The electronic and magnetic properties of cobalt-based perovskites are largely determined by the electronic filling of the Co 3d valence band. The characteristic spin state degree of freedom in many cobaltites is correlated to the electron mobility and thus it can play an important role in metal-insulator transitions (MIT). MIT are found in a wide range of compositions of the $(Pr_{1-x}Y_x)_{1-x}Ca_xCoO_3$ series, coupled to magnetic and structural changes [1,2]. At low temperatures, x-ray diffraction confirms a crystal cell volume contraction occurs due to the appearance of a certain quantity of Pr⁴⁺ ions. The electrons lost by Pr ions move to Co sites. The expected increase of the average Co-O distance is not observed, may be due to a compensation effect by a likely Co ions spin state change [3]. We present here a comprehensive study of these compounds by means of x-ray absorption and emission spectroscopies, which leads us to confirm these hypothesis also quantifying the intersite charge donation across the MIT [4]. The observed photoinduced phase transition in Pr_{0.5}Ca_{0.5}CoO₃ under illumination by laser radiation, where metallic domains can be stimulated [5], could thus be related to induced spin state changes.

[1] Tsubouchi et al, Phys. Rev. B 66, 052418 (2002) [2] J. Hejtmanek et al, Phys. Rev. B 82, 165107 (2010) [3] A. Baron-Gonzalez et al, Phys. Rev. B 81, 054427 (2010) [4] J. Herrero-Martin et al, Phys. Rev. B 84, 115131 (2011); J. Herrero-Martin et al (in preparation) [5] Y. Okimoto et al, Phys. Rev. Lett. 103, 027402 (2009)

EC05

Spin transport in the anisotropic Heisenberg chain at finite temperature and momentum

Wolfram Brenig^{1*} and Robin Steinigeweg²

¹ Technical University Braunschweig, Institute for Theoretical Physics, Germany

² J. Stefan Institute Ljubljana, Slovenia

Magnetic transport in one-dimensional quantum spin systems displays many new features beyond a conventional Boltzmann description. Among them is the dissipation of spin currents. At zero momentum, integrability, such as for the one-dimensional Heisenberg (XXZ) model, can lead to ballistic transport. Transport at finite momentum is an open issue. Here we investigate the role of momentum for the transport of magnetization in the spin-1/2 Heisenberg chain above the isotropic point at finite temperature and momentum. Using numerical and analytical approaches, we analyze the autocorrelations of density and current and observe a finite region of the Brillouin zone with diffusive dynamics below a cut-off momentum, and a diffusion constant independent of momentum and time, which scales inversely with anisotropy. Lowering the temperature over a wide range, starting from infinity, the diffusion constant is found to increase strongly while the momentum space cut-off for diffusion decreases. Above the cut-off momentum diffusion breaks down completely.

Phys. Rev. Lett. 107, 250602 (2011)

ED01

Growth of metastable fcc-Fe film on Cu(100) single-crystal underlayer and phase transformation from fcc to bcc

Mitsuru Ohtake*, Kohei Shimamoto and Masaaki Futamoto

Faculty of Science and Engineering, Chuo University, Japan

Theoretical studies suggest that the magnetic property of metastable fcc iron (Fe) varies in a wide range from nonmagnetic to high-spin ferromagnetic state depending on the distance between Fe atoms [1]. The structure of bulk Fe crystal is bcc up to 912 °C, whereas metastable fcc structure can be stabilized in a form of film at RT. However, the metastable fcc structure is reported to transform into more stable bcc structure with increasing the film thickness [2]. In the present study, Fe films were prepared on Cu(100) single-crystal underlayers at RT by UHV-MBE in order to investigate the growth behavior of fcc-Fe crystal and the fcc-bcc phase transformation process. In an early stage of film growth, metastable fcc-Fe(100) structure was stabilized through hetero-epitaxial growth. With increasing the thickness, the fcc structure started to transform into bcc structure. High-resolution cross-sectional TEM and pole-figure XRD analyses showed that the fcc structure transformed into bcc structure by atomic rearrangement from fcc{100} to bcc{100}. The transformation orientation relationship was thus bcc{100}<011> || fcc{100}<001>. The transformation occurred not only along the perpendicular direction but also along the in-plane directions. The relationship between film thickness and magnetic property will also be discussed at the conference.

[1] L. T. Kong and B. X. Liu: J. Alloys Comp., 414, 36 (2006). [2] T. Detzel et al.: Surf. Sci., 293, 227 (1993).

ED02

Neel temperature and the thickness of surface NiO

Wei Pan*, Ying-ta Shih and Chien-yu Su

National Chung Cheng University, Taiwan

The surface oxidation on Ni/Cu(001) or CoNi alloy on Cu(001) have been studied for the spin reorientation transition and other magnetic interactions, such as magnetic demolishment, canted state, coercivity enhancement, and antiferromagnetic induced ferromagnetism. It is found that a transition temperature of 200 K for these phenomena. This study is to confirm that the transition temperature of 200 K is the Neel temperature of NiO formed by oxygen treatment on the surface of Ni/Cu(001) films. We deposited films of x ML Ni/10 ML Co/Cu(001), where x = 0, 2, 3, 4, and 6. The films were then treated by oxygen exposure of 1800 Langmuir for the formation of y ML NiO(x-y) ML Ni/10 ML Co/Cu(001). The coercivity is enhanced for all x below 200 K after field cooling. For x of 3, 4, and 6, the coercivity is the same and the coercivity enhancement phenomenon disappears when the temperature is above 200 K. It indicates that the thickness of the surface NiO is 3 ML and the Neel temperature is 200 K. Thus, all the phenomena mentioned above is induced by the formation of antiferromagnetic ordering of the surface NiO.

ED03

Reduced exchange bias field in antiferromagnet-patterned FeF₂/Ni stripes

R. Morales^{1*}, J. E. Villegas², D. Navas³, N. Soriano⁴, E. Castellano-hermandez², X. Battle⁴, F. Castano³ and Ivan K. Schuller⁵

¹ University of the Basque Country and IKERBASQUE Basque Foundation for Science, Bilbao, Spain

² Unite Mixte de Physique CNRS/Thales and Universite Paris Sud, Orsay, France

³ University of the Basque Country, Leioa, Spain

⁴ Universitat de Barcelona, Barcelona, Spain

⁵ University of California San Diego, La Jolla, USA

The exchange interaction in antiferromagnetic/ferromagnetic (AF/FM) bilayers gives rise to the exchange bias phenomenon. In addition to the shift of the FM hysteresis loop, the exchange coupling can also modify the magnetization reversal mechanism. Incomplete domains walls (IDWs) have been observed in FeF₂/Ni below the AF Neel temperature [1,2]. However, reversal of the FM moments is expected to have little effect on the FeF₂ spin structure due to the strong AF anisotropy [3]. We show using variable thickness FM layers that this scenario changes as the AF becomes patterned. A wedged substrate/FeF₂ (70nm)/Ni (Ni=2-74 nm)/Al (4nm) sample was patterned into stripes by photolithography. Only the FM layer was patterned for the thickest Ni whilst the FeF₂ layer becomes gradually patterned as Ni decreases. The exchange-bias field-dependence Heb (Ni) shows an increasing difference compared to the value expected with decreasing Ni thickness. This result originates from spring-like DWs parallel to the AF/FM interface formed in both the Ni and FeF₂ layers. Simulations of IDWs account for the experimental values of Heb(Ni). Work supported by MICINN grants FIS2008-06249, MAT2010-20798, MAT2009-08667 and the US Department of Energy DE-FG03-87ER-45332.

[1] R. Morales, Z.-P. Li, O. Petravic, X. Battle, and Ivan K. Schuller, Appl. Phys. Lett. 89, 072504 (2006) [2] R. Morales et al., Appl. Phys. Lett. 95, 092503 (2009) [3] M. Kiwi, J. Mejia-Lopez, R. D. Portugal, and R. Ramirez, Europhys. Lett., 48, 573 (1999)

ED04

Experimental verification of the magnetic interactions between Co particles in C₆₀-Co granular films

Shuhei Toyokawa*, Eiiti Tamura, Eiji Shikoh, Teruya Shinjo and Masashi Shiraishi

Osaka Univ., Japan

Spintronics devices using molecular materials have attracted growing attention over the past decade because of their long spin coherence. Various researches have accomplished about the electrical conduction characteristic and the magnetic transportation characteristic of the C₆₀-Co granular film[1-5], which has a structure that Co nanoparticles are dispersed in C₆₀ matrix. We observed the following two phenomena below the blocking temperature in the sample (C₆₀:Co = 9.2:1): 1) Hysteresis of the magnetization curve. (Ferromagnetic characteristic.), and 2) Magnetic field dependence of the coulomb blockade-electric field characteristic. (This characteristic require the antiferromagnetic basis in our idea) These contradictory characteristics were assumed due to the dipole interaction between the Co nanoparticles, and identified by the following method. We calculated the two particles model with dipole interaction and compared the numerical results and magnetization curve of the samples(C₆₀:Co = 6.0:1, 9.0:1). The measured M-H curves are good agreement with the theoretical curves. The above 1) and 2) can be explained with this model. In this way, the dipole interactions between Co nanoparticles in C₆₀ matrix were identified.

[1] S.Miwa, M.Shiraishi, et al., Jpn. J. Appl. Phys. (2006). [2] S.Sakai, et al., Appl. Phys. Lett. (2006). [3] S.Miwa, M.Shiraishi, et al., Phys. Rev. B (2007). [4] S.Sakai, et al., Appl. Phys. Lett. (2007). [5] Y.Matsumoto, et al., Chem. Phys. Lett. (2009).

ED05

Emergent magnetic switching in spin glass La_{0.7}Sr_{0.3}(Mn,Fe)O₃/La_{0.7}Sr_{0.3}MnO₃ thin films

Zhi-hong Wang^{1*}, Bao-gen Shen¹, Ji-rong Sun¹, G. Cristiani² and H. -U. Habermeier²

¹ Institute of Physics, Chinese Academy of Sciences, P. O. Box 603, Beijing 100190, China

² Max-Planck-Institute for Solid State Research, Heisenbergstrasse 1, D-70569, Stuttgart., Germany

The emergent magnetic switching has been investigated in exchange coupled bilayers composed of spin glass (La_{0.7}Sr_{0.3}Mn_{1-y}Fe_yO₃, y=0.18-0.20) and ferromagnet (La_{0.7}Sr_{0.3}MnO₃) epitaxial thin films. It was found that, i) the magnetization reversal develops from single magnetic switching into double magnetic switching as the sample is cooled below the spin freezing temperature; ii) both the critical field and the transition region for the second magnetic switching (SMS) increase upon cooling but decrease with increasing the cooling magnetic field; iii) at 1.8 K the SMS is only exhibited in the descending branch of the hysteresis loop; however its presence in the ascending branch can be partially restored via enlarging the cooling field; iv) there occurs an obvious training effect for the SMS observed at 1.8 K. The rich features and the micro-origin of the emergent magnetic switching are discussed in terms of a phenomenological domain wall model which involves the exchange anisotropy depending on the alterable spin frustration due to the frozen and activated spins at the spin glass-ferromagnet interface.

ED06

FM-AFM crossover in vanadium oxide nanomaterials.

Sergey Demishev^{1*}, Alexey Chernobrovkin¹, Vladimir Glushkov¹, Nickolay Sluchanko¹, Nickolay Samarin¹, Alexey Semeno¹, Sergey Balakhonov², Bulat Churagulov², Anastasiya Grigorieva² and Evgenii Goodilin²

¹ Low Temperatures and Cryogenic Engineering, General Physics Institute of RAS, Russia

² Faculty of Materials Sciences, Moscow State University, Moscow, 119991 Russia, Russia

The magnetic properties of nanomaterials based on vanadium oxide (multiwall nanotubes, nanorods, whiskers and nanolayers) have been investigated in the temperature range of 1.8-220 K by high frequency (60 GHz) EPR. A transition from a ferromagnetic temperature dependence to an antiferromagnetic temperature dependence has been observed in nanorods, whiskers and nanotubes with a decrease in the temperature. The FM-AFM crossover observed near 100 K is accompanied by a low temperature increase in the Curie constant by a factor of 2.7-7. The comparison of the experimental data for various VO_x nanoparticles indicates that the most probable cause of the change in the type of magnetic interaction is a change in the concentration of V⁴⁺ magnetic ions due to temperature dependent electron localization [1].

1. S.V.Demishev et al., JETP Letters, 91, 11 (2010)

EE01

Spin Hall effect from first principles

Christian Hirschbach¹, Katarina Tauber¹, Dmitry Fedorov¹, Martin Gradhand² and Ingrid Mertig^{3*}

¹ Theory Department, Max Planck Institute of Microstructure Physics Halle, 06120 Halle, Germany

² H. H. Wills Physics Laboratory, University of Bristol, Bristol BS8 1TH, United Kingdom

³ Institute of Physics, Martin Luther University Halle, 06099 Halle, Germany

Spintronics without magnetic materials would be an interesting alternative to the existing spintronics applications. The spin Hall effect creates spin currents in nonmagnetic materials and avoids the problem of spin injection. Future applications of the spin Hall effect require two properties of the materials used in the spin Hall device, a large spin Hall angle and a long spin diffusion length. Ab initio calculations based on density functional theory are a powerful tool to design the desired materials and to get insight into the underlying microscopic processes. We investigated the spin Hall effect in dilute alloys, in particular the intrinsic effect based on the Berry curvature as well as the skew scattering contribution. By means of a relativistic Korringa-Kohn-Rostoker method we calculated the scattering potentials of several impurities in Cu, Ag, Au, and Pt hosts self-consistently. We solve the linearized Boltzmann equation to calculate the conductivity tensor taking as well as the scattering-out and the scattering-in term into account. We identify systems, e.g. Cu(Bi) and Au(C) with a Hall angle larger than 0.06 and a spin diffusion length of about 100 nm.

M. Gradhand, D. V. Fedorov, P. Zahn, and I. Mertig, Phys. Rev. Lett. 104, 186403 (2010); S. Lowitzer, M. Gradhand, D. Koddertzsch, D. V. Fedorov, I. Mertig, and H. Ebert, Phys. Rev. Lett. 106, 056601 (2011); M. Gradhand, D. V. Fedorov, F. Pientka, P. Zahn, I. Mertig, and B. Gyorffy, Phys. Rev. B 84, 075113 (2011)

EE02

Spin transfer torques in magnetic bilayers with strong spin orbit coupling

Mark D. Stiles^{1*}, Paul M. Haney¹, Kyung-jin Lee² and Hyun-woo Lee³

¹ Center for Nanoscale Science and Technology, National Institute of Standards and Technology, USA

² Department of Materials Science and Engineering, Korea University, Korea

³ PCTP and Department of Physics, Pohang University of Science and Technology, Korea

Current driven magnetic dynamics in ferromagnetic thin films on top of non-magnetic films with strong spin orbit coupling combines several topics of significant recent interest. The current flowing through the ferromagnetic layer gives rise to adiabatic and non-adiabatic spin transfer torques when the magnetization is non-uniform. The current flowing through the non-magnetic layer gives rise to a spin Hall current, leading to a spin current incident on the interface between the two layers. This spin current causes spin transfer torques similar to those that are important in magnetic multilayers with current flowing perpendicular to the plane. Recent experiments, models, and simulations raise the possibility of an additional torque due to the spin-orbit coupling at the interface where the inversion symmetry found in the bulk materials is broken. All of the currents and torques are coupled to each other and are non-uniform in the layers. We compute this coupling and spatial variation using a Boltzmann equation approach. We determine the dependence of the torque on the thickness of the layers and study how the torque changes as the contribution from the interfacial spin orbit coupling is increased.

EE03

Diffusive spin dynamics in ferromagnetic thin films with a Rashba interaction

Xuhui Wang* and Aurelien Manchon

KAUST, Saudi Arabia

Injection of a charge current into an asymmetrically sandwiched thin magnetic layer generates an effective Rashba field that reverses the magnetization [1, 2] and improves current-driven domain wall motion [3]. In a ferromagnetic metal layer, we study theoretically the coupled charge and spin diffusion equations in the presence of both Rashba spin-orbit interaction and magnetism. The mis-alignment between the magnetization and the non-equilibrium spin density induced by the Rashba field gives rise to Rashba spin torque acting on the ferromagnetic order parameter. Using Keldysh formalism and gradient expansion, we find that the Rashba torque consists of both in-plane and out-of-plane components [4]. This provides an explanation to the magnetization switching mechanism in a single ferromagnet as observed in the recent experiments [5]. While providing a coherent framework to describe the diffusive spin dynamics in magnetic media with or without Rashba spin-orbit interaction, we also show particularly that the in-plane Rashba torque can be tuned by varying the width of the magnetic nano-wire and its materials parameters.

[1] A. Manchon and S. Zhang, Phys. Rev. B. 78, 212405 (2008); 79, 094422 (2009). [2] I. M. Miron et al., Nature Mater. 9, 230 (2010); 10, 419 (2011). [3] K. Obata and G. Tatara, Phys. Rev. B 77, 214429 (2008). [4] X. Wang and A. Manchon, arXiv:1111.1216; arXiv:1111.5466. [5] I. M. Miron, et al. Nature (London) 476, 189 (2011).

EE04

Emergence of magnetic monopoles in magnetic systems with spin-orbit coupling

Akihito Takeuchi* and Gen Tatara

Department of Physics, Tokyo Metropolitan University, Japan

In spintronics, a spin current plays an essential role. Today, various spin-related phenomena have been discovered and understood through the spin current. However, the spin current is not conserved, and the relation between spintronics and electromagnetism is still an open question. For overcoming this difficulty, we theoretically analyze the spintornic phenomena from the viewpoint of the Maxwell's equations. In particular, we focus on the electron transport driven by a dynamic magnetization or an electric field in the presence of spin-orbit interactions. We calculate an electric current and density, and derive the Maxwell's equations. The Maxwell's equations constructed by this way involve a magnetic monopole contribution [1]. We will discuss this magnetic monopole generated by the magnetization dynamics or the applied electric field in a ferromagnetic-nonmagnetic junction, and we will discuss also the magnetic monopole induces an electric current via the Ampere's law for the monopoles. Therefore, the monopole signal is expected in a similar geometry as the inverse spin Hall signal [2,3].

[1] A. Takeuchi and G. Tatara, arXiv:1104.4215 (to be published in J. Phys. Soc. Jpn.). [2] E. Saitoh et al., Appl. Phys. Lett. 88, 182509 (2006). [3] T. Kimura et al., Phys. Rev. Lett. 98, 156601 (2007).

EE05

Generalization of Gilbert damping in Rashba systems

Kyoung-whan Kim^{1*}, Jung-hwan Moon², Kyung-jin Lee² and Hyun-woo Lee¹

¹ Department of Physics, POSTECH, Korea

² Department of Materials Science and Engineering, Korea University, Korea

Mutual interaction between spin current and magnetization dynamics is described by spin-transfer torque (STT) [1] and spin motive force (SMF) [2]. Spin-transfer torque results in magnetization dynamics due to spin current. In contrast, SMF is spin dependent motive force induced by magnetization dynamics. As a result of combination of these two, magnetization dynamics affects magnetization dynamics itself mediated by spin current. This self-feedback of magnetization dynamics give rise to generalization of Gilbert damping as a second rank tensor [3], but it has been almost ignored since it is negligibly small. However, in an ultrathin magnetic system with strong Rashba spin-orbit coupling (RSOC) [4], which is of recent interest in spintronics, we demonstrate that SMF can be orders of magnitude enhanced so the self-feedback becomes now relevant. We derive the generalized Gilbert damping tensor including RSOC-induced SMF and discuss its effects on magnetization dynamics qualitatively. Our work implies that ultrathin magnetic films are not mere thin limits of thicker ferromagnets but systems governed by qualitatively different physics.

[1] J. C. Slonczewski, *J. Magn. Mag. Mater.* 159, L1 (1996). [2] L. Berger, *Phys. Rev. B* 33, 1572 (1986). [3] S. Zhang and S.-L. Zhang, *Phys. Rev. Lett.* 102, 086601 (2009). [4] Y. A. Bychkov and E. I. Rashba, *J. Exp. Theor. Phys. Lett.* 39, 78 (1984).

EF01

Superconducting, antiferroquadrupolar, and structural transitions in caged compounds PrT₂Zn₂₀ (T=Ru, Rh, and Ir)

T. Onimaru¹, K. T. Matsumoto¹, N. Nagasawa¹, Y. F. Inoue¹, K. Umeo²,

S. Kittaka¹, T. Sakakibara¹, Y. Karaki¹, M. Kubota¹ and T. Takabatake^{1,3}

¹ADSM, 2N-BARD, 3IAMRHiroshima Univ., Higashi-Hiroshima, Japan

⁴ISSP, Univ. of Tokyo, Kashiba, Japan

⁵Fac. Edu., Univ. of the Ryukyus, Okinawa, Japan

There has been considerable interest in praseodymium-based intermetallic compounds, because an abundance of unusual phenomena has been intensively studied such as ferromagnetic order of hyperfine-enhanced nuclear-spins in PrNi₂[1], incommensurate antiferroquadrupolar order in PrPb₂[2], and heavy-fermion superconductivity in filled-skutterudite PrOs₃Sb₃[3]. We have recently focused on Pr-based compounds with caged structures, where large coordination number of the Pr ion leads to weak crystalline electric field effect, whereas hybridization of the f electrons with electrons of cage atoms is strengthened. Such conditions may enable the compounds to show strongly correlated electronic phenomena. Keeping this in mind, we have synthesized and studied a new family of caged compounds PrT₂Zn₂₀ (T=Ru, Rh, and Ir). PrRh₂Zn₂₀ and PrIr₂Zn₂₀ with a nonmagnetic gamma₃ doublet ground state undergo superconducting transitions at TSC=0.06 K and 0.05 K, respectively, in the presence of antiferroquadrupolar order below TQ=0.06 K and 0.11 K[4,5]. The entropy releases at TQ are 6% and 20% of Rln, for PrRh₂Zn₂₀ and PrIr₂Zn₂₀, respectively, suggesting interplay between the quadrupolar fluctuations and formation of the superconducting pair. On the other hand, in PrRu₂Zn₂₀, the symmetry of the Pr ion is lowered by the structural phase transition at TS=138 K. Therefore, no phase transition manifests itself down to 0.04K

[1] M. Kubota et al., *Phys. Rev. Lett.* 51,1382 (1983). [2] T. Onimaru et al., *Phys. Rev. Lett.* 94, 197201 (2005). [3] E. D. Bauer et al., *Phys. Rev. B* 65, 100506 (2002). [4] T. Onimaru et al., *J. Phys. Soc. Jpn.* 79, 033704 (2010). [5] T. Onimaru et al., *Phys. Rev. Lett.* 106, 177001 (2011)

EF02

Structural and magnetic phase separation in PrMn₂Ge_{2-x}Si_x and related compounds

Shane Joseph Kennedy^{1*}, Jiani Wang², Stewart Campbell¹, Michael Hofmann¹ and Shixue Dou³

¹ Brogg Institute, Australian Nuclear Science and Technology Organisation, Lucas Heights, NSW 2234, Australia

² Brogg Institute, Australian Nuclear Science and Technology Organisation, Lucas Heights, NSW, 2234, Australia

³ School of Physical, environmental and Mathematical Sciences, The University of NSW, Canberra, ACT 2600, Australia

⁴ FRM-II, Technische Universität München, 85747 Garching, Germany

⁵ Institute of Superconducting and Electronic Materials, The University of Wollongong, Wollongong NSW, 2522, Australia

We report a comprehensive study of the thermal and magnetic properties of PrMn₂Ge_{2-x}Si_x compounds along with neutron and synchrotron X-ray diffraction studies of their atomic and magnetic structure. Generally, the Mn atoms display the same antiferromagnetic configurations as the broad family of RMn₂X₂ compounds (R = rare-earth, X = Si, Ge). However, between x= 1.0 and 1.4 we see phase separation at low temperatures, into Fmc and AFmc forms. This is caused by spontaneous magnetostriction which differs greatly between the two magnetic phases, and is linked to a subtle structural phase separation over a broader concentration range (from x= 0.4 to 1.6). Clearly two separate & unique structures exist depending on the local concentration of Silicon and Germanium on the mixed (X) site. Our interpretation brings into question whether a random substitution on the X site could produce such remarkable magneto-elastic phenomena or whether atomic short range order plays a significant role in the physical properties of the mixed 122 compounds. Indeed we find ample evidence in the broader family of RMn₂X₂ compounds to support a claim that systematic variation in local order of the R & X sites drives the complicated magnetic and physical properties observed in this system

EF03

Observations of magnetic and ferroelastic nanoclusters in RCo₂

Julia Herrero-albillos¹, Marcela Bonilla^{2*}, Sarah L Driver³, Irene Calvo², Celia Castan², Adriana I Figueroa², Juan Bartolome², Michael A Carpenter¹, Luis Garcia³ and Fernando Bartolome²

¹ CUD, Centro Universitario de la Defensa de Zaragoza, C/ Huesca s/n, Zaragoza, Spain

² ICMA and Dpto. de Fisica de la Mat. Cond. CSIC - Universidad de Zaragoza, Pedro Cerbuna 12, Zaragoza, Spain

³ Department of Earth Sciences, University of Cambridge, Downing Street, Cambridge CB2 3EQ, United Kingdom

New findings of short-range order (SRO) correlations in magnetic materials have recently been reported, even on compounds previously studied for decades, as a result of the use of new and improved experimental techniques. In particular, X-ray Magnetic Circular Dichroism (XMCD) and transverse susceptibility have revealed the existence of several new magnetic configurations in the phase diagram of the family of compounds RCo₂ (R = Er, Ho, Tb, Tm). The presence of magnetic SRO (magnetic nanoclusters) has been shown to be a prerequisite for the existence of these configurations. Relaxation of the magnetic nanoclusters leads to anomalies in the ac susceptibility, observed within the paramagnetic phase of RCo₂ compounds. Additionally, Resonant Ultrasound Spectroscopy (RUS) studies have shown the presence of fluctuations in local strain, also described as ferroelastic clusters, above the magnetic ordering temperature. Comparing RUS and magnetic measurements sheds light on the interrelationship between ferroelastic and magnetic nanoclusters.

EF04

First-principles molecular dynamics study on the magnetic structure of Mn₃Pt

Takashi Uchida^{1*}, Yoshiro Kakehashi² and Nobuyuki Kimura¹

¹ Hokkaido Institute of Technology, Japan

² University of the Ryukyus, Japan

The ordered Mn₃Pt is a three-dimensional frustrated magnet with an octahedral configuration of Mn local magnetic moments, and exhibits two ordered phases below the Neel temperature: collinear antiferromagnetic (AF) phase for 400K < T < 475K, and noncollinear AF phase for T < 400 K. To investigate the origin and details of the magnetic structures of Mn₃Pt, we have applied the first-principles molecular dynamics (MD) approach to this alloy. The theory is based on the first-principles TB-LMTO Hamiltonian, the functional integral method and the isothermal MD technique, and can determine automatically the magnetic structures of itinerant magnets at finite temperatures. Numerical results at 25 K using 4*4*4 FCC unit cell reveal the triangular shaped noncollinear magnetic structure, being consistent with experiment. It is found that with increasing temperature up to 300 K, the amplitude and the thermal average of Mn local moment decrease gradually, and the d-electron density of states (DOS) near the Fermi energy increases. Based on the numerical results for further increasing temperature above 400 K, a discussion is given as to the relationship between frustration, the d-electron DOS, the magnetic structures, and their temperature dependence.

EF05

One-dimensional magnetism in metallic MnB₄

Sergii Khmelevskiy, Josef Redinger and Peter Mohn

Institute of Applied Physics, Vienna University of Technology, Austria

We have investigated from first-principles an electronic structure and magnetism in MnB₄ compound with experimentally observed orthorhombic C_{2v}/m1 structure. It is found that Mn tetra-borides (MnB₄) is found to have metallic ground state with well defined local Mn magnetic moments. This conclusion was drawn from calculation within full potential Linear Augmented Plane Wave method and Korringa-Kohn-Rostocker method using Disordered Local Moment Approximation. We have shown using Lichtenstein Green function method for first-principle calculation of the exchange constants that magnetic exchange interactions between Mn moments are strongly ferromagnetic along 1D-chains of Mn atoms and they are practically vanishing between the chains. The metallic state appears to exhibit a strongly one-dimensional character since the metallic bands show dispersion only in one reciprocal lattice dimension. Thus it is appears that MnB₄ is a novel one-dimensional metallic magnet.

EG01

Negative spin current polarization in amorphous CoFeB measured via the spin-wave Doppler effect

Konrad Hsu Aschenbach¹, Meng Zhu¹ and Robert D McMichael^{2*}

¹ Center for Nanoscale Science and Technology, NIST / Maryland Nanocenter, University of Maryland, USA

² Center for Nanoscale Science and Technology, NIST, Gaithersburg, MD 20899, USA

We use the spin-wave Doppler technique[1-4] to measure and compare the spin polarization of the current (P) of Co₂Fe₁₀B₁₀ before and after thermal annealing. The technique involves inductively launching and detecting spin waves in ferromagnetic wires carrying electrical current. The adiabatic spin transfer torque produces a transmission frequency Doppler shift of Δf = v/λ, where λ is the spin wave wavelength and v = J μB P/(e Ms) is the spin drift velocity, which is a function of the current density J, and the magnetization Ms. We find that the as-deposited amorphous film has a small negative value of P, in contrast to the positive values obtained via point-contact Andreev reflection (PCAR)[5]. Measurements on several other CoFeB samples with different composition also yield small or slightly negative values of P. On the other hand, the annealed film has a positive value of P, in agreement with other techniques[5,6], and as measured for Co₉₀Fe₁₀ without boron[3]. Relatively little has been reported about the current polarization properties of amorphous CoFeB. The spin wave Doppler technique, with its immunity to interfacial effects, yields bulk polarization results that challenge the previous Andreev reflection results.

[1] Vlaminck, V. & Bailleul, Science 322, 410–413 (2008). [2] Zhu, M., Dennis, C. L. & McMichael, R. D. *Phys. Rev. B* 81, 140407 (2010). [3] Zhu, M. et al. *Appl. Phys. Lett.* 98, 072510 (2011). [4] Thomas, R. L., Zhu, M., Dennis, C. L., Misra, V. & McMichael, R. D. *Journal of Applied Physics* 110, 033902-033902-4 (2011). [5] Huang, S. X., Chen, T. Y. & Chien, C. L. *Applied Physics Letters* 92, 242509-242509-3 (2008). [6] Fukami, S. et al. *Applied Physics Letters* 98, 082504-082504-3 (2011). [†] Current Address: Seagate Technology, Bloomington MN 55435

EG02

Switching the conductance of a magnetostrictive nanocontact by magnetic field

Marc Mueller, Christoph Suergers*, Richard Montbrun and Hilbert V. Lohneysen

Physikalisches Institut und DFG Center for Functional Nanostructures, Karlsruhe Institute of Technology (KIT), Germany

The electrical conductance G of magnetostrictive nanocontacts fabricated from Dy break junctions has been investigated at 4.2 K where Dy is in the ferromagnetic state. In addition to the variation of the conductance while breaking the wire mechanically, the conductance can be changed by variation of an applied magnetic field H due to the large magnetostriction of Dy. The behavior of G(H) and its angular dependence can be explained by taking into account the magnetostrictive properties of Dy. This demonstrates the possibility of tuning the conductance of magnetic nanocontacts by a magnetic field [1]. We also investigate the effect of a magnetic field on the contact shape created during mechanical training and find that the shape can be controlled by the applied field due to the strong magnetoelastic coupling of Dy.

[1] M. Mueller, R. Montbrun, M. Marz, V. Fritsch, C. Suergers, H. v. Lohneysen, *Nano Letters* 11, 574 (2011)

EG03

Spin wave and spin pumping in permalloy strips

Sankha Subhra Mukherjee, Jae Hyun Kwon, Mahdi Jamali, Praveen Deorani and Hyunsoo Yang*

National University of Singapore, Singapore

Microfabrication techniques have made it possible to characterize both the resonant as well as the travelling characteristics of spin waves in permalloy [1, 2]. Among variety of methods for measuring spin waves, pulse inductive microwave magnetometry [3-5] is the electrical technique for travelling spin waves. We investigate the effect of the pulse width of excitation pulses on the generated spin wave packets using both experimental results and micromagnetic simulations. We show that spin wave packets generated from electrical pulses are a superposition of two separate spin wave packets, one generated from the rising edge and the other from the falling edge, which interfere either constructively or destructively with one another, depending upon the magnitude and direction of the field bias conditions. A method of spin wave amplitude modulation is also presented by the linear superposition of spin waves. We use interfering spin waves resulting from two closely spaced voltage impulses for the modulation of the magnitude of the resultant spin wave packets. We also investigate the contribution of the surface spin waves to spin pumping. We show that spin waves can be used as a very efficient method for increasing the spin pumping signal compared to the ferromagnetic resonance case.

1. M. Covington, T. M. Crawford, and G. J. Parker, *Physical Review Letters* 89, 237202 (2002). 2. M. Bailleul, D. Olligs, and C. Fermon, *Applied Physics Letters* 83, 972 (2003). 3. T. J. Silva, C. S. Lee, T. M. Crawford, and C. T. Rogers, *Journal of Applied Physics* 85, 7849 (1999). 4. S. S. Kalarickal, P. Krivosik, M. Wu, C. E. Patton, M. L. Schneider, P. Kabos, T. J. Silva, and J. P. Nibarger, *Journal of Applied Physics* 99, 093909 (2006). 5. J. H. Kwon, S. Mukherjee, M. Jamali, M. Hayashi, and H. Yang, *Applied Physics Letters* 99, 132505 (2011).

EG04

Clarification of oxygen impurity effect on NCMR with the film resistivity and bulk scattering spin asymmetry for [FeCo/Natural Oxidation] multi-layers

Yohei Shiokawa

Tohoku university, Japan

Nano-Contacts Magnetoresistance (NCMR) with Fe_{0.5}Co_{0.5} AlOx-NOL (Nano-Oxide-Layer) has been reported to show MR ratio of more 30 % at RA of 0.3 Ωμm²[1]. However, NCMR-SV is predicted to have potentially huge MR ratio of more than 100 % using high bulk spin scattering asymmetry β of ferromagnetic material Fe_{0.5}Co_{0.5} with 0.81[2]. It was surmised this difference of MR ratio between experiments and theory is caused by the impurity of oxygen in FeCo NCs. we investigated the quantitative evaluation of oxygen impurity effect on NCMR with the relation between the resistivity and bulk scattering spin asymmetry for [FeCo/Natural Oxidation] multi-layers. We estimated the resistivity and β of FeCo(O). The resistivity and β of FeCo(O) with [FeCo 2 nm / N.O.]n were 37.4 μΩcm and 0.75, and those of FeCo(O) with [FeCo 1 nm / N.O.]n were obtained 76.7 μΩcm and 0.35. These results suggest the increase of the resistivity by oxygen impurity decreases the β. On the other hand, the resistivity of the single NC in our NCMR was estimated 60 μΩcm by conductive-AFM. The cause of low NCMR ratio is considered to be the impurity of oxygen in NCs. So, reducing oxygen impurity in NC leads to higher NCMR ratio.

[1] H. Iwasaki, and M. Sahashi et al, *MMM 2011, AS-05 (2011)* [2] H. Imamura, et al, *J. Phys. Conf. Seri.* 266, 012090 (2011)

EG05

Room-temperature magnetoresistance properties of planar-type Ni nanostructures controlled from nanoconstrictions to nanogaps

Jun Kitagawa, Ryutaro Suda and Jun-ichi Shirakashi*

Department of Electrical and Electronic Engineering, Tokyo University of Agriculture and Technology, Japan

Innovative devices called ferromagnetic single-electron transistors (FMSETs), which are based on the interplay of single-electron charging phenomena and spin-dependent tunneling effects, have attracted much interest. For the realization of FMSETs, we have reported the magnetoresistance (MR) properties of planar-type tunnel junctions with ferromagnetic nanogap system at 16 K, formed by electromigration methods. [1, 2]. In this paper, we study the room-temperature MR properties of planar-type Ni nanostructures controlled from nanoconstrictions to nanogaps using novel electromigration method, with the aim of fabricating FMSET with higher operation temperature. The stepwise feedback-controlled electromigration (SFCE) methods [3] were performed at room temperature in a vacuum chamber for Ni initial nanochannels with a constriction of a few hundreds of nanometers. We obtained anisotropic MR (AMR) of 0.14 % in the Ni initial nanochannel before performing SFCE procedure. Then, the resistance of the Ni nanochannel was gradually increased from 60 Ω to 76 kΩ by SFCE approach with atomic scale controllability. Positive tunnel MRs (TMRs) with the ratios of between 6 % and 9 % were observed from the controlled structures at room temperature. These results strongly suggest the possibilities of room-temperature operation of planar-type FMSETs with Ni/vacuum/Ni ferromagnetic tunnel junctions.

[1] Y. Tomoda, M. Hanada, W. Kume, S. Itami, T. Watanabe and J. Shirakashi, *J. Phys. Conf. Ser.* 200, 062035 (2010). [2] T. Watanabe, K. Takiya, and J. Shirakashi, *J. Appl. Phys.* 109, 07C919 (2011). [3] S. Itami, Y. Tomoda, R. Yasutake, and J. Shirakashi, *J. Nanosci. Nanotechnol.* 45, 3480 (2010).

EH01

New materials for enhancing device performance in spintronics

Koichiro Inomata, Hiroaki Sukegawa, Zhechao Wen and Seiji Mitani

Magnetic Materials Unit, National Institute for Materials Science (NIMS), Japan

Spin current creates significant effects such as tunneling magnetoresistance (TMR), current perpendicular to plane magnetoresistance (CPP-GMR) and spin transfer torque (STT), which are key factors in spintronics. They are anticipated to be applied for spintronic devices such as ultrahigh density HDD exceeding Tb/in², STT-MRAM, high frequency oscillators, spin logics etc. Perfectly spin-polarized half-metals are essential materials for enhancing the polarization of spin currents and the resultant device performance in spintronics. Full-Heusler alloys with L21 structure have been practically expected as half-metals, because they have a large Curie temperature, and their Fermi level can be tuned by the composition. We have demonstrated that Fermi-level-tuned Co₂FeAl_{0.5}Si_{0.5} Heusler alloy provides half-metallicity even at room temperature [1]. MgO barrier has been used in MTJs because it exhibits a large TMR due to the coherent tunneling in epitaxial MTJs. Very recently we have discovered a new tunnel barrier, spinel (MgAl₂O₄), bringing a large TMR due to coherent tunneling as MgO barrier [2]. Spinel barrier has a benefit of very good lattice matching with bcc metals and Heusler alloys. In this talk we will show half-metallic full-Heusler alloys and their applications to MTJs with in-plane and out-of plane magnetizations [3], and MTJs with an MgAl₂O₄ barrier.

[1] R. Shan et al., *Phys. Rev. Lett.* 102, 246601 (2009). [2] H. Sukegawa et al., *Appl. Phys. Lett.* 96, 212505 (2010). [3] Zhenchao Wen et al., *Appl. Phys. Lett.* 98, 242507 (2011).

EH02

Organic high temperature ferromagnetic compositions

Young-wan Kwon^{*}, Chang Hoon Lee², Dong Hoon Choi¹, Jung-il Jin¹, Eui-kwan Koh³ and Y. H. Geerts⁴
¹ *Chemistry, Korea University, Korea*
² *Polymer Science & Engineering, Chosun University, Korea*
³ *Seoul Branch, Korea Basic Science Institute, Korea*
⁴ *Chemistry, Universite Libre de Bruxelles, Belgium*

Developments of the high temperature organic ferromagnetic materials have been attempted by many researchers. To achieve the ferromagnetic ordering by using organic materials, the high spin multiplicity polymers are also proposed by Itoh et al.[1] in 1968, because they may realize the magnetic storage devices with a versatile processability. Recently, we found that high temperature ferromagnetism could be achieved by intercalating an organic discotic liquid crystalline (DLC) compound with an iron-phthalocyanine [Fe(III)Pc] complex[2] and also with stable organic free radicals. This discovery is originated from our earlier studies[3-5] on the magnetic properties of DNA. We find an analogy between the ferromagnetic properties of inorganic dilute magnetic semiconductors and DNA and DLC compositions. Herein, we will discuss the high temperature ferromagnetic properties of DLC compositions doped with Fe(III)Pc complexes and also with organic free radicals. We also will discuss a preliminary result on the room temperature ferromagnetic properties of polymeric composites consisting of some of polyconjugated polymers and paramagnetic dopants. We studied in details their magnetic properties by electron paramagnetic resonance and SQUID studies. These findings are expected to open a new research field as well as high technological applications of organic materials.

[1] S. Morimoto, K. Itoh, F. Tanaka, and N. Mataga, *Preprints of symposium on the Molecular Structure, Tokyo, 1968*, [2] C. H. Lee, Y.-W. Kwon, D. H. Choi, E. K. Koh, Y. H. Geerts, and J.-I. Jin, *Adv. Mater.*, 2010, 22(39), 4405-4409. [3] C. H. Lee, Y.-W. Kwon, E.-D. Do, D. H. Choi, J.-I. Jin, D.-K. Oh, and J. Kim, *Phys. Rev. B*, 2006, 73, 224417. [4] Y.-W. Kwon, E.-D. Do, D. H. Choi, J.-I. Jin, C. H. Lee, J. S. Kang, and E.-K. Koh, *Bull. Korean Chem. Soc.*, 2008, 29, 1233-1242. [5]

EH03

Structure and magnetic properties of the new ferrimagnetic AFe₂O(PO₃)₂ (A=Ca,Sr,Cd,Pb) compounds

Hassan El Hafid¹, Matias Velazquez^{1*}, Olivier Perez², Abdelaziz El Jazouli³, Alain Pautrat⁴, Rodolphe Decourt¹, Philippe Veber¹, Oudomsack Viraphong¹, Emmanuel Veron¹ and Claude Delmas¹

¹ *Institut de la Chimie de la Matière Condensée de Bordeaux, CNRS, France*
² *CRISMAT, CNRS/ENSICAen, France*
³ *LCMS, Université de Casablanca, Morocco*
⁴ *CEMHTI-CNRS, France*

The crystal structure of the novel monoclinic oxyphosphate PbFe₂O(PO₃)₂ was characterized by single crystal (SC) XRD between 293 and 973 K. χ measurements performed on SCs unveiled an unusual sequence of ferromagnetic-like divergences at Tc1=31.8 K, Tc2=23.4 K and Tc3=10 K, whereas Cp measurements performed on SCs confirmed only the two phase transitions at Tc1 and Tc3, and a slight cusp around Tc2. In powder samples however, the second χ divergence at Tc2 is absent, but they do exhibit a λ -type peak on the Cp(T) curve. A set of γ c measurements, (logarithmic) long time remanent magnetization decay measurements, modified ZFC magnetization measurements, were performed on both powders and SCs. Mean-field critical exponents were obtained in powders and SCs above Tc1, consistently with the low development of magnetic correlations observed in χ curves, but not with the asymmetric λ -type Cp peak. We have clear evidence for two dissipative mechanisms, giving peaks at 27 and 13 K on γ c measurements. While the former spectrum shows a Debye profile with a well defined Eact=240 K, the latter one shows a distribution of Eact typical of spin glass systems. Finally, FC/ZFC magnetization cycles and γ measurements in the AFe₂O(PO₃)₂ (A=Ca,Sr,Cd,Pb) compounds will be presented.

EH04

Magnonic metamaterials formed by arrays of Co antidots on continuous NiFe films

Ehsan Ahmad, Yat-yin Au, Toby Davison, Mykola Dvornik and Volodymyr Kruglyak*
University of Exeter, United Kingdom

Magnonic crystals periodic magnetic media represent one of the central objects in the research field of magnonics [1]. Usually, the periodic modulation of the effective magnetic field in magnonic crystals is achieved as a compositional modulation created either during growth or using lithographic processing. In this report, we demonstrate a method of producing magnonic crystals by periodically modulating the internal magnetic field inside a continuous thin film of NiFe (Permalloy). The modulation of the internal magnetic field is achieved via fabrication of a Co nanostructure (an array of antidots) on top of the Permalloy film, with the latter experiencing the stray magneto-dipole field from uncompensated magnetic charges in Co. The dynamical properties of the fabricated magnonic crystals are characterized using the time resolved scanning Kerr microscopy (TRSKM) [2]. The measurements reveal a strong modification of the magnonic spectrum the strength of which increases as the value of the bias magnetic field decreases. The finding opens new ways for creation of magnonic metamaterials. The research leading to these results has received funding from the EC's 7th Framework Programme (FP7/2007-2013) under GA 228673 (MAGNONICS) and from EPSRC of the UK under project EP/E055087/1.

I. Y. V. Kruglyak, S. O. Demokritov, and D. Grundler, *J. Phys. D: Appl. Phys.* 43, 264001 (2010). 2. Y. Au, T. Davison, E. Ahmad, P. S. Keatley, R. J. Hicken, and V. V. Kruglyak, *Appl. Phys. Lett.* 98, 122506 (2011).

EH05

Formation of FeSi thin films and magnetic properties

Yooleemi Shin¹, Tuan Anh Duong¹, Seungmok Jeon¹, Dung Duc Dang², Thiet Van Duong¹ and Sunglae Cho^{3*}
¹ *Department of Physics, University of Ulsan, Korea*
² *Department of General Physics, School of Engineering Physics, Ha Noi University of Science and Technology, Viet Nam*

The deposition of transition metal layers on silicon and their reaction with substrate are important issues in semiconductor device technology. The interface between metal and semiconductor determines the device performance. whereby both an ohmic contact and a Schottky barrier, i.e., an active electronic element can be realized. The 3d transition metal monosilicides such as FeSi, CoSi, MnSi and CrSi have attracted much attentions because they are easily formed in the interface between transition metal and Si. FeSi is a narrow band gap semiconductor. The activation energy for exciting electrons from the filled band to the empty band is estimated to be 0.05 eV from the experiments on the temperature dependence of the Mossbauer effect, magnetic susceptibility and NMR shift. In this work, Fe thin films were grown on Si(100) substrates using MBE. The structure and surface morphologies of Fe films were determined by X-ray diffraction and atomic force microscopy measurements, respectively. We have observed that all samples grown at 100, 400 and 600 oC have a phase of CsCl crystal structure (c-FeSi). In order to investigate the correlation between magnetization and charge carrier transport, we performed magnetoresistance and Hall resistance measurements by using a physical property measurement system.

[1] U. Starke, W. Weiss, M. Kutschera, R. Bandorf, and K. Heinz, *J. Appl. Phys* 91, 6154 (2002).

EI01

Perpendicular magnetic anisotropy in Fe/Fe_{1-x}Co_x multilayers

Maciej Dabrowski¹, Pedro Gastelois¹, Fikret Yildiz¹, Takeshi Nakagawa², Yasushi Takagi², Toshihiko Yokoyama², Marek Przybylski^{1*} and Jurgen Kirschner¹
¹ *Max-Planck-Institut für Mikrostrukturphysik, Halle, Germany*
² *Institute for Molecular Science, Okazaki, Japan*

A uniaxial anisotropy of a volume character that can keep perpendicular magnetization in relatively thick films is rare. The concept relates to the lattice distortion that modifies the electronic band structure. A model system is provided by Fe_{1-x}Co_x alloy films tetragonally distorted due to their pseudomorphic growth on fcc mismatching substrates like Rh(001) and Ir(001) [1]. In particular, the Fe_{0.5}Co_{0.5} films show perpendicular magnetic anisotropy, whereas Fe layers (x=0) are magnetized in-plane. The Fe_{1-x}Co_x and Fe layers can be separated by a spacer that mediates a ferro- or antiferromagnetic exchange coupling [2]. As MOKE measurements provide only a signal from the average magnetization, a layer resolved knowledge of the spin structure is required. Soft x-ray magnetic circular dichroism allows us to probe the magnetization separately for Fe_{1-x}Co_x (measurements at the Co edges enabled us to investigate the magnetism of the alloy layer independently from the pure Fe layer). We found that non-collinear magnetization configurations can be produced also if there is no spacer, but there is a direct exchange coupling between the Fe and Fe_{1-x}Co_x layers. A final magnetization distribution depends on the composition of the constituent layers, and how thick Fe is with respect to Fe_{1-x}Co_x.

[1] F. Yildiz, M. Przybylski, X.-D. Ma, J. Kirschner, *Phys. Rev. B* 80, 064415 (2009). [2] F. Yildiz, M. Przybylski, J. Kirschner, *Phys. Rev. Lett.* 103, 147203 (2009).

EI02

Effect of annealing temperature on L1o ordering and perpendicular magnetic anisotropy of FePd/CoFeB films

Mohammed Nazrul Islam Khan*, Hiroshi Naganuma, Nobuhito Inami, Yusuke Ohdaira, Mikihiko Oogane and Yasuo Ando
Applied Physics, Tohoku University, Japan

Spin-transfer-torque random access memory (STT-RAM) using perpendicular magnetized L1o-ordered alloy for magnetic tunnel junctions (p-MTJs) has considerable interest because of advantages for scalability and stability of memory. However, tunnel magnetoresistance (TMR) ratio was a few percent at room temperature using L1o-ordered alloys. [1,2] A high TMR ratio as well as perpendicular magnetic anisotropy (PMA) was obtained using the thin CoFeB combined with MgO barrier due to interfacial effect. [3] In this study, we systematically investigated annealing temperature effects on PMA with the insertion of thin CoFeB layer between L1o-FePd and MgO films for use as free layer in the p-MTJs. Stacking structure is Cr₅₀/Pd₁₀/FePd/CoFeB₂₀/MgO₂/Ta₂ (unit in nm, and t=1.5-5.0) and these were epitaxially grown on MgO (100) substrates. FePd and CoFeB were deposited at 300°C and ambient temperature, respectively. After post-annealing, the perpendicular anisotropy was observed at Ta≥ 300°C and 250°C for t= 2.0 nm and 2.5 nm, respectively, whereas it was observed for all samples above t ≥3.0 nm which might be attributed to the crystallization of CoFeB and increased of PMA. The results show that annealing is an effective method to improve the PMA of a FePd/CoFeB system. Acknowledgement: This study was supported by FIRST program from JSPS.

[1] N. Inami et al., *J. Mag. Sco. Jpn.* 34, 293 (2010) [2] G. Kim et al., *Appl. Phys. Lett.* 92, 172502 (2008). [3] S. Ikeda et al., *Nat. Mat.* 9, 721 (2011).

EI03

Magnetic properties of tetragonally strained Fe/(W,Re) multilayers

Cristina Bran¹, Matthias Hudl², Matts Björck¹, Vassilios Kapaklis¹ and Gabriella Andersson^{1*}
¹ *Department of Physics and Astronomy, Uppsala University, Sweden*
² *Department of Engineering Sciences, Uppsala University, Sweden*

Following recent theoretical predictions on perpendicular uniaxial magnetocrystalline anisotropy in multilayers of 5 monolayers of Fe and 2 monolayers of (W,Re) with tetragonally strained components [1], we have investigated the magnetization and detailed atomic structure in a series of samples with 20-80 at% W. Experimental techniques used were SQUID magnetometry, Magneto-Optic Kerr Effect, Energy Dispersive X-ray Spectroscopy, and X-ray Diffraction including reciprocal space mapping around (002) and (103) body-centered-tetragonal Bragg peaks to measure in-plane atomic distances. Although all the samples exhibit considerably smaller strain in the (W,Re) alloy layers than the previously modelled multilayers, and consequently in-plane easy magnetization axes, we do observe an enhancement of the saturation magnetization that corresponds well to the predicted hybridization-induced moments on individual Fe and (W,Re) atomic layers.

[1] S. Bhandary et al., *Phys. Rev. B* 84, 092401 (2011)

EI04

Alloying as a possible mechanism in annealing induced perpendicular magnetic anisotropy in alumina/Co/M (where M= Pd,Pt or Au) trilayers

Patrick Warin, Alain Marty, Ariel Brenac, Lucien Notin, Stephanie Pouget, Celine Vergnaud, Cyrille Beigne and Matthieu Jamet*
INAC, Commissariat a l'Energie Atomique et aux Energies Alternatives, France

Since the work of Garcia[1], perpendicular magnetic anisotropy (PMA) in ferromagnetic/non-magnetic trilayers or multilayers has attracted much attention. Spin-orbit interaction is the main cause for PMA. Recently it has been shown that in MgO/CoFeB/Ta₂ and Oxide/Co/Pt_x, PMA can be induced by annealing. In particular, it has been argued in [4] that the origin of this PMA is the hybridization between Co and O orbitals enhanced by annealing. We demonstrate in this work that another explanation is alloying between cobalt and the capping layer. We have grown and annealed at different temperatures trilayers of alumina(3nm)/Co(tm)/M(3nm) where t varies from 1 to 2 nm and M= Pd, Pt and Au. For Ta=300°C, PMA is observed in Co/Pd and Co/Pt for t<1.6 nm and 1.4 nm respectively. However no PMA is observed for any thickness in Co/Au. At Ta= 400 °C Co/Pd and Co/Pt show PMA for all thicknesses whereas for Co/Au no PMA is observed. It seems that the influence of Co-O bonds is not enough to drive the magnetization out-of-plane in Co/Au. We propose that the observed effect is due to alloying between Co and Pt or Pd, as Co and Au are immiscible no effect is observed in Co/Au.

[1] Garcia et al, *Appl. Phys. Lett.* 47, 178 (1985). [2] Ikeda et al, *Nature Mater.* 9, 721 (2010). [3] Nistor et al, *Appl. Phys. Lett.* 94, 012512 (2009). [4] Rodmacq et al, *Phys. Rev. B* 79, 024423 (2009)

EI05

High perpendicular magnetic anisotropy at Co_xNi_{1-x} (x = 0.0~1.0)/α-Cr₂O₃ interface

Yu Shiratsuchi*, Hiroto Oikawa, Shin-ichi Kawahara and Ryoichi Nakatani
Osaka University, Japan

α-Cr₂O₃(0001) surface offers a high perpendicular exchange bias when it is attached to a ferromagnetic layer [1] because the topmost Cr spins on the α-Cr₂O₃(0001) surface are fully uncompensated and align normal to the surface. In particular to the perpendicular exchange bias, the perpendicular magnetic anisotropy (PMA) at a ferromagnetic(FM)/antiferromagnetic(AFM) interface is essential, which has not been reported. In this work, we have investigated the interface magnetic anisotropy of the Co_xNi_{1-x}(111)/α-Cr₂O₃(0001) interface with the Co composition x = 0-100 at %. From the structural characterizations, we confirmed that the fabricated samples were in the epitaxial manner, i.e. Pt(111) || Co_xNi_{1-x}(111) || α-Cr₂O₃(0001) || Pt(111) || α-Al₂O₃(0001)-sub. We precisely determined the PMA at the Co(111)/α-Cr₂O₃(0001) interface through the change in the PMA energy with the number of stacking-period of Pt/[Co/Pt]n/α-Cr₂O₃/Pt epitaxial superlattices. The PMA energy increases with increasing the number of stacking-period, which indicates that the strong PMA is generated at the Co(111)/α-Cr₂O₃(0001) interface and that the PMA energy of the Co(111)/α-Cr₂O₃(0001) interface is comparable to that of the Co/Pt interface. For the Pt/Co_xNi_{1-x}(111)/α-Cr₂O₃(0001)/Pt films, the PMA energy monotonically decreases with increasing Ni composition. The change in the PMA with the Ni composition is similar to that of Pt/Co_xNi_{1-x}/Pt multilayer [2].

[1] Y. Shiratsuchi, T. Fujita, H. Oikawa, H. Noutom and R. Nakatani, *Appl. Phys. Exp.*, Vol. 3, pp. 113001 (3pp) (2010). [2] R. Krishnan and H. Lassri, *J. Magn. Magn. Mater.*, Vol. 133, pp. 453-456 (1994).

EI06

Controlling domain wall motion by electric fields in perpendicularly magnetized materials

Adrianus Schellekens*, Arno Van Den Brink, Jeroen Franken, Henk Swagten and Bert Koopmans
Applied Physics, Eindhoven University of Technology, Netherlands

Magnetic domain walls (DWs) are excellent candidates to store and transport information in future memory devices [1]. Up until now, control of DWs has only been possible through the application of a magnetic field or current. Here, we demonstrate a novel approach to control DW motion, namely by altering the magnetic properties with an electric field [2]. Pt/Co/AIO_x wires exhibiting perpendicular magnetic anisotropy (PMA) are fabricated to investigate the influence of the electric field on DW propagation. By applying a voltage over the insulating AlO_x barrier charges are induced at the Co/AIO_x interface, locally changing the magnetic properties. Depending on the sign of the voltage, it is observed that DW velocities can be increased or decreased up to an order of magnitude. By analyzing the experimental results with the DW creep law, we were able to attribute the voltage-induced changes in DW motion to the sensitivity of PMA to an electric field. Comparing the obtained changes in PMA to values in the literature [2], we estimate that controlling DW motion over five orders of magnitude should be well within experimental reach.

[1] S. Parkin, *Science* 320, 190 (2008). [2] T. Maruyama, *Nature Nanotechnology* 4, 158 (2009).

EJ01

Evaluation of interlayer exchange coupling in α-Fe(100)/Nd₂Fe₄B(001) Films

Daisuke Ogawa¹, Kunihiro Koike¹, Shigemi Mizukami², Takamichi Miyazaki³, Mikihiko Oogane³, Yasuo Ando³ and Hiroaki Kato³
¹ *Graduate School of Science and Engineering, Yamagata University, Japan*
² *WPI-AIMR, Tohoku University, Japan*
³ *Graduate School of Engineering, Tohoku University, Japan*

Exchange-coupled hard/soft nanocomposite magnets have a potential to exhibit a large maximum energy product[1]. Recently, a new issue has been proposed by the first-principle calculations[2] for the α-Fe/Nd₂Fe₄B system, which suggest that a magnitude of the hard/soft exchange-coupling depends strongly on the Miller indices of the crystallographic planes at the interface between the two phases, and that even antiparallel coupling would be stabilized in particular combination of planes. Recently, we fabricated the α-Fe(100)/Nd₂Fe₄B(001) bilayer on the MgO(100) substrate by using UHV magnetron sputtering system. Q-band FMR measurements revealed the positive interlayer coupling in this sample [3]. In this work, similar films with different values of the α-Fe layer thickness t_{Fe} were fabricated in order to evaluate the exchange-coupling constant more precisely. With increasing t_{Fe}, the shift in the α-Fe resonance field decreased, as compared with the resonance field for the α-Fe single layer film. These FMR spectra and the magnetization curves are found to be in consistent with the simulation assuming the positive exchange coupling in the α-Fe(100)/Nd₂Fe₄B(001) interfaces.

[1] R. Skomski and J. M. D. Coey, *Phys. Rev. B*48 (1993) 15812. [2] Y. Toga, H. Tsuchiura and A. Sakuma, *J. Phys. Conf. Ser.* 266, 012046 (2011). [3] D. Ogawa, K. Koike, S. Mizukami, M. Oogane, Y. Ando, T. Miyazaki, H. Kato, *J. Magn. Soc. Jpn.*, 36, 5 (2012).

EJ02

Morphology and magnetic properties of S_nCo₃/Fe and Sm₂Co₇/FeCo nanocomposite magnets prepared via severe plastic deformation

Narayan Poudyal, Nguyen Van Vuong, Ying Zhang and J. Ping Liu*
Department of Physics, University of Texas at Arlington, USA

SmCo₅ and Sm₂Co₁₇ compounds have been widely applied as the first and the second generations of rare-earth permanent magnets respectively. There are other Sm-Co intermetallic phases with lower Co concentration that have been ignored as permanent magnetic materials for their relatively low magnetization and anisotropy. Those phases, including SmCo₃ and Sm₂Co₇, have been systematically investigated in our recent research as the hard-phase component in hard/soft nanocomposite systems. It has been found that the nanocomposites magnets having SmCo₃ and Sm₂Co₇ as the hard phases have excellent properties. The composites can incorporate more soft phase compared to SmCo₅ and Sm₂Co₁₇. Here, we report SmCo₃/Fe and Sm₂Co₇/FeCo nanocomposites prepared by high energy ball-milling and subsequent heat treatments. The evolution of morphology and magnetic properties with ball milling time and the soft phase content has been studied. The α-Fe phase distributed in the matrix of hard magnetic Sm-Co phases has grain size less than 20 nm after the severe plastic deformation. Enhanced remanence and maximum energy product up to 13.5 and 17.6 MGOe in the nanocomposites with 25 and 40 % of the soft phase are obtained for SmCo₃ and Sm₂Co₇ respectively, which is up to 300 % higher than that of single-phase counterparts.

EJ03

Atomic scale investigation of Sm-Co/Fe nanocomposites: Influence of Fe/Co interdiffusion on the magnetic properties

Jean-marie Le Breton^{1*}, Rodrigue Larde¹, Adeline Maitre¹, Denis Ledue¹, Olivier Isnard², Ionel Chicanas³, Viorel Pop⁴ and Dominique Givord²
¹ *Groupe de Physique des Materiaux - UMR 6634, CNRS - Universite de Rouen, France*
² *Institut Neel, CNRS - Universite Joseph Fourier Grenoble, France*
³ *Materials Science and Technology Department, Technical University Cluj-Napoca, Romania*
⁴ *Faculty of Physics, Babes-Bolyai University Romania, Romania*

The nanostructure of SmCo₂/Fe nanocomposites elaborated by high energy ball milling was investigated using atom probe tomography. This high resolution technique allowed obtaining in the real space a three dimensional mapping of the chemical species (Sm, Co and Fe) at the atomic scale [1]. 3D reconstructions of the nanostructure of the analysed samples were realised from the data and show that the majority of the SmCo₂/Fe nanocomposite is composed of Fe(Co) soft magnetic nano-sized crystallites embedded in a Sm-(Co,Fe) hard magnetic matrix. These results confirm the formation of the Fe(Co) phase and the contamination of the initial SmCo₂ by Fe atoms. The interfaces between the Fe(Co) soft magnetic phase and the Sm-(Co,Fe) hard magnetic phase were also chemically analysed at the atomic scale. Large graded interfaces were evidenced. These observations were correlated with Monte Carlo simulations and confirm the benefit of the Fe/Co interdiffusion on the magnetic exchange coupling.

[1] J.M. Le Breton, R. Larde, H. Chiron, V. Pop, D. Givord, O. Isnard, I. Chicanas, *Journal of Physics D: Applied Physics*, 43 (2010) 083001

EJ04

Effect of particle size on the coercivity of Nd-Fe-B and Sm-Co nanoparticles prepared by surfactant-assisted ball milling

Nilay Gunduz Akdogan^{1*}, Wanfeng Li¹, Dimitrios Niarchos² and George Hadjipanayis¹
¹ *Physics and Astronomy, University of Delaware, USA*
² *Institute of Material Science, N. C. S. R., Greece*

Anisotropic Nd₂Fe₁₄B and SmCo₅ nanoparticles have been produced by surfactant-assisted high-energy ball milling (HEBM) of nanocrystalline precursor alloys. A two-stage HEBM was performed to obtain the nanoparticles; first the coarse powders were made nanocrystalline by milling, and then were subjected to surfactant-assisted milling for different time. Nanoparticles with different shape (irregular, square and spherical shapes) and size have been obtained by varying the grain size of nanocrystalline precursors. The size of the nanoparticles is found to depend strongly on the grain size of nanocrystalline precursors. For a surfactant-free wet milling of 0.5 to 4 hr, anisotropic Nd₂Fe₁₄B and SmCo₅ nanoparticles have been found with a size from 25 to 2.8 nm. The nanoparticles had coercivity values at 50 K of 9 kOe for the 15 nm Nd₂Fe₁₄B and 15 kOe for the 25 nm SmCo₅. The room temperature coercivities were lower with the values of 2.5 and 5 kOe, respectively. The coercivity was found to decrease with the particle size suggesting a decrease in the overall anisotropy because of surface effects. In the Nd₂Fe₁₄B nanoparticles, a lower spin reorientation temperature was observed (117 K) as compared to bulk (135 K).

Work supported by NSF DMR-1005871 and Marie Curie.

FA01

Dynamical generation of spin currents

Eiji Saitoh
Institute for Materials Research, Tohoku University, ASRC, Japan Atomic Energy Agency, Japan

Spin current, a flow of electrons' spins in a solid, is the key concept in spintronics that will allow the achievement of efficient magnetic memories, computing devices, and energy converters. I here review phenomena which allow us to use spin currents in insulators [1]: inverse spin-Hall effect [2,4], spin pumping, and spin Seebeck effect [4-6]. We found that spin pumping and spin torque effects appear at an interface between an insulator YIG and Pt. Using this effect, we can connect a spin current carried by conduction electrons and a spin-wave spin current flowing in insulators. We demonstrate electric signal transmission by using these effects and interconversion of the spin currents [1]. Seebeck effect (SSE) is the thermal spin pumping [5]. The SSE allows us to generate spin voltage, potential for driving nonequilibrium spin currents, by placing a ferromagnet in a temperature gradient. Using the inverse spin-Hall effect in Pt films, we measured the spin voltage generated from a temperature gradient in various ferromagnetic insulators. This research is collaboration with K. Ando, K. Uchida, Y. Kajiwara, S. Maekawa, G. E. W. Bauer, S. Takahashi, and J. Ieda.

References 1. Y. Kajiwara & E. Saitoh et al. *Nature* 464 (2010) 262. 2 E. Saitoh et al., *Appl. Phys. Lett.* 88 (2006) 182509. 3 A. Ando & E. Saitoh et al., *Nature materials* 10 (2011) 655 -659. 4 K. Uchida & E. Saitoh et al., *Nature* 455 (2008)/778. 5 K. Uchida & E. Saitoh et al., *Nature materials* 9 (2010) 894 - 897. 6 K. Uchida & E. Saitoh et al., *Nature materials* 10 (2011) 737-741.

FA02

Domain wall motion by the magnonic spin Seebeck effect

Ulrike Ritzmann, Denise Hinzke and Ulrich Nowak
Department of Physics, University of Konstanz, Germany

In the last years it was demonstrated that in ferromagnetic materials spatial temperature gradients can lead to spin accumulation [1], even in magnetic insulators [2]. In this context, it is important to note that in addition to a spin polarized charge current also a chargeless angular momentum current driven by spin waves can exist. Here, we propose the existence of domain wall (DW) dynamics driven by magnonic spin currents due to temperature gradients. To get some insight into this effect we introduce two different approaches: the stochastic Landau-Lifshitz-Gilbert equation, applied to spin models, and the Landau-Lifshitz-Bloch equation describing the dynamics of the thermally averaged spin polarization on micromagnetic length scales. We show that these approaches describe this new type of DW motion, where chargeless spin currents following from a temperature gradient drag a DW into the hotter region [3]. Furthermore, for a better understanding of the relevant length scales, we investigate the propagation and frequency range of thermally induced magnons. We acknowledge financial support by the Deutsche Forschungsgemeinschaft through Schwerpunktprogramm SpinCaT.

[1] K. Uchida et al., *Nature* 455, 778 (2008). [2] K. Uchida et al., *Nat. Mater.* 9, 894(2010). [3] D. Hinzke and U. Nowak, *Phys. Rev. Lett.* 107, 027205(2011)

FA03

Phonon-drag spin Seebeck effect

Hiroto Adachi¹, Jun-ichiro Ohe², Saburo Takahashi³ and Sadamichi Maekawa¹
¹ *Japan Atomic Energy Agency, Japan*
² *Toho University, Japan*
³ *Tohoku University, Japan*

Spin Seebeck effect refers to a thermal spin injection from a ferromagnet into an attached nonmagnetic metal that occurs over macroscopic scale of several millimeters [Uchida et al., *Nature* 455, 778 (2008)]. The spin Seebeck effect is now established as a universal aspect of ferromagnets since it is observed in a variety of materials ranging from a metallic ferromagnet (NiFe) and semiconducting ferromagnet (GaMnAs) to an insulating magnet (YIG). Recent theoretical and experimental efforts have clarified that the phonon degrees of freedom are of crucial importance in this intriguing phenomenon. Here we theoretically discuss the phonon-drag contribution to the spin Seebeck effect [Adachi et al., *Appl. Phys. Lett.* 97, 252506 (2010)]. The spin Seebeck effect is driven by nonequilibrium phonons that drag the low-lying spin excitations. This scenario explains simultaneously the local nature of the spin Seebeck effect [Jaworski et al., *Nature Materials* 9, 898 (2010); Uchida et al., *Nature Materials* 10, 737 (2011)] and the signal enhancement at low temperatures [Jaworski et al., *Phys. Rev. Lett.* 106, 186601 (2011)].

FA04

Entanglement of spin Seebeck effect and anomalous Nernst effect

Chia-ling Chien
Department of Physics and Astronomy, The Johns Hopkins University, Baltimore MD 21218, USA

Spin Seebeck effect (SSE) is a spin caloritronic effect that generates a pure spin current. The studies of SSE have often been made on a patterned Pt strip on a ferromagnetic (FM) thin metallic film on substrate, where the in-plane temperature gradient ($\nabla_x T$) generates in the FM film a spin current, which is detected by the inverse spin Hall effect as a voltage in the Pt strip. However, there is also the propensity of an out-of-plane temperature gradient ($\nabla_z T$), which gives rise to the anomalous Nernst effect (ANE) due to the larger thermal conduction through the substrate. While SSE with $\nabla_x T$ and ANE with $\nabla_z T$ are two different effects, they can be simultaneously present. More importantly, the voltages of the two effects are additive with the same field dependence and symmetry, and therefore cannot be easily separated. In such cases, the establishment of the SSE is contingent upon the ANE measurements before the Pt strip is in place.

Work supported by the US NSF DMR 05-20491 and Taiwan NSC 99-2911-I-007-510. 1 S. Y. Huang, W. G. Wang, S. F. Lee, R. Kwo, and C. L. Chien, Phys. Rev. Lett., 107, 216604 (2011).

FB01

Textured superconductivity in the heavy fermion CeRhIn5

Xin Lu¹, Tuson Park², Han-oh Lee¹, I. Martin¹, V. A. Sidorov², K. Gofryk¹, F. Ronning¹, E. D. Bauer¹ and J. D. Thompson¹
¹ *Los Alamos National Lab, USA*
² *Department of Physics, Sungkyunkwan University, Korea*
³ *Vereshchagin Institute of High Pressure Physics, RAS, 142190 Troitsk, Russia*

In the coexistence region of antiferromagnetism (AFM) and superconductivity (SC) of CeRhIn₅, the superconducting transition temperatures determined resistively and thermodynamically display a significant difference while the difference disappears at higher pressures where AFM is suppressed and only SC exists. In the coexisting state of AFM and SC, anisotropic transport near the SC transition reveals the emergence of textured SC planes that appear without a change in translational symmetry of the lattice. Similar behaviors have also been observed in other strongly correlated electron systems where there are coexisting and competing orders with SC.

Tuson Park et al. Phys. Rev. Lett. in press.

FB02

Exotic superconductivity of heavy electrons in artificial two-dimensional Kondo lattices

Takasada Shibauchi
Department of Physics, Kyoto University, Japan

When interacting electrons are confined to low-dimensions, the electron-electron correlation effect is enhanced dramatically, which often drives the system into exhibiting behaviours that are otherwise highly improbable. Superconductivity with the strongest electron correlations is achieved in heavy-fermion compounds, which contain a dense lattice of localized magnetic moments interacting with a sea of conduction electrons to form a three-dimensional (3D) Kondo lattice. It had remained an unanswered question whether superconductivity would persist upon effectively reducing the dimensionality of these materials from three to two. We report on the observation of superconductivity in such an ultimately strongly-correlated system of heavy electrons confined within a 2D square-lattice of Ce-atoms (2D Kondo lattice), which was realized by fabricating epitaxial superlattices[1] built of alternating layers of heavy-fermion CeCoIn₃ and conventional metal YbCoIn₃ [2]. The field-temperature phase diagram of the superlattices exhibits highly unusual behaviours, including a striking enhancement of the upper critical field relative to the transition temperature. Possible origins of this enhancement will be discussed, including extremely strong coupled nature as a result of two-dimensionalization[2], formation of FFLO state, and local spatial inversion symmetry breaking [3].

[1] H. Shishido, T. Shibauchi, K. Yasu, T. Kato, H. Kontani, T. Terashima, and Y. Matsuda, *Science* 327, 980-983 (2010). [2] Y. Mizukami, H. Shishido, T. Shibauchi, M. Shimozawa, T. Yasumoto, M. Yamashita, H. Ikeda, T. Terashima, H. Kontani, and Y. Matsuda, *Nature Physics* 7, 849-853 (2011). [3] D. Maruyama, M. Sigrist, and Y. Yanase, *arXiv:1111.4293*.

FB03

Evolution of quasiparticle entropy in high-field superconducting phase in CeCoIn₅

Yoshi Tokiwa¹, Philipp Gegenwart¹ and Eric D Bauer²
¹ *I. Physikalisches Institut, Georg-August-Universitaet Goettingen, 37077 Goettingen, Germany*
² *Los Alamos National Laboratory, Los Alamos, New Mexico 87545, USA*

Unambiguous detection of Fulde and Ferrell and Larkin and Ovchinnikov (FFLO) superconducting (SC) phase in solid state systems is still a challenge in the community of strongly correlated electron systems (SCES). A heavy fermion superconductor, CeCoIn₅, is one of the best candidates for the formation of FFLO state. Existence of FFLO phase in this material has been extensively discussed in the past decade and is still one of the most debated current topics in the field of SCES[1]. Entropy as a function of field can capture the characteristic nature of FFLO state, namely the additional increase of quasi-particles, leading to a steep increase of entropy at the transition field from uniform to FFLO SC state. We have obtained the entropy, derived from combined specific heat and magnetocaloric effect measurements at temperatures T_g ≈ 1005-mK and fields H_l ≈ 125-T aligned parallel, perpendicular and S₁₈₀ off the tetragonal [100] direction. In any direction, we do not observe an additional quasiparticle entropy expected in a FFLO SC state. By contrast, for H_l parallel [100] a negative entropy contribution, compatible with spin-density-wave (SDW) ordering, is found. Our data exclude the formation of a FFLO state in CeCoIn₅ for out-of-plane field directions, where no SDW order exists.

[1] Y. Matsuda and H. Shimahara, *J. Phys. Soc. Jpn.*, 76, 051005 (2007)

FB04

Electronic structure of ferromagnetic heavy fermion YbNi₄P₂

Sven Friedemann^{1*}, Sweeney K Goh¹, Lina Klintberg¹, F Malte Grosche¹, Cornelius Krellner², Christoph Geibel², Frank Steglich² and Helge Roßner²
¹ *Cavendish Laboratory, University of Cambridge, United Kingdom*
² *Max Planck Institute for Chemical Physics of Solids, Dresden, Germany*

Quantum critical phenomena can be studied in great detail in lanthanide based heavy-fermion systems. Up to now, however, only materials with antiferromagnetic ground state were found among the 4f based heavy fermions. In the new heavy fermion material YbNi₄P₂, a clear ferromagnetic transition is observed at TC = 0.17 K. YbNi₄P₂ has the prospect to study ferromagnetic quantum criticality accessible by either composition tuning or transverse-field tuning. Above the transition temperature in YbNi₄P₂ strong evidence is found for its vicinity to a quantum critical point, the specific heat diverges in a power-law form and the resistivity follows a linear temperature dependence. We present first Shubnikov-de Haas measurements in combination with electronic band structure calculations. The electronic structure is dominated by parallel disconnected sheets in accordance with the crystal structure featuring quasi-one-dimensional chains of Yb. The observed Shubnikov-de Haas oscillations are assigned to quasi-two-dimensional features of the Fermi surface. The experimentally observed mass enhancement of these orbits reflects the heavy-fermion character of YbNi₄P₂.

FC01

Models of spin dynamics; ultrafast heat pulses as a sufficient stimulus for reversal in a ferrimagnet

Roy W Chantrell¹, J Barker¹, Rfl Evans¹, U Atxitia², O Chubykalo-fesenko² and Rw Chantrell¹
¹ *Physics, University of York, United Kingdom*
² *ICMM, Spain*

The response of magnetic materials to the heating effect of ultrafast laser pulses is a challenging problem which is giving important insight into spin dynamics at elevated temperatures and sub-picosecond timescales. We have developed a model of ultrafast spin dynamics using an atomistic model based on the Heisenberg exchange Hamiltonian and using the Landau-Lifshitz-Gilbert equation with Langevin dynamics to calculate the evolution of the magnetisation following a laser pulse. Here we describe studies of the properties of amorphous ferromagnetic Rare Earth (RE) Transition Metal (TM) alloys, which are shown to exhibit interesting and unexpected properties. Firstly, the model demonstrates differential sublattice dynamics, specifically a different rate of demagnetisation for the RE and TM sub-lattices, even though these are coupled by a strong exchange interaction. Even more surprising is the existence of a transient ferromagnetic state, stable for around 300fs. It is shown theoretically that this leads to magnetisation reversal, in the absence of a magnetic field, driven by a heat pulse alone. The underlying physics of this effect and its confirmation in recent experiments [1] will be discussed.

[1] T Ostler et al., *Nat. Commun.*, 3:666 doi: 10.1038/ncomms1666 (2012)

FC02

Coherent spin-photon interaction and ultrafast magnetism: From principles to applications

Jean-Yves Bigot, Ji-Wan Kim, Mircea Vomir, and Marie Barthelemy
IPCMS, CNRS, Universite de Strasbourg, France

How fast can one manipulate the magnetization of materials using ultrashort optical pulses? This question is at the heart of several fundamental and applied researches with the prospective of making ultrafast magnetic devices. An important related topic is the coherent time dependent interaction between spins and photons. In the present talk we review the state of the art understandings in that field, describing the spin dynamics from first principles and showing some applications. First, we show that the spin-orbit interaction is a crucial concept when manipulating the spins with a laser field. Second, we distinguish between different mechanisms resulting from the time ordering between a sequence of pump and probe pulses when performing a time resolved magneto-optical experiment. In particular we distinguish between the coherent and population components associated to the spins dynamics. Third, we demonstrate the validity of these theoretical concepts by considering the time dependent magneto-optical response of garnets or transition metals (Ni, CoPt) excited by femtosecond laser pulses. In the case of ferrimagnetic Bi-doped garnets the coherent contribution is most important, leading to the generation of efficient magneto-optical four-wave mixing signals. In the case of ferromagnetic transition metals, the population dynamics dominates with a weaker coherent response.

FC03

Ultrafast switching of ferrimagnets

Sonke Wienhold¹, Denise Hinzke¹, Peter Openeer² and Uli Nowak¹

¹ Department of Physics, University of Konstanz, Germany

² Department of Physics, Uppsala University, Sweden

The ultrafast manipulation of magnetisation by fs laser pulses promises to become a real alternative to conventional techniques based on magnetic fields. It was demonstrated that a 80 fs, circularly polarised laser pulse is able to reverse magnetisation on a ps time scale, as if it acts as a short magnetic field pulse caused by the inverse Faraday effect [1]. In single-shot time-resolved imaging of magnetic structures [2] it has been shown that the magnetisation reverses via a linear pathway [3] without any precession. Even with linearly polarized light switching was demonstrated recently [4], probably on a purely thermal basis. These new types of switching have been demonstrated only in ferrimagnetic materials like GdFeCo, probably because of the antiferromagnetic coupling of the two different sub-lattices in these materials, leading to completely different dynamics as compared to a ferromagnet. To understand this new type of dynamics we perform atomistic spin model simulations of ferrimagnets and investigate their switching mechanisms in detail. Funded by the EU project FemtoSpin and the CAP in Konstanz.

[1] C. D. Stanciu et al., *Phys. Rev. Lett.* **99**, 047601 (2007). [2] K. Vahaplar et al., *Phys. Rev. Lett.* **103**, 117201 (2009) [3] N. Kazantseva et al., *Europhys. Lett.* **86**, 27006 (2009) [4] I. Radu et al., *Nature* **472**, 205 (2011)

FD01

Spin wave mediated magnetic vortex core reversal. Towards a 100 ps V(ortex)MRAM

Hermann Stoll*

MPI for Intelligent Systems (formerly MPI for Metals Research), Germany

The discovery of magnetic vortex core reversal by excitation of the sub-GHz gyromode [1] not only opened a new chapter in vortex dynamics but also enabled the use of the magnetic vortex core polarization p as memory bit for spintronic applications. Suggestions for V(ortex)MRAMs published so far [2-6] are based on the excitation of the vortex gyromode at sub-GHz frequencies and allow switching times of a few ns. Last year we have demonstrated [7] that much faster vortex core reversal can be achieved by exciting azimuthal spin wave modes with external alternating magnetic fields at multi-GHz frequencies. Depending on the sample geometry, lower limits exist [8] for the time needed for spin wave mediated vortex core reversal, which cannot be overcome by shortening the excitation length or by increasing the excitation amplitude. These limits are explained by a finite time needed for the energy transfer of the global excitation towards the center of the sample [8]. In the present talk it will be demonstrated by experiments [9] and micromagnetic simulations, how both, the duration of excitation and the time needed for unidirectional vortex core reversal can be reduced to well below 100 ps, allowing a fast writing of V(ortex)MRAMs.

[1] B. Van Waeyenberge et al., *Nature* **444**, 461 (2006), [2] S. Kim et al., *Appl. Phys. Lett.* **92**, 022509 (2008), [3] S. Bohlens et al., *Appl. Phys. Lett.* **93**, 142508 (2008), [4] B. Pigeau et al., *Appl. Phys. Lett.* **96**, 132506 (2010), [5] Y-S. Yu et al., *Appl. Phys. Lett.* **98**, 052507 (2011), [6] K. Nakano et al., *Appl. Phys. Lett.* **99**, 262505 (2011), [7] M. Kammerer et al., *Nature Communications* **2**, 279 (2011), [8] M. Kammerer et al., <http://arxiv.org/abs/1112.1903>, [9] Performed by scanning transmission X-ray microscopy (STXM) at the MAXYMUS endstation at BESSY II, Berlin, Germany.

FD02

Magnetic vortices and antivortices - From time-resolved imaging to the influence of temperature

Thomas Kamionka, Michael Martens, Andre Drews, Benjamin Krueger, Ole Albrecht and Guido Meier*

University of Hamburg, Germany

Subnanosecond dynamics and potential memory applications give rise to a broad scientific interest in properties of ferromagnetic microstructures with vortex and antivortex magnetization configuration. Such singularities can be excited to gyrate resonantly at a characteristic eigenfrequency. Dynamics are studied by time-resolved scanning transmission X-ray microscopy and broadband-ferromagnetic resonance measurements. The influence of temperature on the gyrotropic eigenfrequency of vortices in micrometer-sized permalloy squares is studied [1]. Ferromagnetic absorption measurements around room temperature show that the eigenfrequency is decreased by 5.4% when the temperature is increased by 100 °C. The lowering of the saturation magnetization and the associated modification of the potential of gyration is discussed as a reason for the frequency shift within the model of the harmonic oscillator. Micromagnetic simulations confirm a linear relation between the eigenfrequency and the saturation magnetization. Absorption measurements under application of static external magnetic fields yield the same percentage frequency shift as without external field when gyrations around equally displaced equilibrium positions are compared. Financial support by the DAAD via the Project 50725506 and by DFG via the SFB 668 and the GrK 1286 as well as the Forschungs- und Wissenschaftsstiftung Hamburg via the Exzellenzcluster “Nano-Spintronik” is gratefully acknowledged.

[1] T. Kamionka, M. Martens, A. Drews, B. Krueger, O. Albrecht, and G. Meier, *Phys. Rev. B* **83**, 224424 (2011).

FD03

Oersted field contribution on the magnetic vortex core dynamics probed by homodyne detection

June Seo Kim¹, Martin Staerk², Jungbum Yoon³, Chun Yeol You³, Florian Kronast⁴, Christian Ulysse⁵, Giancarlo Faini⁵ and Mathias Kläui^{1*}

¹ Institut fuer Physik, Johannes Gutenberg-Universitaet Mainz, Germany

² Fachbereich Physik, Universitaet Konstanz, Germany

³ Department of Physics, Inha University, Korea

⁴ Helmholtz-Zentrum Berlin fuer Materialien und Energie GmbH, Germany

⁵ Phynano Team, Laboratoire de Photonique et de Nanostructures, CNRS, France

The recent discovery that a spin-polarized current can induce magnetic vortex dynamics opened a new way to manipulate magnetization. Here, we report on the resonant excitation of a magnetic vortex core in a permalloy disc due to the injection of the high frequency current. The Oersted field contribution due to the inhomogeneous current distribution in the magnetic vortex core dynamics on a magnetic circular disc is experimentally investigated using a homodyne detection scheme. The homodyne technique allows us to obtain the resonance frequency, the amplitude of the vortex core gyration, and the phase shift between the microwave current and the magnetoresistance oscillation. By the vortex core position dependent measurements, the amplitude of the vortex core gyration obviously increases due to the enhancement of the Oersted field contribution. From systematic phase measurements as a function of microwave frequency, two phenomena are observed: (i) the trajectory of the vortex core gyration is distorted by the bounding effect due to the strong shape anisotropy close to the edge and (ii) the Oersted field contribution is dominant driving the vortex core close to the edge.

FD04

Vortex core switching driven by the novel inverse Faraday effect

Katsuhisa Taguchi^{1*}, Jun-ichiro Ohe² and Gen Tatara¹

¹ Physics, Tokyo Metropolitan University, Japan

² Physics, Toho University, Japan

Many researchers have investigated the mechanisms of the ultrafast vortex core switching by electric current experimentally and theoretically [1]. In this presentation, we theoretically predict a novel mechanism of the core switching by an optical means. We show that for vortex structures, an unconventional inverse Faraday effect [2] without the spin-orbit interaction induces strong magnetic field when a circularly polarized light is applied and is useful for fast core reversal. The magnetic dynamics of the vortex core is calculated with the help of the simulation in the framework of the Landau-Lifshitz-equation, and the switching time is obtained to be 0.2 ns. This switching time is two orders shorter than one for the electrical switching, 20ns [1]. This ultrafast optical core switching is realized in the following process: first the orbital angular momentum of the circularly polarized light is converted to the electron’s orbital angular momentum, and then the spin chirality, which is a solid angle of the vortex spin structure, converts it to the spin angular momentum.

[1] K. Yamada, S. Kasai, Y. Nakatani, K. Kobayashi, and T. Ono, *Nature Mater.* **6**, 270 (2007). [2] A. Kirilyuk, A. V. Kimel, and Th. Rasing, *Rev. Mod. Phys.* **82**, 2731 (2010).

FE01

Ab initio studies of strongly correlated electron systems

Masatoshi Imada

Department of Applied Physics, University of Tokyo, Japan

Recent trends of ab initio studies and progress in methodologies for electronic structure calculations of strongly correlated electron systems are discussed. The interest for developing efficient methods is motivated by recent discoveries and characterizations of strongly correlated electron materials and by requirements for understanding mechanisms of intriguing phenomena beyond a single-particle picture. A multi-scale ab initio scheme for correlated electrons (MACE) is developed by utilizing the hierarchical electronic structure in the energy space[1]. It provides us with a first-principles downfolding of the global band structure into low-energy effective models followed by accurate low-energy solvers for the models. The applications of MACE is illustrated with examples of several materials. In particular, we focus on electron correlations in iron-based superconductors[2], interplay of spin-orbit interaction in 5d systems such as Sr₂IrO₄[3], and Mott physics in organic conductors [4].

[1] M. Imada and T. Miyake, *J. Phys. Soc. Jpn.* **79** (2010) 112001. [2] T. Misawa, K. Nakamura and M. Imada, *arXiv:1112.4682*. [3] R. Arita, J. Kunes, A.V. Kozhevnikov, A.G. Eguiluz, and M. Imada, *arXiv:1107.0835*. [4] H. Shinaoka, T. Misawa, K. Nakamura, and M. Imada, *arXiv:1110.6299*.

FE02

Coarse graining tensor renormalization by the higher-order singular value decomposition

Tao Xiang

Institute of Theoretical Physics/Institute of Physics, Chinese Academy of Sciences, China

We propose a novel coarse graining tensor renormalization group method based on the higher-order singular value decomposition (HOSVD). This method provides an accurate but low computational cost technique for studying two- or three-dimensional (3D) lattice models. The method is demonstrated using the Ising model on the square and cubic lattices. By keeping up to 16 bond basis states, we obtain by far the most accurate numerical renormalization group results for the 3D Ising model.

FE03

Monte-carlo approach to stationary non-equilibrium of mesoscopic systems

Thomas Pruschke^{1*} and Andreas Dirks²

¹ Theoretical Physics, Universtat Göttingen, Germany

² Theoretical Physics, University of Göttingen, Germany

Calculating properties of correlated systems out of equilibrium is a challenging task, even if on targets only stationary situations. In particular, transport through nano-objects like molecules or quantum dots is of strong interest, and a theory to calculate transport properties or merely local quantities in a reliable way for reasonably strong correlations very desirable. Based on a suggestion by Han and Heary [1] we use advanced quantum Monte-Carlo techniques to calculate quantities for stationary non-equilibrium of a single-impurity Anderson model with high accuracy [2]. Employing a two-dimensional analytical continuation based on maximum entropy, we are able to calculate different local quantities like current, magnetization or double occupancy. We compare our results to those obtained by different methods like time-dependent numerical renormalization, real-time quantum Monte-Carlo or real-time density-matrix renormalization group.

[1] J.E. Han and R.J. Heary, *Phys. Rev. Lett.* **99**, 236808 (2007). [2] A. Dirks, Ph. Werner, M. Jarrell, and Th. Pruschke, *Phys. Rev. E* **82**, 26701 (2010).

FE04

SU(4) symmetry for strongly correlated electrons: Kondo and mixed-valence effects in terms of gell-mann matrices

Konstantin Kikoin

School of Physics and Astronomy, Tel-Aviv university, Israel

The concept of dynamical symmetries [1] is used for formulation of the renormalization group approach to the Kondo effect in the Anderson model with repulsive and attractive interaction U in the Kondo and mixed valence regimes. It is shown that the generic local symmetry of the Anderson Hamiltonian is determined by the SU(4) Lie group. The Anderson Hamiltonian is rewritten in terms of the Gell-Mann matrices of 4-th rank, which form the set of group generators and the basis for construction of the irreducible vector operators describing the excitation spectra in the charge and spin sectors. The multistage Kondo screening is also interpreted as a manifestation of the local SU(4) dynamical symmetry. It is shown that the similarity between the conventional Kondo cotunneling effect for spin 1/2 in the positive U model and the Kondo resonance for pair tunneling in the negative U model is a direct manifestation of implicit SU(4) symmetry of the Anderson/Kondo model. The transformation from local SU(4) symmetry to the global SO(4) symmetry in the Hubbard chain model is also discussed.

[1] K. Kikoin, M.N. Kiselev, and Y. Avishai, *Dynamical Symmetries for Nanostructures (Springer, Wien, 2012)*.

GA01

Detection of orbital fluctuations above the structural transition temperature in iron pnictides and chalcogenides

L. H. Greene^{1*}, H. Z. Arhan¹, C. R. Hunt¹, W. K. Park¹, J. Gillett², S. D. Das², S. E. Sebastian², Z. J. Xu³, J. S. Wen³, Z. W. Lin³, Q. Li³, G. Gu³, A. Thaler⁴, S. Ran⁴, S. L. Bud'ko⁴, P. C. Canfield⁴, D. Y. Chung⁵, M. G. Kanatzidis⁵, Wei-cheng Lee¹ and P. Phillips¹

¹ Physics, University of Illinois at Urbana-Champaign, USA

² Physics, Cavendish Laboratory, University of Cambridge, United Kingdom

³ Physics, Brookhaven National Laboratory, USA

⁴ Physics and Astronomy, Ames Laboratory and Iowa State University, USA

⁵ Materials Science, Argonne National Laboratory, USA

The electronic structure of AEF₂As₂ (AE=Ca,Sr,Ba) and Fe_{1-x}Te is studied using point contact or quasiparticle scattering spectroscopy (QPS). [1] For AE=Sr,Ba and Fe_{1-x}Te, a conductance enhancement reproducibly appears at T₀, well above the structural transition temperature, T_S. For Ba(Fe_{1-x}Co_x)₂As₂, the conductance enhancement exists only in the underdoped regime. Thus, we add a new region of strong correlations to the phase diagram: For x = 0 to 5.5, T₀ ~ 175 K to ~ 150 K, respectively. These strong correlations arise from orbital fluctuations, and the prediction [2] that the excess conductance above T_S is only observed in detwinned crystals that exhibit resistance anisotropy above T_S [3] has been verified [1]. The role of orbital fluctuations and nematicity in quantum criticality of these materials will be discussed. [4] Supported by the Center for Emergent Superconductivity, an EFRC, US DOE, DE-AC0298CH1088; Cambridge EPSRC, and Ames Lab US DOE, DE-AC02-07CH11358.

1. H. Z. Arham et al, *arXiv:1201.2479*. 2. W.-C. Lee and P. Phillips, *arXiv:1110.5917*. 3. I. R. Fisher et al., *Rep. Prog. Phys.* **74**, 124506 (2011) and references therein. 4. S. Kasahara et al, *Phys. Rev. B* **81**, 184519 (2010); S. Kasahara et al., *Bull. Am. Phys. Soc.* **56**, Z26.00010 (2011); Y. Matsuda, private communication.

GA02

Nature of magnetic excitations in superconducting iron superconductors

Pengcheng Dai

U. of Tennessee/Institute of Physics, CAS, USA

Since the discovery of the metallic antiferromagnetic (AF) ground state near superconductivity in iron-pnictide superconductors, a central question has been whether magnetism in these materials arises from weakly correlated electrons, as in the case of spin-density-wave in pure chromium, requires strong electron correlations, or can even be described in terms of localized electrons such as the AF insulating state of copper oxides. We use inelastic neutron scattering to determine the absolute intensity of the magnetic excitations throughout the Brillouin zone in a number of iron-based superconductors, which allows us to obtain the size of the fluctuating magnetic moment in absolute units. We find that superconducting BaFe₂Ni_{0.11}As₂ and AF BaFe₂As₂ both have fluctuating magnetic moments similar to those found in the AF insulating copper oxides. The common theme in both classes of high temperature superconductors is that magnetic excitations have partly localized character, thus showing the importance of strong correlations for high temperature superconductivity.

GA03

Universal microscopic description of the infrared conductivity of 122 iron arsenides

Aliaksei Charnukha^{1*}, O. V. Dolgov¹, A. A. Golubov², Y. Matiks¹, D. L. Sun¹, C. T. Lin¹, B. Keimer¹ and A. V. Boris¹

¹ Max Planck Institute for Solid-State Research, Germany

² Faculty of Science and Technology and MESA+ Institute of Nanotechnology Enschede, Netherlands

We report the full complex dielectric function of high-purity Ba_{0.68}K_{0.32}Fe₂As₂ single crystals with T_c=38.5K determined by wide-band spectroscopic ellipsometry at temperatures 10<=T<=300K. We discuss the microscopic origin of superconductivity-induced infrared optical anomalies in the framework of a multiband Eliashberg theory with two distinct superconducting gap energies 2Δ_A = 6k_BT_c and 2Δ_B = 2.2k_BT_c. The observed unusual suppression of the optical conductivity in the superconducting state at energies up to 14k_BT_c can be ascribed to spin-fluctuation--assisted in the clean limit of the strong-coupling regime. We further demonstrate that the same model provides a good description of the infrared conductivity of electron-doped compounds in this class of superconductors.

GA04

Various fabricating conditions of potassium doped BaFe₂As₂ films by pulsed laser deposition system

Nam Hoon Lee, Soon-gil Jung and W. N. Kang*
Department of Physics, SungKyunkwan Univ., Korea

Among the various Fe-based superconductors, potassium doped BaFe₂As₂ is favorable for application because of its higher transition temperature and a low anisotropy compared to other iron based superconductors. To study the superconductivity and applicable aspects, high quality thin films should be fabricated. However, it is difficult to fabricate thin films because of the high volatility of potassium. In this paper, we show the details of fabricating technique of Ba_{1-x}K_xFe₂As₂ films by ex-situ PLD method in various conditions and physical properties of these films. Barium ratio in target is controlled to make films with various potassium doping rate. An annealing temperature and amount of potassium are also controlled to find out optimal condition of fabricating films.

GB01

Nonreciprocal directional dichroism and toroidalmagnons in multiferroic materials

Nobuo Furukawa^{1*} and Shin Miyahara²
¹ Department of Physics, Aoyama Gakuin University, Japan
² ERATO-Multiferroics Project, Japan Science and Technology Agency, Japan

We investigate dynamical magnetolectric effect at electromagnon resonances in multiferroic materials. One of the typical phenomena caused by interferences between the magnetic and electric responses is the nonreciprocal directional dichroism (NDD), where differences in the absorption spectra of electromagnetic wave are observed when propagation directions of the incident wave are inverted. We show that NDD is observed at a magnon excitation that is accompanied by a dynamical toroidal moment, i.e., at a toroidalmagnon excitation. As examples, we discuss toroidalmagnons in multiferroic materials RMnO₃ and Ba₂CoGe₂O₇.

S. Miyahara and N. Furukawa, J. Phys. Soc. Jpn. 81 (2012) 023712/1-4. S. Miyahara and N. Furukawa, J. Phys. Soc. Jpn. 80 (2011) 073708/1-4.

GB02

Electronic ferroelectricity in correlated electron systems

Sumio Ishihara*, Makoto Naka and Akihiko Sekine
Department of Physics,, Tohoku University, Japan

Exotic ferroelectrics and multiferroics are one of the attractive topics in recent correlated electron systems. It is widely known that ionic lattice distortions responsible for the electric dipole moments in conventional ferroelectric compounds. Recently new class of ferroelectricity, termed "electronic ferroelectricity" where electronic charge order brings about the electric polarization, has attracted much attention from fundamental and application view points. We study theoretically ferroelectric and multiferroelectric properties of the electronic ferroelectricity in correlated electron systems. We mainly focus on the layered iron oxides, LuFe₂O₆, and the low-dimensional organic salts, kappa-(BEDT-TTF)₂Cu₂(CN)₂. In the iron oxide, we examine the electronic and dielectric properties by analyzing the model Hamiltonian. It is found that a low-lying charge fluctuation due to a geometrical frustration plays a key role on an origin of ferroelectricity. This fluctuation is expected to be detected by the inelastic x-ray scattering experiments. As for the molecular organic salts, we found that the ferroelectric charge order strongly competes with a Mott insulator based on molecular dimerization, termed a dimmer Mott insulating phase, as well as a metallic phase. A collective excitation mode for an electric polarization and superconductivity due to polarization fluctuation are examined near the phase boundaries.

[1] A. Nagano, M. Naka, J. Nasu, & S. Ishihara, Phys. Rev. Lett. 99, 217202 (2007). [2] M. Naka, A. Nagano, & S. Ishihara, Phys. Rev. B 77, 224441 (2008). (Editor's suggestion) [3] J. Nasu, A. Nagano, M. Naka, & S. Ishihara, Phys. Rev. B 78, 024416 (2008). [4] T. Watanabe, & S. Ishihara, J. Phys. Soc. Jpn. 78, 113702 (2009). [5] S. Ishihara J. Phys. Soc. Jpn. 79, 011010 (2010) (Review) [6] M. Naka, & S. Ishihara, J. Phys. Soc. Jpn. 79, 063707 (2010) (Editor's choice). [7] T. Watanabe, & S. Ishihara, J. Phys. Soc. Jpn. 79, 114714 (2010)

GB03

Interplay between electronic ferroelectricity and magnetism in molecular TMTTF salts

Kazuyoshi Yoshimi¹, Hitoshi Seo^{2*}, Shoji Ishibashi³ and Stuart E. Brown⁴
¹ University of Tokyo, and AIST, Japan
² RIKEN and JST-CREST, Japan
³ AIST, Japan
⁴ UCLA, USA

We theoretically investigate the interplay between charge ordering and magnetic states in quasi-one-dimensional molecular conductors TMTTF₂X, motivated by the observation of a complex variation of competing/coexisting phases. We show that the ferroelectric-type charge order (electronic ferroelectricity) increases two-dimensional antiferromagnetic spin correlation, whereas in the one-dimensional regime two different spin-Peierls states are stabilized. By using first-principles band calculations for the estimation for the transfer integrals and comparing our results with the experiments, we identify the controlling parameters in the experimental phase diagram to be not only the inter-chain transfer integrals but also the amplitude of the charge order. We also discuss the effect of a diagonal inter-chain transfer integral, which causes spin frustration in the dimer-Mott insulating state, but conversely enhances the magnetic ordering in the charge ordered phase.

K. Yoshimi, H. Seo, S. Ishibashi, and S. E. Brown, arXiv:1110.3573 (to be published in Phys. Rev. Lett.); arXiv:1110.3575 (to be published in Physica B).

GB04

Dielectric anomaly in dimer-Mott insulator β¹-(BEDT-TTF)₂ICl₂ with square lattice

Satoshi Iguchi¹, Satoru Sasaki¹, Naoki Yoneyama², Hiromi Taniguchi³ and Takahiko Sasaki⁴
¹ IMR, Tohoku Univ., Japan
² Univ. of Yamanashi, JST-CREST, Japan
³ Saitama Univ., Japan
⁴ IMR, Tohoku Univ., JST-CREST, Japan

Organic dimer-Mott insulator κ-(BEDT-TTF)₂Cu₂(CN)₂ with triangular lattice has been extensively investigated as a candidate for spin liquid materials. Moreover, the recent discovery of a relaxor-like dielectric response [1] in this system paved the way to a new phenomenon of purely electronic ferroelectricity as well as the strong charge fluctuation or charge disproportionation on dimers [2, 3]. Here, we have investigated the dielectric property of a typical antiferromagnetic dimer-Mott insulator β¹-(BEDT-TTF)₂ICl₂ with square lattice, which is compared to that of a spin liquid candidate κ-(BEDT-TTF)₂Cu₂(CN)₂. Anomalous broad peak structure in dielectric constant was observed in β¹-(BEDT-TTF)₂ICl₂, which shows a Curie type temperature dependence with higher Curie temperature than the antiferromagnetic transition and a strong frequency dependence similar to ferroelectric relaxors. The dielectric constant parallel to the BEDT-TTF dimer layer is larger than perpendicular to it, which suggests that the charge degrees of freedom within a dimer of BEDT-TTF molecule has significant role in the dielectric anomaly in dimer-Mott type organic insulator. The coupling between the charge and spin degrees of freedom will be discussed.

[1] M. Abdel-Jawad, I. Terasaki, T. Sasaki, N. Yoneyama, N. Kobayashi, Y. Uesu, and C. Hotta, Phys. Rev. B 82 (2010) 125119. [2] M. Naka and S. Ishihara, J. Phys. Soc. Jpn. 79 (2010) 063707. [3] C. Hotta, Phys. Rev. B 82 (2010) 241104(R).

GB05

Multiferroic transition in a quasi-layered bismuth ferrite

Chan-ho Yang
Physics, KAIST, Korea

Usually magnetic transition temperature is insensitive to structural modification by external strain, while ferroelectric transition temperature can be largely tuned by strain. As a counter-example of the generic tendency of the magnetic transition, we will focus on a highly elongated multiferroic BiFeO₃ thin film, which has been newly discovered as a quasi-layered perovskite phase stabilized through a misfit strain. Special attention has been paid to the phase competition between the new highly elongated phase and the normal phase leading to colossal electron-strain. However the magnetic properties of the new highly elongated phase has not been fully unveiled yet. Here we will provide experimental evidence for the large suppression of the magnetic order indicating strong spin-lattice coupling and discuss underlying physics inherent in the highly-elongated quasi-layered perovskite.

GC01

Field-dependent Fermi surface and high-field superconductivity in URhGe

Ed Yelland^{1,2*}, J. M. Barraclough¹, M. Kepa¹, I. Sheikin¹, D. Sokolov¹, W. Wang¹, K. V. Kamenev³ and A. D. Huxley^{1,2}
¹ School of Physics and Astronomy and Centre for Science at Extreme Conditions, University of Edinburgh, United Kingdom
² School of Physics and Astronomy, University of St. Andrews, United Kingdom
³ School of Engineering and Centre for Science at Extreme Conditions, University of Edinburgh, United Kingdom
⁴ LNCMI, CNRS, Grenoble, France

We present the first observation of the Fermi surface in the ferromagnetic superconductor URhGe [1]. A small class of heavy fermion ferromagnets including URhGe show bulk superconductivity deep within the ferromagnetic state. Existing results for URhGe [2] strongly suggest that the superconductivity arises from p-wave Cooper pairing of electronic quasiparticles with equal spin. Uniquely within this class, URhGe shows a second, field-induced superconducting phase with critical fields in excess of 32 tesla [3]. Our measurements of the Shubnikov-de Haas effect, made on the verge of field-induced superconductivity, reveal a small Fermi surface pocket that shrinks with increasing applied magnetic field, eventually disappearing at a topological transition of the Fermi surface (a Lifshitz transition). The quasiparticle mass decreases and remains finite, implying that the Fermi velocity vanishes due to the collapse of the Fermi wavevector. A simple model calculation of the orbitally limited critical field for the shrinking Fermi pocket reproduces the experimental phase diagram for high-field superconductivity, suggesting that it is the slowing down of quasiparticles at a Lifshitz transition that allows superconductivity to survive above 30 T, without a divergence of the quasiparticle mass. This represents an important departure from all present theoretical treatments of the phase formation.

[1] E. A. Yelland et al., Nature Physics 7, 890 (2011) [2] F. Hardy and A. D. Huxley, Phys. Rev. Lett. 94, 247006 (2005) [3] F. Levy, I. Sheikin, and A. Huxley, Nature Physics 3, 460 (2007)

GC02

Conventional quantum criticality in CeCu₂Si₂

Oliver Stockert*
Max-Planck-Institute for Chemical Physics of Solids, Germany

The heavy-fermion compound CeCu₂Si₂ displays unconventional superconductivity around the magnetic quantum critical point (QCP) where antiferromagnetic order vanishes. The superconducting state is characterized by a spin excitation gap, and almost critical spin fluctuations are responsible for the Cooper pair formation. The energy and wave-vector dependence of the normal state spin fluctuations as measured by inelastic neutron scattering indicate a three-dimensional spin-density-wave QCP in agreement with macroscopic properties. Furthermore, muon spin rotation under pressure allowed to tune through the QCP and to study the interplay between magnetism and superconductivity in more detail. Both phenomena are connected by a first-order transition with the occurrence of phase separation. Small magnetically ordered regions are observed well below the superconducting T_c. The results are in line with the findings obtained by neutron scattering and will be compared to other quantum-critical heavy-fermion compounds.

GC03

Shubnikov-de Haas oscillation in PuIn₃

Yoshinori Haga¹, Oscar Ayala-valenzuela², Ross McDonald², Chuck Mielke², Eric D. Bauer², J N Mitchell², P. H. Tobash², Joe D. Thompson² and Zachary Fisk¹
¹ Advanced Science Research Center, Japan Atomic Energy Agency, Japan
² Los Alamos National Laboratory, USA

Highly correlated f-electron systems are extensively studied because of their unusual physical properties. While the electronic state of 4f rare earth compounds is understood based on the localized 4f state hybridized with conduction bands, that of 5f electrons in actinide compounds is not well defined. In this context, direct observation of Fermi surface provides strong implication whether the 5f electrons are localized or delocalized to participate in Fermi surface. In the present study, we report Shubnikov-de Haas (SdH) study in a plutonium compound PuIn₃ with the cubic AuCu₃-type structure. We succeeded in observing a clear SdH oscillation as a function of inverse magnetic field, where the SdH frequency is proportional to the cross sectional area of the Fermi surface along the magnetic field direction. The obtained SdH frequency can be explained by the band calculations assuming the 5f electrons are delocalized. The SdH oscillation was only observed when the field is applied near the <111> direction and suddenly vanishes, which cannot be explained from the calculated Fermi surface properties and needs further investigations.

GC04

Spin fluctuations and Lifshitz transition in UGe₂ probed by Larmor neutron diffraction under pressure

Dmitry Sokolov^{1*}, Robert Ritz², Christian Pfleiderer², Thomas Keller³ and Andrew Huxley¹
¹ The University of Edinburgh, United Kingdom
² Technische Universität München, Germany
³ MPI Stuttgart, Germany

We present high resolution measurements of the lattice constants of UGe₂ under pressure probed by a novel technique that utilizes Larmor precession of polarized neutrons to surpass the resolution of conventional scattering methods by an order of magnitude. At low temperature UGe₂ is ferromagnetic up to critical pressure p_c but superconductivity is peaked at a lower pressure p_x coinciding with a less understood transition within the ferromagnetic state [1]. At ambient pressure we observed sharp anomalies in the lattice parameters at the Curie temperature, T_c. At higher pressure sharp anomalies in the lattice parameters at both T_c and T_x (the characteristic temperature for the transition that occurs at p_x) shift to lower temperatures in agreement with the known phase diagram. We show that the magnetic thermal expansion is dominated by the critical fluctuations near T_c and is well explained by the spin fluctuation theory at p<p_x, however at p=p_x we identify an additional contribution to the magnetic thermal expansion which is due to pressure driven Lifshitz transition [2] in spin bands of UGe₂. Together with the magnetic correlation length diverging under pressure, this may play an important role in stabilising superconductivity.

[1] S. S. Saxena, et al., Nature 406, 587 (2000) [2] I. M. Lifshitz, Sov. Phys. JETP 11, 1130 (1960)

GD01

Ultrafast manipulation of magnetic order

Theo Rasing
SSI, Radboud University, Netherlands

The interaction of sub-picosecond laser pulses with magnetically ordered materials has developed into an extremely exciting research topic in modern magnetism and spintronics. From the discovery of sub-picosecond demagnetization over a decade ago to the recent demonstration of magnetization reversal by a single 40 femtosecond laser pulse, the manipulation of spins by ultra short laser pulses has become a fundamentally challenging topic with a potentially high impact for future spintronics, data storage and manipulation and quantum computation. In addition, when the time-scale of the perturbation approaches the characteristic time of the exchange interaction (~10-100 fs), the magnetic dynamics enters a novel, highly non-equilibrium, regime where the exchange interaction might even become time dependent. Using ultrashort excitations, we may be able to manipulate the exchange interaction itself or use it strength to manipulate or even switch magnetization. Such studies require the excitation and probing of the spin and angular momentum contributions to the magnetic order at timescales of 10fs and below, a challenge that could be met by the future fs X-ray FEL's.

A.V.Kimel, et al, Nature 435 (2005), 655-657 C.D.Stanciu, et al, Phys.Rev.Lett.99, 047601 (2007) A.V.Kimel, et al, Nature Physics 10, 727-731 (2009) K.Vahaplar, et al, Phys.Rev.Lett.103, 117201 (2009) A.Kirilyuk, et al, Rev. Mod. Phys. 82, 2731-2784 (2010) I.Radu et al, Nature 472, 205 (2011) T. Ostler et al, Nature Comm. 3, #666 (2012)

GD02

Ultrafast emergence of nanoscale ferromagnetism far from equilibrium

Hermann Andreas Durr
Photon Science, SLAC National Accelerator Laboratory, USA

Long-range magnetic order in solids is usually ascribed to the exchange interaction between electron spins. Close to equilibrium this leads to spontaneous magnetization when the system cools below the magnetic ordering temperature. We show that the far from equilibrium flow of angular momentum via spin currents can also achieve long-range ferromagnetic order even above the ordering temperature. To reveal this process, we use ultrafast x-ray diffraction at SLAC's Linac Coherent Light Source to probe the nucleation, growth and transient existence of ferromagnetic order on the nm length and fs timescale after fs optical laser excitation has brought a metallic 3d - 4f alloy system into a highly non-equilibrium chaotic spin state. The technological exploitation of this effect could pave the way for novel ways to manipulate and transport information within the smallest space-time dimensions.

GD03

Modeling of ultra-fast magnetisation dynamics

O. Chubykalo-Fesenko^{1*}, U Atxitia^{1,2}, T.Ostler², R.Evans² and R.W.Chantrell²
¹Material Science Institute of Madrid, CSIC, Spain
²Physics Department, University of York, UK

The ultra-fast laser-induced magnetisation dynamics is currently an attractive topic of modern magnetism due to a new physical phenomena appearing during these strongly non-equilibrium processes and the possibility to extend magnetic switching speed down to femtoseconds. While in ferromagnetic metals such as Ni, Fe, Gd only ultra-fast demagnetisation has been observed, in ferrimagnetic materials such as FeCoGd the controllable magnetization switching in several ps has been reported [1]. Recently we have reported that this switching occurs under ultra-fast heat alone without the necessity of any other external stimulus [2]. Our modeling of the underlying processes is based on two approaches: (i) atomistic simulations using the Landau-Lifshitz-Gilbert equation and (ii) micromagnetic approach using classical and quantum Landau-Lifshitz-Bloch (LLB) equation. Both models assume thermal magnetization dynamics via the coupling to electron (and phonon for Gd) temperature bath. The comparison of our modeling based on the LLB approach with the experiments in Ni [3] and Gd shows an excellent agreement providing a validation of thermal magnetization dynamics mechanism. In agreement with the experiment the modeling reveals different timescales for demagnetisation: fast (100 fs) in Ni and slow (50 ps) in Gd. We will present our atomistic modeling on the switching of a ferrimagnetic CoFeGd compound with the only external stimulus provided by the ultra-fast heating. The atomistic results will be explained in terms of the dynamical system based on the recently-derived two-component LLB micromagnetic equation.

1. K. Kahaplar et al, Phys. Rev. Lett. 103, 117201 (2009) 2. T.Ostler et al., Nature Commun., 3, 666 (2012) 3. U.Atxitia et al., Phys. Rev. B 81, 174401 (2010)

GD04

Ultrafast inverse Faraday effect in paramagnetic dielectrics

Rostislav V. Mikhaylovskiy*, Euan Hendry and Volodymyr V. Kruglyak
 School of Physics, University of Exeter, United Kingdom

We present a critical and thorough analysis of the concept of a light induced effective magnetic field. The analysis reveals incontinuity in the theoretical interpretation of ultrafast femtomagnetic phenomena in paramagnetic dielectrics. Furthermore, we discuss the validity of the assumption of equivalence of origins of opto-magnetic and magneto-optical effects, which has not been rigorously tested so far. We support our arguments by the all-optical femtosecond time-resolved measurements of the ultrafast inverse Faraday Effect in terbium gallium garnet crystal. The measurement of the transient rotation of polarization of the probe pulse induced by a pump pulse allows us perform a systematic study of the full nonlinear optical response of the sample. The magneto-optical contribution attributed to inverse Faraday effect is then extracted by thoroughly studying the dependence of the signal upon the pump polarization. The amplitude of the Faraday rotation was found to significantly exceed that predicted by phenomenological theory relying on the static Verdet constant value. The discrepancy demonstrates that the nature of the inverse Faraday Effect on femtosecond timescale is different from that of the quasi-static inverse Faraday Effect observed by Pershan and coworkers [1,2] and that it cannot be described in terms of the effective magnetic field.

1. J. P. van der Ziel, P. S. Pershan, and L. D. Malmstrom, Phys. Rev. Lett. 15, 190 (1965) 2. P. S. Pershan, J. P. van der Ziel, and L. D. Malmstrom, Phys. Rev. 143, 574 (1966).

GE01

Detection of domain wall position and magnetization reversal in nanostructures using the magnon contribution to the resistivity

Jean-philippe Attane, Van Dai Nguyen, Alain Marty, Piotr Laczkowski, Cyrille Beigne, Lucien Notin, Matthieu Jamet, Williams Savero-torres, Murat Cubukcu and Laurent Vila*
 Universite Joseph Fourier, BP 53, 38041, Grenoble and INAC/CEA Grenoble, France

We present a new magnetoresistance (MR) based on the contribution of the magnons to the resistivity, i.e., Magnon Magnetoresistance (MMR). We show that the MMR can be used to study the magnetization reversal in systems with either perpendicular (FePt) or in-plane anisotropy (NiFe), including domain wall (DW) position detection. MMR measurement exhibits a linear dependence of the resistivity on the applied field, originating from electron-magnon scattering. The drop of resistivity, due to the abrupt change of magnon density, corresponds to the magnetization switching. MMR measurement allows detecting precisely the position of a DW along a FePt nanowire, and following the dynamic of DW motion. In system with in-plane magnetization as NiFe nanowires, we show that the enhancement of the shape anisotropy in the narrowest widths leads to the disappearance of the AMR, the remaining contribution to the MR being that of the MMR. We also show that the MMR signal allows detecting the position of the DW along the NiFe wire. We emphasize that the observation of MMR in in-plane anisotropy nanowires can provide a change of paradigm in the study of in-plane magnetized nanowires: for certain field directions the magnon contribution dominates the MR, clearly overcoming the AMR.

V.D. Nguyen et al., Phys. Rev. Lett. 107, 136605 (2011) V.D. Nguyen et al., Appl. Phys. Lett. 99, 262504 (2011)

GE02

Tunable resistivity of individual magnetic DWs

Jeroen Franken*, Mark Hoeijmakers, Henk Swagten and Bert Koopmans
 Department of Applied Physics, Eindhoven University of Technology, Netherlands

Despite the broad interest in current-induced magnetic domain wall (DW) motion, the current-DW interaction is still not fully understood. A property strongly related to this interaction is the intrinsic DW resistivity. Measuring this property is therefore an important step in unraveling the physics behind DW motion and in particular the non-adiabatic spin torque. However, measurements of the DW resistivity as a function of the main property of the DW, its width, are still lacking. Here, we investigate in a unique way how the resistivity of individual DWs depends on their width [1], by using focused ion beam irradiation to tune the DW width D in perpendicularly magnetized Pt/Co/Pt strips. We use a very direct way to measure the resistivity of individually appearing domain walls, by monitoring in real-time the domain structure in a Kerr microscope. We find that convincingly, the DW resistivity scales with 1/D², in quantitative agreement with the theory of Levy and Zhang [2].

[1] J. H. Franken, M. Hoeijmakers, H. J. M. Swagten, and B. Koopmans, Phys. Rev. Lett. 108, 037205 (2012). [2] P. M. Levy and S. Zhang, Phys. Rev. Lett. 79, 5110-5113 (1997).

GE03

Observation of domain-wall capacitance in permalloy nanowires

Kulothungasagaran Narayanapillai, Mahdi Jamali, Ajeesh Sahadevan and Hyunsoo Yang*
 Electrical and Computer Engineering, National University of Singapore, Singapore

Studies on domain walls have attracted interest due to its potential applications on storage and logic devices. Domain walls can be detected by magneto-resistance effect such as the giant magneto-resistance effect and by magnonic effect [1]. We here report the detection of a domain wall by employing the capacitive effect of a single domain wall in a Permalloy nanowire. Spin-capacitance has been reported as a phenomenon in magnetic tunnel junctions and interfacial oxides where the spin configuration affects not only the resistance across the tunnel junction, but also the capacitance known as magneto-capacitance [2]. Semi-circular nanowires are patterned with the film structure of Ta (5 nm)/ NiFe (30 nm)/ Ta (5 nm) and the capacitance and magneto-resistance is measured. We observe that the magneto-capacitance is a reciprocal of the magneto-resistance. In addition to the resistive component, the capacitance due to the domain wall spin structure enables us to detect the presence of a domain wall. In angular measurements with externally applied magnetic fields, large changes in the field dependent capacitance are discussed.

[1] V. D. Nguyen et al., Phys Rev Lett 107, 136605 (2011). [2] J. M. Rondinelli, M. Stengel, and N. A. Spaldin, Nat Nanotechnol 3, 46 (2008).

GE04

Proposal new type of low current driven spin logic in PMA TbFeCo wire

Toma Kanehira and Hiroyuki Awano
 Toyota Technological Institute Information Storage Material Lab., Japan

We have performed a current driven magnetic domain AND logic circuit by designing a TbFeCo wire which has a large perpendicular magnetic anisotropy and high domain wall motion seed in ‘Y’ shape with two inputs and an output. The TbFeCo wire thickness is 4.8 nm. Well-defined starting states of as single domain wall from two inputs were recorded by pulse currents. The domain walls propagate into the output as a combined domain wall and detected by anomalous Hall voltage through a pair of electrodes (J=3.8×10¹⁰ [A/m²]). In the case of two input domain walls are recorded as a couple bits of ‘1’/‘1’, a sharp-changed anomalous Hall voltage is detected as a bit of ‘1’. In another case of only one input domain wall is recorded, there is no change in anomalous Hall voltage which corresponds to a bit of ‘0’ due to a different width of input and output wires which causes annihilated the domain wall. These results indicated that the circuit of TbFeCo wire work as a logic AND function. Moreover, OR and NOT function can be also designed. This technique expectedly promises lower-powered, higher-speed, nonvolatile devices with which to build the next generation of computing technology.

GE05

Current-induced domain wall motion in perpendicularly magnetized nanowire

Teruo Ono
 Kyoto University, Japan

Electrical displacement of a domain wall (DW) is a prospective method for information processing in new type of magnetic non-volatile memories and logic devices. Such novel spintronic devices require a low DW drive current and a high DW de-pinning field for stable information retention. We show that Co/Ni multilayer with perpendicular magnetic anisotropy is a promising material that satisfies these requirements. An electric current can drive a DW in one direction regardless of the polarity of a magnetic field in a Co/Ni nano-wire with perpendicular magnetization, i.e., the current can drive a DW against a magnetic field. Furthermore, both the DW velocity and the threshold current density for the DW motion show almost no dependence on the external magnetic field. These counter-intuitive behaviors can be interpreted as the consequence that the intrinsic pinning mechanism determines the threshold current, and the adiabatic spin torque dominates the DW motion in this system [1-6]. The established field-insensitivity of the electrical DW motion is promising for future spintronics applications based on the DW motion. This work was partly supported by the NEDO Spintronics nonvolatile devices project and a Grant-in-Aid for Scientific Research (S) from the Japan Society for the Promotion of Science.

[1] T. Koyama et al., Nature Materials, 10 (2011) 194. [2] T. Koyama et al., Appl. Phys. Lett. 98 (2011) 192509. [3] K. Ueda et al., Appl. Phys. Express 4 (2011) 063003. [4] D. Chiba et al., Appl. Phys. Express 3 (2010) 073004. [5] H. Tanigawa et al., Appl. Phys. Express 2 (2009) 053002. [6] T. Koyama et al., Appl. Phys. Express 1 (2008) 101303.

GF01

Melting spin ice

Sarah Ruth Dunsiger¹, A. A. Aczel², C. Arguello³, H. Dabkowska⁴, A. Dabkowski⁵, M-H Du⁶, T. Goko³, B. Javanparast⁷, T. Lin¹, F. L. Ning³, H. M. L. Noad², D. J. Singh⁸, T. J. Williams², Y. J. Uemura⁹, M. J. P. Gingras² and G. M. Luke²
¹ Physics Department E21, Technical University of Munich, Germany
² Dept of Physics and Astronomy, McMaster University, Canada
³ Dept of Physics, Columbia University, USA
⁴ Brockhouse Institute for Materials Research, McMaster University, Canada
⁵ Brockhouse Institute for Materials Research, McMaster University, Canada
⁶ Materials Science and Technology Division, Oak Ridge National Laboratory, USA
⁷ Dept of Physics and Astronomy, University of Waterloo, Canada

Geometric magnetic frustration is a ubiquitous phenomenon within condensed matter physics. The magnetic ground states are highly degenerate, leading to competing low temperature phases and enhanced quantum fluctuations. The nature of the magnetic fluctuations in these systems is currently the subject of lively investigation. ‘Spin ice’ model magnetic systems combine the rich phenomenology associated with geometric frustration with the theoretically tractable nature of Ising models, drawing on a close analogy with the statistical mechanics of proton disorder in water ice. Theory predicts the low-temperature magnetic excitations in spin ices consist of deconfined magnetic charges, or monopoles. A recent transverse-field (TF) muon spin rotation (μSR) experiment [S T Bramwell et al, Nature 461, 956 (2009)] reports results claiming to be consistent with the temperature and magnetic field dependence anticipated for monopole nucleation - the so-called second Wien effect. We demonstrate via a new series of μSR experiments in Dy₂Ti₂O₇ that such an effect is not observable in a TF μSR experiment. Rather, as found in many highly frustrated magnetic materials, we observe spin fluctuations which become temperature independent at low temperatures, behaviour which dominates over any possible signature of thermally nucleated monopole excitations.

GF02

Artificial spin ice: Dimensional reduction, avalanches and disorder

Remo Viktor Hugli, Gerard Duff and Hans - Benjamin Braun*
 Physics, University College Dublin, Ireland

Regular arrays of nanomagnets have proven to serve as ideal models for the study of spin-ice phenomena [1]. In contrast to their 3D analogues, the pyrochlore systems, the magnetic moments in 2D artificial spin ice systems exhibit high anisotropies which renders them stable at room temperature. This allows imaging with various experimental techniques in real space and at room temperature, which makes such metamaterials ideal candidates for comparison with theoretical models. Here we explore the nonequilibrium properties of a model that combines long range dipolar interaction, frustration and disorder which explains experiments on 2D artificial kagome spin ice [2]. We show how frustration induced by dipolar interaction leads to unusual 1D avalanches, an example of dimension reduction due to frustration. In particular, magnetization reversal proceeds via nucleation and subsequent avalanche-type dissociation of emergent monopole-antimonopole pairs along 1D Dirac strings. We show how the flow of these emergent monopoles or charges can be controlled via judicious modification of the islands’ anisotropy and magnetic fields, thus paving the way for magnetic information processing devices.

[1] R.F. Wang et al., Nature 439, 303 (2006). [2] E. Mengotti, L. J. Heyderman, A. Fraile Rodriguez, F. Nolting, R.V. Hugli, and H. B. Braun, Nature Physics 7, 68 (2011).

GF03

Low temperature magnetic studies of geometrically frustrated SrHo₂O₄

Olga Young^{1*}, Geetha Balakrishnan¹, Andrew R. Wildes², Laurent C. Chapon² and Oleg A. Petrenko¹
¹ Department of Physics, University of Warwick, Coventry, CV4 7AL, United Kingdom
² Institut Laue-Langevin, Jules Horowitz, BP156, 38042 Grenoble Cedex 9, France

SrHo₂O₄ is a geometrically frustrated compound as its structure allows the magnetic ions to be arranged in a network of triangles and hexagons [1]. Magnetic susceptibility measurements on single crystals of SrHo₂O₄ show a disparity between the Curie-Weiss constant (-16.9 K) and the establishment of Neel order at 0.68 K [2], which is typical for frustrated systems. Low-temperature measurements of magnetisation [3] show the highly anisotropic nature of this crystal, and more intriguingly, the dM/dH curve for H//b shows double peak behaviour indicating a rich H-T phase diagram. We have performed powder neutron diffraction experiments using the GEM diffractometer (ISIS) [2]. At low temperatures, both k=0 magnetic Bragg reflections and a strong diffuse scattering feature - a broad peak near the position (0 0 1/2) - were observed. Recent experiments on single crystals of SrHo₂O₄ using the D7 instrument (ILL), reveal that this feature can be attributed to a one-dimensional collinear ordering with the spins pointing along the b-axis. This suggests a highly unusual magnetic ground state for SrHo₂O₄, as it is made up of two distinct components: one of the crystallographically inequivalent Ho³⁺ sites orders in a long-range magnetic structure, while the other orders in a short-range one-dimensional structure.

[1] H. Karunadasa et al., Phys. Rev. B 71, 144414 (2005) [2] O. Young et al., arXiv:1110.3521 (2011) [3] T.J. Hayes et al., J. Phys. Soc. Japan 81 024708 (2012)

GF04

Spin densities in manganese molecular cluster : [Mn₃L₄](ClO₄)₂(H₂O)₂

Clara Rodriguez-blanco¹, Javier Campo^{1*}, Jose Alberto Rodriguez-velamazán¹, Beatrice Gillon², Javier Luzon³ and Jose Sanchez-costa⁴
¹ Materials Science Institute of Aragon, (CSIC-University of Zaragoza), Spain
² Laboratoire Leon Brillouin, CEA-Saclay, France
³ Centro Universitario de la Defensa, Zaragoza, Spain
⁴ University of Barcelona, Spain

The molecular cluster [Mn₃L₄](ClO₄)₂(H₂O)₂, (HL=2-methoxy-6-(pyridine-2-ylhydrazono-methyl)-phenol) has been described as an almost linear trimer of Mn(II) in a high spin configuration with two isotropic magnetic interactions: nearest neighbours and next nearest neighbours interactions. One striking fact is the experimental EPR g factor of 2.14 for such an isotropic system. Due to its isotropic and not degenerated nature, the system is an ideal benchmark to investigate the interplay of the magnetic interactions in systems with several magnetic centers and more than one electron per magnetic center. In this contribution we will show how an in deep study of the system through the combination of several experimental and theoretical methods (polarized neutron diffraction at ILL and LLB, magnetic measurements, Density Functional Theory and spin Hamiltonian models) has allowed us to demonstrate the isotropic nature of the system and the anti-ferromagnetic character of the intra-molecular magnetic interactions.

[1] J. Tang et al., 2007 Eur. J. Inorg. Chem 4119

GF05

Electronic structure and magnetic properties of Cr-doped rutile TiO₂: Charge and magnetic state of Crimpurity

Rokyeon Kim¹, Suyeon Cho¹, Wongoo Park¹, Je-geun Park¹, Se-jung Oh¹, Patrick Berthet² and Jaeyun Yu^{1*}
¹ Department of Physics and Astronomy, Seoul National University, Korea
² University of Paris-Sud, France

We report theoretical and experimental studies of Cr-doped rutile TiO₂. In experiment we observe that the electronic and magnetic properties of Cr-doped rutile TiO₂ are highly dependent on the growth conditions. The ferromagnetic component in magnetic susceptibility and the Cr defect concentration are enhanced for the sample grown under the oxygen flow in comparison with those grown under the Ar flow. To understand the charge state of Cr dopants and their role in response to the external magnetic field, we carried out density functional theory (DFT) calculations for the Cr-doped rutile TiO₂. From the results of the formation energy calculations for the Cr atom substituting the Ti site and the O vacancy, assuming the thermodynamic equilibrium, we demonstrate that the Cr³⁺ state is a source of Curie-Weiss-type magnetic response in the O-poor limit, whereas the Cr²⁺ defect states contribute to the ferromagnetic component in the moderately reduced condition. We also provide the electronic structures of various defect configurations and attempt to explain the optical and electronic properties of the Cr-doped system.

GG01

Magnetic nanoparticle arrays by nanomasking pattern transfer

Sara Majetich
Physics, Carnegie Mellon University, USA

In nanomasking, self-assembled nanoparticle monolayers are used as etch masks to pattern underlying thin films [1]. Here we apply this technique to prepare two types of magnetic nanodot arrays, and characterize their structural and magnetic properties. Large area nanoparticle arrays were fabricated by a Langmuir film method and transferred to a solid substrate. After electron irradiation curing and brief exposure to an oxygen plasma, most of the surfactant has been removed yet the ordered pattern of the particle cores has been preserved. We examined direct pattern transfer by methanol-based reactive ion etching into a FePt film. A second strategy prepares nanodot arrays by filling an antidot lattice. Here 2 nm of titanium is deposited on the array of bare nanoparticle cores, which are then removed with phosphoric acid to leave an alumina antidot mask. Here the mask was prepared on a silica film. RIE was then used to generate an array of pits, and permalloy was sputtered to overfill the pits. Magnetic measurements as a function of methanol etching show the transition from a continuous film to an array of nanodots.

I. C. R. Hogg, S. A. Majetich, and J. A. Bain, *IEEE Trans. Magn.* 46, 2307-2310 (2010)

GG02

Spin wave bands and bandgaps in a two-dimensional ferromagnetic antidot array

Roberto Zivieri^{1*}, Silvia Tacchi², Federico Montoncello¹, Loris Giovannini¹, Fabrizio Nizzoli¹, Marco Madami², Gianluca Gubbiotti², Giovanni Carlotti², Sebastian Neusser³, George Duerr³ and Dirk Grundler³

¹ Department of Physics, University of Ferrara, Italy
² Department of Physics, University of Perugia, Italy
³ Department of Physics, University of Muenchen, Germany

The spin wave band structure of a two-dimensional square array of NiFe circular antidots having diameter of 120 nm and periodicity of 800 nm has been investigated by using Brillouin light scattering and micromagnetic calculations based on the dynamical matrix method. The external magnetic field was applied in the plane and perpendicularly to the transferred wave vector. Extended and localized spin modes having a propagative nature were found. Opening of bandgaps is interpreted in terms of Bragg diffraction of spin waves from the antidot lattice and this effect is explained by studying the behavior of the internal field. According to an analytical model, the relevant scattering potential for Bragg reflection is not provided by the holes themselves, but by the concomitant internal field inhomogeneity between holes [1]. This is in contrast to antidots in photonics and electronics where the back-reflection is directly caused by the presence of holes. The research leading to these results has received funding from the European Community's Seventh Framework Programme (FP7/2007-2013) under Grant Agreement n228673 (MAGNONICS).

[1] R. Zivieri, S. Tacchi, F. Montoncello, L. Giovannini, F. Nizzoli, M. Madami, G. Gubbiotti, G. Carlotti, S. Neusser, G. Duerr, and D. Grundler, *Phys. Rev. B* 85, 012403 (2012).

GG03

Ratchet effect in magnetic domain wall motion induced by 2D arrays of triangular submicrometric holes

Celia Castán-Guerrero^{1*}, Aurelio Hierro-Rodríguez², Fernando Valdés-Bangó², Jose Ignacio Martín², Javier Sese², Julia Herrero-Albillos⁴, Fernando Bartolome¹, Juan Bartolome¹, Jose Maria Alameda³ and Luis Miguel Garcia¹
¹ Instituto de Ciencia de Materiales de Aragon (Universidad de Zaragoza - CSIC), Spain
² Departamento de Física, Universidad de Oviedo - CINN, Spain
³ Instituto de Nanociencia de Aragon (Universidad de Zaragoza), Spain
⁴ Centro Universitario de la Defensa, Academia General Militar, Spain

Controlling magnetic domain wall motion in ferromagnetic materials is essential for the development of spintronics. The introduction of asymmetric pinning potentials has proved itself as an efficient tool to induce ratchet effects in domain wall motion, as observed in nanowires with triangular section [1] or asymmetric notches [2]. Similar effects can be induced in extended ferromagnetic thin films when introducing 2D arrays of asymmetric holes[3], although the study is rather more complex due to the higher dimensionality of domain walls [4]. In the present study, antidot arrays have been fabricated on amorphous thin films of Co₂Si₂, with in-plane uniaxial anisotropy. Arrays of triangular antidots of size 500nm and lum and edge-to-edge separation of three, four and five times their size have been studied. Equivalent arrays with rhombohedral antidots have been fabricated for comparison. A Kerr effect microscope has been used for the magnetic imaging. Magnetic domain walls are observed to move through the triangular antidot arrays only in the forward direction, defined from the base of the triangles to the vertex. The cause of the ratchet effect is confirmed to be the holes asymmetry, as domain wall motion is symmetric when crossing rhombohedral (symmetric) antidot arrays.

[1] D. A. Allwood et al., *Appl. Phys. Lett.* 85, 2848 (2004) [2] A. Himeno et al., *J. Appl. Phys.* 97, 066101 (2005); M. Hayashi et al., *Phys. Rev. Lett.* 97, 207205 (2006) [3] A. Perez-Junquera, V. I. Marconi, A. B. Kolton, L. M. Alvarez-Prado, Y. Souche, A. Alija, M. Velez, J.V. Anguita, J. M. Alameda, J. I. Martin, and J. M. R. Parrondo, *Phys. Rev. Lett.* 100, 037203 (2008) [4] A. Alija, A. Hierro-Rodriguez, A. Perez-Junquera, J. M. Alameda, J. I. Martin and M. Velez, *J. Phys. D: Appl. Phys.* 44, 325002 (2011)

GG04

Tailored magnetic anisotropy of Py /Co bilayer ordered nanohole arrays

Karla J. Merazzo, Giovanni A. Badini Confalonieri, Rafael P. Del Real and Manuel Vazquez
Materials for Information Technologies, Instituto de Ciencia de Materiales de Madrid, CSIC., Spain

Highly ordered arrays of magnetic nanoholes show a great potential for technological applications, as high-density magnetic storage media [1] or magnonic devices [2]. Magnetism of ordered nanohole arrays is determined by composition and particularly by geometry characteristics [3]. In this work, magnetic nanohole arrays have been sputtered onto hexagonally self-assembled anodic alumina membranes (AAM) [4] with 35 nm hole diameter and 105 nm interhole distance. Thickness of Py/Co bilayer nanohole arrays were: 10nm, 20nm and 43 nm for the Py layer, with a constant thickness of 28 nm for Co layer. Their magnetic properties were determined by vibrating sample magnetometer and magneto optical Kerr effect. The in-plane angular dependence of coercivity shows that the magnetic behaviour of the Py layer strongly depends on its interaction with the Co, which reminds that of a spring-like system. The sample with thinnest Py layer exhibits highest coercivity (Hc=140 Oe) which decreases with Py thickness (Hc=16 Oe). A bimagnetic-like behaviour is observed in some samples indicating the relevance of local magnetostatic interactions. The overall results have been compared to those of continuous Py/Co bilayer films, showing an increase of five times its coercivity by the only presence of the nanoholes.

J.R. P. Cowburn, A. O. Adeyeye, J. A. Bland, *Appl. Phys. Lett.* 1997, 70, 2309. 2. V. V. Kruglyak, S. O. Demokritov, D. Grundler, *J. Phys. D: Appl. Phys.* 2010, 43, 264001 3. M. Vázquez, K.R. Pirota, D. Navas, A. Asenjo, M. Hernandez-Vélez, P. Prieto and J.M. Sanz *JMMM*, 320 (2008)1978-1983 4. K J Merazzo, D C Leitao, E Jimenez, J P Araujo, J Camarero, R P del Real, A Asenjo and M Vazquez. 2011 *J. Phys. D: Appl. Phys.* 44 505001

GG05

Tailoring magnetic properties of Co thin films through antidot arrays: crossover from antidot to dot regime

Celia Castán-Guerrero^{1*}, Javier Sese², Julia Herrero-Albillos^{1,3}, Florian Kronast⁴, Luis Alfredo Rodríguez², Cesar Magen², Karla J. Merazzo¹, Manuel Vazquez², Juan Bartolome¹, Fernando Bartolome¹, Pavel Strichovanez², Paolo Vavassori⁵ and Luis Miguel Garcia¹
¹ Instituto de Ciencia de Materiales de Aragon (Universidad de Zaragoza - CSIC), Spain
² Instituto de Nanociencia de Aragon (Universidad de Zaragoza), Spain
³ Centro Universitario de la Defensa (Academia General Militar), Spain
⁴ Helmholtz-Zentrum Berlin für Materialien und Energie GmbH, Germany
⁵ Instituto de Ciencia de Materiales de Madrid (CSIC), Spain
⁶ CIC nanoGUNE Consolider, IKERBASKE, Spain

Magnetic properties of thin films are hardly controllable, since they depend strongly on the microstructure and the presence of defects. Nanopatterning of dot [1] and antidot [2] arrays are two different approaches to tailor magnetic properties only as a function of geometry. In this study, a series of antidot arrays have been fabricated with square symmetry, varying the periodicity from 500nm, that is in the diluted regime, to 105nm, almost in the percolation limit. The holes were etched using a focused gallium ion beam, that allows the control of the geometrical parameters with nanometric resolution. Magnetic characterization by MOKE and magnetic imaging by XPEEM show a change in the dependence of coercivity with periodicity below 140nm that can be correlated with a change in the magnetic domain configuration. HRTEM chemical and morphological analysis show gallium ion implantation and amorphization in the cobalt around the holes, that could have turned it into non-magnetic. Then, the effective diameter of the non-magnetic area becomes greater than the antidot one itself. As antidot-antidot distance decreases, the magnetic percolation is lost and a crossover from antidot to dot regime is encountered.

[1] L. J. Heyderman, H. H. Solak, C. David, D. Atkinson, R. P. Cowburn and F. Nolting, *Appl. Phys. Lett.* 85, 4989 (2004) [2] I. Ruiz, L. Lopez, A. Hiverrate, J. Rothman, C. M. Guertler, J. A. C. Bland, L. M. Garcia, J. M. Torres, J. Bartolome, F. Bartolome, M. Natali, D. Decanini, Y. Chen, *J. Magn. Magn. Mater.* 2002, 242-245, 597-600; L. J. Heyderman, F. Nolting, D. Backes, S. Czekaj, *Phys. Rev. B* 2006, 73, 214429; X. K. Hu, S. Sievers, A. Müller, V. Janke and H. W. Schumacher, *Phys. Rev. B* 2011, 84, 024404

GH01

Bio-functional magnetic nanoparticles in biomedical applications

Herg-er Horn*
National Taiwan Normal University, Taiwan

With distinctive characteristics of magnetic properties and a variety of bio-functions by conjugated some specific bio-probes, bio-functional magnetic nanoparticles (MNPs) have been widely investigated in the biomedical applications currently. In this report, several applications using MNPs will be mentioned as examples of such applications. For the immunoassay, an innovative method, ImmunoMagnetoreduction (IMR)(1), will be introduced at first. Secondly, the cancer images by using low field MRI(2-3) will be demonstrated to reveal the possibility of this instrument in the cancer study. Next, the hyperthermia with MNPs, including metabolism of MNPs study(4) , the instrument and the temperature manipulation etc., will be declared. Finally, some other examples, such as magnetofection(5) etc., will be also reviewed in this talk.

References: 1. Wash-free immunomagnetic detection for serum through magnetic susceptibility reduction, *Appl. Phys. Lett.*, 90, 74105 (2007). 2. Bio-functionalized magnetic nanoparticles for in-vitro labeling and in-vivo locating specific bio-molecules, *Appl. Phys. Lett.*, 92, 142504(2008). 3. Characterization of tumors using high-Tc SQUID-detected nuclear magnetic resonance and imaging, *Appl. Phys. Lett.* , 97, 263701, 2010.(Cover page) 4. In-vivo and real-time measurement of magnetic-nanoparticles distribution in animals by scanning SQUID Biosusceptometry for biomedicine study, *IEEE Transactions on Biomedical Engineering* ,58, 2719-2724, 2011. 5. Ex Vivo Magnetofection With Magnetic Nanoparticles: A Novel Platform for Nonviral Tissue Engineering, *Artificial Organs*, 32, 195-204 (2008).

GH02

Spin resolved measurements of single molecular magnets on surfaces

Jens Brede^{1*}, Jorg Schwobel¹, Regis Decker¹, Andrew Dilullo², Germar Hoffmann¹, Svetlana Klyatskaya¹, Mario Ruben³ and Roland Wiesendanger¹
¹ Institute of Applied Physics, University of Hamburg, Germany
² Department of Physics and Astronomy, Ohio University, Germany
³ Institute of Nanotechnology, Karlsruhe Institute of Technology, Germany

The use of magnetic molecules opens a gateway to a flexible design of novel spintronic devices to store, manipulate, and read spin information at the nanoscale. Crucial is the precise knowledge of molecular properties at the interface towards an electrode. Progress in this field relies on resolving and understanding the physics at the relevant interfaces. In particular the role of individual molecular constituents and the impact of the atomic environment on molecular properties, determine device relevant parameters, such as conductance and spin polarization. Here, we applied spin-polarized scanning tunneling microscopy to resolve the physics of the molecule-ferromagnet interface. The analysis focuses on different phthalocyanine molecules. The phthalocyanine constitutes of an organic macrocyclic ligand and can be functionalized with various metal ions in order to modify, e.g. the molecular spin state. We will discuss the spin-dependent transport from magnetic surfaces through such molecules. In particular, spin-split molecular orbitals were resolved with sub-molecular spatial resolution. The magnitude of the exchange splitting is directly determined by spin-resolved tunneling spectroscopy.

GH03

MgO tunnel junction magnetic field sensors at high frequencies

Mustafa Arikan^{1*}, Matthew Carter², Gang Xiao³ and Snorri Ingvarsson¹
¹ Science Institute, University of Iceland, Iceland
² Micro Magnetics, Inc., USA
³ Department of Physics, Brown University, USA
⁴ Science Institute, University of Iceland, Iceland

Micron sized MgO magnetic tunnel junctions with 1.7 nm tunnel barrier were fabricated and characterized at DC and high frequencies to be used as magnetic field sensors. Both DC and AC properties of the sensors were measured by tunneling magnetoresistance (TMR) and impedance spectroscopy between 100 Hz and 40 MHz as a function of applied external magnetic field. Several different types of sensors were investigated: Single and multiple MTJ-sensors. In the first case, single junctions were measured. A simple RLC circuit model was applied to impedance spectroscopy results to investigate magnetocapacitance properties in order to evaluate and compare different sensing schemes such as resistive and capacitive sensing. Contrary to the previous reports in the literature we didn't observe field dependent spin capacitance despite excellent agreements in other parameters such as resistance of the junction and interface capacitance. We attribute this discrepancy to the size of our junctions and reach a conclusion that limits the applicability of the spin-capacitance concept to large area devices. Then multiple tunnel junctions in serpentine geometry were measured. Using the same circuit model, we measured non-zero magnetocapacitance in multiple junction sensors unlike single junction devices. We explain this as a result of the sensor geometry.

S. Ingvarsson et al., *Appl. Phys. Lett.* 96, 232506 (2010). X. Liu et al., *Appl. Phys. Lett.* 89, 023504 (2006). P. Padhan et al., *Appl. Phys. Lett.* 90, 142105 (2007). H. Kaiju et al., *J. Appl. Phys.* 91, 7430 (2002).

GH04

LaSrVMoO₆ : a compensated half metal or not?

Zhijian Wu and Jing Wang
Changchun Institute of Applied Chemistry, Chinese Academy of Sciences, China

LaSrVMoO₆ was first synthesized in 2004. The crystal structure is uncertain and was suggested to be cubic (Fm-3m). compensated half metal (i.e., half metallic compound with zero magnetization) is suggested. Theoretical study in 2005 indicated that it is a normal metal and ferrimagnet. In 2009, LaSrVMoO₆ has been revisited by the experimental study. The crystal structure is determined to be cubic (Fm-3m). It was concluded that LaSrVMoO₆ is a compensated half metal. Theoretical study in 2010 based on the cubic structure indicated that LaSrVMoO₆ is a ferrimagnetic half metal, in contrast to compensated half metal suggested experimentally. Recently in 2010, LaSrVMoO₆ was found to be orthorhombic (Pnma) and metallic. Further theoretical study in 2011 indicated that LaSrVMoO₆ in disordered states for V and Mo is compensated half metal. So the studied system poses great challenge for both experiment and theory.

GH05

Pressure effects on the magnetic properties of Emim[FeCl₄], a magnetic ionic liquid with antiferromagnetic ordering

A. Garcia-saiz¹, I. De Pedro¹, J. C. Gomez Sal¹, J. A. Blanco² and J. Rodriguez Fernandez^{1*}
¹ CITIMAC, Fac. de Ciencias, Universidad de Cantabria, Spain
² Departamento de Física, Universidad de Oviedo, Spain

The magnetic ionic liquids (MILs) are a new class of materials which can favourably combine the properties of ionic liquids with the magnetism that is originated from the metal incorporated in the complex anion [1]. Most of the MILs are paramagnetic, being the Emim[FeCl₄] the first one in which a long-range magnetic order was found at low temperatures [2]. The physical properties of 1-ethyl-3-methylimidazolium tetrachloroferrate Emim[FeCl₄] clearly show antiferromagnetic ordering when it is solidified (in polycrystalline state at 285 K), with a Neel temperature TN ~ 3.8 K [3]. Recent Mossbauer and muon spin relaxation spectroscopies, as well as neutron powder diffraction experiments [4], confirm the three-dimensional magnetic ordering. In this work, we present the effects of pressure on the X(T) and M(H) curves up to 10 kbar. It is observed that the pressure modifies the magnetic interactions, increasing the order temperature and inducing a ferrimagnetic behaviour. Additionally, from the X(T), it is observed that the solid-liquid transition is very sensitive to pressure, being above 300 K for pressures larger than 0.72 kbar.

[1] R. E. de Sesto et al. *Chemical. Communications* (2008) 4, 447. [2] I. de Pedro et al., *J. Phys: Condens. Matter*, (2010) 22, 296006. [3] I. de Pedro et al., *J. Magn. Magn. Mat.* (2011) 323, 1254. [4] A. Garcia Saiz et al., to be published.

GIO1

Magnetic proximity and spin behavior at organic semiconductor/ferromagnet interfaces towards molecular spintronics

Jagadeesh S. Moodera
Massachusetts Institute of Technology, USA

Information storage bit size and computing is inching towards molecular level. Spin transport in organic semiconductors (OS) has the potential in realizing this goal in a straightforward way. The charge and spin transport at OS and ferromagnetic (FM) metal interface, although complex, has the needed ingredients for achieving to reach molecular level spintronics. Spin tunneling through a few monolayers to 30nm thick films of several types of OS, all the way to room temperature combined with spectroscopic and polarized neutron reflectometry studies show unique morphology driven signatures of weakened magnetic behavior of OS/ferromagnet interfaces. However, our recent studies show surprising magnetic interaction of the phenalenyl molecules over the surface of a ferromagnet (Co, permalloy etc), driving the molecular layer to be magnetic and coupled. In addition, the second molecular layer shows spin-filtering property, serving as a spin-sensing layer. As such the FM surface layer and the adjacent two molecular layers of phenalenyl combination demonstrates a well-defined and large interface magnetoresistance (IMR), persisting to near room temperature. With spin valve structures such as Co/Zn-methyl phenalenyl/permalloy an IMR of 50% is measured at 4K which only reduced to ~22% by 250K. With this study the potential for molecular level spintronics is demonstrated.

This work was done with Karthik Raman*1,2,†, Tiffany Santos, Jenny Shim, Shannon Watson, Julie Borchers, Alexander Kamerbeek, Nicolae Atodresci, Arup Mukherjee, Tamal Sen, Predrag Lazic, Vasilie Caciuc, Reem Michel, Dietmar Stalke, Swadhin Mandal, Stefan Blugel and Markus Munzenberg. Research is supported by grants from ONR, NSF and KIST-MIT program.

GIO2

Spin specific transport properties of chiral molecules

Ron Naaman
Dep. of Chemical Physics, Weizmann Institute, Israel

Spin effects normally are seen either in magnetic materials or in systems containing heavy atoms that facilitate spin-orbit coupling. We report spin-selective transmission of electrons through self-assembled monolayers of double-stranded DNA. The spin polarization exceeds 60% at room temperature. The spin filtration efficiency depended on the length of the DNA. In addition, we show that conduction through double stranded DNA oligomers is spin selective, demonstrating a true organic spin filter. The selectivity exceeds that of any known system at room temperature. The spin dependent resistivity indicates that the effect cannot result solely from the atomic spin-orbit coupling and must relate to a special property resulting from the chirality symmetry. A theoretical model indicates that the spin selectivity is related to relative narrow resonances through which the electrons are transmitted. Based on the theory new type of spintronics devices are constructed. The results may reflect on the importance of spin in determining electron transfer rates through biological systems.

1) B. Gohler,V. Hamelbeck, T.Z. Markus, M. Kettner, G.F. Hanne,Z. Vager, R. Naaman,H. Zacharias, *Science*331,894-897 (2011). 2) Z. Xie, T. Z. Markus, S. R. Cohen, Z.Vager, R. Gutierrez, R. Naaman, *Nano Letters*, 11, 4652-4655 (2011).

G103

Reversible and deterministic spin state switching of individual spinrossover molecules on a surface

Toshio Miyamachi^{1*}, Manuel Gruber², Vincent Davesne², Eric Beurepaire² and Wulf Wulfhekel¹

¹ *Physikalisches Institut, Karlsruhe Institute of Technology, Germany*
² *Institute of Physics and Chemistry of Materials of Strasbourg (IPCMS), UMR 7504 UDS-CNRS, France*

A nano-scale molecular switch composed of a single molecule mainly utilizes its conductance change by external stimuli. Adding spin switching functionality to molecular switches is the key concept for realizing molecular spintronics devices with ultimate density. For this purpose, spinrossover (SCO) molecules are promising since their spin state is also switchable between a high spin (HS) state and a low spin (LS) state, in addition to the conductance. We show scanning tunneling microscopy (STM) study of individual SCO molecules, Fe(phen)2(NCS)2 (phen = 1,10-phenanthroline). While the molecules lose their switching functionality on a metallic Cu(100) surface due to a strong coupling of the NCS-groups to the surface, reducing the interaction with the surface by introducing thin CuN layer enables them to switch. Injecting a current with a tip of STM changes the conformation of the molecules between two states, resulting in on (HS-state) and off (LS-state) of a Kondo resonance accompanied with a conductance change. Observed reversible and deterministic switching behaviors of the molecules, which are vital for memory operation, give perspective on future molecular spintronics devices with the smallest unit.

G104

Graphene-based spintronic components

Lei Shen, Minggang Zeng and Yuanping Feng*
Physics, National University of Singapore, Singapore

Using non-equilibrium Green's function method combined with density functional theory, we propose a complete set of basic spintronics devices including bipolar spin diode, transistor and logic gates based on zigzag graphene nanoribbons (ZGNRs). Nearly ±100% spin-polarized current can be generated and tuned by a source-drain voltage in the bipolar spin diode. This transport property is attributed to the intrinsic transmission selection rule of the spin subbands near the Fermi level in ZGNRs. The bias voltage and magnetic configurations of the two-terminal ZGNR-based spin diodes provide a rich variety of ways to control the spin current which can be used to design three-terminal spin transistors and logic gates. These spintronic components make possible the manipulation of spin-polarized current, such as rectification, amplification and logic operation.

1) M. G. Zeng, L. Shen, M. Zhou, C. Zhang, and Y. P. Feng. "Graphene-based bipolar spin diode and spin transistor: Rectification and amplification of spin-polarized current" *Phys. Rev. B* 83, 115427 (2011). 2) M. G. Zeng, L. Shen, H. B. Su, C. Zhang, and Y. P. Feng. "Graphene-based logic devices" *App. Phys. Lett.* 98, 092110 (2011).

G105

Detection and manipulation of spin currents in graphene with non-magnetic electrodes

Ivan J. Vera-marun*, Vishal Ranjan, Paul J. Zomer, Marcos H. D. Guimaraes and Bart J. Van Wees
Physics of Nanodevices, Zernike Institute for Advanced Materials, University of Groningen, Netherlands

We present an interplay between charge currents and spin currents which allows the use of nonmagnetic contacts for both detection [1] and manipulation of spin accumulation in a paramagnet. These effects are the result of a nonlinear interaction between spin and charge transport solely given by the energy dependence of the conductivity [2], analogous to the case of thermoelectrics. A conductivity spin polarization is induced by the presence of a spin accumulation, even in a paramagnet, when the conductivity is energy dependent. We use graphene as a model system to study these effects in nonlocal spin valve devices, including its dependence on charge carrier density and spin amplification under nonmagnetic contacts and in bipolar graphene p-n junctions. The general concept is applicable to the field of semiconductor spintronics.

[1] I.J. Vera-Marun, V. Ranjan and B.J. van Wees, *Nature Phys.* (accepted) [2] I.J. Vera-Marun, V. Ranjan and B.J. van Wees, *Phys. Rev. B* 84, 241408(R) (2011)

GJ01

Science and technology of modern permanent magnet materials

George C. Hadjipanayis*
Physics and Astronomy, University of Delaware, USA

Permanent magnets (PMs) are indispensable for the electric, electronic and automobile industries, information technologies, automatic control engineering and many other commercial and military applications. In most of these applications, an increase in the magnetic energy density of the PM, usually presented via the maximum energy product (BH)max, immediately increases the efficiency of the whole device and makes it smaller and lighter. Worldwide demand for high performance PMs has increased substantially in the past few years driven by hybrid and electric cars, wind turbines and other power generation systems. This talk will cover the major principles guiding the development of PMs, including the important role of microstructure on coercivity, and overview state-of-the-art theoretical and experimental research. Recent progress in the development of nanocomposite PMs, consisting of a fine (at the scale of magnetic exchange length) mixture of phases with high magnetization and large magnetic hardness will be discussed. Fabrication of such PMs is currently the most promising way to boost the (BH)max, while simultaneously decreasing, at least partially, the reliance on the rare earth elements. Current efforts in the development of high performance non-rare earth magnets and their future prospects will also be discussed.

Work supported by DOE and ARPA-E

GJ02

Differential thermal analysis on MnBi in high magnetic fields up to 45 T

Keiichi Koyama^{1*}, Yoshifuru Mitsui², Eun Sang Choi³, Yuki Ikehara², Eric Palm³ and Kazuo Watanabe²

¹ *Kagoshima University, Japan*
² *Tohoku University, Japan*
³ *National High Magnetic Field Laboratory, USA*

Differential thermal analysis was carried out for hard magnetic material MnBi in the temperature range 300-773 K in magnetic fields up to 45 T to investigate the effect of high magnetic fields on its decomposition process and corresponding phase diagram. The decomposition temperature Tt (MnBi → Mn_{1.08}Bi + liquid Bi) increases from 632 K (at a zero field) to 714 K by applying a magnetic field of 45 T. Furthermore, the magnetocaloric effect of MnBi is observed in 11.5-45 T in the vicinity of 689 K, showing that a field-induced composition process occurs. The obtained results show that the equilibrium state of MnBi can be controlled by a high magnetic field [1].

[1] K. Koyama et al., *J. Alloys. Comp.* 509 (2011) L78-L80.

GJ03

Magnetization of Dy₂Fe₁₇ in fields up to 85 Tesla

Y. Skourski¹, A.V. Andreev², M.D. Kuz'min³, Y. Narumi⁴, K. Kindo⁵, N.V. Kudrevatykh⁶ and J. Wosnitza¹

¹ *Dresden High Magnetic Field Laboratory, Germany*
² *Institute of Physics ASCR, Prague, Czech Republic*
³ *IFW Dresden, Germany*
⁴ *IMR, Tohoku University, Sendai, Japan*
⁵ *ISSP, Tokyo University, Kashiwa, Japan*
⁶ *Ural Federal University, Ekaterinburg, Russia*

Dy₂Fe₁₇ is an easy-plane rare-earth ferrimagnet. Applying sufficiently high magnetic field one can break the antiparallel alignment of the sublattice moments and drive the system towards the ferromagnetic state via intermediate non-collinear phases. In this particular case, if the magnetic field is applied within the easy plane, the moment direction of the Fe sublattice deviates only slightly from the field direction. The Dy-moment instead starts from the direction opposite to the field and the Fe moment, and subsequently passes several energetic minima. This manifests itself in corresponding jumps on the magnetization curve. Measurements in fields up to 67 Tesla have shown a field-induced jump on the magnetization curve for field aligned along the a axis. According to a theory developed for hexagonal ferrimagnets and having the field and the jump height along the a axis, we expected the jump along the b direction to appear at 78 T. To check this prediction, we have measured the high-field magnetization curve of a Dy₂Fe₁₇ single crystal for fields up to 85 Tesla along the b axis. We have observed a sharp magnetization jump at 77.8 Tesla, which agrees perfectly with the theory.

GJ04

Electrodeposited FePt films on Ag underlayer with high coercivity

Sirikanjana Thongmee
Department of Physics, Faculty of Science, Kasetsart University, Thailand

FePt films with a composition close to Fe₅₀Pt₅₀ were fabricated following with post annealing. The films were deposited onto Si substrate with a under layer of Ag. The phase formation temperature, microstructure evolution by annealing and the magnetic properties were investigated in detail. The L10 FePt phase started to form after annealing at 500 °C. From TEM results, as-deposited FePt films consisted of randomly oriented nanograin. The average grain sizes are about 5-10 nm. The increasing of temperature led to grain growth. The grain sizes of FePt films on Ag underlayer were about 50 nm after the film was annealed at 800 °C and SAED result was consistent with XRD. High coercivity of 15 kOe was obtained after annealing at 600 °C. After annealing at 800 °C, the coercivity increased to 18 kOe with a significant perpendicular anisotropy of FePt films. Out of plane anisotropy was observed in relatively thick film (800 nm). The work has shown that FePt film with a high coercivity can be achieved by electro-deposition and the thickness, anisotropy can be tuned, which may provide a method to fabricate FePt film for the potential applications both recording media and MEMS.

[1]. O. Gutflaisch, J. Lyubina, K. H. Muller, and L. Schultz, *Adv. Eng. Mater.* 7, 208 (2005) [2]. T. Maeda, T. Kai, A. Kikitsu, and J. I. Akiyama, *Appl. Phys. Lett.* 80, 2147 (2002). [3]. C. P. Luo and D. J. Sellmyer, *Appl. Phys. Lett.* 75, 3162 (1999) [4]. K. Leistner, M. Weisheit, L. Schultz, and S. Fahlke, *Appl. Phys. Lett.* 85, 3498 (2004) [5]. S. Inoue, T. Namazu, and K. Inoue, *Mater. Res. Soc. Symp. Proc.*, 426, 2213 (2003) [6]. Z.L. Zhao, J. Ding, K. Inaba, J.S. Chen, J.P. Wang, *Appl. Phys. Lett.* 83, 2196 (2003)

GJ05

Magnetic properties of BaMg_{0.4}Al_{0.4}Fe_{11.2}O₁₉+SiO₂ nanocomposites for high frequency applications

K Sadhana and K Praveena
Materials Research Centre, Indian Institute of Science, Bangalore-560012, India

The nanomcomposites of Ba_{0.3}Mg_{0.4}Al_{0.4}Fe_{11.2}O₁₉/SiO₂ were prepared using Microwave-Hydrothermal method at 160°C/45min. The as synthesized composites were characterized using X-ray diffraction and Transmission Electron microscopy (TEM). The average particle size is found to be 62nm. The present composites were densified using microwave sintering method at 900°C/60min. The frequency dependent complex permeability of the composites were measured in the range of 1MHz to 1.8GHz. The real part of permeability of the composites found to decreases with an addition of SiO₂ but the resonant frequency is shifted towards higher frequency side. The magnetic properties such as saturation magnetization and coercive field of sintered composites were calculated based on M-H curves. A possible relation between the magnetic hysteresis curves and the microstructure of the sintered composites was investigated.

HA01

Coexistence of competing orders in unconventional superconductors

Setsuko Tajima*, E. Uykur, K. Tanaka, T. Masui and S. Miyasaka
Dept. of Physics, Osaka University, Japan

In my talk, I will focus on the problem of the coexistence of competing orders which is probably inevitable in strongly interacted systems. A typical example is the pseudogap state in high Tc superconducting cuprates, which has been a long-standing puzzle. In order to address this problem, we have carefully measured the c-axis polarized optical spectra of YBa₂(Cu,Zn)₃O_y. Removing an additional spectral feature due to the transverse Josephson plasma by Zn-doping, we could unambiguously discuss the spectral weight transfer. The result clearly showed that the pseudogap originates from some competing order but not a precursor of superconductivity. Moreover, we found that the pseudogap persists even below Tc, which becomes pronounced by Zn-substitution. This indicates that the pseudogap and the superconducting gap are coexisting, presumably in a phase separated form. The most interesting problem is whether or not such a coexistence of competing order plays a positive role in superconductivity mechanism. One of the interesting facts is that the onset temperature for superconducting fluctuation increases with decreasing doping. Its energy scale is unusually large (~ 0.4eV). This suggests that the competing order with a large energy scale contributes to superconducting fluctuation and possibly to pairing mechanism.

HA02

Ultrafast transient generation of spin density wave order in the normal state of BaFe₂As₂ driven by coherent lattice vibrations

Kyungwan Kim^{1*}, Alexej Pashkin¹, Hanjo Schaefer², Markus Beyer², Michael Porez², Thomas Wolf³, Christian Bernhard⁴, Jure Demsar², Rupert Huber³ and Alfred Leitnerstorfer²
¹ *Department of Physics, Chungbuk National University, Korea*
² *Department of Physics, University of Konstanz, Germany*
³ *Department of Physics, University of Regensburg, Germany*
⁴ *Karlsruhe Institute of Technology, Institute for Solid-State Physics, Germany*
⁵ *Department of Physics, University of Fribourg, Switzerland*

The proximity of magnetic ground states to the superconductivity in cuprates and pnictides as well as in other unconventional superconductors has put the magnetism at the heart of the discussion concerning the mechanism of high temperature superconductivity. The recent development of the pump-probe time domain spectroscopy, which was typically limited in the terahertz region below 10 meV, has extended its spectral window to the infrared (IR) region allowing a resonant probe of important elementary excitations such as phonons, excitations across a superconducting gap as well as a density wave gap. We study the ultrafast dynamics of the spin density waves (SDWs) in BaFe₂As₂, a parent compound of pnictide high temperature superconductors. We monitor the SDW gap resonantly by the near-infrared (NIR) pump-IR probe technique. In the SDW state, we observe that the NIR excitation of the carriers breaks the SDW order. The excitation with yet higher fluence launches strong coherent lattice vibrations. Strikingly, these coherent oscillations give rise to a transient SDW order even in the normal state. We discuss that the strong electron-phonon/spin-phonon coupling effects in pnictides result in the modulations of the SDW order parameter in real time in response to the coherent phonon vibrations.

K. W. Kim et al., Nature Materials (2012, to be published)

HA03

High- and low-energy ARPES study of spin-density wave order in FeTe single crystals and FeTeOx films

Martin Mansson^{1*}, Yuefeng Nie², Yasmine Sassa¹, Christof Niedermayer¹, Genda Gu¹, Masaki Kobayashi¹, Vladimir Strokov³, Johan Chang², Magnus Bernsten¹, Olof Gotberg¹, Bastian M. Wojek¹, Oscar Tjernberg¹, Joseph I. Budnick⁴ and Barrett O. Wells⁵
¹ *Lab. for Solid State Physics, ETH Zurich, Switzerland*
² *Department of Physics, University of Connecticut, USA*
³ *Lab. for Neutron Scattering, Paul Scherrer Institut, Switzerland*
⁴ *Brookhaven National Laboratory, USA*
⁵ *Swiss Light Source, Paul Scherrer Institut, Switzerland*
⁶ *LSNS, EPPF Lausanne, Switzerland*
⁷ *Materials Physics, Royal Institute of Technology, KTH Stockholm, Sweden*

We have performed a high-resolution (synchrotron- and laser-based) ARPES investigation of FeTe single crystals/films, as well as thin films of the novel superconductor FeTeOx [1]. Our results from the single crystals reflect the previously reported Fermi surface pocket around the X-point [(π, 0)], possibly connected to a spin-density wave (SDW) order [2]. Unlike such previous report, our results also reveal the presence of an energy gap (Δ), which would be expected from the SDW order. The temperature dependence shows that Δ closes in the vicinity of the magnetic transition temperature, supporting its interpretation as reflecting the SDW state. We also present bulk sensitive results acquired using a soft x-ray ARPES technique. Photon-energy (i.e. kz) dependent measurements reveal a strongly 3D electronic structure that can be uniquely connected to the SDW-gap symmetry found in the low-energy data. Our results clearly illustrate the importance of acquiring not only the true intrinsic bulk-electronic structure but also that it is imperative to consider the full 3D band dispersion in iron-based superconductors and their parent compound in order to obtain an adequate theoretical understanding. Finally, we also acquired novel ARPES data from cleaved FeTe and FeTeOx thin films.

[1] Y.F. Nie et al., *Phys. Rev. B* 82, 020508(R) (2010) [2] Y. Xia, *PRL* 103, 037002 (2009) Funding Source: DOE-BES through contract DE-FG02-00ER45801 and the Swiss National Science Foundation (Project 6, NCCR MaNEP).

HA04

Magnetic fluctuations - a driving force for superconductivity Neutron scattering investigations in Fe-based superconductors.

Alice Elizabeth Taylor^{1*}, Russell A. Ewings², Toby G. Perring², Simon J. Clarke³ and Andrew T Boothroyd⁴
¹ *Department, University of Oxford, United Kingdom*
² *ISIS Facility, Rutherford Appleton Laboratory, STFC, United Kingdom*
³ *Department of Chemistry, University of Oxford, United Kingdom*
⁴ *Department of Physics, University of Oxford, United Kingdom*

One of the most exciting findings in investigations of High-Tc superconductivity has been the discovery of a magnetic resonance in the superconducting state, associated with a spin excitation with a characteristic position in wavevector and energy space [1]. This resonance has been investigated across the families of Fe-based superconductors with several common features observed such as the scaling of the resonant energy with Tc (Er ~ 4.3 Tc in (Ba,K)Fe₂As₂ [1]) and the position of the resonance either at, or incommensurate about, the antiferromagnetic wavevector [1,2,3]. This work presents results of inelastic neutron scattering experiments on a broad range of Fe-based superconducting materials in order to address the question - are these features really common to all these materials? Results from the characteristic 122-arsenide family [4] are contrasted with LiFeAs [2], CsxFe_{2-x}Se₂ and phosphorus containing materials.

[1] A. D. Christianson et al., *Nature* 456, 930 (2008) [2] A. E. Taylor et al., *Phys. Rev. B* 83, 220514(R) (2011) [3] J. -P. Castellan et al., *Phys. Rev. Lett.* 107, 177003 (2011) [4] R. A. Ewings et al., *Phys. Rev. B* 83, 214519 (2011)

HA05

Low-energy quasiparticles probed by heat transport in the iron based superconductor lafepo

Michael Sutherland¹, J. Dunn², W. H. Toews³, Eoin O' Farrell¹, James Analytis⁵, Ian Fisher⁵ and R. W. Hill¹

¹ Department of Physics, Univeristy of Cambridge, United Kingdom

² Department of Physics, University of Waterloo, Canada

³ Department of Physics, Univeristy of Waterloo, Canada

⁴ I.S.S.P., University of Tokyo, Japan

⁵ Geballe Laboratory for Advanced Materials and Department of Applied Physics, Stanford University, USA

Measurements of ultra-low temperature heat transport are an extremely effective probe of the presence of nodes in the superconducting order parameter. In this study we report the thermal conductivity of the iron pnictide superconductor LaFePO down to temperatures as low as T=60mK and in magnetic fields up to 5 T. The data shows a large residual contribution that is linear in temperature, consistent with the presence of low-energy electronic quasiparticles [1]. We interpret the magnitude of the linear term, as well as the field and temperature dependence of thermal transport in several pairing scenarios, with the aim of distinguishing between accidental or symmetry imposed nodes. The presence of an unusual supralinear temperature dependence of the electronic thermal conductivity in zero magnetic field, and a high scattering rate with minimal Tc suppression argues for a sign-changing nodal s+/- state. We compare these results to recent thermal transport studies in related iron-based superconductors.

M. Sutherland et al. Phys. Rev. B 85, 014517 (2012)

HB01

Domains and magnetization processes in electrical steel

Rudolf Schaefer

Leibniz Institute for Solid State and Materials Research (IFW) Dresden, Germany

Understanding and lowering of energy loss in electrical steel requires knowledge about the magnetic domains and magnetization processes. In this presentation some aspects of domains and processes will be addressed, based on domain analysis by Kerr microscopy and neutron imaging. The former provides information on the surface domains and requires the support of domain theory to come up with conclusive models. Examples will be shown for oriented and non-oriented material, including the effects of mechanical stress [1]. The volume domains, which are relevant for key magnetic properties like susceptibility, energy loss, noise or coercivity, can be analysed by the novel method of neutron dark-field microscopy [2,3]. By this grating interferometry technique, the domains and magnetization propagation in bulk FeSi material can be imaged non-destructively and even tomographic analysis becomes possible [4] with a lateral resolution down to 10 µm. The method has the unique potential to visualize the magnetic field penetration in bulk material [3].

[1] O. Perervetov and R. Schaefer: Influence of applied compressive stress on the hysteresis curves and magnetic domain structure of grain-oriented transverse Fe-3%Si steel. Accepted for J. Phys. D: Applied Physics (2012) [2] C. Grunzweig, et al.: Neutron decoherence imaging for visualizing bulk magnetic domain structures. Phys. Rev. Lett. 101, 025504 (2008) [3] C. Grunzweig, et al.: Visualizing the propagation of volume magnetization in bulk ferromagnetic materials by neutron grating interferometry (invited). J. Appl. Phys. 107, 09D308 (2010) [4] I. Manke, et al.: Three-dimensional imaging of magnetic domains. Nature Communications, 1:125 doi: 10.1038/ncomms1125 (2010)

HB02

Iron loss behaviors in 6.5 wt% grain-oriented silicon steel

Jongryoul Kim* and Heejong Jung

Department of Metallurgy and Material Science, Hanyang University, Korea

6.5 wt% silicon steel has great potential for electrical appliances and devices, such as transformer and motor cores, due to its high electrical resistance, extremely low magnetostriiction, low magnetocrystalline anisotropy, and low iron loss [1-2]. However, the presence of ordered phases, i.e. B2, D03, deteriorates the workability of the 6.5 wt% silicon steel, which impedes the mass production using the conventional rolling technique [2]. In addition, there is a lack of research on the effect of the ordered phases on the magnetic behaviors of high silicon steels. In this paper, we, therefore, investigated the relationship between the ordered phases and the iron loss behaviors in high silicon steels using transmission electron microscopy and Kerr microscopy. In order to obtain the high silicon steels, 3 wt% grain-oriented silicon steels inserted between SiO₂ textiles were annealed for the decomposition of the textiles and the diffusion of Si. The size, shape and amount of the ordered phases were controlled by thermo-mechanical treatment. The microscopical analyses showed that the antiphase boundaries of the ordered phases cut magnetic domains, which strongly affected the iron loss behaviors of the high silicon steels.

[1] P. R. Swann, W. R. Duff, and R. M. Fischer, Phys. Stat. Sol., 37 (1970) 577-583 [2] B. Viala, J. Degauque, M. Barico, E. Ferrara, and F. Fiorillo, Mater. Sci. Eng. A, 212 (1996) 62-68

HB03

FeCoB films with large saturation magnetization and high magnetic anisotropy field to attain high ferromagnetic resonance frequency

Shigeki Nakagawa

Dept. of Physical Electronics, Tokyo Institute of Technology, Japan

FeCoB films prepared on a Ru underlayer using the Oblique incidence of sputtered and backscattered particles have a high in-plane magnetic anisotropy field of 500 Oe. Facing targets sputtering system is suitable to attain such deposition condition. In-plane X-ray diffraction analysis clarified that there is anisotropic residual stress, which is the origin of the high in-plane magnetic anisotropy. The directional crystalline alignment and inclination of crystallite growth were also observed. Such anisotropic crystalline structures may affect the anisotropic residual stress in the FeCoB layer. The B content of 6 at.% was appropriate to induce such anisotropic residual stress. The anisotropic residual stress develops according with the film growth. The film with large saturation magnetization of 22 kG and high magnetic anisotropy field of 500 Oe exhibited high ferromagnetic resonance frequency of 9.2 GHz. The large saturation magnetization and the low coercivity along the hard axis direction assure that the film can be operated in the high frequency range up to 8 GHz with maintaining high relative permeability.

HC01

Magnetism where you least expect it

Priya Mahadevan

Department of Condensed Matter Physics and Material Science, S.N.Bose National Centre for Basic Sciences, India

The picture of magnetism that has prevailed over the years has centered around the existence of localized electrons and their ordering leading to different types of magnetic order. Recently several unconventional examples of magnetism have been emerged such as p-band magnetism in alkali metal oxides - a system with no traditional magnetic ions in them. Unfortunately high magnetic ordering temperatures were not possible and this was traced to an orbital ordering transition [1]. While orbital ordering is usually found to reinforce one type of magnetic order over another, in the present case one found it led to the loss of any possibility of high magnetic ordering temperature. In another example, we consider the example of a 4d oxide SrTeO₃ where recent experiments [2] have found a Neel temperature of 1023 K, far higher than its 3d counterpart SrMnO₃. A detailed analysis [3] within a microscopic multiband Hubbard model reveals a rather surprising result of higher bandwidth and smaller Hund's exchange coupling strength resulting in higher magnetic ordering temperatures in 'SrTeO₃-type' oxides. This is work done in collaboration with A.K. Nandy, S. Middey, P. Sen and D.D. Sarma.

[1] A. K. Nandy, Priya Mahadevan, P. Sen and D. D. Sarma. Phys. Rev. Lett. 105, 056403 (2010). [2] E.E. Rodriguez, F. Poineau, A. Llobet, B. J. Kennedy, M. Avdeev, G. J. Thorogood, M. L. Carter6, R. Seshadri, D. J. Singh, and A. K. Cheetham, Phys. Rev. Lett. 106, 067201 (2011). [3]. S. Middey, A.K. Nandy, P. Mahadevan and D.D. Sarma, cond-mat arXiv:1112.5587.

HC02

Exotic magnetism of s-electron cluster array: Ferromagnetism, ferrimagnetism and antiferromagnetism

Takehito Nakano¹, Nguyen Hoang Nam², Truong Cong Duan³, Duong Thi Hanh³, Shingo Araki⁴ and Yasuo Nozue^{1*}

¹ Department of Physics, Graduate School of Science, Osaka University, Japan

² Hanoi University of Science, Viet Nam

³ FPT University, Viet Nam

⁴ Graduate School of Natural Science and Technology, Okayama University, Japan

Alkali metal nanoclusters can be stabilized in the regular cages of zeolite crystals by the loading of guest alkali metals. Cages are connected by the sharing of windows of aluminosilicate framework, and arrayed in simple cubic, diamond and body centered cubic structures in zeolites A, X and sodalite, respectively. The s-electrons have the localized nature of nanoclusters with magnetic moments and the mutual interaction through windows. They show exotic magnetism depending on the structure type of zeolite, alkali metal and the average loading density of alkali atoms per cage, n. In zeolite A, potassium clusters are formed in alpha-cages. They exhibit spontaneous magnetization at n > 2. Ferromagnetic properties are explained by the canted antiferromagnetism of the Mott insulator, where the canting provided by Dzyaloshinsky-Moriya interaction is strongly enhanced by the 1p-like degenerate molecular orbitals of clusters[1] and the superlattice structure. Rb clusters generated at alpha- and beta-cages of zeolite A exhibit ferrimagnetic properties[2]. Na-K alloy clusters generated at supercages and beta-cages of low-silica X zeolite exhibit ferrimagnetism at specific loading densities of alkali metals, where clusters are in the metallic phase[3]. Alkali metal clusters in sodalite show the Heisenberg antiferromagnetism of the Mott insulator[4].

[1] T. Nakano and Y. Nozue, J. Comp. Meth. Sci. Engin. 7, 443 (2007). [2] T.C. Duan, T. Nakano and Y. Nozue, e-J. Surf. Sci. Nanotech. 5, 6 (2007). [3] D.T. Hanh, T. Nakano and Y. Nozue, J. Phys. Chem. Solids 71, 677 (2010). [4] T. Nakano, R. Suehiro, A. Hamazawa, K. Watanabe, I. Watanabe, A. Amato, F.L. Pratt and Y. Nozue, J. Phys. Soc. Jpn. 79, 73707 (2010).

HC03

Spin-dependent molecular arrangement of O₂-O₂ dimer in nanoporous metal-organic solids

Tatsuo C. Kobayashi¹, Akihiro Hori², Yoshiki Kubota³, Akira Matsuo⁴, Koichi Kindo⁴, Jungeun Kim⁵, Masaki Takata², Hirotoishi Sakamoto⁶, Ryotaro Matsuda⁶ and Susumu Kitagawa⁷

¹ Department of Physics, Okayama University, Japan

² RIKEN SPring-8 Center, Japan

³ Department of Physical Science, Osaka Prefecture University, Japan

⁴ ISSP, The University of Tokyo, Japan

⁵ JASRI/SPring-8, Japan

⁶ ERATO, JST, Japan

⁷ ICeMS, Kyoto University, Japan

O₂ is a molecular magnet with S = 1. The characteristic magnetic properties related to the molecular arrangement can be expected since the magnetic exchange interaction between O₂ is comparable to the electric interaction between the quadrupole moments. [1] Recently, for a model system of isolated O₂-O₂ dimer confined in the nanopores of Cu-cyclohexanedicarboxylic acid, the molecular arrangement structure relating to its magnetic properties was investigated by precise x-ray diffraction analysis. The obtained charge density level structures revealed that the significant orientational change of the molecular axes occurs with changing temperature, coupling with the spin states of O₂-O₂ dimer. The temperature dependence of magnetic susceptibility and the magnetization process characterized by the absence of half-plateau (S_{dimer} = 1) can be consistently explained by a simple model taking into account the orientational change of molecular axes. Consequently, the present results experimentally proved that the molecular orientation depends on the spin state, the rectangular parallel H-geometry for the singlet ground state (S_{dimer} = 0) and the shifted parallel S-geometry for the thermally excited quintet state (S_{dimer} = 2), due to the spin-dependent intermolecular potential which has not been discussed for solid O₂.

R. Kitaura et al. Science 298, 2358 (2002).

HC04

Indications for a field-induced 2d collectively-coupled dimer state in nitronyl-nitroxid biradicals

Michael Lang^{1*}, Bernd Wolf¹, Pham Thanh Cong¹, Ulrich Tutsch¹, Martin Baumgarten², Yulia Borozdina², Dominik Strassel¹ and Sebastian Eggert¹

¹ Physics Institute, Goethe-University Frankfurt (M), SFB/TR 49, D-60438 Frankfurt (M), Germany, Germany

² Max-Planck-Institute for Polymer Research, SFB/TR 49, D-55128 Mainz, Germany, Germany

³ Physics Department and Research Center OPTIMAS, University of Kaiserslautern, D-67663 Kaiserslautern, Germany

Arrays of coupled spin S = ½ dimers, exposed to a magnetic field, are of general interest as they can be considered as the source for generating a gas of interacting bosons [1]. We present a novel coupled spin-dimer system with a double-layer structure based on nitronyl-nitroxid stable radicals bridged via tolan molecules. The intra-dimer coupling constant is around 10 K, whereas the inter-dimer couplings, mediated via H-bonds, are of the order of 1 K. The moderate size of these couplings enables us to study the field-induced ordered phase forming for T < 0.3 K and 8T ≤ B ≤ 9.5 T. The anomaly observed in the ac-susceptibility χ(B) differs significantly from ordinary B-induced 3d ordering, tantamount to Bose-Einstein condensation of magnetic excitations, where χ(B) shows sharp peaks at the on- and offset fields. Rather we find a rounded double-peak structure where the peaks remain rounded down to 75 mK, the base temperature of our experiment. These features indicate the formation of a 2d collectively-coupled dimer state, implying topological order for T → 0. In order to analyze the nature of the B-induced ordered state, the experimental data are compared with the results of Quantum-Monte-Carlo calculations.

[1] T. Giamarchi, Ch. Ruegg, O. Tchernyshyov, Nature Physics 4, 198 (2008).

HD01

Magnon caloritronics

Burkard Hillebrands*, Vitaliy Vasyuchka, Bjorn Obyr and Aleksandr Serga

Department of Physics, TU Kaiserslautern, Germany

Eigen excitations of a magnetic system, e. g. spin waves and their quanta, magnons, are expected to play an important role in spin-caloric effects. The recently observed spin Seebeck effect in a magnetic insulator demonstrates the strong connection between magnon and heat transport processes. I will address the interplay between magnon and heat transport phenomena and present recent Brillouin light scattering experiments from magnons in an yttrium iron garnet (YIG) waveguide subject to a temperature gradient. Two issues are addressed in a thermal gradient field: first the propagation of spin waves, and, second, the distribution of thermal magnons. We find, that, first, magnons adapt their wavelength in a thermal gradient field and stopping effects may occur. Second, we report direct measurements of the magnon distribution and show, that it does not follow the phonon temperature.

HD02

Temperature dependence of spin wave resonance frequency in a magnetostatic surface wave mode

Jae Hyun Kwon¹, Sankha Subhra Mukherjee² and Hyunsoo Yang^{1*}

¹ Electrical and Computer Engineering, National University of Singapore, Korea

² Electrical and Computer Engineering, National University of Singapore, India

Propagating spin waves in a 20 nm NiFe film, in the magnetostatic surface wave (MSSW) mode, have been measured at various temperatures in a time domain. Pulse inductive microwave magnetometry (PIMM) is used for the detection of spin wave packets. Impulse voltages were applied to the excitation coplanar waveguide (CPW) by a pulse generator, while the resultant dynamic responses were observed through a sampling oscilloscope at the detection CPW. The spin wave resonance frequencies (fR) increases with decreasing temperature. The saturation magnetization (MS) increases at low temperature, and consequently fR increases in accordance with the dispersion relation of MSSWs. The change in fR from 300 K to 12 K is approximately 400 MHz at a bias field of 280 Oe. A second mode is also observable below 100 K, and becomes progressively clearer at lower temperatures. At higher temperature, there is significant magnon-phonon interaction. However, the lattice vibrations become subsided at low temperatures, and magnon-phonon interaction reduces, while electron-electron scattering decreases. This causes a change in the nature of the damping phenomenon. The nature of the intrinsic damping has been investigated as a function of temperature and has been correlated to the difference in the damping mechanisms.

HD03

Nanoscale spin wave switches and phase shifters

Yat-yin Au and Volodymyr Kruglyak*

University of Exeter, United Kingdom

The short wavelength of spin waves propagating in nanoscale magnonic waveguides at microwave frequencies could potentially provide a device miniaturization opportunity via accomplishing certain tasks with a reduced number of physical devices as compared to semiconductor circuitry. To utilize this promise of magnonics, it is important to learn to manipulate the spin wave phase and perhaps magnitude, which is highly related to data encoding and logical operation, etc. Here, we use OOMMF simulations to demonstrate a new method of achieving controlled phase shift of spin waves that relies on the reverse of the recently discovered spin wave emission mechanism [1]. The method could be highly useful for magnonic applications since it depends heavily on the static magnetization of the control element in the structure. Hence, by changing static magnetization direction in the element, it is possible to control the magnitude and phase of propagating spin waves. These switchable, non-volatile devices could serve as either spin wave valves or phase shifters, all at the nanoscale and low energy cost. The research leading to these results has received funding from the EC's Seventh Framework Programme (FP7/2007-2013) under GAs 233552 (DYNAMAG) and 228673 (MAGNONICS) and from the EPSRC of the UK (EP/E055087/1).

[1] Y. Au, E. Ahmad, O. Dmytriev, M. Dvornik, T. Davison, and V. V. Kruglyak, (submitted).

HD04

Optically induced tunable magnetization dynamics in nanoscale Co antidot lattices

Ruma Mandal, Susmita Saha, Dheeraj Kumar, Saswati Barman, Semanti Pal, Kaustuv Das, Arup Kumar Raychaudhuri, Yasuhiro Fukuma, Yoshichika Otani and Anjan Barman*

Condensed Matter Physics and Material Sciences, S. N. Bose National Centre For Basic Sciences, India

We present the fabrication of high quality Co antidot lattice structures with 100 nm antidot diameter and with varying lattice constants S between 200 and 500 nm by using focused ion beam lithography. We have excited and detected the magnetization dynamics in those antidot lattice structures by an all-optical time-resolved Kerr microscope. The dynamics shows two prominent magnonic bands for sparsely packed lattices with a clear bandgap. The bandgap increases with the decrease in the lattice constant and at the lowest value of the lattice constant S = 200 nm, four distinct magnonic bands appear. The observations are qualitatively reproduced by micromagnetic simulations and the resonant mode profiles are calculated and interpreted. The lower frequency mode corresponds to the magnetostatic surface wave mode while the higher frequency modes are quantized modes with varying quantization number. We further demonstrate the tunability of magnonic spectra in composite structures constructing of antidot lattices with varying lattice constants arranged in varying geometry. The observations are important for potential applications of the antidot lattices in nanoscale magnonic crystals in the form of composite antidot structures with tunable bandgaps.

I. Kruglyak, V. V. Demokritov, S. O. Grundler, D. Magnonics, J. Phys. D: Appl. Phys. 2010, 43, 264001. 2. Neusser, S.; Duerr, G.; Bauer, H. G.; Tschli, S.; Madami, M.; Woltersdorf, G.; Gubbiotti, G.; Back, C. H.; Grundler, D., Anisotropic Propagation and Damping of SpinWaves in a Nanopatterned Antidot Lattice. Phys. Rev. Lett. 2010, 105, 067208. 3. Tschli, S.; Madami, M.; Gubbiotti, G.; Carloti, G.; Adeyeye, A. O.; Neusser, S.; Boters, B.; Grundler, D., Angular Dependence of Magnetic Normal Modes in NiFe Antidot Lattices with Different Lattice Symmetry; IEEE Trans. Magn. 2010, 46, 1440-1443.

HD05

Plasmonic and quantum plasmonic enhancement of magneto-optics

Alexey P. Vinogradov*, Denis G. Baranov¹ and Alexander A. Lisyansky²

¹ ITAE RAS, Russia

² Department of Physics., Queens College of the City University of New York, USA

We consider two scenarios of magneto-optical transmission lines build on the basis of an array of plasmonic nanoparticles. The first scenario corresponds to the well-known transmission line of the plasmonic nanoparticles embedded into a magneto-optical medium. We show that the propagation of the dipole-plasmonic mode travelling along the array is accompanied by the rotation of the polarization (the Faraday effect). The angle of rotation is dozens times greater than that in the uniform magneto-optical material. In the second case, we consider a chain of metallic nano-particles exhibiting magneto-optical properties embedded into a dielectric matrix. When the matrix is passive, in spite of the plasmonic resonance, the Faraday rotation enhancement is small due to the small propagation length of the dipole-plasmonic mode. In an active matrix, the metal nanoparticles are surrounded by active centers (quantum dots or active molecules) forming magneto-optical spasers. The dipole-plasmonic mode in such an array of spasers exhibits high values of the Faraday rotation and the propagation length.

HE01

Pure spin current generation using highly spin polarized Co₂FeSi electrodes

Takashi Kimura*, Soichiro Oki, Shinya Yamada, Masanobu Miyao and Kohei Hamaya

Kyushu University, Japan

Pure spin current provides attractive means for the efficient operation of spin-based electronic devices. Efficient generation of the pure spin current may be a key for developing the future spin-based devices. However, the generation efficiency of the pure spin current using the conventional ferromagnetic metal electrodes such as NiFe and Co is extremely low. This is because most of the injected spin currents return back to the spin injector with the low spin polarization. Such back flows of the spin currents can be effectively reduced by using highly spin polarized ferromagnetic electrodes. In the present study, we fabricated lateral spin valves with Co₂FeSi electrodes, which is one of the Heusler compounds expecting half metallicity. Large nonlocal spin valve signals were observed at room temperature, revealing the high spin polarization of the Co₂FeSi electrodes. From the analysis based on one-dimensional spin diffusion model, the generation efficiency of the pure spin current is found to be significantly enhanced compared to those with the conventional ferromagnetic electrodes. [1] Moreover, from the systematic study of numerous number of the devices, we found the correlation between the electrical resistivity and the spin polarization. [2]

[1] T. Kimura, N. Hashimoto, S. Yamada, M. Miyao and K. Hamaya, *NPG asia materials*, To be published [2] K. Hamaya, N. Hashimoto, S. Oki, S. Yamada, M. Miyao and T. Kimura, *Phys. Rev. B*, (Rapid comm.), in press

HE02

Highly reproducible lateral spin valves for the study of spin injection in metals

Estitxu Villamor¹, Miren Isasa¹, Luis E. Hueso² and Felix Casanova^{2*}

¹ CIC nanoGUNE, Spain

² CIC nanoGUNE and IKERBASQUE, Basque Foundation for Science, Spain

Creation and transport of pure spin currents is a key ingredient in spintronics, which can be achieved by electrical spin injection using lateral spin valves (LSV) [1]. We fabricated highly reproducible LSV devices by using a two-step electron-beam lithography process. In the first step, ferromagnetic (FM) electrodes (Co or Py) were deposited and, in the second one, the non-magnetic (NM) metal (Cu, Au or Ag) was put on top. In these devices, the spin signal was measured at different distances and temperature (T), from which the spin polarization of the FM (α) and the spin diffusion length of the NM (λ) are obtained as a function of T. Whereas $\lambda(T)$ shows the role of surface spin-flip scattering [2] in the various NM, the results in $\alpha(T)$ for the various FM metals help understanding the role of the FM/NM interface in the electrical spin injection. Furthermore, due to the high reproducibility of our LSV devices, $\lambda(T)$ for Co can be independently obtained. The latter parameter has been controversial for its anomalously large value [3]. These results are relevant to control the role of FM metals in electrical spin injection and of NM metals in spin transport.

[1] F. J. Jedema, M. S. Nijboer, A. T. Filip, B. J. van Wees, *Phys. Rev. B* 67, 085319 (2003) [2] T. Kimura, T. Sato, Y. Otani, *Phys. Rev. Lett.* 100, 066602 (2008) [3] J. Bass and W. P. Pratt, *J. Phys.: Condens. Matter* 19, 183201 (2007)

HE03

Extrinsic SHE induced by small impurities in copper

Yoshichika Otani*, Yasuhiro Niimi, Yohei Kawanishi and Dahai Wei

ISSP, University of Tokyo, Japan

Spintronic devices manipulating pure spin currents, flow of spins with no net charge flow, must play an important role in low energy consumption electronics of next generation. This explains the current interest for the spin Hall effect (SHE) which provides a purely electrical way to generate spin currents without ferromagnets and magnetic fields. The inverse SHE (ISHE) is the only means to generate electrical signals from spin currents. It is indispensable for practical applications to have a large spin Hall (SH) angle which characterizes the efficiency in conversion between charge and spin currents. Today platinum is adopted as the best material for this conversion. The ISHE of Pt, for instance, has been used for the detection of spin currents produced from heat flows by the spin Seebeck effect. Thus it is a prime task to find materials with large SH angles and preferably lower cost than Pt. Here we discuss how a giant SH angle (-12%) can be obtained by simply doping copper with a small amount of bismuth impurities.

HE04

Spin Injection at the LaAlO₃/SrTiO₃ Interface

Nicolas Reyren, Manuel Bibes, Edouard Lesne*, Jean - Marie George, Cyril Deranlot,

Sophie Collin, Agnes Barthelemy and Henri Jaffres

Unite Mixte de Physique CNRS/Thales, France

Future spintronics devices will be built from elemental blocks allowing the electrical injection, propagation, manipulation and detection of spin-based information. Owing to their remarkable multifunctional and strongly correlated character, oxide materials already provide such building blocks for charge-based planar devices such as ferroelectric field-effect transistors, as well as for spin-based vertical devices like magnetic tunnel junctions, with giant responses in both cases. In an attempt to bridge these two areas, we report results of electrical spin injection at the high-mobility quasi-two-dimensional electron system (2-DES) that forms at the LaAlO₃/SrTiO₃ interface [1]. In a non-local, three-terminal measurement geometry, we analyze the voltage variation associated with the precession of the injected spin accumulation driven by perpendicular or transverse magnetic fields (Hanle and inverted Hanle effect) [2]. The influence of bias and back-gate voltages reveals that the spin accumulation signal is amplified by resonant tunneling through localized states in the LaAlO₃, strongly coupled to the 2-DES by tunneling transfer.

[1] A. Ohtomo, and H. Y. Hwang, *Nature* 427, 423 (2004). [2] S.P. Dash et al., *Phys. Rev. B* 84, 054410 (2011).

HE05

Coherence in collective spin precession in lateral spin valves

Hiroshi Idzuchi^{1*}, Yasuhiro Fukuma² and Yoshichika Otani³

¹ ISSP, U Tokyo; ASI RIKEN, Japan

² ASI RIKEN; Department of Computer Science and Electronics, Kyushu Institute of Technology, Japan

³ ISSP U Tokyo; ASI RIKEN, Japan

Pure spin current is a diffusive flow of spins with no charge flow, which has drawn much attention worldwide due to spintronic application as well as fundamental interests. Non-local spin injection in a lateral spin valve generates a pure spin current, of which polarization direction can be modulated via Larmor precession [1]. During the diffusive transport between injector and detector, however, spins lose phase coherency with frequent collisions, because these events lead to a broad distribution of dwell time. Here we show that the lateral spin-valves with dual injector Permalloy/MgO/Ag enable us to detect highly coherent spin precession over a distance of 10 μ m with keeping spin accumulation vector in plane against out of plane magnetization process, which results in genuine signal of the in-plane precession. We also experimentally found that the better the phase coherency becomes the longer the spins travel. This tendency appears to fall on a material independent universal curve when the coherence is plotted against the reduced parameter of the injector-detector distance over spin diffusion length. This is useful for the material design of spintronics devices based on pure spin current.

[1] Y. Fukuma, L. Wang, H. Idzuchi, S. Takahashi, S. Maekawa, and Y. Otani, *Nature Materials*, 10, 527 (2011).

HF01

Bias-dependence of the spin-transfer torques in MgO-based magnetic tunnel junctions

Soeren Boyn¹, Rie Matsumoto¹, Joao Sampaio¹, Vincent Cros¹, Julie Grollier¹, Akio Fukushima², Hitoshi Kubota², Kay Yakushiji² and Shinji Yuasa²

¹ Unite Mixte de Physique CNRS/Thales, France

² National Institute of Advanced Industrial Science and Technology, Japan

Understanding the bias dependence of the two spin-transfer torques (IP in-plane and OOP out-of-plane) in Magnetic Tunnel Junctions (MTJs) is important from the fundamental point of view and for applications. For example, back-hopping phenomena at large bias, unwelcome for MRAM applications, has been ascribed to a competition between IP and OOP torques [1]. There is still a debate on the expected bias dependence of both torques. In symmetric tunnel junctions (same thickness and composition for both ferromagnetic electrodes), some results report a OOP torque linear with bias [2], and others quadratic [3]. It has also been shown that by voluntarily introducing an asymmetry in the MTJ, it was possible to control the sign of the linear part of the OOP torque [4,5]. The presented work is a systematic study of the bias-dependence of the two torques in MTJs with different compositions for the electrodes, ranging from symmetric CoFeB/MgO/CoFeB to asymmetric CoFeB/MgO/NiFe MTJs. We will present the switching phase diagrams of the different MTJs, from which we infer the evolution of the two torques by comparing our experimental results to numerical simulations. Financial support by JSPS Postdoctoral Fellowships For Research Abroad and the ERC 2010 Stg 259068 is acknowledged.

[1] J.Z. Sun et al., *J. Appl. Phys.* 105, 07D109 (2009) [2] O. Heinonen et al., *Phys. Rev. Lett.* 105, 066602 (2010) [3] H. Kubota et al., *Nature Phys.* 4, 37 (2007) and *J. Sankey, Nature Phys.* 4, 67 (2007) [4] S.-C. Oh et al., *Nature Phys.* 5, 898 (2009) [5] A. Chanthbouala et al., *Nature Phys.* 7, 626 (2011)

HF02

Spin torque assisted magnetization switching in thermally activated region

Tomohiro Taniguchi and Hiroshi Imamura*

Nanosystem Research Institute, National Institute of Advanced Industrial Science and Technology, Japan

Thermal stability is an important quantity of ferromagnets because it determines performances of spintronics devices. The value of the thermal stability has been determined by analyzing the spin torque switching in the thermally activated region with the switching probability formula, $P=1-\exp[-f\exp(-\Delta(1-Ic)^b)]$, where Δ , I , and Ic are the thermal stability, current, and spin torque critical current at zero temperature, respectively. The value of the exponent, b , has been assumed to be unity. However, recently, several authors, including us, argued that $b=2$. The determination of b is important because it significantly affects the estimation of the thermal stability. Recently, Heindl et al. (JAP 109) experimentally found that the current pulse duration time dependence of the switching current shows nonlinearity, while the theory with $b=1$ predicts linear dependence. They concluded that the discrepancy arises from the breakdown of the thermal model. In this study, we theoretically studied the spin torque switching in the thermally activated region. We employed the mean first passage time approach which reduces the exact solution of the switching probability in the whole range of the thermally activated region and gives $b=2$ in several limits. Our theory reproduced the nonlinearity of the switching current obtained by Heindl et al.

HF03

Joule heating and spin-transfer torque investigated on the atomic scale

Stefan Krause*, Gabriela Herzog, Anika Schlenhoff, Andreas Sonntag and Roland Wiesendanger

Institute of Applied Physics, University of Hamburg, Germany

Reorienting the magnetization of a nanostructure by injecting a spin-polarized current is in the focus of ongoing research because of its relevance for future spintronic and magnetic memory devices. Recent experiments using spin-polarized scanning tunneling microscopy (SP-STM) demonstrated current-induced magnetization switching (CIMS) across a vacuum barrier, driven by Joule heating, spin-transfer torque and Oersted field [1,2]. In our study, we specially utilize a superparamagnetic Fe/W(110) nanoisland to explore CIMS with SPSTM. By simultaneously observing and manipulating its switching behavior with a spin-polarized tunnel current, we separate and quantitatively determine the individual contributions of Joule heating and spin-transfer torque, with the nanoisland serving as a combined local thermometer and spin-transfer torque analyzer. Comparing our results to experiments performed on nanopillar MTJs reveals a very high spin-transfer torque efficiency for SP-STM MTJs. Our studies allow for a detailed investigation of Joule heat generation and spin-transfer torque switching on the atomic scale, thereby providing new insight into the details of CIMS.

[1] S. Krause, L. Berbil-Bautista, G. Herzog, M. Bode, and R. Wiesendanger, *Science* 317, 1537 (2007). [2] G. Herzog, S. Krause, and R. Wiesendanger, *Appl. Phys. Lett.* 96, 102505 (2010).

HF04

Spin-transfer torque and joule heating of field-emitted electrons

Anika Schlenhoff*, Andreas Sonntag, Stefan Krause and Roland Wiesendanger

Institute of Applied Physics, University of Hamburg, Germany

Applying a high electrostatic field results in the emission of electrons from a solid surface into vacuum. These field-emitted electrons are used for microscopy purposes [1]. For magnetic emitters the spin polarization of the field-emission current has been detected since the 1960's [2]. However, the microscopic details of the interaction of spin-polarized field-emitted electrons with magnets remain to be discovered. Here, we utilize spin-polarized scanning tunneling microscopy (SP-STM) in the field emission mode [3] for the direct observation and manipulation of atomic-scale superparamagnets. Injecting high spin-polarized currents into the first field emission resonance (FER) of individual magnets reveals the switching behavior being strongly affected. Telegraphic noise experiments allow for a current-dependent lifetime analysis [4], thereby quantifying the spin-transfer torque and Joule heating of the field-emitted electrons. Switching the magnetization of quasistable nanomagnets is realized by ramping field emission currents. Our experiments demonstrate the capability of field-emitted electrons for magnetic observation and manipulation on the atomic scale at nm distances.

[1] E. W. Muller, *Z. Physik* 108, 668 (1938). [2] M. Hofmann et al., *Phys. Lett.* 25A, 270 (1967). [3] A. Kubetzka et al., *Appl. Phys. Lett.* 91, 012508 (2007). [4] S. Krause et al., *Phys. Rev. Lett.* 107, 186601 (2011).

HF05

Perpendicular spin torque at high bias in MgO-based magnetic tunnel junctions

Kyung-jin Lee^{1*}, Seung-young Park², Younghun Jo² and Soo-man Seo¹

¹ Korea University, Korea

² Korea Basic Science Institute, Korea

This talk will consist of two parts. One is an experimental study on bias-dependence of perpendicular spin torque in MgO-based magnetic tunnel junctions (MTJs) and the other is a numerical study on current-induced self-resonant switching of magnetization. In the first part, we show an experimental method to estimate the bias dependence of the perpendicular spin torque in MTJs based on the switching phase diagrams [1]. A special attention is paid for high-bias range. Our method utilizes the pulse-width-dependent change in the switching phase diagram and addresses the perpendicular-torque-driven precessional switching at high-bias ranges where the in-plane spin torque acts as an additional damping. The bias dependence of the perpendicular spin torque at high bias was found to be linear for a voltage polarity. This method will be useful to address spin torque effects in MTJs at high bias. In the second part, we propose a new type of current-induced magnetization switching in multilayers. It utilizes spin torques caused by DC current injection and consequent RF fields caused by magnetization dynamics. We show that this way of switching magnetization is more efficient than the conventional ways. It allows a large reduction in the switching current with keeping the thermal stability.

[1] S.-C. Oh et al., *Nature Phys.* 5, 898 (2009); S.-Y. Park et al., *J. Phys. D: Appl. Phys.* 44, 064008 (2011); S.-Y. Park, Y. Jo, and K.-J. Lee, *Phys. Rev. B* 84, 214417 (2011).

HG01

Recent progress in spin sem

Kazuyuki Koike

Division of Physics, Graduate School of Science, Hokkaido University, Japan

Spin-polarized scanning electron microscopy (spin SEM) is a magnetic domain observation method. It has excellent capabilities, including high spatial resolution, high sensitivity to a thin or even a monolayer film, a large dynamic observation range, and detection of magnetization direction. Since the initial development of spin SEM by Koike et al. in 1984[1], its capabilities have been greatly improved. The spatial resolution is now 3 nm[2], the sample can be cooled down to 10 K, and images of three magnetization components and surface topography can be obtained simultaneously[3]. Moreover, images of elements and crystallographic orientation can be obtained for the same area as the magnetic domain image. Taking advantage of these capabilities, we have studied recorded bits of high density magnetic recording media, magnetic coupling between a ferromagnetic Fe thin film and a single-crystal NiO antiferromagnet[4], a patterned magnetic island array[5], and the temperature-dependent spin structure of a strongly correlated magnetic material: La_{2-2x}Sr_{1-2x}Mn₂O₇ ($x = 0.30, 0.32$)[6][7]. In this talk, I will discuss the above topics in detail, and demonstrate the applicability of spin SEM to various fields related to magnetism.

[1] K. Koike et al. *Jpn. J. Appl. Phys.* 23 (1984) L187. [2] K. Koike et al. in preparation [3] T. Kohashi et al. *Rev. Sci. Instrum.* 75 (2004) 2003. [4] H. Matsuyama et al. *Phys. Rev. Lett.* 85 (2000) 646. [5] N. Kida et al. *Phys. Rev. Lett.* 94 (2005) 077205. [6] M. Konoto et al. *Phys. Rev. Lett.* 93 (2004) 107201. [7] M. Konoto et al. *Phys. Rev. B* 71 (2005) 184441.

HG02

Asymmetries in the formation process of magnetic vortex states in a permalloy nanodisk

Mi-young Im¹, Tomonori Sato², Yoshinobu Nakatani², Keisuke Yamada³, Teruo Ono³, Shinya Kasai⁴, Andreas Vogel⁵, Guido Meier⁶ and Peter Fischer¹
¹ LBNL/CXRO, USA
² University of Electro-Communications, Japan
³ Kyoto University, Japan
⁴ NIMS, Japan
⁵ Universitat Hamburg, Germany

Magnetic vortices in nanopatterned elements are attracting increased interest because they offer fascinating topological spin structures and great potential as novel concepts for data storage technologies [1]. A-priori, one would assume that a magnetic vortex is degenerate with four energetically equal ground states and therefore the formation of a magnetic vortex state (VS) should exhibit perfect symmetry. In our work, the formation process of VSs in Ni₈₀Fe₂₀ nanodisks has been investigated by direct imaging of in-plane and out-of-plane magnetic components in vortex structures utilizing high resolution magnetic transmission soft X-ray microscopy (MTXM). We observe a symmetry breaking in the formation process of VS in individual nanodisks. Micromagnetic simulations confirm that the Dzyaloshinskii-Moriya interaction on the full surface of nanodisks and surface-related inhomogeneities cause the observed asymmetric phenomenon [2]. In addition, we have expanded the study of the formation process of VS to include nanodots with asymmetric geometry. Based on our experimental observation, we will discuss the possibility to control the generation process of VS by directed modifications of nanodot geometry.

[1] P. Fischer et al., Phys. Rev. B 83 212402 (2011), [2] M.-Y. Im et al., submitted to Nature Communications (2011). This work was supported by the DOE, No. DE-AC02-05CH11231.

HG03

Magnetization switching utilizing the magnetic exchange interaction

Rene Schmidt*, Alexander Schwarz and Roland Wiesendanger
 Institute of Applied Physics, University of Hamburg, Germany

Magnetization reversal is usually induced by applying sufficiently large external magnetic fields. More recently, spin transfer torque using a spin polarized current has been successfully introduced as an alternative approach [1]. Here, we demonstrate the feasibility to utilize the magnetic exchange interaction with a Magnetic Exchange Force Microscopy (MEXFM) set-up to reverse the magnetization direction of a magnetic specimen. MEXFM opened up the possibility to map spin structures of insulating [2] as well as conducting surfaces [3] in real space. We use the distance dependence of the magnetic exchange interaction, measured with Magnetic Exchange Force Spectroscopy (MEXFS) [4], to induce magnetization reversals. In our case the magnetic tip apex switches its magnetization direction during scanning an antiferromagnetic surface with atomic resolution. The apex actually behaves like an independent superparamagnetic cluster with uniaxial anisotropy [5]. We are able to study switching lifetimes, exchange interaction dependent energy barriers and the influence of magnetic fields. Our findings suggest that the magnetic exchange interaction can be employed to monitor and control magnetization reversal processes with atomic resolution on conducting as well as on insulating surfaces.

[1] S. Krause et al., Science 317, 1537 (2007), [2] U. Kaiser, A. Schwarz, and R. Wiesendanger, Nature 446, 522 (2007), [3] R. Schmidt et al., Nano Lett. 9, 200 (2009), [4] R. Schmidt et al., Phys. Rev. Lett. 106, 257202 (2011), [5] R. Schmidt, A. Schwarz, and R. Wiesendanger, submitted.

HG04

X-ray spectroscopy in pulsed high magnetic fields

Cornelius Strohm^{1*}, Olivier Mathon¹, Marcin Sikora², Peter J. E. M. Van Der Linden¹, Thomas Roth¹, Tom T. A. Lummen¹, Paul H. M. Van Loosdrecht¹ and Rudolf Rueffer¹
¹ European Synchrotron Radiation Facility, 6 rue Jules Horowitz 38000 Grenoble, France
² Department of Solid State Physics, Faculty of Physics and Applied Computer Science, AGH University of Science and technology, Krakow, Poland
³ Department of Materials Science and Engineering, The Pennsylvania State University, 121 Steidle Building, University Park, PA, USA
⁴ Zernike Institute for Advanced Materials, University of Groningen, Nijenborgh 4, 9747 AG Groningen, Netherlands
⁵ European Synchrotron Radiation Facility, France

The combination of synchrotron x-ray spectroscopy and pulsed high magnetic fields provides new opportunities for the study of magnetic materials. We have developed X-ray magnetic circular dichroism (XMCD) [1] for element [2] and orbital [3] selective studies of magnetism, and Nuclear Forward Scattering (NFS) of synchrotron radiation [4] to perform isotope selective hyperfine spectroscopy in high magnetic fields. A miniature coil developed by the ESRF Sample Environment Support Laboratory reaches fields of 30 T with a total duration of 1 ms at repetition rates of 5 pulses per minute, and the integrated sample cryostat provides optical access to the sample along the field direction and covers temperatures from 5 K to 250 K [5]. In this contribution we present the coil [5] and detection schemes [1,2,4] along with application examples such as element selective magnetometry in Erbium Iron Garnet [2], the mapping of a magnetostructural phase transition in double Perovskites [3], the high field magnetization of alpha iron [4] and a study of the spin structure in Copper Iron Oxide [6].

[1] O. Mathon et al. J. of Synchrotron Rad. 14, 409, (2007), [2] C. Strohm et al. J. of Synchrotron Rad. 18, 224, (2011), [3] M. Sikora et al. Phys. Rev. B 79, 220402R, (2009), [4] C. Strohm, P. van der Linden and R. Rueffer Phys. Rev. Lett. 104, 087601 (2010), [5] P. J. E. M. van der Linden et al. Rev. Sci. Instrum. 79, 075104, (2008), [6] C. Strohm, T.T.A. Lummen, P.H.M. van Loosdrecht et al. unpublished.

HH01

Recent developments in magnetic measurements: From technical method to physical knowledge

Vittorio Basso, Fausto Fiorillo*, Alessandro Magni, Cinzia Beatrice, Ambra Caprile, Michaela Kuepferling and Carlo Paolo Sasso
 Istituto Nazionale di Ricerca Metrologica, Italy

Novel magnetic materials and applications call for enhanced measurement methods, where the goal of increased physical insight is pursued against the requirements of reproducibility and traceability. We discuss a few examples of measuring techniques where advances have been recently achieved. We shall deal, in particular, with the following topics: 1) High-speed magneto-optical microscopy, where nanosecond time-resolved Kerr microscopy reveals the high-frequency domain wall dynamics in a variety of samples: thin films, amorphous ribbons, patterned magnets. It concurrently allows for pulsed inductive magnetometric techniques, by which the spin precessional modes and their damping behavior can be observed. 2) Calorimetry under magnetic field, a technique permitting one to directly measure the entropy s(Ha,T) as a function of temperature T and applied magnetic field Ha. It is especially attractive for the characterization of magnetocaloric materials and the determination of first order phase transitions with hysteresis. The discussion will focus on the magnetic field induced transition in La-Fe-Co-Si alloys, Heusler alloys, and materials with spin reorientation transition, like Er₂Fe₁₇B and W-type Co-Zn substituted Ba ferrites. 2) Pulsed field magnetometry in permanent magnets, an industrially attractive method of characterization of extra-hard rare-earth based magnets, overcoming the intrinsic fieldstrength limitations of the standard electromagnet-based characterization.

HH02

So, you need reliable magnetic measurements you can use with confidence? How the magnetic measurement capabilities at NPL can help

Michael Hall
 National Physical Laboratory, United Kingdom

Magnetic quantities have an impact on many aspects of our everyday life; in health and safety, the magnetic field levels produced by the domestic appliances we use so regularly is carefully monitored by the manufacturers to meet EMC regulations (we provide measurements that are compliant up to 120 kHz with EN 50366). In the aerospace industry, soft magnetic materials are used in extreme conditions (temperatures up to 450 °C and stress levels up to 450 MPa) and the material can be characterised at NPL using unique measurement techniques. In the car industry, the material properties of permanent magnets have become very important; some cars now contain in excess of 70 magnets. The demand for traceable electrical and magnetic measurements is broadening as new materials and techniques have brought the need for these measurements to new areas of industry. In this talk the magnetic measurement facilities, capabilities and field standards available at NPL will be presented. How these are being developed to meet the demanding conditions of use of instruments and materials will be presented and illustrated with case studies.

HH03

Application of pulsed eddy current technique to inspect the pipeline of nuclear plants

D. G Park
 korea atomic energy research institute, Korea

The local wall thinning is a point of concern in almost all steel structures such as the pipe lines. The present research describes the application of Pulsed Eddy Current (PEC) for wall thickness monitoring. We have built a PEC system which has the ability to detect the wall-thinning or corrosion, and sub-surface defects. In our PEC probe an exciting coil in conjunction with a Hall-sensor has been used. The PEC response to varying metal thickness was measured at various thicknesses of insulations on the tested sample. Excitation coil in the probe is driven by a rectangular current pulse; the time domain features of the detected pulse, such as 'peak value' and 'time to zero' were used to describe the wall thinning in the tested sample. A real time LabVIEW program was developed for the data acquisition and scanning the probe on the insulated sample. The scanning results were continuously displayed on the computer monitor. Signal processing techniques such as energy and power spectrum density (PSD) were devised to infer the PEC response signal. The results show that the proposed PEC differential probes.

HI01

Probing the exotic surface states in topological insulators and superconductors

Yoichi Ando*
 ISIR, Osaka University, Japan

A topological state of matter is characterized by a nontrivial topological structure of the quantum-mechanical wavefunctions in the Hilbert space. Due to the bulk-edge correspondence, a gapless surface state always accompanies a topologically nontrivial bulk state. In topological insulators (TIs), a nontrivial Z2 topology of the bulk state leads to the emergence of Dirac fermions on the surface. Similarly, topological superconductors (TSCs) are accompanied by surface Andreev bound states that often consist of Majorana fermions. In this talk, I will present our experiments to address those exotic surface states. For TIs, we discovered that the chalcogen-ordered tetradymite Bi₂Te₂Se presents a high bulk resistivity, allowing one to observe clear surface quantum oscillations [1]; more recently, we demonstrated that in a related solid-solution system Bi_{2-x}Sb_xTe_{3-x}Se_x, it is possible to achieve a surface-dominated transport even in a bulk crystal [2]. For TSCs, in a superconducting doped-TI material Cu₂Bi₂Se₅, we have succeeded in observing an unconventional surface Andreev bound state, which gives evidence for a new type of topological superconductivity associated with helical Majorana fermions [3]. These works were done in collaboration with A. A. Taskin, Z. Ren, S. Sasaki, and K. Segawa.

[1] Z. Ren et al., PRB 82, 241306(R) (2010), [2] A.A. Taskin et al., PRL 107, 016801 (2011), [3] S. Sasaki et al., PRL 107, 217001 (2011).

HI02

Electronic structure study of bulk HgTe via angle resolved photoemission spectroscopy

Chang Liu¹, Suyang Xu¹, Madhab Neupane¹, Helin Cao², Ireneusz Miotkowski², L. Andrew Wray², Hsin Lin⁴, R. S. Markiewicz², A. Bansil¹, Yong P. Chen² and M. Zahid Hasan¹
¹ Joseph Henry Laboratory and Department of Physics, Princeton University, USA
² Department of Physics, Purdue University, USA
³ Advanced Light Source, Lawrence Berkeley National Laboratory, USA
⁴ Department of Physics, Northeastern University, USA



HI03

Hidden topological order in URu₂Si₂

Tanmoy Das
 Theoretical Division, Los Alamos National Laboratory, USA

Recently breakthrough studies have discovered series of new state of matters, including topological insulators, topological Mott insulators, topological Kondo insulators, topological antiferromagnetic insulators and others. Here we present an analogous, yet fundamentally novel topological order which arises due to spin-orbit coupling density wave in the heavy-fermion material URu₂Si₂. [1] We show via ab-initio calculations that an incommensurate Fermi surface 'nesting' in the partially-filled f-states causes a staggered spin-orbit coupling in the hidden-order state. In this cause neither the spin (S) nor the orbital (L) alone causes ordered state, rather a modulated spin-momentum locked density wave propagates along the unidirectional nesting direction with a polarized total angular momentum ?mJ = ±2, in excellent agreement with neutron scatterings. This is a radically new order parameter and a novel phase of matter. It breaks spontaneous rotational symmetry, but not the time-reversal symmetry and is thus immune to any time-reversal invariant perturbation such as pressure, whereas magnetic field will destroy it. We compute the topological quantum number to show that the hidden-order gap opening causes a trivial to non-trivial topological phase transition, and hence defines a novel 'topological quantum critical point' as a function of magnetic field.

HI04

Robustness of 1D topological superconductors with Majorana edge states against lattice modulation

Masaki Tezuka* and Norio Kawakami
 Department of Physics, Kyoto University, Kitashirakawa, Sakyo-ku, Kyoto 606-8502, Japan

Recently there has been a substantial amount of effort to observe Majorana edge states at the edges or vortex cores of topological superconductors. The robustness of such states against spatial inhomogeneity and electron correlation will be particularly important in observing and manipulating them. We have studied a one-dimensional quantum wire to analyze the condition for a topological phase with edge Majorana fermions to appear when an incommensurate (quasiperiodic) lattice modulation is applied. We have adopted the tight-binding model Hamiltonian by Stoudenmire and coworkers [1], which incorporates the Zeeman effect, the spin-momentum coupling, the proximity effect induced by a bulk superconductor, and the on-site electron-electron interaction U, and analyzed its low-energy behavior when the lattice modulation is applied by the density-matrix renormalization group method. For U=0 we have found multiple reentrant transitions between topological phases with edge Majorana fermions and non-topological phases [2]. The number of transitions increase as the modulation becomes stronger. For U>0, as in the case without the lattice modulation [1], the region with Majorana fermions is broadened in the phase diagram [2]. The effects of other types of spatial inhomogeneities, such as a harmonic trapping potential, will also be presented.

[1] E. M. Stoudenmire, J. Alicea, O. A. Starykh, M. P. A. Fisher: Phys. Rev. B 84, 014503 (2011), [2] M. Tezuka and N. Kawakami: Phys. Rev. B 85, 140508(R) (2012).

HI05

Floquet theory of photo-induced topological phase transitions: Application to graphene

Takashi Oka
 The University of Tokyo, Japan

The effect of strong lasers on the topology of electron systems is becoming a hot topic [1-3]. Recently, a theoretical proposal was made in two dimensional Dirac systems where an application of circularly polarized light was shown to turn the system into a quantum Hall state with a non-trivial photo-induced Chern number and an emergence of photo-induced edge channels [1,2]. One can see this as a dynamical realization of the Haldane model of a quantum Hall state without Landau levels [4], i.e., the circularly polarized light plays the role of the local magnetic fields. This proposal applies to a broad class of multi-band systems including graphene, graphite and surface states of topological insulators as well as cold atoms in optical lattices with synthetic gauge fields. Theoretically, this prediction is based on the Floquet extension of linear response theory and the TKNN formula[1] as well as the Landauer theory of transport[2]. We also explain possible experimental setups to detect this state using transport, photo-emission, and orbital Kerr effect. * This work was done in collaboration with H. Aoki, T. Kitagawa, T. A. Brataas, L. Fu and E. Demler.

[1] T. Oka and H. Aoki: Phys. Rev. B 79, 081406 (2009), [2] T. Kitagawa, T. Oka, A. Brataas, L. Fu, E. Demler: Phys. Rev. B 84, 235108 (2011), [3] N. H. Lindner, G. Refael, V. Galitski: Nat. Phys. 7 490 (2011), [4] F. D. M. Haldane: Phys. Rev. Lett. 61 2015 (1988).

HJ01

Strong coupling of spin, orbital and lattice degrees of freedom in Ru oxides

Je Geun Park
 Department of Physics & Astronomy, Seoul National University, Korea

Being a 4d transition element, Ru has more extended wavefunction compared to those of 3d transition metal elements, and so is likely to have relatively smaller correlation effects. However, it turns out that this relatively broader wavefunction produces strikingly different physical properties from those of 3d transition metal oxides. In this talk, we will highlight the unique physical properties of two Ru oxides emphasizing its difference from 3d transition metal oxides. First example is Ti₂Ru₂O₇, which exhibits a metal-insulator transition at 120 K. We will examine the nature of the metal-insulator transition both experimentally and theoretically, and are going to discuss how a spin-driven spontaneous orbital ordering produces the experimentally observed structural transition and leads to the metal-insulator transition at the exactly same temperature. The second example is the ferromagnetic transition of SrRuO₃ with Tc=165 K. Although it has been known over a half century, the true nature of the ferromagnetic transition is poorly understood. Here combining both neutron diffraction and inelastic neutron scattering we will show how the ferromagnetic ground state is intimately coupled to the unusual volume anomaly, i.e. Invar behavior at an atomic scale.

HJ02

Competing magnetic interactions in eta-carbide-type transition-metal compounds: New class of itinerant-electron frustrated magnets
 Hiroyuki Nakamura*, Takeshi Waki and Yoshikazu Tabata
Department of Materials Science and Engineering, Kyoto University, Japan

Although a number of ternary transition metal compounds with the cubic eta-carbide-type structure, M_3T_3X and M_6T_6X with $M = Mo, W, etc.$, $T = Fe, Co, Ni, etc.$, and $X = C$ or N have been known to exist, their magnetic properties have been less studied. The T sublattice forms the 'stella quadrangula' lattice, which is a newly found geometrically frustrated corner-shared lattice of two nested regular tetrahedrons. Although the stella quadrangula lattice is one of pyrochlore-derived lattices, we anticipate the unique nature of the frustration due to the competition between first- and second-neighbor interactions, J1 and J2, possibly of direct exchange type. Because of the delicate balance between J1 and J2, the eta-carbide-type compounds shows various magnetic ground states such as nonmagnetic non-Fermi liquid, ferromagnetism, antiferromagnetism, etc. [1]. In addition, various types of field-induced transitions are often observed [2]. Here we summarized comprehensively the magnetism of the eta-carbide-type transition metal carbides and nitrides together with resent experimental data.

[1] T. Waki et al., *J. Phys. Soc. Jpn.* 79 (2010) 043701, *EPL* 94 (2011) 37004, *J. Alloys Compd.* 509 (2011) 9451. [2] T. Waki et al., *J. Phys. Soc. Jpn.* 79 (2010) 093703, *J. Phys.: Conf. Ser.* 320 (2011) 012069.

HJ03

Long-time variation of magnetic structure in (Ce-La)Ir₃Si₂: Effect of randomness
 Kiyochiro Motoya^{1*}, Taketo Moyoshi¹ and Masaaki Matsuda²
¹ *Department of Physics, Faculty of Science and Technology, Tokyo University of Science, Japan*
² *Quantum Condensed Matter Division, Oak Ridge National Laboratory, USA*

Long-time variations of magnetic properties observed in spin-glasses have been regarded as due to the multi-valley structure of the free energy surface arising from random magnetic interactions. Therefore, in a system without randomness or imperfections we have not expected to observe a time variation of magnetic property within an attainable time scale. Contrary to all expectations, we found a long-time variation of magnetic structure in a non-diluted uniform magnet CeIr₃Si₂ by means of time-resolved neutron scattering measurements.[1,2] We examined other materials and have found similar long-time variations of magnetic structure in PrCo₃Si₂, TbNi₃Si₂, Ca₃Co₃O₄ and some other compounds.[3,4] All these compounds exhibit successive magnetic transitions and multi-step metamagnetic transitions, which suggest that the frustrations coming from competing magnetic interactions causes the long-time variation of magnetic structure. In order to show that randomness caused by inevitable impurities or imperfections is not the main cause of the long-time variation, we have made macroscopic and neutron scattering measurements of a random system (Ce-La) Ir₃Si₂. The time variation behavior of this random system is basically identical to that of CeIr₃Si₂. These results have shown that the long-time variation of magnetic structure in CeIr₃Si₂ does not originate in randomness.

1. K. Motoya et al.: *J. Phys. Conference Series* 200 (2010) 032048. 2. T. Moyoshi et al.: *J. Phys. Soc. Jpn.* 81 (2012) 014704. 3. K. Motoya et al.: *J. Phys. Conference Series* 273 (2011) 012124. 4. T. Moyoshi and K. Motoya: *J. Phys. Soc. Jpn.* 80 (2011) 034701.

HJ04

Influence of symmetry on Sm magnetism studied in SmIr₂Si₂ polymorphs
 Michal Valiska*, Jiri Pospisil, Martin Divis, Jan Prokleska and Vladimir Sechovsky
DCMP, Charles University, Ke Karlovu 5, 121 16, Prague, Czech Republic

SmIr₂Si₂ crystallizes in two structural polymorphs which make possible unique study of influence of symmetry on Sm magnetism. One polymorph is the primitive tetragonal structure of the CaBe₂Ge₂ structure type stable at high temperatures (high temperature polymorph-HTP) and the other is a body centered tetragonal structure of the ThCr₂Si₂ structure type stable at low temperatures (low temperature phase-LTP). The HTP exists at room temperature as a metastable phase in the quenched samples while the LTP can be obtained by proper annealing. We have found three magnetic phase transitions in both structure polymorphs in specific heat data. The transitions at temperature 1.7, 6.2 and 18.8 K have been found for the HTP and the LTP exhibits transitions at 1.9, 6.1 and 38.9 K. Magnetic moment of 0.034 μB/f.u. has been found for both polymorphs (in the field of 7 T at 2 K). Magnetic features of both polymorphs are discussed on the basis of the strong influence of the crystal field and the admixture of the low lying excited multiplet J = 7/2 with the ground multiplet J = 5/2. All experimental results are supported by first principles calculations.

HJ05

Unconventional thermal expansion of BaIrO₃ investigated by temperature dependent x-ray and neutron diffractions
 Jinwon Jeong¹, Bin Chang¹, Dahee Jung¹, Han-jin Noh^{1*} and Seongsu Lee²
¹ *Department of Physics, Chonnam National University, Korea*
² *Korea Atomic Energy Research Institute, Korea*

We have studied the temperature dependence of the unit cell volume of 9R-type BaIrO₃ by X-ray and neutron diffractions. The volume and the unit cell parameters show a strong correlation with the weak ferromagnetic charge-density-wave phase of this 5d transition metal compound. The volume vs. temperature curve is not well described by a Debye function, which indicates that the interplay between charge, spin, and lattice plays an important role in the thermal expansion behavior. A possible scenario will be presented in order to understand this unconventional behavior.

IA01

A quantum phase transition hidden beneath the superconducting dome of iron-pnictides
 Yuji Matsuda
Physics, Kyoto University, Japan

An enduring question in strongly correlated electron systems is whether high-Tc superconductivity is driven by an underlying quantum critical point (QCP) separating different ground states. In particular, whether a QCP lies beneath the superconducting dome or the criticality is avoided by the transition to the superconducting state has been a central issue. Among iron-based superconductors, the isovalent pnictogen substituted system BaFe₂(As_{1-x}P_x)₂ appears to be the most suitable system to discuss many physical properties, because BaFe₂(As_{1-x}P_x)₂ can be grown with very clean and homogeneous, as evidenced by the quantum oscillations observed over a wide doping range even in the superconducting dome giving detailed knowledge on the electronic structure. We report a sharp peak in the x-dependence of zero-temperature London penetration depth L(0) in BaFe₂(As_{1-x}P_x)₂ at the optimum composition x=0.30 (Tc=30 K). This peak structure most likely results from pronounced quantum fluctuations associated with the QCP which separates two distinct superconducting phases, giving the first convincing signature of a second-order quantum phase transition deep inside the superconducting dome. Moreover, the ratio of Tc to the superfluid density at x=0.30 is strikingly enhanced and even approaches the superfluid-4He value, implying a possible crossover towards the Bose-Einstein condensate limit driven by quantum criticality.

This work has been done in collaboration with T. Shibauchi, K. Hashimoto, S. Kasahara, Y.Mizukami, T. Terashima, H. Ikeda (Kyoto), A. Carrington (Bristol), K. Cho, R. Prozorov, M. Tanatar (Ames), N. Salovich, R. W. Giannetta(Illinois at Urbana-Champaign), and H. Kitano (Aoyama Gakuin)

IA02

Re-entrant quantum criticality in pressurized Yb₂Pd₂Sn and Yb₂Pd₂In_{1-x}Sn_x
 Tahir Rao Khan¹, Herwig Michor¹, Ernst Bauer^{1*}, Rustem Khasanov², Alex Amato³, Veljko Zlatić⁴, Ivica Aviani⁴, Mydeen Kamal⁵, Michael Nicklas⁵ and Mauro Giovannini⁶
¹ *Institute of Solid State Physics, Vienna University of Technology, Austria*
² *Laboratory for Muon-Spin Spectroscopy, Paul Scherrer Institute, Switzerland*
³ *Laboratory for Muon-Spin Spectroscopy, PSI, Paul Scherrer Institute, Switzerland*
⁴ *Institute of Physics, Zagreb, Croatia*
⁵ *Max Planck Institute for Chemical Physics of Solids, Dresden, Germany*
⁶ *Dipartimento di Chimica e Chimica Industriale, University of Genova, Italy*

Recently we reported on the discovery of two consecutive, pressure driven magnetic instabilities in Yb₂Pd₂Sn [1]. They emerge in a non-Fermi liquid environment at the initial and the final point of a dome-like, single magnetic phase at pressures pc1 ~ 1 GPa and pc2 ~ 4 GPa. This unique behavior of Yb₂Pd₂Sn is supposed to result from mutually competing, pressure modified energy scales, which in case of Yb₂Pd₂Sn cause a sign change in the pressure dependence of the Kondo temperature TK and magnetic ordering temperature TN. An earlier study [2] demonstrated the occurrence of long range magnetic order in a dome-like phase space for a narrow concentration range of Sn-rich samples in Yb₂Pd₂In_{1-x}Sn_x. Ordered moments of the order of 1 μB are attained and the transition temperature reveals values above 3 K, although both Yb₂Pd₂In and Yb₂Pd₂Sn exhibit paramagnetic ground states. The aim of the present work is a detailed study of the pressure and field response of Yb₂Pd₂Sn and of alloys with concentrations in the "magnetic dome" of Yb₂Pd₂In_{1-x}Sn_x. We show how the transition temperatures and the ground states modify when applying both pressure and magnetic fields.

[1] T. Muramatsu et al., *Phys. Rev. B* 83, (2011) 180404(R). [2] E. Bauer et al., *J. Phys.: Cond. Mat.* 17 (2005) S999.

IA03

Coupled fermi-bose renormalization group flow for a two-flavor spin-fermion model close to its antiferromagnetic quantum critical point
 Junhyun Lee, Philipp Strack and Subir Sachdev*
Department of Physics, Harvard University, USA

The strong correlations emerging in proximity of antiferromagnetic quantum critical points (QCP) in low-dimensional electronic materials are believed to be one of the main causes for their striking non-Fermi liquid behavior. In this quantum-critical regime, metallic electrons are strongly coupled to gapless, collective spin fluctuations rendering theoretical approaches a challenging affair. In this talk, we will present first results of a renormalization group (RG) analysis of a new, prototypical two-flavor spin-fermion model in the vicinity of its quantum critical point. This model is free of the sign-problem and therefore ideally suited to compare results of analytical methods with quantum Monte Carlo simulations [1]. Our RG method is based on an exact flow equation for the effective Fermi-Bose action. It allows us to treat the electrons and spin fluctuations on equal footing, and to extract correlation functions consistently ordered along a joint energy scale. Solving our flow equations, we present results for renormalized observables such as the fermion self energy and the magnetic susceptibility when approaching the QCP from the paramagnetic phase.

[1] arXiv.org:1206.0742

IA04

Magnetism and filling-controlled mott transition in strongly spin-orbit-coupled iridium oxide
 Kenya Ohgushi^{1*}, Jun-ichi Yamaura¹, Hiroyuki Ohsumi², Soshi Takeshita², Hidenori Takagi¹, Taka-hisa Arima³ and Yutaka Ueda¹
¹ *Institute for Solid State Physics, University of Tokyo, Japan*
² *RIKEN Spring-8 Center, Japan*
³ *University of Tokyo, Japan*

By performing resonant x-ray diffraction experiments for the post-perovskite-type compound CaIrO₃, we revealed that the magnetic structure is a striped-typed order, which is stabilized by the unique superexchange interaction across the edge-sharing bonds in the strongly spin-orbit-coupled Jeff = 1/2 state. Moreover, by introducing hole carriers into CaIrO₃ through the chemical substitution, we have successfully developed a novel metallic state, where bandwidth, Coulomb repulsion, spin-orbit coupling, and Hund coupling are competing.

[1] K. Ohgushi, et al., arXiv:1108.4523v1. [2] K. Ohgushi, et al., *Phys. Rev. B* 74, 241104(R) (2006).

IA05

Magnetic field tuned QCP in YbPtBi
 E. D. Mun¹, H. Kim¹, M. A. Tanatar¹, G. M. Schmiedeshoff², J. H. Park³, T. Murphy³, N. Dilley⁴, S. L. Bud'ko^{1*}, R. Prozorov¹ and P. C. Canfield¹
¹ *Ames Laboratory/Iowa State University, Ames, IA, USA*
² *Occidental College, Los Angeles, CA, USA*
³ *NHMFL, Tallahassee, FL, USA*
⁴ *Quantum Design Inc., San Diego, CA, USA*

Magnetic field dependence of thermodynamic and transport properties of single crystals of stoichiometric, heavy fermion ($\gamma \sim 8$ J/mol K2), antiferromagnetic (TN ~ 0.4 K) compound YbPtBi was studied down to 20 mK. The magnetic order is suppressed on application of ~ 4 kOe magnetic field. The Fermi-liquid state appears to be separated from the quantum critical point. The H* crossover line ("Hall line") marks the emergence of the Fermi-liquid state. The H-T phase diagram will be discussed in context of results on other Yb-based heavy fermions.

IB01

Field-annealed Fe-Ni-Nb-B amorphous and nanocrystalline alloys for magnetic sensor applications
 Marek Varga¹, Jozef Marcini¹, Marek Capik¹, Jozef Kovac¹, Peter Svec² and Ivan Skorvanek^{1*}
¹ *Institute of Experimental Physics SAS, Kosice, Slovakia*
² *Institute of Physics SAS, Bratislava, Slovakia*

The amorphous and nanocrystalline alloys have attracted a great deal of technological interest due to their applicability in various types of magnetic sensors. These alloys often require specific annealing conditions to achieve the desired response to applied magnetic field. In this work, we report on the effects of both longitudinal and transverse magnetic field applied during the heat treatment on the soft magnetic behaviour and the giant magnetoimpedance (GMI) effect in the series of (Fe_{1-x}Ni_x)₈₁Nb₇B₁₂ (x=0.25, 0.33 and 0.5) amorphous and nanocrystalline alloys. The melt-spun ribbons were isothermally annealed under high vacuum in the presence of transverse (TF) or longitudinal (LF) magnetic field with the magnitude up to 640 kA/m. The heat treatment under LF-conditions results in an appreciable reduction of the coercivity. Sheared loops with good field linearity were achieved after TF-annealing. The GMI measurements were performed in dc magnetic field up to ± 9600 A/m over a frequency range 0.1 - 10 MHz. The nanocrystalline samples show markedly larger values of GMI ratio ($\Delta Z/Z$) as compared to their amorphous counterparts. The field annealing results in the modified the GMI response of both amorphous and nanocrystalline ribbons, which can be used for tuning their characteristics for magnetic sensor applications.

IB02

Amorphous and nanocrystalline magnetic materials: Research and production in china
 Shaoxiang Zhou
China Central Iron and Steel Research Institute Group, Advanced Technology and Materials Co., Ltd., China

The planar-flow casting (PFC) is a continuous casting method for the production of a large quantity of rapidly solidified metallic ribbons. In particular, the PFC attracted great interests in the production of amorphous and nanocrystalline thin and wide ribbons because of the cost savings process in a single stage and the novel properties arising from the microstructure of rapidly solidified ribbons. Amorphous and nanocrystalline ribbons are widely used in electrical and electronic system such as distribution transformers and inductive devices because of low core loss. This paper seeks to summarize the recent progress in synthesis methods, properties, and applications in the field of amorphous and nanocrystalline soft magnetic materials in forms of ribbon, the emphasis is focused on some key technologies for producing wide amorphous ribbon and thin nanocrystalline ribbon. In the summary, the total market demands of amorphous and nanocrystalline alloy ribbons in China are predicted.

IB03

Recent status of soft magnetic material applications for renewable energy and eco-friendly vehicle
 In-bum Jeong
Changsung Corporation, Korea

Soft magnetic materials have been widely used in electrical and electronic devices such as inductor, transformer, sensor, motor, EMI absorber and others. Ideal soft magnetic material which is relevant to modern high power electronics should have the best combination of high permeability under DC excitation, low loss, good thermal stability, good frequency behavior, and reasonable cost. But, unfortunately, all the commercialized soft magnetic materials such as ferrite, laminated silicon steel sheet, wound amorphous and nanocrystalline ribbon, and compressed metallic alloy powder core do not meet all the requirements perfectly so far. In Renewable energy and electric vehicle applications, especially the soft magnetic materials are getting important for high efficiency and reliability. Therefore, there are strong market demands for strengthening each material's forte and overcoming each material's limitations and shortcomings. This presentation is focused on Recent Status of Soft Magnetic Material Applications for Renewable Energy and Eco-friendly Vehicle.

IC01

Random fields in molecular magnets

Myriam P. Sarachik*

Physics Department, City College of New York-CUNY, New York, NY 10031, USA

Measurements of the magnetic susceptibility of single crystals of the usual form of Mn₁₂-acetate and of a new high-symmetry variant, Mn₁₂ac-MeOH, indicate a transition to dipolar ferromagnetism below ~ 0.9 K in both materials [1]. In the case of Mn₁₂ac-MeOH, the suppression of ferromagnetism by a magnetic field applied transverse to the easy axis is consistent with mean-field theory for an ordered single crystal: Mn₁₂ac-MeOH is a realization of a “Transverse-Field Ising Ferromagnet” (TFIFM). By contrast, the suppression of ferromagnetism by transverse field is considerably more rapid in Mn₁₂-acetate, resembling instead the behavior observed in randomly site-diluted LiHo_{1-x}Y_xF₄, the only heretofore known realization of a “Random-Field Ising Ferromagnet” (RFIFM) [2]. The randomness in Mn₁₂-acetate derives from the intrinsic distribution of locally tilted magnetic easy axes known to exist in these crystals, suggesting that this prototypical molecular magnet is a realization of the random field Ising ferromagnet (RFIFM) in which the random field can be tuned by a field applied transverse to the easy axis.

* Supported by NSF-DMR-0451605; work done in collaboration with B. Wen, P. Subedi, A. D. Kent, Y. Yeshurun, A. Millis, and G. Christou. [1] B. Wen, P. Subedi, L. Bo, Y. Yeshurun, M. P. Sarachik, A. D. Kent, C. Lampropoulos, and G. Christou, *Phys. Rev. B* **82**, 014406 (2010); P. Subedi, A. D. Kent, B. Wen, M. P. Sarachik, Y. Yeshurun, A. J. Millis, S. Mukherjee, and G. Christou, *arXiv:condmat/1202.4963* (2012).

IC02

Stability of incommensurate field-induced magnetic order via site-disorder

Francesco Casola^{1*}, Toni Shiroka¹, Shuang Wang¹, Christian Rüegg², Henrik Moodysson Rønnow², Michael Gribic², Mladen Horvatic², Steffen Krämer³, Sutirha Mukhopadhyay⁴, Claude Berthier⁵, Hans Rudolf Ott¹ and Joel Mesot¹

¹ *Laboratorium für Festkörperphysik, ETH Hönggerberg, CH-8093 Zürich, Switzerland*

² *Laboratory for Quantum Magnetism, Ecole Polytechnique Fédérale de Lausanne, Switzerland*

³ *Laboratory for Neutron Scattering, Paul Scherrer Institute, CH-5232 Villigen PSI, Switzerland*

⁴ *Laboratoire National des Champs Magnétiques Intenses, LNCMI - CNRS (UPR3228), UJF, UPS and INSA, BP 166, 38042 Grenoble Cedex 9, France*

⁵ *Paul Scherrer Institute, CH-5232 Villigen PSI, Switzerland*

Low-dimensional spin-gapped antiferromagnets (AF) can be driven out of their quantum-disordered (QD) regime not only through the application of pressure or magnetic fields, but also via the introduction of disorder. Despite previous observations of these phenomena in a variety of materials such as Haldane chains, spin ladders or spin-Peierls systems, a limited number of studies has considered the impact of defects on the field-induced magnetic order. It was found that disorder can affect the quantum-critical behaviour of these materials, induce new phases dominated by triplet confinement or even destroy completely any phase transition in case of incommensurate correlations in the QD regime. Extending low-field 31P NMR experiments on the frustrated two-leg spin-1/2 ladder Bi(Cu_{1-x}Zn_x)PO₆ [1] to magnetic fields up to 31T we observed for x=0 the onset of incommensurate field-induced magnetic order at Hc = 20.96 T. The critical exponent for the transition temperature Tc(H)∝ (Hc(T)-Hc(0))^ν is ν = 0.42. Remarkably, the same critical behaviour is found for the compound with x=0.01, but with an enhanced Hc(0) of about 24 T. Site disorder introducing non magnetic Zn ions on regular Cu sites opens the possibility to study finite-size effects in quasi-1D spin systems by directly tuning the chain length via defect concentration.

[1] - F. Casola, T. Shiroka, S. Wang, K. Conder, E. Pomjakushina, J. Mesot and H.-R. Ott, *Phys. Rev. Lett.* **105**, 067203 (2010).

IC03

Low-temperature heat transport and field-induced quantum phase transitions of spin gapped quantum magnetsX. F. Sun^{1*}, C. Fan¹, L. M. Chen², W. P. Ke Ke¹, Z. Y. Zhao¹ and X. M. Wang¹¹ *Hefei National Laboratory for Physical Sciences at the Microscale, University of Science and Technology of China, China*² *Department of Physics, University of Science and Technology of China, China*

Low-dimensional or frustrated quantum magnets were revealed to exhibit exotic ground states, magnetic excitations, and quantum phase transitions (QPTs). In the spin-gapped antiferromagnets, the external magnetic field can close the gap in the spectrum, which results in a QPT between a low-field disordered paramagnetic phase and a high-field long-range ordered one. An intriguing finding is that this ordered phase can be approximately described as a Bose-Einstein condensation (BEC) of magnons. In this work, we study the low-temperature and high-field thermal conductivity (κ) of several spin gapped quantum magnets, including the quasi-one-dimensional S=1 chain compound NiCl₂-4SC(NH₂)₂ (DTN), the quasi-one-dimensional ladder compound (CH₃)₂CHNH₂CuCl₂(IPACuCl₂), and the layered spin-dimer compound Ba₃Mn₂O₈ [1-3]. It is found that the magnetic excitations can contribute to the heat transport rather strongly in these materials, particularly at the field-induced QPTs, by either transporting heat or scattering phonons.

[1] X. F. Sun, W. Tao, X. M. Wang, and C. Fan, *Phys. Rev. Lett.* **102**, 167202 (2009). [2] W. P. Ke, X. M. Wang, C. Fan, Z. Y. Zhao, X. G. Liu, L. M. Chen, Q. J. Li, X. Zhao, and X. F. Sun, *Phys. Rev. B* **84**, 094440 (2011). [3] L. M. Chen, X. F. Sun et al., *unpublished*.

IC04

Review talk about spin superfluidity

Yury Bunkov

Institut NEEL, France

There is a complete analogy between the Bose-Einstein condensation of atomic gases and the Bose-Einstein condensation of magnons in antiferromagnets. Five different states of magnon condensation with Spin Supercurrent have been found in different states of antiferromagnetic superfluid 3He [1]. All these cases are examples of the Bose-Einstein condensation of magnons with the interaction potential provided by specific spin-orbit coupling. The BEC phenomenon in the gas of magnons is readily accessible owing to the possibility of modifying the spin-orbit coupling. In some cases the BEC of magnons corresponds to almost 100% condensation. Recently the magnon BEC state and Spin Supercurrent was found on a 55Mn nuclear in antiferromagnetic monocristals CsMnF₃ and MnCO₃ [2].

[1] Yuriy M. Bunkov and Grigoriy Volovik, *J. Phys.: Condens. Matter* **22** 164210 (2010) [2] Yuriy M. Bunkov et al., *Phys. Rev. Lett.* **108**, 177002 (2012).

IC05

The spin-1/2 Heisenberg antiferromagnetic chain experimental confirmation of 2 and 4 spinon termsBella Lake^{1*}, D. Alan Tennant¹, Jean-sebastien Caux² and Christopher D Frost³¹ *Helmholtz-Zentrum Berlin für Materialien und Energie, Germany*² *Instituut voor Theoretische Fysica, Universiteit van Amsterdam, Netherlands*³ *ISIS Facility, Rutherford Appleton Laboratory, United Kingdom*

The Spin-1/2 Heisenberg antiferromagnetic chain is the fundamental example of a correlated quantum system and has been a long-standing problem in condensed matter physics. The problem was first tackled by Hans Bethe in 1931 who found that the ground state is quantum disordered down to lowest temperatures [1]. In 1981 Faddeev and Takhtajan realized that the basic excitations are spinons [2] which have fractional spin quantum number (S=1/2) and are necessarily created in pairs. In neutron scattering experiments the excitations are observed as a multi-spinon continuum consisting of 2,4,6,8,... spinon states. The dynamical structure factor which is measured by the neutrons has however only recently been calculated [3,4,5]. Caux, Hagemans and Maillet have determined it to high precision and were able to show that while the 2-spinon contribution accounted for 73% of the spectral weight, the 4-spinon contribution was also substantial at 25%. Here we use inelastic neutron scattering to obtain the dynamical structure factor of the spin-1/2 Heisenberg antiferromagnetic chain compound KCuF₃ to high accuracy and in absolute units. The data show much better agreement with this recent theoretical work than earlier theories (Muller Ansatz and field theory) and is able to confirm the presence of the 4-spinon term.

[1] H. Bethe, *Zeit. für Physik* **71**, 205 (1931). [2] L. D. Faddeev and L. A. Takhtajan, *Phys. Lett. A* **85**, 375 (1981). [3] J.-S. Caux and R. Hagemans, *J. Stat. Mech: Th. Exp. p. P12013* (2006). [4] J.-S. Caux and J. M. Maillet, *Phys. Rev. Lett.* **95**, 077201 (2005). [5] J.-S. Caux, R. Hagemans, and J. M. Maillet, *J. Stat. Mech.: Th. Exp.* **2005**, P09003 (2005).

ID01

X-ray microscopy of nanoscale spin dynamics

Peter Fischer

CXRO, LBNL, USA

One of the scientific and technological challenges in nanomagnetism research is to image magnetism down to fundamental length and time scales with elemental sensitivity in advanced multicomponent materials. Magnetic soft X-ray microscopy is a unique analytical technique combining X-ray magnetic circular dichroism (X-MCD) as element specific magnetic contrast mechanism with high spatial resolution down to almost 10nm and a temporal resolution below 100ps [1]. This allows to investigate in detail precessional and relaxation phenomena, which occur e.g. in domain wall motion [2-3] and vortex dynamics [4-8]. In this talk I will review the achievements and future perspectives of using soft X-rays for magnetic imaging by selected examples from current research. The collaboration with many colleagues in particular M.-Y.Im, S.-K. Kim, D.-H. Kim, G. Meier, S. Kasai, T. Ono, D. Allwood, K. Buchanan, B. Mesler and S.-C. Shin is highly appreciated. This work is supported by the Director, Office of Science, Office of Basic Energy Sciences, Materials Sciences and Engineering Division, of the U.S. Department of Energy under Contract No. DE-AC02-05-CH11231.

[1] P. Fischer, *Materials Today* **13**(9) 14 (2010) [2] L. Bocklage, et al. *Phys Rev B* **81**, 054404 (2010) [3] M.T. Bryan, et al. *IEEE Trans Mag* **46**(4) 963 (2010) [4] P. Fischer et al. *Phys Rev B Brief Report* **83** 212402 (2011) [5] S. Kasai, et al. *Phys Rev Lett* **101**, 237203 (2008) [6] Y.-S. Yu, et al. *Appl. Phys. Lett.* **98**, 052507 (2011) [6] H. Jung, et al. *NPG - Scientific Reports* **1** 39 (2011) [7] B. Mesler et al. *J. Appl. Phys.* (2012) in print [8] J.-H. Shim, et al., *J. Appl Phys* **107** 09D302 (2010)

ID02

Non linear spin transfer induced vortex dynamicsV. Cros¹, A. Dussaux¹, P. Bortolotti¹, E. Grimaldi¹, J. Grollier¹, A.v. Khvalkovskiy², K.a Zvezdin³, A. Fukushima⁴, H. Kubota⁴, K. Yakushiji⁵, S. Yuasa⁴, K. Ando⁴ and A. Fert¹¹ *Unité Mixte de Physique CNRS/Thales, France*² *Unité Mixte de Physique CNRS/Thales and A.M. Prokhorov GPI, Moscow and Istituto P.M., Torino., France*³ *Istituto P.M., Torino, and A.M. Prokhorov GPI, Moscow, Russia, Italy*⁴ *AIST, Tsukuba, Japan*

A magnetic vortex can be excited into precessional motion around its equilibrium position through spin transfer torque[1,2]. The associated microwave emission is weak but very coherent. Here we present experimental evidences of high power, low linewidth spin-transfer induced vortex oscillations in MgO based magnetic tunnel junctions with a large TMR ratio[3]. Indeed, a clear picture of how the spin transfer torque influences the frequency and the amplitude of the gyrotropic vortex motion in a nano-pillar is still lacking. Here we derive an analytical model that takes into account the non-linearity of the vortex core confining force and the non-linearity of the effective damping that will be compared to experimental results and micromagnetic simulations. Therefore it allows us to determine the evolution of the vortex core dynamics with perpendicular field and current. Finally, we show that a very efficient coupling[4] to an external microwave current can be obtained in such spin transfer vortex oscillators (STVOs) and compare these results to theoretical locking range, taking into account all possible components of spin transfer torques. Support from ANR through VOICE PNANO-09-P231-36 and EU MASTER No. NMP-FP7-212257 and Canon-Anelva for MTJ films is acknowledged. E. G. acknowledges support from CNES and DGA.

[1] K. Yu Guslienko, *Journal of Nanoscience and Nanotechnology*, **8**, 2745 (2008) [2] V. Pribiag et al., *Nat. Phys.* **3**, 498 (2007); Q. Mistral et al., *Phys. Rev. Lett.* **100**, 257201 (2008) [3] A. Dussaux et al., *Nat. Commun.* **1**, 8 (2010) [4] A. Dussaux et al. *App. Phys. Lett* **98**, 132506 (2011)

ID03

Study of spin transfer induced coupled vortices dynamics in a single spin-valveNicolas Locatelli¹, Paolo Bortolotti¹, Alexey Khvalkovskiy², Grisha Avanesyan³, Vladimir V. Naletov³, Julie Grollier⁴, Gregoire De Loubens⁵, Konstantin Zvezdin⁶, Olivier Klein⁴, Vincent Cros^{1*} and Albert Fert¹¹ *Unité Mixte de Physique CNRS-Thales et Univ Paris-Sud, Palaiseau, France*² *Grandis Inc, Milpitas, CA, USA*³ *A.M. Prokhorov General Physics Institute of RAS, Moscow, Russia*⁴ *Service de Physique de l'Eiat Condense, CEA, Gif-sur-Yvette, France*

In order to address the problem of low coherence of actual spin-transfer nano-oscillators, recent studies have focused on phase locking phenomena, between an oscillator and an external source, or between assemblies of two or more oscillators. In the latter case, new collective modes have to be differentiated from the modes of isolated single oscillators. These appear to be tuned by the amplitude of the coupling, as well as the parameters of the single oscillators, namely the chirality and polarity in case of a vortex[2,3]. In this work, we suggest to use two vortices, nucleated in both layers of a Py(15nm)/Cu(10nm)/Py(4nm) spin-valve, as two interacting oscillators. Fundamental interests of this system lie in the identification of the excited coupled modes and their selection rules. Besides the observation of highly coherent vortex oscillations, we demonstrate that the dynamic behaviour is highly dependent on the vortices parameters[3]. We will compare the experimental results to analytical predictions and simulations, studying the importance of different sources of coupling between the vortices. A careful study of spin-polarized transport also shows the strong influence of the fast magnetization gradients associated with vortices. This work will be extended further to conditions to synchronize arrays of interacting vortex oscillators.

[1] O.V. Sukhostavets et al., *App. Phys. Express* **4**, 065003 (2011), [2] A.V. Khvalkovskiy, N. Locatelli et al., *Appl. Phys. Lett.*, **96**, 212507 (2010), [3] N. Locatelli et al., *App. Phys. Lett.*, **98**, 062501 (2011)

ID04

Collective excitation of magnetostatically coupled two-adjacent magnetic vortices and their relative phase differenceHiroaki Fujimori¹, Yasuhiro Niimi¹, Satoshi Sugimoto¹, Shinya Kasai² and Yoshichika Otani^{1*}¹ *ISSP, University of Tokyo, Japan*² *National Institute for Material Science, Japan*

A magnetic vortex exhibits a core gyration which produces dynamic dipolar interaction between adjacent magnetic vortices. In our previous experiment, we detected the excitation spectra of magnetostatically coupled two gyrating vortices in a pair of magnetic disks by applying the radio frequency ac current only to one of the disks [1].The excitation mode observed in the single disk splits into two eigenfrequencies. In disk pairs four modes appear depending on the combination of polarities, which are characterized by rotational directions and the phase difference in core gyration. We here investigate the effect of the phase difference in gyration on the excitation of magnetostatically coupled vortices by varying the phase difference between ac excitation currents separately applied to the both disks. Firstly the collective excitation is induced by applying the ac current to one of the disks, and then the ac current with variable phase is applied to another disk to detect its indirect excitation caused by dipolar interaction at the specific phase difference. We found the indirect excitation signal at lower frequency clearly changed with respect to that at higher frequency and also the signal changed depending on chiralities.

[1] S. Sugimoto et al., *Phys. Rev. Lett.* **106** 197203 (2011).

IE01

Spin-orbit coupling induced spin torques in diluted magnetic semiconductors

Hang Li, Fatih Dogan and Aurelien Manchon*

King Abdullah University of Science and Technology, Saudi Arabia

It has been recently demonstrated that appropriately designed spin-orbit coupling (SOC) can be used to generate spin torque (SOC-torque) in a single ferromagnet, without the need of an external polarizer [1,2]. This effect has been observed experimentally in both metallic systems [2] and dilute ferromagnetic semiconductors (DMS) [3]. The case of DMSs is of particular interest due to their tunable bulk inversion asymmetry allowing for the generation of both cubic and linear Dresselhaus SOC [3,4]. A theoretical understanding of the microscopic nature of the SOC-torque in DMSs is still needed to accurately interpret the recently obtained experimental results [4]. The present study addresses the nature of SOC-torque in DMS in the framework of Luttinger Hamiltonian (GaMnAs, InMnAs etc. . .). Based on kinetic-exchange model, the non-equilibrium spin transport in DMS is studied theoretically within the first-order Born approximation [4]. Both cubic and linear Dresselhaus SOC are examined and the angular dependence and magnitude of the SOC-torque are studied for a wide range of parameters. Interestingly, the cubic Dresselhaus SOC does generate a spin torque as long as the Fermi surface is not spherical. The role of the carrier concentration and shape of the Fermi surface are emphasized and experimental implications are discussed.

[1] A. Manchon and S. Zhang, *Phys. Rev. B* **78**, 212405 (2008); **79**, 094422 (2009). [2] I. M. Miron et al., *Nature Mater.* **9**, 230 (2010) ; U. H. Pi, et al. *Appl. Phys. Lett.* **97**, 162507 (2010); I. M. Miron, et al. *Nature (London)* **476**, 189 (2011). [3] A. Chernyshev, et al. *Nature Phys.* **5**, 656 (2009); Fang et al. *Nature Nanotechnology* **6**, 413 (2011). [4] T. Jungwirth, M. Abolfath, J. Sinova, J. Kucera, A. H. MacDonald, *Appl. Phys. Lett.* **81** 4029 (2002); A. W. Rushforth, K. Vyborny, C. S. King et al., *J. Magn. Magn. Mat.* **321** 1001 (2009).

IE02

Spin orbit torque assisted domain wall depinning in Pt/Co/Pt

Elena Mure*, Pascal P. Haazen, Jeroen H. Franken, Henk J. Swagten and Bert Koopmans

Eindhoven University of Technology, Netherlands

It has been shown that, in perpendicular magnetic anisotropy (PMA) materials, the injection of a current results in a torque on the magnetization (SO-torque). This torque could participate to the current-induced (CI) domain wall (DW) motion, which up to now has been described in terms of spin transfer torque (STT) effect. This experiment aims at a comparison of SO-torque and STT in a Pt/Co/Pt stack. Using a focused ion beam technique we create a soft magnetic domain in the center of the stripe, and we study its evolution under the application of current and magnetic field. The measurements are done using a pump-probe detection scheme, suitable for stroboscopic experiments with sub-1 ns time-resolution. Our results show that the effect of the current is a broadening/narrowing of the magnetic domain, indicating that the SO-torque is dominant over STT and Joule heating. Moreover, we observe some features that are signature of SO-torque, notably the dependence of the CI-effect on the sign of the in-plane magnetic field and on the relative thickness of the two Pt buffer layers. Finally, we emphasize the potential of our set-up for time-resolved study of CI magnetization dynamics, which could help in determining the origin of the SO-torque.

IE03

Piezo-electric control of the motion of a single domain wallElisa De Ranieri¹, Pierre Roy¹, Dong Fang¹, Erin Vethstedt², Andrew C. Irvine³, Dominik Heiss⁴, Richard Campion⁴, Tomas Jungwirth⁵ and Joerg Wunderlich^{6*}¹ *Hitachi Cambridge Laboratory, JJ Thomson Avenue, Cambridge, CB3 0HE, UK, United Kingdom*² *Department of Physics, Texas A&M University, College Station, Texas 77843-4242, USA, USA*³ *Microelectronics Group, Cavendish Laboratory, University of Cambridge, JJ Thomson Avenue, Cambridge, United Kingdom*⁴ *School of Physics and Astronomy, University of Nottingham, United Kingdom*⁵ *Institute of Physics ASCR, v.v.i., Cukrovarnicka 5 10, 162 53 Praha 6, Czech Republic*⁶ *(a) Hitachi Cambridge Lab, Cambridge, UK (b) Institute of Physics ASCR, Prague, Czech Republic, United Kingdom*

We report piezo-electric control of a single domain wall (DW) driven by electrical current in a microbar fabricated in a perpendicularly magnetized GaMnAsP epilayer and by a magnetic field in the unpatterned film. By applying the piezo-voltage we tune in situ the magneto-crystalline anisotropy and thus modulating the stability of the internal wall structure which determines the value of the Walker breakdown. The low defect density in our high-quality GaMnAsP epilayer allows to study DW propagation in both the viscous and precessional regimes, before and after the Walker breakdown critical current, respectively. This combined with the piezo-electric controlled DW stability allows us to experimentally identify the adiabatic torque as the dominant spin-transfer mechanism and to vary the DW velocity by up to 500% at a fixed driving current and by more than two orders of magnitude at a fixed applied magnetic field. Our experimental conclusions are supported by a one-dimensional DW motion model and detailed micro magnetic simulations taking into account the individually measured complex magnetic anisotropies of the specific microbars. We conclude that our results are generic and applicable to DW motion in magnetic films with tunable magnetic anisotropy and Curie temperatures above room temperature.

IE04

Domain wall manipulation by spin currents in magnetic tunnel junctions
Julie Grollier¹, Peter Metaxas¹, Joao Sampaio¹, Rie Matsumoto¹, Andre Chanthbouala¹, Alexey Khvalkovskiy¹, Vincent Cros¹, Abdelmajid Anane¹, Albert Fert¹, Konstantin Zvezdin², Akio Fukushima¹, Hitoshi Kubota¹, Kay Yakushiji¹ and Shinji Yuasa¹

¹ *Unite Mixte de Physique CNRS/Thales, France*
² *Istituto P.M. s.r.l., Italy*
³ *National Institute of Advanced Industrial Science and Technology, Japan*

The spin transfer effect allows the manipulation of magnetic domain walls (DWs) in ferromagnetic wires by injection of dc currents, which has led in recent years to the proposal of a number of potentially revolutionary devices [1,2]. In most of these systems, the current is injected along the direction of DW propagation, and the current density required to move the DW has generally remained prohibitively high for applications. Recently, it was predicted [3] that higher efficiency could be obtained by using vertical current injection through multilayer devices, specifically in magnetic tunnel junctions (MTJ). Our group has experimentally verified the higher efficiency DW motion with perpendicularly injected dc currents in MTJs, which was attributed to the out-of-plane spin transfer torque and the Oersted field [4]. We now present time-resolved measurements of DW motion under vertically injected pulsed currents, and demonstrate that DW speeds in excess of 500 m/s can be attained using current densities that are up to 2 orders of magnitude less than those required in devices that use lateral current injection. As such, this work represents an important advance in the race towards energy-efficient, high speed domain wall devices. We acknowledge the European Research Council (Stg 2010 No.259068).

[1] S.S.P. Parkin et al., "Magnetic domain wall racetrack memory", *Science*, vol. 320 pp. 190-194, 2008. [2] X. Wang et al., "Spintronic memristor through spin-torque-induced magnetization motion", *IEEE Elec. Dev. Lett.*, vol. 30, pp. 294-297, 2009. [3] A.V. Khvalkovskiy et al., "High domain wall velocities due to spin currents perpendicular to the plane", *Phys. Rev. Lett.*, vol. 102, p.067206, 2009. [4] A. Chanthbouala et al., "Vertical-current-induced domain-wall motion in MgO-based magnetic tunnel junctions with low current densities", *Nature Physics*, vol. 7, pp. 626-630, 2011.

IF01

Large magnetoresistance in antiferromagnet tunnel junctions

Byong-guk Park^{1*}, Joerg Wunderlich², X. Marti³, J. Hayakawa⁴, H. Takahashi⁵ and T. Jungwirth⁵

¹ *Material Science and Technology, KAIST, Korea*
² *Hitachi Cambridge Laboratory, United Kingdom*
³ *Faculty of Mathematics and Physics, Charles University, Czech Republic*
⁴ *Hitachi Central Laboratory, Japan*
⁵ *Institute of Physics, ASCR, Czech Republic*

Antiferromagnets (AFM's) have been used in spintronics devices so far only to pin the magnetization direction of a ferromagnetic electrode through the exchange-bias effect. Spintronics devices whose transport is governed by AFM's have been theoretically proposed, but remain a great challenge for experimental realization. Here, we demonstrate a large magnetoresistance effect in a tunnel junction with an AFM electrode of IrMn and a nonmagnetic counter electrode [1]. In the device, the tunneling resistance depends on the magnetization direction of the IrMn electrode, so-called tunneling anisotropic magnetoresistance (TAMR) effect, which is based on the spin-orbit coupling. This is quite different from the conventional spin-valves where the resistance depends on the relative magnetization directions of two ferromagnetic electrodes. The magnetization direction of the AFM IrMn layer was manipulated with a relatively small magnetic field of 50mT by the exchange spring effect of coupled soft NiFe. In addition, the AFM TAMR provides a means to study the exchange-bias effect by an electronic transport measurement [2].

[1] B. G. Park et al., *Nature Materials* 10, 347 (2011) [2] X. Marti, B. G. Park, et al., *Phys. Rev. Lett* 108, 017201 (2012)

IF02

A first-principles study on spin-dependent tunneling conductance in magnetic tunnel junctions with spinel-type MgAl₂O₄ barrier

Yoshio Miura^{1*}, Shingo Muramoto², Kazutaka Abe¹ and Masafumi Shirai¹

¹ *RIEC & CSIS, Tohoku University, Japan*
² *RIEC, Tohoku University, Japan*

Recently, a normal-spinel type MgAl₂O₄ was grown on and Co₂FeAl_{0.5}Si_{0.5} and bcc-Fe electrodes to explore new materials as a barrier layer in magnetic tunnel junctions(MTJs) [1,2]. The MgAl₂O₄ showed a great advantage in the epitaxial growth compared to the MgO because of a small lattice mismatch less than 1% with bcc-type ferromagnetic metals at (001) face. In this study, we investigated the transport properties of Fe/MgAl₂O₄/Fe(001) MTJs using the first-principles calculations. We found that Fe/MgAl₂O₄/Fe(001) MTJ showed the coherent tunneling conductance through the delta 1 evanescent state as well as Fe/MgO/Fe(001) MTJs. However, the calculated tunneling magnetoresistance (TMR) ratio of Fe/MgAl₂O₄(1nm)/Fe(001) MTJ was about 160%, which was much smaller than that of Fe/MgO(1nm)/Fe(001) MTJ (1600%). This can be attributed to appearance of new conductive channels in the antiparallel magnetization configuration by the band-folding in the two dimensional Brillouin zone of in-plane wave vector of bcc-Fe, because the in-plane cell-size of MgAl₂O₄ is twice of that of bcc-Fe. These results indicate that suppression of band-folding is essential to obtain a large TMR ratio in Fe/MgAl₂O₄/Fe(001) MTJs. This work was partially supported by JSPS through the FIRST Program and by JST through ASPIMATT program.

[1] R. Shan, et al., *Phys. Rev. Lett.* 102, 246601 (2009). [2] H. Sukegawa, et al., *Appl. Phys. Lett.* 98, 212505 (2010).

IF03

Enhanced tunnel magnetoresistance in magnetic tunnel junctions with an epitaxial Mg-Al-O barrier

Hiroaki Sukegawa, Seiji Mitani, Tomohiko Niizeki, Tadakatsu Ohkubo, Koichiro Inomata and Kazuhiro Hono

Magnetic Materials Unit, National Institute for Materials Science (NIMS), Japan

Achievement of defect-free heterostructure is essential to establishment of high performance spintronics devices such as magnetic tunnel junctions (MTJs), spin-transfer devices and spin-transistors. A spinel MgAl₂O₄ has a potential for a future tunnel barrier because of the small in-plane lattice mismatch (< 1%) between MgAl₂O₄ and bcc ferromagnetic alloys such as CoFe alloys and Heusler alloys. In addition, MgAl₂O₄ is a nondeliquescent material, which is favorable for practical applications. Recently a large tunnel magnetoresistance (TMR) ratio of 117% was observed at room temperature (RT) in a fully epitaxial Fe/MgAl₂O₄/Fe(001) MTJ, indicating the enhancement of TMR by an epitaxial MgAl₂O₄ barrier as well as an MgO barrier [1]. In this study we achieved a fully epitaxial CoFe/Mg-Al-O/CoFe(001) MTJ using a sputter deposition and a plasma oxidation of Mg-Al alloy layers. We demonstrated the very large TMR ratio of 308% at RT in the MTJ even though the barrier layer had an off-stoichiometric MgAl₂O₄ composition (Mg₄₀Al₆₀O_x). This result suggests that Mg-Al-O is promising for a tunnel barrier of future spintronics devices using coherent tunneling.

[1] H. Sukegawa et al., *Appl. Phys. Lett.* 96, 212505 (2010).

IF04

The memristive magnetic tunnel junction as a nanoscopic synapse-neuron system

Andy Thomas, Patryk Krzysteczko, Gunter Reiss, Jana Munchenberger and Markus Schafers

Physics, Bielefeld University, Germany

Memristors cover a gap in the capabilities of basic electronic components by remembering the history of the applied electric potentials, and are considered to bring neuromorphic computers closer by imitating the performance of synapses. We used memristive magnetic tunnel junctions based on MgO to demonstrate that the synaptic functionality is complemented by neuron-like behavior in these nanoscopic devices. The synaptic functionality originates in a resistance change caused by a voltage-driven oxygen vacancy motion within the MgO layer. The additional functionality provided by magnetic electrodes enabled a current-driven resistance modulation due to spin-transfer torque. We report on memristive magnetic tunnel junctions characterized by the simultaneous occurrence of resistive switching and tunnel magnetoresistance. Since resistivity provides a natural measure of the synaptic strength, and because of the bipolar nature of the resistance change, long term potentiation and long term depression were emulated. Furthermore, we show that the flux is a good variable for describing voltage-induced resistance variation, which provides the scope for the emulation of spike timing dependend plasticity as well.

[1] Krzysteczko et al., *The memristive magnetic tunnel junction as a nanoscopic synapse-neuron-system*, *Adv. Materials*, DOI: 10.1002/adma.201103723

IF05

Tunnel magnetoresistance in perpendicularly magnetized Co₂FeAl/MgO/CoFeB magnetic tunnel junctions

Zhenchao Wen*, Hiroaki Sukegawa, Shinya Kasai, Masamitsu Hayashi, Seiji Mitani and Koichiro Inomata

National Institute for Materials Science (NIMS), Japan

Perpendicular magnetization of Co₂FeAl (CFA) full-Heusler alloy thin film was achieved with the high perpendicular magnetic anisotropy (PMA), Ku of 2 ~ 3×10⁶ erg/cm³ in the structures of CFA/MgO, which is comparable to that of the conventional PMA materials[1]. The CFA thickness dependence of Ku was investigated at different annealing temperatures, which indicated that the Ku of CFA is contributed by the interfacial anisotropy between CFA and MgO. Furthermore, we successfully fabricated perpendicularly magnetized tunnel junctions (p-MTJs) using CFA full-Heusler alloy. The out-of-plane tunneling magnetoresistance (TMR) ratio of 53% at room temperature was observed in CFA/MgO/Co₂₀Fe₈₀B₂₀ p-MTJs on Cr-buffered MgO(001) substrates. By inserting 0.1 nm Fe (Co₉₀Fe₁₀) between MgO and Co₂₀Fe₈₀B₂₀, TMR ratio was significantly enhanced to 91% (82%) due to the improved interface. The annealing temperature dependence of TMR ratio was also investigated. Comparison of the bias voltage dependence of the differential conductance was carried out between MTJs with the core structures of CFA(1)/MgO(1.8)/Co₂₀Fe₈₀(5) and CFA(30)/MgO(1.8)/Co₂₀Fe₈₀(5) (unit: nm), which suggested that the improvements of B2 ordering of ultrathin CFA and interface structures are required for enhancing coherent tunneling in order to achieve a higher TMR ratio. This work opens up a way for perpendicularly magnetized MTJs using full-Heusler alloys.

[1] Zhenchao Wen, Hiroaki Sukegawa, Seiji Mitani, and Koichiro Inomata, *Appl. Phys. Lett.* 98, 242507 (2011).

IG01

Transport anomalies due to critical valence fluctuations

Kazumasa Miyake

Department of Materials Engineering Science, Osaka University, Japan

It has been gradually turned out in this decade that some Ce- and Yb-based heavy fermion metals exhibit quantum critical phenomena associated with critical end point of valence transition [1]. In particular, temperature dependences of the specific heat, the uniform susceptibility, the longitudinal relaxation rates of NMR, and the resistivity have critical exponents quite different from those of conventional magnetic critical phenomena of a la Moriya-Hertz-Millis, giving possible explanations of behaviors observed in beta-YbAlB₃, YbAuCu₄, YbRh₂Si₂, CeCu₂(Si,Ge)₂, CeRhIn₅, and so on [2,3]. In this talk, we briefly summarize previous studies on the above aspects, and discuss transport anomalies due to the critical valence fluctuations (CVF). Namely, the effect of collective modes beyond the Boltzmann transport due to quasiparticles is analyzed generalizing the case of superconducting fluctuations near the transition point [3]. It is shown that the Hall coefficient, the Nernst coefficient, the Seebeck coefficient, and the thermal conductivity are greatly affected by the CVF, explaining some anomalies of the Hall coefficient, the Nernst coefficient, and the Seebeck coefficient observed in CeCu₂Si₂ and CeRhIn₅ under pressure. This talk is based on collaborations with Shinji Watanabe and Osamu Narikiyo who are gratefully acknowledged.

[1] K. Miyake: *J. Phys.: Condens. Matter* 19, (2007) 125201. [2] S. Watanabe and K. Miyake: *Phys. Rev. Lett.* 105, 186403 (2010). [3] S. Watanabe and K. Miyake: *J. Phys.: Condens. Matter* 23, 094217 (2011).

IG02

Fluctuations and quantum criticality in Eu ternary pnictides

Yuriy Vladimirovich Goryunov^{1*} and Alexandr Nikolaevich Nateprov²

¹ *Russian Academy of Sciences, Kazan Physical-Technical Institute of the Russian Academy of Sciences, Russia*

² *Academy of Sciences of Moldova, Institute of Applied Physics, Moldova*

We have studied the magnetic properties of the Zintl compounds EuZn₂(P, As, Sb)₂ by ESR. The ESR was measured on frequency 9.3 GHz in TE102 rectangular cavity at 4.2 - 300 K. Above 150 K in all cases, we observed the symmetric resonance lines Eu²⁺ with ideal Lorentzian lineshape. At the temperature decreasing well before the antiferromagnetic ordering temperature we have observed an increasing of lineswidth and a decreasing of the resonance fields, which in our case very good described by Landau's theory of magnetic fluctuations. The fluctuational nature of such behaviour is confirmed by changing the shape of the resonance line from Lorentzian to Gaussian. The paramagnetic temperature θ_p, obtained from the temperature dependence of the ESR signal intensity, has the positive sign. We believe such behaviour of θ_p is connected with the proximity to quantum critical point and with the relevant instability of magnetic and crystal structures (instability B₂X₂-layers, competition nonmagnetic 4f₆ and magnetic 4f₇ states of Eu) The obtained ESR data are interpreted in terms of Bloembergen-Rowland's indirect exchange interaction through the valence electrons and the Falicov-Kimball-Kugel model the hybridization of localized electrons with itinerant electrons. Work was supported by Grants of RFBR and RAS.

[1] Yu C. Zhu T.J. Zhang S.N. et al. *J. Appl. Phys.* 104 013705(2008) [2] C. Zheng, R. Hoffmann, *J. of Solid State Chemistry* 72 58 (1988) [3] N. Bloembergen, T.J. Rowland, *Phys. Rev.* 97, 1679 (1955) [4] L.M. Falicov, J.C Kimball, *Phys.Rev.Lett.* 22 997 (1969) [5] K.I Kugel, A.L. Rakhmanov, *A O Sboychakov, Phys.Rev.Lett.* 95, 267210 (2005)

IG03

Synchrotron x-ray spectroscopy study on the valence state in α- and β-YbAlB₃ at low temperatures and high magnetic fields

Yasuhiro H. Matsuda^{1*}, Toshiyuki Nakamura¹, Kentaro Kuga¹, Satoru Nakatsujii¹, Shinji Michimura², Toshiya Inami², Naomi Kawamura³ and Masachiro Mizumaki³

¹ *Institute for Solid State Physics, University of Tokyo, Japan*

² *Japan Atomic Energy Agency, Japan*

³ *Spring-8/JASRI, Japan*

Valence fluctuation phenomena in β-YbAlB₃ and its polymorph α-YbAlB₃ have attracted much attention. [1, 2] The possible quantum criticality due to the valence transition is theoretically predicted. [3] In the present study, valence states of α- and β-YbAlB₃ have been investigated by the x-ray absorption spectra (XAS) in SPring-8 at temperatures from 2 to 280 K. The partial fluorescence yield mode and direct transmission method were used. High magnetic field XAS measurement was done on β-YbAlB₃ at 40 K in pulsed magnetic fields. Observed Yb valence is 2.8 ± 0.05 in α- and β-YbAlB₃ at 5 and 2 K, respectively. This value is slightly higher than the previously reported results 2.73± 0.02 for α-YbAlB₃ and 2.75± 0.02 for β-YbAlB₃. [1] The valence is found to gradually increase with increasing temperature toward the trivalent state; the valence increment from the low temperature to 200 K is about 0.02 in both materials. We also found a small increase of Yb valence by a magnetic field of 31 T.

[1] M. Okawa et al., *PRL* 104, 247201 (2010). [2] Y. Matsumoto et al., *Science* 331, 316 (2011). [3] S. Watanabe et al., *PRL* 105, 186403 (2010).

IG04

Metal-Insulator crossover accompanied by the dual nature of 5f electrons with localized and itinerant character in US2

Naoto Metoki¹, Etsuji Yamamoto², Hironori Sakai², Yoshinori Haga², Tatsuma D Matsuda² and Shugo Ikeda²

¹ *QBus, JAEA, Japan*
² *ASRC, JAEA, Japan*

Uranium dichalcogenide β-US2 is a low carrier system with metallic behavior at room temperature, while insulating with opening a charge gap Eg~90K at low temperatures with colossal magneto-resistance effect 10⁸ for H~10 T. The magnetic properties can be well described by a localized model. In fact clear CEF excitations have been observed at ~7 meV, indicative of the localized character of 5f electrons at low temperatures. With elevating temperature (> 100 K) above the conduction and magnetic excitation gap, however, we observed magnetic quasi-elastic response accompanied by the metal-insulator crossover with a large resistivity drop in the order of 10⁸. This suggests a new mechanism of metal-insulator crossover as a consequence of the change in 5f character between localized and itinerant. We succeeded to separate the magnetic susceptibility into two parts, the contribution from the localized and itinerant part, by carrying out Kramers-Kronig transformation of the imaginary part of the dynamical susceptibility measured by magnetic excitation with neutron inelastic scattering. We revealed a dual nature of 5f electron system, growing itinerant character with elevating temperature beyond the charge gap.

IG05

Valence transition induced by pressure and magnetic field in antiferromagnet EuRh₂Si₂

Akihiro Mitsuda*, Suguru Hamano and Hirofumi Wada

Department of Physics, Kyushu University, Japan

EuRh₂Si₂, which crystallizes in the tetragonal ThCr₂Si₂ type structure, is an antiferromagnet with TN=23K and the Eu ion is in the divalent state (4f₇, J=7/2). Recently, we have found that the application of pressure of 1.0GPa collapses the antiferromagnetism and simultaneously induces a first-order valence transition at Tv~30K [1]. Under higher pressure than 1.0GPa, the sample shows a temperature-independent Pauli-paramagnetic behavior (a non-magnetic phase) below Tv while a Curie-Weiss paramagnetism corresponding to Eu²⁺ (a magnetic phase) above Tv. In this study, we have measured M-B curves under pressure to examine influences of magnetic field on the non-magnetic phase. A metamagnetic transition accompanied by a large hysteresis is observed at 20K under 1.0GPa. The magnetization jumps from 1.0μB/Eu at B=3.6 T to 1.6μB/Eu at B=5.0 T with increasing magnetic field. This phenomenon corresponds to a field-induced valence transition from the non-magnetic phase to the magnetic divalent phase.

[1] A. Mitsuda et al. *J. Phys. Soc. Jpn.* 81 (2012) 023709

IH01

Orbital ordering and multiphase separation at manganite interfaces

Sergio Valencia¹, Defleft Schmitz¹, Luis Pena², Zorica Konstantinovic², Lluis Balcells², Regina Galceran², Felip Sandiumenge², Marie-jose Casanove³ and Benjamin Martinez*

¹ *Helmholtz-Zentrum-Berlin fur Materialien und Energie, BESSY, Germany*

² *Magnetic Materials and Functional Oxides, ICMAB - CSIC, Spain*

³ *Centre d'Elaboration de Materiaux et d'Etudes Structurales, CNRS - CEMES, France*

Interfacial effects between La_{0.7}Sr_{0.3}MnO₃ (LSMO) thin films and different capping layers are analyzed by using x-ray absorption techniques, x-ray diffraction and transport measurements. We make use of x-ray linear dichroism (XLD) to show that, independently of the capping layer, LSMO films exhibit a preferential occupation of Mn 3d 3z²-r² eg orbitals at the interface. The strength of such an orbitally ordered phase does not depend on the capping layer material neither is related to the previously observed degradation of the Mn oxidation state nor to the magnetic properties. Moreover, its intensity is similar to that observed in uncapped films thus indicating its origin lies on the symmetry breaking at the LSMO surface. Transport measurements across LSMO/capping layer interfaces allow estimating the scale length of this effect showing that the disruption of the double exchange ferromagnetic (DE-FM) phase occurs only by the interface, in fact around 2 to 4 unit cells. Thus, XAS local techniques point to a complex scenario at the manganite's interfaces in which orbital ordering and multiphase segregation coexist.

IH02

Conical spin-spiral state in an ultra-thin film driven by higher-order spin interactions

Yasuo Yoshida^{1*}, Silke Schroeder², Paolo Ferriani², David Serrate³, Kirsten Von Bergmann⁴, Andre Kubetzka⁴, Stefan Heinze² and Roland Wiesendanger⁴
¹ Institute for solid state physics, The University of Tokyo, Japan
² Institute for Theoretical Physics and Astrophysics, Christian-Albrechts-Universitaet zu Kiel, Germany
³ Instituto de Nanociencia de Aragon, Universidad de Zaragoza, Spain
⁴ Institute of Applied Physics, University of Hamburg, Germany

The magnetic properties of transition-metal nanostructures are commonly explained based on the interplay of Heisenberg exchange, Dzyaloshinskii-Moriya (DM) interaction and magnetocrystalline anisotropy while higher order terms such as the biquadratic exchange and the four-spin interaction are typically neglected due to their small strength. Here, we demonstrate that higher-order terms can play a crucial role for the magnetic ground state and report as an example a transverse conical spin-spiral state in an ultra-thin film composed of two atomic layers of Mn on W(110) [1]. This spin structure is characterized by magnetic moments rotating on a cone that is perpendicular to the [001] propagation direction of the spin-spiral with a periodicity of 2.4 nm. The cones of nearest-neighbor Mn atoms point into opposite directions which results in nearly antiferromagnetic alignment. This intriguing spin structure has been resolved on the atomic-scale using spin-polarized scanning tunneling microscopy and confirmed to be the ground state by first-principles calculations based on DFT. Our calculations also reveal that the canting of the spins is induced by higher-order exchange interactions while the spiraling along the [001]-direction is due to frustrated Heisenberg exchange and DM interaction.

[1] Y. Yoshida et al., Phys. Rev. Lett. (in press)

IH03

Non-collinear magnetic ground state in finite metallic chains

Matthias Menzel^{1*}, Yuriy Mokrousov², Robert Wieser¹, Jessica E. Bickel¹, Elena Vedmedenko¹, Stefan Blugel¹, Stefan Heinze³, Kirsten Von Bergmann¹, Andre Kubetzka¹ and Roland Wiesendanger¹
¹ Institute of Applied Physics, University of Hamburg, Germany
² Forschungszentrum Julich, Germany
³ Institute of Theoretical Physics and Astrophysics, University of Kiel, Germany

The investigation of one-dimensional magnetic structures on the atomic scale is a quite challenging task, since they are very prone to thermal and quantum fluctuations [1]. Here, we present spin-polarized scanning tunneling microscopy (SP-STM) measurements of bi-atomic Fe chains on (5x1)-Ir(001). The chains exhibit a modulation along the chain axis with a three atom periodicity in an external magnetic field perpendicular to the surface which is not present without the magnetic field [2]. This is due to a spin spiral ground state, whose thermally induced magnetization switching leads to a time-averaged SP-STM signal, with the external field preferring one of the magnetization directions. However, due to the rigid coupling of the Fe atoms' magnetic moments along the chain axis, the spin spiral order is not affected by thermal fluctuations at the measurement temperature. Therefore, changes in the spin direction of one chain end can be probed tens of nanometers away, suggesting a new way of transmitting information about the state of magnetic objects on the nanoscale.

[1] N.D. Mermin and H. Wagner, Phys. Rev. Lett. 17, 1133 (1966). [2] M. Menzel et al., submitted.

IH04

Magnetism and the thermodynamics of Fe-Pt surface alloy formed at Pt(110) surface

Byong Sun Chun, Wondong Kim and Chanyong Hwang*
 Korea Research Institute of Standards and Science, Korea

Surface alloy formation at noble metal surface shows very interesting phenomena. If one of the constituent atoms is magnetic, then its magnetic behavior evolves depending on the ratio of composition and the temperature. We will show atomistic view of Fe-Pt surface alloy formation at Pt(110)-missing low surface using scanning tunneling microscopy. When the external Fe atoms are deposited on top of Pt(110)-(2x1) surface, they are located at the missing row position. When the temperature increases, they exchange the position with the Pt atoms nearby due to the increase of the entropy term to minimize the free energy. Pt atoms located at the missing row position is energetically unstable. The change of magnetic characteristics through this order-disorder phase transition has been probed with the surface magneto-optic Kerr effect. With the aid of density functional theory, all the nanoscopic description of this magnetic surface alloy formation will be discussed.

IH05

A study of antiferromagnetic/ferromagnetic systems using x-ray magnetic dichroism

Z. Q. Qiu¹ and Chanyong Hwang^{2*}
¹ Dept. of Physics, University of California at Berkeley, Berkeley, CA 94720, USA
² Korea Research Institute of Standards and Science, Yuseong, Daejeon 305-340, Korea

Epitaxial CoO/Fe/Ag(001) system was investigated using X-ray Magnetic Circular Dichroism (XMCD) and X-ray Magnetic Linear Dichroism (XMLD). XMCD measurement was used to measure the Fe hysteresis loops and to determine the unidirectional (exchange bias), uniaxial, and the 4-fold anisotropy. XMLD measurement was used to determine the response of the CoO spins. We find that the CoO spins consist of rotatable and frozen spins with respect to the Fe spin rotation, and only the Fe uniaxial magnetic anisotropy follows the CoO frozen spins. We find that only uniaxial magnetic anisotropy is correlated to the frozen spins.

IH06

Magnetic properties and microscopic structures of ultrathin Co/√3x√3-R30°-Ag/Si(111) films

Jyh-shen Tsay¹, Tsu-yi Fu^{1*}, Chih-kuei Kao¹, Xiao-lan Huang¹, Jyh-ron Shue¹, Wei-hsiang Chen¹ and Yeong-der Yao²
¹ physics, National Taiwan Normal University, Taiwan
² physics, Academia Sinica, Taiwan

Combined scanning tunneling microscopy and surface magneto-optic Kerr effect studies were employed to study the relation between magnetic properties and microscopic interfacial structures of ultrathin Co/√3x√3-R30° -Ag/Si(111) films. On the top of √3x√3-R30° -Ag/Si(111), pure Co clusters form without disrupting the √3x√3-R30° structure of the Ag buffer layer. The great strain due to the large mismatch between Co and the substrate influences the nucleation of Co atoms to form large clusters. No magnetic hysteresis in the polar configuration was observed for films thinner than 10 monolayers. The easy axis of magnetization is in the surface plane. Capping √3x√3-R30° -Ag on the top of Si(111) surface before the deposition of Co overlayers can efficiently reduce the nonferromagnetic Co-Si compound to zero thickness. For Co coverage between 2.9 and 4.2 monolayers, the lowered Curie temperature in ultrathin films is observed. Due to the existence of a smooth interface between Co and the √3x√3-R30° -Ag buffer, the coercivity for Co/√3x√3-R30° -Ag/Si(111) is smaller than that for Co/Si(111).

IH01

Giant anomalous Hall effect in magnetic topological insulator

Qi-kun Xue
 Tsinghua University, China

Topological insulator (TI) is a time-reversal-invariant and therefore magnetic field free version of the quantum Hall system. Breaking the time-reversal symmetry by ferromagnetic order in TIs can induce quantum Hall effect in the absence of external magnetic field, known as quantized anomalous Hall (QAH) effect. Here we report the realization of the carrier-independent ferromagnetism in thin films of Cr-doped TI (Bi₂Sb_{1-x})₂Te₃. Despite the opposite types of carriers and one order of magnitude change in carrier density, robust ferromagnetism with nearly constant Curie temperature is observed. Remarkably, anomalous Hall effect is significantly enhanced with decreasing carrier density, with the anomalous Hall angle reaching an unusually large value of 0.2 and the zero field Hall resistance reaching one quarter of the quantum resistance (h/e²), indicating the approaching QAH regime. The work paves the way to realize the QAH effect.

IH02

A rich rashba system created on the surface of a topological insulator

Phil King^{1*}, A De La Torre¹, Felix Baumberger¹, M. Bianchi², R. Hatch², Philip Hofmann², M.S. Bahramy³, R. Arita³, N. Nagaosa³, J. I. Mi⁴, B. Iversen⁴ and G. Balakrishnan⁵
¹ School of Physics and Astronomy, University of St Andrews, United Kingdom
² Department of Physics and Astronomy, Aarhus University, Denmark
³ Correlated Electron Research Group, RIKEN-ASI, Japan
⁴ Department of Chemistry, Aarhus University, Denmark
⁵ Department of Physics, University of Warwick, United Kingdom

Topological insulators are famed for their unconventional surface states which span from the bulk valence to conduction bands [1]. Adsorbing n-type dopants at the surface of these compounds in ultra-high vacuum, analogous to the application of an external gate voltage in a device, we show that new electronic states emerge that co-exist with the topological surface state [2,3]. A strong downward band bending causes quantization of the bulk conduction band states into a two-dimensional electron gas (2DEG) [2], while the bulk valence band states also become quantized due to the narrow valence bandwidth at the zone centre. This provides a novel opportunity to probe the interplay of dimensionality and topological order. Moreover, the 2DEG states can be driven to develop a large Rashba spin splitting [3]. The resulting multi-subband 2DEG provides a very rich Rashba system. The inner-most Fermi surface sheets display the chiral in-plane spin texture characteristic of classic Rashba states such as the L-gap surface state on Au(111). However, the outermost Fermi pockets display increasing degrees of hexagonal warping, resulting in an increasing out-of-plane spin canting. We investigate this system by angle-resolved photoemission and model calculations.

[1] M.Z. Hasan & C.L. Kane, Rev. Mod. Phys. 82 (2010) 3045 [2] M. Bianchi, et al., Nature Commun. 1 (2010) 128 [3] P.D.C. King et al., Phys. Rev. Lett. 107 (2011) 096802

IH03

From topological semimetals towards insulators. First-principles study

Stanislav Chadov^{1*}, Claudia Felser¹, Kristina Chadova², Diemo Kodderitzsch² and Hubert Ebert²
¹ Dept. Inorganic Chemistry, Max-Planck-Institute for Chemical Physics of Solids, Dresden, Germany
² Dept. Chemistry and Biochemistry, Ludwig Maximilians University, Munich, Germany

The presence of disorder is often seen as a destructive mechanism which must be reduced by any means. In present study we attempt to make it constructive using the robustness of the spin current in topologically non-trivial systems with respect to the time-reversal symmetric perturbations. Based on the fully-relativistic first-principles calculations involving the Coherent Potential Approximation (CPA) and Kubo-Greenwood formalism, we inspect the disorder-affected transport properties of random alloys between topologically non-trivial and trivial materials. The subsequent analysis encounters few interesting aspects. First, it straightforwardly leads to an alternative scheme improving the spin-Hall transport in a large class of topological semimetals and indicates the possibility of the topological Anderson insulator state. Second, we obtain the quantized measure of the spin-Hall conductivity in 3D without explicit calculation of the topological invariants. In addition, the CPA technique provides a very practical recipe to validate the non-trivial topological state of the material based on a purely bulk information.

IH04

Engineering and manipulating topological qubits in 1D quantum wires

Panagiotis Kotetes¹, Alexander Shnirman² and Gerd Schon¹
¹ Institut für Theoretische Festkörperphysik, Karlsruhe Institute of Technology, Germany
² Institut für Theorie der Kondensierten Materie, Karlsruhe Institute of Technology, Germany

Recently, the interest in topological quantum computing has grown due to the appearance of promising platforms for realizing the long sought Majorana bound states. Among the proposals that seem suitable for engineering Majorana bound states, the most prominent involves a 1D semiconducting quantum wire in proximity to a bulk s-wave superconductor, where in addition a Zeeman field is applied. In this work we explore novel routes for realizing topological qubits and we further investigate alternative possibilities for performing qubit operations without for instance the use of electrostatic gates. Specifically we focus on the interplay of the phases of the magnetic field and the superconducting order parameter, illuminating the significance of keeping intact the spin degree of freedom for engineering and braiding the topological qubits. Finally, by considering an appropriate junction setup, we demonstrate novel features in the Josephson effect of these systems, such as the magnetic control of the supercurrent.

IJ01

Magnetic structure of iron borate SmFe₂(BO₃)₄ : A neutron diffraction study

Clemens Ritter^{1*}, Anatolii Pankrats², Irina Gudim² and Alexander Vorotynov²
¹ Institut Laue Langevin, Boite Postale 156, F-38042 Grenoble, France
² Kirenskii Institute of Physics, Siberian Branch of RAS, Krasnoyarsk, 660036, Russia

Rare earth ferrobates RFe₂(BO₃)₄ have recently attracted widespread interest due to their interesting magnetic, magnetoelectric and multiferroic properties [1]. The magnetic structure is determined by a low dimensional element in the crystallographic structure which sees well separated chains of helicoidally arranged Fe atoms running along the crystallographic c-axis. No direct R-R or R-O-R interactions exist and the development and arrangement of long range magnetism is determined by the strongly polarizing Fe-sublattices and the competition between the iron and the rare earth anisotropies [2]. We determined the magnetic structure of SmFe₂(BO₃)₄ by neutron powder diffraction using a double wall container and diluting the sample with Al-powder in order to reduce the strong natural neutron absorption of Sm. The antiferromagnetic structure developed below TN=33K is of the easy plane type as already found for the R=Er, Y and Ho (above 6K) compounds [3,4]. The fit of the magnetic peaks was best using a magnetic formfactor for Sm³⁺ where C2=5.42 giving a total magnetic moment of μSm=0.24μB composed of an orbital moment of μSmL=1.3μB and an spin moment of μSmS=1.06μB.

[1] e.g. : R.P. Chaudhury et al., PRB 81, 2010, 220402 [2] C. Ritter et al., J. Phys. : Condens. Matter 19, 2007, 196227 [3] C. Ritter et al., J. Phys. : Condens. Matter 20, 2008, 365209 [4] C. Ritter et al., J. Phys. : Condens. Matter 22, 2010, 206002

IJ02

Preparation and characterization of Sr₃Fe₂O_{7-x} for different oxygen contents

Darren Peets^{1*}, Junghwa Kim¹, Andrey Maljuk², Chengtian Lin¹ and Bernhard Keimer¹
¹ Max-Planck-Institut für Festkörperforschung, Germany
² IFW Dresden, Helmholtzstr. 20, D-01069 Dresden, Germany

Iron(IV)- and ruthenium(IV)-based perovskite phases have proven rich in novel physics. The SrFeO_{3-y} system exhibits a wide range of unusual magnetic phases, from five distinct forms of helical magnetism when fully oxygenated [1] to a phase with frustrated, disordered Fe⁴⁺ moments for an oxygen content of 2¼ [2]. The Ru-based intergrowth phase Sr₃Ru₂O₇ exhibits metamagnetic quantum critical points in applied field [3]. However, the magnetic phase diagram of its Fe⁴⁺ analogue Sr₃Fe₂O_{7-x} remains largely unexplored. We describe single crystal growth by the floating zone technique, oxygen annealing, and transport and magnetic measurements of large Sr₃Fe₂O_{7-x} crystals suitable for neutron diffraction experiments. This work lays the foundation for comprehensive doping-dependent studies of Sr₃Fe₂O_{7-x}'s magnetic phase diagram and magnetic excitations.

[1] S. Ishiwata et al., Phys. Rev. B 84, 054427 (2011) [2] M. Schmidt et al., J. Phys.: Condens. Matter 15, 8691 (2003) [3] R.A. Borzi et al., Science 315, 214 (2007)

IJ03

The magnetic structures of CoPS₃ and NiPS₃

Andrew Wildes^{1*}, Virginie Simonet², Garry Mcintyre³, Eric Ressouche⁴, Emmanuelle Suard¹, Giulio Pepe⁵, Maxim Avdeev⁶ and Trevor Hicks⁶
¹ Institut Laue-Langevin, 6 rue Jules Horowitz, BP 156, 38042 Grenoble, France
² Institut Neel, 25 avenue des Martyrs, BP 166, 38042 Grenoble cedex 9, France
³ Bragg Institute, ANSTO, Locked Bag 2001, Kirrawee DC NSW 2232, Australia
⁴ INAC/SPSMS-MDN, CEA/Grenoble, 17 rue des Martyrs, 38054 Grenoble Cedex 9, France
⁵ Department of Physics & Astronomy, University College London, Gower Street, London, WC1E 6BT, United Kingdom
⁶ School of Physics, Monash University, PO Box 27, Vic 3800, Australia

The compounds CoPS₃ and NiPS₃ are candidates for two dimensional (2D) antiferromagnets, with the transition metal atoms lying on a honeycomb lattice. Magnetic structures for them were published in the 1980s, based on neutron powder diffraction data. Both materials were believed to be collinear antiferromagnets, although the antiferromagnetic axis differed between the compounds, with a magnetic propagation vector of [0 1 0]. We have made a careful study of the magnetization and neutron diffraction from single crystals, taking advantage of recent developments in instrumentation for neutron Laue diffraction, and have also measured neutron powder diffraction for comparison. Our data show that the powder diffraction has very few observable peaks and can, indeed, be fitted with the quoted magnetic structure. However, our single crystal data prove that the reported magnetic structures are erroneous, with the observation of many new Bragg peaks that could be indexed with [1/2 1/2 1/6]. Our experiments have an impact on the interpretations of the magnetic Hamiltonians, and we will contrast our findings with two other members of the family: MnPS₃, which is a good example of a 2D Heisenberg antiferromagnet; and FePS₃, which is a good example of a 2D Ising antiferromagnet.

IJ04

Magnetic properties in Fe-doped LnCo_{1-x}Fe_xAsO (Ln=La, Sm) systems

Yuke Li¹, Chenyi Shen², Yongkang Luo², Chen Lv², Qian Tao², Jianhui Dai¹, Guanghan Cao² and Zhuan Xu^{2*}

¹ Department of Physics, Hangzhou Normal University, China
² Department of Physics, Zhejiang University, China

We study the effect of Fe doping in Co-rich side of LnCo_{1-x}Fe_xAsO (Ln=La,Sm) systems. As Co is replaced partially by Fe ions, the FM transition temperature Tc was seriously suppressed to lower temperatures and it disappears around x = 0.3. In the SmCo_{1-x}Fe_xAsO system, the undoped SmCoAsO undergoes three magnetic phase transitions with decreasing temperatures, a FM transition around Tc of 80 K, and a FM to AFM transition below TN1 of about 45 K, and finally an AFM order of Sm³⁺ ion at TN2 of 5.6 K. With increasing Fe content, both Tc and TN1 gradually decreases. Around x = 0.3, the FM order of Co ions disappears above 2 K, and meanwhile, the FM-to-AFM transition cannot be observed either. However, the AFM order of Sm³⁺ ion is robust, and TN2 slightly decreases in for x =0.3. We concluded that in the 1111 type Co-based LnCo_{1-x}Fe_xAsO systems, 4f electrons of rare earth elements have an important effect on the magnetic behaviors of 3d electrons. On the contrast, the magnetism of rare earth elements is robust to the variations of 3d electrons. A rich magnetic phase diagram of the LnCo_{1-x}Fe_xAsO systems is established.

IJ05

Symmetry argument of cyano-bridged copper-molybdenum complexes

Jun Ohara* and Shoji Yamamoto
 Department of Physics, Hokkaido University, Japan

Photoreactive magnets of general formula Cu₂[Mo(CN)₆]·nH₂O [1] are composed of octacyanomolybdate ions of square antiprism configuration assembled within a tetragonal lattice. CuI₂[MoIV(CN)₆]·nH₂O irradiated with blue light turns into Cu[CuII[MoV(CN)₆]·nH₂O exhibiting a spontaneous magnetization. The induced magnetization is stable for long time below 100 K and is photoreversible. We group-theoretically study competing magnetic phases in this intriguing material. While individual octacyanomolybdate ions of square antiprism configuration are D4d-invariant, the point symmetry of their assembly reads C4h. A single octacyanomolybdenum complex is invariant to polyaxial rotations but has no inversion symmetry. The assembly is merely invariant to uniaxial rotations but is further symmetric with respect to inversion. Besides the paramagnetism (PM) and ferromagnetism (FM), which correspond to the major states before and after photoirradiation, respectively, we find three antiferromagnetic (AFM) states as well as nonmagnetic charge-density-wave and bond-order-wave states of no major interest. The AFM states consist of a spin density wave within the molybdenum sublattice, that within the copper sublattice, and that spreading out in both sublattices, respectively, the latter two of which closely compete with both PM and FM states and therefore possibly have significant effects on the photoreactive magnetization mechanism.

[1] S. Ohkoshi et al., JACS 128, 270 (2005).

IJ06

Phase diagram of the dzyaloshinskii-moriya helimagnet Ba₂CuGe₂O₇ in canted magnetic fields

Sebastian Clemens Muehlbauer*, Severian Gvasaliya², Eric Ressouche², Ekaterina Pomjakushina⁴ and Andrey Zheludev²

¹ Neutron Scattering and Magnetism Group, Laboratory for Solid State Physics, ETH Zurich, Switzerland
² Neutron Scattering and Magnetism Group, Laboratory for Solid State Physics, ETH Zurich, Switzerland
³ INAC/SPSMS-MDN, CEA Grenoble, France
⁴ Laboratory for Developments and Methods, Paul Scherrer Institute, Switzerland

The evolution of different magnetic structures of the non-centrosymmetric tetragonal antiferromagnet Ba₂CuGe₂O₇ is systematically studied as function of the orientation of the magnetic field H. Neutron diffraction in combination with measurements of magnetic susceptibility and specific heat shows a virtually identical phase diagram of Ba₂CuGe₂O₇ for H confined in both the (1,0,0) and (1,1,0) plane. The existence of a recently proposed incommensurate double-k AF-cone phase [1] is confirmed in a narrow range for H close to the tetragonal c-axis. In contrast, for large angles enclosed by H and the c-axis, a complexly distorted non-sinusoidal magnetic structure has recently been observed [1]. We show that its critical field systematically increases for larger canting. Measurements of magnetic susceptibility and specific heat finally indicate the existence of an incommensurate/commensurate (I/C) transition at H =9 T, applied in the basal (a,b)-plane [2]. The observation of this transition in combination with both odd and even harmonics of the propagation vector agree with a non-planar, distorted magnetic structure, possibly caused by the staggered component of the Dzyaloshinskii-Moriya vector.

[1] S. Muehlbauer et al. Phys. Rev. B 84, 180406 (2011) [2] S. Muehlbauer et al. in preparation (2012)

JA01

Close relationship between superconductivity and the bosonic mode in Ba_{0.6}K_{0.4}Fe₂As₂: A pairing glue for superconductivity

Hai-hu Wen*
 Nanjing University, China

Center for Superconducting Physics and Materials, National Laboratory of Solid State Microstructures and Department of Physics, Nanjing University, Nanjing 210093, China Since the discovery of high temperature superconductivity in the iron pnictides and chalcogenides in early 2008, it remains unclear whether there is a glue for the pairing and what it is. There is a debate at this moment about whether the pairing is due to a retarded electron-boson interaction, as in the conventional phonon-mediated superconductors, although here the bosonic excitations may be the antiferromagnetic spin fluctuations. In this paper, we show the clear evidence of the bosonic mode with the energy identical to that of the neutron resonance, and its close relationship with superconductivity in a strongly coupled superconductor Ba_{0.6}K_{0.4}Fe₂As₂ based on the measurements of scanning tunneling microscopy. Our data also indicate an interesting asymmetric feature of the tunneling spectrum, i.e., both the superconducting coherence peak and the peak related to the bosonic mode are always stronger on the positive-bias side, and vanish simultaneously within the vortex cores. Collaborated with Zhenyu Wang, Huan Yang, Delong Fang, Bing Shen

JA02

Broken time-reversal symmetry superconducting state in LiFeAs

Gang Li¹, Ricardo R. Urbano¹, C. Tarantini², Bin Lv³, Phil Kuhns¹, Arneil P. Reyes¹, David Larbalestier², Alexander Gurevich⁴, Ching-wu Chu³ and Luis Balicas^{1*}

¹ Condensed Matter Sciences, NHMFL, USA
² Center for Applied Superconductivity, NHMFL, USA
³ Texas Center for Superconductivity, University of Houston Houston, Texas, USA
⁴ Physics Dept., Old Dominion University, USA

Here, and despite the current experimental support for s-wave superconductivity, we show clear evidence for broken time reversal symmetry within the superconducting state of LiFeAs through magnetic torque and magnetization measurements at high fields and in high quality single crystals close to optimal doping. Both the torque and the magnetization reveal a change in the sign of the magnetic irreversibility/hysteresis as one approaches the upper critical Hc2, from a clear diamagnetic like response dominated by the pinning of vortices according to the Bean model, to a state with a 1000 times smaller paramagnetic like irreversibility which disappears at Hc2. If diamagnetism results from screening super-currents, the paramagnetic like response results from currents circulating in the opposite sense mimicking a field-dependent magnetic moment below Hc2. The quality of our samples is indicated by the observation of the de Haas van Alphen effect and the 75As NMR spectrum which reveals a single Lorentzian line, indicating the absence of magnetism or inhomogeneities. We conclude that the superconducting state in LiFeAs must undergo a field-induced phase-transition towards a chiral superconducting state as the smaller superconducting gap(s) is suppressed by the field. Small anomalies in the reversible component of the magnetization supports this scenario

JA03

Observation of anomalous magneto-resistance behavior near the in-plane upper critical field in Sr(Fe,Ni)₂As₂ single crystals

Seunghyun Kim¹, Bumsung Lee¹, Ki-young Choi¹, Kyung Jun Yoo¹, Ji Hoon Shim² and Kee Hoon Kim^{1*}

¹ Department of Physics and Astronomy, Seoul National University, Korea
² Department of Chemistry, Pohang University of Science and Technology, Korea

We have investigated Hc2 behaviors in various iron based SC including Sr(Fe,Co)₂As₂, Fe(Se,Te) and LiFeAs [1-3]. In this particular work, we measured the resistivity of Sr(Fe,Ni)₂As₂ up to 35 T and report our unexpected findings in the magneto-resistance just above the upper critical fields around the H // ab direction at low temperatures. Apart from the transition in H // c direction, in which the resistivity is saturated after abruptly appearing from the zero resistive superconducting state with increasing magnetic field, the resistivity gradually increases after it rapidly appears until it reaches the value saturated for the H // c direction. This can be interpreted as 1) the rate of superconducting pair breaking changes or 2) the normal state resistivity is suppressed with emerging an abnormal state with the strong magneto-resistance with the in-plane field component. We will discuss the origin of this anomalous magneto-transport behavior based on the band calculation result, in connection with the possible Fulde-Ferrel-Larkin-Ovchinnikov (FFLO) ground state or the competing ground state.

[1] S. Kim et al., Physica C 470, S317 (2010). [2] S. Kim et al., Phys. Rev. B 81, 184511 (2010). [3] S. Kim et al., Phys. Rev. B 84, 104502 (2011).

JA04

Superconductivity in an Einstein solid: A_xV₂Al₂₀ (A = Ga, Al)

Atsushi Onosaka, Junichi Yamaura, Yoshihiko Okamoto and Zenji Hiroi*
 ISSP, University of Tokyo, Japan

We study a series of intermetallic compounds A_xV₂Al₂₀ with A = Ga, Al, Sc, Y, La, and Lu. They crystallize in the CeCr₂Al₂₀ structure which contains a large atomic cage partially occupied by Ga/Al/Sc atoms and completely occupied by Y/La/Lu atoms. Low-energy local modes, which may be similar with what is now called rattling, have been observed for A = Ga and Al. Superconductivity was also reported at 1.6 K for A = Al and Ga, though experimental data was not given. In order to investigate the rattling and its effect on the superconductivity, we synthesized a series of polycrystalline samples and measured heat capacity, resistivity and magnetic susceptibility. Superconductivity is observed at T_c = 1.66, 1.50, 1.84, and 0.69 K for A = Ga_{0.2}, Al_{0.3}, Sc_{0.2}, and Y, respectively, and not above 0.5 K for A = La and Lu. It is suggested that the enhancement in Tc for the Ga, Al and Sc compounds is due to the rattling. In addition, we found a markedly large diamagnetism for A = Y and La, but not for A = Ga, Al, Sc, and Lu, despite the apparent similarity of the electronic structures among these compounds.

JA05

Non-unitary triplet pairing in the centrosymmetric superconductor LaNiGa₂

Adrian Hillier⁴, Jorge Quintanilla², Bayan Mazidian³, James Annett⁴ and Robert Cywinski¹
¹ ISIS facility, STFC, Oxfordshire, United Kingdom
² SEPnet and Hubbard Theory Consortium, School of Physical Sciences, University of Kent, Canterbury CT2 7NH, United Kingdom
³ H. H. Wills Physics Laboratory, University of Bristol, Tyndall Avenue, Bristol BS8 1TL, United Kingdom
⁴ H. H. Wills Physics Laboratory, University of Bristol, Tyndall Avenue, Bristol BS8 1TL, United Kingdom
⁵ School of Applied Sciences, University of Huddersfield, Queensgate, Huddersfield, HD1 3DH, United Kingdom

Symmetry breaking is a central concept of physics for which superconductivity provides a paradigm. In a conventional superconductor gauge symmetry is broken, while unconventional superfluids and superconductors break other symmetries as well. Recently, we showed experimentally time-reversal symmetry (TRS) breaking in the non-centrosymmetric superconductor LaNiC₂ [1]. Using group theory analysis we concluded that LaNiC₂ has only four possible symmetry states consistent with this observation, all of which are non-unitary [2]. This hinges on the low symmetry, C2v, of this material in which all of the irreducible representations are one dimensional. Here, we report the results from muon spin relaxation/rotation experiments on the intermetallic superconductor LaNiGa₂ (Tc=2K) which, although centrosymmetric, has a similarly low-symmetry structure D2h. We find again that the onset of superconductivity coincides with the appearance of spontaneous magnetic fields, implying that in the superconducting state TRS is broken. Group-theoretic analysis of the possible pairing symmetries again suggests only four triplet states compatible with this observation, all of which are also non-unitary [3]. A comparison will be made between LaNiGa₂ and LaNiC₂, and we will propose that these superconductors represent a new family of paramagnetic non-unitary triplet superconductors.

[1] A. D. Hillier et al Phys. Rev. Lett. 102 117007 (2009) [2] J. Quintanilla et al Phys. Rev. B 82 174511 (2010) [3] A. D. Hillier et al submitted to Phys. Rev. Lett.

JB01

Magnetoelectric effects and related phenomena in non-collinear spiral-spin systems

Tsuyoshi Kimura
 Osaka University, Japan

Among various multiferroics, extensive studies of ferroelectrics originating from magnetic orders, i.e., magnetically-induced ferroelectrics in which the inversion symmetry breaking and resultant ferroelectricity are induced by complex magnetic orders (e.g., noncollinear spiral order), have been triggered almost a decade ago by the discovery of multiferroic nature in a perovskite-type rare-earth manganites TbMnO₃. Because the complex magnetic orders often arise from the competition between nearest-neighbor and further-neighbor magnetic interactions, systems containing competing magnetic interactions are promising candidates for magnetoelectric multiferroics [1]. Thus, it is no longer so difficult to find new magnetoelectric multiferroics. Indeed, on the basis of this strategy several new magnetoelectric multiferroics related to noncollinear spiral-spin orders have been discovered in the past few years. In this presentation, I show recent progress on our studies of magnetoelectric effects and related phenomena in noncollinear spin-spiral systems [2].

[1] T. Kimura, "Spiral magnets as magnetoelectrics" Annu. Rev. Mater. Res. 37, 387 (2007). [2] T. Kimura, "Magnetoelectric hexaferrites", Annu. Rev. Condens. Matter Phys. (to be published).

JB02

Electric field control of nonvolatile four-state magnetization at room temperature

Sae Hwan Chun¹, Yisheng Chai¹, Byung-gu Jeon¹, Hyung Joon Kim¹, Yoon Seok Oh¹, Ingyu Kim¹, Hanbit Kim¹, Byeong Jo Jeon¹, So Young Haam¹, Ju-young Park¹, Suk Ho Lee¹, Jae-ho Chung², Jae-hoon Park³ and Kee Hoon Kim^{1*}

¹ Department of Physics and Astronomy, Seoul National University, Korea
² Department of Physics, Korea University, Korea
³ Department of Physics and Division of Advanced Materials Science, POSTECH, Korea

The control of magnetization by an electric field at room temperature remains as one of the great challenges in materials science. We demonstrate the realization of this long-sought capability in a multiferroic hexaferrite Ba_{0.52}Sr_{1.48}Co₂Fe₂₄O₄₁ single crystal. The electric polarization in this crystal rapidly increases in low magnetic fields (~5 millitesla), and its magnetoelectric susceptibility reaches the highest value (3200 picosecond per meter) among single-phase materials. The magnetization is then modulated up to 0.62 μB per formula unit in an electric field of 1.14 MV/m. Furthermore, this compound allows nonvolatile, magnetoelectric read-and-write operations entirely at room temperature. Four different magnetic/electric field writing conditions generate repeatable, distinct magnetization versus electric field curves without dissipation, offering an unprecedented opportunity for multi-bit memory- or spintronic device-applications.

JB03

Low magnetic field reversal of electric polarization in Y-type hexaferrites

Fen Wang, Tao Zou, Li-qin Yan, Yi Liu and Young Sun*
 Institute of Physics, Chinese Academy of Sciences, China

Hexaferrites with spiral magnetic structures provide great opportunities for searching for new multiferroic materials with a high operating temperature and great magnetoelectric sensitivity. Here we report on the magnetically tunable ferroelectricity and the giant magnetoelectric sensitivity up to 250 K in a series of Y-type hexaferrite with the formula of BaSrZnCoFe_{12-3x}Al_xO₂₂. Not only the magnitude but also the sign of electric polarization can be effectively controlled by applying low magnetic fields (a few hundreds of Oe) that modifies the spiral magnetic structures. The magnetically induced ferroelectricity is stabilized even in zero magnetic field. Decayless reproducible flipping of electric polarization by oscillating low magnetic fields is shown. The maximum magnetoelectric coefficient reaches a high value of ~ 3.0×10³ ps/m at 200 K.

JB04

Nearest - next-nearest neighbor exchange frustrated quantum chain antiferromagnets: Recent results

Reinhard Kremer*
 MPI for Solid State Research, Stuttgart, Germany

Lately, one-dimensional quantum chain antiferromagnets which feature magnetic frustration due to the presence of nearest and next-nearest-neighbor superexchange and super-superexchange interaction have attracted considerable attention. Such systems can e.g. be realized in compounds which contain MX₂ ribbon chains where the magnetic species M are located in a square planar anion environment (X = an oxygen or a halogen atom). Some of these ribbon-chain antiferromagnets exhibit unusual magnetic ground states which e.g. support effective magnetoelectric coupling and multiferroic behavior. I review some of our recent investigations on the well-known nearest - next-nearest neighbor quantum chain antiferromagnetic LiCuVO₄ and report first results gained on some new systems, CuCrO₄, TiPO₄ and CuCl₂.

JB05

Multiferroic properties of layered triangular compounds

Francoise Damay¹, Christine Martin², Maria Poienar², Gilles Andre², Sylvain Petit¹, Julien Robert¹, Vincent Hardy² and Antoine Maignan²
¹ Laboratoire Leon Brillouin, CEA-CNRS UMR 12, 91191 GIF-SUR-YVETTE CEDEX, France
² Laboratoire CRISMAT, CNRS UMR 6508, 6 bvd Marechal Juin, 14050 CAEN CEDEX, France

One of the most puzzling families of multiferroics is characterized by stackings of triangular planes, on which geometrically induced frustration of antiferromagnetic exchanges leads to complex non-collinear magnetic structures, like in the delafossite CuCrO₂ [1, 2]. The proposed microscopic origin of this spin-driven ferroelectricity is based on the variation of the ligand-metal orbital hybridization, as a result of spin-orbit coupling [3]. In this context, tuning hybridization by changing the oxygen ligand ion could give clues in the understanding of the physics of multiferroics. The chalcogenide AgCrS₂ has a rhombohedral structure at 300 K [4], in which the Cr²⁺ ions form a perfect triangular lattice. Our recent neutron scattering study [5] has shown that a large magneto-elastic effect leads to a crystal symmetry lowering at T₀, which releases the geometric frustration of the magnetic lattice : below T₀=41.5 K, the antiferromagnetic arrangement is an unconventional collinear one, made of double ferromagnetic stripes coupled antiferromagnetically. Drastic changes in the correlations between spins on cooling through TN are observed. Unlike CuCrO₂, ferrocity in AgCrS₂ is related to the spin-lattice coupling of electric dipoles and magnetic moments, which results in a polar (P~20 μC/m² at 5 K [6]) structure below T₀.

[1] M. Poienar et al., Phys. Rev. B 79, 014412 (2009), [2] S. Seki et al., Phys. Rev. Letters 101, 067204 (2008,), [3] C. Jia et al., Phys. Rev. B 76, 144424 (2007) ; T. Arima, J. Phys. Soc. Japan 76, 073702 (2007), [4] P.F. Bongers et al., J. Phys. Chem. Solids 29, 977 (1968), [5] F. Damay et al., Phys. Rev. B 83, 184413 (2011), [6] K. Singh et al., Chem Mater. 21, 5007 (2009)

JC01

STM and magnetotransport investigations on the heavy fermion metals YbRh₂Si₂ and CeMn₅ (M = Co, Ir)

Steffen Wirth^{*,}, Andrea Bianchi², Stefan Ernst¹, Christoph Geibel¹, Zachary Fisk³, Stefan Kirchner⁴, Cornelius Krellner¹, Joe D Thompson³ and Frank Steglich¹
¹ Max Planck Institute for Chemical Physics of Solids, Dresden, Germany
² Departement de Physique, Université de Montreal, Quebec H3C 3J7, Canada
³ University of California, Irvine, California 92697, USA
⁴ Max Planck Institute for Physics of Complex Systems, Germany
⁵ Los Alamos National Laboratory, Los Alamos, New Mexico 87545, USA

Heavy fermion metals are often characterized by a variety of relevant energy scales and competing interactions which may result in such fascinating phenomena as quantum criticality and unconventional superconductivity. Here, we focus on results obtained by Scanning Tunneling Microscopy and Spectroscopy (STM/S) and Hall effect measurements. YbRh₂Si₂ and its doped counterparts Yb(Rh_{1-x}M_x)₂Si₂ (M = Co, Ir) exhibit a quantum critical point which results from a competition between RKKY and Kondo interaction [1]. The Kondo interaction is visualized by Scanning Tunneling Spectroscopy on YbRh₂Si₂ [2]. The hybridization of conduction and 4f electrons results in a gap-like feature of the tunneling conductance. Importantly, the crystal field excitations are unambiguously reflected by STS. A strongly temperature dependent peak in tunneling conductance is attributed to a resonance resulting from the Kondo lattice. At even lower temperature, Hall effect measurements reveal a Kondo break-down of the heavy quasiparticles [3]. In the CeMn₅ class of compounds the relation between superconductivity and antiferromagnetism will be discussed [4]. Magnetotransport measurements on CeIn₃ indicated a precursor state to superconductivity. A gap detected by low-temperature STS in CeCoIn₃ is compatible with Sd_x(x² - y²) symmetry of the superconducting order parameter and is, again, consistent with a precursor state to superconductivity.

[1] S. Friedemann [i] et al., Nature Phys. [bf 5] (2009) 465. [2] S. Ernst [i] et al., Nature [bf 474] (2011) 362. [3] S. Friedemann [i] et al., Proc. Natl. Acad. Sci. USA [bf 107] (2010) 14547. [4] S. Nair [i] et al., Proc. Natl. Acad. Sci. USA [bf 107] (2010) 9537.

JC02

Fermi surface of URu₂Si₂ in the hidden order state and in the antiferromagnetic state

Elena Hassinger, Georg Knebel, Dai Aoki, Frederic Bourdarot, Liam Malone, Tatsuma Matsuda, Valentin Taufour and Jacques Flouquet
 INAC/CEA Grenoble, France

The heavy fermion compound URu₂Si₂ is famous for its hidden order state appearing below T₀ = 17.5 K at ambient pressure. Inside this phase superconductivity sets in at 1.5 K. Up to now, the order causing huge signatures in macroscopic quantities at the transition temperature has not been detected experimentally with microscopic probes. The proximity of the hidden order state to a usual antiferromagnetic state appearing under pressure allows a comparison of the two. In this talk a Fermi surface study of URu₂Si₂ is presented. New Fermi surface sheets have been detected which puts constrains for theory. The pressure dependence shows that the Fermi surface is the same in the hidden order state and in the antiferromagnetic state. As a conclusion, the hidden order must reconstruct the Fermi surface in the same way the antiferromagnetism does.

JC03

Switching of magnetic ordering near the quantum critical point of the heavy fermion superconductor CeRhIn₅

Hyun Jung Lee^{1,*} and Tetsuya Takimoto²
¹ School of Physics, Korea Institute for Advanced Study, Seoul, Korea
² Asia Pacific Center for Theoretical Physics, POSTECH, Pohang, Korea

The nuclear quadrupole resonance(NQR) and the magnetic neutron diffraction experiments in CeRhIn₅ clearly indicate that the antiferromagnetic long-range order takes place uniformly over the entire sample where the bulk superconductivity appears. The most intriguing feature in this compound is the switching of magnetic ordering near the quantum critical point, where the spin-density waves (SDW) with different wave vectors are simultaneously observed in the NQR spectrum as well as the neutron diffraction profile. In order to understand the switching mechanism, we have calculated the spin excitation spectrum in the presence of antiferromagnetic and superconducting long-range order using the RPA and found that the concurrence of commensurate and incommensurate SDW is associated with the van-Hove singularity that occurs with the superconducting gap opening.

JC04

Resonant magnetic exciton mode in the heavy-fermion antiferromagnet CeB₆

Gerd Friemel¹, Yuan Li¹, A. Dukhnenko², N. Yu. Shitsevalova², N. E. Sluchanko³, Alexandre Ivanov⁴, V. B. Filipov², Bernhard Keimer¹ and Dmytro Inosov^{1,*}
¹ Max Planck Institute for Solid State Research, Stuttgart, Germany
² I. M. Frantsevich Institute for Problems of Material Sciences of NAS, Kiev, Ukraine
³ A. M. Prokhorov General Physics Institute of the Russian Academy of Sciences, Moscow, Russia
⁴ Institut Laue-Langevin, Grenoble, France

Resonant magnetic excitations are widely recognized as hallmarks of unconventional superconductivity. Numerous model calculations have related these modes to the microscopic properties of the pair wave function, but the mechanisms underlying their formation are still debated. Here we report the discovery of a similar resonant mode in the non-superconducting, antiferromagnetically ordered heavy-fermion metal CeB₆. Unlike conventional magnons, the mode is non-dispersive, and its intensity is sharply concentrated around a wave vector separate from those characterizing the antiferromagnetic order. The mode energy increases continuously below the onset temperature for antiferromagnetism, in parallel to the opening of a nearly isotropic spin gap throughout the Brillouin zone. These attributes bear strong similarity to those of the resonant modes observed in unconventional superconductors below their critical temperatures. This unexpected commonality between the two disparate ground states throws new light on the interplay between antiferromagnetism, superconductivity, and 'hidden' order parameters in correlated-electron materials.

JD01

Magnetostriction to 97.4T in frustrated Shastry-Sutherland compound SrCu₂(BO₃)₂

Marcelo Jaime^{*,} Ramzi Daou², Scott A Crooker¹, Franziska Weickert¹, Atsuko Uchida¹, Adrian Feiguin¹, Cristian D Batista¹, Hanna A Dabkowska¹ and Bruce D Gaulin¹
¹ NIMFL, Los Alamos National Laboratory, Los Alamos, New Mexico 87544, USA
² Max Planck Institute for Chemical Physics of Solids, 01187 Dresden, Germany
³ MPA-CMMS, MPA-CMMS, Los Alamos National Laboratory, Los Alamos, New Mexico 87544, USA
⁴ Department of Physics & Astronomy, University of Wyoming, Laramie, Wyoming 82071, USA
⁵ Theory Division, Los Alamos National Laboratory, Los Alamos, New Mexico 87544, USA
⁶ Brockhouse Institute for Materials Research, McMaster University, Hamilton, ON, L8S 4M1, Canada
⁷ Department of Physics & Astronomy, McMaster University, Hamilton, ON, L8S 4M1, Canada

Strong geometrical frustration in magnets leads to exotic states, such as spin liquids, spin supersolids and complex magnetic textures. SrCu₂(BO₃)₂, a spin-1/2 Heisenberg antiferromagnet in the archetypical Shastry-Sutherland lattice, exhibits a rich spectrum of magnetization plateaus and stripe-like magnetic textures in applied fields [1]. The structure of these plateaus is still highly controversial due to the intrinsic complexity associated with frustration and competing length scales [2,3]. We reveal new magnetic textures in SrCu₂(BO₃)₂ via magnetostriction and magnetocaloric measurements in fields up to 97.4 Tesla [4]. In addition to observing the low-field fine structure of the plateaus with unprecedented sub-microstrain resolution, the data also reveal lattice responses at 82 T and at 73.6 T which we attribute, using a controlled density matrix renormalization group approach, to the long-predicted 1/2-saturation plateau, and to a new 2/5 plateau. -AF acknowledges NSF funding under grant DMRG-0955707. Experiments at the High Magnetic Field Laboratory Dresden (HLD) were sponsored by Euro-MagNET II under the EU contract 228043. Work at the NIMFL was supported by the National Science Foundation, the US Department of Energy through the BES*Science at 100T program, and the State of Florida.

[1] K. Kodama, et al. Science 298, 395 (2002). [2] S.E. Sebastian, et al. Proc. Natl. Acad. Sci. 105, 20157 (2008). [3] F. Levy, et al. Europhys. Lett. 81, 67004 (2008). [4] M. Jaime, et al. arXiv:1202.0812v1

JD02

Unconventional spin-glass behaviors in pyrochlore Heisenberg antiferromagnets coupled with lattice distortions

Hiroshi Shimaoka¹, Yusuke Tomita² and Yukitoshi Motome³
¹ Nanosystem Research Institute, National Institute of Advanced Industrial Science and Technology, Japan
² Institute for Solid State Physics, University of Tokyo, Japan
³ Department of Applied Physics, University of Tokyo, Japan

Spin glass, in which spins are frozen randomly, is one of low-temperature phases widely observed in geometrically frustrated magnetic materials. However, it is unclear so far how its nature is different from the canonical one driven solely by randomness. Experimentally, several puzzling spin-glass behaviors have been pointed out for pyrochlore-based magnets, such as R₂Mo₂O₇ and ACr₂O₇, i.e., the transition temperature appears to be almost independent of the strength of randomness, and the value is much higher than the theoretical prediction. Motivated by these puzzles, we investigate the effect of magnetoelastic coupling in a bond-disordered Heisenberg antiferromagnet on a pyrochlore lattice [1,2]. Through classical Monte Carlo simulations using the extended loop algorithm [3,4], we show that the magnetoelastic coupling largely enhances the spin-glass transition temperature. Furthermore, in a wide range of bond disorder, the transition temperature is set by the magnetoelastic coupling, and becomes almost independent of bond disorder, as observed in experiments. These peculiar behaviors are ascribed to spin collinearity induced by the magnetoelastic coupling. We also compute the specific heat and (non)linear susceptibility and compare the results with experiments as well as the canonical spin-glass behaviors. The present theory qualitatively explains the puzzling spin-glass behaviors observed in experiments.

[1] H. Shimaoka, Y. Tomita and Y. Motome, Phys. Rev. Lett. 107, 047204 (2011). [2] H. Shimozuka, Y. Tomita and Y. Motome, arXiv:1107.4144. [3] H. Shimaoka, Y. Tomita and Y. Motome, J. Phys.: Conf. Ser. 320, 012009 (2011). [4] H. Shimaoka and Y. Motome, Phys. Rev. B 82, 134420 (2010).

JD03

Theory of spin liquids in integer spin pyrochlores

Sungbin Lee^{*,} Shigeki Onoda² and Leon Balents³
¹ University of California, Santa Barbara, USA
² Condensed matter theory Laboratory, RIKEN, Japan
³ Kavli Institute for Theoretical Physics, University of California, Santa Barbara, USA

Rare earth pyrochlores, with a chemical formula A₂B₂O₇, exhibit many interesting features. Depending on A site rare earth elements, spin ice and magnetically ordered phases are shown in several experiments. Moreover, they have been also focused as possible candidates of U(1) spin liquid. In order to explore such versatile phases, we study the pseudospin-1/2 model, which is quite generic to describe rare earth pyrochlores with integer spins, in the presence of spin-orbit coupling and crystalline electric field. Using a new 'gauge mean field theory', we show the possible ground states, corresponding to several phases listed above.

JD04

Field-induced spin nematic and spin density wave orders in spatially anisotropic frustrated magnets

Masahiro Sato¹, Toshiya Hikihara² and Tsutomu Momoi³
¹ Department of Physics and Mathematics, Aoyama Gakuin University, Japan
² Faculty of Engineering, Gunma University, Japan
³ Condensed Matter Theory Laboratory, RIKEN, Japan

Magnetic multipolar order including spin nematic (magnetic quadrupolar) order is one of the current topics in frustrated magnetism. Recently, frustrated spin-1/2 chains with ferromagnetic nearest neighbor coupling J1(-0) and antiferromagnetic next nearest neighbor one J2(-0) have been theoretically shown to exhibit multipolar quasi long range orders in the wide region of J1/J2 as an external magnetic field is applied [1,2]. In addition, it is known that several kinds of quasi one-dimensional (1D) cuprates [3] can be described by this J1-J2 spin chain [4,5]. Particularly, recent experiments show that LiCuVO₃, one of the quasi-1D cuprates, possesses a new phase near saturation, and it is expected to be a spin nematic long-range ordered phase [6]. Motivated by these results, we have completed the field-temperature phase diagram for spatially anisotropic magnets consisting of weakly coupled J1-J2 spin chains, making use of the accurate results of the single J1-J2 spin chain [1,4]. The phase diagram contains spin nematic and spin-density-wave ordered phases, and these two orders compete with each other. We will discuss some universal features of the phase diagram and the relevance of our result to LiCuVO₃.

[1]T.Hikihara, L.Kecke, T.Momoi, and A.Furusaki, PRB78, 144404 (2008). [2]J.Sudan, A.Lauser, and A.M.Lauchli, PRB80, 140402(R) (2009). [3]See, for example, M.Hase, et al, PRB70, 104426 (2004); M.Enderle, et al, EPL70, 237 (2005); Y.Yasui, et al, JPSJ80, 033707 (2011); T.Masuda, et al, JPSJ80, 113705 (2011). [4]M.Sato, T.Momoi, and A.Furusaki, PRB79, 060406(R) (2009); M.Sato, T.Hikihara, and T.Momoi, PRB83, 064405 (2011). [5]S.Furukawa, M.Sato, and S.Onoda, PRL105, 257205 (2010). [6]L.E.Svistov, et al, JETP Lett. 93, 21 (2011).

JD05

Spin liquids for spin 1/2 systems with strong charge fluctuation on the triangular lattice

Eun-gook Moon and Cenke Xu
 Physics, UCSB, USA

We describe a new class of spin liquids for organic spin 1/2 triangular lattice systems. Adopting the Fermionic-spinon representation, d-wave pairings between spinons are considered, which makes U(1) gauge symmetry down to Z2 one. Finite amount of energy gap of the Z2 gauge theory prohibits coupling between the emergent gauge field and external electro-magnetic field at low energy. Thus external magnetic field only couples to the Zeeman term and it is argued that the ground state does not show thermal Hall conductance. Also, the fermionic band structure allows both Dirac-fermi points and a quadratic band touching point. It is shown how the fermionic band structure could resolve various puzzling experiments, for example, metallic thermal conductivity without thermal Hall conductivity.[1,2,3]

[1]M. Yamashita, et al., Science 328,1246(2010) [2]S. Yamashita, et al., Nature Communication 2,275(2011) [3]E. Pratt, et al., Nature 471, 612(2011)

JD06

Emergent criticalities and phase transitions in monomer-dimer mixture system on a honeycomb lattice

Hiroimi Otsuka^{*}
 Department of Physics, Tokyo Metropolitan University, Japan

The frustrated magnets such as Dy₂Ti₂O₇ are called as the spin ice, and have received much attention [1]. In particular, a defect representing a breaking the ice rule can be regarded as the magnetic monopole in solids, so its property is a current interest [2]. Here, we study the spin ice in a magnetic field using a toy model, i.e., a monomer-dimer mixture defined on a honeycomb lattice. In a low-doping region of monomers, its effective description is given by the dual sine-Gordon model [3]. In intermediate- and strong-doping regions, the Potts lattice gas theory can be employed [4]. Synthesizing these, we construct a renormalization-group flow diagram, which includes the stable and unstable fixed points corresponding to M5 and M6 in the minimal models of the conformal field theory. We perform numerical calculations to determine a phase diagram and also to proffer evidence to check our prediction [5].

[1] M.J. Harris, et al., Phys. Rev. Lett. 79, 2554 (1997). [2] C. Castelnovo, et al., Nature 451, 42 (2008). [3] P. Lecheminant, et al., Nucl. Phys. B 639, 502 (2002). [4] B. Nienhuis, J. Phys. A 15, 199 (1982). [5] H. Otsuka, Phys. Rev. Lett 101, 227204 (2011).

JE01

Domain-wall physics and devices using focused electron and ion beams

Henk Swagten^{*}, Jeroen Franken, Christian Geurts, Mark Van Der Heijden, Mark Hoeijmakers, Tim Ellis, Elena Mure, Beatriz Barcones, Juergen Kohlhepp and Bert Koopmans
 Applied Physics, Eindhoven University of Technology, Netherlands

In domain-wall (DW) devices with perpendicular magnetic anisotropy (PMA) using e.g. ultrathin Co, a number of exciting phenomena have been observed very recently. Ion irradiation is shown to be an effective tool to locally modify PMA properties, with which a kaleidoscope of new DW physics or device directions may be explored. For example, we have used ion irradiation in PMA strips for (1) controlled pinning of DWs (2) predictions of a novel domain-wall oscillator, (3) intrinsic DW resistivity as a function of the width of the DW, and (4) a novel ratchet DW memory device by sawtooth shaping of the DW potential. After shortly introducing these developments, the presentation will focus on the use of electron-beam-induced-deposition (EBID) for growing Co and Fe-rich nanopillars on top of our magnetic strips, with a diameter typically 50-150nm. After nucleation of a DW at an ion-irradiated part of the strip, the DW is moved towards the position of the pillar, at which it may be pinned/depinned using a variable strength of the applied perpendicular field. Apart from controlled (de) pinning due to the altered DW energy landscape induced by the pillar stray field, we could also uniquely extract the switching fields of these nanopillars.

JE02

Real time analysis of spinmotive forces due to domain wall motion

Jun'ichi Ieda*, Yuta Yamane and Sadamichi Maekawa
Advanced Science Research Center, Japan Atomic Energy Agency, Japan

Spinmotive force, which is induced by motion of a nonuniform magnetic nanostructure, reflects real time dynamics of the magnetization texture [1,2]. It is well-known that domain wall motion in a permalloy nanowire exhibits nontrivial magnetic field dependence. In particular, in high field regime far above the Walker breakdown field, the domain wall shows structural deformation including annihilation and creation of magnetic vortex cores [3]. Using numerical simulations we study the spinmotive force in such a circumstance and find that its dc component scales with an applied magnetic field even in a field range where the wall motion is no longer associated with periodic angular rotation of the wall magnetization. This feature has been confirmed in a recent experiment [4]. As the field is increased, spikes in the voltage signals start to appear, which are mainly associated with vortex core nucleation and annihilation, and this tendency is enhanced with further increase in the field. At high fields, the slope of the generated dc voltage with the applied field is expected to be only dependent on the spin polarization of conduction electrons and thus can be used to accurately determine the degree of spin polarization in various materials.

[1] S. E. Barnes and S. Maekawa, *Phys. Rev. Lett.* **98**, 246601 (2007). [2] Y. Yamane et al., *J. Appl. Phys.* **109**, 07C735 (2011). [3] M. Hayashi et al., *Appl. Phys. Express* **3**, 113004 (2010). [4] M. Hayashi, J. Ieda et al., submitted.

JE03

Spin-current induced magnetization dynamics

Mathias Klaui
Institute of Physics, Johannes Gutenberg-Universitaet Mainz, Germany

Since conventional approaches of manipulating magnetization using magnetic fields exhibit unfavourable scaling and results in limited switching speed, alternative approaches based on spin-currents have emerged. The transfer of angular momentum ("spin transfer torque effect") leads for instance to current-induced domain wall motion (CIDM), which has become the focus of intense research in the last few years. We have comprehensively investigated CIDM and determined the acting adiabatic and non-adiabatic torque terms [1]. We find that the previously neglected diffusive torque term [2] can play an important role for vortex core displacement. For out-of-plane magnetized Co/Pt a large non-adiabatic torque is found, while in Co/Ni the adiabatic torque dominates [3]. By separating charge and spin transport we can generate pure diffusive spin currents with no associated net charge current. Using such diffusive spin currents we find large efficiencies for domain wall displacement due to strong spin accumulation absorption [4]. To increase the spin diffusion length, we use robust turbostratic graphene and find spin injection across transparent contacts. Beyond generating spin currents by spin injection, we have also used the Spin Seebeck Effect, where temperature gradients generate spin currents that then affect for instance domain wall propagation [5].

[1] L. Heyne et al., *Phys. Rev. Lett.* **105**, 187203 (2010); M. Eltschka et al., *Phys. Rev. Lett.* **105**, 056601 (2010). [2] A. Manchon, W.-S. Kim, and K.-J. Lee, arXiv:1110.3487 [3] J. Heinen et al., *J. Phys. Cond. Mat.* **24**, 24220 (2012); T. Koyama et al., *Nature Mat.* **10**, 194 (2011). [4] D. Ilgaz et al., *Phys. Rev. Lett.* **105**, 076601 (2010). [5] P. Mohrke et al., *Sol. Stat. Com.* **150**, 489 (2010); J. Franken et al., *Appl. Phys. Lett.* **95**, 212502 (2009).

JE04

External magnetic field dependence of the magnetic wall drive current density in a TbFeCo magnetic nanowire

Hiroyuki Awano, Ryo Eguchi, Toma Kanehira and Do Bang
Toyota Technological Institute, Japan

Low current driven domain wall by using amorphous TbFeCo wire has been reported (1), the current density was 5×10^6 A/cm². Most reported magnetic wire samples of domain wall drive by current are prepared by using EB or Photo lithography and etching process. However, this process damages the edge of a magnetic wire and increase resistance for domain wall displacement. To reduce the resistance, we propose a new fabrication method of magnetic wire without any etching process. It is named as nano-imprint magnetic wire method. Using the method, the improved TbFeCo wire was fabricated by magnetron sputtering on to the plastic substrate with a groove shape like a wire pattern. Therefore, relatively smooth roughness nanowire can be made. This new fabrication method of nanowire can be reduced number of pinning site. Then, the current density for domain wall driving can be also decreased to 6×10^5 A/cm². Moreover, applying an external field to the sample, the current density can be reduced more. Thus, this new fabrication method of nanowire is attractive for nanowire memory device.

(1) Duc The Ngo, Kotaro Ikeda, and Hiroyuki Awano : *Appl. Phys. Express* **4**, 093002 (2011)

JF01

Disentangling and manipulating intrinsic and extrinsic contributions in the anomalous hall effect

Xiaofeng Jin*
Physics Department, Fudan University, China

The anomalous Hall effect is one of the most prominent phenomena existing in magnetic materials. It has remained unsolved for more than a century because its rich phenomenology defies the standard classification methodology, prompting conflicting reports claiming the dominance of various processes. Working with epitaxial films of Fe, Ni, and Ni_{1-x}Cu_x, we succeeded in independent controls of different scattering processes through temperature and layer thickness, which allows an unambiguous identification and control of the intrinsic mechanism as well as the extrinsic mechanisms of the anomalous Hall effect.

JF02

Spinmotive forces in spin-orbit coupling systems

Yuta Yamane*, Jun'ichi Ieda and Sadamichi Maekawa
Japan Atomic Energy Agency, Japan

Spinmotive force in ferromagnetic conductors with spin-orbit interaction is theoretically studied. We have derived the expression for the spinmotive force including the contribution from a general form of spin-orbit interaction. We have found that, in addition to the conventional spinmotive force which reflects the time- and spatial-dependent magnetization, time variation of the vector product of the magnetization and an electric field gives rise to a spinmotive force. Therefore, a time-varying electric field can induce a spinmotive force even in a static and uniform magnetization configuration. In order to detect this phenomenon, we propose an experimental setup with a metallic film which is thin enough for an electric field to penetrate. In addition, considering a two dimensional electron system with the Rashba and Dresselhaus spin-orbit couplings, the spinmotive force signals are different for each origin. Therefore this spinmotive force offers a method to determine the ratio of spin-orbit couplings.

JF03

Theory of the spin Hall effect in ferromagnetic metals: Nonlinear behaviors around the curie temperature

Bo Gu^{1*}, Timothy Ziman² and Sadamichi Maekawa¹
¹ *Advanced Science Research Center, Japan Atomic Energy Agency, Japan*
² *CNRS and Institut Laue Langevin, France*

We give a theory of the spin Hall effect in ferromagnetic metals near the Curie temperature. We do this by extending Kondo's theory of the Anomalous Hall Effect in ferromagnetic metals to include the short range spin-spin correlations. We find a novel relation between the Spin Hall Effect and a second order nonlinear spin fluctuation in ferromagnetic metals near Curie temperature T_c . In 1962 Kondo gave a relation between the Anomalous Hall Effect and the first order nonlinear spin fluctuation in pure ferromagnetic metals near T_c . Thus our results show an essential difference between the Anomalous and Spin Hall Effects in terms of the nonlinear spin correlations that are probed. Our theory can be compared to experiments in ferromagnetic alloys near T_c by Y. Otani et al.

[1] J. Kondo, *Prog. Theor. Phys.* **27** 772-792 (1962). [2] D. H. Wei, Y. Niimi, B. Gu, T. Ziman, S. Maekawa, and Y. Otani, unpublished.

JF04

Minority band gap and magnetic properties of Co₂(Fe,Mn)Z (Z=Al, Ga ; Si, Ge) in the context of CPP-GMR transport

Faleev Sergey and Oleg N. Mryasov*
Physics and Astronomy and MINT Center, Physics and Astronomy and MINT Center, USA



JF05

Anisotropy in the intrinsic anomalous Hall effect

Lin Wu, Yufan Li, Jianli Xu and Xiaofeng Jin*
Surface Physics Laboratory and Physics Department, Fudan University, China

A new scaling for the anomalous Hall effect was recently proposed [Phys.Rev. Lett.103,087206 (2009)], which can disentangle the intrinsic and extrinsic contributions in the anomalous Hall effect. Based on the new scaling, we have investigated in experiment the anisotropic effect of the intrinsic anomalous Hall contribution. Comparing with Fe(001)/GaAs(001), we find the value of intrinsic AHE contribution is different in Fe(111)/GaAs(111), which is directly related to the electronic band structure of Fe.

JG01

Propagation and scattering of spin waves in curved magnonic waveguides

Vira Tkachenko¹, Andriy Kuchko¹, Mykola Dvornik² and Volodymyr Kruglyak^{2*}
¹ *Donetsk National University, Ukraine*
² *University of Exeter, United Kingdom*

Usually, the modulation of the effective magnetic field in magnonic crystals and devices is achieved as a compositional modulation created either during growth or using lithographic processing. In this report, we develop a continuous medium theory of dispersion and scattering of spin waves propagating in thin cylindrical nanowires (therefore acting as magnonic waveguides) with curved regions. The theory predicts that, assuming that the static magnetization is aligned along the waveguide, the curvature makes a significant contribution to the effective magnetic field in the waveguide, scaling inversely with its radius of curvature squared. We calculate the spectrum and coefficients of reflection and transmission of spin waves that are created due to this topological nonuniformity and discuss problems arising from and opportunities offered by the discovered effect. The research leading to these results has received funding from the EC's 7th Framework Programme (FP7/2007-2013) under GA 247556 (NoWaPhen) and from EPSRC of the UK under project EP/E055087/1.

JG02

Theory of static and dynamic properties of magnetic dot arrays coupled by dipole-dipole interaction

Roman Verba¹, Gennady Melkov¹, Vasil Tiberkevich² and Andrei Slavin^{2*}
¹ *Radiophysics, Kiev National University, Ukraine*
² *Physics, Oakland University, USA*

Arrays of magnetic nano-dots are promising candidates for applications in microwave signal processing and in magnetic recording technology. Since ground state of an isolated dot is double-degenerate, there are many possible ground states of an array. Different ground states, which can be controlled dynamically [1], correspond to different spin-wave (SW) spectra of an array. Thus, using dot arrays it is possible to develop new artificial magnetic materials: dynamic magnonic crystals. In this paper we present a general theory of static and linear dynamic properties of magnetic dots arrays coupled by a magneto-dipolar interaction. In contrast with the majority of previous analytical methods the theory presented here is not limited to macrospin approach, as spatially nonuniform static and dynamic magnetization profiles are taken into account by introducing static-static, static-dynamic and dynamic-dynamic effective mutual demagnetization tensors. We show that all the possible ground states of a finite or infinite array with given periodicity can be found as solutions of a system of linear equations. The developed theory provides a simple way to calculate mode structure, damping rates and excitation efficiency of SWs, and microwave response of a magnetic dot array.

[1] J. Topp et al., *Phys. Rev. Lett.* **104**, 207205 (2010).

JG03

Theoretical study on ferromagnetic resonance of FePt/Py bilayers

Hiroshi Imamura¹, Takeshi Seki², Kazuhisa Utsumiya², Yukio Nozaki³ and Koki Takanashi²
¹ *NRI-AIST, Japan*
² *IMR, Tohoku Univ., Japan*
³ *Keio Univ., Japan*

Twisted magnetic structures such as a domain wall and a magnetic vortex attract much attention for applications in nano spionormics. It has been widely known that we can make a twisted magnetic structure in a ferromagnetic bilayer consisting of materials with different magnetic anisotropies, which is called an exchange spring bilayer (ESB). We can control its twist angle by applying an external magnetic field. Recently the spin dynamics in ESB has attracted much attention since the microwave assisted switching was proposed by Fal et al. [1]. However the spin dynamics in ESB under oscillating magnetic field is not fully understood. We theoretically studied the ferromagnetic resonance of FePt/Py bilayers of which material properties were well studied experimentally in [2]. We solved the Landau-Lifshitz-Gilbert equation and found that the resonance frequency of the perpendicular standing spin wave [3] is lowered by twisting the spins in ESB. The decrease of the resonance frequency is enhanced when ESB is about to switch. We shall show the details of our calculation and comparison with experimental results in our talk.

[1] T. Fal et al., *J. Appl. Phys.* **109**, 093911 (2011) [2] K. Utsumiya et al., *J. Appl. Phys.* **110**, 103911 (2011) [3] S.O. Demokritov et al., *Phys. Rep.* **384**, 441 (2001)

JG04

NMR observations of level crossings in a Cr₃F₈ pivalate single crystal: The solution to the structured enhancement of 1/T1

Shoji Yamamoto*
Department of Physics, Hokkaido University, Japan

Micotti et al. [1] measured 1/T1 of a single crystal of the antiferromagnetic ring [Cr₃F₈(piv)16] up to 15.6 T at 0.3 K. Interestingly enough 1/T1 is single- and double-peaked at the first and second level crossings, respectively. A single but twinned crystal would produce such a split peak, but this possibility is ruled out by x-ray measurements. There is no other observation of such a structured peak. 1/T1 observations of decanuclear ferric wheels [2] are obtainable beyond the third crossing field, but each structure, if any, could not be resolved due to the use of a powder sample. Those of hexanuclear [3] and octanuclear [4] ferric wheels are restricted to the first level crossing. Diagonalizing a well-equipped microscopic spin Hamiltonian of each cluster and then inquiring further into intercluster coupling effects, we reproduce the spin dynamics in the Cr₃ single crystal at sufficiently low temperatures. Here is a solution to the wide-split peak of 1/T1 at the second, rather than the first, level crossing.

[1] E. Micotti et al., *PRB* **72**, 020405(R) (2005). [2] M.-H. Julien et al., *PRL* **83**, 227 (1999). [3] M. Affronte et al., *PRL* **88**, 167201 (2002). [4] L. Schmelzer et al., *PRL* **99**, 087201 (2007).

JG05

Spin state of ferric chloride investigated by Fe NMR

Byeongki Kang, Changsoo Kim, Euna Jo, Sangil Kwon and Soonchil Lee*
Physics, KAIST, Korea

It was reported that ferric chloride(FeCl₃) has helical spin structure with period of 15 in the ground state and undergoes two quantum phase transitions at 1.5 T and 4.0 T as magnetic field increases. Between 1.5 - 4 T, the spins of Fe ions are arranged in two directions canted along the axis parallel with magnetic field and above 4.0 T, spins flop. We have measured magnetization curve and magnetic field and temperature dependences of Fe NMR spectrum of polycrystalline FeCl₃. The temperature dependence of the NMR resonance frequency in zero magnetic field reveals sublattice magnetization. The result fits well to Bloch's T² law which is expected for a simple antiferromagnet having no anisotropy. The magnetic field dependence of the NMR signal line width shows that the directions of the spins hardly change below 2.5 T. From the field dependence of NMR frequency and line width, we conclude that the spins are almost perpendicular to the field above 5 T. The results are compatible with the previously reported transition at 1.5 T but not with that at 4 T. We estimated the exchange coupling constant from the measured angles between the magnetic field and the spins above 5 T.

JG06

Spin dynamics of ferrite nanoparticles studied by 57Fe Mossbauer spectroscopy

Mathias Kraken^{1*}, Jochen Litterst¹, Ilka Marina Grabs², Ingke Christine Masthoff² and Georg Garnweitner²
¹ IPKM, TU Braunschweig, Germany
² IPAT, TU Braunschweig, Germany

Due to its specific timescale, Mossbauer spectroscopy is highly suitable to investigate the dynamic properties of magnetic nanoparticles. The hyperfine magnetic spectra between the blocking temperature and very low temperatures may exhibit a broad variety of different shapes. Accordingly, to describe this rich behaviour a whole range of different, controversially discussed models can be found in literature [1-4]. We performed measurements on ZnFe₂O₄ nanoparticles, prepared by a non-aqueous sol gel method and characterized by x-ray scattering, dynamic light scattering and TEM. The spectra were taken on strongly and weakly interacting particles and the fits to the spectra with the different models are compared in order to gain information about the suitability of the applied models.

[1] D.H. Jones and K.K.P. Srivastava, J. Magn. Magn. Mater. 78, 320 (1989). [2] S. Morup et al., J. Magn. Magn. Mater. 40, 163 (1983). [3] S. Bocquet and S.J. Kennedy, J. Magn. Magn. Mater. 109, 260 (1992). [4] M. F. Hansen et al., Phys. Rev. B 62, 1124 (2000).

JH01

Multi-layered nanocomposite thick film-magnet for power MEMS applications

Hirotohi Fukunaga^{1*}, Masaki Nakano¹, Takeshi Yanai¹ and Fumitoshi Yamashita²
¹ Graduate School of Engineering, Nagasaki University, Japan
² Rotary Component Technology Development Division, Minebea Co., Ltd., Japan

An isotropic nanocomposite thick film-magnet is one of candidates for a magnet used in power MEMS because of its high remanence and the easiness of multi-polar magnetization [1]. Previously, we developed a method of synthesizing multi-layered nanocomposite thick film-magnets composed of several hundred layers by using PLD (Pulsed Laser Deposition) method, and reported magnetic properties of Nd-Fe-B/Fe₂B and Nd-Fe-B/ α -Fe multi-layered thick film-magnets [2,3]. In this investigation, we improved magnetic properties of Nd-Fe-B/ α -Fe multi-layered thick film-magnets and their reproducibility by controlling preparation conditions of films such as energy density of laser beam and stacking periods of Nd-Fe-B/ α -Fe layers, tp. Superior magnetic properties were obtained for the films with tp of 10-20 nm. This tp value is consistent with the results of the previous computer simulation. It is also clarified that decrease in the number and/or size of droplets improve(s) magnetic properties, because the presence of droplets degrades a layered structure and resultantly reduces effective exchange interaction between soft and hard phases. The obtained (BH)_{max} value, 112 kJ/m³, is the larger than the values obtained in previous studies for isotropic film-magnets thicker than 10 μ m, which suggests that multi-layered nanocomposite thick film-magnets are promising for power MEMS applications.

[1] F. Yamashita et al., IEEE Trans. Magn. 46, 2012 (2010). [2] H. Fukunaga et al., J. Alloys and Compounds, 408-412, 1355 (2006). [3] H. Fukunaga et al., J. Phys.: Conf. Ser. 266, 012027 (2011).

JH02

Development of high performance micron-scaled hard magnetic structures for micro-system applications

Nora Dempsey¹, F. Dumas-bouchiat¹, Y. Zhang¹, G. Ciuta¹, L. F. Zanini^{1,2} and D. Givord¹
Institut Neel CNRS/UJF, France

Micro-systems incorporating magnetic materials have many potential applications in the fields of bio-medicine, information technology, energy transformation/management. As the size of the magnetic element is downscaled, the strength of the magnetic field gradient it produces is up-scaled, and values as high as 10 exp 6 T/m can be achieved with micron scaled structures. Hard magnetic materials offer the distinct advantage that they need neither an external magnetic field source nor power supply, and thus they are particularly well suited for use in autonomous, mobile devices or where space is limited. The development of hard magnet based systems has been hindered to-date by the challenges faced in integrating these materials at the appropriate scale using techniques compatible with today's micro-system technologies. In this presentation we will report on the preparation and patterning of high performance hard magnetic materials in film and polymer-powder composite form. We will present their magnetic, structural and mechanical properties and will give examples of a range of bio-related applications now being developed using these micron-scaled hard magnetic structures.

JH03

Exchange spring magnet for rare earth free permanent magnet

Dongyoo Kim and Jisang Hong*
Department of Physics, Pukyong National University, Korea

Using the full potential linearized augmented plane wave (FLAPW) method, we have investigated the thickness dependent magnetic properties of rare earth free exchange spring magnet FeCo/FePt(001). The FeCo adlayer thickness is increased from one monolayer (ML) to four ML coverage. It is observed that the FeCo adlayers and Fe atoms in FePt substrate show almost half metallic behavior, while an ordinary metallic feature is found in Pt atoms. The average magnetization increases with FeCo thickness and the estimated energy product reaches 65.61 MGOe in FeCo(4ML)/FePt(001). A giant perpendicular magnetocrystalline anisotropy (MCA) energy is found in pure FePt(001) and the MCA energy in FeCo/FePt(001) systems also show quite large values. For instance, the calculated MCA energy of pure FePt(001) is about 18.2 meV/cell, and it is about 17.35 meV/cell for FeCo(4ML)/FePt(001). Both MCA energy and estimated energy product values of FeCo/FePt(001) exchange spring magnet structure are comparable with those found in rare earth substituted permanent magnet. This may imply that the FeC/FePt can be utilized for potential rare earth free exchange spring magnet material This work was supported by the KCAP located in Sogang University funded by MEST through (NRF-2011-C1AAA001-2011-0030278), and by KOSEF grant founded by MEST (No.R01-2008-000-20014-0).

JH04

Prediction of maximum energy product for exchange coupled core-shell nanomagnets

Jihoon Park¹, Yang-ki Hong^{1*}, Jaemin Lee¹, Jeevan Jalli², Gavin Sky Abo¹, Woncheol Lee¹, Chul-jin Choi¹ and Junggoo Lee²
¹ Department of Electrical and Computer Engineering and MINT Center, The University of Alabama, Tuscaloosa, Alabama 35487, USA
² Schweitzer Engineering Laboratories, 2350 NE Hopkins Court, Pullman, Washington 99163, USA
³ Korea Institute of Materials Science, Changwon, Kyungsangnam-do, Korea

Ferromagnetic τ -phase MnAl possesses a high magnetic moment of 2.4 μ B per unit cell [1] and the Curie temperature (T_c) of 655 K [2], and is also rare-earth free. However, its maximum energy product, (BH)_{max}, is about 12.3 MGOe at 300 K. This maximum energy product is not enough for high-energy magnetic device applications. Therefore, we have proposed core (τ -phase MnAl hard magnet)/shell (soft magnet) nanostructure to enhance the (BH)_{max}, which is higher than that of Sm₂Co₇. We have modified the Skomski's approach [3], that is exchange hardening in nanoscale combination of a soft phase and an oriented hard phase, to predict the theoretical limit of (BH)_{max} for the τ -phase MnAl core-shell nanomagnet. It was found that (BH)_{max} of core (70 nm τ -phase MnAl hard magnet)/shell (18 nm thick 1.6 T soft magnet) nanomagnet exceeds 40 MGOe at 300 K, where the soft shell thickness is thinner than two times of MnAl domain wall thickness. It is noted that the magnetization of soft shell plays a key role in enhancement of (BH)_{max}. Detailed calculations for (BH)_{max} will be discussed for various hard-core sizes and soft-shell thickness.

[1] A. Sakuma, J. Phys. Soc. Japan, 63, 1422 (1993). [2] Q. Zeng, I. Baker, J. B. Cui, and Z. C. Yan, J. Magn. Magn. Mater. 308, 214 (2007). [3] R. Skomski and J.M.D. Coey, Phys. Rev. B, 48, 21 (1993).

JI01

Ferromagnetic properties of Co-Pd-SrTiO₃ alloy films with high magnetic anisotropy

Yiwen Zhang^{1*}, Syousuke Fukushi¹, Hanae Kijima¹, Nobukiyo Kobayashi², Atsushi Yokoi², Shigehiro Ohnuma² and Hiroshi Masumoto¹
¹ Center for Interdisciplinary Research, Tohoku University, Japan
² Research Institute for Electromagnetic Materials, Japan

Developments of electromagnetic devices require higher frequency soft-magnetic materials with high magnetic anisotropy (Hk) and electrical resistivity (ρ). Early work has found Co-based nanocomposite films show good high-frequency magnetic properties[1]. However, it's difficult to obtain both high Hk and ρ simultaneously. In this work, Pd is induced to form Co-Pd alloy nanoparticles to enlarge Hk and SrTiO₃ (STO) is employed as nonmagnetic structural phase due to its high ρ . The effect of Pd on structure and magnetic properties has been investigated. The Co-Pd-STO alloy films were deposited onto Si and quartz substrates by reactive magnetron sputtering, using a composite target composed of a STO disk and Co, Pd chips. Film structures were investigated by XRD. The chemical composition of the films was analyzed by EDS and EPMA. The magnetization was measured with VSM. The Co-Pd-STO film structures and magnetic properties are strongly affected by Pd content. At the optimal composition, the films exhibit Bs of about 7kG, ρ in order of 103 $\mu\Omega$ cm, and Hk of around 150 Oe. The film shows good frequency response of permeability at GHz range. Co-Pd-STO alloy film is a good candidate for the GHz range electromagnetic devices.

1. Y. W. Zhang, S. Ohnuma, and H. Masumoto, IEEE Transactions on Magnetics, vol. 47, pp. 3795-3798 (2011).

JI02

Effect of change in thickness on the structural and magnetic properties of L10-ordered FePd films with (001) texture

Jungho Ko, Taejin Bae and Jongill Hong*
Materials science and engineering, Yonsei Univ., Korea

L10-ordered films with strong perpendicular magnetic anisotropy (PMA), such as CoPt, FePt and FePd, have received considerable attention since they are a superior candidate that can overcome superparamagnetism as they become smaller [1, 2]. To form L10-ordered FePd on an MgO (001) substrate, we prepared samples having a repetition of a bi-layer composed both Fe and Pd monolayers by a dc ultra-high vacuum magnetron sputtering system at room temperature, and annealed them under a perpendicular magnetic-field of 4 kOe. The total thickness of [Fe/Pd]n was changed from 3 to 20 nm. As-deposited FePd had a (100) textured FCC disordered phase and showed in-plane magnetic anisotropy. Interestingly, after annealing at 500 °C for 2 h, FePd was transformed to a (001) textured FCT L10-ordered phase and showed PMA. Especially, 3- and 5-nm-thick FePd showed strong PMA with a squareness of unity. With increasing of thickness of FePd, the FCC (100) texture was gradually increased, resulted in a decrease in PMA. In fact, the 20-nm-thick L10-FePd showed mixed anisotropy with both in-plane and out-of-plane magnetic anisotropy components. This research was supported in part by the IT R&D program of MKE/KEIT. (KI002189, Technology Development of 30 nm level High Density Perpendicular STT-MRAM)

[1] M. R. Visokay and R. Sinclair, APL 66 1692 (1995). [2] H. Shima, K. Oikawa, A. Fujita, K. Fukamichi, and K. Ishida, JMMM 272 2173 (2004).

JI03

Mechanism of large magnetic anisotropy of thin film m-DO19 Fe₃Pt and analogous 3d-5d compounds

Oleg Mryasov* and Takao Suzuki
Materials for Information Technology (MINT) Center, University of Alabama, USA



JI04

Fabrication of highly ordered L10 type FePt thin films by rapid thermal annealing

Masaki Mizuguchi*, Takashi Sakurada and Koki Takanashi
Institute for Materials Research, Tohoku University, Japan

Large uniaxial magnetic anisotropy materials are extremely promising for the application to high-density magnetic storage devices or permanent magnets. In particular, an L10 type FePt alloy reveals extremely large magnetic anisotropy, therefore numerous studies on the fabrication of FePt films have been reported. However, it is a fatal problem that a high growth-temperature or a high postannealing-temperature is needed to obtain an ordered FePt phase. In this paper, we employed a rapid thermal annealing to promote an L10 ordering of sputtered FePt films even at a relatively low temperature, and investigated their crystallographic and magnetic properties. Fe and Pt were deposited simultaneously on thermally oxidized Si substrates. The thickness of FeNi films was 6.5 nm. After the deposition, films were rapidly annealed by a temperature elevation with a rate of 10°C/sec in high vacuum. It was found that a magnetic anisotropy increased by annealing, and a uniaxial magnetic anisotropy energy (Ku) was estimated to be 3.5×10⁷ erg/cc from magnetization curves. Ku and coercivity drastically increased with higher rates up to 50°C/sec. On the other hand, it was revealed that a chemical order parameter estimated from X-ray diffraction pattern slightly decreased with the rate. Detailed structural analysis will be also discussed.

JI05

Competing intrinsic and side-jump anomalous Hall effects in Isoelectric L10 FePtPd ternary alloy films

Pan He¹, Li Ma¹, Zhong Shi¹, Guan Yu Guo² and Shiming Zhou^{1*}
¹ Department of Physics, Tongji University, China
² Department of Physics and Center for Theoretical Sciences, National Taiwan University, Taiwan

We have for the first time studied the anomalous Hall effect for isoelectric L10 Fe_{0.5}(Pt,Pd_{1-x})_{0.5} ternary alloy films. When the spin-orbital coupling strength is feasibly controlled changing the concentration ratio of Pd to Pt atoms, anomalous Hall conductivity (AHC) can be continuously tuned from 300 S/cm for x = 0 (L10 FePd) to 930 S/cm for x = 1 (L10 FePt). Calculations have shown the intrinsic AHC increases significantly whereas the side-jump AHC decreases weakly. In particular, the present results of the side-jump AHC for L10 FePt and FePd films reproduces the calculated results based on scattering-independent model. Our results will generate new theoretical interest in the L10-ordered ternary alloys.

[1] N. Nagaosa, Rev. Mod. Phys. 82, 1539-1592 (2010). [2] K. M. Seemann, Y. Mokrousov, A. Aziz, J. Miguel, F. Kronast, W. Kuch, M. G. Blamire, A. T. Hindmarch, B. J. Hickey, I. Souza, and C. H. Marrows, Phys. Rev. Lett. 104, 076402 (2010). [3] Y. Tian, L. Ye, and X. Jin, Phys. Rev. Lett. 103, 087206 (2009). [4] M. Chen, Z. Shi, W. J. Xu, X. X. Zhang, J. Du and S. M. Zhou, Appl. Phys. Lett. 98, 082503(2011)

JI06

Effect of deposition temperature on the crystallographic structure and first-order magnetic phase transition of FeRh thin films on glass substrate

Wei Lu¹, Chenchong He², Zhe Chen² and Biao Yan²
¹ School of Materials Science and Engineering, Tongji University, Shanghai, China
² Tongji University, China

Ordered B₂(CsCl)-type FeRh alloy and its nearby compositions have been subject of extensive theoretical and experimental studies due to a first-order magnetostructural phase transition from an antiferromagnetic (AFM) to ferromagnetic (FM) state when heating beyond a critical transition temperature. Recently, there are many literatures investigating the first-order AFM/FM transition in FeRh-based thin films. Generally, deposition temperature is expected to influence the structure and consequently the magnetic properties of magnetic thin films. In this presentation, the effect of deposition temperature on the structure and AFM/FM phase transition is investigated in details. XRD results show that the films fabricated at Ts = 350 and 400 oC are grown with FeRh(001) planes parallel to the MgO(100) substrate. The temperature dependent magnetization curves indicate that the as-deposited thin film at Ts = 350oC did not show any AFM/FM phase transition although it has ordered B₂ structure as shown in XRD results. While for the FeRh film deposited at 400oC, it shows a clear AFM/FM phase transition when heating from low temperature to high temperature. But the transition is very broad (range from -50oC to about 100oC) due to the composition variation, internal stress, defects and so on in the thin films.

JJ01

Some new physics and magnetism of rare earth-rich R₅T₄ and R₅T₃ compoundsVitalij Pecharsky^{1*}, Yaroslav Mudryk², Durga Paudyal² and Karl Gschneidner, Jr.¹¹ Ames Laboratory and Department of Materials Science and Engineering, Iowa State University, USA² Ames Laboratory, Iowa State University, USA

Intermetallic compounds of the rare earth metals (R) with group 14 elements (T) at the R₅T₄ and R₅T₃ stoichiometries provide numerous opportunities to clarify structure-property relationships that are generally elusive in compounds formed by metals, and in the future, to exploit this knowledge. The uniqueness of R₅T₄ compounds lies in well-defined, self-assembled layers composed of R and T atoms coupled with the flexibility to modify their arrangements in closely related structures using a variety of triggers. Interestingly, the R₅T₃ compounds that also adopt distinctly layered but different crystal structures exhibit an interesting interplay between their crystal and magnetic sublattices. In this presentation we will be concerned with some recently discovered, extraordinarily interesting structural, magnetic, and electronic transport phenomena that are related to structural and microstructural modifications that facilitate an unprecedented level of control over the physical behaviors of these compounds. This work is supported by the U.S. Department of Energy, Materials Sciences and Engineering Division of the Office of Basic Energy Sciences under contract No. DE-AC02-07CH11358 with Iowa State University.

JJ02

Morphotropic phase boundary in ferromagnets - A way leading to large magnetostriction

Sen Yang^{1*}, Xiaobing Ren² and Xiaoping Song¹¹ Department of Materials Physics, Xi'an Jiaotong University, China² National Institute for Materials Science, Japan

Morphotropic phase boundary (MPB), a phase boundary separating two ferroelectric phases of different crystallographic symmetries in the composition-temperature phase diagram, is crucially important in ferroelectric materials, because MPB can lead to a great enhancement of piezoelectricity, the most useful property of this large class of functional materials. From the parallel physics between ferroelectricity and ferromagnetism, it is tempting to ask if similar MPB can exist in another large class of functional materials ferromagnetic materials, and if it can lead to significant enhancement of the corresponding properties (magnetostrictive effect, or magnetic-field-induced distortion). Here we report the existence of a MPB in a ferromagnetic system TbCo₂-DyCo₂ between a ferromagnetic rhombohedral phase and a ferromagnetic tetragonal phase. Such a magnetic MPB involves a first-order magnetoelastic transition, at which both magnetization direction and crystal structure change simultaneously. The MPB composition demonstrates a 3-6 time larger "figure of merit" of magnetostrictive response compared with that of the off-MPB compositions. In-situ observation by high-resolution synchrotron x-ray diffractometry (XRD) reveals that the MPB region is composed of co-existing rhombohedral and tetragonal phases, indicating the bi-stability of both magnetization vector and lattice distortion. This accounts for the maximum magnetostrictive property at the MPB.

[1] S. Yang, H. Bao, C. Zhou et al., *Phys. Rev. Lett.*, **104**, 197201 (2010). [2] S. Yang, and X. Ren, *Phys. Rev. B*, **77**, 014407 (2008).

JJ03

Magnetostriction in geometrically frustrated Co₃V₂O₈ single crystalsRyszard Zuberek¹, Ritta Szymczak¹, Jan Fink- Finowicki¹, Victor Nizhankovskii² and Henryk Szymczak¹¹ Institute of Physics Polish Academy of Sciences, Warsaw, Poland² International Laboratory of High Magnetic Fields and Low Temperatures, Wrocław, Poland

In our previous papers (Phys.Rev.B,2006, 2009) we have shown that frustrated Co₃V₂O₈ single crystals are characterized by a strong magnetocrystalline anisotropy and that this anisotropy arises due to presence of Co²⁺ ions strongly connected to the lattice. In order to check this single-ion mechanism we decided to perform magnetostriction measurements in Co₃V₂O₈ single crystals. The high-resolution capacitive dilatometry was used to determine linear (longitudinal and transverse) and volume magnetostriction as a function of temperature in low temperature region and in magnetic field up to 12 T directed along the main crystallographic directions. The single crystals of Co₃V₂O₈ were grown by floating zone technique using an optical image furnace. The results of measurements are discussed in terms of the single-ion model taking into account the competing first and second neighbor Heisenberg exchange interactions and magnetocrystalline anisotropy constants determined in our previous studies. The satisfactory agreement with experimental results shows that the magnetostriction in geometrically frustrated Co₃V₂O₈ is dominated by the single-ion mechanism . The paper was partly supported by the Ministry of Science and Higher Education (Poland) through grant No. N202 125135 .

JJ04

Magneto-volume anomalies and low-temperature inverse magneto-caloric effect in Er₂Fe₁₇Pablo Alvarez², Pedro Gorria^{3*}, Jose Luis Sanchez Llamazares², Jorge Sanchez Marcos², Gabriel Cuello², Ines Puento-oreñch¹, Gaston Garbarino⁴, Imanol De Pedro¹, Jesus Rodriguez Fernandez² and Jesus A. Blanco¹¹ Department of Physics, University of Oviedo, c/ Calvo Sotelo, s/n, 33007 Oviedo, Spain² Division de Materiales Avanzados, IPCYT, Camino a la presa San Jose 2055, 78216, San Luis Potosi, Mexico³ Instituto de Ciencia de Materiales de Madrid, CSIC, Cantoblanco, 28049 Madrid, Spain⁴ Institute Laue Langevin, 6 rue Jules Horowitz, 38042 Grenoble, France⁵ Instituto de Ciencia de Materiales de Aragon, CSIC-Univ Zaragoza, 50009 Zaragoza, Spain⁶ European Synchrotron Radiation Facility, BP 220, 6 rue Jules Horowitz, 38043 Grenoble, France⁷ Department CITIMAC, University of Cantabria, 39005 Santander, Spain

Most of the magnetic properties of Er₂Fe₁₇, intermetallic can be understood using a two-sublattice model, corresponding to the erbium and iron elements, respectively. This compound crystallizes in the hexagonal Th₃Ni₁₇-type structure (P6₃/mmc space group) and exhibits ferrimagnetic behaviour with the Er sublattice moments antiparallel to those of the Fe-sublattice, and a Curie temperature TC=300K. Combining different experimental techniques, such as neutron powder thermo-diffraction, x-ray powder diffraction under high hydrostatic pressure (20GPa) and magnetization measurements as a function of temperature (2-350K), magnetic field (up to 80kOe) and hydrostatic pressure up to 1GPa), we show the presence of strong magneto-volume anomalies, including Invar effect, from low temperature up to 450 K, indicating the existence of short-range magnetic correlations well above TC. In addition, this compound exhibits a direct magneto-caloric effect (MCE) around room temperature as well as an inverse MCE below 100K. A mean field Hamiltonian, that incorporates both crystalline electric field and exchange interactions, has been used to describe the main experimental trends for the temperature dependences of the MCE and the atomic magnetic moments. Therefore, it seems that a correlation between the magneto-volume anomalies and the MCE is the key to understand the physical properties of this intermetallic compound.

D. Givord and R. Lemaire, *IEEE Trans. Magn.*, **10**, 109 (1974). F. Grandjean, O. Isard, D. Hautot, and G. Long, *Phys. Rev. B*, **63**, 014406 (2000). P. Gorria, P. Alvarez, J.Sanchez-Marcos, J.L. Sanchez-Llamazares, M.J. Perez, and J.A. Blanco, *Acta Mater.* **57**, 1724 (2009). P. Alvarez, P. Gorria, and J.A. Blanco, *Phys. Rev. B*, **84**, 024412 (2011).

JJ05

Neutron diffraction study of rare-earth compound Ho₅Pd₂ with large magnetocaloric effectHideaki Kitazawa¹, Yukihiko Kawamura², Noriki Terada¹, Hiroaki Mamiya¹, Hiroyuki S Suzuki¹, Andreas Doenni¹, Koji Kaneko³, Naoto Metoki¹ and Naoki Igawa³¹ Quantum Beam Unit, National Institute for Materials Science, Japan² CROSS-Tokai, Japan³ Japan Atomic Energy Agency, Japan

In recent years, more efficient magnetic refrigerant materials are desired due to potential application in energy-efficient environment-friendly refrigeration technology. Samanta et al. discovered that the rare-earth compound Ho₅Pd₂ shows large magnetocaloric effect (MCE) [1]. The interesting point is that the large MCE might be originated from field-induced metamagnetic transition below antiferromagnetic transition temperature TN of 28 K. However, it is not easy to judge whether Ho₅Pd₂ is antiferromagnetic or not only from magnetization data. In order to determine its magnetic structure, neutron diffraction is most powerful technique. We have performed neutron powder diffraction experiments at JRR-3, Japan using polycrystalline Ho₅Pd₂. Ho₅Pd₂ was prepared by arc-melting and annealed at 850 degrees for 72 hours in a vacuum. In this paper, we will present powder neutron diffraction patterns as a function of temperature. The magnetic peaks with a propagation vector k = (δ, δ, δ) (δ = 0.18) are gradually developing below about 100 K. The peak width is significantly broader than an experimental resolution even temperature is 5 K. These results indicate that Ho₅Pd₂ is a short-range ordered antiferromagnet with a long wave length.

[1] T. Samanta et al., *Appl. Phys. Lett.*, **91**, 082551 (2007).

KA01

Probing the Kondo effect on the atomic scale by mapping the itinerant electrons

Martin Wenderoth

University of Gottingen, 4. Physikalisches Institut, Germany

Scanning tunneling spectroscopy (STS) has provided an approach to study the Kondo effect - one of the oldest many particle phenomena known in condensed matter physics - in real space [1]. In the present work we follow a novel route to investigate Kondo bulk impurities. It has been shown recently [2] that the anisotropy of the copper Fermi surface leads to a strongly directional propagation of quasi particles called electron focusing which gives access to individual bulk impurities in a metal. Using low temperature scanning tunnelling spectroscopy (STS) we have studied the energy-dependent scattering characteristics for single isolated atoms of Co and Fe buried under a Cu(100) surface. For both magnetic impurity atoms we observe a long range Kondo signature which is periodic with the distance to the impurity [3]. The comparison of Co and Fe atoms demonstrates that both impurity species show similar behavior on completely different energy scales, which is determined by the Kondo temperature. We investigate the scattering amplitude as well as the phase. A theoretical interpretation based on a combined approach of band structure and many-body numerical renormalization group calculations is able to describe the rich spatially and spectroscopically resolved experimental data.

[1] M. Ternes et al., *Journal of Physics: Condensed Matter* **053001** (2009) [2] A. Weismann et al., *Science* **323**, 1190 (2009) [3] H. Prueser et al., *Nature Physics* **7**,203 (2011)

KA02

Coexistence of antiferromagnetic order and hybridization gap in Ce-based kondo semiconductors

D.T Adroja^{1*}, T. Takahatake², Y. Muro³, K. Yutani², J. Kajino², K. Urneo³, S. Kimura⁴, A. D. Hillier¹, D. D. Khalyavin¹ and A. Severing⁶¹ ISIS Facility, Rutherford Appleton Laboratory, Chilton, OX11 0QX, United Kingdom² Dept. Quantum Matter, AdSM, Hiroshima University, Higashi-Hiroshima, Japan³ Liberal Arts and Sciences, Toyama Prefectural University, Imizu, Japan⁴ 4N-BARD, Hiroshima University, Higashi-Hiroshima, Japan⁵ UTSOR Facility, Institute for Molecular Science, Okazaki, Japan⁶ Institute of Physics II, University of Cologne, Cologne, Germany

The mechanism of the gap formation in so called Kondo semiconductors (KSS) such as SmB₆, YbB₁₂, and CeRhAs remains elusive. The anisotropic gap structure is thought to originate from the k-dependence of hybridization of a crystal field ground state of the rare-earth ion with a conduction band. The ground states of all the KSS are paramagnetic except for CeOsSb₂ which undergoes an SDW transition at 0.9 K. Recently, the compounds CeT₂Al₁₀ (T = Ru, Os) have been found to have transport gaps of approximately 50 K and order antiferromagnetically at exceptionally high temperature, 28 K [1-5]. It is puzzling that the ordering temperature is much higher than those of the Gd counterparts in spite of the small ordered moment of 0.3-0.4 B/Ce. To answer this puzzle, we have performed bulk and microscopic measurements on single crystalline samples of CeT₂Al₁₀ (T = Fe, Ru, Os) and alloys. We will present the results of magnetic, transport, and optical conductivity measurements [6] as well as neutron scattering, SR, and XAS experiments. The relation between the anisotropic charge/spin gaps, the wave functions of the crystal field ground state, and anisotropic electronic states will be discussed.

[1] A. M. Strydom, *Physica B* **404**, 2981(2009). [2] T. Nishioka et al., *JPSJ* **78**, 123705 (2009). [3] Y. Muro et al., *PRB* **81**, 214401 (2010). [4] D. D. Khalyavin et al., *PRB* **82**, 100405 (2010). [5] D. T. Adroja, et al., *PRB* **82**, 104405 (2010). [6] S. Kimura, et al., *PRL* **106**, 056404 (2011).

KA03

Kondo scattering investigated by Nernst-effect measurements

Peijie Sun¹, Christoph Geibel² and Frank Steglich²¹ Institute of Physics, Chinese Academy of Science, Beijing 100190, China² Max Planck Institute for Chemical Physics of Solids, Dresden, Germany

The transverse thermoelectric response, known as Nernst effect, was investigated for (CeLa)₂Cu₂Si₂ with varying Ce concentrations from 2 K to room temperature. Except for the non-magnetic LaCu₂Si₂, all compounds exhibit largely enhanced Nernst signal in the whole temperature range investigated. Within the standard Boltzmann transport theory, the Nernst effect measures the relaxation-time spectra of charge carriers as a function of energy at the Fermi level. This, however, is hardly accessible by the longitudinal thermoelectric effect, which is mostly dominated by the asymmetric feature of the electronic density of states. With these considerations in mind, we hope to gain new insights into the charge-carrier relaxation related to Kondo scattering by studying the Nernst effect, as well as its correlation with the enhanced thermoelectricity generally observed in heavy-fermion systems. Our observations of large Nernst signals in (CeLa)₂Cu₂Si₂ point to a remarkable asymmetric character of the charge-carrier relaxation time attributable to the Kondo effect. Furthermore, our analysis shows that the asymmetric relaxation can account for a major part of the enhanced thermopower observed in the current systems over a large temperature range, leading to the conclusion that the asymmetric density of states is of only minor importance in this respect for Kondo systems

KA04

Electron spin resonance in antiferro-quadrupolar ordered CeB₆

Pedro Schlottmann*

Department of Physics, Florida State University, USA

CeB₆ is the first heavy fermion compound without ferromagnetic short-range correlations displaying an ESR signal [1]. The ferromagnetic correlations among Ce or Yb spins in all other compounds showing an ESR signal narrow the resonance width rendering it observable [2]. CeB₆ is a cubic compound with a Gamma₈ ground-quartet. The orbital content of the quartet gives rise to an antiferro-quadrupolar ordered phase below 4 K. Single ions with a Gamma₈ ground-multiplet are expected to display four transitions, however, only one was observed. Two fundamental questions arise: (1) why is only one transition seen, and (2) why is this transition observed if the Kondo temperature is larger than the linewidth and there are no ferromagnetic correlations between the ions? While for other Ce and Yb compounds with ESR-signal it is not possible to distinguish if the resonance is due to localized spins or conducting heavy electron spins, an itinerant picture within the antiferro-quadrupolar state is necessary for CeB₆. Work supported by the Department of Energy under grant DE-FG02-98ER45707.

[1] S.V. Demishev et al., *Phys. Rev. B* **80**, 245106 (2009). [2] E. Abrahams and P. Wolfle, *Phys. Rev. B* **78**,104423 (2008); **80**, 235112 (2009); P. Schlottmann, *Phys. Rev. B* **79**, 045104 (2009).

KB01

Aligning and measuring the magnetic easy axis direction of superparamagnetic nanoparticles at temperatures much greater than the blocking temperature

Jean-charles Eloi, Mitsuhiro Okuda, Sarah Ward Jones and Walther Schwarzacher*

H. H. Wills Physics Laboratory, University of Bristol, United Kingdom

Cobalt-doped magnetite nanoparticles with diameter ~8nm and blocking temperature ~60K were fabricated using the protein ferritin as a template. Magnetic measurements of a solution of the nanoparticle-containing ferritin (magnetoferritin) in 50 mM Tris-HCl reveal unusual dynamic behaviour. The magnetoferritin is free to rotate at temperatures down to ~210K, although differential scanning calorimetry shows that the bulk of the solution starts to freeze at ~269K. Cooling the sample through 210K in a 5T applied field aligns the easy axes of the magnetoferritin, even though 210K is considerably higher than the blocking temperature. At low temperatures (5K) the magnetoferritin with aligned easy axes has significantly higher remanence and coercivity than when the easy axes are randomly oriented. For temperatures 60<<T<210K, the aligned magnetoferritin also has a much higher susceptibility than when the easy axes are randomly oriented. Warming the sample through 210K, the loss of easy axis alignment is observed as a decrease in the susceptibility from the aligned towards the randomly oriented value. The time constant for this decrease depends on the effective viscosity, and is extremely sensitive to temperature. This work has received funding from the European Community's Seventh Framework Programme (FP7/2007-2013) under Grant Agreement n°228673 (MAGNONICS).

KB02

Exchange-bias in iron-based nanoparticles

Emeric Folcke¹, Jean-marie Le Breton^{1*}, Williams Lefevbre¹, Rodrigue Larde¹ and Jeffrey E Shield²¹ Groupe de Physique des Materiaux - UMR 6634, CNRS - Universite de Rouen, France² Nebraska Center for Materials and Nanoscience, University of Nebraska Lincoln, USA

Iron-based magnetic alloys are much investigated for their good magnetic properties, especially their high saturation magnetisation. However, large magnetocrystalline anisotropy is necessary to obtain a support for magnetic recording. This can be achieved in particular for FePt nanoparticles with the L10 structure [1,2]. In this work, we investigated the magnetic properties of FePt, FeAu and FeW nanoparticles embedded in a metallic matrix (Cr or W). The samples were elaborated by inert-gas condensation. The structural properties have been investigated by high resolution transmission electron microscopy (HRTEM) and laser assisted atom probe tomography (APT) [3]. Their magnetic properties were characterised by SQUID magnetometry and Mossbauer spectrometry. SQUID measurements revealed in some cases an exchange-bias effect which could be due to the occurrence of a core-shell structure in the nanoparticles or to the presence of RKKY interactions through the metallic matrix. This point will be discussed in relation with the nanostructure characterised by HRTEM and APT.

[1] D.J Sellmyer, C.P. Luo, M.L. Yan, Y. Liu, *IEEE Trans. Mag.*, **4** (2001) 1286-1291. [2] Y.F. Xu, M.L. Yan, D.J. Sellmyer, *J. Nanosci. Nanotechnol.*, **7** (2007) 206-224. [3] D. Blavette, B. Decoinhout, A. Bostel, J. M. Sarrau, M. Bouet, and A. Menand, *Review of Scientific Instruments*, **64**(10) (1993) 2911-2919.

KB03

Photocontrolled magnetism through interface strain in core-shell prussian blue analogues

Elisabeth S. Knowles¹, Carissa H. Li², Matthieu F. Dumont¹, Marcus K. Peprah¹, Daniel R. Talham² and Mark W. Meisel^{1*}¹ Department of Physics and NHMFL, University of Florida, USA² Department of Chemistry, University of Florida, USA

Cubic heterostructured (BA) particles of Prussian blue analogues, composed of a shell of ferromagnetic K₃Ni[Cr(CN)₆]₂ · nH₂O (A), Tc ~ 70 K, surrounding a bulk core of photoactive ferrimagnetic RbCo[Fe(CN)₆]₂ · mH₂O (B), Tc ~ 20 K, have been studied. Below Tc ~ 70 K, these samples exhibit a persistent photoinduced decrease in low-field magnetization, and these results resemble data from other core-shell particles [1] and analogous ABA heterostructured films [2]. This net decrease suggests that the photoinduced lattice expansion in the B layer generates a strain-induced decrease in the magnetization of the A layer, similar to a pressure-induced decrease observed by others in a pure A-like material [3] and by us in our BA cubes. Photocontrol at higher temperatures is being pursued by applying this strain from the B material to other hexacyanochromate analogues, which possess higher ordering temperatures for some stoichiometries. Work supported by NSF DMR-1005581 (DRT) and the NHMFL.

[1] M.F. Dumont, et al., *Inorg. Chem.* **50** (2011) 4295. [2] D.M. Pajerowski, et al., *J. Am. Chem. Soc.* **132** (2010) 4058. [3] M. Zentkova et al., *J. Phys.: Condens. Matter* **19** (2007) 266217.

KB04

Confinement effect on the Al1 to L10 phase transformation of FePt

Andrew Gallagher*, Levent Colak, Ozan Akdogan and George Hadjipanayis
Physics and Astronomy, University of Delaware, USA

The major challenge for the application of chemically synthesized FePt nanoparticles (NPs) in magnetic storage media is the sintering problem encountered during the required high temperature annealing to obtain the high anisotropy L10 phase. In this work, we have used two different methods to avoid sintering; coating the NPs with a protective layer of silica (SiO₂) and using porous aluminum oxide (Al₂O₃) as a template to embed the NPs. The NPs were synthesized via the synthesis method of Sun et al.[1] The NPs were embedded into the Al₂O₃ by in-situ suctioning of the reaction solution into the porous Al₂O₃ template followed by annealing at high temperatures. Monodispersed FePt NPs with a size of 5.8 and 15 nm were coated with SiO₂ shells using a water-in-oil micro emulsion method. High room temperature coercivities were only obtained after annealing the samples at 900°C for long times (24-48 h) under forming gas flow as compared to the usual heat treatment at 600-700°C. Values of 4.7 and 7.8 kOe were observed in SiO₂ and Al₂O₃ samples, respectively after annealing for 24 h at 900°C. This behavior suggests that the restricted geometry of the samples suppresses the atomic ordering and the phase transformation drastically.

Work supported by DOE DE-FG02-04ER4612 [1] S. Sun, C. B. Murray, D. Weller, L. Folks, A. Moser Science 2000, 287, 1989.

KB05

Are small CoPt and FePt nanoparticles mono-L10 domain?

Florent Tournus^{1*}, Kazuhisa Sato², Toyohiko J. Konno², Thierry Epicier³ and Veronique Dupuis¹
¹ LPMCN, CNRS & Univ. Lyon 1, France
² Institute for Materials Research, Tohoku University, Japan
³ MATEIS, CNRS & INSA-Lyon, France

Despite the many experimental and theoretical studies, open questions regarding the structure of small CoPt and FePt nanoparticles remain (threshold size for L10 ordering, preferential segregation, most favourable geometry). Moreover, while well known planar defects (c-domain boundaries, antiphase boundaries) are met in macroscopic materials or thin films, their relevance for particles of a few nanometers has not been examined. Therefore, an implicit belief is that small CoPt or FePt nanoparticles, if they can be chemically ordered, would be mono-L10 domain. CoPt and FePt nanoparticles, with a diameter between 2 and 5 nm, have been prepared by cluster deposition and annealed. For both alloys, we observe using transmission electron microscopy a coexistence of fcc nanocrystals and multiply-twinned particles with decahedral or icosahedral shapes. In addition to mono-L10 domain particles, we put into evidence that even small particles can display several L10 domains. In particular, the chemical order can be preserved among twinning which can give rise to spectacular chemically ordered decahedral particles made of five L10 domains. The stability of such structures, which had been recently predicted from theoretical simulations, is thus experimentally confirmed. These observations are then confronted to recent experimental results of magnetometry and synchrotron measurements (XMCD, EXAFS).

KB06

Magneto-structural correlations in antiferromagnetic and ferrimagnetic nanoparticles

Nuno Silva^{1*}, Vitor S. Amaral¹, Luis D. Carlos¹, Ainhoa Urizberoa², Rodney Bustamante², Angel Millán¹, Fernando Palacios², Erik Kampert¹, Uli Zeitler¹, Sophie De Brion¹, Yuki Komori³, Masaki Mito³, Oscar Iglesias⁴, Amikar Labarta¹, Ines Puente Orenchi¹ and Javier Campo¹
¹ Dep. Fisica and CICECO, Universidade de Aveiro, Portugal
² Departamento de Fisica de la Materia Condensada and ICMA Universidad de Zaragoza, Spain
³ Radboud University Nijmegen, High Field Magnet Laboratory, Netherlands
⁴ CNRS, Inst. Neel, F-38042 Grenoble 9, France and Univ. Grenoble, Grenoble, France
⁵ Faculty of Engineering, Kyushu Institute of Technology, Kitakyushu, Japan, Japan
⁶ Departament de Fisica Fonamental and Institut de Nanociencia i Nanotecnologia, Univ. Barcelona, Spain
⁷ ICMA-CSIC/Univ. Zaragoza, Zaragoza Spain and Institut Laue-Langevin, Grenoble, France, Spain

We present structural and magnetic studies performed in ferrimagnetic[1,2] and antiferromagnetic[3-7] nanoparticles. We focus our attention on the antiferromagnetic ferritin and cobalt oxide and on the ferrimagnetic maghemite. High-field studies in ferritin reveal that the temperature dependence of the antiferromagnetic susceptibility decreases with temperature when correctly determined from high-field data.[5] High-field hysteresis loops also show that coercivity and loop-shifts are a function of the maximum field, which can be understood in the frame of coherent rotation models considering a field-dependent anisotropy energy.[7] Neutron diffraction is particularly effective in the study of structural and magnetic coherence sizes of antiferromagnetic nanoparticles. In the case of cobalt oxide, we found that the difference between both sizes is consistent with a core-shell model where the shell is structurally ordered but magnetically disordered with a thickness of ~2 nm.[6] This core-shell model was also successfully applied to a series of maghemite nanoparticles, based on small-angle X-ray scattering and magnetization results, yielding, in this case, a magnetically disordered shell with about 1 nm.[1] Surface and core contribution to anisotropy energy in maghemite can be elegantly separated by using pressure, since the core/shell volume ratio changes with pressure inducing a change in the average anisotropy energy.[2]

[1] A. Millan et al. *J. Mag. Mag. Mater.* 312, L5-L9 (2007). [2] Y. Komori et al. *Appl. Phys. Lett.* 94, 202503 (2009) [3] N. J. O. Silva et al. *Phys. Rev. B* 71 184408 (2005). [4] N. J. O. Silva et al. *Phys. Rev. B* 77, 134426 (2008). [5] N. J. O. Silva et al. *Phys. Rev. B* 79, 104405 (2009). [6] N. J. O. Silva et al. *Phys. Rev. B* 82, 094433 (2010). [7] N. J. O. Silva et al. *Phys. Rev. B* 84, 104427 (2011).

KC01

360 degree domain walls in various magnetic ring thin films

Chunghye Nam¹ and Caroline A. Ross²
¹ Physics, Hannam University, Korea
² Materials Science and Engineering, MIT, USA

Magnetic domain wall (DW), which is an interface between differently oriented magnetization regions, becomes an important physical property as the size of magnetic materials is reduced. DW can be regarded as a rigid particle, which has been verified in experiments and theoretical study, so that diverse applications have been introduced. In this presentation, the authors report that 360 degree magnetic domain walls(360DW) are formed in a circular or ellipse Co rings. In theoretically, 360DWs have been recently studied in terms of the formation and dynamic as a function of applied magnetic fields and electrical currents.[1,2] 360DWs are consisted of two transverse DWs with opposite polarities but the same chirality. Thus 360DWs are locally in a flux-closure state at remanence, which reduce the magnetostatic energy. Magnetic force microscopy(MFM) is used to see the formation of 360DWs. Based on the MFM measurements, the formation of 360DWs gives rise to monitoring the vortex chirality in various ring-structured thin films. Furthermore, 360DWs generate a low stray field, which is useful for high density magnetic devices without proximity effects. The interaction between 360DWs and a tip of MFM will be shown to verify properties of 360DWs in detail.

[1]P. E. Roy, T. Trypiniotis and C. H. W. Barnes, *Phys. Rev. B* 82, 134411 (2010) [2]Mark D. Mascaro and C. A. Ross, *Phys. Rev. B* 82, 214411 (2010)

KC02

Magneto-optical effect of rare earth doped zinc ferrite thin films prepared using PLD

Naoki Wakiya^{1*}, Tekeshi Misu¹, Nobuyasu Adachi², Naonori Sakamoto¹, Kazuo Shinozaki³ and Hisao Suzuki¹
¹ Shizuoka University, Japan
² Nagoya Institute of Technology, Japan
³ Tokyo Institute of Technology, Japan

Rare earth elements have large orbital interactions. In addition, electron transition of trivalence rare earth ions exists in the ultra violet regions, and suppresses the absorption in the visible light region. Therefore, large magneto-optical effect is expected for ZnFe₂O₄ thin films doped with rare earth elements even in the visible region. In this work, ZnFe₂O₄ thin films doped with rare earth elements (La, Nd, Sm, Eu, Gd, Dy, Ho, Yb) in the Fe site were prepared on fused SiO₂ substrate using pulsed laser deposition. All films were polycrystalline. Ho doped ZnFe₂O₄ thin film showed relatively high optical transmittance in the visible light region (400-800 nm). Faraday rotation angle changes with the kind of rare earth elements, and maximum angle (12000 deg/cm) was obtained for Ho doped ZnFe₂O₄ thin film. This results reflects the large spin orbital interactions.

KC03

Electric field control of coercivity of Pt / Co / Al-O trilayer structures

Tatsuro Ohashi¹, Junichi Shioagai¹, Tim Yang¹, Makoto Kohda^{1*}, Takeshi Seki², Kesami Saito², Koki Takanashi² and Junsaku Nitta²
¹ Department of Materials Science, Tohoku university, Japan
² Department of Materials Science, IMR, Tohoku university, Japan

In recent years, much attention has been focused on studies of effective magnetization switching by electric current[1-4] because of lower power consumption and zero-magnetic field operation. Due to its compatibility with conventional technology, the electric field control of magnetic properties is more attractive[5-8]. Here we demonstrated the electrical gate control of coercivity in an ultrathin Co layer sandwiched between Pt and Al-O. A single wafer, which consists of Pt (3 nm) / Co (0.6 nm) / Al-O (1.0 nm) trilayer on SiO₂ substrate, was prepared. In order to investigate magnetic properties by anomalous Hall effect (AHE), the wafer was processed into a Hall bar geometry. Subsequently, a 20nm-thick Al-O insulating layer was formed by atomic layer deposition at 200 °C. Finally, an AuGeNi / Au gate electrode was evaporated on top. The Curie temperature of our sample was determined to be 340 K at VG = 0 V from the temperature dependence of AHE. The coercivity change of ± 3.0 Oe was observed at 280K by applying the gate voltages of ± 8 V, which correspond to electric fields of ± 3.83 MVcm⁻¹. We successfully modulated the coercivity of the Pt / Co layer by the electric field application.

[1] S. Mangin et al., *Nature Mater.* 5, 210 (2006). [2] T. Seki et al., *Appl. Phys. Lett.* 88,172504 (2006). [3] M. Misiorny et al., *Phys. Rev. B* 76, 054448 (2007). [4] I. M. Miron et al., *Nature Mater.* 9, 230 (2010). [5] D. Chiba et al., *Nature Mater.* 10, 853 (2011). [6] Y. Shiota et al., *Nature Mater.* 11, 39 (2011). [7] T. Seki et al., *Appl. Phys. Lett.*, 98, 212505 (2011). [8] W. G. Wang et al., *Nature Mater.* 11, 64 (2012).

KC04

Microstructure and magnetic property of epitaxial Fe/MgO layer on GaAs and InAs (001) substrates

Kyung Ho Kim¹, Hyung-jun Kim^{1*}, Jun Woo Choi¹, Joonyeon Chang¹ and Young Keun Kim²
¹ Spin Convergence Research Center, Korea Institute of Science and Technology, Korea
² Department of Materials Science and Engineering, Korea University, Korea

Epitaxial growths of Fe/MgO layers on GaAs and InAs heterostructures have been extensively studied for efficient spin injection from ferromagnetic metals into semiconductors. Structural property related to magnetic anisotropy of the Fe layers is mainly determined by underlying strain of MgO tunnel barrier due to the large lattice mismatch between MgO and substrates. In this presentation, we investigated the microstructural evolution and the effect on in-plane magnetic anisotropy of epitaxial Fe/MgO layers grown on GaAs and InAs(001) substrates with respect to the growth temperature and thickness of the MgO tunnel barrier. The Fe layer grew in three-dimensional(3D) islands with two different in-plane textures of [010] and [110] on the MgO layers grown at low temperatures, while it grew in two-dimensional(2D) layer on the MgO layers grown at high temperatures. As the MgO growth temperature and the thickness increase, the strain of the MgO and the subsequent Fe layers are simultaneously relaxed. The partial strain relaxation of the Fe leads to the transition from 3D islands of no magnetic anisotropy to 2D layer of in-plane cubic anisotropy. Furthermore, the islands coalesce as the nominal thickness of Fe increases, resulting in the continuous 2D layer of Fe with the cubic anisotropy.

[1] Kim, K. H. et al., *Appl. Phys. Lett.*, V.95, pp. 164103 (2009) [2] Kim, K. H. et al., *Cryst. Growth Des.*, V.11, pp. 2889 (2011) [3] Kim, K. H. et al., *J. Appl. Phys.*, V.110, pp. 114910 (2011) [4] Kim, K. H. et al., *J. nano sci. nano tech.*, V.12, pp. 1573 (2012)

KC05

Magnetic and transport properties of epitaxial discontinuous Fe/MgO multilayers

A. Garcia - Garcia¹, J. A. Pardo², P. Strichovanec³, A. Vovk⁴, J. M. De Teresa¹, G. N. Kakazei⁵, Yu. G. Pogorelov⁶, P. A. Algarabel^{1*} and M. R. Ibarra²
¹ ICMA, Universidad de Zaragoza-CSIC, 50009 Zaragoza, Spain
² INA, Universidad de Zaragoza, 50018 Zaragoza, Spain
³ INA, Universidad de Zaragoza, 50018, Spain
⁴ CFMC, Universidade de Lisboa, 1749-016 Lisboa, Portugal
⁵ IFIMUP Universidade do Porto, 4169-007 Porto, Portugal

Discontinuous metal-insulator multilayers (DMIMs) are cermet structures prepared by repeated alternate deposition of a continuous insulating and a discontinuous metal layer [1]. However, little attention has been paid to the influence of the substrate nature, deposition temperature, and degree of crystallinity of the insulator layer on transport properties of DMIMs. In recent work [2] we reported tunnelling magnetoresistance (TMR) values for epitaxial Fe/MgO DMIMs deposited on single-crystalline MgO(001) substrates. Here we report a comparison of the magnetic and transport properties of DMIMs [Fe (0.6 nm)/MgO (3 nm)]₁₀ deposited on two different substrates: Corning Glass (CG) and single-crystalline MgO(001) with deposition temperatures (Ts) ranging from 20 °C to 250 °C. Zero field cooled and field cooled magnetic susceptibility measurements were carried for H=50 Oe and 5K<T<300K. The samples exhibit superparamagnetic behaviour. For temperatures higher than the bifurcation temperature (TB) the susceptibility measurements were fitted using a Curie-Weiss law and the average size (Davg) of the magnetic grains was obtained. More precise determination of Davg and their distribution was done by measuring magnetization isotherms for T>TB. We observed that the Fe grains volume is bigger for the samples prepared on MgO substrates. The relationship between transport and magnetic properties will be discussed.

[1]H. G. Silva, A. M. Pereira, J. M. Teixeira, J. M. Moreira, G. N. Kakazei, J. P. Araujo, Yu. G. Pogorelov, J. B. Sousa, M. E. Bragan, B. Raquet, H. Rakoto, C. Gatel, E. Snoeck, S. Cardoso, and P. P. Freitas *Phys. Rev. B* 82, 144432 (2010). [2]A. Garcia-Garcia, J. A. Pardo, P. Strichovanec, C. Magen, A. Vovk, J. M. De Teresa, G. N. Kakazei, Y. G. Pogorelov, L. Morellon, P. A. Algarabel, and M. R. Ibarra *Appl. Phys. Lett.* 98, 122502 (2011).

KC06

Magnetic and transport properties of submicron Gd strip

Seiji Nonoguchi¹, Tatsuya Nomura¹, Takahiro Matsunaga², Kohsuke Furukawa², Masahiro Hara² and Takashi Kimura^{2*}
¹ Kyushu University, Japan
² Kumamoto University, Japan

Magnetic refrigeration utilizing magnetocaloric effects is expected as future environment-friendly refrigeration system. So far, the magnetocaloric effects have been investigated mainly in bulk systems. Recent nanofabrication techniques enable us to make the magnetocaloric materials with reduced dimensions. However, physical properties in such materials have not been investigated intensively. Here, we investigate the magnetic and transport properties of the Gd with reduced dimensions. Submicron-wide Gd strips have been prepared by the conventional lift-off technique combined with the electron-beam lithography. The magnetic properties have been evaluated by using a micro Hall cross based on GaAs/AlGaAs two dimensional electron gas (2DEG) system, and the transport properties have been evaluated by the magnetoresistance measurements. Clear magnetic hysteresis loops with the shape anisotropy were observed by the 2DEG Hall measurements, meaning that the Gd maintains still ferromagnetism even in the reduced dimension. On the other hand, the resistance change related to the magnetization was not observed. Since the f-electrons play an important role in the magnetocaloric effect of the Gd, this result implies that the correlation between the conduction electrons and f-electrons is very small.

KD01

Spin coupling, orbital angular momentum quenching, and electron localization in size-selected free transition metal clusters

Konstantin Hirsch¹, Markus Niemeyer¹, Vicente Zamudio-Bayer¹, Andreas Langenberg¹, Arkadiusz Lawicki¹, Bruno Langbehn¹, Henning Schroeder¹, Martin Kossick², Akira Terasaki³, Thomas Moeller², Bernd Von Issendorff¹ and Tobias Lau^{1*}
¹ Institut fuer Methoden und Instrumentierung der Forschung mit Synchrotronstrahlung, Helmholtz-Zentrum Berlin fuer Materialien und Energie GmbH, Germany
² Institut fuer Optik und Atomare Physik, Technische Universitaet Berlin, Germany
³ Cluster Research Laboratory and Department of Chemistry, Toyota Technological Institute and Kyushu University, Japan
⁴ Fakultae fuer Physik, Universitaet Freiburg, Germany

X-ray magnetic circular dichroism (XMCD) spectroscopy is a local and element specific technique to study spin and orbital magnetization. By applying XMCD spectroscopy to size-selected free clusters, we are able to resolve spin and orbit contributions to the magnetization in particles without any interaction with a support or matrix. This experimental technique allows us to study magnetic coupling in transition metal clusters, follow the quenching of the orbital angular momentum, and gain insight into the interaction of a magnetic impurity with a finite, few-atom free electron gas. Recent highlights will be discussed, including antiferromagnetic coupling of the central atom in Fe 13⁺, ferromagnetic spin coupling in Cr 2⁺, and the complex interplay of hybridization and on-site coulomb repulsion which determines the magnetic moment of impurity atoms in transition metal-doped gold clusters.

M. Niemeyer, K. Hirsch, V. Zamudio-Bayer, A. Langenberg, M. Vogel, M. Kossick, C. Ebrecht, K. Egashira, A. Terasaki, T. Moeller, B. v. Issendorff, J. T. Lau, *Phys. Rev. Lett.* 108 (2012) 057201

KD02

Nm-sized magnetic domains observed by small angle neutron scattering in exchange coupled superlattices

Karine Dumesnil^{1*}, Catherine Dufour¹, Mike Fitzsimmons², Julie Borchers³, Kathryn Krycek³, Mark Laver⁴ and Jonghan Won⁵
¹ Institut Jean Lamour - Lorraine University, France
² LANSCE, USA
³ NIST, USA
⁴ PSI, Switzerland

WITHDRAWN

KD03

Optical and magneto-optical characterization of Y_{0.3}Bi_{2.3}Fe₂O₁₂ and Bi₃Fe₂O₁₂ thin films prepared by metal-organic decomposition

Shengjun Tang¹, Tomohiko Yoshida¹, Martin Veis², Martin Zahradnik², Roman Antos², Takumi Moriyama³ and Takayuki Ishibashi^{1*}
¹ Department of Materials Science of Technology, Nagaoka University of Technology, Japan
² Faculty of Mathematics and Physics, Charles University at Prague, Czech Republic
³ HORIBA, Ltd., Japan

In this work, optical and magneto-optical (MO) properties of Y_{0.3}Bi_{2.3}Fe₂O₁₂ (Bi:YIG) and Bi₃Fe₂O₁₂ (BIG) thin films prepared by a metal-organic decomposition (MOD) method [1] have been studied. The Bi:YIG and BIG thin films were prepared on Gd₃Ga₅O₁₂ (100) substrates. After a spin-coating process, the samples were placed in a furnace with pre-annealing temperatures of 450°C and 400°C for 30 minutes and annealed at 750°C and 490°C for 3 hours to crystallize. Spectroscopic ellipsometry and magneto-optical spectroscopy were employed to derive a spectral dependence of permittivity tensor at photon energy range from 0.6 to 5 eV. Magneto-optical spectra displayed spectral features typical for Bi substituted garnets [2] reflecting fully developed garnet structure in all investigated films. At the energy range of 3.2–5 eV, Bi:YIG film showed higher amplitude of Kerr rotation than BIG, which is opposite to Faraday rotation measurements at the energy range 1.7–3.1 eV. This can be explained by higher surface roughness of BIG film according to atomic force microscopy measurements. Presented results showed high quality of investigated Bi:YIG films which demonstrates MOD as an effective technique to prepare highly substituted garnet films suitable for MO applications.

[1] T. Kosaka, et al., *J. Magn. Soc. Jpn.*, 35, 194-198 (2011). [2] S.Wetchoek, et al., *Phys. Rev. B*, 12, 2777-2788 (1975).

KD04

Fabrication of the epitaxial growth of (100) and (110) oriented Heusler alloy films for magnetic damping measurement.

Augustin Lutondo Kwilu, Mikiko Oogane, Hiroshi Naganuma and Yasuo Ando
Department of Applied Physics, Tohoku University, Japan

It has been reported [1] that the critical current density of MRAM is proportional to the damping parameter. Various investigations have reported a small damping parameter on the half metallic heusler alloy but the mechanism of magnetic damping is not yet clarified [2]. The present work aims at fabricating the epitaxial growth films for the damping measurement. Thus, Cr/Co₂MnSi/Ru and Ta/Cr/ Co₂MnSi/ Ta films were fabricated by sputtering respectively on MgO (100) substrate and on a-sapphire substrate at annealing temperatures ranging from 350 to 5500C. The pole figure analysis of the fabricated films show an epitaxial growth of Co₂MnSi layer on MgO (100) and a-sapphire substrate. We thus, have successfully fabricated (100) and (110) oriented Heusler alloy films. The films contain also L21 order structure. In addition, the FMR and the VSM measurements were conducted in order to investigate the magnetic properties of those films. The line widths of ferromagnetic resonance spectrum depend on the annealing temperature of Co₂MnSi layer. Those measurements displayed optimal conditions (a high Magnetization and a small damping constant) for the sample with Co₂MnSi layer annealed at 4500C. The samples will have Co₂MnSi layer annealed at 450 0C for further investigations.

[1] D. Kim et al. *Applied physics letter*99, 072502(2011) [2] Mizukami et al. *Journal of Magnetism and Materials* 226-230(2001) 1640-1642

KE01

Thermalised and frozen magnetization dynamics in artificial spin ice

Jason Morgan¹, Zoe Budnikis², Johanna Akerman³, Aaron Stein⁴, Paolo Politi⁵, Sean Langridge⁶, Robert Stamps⁷ and Christopher Marrows^{8*}

¹ School of Physics and Astronomy, University of Leeds, United Kingdom
² School of Physics, University of Western Australia, Australia
³ ISOM, Universidad Politecnica Madrid, Spain
⁴ Center for Functional Nanomaterials, Brookhaven National Laboratory, USA
⁵ Istituto dei Sistemi Complessi, CNR, Italy
⁶ ISIS, STFC Rutherford Appleton Laboratory, United Kingdom
⁷ SUPA School of Physics and Astronomy, University of Glasgow, United Kingdom

Spin ices are rare earth pyrochlores where the crystal geometry leads to frustration of the rare earth moments [1], which meet at tetrahedra in the lattice. Nanotechnology allows many of the essential features of this physical system can be reproduced in arrays of nanomagnets [2]. This approach offers the opportunity to continuously tune the various parameters controlling the magnetic microstate, and also to inspect that microstate using advanced magnetic microscopy [3,4]. A significant difference with the naturally occurring spin-ices is that the change in symmetry gives rise to a true long-range ordered ground state, although the frustrated interactions in these athermal systems mean that its observation is extremely difficult [5]. Most attempts to achieve it rely on a rotating field demagnetisation protocol that produces states that show reasonably good ice rule fidelity but only short range correlations [2,5]. Here I will describe our recent work on an array of 250 nm × 80 nm Permalloy islands in the square ice geometry, including the achievement of a thermalised ground state during fabrication and the observation of the effects of fractionalised monopoles on excitations out of it [6], and athermal achievement of the ground state using a suitable field protocol [7].

[1] S. T. Bramwell and M. J. P. Gingras, *Science* 294, 1495 (2001). [2] R. F. Wang et al., *Nature* 439, 303 (2006). [3] S. Ludak et al., *Nature Physics* 6, 359 (2010). [4] E. Mengotti et al., *Nature Physics* 7, 69 (2011). [5] X. Ke et al., *Phys. Rev. Lett.* 101, 037205 (2008). [6] J. P. Morgan, A. Stein, S. Langridge, and C. H. Marrows, *Nature Physics* 7, 75 (2011). [7] Z. Budnikis, J. P. Morgan, J. Akerman, A. Stein, R. L. Stamps, P. Politi, S. Langridge, and C. H. Marrows, arXiv:1111.6491v1 [cond-mat.mes-hall].

KE02

Towards fully 3-dimensional MRAM

Russell Cowburn
Cavendish Laboratory, University of Cambridge, United Kingdom

Spintronics could have a revolutionary impact on microelectronics and data storage if it provides the enabling step for transforming today's planar 2-dimensional devices into volume-filling 3-dimensional devices, where the data storage and processing capacity are related to the minimum feature size of the fabrication process, F, by F⁻³ instead of F⁻². Recently, we proposed a new approach to 3-dimensional spintronics in which topological kink solitons in multi-layered magnetic nanostructures are used to code and move data. Such solitons can be extremely stable at room temperature, highly compact, and easily injected, detected and synchronously propagated. As such, they are interesting candidates for use in ultrahigh density 3-dimensional MRAM devices. During this talk I will show the first experimental demonstration of a vertical shift register based on this principle and operating at room temperature. Eleven perpendicularly magnetised CoFeB layers coupled by Ru interlayers allow solitons coding binary '0' and '1' to be injected into the bottom layer and then propagated during eight successive clock edges up the stack, eventually exiting at the top layer.

KE03

Spin-transfer-torques-induced domain-wall motion in ferromagnetic Pt/Co/Pt nanowires with perpendicular magnetic anisotropy

Kab-jin Kim¹, Jae-chul Lee¹, Jisu Ryu², Kyoung-woong Moon¹, Sang-jun Yun¹, Kyung-ho Shin³, Hyun-woo Lee² and Sug-bong Choe^{1*}

¹ Department of Physics, Seoul National University, Korea
² Department of Physics, POSTECH, Korea
³ KIST, Korea

The spin-current-based electric controllability of ferromagnetic domain walls (DWs) has been of great interest because of its feasible applications. In particular, nanowires with perpendicular magnetic anisotropy have been predicted as more suitable materials for practical applications. However, the experimental verification with multiple DWs control in such materials has not been explored yet. And also, the physical driving mechanism resulting from the competition between the spin transfer torques (STTs) adiabatic and nonadiabatic STTs and disorders is still controversial. By using Pt/Co/Pt nanowires, here we experimentally demonstrate that the purely current driven multiple DWs motion can be obtained at current densities less than 10⁷ A/cm², allowing random magnetic bits recording and transferring. Furthermore, based on the DWs motion driven by magnetic field and/or current, we can unambiguously distinguish the role of STTs on thermally activated magnetic domain wall motion. The adiabatic STT resulting in quadratic contribution to effective field is found to be dominant for large current densities, whereas the nonadiabatic STT playing the same role as magnetic field subsisted at low current densities. This finding will provide a step to the complete understanding of STT induced DW dynamics as well as the technological progress in DW based emerging nanodevices.

[1] K.-J. Kim et al., *Appl. Phys. Express* 3, 083001 (2010). [2] J.-C. Lee et al., *Phys. Rev. Lett.* 107, 067201 (2011). [3] K.-J. Kim et al., *Phys. Rev. Lett.* 47, 217205 (2011).

KF01

Non-linear dynamics and high RF detection sensitivity in MgO-based spin-torque diode

Yoshishige Suzuki¹, Shinji Miwa¹, Shota Ishibashi¹, Hiroyuki Tomita¹, Takayuki Nozaki², Eiichi Tamura¹, Ken Ando¹, Takeshi Saruya², Hitoshi Kubota², Kay Yakushiji², Akio Fukushima² and Shinji Yuasa²

¹ Graduate School of Engineering Science, Osaka University, Japan
² Spintronics Research Center, National Institute of Advanced Industrial Science and Technology (AIST), Japan

In the emerging field of 'spintronics', two electron attributes, namely, charge and spin, are simultaneously manipulated to obtain new, desirable characteristics, such as large magnetoresistance, spin-transfer induced magnetization switching, and precession in magnetic nano-materials. In 2005, a phenomenon called the spin-torque diode effect [1] was demonstrated, which enabled the rectification of RF signals in magnetic tunnel junctions (MTJs); the rectification output, however, was several thousand times smaller than that of semiconductor diode detectors. Many efforts, such as the control of magnetic field direction [2,3] and the use of stochastic resonance [4], have significantly enhanced the sensitivity; nevertheless, the sensitivity of MTJs remain far lower than that of semiconductor diode detectors. In this study, we show that applying a DC bias current to MTJs while precisely controlling their magnetic potential profiles provides a high RF detection sensitivity of 12,000 V/W at room temperature, which exceeds that of semiconductor diode detectors (3,800 V/W). Analysis based on a macro-spin model reveals that this increase is caused by rotation of the precession axis that depends on RF input power. This rotation, a type of non-linear ferromagnetic resonance, causes a change in resistance and affords the high sensitivity.

[1] A. A. Tulapurkar, Y. Suzuki et al., *Nature* 438, 339 (2005). [2] C. Wang et al., *J. Appl. Phys.* 106, 053905 (2009). [3] S. Ishibashi, Y. Suzuki et al., *IEEE Trans Magn.* 47, 3373 (2011). [4] X. Cheng et al., *Phys. Rev. Lett.* 105, 047202 (2010).

KF02

Finite tunnel magnetoresistance in junctions with a zero magnetization ferromagnetic electrode

Karine Dumesnil*, Mathias Bersweiler, Mathieu Da Silva, Catherine Dufour, Michel Hehn, Daniel Lacour and Francois Montaigne
Institut Jean Lamour - Lorraine University, France



KF03

Effects of mechanical rotation and vibration on spin currents

Mamoru Matsuo*, Jun'ichi Ieda, Eiji Saitoh and Sadamichi Maekawa
Advanced Science Reserch Center, Japan Atomic Energy Agency, Japan

In the frontier of spintronics, much attention is paid on the control of spin currents. Due to the recent progress of nanoelectromechanics, mechanical manipulation of spins increases its importance. We discuss theoretically the generation of spin currents in both rotationally and linearly accelerating systems. The spin-orbit interaction argued by inertial effects is derived from the low energy limit of the generally covariant Dirac equation. It is shown that the spin-orbit interaction is responsible for the generation of spin currents by mechanical rotation and vibration. We also investigate SU(2) x U(1) gauge theory in accelerating systems, which allows us to extend the spintronic theory in inertial frame to non-inertial frames.

M. Matsuo, J. Ieda, E. Saitoh, and S. Maekawa, *Physical Review Letters* 106, 076601 (2011); *Applied Physics Letters* 98, 242501 (2011); *Physical Review B* 84, 104410 (2011).

KF04

Design of self-organized nanostructures to achieve high blocking temperatures in MgO-based d⁰ ferromagnets

Masayoshi Seike^{1*}, Tetsuya Fukushima², Kazunori Sato² and Hiroshi Katayama-yoshida²

¹ Grad. School of Eng. Sci., Osaka Univ. and Cent. Research Labs., Sysmex Corp., Japan
² Grad. School of Eng. Sci., Osaka Univ., Japan

d⁰ ferromagnetism, a new class of magnetism wherein the ferromagnets contain no magnetic elements, has created significant interest in the field of dilute magnetic semiconductors [1]. In this study, we present a materials design of MgO-based d⁰ ferromagnets with high blocking temperature (T_b) based on multi-scale simulations [2-4]. Chemical pair interactions between N atoms in Mg(O,N) and V_{Mg} in (Mg,V_{Mg})O were calculated using a generalized gradient approximation and the VASP code. Using the Ising model, Monte Carlo simulations of the crystal growth were performed to predict the configurations of dopant distribution. In Mg(O,N), a strong attractive interaction was found between the 1st and 4th nearest neighbors (NN) in which the 1st-NN interaction is approximately twice as strong as the 4th-NN interaction. In (Mg,V_{Mg})O, a strong attractive interaction only occurs between the 2nd NN. Our simulation showed that self-organized nanostructures can be formed both in Mg(O,N) and (Mg,V_{Mg})O under layer-by-layer crystal growth, suggesting that these d⁰ ferromagnets can obtain high T_b due to superparamagnetic blocking. Furthermore, depending on the simulation condition corresponding to the interval time between layers in deposition, various self-organized nanostructures can form, such as quasi-one-dimensional nanowires, two-dimensional nanoplates and three-dimensional nanoclusters.

[1] H. Yoshida, et al., P2006-510484 (registered in 2011). [2] M. Seike, et al. *Jpn. J. Appl. Phys.* 50, 090204 (2011). [3] M. Seike, et al. *Physica B* (in press). [4] K. Sato, et al. *Rev. Mod. Phys.* 82, 1633 (2010).

KF05

Negative spin-polarization of Fe₂N observed by spin-resolved photoemission spectroscopy

Keita Ito¹, Kazunori Haraeda¹, Tatsunori Sanai¹, Kaoru Toko¹, Kazuaki Okamoto², Shigenori Ueda³, Yoji Imai⁴, Koji Miyamoto⁵, Taichi Okuda⁵, Akio Kimura² and Takashi Suemasu¹

¹ Institute of Applied Physics, University of Tsukuba, Japan
² Graduate School of Science, Hiroshima University, Japan
³ Synchrotron X-ray Station at SPring-8, NIMS, Japan
⁴ AIST, Japan
⁵ HSRC, Hiroshima University, Japan

Ferromagnetic (Co,Fe)₂N has attracted a growing interest for application to spintronics devices because the large negative spin polarization at the Fermi level (EF) is expected. However, there have been no experimental reports confirming negative spin-polarization in (Co,Fe)₂N by photoemission spectroscopy. In this study, we investigate the valence band (VB) electronic band structure and spin-polarization of Fe₂N using hard x-ray photoemission spectroscopy (HX-PES) and spin resolved photoemission spectroscopy (SRPES) at room temperature. CaF₂(1 nm)/Fe₂N(5 nm) layered structure was epitaxially grown on SrTiO₃(001) by molecular beam epitaxy. We measured VB structure of the Fe₂N layer using HX-PES (hv = 5953 eV) at BL15XU of SPring-8, and compared the obtained spectrum with the calculated photoemission spectrum. After removing the CaF₂ capping layer by Ar ion sputtering, we measured spin resolved density of states (DOS) below EF of the Fe₂N using SRPES (hv = 21.2 eV) at HISOR, Hiroshima University. The peak position of measured Fe 3d electron photoemission spectrum by HX-PES was well explained by the theoretical DOS. We deduced spin-polarization from the obtained SRPES spectrum by eliminating the background signals of secondary electrons caused by He II resonance line (hv = 40.8 eV), and confirmed negative spin-polarization at EF in Fe₂N.

KG01

Hidden order pseudogap and hybridization modulation in URu₂Si₂

Alexander Balatsky¹, Jason Haraldsen¹, Yoni Dubi², Jian Xin Zhu³, Peter Wolfle⁴ and Matthias Graf⁴
¹ Center for Integrated Nanotechnologies, LANL, USA
² Center for Integrated Nanotechnologies, LANL, Israel
³ Theory division, LANL, USA
⁴ Institute for Theory of Condensed Matter and Center for Functional Nanostructures, Karlsruhe Germany, Germany

A. Balatsky (Los Alamos) URu₂Si₂ proved to be a compound that has exhibited similarities with other correlated materials like HighTc oxides in that it has strong correlations, competing phases and intense nanoscale inhomogeneity in Kondo lattice. We point out that Hidden order transition is not a mean field transition, in contrast to prevailing discussion to date. It has significant precursor effects, so called pseudogap. Through an analysis and modeling of data from various experimental techniques, we present evidence for the presence of a hidden order pseudogap in URu₂Si₂ in the temperature range between 25 K and 17.5 K. We evaluate the effects that gap fluctuations would produce on observables like tunneling conductance, neutron scattering and nuclear resonance, and relate them to the experimental findings. We show that the transition into hidden order phase is preceded by the onset of non-coherent hidden order fluctuations. We also discuss nanoscale inhomogeneity seen in URu₂Si₂ with STM as an evidence for hybridization modulation due to local defects and discuss the role of hybridization modulations in Hidden Order.

Hidden order pseudogap in URu₂Si₂, J. Haraldsen, 10.1103/PhysRevB.84.214410 (2011) Electronic inhomogeneity in a Kondo lattice, E. Bauer et al. PNAS 108, 6857 (2011) How Kondo Holes Create Intense Nanoscale Heavy-Fermion Hybridization Disorder.PNAS 2011 108 (45) 18233-18237; published ahead of print October 17, 2011. doi:10.1073/pnas.1115027108 Anomalous femtosecond quasiparticle dynamics of hidden order state in URu₂Si₂ Georgi L. Dakovski et al. Phys. Rev. B 84, 161103 (2011) Hybridization Wave as the "Hidden Order" in URu₂Si₂, Y. Dubi et al. Phys. Rev. Lett. 106, 086401 (2011) Incommensurate spin resonance in URu₂Si₂, A. V. Balatsky, et al. Phys. Rev. B 79, 214413

KG02

Strain-effect on topological quantum phase transition in Ir-oxides

Jaeyun Yu
Department of Physics and Astronomy and CSCMR, Seoul National University, Korea

We predict that a three-dimensional strong topological insulator (TI) phase can be realized by controlling the electron hopping terms in Na₂IrO₃. From a realistic tight-binding Hamiltonian, constructed from the results of first-principle calculations, we identified the crucial parameters of the effective low-energy Hamiltonian, which determine the topological nature of the spin-orbit coupled ground state. We present a phase diagram exhibiting a quantum phase transition from normal-to-topological insulators in terms of the spin-orbit coupling strength and the hopping parameter. The existence of the TI phase has also been verified by the parity analysis from the first-principles calculations with a modified crystal structure corresponding to the predicted tight-binding parameters. We clarified that the topological nature of the Na₂IrO₃ band structure is sensitive to the structural variation. The long-range hopping and trigonal crystal field play a crucial role in addition to the strong spin-orbit coupling in Na₂IrO₃. The TI phase realized in Na₂IrO₃ can be a "good" playground for the study of the interplay between spin-orbit coupling and on-site Coulomb interaction.

This work was done in collaboration with Choong H. Kim, Heung-Sik Kim, Hognyun Jeong, and Hosub Jin and supported by the NRF through the ARP (R17-2008-033-01000-0).

KG03

Hollandites - theoretical aspects of their unique electronic properties

Tatsuya Toriyama¹, Masayuki Watanabe¹, Takehisa Konishi² and Yukinori Ohta^{1*}
¹ Department of Physics, Chiba University, Japan
² Graduate School of Advanced Integration Science, Chiba University, Japan

Density-functional-theory-based electronic structure calculations are made to clarify the mechanisms of the observed anomalous electronic properties in transition-metal oxides with hollandite-type crystal structure. We first discuss some general aspects of the electronic structures of the 3d and 4d series of hollandites, focusing on the validity and insufficiency of the rigid-band filling of electrons in the series. Then, we in particular discuss (i) the Peierls mechanism of the metal-insulator transition in ferromagnetic hollandite K₂Cr₃O₁₆ [1], (ii) superatomic-crystal-type electronic structure emerging in molybdenum hollandites K₂Mo₃O₁₆ and Rb_{1-x}Mo₃O₁₆ [2], and (iii) Tomonaga-Luttinger-liquid properties emerging in ruthenium hollandite K₂Ru₃O₁₆ [3]. We also consider the essential role of electron correlations played in the metal-insulator transition of vanadium hollandite K₂V₃O₁₆.

[1] T. Toriyama et al., *Phys. Rev. Lett.* 107, 266402 (2011). [2] M. Watanabe et al., unpublished. [3] T. Toriyama et al., *Phys. Rev. B* 83, 195101 (2011).

KG04

Inter-band pairing and inhomogeneous superconductivity in multi-orbital systems

Mucio A. Continentino¹ and Heron Caldas²
¹ *Theory, Centro Brasileiro de Pesquisas Físicas, Brazil*
² *Physics, Universidade Federal de S. J. del Rei, Brazil*

In multi-band systems, electrons from different orbitals coexist at a common Fermi surface. An attractive interaction among these quasi-particles gives rise to inter-band or hybrid pairs, which eventually condense in a superconducting state. These quasi-particles have a natural mismatch of their Fermi wave-vectors, δk_F which depends on the strength of the hybridization between their orbitals. The existence of this natural scale leads us to consider the possibility of inhomogeneous superconducting ground states in these systems, even in the absence of an applied magnetic field. Furthermore, since hybridization V depends on pressure, this provides an external parameter to control the wave-vectors mismatch at the Fermi surface. In this work, we study the zero temperature phase diagram of a two-dimensional, two-band superconductor with inter-band pairing. We show that as the mismatch between the Fermi wave-vectors of the two-bands is reduced, the system presents a normal-to-inhomogeneous superconductor quantum phase transition of unusual character at a critical value of the hybridization, $V_c = \Delta_0$, below which the system condenses in pair-wave superconducting state characterized by a wave-vector $q_c = \Delta_0/v_f$ (Δ_0 is the homogeneous superconducting gap and v_f the Fermi velocity).

KH01

High performance permanent magnets for energy applications

Oliver Gutfleisch¹, Tom G Woodcock², Simon Sawatzki², Konrad Lowe² and Konrad Guth²
¹ *Material Science, TU Darmstadt, Germany*
² *IFW Dresden, Germany*

A new energy paradigm, consisting of greater reliance on renewable energy sources and increased concern for energy efficiency in the total energy lifecycle, has accelerated research in energy-related technologies. Due to their ubiquity, magnetic materials play an important role in improving the efficiency and performance of devices in electric power generation, conversion and transportation. Magnetic materials are essential components of energy applications (i.e. motors, generators, transformers, actuators, etc.) and improvements in magnetic materials will have significant impact in this area, on par with many “hot” energy materials efforts. The lecture focuses on the synthesis, characterization, and property evaluation of high performance permanent magnets. Using multi-scale characterization and modeling the structure-property relationships will be examined. Options for the development of novel resource efficient magnets will be discussed in the context of drastically reducing the rare-earth contents or developing rare earth free magnets. Finally, considering future bottle-necks in raw materials and in the supply chain, options for recycling of rare-earth metals will be analyzed.

O. Gutfleisch, J.P. Liu, M. Willard, E. Bruck, C. Chen, S.G. Shankar, Magnetic Materials and Devices for the 21st Century: Stronger, Lighter, and More Energy Efficient (review), Adv. Mat. 23 (2011) 821-842.

KH02

Influence of surface anisotropy on orientation of crystal grain in rare-earth permanent magnet

Chiharu Mitsumata*, Hiroki Tsuchiura and Akimasa Sakuma
Tohoku University, Japan

The coercive force of Rare-Earth permanent magnets has been investigated. In general, the nucleation and the domain wall pinning are discussed to understand the magnetization reversal process [1]. However, the large discrepancy between the ideal anisotropy field (Hk) and the coercivity (Hc) still remains in an unsolved problem of the permanent magnet. Recently, we proposed the possible mechanism of the reduction for Hc in NdFeB system, that was realized owing to the negative anisotropy of the rare-earth ion at the surface of a crystalline [2, 3]. In this paper, we discuss the influence of the surface anisotropy on the mis-orientation of the crystal grain in the permanent magnets. In the case of simultaneous rotation of the magnetization, the steep reduction of Hc is obtained when the angle between the direction of external applied field and the magnetic easy axis increases. For comparing the ideal simultaneous rotation, we assume the polycrystalline magnet in which the surface anisotropy effects on the crystal grains. As the result, the surface anisotropy causes the large reduction of Hc from Hk, however, a tolerance of Hc reduction against the mis-orientation of crystal grains becomes promising.

[1] H. Kronmüller, K.-D. Durst and M. Sagawa, *J. Magn. Magn. Mater.*, 74 (1988) 291. [2] C. Mitsumata, H. Tsuchiura and A. Sakuma, *Appl. Phys. Express*, 4 (2011) 113002. [3] H. Moriya, H. Tsuchiura and A. Sakuma, *J. Appl. Phys.*, 105 (2009) 07A70.

KH03

International comparison of the properties of permanent magnets measured using an electromagnet and a pulse field magnetometer

Michael Hall
National Physical Laboratory, United Kingdom

An IEC TC 68 comparison on the measurement of the magnetic properties of permanent magnets was recently completed. With permanent magnets being used in safety critical situations it is necessary to perform 100% quality control at the operating temperature. An established method using an electromagnetic to measure the demagnetising curve is not practical for these measurements due to the time taken, the difficulty in raising the temperature and the operator skill required. A Pulsed Field Magnetometer (PFM) has been developed that can determine the full BH curve in as little as 100 ms. By comparing measurement made using electromagnet and pulse methods, the influence of the dynamic effects of the latter could be established. It was found that for the technology significant parameter of intrinsic coercivity a significant difference exist between the methods. The talk will present the results from measurements on 6 NdFeB magnets with intrinsic coercivities ranging from 1000 to 2600 kA/m by 8 institutes based in China, Japan, Italy, Belgium, Germany and the UK. For the electromagnet method, the Influence of local pole piece saturation on the measurement of the intrinsic coercivity will be discussed.

KH04

Ab initio calculations of magnetic moment and magneto-crystalline anisotropy: New ternary alloy Mn-Bi-Co permanent magnet

Yang-ki Hong^{1*}, Jihoon Park¹, Oleg N Mryasov², Jaejin Lee¹, Seong-gon Kim³, Sungho Kim³, Chul-jin Choi⁴ and Jung-goo Lee⁴
¹ *Department of Electrical and Computer Engineering and MINT Center, The University of Alabama, USA*
² *Physics and Astronomy and MINT Center, The University of Alabama, USA*
³ *Department of Physics & Astronomy and Center for Computational Sciences, Mississippi State University, USA*
⁴ *Korea Institute of Materials Science, Korea*

There are two important issues to address for full utilization of permanent magnets in electric vehicle, windmill generator, and other motors. One is a technical issue such as low operation temperature of permanent magnet, and the other is rare-earth metal source and price. Rare-earth permanent magnets, including Nd₂Fe₁₄B and Dy-doped Nd₂Fe₁₄B, Sm₂Co₁₇, and Sm₂Fe₁₇N₃, have been used for motors for hybrid vehicle and electric vehicle. The Nd₂Fe₁₄B possesses 60 MGOe of the highest maximum energy product (BH)_{max}. All these permanent magnets contain rare-earth metals. Therefore, in order to address the second issue, we have proposed rare-earth-free Mn-Bi-Co ternary alloy and performed first principles calculations to investigate the effects of the alloying element Co on magnetic properties of conventional Mn-Bi binary alloy magnet. Our calculations predict that an addition of Co to the Mn-Bi magnet will likely to increase the magneto-crystalline anisotropy by more than 300%, while the saturation magnetization will be increased by 20%. Accordingly, it is predicted that the (BH)_{max} increases to 21 MGOe from 17 MGOe of the Mn-Bi permanent magnet. The proposed Mn-Bi-Co magnet exhibits a much higher maximum energy product than the conventional Mn-Bi magnet. Experimental verification of these results is in progress.

KI01

First-principles prediction of large perpendicular magnetocrystalline anisotropy of 4d-monolayers on bcc-Fe(001) surface

Dorj Odkhuu, Tumurbaatar Tselvelmaa, Won Seok Yun, Oryong Kwon, Bharat Kumar Sharma and Soon Cheol Hong*
Department of Physics, University of Ulsan, Korea

Using the highly precise full-potential linearized augmented plane-wave method based on general gradient approximation, we investigated the magnetism and magnetocrystalline anisotropy energy (E_{MCA}) of 4d Ru, Rh, and Pd monolayers (MLs) on a bcc-Fe(001) surface. Coupling with Fe ferromagnetically, the Ru, Rh, and Pd monolayers are induced to have the magnetic moments of 0.43, 0.92, and 0.36 μ_B , respectively, in consistent with experimental [1,2] and previous theoretical results [3]. The calculated magnetic moments of Fe at the interface are significantly enhanced 2.8 μ_B for Rh and 2.92 μ_B for Pd, compared to the bulk bcc-Fe value, but Ru makes the Fe atoms to retain the bulk value (2.2 μ_B). We predict that the Ru and Rh MLs have the perpendicular huge E_{MCA} of 2.2 and 3.0 meV/atom, whereas the Pd ML has the in-plane E_{MCA} of -0.2 meV/atom. The huge positive E_{MCA}s with induced magnetic moments of the Ru and Rh MLs on a Fe(001) surface are expected to be promising in application to devices such as high-density magnetic recording media and random access memory. The electronic origins of the induced magnetism and E_{MCA} will be discussed with the density of states.

[1] K. Tørlund, P. Fuchs, J. C. Groth, and M. Landolt, *Phys. Rev. Lett.* 70, 2487 (1993). [2] Z. Celinski, B. Heinrich, J. F. Cochran, W. B. Muir, A. S. Arrott, and J. Kirschner, *Phys. Rev. Lett.* 65, 1156 (1990). [3] L. Zhong and A. J. Freeman, *J. Appl. Phys.* 81, (1997).

KI02

Ferromagnetic phase at the LaAlO₃/SrTiO₃ (001) interface induced by SrTiO₃ lattice deformation

Jichao C Li and Carmen Munoz*
ICMM- Consejo Superior de Investigaciones Científicas, Spain

We address the origin of the ferromagnetic phase formed at the LaO/TiO₂ interface in LaAlO₃/SrTiO₃ (001) heterostructures [1]. Using first-principles density functional calculations we show that the charge transfer to the Ti t_{2g} conduction band, induced by the polar mismatch at the interface, combined with the incipient ferroelectric character of the SrTiO₃, lead to a substantial lattice deformation. The ferroelectric-like distortion of the SrTiO₃ slab generates the spontaneous spin-polarization of the lowest dxy orbital parallel to the interface and the emergence of a ferromagnetic ground state. Moreover, it yields differential occupation of the non-degenerated dxy and degenerated dxz-yz orbital states. We predict the existence of three different types of electrons, magnetic two-dimensional (2D) dxy electrons and non-magnetic higher-lying dxy and dxz-yz quasi-2D electrons. While the former, with a 2D-light effective mass (m*), are confined to the TiO₂ interface plane, the non-spin polarized higher-lying dxy, also with a light m*, and the Bloch dxz-yz electrons spread over several SrTiO₃ layers. Their differences could explain the coexistence in the same sample of superconductivity and magnetism [2-5]. Furthermore, since ferroelectric distortions and orbital magnetism are coupled, the magnetic state can be controlled by an electric field.

[1] A. Brinkman, M. Huijben, M. van Zalk, J. Huijben, et al., *Nature Materials* 6, 493 (2007). [2] Ariando, X. Wang, G. Baskaran, Z. Q. Liu, et al., *Nature Communications* 2, 188 (2011). [3] D. A. Dikin, M. Mehta, C. W. Bark, C. M. Folkman, et al., *Phys. Rev. Lett.* 107 (2011). [4] L. Li, C. Richter, J. Mannhart, and R. C. Ashoori, *Nature Physics* 7, 762 (2011). [5] J. A. Bert, B. Kalisky, C. Bell, M. Kim, et al., *Nature Physics* 7, 767 (2011).

KI03

Interfacial magnetic anisotropy of junctions between Fe and transition-metal nitrides or carbides: A first-principles study

Masahito Tsujikawa¹, Miura Yoshio² and Masafumi Shirai³
¹ *CSIS, Tohoku University, Japan*
² *RIEC and CSIS, Tohoku University, Japan*
³ *RIEC and CSIS, Tohoku University, Japan*

Recently, CoFeB/MgO-based perpendicular magnetic tunnel junctions (MTJ) with high thermal stability have been fabricated[1]. For further reduction of MTJ size, larger perpendicular magnetic anisotropy (PMA) is required. In the MgO/Fe(001) interface, the hybridization between O-2p and Fe-3d orbital decreases the in-plane magnetic anisotropy (IMA) component. This effect is also expected for Fe/nitride(carbide) interfaces. In order to design large PMA film, we investigated magnetic anisotropy of Fe(001) and NaCl-type transition-metal nitride(carbide) interfaces (Fe/MN(C): M=Sc, Ti, V, Cr, Zr, Nb, Hf, and Ta) by using a first-principles density-functional calculations. Large PMA energy is obtained for the Fe/ScN (1.21 mJ/m²) and Fe/ScC (0.89 mJ/m²) film. The origin of PMA component of these films is attributed to the surface PMA of Fe(001) (0.60 mJ/m²). In other films, weak PMA or IMA is obtained due to the reduction of PMA component caused by the strong hybridization between interfacial Fe-3d and transition-metal-d orbitals. We also discuss the influence of boron atoms at the interfaces. This work was supported by JSPS though the FIRST Program initiated by the CSTP and a Grant-in-Aid for Scientific Research (Grant No. 22360014) from JSPS.

[1] S. Ikeda et al., *Nature Mater.* 9, 721 (2010).

KI04

Enhancement of exchange coupling by incoherent quantum resonance

Ching Hao Chang
National Tsing Hua University, Taiwan

By simulating the nanoscale Fe/Ag/Fe trilayer in the quantum well potential, the coupling strength is found to oscillate with Fe thickness. This is generated by the competition between quantum interferences for majority carriers in ferromagnetic configuration and for carriers in anti-ferromagnetic configuration. Furthermore, we fix the Fe side-layer thickness and study the coupling as the function of spacer width. The strength oscillates with the period determined by quantum well states of minority carriers in ferromagnetic configuration while the amplitude decided by this competition of interferences. This amplitude can be enhanced almost one time by choosing the proper side-layer thickness that satisfies (1) the conditions for incoherent quantum interferences and (2) much thinner than the spacer width.

KI05

Scrolling effects in vanadium oxide nanotubes and nanolayers

Sergey Demishev^{1*}, Alexey Chernobrovkin¹, Vladimir Glushkov¹, Nickolay Sluchanko¹, Nickolay Samarin¹, Alexey Semeno¹, Anastasiya Grigorjeva², Evgenii Goodilin², Hitoshi Ohta³, S. Okubo³, M. Fujisawa³ and T. Sakurai³
¹ *Low Temperatures and Cryogenic Engineering, General Physics Institute of RAS, Russia*
² *Faculty of Materials Sciences, Moscow State University, Moscow, 119991 Russia*
³ *Molecular Photoscience Research Center, Kobe University, 1-1 Rokkodai, Nada, Kobe 657-8501, Japan*

The comparative analysis of the ESR together with the magnetic susceptibility data [1] has allowed elucidating effects of scrolling the VO_x nanolayers, NLs, (stacks of 4 to 8 distorted layers of vanadium oxide separated by an organic template) into VO_x nanotubes, NTs. First, scrolling leads to formation of the antiferromagnetic dimers consisting of almost half of the vanadium ions with a spin gap near 720 K. The second effect, specific to NTs, is the correlated change in the Curie constant for the nondimerized V⁴⁺ quasifree spins and in variations of the background formed by Van Vleck and Pauli terms: the decreasing temperature in the interval 70<T<120K induces an initial 1.8-fold growth of the Curie constant followed by a decrease, along with a change of the sign of the background. Third, it is found that scrolling results in reduction of the quasifree electron concentration in the VO_x plane by a factor of 2-4. It is found that the number of electrons in the V⁴⁺ state is always less than the total electron concentration, and the concentration of the “excessive” electrons may vary in the range 0.11-0.46 per vanadium site.

S.I.V.Demishev et al., Phys. Rev. B 84, 094426 (2011)

KJ01

THz Emission from High-T_c Superconductor Bi₂Sr₂CaCu₂O_{8+x} Intrinsic Josephson Junctions

K. Kadowaki^{1,2}, T. Kashiwagi^{1,2}, M. Tsujimoto^{1,2}, K. Delfanazari^{1,2}, T. Kitamura^{1,2}, M. Sawamura^{1,2}, K. Ishida^{1,2}, S. Sekimoto^{1,2}, C. Watanabe^{1,2}, R. A. Klemm³ and M. Tachiki¹
¹ *Graduate School of Pure and Applied Sciences, University of Tsukuba, Japan*
² *CREST & WPI-MANA, Japan*
³ *Department of Physics, University of Central Florida, USA*

After the discovery of THz emission of radiation from high-T_c superconductor Bi₂Sr₂CaCu₂O_{8+x} in 2007, intensive studies on the mechanism of radiation from high-T_c superconductors have been carried out both theoretically and experimentally. So far, two important ingredients are found for the necessary condition of radiation: One is the ac-Josephson effect working in the individual intrinsic Josephson junction existing in a unit cell of the crystal structure of high-T_c superconductors. This generates the electromagnetic waves at a fixed frequency according to the ac-Josephson effect and the power of the radiation at the frequency can be enhanced by the cavity resonance, which is determined by the geometry of the mesa structure. This mechanism works as a second important mechanism for the radiation. We show experimental results confirming these important ingredients for the emission of radiation. In addition by knowing these mechanisms we intend to extend the power of radiation to nearly 1 mW level by the array of three mesas synchronized together quantum mechanically. We will also show a prototype imaging machine for the applications.

KJ02

Electric field control of magnetization in spiral magnets

Kee Hoon Kim
CeNSCMR, Department of Physics and Astronomy, Seoul National University, Seoul 151-747, Korea

The control of magnetization by an electric field remains as one of great challenges in materials science. Multiferroics, in which magnetism and ferroelectricity coexist and couple to each other, could be the most plausible candidate to realize this long-sought capability. While recent intensive research on the multiferroics has made significant progress in the sensitive magnetoelectric (ME) effects, the electrical control of magnetization, the converse effect, has been observed only in a limited range far below room temperature. Here I will summarize recent developments on how the spiral magnets, particularly based on the hexagonal ferrites, can realize the viable, converse ME effect in a broad temperature range including room temperature. Starting with the chemical aspect of the hexaferrite materials, I discuss the importance of the strong magnetoelectric (ME) coupling to achieve the significant converse ME effect. The three key material parameters, magnetic anisotropy, spin frustration, and spin exchange interaction, will be pointed out. By controlling those key parameters, we demonstrate that the four state magnetization curves can be obtained at room temperature by an electric field. We also show based on the similar mechanism that the magnetization reversal by an electric field can be realized with fast switching time.

Sae Hwan Chun et al., Phys. Rev. Lett. 108, 177201 (2012); *ibid*, 104, 037204 (2010); Y. S. Chai et al., (unpublished).

Oral Friday

Oral Friday

ORAL PRESENTATION

KJ03

Novel Josephson effect in triplet Josephson junctions: The story begins

Dirk Manske

Max Planck Institute for Solid State Research, Germany

In the theoretical study of Josephson junctions, it is usually assumed that the properties of the tunneling barrier are fixed. This assumption breaks down when considering tunneling between two triplet superconductors with misaligned d-vectors in a TFT-junction (triplet ferromagnet triplet) [1,2]. Such a situation breaks time-reversal symmetry, which radically alters the behaviour of the junction, stabilizing it in a fractional state, i.e. the free energy minimum lies at a phase difference intermediate between 0 and π . Fractional flux quanta are then permitted at the junction [3]. A further consequence of the d-vector misalignment is the appearance of a Josephson spin current, which flows even in the absence of an equilibrium charge current. Not only do our calculations enhance the physical understanding of transport through triplet superconductor junctions, but they also open the possibility of novel spintronic Josephson devices [4].

[1] B. Kastening, D.K. Morr, D. Manske, and K.H. Bennemann, *Phys. Rev. Lett.* 96, 047009 (2006)
[2] P. M. R. Brydon, B. Kastening, D. K. Morr and D. Manske, *Phys. Rev. B* 77, 104504 (2008). [3] P.M.R. Brydon, C. Iniotakis, D. Manske, and M. Sigrist, *Phys. Rev. Lett.* 104, 197001 (2010). [4] P.M.R. Brydon and D. Manske, *Phys. Rev. Lett.* 103, 147001 (2009).

KJ04

Field-induced polarization of dirac valleys in bismuth

Zengwei Zhu¹, Aurelie Callaudin¹, Benoit Fauque¹, Woun Kang², Kamran Behnia^{1*} and Yuki Fuseya³

¹ CNRS, France

² Ewha Womans University, Korea

³ Osaka University, Japan

The principal challenge in the field of "valleytronics" is to lift the valley degeneracy of electrons in a controlled way. In bulk semi-metallic bismuth, the Fermi surface includes three cigar-shaped electron valleys lying almost perpendicular to the high-symmetry axis known as the trigonal axis. The in-plane mass anisotropy of each valley exceeds 200 as a consequence of Dirac dispersion, which drastically reduces the effective mass along two out of the three orientations. According to our very recent study of angle-dependent magnetoresistance in bismuth [1], a flow of Dirac electrons along the trigonal axis is extremely sensitive to the orientation of in-plane magnetic field. Thus, a rotatable magnetic field can be used as a valley valve to tune the contribution of each valley to the total conductivity. As a consequence of a unique combination of high mobility and extreme mass anisotropy in bismuth, the effect is visible even at room temperature in a magnetic field of 1 T. At high temperature and low magnetic field, the three valleys are interchangeable and the three-fold symmetry of the underlying lattice is respected. As the temperature is decreased or the magnetic field increased, this symmetry is lost.

1. Z. Zhu, A. Callaudin, B. Fauque, W. Kang and K. Behnia, *Nature Phys.* 8, 89 (2012)



POSTER PRESENTATION

- July 9 (PA~PO) • 116
- July 10 (QA~QP) • 182
- July 12 (RA~RR) • 249
- July 13 (SA~SO) • 316

PA01

Magnetolectric polarization in the field-induced commensurate phase of Y-hexaferrite $Ba_{0.7}Sr_{1.3}Zn_2(Fe_{1-x}Al_x)_{12}O_{22}$
 Hak Bong Lee, Hun Chang, Young Sang Song, Jae-ho Chung
Department of Physics, Korea Univ., Korea

Hexagonal ferrites containing Fe^{3+} ($S = 5/2$) ions are attracting much attention because it is expected that solutions for high-temperature low-field multiferroics can be found in these materials. Y-type $Ba_{0.7}Sr_{1.3}Zn_2Fe_{12}O_{22}$ possesses proper-screw antiferromagnetic order in zero field, which does not allow spin-current ferroelectric polarization. Electric polarization can, however, be induced when a strong external field is applied perpendicular to its c axis. The field-response can greatly be improved upon Al doping, which is ascribed to the formation of conical spin structures. In this work, we investigated the magnetic phase transitions of single crystal $Ba_{0.7}Sr_{1.3}Zn_2(Fe_{1-x}Al_x)_{12}O_{22}$ ($x = 0.04$ & $x = 0.08$) in external magnetic field. Both samples exhibited incommensurate helical antiferromagnetic order in zero-field cooling down to 10 K. When the external magnetic field was applied so that electric polarization was induced, however, the incommensurate order was replaced by a commensurate order in all samples. Our analysis shows that the commensurate order plays the role of breaking inversion symmetry, thereby allowing finite electric polarization. We argue that two different magnetic anisotropies, easy-axis and easy-plane, play an important role in establishing stable field-induced electric polarization in the observed commensurate magnetic phase.

PA02

Temperature- and field-tuning of magnetic phases in multiferroic $NdFe_3(BO_3)_4$
 Christie S. Nelson^{1*}, Leonard N. Bezmaternykh² and Irina A. Gudim²
¹*Photon Sciences Directorate, Brookhaven National Laboratory, USA*
²*L.V. Kirensky Institute of Physics, Siberian Branch of RAS, Russia*

We report the low-temperature coexistence of magnetic phases in $NdFe_3(BO_3)_4$, which is a field-induced multiferroic material. The ground state incommensurate magnetic phase coexists with a strained commensurate magnetic phase that is primarily at the surface of the crystal. Increasing the temperature or magnetic field decreases the incommensurability and stabilizes the commensurate magnetic phase above $T_c \approx 14$ K or $H_c = 0.9$ T. A comparison to published studies indicates the onset of longitudinal magnetostriction and electric polarization at the field-induced transition, which may arise due to a basal plane spin-flop and canting of moments along the field direction. Use of the National Synchrotron Light Source, Brookhaven National Laboratory, was supported by the U.S. Department of Energy, Office of Science, Office of Basic Energy Sciences, under Contract No. DE-AC02-98CH10886.

PA03

Control of magnetic anisotropies for stable electric polarization in multiferroics hexaferrites
 Hun Chang, Hak-bong Lee, Young-sang Song and Jae-ho Chung^{*}
Department of physics, Korea Univ., Korea

Hexaferrites are widely studied for the hopes of realizing multiferroics working at room temperature and under low field. It was shown recently that Al-doping can effectively enhance magnetolectric susceptibility and low-field behaviors of Y-type hexaferrite $Ba_{0.5}Sr_{1.5}Zn_2Fe_{12}O_{22}$. The key for such enhancement has been suspected to be the formation of heliconical spin ordering via reduction of planar anisotropy. Using single crystal neutron diffraction, we investigated in detail the Al-doping dependence of the magnetic phase transitions in $Ba_{0.7}Sr_{1.3}Zn_2(Fe_{1-x}Al_x)_{12}O_{22}$. We confirm that the heliconical phases indeed appear upon Al doping, and finally collapse into commensurate phases at excessive doping concentrations. The observed evolution of magnetic order coincides with the doping dependence of the magnetolectricity previously reported. Analysis of magnetic energy shows, however, that planar anisotropy alone will not allow the heliconical order to stabilize. We argue that it is important to have a competition between easy-axis and easy-plane anisotropies in order to stabilize the heliconical order, and thereby establish the optimum magnetolectric property.

PA04

Chemical control of ferroelectric polarization in $Mn_{1-x}Co_xWO_4$
 Young-sang Song¹, Jae-ho Chung^{1*}, Sung-beak Kim², Jurg Scheffer³, Li Qin Yan⁴, Bumsung Lee⁵, Sae-hwan Chun¹, Kee Hoon Kim¹, A. Nogami³ and T. Katsufuji³
¹*Department of Physics, Korea University, Seoul, 136-713, Korea*
²*Advancement for College Education Center, Konyang University, Chungnam 320-711, Korea*
³*Laboratory for Neutron Scattering, Paul Scherrer Institut, Villigen, Switzerland*
⁴*Department of Physics, Seoul National University, Seoul, 151-742, Korea*
⁵*Department of Physics, Waseda University, Tokyo 169-8555, Japan*

$MnWO_4$ is one of the best known magnetolectric multiferroics, in which ferroelectric polarization appears due to long-range spin order. Whereas it exhibits three different antiferromagnetic phases at low temperatures, ferroelectric polarization along the b axis is observed only in the intermediate phase with an elliptical spiral incommensurate spin structure. In this work, we present the effect of Co doping on the magnetic phase transitions and multiferroic properties of $Mn_{1-x}Co_xWO_4$ using neutron diffraction, magnetization and ferroelectric measurements. The main results include the stabilization of the incommensurate phase at $x \approx 0.03$ and the flop of its spiral plane for $x > 0.05$. Subsequently, the ferroelectric polarization appears mainly along the a axis in this range. These results indicate that the multiferroic properties of $MnWO_4$ can be controlled via Co doping.

PA05

Multiferroic phase competition in orthorhombic $RMnO_3$: Monte Carlo approaches
 Jun-ming Liu^{*}
Department of Physics, Nanjing University, China

For type-II multiferroic oxide compounds, the ferroelectricity is believed to be induced by specific spin orders which can break the spatial inversion symmetry, allowing an electric polarization to respond significantly to external magnetic field. These phenomena have been receiving attentions due to the underlying physics and promising application potentials. Nevertheless, conventional understanding of these multiferroics remains in an early stage since these materials exhibit typical features of strongly correlated electron systems in which the spin, charge, orbit, and phonon degrees of freedom are intrinsically coupled together. So far, rare models other than the Mochizuki-Furukawa (M-F) model specifically addressing orthorhombic $RMnO_3$ are available. In this talk, we present our Monte Carlo simulations on the multiferroic behaviors of orthorhombic $RMnO_3$, based on this model. Our simulations address the phase competition between the ab-plane spiral spin order and bc-plane spiral spin order as well as their coexistence, including the following cases: (1) nonmagnetic Mn-site substitution; (2) R-site substitution; (3) interaction between multiferroic $RMnO_3$ thin films and magnetic substrates. We will further extend our simulation based on the semi-quantum two-orbit double exchange model to the above issues.

PA06

Spin-driven electric polarization in akermanite $Sr_2MSi_2O_7$ crystals
 Mitsuru Akaki^{1*}, Tomoya Tadokoro¹, Takumi Kihara², Masashi Tokunaga² and Hideki Kuwahara¹
¹*Department of Physics, Sophia University, Japan*
²*The Institute for Solid State Physics, The University of Tokyo, Japan*

Since the magnetolectric effect was observed in akermanite $Ca_2CoSi_2O_7$ [1] and $Ba_2CoGe_2O_7$ [2,3], the multiferroicity in these materials has been attracting much attention. The akermanite materials show the magnetic-field-induced electric polarization which can be explained by the transition-metal-ligand (p-d) hybridization depending on the spin direction [4]. The multiferroicity of akermanite materials is, therefore, expected to be influenced by substitution on the transition-metal site. In this study, we have investigated magnetic and dielectric properties of akermanite $Sr_2MSi_2O_7$ (M: transition-metal ion) single crystals. In $Sr_2CoSi_2O_7$, the electric polarization was not observed in a zero magnetic field. By applying the magnetic field along the [110] direction, the electric polarization emerges along the c axis below the magnetic transition temperature. According to the p-d hybridization mechanism, the electric polarization is proportional to the spin quantum number S. However, the induced electric polarization in $Sr_2MnSi_2O_7$ (Mn^{2+} ; $S=5/2$) is almost two orders of magnitude smaller than that of $Sr_2CoSi_2O_7$ (Co^{2+} ; $S=3/2$). These results suggest that the electronic configuration of the transition-metal ion is of crucial importance for the appearance of electric polarization. We will also present and discuss the results of the comparative study of magnetolectric properties in other $Sr_2MSi_2O_7$ crystals.

[1] M. Akaki et al., *Appl. Phys. Lett.* 94, 212904 (2009). [2] H. T. Yi et al., *Appl. Phys. Lett.* 92, 212904 (2008). [3] H. Murakawa et al., *Phys. Rev. Lett.* 105, 137202 (2010). [4] T. Arima, *J. Phys. Soc. Jpn.* 76, 073702 (2007).

PA07

Magnetolectric effects in antiferromagnet $Ba_2CoGe_2O_7$
 Shin Miyahara¹ and Nobuo Furukawa²
¹*JST ERATO-MF, Japan*
²*JST ERATO-MF, Aoyama Gakuin University, Japan*

We have investigated magnetolectric effects in $Ba_2CoGe_2O_7$, which is a quasi two-dimensional antiferromagnet[1]. By applying the external magnetic field along certain directions, electric polarization is induced[2,3]. We consider a spin-dependent d-p hybridization mechanism[4], where the electric polarization couples to a single spin structure via the spin-orbit interaction, and we can explain the novel magnetolectric behaviors in $Ba_2CoGe_2O_7$ [3]. In this compound, it is recently reported that there exist magnetic excitations induced by electric components of electromagnetic wave at THz frequencies[5]. In addition, the magneto-electric excitation in $Ba_2CoGe_2O_7$, accompanies a non-reciprocal linear directional dichroism, where absorption coefficient depends on the direction of the incident electromagnetic wave (+k or -k). We theoretically clarify the origin of the peculiar features in these dynamical magnetolectric phenomena[6]. The non-reciprocal dichroism observed in $Ba_2CoGe_2O_7$, can be explained by cross-correlated effects, i.e., the interference between the magnetic and the electric responses.

[1] A. Zheludev et al., *Phys. Rev. B* 68 024428 (2003). [2] H.T. Yi et al., *Appl. Phys. Lett.* 92 212904 (2008). [3] H. Murakawa et al., *Phys. Rev. Lett.* 105 137202 (2010) [4] T. Arima, *J. Phys. Soc. Jpn.* 76 073702 (2007). [5] I. Keszmerki et al., *Phys. Rev. Lett.* 106 057403 (2011) [6] S. Miyahara and N. Furukawa, *J. Phys. Soc. Jpn* 80 073708 (2011)

PA08

X-ray non-reciprocal effects in multiferroic single crystal of $GaFeO_3$
 Andrei Rogalev^{*}, Fabrice Wilhelm and Alexei Bosak
European Synchrotron Radiation Facility, France

Ferroelectric and ferrimagnetic ordering coexist in gallium ferrate - $GaFeO_3$. The ferroelectric properties of this compound have been extensively studied since early sixties by many different experimental techniques. In order to study these properties on a microscopic level we have measured various X-ray reciprocal and non-reciprocal dichroisms at the Fe K-edge. The results of these experiments carried out at the ESRF beamline ID12 on a high quality untwined single crystal of $GaFeO_3$ are presented here. X-ray magnetochiral dichroism and X-ray non-reciprocal magnetic linear dichroism, which are a direct measure of the Fe orbital anapole and higher order magnetolectric multipole, are disentangled experimentally for the first time. These two dichroic signals are compared to usual X-ray magnetic circular dichroism which is a measure of orbital magnetic moment carried by Fe atoms. Moreover, X-ray natural circular dichroism has been also measured on this biaxial non-enantiomorphous crystal. All these dichroisms are analyzed with the help of a set of the sum rules. This analysis allowed us to deduce the expectation values of different effective operators related to multiferroic properties of $GaFeO_3$.

PA09

NMR study on $Ba_{0.5}Sr_{1.5}Zn_2(Fe_{0.92}Al_{0.08})_{12}O_{22}$
 Sangil Kwon¹, Soonchil Lee^{1*}, Dong Young Yoon¹, Sae Hwan Chun², Yi Sheng Chai², Kee Hoon Kim², Euna Jo¹, Changsoo Kim¹ and Byeongki Kang¹
¹*Department of Physics, Korea Advanced Institute of Science and Technology, Daejeon 305-701, Korea*
²*CeNSCMR, Department of Physics and Astronomy, Seoul National University, Seoul 151-747, Korea*

We did zero-field NMR study on the annealed single crystal of multiferroic helimagnets $Ba_{0.5}Sr_{1.5}Zn_2(Fe_{0.92}Al_{0.08})_{12}O_{22}$ (Al-BSZFO). This material shows extremely high magnetolectric susceptibility so that the critical field for switching electric polarization is less than 1 mT below 90 K [1]. NMR frequency change by the temperature follows Bloch's T^{3/2} law which presents the low temperature excitation is ferromagnetic spin wave. The nuclear spin-lattice relaxation rate and the nuclear spin-spin relaxation rate were also measured. Both increased rapidly as the temperature increases above 60 K at which the spin structure changes from normal longitudinal cones (NLCs) to alternating longitudinal cones (ALCs) for the case of as-grown (not annealed) sample [2]. Due to rapid shortening of spin-spin relaxation time, the NMR signal intensity abruptly reduced above 60 K. We also studied rf pulse width and power dependence and revealed that most of the signal came from the domain walls.

[1] S. H. Chun et al., *Phys. Rev. Lett.* 104, 037204 (2010). [2] H. B. Lee et al., *Phys. Rev. B* 83, 144425 (2011).

PA10

Magnetic ordering in multiferroic $TbFe_xMn_{2-x}O_3$ with $x=0.18$
 Nadir Aliouane¹, Andrey Malyuk² and Dimitri N. Argyriou³
¹*Laboratory for Neutron scattering, Paul Scherrer Institut CH-5232, Villigen-PSI, Switzerland*
²*IFW Dresden, Institute for Solid State Research Helmholtzstr. 20 DE-01069 Dresden, Germany*
³*Swedish Directorate, European Spallation Source ESS AB P.O. Box 176, SE-221 00 Lund, Sweden*

Manganite compounds present a large range of functional properties from colossal magnetoresistor to multiferroic properties. $TbMn_2O_3$ is well known multiferroic materials that exhibit complex magnetic phase transitions [1] and multifunctional properties which are tunable by a magnetic field [2,3]. Below 38K, the long range incommensurate anti-ferromagnetic ordering induces the ferroelectric behavior through either an exchange striction mechanism between neighboring spins wave ($SiSj \neq 0$) [4] or inverse Dzyaloshinskii-Moriya interaction due to cycloidal spin arrangement [5]. All the magnetic properties in these systems are controlled by frustrations. The frustration can be tuned in increasing or decreasing the interactions by substituting Mn^{3+}/Mn^{4+} with Fe^{3+}/Fe^{4+} ($HS, S=5/2$) without structural distortion. Fe doped materials in ceramics sample at similar composition have shown enhancement of Ps. Large single crystals of $TbMn_{2-x}Fe_xO_3$ ($x=0.18$) have been grown by flux method and characterized by (ac and dc) susceptibility measurements. Single crystal neutron diffraction on E4 and TriCS diffractometer have been carried out respectively at the Helmholtz Zentrum Berlin and Sing. Paul Scherrer Institut. Below 38K, Mn/Fe spins order antiferromagnetically ($\tau(0.5,0,qz)$ $qz \approx [0.21,0.245]$). Below 15K, Tb sublattice is polarized by Mn/Fe one and orders antiferromagnetically below 5K. Nuclear and magnetic structure has investigated at 5 and 20K and be presented in this work.

[1] E. F. Bertaut et al., *Solid. Stat. Comm.* 5,25 (1925) [2] I. Akinobu and K. Kay, *Ferroelectrics* 169, 75 (1995) [3] N. Hur et al., *Nature* 429, 392 (2004). [4] L. C. Chapon, *Phys. Rev. Lett.* 96, 976001 (2006). [5] H. Kimura, *J Phys Soc Jpn* 76, 074706 (2006).

PA11

Strain-induced ferroelectric instabilities in the epitaxial RMn_2O_5 (R=Dy and Tb) thin films
 Jong Hyun Song¹, Jae Young Kim², Sun Hee Kang³, Ill Won Kim³, Yoon Hee Jeong⁴ and Tae Yeong Koo^{2*}
¹*Physics Department, Chungnam National University, Korea*
²*Pohang Accelerator Laboratory, Korea*
³*Physics Department, Ulsan University, Korea*
⁴*Physics Department, Pohang University of Science and Technology, Korea*

Epitaxial thin films of $DyMn_2O_5$ (DMO) and $TbMn_2O_5$ (TMO) were successfully grown on Nb-doped TiO_2 (110) substrates by the pulsed laser deposition to investigate the effects of substrate-induced strains on multiferroic properties. Synchrotron X-ray azimuthal angle scans and reciprocal space mappings confirmed the epitaxial qualities of the films. Magnetic phase transitions of the films were observed at $T_m = 43$ K, showing consistent values with those of the bulk samples. Dielectric constant showed a steplike anomaly around 16 K, where a magneto-capacitance effect about 10 % at 8 T was detected. Magnetization-induced ferroelectric phases below Tn appear to become unstable in the epitaxial thin films due to the substrate-induced tensile strains which make the magnetic exchange interactions between nearby manganese ions weaker.

PA12

Magnetically driven ferroelectric atomic displacements in perovskite-type $YMnO_3$ determined by single-crystal structure analysis
 Daisuke Okuyama¹, Shintaro Ishiwata², Youtarou Takahashi³, Kumihiro Yamachi⁴, Silvia Picozzi⁴, Kumihsa Sugimoto⁵, Hideaki Sakai⁶, Masaki Takata⁷, Ryo Shimano⁸, Yasujiro Taguchi⁹, Taka-hisa Arima¹ and Yoshinori Tokura¹
¹*Cross-Correlated Materials Research Group (CMRG), and Correlated Electron Research Group (CERG), RIKEN-ASI, Japan*
²*Department of Applied Physics and Quantum-Phase Electronics Center (QPEC), University of Tokyo, Japan*
³*The Institute of Scientific and Industrial Research (ISIR)-Sanken, Osaka University, Japan*
⁴*Consiglio Nazionale del le Ricerch-Superconducting and Innovative materials and device (CNR-SPIN), Italy*
⁵*JASRI, Spring-8, Japan*
⁶*School of Physics & Astronomy, University of St Andrews North Haugh, United Kingdom*
⁷*RIKEN, Spring-8 Center, Japan*
⁸*Department of Physics, University of Tokyo, Japan*
⁹*Department of Advanced Materials Science, University of Tokyo, Japan*

Multiferroic materials have been intensively studied with a particular focus on the driving mechanism of cross-correlated interactions between the magnetism and electricity [1]. Many theoretical and experimental works have clarified the origin of the interplay between magnetism and electricity. However, the lack of information about the crystal structure in the multiferroic phase has prevented quantitative discussion of the ferroelectricity driven by magnetic order. In order to quantitatively discuss the microscopic origin of the ferroelectricity of multiferroic perovskite- $YMnO_3$, in which the up-down-down-type (E-type) antiferromagnetic order causes a ferroelectric polarization below 30 K [2], we performed the crystal structural analysis for a twin-free single crystal by using synchrotron x-ray diffractometer at BL02B1 in Spring-8, and successfully determined the ferroelectric atomic displacements of the order of 0.001 Angstrom. The refined polar structure shows the characteristic bond alternation, which is consistent with that expected for the exchange striction mechanism giving rise to a ferroelectric polarization along the a-axis. From the experimental results of x-ray diffraction and a theoretical first-principles calculation, we quantitatively discuss the origin of the ferroelectricity in multiferroic $YMnO_3$ [3].

[1] Y. Tokura and S. Seki, *Adv. Mater.* 22, 1554 (2010). [2] S. Ishiwata, Y. Tokunaga, Y. Taguchi, and Y. Tokura, *J. Am. Chem. Soc.* 133, 13818 (2011). [3] D. Okuyama, S. Ishiwata, Y. Takahashi, K. Yamachi, S. Picozzi, K. Sugimoto, H. Sakai, M. Takata, R. Shimano, Y. Taguchi, T. Arima, and Y. Tokura, *Phys. Rev. B* 84, 054440 (2011).

July 9 (Mon)

July 9 (Mon)

PA13

Magnetic symmetry and electric polarization on $Mn_{1-x}Co_xWO_4$ multiferroics
 Irene Urcelay - Olabarria*, Eric Ressouche¹, Jose Luis Garcia - Munoz², Vassil Skumryev³, Alexander Mukhin⁴ and Juan Manuel Perez - Mato⁵
¹Institut Laue Langevin, 38042 Grenoble, Cedex 9, France
²Instituto de Ciencia de Materiales de Barcelona, ICMAB-CSIC, E-08193 Bellaterra, Spain
³Institut Catala de Recerca i Estudis Avancats (ICREA), E-08193 Barcelona, Spain
⁴Prokhorov General Physics Institute of the Russian Acad. Sci., 119991 Moscow, Russia
⁵Dpto. De Fisica de la Materia Condensada, Fac. de Ciencia y Tecnologia, Universidad del Pais Vasco, Spain

$MnWO_4$ exhibits magnetoelectric effects and belongs to the new class of frustrated multiferroics in which magnetic and ferroelectric order coexist [1-3]. It undergoes three successive magnetic phase transitions [1,2]. Below $T_N = 13.5$ K the spins are collinear and sinusoidally modulated, (AF3, paraelectric). In the AF2 phase (7.5 K < T < 12.5 K) a spontaneous polarization along b axis coexists with a cycloidal spin structure, $k = (-0.214, 1/2, 0.457)$. Below 7.5 K the system is in the AF1 collinear commensurate phase, $k = (\pm 1/4, 1/2, 1/2)$. Addition of Co²⁺ ions (S=3/2) modifies the overall magnetic interactions, produces changes in the magnetic anisotropy at 3d-site and stabilizes the multiferroic behaviour [3-5]. We have studied the temperature induced phase transitions of $Mn_{1-x}Co_xWO_4$ (x = 0, 0.1) multiferroics by single crystal neutron diffraction experiments, magnetic and polarization measurements, and we have analyzed the results in the light of the symmetry. All the magnetic models have been refined with JANA2006 [6] using the superspace formalism which allows predicting the crystal tensor properties, such as the electric polarization. We have observed that compared to pure $MnWO_4$, the magnetic symmetry of the multiferroic phase changes in agreement with the experimentally observed flip of the electric polarization.

I.-G. Lantierschlaeger et al., Phys. Rev. B 48, 6087 (1993). 2.-H. Sagayama et al., Phys. Rev. B 77, 220407(R) (2008). 3.-K. Taniguchi et al., Phys. Rev. Lett. 102, 147201 (2009). 4.-F. Ye et al., Phys. Rev. B 78, 193101(2008). 5.-Y.-S. Song et al., Phys. Rev. B 79, 224415 (2009). 6.-Petrick, V., Dusek, M. & Palatinus, L. (2006). Jana2006. The crystallographic computing system. Institute of Physics, Praha, Czech Republic.

PA14

Crystal and magnetic structure of multiferroic $Ba_2CoGe_2O_7$
 Vladimir Hutani*, Andrew Sazonov², Martin Meven¹, Dmitry Chernyshov³, H. Murakawa⁴, Y. Tokura⁴, Istvan Kézsmarki⁵, Balint Nafradi⁶ and Georg Roth¹
¹Institut für Kristallographie, RWTH Aachen University, Germany
²Laboratoire Leon Brillouin, CEA, Centre de Saclay; DSM/IRAMIS, France
³Swiss-Norwegian Beam Lines, ESRF, France
⁴Multiferroics Project, ERATO, JST, University of Tokyo, Japan
⁵Department of Physics, Budapest University of Technology, Hungary
⁶Max Planck Institute for Solid State Research, Stuttgart, Germany

The crystal structure of $Ba_2CoGe_2O_7$ has been precisely determined by single crystal diffraction at four different temperatures. Room temperature as well as 90 K structure determinations were performed using x-ray synchrotron radiation. The observation of the superstructure reflections commensurate with the tetragonal cell and violating the 2-1 axis lead to the conclusion that P-421m is a rather good approximation of the average structure, but the real structure has lower symmetry and most probably corresponds to the Cmm2 SG [1]. Crystal structure above (10 K) and crystal and magnetic structures below (2 K) the antiferromagnetic transition temperature of 6.7 K have been determined using neutron diffraction on single crystal. The structural results show no significant changes with the temperature indicating no structural phase transition down to the multiferroic phase. Antiferromagnetic non-collinear magnetic order has been found in the ground state contrary to the previous literature data [2]. The canting angle and the magnitude of the ordered moment have been refined. The possibility of the existing of polar structure and weak ferromagnetic component in the (a,b) plane shed a new light in the understanding of the multiferroicity in the $Ba_2CoGe_2O_7$.

[1] V. Hutani et al. Phys. Rev. B 84, 212101 (2011) [2] A. Zheludev, et al, Phys. Rev. B, 68, 024428 (2003)

PA15

The role of Co-doping in $Mn_{0.85}Co_{0.15}WO_4$ studied by magnetic X-ray scattering
 Javier Herrero-martin*, Alexey Dobrynin², Paul Steadman³, Peter Bencok², Raymond Fan², Claudio Mazzoli³, A. M. Balbashov⁴ and A. A. Mukhin⁵
¹Institute of Materials Science of Barcelona - CSIC, Spain
²Diamond Light Source, Didcot, Oxfordshire, United Kingdom
³Dpto. Fisica, Politecnico di Milano, Milano, Italy
⁴Moscow Power Engineering Institute, Moscow, Russia
⁵Prokhorov General Physics Institute of the Russian Acad. Sci., Moscow, Russia

$MnWO_4$ is known to show a multiferroic (MF) behaviour at low temperatures (~8-13 K) where the development of an incommensurate (ICM) Mn cycloidal spin structure (AF2 phase) is responsible for the appearance of a net electric polarization along the crystal b-axis [1-3]. The partial substitution of Mn by Co in small quantities stabilizes AF2 down to the ground state. A further Co doping produces the appearance of a new ICM phase, defined as AF2 [4,5]. We have performed resonant magnetic x-ray scattering (RMXS) with soft x-rays (Mn, Co 2p → 3d) on $Mn_{0.85}Co_{0.15}WO_4$ to independently analyze the spins orientation in Mn and Co ions in antiferromagnetically (AFM) ordered phases. A full polarization analysis of the incident and scattered x-rays permits us to provide an accurate complete picture of the magnetic structure in the collinear AF4 phase. The latter points to a strong influence of Co doping on the Mn spins alignment direction. We discuss these results in the frame of a large Co single ion anisotropy as reported in $CoWO_4$ [6].

[1] G. Lantierschlaeger et al, Phys. Rev. B 48, 6087 (1993) [2] D. Meier et al, Phys. Rev. Lett. 102, 147201 (2009) [3] H. Sagayama et al, Phys. Rev. B 77, 220407(R) (2008) [4] Y.-S. Song et al, Phys. Rev. B 79, 224415 (2009) [5] R. P. Chaudhury et al, Phys. Rev. B 82, 184422 (2010) [6] N. Hollmann et al, Phys. Rev. B 82, 184429 (2010)

PA16

Magnetic and electronic properties of hexagonal $RMnO_3$ (R = Y, Tb) quantum-wells
 Ambrose Seo*
 Physics and Astronomy, University of Kentucky, USA



PA17

Magnetic properties of the pyroxenes
 Sergey Streltsov¹ and Daniel Khomskii²
¹Institute of metal Physics, Russia
²University of Cologne, Germany

Pyroxenes, silicates of composition $AMSi_2O_6$, comprise one of the most important classes of minerals both in the Earth's crust and upper mantle, and as typical (extra) terrestrial rock-forming materials (A=Li,Na,Ca, and M is a transition metal ion). Interestingly enough these materials exhibit very different magnetic properties. Some of them have a spin-gapped ground state, like $NaTiSi_2O_6$, others show AFM or FM (which is unusual for transition metal insulator) long range magnetic order, Fe-based pyroxenes were found to be multiferroic and possibly have the spin-state transition under a high pressure. In the present talk we will review magnetic properties of the pyroxenes and provide a theoretical description for some of their properties. This work was supported by grants RFBR 10-02-00046 and 10-02-96011.

[1] S. Jodlauk et al. J. Phys.: Condens. Matter, 19, 432201 (2007) 2) S.V. Streltsov and D.I. Khomskii Phys. Rev. B, 77, 064405 (2008) 3) S.V. Streltsov, J. McLeod, A. Moewes, G.J. Reilhammer and E.Z. Kurmaev Phys. Rev. B 81, 045118 (2010) 4) Streltsov S.V. and Skorikov N.A. Phys. Rev. B 83, 214407 (2011)

PA18

High-field study of multiferroic $Ni_3V_2O_8$
 Junfeng Wang¹, Masashi Tokunaga², Zhangzhen He³ and Koichi Kindo³
¹Wuhan National High Magnetic Field Center, China
²The Institute for Solid State Physics (ISSP), The University of Tokyo, Japan
³Fujian Institute of Research on the Structure of Matter, Chinese Academy of Sciences, China



PA19

Control of coexisting ferroelectric phases in $RMnO_3$ crystals with fine tuning of 4f moment
 Tomoya Tadokoro*, Mitsuru Akaki, Haruhiko Kuroe, Tomoyuki Sekine and Hideki Kuwahara
 Department of Physics, Sophia University, Japan

Recently, a new class of multiferroics with a coexistence of magnetic and ferroelectric ordering has been attracting revived interests. $RMnO_3$ (R: rare earth) with distorted orthorhombic structure is one of the most canonical examples for such a multiferroic material. In $TbMnO_3$ [1], the electric polarization lies along the c axis in the ferroelectric ground state, and the polarization does not flop without a magnetic field. Meanwhile, in $Eu_{0.995}Y_{0.005}MnO_3$ without 4f moment [2], the magnetoelectric properties are quite different from those of $TbMnO_3$, although they have the same ionic radius of R-site. This result suggests that the magnetoelectric properties of the $RMnO_3$ strongly depend on the characteristics of the R-site 4f-moments [3]. In this study, we have systematically investigated magnetic and dielectric properties of $Eu_{0.995}(Y_{1-x}Ho_x)MnO_3$ ($0 \leq x \leq 1$) single crystals with control of 4f moments while keeping the average size of the R-site. In the x = 0.3 crystal, the ferroelectric polarization along the c axis (Pc) emerges at 25K, and then Pc is suppressed and Pa appears simultaneously with decreasing temperature. On further decreasing temperature, Pa disappears and Pc appears again. The observed reentrant behavior of the Pc phase indicates that Pa and Pc phases are strongly competing with each other.

[1] T. Kimura et al., Nature 426, 55 (2003). [2] K. Noda et al., J. Appl. Phys. 99, 08S905 (2003). [3] M. Hitomi et al., J. Phys. Soc. Jpn. 79, 054704 (2010).

PA20

$SmCr_3(BO_3)_4$ - A new multiferroic?
 Kirill N. Boldyrev*, Marina N. Popova¹, Viktor V. Mal'tsev² and Nicolay I. Leonyuk²
¹Solid State Spectroscopy, Institute of spectroscopy RAS, Russia
²Faculty of Geology, Moscow State University, Russia

Rare-earth borates with general formula $RM_3(BO_3)_4$ (R = Y, La-Lu; M = Al, Fe, Cr) are interesting for science and technology. Iron borates have rich magnetic properties stipulated by the presence of two interacting magnetic subsystems. It has recently been shown that $RFe_3(BO_3)_4$ belong to a new class of multiferroics [1,2]. For this reason it is interesting to study rare-earth borates with other magnetic ion chromium. At present, little is known about these compounds. Antiferromagnetic phase transition has been found in $NdCr_3(BO_3)_4$ at $T_N=8.0$ K [3]. This work describes an optical study in a wide spectral and temperature range of the $SmCr_3(BO_3)_4$ crystal, both pure and doped with erbium or neodymium. We have found that $SmCr_3(BO_3)_4$ undergoes a cascade of phase transitions at temperatures of 8.0 K, 6.7 K and 4.3 K. The first two ones are second-order phase transitions and, supposedly, correspond to the antiferromagnetic and (anti) ferroelectric ordering, respectively. First-order phase transition at 4.3 K is, most probably, the spin reorientation of the chromium magnetic moments. The presence of the magnetic and ferroelectric order allows us to talk about samarium chromium borate as a new multiferroic crystal.

[1] A.E. Zvezdin, S.S. Krotov, A.M. Kadomtseva, G.P. Vorob'ev, Yu.F. Popov, A.P. Pyatakov, L.N. Bezmaternyykh, E.A. Popova, JETP Lett. 81, 272 (2005). [2] A.M. Kadomtseva, Yu.F. Popov, G.P. Vorob'ev, A.P. Pyatakov, S.S. Krotov, K.I. Kamilov, J. Low Temp. Phys. 36(6), 640 (2010). [3] E.A. Popova, N.I. Leonyuk, M.N. Popova, E.P. Chukalina, K.N. Boldyrev, N. Tristan, R. Klingeler, B. Buchner, Phys. Rev. B, 76, 054446 (2007).

PA21

Magnetodielectric effect in the antiferromagnet $SrNdFeO_4$
 Jungmin Hwang¹, Eun Sang Choi², Haidong Zhou², Yan Xin², Jun Lu² and Pedro Schlottmann¹
¹Florida State University/NHMF, USA
²NHMF (National High Magnetic Field Laboratory), USA

We investigated the magnetic phase diagram of single crystals of the compound $SrNdFeO_4$ by measuring the magnetic susceptibility, the magnetization, the specific heat and the dielectric constant. The system has two magnetically active ions, namely Fe^{3+} and Nd^{3+} . The Fe^{3+} spins are antiferromagnetically ordered below 360 K with the moments lying in the ab-plane, and undergo a reorientation transition at about 35-37 K to an antiferromagnetic order with the moments along the c-axis. A short-range, antiferromagnetic ordering of Nd^{3+} along the c-axis was attributed to the reorientation of Fe^{3+} followed by a long-range ordering at lower temperature.[1] At low temperatures and magnetic fields above 8 T the Nd^{3+} moments are completely spin-polarized. The dielectric constant also shows anomalies associated with spin configuration changes. Remarkably, the sign of the dielectric changes are dependent on the direction of the probing electric field. A possible magnetic structure explaining all the data is presented.

[1] S. Oyama, M. Wakeshima, Y. Hinatsu, and K. Ohoyama, J. Phys.: Condens. Matter. vol. 16, 1823 (2004).

PA22

Mössbauer studies of Y-type hexaferrite by Aluminum doping
 Jung Tae Lim, Chin Mo Kim, Sung Wook Hyun, Mi Hee Won, Taejoon Kouh and Chul Sung Kim*
 Department of Physics, Kookmin University, Korea

In recent years, the magnetoelectric effect observed in some of helical magnets has been of great interest. With Al substitution, the improvement of magnetoelectric effect has been reported due to reduction of the in-plane orbital moment originating from lowering magnetic anisotropy [1-2]. Therefore, it is important to understand the origin of magnetic properties in conjunction with the site distribution in hexagonal structure. The crystal structure of polycrystalline $Ba_2Co_{1-x}Mg_{0.5}(Fe_{1-x}Al_x)_{12}O_{22}$ (x = 0, 0.01, 0.02) samples were determined to be rhombohedral with the space group of R-3m. From the temperature-dependent of magnetization curves under 100 and 300 Oe, all samples showed ferrimagnet-to-paramagnet and helimagnet-to-ferrimagnet transitions. Base on the applied-field dependent magnetization measurements up to 10 kOe at 295 K, the saturation magnetization (Ms) and coercivity (Hc) of $Ba_2Co_{1-x}Mg_{0.5}(Fe_{1-x}Al_x)_{12}O_{22}$ (x = 0, 0.01, 0.02) samples were found to be Ms = 28.0, 24.7, 23.4 emu/g and Hc = 255.4, 222.0, 196.2 Oe, respectively. Also, from Mössbauer spectra of 295 K, Isomer shift values of all samples indicate that the charge states are Fe^{3+} . We expect that the decrease in the Ms with Al ion doping is due to the fact that Al ions preferentially occupy the 3bVI, 18hVI and 3aVI octahedral sublattices of up-spin sites [3].

[1] S. Ishiwata, Y. Taguchi, H. Murakawa, Y. Onose, and Y. Tokura, Science 319, 1643 (2008). [2] H. B. Lee, Y. S. Song, J. H. Chung, S. H. Chun, Y. S. Chai, K. H. Kim, M. Reehuis, K. Prokes, and S. Matas, Phys. Rev. B 83, 144425 (2011). [3] A. Collomb, M. A. Hadj Farhat and J. C. Joubert, Mat. Res. Bull. 24, 453 (1989).

PA23

Optical spectroscopy of the triangular lattice antiferromagnets $CuCrO_2$ and alpha- $CaCr_2O_4$
 Michael Schmidt*, Zhe Wang¹, Franz Mayr¹, Sandor Toth², Bella Lake², A. T. M. Nazmul Islam², Vladimir Tsurkan¹, Alois Loidl¹ and Joachim Deisenhofer¹
¹Experimental Physics V, EKM, Institute of Physics, University of Augsburg, Germany
²Helmholtz Zentrum Berlin für Materialien und Energie, Germany

We will compare and discuss our results obtained by optical spectroscopy on $CuCrO_2$ and alpha- $CaCr_2O_4$. While $CuCrO_2$ is famous for its multiferroicity [1], in alpha- $CaCr_2O_4$ a polarization can only be observed under the application of electric or magnetic field, despite having a closely related structure [2]. In alpha- $CaCr_2O_4$ we can see a strong, broad absorption at 57 cm^{-1} in the magnetically ordered state. The other compound shows two excitations at 11 and 48 cm^{-1} below the magnetic ordering temperature. At near infrared and visible light frequencies we observe Cr^{3+} crystal field absorptions and below T_N excitons and exciton-magnon-transitions appear. The width of these exciton-magnon transitions is analyzed with respect to the existence of Z2 vortices as proposed by Kojima et al. [3].

[1] S. Seki et al., Phys. Rev. Lett. 101, 067240 (2008) [2] K. Singh et al., Phys. Rev. B 84, 064129 (2011) [3] N. Kojima et al., J. Phys. Soc. Jpn. 62, 4137 (1993)

PA24

Nuclear forward scattering in high magnetic fields; spin structures in the magnetic staircase of frustrated multiferroic $CuFeO_2$
 Cornelius Strohm*, Tom T. A. Lummen², Puri I. Handayani³, Thomas Roth¹, Peter J. E. M. Van Der Linden¹ and Paul H. M. Van Loosdrecht¹
¹European Synchrotron Radiation Facility, 6 rue Jules Horowitz 38000 Grenoble, France
²Department of Materials Science and Engineering, The Pennsylvania State University, 121 Steidle Building, University Park, PA, 16802, USA
³Zernike Institute for Advanced Materials, University of Groningen, Nijenborgh 4, 9747 AG Groningen, Netherlands

Geometrically frustrated magnets often show a multitude of nearly degenerate ground states, which may be stabilized individually by the presence of small internal or external perturbations. In Copper Iron Oxide, the combination of geometrically frustrated interactions, with uniaxial anisotropy and spin-lattice coupling lead to a staircase of metamagnetic phases as a function of applied field [1-3]. We used Nuclear Forward Scattering of synchrotron radiation in magnetic fields up to 30 T [4, 5] to probe the spin structure of these phases up to the 1/3-plateau for fields parallel and perpendicular to the c axis [6]. The low field data and all transition fields agree with previous work. For the parallel configuration, we confirm the low field collinear spin structure. The data for the ferroelectric phase does not support a cycloid structure, while a 3D distribution approximating a multi-domain transverse proper helix structure gives qualitative agreement. For the 1/3-plateau, the anticipated collinear 3-sublattice structure best represents the data. In the perpendicular configuration we directly evidence the stability of the canted 4-sublattice phase up to the 1/3-plateau, where a collinear three sublattice configuration provides the best fit when a small amount of the spins oriented in the H-c plane is allowed for.

[1] R. S. Fishman Phys. Rev. Lett. 106, 037206 (2011). [2] T. T. A. Lummen et al. Phys. Rev. B 80, 012406 (2009). [3] T. T. A. Lummen et al. Phys. Rev. B 81, 224420 (2010). [4] P. J. E. M. van der Linden et al. Rev. Sci. Instrum. 79, 073104, (2008). [5] C. Strohm, P. van der Linden and R. Rueffer Phys. Rev. Lett. 104, 087601 (2010). [6] C. Strohm, T.T.A. Lummen, P.H.M. van Loosdrecht et al. unpublished.

July 9 (Mon)

July 9 (Mon)

PA25

Magnetic dispersion of the quasi-1D, spin-1/2, multiferroic CuO

Stephen Michael Gaw
Oxford University, United Kingdom

Cupric Oxide (CuO) exhibits a magnetoelectric multiferroic phase over the narrow but relatively high temperature range of 213-230K [1]. The mechanism for this magnetoelectric coupling is not fully understood and there have been various theoretical models proposed [2]. The excitation spectra of CuO in the collinear antiferromagnetic phase (T<213K) was measured using inelastic neutron scattering. We have observed three-dimensional magnetic behaviour transform into a spin-1/2 chain regime with increasing energy. Through comparison of the data to a semi-classical spinwave model and a quantum spinon model, we have extracted values of the magnetic exchange constants. With these values we can refine the existing theoretical models of the magnetoelectric mechanism as well as unravel the nature of one-dimension quantum magnetism in CuO.

[1] T. Kimura et al., Nature Materials, 7, 291 (2008) [2] G. Giovannetti, et al, Phys. Rev. Lett., 106, 026401 (2011); G. Jin, et al, ArXiv:1007.2274v2 (2007); A-M. Pradipto, et al, Phys. Rev. B, 85 014409 (2012)

PB01

Hole-doped cuprate panorama and the second neighbor hopping

Partha Goswami*
Physics department, D.B.College(University of Delhi),New Delhi, India

We consider the coexistent id-density wave (DDW) order, at the anti-ferromagnetic wave vector Q = (π,π), representing the pseudo-gap (PG) state, and d-wave superconductivity (DSC), driven by an assumed attractive interaction, within the BCS framework for the two-dimensional (2D) fermion system on a square lattice starting with a mean-field Hamiltonian involving the singlet DDW and the DSC pairings. The second-neighbor hopping, which is known to be important for cuprates [K. Tanaka et al.,Phys. Rev. B 70 , 092503(2004)]and frustrates the kinetic energy of electrons, leads to Fermi surface sheets being not connected by Q. The particle-hole asymmetry in the single-particle excitation spectrum of the pure DDW state is reflected in the coexisting DDW and DSC states though the latter is characterized by the Bogoliubov quasi-particle bands- a characteristic feature of SC state. Quite significantly, we find that the coexistence is possible due to the non-nesting property.

PB02

Quantum oscillations from nodal bilayer magnetic breakdown in the underdoped high temperature superconductor YBa₂Cu₃O_{6+x}

Neil Harrison
Los Alamos National Laboratory, USA

We report quantum oscillations in underdoped YBa₂Cu₃O_{6.56} in magnetic fields over a significantly large range in magnetic field extending from ~25 to 94-T, enabling three well-spaced low frequencies at ~462-T, 532-T, and 602-T to be clearly resolved. We show that a small nodal bilayer coupling that splits a nodal pocket into bonding and antibonding orbits yields a sequence of frequencies, F₀-Δ F, \$F_0\$ and F₀+Δ F and accompanying beat pattern similar to that observed experimentally on invoking magnetic breakdown tunneling at the nodes. The relative amplitudes of the multiple frequencies observed experimentally in quantum oscillation measurements are shown to be reproduced using a value of nodal bilayer gap quantitatively consistent with that measured in photoemission experiments in the underdoped regime. A clear consistency between the experimental data and a Fermi surface consisting of nodal pockets is revealed.

PB03

Influence of BaSnO₃ nanoparticle dispersions on flux pinning property of GdBa₂Cu₃O_{7-x} multilayered thin films

Duc H. Tran¹, Witha B. K. Putri¹, Byeongwon Kang^{1*}, N. H. Lee², W. N. Kang², J. Y. Lee³ and W. K. Seong³
¹ Physics, Chungbuk National University, Korea
² Physics, Sungkyunkwan University, Korea
³ Convergence Technology Laboratory, Korea Institute of Science and Technology, Korea

Flux pinning property of GdBa₂Cu₃O_{7-x} (GdBCO) thin films with embedding BaSnO₃ (BSO) nanoparticle pseudo-layers structured as (BSO/GdBCO) x N layers was investigated. The multilayered films whose entire thickness of approximately 200 nm were fabricated on SrTiO₃ (STO) substrate by using the pulsed laser deposition (PLD) technique. Number of BSO pseudo-layers was varied from 1 to 5 in order to increase the density of pinning centers along the c-axis of the films. BSO nanoparticle density per layer was estimated to be approximate 114/μm² by using an atomic force measurement (AFM). A minor decrease in the transition temperature T_c was observed for (BSO/GdBCO) multilayered films. Magnetization data showed that BSO pseudo-layers provides enhanced in-field critical current density J_c up to certain magnetic fields. J_c enhancements were attributed to the dispersions of BSO nanoparticle pseudo-layers confirmed by cross sectional TEM image.

I. A. A. Gapud, D. Kumar, S. K. Viswanathan, C. Cantoni, M. Varela, J. Abiade, S. J. Pennycook and D. K. Christen, Supercond. Sci. Technol. 18 (2005) 1502-1505. 2. T. A. Campbell, T. J. Haugan, I. Maartense, J. Murphy, L. Brunke and P. N. Barnes, Physica C 423 (2005) 1-8

PB04

Highly anisotropic dielectric behavior of insulating Bi₂Sr₂RECu₂O_{8+x} (RE = Dy, Y)

Makoto Maki, Chikano Yukitake and Shigeyuki Yufu
Department of Physics, Saga University, Japan

The low-frequency dielectric measurements on lightly-doped Bi₂Sr₂RECu₂O_{8+x} (RE = Dy, Y) single crystals were carried out in order to investigate the electronic structure and carrier dynamics near the insulator-to-metal transition. We found the unusually large dielectric polarization in the ab plane, whereas the out-of-plane dielectric constant was reasonably small at low temperatures. With increasing temperature above about 230 K, the out-of-plane dielectric constant shows a rapid increase followed by a sharp peak. The large anisotropy and unusual temperature dependence of the dielectric response probably reflect the hopping polarization induced by localized charge carriers and the spatial charge distribution peculiar to the insulating Bi2212. Our results seem to imply that the carrier movement is limited within the CuO₂ planes at low temperatures below about 230 K, and the confined carriers start to hop toward the perpendicular direction at higher temperatures [1, 2]. We also present data for Zn-doped Bi₂Sr₂RECu₂O_{8+x} samples to discuss the relationship between the enhanced dielectric polarization and a long-range antiferromagnetic ordering of Cu magnetic moments in the CuO₂ planes.

[1] M. Maki, S. Nakao, K. Machida, M. Shiraishi, X. G. Zheng, T. Naito, and H. Iwasaki, J. Phys. Soc. Jpn. 76, 044711 (2007) [2] S. Yufu, M. Shu-nan, S. Nakao, and M. Maki, J. Phys. Soc. Jpn. 79, 054709 (2010)

PB05

Pressure effect on the superconductivity and crystal structure for Hg cuprate

Yukihiro Kamada¹, Tomoko Kagayama^{1*}, Katsuya Shimizu¹, Akira Iyo² and Shin-ichi Uchida³
¹ KYOKUGEN, Osaka Univ., Japan
² AIST, Japan
³ Dept. of Phys., The Univ. of Tokyo, Japan

18 years ago, Hg cuprate recorded the highest T_c=164 K under high pressure (31 GPa) in 1994 [1]. But the record has not broken yet. We try to make new world record of T_c with the high purity Hg₁₂₂₃ (HgBa₂Ca₂Cu₃O_{8+x}) samples and the high purity Hg₁₂₃₄ (HgBa₂Ca₂Cu₄O_{10+x}) sample. We measured electrical resistance and X-ray diffraction under the pressure with a diamond-anvil cell (DAC). We measured two different Hg₁₂₂₃ samples, which were under doped sample (Hg₁₂₂₃ UD) and optimal doped sample (Hg₁₂₂₃ OPT), and one Hg₁₂₃₄ sample which was optimal doped sample. We measured two different pressure conditions, using pressure medium (NaCl) or not (None). The resistance drop of superconducting transition becomes broader by increasing pressure. At 80 GPa, we can not find the drop of superconducting transition above 10 K. The T_c have a maximum at 20-30 GPa accompanied with the anomaly in crystal structure.

[1] L. Gao et al., Phys. Rev. B 50, 4260 (1994)

PB06

Hole doping effect for the T'-Ln₂CuO₄ (Ln = La,Nd) cuprate

Wataru Ito, Kenji Kawashima, Suguru Igarashi, Michinori Fukuma and Jun Akimitsu
Physics and Mathematics, Aoyama Gakuin University, Japan

The Ln₂CuO₄ (Ln=La,Nd) cuprate has two different structure types and shows the superconductivity for hole doping of La₂CuO₄ and electron doping of Nd₂CuO₄. From the Madelung energy calculation in hole doping cuprate, T_c is enhanced with increasing the distance between Cu²⁺ ions in CuO₂-layer and apical oxygens. Nd₂CuO₄ with T'-type structure has exhibited superconductivity by electron carrier doping in CuO₂-layer. We focused on our attention to synthesize the hole doping to T'-Ln₂CuO₄, in which there is no oxygen atom at apical site of CuO₂-layer. We successfully synthesized the polycrystalline samples of T'-(Ln²⁺,M²⁺)₂CuO₄ (Ln=La,Nd, M=Ca,Sr). In particular, T'-(La²⁺,Sr²⁺)₂CuO₄ was synthesized using CaH₂, which is a strong reducing agent at annealing temperature of 573 K [1]. The powder X-ray diffraction patterns showed that the samples were a single phase, and diffraction peaks indexed by a tetragonal symmetry of T'-type cuprate of Nd₂CuO₄. The lattice constants a and c show the systematic changes by increasing the M²⁺ concentration. We determined the copper ion's valence state using iodometry method for substituted sample of T'-(Ln²⁺,M²⁺)₂CuO₄ and confirmed that the valence of Cu ion is closed to 2+. These facts indicate that there is oxygen deficiency in Ln₂O₂ or CuO₂-layer of T'-(Ln²⁺,M²⁺)₂CuO₄ and canceled hole carriers.

T. Takamaysu, M. Kato, T. Noji, and Y. Koike, Physica C 471 (2011) 679-681

PB07

Thermodynamic properties of copper oxide Cu₆O₈YCl_{1-x}Br_x

Kenji Kawashima, Hiroki Takeda and Jun Akimitsu
Physics and Mathematics, Aoyama Gakuin University, Japan

Copper-oxide family Cu_nO_mMCl (M=cation) has a cubic structure (Fm-3m) with Cu_nO_m-cage including Cl ion in its crystal structure [1,2]. Cations of M ions are located in the cuboid space between Cu_nO_m-cages. The Cu_nO_m-cages share their face to form a three-dimensional network. Cu₆O₈YCl shows the metallic and paramagnetic behavior at low temperature. Moreover, Y and Cl ions have large atomic displacement parameters, suggesting the anharmonic vibrations like rattling phenomena of other cage structured compounds. We synthesized the polycrystalline samples of Cu₆O₈YCl_{1-x}Br_x as a single phase to clarify relationship between the thermodynamic properties including its ground state and Cu_nO_m cage size. In thermo-electronic measurements of Cu₆O₈YCl, seebeck coefficient is relatively high value (-14 μV/K at 350K), and thermal conductivity exhibits of low value (~0.3W/Km at 350K). The lattice constant a increases with increasing Br concentration, indicating expansion of Cu_nO_m-cage. The temperature dependence of electrical resistivity of Cu₆O₈YBr exhibits semiconducting behavior, suggesting that the ground state of Cu₆O₈YCl_{1-x}Br_x changes from metallic to semiconducting by increasing Br concentration. Thermal conductivity undergoes very little change. However, S is enhanced by substituting Br. These facts indicate that the ground state and physical properties are sensitive on the Cu_nO_m-cage size in Cu_nO_mYCl_{1-x}Br_x system.

[1] G.Zouganell, K.Bushida, I.Yazawa N.Terada, M.Jo, H.Hayakawa, and H.Ihara, Sol. St. Comm. 80 (1991) 709. [2] K.Bushida, I.Yazawa, G.Zouganell, T.Connard, N.Terada, K.Kaneko, M.Hirabayashi, and H.Ihara, Physica C 185-189 (1991) 2727.

PB08

Nodal superconducting gap in Bi₂₂₀₁ investigated by low temperature specific heat measurements

Naoki Momono^{1*}, Nobutaka Saikai¹, Tohru Kurosawa², Yusuke Amakai¹, Sigeyuki Murayama¹, Hideaki Takano¹, Migaku Oda² and Masayuki Ido²
¹ Applied Sciences, Muroran Institute of Technology, Japan
² Department of Physics, Hokkaido University, Japan

In order to examine the gap magnitude near nodes in Bi₂₂₀₁ cuprate superconductors, we have measured the magnetic field dependence of low temperature electronic specific heat Cel(T, H), which is much more bulk-sensitive than standard ARPES and STS. In optimally doped Bi₂₂₀₁, the coefficient of T-linear term in Cel at T<<T_c, which is almost vanished in zero field, shows a square-root dependence of magnetic field H as is expected in d-wave superconductors. We determined the nodal gap slope v, reflecting the gap magnitude near nodes, from the square-root dependence of H; v~4.4x10⁻⁵ cm/s. In heavily underdoped Bi₂₂₀₁, the coefficient of T-linear term is not zero even in zero field, and is nearly independent of H up to 6 T. The comparison of these results with recent ARPES and STS results will be discussed in detail.

PB09

Chemically introduced disorder effects on the critical current density and pinning force of YBa₂Cu₃O_{7-δ} single crystals

Rovan Fernandes Lopes^{1*}, Valdemar Das Neves Vieira¹, Ana Paula Aguiar De Mendonca¹, Fabio Teixeira Dias¹, Douglas Langie Da Silva¹, Paulo Pureur², Jacob Schaf² and Frederik Wolff-fabris³
¹ Universidade Federal de Pelotas, Brazil
² Universidade Federal do Rio Grande do Sul, Brazil
³ HZ Dresden-Rossendorf, Germany

We report isotherm dc magnetization hysteresis loops of a series of YBa₂Sr_xCu₃O_{-δ} (x=0, 0.1, 0.25, 0.37 and 0.5) single crystals with the aim to study the influence of the chemically introduced site disorder on the YBa₂Cu₃O_{-δ} critical current density, J_c and flux pinning properties, FP. [1,2] The Sr ion size chemical disorder is introduced in YBa₂Cu₃O_{-δ} structure by lattice distortion. Transmission electronic microscopy (TEM) observations of our samples structure reveals the existence of a high density of twins, probably, decorated by many small local precipitates. The J_c were determined by application of the modified Bean critical state model.[3-5] Preliminary magnetization data analysis shows a significant and a systematically decrease of the critical current density and pinning force intensities as Sr concentration level increases up to 25%. The normalized FP curves showed no reasonable scaling as a function of the Sr doping level or temperature range.[4,5] The application of the Dew Hughes law to the normalized FP curves reveals that pinning mechanism in the doped samples are strongly temperature and level doping dependent. We consider the particular defect structure introduced by Sr substitution as a responsible to the flux pinning properties.

I. K. Saito, H. U. Nissen, C. Beeli, T. Wolf, K. H. Schauer, Physical Review B 58, 6645 (1998). 2. V. N. Vieira, J. Schaf, Physica C 408, 533 (2004). 3. L. Cvale, M. V. Mcelfresh, A. D. Marwick, F. Holtzberg, C. Field, J. R. Thompson, D. K. Christen, Physical Review B 43, 13732 (1991). 4. T. Masai, Y. Takano, K. Yoshida, K. Kajita, S. Tajima, Physica C 412, 515 (2004). 5. G. Fuchs, K. Nenkov, G. Krabbes, R. Weinsten, A. Gandini, R. Savh, B. Mayer, D. Parks, Superconductor Science and Technology 20, 197 (2007).

PB10

The correlation between the magnetic irreversibility and the zero resistance temperatures in granular YBa₂Cu₃O_{7-x} single crystals

Daniela Goetzke Macedo^{1*}, Valdemar Vieira¹, Fabio Dias¹, Douglas langie¹, Paulo Pureur², Jacob Schaf² and Frederik Fabris³
¹ Instituto de Fisica e Matematica, UFPEL, Brazil
² Instituto de Fisica, UFRGS, Brazil
³ Dresden High Magnetic Field Laboratory, HZ Dresden-Rossendorf, Brazil

We report on dc magnetization and ac magnetoresistance measurements of the Y_{0.00}Ca_{0.01}Ba₂Cu₃O_{7-x}, YBa₂Sr_{0.05}Cu₃O_{7-x} and YBa₂Cu_{2.97}Zn_{0.03}O_{7-x} single crystals with the propose of to study the role of the superconducting granularity on the correlation between the magnetic irreversibility, T_{irr}(H) and the zero resistance, T_r(H) temperatures.[1-3] The results show that in the low field region of the H-T diagram that the T_r(H) data falls systematically underneath of the T_{irr}(H) data and at H-T high field region the T_r(H) data matches the T_{irr}(H) data. In this scenario, T_{irr}(H) and T_r(H) do not depend on the same parts of the sample. While the T_{irr}(H) depends on wellcoupled grain clusters, the T_r(H) depends on grain arrays traversing the whole sample. Along such long range paths, the T_r(H) can be attained only at some temperature below the T_{irr}(H). On the other hand, in fields above several kOe, for which the magnetic field penetrates the grains, the T_{irr}(H) is dominated by the intragrain Abrikosov flux dynamics while the T_r(H) is still ruled by the grain junctions. It can vanish only after long-range coherence is achieved. The granular aspects of our results are discussed in terms of the superconducting glass theories.[1-4]

I. V. N. Vieira, J. Schaf, and P. Pureur, Phys. Rev. B 66, 224506 (2002). 2. R. Menegotto Costa R. P. Pureur et al, Phys. Rev. B 64, 214513 (2001). 3. V. N. Vieira, I. C. Rigel, and J. Schaf, Phys. Rev. B 76, 024518 (2007). 4. V. N. Vieira and J. Schaf, Phys. Rev. B 64, 094516 (2001).

PB11

Paramagnetic Meissner effect and strong time dependence at high fields in melt-textured high-TC superconductors

Cristol De Paiva Gouvea^{1*}, Fabio Teixeira Dias¹, Valdemar Das Neves Vieira¹, Douglas Langie Da Silva¹, Frederik Wolff-Fabris², Erik Kampert², Jacob Schaf² and Joan Josep Roa Rovina⁴
¹ Universidade Federal de Pelotas, 96010-900, Pelotas, Brazil
² Dresden High Magnetic Field Laboratory, HZ Dresden-Rossendorf, 01314, Dresden, Germany
³ Universidade Federal do Rio Grande do Sul, 91501-970, Porto Alegre, Brazil
⁴ Universite de Poitiers, 86962, Poitiers, France

The conventional Meissner effect is characterized by a diamagnetic response of the superconducting material when a magnetic field is applied, but in several cases this magnetic response in field-cooled experiments can be paramagnetic. This effect is known as paramagnetic Meissner effect (PME) [1]. Sometimes the PME presents a time dependence of the FC magnetization and a paramagnetic signal can be observed when the field-cooled moment relaxes at constant magnetic field and temperature [2,3]. In this work we report on systematic field-cooled magnetization experiments in melt-textured YBaCuO samples containing Y211 precipitates. Magnetic fields up to 14 T were applied either parallel or perpendicular to the ab planes and a strong paramagnetic response related to the superconducting state was observed. The magnitude of the PME increases when the field is augmented. This effect shows a strong paramagnetic relaxation, such that the paramagnetic moment increases as a function of the time. The pinning by the Y211 particles plays a crucial role in the explanation of this effect and our results suggest that the pinning capacity [4] can produce a strong flux compression [5] into the sample, originating the PME and the strong time dependence.

[1] P. Svellinsh, K. Niskanen, P. Norling, P. Nordblad, L. Lundgren, B. Lonnberg, and T. Lundstrom. Physica C 162/164, 1365 (1989). [2] A. Terentiev, D. Watkins, L. De Long, D. Morgan, and J. Keterson, J. Phys. Rev. B 60, R761 (1999). [3] F. Dias, P. Pureur, P. Rodrigues Jr, and X. Obradors. Phys. Rev. B 70, 224519 (2004). [4] F. Dias, V. Vieira, M. de Almeida, A. Falck, P. Pureur, J. Pimenel Jr, and X. Obradors. Physica C 470, S111 (2010). [5] A. Koshelev, and A. Larkin. Phys. Rev. B 52, 13559 (1995).

PB12

Enhancement of Ti-Se bonding length in CuxTiSe2

Sang Wook Han¹, Han-jin Noh², Daehyun Kim¹, Jihoon Hwang³, Jeong Soo Kang³, W. F. Pong⁴ and Soon Cheol Hong^{1*}

¹Department of Physics and EHSRC, University of Ulsan, Korea

²Department of Physics, Chonnam Nation University, Korea

³Department of Physics, The Catholic University of Korea, Korea

⁴Department of Physics, Tamkang University, Taiwan

Titanium diselenide (TiSe₂) undergoes a charge-density-wave (CDW) instability characterized by a 2x2x2 real-space superstructure [1]. TiSe₂ is not superconducting at low temperature, but CDW is suppressed and superconductivity stabilized either by Cu intercalation (maximum Tc =4.5 K) [1] or pressure (maximum Tc = 1.8 K) [2]. The resulting phase diagram looks similar to that of cuprates with the difference that the spin-density wave order has been replaced by a CDW one. The mechanism at the origin of the CDW and superconducting phases in TiSe₂ is currently unknown. The charge-order instability in pure TiSe₂ is known to involve both exciton formation and a strong electron-phonon coupling, it may be expected that the superconducting phase will likewise involve a combination of both excitonic [3] and phonic [4] contributions. In order to elucidate the role of Cu atoms, we have investigated the Cu-doped TiSe₂ by employing both x-ray absorption near-edge structure (XANES) and extended x-ray absorption fine-structure (EXAFS). The Cu atoms enhance the bonding length of Ti and Se atoms with lowering temperature. Concurrently, the Debye-Waller factors change at the transition temperatures of CDW and superconductivity, respectively.

[1] E. Morsan et al., Nature Phys. 2, 544 (2006). [2] A. F. Kusmartseva et al., Phys. Rev. Lett. 103, 236401 (2009). [3] C. Morney et al., Phys. Rev. Lett. 106, 106404 (2011). [4] M. Calandra and F. Mauri, Phys. Rev. Lett. 106, 196406 (2011).

PB13

Para-conductivity of (Bi_{0.25}Cu_{0.25}Li_{0.25}Tl_{0.25})Ba₂Ca₂Cu₃O_{10-δ} superconductors

Qurat-ul Ain and Nawazish Ali Khan

Physics, Quaid-i-azam university islamabad pakistan, Pakistan

Excess conductivity analyses of as-prepared and oxygen post-annealed (Bi_{0.25}Cu_{0.25}Li_{0.25}Tl_{0.25})Ba₂Ca₂Cu₃O_{10-δ} samples were carried out by following Lorentz-Danish (LD) model beyond the transition region and Ginzburg-Landau (GL) equations in the critical regime. In these studies the effect of oxygen annealing on the thermodynamic fluctuations of the Cooper pairs just above the Tc is performed by using Aslamazov-Larkin (AL) theory. We have observed a major increase in the width of 3D AL and 2D LD regimes after post-annealing in oxygen atmosphere. Moreover, with the oxygen post-annealing the coherence length along the c-axis has also been found to increase along with inter-plane coupling. The thermodynamic critical magnetic field, the lower critical magnetic field, the upper critical magnetic field, the critical current density and penetration depth are also calculated from the analysis of four regions namely critical (cr), three dimensional (3D), two dimensional (2D) and zero dimensional (0D) region that appeared as the temperature increases. The values of Fermi velocity, phase relaxation time, penetration depth, κ values and energy required to break apart the cooper pairs are increased with the annealing of oxygen. This shows that in (Bi_{0.25}Cu_{0.25}Li_{0.25}Tl_{0.25})Ba₂Ca₂Cu₃O_{10-δ} sample, the optimum density of carriers in the conducting CuO2 is essential for enhanced superconductivity in these compounds.

[1] Qiang Lia, M. Suenaga, Junho Gohng, D.K.Finnemore, T. Hikata and K. Sato Phys.Rev. B 46, 3195-3198 (1992). [2] V. V. Schmidt, The physics of superconductors (Springer, New York, 1997), p. 45. [3]A.L. Solovjov; V.M. Dmitriev; and H.-U. Habermeier, Phys. Rev. B 55, 8551 (1997). [4]A.L. Solovjov, H.-U. Habermeier, and T. Haenge, Fiz Nizk Temp. 28, 144 (2002) [Low Temp. Phys. 28, 99 (2002)] [5] C. J. Lobb, Phys. Rev. B 36 (1987) 3930. [6] A. I. Abu Aly, I. H. Ibrahim, R. A. Awad and A. El-Harizy, J. of Supercond. Nov. Magn. 23 (2010) 1325.

PB14

Charge transfer instability governs unconventional behavior of doped cuprates

Alexander Moskvín and Alexey Korolev

Department of Theoretical Physics, Ural Federal University, Russia

A large body of experimental data points towards an unique charge transfer (CT) instability of parent insulating cuprates. True CT gap in these compounds is believed to be as small as 0.4-0.5 eV as derived from the midinfrared absorption measurements [1] rather than 1.5-2.0 eV as usually derived from the fundamental absorption measurements. Actually we deal with a competition of the conventional (3d9) ground state and a CT state with formation of electron-hole dimers which evolves under doping to an unconventional bosonic system [1-3]. Making use of a quantum Monte-Carlo (QMC) technique we study the evolution of the phase state of CuO₂ planes in a model CT unstable cuprate La_{2-x}Sr_xCuO₄. Nonisovalent doping gives rise to a suppression of parent antiferromagnetic phase with the nucleation of the inhomogeneous supersolid CO+BS phase characterized by a charge (CO) and off-diagonal Bose superfluid (BS) order parameters which competition results in a generic T-x phase diagram with a distinct pseudogap regime due to a charge ordering and emergence of a local superconductivity. Our QMC simulation does reproduce all the main features of the T-x phase diagrams for doped cuprates.

1. A.S. Moskvín, Phys. Rev. B 84, 075116 (2011). 2. A.S. Moskvín, Low Temp. Phys. 33, 234 (2007). 3. A.S. Moskvín, Phys. Rev. B 69, 214505 (2004).

PB15

The effect of CdO nanoparticles doping and sintering time on the structure and critical temperature of Bi_{1.223} superconductor

Morteza Zargar Shoushtari*, S Ebrahim Musavi Ghahfarokhi and Nahid Hossinzadeh Physics, Shahid Chamran University of Ahvaz, Iran

The effect of CdO nanoparticles doping and sintering time on the structure and critical temperature of Bi_{1.223} superconductor M. Zargar shoushtari 1, S. E. Musavi Ghahfarokhi, N. Hossinzadeh 1 Department of physics, Shahid Chamran University of Ahvaz, Ahvaz, I. R. Iran Presenting author: zargar@scu.ac.ir In this paper, Bi_{1.64}Pb_{0.36}Sr₂Ca₂xCd_{1-x}Cu₃O₇ (x= 0.0, 0.01, 0.02, 0.03, 0.04, 0.1) superconductor is prepared by using the solid state method. The effect of doping CdO nanoparticles for different sintering times (t= 90, 180 and 270 h) on the structure and critical temperature has been studied. The structural analysis was carried out using XRD and SEM measurements. The critical temperature was measured by the standard four-probe method. The results showed that the more sintering time increases the critical temperature such that the samples prepare at 270h have maximum critical temperature. Also, our results reveal that, the Bi_{1.64}Pb_{0.36}Sr₂Ca_{1.97}Cd_{0.03}Cu₃O₇ sample has the highest Tc (Tc= 137.5k) in between the doped samples.

PB16

Charging/Discharging and overcurrent characteristics of GdBCO coils using various partial insulation winding methods

Yoon Hyuck Choi, Kwang Lok Kim, Oh Jun Kwon, Hyun-jin Shin and Haigun Lee*

Department of Materials Science and Engineering, Korea University, Korea

Eliminating the insulation in high temperature superconducting (HTS) windings can allow a system to be compact and well protected by bypassing the excessive current flow that occurs through the turn-to-turn contact between uninsulated turns. However, the time constant of coils without insulation is much higher than that of completely insulated coils due to the absence of insulation resistance, resulting in a coil charge-discharge rate that becomes quite slow. Therefore, this study examined the charging, operating, and discharging behaviors of Gd-Ba-Cu-O (GdBCO) HTS coils with Kapton insulation every 3, 6, or 9 turns to investigate the effect of changes in insulated turns on the coil's time constant. Furthermore, to verify the demagnetization phenomena of the coils in the excessive current condition, the overcurrent characteristics of partially insulated GdBCO coils were evaluated and discussed in detail.

<Acknowledgment> This work was supported by the International Collaborative R&D Program of the Korea Institute of Energy Technology Evaluation and Planning (KETEP) grant funded by the Korean government Ministry of Knowledge Economy (20118520020020).

PB17

Effect of filter shape on the capture efficiency of a high gradient magnetic separation (HGMS) system

Young-gyun Kim, Jung-bin Song, Dong Gyu Yang, Jongseok Lee and Haigun Lee*

Department of Materials Science and Engineering, Korea University, Korea

High gradient magnetic separation (HGMS) using a ferromagnetic filter enables the capture of fine particles of even weakly magnetic materials by the high gradient of the magnetic field. In general, such a field gradient, which can determine the capture capability of the HGMS system, is mainly affected by the filter's mesh size, wire diameters, and materials. Therefore, this study examined the capture efficiency of the HGMS system with respect to mesh size and wire diameter to investigate the effect of filter shape on gradient magnitude. Furthermore, the capture efficiency of various filter shapes was also examined and compared with the simulation.

<Acknowledgment> This study was supported by the Ministry of Knowledge Economy (MKE), Korea, under the IT R&D Infrastructure Program supervised by the National IT Industry Promotion Agency (NIPA-2011-(B1110-1101-0002)).

PB18

Effects of various epoxy impregnations on the electrical properties of GdBCO-coated conductor racetrack pancake coils

Hyun-jin Shin, Kwang Lok Kim, Yoon Hyuck Choi, Oh Jun Kwon, Yeonjoo Park and Haigun Lee*

Department of Materials Science and Engineering, Korea University, Korea

A high temperature superconducting (HTS) field coil in a wind turbine generator is generally impregnated with epoxy resin to provide high mechanical integrity against the rotational vibrations. However, if cooled down, the epoxy-impregnated coil wound with second generation (2G) HTS tape usually encounters superconducting property degradation and delamination due to the thermal contraction mismatch between the epoxy and the HTS tape. Therefore, to investigate the effect of various epoxies on the coil's electrical properties, the GdBCO racetrack pancake coils impregnated with Stycast 2850-FT, Epikote 828R, or Epon 815 were characterized using Ic testing. Furthermore, degradation of the coils' superconducting properties was also examined using repetitive cooling tests.

<Acknowledgment> This work was supported by the International Collaborative R&D Program of the Korea Institute of Energy Technology Evaluation and Planning (KETEP) grant funded by the Korean government Ministry of Knowledge Economy (20118520020020).

PB19

Crystal structure of (Ru_{0.5}Cu_{0.5})(Sr_{1.47}Ba_{0.2}Nd_{0.33})(NdCe)Cu₂O_{10-δ} compound

H.K. Lee¹ and Y.I. Kim²

¹Physics, Kangwon National University, Department of Physics, Korea

²Korea Research Institute of Standards and Science, Korea



PB20

Absence of broken time reversal symmetry below the surface of (110)-oriented YBCO superconductors

Hassan Saadaoui*, Zaher Salman¹, Thomas Prokscha¹, Hannu Huhtinen² and Elvezio Morenzoni¹

¹Laboratory for Muon Spin Spectroscopy, Paul Scherrer Institut, 5232 Villigen PSI, Switzerland

²Department of Physics, Wihuri Physical Laboratory, University of Turku, FI-20014 Turku, Finland

Low-energy muon spin rotation (LE-μSR) is a very sensitive local magnetic probe to study magnetism on a nanometer length scale near the surface of materials and thin films. Here, we report the results of a search for spontaneous magnetization due to a time reversal symmetry breaking phase in the superconducting state of (110)-oriented YBCO films, expected to develop near the surface in this orientation. Zero field and weak transverse field measurements performed using LE-μSR few nm inside optimally-doped YBCO-(110) films showed no appearance of spontaneous magnetization below the superconducting temperature up to 2.9 K, contrary to tunneling measurements. Our results give an upper limit of 0.01 mT for spontaneous internal fields in these films.

PB21

Transport properties of the twin boundary of YBa₂Cu₃O₇ thin films on LaAlO₃ substrates

Sung Hoon Lee¹, Sung-hak Hong¹, Jae-hyuk Choi² and Soon-gul Lee^{1*}

¹Department of Display and Semiconductor Physics, Korea University, Korea

²Division of Convergence Technology, Korea Research Institute of Standards and Science, Korea

We have fabricated superconducting YBa₂Cu₃O₇ (YBCO) twin-boundary junctions and studied their critical transport properties. The twin boundary junctions were fabricated by using a focusd-ion-beam (FIB) etching technique and of the size of nominally 150 nm in width, 100 - 120 nm in length, and 100 nm in thickness. The junctions showed Tc = 91 K with 1 K transition width and a high critical current density of Jc = 15 MA/cm² at 77 K. Measured current-voltage (I-V) curves showed the resistively-shunted-junction (RSJ) characteristics near the transition with excess current associated with flux-flow effect. High-resolution X-ray diffraction (HR-XRD) spectra strongly indicated the possibility that the epitaxially-grown YBCO film was also twinned in commensurate with the twinning of the LAO substrate. Misorientation of the c-axis of YBCO at the twin boundary is believed to be the major cause of the weak link behavior of the bridge across the twin boundary.

PB22

Displacement waves of oxygen atoms in the Bi, Pb₂₂₂₃ lattice of superconducting composites annealed in an oxygen reduced atmosphere

Tatiana Krinitsina*, Svetlana Sudareva, Elena Kuznetsova and Julia Blinova Institute of Metal Physics, Ural Branch of Russian Academy of Sciences, Russia

The Bi, Pb²²²³/Ag composites annealing in oxygen-nitrogen atmosphere is believed to reduce the number of the accompanying phases, to make contacts between crystallites closer and to increase the critical current. The goals of this study were determining the 2223 lattice changes at annealing in the reduced oxygen atmosphere, revealing the reasons of these changes and their effect on the ceramics superconductivity. After such annealing the transversely-polarized waves of oxygen atoms displacement in [010] direction are observed in the 2223 phase by electron diffraction analysis. These waves may appear due to the lack of oxygen in the 2223 lattice or to the nitrogen penetration in it. As demonstrated by the X-ray photo-electron spectroscopy and nuclear microanalysis, nitrogen does not interact with the 2223 lattice, and the oxygen index decreases to 9.67, which is lower than the stoichiometric. Thus, the atomic displacement waves result from the lack of oxygen in Bi-O bilayers.

PB23

Irreversibility line in the CNT and carbon doped YBCO superconductors

Sedigheh Dadras^{1*}, Nallayian Manivannan², Vahid Daadmehr¹ and Kee Hoon Kim³

¹physics, Other Academic, Iran

²physics, Other Academic, India

³Other Academic, Korea

Irreversibility Line in the CNT and Carbon Doped YBCO Superconductors S. Dadras^{1*}, N. Manivannan², V. Daadmehr¹, and K. H. Kim³ ¹Magnetic and Superconducting Res. Lab., Department of Physics, Alzahra University, P.C.1993891176, Tehran, Iran. ²eXtreme Multifunctional Physics Laboratory, FPRD, School of Physics and Astronomy, Seoul National University, Seoul 151-747, Republic of Korea. *dadras@alzahra.ac.ir s_dadras2001@yahoo.com Abstract. We investigated the irreversibility line (IL) of the carbon nano tube (CNT) and carbon doped YBa₂Cu₃O_{7-δ} superconductor samples using magneto-resistive measurement results. Irreversibility line moves to higher magnetic fields for CNT doped and to lower magnetic field for carbon doped YBCO samples respect to the undoped sample.

PB24

Nonlocal excitations and 1/8 singularity in cuprates

Yoshiro Kakehashi*, M. Atiqur R. Patoary and Sumal Chandra
Department of Physics, University of the Ryukyus, Japan

Low energy excitations and unusual behaviors of electrons in the 2D cuprates have been the question under debates. Especially the non Fermi liquid behaviors and the pseudogap remain unresolved theoretically because of the limited range of the inter-site correlations and the limitation of the momentum and energy resolutions in the theory. We present here our results for the momentum-dependent single-particle excitation spectra of the 2D Hubbard model, which are based on the full self-consistent projection operator method. The theory self-consistently takes into account the long-range intersite correlations with use of the off-diagonal effective medium, and allows us to calculate the excitation spectra with high energy and momentum resolutions. We obtained the excitation spectra being consistent with the QMC results and found at T=0 that the nonlocal excitations enhance the Mott-Hubbard gap and create the shadow-band excitations due to strong antiferromagnetic correlations. The present theory yields the characteristic hole concentration $1-n^* = 0.123$ (=1/8) at which the van Hove type singular peak appears just on the Fermi level at T=0, while it is $1-n^* = 0.15$ at finite temperatures in the 4x4 DCA. The present result suggests the emergence of the 1/8 stripe phase due to the Fermi surface instability.

PB25

Magnetic memory in a ceramic YBCO superconductor composed of sub-micron size grains

Hiroyuki Deguchi^{1*}, Takuya Ashida¹, Mitsuhiro Syudou¹, Masaki Mito¹, Makoto Hagiwara², Kuniyuki Koyama³ and Seishi Takagi¹
¹*Faculty of Engineering, Kyushu Institute of Technology, Japan*
²*Faculty of Engineering and Design, Kyoto Institute of Technology, Japan*
³*Faculty of Integrated Arts and Science, The University of Tokushima, Japan*

The nonequilibrium nature of a ceramic YBCO composed of sub-micron size grains is investigated by measurements of the dc magnetizations. The ceramic YBCO is considered as random Josephson-coupled networks of 0 and π junctions and shows successive phase transition. The first transition occurs inside each grain at Tc1= 81 K and the second transition occurs among the grains at Tc2=47 K. The magnetic glass behavior similar to those of spin-glasses is observed below Tc2.[1] Theoretically, the frustration effect due to the random distribution of π junctions should lead to the chiral-glass state, as predicted by Kawamura and Li.[2] The memory phenomena are investigated by recording the zero-field-cooled and thermoremanent magnetization temperature dependence measured on heating after the cooling process with and without field switches.[3] There are memory effects of the halt at T=44 K imprinted in the system on the re-heating the sample. In the case without field switches at Ts, the influence of the halt is confined to a narrow temperature region near the halt temperature, whereas the memory effects of the halt employing a field switch is extended over a wide temperature region below Ts. The results suggest that chiral-glass ordering occurs at Tc2 in the ceramic YBCO.

[1] H.Deguchi et al., *J. Phys. Conference Series* 320 (2011) 012076. [2] H.Kawamura and Li, *J. Phys. Soc. Jpn.* 66 (1997) 2110. [3] E.L.Papadopolou and P.Nordblad, *Eur. Phys. J. B* 22 (2001) 187.

PB26

Phase diagram of high-Tc superconductivity and antiferromagnetism revealed by Cu-NMR in multilayered cuprates

Hidekazu Mukuda^{1*}, Sunao Shimizu¹, Akira Iyo² and Yoshio Kitaoka¹
¹*Osaka University, Japan*
²*National Institute of Advanced Industrial Science and Technology (AIST), Japan*

We present site-selective nuclear magnetic resonance (NMR) studies on multilayered cuprates, which have uncovered the intrinsic phase diagram of antiferromagnetism (AFM) and high-temperature superconductivity (HTSC) for a disorder-free CuO₂ plane with hole carriers. We revealed the existence of the AFM metallic state in doped Mott insulators, the uniformly mixed phase of AFM and HTSC, and the emergence of d-wave SC with a maximum Tc just outside a critical carrier density, at which the AFM moment on a CuO₂ plane disappears. These results can be accounted for by the Mott physics based on the t-J model, where the superexchange interaction J among spins within the plane plays a vital role as a glue for Cooper pairs or mobile spin-singlet pairs.

PB27

Magnetism and superconductivity in CeCu₂Ge₂ under high pressures and magnetic fields

Fuminori Honda^{1*}, Takashi Maeta², Yusuke Hirose², Atsushi Miyake³, Tetsuya Takeuchi⁴, Katsuya Shimizu³, Tomoko Kagayama³, Rikio Settai² and Yoshichika Onuki²
¹*Graduate School of Engineering Science, Osaka University, Japan*
²*Graduate School of Science, Osaka University, Japan*
³*KYOKUGEN, Osaka University, Japan*
⁴*Low Temperature Center, Osaka University, Japan*

CeCu₂Ge₂ with the ThCr₂Si₂ type tetragonal structure is an antiferromagnet with TN = 4.2 K (AF1) and shows two kinds of superconducting phases named a low-Tsc phase (SC1) and a high-Tsc phase (SC2) under high pressures [1]. We have grown CeCu₂Ge₂ single crystals by Sn-flux method and studied an electronic state under high pressures and magnetic fields by means of the electrical resistivity measurement. We have found two anomalies at TN = 4.1 K and TN'= 1.3 K at 2.6 GPa for example, implying a Neel temperature and a change of magnetic structures with the first order. In the temperature-pressure phase diagram, two kinds of magnetic phases named AF1 and AF2 appear and merge at 5 GPa. At pressures higher than 5 GPa, the AF2 phase becomes dominant. The AF2 phase can be another antiferromagnetic phase, since the metamagnetic transition to the AF1 phase is observed around 3 T for the H || [001] direction. At 8.2 GPa, pressure-induced superconductivity (SC1) is induced below Tsc(onset) = 0.5 K. The upper critical field is 30 kOe for H || [001]. The AF2 phase coexists with SC1 below 10 GPa and the AF2 phase disappears above 11 GPa, revealing only SC1 phase.

[1] E. Vargoz and D. Jaccard: *J. Magn. Magn. Mater.* 177-181 (1998) 294.

PB28

Doping and temperature dependence of Fermi arc in cuprate superconductors

Shipping Feng*, Huaisong Zhao and Lulin Kuang
Department of Physics, Beijing Normal University, China

The pseudogap observed in the excitation spectrum as a suppression of spectral weight in the normal-state of cuprate superconductors is thought to be key to understanding the mechanism of superconductivity. Within the framework of the kinetic energy driven superconducting mechanism [1], we [2] study the evolution of the Fermi arc with doping and temperature by considering the interplay between the superconducting gap and normal-state pseudogap [3]. It is shown that the system in the underdoped regime is a nodal liquid, and the length of the Fermi arc increases with increasing temperatures, in qualitative agreement with the experimental observation on cuprate superconductors [4]. Our results also show that the unusual behavior of the quasiparticle dispersion and Fermi arc in cuprate superconductors is intriguingly related to the effect of the normal-state pseudogap.

[1] Shipping Feng, *Phys. Rev. B* 68, 184501 (2003); Shipping Feng et al., *Physica C* 436, 14 (2006). [2] Huaisong Zhao, Lulin Kuang, and Shipping Feng, unpublished. [3] Shipping Feng, Huaisong Zhao, and Zheyu Huang, arXiv:1109.3973. [4] A. Kanigel et al., *Nature Phys.* 2, 447 (2006); U. Chatterjee et al., *Nature Phys.* 6, 99 (2010).

PB29

Static spin correlation in Pr_{2-x}Ca_xCuO₄ Studied by neutron scattering

Kenji Tsutsumi^{1*}, Tomohiro Miura¹, Masanori Enoki², Kentaro Sato³, Masato Matuura⁴, Kazuyoshi Yamada⁵ and Masaki Fujita⁶
¹*Department of Physics, Tohoku University, Japan*
²*Kyushu Institute Technology, Japan*
³*Department of Physics, Tohoku university, Japan*
⁴*IMR, Tohoku University, Japan*
⁵*WPI, Tohoku University, Japan*
⁶*IMR, Tohoku Univesity, Japan*

It is well known that a small amount of hole-doping into La₂CuO₄ having K₂NiF₄-type (attributed as T) crystal structure destroys the antiferromagnetic (AF) order and superconducting phase appears with further hole doping. On the other hand, recent experimental study on Nd₂CuO₄-type (attributed as T') structured La₂CuO₄ with no apical oxygen clarified contrasting properties to that in T-structured La₂CuO₄; that is Neel temperature is different in two structured systems. [1] Therefore, the crystal structure is an important factor to determine the physical properties. In order to gain further insight into the physics of doped Mott insulator, we performed neutron-scattering measurement on T'-Pr_{2-x}Ca_xCuO₄. The as-grown and annealed x=0.10 samples shows the long-range AF order below TN~290 K. This result suggests a weak Ca doping effect on the AF order, which is contrast to the results in T-La_{2-x}Sr_xCuO₄. In my poster, the details of doping dependence of magnetic order will be presented.

[1] R. Hord et al., *Phys. Rev. B* 82, 180508 (2010).

PB30

High-energy neutron scattering study of spin excitation in slightly-overdoped La_{1.82}Sr_{0.18}CuO₄

Kentaro Sato^{1*}, Masato Matsuura², Masaki Fujita², Kenji Tsutsumi¹, Masanori Enoki³ and Kazuyoshi Yamada⁴
¹*Physics, Tohoku University, Japan*
²*IMR, Tohoku University, Japan*
³*Kyushu Institute of Technology Graduate School of Life Science and Systems Engineering, Japan*
⁴*WPI, Tohoku University, Japan*

Antiferromagnetism in the doped cuprate Mott-insulator has been investigated due to its rich physics and close connection with the high-Tc superconductivity. A finding of a generic form of spin excitations showing the "hourglass" shape in the different class of superconductors La_{2-x}(Sr,Ba)_xCuO₄ (La²⁺) [1] and YBa₂Cu₃O_{7-x} [2] suggests a common role of spin fluctuations in the mechanism of high-Tc superconductivity. Recently, Vignolle and co-workers revealed the existence of two energy scales in the spin excitations of optimally-doped La²¹⁴ [3] and pointed out the possibility of different origins for the excitation separated by energy. To study the dual nature of spin excitations in more detail, we have performed a high-energy neutron scattering measurement on slightly-overdoped La_{1.82}Sr_{0.18}CuO₄. The constant-energy spectrum at low temperature is a broad single-peak in a wide energy range below ~150meV, although the peak-slitting was observed below ~10meV. This feature is somehow similar to the dispersion of spin excitation in the overdoped La²¹⁴. On the other hand, the integrated intensity shows sharp and broad maximums at ~18meV and ~45meV, respectively, as is the case of optimally-doped system. In the poster, we will present the temperature dependence of the overall excitation spectrum and discuss the dual nature of the hourglass-shaped excitation.

[1] J. M. Tranquada et al., *Nature* 429, 534 (2004). [2] S. M. Hayden et al., *Nature* 429, 531 (2004). [3] B. Vignolle et al., *Nature Physics*, 3, 163 (2007).

PB31

Quantized massive gauge fields around the doped holes in high-Tc cuprates and the relation to iron pnictides

Ikuzo Kanazawa*
Physics, Tokyo Gakugei University, Japan

Recently Yazdani[1] has suggested strongly that the high-energy(up to about 400meV) hole-like excitations of the normal state are a direct predictor of the strength of pairing, although he cannot present a model for the excitations. The present author has proposed the mechanisms of evolution of the Fermi arc with increasing temperature[2] and with increasing of hole-doping[3] in high-Tc cuprates. In this study, we present one model for the high-energy excitations, which play an important role on strength of Cooper pairing, and show that quantized massive gauge fields induce short-range spin-fluctuations and short-range orbital fluctuations[4,5].

[1] A.Yazdani, *J.Phys.Condense Matters* 21,164214(2009) [2]I.Kanazawa, *J.Phys.Chem.Solids* 66,1388(2005) [3]I.Kanazawa, *Physica C* 470,5183(2010) [4]H.Kontani and S.Onari,*Phys.Rev.Lett.*104,157001(2010) [5]Y.Yanagi et al. *J.Phys.Soc.Jpn.* 79,123707(2010)

PB32

Ho-doping effect on the static stripe order in La₂₁₄ superconductor

Masaki Fujita*, Masanori Enoki², Satoshi Iikubo², Kenji Tsutsumi³, Kentaro Sato³, Masato Matsuura¹ and Kazuyoshi Yamada¹
¹*Institute for Materials Research, Tohoku University, Japan*
²*Graduate School of Life Science and Systems Engineering, Kyushu Institute of Technology, Japan*
³*Department of Physics, Tohoku University, Japan*
⁴*World Premier International Research Center, Tohoku University, Japan*

We have performed elastic neutron scattering experiments on the superconducting La_{1.8x}Ho_{0.0x}Sr_{0.12}CuO₄ to study the substitution effect of cation with the large magnetic moment at La site on the static spin correlation. In the Ho-free sample with the hole concentration of 0.12, spatially modulated magnetic order is known to be stabilized below T_{spin} ~ 30K [1]. In the present Ho-doped sample, we found the appearance of magnetic peaks at (0.5, 0.5±0.118, 0) positions below T_{spin} ~ 35K, which is similar to the observation in the pristine sample. Furthermore, the volume corrected intensity in the Ho-free and Ho-doped samples is comparable, suggesting a negligible effect of Ho-substitution at La site. These results are quite contrast to the huge enhancement of magnetic intensity and the increase of T_{spin} by substituting magnetic Fe³⁺ ions onto CuO₂ planes [2]. Therefore, the stability of stripe order induced by the cation substitution is sensitive to the substituted site.

[1] H. Kimura et al., *Phys. Rev. B* 59, 6517 (1999). [2] M. Fujita et al., *J. Phys. and Chem. Solids* 69, 3167 (2008).

PB33

High field paramagnetic meissner effect in Ca doped YBa₂Cu₃O_{7-x} single crystals

Valdemar Vieira^{1*}, Augusto Falck¹, Fabio Dias¹, Douglas Da Silva¹, Paulo Pureur², Jacob Schaf³ and Frederik Fabris³
¹*Instituto de Fisica e Matematica, UFPEL, Brazil*
²*Instituto de Fisica, UFRGS, Brazil*
³*Dresden High Magnetic Field Laboratory, HZ Dresden-Rossendorf, Germany*

We report on dc magnetization of a series of Y_{1-x}Ca_xBa₂Cu₃O_{7-x} (x = 0, 0.0025, 0.05, 0.1) single crystals with the goal to study the role of the hole doping on the paramagnetic Meissner effect (PME). [1] The magnetization as a function of the temperature, under constant magnetic field, was recorded adopting the field-cooled procedure. Mfc(T) as well as magnetic relaxation, Mfc(t) for a measurement time up to 50.000s. The Mfc(T) data of our single crystals shows the usual superconductor diamagnetic response when magnetic fields up to 0.5 kOe are applied. In contrast, when H > 0.5 kOe are applied, the Mfc(T) data displays a systematic reduction of the superconductor diamagnetic response until it became predominantly paramagnetic at higher fields not showing tendency to a temperature saturation behavior in the doped samples. This behavior is a signature of the high field paramagnetic Meissner effect (HPPME) in HTSC. [2,3] The Mfc(t) data reveals that the paramagnetic moment of the samples increase continuously as a function of the time. In specific, the Ca doping promotes an enhancement of the HPPME intensity as compared with no doped sample. We suggest the flux compression scenario to explain the HPPME in your samples. [4]

[1] V. N. Vieira et al. *Phys. Rev. B* 76 (2007) 024518-1. [2] F. T. Dias, et al. *Physica C* 470, S111 (2010). [3] F.T. Dias et al. *Phys. Rev. B* 70 (2004) 224519. [4] A.K. Geim et al. *Nature* 396 (1998) 144.

PB34

Growth of a-axis oriented thin films of infinite-layer Sr_{1-x}La_xCuO₂

Hiroyuki Akatsuka*, Keita Sakuma, Kenji Ueda and Hidehumi Asano
Crystalline Materials Science, Nagoya University, Japan

Electron-doped infinite-layer compound Sr_{1-x}La_xCuO₂ has the simplest crystal structure, and is suitable for fundamental studies of high-Tc superconductivity as well as device applications. The epitaxially grown c-axis oriented Sr_{1-x}La_xCuO₂ thin films with Tc of around 40 K were fabricated on the lattice matched substrates like DyScO₃ and KTaO₃[1]. Since the in-plane coherence length ξ_{ab}(4.5nm) of Sr_{1-x}La_xCuO₂ is larger than the out-of-plane coherence length ξ_c(0.3nm)[2], the a-axis oriented film is favorable for junction fabrication. In this paper, we will make the first report on the preparation and properties of a-axis oriented thin films. Sr_{0.9}La_{0.1}CuO₂(a0=0.3949nm, c0=0.341nm) thin films were prepared by magnetron sputtering. KTaO₃(a0=0.3989nm), SrTiO₃(a0=0.3905nm), (La0.18Sr0.82)(Al0.59Ta0.41)O₃(LSAT)(a0=0.3868nm) and LaAlO₃(a0=0.3791nm) substrates were used to investigate the effect of the lattice mismatch. On KTaO₃, LSAT and SrTiO₃ substrates, c-axis oriented films were obtained. In contrast, on LaAlO₃ substrates with a large lattice mismatch (-4.2%), a-axis oriented films were obtained. One possible reason for the a-axis growth is due to a higher-order lattice matching, that is, lattice mismatch between ten unit cell of Sr_{0.9}La_{0.1}CuO₂(001)(3.10nm) and nine unit cell of LaAlO₃(100)(3.412nm) is 0.03%. As-grown thin films showed a semiconducting behavior. Post deposition annealing resulted in the a-axis oriented films with Tconset of around 30 K.

[1] S. Karimoto and M. Naito, *Appl. Phys. Lett.* 84, (2004) 12. [2] V. P. Jovanovic, Z. Z. Li, and H. Raffy, *Phys. Rev. B* 80, (2009) 024501.

PB35

Thermal stability of an epoxy-impregnated HTS racetrack coil without turn-to-turn insulation for rotating machines

Oh Jun Kwon, Kwang Lok Kim, Yoon Hyuck Choi, Hyun-jin Shin and Haigun Lee*
Department of Materials Science and Engineering, Korea University, Korea

Since use of the no-insulation (NI) technique creates a compact system with better thermal and electrical stability, use of a high temperature superconducting (HTS) coil without turn-to-turn insulation is now being proposed for the field coil in HTS rotating machines. Epoxy impregnation of field coils is generally needed to protect the coil against mechanical disturbances by time-varying magnetic fields and to provide high mechanical integrity against the rotational vibrations. Therefore, to use the NI technique on the practical HTS field coil of a rotating machine, it is essential to obtain sufficient information on the thermal and electrical behaviors of the epoxy-impregnated NI coil. In this study, the quench characteristics of epoxy-impregnated HTS racetrack coils without turn-to-turn insulation were investigated using overcurrent tests. Furthermore, the thermal stability of the epoxy-impregnated NI coil at various current charging rates was also investigated and discussed.

<Acknowledgement> This work was supported by a grant from the International Collaborative R&D Program of the Korea Institute of Energy Technology Evaluation and Planning (KETEP) funded by the Korean government Ministry of Knowledge Economy (20118520020020).

July 9 (Mon)

July 9 (Mon)

PB36

Design, fabrication, and testing of a cooling system using solid nitrogen for a 3 T/60-mm RT bore superconducting HGMS

Jung-bin Song, Kwang Lok Kim, Dong Gyu Yang, Yoon Hyuck Choi, Jongseok Lee and Haigun Lee*
Department of Materials Science and Engineering, Korea University, Korea

To develop a compact and stable superconducting high gradient magnetic separator (HGMS) for the removal of copper and silica from chemical mechanical polishing wastewater, a 3 T/60-mm room temperature bore HGMS using solid nitrogen cooling system was fabricated. The HGMS's magnet was assembled using 18 GdBCO-coated conductor double pancake coils, each of which was wound without turn-to-turn insulation. The cooling capabilities of the solid nitrogen cooling system for the superconducting HGMS were examined using cool-down, warm-up, and charging-discharging tests in the temperature range of 10-20 K. The capture efficiency of the superconducting HGMS using the solid nitrogen cooling system was also evaluated using a filtration test.

<Acknowledgment> This work was supported by the International Collaborative R&D Program of the Korea Institute of Energy Technology Evaluation and Planning (KETEP) grant funded by the Korean government Ministry of Knowledge Economy (20118520020020).

PB37

Purification of chemical mechanical polishing wastewater using a 2G HTS high gradient magnetic separation system

Dong Gyu Yang, Jung-bin Song, Young-gyun Kim, Jongseok Lee, Yeonjoo Park and Haigun Lee*
Department of Materials Science and Engineering, Korea University, Korea

Magnetic separation efficiency is related to the strength of the applied magnetic field and the field gradient used to trap the magnetic particles. The use of a magnet wound with high temperature superconducting (HTS) tape enables the magnetic separation system to more efficiently remove wastewater contaminants than their conventional counterparts due to the facile generation of a higher magnetic field due to the absence of Joule heating losses. In this study, we fabricated and tested the second generation (2G) HTS high gradient magnetic separation (HGMS) system for the purification of chemical mechanical polishing wastewater. The capturing efficiencies of the 2G HTS HGMS system were investigated in terms of the wastewater flow velocity and turbidity using repetitive separation tests. Furthermore, the appropriate purification process for enhancing removal efficiency was also discussed.

<Acknowledgment> This study was supported by the Ministry of Knowledge Economy (MKE), Korea, under the IT R&D Infrastructure Program supervised by the National IT Industry Promotion Agency (NIPA-2011-(B1110-1101-0002)).

PB38

Effect of liquid cryogen on a 2G HTS magnet using a mixed cryogen cooling system

Kwang Lok Kim, Jung-bin Song, Yoon Hyuck Choi, Dong Gyu Yang and Haigun Lee*
Department of Materials Science and Engineering, Korea University, Korea

A cooling system employing a mixture of solid cryogen with small amounts of liquid cryogen was reported for use in high temperature superconducting (HTS) applications. Although the liquid cryogen in the mixed cryogen cooling system can improve the thermal contact between the solid cryogen and the HTS magnet, it is essential that further studies be performed because there are insufficient data about the thermal/electrical behaviors of the HTS magnet that has been subjected to mixed cryogen. Therefore, in this study, the quench/recovery characteristics of mixed cryogen-cooled 2G HTS magnets with respect to liquid cryogen amount were examined to investigate the influence of the solid/liquid ratio on the thermal/electrical stabilities of the HTS magnet.

<Acknowledgment> This work was supported by the International Collaborative R&D Program of the Korea Institute of Energy Technology Evaluation and Planning (KETEP) grant funded by the Korean government Ministry of Knowledge Economy (20118520020020).

PB39

Removal of silica and copper ions from CMP wastewater via magnetic seeding aggregation using superconducting HGMS

Jongseok Lee, Jung-bin Song, Dong Gyu Yang, Yeonjoo Park and Haigun Lee*
Department of Materials Science and Engineering, Korea University, Korea

With the increased demand for semiconductor devices, the purification of chemical mechanical polishing (CMP) wastewater in the semiconductor industry has become of great importance for worldwide environmental protection. Superconducting high gradient magnetic separation (HGMS) is one promising technique due to its compact design and efficient and accurate removal of particles. For the HGMS, various ferromagnetic materials were required to coagulate non-magnetic heavy metal ions and various nanoparticles in CMP wastewater. In this study, we suggested the use of a coagulation process optimized by magnetic seeding aggregation at various pH values for the separate yet simultaneous removal of copper ions and silica nanoparticles. The filtration efficiency of the flocculated substances in an HGMS was evaluated using turbidity measurements.

<Acknowledgment> This study was supported by the Ministry of Knowledge Economy (MKE), Korea, under the IT R&D Infrastructure Program supervised by the National IT Industry Promotion Agency (NIPA-2011-(B1110-1101-0002)).

PB40

Joint characteristics of ReBCO-coated conductors using various fusion splicing techniques

Yeonjoo Park¹, Hyun-jin Shin¹, Young-gyun Kim¹, Young Kun Oh² and Haigun Lee^{1*}
¹Department of Materials Science and Engineering, Korea University, Korea
²K-joins Co., Korea

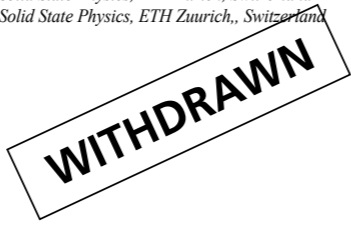
For superconductor splicing, it is essential that joint resistance be minimized between superconducting tapes to operate with the persistent current mode and lengthen them. We have already proposed the concept of RE-Ba₂Cu₃O_{7-x} (ReBCO) tape fusion splicing technology that is based on the unique ReBCO thermal and structural properties. The melting point of ReBCO decreases as the surrounding oxygen partial pressure decreases, allowing for low temperature splicing and recovery of the superconductivity lost during the joining process by a subsequent oxygenation annealing process. In this study, the fusion splices with changing joining parameters, such as PO₂, heating rate, peak temperature and holding time, cooling rate, oxygen flow rate, temperature and holding time for oxygenation annealing, tape clamping pressure, and so on were performed using the following two splicing methods: 1) the ReBCO-ReBCO interface was directly connected by fusion, and 2) the Ag layer was diffused in a face-to-face manner without solder. The joint characteristics were evaluated in terms of joint resistances, critical currents, and index numbers. Furthermore, the sample morphologies and structures were analyzed by scanning electron microscopy (SEM) and X-ray diffraction (XRD), respectively.

<Acknowledgment> This work was supported by the International Collaborative R&D Program of the Korea Institute of Energy Technology Evaluation and Planning (KETEP) grant funded by the Korean government Ministry of Knowledge Economy (20118520020020).

PC01

Bulk electronic structure of LaRu₂P₂ probed by soft X-ray angle-resolved photoemission spectroscopy (SX-ARPES)

E. Razzoli¹, M. Kobayashi¹, V. N. Strocov¹, B. Delley¹, Z. Bukowski², J. Karpinski³, N. C. Plumb¹, M. Radovic¹, J. Chang¹, T. Schmitt¹, L. Patthey¹, J. Mesot¹ and M. Shi^{1*}
¹Paul Scherrer Institute, Switzerland
²Laboratory for Solid State Physics, ETH Zurich, Switzerland
³Laboratory for Solid State Physics, ETH Zuurich., Switzerland



PC02

Superlattice quantum critical point in the cubic metal (Sr/Ca)₃Ir₂Sn₁₃

Lina Esther Klintberg¹, Swee Kuan Goh^{1*}, Patricia Alireza¹, Paul Saines¹, David Tompsett¹, Peter Logg¹, Jinhu Yang², Bin Chen², Kazuyoshi Yoshimura² and Malte Grosche¹
¹University of Cambridge, United Kingdom
²University of Kyoto, Japan

Structural self-organisation is a central theme in condensed matter physics. Often, the symmetry of a given parent structure is lowered by subtle structural variations which decrease the electronic degeneracy and thereby the total energy. Examples include Jahn-Teller and Peierls distortions and, more generally, modulated lattice distortions, or superlattices. The quasi-skutterudite compounds R3T4X13, where R is an earth alkaline or rare-earth element, T is a transition metal and X is a group-IV element, form either in a simple cubic structure, called the I-phase, or in the variant I'-phase, which can be viewed as a superlattice distortion of the I-phase. Here, we investigate the borderline system (Sr/Ca)₃Ir₂Sn₁₃, which we report forms in the I-phase, but transforms into the I'-phase on cooling. Hydrostatic pressure is used to suppress the second order structural transition enabling the first comprehensive investigation of a structural quantum critical point in a three-dimensional charge density wave driven superconductor.

PC03

Unconventional superconductivity in PuCoIn₅: An NQR investigation.

Hiroshi Yasuoka¹, Georgios Koutroulakis^{1*}, Hiroyuki Chudo², Eric D. Bauer¹ and Joe D. Thompson¹
¹Los Alamos National Laboratory, USA
²Advanced Science Research Center, Japan Atomic Energy Agency, Japan



PC04

Pressure effect on the structural and superconducting transitions in a caged compound PrRh₂Zn₂₀

Y Sugano¹, T Ohsuka¹, K Umeo^{2*}, N Nagasawa¹, T Onimaru¹ and T Takabatake¹
¹AdSM, Hiroshima University, Kagamiyama 1-3-1, Higashi-Hiroshima 739-8530, Japan
²N-BARD, Hiroshima University, Kagamiyama 1-3-1, Higashi-Hiroshima 739-8526, Japan

PrRh₂Zn₂₀ crystallizes in a cubic CeCr₂Al₂₀-type structure, where the Pr³⁺ ion is encapsulated in a polyhedron formed by 16 zinc atoms. The crystalline electric field ground state of 4f2 electrons in the Pr ion was found to be a nonmagnetic Γ3 doublet [1]. The resistivity of this compound shows a superconducting transition at TSC = 0.060 K and a hysteretic behavior in the temperature range from 140 K to 470 K, which originates from a structural phase transition. In order to reveal the interplay between the structural and superconducting transitions, we have measured the electrical resistivity ρ for a single crystalline sample under pressures up to 2 GPa and at temperatures down to 0.052 K. With increasing pressure up to 2 GPa, the anomaly in ρ(T) at TS = 160 K shifts to higher temperatures by the ratio of 3 K/GPa. This indicates that the low-temperature phase (T<TS) is stabilized under pressure. At P = 0.85 GPa, TSC was not observed down to 0.052 K, indicating that the superconducting state is suppressed under pressure. The opposite responses to the pressure imply that the superconducting state is in competition with the low-temperature phase below TS.

[1] N. Nagasawa, to be published in the proceedings of SCES 2011.

PC05

Phonon raman scattering of YB6

Koichi Yukawa^{1*}, Hisamitsu Bandou¹, Norio Ogita¹, Masayuki Udagawa¹, Fumitoshi Iga² and Takumi Hasegawa¹
¹Graduate School of Integrated Arts and Sciences, Hiroshima University, Higashi-Hiroshima 739-8521, Japan
²Graduate School of Science & Engineering, Ibaraki University, 2-1-1 Bunkyo, Mito 3 10-0056, Japan

YB6 becomes superconducting state below 7.5K. Both tunneling and photoemission measurements suggested that YB6 is the strong coupling superconductor with 2Δ/kBTc = 3.8 and phonons with 8meV play an important role for superconductivity. We once reported the results of Raman scattering using 514.5nm laser in SCES2010. Very recently we have measured the Raman scattering spectra with the high resolution using 674.1nm laser. Three Raman active phonons are similar with the previous report, that is, the doublet spectra of the T2g and Eg modes suggest that the crystal symmetry of YB6 is F4/mmm as already reported. The remarkable change has been observed in the low energy spectra below 200cm-1, where the vibration due to Y is dominant. Below 100K, the peak at about 100cm-1 disappears and two new peaks appear. At this temperature the resistivity deviated from the linear dependence. This implies the structural change at low temperature. Furthermore, the energy of two lowest-energy peaks at 50 and 70cm-1 decreases with decreasing temperature. Below Tc, their energies become constant. These results are the experimental evidences that the Y vibration is highly anharmonic and that the anharmonic vibration or rattling mode due to Y is important for superconductivity.

PC06

Vortex lattice structures in spin-triplet superconductors with weak spin-orbit coupling

Shuhei Takamatsu^{1*} and Youichi Yanase²
¹Graduate School of Science and Technology, Niigata University, Japan
²Faculty of science, Niigata University, Japan

The oxide Sr₂RuO₄ was discovered to be superconducting by Maeno et al. in 1994[1]. Sr₂RuO₄ is considered to be a spin-triplet superconductor from both theoretical and experimental point of view. Recently, the direction of d-vector in the superconducting state of Sr₂RuO₄ subjected to the magnetic field is discussed. In order to determine the direction of d-vector, we investigate the vortex lattice structure of Sr₂RuO₄ with a weak spin-orbit coupling for the magnetic field along c-axis. We will report the difference in vortex lattice structures between chiral state and helical state.

[1] Superconductivity in a layered perovskite without copper, Y. Maeno, H. Hashimoto, K. Yosida, S. Nishizaki, T. Fujita, J. G. Bednorz and F. Lichtenberg, Nature (London) 372, 532 (1994)

PC07

Effect of the magnetic trapped flux on the heat capacity of the low-temperature superconductors: Pb, La, Sn

Sergey Mikhailovich Podgornykh^{1*}, Veronika Myakon'kikh² and Veronika Dyakina³
¹Institute of Metal Physics, Ural Federal University, Russia
²Ural Federal University, Russia
³Institute of Metal Physics, Russia

Effect of the magnetic prehistory on the temperature dependence of the heat capacity of the superconducting Pb, La, Sn has been studied. The intermediate state is characterized by a subdivision of the specimen into superconducting and normal regions that the relative total volumes of these two types of region are determined by the mean induction. The trapped flux was produced after the magnetic field was turned off. We observed a difference of the heat capacity between zero field cooling (ZFC) and field cooling (FC) states in zero magnetic field for the ring specimen. It was found that the FC heat capacity has a smaller value than the heat capacity both in the normal and in superconducting states. We believe that the surface energy changes between the normal and superconducting phases and gives rise to the change of the heat capacity of the specimen. This result is the first experimental evidence of the surface energy contribution to the heat capacity. The work was supported by Russian Foundation For Basic Research Grant No. 10-02-96019-r-ural-a.

July 9 (Mon)

July 9 (Mon)

PC08

A novel superconductivity in Ir oxides with large spin-orbit coupling

Hiroshi Watanabe*, Tomonori Shirakawa and Seiji Yunoki
RIKEN, Japan

Recently, the 5d transition metal oxides such as Sr₂IrO₄ and Ba₂IrO₄ have attracted much attention as a novel Mott insulator. In these materials, three t_{2g} orbitals of Ir atoms are hybridized with each other by the spin-orbit coupling of 5d electrons. As a result of the quantum entanglement of spin and orbital degrees of freedom, an anomalous Jeff=|L-S|=1/2 state is realized, which causes interesting properties [1]. To clarify the properties of this system, we have studied the ground state of the three-orbital Hubbard model with a spin-orbit coupling term using variational Monte Carlo method and variational cluster approximation [2]. Here, we study the electronic states when carriers are doped in this three-orbital system and discuss the possibility of superconductivity. The obtained ground state phase diagram reveals the antiferromagnetic state, stable around the electron density n=5, is destabilized by carrier doping and the ground state turns to be superconducting under a certain condition. Similar to the high-Tc cuprates, a large asymmetry between electron doping (n>5) and hole doping (n<5) is also observed. Due to the large spin-orbit coupling, the spin is no longer a good quantum number. Instead, the pseudospins form a singlet pairing and a “d-wave like” superconductivity is realized.

[1] B. J. Kim et al., *Science* 323, 1329 (2009). [2] H. Watanabe et al., *Phys. Rev. Lett.* 105, 216410 (2010)

PC09

Fermi surface studies of Sr₃Ir₄Sn₁₃ via the Shubnikov-de Haas effect

Swee K. Goh^{1*}, Lina Klntberg¹, David A. Tompsett¹, Sven Friedemann¹, Stan Tozer², Jinhu Yang³, Bin Chen³, Kazuyoshi Yoshimura³ and Malte Grosche¹

¹University of Cambridge, United Kingdom
²National High Magnetic Field Laboratory, Florida State University, USA
³Kyoto University, Japan

The ternary stannide system (Ca,Sr)₃Ir₄Sn₁₃ is recently reported to feature a superlattice quantum critical point, where the superlattice distortion transition temperature T* is suppressed to 0 K [1]. Sr₃Ir₄Sn₁₃ lies on the part of the phase diagram where T*~147 K, and hence the low temperature phase is the superlattice phase. Using the Shubnikov-de Haas effect, we directly study the Fermiology of this superlattice phase, and compare the results with bandstructure calculations performed both with and without the superlattice distortion. The effective mass and the mean free path associated with various Shubnikov-de Haas frequencies will be presented. The relevance of the present study to superconductivity and quantum criticality will be discussed.

[1] L. E. Klntberg, S. K. Goh, P. L. Alireza, P. J. Saines, D. A. Tompsett, P. W. Logg, J. Yang, B. Chen, K. Yoshimura and F. M. Grosche, submitted (2012)

PC10

Magnetism in CeIr(Si_{1-x}Ge_x)₃ compounds

Jan Prokleska*, Jiri Pospisil, Marie Kratochvilova and Vladimir Sechovsky
DCMP, Charles University, Ke Karlovu 5, 121 16, Prague, Czech Republic

The CeMX₃ intermetallics adopting the noncentrosymmetric tetragonal BaNiSn₃-type crystal structure recently attracted much attention mainly owing to unconventional superconductivity observed in some of them [1]. CeIrSi₃ and CeIrGe₃ were reported to exhibit antiferromagnetic ordering with TN = 5.0 K and 8.5 K, respectively. CeIrGe₃ also undergoes an order-order transition at T1 = 4.7 K. When applying hydrostatic pressure TN gradually decreases and a superconducting dome appears in the vicinity of QCP for the pressure Pc = 2.2 and 23 GPa, respectively [1, 2]. Our work has been motivated by the desire to know how the magnetism and superconductivity evolve with the composition of the SiGe sublattice. For this purpose we have prepared polycrystalline samples of selected compositions of the SiGe sublattice by arc melting, annealed and characterized them and measured magnetization, resistivity and specific heat in a wide temperature range and various magnetic fields. The solutions keep the crystal symmetry of the parent compounds and the lattice parameters follow Vegard’s law. The TN vs. x dependence is not entirely monotonous; a minimum TN is observed for x between 0.75 and 1. The results of powder neutron diffraction will be presented as well.

[1] Ch. Pfeleiderer, *Rev. Mod. Phys.* 81, 1551 (2009) and ref. therein [2] F. Honda et al., *PRB* 81, 140507 (2010)

PC11

Superconductivity at 5.2K in ZrTe₃ polycrystals

P. L. Paulose* and C. S. Yadav
Tata Institute of Fundamental Research, India

Interplay of the Charge Density Wave (CDW) and Superconducting (SC) states is a subject of significant interest. Low dimensional chalcogenides of transition metals are one of the well studied systems that show the coexistence of these competing phenomena. Recently Cu and Ni intercalated single crystals of ZrTe₃ are reported to show bulk SC at 3.8K and 3.1K respectively. However single crystalline ZrTe₃ show only filamentary SC below 2K, along with CDW at 63K. We have studied the polycrystalline ZrTe₃, and the effect of intercalation of Cu and Ag on the superconducting and CDW states of the compound. Our main finding is the occurrence of filamentary superconductivity at enhanced temperature of 5.2K in the polycrystalline ZrTe₃, at ambient pressure, and the SC coexists with the CDW phase. Enhancement in Tc mimics the effect of external pressure on SC in ZrTe₃ single crystals. The strains between the agglomerated small single crystallites in polycrystalline samples could be one possible reason. The intercalation of Cu or Ag, does not affect the transition temperatures but suppresses the CDW state. We have analyzed the resistivity data to estimate the relative loss of carriers and reduction in the nested Fermi surface area upon CDW formation in these

1. Zhu X, Lei H, and Petrovic C 2011 *Phys. Rev. Lett.* 106 246404 2. Lei H, Zhu X, and Petrovic C 2011 *Euro Phys. Lett.* 95 17011 3. Takahashi S and Sambongi T 1983 *J. Physique* 44 C-3 1733 4. Yomo R, Yamya K, Abliz M, Hedo M, and Uwamoto Y 2005 *Phys. Rev. B* 71 132508 5. Ido M, Okayama Y, Jjiri T and Okajima Y 1990 *J. Phys. Soc. Jap.* 59 1341

PC12

Coexistence of superconductivity and antiferromagnetism in CeNi_{0.8}Bi₂

Soo-whan Kim¹, Soohyun Kim¹, Kyujoon Lee¹, Adrian Hiller², Devashibhai Adroja² and Myung-hwa Jung^{1*}

¹Department of Physics, Sogang University, Korea
²Science and Technology Facilities Council, United Kingdom

There have been some reports on RNiBi₂ (R=rare-earth elements) with ZrCuSiAs-type structure[1,2]. Both superconductivity and antiferromagnetism were observed in CeNi_{0.8}Bi₂. The previous studies suggested two types of carriers with different masses; a light electron responsible for superconductivity and a heavy electron for antiferromagnetism[3]. However, the antiferromagnetic transition was not found in specific heat data. Thus, we have also studied RNi_{0.8}Bi₂ (R = La, Ce) in order to take a close look at the possible coexistence of superconducting and antiferromagnetic order parameters. As observed previously, both samples are type-II superconductors with the superconducting transition temperature TC = 4 K. For CeNi_{0.8}Bi₂ the lower and upper critical fields are found to be 62 Oe and 660 Oe. Two antiferromagnetic transitions are observed at TN1 = 5 K and TN2 = 7 K. These results well agree with the magnetization versus field data showing two metamagnetic transitions around 5 kOe and 40 kOe. We suggest that they correspond to commensurate and incommensurate antiferromagnetic transitions, respectively. These results are also in good agreement with the neutron experiments.

1. K. Kodama, S. Wakimoto, N. Igawa, S. Shamoto, H. Mizoguchi, and H. Hosono, *Phys. Rev. B* 83, 214512 (2011) 2. M. H. Jung, A. H. Lacerda, and T. Takabataka, *Phys. Rev. B* 65, 132405 (2002) 3. H. Mizoguchi, S. Matsuiishi, M. Hirano, M. Tachibana, E. Takayama-Muromachi, and H. Karagi, *Phys. Rev. Lett.* 106, 057002 (2011).

PC13

Optical studies of superconducting InN thin film

H. L. Liu^{1*}, C. Y. Liu¹, C. R. Lu¹, D. C. Ling² and P. H. Chang³

¹Department of Physics, National Taiwan Normal University, Taiwan
²Department of Physics, Tamkang University, Taiwan
³Department of Materials and Mineral Resources Engineering, National Taipei University of Technology, Taiwan

The indium nitride (InN) thin film (thickness about 220 nm) was grown on (0001) sapphire substrate by metal-organic vapour phase epitaxy technique. The superconducting transition temperature determined by dc resistivity and magnetization gave a Tc about 2 K. Near-infrared photoluminescence from InN thin film can be clearly observed at room temperature. The optical reflectance was measured over a wide frequency range (50 ~ 52000 cm-1) and at temperature between 10 and 340 K. To extract the optical constants of the films, the Drude-Lorentz model was used to fit all of the layers of this thin-film structure. From the parameters obtained, the optical constants were computed. The vibrational spectrum of InN thin film consists of a A1(TO) and a E1(TO) at about 448 cm-1 and 478 cm-1. The temperature variation of the phonon parameters can be explained by the anharmonic effect. Notably, the Drude plasma frequency (~ 3200 cm-1) and the position of the band absorption (~ 6500 cm-1) exhibit little temperature dependence, whereas the scattering rate monotonically decreases with decreasing temperature. All of these observables suggest the unusual normal-state behavior in this superconducting thin film.

PC14

Lateral Josephson junction induced by inverse proximity effect

Lu-kuei Lin¹, Ssu-yen Huang¹, Jin-hua Huang² and Shang-fan Lee^{3*}
¹Institute of Physics, Academia Sinica, Taiwan
²Materials Science and Engineering, National Tsing Hua University, Taiwan

A Josephson junction is characterized by a phase coherent transfer of the Cooper pairs across a weak link between two superconducting electrodes. The proximity effect at the interface between a superconductor and a ferromagnetic metal occurs, implying that the Cooper pairs penetrate into the ferromagnet. It results in spatial oscillations of the superconducting order parameter in the ferromagnet. Recently an opposite effect so-called “inverse proximity effect”, i.e. the induction of a magnetic moment in a superconductor in contact with a ferromagnet attracted much attention. We utilize the inverse proximity effect in superconductor-ferromagnet bilayer to generate lateral Josephson junctions. The weak link is created by a strong ferromagnet Py strip across a superconductor Nb bridge due to inverse proximity effect and forms a region S’. Samples with different size of weak link region S’ were fabricated by varying the Py strip width from 0.5 to 2 μm. The junctions exhibit a modulation of the critical current in perpendicular magnetic field similar to a Fraunhofer interference pattern even when the S’ has such long distance as 2 μm, which proves the dc Josephson effect and spin triple component taking place.

PC15

13C NMR study of charge fluctuation induced superconductivity in beta''-(BEDT-TTF)4[(H₂O)Ga(C₂O₄)₂]-C₆H₅NO₂

Yoshihiko Ihara*, Harumi Seki and Atsushi Kawamoto
Department of Physics, Graduate School of Science, Hokkaido university, Japan

Superconductivity emerging near antiferromagnetism has been thoroughly investigated. The antiferromagnetic fluctuations in the vicinity of quantum critical point are believed to induce such superconductivity. In this paper, we report experimental evidence that points to the novel possibility of superconducting state, that is, charge fluctuation induced superconductivity. The molecular superconductor beta''-(BEDT-TTF)4[(H₂O)Ga(C₂O₄)₂]-C₆H₅NO₂ demonstrates a charge instability at 100 K, before showing the superconducting transition at 7.5 K [1]. Besides, this salt is intriguing because of its high upper critical field of 33 T, which is almost three times the Pauli limiting field [2]. We performed the 13C NMR experiment and revealed on the basis of the Knight shift measurement that the spin-singlet superconductivity is realized in the charge disproportionated state. The nuclear spin-lattice relaxation rate measurement detects the strong electron-electron correlations slightly above superconducting transition temperature. Since 13C NMR technique can probe only the magnetic properties, we measured in-plane resistivity as a complementary probe and found an abrupt increase below 10 K. These results lead us to address the importance of charge fluctuations to induce superconductivity.

[1] A. I. Coldea et al., *PRB* 69, 085112 (2004). [2] A. F. Bangura et al., *PRB* 72, 014543 (2005).

PC16

Ac susceptibility components of a thin type-II superconducting annulus carrying a radial current

Aliakbar Babaei Brojeny*, Mostafa Molavi, Asghar Sharbaf Zadeh and Mahdi Sohrabi
Department of Physics, Isfahan University of Technology, 84156-83111, Iran

By assuming a spatial dependence on the sheet-current density, we have investigated the real (χ') and imaginary parts (χ'') of the susceptibility of a thin type-II superconducting annulus in the absence and also in the presence of a transport radial current, using the Bean critical state model in which the critical current density is assumed to be independent of the local magnetic field. The results of our calculations on the components of the magnetic susceptibilities in two cases and for the different aspect ratios are compared with each other. The comparison shows that by applying a radial current to the sample, the imaginary part of the susceptibility is increased. We have also studied the variations of the χ'' with respect to χ' for a several aspect ratios.

1-Ali A. Babaei-Brojeny and John R. Clem, *Phys. Rev. B* 68, 174514 (2003). 2-Ali A. Babaei-Brojeny, Asghar Sharbaf Zadeh and Mostafa Molavi, *Journal of Physics:Conference Series...*(2012).

PC17

Pressure evolution of superconductivity in β-pyrochlore oxides

Takeshi Matsubara¹, Takayuki Isono², Daisuke Iguchi¹, Yo Machida¹, Koichi Izawa^{1*}, Bernard Salce³, Jacques Flouquet², Hiroki Ogusu², Jun-ichi Yamaura² and Zenji Hiroi²
¹Department of physics, Tokyo Institute of Technology, Meguro, Tokyo 152-8551, Japan
²ISSP, University of Tokyo, Kashiwa, Chiba 277-8581, Japan
³SPSMS, CEA-Grenoble, 38054 Grenoble Cedex 9, France

The β-pyrochlore oxides AO₅O₆ (A = K, Rb and Cs) have attracted much interest because of their unusual electronic properties including the superconductivity[1]. A unique feature of this system is the presence of the remarkable anharmonic vibration of an A ion, called ‘rattling’ motion. Although it has been pointed out by various studies that the rattling motion plays an important role for the occurrence of superconductivity in this system, its concrete role for superconductivity have not been understood yet. In order to clarify the interplay between the rattling motion and superconductivity, we study the pressure (P) evolution of superconductivity in magnetic field (H) at low temperatures (T). The rattling motion could be affected by pressure through the modification of the crystal lattice. In this paper, we report the T-H-P phase diagram of AO₅O₆ and K_{0.8}Rb_{0.2}Os₅O₆ obtained by specific heat measurements and discuss the pressure variation of the electron-phonon coupling and phonon frequency. We demonstrate that the non-monotonous pressure dependence of the transition temperature can be explained in terms of the competition between the enhancement of the electron-phonon coupling and the suppression of the phonon frequency.

[1]Y.Nagao et al., *J.Phys.Soc.Jpn.* 78 064702 (2009)

PC18

Inverse magnetic proximity effects in superconducting Sn-Ni nanoparticle assemblies

Chi-hung Lee, Yen-cheng Chen, Chin-wei Wang and Wen-hsien Li*
Physics, National Central University, Taiwan

Although the superconductivity of the element Sn, in their bulk form, is believed to be associated with the spin-singlet s-wave pairing, it is now known that the superconducting parameters are strongly dependent on the physical size of the system. Here, we report on the results of magnetization, magnetic susceptibility and resistivity measurements made on Sn, Sn-Ni and Sn-Au nanoparticle assemblies. The thermal profiles of the magnetic susceptibility of Sn nanoparticle assemblies can be described by Scalapino’s expression. Inverse magnetic proximity effect is observed, as the TC of the superconducting nanoparticles is found to be noticeably increased, when magnetic Ni nanoparticles are introduced into the vicinity of the superconducting nanoparticles. Closing up the spatial separations between Sn and Ni nanoparticles leads to a further increase in TC. There is a critical Ni composition and a critical spatial separation between the magnetic and superconducting nanoparticles that must be reached before their magnetic proximity will suppress the superconductivity. On the other hand, the inverse proximity effect of the In-Ni nanoparticle assemblies is not observed in the (Sn-C)14(Au-A)86 nanoparticle assembly, where TC of Sn remains essentially unaltered by cold pressing. A qualitative mechanism is proposed to understand the present observations.

PC19

Pressure study on anisotropic electrical resistivity of Hg-doped CeRhIn₅

Soonbeom Seo¹, Sol Ju¹, E.d. Bauer², J.d. Thompson² and Tuson Park^{1*}
¹Physics, Sungkyunkwan University, Korea
²Physics, Los Alamos National Laboratory, USA

The stoichiometric compound CeRhIn₅ is a prototypical antiferromagnet where Ce 4f moments align below 3.8 K. With increasing pressure, the antiferromagnetic ordering of CeRhIn₅ disappears and the superconducting state emerges. When doped with Hg, the antiferromagnetic transition TN initially decreases and develops a different magnetic structure with further increasing Hg concentration. In this research, we focused on a 0.45 % Hg-doped CeRhIn₅, where TN is suppressed from 3.8 K to 3.4 K and the magnetic structure is same as that of the undoped compound with Q=(1/2, 1/2, 0.298). By applying hydrostatic pressure, we suppressed TN to zero and measured the anisotropic electrical transport measurements for the electrical current applied within and perpendicular to the Ce-In plane. Evolution of the anisotropic transport property across the quantum critical point will be discussed.

PC20

Control of superconductivity in parity mixing superconductors Li₂T₃B(T:Pt,Pd) by non-magnetic impurity and defect doping

Guizhi Bao¹, Gaku Eguchi², Akiko Ono³, Yoshihiko Inada⁴, Yoshiteru Maeno² and Guo-qing Zheng¹
¹Department of Physics, Okayama University, Japan
²Department of Physics, Graduate School of Science, Kyoto University, Japan
³Graduate School of Education, Okayama university, Japan
⁴Graduate school of Natural Science and Technology, Graduate School of Education, Okayama university, Japan

Recently, superconductors with noncentrosymmetric crystal structures like Li₂T₃B (T:Pt, Pd) have been the focus of in-depth research with its parity mixing nature. Previous studies of NMR and penetration depth measurements suggested that Li₂T₃B is a spin triplet dominant and Li₂Pd₃B is a s-wave spin singlet dominant superconductor, approximately 2:3 and 4:1 ratio of spin singlet and spin triplet order parameters, respectively [1-3]. It is known that s-wave superconductor without the sign inversion of the order parameter on the Fermi surface is not affected by non-magnetic impurity and defects doping as contrasted to that of a non s-wave superconductor. In this research, we prepared different quality samples by substituting B with Al. Sample qualities were estimated by residual resistivity. Li₂Pd₃B exhibits the small T_c suppression attributed by the non-magnetic impurities and defects, while H_{c2}(0) value increased. This behavior is similar in ordinary s-wave superconductor. While results for Li₂Pt₃B show that T_c and H_{c2}(0) value were found to be suppressed by disorder. However, the rate of T_c-suppression by disorder has been found to be not so large to be explained by the pair-breaking effect expected for the non s-wave superconductor. Further details will be outlined during the actual presentation.

[1] Nshiyama M, Inada Y, and Zheng Guo-qing, 2007 Phys.Rev. Lett. 98, 047002 [2] Nshiyama M, Inada Y, and Zheng Guo-qing, 2005 Phys.Rev. B 71, 220505 [3] H. Q. Yuan et al., Phys. Rev. Lett. 97 (2006) 017006

PC21

Pressure-induced metal-insulator transition of Mott insulator Ba₂IrO₄

Daisuke Orii^{1*}, Masafumi Sakata¹, Atsushi Miyake¹, Katsuya Shimizu¹, Hiroataka Okabe², Masaaki Isobe², Eiji Muromachi² and Jun Akimitsu³
¹KYOKUGEN, Osaka Univ., Japan
²NIMS, Japan
³Aoyama Gakuin Univ., Japan

Ba₂IrO₄ is an antiferromagnetic Mott insulator, because the large spin-orbit interactions of the 5d electrons in Ir atoms lift the energy levels. The magnetic moment is suppressed to ~ 0.34 μB/Ir atom because of the spin fluctuation, and the Neel temperature TN is ~ 240 K. These magnetic properties are similar to ones of La₂CuO₄, which is the parent material of a high-T_c superconductor [1-3]. The crystal structures are also similar. Here, in order to inhibit the insulating state and to search the superconducting phase, the electrical resistivity of Ba₂IrO₄ has been performed under high pressure. According to the present results, metal-insulator transition was observed at 28 GPa, but not the superconducting transition above 50 mK.

[1] H. Okabe et al.: Phys. Rev. B, 83, 155118 (2011). [2] D. Vaknin et al.: Phys. Rev. Lett., 58, 2802 (1987). [3] T. Freltoft et al.: Phys. Rev. B, 36, 826 (1987).

PC22

Charge and spin order of charge stripe ordered La_{2-x}Sr_xCoO₄

Paul G. Freeman¹, E. Wechke², E. Schierle², A. T. Boothroyd³ and D. P³
¹Helmholtz-Zentrum Berlin, Germany; EPFL, Lausanne, Switzerland; ILL, Grenoble, France
²Helmholtz-Zentrum Berlin, Germany
³Department of Physics, Oxford University, United Kingdom

Since the discovery of charge stripe order in the cuprates, the role of stripes in high temperature superconductivity, and whether charge stripes are ubiquitous to the cuprates has been under intensive debate[1]. Recent neutron scattering studies of cobalt and manganese based charge-stripe ordered materials have demonstrated how the striking hourglass excitation spectrum of the cuprates is consistent with charge-stripe order[2,3]. One important experimental observation in charge-stripe ordered La_{2-x}Sr_xCoO₄ is however presently missing, direct observation of stripe charge order itself. Although alternative forms of charge order has been observed in cobaltates in the form of a checkerboard charge ordered state and a proposed charge river state[4,5]. Here we use the technique of resonant soft x-ray scattering to study by diffraction the spin and charge ordering of the charge-stripe phase of La_{2-x}Sr_xCoO₄. We report our analysis of the diffuse order recorded in our study, this study completes the evidence for the charge-stripe model of this system that is used to explain the hourglass spin excitation spectrum.

[1] M. Tranquada, et. al., Nature 375, 561 (1995). [2] A. T. Boothroyd, et. al., Nature 471, 341-344 (2011). [3] H. Ulbrich, et. al., arXiv:1112.1799. [4] I. A. Zaloznyak, et. al. Phys. Rev. Let. 85, 4353 (2000). [5] N. Sakiyama, et. al. Phys. Rev. B 78, 180406(R) (2008).

PC23

Strong enhancement of superconductivity in inorganic electride 12CaO•7Al₂O₃:e- under high pressure

Shigeki Tanaka^{1*}, Tomoki Kato¹, Atsushi Miyake¹, Tomoko Kagayama¹, Katsuya Shimizu¹, Sung Wng Kim², Satoru Matsuishi³ and Hideo Hosono⁴
¹KYOKUGEN, Osaka University, Japan
²Frontier Research Center, Tokyo Institute of Technology, Japan
³Materials and Structures Laboratory, Tokyo Institute of Technology, Japan
⁴Frontier Research Center, Materials and Structures Laboratory, Tokyo Institute of Technology, Japan

The nanoporous main group oxide 12CaO•7Al₂O₃ (C₁₂A₇) is a compound in the system CaO-Al₂O₃ and is used widely as a constituent of aluminous cements. It can be transformed from a wide-gap insulator to a metal with substituting electrons for anions in cages constituting a positive frame. A superconducting transition was found at T_c = 0.2-0.4 K for C₁₂A₇ electride (C₁₂A₇:e-) doped with anionic electrons to 2*10²¹ per cubic centimeter[1]. We carried out the ac-susceptibility measurement of single crystalline C₁₂A₇:e- under high pressure using a piston-cylinder cell and a diamond anvil cell. With increasing pressure, T_c monotonically increases up to 1.0 K at 2.4 GPa. In addition, the upper critical field H_{c2} (T) and -dH_{c2}/dT becomes larger. The density of states at the Fermi level is estimated to increase under high pressure, in agreement with dTc/dP > 0.

[1] M. Miyakawa et al., J. Am. Chem. Soc. Vol. 129 (2007) 7270.

PC24

Superconductivity in conical magnets

Gertrud Zwicknagl
 Technische Universitaet Braunschweig, Germany

The influence of spatially modulated exchange fields on superconducting properties is discussed. Of particular interest are conical magnets where the non-collinear magnetic structure permits to control the symmetry of the pair wave function. The limiting cases - homogeneous ferromagnetic and anti-ferromagnetic exchange field - have been extensively studied. The central focus of the present work is the variation with modulation length of the superconducting properties. I discuss the evolution of the induced triplet components and analyze their orbital structures. Spin-resolved tunnelling spectra highlight the cross-over from typical pair-breaking to pair-weakening which occurs when the magnetic modulation length is comparable to the superconducting coherence length in the absence of exchange fields.

PC25

Observation of Bose-metallic phase in Ta Films

Sungyu Park* and Eunseong Kim
 Center for Supersolid & Quantum matter Research, Department of Physics, KAIST, Daejeon, 305-701, Korea

Superconductor-insulator transition has been induced by tuning film thickness or magnetic field [1-3]. Recent electrical transport measurements of Ta thin films revealed an interesting intermediate metallic phase which intervened superconducting and insulating phases in the zero temperature limit [4]. The resistance of Ta films in this regime exhibited a sharp drop at the transition temperature but a finite saturated value at low temperatures. In addition, IV characteristic curves showed non-linear response, indicating possible appearance of a new metallic phase. The intriguing quantum metallic phase can be interpreted as a consequence of vortex dynamics or dislocation response in the vortex lattice [5]. Here we present systematic studies on the superconductor-metal-insulator transition and nonlinear transport in two dimensional Ta films.

[1] M. P. A. Fisher, PRL 65, 923 (1990) [2] D. B. Haviland, et al. PRL 62, 2180 (1989) [3] V. F. Gantmakher, et al. JETP Letters 71, 160 (2000) [4] Y. Li, et al. PRB 81, 020505 (2010) [5] D. Ephron, et al. PRL 76, 1529 (1996)

PC26

Non-trivial vortex dynamics in a superconducting Corbino disk

Masaru Kato and David E. Fujibayashi
 Department of Mathematical Sciences, Osaka Prefecture University, Japan

Using the molecular dynamics method for vortex motion and the finite element method for heat transport, we investigate the vortex motion in a superconducting corbino disk, where an external current is injected at the center of the disk and flows toward the perimeter of the disk. For this geometry, vortices move circularly, but velocity of the vortices is large around the center and small at the edge of the disk, according to the magnitude of the external current density. Moving vortices cause resistivity and heat, and therefore there appear non-uniform temperature distribution. This non-uniform temperature distribution makes the vortices out of their circular motion through entropy force. Therefore the motion in the superconducting corbino disk becomes non-trivial one. We focused on the how heat transport to the outside of superconductors, such as a substrate under the superconductor, affect the vortex motion. And we find that firstly the vortices move toward the edge of the disk, but finally they form laminar flow for large heat resistance to the substrate but they show a peculiar ordered state for small heat resistance. We show details of these vortex motions.

PC27

Coexistence of ferromagnetism and superconductivity in single-phase Bi₂Ni nanostructures

Thomas Herrmannsdorfer^{1*}, Richard Skrotzki¹, Rico Schoenemann¹, Yurii Skourski¹, Joachim Wosnitza¹, Daniel Koehler², Regine Boldt² and Michael Ruck²
¹Dresden High Magnetic Field Laboratory, Helmholtz-Zentrum Dresden-Rossendorf, Germany
²Department of Chemistry and Food Chemistry, TU Dresden, Germany

We have demonstrated the coexistence of superconductivity and ferromagnetism in Bi₂Ni nanostructures which have been prepared by making use of novel chemical-reaction paths [1]. We have characterized their magnetic and superconducting properties by means of SQUID magnetometry, ac susceptometry, and electrical-transport measurements in a wide field and temperature range. Here, we also present recent experiments on novel nanostructures, such as monodisperse spherical clusters with a diameter of 8 nm as well as nanofibers. Pulsed-field susceptibility data up to 60 T allow for a determination of the saturation magnetization of Bi₂Ni nanostructures. Resistivity measurements performed on moderately compacted Bi₂Ni nano fibers down to 40 mK have shown clear evidence for the existence of an isosbestic point. Superconductivity in confined Bi₂Ni emerges in the ferromagnetically ordered phase and is stable up to remarkably high magnetic fields. This coexistence would most likely be possible in the case of triplet pairing. The absence of an inversion center of the lattice of Bi₂Ni nanostructures would allow for the formation of an antisymmetric spatial component of the electron-wave function and could lead to a significant admixture of a spin-triplet component of the order parameter. Part of this work was supported by EuroMagNET, EU-contract No. 228043.

[1] T. Herrmannsdorfer, R. Skrotzki, J. Wosnitza, D. Koehler, R. Boldt, M. Ruck, Phys. Rev. B 83, 140501(R) (2011)

PC28

Observation of twofold symmetry breaking in the gap function of heavy-fermion superconductor UPt₃

Yo Machida¹, Atsushi Itoh¹, Yoshitaka So¹, Koichi Izawa^{1*}, Yoshinori Haga², Etsuji Yamamoto², Noriaki Kimura³ and Yoshichika Onuki⁴
¹Department of Physics, Tokyo Institute of Technology, Meguro, Tokyo 152-8551, Japan
²Advanced Science Research Center, Japan Atomic Energy Agency, Tokai, Ibaraki 319-1195, Japan
³Graduate School of Science and Center for Low Temperature Science, Tohoku Universit, Miyagi 980-8577, Japan
⁴Graduate School of Science, Osaka University, Toyonaka, Osaka 565-0871, Japan

WITHDRAWN

PC29

Investigation of the three-dimensional electronic structure of MgB₂ by soft X-ray angle-resolved photoelectron spectroscopy

Y. Sassa^{1*}, M. Mansson¹, B. M. Wojek², M. Kobayashi³, V. Strocov³, O. Tjernberg², N. D. Zhigadlo¹ and B. Batlogg¹
¹Laboratory of Solid State Physics, ETH Zurich, CH-8093 Zurich, Switzerland
²Materials Physics, Royal Institute of Technology KTH, S-16440 Kista., Sweden
³Swiss Light Source, Paul Scherrer Institute, CH- 5234 Villigen PSI, Switzerland

WITHDRAWN

PC30

Vortex channeled effect in Nb thin film with artificial pinning array

Tian-chiuan Wu^{1*}, Lance Horng², Jong-ching Wu² and Rong Cao²
¹Department of Electrical Engineering, Nation Formosa University, Taiwan
²Department of Physics, National Changhua University of Education, Taiwan

The vortex pinning effect is a fundamental characteristic in type II superconductors. Vortex dynamics in the mixed state in type-II superconductors is strongly influenced by the pinning centers. We have studied a channeled-like pinning potential in Nb thin films which is formed by the pinned vortices. Nb films with periodic pinning arrays show matching effects in the magnetic field dependence of the resistivity and Hall Effect. It is suggested that the motion of interstitial vortices has great influence by the channel. When vortices propagate through these arrays, both the longitudinal and transversal voltages show cusp-like anomalies at matching fields. Vortices can be guided by the channel formed between pinned vortices.

[1] R. Cao, T.C. Wu, P.C. Kang, J.C. Wu, T.J. Yang, Horng Lance, Solid State Comm. 143 (2007) 171. [2] M. Baert, V.V. Metlushko, R. Jonckheer, V.V. Moshchalkov, Y. Bruynseraede, Phys. Rev. Lett. 74 (1995) 3269. [3] J.E. Villegas, E.M. Gonzalez, M.I. Montero, Ivan K. Schuller, J.L. Vicent, Phys. Rev. B 68 (2003) 224504.

PC31

Role of the third dimension on the spectral property and transport behaviour in layered cuprates

Bhagya Sindhu Tewari
 Physics, University of Petroleum and Energy Studies, Dehradun, India

In the present work, we have analyzed the influence of the third dimension coupling on the normal state electronic spectra of bilayer cuprates employing Green's function equations of motion approach within tight binding extended Hubbard model and model, which necessarily includes the three site exchange interaction (J3) and the inter unit cell resonant tunneling (T12). The influence of inter unit cell resonant tunneling on the out of plane (c-axis) conductivity has also been analyzed for cuprates employing Kubo formula and Green's function technique. On the basis of numerical computation, it is found that the inter cell resonant tunneling (T12) introduces a broadening in the spectral function and increases the c-axis conductivity. It is also found that the J3 term suppresses the bilayer splitting in the electronic spectra. These results are viewed in terms of recent ARPES measurements.

[1] S. Chakravarty, et. al, Science 61 (1993) 337 [2] E.Dagotto, Rev. Mod. Phys. 68(1994)763 [3] Y.D.Chaung, et.al, Phys. Rev. Lett. 87 (2001) 117002. [4] B.S. Tewari et. al, Eur.Phys.J. B, 66(2008)67 [5] Q.P.Li, et. al, Phys. Rev. B, 48(1993) 437 [6] R.kubo, J.Phys soc. Japan, 28, (1957) 1402 [7] W.C. Wu, et. Al, J. Supercond. 11, 305 (1998) 305 [8] B.S. Tewari et. al, Physica C 468 (2008) 237 [9] B.E.C. Kollentbah, et. Al, Rev. Mod. Phys. 60 (1997) 23

PD01

Ground dielectric state of the Mott-doped material

Vladimir Gavrichkov*
Krasnoyarsk, Kirensky Institute of Physics, Russia

Using analytic calculations, within the framework of the Russell-Saunders scheme we investigated the dependence of the number of valence states on a doping level x in the full package of the valence bands for the Mott-doped material. According to our calculations the total number of valence states $N_v(x)$ coincides with the number of electrons per unit cell ($N-x$) if there is a ban (both spin S_z - and orbit L_z -) on the first removal quasiparticle states (frs). Thus is formed an insulating ground state of the doped material at the $T=0K$. We believe that such materials with the forbidden frs states can be attributed the manganites with the L -forbidden states and cobaltites with the S -forbidden states.

PD02

Temperature-dependent phonon anomalies in uranium and plutonium compounds

Peter S Riseborough*
Physics, Temple University, USA

There is evidence that a number of heavy-fermion/mixed-valent materials show strongly renormalized hybridization gaps either at the Fermi-energy or close to the Fermi-energy. In the former case, a heavy-fermion semiconducting state ensues and in the later case, the system remains metallic at low temperatures. Due to the temperature-dependence of the electronic correlations, the magnitudes of the hybridization gaps decrease with increasing temperatures. The existence of a temperature-dependent low-energy electronic energy scale opens up the possibility that the Born-Oppenheimer approximation may fail and that there may be a resonant coupling between the phonons and the electronic excitations. It is argued that such a mechanism may be the cause of the anomalous temperature-dependence of the phonon spectrum in Pu and the anomalous phonon mode observed in α -uranium.

PD03

Non-linear conductivity of resistive oxides: truths and myths

B. - Fisher*, J. - Genossar, L. - Patlagan and G. M. Reisner
Physics, Technion, Israel

WITHDRAWN

PD04

The modulated spin liquid and hidden order in URu₂Si₂

Sebastien Burdin
Bordeaux University, France

We have shown that near a Kondo breakdown critical point, a spin liquid with spatial modulations is likely to be formed. Unlike its uniform counterpart, we find that this occurs via a second order phase transition. The amount of entropy quenched when this ordering is manifest is of the same magnitude as for an antiferromagnet. Moreover, these two states are in direct competition with each other, and at low temperatures they are separated by a first order phase transition. This suggests that the modulated spin liquid is indeed a viable candidate for the unique phase of matter which is observed in the hidden order phase of URu₂Si₂. We investigate the modulated spin liquid proposal taking full account of the tetragonal-body-centered lattice structure which characterizes URu₂Si₂. We find that the physical quantities predicted from the model are in very good qualitative and quantitative agreement with recent experiments, including thermodynamic properties, inelastic neutron scattering, and Fermi surface measurements. We also present an overview of other f -electron compounds where similar phases have been observed.

Refs. : C. Pepin, M.R. Norman, S. Burdin, and A. Ferraz, Phys. Rev. Lett. 106, 106601 (2011) C. Thomas, S. Burdin, C. Pepin, and A. Ferraz, in preparation.

PD05

Fermi-surface evolution in Yb-substituted CeCoIn₅

Joachim Wosnitza*, Andrey Polyakov¹, Andrea D. Bianchi², S. Blackburn², B. Provost², G. Seyfarth² and Michel Cote²
¹Hochfeld-Magnetlabor Dresden, Helmholtz-Zentrum Dresden-Rossendorf, Germany
²Department de Physique and RQMP, Universite de Montreal, Montreal H3C 3J7, Canada

In CeCoIn₅, substitution on the rare-earth site has been found to influence the Kondo-lattice coherence and Cooper pairing in a rapid and uniform way. Yb substitution, however, shows a different behavior in that T_c and the Kondo-coherence temperature do not scale, in contrast to other heavy-fermion compounds. We performed a comprehensive dHVA study on Ce_{1-x}Yb_xCoIn₅. For small Yb concentration, $x = 0.1$, the band-structure topology and the effective masses remain nearly unchanged compared to CeCoIn₅. This contrasts clearly modified Fermi surfaces and light, almost unrenormalized effective masses for $x = 0.2$ and above. These observations cannot explain the heavy-fermion physics observed in specific-heat and resistivity data even for high Yb concentrations. Thus, we suggest the existence of heavy quasiparticles with short mean free paths, not detectable by dHVA experiments. However, the mechanism by which superconductivity can emerge from these charge carriers remains elusive. Work done in cooperation with K. Gotze, D. Hurt, Z. Fisk, R. G. Goodrich, I. Sheikin, M. Richter. Part of this work was supported by EuroMagNET II (EU contract No. 228043).

PD06

Spin exciton formation inside the hidden order phase of CeB₆

Alireza Akbari and Peter Thalmeier
MPI-CPfS, Germany

The heavy fermion metal CeB₆ exhibits hidden order of antiferroquadrupolar (AFQ) type below $T_Q=3.2K$ and subsequent antiferromagnetic (AFM) order at $T_N=2.3K$. It was interpreted as ordering of the quadrupole and dipole moments of a Γ_8 quartet of localised Ce 4f electrons. This established picture has been profoundly shaken by recent inelastic neutron scattering[1] that found the evolution of a feedback spin exciton resonance within the hidden order phase at the AFQ wave vector appears and is stabilized by the AFM order. We develop an alternative theory based on a fourfold degenerate Anderson lattice model, including both order parameters as particle-hole condensates of itinerant heavy quasiparticles. This explains in a natural way the appearance of the spin exciton resonance and the momentum dependence of its spectral weight, in particular around the AFQ vector and its rapid disappearance in the disordered phase. Analogies to the feedback effect in unconventional superconductors and Kondo semiconductors are pointed out.

[1] G. Friemel, et al, Nature Communications 3, 830 (2012).
[2] A. Akbari and P. Thalmeier, Phys. Rev. Lett. 108, 146403 (2012).

PD07

Antiferromagnetic fluctuation in hidden order phase of U(Ru,Rh)₂Si₂

Makoto Yokoyama*, Kenichi Tenya² and Hiroshi Amitsuka³
¹Faculty of Science, Ibaraki University, Japan
²Faculty of Education, Shinshu University, Japan
³Graduate School of Science, Hokkaido University, Japan

The origin of so-called hidden-order (HO) transition observed at $T_0=17.5K$ in URu₂Si₂ has been one of the longstanding issues in physics of heavy-fermion systems. In the mixed compounds U(Ru_{1-x}Rh_x)₂Si₂, it is found that a large-moment antiferromagnetic (AF) order replaces HO for $0.02 \leq x \leq 0.03$ via a first-order phase transition, and both orders disappear above $x \geq 0.04$. To clarify microscopic features of magnetic fluctuation in both HO and AF phases, we have performed inelastic neutron scattering experiments for U(Ru_{1-x}Rh_x)₂Si₂ ($x \leq 0.03$). At the AF wave vector $Q=(1,0,0)$, the AF excitation peak is clearly observed in HO phase for $0 \leq x \leq 0.02$, but it disappears in the AF phase for $0.02 \leq x \leq 0.03$. The excitation gap at 1.4K is found to be weakly reduced from 2.4meV ($x=0$) to 1.8meV ($x=0.015$) as x is increased. Temperature variations of the staggered susceptibility $\chi(Q,T)$ at $x=0$ estimated from the inelastic-peak intensities show a weak enhancement in HO phase and a cusp-like anomaly at T_0 . By doping Rh, the enhancement of $\chi(Q,T)$ in HO phase becomes pronounced, but a cusp-like anomaly at T_0 is reduced. These features indicate that the AF fluctuation develops on the verge of the first-order phase boundary in HO phase, while it is suppressed in the AF phase.

PD08

Pressure effect on the field-induced ordered phase in heavy fermion compound YbCo₂Zn₂₀

Tetsuya Takeuchi¹, Yuki Taga², Shingo Yoshiuchi², Masahiro Ohya², Yusuke Hirose², Fuminori Honda², Rikio Settai² and Yoshichika Onuki²
¹Low Temperature Center, Osaka University, Japan
²Graduate School of Science, Osaka University, Japan

We succeeded in growing high-quality single crystals of heavy fermion compounds YbT₂Zn₂₀ with T = Co, Rh, and Ir, and found a metamagnetic behavior at H_m below the characteristic temperature $T_{\gamma max}$, where the magnetic susceptibility takes a broad maximum. For YbCo₂Zn₂₀, $H_m = 6$ kOe and $T_{\gamma max} = 0.32$ K, for example. H_m and $T_{\gamma max}$ in these compounds were found to satisfy a universal relation H_m (kOe) = $15T_{\gamma max}$ (K). Recently, we found a field-induced ordered phase (FIOP) above $H_0 = 60$ kOe for $H // <111>$ in YbCo₂Zn₂₀ below $T_0 = 0.6$ K and suggested an antiferro-quadrupole order for the FIOP. In this work, we performed pressure experiments in YbCo₂Zn₂₀ with $H // <111>$ in order to study the pressure effect on the FIOP as well as the pressure-induced antiferromagnetic phase (PIAF) above $P_c \sim 2$ GPa. When the pressure is applied, the transition field H_0 was found to decrease with increasing pressure up to around P_c . Above P_c , there is a pressure region where the PIAF and FIOP were observed under the same pressure. In order to investigate how the FIOP disappears or merges with the PIAF, further pressure experiments are in progress under higher pressures.

PD09

29Si-NMR Study of antiferromagnet CeRh₂Si₂ using single crystals

Hironori Sakai, Yo Tokunaga, Shinsaku Kambe, Yuji Matsumoto, Tatsuma D Matsuda and Yoshinori Haga
Advanced Science Research Center, Japan Atomic Energy Agency, Japan

29Si-NMR Study of antiferromagnet CeRh₂Si₂ has been performed using single crystals. Heavy fermion material CeRh₂Si₂ is known to be an antiferromagnet with strong uniaxial magnetic anisotropy along the crystallographic c-axis under ambient pressure. From our measurements of Knight shifts and relaxation rates, the spin dynamics of this material have been investigated. At ambient pressure, as seen in the static susceptibility, the Ising-type antiferromagnetic spin fluctuations along the c-axis has been found to be enhanced. In this presentation, we will show our latest data and discuss about the anisotropy of hyperfine couplings and spin dynamics.

PD10

Bulk compressibility of orthorhombic YbFe₂Al₁₀-type CeRu₂Al₁₀

Yukihiro Kawamura*, Kazuki Matsui¹, Keiichi Yamamoto¹, Yusuke Hori¹, Junichi Hayashi¹, Keiki Takeda¹, Chihiro Sekine¹ and Takashi Nishioka²
¹Muroran Institute of Technology, Japan
²Kochi University, Japan

Orthorhombic YbFe₂Al₁₀-type CeRu₂Al₁₀ shows antiferromagnetic transition at $T_0=27$ K[1]. This antiferromagnetic transition has various unusual features. One of them is reduced magnetic moment; The neutron experiment reveals that the magnetic moment of Ce in the ordered phase on CeRu₂Al₁₀ is 0.34 μ_B /Ce[2]. Considering this reduced magnetic moment, T_0 should be much lower. Another unusual feature is abrupt disappearance of antiferromagnetic transition by applying pressure[3]. Structural modulation might be occurred at around the pressure of disappearing T_0 . Thus, we performed synchrotron X-ray study at room temperature under pressure by using diamond anvil pressure cell and investigated bulk compressibility of CeRu₂Al₁₀. We revealed that lattice parameters a, b and c monotonically decreases with increasing pressure, which indicates that there is no structural modification up to 9.2 GPa at room temperature. We also revealed that the decrease ratio of b is smaller than that of a and c.

[1] A. M. Strydom, Physica B 404 (2009) 2981-2984 [2] D. D. Khayavin et al., Phys. Rev. B 82 (2010) 100405 [3] T. Nishioka et al., J. Phys. Soc. Jpn 78 (2009) 123705

PD11

Ultrasound measurements on the skutterudite compound SmOs₄P₁₂

Yoshiki Nakanishi*, Gen Koseki¹, Dai Tamura¹, Kohei Kurita¹, Takeshi Saito¹, Minoru Koseki¹, Mitsuteru Nakamura¹, Masahito Yoshizawa¹, Masahito Yoshizawa¹, Yuya Koyota², Chihiro Sekine² and Takehiko Yagi³
¹Iwate University, Japan
²Muroran Institute of Technology, Japan
³ISSP The University of Tokyo, Japan

We present an ultrasound study on the Sm-based filled skutterudite compound SmOs₄P₁₂ for the first time. The measurements were performed on a polycrystalline sample using a phase-sensitive detection technique. The ternary compound SmOs₄P₁₂ were prepared at high temperature and high pressures using a wedge-type cubic-anvil high-pressure apparatus. SmOs₄P₁₂ exhibits antiferromagnetic ordering below 4.5 K. A clear decrease was observed at 4.5 K in the temperature dependence of both longitudinal and transverse elastic constants. However, less or no elastic softening toward the transition temperature was observed in the both elastic constants. Absence of the precursor behavior reminds us a multipolar ordering, possibly octupolar ordering observed in the isostructural system SmRu₄P₁₂, reported previously by our group. The transition is robust against the external magnetic field. To be more interesting, the elastic constants show a minimum around 180 K, possibly related to a rattling motion due to weakly bounded Sm ion in an oversized P cage. We argue a low-lying degenerated levels derived from 4f-multiplets ground state of Sm ion split by crystalline electric field effect in SmOs₄P₁₂. Furthermore, we discuss the phononic properties in comparison with other isostructural systems which include an ionic degrees of freedom of the rattling motion.

PD12

YbRh₂Si₂: Fermi surface and crystal-field splittings of a heavy-Fermion compound

Steffen Danzenbacher¹, Denis V. Vyalikh¹, Kurt Kummer², Yuri Kucherenko³, Cornelius Krellner⁴, Christoph Geibel⁵, Serguei L. Molodtsov⁶, Ming Shi⁷, Luc Patthey⁷ and Clemens Laubschat^{1*}
¹Institut für Festkörperphysik, Technische Universität Dresden, D-01062 Dresden, Germany
²European Synchrotron Radiation Facility, FR-38043 Grenoble Cedex, France
³Institute of Metal Physics, National Academy of Sciences of Ukraine, UA-03142 Kiev, Ukraine
⁴Max-Planck-Institut für Chemische Physik fester Stoffe, D-01187 Dresden, Germany
⁵Max-Planck-Institut für Chemische Physik fester Stoffe, D-01187 Dresden, Germany
⁶European XFEL GmbH, D-22671 Hamburg, Germany
⁷Swiss Light source, Paul Scherrer Institute, CH-5232 Villigen-PSI, Switzerland

YbRh₂Si₂ is a well known heavy Fermion system with a Kondo temperature of 25 K and a mean valence of 2.9. Due to the mixing of 4f14 and 4f13 configurations in the ground state, the 4f13 state is reproduced as a final state in a photoemission experiment allowing for direct observation of near ground state properties. Angle-resolved photoemission spectra reveal a general dispersion of the 4f13 state with a Fermi-level crossing around the Γ -point. A clear wave-vector dependence of the crystal-field split states is observed that leads to a variation of the energy splittings across the Brillouin zone and even to an interchange of the sequence of states. The bulk Fermi surface reveals strong similarities with the one expected for a stable trivalent compound, but is slightly larger, reveals strong 4f character, and deviates from LDA results by a larger region without states around the Γ -point. These properties are well described in the framework of a simple fd-hybridization model.

PD13

Single crystal growth and various electronic states in Yb-based compounds

Yusuke Hirose^{1*}, Shingo Yoshiuchi¹, Naoto Nishimura¹, Jyunya Sakaguchi¹, Kentaro Enoki¹, Ken Iwakawa¹, Yasunao Miura¹, Tetsuya Takeuchi², Kiyohiro Sugiyama¹, Fuminori Honda³, Etsuji Yamamoto⁴, Yoshinori Haga⁴, Masayuki Hagiwara⁴, Koichi Kindo⁵, Rikio Settai⁶ and Yoshichika Onuki²
¹ Graduate School of Science, Osaka University, Japan
² Low Temperature Center, Osaka University, Japan
³ Graduate School of Engineering Science, Osaka University, Japan
⁴ Advanced Science Research Center, Japan Atomic Energy Agency, Japan
⁵ KYOKUGEN, Osaka University, Japan
⁶ ISSP, University of Tokyo, Japan

To clarify the various electronic states of Yb compounds, we grew single crystals of several Yb compounds such as YbTlIn₂ (T: Co, Rh, Ir), YbCoGa₂, YbT₂Zn₂₀ (T: Co, Rh, Ir) and Yb₂Pt₂Pb by the flux method, and YbPdGe and YbPdAl₂ by the Bridgman method. YbTlIn₂ and YbCoGa₂ are Pauli paramagnets, but the cyclotron effective mass of YbCoGa₂ is by four times larger than that of YbTlIn₂. YbT₂Zn₂₀ (T: Co, Rh, Ir) compounds are heavy fermion compounds. In fact, the electronic specific heat coefficient γ is 8000 mJ/K²mol in YbCo₂Zn₂₀, very close to the quantum critical point. YbPdGe is an Ising-type ferromagnet with the Curie temperature TC = 11.4 K and a saturated magnetic moment μ S = 1.7 μ B/Yb, but possesses a relatively large value of γ = 150 mJ/K²mol. Yb₂Pt₂Pb is a Shubny-Sutherland-type antiferromagnet with the Neel temperature TN = 2.1 K. Finally, YbPdAl₂, of which the analogue is a heavy fermion superconductor NpPd₂Al₃ is a well-known heavy fermion superconductor[1] is an antiferromagnet with a very small Neel temperature TN = 0.19 K.

[1] D. Aoki et al. : J. Phys. Soc. Jpn. 76 (2007) 063701.

PD14

Physical properties under pressure in a heavy fermion superconductor CeIrIn₅

Naofumi Aso^{1*}, Yuki Tamaki¹, Yoshinao Takaesu¹, Masato Hedo¹, Takao Nakama¹, Kiyoharu Uchima², Kazuyuki Matsubayashi³, Yoshiya Uwatoko³, Yusuke Ishikawa⁴, Kazuhiko Deguchi⁴ and Noriaki K. Sato⁴
¹ Faculty of Science, University of the Ryukyus, Japan
² General Education, Okinawa Christian Junior College, Japan
³ ISSP, University of Tokyo, Japan
⁴ Graduate School of Science, Nagoya University, Japan

CeIrIn₅ is a heavy fermion superconductor with Tc = 0.4 K and the electronic specific heat γ = 700 mJ/(K²mol) [1]. To investigate the nature and the pressure effect of the Kondo effect on CeIrIn₅, electrical resistivity ρ and magnetization M under pressure in CeIrIn₅ have been measured using the single-crystalline CeIrIn₅, which were grown by the In-flux method. The temperature dependence between 2.0 K and 300 K of the a-axis and c-axis electrical resistivity ρ of CeIrIn₅ under pressure up to 8.0 GPa, which were obtained using a cubic anvil device, exhibits the typical dense Kondo behavior: on cooling from room temperature at P = 1.0 GPa, the ρ increases and shows a maximum of the coherence peak, and then goes down into the coherent Kondo state. We also find that the coherence peak moves to higher temperatures with pressure, indicating that the Kondo temperature of CeIrIn₅ increases by applying the pressure. In the conference, we will also report the M data under pressure up to 1.5 GPa and compare the ρ data with our recent thermoelectric power S measurements, which exhibit a large positive value up to 90 μ V/K with a sharp maximum in its temperature dependence. [2]

[1] C. Petrovic et al., Europhys Lett., 53, 354, (2001). [2] Y. Takaesu et al., J. Phys.: Conf. Series, 273, 012058, (2011).

PD15

Periodic Anderson model with correlated conduction electrons

Imre Hagymasi*, Kazumasa Itai and Jenő Solymos
 Theoretical Solid State Physics, Wigner Research Centre for Physics, Hungarian Academy of Sciences, Hungary

We investigate the so-called periodic Anderson-Hubbard model with the aim to understand the role of interaction between conduction electrons in the formation of the heavy-fermion and mixed-valence states [1]. We perform variational calculation using the Gutzwiller wave function and exact diagonalization of the Hamiltonian for short chains. The f-level occupancy and the renormalization factor of the quasiparticles are calculated as a function of the energy of the f-orbital for a wide range of the interaction parameters. The results obtained by the two methods are in reasonably good agreement for the periodic Anderson model. The agreement remains even for the Anderson-Hubbard model, except for the half-filled case. We find that due to this interaction the energy range of the bare f-level, where heavy-fermion behavior can be observed, shifts and widens. The Gutzwiller method indicates a robust transition from Kondo insulator to Mott insulator in the half-filled model, while this interaction enhances the quasi-particle mass when the filling is close to half filling.

[1] I. Hagymasi, K. Itai and J. Solymos Periodic Anderson model with correlated conduction electrons: variational and exact diagonalization study, arXiv:1106.4999

PD16

Thermoelectric study of the metamagnetic behavior in YbCo₂Zn₂₀

Yo Machida¹, Tohru Ikeura¹, Koichi Izawa^{1*}, Shingo Yoshiuchi², Fuminori Honda², Rikio Settai² and Yoshichika Onuki²
¹ Department of Physics, Tokyo Institute of Technology, Japan
² Department of Physics, Osaka University, Japan

Despite the intensive studies on the metamagnetic behavior which has been found in a wide variety of heavy fermion materials such as CeRu₂Si₂, CeCu₆, and UPt₃, the origin remains under debate. The recent discovered heavy fermion compound YbCo₂Zn₂₀ exhibits the metamagnetic behavior under unexpectedly small magnetic field ~ 0.6 T, providing a new platform for elucidation of the metamagnetism. We have addressed this issue by means of the thermoelectric transport, which has been a promising probe to unveil the low-energy itinerant excitations and the electronic transformation across the metamagnetic transition. We measured the Seebeck and Nernst coefficients of YbCo₂Zn₂₀ down to very low temperature. Remarkably, we found a huge Seebeck coefficient ~ -250 μ V/K² under zero field, as an indication of the “super” heavy fermion state. Moreover, on passing through the metamagnetic field the Seebeck coefficient shows dramatic suppression, being distinct from that observed in CeRu₂Si₂ in which the Seebeck coefficient is largely enhanced at the metamagnetic field. In our presentation, we will discuss the thermoelectric response of YbCo₂Zn₂₀ and its implication to the metamagnetism. The comparison to the other metamagnetic materials will be also made.

PD17

Raman scattering study of the hidden order state of URu₂Si₂

Jonathan Buhot¹, Marie-aude Measson^{1*}, Yann Gallais¹, Maximilien Cazayous¹, Alain Sacuto¹ and Dai Aoki²
¹ Laboratoire Matériaux et Phénomènes Quantiques, UMR 7162 CNRS, Université Paris Diderot, France
² SPSMS, UMR-E CEA / UJF-Grenoble 1, INAC, 38054 Grenoble, France

For over 25 years, researchers attempt to understand the microscopic origin of the Hidden Order that appears below T0=17.5 K in the heavy fermions compound URu₂Si₂. Mainly, optical measurements on URu₂Si₂ are far-infrared reflectance experiments[1,2]. Only few Raman scattering studies have been performed [3,4] and only for c axis. We have studied URu₂Si₂ for both axes, down to low temperature (2K). We have probed the phononic and electronic properties and their interaction. Softening of phonon modes together with Fano-shape were observed, implying that a phonon-electron coupling is at play. At low energy, electronic Raman signal shows either fluctuations or more conventional Drude shape for different symmetry. We have studied both signals through the Hidden Order temperature.

D.A. Bonn et al., PRL 61 1305 (1988), J. Levallois et al., PRB 84, 184420 (2011) S. Cooper et al., PRB 36 5743 (1987), D. Lampakis et al., PHYSICA B 378-380, 578 (2006)

PD18

The evolution of superconductivity and magnetism in Pd-doped CeRhIn₅ and Ce₂RhIn₅

Marie Kratochvilova*, Klara Uhlírova, Jiri Prechal, Alexandra Rudajevova, Jeroen Custers and Vladimir Sechovsky
 Department of Condensed Matter Physics, Faculty of Mathematics and Physics, Charles University, Czech Republic

CeRhIn₅ and Ce₂RhIn₅ are heavy fermion antiferromagnets. Unconventional superconductivity can be induced by hydrostatic pressure or doping [1,2]. By contrast, Ce₂PdIn₅ is a heavy fermion superconductor (Tc=0.7K) at ambient pressure. We have examined the influence of Pd doping in single crystals of CeRh_{1-x}Pd_xIn₅ and Ce₂Rh_{1-x}Pd_xIn₅. Since the synthesis of Ce₂PdIn₅ is connected either to intergrowth of CeIn₃ and PdIn₃, or variation of critical temperature, growth conditions were studied by differential thermal analysis. By this, we have succeeded in obtaining high-quality single crystals free of CeIn₃ and with a critical temperature Tc=0.7K. The crystals have been subjected to specific heat, resistivity and AC susceptibility measurements. In addition, resistivity experiments under hydrostatic pressures up to 3GPa were performed. Surprisingly, at ambient pressure the Neel temperature of CeRh_{1-x}Pd_xIn₅ has only slightly decreased with increasing Pd content. And moreover, the pressure influence on magnetism in CeRh_{1-x}Pd_xIn₅ does not significantly differ from CeRhIn₅. Contrary, the superconducting transition increases significantly compared to its 115-counterpart. The less two-dimensional Ce₂Rh_{1-x}Pd_xIn₅ behaves different. Here, the antiferromagnetic ordering is immediately lowered upon Pd substitution and vanishes completely at x=0.35 already. The obtained magnetic field-temperature phase diagrams will be discussed in context of the physical properties of other CeTlIn_{3n+2} compounds.

[1] H. Hegger et al., Phys. Rev. Lett. 84, 4986 (2000). [2] M. Nicklas et al., Phys. Rev. B 67, 020506 (2003).

PD19

Magnetic phase diagram of the new heavy fermion compound Ce₂PtIn₈₁

Marie Kratochvilova^{1*}, Klara Uhlírova¹, Jiri Prechal¹, Ivana Cisarova², Jeroen Custers¹ and Vladimir Sechovsky¹
¹ Department of Condensed Matter Physics, Faculty of Mathematics and Physics, Charles University, Czech Republic
² Department of Inorganic Chemistry, Faculty of Science, Charles University, Czech Republic

CeTmIn_{3n+2m} (n=1,2; m=1; T=transition metal) type compounds are subject of intense interest in the condensed-matter community [1]. They are predestinated to investigate the interplay between magnetism and superconductivity. Recently, two new compounds from this heavy fermion family have been found. Ce₂PdIn₈₁ is an ambient pressure superconductor while CePtIn₈₁ orders antiferromagnetically [2]. We report on the existence of a new compound Ce₂PtIn₈₁. Similar to Ce₂PdIn₈₁, the synthesis of Ce₂PtIn₈₁ is rather complicated. However, from our studies of solution growth of Ce₂PdIn₈₁ and the support by differential thermal analysis, optimal conditions for growing Ce₂PtIn₈₁ were deduced. Single-crystal X-ray diffraction confirmed that Ce₂PtIn₈₁ crystallizes in Ho₂CoGa₈-type structure with lattice parameters a=4.699Å and c=12.185Å. We will present specific heat, resistivity (ambient and under hydrostatic pressure) and magnetization measurements. Ce₂PtIn₈₁ orders magnetically below 2.1K. A second transition, likely into a magnetic commensurate ordering, is observed just below at 2K. Contrary to Ce₂RhIn₈₁, the magnetic transitions shift to lower temperatures in applied magnetic field along both principal crystallographic axes suggesting different character of magnetic ordering. Specific heat measurements reveal an enhanced Sommerfeld coefficient (γ ~740 mJ/mol.K²). The magnetic field-temperature phase diagram will be discussed in the context of superconductivity and magnetism evolution in related compounds.

[1] Ch. Pfeleiderer, Rev. Mod. Phys. 81, 2009 [2] E. D. Bauer, et al., Phys. Rev. B 81, 180507 (2010)

PD20

Coexistence and competition of superconductivity, magnetism and charge density waves in rare-earth tri-telluride TbTe₃

Kazuhiko Deguchi, Hiroaki Iwase, Yuya Imai, Koji Yamamoto and Noriaki Sato
 Department of Physics, Graduate School of Science, Nagoya University, Japan

Rare-earth tri-telluride RTe₃ (R = Y, La-Sm, Gd-Tm) forms a weakly orthorhombic crystal lattice, consisting of alternating double layers of corrugated double RTe layers and nominally square-planar Te sheets. The RTe layers are responsible for magnetism while the square Te sheets contribute to strongly anisotropic conduction. Interestingly, the two-dimensional conduction bands originating from Te-5px and 5py orbitals give rise to Fermi surface nesting, and this hidden one-dimensionality leads to a charge density waves (CDW) with a high transition temperature. Because of this intriguing feature, RTe₃ attracts great interest in recent years. TbTe₃ has localized 4f electrons, and exhibits successive phase transitions of magnetic origin, which all coexist with the CDW. Surprisingly, superconductivity emerges under high pressure. The question is whether the superconductivity coexists or competes with the other long range orders. Therefore, we investigated the long-range orders by the electrical resistivity and ac magnetic susceptibility at high pressures up to 8 GPa and at low temperatures down to 2 K using a constant-load cubic-anvil cell with single crystalline samples that were grown from Te-fluxes. We found that the antiferromagnetism survives even at the highest pressure of the present experiment. We also confirmed the emergence of the superconductivity at high pressures.

PD21

Magnetic properties of Ce₃Rh₄Sn₁₃ and Ce₃Co₄Sn₁₃; a comparative study

Andrzej Słebarski*, Marcin Fijałkowski and Jerzy Góraś
 Institute of Physics, University of Silesia, Poland

We report on the electronic structure (XPS) and basic thermodynamic properties of Ce₃Rh₄Sn₁₃ and Ce₃Co₄Sn₁₃, and the reference La-based compounds. The both compounds were classified as a heavy fermion materials with extremely large low temperature electronic specific heat C/T [1] of about 4 J/molK². The data show that either Ce₃Rh₄Sn₁₃ or Ce₃Co₄Sn₁₃ are very sensitive to applied magnetic fields and exhibit a cross-over from magnetically correlated state to a single impurity state, when the applied magnetic field increases. We noted that the low temperature properties are dependent on the stoichiometry of the sample. We also present and discuss the low temperature properties of Ce₃Co₄Sn₁₃ doped with La.

[1] U. Kohler et al. J. Phys.:Condens. Matter 19 (2007) 386207

PD22

Thermoelectric properties of Kondo semiconductor CeRu₄As₁₂ prepared under high pressure

Chihiro Sekine^{1*}, Tomokazu Kawata¹, Yukihiko Kawamura¹ and Takehiko Yagi²
¹ Graduate School of Engineering, Muroran Institute of Technology, Japan
² Institute for Solid State Physics, The University of Tokyo, Japan

The filled skutterudite compound CeRu₄As₁₂ exhibits a hybridization gap insulating state, with a small activation energy Δ /kB of 50K [1]. We report further results for CeRu₄As₁₂ prepared under high pressure (4GPa). Thermoelectric power and thermal conductivity measurements have been performed on this material. The temperature dependence of thermoelectric power for CeRu₄As₁₂ shows two peaks (around 80K, 200K). The phenomena could be related to Kondo behavior at high temperature and hybridization-gap-formation process at low temperature.

[1] C. Sekine et al., J. Mag. Mag. Mater., 310 (2007) 260.

PD23

Single crystal growth and physical properties of UT₂Al₂₀ (T=transition metal)

Yuji Matsumoto¹, Tetsuya D Matsuda¹, Naoyuki Tateiwa², Etsuji Yamamoto¹, Yoshinori Haga¹ and Zachary Fisk³
¹ advanced science research center, Japan atomic energy agency, Japan
² Japan atomic energy agency, Japan
³ University of California, USA

Many anomalous physical properties have been observed in RT₂X₂₀ (R=Rare metal, T=transition metal, X=Al, Zn) system. For example, the quadrupolar order takes place in PrT₂X₂₀ system, and the extreme heavy fermion state takes place in YbCo₂Zn₂₀. In the uranium analogue, for example, UT₂Al₂₀ is worth investigating because the extended 5f wave function in uranium would lead to peculiar features due to strong hybridization. Therefore we have studied single crystal growth and physical properties of UT₂Al₂₀. The sample preparation is performed by using Al-self flux method. We have succeeded to prepare the single crystal of UT₂Al₂₀ (T=Ti, Nb). We are going to present about the physical properties of the prepared samples in the Conference.

PD24

Anisotropic c-f hybridization in a Kondo semiconductor CeFe₂Al₁₀

Yuji Muro¹, Keisuke Yutani², Jumpei Kajino², Takahiro Onimaru² and Toshiro Takabatake³
¹ Liberal Arts and Sciences, Toyama Prefectural University, Kurokawa 5180, Imizu 939-0398, Japan
² AdSM, Hiroshima University, Kagamiyama 1-3-1, Higashi-Hiroshima 739-8530, Japan
³ AdSM and IAMR, Hiroshima University, Kagamiyama 1-3-1, Higashi-Hiroshima 739-8530, Japan

We report anisotropic properties of a Kondo semiconductor CeFe₂Al₁₀. This compound is the non-magnetic counterpart of Kondo semiconductors CeT₂Al₁₀ (T=Ru and Os) that exhibit an unusual antiferromagnetic transition at about 28 K[1-5]. The magnetic susceptibility for B//a, χ (T), shows a broad peak at 70 K due to the strong c-f hybridization. The anisotropy in χ , $\chi_a - \gamma c > \chi_b$, is in common with those for T = Ru and Os. Electrical resistivity ρ (T) has a broad maximum at 45, 35 and 110 K for l//a, l//b and l//c, respectively. Below 20 K, ρ 's along all axes show an upturn due to the opening of a pseudo gap. Thermopower S(T) also shows a maximum at 190, 150 and 200 K for a-, b- and c-axis, respectively. The temperatures at the maximum in ρ and S suggest the anisotropy of c-f hybridization strength Vc>Va>Vb in CeFe₂Al₁₀ as reported in the study of optical conductivity[6]. Furthermore, only S_c(T) changes the sign from positive to negative at 100 K on cooling and shows a minimum at 50 K. The negative minimum was also observed in S_c(T) for T=Ru and Os[7]. This behavior indicates the development of antiferromagnetic correlation along the c-axis in CeT₂Al₁₀.

[1] Y. Muro et al. J. Phys. Soc. Jpn. 78 (2009) 083707. [2] T. Nishioka et al. J. Phys. Soc. Jpn. 78 (2009) 123705. [3] Y. Muro et al. Phys. Rev. B 81 (2010) 214401. [4] D. D. Khalyavin et al. Phys. Rev. B 82 (2010) 100405R. [5] D. T. Adroja et al. Phys. Rev. B 82 (2010) 104405. [6] S. Kimura et al. J. Phys. Soc. Jpn. 80 (2011) 033702. [7] H. Tamida et al. J. Phys. Soc. Jpn. 79 (2010) 063709.

PD25

Cu-NMR studies of heavy-Fermion compound CeCu₆ under high magnetic fields

Keisuke Kuroda, Kyohei Morita, Hisashi Kotegawa, Hitoshi Sugawara and Hideki Tou*
Department of Physics, Kobe University, Japan

It is known that the intermetallic compound CeCu₆ is a heavy fermion system showing a huge specific heat coefficient $\gamma \sim 1600$ mJ / K² mol, without magnetic order or superconductivity at low temperatures down to 10 mK[1,2]. The electric resistivity shows characteristic temperature dependence of $\rho \sim \log T$ above 10 K, which is ascribed to the Kondo effect, and it has a maximum around 10 K. No detailed NMR results have been reported yet because of a drawback of the complicated Cu NMR spectrum due to a peculiar orthorhombic crystal structure. We have carried out Cu-NMR measurements to clarify the heavy fermion state of a single crystal CeCu₆ under several magnetic fields. We have measured Knight shift and the nuclear spin-lattice relaxation time T₁ under magnetic fields up to 15 T along the a-axis and c-axis in the temperature range of 100-1.5 K. At low temperatures, the Cu-NMR Knight shifts are suppressed as magnetic field increases. Simultaneously, 1/T₁ is suppressed. These features are understood by the concept that the heavy fermion state in CeCu₆ is formed through Kondo effect. We will report detailed field dependence of the heavy fermion state of CeCu₆ for the first time.

[1] Y. Omuki, et al.: JPSJ 53 (1984) 1210 [2] Y. Omuki, et al.: JMMM 63-64 (1987) 281

PE01

The underscreened Anderson lattice : A model for uranium compounds.

Peter S Riseborough^{1*}, Sergio Magalhaes² and Bernard Coqblin³
¹ *Physics, Temple University, USA*
² *Inst. Fis., Univ. Fed. Fluminense, Rio de Janeiro, Brazil*
³ *L.P.S., CNRS-Universite Paris-Sud, 91405 Orsay, France*

We present a model based on the Underscreened Anderson Lattice (UAL) with two 5f electrons per site to account for the Kondo-ferromagnetism co-existence observed in some actinide compounds. The UAL model allows a description of the decrease of the number of f-electrons and we present a calculation which explains the pressure dependence observed in some Uranium compounds and particularly in Uranium monochalcogenides. On the other hand, we have developed a novel type of phase transition within the UAL model and we suggest that this model might describe the "Hidden Order" transition in URu₂Si₂. The gaps that appear in the electronic dispersion relations of bands of different orbital character are in agreement with experimental photoemission results.

PE02

Transport properties of intermetallic compounds RCoGe₂ (R = Ce and La)

Yung-kang Kuo^{1*}, P. C. Chang² and C. S. Lee³
¹ *National Dong Hwa University, Department of Physics, Taiwan*
² *Department of Physics, National Dong Hwa University, Taiwan*
³ *National Cheng Kung University, National Dong Hwa University,, Taiwan*

The electronic and magnetic properties of the cerium-based ternary intermetallic compound compounds with the general formula CeMSi₂ (M = transition metals) has been of considerable interest recently. Among those compounds, CeCoGe₂ is of particular interest due to its peculiar physical properties, such as it has a rather high Kondo temperature TK ~ 250 K, and it is the first Kondo system clearly interpreted by the Coqblin-Schrieffer model with j = 5/2. In this study, measurements of the electrical resistivity, Seebeck coefficient, and thermal conductivity on CeCoGe₂ have been performed in the temperature range 10 - 300 K to investigate the electronic structure. For comparison, the nonmagnetic counterpart LaCoGe₂ has also been studied. It is found that CeCoGe₂ exhibits a broad maximum in Seebeck coefficient at about 75 K, at which the sudden drop in electrical resistivity occurs. This is a typical behavior commonly seen in Ce-based Kondo lattice compounds. A theoretical attempt was made and found that the electrical transport and thermoelectric properties of CeCoGe₂ can be well described by a two-band model with reliable physical parameters. On the other hand, both electrical resistivity and Seebeck coefficient show a typical metallic-like behavior for the nonmagnetic LaCoGe₂.

PE03

The lattice Kondo effect - A fabric for superconducting correlations?

Oliver Bodensiek^{1*}, Thomas Pruschke¹ and Rok Zitko²
¹ *Department of Physics, University of Goettingen, 37077 Goettingen, Germany*
² *Jozef Stefan Institute, Jamova 39, SI-1000 Ljubljana, Slovenia*

Although the simple Kondo lattice model constitutes one of the paradigms for understanding the physics of heavy-fermion materials, a reliable theoretical investigation of superconductivity in this model is still lacking. We present results based on the dynamical mean-field approximation in combination with the numerical renormalization group as impurity solver. While superconducting order is commonly not expected for a correlated lattice model without additional bosonic degrees of freedom, we observe strong superconducting order in the plain Kondo lattice model away from half filling. The possible origin of this superconducting order is discussed in view of the frequency dependence of the order parameter. In addition, close to half filling we find this ordered phase to appear most pronounced in the vicinity of the antiferromagnetic quantum critical point. Since a characterization of quantum criticality within dynamical mean-field theory is not possible, we rather discuss questions of principle such as the actual nature of the ordered states, that is, local moment or heavy-fermion physics. The latter issue is of considerable interest addressing the question whether the ordered states stay in direct competition or even cooperate with the coherent Kondo effect in the lattice.

PE04

Lifshitz transition with interactions in high magnetic fields: application to CeIn₃

Pedro Schlottmann*
Department of Physics, Florida State University, USA

The Neel ordered state of CeIn₃ is suppressed by a magnetic field of 61 T at ambient pressure. There is a second transition at ~45 T, which has been associated with a Lifshitz transition. Skin depth measurements indicate that the transition is discontinuous as T -> 0 and that the transition has a weak pressure dependence until it merges with the Neel transition. We study the effects of Landau quantization and interaction among carriers on a Lifshitz transition. The Landau quantization leads to quasi-one-dimensional behavior for the direction parallel to the field. Repulsive Coulomb interactions give rise to a gas of strongly coupled carriers. The density correlation function is calculated for a special long-ranged potential [1]. For the lowest Landau level the problem can be mapped onto the interacting one-dimensional electron gas. It is concluded that in CeIn₃ (a) an electron or hole pocket is being emptied as a function of field and (b) in the ground state the pocket is emptied in a discontinuous fashion. This discontinuity is gradually smeared by the temperature in agreement with the skin depth experiments. Work supported by the Department of Energy under grant DE-FG02-98ER45707.

[1] P. Schlottmann, Phys. Rev. B 83, 115133 (2011).

PE05

Dynamical mean-field theory of indirect exchange between magnetic adatoms on metallic surfaces

Irakli Titvinidze*, Andrej Schwabe, Niklas Rother and Michael Potthoff
¹ *Institute of theoretical physics, University of Hamburg, Germany*

Two magnetic impurities on a metallic substrate surface experience the Ruderman-Kittel-Kasuya-Yosida (RKKY) exchange interaction. This indirect non-local magnetic exchange competes with the local Kondo effect. While the latter is described in principle exactly within single-site dynamical mean-field theory, the effects of the RKKY coupling are taken into account approximately only. Here, this is demonstrated by comparing the DMFT results with numerically exact data obtained by the density-matrix renormalization group for a one-dimensional model with two Anderson impurities. With the two-site DMFT, we also benchmark a simplified DMFT variant. Varying the inter-impurity distance d and the local exchange coupling J, different parameter regimes with dominating Kondo physics or with dominating RKKY interaction are studied. For the Kondo regime, our calculations show that DMFT is able to reliably describe magnetic nanostructures on metallic surfaces. The prospects of DMFT (and two-site DMFT) as a reliable approach to study nanomagnetism of more complex RKKY-interacting systems are discussed.

PE06

Kondo effect near the Van Hove singularity in biased bilayer graphene

Stanislaw Lipinski* and Damian Krychowski
Institute of Molecular Physics, Polish Academy of Sciences, Poland

We study Kondo impurity in a bilayer graphene with Bernal stacking for adatom adsorbed on the outside of the bilayer or intercalated between the two graphene layers. The density of states (DOS) close to the gap diverges as the square root of energy - Van Hove singularity (VHS). The system is modeled by the generalized Anderson hamiltonian with bilayer described by Hubbard model. The many-body problem is studied within the mean field Kotliar-Ruckenstein slave boson approach for SU(2) and SU(4) symmetries. We examine the impact of tuning the Fermi level (EF) through the VHS. Increase of the DOS at EF increases hybridization of the impurity, what moves the system towards mixed valence regime or even completely suppresses the many body peak of DOS. Additionally a competitive influence of magnetic instability is analyzed. Crossing of the Fermi level with a Van Hove singularity leads to weak ferromagnetism of the bilayer graphene with strong spin polarization at EF. The spin symmetry is broken, what for the case of spin-orbital degeneracy results in a crossover from SU(4) Kondo effect to SU(2) and in the case of only spin degeneracy it leads to a strong suppression of SU(2) Kondo effect.

PE07

Indirect exchange between magnetic atoms on surfaces: From two impurities to diluted chains

Andrej Schwabe*, Irakli Titvinidze, Daniel Gutersloh, Anke Braun and Michael Potthoff
¹ *Institute of theoretical physics, University of Hamburg, Germany*

Magnetic atoms on metallic surfaces are subject to the competition between Kondo screening and indirect magnetic (RKKY) exchange. To study the crossover of the magnetic properties from the case of a single or two magnetic adatoms to the limit of a dense chain of indirectly coupled adatoms, we model the metal surface as a one-dimensional tight-binding system and apply the density-matrix renormalization group (DMRG) to the resulting Kondo model. The case of three magnetic atoms turns out to be particularly interesting as finite-size gaps are found to qualitatively affect the balance between Kondo physics and RKKY. With the transition from the diluted case with a few magnetic atoms to the dense chain with all atoms RKKY-coupled ferro- or antiferromagnetically, magnetic long-range order becomes possible. The resulting phase diagram is studied in the weak (RKKY) but also in the strong-coupling (Kondo) limit. Besides DMRG we employ real-space dynamical mean-field theory (R-DMFT) in addition and thereby extend the results to higher dimensions.

PE08

ESR study of hybridization in some undoped Yb-based alloys

Vladimir Ivanshin*, Tatyana Litvinova and Eduard Gataullin
Institute of Physics, Kazan University, Russia

The hybridization between a wide conduction band and correlated f-electrons localized at lattice sites is investigated using method of electron spin resonance (ESR) in some dense heavy-fermion compounds. ESR signals arise here both from the local moment spins and conduction electrons (CE) due to the strong electronic correlations because of the hybridization between 4f-electrons and CE in the presence of ferromagnetic (FM) fluctuations [1]. We review very recent ESR experiments in several undoped Yb-based intermetallics [2, 3] and discuss the role of chemical composition, Kondo effect, anisotropy, and RKKY interactions for the ESR linewidth. It is shown that an increase of the Kondo interaction and FM correlations leads to a stronger hybridization and an essential ESR line narrowing. Possible hybridization mechanisms are proposed.

[1] P. Wölfle, E. Abrahams, Ann. Phys. (Berlin) 523 598 (2011) [2] V.A. Ivanshin et al., J. Phys.: Conf. Ser. 324 012019 (2011) [3] T. Gramer et al., Phys. Rev. B 85 035119 (2012)

PE09

ESR study of influence of anionic and cationic substitutions in EuB₆ on the magnetic phase separation

Tatiana Semenovna Altshuler^{1*}, Yuriy Vladimirovich Goryunov¹, Anna Vasilievna Levchenko² and Vladimir Borisovich Filippov²
¹ *Russian Academy of Sciences, Kazan Physical-Technical Institute, Russia*
² *National Academy of Sciences of Ukraine, Institute of Problem of Material Science, Ukraine*

We performed a comparative study of the features of the magnetic phase separation in europium hexaboride with anionic and cationic substitution with donor impurities. The ESR (electron spin resonance) were measured on the single crystal plates EuB_{6-x}C_x and Eu_{1-x}Gd_xB₆ with x < 0.07 in X-band in the temperature range T = 10-300 K. Both types substitution keep integrity of the magnetic sublattice and they add one electron per the impurity atom in the conduction band of EuB₆. The magnetic field was oriented perpendicular to the sample plane and along various crystal axis. In all case we observed the magnetic phase separation and phase transitions. However, the ratio of the magnetic phases and their behavior is slightly different for substitution boron in carbon and europium gadolinium. In the latter case, there was the coexistence of ferromagnetic and antiferromagnetic phases. The obtained ESR data are discussed in frame Falicov-Kimball model the hybridization of the localized electrons with two band (valence and conduction band) itinerant electrons and formation of Kondo-like electron states. Work was supported by Grants of RFBR and Presidium of RAS.

[1] Altshuler T.S., Goryunov Y.V., Shitsevalova N.Y., Dukhnenko A., JETP Lett. 88, 779 (2008) [2] Kunes J., Pickett W.E., Phys.Rev. B 69, 1651 (2004) [3] Falicov L.M., Kimball J.C., Phys.Rev.Lett. 22 997 (1969) [4] Kugel K.I., Rakhamanov A.L., Shoychakov A.O., Phys.Rev.Lett. 95, 267210 (2005)

PE10

High pressure synthesis of novel boron-cage compounds RB₁₂ (R=Gd, Sm)

Fumitoshi Iga^{1*}, Yusaku Egashira², Tomoaki Noguchi², Toshiro Takabatake², Akinori Kondo³, Koichi Kindo³, Shoji Yamanaka⁴, Kei Inumaru⁴, Norimasa Nishiyama⁵, Tetsuo Irfune⁶ and Hitoshi Yusa⁶
¹ *Faculty of Science, Ibaraki University, Japan*
² *Graduate School of ADSM, Hiroshima University, Japan*
³ *Institute for Solid State Physics, University of Tokyo, Japan*
⁴ *Graduate School of Engineering, Hiroshima University, Japan*
⁵ *Geodynamics Research Center, Ehime University, Japan*
⁶ *High pressure Science, National Institute Material Sciences, Japan*

Rare-earth compounds with cage structures recently attract much attention because of possibility of new heavy fermion mechanism using the lattice vibration [1]. Rare-earth borides such as RB₆ and RB₁₂ also have such cage structures composed by boron. However, RB₁₂ series are known from R = Tb to Lu. Cannon has succeeded in high-pressure synthesis of GdB₁₂ in pressure of 6.6 GPa and 2,400 C, and reported lattice parameter a = 7.523 Å in the UB₁₂-type structure [2]. We have also succeeded in high-pressure synthesis of polycrystalline GdB₁₂ and SmB₁₂. Magnetic susceptibility of GdB₁₂ shows a kink at 38 K indicating of antiferromagnetic ordering. High-field magnetization of GdB₁₂ shows the saturation moment is 7 μB. All the reported Neel ordering temperatures of RB₁₂ well agree to the values estimated from the trivalent rare-earth dependence of de Gennes factor. From the x-ray powder diffraction of SmB₁₂, this compound also has the UB₁₂-type structure with lattice parameter of a = 7.541 Å. Magnetic susceptibility shows two anomalies at 9 K and 19 K different from other RB₁₂.

[1] T. Hotta and K. Ueda: Phys. Rev. B 67 (2003) 104518. [2] J. F. Cannon, et al.: J. Less-Common Metals 56 (1977) 83.

PE11

Magnetic anisotropy of tetragonal rare-earth compounds RRu₂Al₂B (R: rare-earth metals)

Eiichi Matsuoka^{1*}, Yo Tomiyama¹, Kotaro Iwasawa¹, Hitoshi Sugawara¹, Takahiro Sakurai² and Hitoshi Ohta³
¹ *Department of Physics, Graduate School of Science, Kobe University, Japan*
² *Center for Supports to Research and Education Activities, Kobe University, Japan*
³ *Molecular Photoscience Research Center, Kobe University, Japan*

Recently, we succeeded to synthesize polycrystalline samples of new tetragonal rare-earth compounds CeRu₂Al₂B and PrRu₂Al₂B and reported magnetic properties of these compounds [1]. Both compounds show successive phase transitions of an antiferromagnetic and a ferromagnetic ordering. The Neel and Curie temperatures for CeRu₂Al₂B are 14.3 K and 13 K, respectively, and those for PrRu₂Al₂B are 26 K and 11 K, respectively. The values of magnetization vary when the angle between sample direction and applied magnetic field is changed even in the polycrystalline samples. This fact implies that the grains of polycrystalline samples are oriented partially and the variation of magnetization values is due to the magnetic anisotropy. In this study, we will report on the results of magnetization and magnetic-susceptibility measurements of grain-oriented powder samples of RRu₂Al₂B (R: rare-earth metals) and will discuss the magnetic anisotropy.

[1] E. Matsuoka, Y. Tomiyama, H. Sugawara, T. Sakurai, and H. Ohta, J. Phys. Soc. Jpn. 81 (2012) 043704.

PE12

Collective magnetic resonance mode in CeB₆

A. V. Semeno^{1*}, V. V. Glushkov¹, N. E. Sluchanko¹, N. Yu. Shitsevalova², V. B. Filipov², A. V. Dukhnenko² and S. V. Demishev¹
¹ *A.M.Prokhorov General Physics Institute RAS, Russia*
² *Institute for Problems of Materials Science NAS, Ukraine*

The observation of the electron spin resonance (ESR) in low temperature phase (phase II) of CeB₆ has risen up new questions about the nature of its ground state [1]. In the present work we study the effects of La doping on the ESR parameters in Ce_{1-x}La_xB₆. Experiments in the doping range 0<x<0.1 have shown that even small La concentrations x~0.03 cause strong broadening as well as suppression of the ESR line. Such behavior is accompanied by a tendency of g-factor increase from g~1.6 in CeB₆ to higher values with La doping. The resonance line gets unobservable with further concentration increase up to x~0.05. At the same time the phase border between the phase II and the paramagnetic phase I observed as a kink in microwave conductivity remains almost independent on the La concentration in the studied range. Such strong sensitivity of the ESR parameters to the doping concentration allows suggesting the collective origin of the electron spin resonance mode.

[1] S. V. Demishev et. al., Phys. Rev. B 80, 245106 (2009)

PE13

Transport and magnetic properties of CeFe₄Sb₁₂ synthesized under high pressure

Hitoshi Sugawara^{1*}, Masahito Sakoda¹, Eiichi Matsuoka¹, Takashi Saito², Sho Tatsuoka², Kenya Tanaka² and Hideyuki Sato²
¹ *Department of Physics, Kobe University, Japan*
² *Department of Physics, Tokyo Metropolitan University, Japan*

The filled skutterudite compounds have attracted much attention, since they exhibit a variety of novel features such as the heavy fermion behavior, hybridization-gap semiconducting behavior, and unconventional superconductivity [1]. The filling fraction of rare-earth site plays the important role for the ground state in certain compounds, such as PrxFe₄Sb₁₂, in which the ferromagnetic ground state for x~0.8 is changed to the non-magnetic one by increasing to x~1 [2]. In this work, we have succeeded in synthesizing the filled skutterudite CexFe₄Sb₁₂ with the Ce-site filling fraction x~1 under high pressure, and found the semiconducting behavior in this compound.

[1] H. Sato, H. Sugawara, Y. Aoki and H. Harima: Handbook of Magnetic Materials, Vol. 18, "Magnetic Properties of Filled Skutterudites" ed. by K.H.J. Buschow. (Amsterdam, Elsevier), p.1-110, 2009. [2] K. Tanaka, Y. Kawahito, Y. Yonezawa, D. Kikuchi, H. Aoki, K. Kiawahara, M. Ichihara, H. Sugawara, Y. Aoki and H. Sato: J. Phys. Soc. Jpn. Vol. 76 (2007) 103704.

PE14

Interplay of Kondo effect and spin orbit coupling

Kalobaran Maiti^{*}, Swapnil Patil, V R R Medicherla, R S Singh and E V Sampathkumaran
Department of Condensed Matter Physics, Tata Institute of Fundamental Research, India

Physics near quantum critical point (QCP) has been an interesting unresolved problem for many decades now. While the ground states on either sides, away from QCP are reasonably well understood, the physics in the vicinity of QCP is a long standing puzzle. The question is, how the quantum critical fluctuations affects the electronic excitations and evolves as one goes across QCP. We studied the electronic structure of Ce_{1-x}Rh_xCo₂Si₃ with varying x using high resolution photoemission spectroscopy. Co substitution at the Rh sites in antiferromagnetic Ce₂RhSi₅ leads to transition to a Kondo system, Ce₂CoSi₅ via QCP at x = 0.6. High resolution spectra reveal signature of Kondo resonance feature (KRF) and its spin orbit split component (SOC) in the whole composition range indicating finite Kondo temperature scale at QCP and applicability of spin density wave picture at the approach to QCP. Interestingly, the intensity ratio of the Kondo resonance feature and its spin orbit split component, KRF/SOC gradually increases with the decrease in temperature suggesting importance of spin-orbit interactions in this regime.

PE15

Insulator-to-metal transition and magnetism of potassium metals loaded into regular cages of zeolite LSX

Takehito Nakano¹, Duong Thi Hanh¹, Nguyen Hoang Nam², Yasuhiro Owaki¹, Shingo Araki³ and Yasuo Nozue^{1*}
¹ *Department of Physics, Graduate School of Science, Osaka University, Japan*
² *Hanoi University of Science, Viet Nam*
³ *Graduate School of Natural Science and Technology, Okayama University, Japan*

Zeolite low-silica X (LSX) crystals have an aluminosilicate framework with the regular nanospace of supercages and beta-cages. They are connected by the double diamond structure. Many K-cations are distributing among negatively charged framework in K-type LSX. 4s-electrons of guest alkali atoms are shared with K-cations of zeolite. Loading density of guest K atoms per unit cage, n, can be controlled from 0 to 9. At n < 2, samples are nonmagnetic and insulating[1]. When n is just above 2, number density of magnetic moments suddenly increases and electrical resistivity decreases as semiconductive materials. For n > 6, electrical resistivity shows metallic properties suddenly. When n > 8.5, ferrimagnetic properties is observed at low temperatures. A remarkable increase in resistivity is observed at low temperatures likely Kondo semiconductor. In materials with the strong electron-phonon interaction, excess electrons are self-trapped quantum mechanically at the deformation potential well[2]. These immobile electrons are small polarons with magnetic moments. If the electron-phonon interaction is much stronger than the repulsive interaction between two electrons, nonmagnetic small bipolarons are stabilized. Observed novel properties are explained by small bipolarons, small polarons, metallic large polarons, and Kondo-like mixing between metallic electrons in supercages and localized electrons in beta-cages.

[1] Y. Ikemoto, T. Nakano, M. Kuno, Y. Nozue and T. Ikeda, J. Mag. Mag. Mat. 226-230, 229 (2001). [2] Y. Toyozawa, Prog. Theor. Phys. 26, 29 (1961).

PE16

1/(N-1) expansion for a finite U Anderson model with an SU(N) symmetry

Akira Oguri¹ and Rui Sakano²
¹ *Physics, Osaka City University, Japan*
² *Applied Physics, University of Tokyo, Japan*

We apply recently developed 1/(N-1) expansion to a particle-hole asymmetric SU(N) Anderson model with finite Coulomb interaction U. This approach is completely different from the conventional 1/N expansion, or the non-crossing approximation. In our approach the factor N-1 corresponds to the number of interacting orbitals, excluding the one prohibited by the Pauli principle. To leading order in 1/(N-1) it describes the Hartree-Fock random phase approximation (HF-RPA), and the higher-order corrections describe systematically the fluctuations beyond the HF-RPA. The low-energy local Fermi-liquid behavior is described properly with this approach. We show that the next-leading order results of the renormalized parameters agree closely with the numerical renormalization group results at N=4 in a wide range of the electron fillings, from the empty to fully occupied orbitals, specifically in the mixed-valence regions. This ensures the reliability of the next-leading order results for N > 4. Our expansion scheme uses the standard Feynman diagrams, and thus has wide potential applications. It can be applied to the Keldysh formalism, and to lattice systems such as the Hubbard model.

[1] A. Oguri, R. Sakano, and T. Fujii, Phys. Rev. B 84, 113301 (2011). [2] A. Oguri, arxiv:1112.6051.

PE17

Formation of the Kondo resonance band in CeCoGe₂: DFT+DMFT approach

Hong Chul Choi¹, B. I. Min², K. Halue³, G. Kotliar³ and J. H. Shim^{1*}
¹ *Department of Chemistry, Pohang University of Science and Technology, Korea*
² *Department of Physics, Pohang University of Science and Technology, Korea*
³ *Department of Physics, Rutgers University, USA*

We have investigated the formation of the Kondo resonance (KR) band in the heavy fermion CeCoGe, using the combined approach of the density functional theory (DFT) and the dynamical mean field theory (DMFT). The low temperature (T) spectral function shows the dispersive KR states in momentum space, which is well consistent with the experimental observation. The size of the induced hybridization gap is rather insensitive to T. During the evolution from the spd bands at high T to the dispersive KR bands at low T, whose topologies are different each other, we have found the existence of kinks in the spectral function near EF. We suggested that the kink can be intrinsically observed in measuring spdcduction bands during the formation of the fully coherent KR band.

PE18

Charge ordering in the Kondo lattice model at quarter filling

Junki Yoshitake^{*}, Takahiro Misawa and Yukitoshi Motome
Department of Applied Physics, The University of Tokyo, Japan

The Kondo lattice model is one of the fundamental models for heavy-fermion systems, where exchange interactions between itinerant electrons and localized spins play an important role. Among many different phases described by this model, emergence of charge-ordered state [1,2] is interesting possibility, because this model does not include any bare inter-site repulsions between electrons. The possibility was first pointed out by a perturbation expansion in the strong Kondo coupling limit at quarter filling in 1D [1], and recently examined by the dynamical mean-field theory in infinite dimensions [2]. However, it remains unclear whether the charge-ordered state appears in two and three dimensions and what type of magnetic order is accommodated in the charge-ordered state. To clarify these issues, we investigate both the ground state and finite-temperature properties of the quarter-filled Kondo lattice model on a square lattice by complementarily using the variational Monte Carlo simulation and cluster dynamical mean-field theory. We found that charge-ordered state appears in a wider region than the previous result in infinite dimensions, and that the antiferromagnetic order between charge poor sites is accommodated in the charge-ordered state. We discuss the stabilization mechanism of charge ordering by carefully analyzing the electronic and magnetic properties.

[1] J. E. Hirsch, Phys. Rev. B 30, 5383 (1984). [2] J. Otsuki et al., J. Phys. Soc. Jpn. 78, 034719 (2009).

PE19

Angular-dependent magnetoresistance of the filled skutterudite CeOs₄As₁₂

Lukasz Bochenek^{*}, Zygmunt Henkie and Tomasz Cichorek
Division of Magnetic Research, Institute of Low Temperature and Structure Research, Polish Academy of Sciences, Wroclaw, Poland, Poland

The filled skutterudite CeOs₄As₁₂ compound is a narrow-gap semiconductor whose low-temperature properties originate from a hybridization between 4f and conduction electrons. Nonmagnetic CeOs₄As₁₂ is the cubic system showing a nodal structure of hybridization energy gap(s) as evidenced from low-temperature (T > 0.08 K) and high-magnetic field (B < 14 T) studies of a directional dependence of the electrical resistivity ρ(T): At T < 3 K and for j || B, we found remarkable dissimilarities along the [001] and [111] directions, indicative of an anisotropic suppression of energy gap(s). Additionally, differences observed between the transverse and longitudinal magnetoresistivity cannot be ascribed to the Lorentz force and thus, provide a further evidence for magnetic-field-induced anisotropy of hybridization gap in CeOs₄As₁₂. High-quality single crystals of CeOs₄As₁₂ enable studies of a change of Fermi surface via the angular-dependent magnetoresistivity both in the field-induced metallic as well as semiconducting state. Our experiments with the use of the commercial one-axis rotator (PPMS) provide an additional evidence for strongly correlated electron phenomena in CeOs₄As₁₂ that we tentatively relate to the quartet Γ67 ground state of the Ce³⁺ ion in the Th symmetry.

PF01

Spin and charge correlation of electrons at variation of interorbital Coulomb interaction

Sergey Stepanovich Aplesnin¹ and Nataly Ivanovna Piskunova²
¹ *M.V. Reshetnev Siberian State Aerospace University, Russia*
² *Omsk State Agrarian University, Russia*

Of great interest for the researches is the ions with orbital degeneration and electron shell with filling more than half. The aim of our work is to evaluate spin and charge correlation at variation of interorbital Coulomb interaction and competition of electron hopping parameters between nearest sites on the same and different orbitales arising as a result of variation of orbitales filling. Variation of charge gap may be also cause a radical change in the electronic density and spin correlation functions. We calculated electron spectrum in the Hubbard model with electron filling n=1.5 and following parameters: energy level of ions, the matrix element of the hopping between the nearest sites and orbitales, U and V is the Coulomb repulsion of the electrons on site and between orbitales. We calculated the eigenvalue spectrum and the corresponding state vectors by exact diagonalization for small cluster, based on which we determined the spin correlation functions on the longitudinal and transverse spin components, correlator of electron density. As a results, critical parameters Vc of the interorbitales Coulomb interaction and hopping integral are found at which reveal change in the value and sign of exchange interaction and in the correlator of electron density.

PF02

Superfluid state of repulsively interacting three-component fermionic atoms in optical lattices

Seiichiro Suga^{1*} and Kensuke Inaba²
¹ *University of Hyogo, Japan*
² *NTT Basic Research Laboratories and JST CREST, Japan*

We investigate the superfluid state of repulsively interacting three-component (color) fermionic atoms in optical lattices. We first discuss the effective interactions using diagrammatic approaches. We then investigate the superfluid properties using complementary two methods: the dynamical mean-field theory with a perturbative approach and the self-energy functional approach. We show that when the anisotropy of the three repulsive interactions is strong, atoms of two of the three colors form Cooper pairs and atoms of the third color remain a Fermi liquid. An effective attractive interaction is induced by density fluctuations of the third-color atoms. This superfluid state is similar to the color superfluid of the attractively interacting three-component systems. We show from dynamical properties that the Cooper-pairing mechanism is basically similar to that of the conventional phonon-mediated superconductivity. The superfluid state is stable against changes in filling close to half filling. We determine the phase diagrams in terms of temperature, filling, and the anisotropy of the repulsive interactions. We also discuss the relation between the theoretical results and experiments.

PF03

Magnetism in complex oxides: A challenge for advanced ab-initio methods

Alessio Filippetti
Dept. of Physics, CNR-IOM, University of Cagliari, Italy

The accurate description of magnetic properties in complex oxides by first-principles is tantamount with the possibility of achieving reliable theoretical design of oxide-based spintronic devices. Alas, standard first-principles approaches fails to properly describe strong correlated systems, and more sophisticated approximations are required. Recently the novel variational pseudo-self-interaction corrected density functional theory (VPSIC) has been introduced, showing great potential as theoretical tool for the study of complex oxides and strong-correlated systems in general, and promising to open the field to reliable designs of magnetic oxide-based devices. Here we apply the new approach to investigate two prototypical oxide families, i.e. transition metal monoxides (MnO, NiO) and perovskite titanates (LaTiO₃, YTiO₃). We give evidence that the new theory is capable to furnish an unprecedentedly accurate description of both ground-state and finite-temperature magnetic properties, both at equilibrium and under pressure. As highlights of the results obtained in the work, we mention the correct determination of critical temperature and the accurate description of orbital ordering in transition metal oxides.

PF04

Resonating Hartree-Fock Studies for spin fluctuations in the Hubbard model on triangular lattice

Norikazu Tomita^{*}
Yamagata University, Japan

Electron correlation effects in geometrically frustrated systems have attracted much attention in condensed-matter physics. In fact, these systems show a variety of interesting and non-trivial ground states. On the other hand, theoretical description on the electron correlations in these systems is difficult, and origins of such non-trivial states are not yet clarified. In this research, the electron correlations are visualized from the viewpoint of quantum fluctuations. Such visualization is important for the fundamental understanding and applications of the frustrated system. A resonating Hartree-Fock method constructs a many-body wave-function by superposition of non-orthogonal Slater determinants, where superposition coefficients and orbitals in all the Slater determinants are simultaneously optimized. We can visualize quantum fluctuations from the structures of Slater determinants generating the wave-function. We have previously demonstrated that quantum fluctuations in the doped Hubbard model on a square lattice are described by vibrations and translations of polarons. [Phys. Rev. Lett. 103(2009)116401.] Now, the half-filled Hubbard model on a uniform triangular lattice are considered. The ground state is metallic and non-magnetic when U is weak. We show that non-magnetic ground state is realized by the large quantum fluctuations due to hybridization of two different co-linear spin-density waves and their modulations. [Phys. Rev. B84(2011)245101.]

PF05

Theory of momentum-dependent variational ansatz to strongly correlated electron system

M. Atiqur R. Patoary* and Yoshiro Kakehashi
Univ. of the Ryukyus, Nishihara, Okinawa, Japan

We have recently developed Momentum dependent Local-Ansatz wavefunction (MLA) approach to describe the correlated electron system in the weak and intermediate Coulomb interaction (U) regime. The theory did not work best in the strong U regime because we started from the Hartree-Fock (HF) wavefunction. To overcome the difficulty, we propose here a new hybrid wavefunction in which the starting wavefunction can vary via a new variational parameter w from the HF wavefunction (w=0) suitable for the weak interaction regime to the alloy-analogy (AA) wavefunction (w=1) suitable in the strong interaction regime. The extended method overcomes the standard variational method such as the Gutzwiller wavefunction approach (GA) irrespective of U. We have demonstrate that the energy for the MLA-AA (w=1) is lower than those of the MLA-HF (w=0) in the strong U region for the half-filled band Hubbard model for the hypercubic lattice in infinite dimensions. Moreover, the energy of the MLA (w=0 and 1) is always lower than the GA. We have also verified that the double occupation number, quasi-particle weight and momentum distribution function are much improved by the new MLA.

PF06

Metal-insulator transition in orthorhombic Perovskite PbRuO₃

Young-joon Song¹ and Kwan-woo Lee^{2*}
¹ *Department of Applied Physics, Graduate School, Korea University, Sejong, Korea*
² *Department of Display and Semiconductor Physics, Korea University, Sejong, Korea*

Transition metal oxide perovskites show abundant physical phenomena such as superconductivity, CMR, ferroelectricity, and unusual magnetic behavior. Recently, the orthorhombic perovskite PbRuO₃, which was first synthesized 40 years ago, has been revisited by two experimental groups. Commonly, the measurements of temperature-dependent magnetic susceptibility show a kink at 90 K, where a structural transition occurs, but no magnetic ordering has been observed even at very low T. Remarkably, the resistivity measurements of Kimber et al. indicate a metal-insulator transition, but ones of Cheng et al. shows a metal-metal transition though a kink appears at 90 K. To understand this discrepancy, we have carried out first principles calculations using various approaches: correlated band theory (LDA+U), LDA+U+SOC (spin-orbital coupling), modified BJ, and fixed spin moment calculations. In this presentation, we will address the electronic and magnetic structures on PbRuO₃ in more detail and a scenario on the discrepancy.

PF07

Ferromagnetic semiconductor-metal transition in heterostructures of europium monoxide

Tobias Stollenwerk* and Johann Kroha
Physikalisches Institut, University of Bonn, Germany



PF08

The temperature dependence of the staggered magnetisation in itinerant weak antiferromagnets

Nobukuni Hatayama¹, Rikio Konno^{1*} and Yoshinori Takahashi²
¹ *Kinki University Technical College, Japan*
² *Graduate School of Material Science, University of Hyogo, Japan*

Effect of spin fluctuations on the staggered magnetisation in itinerant weak antiferromagnets is investigated below the Neel temperature T_N. It is known that the discontinuous change of the magnetisation occurs at the critical temperature in the rotationally invariant treatment in the self-consistent renormalization spin fluctuation theory. The difficulty is resolved in itinerant weak ferromagnets by Takahashi [J. Phys.: Condens. Matter 13 (2001) 6323.]. In this paper, we extend his theory to the case of weak antiferromagnets. We have succeeded in deriving the temperature dependence of the staggered magnetisation below T_N, by taking account the effects of spin-waves excitations into the transverse component of the dynamical magnetic susceptibility within the small area of wave-vector space around the staggered wave-vector. We found T^{3/2}-linear behaviour of the staggered magnetisation at low temperatures compared with T_N.

PF09

Theory of excitonic insulator in the two orbital Hubbard model: Variational cluster approach

Tatsuya Kaneko^{1*}, Kazuhiro Seki¹, Satoshi Nishimoto² and Yukinori Ohta¹
¹ *Department of Physics, Chiba university, Japan*
² *Institut für Theoretische Festkörperphysik, IFW Dresden, Germany*

Motivated by the recent experimental and theoretical studies of excitonic insulators, we investigate the spontaneous symmetry breaking of the excitonic insulator state in the two-orbital Hubbard model defined on the two-dimensional square lattice. Using the variational cluster approximation (VCA) and Hartree-Fock approximation (HFA), we evaluate the number of particles on each orbital, staggered magnetization in the Mott insulator phase, the order parameter indicating the coherence between electrons and holes in the excitonic insulator phase, and the ground-state phase diagram as functions of intra-orbital and inter-orbital Coulomb interactions. We also calculate the single-particle excitation spectra of the band insulator, Mott insulator, and excitonic insulator phases. We thereby argue that the normal metallic phase is unstable to the formation of the excitonic insulator phase, which should appear in a wide parameter region between the band insulator and Mott insulator phases.

PF10

Layered chalcogenide Ta₂NiSe₅ as a candidate for excitonic insulators - theoretical aspects

Tatsuya Kaneko^{1*}, Tatsuya Toriyama¹, Takehisa Konishi² and Yukinori Ohta¹
¹ *Department of Physics, Chiba university, Japan*
² *Graduate School of Advanced Integration Science, Chiba university, Japan*

The electronic structure of layered chalcogenide Ta₂NiSe₅, a candidate for excitonic Insulators, is calculated using the generalized gradient approximation in the density functional theory, where the Hubbard-type repulsive interaction is taken into account. We find for the low-temperature monoclinic phase that the conduction band has a cosinelike quasi-one-dimensional (1D) band dispersion coming mainly from the 5dxy orbitals of Ta ions arranged along the a-direction of the lattice, whereas the top of the valence band has a quasi-1D dispersion coming mainly from the Ni 3dxz+3dyz and Se 4px+4py orbitals arranged alternately along the a-direction. The electronic state near the Fermi level is thus described by the quasi-1D structural unit consisting of these orbitals. The electronic structure of Ta₂NiS₅, which has the orthorhombic crystal structure, is also calculated to clarify the role of the lattice distortion. Three scenarios are suggested to explain the characteristic temperature dependence of the band structure observed in the angle-resolved photoemission: a scenario of the band deformation due to the monoclinic lattice distortion, a scenario of the formation of the excitonic insulator state, and a scenario made from the combination of the former two where the monoclinic lattice distortion and formation of the excitonic insulator state occur cooperatively.

PF11

Electric dipolar susceptibility of the Anderson-Holstein model

Takahiro Fuse* and Takashi Hotta
Department of Physics, Tokyo Metropolitan University, Japan

Recently, cage structure materials have attracted much attention due to intriguing magnetic phenomena induced by the coupling effect between electrons and rattling, i.e., anharmonic local oscillation of guest ion in a cage. When the guest ion oscillates in the cage, there should occur electric dipole moment P, given by P=Zex, where Z denotes the valence of the guest ion, e indicates electron charge, and x is ion displacement. In order to investigate properties of electron-rattling system, we evaluate electric dipolar susceptibility χ_P on the basis of the Anderson-Holstein model, which consists of conduction electron term, hybridization between conduction and localized electrons, Coulomb interaction between localized electrons, and coupling between ion oscillation and local charge density. We analyze the model by using the numerical renormalization group (NRG) method. Note that χ_P is directly related to the phonon Green's function D. For the evaluation of D, we pay due attention to the phonon excited states kept in the renormalization process. We carefully evaluate D with the use of NRG and compare it with that obtained from charge susceptibility in the combination with the Dyson equation. Then, we discuss the effects of anharmonicity and Coulomb interaction on χ_P.

PF12

Insulator version of the double-exchange ferromagnetism

Yukinori Ohta^{1*}, Satoshi Nishimoto² and Kyohei Nakano¹
¹ *Department of Physics, Chiba University, Japan*
² *Institute for Theoretical Solid State Physics, IFW-Dresden, Germany*

The double-exchange ferromagnetism is known to appear when the coherent motion of electrons occurs in the conduction band that is coupled with the localized spins via the ferromagnetic Heisenberg-type exchange interaction, i.e., the Hund's rule coupling. A natural and realistic issue that arises is then what happens with the ferromagnetism when a gap opens in the conduction band and coherent motion of electrons ceases. To answer this question quantitatively, we apply the density-matrix renormalization group method to the study of the one-dimensional double-exchange model, where we introduce the Peierls-type lattice distortion in the conduction band to make the system an insulator with the band gap. We find from the analysis that the double-exchange ferromagnetism persists strongly into the strength of the lattice distortion exceeds a certain critical limit; we thus call this an insulator version of the double-exchange ferromagnetism. We note that this type of ferromagnetism actually occurs in a chromium hollandite K₂Cr₂O₁₆, where a half-metallic ferromagnet due to the double-exchange mechanism undergoes a metal-insulator transition, resulting in the realization of a ferromagnetic insulator [1].

[1] Toriyama et al., Phys. Rev. Lett. 107, 266402 (2011).

PF13

Metallic ferromagnetism in the 3D Hubbard model at finite temperature

Andre Neves Ribeiro and Claudio Andrade Macedo*
Departamento de Fisica, Universidade Federal de Sergipe, Brazil

The dynamical mean-field approximation (DMFA), when used to study strongly correlated electron systems (SCES), allows the obtainment of thermodynamic properties in a nonperturbative regime. The Hubbard model is the simplest model capable of describing the essential physics of SCES. Thus, we investigated the existence of ferromagnetism in the Hubbard model on fcc lattices, at finite temperatures, using the DMFA with effective parameters solved by exact numerical diagonalization. We calculated the magnetization for 0.3 n 0.9 (where n is the number of electrons per site), with temperature of 0.04t/kB (where t is the hopping integral between nearest-neighbor sites) and the value of the on-site Coulombian interaction U equal to 3W (where W denotes the noninteracting energy bandwidth). Our results reveal a significant magnetization for n = 0.6, 0.7 and 0.8. The densities of states indicate that these systems are metallic. In the particular case for n = 0.6, magnetization, internal energy and specific-heat curves versus temperature were calculated to that value of U. This work provides an affirmative answer to the question whether the Hubbard model with only nearest-neighbor hopping, on a three-dimensional lattice, and finite both temperature and on-site Coulombian interaction, exhibits ferromagnetism when solved using the DMFA.

PF14

BCS-BEC crossover in the extended Falicov-Kimball model: Variational cluster approach

Kazuhiro Seki^{1*}, Robert Eder² and Yukinori Ohta¹
¹ *Department of Physics, Chiba University, Japan*
² *Institut fuer Festkoerperphysik, Karlsruhe Institute of Technology, Germany*

We study the spontaneous symmetry breaking of the excitonic insulator state induced by the Coulomb interaction U in the two-dimensional extended Falicov-Kimball model. Using the variational cluster approximation (VCA) and Hartree-Fock approximation (HFA), we evaluate the order parameter, single-particle excitation gap, momentum distribution functions, coherence length of excitons, and single-particle and anomalous excitation spectra as functions of U at zero temperature. We find that in the weak-to-intermediate coupling regime, the Fermi surface plays an essential role and calculated results can be understood in close correspondence with the BCS theory, whereas in the strong-coupling regime, the Fermi surface plays no role and results are consistent with the picture of a Bose-Einstein condensate (BEC). Moreover, we find that HFA works well in both the weak and strong-coupling regimes, and that the difference between the results of VCA and HFA mostly appears in the intermediate-coupling regime. The reason for this is discussed from a viewpoint of the self-energy. Details are reported in Ref. [1].

[1] K. Seki, R. Eder, and Y. Ohta, Phys. Rev. B 84, 245106 (2011).

PF15

Theory of the metal-insulator transition and charge/orbital states in V₂O₁₃

Takayoshi Nakayama^{1*}, Tatsuya Toriyama¹, Takehisa Konishi² and Yukinori Ohta¹
¹ *Department of Physics, Chiba University, Japan*
² *Graduate School of Advanced Integration Science, Chiba University, Japan*

The Wadsley-phase vanadium oxide V₂O₁₃ has the crystal structure composed of the two-dimensional single and double trellis lattices, where the V ions are in the mixed valent state with an average valence of V4.33+ (3d0.66); i.e., there are formally V5+ (3d0) and V4+ (3d1) in a 1 : 2 ratio. This material undergoes a metal-insulator transition (MIT) at 150K, which is accompanied by the structural distortion, and shows an antiferromagnetic order below 55K. To clarify the electronic structure of this material, we make the density-functional-theory-based electronic structure calculations and discuss the mechanism of the MIT, as well as its charge and orbital states above and below the MIT. We find that the band structure obtained is in reasonable agreement with the observed angle-resolved photoemission spectra but that the characteristic distribution of valence electrons is not necessarily compatible with the results of a recent NMR experiment. We also find that, if we assume the observed low-temperature crystal structure in the calculations, we obtain the insulating solution with an antiferromagnetic order, which is in agreement with experiment.

PF16

Statistical dynamical mean field study of correlated fermions with disorder

Masaru Sakaïda*, Kazuto Noda and Norio Kawakami
Kyoto university, Japan

Disordered systems with strong correlation effects have been studied in solid state physics, and even now have attracted much interest. Various experiments have been performed extensively, and in particular a disordered system of strongly interacting cold atoms has been experimentally realized recently[1]. Statistical dynamical mean-field theory[2,3] to treat disorders and strong correlation effects on equal footing and non-perturbatively makes it possible to capture essential features of the Anderson transition beyond the coherent-potential approximation. In this work, we analyze the tight-binding fermion model on the Bethe lattice in which the box disorder manifests itself by random on-site energies. We systematically investigate characteristic behaviors of the density of states and the conductivity to estimate competitions between disorders and correlation effects in this system.

[1] L. Fallani et al., Phys. Rev. Lett. 98, 130404 (2007) [2] V. Dobrosavljevic et al., Phys. Rev. Lett. 78, 3943 (1997) [3] D. Semmler et al., Phys. Rev. B 84, 115113 (2011)

July 9 (Mon)

July 9 (Mon)

PF17

Analysis of many-body effects on anisotropic magnetic properties of YbB₁₂

Yoshihiro Kikuchi*, Yoshiki Imai and Tetsuro Saso
Department of Physics, Saitama University, Japan

YbB₁₂ is one of the typical Kondo insulator and many experiments are already reported. Although it has cubic structure, critical magnetic fields of insulator-to-metal transition are anisotropic[1]. Moreover anisotropic magnetization is observed above the critical field[2]. One of the authors studied the magnetic properties by means of tight binding model, composed of Yb 5d_z and 4f Γ_8 orbitals[3]. The results were qualitatively in agreement with the experiments but a quantitative disagreement was left, because many-body effects were not taken into account. Therefore, we introduce coulomb repulsion between f-electrons in the tight binding model. We apply the dynamical mean field theory, in which we solve the effective impurity problem by using the continuous-time quantum Monte Carlo method. We compare obtained result with the experimental one's quantitatively, and discuss the many-body effects in the magnetic properties of YbB₁₂.

[1] F. Iga et al. : Jpn. J.Appl. Phys. Series 11(1999)88 [2] S. Hiura, et al.: Physica B 281&282(2000)271 [3] T. Izumi, Y. Imai, T. Saso : J. Phys. Soc. Jpn. 76(2007)084715

PF18

The ground state energies of spinless free fermions and hard-core bosons in 2D square lattices

Wenxing Nie¹ and Masaki Oshikawa^{2*}

¹ The Institute for Solid State Physics, The University of Tokyo, Japan
² The institute for Solid State Physics, The University of Tokyo, Japan

We compare the ground state energies of hard-core bosons and spinless free fermions on the same lattice. Ground state energy of bosons is usually expected to be lower than that of fermions, because bosons can condense into the lowest energy state. However, in the presence of hard-core interaction among bosons, the condensation is not perfect and comparison is nontrivial. We find that, in the absence of frustration, the ground state energy of hard-core bosons is indeed lower than that of free fermions. In general, however, the hard-core bosons could have higher ground state energy than the fermions on the same lattice if there is a frustration. In fact, there is an exactly solvable one-dimensional model, in which the ground state energy of bosons is proved to be higher. However, the difference vanishes in the thermodynamic limit. We also studied the two-dimensional square lattice with uniform magnetic flux perpendicular to the lattice, by numerical diagonalization. As the magnetic flux introduces frustration, we actually find the ground state energy of hard-core bosons is higher for a range of flux and particle density. In the two dimensional case, this difference seems to persist in the thermodynamic limit, in contrast to the one-dimensional case.

[1]Phys. Rev. B 14, 2239 (1976) [2]Phys. Rev. Lett. 83, 2246(1999) [3]Phys. Rev. Lett. 96, 036406 (2006)

PF19

Correlation effect in ferromagnetic 3d transition metals

Muneyuki Nishishita¹, Sudhakar Pandey² and Dai Hirashima^{1*}

¹ Nagoya University, Japan
² APTPC, Korea

Selfconsistent perturbation theory is applied to ferromagnetic 3d transition metals, Fe and Ni. Realistic tight-binding model is used to describe the electronic states of the system. It is found that a reasonable value of the Curie temperature for Fe is obtained for realistic strength of the Coulomb interaction. Dynamical transverse susceptibility is also calculated. Here, vertex corrections are considered so that the spin rotational symmetry is preserved. Then, the spin-wave energy correctly vanishes in the long-wavelength limit. The effect of the electron correlation on the spin stiffness is clarified. We also compare the spin fluctuation spectra below and above the Curie temperature and discuss the possible short-range order above the Curie temperature.

PG01

Ferrimagnetic compensation in a Fe₆₄Er₁₉B₁₇ glass, - the head of a dandelion, or the spokes of a wheel?

Andrew R. Wildes^{1*}, Neil Cowlam² and Nourh A. Al-senany³

¹ Institut Laue-Langevin, BP 156, 6 rue Jules Horowitz, 38042 GRENOBLE Cedex 9, France
² Department of Physics and Astronomy, University of Sheffield, SHEFFIELD, S3 7RH, United Kingdom
³ Department of Physics and Astronomy, University of Sheffield, SHEFFIELD, S3 7RH, King Abdulaziz University, Jeddah, Saudi Arabia, United Kingdom

Magnetization and neutron scattering measurements with polarization analysis were made on a Fe₆₄Er₁₉B₁₇ glass to investigate its ferrimagnetic compensation at T(comp) = 112 ± 2K. The measurements prove that the glass has a non-collinear magnetic structure. The two non-spin flip cross-sections interchange between 100K and 125K, proving the magnetic structure flips at T(comp). They are identical at 112K where the forward limit of the spin flip cross-sections was greatest. The mean collinear components of the moments therefore go to zero at T(comp). If the moment vectors were mapped to originate at a point, the data correspond either to the moments being randomly oriented like the head of a dandelion, or with a collapse of the moments into a plane normal to the field, like the spokes of a wheel. The data will be presented and the possible driving mechanisms for the ferrimagnetic compensation will be discussed.

PG02

Evolution of reverse magnetized seed in monodomain uniaxial garnet film elements

Vladimir Skidanov*

Nanoelectronics and Spintronics Department, Institute for Design Problems in Microelectronics RAS, Russia

Evolution of cylindrical domain seeded in monodomain film and film circular element was investigated numerically and experimentally. It is found that in continuous film in zero external magnetic field cylindrical domain may expand unlimitedly or collapse independently on initial diameter of the seed. Single seed expansion followed by film magnetization reversal is observed if l/h < 1.38 (where l is garnet characteristic length, h is film thickness). Constant positive external magnetic field antiparallel to magnetization inside seed supports stable domain diameter which is inverse proportional to field intensity H. Cylindrical domain inside disk is found stable in zero and negative external magnetic field due radial gradient of inhomogeneous stray field of the disk boundary. If l/h > 1.38 reverse magnetized seed collapses in zero external field. Stable domain doesn't exist in constant negative external field parallel to seed magnetization this case. Unlimited domain expansion takes place if modulus of negative H exceeds critical value which is inverse proportional to initial seed diameter. Domain is stable if domain wall embraces circular hole in garnet film. This case garnet boundary stray field prevents from domain contraction in zero and positive external field. Two-domain ring-shape elements can be utilized as fast magneto-optical modulators.

PG03

Re-entrant structure and critical behaviour of Fe-Cr and Fe-V sigma-phase alloys

Reginaldo Barco¹, Paulo Pureur¹, G L F Fraga¹ and Stanislaw M Dubiel²

¹ Physics, UFRGS Porto Alegre, Brazil
² Physics and Applied Computer Science, AGH University Krakow, Poland

The σ -phase (tetragonal unit cell, space group D144h-P42/mnm) belongs to a family of a complex Frank-Kasper phases. It can be formed in transition-metal alloys. Only two alloys, among about 50 examples of σ known to occur in binary systems, viz. Fe-Cr and Fe-V have well-evidenced magnetic properties. The magnetic ordering of σ has been regarded as ferromagnetic (FM) with the Curie temperatures, T_c, below ~40 K for σ -FeCr and below ~315 K for σ -FeV. Here we report a clear evidence that the ground state of the σ -phase Fe_{0.53}Cr_{0.47} and Fe_{0.52}V_{0.48} alloys is a re-entrant spin-glass (RSG). The evidence was found from a study of magnetization versus temperature, T, and magnetic field, H. Based on the field-cooled and zero-field-cooled magnetization curves recorded in different fields, H, phase diagrams in the H-T plane could have been drawn. They display the location of the paramagnetic (P), FM and RSG states, and are in a qualitative accord with predictions of the mean-field theory. Critical behaviour near T_c was also studied with both conventional and extended protocols, and the critical exponents β , γ , δ were determined.

PG04

Pressure effects in the ferromagnetic shape memory alloys Ni₂Mn_{1-x}Cu_xGa

Tomoya Miura¹, Yoshiya Adachi^{1*}, Keita Endo², Ryosuke Kainuma² and Takeshi Kanomata³

¹ Graduate School of Science and Engineering, Yamagata University, Japan
² Department of Materials Science, Tohoku University, Japan
³ Faculty of Engineering, Tohoku Gakuin University, Japan

The Heusler alloy Ni₂MnGa attracts attention as an actuator material because the magnetic distortion of about 10% is observed just below the martensitic transition temperature (TM). The pressure dependence coefficient of the Curie temperature of Ni₂MnGa is +1.0×10⁻⁸ K/Pa.[1] In the Ni₂Mn_{1-x}Cu_xGa alloy system, TC and TM were reported by Kataoka et al.[2] that the samples with the range of x < 0.23, 0.23 < x < 0.30 and x > 0.30 are characterized TC > TM, TC = TM and TC < TM, respectively. We carried out the initial permeability measurements under pressure up to 1 GPa for Heusler Ni₂Mn_{1-x}Cu_xGa system. TM and TC were determined from the change of the initial permeability under each pressure. It was found that TM was considered to coincide with TC in 0.23 < x < 0.30. Moreover it was obtained dTC/dp is positive in x < 0.23 and dTC/dp is negative in x > 0.30. As a result, the temperature-pressure magnetic phase diagram was obtained. We'd like to discuss the mechanism of the martensitic transformation in Heusler alloy Ni₂Mn_{1-x}Cu_xGa system.

[1] T.Kanomata et al.: J. Magn. Magn. Mater 65 (1987) 76. [2] M. Kataoka et al.: Phys. Rev B 82 (2010) 214423.

PG05

Electronic state of Cr and collapse-like decrease of Fe magnetic moment in amorphous (Fe-Cr)B alloys

Kazuo Yano^{1*}, Tastuo Kamimori², Hiroaki Kanetsuki², Hatsuo Tange², Masayoshi Itou¹, Yoshiharu Sakurai¹, Eiji Kita³ and Hiromitsu Ino⁵

¹ College of Science and Technology, Nihon University, Japan
² Faculty of Science, Ehime University, Japan
³ JASRI/SPring8, Japan
⁴ Applied Physics, University of Tsukuba, Japan
⁵ Faculty of Engineering, University of Tokyo, Japan

Magnetic properties in amorphous alloys have been extensively investigated in rare earth (RE)-transition metal (TM) systems and transition metal (TM)-metalloids systems. Many interesting and important problems have been investigated and solved, however, some of the important problems seem to be hard nuts to crack and remain unsolved. One of the unsolved and interesting problems is an anomaly in Slater-Pauling curve discovered by Mizoguchi et al. and the Fe magnetic moment decreases abruptly, for example in (Fe-Cr)₈₀B₂₀ amorphous alloys. For instance, the substitution of Fe by only 10 at% of Cr causes about 50 %decrease of Fe magnetic moment. Mizoguchi et al. suggested that the Cr retained magnetic moment and coupled anti-parallel to that of Fe, however there have been no decisive experimental results. In order to detect and examine the Cr magnetic moment, one of the powerful tools for this aim, is the magnetic Compton scattering profile (MCP) method which can obtain the informations of 3d electrons and the spin-polarized outer 4s, 4p electrons, separately. The MCP measurement was carried out for (Fe-Cr)₈₀B₂₀ (Cr=0.1, 0.2, 0.3) and the result suggest the existence of Cr magnetic moment coupling antiparallel to that of Fe. Macroscopic magnetic properties were also measured and analyzed.

PG06

Micromagnetic simulation of CNT-MFM probes under magnetic field

Takashi Manago^{1*}, Hironori Asada² and Hiromi Kuramochi³

¹ Department of Applied Physics, Fukuoka university, Japan
² Graduate School of Science and Engineering, Yamaguchi university, Japan
³ International Center for Materials Nanoarchitectonics, National Institute for Materials Science(NIMC), Japan

Ferromagnetic-film-coated carbon nanotube in a magnetic force microscope (CNT-MFM) demonstrated the high spatial resolution of about 10 nm and low perturbation. The magnetic structures of CNT-MFM probes were investigated using three-dimensional micromagnetic simulation and it showed the advantages of the CNT-MFM probes [1]. In this paper, the stability of the magnetic structure in external magnetic field was investigated to confirm magnetic robustness using micromagnetic simulation. At a remanent state, the magnetic moments of the CNT-MFM probe align almost along the longitudinal direction of the CNT lod due to the shape anisotropy. When the opposite magnetic field applied, the magnetic moments of the probes reversed all at once at about 200 mT. In the pyramidal probe, the vortex core was appeared around the tip at a remanent state. When the opposite magnetic field applied, the magnetization of the side wall gradually tilted, and at last the vortex core was reversed. Thus magnetization reversal process is quite different because of large difference in magnetic structures between the CNT-MFM and pyramidal probes. We found that the CNT-MFM probes have better magnetic robustness than the conventional pyramidal probes.

[1] T. Manago et al., Nanotechnology, 23, 035501 (2012).

PG07

Pressure effect of metamagnetic shape memory alloy Pd₂Mn_{1-x}Sn_{1-x}

Yohei Yamazaki¹, Takamitsu Akama², Hironari Okada^{1*}, Takeshi Kanomata¹ and Ryosuke Kainuma³

¹ Division of Engineering Graduate School, Tohoku Gakuin University, Japan
² Faculty of Engineering, Tohoku Gakuin University, Japan
³ Graduate School of Engineering, Tohoku University, Japan

Recently, it has been reported that NiMnX (X = In, Sn and Sb) Heusler alloys show metamagnetic shape memory effect. In these alloys, the martensitic transformation temperature decreases with increasing magnetic field, and magnetic field-induced reverse martensitic transformation associated with metamagnetic transition occurs below the martensitic transformation temperature. Since the magnetic field-induced transformation leads an almost perfect shape memory effect, these alloys attract attention as new type of ferromagnetic shape memory alloys. Very recently, similarly to NiMnX Heusler alloys, it has been found that PdMnSn Heusler alloys show metamagnetic shape memory effects and a drastic change with martensitic transformation in magnetic and transport properties. In this study, in order to investigate pressure effect on martensitic transformation in PdMnSn Heusler alloys, we performed electrical resistivity measurements under high pressure. As a result, it was found that the pressure-temperature phase diagram is similar to the temperature-Mn content phase diagram. These results suggest that the atomic distance plays an important role for martensitic transformation in PdMnSn Heusler alloys.

PG08

Engineering of Co atomic 1-D chains on Ag(111) with tailored magnetic ground state

David Serrate^{1*}, Maria Moro¹, Marten Piantek², Jose Ignacio Pascual³ and Manuel Ricardo Ibarra¹

¹ Instituto de Nanociencia de Aragon, University of Zaragoza, Spain
² Instituto de Ciencia de Materiales de Aragon, CSIC-University of Zaragoza, Spain
³ Institut für Experimentalphysik, Freie Universität Berlin, Germany

Certain magnetic adatoms lying on a metal surface give rise to a Kondo resonance. We used the model system of Co atoms on Ag(111) to investigate their magnetic interactions through the Kondo resonance [1,2]. The Co atoms architecture and the substrate LDOS landscape are artificially arranged by means of lateral manipulation with a scanning tunneling microscope (STM) tip at 4.8 K. The resonance is subsequently characterized by means of STM spectroscopy. Individual Co atoms in natural equilibrium positions at minima of the surface LDOS exhibit Kondo temperature TK=90 K in agreement with earlier studies [3]. TK can be gradually varied from 60 to 145 K by positioning the same atom in different Ag LDOS values of the interference patterns. The coordination with neighboring Co atoms increases TK when their distance decreases below four Ag(111) lattice parameters (2.9 Å). In Co chains with N atoms (N=2,3,...,19), both the amplitude and the spatial extent of the many-body wave function of the Kondo resonance are reduced with increasing coordination. In the frame of the two impurity Kondo theory, our data unveil the nature of direct Co-Co and substrate mediated magnetic interactions as a function of the local electronic and structural environment.

[1] A. Otte et al., Nature Phys. 4, 847 (2008) [2] J. Bork et al., Nature Phys. 7, 901 (2011) [3] M.A. Schneider et al., Phys. Rev. B 65, 121406R (2002)

PG09

Pressure-induced suppression of magnetic ordering in a chiral magnet Cr_{1/3}NbS₂

Takumi Imakure¹, Kousuke Nagai¹, Masaki Mito¹, Hiroyuki Deguchi¹, Jun-ichiro Kishine¹, Takayuki Tajiri², Katsuya Inoue³, Yuya Nakao⁴, Yusuke Kousaka⁴ and Jun Akimitsu⁴

¹ Faculty of Engineering, Kyushu Institute of Technology, Japan
² Faculty of Science, Fukuoka University, Japan
³ Department of Chemistry and Institute for Advanced Materials Research, Hiroshima University, Japan
⁴ Department of Physics and Mathematics, Aoyama-Gakuin University, Japan

Cr_{1/3}NbS₂ is a chiral magnet without structural inversion center. The magnetic property is attributed to the localized moment of Cr, and metallic conductivity is attributed to conduction electrons of Nb. We expect that Cr_{1/3}NbS₂ would become a non-centrosymmetric superconductor after disappearance of magnetic ordering at high pressure. Thus we carried out the AC susceptibility measurements at pressures up to 10 GPa and powder X-ray diffraction experiments at room temperature up to 7 GPa for the powder sample of Cr_{1/3}NbS₂. In the pressure region of below 3 GPa, the anomaly of magnetic susceptibility due to the magnetic ordering shifted toward low temperature side and the magnitude was gradually suppressed. At present, the Meissner signal has not yet been observed in the temperature region down to 2 K and the pressure region up to 10 GPa. The lattice parameters exhibited the change of contraction at around 3 GPa, where it became difficult to evaluate the magnetic ordering temperature.

PG10

Multiple ESR spectra in a chiral molecule-based magnet [Cr(CN)₆][Mn(R)-pnH(H₂O)](H₂O)

Takuma Nagano¹, Masaki Mito¹, Seishi Takagi¹, Hiroyuki Deguchi¹, Jun-ichiro Kishine¹, Yusuke Yoshida² and Katsuya Inoue²

¹ Faculty of Engineering, Kyushu Institute of Technology, Japan
² Department of Chemistry and Institute for Advanced Materials Research, Hiroshima University, Japan

A molecule-based magnet [Cr(CN)₆][Mn(R)-pnH(H₂O)](H₂O) (abbreviated as R-GN) is a chiral magnet without inversion center and mirror reflection. The magnetic network is constructed with the help of a chiral ligand diaminopropane. In R-GN, multiple spectra of ESR were observed below magnetic order temperature by Morgunov et al. [1]. They concluded that the phenomenon was caused by the formation of a chiral soliton lattice, which originated from incommensurate magnetic structure. However, we have a suspicion against their interpretation, because R-GN indeed exhibits no incommensurate magnetic structure. Now, we conducted the experiment of X-band ESR measurement in the condition similar to the experiment by Morgunov et al., and performed the detailed spectrum analyses. In order to reproduce the main ESR spectra, at least two Lorentz spectra are required, and the multiplicity was explained by assuming the existence of two characteristic modes when each periodicity is defined as f or f' ($f' < f$), there is a relation of $f = 2f'$. We consider that the magnetic fine structure originates from the existence of at least two nonequivalent magnetic sites owing to the diaminopropane with electric dipole moment.

[1] R. Morgunov et al., Phys. Rev. B 77 (2008) 184419.

PG11

Valence and spin structures of TFe₂O₄ spinel oxides (T=Mn, Co, Ni, Cu) investigated by using synchrotron radiation

Jihoon Hwang¹, D. H. Kim¹, Eunsook Lee¹, J.-S. Kang¹, B.-G. Park², J.-Y. Kim³, S. W. Han³, S. C. Hong³, S. B. Kim¹, Bongjae Kim³ and B. I. Min³

¹ Department of Physics, The Catholic University of Korea (CUK), Bucheon 420-743, Korea
² Pohang Accelerator Laboratory, POSTECH, Pohang 790-784, Korea
³ Department of Physics, Ulsan University, Ulsan 680-749, Korea
⁴ ACE center, Konyang University, Nonsan 320-711, Korea
⁵ Department of Physics, POSTECH, Pohang 790-784, Korea

AB₂O₄-type spinel oxides have attracted much attention because of the interesting physical phenomena, such as Jahn-Teller (JT) effects, multiferroic phenomena, and phase separations [1]. In normal spinels of AB₂O₄, A and B ions occupy the tetrahedral (Td) and octahedral (Oh) sites, respectively. When both A and B ions are magnetic ions, a ferrimagnetic (FiM) ordering is often observed because the A-B interaction is mainly antiferromagnetic. In this work, we have investigated the electronic structures of FiM spinels of TFe₂O₄ (T=Mn, Co, Ni, Cu) by employing soft x-ray absorption spectroscopy (XAS) and soft x-ray magnetic circular dichroism (XMCD). It is found that the valence states of Fe ions are nearly trivalent (-Fe³⁺) and those of T ions are nearly divalent (-T²⁺). The 2p XMCD spectra of MnFe₂O₄ show that the magnetic moments of Mn²⁺ and Fe²⁺ ions are antiparallel to each other. On the other hand, the magnetic moments of Co²⁺, Ni²⁺, and Cu²⁺ ions are parallel to those of B(Oh)-site Fe³⁺ ions, but are antiparallel to those of A(Td)-site Fe³⁺ ions, implying that Fe³⁺ ions occupy both A and B sites while Co, Ni, Cu ions occupy mainly B sites. *Corresponding Author: kangjs@catholic.ac.kr

[1] J.-S. Kang, et al., Phys. Rev. B 77, 035121 (2008).

PG12

Probing the distance dependence of the magnetic exchange interaction with atomic resolution

Alexander Schwarz^{1*}, Rene Schmidt¹, Roland Wiesendanger¹, Cesar Lazo² and Stefan Heinze³

¹ Institute of Applied Physics, University of Hamburg, Germany
² Christian-Albrechts-Universität zu Kiel, Germany
³ Christian-Albrechts-Universität zu Kiel, Germany

Quantifying strength and distance dependence of magnetic interactions between atoms is crucial to gain a deeper understanding of magnetic phenomena on the nanoscale. Magnetic exchange force microscopy (MExFM) [1] is a new and very versatile tool to study magnetism with atomic resolution in real space. It utilizes an atomically sharp magnetic tip at the free end of a cantilever to detect the short-ranged electron-mediated magnetic exchange interaction between tip apex and surface atoms. This force microscopy based technique can be employed to map spin structures of insulating [1] as well as conducting [2] magnetic samples with atomic resolution. Here we demonstrate that its spectroscopic mode, i.e., magnetic exchange force spectroscopy (MExFS), is able to measure the distance dependence of the magnetic exchange interaction in a very direct and elegant fashion [3]. Results obtained on the antiferromagnetic Fe monolayer on W(001) are compared with theoretical calculations based on density functional theory. They were performed for realistic multiatom tips and agree very well with data acquired using non-dissipative stable tips.

[1] U. Kaiser, A. Schwarz, and R. Wiesendanger, Nature 446, 522 (2007). [2] R. Schmidt, C. Lazo, H. Holscher, U. H. Pi, V. Caciuc, A. Schwarz, R. Wiesendanger, and S. Heinze, Nano. Lett. 9, 200 (2009). [3] R. Schmidt, C. Lazo, U. Kaiser, A. Schwarz, S. Heinze, and R. Wiesendanger, Phys. Rev. Lett. 106, 257202 (2011).

PG13

Electron correlation in a mixed valence perovskite system of Sr_{1-x}Ca_xRu_{0.5}Mn_{0.5}O₃

Tomohiro Ohnishi¹, Soichiro Mizusaki¹, Makoto Naito¹, Yoshihiko Noro², Masayoshi Itou³, Yoshiharu Sakurai³ and Yujiro Nagata¹

¹ Electrical Engineering and Electronics, Aoyama Gakuin Univ., Japan
² Kawazoe Frontier Technologies Co. Ltd., Japan
³ Japan Synchrotron Radiation Research Institute, Japan

Mixed valence systems are interesting for their fundamental and practical properties. Perovskite-type oxides Sr_{1-x}Ca_xRu_{0.5}Mn_{0.5}O₃ is a typical mixed valence system.¹ The host itinerant system Sr_{1-x}Ca_xRuO₃ shows various interesting properties such as ferromagnetism and paramagnetism.^{2,3} Mn-substitution induces a mixed valence state of Ru⁴⁺, Ru³⁺, Mn⁴⁺ and Mn³⁺ ions and localized ferromagnetism.^{1,4} However, understanding of the electron correlation in the mixed valence systems is not yet enough. In this work, we studied the relationship between electron correlation and mixed valence state through the experiments for Sr_{1-x}Ca_xRu_{0.5}Mn_{0.5}O₃ using the traditional experimental methods and the synchrotron-based magnetic Compton scattering. Sr_{1-x}Ca_xRu_{0.5}Mn_{0.5}O₃ is a good system since the Ca-substitution will modify crystal symmetry and change the electron correlation. The following results have been obtained; 1. Cell volume decrease for Ca substitution. 2. insulator-metal transition occurs for Ca substitution. 3. Ferromagnetism appears at $x \sim 0.3$. 4. Antiferromagnetic coupling between Ru and Mn. These facts can be explained as follows. The decrease in the cell volume enhances the hybridization between Ru and O orbitals inducing itinerant electrons. The itinerant electrons enhance the formation of a ferromagnetic order of Ru ions. Mn ions couples antiferromagnetically with Ru ions by a superexchange interaction via O 2p orbitals.

1. M. Naito et al., J. Appl. Phys. 103 (2008) 07C906-1. 2. A. Kanbayashi, J. Phys. Soc. Jpn. 44 (1978) 108. 3. T. Kiyama et al. Phys. Rev. B 54 (1996) R756. 4. T. Taniguchi et al. Phys. Rev. B 77 (2008) 014406-1.

PG14

An x-ray scattering study of magnetic order in a pyrochlore iridate Eu₂Ir₂O₇

Daisuke Uematsu^{1*}, Hajime Sagayama¹, Taka-hisa Arima¹, Jun J Ishikawa² and Satoru Nakatsuji²

¹ Department of Advanced Materials Science, The University of Tokyo, Japan
² Institute of Solid State Physics, The University of Tokyo, Japan

The pyrochlore iridate Eu₂Ir₂O₇ undergoes a metal-insulator transition at T_c[MI] = 120 K [1]. Since the magnetic Ir⁴⁺ ions occupy the pyrochlore B-site, strong geometrical spin frustration is predicted. Nevertheless, a muon spin rotation study [2] indicated long-range orderings spins of Ir⁴⁺. To determine the spin configuration, we have performed the resonant X-ray diffraction measurement at the LIII edge of Ir. A clear magnetic reflection was found at (10,0,0) below T_c[MI]. The result proposes the all-in-all-out-type magnetic structure.

[1] K. Matsuhiro et al., J. Phys. Soc. Jpn. 76, 043706 (2007). [2] S. Zhao et al., Phys. Rev. B. 83, 180402 (2011).

PG15

Magnetic structure analyses by small-angle electron diffraction

Yoshihiko Togawa^{1*}, Tsukasa Koyama², Shigeo Mori² and Ken Harada²

¹ Nanoscience and Nanotechnology Research Center (N2RC), Osaka Prefecture University, Japan
² Department of Materials Science, Osaka Prefecture University, Japan

Electrons are deflected at small angles by Lorentz force in magnetic materials. In magnetic elements in functional materials and spintronic devices, observation of Lorentz deflection of electrons at the small angle turns to be of significance because Lorentz deflection angle of electrons becomes smaller in modern miniaturized magnetic devices composed of thinner magnetic films. In the present work, electron optical system is constructed in order to obtain small angle diffraction and Lorentz deflection of electrons at the order of down to 10-6 radian in the reciprocal space[1]. Long-distance camera length up to 3000 m is achieved in a conventional transmission electron microscope with LaB6 thermal emission type. The diffraction pattern at 5 × 10-6 radian is presented in a carbon replica grating with 500 nm lattice spacing while the magnetic deflection pattern at 2 × 10-5 radian is exhibited in Permalloy elements. A simultaneous recording of electron diffraction and Lorentz deflection is also demonstrated in 180 degree striped magnetic domains of La_{0.825}Sr_{0.175}MnO₃[2]. We believe that small-angle Bragg diffraction and Lorentz deflection analyses provide a quantitative way to analyze structural and magnetic properties in the reciprocal space. This study is partly supported by SCOPE project from the MIC in Japan.

[1] T. Koyama, K. Takayanagi, Y. Togawa, S. Mori, and K. Harada, submitted. [2] T. Koyama, Y. Togawa, K. Takenaka, and S. Mori, to appear in J. Appl. Phys.

PG16

Raman scattering of metal-insulator transition in Cd₂Os₂O₇

Takumi Hasegawa^{1*}, Norio Ogita¹, Jun-ichi Yamaura², Zenji Hiroi² and Masayuki Udagawa¹

¹ Graduate School of Integrated Arts and Sciences, Hiroshima University, Higashi-Hiroshima, Hiroshima 739-8521, Japan
² Institute for Solid State Physics, The University of Tokyo, Kashiwa, Chiba 277-8581, Japan

Cd₂Os₂O₇ is a pyrochlore oxide showing metallic behavior at room temperature, and it shows metal-insulator transition at 225 K [1]. It has been suggested that this metal-insulator transition is caused by magnetic order [1,2], because any superlattice reflection has not been observed by x-ray and neutron [3] diffraction measurements. However, to conclude no structural distortion precisely below the transition temperature, it is necessary to perform symmetry sensitive measurements rather than diffractions. Raman scattering method is a sensitive tool to observe small lattice distortion with symmetry breaking. We have measured Raman spectra of Cd₂Os₂O₇ from 4 K to 300 K to investigate possibility of structural distortion in the insulator phase. Below the transition temperature, we have not observed any new peak indicating symmetry breaking from the pyrochlore structure with the space group Fd3m.

[1] A. W. Sleight, J. L. Gillson, J. F. Weiher and W. Bindloss, Solid State Commun. 14, 357(1974). [2] D. Mandrus, et al., Phys. Rev. B 63, 195104(2001). [3] J. Reading and M. T. Weller, J. Mater. Chem. 11, 2373(2001).

PG17

Effects of impurities in the chromic compound CuMoO₄

Takayuki Asano^{1*}, Taizo Nishimura¹, Katsutaka Kubo¹, Minoru Sanda¹, Keisuke Matsuura¹, Akira Matsuo², Yasuo Narumi³ and Koichi Kindo²

¹ Department of Physics, Kyushu University, Japan
² Institute for Solid State Physics, University of Tokyo, Japan
³ Institute for Materials Research, Tohoku University, Japan

Recently interest in "Chromism" phenomena for compounds may be attributed to the fact that a reversible color change of organic and inorganic materials can occur as the compound experiences various changes in its environmental conditions. Copper molybdate, CuMoO₄, has demonstrated attractive properties of both thermochromism and piezochromism that are induced by a structural phase transition. We report a tunable structural phase transition and magnetic phenomena using substitutional effects in Cu_{1-x}Zn_xMoO₄ (0 ≤ x ≤ 0.1), CuMo_{1-y}W_yO₄ (0 ≤ y ≤ 0.1), and CuMo_{1-z}Cr_zO₄ (0 ≤ z ≤ 0.1) over wide ranges of temperatures and magnetic fields. The substitution of magnetic Cu²⁺ ions for nonmagnetic Zn²⁺ ions causes the hysteresis in the structural phase transition to shift to remarkably lower temperatures as x increases by means of magnetic susceptibility measurement. In contrast, replacing Mo⁶⁺ ions with W⁶⁺ ions results in a shift of the hysteresis and the structural phase transition to higher temperatures as y increases. However, in the case of replacing the Mo⁶⁺ ions with Cr⁶⁺ ions, the structural phase transition around 200K is completely disappeared and a ferromagnetic component is induced below 150K as z increases. We are going to discuss the reason of the shifting structural phase transitions and also show the magnetic properties under extreme conditions.

PG18

Effective exchange interactions in 5d transition metal oxides

Tomonori Shirakawa¹, Hiroshi Watanabe and Seiji Yunoki
Computational Condensed Matter Physics Laboratory, RIKEN, Japan

5d transition metal oxides, Sr₂IrO₄ and Ba₂IrO₆, have attracted much attention because of their unique properties caused by a strong spin-orbit coupling for 5d transition element. Both of these compounds behave as Jeff=1/2 Mott insulator at low temperature [1,2,3]. Recently, these compounds are expected to be a superconductor as an analogous system to high-Tc cuprates. According to recent experimental results on magnetic susceptibility and μSR studies, the effective exchange interactions in Sr₂IrO₄ and Ba₂IrO₆ are expected to be very large, and comparable to the ones of high-Tc cuprates [3]. Motivated by these experiments, we have studied theoretically the electronic and magnetic properties of Sr₂IrO₄ and Ba₂IrO₆ using a three-band Hubbard model with the spin-orbit coupling [4]. We first obtain the phase diagram of 8-site cluster in a wide parameter region using exact diagonalization technique. We find that there are several phases including the Jeff=1/2 Mott insulating phase which is realized in Sr₂IrO₄ and Ba₂IrO₆. We then calculate the dynamical spin structure factor composed by the Jeff=1/2 state in the Jeff=1/2 Mott insulating phase. We then estimate the values of effective exchange interactions by comparing the results with the ones of an effective spin model.

[1] B. J. Kim et al., Science 323 (2009) 1329. [2] B. J. Kim et al., Phys. Rev. Lett. 101 (2008) 076402. [3] H. Okabe et al., Phys. Rev. B 83 (2011) 155118. [4] H. Watanabe et al., Phys. Rev. Lett. 105 (2010) 216410.

PG19

Magnetic and electrical transport behavior of Ir substituted NiTi shape memory alloy

Sandhya Dwevedi^{1*} and A.k Nigam
Department of Condensed Matter Physics and Material Sciences, Tata Institute of Fundamental Research(TIFR), Mumbai 400 005, India

NiTi shape memory alloys (SMAs) show attractive functional properties for a number of engineering and medical applications [1]. Recently, Somsen et al [2] have synthesized the novel Ni-Ti-Ir alloys and have studied its structural properties. This motivates us to study the other properties of the alloy. In the present work, we have systematically studied the structural, kinetics, magnetic and transport properties of the Ni-Ti-Ir alloy. The alloy is formed in the B2- type phase with a small amount of Ti₂NiIr as an additional phase. In the DSC curve, two distinct peaks are observed on heating and cooling. These peaks correspond to the Martensitic transformations (MT) from the B2 to R-phase and from R to B19'-phase on cooling and, a reverse transformation from B19'-R-B2 phase on heating, respectively. From the temperature dependence of resistivity curve, the Martensitic Start (MS), Martensitic Finish (Mf), Austenite Start (AS) and Austenite Finish (Af) temperatures are found to be 193 K, 153 K, 267 K and 293 K respectively. In the Magnetization versus temperature (M-T) curve, no evidence of the ferromagnetic ordering temperature is observed. However, the Magnetization versus Field (M-H) curve at 5 K and 300 K shows existence of ferromagnetic order in the alloy.

[1]K. Otsuka, C. M. Wayman, Shape Memory Materials(Cambridge University Press) [2]Ch. Somsen, J. Khalil-AllaFib, E.P. George, Mater. Sci. Eng. A, 378, 170-174 (2004)

PG20

X-ray diffuse scattering of pyrochlore niobium oxides R₂Nb₂O₇

Shingo Toyoda¹, Hajime Sagayama¹, Kunihisa Sugimoto² and Takahisa Arima^{1*}
¹ Department of Advanced Materials Science, The University of Tokyo, Japan
² Spring-8, Japan

It was reported that Y₂Nb₂O₇ is a non-magnetic insulator, although the electron configuration of Nb⁴⁺ is 4d1 with S=1/2. To reveal the origin, we have performed X-ray scattering measurement of single crystals of R₂Nb₂O₇ (R=Y,Sm,Dy,and Ho). All the compounds show diffuse scattering, indicating that there exists short-range order. Analysis of the average structure suggests that Nb ions are displaced along the (111) direction. The formation of spin-singlet tetramers cannot explain the observed diffuse pattern. The short-range correlation implies the formation of spin-singlet dimmers, because the configuration of dimmers in a pyrochlore lattice can be mapped on the ice rule problem. In addition, the diffuse pattern changes with R. The diffuse of Y₂Nb₂O₇ is the broadest, while that of Dy₂Nb₂O₇ is narrowest and almost spot.

[1] H. Fukazawa, Y. Maeno, Phys. Rev. B 67, 054410 (2003)

PG21

Freezing of local lattice strains in the magnetic martensitic/ferroelastic material system

Yu Wang^{1*}, Chonghui Huang, Xiaoping Song and Xiaobing Ren
Xi'an Jiaotong University, China

Glass state is a frozen disordered state, in which the long range order is destroyed but short range order persists. Recently, a new glass phenomenon called strain glass was found in the martensitic/ferroelastic material system [1]. The strain glass state is a frozen disordered state of local lattice strains (nanosized martensitic/ferroelastic domains). Experimental measurements show that strain glass possesses obvious glassy features including dynamic freezing and breaking down of ergodicity in its mechanical properties [1, 2], being similar to the glassy features of the cluster-spin glass with froze local spin order. Strain glass can be obtained by doping point defects into normal martensitic/ferroelastic system [1]. However, whether strain glass can be achieved in the defect doped magnetic martensitic/ferroelastic system is unknown so far. In this study, we report that a strain glass transition with freezing of local lattice strains can exist in the Co doped magnetic martensitic system Ni-Mn-Ga by using dynamic mechanical analysis. Moreover, our magnetic measurements show that the strain glass in the Co doped Ni-Mn-Ga system is ferromagnetic, which is a new form of strain glass. The finding of the strain glass in magnetic martensitic/ferroelastic system may lead to novel applications.

[1] S. Sarkar, X. Ren and K. Otsuka, Phys. Rev. Lett. 95, 205702(2005) [2] Y. Wang, X. Ren, K. Otsuka, and A. Saxena, Phys. Rev. B 76, 132201(2007)

July 9 (Mon)

July 9 (Mon)

PG22

Magnetic structure of the new chiral compound [Cr(CN)₆][Mn(S)-pnH(DFM)](H₂O)

Cristina Saenz De Pipaon¹, Javier Campo^{1*}, Fernando Palacio¹, Jose Alberto Rodriguez-velamazán¹, Katsuya Inoue² and Hiroyuki Honda²

¹ Materials Science Institute of Aragon (CSIC-University of Zaragoza), Spain
² Hiroshima University, Japan

Research on magnetic molecular materials has received strong attention in the last years for several reasons, among them, the possibility of these materials to be multifunctional, thus exhibiting more than one functional property at the same time. A very interesting possibility in a molecular material is magneto-chirality. Despite this interest, very few molecular candidates with likely possibilities have been synthesized, because chirality must be controlled in the molecular structure and at the same time the crystal must exhibit nuclear chirality. In addition, the arrangement of the magnetic moments must also be chiral. Nowadays, single crystals of the cyano-bridged bimetallic complexes have been grown, a 2D chiral ferrimagnet [Cr(CN)₆][Mn(R)-pnH(DMF)]·(2H₂O) (1) and a racemic one [Cr(CN)₆][Mn(rac)-pnH(DMF)]·(2H₂O) (2), where DFM is N,N-dimethylformamide. Compound 1 consists of two-dimensional bimetallic sheets, with the same space group P212121, whereas compound 2 crystallizes under Pnma [1]. These compounds have been studied employing neutron diffraction techniques at the Institute Laue Langevin. In this communication, we present the nuclear and magnetic structures for (1) and (2). The coexistence of nuclear and magnetic chirality has been demonstrated.

[1] H. Imai, K. Inoue, K. Kikuchi, *Polyhedron* 24, 2808-2812(2005)

PG23

Origin of spin scalar chiral order in frustrated Kondo lattice model - higher-order Kohn anomaly and hidden positive biquadratic interaction -

Yutaka Akagi^{1*}, Masafumi Udagawa² and Yukitoshi Motome¹

¹ University of Tokyo, Japan
² University of Tokyo, MPI PKS, Japan

Recently, noncoplanar spin configurations with scalar chirality have drawn considerable attention as an origin of the anomalous Hall effect. In this mechanism, itinerant electrons acquire an internal magnetic field through the Berry phase according to the solid angle spanned by three spins, which can result in the anomalous Hall effect. In order to clarify how such nontrivial magnetic states appear in spin-charge coupled systems, we investigate a ferromagnetic Kondo lattice model on a triangular lattice by variational and perturbative calculations. As a result, we find that a noncoplanar four-sublattice spin ordering emerges near 1/4-filling [1], in a wider parameter region compared to the nesting-driven 3/4-filling phase predicted in the previous study. We unveil that a kinetic-driven positive biquadratic interaction is critically enhanced and plays a crucial role on stabilizing a chiral ordering near 1/4-filling. The origin of large positive biquadratic interaction is ascribed to the Fermi surface connection by the four-sublattice ordering wave vectors, which we call the higher-order Kohn anomaly [2]. Similar hidden interactions and resultant noncoplanar states are also found in other frustrated lattices, such as fcc and pyrochlore lattices. Our results suggest a universal mechanism underlying nontrivial spin configurations in frustrated spin-charge coupled systems.

[1] Y. Akagi and Y. Motome, *J. Phys. Soc. Jpn.* 79 (2010) 083711. [2] Y. Akagi, M. Udagawa, and Y. Motome, preprint (arXiv:1201.3053), accepted for publication in *Phys. Rev. Lett.*

PG24

Doping effects on the metal-insulator transition of Li_{1-x}RuO₃

Seongil Choi¹, Junghwan Park¹, Sanghyun Lee¹, Deo-kyong Cho¹, T. Morioka², H. Nohjiri³ and J.-G. Park^{3*}

¹ Center for Strongly Correlated Materials Research, Seoul National University, Seoul 151-742, Korea
² Institute for Materials Research, Tohoku University, Sendai 980-8577, Japan
³ Department of Physics & Astronomy, Seoul National University, Seoul 151-742, Korea

Li_{1-x}RuO₃ has a layered rocksalt-type structure and has attracted much attention because of its interesting physical properties. In particular, it exhibits a metal-insulator transition at a very high temperature around 540 K. At the same temperature, the magnetic susceptibility shows a big drop implying the formation of a spin gap. It is also interesting to note that all of these physical properties occur on the unusual honeycomb lattice of Ru ions. In order to understand the origin of the metal-insulator transition and its related physical properties better, we have carried some extensive studies ranging from bulk properties to neutron scattering experiments. First, we have investigated the doping effects on the metal-insulator transition by varying Li content. Second, we have examined the field dependence of the physical properties by measuring resistivity and magnetization over a wide temperature range. In this report, we are going to summarize our experimental results and its importance with respect to the reported metal-insulator transition.

PG25

Ferromagnetism in hydrothermally treated glassy carbon

Hyun Jin Cho, Kyu Won Lee and Cheol Eui Lee*

Department of physics and institute for Nano Science, Korea University, Korea

We have investigated the magnetic properties of pristine and hydrothermal-treated glassy carbon by means of superconducting quantum interference device (SQUID) and electron spin resonance (ESR) measurements. The magnetic properties of the hydrothermally treated glassy carbon showed a sensitive dependence on the solvents and the treatment time. In particular, prominent ferromagnetism was observed in samples hydrothermally treated in ethanol for a properly chosen time, with the saturation moment and coercive force being comparable to those of iron. The ferromagnetism in the hydrothermally treated glassy carbon may have to do with the relative fractions of the sp³- and sp²-bonds.

[1] X Wang et al 2002 *J. Phys.: Condens. Matter* 14 10265

PG26

On the structure and symmetry of the spin glass state (SGS)

Jerzy Warczewski*, Pawel Gusin and Daniel Wojcieszuk

Institute of Physics, University of Silesia, Poland

The explanation of uniqueness of SGS has roots in the appearance of a certain probability function in the second term of the assumed Hamiltonian [1, 2]. This term describes the random distribution of either dopants or defects in the ferromagnetic matrix under the percolation threshold. The Gaussian type randomness was derived for both the global magnetic coupling constant and the magnetization vector M, the latter effect bringing to the statistical features of the magnetic structure and the magnetic symmetry group of SGS. In both cases the use has been made of the central limit theorem of the theory of probability (the Lyapunov theorem) [3]. The authors have earlier proved that a certain spontaneous minimum magnetic field H is necessary for the stability of SGS [4]. The structure of SGS can then be described in such a way that M is situated along a generatrix of a given cone whose axis coincides with the direction of H [4]. Let us call φ the angle between M and H. Any precession of M around the direction of H at φ = const (at constant energy) makes the symmetry operation of SGS. Thus the symmetry group of this precession is SO(2) [3].

[1] J. Warczewski, P. Gusin et al., *Journal of Non-Linear Optics, Quantum Optics* 30 (2003), 301-320 [2] P. Gusin, J. Warczewski, *Mol. Cryst. Liq. Cryst.* 521 (2010), 288-292 [3] J. Warczewski, P. Gusin, D. Wojcieszuk, *Mol. Cryst. Liq. Cryst.* 554 (2012), 209-220 [4] J. Warczewski, P. Gusin et al., *J. Phys.: Condens. Matter*, 21 (2009), 035402-035407

PG27

Magnetic study of Fe/MgO/Fe and Fe/MgO/Fe/Co multilayer systems

Jitendra Pal Singh¹, Sanjeev Gautam², K Asokan¹, D. Kabiraj¹, D. Kanjilal¹, M Raju³, Braj Bhusan Singh⁴, S. Chaudhary⁵, R. Kotnala⁴ and Keun Hwa Chae^{2*}

¹ Inter University Accelerator Centre, Aruna Asaf Ali Marg-110067, New Delhi, India
² Advanced Analysis Center, Korea Institute of Science and Technology (KIST), Seoul 136-791, Korea
³ Department of Physics, Indian Institute of Technology, New Delhi - 110 016, India
⁴ National Physical Laboratory, Dr. K. A. Krishnan Marg, New Delhi - 110 012, India

Theoretical calculations [1-3] show high TMR up to 1000% for Fe/MgO/Fe MTJ's however TMR ratios of 200% at room temperature could be realized in these systems [4]. The discrepancy between theoretical and experimental values of TMR is probably due to the interface properties of the heterostructures, as spin dependent tunneling is sensitive to the interface [3]. In present work, we investigated the magnetic properties of Fe/MgO/Fe (MfE) and Fe/MgO/Fe/Co (MfECo) multilayers by vibrating sample magnetometer (VSM) deposited by electron beam evaporation method [6]. Attributes of perpendicular magnetic anisotropy (PMA) are observed in MfE multilayer. The PMA arises due to Fe(3d) and O(2p) hybridization at metal-oxide layer interface and generally observed in MTJs [6]. The asymmetric coercivity observed in this structure is due to the presence of exchange bias which arises probably due to oxidation of Fe at surface; resulting in antiferromagnetic Fe₂O₃. The positive vertical shift along magnetization axis may be due to the pinned interfacial uncompensated spins of unwantedly formed Fe₂O₃ [7]. Apart from this MfECo multilayer do not exhibit any feature observed in MfE multilayers. The absence of these is expected almost 3 times increase of Fe layers in MfECo system [5].

References: 1. A. Lyle, et al. *App. Phys. Lett.* 97 152504 (2010) 2. J.-G. Zhu and C. Park, *Materials Today*, 9 36 (2006) 3. J. Mathon and A. Umerski, *Phys. Rev. B* 63 220403 (2001), 4. S.S.P. Parkin, et al., *Nat Mater*, 3 862 (2004) 5. J. P. Singh et al., *AIP Conf. Proc.* (in Press) 6. S. Ikeda et al. *Nature Mater.* 9 (2010) 721-722 7. H. Ohldag et al. *Phys. Rev. Lett.*, 91, 017203, 2003

PH01

Ionic size effect on the spin gap nature of SrCu₂(TeO₃)₂Cl₂

C. N. Kuo, S. C. Chen and C. S. Lue*

Department of physics., National Cheng Kung University, Tainan 70101, Taiwan, Taiwan

We report the effects of partial substitution of Br onto the Cl sites of SrCu₂(TeO₃)₂Cl₂ by means of magnetic susceptibility measurements. This material has been a subject of current interest due to indications of spin gap behavior. However, the magnetic spin couplings responsible for the spin gap nature remains unclear. For each composition of SrCu₂(TeO₃)₂(C_{1-x}Br_x)₂, the temperature-dependent susceptibility exhibits a character of low-dimensional magnetism with a broad maximum at T_{max}. The magnitude of T_{max} gradually shifts to higher temperatures as increasing the Br concentration. The experimental data can be well fitted to a coupled spin dimer model, yielding an increasing trend for the spin gap size from 170 K to 190 K. It thus points out that the substitution of Br ions has an effect to reduce the distance between Cu(1) and Cu(2), leading to a stronger antiferromagnetic spin interaction. On the other hand, the variation of the interdimer coupling is marginal, indicative of weak effects on the distances of Cu(1)-Cu(1) and Cu(2)-Cu(2) in SrCu₂(TeO₃)₂Cl₂.

PH02

Magnetism of SrM₃P₄O₁₄ (M²⁺ = 3d ions) investigated using neutron-scattering measurements

Masashi Hase^{1*}, Vladimir Yu. Pomjakushin², Lukas Keller², Andreas Doenni¹, Osamu Sakai¹, Tao Yang³, Rihong Cong³, Jianhua Lin³, Kiyoshi Ozawa¹ and Hideaki Kitazawa¹

¹ National Institute for Materials Science (NIMS), Japan
² Paul Scherrer Institut (PSI), Switzerland
³ Peking University, China

One of intriguing phenomena in magnetism is appearance of qualitatively different magnetism in isostructural substances. In AM₃P₄O₁₄ (A = Ca, Sr, Ba or Pb, M²⁺ = Ni²⁺, spin-1, Co²⁺, spin-3/2, Fe²⁺, spin-2 or Mn²⁺, spin-5/2), magnetism in AM₃P₄O₁₄ is qualitatively different from magnetism in the other substances. A 1/3 quantum magnetization plateau was observed only in AM₃P₄O₁₄. An antiferromagnetic (AFM) long-range order (LRO) without a spontaneous magnetization appears in AM₃P₄O₁₄, while a canted AFM LRO appears in the other substances. We studied magnetism of SrM₃P₄O₁₄ using neutron-scattering measurements. In SrM₃P₄O₁₄, we determined the coplanar spiral magnetic structure that had no spontaneous magnetization. We confirm that the spin system is a frustrated J1-J1-J2 trimerized spin chain with dominant AFM J1, small AFM J2, and small next-nearest-neighbor exchange interactions. The magnetization plateau is possible. In SrM₃P₄O₁₄ (M = Co or Ni), we determined the canted magnetic structure (the irreducible representation τ₁ in the space group P21/c). We consider that the spin system consists of ferromagnetic dimers formed by the dominant J2 interaction and monomers. The magnetization plateau is impossible.

PH03

Spin-Peierls-like lattice distortion and incommensurate magnetic structure of geometrically frustrated spinel CdCr₂O₄

J. H. Chung¹, J. M. S. Park², K. P. Hong², M. Matsuda³, H. Ueda⁴, Y. Ueda⁴ and S. H. Lee^{5*}

¹ Department of Physics, Korea University, Korea
² Korea Atomic Energy Research Institute, Korea
³ Oak Ridge National Laboratory, Korea
⁴ The University of Tokyo, Japan
⁵ University of Virginia, USA

ACr₂O₄ spinels (A = Zn, Cd, Hg) with antiferromagnetic Cr²⁺ (S = 3/2) on B sites are well known for strong geometrical frustration preventing long-range order. The frustrations in their cubic phases are finally lifted via spin-Peierls-like lattice distortions at low temperatures. In spite of their similarities in the cubic phases, each of them undergo distinctive lattice distortions and exhibit unique magnetic order. The nature of their magnetic ground states is thus of great importance in order to understand these novel transitions. Nevertheless, the exact spin structure of CdCr₂O₄ has so far never been reported. We revisited this issue by performing neutron powder diffraction measurement of isotope-enriched sample for reduced neutron absorption. We observed the cubic-to-tetragonal distortion and the subsequent incommensurate magnetic order that are consistent with previous reports. Using representation analysis, we found that the spins on different sublattices maintain nearly collinear arrangements within a single tetrahedron. Whereas the obtained spin structure is different from the one previously conjectured based on spin wave frequencies, it is consistent with the idea that quantum fluctuation plays an important role in the magnetic ground state of CdCr₂O₄.

PH04

Interplay of magnetic order and structural distortions in multiferroic GdMnO₃ single crystals

Mathias Doerr^{1*}, Sahana Roessler², Martin Rotter², Aditya A. Wagh³, P. S. Anil Kumar³, Suja Elizabeth¹, Steffen Wirth² and Michael Loewenhaupt¹

¹ Institut für Festkörperphysik (IFP), Technische Universität Dresden, Germany
² Max-Planck-Institut für Chemische Physik fester Stoffe Dresden, Germany
³ Department of Physics, Indian Institute of Science Bangalore, India

Multiferroics are candidates for magneto-electrical applications. Magnetic and dielectric phenomena in orthorhombic GdMnO₃ are strongly intertwined. In addition, electrically induced magnons exist. Magnetostriction measurements by high-resolution capacitive dilatometry, performed in the different AFM phases below T_N = 42 K, show lattice distortions with striction of about 10⁻⁴. All longitudinal and transversal components of the magnetostriction tensor were measured for the first time. Although no changes of the lattice symmetry exist, the measurements reveal magneto-structural phenomena, especially in the canted-AFM phase. A strong anisotropy of the magnetoelastic properties was found, in good agreement with the type and propagation of the magnetic structure. As the capacitive method is sensitive to expansion effects and changes of permittivity, dielectric anomalies could be detected and compared to the critical values of H and T of the magnetic transitions. The anomalies especially exist in the range 10...22 K in which the structure is characterized by magnetic order on both the Gd- and Mn-sites. This demonstrates the strong interplay of magnetic, charge and lattice degrees of freedom. First steps in modelling the magnetization of GdMnO₃ by the simulation program McPhase are presented and exchange mechanisms are discussed. These results are examined in connection with the magnetostriction data.

PH05

Uniaxial pressure effect on magnetic ordering in a frustrated ising antiferromagnet CoNb₂O₆

Satoru Kobayashi^{1*}, Hiromu Tamatsukuri², Chikafumi Kaneko², Yuki Honma², Taro Nakajima² and Setsuo Mitsuda²

¹ Department of Materials Science and Engineering, Iwate University, Japan
² Department of Physics, Faculty of Science, Tokyo University of Science, Japan

Uniaxial pressure effect on magnetic ordering has been investigated by magnetization measurements for a frustrated Ising antiferromagnet CoNb₂O₆ where quasi-one-dimensional ferromagnetic chains along the c axis form a frustrated isosceles triangular lattice on the a-b plane. Under uniaxial pressure and magnetic field along the a axis, a critical field of magnetic phase transitions from antiferromagnetic to incommensurate magnetic (ICM) phase as well as from ICM to ferromagnetic phase monotonically increases, indicating the strengthening of antiferromagnetic interchain exchange interactions. Above 700 MPa, a step-like behavior of the magnetization curve shows up at around the half of the saturation magnetization. This behavior implies the appearance of a pressure-induced magnetically ordered phase characterized by the propagation wave vector of qM=(0,0.5,0) and/or (0,0.25,0). These observations were explained within mean field calculations with nearest-neighbor and next-nearest-neighbor interchain exchange interactions.

PH06

Thermal and magnetic properties of LiNiPO₄ olivine

J. Wiecekowsk^{1*}, M. U. Gutowska¹, A. Szweczyk¹, Yu. Kharchenko², M. F. Kharchenko², M. Kowalczyk², N. Nedelko³, S. Lewinska⁴, A. Slawska - Waniewska⁴, A. Kulka⁵ and J. Molenda⁴

¹ Institute of Physics, Polish Academy of Sciences, Warsaw, Poland
² B.Verkin Inst. for Low Temp. Phys. and Engineering, National Academy of Sciences of Ukraine, Kharkiv, Ukraine
³ Faculty of Materials Engineering, Warsaw University of Technology, Warsaw, Poland
⁴ Department of Hydrogen Energy, AGH University of Science and Technology, Cracow, Poland

On the contrary to LiMPO₄, olivines with M = Mn, Fe, Co, in LiNiPO₄ two step transformation between the paramagnetic and a uniform in space antiferromagnetic phase occurs. At first, a long-range magnetic order develops in the form of an incommensurate antiferromagnetic phase (via a second-order transition at 21.8 K) and then a first-order transition to the antiferromagnetic phase occurs at 20.9 K. To study thermal properties of LiNiPO₄, and an influence of magnetic field, B, on the magnetic structure, specific heat measurements of a single crystal were carried out from 3 K to 60 K, in B=0 and in B (up to 9 T) applied along three main crystallographic directions. It was found that B applied along a and b directions has no effect on the transitions, whereas B directed along c axis shifts both transitions towards lower temperatures (with the transition temperatures depending parabolically on B). To elucidate these effects, supplementary studies of magnetic torque were performed for several B values, for B rotating within a-c and b-c planes, for a series of fixed temperatures. This work was partly supported by the European Regional Development Fund, through the Innovative Economy Grants: POIG.01.01.02-00-108/09 and POIG.02.02.00-00-025/09.

July 9 (Mon)

July 9 (Mon)

PH07

Cr- and mo-doping effects on structural and orbital order phase transition in spinel-type MnV₂O₄

Kazuhiro Hemmi^{1*}, Ryuichiro Fukuta¹, Ece Uykur¹, Shigeki Miyasaka¹, Setsuko Tajima¹, Akiko Nakao², Hironori Nakao², Reiji Kumai² and Youichi Murakami²

¹ Physics, Osaka University, Japan
² PF/CMRC, KEK, Japan

MnV₂O₄ has orbital degrees of freedom of t_{2g} electrons in V³⁺ (3d²), and undergoes magnetic and orbital order. In this study, we investigated the doping effects of Cr³⁺ (3d³) and Mo³⁺ (4d³), which have no orbital degrees of freedom, for the V³⁺ site of MnV₂O₄, in order to clarify the Cr- and Mo-doping effect on the electronic properties in this system. In MnV₂O₄, the paramagnetic to collinear ferrimagnetic phase transition and the collinear to noncollinear ferrimagnetic phase transition occur at TN=59K and TOO=54K, respectively. The structural phase transition from cubic to tetragonal lattices takes place at TOO concomitantly with the orbital order. From the magnetic susceptibility and powder X-ray diffraction measurements, it is clarified that the orbital order is suppressed by Cr- and Mo-doping and disappears above x=0.12 (x=0.08) in Cr (Mo)-doped samples. The resistivity and optical reflectivity measurements have clarified that the system becomes almost metallic with increasing Mo content, while the Cr-doped samples are still Mott insulators. These results indicate that the doped Cr and Mo with no orbital degrees of freedom suppress the orbital order in MnV₂O₄. The introduced 3d electrons remain localized in the Cr-doped system, while 4d electrons become nearly itinerant in the Mo-doped one.

R. Plumier and M. Sougi, Solid State Commun. 64, 53 (1987). S. Suzuki et al., Phys. Rev. Lett. 98, 127203 (2007).

PH08

Dopant-dependence on charge/orbital order in impurity doped layered manganites

Yuki Yamaki¹, Hironori Nakao², Yuichi Yamasaki², Youichi Murakami², Yoshio Kaneko³ and Yoshinori Tokura⁴

¹ Tohoku University CMRC/PF, KEK, Japan
² CMRC/PF, KEK, Japan
³ ERATO-MF, JST CERG, RIKEN, Japan
⁴ ERATO-MF, JST CERG/CMRG, RIKEN University of Tokyo, Japan

A layered manganite La_{0.5}Sr_{1.5}MnO₃ shows charge/orbital order and CE-type antiferromagnetic structure below 240 K and 110 K, respectively. We have studied how the ordering state is changed by the substitution of Cr, Fe and Ga ions for Mn ions using a resonant x-ray scattering (RXS) technique and magnetization measurement. In trivalent ions these impurity ions have no orbital degree of freedom and different spin values, in fact Cr³⁺, Fe³⁺, and Ga³⁺ have S = 3/2, S = 5/2, and S = 0, respectively. As a result, the magnetization for Ga doped compound shows the same temperature dependence as pure compound, but in Cr and Fe doped compounds the magnetizations increase below 90 K and 70 K, respectively. On the other hand, in all doped compounds the RXS intensities which reflect charge/orbital order are smaller than that in pure compound, but degrees of decrease are different according to the dopants. Namely, RXS intensity of Ga-doped compound has the same temperature dependence as pure compound, while RXS intensities of Cr- and Fe-doped compounds drastically decrease below 90 K and 70 K, respectively.

PH09

Magnetic and nonmagnetic impurity effect on magnetic orderings of isosceles triangular lattice antiferromagnet CuMnO₂

Noriki Terada¹, Yoshinori Tsuchiya¹, Hideaki Kitazawa¹ and Naoto Metoki²

¹ National Institute for Materials Science, Japan
² Japan Atomic Research Agency, Japan

In recent years, chemical substitution effect on magnetic and dielectric properties in frustrated magnetic systems has been a vast field of challenging new physics. Good illustrations are the drastic and various effects of a small level of chemical substitution upon the magnetic and dielectric properties on frustrated magnetic systems such as CuFeO₂ and MnWO₄. These magnetic ground states stabilized with strongly competing exchange interactions should be easily changed by slight chemical disturbance. In the present study, we have investigated magnetic and nonmagnetic impurity substitution effects on magnetic ordering of a frustrated isosceles triangular lattice antiferromagnet CuMnO₂ by means of the magnetic neutron diffraction measurements on Cu(Mn_{1-x}Cu_x)O₂ and Cu(Mn_{1-x}Ga_x)O₂. While the magnetic wave vector of Cu(Mn_{1-x}Cu_x)O₂ the magnetic ground state of "magnetically" substituted with x=0.04 is Q=(-1/2 1/2 0)[1-3], that in the "nonmagnetically" substituted Cu(Mn_{1-x}Ga_x)O₂ with y=0.05, 0.15 and 0.20 is Q=(-1/2 1/2 1/2) that is identical to that of pure CuMnO₂. We discuss an influence of magnetic or nonmagnetic impurity substitution on the magnetic ordering of CuMnO₂ by comparing the results of Cu(Mn_{1-x}Ga_x)O₂ with Cu(Mn_{1-x}Cu_x)O₂.

[1]N. Terada, Y. Tsuchiya, H. Kitazawa, T. Osakabe, N. Metoki, N. Igawa and K. Ohoyama, Phys. Rev. B 84 064432 (2011). [2]M. Poienar, C. Vecchini, G. Andre, A. Daoud-Aladine, I. Margiolaki, A. Maignan, A. Lappas, L. C. Chapon, M. Hervieu, F. Damay, and C. Martin, Chem. Mater. 23, 85 (2011). [3]V. O. Garlea, A. T. Savici, and R. Jin, Phys. Rev. B 83, 172407 (2011).

PH10

Resonant soft X-ray scattering studies on half-doped manganite LaSr₂Mn₂O₇

J.-s. Lee^{1*}, C.-c. Kao¹, C.s. Nelson², H. Jang³, K.-t. Ko³, S.b. Kim⁴, Y.j. Choi⁴, S.w. Cheong⁴, S. Smadici⁵, P. Abbamonte⁵ and J.-h. Park³

¹ SSRL, SLAC National Accelerator Laboratory, USA
² BNL, USA
³ POSTECH, Korea
⁴ Rutgers university, USA
⁵ UIUC, USA

Recently, a careful doping control study, however, reported that the La_{2-2x}Sr_{1+2x}Mn₂O₇ system has an exotic spin phase diagram very near the half doping with extremely narrow antiferromagnetic (AFM) phase boundaries at x ~ 0.5 +/- 0.005: the CE-type within the boundaries but the A-type outside. To elucidate complication of this spin phase diagram, we investigated the orbital and AFM ordering behaviors of the half-doped bilayer manganite LaSr₂Mn₂O₇ by using Mn L-edges resonant soft x-ray scattering. We confirmed the predicted CE-type AFM order for the true half-doped (x = 0.5) case. Furthermore, we found that such a narrow phase boundary is due to the close competition of the two AFM phases via 3d Mn eg orbital instability.

PH11

On the non-idle-spin behavior and the field-induced magnetic transitions of the trimer chain magnet Cu₃(OH)₄SO₄

Hyun-joo Koo¹, Reinhard K Kremer² and Myung-hwan Whangbo³

¹ Chemistry, Kyung Hee University, Korea
² Max-Planck-Institut für Festkörperforschung, Stuttgart, Germany
³ Chemistry, North Carolina State University, USA

The magnetic properties of the Cu(2)-Cu(1)-Cu(2) trimer chain magnet Cu₃(OH)₄SO₄ were examined by evaluating the spin exchange constants, the Dzyaloshinskii-Moriya (DM) vectors, and the magnetic anisotropy energies of the Cu(1) and Cu(2) sites on the basis of density functional calculations. Cu₃(OH)₄SO₄ is not a idle-spin magnet, the Cu(1) spins have a strong antiferromagnetic coupling in the Cu(1) chain, and the Cu(2) spin arrangements of a Cu(2)-Cu(1)-Cu(2) trimer chain result from the presence of two non-equivalent sets of AFM interactions between the Cu(1) and Cu(2) chains. We propose the probable spin arrangements of a trimer chain responsible for the field-induced successive magnetic transition, and suggest that the nature of the magnetic transition depends on the field-direction because of the DM interactions associated with two strong spin exchange paths.

PH12

Spin state of LaCoO₃ investigated from non-magnetic-ion substitution effect of Co sites

Shinichiro Asai^{*}, Ryuji Okazaki, Yukio Yasui and Ichiro Terasaki

Department of Physics, Nagoya University, Japan

The perovskite oxide LaCoO₃ is a fascinating material because of a dramatic change of its spin state with temperature variation. In low-temperature range, LaCoO₃ is non-magnetic because the d electrons of Co³⁺ (3d⁶) fully occupy the lower t_{2g} orbitals (LS). On the other hand, the nature of its excited state is controversial. The spin state of this system is also sensitive to the chemical substitutions. Most interestingly, non-magnetic Rh³⁺ (4d⁶: LS) substitution increases the magnetization at low temperature, which is different from Ga³⁺ (3d¹⁰) substitution effect. We have measured the magnetization and x-ray diffraction of LaCo_{1-x}Rh_xO₃ [1]. We have found a weak ferromagnetic ordering for 0.1 < x < 0.4, indicating that the Rh substitution stabilizes the magnetic state of Co³⁺ at low temperatures. The effective magnetic moment of LaCo_{1-x}Rh_xO₃ evaluated at room temperature is independent of x for 0 < x < 0.5, and rapidly decreases above x = 0.5. It indicates that the excited state of Co³⁺ is well described as a mixture of the low- and the high-spin Co³⁺ ions, and that a Rh³⁺ ion favors to substitute for a low-spin Co³⁺ ion.

[1]. S. Asai et al.; J. Phys. Soc. Jpn. 80 (2011) 104705.

PH13

First-Principles Calculation of the A-Site Ordered Perovskite CaCu₃Fe₂O₁₂

Takuya Ueda¹, Mitsuru Kodera¹, Kunihiko Yamauchi¹ and Tamio Oguchi^{2*}

¹ Osaka University, Japan
² Osaka University & JST-CREST, Japan



PH14

Soft x-ray absorption spectroscopy study of Prussian blue analogue MCo[Fe(CN)₆]H₂O Nano-particles (M=Na, K, Rb)

Eunsook Lee¹, D.h. Kim¹, Jihoon Hwang¹, Nguyen Van Minh², In-sang Yang³, M. Sawada⁴, T. Ueno⁴ and J.-s. Kang^{1*}

¹ Department of Physics, The Catholic University of Korea, Bucheon 420-743, Korea
² Department of Physics, Hanoi National University of Education, Hanoi, Viet Nam
³ Department of Physics, Ewha Womans University, Seoul 120-750, Korea
⁴ Hiroshima Synchrotron Radiation Center, Hiroshima University, Higashi-Hiroshima 739-0046, Japan

Molecular-based magnetic materials have been studied for their possible applications as nano-magnetic devices as well as for the understanding of the fundamental physics of their magnetic phenomena. Molecular magnetic materials of Prussian Blue (PB) analogues, which are represented by the general formula, An[B(CN)₆]_mxH₂O, where A and B are transition-metal ions [1], show various characteristic magnetic properties depending on their transition metal ions. PB crystallizes in the fcc structure with space group Fm3m [2]. Of special interest is the photo-induced spin transition. However, the origin of the photo-induced spin transition has not been understood well yet. In this work, we have studied the valence states of PB analogue MCo[Fe(CN)₆]H₂O (M=Na, K, Rb) nano-size particles by employing synchrotron-radiation soft x-ray absorption spectroscopy (XAS). The measured Fe and Co 2p XAS spectra of MCo[Fe(CN)₆]H₂O (M=Na, K, Rb) reveal the systematic changes as the size of M ion changes, from the Fe²⁺-Fe²⁺ mixed-valent states and the nearly divalent Co²⁺ states to the nearly trivalent Fe³⁺ states and the Co²⁺-Co³⁺ mixed-valent states. This finding suggests that the electronic structures of PB nano-particles play an important role in determining their magnetic properties.

[1] Amit Kumar and S M Yusuf, Pramana - J. Phys., 63, 239 (2004). [2] Nguyen Van Minh, Phung Kim Phu, Nguyen Minh Thuan, and In-Sang Yang, J. Magnetism, 13, 149 (2008).

PH15

Long-time variation of magnetic structure in multistep metamagnets Ca₃(Co-M)₂O₆: Effect of disorder

Taketo Moyoshi^{*}, Rui Takahashi, Yuichiro Ito, Ryotaro Irie, Tetsuto Ide, Daiki Syoji and Kiyochiro Motoya

Faculty of Science and Technology, Tokyo University of Science, Japan

We have reported that CeIr₂Si₂, Ca₃Co₂O₆ and some other materials show long-time variation of magnetic structure [1-4]. These materials are uniform compounds including no appreciable randomness or imperfections. All of these compounds show successive magnetic transitions and metamagnetic transitions at low magnetic field, which indicate the presence of competing magnetic interactions. Therefore, we think that the long-time variation of magnetic structure in these materials is caused by the competing magnetic interactions. To ensure that randomness or imperfections are not the main factor causing the long-time variation of magnetic structure, we have investigated the element substitution effects. In this presentation, we show the time dependence of the magnetization in Ca₃(Co_{1-x}M_x)₂O₆ (M=Ga, Mg, Al and Ti). The time variations of magnetization were measured after the sample was cooled to various target temperatures from T=30 K (T>Tc1) at B=5 mT. Characteristics of the time variation behavior were not much modified by the disorder produced by the substitution of non-magnetic elements. These results show that the long-time variation of the magnetic structure in Ca₃Co₂O₆ is not caused by randomness or imperfections.

[1]K. Motoya et al. J. Phys. Conf. Series 200 (2010) 032048 [2]T. Moyoshi et al., J. Phys. Soc. Jpn. 81 (2012) 014704 [3]T. Moyoshi and K. Motoya, J. Phys. Soc. Jpn., 80 (2011) 034701 [4]K. Motoya et al. J. Phys. Conf. Series 273 (2011) 012124

PH16

Study of magnetic properties of NdCo_{1-x}Ni_xO₃ (x = 0, 0.2, 0.4)

Ravi Kumar¹, Vinod Kumar², Rajesh Kumar³, Dinesh Kumar Shukla⁴, Sunil Kumar Arora⁵ and I V Schvets⁶

¹ Centre for Materials Science and Engineering, National Institute of Technology, Hamirpur 177005 (H.P.), India
² Department of physics, National Institute of Technology, Hamirpur 177005 (H.P.), India
³ Department of physics, National Institute of Technology, Hamirpur 177005 (H.P.), India, India
⁴ Deutshes Elektronen Synchrotron DESY, 22607 Hamburg, Germany, Deutshes Elektronen Synchrotron DESY, 22607 Hamburg, Germany, Germany
⁵ School of Physics, Trinity College Dublin 2, 3School of Physics, Trinity College Dublin 2, Ireland
⁶ School of Physics, Trinity College Dublin 2, School of Physics, Trinity College Dublin 2, Ireland

We report here the magnetization studies of the NdCo_{1-x}Ni_xO₃ (x = 0, 0.2, 0.4) samples synthesized using conventional solid state reaction method. X-ray diffraction followed by Rietveld refinement, confirms the single phase orthorhombic structure with Pbnm space group for all the samples. X-ray absorption spectroscopy studies revealed that both Co and Ni exist in trivalent state. The zero field cooled and field cooled magnetization measurements show that below room temperature the magnetization has strong influence of paramagnetic rare earth ion inhibiting magnetic ordering of cobalt ions. Below a certain low temperature (T< 50K), samples with x = 0, 0.2, show paramagnetic to anti ferromagnetic transition but the sample with x = 0.4 shows paramagnetic to Spin glass transition. Isothermal magnetization hysteresis measurements revealed the similar behavior at low temperature. The overall magnetic behavior has on the basis of various magnetic interactions between Nd-sublattice and those of transition metal networks.

PH17

Fluctuations of charge, orbital, and spin order in single layer manganite Pr_{0.5}Ca_{1.5}MnO₄

Ismudiaty Puri Handayani^{*}, Agung Nugroho², Nandang Mufti³, Syarif Riyadi¹, May On Tjia⁴, T.t.m Palstra⁵ and P.h.m Van Loosdrecht¹

¹ Zernike Institute for Advanced Material, Netherlands
² Bandung Institute of Technology, Indonesia
³ State University of Malang, Indonesia

The magnetic and transport properties of doped manganite oxides are intimately related to the dimensionality of the MnO₂ network. A three dimensional system tends to lead to metallic-ferromagnetic properties, whereas the two dimensional (2D) systems is dominated by charge-orbital order (COO) leading to insulating-antiferromagnetic properties. Pr_{0.5}Ca_{1.5}MnO₄ is one of the more interesting members of the 2D manganite family showing a charge and orbital ordering transition above room temperature (TCOO = 320 K) with distinct changes in the magnetic, transport, and structural properties, evidencing a strong coupling between the orbital, structural, charge, and spin degrees of freedom. We study the structural, magnetic susceptibility, transport, specific heat, and Raman spectroscopy of this material. The metal insulator transition observed at TCOO is found to be more pronounced in comparison to the well studied isostructural La_{0.5}Sr_{1.5}MnO₄ compound. The same holds for the changes in the magnetic susceptibility at the antiferromagnetic transition (TN=120 K). Even though the COO is accompanied by rather abrupt changes in the physical properties, our data shows that no full ordering occurs at the transition temperature. The system exhibits orbital fluctuations down to a temperature of about 200K, leading to an unusual temperature dependence of the vibrational, magnetization, and transport properties.

PH18

Magnetic properties of spinel oxide CuCr₂O₄ investigated by NMR

Euna Jo, Soonchil Lee^{*}, Changsoo Kim, Byeongki Kang and Sangil Kwon

Physics, KAIST, Korea

Spinel oxide CuCr₂O₄ is known to have non-collinear spin structure and orbital ordering in its ground state. NMR spectrum for the magnetic ions Cr³⁺ and Cu²⁺ was measured at liquid helium temperature to investigate magnetic properties of CuCr₂O₄. Temperature dependence of the Cr NMR frequency shows that there exist initial energy gap in the dispersion relation of the spin wave. This energy gap is larger than that of the Cu ion, implying that spin-orbit coupling of the Cr ion is stronger than that of the Cu ion. This is consistent with theory that predicts orbital order for the Cu ion in CuCr₂O₄. The canting angle of the Cr³⁺ spin was estimated to be 80° by external magnetic field dependence of the Cr NMR frequency. Also the line width of the Cr NMR spectrum was measured in 7T external magnetic field. The broadening of the spectrum is induced by the anisotropy field. The broadening of the Cu NMR spectrum is larger than that of the Cr NMR spectrum, implying that orbital ordering, rather than anisotropy field, is the main reason of the Cu NMR spectrum broadening.

July 9 (Mon)

July 9 (Mon)

PH19

Magnetic frustration effects in the new colossal magnetoresistance oxide NaCr₂O₄

Hikaru Takeda^{1*}, Yasuhiro Shimizu¹, Masayuki Itoh¹, Hiroya Sakurai² and Eiji Takayama- Muromachi²

¹ Department of Physics, Graduate School of Science, Nagoya University, Japan
² National Institute for Materials Science, Japan

In itinerant electron systems on a geometrically frustrated lattice, the magnetic frustration is considered to play a crucial role for their transport properties as seen in LiV₂O₄ which shows the heavy fermion-like behavior [1]. Recently, a new chromium oxide NaCr₂O₄ with geometrically frustrated double chains was reported to show the unconventional colossal magnetoresistance (CMR) effect [2]. Unlike the conventional CMR materials represented by the ferromagnetic manganites, NaCr₂O₄ is an antiferromagnet with the Neel temperature TN = 125 K. The origin of the CMR effect in NaCr₂O₄ is expected to be closely related to the unconventional spin structure generated by the magnetic frustration. In this study, we have performed ²³Na NMR measurements on NaCr₂O₄ to investigate the spin structure in the antiferromagnetic phase and the magnetic correlations. We found the presence of a ferromagnetic interaction, which competes with an antiferromagnetic one, from the temperature dependence of the nuclear spin-lattice relaxation rate 1/T₁. Below TN, ²³Na NMR spectra, which change with increasing the external magnetic field, cannot be explained by a conventional spin structure. The CMR effect may be related to the instability of the spin structure in the external field due to the magnetic frustration.

[1] S. Kondo, et al., PRL 78, 3729 (1997). [2] H. Sakurai, et al., (unpublished).

PH20

Site-dependent metal-insulator transition and orbital order in quasi-one-dimensional V₆O₁₃

Satoshi Aoyama¹, Yasuhiro Shimizu¹, Masayuki Itoh^{2*} and Yutaka Ueda³

¹ Department of Physics, Graduate School of Science, Nagoya University, Furo-cho, Chikusa-ku, Nagoya, Japan
² Department of Physics, Graduate School of Science, Nagoya University, Japan
³ Institute for Solid State Physics, University of Tokyo, 5-1-5 Kashiwanoha, Kashiwa, Japan

Vanadates are prototypes of metal-insulator transitions with orbital degrees of freedom. In a quasi-one-dimensional compound V₆O₁₃, the mixed valence gives non-uniform spin-charge distributions on inequivalent V sites even for the metallic state. Our sophisticated 51V NMR measurements using a single crystal distinguished the site-dependent orbital order and the local spin susceptibilities on two inequivalent chains. One chain behaves as a metallic one with the moderately depressed susceptibility, whereas another behaves as an insulating one with the magnetically active local moment. The result arises from the site dependent electron correlation, giving the net duality in the conducting and magnetic properties. A metal-insulator transition occurring at -150 K accompanies with dramatic changes in the charge and orbital ordering textures, as we observed in the 51V nuclear quadrupole splitting anisotropy. Such ordering separates the metallic chain into magnetic and nonmagnetic sites, giving a complex antiferromagnetic spin structure below -50 K.

PH21

Synthesis and characterization of CoMn₂O₄ nanopowders by a reverse Micelle processing

Hojung Kim and Dong Sik Bae*

Department of Convergence Materials Science and Engineering, Changwon National Univ., Korea

CoMn₂O₄ nanoparticles was synthesized by reverse micelle processing the mixed precursor (consisting of Co(NO₃)₃ and MnCl₂·4H₂O). The CoMn₂O₄ was prepared by mixing the aqueous solution at a molar ratio of Co : Mn = 1 : 2. The synthesized powders were calcined at 600°C for 2h. The average size and distribution of synthesized powders were in the range of 10-20nm and narrow, respectively. The average size of the synthesized powders increased with increasing water to surfactant molar ratio. The XRD diffraction patterns show that the phase of CoMn₂O₄ was spinel (JCPDS no.77-0471). The synthesized and calcined powders were characterized by thermo gravimetry- differential scanning calorimeter (TG-DSC), X-ray diffraction analysis (XRD) and transmission electron microscopy (TEM). The magnetic property of the powder was measured by Vibrating Sample Magneto-meter (VSM) at 298K. The effect of synthesis parameter, such as the molar ratio of water to surfactant, is discussed.

PH22

The patterning with a circular magnet array, its observation and domain switching in ferromagnetic ZnCoO:H

Won-kyung Kim, Seunghun Lee, Sang-uk Cho, Yong-chan Cho, Hideomi Koinuma and Se-young Jeong*
 Cogno-Mechatronics Engineering, Pusan National University, Korea

Today's spintronic technologies are considered to be the most progressive solution for overcoming the typical semiconductor electronics. Many researchers have extensively studied the effect of size, shape, structure on single-domain magnet and its wall motion with permanent magnetic metal for high-density magnetic memory and logic devices[1,2]. However, the fact that permanent magnetic metals could not reprogram after the first design for logic devices is still remaining as an important issue. Thus, hydrogen-mediated Co-doped ZnO(ZnCoO:H) having reversible room-temperature ferromagnetism has been considered as a strong candidate material for spintronic devices[3]. In this study, we observed domain switching in a ZnCoO:H in real-space and simulate it using object-oriented micromagnetic framework(OOMMF). ZnCoO circular patterns are fabricated by rf-sputtering and various lithography processes, and hydrogen is injected by plasma and hot isostatic pressing(HIP) methods. The reversible magnetic single-domain behavior is activated and deactivated by hydrogen manipulation, which are investigated with superconducting quantum interference device(SQUID) and magnetic force microscopy(MFM) measurements, and the results are compared with the OOMMF simulation. This reversible room-temperature magnetic switching of the oxide materials could greatly contribute to the development of reprogrammable spin logic devices.

[1] S. Y. Chou, Proc. IEEE 85, 652 (1997); G. A. Prinz, Science 282, 1660 (1998) [2] E. R. Lewis et al., Nat. Mater. 9, 980 (2010); J.-C.Lee et al., Phys. Rev. Lett. 107, 067201 (2011) [3] H. J. Lee et al., Appl. Phys. Lett. 88, 062504 (2006); S. Lee et al., Appl. Phys. Lett. 94, 212507 (2009); Y. C. Cho et al., Appl. Phys. Lett. 95, 172514 (2009); S. J. Kim et al., Phys. Rev. B 81, 212408 (2010); S. Lee et al., J. Appl. Phys. (accepted); J. M. Shin et al., Phys. Rev. Lett. (submitted)

PH23

Orbitally induced molecule formations in itinerant triangular vanadates

Yasuhiro Shimizu^{1*}, Ken-ichiro Matsudaira¹, Masayuki Itoh¹ and Yutaka Ueda²

¹ Nagoya University, Japan
² University of Tokyo, Japan

An intriguing route that eliminates the geometrical frustration is the orbitally-induced symmetry breaking usually described by the Kugel-Khomskii model. In itinerant systems, however, the model for localized electrons may not be guaranteed, and the degenerated d orbitals can be partially occupied. We show that the orbital occupation continuously changes into a valence-bond-solid ground state in an itinerant vanadate BaV₁₀O₁₅ with a triangular lattice, based on the orbital-resolved nuclear magnetic resonance technique. Owing to the odd number of d electrons, i. e., eleven electrons for a five-V unit, all the V sites cannot form the valence bonds. Instead, two of the five V sites, sharing five electrons, remain magnetic with the ferro-orbital ordering [1]. In clear contrast, no commensurate spin order and orbital order are stabilized in SrV₁₀O₁₅. The result suggests fractional and incommensurate spin-orbital orders that cannot fully remove the geometrical frustration.

[1] Y. Shimizu, K. Matsudaira, M. Itoh, T. Kajita, and T. Katsufuji, Phys. Rev. B. 84, 064421 (2011).

PH24

Investigation of magnetocaloric effect in La_{0.45}Pr_{0.25}Ca_{0.3}MnO₃ by differential scanning calorimetry and thermal analysis

Aparnadevi M, Sujit Kumar Barik and Ramanathan Mahendiran*

Department of Physics, National university of Singapore, Singapore

We investigated magnetocaloric effect in La_{0.45}Pr_{0.25}Ca_{0.3}MnO₃ by direct (changes in temperature and latent heat) and indirect methods (magnetization isotherms). This compound undergoes a first-order paramagnetic to ferromagnetic transition with T_c = 200 K upon cooling. The paramagnetic phase becomes unstable and it transforms into a ferromagnetic phase under the application of magnetic field, which results in field-induced metamagnetic transition (FIMT). The FIMT is accompanied by release of latent heat and change in temperature of the sample as evidenced from differential scanning calorimetry and thermal analysis experiments. A large magnetic entropy change of ΔSm = -7.3 J/kg-K-1 at T_c = 212.5 K and refrigeration capacity of 228 J/kg are observed for a field change of ΔH = 5 T. It is suggested that the nanometer sized ferromagnetic clusters co-exist with short-range charge-ordered clusters in the paramagnetic state, resulting in a large value of ΔSm above the T_c.

PH25

Specific heat and magnetic properties of spinel compound FeV₂O₄

Shogo Kawaguchi*, Yoshiki Kubota and Hiroki Ishibashi
 Department of Physical Science, Graduate School of Science, Osaka Prefecture University, Japan

The spinel compound FeV₂O₄ has the orbital degrees of freedom at both eg (Fe²⁺) and t_{2g} (V³⁺) orbitals. This compound shows successive structural phase transitions at about 140 K, 110 K accompanied by ferrimagnetic ordering, 70 K and 35 K. However, the details of the phase transitions below 110 K are still not understood. In order to clarify the origin of these phase transitions, we measured magnetization and specific heat capacity for polycrystalline and single crystal of FeV₂O₄. We first observed three anomalies at 140 K, 109 K and 68 K with decreasing temperature in the specific heat measurements using the polycrystalline sample. The λ-type anomaly at 109 K indicates the second order phase transition, which is related to the ferrimagnetic ordering. Moreover, the anomaly at 68 K has a sharp peak, which conforms to the anomaly on the temperature dependence of magnetic susceptibility. The electronic specific coefficient γ = 1.8 mJ/molK² of FeV₂O₄ is smaller than that of MnV₂O₄ (γ = 12 mJ/molK²)[2] because the Jahn-Teller effect of Fe²⁺ for FeV₂O₄ may weaken the electron-electron interactions. The details of the measurements using single crystal and the correlation between the crystal and the magnetic structures are also discussed.

[1] T. Katsufuji et al., J. Phys. Soc. Jpn. 77 (2008) 053708 [2] K. M. Whun et al., Phys. Rev. B 83 (2011) 024403

PH26

The crossover to checkerboard charge order: Magnetic excitations of charge-stripe ordered of La_{2-x}Sr_xNiO₄

Paul G Freeman¹, A. T. Boothroyd², D. Prabhakaran³, K. Hradil⁴, R. A. Mole⁴ and S. R. Giblin⁵
¹ Helmholtz-Zentrum Berlin, Germany; EPFL, Lausanne, Switzerland; ILL, Grenoble, France
² Department of Physics, Oxford University, United Kingdom
³ Technische Universität Wien, Austria; Institut für Physikalische Chemie, Universität Göttingen, Germany
⁴ Bragg Institute, ANSTO, Australia; FRM II, Germany
⁵ ISIS Facility, Rutherford Appleton Laboratory, United Kingdom

Are stripes ubiquitous to the cuprates, and what is the role of stripes in high temperature superconductivity, are two questions that have been intensively debated since the discovery of charge stripe order in the cuprates[1]. From studying the magnetism of charge-stripe ordered La_{2-x}Sr_xNiO₄ (LSNO) the magnetic interactions of a charge-stripe ordered phase have been quantitatively described[2], although our knowledge is incomplete[3]. For x = 1/2 the ground state order of LSNO is part stripe and part checkerboard like in character, with both the magnetic excitations from the ordered moments and charge stripe electrons showing dramatic differences compared to lower doping levels [2,3]. Variations of the charge-stripe periodicity, discommensurations, create additional magnetic excitations from the ordered moments in the x = 1/2 compared to damping the excitations at x = 1/3. While the magnetic excitations from the charge stripe electrons have a different wavevector centring in the x = 1/2 [3,4]. We report a neutron scattering study of the magnetic excitations in LSNO x = 0.4 and 0.45. Between these two doping levels the magnetic excitations show a dramatic crossover in character. We discuss this crossover behaviour with regards to charge-stripe materials with larger charge stripe spacing.

[1] M. Tranquada, et al., Nature (London) 375, 561 (1995). [2] H. Woo et al. Phys. Rev. B 72, 064437 (2005). [3] P. G. Freeman, et al. Phys. Rev. B 71, 174412 (2005). [4] A. T. Boothroyd, et al., Phys. Rev. Lett. 91 257201 (2005).

PH27

Magnetic properties of low-dimensional α and γ CoV₂O₆

Marc Lenertz*, Jonathan Alaria, Daniel Stoeffler, Silviu Colis and Aziz Dinia
 DCMI, Institut de Physique et Chimie des Matériaux de Strasbourg, CNRS - Université de Strasbourg, France

CoV₂O₆ is a low dimensional oxide existing in two allotropic phases, generally called α and γ, and showing monoclinic and triclinic structures, respectively. We synthesized this oxide by solid state reaction and performed neutrons diffraction and magnetic measurements in order to understand the magnetic behavior in correlation with the low dimensional structure. The magnetic properties were supported by ab initio calculations. Both phases are constituted of parallel 1D Co chains organized in planes that are separated by vanadium oxide thin layers and are antiferromagnetic in the ground state. The magnetization curves recorded at 5 K show a stepped variation with sharp field-induced magnetic transitions and a magnetization plateau at one-third of the saturation magnetization. In α-CoV₂O₆, additional steps are evidenced at 1.8 K. The magnetic moment per Co ion is larger in the α phase (4.5 μB) than in the γ phase (3 μB), although Co has the same octahedral environment in both cases. Ab initio calculations show that α-CoV₂O₆ is an antiferromagnetic semiconductor with a gap of 1.1 eV in which the magnetic moment is essentially carried by Co and can reach a maximum value of about 4.2 μB for a meta-stable solution.

M. Lenertz, J. Alaria, D. Stoeffler, S. Colis and A. Dinia, J. Phys. Chem. C, 2011, 115, 17190-17196

PH28

Structural and magnetic properties of the parent compound T'-La₂CuO₄ of electron-doped cuprates

Gwendolyn Pascua¹, Hubertus Luetkens¹, Marco Guenther², Roland Hord³, Lukas Keller¹, Vladimir Pomjakushin¹, Andreas Suter¹, Hemke Maeter², Alexander Buckow², Barbara Albert¹, Hans-henning Klaus² and Lambert Alff²
¹ Laboratory for Muon Spin Spectroscopy, Paul Scherrer Institute, CH-5232 Villigen PSI, Switzerland
² Institut fuer Festkoerperphysik, TU Dresden, DE-01069 Dresden, Germany
³ Eduard-Zintl-Institute of Inorganic and Physical Chemistry, TU Darmstadt, Petersenstr. 18, DE-64287, Darmstadt, Germany
⁴ Laboratory for Neutron Scattering, Paul Scherrer Institute, CH-5232 Villigen PSI, Switzerland
⁵ Institute of Materials Science, TU Darmstadt, Petersenstr. 23, DE-64287 Darmstadt, Germany

Recently, we found that the newly synthesized metastable T'-La₂CuO₄ exhibits much lower Neel temperature (TN) and increased magnetic fluctuations compared to other mother compounds of electron-doped superconductors like Nd₂CuO₄ or Pr₂CuO₄. Muon spin rotation (μSR) reveals a gradual slowing down of dynamic magnetic fluctuations below TN1=220K and static magnetic order below TN2=115K in contrast to T-La₂CuO₄ where TN2=300K. In comparison to our T'-La₂CuO₄ measurements were done on T'-Pr₂CuO₄ to study the effect of a magnetic rare earth ion on the magnetism. Zero-field μSR on T'-Pr₂CuO₄ shows oscillations at high temperatures up to 220K in sharp contrast to the predominantly dynamic character of the depolarization in T'-La₂CuO₄ in the same temperature range. This clearly demonstrates that the magnetism of T'-La₂CuO₄ is much more 2-dimensional than in T'-Pr₂CuO₄. Interestingly, there is also an abrupt change of the internal field distribution at TN3=40K for both the T'-La₂CuO₄ and the T'-Pr₂CuO₄ compounds consistent with a reorganization of the magnetic structure at this temperature. La-NMR results for the T'-La₂CuO₄ also display anomalies at the abovementioned characteristic temperatures. In addition, μSR and neutron scattering results on T'-Pr₂CuO₄ indicate a similar behaviour previously observed for Nd₂CuO₄ pointing to, up-to-now undetected spin reorientation transitions.

[1] R. Hord, H. Luetkens, et al., Phys. Rev. B 82, 180508(R) (2010). [2] G. M. Luke et al., Phys. Rev. B 42, 7981 (1990). [3] I.W. Sumarlin, et al., Phys. Rev. B 51, 5824 (1990). [4] V.P. Plakhy et al., Phys. Lett. A 250, 201 (1998). [5] R. Sachidanandam et al., Phys. Rev. B 56, 260 (1997). [6] S. Katano, et al., Physica C 215, 92 (1993).

PH29

Microscopic magnetic nature of the quasi-one-dimensional antiferromagnet BaCo₂V₂O₆

Martin Mansson^{1*}, Krunoslav Prsa¹, Jun Sugiyama², Hiroshi Nozaki², Alex Amato³, Shojiro Kimura⁴, Kumiko Omura⁵, Masayuki Hagiwara⁶ and Andrey Zheludev¹
¹ Lab. for Solid State Physics, ETH Zurich, Switzerland
² Toyota Central Research and Development Labs. Inc., Japan
³ LMU, Paul Scherrer Institut, Switzerland
⁴ Institute for Materials Research, Tohoku University, Japan
⁵ KYOKUGEN, Osaka University, Japan

BaCo₂V₂O₆ belongs to a wide group of quasi-1D antiferromagnets (AF). The Q1D compounds display a variety of fascinating ground states governed by the strong spin-spin coupling along the 1D direction and a much weaker coupling along other directions. BaCo₂V₂O₆ display a long-range AF order below TN=5 K and possibly short-range order all the way up to 30 K. Further, a novel type of field induced magnetic order has been found for T<1.8 K and H<3.9 T [1,2]. It was determined to be an incommensurate spin structure caused by quantum fluctuations, fitting well to theoretical predictions for a so-called Tomonaga-Luttinger liquid (TLL). To the best of our knowledge, we present here the first μSR investigation of the microscopic magnetic nature of single crystalline BaCo₂V₂O₆ samples. Our data reveal several clear muon frequencies below TN indicating the onset of a long-range order. Above 5 K, the μSR spectra are well fitted to a simple power-exponential relaxing function. The temperature dependence of the relaxation-rate as well as the power display a clear anomaly around T=40 K, indicating the onset of short-range 1D correlations. Finally we also present initial and intriguing field dependent data.

[1] S. Kimura et al. PRL 100, 057202 (2008) [2] S. Kimura et al. PRL 101, 207201 (2008) Funding Source: Swiss National Science Foundation (Project 6, NCCR MaNEP) and Toyota CRDL.

PH30

Detection of orbital wave in YVO₃ using inelastic neutron scattering

Daichi Kawana¹, Youichi Murakami¹, Tetsuya Yokoo², Shinichi Itoh², Andrei T Savici³, Garrett E Granroth⁴, Kazuhiko Ikeuchi⁴, Hironori Nakao⁴, Kazuaki Iwasa⁵, Ryuichiro Fukuta⁶, Shigeki Miyasaka⁶, Setsuko Tajima⁶, Sumio Ishihara⁶ and Yoshinori Tokura⁷
¹ Condensed Matter Research Center, Institute of Materials Structure Science, KEK, Japan
² Neutron Science Division, Institute of Materials Structure Science, KEK, Japan
³ Neutron Scattering Sciences Division, Oak Ridge National Laboratory, USA
⁴ Comprehensive Research Organization for Science and Society, Japan
⁵ Department of Physics, Tohoku University, Japan
⁶ Department of Physics, Osaka University, Japan
⁷ Department of Applied Physics, University of Tokyo, Japan

We focus on an orbital excitation in YVO₃, which shows the complex magnetic and orbital orderings in the low temperatures [1]. In the phase where the G-type orbital order accompanied with the C-type spin order (G-OC-SO) appears, the existence of the large orbital fluctuation is suggested [2]. Additionally, a large dispersive orbital-wave along the c-axis, due to the strong one-dimensional spin-orbital correlation, is calculated [3]. In consideration of the neutron scattering cross-section obtained from the correlation function for the orbital angular moment, we have attempted to detect the orbital excitation using inelastic neutron scattering spectrometers. We observed a magnetic excitation up to 35 meV. This energy range is higher than that reported previously [3]. On the other hand, weak excitations are observed in the range of 40-70 meV. In this Presentation, we discuss whether these are originated from orbital excitation or not.

[1] S. Miyasaka et al., Phys. Rev. B 73, 224436 (2006). [2] C. Ulrich et al., Phys. Rev. Lett. 91, 257202 (2003). [3] S. Ishihara, Phys. Rev. B 69, 075118 (2004).

July 9 (Mon)

July 9 (Mon)

PI08

Orbital occupation and magnetism of tetrahedrally coordinated Fe in CaBaFe₂O₇
 Nils Hollmann¹, Martin Valldor², Hua Wu², Zhiwei Hu¹, Navid Qureshi², Thomas Willers², Yi-ying Chin³, Julio Cezar⁴, Arata Tanaka³, Nicholas Brookes⁴ and Liu Hao Tjeng⁵

- ¹ Max-Planck-Institute for Chemical Physics of Solids, Dresden, Germany
- ² II. Institute of Physics, University of Cologne, Germany
- ³ Max-Planck-Institute for Chemical Physics of Solids, Germany
- ⁴ European Synchrotron Radiation Facility, Grenoble, France
- ⁵ Department of Quantum Matter, ADSM, Hiroshima University, Japan

CaBaFe₂O₇ is a new mixed-valent transition metal oxide from the class of Swedenborgites [1,2] having both Fe²⁺ and Fe³⁺ ions in tetrahedral coordination situated in a Kagome lattice. This class of materials could be an interesting starting point to study orbital physics in tetrahedral coordination. Here we characterize its magnetic properties by magnetization measurements and investigate its local electronic structure using soft x-ray absorption spectroscopy at the Fe L_{2,3} edges, in combination with multiplet cluster simulations and band structure calculations [3]. We found that the Fe²⁺ ion in the unusual tetrahedral coordination is Jahn-Teller active having a minority-spin electron with an x2-y2 character. We deduce that there is an appreciable orbital moment caused by multiplet interactions, thereby explaining the observed magnetic anisotropy.

[1] B. Raveau et al., Chem. Mat. 20, 6295 (2008) [2] B. Raveau et al., Z. Anorg. Allg. Chem. 635, 1869 (2009) [3] N. Hollmann et al., Phys. Rev. B 83, 180405 (2011)

PI09

Search for topological spin order in the multiferroic insulator Cu₂OSeO₃

M. Wagner¹, T. Adams¹, A. Chacon², G. Brandl², H. Berger³, P. Lemmens⁴ and C. Pfleiderer⁵
¹ Physik-Department, Technische Universitaet Muenchen, D-85748 Garching, Germany
² Physik-Department and Forschungsneutronenquelle Heinz-Maier Leibniz, TU Muenchen, D-85748 Garching, Germany
³ Ecole Polytechnique Federale Lausanne, CH-1015 Lausanne, Switzerland
⁴ Institut fuer Physik, Technische Universitaet Braunschweig, Germany

We report a comprehensive study of the magnetic properties of single crystals of the multiferroic insulator Cu₂OSeO₃. Our study was motivated by the recent discovery of a skyrmion lattice phase in the B₂₀ transition metal Si and Ge transition metal compounds [1], which are isostructural siblings of Cu₂OSeO₃. For our study large high-quality single crystals were grown by vapour transport. The magnetisation, ac susceptibility and specific heat were measured down to 2K under magnetic fields up to 9T. The magnetic properties were studied with small angle neutron scattering. We find a paramagnetic to helimagnetic transition at T_c = 58K. The magnetic phase diagram of Cu₂OSeO₃ shares remarkable similarities with the B₂₀ transition metal silicides, including the existence of a small phase pocket below T_c. The putative evidence for topological spin order is compared with the evidence for a skyrmion lattice in B₂₀ transition metal Si and Ge compounds.

[1] S. Muehlbauer et al., Science 323, 915 (2009).

PI10

Studies of neutron scattering and bulk properties of honeycomb lattice Li₂MnO₃

Sanghyun Lee¹, Sungil Choi¹, Jiyeon Kim¹, Choongjae Won², Seongsu Lee³, Shin-ae Kim³, Namjung Hur² and Je-geun Park^{4*}
¹ Center for Strongly Correlated Materials Research, Seoul National University, Seoul 151-742, Korea
² Department of Physics, Inha University, Incheon 402-751, Korea
³ Neutron Science Division, Korea Atomic Energy Research Institute, Daejeon 305-353, Korea
⁴ Department of Physics & Astronomy, Seoul National University, Seoul 151-742, Korea

Li₂XO₃ with transition metal ions occupying the X position forms an interesting honeycomb lattice. Among Li₂XO₃, Li₂RuO₃ was recently found to have an unusual structural phase transition involving probably Ru dimerization. For example, it was reported that the crystal structure changes from P21/m to C2/m near 540 K, accompanied by a concomitant metal-insulator transition and an abrupt change in the magnetic susceptibility. Li₂MnO₃ is another example having the C2/m crystal structure with the honeycomb lattice. In order to investigate the magnetic properties of Li₂MnO₃, we have successfully grown single crystal Li₂MnO₃ by using a flux method. Using these single crystals, we have carried out both bulk measurements and neutron diffraction studies with high resolution powder diffractometer (HRPD) and single crystal diffractometer (FCD) at HANARO, Korea. We also measured the magnetization and heat capacity of the single crystals.

PI11

Magnetic and calorimetric properties of Mn₂GeO₄ single crystals
 Natalia Mihashenok*, Nikita Volkov, Klara Sablina, Alexander Balaev, Maxim Molochev, Sergei Popkov and Dmitriy Velikanov
 L.V. Kirensky Institute of Physics SB RAS, Russia

Within the framework of our research of manganese oxides the single crystals Mn₂GeO₄ have been grown by the flux method using the original technique [1]. The crystal structure, an isomorph of olivine, was determined on single crystal by X-ray diffraction method: cell parameters, a=10.7401 Å, b=6.3116 Å, c=5.0766 Å, and the space group Pnma. Magnetic measurements were performed in the temperature range from 2 to 300 K and in magnetic fields up to 50 kOe with the exact orientation of the applied magnetic field relative to the crystallographic directions of the crystal. There are three sharp magnetic phase transition at T1=47 K, T2=17.5 K and T3=5.5 K, with phase transition at T2 depended on applied magnetic field. Also the specific heat measurements of single crystals were carried out. The heat capacity of Mn₂GeO₄ exhibits three sharp maxima, which exactly correlate with the magnetic phase transition.

[1] Sapronova N.V., Volkov N.V., Sablina K.A., Petrakovskii G.A., Bayukov O.A., Vorotyynov A. M., Velikanov D.N., Bovina A.F., Vasilyev A.D., Bondarenko G.V. Phys. Stat. Sol. B, 246 (2009) 206

PI12

Effect of doping on the magnetic structure of YMn_{1-x}M_xO₃ (M = Ga, Ti, x ≤ 0.1)

Neetika Sharma¹, Poonam Kumari², A. Das^{1*} and G. Ravi Kumar³
¹ Solid State Physics Division, Bhabha Atomic Research Centre Mumbai, India
² UM - DAE Centre for Excellence in Basic Sciences University of Mumbai, Mumbai, India
³ Technical Physics Division, Bhabha Atomic Research Centre Mumbai, India

The effect of doping at the Mn site of multiferroic manganites, YMn_{1-x}M_xO₃ (M = Ga, Ti, x ≤ 0.1) have been studied by neutron powder diffraction and magnetic measurements. These compounds have been prepared by solid state synthesis techniques. All the compounds studied are isostructural and crystallizes with hexagonal structure in P63cm space group. We find that both Ga³⁺ (d10) and Ti²⁺ (d0) doping leads to significant reduction in the magnetic transition temperature (TN) while they influence the magnetic structure of YMnO₃ differently. The magnetic structure of YMnO₃ is described by the irreducible representation Γ1 (or Γ3) with moment on Mn~3μB at 5K, in agreement with previously reported values on this compound [1]. We find that the representation remains the same on doping with Ga in YMnO₃ albeit with a decrease in the value of the moment to 2.5μB at 6K. However, the irreducible representation changes on doping with Ti, and this modified structure is given by the basis vectors of the irreducible representation Γ2 with moment 2.1μB at 6K. The geometrical frustration parameter, f = θp/Tn, ~ 7 and reduces with doping. These observations are different from the earlier reported doping studies carried out in this compound [2].

[1] J.A. Alonso et al. Phys. Rev. B 62 9498 (2000) [2] J. Park et al., Phys. Rev. B 79 064417 (2009)

PI13

Neutron diffraction and magnetic properties of Ba₂Co₂Fe₁₂O₂₂: Co₂Y

Chan Hyuk Rhee¹, Jung Tae Lim¹, Sung Wook Yoon¹, Kwang Lae Cho¹, Sung Baek Kim² and Chul Sung Kim^{1*}
¹ Department of Physics, Kookmin University, Korea
² Advancement for College Education Center, Konyang University, Korea

Y-type hexa-ferrites with non-collinear magnetic structure have been studied for magnetoelectric effect, showing induced electric polarization under external magnetic field. The helical magnetic structure of these ferrites depends on the temperature and magnetic field [1]. Here, polycrystalline Y-type barium cobalt ferrite (Ba₂Co₂Fe₁₂O₂₂: Co₂Y) was synthesized by conventional ceramic method in O₂ gas atmosphere to reduce the oxygen defect. The temperature and magnetic field dependence of magnetic structure was investigated by neutron diffraction and vibration sample magnetometer. At temperature below TN = 615 K, the crystal structure of Co₂Y was determined to be rhombohedral with the space group R-3m. It showed soft ferrimagnetic behavior with Hc of 145 Oe at 297 K. Most of super-lattice peaks from spin structure decreased with increasing temperature. However, the peak at 21.1o increased with increasing temperature at temperatures above 205 K. In addition, the slope of zero-field cooled magnetization under low field of 0.01 T changed at 205 K. This magnetic structure transition temperature of Co₂Y is higher than that of Ba₂Mg₂Fe₁₂O₂₂ [1] due to the presence of cobalt ion with strong magnetic anisotropy.

[1] S. Ishiwata, Y. Taguchi, H. Murakawa, Y. Onose, and Y. Tokura, Science 319, 1643 (2008).

PI14

Mössbauer studies of olivine Fe_{1-y}Mn_yPO₄
 Woo Jun Kwon, In Kyu Lee, Hee Seung Kim, In-bo Shim and Chul Sung Kim*
 Department of Physics, Kookmin University, Korea

The olivine structured Fe_{1-y}Mn_yPO₄ (y = 0.1, 0.3), a possible cathode material for lithium ion secondary battery, have been studied by x-ray diffraction and Mössbauer spectroscopy. These Fe_{1-y}Mn_yPO₄ samples were prepared by chemical deintercalation lithium from the LiFe_{1-y}Mn_yPO₄. The crystal structures of the Fe_{1-y}Mn_yPO₄ samples were determined to be orthorhombic (space group Pnma) at 295 K by Rietveld refinement method. The lattice constants of the Fe_{1-y}Mn_yPO₄ samples increased from a0 = 9.833 Å, b0 = 5.811 Å and c0 = 4.786 Å for y = 0.1 to a0 = 9.979 Å, b0 = 5.895 Å and c0 = 4.799 Å for y = 0.3 with the increasing Mn concentration. From the Mössbauer spectra at 295 K, the electric quadrupole splitting (ΔEQ) and isomer shift (δ) values of the Fe²⁺-yMnyPO₄ were determined to be ΔEQ = 1.50 mm/s, δ = 0.31 mm/s for y = 0.1 and ΔEQ = 1.35 mm/s, δ = 0.31 mm/s for y = 0.3. The decrease in ΔEQ of Fe_{1-y}Mn_yPO₄ samples can be explained by the exchange interaction due to the asymmetry in FeO₆ octahedral sites depending on the Mn concentrations.

[1] B. C. Melot, G. Rousse, J.-N. Chotard, M. Ati, J. Rodriguez-Carvajal, M. C. Kemei, and J.-M. Tarascon, Chem. Mater. 23, 2922 (2011). [2] W. Kim, C. H. Rhee, H. J. Kim, S. J. Moon, and C. S. Kim, Appl. Phys. Lett. 96, 242505 (2010).

PI15

Three- dimensional electronic structure of Na_{0.85}CoO₂

Y. Sassa^{1*}, M. Mansson¹, B. M. Wojek², J. Chang³, M. Kobayashi⁴, J. Kanter¹, V. Strocov⁴, K. Mattenberger¹ and B. Batlogg¹
¹ Laboratory of Solid State Physics, ETH Zurich, CH-8093 Zurich, Switzerland
² Materials Physics, Royal Institute of Technology KTH, S-16440 Kista, Sweden
³ Laboratory for synchrotron and neutron spectroscopy, Paul Scherrer Institute, CH-5234 Villigen PSI, Switzerland
⁴ Swiss Light Source, Paul Scherrer Institute, CH-5234 Villigen PSI, Switzerland



PI16

Formation of stoichiometric of FeO synthesized under high pressure

Yasushi Kanke¹, Takuro Yoshikawa², Hideto Yanagihara², Eiji Kita², Yorihiro Tsunoda³, Kiiti Siratori² and Kay Kohn¹
¹ National Institute of Materials Science, Japan
² Institute of Applied Physics, University of Tsukuba, Japan
³ School of Science and Engineering, Waseda University, Japan

FeO has the simplest NaCl crystalline structure and one electron exists in the degenerated d_{z²} orbitals due to the regular octahedral ligands. Even such simple structure, the partial quenching of the orbital angular momentum (S = 2 and L = 1) bring the electronic structure complex.[1] Difficulty in the sample preparation, only the samples Fe_xO with X ≤ 0.96 have been obtained, makes the experimental investigation of FeO hard. We have prepared the stoichiometric FeO with the high pressure synthesis technique.[2] The starting material of the mixture of α-Fe and Fe₂O₃ powder was sealed in a Pt capsule and was heated up to 1000 °C and 1200 °C under 5.5GPa for 1 hour. The residual ferromagnetic parts were estimated to be less than 0.69 at%. Higher reaction temperature may bring lower concentration of ferromagnetic components. From Mossbauer study, it is found that the Koch-Cohen cluster does exist especially when the reaction temperature is high. We present the influence of post annealing with various conditions for the improvement of degree of stoichiometry.

[1] J. Kanamori: Prog. Theo. Phys. 17, 177 (1957) [2] T. Katsura, B. Iwasaki, S. Kimura, S. Akimoto : J. Chem. Phys. 47, 4559 (1967)

PI17

Charge and spin ordering in Sr₂Fe₂O₁₁ system
 Qiang Liu^{1,2,3}, Gwendolyne Pascua⁴, Alexander Komarek², Zhiwei Hu¹, Nils Hollmann³, Olivier Toulemonde², Hubertus Luetkens⁴, Gwilherm Nener⁴, Alain Wattiaux², Liu Hao Tjeng³

- ¹ II. Physikalisches Institut, Universität zu Köln, Germany
- ² Institut de Chimie de la Matière Condensée de Bordeaux, France
- ³ Max-Planck-Institut für chemische Physik fester Stoffe, Dresden, Germany
- ⁴ Laboratory for Muon Spin Spectroscopy, Paul Scherrer Institute, CH-5232 Villigen PSI, Switzerland.
- ⁵ Institut Laue-Langevin, 38042 Grenoble Cedex 9, France

Ordering and disordering of charge, spin, lattice and orbital degrees of freedom play an important role in the physics of strongly correlated electron systems. In the mixed valence (Fe²⁺/Fe³⁺) compound Sr₂Fe₂O₁₁, the spin and charge ordering have recently generated a debate arising from its two crystallographic (pyramidal and octahedral) sites and the distribution of Fe²⁺ and Fe³⁺ species [1-5]. Due to symmetry reasons, either the Fe²⁺ sublattice is frustrated while Fe³⁺ ions order antiferromagnetically or the opposite. We are trying to explore this puzzle by X-ray Absorption Spectroscopy, Photoemission Spectroscopy, μSR, Neutron, Synchrotron X-ray diffraction and Mossbauer measurement on precisely adjusted oxygen stoichiometric polycrystalline samples and single crystals.

[1] P. Hodges, S. Short, J. D. Jorgensen, X. Xiog, B. Dabrowski, S. M. Mini, and C. W. Kimball, J. Solid State Chem. 151, 190-209 (2000) 2 M.Schmidt, M Hofmann and S J Campbell, J. Phys.: Condens.Matter 15, 8691-8701 (2003) 3 P. Adler, A Lebon, V Damjanovic, C Ulrich, C Bernhardt, AV Boris, A Maljuk, CT Lin, and B Keimer, Phys. Rev. B 73, 094451(2006) 4 R. Vidy, P. Ravindran, H. Fjellvag, and A. Kjekshus, Phys. Rev. B 74, 054422 (2006) 5 P-Adler Comment Phys. Rev. B 77, 136401 (2008) and R. Vidy Reply Phys. Rev. B 77, 136402 (2008)

PI18

Catalyst structure determination from magnetic properties

Jorge Hernandez-velasco^{1*}, Javier Garcia-garcia² and Angel Landa-canovas¹
¹ Energy, ICMM CSIC, Spain
² CME UCM, Spain

SbVO₄ series of compounds could be used as oxidation catalysts of industrial interest yielding 20% cheaper acrylonitrile (production 8 million ton/year) by the ammoxidation of propane compared to current method based on propylene as starting reactant. SbVO₄ structure was just known to be related to tetragonal rutile. Nevertheless we have shown that actually there is a non-stoichiometric flexible series described as Sb_{0.9-x}V_{0.9-x}O₄ (0<x<0.2), where cation vacancies (□) are introduced in the basic rutile type-structure following the mechanism: 4V(3+)→3V(4+)+□, while antimony remains as Sb(5+). In this sense, for the compounds synthesized in oxidizing conditions the presence of vacancies has been confirmed, however no cation vacancies have been observed in the reduced phase but alternating Sb/V cation order along the crystallographic c-axis. On the other hand, our magnetic susceptibility studies could distinguish between different phases including possible existence of magnetic order. Using neutron diffraction we determined the magnetic structure of reduced SbVO₄ coming from the ordering of vanadium magnetic moments, taking place at TN~50K, and we studied how the substitution of V³⁺ (S=1) by V⁴⁺ (S = ½), while the synthesis conditions become more oxidizing, affects the spin arrangement in SbVO₄. The structure-property relationship could be evaluated thanks to the magnetic behaviour.

PI19

Synthesis and characterization of the mixed perovskite Ba_{1-x}La_xTi_{1/2}Mn_{1/2}O₃ as a function of La-doping

Raimundo Lora-serrano^{1*}, Ulisses F Kaneko², Eduardo Granado³, Ali F. Garcia-flores², Pablo Marques-ferreira¹, Fernando A. Garcia³ and Jose G. S. Duque⁴
¹ Instituto de Fisica, Universidade Federal de Uberlandia, 38400-902 Uberlandia-MG, Brazil
² Instituto de Fisica 'Gleb Wataghin' UNICAMP, CP 6165, 13083-970 Campinas, SP, Brazil
³ Max Planck Institute for Chemical Physics of Solids, D-01187 Dresden, Germany
⁴ Nucleo de Fisica, Campus Itabaiana, UFS, 49500-000, Itabaiana, SE, Brazil

Oxides materials with perovskite structure are outstanding examples of materials used in technological applications, as well as in fundamental studies in condensed matter physics due to the great number of observed ground states such as: multiferroicity, high-temperature superconductivity, colossal magnetoresistive effects, multiferroicity, and many others. One possible way to work and study on the coexistence of electric and magnetic orders within metal oxides perovskites may be making "mixed" perovskites with dⁿ0 and dⁿ ions. In this work we present the results of the synthesis and structural characterization (x-ray powder diffraction and Raman spectroscopy analysis) within the family of transition metal oxides Ba_{1-x}La_xTi_{1/2}Mn_{1/2}O₃ (x = 0, 0.1, 0.2, 0.3, 0.4, 0.5, 0.6) as we dope the 12R-type perovskite BaTi_{1/2}Mn_{1/2}O₃ with the non-magnetic ion La³⁺. Our results show the evolution of the structure symmetry from the hexagonal one for the non-doped (x=0) sample [1] to a tetragonal one for the highest La concentration as well as the mixture of these two phases for intermediate doping. These results are compared with the appearance of ferromagnetic and antiferromagnetic orders as a function of La-content, temperature and magnetic field.

[1] G. M. Keith, C. A. Kirk, K. Sarma et al., Chem. Mater. 16, 2007 (2004).

PI20

Theoretical modeling of the magnetic properties and magnetocaloric effect in $\text{La}_{0.1}\text{Ca}_{0.9}\text{MnO}_3$ manganite by Monte Carlo study
Oksana Pavlukhina*, Vacily Buchelnikov and Vladimir Sokolovskiy
Chelyabinsk State University, Russia

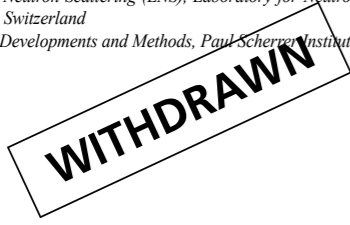
Manganites have a special place among various materials which have a magnetocaloric effect. This materials, first, allow varying temperature of phase transitions in wide region of temperatures, and secondly, they are cheap and ecological. Experimental studies have shown that the manganites are also attractive for the application in magnetic refrigeration [1]. In this work, using the Heisenberg's Hamiltonian, we investigated by Monte Carlo method magnetic and magnetocaloric properties of $\text{La}_{0.1}\text{Ca}_{0.9}\text{MnO}_3$. In the simulation, magnetic Mn^{4+} and trivalent Mn^{3+} ions are described by classical Heisenberg spins, while oxygen and calcium ions are considered as non-magnetic. Mn magnetic ions are distributed on a lattice according to the perovskite structure of the manganite. For the modelling lattice samples of size L3 with L=15 were used. Around 5x105 Monte Carlo steps per spin were considered in order to compute equilibrium averages. Curie temperature obtained during the theoretical simulations (TC ~150 K) agrees well with theoretical result for this compound (TC ~150 K) [2]. The Curie temperature and magnetocaloric effect obtained during the theoretical simulations agree well with experimental data. Support by RFBR grants 10-02-96020-r-ural, 11-02-00601 and Federal Target Program № 14.740.11.1442 (03.11.2011) is acknowledged.

1 Phan, Manh-Huong, 2007, Review of the magnetocaloric effect in manganite materials, J. Magn. Magn. Mater. 308: 325-340. 2 Restrepo-Parra E. 2011, Magnetic phase diagram simulation of $\text{La}_{1-x}\text{Ca}_x\text{MnO}_3$ system by using Monte Carlo, Metropolis algorithm and Heisenberg model, J. Magn. Magn. Mater. 323:1477-1483.

PI21

Pressure effects on magnetic ordering transitions of bilayer manganites $\text{Pr}(\text{Sr}_{1-x}\text{Ca}_x)_2\text{Mn}_2\text{O}_7$ ($x=0,1$) by neutron diffraction and muon spin rasonance

Guochu Deng^{1*}, Denis Cheptakov², Ekaterina Pomjakushina³ and Kazimierz Conder³
¹ *Bragg Institute, Australian Nuclear Science and Technology Organization, Australia*
² *Laboratory for Neutron Scattering (LNS), Laboratory for Neutron Scattering, Paul Scherrer Institut, Switzerland*
³ *Laboratory for Developments and Methods, Paul Scherrer Institute, Switzerland*



PI22

Magnetization reversal and chemical pressure effect in the electron doped manganite $\text{Ca}(\text{Mn}_{1-x}\text{Sb}_x)\text{O}_3$

Syuya Ohuchi¹, Michiaki Matsukawa*, Satoru Kobayashi¹, Shigeki Nimori² and Ramanathan Suryanarayanan³
¹ *Dep. of Materials Science and Engineering, Iwate University, Japan*
² *National Institute for Materials Science, Japan*
³ *Universite Paris-Sud, France*

In ref.1, we have demonstrated the effect of hydrostatic pressure of magnetic and transport properties, and thermal transport properties in the electron doped manganite $\text{Ca}(\text{Mn}_{1-x}\text{Sb}_x)\text{O}_3$. The substitution of Sb^{5+} ion for Mn^{4+} site of the parent matrix causes one-electron doping since the X-ray photoemission spectroscopy of Sb substituted CaMnO_3 sample reveals that the valence of Sb ion is 5+. Anomalous magnetization reversals are observed at $x=0.05$ and 0.08 in the field cooled magnetization while the application of external pressure induces a suppression of the negative magnetization. The effect of chemical pressure on magnetization of $\text{Ca}(\text{Mn,Sb})\text{O}_3$ are examined through the substitution of Ca ion for Sr with larger ion radius and are compared with the effect of external pressure on that of the same compound. We believe that the magnetization reversal is not caused by ferrimagnet model but is associated with the presence of the Jahn-Teller type orbital lattice coupling between 3d eg electron and MnO_6 octahedron, giving stabilization of negative canted spin state through the Dzyaloshinsky-Moriya interaction.

Ref.1, Y.Murano et al., Phys.Rev.B83,054437 (2011).

PI23

The effect of cu substitution on the structural, electrical and magnetic properties of $\text{LaMn}_{1-x}\text{Cu}_x\text{O}_3$ manganites

Parviz Kameli*, H. Vaezi, B. Aslibeiki and H. Salamati
Isfahan University of Technology, Iran

The hole-doped manganites, $\text{La}_{1-x}\text{A}_x\text{MnO}_3$ (A = Sr, Ca, Ba or vacancies) with a Perovskite structure have attracted considerable attention due to the discovery of the phenomenon of colossal magnetoresistance (CMR) and its potential application [1-3]. In this study, the effect of Cu substitution on structural, electrical and magnetic properties of $\text{LaMn}_{1-x}\text{Cu}_x\text{O}_{3-\delta}$ ($0 \leq x \leq 0.075$) manganites are investigated by XRD, electrical resistivity and Ac susceptibility measurements. The XRD refinement result indicates that the samples are single phase and the lattice parameters and volumes increase by the increase of the Cu doping level. The resistivity measurement results show that by increasing Cu doping level, the resistivity decreases and the heavily doped samples show metal - insulator transition at low temperatures. The paramagnetic- ferromagnetic transition temperature, T_c increases for low level doped samples and decreases for heavily doped samples. The analysis of the frequency dependent Ac susceptibility measurements by critical slowing down model, indicates that the reentrant spin glass (RSG) state exists in $x=0.025, 0.05$ and 0.075 samples. The RSG state is mainly ascribed to the coexistence of ferromagnetic (FM) and antiferromagnetic (AFM) phases and increase of disorder in the FM matrix induced by the random Cu impurity.

PI24

Investigation of the structural and magnetic peroperties of $\text{La}_{0.9}\text{Sr}_{0.1}\text{MnO}_3$ nanoparticles

M. Eshraghi*, M. Roshanmehr¹, F. Khademi², P. Kameli² and H. Salamati²
¹ *Department of Physics, Payame Noor University, Iran*
² *Department of Physics, Isfahan University of Technology, Iran*

In recent years, magnetic nanoparticles have been the subject of intense research not only for their fundamental scientific interest such as superparamagnetism, but also for their potential applications in magnetic storage media, biosensor devices and medical applications, such as targeted drug delivery and hyperthermia [1-3]. In a large number of magnetic nanoparticles applications, it is important to know the effects of interaction between nanoparticles on physical properties of these systems. In this paper, we studied the structural and magnetic properties of $\text{La}_{0.9}\text{Sr}_{0.1}\text{MnO}_3$ nanoparticles. Magnetic nanoparticles of $\text{La}_{0.9}\text{Sr}_{0.1}\text{MnO}_3$ manganite with mean particle sizes of 20 nm were prepared by the Microwave synthesis method. The crystal structure of the samples were analyzed, using X-ray diffractometer with Cu- α (0.154 nm) radiation. The morphology of the samples was characterized by a scanning electron microscope (FESEM). Magnetic dynamics of the samples was studied by the measurement of ac magnetic susceptibility versus temperature and frequency. The XRD pattern along with Rietveld analysis indicates that the samples are nearly single phase. By fitting the experimental data with Vogel-Fulcher law, the relaxation time, characteristic temperature, magnetic anisotropy energy and effective magnetic anisotropy constant have been estimated.

PJ01

Magnetotransport properties of anisotropic $\text{Co}(\text{tCo})/\text{Au}(\text{tAu})$ multilayers

Conrad Rizal¹, Parshu R. Gyawali² and Ramesh K. Pokharel³
¹ *Electrical and Computer Engineering, University of British Columbia, Canada*
² *Laboratory for Nanospintronics and Nanoelectronics, Catholic University of America, USA*
³ *Electrical and Communication Engineering, Kyushu University, Japan*

Artificially tailored Co/Au multilayers have been the subject of intense research in search of novel properties for potential applications [1] [2]. Earlier, we reported various components of giant magnetoresistance (GMR) effects and correlated them with microstructure of the isotropic multilayers [2]. In this work, we have investigated the effects of incident angle of deposition and magnetic annealing on GMR and magnetic properties of anisotropic Co/Au multilayers as the layer thicknesses of Co and Au are changed. We have investigated physical mechanisms responsible for various MR effects and correlated them with the existing models. The multilayers deposited at an oblique incident angle of 45 degree exhibited strong magnetic anisotropy. The maximum MR ratio is found to be 2.1 %. The transverse MR effect is always found to be larger than the longitudinal MR effect. These multilayers have been considered potential in developing biomagnetic technology.

[1] E. T. Papaioannou et al. 'Magnetic, magneto-optic and magnetotransport properties of nanocrystalline Co/Au multilayers with ultrathin Au interlayers,' J. Nanosci. Nanotechnol, vol. 8, pp. 4323-4327, 2008. [2] C. Rizal, 'Study of magnetic anisotropy and magnetoresistance effects in ferromagnetic Co/Au multilayer films,' J. Magn. Magn. Mater., vol. 310, pp.646-e648, 2007.

PJ02

The new type of current and spin polarization oscillations

Alexander I Kopeliovich and Pavel V Pyshkin
theoretical physics, B.Verkin Institute for Low Temperature Physics and Engineering of the National Academy of Sciences, Ukraine

In our work we found new type of spin polarization and current oscillations in conducting rings with inhomogeneous magnetic properties. In case of hydrodynamic electron transport (when frequency of electron-electron collisions is more than frequency of collisions that does not conserve momentum of electrons) we obtained spin hydrodynamics equations for non equilibrium electron spins when the electron spectrum was spatially inhomogeneous. We showed that in case of close conductor these equations had non zero solution in form of "spin pendulum" oscillations, i.e. oscillations of full current and spin polarization with frequency determined by characteristics of magnetic inhomogeneity. We found own oscillations of electron system in conducting ring consisting of two parts with different magnetic properties. For example it could be realized by connecting DMS and NMS conductors into a ring and placing it in magnetic field. We used equations similar to well-known two-current model and we showed that conductance of this system as a function of external EMF frequency had one maximum in hydrodynamic regime and this case was conform to 'spin pendulum', and conductance had many maximums in a case of ballistic regime. These maximums vanished when magnetic properties of parts of the ring were identical.

PJ03

Pressure-enhanced giant magnetoresistance in Fe/Cr magnetic multilayers

Gendo Oomi*
Kurume Institute of Technology, Japan

Pressure-enhanced Giant Magnetoresistance in Fe/Cr Magnetic Multilayers G Oomi1),S.Higashihara2),K. Suenaga2),K.Saito3),S.Mitani3) and K.Takanashi4) 1)Kurume Institute of Technology,Kurume,Fukuoka,Japan 2)Department of Physics,Kyushu University,Fukuoka,Japan,3)Institute of Materials Research,Tohoku University,Sendai,Japan The giant magnetoresistance(GMR) of Fe/Cr magnetic multilayers has been measured under high pressure at low temperatures. It is found that the GMR on the second peak samples is enhanced strongly by applying pressure:the magnitude of GMR becomes twice at 2 GPa compared with the value at ambient pressure.The saturation magnetic fields of these samples decreases with increasing pressure.However the GMR of the first peak samples decreases with increasing pressure and the saturationfields increases with pressure. These sharp differences in the behaviour against pressure will be discussed phenomenologically.

PJ04

Spin current-induced by sound wave

Igor Ivanovich Lyapilin
Institut Metal Physics RAS, Russia

In recent years, increased interest in studying the effects that arise in response to spin degrees of freedom of electrons, when the external perturbation acts on the kinetic degrees of freedom. As rule, the external perturbation (electric field) directly affects only the kinetic degrees of freedom of electrons and through spin-orbital interaction is transferred to the spin subsystem. There are other ways of influencing the system of conduction electrons, which are also reflected in the response of the spin degrees of freedom. So, in the ferromagnetic metals temperature gradient leads to the spin Seebeck effect. It is interesting to consider the mechanisms of interaction with external fields, in which the energy of the external field is transmitted simultaneously in both electronic subsystems (kinetic and spin). An example of such interaction is the interaction of conduction electrons with the field of sound waves. We studied the evolution of the electronic system for their interaction with the field of sound wave analysis of the conditions of occurrence and the the responce of the spin subsystem in a constant magnetic field. It is shown that in this case the longitudinal sound wave propagation arises transverse spin current, which has a resonant character.

PJ05

Enhancement of magnetocaloric width in $\text{La}_{2/3}\text{Ca}_{1/3}\text{MnO}_3$ compounds with remain the composition ratio between Mn^{3+} and Mn^{4+}

Qing Ji and Xiaoshan Wu*
Physics, Nanjing University, China

Large magnetic entropy in a relative narrow transition temperature in manganites has been reported. To explore the enhancement of transition temperature width with large magnetocaloric properties, we here designed the samples with the same composition ratio of Mn^{3+} and Mn^{4+} , and the same averaged radius at each lattice sites, which we previously used to find the roles of the local Jahn-Teller distortion on the magnetic properties in manganites. Here, Y and Sr are used together to replace for La and Ca in $\text{La}_{2/3}\text{Ca}_{1/3}\text{MnO}_3$ (i.e., ABO3) to remain the average radius and the average valance at A-site. Results show that the averaged unit cell lattice parameters are unchanged. The ferromagnetic-to-paramagnetic transition temperature T_c increases abruptly owing to the increase of the competition between σ_2 and double-exchange interaction resulting from Mn-O-Mn bond angle. The disordered distribution of cations at A-site broaden the phase transition temperature range (~T~10K or more) with large magnetic entropy of $\Delta\text{SM}=1.3 \text{ J/Kg K}$, which may be used as a promising candidate for magnetic refrigerant near room temperature.

PJ06

Output voltage calculations in double barrier magnetic tunnel junctions with asymmetric voltage behavior

Artur Useinov, Jurgen Kosel and Aurelien Manchon
King Abdullah University of Science and Technology, Saudi Arabia

We studied the asymmetric voltage behavior of the tunnel magnetoresistance (TMR) for single and double barrier magnetic tunnel junctions (S&DMTJ) in range of a quasi-classical tunneling model. Numerical calculations of the TMR-V curves, output voltages and I-V characteristics for the negative and positive applied voltages were carried out using MTJs with CoFeB/MgO interfaces. Asymmetry is explained by different values of the minority and majority Fermi wave vectors for the left and right sides of the tunnel barrier, which can arises due to different annealing regimes. Electron tunneling in DMTJs was simulated in two ways: (I) Coherent tunneling, where the DMTJ is modeled as one tunnel system and (II) consecutive tunneling, where the DMTJ is modeled by two SMTJ connected in series. We found that DMTJs, in range of model I, the output voltage peaks will be shifted into the region of low voltages. For the model II, we found that, in order to provide symmetric output voltage branches in DMTJ, the conditions of equal Fermi vectors ratios have to be fulfilled for the left and right magnetic layers while ratio in the middle layer can be different.

PJ07

Spin-current manipulation by domain wall motion in the non-local spin valve

Ryoko Sugano¹, Masahiko Ichimura¹, Saburo Takahashi² and Sadamichi Maekawa³
¹ *Central Reserach Laboratory, Hitachi, Ltd., Japan*
² *Institute for Materials Research, Tohoku University and CREST-JST, Japan*
³ *Advanced Science Research Center, Japan Atomic Energy Agency and CREST-JST, Japan*

A spatially- and time-dependent magnetic spin texture exerts a spin-dependent force on conduction electrons[1]. In particular, spin-motive force generated by a domain wall motion has been theoretically investigated and experimentally observed by detection of electric voltage[2,3]. The spin-dependent field generated by spin-motive force is also expected to directly affect the non-equilibrium magnetization such as spin accumulation. In order to study the effect of the spin motive force on the spin accumulation in a lateral non-local spin-valve (NLSV) structure, we treat the NLSV device attached with a magnetic wire. The device consists of spin injector F1 and detector F2 strips bridged by a non-magnetic strip N and the magnetic wire is attached on N through the insulating layer in-between two magnetic stripes. A domain wall is introduced into F3 and driven by external magnetic fields. The spin-dependent field drives the pure spin current flowing in the N-channel. This effect can be detected as increase or decrease in the nonlocal spin-accumulation signals depending on the domain wall motion. We evaluated the spin-dependent field based on the LLG approach and calculate the spatial distribution of spin/charge current of this NLSV by applying a finite element method in three-dimensions.

[1] S. Barnes and S. Maekawa, Phys. Rev. Lett. 98, 246601 (2007). [2] S. A. Yang et al., Phys. Rev. Lett. 102, 067201 (2009). [3] P. N. Hai et al., Nature 458, 489 (2009).

July 9 (Mon)

July 9 (Mon)

PJ08

The study of microwave assisted magnetization reversal via spin pumping

Sankha Subhra Mukherjee, Siddharth Rao, Praveen Deorani, Jae Hyun Kwon, Charanjit Singh Bhatia and Hyunsoo Yang*
ECE, National University of Singapore, Singapore

There has been a significant interest to switch high coercivity magnetic bits for the future magnetic media by lowering the coercivity during the writing process. MAMR is a popular method of reducing the coercivity. We present a novel method of studying MAMR via spin pumping and the inverse spin Hall effect (ISHE). In this method, a Pt layer was placed in contact with a ferromagnetic (Py) layer, and an rf signal was applied to the Py via a coplanar waveguide during loop measurements. Due to the presence of the rf power, magnetization dynamics in the Py layer pumps spin in the adjacent nonmagnetic Py layer, which creates a measurable dc voltage across the Pt due to the ISHE. The measured signal is of the order of several microvolts and thus does not affect the magnetization by any significant amount. It also effectively decouples the input rf input from the dc output. The coercivity can be easily detected by the field at which there is a change in the polarity of the measured voltage. The coercivity as a function of the applied rf power is studied.

PJ09

Contributions of domain walls on large magnetoresistance effect in ultrathin TbFeCo wires

Bang Do and Hiroyuki Awano
Toyota Technological Institute, Japan

Perpendicular anisotropy magnetic materials such as TbFeCo are expected to introduce large effectivity of spin-transfer torque and high domain wall (DW) motion speed as well as high magnetoresistance (MR) values. We investigated the size dependence of MR effect in TbFeCo wires. The 80-µm-length and different widths (1 to 80 µm) of Tb₂₀Fe₆₈Co_{7.2} wire-patterns were designed by using electron beam lithography technique. The Tb₂₀Fe₆₈Co_{7.2} films with different thicknesses of 6, 18 nm were grown by RF sputtering. It is found that MR values are strongly depend on injection current for all applied fields. Large MR values which up to 100% were observed at a low bias current and depend on DW structure inside the TbFeCo wires. On the other hand, the MR values rapidly reduced at large bias currents which induce magnon and phonon scattering effects. The introduction of DWs in a magnetic wire causes an increase in spin-dependent scattering inside the DWs and leads to an enhancement of resistivity expectedly. The well defined and controllable number of DWs inside magnetic nanowires will expectedly introduce a new technique to obtain high and multi-level MR values as well as high potentials on future magnetic devices.

PJ10

First-principles study of conductivity tensor in transition metals and alloys

Yohei Kota* and Akimasa Sakuma
Department of Applied Physics, Tohoku University, Japan

Spin-orbit interaction which is a relativistic correction to electron motion influences the transport properties, so the resistance anisotropy and Hall effect appear in conductivity tensor. In the present work, we calculate the conductivity tensor of transition metals and alloys in first-principles by the Fermi-surface term of Kubo-Streda formula. To calculate the conductivity tensor and electronic structure with spin-orbit interaction, we employ the tight-binding linear muffin-tin orbital method based on the local spin-density approximation [1]. The substitution disorder of alloys is treated using the coherent potential approximation. The obtained anomalous Hall conductivity, anisotropic magnetoresistance ratio, and also normal resistivity in ferromagnets such as Fe-Co and Fe-Ni as a function of the alloys composition are quantitatively consistent with the available experimental measurements in terms of their magnitude and sign. In particular we find that the Hall resistivities reveal the nontrivial behavior against the magnetization which can be varied by the modification of the composition ratio. Furthermore, the intrinsic and extrinsic contribution of the Hall conductivity is comparable in these alloys systems. Also we show the calculation results about the spin Hall conductivity of nonmagnetic compounds obtained in similar frameworks.

[1] I. Turek, et al., *Philos. Magaz.* 88, 2782 (2008); I. Turek, et al. *Phys. Rev. B* 65, 125101 (2002).

PJ11

Magnetoresistance of CoFe/Pt nano-contacts

Muftah Al-mahdawi* and Masashi Sahashi
Department of Electronic Engineering, Tohoku University, Japan

Using an alumina-based Nano-Oxide Layer (AlO_xNOL) between with many nano-holes between two ferromagnets [1] has gained more interest in recent years both in their fundamental physics of spin-scattering off the confined domain-walls and in their applicability for next-generation hard-disk-drive reading heads. Also, spin-torque driven oscillations of the confined domain-walls has been reported [2]. Following the report by [3] that Pt is magnetized at the interface with Co, we examined the insertion of AlO_xNOL between the Co-rich Co₉₀Fe₁₀ and Pt. Film stack was (in nm): Underlayer/Co₉₀Fe₁₀ 3/AlO_xNOL/Pt 2/cap. It was deposited using ion-beam sputtering and dc magnetron sputtering deposition. AlO_xNOL was prepared using Ion-Assisted Oxidation (IAO) process[1]. IAO process forms direct nano-contacts (NC) in NOL between the CoFe and Pt (1~2 nm in diameter, with <1% areal density). One film was pin-annealed in a 10 kOe field at 270°C for 1.5 hours and the other was left as is. Magnetization curve was measured using VSM at room-temperature and showed only the curve of CoFe. Current-In-Plane Tunneling (CIPT) at room-temperature showed that CPP RA product were around 0.24 Ωµm² for both films, and MR ratio was 3% (as-depo film) and 5% (pin-annealed film). Further discussion and data will be presented.

[1] M. Takagishi et al., *Journal of Applied Physics*, vol. 105, no. 7, 2009. [2] H. Suzuki et al., *Journal of Applied Physics*, vol. 105, no. 7, 2009. [3] M. Suzuki et al., *Physical Review B*, vol. 72, no. 5, p. 054430, 2005.

PJ12

Inversion of magenetoresistance in La_{1-x}Sr_xMnO₃/Nb-doped SrTiO₃/CoFe junctions

Kenji Ueda*, Katsunori Tozawa, Keita Sakuma, Naoto Fukatani, Tetsuya Miyawaki and Hidefumi Asano
Graduate school of engineering, Nagoya University, Japan

Understanding of the spin transport thorough ferromagnet/semiconductor interfaces is a critical issue to realize novel spintronic devices such as spin transistors. Specially, spin transport in degenerated semiconductors, which becomes metallic by heavy doping, is important for avoiding conductivity mismatch problems. In this study, magnetic junctions using degenerated semiconductors, Nb-doped SrTiO₃ (Nb-STO), as intermediate layers were fabricated. XRD measurements indicate 15mol% Nb-STO and La_{0.7}Sr_{0.3}MnO₃ (LSMO) films were epitaxially grown on MgO substrates (MgO(001) [100]/Nb-STO(001)[100]/LSMO(001)[100]). In the hysteresis curves of the LSMO/Nb-STO/CoFe at 4.2 K, two step magnetization correspond to the Hc of LSMO and CoFe were observed. The junctions using the trilayers showed magnetoresistance (MR) of ~5 % at 4.2 K. The sign and the magnitude of the MR were changed depending on the thickness of Nb-STO. Typically, positive MR of ~2% for 10 nm and negative MR of ~1% for 15 nm were observed. The origin of the MR is under investigation, however we consider these behaviours can be explained by regarding the trilayers as magnetic tunnel junctions with double tunnelling barriers (FM/I/NM/I/FM), which show oscillation of MR [1]. The depletion layers (~2 nm) at the interface between Nb-STO and ferromagnets seem to be behaved as insulative barriers in the junctions.

[1] Y. Yuasa et al., *Science* 297 (2002) 234.

PJ13

Spin transfer torques in antiferromagnets

Hamed Ben Mohamed Saidaoui¹, Aurelien Manchon^{2*} and Xavier Waintal³
¹ Physical Science and Engineering, King Abdullah University of Science And Technology KAUST, Saudi Arabia
² Physical Science and Engineering, King Abdullah University of Science And Technology KAUST, Saudi Arabia
³ Departement de Physique, SPSMS-INAC-CEA, France

Current-driven magnetization switching through spin transfer torque [1] has been widely studied in ferromagnetic (F) spin-valves [2,3]. Recently, Nunez et al. [4] theoretically showed that spin-valves based on antiferromagnetic (AF) electrodes also display outstanding spintronics properties such magnetoresistance and spin torque. Whereas the nature of current-driven torque has been theoretically examined in AF spin-valves [6,7], promising experimental results have been obtained on F/N/F/AF spin-valves structures (F is a ferromagnet and N is a normal metal) [5]. However, the microscopic origin of the spin torque between F and AF layers has not been addressed. In the present study, we apply non-equilibrium Green's function formalism in the tight-binding approach to investigate the spin transport in spin-valves consisting in N/AF/N/AF/N and N/F/N/AF/N. Whereas the spin torque calculated in the AF spin-valve is consistent with previous results [4,6,7], it presents significant differences in the latter structure (angular dependence, spatial distribution and relative magnitude between the in-plane and out-of-plane torque). Interestingly, we find that the AF layer exerts a torque on the F layer. Finally, we analyze the contribution of the in-plane torque and out-of-plane torques on the different sub-lattices of the AF layer and discuss the implications in terms of magnetization dynamics.

[1] J. C. Slonczewski, *J. Magn. Magn. Mater.* 159, L1 (1996) [2] E. B. Myers et al., *Science* 285, 867 (1999). [3] J. A. Katine et al., *Phys. Rev. Lett.* 84, 3149-3152 (2000). [4] A. S. Nunez, R. A. Duine, P. Haney and A. H. MacDonald, *Phys. Rev. B* 73, 214426 (2006). [5] Z. Wei, A. Sharma, et al., and M. Tsoi, *Phys. Rev. Lett.* 98, 116603 (2007). [6] R. A. Duine et al., *Phys. Rev. B* 75, 014433 (2007) [7] Yuan Xu, Shuai Wang, and Ke Xia, *Phys. Rev. Lett.* 100, 226602 (2008).

PJ14

Domain wall configuration and magneto-transport properties in dual spin-valve with nanoconstriction

Byong Sun Chun¹, Chan Yong Hwang¹, Han Chun Wu², Mohamed Abid³, Su Jung Noh⁴ and Young Keun Kim⁴
¹ Korea Research Institute of Standards and Science, Korea
² Trinity College Dublin, Ireland
³ Ecole Polytechnique Federale de Lausanne/IPMC, Switzerland
⁴ Korea University, Korea

In this work, we use a synthetic antiferromagnet-based dual spin-valve (SAF-DSV) structure (i.e. the SV structure is doubled symmetrically with respect to the FM) and present the effect of the direction of the applied magnetic field with respect to nanoconstriction shapes on the magneto-transport properties including domain wall (DW) configuration and reversal process. We can tune the DW configuration and its reversal process from a vortex to a transverse type by changing the direction of applied magnetic field respect to the nanoconstricted SAF-DSV. When the field is applied in the perpendicular direction to the nanoconstricted SAF-DSV, the perpendicular magnetic moments are developed due to the transverse magnetization reversal mode and result in a multistep switching process. This multi step switching process reflects the pinning and depinning of a DW at the nanoconstriction. Our results also show an asymmetric depinning field. We demonstrate, if nanoconstriction is asymmetric along its length, i.e. expansions from both sides of the neck into the two nanowires are not identical, and then an asymmetric energy barrier to domain wall propagation is formed. This is due to the difference in DW width, which leads to an asymmetry in the domain wall depinning forces.

PJ15

Giant magnetocaloric effect of Mn_{0.91}Ca_{0.09}As thin film on Al₂O₃ (0001)

Duong Anh Tuan¹, Cho Sunglae^{1*}, Dang Duc Dung², Shin Yooleemi¹ and Jeon Seung Mok¹
¹ Physics, University of Ulsan, Korea
² Physics, Depart of General Physics, School of Engineering Physics Hanoi University of Science and Technology., Viet Nam

The MnAs compound is promising to magnetocaloric effect (MCE) application [1]. It presents the first order phase transition from a ferromagnetic to paramagnetic ~ 318 K, which is accompanied by a structural transition from a hexagonal NiAs-type (α-MnAs) to orthorhombic MnP-type structure (β-MnAs) [2]. Recently, the room temperature giant magnetocaloric effect was obtained by substitution of Mn by Fe, Co, Cu or Cr in MnAs: Co-25 J/kgK at 4T, Cu-175 J/kgK at 5T, Cr and Fe-42 J/kgK at 5T [3-5]. However, there is less information about group II dopants such as Ca, Ba, and Sr in MnAs. In this work, we report the magnetism and transport properties of epitaxial Ca_{0.09}Mn_{0.91}As thin film on Al₂O₃(001) substrate. The RHEED and XRD results indicated that film were epitaxially grown on Al₂O₃(0001). The temperature dependent resistivity showed metallic and the temperature dependent magnetoresistance at 7 kOe showed a peak around 325K. The negative anomalous Hall effect was observed in Hall measurement. The magnetic measurement indicates that the sample is ferromagnetic with TC was around 340K and display the giant magnetocaloric signal. The magnetization hysteresis loops exhibited the saturation magnetization (MS) was around 300 (emu/cm3) at 10K and 180 (emu/cm3) at 300 K.

[1] L. Daweritz, *Pep. Prog. Phys.* 69, 2581 (2006). [2] J. Mira et al., *Phys. Rev. Lett.* 90, 097203 (2003). [3] Wang et al., *Appl. Phys. Lett.* 97, 042502 (2010) [4] D. L. Rocco et al., *Appl. Phys. Lett.* 90, 242507 (2007). [5] C. S. Mejia et al., *Appl. Phys. Lett.* 98, 102515 (2011).

PJ16

Anomalous Hall effect of [Amorphous CoSiB/Pt] multilayer films

Hana Lee, Insung Park, Hyungjun Kim, Sungyong Kim, Youngkwang Kim, Hwayong Noh and Taewan Kim*
Sejong university, Korea

We have quantitatively investigated the Anomalous Hall effect (AHE) in [CoSiB/Pt] multilayer films. The [CoSiB/Pt] multilayers exhibited large Hall effect. In this study, we compared with the effects of the before and after of patterning. The [amorphous CoSiB 6A/Pt 14 A]n multilayers were deposited on SiO_x substrate with a 30 Å Pt and 50 Å Ta buffer layer at the room temperature using a DC magnetron sputtering system. Thereafter the sample was patterned into a hall bar with the line width of 10 µm. Hall effect measurements at room temperature were made up to 3 kOe with the applied magnetic field perpendicular to the film plane. The samples for the Hall effect measurement were prepared with a square geometry for the easy application of the Van der Pauw method to measure the Hall voltage of the samples. The applied current was 50µA ~ 1 mA and the measured Hall voltage was in the range of several mV.

PJ17

Spin transport phenomena through MgO/CuPc hybrid barrier in magnetic tunnel junctions

Yu Jeong Bae¹, Nyun Jong Lee¹, Tae Hee Kim^{1*}, Hyunduck Cho², Changhee Lee², Luke Fleet³, Atsumi Hirohata³, Yeong-ah Soh⁴ and Gabriel Aeppli⁴
¹ Physics, EWha Womans University, Korea
² School of Electrical Engineering and Computer Science, Seoul National University, Korea
³ Electronics, The University of York, United Kingdom
⁴ London Centre for Nanotechnology, United Kingdom

For realistic applications of organic spintronic devices, the investigation of the growth mechanism and electrical properties is of great importance to understand the spin transport phenomena in metal-organic hybrid systems. As the first step, we focused on surface morphology, growth mode, and thermal stability of thin Cu-phthalocyanine (CuPc) organic layers grown on metal surfaces covered with a few monolayer thick insulating films, such as MgO(001). Recent reports of achieving spin polarized tunneling across organic-inorganic hybrid barrier with significant magnetoresistance (MR) values at low temperature (< 10 K) led us to study the organics semiconductor (OSC) thin films for substituting highly performing inorganic barriers. Therefore, we investigated systematically the spin transport phenomena through the OSC CuPc barrier with and without MgO(001) layer as a function of CuPc thickness. An epitaxial Fe(001)/MgO(001) layer was utilized as a spin injection layer, while a polycrystalline Co film as a spin detector. Here, we observed, for the MgO/CuPc hybrid barrier with a total thickness of ~ 3 nm, the high MR (> 200 %) values at 77 K and ~ 10 % MR at 300 K in the Si(001)/MgO/Fe/MgO(001)/CuPc/Co hybrid tunnel junctions.

PJ18

Theoretical approach to spin-current absorption at an interface

Kazuhiro Tsutsui¹, Kazuhiro Hosono² and Takehito Yokoyama^{1*}
¹ Dept. of Physics, Tokyo Institute of Technology, Japan
² Dept. of Physics, Tokyo Metropolitan University, Japan

In the development of spintronic devices, techniques to detect spin currents efficiently are indispensable as well as the generation of spin currents. In general, the spin-current detection is demonstrated via the inverse spin Hall effect and the absorption of the spin current [1]. In this presentation, we theoretically examine the spin current induced by an inhomogeneous spin-orbit coupling due to impurities [2]. Using the Keldysh Green's function formalism, we propose analytical expressions of the diffusive spin currents under an external electric field and find a spin-current generation in the presence of both gradient of the spin-orbit strength and that of the external field. The resulting diffusive spin current indicates the absorption of the spin current at the interface between materials with different spin-orbit strengths, which is exemplified with an experimentally relevant setup.

[1] T. Kimura, Y. Otani, T. Sato, S. Takahashi, and S. Maekawa, *Phys. Rev. Lett.* 98, 156601 (2007). [2] K. Hosono, A. Yamaguchi, Y. Nozaki, and G. Tatara, *Phys. Rev. B* 83, 144428 (2011).

PJ19

Magneto-transport properties of Al₂O₃-doped Mn-Zn ferrites

Hyo-jin Kim and Sang-im Yoo*
Department of Materials Science and Engineering, Seoul National University, Korea

We report the magneto-transport properties of Al₂O₃-doped Mn-Zn ferrites prepared by the conventional solid state reaction. Various amounts of Al₂O₃ were doped to a pure Mn-Zn ferrite to have the nominal composition of (Mn_{0.8}, Zn_{0.2})_{1-x}Al_xFe₂O₄ (x = 0.03-0.1). Field dependency of magnetization was measured with a SQUID (superconducting quantum interference device) magnetometer, and low field magnetoresistance (LFMR) was also measured with the SQUID magnetometer using an external current source and voltmeter. The X-ray diffraction analyses revealed that all Al₂O₃-doped Mn-Zn ferrites of the spinel structure were a pure phase without the second phase. From the transport measurements of our samples in the temperature region of 100~300 K, it was found that with the addition of the Al₂O₃ dopant the resistivity level of the pure Mn-Zn ferrite was abruptly dropped over four orders of magnitude and further the LFMR ratio was greatly improved. High LFMR ratio over 1.7% at 300 K in 0.5 kOe was achievable from 3mol% Al₂O₃-doped Mn-Zn ferrite without an appreciable increase in its resistivity. Detailed effects of the Al₂O₃ dopant on the microstructures, magnetic and magnetotransport properties of the Mn-Zn ferrite will be presented for a discussion.

PJ20

Current induced fluctuation of switching fields in Co/Pd nanowires
Mahdi Jamali, Xuepeng Qiu, Kulothungasagan Narayanapillai and Hyunsoo Yang*
Electrical and Computer Engineering, National University of Singapore, Singapore

Current induced effective magnetic fields in a thin metallic film of a ferromagnetic material sandwiched by two nonmagnetic materials have been studied intensively due to its potential applications for the magnetic random access memory [1, 2]. There is a controversy about the origin of the effective field such as the Rashba effect [3] or spin torque induced by the spin Hall effect [4]. We have recently observed current induced effective fields in nanowires made of Co/Pd multilayer [5]. The further investigation of the switching fields of nanowires reveals fluctuation in the switching fields upon an injection of different current densities. We have applied current pulses with a width of 2 ns and repetition of less than 1 Hz to minimize the Joule heating effect. At low current densities ($J < 10^{11}$ A/m²) there is a fluctuation in the switching field of the nanowire. For a certain value of the input current, the switching field of the Co/Pd nanowire increases (>6%). Furthermore, the switching fields in the positive and negative fields are not the same. The relative angle between the sample and magnetic field has changed and the effect of the angle on this fluctuation has been studied.

[1] I. M. Miron, K. Garello, G. Gaudin, P. J. Zermatten, M. V. Costache, S. Auffret, S. Bandiera, B. Rodmacq, A. Schuhl, and P. Gambardella, *Nature* 476, 189 (2011). [2] T. Suzuki, S. Fukami, N. Ishiwata, M. Yamanouchi, S. Ikeda, N. Kasai, and H. Ohno, *Appl. Phys. Lett.* 98, 142505 (2011). [3] I. M. Miron, G. Gaudin, S. Auffret, B. Rodmacq, A. Schuhl, S. Pizzini, J. Vogel, and P. Gambardella, *Nat. Mater.* 9, 230 (2010). [4] <http://arxiv.org/abs/1110.6846>. [5] K. Narayanapillai, M. Jamali, and H. Yang, *MMM conference, Arizona* (2011).

PJ21

Role of structural inversion asymmetry on current-induced effective field in perpendicular magnetized trilayers
Xuepeng Qiu, Kulothungasagan Narayanapillai and Hyunsoo Yang*
Electrical and Computer Engineering, National University of Singapore, Singapore

The fact that a current pulse can switch the magnetic moment of a perpendicular magnetized nanodot has attracted much attention for the next generation spintronic devices [1]. However, the physical origin of this effect is still under debate. Here we report the pulse delta measurements in perpendicular magnetized substrate/2 MgO/ Pt_{0.8} CoFeB, MgO (sample A) and substrate/2 MgO_{0.8} CoFeB, Pt (in nm) micro-sized hall bar samples with opposite structural inversion asymmetry (SIA). For both structures, when the magnetic field applied along the current direction tilted off-plane by 2°, positive (negative) current induces a downward (upward) effective field with positive magnetic fields and the effective field direction switches with negative magnetic fields. The effective field is around 2,388 Oe per 10¹² A/m² in the sample A. For the other structure, the effective field shows a nonlinear correlation with the intensity of current. With small in-plane external fields, the magnetization can be switched by pulse current and the switching hysteresis was the same in the two structures. Our results suggest that the main contribution of the current induced effective field arises from the spin Hall effect rather than the Rashba or other SIA related effects.

[1] Ioan Mihai Miron, Kevin Garello, Gilles Gaudin, Pierre-Jean Zermatten, Marius V. Costache, Stephane Auffret, Sebastian Bandiera, Bernard Rodmacq, Alain Schuhl and Pietro Gambardella, *Nature*. 476, 189 (2011)

PJ22

Characterization of mechanically milled Cu-Co powder by 3D-FIB and atom probe tomography : effect of oxidation on the magnetoresistance
Julien Bran, Rodrigue Larde, Malick Jean and Jean-marie Le Breton*
Groupe de Physique des Materiaux - UMR 6634, CNRS - Universite de Rouen, France

The Giant MagnetoResistance (GMR) effect discovered in 1988 [1] had inspired many researches on magnetoresistive materials. The resistance of the device is reduced with the application of a magnetic field and it is due to the spin dependent scattering effect. However, an inverse effect has been observed after an oxide phase introduction by Khan et al. [2]. This effect appears at low magnetic field and could be interesting for improving the sensitivity of magnetoresistive devices. In our study, a Cu₈₀Co₂₀ powder was elaborated by mechanical alloying under ambient atmosphere to investigate the oxide formation and its influence on magnetoresistive properties. 3D-Focused Ion Beam tomography (3D-FIB) and Atom Probe Tomography (APT) [3] were used to characterize our samples. It was shown with 3D-FIB that after 1h30 of milling, the powder exhibits a lamellar structure with micro-sized Co rich regions. The APT experiments have revealed that after 20h of milling 1/3 of Co atoms is oxidized leading to the formation of nano-sized CoO clusters embedded in a Cu₈₈Co₁₂ matrix. These results bring crucial informations to correlate the structural properties with magnetoresistive properties of the Cu-Co-O powder and to understand the influence of the nano-sized oxide clusters on the inverse magnetoresistance.

[1] M. N. Baibich, J. M. Broto, A. Fert, F. Nguyen Van Dau, F. Petroff, P. Etienne, G. Creuzet, A. Friederich, and J. Chazelas, *Phys. Rev. Lett.*, 61(21) (1988) 2472-2475. [2] H. R. Khan, A. Granovsky, M. Prudnikova, V. Prudnikov, F. Bruers, A. Vedyayev, A. Radkouskaya, *J. Magn. Magn. Mater.* 183 (1998) 379-386. [3] D. Blavette, B. Decrochant, A. Bostel, J. M. Sarrau, M. Bouet, and A. Menand, *Review of Scientific Instruments*, 64(10) (1993) 2911-2919.

PJ23

Effect of pressure on magnetotransport properties in Fe/MgO granular films
A. Garcia - Garcia¹, J. A. Pardo², P.A. Algarabel^{1*}, Z. Arnold³, J. Kamarad³ and M. R. Ibarra²

¹ ICMA, Universidad de Zaragoza-CSIC, 50009 Zaragoza, Spain
² INA, Universidad de Zaragoza, 50018 Zaragoza, Spain
³ Institute of Physics AS CR, 162 53 Praha 6, Czech Republic

A special example of granular thin films is the discontinuous metallic and insulator multilayers (DMIMs) consisting of metallic layers with different degrees of discontinuity intercalated between insulating layers. However, the studies about the effect on the magneto-transport properties of the hydrostatic pressure are scarce[1]. In this work we report the effect of hydrostatic pressure on the resistance and magnetoresistance of a DMIM of nominal composition [Fe(t=0.7nm)/MgO(t=3 nm)]₁₅ ,deposited on a substrate of coming glass. The DMIM has been characterized previously showing a superparamagnetic behaviour [2]. The resistivity has been measured at room temperatures with hydrostatic pressure (Ph) up to 7 Kbar. The resistivity decreases linearly with pressure, indicating an increase in conduction via tunneling. The value of the coefficient, (1/ρ)dp/dPh =-3.9 10-2 kbar-1 is higher than the value obtained in other granular films. This result implies that the electronic state of the DMIM is near the percolation threshold. Magnetoresistance (MR) isotherms have been measured at room temperatures for Ph=1bar and Ph=7Kbar. At the maximum applied magnetic field (3KOe) the MR increases from 0.6% at ambient pressure to 1.1% at 7 Kbar. This result will be explained due to the reduction of the tunnel barrier induced by the hydrostatic pressure.

[1] G. Oomi, Miyawaga H., Sakai T., Saito K., Takanashi K., and Fujimori Hl. *Physica B* 284 1245 (2000) [2] A. Garcia-Garcia, A. Vovk, J. A. Pardo, P. Strichovanec, C. Magen, E. Snoeck, P. A. Algarabel, J. M. De Teresa, L. Morellon, and M. R. Ibarra *J. Appl. Phys.* 105, 063909 (2009)

PJ24

Measurement of anomalous nernst effect in [CoSiB/Pt] multilayer films
Ozgur Kelekci¹, Ha Na Lee², K. J. Min², H. M. Waseem Khalil¹, Tae Wan Kim² and Hwayong Noh^{1*}
¹ Physics Department and Graphene Research Institute, Sejong University, Korea
² Department of Advanced Materials Engineering, Sejong University, Korea

Recently, a new research field taking advantage of both spintronics and thermoelectronics, called spin caloritronics, has started to attract a great deal of attention [1]. In contrast to the Anomalous Hall Effect driven by electrical currents, Anomalous Nernst Effect includes combination of thermal and spin transport driven by a temperature gradient in ferromagnets. We have investigated Anomalous Nernst Effect in [CoSiB/Pt] multilayer films with perpendicular magnetic anisotropy. The layer structure of samples was SiO₂/Ta₅₀Pt₅₀(CoSiB_xPt_{4-x})_n. Standard Hall bars were patterned on the samples. Additionally, heating element was also patterned on the samples in order to apply temperature gradient. Nernst effect measurements were made up to 1.5 kGauss with the applied magnetic field perpendicular to the film plane. We obtained significant Nernst voltages (VN) by applying temperature gradient ∇T to the samples. Nernst voltage exhibited similar characteristic as AHE voltage due to the spontaneous magnetization. Samples with different number of [CoSiB/Pt] multilayers were measured and compared. VN increased with increasing number of layers. Dependence of VN on the heating power (P) and the distance from the heating element (d) have been investigated. We have extracted [VN] α [P] and [VN] α [1/d] dependencies from the measured samples.

[1] G. E. W. Bauer, A. H. MacDonald, S. Maekawa, *Solid State Commun.*, 150, 459, (2010).

PJ25

GMR effect in Co-Cu microwires
Valentina Zhukova^{1*}, Rastislav Varga², Carlos Garcia³, Juanjo Del Val¹, Mihail Ipatov¹ and Arcady Zhukov⁴
¹ Dpto. de Fisica de Materiales, UPV/EHU, Spain
² Inst. Phys., Fac.Sci., UPJS, Slovakia
³ Dept Phys, Bogazici Univ, Turkey
⁴ Dept. de Fisica de Materiales, UPV/EHU San Sebastian and IKERBASQUE, Basque Foundation for Science, Bilbao, Spain

Granular materials exhibiting giant magnetoresistance (GMR) effect attracted considerable attention. For obtaining of the granular structures, melt spinning technique allowing rapid quenching from the melt is quite suitable. During last years considerable attention has been paid to the studies of glass-coated microwires produced by Taylor-Ulitovski technique allowing to achieve high quenching rate and producing amorphous, nanocrystalline, microcrystalline or even granular thin microwires. In this paper, we studied magnetic properties and GMR effect of Co^xCu_{100-x} (10≤x≤30 at%) microwires and observed considerable magnetoresistance (MR), ΔR/R. For Co₁₀Cu₉₀ microwires, ΔR/R increases when the temperature decreases, exhibiting negative MR, tending to saturate in high magnetic fields, H. On the other hand, for Co₃₀Cu₇₀ samples ΔR/R(H) dependences showed non-monotonic behavior, exhibiting ΔR/R increase with H at low H-values (up to 5 KOe) and also considerable GMR effect. X-ray diffraction (XRD) results reveal that the structure of the metallic core is granular with two phases: the main one, fcc Cu (lattice parameter 3.61 Å) and fcc α-Co (lattice parameter 3.54 Å) which is present in microwires with higher Co content. In the case of low Co content, XRD indicates that Co atoms are distributed within the Cu crystals.

PJ26

Domain wall quantum interferometer
John Eves, N. Grisewood and H. B. Braum
School of Physics, UCd, Ireland

Ferromagnetic nanosized toroidal rings have recently attracted much interest as potential storage elements for conventional bit storage. Here we consider quantum transport properties of such rings, and their dependence on the intrinsic domain structure of the ferromagnetic materials. Considering samples with realistic anisotropies we study the propagation of conduction electrons in the background of nontrivial domain configurations. Due to sd-coupling, the propagating electrons experience a domain dependent phase shift due to Berry's phase. Using exact solutions for domain configurations on a ring we use a path integral approach to determine exactly how this phase depends on the domain configuration in the ring. We find that the transmission through the ring can be controlled by the relative position of the domain walls, giving rise to a novel domain wall interferometer.

PJ27

Synthesis and magnetic properties of trilayer NiFe/Bi/NiFe films
Konstantin Patrín¹, Viktor Yakovchuk¹, Gennady Patrín² and Stanislav Yarikov²
¹ Institute of Physics of Siberian Branch of Russian Academy of Sciences, Russia
² Siberian Federal University, Russia

Earlier, it was found [1] that the bismuth spacer formation influences essentially the system magnetization. The shape of m(H) curve is changed with bismuth spacer thickness increasing. In particular, the test film with tBi = 0 has the narrow hysteresis loop and magnetization curve of a ferromagnetic type. For the films with tBi ≠ 0 the magnetization curves are typical for films possessing either by intra-layer anisotropy or by antiferromagnetic interlayer coupling. Since anisotropy is not experimentally observed, we attribute such a behavior to the presence of interlayer antiferromagnetic exchange. The investigations of electron magnetic resonance were made in NiFe/Bi/NiFe films. It was established that the magnetic resonance spectrum consists of solitary line for films with tBi = 0 nm and tBi = 15 nm, whereas for films with intermediate value of semi metal spacer the spectrum is superposition of two lines. Theoretical treatment of temperature dependences of resonance fields gives conclusion that the interlayer coupling depends on both bismuth interlayer thickness and temperature. Also, the magnetoresistivity of order of percent units and dependence of its value on thickness of bismuth spacer were found in these films at helium temperatures [2].

[1] G.S. Patrín, V.Yu. Yakovchuk, D.A. Velikanov. *Phys. Lett. A*, 363, 164 (2007) [2] G. S. Patrín, V. Yu. Yakovchuk, D.A. Velikanov, K.G. Patrín, and S.A. Yarikov. *Bull. Russ. Acad. Sci. Phys.*, 76, 177 (2012)

PJ28

A study on the pulsed laser deposited metallic spin valve structures
Sayak Ghoshal^{1*} and P. S. Anil Kumar²
¹ Physics, Indian Institute of Science, India
² Indian Institute of Science, India

It is envisaged that the conventional Spin Valve (SV) structures will be more advantageous over Tunneling Magneto-resistance (TMR) for the perpendicular magnetic recording due to the suitable RA product. Here Pulsed Laser Deposited (PLD) Spin Valve (SV) and Pseudo Spin Valve (PSV) samples are grown at room temperature with moderately high MR values using simple NiFe/Au/Co/FeMn structure. Although PLD is not a popular technique to grow metallic SVs because of its expected large intermixing of the interfaces, particulate formation etc., still by suitably adjusting the deposition parameters we could get exchange bias as well as more than 3% MR in the Current In Plane (CIP) geometry. Different SV and PSV samples are grown to study anisotropy effects, exchange coupling and exchange bias with anti-ferromagnet. Angular variation of the MR is also obtained which shows that the hard layer (Co) has a four-fold anisotropy in the NiFe/Co/Au/Co structures which becomes two-fold in presence of anti-ferromagnet. In this presentation, properties of these PLD grown SVs will be discussed in terms of the angular variation of MR, intermixing at the interfaces as well as details of exchange bias.

(1) S. Yuasa et. al. *J. Phys. D: Appl. Phys.* 40 R337 (2007) (2) Y. Sakuraba et. al. *Appl. Phys. Lett.* 94, 012511 (2009)

PJ29

Spin torque in a finite two-dimensional ferromagnet with Rashba interaction
Christian Ortiz, Xuhui Wang and Aurelien Manchon*
Physical Science and Engineering Division, King Abdullah University of Science and Technology, Saudi Arabia

The interaction between a ferromagnetic exchange coupling and a Rashba spin-orbit interaction has shown its potential in magnetization switching [1, 2]. For such a system, a coherent theoretical framework has been developed to study the coupled spin-charge diffusive dynamics [3]. Using finite element method, we numerically solve, in a two-dimensional (2D) electron system with appropriate boundary conditions, the generalized equations for the diffusive charge and spin dynamics. This numerical approach allows for an accurate description of the spin and charge dynamics (i.e. non-equilibrium accumulation and current) for a wide range of parameters beyond the limit of weak Rashba interaction [1,3]. The spatial profile of the spin accumulation exhibits a strong presence of a spin precession arising from both the s-d exchange and the effective Rashba field. Spin relaxations due to random magnetic impurities as well as the D'yakonov-Perel mechanism are embedded in the solution. We also discuss the diffusive dynamics and the spin torques in different regimes with respect to the magnitude of the Rashba spin-orbit interaction.

[1] A. Manchon and S. Zhang, *Phys. Rev. B*. 78, 212405 (2008); 79, 094422 (2009). [2] I. M. Miron, et al. *Nature (London)* 476, 189 (2011). [3] X. Wang and A. Manchon, *arXiv:1111.1216* (to appear on *Phys. Rev. Lett.*); *arXiv:1111.5466*.

PJ30

Spin transport of Py/Au/Py spin valves with different Au channel widths
Jang Hae Ku¹, Joonyeon Chang^{1*}, Hyun Cheol Koo¹, Jonghwa Eom², Suk-hee Han¹ and Gytuae Kim³
¹ Spin Convergence Research Center, Korea Institute of Science and Technology (KIST), Korea
² Department of Physics, Sejong University, Korea
³ Department of Electrical Engineering, Korea University, Korea

Most previous studies on spin injection and transport were dealt with one dimensional diffusive model and two-dimensional consideration has been neglected for simplicity [1-2]. However, all of the lateral spin valve devices experimentally demonstrated are fabricated based on thin film technology so that it is indispensable to have spatial distribution of spin current in a non-magnetic channel [1-2]. Actually, some of the experimental data can't be understood in terms of one-dimensional conduction model. Injected spin current usually produce inhomogeneous spin accumulation which appears to a different magnitude of spin signal (ΔR) depending on the position of voltage probes on the detector [3-4]. In this study, nonlocal spin valve (NLSV) measurements for lateral Permalloy(Py)/Au/Py spin valve devices with different Au channel widths were carried out in two viable voltage probe configurations. The larger channel width is at a fixed center to center channel length, the lower the magnitude of ΔR is in the NLSV, which is attributed to the increase in junction area and enhanced spatial distribution of spin accumulation. The voltage probe configuration strongly affects the spin valve signal owing to the non-uniform spin current distribution in lateral Au channel.

[1] M. Johnson, *Phys. Rev. Lett.* 70, 2142 (1993). [2] F.J. Jedema, A.T. Filip, and B.J. van Wees, *Nature* 410, 345 (2001). [3] T. Kimura, Y. Otani, and J. Hamrle, *Phys. Rev. B*. 73, 132405 (2006). [4] J. Ku, J. Chang, J. Eom, H. Koo, S. Han, and G. Kim, *phys. stat. sol. (b)* 244, No. 12, 4530 (2007).

PJ31

The effect of magnetic impurities in magnetic tunnel junction
Sungjung Joo¹, K.y. Jung¹, B.c. Lee², Tae-suk Kim¹, K.h. Shin¹, Mung-hwa Jung³, Jinki Hong¹ and K. Rhie^{4*}
¹ Department of Display and Semiconductor Physics, Korea University, Korea
² Department of Physics, Inha University, Korea
³ Department of Physics, Chonnam national University, Korea
⁴ Spintronics Device Research Center, Korea Institute of Science and Technology, Korea
⁵ Department of Physics, Sogang University, Korea

Magnetic tunnel junctions (MTJs) have been extensively investigated for more than a decade, not only because of potential applications such as next generation memory devices or high frequency spin oscillators, but also due to scientific interest. The physical properties of MTJs are very sensitive to the conditions of interface formation and, therefore, it is essential to understand the various influencing factors to control interface quality. The effect of oxidizing the ferromagnetic layer on tunneling magnetoresistance (TMR) is one of the most interesting problems in MTJs. The ferromagnetic layer in MTJs was oxidized with varying O₂ concentrations and the corresponding effect on spin-dependent transport was studied. As expected from our previous results for MTJs with an over-oxidized AlOx tunnel barrier, a partially oxidized ferromagnetic layer plays an important role in spin-dependent transport. As the temperature is lowered, the junction resistance increases dramatically and the TMR is strongly suppressed. Increasing the O₂ concentration enhances the increase of resistance and suppression of TMR. This work supports our previous conclusion that oxidizing the ferromagnetic layer generates localized magnetic moments, which act as a scattering center for spin-polarized tunneling electrons.

I. K.J. Rho, J.-S. Lee, K.B. Lee, J.-H. Park, J.Y. Kim, Y. Park, K. Kim, S. Joo, and K. Rhie, *Phys. Rev. B* 83, 172408 (2011). 2. K. Lee, S. Joo, J. Lee, K. Rhie, T.-S. Kim, W. Lee, K. Shin, B. Lee, P. Leclair, J.-S. Lee, and J.-H. Park, *Phys. Rev. Lett.* 98, 107202 (2007). 3. T.-S. Kim and D.L. Cox, *Phys. Rev. Lett.* 75, 1622 (1995).

July 9 (Mon)

July 9 (Mon)

PJ32

Effect of cobalt layer thickness on the magnetic and magnetoresistance properties of asymmetrical Co/Cu multilayers

Srikrishna Pandey, Pavel Nikolaev and Sivaram Arepalli*
Department of Energy Science, Sungkyunkwan University, Korea

A series of asymmetrical multilayer thin films of Co/Cu with a systematically varying cobalt layer thickness (tCo= 10, 15, 20, 30, 40 and 50 Å) was prepared by DC magnetron sputtering technique to study the effect of tCo on its magnetization and magnetoresistance properties. The XRD pattern of the multilayers showed the polycrystalline nature with texture (111). The magnetization measurements at different temperatures of the series showed that change in tCo leads to the change in magnetic anisotropy of the multilayers and thus change in coercive field (HC). The magnetoresistance measurements at different temperature of the series of multilayer showed a temperature dependent giant magnetoresistance (GMR) due to the inelastic scattering of electrons by phonons and magnons. Moreover, an asymmetry in GMR curves at low temperature was observed because of the asymmetrical (pseudo spin valve) structure of the multilayer.

PJ33

Current-induced motion of a transverse magnetic domain wall in the presence of spin Hall effect

Soo-man Seo¹, Kyung-whan Kim², Jisu Ryu², Hyun-woo Lee² and Kyung-jin Lee*
¹Materials Science and Engineering, Korea university, Korea
²Physics, Pohang University of Science and Technology, Korea

The electric manipulation of a domain wall (DW) in a magnetic nanowire is subject to the spin-transfer torque (STT) effect due to the coupling between local magnetic moments of the DW and spin-polarized currents [1]. Numerous studies on this subject have been performed to understand its fundamental physics [2] and to extend its potential to applications such as data storage and logic devices [3]. In this work, we study theoretically current-induced dynamics of a transverse magnetic domain wall in bi-layer nanowires consisting of a ferromagnet on top of a nonmagnet having strong spin-orbit coupling. Domain wall dynamics is characterized by two threshold current densities, J(WB) and J(REV), where J(WB) is a threshold for the chirality switching of the domain wall and J(REV) is another threshold for the reversed domain wall motion caused by spin Hall effect. The domain wall with a certain chirality may move opposite to the electron-flow direction with high speed in the current range J(WB) < J < J(REV) for the system designed to satisfy the conditions J(WB) > J(REV) and $\alpha > \beta$ where α is the Gilbert damping constant and β is the nonadiabaticity of spin torque. Micromagnetic simulations confirm the validity of analytical results.

[1] J. C. Slonczewski, *J. Magn. Mag. Mater.* 159, L1 (1996); L. Berger, *Phys. Rev. B* 54, 9353 (1996). [2] A. Yamaguchi et al., *Phys. Rev. Lett.* 92, 077205 (2004); M. Yamanouchi et al., *Nature (London)* 428, 539 (2004); M. Klaui et al., *Phys. Rev. Lett.* 94, 106601 (2005). [3] S. Parkin et al., *Science* 320, 190 (2008).

PJ34

Universal spin-hall effect in metallic thin films

Xuhui Wang¹, Jiang Xiao², Aurelien Manchon¹, and Sadamichi Maekawa^{3,4}
¹King Abdullah University of Science and Technology (KAUST), Physical Science and Engineering Division, Thuwal 23955-6900, Saudi Arabia
²Department of Physics and State Key Laboratory of Surface Physics, Fudan University, Shanghai 200433, China
³Advanced Science Research Center, Japan Atomic Energy Agency, Tokai 319-1195, Japan
⁴CREST, Japan Science and Technology Agency, Tokyo 102-0075, Japan

Spin-orbit interaction fills the academic and industrial pursuit for an electrical manipulation of spins. Fabricated using the state-of-art nanotechnology, semiconductor and metallic thin films embedded between two asymmetric interfaces in the presence of spin-orbit interaction have attracted intensive theoretical and experimental interest in recent years. Spin Hall effect [1], voltage-controlled spin precession [2] as well as the recently observed spin-orbit torque [3] all stem from a careful design of spin-orbit coupling in the bulk or at the interfaces. We predict a large spin-Hall conductivity due to interfacial spin-orbit interactions in an ultrathin normal metal film that is sandwiched by two insulators. While providing a confinement, the insulator/metal interfaces also serve as a source to the spin-orbit interaction due to inversion symmetry breaking. More interestingly, the interfacial spin-orbit coupling gives rise to a universal spin-Hall conductivity that is independent of microscopic details of the interfacial spin-orbit interaction and is predicted to be much larger than that induced by bulk impurities.

[1] Y. K. Kato, et al. *Science* 306, 1910 (2004). [2] H. C. Koo et al., *Science* 325, 1515 (2009) [3] A. Manchon and S. Zhang, *Phys. Rev. B*, 78, 212405 (2008); A. Chernyshov, et al., *Nature Physics* 5, 656 (2010); I. M. Miron, et al. *Nature (London)* 476, 189 (2011).

PK01

Controlling magnetic isolation and moment reversal of FePt (001) films by Cu capping nanoislands

D. H. Wei^{1*}, C. H. Chao¹ and Y. D. Yao²
¹Institute of Manufacturing Technology and Graduate Institute of Mechanical AND Electrical Engineerin, National Taipei University of Technology, Taiwan
²Institute of Applied Science and Engineering, Fu Jen University, Taiwan

We aimed to control the magnetic interaction of FePt(001) films by introducing Cu capping nanoislands for applications in magnetic recording and permanent magnets. Fe/Pt multilayers were prepared by e-beam evaporation onto MgO substrates, and the thickness of Cu capping layers was varied from 1 to 6 nm. Out-of-plane coercivity increases with increasing growth temperature, and the reduction of grain/domain size and intergrain interaction of FePt can be achieved. Cu could penetrate into FePt nanostructures along the grain boundaries and create a strain-energy modulation at the interface due to its lower surface energy. Studies of angular dependent coercivity show a tendency of a domain-wall motion shift toward rotation of reverse-domain type with Cu capping nanoislands. The intergrain interaction was confirmed from the Kelly-Henkel plot that indicated the strong exchange coupling between neighboring grains in pure FePt films, and the negative δM value was obtained while FePt films capped with Cu nanoislands.

PK02

Perpendicular magnetic anisotropy for annealed Co/Ir(111) ultrathin films

Wen-yuan Chan, Du-cheng Tsai, Cheng-hsun Chang and Jyh-shen Tsay*
National Taiwan Normal University, Taiwan

Compositions and magnetic properties of Co/Ir(111) ultrathin films thinner than 4 monolayers (ML) have been investigated. As the Co thickness increases to above 2 ML, magnetic hysteresis appears in both the longitudinal and polar configurations as revealed using surface magneto-optic Kerr effect (SMOKE) technique. After annealing treatments, the observations of the attenuation of Co LMM Auger signal and chemical shifts to lower kinetic energy show that Co atoms diffuse into the Ir(111) substrate. At higher temperatures, the Kerr intensities in both the longitudinal and polar configurations decrease due to the reduction of Co overlayer. At a temperature interval, magnetic hysteresis appears only in the polar configuration. This shows that the magnetic easy axis of Co/Ir(111) could be stabilized in the direction of the surface normal by thermal annealing treatments. By systematical investigations for Co/Ir(111) ultrathin films thinner than 4 ML, a magnetic phase diagram has been established. Several phases are observed, including a nonmagnetic phase, canted out-of-plane anisotropy and perpendicular magnetic anisotropy. On the top of the Co/Ir(111), the introduction of Ag overlayer shows an oscillatory behavior of the Kerr intensities. Possible mechanisms of the charge transferring, quantum well effects and completeness of the Ag layer are discussed.

PK03

Anomalous easy-plane magnetocrystalline anisotropy of compressive strained (La,Ba)MnO₃ films

Hong Zhu*, Jinzeng Tian, Lei Yang, Qingyong Duanmu, Lin Hao and Xiaoping Wang
Department of Physics, University of Science and Technologh of China, China

Magnetic anisotropy of manganite films is sensitive to the epitaxial strain. So far, in Ca- and Sr-doped manganite films, many authors reported that a lattice expansion induces easy magnetization in the corresponding direction. In this work, magnetocrystalline anisotropy of La_{0.67}Ba_{0.33}MnO₃ epitaxial films suffering large compressive strain on LaAlO₃ substrates (LBMO/LAO) has been investigated by using ferromagnetic resonance (FMR) technique. By mapping out the dependence of the FMR position on the angle between the applied magnetic field and crystallographic axes of the films, a large easy-plane anisotropy has been found in such compressive strained LBMO films, which is in contrast to the common tendency reported before. The excellent epitaxial crystallographic orientation gives rise to an observable fourfold symmetry of the in-plane anisotropy. The results are discussed by taking large tolerance factor and giant magnetostriction of Ba-doped manganites into account. In the phase diagram of temperature vs. tolerance factor for doped manganites, we noticed that LBMO has a larger tolerance factor but a lower Curie temperature than Sr-doped manganite, meaning that shrinkage of Mn-O-Mn bond length in LBMO is in favor of spontaneous magnetization, which in turn results in the anomalous easy-plane anisotropy in the compressive strained LBMO films.

PK04

Magnetic reversal of Co/Pt multilayer depending on Co thickness and annealing temperature

Seung-ha Yoon, Seungkyo Lee, Joonhyun Kwon, Junghyon Lee and B. K. Cho*
Materials Science and Engineering, Gwangju Institute of Science and Technology, Korea

Magnetic reversal behaviors in ferromagnetic thin films are continuously studied to achieve high performance of technological applications. Recently, CoPt multilayers and alloys have been an important issue in perpendicular magnetic anisotropy (PMA) applications. However, fundamental studies of the magnetic properties were not much presented. In this work, we present a magnetic reversal behavior of Ta(3.0 nm)/[Co(x nm)/Pt(1.0 nm)]x3 /Ta(1 nm) multilayers, when the Co thickness varied from 0.3 nm to 2.0 nm. The multilayers were deposited using DC magnetron sputter on Si/SiO₂ substrate, and annealed with various temperature after deposition. The magnetic and structural properties of the multilayers were measured using vibrating sample magnetometer (VSM) and x-ray diffraction (XRD) at room temperature. In addition, we observed the magnetic reversal behavior with magneto-optic Kerr effect (MOKE) microscope system, capable time-resolved domain observation.

PK05

Annealing effect on the microstructures and magnetic properties of [Fe/Pt]16 multilayers on MgO (001) substrate

Aimei Zhang¹, Weihua Zhu² and Xiaoshan Wu³
¹College of Science, Hohai University, China
²College of Science, Hohai University, China
³Physics, Nanjing University, China

[Fe/Pt]16 multilayers are deposited on MgO (001) single crystal substrate by magnetic sputtering layer by layer with varying the substrate temperature from 150-500°C to explore the annealing effect on the microstructures and magnetic properties of the films. Results show that FePt alloy with L₁₀ phase forms at about 300°C, and reaches a completely ordered state at about 400 °C. FePt film depositing at above 300°C has (001)-preferred texture which shows that L₁₀-FePt film has perpendicular magnetic anisotropy. The out-of-plane coercivity increases with sample transforming from [Fe/Pt]16 multilayers to L₁₀-FePt alloy. The out-of-plane coercivity for the morphology, which is confirmed to have the effects on the out-of-plane coercivity, with the continuing surface has an order higher than that for the granular surface.

PK06

Preparation and magnetic studies of room-temperature sputtered [Co/Pt] multilayer films on glass substrates with perpendicular magnetic anisotropy

Chiuan-fa Huang¹, Hsian-yuan Wu¹, An-cheng Sun^{1*}, Fu-te Yuan², Jen-hwa Hsu², S. N. Hsiao³ and H. Y. Lee³
¹Department of Chemical Engineering & Materials Science, Yuan Ze University, Taiwan
²Department of Physics, National Taiwan University, Taiwan
³National Synchrotron Radiation Research Center (NSRRC), Taiwan

Multilayer [Co_n/Pt_n]n films were deposited at room temperature (RT) on glass substrates with and without a Pt(111) underlayer. The thicknesses of each Co and Pt layer were set at 1 and 0.75 nm respectively. The stacking period, n, was varied from 1 to 6, leading to the total thickness of [Co₁₀/Pt_{7.5}]n films from 1.75 to 10.5 nm. The results of magnetic studies indicate that the perpendicular magnetic anisotropy (PMA) of [Co_n/Pt_n]n films is strongly influenced by inserting a Pt(111) underlayer and the number of n. Surprisingly, [Co/Pt]n films exhibit PMA behavior with a Pt(111) underlayer when n exceeds 3 even the films were deposited at room temperature. However without a Pt(111) underlayer, the films will not exhibit PMA in all cases. The appearance of L11 phase is found related to the appearance of PMA in [Co_n/Pt_n]nPt(111) films. The [Co/Pt]n film is grown along Pt(111) resulting in the L11(222) orientation, which causes the easy axis <111> along the plane normal. In this study, the microstructure at [Co_n/Pt_n]nPt(111) interface is also studied and will be presented, which is helpful for understanding the formation mechanism of PMA behavior in multilayer [Co_n/Pt_n]n structure prepared at room temperature.

PK07

Magnetic anisotropy in FeCo thin films

Xiaoxi Liu*, Shinsaku Isomura and Akimitsu Morisako
Department of Information Engineering, Shinshu University, Japan

Sputtered FeCo films normally show magnetic anisotropy inside the film plane. It is believed that the magnetic anisotropy are due to the stray field of the magnet of the target. However, the details of the induced magnetic anisotropy are yet to be fully understood. In the present work, we have prepared FeCo films by both DC magnetron sputtering system and facing targets sputtering system. The magnetic properties, crystallographic properties, and microstructure of the films have been investigated. Films deposited by DC magnetron sputtering show isotropic magnetic properties in the film plane. However, films deposited by facing targets sputtering show strong magnetic anisotropy in the film plane. The magnetic anisotropy field increases from 40 Oe to 540 Oe with the increase of the film thickness from 10 nm to 150 nm for films deposited by facing targets sputtering system. XRD results show that the (110) lattice spacing of FeCo films increases with the increase of films thickness from 10 nm to 40 nm. However, lattice spacing almost not changes with further increase of the film thickness. Of particular interest is that internal stress of the films increased with the decrease of the film thickness.

PK08

Magnetic domain wall energy of Co/Ni superlattice with perpendicular magnetic anisotropy

Kentaro Toyoki, Yu Shiratsuchi* and Ryoichi Nakatani
Osaka University, Japan

Co/Ni superlattice is a promising material for spintronics devices, in which the magnetic domain walls carry information stored, owing to a perpendicular magnetic anisotropy and a high saturation magnetization. Despite the numerous studies on the magnetic domain wall motion of the Co/Ni superlattice, the magnetic domain wall energy density has not been reported. In this work, we present the experimental determination of the magnetic domain wall energy density of the Co/Ni superlattice with perpendicular magnetic anisotropy (PMA). We confirmed that the epitaxial growth of Co(111)/Ni(111) superlattice on the Ag(111)-buffered Si(111) substrate. Several parameters were determined to obtain the magnetic domain wall energy σW [1], i.e. the saturation magnetization MS, the PMA energy, and the magnetic domain period. From the dependence of the magnetic domain period on the ferromagnetic layer thickness, the dipole length, D0 ($= \sigma W / 2\pi MS^2$), is estimated as 22.5±2.5 nm. Using the experimentally obtained MS (≈ 660 emu/cc), the magnetic domain wall energy density is estimated as $\sigma W = 6.4 \pm 1.4$ erg/cm². The estimated σW is about three-times higher than those for L12-CrPt3[2], and about one-third of that for L10-FePt[3]. From the obtained values, the exchange stiffness constant is calculated as about 4.8×10⁻⁶ erg/cm, which is comparable to that of bulk-Co.

[1] C. Kooy and U.ENZ, *Phil. Re. Rept.* 15, 7 (1960). [2] Y. Shiratsuchi, M. Yamashita, R. Nakatani and M. Yamamoto, *J. Mag. Soc. Jpn.* 33, 447 (2009). [3] S. Okamoto, N. Kikuchi, O. Kitakami, T. Miyazaki, Y. Shimada and K. Fukamichi, *Phys. Rev. B* 66, 024413 (2002).

PK09

Anisotropic Magnetoresistance of Co/Ni multilayers

Chih_yung Chen¹, James C Eckert¹, Natalia Fear¹, Sheena K. K. Patel¹, Richard Sayanagi¹, Patricia D Sparks¹, E Shipton² and Eric E Fullerton²
¹Harvey Mudd College, USA
²University of California, San Diego, USA

Co/Ni multilayers exhibit perpendicular magnetic anisotropy, relatively low magnetic damping and unusual magneto-transport characteristic that make them useful for spintronic devices. Anisotropic magnetoresistance was measured for sputtered Ni/Co films: SiO₂/Ta₆₀/Pd₄₀/(Co₂Ni_{1-x})₁₀/Ta₆₀, with Ni thicknesses from Y=2-14Å. Three AMR configurations were studied. Two configurations, varying the applied field vs. current angle, the applied field always in the plane of the sample, AMR1, and varying the applied field from in plane to out of plane, AMR2, provide similar information. The %AMR1 or 2 increases monotonically as the fraction of Ni increases and shows the expected cos² dependence. Rotating the sample with the field always perpendicular to the current, AMR3, we see anomalous angle-dependence for all samples, at all temperatures. At the sample orientation where a peak in the AMR is expected, there is a dip. The relative magnitudes of these contributions vary with temperature and Ni thickness. The magnitude of the AMR3 is approximately half the AMR2. At 5K, the magnitudes of all AMRs increase with Ni thickness except the AMR3 for the sample with 3Å of Ni is anomalously low. The temperature variations for AMR2 and AMR3 are quantitatively different but each varies by approximately a factor of 3 from 5K to 305K.

PK10

Interface perpendicular magnetic anisotropy in thick amorphous CoSiB film by Pt layer

Insung Park, Hana Lee, Hyung Jun Kim, Sung Yong Kim, Young Kwang Kim and Taewan Kim*
Department of Advanced Materials Engineering, Sejong Univ., Korea

Recently, magnetic tunnel junctions (MTJs) with perpendicular magnetic anisotropy (PMA) have attracted a lot of research interest, because they have a potential for spin transfer torque magnetic random access memories (MRAMs). Devices with perpendicular magnetic anisotropy have lower switching currents than devices with in-plane magnetic anisotropy. We have investigated the interface perpendicular magnetic anisotropy (IPMA) of amorphous CoSiB thin film. CoSiB/Pt exhibited perpendicular magnetic anisotropy. The structure of samples was SiO₂/Ta_{50Å}Pt_{30Å}CoSiBx/Pt_{30Å} and SiO₂/Ta_{50Å}Pt_{30Å}CoSiBx. The thickness of CoSiB were varied in the range of from 2 to 40Å. The sample without Pt capping layer exhibited perpendicular magnetic anisotropy at tCoSiB=10Å but the sample with Pt capping layer exhibited perpendicular anisotropy at lower thickness tCoSiB=5Å. Therefore, it was expected that IPMA properties of amorphous CoSiB on Pt layer was suitable for STT-MRAM.

PK11

Perpendicular magnetic anisotropy and superparamagnetism in Ta/CoFeB/MgO structures

C. C. Tsai¹, H. M. Chen², Chih-wei Cheng², C. H. Shue², M.C. Tsai², J. P. Singh², C.W. Su³ and G. Chem^{2*}
¹Department of Engineering and Management of Advanced Technology, Chang Jung Christian University, Tainan 71101, Taiwan
²Department of Physics, National Chung Cheng University, ChiaYi 62102, Taiwan
³Department of Electrophysics, National Chiayi University, ChiaYi, 60004, Taiwan

Collapses of tunnel magnetoresistance in perpendicular magnetic tunnel junctions have been reported recently[1-2]. These observations indicate that the coercivity of the reference layer and sensing layer behaves differently at low temperature. We extend to study the temperature dependence of a series of films with SiO₂ substrate/Ta_{5nm}CoFeB_{xnm}MgO_{1nm} 1.5<x<1.9, structures by sputtering. The perpendicular magnetic anisotropy (PMA) is revealed as the thickness of CoFeB < 1.7 nm after a post annealing process. In this report, we focus on the magnetic response of Ta/CoFeB_{7nm}/MgO which has a critical thickness of the transition from perpendicular to in-plane. Although the magnetic hysteresis shows weak in-plane anisotropy at room temperature the magnetic anisotropy changes to perpendicular at low temperature. The magnetization vs. temperature further indicates a superparamagnetic behavior with blocking temperature ~ 150K. The characteristic of a super-paramagnetism suggests a pancake shape nanostructure with diameter ~ 40 nm exists at the interface. The present study demonstrates that small ferromagnetic particles may exist even after a post annealing process and the temperature-dependent coercivity is associated with an "intrinsic" structure of the interface in Ta/CoFeB/MgO structures.

1 G. Feng, H.C. Wu, J.F. Feng, and J.M.D. Coey, Appl. Phys. Lett. 99, 042502 (2011), 2 H.D. Gan, H. Sato, M. Yamamoto, S. Ikeda, K. Miura, R. Koizumi, F. Matsukura, and H. Ohno, Appl. Phys. Lett. 99, 252507 (2011).

PK12

Observation of symmetry of wavefunction in interface controlled Co/Pd multilayer using magnetic Compton profile

Kosuke Suzuki^{1*}, Naoto Go¹, Shun Emoto¹, Masayoshi Ito², Yoshiharu Sakurai² and Hiroshi Sakurai¹
¹ Graduate School of Engineering, Gunma University, Japan
² JASRI/Spring-8, Japan

Co/Pd multilayers have attracted attention as a potential application in high-density magnetic recording media because of their strong perpendicular magnetic anisotropy (PMA)[1,2]. It has been reported that thin Co layer and thicker Pd layer enhance the PMA energy[2,3]. In this paper two Co/Pd multilayers which have smooth and rough interfaces, respectively, were studied. A Co_{1.5nm}Pd_{2.5nm} multilayer with smooth interfaces was fabricated by the MBE technique. A Co_{1.5nm}Pd_{2.5nm} multilayer with rough interfaces was fabricated by the sputter technique[4]. Both multilayers had almost the same PMA energy, 1.15Merg/cc for the Co_{1.5nm}Pd_{2.5nm} multilayer and 1.20Merg/cc for the Co_{1.5nm}Pd_{4nm} multilayer, respectively. The symmetry of the wavefunction was measured using the magnetic Compton profile measurement. The symmetry of wavefunction of both the multilayers is almost the same. Population analysis of Co-3d shows that the population of magnetic quantum number |m|=2, 1 and 0 is 50%, 36% and 14%, respectively. This suggests that the smooth interface enhances the population of |m|=2 symmetry and hence enhances the PMA energy[5-7]. In conclusion smooth interface enhances |m|=2 symmetry and hence enhances the PMA energy even if a Co/Pd multilayer has a thinner Pd layer.

[1] P. F. Garcia, A. D. Meinhaldt and A. Sina: Appl. Phys. Lett.47, 178 (1985) [2] P. F. Garcia: J. Appl. Phys.63, 5066 (1988) [3] H. Nemoto and Y. Hosoe: J. Appl. Phys. Vol.97, 10U109 (2005) [4] M.Ota: Master's Thesis, Gunma University (2002), in Japanese [5] K. Kyuno, J.-G. Ha, R. Yamamoto and S. Asano: Phys. Rev. B54, 1092 (1996) [6] H. Sakurai, M. Ota, F. Itoh, M. Ito, Y. Sakurai and A. Koizumi: Appl. Phys. Lett. Vol.88, 062507 (2006) [7] M. Ota, M. Ito, Y. Sakurai, A. Koizumi and H. Sakurai: Appl. Phys. Lett.96, 152505 (2010)

PK13

Tunable spin configuration in [Co/Ni] adjoined NiFe exchange spring structures

Sunjae Chung^{1*}, S. M. Mohseni¹, T. N. Anh Nguyen¹, N. Benatmane¹, R. K. Dumas² and Johan Akerman²
¹ Materials Physics, School of ICT, KTH - Royal Institute of Technology, Electrum 229, 164 40, Kista, Sweden
² Department of Physics, University of Gothenburg, 412 96 Gothenburg, Sweden

Future spintronic devices based on spin-transfer torque require a delicate engineering of constituent magnetic layers. More specifically, realization of a tunable spin configuration is expected to allow for operation in zero magnetic field, as well as increased output efficiency and quality, e.g. linewidth, of the device.[1] Here, we report on a tunable spin configuration in exchange coupled NiFe, with in-plane magnetic anisotropy (IMA), to a [Co/Ni]x4 multilayer, with perpendicular magnetic anisotropy (PMA). A set of sputter deposited [Co/Ni]x4/NiFe samples (series 1) is compared with the reverse structure, NiFe/[Co/Ni]x4 (series 2), with various NiFe thicknesses (tNiFe) of 0.5, 1, 2 and 3 nm. Both series show the same eventual transition from dominant PMA to IMA as tNiFe is increased. However, this transition appears for smaller tNiFe in series 2, most likely due to the initially sputtered NiFe modifying the PMA and the [Co/Ni] multilayer. Most importantly, due to the competition between PMA and IMA, a tilted spin configuration can be stabilized and tuned for intermediate tNiFe.

[1] T. N. Anh Nguyen, Y. Fang, V. Fallahi, N. Benatmane, S. M. Mohseni, R. K. Dumas, and J. Akerman, Appl. Phys. Lett. 98, 172502 (2011).

PK14

Large perpendicular magnetic anisotropy in the MgO/CoFeB/Ta with thick Ta layer

Tao Zhu
Institute of Physics, Chinese Academy of Sciences, China

It is widely recognized that current-induced spin transfer torque (STT) plays an important role in spintronic devices [1]. The magnetic tunnel junction with a perpendicular magnetic anisotropy (PMA) is a candidate for such STT devices because the PMA enables a small critical current density for current induced magnetization switching. The perpendicular magnetic anisotropy (PMA) in the Ta capping film, MgO/CoFeB/Ta, has been investigated by using anomalous Hall effect. Ta capping structures, MgO_{1.1}CoFeB_{1.22}Ta_{0.55-4.4} (numbers are the nominal thicknesses in nanometers, Ta=300°C), were prepared. The out-of-plane squareness increases with the Ta cap layer thickness from 0.55 to 0.94 nm and reaches unity at Ta thickness of 0.94 nm. Different from the previous report [2], the perpendicular anisotropy of CoFeB retains at which Ta thickness is larger than 0.94 nm. Unity squareness can be observed at the Ta cap layer thickness up to 4.4 nm. It is clear that there is no strong relationship between PMA and the Ta cap layer thickness. Moreover, a large PMA in the Ta capping film is due to the large effective anisotropy.

[1]S. Ikeda et al., Nature Mater. 9, 721 (2010). [2]C. W. Cheng et al., J. Appl. Phys. 110, 033916 (2011).

PK15

Strain induced overlayer effect on perpendicular magnetic anisotropy in Ta/CoFeB/MgO structures

C.W. Su¹, H.M. Chen², Chih-wei Cheng², C.H. Shue², J. P. Singh², C.C. Tsai³ and G. Chem^{2*}
¹ Department of Electrophysics, National Chiayi University, Chiayi, 60004, Taiwan
² Department of Physics, National Chung Cheng University, Chiayi 62102, Taiwan
³ Department of Engineering and Management of Advanced Technology, Chang Jung Christian University, Tainan 71101, Taiwan

The perpendicular magnetic anisotropy (PMA) in ultrathin CoFeB-MgO based structure is an important feature for the applications on magnetic random access memory. However, the interface structure is sensitive to seed (cap) metal layer and the annealing treatment. In this study, we fabricated a series of structures of Sub/Ta_{nm}CoFeB_{1.2nm}MgO(0<x<5 nm)/Ta(0<y<5 nm) and found that the PMA not only depends upon the thickness of MgO but also depends upon the Ta overlayer on top of MgO. In Ta/CoFeB/MgO(0<x<5 nm)/Ta(5 nm), PMA is observed as the thickness of MgO is over 0.75 nm (~3 atomic monolayer) and a maximum of Hk ~ 5 kOe at MgO thickness ~1nm is identified. In Ta/CoFeB/MgO_{nm}Ta(0<y<5 nm), we found both Hk and coercivity increases from 2.5 kOe to 5 kOe and 15 Oe to 30 Oe, respectively as the thickness of Ta varies from 1 to 5 nm. These results may conclude that the match of the lattice parameter between CoFe and MgO is crucial for the PMA in the CoFeB-MgO based structure after a post anneal process. The strain induced by MgO layer and by Ta overlayer may substantially improve the (001) texture of CoFe and thus improves the PMA in these structures.

1 S. Ikeda et al., Nat. Mater. 9, 721 (2010). 2 D. C. Worledge et al., Appl. Phys. Lett. 98, 022501 (2011).

PK16

Ultrathin Co/Pt films with high thermal stability and large effective magnetic moment

Prasanta Chowdhury*, Prabhajan Dilip Kulkarni, Murali Krishnan and Harish C Barshilia
Surface Engineering Division, National Aerospace Laboratories (CSIR), India



PK17

Magnetic characteristics of amorphous [CoSiB/Pt]n multilayers

Woosuk Yoo¹, Kyujoon Lee¹, Myung-hwa Jung^{1*}, Insung Park², Taewan Kim², E.h.m. Van Der Heijden³ and H.j.m. Swagten³
¹ Dept of Physic, Sogang University Seoul, Korea
² Dept of Physic, Sejong University Seoul, Korea
³ Department of Applied Physics, Eindhoven University of Technology, Netherlands

The development of electronics demands an increasing effort in attaining more efficient electronic memories. The materials with perpendicular magnetic anisotropy (PMA) are important in applications of electronic memories. One promising new material is amorphous PMA multilayers [CoSiB/Pt]n with n the number of repeated bilayers. By using a VSM-SQUID measurement setup, the magnetic characteristics of the [CoSiB/Pt]n are gained. The anisotropy constants k1eff, K1, K2 are obtained by fitting the hard-axis magnetization curve with GST equation. The hysteresis loops appear slanted increasing n. Furthermore magneto- optical Kerr effect (MOKE) imaging confirms magnetic domain wall motion. The coercive field is first increasing with n and after a maximum, decreasing with n. This result is caused by the RKKY coupling between the magnetic layers and the balance between the domain wall energy scaling with n and the magnetostatic energy scaling with n². In addition the reversal process is not depending on the strength of the initial magnetization field.

PK18

Effects of phase distribution and grain size on the effective anisotropy and coercivity of nanocomposite PtCo permanent alloy

Tao Liu¹, Pei Zhao², Zhaohui Guo¹, Wei Li¹, Wei Sun¹ and Jingdai Wang¹
¹ Division of Functional Materials, Central Iron & Steel Research Institute, China
² Central Iron & Steel Research Institute, China

Phase distribution and grain size are the key factors controlling the coercivity of nanocomposite permanent magnets. Feng et al. have investigated the effective anisotropy and coercivity of nanocomposite Nd₂Fe₁₄B/α-Fe magnets. [1] The latest research shows that the PtCo alloy is composed of nano-structured soft and hard magnetic phases. [2] This system can be used as an ideal model system for studying exchange coupling between the magnetically hard and soft phases. There exist three types of grain interfaces with different exchange-coupling strengths in nanocomposite PtCo permanent magnets. It is necessary to describe the proportions of the three kinds of grain interfaces for analyzing the influences of the exchange-coupling interactions on the magnetic properties. We assume that soft and hard phases distribute randomly in nanocomposite permanent magnets and that all grains have cubic shapes. We calculate the dependence of the coercivity Hc of a nanocomposite on the hard-grain size Dh. For a given volume fraction vh and soft-grain size Ds, Hc shows a maximum value as a function of the hard-grain size Dh, and the maximum position shifts to a smaller Dh with the decreasing volume fraction of the hard phase. We shows the comparisons between the calculated coercivity Hc and experimental results.

[1] W.C. Feng, W. Li, et al., J. Appl. Phys. 98, 044305(2005) [2] Xiao Q F, Bruck E, de Boer F R et al., J. Alloys Compd., 364,64(2004)

PK19

Perpendicular magnetic anisotropy and metal layer effect in MgO/CoFeB/cap (cap = Ta, Ru, and Nb)

Chih-wei Cheng, Tsung-I Cheng and G. Chern*
Department of Physics, National Chung Cheng University, Chiayi 62102, Taiwan

Perpendicular magnetic anisotropy (PMA) has been observed in MgO/CoFeB/Ta but not in MgO/CoFeB/Ru, indicating that the metal cap layer is crucial¹⁻². In this report, we extend the study to MgO/CoFeB_{1.2nm}Nb(1 - 5 nm) by sputtering and find again that PMA can be induced by Nb cap layer. Our experimental results also show that Nb and Ta have strong interface effect but the PMA occurs in a small window (~ 1 - 3 nm) while Ru shows much weaker effect and the induced interface anisotropy constant (Ki) is basically not high enough to overcome the bulk anisotropy contribution.

PK20

Dependence of perpendicular magnetic anisotropy of CoFeB thin films on thickness of MgO overlayer

Duong Duc Lam¹, Frederic Bonell¹, Shinji Miwa¹, Yoichi Shiota¹, Kay Yakushiji², Hitoshi Kubota², Takayuki Nozaki², Akio Fukushima², Shinji Yuasa² and Yoshishige Suzuki^{1*}
¹ Graduate School of Engineering Science, Osaka University, Toyonaka, Osaka 560-8531, Japan
² National Institute of Advanced Industrial Science and Technology (AIST), Spintronics Research Center, Japan

The CoFeB/MgO interface is known to favor perpendicular magnetic anisotropy (PMA) which is already found application in the efficient magnetic tunnel junctions and electric field control the magnetization. Recently, the PMA of CoFeB/MgO structure has been achieved in both experiment [1,2] and theory [3], however the origin of PMA is still ambiguous. In this scope, the structure Ta_{nm}Co_{0.9}Fe_{0.1}B_{2.0nm}MgO_(0.6-0.9nm)Ta_{nm} (unit in nm) was investigated. All samples were fabricated by sputtering method on thermally oxidized Si substrates. We studied the dependence of the total magnetic moment and the effective magnetic anisotropy energy of the Co_{0.9}Fe_{0.1}B_{2.0} layer. Magnetic anisotropy is found to be very sensitive to MgO thickness, favouring to perpendicular direction with thin MgO film (the maximum interface anisotropy was 1.74 erg/cm² with the CoFeB/MgO_{nm} structure. Although thin MgO samples have thick magnetic dead layer, resulting in the reduction of total magnetic moment, only the existence of the magnetic dead layer cannot explain the change of the PMA. We found that the thickness of MgO overlayer plays the very important role for the direction of magnetic anisotropy easy axis. This work is supported by CREST, Japan Science Technology Agency, Japan.

[1] S. Yakata et al., J. Appl. Phys., 105, 07D131 (2009) [2] S. Ikeda et al, Nature Materials., 9, 721-724 (2010) [3] H. X. Yang et al. Phys. Rev. B, 84, 054401 (2011)

PK21

The study of MgO based surface anisotropy of CoFeB layer

Dongseok Kim¹, Kuyeol Jung¹, Sungjung Joo¹, Youngjae Jang¹, Byungchan Lee², Jinki Hong¹ and Kungwon Rhie^{1*}
¹ Display and Semiconductor Physics, Korea University, Korea
² Department of Physics, Inha University, Korea

STT-MRAM (Spin transfer torque-magneto-resistive random access memory)[1] has considered as an outstanding candidate for the next generation memory device. Higher anisotropy constant K and low saturation magnetization Ms are required for the perpendicular magnetic layers to satisfy the high thermal stability and low current density for current induced magnetic switching. The PMA(perpendicular magnetic anisotropy) have been reported in Fe-Pt alloy[2] ordered by L10, Co/Pd multi-layer[3] and CoFeB-MgO[4,5]. We report the PMA of CoFeB based with MgO using amorphous paramagnetic FeZr buffer layer. Samples are deposited on SiO₂ substrate by RF magnetron sputtering machine at room temperature. The structures are SiO₂FeZr_{nm}CoFeB(tCoFeB:0.5-2)MgO_{2.5nm}Ta_{nm} (in nm) and annealing for 1 hour at 400°C. Figure 1 shows Hall resistance of PMA of CoFeB after annealing. During the annealing treatment, the lattice of CoFeB became BCC lattice structure along with crystal structure of upper MgO. Therefore, the interface anisotropy is formed between CoFeB and MgO layers in rather thin thickness. In summary, we observed the PMA in CoFe/MgO using the FeZr buffer layer. We obtain a high anisotropic constant K with a various conditions. This method can be an excellent candidate for PMA- MTJ with low critical current density.

[1] Kishi, T. et al. IEDM Tech. Dig. 309 (2008) [2] Yoshikawa, M. et al. IEEE Trans. Magn. 44,25732576 (2008) [3] Mizunuma, K. et al. APL. 95, 232516 (2009) [4] S.Yasuda, et al. Nat. Mater. 3, 868 (2004) [5] S.Ikeda, et al. Nat. Mater. 9, 721 (2010)

July 9 (Mon)

July 9 (Mon)

PL01

BiFeO₃ thickness dependence of exchange bias in polycrystalline BiFeO₃/FeNi bilayers

Xiaobo Xue¹, Xueyong Yuan², Wenbing Rui¹, Biao You¹, Qingyu Xu² and Jun Du^{1*}
¹ National Laboratory of Solid State Microstructures and Department of Physics, Nanjing University, China
² Department of Physics, Southeast University, China

Due to both ferroelectric and antiferromagnetic transition temperatures above room temperature, multiferroic BiFeO₃ has attracted much attention for uses in the electrical control of magnetic random access memory. Exchange bias in ferromagnet (FM)/antiferromagnet (AFM) bilayers has also attracted much attention because of its importance in developing magneto-electronic devices. Although there have been some reports on the exchange bias employing BiFeO₃ as antiferromagnetic layer, most of them the BiFeO₃ layers were grown epitaxially. In this presented work, single phase polycrystalline BiFeO₃ films were successfully grown on Si substrate with LaNiO₃ buffer layer. Clear exchange bias were observed at room temperature in a series of BiFeO₃/FeNi(3.6nm) bilayers, in which t varies from 8 nm to 240 nm. With increasing t, both the exchange bias field and the coercivity increase sharply and approach maxima when t is about 40 nm, which is close to one half of the spin cycloidal modulation period (64 nm) of the bulk BiFeO₃ material. Our results suggest that the cycloidal spin structure may still exist in the polycrystalline BiFeO₃ film and the interfacial uncompensated pinned spins may be responsible for exchange bias in the BiFeO₃/FeNi bilayer films.

PL02

Temperature-dependent magnetic anisotropies in epitaxial Fe/CoO/MgO(001) system studied by the planar Hall effect

J. Zhu¹, J. Li¹, W.n. Cao², J. Zhu¹ and Yizheng Wu^{2*}
¹ Physics department, Fudan university, China
² physics department, Fudan university, China

The exchange coupling between ferromagnet (FM) and antiferromagnet (AFM) has been intensively explored due to fundamental interest and its technological applications. The effect of the magnetic anisotropy of the AFM layer on the exchange coupling has not been well studied, which can only be performed in single-crystalline FM/AFM system. In this contribution, we investigated the exchange-induced in-plane magnetic anisotropies in a single-crystalline Fe/CoO/MgO(001) system in the temperature range of 10-400K. The temperature-dependent magnetic anisotropies of the Fe film were quantitatively measured with the torque technique utilizing the planar Hall effect. We found the field cooling can induce a very strong uniaxial anisotropy up to 0.196erg/cm² in Fe film with the easy axis(EA) // CoO<110>, and also a 4-fold anisotropy with the EA//CoO<100>. Such EA of the exchange-induced anisotropy was found insensitive to the cooling field orientation and only related to the CoO crystalline axis. The CoO thickness dependent exchange-induced anisotropy will be discussed in this contribution.

I.W. N. Cao, J. Li, G. Chen, J. Zhu, C. R. Hu, and Y. Z. Wu, Appl. Phys. Lett. 98, 262506 (2011)

PL03

Structural changes and magnetic properties of ultrathin Fe/Pt(111) films influenced by oxygen exposure

Jyh-shen Tsay^{1*}, Hau-chun Jhang¹, Ying-chen Lee¹, Wei-hsiang Chen¹, Yao-jung Chen² and Huei-ying Ho³
¹ National Taiwan Normal University, Taiwan
² Taipei College of Maritime Technology, Taiwan
³ National Taipei University of Education, Taiwan

Magnetic properties of Fe/Pt(111) films have received much attention in the past decade [1-2]. In this contribution, we focus on the structures and magnetic properties of ultrathin Fe/Pt(111) films influenced by oxygen exposure. Fe atoms in the submonolayer region adapt a smaller layer distance as compared to the BCC structure of a Fe layer above one monolayer (ML). At saturation conditions for absorbed oxygen on Fe/Pt(111), the increase of oxygen in the films coincides with the Fe thickness while the amount of adsorbed oxygen in the submonolayer range is rather small. In addition, the amount of oxygen exposure to achieve a saturation condition increases to a maximum value followed by a reduction for Fe/Pt(111) thicker than 1 ML. This shows the structure related oxidation efficiency of Fe/Pt(111). The growth of Fermi edge at 620 K shows the segregation of Pt atom to the top layers. Only the Fe/Pt(111) thicker than 3 ML shows the enhanced coercive force after thermal annealing. This could be explained by the blocking of the formation of FePt alloy by the iron oxides.

[1] T.U. Nahm, et al., J. Korean Phys. Soc. 46 (2005) S125; [2] Y.J. Chen, et al, APL, 93 (2008) 012503.

PL04

Initial growth of bcc Co films on Au(001) studied by STM/BH imaging

T. Kawagoe*, E. Wakabayashi, Y. Murasawa and T. Sakata
 Osaka Kyoiku University, Japan

We have studied the surface structure and magnetism of metastable bcc Co films (>1 ML) on Au(001) [1]. Here we report the initial growth of submonolayer Co films by means of barrier height (BH) imaging using STM, which has capability of element discrimination. The experiments were performed in a UHV-MBE system equipped with an STM unit. After the clean Au(001) reconstructed surface was confirmed by STM, a submonolayer Co was deposited on it at RT. Spatially resolved BH maps, together with the topographic images were obtained at RT using a tip-sample distance modulation technique. We have observed numerous islands with different sizes and heights after 0.15 ML Co coverage and successfully obtained, from the BH imaging, an element-specific contrast, i.e. recognizing aggregated Au islands and Co islands, and information about inhomogeneities of BH with proper consideration of the artifacts near the step edges. BH of metastable bcc Co film was observed for the first time, and that showed a large BH value (~6 eV), whereas the observed BH of the Au(001) surface (~3.5 eV) was consistent with the previous results.

[1] T. Kawagoe et al., Surf. Sci. 602, L15 (2008).

PL05

Magnetic field induced “switching” of the nanodomain state of ferromagnet - antiferromagnet frustrated system

Alexander I Morosov and Alexander S Sigov
 Electronics Department, MSTU MIREA, Russia

The presence of atomic steps on the interface between the nanolayers of ferromagnet and antiferromagnet with uncompensated atomic planes parallel to the interface causes frustrations of the interlayer exchange interaction. If the exchange integral for the ferromagnet is less than that one for the antiferromagnet, then, for the layers of equal thickness, and in the case where the characteristic distance R between the neighboring edges of the steps on the interface exceeds the layer thickness, the ferromagnetic layer appears to be broken down into 180° domains. The domain walls separating such domains generated by frustrations arise at the atomic step edges and penetrate the ferromagnetic layer, the domain wall thickness increases with increasing distance from the interface. An external magnetic field applied parallel to the magnetizations of the domains, being in excess of some critical value B*, makes the monodomain state of the ferromagnetic layer more favorable. If so, the domain walls with more complicated structure depending on the field magnitude arise between 180° domains in the antiferromagnet layer. The B* value can be obtained from the equality of the gain in the Zeeman energy and the difference between the energies of the domain walls in different layers.

PL06

Stable structural and electronic properties of adsorption Tl on the clean Ti/Si(111) surface

Haruki Kato^{1*}, Liang Li¹, Shinya Haraguchi¹, Junpei Goto¹, Masahito Tsujikawa² and Tatsuki Oda³
¹ Graduate School of Natural Science and Technology, Kanazawa University, Japan
² Center for Spintronics Integrated Systems, Tohoku University, Japan
³ Institute of Science and Engineering, Kanazawa University, Japan

The structural inversion asymmetry shows up surfaces or interfaces. It leads to spin split electronic state (Rashba-Bychkov effect) in the material. In particular, heavy metals on the light elements like Si show strong spin-orbit splitting [1] and such property in Ti/Si(111) has also been confirmed both in simulation and experiment [2]. This surface has been observed as a clean one, indicating the stability due to the insulating property verified by the experiments and theoretical approaches [3,4]. By donating (or accepting) electrons, one can introduce carriers with spin polarization at the part of states, implying an interesting basis for spintronics devices. In this work, as a method of donating electrons, Tl atom which is the same element as the top surface of Ti/Si(111) is considered within the density functional first-principles approach of fully relativistic pseudo-potential and planewave basis. First, the stable adsorption site has been investigated with using the √3×√3 superlattice of Ti/Si(111). It was found that one of hollow site models is most stable in the adsorption models investigated. In the presentation, we report details of the stable structure and, for typical systems, we also present electronic structures and spin splitting in the band dispersion relations.

[1] C. R. Ast et al., Phys. Rev. Lett. 98, 186807 (2007). [2] K. Sakamoto et al., Phys. Rev. Lett. 102, 096805 (2009). [3] J. Ibanez-Azpiroz et al., Phys. Rev. B 84, 125435 (2011). [4] S. S. Lee et al., Phys. Rev. B 66, 233312 (2002).

PL07

Exchange bias effect in Ni(Zn)O film

R. Ray^{1*}, S. Biswas¹, S. Das², S. Majumdar² and S. Giri²
¹ Department of Physics, Jadavpur University, India
² Solid State Physics, Indian Association for the Cultivation of Science, India

Exchange bias (EB) has received significant attentions for fundamental interest and potential applications in magnetic memory and read heads. Recently, EB is observed in various alloys and compounds [1]. Magnetic nanoparticles have been found promising for significant EB effect where surface spins were found to have different magnetic anisotropy than core spins, causing sizable EB effect. Compared to the studies of EB in nanoparticles, these studies in film geometry having chemically single phase are rarely investigated, which is rather promising for technological applications. Here, we report EB in Ni_xZn_{1-x}O films where Zn substitution in NiO significantly modifies magnetic properties and EB effect. Atomic Force Microscopy exhibits formation of granular films of average grain size ≈25 nm. We note that EB field (HE) and coercivity (HC) decrease considerably with Zn substitution at x = 0.3 and HE vanishes at x = 0.5. Appearance EB in NiO film is suggested due to significant difference in anisotropy between core and surface spins, as it has been conjectured for NiO nanoparticles. The Zn substitution appreciably decreases the difference between core and surface anisotropy causing the reduction of HE as well as HC.

[1] S. Giri et al. J. Phys.: Condens. Mater 23 (2011) 073201.

PL08

Electronic properties of transition metal oxides interface between GdTiO₃/SrTiO₃

Sungbin Lee^{1*} and Leon Balents²
¹ University of California, Santa Barbara, USA
² Kavli Institute for Theoretical Physics, University of California, Santa Barbara, USA

The creation of a two dimensional electron gas (2DEG) at the interface between two insulating oxides has been a subject of great interest, and much experimental activity has centered on the LaAlO₃/SrTiO₃ interface. The (001) GdTiO₃/SrTiO₃ interface has the same naive polarization discontinuity as the former system, but unlikely it actually exhibits a 2DEG with the expected e/2 charge per planar unit cell.[1] Motivated by recent experiments, which show that the 2DEG primarily lives in the SrTiO₃, we construct a theoretical tight-binding model and discuss the electronic properties in comparison with experiment, and consider possible magnetism in this system at low temperature.

[1] P. Moetakef et al., Appl. Phys. Lett. 99, 232116 (2011)

PL09

Parallel ferromagnetic resonance and spin wave excitation in exchange-biased NiFe/IrMn bilayers

Marcos Sousa^{1*}, Fernando Pelegrini¹, Justiniano Marcatoma², Willian Alayo² and Elisa Baggio-saitovitch²
¹ Universidade Federal de Goias - UFG, Brazil
² Centro Brasileiro de Pesquisas Fisicas, Brazil

Ferromagnetic Resonance (FMR) investigation of magnetron sputtered exchange-biased Si₁₁₁Ru_xNiFe_{1-x}IrMn_{1-x}Ru_x bilayers reveals that spin wave and uniform resonance modes are excited by the microwave field. The samples studied were produced in the presence of a 400 Oe magnetic field to set the unidirectional anisotropy and the thickness t of the NiFe layer varied in the range 55-120 nm. The FMR experiments were done at room temperature using a commercial spectrometer with swept static magnetic field and the usual detection techniques. In-plane angular variation of resonance fields of spin wave and uniform modes reveal for both modes the dependence on cosθ, where θ is the field angle with respect to the anisotropy axis. The unidirectional anisotropy field for the spin wave mode is twice larger than that for the uniform mode; they are equal to 40 and 20 Oe, respectively, for the Si₁₁₁Ru_xNiFe_{1-x}IrMn_{1-x}Ru_x sample. Spin wave resonance theory give for the NiFe layer of this sample the exchange constant of 1.2 × 10⁻⁶ erg/cm. The parallel FMR results at microwave frequencies of 9.45 and 34.1 GHz agree with the values given by the resonance fields of spin wave and uniform modes also excited in perpendicular FMR at a frequency of 9.45 GHz.

[1] W. Stoeklein, S. S. Parkin and J. C. Scott, Phys. Rev. B 38, 6847 (1988). [2] M. Nisenoff and R. W. Terhune, J. Appl. Phys. 36, 733 (1964). [3] V. S. Speriosu, S. S. P. Parkin, and C. H. Wilt, IEEE Trans. Magn. 23, 2999 (1987).

PL10

Morphological consideration for post-annealed Cr2O3 surface and exchange bias in bilayer system

Tomohiro Nozaki*, Naoki Shimomura, Takuya Ashida, Yuji Sato and Masashi Sahashi
 Graduate school of Electronic Engineering, Tohoku University, Japan

Magnetolectric Cr₂O₃ has been received renewal of attentions as a promising material for the low energy consumption electric controlled spintronic devices such as MERAM [1]. High exchange bias field (Hex) between ferromagnetic layer and Cr₂O₃ thin film layer, and low coercivity (Hc) are essential for the applications. Previously we reported the high Hex (~500 Oe) at the wide temperature range from 10 K to 250 K and the low Hc (~30 Oe) at 250 K for post-annealed Cr₂O₃ thin film system [2]. In this study we compared the morphology and magnetic properties of the post-annealed sample with that of samples fabricated by other manners and examined the origin of the high Hex and low Hc of the post-annealed sample. The post-annealed sample was identified to be polycrystalline, which would contribute to the low Hc. From TEM and AFM images, flat (1-102) planes (r-planes) were observed diagonally to the film surface which are formed during the post annealing by grain growth due to the low surface energy [3]. From the fact that Cr₂O₃ has uncompensated spin not only c-plane but also r-plane, we conclude that the origin of the high Hex is the uncompensated r-plane.

[1] X. Chen et al., Appl. Phys. Lett., 89 (2006) 202508. [2] T. Ashida et al., The 56th MMM Conference, (2011) FE-05. [3] J. Sun et al., Surf. Coat. Tech., 201 (2006) 4205.

PL11

Magnetic properties of [NiFe/NiFeCuMo/NiFe]/FeMn-multilayers depending on a thickness of NiFeCuMo layer

Jong-gu Choi¹, Kwang-jun Park², Jang-rho Rhee³ and Sangji-suk Lee^{2*}
¹ Eastern-Western Biomedical Engineering, Sangji University, Korea
² Oriental Biomedical Engineering, Sangji University, Korea
³ Physics, Sookmyung Women' University, Korea

Variations in the exchange bias field (HEX) and coercivity (HC) of the intermediately super-soft magnetic NiFeCuMo layer were investigated for different thicknesses of the bottom NiFe layer. HEX of the triple pinned NiFe_{4nm}NiFeCuMo (tNiFeCuMo = 1 nm)/NiFe_{1nm}FeMn multilayer has a maximum value that is more less than that of a single pinned NiFe_{8nm}FeMn layer. If a NiFeCuMo layer is inserted between the pinned and free NiFe layers, this multilayer system can be used as a giant magnetoresistive spin-valve (GMR-SV) device for biosensors with improved magnetic sensitivity.

[1] J. G. Choi, D. G. Hwang, S. S. Lee, J. H. Choi, K. A. Lee, and J. R. Rhee, J. Kor. Magn. Soc. 19, 197 (2009). [2] J. G. Choi, D. G. Hwang, S. S. Lee, and J. R. Rhee, J. Kor. Magn. Soc. 19, 142 (2009). [3] J. G. Choi, D. G. Hwang, J. R. Rhee, and S. S. Lee, J. Magn. Magn. Mater. 322, 2191 (2010). [4] W. F. Egelhoff Jr., R. D. McMichael, C. L. Dennis, M. D. Stiles, F. Johnson, A. J. Shapiro, B. B. Maranville, C. J. Powell, Thin Solid Films 505, 90 (2006).

PL12

Structural and magnetic properties of antiferromagnetic Heusler Ru₂MnGe epitaxial thin films

Naoto Fukutani*, Hirohito Fujita, Tetsuya Miyawaki, Kenji Ueda and Hidefumi Asano
 Nagoya University, Japan

Recently, it is suggested that spin transport phenomena observed in conventional spintronics ought to occur in systems where all FM materials are replaced by antiferromagnetic (AFM) materials. Although various studies have investigated FM Heusler alloys, very few studies have been made on AFM Heusler alloys in terms of spintronic applications. The AFM transition temperatures (TN) of Heusler alloy such as Fe₂VSi can be controlled by inducing biaxial strain[1]. Thus we investigate the correlation between structural and magnetic properties of epitaxial thin films of AFM Ru₂MnGe. Structural characterization revealed that Ru₂MnGe films on MgO were subjected to compressive strain (c/a = 1.0042). The strained Ru₂MnGe exhibited markedly enhanced TN of 353 K compared to the bulk value (316 K)[2]. The in-plane Mn-Mn distance for the strained Ru₂MnGe is slightly smaller than that of bulk Ru₂MnGe, which may contribute to reducing the total J2 values, resulting in the enhancement of TN. We also observed the exchange coupling between Heusler-type FM half-metal Fe₂CrSi and AFM metal Ru₂MnGe. The present AFM Heusler alloy with relatively high TN is useful to fabricate high-quality all Heusler-type half-metal FM/AFM junctions and is a promising material for the emerging field of AFM spintronics.

[1] N. Fukutani, C. Shishikura, Y. Takeda, and H. Asano, Appl. Phys. Expr. 2, (2009) 053001. [2] T. Kanomata, M. Kikuchi, and H. Yamauchi: J. Alloys Compd. 414 (2006) 1-7.

PL13

Exchange-spring phenomenon of ultrathin Fe/CoPt bilayer

Wei-hsiang Chen¹, Hsing-hsuane Wu¹, Huei-ying Ho² and Jyh-shen Tsay^{1*}
¹ Physics, National Taiwan Normal University, Taiwan
² Physics, Department of Science Education, National Taipei University of Education, Taiwan

A large enhancement in the polar magneto-optic Kerr signal was observed after one monolayer (ML) of Co adatoms on Pt(111) was annealed above 600 K to form a Co-Pt alloy at the interface [1]. In this contribution, the composition, surface structure and magnetic properties of ultrathin Fe films on the top of a Co-Pt(111) surface alloy has been investigated. As the Fe coverage increases on the top of the Co-Pt alloy, the polar Kerr rotation increases. By way of systematically changing the Fe thickness, the magnetic properties of Fe/CoPt in both the polar and longitudinal configurations are investigated for Fe thinner than 7 ML. At an optimal condition for both the Fe thickness and the annealing temperature for preparing the Co-Pt alloy, the polar coercive force remains the same as the Fe coverage increases. The Fe/CoPt system exhibits magnetic exchange-spring behavior in the polar configuration. The interfacial conditions for the Fe/CoPt system are demonstrated to play an important role on the exchange-spring phenomenon and will be discussed in this contribution.

[1] C.S. Shern, J.S. Tsay, H.Y. Her, Y.E. Wu, and R.H. Chen, Surf. Sci. Lett. 429 (1999) L497.

PL14

Neutron magnetic scattering study in manganite thin film system

H. Nakao^{1*}, H. Yamada², K. Iwasa³, J. Okamoto¹, Y. Yamasaki¹, Y. Murakami¹ and A. Sawa²
¹ Condensed Matter Research Center and Photon Factory, IMSS, KEK, Japan
² Electronics and Photonics Research Institute, AIST, Japan
³ Department of Physics, Tohoku University, Japan

Perovskite manganites show various interesting phenomena including colossal magnetoresistance (MR) due to a close interplay among charge, orbital, spin, and lattice degrees of freedom. The superlattice [(LaMnO₃)_n(SrMnO₃)_m]_z was investigated as a stage to control the Mn valence artificially. The physical properties were reported to strongly depend on the periodicity m, and the interface state between LaMnO₃ and SrMnO₃ layer was noted.[1] The stacking structure of Mn valence state by resonant x-ray scattering technique has been studied.[2] It elucidated that the physical properties just depend on the quality of the film. Recently, however, new large MR effect was discovered in the high quality superlattice system.[3] To understand the MR effect microscopically, the Mn valence state and the magnetic field effect were studied. Here the magnetism is also important, and then neutron magnetic scattering experiment was started using the neutron spectrometer TOPAN in JRR-3. As a first step, SrMnO₃ film with 80 nm thickness has been investigated. A signal with about 2 cps at (0.5, 0.5, 0.5) corresponding G-type AFM was certainly discovered. The temperature dependence of the signal intensity was also measured. Consequently we have succeeded in observing magnetic scattering from thin film system.

[1] T. Koida et al., Phys. Rev. B 66 (2002) 14418. [2] H. Nakao et al., J. Phys. Soc. Jpn. 78 (2009) 024602. [3] H. Yamada et al., Phys. Rev. B 81 (2010) 014410.

PL15

Direction and temperature dependences of exchange bias and coercivity of NiFe/Cr_{2(1-x)Fe_{2x}O₃(x= 0.25, 0.4) bilayers}

Sanghoon Ki, Byeong-geon Kim and Joonghoe Dho^{*}
 Kyungpook National University, Korea

The antiferromagnets α-Fe₂O₃ and α-Cr₂O₃ have the same crystal structure but different magnetic orderings. The AF spin structure for α-Cr₂O₃(TN~307 K) is represented by the up-down-up-down spin ordering along c-axis, while that for α-Fe₂O₃(TN~953 K) is done by the up-down-down-up one. As reported in previous neutron diffraction study for the solid solution Cr_{2(1-x)Fe_{2x}O₃(CFO), such contradictory spin structures may result in a new type AF structure such as spiral order or cycloidal order. Here, we report exchange bias in NiFe/Cr_{2(1-x)Fe_{2x}O₃(x= 0.25, 0.4) bilayers grown on c-plane and r-plane Al₂O₃. The direction and temperature dependences of magnetic property of NiFe/CFO layer substrates were checked by a surface magneto-optical Kerr effect (SMOKE) setup. At room temperature, the M(H) loop of the NiFe layer exhibited enhanced coercivity and exchange bias depending on the measurement direction and the temperature. In order to see the direction dependence of magnetic property of NiFe layer, the magnetic field was applied to two orthogonal directions within the plane. Interestingly, the temperature dependence of M(H) loop exhibited some features of spin reorientation of CFO layer below antiferromagnetic transition temperature.}}

PL16

Structure and magnetic properties of epitaxial Fe/MgO/Si (001) heterostructures

Jeong Hong Jo¹, Kyung-ho Kim², Yoon Jae Nam³, Hyung-jun Kim², Joonyeon Chang² and Sang Ho Lim^{1*}
¹ Department of Materials Science and Engineering, Korea University, Seoul 136-713, Korea
² Spin Convergence Research Center, Korea Institute of Science and Technology, Seoul 136-791, Korea
³ Department of Nano Semiconductor Engineering, Korea University, Seoul 136-713, Korea

The ferromagnetic metal/semiconductor structures with inserting a thin MgO tunneling barrier are expected to play a key role in spin-based electronic applications to enhance spin injection efficiency. Recently, spin-based devices using silicon channel enable seamless integration with conventional MOS-FET technology. However, there are only a few reports on ferromagnetic metal/MgO/Si system due to large lattice mismatch (3.5%) between Si and MgO. The study on strain induced microstructure of the Fe and MgO layers is essential because the lattice mismatch between Si and MgO results in distortion in both MgO and Fe layers. In addition, the magnetic property of the ferromagnetic metal with respect to its microstructure evolution is also of importance in terms of spin injection. In this study, Fe thin films of thinner than 2 nm, were prepared on Si (001) substrates with 4 nm thick MgO buffer layer by a molecular beam epitaxy system at room temperature and 200 °C, respectively. X-ray diffraction and reflection high-energy electron diffraction results show epitaxial relationship of the system. In-plane four-fold magnetic anisotropy was observed by vibrating sample magnetometer, suggesting that elevated growth temperature of the Fe films leads to the strain relaxation and the suppression of two-dimensional Fe layer formation.

PL17

Uncompensated magnetic moment around Mn₃Ir / Fe-Co-Ni bilayer interface

Yohei Kota^{*}, Hirokazu Takahashi, Masakiyo Tsunoda and Akimasa Sakuma
 Graduate School of Engineering, Tohoku University, Japan

We study the microscopic origin of the uncompensated moment in Mn₃Ir / Fe-Co-Ni bilayer, which is practically utilized system due to the excellent property of exchange anisotropy, by the theoretical and experimental approach. In order to induce exchange anisotropy, the magnetic structure in the ferromagnetic / antiferromagnetic bilayer needs to have some asymmetry against the field reversal, and the uncompensated moments around the interface is a candidate for the spin asymmetry. We previously reported that there is a linear correlation between the exchange anisotropy and uncompensated moments measured by the x-ray magnetic circular dichroism (XMCD) experiment in Mn-Ir / Co-Fe bilayer [1]. Therefore, in the present work, we investigate the composition dependence of the uncompensated moment in Mn₃Ir / Fe-Co-Ni by performing the first-principles calculation and the XMCD measurement to clarify the origin of the uncompensated moment. In the comparison of the calculation and experimental results, the obtained uncompensated moments are in good agreement for their sign and relative magnitude [2]. Furthermore, the calculated result reveals that the uncompensated moment originates from the local magnetic correlation near the interface. So we find that the reorientation of the magnetic moments of Mn occur at the very interface with the ferromagnetic layer.

[1] M. Tsunoda, H. Takahashi, T. Nakamura, C. Mitsumata, S. Isogami, and M. Takahashi, Appl. Phys. Lett. 97, 072501 (2010). [2] H. Takahashi, Y. Kota, M. Tsunoda, T. Nakamura, K. Kodama, A. Sakuma, and M. Takahashi, J. Appl. Phys. 110, 123920 (2011).

PL18

Unusual exchange bias effects in NiFe/Mn thin films induced via ion-beam bombardment

Chi-hsin Liu¹, Chin Shueh¹, Yi-wen Ting¹, Wen-chen Chen², Te-ho Wu², Johan Van Lierop³ and Ko-wei Lin^{1*}
¹ Dept of Materials Science and Engineering, National Chung Hsing University, Taiwan
² Graduate School of Material Science, National Yunlin University of Science and Technology, Taiwan
³ Department of Physics and Astronomy, University of Manitoba, Canada

When spins at the interface between a ferromagnet (FM) and an antiferromagnet (AF) couple, a unidirectional anisotropy occurs, resulting in exchange bias [1,2]. In this study, we wish to identify the dependence of the exchange bias on the interface microstructure in NiFe/Mn thin films. A series of [NiFe/Mn] multilayer thin films were fabricated using a dual ion-beam deposition technique [3]. Different Ar-ion deposition voltages created striking differences in magnetic properties. The [NiFe/Mn] (VEH= 0 V, i.e. un-bombarded) thin film (~200 nm) at 5 K when 20 kOe field-cooled (FC), exhibited an enhanced coercivity (Hc~ 935 Oe) and positive exchange bias field, Hex~ +130 Oe. By contrast, the [NiFe/Mn] (VEH= 150 V) Ar-ion bombarded thin film (~20 nm) at 5 K when 20 kOe field cooled showed a larger positive Hex (~ +160 Oe) with smaller Hc (~ 610 Oe) accompanied by an asymmetric hysteresis loop. The observed enhanced positive Hex indicated that the transition from FM to AF coupling was made possible by changing the ion-beam bombardment voltages. Further, the role of Ar ion-bombardment seems to change both the spin orientations in FM NiFe and AF Mn and thus gives rise to the positive enhanced Hex.

[1] T. Sauerbeck, F. Klose, D. Lott, G.J. Mankey, Z. Lu, P.R. LeClair, W. Schmidt, A. Stamm, S. Danilkin, M. Yethiraj, A. Schreyer, Phys. Rev. B 82, 134409 (2010). [2] H. Ouyang, Y.-H. Han, S.-C. Lo, C.-H. Su, Y.-R. Shiu, K.-W. Lin, R. D. Desautels, and J. van Lierop, Phys. Rev. B 81, 224412 (2010). [3] K.-W. Lin, V. V. Volobuev, J.-Y. Guo, S.-H. Chung, H. Ouyang, and J. van Lierop, J. Appl. Phys. 107, 09D712 (2010).

PL19

Exchange bias effect in BiFeO₃ thin films

Kil-dong Sung and Jonghoon Jung^{*}
 Physics, Inha University, Korea

We fabricated BiFeO₃ thin films with Bi₂O₃ or γ-Fe₂O₃ impurities by changing oxygen partial pressures and characterized their magnetic properties. Since Bi₂O₃ impurity is a non-magnetic material, only antiferromagnetic spins of BiFeO₃ will contribute to whole magnetic properties. But γ-Fe₂O₃ impurity is a well known ferrimagnetic material, so there is a possibility to show exchange bias effect with antiferromagnetic spins of BiFeO₃. We measured M(H) loop at various temperatures after zero- and ±5 T-field cooling. Almost no but very small amount of M(H) hysteresis loop was appeared in BiFeO₃ with Bi₂O₃ impurity. Which indicate that there is uncompensated spins in BiFeO₃ which generate exchange bias effect with γ-Fe₂O₃. Significant hysteresis loop was appeared in BiFeO₃ with γ-Fe₂O₃ impurity. Depending on the field cooling direction, the M(H) loops also shifted to the opposite directions. But unlike other conventional exchange bias systems, the interaction between ferrimagnetic spins of γ-Fe₂O₃ and antiferromagnetic spins of BiFeO₃ is not so strong as shown in the training effect result.

PL20

Experiment evidence to the existence of interaction between antiferromagnetic domains in IrMn/Pt/Co/Pt multilayers

X. J. Bai¹, Z. Shi², S. M. Zhou^{2*}, X. R. Zhao¹ and C. D. Cao¹
¹ Key Laboratory of Space Applied Physics and Chemistry, Northwestern Polytechnical University, Xi'an, China
² Department of Physics, Tongji University, Shanghai 200092, China

Exchange bias phenomenon has become an integral part of the modern magnetism, with implications in basic research and applications in magnetoelectronic devices. In the numerous experimental and theoretical studies, the surface layer of antiferromagnetic (AFM) material is often regarded as an assembly of uniaxial domains, which are independence from each other. This basic assumption is really suspect. In our presented work, experiment evidence of interaction between AFM domains has been found. The IrMn/Pt/Co/Pt perpendicular exchange bias systems were fabricated and treated by AC demagnetization (ACDM) parallel to the film plane at high temperature. The purpose of ACDM is to get the pinned demagnetization state in ferromagnetic layer. In the corresponding hysteresis loop, two minor-loops shift oppositely along the magnetic field axis and locate totally on one side of the vertical axis. Compare the training effects of the minor-loop and full-loop, we found that one minor-loop measurement gives influence to the other. It is reasonable that the influence is attributed to the interaction between the IrMn surface domains. Our experiment facts can not be explained by the past theory models, new energy item of interaction between AFM domains should be considered.

[1] C. H. Lui, W. E. Bailey, R. L. White, T. C. Anthony, J. Appl. Phys. 81 4990 (1997) [2] T. Hanet, S. Mangin, J. McCord, F. Montaigne, and E. E. Fullerton, Phys. Rev. B 76, 144423 (2007) [3] X. P. Qiu, D. Z. Yang, S. M. Zhou, R. Chantrell, K. O'Grady, U. Nowak, J. Du, X. J. Bai, and L. Sun, Phys. Rev. Lett. 101, 147207 (2008) [4] E. Fulcomer, S.H. Charap, J. Appl. Phys. 43, 4190 (1972)

PL21

Nanoscale investigation of the Cr/Fe(001) interface grown by oxygen assisted epitaxy

Alberto Brambilla^{1*}, Andrea Picone¹, Guido Fratesi², Alberto Calloni¹, Michele Riva¹, Gianlorenzo Bussetti¹, Alberto Ferrari¹, Lamberto Duo¹, Marco Finazzi¹, Mario Italo Trioni¹ and Franco Ciccacci¹
¹ Dipartimento di Fisica, Politecnico di Milano, Piazza Leonardo Da Vinci 32, 20133 Milano, Italy
² Dipartimento di Scienza dei Materiali, Università di Milano-Bicocca, Via Cozzi 53, 20125 Milano, Italy
³ CNR, National Research Council of Italy, ISTM, Via Golgi 19, 20133 Milano, Italy

Cr deposition on Fe(100) has been the subject of intense investigations in the past, being an excellent model system for thin film magnetism, and also because Fe/Cr multilayers played a fundamental role in the development of giant magneto resistive devices [1]. The magnetic properties of such systems can be affected by parameters like interfacial mixing, strain and defects. For instance, previous investigations have shown that, within the atom distribution resulting from Cr incorporation into the Fe substrate, nearest neighbour Cr-Cr coupling is energetically less favorable than next nearest neighbor coupling, due to magnetic frustrations [2]. Here we employ experimental and theoretical methods to highlight and characterize deviations in the micromagnetic structure of the Cr/Fe interface due to the presence of adsorbed O, which induces a layer-by-layer Cr growth at room temperature, as we recently demonstrated [3]. Scanning tunnelling microscopy (STM) is used to investigate the deposition of Cr on the Fe-p(1x1)O surface since the first stages of interface formation. Atomic resolution STM images reveal the occurrence of different magnetic configurations, including first-neighboring Cr atoms in the Fe matrix. The observations are discussed in the light of density-functional simulations with the generalized gradient approximation and plane waves basis set [4].

[1] B. Heinrich, J.A.C. Bland (Eds.), Ultrathin Magnetic Structures, Springer Verlag, Berlin, (1994). [2] A. Davies, Joseph A. Sroscio, D.T. Pierce, and R. J. Celotta, Phys. Rev. Lett. 76, 4175 (1996). [3] A. Calloni, A. Picone, A. Brambilla, M. Finazzi, L. Duo, F. Ciccacci Surf. Sci. 605, 2095 (2011). [4] P. Giannozzi, N. Baroni, M. Bonini et al., J. Phys.: Condens. Matter 21, 395502 (2009).

PM01

Correlation of soft magnetic properties with free volume and medium range ordering in metallic glasses

Amit P Srivastava^{1*}, D Srivastava¹, P K Pujari¹, K G Suresh² and G K Dey¹
¹ Bhabha Atomic Research Centre, Mumbai, India
² Indian Institute of Technology Bombay, Mumbai, India

The effect of cooling rate on thickness and soft magnetic properties of the metallic glass of alloy composition Co_{64.5}Fe_{3.5}Si₁₆B₁₄Ni₂ have been studied. The amorphous structure has been characterized by positron annihilation spectroscopy (PAS) and fluctuation electron microscopy (FEM) techniques. These studies suggest that the first lifetime component is associated with MRO present in the amorphous structure. Theoretical calculations showed that second component is associated with nanovoids having free volume equivalent to that of a vacancy defect consisting of 4 and more atom vacancy cluster. Coercivity of the samples showed small variations with wheel speed and it was found to decrease with the decrease in effective size of the defects present in the samples. This study reveals that, in case of amorphous metallic glass, the variation in coercivity is mainly controlled by the defects formed during processing rather than the small variations in MRO introduced due to different cooling rates.

PM02

Microscopic magnetic hysteresis measurement of amorphous Tb-TM (TM=Fe and Co) thin films by magnetic Compton scattering

Akane Agui^{1*}, Tetsuya Unno², Sayaka Matsumoto², Kousuke Suzuki² and Hiroshi Sakurai²
¹ Japan Atomic Energy Agency, Japan
² Dept. Production Sci & Technol., Gunma Univ., Japan

Rare earth transition metal (RE-TM) alloys have attracted considerable attention from the viewpoint of fundamental research and technology. For instance, they have been studied as candidate heat-assisted magnetic recording media for high-density magnetic storage. It is known that magnetic moment of RE and TM form ferrimagnetisms and have anisotropy dispersion along magnetic easy axes, so-called sperrri-magnetism [1]. The magnetic switching process of sperrri magnetism is considered not to be simple. In this report, we have study spin, orbital and also element specific magnetic switching process of amorphous Tb-TM (TM=Fe and Co) films by means of combination of magnetic Compton scattering [2, 3] and conventional macroscopic magnetization measurements. As specimen, amorphous Tb₄₅Co₅₅ and Tb₃₅Fe₆₅(O₁₀) thin films were fabricated by an RF sputtering onto a thin Al foil substrates. The macroscopic magnetization curves were measured by SQUID and VSM magnetometers. Magnetic Compton scattering measurements were carried out at AR-NE1A of KEK [2] and at BL08W of SPring-8 [3], Japan. The present results suggest that magnetic switching can be different among the spin moment, the orbital moment, and even the states of electrons, e.g., the Tb 4f electron, TM 3d electron, and itinerant electron.

References: [1] J. M. D. Coey, J. Chappert, J. P. Rebouillat, and T. S. Wang, Phys. Rev. Lett. 36 (1976) 1061. [2] A. Agui, H. Sakurai, T. Tamura, T. Kurachi, M. Tanaka, H. Adachi, and H. Kawata, J. Synchrotron Rad., 17 (2010) 321. [3] A. Agui, S. Matsumoto, H. Sakurai, N. Tsuji, S. Honma, Y. Sakurai, and M. Ito, APEX 4 (2011) 083002.

PM03

A significant reduction of hysteresis in MnFe(P,Si) compounds

O. Tegus^{1*}, Y. X. Geng¹ and J. H. Huang²
¹ Physics and Electronic Information College, Inner Mongolia Normal University, Hohhot 010022, China
² Baotou Research Institute of Rare Earths, Baotou 014030, China

The magnetocaloric effects in Mn_{1-x}Fe_{0.7-x}Co_{0.46}Si_{0.54} compounds with x = 0, 0.025, 0.05 and 0.1 are studied systematically. X-ray diffraction shows that the compounds in the range from x = 0 to 0.1 crystallize in the Fe₂P-type hexagonal structure with space group P-62m symmetry. Magnetic measurements show that the paramagnetic-ferromagnetic transition temperatures range from 247 to 298 K. The maximum of magnetic entropy changes in Mn_{1-x}Fe_{0.7-x}Co_{0.46}Si_{0.54} compound reaches 8.3 J/kgK in a field change of 0 to 1.5 T, and the thermal hysteresis of these compounds is less than 3 K. The maximum adiabatic temperature change is 2.2 K in Mn_{1-x}Fe_{0.7-x}Co_{0.46}Si_{0.54} and Mn_{1-x}Fe_{0.65}Co_{0.05}P_{0.46}Si_{0.54} compounds for a field change from 0 to 1.48 T.

PM04

Temperature dependence of creep-induced anisotropy in nanocrystalline FeCuNbSiB alloys

Giselher Herzer*, Mie Marsilius and Christian Polak
R&D Rapid Solidification Technology, Vacuumschmelze GmbH & Co. KG, Germany

We have investigated the creep induced anisotropy in nanocrystalline Fe₇₅Cu₁Nb₅Si₁B_{21-x} alloys as a function of the measuring temperature. The samples were produced by annealing originally amorphous ribbons for about 4 s between 500°C and 700°C with a tensile stress applied along the ribbon axis. For Si-contents equal or larger than 9 at% the annealed ribbons reveal a linear hysteresis loop indicative of an easy magnetic plane perpendicular to the stress axis. For lower Si-contents, stress annealing results in a square loop indicative of an easy magnetic axis parallel to the stress axis. This transition from an easy plane to an easy axis as a function of the Si-content is well-known from previous investigations and is related to the dependence of local magnetostriction of the nanocrystals on the Si-content. However, the investigations so far have been only carried out at room temperature. The present work, for the first time, reveals that the Si-contents where the easy axis changes its direction shifts to higher concentrations as the temperature increases. This is also nicely reflected in a reversible change from a linear hysteresis loop with low remanence to a square loop as a function of the measuring temperature.

PM05

Magnetocaloric properties of Ni-Co-Mn-In ribbon

M. U. Gutowska^{1*}, J. Wiecekowsk¹, A. Szewczyk¹, W. Maziarz², N. Nedelko¹, S. Lewinska¹, A. Slawska - Waniewska¹, M. Kowalczyk³ and A. Kolano - Burian⁴

¹ Institute of Physics, Polish Academy of Sciences, Warsaw, Poland
² Institute of Metallurgy and Materials Science, Polish Academy of Sciences, Cracow, Poland
³ Faculty of Materials Engineering, Warsaw University of Technology, Warsaw, Poland
⁴ Institute of Non-Ferrous Metals, Gliwice, Poland

Temperature dependences of two parameters characterizing magnetocaloric effect (isothermal change in entropy and adiabatic change in temperature) were determined for a Ni₄₀Co₃₀Mn₂₅In₄ ribbon. Two experimental methods were used, i.e., measuring temperature dependences of a specific heat (from 3 to 380 K) in zero magnetic field and in the field B=1 T, and measuring dependences of magnetization on temperature and on B. In the former method, both parameters were determined by analyzing the system entropy (determined by integrating the measured specific heat). In the latter method, the Maxwell relation was applied to get the isothermal change in entropy. The magnetocaloric effect shows two extrema of opposite sign, one near the transition between martensitic and austenitic phases, and the other one at the Curie temperature. The parameters characterizing the magnetocaloric effect near room temperature in relatively low B (1 T) make this material promising for application in magnetic refrigerators. The magnetocaloric effect was found to be highly anisotropic, being much larger for B applied in the ribbon plane. This property is particularly useful for designs, in which the active medium rotates in the field. This work was supported by the European Regional Development Fund, Innovative Economy Grants POIG.01.01.02-00-108/09, POIG.01.03.01-00-058/08 and POIG.02.02.00-00-025/09.

PM06

Influence of bismuth substitution on the magnetocaloric properties of Gd₅Si₂Ge₂ compound

Comeliu Bazil Cizmas^{1*}, Rim Guetari², Lotfi Bessais³, Najeh Thabet Mliki² and Sorin Adam¹
¹ Department of Electrical Engineering and Applied Physics, Transilvania University of Brasov, Bd. Eroilor 29, 500036 Brasov, Romania
² LMOP, Department of Physics, Faculty of Sciences of Tunis, Tunis El Manar University, 2092 El Manar, Tunisia
³ ICMPE, UMR7182 CNRS, Universite Paris-Est Creteil, 2/8 rue Henri Dunant, B.P. 28 F-94320 Thiais, France

In order to study the influence of relative small Bi addition on the magnetocaloric effect of Gd₅Si₂Ge₂, a series of Gd₅Si_{2-x}Ge_{2+x}Bi_{2x} (2x=0, 0.02, 0.04, 0.06 and 0.08) alloys was prepared by arc melting method. Investigations of Gd₅Si_{2-x}Ge_{2+x}Bi_{2x} properties were carried out using X-ray diffraction, thermomagnetic analysis, magnetization isotherms measurements and differential scanning calorimetry (DSC). After a heat treatment at 1250°C for 200 min., all the alloys have, at room temperature, a monoclinic structural phase of Gd₅Si₂Ge₂ type (S.G.: P112₁/a) with a small amount of hexagonal structural phase of Gd₅Si₃ type (S.G.: P63/mcm). The Curie temperature is around ~ 285K (±2K). The results of the DSC measurements show a difference of ~10K in the peak of the heating and cooling curves associated with a first order structural phase transition. The peak slightly decreases with Bi content. This is expected to be related to the increasing of the Si/Ge bond distance in the monoclinic phase with Bi addition. The maximum isothermal magnetic entropy change decreases with Bi addition, however a giant magnetocaloric effect was obtained for all alloys. As an example, the maximum magnetic entropy change for the Gd₅Si_{1.98}Ge_{2.02}Bi_{0.04} was found to be 12.6 J/kgK under an applied field of 5T.

PM07

Ion incident energy effects on the giant magnetoimpedance enhancement

Hoon Song and D. G. Park*
korea atomic energy research institute, Korea

The present experiment investigates the physical effects of ion irradiation on the magnetic properties of the amorphous ribbon. Samples were commercial amorphous ribbon with sizes of 2 mm x 40 mm x 20 μm. The Ar ions were provided by an ion implanter at various dosages from 100 keV to 200 keV at the 1.0 x10¹⁸ ion/cm². The GMI ratio was measured as a function of the DC magnetic field (Hmax=35 Oe) at different driving frequencies up to 10 MHz with a 5 mA amplitude applied to the sample irradiated with different energy. The irradiated samples show a clear change in the impedance response with applied field. When energetic ions with energies of several tens of keV penetrate into a thin film, the collision cascade cause displacements of the target atoms that induce a uniaxial anisotropy in the sample. Ion irradiation induces uniaxial anisotropy along the transverse direction, which is accompanied by an effective transverse susceptibility. Therefore, the increase in the GMI ratio in an ion-irradiated sample is attributed to the increase in associated uniaxial anisotropy created by ion bombardment. We found that controlling the ion energy can be one of the effective ways of controlling the GMI property for ion

[1] E. Lee, S. Lee, W. Lee and C. E. Lee, *J. Korean Phys. Soc.* 56, 2108 (2010). [2] D. Pathak and R. K. Bedi, *J. Korean Phys. Soc.* 57, 474 (2010).

PM08

Investigation of electrodeposited FeNi film prepared from tartaric acid based bath

Takaya Shimokawa*, Takeshi Yanai, Ken-ichiro Takahashi, Masaki Nakano and Hirotohi Fukunaga
Nagasaki University, Japan

FeNi films have been plated by using boric acid as pH buffer agent. However, the boric acid is needed to be replaced by another one which does not include boron, because boron is an environmentally hazardous substance. In order to achieve boron-free electroplating of FeNi, we applied the method proposed by Luisa et al for the CuNi electroplating [1] to that of FeNi, in which they successfully plated CuNi with good surface morphology by using tartaric acid. We electroplated FeNi films with Fe content of 17-45 at.% from the bath including NiSO₄·6H₂O, FeSO₄·7H₂O, NaCl, C₄H₄NNaO₆·2H₂O and C₄H₆O₆ (tartaric acid). The content of Fe was controlled by varying the amounts of tartaric acid between 0-200 g/L. The coercive force of the as-deposited films varied with the content of Fe, and showed a sharp bottom of 20 A/m at around 22 at.% of Fe. This result is consistent with the fact that FeNi alloys have nearly zero values of magnetocrystalline anisotropy and saturation magnetostriction at around 22 at.% of Fe. From the above result, we concluded that tartaric acid based bath film is one of hopeful plating bath for electroplating of FeNi films.

[1] Luisa et al, *J. Appl. Electrochem*, 41 (2011) 415.

PM09

Electrodeposited Fe-Co film prepared from citric acid-based plating bath

Takeshi Yanai*, Haruka Uto, Takaya Shimokawa, Ken-ichiro Takahashi, Masaki Nakano and Hirotohi Fukunaga
Nagasaki University, Japan

Although a lot of the electrodeposited Fe-Co films with good soft magnetic properties were reported [1-3], boron, which is harmful and restricted by the regulation of environmental protection in Japan, was included in the plating bath as boric acid for controlling pH. Therefore, in order to remove boron, we focused on the citric acid-based plating bath and investigated effect of citric acid for the electrodeposited Fe-Co films. The plating bath was consisted of FeSO₄·7H₂O(100 g/L), CoSO₄·7H₂O(100 g/L), NaCl(50 g/L), C₆H₈O₆·H₂O(0 - 270 g/L). An Fe plate as anode and a Cu plate as cathode were used, and Fe-Co film was deposited on the Cu plate. Current density was kept at 2 mA/mm² and bath temperature was set at 50 °C during the deposition. The coercivity of the deposited film was drastically reduced from 1700 to 200 A/m with increasing content of citric acid from 0 to 100 g/L, and then slightly increased. The Fe-Co film prepared from the bath with citric acid of 100 g/L has high saturation magnetization of over 2.2 T and we can conclude that citric acid-based plating bath is one of hopeful plating ones to obtain good soft magnetic film with high saturation magnetization.

[1] Qiang et al., *Appl. Surf. Sci.*, 257 (2010) 1371. [2] Kockar et al., *J. MMM*, 322 (2010) 1095. [3] Teh et al., *IEEE Trans. Magn.*, 47 (2011) 4398.

PM10

Magnetic and magnetocaloric properties of polycrystalline Fe₂P under hydrostatic pressure

Luana Caron^{1*}, Viktor Hoglin², Yvonne Andersson², Per Nordblad³ and Ekkes Bruck⁴
¹ Fundamental Aspects of Materials and Energy, Faculty of Applied Sciences, TU Delft, Mekehweg 15, 2629 JB Delft, Netherlands
² Department of Materials Chemistry, Uppsala University, Box 538, 751 21 Uppsala, Sweden
³ Department of Engineering Sciences, Uppsala University, Box 534, 751 21 Uppsala, Sweden
⁴ Fundamental Aspects of Materials and Energy, TU Delft, Mekehweg 15, 2629 JB Delft, Netherlands

Magnetocaloric-based refrigeration presents itself as an environmentally-friendly energy-efficient technology capable of beneficially replacing the current gas compression-based technology. Some of the most promising magnetocaloric working materials found to date, such as Fe₂(Mn)2(P,Si), are based on the Fe₂P binary compound. Fe₂P itself presents a first order magnetoelastic transition between FM and PM states at around 219 K and a low magnetic entropy change spanning a large temperature range. What makes Fe₂P so unique is the coupling presented by its magnetic and crystal lattices which gives rise to the so-called mixed magnetism[1]. We believe that the mixed magnetism is responsible for the giant magnetic entropy change present in Fe₂P-based compounds. To further advance our understanding of this coupling we performed magnetization experiments under hydrostatic pressures up to 8 kbar on pure Fe₂P in its polycrystalline form. Pressure is found to decrease Tc at a rate of 6 K/kbar, about twice the rate reported in literature[2]. The T dependence on field is found to be non-linear and is only weakly affected by pressure. The magnetic entropy change peak is slightly decreased by increasing pressure whereas the total entropy increases by ~6%.

[1] Dung, N.H. et al. *Advanced Energy Materials* 1, 1215 (2011). [2] Fujii, H., Hokabe, T., Kamigaiichi, T. & Okamoto, T., *J. Phys. Soc. Jpn.* 43, 41-46 (1977).

PM11

Influence of Er doping on magnetic and magnetocaloric properties of (NiCo)₂MnGa

Jiří Kaštil^{1*}, Jiří Kamarád² and Zdeněk Arnold²
¹ Faculty of Mathematics and Physics, Charles University, Prague, Czech Republic
² Institute of Physics ASCR, Prague 8, Czech Republic., Czech Republic

Recently, an attention has been paid to magnetocaloric properties of the Co-doped Heusler Ni₂MnGa alloys with a paramagnetic gap in martensitic phase that can be tuned by their composition [1]. The strong influence of a rare-earth doping has been calculated and observed on the valence orbitals of Mn that makes the main contribution to the magnetic properties of these alloys [2]. We have prepared Co-doped Ni₂MnGa alloys with a very small amount of Er. The polycrystalline sample of Ni₄₉Co₃₀Mn₁₁Ga₁₀Er_{0.1} was checked by the EDX analysis and a segregation of Er was discovered on grain boundaries as it was expected in [2]. Saturated magnetization M(5K,0)=2.38μB/f.u. and the Curie temperatures TCM=318 K and TCA=440 K of martensite and austenite, respectively, were observed in Er free sample by a SQUID magnetometer. The inverse magnetocaloric effect at vicinity of martensitic transition, TM-A=379 K, was measured by direct method with ΔT=1.2K. In the Er-doped alloy, M(5K,0)=2.83μB/f.u. and paramagnetic gap was diminished in martensitic phase. TCA=450 K has been detected only and magnetic susceptibility obey nicely the Curie-Weiss law with paramagnetic moment of mP=5.09 μB/f.u. above TCA. The effect of the Er-segregation on crystal texture and magnetic behaviour of the Co-doped Ni₂MnGa alloys will be discussed.

[1] S. Fabbri, J. Kamarad, Z. Arnold, F. Casoli, A. Paoluzi, F. Bolzoni, R. Cabassi, M. Solzi, G. Porcari, C. Pernechele, F. Albertini, *Acta Materialia* 59 (2011) 412-419 [2] J. Wan, Y. Fei, J. Wang, *Journal of Rare Earths* 24 (2006) 373-375

PM12

Structural and magnetic properties of FeMnAl nanocrystalline alloys

Kontan Tarigan, Young-yeal Song and Seong-cho Yu*
BK21 Physics Program and Department of Physics, Chungbuk National University, Cheongju 361-763, Korea

Nanocrystalline magnetic alloys have been promising materials for magnetic device applications requiring high saturation magnetic flux density, high permeability, and low core loss. Among the magnetic alloys, Fe-Mn-Al system has been one of the most interesting ternary alloys with several magnetic phases. The magnetic properties were studied in one particular compound in previous works [1,2]. More systematic research of Fe-Mn-Al alloys would contribute to better understanding with Al contents. Nanocrystalline Fe₉₀Mn₁₀Al, prepared via mechanical alloying using Fe, Mn, and Al powder with 48 hrs milling time. The structural and magnetic properties were studied. All peaks of XRD data are broader and shifted to smaller angle with increasing Al contents depending on the crystalline size and the lattice parameter, respectively. All the samples exhibit alloy behavior with an average crystallite size around 10 nm. The magnetic saturation, the coercivity, and the permeability, obtained from measurements by vibrating sample magnetometer showed strong dependence on the Al contents, and these dependences were related to the changes in structure and crystallite size. In addition Mossbauer experiments confirm the Al diffuses into Fe bcc grains. Furthermore, these results suggest that, by adjusting the Al content, appropriate structural transformation and appropriate magnetization values can be obtained.

[1] Kontan Tarigan, Yong-Goo Yoo, Dong-Seok Yang, J. M. Grenèche, and Seong-Cho Yu, *IEEE Trans. Mag.* 45, No. 6 (2009) 2492-2495. [2] E.A. Vela 'squez, L.F. Duque, J. Mazo-Zuluaga, J. Restrepo, *Physica B* 398 (2007) 364-368.

PM13

Magnetocaloric effect in Fe doped La_{0.67}Ba_{0.33}MnO₃ system

Hirofumi Kawanaka^{1*}, Hiroshi Bando¹ and Yoshikazu Nishihara²
¹ Advanced Industrial Science and Technology, Japan
² Ibaraki Univ., Japan

The perovskite-type oxides of La_{0.67}Ba_{0.33}Mn_{1-x}Fe_xO₃ were synthesized by the conventional solid-state reaction method. The Curie temperature Tc and magnetic entropy change (MCE) in these samples are determined and compared to those of Gd-doped systems. [1,2] The Curie temperature Tc decreases from 350 K to 290 K with increasing Fe concentration x from 0 to 0.05. The relatively large MCE with a broad peak around Curie temperature compared with other oxides is observed in this system. These results suggest this system is a suitable candidate as magnetic refrigerator material working at room temperature.

[1] Z. Juan, W. Gui, *J. Magn. Magn. Mater.* 321 (2009) 43-46 [2] M. H. Phan, S. C. Yu, *J. Magn. Magn. Mater.* 308 (2007) 325-340

PM14

Study of magnetic transition and magnetic entropy changes of La_{0.7}Sr_{0.3}MnO₃ and La_{0.7}Ca_{0.1}Sr_{0.2}MnO₃

Anwar Mohammad Shafique, Shalendra Kumar, Faheem Ahmed, G. W. Kim and Bon Heun Koo*
School of Nano & Advanced Materials Engineering, Changwon national university, Korea

Magnetocaloric effect (MCE) and its most straightforward application, magnetic refrigeration, are becoming fields of increasing research interest. On the one hand, there are reasonable expectations that these subjects will give rise to energy-efficient, environmentally friendly technological applications. On the other hand, the study of some model materials gives some more insight into the physics underlying these phenomena. In this paper, complex magnetic materials La_{0.7}Sr_{0.3}MnO₃, La_{0.7}Ca_{0.3}MnO₃ and La_{0.7}Ca_{0.1}Sr_{0.2}MnO₃, suitable for the magnetic refrigeration, has been investigated. We have found that the substitution of the Sr with Ca leads to an important decrease of the Curie temperature (TC) from 374 K to 345 K. The magnetocaloric study exposes a quite large value of the magnetic entropy changes for La_{0.7}Ca_{0.3}MnO₃ and La_{0.7}Ca_{0.1}Sr_{0.2}MnO₃. In cooling applications, another important parameter is relative cooling power (RCP), a good indicator of cooling efficiency of a magnetic refrigerator. For an applied magnetic field of 2 T, the RCP value is found to be 203 J/kg for La_{0.7}Ca_{0.1}Sr_{0.2}MnO₃. As a result, the studied compounds could be considered as potential material for magnetic refrigeration near and above room temperature.

PM15

Perpendicular magnetic anisotropy of amorphous ferromagnetic CoSiB multilayer

Sol Jung¹, H. I. Yim^{1*}, Ahri Kim² and Sumin Kim²
¹ Physics, Sookmyung Women's University, Korea
² Nano-Physics, Sookmyung Women's University, Korea

Perpendicular magnetic anisotropy (PMA) is worthy of notice in both fields of science and industry due to its high integrate. In the previous study, we used CoSiB (75:15:10, atn%) and CoSiB/Pt multilayer showed the strong dependence on both the thicknesses of CoSiB and Pt. For the [CoSiB 3A/ Pt 14A]x5 multilayer, the maximum coercivity was ~ 224 Oe and the maximum PMA constant was obtained as ~ 2 × 10⁶ erg/cm³¹. In addition, this film has the coercivity (Hc) and the saturation magnetization (Ms) with respect to 1.6 Oe and 407 emu/cm³. Considering this result, we suggest the new idea of CoSiB/Au/CoSiB sandwich structure and CoSiB/Pd multilayer. 1 mono-layer-thick of Au and Pt are 144pm, 139pm and they are diamagnetic and ferromagnetic materials, respectively. CoSiB/Au/CoSiB sandwich structure and CoSiB/Pd multilayer is expected to show PMA and it can be developed to the magnetic random access memory (MRAM).

[1] J. Y. Hwang, S. S. Kim, and J. R. Rhee, *J. Magn. Magn.* 310, 1943 (2007). [2] J. S. Park, H. I. Yim, J. Y. Hwang, S.B. Lee, T. W. Kim, *J. Phys. Soc.* 57, 1672 (2010). [3] S. Jeong, H. I. Yim, *J. Phys. soc.* 60, 450 (2012).

PM16

Thickness dependence of magnetic induction in inhibitor-free 3% silicon steels

Sang-beom Kim^{1*}, Joon-young Soh¹, Sang-yun Lee¹, Heejong Jung² and Jongryoul Kim²

¹ Korea Electric Power Corporation Research Institute, Korea

² Department of Metallurgy and Materials Science, Hanyang University, Korea

Cold-rolled sheets of differing thicknesses were prepared through the conventional hot and cold rolling process. After annealing at 1200°C, final texture greatly varied with heating rate and sheet thickness. The 0.2 mm thick samples contained no or few {110} grains within the tested range of heating rates, yielding a poor magnetic induction. On the contrary, the 0.15 mm thick samples consisted entirely of {110} grains, and consequently resulted in a very high magnetic induction of over 1.95 Tesla. The 0.1 mm samples were also composed of {110} grains either at a very slow or at a very fast heating rate, but they unexpectedly exhibited a poor magnetic induction due to the deviated <001> direction of {110} grains from rolling direction. Orientation distribution functions of the samples taken from each cold rolling pass revealed that initial {111}<112> texture components started to move toward {111}<110> at a thickness of 0.13 mm. According to the nucleation and selective growth mechanism [1], primarily recrystallized texture takes after cold rolling texture, and hence the deviated final texture was obtained. This study indicates that there exists an optimum thickness for obtaining high magnetic induction and low iron loss.

[1] N. H. Heo et al., Acta Mater. 51 (2003), 4953-4964.

PM17

Effect of M (= Ge, Y, Hf) addition on soft magnetic properties of Fe-B-Si-M metallic glass alloys

Juho Lee¹, Hwijun Kim¹, Jungchan Bae¹ and Dohyang Kim^{2*}

¹ Korea Institute of Industrial Technology, Korea

² Center for noncrystalline Materials, Yonsei University, Korea

Fe-based metallic glass (MG) alloys exhibit good soft magnetic properties such as low coercivity and core loss but have the limits for industrial application because of low saturation flux density below 1.5T. Therefore, Fe-based MG alloys with high saturation flux density above 1.7T are very attractive soft magnetic alloy systems. In order to investigate the effect of M(= Ge, Y, Hf) addition on soft magnetic properties of Fe-B-Si-M metallic glass alloys, structural variations and magnetic properties of Fe_{83-x}B₁₀Si₇M_x (X=1~5 at atomic percent) MG alloys were examined by X-ray diffraction(XRD) and vibration sample magnetometer(VSM) after fabricating Fe_{83-x}B₁₀Si₇M_x MG ribbons by a single-roller melt-spinning technique under argon atmosphere. The thermal stability was measured by Differential Scanning Calorimetry(DSC) at a heating rate of 20K/min. Fe_{83-x}B₁₀Si₇M_x MG alloys added Ge, Y or Hf exhibited a fully amorphous structure. Saturation flux density and coercive force of these alloys were Bs = 1.6~1.8T and Hc = 20~40 A/m, respectively. After annealing for 1 hr at 773K, Fe80B10Si7Ge3 MG alloy displayed excellent soft magnetic properties such as saturation flux density of 1.8T and corecivity of 20A/m.

PM18

Effects of film composition and substrate temperature on the structure and magnetic properties of FeCoB alloy films formed on MgO single-crystal substrates

Yugo Asai*, Mitsuru Ohtake, Tetsuroh Kawai and Masaaki Futamoto

Chuo University, Japan

Tri-layer films consisting of FeCoB and MgO layers have been investigated for MTJ applications. Theoretical studies show that the TMR ratio of MTJ prepared using epitaxial layers is one order of magnitude greater than that obtainable with amorphous layers [1,2]. The structure of bulk FeCoB alloy changes from crystalline to amorphous as the B content exceeds around 10 at. %. However in a form of thin film, there is a possibility of crystallization for B rich compositions. In the present study, (Fe_{93-x}Co_{0.3})_{100-x}B_x (x = 0-15 at. %) films were sputter deposited on MgO substrates of (100), (110), and (111) orientations at different substrate temperatures to investigate the effects of film composition, temperature, and substrate orientation on the structure and magnetic properties. Epitaxial films were obtained for all compositions by adjusting substrate temperature. For example, (FeCo)₉₃B₅ and (FeCo)₉₃B₁₅ epitaxial films were respectively obtained at temperatures higher than 200 and 600 °C, while amorphous films were formed below these temperatures. The epitaxial films formed on MgO (100), (110), and (111) orientations consisted of bcc(100), bcc(211), and bcc(110) crystals, respectively. The magnetocrystalline anisotropy decreased with increasing the B content. Improved soft magnetic properties were realized in films with high B contents.

[1] W. H. Butler, X.-G. Zhang, T. C. Schulthess, and J. M. MacLaren: Phys. Rev. B., 63, 054416 (2001). [2] J Mathon and A Umerski: Phys. Rev. B., 63, 220403 (2001).

PM19

Arrangement of different magnetic alloy sheets for effective magnetic shielding

Sang-yun Lee, Yun-seog Lim, Ho-seong Ahn, Dong-il Lee and Sang-beom Kim*

Korea Electric Power Corporation Research Institute, Korea

The purpose of this study is to provide an effective shielding method for power frequency magnetic field emanating from a neutral ground reactor (NGR). The 0.35 mm thick commercial grade grain-oriented electrical steel (GO), non-oriented electrical steel (NGO), and permalloy (PC) were used as shielding materials. The area of 1200x1200 mm² was blocked with the alloy sheets at a place 600 mm away from the NGR. In a weak magnetic field, PC is the best in shielding performance, whereas GO is the best in a strong magnetic field. NGO is worse than GO, but is better than PC in a very strong magnetic field. For multi-layered shields, it was observed that GO/PC pair (GO is close to source) was most effective, yielding a shielding factor less than 0.06 in the wide range of magnetic fields. These results are explained by variation of shielding effectiveness of a magnetic material with magnitude of magnetic field. The inner GO sheet effectively shields a strong magnetic field first, and then the outer PC sheet effectively shields the weakened field. Furthermore, this study demonstrates some spacing between laminations is essential to achieve best shielding performance in the 'shunt' mechanism of magnetic shielding.

PM20

Fabrication of pariculated Fe-Mg thin films by selective oxidation and their magnetic properties

Pyungwoo Jang*

College of Science and Engineering, Cheongju university, Korea

It is impossible to manufacture Fe-Mg bulk alloys even in vacuum melting system because of very low melting temperature, high affinity with oxygen, and very high vapor pressure of Magnesium. However, it is very easy to fabricate Fe-Mg thin films by sputtering. Because of big difference of enthalpy of Fe-O and MgO, Mg can be selectively oxidized in a mixture atmosphere of hydrogen and water vapor. 10 - 200 nm thick sputtered Fe-Mg films were selectively oxidized in a damp atmosphere and annealed at 800-900oC for 10 - 200 min. With increasing oxidation time, saturatio magnetizatin of Fe-Mg films increased due to selective oxidation of Mg. Furthermore, Initial permeability as well as the slope of magnetizatio loops of the films decreased, which was attributed from the facts that morphology of the films were changed from continuous type to pariculated type. when the films were annealed in pure hydrogen atmosphere the rate of change is very slow. The reason for the expedited change is probably due to energy transfer to Fe atoms during migration of Mg atoms to film surface .

PM21

Optimum spacing of magnetic alloy strips in open-type magnetic shielding

Yun-seog Lim, Sang-yun Lee, Ho-seong Ahn, Dong-il Lee and Sang-beom Kim*

Korea Electric Power Corporation Research Institute, Korea

This study suggests an effective shielding method for power frequency magnetic field in open-type magnetic shielding, which secures the clear view of field sources by aligning magnetic alloy strips sparsely. A neutral ground reactor (NGR) was used as a field source. The 0.35 mm thick commercial grade grain-oriented electrical steel (GO) and permalloy (PC) were cut into a size of 50x1200 mm² and then placed vertically 600 mm away from the center of the NGR. In a weak magnetic field, PC was the best in shielding performance, whereas GO was the best in a strong magnetic field due to change in hierarchy of material permeability with increasing magnetic field strength. In case of multi-layered shields, it was observed that combination of GO/PC/GO was more effective than the triple-layered shield of the same material. However, closely conjoined GO/PC/GO shield showed worse shielding performance than the same layered shield seperated from each other, which demonstrates it acts as one body regardless of presence of thin surface insulation layers. This study reports that introducing air gap between laminations of each layered shield is important to obtain desired shieding performances and optimum spacing between alloy strips exists in open-type magnetic shielding.

PM22

Magnetocaloric effect in Ni_{2.27}Mn_{0.73}Ga Heusler alloy

Mikhail Drobosyuk, Vasily Buchelnikov, Sergey Taskaev and Rafael Fayzullin

Chelyabinsk state university, Russia

Drobosyuk Mikhail, Buchelnikov Vasily, Taskaev Sergey, Fayzullin Rafael Chelyabinsk State University, Chelyabinsk, Russia m.syuk@mail.ru type of presentation: poster There are many theoretical and experimental works devoted a possibility any magnetic materials to change its temperature after applying an external magnetic field. This effect is called the magnetocaloric effect (MCE). Recent experimental studies have shown that Ni-Mn-Ga Heusler alloys have unique properties such as the shape memory effect, the large magnetostriction, the large magnetoresistance and other magnetic properties. In this work we present the experimental studies of the MCE for Ni_{2.27}Mn_{0.73}Ga Heusler alloy. Polycrystalline ingot was prepared by a conventional arc-melting method. Samples for measurements were cut from the middle part of the ingot. The magnetocaloric measurements were performed by the Magnetocaloric Measuring Setup produced by AMT&C. The results of measurements will be shown on the poster.

PM23

Soft magnetic properties of Fe-6.5wt.%Si alloy sheets fabricated by powder hot-rolling

Hunju Lee¹, Hwijun Kim² and Mooyoung Huh^{1*}

¹ Department of Materials Science and Engineering, Korea University, Korea

² Korea Institute of Industrial Technology, Korea

It is widely known that Fe-6.5 wt.% Si alloys have excellent soft magnetic properties. In this work, Fe-6.5 wt.% Si sheets were rolled by powder hot-rolling process without cracking and soft magnetic properties were investigated with microstructural defects. The cylindrical preforms were prepared by inert gas atomization and subsequent spark plasma sintering of Fe-6.5 wt.% Si powders at 1223K. The Fe-6.5 wt.% Si sheets were fabricated by hot rolling of copper canned preforms at 1173K with total reduction of 70%, 80% and 90%, respectively. The hot rolled sheets were annealed at 1073K in an argon atmosphere. Microstructures and magnetic properties (magnetic flux density, coercivity and core loss) of the hot rolled and annealed Fe-6.5 wt.% Si sheets were examined by scanning electron microscopy (SEM), vibration sample magnetometer (VSM) and B-H analyzer. The hot rolled Fe-6.5wt.% Si sheet with reduction of 90% and subsequent annealing exhibited soft magnetic properties such as magnetic flux density of 1.8 T and coercivity of 20 A/m. This result is due to the elimination of microstructural defects and the increase of the average grain size and density.

PM24

Structure and magnetic properties of nano/micro-sized Mn-Al alloy powders produced by plasma arc-discharge and gas atomization

Junggoo Lee^{1*}, Younkyoung Baek¹, Hwijun Kim² and Chuljin Choi¹

¹ Powder & Ceramics Division, Korea Institute of Materials Science, Korea

² Eco-Materials and Processing Division, Korea Institute of Industrial Technology, Korea

The ϵ -phase in the Mn-Al system has attracted great attention due to the remarkable magnetic properties superior to the Alnicos and hard ferrites, low cost, as well as good machinability and corrosion resistance. Due to these reason, several methods have been employed to produce ϵ -phase Mn-Al alloy powder until now. On the other hand, plasma arc-discharge and gas-atomization method has been widely used for the production of nano-sized and micro-sized powders, respectively. To our best knowledge, however, there is no comparison study of Mn-Al alloy powder produced by these two methods. In the present study, Mn-Al alloy powders were prepared by the methods of plasma arc-discharge and gas-atomization and influence of process parameters on composition, particle size, and magnetic properties of the powders was systematically investigated. Mn-Al powder produced by plasma arc-discharge was smaller than its single magnetic domain and exhibited the coercivity of 5.6 kOe, which is the highest among the values reported until now. It was also confirmed that the magnetic properties of micro-sized powder produced by gas-atomization have been improved by subsequent treatments such as annealing and mechanical milling Based upon these results, the magnetic properties of these two types of Mn-Al alloy powders will be discussed.

This research was supported by a grant from the Fundamental R&D Program for Core Technology of Materials funded by the Ministry of Knowledge Economy, Republic of Korea.

PM25

Ultra high speed pm type synchronous motor-generator with amorphous core for micro turbine

Do-kwan Hong*, Yeon-ho Jeong, Dae-suk Joo, Byung-chul Woo and Dae-hyun Koo

Electric Motor Research Center, Korea Electrotechnology Research Institute, Korea



PM26

Temperature dependence of magnetic domains in grain-oriented silicon steel

H. L. Park¹, R. Schaefer², O. Y. Kwon³ and Y. H. Jeong^{1*}

¹ Physics, POSTECH, Korea

² IFW Dresden, Institute for Metallic Materials,, Germany

³ Pohang Iron and Steel Company, Korea

Abstract: Silicon steels are essential for transformers and the reduction of loss in them is of utmost importance in this green age. Since the loss in steels are closely related to their magnetic domain structures, the magnetic domain structures in turn are of exceeding interest. We studied magnetic domains of 3% silicon steel single crystals with (110) [001] texture as a function of temperature via magneto-optical Kerr effect (MOKE) microscopy. Generally, the silicon steels (110) [001] have 180° main domains oriented along the [001] axis, and they also have complimentary Lancet domains in case of misorientation. [1, 2, 3] The MOKE images shown in Figure 1 clearly reveal that the domain patterns change as temperature is changed. The width of the 180° main domains, for instance, decreases with increasing temperature. In order to go one step further from mere qualitative observations, we analyzed the MOKE images quantitatively, and, in particular, investigated temperature dependence of the 180° domain width and the Lancet domain density. These temperature characteristics will be interpreted from the standpoint of total energy minimization.

[1] A. Hubert, R.Schaefer, Magnetic domains(1998),Springer [2] Y. Ushigami, J. Magn. Magn. Mater. 254-255(2003), 307-314 [3] M. Imamura, Physica Scripta. T 24 (1988)

PM27

A tri-layer stress impedance sensor using amorphous magnetostrictive thin film

Bodong Li*, Ahmed Alfadhel and Jurgen Kosel

KAUST, Saudi Arabia

Mechanical stress sensors have a wide area of applications in strain and torque measurements. Thin film stress impedance (SI) sensors have several advantages over other stress sensors such as high sensitivity in small stress range, miniaturization possibility as well as the integration capability with other devices. Stress sensors that utilize amorphous magnetostrictive thin films have been proposed previously. The permeability change of the magnetostrictive material upon the applied external stress was evaluated throughout an impedance measurement. In this work, a tri-layer thin film stress sensor is fabricated and analyzed. The sensor has a Fe₈₀Ni₁₈Mo₂B₁₈/Ti/Fe₈₀Ni₁₈Mo₂B₁₈ tri-layer structure with 900 nm thickness each and dimensions of 10×0.1 mm². After the deposition, the sensor is annealed at 300 °C with a magnetic field of 500 Oe applied in the transverse direction to induce an in-plane transverse anisotropy. The magnetic behavior is studied with a vibrating sample magnetometer and the crystallographic structure is studied with using X-ray diffraction. The sensor is tested by applying compressive and tensile stresses and the sensor response was obtained from an impedance analyzer. The results show high sensitivity at strains between 0-80 ppm with a maximum impedance change of 16% at 50 MHz.

Frommberger, M.; Glasmachers, S.; Schmutz, C.; McCord, J.; Quandt, E., IEEE Trans. Magn., vol. 41, pp.3691 - 3693, 2005

July 9 (Mon)

July 9 (Mon)

PM28

Magnetoimpedance(GMI) effect in the NiFe shell/Cu core wires fabricated by electrodeposition

Dong Young Kim, Sung Jae Jeon, Jung Dong Kim and Seok Soo Yoon*
Physics, Andong National University, Korea

Microwires with NiFe shell on Cu core of 90 μm diameter were fabricated by electrodeposition method. The thickness of NiFe shell was well controlled by deposition time in the range of 4 μm ~18 μm. Giant magnetoimpedance(GMI) effect in the NiFe/Cu core shell wire was measured in frequency range of 10 kHz ~ 10 MHz and in the magnetic field range of -300 Oe ~ 300 Oe. The variations GMI ratio with frequency and NiFe shell thickness were analyzed in terms of magnetic relaxation and skin depth at ac field. We obtained maximum GMI ratio of 250 % at 300 kHz in the wire with NiFe shell of 11.5 μm thickness.

PN01

SQUID, XRD and Raman studies of Mn implanted gallium nitride at elevated temperature

N. S. Pradhan¹, Sheshmani K. Dubey², A. D. Yadav¹, B. K. Panigrahi³, K. G. M. Nair⁴ and M. Roy⁵

¹ Department of Physics, University of Mumbai, Mumbai, India
² Department of Physics, University of Mumbai, India
³ Materials Science Division, Indira Gandhi Centre for Atomic Research, Kalpakkam-603 102, India
⁴ Materials Science Division., Indira Gandhi Centre for Atomic Research, Kalpakkam-603 102, India
⁵ Chemistry Division, Bhabha Atomic Research Center, Mumbai - 400 005, India

The magnetic and structural properties of GaN samples implanted with 325 keV Mn²⁺ ions at 350 °C substrate temperature for various fluences varying from 1.75 x 10¹⁵ to 2.0 x 10¹⁶ ions cm⁻² were studied using SQUID, XRD and Raman scattering techniques. Magnetic properties were found to vary with the ion fluence. The 5 MeV Si³⁺ ion irradiation with fluence of 1 x 10¹⁶ ions cm⁻² was performed on the sample implanted for ion fluence 2 x 10¹⁶ cm⁻². The Curie temperature estimated for as-implanted and after irradiated with 5 MeV Si³⁺ ion samples was found to 301 and 326 K respectively. XRD spectra showed GaN peak at (002) reflection, this peak shifted toward lower angle indicated the incorporation of Mn ion in GaN film. Raman spectra of the samples showed bands at ~300 and 670 cm⁻¹ were attributed to the local vibration modes of gallium and nitrogen vacancies related defects respectively.

PN02

Oxidation of monovacancies in graphene by oxygen

Thaneshwor Prasad Kaloni and U. Schwingenschlög
King Abdullah University of Science and Technology, Saudi Arabia

We study the oxidation of monovacancies in graphene by oxygen molecules using first principles calculations. In particular, we address the local magnetic moments which develop at monovacancies and show that they remain intact when a molecule is adsorbed such that the dangling carbon bonds are not fully saturated. The observed value of magnetic moment is 1.35 Bohr Magnetons for monovacancy and it becomes 1.86 Bohr Magnetons by oxygen adsorption on monovacancy in graphene. However, the lowest energy configuration does not maintain dangling bonds and is found to be semiconducting. Our data can explain the experimentally observed behavior of graphene under exposure to an oxygen plasma.

PN03

Structural , compositional and magnetic study of bulk Fe doped ZnO system and impurity phase formation

Shumaila Karamat^{1*}, Rajdeep Singh Rawat², Paul Lee³, Tan Tuck Lee Augustine⁴ and Muhammad Ghaffar⁵

¹ Physics, 1. NIE, Nanyang technological University, Singapore 2. COMSATS Islamabad, Pakistan
² NSSE-NIE, Nanyang Terchnological University, Singapore
³ NSSE-NIE, Nanyang Technological Unievrsty Singapore
⁴ Physics, Nanyang Technological University, Singapore
⁵ EEE, Nanyang Technological University, Singapore

Structural, compositional, optical, vibrational and magnetic properties have been studied for (ZnO)_{1-x}(Fe₂O₃)_x series of bulk samples. The ZnO based ceramic samples with different doping percentage of Fe₂O₃ were prepared by ball milling process. The phase composition of the pellets was determined via X-ray diffraction analysis. Raman spectroscopy give information about the additional modes appear in the ZnO spectrum having Fe doping which assures the presence of Fe in the ZnO matrix. The de-convolution of XPS spectra of core peaks of different elements indicated the presence of different bond breakage due to Fe substitution in ZnO lattice. The appearance of shaking satellites in XPS spectra also confirmed the presence of different valance states of Fe ions. The red shift in energy band gap estimated from reflectance UV-VIS spectroscopy was observed for all bulk samples. The magnetic behavior of the samples was examined by using Vibrating Sample Magnetometer (VSM) indicating ferromagnetic behavior at room temperature. The effective magnetic moment per Fe atom decreases with the increase in doping percentage which indicates that ferromagnetic behavior is due to substitution of Fe ions in the ZnO lattice.

PN04

Enhanced magnetization and spin injection in Co/ZnO films by Al doping

Zhiyong Quan, Wei Liu and Xiaohong Xu*
School of Chemistry and Materials Science, shanxi normal university, China

An important hurdle in the development of semiconductor spintronic devices is the inefficient injection of spin polarized currents from metallic ferromagnets into semiconductors due to the large conductivity mismatch. Inserting a magnetic semiconductor at the interface was regarded as an effectively route for spin injection into semiconductors. In this work, we investigate the magnetism and electrical spin injection into ZnO and Al-doped ZnO (Al 2at.%) matrix from Co particles in Co/ ZnO and Co/ZnAlO films, which were prepared by depositing ultrathin Co layers and semiconductor layers at room temperature. The films consist of Co particles dispersed in the semiconductor matrix. The graded magnetic semiconductors were formed at the transition region between metallic Co particles and semiconductor matrix with the substitution of Zn²⁺ with Co²⁺ ions. The increasing of magnetization of Co/ ZnAlO films compared to the corresponding Co/ZnO films is probably due to the enhanced magnetization of graded magnetic semiconductors with Al enhancing carrier concentration. The room temperature magnetoresistance of Co/ZnAlO film with 1.0 nm of ZnAlO layer reaches -12.3% which is higher than -8.4% of the corresponding film without Al, probably due to the large spin filter effect occurring in the graded magnetic semiconductors having a relative larger polarization.

PN05

Structure, magnetic, and transport properties in Cu_{1-x}Mn_xO compounds

Jinzu Cai, Li Li, Bin Lv, Shen Wang, Wenqin Zou, Fengming Zhang* and Xiaoshan Wu
Physics, Nanjing University, China

By annealing at air, O₂, N₂ atmosphere, the polycrystalline Cu_{1-x}Mn_xO powders, which are prepared by sol-gel method with the concentration range of 0 ≤ x ≤ 0.2, are synthesized. The phase component and atomic structure of the main phase are obtained by X-ray diffraction (XRD) with Rietveld refinements. The bond length of Cu(Mn)-O decreases, and the bond-angle of Cu(Mn)-O-Cu(O) increases, with increasing the dopant. Magnetism measurements (SQUID) show that the ferromagnetic transition temperature, T_c, and the saturation moment, M_s, increase with the doped concentration of Mn, although all the samples show that the T_c is less than 100 K. All samples show the well defined thermal active mechanism with the thermal active energy varying with the annealing atmosphere. Results reveal that annealed in O₂ may increase the carrier concentration of the prepared samples while annealed in N₂ the reverse.

PN06

A probe into the structural, magnetic and dielectric properties of barium and lithium substituted pseudobrookites

Pushpinder Gupta Bhatia^{1*} and Radha Srinivasan²
¹ Physics, Department of Physics, Guru Nanak college, Mumbai-37, India
² Physics, Department of Physics, University of Mumbai, Mumbai-98, India

The versatile nature of the Fe-Ti oxides makes them attractive candidates in applications in which their coupled semiconductor, magnetic and dielectric properties can be exploited and they appear to be good candidates for emerging technologies such as spintronics, magneto-electronics, and radar electronics. In the present work, pure pseudobrookite Fe₂TiO₅ and its lithium and barium substituted varieties namely Ba_xFe_{2-x}Li_{3x}Ti_{1-x}O₅ and Ba_{x/2}Fe_{2-x}Li_yTi_{1-x}O₅ (x = y = 0.05) are synthesized by the solid-state reaction method. Powder x-ray diffraction studies show the single phase orthorhombic structure. Substitution has reduced the crystallite size but enhanced the grain size. A new intense plane (122) is observed in the barium-substituted sample. Lithium intercalation is also observed. Room temperature dielectric studies have confirmed the Maxwell-Wagner interfacial polarization and space charge is seen to have almost doubled with doping. The magnetic hysteresis loops show an asymmetric shift and constriction of loops. Variation of normalised susceptibility with absolute temperature is plotted. Presence of barium and lithium have also brought about a long range magnetic ordering in the pseudobrookite. Susceptibility measurements also show that the Curie temperature in the barium-rich pseudobrookite approaches room temperature making it a potential switch material.

PN07

Oxygen vacancy and magnetism of a room temperature ferromagnet Co-doped TiO₂

Ikuo Nakai^{1*}, Masashi Sasano¹, Yingjie Li², Ken Inui¹, Tomoya Korekawa¹, Hiroyuki Ishijima¹, Hisashi Katoh¹ and Makio Kurisu³
¹ Department of Electrical and Electronic Engineering, Graduate School of Engineering, Tottori University, Japan
² Inner Mongolia Key Laboratory for Physics and Chemistry of Functional Materials, Inner Mongolia Normal University, China
³ Department of Physics, Graduate School of Science and Engineering, Ehime University, Japan

We report the magnetic and local structural study of a room temperature ferromagnetic Co-doped TiO₂ prepared by the solid state reaction. The ferromagnet with 5% Co shows a rutile-type structure and has a saturation magnetization of 0.005 JT-1kg-1 and a coercive force of 0.02 T. We have found that it has some oxygen vacancy sites around a Co atom only from the extended x-ray absorption fine structure (EXAFS) measurement. The charge compensation makes the oxygen vacancy around Co²⁺ and/or Co³⁺ substituted with Ti⁴⁺.

PN08

Effect of annealing on the magnetic anisotropy of GaMnAs film with low Mn concentration

Hyehyeon Byeon¹, Yoonjung Gwon¹, Jaehyuk Won¹, Taehee Yoo¹, Sanghoon Lee^{1*}, X. Liu² and J. K. Furdyna²
¹ Physics Department, Korea University, Korea
² Physics Department, University of Notre Dame, USA

We have investigated the effect of annealing on the magnetic anisotropy of a GaMnAs film with a low Mn composition of 2 %. Three pieces of samples were cleaved from the sample and two of them we are annealed at 200 and 300 °C, respectively, for 3 hours in air. In case of as-grown sample, abrupt transitions in the Hall resistance appeared with a negative coercive field, when field strength was swept at a fixed direction in the film plane. The phenomenon turned out to be related to the presence of magnetic domains with a vertical easy axis in the film, which was identified via the Hall measurement that was performed with a field direction that was normal to the plane. The portion of domain with dominant out-of-plane magnetic anisotropy in the GaMnAs film was systematically decreased with an increasing annealing temperature. Especially, the negative coercive field disappeared in the sample annealed at 300 °C and two abrupt positive switching fields we are observed in the field scan of the planar Hall resistance. This indicates that the annealing significantly affects the magnetic anisotropy of GaMnAs film by changing from out-of-plane dominant to in-plane dominant anisotropy.

PN09

Low field magnetization reversal behavior of ferromagnetic GaMnAs film

Yoonjung Gwon¹, Hyehyeon Byeon¹, Jaehyuk Won¹, Hakjoon Lee¹, Sanghoon Lee^{1*}, X. Liu² and J. K. Furdyna²
¹ Physics Department, Korea University, Korea
² Physics Department, University of Notre Dame, USA

We have investigated magnetization reversal process of a GaMnAs film by using planar Hall effect. The angle-dependent measurements of the planar Hall resistance (PHR) showed sinusoidal behavior without hysteresis between clockwise and counter clockwise rotation with strong field. However, the magnetization reversal behavior changes significantly by showing abrupt transition at the <110> directions as the field strength reduced to 200 Oe. Furthermore, when a smaller field is used, the PHR displays four stable values arising from the formation of four different multidomain states during the rotation of the external field direction over 360°. Two of these states, showing maximum and minimum values of the PHR, correspond to the sample fully magnetized along one of the easy axes. Other two intermediate states are multi-domain states in which a fraction of the domains populates one easy [100] direction, and the remaining fraction populates an orthogonal easy [010] direction. We showed that the relative populations of the magnetic domains corresponding to the two orthogonal easy axes can be controlled by the value of the applied field during the process of magnetization reversal. This phenomenon was understood by considering the differences in domain-pinning fields and their distributions required for crossing the two hard axes.

PN10

Half-metallic antiferromagnetism in the ordered Cr_{1-x}Ca_xSb alloy from first-principles calculations

Guoying Gao* and Kailun Yao
School of Physics, Huazhong University of Science and Technology, China

Compared to half-metallic ferromagnets, half-metallic antiferromagnets (precisely called half-metallic fully compensated ferrimagnets) are more promising candidates for spintronic applications since their zero magnetization leads to lower stray fields and thus tiny energy losses. Using the first-principles calculations, we have systematically investigated the electronic and magnetic properties of the ordered Cr_{1-x}Ca_xSb alloy. It is found that Cr_{1-x}Ca_xSb with x = 0.125, 0.25, 0.5 and 0.75 all are half-metals like zinc-blende CrSb and CaSb which have been fabricated experimentally or predicted theoretically. Interestingly, Cr_{0.25}Ca_{0.75}Sb is a half-metallic antiferromagnet with complete spin polarization, and the half-metallic antiferromagnetism is robust against the lattice compression and expansion and the choice of electronic exchange and correlation functional.

[1] H. Akai, M. Ogura, Phys. Rev. Lett. 97, 026401 (2006). [2] B.-G. Liu, Phys. Rev. B 67, 172411 (2003). [3] M. Sieberer, et al., Phys. Rev. B 73, 024404 (2006). [4] G.Y. Gao, et al., Phys. Rev. B 75, 174442 (2007); [5] J.H. Zhao, et al., Appl. Phys. Lett. 79, 2776 (2001). [6] G. Y. Gao, J. Chen, and K.L. Yao, Phys. Lett. A 375, 4053 (2011).

PN11

Translation & rotation of diamagnetic material induced by a low field of a permanent magnet and terminal identification of a micron-sized particle

Keiji Hisayoshi and Chiaki Uyeda
Osaka university, Japan

It has been generally believed that field-induced motion of an ordinary diamagnetic material can be induced only at high field above several Tesla. However, translations were recently observed on various diamagnetic crystals in a direction of monotonously decreasing field produced by a permanent magnet [1]; the crystals were released in diffused micro-gravity area. In a given field distribution, terminal velocity of translation is uniquely determined by intrinsic susceptibility of material; the velocity is independent to mass of particle. Rotational oscillation, caused by diamagnetic anisotropy energy, was also reported for the crystals [1]. When the above motions are observable, diamagnetic susceptibility & anisotropy of a small particle can be detected, irrespective of its size, since the measurements are both free from interference of a sample holder and from mass measurement of sample. Material identification of particle is easily performed by comparing the obtained susceptibility (& anisotropy) with published values. A simple and nondestructive method to identify the material of a small particle is desired in various fields of nano-science. By introducing a compact NdFeB magnet, the measurement was realized in an ordinary laboratory using a chamber-type drop shaft.

[1] C. Uyeda et al: Jpn. Phys. Soc. Jpn. 79, 064709 (2010). 246

PN12

Magnetoresistance effect in electron-injected p-type silicon

Michael P. Delmo*, Eiji Shikoh, Teruya Shinjo and Masashi Shiraishi
Graduate School of Engineering Science, Osaka University, Japan

Magnetoresistance (MR) effect in silicon has gained a renewed interest in recent years because it is large and non-saturating [1-3]. It is known that the presence of "static" inhomogeneity, like phosphorus in low-doped silicon, generates large and non-saturating MR effect [2,4]. Inhomogeneity can also be introduced "dynamically" by injecting electrons or holes into a low-doped silicon [1,3]. In n-type silicon (n-Si), electron injection generates space-charge effect [1], whereas, the hole injection induces the formation of a hole-electron (p-n) boundary [3]. These dynamic inhomogeneities induce large MR effect even up to room temperature. Most of the silicon devices used in inhomogeneity-induced MR effect studies are n-type, and no study has ever been reported for p-type, so far. In this study, we investigated the MR effect in indium (In)/p-type silicon (p-Si)/In devices. Current (I)-voltage (V) characteristic of the device shows an Ohmic and non-Ohmic I-V regime (I is proportional to the square root of V), which indicates electron space-charge injection into p-type silicon [5]. MR of the In/p-Si/In device is small (10%) compared to that of In/n-Si/In device (1,000%) for the same condition (3 T, 300 K). This suggests that the electron-hole compensation or recombination suppress inhomogeneity formation in the silicon device.

[1] Delmo, M.P. et al. *Nature* 457, 1112 (2009). [2] Porter, N.A. & Marrows, C.H., *arXiv:1105.2174 [cond-mat.mtrl-sci]*. [3] Wan, Caihua et al. *Nature* 477, 304 (2011). [4] Herring, C. J. *Appl. Phys.* 31, 1939 (1960). [5] Roberts, G.G. *Phys. Stat. Sol.* 27, 209 (1968).

PN13

First-principles investigation of the influence of adsorbed atom on the defect and impurity substitute graphene

Kengo Nakada¹ and Akira Ishii²

¹ JST-CREST, Japan
² Department of Applied Mathematics and Physics, Tottori University, Japan

Graphene is well-known to be two-dimensional material made of carbon atoms. Graphene is a substance that attracts attention not only as parts of the nanocarbons but also for its own interesting electronic and mechanic properties. It is important for the application that charge and magnetic are controlled by defect and impurity in the graphene. Furthermore, influence of defect and the impurity are important in the growth of the compound on the graphene. The technological uses of controllable charge and magnetic carbon systems are extensive, and it is important that the mechanism is known. In previous study, we investigated the adsorption energies and magnetism in adsorption sites on graphene from atomic number 1 to 83, using the DFT. We discussed the charge transfer and the magnetism. When several adatoms is adsorbed, the defect graphene develops magnetic. In this study, we performed atom substitute in the graphene and atomic adsorption on the graphene with the defect. The aim of the research is discussion about the magnetic and stability when several adatoms adsorbed on defects and impurities substitute in graphene. In addition, we discuss the growth mechanism of the nitrated compounds. We used a band calculation technique based on the DFT calculation.

PN14

Room-temperature fabrication of highly transparent magnetic nanocomposite systems by aerosol deposition

Jae-hyuk Park* and Akedo Jun
National Institute of Advanced Industrial Science and Technology (AIST), Japan

Nanocomposite systems, materials containing particles of nanometer dimensions have shown interesting properties related to its extremely small size. Some of their optical, magnetic, electronic, mechanical, and chemical properties are different from those exhibited by the same composition in bulk material[1]. We have proposed novel concept for materializing nanocomposite systems using aerosol deposition (AD) process[2-3]. Our concept can apply various sizes of nanoparticles, and achieves desirable distribution of nanoparticles in host matrix because the structure of deposited layer is similar to that of composite powder. In this report, we developed highly transparent magnetic nanocomposite thick films consisting of cobalt nanoparticles embedded in a host matrix of ferroelectric lead zirconate titanate (PZT) by AD process at room temperature. Transparent thick nanocomposite cobalt/PZT films display very dense without any pores as well as any cracks. As the wt% of nanocobalt increased, magneto-optic effect measured in the transmission mode, especially Faraday rotation effect of nanocomposite layers gradually increases with good linearity. The 0.1 wt% nanocobalt-containing nanocomposite film acquired the Faraday rotation angle of approximately 0.2 degree. These results would strongly show potential of optical multiferroics on transparent nanocomposite systems.

[1] M. Abe, M Gomi, and F. Yokoyama, *J. Appl. Phys.*, Vol. 57, pp. 3909-3911, 1985. [2] J. Akedo, *J. Am. Ceram. Soc.*, Vol. 89, pp. 1834-1839, 2006. [3] Jae-Hyuk Park, Jun Akedo and Masafumi Nakada, *Jpn. J. Appl. Phys.*, Vol.45, pp. 7512-7515, 2006

PN15

Effect of transition metal (Co, Ni and Cu) doping on lattice volume, band gap, morphology and saturation magnetization of ZnO nanostructures

Faheem Ahmed, Shalendra Kumar, Nishat Arshi, M S Anwar and Bon Heun Koo*
Changwon National University, Korea

The interest in transition-metal (TM)-doped ZnO has increased because of promising applications in the field of semiconductor spintronics, which seeks to extend the properties and applications of established electronic devices by using the spin of electrons in addition to their charge. In this work, the effect of different TM (Co, Ni and Cu) doping on structural, optical and magnetic properties of ZnO nanostructures have been studied. Zn_{1-x}TM_xO (TM=Co, Ni and Cu) nanostructures were prepared by a microwave assisted chemical route and characterized by X-ray diffraction (XRD), field emission scanning electron microscopy (FESEM), transmission electron microscopy (TEM), Raman spectroscopy, UV-Vis and magnetization measurements. The X-ray diffraction (XRD) and TEM analysis showed that the TM-doped nanostructures had single phase nature with the wurtzite structure. There is a strong correlation between changes in the lattice parameters, bandgap energy, morphology and the saturation magnetization of Zn_{1-x}TM_xO nanostructures. Lattice volume and bandgap determined from XRD and UV-Vis, respectively, were found to decrease as the atomic number of the dopant moved away from Co. Magnetic studies showed that all the TM-doped ZnO exhibit room temperature ferromagnetism and the decreasing trend of saturation magnetization was observed with the increase of 3d electrons number from Co to Cu.

PN16

Functionalized graphene as a room-temperature ferromagnetic semiconductor

Jeongmin Hong*, Sandip Niyogi², Elena Bekyarova², Mikhail E. Itkis², Palanisamy Ramesh², Claire Berger³, Walt A. Deheer⁴, Robert C. Haddon² and Sakhrat Khizroev²

¹ Electrical and Computer Engineering, Florida International University, USA
² Department of Chemistry, Department of Chemical Engineering, Center for Nano Scale Science and Eng, University of California-Riverside, USA
³ CNRS, Institut Neel, France
⁴ School of Physics, Georgia Institute of Technology, USA
⁵ Department of Electrical and Computer Engineering, Florida International University, USA

Low-temperature magneto-transport and vibrating sample magnetometry (VSM) combined with superconducting quantum interference device (SQUID) measurements indicated that graphene, when functionalized with aryl radicals, behaved as a room-temperature ferromagnet and therefore might form the basis for a new approach to semiconducting ferromagnetism. After radical functionalization, epitaxially grown graphene samples became semiconductors and at the same time displayed high-density magnetism, with a room temperature saturation magnetization of approximately 0.1 Bohr magnetons per carbon atom. The bulk measurements with VSM and SQUID were corroborated with local studies using atomic force microscopy (AFM), electrostatic force microscopy (EFM), magnetic force microscopy (MFM), scanning tunneling microscopy (STM), and Raman Spectra measurements. Both local and bulk measurements indicated a strong dependence on the degree of coverage of the graphene surface with functionalized sites. The measurements showed the presence of a superparamagnetic order in the graphene regions with a relatively low-density of functionalized sites in the entire temperature range from 2 to 300 K. In contrast, the regions with a relatively high-density of functionalized sites displayed a ferromagnetic order even at room temperature. In summary, the measurements indicated that aryl radical functionalized multi-layered graphene on Silicon Carbide could simultaneously be a semiconductor and a ferromagnet at room temperature.

PN17

Tuning of the curie temperature by varying reduction potential in electrochemically prepared thin films of Prussian blue analogue based molecular magnets

Pramod Bhatt*, M. D. Mukadam and S. M. Yusuf
Solid State Physics Division, Bhabha Atomic Research Centre, Mumbai-400085, India

The quest for molecular magnets with ordering temperature at or above room temperature is highly desirable for their practical applications at ambient conditions. In order to increase the ordering temperatures, many efforts have been devoted to synthesizing compounds with appropriate choice of organic/inorganic ligands, their valence modulation and spin centers, and alkali metal ion doping, etc., using organometallic and/or coordination chemical methods. However, we have shown that, the magnetic ordering temperature in PBAs (Prussian blue analogues) can be enhanced by varying reduction potential in electrodeposition method. In this regard, the electrochemically prepared films of PBAs, X_jFe₁₁k[CrIII(CN)₆]_l.mH₂O with varying reduction potential are investigated using dc magnetization measurements. The magnetization data for film deposited at lower reduction voltage shows ferromagnetic ordering with TC (Curie temperature) of ~ 21 K, similar to previously reported ordering temperature for this compound. However, an increase in TC up to ~50 K has been observed for film deposited at higher reduction potential. The observed variation in TC is mainly attributed to the inclusion of potassium ion (K+) at higher reduction potential, which changes stoichiometry of the film. The ability of tuning TC just by changing reduction potential could be useful for designing future device applications.

PN18

Evolution of multifunctional behavior in site specific cation substituted Na_{0.5}Bi_{0.45}Gd_{0.05}Ti_{0.95}Mn_{0.05}O₃ ceramics

T Karthik^{1,2} and Saket Asthana^{1*}
¹ Advanced Functional Materials Laboratory, Department of Physics, Indian Institute of Technology Hyderabad, Andhra Pradesh - 502205, India
² Department of Materials Science and Engineering, Indian Institute of Technology Hyderabad, Andhra Pradesh - 502205, India

A novel multifunctional behavior was observed by site specific cation substitution in NBT ceramics prepared by conventional solid state reaction technique. X-ray diffraction studies revealed the co-existence of orthorhombic reflections in co-substituted NBT system along with the primary R3c phase. Raman spectroscopy of NBT-GM ceramics reveals a substantial change in all phonon modes in terms of suppression and shift indicates that the substitution affects nature of the cation displacement, octahedral tilt and hybridization. Reduced polarization value in NBT-GM ceramics with non-saturated hysteresis loops gives evidence for the suppression of ferroelectricity. Temperature dependent magnetization measurements from R.T to 2.5K in NBT-GM ceramics show the occurrence of spin-paramagnetic behavior. Susceptibility plots show some evidence for weak interaction between Mn⁴⁺ ions at low temperatures below 30K. UV-Vis spectroscopy measurements reveal the indirect transition allowed band gap nature for both NBT and NBT-GM ceramics with a slight increase in band gap (E_g) value for NBT-GM ceramics. Photoluminescence measurements show a strong blue emission at ~390nm (3.18 eV) in Gd-Mn substituted NBT system, which corresponds to radiative transition from ⁴T_{1g} → ⁴A_{2g} energy levels of Mn⁴⁺-ions.

PN19

Magnetic doping effect on physical properties of PbPdO₂

Kyujoon Lee, Seongmin Choo and Myung-hwa Jung*
Sogang University, Korea

The exotic features of gapless semiconductors have attracted many researchers in solid state physics. Materials such as HgCdTe have been studied as a gapless semiconductor. Recently PbPdO₂ has been theoretically proposed to be a gapless semiconductor. In addition, by substituting Co for Pd ions the material becomes a spin gapless semiconductor which has full spin polarization. In this study we have experimentally shown the changes in the physical properties of PbPdO₂ by doping different magnetic ions such as Co, Mn, and Zn. PbPdO₂ shows a metal-insulator-like transition at TMI=100 K in the resistivity vs. temperature measurements. The magnetic properties show a diamagnetic behavior at high temperatures and a ferromagnetic behavior at low temperatures. The TMI increases to 150 K by Co doping and the diamagnetic behavior changes to paramagnetic behavior. By Mn doping, the TMI decreases to 73 K and the magnetic behavior changes drastically to show antiferromagnetic ordering at low temperatures. However no difference has been found by Zn doping. The common feature for all materials is that the charge carrier density increases with doping. The easily tuned properties of PbPdO₂ show evidence that PbPdO₂ is a gapless semiconductor and could be tuned to be a spin gapless semiconductor.

PN20

An experimental approach using EPR and XMCD to explore hydrogen mediated ferromagnetism

Seunghun Lee¹, Bun-su Kim¹, Yong Nam Choi², Naoki Ishimatsu³, Masahiro Sawada³, Won-kyung Kim¹, Ji Hun Park¹, Yong Chan Cho¹ and Se-young Jeong^{1*}
¹ Cogno-Mechatronics Engineering, Pusan National University, Korea
² Korea Atomic Energy Research Institute, Korea
³ Hiroshima University, Japan

Since the ferromagnetism of III-VI based DMS materials such as GaMnAs was turned out to be based on carrier induced model, much progress has been made in developing its applicability but low operation temperature has limited the approach to functional devices[1]. Among other materials, Co doped ZnO has been regarded as strong candidate for room temperature DMS but the origin of ferromagnetism has been on controversy[2]. Previously, we reported experimental results on Co-H-Co responsible for ferromagnetism depending on hydrogen contents and position[3-5]. Here, in order to apply these phenomena for new functional devices, more convincing experimental evidence for Co-H-Co is necessary. In this study, we show the experimental approaches to hydrogen mediated ferromagnetic spin ordering in ZnCoO through electron paramagnetic resonance(EPR) and x-ray magnetic circular dichroism(XMCD). The signal intensity of ferromagnetic resonance is attributed to hydrogen contents and spin/angular magnetic moments compared with theoretical model of Co-H-Co are calculated from XMCD spectrum. In addition, the results of photoluminescence and spectrum of magnetic circular dichroism within UV-Vis range suggests the possibility for creating and manipulating spin-polarized carrier using hydrogenated ZnCoO. Through advanced theoretical calculation for Co-H-Co model, we are expecting to obtain the direct evidence for Co-H-Co unit.

[1] D. A. Allwood et al., *Science*, 309, 1688 (2005) [2] S. Lee et al., *Appl. Phys. Lett.* 94, 212507 (2009) [3] Y. C. Cho et al., *Appl. Phys. Lett.* 95, 172504 (2009) [4] S. J. Kim et al., *Phys. Rev. B* 81, 212408 (2009) [5] S. Lee et al., *J. Appl. Phys.* (in press, 2012)

PN21

A role of mobility in hydrogen mediated ferromagnetism of ZnCoO

Ji Hun Park¹, Seunghun Lee¹, Won-kyung Kim¹, Jong Moon Shin², Yong Chan Cho¹, Chae Ryong Cho², Hideomi Koinuma¹ and Se-young Jeong^{1*}
¹ Dept. of Cogno-Mecatronics Engineering, Pusan National University, Korea
² Dept. of Nano Fusion Technology, Pusan National University, Korea

Diluted magnetic semiconductors (DMSs) have recently been attracting much attention for their potential as spin manipulation layers [1]. Although there have been reported several authorized DMSs, such as Mn doped GaAs, their limited operating temperature requires new DMS materials with high Curie temperature. Up to now, many theoretical and experimental studies about hydrogen mediated ferromagnetism in ZnCoO have been introduced [2-3]; however, the interaction between such magnetic units as Co-H-Co complexes has not yet been confirmed. Delocalized electron in ZnCoO lattice is possibly considered to play a crucial role in the correlation [4]. In this work, we investigated the correlation between carrier mobility and ferromagnetic spin ordering in ZnCoO. Electron mobility was artificially controlled with the manipulation of crystallinity and hydrogen contents. Hydrogen treatment is carried out using hot isostatic pressing (HIP) system. The correlation between carrier mobility and ferromagnetic spin ordering was analyzed in terms of Co-H-Co magnetic units. Mobility-dependent ferromagnetic spin ordering is discussed in our experiment.

[1] H. Ohno, *Science*, 281, 951 (1998). [2] C. H. Park and D. J. Chadi, *Phys. Rev. Lett.* 94, 127204 (2005). [3] S. Lee et al., *Appl. Phys. Lett.* 94, 212507 (2009); Y. C. Cho et al., *Appl. Phys. Lett.* 95, 172514 (2009); S. J. Kim et al., *Phys. Rev. B* 81, 212408 (2010). [4] Z. Lu et al., *Appl. Phys. Lett.* 94, 152507 (2009).

PN22

Magnetic and magneto-optical properties of TiO₂:V semiconductor oxide films with various resistivity

Andrey F Orlov¹, Leonid A Balagurov¹, Ivan V Kulemanov¹, Elena A Petrova¹, Nikolai Perov^{2*}, Elena A Gan'shina², Leonid Yu Fetisov², Anna S Semisalova², Anastasia D Rubacheva², Andrei Rogalev², Alevtina G Smekhova² and Lada V Yashina²
¹ Institute for Rare Metals, Moscow, 119017, Russian Federation, Russia
² Lomonosov Moscow State University, Russia
³ European Synchrotron Radiation Facility, Grenoble Cedex, France
⁴ European Synchrotron Radiation Facility, Grenoble Cedex, France; Lomonosov Moscow State University, Russia

We present the investigation results of semiconducting films TiO₂:V with 3-18%at. of vanadium, which develop our previous research of doped titanium oxide [1,2]. The films have been grown by RF magnetron sputtering on either LaAlO₃ or rutile TiO₂ substrates and revealed the room temperature ferromagnetic ordering in the wide range of resistivity (10³-10⁶ Ωcm). For degenerate semiconductors the values of magnetization were found to be lower. Magnetization of TiO₂ doped with vanadium is maximum for all semiconductor oxides doped with transition metal impurities. Maximum values of magnetization were observed in the films with a small content of V impurity and corresponded to 4.8 Bohr magneton per V atom. The V impurity was found to be utterly in the oxidized state only in the films with a small V concentration. The magneto-optical response in the 1.5-3.0 eV energy range was observed in samples with a high magnetic moment only. The results are discussed within the model of charge-transfer ferromagnetism suggested by Coey et al. [3,4]. Supported by RFBR and Ministry of Science and Education No.16.513.11.3088.

[1] A.F. Orlov et al., *JMMM*, 320, 895 (2008); [2] E.A. Gan'shina et al., *JMMM*, 321, 723 (2009); [3] J.M.D. Coey et al., *J. Phys. D: Appl. Phys.*, 41, 134012 (2008); [4] J.M.D. Coey et al., *New J. Phys.*, 12, 053025 (2010).

PN23

Magnetic properties and electrical conductivity on oxygen-deficient europium monoxide

Jun-young Kim^{1*}, Pedro M.d.s. Monteiro¹, Kiyoung Lee¹, Adrian Ionescu¹, Stuart N Holmes², Crispin H.w. Barnes¹, Peter J Baker¹, Sean Langridge¹, Zaher Salman¹, Andreas Suter¹ and Thomas Prokscha¹
¹ Department of Physics, Cavendish Laboratory, University of Cambridge, J J Thomson Avenue, Cambridge, CB3 0HE, United Kingdom
² Toshiba Cambridge Research Laboratory, 208 Cambridge Science Park, Milton Road, Cambridge, CB4 0GZ, United Kingdom
³ ISIS, Harwell Science and Innovation Campus, STFC, Oxon OX11 0QX, United Kingdom
⁴ Laboratory for Muon-Spin Spectroscopy, Paul Scherrer Institut, CH-5232 Villigen PSI, Switzerland

Pristine europium monoxide (EuO) is a ferromagnetic semiconductor with a Curie temperature (T_c) of 70 K. Below T_c, the conduction band is 100% spin-polarised [1] while at T_c it undergoes a metal-to-insulator transition [2]. These properties render it a promising material for future spintronic devices such as spin injection electrodes or filters [3]. Tunable control of magnetic properties is obtained by doping with oxygen vacancies. We present results on co-sputtered EuO_{1-x} films with T_c as high as 140 K. The films were characterized by SQUID magnetometry, x-ray and polarized neutron reflectometry. The magnetic moment was found to increase monotonically with oxygen vacancy concentration. Density-functional theory calculations of EuO_{1-x} show that oxygen vacancies act as n-type dopants and that the excess electrons preferentially populate the majority spin branch of the conduction band [4]. We also present thickness-dependent magnetic properties of EuO_{1-x} thin films, where surface-induced changes were observed in films with below 5 nm thickness [5]. Muon spin rotation measurements investigated microscopic magnetic behaviour and magnetic volume fraction as a function of temperature. Electrical transport measurements in the Hall geometry will also be presented.

[1] R. P. Panguluri, T. S. Santos, E. Negusse, J. Dvorak, Y. Izderka, J. S. Moodera, and B. Nadjgorny, *Phys. Rev. B* 78, 125307 (2008) [2] G. Ferrich, S. von Molnar, and T. Pernes, *Phys. Rev. Lett.* 26, 885-888 (1971) [3] A. Schmelz et al., *Nature Materials* 6, 882-887 (2007) [4] M. Barbagallo et al., *Phys. Rev. B* 81, 235216 (2010) [5] M. Barbagallo et al., *Phys. Rev. B* 84, 075219 (2011)

PN24

Magnetism and optical properties of diluted magnetic semiconductor superlattice GaGdAs/GaAs with GaGdAs nanograins

Miyagawa Hayato*, Yuuki Uda, Shoutaro Matsumoto, Nakaba Funaki and Shyun Koshiha
Faculty of Engineering, Kagawa University, Japan

We found ferromagnetic coupling in the rare earth elements Gd doped GaAs DMS, abbreviated as GaGdAs, which was grown by molecular beam epitaxy (MBE). However, GaGdAs is easy to have distortions or dislocations, because the atomic size of Gd is large compared to GaAs matrix, and also there is lattice mismatch between GaGdAs layer and substrate. Superlattice (SL) structure of GaGdAs/GaAs, in which GaGdAs layers are interleaved with a few ML thick GaAs layer, is considered to have a good crystallinity. We fabricate magnetic semiconductor superlattice GaGdAs/GaAs and mono layer GaGdAs by MBE and analyze the crystal structure by means of Transmission Electron Microscopy (TEM) and measured the macroscopic magnetic properties by Alternating Gradient Magnetometer (AGM). In high resolution TEM images, there are GaGdAs grains of 2-3 nm, which has high Gd concentration and lattice-matching in GaAs Matrix. The result of magnetic measurements shows that superlattice structures have larger saturated magnetization and smaller coercive field than that of monolayers. We think that the GaGdAs grains, which are observed only in SL structures, possibly has main contribution to generate ferromagnetism in room temperature. We also measured Photoluminescence of GaGdAs samples and found the energy band gap is larger than GaAs.

PN25

Ferromagnetism in hydrogenated fullerene

Kyu Won Lee, Gi-wan Jeon and Cheol Eui Lee*
Physics, Korea University, Korea

We identify Stoner ferromagnetism in fcc C₆₀H_n (n=odd) by using a local density approximation in the framework of the density functional theory. Hydrogen chemisorption on fullerenes creates quasilocalized π-electrons on the fullerene surface, overlapping of their wave functions giving rise to a narrow half filled impurity band in the fcc C₆₀H_n. The Stoner-type ferromagnetic exchange between the itinerant electrons leads to spin-split impurity bands. The magnetic moment per C₆₀H_n molecule is 1 μB (for n=odd) or 0 (for n=even, including zero), only one of the hydrogens contributing to the spin-split states. Direct overlapping of the quasilocalized π-electron orbitals is essential for the ferromagnetism.

1. T. L. Makarova, B. Sundqvist, R. Hořne, P. Esquinazi, Y. Kopelevich, P. Scharff, V. A. Davydov, L. S. Kashevarova, and A.V. Rakhmanina, *Nature (London)* 413, 716 (2001). 2. T. L. Makarova, B. Sundqvist, R. Hořne, P. Esquinazi, Y. Kopelevich, P. Scharff, V. Davydov, L. S. Kashevarova, and A.V. Rakhmanina, *Nature (London)* 440, 707 (2006). 3. S. Okada and A. Oshiyama, *Phys. Rev. B* 68, 235402 (2003).

PN26

Enhancement of the magneto-optical effect by an addition of Co in pseudo-quaternary II-VI magnetic semiconductor CdMnCoTe films

Masaaki Imamura* and Keisuke Ninomiya
Electrical Engineering, Fukuoka Institute of Technology, Japan

Magneto-optical properties with pseudo-quaternary magnetic semiconductor CdMnCoTe films deposited on quartz glass substrates by using MBE equipment [1] have been studied at a visible wavelength region at room temperature. Deposition was made at an average rate of ~1 Å/sec for 8h using a 4N Co target sputtered by an electron gun having an emission-current of 20 mA, a 5N CdTe effusion cell heated at 490°C and a 4N MnTe cell at 1020°C. Using this system, ~2-μm-thick CdMnTe and CdMnCoTe films were prepared on 0.5-mm-thick QG substrates. These films exhibited the preferred (111) growth and paramagnetic characteristics. The magnetization intensity at 15 kOe at room temperature was approximately 2.5x10⁻⁴ emu for the Cd_{0.65}Mn_{0.35}Te film and 2.8x10⁻⁴ emu for the Cd_{0.52}Mn_{0.39}Co_{0.05}Te film, showing the values that were almost the same for two films. Faraday rotation measured at 620 nm in the CdMnCoTe film was -0.32 deg/cm-G and that in the CdMnTe film was -0.10 deg/cm-G. Thus the Faraday rotation in the CdMnCoTe films was largely enhanced compared to that in the CdMnTe films. A direct ac Faraday rotation observation under 1.27 kHz ac fields generated by a ring magnet [2] has successfully been carried out for the CdMnCoTe films.

[1] A. Okada et al., *IEEE Trans. Magn.* 39, 3175 (2003). [2] A. Okada et al., *J.Magn. Soc. Jpn.*, 31, 328 (2007).

PN27

Origin of ferromagnetism in Co-doped (La,Sr)TiO₃ diluted magnetic semiconductors

Xuefeng Wang¹, Fengqi Song², Yi Shi¹, Rong Zhang¹ and Jianbin Xu³
¹ School of Electronic Science and Engineering, Nanjing University, China
² Department of Physics, Nanjing University, China
³ Department of Electronic Engineering, The Chinese University of Hong Kong, China

Diluted magnetic semiconductors (DMSs) are one of the important supporting materials for the new-generation of spintronic devices. We prepared (La,Sr)TiO₃ (LSTO) and Co-doped LSTO DMS nanocrystals through solvothermal technique combined with post-annealing process. After that, the effects of concentration of Co dopant, the annealing atmosphere, temperature, duration and other conditions on the microstructures and magnetic properties were investigated. When the doping concentration is lower than 5 at.%, the observed room-temperature ferromagnetism (RTFM) of our samples is of intrinsic property. Meantime, it is found that the magnetism has the close relation with the concentration of Co dopant and the amorphous carbon which is remained after annealing. Through controlling the annealing atmosphere and duration, we can synthesize single-phase Co-doped LSTO nanocrystals. It is demonstrated that the RTFM is correlated with the structural defects induced in the Ar annealing process. It is also shown that Co-doped LSTO nanocrystals will have the CoO secondary phase when the Co doping concentration is higher than 5 at.%. According to the interesting exchange biasing phenomenon, the RTFM of our samples is ascribed to the collection of the CoO nanophase or amorphous Co metallic impurities.

PN28

Two dimensional growth of Nb doped SrTiO₃ thin films and its superlattices

Abhijit Biswas, Yong Woo Lee, Min Hwa Jung and Yoon Hee Jeong*
Department of Physics, Pohang University of Science and Technology, Korea

Two dimensional growth modes were obtained for Nb doped SrTiO₃ thin films grown on TiO₂ terminated SrTiO₃ (001) substrates; as monitored by in-situ reflection high-energy electron diffraction (RHEED). At low substrate temperature ordinary RHEED oscillation was observed, indicating layer by layer growth. At high temperature, recovery of RHEED intensity after switching off laser pulses indicated the step flow growth mode. In both cases, films show metallic behavior with resistivity (ρ)~10-3 Ω-cm. Nb:SrTiO₃/SrTiO₃ (NSTOm/STON) superlattices were also being fabricated at low temperature containing five unit cell thick NSTO layers with various stacking sequences. Film surfaces were characterized by atomic force microscopy (AFM), showing high crystalline quality having steps of 3.9 Å. At room temperature, resistivity was found to be 1~2 Ω-cm. The oxide superlattice growth approach might provide a useful way to control the charge carrier and resistivity for novel device applications.

PN29

Anomalous hall effect in ferromagnetic nanocomposite FeGa/Fe₃Ga thin films

Dang Duc Dung¹, Duong Anh Tuan², Yooleemi Shin² and Sunglae Cho^{2*}
¹ Department of General Physics, School of Engineering Physic, Ha Noi University of Science and Technology, 1 Dai Co Viet road, Ha Noi, Viet Nam
² Department of Physics, University of Ulsan, Ulsan 680-749., Korea

The anomalous Hall effect (AHE) is a central topic in the study of the ferromagnetic materials because it exhibit one of the strong evidence for spin polarization [1]. There are three main mechanisms for AHE including intrinsic deflection, side jump and skew scattering. The AHE in intrinsic homogeneous magnetic material is related to spin polarize due to difference state of spin up and spin down at the Fermi energy level and matched to the Berry phase theory [2]. In inhomogeneous magnetic material, AHE implies the presence of spin dependent scattering mechanism. The skew scattering dominates at low temperature, while the side jump becomes important at high temperature [3]. Recently, we reported the observation of weak AHE in FeGa epitaxial thin film on GaAs(001) substrate where FeGa displayed the A2 structure [4]. The FeGa were recently rapidly studied because of its giant magnetostrictive characteristics [5, 6]. In this work, we report the observation of AHE in nanocomposite FeGa/Fe₃Ga epitaxial thin film on GaAs(001). Unlike FeGa (A2-structure), the strong AHE were shown up to 400 K. Interestingly, the nanocomposite FeGa/Fe₃Ga film exhibited strong out-of-plane magnetization. We suggest that the origin of strong AHE are magnetization orientation of epitaxial Fe₃Ga (DO3-structure).

[1] N. Nagasua et al., *Rev. Mod. Phys.* 82, 1539 (2010). [2] M. V. Berry, *Proc. Roy. Soc. of London* 392, 45 (1984). [3] P. Xiong et al., *Phys. Rev. Lett.* 69, 3220 (1992). [4] D. A. Tuan et al., to be printed in *JAP*. [5] J. Anlasimha et al., *Smart Mater. Struct.* 20, 043001 (2011). [6] O.M.J. van Erve et al., *Appl. Phys. Lett.* 91, 122515 (2007), and reference therein.

PN30

MnAs nanoclusters embedded in GaAs: Magnetism and transport properties

Duong Van Thiet¹, Dang Duc Dung², Yooleemi Shin³ and Sunglae Cho^{2*}
¹ Department of Physics, University of Ulsan, Ulsan 680-749, Korea
² Department of General Physics, School of Engineering Physics, Ha Noi University of Science and Technology, 1 Dai Co Viet road, Ha Noi, Viet Nam
³ Department of Physics, University of Ulsan, Ulsan 680-749., Korea

The fabrication of magnetic nanocluster embedded in conventional semiconductor is a research trend because of their unique physical properties in electronics, optics and magnetism. The understanding of magnetic clusters effect on the transport and magnetic properties in semiconductor is timely demanded for the spintronic device application. In this work we embedded MnAs nanoclusters in GaAs(001) by growing MnAs/GaAs multilayer structure using molecular beam epitaxy. After growing 2000 Å GaAs buffer layer on GaAs (100) substrate, the [MnAs (20 Å)/GaAs (tGaAs)]₄ multi-layer configurations were grown at 400 oC, finally followed by the growth of 200 Å-thick GaAs capping layer to avoid the oxidation of inner layer. The GaAs was selected as 100, 200 and 300 Å. The reflection high energy diffraction (RHEED) exhibited spotty patterns, indicating the island-growth of MnAs nanocluster. The result of cross-sectional TEM measurement also showed that MnAs nanocluster are embedded in GaAs matrix successfully. The resistance was increased rapidly with decreasing temperature, indicating that the samples demonstrate semiconductor behavior. The magnetic properties were carried out by the superconductor quantum interface devices (SQUID) measurement, which showed the TC above room temperature. The detail sample growth, and magnetic and transport properties of MnAs nanocluster embedded on GaAs will be discussed.

PN31

Half-metallic and ferromagnetic properties of carrier doping in Zn_{1-x}Cu_xO

Byung-sub Kang¹, Kie-moon Song¹, Yong-sik Lim¹, Kyeong-sup Kim², Young-yeal Song² and Seong-cho Yu²
¹ Dept. of Nano science and Mechanical engineering, Konkuk University, Korea
² Dept. of Physics and BK21 Physics Program, Chungbuk National University, Korea,

Diluted magnetic semiconductors (DMSs) have attracted a great deal of attention because of the possibility of incorporating magnetic degrees of freedom in traditional semiconductors. However, it is one of the primary challenges to create the ferromagnetic semiconductors due to the difficulty in the spin-injection into the semiconductors to form DMSs at room temperature or above room temperature. Since ZnO is a direct wide-band gap semiconductor which is piezoelectric, ZnO-based DMS would be useful for transparent thin film transistors, blue and UV light-emitting diodes and laser diodes. The precipitates of nonmagnetic Cu dopants do not contribute to the magnetism. In our work, the stability of ferromagnetic state in ZnO-based DMSs with a concentration of 2.77%, 5.55%, and 8.33% has been investigated by first-principles calculations. The magnetic moments are not affected by changing the doping concentrations, while the band gap is decreased as for increasing of Cu concentration. The band gaps in Cu-doped ZnO are 0.65, 0.22, and 0.08 eV for the Cu concentration of 2.77%, 5.55%, and 8.33%, respectively. The half-metallic character shows at low Cu concentration, while it is disappeared as for increasing of Cu concentration. The effects on the electronic state by the hole (Nitrogen) doping have been investigated.

PO01

Synthesis and characterization of surface functionalized magnetic polymer microspheres with multi-shell structure

Zuli Liu*, Qing Li and Kailun Yao
Physics, Huazhong university of science and technology, China

We synthesize magnetic polymer microspheres with amino/ carboxyl groups on the surface. We also fabricate the microspheres by incorporating magnetite nanoparticles(MPs) into a silica shell around preformed polystyrene(PSt)/SiO₂ core/shell microspheres. Due to the silicization reaction with 3-aminopropyl triethoxysilane(APTES), the outermost silica shell is formed and linked with amino group at the same time. And we use PEG diacid to obtain carboxyl functionalized microspheres via the reaction between -NH₂ and -COOH. Optical microscope and scanning electron microscopy(SEM) show that the microspheres are monodisperse with the average diameter about 2μm; vibrating sample magnetometer(VSM) indicates that the synthesized sample with amino-group on the surface exhibits superparamagnetism with the saturation magnetization 7emu/g; thermogravimetry(TG) reveals that the microspheres are thermally stable when temperature is below 300°C and the Fe₃O₄ content is 20.68%. Last, the fluorescence microscope shows that the microspheres obtained can be successfully conjugated with biomolecular, including streptavidin and antibody.

PO02

Production of Fe_{3-x}Zn_xO₄ nanoparticles for agents in hyperthermia treatment

Hiromasa Takeuchi*, Akinobu Kurokawa, Takuya Yanoh, Shinya Yano and Yuko Ichiyanagi
Yokohama National University, Japan

Fe_{3-x}Zn_xO₄(x=0.2, 0.4, 0.6, 0.8, 1) nanoparticle with average diameters 12nm were produced by our novel wet chemical method. The crystal structure and magnetic property of the obtained particle were investigated by X-ray diffraction and SQUID magnetometer. DC magnetization measurement showed that the coercive force Hc and saturation magnetization Ms decreased as the composite parameter x increased. This phenomenon suggests that Zn²⁺ ions located on A-sites weaken the superexchange interaction between A and B sites. From the AC magnetic susceptibility, a sample with composition of x=0.4 is expected for heating by external field. Temperature increase depending on the magnetic field strength and frequency supported that samples with composition of x=0.2, 0.4 were appropriate for use as an agent in hyperthermia treatment.

PO03

Gene delivery using polyethylenimine-coated magnetic nanoparticles by static and oscillating magnetic field

Yoshiyuki Takahashi¹, Satoshi Ota¹, Asahi Tomitaka¹, Tsutomu Yamada¹, Daisuke Kami², Shogo Takeda³, Masatoshi Watanabe³ and Yasushi Takemura¹
¹ Electrical and Computer Engineering, Yokohama National University, Japan
² Kyoto Prefectural University of Medicine, Japan
³ Materials and Chemical Engineering, Yokohama National University, Japan

Recently gene delivery without viral vectors attracts rising attention. Low transfection efficiencies of nonviral gene vectors such as transfection reagent limit their utility in gene therapy. To overcome this disadvantage, we report a transfection method using cationic polymer polyethylenimine(PEI)-coated magnetic nanoparticles and an external magnetic field. It shows high transfection efficiency as well as low cytotoxicity. In this study, transfection efficiency of plasmid DNA in complex with PEI-coated magnetic nanoparticles was studied. HeLa cells were seeded the day before transfection. Immediately before transfection, the PEI-coated magnetic nanoparticles (γ-Fe₂O₃) were mixed with plasmid DNA. The complexes were incubated and added to HeLa cells on a NdFeB magnet and a coil. After 48 hours, transfection efficiency of plasmid DNA to HeLa cells was evaluated by the average percentage of the fluorescent cells imaged by a fluorescent microscope in triplicate. The optimal amount of magnetic nanoparticles was 3.0 μg/sample on a magnet for 4 h. The transfection efficiency was increased five-times compared without magnetic nanoparticles (only PEI). Higher transfection efficiency was obtained by applying an ac magnetic field. Further analysis on other parameters of an applied magnetic field and endocytosis are reported.

PO04

Fabrication of QD-anchored magnetic nanocomposites for biomedical applications

Hangdeok Oh and Sang-wha Lee*
Department of Chemical and Bio Engineering, Kyungwon University, Korea



July 9 (Mon)

July 9 (Mon)

PO05

Determination of biomolecule interaction in magnetic particle by voltammetry and ac impedance

Hoon Song and D. G. Park*
korea atomic energy research institute, Korea

Magnetic biochip based immunoassay have potential in many fields, such as environmental immunoassay, diagnostic immunoassay, and biochemical studies and immunosensors [1]. In the field of immunoassays, cyclic voltammetry (CV) technique have become known independently as methods suitable for the detection of immunological reactions. CV measurements are the current signals based on the electrochemical species consumed and/or generated during a biological and chemical interaction process of a biologically active substance and substrate. To apply to the real biomarker and verify the sensitivity of CV-based sensor, we used the biomarker scheme using the applied the real protein on the gold surface. The capture antibodies (P21 mono antibody) are first immobilized on the positive gold sensor surface. The samples with biomarkers (P21 recombination protein) to give antibody and antigen reaction are applied on gold surface. After the non specific binding labels were successfully removed through the washing progress, only the chemically bounded bio molecules were remained on the Au surface. This enables to increase the sensitivity of the sensor for the binding of biomolecules on the gold surface. The difference in the CV represents the quantity of the antigen of interest and could be applied to the biosensor.

[1] Choi JW, Chun BS, Oh BK, Lee W, Lee WH (2005) Fabrication of DNA-protein conjugate layer on gold-substrate and its application to immunosensor. *Colloid Surf B* 40:173-177

PO06

The effects of pulsed magnetic field stimulus on electromyographic activity

Juyeon Seo¹, Yongjin Kim¹, Jaehyun Kim¹, Sunghyun Kim¹, Do Gwen Hwang¹, Yun-yeop Cha² and Hyun Sook Lee^{1*}
¹ Department of Oriental Biomedical Engineering, Sangji University, Korea
² Department of Oriental rehabilitation medicine, Sangji University, Korea

Pulsed magnetic fields (PMF) conducting impulses toward the deep tissues as well as transcutaneous tissues are well known to be alternative non-invasive medical treatment for influencing human physiology as compared with acupuncture. In traditional Chinese medicine, acupuncture is used clinically to relieve myalgia and many studies have attempted to elucidate its mechanism of action [1]. The aim of the present study was to examine the immediate effects of PMF stimulus on the electromyographic (EMG) activity at acupoint HT2, Qingling, which is a trigger point as hyperirritable spots in biceps brachii muscle on the arm [2]. Six healthy volunteers were asked to perform four repetitions of withstanding maximal isometric contraction with 5-kg load and an elbow angle of 90° to cause fatigue in biceps brachii muscle on the arm. Analyzing power density spectrum from fast Fourier transformation of EMG signal, we observed that median power frequency (MDF) decreased and median power increased due to muscle fatigue during isometric contractions. It was proved that PMF stimulus on acupoint was effective in relieving muscle pain by means of increased MDF and amplitude probability distribution of RMS EMG shifted to high amplitude. Therefore, it may be concluded that appropriate PMF stimulus affects neuromuscular function.

[1] K. Toma, R. Conatser, R. Gilders, and F. Hagerman, *J. Strength & Condit. Res.* 12(4), 253-257(1998). [2] J. Majlesi & H. Unalan, *Curr Pain Headache Rep* 14,353-360(2010)

PO07

Magnetic anisotropy of Co₃Fe_{3-d}O₄ nanoparticles for applications in magnetic hyperthermia

Costica Caizer*
Electricity and Magnetism, West University of Timisoara, Romania

The magnetic behaviour of the Co₃Fe_{3-d}O₄ (d = 0 ~ 1.5) nanoparticles strongly depends on the concentration (d) of the cobalt ions within the spinel ferrite structure; this is a superparamagnetic behaviour for low d, a soft magnetic behaviour for moderate d, and a hard magnetic behaviour for high d. The d parameter determines a certain value of the magnetocrystalline anisotropy [1]. The effective magnetic anisotropy in the case of nanoparticles is a very important intrinsic parameter (besides their diameter) to obtain the magnetic hyperthermia (MHT), with a great influence on the specific absorption rate (SAR), in the case of their usage in medicine to obtain tumour magnetic hyperthermia (to destroy tumour cells) [2,3]. The purpose of this research is to determine the magnetic anisotropy of the Co₃Fe_{3-d}O₄ nanoparticles, having the diameters of 2 ~ 17 nm, to identify its origin (magnetocrystalline or/and other nature (surface anisotropy or/and shape anisotropy)), and also to establish, based on the experimental results, the most suited nanoparticles (as anisotropy and diameter) in order to use them in intracellular MHT [4]. The obtained results are presented and discussed in detail in the paper.

Acknowledgement: This work was supported by PCCA-2012 project from the UEFISCDI-ANCS Romania. References [1] R. Valenzuela, *Magnetic Ceramics* (Cambridge Univ. Press, Cambridge) (1994). [2] C.L. Oudeck, A.H. Habib, P. Ohodnicki, K. Miller, C.A. Sawyer, P. Chaudhary, M.E. McHenry, *J. Appl. Phys.* 105 (2008) 07B324. [3]. C. Caizer, N. Hadaruga, D. Hadaruga, G. Tanasie, P. Vlazan, 7th Int. Conf. on Inorganic Materials, 12 - 14 Sept. 2010, Biarritz, France. [4] J.P. Fortin, F. Gazeau, *Eur. Biophys. J.* 37 (2008) 223.

PO08

Magnetic nanoemulsion as advanced drug delivery system applied to synergic procedures in the photodynamic therapy and hyperthermia trials using human mesenchymal stem cells as biological model

Fernando Lucas Primo¹, Daniela Regina Jardim¹, Paulo Cesar Moraes² and Antonio Claudio Tedesco^{1*}
¹ Chemistry, Nanotechnology and Tissue Engineering Center, FFCLRP, Sao Paulo University, Ribeirao Preto, SP, Brazil
² Physical, Brasilia University - UnB, Physical Institute, Brasilia-DF, 70910-900, Brazil

Tissue engineering and nanotechnology are important research fields in the future development of biological models useful for the understanding of wound healing processes, extracellular matrix activity and other biological skin activities[1]. This study reports on the synthesis and characterization of advanced drug delivery system with magnetic properties useful to Photodynamic Therapy (PDT) and Hyperthermia (HPT). Magnetic-Nanoemulsion (MNE) was obtained from spontaneous nanoemulsification to entrapment/controlled-release of lipophilic drugs as described by Siqueira-Moura[2]. The results demonstrated appropriated physical-chemistry stability to MNE biomaterial with size < 200 nm, exhibited a narrow size distribution (polydispersity index < 0.1) and zeta potential with modular value > |40| mV. Biological studies were carried out on human bone mesenchymal stem cells determination of in vitro biocompatibility after incubation with MNE which shown a safe concentration drug specific for each cellular type. Besides, the in vitro synergic effect of PDT and HPT were evaluated after simultaneous induction of photodynamic effects and magnetic field (40 Oe) application. These results confirmed that the use of nanotechnology associated with PDT and HPT procedures led to in vitro tumor inactivation by advanced protocols that can be useful to future oncological treatment. Financial grant CNPq (D.R.J.) and FAPESP projects 2009/15363-9 and 2008/53719-4 (F.L.P.).

[1] Primo, F.L.; Reis, M.B.C.; Porcionato, M.A.; Tedesco, A.C. In vitro Evaluation of Chloroaluminum Phthalocyanine Nanoemulsion and Low-Level Laser Therapy on Human Skin Dermal Equivalents and Bone Marrow Mesenchymal Stem Cells. *Current Medicinal Chemistry*. 18, 3376-3381, 2011. [2] Siqueira-Moura, M.P.; Primo, F.L.; Peti, A.P.F.; Tedesco, A.C. Validated spectrophotometric and spectrofluorimetric methods for determination of chloroaluminum phthalocyanine in nanocarriers. *Pharmazie*, 65, 1-6, 2010.

PO09

The morphological change of red blood cells in the hand exposed to the stimulus of strong pulse magnetic field

Jinyong Lee¹, Hyun Sook Lee¹, Jun Sang Yu² and Do Guwn Hwang^{1*}
¹ Oriental Medical Engineering, Sangji University, Korea
² Oriental Medical, Sangji University, Korea

The influence of magnetic field on human body has been studied to use as application of therapeutic equipment for a long time. Some studies have carefully suggested that vascular blood flow volume can be increased by an electromagnetic field stimulus [1-3]. In this study, live blood analysis (LBA) of blood collected in the hand stimulated by strong pulsed magnetic field was used in vitro to get the morphological change of red blood cells before and after magnetic stimulus. The LBA is a test methodology to approach the risk factors of illness, states of immunity, nutritional states of cells, degrees of hidden lesions, or treatments over time. The analysis can accomplish these goals functionally and preventively by observing morphological changes of ingredients constituting blood, which is alive without being chromated and collect through peripheral blood vessel. Our system was designed to generate a pulsed magnetic field that had a maximum intensity variation of 0.48 T and a transition time of 0.102 msec. LBA were done in the blood collected before and after the stimulation of 10 minutes in the hand. As a result, the hemadsorption (adhesion of red blood cells) observed before stimulus were normally distributed after stimulus of blood.

[1] D. Roland, M. Ferder, R. Kothura, T. Faiernan, and B. Strauch, *Plast. Reconstr. Surg.* 105, 1371 (2000). [2] H. N. Mayrovitz and P. B. Larsen, *Wounds* 4, 197 (1992). [3] H. N. Mayrovitz and P. B. Larsen, *Wounds* 7, 90 (1995).

PO10

An analytical comparison in electroencephalography and electrocardiography during stimulus of pulsed magnetic field and acupuncture on acupoint PC9

Jinyoung Lee¹, Do Guwn Hwang¹, Yun-Yeop Cha² and Hyun Sook Lee^{1*}
¹ Department of Oriental Biomedical Engineering, Sangji University, Korea
² Department of Oriental rehabilitation medicine, Sangji University, Korea

With recent increasing attention on the pulsed magnetic field stimulus as non-invasive medical treatment, diverse studies are being conducted to elucidate its effects on human physiology [1]. Among several bio-signals obtained from human body, electroencephalography and electrocardiography are known to have no side effect and provide real-time information on autonomic nervous activity with spectral analysis. The aim of the present study was to compare the changes of EEG and ECG during the PMF and acupuncture stimulus on acupoint, which is known to sedation and tonification point. In order to compare qualitatively the effect of PMF and acupuncture stimulus, the difference of alpha activities are calculated from EEG spectra compared with before, during and after stimulus, and the spectrum curves of ECG were analyzed in the frequency domain of heart rate variability. The increase of alpha activities after both stimuli could be explained that the impulse of stimulus on PC9 might pass through sensory nerve following meridian and approach the cerebral cortex, causing the CNS to be activated for pacifying emotion and calming the mind [2]. The decrease in index of sympathovagal activity after both stimuli indicates that parasympathetic nerves were activated and the sympathetic nerves were in constrained condition.

[1] N.M. Shupak, F.S. Prato, and A.W. Thomas, *Neurosci. Lett.* 363, 157 (2004). [2] H.S. Lee, S.W. Kim, D.G. Hwang, *IEEE transaction on Magn.* 47(10), 3060 (2011).

PO11

Reliability of a head movement compensation method based on minimum norm estimation for magnetoencephalographic recordings

Sanghyun Lim and Kiwoong Kim*
Brain and Cognition Measurement Lab, KRISS, Korea

Non-invasive multi-channel recordings of neuronal activity of brain play an important role in brain research fields. Magnetoencephalography (MEG) which measures magnetic field generated by synchronous firing of group of neurons, has superior spatial and temporal resolutions with quick and easy recording procedures. However, a movement of subject's head during recordings makes significant data distortions, since the array of multi-channel sensors is not physically fixed to subject's head. One approach compensating these distortions is to utilize a singular-value-truncated minimum norm estimation (MNE) method to generate virtual MEG signals at a common reference head position. Since MNE is biased to minimize the total output power, this approach can be applied to signals which have a number of distinct sources generating event related fields (ERF), but not to spontaneous neuronal recordings. In this study, we calculated compensation errors of ERF recordings and spontaneous neuronal recordings, by comparing real sensor signals to virtually-generated signals, to see the reliability of the method for spontaneous recordings. MEG data were recorded using a 152-channel whole head helmet MEG system (KRISSE MEG system) within a magnetically shielded room, and each channel was simulated and compared with each time trials.

PO12

The effect of small quantities of irradiation damage on the magnetic properties of Steel 316.

Robert Aldus¹, Jack Muir¹, Greg Lumpkin² and Paolo Imperia^{1*}
¹ bragg institute, ANSTO, Australia
² IME, ANSTO, Australia

The Steel 300 series is often used in applications where a non-magnetic steel is required. The materials take the austenite FCC crystal structure as opposed to the ferrite structure common in magnetic steels. It has previously been suggested that large doses of radiation (approximately 1022 ions/cm2) can cause a change in the local crystal structure of steel-316 to the ferrite structure and thus creating a magnetic signal [1]. We have performed x-ray absorption, x-ray dichroism and neutron scattering using WOMBAT at ANTOSO where we also commissioned the new ANSTO Oxford Instruments cryomagnet. The samples of steel-316 were irradiated to only about 10¹⁵ ions/cm2 using He⁺ ions. This level of irradiation should not be enough to change the bulk crystal structure and yet we observe some magnetic signal. We present our results and explanation for our findings.

PO13

Study of a hybrid magnet array for an electrodynamic maglev control

Chan Ham¹, Kurt Lin², Younghoon Joo³ and Wonsuk Ko^{4*}
¹ Mechatronics Engineering, Southern Polytechnic State University, USA
² Mechanical, Materials, and Aerospace, University of Central Florida, USA
³ Kunsan Nat'l University, Korea
⁴ Kyungwon Univ. Korea

This paper introduces an innovative hybrid array consisted of both permanent and electro magnets that would enable us to develop an active control mechanism for underdamped EDS Maglev systems. The proposed scheme is based on the Halbach array configuration in order to take the major technical advantage from the original Halbach characteristics: a strongly concentrated magnetic field on a side of the array and a cancelled field on the opposite side. The magnetic force produced by the proposed hybrid array can also be actively controlled. This force controllability resulted from a variable magnetic field is instrumental to provide a dynamic damping force to compensate the instability of EDS Maglev system caused by external perturbations and guideway irregularities. In this study, the magnetic characteristics and capability of the proposed array compared to the basic Halbach concept are focused. The results show that the proposed array is capable to produce an equivalent suspension force of the basic Halbach permanent magnet array but in a controlled mode. The effectiveness of the proposed array confirms that this study can be used as a technical framework to develop an active control mechanism for an EDS Maglev system.

[1] Donald M. Rote and Yigang Cai, "Review of Dynamic Stability of Repulsive-Force Maglev Suspension Systems," *IEEE Transactions On Magnetics*, Vol. 38, No. 2, 1383-1390, March 2002 [2] R. F. Post and D. D. Ryator, "The Inductrack: A Simpler Approach to Magnetic Levitation," *IEEE Transactions on Applied Superconductivity*, Vol. 10, 901-904, 2000

PO14

FEM simulation of magnetic treatment of surface vessel

Yongmin Kim¹, Hwiseok Kim², Kwan-seob Yoon³, Seon-ho Lim³, Jaewon Doh², Young-hak Kim¹ and Kwang-ho Shin^{1*}
¹ Dept. of Information and Communication Engineering, Kyungsoong University, Korea
² S/W R&D Center, Project 5 team, LIGNexI, Korea
³ S/W R&D Center, Project 4 team, LIGNexI, Korea
⁴ Dept. of Information and Communication Engineering, Pukyong National University, Korea

Since most of surface vessels and submarines are constructed with ferromagnetic materials, mainly Fe-C, Magnetic treatment (Deperm) of surface vessels and submarines is required to camouflage them against magnetic detection from enemy marine force. We investigated whether we could analyze practically magnetic treatment process of a surface vessel with FEM simulation. Because a surface vessel has non-linear ferromagnetic property as well as complicated structure with very large dimension, it is impossible to analyze the magnetic treatment process through conventional FEM using scalar material constants. We tried to do the FEM analysis a hysteresis model. The magnetic property including hysteresis of the constructing material of the submarine was calculated with the hysteresis model, and compared with the material property measured with the ferrite yoke method. The alternating magnetic field applied to the submarine in FEM analysis had several tens steps, and the maximum field was 1000 A/m. The analysis results showed that overall magnetic remanence was almost the same with that of hysteresis model. However, it was found that the magnetization in the endpiece of the vessel was changed non-linearly. The simulated results could be analyzed with the ferromagnetic exchanging coupling of magnetic nodes in FEM model.

PO15

Magnetically exchange-coupled nanoparticles as efficient heat inductor

Seung Ho Moon, Jung-tak Jang, Seung-hyun Noh, Jae-hyun Lee and Jinwoo Cheon*
Chemistry, Yonsei University, Korea

The conversion of electromagnetic energy into heat by nanoparticles has the potential to be a powerful, non-invasive technique for biotechnology, but poor conversion efficiencies have hindered practical applications so far. We demonstrate a significant increase in the efficiency of magnetic thermal induction by nanoparticles. We take advantage of the exchange coupling between a magnetically hard core and magnetically soft shell to tune the magnetic properties of the nanoparticle and maximize the specific loss power (SLP), which is a gauge of the conversion efficiency. We simulated SLP as a function of magnetocrystalline anisotropy K, diameter of the nanoparticle D, and magnetization M. The dependency on K chiefly results from the internal magnetic spin fluctuation (Neel relaxation), and the dependency on D is due to both Neel and Brownian relaxation. Our simulation indicates the optimal range of K and D for nanoparticles with high SLP values. High magnetization M is beneficial, too. The optimized core-shell magnetic nanoparticles have SLP values that are an order of magnitude larger than conventional iron-oxide nanoparticles. We also perform an antitumour study in mice, and find that the therapeutic efficacy of these nanoparticles is superior to that of a common anticancer drug.

Nature Nanotech. 2011, 6(7), 418-422

PO16

Theranostic magnetic nanoparticles

Seung-hyun Noh, Dongwon Yoo, Jae-hyun Lee, Jung-tak Jang, Seung Ho Moon and Jinwoo Cheon*
center for evolutionary nanoparticles, Korea

The property of magnetic materials can be defined using some parameters such as saturation magnetization(Ms), coercivity(Hc), and magnetocrystalline anisotropy(K). Understanding the interplay of these parameters is critical for optimizing magnetic characteristics we need for their effective use. We can control these parameters by changing the shape, size and composition of nanoparticles. Because there are various species of application of nanoparticles and magnetic properties needed to be optimized in each field of application are all different flexible tuning of magnetic parameters is very important. Important capabilities of magnetic nanoparticles are the external controllability of magnetic heat generation and magnetic attractive forces for the transportation and movement of biological objects. We show that these functions can be utilized not only for therapeutic hyperthermia of cancer but also for controlled release of drugs through the application of an external magnetic field. Additionally, the use of magnetic nanoparticles to drive mechanical forces is demonstrated to be useful for molecular-level cell signaling and for controlling the ultimate fate of the cell. The wide range of accessible features of magnetic nanoparticles underscores their potential as the most promising platform material available for theranostics.

PO17

Ion-texturing & Dynamics in Layered Compounds: From Electric Automobiles to Frustrated Magnetism
 Martin Mansson^{1*}, Jun Sugiyama², Kazuhiko Mukai³, Yutaka Ikegō², Hiroshi Nozaki², Kazuya Kamazawa², Masashi Harada², Marisa Medarde⁴, Fanni Juranyi¹, Jorge Gavilano¹, James S. Lord⁵, Isao Watanabe⁶, Ekaterina Pomjakushina⁷, Kazimierz Conder⁸, Vladimir Pomjakushin⁹, Tsutomu Ohzuku¹ and Tsunehiro Takeuchi¹

¹ Lab. for Solid State Physics, ETH Zurich, Switzerland
² Toyota Central Research and Development Labs. Inc., Japan
³ Muon Science Laboratory, KEK, Japan
⁴ LDM, Paul Scherrer Institut, Switzerland
⁵ Lab. for Neutron Scattering, Paul Scherrer Institut, Switzerland
⁶ ISIS, Rutherford Appleton Laboratory, United Kingdom
⁷ Muon Science Laboratory, RIKEN, Japan
⁸ Department of Applied Chemistry, Osaka City University, Japan
⁹ Department of Applied Physics, Nagoya University, Japan

The drastic change from an antiferromagnetic to a superconducting state in cuprates exemplifies how a slight change in carrier-density strongly governs magnetic and electronic properties. In cuprates the intermediate ion-layers are thought to only serve as 'passive' charge-reservoirs. However, it has become increasingly clear that also ion-order within these layers is of great importance [1]. Further, it was recently demonstrated that also ion-dynamics needs to be considered. In the Na_xCoO₂ compound it was shown that the low-T magnetic properties could be connected to Na dynamics a much higher temperatures [3,4]. From the context of rechargeable Li-ion batteries for electrical cars, our group has recently presented a novel experimental method [5] to investigate microscopic ion-dynamics in lithium-transition-metal-oxides (Li-TMO). By using the μSR technique we have obtained results regarding ion-dynamics in a wide range of Li-TMO's [6-7]. We will here give an overview of the method/results as well as discuss their importance for the development of thin-film batteries for the future. Finally, we will also present our latest results regarding Na-dynamics in magnetically frustrated compound Na_xCoO₂. With the use of μSR, neutron quasi-elastic neutron scattering and diffraction, we show how solid state dynamics is imperative for tuning this compound's magnetic/electronic/thermoelectric properties.

[1] Y. Sassa et al., PRB 83, 140511(R) (2011) [2] W. Bao et al., arXiv:1102.3674v1 (2011) [3] T. F. Schube et al., PRL 100, 026407 (2008) [4] M. Weller et al., PRL 102, 056401 (2009) [5] J. Sugiyama et al., PRL 103, 147601 (2009) [6] J. Sugiyama et al., PRB 82, 22412 (2010) [7] J. Sugiyama et al., PRB 84, 054430 (2011) Funding Source: Swiss National Science Foundation (Project 6, NCCR MaNEP) and Toyota CRDL.

PO18

Large resistive switching phenomenon induced by magnetic field in nano conduction path formed in SiO₂
 Shintaro Otsuka, Tomohiro Shimizu*, Takashi Kato, Takuya Kyomi and Shoso Shingubara
 Kansai University, Japan

A large magnetoresistance (MR) exceeded 800% was observed in a nano conduction path (NCP) formed in SiO₂ layer sandwiched between Co film and Si substrate. Applied a high voltage of 20 MV / cm between the Co film and the backside of Si substrate, the NCP was formed by dielectric breakdown of SiO₂ layer. The Magnetoresistance of the NCP in in-plane magnetic field for NCP was measured. Using Ni layer instead of Co, the large MR also appeared, but could not be observed in the case of using non-magnetic materials. The structure of the device was similar to the resistive switching memory device, regarding Co layer and Si substrate as top and bottom electrode. Therefore we also measured I-V characteristic of the NCP device, and the resistive switching effect was observed. We haven't fully understood the mechanism of this large MR switching phenomenon yet. However, it is speculated that the atomic scale NCP consisted of Co atoms was formed due to dielectric breakdown of SiO₂, and the nano gap in NCP was formed by magnetic field.

Jpn. J. Appl. Phys., 50 (2011) 06GG15.

PO19

Size dependence simulation of saturated field in circular permalloy
 Xinghao Hu, Byunghwa Lim, Ilgyo Jeong and Cheolgi Kim*
 Department of Materials Science and Engineering, Chungnam National University, Korea

Manipulation of magnetic beads for biomoleculars and cells separation, purification and sensing application is of great fundamental and practical interest [1]. On-chip magnets of soft magnetic structure of permalloy is a classic manipulation systems for magnetic beads, which utilizes external magnetic fields for control of the magnetic beads [2]. The maximum of magnetic force generated by on-chip magnet in an applied field should be obtained for transportation of magnetic beads. We present a simulation method that is available to enable a maximum value of magnetic force under an advisable field. As shown in simulations, when the applied field is gradually increased to 130 Oe on the on-chip magnet of 5 μm radius, the magnetization of the on-chip magnet is saturated that means a maximum value of magnetic force is obtained. Therefore, this simulation method can assist researchers to obtain the advisable field for maximum of magnetic force in designing variform on-chip magnets.

[1] J. Dobson, Nat. Nanotech., 2008, 3, 139. [2] K. Gunnarsson, P. E. Roy, S. Felton, J. Pihl, P. Svedlindh, S. Berner, H. Lidbaum, and S. Oscarsson, Adv.Mater., 2005, 17, 1730.

PO20

A new definition of magneto-mechatronics and applications
 Sung Hoon Kim*, Jaewon Shin, Shuichi Hashi and Kazushi Ishiyama
 Research Institute of Electrical communication, Tohoku University, Japan

Recently, magnetic wireless sensors and actuators have been developed for use in biomedical fields. In particular, their mechanisms depend on magnetics, such as magnetic material and physical phenomena. However, their research boundary has not been clear. Researchers talk of magnetic micro-robots, magnetic actuators and sensors, and so on [1-3]. Therefore, a new and correct definition is required. Magneto-mechatronics is synergistic integration of magnetic engineering, mechanical engineering, and electronics/computer engineering in the design, manufacturing, and control process. In particular, magneto-mechanical mechanisms are directly controlled by external magnetic fields. Magneto-mechatronics is offered as a new definition of magnetic sensors and actuators. In this study, we introduce and investigate methods of magnetic field control and their suitable magnetic mechanisms. In general, the control methods and mechanisms are determined according to the types of magnetic field: gradient, alternating, and rotating magnetic fields. Because the magnetic field controls are suitable for use in the restricted spaces, magnetic devices based on magneto-mechatronics can be widely used medical applications. In magneto-mechatronics, the combination of magnetic, mechanical, and computer engineering provides physical hardware, system modeling, and analysis, whereas the combination of magnetic, electrical, and computer engineering provides control methods and its algorithm, and an interface, and so on.

[1] K. Ishiyama, M. Sendoh, A. Yamazaki, and K. I. Arai, "Swimming Micro-machine driven by Magnetic Torque," Sens. Actuators A, Phys. 91, 141-4, 2001. [2] L. Zhang, J. J. Abbott, L. Dong, K. E. Peyer, B. E. Kratochvil, H. Zhang, C. Berges, and B. J. Nelson, "Characterizing the Swimming Properties of Artificial Bacterial Flagella," Nano Letters 9, 3663-3667, 2009. [3] S. Hashi, M. Toyoda, M. Ohya, Y. Okazaki, S. Yabukami, K. Ishiyama, and K. I. Arai, "Magnetic motion capture system using LC resonant magnetic marker composed of Ni-Zn ferrite core," J. Appl. Phys. 99, 08B312, 2006.

PO21

AC magnetic field frequency dependence of drug release characteristics for magnetic hyperthermia based polymer-drug encapsulate system for cancer treatment applications
 Tejabhiram Yadavalli¹, Shivaraman Ramasamy¹, Gopalakrishnan Chandrasekaran¹ and Ramasamy R²

¹ Nanotechnology Research Centre, SRM University, India
² School of Pharmacy, SRM University, India

Ferromagnetic nickel, cobalt and gadolinium ferrite nanomaterials with Curie temperature values in the range of 40-50°C have been synthesized by wet chemical routes. These nanoparticles were then coated with Poly n-isopropyl Acrylamide thermo-sensitive polymer and doxorubicin drug forming a drug-polymer-nanoparticle conjugate. The conjugate was then tested for the drug release characteristics in-vitro by the application of alternating magnetic field to it. The study was conducted to understand the heating rate of the nanoparticles in the conjugate system and the quantitative drug release due to the heating of the nanoparticle. The quantitative study was conducted using a homemade magnetic hyperthermia setup and High Precision Liquid Chromatography (HPLC) with doxorubicin standards. The study was conducted in the range of 100 to 1000 kHz with 20 W power rating. The maximum heating rate and the drug release rate per minute was seen at around 900 kHz which was in concurrence with the theoretical calculations done using the hysteresis loop area of the material. These results will later be useful for testing on animal models to analyze in-vivo drug release characteristics of the conjugate.

PO22

Account of the image forces in the Bi_{1-x}Sb_x-insulator film structures.
 Konstantin Nicolaevich Kashirin
 The Russian State Agrarian University-Moscow Timiryasev Agricultural Academy, Kaluga Branch, Russia

Semiconducting alloy Bi_{1-x}Sb_x (x=0,11) films of the different fixed thickness with a thin layer of insulating coating (SiO₂) of variable thickness are investigated. The measuring of kinetic parameters was conducted in a superconducting solenoid gap (with magnetic induction to 9 T) and on the different temperatures (4,2÷200 K). The calculations of magnetic resistance, of the carries mobility and the Hall coefficient was done. The resistance oscillations is observed depending on the thickness of insulating coating for all films. The kinetic parameters oscillations was observed as function of coating thickness at different temperature and on magnetic field. So, the following should be noted by the results of experimental investigations: - the resistance oscillations of all investigated bismuth-antimony alloy films is observed depending on the thickness of dielectric coating and the period of oscillations is amounts 80-100 Å average; - the magnetic resistance and the Hall coefficient oscillate with the variation of the dielectric coating thickness in antiphase with the analogous oscillation resistance; - the sphere of negative magnetic resistance is observed. One of the possible mechanisms accounting for the oscillations of the kinetic parameters of semiconducting films with insulator coating is taking into accounts the image forces.

Semiconducting alloy Bi_{1-x}Sb_x (x=0,11) films of the different fixed thickness with a thin layer of insulating coating (SiO₂) of variable thickness are investigated. The measuring of kinetic parameters was conducted in a superconducting solenoid gap and on the different temperatures. The calculations of magnetic resistance, of the carries mobility and the Hall coefficient was done. The assumptions that the one of the possible mechanisms accounting for the oscillations of the kinetic parameters of semiconducting films with dielectric coating is taking into accounts the reflection forces were done.

PO23

Time-resolved pump-probe measurement of polarization rotation in nano-structured chiral metamaterial

J. H. Woo¹, H. -Y. Shin¹, M. J. Gwon¹, M. Vomir², M. Barthelemy², D. -W. Kim¹, S. Yoon¹, J.-Y. Bigot² and J. W. Wu^{1*}
¹ Department of Physics & CNRS- Ewha International, Ewha Womans University, Korea
² CNRS-IPCMS, University of Strasbourg, France

In this study, we performed time resolved pump-probe measurement in two nano-structured metamaterials with opposite chirality which were fabricated by e-beam lithography on 30nm thick gold film. Transient absorption was measured to investigate the temporal behavior of the polarization rotation in metamaterial. It is well known that surface plasmonic resonances in metamaterial are originated from its structure rather than composition [1,2]. Surface plasmonic resonances in metamaterials which were used in this study were located in the visible spectral range with resonance peaks at 625nm and 670nm and an optical rotatory dispersion was observed. Time resolved pump-probe measurements were carried out with 35fs Ti:sapphire laser operating at 800nm. BBO crystal was used to generate a 400nm pump pulses. For the probe, a sapphire crystal plate was used to generate a white light continuum. With linearly polarized pump beam, the electron dynamics in the metamaterial structure was studied. Also with right and left circularly polarized pump, we investigated the time dependent rotation of polarization of the probe beam in a polarization bridge configuration.

[1] V. A. Fedotov, M. Rose, S. L. Prosvirnin, N. Papasakakis, and N. I. Zheludev, "Sharp trapped-mode resonances in planar metamaterials with a broken structural symmetry", Phys. Rev. Lett. 99, 147401 (2007). [2] Boyoung Kang, E. Choi, Hyun-Hee Lee, E.S. Kim, J. H. Woo, J. Kim, Tae Y. Hong, Jae H. Kim, and J.W. Wu, "Polarization angle control of coherent coupling in metamaterial superlattice for closed mode excitation", Opt. Express 18, 11552 (2010).

PO24

Structural and magnetic properties of glassy like carbon synthesized by pyrolysis of sucrose
 Shivaraman Ramaswamy* and C Gopalakrishnan
 Nanotechnology Research Center, SRM University, India

The structure and properties of glassy carbon (GC), a technologically important and widely used material, is still not well established. The glassy carbon samples were produced by a low-temperature pyrolysis of sucrose. The thermal destruction occurred in five stages to minimize carbon losses. At the first stage (175 °C, 3 h) a viscous melt was obtained due to detachment of volatile components and water. After the second and the third stages (300 °C, 1 h and 400 °C, 0.5 h, respectively) the material becomes solid. The next stage (525 °C, 1h) and the last stage (700 °C, 1 h) are performed to complete removal of all volatile impurities. The samples were then characterized using AFM and SEM to determine its structure and morphology. The magnetic properties were studied using vibrating sample magnetometer. It was found that the glassy carbon sample has an inherent fullerene like morphology whose concentration increases with increased heat treatment. Further, the samples also exhibited a distinct change in magnetic properties based on the pyrolysis. Paramagnetic and diamagnetic properties were found in the samples. The same has been explained based on the composition of the samples and structural properties.

[1] A.A. Ovchinnikov and V.N. Spector, "Organic ferromagnets. New results." Synth. Met., vol. 27, pp. 615-624, Dec. 1988. [2] H. Ohldag, et al., "Electron Ferromagnetism in Metal-Free Carbon Probed by Soft X-Ray Dichroism", Phys. Rev. Lett., vol. 98, May 2007.

PO25

Simulation of energy dispersive mode for RITA-type cold neutron triple axis spectrometer SIKA

Guochu Deng^{1*}, Peter Vorderwisch², Chun-ming Wu², Garry Mcintyre¹ and Wen-hsien Li²
¹ Bragg Institute, Australian Nuclear Science and Technology Organization, Australia
² Department of Physics, National Central University, Zhongli 32054, Taiwan, Australia

SIKA is a high flux cold-neutron triple axis spectrometer in Bragg Institute. Equipped with a multi-blade analyser system (13 PG(002) blade) and position sensitive detector, SIKA possesses high flexibility to efficiently run in a traditional step-by-step mode or various mapping (or dispersive) modes by changing the configuration of analysers and detectors. In this study, the energy dispersive modes, namely the so-called E1 mode [1] at two different energy transfers is simulated using Monte Carlo ray-trace package SIMRES. [2] The simulated results show that SIKA could effectively work on E1 mode at low and intermediate energy transfer with reasonable energy and Q resolutions. The energy resolution is around 0.23meV at Ei=5meV while it increases to 1.8meV at Ei=15meV. This simulation shows SIKA has the potential in operation flexibility and data-acquisition efficiency, and provides valuable references to the future inelastic neutron scattering experiments on SIKA.

[1] Lefmann K, McMorrow D F, Romow H M et al. 2000 Physica B 283 343 [2] ©aroun J and Kulda J 1997 Physica B, 234-236 1102 [3] Shirane G, Shapiro Stephen M, and Tranquada John M, 2002, Neutron scattering with a triple-axis spectrometer, (Cambridge University Press) p 123 [4] Clausen K N et al. 1998 Physica B 241-243 50 [5] Demmel F, Grach N and Romow H M 2004 Nuclear Instruments & Methods in Physics Research Section A 530 404

PO26

Efficiency of Energy base depermm protocol
 Yongmin Kim¹, Young-hak Kim² and Kwang-ho Shin^{1*}
¹ Dept. of Information and Communication Engineering, Kyungsoong University, Korea
² Pukyong National University, Korea

Magnetic treatment of surface vessels and submarines (Depermm) is a required to camouflage them against magnetic detection from enemy marine force. So far, depermm has been accomplished by applying an alternating magnetic field of which amplitude decreases linearly. However, the reduction of the residual flux density in the direction of magnetic field is not linear in the case of the linear protocol, since the ferromagnetic material used to construct a surface vessel, mainly Fe-C, shows a nonlinear behavior in an alternating magnetic field. This is one of main reasons to make an ordinary depermm protocol inefficient. In this paper, we propose an energy base depermm protocol which calculated by an algebraic hysteresis model, and present how to optimize the depermm protocol with the minor loops of magnetic hysteresis. We found out that step number could be reduced in the energy base depermm protocol compare with in the linear protocol, because the larger numbers of depermm steps are dedicated in the irreversible domain process region on the magnetic hysteresis.

PO27

Effect of a magnetic field on mixed convection of a nanofluid in a square cavity
 G. A. Sheikhzadeh^{1*}, S. Mazrouei Sebdani¹, M. Mahmoodi², Elham Safaeizadeh³ and Sayed Ebrahim Hashemi¹
¹ Mechanical Engineering Department, University of Kashan, Iran
² Mechanical Engineering Department, Amirkabir University of Technology, Iran
³ Department of Mathematics, Payame Noor University, Najafabad, Isfahan, Iran

The problem of mixed convection in a differentially heated lid-driven square cavity filled with Cu-water nanofluid under effect of a magnetic field is investigated numerically. The left and right walls of the cavity are kept at temperatures of Th and Tc respectively while the horizontal walls are adiabatic. The top wall of the cavity moves in own plane from left to right. The effects of some pertinent parameters such as Richardson number (ranging from 0.1 to 10), the volume fraction of the nanoparticles (ranging 0 to 0.1) and the Hartmann number (ranging from 0 to 100) on the fluid flow and temperature fields and the rate of heat transfer in the cavity are investigated. It must be noted that in all calculations the Prandtl number of water as the pure fluid is kept at 6.8, while the Grashof number is considered fixed at 10⁴. The obtained results show that the rate of heat transfer increases with an increase of the Rayleigh number, while but it decreases with increase in the Hartmann number. Moreover it is found that by increase in volume fraction of the nanoparticles the rate of heat transfer can be enhanced or deteriorated compared to the based fluid.

PO28

Magneto-hydrodynamic free convection in a square cavity heated from below and cooled from other walls
 Ali Akbar Abbasian Arani*, Mostafa Mahmoodi and Saeed Mazrouei Sebdani
 Mechanical Engineering, University of Kashan, Iran

Magneto-hydrodynamic free convection fluid flow and heat transfer in a square cavity filled with an electric conductive fluid with Prandtl number of 0.7 has been investigated numerically. The horizontal bottom wall of the cavity was kept at Th while the side and top walls of the cavity were maintained at a constant temperature Tc with Th>Tc. The governing equations were solved numerically while the SIMPLER algorithm was used. A parametric study was performed, and the effects of the Rayleigh number and the Hartman number on the fluid flow and heat transfer were investigated. The results showed that temperature distribution and flow pattern depended on both strength of the magnetic field and Rayleigh number. For all cases two rotating eddies were formed. Using the longitudinal magnetic field results in a force (Lorentz force) opposite to the flow direction that tends to decrease the flow velocity. The magnetic field decreased the free convection and flow velocity. Also it was found that for higher Rayleigh numbers a relatively stronger magnetic field was needed to decrease the heat transfer. Moreover for low Rayleigh numbers, by increase in the Hartman number, free convection is suppressed and heat transfer occurs through conduction mainly.

July 9 (Mon)

July 9 (Mon)

PO29

Interaction of a magnetic field and buoyancy force in a square cavity filled with a fluid with low Prandtl number

G. A. Sheikhzadeh^{1*}, S. E. Hashemi¹, S. Mazrouei Sebdani¹, M. Mahmoudi² and Elham Safaeizadeh³

¹ Mechanical Engineering Department, University of Kashan, Iran

² Mechanical Engineering Department, Amirkabir University of Technology, Tehran, Iran

³ Department of Mathematics, Payame Noor University, Najafabad, Isfahan, Iran

In this paper, influences of Lorentz force due to a magnetic field on buoyancy driven heat transfer in a square cavity containing a fluid with low Prandtl number is investigated numerically. The left and right walls of the cavity are kept at temperatures of T_c and T_h respectively, while the horizontal walls are kept adiabatic. Effect of existence of an adiabatic body in the middle of the cavity is considered too. The dimensionless governing equations associated with the boundary conditions are solved numerically using the finite volume method. Streamlines and isotherms are shown for Grashof number (ranging from 10^5 to 10^7), Hartman number (ranging from 0 to 100) and Prandtl number (ranging from 0.005 to 0.1). The results show that variations of magnetic field donot have noticeable effect on buoyancy force, while increase in magnetic field increases Lorentz force. Moreover buoyancy and Lorentz forces increase by increase in Grashof number in a constant Hartman and Prandtl numbers.

PO30

Numerical study of magnetic field effects on flow field and heat transfer in a cavity filled with porous materials

G. A. Sheikhzadeh*, M. Aliakbari Miyan Mahaleh, A. A. Abbasian Arani and S. Mazrouei Sebdani

Mechanical Engineering Department, University of Kashan, Iran

Natural convection flows in a square cavity filled with a fluid-saturated porous medium under the effect of magnetic field has been studied numerically. A square hot body with length W is placed in the center of the cavity (with length L). The ratio of W/L is assumed to be 0.5. Continuity, momentum and energy equations are solved using the finite volume technique under the boundary conditions. The two vertical sides of the cavity are cooled and two horizontal bottom and top walls are adiabatic. The Prandtl number is 0.71, the Rayleigh number changes from 10^4 to 10^6 , the Darcy number varies from 10^{-5} to 10^{-3} and the Hartmann number alters from 0 to 100. Numerical results are presented in terms of stream functions, temperature profiles. The results say increasing the braking effect of magnetic field as increasing the Hartman number; lead to decreases the heat transfer. Also at low Darcy number, fluid circulation is weak due to high hydraulic resistance offered by porous medium for Darcy number down to 10^{-5} . Average Nusselt number increases with enhancement of Rayleigh number and decreasing the Hartmann number.

PO31

Numerical simulation of magnetohydrodynamic Benard convection in a shallow enclosure

G. A. Sheikhzadeh*, M. Mahmoudi and S. Mazrouei Sebdani

Mechanical Engineering Department, University of Kashan, Iran

In this paper the problem of magnetohydrodynamic Benard convection in a shallow rectangular enclosure with aspect ratio of 10 (width to height ratio) has been investigated numerically. The enclosure is filled with an electric conductive fluid with Prandtl number of 1. The bottom and the top walls of the cavity are maintained at a constant temperature T_h and T_c respectively, with $T_h > T_c$, while; the side walls of the cavity are kept insulated. The governing equations written in terms of the primitive variables are solved numerically using the finite volume method and the SIMPLER algorithm is employed to couple velocity and pressure fields. Using the developed code, a parametric study is performed, and the effects of the Rayleigh number and the Hartman number on the fluid flow and heat transfer inside the enclosure are investigated. The results show that temperature distribution and flow pattern inside the enclosure depend on both the strength of the magnetic field and Rayleigh number. Moreover it was found that at low Rayleigh number with increase in Hartman number the flow intensity decreases and fluid becomes stagnant. At high Rayleigh numbers number of the Benard cell decreases by increase in Hartman number.

PO32

Near-electrode effects of magnetic fields in electrochemistry

Michael Coey and Peter Dunne

Physics, Trinity College dublin, Ireland

Remarkable influences of magnetic fields have been discovered on the diffusion layer and on the electrochemical double layer. The former are mainly due to magnetic pressure, which allows the patterning of deposits from both paramagnetic and diamagnetic ions (using a nonelectroactive paramagnetic species such as Dy^{3+}). The effects of small cylindrical [1] and linear magnet arrays are demonstrated. The magnetic patterning is estimated to be effective down to about the 100 micron scale. The essential requirement for patterning of this type are orthogonal concentration gradients and magnetic field gradients. More surprising is the evidence we have found for an influence of a static magnetic field on the electrochemical double layer, a poorly understood region about 1 nm thick at the cathode. Using a nitrobenzene model redox system, we show that the double layer capacitance can be modified by a factor of two at an appropriate potential. The influence of Maxwell stress on the free radicals in solution is discussed as a possible explanation. More remarkable are

[1] P. Dunne, L. Mazza and J. M. D. Coey, Phys Rev Letters 107 042501 (2011)

QA01

Resonant magnetic x-ray scattering: Beamline P09 at PETRA III at DESY

Joerg Stropfner, Sonia Francoual, Dinesh K. Shukla and Arvid Skaugen

DESY, Germany

Resonant and non-resonant magnetic scattering are complementary tools to magnetic neutron diffraction for the investigation of magnetic properties in solids. Resonant magnetic x-ray scattering opens the possibility to investigate magnetic order in single crystals and layered systems element selectively. Also the interference of magnetic order with orbital or charge order can be determined through the polarization properties of the x-ray and the special form of the scattering cross sections, describing the variation of the polarization states through the scattering process. The new beamline for Resonant Scattering and Diffraction (RSD), P09 at PETRA III, is designed especially to address the above mentioned issues. Low temperature cryostats and high magnetic fields of up to 14T allow the investigation of magnetic properties of materials as function of polarization, temperature and field. Two diffractometers are available to conduct experiments using the highly brilliant synchrotron beam available at PETRA III. The polarization of the incident x-ray beam can be varied arbitrarily through x-ray phase-plates and the polarization of the scattered beam is analyzed by a polarization analyzer. Examples for the performance of the beamline and experimental results on magnetic scattering from multiferroic systems will be presented.

QA02

Magnetic and dielectric properties of FeTiO₃

Takayasu Kiyokawa^{1*}, Shigeki Yamada¹ and Takatsugu Masuda²

¹ Nanosystem Science, Yokohama City University, Japan

² Institute for Solid State Physics, University of Tokyo, Japan

The magnetic and dielectric properties of single crystal iron ilmenite FeTiO₃ have been investigated. The temperature dependence of the magnetization for H parallel to the c axis (M//c) has a sharp peak at 58 K (T_N) and abruptly decreases below T_N , while the magnetization for H perpendicular to the c axis (M \perp c) is almost independent of the temperature. These features indicate that the ground state is Neel state with the easy axis in the c direction. Above T_N the value of M//c is larger than that of M \perp c due to the magnetic anisotropy. These results are consistent with previous report by Kato et al.. The temperature dependence of the dielectric constant for E parallel to the c axis also shows a kink at T_N . Furthermore the dielectric polarization for E parallel to the c axis abruptly increases at T_N . Hence this kink is ascribed to ferroelectric phase transition. These results indicate that FeTiO₃ is a strong candidate for a new type of multiferroic materials.

QA03

Theoretical study of tuning polarization and magnetism of BiCoO₃

Yu-jun Zhao and Xing-yuan Chen

Department of Physics, South China University of Technology, China



QA04

Soft x-ray synchrotron radiation spectroscopy study of Co_{0.6}Fe_{0.9}Mn_{1.5}O₄ spinel with nano-checkerboard patterns

D.H. Kim¹, Jihoon Hwang¹, Eunsook Lee¹, S.-W. Cheong², B.-G. Park³, J.-Y. Kim³ and J.-S. Kang^{1*}

¹ Department of Physics, The Catholic University of Korea, Korea

² Department of Physics and Astronomy, Rutgers University, USA

³ Pohang Accelerator Laboratory, POSTECH, Korea

In the AB₂O₄-type spinels, transition-metal ions occupy either the tetrahedral (Td) A site or the octahedral (Oh) B site. Recently, nano-checkerboard (CB) patterns have been observed in ZnMnGaO₄, MgMn_{1/2}Fe_{3/2}O₄, and Co_{0.6}Fe_{0.9}Mn_{1.5}O₄ [1]. When properly annealed, these spinels show two different structures with different chemical phases, where one is cubic and the other is tetragonal or orthorhombic. This structural and chemical phase separation has been explained by the Jahn-Teller (JT) distortion. To confirm this idea, it is important to determine the valence states of the transition-metal ions that constitute these spinel oxides. In this work, we have studied the electronic structure of checkerboard Co_{0.6}Fe_{0.9}Mn_{1.5}O₄ single crystal by employing soft x-ray absorption spectroscopy (XAS) and soft x-ray magnetic circular dichroism (XMCD). The measured T 2p XAS spectra (T=Co, Fe, Mn) of Co_{0.6}Fe_{0.9}Mn_{1.5}O₄ reveal that the valence states of Co, Fe, and Mn ions are nearly divalent (Co²⁺), trivalent (Fe³⁺), and mixed-valent (Mn²⁺-Mn³⁺), respectively. Very weak XMCD signals are observed in checkerboard Co^{0.6}Fe^{0.9}Mn^{1.5}O₄. *Corresponding Author : kangjs@catholic.ac.kr

[1] C.L. Zhang, et al., Appl. Phys. Lett. 91, 233110 (2007).

QA05

Zn-substitution effects in multiferroic Cu₂Mo₂O₆

Haruhiko Kuroe^{1*}, Kento Aoki¹, Ryusuke Itoh¹, Tomohiro Hosaka¹, Takuya Hasegawa¹, Suguro Hachiuma¹, Mitsuru Akaki¹, Hideki Kuwahara¹, Tomoyuki Sekine¹, Masashi Hase², Kunihiko Oka³, Toshimitsu Ito³ and Hiroshi Eisaki³

¹ Department of Physics, Sophia University, Japan

² National Institute for Material Science (NIMS), Japan

³ National Institute of Advanced Industrial Science and Technology (AIST), Japan

We present the Zn substitution effects on the quasi-one dimensional frustrating spin system Cu₂Mo₂O₆. This material has S = 1/2 distorted tetrahedral spin chains and undergoes the multiferroic phase below 7.9 K without magnetic field [T. Hamasaki et al., Phys. Rev. B 77 (2008) 134419, H. Kuroe et al., J. Phys. Soc. Jpn. 80 (2011) 083705]. The S = 0 Zn²⁺ ions substitute for the S = 1/2 Cu²⁺ ions at the three crystallographically different sites, namely Cu₁, Cu₂, and Cu₃. The spins at the Cu₂ and Cu₃ sites form nearly spin-singlet spin dimers at the bisectors of the nearest neighbor Cu₁ sites in the quasi-one dimensional spin chain [H. Kuroe et al., J. Phys.: Conf. Ser. 200 (2010) 022028, H. Kuroe et al., Phys. Rev. B 83 (2011) 184423]. In this study, we focus on the magnetic, electric, and thermodynamical properties of the single crystal of (Cu,Zn)₂Mo₂O₆. Comparing our previous results in polycrystalline samples [M. Hase et al., J. Phys. Soc. Jpn. 77 (2008) 034706], we discuss the reduction of the antiferromagnetic correlation and the singlet-pair breaking effect on the Cu₂-Cu₃ spin dimers. The dielectric constant and the specific heat in (Cu,Zn)₂Mo₂O₆ will also be discussed in this study.

QA06

Effects of bismuth substitution on the magnetic properties of Bi_{1-x}Co_xMnO₄

Maria Elenice Dos Santos¹, Paulo Noronha Lisboa-filho² and Octavio Pena¹

¹ Institut des Sciences Chimiques de Rennes, Universite de Rennes 1, France

² Laboratorio de Materiais Eletronicos, Universidade Estadual Paulista, Brazil

Coexistence of magnetism and ferroelectricity, along with coupling between them, ensures many technological applications of materials named multiferroics. Transition metal and/or rare earth oxides with ABO₃ perovskite and AB₂O₄ spinel structures are good candidates due to the substitution of magnetic and non-magnetic ions at the A and/or B sites [1]. Bi-substituted Bi_{1-x}MnO₄ multiferroic samples, well-characterized structurally by XRD and Rietveld refinement together with SEM-EDX techniques, were synthesized by a polymeric precursors method. A gradual expansion of the lattice parameter due to the substitution of Co³⁺ by Bi³⁺ is observed for x = 0.1, 0.2 and 0.3. Magnetic characterization was carried out by SQUID measurements. The inverse susceptibility exhibited ferrimagnetic behaviour, as also proved by the strong antiferromagnetic and ferromagnetic interactions shown by the ZFC and FC curves. The M(H) loops performed at various temperatures below T_c showed larger loop areas when decreasing the temperature, indicating an increasing ferromagnetism. The inclusion of Bi in Co_xMnO₄ creates fluctuating valence states of both Co and Mn ions (Co²⁺/Co³⁺, Mn²⁺/Mn³⁺/Mn⁴⁺) which occupy the tetrahedral and octahedral sites [2]. Magnetization measurements showed that T_c and M_s increase with increasing Bi³⁺ concentration due to the redistribution of the magnetic cations, in particular the Mn³⁺ and Mn⁴⁺ ones.

[1] P. Barahona, et al. J. Chil. Chem. Soc. 50, N 2 (2005) 495. [2] N. E. Rajeevan, et. al. Mater. Sci. Eng. B 163(2009) 48.

QA07

Cross-correlation effects in multiferroic Cu₃Mo₂O₉

Ryusuke Itoh^{1*}, Tomohiro Hosaka¹, Takuya Hasegawa¹, Haruhiko Kuroe¹, Tomoyuki Sekine¹, Masashi Hase², Kunihiko Oka³, Toshimitsu Ito³ and Hiroshi Eisaki³

¹ Sophia University, Japan

² National Institute for Materials Science (NIMS), Japan

³ National Institute of Advanced Industrial Science and Technology (AIST), Japan

We present the cross correlation effects in a multiferroic material Cu₃Mo₂O₉. This material contains spin tetrahedra made from the Cu²⁺ ions which form a edge sharing spin chain. The quasi-one dimensional magnon dispersion curve, the ferroelectric properties caused by the geometrical magnetic frustration, and a strong magnetocapacitance effect have been reported [H. Kuroe et al., Phys. Rev. B 83 (2011) 184423, H. Kuroe et al., J. Phys. Soc. Jpn. 80 (2011) 083705]. In this study, we focus on the change of the longitudinal magnetization under the electric field. Using a SQUID magnetometer which has two electric leads, we measured the longitudinal magnetization M_a along the a axis and the electric polarization P_c along the c axis of a plate-like single crystal of Cu₃Mo₂O₉ simultaneously. We measured the longitudinal magnetization along the a axis (Ma-Ha loop) under the static electric field E_c along the c axis, and the Ma-Ec loop under the static H_a . The details of our results including the change of the Ma-Ha loop under the static electric field and butterfly-loop in the Ma-Ec loop will be presented in this study.

QA08

Nonlinear current-voltage characteristics of (La_{0.5}Eu_{0.5})_{0.7}Pb_{0.3}MnO₃ Single crystals: Possible manifestation of the internal heating of charge carriers

Kirill Shaykhtudinov*

Kirensky Institute of Physics, Russia

Current-voltage characteristics of the polycrystalline substituted lanthanum manganite La_{0.7}Ca_{0.3}MnO₃ were experimentally studied at T = 77.4 K in magnetic fields up to 13 kOe. In these characteristics, a portion of negative differential resistivity was observed above a certain threshold value of critical current density j_c caused, in our opinion, by nonequilibrium heating of the electron gas due to low thermal conductivity of the manganite material. Because of the nonlinearity of the current-voltage characteristics, the field dependences of resistivity $\rho(H)$ appear extremely sensitive to the value of a transport current. In this case, the $\rho(H)$ dependences reveal both ordinary negative and positive magnetoresistance.

QA09

High field phase diagram in multiferroic $\text{Cu}_3\text{Mo}_2\text{O}_9$

Haruhiko Kuroe^{1*}, Ryo Kino¹, Ryusuke Itoh¹, Tomohiro Hosaka¹, Takuya Hasegawa¹, Tomoyuki Sekine¹, Takumi Kihara², Masashi Tokunaga², Masashi Hase³, Kanji Takehana³, Hideaki Kitazawa³, Kunihiko Oka⁴, Toshimitsu Ito⁴ and Hiroshi Eisaki⁴
¹ Department of Physics, Sophia University, Japan
² The Institute for Solid State Physics, The University of Tokyo, Japan
³ National Institute for Materials Science (NIMS), Japan
⁴ National Institute of Advanced Industrial Science and Technology (AIST), Japan

We present the multiferroic behavior in the quasi-one dimensional antiferromagnet $\text{Cu}_3\text{Mo}_2\text{O}_9$. This material has spin chains of the distorted spin tetrahedra made from $S = 1/2 \text{ Cu}^{2+}$ ions. In ICM2009, we have presented that the magnon dispersion relation in $\text{Cu}_3\text{Mo}_2\text{O}_9$, which is well explained by the hybridization effects between a magnon excitation from the quasi-one dimensional spin system and that from the isolated spin dimers [H. Kuroe et al., J. Phys.: Conf. Ser. 200 (2010) 022028, H. Kuroe et al., Phys. Rev. B 83 (2011) 184423]. Recently, we found that this material shows a multiferroic behavior [H. Kuroe et al., J. Phys. Soc. Jpn. 80 (2011) 083705]. We proposed that the origin of the multiferroic behaviors in $\text{Cu}_3\text{Mo}_2\text{O}_9$ is the charge redistribution effect in a frustrated Mott insulator studied by Bulaevskii et al [L. N. Bulaevskii et al., PRB 78 (2008) 024402], which is presented by Khomskii as an invited talk in ICM2009 [D. I. Khomskii, J. Phys.: Condens. Matter 22 (2010) 164209]. In this study, we present the magnetic-field-temperature phase diagram up to 55 T obtained from the temperature and magnetic-field dependences of the magnetization, the dielectric constants, the electric polarization, the pyroelectric current, and the specific heat.

QA10

Magnetoelectric effect in $\text{Ca}_2\text{FeAlO}_5$

Nobuyuki Abe^{1*}, Khanh Duy Nguyen², Yoichi Nii², Yutaro Kitagawa³ and Taka-hisa Arima¹
¹ Department of Advanced Materials Science, The University of Tokyo, Japan
² Department of Physics, Tohoku University, Japan
³ Department of Applied Physics, The University of Tokyo, Japan

$\text{Ca}_2\text{FeAlO}_5$ has the same crystal structure as mineral Brownmillerite. The oxygen deficient perovskite type structure is constructed by the alternate stacking of $(\text{Fe,Al})\text{O}_6$ octahedra and $(\text{Fe,Al})\text{O}_4$ tetrahedra. An early structure analysis showed that $\text{Ca}_2\text{FeAlO}_5$ belongs to a non-centrosymmetric space group $Ibm2$ [1], which originates from the in-phase stacking of $(\text{Fe,Al})\text{O}_4$ tetrahedra. This compound shows antiferromagnetic order below 350 K. Mossbauer spectroscopy measurements conclude that the magnetic moments of Fe^{3+} align along the a-axis[2]. Because the crystal structure lacks the inversion symmetry, $\text{Ca}_2\text{FeAlO}_5$ is a candidate material which has a magnetoelectric coupling. Here we show the measurements of magnetoelectric effect in single crystalline $\text{Ca}_2\text{FeAlO}_5$. The field dependence of the magnetization along the a-axis shows a metamagnetic transition caused by the spin flop of Fe^{3+} moments. Moreover, the dielectric constant and electric polarization show an anomaly at around the phase transition. These results indicate that $\text{Ca}_2\text{FeAlO}_5$ shows magnetoelectric effect in a magnetic field induced spin flop phase, which is one example of a new route to realize a magnetoelectric coupling above the room temperature.

[1] A. A. Colville and S. Geller, *Acta Cryst.*, B27, 2311(1971) [2] R. W. Grant et al., *J. Appl. Phys.* 39, 1122 (1968)

QA11

Electronic and magnetic phase separation in the semimetallic ferromagnet EuB_6

Pintu Das¹, Adham Amyan¹, Jens Brandenburg¹, Jens Mueller^{1*}, Peng Xiong², Stephan Von Molnar² and Zachary Fisk³
¹ Institute of Physics, Goethe University Frankfurt, Germany
² Dept. of Physics, Florida State University, Tallahassee, USA
³ Dept. of Physics, University of California, Irvine, USA

EuB_6 is a low-carrier semimetal, which undergoes a unique paramagnetic to ferromagnetic transition displaying two consecutive features at $T_{c1} = 15.5 \text{ K}$ and $T_{c2} = 12.6 \text{ K}$ in electrical transport, magnetization and specific heat. Its structural and electronic simplicity makes EuB_6 an ideal model system for studying the effect the magnetic state of a system has on its electronic transport properties. In particular, the fundamentals of intrinsic electronic and magnetic phase separation can be studied, which play a critical role for the colossal magnetoresistance (CMR) in magnetic semiconductors and manganites. In explaining CMR in EuB_6 , being largest at T_{c1} , the concept of magnetic polaron (MP) percolation has been invoked. We report resistance noise and weakly nonlinear transport measurements, being sensitive to the microgeometry of the electronic system. We find direct evidence for electronic phase separation when cooling through T_{c1} and a diverging noise level at T_{c2} , which we interpret as magnetically-driven percolation resulting from the overlap of spatial inhomogeneities in conductivity produced by MP. Interestingly, MP percolation can be induced also by applying magnetic fields in the paramagnetic region. We find that the density of MP can be described by a universal scaling function, being related to a single critical magnetization.

QA12

Study of magnetic and magnetodielectric properties of perovskite YbCrO_3

Jong-suck Jung, Ayato Iyama*, Hiroyuki Nakamura, Yusuke Wakabayashi and Tsuyoshi Kimura
 Division of Materials Physics, Osaka University, Japan

Perovskite YbCrO_3 shows the G-type antiferromagnetic ground state for Cr^{3+} moments ($T_N \sim 118 \text{ K}$). Because of the Dzyaloshinskii-Moriya interaction, the G-type structure becomes canted, and then YbCrO_3 exhibits weak ferromagnetism. When weak magnetic fields are applied ($B \leq 0.3 \text{ T}$), temperature-induced magnetization reversal is observed. The magnetization reversal is probably associated with a keen competition between antiferromagnetically coupled Cr^{3+} - Yb^{3+} moments. Recently, a distinct magnetodielectric effect was observed in another perovskite SmMnO_3 which also shows temperature-induced magnetization reversal due to the competition between antiferromagnetically coupled Mn^{3+} - Sm^{2+} moments [1]. Thus, it is intriguing to study magnetodielectric properties of YbCrO_3 . In this study, we investigated magnetic and magnetodielectric properties for single crystals of YbCrO_3 grown by the flux method. The comparison of magnetodielectric properties between YbCrO_3 and SmMnO_3 provides useful information to understand the distinct magnetodielectric effect observed in SmMnO_3 .

[1] J.-S. Jung et al. *Phys. Rev. B* 82, 212403 (2010)

QA13

Interplay among spin, orbital, and lattice degrees of freedom in a frustrated spinel Mn_2O_4

Yoichi Nii^{1*}, Hiroshi Umetsu¹, Hajime Sagayama², Nobuyuki Abe², Kouji Taniguchi² and Taka-hisa Arima²
¹ Dept. of Phys., Tohoku University, Japan
² Dept. of Advanced Mater. Sci., The University of Tokyo, Japan

Spinel oxides, AB_2O_4 , are one of the typical systems for studying the effects of geometrical frustration and the possible coupling among spin, orbital and lattice degrees of freedom. Mn_2O_4 exhibits the cooperative Jahn-Teller (JT) transition from cubic to tetragonal structure at 1443 K with the 3z²-r² ferro-orbital order at B-site Mn^{3+} . The gigantic JT distortion (~16 %) would encourage the formation of one-dimensional (1D) antiferromagnetic spin chains at B-site Mn^{3+} normal to the c-axis. A macroscopic degeneracy of the arrangements of 1D-spin-chains still remains, even if one considers the magnetic interaction between the nearest neighbor 1D-chains. It was reported that Mn_2O_4 exhibits successive magnetic phase transitions from paramagnetic to Yafet-Kittel (43 K), incommensurate (IC) (40 K) and commensurate (C) phase (34 K)[1], which is an indicative of the surviving magnetic frustration. Another phase transition is induced by applying magnetic field in the low-temperature C phase [2]. In order to elucidate the magnetic-field induced phase transition, we have measured synchrotron x-ray diffraction and neutron scattering in a magnetic field along [100] c. We propose a scenario of the magnetic-field induced phase transition, where the rearrangement of 1D-spin-chains is triggered by orbital hybridization at B-site Mn^{3+} through the spin-orbit coupling.

[1] R. Tackett et al., *Phys. Rev. B* 76, 024409 (2007). [2] T. Suzuki et al., *Phys. Rev. B* 77, 220402(R) (2008)

QA14

Structural and dielectric study of hexagonal $\text{Y}_{0.8}\text{Sr}_{0.2}\text{MnO}_3$ Compound

Rajesh K. Thakur^{1*}, Rasna Thakur², A. Bharathi³ and N.k. Gaur²
¹ Department of Physics, Barkatullah University, Bhopal, India
² Department of Physics, Barkatullah University, Bhopal, India
³ Condensed Matter Physics Division, Materials Science Group, Indira Gandhi Centre for Atomic Research, Kalpakkam, India

Strontium doped YMnO_3 compound have been prepared in single-phase form by using high temperature solid state reaction method. The structural and dielectric properties of the prepared sample have been carried out in the wide range of temperature and frequency. Temperature and frequency variations of dielectric permittivity measurements show that the present hole doped YMnO_3 compound exhibits a competing interaction in between the ferromagnetic double - exchange and antiferromagnetic super-exchange interactions, further a weak signature of ferromagnetic ordering at lower temperature has been witnessed. Our resistivity measurement reveals that the material is highly insulating at lower temperature just below the reported AFM transition in this class of materials.

QA15

Controlling the superparamagnetic limit using the magnetoelectric effect

Hyungsuk K. D. Kim¹, Laura Schelhas², Sarah Tolbert² and Gregory P. Carman^{3*}
¹ Department of Materials Science and Engineering, UCLA, USA
² Department of Chemistry and Biochemistry, UCLA, USA
³ Department of Mechanical and Aerospace Engineering, UCLA, USA

MRAM (Magnetic Random Access Memory) is attracting considerable attention as a possible candidate for next generation of non-volatile memory devices. Major challenges facing scientists today are overcoming thermal instability and reducing the writing energy. As bit density increases, this requires smaller magnetic regions to be written magnetically at small scales and external energies become a dominant feature. For example in the small scale, thermal energy becomes larger than magnetic anisotropy, resulting in superparamagnetic behavior. For a given small scale size, the temperature above which superparamagnetism begins is referred to as the blocking temperature. Superparamagnetic behavior is undesirable due to limits it places on the size of a bit of information. Recently, researchers have begun to study magnetoelectric (ME) memory related to some issues with memory. Their focus has been on writing processes using electric field-induced strain rather than addressing the more challenging topic of controlling superparamagnetism. Here we report experimental results showing the introduction of a magnetoelectric anisotropy energy to alter the blocking temperature and thus control the superparamagnetic behavior. This is achieved via an electric field-induced strain in a ME composite. Our results show 50 K increase of the blocking temperature with the application of an electric field.

1. Y. Jun, J. Seo, J. Cheon, *Accounts of chemical research* 41, 179 (2008). 2. F. Zavaliche et al., *Nano letters* 7, 1586 (2007). 3. T. Wu et al., *Applied Physics Letters* 98, 012504 (2011). 4. M. Bibes, A. Barthelemy, *Nature Materials* 7, 425 (2008).

QA16

Magneto-Capacitance Effect and Electric Polarization in Spinel Co_2MnO_4

Sun Hee Kang¹, San Youn Park², Ill Won Kim¹, Yoon Hee Jeong³ and Tae Yeong Koo^{3*}
¹ Physics Department, Ulsan University, Korea
² Physics Department, Pohang University of Science and Technology, Korea
³ Physics Department, Pohang University of Science and Technology, Korea
⁴ Pohang Accelerator Laboratory, Korea

Structural phase diagram of spinel $\text{Co}_{x-1}\text{Mn}_x\text{O}_4$ ($1.0 \leq x \leq 2.0$) was reexamined at the room temperature with a focus on the cubic-tetragonal phase boundary. A specific composition of Co_xMnO_4 ($x=1.0$) was selected from the phase diagram study under the requirement of both high ferrimagnetic transition temperature (T_c) and non-mixed structural phase condition. Experimental result of magnetization measurements and local distortions due to the Jahn-Teller Mn^{3+} ions support the stabilization of Yafet-Kittel type magnetic configuration in the cubic inverse spinel Co_2MnO_4 . Correlation between the observed forced magnetization - a continual increment of magnetization above the saturation field - and magneto-capacitance effect (MCE) was clarified. MCE of up to 7 % at 8 T around T_c was observed without an appreciable hysteresis and nonlinearity in the field variation. Diffraction-spectroscopy techniques were also used to identify the local chemical and structural environments of both Co and Mn ions at two crystallographic sites of the spinel structure.

QA17

Magnetically induced polarization in copper metaborate CuB_2O_7

Khanh Duy Nguyen¹, Nobuyuki Abe², Masashi Tokunaga³, Mitsuru Saito¹ and Taka-hisa Arima^{2*}
¹ Department of Physics, Tohoku University, Japan
² Department of Advanced Materials Science, The University of Tokyo, Japan
³ Institute for Solid State Physics, The University of Tokyo, Japan

Intriguing electro-magneto optic effect of non-centrosymmetric magnet copper metaborate has attracted huge consideration during last time [1]. In here we report the magneto-electric behavior of CuB_2O_7 under external magnetic field. It is well known that CuB_2O_7 undergoes a phase transition from paramagnetic state to canted-antiferromagnet at 21 K, then followed by a second transition to spiral order around 10 K. Although the magnetic structure at low temperature below 10 K has not completely been made clear yet, some evidences of incommensurate helical order in this range of temperature have been observed [2]. Result of magnetization measurement points out the existence of an anomaly around 1, 3 T at 2 K, then disappeared when increasing temperature above 10 K, which may be attributed to the transition from commensurate to incommensurate phase. Furthermore, electric polarization was also observed by applying a magnetic field along the [110] and [1-10] axes without poling electric field in low temperature regime. The magnitude of polarization in static field was found to be compatible with the measurement in pulse magnetic field. Besides novel optical characteristic, these results show the ability of generation and control electric polarization by magnetic field in CuB_2O_7 as well as application to opto-electronic devices.

[1] M. Saito, K. Ishikawa, S. Korno, K. Taniguchi and T. Arima, *Nature Mater.* 8, 634 (2009) [2] M. Boehm, B. Roessli, J. Schefer, A. S. Willis, B. Ouladdiaf, E. Lelièvre-Berna, U. Staub and G. A. Petrakoskii, *Phys. Rev. B* 68, 024405 (2003)

QA18

Impedance spectroscopy of ferromagnetic oxide: $\text{Pr}_{0.6}\text{Sr}_{0.4}\text{MnO}_3$

D V Maheswar Repaka¹ and Mahendiran Ramanathan²
¹ PHYSICS, National University of Singapore, Singapore
² Physics, National University of Singapore, Singapore

In recent years, coupling between electrical and magnetic polarizations in multiferroic-magnetoelectrics have become a topic of considerable interest due to novel applications and fundamental physics involved [1]. Impedance spectroscopy has been extensively used to investigate cross coupling between magnetic and electrical dipole ordering. Anomalies in low-frequency ($f = 1-10 \text{ kHz}$) dielectric constant at magnetic transition have been reported in YMnO_3 [2], BiMnO_3 [3] etc. However, measurement in MHz range has been hardly reported. In this work, we report temperature, frequency and magnetic field dependence of impedance in $\text{Pr}_{0.6}\text{Sr}_{0.4}\text{MnO}_3$ which shows ferromagnetic transition near room temperature ($T_c = 303 \text{ K}$). It is found that with increasing frequency of the ac current, an anomaly in the form of a sharp peak appears at the Curie temperature. A second anomaly in the form of an abrupt decrease occurs at $T = 100 \text{ K}$ much below the Curie temperature. These anomalies are suppressed under external magnetic field. It is suggested that the observed anomalies are not necessarily caused by ordering of electrical dipoles. The observed features in impedance closely correlate with the magnetization. We suggest that impedance spectroscopy in these materials can probe magnetization dynamics, which is often neglected in studies of magnetocapacitance effect in multiferroic materials.

[1] S.W. Cheong and M. Mostovoy, *Nat.Mater.* 6 (2007) 13. [2] S. Lee, A. Pirogov, M. Kang, K.H. Jang, M. Yonemura, T. Kamiyama, S.W. Cheong, F. Gozzo, N. Shin, H. Kimura, Y. Noda, and J.G. Park, *Nature (London)* 451, (2008) 451. [3] R. Seshadri and N. A. Hill, *Chem.Mater.* 13, (2001) 2892.

QA19

Structures and magnetic properties of $\text{Tm}_{1-y}\text{Y}_y\text{Mn}_{1-x}\text{Co}_x\text{O}_3$

Toshiyuki Tanaka, Yusuke Amakai, Naoki Momono, Shigeyuki Murayama and Hideaki Takano*
 Department of Applied Sciences, Muroran Institute of Technology, Japan

The structure and magnetic properties of $\text{Tm}_{1-y}\text{Y}_y\text{Mn}_{1-x}\text{Co}_x\text{O}_3$ with $0 \leq x \leq 0.5$ and $0 \leq y \leq 0.3$ were investigated by X-ray diffraction, specific heat and magnetization measurements. A thulium manganite TmMnO_3 prepared by the solid state synthesis method in ambient pressure is hexagonal and antiferromagnetic with Neel temperature $T_N = 86 \text{ K}$. The substitution of Y for Tm in TmMnO_3 does not largely affect the fundamental hexagonal structure. We can roughly understand the results of the magnetization and the specific heat of $\text{Tm}_{1-y}\text{Y}_y\text{MnO}_3$ in terms of a dilution effect of Tm by Y. On the other hand, the structure of $\text{TmMn}_{1-x}\text{Co}_x\text{O}_3$ gradually changes from hexagonal to orthorhombic with the substitution of Co for Mn and hexagonal and orthorhombic phases coexist in samples for $x \leq 0.3$, and $\text{TmMn}_{0.6}\text{Co}_{0.4}\text{O}_3$ become almost orthorhombic single phase. The magnetization of $\text{TmMn}_{0.6}\text{Co}_{0.4}\text{O}_3$ in a field of 250 Oe increases rapidly below about 60 K with decreasing temperature. The discrepancy of the zero-field-cooled (ZFC) and the field-cooled (FC) magnetization remarkably expands below about 60 K. Moreover, temperature dependence of ZFC and FC magnetization show peaks at 40 K and 27 K, respectively. $\text{TmMn}_{1-x}\text{Co}_x\text{O}_3$ we obtained shows complicated magnetic properties.

QA20

Complex magnetic and electric orders in multiferroic Co_3TeO_6

Chin-wei Wang¹, Chih-jen Wang¹, Wen-hsien Li^{1*}, Chih-chieh Chou², Hung-duen Yang², Yang Zhao³, Sung Chang³, Jeffrey W. Lynn³ and Helmut Berger⁴
¹ Department of Physics and Center for Neutron Beam Applications, National Central University, Taiwan
² Department of Physics and Center for Nanoscience and Nanotechnology, National Sun Yat-Sen University, Taiwan
³ NIST Center for Neutron Research, National Institute of Standards and Technology, Gaithersburg, USA
⁴ Institute of Physics of Complex Matter, EPFL, Lausanne, Switzerland

Multiferroics, where both ferroelectric and magnetic order coexist, are quite uncommon, but are of particular interest both to understand the fundamental interactions between the two types of order as well as for the potential for practical applications. The novel metal tellurates M_3TeO_6 , where M is a first-row transition metal, have been shown to be rich in crystalline chemistry. Ferroelectricity and magnetic-field-driven polarization have been observed. Here, we report on the results of neutron diffraction, magnetic susceptibility, specific heat, and dielectric constant measurements made on a single crystal Co_3TeO_6 to study the interplay between the ferroelectricity and magnetic order. A strong interplay between the order parameters of ferroelectricity and both commensurate and incommensurate magnetic order are observed. Long range incommensurate magnetic order develops below $\text{TM}_1 = 26 \text{ K}$, which is followed by three additional zero-field phase transitions at $\text{TM}_2 = 19.5 \text{ K}$, $\text{TM}_3 = 18 \text{ K}$, and $\text{TM}_4 = 16 \text{ K}$ where the incommensurate order changes and commensurate order develops. In magnetic fields up to 14 T we find that the magnetic intensities and incommensurate wave vector are dramatically altered as ferroelectricity develops, with a fifth abrupt transition around 10 T. The overall behavior characterizes Co_3TeO_6 as a type-II multiferroic.

QA21

Annealing induced colossal magnetocapacitance and colossal magnetoresistance in in-doped CdCr₂S₄

Zhaorong Yang*
Institute of Solid State Physics, Chinese Academy of Sciences, China

Colossal magnetocapacitance (CMC) and colossal magnetoresistance (CMR) induced by annealing polycrystalline Cd_{0.97}In_{0.03}Cr₂S₄ are reported. In agreement with the appearance of CMR near the Curie temperature T_c, a insulator-metal transition is observed with decreasing temperature at zero magnetic field. On the contrary, after the same annealing treatment, CdCr₂S₄ displays typical semiconductor behavior and does not show magnetic field dependent dielectric and electric transport properties. Accordingly, the simultaneous occurrence of CMC and CMR effects implies that the CMC in the annealed Cd_{0.97}In_{0.03}Cr₂S₄ could be explained qualitatively by a combination of CMR and Maxwell-Wagner effect.

QA22

Critical dynamics in LiCuVO₄

Christoph Grams¹*, Maximilian Schalenbach¹, Daniel Niermann¹, Petra Becker² and Joachim Hemberger¹
¹ II. Physikalisches Institut, University of Cologne, Germany
² Institut für Kristallographie, University of Cologne, Germany

QA24

Anomalous magnetodielectric and magnetostrictive effect via spin reorientation in terbium iron garnet

Ki-myung Song¹, Seongsu Lee² and Namjung Hur¹*
¹ Dept. of physics, Inha univ., Korea
² Neutron Science Division, Korea Atomic Energy Research Institute, Korea

We have investigated the relationship among the magnetic, dielectric and magnetostrictive properties of terbium iron garnet (TbIG). In this presentation, we report experimental observations which are extraordinary magnetostriction and magnetodielectric effects in TbIG with a non-collinear spin structure in a single unit cell. The distinct effects of magnetism on the lattice are also demonstrated by the unprecedented magnetostriction with a negative poisson ratio. We attribute the observed magnetodielectric effects and the huge magnetostriction to the magnetic field induced spin reorientation from non-collinear to collinear. In this study, we analyzed crystallographic and spin structure of TbIG in various temperatures by the Fullprof program. We investigated the effect of the non-collinear spin structure on the crystal structure of TbIG to elucidate the relation between them through analyzing neutron diffraction data.

QA25

Template based synthesis of multiferroic BiMnO₃ nanotubes and shape dependent study of its magnetic properties

Geo George Phillip, Anuraj Sundar, Mahdiyar Bagheri, Helen Annal Therese* and Gopalakrishnan Chandrasekaran
Nanotechnology Research Centre, SRM University, India

The synthesis of Bismuth manganite nanotubes was done by templating precursors of bismuth and manganese on titanium dioxide nanotubes. The yield was post treated to remove the template material and sintered at 400°C. The resulting powders were studied using X-ray Diffractometer and Scanning Electron Microscope, which revealed the formation of perovskite nanotubes. The BiMnO₃ nanotubes were characterized for its magnetic properties by Vibrating sample magnetometer that revealed the intrinsic ferromagnetic nature with increase in its magnetic saturation that could have been due to the shape anisotropy of the nanotubes. The magnetization under field cooled and zero-field cooled was also found to differ significantly with applied magnetic field. These results indicate the co-existence of antiferromagnetic behavior at higher temperatures along with its intrinsic ferromagnetic nature which deviate from its bulk counterpart that only exhibits ferromagnetic nature.

1. Srihala, D., Singh, V.N., Banerjee, A., Mehta, B.R. Effect of induced shape anisotropy on magnetic properties of ferromagnetic cobalt nanocubes (2010) *Journal of Nanoscience and Nanotechnology*, 10 (12), pp. 8088-8094. 2. Tajiri, T., Harazono, M., Deguchi, H., Mito, M., Kohno, A., Kohiki, S. Synthesis and magnetic property of multiferroic BiMnO₃ nanoparticles in the pores of mesoporous silica (2010) *Japanese Journal of Applied Physics*, 49 (6 PART 2), pp. 06GH041-06GH044. 3. Xu, E., Qian, T., Zhang, G., Zhang, T., Li, G., Wang, W., Li, X. Fabrication and magnetic properties of multiferroic BiFeO₃ nanotube arrays (2007) *Chemistry Letters*, 36 (1), pp. 112-113.

QA26

Solitary reentrant superconductivity prediction in asymmetrical ferromagnet-superconductor-ferromagnet trilayer

Yurii N. Proshin*, Marat M. Khusainov, Arthur Minnullin and Mansur G. Khusainov
Theoretical Physics Department, Kazan Federal University, Russia

The theory of proximity effect for thin bilayer FS, trilayer FSF and fourlayered system FSFS, where F is a ferromagnetic metal, and S is superconductor, is proposed on the base of new boundary-value problem for the Eilenberger function. For all systems the dependencies of critical temperature on an exchange field of the F metal, electronic correlations in the S and F metals, and thicknesses of layers F and S are derived. It is shown that the possibility of the Fulde-Ferrell-Larkin-Ovchinnikov (FFLO) state observation is especially increased in the asymmetrical systems (FSF* and FSF'S) for which solitary reentrant superconductivity is predicted. On the basis of a proximity effect we propose new method of probe of electronic parameters of contacting materials. If well known BCS superconductor S is used as a probe, one can determine the exchange field, the electron-electron constant in various magnetics F for the FS structures. It allows us to predict the sign and value of the constant of electron-electron interaction in gadolinium and to explain a surprisingly high critical temperature T_c ~ 5K in the short-periodic Gd/La superlattice [1].

P.P. Deen, et al. *J. Phys.: Cond. Matt.* 17, 3305 (2005).

QA23

High quality crystal growth and Low temperature diffuse scattering studies

Shilpa Adiga*, Yixi Su, Jrg Persson and Manuel Angst
PGI-4, Forschungszentrum Juelich, Germany

The 120 K Verwey-transition [1] in magnetite Fe₃O₄ is the classical example for charge ordering, but the complex low-temperature structure was unresolved during decades. Early experimental studies and recent calculations suggest ferroelectricity (FE) due to charge ordering, which would be significant if confirmed. Very recent structural refinement [2] supports the necessary polar structure. Recently, signatures of relaxor FE were observed below 40 K [3]. Specific diffuse scattering would be expected in such a case [4], best re- solved on high quality single crystals. The Verwey transition depends sensitively oxygen stoichiometry [5] and the high quality crystals are obtained by the direct synthesis in an appropriate CO/CO₂ flow [6]. We have grown high quality single crystals of magnetite under the tailored growth conditions by optical floating zone method and characterized them primarily by specific heat measurement. We present the results of high energy x-rays and neutrons diffuse scattering experiments, performed to test the proposed relaxor FE. The presence of weak diffuse scattering at very low temperature is observed only by neutron scattering, and thus likely magnetic, not supporting relaxor FE. Proof of the latter would require time resolved scattering.

1. E.J.W.Verwey, *Nature* 144, 327 (1939). 2. Mark S.Senn et al, *Nature Letter* (2011). 3. F.Schrettle et al, *Phys. Rev. B*, 83 195109 (2011). 4. Grace Yong et al., *Phys. Rev. B*, 62, 14763 (2000). 5. P. Shepherd et al., *Phys. Rev. B* 43, 8461 (1991). 6. R. Aragon et al., *J. crystal growth*, 61, 221 (1983)

QA27

Tuning magnetic order, electromagnons and exchange bias by epitaxial strain in BiFeO₃ thin films

Manuel Bibes¹*, Daniel Sando¹, Arsene Agbelele², Maximilien Cazayous³, Ingrid Infante⁴, Wei Ren⁵, Sergey Lisenkov⁶, Cecile Carretero¹, Agnes Barthelemy¹, Laurent Bellaiche⁵, Jean Jurazsek² and Brahim Dkhil¹
¹ Unite Mixte de Physique CNRS/Thales, France
² Universite de Rouen, France
³ Universite Paris Diderot, France
⁴ Ecole Centrale Paris, France
⁵ University of Arkansas, USA
⁶ University of South Florida, USA

With a ferroelectric Curie temperature of 1100 K and a Neel temperature of 640K, BiFeO₃ is one of the very few room-temperature multiferroics [1]. Its ferroelectric polarization is as high as 100 μC/cm² and in the bulk it is a G-type antiferromagnet, with a superimposed cycloidal modulation. In addition to showing magnetoelectric coupling between its ferroic orders, BiFeO₃ also exhibits coupling between dynamic lattice and spin excitations (electromagnons), enabling an electrical control of spin waves [2]. We have explored the influence of epitaxial strain [3] on the antiferromagnetic properties of BiFeO₃ thin films. Combining Mossbauer spectroscopy and Raman scattering, we have found that the harmonic cycloidal order is stable at low strain but is replaced at higher strain by conventional antiferromagnetism. This is accompanied by strong changes in the electromagnon spectra and on their dependence on external stimuli. In addition, the mean antiferromagnetic vector progressively rotates as strain varies, offering novel strategies to control exchange bias with ferromagnetic overlayers.

[1] G. Catalan et al, *Adv. Mater.* 21, 2463 (2009); [2] P. Rovillain et al, *Nature Mater.* 9 975 (2010); [3] I.C. Infante et al, *Phys. Rev. Lett.* 105, 057601 (2010)

QB01

Magnetic-enhanced electron-phonon coupling and vacancy effect in '111' type iron pnictides from first-principles calculations

Mei Liu¹ and Bin Li²
¹ Dept. of Physics, Southeast University, China
² Department of Physics, Southeast University, China

We investigate the lattice dynamics in both nonmagnetic and striped antiferromagnetic states of '111' type iron pnictides using the density-functional perturbation theory. The anisotropic spin-phonon effects lead to the softening of phonon frequencies and the renormalization of electron-phonon matrix elements, so as to increase the electron-phonon couplings by 68%, 65%, and 0.9% for LiFeAs, NaFeAs, and LiFeP, respectively. Taking into account the vacancy effects in the three iron pnictides, we find that the electron-phonon couplings are further enhanced by hole doping, yielding superconducting transition temperatures close to their experimental values.

QB02

Penetration depth and knight shift in iron-based superconductor Ba_{1-x}K_xFe₂As₂

Kazuki Ohishi¹*, Yasuyuki Ishii², Isao Watanabe³, Taku Saito⁴, Hideto Fukazawa⁴, Yoh Kohori⁴, Kunihiro Kihou⁵, Chul-ho Lee⁵, Hijiri Kito⁵, Akira Iyo⁵ and Hiroshi Eisaki²
¹ Research Center for Neutron Science and Technology, CROSS, Japan
² Department of Physics, Tokyo Medical University, Japan
³ Advanced Meson Science Laboratory, RIKEN, Japan
⁴ Department of Physics, Chiba University, Japan
⁵ AIST, Japan

We have observed temperature and magnetic field dependence of penetration depth λ in single crystalline samples of Ba_{1-x}K_xFe₂As₂ (x = 0.27, 0.64, 0.7, 0.8, 0.94 and 1.0) in order to clarify the superconducting gap mechanism. We have found that T dependence of 1/λ² in KFe₂As₂ with H//c and H⊥c are completely different. While the T dependence of 1/λ² observed with H//c is well fitted by a two-full-gap model, T-linear behavior is clearly observed below ~T_c/2 with H⊥c, suggesting the existence of line node. These results are well interpreted when we take into account the horizontal line node (line node in ab-plane) in KFe₂As₂. At the presentation, we will also report the T and H dependence of λ and Knight shift over a wide x region of Ba_{1-x}K_xFe₂As₂.

QB03

Raman scattering study of the lattice dynamics in LiFeAs and Fe_{1-x}Te_{1-x}Se_x

Youngje Um
Max-Planck institute, Stuttgart, Germany

Following the recent discovery of superconductivity in F doped LaFeAsO with T_c of 26 K, numerous families of the Fe-based superconductors such as REFeAs(O_{1-x}F_x) (RE = rare earth), MFe₂As₂ (M = Ba, Ca, Sr, K, ...), LiFeAs/NaFeAs and Fe_{1-x}Te_{1-x}Se_x have been found and investigated. Most of these compounds have closely related phase diagrams and present an antiferromagnetic parent compound at low temperature, which turns superconductor upon doping. A noticeable exception is LiFeAs, in which superconductivity is observed already in the parent compound. Recent ARPES results suggest strong electron-phonon coupling in LiFeAs, but so far no experimental study of its lattice dynamics is available. Here, we present first Raman light scattering investigations of lattice dynamics on superconducting LiFeAs. Five of the six expected phonon modes are observed, and show a conventional anharmonic behavior. No clear evidence for coupling of electron with zone center phonon is observed. Then, we present a systematic study of the lattice dynamics in Fe_{1-x}Te_{1-x}Se_x as a function of Se and excess Fe contents, with special emphasis on the Fe phonon. A peculiar doping dependence of the mode is observed, which suggests an original coupling of this phonon to the low energy spin excitations induced by excess iron.

QB04

Magnetism and Superconductivity in Rb_{1-x}Fe_{2-x}Se₂

Kazuki Ohishi¹*, Shouhei Kototani², Shunsuke Saiki², Yoshiaki Kobayashi², Masayuki Itoh² and Masatoshi Sato¹
¹ Research Center for Neutron Science and Technology, CROSS, Japan
² Department of Physics, Nagoya University, Japan

The recent discovery of superconductivity in A₂Fe_{2-y}Se₂ (A = alkali metal), with transition temperatures up to T_c ~ 32 K, has led to a renewed interest for iron based chalcogenide systems. A remarkable observation is that, beside the superconducting state, a strong antiferromagnetic (AFM) state with magnetic moments up to 3.3 μB per Fe ion is observed below TN ~ 550 K. The key issue in A₂Fe_{2-y}Se₂ is whether AFM order and superconductivity cohabit due to phase separation or share a microscopic coexistence. We have performed muon spin relaxation/rotation measurements in single crystalline samples of superconducting (SC) Rb_{0.8}Fe_{1.6}Se₂ (T_c = 29 K) and non-SC Rb_{1-x}Fe_{2-x}Se₂, which doesn't show superconductivity, in order to elucidate whether there is difference of magnetic state between SC and non-SC samples. In SC sample, we found that SC volume fraction is only ~6% and the rest of amount is AFM ordered phase, suggesting SC and AFM ordered phases are separated. We found that muon spin depolarization increases with decreasing temperature in non-SC sample, while no change was observed in SC sample. It suggests the appearance of new magnetic state below 40 K in non-SC sample.

QB05

Magnetic Resonant mode in the Spin-Excitation Spectrum of Superconducting Rb2Fe4Se5 Single Crystals

Jitae Park
Max-Planck-Institute for Solid State Research, Germany



QB06

Magnetic field-induced superconductivity in the canted antiferromagnet Eu(Fe_{0.81}Co_{0.19})₂As₂

Vinh Hung Tran^{1*}, T A Zaleski², Z Bukowski¹, L M Tran¹ and A J Zaleski¹
¹ Institute of Low Temperature and Structure Research, Polish Academy of Sciences, 50-950 Wroclaw, Poland
² Institute of Low Temperature and Structure Research, Polish Academy of Sciences, 50-950, Poland

We present results of ac-magnetic susceptibility, dc-magnetization, specific heat and magnetotransport measurements on a single crystal of magnetic Eu(Fe_{0.81}Co_{0.19})₂As₂ superconductor. The compound undergoes multiple phase transitions; from paramagnetic to a spin-density-wave (SDW) at TSDW = 80 K, to canted antiferromagnetic (C-AF) state at TN = 16.5 K and superconducting (SC) state at Tc = 5.15 K at zero field. Upon applying fields both the C-AF and SC states evolve in an unconventional manner. Magnetic field distinctly affects the spin canting, resulting in separation of the C-AF into two a new C-AF and ferromagnetic phases. The unusual behavior of the SC state deserves the observation that Tc can be increased up to 6.5 K with magnetic fields applied parallel to the ab-plane of crystals. The observed field-induced superconductivity is interpreted as a result of a weakening of the orbital pair-breaking effect. From the experimental data we propose the field-temperature phase diagrams for Eu(Fe_{0.81}Co_{0.19})₂As₂.

QB07

Superconductivity and spin fluctuations in Ca_{1-x}Pr_xFe₂As₂ superconductors studied by 75As NMR

Long Ma^{*}, Gaofeng Ji¹, Jia Dai¹, S. R. Saha², J. Paglione² and Weiqiang Yu¹
¹ Department of Physics, Renmin University of China, China
² Center for Nanophysics and Advanced Materials, Department of Physics, University of Maryland, USA

The observation of superconductivity in the rare earth doped CaFe₂As₂ with Tc as high as 47 K is still not understood. Here we report the first NMR study on the newly discovered Ca_xPr_{1-x}Fe₂As₂ (x=0.075, 0.15) single crystals. The magnetization shows superconductivity at ~25 K with a small volume ratio for both samples. A first order structural transition from the tetragonal to the collapsed tetragonal phase in both crystals is shown by 75As spectra. Residual tetragonal phase is seen in the x = 0.075 sample with a finite volume, but not seen in the x = 0.15 sample. We also observed a sharp drop of Knight shift below Ts in both samples, suggesting a suppression of local moments in the collapsed phase. However, the 1/75T1 is enhanced below 50 K and shows a prominent peak at about 25 K. Such behaviors indicate strong low-energy antiferromagnetic spin fluctuations, with static or quasi-static magnetic ordering at low temperatures, which is probably caused by Pr³⁺ doping. The absence of the residual tetragonal phase and the observation of antiferromagnetic spin fluctuations in the x=0.15 sample suggest that superconductivity in Ca_xPr_{1-x}Fe₂As₂ is not tied to the tetragonal phase and may have a magnetic origin.

QB08

Importance and details of the spin excitation spectra in high-Tc pnictide superconductors

Tanmoy Das and A. V. Balatsky
 Theoretical Division, Los Alamos National Laboratory, USA

One common feature that underlies all high-Tc superconductor families is the development of a magnetic resonance peak at or around the antiferromagnetic ‘hot-spot’ vector. This feature has proven to give valuable information about the pairing symmetry, and bulk Fermi surface properties. We provide a random-phase approximation (RPA) based BCS susceptibility calculation using material specific band structure for 122 family of iron-pnictide and layered iron selenide superconductors. (i) In iron-pnictide, we show that when two hole-pockets at Gamma point and the electron pockets at M point are present on the Fermi surface, the spin-excitation spectra split into two distinct resonance branches. [1] The energy separation between the two resonances is related to the differences in the superconducting gaps on two hole-pockets. Again, the momentum resolution between the two modes comes from the differences in Fermi surface areas of the two hole-pockets. (ii) We also show that when one hole-pocket disappears, one of the resonances disappears. Furthermore, when both hole pockets vanish, the magnetic scattering between the remaining electron-pockets lead to a change in the gap symmetry from s± to d-wave. The latter is observed in the newly discovered iron-selenide superconductors. [2] Finally, we will present the resulting spin-excitation spectra for both materials.

[1] T. Das, and A. V. Balatsky, Phys. Rev. Lett. 106, 157004 (2011). [2] T. Das, and A. V. Balatsky, Phys. Rev. B 84, 014521 (2011).

QB09

Angular dependence of the resistive upper critical field of an iron-based superconductor Fe(Te,Se) in high magnetic fields

Takanori Kida¹, Yoshikazu Mizuguchi², Yoshihiko Takano³ and Masayuki Hagiwara¹
¹ KYOKUGEN, Osaka university, 1-3 Machikaneyama, Toyonaka, Osaka 560-8531, Japan
² Grad. Sch. Sci. Eng., Tokyo Metropolitan University, 1-1 Minami-Osawa, Hachioji, Japan
³ National Institute for Materials Science, 1-2-1 Sengen, Tsukuba 305-0047, Japan

The 11-system FeCh (Ch=S, Se, Te) superconductors are of great importance in understanding the mechanism of superconductivity in iron-based superconductors owing to their simple structures. Previously, we have reported the temperature dependence of the resistive upper critical field (Hc2) on Fe_{1.05}Te_{0.85}Se_{0.15}, which exhibits superconductivity at T = 14 K [1,2]. The Hc2 of this compound at low temperature is considerably smaller than that expected from the Werthamer-Helfand-Hohenberg model, manifesting the Pauli limiting behavior. It suggests that this compound shows the spin-singlet pairing in the superconducting state. The anisotropy coefficient of Hc2 decreases from 2.4 near Tc to ~1 (nearly isotropic) at low temperatures. In this study, we have investigated an angular dependence of Hc2 of a single crystal of Fe_{1.05}Te_{0.85}Se_{0.15} in pulsed high magnetic fields up to 52 T. At T = 10 K, the Hc2 increases with increasing Θ, which is the angle between the c-axis and applied magnetic fields direction. We have found that the angular dependence of Hc2 is well agreement with the Ginzburg-Landau effective-mass prediction.

[1] T. Kida et al., J. Phys. Soc. Jpn. Vol.78 (2009) 113701. [2] T. Kida et al., J. Phys. Soc. Jpn. Vol.79 (2010) 074706.

QB10

Ab initio evidence of strong correlation and large Mott proximity in iron-based superconductors

Takahiro Misawa, Kazuma Nakamura and Masatoshi Imada
 Dept. Applied Physics, Univ. of Tokyo, Japan

Recently discovered iron-based superconductors have attracted much interest in their high superconducting critical temperatures (Tc). Although it is believed that electron correlations mediate the unconventional high-Tc superconductivity, their roles are not fully understood yet. To clarify electron correlation effects from a microscopic point of view, we study the ab initio low-energy effective model for iron-based superconductors by using multi-variable variational Monte Carlo method. From this ab initio calculations, we show that iron-based superconductors discovered near d6 configuration (5 Fe 3d orbitals filled by 6 electrons) is located on the foot of an unexpectedly large dome of correlated electron matter centered at the Mott insulator at d5 (namely, half filling). The d5 Mott proximity extends to subsequent emergence of incoherent metals, orbital differentiations due to the Mott physics and Hund’s-rule coupling, followed by antiferromagnetic quantum criticality, in quantitative accordance with available experiments.

QB11

As-NQR study of LaFeAsO_{1-x}F_x

Toshihide Oka^{*}, Z Li², S Kawasaki¹, G F Chen², N L Wang² and G-Q Zheng¹
¹ Department of Physics, Okayama university, Japan
² Beijing National Laboratory for Condensed Matter Physics, Institute of Physics, Chinese Academy of Science, China

The discovery of superconductivity in LaFeAsO_{1-x}F_x at superconducting transition temperature Tc=26K, followed by that in ReFeAsO_{1-x}F_x(Re:Ce,Pr,Nd,Sm) with Tc as high as 55K, has gained much attention. We have performed systematic As-nuclear quadrupole resonance(NQR) measurements on LaFeAsO_{1-x}F_x to elucidate its superconducting gap structure and mechanism of the Cooper pair formation. For x=0.03, we find the spin-lattice relaxation rate(1/T1) exhibits a small upturn at TN=58K, below which the spectra become broadened due to the internal magnetic field attributed to an antiferromagnetic ordering. Above TN, 1/T1T increases with decreasing T due to the antiferromagnetic spin fluctuation(AFSF), which persists in the x=0.04,0.06, and 0.08 compounds. A dome-shaped x dependence of Tc is found, with the highest Tc=27 K at x=0.06, which is realized under significant AFSF. With increasing x further, AFSF decreases, and so does Tc. These features resemble the cuprates La_{2-x}Sr_xCuO₄, which suggests that AFSF is also important in producing high Tc superconductivity in LaFeAsO_{1-x}F_x. In the superconducting state, we find that 1/T1 decreases exponentially below Tc down to 0.13Tc for x=0.06, which suggests that the energy gaps are fully opened. Meanwhile, 1/T1 below Tc decreases nonexponentially for x either smaller or larger than 0.06, which is accounted for by impurity scattering.

QB12

Interplay between 3d- and 4f-electrons in ReFe_{1-x}Co_xAsO (Re = Ce,Gd)

T. Shang¹, L. Yang¹, Y. Chen¹, L. Jiao¹, J. L. Zhang¹, J. Chen¹, H. Q. Yuan^{1*}, N. Cornell², A. Howard², A. Zakhidov², M. B. Salamon², F. Ronning³, E. D. Bauer³ and J. D. Thompson³
¹ Department of Physics and Center for Correlated Matter, Zhejiang University, China
² UTD-NanoTech Institute, The University of Texas at Dallas, USA
³ Los Alamos National Laboratory, USA

In order to study the evolution from a high Tc superconductor to a strongly correlated system with largely enhanced effective mass in iron pnictides, we have synthesized a series of ReFe_{1-x}Co_xAsO (x=0-1) polycrystalline samples and characterized their physical properties by means of electrical resistivity, magnetization and specific heat. It is shown that, for CeFe_{1-x}Co_xAsO, the SDW transition of the 3d-electrons is quickly suppressed upon substituting Fe with Co and superconductivity appears in a narrow doping range of 0.05<x<0.20. On the other hand, the 4f-electrons of Ce is antiferromagnetically ordered with a nearly unchanged TN~4K over a wide doping concentration (0<x<0.8). Remarkably, the 3d- and 4f-electrons become ferromagnetically ordered above x~0.75 and x~0.80, respectively. Similar results are derived for the GdFe_{1-x}Co_xAsO upon partially substituting Fe with Co. However, the 4f-electrons are antiferromagnetically ordered over the entire doping concentration and likely undergo a spin reorientation above x~0.6. On the Co-side (x<0.8), the 3d-electrons undergo a FM transition, followed by an AFM transition upon decreasing temperature. These results suggest that the interplay of 3d- and 4f-electrons may play an important role in ReFe_{1-x}Co_xAsO, giving rise to rich physical properties attributed to the the Kondo scattering and the polarization between the 3d-and 4f-electrons.

QB13

Anisotropic Hc2 curves determined up to 92 T and two-band superconductivity in Ca₁₀(Pt₄As₈)((Fe_{1-x}Pt_x)₂As₂)₅ superconductor

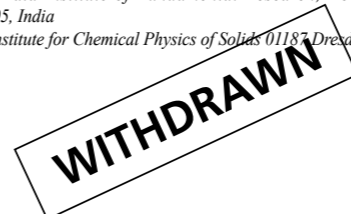
Eundeok Mun¹, Ni Ni², Jared M Allred², Robert J Cava², Oscar Ayala¹, Ross D McDonald¹, Neil Harrison¹ and Vivien S Zapf¹
¹ Nationa High Magnetic Field Lab, Los Alamos National Lab, USA
² Department of Chemistry, Princeton University, USA

The upper critical fields, Hc2(T), of single crystals of the novel superconductor Ca₁₀(Pt₄As₈)((Fe_{1-x}Pt_x)₂As₂)₅ with x=0.02 were determined over a wide range of temperatures down to T = 1.42 K and magnetic fields up to H = 92 T. The measurements of anisotropic Hc2(T) curves are performed in pulsed magnetic fields using radio-frequency contactless penetration depth measurements for magnetic field applied both parallel and perpendicular to the ab-plane. The high magnetic fields up to 92 T and temperatures down to 1.42 K, used in this study, enable access to the complete evolution of the Hc2(T) curves. Whereas a clear upward curvature in Hc2c(T) along H||c is observed with decreasing temperature, the Hc2ab(T) along H||ab shows a flattening at low temperatures. The rapid increase of the Hc2c(T) suggests that the superconductivity can be described by two dominating bands. The anisotropy parameter, Hc2ab(T) / Hc2c(T) , is ~7 close to Tc and decreases considerably to ~1 with decreasing temperature, showing rather weak anisotropy at low temperatures.

QB14

Effect of Ni-doping on superconductivity and magnetism in Eu_{0.5}K_{0.5}Fe₂As₂

Anupam Guleria¹, Vivek Kumar Anand², P.I. Paulose², S. Ramakrishnan², C. Geibel³ and Z. Hossain^{1*}
¹ Department of Physics, Indian Institute of Technology, Kanpur, India
² DCMP&MS, Tata Institute of Fundamental Research, Homi Bhabha Road, Mumbai-400 005, India
³ Max-Planck Institute for Chemical Physics of Solids 01187 Dresden, Germany



QB15

75As NMR/NQR study of hole-doped superconductor Ba_{1-x}K_xFe₂As₂

Masanori Hirano¹, Yuji Yamada¹, Taku Saito¹, Ryo Nagashima¹, Hideto Fukazawa¹, Yoh Kohori^{1*}, Yuji Furukawa², Kunihiro Kihou², Chul-ho Lee², Akira Iyo³ and Hiroshi Eisaki³
¹ Department of Physics, Chiba University, Japan
² Ames Laboratory and Department of Physics and Astronomy, Iowa State University, USA
³ National Institute of Advanced Industrial Science and Technology, Japan

We have performed 75As NMR and NQR on single crystalline Ba_{1-x}K_xFe₂As₂ for x = 0.27-1. The Knight shift K in normal state shows Pauli paramagnetic behavior with slight temperature T dependence. The value of K increases gradually with increasing x. By contrast, nuclear spin- lattice relaxation rate 1/T1T in normal state has a large T-dependence, which indicates existence of large antiferromagnetic (AF) spin fluctuations for all x. The T-dependence of 1/T1T shows a gap-like behavior below approximately 100 K for 0.6 < x < 0.9. These behaviors are well explained by the change of band structure with expansion of hole Fermi surfaces and shrink and disappearance of electron Fermi surfaces at Brillouin zone (BZ) with increasing x. The T dependence of 1/T1 in SC state indicates multiple-SC-gap feature. A simple two gap model analysis shows that the larger superconducting gap gradually decreases with increasing x from 0.27 to 1 and smaller gap decreases rapidly and nearly vanishes for x > 0.6 where the electron pockets in BZ disappear.

QB16

Homogeneous coexistence and phase segregation in the 1111 iron-based pnictides studied via NMR

Naoki Fujiwara^{1*}, Satoru Matsuiishi², Yoichi Kamihara³ and Hideo Hosono²
¹ Graduate School of Human & Environmental Studies, Kyoto University, Japan
² Frontier Research Center (FRC), Tokyo Institute of Technology, Japan
³ Faculty of Science & Technology, Keio University, Japan

In iron-based pnictides, one of the interesting topics is homogeneous coexistence or phase segregation between antiferromagnetic (AF) and superconducting (SC) states, because these phenomena are deeply related to the pairing symmetry. We addressed this problem on a microscopic level by means of 75As NMR measurements in LaFeAsO_{1-x}F_x (La1111 series), and CaFe_{1-x}Co_xAsF (Ca1111 series) having an intermediate electronic phase diagram between Ba(Fe_{1-x}Co_x)₂As₂ and the La1111 series [1]. The spectra for 6%-Co Ca1111 samples exhibited 75As signals similar to the undoped samples even below Tc [1], whereas those for 2.6%-F La1111 samples exhibited signals arising from both AF and SC phases at 3.0 GPa. At ambient pressure, we observed signals arising from AF and paramagnetic metallic (PM) states. These results indicate that homogeneous coexistence between AF and SC states is realized in the Ca1111 series, whereas SC or PM domains are formed other than AF domains in the La1111 series. The separation of two phases at ambient pressure indicates that the SC phase is not directly related to the AF phase and some pairing mechanism other than spin fluctuation would be important.

[1] T. Nakano, S. Tsutsumi, N. Fujiwara, S. Matsuiishi, and H. Hosono, Homogeneous coexistence of superconducting and spin-density-wave states in CaFe_{1-x}Co_xAsF as seen via nuclear magnetic resonance, Phys. Rev. B 83 (2011) 180508(R)

QB17

NMR study of Fe-based superconductors K_xFe_{2-y}Se₂

Yuusuke Tomita¹, Hisashi Koteawa^{1*}, Hideki Tou¹, Yoshikazu Mizuguchi², Hiroyuki Takeya² and Yoshihiko Takano²
¹ Department of physics, Kobe University, Japan
² NIMS, Japan

K_xFe_{2-y}Se₂ with a transition temperature Tc of 32K is an unique example among Fe-based superconductors.[1] Angle-resolved photoemission spectroscopy studies suggest that the electronic structure is distinct from other Fe based superconductor in the absence of hole-like Fermi surface around Γ point. [2]On the other hand, the diffraction studies suggest a phase separation of an antiferromagnetic (AF) phase and a superconducting phase.[3] We measured nuclear spin-lattice relaxation time T1 and Knight shift using 77Se-NMR in a single crystal K_xFe_{2-y}Se₂. Their anisotropy for H// ab and H//c including the field dependence were measured in a wide temperature range down to the SC state. In the SC state, the field dependence of 1/T1 was weak, suggesting that the relaxation is dominated by the SC quasiparticle and the contribution from the AF phase and the phase boundary is weak. Knight shift in the normal state is almost isotropic, but it consists of the spin part and the orbital part. From a measurement at low temperatures, we found that the orbital part is anisotropic, and hence the anisotropic spin part. We will discuss the SC gap symmetry and the character of spin fluctuations in K_xFe_{2-y}Se₂.

[1] J. Gio et al. Phys. Rev. B 82, 180520(R) (2010) [2] J.L.Marzin et al Phys. Rev. B 84, 024529 [3] W.Bao et al Chinese Phys. Lett. 28, 086104

QB18

Spectroscopy and anisotropies in the magnetic state of iron pnictides
 Belen Valenzuela, Maria Jose Calderon, Gladys Leon, Noel A. Garcia and Elena Bascones*
Theory and Simulations of Materials, Instituto de Ciencia de Materiales de Madrid, Spain



QB19

Magnetic interactions in iron pnictides
 Maria Jose Calderon, Gladys Leon, Belen Valenzuela and Elena . Bascones*
Theory and Simulations of Materials, Instituto de Ciencia de Materiales de Madrid, Spain



QB20

Te-doped $K_{0.80}Fe_{1.81}Se_{2-x}Te_x$ single crystals
 C T Lin*
Crystal Growth, Max Planck Institute for Solid State Research, Germany

We report the growth a serious of Te-substituted $K_{0.80}Fe_{1.81}Se_{2-x}Te_x$ ($x=0, 0.09, 0.16, 0.34$ and 0.55) single crystals using optical floating-zone technique under application of 8 bar of argon pressure. Study of XRD indicated that the undoped single crystals contain a significant intergrowth of two sets of the c-axis characterized by slightly different lattice constants, i.e., the phase separation phenomenon. Our results demonstrate that the partial substitution of Se by Te atoms can lead to the expansion of the c-lattice constant, whereas the phase separation phenomenon is suppressed continuously with the increase of substitution level and vanished at $x=0.55$. The magnetization data show the superconducting transition temperature is gradually depressed for Tc ~32, 27, 25, 15, and 0 K with the substitution level $x=0, 0.09, 0.16, 0.34$ and 0.55 , respectively.

QB21

High-pressure resonant x-ray emission study of $Fe_{1.01}Se$ superconductors
 Jin-ming Chen, S. C. Haw, J. M. Lee, S. A. Chen, K. T. Lu, N. Hiraoka, H. Ishii and K. D. Tsuei
National Synchrotron Radiation Research Center, Taiwan

The Fe 3d valence states, electron structures and spin states of iron-chalcogenide $Fe_{1.01}Se$ superconductors under pressure up to 45 GPa were probed by resonant x-ray emission spectroscopy (RXES) and and x-ray absorption spectra. The Fe 1s3p-RXES spectra of $Fe_{1.01}Se$ at ambient pressure, 6 GPa and 45 GPa were measured to deduce the variation of Fe 3d valence states. The 1s3p-RXES data obtained at the Fe K edge clearly reveal that unoccupied Fe 3d states exhibit a relatively delocalized character, stemming from hybridization of the Fe 3d states with the Fe 4p orbitals. The pronounced pre-edge peak at ~7112.7 eV in Fe K-edge x-ray absorption spectra of $Fe_{1.01}Se$ predominantly originates from the dipole transition of a Fe 1s electron to unoccupied Fe 3d-4p hybrid bands. The larger compression accompanied with a significant distortion around the Fe atoms along the c axis in $Fe_{1.01}Se$ upon applying pressure suppresses the Fe 3d-4p and Fe 4p-4d hybridization. The applied pressure suppresses the nearest-neighbor ferromagnetic superexchange interaction and enhances spin fluctuations on the Fe sites in $Fe_{1.01}Se$. $Fe_{1.01}Se$ shows a small net magnetic moment of Fe^{2+} at ambient pressure.

QB22

Microscopic coexistence and competition of magnetism and superconductivity in $Ba_{1-x}K_xFe_2As_2$: A structural, magnetic, and superconducting phase diagram
 Gwendolynne Pascua¹, Hubertus Luetkens¹, Erwin Wiesenmayer², Zurab Shermadini¹, Rustem Khasanov¹, Alex Amato¹, Hans-henning Klaus³ and Dirk Johrendt¹
¹Laboratory for Muon Spin Spectroscopy, Paul Scherrer Institute, CH-5232 Villigen PSI, Switzerland
²Department Chemie, Ludwig-Maximilians-Universität München, D-81377 München, Germany
³Institut fuer Festkoerperphysik, TU Dresden, DE-01069 Dresden, Germany

It is widely believed that in contrast to its electron-doped counterparts, the hole-doped compound $Ba_{1-x}K_xFe_2As_2$ exhibits a mesoscopic phase separation of magnetism and superconductivity in the underdoped region of the phase diagram. Here, we report a combined high-resolution X-ray powder diffraction and volume-sensitive muon spin rotation (μ SR) study of $Ba_{1-x}K_xFe_2As_2$ showing that this paradigm does not hold true in the underdoped region of the phase diagram ($0 \leq x \leq 0.25$). Instead, we find a microscopic coexistence of the two forms of order. A competition of magnetism and superconductivity is evident from a significant reduction of the magnetic moment and a concomitant decrease of the magnetoelastically coupled orthorhombic lattice distortion below the superconducting phase transition. The doping dependence of structural, magnetic, and superconducting properties is completed in a phase diagram ($0 \leq x \leq 1$) herein presented and discussed.

[1] E. Wiesenmayer, H. Luetkens et al., Phys. Rev. Lett. 107, 237001 (2011). [2] M. Rotter et al., Nature Physics 5, 141 (2009). [3] A. A. Aczel et al., Phys. Rev. B 78, 214503 (2008). [4] T. Goko et al., Phys. Rev. B 80, 024508 (2009).

QB23

Anomalous superconducting phase in $LaFeAsO_{1-x}F_x$ studied via 75As NMR
 N. Fujiwara^{1*}, S. Tsutsumi¹, S. Iimura², S. Matsuishi² and H. Hosono²
¹Graduate School of Human & Environmental Studies, Kyoto University, Japan
²Frontier Research Center (FRC), Tokyo Institute of Technology, Japan

$LaFeAsO_{1-x}F_x$ (La1111 series) is a prototype of high-Tc pnictides and has been investigated extensively by means of various experimental techniques. The electronic phase diagram is unique compared to other high-Tc pnictides in that the antiferromagnetic (AF) phase hardly overlaps the superconducting (SC) phase, and the optimal doping level is located away from the AF phase boundary. The latter feature is common to the R1111 series (R = Ce, Nd, etc.). Recently, an exotic phase diagram has been obtained in $LaFeAsO_{1-x}F_x$ in which a high Tc is maintained even in an overdoping regime, and the second SC dome emerges upon excess H doping. To investigate the exotic electronic state on a microscopic level, we performed 75As NMR measurements for 20% and 40% doped samples. The former doping level corresponds to the boundary between two SC domes, and the latter corresponds to the optimal doping level of the second dome. The relaxation rates for 20% doped samples are comparable with those of $LaFeAsO_{1-x}F_x$ ($x = 14\%$), however rates for 40% doped samples enhanced at a fixed temperature implying that some spin fluctuations return and some magnetic ordering would occur upon excess H doping.

QB24

Multi-frequency ESR in $EuFe_2As_2$
 Masami Ikeda¹, Tatsuya Kobayashi², Wataru Hirata², Shigeki Miyasaka², Setsuko Tajima² and Masayuki Hagiwara¹
¹KYOKUGEN, Osaka University, 1-3 Machikaneyama, Toyonaka, Osaka 560-8531, Japan
²Dep. of Phys., Faculty of Science, Osaka University, 1-1 Machikaneyama, Toyonaka, Osaka 560-0043, Japan

One kind of the iron based superconductors is called '122' system. Most parent materials of the '122' system exhibit a spin-density wave (SDW) transition that is accompanied by a structural phase transition [1]. $EuFe_2As_2$ shows the SDW transition at TSDW=190 K, and the large local moment Eu^{2+} (S =7/2, L =0) orders antiferromagnetically below TN=19 K. Above TSDW, it is believed that Eu^{2+} localized magnetic moments interact with itinerant electrons. Below TSDW, the interlayer interaction turns to be weak and the system becomes anisotropic [2]. To study the above natures of $EuFe_2As_2$, in more details, we have performed multi-frequency (20-35 GHz) electron spin resonance (ESR) measurements. Above TN, the resonance signal can be fitted with the Dysonian function, and the temperature dependence of the linewidth obtained by this fitting obeys the Korringa relation above TSDW as observed at X-band ESR [2]. From this relation, we will discuss the exchange interaction between Eu^{2+} moments and conduction electron spins.

[1]Y. Xiao et al., Phys. Rev. B 80 (2009) 174424. [2]E. Dengler et al., Phys. Rev. B 81 (2010) 024406.

QB25

Analysis of the critical current density and flux pinning properties in iron-based $Ba_{0.55}K_{0.45}Fe_2As_2$ high Tc superconductor
 Dawood Ahmad¹, I S Park¹, G C Kim¹, Rock Kil Ko^{1,2}, J H Lee¹, and Y C Kim¹
¹Department of Physics, Pusan National University, Korea
²Korea Electrotechnology Research Institute, Changwon 641-120, Korea

The critical current density and flux pinning properties of the $Ba_{0.55}K_{0.45}Fe_2As_2$ high Tc superconductor with $T_c = 37K$ are studied using field and time dependence of the magnetization. The temperature dependence of the critical current density $J_c(T)$ have been found to follow the form $J_c \propto (1-T/T_c)^n$ and is consistent with δT_c type pinning due to the randomly distributed defects larger than the coherence length ξ . The temperature dependence of the magnetic relaxation rate S exhibits a peak at much lower temperature which corresponds to the smaller pinning energy in the $Ba_{0.55}K_{0.45}Fe_2As_2$ superconductor. Moreover, the effective pinning potential U_p increases with the increase in temperature this behavior is in agreement with those of high T_c cuprate superconductors.

QB26

In-plane anisotropy of magnetic and electric properties of the Fe pnictide $Ba(Fe_{1-x}Co_x)_2As_2$
 Yoshiaki Kobayashi^{1*}, Akihiro Ichikawa¹, Masayuki Itoh¹ and Masatoshi Sato²
¹Department of Physics, Graduate School of Science, Nagoya University, Japan
²Research Center For Neutron Science And Technology, CROSS, Japan

The anisotropy of electronic and magnetic properties within FeAs-planes of Co(2%) doped $BaFe_2As_2$ was investigated by 75As-NMR measurements of the As sites As0 with all four nearest neighbor sites occupied by Fe. Interestingly, even in the tetragonal phase (T >100 K), two sets of NMR spectra with two fold symmetry of in-plane Knight shifts and electronic nuclear quadrupole frequencies were observed. They originate from the existence of two domains with their symmetry axes lying at right-angles to each other. The anisotropy of the electronic and magnetic properties become pronounced on cooling at ~140 K, below which the in-plane anisotropy was reported to appear for the electrical resistivity under the pressure along one of Fe-Fe directions [1]. 75As-NMR was also carried out at the As site As1 surrounded by one Co and three Fe. From the data, we can see that the spin susceptibility at As1 is ~1/3 of the value at As0 and that the antiferromagnetic spin fluctuation at As1 is fairly suppressed as compared with the value at As0. We discuss these behaviors of the FeAs layer in connection with the impurity-induced local orbital ordering suggested by the theoretical studies.

[1] J.-H. Chu, J. G. Analytis, K. D. Greve, P. L. McMahon, Z. Islam, Y. Yamamoto and I. R. Fisher :Science 329 (2010) 824.

QB27

Vortex tunneling spectra of iron-pnictide superconductors
 Yuhei Kikuchi* and Hiroki Tsuchiura
Applied Physics, Tohoku University, Japan

Symmetry and structure of the superconducting gap functions in iron-pnictides have been still under spirited debate. Quasi-particle states around surfaces/interfaces or impurities have played a crucial role for identifying the gap functions in several unconventional superconductors such as cuprates or Sr_2RuO_4 . However, the gap symmetry of iron-pnictide is believed to be s-wave, and the point at issue is to identify whether the gap structure has inter-band sign reversal (s⁻) or not (s⁺⁺). Thus, it will be difficult to distinguish these gap structures based on surfaces/interfaces information. There exist several studies on impurity-induced states in iron-pnictides. However, because of the complex band-structures of such systems, theoretical-modeling of impurities in iron-pnictide is not free of ambiguity. Vortex core states can be another "probe" to identify the gap symmetries and structures in unconventional superconductors. Since a vortex core is not a chemical substance, there are no ambiguities in theoretical modeling. Thus, in this work, we theoretically study the quasi-particle states induced around a vortex core in iron-pnictides using two- or five-band effective two-dimensional lattice models [1][2] within the Bogoliubov-de Gennes theory. We will also examine the impurity-induced quasi-particle states, and discuss the relation between present results and recent STM/S experimental results.

[1]T. Kariyado and M. Ogata, J. Phys. Soc. Jpn. 79, 083704 (2010). [2]S. Raghu et al., Phys. Rev. B 77, 220503 (2010).

QB28

Direct observation of superconducting gaps and their anisotropies in $Ba_{1-x}K_xFe_2As_2$
 Y. Ota^{1*}, K. Okazaki², Y. Kotani², T. Shimoyama³, T. Kiss⁴, C.-T. Chen⁵, S. Watanabe⁶, K. Kihou⁷, C. H. Lee⁸, A. Iyo⁹, H. Eisaki¹⁰, T. Saito¹, H. Fukazawa¹, Y. Kohori⁹ and S. Shim¹⁰
¹ISSP, Japan
²ISSP, JST-CREST, Japan
³Univ. of Tokyo, Japan
⁴Osaka Univ., Japan
⁵CAS, China
⁶Tokyo Univ. of Sci., Japan
⁷AIST, JST-TRIP, Japan
⁸Chiba Univ., Japan
⁹JST-TRIP, Chiba Univ., Japan
¹⁰ISSP, JST-CREST, JST-TRIP, RIKEN, Japan

Among the iron-pnictides, $(Ba,K)Fe_2As_2$ (BaK122) system is the most interesting: while the optimally-doped BaK122 has a full gap (no node in the superconducting(SC) gap), the extremely hole-doped KFe_2As_2 (K122), which has no electron pocket, has been suggested to have SC-gap nodes from several experiments. From the previous studies of laser-excited angle-resolved photoemission spectroscopy (laser ARPES), the optimally doped BaK122 has no anisotropy and Fermi surface (FS) sheet dependence in SC-gap sizes on the three hole FS around the Brillouin zone center. On the other hand, we found that K122 has clear anisotropies and sheet dependence. In addition, we found that the middle hole FS has eight nodes and identified their Fermi momenta. It should be important to investigate doping dependence of anisotropies and FS-sheet dependence of SC-gap sizes, and node existence to clarify the pairing mechanism at each doping level. We have directly observed superconducting gaps and their anisotropies in the overdoped BaK122 utilizing laser ARPES. We will discuss these results and contrast them with other experimental and theoretical results available in literature.

QB29

Contrasting superconducting property in Fe-based superconductors $(Ca_4Al_2O_{6y})(Fe_2Pn_2)[Pn=As \text{ and } P]$
 Hiroaki Kinouchi¹, Hidekazu Mukuda¹, Mitsuharu Yashima¹, Yoshio Kitaoka¹, Chulho Lee², Parasharam M. Shirage², Hiroshi Eisaki² and Akira Iyo²
¹Department of Materials Engineering Science, Graduate School of Engineering Science, Osaka University, Japan
²National Institute of Advanced Industrial Science and Technology (AIST), Japan

We report As-nuclear quadrupole resonance (NQR) study on $(Ca_4Al_2O_{6y})(Fe_2As_2)$ with $T_c=27K$, and P-nuclear magnetic resonance (NMR) study on $(Ca_4Al_2O_{6y})(Fe_2As_2)$ with $T_c=17K$. $(Ca_4Al_2O_{6y})(Fe_2As_2)$ possesses the characteristic structural parameters such as short a-axis length, high pnictgen height, narrow As-Fe-As angle, and thick perovskite-type blocking layer. A measurement of the nuclear spin relaxation rate 1/T1 revealed a significant evolution of antiferromagnetic (AFM) spin fluctuations in normal state, which originates from the possible well nested hole and electron Fermi surfaces. Below Tc, the 1/T1 decreases steeply upon cooling without any trace of Hebel-Slichter peak, which is consistently accounted for within the framework of nodeless s⁽⁺⁾-wave multiple gap model. On the other hands, $(Ca_4Al_2O_{6y})(Fe_2As_2)$ is characterized by lower pnictgen height and wider As-Fe-As angle than that of $(Ca_4Al_2O_{6y})(Fe_2As_2)$, where FeP₄ forms nearly regular tetrahedron. The P-NMR- 1/T1 measurement revealed the presence of AFM spin fluctuations in normal state and gapless SC state. These facts indicate the close relationship between the local structural characters of FePn₄ and the SC properties.

H. Kinouchi, H. Mukuda, M. Yashima, Y. Kitaoka, P. M. Shirage, C-H. Lee, H. Eisaki, and A. Iyo

QB30

Superconducting properties of FeTe_{1-x}Se_x single crystals: impact of disorder and hydrostatic pressure

Roman Puzniak*, Dariusz J. Gawryluk, Marek Berkowski, Piotr Dłuzewski, Jarosław Pietosa, Aleksander Wittlin and Andrzej Wisniewski
Institute of Physics, Polish Academy of Sciences, Aleja Lotników 32/46, PL-02-668 Warsaw, Poland

It was found that chemical and structural disorder in superconducting single crystals of Fe(Te,Se), originating from kinetics of crystal growth process, strongly influences superconducting properties. The sharpness of a transition to the superconducting state is evidently inversely correlated with crystallographic quality. Ions inhomogeneous spatial distribution seems to enhance the superconductivity and inhomogeneous distribution of host atoms might be an intrinsic feature of superconducting chalcogenides. Small disorder introduced into magnetic sublattice, by partial replacement of Fe ions by slight amount of nonmagnetic ions of Cu or by magnetic ions of Ni and Co with spin value different than that of Fe ion, completely suppresses superconductivity. Even if superconductivity is observed in the system containing magnetic ions it can not survive when the disorder in magnetic ions sublattice is introduced. We have found pressure-induced enhancement of all of the superconducting state properties of FeTe_{0.95}Se_{0.05} single crystals, which entails a growth of the density of superconducting carriers. We noticed more pronounced increase in superconducting carrier density under pressure than that in the critical temperature what may indicate an appearance of a mechanism limiting the increase of Tc with pressure. The critical current density increases under pressure by at least one order of magnitude.

QB31

The influence of superconductivity with magnetism in superconductor/magnetic heterostructures

Jeehoon Kim*, R. Baumbach, N. Haberkorn, J. Lee, L. Civale, Q. Jia, A. J. Taylor, E. Bauer, J. D. Thompson and R. Movshovich
Los Alamos National Laboratory, USA

Interplay between superconductivity and magnetism continues to be one of the central themes in Condensed Matter Physics. We have investigated a variety of superconductor/ferromagnetic heterostructures, such as YBCO/LSMO, Nb/GCMO, and Nb/CeRu₂Al₃B using low temperature magnetic force microscopy, addressing mainly magnetic pinning and domain wall superconductivity. In YBCO/LSMO, we focused on the critical state and observed effects of magnetism on superconductivity. In Nb/GCMO, we found that magnetic domains provide weak pinning centers, and act as magnetic templates. A recently discovered CeRu₂Al₃B system shows a variety of magnetic phases such as antiferromagnetic, ferromagnetic, and ferrimagnetic domains in the field/temperature plane. We will discuss how we can manipulate superconducting domains in superconducting film (Nb) via these magnetic phases in close proximity.

QC01

The influence of the magnetic moment on the atomic distance in amorphous CexRu_{100-x}

Yingjie Li¹, Nakai Ikuo^{2*}, Amakai Yusuke³ and Shigeyuki Murayama³
¹ Inner Mongolia Key Laboratory for Physics and Chemistry of Functional Materials, Physics and Electronic Information College, Inner Mongolia Normal University, Hohhot 010022, China
² Department of Electrical and Electronic Engineering, Graduate School of Engineering, Tottori University, Tottori 680-8552, Japan
³ Department of Materials Science and Engineering, Muroran Institute of Technology, Hokkaido 050-8585, Japan

The extended x-ray absorption fine structure (EXAFS) measurement was performed in amorphous alloys CexRu_{100-x} (x=9, 43 and 80). We found that the Ce-Ce interatomic distance increases with increasing the Ce content while those of Ce-Ru and Ru-Ru pairs are unchanged and that the Ce-Ce interatomic distance is exactly proportional to the Ce effective magnetic moment. We discuss the relation between the Ce-Ce atomic distance and the effective magnetic moment 1) from the point of view of the magnetovolume effect.

1) Y. Amakai et al., *J. Phys. : Conf. Ser.* 150 (2009) 042004.

QC02

Theoretical studies of the superconductivity and antiferromagnetism coexistence and the divergence of effective electron mass near quantum critical point in CeRhIn₅

Valery V. Val'kov and Anton O. Zlotnikov
Laboratory of Theoretical Physics, L.V. Kirensky Institute of Physics, Russia

Competition and coexistence of superconductivity and antiferromagnetism have been studied in the framework of the periodic Anderson model taking into account the superexchange interaction between localized 4f electrons. It has been shown that pressure-induced energy change of the localized states leads to modifying antiferromagnetic and superconducting order parameters. This modification of the order parameters develops in such way that a strong competition is suggested between antiferromagnetism and superconductivity. It has been proposed that the energy increase is caused by pressure growth. In spite of the competition mentioned above, conditions have been found for the coexistence of superconductivity and antiferromagnetism in the model. Theoretical results of the pressure effects on the ground state character of the heavy-fermion systems are in good agreement with specific heat data for CeRhIn₅ [1, 2]. In the coexistence phase there occur two types of Cooper pairing due to the antiferromagnetic exchange field. The divergence of the effective electron mass produced by suppressing antiferromagnetic order has also been analyzed in the same framework. Further it has been shown that at quantum critical point there occurs the transition from small to large Fermi surface. Such features have been found in the de Haas-van Alphen experiments for CeRhIn₅ [3].

1. H. Hegger, C. Petrovich, E.G. Moshopoulou, M.F. Hundley, J.L. Sarrao, Z. Fisk, J.D. Thompson, *Phys. Rev. Lett.* 84, 4986 (2000). 2. T. Park, J.D. Thompson, *New Journal of Physics* 11, 055062 (2009). 3. H. Shishido, R. Settai, H. Harima, Y. Onuki, *J. Phys. Soc. Jap.* 74, 1103 (2005).

QC03

Josephson effect between UPt₃ and Nb under pressure

Akihiko Sumiyama^{1*}, Jun Gouchi¹, Gaku Motoyama¹, Akira Yamaguchi¹, Noriaki Kimura², Etsuji Yamamoto³, Yoshinori Haga³ and Yoshichika Onuki⁴
¹ Univ. of Hyogo, Japan
² Tohoku Univ., Japan
³ JAEA, Japan
⁴ Osaka Univ., Japan

The heavy-fermion compound UPt₃ is an odd-parity superconductor and possesses a complex field-temperature (H-T) phase diagram with three phases: A (low H and high T), B (low H and low T) and C (high H and high T) phases. We have investigated the Josephson effect between UPt₃ and Nb and observed an anisotropic temperature dependence of Josephson critical current Ic at the transition from A to B phases[1]. However, the Josephson effect, which is easily destroyed by a small magnetic field, has not been measured in C phase. Considering that C phase appears even in zero field by applying pressure[2], we have investigated the pressure dependence of Josephson effect together with resistance and Meissner effect of UPt₃. The superconducting transition occurs at lower temperature and becomes broader by applying pressure. As the pressure is increased, the Josephson effect appears at lower temperature than the zero-resistivity temperature of UPt₃, while Ic increases more rapidly; the increasing rate -dIc/dT is a linear function of pressure. Although the Josephson effect in C phase has been observed for the first time, an abrupt change in the temperature dependence of Ic caused by the transition to C phase has not been found yet.

[1] A. Sumiyama et al.: *Phys. Rev. Lett.* 81 (1998) 5213; A. Sumiyama et al.: *Jpn. J. Appl. Phys. Series 11* (1999) 47. [2] M. Boukhny et al.: *Phys. Rev. Lett.* 73 (1994) 1707.

QC04

Hidden order in URu₂Si₂ --- Analysis based on the first-principles approach

Hiroaki Ikeda^{1*}, Michi-to Suzuki², Ryotaro Arita³, Tetsuya Takimoto⁴, Takasada Shibauchi¹ and Yuji Matsuda¹
¹ Department of Physics, Kyoto university, Japan
² CCSE, Japan Atomic Energy Agency, Japan
³ Department of Applied Physics, University of Tokyo, Japan
⁴ Asia Pacific Center for Theoretical Physics, POSTECH, Korea

The so-called 'hidden-order' phase transition at ST₁{HO}=17.55K in the heavy-electron metal URu₂Si₂, specified by a clear jump in the specific heat measurement, is a long-standing mystery in the condensed-matter physics since the discovery in 1985. In spite of every effort, it remains still dark what kind of symmetry is broken below ST₁{HO}\$. So far, there are no evidence for magnetic/structural and any low-rank multipole orders. Recent advanced angle-resolved photo-emission spectroscopy indicates that 5f5 electrons appears to be itinerant rather than localized. Thus, the detailed analysis of the complicated band structures including the spin-orbit coupling has been strongly desired. We show here the first report of the complete set of itinerant multipole correlations up to the fifth rank within the random-phase approximation and beyond. The itinerant Hamiltonian is obtained by the advanced Wannier method from the first-principles calculations. From the most divergent correlations, we obtain nearly degenerate two staggered-ordered states of rank-1 dipole with SA₂'-\$ and rank-5 dotriacontapole with SE²'-\$; the former corresponds to the antiferromagnetic state realized under high pressures, and the latter the hidden-order state. This novel high-rank electronic state provides natural explanations of the key features for the hidden order including spontaneous fourfold symmetry breaking.

QC05

Sb NQR study of filled skutterudite CeFe₃Sb₁₂ synthesized under high pressure

Ko-ichi Magishi^{1*}, Hitoshi Sugawara², Masahiro Takahashi¹, Takahito Saito¹, Kuniyuki Koyama¹, Takashi Saito³, Sho Tatsuoka³, Kenya Tanaka³ and Hideyuki Sato³
¹ Institute for Socio-Arts and Sciences, The University of Tokushima, Japan
² Graduate School of Science, Kobe University, Japan
³ Graduate School of Science, Tokyo Metropolitan University, Japan

Among filled skutterudites, the influence of the filling fraction of R ion on the physical properties has been argued, especially in Sb-based filled skutterudites with a large pnictogen cage. On RFe₃Sb₁₂ system, the drastic effect of the R-site vacancy on the basic properties has been pointed out. Recently, it has been reported that CeFe₃Sb₁₂ synthesized under high pressure (HP) in order to increase the Ce-site filling fraction shows the semiconducting transport property at low temperatures, in contrast that the sample synthesized under ambient pressure (AP) shows the metallic behavior. At the presentation, we report on the result of the Sb NQR measurements for the HP sample of CeFe₃Sb₁₂, and compare with that for the AP sample in order to understand the influence of the Ce-site filling fraction. In the high temperature range, the nuclear spin-lattice relaxation rate for the HP sample decreases on cooling, and follows the exponential decrease above 100 K with the energy gap of 270 K. The value of the gap for the HP sample is larger than that for the AP sample, which suggests that the hybridization is enhanced by increasing the Ce-site filling fraction. More detailed results and analyses will be presented at the conference.

QC06

High-mobility magnetotransport of the narrow-gap semiconductor FeSb₂

Hidefumi Takahashi*, Ryuji Okazaki, Yukio Yasui and Ichiro Terasaki
Department of Physics, Nagoya University, Japan

Recently, a huge Seebeck coefficient S (-45 mV/K at 10 K) was reported for single-crystalline FeSb₂ samples. Such a huge value seems beyond conventional semiconductor physics, indicating a novel mechanism to enhance the Seebeck coefficient such as a strong electron correlation expected in so-called 'Kondo insulators'. We study the magnetotransport properties of FeSb₂ single crystals to investigate its electronic state at low temperatures[1]. The conductivity tensor is well analyzed using a two-carrier model, leading to proper evaluation of the mobility and carrier concentration. The mobility significantly increases with decreasing temperature and reaches 28000 cm²/Vs at 4 K. The carrier concentration decreases from 1 down to 10-4 ppm/unit cell with decreasing temperature from 30 down to 4 K, which is well described by thermal activation with a small gap of 6 meV. We also find that the magnetoresistive behavior dramatically changes from positive to negative at lower temperatures. The negative magnetoresistance is generally observed in doped semiconductors and derives from a weak localization of carriers, indicating a considerable impurity level in the electronic structure. Our magnetotransport measurements, as well as the impurity-effect study[2], strongly suggest that the low-temperature transport is well understood within an extrinsic semiconductor picture with ppm-level impurity.

[1] H. Takahashi et al. *Phys. Rev. B* 84, 205215 (2011). [2] H. Takahashi et al. *J. Phys. Soc. Jpn.* 80, 054708 (2011).

QC07

A possible ferromagnetic quantum critical point in CeFe_{1-x}Ru_xPO

Tetsuro Nakamura¹, Takashi Yamamoto², Masanori Matoba¹, Yasuaki Einaga³ and Yoichi Kamihara¹
¹ Department of Applied Physics and Physico-Informatics, Keio University., Japan
² Department of Chemistry, Keio University., Japan

Many materials have their own magnetic transition temperature, and it is controllable by the application of a pressure, field or through chemical substitution. In particular, phase transitions which take place at absolute zero are called quantum phase transitions, and the transition point is called a quantum critical point. Quantum critical points have attracted much attention since some materials exhibit superconductivity in proximity to a magnetic quantum critical point. [1] Both CeFePO and CeRuPO are heavy-fermion materials containing Ce 4f-electron's sublattice inducing Kondo effects. Although CeFePO exhibits no magnetic transition down to 0.4 K, CeRuPO is one of rare examples of a ferromagnetic Kondo lattice, whose transition temperature is 15 K [2]-[5]. In this study, we synthesized CeFe_xRu_{1-x}PO by a solid reaction to quantify a chemical composition which is a boundary between ferromagnetic phase and paramagnetic phase indicating the quantum critical point. Electrical resistivity and magnetic susceptibility are measured at temperatures from 4 K to 300 K. Furthermore, 57Fe Mossbauer spectroscopy was applied to CeFe_xRu_{1-x}PO to confirm the ordering of the magnetic sublattice. Our results tentatively indicate that CeFe_xRu_{1-x}PO is heavy-fermion metal, and the magnetic quantum critical point exists at x=0.15.

1) A. J. Millis: *Phys. Rev. B* 48 7183 (1993). 2) E. M. Bruning, C. Krellner, M. Baenitz, A. Jesche, F. Steglich, and C. Geibel: *Phys. Rev. Lett.* 101 117206 (2008). 3) S. Kitagawa, H. Ikeda, Y. Nakai, T. Hattori, K. Ishida, Y. Kamihara, M. Hirano, and H. Hosono: *Phys. Rev. Lett.* 107 277002 (2011). 4) Y. Kamihara, H. Hirata, M. Hirano, H. Yonagi, T. Kamiya and H. Hosono: *J. Phys. Chem. Solids.* 69 2916 (2008). 5) C. Krellner, N. S. Kini, E. M. Bruning, K. Koch, H. Rosner, M. Nicklas, M. Baenitz, and C. Geibel: *Phys. Rev. B* 76 104418 (2007).

QC08

Ru doping evolution of magnetic properties in Ce(Fe_{1-x}Ru_x)PO studied by 31P-NMR

Shunsaku Kitagawa^{1*}, Yusuke Nakai², Kenji Ishida¹, Hiroaki Ikeda³, Kensuke Iritani⁴, Masanori Matoba⁴, Youichi Kamihara⁴, Masahiro Hirano⁵ and Hideo Hosono⁶
¹ Department of Physics, Kyoto University JST-TRIP, Japan
² Department of Physics, Kyoto University JST-TRIP *present address Graduate School of Science, Tokyo Metropolitan Univ., Japan
³ Department of Physics, Kyoto University, Japan
⁴ Departments of Applied Physics and Physico-Informatics, Keio University, Japan
⁵ Frontier Research Center, Tokyo Institute of Technology, Japan
⁶ Frontier Research Center, Materials and Structures Laboratory, Tokyo Institute of Technology, Japan

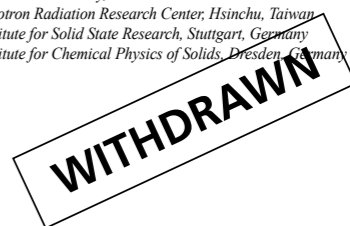
CeFePO and CeRuPO have the same layered crystal structure as iron pnictide superconductors RFeAs(O_{1-x}F_x) (R: rare earth). CeFePO is a paramagnetic down to 80 mK and possesses a large Sommerfeld coefficient gamma ~ 700 mJ/mol K² at low temperatures, indicating that CeFePO is a heavy fermion compounds originated from Ce 4f electrons[1]. On the other hand, CeRuPO is a ferromagnetic Kondo lattice system with TCurie = 15 K and coherent temperature TK ~ 10 K[2]. We have performed 31P-NMR on Ce(Fe_{1-x}Ru_x)PO system to investigate the evolution of magnetic properties at low temperatures. Knight shift and spin-lattice relaxation rate 1/T1 shows extremely large anisotropy. In CeFePO, we found a metamagnetic transition at around mu0H = 4 T and below 5 K characterized by the sudden increase in Knight shift when fields are applied perpendicular to the c axis[3]. As far as we know, this is the first example of the metamagnetic behavior in a heavy fermion observed with XY spin anisotropy. Moreover, Ce(Fe_{1-x}Ru_x)PO shows ferromagnetic ordering at ~ 3 K with strong two dimensional ferromagnetic fluctuations. We will show the phase diagram in Ce(Fe_{1-x}Ru_x)PO and discuss how two dimensional ferromagnetic fluctuations are changed with the Ru doping.

[1] E. M. Bruning et al., *Phys. Rev. Lett.* 101, 117206 (2008). [2] C. Krellner et al. *J. Cryst. Growth* 310, 1875 (2008). [3] S. Kitagawa et al., *Phys. Rev. Lett.* 107, 277002 (2011).

QC09

Determining the orientation of the 4f ground state orbital in CeCu₂Si₂ with vector q dependent non-resonant inelastic X-ray scattering (NRIXS).

Thomas Willers^{1*}, Fabio Strigari¹, Yong Cai², Nozomu Hiraoka³, Ku-ding Tsuei³, Yen-fa Liao³, Maurits Wilm Haverkort⁴, Silvia Seiro⁵, Christoph Geibel⁶, Frank Steglich⁶, Liu Hao Tjeng⁶ and Andrea Severing⁶
¹ Institute of Physics II, University of Cologne, Germany
² Brookhaven National Laboratory, USA
³ National Synchrotron Radiation Research Center, Hsinchu, Taiwan
⁴ Max Planck Institute for Solid State Research, Stuttgart, Germany
⁵ Max Planck Institute for Chemical Physics of Solids, Dresden, Germany



QC10

Possible superconducting fluctuation in pressure-induced heavy-fermion superconductor CeRhSi₃

Noriaki Kimura*, Tetsuya Sugawara, Hiroki Iida and Haruyoshi Aoki
Department of Physics, Tohoku University, Japan

CeRhSi₃ is a heavy fermion antiferromagnet whose transition temperature is 1.6K. The itinerant f electron is thought to be responsible for the magnetism in this material. Application of pressure suppresses the magnetism and simultaneously induces the superconductivity. At pressures from 0.2GPa to 2.4GPa, the superconductivity coexists with the antiferromagnetism. In this pressure region, a broad drop of the electrical resistivity and weak shielding in the ac-susceptibility are observed at the superconducting transition temperature. We argue a possibility of the superconducting fluctuation realized in the coexisting region of the superconductivity and antiferromagnetism.

QC11

Thermoelectric power in a single-crystalline CeRhSi₃

Hidekazu Tanaka^{1*}, Naofumi Aso², Yoshinao Takaesu¹, Masato Hedo², Takao Nakama³, Hiroki Iida³, Noriaki Kimura³ and Haruyoshi Aoki³
¹ Graduate School of Engineering and Science, University of the Ryukyus, Japan
² Faculty of Science, University of the Ryukyus, Japan
³ Graduate School of Science, Tohoku University, Japan

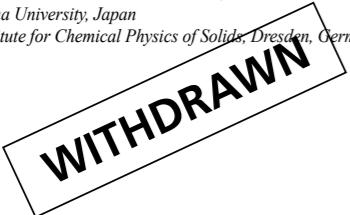
CeRhSi₃ is a non-centrosymmetric heavy fermion superconductor.[1] The a- and c-axis thermoelectric power S_a and S_c of a single-crystalline CeRhSi₃ were measured under pressure up to around 2.7 GPa in the temperature range from 1.5 K to 300 K. Both S_a and S_c exhibit a large positive value up to around 60 μV/K, which is characteristic of heavy-fermion systems. S_a and S_c show a maximum in its temperature dependence due to the Kondo effect and its maximum temperature T_{Smx} gradually moves to higher temperatures from about 90 K (at ambient pressure) to about 130 K (at 2.7 GPa) by applying the pressure. In both directions, such behaviors of thermoelectric power are very similar to those in the CeIrSi₃. [2] In the conference, we will discuss the anisotropy of the thermoelectric power in connection with the superconductivity in CeRhSi₃.

[1] N.Kimura et al., Phys. Rev. Lett. 95 (2005) 247004. [2] Y.Takaesu et al., J. Phys. Soc. Jpn. 80 (2011) S4068.

QC12

Valence of CeM₂Al₁₀ (M=Ru, Os, and Fe) determined with hard X-ray photo emission spectroscopy (HAXPES).

Fabio Strigari¹, Thomas Willers¹, Ku Ding Tsuei², Yen Fa Liao², Arata Tanaka³, K. Yutani³, Y. Muro³, Toshiro Takabatake³, Liu Hao Tjeng³ and Andrea Severing^{3*}
¹ University of Cologne, Germany
² National Synchrotron Radiation Research Center, Taiwan
³ ADSM, Hiroshima University, Japan
⁴ Max Planck Institute for Chemical Physics of Solids, Dresden, Germany



QC13

Studies on novel tetragonal Ce₂RhGa₁₂ heavy fermion compound

Ramamoorthi Nagalakshmi^{1*}, Sengodan Nallamuthu¹, Varadharajan Krishnakumar², Celine Besnard³, Hans Hagemann⁴ and Marian Reiffers⁵
¹ Physics, National Institute of Technology, Tiruchirappalli, India
² Physics, Periyar University, Salem, India
³ Laboratory of Crystallography, Laboratory of Crystallography, University of Geneva, 24 Quai Ernest-Ansermet, CH-1211 Geneva 4, Svit, Switzerland
⁴ Physical Chemistry, University of Geneva, Geneva, Switzerland, Switzerland
⁵ Physics, Institute of Experimental Physics, Slovakia Academy of Sciences, Kosice, Slovakia

Single crystals of Ce₂RhGa₁₂ have been synthesized using Ga flux and their structure was determined by single-crystal X-ray diffraction. The Ce₂RhGa₁₂ crystallizes in the tetragonal P4/nbm space group (No. 125), which is isostructural to Ce₂PdGa₁₂, with Z = 2 and lattice parameters a = 6.0405 Å and c = 15.706 Å. Data were collected at the Swiss Norwegian Beam Line at the European Synchrotron Facility, Grenoble France. Also the Laue diffraction was carried out to confirm the single crystal quality possessing tetragonal symmetry. The tetragonal structure of Ce₂RhGa₁₂ is composed of Ce-Ga and PdGa₈/2 layers similar to CePdGa. [1]. The structure is isomorphous to Ce₂MGa₁₂, M=(Ni, Cu[2], Pd). Along the c axis slabs of edge-sharing rectangular prism of RhGa₈ alternates with Ga rich areas in which Ce atoms occupy cavities made of Ga atoms. The bulk anti ferromagnetic transition of Ce₂RhGa₁₂ at 3.5 K is exhibited by a big jump up to 12 J/mol K. The value of γ above magnetic transition in specific heat measurements suggests that it is a heavy-fermion system with γ = 420 mJ mol⁻¹ K⁻². The magnetic measurements are in progress to confirm the consistency of the ordering temperature and the further studies are in progress.

[1] R. Robin T. Macaluso, S. Nakatsuji, H. Lee, Z. Fisk, M. Moldovan, D.P. Young, and Julia Y. Chan Journal of Solid State Chemistry 174, 296-301(2003) 2. J.Y. Cho, J.N. Millican, C. Capan, D.A. Solokov, M. Moldovan, A.B. Karki, D.P. Young, M.C. Aronson, J.Y. Chan, Chem. Mater. 20, 6116-6123(2008)

QC14

Electronic structures of plutonium compounds with the NaCl-type monochalcogenides structure

Takahiro Maehira^{1*}, Yasutomi Tatetsu² and Eijiro Sakai¹
¹ Faculty of Science, University of the Ryukyus, Nishihara, Okinawa 903-0213, Japan
² Graduate school of Engineering and Science, University of the Ryukyus, Nishihara, Okinawa 903-0213, Japan

Some of the uranium and the transuranium compounds are characterized as strongly correlated f electron systems and have attracted particular interest because of rich variety of anomalous physical phenomena such as the valence fluctuation, the Kondo lattice, exotic magnetism, unconventional superconductivity, etc. Among such compounds, the plutonium monochalcogenides display a variety of anomalous physical properties. For PuX (X=S, Se, Te) have been studied intensively both theoretically and experimentally[1,2]. To understand the electronic properties of these materials, the features of the ground state should be first clarified. The calculations for the energy band structure have been done by using the relativistic linear augmented-plane-wave (RLAPW) method. Note here that relativity should be taken into account, because of large atomic numbers of the constituent atoms. In the presentation, we try to understand what the key issues are to construct the energy band structures around the Fermi energy for PuS, PuSe and PuTe.

[1] A. Hasegawa, and H. Yamagami, J. Magn. Magn. Mater. 104-107, 65 (1992). [2] P. M. Oppeneer, T. Kraft, and M. S. S. Brooks, Phys. Rev. B61, 12825 (2000).

QC15

Electronic property of ThSn₃ in comparison with uranium and transuranium compounds

Yasutomi Tatetsu^{1*}, Takahiro Maehira² and Eijiro Sakai²
¹ Graduate school of Engineering and Science, University of the Ryukyus, Japan
² Faculty of Science, University of the Ryukyus, Japan

Recent rapid expansion of the research frontier of condensed matter physics from uranium to transuranium compounds has stimulated renewed attention and much interest on exotic properties of actinides and related compounds. It is a challenge to modern electronic-structure theory to understand the appearance of a large number of exceptionally complicated crystal structures of actinide metal. It is important to clarify electronic structure of actinide compounds which exhibit exotic magnetism and unconventional superconductivity. By using a relativistic linear augmented-plane-wave (RLAPW) method with the one-electron potential in the local-density approximation, we investigate energy band structures and the Fermi surfaces of transuranium compounds ThSn₃, USn₃, NpSn₃ and PuSn₃. It is found in common that the energy bands in the vicinity of the Fermi level are mainly due to the large hybridization between 5f and Sn 5p electrons. Thorium contains no occupied 5f states, thorium compounds provide good comparative systems for investigating the role of 5f electrons. In the presentation, we try to understand what the key issues are to construct the energy band structures around the Fermi energy for ThSn₃, USn₃, NpSn₃ and PuSn₃, we attempt to unveil 5f electron properties purely originating from actinide atoms.

QC16

Multipolar phase transition of the 4f2 nonmagnetic doublet in a caged compound PrRh₂Zn₂₀

Nagasawa Naohiro¹, Matsumoto T Keisuke¹, Wakiya Kazuhei¹, Onimaru Takahiro¹, Umeo Kazunori¹, Kittaka Shunichiro², Sakakibara Toshiro² and Takabatake Toshiro¹
¹ Hiroshima University, Japan
² The University of Tokyo, Japan

The caged compound PrRh₂Zn₂₀ with the Pr³⁺ ion in the Γ3 doublet ground state exhibits a superconducting transition at TSC=0.05K in the presence of an antiferroquadrupolar (AFQ) order below TQ=0.11K [1, 2]. The entropy release up to TQ is only 20% of Rln₂, which is expected for the Γ3 doublet with the quadrupolar degrees of freedom. It suggests that quadrupolar degrees of freedom remain active even below TQ and quadrupole fluctuations play an important role in forming the Cooper pair in the superconducting state. In the present work, we have focused an isostructural and isoelectronic compound PrRh₂Zn₂₀. The electrical resistivity shows a hysteretic behavior between 140K and 470K, suggesting a first-order structural transition. In spite of the possible structural transition, a Schottky-like peak at around 10K in the specific heat and anisotropic behavior of the isothermal magnetization at 1.8K indicate the crystalline electric field ground state to be the Γ3 doublet. The specific heat exhibits a peak at TQ=0.06K, where the entropy release is evaluated to be only 6% of Rln₂. Because of the increment of TQ in the magnetic fields and the anisotropic B-T phase diagram, the phase transition at TQ should be an AFQ order.

[1] T. Onimaru et al., J. Phys. Soc. Jpn. 79 033704 (2010). [2] T. Onimaru et al., Phys. Rev. Lett. 106 177001 (2011).

QC17

Crystal growth and low temperature properties of non-centrosymmetric heavy-fermion compound CeTAI₃ (T = Cu, Ag, Au)

Christian Franz, Alexander Regnat, Andreas Bauer and Christian Pleiderer
 Department für Physik, Technische Universität München, Germany

For a long time full inversion symmetry was thought to be a precondition for heavy-fermion superconductivity. The discovery of heavy-fermion superconductivity in the antiferromagnetic state of CePt₃Si at ambient pressure and CeRhSi₃, CeIrSi₃ and CeCoGe₃ at high pressure contradicted these paradigms. All compounds in this class crystallize in a P4mm or subclass crystal structure. Here we report on the single crystal growth of CeTAI₃ (T = Cu, Ag, Au) with crystal structure I4mm, being isostructural to CeRhSi₃ and CeIrSi₃. High purity elements (>5N) have been used as starting materials. A special build image furnace was used for crystal growth. Crystal quality was determined by Laue x-ray scattering, x-ray powder diffraction and edx. Low temperature properties have been investigated by measurements of bulk properties including magnetisation, heat capacity and electrical resistivity.

QC18

Enhancement of the hall coefficient under pressure in CeCu₂Si₂

Shingo Araki^{1*}, Naoto Nishiumi¹, Minami Hayashida¹, Takafumi Shinohara¹, Yoichi Ikeda¹, Tatsuo C. Kobayashi¹, Silvia Seiro², Christoph Geibel² and Frank Steglich²
¹ Department of Physics, Okayama University, Japan
² Max Planck Institute for Chemical Physics of Solids, Germany

CeCu₂Si₂ is the heavy fermion superconductor discovered in 1979. The unconventional superconductivity with T_c ~ 0.6 K at ambient pressure is believed to be mediated by antiferromagnetic spin fluctuation around the AFM quantum critical point. With increasing pressure, T_c increases to reach the maximum at 4.2 GPa, although antiferromagnetic spin fluctuation decreases. The existence of the critical valence fluctuation around the critical valence transition is proposed to explain the enhancement of T_c under pressure [1]. However, there is no direct evidence to reveal the existence of the valence fluctuation. In this study, we investigated the Hall effect on single crystal of CeCu₂Si₂ under high pressure. The temperature dependence of the Hall coefficient at ambient pressure shows a peak at T_ML = 4 K for H // [001] and [100]. In addition, the Hall coefficient shows the other peak at T₁max for H // [100]. The magnitude of the Hall coefficient at T_ML increases with increasing pressure and reaches the maximum at around 4 GPa, coincident with the enhancement of T_c. We will discuss the relation between the enhancement of the Hall coefficient and T_c.

[1] K. Miyake et al.: J. Phys.: Condens. Matter 19 (2007) 125201.

QC19

Saturation moment in the ferromagnetic state of EuB₆

Vladimir V. Glushkov^{1*}, Alexey V. Bogach¹, Alexey V. Semenov¹, Sergey V. Demishev¹, Vsevolod Yu. Ivanov¹, Nickolay E. Sluchanko¹, Alexey V. Kuznetsov², Sergey Yu. Gavrilkin¹, Kirill V. Mitsen¹, Natalja Yu. Shitsevalova³, Vladimir B. Filipov⁴, Johan Vanacken⁴ and Victor Moshchalkov⁵
¹ Low Temperatures and Cryogenic Engineering Dept., A.M.Prokhorov General Physics Institute of RAS, Russia
² National Research Nuclear University MEPhI, Russia
³ P.N.Lebedev Physical Institute of RAS, Russia
⁴ I. Frantsevich Institute for Problems of Materials Science NASU, Ukraine
⁵ Institute for Nanoscale Physics and Chemistry, Katholieke Universiteit Leuven, Belgium

Two consecutive phase transitions featuring the onset of ferromagnetism in europium hexaboride [1-4] are commonly associated with percolation in the system of linked magnetic polarons at T_M ~15.6 K and with long range magnetic ordering below T_C =12.6-13.9 K [1]. However, the recent study of high frequency electron spin resonance [5] showed neither magnetic phase separation nor MP formation features in the system of localized magnetic moments of Eu²⁺. To shed more light on the nature of ferromagnetism we studied the magnetic and thermal properties of the EuB₆ single crystals in pulsed (up to 40 T) and steady (up to 9 T) magnetic fields at temperatures 2-40 K. The estimated saturation moment M_{sat} ~7.4μ_B is found to exceed noticeably the magnetic moment of Eu²⁺ ion. The difference is shown to be induced by an additional contribution to magnetization due to the formation of intermediate magnetic phase below T_M. The observed renormalization of M_{sat} is discussed in terms of the effects of the spin polarization in 5d-band and the short range magnetic ordering in the system of Eu²⁺ ions. Support from RFBR 11-02-00623 project, Federal Programme "Scientific and Educational Human Resources of Innovative Russia" and the Methusalem Funding by the Flemish Government is acknowledged.

[1] U.Yu. B.I.Mim. Phys. Rev. B, v.74, p.094413 (2006). [2] S.Sullow et al., Phys. Rev. B, v:57, p.5860 (1998). [3] V.V.Glushkov et al., JETP v.105, p.32 (2007). [4] J.Kim et al., Phys Rev B, v:78, p.165120 (2008). [5] A.V.Semenov et al., Phys Rev B, v:79, p.014423 (2009).

QC20

Magnetization of Tm_{1-x}Yb_xB₂ in strong pulsed and steady magnetic fields

Alexey Bogach^{1*}, Nickolay Sluchanko¹, Vladimir Glushkov¹, Sergey Demishev¹, Andrey Azarevich¹, Vladimir Filipov², Natalia Shitsevalova², Slavomir Gabani³, Karol Flachbart⁴, Johan Vanacken⁴ and Victor Moshchalkov⁴
¹ Low temperature and cryogenic engineering, A.M.Prokhorov General Physics Institute RAS, Russia
² Institute for Problems of Materials Science NASU, Ukraine
³ Institute of Experimental Physics, Slovakia Academy of Sciences, Slovakia
⁴ Institute for Nanoscale Physics and Chemistry of KUL, Belgium

The magnetization of solid solutions Tm_{1-x}Yb_xB₂ (0<x≤0.8) crossing metal-insulator transition point at x_{c}~0.3 have been studied at low temperatures 1.8-40 K in strong steady (up to 11T) and pulsed (up to 50T, pulse duration ~20-100 ms) magnetic fields. The analysis of the magnetization data allows extracting three contributions to the paramagnetic response. Itinerant electron components are attributed to heavy fermion and ferror type manybody states at EF with densities of states N(E_F)= 1div 4?10²² cm⁻³meV⁻¹ and 3div 4?10²¹ cm⁻³meV⁻¹, correspondingly. The third contribution may be identified as the response from the localized magnetic moments of the rare earth ions (~0.8-3.7 μB per unit cell) which saturates at helium temperatures in strong magnetic fields. The reduced intensity of the manybody resonance at E_F is shown to increase with Yb concentration reaching 2 electrons per unit cell for x>0.7. Comparison between the steady and pulsed field magnetization behavior provides additional arguments in favor of magnetic nanoclusters formation, short range ordering and electron phase separation effects in Tm_xYb_{1-x}B₂.

QC21

Stabilization of ferromagnetism and existence of ferromagnetic quantum criticality in UCo_{1-x}Ru_xGe system

Michal Valiska^{*}, Jiri Pospisil, Martin Divis, Jan Prokleska and Vladimir Sechovsky
 DCMF, Charles University, Ke Karlovu 5, 121 16, Prague, Czech Republic

We have prepared polycrystalline samples of UCoGe doped by Ru on the Co-site about nominal stoichiometry UCo_{1-x}Ru_xGe where x = 0.01-0.35 with step 0.01 to studied the magnetic state and ferromagnetic instability in UCoGe. The whole series of doped materials keeps the orthorhombic TiNiSi-type structure. The evolution of the lattice parameters well follows Vegard's law respecting the pure parent UCoGe and URuGe. While the UCoGe is well known ferromagnetic superconductor (T_C = 2.5 K, T_{SC} = 0.6 K) the URuGe is paramagnetic down the lowest temperatures. Nevertheless the ruthenium doping of UCoGe leads to surprising stabilization of the ferromagnetic state when the maximum T_C = 8.5 K has been found in 12 % Ru doped sample. The further increase of the Ru content destabilizes previous ferromagnetic state and it is terminated by ferromagnetic quantum critical point at concentration of 30 % of Ru. We have prepared single crystal of the UCo_{0.88}Ru_{0.12}Ge and UCo_{0.70}Ru_{0.30}Ge for detail study of the ferromagnetic state, individual contributions of the U, Co and Ru components to total magnetic moment, magnetic anisotropy and destabilization of the ferromagnetism in UCoGe in relation to superconductivity. The results are discussed on the basis of the change of electronic structure.

QC22

Thermal properties of RB₆ (R-La, Ce, Pr, Nd)

M. A. Anisimov^{1*}, A. V. Bogach¹, V. V. Glushkov¹, S. V. Demishev¹, N. A. Samarin¹, S. Gavrilkin², N. Yu. Shitsevalova³, A. V. Levchenko³, V. B. Filipov³, S. Gabani⁴, K. Flachbart⁴ and N. E. Sluchanko¹
¹ Low Temperatures and Cryogenic Engineering Dept., A.M.Prokhorov General Physics Institute of RAS, Russia
² P.N.Lebedev Physical Institute of RAS, Russia
³ Institute for Problems of Materials Science NAS, Ukraine
⁴ Institute of Experimental Physics of SAS, Slovakia

Rare earth (RE) hexaborides RB₆ represent a class of compounds with variety of magnetic properties including antiferromagnetic (R-Ce, Pr, Nd, Gd, Dy, Tb, Ho), ferromagnetic (EuB₆), intermediate valence (SmB₆) and heavy fermion behavior (CeB₆). Here we investigate the heat capacity C_P(T) on the high quality single crystals of light hexaborides (R-La, Ce, Pr, Nd) in the wide range of temperatures 2-300K. The data obtained allow to estimate correctly (i) the electronic component with γ(LaB₆)=2.4mJ/(molK), (ii) contribution from quasilocal vibrational mode of R³⁺ ion with Θ_E=119 - 152K, (iii) the Debye-type term from rigid boron cage with Θ_D=1160K. Our data also suggest the additional (iv) defect mode component which is provided by the contribution of the boron vacancies. The estimated values of residual concentration N_{vac}~1-4% agrees with the results of X-ray studies of RB₆ [1], [2]. The analysis of magnetic contribution shows that magnetic entropy S=ΔC_{mag}/TdT reaches the value corresponding to the ground state of 4f-multiplet in the range 2-4T_N. Taking into account the results of previous thermal investigations [3] we conclude in favour of the spin-polaron formation (see [4], [5] for details) in the paramagnetic vicinity of Neel temperature.

[1] V.A.Trunov, A.L.Malyshov et al., J. Phys.: Cond. Mat. v. 5, p. 2479 (1993). [2] M.M.Korsukova, V.N.Gurin et al., J. Less-Common. Met. v. 117, p. 73 (1986). [3] M.Sera, S.Kobayashi et al., Phys. Rev. B v. 54, p. R5207 (1996). [4] N.E.Sluchanko, A.V.Bogach et al., JETP v. 104, p. 120 (2007). [5] M.A.Anisimov, A.V.Bogach, V.V.Glushkov et al., JETP v. 109, p. 815 (2009).

July 10 (Tue)

July 10 (Tue)

QC23

Magnetic penetration depth and skin depth study of superconductivity and quantum criticality in Ce_{1-x}R_xCoIn₅ (R=La and Nd)

H. Kim¹, M. A. Tanatar¹, K. Cho¹, J. Murphy¹, R. Hu², C. Petrovic² and R. Prozorov^{1*}
¹ *The Ames Laboratory, USA*
² *Brookhaven National Laboratory, USA*

A heavy fermion superconductor CeCoIn₅ shows different responses to Nd- or La-substitutions for Ce, with the former inducing long range magnetic order coexisting with superconductivity. To understand the origin of the differences, we studied the temperature and field dependent in-plane magnetic penetration depth, $\lambda_{ab}(T)$, in single crystals of (Ce,R)CoIn₅ (R=La, Nd). Measurements were performed with a tunnel diode resonator down to 50-mK in a dilution refrigerator, in magnetic field up to 14 T parallel to the c -axis. These low-temperature and high field measurements allowed for the exploration for the full domain of superconductivity and quantum criticality in the T_H phase diagram. Some previously unreported features were observed and will be discussed from the point of view of measured differential magnetic susceptibility. These measurements bring new insight into the interplay between superconductivity and magnetism as well as field-tuned quantum critical behavior of doped 115 systems.

QC24

Low energy spin excitations in single-crystalline CeCu₂Ge₂ in magnetic fields up to 10T

Astrid Schneiderwind^{1*}, Michael Loewenhaupt², Oliver Stockert³ and Enrico Faulhaber³
¹ *Helmholtz-Zentrum Berlin für Materialien und Energie, Germany*
² *IFP, TU Dresden, Germany*
³ *MPI-CPFS Dresden, Germany*

CeCu₂Ge₂ is Kondo lattice with a moderately enhanced Sommerfeld coefficient of the specific heat $\gamma = 140$ mJ/molK². It exhibits antiferromagnetic order below T_N = 4.1 K. The incommensurate magnetic structure can be explained by the nesting properties of the calculated Fermi surface when taking into account an itinerant component of the Ce 4f-moments in addition to their local character. We performed low-energy inelastic neutron scattering experiments on a 2g single crystal of CeCu₂Ge₂ using the cold three-axis spectrometer PANDA at FRM II. Data were taken at 1.5 K and in magnetic fields up to 10T applied perpendicular to the (110/001) scattering plane. At zero field the spin excitations show an energy gap of 0.5 meV at the magnetic zone center. Away from the magnetic excitations become dispersive merging into a band of excitations around 1 meV. For increasing magnetic fields, the gap energy is lowered indicating opposite action of external and internal fields. The results will be discussed in the framework of local, crystal-field related, and non-local, spin-wave-like, magnetic excitations.

QC25

Magnetization measurements under high pressure on incommensurate-commensurate phase transitions on UPd₂Si₂

Hiroyuki Hidaka, Hideki Igarashi, Yusei Shimizu, Chihiro Tabata, Tatsuya Yanagisawa and Hiroshi Amitsuka
Graduate School of Science, Hokkaido University, Japan

UPd₂Si₂ has the ThCr₂Si₂-type body-centered tetragonal structure. This compound shows an incommensurate-antiferromagnetic (IC-AFM) ordering with a propagation vector Q = 0.73c* at 135 K (= TNh), and successively undergoes a simple commensurate (C) type-I AFM ordering at 108 K (=TNl). It is known that the phase transitions are of second order at TNh and of first order at TNl. In addition, an anti-phase ordering state (Q = 2/3c*) becomes stable in high magnetic field applied along the c-axis. The magnetism of UPd₂Si₂ is phenomenologically well explained in terms of the one-dimensional Ising model assuming localized 5f spins, whereas Fermi liquid behavior with a moderately large electric-specific-heat coefficient ~ 30 mJ/molK² is also seen at low temperature [1]. In the present study, we have measured magnetization of UPd₂Si₂ under high pressure up to 5.5 GPa and high magnetic field up to 7 T in order to investigate the duality between the localized and the itinerant features of the 5f-electronic states in U compounds. From the results of the magnetization and previous resistivity measurements under high pressure [2], we will discuss about the 5f-electronic states of the compound.

[1] H. Honma et al., *J. Phys. Soc. Jpn.* 67 (1998) 1017. [2] H. Hidaka et al., *J. Phys.: Conf. Ser.* 273 (2011) 012032.

QD01

Fe doping and magnetic field effect in the valence fluctuating heavy fermion system α -YbAlB₄

Kentarō Kuga, Keita Sone, Yosuke Matsumoto, Eoin Conon O'farrell and Satoru Nakatsuji
Institute for Solid State Physics, Japan

The Yb-based heavy fermion system, α -YbAlB₄, has a noncentrosymmetric crystal structure, while the structure of the isostructural system, β -YbAlB₄ is centrosymmetric [1]. β -YbAlB₄ is a unique example of the Yb based heavy fermion systems that shows pronounced non Fermi liquid behaviors and a superconducting transition at 80 mK under ambient pressure and field [2,3,4]. On the other hand, α -YbAlB₄ at low temperatures is well fit to a Fermi liquid type description. Both α and β -YbAlB₄ are valence fluctuating systems with the Yb valence of 2.73 for α -YbAlB₄ and 2.75 for β -YbAlB₄ [5]. We succeeded in substituting Fe for Al in α -YbAlB₄, and found an antiferromagnetic order at 10 K. By a small substitution to α -YbAlB₄, we also succeeded in inducing non-Fermi liquid behaviors. The antiferromagnetic ordering temperature is suppressed by magnetic field and non-Fermi liquid behaviors are induced where the Neel temperature vanishes. In this presentation, we will discuss the difference of the two non-Fermi liquid behaviors in Fe doped α -YbAlB₄ showing thermodynamic and transport properties.

[1] R. T. Macaluso et al., *Chemistry of Materials* 19, 1918 (2007). [2] S. Nakatsuji et al., *Nature Physics* 4, 603 (2008). [3] K. Kuga et al., *Physical Review Letters* 101, 137004 (2008). [4] Y. Matsumoto et al., *Science* 21, 316 (2011). [5] M. Okawa et al., *Physical Review Letters* 104, 247201 (2010).

QD02

Magnetic and electric properties of single crystal SmBaMn₂O₆

Youichi Maeda^{1*}, Shigeki Yamada¹ and Takahisa Arima²
¹ *Yokohama city university, Japan*
² *University of Tokyo, Japan*

We have succeeded in growth of single crystals of an A-site ordered perovskite manganese oxide, SmBaMn₂O₆, and investigated the magnetic and electric properties. Since Sm and Ba ions alternately occupy the perovskite A-site, it is expected that the magnetic and electric properties should be anisotropic. Moreover, the anisotropy may be modified with the charge orbital ordering. We also found that a peak in magnetic susceptibility of polycrystals at about 250 K. The magnetic susceptibility of a single crystal shows an anomaly which is accompanied by a hysteresis between 170 K and 210 K. This anomaly is caused by a rearrangement of charge orbital ordering. A clear magnetic anisotropy is observed below this temperature indicating that this rearrangement of charge orbital ordering accompanies the simultaneous antiferromagnetic spin ordering. Temperature dependence of the dielectric constant along the c axis also shows an anomaly at the rearrangement temperature, while no clear anomaly is observed for E perpendicular to the c axis. This result is consistent with the rearrangement of the stacking of the charge- and orbital-ordered sheets along the c axis.

QD03

Phase diagram and Eu valence state in EuPt_{1-x}As_x

Masaki Sugishima¹, Akihiro Mitsuda¹, Hirofumi Wada^{1*}, Masahiko Isobe² and Yutaka Ueda²
¹ *Department of Physics, Kyushu University, Japan*
² *Institute for Solid State Physics, University of Tokyo, Japan*

EuPtP is known to exhibit two valence order transitions at T₁ = 235 K and T₂ = 190 K [1]. At T > T₁, the Eu ions have a single valence state with the mean valence of 2.16. At T₂ < T < T₁, the Eu valence state is ordered with the sequence of -Eu²⁺-Eu³⁺-Eu³⁺-Eu²⁺-Eu²⁺-Eu³⁺- along the c-axis. Moreover, the stacking is replaced by another sequence with -Eu²⁺-Eu³⁺-Eu²⁺-Eu³⁺- below T₂ [2]. Consequently, the successive valence order transitions are accompanied by increase in the Eu mean valence upon cooling. The substitution of As for P expands the lattice and decreases both T₁ and T₂ [3]. In this study, we report a phase diagram and the Eu valence state in EuPt_{1-x}As_x. For 0 < x < 0.4, the resistivity, ρ , decreases with decreasing temperature, and shows an abrupt increase at T₁, followed by a sharp drop below T₂. For x = 0.55 and 0.6, only a sharp increase in ρ was observed with decreasing temperature, suggesting a single valence order transition at T₁. For x = 0.7, a slight upturn was observed in the ρ - T curve. Based on these results, we will present a phase diagram of EuPt_{1-x}As_x.

[1] N. Lossau et al., *Z. Phys. B* 74 (1989) 227. [2] T. Inami et al., *Phys. Rev. B* 82 (2010) 195133. [3] A. Mitsuda et al. To be published in EPJB.

QD04

Investigation of crystal structure, magnetism and transport properties of SrFe_{1-x}Ti_xO_{3- δ} systems

Sendilkumar A¹, Babu P. D.², Manivelraja M³, R. Reddy V.⁴ and Srinath S^{1*}
¹ *School of Physics, University of Hyderabad, India*
² *UGC-DAE Consortium for Scientific Research, R-5 Shed, B.A.R.C.Mumbai, 400 085, India*
³ *School of Physics, Advanced Magnetics Group, DMRL, Hyderabad, 500 046, A.P., India*
⁴ *UGC-DAEF, Khandwa Road, Indore, 425017, M.P, India*

SrFeO₃ has attracted lot of attention in the recent past due to the exciting electric and magnetic properties that can be achieved by varying oxygen stoichiometry. In this investigation, partial replacement of Fe²⁺ with a non-magnetic ion of Ti³⁺ in SrFeO_{3- δ} is carried out to reduce the magnetic complexity of the helical structure and determine the resulting chemical and magnetic structure using neutron powder diffraction and Mossbauer spectroscopy. Rietveld refinement of the neutron data indicated the presence of tetragonal symmetry with I4/mmm space group in δ -0.125. Our neutron and Mossbauer measurements confirm that Fe exists in three different sites both crystallographically as well as magnetically in all four compositions. Oxygen deficient SrFe_{1-x}Ti_xO_{3- δ} (x = 0 to 0.3) show an insulating behavior with a canted antiferromagnetic spin ordering, in comparison to a metallic, helical spin arrangement of x=0. Resistivity of x = 0 to 0.3 follows the Mott's 2-dimensional variable range hopping (VRH), $\rho = \rho_0 \exp(T_0/T)^{1/3}$. The composition dependence of ac conductivity is carried out in the frequency range 40 Hz to 1 MHz and the Cole-cole plots show a single semicircular arc representing the grain contribution. The temperature coefficient of resistance (TCR) changes from negative to positive (PTCR) for x = 0.2.

[1] J.P.Hodges, S.Short, J.D.Jorgensen, X.Xiong, B.Dabrowski, S.M.Mini and C.W.Kimball *Journal of Solid State Chemistry* 151,(2000) 190-209. [2] P.K.Gallagher, J.B.Mac.Chesney and D.N.E.Buchanan, *The Journal of Magnetic Physics* 41, 8(1964) 2429. [3] Y.Takeda, K.Kanno, T.Takeda, O.Yamamoto, M.Takano, N.Nakayama and Y.Bando, *J.Solid State Chemistry* 63,(1988) 237-249. [4] M.Takano, T.Okita, N.Nakayama, Y.Bando, Y.Takeda, O.Yamamoto and J.B.Goodenough, *J.Solid State Chemistry* 73,(1988) 149-150. [5] A.Lehon, P.Alder, C.Bernhard, A.V.Boris, A.V.Pimenov, A.Majuk, C.T.Lin, C.Ulrich and B.Keimer *Phys.Rev.Lett.* 92,3(2004) 037202. [6] Peter Alder and Sten Eriksson, *Z.Anorg. Allg. Chem.* 626 (2000) 118-214. [7] S. Srinath, M. Mahesh Kumar, M. L. Post, and H. Srikanth, *Phys. Rev. B* 72 (2005)

QD05

Evolution from a localized to an intermediate valence regime in Ce₂Cu_{2-x}Ni_xIn

Adam Pikul^{*} and Dariusz Kaczorowski
Institute of Low Temperature and Structure Research, Polish Academy of Sciences, Poland

Ce₂Cu₂In and Ce₂Ni₂In crystallize in a primitive tetragonal structure of the Mo₂FeB₂ type. The former compound orders antiferromagnetically at the Neel temperature of 5.5 K, while the latter one is a system with fluctuating valence [1]. Here we report on low temperature physical properties of the solid solution Ce₂Cu_{2-x}Ni_xIn studied by means of x-ray powder diffraction, magnetic susceptibility and electrical resistivity measurements, using polycrystalline specimens. We show that partial substitution of Cu by Ni results in a quasi-linear decrease of the lattice parameters and unit cell volume of the system. The lattice compression leads to an increase in the exchange integral and yields a reversal in the order of the magnetic 4f1 and nonmagnetic 4f0 states, being in line with the Doniach phase diagram. In the localized regime, where an interplay of the Kondo scattering and the crystalline electric field effect occurs, the rise in the hybridization strength is accompanied by a relative reduction in the scattering conduction electrons on excited crystal field levels.

[1] D. Kaczorowski, P. Rogl and K. Hiebl, *Phys. Rev. B* 54 (1996) 9891.

QD06

Substitution effect in CeFe₂Al₁₀

Takashi Nishioka¹, Yuta Oogane¹, Daishi Hirai¹, Harukazu Kato¹, Masahiro Matsumura¹, Yukihiko Kawamura² and Chihiro Sekine²
¹ *Physics, Kochi University, Japan*
² *Physics, Muroran Institute of Technology, Japan*

CeFe²Al¹⁰ is an important reference material as CeRu²Al¹⁰ which indicates a mysterious phase transition. We have performed the electrical resistivity and magnetic susceptibility of substituted systems, i.e., (Ce,La)Fe²Al¹⁰ and Ce(Fe,Co)Ru²Al¹⁰. The former system reveals the effect of periodicity and the latter one reveals that of electron number. A broad peak, which is attributed to Kondo effect, monotonically shifts to higher and lower temperatures with La- and Co-substitution, respectively. The electrical resistivity of CeFe²Al¹⁰ shows a broad peak at 60 K and sharp increase below 15 K. A slight substitution of Ce by La and Fe by Co site remove the broad peak and the increase at low temperatures. These results indicate the broad peak is due to coherence effect and the increase is due to a semiconducting gap.

QD07

Fermi surface and electronic correlations in a valence fluctuating Eu-system: an experimental and theoretical study of EuIr₂Si₂

Silvia Seiro¹, Oleg Ignatchik², Violeta Guritanu¹, Vivien Petzold¹, Takuya Iizuka³, Kathrin Gotze², Jorg Sichelschmidt¹, Shin-ichi Kimura³, Horst Borrmann¹, Jochen Wosnitza², Helge Rosner¹ and Christoph Geibel^{1*}
¹ *Max Planck Institute for Chemical Physics of Solids, Germany*
² *High Magnetic Field Laboratory Dresden, Helmholtz Center Dresden-Rossendorf, Germany*
³ *Institute for Molecular Science, UVSOR Facility, Okazaki 444-8585, Japan*

Electronic correlations can induce strong changes in electronic states, especially those at the Fermi level. These effects are presently the subject of intense theoretical and experimental investigations, especially on Ce- and U-based heavy fermion systems as well as on High T_c cuprates. In contrast valence fluctuating Eu-systems have yet not been investigated in this respect, although the valence fluctuations of Eu should have a strong impact. We have recently grown high quality single crystals of the valence fluctuating compound EuIr₂Si₂ and started a thorough investigation of its electronic properties. From previous Moessbauer studies the valence v of Eu in EuIr₂Si₂ was reported to decrease continuously with temperature, from v = 2.3 at 300 K to v = 2.8 below 20 K [1, 2]. Our T-dependent XRD, susceptibility, resistivity, and specific heat measurements on these single crystals confirm such a strong evolution of the valence and give insight into global effects of the strong correlations. These single crystals allowed the first observation of de Haas-van Alphen oscillations in a valence fluctuating Eu-system, as well as the first determination of the optical conductivity in such a system. Comparing these results with DFT-based calculations give a deeper insight into the correlation effects.

[1] B. Chevalier, J.M.D Coey, B. Lloret, and J. Etourneau, *J. Phys. C: Solid State Phys.* 19 (1986) 4521. [2] S. Patil, R. Nagarajan, L. C. Gupta, R. Vijayaraghavan, and B.D. Padalia, *Solid State Comm.* 63 (1987) 955

QD08

Heat capacity and electrical resistivity of CeNi_{1-x}Ge_x

Mariana Zapotokova¹, Ivan Curlik², Marian Reiffers³ and Mauro Giovannini⁴
¹ *Institute of Experimental Physics, Watsonova 47, SK 043 53 Kosice, Slovakia*
² *Centre od Low Temperature Physics, Institute of Experimental Physics, Watsonova 47, SK 043 53 Kosice, Slovakia, Slovakia*
³ *Centre od Low Temperature Physics, Institute of Experimental Physics, Slovakia Academy of Sciences, Kosice, Slovakia, Slovakia*
⁴ *CNR-SPIN and Department of Chemistry, CNR-SPIN and Department of Chemistry, University of Genova I-16146 Genova, Italy*

Metallic Ce compounds are of great interest for the intriguing physical properties associated with the 4f electrons. One notable example of compound intensively studied for many years is CeNi₃ crystallizing in the hexagonal CaCu₃ type, which results to be a Stoner enhanced paramagnet characterized by a spin fluctuation contribution on its transport properties. Here the effect of the Ni/Ge substitution on the ground state of CeNi₃ is presented. Several ternary germanides CeNi_{3-x}Ge_x (x=0.1, 0.2, 0.5, 0.8) were prepared by arc melting method. All the alloys crystallize in the CaCu₃ structure. Single phase of the polycrystalline samples was confirmed by X ray diffraction. The measurements of resistivity between 2-300 K and heat capacity between 0.4-300 K were provided and the results are presented. The resistivity measurements show typical metallic behaviour. No phase transition was observed in resistivity and heat capacity measurements.

QD09

Antiferromagnetic order in Yb₂Rh₂Ge₁₀

Kazunori Umeko^{1*}, Kenichi Katoh² and Toshiro Takabatake³
¹ *N-BARD, Hiroshima University, Kagamiyama 1-3-1, Higashi-Hiroshima 739-8526, Japan*
² *Department of Applied Physics, National Defense Academy, Yokosuka 239-8686, Japan*
³ *AdSM and IAMR, Hiroshima University, Kagamiyama 1-3-1, Higashi-Hiroshima 739-8530, Japan*

The titled compound has three Yb sites in the tetragonal Sc₂Co₂Si₁₀-type structure. The magnetization process shows strong anisotropy [1]. At 2 K, M (B/a) is saturated to 4.5 μ B/f.u. in 5 T, whereas M (B/c) increases linearly up to 0.9 μ B/f.u. at 5 T. The effective magnetic moment for B/a is 4.25 μ B/Yb, which is close to the value of 4.53 μ B/Yb expected for the Yb³⁺ free-ion [1]. The continuous increase in the specific heat down to the lowest measured temperature 2 K suggests a magnetic order below 2 K [1]. Therefore, we have measured the temperature dependence of the magnetization M, specific heat C and resistivity down to 0.3 K. A cusp in M (B/a) and sharp peak in C(T) were observed at 0.5 K, both of which were suppressed by applying magnetic fields up to 0.8 T. These findings indicate an antiferromagnetic order at TN = 0.5 K. However, the magnetic entropy Sm at TN is only 60 % of Rln₂. This observation suggests a heterogeneous mixed valence state where three of five Yb ions in formula unit are in trivalent state and the rest two are in divalent state.

[1] K. Katoh et al., *Physica B* 373 (2006) 111.

QD10

Magnetic field dependence of the resistivity minimum of nanosized YbAl₃
 C. Echevarria-Bonet^{1*}, D. P. Rojas², L. Fernandez Barquin¹, J. C. Gomez Sal¹, S. N. Kaul³, B. Coqblin⁴, S. G. Magalhães⁵ and E. Bauer⁶
¹ CITIMAC, Universidad de Cantabria, Spain
² Departamento de Física, Universidad Carlos III de Madrid, Spain
³ School of Physics and Centre for Nanotechnology, University of Hyderabad, India
⁴ Laboratoire de Physique des Solides, CNRS-Universite Paris-Sud, France
⁵ Instituto de Física, Universidade Federal Fluminense, Brazil
⁶ Institute of Solid State Physics, TU Wien, Austria

Yb-based alloys follow the Doniach phase diagram where the competition between RKKY and Kondo interaction plays a predominant role. Among them, a simple cubic compound (Pm-3m) YbAl₃ is a fine example of strong electron correlations leading to intermediate valence behavior [1]. Recently, we have investigated the effect of crystallite size on the electronic and magnetic properties of the nanometric samples of this alloy, prepared by high-energy milling of arc-melted ingots. Milling yields massive quantities of 4f-alloys in nanocrystalline (nc-) form with a relatively narrow size distribution [2]. In nc-YbAl₃, the variation of valence is due to a modification of the fraction of surface atoms compared to the total number of particles. This affects both specific heat and susceptibility data [3]. Here, we present a magnetic field (H)-dependent study of the electrical resistivity, ρ, of annealed and pressed pellets of nc-YbAl₃. The XRD Rietveld refinements yield particle sizes of maximum ~10 nm whereas slightly smaller values are detected by HRTEM. The results are striking in that the physical properties change drastically compared to the bulk [4] and an unexpected minimum in ρ(T) occurs around 15 K. With increasing H, the minimum becomes more pronounced and shifts to higher temperatures.

[1] E. Bauer et al., Phys. Rev. B 52, 4327 (1995). [2] D. P. Rojas et al., J. Phys.: Cond. Matter 19, 186214 (2007). [3] D. P. Rojas et al., Phys. Rev. B 78, 094412 (2008). [4] D. M. Rowe et al., J. Phys. D: Appl. Phys. 35, 2183 (2002).

QD11

Electronic states of Eu₄As₃ under high pressure
 Hisao Kobayashi^{1*}, Yoshitaka Yoda² and Akira Ochiai³
¹ Graduate School of Material Science, University of Hyogo, Japan
² Japan Synchrotron Radiation Institute, Japan
³ Department of Physics, Tohoku University, Japan

The mixed valence Eu₄As₃ compound with an anti-Th₃P₄ structure shows the charge ordering at 345 K and ambient pressure accompanied by trigonal distortion, which is similar to those in Yb₄As₃ and Sm₄Bi₃ [1-3]. The hybridization of a narrow 4f band with broad conduction bands is one of the important parameters in these charge-ordering compounds, which is possible to be controlled by hydrostatic pressure. We observed the melting of the static charge order at about 10 GPa and room temperature without structural change using high-pressure X-ray diffraction [4]. We have carried out 151Eu nuclear forward scattering (NFS) measurements using synchrotron radiation under high pressures at low temperatures to investigate the magnetic properties of Eu₄As₃. Clear quantum beats due to magnetic hyperfine field were observed in 151Eu NFS spectra at 6 K under pressure up to 14.5 GPa. The results of temperature dependences of 151Eu NFS spectra reveal that a magnetic ordering temperature increases linearly with pressure up to 10 GPa. Above 10 GPa, the magnetic ordering temperature decreases gradually with pressure. Consequently, the pressure dependence of the magnetic ordering temperature is related to the melting of the static charge order.

[1] A. Ochiai, et al., J. Phys. Soc. Jpn. 72, 3174 (2003). [2] A. Ochiai, et al., J. Phys. Soc. Jpn. 59, 4129 (1990). [3] A. Ochiai, et al., J. Magn. Magn. Mater. 52, 13 (1985). [4] H. Kobayashi, et al., J. Phys.: Condens. Matter 20 415217 (2008).

QD12

Pressure effect on intermediate valence semiconductor SmB₆: 11B-NMR
 Kouhei Nishiyama¹, Gabriel Pristas², Takeshi Mito¹, Takao Kohara¹, Slavomir Gabani², Marian Reiffers², Yasuhiro Komaki³, Mitutane Kokubu³, Hideto Fukazawa³, Yoh Kohori³, Nao Takeshita⁴ and Natalia Shitsevalova⁵
¹ Graduate school of Material Science, University of Hyogo, Japan
² Institute of Experimental Physics, Slovakia Academy of science, Slovakia
³ Graduate School of Science, Chiba University, Japan
⁴ Nanoelectronics Research Institute, National Institute of Advanced Industrial Science and Technology, Japan
⁵ Institute for Problems of Material Science, National Academy of science of Ukraine, Ukraine

The intermetallic compound SmB₆ is one of the most famous compounds in terms of the physics of intermediated valence state, heavy Fermion systems and Kondo insulators. Recent high pressure measurements of 149Sm nuclear forward scattering and resistivity revealed that a pressure-induced insulator-metal transition of SmB₆ is intimately connected with a long-range magnetic order, which has renewed interest in this compound. In order to investigate variations of the ground state and magnetic properties in SmB₆, we have carried out 11B-NMR measurement under pressure. While our group had reported the results of 11B-NMR measurements up to 2.6 GPa with a piston-cylinder type pressure cell, the use of a Bridgman Anvil Cell has recently enabled us to perform NMR measurements at higher pressures than 4.5 GPa. Spin-lattice relaxation rate 1/T1 above 20 K roughly follows an exponential function of temperature, Exp(-Eg/2kBT), consistent with previous reports. 1/T1 between 20 and 100 K increases with increasing pressure, indicating a reduction of the insulating gap. We will discuss detailed pressure dependences of the energy gap and the Sm valence.

QD13

Magnetic properties of ytterbium fluoride sulfide Yb₂F₄S₂
 Masashi Kosaka¹, Takuya Kobiyama¹, Hiroko Aruga Katori² and Naoki Shirakawa³
¹ Graduate School of Science and Engineering, Saitama University, Japan
² Division of Advanced Frontier Applied Physics, Tokyo University of Agriculture and Technology, Japan
³ Nanosystem Research Institute, National Institute of Advanced Industrial Science and Technology, Japan

The ternary ytterbium fluoride sulfide Yb₂F₄S₂ crystallizes in the tetragonal structure with space group I4/mmm. This structure can be described as an alternative stack of one layer of YbF₂ and two layers of YbFS along the c-axis. In a previous paper, it was suggested that there are two different ytterbium cations (Yb²⁺(Yb³⁺)₂(F)₄(S²⁻)₂ present [1]. An anomaly with the long-range magnetic order has not been observed down to 0.4 K by magnetization measurements, and the magnetic susceptibility exhibits a Curie-Weiss behavior above 50 K. However, it has become clear that the estimated value of the effective magnetic moment cannot be explained by a model which assumes that Yb²⁺ and Yb³⁺ occupy the two different crystallographic sites. A Schottky anomaly is found in the temperature dependence of the specific heat around 1.0 K at zero magnetic field. This anomaly is shifted towards higher temperatures with increasing applied magnetic field, and a release of the residual entropy is observed simultaneously.

[1] T. Schleid et al., Z. Anorg. Allg. Chem. 626 (2000) 2429.

QD14

Physical properties of the layered oxypnictides (CeO)MnPn; Pn=As, Sb
 Morosawa Yasuhiro¹, Takase Koichi^{1*}, Onizawa Manami¹, Moriyoshi Chikako², Kuroiwa Yoshihiro¹, Watanabe Tadataka¹ and Takano Yoshiki³
¹ Nihon University, Japan
² Hiroshima University, Japan

Recently, the layered iron oxypnictides (LaO)FePn; Pn = P, As, Sb, which belong to the tetragonal system, have attracted much attention due to the discovery of the superconductors (LaO)FeP [1] and (LaO)FeAs [2]. Many efforts have been dedicated to explore the superconductor with the highest transition temperature. In this tidal stream, many new materials with different physical properties have been found. In case of selection of the cerium atom as a rare earth element, these materials of (CeO)FeP [3], (CeO)FeAs [4], (CeO)CoP [5], (CeO)CoAs [6] show the typical metallic properties and the Fermi liquid behaviors at low temperature. In these systems, the 3d electrons of the iron and cobalt have finite density of state at the Fermi energy, and the cerium atom provides the f electrons as carriers at the same time. Namely, it is difficult to know which effects are dominant. In our group, the semiconductor based materials (LaO)MnPn have been focused and the substitution effects of the rare earth elements on the physical properties have been investigated. (CeO)MnAs and (CeO)MnSb indicate metallic character and the Fermi liquid behaviors below 30K and 8 K, respectively due to the valence fluctuation of the Ce f electrons.

[1] YKamihara et al., PHYSICAL REVIEW B 77, 214515 (2008). [2] Ykamihara et al., J. AM. CHEM. SOC. 130, NO. 11, 3296-3297 (2008). [3] YKamihara et al., Journal of Physics and Chemistry of Solids 69 2916-2918 (2008). [4] G. F. Chen et al., PHYSICAL REVIEW LETTERS 100, 247002 (2008). [5] C. Krellner et al., PHYSICAL REVIEW B 404, 3206-3209 (2009). [6] Rajib Sarkar et al., Phys. Rev. B 82, 054423 (2010).

QD15

31P-NMR study of valence fluctuating compound EuPtP
 Takeshi Mito¹, Koji Nishitani¹, Takehide Koyama¹, Koichi Ueda¹, Takao Kohara¹, Akihiro Mitsuda², Masaki Sugishima² and Hirofumi Wada²
¹ University of Hyogo, Japan
² Kyushu University, Japan

We report the results of the first 31P-NMR measurements on the hexagonal layered compound EuPtP. This compound exhibits two valence transitions at T1= 235 K and T2= 190 K. Various experiments, including magnetization, Eu Mossbauer, and x-ray diffraction measurements [1-5], have been carried out in order to investigate the valence transitions so far, however the ordered structures below T1 and T2 have not been fully clarified. We observed 31P-NMR signals in all three phases. They show anomalies at T1 and T2, and the Knight shift of the 31P-NMR lines reach ~ 20 % at low temperatures due to large effective moments of magnetic Eu²⁺ ions. Below T2, three resonance lines of 31P-NMR were observed, which should reflect local symmetry at the P-site. Based on these information obtained from the NMR measurements (spectrum and spin lattice relaxation time T1, and so on), we discuss possible ordered structures at low temperatures of EuPtP.

[1] N. Lossau et al., Z. Phys. B 74, 227 (1989). [2] N. Lossau et al., Z. Phys. B 77, 393 (1989). [3] G. Michels et al., Z. Phys. B 98, 75(1989). [4] A. Mitsuda et al., J. Phys.: Condens. Matter 22, 226003 (2010). [5] T. Inami et al., Phys. Rev. B 82, 195133 (2010).

QD16

Magnetic behavior of polycrystalline Eu₂Si₃ compound
 Sujata M. Patil^{1*}, P. L. Paulose² and E. V. Sampathkumaran²
¹ Wilson College, Mumbai 400007, India
² Tata Institute of Fundamental Research, Colaba, Mumbai 400005, India

The series R₂X₃ (R= light rare earth and X = Ga, Si, Ge, Sn, Sb), form in Cr₂B₃-type tetragonal structure. There are two inequivalent ‘R’ sites in this structure, one of them showing a very short distance between rare-earth atoms. Single crystal studies of Ce₂Si₃ show that metamagnetic transition temperature is different along ‘a’ axis and ‘c’ axis, which was attributed to the two inequivalent sites of Ce atoms. Studies of R₂X₃ have been extensively reported for different rare earths with exception of Eu₂Si₃. Rietveld analysis of x-ray diffraction shows the formation Eu₂Si₃ in the Cr₂B₃-type tetragonal structure (space group I4/mcm). Magnetization display a prominent cusp around 32K corresponding to antiferromagnetic ordering. Zero field cooled and field cooled magnetization is different below 30K, thereby showing a complex magnetic structure. Magnetization for applied magnetic fields up to 12 T shows that this sample does not undergo metamagnetic transition like that in Ce₂Si₃. Heat capacity shows a peak below 32K which shifts to lower temperatures upon application of magnetic fields, like in a typical antiferromagnet. Specific heat also shows a strong magnetic field dependence below 20K, revealing the complex nature of magnetic ordering.

1. R. Pottgen et. al.Z. Anorganische und allgemeine Chemie, 624, 1998, 945. 2. Y. Ushida, M. Kontani, Physica B, 281-282, (2000), 86-87. 3. Y. Ushida et. al. J. Phys. Soc. Japan, 70, (2001) 513. 4. F. Canepa et al. J. Alloys and Comp. 203, (1994) L11.

QD17

Valence fluctuation study by using X-ray absorption and emission spectroscopies at Yb L3-edge in YbNi₂X₆ (X=Al and Ga)
 Naomi Kawamura¹, Masaichiro Mizumaki¹, Hisashi Hayashi², Noriko Kanai², Kazuyuki Matsubayashi³, Yoshiya Uwatoko³, Tetsuro Yamashita⁴ and Shigeo Ohara⁴
¹ Japan Synchrotron Radiation Research Institute (JASRI/Spring-8), Japan
² Department of Chemical and Biological Science, Japan Women's University, Japan
³ Institute for Solid State Physics, University of Tokyo, Japan
⁴ Department of Engineering Physics, Nagoya Institute of Technology, Japan

Quantum criticality of Ce- and Yb-based heavy fermion system has been recently discussed from a viewpoint of valence fluctuation [1], thus the estimation of valence guides in the solution for several anomalies observed near the quantum critical point (QCP). Recently, high-quality YbNi₂X₆ (X = Al and Ga) is newly synthesized [2,3] and is desired to investigate the electronic states including the valence state as a heavy fermion system. In order to clarify the Yb valence state in YbNi₂X₆, X-ray absorption and emission spectroscopies at the Yb L3-edge have been performed at BL39XU of SPring-8. For YbNi₂Ga₆, the Yb valence of 2.71 at room temperature almost linearly decreases to 2.60 at 55 K with decreasing temperature, and then the valence maintains a constant value at 2-55 K, while the valence of YbNi₂Al₆ is almost trivalent in a temperature range of 2-300 K. Moreover, the XES spectra for YbNi₂X₆ give us detail information of Yb electronic states by comparison with the result in several Yb-based compounds.

[1] S. Watanabe, et al., Phys. Rev. Lett. 105, 186403 (2010). [2] S. Ohara, et al., J. Phys.: Conf. Ser. 273, 012048 (2011). [3] T. Yamashita, et al., J. Phys. Soc. Jpn. 81, 034705 (2012).

QD18

Angle-resolved photoemission spectroscopy of mixed-valence Sm_{1-x}Y_xS
 Keiichiro Imura^{1*}, Tetsuya Hajiri², Masaki Kaneko², Yusuke Nishi², Hiroyuki S. Suzuki³, Noriaki K. Sato², Takahiro Ito², Masaharu Matsunami¹ and Shin-ichi Kimura¹
¹ UVSOR Facility, Institute for Molecular Science, Japan
² Nagoya University, Japan
³ National Institute for Materials Science, Japan

It is known that samarium mono-sulfide (SmS) exhibits an insulator-to-metal transition, so called Black-to-Golden phase transition, by the application of pressure or by the substitution of Sm ions [1,2]. Although extensive studies to investigate the mechanism of this transition as well as the ground state of golden phase have been made, the phase transition has net been perfectly clarified yet. In this study, we focus on Sm_{1-x}Y_xS system in order to investigate the electronic structure of these two phases by an angle-resolved photoemission spectroscopy (ARPES). Single crystals of Sm_{1-x}Y_xS (x = 0, 0.17, 0.33) were grown by the Bridgman technique using a high-frequency induction furnace installed in NIMS. Photoemission spectroscopy measurement on these crystals was performed at UVSOR-II BL5U end station. The obtained ARPES spectrum of pure SmS (x = 0) has an energy gap of about 0.4 eV which is consistent with a previous report [3]. This energy gap decreases with increasing x, and the top of the Sm²⁺ 4f band touches the Fermi level in x = 0.33. This result suggests that the Golden phase induced by the yttrium substitution is a mixed-valence state.

[1] A. Jayaraman, et al., Phys. Rev. Lett. 25 (1970) 1430. [2] L. J. Tao and F. Holtzberg Phys. Rev. B 15 (1975) 3842. [3] T. Ito, et al., Phys. Rev. B 65 (2002) 155202.

QE01

Critical behavior of a spin-1 triangular lattice Ising antiferromagnet
 Milan Zukovic* and Andrej Bobak
 Department of Theoretical Physics and Astrophysics, Faculty of Science, P. J. Safarik University, Slovakiaia

We employ Monte Carlo simulations in order to investigate critical behavior of a frustrated spin-1 Ising antiferromagnet on a triangular lattice in the presence of a single-ion anisotropy. It has been previously found that no long-range order can exist in the system with spin 1/2 [1] but it can occur if the spin is larger than some critical value estimated as 11/2 [2]. We demonstrate that even small amount of the single-ion anisotropy can change this scenario. More specifically, we show that long-range order can exist in the low-temperature region even below this critical value, namely for spin 1, within a certain range of the single-ion anisotropy strength. At higher temperatures we identify another phase of the Berezinsky-Kosterlitz-Thouless type characterized by a power-law decay of the spin correlation function. We perform finite-size scaling analyses to calculate the correlation decay exponent. Subsequently, we estimate the critical boundaries of both phases and plot the phase diagram as a function of the single-ion anisotropy strength. This work was supported by the Scientific Grant Agency of Ministry of Education of Slovakia Republic (Grant No. 1/0234/12).

[1] G.H. Wannier, Phys. Rev. 79 (1950) 357. [2] Y. Yamada et al., J. Magn. Magn. Mater. 140-144 (1995) 1749.

QE02

Selectively diluted triangular lattice Ising antiferromagnet in an external magnetic field
 Andrej Bobak*, Michal Borovsky and Milan Zukovic
 Department of Theoretical Physics and Astrophysics, Faculty of Science, P.J. Safarik University, Slovakiaia

It is well known that the pure Ising model with nearest-neighbor antiferromagnetic interactions on a triangular lattice shows no long-range ordering due to a high degree of frustration. Dilution of one out of three sublattices with nonmagnetic impurities can relieve the geometrical frustration globally and, above a certain dilution threshold, the system starts showing long-range magnetic ordering characterized by the second-order phase transitions [1]. Within the effective-field theory with correlations we demonstrate that the presence of a finite external field in the selectively diluted system can dramatically change its critical behavior. In particular, above a certain field value the system starts displaying tricritical behavior, i.e., as the dilution increases the phase transition becomes initially of first order and only upon further dilution changes to the second order. We confirm the existence of the first-order transition in the region of moderate dilution and relatively high fields by Monte Carlo simulations. An Ising antiferromagnet on a honeycomb lattice is treated as a special case when one sublattice is completely removed by dilution. This work was supported by the Grant VEGA No. 1/0234/12.

[1] H. Kaya, A.N. Berker, Phys. Rev. E 62 (2000) R1469.

QE03

Possible magnetic transition observed in S=1/2 kagome antiferromagnet volborthite by high field ESR
 Hitoshi Ohta^{1*}, Wei-min Zhang¹, Susumu Okubo¹, Takahiro Sakurai², Yoshihiko Okamoto³, Hiroyuki Yoshida⁴ and Zenji Hiroi³
¹ Molecular Photoscience Research Center, Kobe University, Japan
² Center for Supports to Research and Education Activities, Kobe University, Japan
³ Institute for Solid State Physics, University of Tokyo, Japan
⁴ National Institute for Materials Science (NIMS), Japan

Due to the recent discovery of model substances, such as ZnCu₂(OH)₂C₁₂ (herbertsmithite), Cu₃V₂O₇(OH)₂·2H₂O (volborthite) and BaCu₃V₄O₁₆(OH)₂ (vesignieite), S=1/2 kagome antiferromagnet has attracted much interest experimentally, and we suggested a gapless spin liquid state in vesignieite [W. Zhang et al, J. Phys. Soc. Jpn. 79 (2010) 023708.]. In this paper we will report on high field ESR results of volborthite powder sample. For the spin dynamics volborthite shows the g-shift below around 20 K similar to vesignieite [H. Ohta et al., Phys. Status Solidi B 247(2010) 679.]. However, it shows two modes at 1.8 K, mode A with a very small gap of about 40 GHz (1.9 K) and mode B with no gap. Existence of mode B may suggest the spin liquid state with no spin gap at 1.8 K. Moreover, two modes cross at around 4.5 T, which corresponds to magnetization anomaly at 4.3 T. Detailed frequency dependence measurement up to 30 T at 1.8 K shows also new anomaly at 14 T. Possible magnetic transitions at 4.3 and 14 T will be discussed in connection with recent NMR result on volborthite powder. Finally very recent high-field ESR result using single crystal of volborthite will be also presented.

QE04

Field-induced staggered moment stabilization in frustrated quantum magnets

Burkhard Schmidt*, Mohammad Siahatgar and Peter Thalmeier
Max-Planck-Institut für Chemische Physik fester Stoffe, Germany

For low-dimensional frustrated magnets, the dependence of the staggered moment on a magnetic field is nonmonotonic: For small and intermediate fields, quantum fluctuations are gradually suppressed, leading to an increase of the staggered moment as function of the field strength. For large applied magnetic fields, the classically expected field dependence is recovered, namely a monotonous decrease with increasing field strength. The staggered moment is eventually suppressed when reaching the fully polarized state at saturation. The quantitative analysis of this behavior is an excellent tool to determine the frustration parameter of magnetic compounds. We have developed a general finite-size scaling scheme for numerical exact-diagonalization data of low-dimensional frustrated magnets, which we apply to the recently measured field dependence of the magnetic neutron scattering intensity of $\text{Cu}(\text{pz})_2(\text{ClO}_4)_2$ in the framework of the $S=1/2$ two-dimensional J_1 - J_2 Heisenberg model. We also apply linear spin-wave theory to complement our numerical findings. Our results show that $\text{Cu}(\text{pz})_2(\text{ClO}_4)_2$ is a quasi-2D antiferromagnet with intermediate frustration $J_2/J_1=0.2$. A self-consistent RPA theory for the magnetic ordering temperature shows that with this ratio the observed reentrant behavior of the latter as function of the applied magnetic field can be understood as a consequence of the reduced quantum fluctuations as well.

QE05

Structural and magnetic properties of single crystals of volborthite comprising a distorted spin-1/2 kagome lattice

Hajime Ishikawa*, Yoshihiko Okamoto¹, Junichi Yamaura¹, Hiroyuki Yoshida², Goran J. Nilsen¹ and Zenji Hiroi¹
¹ *ISSP, the University of Tokyo, Japan*
² *NIMS, Japan*

In geometrically frustrated magnets, exotic ground states such as a spin liquid are expected to realize as a result of competing magnetic interaction. Volborthite $\text{Cu}_3\text{V}_2\text{O}_7(\text{OH})_2 \cdot 2\text{H}_2\text{O}$ has drawn attention as a model compound for the distorted spin-1/2 kagome antiferromagnet. Previous studies using powder samples showed a peculiar magnetic transition at 1 K. Recently, H. Yoshida et al. synthesized a small single crystal, and found a structural phase transition at 310 K and two magnetic transitions at around 1 K, which have not been observed in powder samples. To clarify the physical properties of volborthite at low temperatures, we tried to synthesize a large and high-quality single crystal and obtained large single crystals of $2.5 \times 1.5 \times 0.1$ mm in size as a result of improving synthesis conditions. By means of single crystal XRD, we found a new crystal polymorph at room temperature which crystallizes in space group $C2/c$, not in $C2/m$ as reported before. There is a phase transition upon cooling at around 290 K to an $I2/a$ phase, similar as in the $C2/m$ phase. In this presentation, we show the differences of structure and magnetic properties between various polymorphs.

QE06

High-field study of multiferroic $\text{Ni}_2\text{V}_2\text{O}_8$

Junfeng Wang¹, Masashi Tokunaga², Zhangzhen He³ and Koichi Kindo²
¹ *Wuhan National High Magnetic Field Center, China*
² *The Institute for Solid State Physics (ISSP), The University of Tokyo, Japan*
³ *Fujian Institute of Research on the Structure of Matter, Chinese Academy of Sciences, China*



QE07

Gapless spin excitation of the triangular-lattice antiferromagnet

Hiroki Nakano^{1*} and Toru Sakai²
¹ *University of Hyogo, Japan*
² *JAEA, SPring8, Japan*

Two-dimensional frustrated magnets including the triangular-lattice antiferromagnet (TLA) have attracted much attention. However, a useful method among unbiased computational methods is limited to being the numerical-diagonalization method that can treat only small systems. In spite of such situation, great efforts have been done for studies of the TLA; it is widely believed that the ground state of TLA has a long-range order of 120-degree structure. The existence of this order indicates that spin excitation is gapless; however, the system size (N) dependence of the singlet-triplet energy difference of finite-size clusters shows a peculiarity that a nonzero spin gap seems to survive in the extrapolation with respect to $N[1]$. Under circumstances, we calculate the singlet-triplet energy difference of possible all the finite-size clusters up to 39 sites by our MPI-parallelized code of the numerical-diagonalization method. The analysis used in the study of the spin-gap issue of the kagome-lattice antiferromagnet[2] is applied to the TLA. The present examination successfully confirms a gapless spin excitation, which is consistent with the existence of the long-range order.

[1] J. Richter et al.: *Phys. Rev. B* 70 (2004) 174454. [2] H. Nakano and T. Sakai: *J. Phys. Soc. Jpn.* 80 (2011) 053704.

QE08

Magnetic properties of the spin-1/2 kagome antiferromagnets: vesignieite $\text{BaCu}_3\text{V}_2\text{O}_8(\text{OH})_2$ and $\text{CdCu}_3(\text{OH})_6\text{Br}_2$

Yoshihiko Okamoto*, Makoto Yoshida¹, Hajime Ishikawa¹, Goran J. Nilsen¹, Hiroyuki Yoshida², Masashi Takigawa¹ and Zenji Hiroi¹
¹ *Institute for Solid State Physics, Univ. of Tokyo, Japan*
² *National Institute for Materials Science, Japan*

An ideal model system for the spin-1/2 kagome antiferromagnet has not yet been obtained and the search for that is still going on. Here we report the magnetic properties of two Cu minerals, vesignieite $\text{BaCu}_3\text{V}_2\text{O}_8(\text{OH})_2$ and $\text{CdCu}_3(\text{OH})_6\text{Br}_2$, both of which comprise spin-1/2 kagome lattices. Vesignieite has a nearly isotropic kagome lattice and was found to show neither Neel order nor a spin-glass transition above 2 K [1]. However, the intrinsic ground state has remained unsolved, because previous samples contained many impurity spins caused by the low crystallinity. Recently, we succeeded in improving the sample quality by optimizing preparation parameters under hydrothermal conditions. The magnetic susceptibility of the new sample increases steeply below 15 K, followed by a sharp peak at 9 K that is indicative of long-range antiferromagnetic order. $\text{CdCu}_3(\text{OH})_6\text{Br}_2$ has an isotropic kagome lattice made of Cu^{2+} ions. The compound is an antiferromagnet with a Weiss temperature of -48 K and shows long-range antiferromagnetic order at 7 K. Thus, both the compounds show long-range order at rather high temperatures, which may be due to significantly large interlayer magnetic interactions.

[1] Y. Okamoto et al., *J. Phys. Soc. Jpn.* 78, 033701 (2009).

QE09

Spin dynamics of triangular spin tubes

Hirohata Manaka^{1*} and Yoko Miura²
¹ *Graduate School of Science and Engineering, Kagoshima University, Japan*
² *Suzuka National College of Technology, Japan*

Triangular spin tubes belong to a new category of one-dimensional Heisenberg antiferromagnets along the tubes coexisting with geometrically frustrated spin systems in the triangular plane. Recently, we discovered that chromium fluoride CsCrF_4 forms ideal equilateral triangular spin tubes with $S=3/2[1]$. All Cr ions are at equivalent sites, and each angle of Cr-Cr-Cr in the triangular plane is 60 deg.[2] Because superexchange interactions through the three Cr-F-Cr paths in each equilateral triangle may be kept in equilibrium at 0 K, we propose resonating spin-singlet pairs in each equilateral triangle. From DC magnetic susceptibility and adiabatic heat capacity data above 1.5 K, we concluded that there is no magnetic phase transition. Therefore, CsCrF_4 consists of a gapless spin-liquid ground state encompassing resonating spin-singlet pairs not only in each equilateral triangle but also along the tubes[2]. To clarify spin dynamics of the spin-liquid ground state, we performed linear and nonlinear AC magnetic susceptibility measurements on CsCrF_4 . As a result, temperature dependence of a linear susceptibility exhibits a positive peak at around 4 K, while a nonlinear susceptibility exhibits a broad and negative peak at around 3.5 K. We found that a spin-glass like state was realized below 4 K.

[1] H. Manaka et al., *J. Phys. Soc. Jpn.* 78, 093701 (2009). [2] H. Manaka et al., *J. Phys. Soc. Jpn.* 80, 084714 (2011).

QE10

Origin of field induced magnetic ordering in frustrated honeycomb lattice antiferromagnet

Susumu Okubo^{1*}, Tomonari Ueda², Wei-min Zhang³, Takahiro Sakurai¹, Masashi Fujisawa¹, Hitoshi Ohta¹, Nozomi Ohnishi³, Masaki Azuma⁴, Yuichi Shimakawa⁵ and Nobuhiro Kumada⁷
¹ *Molecular Photoscience Research Center, Kobe University, Japan*
² *Graduate School of Science, Kobe University, Japan*
³ *Center for Collaborative Research and Technology Development, Kobe University, Japan*
⁴ *Center for Supports to Research and Education Activities, Kobe University, Japan*
⁵ *Institute for Chemical Research, Kyoto University, Japan*
⁶ *Materials and Structures Laboratory, Tokyo Institute of Technology, Japan*
⁷ *Graduate School of Medicine and Engineering, University of Yamanashi, Japan*

The ground state of honeycomb lattice antiferromagnet (HLAF) have been considered theoretically to be the Neel state similar to the square lattice antiferromagnet because both antiferromagnets are bipartite lattices. However, the honeycomb lattice has smaller coordination number 3 than the square lattice of 4 and it is close to the one dimensional chain. Therefore, the stronger spin fluctuation is expected in the HLAF. Actually, anomalous spin dynamics are reported in $S=1/2$ HLAF $\text{InCu}_2\text{V}_2\text{O}_7$ [1]. On the other hand, the spin liquid state is expected in $S=3/2$ HLAF $\text{Bi}_3\text{Mn}_2\text{O}_{12}(\text{NO}_3)$ due to no long range order down to 0.4K despite of the large Weiss temperature. Although no spin gap has been observed in the magnetic susceptibility of $\text{Bi}_3\text{Mn}_2\text{O}_{12}(\text{NO}_3)$, it shows the field-induced magnetic ordering (FIMO) above around 6 T. Neutron diffraction measurements confirmed FIMO state and suggested that Dzyaloshinski-Moriya (DM) interaction plays an important role in the FIMO state. In order to estimate the DM interaction, high-field ESR measurements have been performed. The D-term of DM interaction is estimated to be 1.3K from the analysis of observed antiferromagnetic resonance mode. Origin of FIMO will be discussed in connection with the DM interaction and the other magnetic anisotropy.

[1] S. Okubo et al., *J. Phys. Soc. Jpn.* 80 (2011) 023705

QE11

Semi-classical spin-liquid state as a low-energy excited state in frustrated quantum spin systems on triangle-based lattice system

Makoto Isoda¹, Hiroki Nakano² and T*oru Sakai³
¹ *Kagawa University, Japan*
² *University of Hyogo, Japan*
³ *JAEA SPring-8, Japan*

The magnetic and the thermal properties of the spin-1/2 Heisenberg antiferromagnets on the triangle-based lattice are summarized, focusing on the realization of the semi-classical spin-liquid state of the resonating doublet trimers formed on triangles, through the calculations for various systems such as the triangular, the kagome, the triangulated-kagome(1), the Sierpinski-gasket like(2) and the spatially anisotropic triangular lattices, which interpolates the triangular and the kagome lattices. The calculations have been performed by the numerical diagonalization method. On these systems, the peculiar behaviors have been found in the Heisenberg(3,4) and the Ising(5) models for spin-1/2 on those triangle-based lattices with nearest neighbor (nn) antiferromagnetic interaction. The peculiarities are the bending of the magnetic susceptibility as a function of temperature, the more than two peaks structure on the specific heat and the 1/3 magnetization plateau under magnetic field. Each of these peculiarities appears at the characteristic temperature or magnetic field corresponding to the magnitude of nn interaction, suggesting the predominance of the doublet trimer low energy excited state. The peculiarities reveal as an intrinsic character of the systems with the nn antiferromagnetic interaction depending on whether the lattice is formed by the equilateral triangle as a unit cell or not.

1) M.Gonzalez et al., *Mol. Cryst. Liq. Cryst.* 233 (1993) 317. 2) T. Stosic et al., *Phys. Rev. E* 49 (1994) 1009. 3) M.Isoda, H.Nakano and T.Sakai, *Mod. Phys. Lett. B* 25 (2011) 909. 4) M.Isoda, H.Nakano and T.Sakai, *J. Phys. Soc. Jpn.* 80 (2011) 084704. 5) M.Isoda, *J. Phys.: Condens. Matter* 20 (2008) 315202.

QE12

High pressure and low-temperature 31P NMR study of the two-dimensional frustrated square lattice compound $\text{BaCdVO}(\text{PO}_4)_2$

Yuji Furukawa¹, Beas Roy¹, Ramesh Nath², David C Johnston¹, Yasuhiro Komaki³, Hideto Fukazawa³ and Yoh Kohori³
¹ *Department of Physics and Astronomy, Iowa State University / Ames Laboratory, USA*
² *Indian Institute of Science Education and Research, India*
³ *Department of Physics, Chiba University, Japan*

We report first NMR study under pressures on $\text{BaCdVO}(\text{PO}_4)_2$, a $S = 1/2$ frustrated square-lattice (FSL) compound with a nearest neighbor exchange coupling $J_1 \sim -3.36$ K and a next-nearest neighbor exchange coupling $J_2 \sim 3.53$ K bearing $J_2/J_1 \sim 1.05$. Based on the J_2/J_1 ratio, the system is known to be located close to the disordered ground state (known as 'nematic state') regime of the phase diagram. We have carried out 31P-NMR measurements under high pressure (up to ~ 2 GPa) and at low temperatures (down to ~ 0.1 K) using a dilution refrigerator to investigate the pressure effects on the magnetic properties of the system from microscopic point of view. Under ambient pressure, we observed a sharp peak in 31P spin lattice relaxation rate (1/T1) at $T_N \sim 1.05$ K at $H = 2.67$ T, which corresponds to the antiferromagnetic ordering temperature. With increasing pressure, the peak position of 1/T1 shifts to lower temperature. This indicates that T_N decreases with the application of pressure. We will discuss pressure effects on magnetic state based on the temperature dependence of the NMR spectra and of the 1/T1 under different magnetic fields and pressures.

QE13

Kasteleyn transitions in the spin ice $\text{Dy}_2\text{Ti}_2\text{O}_7$

Hiroaki Kadowaki^{1*}, Naohiro Doi¹, Hiroshi Takatsu¹, Ryuji Higashinaka¹, Yuji Muro², Kiyochiro Motoya³, Rei Morinaga⁴, Taku J Sato⁵, Takashi Tayama⁶, Toshiro Sakakibara¹, Kazuyuki Matsuhira⁷ and Zenji Hiroi¹
¹ *Department of Physics, Tokyo Metropolitan University, Japan*
² *Toyama Prefectural University, Japan*
³ *Department of Physics, Tokyo University of Science, Japan*
⁴ *Institute for Solid State Physics, University of Tokyo, Japan*
⁵ *Department of Physics, University of Toyama, Japan*
⁶ *Department of Electronics, Kyushu Institute of Technology, Japan*

The spin ice model in the pyrochlore lattice, e.g. $\text{Dy}_2\text{Ti}_2\text{O}_7$, consisting of corner sharing tetrahedra has attracted much attention because of its intriguing frustration mechanism. The ground states of this system are macroscopically degenerate with the finite zero-temperature entropy, and the spins freeze in this manifold at low temperatures. The macroscopic degeneracy of the ground states is partly lifted under magnetic fields, where degrees of the degeneracy depend on direction and strength of the field. Interesting theoretical predictions, which have not been seriously investigated to date by experiments, are Kasteleyn transitions [1] in three and two space dimensions, which may occur under magnetic fields along a [100] direction [2] and fields tilted slightly from a [111] direction [3]. These transitions are classified into topological phase transitions which are characterized by line (string) defects. We have investigated these possibilities in the spin ice compound $\text{Dy}_2\text{Ti}_2\text{O}_7$ using magnetization and specific heat measurements.

[1] P. W. Kasteleyn, *J. Math. Phys.* 4, 287 (1963). [2] L. D. C. Jaubert et al. *Phys. Rev. Lett.* 100, 067207 (2008). [3] R. Moessner, S. L. Sondhi, *Phys. Rev. B* 68, 064411 (2003).

QE14

Novel frustrated quantum antiferromagnets in the solid-solution $\text{Cs}_x\text{CuCl}_{4-x}\text{Br}_x$ through site-selective halide substitution

Bernd Wolf*, Pham Thanh Cong, Natalia Kruger, Franz Ritter, Wolf Assmus and Michael Lang
Physics Institute, Goethe-University Frankfurt (M), SFB/TR 49, D-60438 Frankfurt (M), Germany

We report on the magnetic properties of tetragonal and orthorhombic single crystals of the solid solution $\text{Cs}_x\text{CuCl}_{4-x}\text{Br}_x$ ($0 \leq x \leq 4$). Two phase regions, namely an A-type orthorhombic and a B-type tetragonal structure, were detected in this system depending on the growing conditions. The two known orthorhombic end-member compounds Cs_2CuCl_4 and Cs_2CuBr_4 are classified as quasi-two-dimensional quantum antiferromagnets with different degrees of magnetic frustration. By measurements of the magnetic susceptibility $\chi(T)$ on orthorhombic single crystals with different Br concentrations, we found that the in-plane and out-of-plane magnetic correlations, probed by the position and height of a maximum in $\chi(T)$, respectively, do not show a smooth variation with x. Instead three distinct concentration regimes can be identified, which are separated by critical concentrations $x_{c1} = 1$ and $x_{c2} = 2$. This unusual magnetic behaviour can be explained by considering the structural peculiarities of the materials, which support a site-selective replacement of Cl- by Br- ions [1]. Consequently, the critical concentrations x_{c1} (x_{c2}) mark particularly interesting systems, where one (two) halide-sublattice positions are fully occupied. The magnetic properties of the tetragonal phase of $\text{Cs}_x\text{CuCl}_{4-x}\text{Br}_x$ differ strongly from those of the orthorhombic variants, reflecting changes in the Cu-coordination.

[1] P. T. Cong et al., *PRB* 83, 064425, (2011)

QE15

Strong geometrical frustration in Fe oxychalcogenide

Sungdae Ji¹, K. Horigane² and K. Yamada³
¹ *CROSS, Japan*
² *University of Virginia, USA*
³ *Tohoku University, Japan*

After Fe-based superconductors have emerged, it has generated a lot of controversies regarding to low ordered moments in parent compounds which have been explained by itinerant magnetism with Fermi surface nesting vs. magnetic frustration and/or fluctuation effects in a large-local-moment system [1]. Very recently, Fe-oxychalcogenide has drawn attention, because it has been identified as a layered insulating antiferromagnet with the geometrically frustrated, so-called, "double diagonal stripe" spin structure which is realized only in Iron telluride among the family of Fe-based superconductors [2,3]. Here, we report elastic and inelastic neutron scattering study on $\text{La}_2\text{O}_7\text{Fe}_2\text{OSe}_2$. Our elastic neutron measurement at 5 K shows that magnetic Bragg peaks are diffusive and a obtained magnetic moment is $2.2 \mu_B$, which is smaller than a localized spin, $S=5/2$. Inelastic neutron scattering measurement shows that a strong magnetic fluctuation survives even at 300 K far above magnetic transition temperature, $T_N = 90$ K. Moreover, observed dispersive excitation reveals that the 3rd nearest neighbor interaction is the key to explain a magnetic ground state on the geometrically frustrated lattice.

[1]. David C. Johnston, *Adv. in Phys.* 59, 803 (2010). [2]. Jian-Xin Zhu et al., *Phys. Rev. Lett.* 104, 216405 (2010). [3]. David G. Free and John S. O. Evans, *Phys. Rev. B* 81, 214433 (2010).

QE16

Magnetic properties of the frustrated magnet Cu₅(PO₄)₃(OH)₃ on a peculiar spin network composed of pentagons and triangles

Hikomitsu Kikuchi¹, Nguyen Thi Tinh Y¹, Yutaka Fujii², Masashi Fujisawa³, Akira Matsuo⁴ and Koichi Kindo⁴

¹ Department of Applied Physics, University of Fukui, Japan

² Research Center for Development of Far-Infrared Region, University of Fukui, Japan

³ Research Center for Low Temperature Physics, Tokyo Tech, Japan

⁴ ISSP, The University of Tokyo, Japan

Orthorhombic Cu₅(PO₄)₃(OH)₃ (pseudomalachite) is a layered compound. Each Cu-O layer in this compound is well separated by PO₄ tetrahedrons. Spin network in bc-plane of pseudomalachite is composed of triangles and pentagons, which will induce the spin frustration effect. This network can be a new type of geometrically frustrated spin lattice. Magnetic susceptibility, specific heat, high field magnetization are measured to study magnetic properties of Cu₅(PO₄)₃(OH)₃ using natural mineral samples. Magnetic ordering is observed at around 4.2 K. Spin entropy change at the transition temperature is about one fifth times smaller than that expected for a usual long range order. 1/5 magnetization plateau is observed in the high field magnetization curve. The plateau can be explained based on the simple model in which the spin network is assumed to be composed of chain, dimer and monomer units.

QE17

Single crystal growth and magnetic properties of novel kagome compound KMn₃Ge₂O₉

Shigeo Hara* and Hirohiko Sato

Department of Physics, Chuo-univ, Japan

We have succeeded in synthesizing single crystals of a novel manganese oxide KMn₃Ge₂O₉ by a hydrothermal method. This compound has a hexagonal unit cell with lattice constants a = 11.77 Å and c = 13.77 Å. In this structure, edge-shared MnO₆ octahedra form layers separated by GeO₄ tetrahedra. In each layer, Mn ions with S = 2 spin form a rippled kagome lattice. Therefore, we can expect a frustrated magnetism. We measured temperature dependence of the magnetic susceptibility on a single crystal. The result suggests the existence of a strong magnetic frustration. The Curie constant and Weiss temperature are estimated at 3.4 emu K/mol Mn and - 84 K, respectively. The negative Weiss temperature indicates that the nearest-neighbor exchange interaction among Mn ions is antiferromagnetic. At low temperatures, the susceptibility suggests the existence of multiple magnetic phases. For example, the susceptibility shows an antiferromagnetic like transition at 40 K and a spin-glass like transition at 20 K under 0.5 T of magnetic field perpendicular to the kagome lattice. The successive transitions are also observed in other conditions of magnetic field. We consider that these behaviors are driven from the strong magnetic frustration of the kagome lattice.

QE18

Specific heat study of geometrically frustrated magnet botallackite Cu₂(OH)₃Cl

Hiroki Morodomi¹, Yuji Inagaki¹, Tatsuya Kawai¹, Masato Hagihala² and X.G. Zhen²

¹ Department of Applied Quantum Physics, Kyushu University, Japan

² Department of Physics, Saga University, Japan

Specific heat measurements have been performed in the geometrically frustrated magnets botallackite, Cu₂(OH)₃Cl with the triangular structure of the Cu²⁺ ions. This is a different polymorphic form of clinooctamite with the corner-sharing tetrahedral structure, which exhibits the coexistence of spin fluctuation and long range ordering below 6.2 K[1]. The specific heat of botallackite shows a sharp peak at TN=7.0K and approximately exhibits T³-dependence with lowering temperature in zero magnetic field. When a magnetic field is applied, TN shifts to lower temperatures and the peaks disappears at H=8 T. Moreover, no residual entropy is observed at lower temperatures.

[1] X.G. Zheng, et. al., Phys. Rev. Lett. 95 057201 (2005).

QE19

Order and excitations in the frustrated quantum spin ladder BiCu₂PO₆

P. Merchant¹, S. Wang², O. Zaharko³, Ch. Niedermayer³, L. P. Regnault⁴, M. Boehm¹, M. Kenzelmann² and Ch. Ruegg³

¹ London Centre for Nanotechnology, University College London, United Kingdom

² Laboratory for Developments and Methods, Paul Scherrer Institute, Switzerland

³ Laboratory for Neutron Scattering, Paul Scherrer Institute, Switzerland

⁴ Institut Laue-Langevin, France

Quantum spin ladders are exceptional model systems showing non-trivial phenomena ranging from complex spin correlations in the ground state to rich phase diagrams with several quantum critical points. A fully quantitative understanding of their magnetic and thermodynamic properties may be achieved e.g. by powerful computational methods (DMRG, ED, bond operators) [1, 2] and comparison with high-precision experimental data, which may only be possible in such model systems [3]. BiCu₂PO₆ is a new prototypical model material in which the spin ladders are frustrated by next-nearest neighbour exchange along the ladder legs, furthermore it can be doped with non-magnetic Zn²⁺ impurities. The results of comprehensive neutron scattering studies on single crystals are presented of the elementary excitations and spin Hamiltonian of this frustrated ladder compound, as well as of the Zn-induced magnetic order and phase diagrams. The physics in this system is dominated by incommensurate correlations on all energy scales.

[1] P. Bouillot et al., Phys. Rev. B 83, 054407 (2011). [2] B. Normand and Ch. Ruegg, Phys. Rev. B 83, 054415 (2011). [3] e.g. see B. Thielemann et al., Phys. Rev. Lett. 102, 107204 (2009).

QE20

Melting of the spin ice state in Dy₂(Ti_{1-x}Zr_x)₂O₇ without dilution of rare-earth ion

Yuta Kodama, Kousuke Tsuruta, Daisuke Akahoshi and Toshiaki Saito*

Department of Physics, Faculty of Science, Toho University, Funabashi City, Chiba 274-8510, Japan

The pyrochlore Dy₂Ti₂O₇ is a spin ice material, in which the spins reside on the lattice of corner-sharing tetrahedra with single-ion anisotropy along each local <111> axis. The effective ferromagnetic interaction between spins leads to a highly degenerate ground state. Earlier researches [1][2] reported that the magnetic relaxation shows three successive processes; thermally activated Arrhenius process above 13 K, quantum tunneling process between 4 K ~ 13 K, and process with strong spin correlation below 4 K. The relaxation in the medium temperature regime is the Davidson-Cole type [3] characterized by a wide distribution of relaxation time τ with a cut-off τ. The dilution of Dy causes disappearance of the ac susceptibility 15 K peak [1] due to a speeding up of relaxation [2]. In this talk, we examined the magnetic relaxation of Dy₂(Ti_{1-x}Zr_x)₂O₇ through ac magnetic susceptibility measurements in order to study B-site disorder effect. We found, for x above about 0.01, disappearance of the 15 K peak, small frequency dependence, and substantial change of the magnetic relaxation from the Davidson-Cole type into the Cole-Cole one having no cut-off τ, indicating a major effect of B-site disorder on the spin ice state toward melting without dilution of Dy ion.

[1] J. Snyder et al., Phys. Rev. B 70 (2004) 184431. [2] G. Ehlers et al., J. Phys. Condens. Matter 15 (2003) L9. [3] K. Matsuhira et al., J. Phys. Condens. Matter 13 (2001) L737. [4] L.D.Jaubert and P.C.Holdsworth, J. Phys. Condens. Matter 23 (2011) 164222.

QE21

Unusual magnetic ordering of kagome lattice magnet [Cu₂(CO₃)₂(bpe)₃]*₂ClO₄

Hikomitsu Kikuchi¹, Hayato Nakata¹, Yutaka Fujii² and Toshifumi Taniguchi³

¹ Department of Applied Physics, University of Fukui, Japan

² Research Center for Development of Far-Infrared Region, University of Fukui, Japan

³ Graduate School of Science, Osaka University, Japan

Cu²⁺ ions in a hexagonal compound [Cu₂(CO₃)₂(bpe)₃]*₂ClO₄ (space group; P-6) form slightly distorted kagome lattice in its c-plane. Former study[1] reported that the magnetic susceptibility increased rapidly below about 7 K indicating an occurrence of the ferromagnetic transition. Surprisingly, however, no anomaly in the specific heat was observed at the transition temperature in this compound. In order to scrutinize the magnetic properties, we measure the specific heat of this compound using single crystals under an applied magnetic field up to 7 T. IH-NMR measurement is also carried out. NMR spectra-broadening and a divergent behavior of the spin-lattice relaxation rate are observed at around 7 K. Slight anomaly in the specific heat is observed and the anomaly temperature is found to depend on the magnetic field. These results suggest that entropy change associated with the magnetic ordering of this compound is vanishingly small.

1) P. Kanoo et al. Dalton Trans. 2009, 5062.

QE22

Field-induced staggered moments in the spin-gapped antiferromagnet on a deformed kagome lattice, Rb₂Cu₃SnF₁₂

Hiroshi Tashiro*¹, Masahide Nishiyama¹, Akira Oyamada¹, Tetsuaki Itou¹, Satoru Maegawa¹, Midori Yano², Toshio Ono³ and Hidekazu Tanaka²

¹ Graduate School of Human and Environmental Studies, Kyoto University, Japan

² Department of Physics, Tokyo Institute of Technology, Japan

³ Department of Physical Science, Osaka Prefecture University, Japan

Rb₂Cu₃SnF₁₂ is a kagome lattice antiferromagnet in which Cu²⁺ ions with spin 1/2 interact with four exchange interactions, J1~200K>J2>J3~J4~100K. The ground state of this compound is a valence bond solid owing to the quantum and frustration effects, so that no magnetic ordering occurs [1,2]. We have performed 19F-NMR experiments on a single crystal of Rb₂Cu₃SnF₁₂ in order to clarify the microscopic property of the ground state. One sharp 19F-NMR spectrum at high temperature splits to several peaks at low temperatures due to different magnetic sites of 19F. The shifts of these peaks increase steeply below around 70K, whereas the static susceptibility decreases exponentially below this temperature owing to the singlet ground state with the spin-gap. The shifts are proportional to the applied field. These results strongly suggest that the local fields are produced by the staggered moments induced by the external field through Dzyaloshinsky-Moriya interaction. The staggered moments become dominant below 70K, while the parallel moments are remarkably small because of the large exchange interaction. This characteristic temperature differs from the spin-gap of 20K obtained from the susceptibility, because the large density of state in the dispersion curve around 70K contributes to the generation of the staggered moments [3].

[1] K. Morita, M. Yano, T. Ono, H. Tanaka, K. Fujii, H. Uekusa, Y. Narumi, and K. Kindo, J. Phys. Soc. Jpn. 77, 043707 (2008). [2] K. Maan, T. Ono, Y. Fukumoto, T. J. Sato, J. Yamawara, M. Yano, K. Morita, and H. Tanaka, Nature Phys. 6, 865-869 (2010). [3] H. Tashiro, M. Nishiyama, A. Oyamada, T. Itou, S. Maegawa, M. Yano, T. Ono, and H. Tanaka, J. Phys.: Conf. Ser. 320, 012052 (2011).

QE23

Magnetic order in finite size domains of the honeycomb lattice compound InCu_{2/3}V_{1/3}O₃

E. Vavilova*¹, M. Yakovleva¹, M. Yehia², R. Klingeler³, V. Kataev², T. Taetz², U. Loew⁴, A. Moeller⁵ and B. Buechner⁶

¹ Zavoisky Physical Technical Institute, RAS, Kazan, Russia

² IFW Dresden, Dresden, Germany

³ Heidelberg University, Heidelberg, Germany

⁴ Institut für Anorganische Chemie, Universität zu Köln, Germany

⁵ Technische Universität Dortmund, Germany

⁶ University of Houston, Department of Chemistry and Texas Center for Superconductivity, USA

The results of high field electron spin resonance, nuclear magnetic resonance, nuclear quadrupole resonance and magnetization studies addressing the ground state of the quasi two-dimensional spin-1/2 honeycomb lattice compound InCu_{2/3}V_{1/3}O₃ are reported. Uncorrelated finite size structural domains occurring in the honeycomb planes are expected to inhibit long range magnetic order. Surprisingly, magnetic resonance data show the development of two collinear antiferromagnetic (AFM) sublattices below 35K and the presence of the staggered internal field. Magnetization data evidence a spin reorientation transition at 5.7T. Quantum Monte-Carlo calculations show that switching on the coupling between the honeycomb spin planes in a finite size cluster yields a Neel-like AFM spin structure with a substantial staggered magnetization at finite temperatures. ESR, NMR and NQR data allow to retrace the development of staggered magnetization during the crossover to ordered ground state.

A. Yehia, et al., Phys. Rev. B 81, 060414 (2010)

QE24

Z₂ vortices in frustrated background of cuprates

Maciej Fidrysiak and Pawel Rusek*

Wroclaw University of Technology, Poland

La_{2-x}Sr_xCuO₄ (LSCO) in the underdoped regime (x=0.02 - 0.05) is a non-collinear quantum antiferromagnet. The relevant order parameter is a triad of orthonormal vectors. The topology of the order parameter space allows the existence of Z₂ vortices. Randomly distributed Sr dopants introduce holes into the Cu-O planes which are the source of fluctuating dipolar fields resulting in frustrated spin background. We study Z₂ vortices in the system in the framework of non-linear sigma-model coupled to SO(3) gauge fields which represent fluctuating frustrated background. In this model we describe explicitly not only spin degrees of freedom, but also the distribution of frustrations as opposed to pure spin systems. We have found explicitly a finite energy Z₂ vortex solution. Frustrations are concentrated in the soft core of Z₂ vortices and exponentially decrease at large distances. The chirality of spin system changes its sign in the vortex core as expected. Our vortex seems to be more relevant to the study of frustrated Heisenberg spin systems and the charge transport by vortices in cuprates than Z₂ vortices in pure spin degrees of freedom.

QE25

First-principles study of S=1/2 Kagome antiferromagnet

Chung-yuan Ren*

National Kaohsiung Normal University, Taiwan

3-D systems with interacting spins usually develop static long-range order when they are cooled. However, quantum fluctuations are enhanced in low dimensionality system with low spin value and lead to suppress the long-range ordering, and can show some extremely subtle, complex, and sometimes even useful magnetic behavior in solids. Here, using first-principles calculations, we investigated the atomic structural and magnetic properties of S=1/2 Kagome antiferromagnet A₃Cu₃(OH)₂Cl₂ (A=Zn, alkali metal ion). Cu ions are indeed found to locate at the tetragonally elongated intralayer site and Zn ions favorably rest on the higher symmetry interlayer site, in support of experimental contention. The intra- and inter-layer exchange interactions are studied in details. The effect of Dzyaloshinskii-Moriya interaction on the magnetic structure is also discussed.

[1] M. P. Shores, E. A. Nytko, B. M. Bartlett, and D. G. Nocera, J. Am. Chem. Soc 127, 13462, (2005) [2] S. Chu, T.M McQueen, R. Chisnell, D.E. Freedman, P. Muller, Y.S. Lee, and D.G. Nocera, J. Am. Chem. Soc. (2010).

QE26

Exotic phases in the frustrated hexagonal lattice

Daniel C. Cabra*

Physics Department, National University of La Plata, Argentina

We study the phase diagram of the Heisenberg model on the Honeycomb lattice with antiferromagnetic interactions up to third neighbors along the line J2=J3, close to the point where it has macroscopic degeneracy at the classical level. Using the Schwinger boson technique followed by a mean field decoupling and exact diagonalization for small systems we find an intermediate phase with a spin gap and short range Neel correlations even in the strong quantum limit 1/2. We have also studied the magnetization curve for J3=0, close to J2/J1 = 1/2 where the classical ground state is also highly degenerate. The properties of the magnetization curve and phase transitions are studied by means of Montecarlo, which shows many interesting transitions.

QE27

Light scattering in spin liquid systems

Dirk Wulferding¹*, Peter Lemmens¹, Vladimir Gnezdilov², Tianheng Han³, Young S. Lee³, Hiroyuki Yoshida⁴, Yoshihiko Okamoto⁵ and Olga Volkova⁶

¹ IPKM, TU-BS, Braunschweig, Germany

² ILTPE NAS, Ukraine

³ MIT, Massachusetts, USA

⁴ NIMS, Tsukuba, Japan

⁵ ISSP, Tokyo, Japan

⁶ MSU, Moscow, Russia

When quantum spin systems are restricted in dimensionality and coordination they realize spin liquid states with enhanced quantum fluctuations and exotic correlation functions. We compare the experimentally determined excitation spectra of different spin liquid candidates such as the s=1/2 Heisenberg antiferromagnet on a kagome lattice and weakly coupled spin chain system in Herbertsmithite and (NO)Cu(NO₃)₃ using Raman scattering. This technique is sensitive to fractional spinon excitations. The effect of the crystal's lattice structure and defects on the spin dynamics is investigated. The data is also compared with recent theoretical modelling. Work supported by DFG, B-IGSM and NTH School for Contacts in Nanosystems.

D. Wulferding, et al., Phys. Rev. B 82, 144412 (2010) V. Gnezdilov, et al., arXiv:1203.2818 (2012) D. Wulferding, et al., arXiv :1111.2167 (2012)

QF01

Molecular nanomagnets as quantum simulators

Paolo Santini
University of Parma, Italy

Quantum simulators (QSS) are controllable quantum systems that can be used to simulate other quantum systems. QSSs can tackle problems intractable on classical computers. Here we focus on the dynamics of qubits encoded in chains of molecular nanomagnets. For instance, we have shown that Cr₇Ni rings are good candidates for qubits and can be linked to each other either directly or through magnetic complexes [1,2]. We theoretically show that the dynamics of such chains can be controlled by means of uniform magnetic pulsed fields and used to mimic the coherent time evolution of other quantum systems (e.g., spin-one chains) [3]. We propose two significant proof-of-principle experiments [3].

[1] G.A. Timco et al., Nature Nanotechnology 4, 173 (2009) [2] A. Candini et al., Phys. Rev. Lett. 104, 037203 (2010) [3] P. Santini, S. Carretta, F. Troiani, G. Amoretti, Phys. Rev. Lett. 107, 230502 (2011)

QF02

ESR signature of the next-nearest-neighbor interactions in the S = 1/2 chain compound (6MAP)CuCl₂

M. Ozerov¹, A. A. Zvyagin¹, E. Cizmar², F. Xiao⁴, C. P. Landee⁴, J. Wosnitzer¹ and S. A. Zvyagin¹

¹ Dresden High Magnetic Field Laboratory, Helmholtz-Zentrum Dresden-Rossendorf, Dresden, Germany
² Institut für Festkörperphysik, Technische Universität Dresden, Dresden, Germany
³ Centre of Low Temperature Physics, P.J. Safarik University, Kosice, Slovakia
⁴ Department of Physics and Carlson School of Chemistry, Clark University, Worcester, Massachusetts, USA

Electron spin resonance (ESR) studies of the S = 1/2 chain material (6MAP)CuCl₂ [6MAP = C₆H₉N₃] are presented. Two modes with asymmetric with respect to a simple gapless Zeeman splitting resonance positions have been observed in the low-temperature ESR spectrum. This shows that the simple S = 1/2 Heisenberg antiferromagnet chain model, employed so far, is not sufficient for a complete description. The frequency-field diagram of magnetic excitations is interpreted in the frame of the recently developed theory for S = 1/2 chains with nearest- and next-nearest-neighbor interactions [A.A. Zvyagin, Phys. Rev. B 79, 064422 (2009)]. A good qualitative agreement with experiment has been achieved. The work was supported in part by DFG and EuroMagNET II (EU Contract No. 228043).

QF03

Electron spin resonance in the spin-ladder compound BPCB

S. Zvyagin¹, E. Cizmar², M. Ozerov¹ and J. Wosnitzer¹
¹ Dresden High Magnetic Field Laboratory (HLB) Helmholtz-Zentrum Dresden-Rossendorf, Dresden, Germany
² Centre of Low Temperature Physics, P.J. Safarik University, Kosice, Slovakia

Magnetic excitations in the spin-ladder material (C₅H₁₂N₂)CuBr₄ (known as BPCB) are probed by means of electron spin resonance (ESR) spectroscopy in magnetic fields up to 16 T. The gap between the ground state and the first excited state, 16.5 K (or 1.42 meV), is detected directly. In addition, our experiments provide clear evidence for a pronounced anisotropy (~ 5% of the dominant exchange interaction), responsible for a shift of the observed ESR line and a specific angular dependence of resonance absorptions. The results are explained in frame of the recently developed theory for ESR in spin-ladders (Furuya et al., arXiv: 1107.5965). The work was done in collaboration with B. Thielemann, K. W. Kramer, Ch. Ruegg, O. Piovesana, M. Klanjssek, M. Horvatic, and C. Berthier. The work was supported in part by DFG and EuroMagNET II (EU Contract No. 228043).

QF04

Non-magnetic impurity effect of S=1/2 spin ladder system (pipdH)₂Cu_{1-x}Zn_xBr₄

Chiori Yokoyama¹, Weimin Zhang², Takahiro Sakurai¹, Susumu Okubo^{4*}, Hitoshi Ohta⁵, Eiichi Matsuoka⁶, Hitoshi Sugawara⁷ and Hikomitsu Kikuchi⁸
¹ Kobe University, Japan
² Center for Collaborative Research and Technology Development, Kobe University, Japan
³ Center for Supports to Research and Education Activities, Kobe University, Japan
⁴ Molecular Photoscience Research Center, Kobe University, Japan
⁵ Molecular Photoscience Research, Kobe University, Japan
⁶ Graduate School of Science, Kobe University, Japan
⁷ Graduate School of Science, Kobe University, Japan
⁸ Department of Applied Physics, University of Fukui, Japan

Low dimensional spin system shows fruitful magnetic properties such as the Bose-Einstein condensation of magnon or the spin liquid state. Non-magnetic impurity effect in a quantum spin chain, which arises as an appearance of magnetic moment with spin correlation at around the impurity, is one of typical quantum effects of correlated spins. (pipdH)₂CuBr₄ is known as a model substance of weakly coupled spin 1/2 Heisenberg antiferromagnetic ladder system. Recently, we succeeded in synthesizing Zn-doped (pipdH)₂Cu_{1-x}Zn_xBr₄ single crystal. Samples were confirmed to be in a single phase and have the same crystal structure as the pure system (pipdH)₂CuBr₄ by X-ray diffraction measurements. To check magnetic properties, the magnetic susceptibility and the magnetization measurements are performed by the SQUID magnetometer. The magnetic susceptibility shows a maximum related to the spin ladder and the Curie increase at low temperature related to the doping of Zn. The Curie term increases as the Zn concentration increase. Observed non-magnetic impurity effect of S=1/2 spin ladder system will be discussed in connection with AKLT model.

QF05

High-field multi-frequency ESR in the S=2 Heisenberg antiferromagnetic chain compound MnCl₃(bpy)

Masayuki Hagiwara^{1*}, Shojiro Kimura², Yuichi Idutsu¹ and Zentaro Honda³
¹ KYOKUGEN, Osaka University, Japan
² IMR, Tohoku University, Japan
³ Graduate School of Science and Engineering, Saitama University, Japan



QF06

High field magnetization of bimetallic chain with alternating ising and Heisenberg spins

Yibo Han¹, Jozef Strecka², Takanori Kida¹, Zentaro Honda¹, Masami Ikeda¹ and Masayuki Hagiwara^{1*}
¹ KYOKUGEN, Osaka University, 1-3 Machikaneyama, Toyonaka, Osaka 560-8531, Japan
² Department of Physics, Faculty of Science, P. J. Safarik University, Park Angelinum 9,040 01 Kosice, Slovakia
³ Department of Functional Materials Science, Graduate School of Science and Engineering, Saitama University, 255 Shimo-Okubo, Sakura-ku, Saitama 338-8570, Japan

3d-4f bimetallic chain [Dy(NO₃)(DMSO)₂Cu(opba)(DMSO)₂] built from alternating dysprosium(3+) and copper(2+) ions has been synthesized and magnetically studied. Magnetic susceptibility as well as high-field magnetization of the polycrystalline sample was measured under the temperature down to 1.3 K and the magnetic field up to 52 T. After performing correction for the temperature independent paramagnetism, the magnetization curve recorded at 1.3 K shows a rapid increase with the magnetic field in the low-field range 0-3 T, followed up with a less steep increase in the field range 5-34 T before tending towards its saturation value at 34 T. The observed magnetization process can be interpreted in terms of the spin-1/2 chain model with alternating Ising and Heisenberg spins, which accounts for both parallel and perpendicular Zeeman's energy of Dy and Cu ions. The good fitting of the experimental data by using the above theoretical model suggest the effective antiferromagnetic exchange constant J/kB= -26 K, the highly anisotropic g-factor of Dy ions and almost isotropic g-factor of Cu ions. It was concluded that a new type of one-dimensional Ising-Heisenberg spin chain was found.

QF07

Thermal conductivity and magnetic susceptibility of the 4-leg spin-ladder system (La_{1-x}Y_x)₂Cu₂O₅ and the 5-leg spin-ladder system (La_{1-x}Eu_x)₂Cu₂O₁₀

Takayuki Kawamata*, Takashi Noji and Yoji Koike
Department of Applied Physics, Tohoku University, Japan

We have measured the thermal conductivity and magnetic susceptibility of the 4-leg spin-ladder system (La_{1-x}Y_x)₂Cu₂O₅ (x = 0.01) and the 5-leg spin-ladder system (La_{1-x}Eu_x)₂Cu₂O₁₀ (x = 0, 0.01). It has been found that the temperature dependence of the thermal conductivity along the spin-ladders of (La_{0.99}Y_{0.01})₂Cu₂O₅, La₂Cu₂O₁₀ and (La_{0.99}Eu_{0.01})₂Cu₂O₁₀ shows only one peak originating from the thermal conductivity due to phonons at ~15K. That is, the thermal conductivity due to spins, kspin, has not been observed in these compounds, though kspin was expected to be large owing to the exchange interaction along the spin-ladders as large as ~1000K. Since the antiferromagnetic transition temperature, TN, is as large as 137K and 103K in La₂Cu₂O₅ [1] and La₂Cu₂O₁₀ [2], respectively, it has been concluded that the comparatively large exchange interaction between spin-ladders disturbs the thermal conduction due to spins along the spin-ladders. Moreover, it has been found that the temperature dependence of the magnetic susceptibility below TN is clearly different between (La_{0.99}Y_{0.01})₂Cu₂O₅ and (La_{0.99}Eu_{0.01})₂Cu₂O₁₀, which may be related to the difference of the ground state between the odd- and even-leg spin-ladder systems.

[1] K. Kudo et al., J. Phys. Soc. Jpn. 72 (2003) 2551. [2] I. A. Zobkalo et al., Physica B 234-236 (1997) 734.

QF08

Magnetic susceptibility of the quasi one-dimensional spin system Sr₂V₃O₉

Takayuki Kawamata*, Masanori Uesaka, Mitsuhide Sato and Yoji Koike
Department of Applied Physics, Tohoku University, Japan

According to the magnetic susceptibility of polycrystalline samples of the quasi one-dimensional spin system Sr₂V₃O₉, this compound undergoes a weak ferromagnetic transition due to the Dzyaloshinsky-Moriya (DM) interaction at TN ~ 5K [1]. We have grown single crystals of Sr₂V₃O₉ [2] and measured the magnetic susceptibility along the [101] direction, χ[101], along the [10-1] direction, χ[10-1], and along the b-axis, χb. It has been found that temperature dependences of χ[101], χ[10-1] and χb show Bonner-Fisher-type behavior and that the anisotropy is very small at high temperatures above TN, indicating that Sr₂V₃O₉ is regarded as an isotropic one-dimensional Heisenberg spin system. At low temperatures below TN, however, both χ[10-1] and χb increase with decreasing temperature, while χ[101] decreases. This anisotropic behavior is consistent with the canted spin state proposed from the ESR measurements [3].

[1] E. E. Kaul et al., Phys. Rev. B 67 (2003) 174417. [2] M. Uesaka et al., J. Phys.: Conf. Ser. 20 (2010) 022068. [3] V. A. Ivanshin et al., Phys. Rev. B 68 (2003) 064404.

QF09

Magnetic property of a single crystal of spin-1/2 triple-chain magnet Cu₃(OH)₄SO₄

Yutaka Fujii^{1*}, Yuya Ishikawa², Hikomitsu Kikuchi², Yasuo Narumi³, Hiroyuki Nojiri³, Shigeo Hara⁴ and Hirohiko Sato⁴
¹ Research Center for Development of Far-Infrared Region, University of Fukui, Japan
² Department of Applied Physics, University of Fukui, Japan
³ Institute for Materials Research, Tohoku University, Japan
⁴ Department of Physics, Chuo University, Japan

A spin-1/2 triple-chain magnet Cu₃(OH)₄SO₄ (antlerite) is a candidate 'idle-spin' system in which magnetic moments on central spin chain seem to disappear, while the rest exhibit a long-range order below TN=5.5 K [1]. Our previous proton NMR study with a powder sample almost supported this scenario, although it was difficult to determine the spin structure [2]. Recently, successive phase transitions and anisotropy of phase diagram were found from the results of magnetization measurements with high-quality single crystals of Cu₃(OH)₄SO₄ [3]. In order to study phase transitions in the present compound in detail, we have performed specific heat measurements under magnetic fields up to 7 T and in the temperature range down to 2 K and proton NMR experiments at several frequencies with single crystals. We found at least three successive phase transitions at zero field around TN. Complicated phase diagrams involving changes of spin structures were suggested.

[1] S. Vilminot et al., J. Solid State Chem., 170, (2003) 255. [2] Y. Fujii et al., J. Phys.: Conf. Ser., 145, (2009) 012061. [3] S. Hara et al., J. Phys. Soc. Jpn., 80, (2011) 043701.

QF10

Thermal conductivity due to magnons in high-quality single crystals of the two-leg spin ladder system (Ca,Sr,La)_{1-x}Cu₂O₄₁

Koki Naruse*, Takayuki Kawamata¹, Mitsuhide Sato¹, Masumi Ohno¹, Kazutaka Kudo², Norio Kobayashi³ and Yoji Koike¹
¹ Department of Applied Physics, Tohoku University, Japan
² Department of Physics, Okayama University, Japan
³ Institute for Materials Research, Tohoku University, Japan

In order to enhance the thermal conductivity due to magnons, kmagnon, in the two-leg spin ladder system (Ca,Sr,La)_{1-x}Cu₂O₄₁, we have grown single crystals using high-purity raw materials, improved the quality of the single crystals by annealing in O₂ and measured the thermal conductivity along the spin ladders. In both Ca_{0.99}La_{0.01}Cu₂O₄₁ and Sr_{1-x}La_xCu₂O₄₁, the thermal conductivity shows a very large peak around 150K owing to the contribution of kmagnon along the spin ladders[1,2]. However, no enhancement of kmagnon has been observed in spite of the increase of the purity of the raw materials and the O₂-annealing. In Sr_{1-x}Cu₂O₄₁, on the other hand, a large enhancement of kmagnon has been observed through the O₂-annealing. These results indicate that the mean free path of magnons, l_{magnon}, has already limited by the disorder of the atomic arrangement due to the substitution of Ca and La for Sr in Ca_{0.99}La_{0.01}Cu₂O₄₁ and Sr_{1-x}La_xCu₂O₄₁, while l_{magnon} is enhanced owing to the decrease of spin defects through the O₂-annealing in non-substituted Sr_{1-x}Cu₂O₄₁. Accordingly, it is necessary for the enhancement of kmagnon to remove the disorder of the atomic arrangement in the spin ladders in (Ca,Sr,La)_{1-x}Cu₂O₄₁.

[1] K. Kudo, S. Ishikawa, T. Noji, T. adachi, Y. Koike, K. Maki, S. Tsuji, and K. Kumagai: J. Phys. Soc. Jpn. 70, 437 (2001). [2] C. Hess C. Baumann, U. Ammerahl, B. Buchner, F. Heidrich-Meisner, W. Brenig, and A. Revcolevschi: Phys. Rev. B 64, 184305 (2001).

QF11

Magnetic property of Ni²⁺ antiferromagnetic perfect triangle cluster

Emika Takata^{1,2*}, Minoru Sando¹, Katsutaka Kubo², Takayuki Asano², Akira Matsuo¹, Koichi Kindo³ and Masaki Oshikawa¹
¹ Institute for Solid State Physics, University of Tokyo, Japan
² Department of Physics, Kyushu University, Japan

The magnetic properties of spin systems with frustration have attracted much attention for a long time. The fundamental structure causing the frustration is "triangle". The magnetic properties of the antiferromagnetic perfect triangular cluster (APTC) with half-integer spins have been already studied well. [1] By contrast, there are little experimental data on the APTC with integer spins. Such an APTC is expected to possess a non-magnetic, singlet ground state. Recently, Liu et al. have investigated magnetic properties of S=1 APTC, [Ni₃(μ₃-N₃)₂(2,2'-bpy)₃](ClO₄)₃·3H₂O. It is believed as one of model materials for the S=1 APTC. [2] We synthesized it and measured the magnetization process (M(H)) and the temperature dependence of the magnetic susceptibility (χ(T)) of the material. We calculated M(H) and χ(T) in the simple ISOTROPIC S=1 APTC. However, the experimental results clearly cannot be accounted for by the calculated results. When the spin is greater than or equal to 1, generally a single ion anisotropy D can present. Thus we consider an anisotropic model Hamiltonian by including D. We will discuss the experimental data based on calculations using the new Hamiltonian with D.

[1] for example T. Yosida et al., J. Phys. Soc. Jpn. 57 (1988) 1428. [2]J.L. Liu et al., Aust. J. Chem. 63 (2010) 1111.

QF12

Thermal conductivity of anisotropic spin ladder

Hamed Rezania*
Razi university, Iran

We have studied the thermal conductivity of anisotropic spin ladder model with antiferromagnetic coupling constants between spins on the both rung and ladder directions. Kubo formalism has been applied to study temperature dependency of thermal conductivity of this model hamiltonian. The bond operator formalism is used to transform the spin model to a hard core bosonic gas. We have used the green's function approach to obtain the temperature dependence of spin excitation spectrum. We have found the temperature dependence of the thermal conductivity for various exchange coupling constants and anisotropies in both coupling strengths. We have obtained the increase of coupling constant along ladder direction leads to decrease of thermal conductivity. Furthermore the effect of local anisotropy anisotropy on the thermal conductivity has more significant in comparison with other one.

1)E. Dagotto and T. M. Rice, Science 271, 618 (1996) 2)A. Klumper and D. C. Johnston, Phys. Rev. Lett, 84, 4701 (2000) 3)A. V. Sologubenko and K. Gianno, H. R. Ott, U. Ammerahl and A. Revolevshchi, Phys. Rev. Lett, 84, 2714(2000) 4)X. Zotos, F. Naef, P. Prelovse, Phys. Rev. B, 55, 11029 (1997) 5)K. Louis, P. Prelovse and X. Zotos, Phys. Rev. B 74, 235118(2006)

QF13

The magnetic properties of the newly synthesized trinuclear copper complex

A. N. Ponomaryov^{1*}, K. Y. Choi¹, N. Kim², S. Yoon², B. J. Suh³ and Z. H. Jang⁴¹ Department of Physics, Chung-Ang University, Seoul, Korea² Department of Chemistry, Kookmin University, Seoul, Korea³ Department of Physics, The Catholic University of Korea, Bucheon, Korea⁴ Department of Physics, Kookmin University, Seoul, Korea

We present magnetic properties of a newly synthesized single molecule magnet (SMM) $\text{Cu}_3(\mu_3\text{-OMe})(\mu\text{-OMe})(\mu\text{-O}_2\text{CAr}^{\text{Rb}})_2(\text{O}_2\text{CAr}_2\text{F-Ph})_2(\text{HOME})_3$. In this compound, three copper ions with $s=1/2$, connected by one μ_3 -bridged methoxide, form a spin triangle, whereby two Cu^{2+} ions are 5 coordinated and the other Cu^{2+} ion is 4 coordinated. By means of SQUID magnetometer, temperature dependence of magnetic susceptibility $\chi(T)$ was measured in the range from 2 K to 300 K at the external field of 100 Oe and field dependence of magnetization $M(H)$ was measured at 2 K and 300 K in the range from 0 to 7 T. From an analysis of the magnetization data of the polycrystalline powder sample using ITO (Irreducible Tensor Operator) method, we obtain the antiferromagnetic exchange coupling constants of $J_1 = -143.65$ K, $J_2 = -143.78$ K, $J_3 = -143.61$ K and the g-factor of $g = 2.66$. A further analysis with a model Hamiltonian including anisotropic exchange interactions is on-going.

QF14

Magnetization process of S=1/2 diamond chain compound $\text{Na}_2\text{Cu}_2\text{Ge}_2\text{O}_{12}$ Minoru Sanda^{1*}, Keisuke Matsuura¹, Takayuki Asano¹, Junfeng Wang², Akira Matsuo², Koichi Kindo², Hiroki Morodomi², Yuji Inagaki² and Tatsuya Kawae³¹ Department of Physics, Kyushu University, Japan² Institute for Solid State Physics, University of Tokyo, Japan³ Department of Applied Physics, Kyushu University, Japan

Frustrated magnetism is one of the most fascinating systems because these systems have a great variety of quantum phenomena, and a lot of research activities are going on. Diamond chain in which spins exist on the Diamond-shaped lattice is one of examples of 1D-frustrated magnet. In this system, it is theoretically expected that not only the frustration but also low-dimensionality induces the quantum phenomena. Experimentally, $\text{Cu}_2(\text{CO}_3)_2(\text{OH})_2$ was reported as an S=1/2 Diamond chain compound, and its magnetic properties are studied actively [1]. Recently, Mo et al. reported the crystal structure of $\text{Na}_2\text{Cu}_2\text{Ge}_2\text{O}_{12}$, which has magnetic ions Cu^{2+} ($3d^9, S=1/2$) arranging in Diamond chain [2]. This compound has a short-range order at $T(\text{SLO}) \sim 10\text{K}$ and a long-range order at $T(\text{N})=2\text{K}$ by means of magnetic susceptibility and heat capacity measurements [2][3]. We performed high field magnetization measurement using pulse magnetic field up to 55T at $T(\text{N}) < T < T(\text{SLO})$. The magnetization curve increase convex downward up to one-third of saturation value, and clearly exhibit a plateau behavior with increasing magnetic field more than 30T. The convex downward curve indicates the components of S=1/2 1D antiferromagnetic phenomena with a spin reduction. More detailed results will be discussed in the conference.

[1] H. Kikuchi et al., Phys. Rev. Lett. 94 (2005) 227201. [2] X. Mo et al. : Inorg. Chem. 45 (2006) 3478. [3] M. Sato et al. : Solid State Science (2009) 1.

QF15

Quantum criticality in a frustrated ising chain columbite

Kazuhiro Igarashi, Yasuhiro Shimizu* and Masayuki Itoh

Nagoya University, Japan

A ferromagnetic Ising model in transverse magnetic field is a textbook example of the quantum phase transition. Nevertheless, few experiments have been accessible to the quantum criticality. CoNb_2O_6 with a triangular lattice of ferromagnetic Ising chains is the highlight compound that has been recently found to exhibit the emergent symmetry in the excitation spectrum. Here we present the NMR observation of the low-energy quantum critical behavior in CoNb_2O_6 . We find that the dynamical critical exponent toward the quantum critical point exhibits close to that of quantum antiferromagnets. Namely, the nuclear spin-lattice relaxation rate is independent of temperature at the critical transverse magnetic field of 5.4 T. The strong field dependence is manifested only in the dynamical susceptibility, whereas the uniform part is almost independent of magnetic field. Our results can be served as the ideal Ising spin dynamics on the quantum phase transition.

QF16

Ligand-driven geometric and electronic structures of FeII spin-crossover molecules

Van Thanh Nguyen and Anh Tuan Nguyen*

Faculty of Physics, Hanoi University of Science, Viet Nam

Transition-metal complexes that exhibit spin-crossover (SCO) between low-spin (LS) state and high-spin (HS) state are now potential candidates for many applications such as display and memory devices. In these applications, thermal hysteresis in SCO of transition-metal complexes is required. Our previous study demonstrated that there is a correlation between thermal hysteresis in SCO and the electrostatic-energy difference (ΔU) of transition-metal complexes [1]. In this work, in order to explore more about the role of ligands in tailoring SCO behavior of transition-metal complexes, we study SCO of a series of FeII molecules with different ligand configurations [2-4]. Our results showed that the ΔU of transition-metal complexes can be determined by pKa constant of ligands. These results should be helpful for designing new SCO complexes.

[1] Nguyen Anh Tuan, Geometric Structure, Electronic Structure and Spin Transition of Several FeII Spin-crossover Molecules, to be published on Journal of Applied Physics, 111, No. 7, (2012), DOI: 10.1063/1.3670044. [2] Birgit Weber, et al., Eur. J. Inorg. Chem. No. 10, 1589 (2008). [3] Birgit Weber, et al., Eur. J. Inorg. Chem. No. 31, 4891 (2008). [4] Birgit Weber, et al., Eur. J. Inorg. Chem. No. 21, 3193 (2011).

QF17

Magnetic properties of S=1/2 zigzag antiferromagnetic chain compounds, $\text{VO}(\text{XO}_4)(2,2'\text{-bpy})$ (X=S, Mo; bpy = bipyridine)Akira Matsuo^{1*}, Yuya Ishikawa², Yutaka Fujii³, Hikomistu Kikuchi² and Koichi Kindo¹¹ The Institute for Solid State Physics, The University of Tokyo, Japan² Department of Applied Physics, University of Fukui, Japan³ Research Center for Development of Far-Infrared Region, University of Fukui, Japan

One dimensional Heisenberg antiferromagnets (1D HAF) with the nearest J1 and second-nearest J2 interactions (zigzag chain) are the simplest frustrated magnets. We measured magnetic susceptibility, specific heat and high field magnetization up to about 60 T of $\text{VO}(\text{XO}_4)(2,2'\text{-bpy})$ (X=S, Mo; bpy = bipyridine), model compounds of the zigzag chain. V^{4+} ions carry S = 1/2 in these compounds. No magnetic long range order is observed in both compounds, assuring low dimensionality of the present compounds. The exchange interactions are determined by comparing the experimental data with calculated results based on the exact diagonalization to the finite spin chain up to N=12. For $\text{VO}(\text{SO}_4)(2,2'\text{-bpy})$, data agree well with the theoretical curve for the simple 1D HAF, thus J2 is found to be zero. On the other hand, for $\text{VO}(\text{MoO}_4)(2,2'\text{-bpy})$, a ratio of J2 to J1 is estimated to be 0.2-0.3.

QF18

Inter-chain coupling and anisotropy in the frustrated chain cuprate Li_2CuO_2 W. E. A. Lorenz^{1*}, S.-I. Drechsler², R. O. Kuzian³, S. Petit⁴, Y. Skourki⁵, R. Klingeler⁶ and B. Buchner²¹ Neutron Scattering and Magnetism Group, Laboratory for Solid State Physics, ETH Zurich, Switzerland² Leibniz Institute for Solid State and Materials Research Dresden, Germany³ Institute for Problems of Materials Science, Kiev, Ukraine⁴ Laboratoire Leon Brillouin, Saclay, France⁵ Dresden High Magnetic Field Laboratory, FZ-Dresden-Rossendorf, Dresden, Germany⁶ Kirchhoff Institute for Physics, University of Heidelberg, Germany

Frustrated spin-chains with nearest neighbor ferromagnetic and next-nearest neighbor antiferromagnetic interactions have recently attracted lots of interest. In this class of materials, Li_2CuO_2 represents a reference system with a particularly simple structure. Here we present a detailed experimental study of this quasi-one-dimensional magnet with focus on the properties at low temperature where long range order sets in due to the present inter-chain interactions. We discuss the magnetic phase diagram as obtained from magnetization, specific heat and lattice expansion measurements. Using inelastic neutron scattering we have further examined the magnetic excitations throughout a vast part of the Brillouin zone and in great detail, revealing an exceptional spectrum. In conclusion, we demonstrate that the low temperature dynamics of this S=1/2 chain material is well described within spin-wave theory and that the observed ground state is largely due to the exchange anisotropy.

QF19

Spectral signatures of magnetic Bloch oscillations in 1D ferromagnets

Sergey Shinkevich and Olav F. Syljuasen

Department of Physics, University of Oslo, Norway

Domain walls in a one-dimensional gapped easy-axis ferromagnet can exhibit Bloch oscillations in an applied magnetic field. We investigate how exchange couplings modify this behavior within an approximation based on non-interacting domain-wall bound states. In particular we obtain analytical results for the spectrum and the dynamic structure factor, and show where in momentum space to expect equidistant energy levels, the Wannier-Zeeman ladder, which is the spectral signature of magnetic Bloch oscillations. We compare our results to previous calculations employing a single domain-wall-approximation, and make predictions relevant for the material cobalt chloride dihydrate ($\text{CoCl}_2 \cdot 2\text{H}_2\text{O}$).

1) Jordan Kyriakidis and Daniel Loss, Phys. Rev. B 58, 5568 (1998). 2) W. Montfrooij, G. E. Granroth, D. G. Mandrus, and S. E. Nagler, Phys. Rev. B 64, 134426 (2001). 3) N.B. Christensen, K. Lefmann, I. Johansen, and O. Jørgensen, Physica B 276, 784 (2000).

QF20

Quasi-one-dimensional magnetic phase as a competing ground state in a frustrated magnet

Krunoslav Prsa¹, Mark Laver², Martin Mansson¹, Ivica Zivkovic³, Peter Derlet⁴, Sebastian Guerrero⁴, Christopher Mudry⁵, Oksana Zaharko⁶, Sang-wook Cheong⁶, Hee-taek Yi⁷, Jorge Gavilano⁸, Joachim Kohlbrecher⁹, Michel Kenzelmann⁹ and Joel Mesot⁹¹ Laboratory for Solid State Physics, ETH Zurich, Switzerland² Laboratory for Neutron Scattering, Paul Scherrer Institute, Switzerland³ Institute of Physics, Croatia⁴ Condensed Matter Theory, Paul Scherrer Institute, Switzerland⁵ Department of Physics and Astronomy, Rutgers University, USA⁶ Laboratory for Developments and Methods, Paul Scherrer Institute, Switzerland

Low-dimensional physics is interesting because it is driven by fluctuations and it may result in exotic phenomena, like the fractionalization of quantum numbers and spinons in magnetic chains. In magnetic systems, the reduction of dimensionality occurs due to anisotropic short-ranged interactions. Generally, transition metal oxides order at low temperatures. Here, in geometrically frustrated $\text{Ca}_2\text{Co}_2\text{O}_6$, we show that by geometric frustration a stable quasi-one-dimensional (Q1D) magnetic phase emerges from a competition of degenerate ground states. This phase coexists and competes with the 3D antiferromagnetism in a large range below the 3D ordering temperature. We show that (i) constituent entities of this Q1D phase are shaped as rods in real space with alternating up and down magnetized sections ($d=15\text{\AA}$, $l=320\text{\AA}$ at 15 K) along the chain axis where (ii) the sections belong to a degenerate ferromagnetic class of ground states, (iii) these magnetic rods are arranged randomly in the frustrated triangular plane, (iv) they occupy a significant volume fraction (estimated 25% of moments at 15K) and (v) they are correlated with the magnetic response of this material. These results provide a new general possibility of a frustration-stabilized one-dimensional phase in physics.

QF21

Crossover of magnetic relaxation from 2D-spin ice like state to ordered state in layered single molecular magnet networks

Yuta Kodama¹, Rikako Ishii², Chihiro Kachi-terajima², Hitoshi Miyasaka³, Daisuke Akahoshi¹ and Toshiaki Saito^{1*}¹ Dept. of Phys., Fac. of Sci., Toho Univ., Funabashi, Chiba 274-8510, Japan² Dept. of Chem., Fac. of Sci., Toho Univ., Funabashi, Chiba 274-8510, Japan³ Dept. of Chem., Div. of Mat. Sci., Grad. Sch. of Nat. Sci. and Tech., Kanazawa Univ., Ishikawa 920-1192, Japan

Layered 2D single molecular magnet (SMM) network $[\text{Mn}(\text{saltmen})_4[\text{M}(\text{CN})_6]\text{ClO}_4 \cdot n\text{H}_2\text{O}$ (M=Mn, Fe[1]) is a strongly frustrated system. The each SMM unit $[\text{M}(\text{CN})_6]$ ($ST=4$) is ferromagnetically connected through the $[\text{M}(\text{CN})_6]$ unit ($S=1$ for Mn, and $S=1/2$ for Fe) within a layer. The origin of the frustration [2] is a competition between the orthogonally oriented two uniaxial axes of the SMM unit and the ferromagnetic interaction, leading to a macroscopically degenerated ground state as the pyrochlore 3D-spin ice. Our previous work [2] for M=Mn showed no transition down to 2 K through the Weiss temperature $\Theta=8.3$ K and Davidson-Cole (DC) type magnetic relaxation as 3D-spin ice [3]. However, for M=Fe, a distinct anomaly of relaxation time is observed at 2.6 K ($\Theta=7.5$ K), and the relaxation is the Cole-Cole (CC) type, suggesting a magnetic order. In this work, we measured ac susceptibility of $M = \text{Mn}1-x\text{Fe}$ ($x=0 \sim 1.0$). We found that the relaxation is not the DC type for $x=0.1$, and changes into CC type for $x > 0.3$ accompanying the distinct anomaly of relaxation time. The results suggest that 2D-spin ice-like state is ordered into a randomly frozen state above $x \sim 0.1$.

[1] H. Miyasaka et al., J. Am. Chem. Soc. 118 (1996) 981. [2] T. Saito et al. (2012), in preparation (partly presented in ICM 2009). [3] K. Matsuhira et al., J. Phys. Condens. Matter 13 (2001) L737.

QF22

Magnetic properties of the novel low-dimensional spin-1/2 magnet $\alpha\text{-Cu}_2\text{As}_2\text{O}_7$ V. Kataev^{1*}, Y. C. Arango¹, E. Vavilova², M. Abdel-Hafiez³, O. Janson⁴, A. Tsirlin⁵, H. Rosner⁶, S.-I. Drechsler⁷, M. Weil⁸, G. Nener⁹, R. Klingeler⁹, O. Volkova⁹, A. Vasiliev⁹ and B. Buechner⁹¹ Leibniz Institute for Solid State and Materials Research IFW Dresden, Germany² Zavoisky Physical Technical Institute of the Russian Academy of Sciences, 420029, Kazan, Russia³ Max Planck Institute for Chemical Physics of Solids, D-01187 Dresden, Germany⁴ Institute for Chemical Technologies and Analytics, Vienna University of Technology, A-1060 Vienna, Austria⁵ Institut Laue-Langevin, Boite Postale 156, 38042 Grenoble Cedex 9, France⁶ Kirchhoff Institute for Physics, University of Heidelberg, D-69120 Heidelberg, Germany⁷ Low Temperature Physics Department, Moscow State University, Moscow 119991, Russia

In copper pyroarsenate $\alpha\text{-Cu}_2\text{As}_2\text{O}_7$, the quantum spins $S = 1/2$ localised at the Cu sites in the structurally well defined dimer chains interact predominantly in one spatial dimension (one-dimensional spin systems). Magnetic properties of this new material have been thoroughly investigated by means of magnetization, heat capacity, electron spin resonance, and nuclear magnetic resonance techniques, as well as by density functional theory (DFT) calculations and quantum Monte Carlo (QMC) simulations. The data reveal that the magnetic Cu-O chains in the crystal structure represent a realization of a quasi-one-dimensional (1-D) coupled alternating spin-1/2 Heisenberg chain model with relevant pathways through nonmagnetic AsO4 tetrahedra. Owing to residual 3-D interactions, antiferromagnetic long range ordering at $T_N \sim 10$ K takes place. The experimental data suggest that substantial quantum spin fluctuations take place at low magnetic fields in the ordered state. DFT calculations and QMC fits enable quantitative evaluation of the exchange couplings. We conclude that the electronic state of the central ion in the nonmagnetic AsO₄ side groups plays a crucial role for determining the relevant interchain pathways which makes $\alpha\text{-Cu}_2\text{As}_2\text{O}_7$ distinct in its magnetic properties from other representatives of this class of compounds [1].

[1] Y.C. Arango, E. Vavilova, M. Abdel-Hafiez et al., Phys. Rev. B 84, 134430 (2011)

QF23

Low temperature magnetic properties of the dilutable frustrated spin-ladder $\text{Bi}(\text{Cu}_{1-x}\text{Zn}_x)_2\text{PO}_8$ Shuang Wang¹, Krunoslav Prsa², Neda Niksereshi², Christian Ruegg³, E. Pomjakushina⁴, Kazimierz Conder⁴ and Henrik M Ronnow⁴¹ Laboratory for Quantum Magnetism/Laboratory for Developments and Methods, Ecole Polytechnique Federale de Lausanne, 1015 Lausanne Paul Scherrer Institut, 5232 Villigen, Switzerland² Laboratory for Quantum Magnetism, Ecole Polytechnique Federale de Lausanne, 1015 Lausanne, Switzerland³ Laboratory for Neutron Scattering, Paul Scherrer Institut, 5232 Villigen, Switzerland⁴ Laboratory for Developments and Methods, Paul Scherrer Institut, 5232 Villigen, Switzerland

Quantum antiferromagnets with a spin-ladder magnetic network show an energy gap in the spin excitation spectrum and may possess an intrinsically disordered (spin liquid) ground state. BiCu_2PO_8 (BCPO) shows a structure where Cu^{2+} magnetic ions ($S=1/2$) form two-leg zigzag ladders along the b-axis, which closely corresponds to theoretical quasi-1D AF spin ladder model. We can reveal quantum nature of low temperature behavior by studying the effect of non-magnetic impurities (e.g. Zn^{2+} , Ni^{2+}) introduced at magnetic Cu-sites. Recently, single crystals of $\text{Bi}(\text{Cu}_{1-x}\text{Zn}_x)_2\text{PO}_8$ ($0 \leq x \leq 0.05$) were successfully synthesized and studied by NMR for the first time [1,2]. We present here the specific heat C_p (H,T), ac susceptibility (f ,T) and dc magnetization M (H,T) on single crystal sample of the undoped BCPO and 5% Zn-doped BCPO ($\text{Zn}005\text{BCPO}$) with field applied along main crystallographic axes focusing on low temperatures $T < 10$ K. We argue that the ground state of the Zn doped compound ($\text{Zn}005\text{BCPO}$) has features of both spin-glass and long range magnetic order, and that glassiness is lost under application of higher magnetic fields. We show the H-T magnetic phase diagram.

[1] S. Wang, E. Pomjakushina, T. Shiroka, G. Deng, N. Niksereshi, Ch. Ruegg, H.M. Ronnow, and K. Conder, J.Crystal.Growth 313, 51-55 (2010) [2] F. Casola, T. Shiroka, S. Wang, K. Conder, E. Pomjakushina, J. Mesot and H.-R. Ott, Phys. Rev. Lett. 105, 067203 (2010)

QF24

51V-NMR study of the quasi-one-dimensional antiferromagnet $\text{BaCo}_2\text{V}_2\text{O}_8$ Yukiichi Ideta¹, Yu Kawasaki¹, Yutaka Kishimoto¹, Takashi Ohno¹, Yoshitaka Michihiro¹, Zhangzhen He², Yutaka Ueda³ and Mitsuru Itoh⁴¹ Institute of Technology and Science, The University of Tokushima, Japan² Fujian Institute of Research on the Structure of Matter, Chinese Academy of Sciences, China³ Institute for Solid State Physics, University of Tokyo, Japan⁴ Materials and Structures Laboratory, Tokyo Institute of Technology, Japan

The double rectangle-like powder pattern has been observed in the 51V-NMR spectrum for the quasi-one dimensional antiferromagnet $\text{BaCo}_2\text{V}_2\text{O}_8$ below $T_N = 5.4$ K. The powder pattern indicates the existence of two V sites with different internal field, 2.1 and 3.8 kOe, although V atoms occupy only one magnetically symmetric site where the scalar type transferred field from the surrounding Co^{2+} magnetic moments is zero. The internal field at V site is explained by taking into account of the classical and the pseudo-dipolar fields from Co^{2+} magnetic moments. In the paramagnetic state, the nuclear spin-lattice relaxation is dominated by the antiferromagnetic spin fluctuation via the dipolar field, which is proved by the linear relation between the nuclear spin-lattice relaxation rate divided by temperature $1/T1T$ and the magnetic susceptibility. The change in the slope of $1/T1T$ against the magnetic susceptibility around 150 K suggests the change in the antiferromagnetic spin fluctuation spectrum. Below 60 K, $1/T1$ shows the thermal activation-type temperature dependence signaling the formation of spin gap.

QF25

Magnetic properties of one-dimensional chain of O₂ confined in nanopores of MFI-zeolite

Akihiro Hori¹, Kanako Kuwana², Tatsuo C Kobayashi², Yasushi Wanikawa³, Yoshiki Kubota³, Kenichi Kato¹, Masaki Takata¹, Ryotaro Matsuda⁴ and Susumu Kitagawa¹

¹RIKEN SPring-8 Center, Japan

²Okayama University, Japan

³Osaka Prefecture University, Japan

⁴Exploratory Research for Advanced Technology (ERATO), Japan

We have studied the molecular arrangement and the magnetic properties in O₂ adsorbed in nanoporous compounds [1-3]. We found that the O₂ adsorbed in MFI zeolite form a one-dimensional chain. The O₂ adsorption isotherm shows a plateau and the step, indicating a phase transition. It is found by means of the x-ray diffraction measurements that the zeolite deforms from monoclinic to orthorhombic corresponding to the step of adsorption isotherm. In the low-adsorption case, the adsorbed O₂ aligns linearly in the straight and sinusoidal channels in MFI zeolite. In the high-field magnetization measurements, the magnetization process does not show the linear field dependence characteristic to one-dimensional Heisenberg antiferromagnet and presents the metamagnetic transition similar to the case of O₂-O₂ dimer reported previously [1, 2]. This result may suggest that the singlet ground state is realized at low fields and the field-induced orientational change of molecular axis occurs. In the high-adsorption case, the adsorbed O₂ seems to align in rows of two. The temperature dependence of susceptibility shows the first-order transition with large hysteresis. By XRD measurement, the structural phase transition from orthorhombic to monoclinic with decreasing temperature was found, which is not observed in N₂ adsorbed compound.

[1] T. C. Kobayashi et al., Prog. Theor. Phys. Suppl. 159 (2005) 271. [2] A. Hori et al., J. Phys. 200 (2010) 0022018. [3] A. Hori et al., J. Low. Temp. Phys. 159 (2010) 122.

QF26

Quantum spin transport in a Heisenberg spin chain

Nan-hong Kuo¹, Sujit Sarkar² and Chong Der Hu^{1*}

¹ Physics, National Taiwan University, Taiwan

² PoornaPragna Institute of Scientific Research, India



QG01

Magnetic transition of plastic deformed Si-doped Ni₃Mn alloy

Kowan-young Ko^{1*}, Sung-won Ko² and John Graham Booth³

¹ Faculty of mechanical engineering, Ulsan College University, Korea

² Department of biological science, Sungkyunkwan University, Korea

³ School of computing, science and engineering, Salford University, United Kingdom

Structural and magnetic properties of plastic deformed Si-doped Ni₃Mn alloy were studied and compared with those of undeformed specimen investigated by powder neutron diffraction and diffuse purely magnetic scattering measurements in which coexistences of ferromagnetic and antiferromagnetic interactions were still existing even far above Neel temperature. Two specimens showed spin glass properties and disordered face-centered cubic structure but lattice parameters were a little different value of 3.5961 Å and 3.5890 Å. Magnetic properties showed very different Neel temperatures of 87.5 K and 62.5 K respectively. The paramagnetic Curie temperature appeared by -325 K and 125 K and therefore effective magnetic moments were calculated by 3.51 μB and 0.41 μB respectively. The reasons for different magnetic transition could be introduced by the elongation of ferromagnetic clusters and change of atomic environments effect after plastic deformation. This report shows two kinds of magnetic properties by plastic deformation.

QG02

Incommensurate-commensurate phase transition in TbNi₅ induced by external magnetic field

Elena Sherstobitova^{1*}, Alexander Pirogov¹, Vadim Sikolenko², Savva Bogdanov¹ and Roland Schedler³

¹ Institute of Metal Physics of UD of RAS, Russia

² Joint Institute for Nuclear Research, Dubna, Russia

³ Hahn-Meiner Institute, Berlin, Germany

The rare earth intermetallic RNi₅ compounds are attractive subjects for the study of the exchange and crystal field interactions due to their simple crystal and magnetic structures. The magnetic ordering in TbNi₅ compound has been interpreted in terms of FAN-like incommensurate structure at temperatures between 23 K and 10 K. On cooling sample down to T = 10 K order-order type magnetic phase transition from the incommensurate phase to a “lock-in” phase takes place. In the present work we report the results of neutron diffraction experiment on TbNi₅ single crystal sample in external magnetic field up to μ₀H = 1T. Abrupt change of the intensity of (001) Bragg peak and satellites (001)± occurs within temperature interval 7 K -10 K due to magnetic phase transition from the incommensurate phase to a “lock-in” phase. It has been found that the application of external magnetic field up to μ₀H = 0.1T at the temperature T = 11K along [100]-axis of TbNi₅ single crystal recovers zero-field low temperature 'lock-in' magnetic structure. The external magnetic field increase up to μ₀H = 0.4T leads to transformation of the modulated magnetic structure to a ferromagnetic structure.

QG03

First-principles dynamical CPA study of ferro- and antiferromagnetism of transition metals

Yoshiro Kakehashi* and Sumal Chandra

Department of Physics, University of the Ryukyus, Japan

Quantitative explanation of the finite-temperature properties of 3d transition metals and alloys has been a long standing problem in metallic magnetism because their Coulomb interactions are comparable to the band widths and simple perturbation approach is not applicable to such systems. We present here the first-principles dynamical CPA combined with the LDA+U Hamiltonian toward quantitative calculations of magnetic properties at finite temperatures and explain quantitatively or semi-quantitatively the finite-temperature magnetism of 3d transition metals from V to Ni. We obtained the Curie-Weiss spin susceptibility with meff=1.8 muB (Expt. 2.1 muB) in V, the Pauli paramagnetic susceptibility in Cr being in agreement with the experimental data, as well as the Curie-Weiss susceptibilities in Fe, Co, and Ni whose meff quantitatively agree with the experimental data (3.2, 3.2, and 1.6 muB). Calculated ground-state magnetizations are 2.58, 1.72, and 0.64 muB for Fe, Co, and Ni, being in good agreement with the experimental data (2.2, 1.74, and 0.62 muB). On the other hand we obtained the Curie temperatures 1900K, 2100K, and 620K for Fe, Co, and Ni which are somewhat overestimated because of the single-site approximation. We also clarify the systematic change of the single-particle DOS in these systems.

QG04

High-coercive metastable ferromagnetic state induced in the Ising antiferromagnet Fe_{0.5}TiS₂

Nikolay Baranov^{1*}, Elizaveta Sherokalova², Alexey Volegov², Alexey Proshkin³, Nadezhda Selezneva², Andrey Gubkin⁴ and Ekaterina Proskurina²

¹ Micromagnetic laboratory, Institute of Metal Physics, Russia

² Institute of Natural Sciences, Ural Federal University, Russia

³ Laboratory of ferromagnetic alloys, Institute of Metal Physics, Russia

⁴ Laboratory of neutron studies of matter, Institute of Metal Physics, Russia

The transition metal (T) dichalcogenides TX₂ (X = S, Se, Te) with a layer crystal structure being intercalated with 3d-transition (M) metals demonstrate different magnetic states depending on the type and concentration of M-atoms as well as on the parent TX₂ matrix [1]. In the present work, the magnetic susceptibility, magnetization, electrical resistivity, magnetoresistance and powder neutron diffraction measurements have been performed for the Fe intercalated compound Fe_{0.5}TiS₂. It has been shown that this compound exhibits an antiferromagnetic (AF) ground state below the Neel temperature TN = 140 K. Application of the magnetic field at T < TN induces a metamagnetic phase transition to the ferromagnetic (F) state, which is accompanied by the large magnetoresistance effect (~ -27 %). The field-induced AF-F transition is found to be irreversible below 100 K. At low temperatures, the magnetization reversal in the metastable F state is accompanied by substantial hysteresis (up to 100 kOe) which is associated with the Ising character of Fe ions. This work was supported by the RFBR (project 12-02-00778) and by the program of the Ural Branch of RAS (project № 12-T-1012).

[1] Baranov N. V. et al. J. Phys. Condens. Matter. 17 (2005) 5255

QG05

Magnetic and thermoelectric properties of the solid solutions Mn_{1-x}Ni_xS

Sergey Aplesnin¹, Oksana Romanova¹, Ludmila Ryabinkina¹, Olga Demidenko², Anatoly Galyas² and Kazimir Yanushkevich²

¹ L.V. Kirensky Institute of Physics, Russia

² Scientific-Practical Materials Research Centre NAS of Belarus, Belarus

In connection with intensive development of a microelectronics and spintronics, interest of researchers to the magnetic semiconductor materials showing magnetoresistivity effect and metal-insulator transition has increased. New sulphide solid solutions Mn_{1-x}Ni_xS (0<X<0.1) are synthesized. The structural, magnetic and thermoelectric properties of the obtained materials have been studied at the temperatures 77-1000 K in magnetic fields up to 10 kOe. The X-ray diffraction analysis has shown that the samples synthesized Mn_{1-x}Ni_xS have a NaCl-type FCC lattice and are observed four reflexes of a weak intensity, associated with γ - modifications of MnS. Solid solutions Mn_{1-x}Ni_xS are antiferromagnetic with the Neel temperature (TN = 180 K for X=0,05 and TN= 200 K for X=0,1). The temperature dependence of magnetization is described by the Curie-Weiss law at T> TN. The effective magnetic moment are found to be μ_{eff}. f=5,04 μB for X=0,05 and μ_{eff}.f=5,16 μB for X=0,1. Change in the conductivity type from the hole to the electronic at X=0,05 is revealed on the basis of measurements of thermoelectric power.

QG06

Field induced anisotropy in NiMn and NiMnPt alloys

Yildirhan Oner

Department of Physics, Istanbul Technical University, Dept. of Physics, 34469, Istanbul, Turkey

We report the detailed characterization of the magnetic properties of polycrystalline disks of Ni_{1-x}Mn_x and Ni_{1-x}Mn_xPt_x (x=1.0, 4.0, and 10.0) at 4.2 K induced by field cooling (FC). It is found that the FC-induced anisotropy field ,HK and coercivity , HC are strongly enhanced by the addition of nonmagnetic Pt impurities. The remanent magnetization in the direction of the initial applied field (in the disk plane) for each samples can be rotated from 0° to 1800 and back to 0° in various stationary fields above and below HK and the parallel component of the rotated remanents are measured. From the analysis of the angular dependence of ML, we show that these results can be accounted for by the coexistence of Mn(Ni)-rich and /or Mn(Ni)-deficient nano scale regions coupled antiferromagnetically. It is found that the unidirectional anisotropy originates from interfacial exchange interactions between these regions. Up to some critical angle rotation (Θ C) relative to H, the unidirectional anisotropy field turns rigidly with the sample, while above Θ C, the coupled regions become unstable and magnetically rearrange such that a unidirectional anisotropy is induced along H .

QG07

X-ray-absorption near-edge structure and X-ray magnetic circular dichroism studies of a Lu₂Fe₁₆Ru_{0.5} single crystal

E. A. Tereshina¹, A. Smekhova², O. Isnard³, A. V. Andreev⁴ and A. Rogalev⁵

¹ Institute of Physics, Academy of Sciences, 18221 Prague, Czech Republic

² Faculty of Physics, Moscow State University, 119991 Moscow, Russia

³ Université Joseph Fourier/Institut Neel (CNRS), 38042 Grenoble Cedex, France

⁴ Institute of Physics, Academy of Sciences, Czech Republic

⁵ European Synchrotron Radiation Facility (ESRF), 38043 Grenoble Cedex, France

The magnetism of R₂Fe₁₇ with the smallest rare-earth R=Lu (hexagonal Th₂Ni₁₇ structure type) is essentially associated with its Fe sublattice behavior. Strong contribution of the local antiferromagnetic (AF) Fe-Fe interactions in the overall ferromagnetic (F) exchange considerably lowers the ordering temperature (TN=274 K) and balances the non-collinear antiferromagnetic phase above the Curie temperature TC=130 K. Generally, various doping elements (M) in Lu₂Fe_{17-x}M_x suppress fully the AF states by strengthening the ferromagnetic ones accompanied by a dramatic TC increase. However, recently a unique case of antiferromagnetism stabilization in the whole range of magnetic ordering in Lu₂Fe_{17-x}Ru_x was reported [1], and this work is dealing with the local studies of intrinsic magnetic properties of Lu₂Fe_{16.8}Ru_{0.5}. A single-crystalline sample of Lu₂Fe_{16.8}Ru_{0.5} has been investigated by X-ray-absorption (XANES) and X-ray magnetic circular dichroism (XMCD) techniques in the applied magnetic field up to ±3 T at 7 K. By probing the lutetium L2,3-, iron K- and ruthenium L2 absorption edges, information on magnetic states of the constituents of Lu₂Fe_{16.8}Ru_{0.5} is obtained. Small but noticeable induced magnetic moments with an antiparallel orientation to Fe moments have been registered on Lu and Ru sites.

[1] E.A. Tereshina et al., J. Appl. Phys. 105 (2009) Art. No. 07A747.

QG08

Study of the metamagnetic behavior of Ni-Co-Mn-Sb alloy in high magnetic fields

Rie Y Umetsu^{1*}, Xiao Xu², Wataru Ito³, Takumi Kihara⁴, Masashi Tokunaga⁴, Kohki Takahashi¹ and Ryosuke Kainuma²

¹ Institute for Materials Research, Tohoku University, Japan

² Department of Materials Science, Graduate School of Engineering, Tohoku University, Japan

³ Department of Materials and Environmental Engineering, Sendai National College of Technology, Japan

⁴ International MegaGauss Science Laboratory, Institute for Solid State Physics, The University of Tokyo, Japan

In order to investigate metamagnetic behavior and temperature dependence of equilibrium magnetic field of the martensitic transformation for Ni-Co-Mn-Sb, magnetization experiments up to 18 T static magnetic field and up to 40 T pulsed magnetic field were performed. Polycrystalline specimen of Ni₄Co₃Mn₃₉Sb₇₁ was prepared by induction melting, and annealed at 1173 K for 1 day. Transformation temperatures, TM, and entropy change, ΔS, between the martensite phase and parent phase were examined with DSC. Magnetic measurements were performed with using a SQUID magnetometer up to 5 T, by extracting method up to 18 T static magnetic fields, and also by induction method up to 40 T pulsed magnetic fields. In the thermomagnetization curves, it was observed that TM decreased with increasing the applying magnetic field, H, with a rate of dTM/dH = 3.8 K/T. An estimated value of ΔS from the Clausius-Clapeyron relation, is about 15.8 J/K-kg, being in good agreement with the value obtained by the DSC. For the isothermal magnetization curves, metamagnetic behavior associated with the magnetic field induced martensitic reverse transformation was observed. Arresting behavior of the martensitic transformation was confirmed in lower temperature, as similar to the Ni(Co)-Mn-Z (Z = In, Sn, Ga) alloys.

QG09

Magnetic Transition and Thermal Expansion in LaFe_{13-x-y}Co_xSi_y

Jianli Wang¹, Stewart James Campbell^{2*}, Shane J Kennedy³, Precious Shamba⁴, Rong Zeng⁴, Shixue Dou⁴ and Guang Heng Wu⁵

¹ Institute for Superconductivity & Electronic Materials, The university of Wollongong, Australia

² School of PEEMS, The University of New South Wales, Canberra, Australia

³ Bragg Institute, ANSTO, Australia

⁴ Institute for Superconductivity and Electronic Materials, The University of Wollongong, Australia

⁵ National Laboratory for Condensed Matter Physics, Institute of Physics., Chinese Academy of Sciences, China

Materials with a large magnetocaloric effect (MCE) continue to attract significant attention for cooling applications with particular interest in the isothermal transition changes at first-order magnetic transitions [1]. The large entropy change in LaFe_{13-x}Si_y is associated with negative lattice expansion and metamagnetic transition behaviour [2]. We have investigated LaFe_{13-x-y}Co_xSi_y to clarify the influence of magneto-structural coupling on the MCE. The Curie temperatures of LaFe_{13-x-y}Si_y increase with Si content from TC=219 K for x=1.6 to TC=250 K for x=2.6 with further enhancement to TC=281 K on substitution of Co to LaFe_{10.4}CoSi_{2.6}. A pronounced positive spontaneous volume magnetostriction has been observed below TC and the anomalous thermal expansion attributed to the volume dependence of the magnetic energy. Our results show that the magnetic transition changes from first order for LaFe_{11.8}Si_{1.6} to second order for LaFe_{10.8}Si_{2.6} and LaFe_{9.4}CoSi_{2.6}. The different natures of the magnetic transitions in LaFe_{13-x-y}Co_xSi_y have been discussed in terms of the classical model for itinerant ferromagnets and the volume dependence of the magnetic energy.

[1] KA Gschneidner, Jr., VK Pecharsky and AO Tsoko, Rep. Prog. Phys. 68, 1479 (2005) [2] FX Hu, BG Shen, JR Sun, ZH Cheng, GH Rao, X Zhang, Appl. Phys. Lett. 78, 3675 (2001)

QG10

The magnetovolume effect of Y₂Fe_{17-x}Ga_x

Daiki Haruna and Tatsuo Kamimori

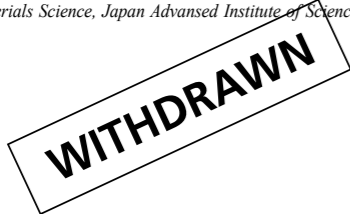
Ehime University, Japan

The unit cell volume and the Curie temperature of Y₂Fe₁₇ increases by substitution of Ga for Fe. This phenomenon is understood as a property of Invar materials, dTc/dV > 0, because the compounds R₂Fe₁₇ have Invar properties. However, in the substitution of Si for Fe, dTc/dV is negative. Kamimori et. al. proposed damping of the Invar properties by these substitutions. In this work, the magnetovolume effect of Y₂Fe_{17-x}Ga_x was investigated by measuring temperature dependence of unit cell volume and forced volume magnetostriction. X-ray diffraction was used to measure unit cell volume at under R.T. and thermal expansion meter at above R.T.. The forced volume magnetostriction was measured by three terminals capacitance method under magnetic field up to 1.5T. The forced volume magnetostriction at R.T. is positive. This shows Y₂Fe_{17-x}Ga_x compounds have Invar property. However, the magnitude of the forced volume magnetostriction decreases violently by the substitution of Ga for Fe. This tells us the substitution of Ga for Fe in R₂Fe₁₇ decreases magnetovolume effect and attenuates Invar characters of the compounds.

QG11

Pressure effect on the electrical resistivity of $\text{La}_{1.09}(\text{Fe}_{0.845}\text{Si}_{0.155})_{13}$ compound

Makio Kurisu^{1*}, D. T. K. Anh² and Go Nakamoto³
¹ Department of Physics, Ehime University, Japan
² School of Materials Science, Japan Advanced Institute of Science and Technology, Japan
³ School of Materials Science, Japan Advanced Institute of Science and Technology, Japan



QG12

One- and two-magnon and exciton raman scattering in antiferromagnetic CoF_2 : Experiment and theory

Eric Meloche¹, Michael Cottam¹ and David Lockwood²
¹ Department of Physics and Astronomy, University of Western Ontario, Canada
² Institute for Microstructural Sciences, National Research Council, Canada

Experimental data are reported for the temperature and polarization dependence of the one- and two-magnon Raman light scattering in the rutile-structure antiferromagnet CoF_2 (Neel temperature = 38 K). A detailed analysis of the one-magnon Stokes and anti-Stokes Raman spectra is presented resulting in comprehensive experimental data for the temperature variation of the one-magnon frequency, line width, and integrated intensity. A similar analysis was carried out for the two-magnon scattering. The low-lying excitons were also investigated at low temperatures and comparisons are made with results from earlier Raman, infrared, and neutron scattering work. The Green's function equation of motion method was employed to derive the excitation energies and spectral intensities over a broad range of temperatures for the magnetic excitations in a spin $S = 3/2$ anisotropic antiferromagnet with strong spin-orbit coupling. Results were obtained using RPA for the product of operators at different sites while the single-anisotropy terms were treated exactly by generating a closed set of coupled Green's function equations. The numerical results are in good agreement with one-magnon Raman light scattering data. Results were deduced for some exchange and anisotropy parameters and the relative magnitudes of the magneto-optical coefficients in the interaction Hamiltonian.

QG13

Thermodynamic and transport properties of $\text{Ru}_{2-x}\text{Fe}_x\text{CrSi}$ ($1.3 \leq x \leq 1.8$)

Masakazu Ito*, Toru Hisamatsu, Tsugumi Rokkaku, Iduru Shigeta and Masahiko Hiroi
 Department of Physics and Astronomy, Graduate School of Science and Engineering, Kagoshima University, Japan

Full-Heusler compounds with the generic chemical formula X_2YZ (X and Y are transition elements, Z is sp element) attract much interests because this system shows a number of physical properties and some of them have a potential for the technological applications. The ferromagnetic Heusler compound $\text{Ru}_{2-x}\text{Fe}_x\text{CrSi}$ is one of candidate materials expected a half metallicity[1] and this system has relatively high Curie temperature $T_C \sim 500$ K for $x > 1.4$ [2]. We have carried out electric resistivity $\rho(T)$ and specific heat $C_p(T)$ measurement of Fe-rich $\text{Ru}_{2-x}\text{Fe}_x\text{CrSi}$ ($x = 1.3, 1.6, \text{ and } 1.8$). For all samples, $\rho(T)$ shows metallic behavior ($\partial\rho/\partial T$) in $20 < T < 300$ K, and upturn at around 20 K. In low-temperature range, $C_p(T)$ can be described by Debye's law. Although a coefficient of lattice specific heat β is insensitive for Fe concentration x , a electronic specific heat part γ decreases slightly with increasing x . For each x sample, we estimated total density of states (DOS) at the Fermi level $D(E_F)$ from γ .

[1] S. Mizutani et al., Mater. Trans. 47, 25 (2006). [2] M. Hiroi et al., Phys. Rev. B 79, 224423 (2009)

QG14

Magnetic structure and excitations of the one-dimensional quantum antiferromagnet RbCoCl_3

Mattia Mena^{1*}, Eva Hirtenlechner², Nora Haenni³, Simon Ward⁴, Karl Kraemer³, Christian Ruegg⁴ and Des Mcmorrow¹
¹ London Center for Nanotechnology, UCL, United Kingdom
² Institut Laue-Langevin, France
³ University of Bern, Switzerland
⁴ Paul Scherrer Institut PSI, Switzerland

RbCoCl_3 is a hexagonal perovskite in which the Co^{2+} ions have an effective spin $S = 1/2$ and form one-dimensional (1D) chains perpendicular to the basal plane. Measurements of the magnetic susceptibility confirm its antiferromagnetic behaviour; the difference between the maximum of the susceptibility and the Neel temperature indicates 1D magnetic correlation. Isostructural materials, such as CsCoCl_3 and TlCoCl_3 , are quasi-1D Ising-like spin systems[1][2]. The lowest-lying magnetic modes in their spectrum consist of pairs of domain-wall excitations and are described by a strongly anisotropic Heisenberg Hamiltonian[3]. Here we report the first results of a comprehensive neutron scattering study of the magnetic structure and excitations in RbCoCl_3 . A neutron diffraction experiment on HRPT (SINQ,PSI,Switzerland) revealed the existence of two phase transitions at $T_{N1} \sim 28$ K and $T_{N2} \sim 14$ K. At T_{N1} there is a paramagnetic-to-antiferromagnetic transition, while at T_{N2} a low-temperature phase with a new propagation vector develops. Inelastic neutron scattering experiments were performed on LET (ISIS,RAL,UK) and IN22 (ILL,Grenoble,FR). Between T_{N1} and T_{N2} , as well as above T_{N1} , excitations characteristic for an Ising magnet are observed. Below T_{N2} an additional splitting of the modes is discovered. Results and analysis of the data from LET will be presented and discussed.

[1] J. P. Goff, D. A. Tennant and S. E. Nagler, Phys.Rev. B 52, 15992 (1995). [2] A. Oosawa, Y. Nishiwaki, T. Kato and K. Kakurai, J. Phys. Soc. Jpn. 75, 15002 (2006). [3] N. Ishimura and H. Shiba, Progr. Theor. Phys. 63, 743 (1980).

QG15

Antiferromagnetic transition in Ru_2CrSi in magnetic fields

Masahiko Hiroi^{1*}, Kaori Uchida¹, Iduru Shigeta¹, Masakazu Ito¹, Keiichi Koyama¹, Shojiro Kimura² and Kazuo Watanabe²
¹ Department of Physics and Astronomy, Kagoshima University, Japan
² Institute for Materials Research, Tohoku University, Japan

Heusler compounds $\text{Ru}_{2-x}\text{Fe}_x\text{CrSi}$ for Fe-rich region were recently found to be ferromagnetic and to be candidates for a half-metal, where conduction electrons are fully spin-polarized.[1] In the Heusler compound Ru_2CrSi , on the other hand, an antiferromagnetic (AF) transition at $T_N = 14$ K was revealed by specific heat and magnetization measurements.[2] In this study electrical resistivity is measured in magnetic fields up to 14.5 T and the AF transition in magnetic fields is investigated. In the temperature dependence of the resistivity at zero field a clear kink is observed at $T_N = 14$ K. With decreasing temperature the resistivity turns upward from the kink at T_N . This kink can be regarded as an indication of the AF transition. With increasing magnetic field the resistivity only slightly changes and even at 14.5 T the clear kink is observed. From the kink T_N is found to decrease just a little in high magnetic fields. T_N at 14.5 T is lower than T_N at zero field by 0.5 K. These results demonstrate that the AF state in Ru_2CrSi is unusually unaffected by strong magnetic field.

[1] M. Hiroi et al., Phys. Rev. B 76, 132401 (2007). [2] M. Hiroi et al., to be published in J. Phys.: Conf. Series.

QG16

Assessment of Curie temperature by magnetization vs. temperature (M-T) scans in a granular magnetic Cu-Fe-Ni alloy

Sung Kang¹, Atsuki Takano², Dong-hae Lee², Mahoto Takeda^{2*}, Zenji Hiroi³ and Masaki Takeguchi⁴
¹ Research Institute of Industrial Science & Technology (RIST), Korea
² Yokohama National University, Japan
³ University of Tokyo, Japan
⁴ National Institute for Materials Science (NIMS), Japan

The present study has investigated the Curie temperature of Cu-Fe-Ni ternary alloy which is known as a granular giant magneto-resistance (GMR) material with a high magneto-resistance (MR) ratio. At first, we surveyed the relationship between the microstructure and the aging temperature of precipitates formed in Cu-Fe-Ni alloys isothermally annealed at 873K and 1073K for various aging times, using a transmission electron microscopy (TEM). According to TEM observations, we have revealed that two or more nano-scale particles with a cubic shape and rod shape precipitates were formed at 873K and 1073K, respectively. The critical temperature of the drastic change of the microstructure coincides with the Curie temperature of magnetism of the alloy. And, the Curie temperature has been determined by the magnetization (M) vs. temperature (T) scans, using the SQUID magnetometer. The experimentally determined temperature of 1028K was as high as a bulk Fe-Ni alloy, even though nano-scale ferromagnetic particles are finely distributed in copper matrices. The high Curie temperature has, however, well explained the temporal evolutions in both microstructure and magnetic properties occurring during isothermal annealing.

[1] S. Kang, M. Takeda, Z. Hiroi, G. W. Kim, C. G. Lee, and B. H. Koo, J. Phys. D: Appl. Phys. 43, 415001 (2010) [2] S. Kang, M. Takeda, M. Takeguchi, and D. S. Bae, J. Alloy. Compds. 496, 196 (2010)

QG17

Design strategy for strongly coupled diradicals: Systematic Approaches of intramolecular magnetic interactions

Kyoung Chul Ko, Daeheum Cho and Jin Yong Lee*
 Department of Chemistry, SungKyunkwan University, Korea

A new series of neutral radicals (DP1-DP6) based on diazaphenalenyl were designed via heteroatomic modifications. As spin sources, the designed radicals were implemented in four different diradical model systems (Model I, II, III, and IV) by changing the reference radical and the linkage, and their magnetic interactions between the designed radicals and the reference radical were investigated by using density functional theory calculations. The trend in strength of magnetic interactions of radicals was found to be identical in different model systems. In particular, as a new family of spin source radical, DP3 could be a potential candidate in designing new organic magnetic materials due to its strong magnetic coupling and high stability in diradical systems.(1) We divided 8 monoradicals into α -group and β -group according to Mulliken spin density values of the connected atoms. The overall trends in the strength of magnetic interactions of diradicals were found to be identical in three different model systems (Model I, II and V). NN-ethylene-PO was calculated to have the strongest magnetic coupling constant with ferromagnetism, and even stronger (more than twice) than NN-ethylene-NN which was reported to have strong antiferromagnetic interactions in a previous experiment.

(1) Ko, K. C.; Son, S. U.; Lee, S.; Lee, J. Y. J. Phys. Chem. B 2011, 115, 8401.

QG18

Single crystal growth and physical properties of metallic antiferromagnet (Mn,Fe)₃Si

So Nara¹, Sun Chang Che¹, Haruhiro Hiraka², Kenji Ohoyama², Yasuo Yamaguchi², Hiroyuki Miki³ and Kazuyoshi Yamada⁴
¹ Dept. of Physics, Tohoku University, Japan
² IMR, Tohoku University, Japan
³ IFS, Tohoku University, Japan
⁴ WPI, Tohoku University, Japan

Heusler alloys $\text{Mn}_x\text{Fe}_y\text{Si}$ ($x+y=3$) have a face centered cubic (DO3 type) structure in the whole x-region from the antiferromagnet Mn₃Si ($T_N=23$ K) to the ferromagnet Fe₃Si ($T_C=85$ K). As a characteristic point, Mn₃Si shows anomalous magnetic excitations so-called "chimney-type" ones, which is difficult to understood by normal spin waves, while Fe₃Si shows typical ferromagnetic spin wave excitations. Our final goal is to clarify how the spin dynamics qualitatively changes from antiferromagnet to ferromagnet in this (Mn,Fe)₃Si system, so that a deep insight into the origin of magnetism would be gained. The purpose of current work is to grow high quality large single crystals of $\text{Mn}_x\text{Fe}_y\text{Si}$ for inelastic neutron scattering experiments, which can reveal generalized magnetic susceptibility directly. Besides, for accurate measurement of bulk properties, such as electric resistivity $\rho(T)$ and magnetic susceptibility $\chi(T)$, minimizing amount of impurities is important. So far, we have succeeded in growing large single crystals of $x=0, 0.2, 0.6, 1.0$, and 1.5 by the Bridgman method. At present, an impurity phase (several-% order) is still observable in X-ray powder diffraction patterns. In this work, we report the details of single crystal growth of $\text{Mn}_x\text{Fe}_y\text{Si}$, assignment of impurity phase, and resultant $\chi(T)$, and $\rho(T)$.

QG19

AC magnetic measurement of LiFeAs at pressures up to 5.2 GPa: Verification of the relation between Tc and structural parameters

Shuhei Yamaguchi¹, Nobuhiro Yamaguchi¹, Masaki Mito¹, Hiroyuki Deguchi¹, Michael. J. Pitcher², Peter. J. Baker³, Stephen. J. Blundell³, Dinah. R. Parker² and Simon. J. Clarke²
¹ Fac. of Eng, Kyushu Inst. of Tech, Japan
² Dep. of Chem, Univ. of Oxford, United Kingdom
³ Dep. of Phys, Univ. of Oxford, United Kingdom

We have already conducted AC susceptibility measurements at pressures up to 1.5 GPa and X-ray diffraction experiment up to 20 GPa for a 111 type of iron-based superconductor, LiFeAs[1]. Now, we have enlarged the pressure range of the AC susceptibility measurement for the same sample up to 5.2 GPa. The superconducting transition temperature T_c decreased from 17 K at 0 GPa to 10 K at 5.2 GPa. T_c has been related to two structural parameters, an As-Fe-As bond angle α and the height of As from the Fe layers (hAs): Lee et al. have suggested that T_c has the highest value at the optimal α of 109.47°[2]. Kuroki et al. have suggested that T_c increases with increasing hAs[3]. According to our previous study, α changes from 101.5° at 0 GPa to 97.8° at 17 GPa, and hAs changes from 0.154 nm at 0 GPa to 0.156 nm at 17 GPa. The present pressure-induced decrease in T_c is not explained by the change in hAs, but is qualitatively consistent with the change in α .

[1] M. Mito et al., J. Am. Chem. Soc., 131 (2009) 2986. [2] C.H. Lee et al., J. Phys. Soc. Jpn. 77 (2008) 083704. [3] K. Kuroki et al., Phys.Rev.B 79 (2009) 224511.

QG20

Fundamental Magnetism of Fe-P Alloys and Fe3P Compounds: A density functional study

Won Seok Yun, Jee Yong Lee and In Gee Kim*
 Graduate Institute of Ferrous Technology, POSTECH, Korea

Phosphorus (P) is quite harmful on the mechanical properties of steel. For instance, the decrease of the strength and plastic properties of G13L steel is nearly half when it contains 0.065 wt.% P compared to the case of 0.028 wt.% P steel. On the contrary, P is an important component in the making phosphor bronze which enhances wear and water corrosion resistant. On the purpose of solid solution strengthening, P containing interstitial free steel is very important in the automotive industry due to their excellent deep drawability. However, there is no systematic first-principles study done for understanding the Fe-P alloys and Fe3P compounds. Thus, we investigated fundamental magnetic and thermodynamic properties of ferrites with the various P concentrations ($\text{Fe}_{1-x}\text{P}_x$ alloys, $x = 0.037, 0.0625, \text{ and } 0.125$) and (L12, D03, and I-4 structured) Fe_3P compounds using the highly precise all-electron full-potential linealized augmented plane wave method. As a result, the ferromagnetic state for I-4 structured Fe_3P compound is more stable than the nonmagnetic one by energy difference of about 809 meV. The calculated magnetic moments are rather overestimated compared to the neutron diffraction study. Detailed discussion on the magnetic and thermodynamic properties of $\text{Fe}_{1-x}\text{P}_x$ alloys and Fe_3P compounds will be given.

QG21

Analysis of spin-polaron formation in Hund lattices

Yesenia Arredondo^{1*}, Emmanuel Vallejo², Oracio Navarro¹ and Michel Avignon³
¹ Instituto de Investigaciones en Materiales, Universidad Nacional Autonoma de Mexico, Mexico
² Facultad de Ingenieria Mecanica y Electrica, Universidad Autonoma de Coahuila, Mexico
³ Institut Neel, CNRS and Universite Joseph Fourier, France

The ferromagnetic Kondo lattice model, also known as Hund lattice model, is a well-established model to study the interplay between charge and spin degrees of freedom in strongly correlated fermionic systems such as transition-metal oxides. Their electronic, magnetic and transport properties have displayed interesting physics such as the phenomenon of magnetoresistance [1]. Their properties depend as well strongly on the doping of the materials, which leads to formation of magnetically ordered regimes [2]. In our work, we study numerically the formation of spin-polarons in one-dimensional systems. We consider a Hund lattice model where a conducting band is coupled to a background of localized spins interacting antiferromagnetically with coupling constant J. Even though the zero-temperature of such lattice model has been intensively studied [3-4], the physics of its phase diagram is still not exhausted. We investigated the ground state phase diagram as a function of the exchange coupling J and as a function of the band filling and found different evolving magnetic orderings. We report measurements of static properties such as spin structure factor. We study the quasi-particle formation and phase separation using the density-matrix renormalization group method, which is a highly efficient method to investigate quasi-one-dimensional strongly correlated systems[5].

1. D. D. Sarma, P. Mahadevan, T. Saha-Dasgupta, S. Ray, A. Kumar, Phys. Rev. Lett. 85, 2549(2000). 2. T. Kumar, M. Greenblatt, In Functional Oxides, John Wiley & Sons, 2010. 3. E. Vallejo, F. Lopez-Urias, O. Navarro, M. Avignon, Solid State Commun. 149, 126(2009). 4. D. J. Garcia, K. Hallberg, B. Alascio, M. Avignon, Phys. Rev. Lett. 93, 177204(2004). 5. U. Schollwock, Rev. Mod. Phys. 77, 259(2005).

QG22

Chiral magnetic orders in chiral helimagnet $\text{Cr}_{13}\text{NbS}_2$

Yoshihiko Togawa^{1*}, Tsukasa Koyama², Shigeo Mori², Yusuke Kousaka³, Jun Akimitsu³, Sadafumi Nishihara⁴, Katsuya Inoue⁵, Alexander Sasha Ovchinnikov⁵ and Jun-ichiro Kishine⁶
¹ Nanoscience and Nanotechnology Research Center (N2RC), Osaka Prefecture University, Japan
² Department of Materials Science, Osaka Prefecture University, Japan
³ Department of Physics, Aoyama Gakuin University, Japan
⁴ Department of Chemistry, Hiroshima University, Japan
⁵ Department of Physics, Ural Federal University, Russia
⁶ Graduate School of Arts and Sciences, The Open University of Japan, Japan

We directly present that chiral magnetic orders emerge in chiral helimagnet $\text{Cr}_{13}\text{NbS}_2$ in small magnetic fields by means of low-temperature Lorenz transmission electron microscopy and small-angle electron diffraction technique. Based on precise analyses in both real and reciprocal space, we undoubtedly demonstrate that chiral magnetic soliton lattice (CSL) develops from chiral helimagnetic structure (CHM) with increasing the spatial period from 48 nm toward infinity in rising magnetic fields perpendicular to the helical axis. CSL and CHM do not exhibit any structural dislocation, indicating their high stability and robustness. This is because chiral magnetic orders are macroscopically induced by the uniaxial Dzyaloshinskii-Moriya (DM) exchange interactions that is allowed in $\text{Cr}_{13}\text{NbS}_2$ hexagonal crystals belonging to noncentrosymmetric chiral space group. Theoretical sides of this talk will be given in this topic category by Prof. Jun-ichiro Kishine from the Open University of Japan.

[1] Y. Togawa, T. Koyama, K. Takayanagi, S. Mori, Y. Kousaka, J. Akimitsu, S. Nishihara, K. Inoue, A. S. Ovchinnikov, and J. Kishine, to appear in Phys. Rev. Lett.

July 10 (Tue)

July 10 (Tue)

QG23

ESR study of AFM - Ordering in the orthorhombic CuMnAs

Yuriy Vladimirovich Goryunov^{1*} and Alexandr Nikolaevich Nateprov²
¹ Russian Academy of Sciences, Kazan Physical-Technical Institute of the Russian Academy of Sciences, Russia
² Academy of Sciences of Moldova, Institute of Applied Physics, Moldova

At the present time the Mn based compounds with elements of I or V group were studied intensively as advances materials for spintronic. One from such compounds is CuMnAs. CuMnAs is ordered antiferromagnetically above room temperature. We have studied electronic spin resonance (X-band) in this compound at temperature range 10 - 400 K At all temperature we observed symmetric Lorentz's shape resonance lines from Mn²⁺ ions with g - factor 2.00. The linewidth increase in 2 times at temperature decreasing to 10 K. The second line with a g-factor of 2.55 has appeared in the spectrum at temperatures below 60 K Non resonant absorption was observed for powder samples. We interpreted our results in terms Mn-Cu-Mn and Mn-As-Mn indirect superexchange interaction. Work was supported by Grants of RFBR and Presidium of the RAS.

[1] F. Maca, J. Masek, O. Stelmakhovych, et al., ArXiv: 1102.5373v1 [cond-mat. matrI-sci] 25 Feb 2011 [2] T. Jeong, Ruben Weht, W. E. Pickett, Phys.Rev. B 71, 184103 (2005) [3] J. Boeuf, C. Pfeleiderer, A. Fajßt, Phys.Rev. B 74, 024428 (2006) [4] T. Jungvirth, V. Novak, X. Marti, M. Cukr, et al., Phys.Rev. B 83, 035321 (2011)

QG24

Elastic properties and stability of Heusler compounds

S.-C. Wu*, S. S. Naghavi, G. H. Fecher and C. Felser
 Max Planck Inst. for Chem. Phys. of Solids; Inst. for Inorg. and Analy. Chem., Uni. Mainz, Germany

The physical properties of Heusler compounds which are promising materials for spintronics are important. Various Heusler compounds are investigated with respect to their malleability and stability. The elastic constants are calculated by applying isotropic strain in different ways to the cubic crystal. We used FP-LAPW implemented in Wien2K to calculate the elastic constants as well as further physical properties (bonding, hardness, velocity of sound, Debye temperature, etc.) that can be derived from the elastic constants. The result of the cubic elastic anisotropy can be used to decide the structural stability. Zener's ratios of the most stable compounds are in the range of 1.0 < Ae < 2.5. Ae < 0 is not stable and Ae = 0 is isotropic. We observed phase transitions in some of Heusler compounds with Ae < 0. It is shown that calculating elastic constants provides an estimate for studying phase transitions.

QG25

Electronic and magnetic properties of ferromagnet/dilute-magnetic semiconductor interfaces

Alessandra Continenza* and Gianni Profeta
 Physics, Universita' degli studi dell'Aquila, Italy

A. Continenza and G. Profeta Experimental findings [1-4] report exchange-bias effects at the Fe/GaMnAs together with interesting possible magnetic proximity effects at the interface between the ferromagnetic (FM) material and the dilute semiconductor (DMS). In this work we perform ab-initio calculations of different FM/DMS geometries (superlattice systems and periodic slab) for Fe/Ge/Mn and Fe/GaAs/Mn interfaces. We examine different interfaces to assess the most stable structures, the magnetic coupling between the magnetic overlayer and the Mn dopant atoms and how the ferromagnetic overlayer affects the interaction between two Mn atoms dispersed in the semiconductor matrix. An antiferromagnetic coupling between the overlayer Fe and the Mn is found for Mn close to the interface layers, fading away with the distance of the Mn atom from the interface. A study of how the magnetic coupling between overlayer and dilute Mn and between dilute Mn's at different locations is performed and discussed. We find a rather large magnetic coupling enhancement in the case of Ge while the situation for GaAs looks to be much more complex due to chemical effects at the GaA/Fe interface. Results are discussed in terms of local densities of states, magnetic moments and total energies.

[1] Phys. Rev. Lett. 101, 267201 (2008) [2] Phys. Rev. B 81, 104402 (2010) [3] Phys. Rev. B 81, 035211 (2011) [4] J. Appl. Phys. 109, 07C505 (2011)

QG26

Mn-Sublattice of YbMn₂Si₂

Stewart J Campbell^{1*}, Michael Hofmann², Richard A Mole³, Karel Prokes⁴, Jianli Wang⁵ and Dirk Wallacher⁶
¹ School of Physical, Environmental and Mathematical Sciences, ADEFA, The University of New South Wales, Australia
² Forschungsneutronenquelle Heinz Maier-Leibnitz (FRM II), Technische Universität München, Germany
³ Bragg Institute, ANSTO, Australia
⁴ Helmholtz Zentrum Berlin, Lise Meitner Campus, Germany
⁵ Institute for Superconducting & Electronic Materia, University of Wollongong, Australia
⁶ Helmholtz Zentrum Berlin, Lise Meitner Campus, Germany

The instability of the f shell in Yb and the small energy difference between the Yb²⁺ divalent and Yb³⁺ trivalent states, has led to the wide range of physical and magnetic properties exhibited by ytterbium-based intermetallic compounds. The ranges of effects are linked with many physical states such as: mixed valence, Kondo effect, heavy fermions, spin wave excitations, superconductivity and magnetic quantum critical point [e.g. 1]. Trivalent YbMn₂Si₂ exhibits a collinear antiferromagnetic AFII structure below TN1 = 526(4) K with a doubling of the magnetic c-lattice below TN2 = 30(5) K; this structure of the Mn-sublattice would therefore be expected to result in different environments for Yb atoms in the doubled unit cell [2]. However 170Yb Mossbauer studies led to the conclusion that the observed spectra are inconsistent with the cell-doubling [3]. To clarify this discrepancy, we have re-investigated the magnetic behaviour of YbMn₂Si₂ over the temperature range ~0.4-50 K using the E6 neutron diffractometer, HZB. The high density of diffraction patterns confirm the cell doubled magnetic behaviour of the Mn-sublattice below 27.3(2) K with the onset of the satellite reflections (propagation vector k = 00½) described well by a power law.

[1] C. Klingner, C. Krellner, M. Brando, C. Geibel, F. Steglich, D. V. Yul'ikh, K. Kummer, S. Danzonbacher, S. L. Molodtsov, and C. Lantschur, T. Kamohsji, Y. Kato, and T. Muro, Phys. Rev. B 83, 144405 (2011). [2] M. Hofmann, S.J. Campbell, A.J. Edge and A.J. Studer, J. Phys.: Condens. Matter 13, 9773 (2001). [3] D. H. Ryan, J. M. Cadogan, and A.J. Edge, J. Phys.: Condens. Matter 16, 6129 (2004)

QG27

Electronic structures and magnetic properties of full and half Fe-Mn-Ga Heusler alloys

Y. V. Kudryavtsev¹, N.v. Uvarov¹, J. Dubowik², I.n. Glavatskiy³, Y. J. Yoo⁴ and Y. P. Lee^{4*}
¹ G.V.Kurdumov Institute of Metal Physics NAS of Ukraine, Ukraine
² Institute of Molecular Physics, PAS, Poland
³ Helmholtz Centre Berlin for Materials and Energy, Germany
⁴ Dept. of Physics, Hanyang University, Korea

Electronic and magnetic structures of bulk and film Fe₂MnGa and FeMnGa alloys near 2:1:1 and 1:1:1 stoichiometric compositions have been investigated theoretically and experimentally. It was experimentally found that unlike most of full stoichiometric Heusler compounds, bulk Fe₂₀4Mn₂₀2Ga₂₅4 alloy with the Curie temperature of 800 K and saturation magnetization of 4.86 μB/f.u. crystallizes in the face-centered-cubic (FCC) ordered lattice of L12 (Cu₃Au)-type with small admixture of B2-phase. According to results of our first-principle calculations of full electron energy ferromagnetic metallic FCC phase (μFCC=6.11 μB/f.u.) is energetically more preferable than ferrimagnetic half-metallic phase with L21 type of structure (μL21=2.04 μB/f.u.) or ferrimagnetic metallic FCC phase (μFCC=0.48 μB/f.u.). Metamagnetic transition in Fe₂₀4Mn₂₀2Ga₂₅4 alloy from antiferromagnetic to ferromagnetic phase was observed at low temperatures. Bulk Fe₃₃Mn₂₇Ga₃₄ alloy has hexagonal structure and saturation magnetization at T=15 K of μ=3.00 μB/f.u. and the Curie temperature of 453 K. Magnetic properties of Fe₃₃Mn₂₇Ga₂₈ alloy films strongly depend on their structure. Atomic disorder in amorphous state significantly reduces the film magnetization nearly to zero at room temperature. Depending on deposition conditions, unlike the bulk alloy, crystalline Fe₃₃Mn₂₇Ga₂₈ alloy films exhibit BCC- or FCC-ordering that result in anomalous temperature dependencies of magnetization in low-temperature region.

QG28

Microscopic analysis of magnetic orders in MnP single crystals

Tsukasa Koyama¹, Shin-ichiro Yano², Yoshihiko Togawa³, Yusuke Kousaka², Shigeo Mori¹, Jun-ichiro Kishine⁴ and Jun Akimitsu²
¹ Department of Materials Science, Osaka Prefecture University, Japan
² Department of Physics, Aoyama Gakuin University, Japan
³ Nanoscience and Nanotechnology Research Center, Osaka Prefecture University, Japan
⁴ Graduate School of Arts and Sciences, The Open University of Japan, Japan

Manganese phosphide (MnP) has been extensively studied because of its richness of magnetically ordered phases in the magnetic phase diagram. In this study, as a first step to understand the mechanism of the magnetic phase transition from the ferromagnetic (FM) phase to the proper screw spiral phase or FAN phase, we have studied FM structures in the FM phase of MnP single crystals by means of low-temperature Lorentz transmission electron microscopy and small-angle electron diffraction[1]. In Lorentz Fresnel micrographs, striped FM domain structures were observed in external magnetic field less than 10 Oe in the specimens with the ab-plane in the plane of the specimen. From real- and reciprocal-space analyses, it was undoubtedly identified that striped FM domains oriented to the c-axis appear with Bloch-type domain walls in the b direction and arrange regularly along the a-axis with 64 nm separation. Moreover, the magnetic chirality reverses in alternate FM domain walls. These specific spin configuration of striped FM domains will affect the magnetic phase transition from the FM phase to the proper screw spiral phase at the low temperature or the FAN phase in the magnetic field in MnP.

[1] T. Koyama, S. Yano, Y. Togawa, Y. Kousaka, S. Mori, K. Inoue, J. Kishine, and J. Akimitsu, submitted.

QH01

Structural and magnetic properties of Fe₂Mn_{0.5}Cu_{0.5}Al Nanocrystalline Alloys

Dwi Nanto¹, Dong-seok Yang², Suhk-kun Oh¹ and Seong-cho Yu^{1*}
¹ Dept. of Physics, BK 21 Physics Program and Dept. of Physics, Chungbuk National University, Cheongju, 361-763, Korea
² Dept. of Physics Education, Physics Division, Chungbuk National University, Cheongju, 361-763, Korea

We synthesized Fe₂Mn_{0.5}Cu_{0.5}Al nanocrystalline alloys by mechanical alloying technique and studied as a function of milling time. The milling times were 1, 3, 6, 9, and 24 hrs. The effect of milling time on structure formation was investigated by X-ray Diffraction (XRD), and magnetic properties was investigated using vibration sample magnetometer (VSM). Alloy nature of Fe₂Mn_{0.5}Cu_{0.5}Al was confirmed after 24 hrs. The crystallite size after 24 hrs of milling time was estimated using Scherer formula, and the value was 24 nm. Magnetic saturation was decreased with increased milling time, which seemed be due to co-existence of Mn and Cu atoms. The magnetic saturation was 86.19 (emu/gr) and the coercivity was 376.59 Oe after 24 hrs of milling time. The coercivity (Hc) was increased with milling time presumably due to magnetic domain growth towards stable structure. Keywords: Heusler compound, nanocrystalline

References: [1] Tanja Graf, Claudia Felser, Stuart S.P. Parkin, Progress in Solid State Chemistry 39 (2011) 1-50 [2] Shane Stadler¹, Mahmud Khan¹, Joseph Mitchell¹, Naushad Ali¹, Angelo M. Gomes², Igor Dubenko³, Armando Y. Takeuchi³, and Alberto P. Guimarães³ Appl. Phys. Lett. 88, 192511 (2006)

QH02

Antiferromagnetic resonance in the one-dimensional magnet IPACu(Cl_{1-x}Br_x)₂ (x=0.83)

Takahito Fujita¹, Masayuki Hagiwara¹ and Hirotaka Manaka²
¹ KYOKUGEN, Osaka university, KYOKUGEN, Osaka university, 1-3 Machikaneyama, Toyonaka, Osaka 560-8531, Japan
² Graduate School of Science and Engineering, Kagoshima University, Graduate School of Science and Engineering, Kagoshima University, 1-21-40 Korimoto, Kagoshima 890-00, Japan

Low-dimensional antiferromagnets with a small spin value exhibit various fascinating properties. IPACuCl₂ and IPACuBr₂ (IPA: isopropyl-amine) having magnetic Cu²⁺ (spin S=1/2) ions form the ladder chain in the b plane. The ground states of IPACuCl₂ and IPACuBr₂ are considered to be the Haldane state [1] and the singlet dimer state [2]. It was reported that IPACu(Cl_{1-x}Br_x)₂ (0.44 < x < 0.87) undergo an antiferromagnetic long-range order (AFLRO) at low temperatures. However, the details of the AFLRO phase have not been clarified yet [3]. Therefore, we have performed electron spin resonance (ESR) measurement on single crystals of IPACu(Cl_{1-x}Br_x)₂ (x=0.83) in magnetic fields of up to 14 T. We have observed the typical antiferromagnetic resonance (AFMR) signals, and successfully explained all the observed resonance modes by the conventional AFMR modes with orthorhombic anisotropy.

[1] T. Masuda et al., Phys. Rev. Lett. 96 (2006) 047210. [2] H. Manaka and I. Yamada, J. Phys. Soc. Jpn. 66 (1997) 1908. [3] H. Manaka et al., Phys. Rev. B 64 (2001) 104408.

QH03

Magnetization steps in Yb₂Pt₂Pb with the Shastry-Sutherland lattice

Yasuyuki Shimura^{1*}, Toshiro Sakakibara¹, Ken Iwakawa², Kiyohiro Sugiyama, and Yoshichika Onuki,
¹ Institute for Solid State Physics, University of Tokyo, Kashiwa, Chiba 277-8581, Japan
² Graduate School of Science, Osaka University, Toyonaka, Osaka 560-0043, Japan

In the tetragonal compound Yb₂Pt₂Pb, Yb³⁺ ions form the Shastry-Sutherland lattice [1]. The Yb moment shows a strong Ising type anisotropy with the easy axis lying along either [110] or [1-10] directions, and exhibit an antiferromagnetic long range order at TN=2.1 K [1]. Surprisingly, the recent H-T phase diagram investigation [2] has revealed that when a sufficiently strong magnetic field is applied along the [110] direction, the system exhibits a partially disordered state below TN; half of the Yb sites remain antiferromagnetically ordered whereas the rest become paramagnetic. This unusual behavior has been interpreted by a decoupling of two Yb sublattices in a [110] magnetic field due to the characteristic crystal structure and the competing Ising anisotropy [2]. In this paper, we measured the DC magnetization of Yb₂Pt₂Pb at very low temperatures down to 0.08 K for H//[100] and [110] in order to further explore its unusual phase diagrams. For both directions, a sequence of sharp magnetization steps is observed at T<0.5 K. Comparison of the differential susceptibility data for the two directions indicates the presence of an intersublattice coupling for H//[100].

[1] M.S. Kim et al., Phys. Rev. B 77 144425 (2008). [2] A. Ochiai et al., J. Phys. Soc. Jpn. 80 123705 (2011).

QH04

Mossbauer study on Fe (Si,Ge) alloys

Yasushi Amako, Yusuke Taniguchi and Miho Nakashima
 Faculty of Science, Shinshu University, Japan

Calculations of electronic structures in FeSi_{1-x}Ge_x with a cubic B20-type structure found that they were narrow-gap semiconductors in the non-magnetic state for x<0.5, however, the metallic state with the magnetic moment of about 1μB per Fe was shown to be more stable for x≥0.5 [1]. In this paper, we report the results of the magnetization measurements and 57Fe Mossbauer effect measurements on FeSi_{1-x}Ge_x compounds. The 57Fe hyperfine fields for x=0.6 and 0.8 estimated by fitting of Mossbauer spectra at 80K were 6.0T and 8.0T, respectively, while they were almost zero for 0≤x≤0.5. The Curie temperature and spontaneous magnetization at 4K were found to be 124K and 0.66μB/f.u. for x = 0.6 and 171K and 0.71μB/f.u. for x = 0.7, respectively.

[1] H.Yamada, K.Terao and T.Goto, Physica B 344 (2004) 451.

QH05

Ab initio and Monte Carlo investigations of the magnetic exchange and curie temperature of Ni₂Mn_{1+x}Sn_{1-x} alloys

Vasily Buchelnikov^{1*}, Vladimir Sokolovskiy¹, Mikhail Zagrebin¹, Peter Entel² and Sergey Taskaev¹
¹ Chelyabinsk State University, Russia
² University of Duisburg-Essen, Germany

The ab initio and Monte Carlo calculations of magnetic exchange constants, magnetic moment and the Curie temperatures of stoichiometric and non-stoichiometric Heusler Ni₅₀Mn_{25-x}Sn_{25-x} alloys have been performed. For the ab initio calculations of magnetic exchange constants and magnetic moment the Munich SPR KKR package was used [1]. The calculations were made for order and disorder structures. We consider two types of disorder. First is a disorder between Ni and Mn atoms and second is a disorder between Mn and Sn atoms. The Curie temperatures have been calculated by mean field approximation and Monte Carlo method using the Heisenberg model. It is shown that the experimental Curie temperature of non-stoichiometric alloys can be explained theoretically by the assumption that in alloys the disorder between Mn and Sn atoms exists. Our calculations have shown that the magnetic moment and Curie temperatures for Ni-Mn-Sn alloys are in qualitative agreement with experimental magnetic moment and transition temperatures [2].

I. H. Ebert, Electronic Structure and Physical Properties of Solids, ed. H. Dreyse, Springer, Lecture Notes in Physics, Berlin, 1999, Vol. 535, p. 191. 2. T. Kanomata, et al., Magnetic and crystallographic properties of shape-memory alloys Ni₂Mn_{1+x}Sn_{1-x}, Materials Science Forum 583 (2008) 119.

QH06

Structural, magnetic, magnetocaloric and magneto-transport properties in Ge doped Ni-Mn-Sb Heusler Alloys

A. K. Nigam¹, Roshnee Sahoo² and K. G. Suresh^{2*}
¹ Physics, TIFR, Mumbai, India
² Physics, IIT Bombay, India

A. K. Nigama, Roshnee Sahoob and K. G. Sureshb* aTata Institute of Fundamental Research, Homi Bhabha Road, Mumbai-400005, India bDepartment of Physics, Indian Institute of Technology Bombay, Mumbai-400076, India Abstract The effect of Ge substitution on the magnetic, magnetocaloric and transport properties of Ni₄₂Co₃Mn₃₈Sb_{12-x}Ge_x (x=0-3) has been investigated. The decrease in the exchange interaction brought by Ge substitution can be seen from the reduction in the magnetization of austenite phase and the increase in the martensitic transition temperature. The hysteresis observed for x=0 between the heating and the cooling curves in the magnetization data decreases considerably for x=3. The reduction in the sharpness of the metamagnetic transition is also observed with Ge doping. From the resistivity data it is found that the disorder in the martensite phase increases with increase in the Ge concentration. It is also found that the martensitic transition can be tuned over a large temperature interval with a small change in Sb/Ge ratio, giving rise to a large MCE and a large MR value over a broad temperature interval. This makes the system as a potential material system for various applications.

QH07

Effect of doped Mn ions in thermoelectric material of Mg₂Sb₂

Soo Hyun Kim¹, Chung Man Kim¹, Junpei Kajino², Toshiro Takabatake² and Myung-hwa Jung^{3*}

¹ Physics, Sogang university, Korea

² Physics, Hiroshima University, Japan

Spin caloritronics is about the physics that control of heat, charge and spin currents in structures, devices, and materials. Here we focus on the spin-related thermoelectric properties and study the effect of magnetic ion doping on the thermoelectric material of Mg₂Sb₂. We have synthesized single crystals of Mg₂Sb₂ and Mn-doped Mg₂Sb₂ by using Bridgeman method. The X-ray diffraction data show that the crystals are single-phased and c-axis oriented. In order to illustrate the thermoelectric performance, we have measured the seebeck coefficient (S), electrical conductivity (σ), and thermal conductivity (κ) as a function of temperature. The efficiency of thermoelectric performance is dominated by the figure of merit, ZT=S²σ/Tκ. The obtained S, σ, and κ values at 300K are 600 μV/K, 16 S/m, and 3.5 W/mK, respectively for Mg₂Sb₂. Because of the lower σ, the ZT value is estimated to be small. However, by doping Mn ions into Mg₂Sb₂, we find the electrical properties to be improved. We will discuss more about the optimal condition of Mn doping rate in Mg₂Sb₂ to promote the thermoelectric performance.

QH08

X-ray diffraction study on crystal structure of Mn_{1-x}Co_{0.2}Sb under high magnetic fields

Hiroki Orihashi^{1*}, Daisuke Mitsunaga¹, Masahiko Hiroi¹, Yoshifuru Mitsui², Kohki Takahashi², Kazuo Watanabe² and Keiichi Koyama¹

¹ Graduate School of Science Engineering, Kagoshima University, Japan

² HFLSM, IMR, Tohoku University, Japan

Measurements of magnetization, electrical resistivity and high field X-ray powder diffraction (XRD) were carried out for polycrystalline Mn_{1-x}Co_{0.2}Sb in magnetic fields up to 5 T in 4.2-300 K temperature range, in order to investigate the structural properties affected by magnetic fields. In a zero field, the compound shows the first-order magnetic transition from the ferrimagnetic (FRI) to antiferromagnetic (AFM) states at Tt = 145 K with decreasing temperature. By applying magnetic fields of 5 T, Tt decreased to 60 K with thermal hysteresis of 35 K. From the XRD measurements, not only the AFM phase but also the residual FRI phase was confirmed even at 10 K in cooling process under 5 T. Results obtained indicate that the residual FRI phase is kinetically arrested [1].

[1] H. Orihashi et al. *Mater. Trans. [Selected Papers from JIM Fall Meeting(2011)]* 76 (2011) in press

QH09

Emergence of Ferromagnetism under pressure in (Mn_xFe_{1-x})₂GaN

S. Iikubo^{1,6}, T. Inagaki², K. Takenaka², K. Matsubayashi³, Y. Uwatoko³, H. Takagi⁴, and H. Ohtani^{1,6}

¹ Graduate School of Life Science and Systems Engineering, Kyushu Institute of Technology, Japan

² Department of Crystalline Materials Science, Nagoya University, Japan

³ Institute for Solid State Physics University of Tokyo, Japan

⁴ RIKEN (The Institute of Physical and Chemical Research), Japan

⁵ Department of Materials Science and Engineering, Kyushu Institute of Technology, Japan

⁶ JST, CREST, Japan

The recent development of “metallic” antiperovskite nitrides Mn_xAN, where A is a metal or a semiconducting element, has promoted research toward practical use. We found an intimate relationship between the large magneto-volume effect (MVE) in cubic Mn_xAN and the Γ^{6g}-type antiferromagnetic (AF) ordering. As a tunable thermodynamic parameter, the external pressure may play an important role in this system, because it can affect not only the crystal structure but also the magnetic structure. We report the pressure effect on the stability of magnetic structure of (Mn_xFe_{1-x})₂GaN. In this system, it was reported that a few percent of Fe dopants at the Mn sites alters the AF spin structure of Mn₂GaN and induces a first-order antiferromagnetic-ferromagnetic phase transition. We have measured the magnetization of (Mn_xFe_{1-x})₂GaN with x=0, 0.05 and 0.07 and Mn₂GaN (x₁, y₁) with y=0, 0.05 and 0.1 under pressure up to 1.3 GPa. A magnetic transition from an AF to an ferromagnetic (FM) state with spontaneous magnetization is observed under pressure. Especially, a spontaneous magnetization in Mn₃GaN is 0.24 μB per Mn under pressure. The application of pressure increases the magnetization in the FM phase for all these compounds.

QH10

First-principles-calculations of the magnetic anisotropy energy of FeCo and FeNi alloys

Masanori Enoki¹, Satoshi Iikubo² and Hiroshi Ohtani³

¹ Graduate School of Engineering, Kyushu Institute of Technology, Japan Science and Technology CREST, Japan

² Graduate School of Life Science and Systems Engineering, Kyushu Institute of Technology, Japan Science and Technology CREST, Japan

³ Department of Materials Science, Kyushu Institute of Technology, Japan Science and Technology CREST, Japan

The calculations of T.Burkert et al. predict an unusually large magnetic anisotropy energy (MAE) of ~700 μeV/atom for the Fe_{0.4}Co_{0.6} random alloy at a ratio of c/a [1]. This result suggests that other transition metal alloys are also candidate for emerging a high MAE with altering the 'c/a'. In order to seek new design of materials, we research MAE and electronic structures for Fe-Co and Fe-Ni alloys with using the first-principles-calculations. The calculations were carried out using the VASP code. At first, we optimized the length of lattice constant 'a' against the fixed 'c/a' at range of 1.10-1.35. The MAE were evaluated by subtracting the energy with polarized spin direction parallel to [100] from that to [001]. For the Fe-Co alloy, the estimated MAE has maximum at c/a=1.25 and Fe_{0.4}Co_{0.6}, which is roughly consistent with the previous result of Burkert et al. On the other hand, Fe-Ni system has the high MAE (~300 μeV/atom) is found at the Fe_{0.75}Ni_{0.25}. We will present the origin of the large MAE from the electronic structures in these systems.

[1]T. Burkert et al. *Phys. Rev. Lett.* 93 027203 (2004)

QH11

Tuning the magnetic properties of amorphous FeZr thin by hydrogen implantation

Atieh Zamani^{1*}, Anders Hall², Per Nordblad³, Bjorgvin Hjorvarsson¹ and Petra Jonsson¹

¹ Physics and Astronomy, Material Physics, Uppsala University, Sweden

² School of Information and Communication Technology (ICT), KTH, Sweden

³ Department of Engineering Sciences, Uppsala University, Sweden

Amorphous FeZr alloys order ferromagnetically, with a maximum in the ferromagnetic transition temperature near 240K for Zr contents between 10-20 at.%. Interestingly, hydrogen can be introduced into the alloy, enhancing its Curie temperature, magnetic moment and soft magnetic properties. In order to understand the magnetism of the Fe(Zr) binary system, and the effect of hydrogen on the magnetic interaction, we have investigated in details the magnetic properties of amorphous thin films of Fe(Zr). Fe1-xZrx films with compositions x=7.5, 9.5, 11.5, 12.5 and 13.5 at.% were grown by co-sputtering on Si substrate in ultra high vacuum (UHV) conditions. The compositions, structural and magnetic properties of the films were investigated by Rutherford Backscattering spectrometry (RBS), X-ray diffraction, and SQUID magnetometry respectively before and after hydrogenation. The hydrogen implanted samples show an increased value of the Curie temperature with increasing hydrogen content. The magnetization curves at low temperature show a continuous increase with increasing x also at quite high temperature confirming the presence of random anisotropy. This anisotropy is heavily suppressed by hydrogen implantation. Keywords: Amorphous Fe(Zr), Magnetization, H-implantation

QH12

Normal and intrinsic anomalous Hall effect in NbFe₂

Sven Friedemann^{1*}, William J Duncan², Andreas Neubauer³, Manuel Brando⁴, Christian Pfeiderer³ and F Malte Grosche¹

¹ Cavendish Laboratory, University of Cambridge, United Kingdom

² Department of Physics, Royal Holloway University of London, United Kingdom

³ Physik Department E21, Technical University Munich, Germany

⁴ Max Planck Institute for Chemical Physics of Solids, Dresden, Germany

Hall effect studies are a powerful probe of the Fermi surface of metals via the normal contribution whilst the anomalous contribution may give substantial insight into spin-orbit interactions. Here, we present Hall effect measurements on selected samples of the band magnet system NbFe₂. In the dilution series Nb_{1-y}Fe_{2+y}, composition tuning allows to access various magnetic ground states including a complete suppression at a quantum critical point. We observe normal and anomalous contributions in the Hall effect. Consistent analysis of the anomalous contribution, however, is only possible for Fe-rich Nb_{0.985}Fe_{2.015} featuring a ferromagnetic ground state. Here, a positive normal Hall coefficient is found at all temperatures with a moderate maximum at the spin-density-wave transition. The anomalous Hall effect is covered by an intrinsic (Berry-phase) contribution which is constant below the ordering temperature TC and continuously vanishes above TC. For samples with antiferromagnetic ground state, i.e., stoichiometric NbFe₂ and Nb-rich Nb_{1.01}Fe_{1.99}, an additional contribution to the Hall resistivity impedes a complete analysis and indicates the need for more sophisticated models of the anomalous Hall effect in itinerant antiferromagnets.

QH13

Magnetovolume effect in the itinerant-electron frustrated magnet Fe₃Mo₃N

Yoshikazu Tabata^{1*}, Masaki Yamamoto¹ Shinsuke Terazawa¹, Takeshi Waki¹, Kenji Ishida² and Hiroyuki Nakamura¹

¹ Department of Materials Science and Engineering, Kyoto University, Japan

² Department of Physics, Kyoto University, Japan

The η-carbide-type compound Fe₃Mo₃N, including the frustrated stella-quadrangula Fe-sublattice, is a novel itinerant-electron frustrated magnet and exhibits intriguing features such as non-Fermi-liquid behavior without parameter-tuning and sharp metamagnetic transition [1]. We performed thermal expansion and magnetostriction measurements of Fe₃Mo₃N up to 15 T. A large volume expansion is found at the metamagnetic transition field and the magnetovolume coupling constant is estimated as about 4 × 10⁻³ μB⁻², being the same of magnitude of those of Co Laves phase compounds [2]. It indicates that the metamagnetic transition of Fe₃Mo₃N is a typical moment-induced-type in nonmagnetic itinerant electron systems. The nonmagnetic ground state of Fe₃Mo₃N at zero field is emergent due to the frustration effect built into the stella quadrangula lattice.

[1] T. Waki et al., *J. Phys. Soc. Jpn.* 79, 043701 (2010).; T. Waki et al., *Europhys. Lett.* 94, 37004 (2011). [2] Y. Muraoka et al., *J. Phys. Soc. Jpn.* 53, 331 (1984).

QH14

NMR studies of magnetic properties in the spinel-type Cu(Cr_{1-x}Hf_x)₂S₄

Haruo Niki^{1*}, Morihito Oshiro¹, Saori Nakamura¹, Ayaka Uechi¹, Mamoru Yogi¹, Shuji Ebisu² and Shoichi Nagata²

¹ Department of Physics, Faculty of Science, University of the Ryukyus, Japan

² Muoran Institute of Materials Research, Japan

A chalcogenide spinel CuCr₂S₄ is a metallic ferromagnet with Tc = 380 K. The increase of x for the mixed spinel Cu(Cr_{1-x}Hf_x)₂S₄ shows a successive change from a ferromagnetic, a re-entrant spin-glass, a spin-glass, and finally to a paramagnetic state. A step-like anomaly in magnetization is also found around 160 K in the range of 0.50 ≤ x ≤ 0.70 due to a spin crossover phenomenon [1]. In order to investigate the magnetic properties of Hf rich side in Cu(Cr_{1-x}Hf_x)₂S₄ from a microscopic point of view, 63Cu NMR have been carried out between 4.2 and 300 K. Temperature dependences of resonance line-width, Knight shift and spin-lattice relaxation time (T1) have been measured. Knight shift in the range of 0.50 ≤ x ≤ 0.70 gradually shifts to negative side down to 130 K, but rapidly shifts to negative side below 130 K due to the core polarization of d conduction electrons. Temperature dependence of 1/T1T in the range of 0.50 ≤ x ≤ 0.70 obeys the Korringa relation (T1T = constant) down to 130 K, as expected in a Pauli-paramagnetic metallic state. However, the values of 1/T1T = constant abruptly change between 130 and 90 K, and keep constant below 90 K.

[1] F. Kariya, K. Ebina, K. Hasegawa, K. Koshimizu, B. Wuritunastu, K. Hondou, S. Ebisu and S. Nagata, *J. Solid State Chem.* 182 (2009) 2018.

QH15

Relationship between microstructure and magnetic properties of nano-scale magnetic particles formed in a Cu-Ni-Co alloy

Donghae Lee¹, Mahoto Takeda^{1*}, Sung Kang² and Takahiro Moriki¹

¹ Department of materials engineering, Yokohama national university, Japan

² Research Institute of Industrial Science & Technology(RIST), Korea

The discovery of Giant Magnetic Resistance (GMR) has invoked strong interest to relationship between microstructure and magnetic properties of nano-scale particles. The magnetic properties of nano-scale particles are strongly dependent on their structures, particle sizes, shapes, and interparticle distances particularly in granular magnets. The present study aimed to investigate the relationship between the microstructure and the magnetic properties of granular Cu-Ni-Co alloys, using transmission electron microscope (TEM), a superconducting quantum interference device (SQUID) magnetometer and thermo gravimetric-differential thermal analysis (TG-DTA). The present TEM observations revealed a specific feature that spherical ferromagnetic precipitates are transformed into cubic ones, and subsequently two or more cubic precipitates are aligned along the <100> orientation of a Cu matrix, which feature was significantly different from previous recognition to conventional precipitation. SQUID measurements shows that the magnetic property of the specimen changes from superparamagnetism to ferromagnetic in character with increasing isothermal annealing period from M-T curves. The present TG/DTA curves showed that a ferromagnetic to paramagnetic transition occurred at low temperatures (~950K) but paramagnetic to ferromagnetic transition at high temperatures(600~700K). This suggests that the coalescence of magnetic atoms and accordingly the Curie point are sensitive to annealing temperature.

QH16

Magnetic study of mechanically deformed FeAlSi alloys

Estibaliz Legarra¹, Estibaliz Apinaniz², Damian Martin-rodriguez³, Jose Javier Garitaonandia⁴ and Fernando Plazaola¹

¹ Department of Electricity and Electronics, Basque Country University, UPV/EHU, p. c. 644, 48080, Bilbao, Spain

² Department of Applied Physics I, Basque Country University, UPV/EHU, Alameda Urquijo s/n, 48013, Bilbao, Spain

³ Julich Centre for Neutron Science and Institute for Complex Systems, Forschungszentrum Julich GmbH, 52425 Julich, Germany

⁴ Department of Applied Physics II, Basque Country University, UPV/EHU, p. c. 644, 48080, Bilbao, Spain

The mechanical deformation of Fe-Al alloys produces order-disorder transition that induces an enlargement of the magnetism of the alloys. It has been demonstrated that this enlargement is related to atomic disorder and cell volume increase [1]. The behaviour of the saturation magnetization with milling and Si content in Fe₇₀Al₂₅-Si₅ and Fe₇₀Al₁₀-Si₁₀ alloys is similar to the behaviour shown by the mean magnetic hyperfine field. Their values increase with disordering in alloys with low Si content, but decrease in alloys with higher Si content. The behaviour observed indicates clearly that the introduction of Si in the binary Fe₇₀Al₂₅ and Fe₇₀Al₁₀ alloys opposes the magnetic behaviour induced by Al in the magnetism of Fe. These opposite behaviours are related to the lower increase of the lattice parameter with disorder for FeSi alloys. Besides, when plotting the normalized variation of lattice parameter produced by the disorder versus the normalized variation of magnetization we observe a linear relationship, showing that lattice parameter and magnetic properties are related. The study of the hyperfine fields also indicates that there is a redistribution of non-ferrous atoms around Fe atoms with the disordering, indeed, there is an inversion of the behaviour of the hyperfine fields.

[1] A. Hernandez, X. Amils, J. Nogues, S. Surinach, M. D. Baro, and M. R. Ibarra, *Phys. Rev. B* 58 11864 (1998).

QH17

The propagation of electromagnetic waves in magnetic with ferromagnetic spiral

Igor Valer'evich Bychkov¹, Vasily Dmitrievich Buchelnikov¹, Dmitry Aleksandrovich Kuzmin¹ and Vladimir Grigor'evich Shavrov²

¹ Cheliabinsk State University, Russia

² The Institute of Radioengineering and Electronics of RAS, Russia

Recently, spiral magnetic materials have attracted researchers' attention for their unusual physical properties. However, the spectrum and dynamic properties of magnets in a phase <<ferromagnetic spiral>> are not studied enough. In the present work the spectrum of the coupled spin and electromagnetic waves in spiral magnetic structure of type <<ferromagnetic spiral>> is investigated. Also the reflection of electromagnetic waves from a layer of magnetic having the ferromagnetic spiral and the Faraday effect are considered. We use approach L >> a, where L - the spiral period, a - the lattice constant. Studies showed that the spectrum of the coupled waves has band structure. The band gap depends on the angle of the ferromagnetic spiral, and hence on the external magnetic field. The frequency dependence of the reflection coefficient of electromagnetic waves from the plate of the magnetic with a ferromagnetic spiral at different angles of the helix has been calculated. As the angle increases the opacity region broadens and shifts to higher frequencies. Thickening of the plate also leads to broadening of the opacity region. The Faraday effect has been observed for different frequencies. The angle of plate-of-polarization rotation increases near the band gap. The Verdet constant has been calculated.

QH18

Magnetism of sigma-phase Fe-Mo and Fe-Re systems

Jakub Cieslak^{1*}, Stanislaw M Dubiel¹, Michael Reissner² and Janusz Tobola¹

¹ Academy of Mining and Metallurgy, AGH al. Mickiewicza 30, 30-059 Krakow, Poland

² Institute of Solid State Physics, Vienna University of Technology, A-1040 Wien, Austria

Sigma phase exists in five binary systems of the Fe-X type viz. for X = Cr, V, Mo, Re and Tc. It is characterized by a lack of chemical order on all five sublattices of the tetrahedral unit cell. Until now, the magnetic properties have been known only for sigma-FeCr and sigma-FeV systems. The newly discovered low temperature magnetic properties of sigma-FeMo and sigma-FeRe phases will be presented and analyzed in detail in the whole concentration range in which this phase occurs. In particular, in both cases, the observed increase in an average magnetic moment and magnetic ordering temperature with increasing of Fe content is evident. Differences in Zero-Field Cooling and Field Cooling magnetization measurements suggest the magnetic ordering of spin-glass type or a large magnetic anisotropy in the measured samples. Electronic structure calculations using the KKR method were carried out for more than a dozen semi-ordered unit cells. The results of these calculations show a linear dependence of magnetic moments and hyperfine fields of Fe atoms at different sites versus the number of Fe atoms being their nearest neighbors. They also suggest a noncollinear magnetic structure in some sublattices.

QH19

Second order magnetization effects in bcc Fe

Dominik Legut*, Jaroslav Hamrle and Jaromir Pistora
Nanotechnology Centre, VSB-Technical University of Ostrava, Czech Republic, Czech Republic

Second order effect in magnetization are becoming an important way of characterization of the magnetic samples. One of the examples of second order effect in magnetization are anisotropic magnetoresistance (AMR), Voigt effect, quadratic magneto-optical Kerr effect (QMOKE) or X-ray magnetic linear dichroism (XMLD). All those effects are originating from conductivity (or permittivity) tensor, which elements are varying with direction of the sample magnetization. This dependence is determined by symmetry arguments describing break of the symmetry by magnetization in the crystal. From first principles we have calculated the complete angular dependence of all elements of the permittivity tensor with respect to the change of magnetization axis in a wide spectral range (from dc to ultraviolet) for a body-centered cubic Fe. The correctness of calculations are verified by careful comparison with expected dependences provided by symmetry arguments. The calculations are based on density functional theorem utilizing one of the most accurate full potential augmented plane-wave code. The effect of the spin-orbit interaction for valence and semicore states is included as well.

QH20

Magnetic structure of nearly equiatomic MnRh alloy

Yuki Matsuoka¹ and Aya Takasaki²
¹ *Nara Women's University, Japan*
² *Graduate School of Humanities and Sciences, Nara Women's University, Japan*

MnRh shows various kind of magnetic state. The magnetic structure and the transition temperature of MnRh are expected to be very sensitive to the atomic composition. At the equiatomic composition, this alloy shows antiferromagnetic - paramagnetic transition. By increasing Mn ratio, this alloy shows complicated magnetic property, ferromagnetic - weak ferromagnetic transition.[1] Yamada et.al. reported that antiferromagnetic structure is most stable in this alloy.[2] To determine the magnetic structure, we performed neutron diffraction measurements and observed some magnetic scattering peaks. The intensities of magnetic scattering peaks were almost same even just below the phase transition temperature. On the other hand, magnetization curve of same component alloy suggests magnetic phase transition. We attempt to determine the magnetic structure and to make magnetic phase diagram of nearly equiatomic MnRh.

[1] Matsuoka Y, 1995 MA Thesis [2] Yamada H, Shimizu H, Yamamoto K, Uebayashi K, 2006 J.Alloys Comp. 415 31

QH21

Magnetic and transport properties of Pd₂Mn_{1+x}In_{1-x} Heusler alloys

Hironari Okada¹*, Yohei Yamazaki², Takashi Yasuda¹ and Takeshi Kanomata¹
¹ *Faculty of Engineering, Tohoku Gakuin University, Japan*
² *Division of Engineering, Graduate School of Tohoku Gakuin University, Japan*

Recently, it was reported that Ni-Mn-In and Ni-Mn-Sn Heusler alloys having a ferromagnetically ordered L21 type structure show a magnetic-field-induced reverse martensitic transformation associated with a metamagnetic transition [1]. The interplay between the martensitic transformation and the magnetic transition gives rise to a magnetic-field-induced shape recovery effect and a magnetoresistance effect. Pd₂MnIn has an antiferromagnetically ordered L21 type Heusler structure [2], which is different from the magnetic ordered state of Ni₂MnIn. In this work, in order to investigate the magnetic and transport properties of the antiferromagnetic Heusler alloys, we performed magnetization and electrical resistivity measurements for Pd₂Mn_{1+x}In_{1-x}. In Pd₂Mn_{1+x}In_{1-x} with x > 0.2, a sudden increase of the resistivity was observed. The temperature at which the anomaly of the resistivity appears shifts to the higher temperature with increasing Mn content, and no anomaly was detected for the Mn content with x = 0.55. The results of powder X-ray diffraction experiment indicate that a martensitic phase appears for the Mn content with x = 0.55 at room temperature. Therefore, it is considered that the anomalous behavior of the resistivity results from the martensitic transformation.

[1] R. Kaimuma et al. Nature 439 (2006) 957. [2] P.J. Webster and R. S. Tebble, Phil. Mag. 16 (1967) 347.

QH22

Structural and magnetic properties of (Co, Fe, Ni), (Fe, Mg, Zn) and (Fe, Mn, Zn) alloys deposited onto Al₂O₃ and SiO₂

Lonzeche Jean Augustin Lodya¹*, Adli Beck², Rudelle White³, Bongani Xaba¹, Siyanda Lubhelwane¹, Khuselwa Vundisa¹ and Jeanette Ngubane¹
¹ *Research & Development, Sasol Technology, South Africa*
² *Chemistry Department, University of Stellenbosch, South Africa*
³ *Chemistry Department, North-West University, South Africa*

Structural and magnetic properties of (Co, Fe, Ni), (Fe, Mg, Zn) and (Fe, Mn, Zn) alloys deposited onto Al₂O₃ and SiO₂ supports are reported. The samples were synthesised by ball milling and characterised using magnetic measurements (MM), Mossbauer spectroscopy (MS), XRD, SEM, TPR and (BET). Granular and irregular shaped particles were formed. MM, MS measurements and XRD data revealed the formation of peculiar solid solutions some of them having spinel structures. In all the samples small crystallites in a superparamagnetic (SPM) state at room temperature were found to coexist with larger ones, their fractions depending on the energy imparted during the ball milling process. That is, crystallites were predominantly in a SPM state at a relatively high ball-to-powder ratio while larger crystallites were prevalent at a relatively low ball-to-powder ratio. The ball milling process resulted also in low surface areas and collapse of pores. Further, the existence of strong metal support interactions (SMSI) was inferred in all the samples; this rendered reduction difficult and/or led to incomplete reduction. Fittings of the Curie-Weiss model to the experimental temperature dependences of AC magnetic susceptibility were used to determine the effective magnetic moments associated with magnetic cations and the nature of their interactions.

QH23

Structure disorder effect of L1₀ FePt within supercell method

Kazuhiko Uebayashi
Section of Natural Science, Akita National College of Technology, Japan

L1₀ FePt alloy is famous for a good candidate of high density magnetic recording media. In my previous work[1], I have performed energy-band calculations for the L1₀ bulk alloy FePt by using the linear muffin-tin orbital method with atomic sphere approximations. This previous calculated study shows that the calculated lattice constants and magnetic moments are good agreement with observed ones. The experimental stable-magnetic state is ferro magnetic, but in the calculation one of the anti-ferro magnetic state is most stable, and the second is ferro magnetic above 1 mRy/ f.u. The difference between the experimental and calculated result for L1₀FePt is known by another work[2]. To improve the difference, I carry out structure-disorder band calculation for FePt with supercell method. I assumed that the supercell is as 8 times large as a formula unit. In the supercell with only one substitution Fe and Pt, the most stable state becomes ferro and the difference between ferro and anti-ferro magnetic state is about 10²mRy. The result indicate that the structure disorder of L1₀ FePt in the supercell makes ferro magnetic stable with observed lattice constants.

[1] K. Uebayashi, JOURNAL OF APPLIED PHYSICS 107, 09A733 (2010) [2] G. Brown, PHYSICAL REVIEW B 68, 052405 (2003)

QH24

Itinerant antiferromagnetism in high-quality single crystal CrB₂

Andreas Bauer¹*, Alexander Regnat¹, Christian Blum², Saskia Gottlieb-schoenmeyer¹, Bjoern Pedersen³, Sabine Wurmehl², Bernd Buechner² and Christian Pfleiderer¹
¹ *Physik-Department E21, Technische Universitaet Muenchen, D-85748 Garching, Germany*
² *Leibniz Institute for Solid State and Materials Research IFW, D-01171 Dresden, Germany*
³ *Forschungsneutronenquelle Heinz-Maier Leibniz, Technische Universitaet Muenchen, D-85748 Garching, Germany*

Transition metal and rare earth diborides with the hexagonal AIB₂ structure form a series of compounds with a remarkably wide range of different electronic ground states. We report the properties of isotopically enriched high-purity single crystals of CrB₂ grown by optical float-zoning. The temperature dependence of the electric resistivity and specific heat provide unambiguous evidence of spin density wave type order with a slightly anisotropic charge gap Δ(001) = 230 K and Δ(100) = 212 K, respectively. We also find that the Neel temperature of 88.5 K remains unchanged under magnetic fields up to 14 T, the highest field studied. A detailed neutron scattering study, made possible through the use of 99% isotopically enriched ¹¹B, provides for the first time unambiguous evidence of antiferromagnetic order, and identifies CrB₂ as a textbook example of itinerant antiferromagnetism. In comparison to the properties of other high-quality single crystal transition metal and rare earth diborides we have prepared, our studies of CrB₂ shed an unexpected new light on the properties of this exciting series of compounds.

QH25

Magnetic orderings in Fe-intercalated TiX₂ (X=S, Se)

Seung Ill Hyun and J.h. Shim*
Chemistry, POSTECH, Korea

Titanium dichalcogenides shares the same layered structure, except TiO₂. Their physical properties, however, are different from each other. TiSe₂, for example, is the only compound that bears an unconventional charge-density wave (CDW) transition under 200K, whereas the others show no distinct structural distortion.[1] Furthermore, Iron-intercalated TiS₂ and TiSe₂ exhibit different types of magnetism. Fe_{0.5}TiS₂ displays a ferromagnetic ordering under 80K, Fe_{0.5}TiSe₂ shows an antiferromagnetic ordering under 135K.[2,3] In order to describe the magnetic interactions between Fe atoms, we apply the first principle calculation on Fe_{0.5}TiX₂ (X=S, Se) and explain the experimental observations correctly. We also discuss the origin of different magnetic behaviors based on the structural & elemental effect.

[1] K. C. Woo, F. C. Brown, W. L. McMillan, R. J. Miller, M. J. Schaffman, and M. P. Sears, Phys. Rev. B 14, 3242 (1976) [2] N. V. Selezneva, N. V. Baranov, V. G. Pleshchev, N. V. Mushnikov, and V. I. Maksimov, Phys. Solid State 53 (2), 329 (2011) [3] N. V. Baranov, V. G. Pleshchev, E. M. Sherokalova, N. V. Selezneva and A. S. Volegov, Phys. Solid State 53 (4), 701 (2011)

QH26

Non-Stoner Itinerant Ferromagnetism of a Transition Metal Monomer

Hanhim Kang, Geunsik Lee, P. Dua, Ji-hoon Shim and Kwang S Kim*
Department of Chemistry, POSTECH, Korea

We investigated the one-dimensional monomer chain of 3d transition metals (Fe, Co, and Ni) by ab-initio band structure calculation with quasiparticle GW method [1]. We also studied the role of pair hopping interaction on the magnetic properties using the extended Hubbard model [2][3]. GW calculation of transition metal monomer shows the spin-dependent band width changes as well as spin-dependent transport properties in ferromagnetic phase. Such behavior is well described by the extended Hubbard model, where the pair hopping enhances the metallic ferromagnetism in one-dimension. We suggest that the electron correlation effect such as pair hopping usually has important role in the metallic ferromagnetism of low dimensional system.

[1] T. Kotani, M. van Schilfgaarde, and S. Faleev, Phys. Rev. B, 76 (2007). [2] J. Hirsch, Phys. Rev. B, 59, 6256 (1999) [3] J. Hirsch, Phys. Rev. B, 43, 701 (1991)

QH27

Magnetic structure variation with structural phase transition in SrMnSb₂

M. Arshad Farhan, Geunsik Lee and Ji Hoon Shim*
Chemistry, POSTECH, Korea

RMnSb₂ system (R = Alkali Earth Metal) is analyzed by first principle DFT calculation using full potential linearized augmented plane wave method while PBE-GGA is used to account for the Exchange-Correlation potential. SrMnSb₂ has zig-zag chains of Sb ions while BaMnSb₂ has square planes of it. The application of pressure on SrMnSb₂ leads to a phase transformation from chain like semi-metal phase to BaMnSb₂ like Square planner structure showing metallic properties. The density of states for AFM SrMnSb₂ changes with the structural phase change indicating a magnetic transition. While for a similar chain to square transition in BaMnSb₂ accompanying an Insulator to Metal transition, no such variation in magnetic structure is observed.

QH28

Magnetoresistance effect of Heusler-type Fe₂VAl single crystal

Rika Hamada¹, Hidetoshi Miyazaki^{2*} and Yoichi Nishino¹
¹ *Department of Frontier Materials, Nagoya Institute of Technology, Japan*
² *Center for Fostering Young and Innovative Researchers, Nagoya Institute of Technology, Japan*

The Heusler-type intermetallic compound Fe₂VAl has attracted strong attention because of a semiconducting behavior of ρ and a large electronic specific heat coefficient γ, 14 mJ/(K²mol). The band calculation revealed that the Fe₂VAl was a semimetal and nonmagnetic with a pseudogap around the Fermi level [2]. Endo et al. discovered the giant magnetoresistance (GMR) effect in the Heusler type alloys Fe_{2-x}V_{1-x}Al poly crystal of about 30 % for Fe_{2.1}V_{0.9}Al at 4.2 K in the field of 55 kOe [3]. Recently we have succeeded in fabricating single crystals of Fe_{2.1}V_{0.9}Al using Czochralski method and investigated their electric and magnetic properties. The temperature dependence of GMR is negative below the Curie temperature (TC). The maximum value of GMR is about 35 % around the TC. The value of GMR in Fe_{2.1}V_{0.9}Al single crystal is similar in that of poly crystal.

[1] Y. Nishino et al., Phys. Rev. Lett. 79, 1909 (1997). [2] G. Y. Guo, G. A. Bottom and Y. Nishino, J. Phys.: Condens. Matter 10 L119 (1998). [3] K. Endo et al., J. Magn. Magn. Mater. 177-181 1437 (1998).

QH29

Electronic structures and magnetic properties of antiferromagnetic BaFe₂As₂

Jae Kyung Chang, Ju Young Kim, Chang Hyun Yi and Joo Yull Rhee*
Department of physics, Sungkyunkwan university, Korea

In low dimensional metals the electrons can be organized into regular patterns, which is known to be the charge-density wave(CDW) or spin-density wave(SDW). The parent compound of iron-based superconductors, BaFe₂As₂, undergoes both structural and magnetic phase transitions. The crystal structure changes from tetragonal to orthorhombic, and the magnetic ground state changes from paramagnetic to antiferromagnetic at ~140 K and neutron scattering measurements show the magnetic moment of 0.87μB per Fe in antiferromagnetic state. SDW anomaly at 140 K, which is believed to be an important prerequisite for high-Tc superconductivity in iron-based superconductors, was also observed. We performed the electronic-structure calculation for the BaFe₂As₂ compound in various antiferromagnetic states, and the electronic structures and Fermi surfaces are carefully investigated. While there have been considerable debates as to whether the antiferromagnetism is due to the Fermi-surface nesting or the second-neighbor superexchange, via comparing our results with experimental and hypothetical cases, we can deduce the correlation between the SDW and the Fermi-surface nesting.

QI01

Development of magnetic order in the TbNi(Al,In) series and magnetocrystalline anisotropy in TbTX compounds

Milan Klicpera¹*, Pavel Javorsky¹, Ines Puente Orench², Eva Santava³ and Stanislav Danis¹
¹ *Department of Condensed Matter Physics, Charles University in Prague, Faculty of Mathematics and Physics, Czech Republic*
² *Institut Laue-Langevin, Grenoble, France*
³ *The Academy of Sciences of the Czech Republic, Czech Republic*

We present recent study of magnetocrystalline anisotropy in TbNi(AlIn) series, crystallizing in hexagonal ZrNiAl structure. The properties of this series were investigated by magnetic measurements, low-temperature x-ray diffraction in magnetic field and mainly by powder neutron diffraction. Parent compounds of our series were previously studied. TbNiAl orders antiferromagnetically with propagation (1/2,0,1/2) and at lower temperatures undergoes another magnetic phase transition when one third of magnetic moments is reduced to almost zero. TbNiIn shows complex magnetic ordering with propagation vector (0,0,0) and other propagation (1/2,0,1/2) occurs at lower temperatures. Our data reveal suppression of the antiferromagnetic structure of TbNiAl with substitution of 10% Al by In. Instead, dominant ferromagnetic order appears, while the direction of Tb magnetic moments along the c-axis is retained. Additional weak antiferromagnetic components arranged within the basal plane and described by k=(1/2,0,1/2) appear at low temperatures. This antiferromagnetic component is presented in the whole rest of series. Dominant component described by (0,0,0) propagation then undergoes change from c-axis ferromagnetic order to a more complex basal-plane structure around 40% of In. Anisotropy change in this series is related to strong change of the c/a ratio of lattice parameters. This behaviour can be generalized for other hexagonal Tb-based compounds.

Q102

Magnetic properties of Ho_{1-x}Lu_xB₁₂ solid solutions

Slavomir Gabani¹, Emil Gazo¹, Gabriel Pristas¹, Marian Reiffers¹, Iveta Takacova¹, Natasha Shitsevalova², Konrad Siemensmeyer³, Nickolay Sluchanko⁴ and Karo Flachbart^{1*}

¹ Institute of Experimental Physics of Slovakia Academy of Sciences, Kosice, Slovakia
² Institute for Problems of Materials Sciences, NASU, Kiev, Ukraine
³ Helmholtz Zentrum Berlin, Berlin, Germany
⁴ General Physics Institute, RAS, Moscow, Russia

Rare earth dodecaborides (REB₁₂) have attracted considerable attention in recent years, above all due to the wide variety of their physical properties. In our contribution we present the magnetic properties of the geometrically frustrated antiferromagnet HoB₁₂ (with ordering temperature T_N = 7.4 K) modified by substitution of magnetic Ho atoms through nonmagnetic Lu ones. In this case, in the so-called solid solution Ho_{1-x}Lu_xB₁₂, both chemical pressure (as Lu³⁺ ions and Ho³⁺ ions have different radii) and magnetic dilution take place with the increasing content of Lu that change the properties of the system. The received results show strong indication for the existence of a quantum critical point close to x = 0.9. This critical point separates the region of magnetic order (starting with HoB₁₂ for x = 0) and the nonmagnetic region (ending with superconducting LuB₁₂ for x = 1). The work was supported by the Slovakia Scientific Agency VEGA (0148-10), the Slovakia Research and Development Agency APVV, and by the Center of Excellence of the Slovakia Academy of Sciences.

Q103

High-field magnetization of Tm₂Fe₁₇ and its deuteride

A. V. Andreev^{1*}, O. Isnard², M. D. Kuz'min³, Y. Skourski⁴, D. I. Gorbunov¹, J. Wosnitza⁵, N. V. Kudrevatykh⁵, A. Iwasa⁶, A. Kondo⁶, A. Matsuo⁶ and K. Kindo⁶

¹ Institute of Physics ASCR, 18221 Prague, Czech Republic
² Institut Neel CNRS and Universite Joseph Fourier, BP166X, Grenoble, France
³ IFW, 01171 Dresden, Germany
⁴ High Magnetic Field Laboratory, 01314 Dresden, Germany
⁵ Ural Federal University, 620083 Ekaterinburg, Russia
⁶ ISSP, Tokyo University, 277-8581 Kashiwa, Japan

A magnetization study of a Tm₂Fe₁₇ single crystal and aligned powder of the deuteride Tm₂Fe₁₇D₂ has been carried out in steady (14 T) and pulsed (60 T) magnetic fields at 1.5-300 K. Tm₂Fe₁₇ is a ferrimagnet with T_c=295 K and a spontaneous moment of 21 μ_B/f.u. Due to competing magnetic anisotropy of the Tm and Fe sublattices, a spin-reorientation occurs at 70-100 K, from the easy-axis to the easy-plane type via a cone of easy axes. Two metamagnetic transitions, at 41 and 53.5 T, are observed at 2 K in fields applied along the c axis. At 60 T the magnetization reaches 43 μ_B/f.u., i.e. the sublattices are not yet parallel (M_c+M_{ab}= 49 μ_B). In the basal plane a wide S-shape magnetization curve is observed. The high-field behavior of Tm₂Fe₁₇ is compared with that of two other easy-axis R₂T₁₇ compounds, Tm₂Co₁₇ and Er₂Co₁₇. Hydrogenation (deuteration) stabilizes easy-plane anisotropy in Tm₂Fe₁₇D₂ over whole ferrimagnetic range (up to T_c=465 K). Despite different types of magnetic anisotropy, the high-field behavior of the deuteride and the parent compound is qualitatively similar. The transitions along the c axis occur in the same fields, being less pronounced in the deuteride.

Q104

RKKY interaction and magnetic properties in (Y-Gd)Ni compounds

Kazuo Yano^{1*}, Katsuhiko Nishimura², Eiji Kita³, Tsuyoshi Ohta³ and Kiyoo Sato⁵
¹ College of Science and Technology, Nihon University, Japan
² Graduate School of Science and Engineering for Research, University of Toyama, Japan
³ Applied Physics, University of Tsukuba, Japan
⁴ Quatum Desighn Japan, Japan
⁵ Faculty of Engineering, Yokohama National University, Japan

CeNi is well known as one of the most famous heavy fermion compounds and shows a peculiar behavior as an enhanced Pauli-paramagnet. That is, both Ce and Ni seem to be non-magnetic in CeNi. On the other hand, GdNi, which has the same structure as that of CeNi, is a ferri-magnet and not only Gd but also Ni are magnetic. It follows that the result that Ni is non-magnetic in CeNi becomes not self-evident and the mechanism of disappearance of Ni magnetic moment is important and interesting problem. Based on such scenario, we have been investigating a (Ce-Gd)Ni compound system. One of the results obtained is a linear relationship in M(T) in Gd-poor content (Gd<20 at%) and it is found that this result reflects the collapse-like decrease of Gd-Gd exchange interaction. In order to examine this collapse-like decrease of RKKY interaction, we have investigated the (Y-Gd)Ni compound system where Ce is replaced by Y. In this system, the exchange interaction between Gd and Gd does not collapse-likely decrease and seems to revive even in Y=15 at%. Furthermore, YNi (Gd=0) seems to be itinerant, however, the substitution of Y by Gd causes localization and Curie-Weise law becomes valid.

Q105

Magnitization curves in high magnetic fields of TbZn₂

Yoshiya Adachi¹, Tetsuo Kitai², Keiichi Koyama³, Hajime Yoshida⁴ and Takejiro Kaneko⁴

¹ Graduate School of Science and Engineering, Yamagata University, Japan
² Faculty of Engineering, Kyushu Institute of Technology, Japan
³ Graduate School of Science and Engineering, Kagoshima University, Japan
⁴ IMR, Tohoku University, Japan

Rare earth Zinc compounds RZn₂ (R=Gd, Tb, Dy, Ho, Er) crystallize in CeCu₂-type structure. In the case of GdZn₂, its magnetism is ferromagnetic, in the other cases, antiferromagnetic. Debray et al. [1] was reported that TbZn₂ is the antiferromagnet with two antiferromagnetic phases which are the high temperature phase AF(a) and the low one AF(b). Two transition points TN(a) = 75 K and TN(b) = 60 K are corresponding to those phases. The magnetic structure of AF(b) is a collinear type and AF(a) is a sinusoidal transverse wave type. The magnetic measurements were performed with a single crystalline sample by Kitai [2]. Two transition points TN and Tt were observed corresponding to TN(a) and TN(b). We performed the measurements of the magnetization curves in high magnetic fields with the single crystalline sample of TbZn₂. The metamagnetic transitions were observed in the directions of all axes. Especially in the direction of c-axis, the metamagnetic behaviors were observed above TN. In this paper, we will discuss the origin of the metamagnetic transitions for TbZn₂.

[1] D. Debray et al.: J. Chem. Phys., 56 (1972) 4325. [2] T. Kitai: J. Phys. Soc. Jpn., 64 (1995) 3403.

Q106

Deuteration induced ferromagnetic metallic properties in R₂Rh₃Dx (R = Tb, Dy)

Koji Shimomura^{1*}, Takanori Tsutaoka¹ and Stanislaw M. Filipek²

¹ Graduate School of Education, Hiroshima University, Japan
² Institute of Physical Chemistry, Polish Academy of Sciences, Poland

Heavy rare earth compounds R₂Rh₃ (R = Gd to Er) show the antiferromagnetic character at low temperature and semimetallic behavior in which the temperature coefficient of electrical resistivity is negative in high temperature region [1]. We studied the magnetic properties of Tb₂Rh₃ and Dy₂Rh₃ hydrides and reported the hydrogenation induced ferromagnetic states in these compounds [2]. At this time, we have investigated the magnetic and electrical properties of the R₂Rh₃D_x deuterides and found the ferromagnetic metallic state in these compounds. Deuteration of Tb₂Rh₃ and Dy₂Rh₃ were carried out using the high pressure apparatus in the pressure range up to 1 GPa at 100 °C for 24 hours and Tb₂Rh₃D₂₇ and Dy₂Rh₃D₂₈ were obtained. Dy₂Rh₃ has an antiferromagnetic phase below TN = 59 K and a semimetallic properties. On the other hand, Dy₂Rh₃D₂₈ shows a ferromagnetic state below TC = 11.5 K and a metallic property below 300 K. In Tb₂Rh₃D₂₇, almost the same changes in magnetic and electrical properties were observed.

[1] T. Tsutaoka, Y. Nakamori, T. Tokanaga, T. Itoh, J. Phys. Soc. Jpn., 70 (2001) 199. [2] R. Sato, T. Tsutaoka, S. M. Filipek, J. Alloys Comp., 446-447 (2007) 610.

Q107

Magnetic properties of Nd₂Pd₃ single crystal

Takuya Matsushita, Koji Shimomura and Takanori Tsutaoka^{*}
 Graduate School of Education, Hiroshima University, Japan

Rare earth intermetallic compound Nd₂Pd₃ shows relatively large magneto-coloric property and magnetoresistance [1]. This time, we have succeeded to make single crystals of Nd₂Pd₃ and investigated the magnetic properties by measuring magnetization and magnetic susceptibility. Single crystals were grown by the Czochralski method from single-phase polycrystalline samples, which were made by arc-melting the constituting 99.9%-pure Nd and 99.95%-pure Pd elements, under high-purity argon atmosphere. The crystal orientation was determined by the back-reflection Laue method. Magnetization curve at 2 K indicates ferromagnetic property for both a- and c-axes; the easy magnetization axis locates in the c-plane. Metamagnetic transitions indicating an antiferromagnetic state were observed above TC = 34 K in the magnetization curves, which were reported so far. A first order magnetic transition from ferromagnetic to antiferromagnetic was observed at TC in the temperature dependence of magnetic susceptibility in both a- and c-axes. Magnetic susceptibility curves for both axes also indicate a small cusp at around TN = 40 K indicating the antiferromagnetic to paramagnetic transition.

[1] N. K. Singh, P. Kumar, Z. Mao, D. Paudyal, V. Neu, K. G. Suresh, V. K. Pecharshy, K. A. Gschneidner Jr., J. Phys. Cond. Mat., 21 (2009) 456004.

Q108

Giant magnetoresistance and field-induced phase transitions in Tb₂Rh₃ single crystal

Takanori Tsutaoka^{1*}, Koji Shimomura¹, Nikolay V. Baranov², Alexey V. Proshkin², Evgeny G. Gerasimov³ and Pavel B. Terentev³

¹ Graduate School of Education, Hiroshima University, Japan
² Institute of Natural Sciences, Ural Federal University, Russia
³ Institute of Metal Physics, Ural Branch of RAS, Russia

The rare earth intermetallic compound Tb₂Rh₃ crystallizes in the Th-Fe3 type hexagonal structure with the space group P63mc in which Tb occupies three non-equivalent sites. Tb₂Rh₃ enters an antiferromagnetic (AF) state below TN = 91 K and shows further magnetic transformations with decreasing temperature below ~ 73 K [1]. Unusual negative temperature coefficient of the resistivity in a wide temperature range above TN [1] and the large magnetoresistance even in paramagnetic state [2] were observed for this compound. In this study, we have performed high field magnetization (up to 350 kOe) and magnetoresistance (up to 120 kOe) measurements on a Tb₂Rh₃ single crystal. The metamagnetic transition along the b-axis is observed to be accompanied by the giant magnetoresistance effect (~ 65 %) in the field interval (70 -110) kOe. The magnetization measurements along the c-axis have revealed multiple phase transitions at fields above 200 kOe. The magnetization curves measured in the paramagnetic state along the c-axis show an inflection point up to 140 K, which may be indicative of the persistence of antiferromagnetic short-range magnetic order in the c-plane.

[1] Y. Nakamori et al. Physica B, 304 (2001) 1. [2] K. Sengupta et al. Solid State Comm., 39 (2006) 351

Q109

Magnetic properties of a GdFe₃Al₇ single crystal

D. I. Gorbunov^{1*}, A. V. Andreev¹ and M. D. Kuz'min²

¹ Institute of Physics ASCR, 18221 Prague, Czech Republic
² IFW, 01171 Dresden, Germany

A magnetization study of a GdFe₃Al₇ single crystal has been carried out in static magnetic fields up to 14 T at temperatures between 2 and 300 K. The compound is found to order ferrimagnetically at T_c = 266 K. The spontaneous magnetic moment is 0.56 μ_B at 2 K. There is no compensation point in GdFe₃Al₇, as distinct from isomorphous compounds DyFe₃Al₇ and HoFe₃Al₇. GdFe₃Al₇ is endowed with an appreciable magnetic anisotropy, the 4-fold axis being a hard magnetization direction. The easy direction is [110] and the anisotropy within the basal plane is also rather strong. The latter is quite remarkable for a system devoid of significant orbital moments. The possible cause of the in-plane anisotropy in GdFe₃Al₇ could be the unusually large crystal field parameter B₄₄, as observed in other compounds with the ThMn₁₂-type structure, e.g., in DyFe₃Ti. The crystal field effect could be mediated by a small admixture of the 4f⁶ configuration to the ground state 4f⁷. The exchange field on the Gd sublattice is determined from the high-field slope of the basal-plane magnetization curves to equal 62 T.

Q110

Study of multipole ordering in CePd₃S₄ by resonant X-ray diffraction with full polarization analysis

Sinji Michimura^{1*}, Toshiya Inami¹, Toru Otsubo², Takeshi Matsumura², Hiroshi Tanida², Masafumi Sera², Eiichi Matsuoka³, Masanori Watahiki⁴, Katsumi Tanigaki⁴ and Hideya Onodera⁴

¹ Condensed Matter Science Division, Japan Atomic Energy Agency, Japan
² AdSM, Hiroshima University, Japan
³ Department of Physics, Kobe University, Japan
⁴ Department of Physics, Tohoku University, Japan

In rare-earth palladium bronzes RPd₃S₄ (R = La-Yb) compounds with a cubic structure, it is expected that the multipole interactions dominate the low temperature properties because the degeneracy of the orbital degree of freedom remains in the crystalline electric field ground states of R³⁺ in RPd₃S₄ except for R = Tm.[1] CePd₃S₄ orders ferromagnetically below the transition temperature TC = 63 K.[2] Recently we revealed that the O20-type quadrupole moments order below TC, and inferred that the magnetic structure is a ferromagnetic structure by resonant x-ray diffraction (RXD) experiments.[3] Since the symmetry of the magnetic and O20-type quadrupole moments differs from each other, simultaneous order of them below TC suggests the involvement of the octupole interaction. We performed full polarization analysis of RXD experiments in magnetic fields to study the contribution of an octupole interaction. The experiments were performed at the Ce-L₃ absorption edge using a single crystal at BL22XU in Spring-8. In our presentation, we will discuss the contribution of multipole interactions for the low temperature properties in detail.

[1] K. abe et al.: Phys. Rev. Lett. 76 (1999) 5366. [2] E. Matsuoka et al.: J. Phys. Soc. Jpn. 77 (2008) 114706. [3] S. Michimura et al., submitted to J. Phys. Soc. Jpn.

Q111

Effect of temperature and magnetic field history on magnetization behavior of NdVO₃ polycrystalline

Zhengcai Xia^{*}
 wuhan national high magnetic field center, huazhong university of science and technology, China

The magnetic properties of NdVO₃ polycrystalline have been studied in the temperature range from 300 to 1.8K and in magnetic fields up to 16 T. It is found that in an applied field less than 1 T remarkable magnetization reversals occurred in field cooling mode: a diamagnetic behavior was observed below a compensation temperature T_{comp}. Most interestingly, the diamagnetic behavior was dependent to both the temperature and applied magnetic field, where the temperature window is 50-100K, and magnetic field below 1T. Beyond the temperature window and above the magnetic field, the diamagnetic behavior disappeared. That is the magnetization always switches to the opposite direction if the sample is cooled through the temperature window in a field less than 1 T. However, the temperature dependence of the resistance has an almost independent to the applied magnetic field in the range from 0 to 16T. A possible mechanismbased on the competition of the single-ion magnetic anisotropy and the antisymmetric Dzyaloshinsky-Moriya interaction accompanied by a change of orbital ordering is discussed.

Q112

Phase diagram and transport properties of Y_{1-x}Nd_xCo₂ pseudo-binary alloys

Alexander T Burkov¹, Masataka Takeda², Ai Nakamura², Yoshinao Takaesu², Kiyoharu Uchima³, Masato Hedo⁴, Takao Nakama^{2*}, Katsuma Yagasaki² and Yoshiya Uwatoko⁴

¹ A. F. Ioffe Physical-Technical Institute, Russian Academy of Sciences, Russia
² Department of Physics and Earth Sciences, Faculty of Science, University of the Ryukyus, Japan
³ General Education, Okinawa Christian Junior College, Japan
⁴ Institute for Solid State Physics, University of Tokyo, Japan

Electrical resistivity ρ and thermopower S of pseudo-binary Y_{1-x}Nd_xCo₂ alloys have been measured at temperatures from 2 K to 300 K, under pressures up to 3.5 GPa. NdCo₂ is a ferromagnet with Curie temperature TC of 99 K. In ferromagnetic phase it undergoes 4f spin-reorientation transition at TR = 40 K. At this transition the easy direction of 4f magnetization is changed from [100] above TR to [110] below TR. The system phase diagram TC(x,P) and TR(x,P) is inferred from the temperature dependencies of the electrical resistivity and thermopower. The Curie temperature of the alloys, TC decreases with decreasing Nd concentration x and vanishes around xc=0.3. Above xc the Curie temperature decreases with pressure. The spin-reorientation temperature is weakly dependent on composition and on pressure until it merges with TC. There is a large region of the phase diagram, partly overlapping with the ferromagnetic phase, where cobalt 3d electron system is non-uniformly magnetized due to spatial fluctuations of the 4f-3d exchange field, related to random distribution of Nd 4f magnetic moments over R-sublattice. In this region, spanning the range 0 < x < xm, large static 3d magnetic fluctuations govern the electronic transport.

Q113

Effect of partial magnetic order on resistivity and thermopower of Ho(Co_{1-x}Al_x)₂ alloys

Takao Nakama^{1*}, Chojun Zukeran¹, Ai Nakamura¹, Atsushi Teruya¹, Sentaro Hirakawa¹, Shintaro Watanabe¹, Masataka Takeda¹, Yoshinao Takaesu¹, Kiyoharu Uchima², Masato Hedo³, Katsuma Yagasaki¹ and Alexander T Burkov³

¹ Department of Physics and Earth Sciences, Faculty of Science, University of the Ryukyus, Japan
² General Education, Okinawa Christian Junior College, Japan
³ A. F. Ioffe Physical-Technical Institute, Russian Academy of Sciences, Russia

The electrical resistivity ρ and thermopower S of Ho(Co_{1-x}Al_x)₂ alloys (x = 0, 0.15 and 0.2) were measured from 2 K to 300 K in magnetic fields up to 10 T and under pressures up to 3 GPa. While ρ(T) and S(T) of the pure HoCo₂ reveal abrupt changes at the magnetic ordering temperature TC, indicating the first order transition, the temperature variation of both properties across the ordering temperature in Ho(Co_{1-x}Al_x)₂ alloys clearly show that the type of the magnetic transition changes under substitution of Al for Co from the first order to the second order. ρ(T) of the Al substituted samples (x = 0.15 and 0.2) has a very unusual variation below TC. Usually, the resistivity of an itinerant ferromagnet decreases below TC with decreasing temperature at higher rate than above TC, its temperature derivative having positive “lambda” anomaly at the ordering point. In contrast, ρ(T) of Ho(Co_{1-x}Al_x)₂ alloys (x=0.15 and x=0.2) increases below TC. Moreover, the magnetoresistance of these alloys is positive around TC, this is also in a sharp contrast to usually observed negative magnetoresistance.

QI14

Breakdown of Hund’s third rule for intrinsic magnetic moments

Julia Herrero-albillos^{1*}, Fernando Bartolome², Luis Miguel Garcia³ and A. T. Young³
¹ *CUD, Centro Universitario de la Defensa, Ctra. de Huesca s/n, E-50090 Zaragoza, Spain, Spain*
² *ICMA, ICMA and Dpto. de Fisica de la Mat. Cond. CSIC - Universidad de Zaragoza, Pedro Cerbuna 12, Spain*
³ *Advanced Light Source, Lawrence Berkeley National Laboratory, University of California Berkeley, CA, USA*

Hund’s rules were originally developed in an atomistic picture, and it is therefore surprising that they also hold, almost universally, for molecules and solids. Here we report the first experimental example of a breakdown of Hund’s third rule in an intrinsic magnetic moment: the Co 3d moment of the unorthodox ferrimagnet ErCo₂. The application of magneto-optical sum rules to X-ray magnetic circular dichroic spectra allows for the determination of the Co orbital and spin magnetic moments both in the ferrimagnetic and paramagnetic phases of ErCo₂. In agreement with the predictions of Hund’s third rule, Co orbital and spin moments are parallel throughout the overall temperature range, except in a narrow temperature window within the paramagnetic phase, in which they are overall coupled antiparallel. A qualitative consideration of the balance between the interatomic and intra-atomic interactions acting on the cobalt atoms explains the phenomenon. This situation also leads to the observation of other exotic forms of magnetism in solids, such as a “pure” spin or a “pure” orbital moment on the same compound at selected temperature and fields.

QI15

Magnetic properties of Y substituted TbB₄

Boyoun Kang¹, Sungsu Lee¹, Juyoung Kim² and B. K. Cho^{1*}
¹ *School of Materials Science & Engineering, Gwangju Institute of Science and Technology, Korea*
² *Advanced metallic materials research department, Research Institute of Industrial Science & Technology, Korea*

We synthesized the single crystals of Tb_{1-x}Y_xB₄ (x=0.0, 0.1, 0.2, 0.3, 0.35, 0.4, 0.5, and 0.6) using metallic flux method. The lattice parameters of these crystals are confirmed by powder x-ray diffraction using Fullprof program. The lattice parameters are decreased with increasing substituted Y ratio, according to Vegard’s law. The measurements of temperature-dependent magnetization M(T) is carried out for the single crystals of Tb_{1-x}Y_xB₄ (x=0.0, 0.1, 0.2, 0.3, 0.35, 0.4, 0.5, and 0.6) in 1 Tesla. The compounds reveal antiferromagnetic ordering and its Neel temperatures are decreased with increasing Y ratio. We confirm the spin direction of antiferromagnetic contribution in Tb_{0.65}Y_{0.35}B₄ using single crystal neutron scattering. The direction of Tb spin magnetic moment is tilted from a axis.

QI16

High pressure effects on antiferroquadrupolar orders in RB₂C₂ (R = Dy and Ho)

Hiroki Yamauchi^{1*}, Toyotaka Osakabe¹, Masashi Kosaka², Eiichi Matsuoka³ and Hideya Onodera⁴
¹ *Quantum Beam Science Directorate, Japan Atomic Energy Agency, Japan*
² *Graduate School of Science and Engineering, Saitama University, Japan*
³ *Department of Physics, Graduate School of Science, Kobe University, Japan*
⁴ *Department of Physics, Graduate School of Science, Tohoku University, Japan*

Single-crystal neutron diffraction experiments under 10 GPa class pressure were performed on tetragonal DyB₂C₂ and HoB₂C₂ compounds showing antiferroquadrupolar (AFQ) and antiferromagnetic (AFM) orders. Both magnetic structures in the ground state phases are basically same and described mainly by the propagation vectors k1 = (1, 0, 0) and k2 = (0, 1, 1/2) for an AFM alignment in the c-plane and an orthogonal arrangement along the c-axis. This characteristic zigzag structure is attributed to the competitive coexistence of the underlying AFQ order with the AFM order. Our purpose is to investigate pressure effects on the AFQ and AFM orders through the alteration of the magnetic structures with k1 and k2. The high pressure experiments revealed that applying pressure enhanced the AFM interactions and simultaneously suppressed the AFQ orders in the both compounds. In addition, we found that applying pressure shrinks the crystal volumes more greatly in the direction of the c-axis even under hydrostatic pressure. Therefore, we presume that the volume shrinkage by applying pressure constrains the buckling accompanied by the AFQ orders, which means a local atomic displacement of (B-C) layers along the c-axis, and leads to the suppression of the AFQ orders in the both compounds.

QI17

Antiferromagnetism of TbPd₂Ge₂ Single Crystals

Takahiro Hasegawa^{1*}, Fujiwara Tetsuya¹, Matsubayashi Kazuyuki², Uwatoko Yoshiya² and Shigeoka Toru¹
¹ *Grad. Sch. Sci. and Eng. Yamaguchi Univ., Japan*
² *ISSP, Univ. Tokyo., Japan*

The compound TbPd₂Ge₂, having the tetragonal ThCr₂Si₂-type crystal structure, exhibits an antiferromagnetic order below TN=4 K [1]. The details are not clear. In order to clarify magnetic behavior, we have grown TbPd₂Ge₂ single crystals, and carried out magnetic and specific heat measurements using the single crystals. The magnetic susceptibility shows an anomaly at 13 K in susceptibility vs. T curves, indicating an antiferromagnetic order. The appearance of anomaly at 13K is confirmed in specific heat. This transition temperature is fairly higher than one reported previously [1]. The easy magnetization direction is the [100] direction in the basal plane within this experimental magnetic field up to 7 T. Three metamagnetic transitions appear in the process at low temperatures. In the [110] magnetization process, two metamagnetic transitions are observed. In magnetization curves along the all directions, downward curvatures can be seen, suggesting a precursor of further transition. From these results, the magnetic behavior of this compound is discussed in detail.

[1] A.Szytula et al., *Solid State Commun.*66 (1988) 309.

QI18

Multi-step metamagnetic processes in PrPd₂Si₂ single crystal

Toru Shigeoka^{1*}, Tetsuya Fujiwara¹, Kazuyuki Matsubayashi², Yoshiya Uwatoko², Shoji Kimura³ and Kazuo Watanabe³
¹ *Yamaguchi University, Japan*
² *ISSP, University of Tokyo, Japan*
³ *IMR., Tohoku University, Japan*

Magnetic studies have been performed in detail on a PrPr₂Si₂ single crystal which is crystallized in the tetragonal ThCr₂Si₂-type structure. The temperature dependence of magnetic susceptibility indicate the compound orders antiferromagnetically below TN=3.0 K. The transition has been confirmed by specific heat. Magnetization measurements up to 18 T have been performed and obtained following results. The easy magnetization direction is the [100] direction in the basal plane. In the magnetization process, four metamagnetic transitions appear; it is a four-step metamagnetic one. The [110] magnetization process is a three-step one. A strong magnetic anisotropy between the [100] and [110] directions is observed within the basal plane in high magnetic fields. Along the hard magnetization direction of the c-axis, a metamagnetic transition appears. A magnetic anisotropy between the [100] and [001] directions is also strong. These behaviors are discussed from an analysis of crystal field effects.

QI19

Anisotropic properties of Tb₂Pd₂In single crystal

Silvie Maskova¹, Ladislav Havela¹, Olexander Kolomiets², Alexander V. Andreev³ and Pavel Svoboda^{1*}
¹ *Department of Condensed Matter Physics, Charles University, Czech Republic*
² *Department of Physics, Lviv Polytechnic National University, Ukraine*
³ *Institute of Physics, ASCR, Czech Republic*

Tb₂Pd₂In (tetragonal Mo₂FeB₂ structure type) was reported to be an antiferromagnet with the Neel temperature TN = 32 K and metamagnetic transition at μ₀Hc = 4 T [1]. On the contrary, our magnetization measurements on polycrystalline sample indicate that the magnetization curve of Tb₂Pd₂In has 4 metamagnetic features in the field range to 14 T. We have succeeded to prepare single-crystalline sample of Tb₂Pd₂In using Czochralski method. The magnetic susceptibility measured on single-crystal in various crystallographic directions shows that magnetic properties of Tb₂Pd₂In are highly anisotropic. c-axis was found to be an easy magnetization direction. The magnetization curve along the c-direction at T = 2 K shows two metamagnetic transitions (μ₀Hc = 5 and 8 T). The magnetization is completely saturated at 14 T (Ms = 19.1 μB/f.u.). We have also observed another metamagnetic transition along the a-direction. The magnetization in the a-direction does not show any tendency to saturation in the highest available fields.

[1] M. Giovannini et al., *J. Alloys Compd.* 280, 26 (1998).

QJ01

Successive magnetic transitions of PrRh₂Ge₂ single crystal

Okawara Yuu^{1*}, Cui Jingwei¹, Fujiwara Tetsuya¹, Matsubayashi Kazuyuki², Uwatoko Yoshiya², Kimura Shoji², Watanabe Kazuo³ and Shigeoka Toru¹
¹ *Grad. Sch. Sci. and Eng. Yamaguchi Univ., Japan*
² *ISSP, Univ. Tokyo., Japan*
³ *IMR, Tohoku Univ., Japan*

The ternary compound PrRh₂Ge₂, having the tetragonal ThCr₂Si₂-type crystal structure, shows an interesting magnetic behavior; it orders antiferromagnetically below TN=45 K and exhibits an additional magnetic transition at T=30 K [1]. The details have been, however, unknown yet. In order to elucidate its magnetic behavior, measurements of magnetization and specific heat have been performed on a PrRh₂Ge₂ single crystal. A much large magnetic anisotropy with the easy magnetization direction of c-axis is observed. Four anomalies appear in the temperature dependence of magnetic susceptibility along the c-axis; a cusp at TN=52 K, a high peak at T3=38 K, a shoulder at T2=33 K and a small peak at T1=4 K are observed. Specific heat also shows four anomalies at corresponding temperatures where magnetic anomalies appear, confirming an occurrence of successive magnetic transitions. A clear two-step metamagnetic process appears along the easy magnetization direction of the c-axis at low temperatures. The magnetization in the first step is almost flat and is corresponding to (1/5)Ms, indicating this field-induce phase has a long period magnetic structure. This behavior is discussed as one of characteristic features for Ising-like system with competing exchange interactions.

[1] A. Szytula et al., *Intermetallics* 18 (2010) 1766.

QJ02

Phase diagram of the magnetically frustrated system SmPd₂Al₃ studied by neutron diffraction

Jiri Pospisil^{1*}, Gwilherm Nenert², Hideaki Kitazawa³, Martin Divis¹, Jan Prokleska¹ and Vladimir Sechovsky¹
¹ *DCMP, Charles University, Ke Karlovu 5, 121 16, Prague, Czech Republic*
² *Institut Laue Langevin, 6 rue Jules Horowitz, BP 156, F-38042 Grenoble Cedex 9, France*
³ *National Institute for Materials Science, Tsukuba, Ibaraki 305-0047, Japan*

SmPd₂Al₃ represents a distinctive example of Sm magnetism exhibiting a complex magnetic behavior [1]. The complexity of magnetism is caused by specific features of the Sm³⁺ ion, namely by nearness of the ground-state multiplet J = 5/2 and the first excited multiplet J = 7/2 in conjunction with strong crystal field. We have established a magnetic phase diagram based on magnetization data. Detailed information regarding the magnetic structure of each magnetic phase was lacking and neutron diffraction was highly desirable. To reduce the neutron absorption by the Sm we have performed an experiment at the ILL Grenoble D9 diffractometer with the short wavelength neutrons which are much less absorbed by the natural Sm. The four successive magnetic phases have been detected within the neutron diffraction experiment providing the values of the critical temperatures 3.5, 4, 4.5 and 12.4. Despite the still strong Sm neutron absorption and the low effective magnetic moment we have determined the magnetic k-vector (1/3 1/3 0) of the phase existing in the temperature interval 12.4-4.5 K which classifies the SmPd₂Al₃ to the unique group of magnetically frustrated systems. Discussion will be drawn in the context of recent theoretical approaches to geometrically frustrated magnetic systems.

[1] J. Pospisil, M. Kratochvilova, J. Prokleska, M. Divis, V. Sechovsky; *Phys. Rev. B* 81, 024413 (2010)

QJ03

Interplay of rare-earth and iron sublattices in NdFeAsO

Gwendolyne Pascua¹, Hubertus Luetkens¹, Yurii G. Pashkevich², Hemke Maeter³ and Hans-henning Klaus³
¹ *Laboratory for Muon Spin Spectroscopy, Paul Scherrer Institute, CH-5232 Villigen PSI, Switzerland*
² *A.A. Galkin Donetsk Physytek, NASU, 83114 Donetsk, Ukraine*
³ *Institut für Festkörperphysik, TU Dresden, DE-01069 Dresden, Germany*

We report zero-field (ZF) muon spin relaxation (μSR) measurements on NdFeAsO polycrystalline samples. We investigate the interaction of the Fe magnetic sublattice with the RE (rare-earth) paramagnetic moment in the nonsuperconducting magnetically ordered Nd oxypnictide by a detailed analysis of the hyperfine fields at the muon site. At high temperatures, the fluctuations of the Nd moments are evident from the observed exponential depolarization of the μSR signal. Microscopic evidence of static commensurate magnetic order of Fe moments is revealed by μSR at temperatures below TN(Fe) = 136K. Drastic slowing down of RE moment fluctuations is observed only below TN(RE) = 2K. In the intermediate temperature range, a Schottky-like polarization of the Nd magnetic sublattice by the ordered Fe system is observed. In the Fe system, a transition between a high- and a low-temperature magnetic structures is proposed on the basis of a detailed symmetry analysis and magnetic dipole-field calculations at the muon site. The observed behavior resembles the one of the spin reorientation in the structurally-related Nd₂CuO₄.

[1] H. Maeter, H. Luetkens, Y. Pashkevich, et al. *Phys. Rev. B* 80 094524 (2009). [2] W. Tian, et al. *Phys. Rev. B* 82, 060514 (2010). [3] Y. Qiu, et al. *Phys. Rev. Lett.* 101, 257002 (2008).

QJ04

Magnetic properties of C15 laves phase compound SmRu₂

Yusuke Amakai^{*}, Mototsugu Sato, Naoki Momono, Hideaki Takano and Shigeyuki Murayama
Graduate School of Engineering, Muroran Institute of Technology, Japan

We report the magnetic properties of polycrystalline C15 laves phase rare-earth compound SmRu₂. The sample of SmRu₂ was made by an arc-melt method and was annealed at 500 °C in vacuumed quartz tube for 50 hours. The susceptibility χ of SmRu₂ follows a typical Curie-Weiss law above 80 K. The effective magnetic moment peff is 1.39 μB/Sm-atom, and the Weiss temperature θ is a positive value of 42 K. The low-temperature χ for T < 70 K increases rapidly with decreasing temperature. In the resistivity ρ and the specific heat Cp, we found a small anomaly and a jump at about 55 K. Furthermore, we observed a hysteresis in the magnetic field dependence of magnetization at 2 K. These experimental results suggest that C15 laves phase SmRu₂ is ferromagnetic material on Tc ~ 55 K. Detailed discussion will be presented at the conference.

QJ05

Pressure effect on the electrical resistivity of a ferromagnetic clathrate Eu₈Ga₁₆Ge₃₀

T Iizuka¹, K Umeo^{2*}, M A Avila³ and T Takabatake¹
¹ *AdSM, Hiroshima Univ., Kagamiyama 1-3-1, Higashi-Hiroshima 739-8530, Japan*
² *N-BARD, Hiroshima Univ., Kagamiyama 1-3-1, Higashi-Hiroshima 739-8526, Japan*
³ *Federal University of ABC, Santo Andre, SP, 09210-170, Brazil*

Eu₈Ga₁₆Ge₃₀ is a unique intermetallic clathrate in which the guest sites are fully occupied by a rare-earth element. The Eu²⁺ ions in the tetrakaidecahedral cages in the type-I structure are rattling among off-center positions [1]. This compound exhibits a ferromagnetic transition at Tc=36K. Both the electrical resistivity ρ and the temperature derivative of magnetization exhibit peaks at Tc and T*. Upon applying pressure of 6GPa at 290K, the off-center rattling state of Eu ions changes to the on-centered state. Furthermore, at Ps=14GPa, a structural transition occurs with the volume reduction of about 4% [2]. In order to examine the pressure dependence of Tc and T*, we have measured the temperature dependence of ρ under various pressures up to 15GPa, by using a Bridgman anvil cell made of sintered diamond. With increasing pressure, Tc shifts to higher temperatures. Broadening of the peak at T* for P>4GPa is attributed to the change from the off-center to on-center state. At 290K, ρ(P) jumps at 13GPa, which must be the manifestation of the structural transition.

[1] B. C. Sales, et al., *Phys. Rev. B* 63, 245113 (2001). [2] T. Kume et al., *unpublished*.

QJ06

Magnetic transitions under pressure in GdCo₂B₂

Guanghai Hu^{1*}, Izuru Umehara¹, Lingwei Li² and Katsuhiko Nishimura³
¹ *Department of Physics, Yokohama National University, Japan*
² *Institute of Materials Physics, Hangzhou Dianzi University, China*
³ *Graduate School of Science and Engineering, University of Toyama, Japan*

The pressure effect on magnetic transitions of GdCo₂B₂ compound was studied by dc susceptibility and ac heat capacity in the temperature range 2 K ~ 300 K. The temperature dependence of dc susceptibility for GdCo₂B₂ under various pressure in 0.1 T magnetic field show two information. First, the Antiferromagnetic transition temperature TN decrease with pressure increasing from 12.5 K in 0GPa decrease to 6.3 K in 1.07 GPa and disappeared near to 1.30 GPa with a slope of dTN/dP about -5.8 K/GPa. Second, ferromagnetic transition TC increases slightly with pressure increasing from 20.4 K in 0 GPa to 22.1 in 1.27 GPa with a slope of dTC/dP about 1.5 K/GPa. They were also found in ac heat capacity measurements. It can be understand that there is a strong interaction in the ferromagnetic state and a very weak interaction in antiferromagnetic state which can easily be destroyed by pressure and magnetic field. The transitions are proved to be the second-order transition. In addition, a transition temperature TM which comes from domains of ferromagnetism in heat capacity measurements was found increase from 17.5 K under 0 GPa to 22.0 K under 2.36 GPa with a ratio dTM/dP about 2.2 K/GPa.

[1] L. Li, K. Nishimura, and H. Yamane, *Appl. Phys. Lett.* 94 (2009) 102509 [2] L. Li, D. Huo, Z. Qian, and K. Nishimura, *J. Phys.: Conf. Ser.* 263 (2011) 012017 [3] I. Felner, *Sol. Sta. Comm.* 52 (1984) 191-195 [4] V. K. Pecharsky, and K. A. Gschneidner, Jr., *Int. J. Refrig.* 29 (2006) 1239 [5] I. Umehara, F. Tomioka, A. Tsuboi, T. Ono, M. Hedo, Y. Uwatoko, *J. Magn. Magn. Mater.* 272-276 (2004) 2301-2302.

QJ07

New ferromagnetic compounds with noncentrosymmetric crystal structures

Yoshihiko Inada^{1*}, Guizhi Bao² and Akiko Ono¹
¹ Graduate School of Education, Okayama University, Japan
² Department of Physics, Okayama University, Japan

Recently, physical properties in noncentrosymmetric crystal structures have attracted considerable attentions. The broken inversion symmetry in the crystal causes finite antisymmetric spin orbit coupling (ASOC). A spin-polarized electrons that originates from the ASOC effect is formed even for nonmagnetic materials. Generally, the electronic states of opposite spin orientation are considered to be degenerate in nonmagnetic materials due to the presence of both time-reversal and space-inversion symmetries. However, this degeneracy will be solved by the ASOC in broken space-inversion symmetries with noncentrosymmetric crystal structures. A pair of split bands is produced in the k-space. Ferromagnetic compounds with noncentrosymmetric crystal structures are interesting materials, because the time-reversal symmetries also broken. We discovered new ferromagnetic compounds, Pr₂Bi₃ and Nd₂Bi₃, with noncentrosymmetric crystal structures. They are crystallized in anti-Th₃P₄ structure (space group I-43d), which has no inversion center. Curie temperature T_c are 48K and 94K, respectively. Large ASOC is expected caused by heavy material of Bi. We will report further results in detail.

QJ08

Singlet-triplet crossover in the two-dimensional dimer spin system YbAl₃C₃

Shunichiro Kittaka^{*}, Tomoyoshi Sugiyama¹, Yasuyuki Shimura¹, Toshiro Sakakibara¹, Saori Matsuda² and Akira Ochiai²
¹ Institute for Solid State Physics, University of Tokyo, Japan
² Department of Physics, Tohoku University, Japan

YbAl₃C₃ has the hexagonal ScAl₃C₃ type structure in which magnetic Yb³⁺ ions form a two-dimensional triangular lattice. At 80 K, it exhibits a structural phase transition to an orthorhombic structure with a slight displacement of the Yb atoms [1]. Interestingly, a dimer ground state with the singlet-triplet energy gap of about 15 K has been suggested from the magnetic susceptibility and the specific heat at low temperatures [2]. Indeed, a direct observation of the singlet-triplet excitations has been reported from the inelastic neutron experiments [3]. To investigate the variation of the ground states in magnetic fields, we measured magnetization of a single crystal of YbAl₃C₃ down to 0.07 K and in fields up to 14.5 T. At low temperatures below 0.8 K, several magnetization steps were clearly observed for H||c in 6 T < μ₀H < 9 T, whereas only two transitions were observed at 4.7 and 6.6 T for H||ab. At fields above 9 T, the magnetization becomes almost saturated for both H||c and H||ab. Our results indicate that the singlet-triplet crossover occurs in a relatively narrow field range, suggesting a rather weak interdimer interaction in spite of the nearly triangular lattice of Yb ions.

[1] T. Matsumura et al., J. Phys. Soc. Jpn. 77, 103601 (2008). [2] A. Ochiai et al., J. Phys. Soc. Jpn. 76, 123703 (2007). [3] Y. Kato et al., J. Phys. Soc. Jpn. 77, 053701 (2008).

QJ09

Magnetic structure transition in PrPd₂

Hiroyuki S. Suzuki^{1*}, Noriki Terada¹, Akiko Kikkawa¹, Koji Kaneko² and Naoto Metoki²
¹ National Institute for Materials Science, Japan
² Japan Atomic Energy Agency, Japan

A complex magnetic phase diagram of PrPd₂ with AuCu₃-type structure was reported [1]. The specific heat shows double peaks at TN = 0. 88 K and 0.77 K, which are relatively low compared with the Curie-Weiss temperature Θ_p ~ 17 K. The temperature of the peak at higher temperature is increased but another decreased with the magnetic field. A large tail above TN in the specific heat is also observed. Considering no geometric frustrations in the simple cubic structure of the Pr site, these behavior suggest a competition of inter-site interactions. The magnetic field dependence of the peak at higher temperature, which is typical in the quadrupole ordering system, also suggests an importance of the multipole effect arising from the crystalline electric field ground state. We have investigated the multipole effect using the single crystal by specific heat, magnetic susceptibility, ultra-sonic and also neutron scattering measurements. In this report, we focus on the magnetic structure and its transition. We have found first the 1st transition of the magnetic phase at 0.5 K. The propagation vector observed in the neutron scattering is changed from the incommensurate to commensurate one. We will discuss the complex magnetic phase based of the multipole effect.

[1] S. Zhang, et al., Journal of Physics : Conference Series, 15 (2009) 042074

QJ10

Competition between magnetic ordering and random spin freezing in Dy₂PtSi₃

D. X. Li^{1*}, T. Yamamura¹, S. Nimori² and T. Shikama¹
¹ Institute for Materials Research, Tohoku University, Japan
² Tsukuba Magnet Laboratory, National Research Institute for Metals, Japan

We have been paying special attention to a new family of the ternary intermetallic compounds R₂PtSi₃. The spin-glass or cluster-glass-like effect can be observed in some R₂PtSi₃ compounds with heavy rare earth element, which have been confirmed to crystallize in the ordered hexagonal structure [1]. The mechanisms of the anomalous magnetic behaviors are very interesting in physics. Recently, we prepared a polycrystalline Dy₂PtSi₃ sample and systematically measured its magnetic properties including ac susceptibility (Xac), FC and ZFC magnetization, magnetic relaxation, electrical resistivity and specific heat. The most important observation is the evident peak in Xac(T) curve near Tc~6 K, which shifts to high temperature with increasing frequency suggesting the presence of random spin freezing effect. The observed long-time magnetic relaxation and the low temperature irreversible magnetism give further evidence for this conclusion. However, specific heat measurement shows an evident peak at Tc and the electrical resistivity drops rapidly as decreasing the temperature just below Tc. In this sense, the long-range magnetic exchange interactions have also important influence on the magnetic behavior. Thus it seems to be appropriate to classify the Dy₂PtSi₃ sample as a large magnetic cluster system with competition between magnetic ordering and random spin freezing.

[1] D. X. Li, S. Nimori, Y. Homma and Y. Shiokawa, J. Phys. Soc. Jpn., 71 (2002) Suppl. 211.

QJ11

Dilatometric investigations on the semimetallic ferromagnet EuB₆

Rudra Sekhar Manna¹, Frank Schnelle¹, Mariano De Souza¹, Michael Lang¹, Pintu Das¹, Adham Amyan¹, Jens Mueller¹, Stephan Von Molnar², Peng Xiong² and Zachary Fisk²
¹ Physics Institute, Goethe-University Frankfurt (M), SFB/TR 49, D-60438 Frankfurt (M), Germany
² Department of Physics, Florida State University, Tallahassee, Florida 32306, USA
³ Department of Physics, University of California, Irvine, California 92697, USA

EuB₆ is a semimetallic correlated electron system, which exhibits a complex sequence of electronic and magnetic phase transitions at ~ 15.5 K (Tc1) and 12.5 K (Tc2). The material also shows a colossal magnetoresistance effect which is largest at Tc1. A percolative transition of magnetic polarons, i.e., clusters of ordered Eu²⁺ moments polarized by the spins of localized charge carriers (holes), is involved in the paramagnetic to ferromagnetic transition. Thermal expansion and magnetostriction measurements have been performed on this material to explore to which extent lattice degrees of freedom are involved in these phase transitions. We find two corresponding anomalies in the thermal expansion, the one occurring at Tc2 being much larger than that at Tc1. By applying a small magnetic field of less than 50 mT, the anomaly at Tc1 is fully suppressed, while the lower-temperature anomaly at Tc2 shifts to higher temperature as the field is increased and finally fades out at a field B > 5 T. These measurements are complemented by magnetostriction measurements for a set of temperatures from below Tc2 to above Tc1, highlighting the extraordinarily large magnetoelastic effects in this material.

QJ12

The magnetic anisotropy and magnetostriction of RAl₂ (R= rare earth) compounds

Masashi Ohashi, Yusuke Araki and Kazuma Sawami
 Kanazawa University, Japan

The RAl₂ (R : rare earth element) intermetallic compounds crystallize in the MgCu₂ cubic Laves phase structure. In most of these compounds the R ions are trivalent 3+ and ferromagnetic ordering has been observed with Curie temperature TC up to 170 K. It is expected that some of structural transition occurs due to magnetic symmetry braking below TC. In the present work, spontaneous magnetostriction of ferromagnetic RAl₂ compounds are studied from the X-ray diffraction measurement at low temperature and the thermal expansion of the single crystal. The X-ray diffraction pattern shows the d-spilling at several peaks of TbAl₂ and DyAl₂ due to the large magnetic anisotropy below TC. From these results, the crystal structures are estimated at ferromagnetic phase of TbAl₂ and DyAl₂. The anisotropic magnetoelastic constants have been calculated by using the results of the magnetization and the magnetostriction at the ferromagnetic phase and at the magnetic field up to 2 T.

QJ13

Influence of weak-magnetic, non-magnetic and disoriented grains on remagnetization processes of Nd-Fe-B alloys

Anna Starikova*, Alexey Lileev and Olga Arinicheva
 National University of Science and Technology 'MISIS' (MISIS), Russia

The uniaxial high-anisotropic materials, in which magnetostatic interaction between volumes have a significant influence were investigated. The analysis of domain structure formation during magnetization reversal these materials in the presence of weak-magnetic, non-magnetic and disoriented grains was carried out. The modeling ensemble simulating magnetic properties of sintered alloy neodymium- iron - boron (Nd_{1-x}Fe_xB₃) was selected. Research of influence of inclusions was conducted on the basis of model experiments with the received ensemble. The program, devised for uniaxial high-anisotropic ferromagnetics, in which the sample is presented by ensemble from 1000 particles having transitive domain structure and following individual characteristics was used. After selection of all parameters of the ensemble simulating this material, for researching the influence of inclusions on magnetic reversal processes, key parameters of some microvolumes (Ms, H_{max}, H_s, Angle) were changed. It was concluded that magnetic reversal is realized by the channels formed at the expense of directed magnetostatic interaction. Weak-magnetic, non-magnetic and disoriented grains are the magnetic reversal centers, i.e. they are the beginning of formation of the channel of magnetic reversal.

QJ14

Cobalt magnetism in HoCo₂ under pressure

Jaroslav Valenta, Jiri Prcchal*, Marie Kratochvilova, Martin Misek and Vladimir Sechovsky
 Department of Condensed Matter Physics, Charles University in Prague, Czech Republic

HoCo₂ belongs to a group of RCo₂ (R = rare earth metal) compounds forming in the cubic Laves phase structure. The Ho localized 4f-electron magnetic moments coexist together with the itinerant Co 3d moments, which appear on the verge of magnetism, similar to the ErCo₂ system [1]. Below TC, the large exchange field due to the ferromagnetically ordered Ho moments polarizes the Co 3d-electron states and the emerged moments in the Co sublattice orient antiparallel to the Ho sublattice. Weak Co moments survive rather far above TC (= 79.5 K) in Co magnetic clusters remaining coupled antiparallel to paramagnetic Ho moments forming a paramagnetic phase. This causes a susceptibility anomaly at the paramagnetic transition temperature Tf (= 125 K). At low temperatures the easy magnetization direction changes at the spin-reorientation temperature TR = (16.4 ± 0.5) K. We will present variations of the three transition temperatures with applying hydrostatic pressure up to 3 GPa. TC and TR coincidentally decrease with increasing pressure whereas TR increases. The results will be discussed in term of suppressing the Co magnetic moments and varying the exchange and crystal-field interactions with applying the hydrostatic pressure.

[1] J. Herrero-Albillos et al., Phys.Rev.B 76 (2007) 094409.

QJ15

High-field magnetization study of ErCo₂

Maurice Guillot¹ and Yildirhan Oner^{2*}
¹ Grenoble High Magnetic Field Laboratory, CNRS, BP166, 38042 Grenoble Cedex 9, France, France
² Department of Physics, Istanbul Technical University, Turkey

In this work are presented new results on the magnetic properties of the ErCo₂ compound in which three magnetic phases (ferrimagnetic, paramagnetic and paramagnetic) were proposed very recently. This study is based on the investigation of the magnetization under continuous high magnetic fields (up to 330 kOe at 4.2K and up to 230 kOe in the 4.2-300K respectively). At low temperatures the stability of the ferrimagnetic structure is shown although the saturation was never found. Special attention was paid to the 35-100K temperature range where the transitions between the different magnetic phases occur confirming of the paramagnetic” orderings. The transition temperature Tc from the ferrimagnetic to the paramagnetic phase increases from ? 34 to 62 K with the applied field. For the values of H smaller than 100 kOe. At H values greater than this Tc remains constant at (62 ±5) K. The atomic magnetic moment of Co is independent of the magnetic structure is and in the order of 1μBatom-1.

QJ16

Resonance, magnetic and neutron investigations of magnetic structures in Pr_{1-x}Y_xFe₃(BO₃)₄ system

A Pankrats¹, V Tugarinov^{1*}, C Ritter², D Velikanov¹, I Gudim¹ and V Temerov¹
¹ Kirensky Institute of Physics SB RAS, Krasnoyarsk, Russia
² Institute Laue-Langevin, Grenoble, France

The rare earth borates RFe₃(BO₃)₄, with the structure of the huntite mineral are interesting as materials with two magnetic subsystems with competing anisotropy. In this work we present data on antiferromagnetic resonance (AFMR), magnetic properties and neutron investigation of Pr_{1-x}Y_xFe₃(BO₃)₄ system. Our AFMR and neutron investigations [1-3] show that the last points of the system, YFe₃(BO₃)₄ and PrFe₃(BO₃)₄ are easy-plane (EP) and easy-axis (EA) antiferromagnets, respectively, confirming the magnetic data for R=Pr [4]. A dilution of the Pr³⁺ subsystem by diamagnetic yttrium reduces the magnetic anisotropy of the Pr subsystem and can lead to a transition from EA to EP state at some yttrium content. The single crystals Pr_{1-x}Y_xFe₃(BO₃)₄ with x=0.25, 0.325, 0.5 and x=0.75 were grown. Magnetic and resonance investigations show that the crystals with x= 0.25 and 0.325 are EA antiferromagnets with the energy gap at T=4.2 K close to 75 and 60 GHz, respectively, but the crystals with x=0.5 and 0.75 are EP ones. Neutron investigations showed that the concentration transition from EP to EA state occurs via an inclined magnetic structure which was found for x=0.325. The concentration dependency of AFMR energy gap is studied at T=4.2K. This work was supported by RFBR grant #10-02-00765.

[1] A.I. Pankrats, G.A. Petukovskii, L.N. Bezmaternykh, V.L. Temerov, Physics of Solid State, 2008, Vol. 50, p. 79. [2] Ritter C., Vorotyнов A., Pankrats A., et al., J. Phys.: Cond. Matter, 2008, V. 20, p. 365209. [3] Ritter C., Vorotyнов A., Pankrats A., et al., J. Phys.: Cond. Matter, 2010, V. 22, p. 206002. [4] A. M. Kadamtseva, Yu. F. Popov, G. P. Vorob'ev et al., JETP Lett., 2008, V. 87, p. 45.

QJ17

Anisotropic transport and magnetic properties of PrGe single crystal

Pranab Kumar Das, Neeraj Goyal, Ruta Kulkarni, Arumugam Thamizhavel and Suresh Kumar Dhar
 Department of Condensed Matter Physics and Materials Science, Tata Institute of Fundamental Research, Mumbai, India

The compounds RGe (R = La, Ce, Pr and Nd) crystallize in the two closely related CrB and FeB-type orthorhombic crystal structures, depending upon R and heat treatment. We have recently reported the anisotropic magnetic properties of CeGe in detail which crystallizes in the FeB-type crystal structure [1]. In continuation of our studies on RGe compounds, we report here the anisotropic properties of a single crystal of PrGe grown by Czochralski method. PrGe exhibits dimorphism in which the high temperature FeB-type structure transforms into CrB-type structure at lower temperatures [2]. From the powder X-ray diffraction we have confirmed that the grown single crystal of PrGe possesses CrB-type crystal structure with the space group Cmc#(63). The anisotropic magnetic properties have been studied along the three principal crystallographic directions. From the magnetic and transport properties we find that PrGe exhibits two magnetic transitions at 44 K and 41.6 K along [100] and [010] directions, whereas along [001] direction only a ferromagnetic ordering at 44 K is observed. The susceptibility data clearly indicate that the high temperature ordering is antiferromagnetic and the low temperature one is ferromagnetic. The specific heat capacity data also confirm the two magnetic transitions in PrGe.

[1] Pranab Kumar Das, Neeraj Kumar, Ruta Kulkarni, S.K. Dhar and A. Thamizhavel, arXiv: 1108.1291 [2] D. Hohnke and E. Parthe, Acta Crys. 20 (1966) 572.

QJ18

Theoretical investigation of the phase transition and the spin-gap behavior of the triangular antiferromagnet YbAl₃C₃

Changhoon Lee^{*}, Myung-hwan Whangbo², Juergen Koehler³ and Ji-hoon Shim¹
¹ Chemistry, Postech, Korea
² Chemistry, North Carolina State University, USA
³ MPI for Solid State Research, Stuttgart, Germany

Ytterbium aluminum carbide YbAl₃C₃, first reported in 1992[1] has recently attracted much attention concerning the nature of its phase transition at T* = 77 K.[2-4] YbAl₃C₃ containing triangular sheets of magnetic ions Yb³⁺ (f13) undergoes a phase transition at T* = 77 K and exhibits a spin-gap behavior. The two model structures of YbAl₃C₃, proposed to explain these observations, give unreasonably short C-Al distances. These model structures were optimized by density functional calculations to find that the Model 2 structure is more stable than the Model 1 structure, with chemically reasonable C-Al distances, and that the phase transition at T* is a cooperative second-order Jahn-Teller distortion involving the layers of corner-sharing CA15 trigonal bipyramids. The spin exchanges between nearest-neighbor Yb³⁺ ions, evaluated by density functional calculations for the optimized Model 2 structure, show that YbAl₃C₃ has a two-dimensional spin lattice described by three antiferromagnetic exchanges, but exhibits a spin-gap behavior because one exchange is substantially stronger than the other two.

(1) Gelsing, T. M.; Potgen, R.; Jeitschko W.; Wortmann, U. J. Alloys Compd. 1992, 186, 321. (2) Kosaka, M.; Kato, Y.; Araki, C.; Mori, N.; Nakanishi, Y.; Yoshizawa, M.; Ohoyama, K.; Martin C.; Tozer, S. W. J. Phys. Soc. Jpn. 2005, 74, 2413. (3) Ochiai, A.; Inukai, T.; Matsumura, T.; Oyamada A.; Katoh, K. J. Phys. Soc. Jpn. 2007, 76, 123703. (4) Kato, Y.; Kosaka, M.; Nowatari, H.; Saiga, Y.; Yamada, A.; Kobiyama, T.; Katano, S.; Ohoyama, K.; Suzuki, H. S.; Aso N.; Iwasa, K. J. Phys. Soc. Jpn. 2008, 77, 053701.

QJ19

First Principle Analysis for Pressure Effect on Charge Density Wave Phases of SmNiC₂

Jae Nyeong Kim and Ji-hoon Shim*
Chemistry, POSTECH, Korea

Using a first principles calculation, we have investigated pressure effect on the electronic structure anisotropies, Fermi surface properties, and transport properties of SmNiC₂ to check their effects on the charge density wave instabilities. Both band structure and electric conductivity results show that SmNiC₂ has quasi 1D electronic structure by Ni 1D chain along a axis. However hybridization between nearest Sm 1D chain makes its charge density wave (CDW) properties 2D like with CDW vector $q_1=(0.5, 0.5, 0)$ and another weak CDW vector $q_2=(0.5, 0.5, 0.5)$ at -6 GPa. With increasing pressure, highly anisotropic change of lattice induces these CDW vector to become incommensurate with flattening Fermi surface (FS) in the [110] plane and suppressing FS in [111] plane. The FS nesting vector q_1 is gradually shifted from $q_1=(0.5, 0.50, 0)$ at -6 GPa to $q_1=(0.5, 0.56, 0)$ at 14 GPa, while $q_2=(0.5, 0.52, 0)$ at 0 GPa, coincide with experimental results. Also, $q_2=(0.5, 0.5, 0.5)$, which is significant local maximum at -6GPa, becomes almost saddle point like with its nesting vector shifting another points. We conclude that CDW strength along q_1 vector become stronger with flattening (more 1D like) FS, but CDW strength along q_2 vector become weak with highly anisotropic change of lattice.

[1] S. Shimomura, C. Hayashi, G. Asaka, N. Wakabayashi, M. Mizumaki, and H. Onodera, *Phys. Rev. Lett.* 102, 076404 (2009). [2] Alexander Wolfel, Liang Li, Susumu Shimomura, Hideya Onodera, and Sander van Smaalen, *Phys. Rev. B* 82, 054120 (2010). [3] J. Laverock, T. D. Haynes, C. Uffeld, and S. B. Dugdale, *Phys. Rev. B* 80, 125111 (2009).

QK01

The magnetoresistance of sandwich-structure organic spin-valve

Feng Li*, Fapei Zhang and Yu Xiao
High Magnetic Field Laboratory, Chinese Academy of Science, China

We studied the magnetoresistance (MR) effect in an organic spin-valve structure of ferromagnetic/organic semiconductor/ferromagnetic system theoretically using the spin-diffusion theory and Ohm's law. Spin polarons and spinless bipolarons are assumed to be the main carriers in organic semiconductors. From the calculation, it is obtained that MR value increases with the increase of the polaron proportion and rapidly decreases with the increase of the thickness of organic layer. MR ratio can be enhanced remarkably when the interfacial resistances are spin related. We also investigated MR value dependence of the effects of the matching conductivity and the spin-polarization of ferromagnetic layer.

QK02

First-principles calculations investigation of interfacial roles in spin-dependent transport properties in OMTJs

Shiheng Liang¹, Dongping Liu¹, Lingling Tao¹, Hong Guo² and Xiufeng Han^{1*}
¹ Beijing National Laboratory for Condensed Matter Physics, Institute of Physics, Chinese Academy of Sciences, China
² Department of Physics and Center for the Physics of Materials, McGill University, Montreal, Quebec, Canada

Organic spin valves and organic magnetic tunnel junctions (OMTJs) are new and promising research fields and show advantages for spin-dependent transport due to relatively weak spin-orbital coupling and hyperfine interaction. Long-chain alkanic acids usually form close-packed monolayer films with alkyl chains highly oriented on substrates. The characterization of stearic acid adsorbed on Ni(111) surface has been studied. Our results suggest that the stearic acid is chemically adsorbed on the Ni surface via a bidentate interaction with a distance of about 1.8 Å. We also investigated spin-dependent transport characterization through two kinds of organic magnetic tunneling junctions (OMTJs), as Ni/1-stearic acid radical (1-SAR)/Ni and Ni/1,18-stearic diacid radical (1,18-SDR)/Ni. We found magnetoresistance (MR) of Ni/1-SAR/Ni is -19.6%, and it is 13.7% for Ni/1,18-SDR/Ni OMTJ. There is a magnetic proximity effect in the interface, and the magnetic decay rate is dissimilar in different interfaces. Due to interaction at hybrid organic/magnetic interface, the electronic properties of interfacial atoms are modified. These effects influence the spin-dependent transport properties, and there appears positive or negative tunneling magnetoresistance (TMR) due to different interface. Our results suggest, the interface between organic barrier and FM electrode play an important role in the transport behavior.

QK03

GMR properties on flexible polymer film with bending stress

Joonhyun Kwon, Seungha Yoon, Seungkyo Lee, Jeonghyeon Lee and B. K. Cho*
School of Materials Science and Engineering, Gwangju Institute of Science and Technology (GIST), Korea

Recently, demands and researches about variable flexible devices have been constant. In other to satisfy such demands, researches about magnetic properties in flexible environment also have been continued. In these researches, the simple giant magnetoresistance (GMR) spin valve structure was deposited on flexible polymer films, then was induced by external tensile stress from repetitive bending fatigue. As bending samples, bending directions were decided whether parallel or transverse directions to easy axis directions of GMR structure. As a result, when increasing parallel bending times, switching field interval range of free layer also increased, inversely as increasing transverse bending times, coercivity of free layer also increased. Such tendency had opposite properties to inverse magnetostriction effect theory from the view of bending direction, because flexible films had larger elastic recovery forces than tensile forces after bending. Therefore we anticipate that such elastic recovery forces was the reason of opposite tendency from the aspect of direction. Based on these results, we clarified possibilities that the coercivity could be controlled without curvature, moreover axis behavior, e.g., easy axis or hard axis, also could be controlled without curvature and extra annealing processes.

QK04

Giant magnetoresistance in graphene nanoribbons: Geometry, interface and dephasing effects

Stefan Krompiewski*
Institute of Molecular Physics, Polish Academy of Sciences, Poznan, Poland

Motivated by the ongoing debate on the role of external contacts on electronic transport through carbon nanostructures [1-3], we theoretically estimate the combined effects - due to (i) geometry, (ii) the way the external contacts are attached and (iii) possible dephasing processes - in graphene nanoribbon (GNR). The method is based on the tight binding model, the Green function technique and the Landauer-type formalism. It is shown that giant magnetoresistance in GNRs depends strongly not only on the aspect ratio of the sample and the current direction, but also on whether ferromagnetic electrodes are attached in the end- or side-contacted manner. Typically the former attachment is favorable for conductivity. However the observed tendency is that the higher conductive systems reveal the lower giant magnetoresistive effect, and vice versa. Accordingly, the dephasing usually decreases conductivity, thereby increasing the GMR.

[1] X. Song et al, *Nanotechnology* 20 195202 (2009). [2] Y. Matsuda et al, *J. Phys. Chem. C*, 114, 17845 (2010). [3] S. Krompiewski, *Nanotechnology*, 22, 445201 (2011). Acknowledgment This work was supported by the Polish Ministry of Science and Higher Education as a research project No. N 202 199239 for 2010-2013.

QK05

Negative magnetoresistance in ferromagnet/semiconductor/ferromagnet structures with cubic dresselhaus spin-orbit-interaction

Kenji Kondo*
Laboratory of Quantum Electronics, Research Institute for Electronic Science, Japan

We have investigated the spin transport in Ferromagnet (FM)/Semiconductor (SC)/Ferromagnet (FM) structures with a central SC barrier exhibiting cubic Dresselhaus spin-orbit-interaction (SOI). The energy profile of the barrier is assumed to be a square with height V and thickness d along z-direction. The magnetoresistance (MR) ratio has been calculated for three different barriers, GaAs, GaSb, and GaAs without SOI as a function of barrier thickness. Both ferromagnets are assumed to be Fe. Intriguingly, MR ratios exhibit negative values for two different barriers in some range of thickness. For GaAs, the MR ratio is negative when the thickness is larger than 0.03 nm. For GaSb, the MR ratio is negative in the range of 0.02 to 0.9 nm, changing the sign gradually from negative to positive at a thickness of about 0.9 nm. Afterwards, its value increases monotonically and reaches a constant value at a thickness of 2.5 nm. We can attribute these phenomena to spin filtering effects caused by both the spin precession and the energy-splitting in the central SC region. Without SOI, the MR ratio shows positive value in all the range since the spin does not rotate in the barrier.

QK06

Spin valve effect of NiFe/graphene/NiFe junctions

Muhammad Zahir Iqbal, Muhammad Waqas Iqbal and Jonghwa Eom*
Department of Physics & Graphene Research Institute, Sejong University, Korea

Novel linear dispersion in graphene makes unique electronic properties such as ambipolar transport and Dirac particle quantum Hall effect. Although graphene was previously considered to be a physically unstable form until it was shown to exist on the Si substrate, various methods to synthesize graphene have been developed. Exploiting such superior electronic properties combined with recently developed large scale growth of graphene by chemical vapor deposition (CVD), has led to field effect devices integrated on a wafer scale showing promise for future electronic applications. In this paper, CVD-grown graphene is used as intervened spacer between two ferromagnetic electrodes. The device is composed of 55 nm thick NiFe film, graphene and 75 nm thick NiFe film. The current-to-perpendicular-to-plane magnetoresistance (MR) shows the spin valve effect. The increased resistance in the antiparallel configurations of magnetizations is due to the spin dependent scattering inside the magnetic films or at interfaces. A positive MR ratio of the order of 0.045% has been observed at 300 K and this signal grows up to 0.14 % at 10 K. The junction resistance is found to be monotonically increasing with temperature. Graphene functions as not a tunnel barrier but a resistive thin film between two NiFe electrodes.

QK07

Giant magnetoimpedance and photoinduced magnetoresistance effects in ferromagnet/SiO₂/p-Si hybrid structures

N. V. Volkov*, A. S. Tarasov, E. V. Eremin, A. V. Eremin, S. N. Varnakov and S. G. Ovchinnikov
L. V. Kirensky Institute of Physics SB RAS, Russia

We report the electron transport properties in the Fe/SiO₂/p-Si hybrid structure. The results of dc studies show that the features of the transport properties of the structure are caused by a metal/insulator/semiconductor transition with a Schottky barrier formed at the SiO₂/p-Si in-terface [1]. The magnetoresistance effect is determined by contributions of the processes occurring in the volume of a semiconductor and in a inversion layer near the SiO₂/p-Si inter-face. Study of the impedance Z = R + iX and magnetoimpedance allows separating the dynamic contributions determined by charge and spin transport in different regions of the hybrid structure. The strongest effect of a magnetic field on R and X is caused by the presence of magnetic impurity centers in the semiconductor near the SiO₂/p-Si interface. Magnetoimpedance originates from spin-dependent tunneling between a ferromagnetic electrode and magnetic impurity centers via a potential barrier (SiO₂). The magnetic impurity centers determine also the change in photoconductivity in a magnetic field. The structure, as a matter of fact, exhibits giant magnetoresistance induced by optical radiation. As a mechanism of this effect, we consider the spin-dependent tunnel photocurrent, i. e., the current of photoexcited electrons, from p-Si to Fe via the SiO₂ barrier.

I. N.V. Volkov, A.S. Tarasov, E.V. Eremin, et al., *J. Appl. Phys.* 109, 123924 (2011).

QK08

Charge imbalance with the same decaying length as spin accumulation

Yao-hui Zhu*
Physics Department, Beijing Technology and Business University, China

Starting from the Valet-Fert theory of the current-perpendicular-to-plane giant magnetoresistance, we study the charge imbalance in ferromagnetic metals by solving Poisson's equation. Our results show that, in ferromagnetic layers, the charge imbalance has two exponential terms with different decaying lengths: the Thomas-Fermi screening length (on the order of angstrom) and the spin diffusion length (tens of nm in 3d ferromagnetic metals). The charge imbalance on the scale of the screening length has been well studied and it is also present in spin-unpolarized transport in nonmagnetic multilayers. However, the charge imbalance on the scale of the spin diffusion length has never been studied before and it shows up only in ferromagnetic layers with spin accumulation, which also decays on the scale of the spin diffusion length. This charge imbalance is essential to the giant magnetoresistance effect and thus one should be cautious when using quasi-neutrality condition, which neglects the charge imbalance.

[1] T. Valet and A. Fert, *Phys. Rev. B* 48, 7099 (1993). [2] Y.-H. Zhu, B. Hillebrands, and H. C. Schneider, *Phys. Rev. B* 78, 054429 (2008). [3] S. Zhang, *Phys. Rev. Lett.* 83, 640 (1999).

QK09

Simulation of spin-dependent transport in GaAs: Effect of electron-electron interactions

Matthew Hodgson, Gianni Marchetti, Roy W. Chantrell and Irene D'amico
Physics, University of York, United Kingdom

We investigate the effect of electron-electron interaction on electronic spin transport in bulk GaAs. We use Ensemble Monte Carlo (EMC) techniques to simulate the electron and spin dynamics. EMC has been successfully used in the study of charge transport and more recently in spin transport. However electron-electron interactions are often neglected, also due to computational costs. Here, in addition to electron-electron scattering we include scattering from optical and acoustic phonon, and charged defect scattering. Spin decoherence occurs due to the spin-orbit interaction (Dresselhaus term), which arises from the lack of inversion symmetry in GaAs. The electron-electron interaction is described by the screened Coulomb potential. At variance with previous simulations, we implement both spin dependent (Mott) and spinless (Rutherford) scattering. We also propose a new, more realistic, method for choosing partners undergoing electron-electron collisions which properly accounts for the dependence on the distance between electrons. We show that, in EMC simulations, electron-electron interactions should not be discarded, as doing so may result in an anomalous drop in the spin relaxation time at temperatures as high as 100K.

QK10

Electrical detection of spin-polarized current in InAs quantum point contacts

Taeyueb Kim^{1,2}, Sungjung Joo¹, Jinki Hong^{1*}, Kungwon Rhie¹, Hyuncheol Koo^{2*}, Jindong Song², Joonyeon Chang², Sukhee Han², Kyungho Shin²
¹ Department of Applied Physics, Korea University, Chochiwon, Korea
² Spin device research center, Korea Institute of Science and Technology, Seoul 136-791, Korea
³ Nano Photonics research center, Korea Institute of Science and Technology, Seoul 136-791, Korea

The controlled generation, manipulation and detection of spin-polarized currents in semiconductor is an important issue in spintronic devices [1]. The Rashba spin-orbit interaction has been focused to manipulate spin currents. Furthermore, the quantum point contact (QPC) having the Rashba interaction was recently proposed as a spin-current generator. [2], [3] In this work QPCs were fabricated from InAs quantum well. Gates were installed on the sides of the quantum well, and narrow conducting channels, i.e. QPC, were formed by application of voltages on these gates. Two QPCs were connected in series and the distance between them was less than 1.6 micro-meter. An external magnetic field was applied in parallel with the line connecting the two QPCs. Oscillations of resistance according to the magnetic field have been observed in this device at 1.8K. We believe that these data can be an evidence for our QPCs to work as a spin polarizer with a following scenario; the first QPC works as a spin-polarizer, and the second does as a detector. The spin-current produced by the first QPC precesses by the external magnetic field, which makes the oscillatory resistance as the magnetic field changes.

[1] Mikio Eto, Tetsuya Hayashi and Yuji Kurotani, *J. Phys. Soc. Jpn.* 74, 7, 193(2005) [2] P. Debray, S. M. S. Rahman, J. Wan, R. S. Newrock, M. Cahay, A. T. Ngo, S. E. Ulloa, S. T. Herbert, M. Muhammad and M. Johnson, *Nature Nanotech.* 4, 759 (2009) [3] A. Reynoso, Gonzalo Usaj, and C.A. Balseiro, *Phys. Rev. B* 75, 085321 (2007)

QK11

Gate dependence of spin-orbit interaction in a two-dimensional hole gas structure

Youn Ho Park¹, Hyun Cheol Koo^{1*}, Sang-hoon Shin¹, Jin Dong Song¹, Hyung-jun Kim¹, Joonyeon Chang¹, Suk Hee Han¹ and Heon-jin Choi²
¹ Spin Device Research Center, Korea Institute of Science and Technology, Korea
² Department of Materials Science and Engineering, Yonsei University, Korea

In order to implement spin-Field Effect Transistor (spin-FET), gate control of spin-orbit interaction parameter (α) is a key factor in a quantum well structure because spin precession is influenced by strength of the α [1]. Many papers utilized n-type channel for the spin transport, however, for the complementary logic device p-type channel should be also necessary. We have investigated the spin-orbit interaction parameter and the effective mass using the Shubnikov-de Haas (SdH) oscillation measurement in a GaSb two-dimensional hole gas (2DHG) structure. The α of 1.71×10^{11} eV/m and effective mass of 0.98m₀ are obtained at T = 1.8 K, respectively. We also found the gate dependence of the α and the hole concentration at 1.8 K. As increasing the gate voltage both the α and the hole concentration are reduced, which indicates the α increases with the carrier concentration in p-type channel. On the order hand, n-type channel shows opposite gate dependence [1, 2]. Therefore, the combined device of p and n-type channel spin transistor would be a good candidate for the complimentary logic device.

[1] H. C. Koo, J. H. Kwon, J. Eom, J. Chang, S. H. Han, and M. Johnson, *Science*, 325, 1515 (2009). [2] J. Nitta, T. Akazaki, and H. Takayanagi, *Phys. Rev. Lett.* 78, 1335 (1997).

QK12

Perpendicular spin transport in ferromagnet/MgO/GaAs structures

Joohyung Bae¹, Kyung-ho Kim¹, Hyun Cheol Koo^{1*}, Hyung-jun Kim¹, Joonyeon Chang¹, Suk Hee Han¹ and Sang Ho Lim²
¹ Spin Device Research Center, Korea Institute of Science and Technology, Korea
² Department of Materials Science and Engineering, Korea University, Korea

The electrical spin transport from TbFeCo/CoFeB into GaAs using MgO tunnel barrier is investigated. The 20 nm thick TbFeCo layer produces perpendicular magnetization and the 0.8 nm thick CoFeB layer, which contacts the MgO/GaAs layer, enhances the spin polarization of the injector. The MgO layer has a role of spin filter for efficient spin injection. In order to reduce the contact resistance, the heavily doped GaAs layer is inserted between TbFeCo/CoFeB/MgO and GaAs substrate. We measured spin accumulation and spin lifetime using three-terminal Hanle measurements with temperature range from 1.8 K to 300 K. In this geometry, the bias current is applied from the top TbFeCo layer to the GaAs channel and the voltage is measured at the interface. The perpendicular spin is injected so the in-plane magnetic field is swept to observe the spin relaxation at the interface. For a bias current of 1.5 mA, the spin signal of 0.12 mV and 0.03 mV are obtained at T = 1.8 K and 300 K, respectively. From the analysis of the Hanle curve, a spin life time of 0.4 ns is extracted at 300 K.

QK13

Spin hall effect in 2DEG in the presence of Rashba spin-orbit interaction

Won Young Choi, Hyung-jun Kim, Joonyeon Chang, Suk Hee Han and Hyun Cheol Koo*
 Korea Institute of science and technology, Korea

Spin Hall effect using an InAs-based 2DEG system with a strong Rasba effect is researched. To make all electric devices, permalloy is used as spin injector on Hall bar geometry. Two kinds of equivalent measurement, inverse and direct spin Hall, are performed. Inverse and direct spin Hall are the conversion of spin to charge and charge to spin, respectively. Also to confirm the effect of precession, dependences of channel length and magnetization direction are systematically investigated. The bias current between ferromagnet and neutral region of channel induces the injection of in-plane spin. Inside the channel, spin precession occurs and then spin orientation is changed to the perpendicular direction at the Hall cross. The spin signal as a function of channel length shows oscillation behavior which is also evidence of spin precession. At 1.8K, a spin Hall voltage of 4 μV is detected for a bias current 0.1 mA and a channel length of 0.64 μm. From this experiment, we confirm the spin Hall effect and spin precession at the same time.

[1] J. Wunderlich, B. G. Park, and A. C. Irvine et al, *Science* 330, 1801 (2010) [2] L. Sheng, D. N. Sheng, and C. S. Ting, *PRL* 94, 016602 (2005) [3] H. C. Koo, J. H. Kwon, J. Eom, J. Chang, S. H. Han, and M. Johnson, *Science* 325, 1515 (2009).

QK14

Spin transport and spin injection into turbostratic graphene

June Seo Kim¹, Sebastian Schweitzer², Ajit K Patra², Yenny Hernandez³, Klaus Muellen¹, Xinliang Feng¹ and Mathias Klau^{1*}
¹ Institut fuer Physik, Johannes Gutenberg-Universitaet Mainz, Germany
² Fachbereich Physik, Universitaet Konstanz, Germany
³ Max Planck Institute for Polymer Research, Germany

The remarkable physical properties of graphene, a monolayer of carbon atoms packed into a two-dimensional hexagonal lattice, make it a promising material for applications. In particular, the high electron mobility [1] and the relatively long spin lifetime (weak interaction of the electrons spin and orbital degree of freedom [2]) resulting in long spin diffusion lengths λ up to 2 μm [3], make it an interesting candidate for spintronics. However, λ is currently limited by the strong interaction between graphene and the underlying substrate and by the intrinsic corrugation of mechanically exfoliated graphene sheets. This can be overcome by using turbostratic graphene (TG), a multilayer graphene stack consisting of tens of electronically decoupled layers. TG combines the exciting properties of graphene with the higher robustness to environmental influences and the absence of inner corrugations of a microstructured material [4]. In this study, we have successfully performed spin injection from ferromagnetic electrodes into TG discs and detected the spin transport using a non-local spin valve configuration [3]. Moreover we can also investigate the correlation between the charge carrier transport properties and the spin injection efficiency.

[1] A. K. Geim et al., *Nature Materials* 6, 183 (2007), *Science* 324, 1530 (2009). [2] Hernando et al., *Phys. Rev. B* 74, 155426 (2006). [3] N. Tombros et al., *Nature* 448, 571 (2007). [4] M. Orlita et al., *Phys. Rev. Lett.* 101, 267601 (2008).

QK15

Spin signal in metallic lateral spin valves made by a shadow evaporation technique

Piotr Laczkowski, Laurent Vila, Williams Savero-torres, Van Dai Nguyen, Juan Carlos Rojas-sanchez, Murat Cubukcu, Alain Marty, Lucien Notin, Cyrille Beigne and Jean-philippe Attane
 Universite Joseph Fourier, BP 53, 38041, Grenoble and INAC/ CEA Grenoble, France

Amidst the large variety of proposed spin structures, Lateral Spin Valves (LSV) devices attracted recently an increasing attention. These lateral devices consist in two ferromagnetic electrodes connected by a non-magnetic metallic wire allowing to tune the transport properties according to the respective magnetic states of the two ferromagnetic electrodes. They allow realizing non-local transport measurements, by separating the spin current from the charge current using a four probe connections to an interface. We are developing non-local spin injection and detection technique in lateral spin valve structure made by electron beam lithography and angle evaporation techniques with a special emphasis on the study of the spin Hall effect. The spin signal depends mainly on the geometry of the LSV, on the quality of the interfaces, and on the choice of the used materials. We present a method used to optimize the spin signal of lateral spin valves using a technique to form and connect nanowires in a single step in vacuum, avoiding interface contamination and oxidation. By using different evaporation angles of materials through a resist mask and by reducing the devices geometry, we succeeded in obtaining spin signals close to 25 mΩ at 77K in devices with transparent interfaces.

P. Laczkowski et al., *Applied Physics Express*, Volume 4, Issue 6, pp. 063007-063007-3 (2011)

QK16

Hanle effect with in-plane magnetic fields in metallic lateral spin valves

Juan-carlos Rojas Sanchez, Laurent Vila, Matthieu Jamet, Piotr Laczkowski, Murat Cubukcu, Williams Savero-torres, Van Dai Nguyen, Alain Marty, Cyrille Beigne and Jean-philippe Attane
 Universite Joseph Fourier, BP 53, 38041, Grenoble and INAC/ CEA Grenoble, France

When a charge current crosses the interface between a ferromagnetic (FM) and a non-magnetic (NM) material, a spin current appears that occurs on the length scale of the spin diffusion. It is possible to detect this spin accumulation by measuring the voltage between the NM wire and the other FM wire. We show that the spin signal amplitude can be enhanced by inserting a natural Al oxide between the interface of Py and Al, achieving spin signals above 150 mOhms at 77 K (instead of 24mOhms with transparent contacts) and 38 mOhms at RT. When the magnetic field is applied perpendicularly to the LSV plane, the injected spins in the normal channel precess around an axe parallel to H. The decoherence and/or the precession induced by the magnetic field can lead to oscillations and disappearance of the spin signal (Hanle effect). Hanle measurements are usually performed by applying H perpendicular to the sample plane [1], the spin precessing in plane. Here we show that it is possible to carry out Hanle measurements by applying H in the sample plane, generating out-of-plane spin precession, and thus gaining a degree of freedom for the control of the spin current.

[1] "Electrical detection of spin precession in a metallic mesoscopic spin valve" F.J. Jedema, H.B. Heersche, A.T. Filip, J.J.A. Baselmans and J. van Wees, *Nature* 416, 713 (2002).

QK17

Detecting the magnetization switching of a ferromagnetic dot using non local spin injection by means of lateral spin valve structures

Williams Savero-torres, Laurent Vila, Alain Marty, Piotr Laczkowski, Van Dai Nguyen, Murat Cubukcu, Juan-carlos Rojas Sanchez, Lucien Notin and Jean-philippe Attane
 Universite Joseph Fourier, BP 53, 38041, Grenoble and INAC/ CEA Grenoble, France

In most researches on Spin Torque, the charge and spin currents cannot be separated. To solve this problem, spin injection using lateral spin-valves, made of magnetic and non magnetic materials, have been proposed [1]. In this context, we study the spin torque generated by pure spin current on a ferromagnetic dot, using lateral spin-valve structures. The nanostructure is composed of two parallel ferromagnetic electrodes, one transversal metallic channel, and one ferromagnetic dot at the middle of the structure. The width of wires and dots is 50 nm. To detect the dot magnetization switching, non-local measurements are performed. The spin polarised current is injected on one side using a ferromagnetic electrode. The spin accumulation produces the splitting of the electrochemical potential, enabling the diffusion of the pure spin current along the channel. The pure-spin current is found to be adsorbed by the ferromagnetic dot, decreasing the spin signal amplitude, which is detected using the second ferromagnetic electrode. The non local geometry enables the spin current and the charge current separation, giving the possibility to test the magnetization switching induced by a pure spin current.

[1] T. Yang, T. Kimura, and Y. Otani, Giant spin-accumulation signal and pure spin-current-induced reversible magnetization switching, *Nat. Phys.* 4, 851 (2008).

QK18

Perfect spin filter and highly spin-polarized current induced by fano antiresonance effect in the multiple-quantum-dot nanodevices

Hua-hua Fu¹, Kai-lun Yao^{2*} and Zu-li Liu²
¹ Department of Physics, Huazhong University of Science and Technology, Wuhan 430074, China
² Physics Department, Huazhong University of Science and Technology, Wuhan 430074, China

To realize perfect spin filter or to generate highly spin-polarized current is one of the fundamental requirements of any applications on spintronics, and in what material or model structure to achieve this goal effectively is still one of the central issues in spintronics. To realize these aims, multiple-quantum-dot system which can be man-made in a controllable way have been attracted much attention. In this report, we propose a practical design to realize perfect spin filter in a periodic diamondlike network composed of multiple quantum dots (QDs). In our design, by producing an energy difference between the site energy between the upper and down QDs in the network, the conductance spectra show a valley structure with a zero point due to the Fano antiresonance effect. As the energy difference increases or the network size increases to a not very large value, the antiresonance valley changes to a well-defined insulating band. Moreover, the conditions for the occurrence of the Fano antiresonance and its relation with the formation of the well-defined insulating band are determined. By a Zeeman effect, the spin-splitting conductance spectra show several highly to 100% spin-polarized windows, strongly proposing that this network can be applied as a perfect spin filter.

1. H. H. Fu, K. L. Yao, *Appl. Phys. Lett.* 110, 013502, 2012. 2. H. H. Fu, K. L. Yao, *J. Chem. Phys.* 134, 054903 (2011). 3. H. H. Fu, K. L. Yao, *J. Appl. Phys.* 108, 084510 (2010); 110, 094502 (2011).

QK19

Transmission of spin polarized photoelectrons across ferromagnet/ semiconductor interfaces using oblique Hanle effect

Yasuhiro Shirahata¹, Toshiyuki Isozaki¹, Ippei Suzuki¹, Eiji Wada¹, Mitsuru Itoh¹, Masahito Yamaguchi² and Tomoyasu Taniyama¹
¹ Materials and Structures Laboratory, Tokyo Institute of Technology, Japan
² Department of Electrical Engineering and Computer Science, Nagoya University, Japan

We demonstrate spin-dependent transmission of photoelectrons from a GaAs quantum well (QW) into a ferromagnetic FeGa layer under optical spin orientation in a small oblique magnetic field. The application of the oblique magnetic field enables us to measure the spin-dependent electron transmission across the interface due to the in-plane spin component of photoelectrons caused by the Larmor precession of electron spins about the magnetic field. A clear field dependence of the spin-dependent photocurrent is observed for a 20-nm-thick FeGa/GaAs QW sample, showing that the filtering of in-plane polarized electron spins which are generated by the Larmor precession occurs at the interface. To get concrete evidence for the spin filtering effect, we measure the magnetic field dependence of the phase shift between the circular polarization of light irradiated and the spin-dependent photocurrent. The phase shift exhibits a hysteresis behavior as a function of magnetic field, in compatible with the in-plane magnetization process of the FeGa layer. These results clearly demonstrate that a very efficient spin filtering effect occurs at the FeGa/GaAs interface even at a low magnetic field, providing a promising basis for designing spin detection technology based on spin filtering effect.

QK20

Electric field tuning and spin coulomb drag in spin field effect transistors (spin-FETs)

George Alexandru Nemes, Lucian Ion and Stefan Antohe
 University of Bucharest, Faculty of Physics, Romania

The quasi-bound states which appear as a consequence of the Rashba spin-orbit (SO) coupling, introduce a strongly irregular behavior of the spin-FET conductance at large Rashba parameter [1]. However, by introducing stray electric fields in addition to the SO couplings, the effect of the SO induced quasi-bound states can be tuned. The oscillations of the spin-resolved conductance become smoother, resulting the possibility to control the spin-FET characteristics [2]. Besides these effects, the Coulomb interaction gives rise to new and interesting many-body phenomena. D'Amico et al. discussed recently the physical origin of spin Coulomb drag effect (SCD) in rather general three-, two- and one dimensional systems. Here, a step closer to a realistic device is made: the SCD effect will be investigated in a nanowire spin-FET structure within the framework of self-consistent calculations for the open quantum system [3]. The spin drag trans-resistivity as a measure for SCD effect will be obtained, in the context of adjusting the spin injection efficiency from the contacts. In addition, the SCD effect in the presence of Rashba spin-orbit coupling will be analyzed. The Coulomb interaction will also be introduced in an exact manner for a few electron system, using the exact diagonalization method [4].

[1] M. M. Gelabert et al., *Phys. Rev. B* 81, 165317 (2010). [2] G. A. Nemes, A. Manolescu, V. Gudmundsson, *IOP - JPCS* (to be published, 2012). [3] G. A. Nemes, L. Ion, and S. Antohe, *J. Appl. Phys.* 106, 113714 (2009). [4] C. Yannouleas and U. Landman, *Rep. Prog. Phys.* 70, 2067 (2007).

QK21

The Rashba-type Spin splitting in Pb monolayer on Si and Ge surfaces: a First-principles study

Hyunjun Lee and Hyoung Joon Choi*
 Department of Physics, Yonsei University, Korea

Rashba spin-orbit splitting of the surface states due to structural inversion asymmetry is a rapidly growing field of research. Specifically, owing to a technological importance in spin-dependent electronics, spin-polarized metallic surface states on semiconductor surfaces would be highly interesting. Along this line, we have performed first-principles calculations of electronic structures of monolayer of heavy element deposited on semiconductor surfaces, Pb/Si(111) and Ge(111)-√3×√3 surfaces, by including the spin-orbit coupling in the form of additional nonlocal pseudopotential projectors. We investigate and compare energy band dispersions and spin polarizations of these systems and simulate angle-resolved photoemission spectra for direct comparison with experimental results. We also discuss our results focusing on the difference from the Rashba splitting in the Shockley surface states on Au(111) surface. This work was supported by the NRF of Korea (Grant No. 2011-0018306), and computational resources have been provided by KISTI Supercomputing Center (Project No. KSC-2011-C3-06).

QK22

Geometry effect on quasi-twodimensional electron system

Kuo-chin Chen, Hsin-han Lee and Ching-ray Chang*
 National Taiwan University, Taiwan

We calculate the local charge density and local spin density in a deformed square lattice system with Rashba spin orbital interaction. Use nonequilibrium Keldysh Green's function formalism, within the tight-binding framework. The system consists of normal metal lead and deformed central part. We treat the deformed system as adding effective magnetic field that introduces Zeeman effect. We also present the charge and spin current. The deformation we adopt is hemispherical shape and Gaussian shape. We will compare the result with the case that deformation vanished.

QK23

Electrical measurement of spin accumulation and transport in Fe/ AlGaAs heterostructures

Joon-il Kim^{1*}, Jennifer Misuraca¹, Kangkang Meng², Jun Lu², Lin Chen², Jianhua Zhao², Stephan Von Molnar¹ and Peng Xiong¹
¹ Physics, Department of Physics, Florida State University, Tallahassee, Florida, USA
² Physics, Institute of Semiconductors, Chinese Academy of Sciences, Beijing, China

Utilizing the persistent photoconductivity effect, we report on spin accumulation and transport in AlGaAs at different carrier densities under the same experimental conditions without the necessity for making replicas to access different doping levels. We conducted non-local 3 and 4 terminal Hanle effect measurements in AlGaAs to measure spin accumulation and spin transport respectively at different carrier densities. We will present our recent results, especially the carrier density dependence of the spin lifetime derived from our non-local spin measurements. We also report the bias current dependence of the spin lifetime. From optical studies, the spin life-time at zero bias and at low temperature was reported to be larger than 100 ns in n-GaAs on the insulating side and ~80 ns on the metallic side [1]. Based on our non-local 3 terminal measurement in Si:Al_{0.3}Ga_{0.3}As, the extrapolated spin life-time at zero bias and at 5 K was found to be as large as ~2 ns on the insulating side and decreased with increasing bias current. This work was supported by NSF DMR-0908625 and NSFC 10920101071.

[1] M. Furis, D.L. Smith, and S.A. Crooker and J.L. Reno, *Appl. Phys. Lett.* 89, 102102 (2006).

QK24

Pure spin current injection into a Gd wire
Seiji Nonoguchi, Tatsuya Nomura and Takashi Kimura*
Kyushu University, Japan

In magnetocaloric effects, the spin entropy is transformed to the thermal entropy because of an interaction between spin and heat. Since the spin entropy can be controlled by the external magnetic field, the environment temperature also can be tuned by the external magnetic field. Although such methods can be operated efficiently, it is difficult to reduce the size of the entire system. An effective magnetic field can be produced also by injecting spin currents via the interaction between the conduction electrons and localized magnetic moments. Therefore, when a pure spin current is injected into the magnetocaloric material, we may control the spin entropy because of the spin transfer torque and/or spin accumulation. Such a cooling effect has a possibility for a highly efficient nanosized refrigeration device. To demonstrate this effect, we prepared a lateral spin valve with the Gd middle wire, which is a magneto-caloric material. We observed the reduction of nonlocal spin signal by inserting the middle Gd wire, meaning the pure spin current was injected into the Gd wire. We also found that the background resistance decreases with increasing DC current. This implies that the device was cooled by the pure spin current injection into the Gd wire.

QL01

Synthesis and characterization of Ba₃Co₂Fe₂O₄₁ by the proteic sol-gel process
Bruna Andrade, Petrucio Silva and Marcelo Macedo*
Physics, Federal University of Sergipe, Brazil

In this work, we show the production of hexagonal Z-type barium ferrite (Ba₃Co₂Fe₂O₄₁) prepared via the proteic sol-gel process as well as their structural characterization and magnetic properties. The precursor materials were iron nitrate, cobalt nitrate and barium carbonate which formed a sol after being stoichiometrically dissolved in coconut water. We carried out a heat treatment at 100°C/24 h for the formation of an amorphous xerogel and a calcination at 1000°C/1 h for phase formation of Z-type barium ferrite. The material exhibited a magnetization curve as a function of temperature characteristic of ferrimagnetic material with T_c > 300 K and a hysteresis at room temperature with low coercive field (142 Oe) and saturation magnetization around 48 emu/g for a field of 7 T. Our results indicate that the proteic sol-gel process may be a route of great potential for obtaining Z-type ferrites.

QL02

Ferromagnetism in vanadium doped ZnO thin films grown by pulsed laser deposition
Shumaila Karamat^{1*}, Rajdeep Singh Rawat², Paul Lee³, Tan Lee Augustine⁴, Raju V Ramanujan⁵ and H.d Sun⁶
¹Physics, I. NIE, Nanyang Technological University, Singapore 2. COMSATS, Islamabad, Pakistan
²Physics, National Institute of Education, Nanyang Technological University, Singapore
³Physics, NIE-NTU, Singapore
⁴Physics, NIE-NTU Singapore
⁵Material Science, MSE-NTU Singapore
⁶SPMS, SPMS-NTU, Singapore

This paper investigates the structural, compositional and magnetic properties of vanadium doped ZnO films (ZnO)_x(V₂O₅)_{1-x}, where x = 0.02, 0.03 and 0.05 deposited by pulsed laser technique (PLD). Thin films were deposited for a constant duration of 1 hr at 2×10⁻² mbar O₂ ambient gas pressure by using frequency doubled Nd:YAG laser at 750 °C substrate temperature. The preferred orientation in thin films is along the (002) plane of ZnO. The lattice parameter c derived from the (002) diffraction peak increases as vanadium content increases, suggesting that vanadium substitutes for Zn in ZnO lattice. The PL measurement at low temperature shows the emission peak at 3.30 eV which is usually caused by acceptor-related transitions such as free electron to neutral acceptor (FA) and donor-acceptor-pair (DAP). The XPS results show that vanadium exist in V³⁺ and V⁴⁺ valence state which is in agreement with the XRD and PL results and points to the fact that the ZnVO phase, desirable in DMS, is formed in thin film samples. Furthermore, the hysteresis curves exhibiting the ferromagnetism for all thin films samples further support the formation of ZnVO phase in thin films samples.

QL03

The magnetic and dielectric properties of multiferroic Bi_{1-x}Gd_xFeO₃
Takuya Yanoh*, Naoki Sakai, Liming Zhu, Akinobu Kurokawa, Hiromasa Takeuchi, Shinya Yano, Kazuki Onuma, Takaya Kondo, Kazunari Miike, Toshiki Miyasaka and Yuko Ichihyanagi
Physics, Yokohama National University, Japan

BiFeO₃ is known as multiferroic material with antiferromagnetic and ferroelectric properties. Especially, ferroelectricity at room temperature is remarkable and BiFeO₃ is expected for new device materials. However, BiFeO₃ has antiferromagnetic ordering, as the result, magnetic values such as remanent magnetization Mr and coercive force HC are rather small for further application. In this study, in order to improve magnetic property and to evaluate dielectric property, we tried to synthesize Bi_{1-x}Gd_xFeO₃ particles where x = 0 to 1.0 by our original wet chemical method. The structural, magnetic and dielectric properties of prepared samples were investigated. Crystal structure change from rhombohedral to orthorhombic was found around x = 0.2 from the X-ray diffraction (XRD) measurement. Lattice constants a and c estimated by XRD decreased as Gd ion increased, supporting that Gd ions were doped exactly in BiFeO₃. The magnetic properties of Bi_{0.9}Gd_{0.1}FeO₃ which has rhombohedral (BiFeO₃ type) structure exhibited canted antiferromagnetism at 5 K. Both remanent magnetization Mr and coercive force HC significantly increased as Gd ion increased compared with BiFeO₃. The dielectric properties of Bi_{0.9}Gd_{0.1}FeO₃ showed that dielectric loss (tanδ) has been drastically improved compared with that of BiFeO₃, for about 90%, while real dielectric constant ε' decreased about 15%.

QL04

Double-exchange interaction in heavily Mn-doped CuO thin films
Li Li, Bin Lv, Shen Wang, Jinzhu Cai, Wenqin Zou, Fengming Zhang* and Xiaoshan Wu
Physics, Nanjing University, China

RKKY exchange, double-exchange interactions are two main mechanisms which are proposed to explain the origin of ferromagnetism of Mn-doped CuO films. Consider that double-exchange interactions cannot produce long-range magnetic order at concentrations of magnetic cations of low percent, Heavily Mn-doped CuO films have been prepared by PEVCD in air and in O₂. The M-T and M-H curves show that the average magnetic moment of the films prepared in O₂ is larger than those prepared in air, which may attribute to the variation of Mn chemical valence state. Double-exchange between Mn²⁺ and Mn³⁺ can be used to understand the ferromagnetism of CuO under heavily Mn-doping. The Curie temperature varies slightly with the growth atmosphere. The structure and magnetic properties vary with the annealing parameters obviously, which may indicate that the strain and carriers may play roles on the double exchange.

QL05

Magnetic properties of Cu-doped GaN films grown by MBE
Philipp R. Ganz¹, Christoph Suergers^{2*}, Gerda Fischer³ and Daniel M. Schaadt⁴
¹ Institut für Angewandte Physik and DFG-Center for Functional Nanostructures, Karlsruhe Institute of Technology (KIT), Germany
² Physikalisches Institut und DFG Center for Functional Nanostructures, Karlsruhe Institute of Technology (KIT), Germany
³ Physikalisches Institut, Karlsruhe Institute of Technology (KIT), Germany
⁴ Institute for Energy Research and Physical Technologies, Clausthal University of Technology, Germany

The magnetic properties of Cu-doped GaN films have been investigated in dependence of Cu doping level and film thickness. The films were epitaxially grown at different Cu-to-Ga beam-equivalent-pressure ratios (BEPR) by molecular beam epitaxy on sapphire substrates with an AlN buffer and were characterized by scanning electron microscopy, energy dispersive x-ray spectroscopy, and x-ray diffraction. Within a narrow range of BEPR around 1 %, a ferromagnetic behavior with a Curie temperature higher than 400 K is observed. For BEPR > 1 %, nonferromagnetic Cu-Ga islands are predominantly formed at the surface. The saturation magnetization of ferromagnetic films with BEPR = 1 % decreases with increasing film thickness. This suggests that the ferromagnetic behavior is due to defects created during the growth process and by the incorporation of Cu into GaN for BEPR ≤ 1 % leading to a long-range magnetic polarization.

QL06

Magnetism and electronic transport of MnAs single nanostructures
Federico Fernandez Baldi¹, Marina Tortarolo², Martin Sirena¹, Laura Steren³, Victor Etgens² and Mahmoud Eddrief²
¹ Centro Atomico Bariloche, Argentina
² Institut des NanoSciences de Paris, France
³ Centro Atomico Constituyentes, Argentina

The magneto-structural properties of MnAs thin films grown onto GaAs have recently drawn much attention due to its potential application in spintronics devices. The MnAs thin films exhibit a coexistence of a low-temperature ferromagnetic hexagonal phase (α) and a paramagnetic orthorhombic (β) one in a finite temperature range below the Curie temperature. When MnAs is grown onto GaAs[100], both phases are self-organized in a regular stripes array. This pattern is affected when the MnAs films are confined laterally to micrometric sizes and depends on the direction of the confinement. In this work, we present an investigation of the temperature dependence of the magnetic domain structure and magneto-transport properties of MnAs nanoribbons in order to determine the anisotropic response of the system, regarding both the magnetism and electronic transport. The confinement effects were examined at the low-temperature pure ferromagnetic phase and at the α-β phase-coexistence regime. Nanoribbons confined along the (I) α-MnAs[1120] and (II) α-MnAs[0001] directions were fabricated by e-beam lithography combined with optical lithography. The magnetic domain imaging was performed with a MFM, home-adapted for variable temperature measurements between 284K and 320K. The magneto-resistance and Hall effect measurements were made between 50K and 320K using a 9 Tesla superconducting magnet.

QL07

The generated antiferromagnetic and ferromagnetic states in nanocrystalline Cu-Cu₂O system and the consequences for spin chemistry
Anatoly Yermakov^{1*}, Michael Uimin¹, Alexandre Korolyov¹, Ilya Byzov¹, Alexey Mysik¹, Vladislav Maikov¹ and Mamoru Senna²
¹ Institute of Metal Physics, Ural Branch of RAS, Russia
² Faculty of Science and Technology, Keio University, Japan

Under investigations of nanocrystalline Cu-Cu₂O oxides it has been established that they actually possess heterogeneous magnetic states in nanoscale range. In nano-structured Cu-Cu₂O oxides, ferromagnetic (FE) and anti-ferromagnetic (AF) states are coexisting at above room temperature. The new idea based on the magnetic phase transformation from AF to FE state at an external field was suggested as a hypothesis to understand the variation of chemical rate transformations. The point is that a metamagnetic phase transition is accompanied by a variation of an electronic state of carrier from localized to delocalized one which can result in a variation of nanoreagents reactivity. In fact, the influence of magnetic field on the rate of chemical transformations, e.g. Cu ammonium complex formation using Cu-Cu₂O nanomaterials, as magneto-controlled reagents, has been reliably observed. Thus, the nanocrystalline copper oxides having a liquid-like potential are a remarkable example of energy-wise degenerated different magnetic states that can be operated by fairly weak external magnetic fields to control a rate of chemical transformations and other properties. We think the principle we here propose could be extended to other transition metal oxide nanoparticles with a similar electronic states. Thanks to RFBR Grants # 10-02-00323 and # 10-02-546 for support.

QL08

Unidirectional anisotropy observed in Fe film grown on GaAs at low temperature
Seonghoon Choi¹, Taehee Yoo¹, S. Khym¹, Sanghoon Lee^{1*}, X. Liu² and J. K. Furdyna²
¹ Physics Department, Korea University, Korea
² Physics Department, University of Notre Dame, USA

The magnetic anisotropy properties of Fe films have been investigated by planar Hall effect (PHE) measurements. A 4 nm thick Fe film was grown on a (001) GaAs substrate by MBE technique at room temperature. The field scans of the planar Hall resistance (PHR) at room temperature show an abrupt transition with hysteresis centered at zero field during the magnetization reversal, indicating the presence of symmetric magnetic easy axes in the film plane. However, the hysteresis in the PHR appeared to be shifted toward one field direction when the temperature decreased to 3 K. This asymmetry in the magnetization reversal process at 3 K can be understood by introducing an unidirectional anisotropy field H_{ud}. Interestingly, the direction of the H_{ud} directly follows the direction of the cooling field. This indicates that the direction of the H_{ud} is not fixed but can be changed by the cooling field. For the case of the cooling field along the [-1-10] direction, we obtained the values of cubic, uniaxial and unidirectional anisotropy fields by analyzing angular dependence of PHR. The magnitude of H_{ud} was one order of magnitude smaller than other anisotropy fields although it caused a significant asymmetry in the PHR hysteresis.

QL09

Magnetic properties of hydrothermally synthesized ZnO nanostructures
H Hadiywarman, Kadek J. Parwanta, Bowha Lee and Chunli Liu*
Department of Physics, Hankuk University of Foreign Studies, Korea

We report the study on the ferromagnetism in ZnO nanostructures fabricated by hydrothermal method at low temperature and with three different pH values. No post-treatment was applied to all samples. X-ray diffraction shows that the samples possess typical wurtzite structure and have no other impurity phases. Magnetization properties of ZnO samples were measured. With the defect analysis based on low temperature photoluminescence spectroscopy, the effective defects contributed to the magnetic properties were investigated. The result suggests that oxygen defects and synthesis conditions play an important role in mediating the magnetic property in the undoped ZnO nanostructures.

QL10

Electrical, magnetic and magnetoimpedance studies of LSMO thin film prepared by sol gel method
Pawan Kumar and Ramanathan Mahendiran
Physics, NUS, Singapore

In this work, we have prepared La_{0.7}Sr_{0.3}MnO₃ by sol-gel method using Si (100) substrate and characterized the sample by XRD, dc magnetization, dc magnetoresistance, and atomic force microscopy. The sample is found to be ferromagnetic below 367 K from the magnetic measurement. Impedance spectroscopy study has been reported on the thin film for the first time. We have studied the ac electrical impedance (Z) in LSMO thin film as function of Temperature (T) and magnetic field in response to radio frequency (f=0.1-5MHz) ac current flowing directly through the sample. DC resistivity and Z (T) shows transition around 365K which is correspond to T_c of LSMO thin film. In Z (T) peaks around T_c decreases in magnitude with applied field (1KOe), which is not affected much in DC resistivity. Magnetoimpedance ΔZ/Z= -30% is observed in MHz frequency range. It is suggested that observed magnetoimpedance results from suppression of the high frequency transverse permeability by an external field. Our study suggests that magnetoimpedance in manganite thin films might find new application in radio frequency regime.

References: (1). Gang Zou , Xian You, Pingsheng He, Materials Letters 62 (2008) 1785-1788.

QL11

Differential conductance measurements in Ni nanoscale contact fabricated by electromigration
Junya Sakai^{1*}, Koichiro Ienaga¹, Yuji Inagaki¹, Hiroyuki Tsujii², Ryuya Nomura³, Seiji Nonoguchi³, Takashi Kimura⁴ and Tatsuya Kawae⁵
¹ Department of Applied Quantum Physics, kyushu university, Japan
² Faculty of Education, Kanazawa university, Japan
³ INAMORI Frontier Research Center, Kyushu University, Japan
⁴ INAMORI Frontier Research Center, Kyushu University, Japan
⁵ Department of Applied Quantum Physics, Kyushu University, Japan

A zero-bias anomaly in differential conductance has been reported in atomic-size contacts fabricated from the ferromagnets, Fe, Co and Ni, which is considered to come from the Kondo effect [1]. This is interesting because the Kondo effect usually requires two species of atom and is thought to be incompatible with ferromagnetic interaction. In order to clarify the origin of Kondo effect in atomic ferromagnetic contact, we have studied the size dependence of the zero-bias anomaly in Ni nanoscale contacts by mechanical controllable break junction technique and observe the anomaly in a large size where the ferromagnetism appears[2]. In this presentation, we study differential conductance in Ni nanoscale contacts with decreasing the size by electromigration. In large size contacts, zero-bias anomaly is not observed. When the conductance is smaller than 200G0 (G0=2e²/h), the anomaly is clearly observed.

[1]M. Reyes-Cabvo et al., Nature 458, 1150 (2009) [2]K. Ienaga et al., to be published.

July 10 (Tue)

July 10 (Tue)

QL12

Magnetoresistance measurements in Pd atomic-scale contact at 4.2K

Koichiro Ienaga^{1*}, Naoya Nakashima¹, Yuji Inagaki¹, Hiroyuki Tsujii² and Tatsuya Kawae¹

¹ Department of Applied Quantum Physics, Kyushu University, Japan

² Faculty of Education, Kanazawa University, Japan



QL13

Differential conductance measurements in Cu-Mn atomic-scale contacts

Koichiro Ienaga¹, Naoya Nakashima¹, Yuji Inagaki¹, Hiroyuki Tsujii² and Tatsuya Kawae^{1*}

¹ Department of Applied Quantum Physics, Kyushu University, Japan

² Faculty of Education, Kanazawa University, Japan



QL14

Tuning the magnetic interaction in carbon nanotube/NiO nanocomposite system

S Chattopadhyay, S Giri and S Majumdar^{*}

Department of Solid State Physics, Indian Association for the Cultivation of Science, India

We have prepared a series of nanocomposite materials with multi-walled CNTs and NiO nanoparticles by varying the concentration of nickel nitrate solution. Transmission electron microscopy shows that the average size of the nanoparticles is about 10 nm and they are predominantly embedded either on the inner or the outer wall of the multi-walled CNTs forming a quasi one dimensional arrangement. It is also observed that the particles are well separated and density of the product NiO nanoparticles increases systematically with increasing concentration of the nickel nitrate solution. DC magnetization measurement shows the presence of thermomagnetic irreversibility in the temperature variation of the magnetization data. In contrary to the antiferromagnetic bulk NiO, field dependence of magnetization reveals the presence of strong ferromagnetic interaction along with prominent exchange bias effect. These materials also show magnetization relaxation which is an indication of non-ergodicity in the magnetic ground state. This system provides a rare opportunity to externally fabricate the degree of isolation among the particles and to tune the interparticle magnetic interactions as well for performing a systematic investigation on the evolution of the magnetic ground state with the variation of the interaction strength.

QL15

Bias-voltage dependence of magnetotransport properties in co-deposited Co-C granular thin films

Jun-goo Kang^{1*}, Masaki Mizuguchi¹, Shiro Entani², Seiji Sakai² and Koki Takanashi¹

¹ Institute for Materials Research, Tohoku University, Japan

² Advanced Science Research Center, Japan Atomic Energy Agency, Japan

Granular systems consisting of ferromagnetic nanoparticles dispersed in a nonmagnetic matrix exhibit giant magnetoresistance (MR) due to spin dependent transport. Carbon-based nanocomposite thin films have large application potential as spin transport materials because long spin relaxation time is expected due to its weak spin-orbit interaction [1]. We have found that co-deposited Co-C films exhibit a large negative magnetoresistance (MR: 27.6% at 2 K) [2]. It is expected that the bias voltage dependence of MR includes significant information on the mechanism of the MR. In this study, the bias-voltage dependence of magneto-transport properties for Co-C granular thin films has been investigated. Co-C granular thin films were fabricated by a co-sputtering technique. The current (I)-bias-voltage (V) characteristics and the MR behavior of the Co-C films were measured at temperatures of 2-30 K in a two-terminal geometry with the electrical current and magnetic fields (up to 70 kOe) in the in-plane direction. It was found that the magnitude of the MR ratio changed remarkably with bias voltage. A clear increase in the MR ratio with bias voltage was observed, and it reached 66.6 % for V=25 V.

[1] S. Sakai, K. Yakushiji, S. Mitani, K. Takanashi, H. Naramoto, P. V. Avramov, K. Narumi, V. Lavrentiev, and Y. Maeda, *Appl. Phys. Lett.* 89, 113118 (2006). [2] R. Tang, M. Mizuguchi, H. Wang, R. Yu, and K. Takanashi, *IEEE Trans. Magn.* 46, 2144 (2010).

QL16

Switchable voltage control of the magnetic anisotropy in heterostructured nanocomposites of CoFe/NiFe/PZT

Thang D. Pham^{1*}, Hong T. M. Nguyen², Dong H. Kim¹, Tiep H. Nguyen³ and Cuong V. Le²

¹ Faculty of Engineering Physics and Nanotechnology, University of Engineering and Technology, Vietnam National University, Hanoi, Viet Nam

² Laboratory for Micro and Nanotechnology, University of Engineering and Technology, Vietnam National University, Hanoi, Viet Nam

³ Department of Physics, Chungbuk National University, Korea

Heterostructures of nanostructured ferromagnetic (FM) and ferroelectric (FE) layers are of increasing interest due to the coupling between the magnetic moment and electric polarizations. In particular electric voltage, rather than the conventional magnetic field, can be directly used to control the magnetic properties of the magnetic layers. This magnetic-electric coupling may open promising applications towards novel spin electronic devices with low power consumption and high-speed data access. In this article, we study on the crystallographic structure and magnetic properties of CoFe/NiFe/PZT heterostructures. In these nanocomposites, the magnetic behaviors, such as magnetization significantly changes in the presence of an applied voltage. The change also depends on the FM layer thickness, the magnetic field direction and it can reaches up to more than 100%. Furthermore we observed the switching in magnetization at suitable applied voltage. Besides, we present a phenomenological approach to investigate stress-induced magnetic anisotropy, which originated from magnetoelectric coupling between two FM and FE phases.

QL17

Origin of the ferromagnetism in scandium-doped ZnO thin films

Mohammed Benali Kanoun^{*}, Souraya Goumri-said, Udo Schwingschlogl and Aurelien Manchon

¹ King Abdullah University of Science and Technology(KAUST), Saudi Arabia

In recent years, there have been more startling discoveries in diluted magnetic semiconductors [1] achieving possible room-temperature ferromagnetism in undoped (ZnO [2]) and non-transition metal-doped (ZnO:C [3]) systems. ZnO-based materials serve as model systems for the dilute magnetic oxides and are among the most intensely studied systems so far [4]. Interestingly, Venkatesan et al [5] have shown that room temperature ferromagnetism is observed in Sc-doped ZnO films. We note that in the bulk phase Sc has different crystal structures and nonmagnetic properties. How different are their magnetic properties when doped in ZnO thin films? Why do experimental results differ so much? To answer these questions, we have carried out comprehensive first-principles theoretical investigations of energetics, electronic structure, and magnetic properties of Sc-doped ZnO (11-20) thin films. In this work, the ZnO thin film was modeled by a (1×2) seven-layer slab supercell having a wurtzite structure along the [11-20] surface orientation. Each slab was separated from the other by a vacuum region of 10 Å along the [11-20] direction. Even though Sc is not magnetic in its natural phase, we found that it is likely to order ferromagnetically in ZnO thin film, in agreement with experiment [5].

[1] T. Dietl et al., *Science* 287, 1019 (2000). [2] Q. Xu et al., *Appl. Phys. Lett.* 92, 082508 (2008). [3] C. Liu et al., *J. Mater. Sci.* 16, 555 (2005). [4] Q. Ma, D. B. Buchholz, and R. P. H. Chang, *Phys. Rev. B* 78, 214429 (2008). [5] M. Venkatesan, C. B. Fitzgerald, J. G. Lunney, and J. M. D. Coey, *Phys. Rev. Lett.* 93, 177206 (2004).

QL18

Magnetic control of the hydrogen storage of hydrogen-injected ZnCoO

Bum-su Kim¹, Seunghun Lee¹, Jong Moon Shin², Yong-chan Cho¹, Yong Nam Choi³, Hee-ju Lee³, Chae Ryong Cho², Hideomi Koinuma¹ and Se-young Jeong^{1*}

¹ Cogno-Mechatronics Engineering, Pusan National University, Korea

² Nano fusion technology, Pusan National University, Korea

³ Korea Atomic Energy Research Institute, Korea

Many researchers have tried to apply ZnO for hydrogen storage through additional doping and nanostructure which increase hydrogen capability[1]. It has been regarded for Zn-O bond center and oxygen vacancy as practicable position for hydrogen storage. Co-Co dimer in ZnCoO has been suggested as appropriate position for its reversibility, and hydrogen placed in Co-Co dimer mediates ferromagnetic spin ordering by Co-H-Co complex[2,3]. In our recent research, we have reported the correlation between hydrogen content and ferromagnetism in Co doped ZnO (ZnCoO) and suggested that ZnCoO can be exploited for hydrogen storage and the tools for the measurement of hydrogen[4]. In this study, ZnCoO powder was fabricated by sol-gel method and annealing process was performed at 300 °C and subsequently 800 °C for removing organic compound. Pt was coated on ZnCoO powder as hydrogen catalyst. The hydrogen absorption and change in structure are characterized by the press composition and temperature (PCT) system and neutron diffraction, in-situ. We investigate the correlation between hydrogen contents and magnetism in ZnCoO and discuss its applicability for hydrogen storage. We also show the hydrogen contents in ZnCoO depending on the Pt layer and the spillover effect between Pt layer and ZnCoO nanocrystal.

[1] Q. Wan et al., *Appl. Phys. Lett.* 84, 124 (2004). [2] S. Lee et al., *Appl. Phys. Lett.* 94, 212507 (2009). [3] Y. C. Cho et al., *Appl. Phys. Lett.* 95, 172514 (2009). [4] S. Lee et al., *J. Appl. Phys.* (in press, 2012).

QL19

Ferromagnetism in Co-doped TiO₂ films probed by low-energy muon spin rotation

Hassan Saadaoui^{1*}, Jiabao Yi², Zaher Salman¹, Thomas Prokscha¹ and Elvezio Morenzoni¹

¹ Laboratory for Muon Spin Spectroscopy, Paul Scherrer Institut, 5232 Villigen PSI, Switzerland

² School of Materials Science and Engineering, University of New South Wales, Kensington, NSW, 2052, Australia

Ferromagnetic semiconductors have been widely studied recently for potential applications in spintronics. In this experiment, we probe the magnetism in Co-doped TiO₂ ferromagnetic semiconducting films using Low-energy muon spin rotation (LE-μSR). This technique is very powerful to probe the magnetic properties of thin films and interfaces on a nanometer length scale. We investigated Co-doped (5%) TiO_{2,3} films grown in different oxygen pressures. We find the internal magnetism in these films to be strongly dependent on the oxygen pressure during growth. The oxygen vacancies, modified by pressure, act as electron donors and alter the electron density. As the pressure increases, the magnetic volume fraction is strongly reduced. In this work, we present the temperature, magnetic field and depth dependence of the internal magnetism, and discuss its origin.

QL20

Structural and magnetic changes induced by high energy ball milling of CdFe₂O₄ oxide

Justice Msomi and Ta Nhlapo

School of Chemistry and Physics, University of KwaZulu-Natal, South Africa

Bulk CdFe₂O₄ ferrite nanoparticles have been synthesized by solid state reaction. The fine powders of CdFe₂O₄ oxide were produced by high energy ball milling. The structural and magnetic changes induced by high energy ball milling are investigated. The oxides have been characterised by XRD, Mossbauer spectroscopy and VSM measurements. A general decrease in lattice constant with increasing milling time is observed. The Mossbauer spectra indicate paramagnetic spin state in all the samples. Magnetization increases with reduction in particle size. This can be explained by the redistribution of Cd ions in both tetrahedral (A) and octahedral (B) sites. The coercive field of the milled CdFe₂O₄ oxide are highly sensitive to temperature compared to that of the bulk compound. An increase in coercive field for 50 hours milled oxide from about 9 Oe at 300 K to 520 Oe at 10 K has been observed. A smaller increase from 9 Oe at 300 K to 200 Oe at 10 K occurs in the coercive field of the bulk oxide. The variation of magnetization as a function of measuring temperature is also presented. An anomalous variation of field cooled magnetization as a function of temperature has been observed.

QL21

Room temperature ferromagnetism in Zn_{1-x}Ni_xS diluted magnetic semiconducting nanocrystalline thin films

M A El-hagary^{1*}, Soltan Soltan², M Emam-ismail¹ and S Althoyaib¹

¹ Physics Department, Qassim University, Saudi Arabia

² Physics Department, Helwan University, Helwan, Cairo, Egypt

We have investigated the magnetic properties of Ni doped Zn_{1-x}Ni_xS diluted magnetic semiconducting nanocrystalline thin films for different doping concentrations (0.005 ≤ x ≤ 0.2) synthesized by electron beam evaporation technique. X-ray diffraction patterns confirm the existence of single phase nature in all the Ni doped Zn_{1-x}Ni_xS samples with cubic zinc blend type structure. Evidence of nanocrystalline nature of the films was observed from the investigation of surface morphology using scanning electron microscopy and atomic force microscopy. Magnetic domains were observed by using magnetic force microscopy at room temperature indicating the existence of ferromagnetism over the film surface. The temperature and field dependent magnetization measurements by using superconducting quantum interface device showed ferromagnetic behavior between room and low temperatures (5 K) with a T_c at or above room temperature for the nanostructure samples with 0.1 ≤ x ≤ 0.2. The saturation magnetization for Zn_{1-x}Ni_xS system is found to increase with the dopant concentration (x). The exchange interaction between local spin polarized electrons (Ni ions) and conductive electrons according to RKKY mechanism, rather than from the Ni oxide impurities, is proposed to be the possible mechanism for ferromagnetism.

QM01

Extraordinary hall measurements of Co/Ni multilayers

Chih-yung Chen¹, James C Eckert¹, Natalia Fear¹, Sheena K. K. Patel¹, Richard Sayanagi¹, Patricia D Sparks¹, E Shipton² and Eric E Fullerton²

¹ Physics, Harvey Mudd College, USA

² University of California, San Diego, USA

Interest in Co/Ni multilayers is driven by their unusual magnetic properties. They exhibit perpendicular magnetic anisotropy, relatively low magnetic damping and unusual magneto-transport characteristics making them well suited for spintronic devices. To understand their magnetic and magneto-transport properties we measured the temperature dependence of the Hall effect for a series of sputtered Ni/Co films: SiO₂/Ta(40Å)/Pd(40Å)/[Co(2Å)/Ni(Y)]x10/Ta(40Å)), with Ni thicknesses from Y=2-14 Å. Because the signs, and the temperature dependence, of the extraordinary Hall effects (EHE) differ for Co and Ni, the behavior for the multilayers is complex. At room temperature the sign of the EHE changes as the Ni thickness increases from 4 to 5Å. For Y=4Å, the sign of the EHE is temperature dependent, going to zero near 220K and changing sign for lower temperatures. The magnitude of the EHE increases with increasing temperature for Y<5Å, decreases for Y=5 and 6Å and then increases for Y>6Å. We used the EHE to measure the magnetization properties finding a decrease in the coercive field for increasing Y. For Y<4Å, a complicated EHE response does not reflect the average magnetization. We discuss this research in term of competing EHE properties of Co and Ni. Work at UCSD supported by DOE-BES Award # DE-SC0003678.

QM02

Magnetic Spin Structure of Fe₃₀Pt_{50-x}Rh_x Films

Jochen Fenske¹, Dieter Lott¹, Gary J. Mankey², Wolfgang Schmidt³, Karin Schmalzl³, Elena V. Tartakovskaya⁴ and Andreas Schreyer¹

¹ Helmholtz-Zentrum Geesthacht, Germany

² MINT Center, University of Alabama, USA

³ Juelich Centre for Neutron Science, Germany

⁴ Institute for Magnetism, National Ukrainian Academy of Science, Ukraine

Ordered FePt alloys with L10 structure are known as materials with FM order and a high magnetic moment of Fe providing a large magnetization. The large atomic number of Pt on the other hand results in a high magnetic anisotropy. If grown in thin films, the high anisotropy often results in perpendicular magnetization which is the preferred orientation for current magnetic recording media. One way to control the magnetic properties in these materials is through the introduction of a third element into the crystal matrix e.g. Rh. When Rh is added to replace Pt in the equiatomic alloy, new magnetic phases emerge. Bulk samples of Fe₃₀Pt_{50-x}Rh_x studied by magnetization measurements refer to an AF-FM transition with decreasing Rh content. An additional temperature driven AF-FM transition was observed in the Fe₃₀Pt_{50-x}Rh₁₀ film. It is also well known that the magnetic properties of a thin film can differ drastically from the bulk behavior due to dimensionality effects. Here we present neutron diffraction studies on the magnetic properties of different 200nm thick Fe₃₀Pt_{50-x}Rh_x films in dependence of temperature and external magnetic fields. The polarized and unpolarized neutron diffraction data allowed us to develop a detailed model of the magnetic structure of the films.

QM03

Cross over from anisotropic magnetoresistance to magnon magnetoresistance in PLD grown permalloy nanowires

Vineeth Mohanan Parakkat and Anil P. S Kumar
Physics, Indian Institute of Science, India

We are able to observe and distinguish Anisotropic-Magnetoresistance(AMR) and Magnon Magnetoresistance(MMR) [1] contributions clearly in Permalloy nanowires by varying their width thereby tuning their shape anisotropy. Nanowires of thickness 20nm and varying widths down to 160nm were prepared by e-beam lithography and Pulsed Laser Deposition. A linear non-saturating longitudinal MR observed in high field regime for NiFe nanowires could never be explained using AMR but only MMR can account for it. MMR follows as $\rho = \alpha(M/M_s)B$, where M is magnetization along the easy axis, M_s saturation magnetization, B magnetic field applied along the easy axis, $\alpha = (d\rho/dB)$ is the slope of $\rho(B)$ at magnetic saturation. A cross over in magnetoresistance at low field from AMR-dominant to MMR-dominant one was observed as wire width reduces since the AMR value is getting reduced from 1.2% for 650nm wide wire to 0.26% for 160nm, however the contributions from the electron-magnon interactions still persist. At 280nm itself the AMR contribution to the longitudinal MR has substantially reduced so that only magnon effect is visible. The MMR proves to be an excellent way of determining M/Ms, understanding the magnetization reversal mechanisms in nanostructures, domain wall dynamics and also fundamental problems like electron magnon interactions.

[1] A. P. Mihai et al Phys. Rev. B 77, 060401 (2008).

QM04

Investigation of magnetic anisotropy of ferromagnetic GaMnAs film by planar Hall effect

Jaehyuk Won¹, Jinsik Shin¹, Yoonjung Gwon¹, Hyehyeon Byeon¹, Sangyeop Lee¹, Sanghoon Lee^{1*}, X. Liu² and J. K. Furdyna²
¹ Physics Department, Korea University, Korea
² Physics Department, University of Notre Dame, USA

Magnetic anisotropy properties of the GaMnAs ferromagnetic film have been investigated by using planar Hall effect measurements. The field scan of the planar Hall resistance (PHR) showed a two-step switching behavior indicating a strong cubic anisotropy along the <100> directions. The difference in the behavior of the PHR for the two applied field directions between the [100] and the [110] was understood via well-known uniaxial anisotropy along the [110] direction. In addition to such known effects, we also found the presence of asymmetry for the field directions between the [010] and the [001] directions. This new asymmetry phenomenon was explained by introducing an additional uniaxial anisotropy field H_{112} along the [100] and the [001] directions, which coincides with the two directions of cubic anisotropy. The values of the anisotropy fields, cubic (H_c), first uniaxial (H_{111}), and second uniaxial (H_{112}), were obtained by analyzing the angle dependence of the PHR. Although the value of H_{112} is small, its effect is clearly observed at high temperature above 25 K, where the transition of magnetization occurred before the field direction is reversed during the magnetization reversal process.

PACS number: 73.50.-h; 75.50.Pp; 75.30.Gw

Keywords: Ferromagnetic semiconductor, Magnetic anisotropy, Planar Hall effect

QM05

A crossover between magnetic vortex state and strip domains in electrodeposited nanogranular nickel films

Alexander Sergeevich Samardak^{1*}, Ekaterina Sukovatsina¹, Alexey Ognev¹, Ludmila Chebotkevich¹, S. M. Janjan² and Farzad Nasirpour²
¹ School of Natural Sciences, Far Eastern Federal University, Institute of Automation and Control Processes FEBRAS, Russia
² Department of Materials Engineering, Sahand University of Technology, Iran

We have investigated the change of magnetization mode of nanogranular nickel films electrodeposited on silicon. The electrodeposition of nickel at a distinct potential starts with the formation of isolated nanogranules with size of 130-190 nm which subsequently tend to coalesce forming a continuous nanogranular film. Assuming nickel nanogranules as oblate spheroids and calculating the critical size for single domain state, we find that the nickel nanogranules are magnetized under vortex ground state. Micromagnetic simulations calculated for this isolated nanogranules and MFM images confirm the magnetic vortex states for electrodeposited nickel nanogranules. Upon the nanogranules joining each other, coercivity increases due to the reduction of intergranular space and strengthening of magnetostatic interaction. Further growth leads to the formation of continuous nanogranular film which is associated with decrease in coercivity and rotation of the easy axis of magnetization to in-plane mode which is characterized by the domain wall displacement and strip-like multidomain pattern. The crossover between vortex ground state and multidomain magnetic pattern leads to the significant decrease in coercive force. Continuous nickel films electrodeposited on silicon have anisotropic magnetoresistance the value of which increases as the thickness and, appropriately, uniformity of film is increased.

QM06

Non-linear susceptibility of nanogranular FeAg films at the verge of superferromagnetism

D. Alba Venero¹, L. Fernandez Barquin^{1*}, S. N. Kaul², J Alonso³ and M. L. Fdez-gubieda³
¹ CITIMAC, Universidad de Cantabria, Santander 39005, Spain
² School of Physics and Centre for Nanotechnology, University of Hyderabad, Hyderabad - 500046, India
³ Electricidad y Electronica, Universidad del Pais Vasco, Bilbao 48080, Spain

A detailed magnetization study of Fe_xAg_{100-x} films, comprising nanoparticles (3 nm) of Fe embedded in a Ag matrix, has recently revealed [1] a crossover from super-spin glass state to superferromagnetic state at x70. This changeover is presumably caused by an interplay between the direct exchange, dipolar and RKKY interactions operating between the particle magnetic moments. In order to gain further insight into the nature of inter-particle interactions and their role, first five harmonics χ_1 - χ_5 of the ac magnetic response were measured at several frequencies and magnetic fields over the temperature range 5-300 K on DC-sputtered Fe_xAg_{100-x} (x = 25, 35, below and above the percolation threshold, respectively) 100 nm thick films. Susceptibilities χ_1 - χ_5 measured in the absence of the superposed dc magnetic field, H_{dc}, exhibit features that are characteristic of a spin glass and a ferromagnet in x = 25, 35. The ferromagnetic fingerprints in the temperature variations of the linear and nonlinear susceptibilities become all the more apparent when H_{dc} is applied. The data are analyzed on the same lines as those in the previous works on magnetically disordered CMR manganites [2, 3] and LiNiO insulators [4].

[1] J. Alonso et al., Phys. Rev. B 82, 54406 (2010). [2] Y. Bitla and S. N. Kaul, EuroPhys. Lett. 96, 37012 (2011). [3] L. Fernandez Barquin and R. Garcia Calderon, J. Phys.: Conf. Ser. 17, 87 (2005). [4] A. Bajpai and A. Banerjee, Phys. Rev. B 62, 8996 (2000).

QM07

Dynamics of Ni-Fe elliptical dot arrays based on CPW-FMR measurements

Yasushi Endo, Naomi Skashita*, Yutaka Shimada and Masahiro Yamaguchi
Graduate School of Engineering, Tohoku University, Japan

The dynamics of nanomagnets have been studied intensively for high-frequency applications in spintronic devices. The dynamics closely correlate with the damping constant α which determines the strength of damping torque in nanomagnets. α has been evaluated by exciting ferromagnetic resonance (FMR) in nanomagnets using microwave cavities and coplanar waveguides (CPWs). Advantages of CPW-FMR measurements are a wide range of radio frequencies and external field intensity and micron-scale samples. Herein to clarify the dynamics of nanomagnets, we employed FMR measurements with CPW to evaluate α in 50-nm-thick Ni-Fe elliptical dot arrays. Effective in-plane anisotropy field $H_{k,eff}$ increases markedly as the dot size decreases, which may be attributed to enhanced magnetostatic energy. Effective saturation magnetization $4\pi M_s,eff$ decreases slightly as the dot size decreases because the demagnetization field coefficient changes as the dot size decreases. Additionally, α increases monotonically from 0.01 to 0.02 as the dot size decreases in a 500 Oe external magnetic field applied in the longitudinal axial direction of the dots. Their values are higher than that of the Ni-Fe film ($\alpha = 0.009$) likely because the inhomogeneity of the demagnetization field distribution near dot edges. Therefore, these results propose that CPW-FMR measurements can evaluate the dynamics of nanomagnets in detail.

QM08

Structure and magnetic properties of SiO₂(Co) granular film on GaAs substrate.

Victor Ukleev^{1*}, Natalya Grigoryeva², Ekaterina Dyadkina¹, Alexei Vorobiev³, Dieter Lott⁴, Leonid Lutsev⁵, Alexandr Stognij⁶, Dirk Menzel⁶, Nicolay Novitskiy⁶ and Sergei Grigoriev¹
¹ Petersburg Nuclear Physics Institute, Russia
² Saint-Petersburg State University, Russia
³ European Synchrotron Radiation Facility, France
⁴ Helmholtz-Zentrum Geesthacht, Germany
⁵ Ioffe Physical-Technical Institute, Russia
⁶ Scientific and Practical Materials Research Centre of NAS of Belarus, Belarus
⁷ Institut für Physik der Kondensierten Materie, TU Braunschweig, Germany

The effect of giant injection magnetoresistance (GIMR) was recently observed in a granular SiO₂/ (54 - 75 at.% Co) film on a semiconductor GaAs substrate in a temperature range near T = 300 K. The magnetoresistance reaches the value of 10000% in the magnetic field of 1.9 T and at the voltage of 90 V [1]. The grazing-incidence small-angle X-ray scattering (GISAXS) data indicated the layer of lower concentration of cobalt particles at the granular film/semiconductor interface if compared to the SiO₂(Co) granular film itself. The thickness of this interface layer is about 70 Å [2]. The polarized neutron reflectometry confirms the existence of the additional layer on the granular film/substrate interface. The temperature dependence of the magnetization M(T) shows the presence of two types of magnetic nanoparticles with different blocking temperatures and magnetization dynamics. The hysteresis curve of the magnetization demonstrates two-loop structure in region of the fields 0 - 80 mT and 80 - 200 mT. Data obtained by polarized neutron reflectometry, GISAXS and SQUID measurements are well correlated with each other and give the possibility to develop the GIMR effect theory paying attention to the interface features.

[1] L.V. Lutsev, A.I. Stognij, and N.N. Novitskii, Phys. Rev. B, 184423 (2009). [2] N. Grigor'eva, A. Vorob'ev, V. Ukleev, E. Dyadkina, L. Lutsev, A. Stognij, N. Novitskii, and S. Grigor'ev, JETP Letters, 92:767 - 773, 2010.

QM09

Magnetic properties and structure of electrodeposited nickel on thin niobium film

Huei-ying Ho^{1*}, Wei-yan Lin¹, Shih-jia Chen¹, Hong-wen Cheng¹ and Yung Liou²
¹ Department of Science Education, National Taipei University of Education, Taiwan
² Institute of Physics, Academia Sinica, Taiwan

Cyclic voltammetry, chronopotentiometry, atomic force microscope, magneto-optical Kerr effect, and X-ray diffraction were used to investigate the magnetic property and structure of thin Ni films electrodepositing onto a 100 nm Nb. Constant-current method was used to grow the Ni films in this study. During the reduction process of Ni, a small amount of β -Ni(OH)₂ is formed; it becomes intense when the applied potential is more cathodic. The average size of the Ni grains grows and the coercivity of the Ni film decreases during the steady-state depositing process. The preferred orientations of the electrodeposited Ni film are fcc-(111) and fcc-(200), the easy axis of the magnetization of it is in the in-plane direction, however. This may due to the formation of the β -Ni(OH)₂. The effects of current density on the magnetism and structure were also studied. The high current density does not make any significant change in the magnetic property if the current density is higher than 5.2 mA/cm². This may due to the intense hydrogen evolution reaction during the high current density deposition. These results could be the foundation of further research in the hydrogen energy area.

QM10

Characterization of epitaxial EuS(111) thin films on BaF₂(111) and SrF₂(111) substrates grown by molecular beam epitaxy

Shinya Senba^{1*}, Naoki Matsumoto², Mitsuhiro Jomura², Hironori Asada², Yasuhiro Fukuma³, Tsuyoshi Koyanagi² and Kengo Kishimoto²
¹ Ube National College of Technology, Japan
² Graduate School of Science and Engineering, Yamaguchi University, Japan
³ Faculty of Computer Science and Systems Engineering, Kyushu Institute of Technology, Japan

A ferromagnetic insulating EuS thin film has received considerable attentions in fundamental studies of spin injection devices because of its very high spin filter efficiency[1]. It has been reported that EuS thin films on Si(100) and GaAs(100) substrates become insulating at a growth temperature(Ts) of 300°C and above, and the resistivity of that decreases with decreasing Ts due to the sulfur deficiency[2]. In this study, we have successfully grown EuS(111) epitaxial films on BaF₂(111) and SrF₂(111) substrates using molecular beam epitaxy at Ts=100-500°C. Pole figures of x-ray diffraction indicate a high degree of in-plane orientation, and all of the samples show very high resistivity. The arithmetic mean deviation of the surface for 10 nm-thick EuS films on BaF₂(111) and SrF₂(111) substrates measured by AFM are 0.122 and 0.092 nm, respectively. The Curie temperature of EuS films increases up to ~16 K with increasing Ts. In order to achieve an anti-parallel state between two ferromagnetic layers in spin injection devices, we try to manipulate the coercive force by Te doping. The obtained coercive force of Te-doped film (110 Oe) is large compared with that of undoped one (20 Oe). Optical properties such as a magnetic circular dichroism are also presented.

[1] P. LeClair et al., Appl. Phys. Lett. 80, 625 (2002). [2] I. J. Gularan et al., Phys. Rev. B 68, 144424 (2003).

QM11

The cation distribution and electrical hopping in Fe_xCo_{1-x}O₄ (0<x<1.65) ferrite films on MgO substrate grown by molecular beam epitaxy

Der-sheng Lee¹ and Gung Chern^{2*}
¹ Electrical Engineering Department, DA-YEH University, Chunghua, Taiwan
² Physics Department and SPIN Research Center, National Chung Cheng University, Chia-Yi, Taiwan



QM12

Magnetic circular dichroism in near-threshold two-photon photoemission

K Hild¹, S A Nephjiko¹, G Schoenhense¹, H J Elmers^{1*}, T Nakagawa², T Yokoyama², K Tarafder³ and P M Oppeneer³
¹ Institute of Physics, University of Mainz, Germany
² Institute for Molecular Science, The Graduate University for Advanced Studies (Sokendai), Japan
³ Department of Physics and Astronomy, Uppsala University, Sweden

Magnetic circular dichroism in near-threshold photoemission (TPMCD) results in large asymmetries similar to values observed in the regime of x-ray magnetic circular dichroism (XMCD). Hence, TPMCD facilitates new routes for microscopy and time-resolved experiments. Here we investigate the microscopic origin of the TPMCD for ultrathin Co films [1]. TPMCD is measured for perpendicularly magnetized Cs/Co/Pt(111) films with work function adjusted by Cs adsorption. For one-photon photoemission (IPPE) TPMCD at a fixed photon energy of $h\nu = 3.06$ eV and varying work function results in an almost constant value of 6.2%. TPMCD in two-photon photoemission (2PPE) with the same photon energy results in 8.4% demonstrating that for 2PPE the first excitation step is the dominant asymmetry-generating process. For 2PPE with reduced work function TPMCD yields an asymmetry of 17% in the photon energy range $h\nu = 1.53$ -1.66 eV, thus revealing the importance of a real intermediate state. The experimental results are in reasonable agreement with ab initio calculations considering energy conservation and all directions of excitation instead of only those conserving parallel momentum. Funded by DFG (EL175/15, EL175/16), Carl-Zeiss-Stiftung and the MAINZ Graduate School of Excellence.

[1] K. Hild, G. Schoenhense, H. J. Elmers, T. Nakagawa, T. Yokoyama, K. Tarafder and P. M. Oppeneer, Phys. Rev. B 85, 014426 (2012).

QM13

Structural and magnetic properties of pseudocubic BaFeO_{3-d} thin films

B. Ribeiro^{1*}, R. P. Borges¹, R. C. Da Silva¹, N. Franco², P. Ferreira³, T. P. Gasche⁴, E. Alves⁵ and M. Godinho¹
¹ CFMC/Dep. Física, Faculdade de Ciências, Universidade de Lisboa, Campo Grande, 1749-016 Lisboa, Portugal
² Unidade de Física e Aceleradores, Instituto Tecnológico e Nuclear, E.N. 10, 2686-953, Portugal
³ Departamento de Engenharia Cerâmica e do Vidro, CICECO, Universidade de Aveiro, Portugal
⁴ CINAMIL, Laboratório de Física da Academia Militar, Lisboa, Portugal

Bulk BaFeO_{3-d} is known to assume different crystal structures (hexagonal, cubic, tetragonal, orthorhombic, monoclinic) depending on the oxygen stoichiometry. For $d < 0.35$ [1] the compound has a hexagonal structure and is antiferromagnetic below 160 K[2], while for higher values of d it assumes a distorted cubic structure and is a magnetically ordered insulator at room temperature that has been considered a potential multiferroic[3]. In order to explore their structural and magnetic properties, thin films of BaFeO_{3-d} were grown by Pulsed-Injection Metal Organic Chemical Vapour Deposition (PI-MOCVD) on cubic SrTiO₃ single crystal substrates using different deposition conditions. The films were characterized using X-Ray diffraction, atomic force microscopy (AFM), SQUID magnetometry and Rutherford Backscattering Spectroscopy (RBS). By tuning the deposition conditions, namely the substrate temperature and the relative concentrations of Ba and Fe precursors, it was possible to obtain films that have a pseudocubic structure, are insulating and show antiferromagnetic properties at room temperature. The results obtained from the experimental characterization of the pseudocubic BaFeO_{3-d} thin films are discussed and compared with the results obtained using density functional theory (DFT) using local spin density approximation (LSDA) and the LSDA+U.

[1] J. C. Grenier, et al, J. Solid State Chem., 80, 6 (1989) [2] J. B. MacChesney, et al, J. Chem. Phys. 43, 3317, 1965 [3] T. Matsui, et al, Appl. Phys. Lett. 81, 2764 (2002)

QM14

Exchange anisotropy and antiferromagnetic coupling in NiFe/FeMn/Co trilayers

Fernando Pelegrini^{1*}, Marcos Antonio De Sousa², Willian Alayo³ and Elisa Baggio-saitovitch³
¹ Universidade Federal de Goiás - Instituto de Física, Brazil
² Universidade Federal de Goiás, Brazil
³ Centro Brasileiro de Pesquisas Físicas, Brazil

Ferromagnetic Resonance (FMR) study of the exchange anisotropy of magnetron sputtered Si₃₀Cu₂₀Ni₅₀ iFe_{nm}FeMn_{nm}CoCu_{nm} trilayers reveals the existence of antiferromagnetic coupling between NiFe and Co layers. The samples studied were produced in the presence of a magnetic field of 400 Oe to set the unidirectional anisotropy and the thickness of the Co layer varied from 3 to 5 nm. The FMR experiments were done at room temperature using a commercial spectrometer operating with microwave frequencies of 9.79 and 34.1 GHz, swept static magnetic field and the usual detection techniques. The FMR spectra display two resonance modes due to Co and NiFe layers with very distinct effective magnetizations. The in-plane angular dependence of the resonance field of the Co layer displays the characteristic bell shape curve due to an exchange-biased bilayer with unidirectional anisotropy larger than the magnetocrystalline anisotropy. At the FeMn/Co interface of the sample with 5 nm thick Co layer, the exchange bias field is 160 Oe. At the NiFe/FeMn interface it is about only 10 Oe and the angular dependence of the resonance field exhibits an asymmetry due to the presence also of uniaxial anisotropy. This additional anisotropy results from an antiferromagnetic coupling between NiFe and Co layers.

[1] J. Zhang, L. Zhou, and P. E. Wigen, Phys. Rev. B 50, 6094 (1994). [2] W. Alayo, M. A. Sousa, F. Pelegrini and E. Baggio-Saitovitch, J. Appl. Phys. 109, 083917 (2011).

QM15

Parallel spin wave resonance in exchange-biased NiFe/FeMn/NiFe trilayers

Fernando Pelegrini^{1*}, Valberto Pedruzi Nascimento², Armando Biondo², Edson Caetano Passamani² and Elisa Baggio-saitovitch³
¹ Instituto de Física, Universidade Federal de Goiás, Brazil
² Departamento de Física, Universidade Federal do Espírito Santo, Brazil
³ Centro Brasileiro de Pesquisas Físicas, Brazil

The Ferromagnetic Resonance (FMR) technique was used to study the magnetic properties of asymmetrical NiFe_{3nm}/FeMn_{15nm}/NiFe_{10nm} trilayers magnetron sputtered under working pressures of 2, 5 and 10 mTorr, in the presence of a 460 Oe magnetic field to set the unidirectional anisotropy. The FMR experiments were done at room temperature using a commercial spectrometer operating with microwave frequencies of 9.79 and 34.0 GHz, swept static magnetic field and the usual detection techniques. At a microwave frequency of 34.0 GHz, the parallel FMR spectra reveal that spin wave and uniform resonance modes are excited by the microwave field. The study of the in-plane angular dependences of the resonance fields reveals for both modes the effect of the unidirectional anisotropy. The dependences of the absorption fields on cosθ, where θ is the field angle with respect to the anisotropy axis, give for the spin wave and uniform modes of the sample produced under the pressure of 2 mTorr the anisotropy fields of 66 and 37 Oe, respectively. The parallel FMR results and spin wave resonance theory imply for this sample the exchange constant of 0.92 x 10⁻⁶ erg/cm. This result agrees with perpendicular FMR measurements at a microwave frequency of 9.79 GHz.

[1] V. P. Nascimento, E. Baggio-Saitovitch, F. Pelegrini, L. C. Figueiredo, A. Biondo and E. C. Passamani, *J. Appl. Phys.* 99 (2006) 08C108. [2] W. Stoeklein, S. S. Parkin and J. C. Scott, *Phys. Rev. B* 38 (1988) 6847. [3] M. Nisenoff and R. W. Terhune, *J. Appl. Phys.* 36 (1964) 733.

QM16

Studies on local structures and magnetism at buried Fe/ Fe₃O₄ interfaces using synchrotron-radiation Mössbauer spectroscopy

Ko Mibu^{1*}, Hideto Yanagihara², Takaya Mitsui³, Ryo Masuda³, Shiori Hori¹, Atsushi Murata¹, Masaaki Tanaka¹, Kazuya Suzuki², Eiji Kita¹ and Makoto Seto⁴
¹ Graduate School of Engineering, Nagoya Institute of Technology, Japan
² Institute of Applied Physics, University of Tsukuba, Japan
³ Japan Atomic Energy Agency, Japan
⁴ Research Reactor Institute, Kyoto University, Japan

Strong antiparallel magnetic coupling was found recently in Fe/ Fe₃O₄ bilayers [1], and attention has been paid as a new and noble-metal-free “synthetic antiferromagnet” for magnetic recording devices. In order to clarify the mechanism of this interfacial magnetic coupling, it is important to elucidate the local crystallographic structure and magnetism at the buried interface experimentally. Mössbauer spectroscopy is a useful method to obtain such information through absorption spectra of gamma-rays (or X-rays) by the constituent Fe nuclei. In this presentation, we report the results we have obtained using recently developed synchrotron-radiation-based Mössbauer spectroscopy with a nuclear Bragg monochromator at BL11XU, SPring-8 [2]. The structures and magnetism at the buried Fe/ Fe₃O₄ interface are discussed on the basis of the obtained spectra.

[1] H. Yanagihara et al., *Appl. Phys. Express* 1 (2008) 111303. [2] T. Mitsui et al., *J. Synchrotron Radiation* 19 (2012), in press.

QM17

Dependence of in-plane magnetic anisotropy of Au/Co/Au heterostructures on thickness of Co-component layer: An FMR study

Leszek Gladczuk, Pawlo Aleshkevych and Piotr Przyślupski
 Institute of Physics, Polish Academy of Sciences, Al. Lotnikow 32/46, PL02-668 Warsaw, Poland

Recently, there was a lot of interest in magnetic tunnel junctions built from electrodes characterized by in-plane magnetic anisotropy. In the present study, ultrathin Mo/Au/Co/Au heterostructures where the cobalt layer is of the wedge shape (i.e. with thickness gradually changing along the sample) were grown on a sapphire substrate by molecular beam epitaxy. Room temperature ferromagnetic resonance (FMR) measurements were used to evaluate the resonance field as a function of (i) the in-plane and the out-of-plane orientation of external magnetic field and of (ii) the cobalt layer thickness. The experiments demonstrates an interesting effect of enhancement of the in-plane anisotropy for heterostructures with wedge-shaped Co layer. This finding provides a method to modify the magnetic anisotropy, which can be of a great importance for the application in magnetic tunneling junctions. A comparison of the obtained results with earlier data on Co anisotropy will be presented.

QM18

Depth dependent chemical and magnetic information of CoFeB/MgO multilayered thin films studied by x-ray and polarized neutron reflectometry

Ki Yeon Kim^{1*}, Il Jae Shin², Byoung Chul Min², Hyeok Cheol Choi³, Chun Yeol You³, Jeong Soo Lee¹, Surendra Singh⁴, M. R. Fitzsimmons⁵ and Sungkyun Park⁵
¹ Neutron Science Division, Korea Atomic Energy Research Institute, Korea
² Center for Spintronics Research, Korea Institute of Science and Technology, Korea
³ Department of Physics, Inha University, Korea
⁴ Los Alamos National Laboratory, USA
⁵ Department of Physics, Pusan National Laboratory, Korea

Magnetic Tunnel Junctions (MTJs), consisting of a crystalline MgO barrier sandwiched by amorphous CoFeB layers, have received much attention owing to novel magnetic and transport properties such as perpendicular magnetic anisotropy and large tunneling magneto-resistance at room temperature [1-2]. With a combined study of x-ray (XRR) and polarized neutron reflectometry (PNR), depth-dependent chemical and magnetic profiles in Co₄₀Fe₆₀B₂₀/MgO multilayered thin films were investigated. The annealing was done at 400°C for half an hour in an applied field of 4 kOe after sample growth. In addition to XRR and PNR, structure characterization was also conducted using high-angle theta/2theta x-ray diffraction, and high resolution tunneling electron microscopy (HR-XTEM), the magnetic property was studied using vibrating sample magnetometer. The boron diffusion and magnetic moment around both CoFeB/MgO interfaces will be discussed in detail.

[1] S. Ikeda, K. Miura, H. Yamamoto, K. Mizumama, H. D. Gan, M. Endo, S. Kanai, H. Hasegawa, J. Hayakawa, F. Matsukura, and H. Ohno, *Nature Mater.* 9, 721 (2010). [2] D. D. Djayaprawira, K. Tsunekawa, M. Nagai, H. Maehara, S. Yamagata, N. Watanabe, S. Yusa, Y. Suzuki, and K. Ando, *Appl. Phys. Lett.* 86, 092502 (2005).

QM19

Depth-resolved rotational hysteresis of exchange-coupled Fe/Cr multilayers

Tatyana Guryeva, Kai Schlage, Hans-christian Wille and Ralf Roehlsberger
 HASYLAB, Deutsches Elektronen-Synchrotron (DESY), Germany



QM20

Magnetization reversal behavior in exchange-coupled NiFe/FeMn/CoFe trilayers: vectorial MOKE & PNR study

Ki Yeon Kim^{1*}, Ji Wan Kim², Hyeok Cheol Choi³, Anke Teichert⁴, Chun Yeol You³, Sungkyun Park⁵, Sung Chul Shin² and Jeong Soo Lee¹
¹ Neutron Science Division, Korea Atomic Energy Research Institute, Korea
² Department of Physics and Center for Nanospinics of Spintronic Materials, Korea Advanced Institute of Science and Technology, Korea
³ Department of Physics, Inha University, Korea
⁴ Helmholtz Zentrum Berlin für Materialien und Energie, Germany
⁵ Department of Physics, Pusan National Laboratory, Korea

With a combination of vector magneto-optic Kerr effect (MOKE) magnetometry and polarized neutron reflectometry (PNR), the detailed magnetization reversal mechanism of the exchange-biased Py(30-nm)/FeMn(t_{AF}=0-30nm)/CoFe(30-nm) trilayers was studied.[1] We found that Py/FeMn(15-nm) and FeMn/CoFe bilayers show completely different magnetization reversal modes, whereas they become very similar to each other in the corresponding Py/FeMn/CoFe trilayers. This is convincing evidence that the 15-nm FeMn layer mediates the magnetization reversal behaviors of Py and CoFe layers through interlayer exchange bias coupling. Furthermore, magnetization reversal of Py and CoFe layers are decoupled for t_{AF}=30 nm, indicating that both Py and CoFe layers separated by an intermediate FeMn layer are exchange-coupled within 30 nm distance. This is in reasonable agreement with the theoretically predicted domain-wall width such as 28 nm for the polycrystalline FeMn/Co bilayers and 50 nm for the perfect Fe₅₀Mn₅₀ crystal.

[1] Ki-Yeon Kim, Ji-Wan Kim, Hyeok-Cheol Choi, A. Teichert, Chun-Yeol You, Sungkyun Park, Sung-Chul Shin, and Jeong-Soo Lee. *Phys. Rev. B.* 84,144410 (2011).

QM21

Uniaxial magnetic anisotropy of La_{0.7}Sr_{0.3}MnO₃ film grown on step-terrace surface SrTiO₃ (100) substrate

Byeong-geon Kim, Sanghoon Ki and Joonghoe Dho*
 Kyungpook National University, Korea

In this work, we used the step-terrace surface STO (100) substrates to control the spin direction of the La_{0.7}Sr_{0.3}MnO₃ (LSMO) film in the atomic level. The shape magnetic anisotropy in the nano scale was induced by using step-terrace surface STO (100) substrates with small vicinal angle of 0.1 degree. Atomically flat STO substrate was prepared by annealing after etching by HCL (hydrochloric acid), and the surface morphology of the STO substrate with molecular step-and-terrace was observed by atomic force microscopy. Here, we simultaneously deposited two La_{0.7}Sr_{0.3}MnO₃ films on the processed and unprocessed STO substrates by using pulsed laser deposition. The direction dependence of magnetic hysteresis within the film plane was investigated by using SMOKE (Surface Magneto-Optical Kerr Effect) system. The magnetic hysteresis loops of the LSMO film on the unprocessed STO substrate showed weak direction dependence within the plane, while those on the step-terrace surface STO did a significant uniaxial magnetic anisotropy along the longitudinal direction of the step-terrace of the STO substrate.

QM22

The effect of compositional ratio on the magnetocaloric effect

Ho-sup Kim¹, Sang-soo Oh¹, Kiran Shinde¹, Seung-kyu Baik¹, Kook-chaeh Chung² and Bhavesh Bharat Sinha²
¹ Korea Electrotechnology Research Institute, Korea
² Korea Institute of Materials Science, Korea

Film type Ni-Mn-Ga alloys were prepared using co-evaporation method in order to investigate the effect of compositional ratio on magnetocaloric effect (MCE). In the deposition process on the metal substrate, Ni was evaporated by an induction heating, and Mn and Ga were evaporated by a resistive heating. The deposition rate of each element was measured by Quartz Crystal Microbalance and the rate was controlled up to 0.1 mm / hour to get a thick Ni-Mn-Ga film. Three crucibles of Ni, Mn, and Ga were arranged triangularly to form the composition gradient of Ni-Mn-Ga film on the surface of whole substrate. Long tape samples with different composition of Ni, Mn, and Ga along the length were prepared. The magnetic property of prepared sample at around transition temperature was continuously evaluated by a reel to reel Hall probe measurement system with a temperature controller. The Hall probe signal is related to the relative value of MCE so that the optimal composition ratio could be obtained by analyzing it. The section which exhibited the highest value in Hall probe measurement was cut and analyzed by XRD and followed by MCE measurement using PPMS equipment. Detailed experimental results will be reported in the presentation.

1. V. Recarte et al., *Appl. Phys. Lett.*, 95, 141908, 2009. 2. Yuepeng Zhang et al., *Smart Mater. Struct.*, 18, 025019, 2009. 3. V. A Chernenko et al., *J. Phys.: Condens. Matter*, 17,5215-5224, 2005.

QM23

Magnetocaloric effect in Ni doped Zn ferrite nanoparticles grown by the combustion method

Kyungdong Lee, Rahul Chandrakant Kambale and Namjung Hur*
 Department of Physics, Inha university, Korea

We studied the magnetocaloric effect (MCE) in two different compositions of Ni-Zn ferrite nanoparticles (Ni_xZn_{1-x}Fe₂O₄, x=0.2 and 0.3) which were prepared by the combustion method. From the temperature and the magnetic field dependent magnetization curves, the magnetic entropy changes (ΔS) and the adiabatic temperature changes (ΔT) were evaluated. Magnetocaloric effect in these nanoparticles is compared to that in bulk system with the same compositions to study the effects of grain size. Although the values of ΔS and ΔT at 2 T magnetic fields in these nanoparticles are lower than the values in the bulk one, wider effect transition windows were observed in nanoparticle systems. As the domain size of Ni-Zn ferrite nanoparticles affects the temperature and magnetic field dependence of magnetization, the maximum ΔS and ΔT are also influenced by the grain size around the magnetic transition temperature (TC). Therefore, the field dependence of ΔT at TC, which can be analyzed by the mean field approximation denoted by the exponential p, was found to be different from the typical one.

QM24

Interlayer interaction in ReCoPO (La, Nd and Sm): 31P NMR Study

M Majumder¹, K Ghoshray^{1*}, A Ghoshray¹, A Pal² and V. P. S Awana²
¹ ECMP Division, Saha Institute of Nuclear Physics, Kolkata, India
² QPA Division, National Physical Laboratory (CSIR) Dr. K.S. Krishnan Marg, New Delhi-110012, India

31P NMR result is presented in Co based non-superconducting members of pnictides family revealing the importance of the interlayer interaction, a key factor that determines the ground state. In ReCoPO (Re = rare earth) series, La and Ce show only PM → FM transition, whereas Nd and Sm show successive PM → FM → AFM transition with varying degree of TC and TN. 31P NMR spectrum in polycrystalline La, Nd and SmCoPO respectively corresponds to a powder pattern for a spin 1/2 nucleus with axially symmetric local magnetic field showing varying degree of shift parameters. In particular, Nd and Sm compound show large temperature dependent shift anisotropy with similar magnitude of Kiso and Kax. However, relaxation rate (1/T1T) in Sm is atleast two orders of magnitude higher than that observed in other two compounds. Our earlier 31P and 139La NMR [1] measurements in LaCoPO (quasi 2D Fermi surface) reveal dominant 2D spin fluctuation of 3d electrons in PM state with non negligible 3D part and in the FM state spin fluctuation is 3D in nature. Whereas, in SmCoPO the present result is able to distinguish the FM in plane spin-correlations from the AFM type out of plane spin-correlations.

1. M. Majumder, K. Ghoshray, A. Ghoshray, B. Bandyopadhyay, M. Ghosh, *Phys. Rev. B* 82, 054422 (2010).

QM25

Jahn-teller distortion and enhancement of curie temperature of Mn_{3-x}Ni_xO₄ films on MgO (001) by molecular beam epitaxy

Der-sheng Lee¹, K. M. Kuo² and Gung Chern^{2*}
¹ Electrical Engineering Department, DA-YEH University, Chunghua, Taiwan
² Physics Department and SPIN Research Center, National Chung Cheng University, Chia-Yi, Taiwan

We report on x-ray diffraction, scanning electron micrograph, and magnetization measurements vs. external field and temperature of Mn_{3-x}Ni_xO₄ (x=0, 0.25, 0.5, 0.75, 1) films grown on MgO (001) and (011) substrates by molecular beam epitaxy. Magnetization vs. temperature measurements reveal that Curie temperature increases from 43 K to 103 K as the Ni composition increasing. This increase of Tc is qualitatively understood as a result of the decrease of the exchange coupling of the cations between B site and B site (JBB). The Jahn-Teller distortion also reduces as the Ni composition increasing and the cubic structure is estimated to be recovered as x approaches ~ 1.2. The cation distribution in the present films is different from the bulk and can be described as [Mn²⁺+1-xMn³⁺+2x/3Ni²⁺+x/3]A[Ni²⁺+2x/3Mn³⁺+2-2x/3]BO₄.

QM26

Anomalous switching of in-plane magnetic anisotropy of Fe and Co thin films grown on curved Pt(001) surface

Wondong Kim^{1*}, Chanyong Hwang¹ and Z.-Q. Qiu²
¹ Korea Research Institute of Standards and Science, Korea
² Physics Department, University of California at Berkeley, USA

We investigated the step-induced magnetic anisotropy of Fe and Co thin films grown on the curved Pt(001) surface using Surface Magneto-Optical Kerr Effect(SMOKE) and Scanning Tunneling Microscopy(STM). The continuous variation of step density of the curved Pt(001) surface are confirmed by STM experiment. From SMOKE measurements on both of Fe and Co thin films, we observed the switching of the magnetic easy axis from the parallel-to-step direction to the step-normal direction with increase of the step-density. We attributed the origin of this anomalous transition to the abrupt change in the step structure at high-step density position, which was revealed by STM measurements.

July 10 (Tue)

July 10 (Tue)

QM27

Magnetic-field and temperature-dependent relaxation in ferrofluids characterized with a high-Tc SQUID-based nuclear magnetic resonance spectrometer

Hong-chang Yang^{1*}, Chieh-wen Liu¹, Shu-hsien Liao², M.¹ Chen¹, K.I. Chen¹, Hsin-hsien Chen², Heng-er Horn², L.m. Wang¹ and S.Y. Yang²

¹ Department of physics, National Taiwan University, Taiwan

² Institute of Electro-Optical Science and Technology, National Taiwan Normal University, Taiwan

In this work the magnetic-field and temperature dependent spin-lattice relaxation rate, 1/T1, and spin-spin relaxation rate, 1/T2, of ferrofluids are characterized using a high-Tc SQUID-based magnetometer as the detector. The ferrofluids are consisted of detrain-coated Fe₃O₄ dispersed in phosphate buffer saline solution. It was found that 1/T1 measured in a magnetic field of 56.8 mT is significantly higher than 1/T2 measured in a magnetic field of 102 μT. We attribute this to the magnetic-field gradients from magnetic nanoparticles that accelerate the T1-relaxation more in a high strength of magnetic fields than they are in a low strength of magnetic fields. Furthermore, 1/T1 and 1/T2 decrease when temperature increases. We attribute this to the improved field-homogeneity seen by protons' spins under the influence of enhanced Brownian motion of magnetic nanoparticles at high temperatures than they are at low temperatures. Characterizing the relaxation rates of ferrofluids in low concentration regimes will be helpful for their future applications such as the low field MR imaging.

QM28

Influence of metal precursor on synthesis and magnetic properties of nanocrystalline strontium hexaferrite thin films

S. M. Masoudpanah, S. A. Seyyed Ebrahimi* and M. Khodaei

Center of Excellence for Magnetic Materials, University of Tehran, Iran

The effects of starting metal salts on the structure and magnetic properties of strontium hexaferrite thin films synthesized by sol gel process have been investigated. Fourier transform infrared and thermal analyses were conducted to determine the chelated species and thermal decomposition of the gels, respectively. X-ray diffraction, scanning electron microscopy and vibrating sample magnetometry techniques were also applied to evaluate the microstructure, composition, crystallite size and magnetic properties of the thin films. The results showed the film prepared from nitrate precursor offered a single phase strontium hexaferrite with nanocrystalline structure and higher saturation magnetization after calcination. However, the films obtained from hydroxide and chloride precursors had higher coercivity due to smaller crystallite size.

QM29

Planar Hall effects measurements of sensitive magnetization response in epitaxial Fe thin films

Anis Faridah Md Nor^{1*}, Tatsuya Matsumoto², Teppei Takashima², Terumitsu Tanaka² and Kimihide Matsuyama²

¹ Physics Department, University of Malaya, Malaysia

² Department of Electronics, ISEE, University of Kyushu, Japan

The Fe thin film is a promising candidate for future magnetic microwave devices, owing to the high ferromagnetic resonance frequency with an order of 10 GHz [1-2]. A high sensitive magnetization response is crucial for the low power device operation. In the present study, we prepared Fe(100) thin films deposited on MgO(100) substrates using magnetron sputtering system and investigate the magnetization process using the planar Hall effect (PHE).The PHE measurements were carried out with several Fe thicknesses and temperatures. In the PHE measurements, alternating external magnetic fields along vertical easy axis were applied with various amplitudes and the sense current was applied along the horizontal easy axis. With increase of alternating magnetic field, the PHE voltage increased due to the disposition of Fe magnetization from easy axis. When the alternating magnetic field exceed a threshold value, the PHE voltage decreased rapidly. The threshold value depend on the thickness of Fe film and the PHE voltage decreased with decreasing temperature. These results suggest that the magnetization rotates exceeding the hard axis direction and reversible susceptibility can be realized. The stochastic aspect of the magnetization process also appears at 10 K.

[1] E. Schloeman et al., J. Appl. Phys., 63, 3140 (1988). [2] N. Cramer et al., J. Appl. Phys., 87, 6911 (2000).

QN01

Antiferromagnetic order and domains in Sr₃Ir₂O₇

S. Boseggia¹, R. Springell¹, H. C. Walker², A. T. Boothroyd³, D. Prabhakaran³, D. Wermeille⁴, L. Bouchenoire⁵, S. P. Collins⁵ and D. F. McMorrow¹

¹ Physics and Astronomy, London Centre for Nanotechnology, UCL, United Kingdom

² European Synchrotron Radiation Facility, France

³ Clarendon Laboratory, University of Oxford, United Kingdom

⁴ 5XMAS, UK-CRG, European Synchrotron Radiation Facility, France

⁵ Diamond Light Source, Didcot, Oxfordshire, United Kingdom

Resonant scattering at the Ir L2, 3 edge has been used to determine that Sr₃Ir₂O₇ is a long-range ordered antiferromagnet below TN~230 K with an ordering wavevector, q = (½, ½, 0). The energy resonance at the L3 edge was found to be a factor of ~30 times larger than that at the L2. This remarkable effect has been seen in the single layer compound Sr₂IrO₆ and has been linked to the observation of a Jeff= 1/2 spin-orbit insulator. Our result shows that despite the modified electronic structure of the bilayer compound, caused by the larger bandwidth, the effect of strong spin-orbit coupling on the resonant magnetic scattering persists. Using the programme SARAh, we have determined that the magnetic order consists of two domains with propagation vectors k1 = (½, ½, 0) and k2 = (½,-½, 0), respectively. A raster measurement of a focussed x-ray beam across the surface of the sample yielded images of domains of the order of 100 μm size, with odd and even l components, respectively. Fully relativistic, monoenergetic calculations (FDMNES) have been employed to calculate the relative intensities of the L2, 3 edge resonances, comparing the effects of including spin-orbit coupling and the Hubbard, U, term.

QN02

High frequency permeability of Fe-Co and Co granular composite materials

Teruhiro Kasagi^{1*}, Aiko Tsurunaga², Takanori Tsutaoka² and Kenichi Hatakeyama³

¹ Tokuyama College of Technology, Japan

² Graduate School of Education, Hiroshima University, Japan

³ Graduate School of Engineering, University of Hyogo, Japan

Relative complex permeability and permittivity spectra of Fe₃₀Co₇₀ (Permendur) and Co granular composite materials have been studied in the microwave frequency range up to 18 GHz. Particles were heat-treated in air using an electric furnace in order to suppress the eddy current effect in the composite structure containing percolated particles. Composite materials were prepared by mixing these particles with Polyphenylene sulfide resin. The 78 vol.% Fe₃₀Co₇₀ granular composite has the larger relative permeability value than that of the 79 vol.% Co composite at 100 MHz. The negative frequency dispersion of permeability was observed above 7 and 8 GHz for Fe₃₀Co₇₀ and Co composites, respectively. The dc magnetic field effect on the permeability spectra revealed that the permeability dispersion of Co composites in the microwave range is mainly attributed to the gyromagnetic resonance. The relative permittivity spectra of 78 vol.% Fe₃₀Co₇₀ and 79 vol.% Co composites show the insulating property up to several GHz; the permittivity value increases with increasing particle content in both composites.

QN03

Magnetic carbonyl iron suspension with nanoclay additive and its magnetorheological properties

Cheng Hai Hong, Ying Dan Liu and Hyoung Jin Choi*

Department of Polymer Science and Engineering, Inha University, Korea

Soft magnetic carbonyl iron (CI) based magnetorheological (MR) fluids with different loadings of nanoclay were prepared, in which the MR fluid is a complex colloidal suspension consisting of magnetic particles dispersed in a liquid, showing its rapid, reversible and tunable change between a liquid-like and solid-like state with an applied external magnetic field. The MR characteristics were measured via rotational tests, in which the flow curves exhibited a non-Newtonian behavior for all investigated samples under applied magnetic fields. Flow curves showed not only the dynamic yield stress change measured as a function of magnetic field strength using a power law fit but also the existence of a solid-like character. Sedimentation of the MR fluid with and without an additive was also examined.

QN04

Hysteresis analysis: A study on the demagnetization by using M-B preisach model for improved stability of numerical analysis

Hyuk Won and Gwan Soo Park*

School of Electrical Engineering, Pusan National University, Korea

It is necessary to describe the hysteresis characteristic of magnetic material precisely for the analysis of design of system with ferromagnetic materials. Although Preisach model is regarded as the most accurate method to describe the hysteresis characteristics, it is not applied widely to the real systems because of some difficulties. The conventional Preisach model shows the numerical instabilities during the iterative computations because the density distribution obtained from the sets of M-H curves are strongly localized. To remove such numerical instabilities, if we use a M-B variable instead of M-H variable would be better the results. In this paper, we suggest method for a M-H variable to change a M-B variable, and also, from the computed results of used normal Preisach, M-H cure method and M-B curve method, we shows better than numerical stabilities by using two dimensional finite element method.

QN05

A study on the design of transmitting coils and receiving coils on active magnetic snesor using finite element method

Hye Sun Ju and Gwan Soo Park*

Pusan National University, Korea

Proximity magnetic sensor is able to detect the object target accurately in close range and it has been widely used in the underwater guided weapon system because there is no countermeasures from the target. In order to increase the damage of target by shock wave due to explosion of the underwater guided weapon system, the maximum detection range of the proximity magnetic sensor needs to be increased. In this paper, we describe the techniques of the optimum transmitting and receiving coils design using the Finite Element Method for the output power enhancement of the transmitter and the sensitivity improvement of the receiver. Finally, the proposed design techniques of the transmitter and the receiver were verified using a experimental setup and a prototype.

QN06

What can we learn from isothermal remanent magnetization curves on diluted nanoparticle assemblies?

Florent Tournus*, Arnaud Hillion, Alexandre Tamion and Veronique Dupuis

LPMCN, CNRS & Univ. Lyon 1, France

Isothermal remanent magnetization (IRM) and direct-current demagnetization (DcD) curves are mainly used to characterize interactions in a granular magnetic media and to determine the switching field distribution. These curves are only sensitive to irreversible changes, i.e. to the particle magnetization switching for samples made of clusters embedded in a matrix. Moreover, at remanence there is no unsuitable contribution (superparamagnetic, diamagnetic or paramagnetic) to the signal. This makes IRM/DcD curves of great interest in the investigation of the intrinsic properties of nanoparticles. The underlying process, i.e. macrospin switching by applying a field, is complementary to the thermal switching observed with ZFC/FC curves where the particle size distribution has a critical influence. Interestingly, IRM curves have a high sensitivity to other characteristics such as an anisotropy constant distribution, non-uniaxial terms of the anisotropy, and of course inter-particle interactions. We show how IRM/DcD curves can be modelled for an assembly of randomly oriented and non-interacting macrospins, thus allowing efficient and realistic simulations of experimental curves (taking into account the size distribution, temperature, etc). This modelling is then confronted to a series of measurements on diluted Co nanoparticle samples prepared by low-energy cluster-beam deposition. Experiment/theory comparison can provide new insights on their magnetic properties.

QN07

On real-time hysteresis compensation for magentostriictive sound transducers

Hae Jung Park and Young-woo Park*

Department of Mechatronics Engineering, Chungnam National Unvers, Korea

Magnetostrictive actuators show inherent hysteresis, and it hinders wide applications. To solve this problem, in the literature, ‘Jiles-Atherton model’ and ‘Preisach model’ have been used mostly. But the methods require huge CPU time, or need complex mathematics. Thus, for real-time, ability of hysteresis compensation using capacitor is proposed by park et al [1]. In this paper, class-D amplifier containing capacitor as hysteresis compensator is proposed. The Class-D amplifier consists of comparator, current supplier and R-C circuit. Hysteresis compensator is implemented by a R-C circuit, because the output voltage of capacitor has similarity to a hysteresis compensated input, and the process of development is as follows: 1. Generation of Hysteresis compensated input by Preisach model; 2. Comparison between hysteresis compensated input and R-C circuit model by non-linear regression; 3. Application found capacitance to the class-D amplifier. Experimental setup is consisted of a capacitance displacement sensor, a digital oscilloscope and a function generator. Hysteresis loss observed about 19 percent before application of hysteresis compensator, and hysteresis loss observed less than 13 percent after application of hysteresis compensator at 10 Hz by using the 3 uF of capacitor.

[1] Ki-Hyun Ji, Hae-Jung Park, and Young-Woo Park, “Semiempirical Approach to Compensate Hysteresis in Magnetostrictive Actuator”, IEEE International Magnetism Conference 2011, 2011

QN08

The investigation on structural and magnetic properties of Ni-Cu-Zn-Mn-Mg-Li ferrites

Chih-wen Chen*, Mean-June Tung and Shi-Yuan Tong

Industrial Technology Research Institute, Taiwan

In this work, addition of seven raw materials inclusive of nickel oxide, copper oxide, zinc oxide, manganese oxide, magnesium oxide, lithium oxide, and iron oxide to form a new multi-component ferrite system. The Ni-Cu-Zn-Mn-Mg-Li substituted ferrites were prepared by conventional solid-state-reaction process and sintered at 1100°C for 2 h in air atmosphere. The influences of Ni-Cu-Zn-Mn-Mg-Li substitution on structural and magnetic properties were investigated by scanning electron microscopy, RF impedance/material analyzer, B-H curve loop tracer, and vibrating sample magnetometer. The experimental results show that the additives with low melting point form precipitates at the grain boundaries.[1] The average grain size of sintered ferrites decreases with a decrease of Ni/Mn ratio. The sintered ferrites, Ni/Mn=0.79, showed largest initial permeability (μi=85), largest saturation magnetism (Bs=3930 gauss), and better saturation magnetization (Ms=74.91 emug-1).

[1]Guiqing Wang, Xufang Bian, Weimin Wang, Junyan Zhang,Mater. Lett., 57 (2003) 4083-4087.

QN09

Magnetorheology of xanthan gum coated soft magnetic carbonyl iron microspheres and their polishing characteristics

Seung Hyuk Kwon¹, Hyoung Jin Choi^{1*}, Jung Won Lee², Kwang Pyo Hong² and Myeong Woo Cho²

¹ Department of Polymer Science and Engineering, Inha University, Korea

² Department of Mechanical Engineering, Inha University, Korea

Magnetorheological fluids, complex colloidal suspensions consisting of magnetic particles dispersed in a liquid, showing their rapid, reversible change between a liquid-like and solid-like state with an applied magnetic field. Among these applications, MR polishing arrests a lot of attention due to its smart controlling polishing characteristics for dedicated MEMS applications. In order to improve polishing characteristics of MR fluids, in this study, carbonyl iron (CI) microspheres coated with xanthan gum (XG) were fabricated via solvent casting method. The morphologies and densities of both pure CI and CI/XG particles were characterized via SEM and pycnometer, respectively. In addition, rheological characteristics of the MR fluids under applied magnetic field strengths were examined via a rotational rheometer, in which shear viscosity, storage modulus, normal force the variation in MR performance under applied magnetic fields. Especially, the normal force was measured for different gap distances to simulate the work condition of MR polishing. MR polishing characteristics were conducted using an MR polishing machine to investigate the surface roughness from the MR polishing with nano ceria slurry abrasives. A series of experiments were performed for fused silica glass using prepared slurry by changing the processing parameters such as a rotating wheel speed and polishing time.

QN10

Cluster-glass-like magnetic state in rare-earth intermetallic compound Tb₃Pd₂

Andrey F. Gubkin^{1*}, Pavel E. Terent'ev², Elena A. Sherstobitova¹ and Nikolai V. Baranov³

¹Laboratory of neutron scattering, Institute of Metal Physics, Russia

²Laboratory of ferrimagnetic alloys, Institute of Metal Physics, Russia

³Laboratory of micromagnetic materials, Institute of Metal Physics, Ural Federal University, Russia

The rare-earth intermetallic Tb₃Pd₂ compound crystallizes in a cubic crystal structure with site disorder and magnetic frustrations due to triangle-like arrangement of Tb atoms [1]. In this work the DC and AC magnetic susceptibility measurements together with powder neutron diffraction have been performed in order to study the Tb₃Pd₂ magnetic state. The susceptibility measurements on a polycrystalline Tb₃Pd₂ sample have revealed a complex highly irreversible behaviour below 58 K, which can be associated with the existence of a spin-glass-like magnetic state. According to our neutron diffraction data the Tb₃Pd₂ compound doesn't exhibit a long-range magnetic down to 5 K. However below and above the freezing temperature T_G ≈ 58 K, the appearance of the broad diffuse maxima of magnetic origin has been detected in the low angle region. The second anomaly of the susceptibility was observed at T_B ≈ 25 K, which can be ascribed to the blocking process of uncompensated magnetic moments of antiferromagnetically short-range correlated regions. The results obtained allow us to suggest that the Tb₃Pd₂ compound exhibits a complex non-ergodic magnetic state of a cluster-glass type associated with frustrations of the RKKY-type exchange interaction. This work was supported by the program of RAS (Projects RAS UB 11-2-HII-26).

1. M. L. Fornasini, A. Palenzon, *J. Less-Common Metals*, 38, (1974) 77-82.

QN11

Microwave absorption properties of polymer composites with amorphous Fe-B and Ni-Zn-Co ferrite nanoparticles

Kazuaki Shimba*, Shozo Yuki, Nobuki Tezuka and Satoshi Sugimoto
Materials Science, Tohoku University, Japan

Recently, many communication devices use GHz-range microwave. It causes serious issue, such as electromagnetic interference and multipath interference. To prevent these problem, microwave absorbers (MA) consisting of polymer composites of magnetic powders are paid attention. With the current trend being to miniaturize devices, thinner MA are now required. We reported that polymer composites with amorphous Fe-B particles (AFBP) and Ni-Zn ferrite nanoparticles showed high permeability of μ'r = 9.5 at 1.0 GHz and good microwave absorption properties at 0.6-1.1 GHz and resulted in thinner MA than reported MA [1]. However, they cannot used as MA over 1.1 GHz, because of their low resonant frequency (fr = 1.2 GHz). In this study, Ni-Zn-Co ferrite nanoparticles (NZCFN) were mixed with AFBP for increasing fr in polymer composites. XRD analyses show that NZCFN exhibit typical spinel structure. The fr of NZCFN increases from 0.7 to 3.6 GHz with increasing Co contents. It indicates that the magneto-crystalline anisotropy of NZCFN is increased by Co addition. The fr of polymer composites with AFBP and NZCFN can be increased to 2.6 GHz. They exhibits good microwave absorption properties at 0.8-1.4 GHz with thicknesses of 2.4-3.9 mm and resulted in thin MA at 1-1.4 GHz.

[1] O. Shimba, N. Tezuka, S. Sugimoto; *Materials Science and Engineering B* 177 (2012) 251-256

QN12

Magnetostrictive properties of Mn substituted sintered cobalt ferrite derived from nanocrystalline materials

Khaja Mohaideen Kamal and P A Joy*
Materials chemistry division, National Chemical Laboratory, India

Magnetostrictive smart materials are of great importance for sensor applications. Cobalt ferrite is well known for its highest magnetostrictive strain at room temperature among the oxide based magnetostrictive materials. The substitution of manganese for iron in cobalt ferrite, CoFe₂O₄, increases the strain derivative even though the magnetostriction value is decreased for the material synthesized through the conventional ceramic route [1,2]. In the present study we have investigated the influence of the initial particle size of the powders of manganese substituted cobalt ferrite on the magnetostrictive coefficient of the sintered ferrite samples with compositions 0 ≤ x ≤ 0.3 in CoFe_{2-x}Mn_xO₄. Nanoparticles of CoFe_{2-x}Mn_xO₄ of size less than 10 nm were synthesized by an autocombustion method and the resulting powders were sintered in air at 1300° C. Magnetic characteristics of the nanocrystalline powders and sintered products have been studied. Magnetostriction measurements were performed on the sintered samples to determine the influence of initial particle size of the starting powders. Higher magnetostriction at low fields is obtained along with enhanced strain derivative for the sintered Mn substituted cobalt ferrite derived from nanocrystalline materials compared to the bulk counterparts.

J. J.A. Paulson et al. *J. Appl. Phys.*, 97, 44502 (2005). 2. S.D. Bhamé and P.A. Joy; *J. Appl. Phys.*, 100, 113911 (2006).

QN13

Magnetic Properties of Co₂Z Ferrite Densified through High BET Powders

Ji Yeon Song and Young Ho Han*
Materials Engineering, Sungkyunkwan University, Korea

Co₂Z is a planar hexagonal ferrite that exhibits high permeability (μi) and high resonance frequency (fr) up to the GHz region. Z-type Ba₃Co₂Fe₂₃O₄₁ hexagonal ferrite was prepared by two-step calcinations [1]. Single phase Co₂Z ferrite powders were possible after post-calcination at 1300°C. Various sintering aids improved densification of ceramic bodies, but lowered magnetic permeability due to non-magnetic characteristics of sintering additives. In order to increase permeability, Co₂Z specimen was sintered without sintering aids. The densities of sintered bodies increased with increasing specific surface area (BET) of calcined powders, and Co₂Z with BET 7.80m²/g led to significantly high densification(5.23g/cm³, 97% theoretical density). Permeability of Co₂Z gradually increased with increasing density, whereas their resonance frequencies decreased with increasing permeability, where the product of μi x fr was estimated to be ~10.3GHz. It was thus confirmed that the calcined powders with high BET could enhance sintering kinetics of Co₂Z hexagonal ferrites without sintering additives and significantly increase magnetic permeability.

[1] J. Jeong, K.W. Cho, D.W. Hahn, B.C. Moon, Y.H. Han, *Mater. Lett.* 59 (2005) 3959-62

QN14

Magnetic properties of Cr³⁺ substituted Mg-Cd ferrites

S A Masti^{1*}, A. K Sharma² and P. N. Vasambekar³
¹ Physics, Dr. Ghali College, Gadhinglaj, India
² Physics, Shivaji University, Kolhapur, India
³ Electronics, Shivaji University, Kolhapur, India

Magnetization and susceptibility of polycrystalline ferrites with general formula Cd_xMg_{1-x}Fe_{2-y}Cr_yO₄ (x = 0, 0.2, 0.4, 0.6, 0.8, 1.0; y = 0, 0.05 and 0.10) were studied. Study of saturation magnetization reveals that the Neels two sublattice model exists up to x = 0.4, for y = 0, 0.05 and 0.1 and a three sublattice model (YK-model) is predominant for x > 0.4, y = 0, 0.05 and 0.10. The saturation magnetization and magnetic moment were found to decrease with the increase of Cr³⁺ contents, which is attributed to the dilution of B-B site interaction. Temperature dependence normalized AC susceptibility study reveals that MgFe₂O₄ exhibits single domain(SD) structure. On substitution of Cd²⁺, single to multi domain transition takes place. Curie temperature decreases with Cd²⁺, was attributed to decrease in A-B intraction. On substitution of Cr³⁺, peak obtained in MgFe₂O₄ was suppressed which is attributed to decrease in grain size and further decrease

QN15

Docking Speaker Based on Magnetostrictive Sound Transducer

Han Sam Kang, Jin Hong Min and Young Woo Park*
Department of Mechatronics Engineering, Chungnam National University, Korea

All docking speakers available in the market are equipped with iDevice cradle and with cone-type sound unit. This paper presents a novel docking speaker without them. It is based on the magnetostrictive sound transducer (MST), which transforms any flat surface into speaker. The docking speaker consists of one MST, two circuit boards, and aluminum housing. One circuit board contains a Bluetooth module, a power amplifier module, Aux, and a recharge adapter. The other board is called a control board, which ATmega128 is used to control a digital clock, a LCD module, four control switches, and a power amplifier module. The reluctance concept is utilized to the magnetic circuit for the MST. Allowable current and number of coil turns are determined through this procedure. The result is compared with the simulation result. Then, circuit board and housing are designed. The assembled docking speaker is subjected to the experiments. For the experiments, the MST is placed and bolted between the wood and glass panels. An accelerometer sensor, ADXL001, is firstly located beneath the center of the MST. Then, the location is placed away by 50 mm from the center of the MST. It is proved that the developed docking speaker works well.

QN16

Characteristics of composite materials Ba_{0.5}Sr_{0.5}Fe_{11.7}Mn_{0.15}Ti_{0.15}O₁₉/La_{0.7}Ba_{0.3}MnO₃ as a microwave absorber

V. Vekky R. Repi* and Azwar Manaf
Graduate Program of Materials Science Study, Universitas Indonesia, Indonesia



QN17

The effect of shape anisotropy to acoustical performance of magnetostrictive sound transducer

Hae Jung Park, Young Woo Park* and Ok Kyun Oh
Department of Mechatronics Engineering, Chungnam National Univvers, Korea

This paper presents the experimental approach to investigate the effect of the shape anisotropy of magnetostrictive material (MM) to acoustical performance of magnetostrictive sound transducer. The assumption is that the volume of MM is kept constant. In the experiments, four MM samples are used with a volume of 295 mm³ and input currents are swept from 20 Hz to 20 kHz. The diameters of MM samples are 4, 5, 6 and 10 mm and the lengths are 23.5, 15, 10.5 and 3.5 mm, respectively. The displacements are measured from 2.1 to 0.8 um at 20 Hz. Forces are measured from 81 to 120 N at 20 Hz. Among the samples, the MM sample of 23.5mm length shows the largest displacement and force. SPL is obtained from forces of MM and a area of vibration panel. The largest SPL is observed at 20 Hz and the SPL is measured to 115dB. Also, the SPL of the samples show the level from 103 dB at 1 kHz to 81 dB at 20 kHz. The displacement and force are measured from 0.36 um and 29N at 1 kHz to 15.3 nm and 2.5 N at 20 kHz.

QN18

Size effects on magnetic properties of nanocrystalline Sr₂CuCo₂Fe₂₄O₄₁ prepared by Co-precipitation method

K Praveena and K Sadhana
Materials Research Centre, Indian Institute of Science, India

The nanocrystalline z-type hexaferrite powders were synthesized by Co-precipitation method using aqueous solutions of strontium, copper, cobalt iron and nitrates. The as synthesized powders were characterized using XRD, TEM and TG/DTA. The average particle size of the powders was found to be 48nm. The effect of calcinations temperature on crystallinity, morphology and magnetic properties have been investigated. The sintered samples were characterized using XRD, FE-SEM and EDS. The hexagonal ferrite formation was observed around 900°C which is confirmed with the TG/DTA curves. The plate shape grains were observed in FE-SEM at 950°C. The grain sizes of sintered hexaferrites are in the range of 220nm to 850nm. The value of Ms= 70 emu/g and Hc=540 Oe was obtained at 900°C/5h.

QN19

Structural and magnetic properties of Mn₂Rh_{1-x}Co_xSn Heusler alloys

Olga Meshcheriakova¹, Jurgen Winterlik¹, Gerhard H. Fecher², Benjamin Balke³ and Claudia Felser³
¹Institute of Inorganic and Analytical Chemistry, Johannes Gutenberg University Mainz, Germany
²Institute of Inorganic and Analytical Chemistry, Johannes Gutenberg University Mainz, Max Planck Institute for Chemical Physics of Solids, Dresden, Germany
³Institute of Inorganic and Analytical Chemistry, Johannes Gutenberg University Mainz, Max Planck Institute for Chemical Physics of Solids, Dresden, Germany

Mn₂-based Heusler compounds are promising candidates for spintronic applications as they are known to crystallize with cubic and tetragonal structures or exhibit cubic-tetragonal phase transitions. Sn-containing compounds have only a small lattice mismatch with MgO thus providing higher symmetry correlation between magnetic film and tunneling barrier. Quaternary Mn₂Rh_{1-x}Co_xSn and Mn_{2-x}Rh_xSn Heusler alloys have been synthesized with a step of x = 0,1 and their magnetic properties were experimentally investigated. In the present work the structural and magnetic properties are discussed depending on the Rh and Co content. The first series undergoes a cubic-tetragonal transition at x = 0,5, while the latter one experiences a hexagonal-tetragonal change of structure. The presence of Co increases the Curie temperature keeping the magnetic moment unchanged. This work is supported by the Graduate School of Excellence Materials Science in Mainz (MAINZ).

[1] Simple Rules for the Understanding of Heusler Compounds, Tanja Graf, Stuart S. P. Parkin, and Claudia Felser, *Progress in Solid State Chemistry* 39 (2011) 1-50, invited review. doi:10.1016/j.progsolidchem.2011.02.001. [2] Electronic, magnetic, and structural properties of the ferrimagnet Mn₂CoSn, Jurgen Winterlik, Gerhard H. Fecher, Benjamin Balke, Tanja Graf, Vajitsh Alijani, Vadim Ksenofontov, Catherine A. Jenkins, Olga Meshcheriakova, and Claudia Felser 83 (2011) 174448. [3] Quaternary half-metallic Heusler ferromagnets for spintronics applications, V Alijani, J. Winterlik, G. H. Fecher, S. S. Naghavi, C. Felser, *Phys. Rev. B* 83 (2011) 184428

QN20

Magnetic properties of Mn₂Sb_{1-x}Ge_x (0.05 ≤ x ≤ 0.2) in high magnetic fields

Daisuke Shimada^{1*}, Hiroki Orihashi¹, Daisuke Mitsunaga¹, Kohki Takahashi², Masahiko Hiroi¹, Masakazu Ito¹, Kazuyuki Matsubayashi², Yoshiya Uwatoko³ and Keiichi Koyama¹
¹Kagoshima University, Japan
²Tohoku University, Japan
³Tokyo University, Japan

The Mn₂Sb compound with a Cu₂Sb-type tetragonal structure is ferromagnetic (FRI) below TC ~ 550 K. The substitution of various elements (V, Cr, Co, Cu and Zn) for Mn as well as (As, Ge and Sn) for Sb results in a first-order magnetic (FOM) transition from the ferromagnetic (FRI) to an antiferromagnetic (AFM) states with decreasing temperature [1]. Mn_{2-x}Co_xSb, it has been reported that the FOM transition occurs accompanied with large change in unit cell volume, resistivity and magnetization etc. However, detailed results on Mn₂Sb_{1-x}Ge_x have not been reported yet. In this study, magnetization and electrical resistivity measurements were carried out for polycrystalline Mn₂Sb_{1-x}Ge_x (0.05 ≤ x ≤ 0.2) in magnetic fields up to 16 T in 4.2-600 K temperature range, in order to investigate the magnetic and electrical properties affected by magnetic fields. Mn₂Sb_{0.92}Ge_{0.08} showed the Curie temperature T_c of 532 K and the FOM transition at T_t = 230 K in a zero magnetic field. With increasing x, T_c decreased and T_t increased. For Mn₂Sb_{0.92}Ge_{0.08}, we observed a matamagnetic transition from the AFM to FRI with a hysteresis of 0.5 T at 200 K.

[1] O. Beckman and L. Lundgren: *Handbook of Magnetic Materials* vol 6, ed K H J Buschow (Amsterdam: Elsevier) chapter 3, (1991) p 181-287

QN21

Microwave magnetic properties of FeNi films prepared by electrodeposition

Dong Zhou¹, Wei Li¹, Minggang Zhu^{1*}, Yanfeng Li¹, Wei Sun¹ and Fashen Li²
¹Central Iron & Steel Research Institute, China
²Lanzhou University, China

With the development of computers and communication devices using the electromagnetic wave of GHz range, the serious electromagnetic interference (EMI) have been emerged. The electromagnetic wave absorbers have been widely investigated to eliminate the EMI problems. Electrodeposition is one of the simplest, most flexible, and cheapest processes available for the fabrication of single component and multilayered thin films. In this study, FeNi alloys thin films have been successfully electrodeposited on Ag films. The morphology, structure, composition, and magnetic property of the FeCo films were characterized by scanning electron microscopy, x-ray diffraction, energy dispersive spectrometer, vibrating sample magnetometer and network analyzer. With the increase of deposition time, the coercivity of deposited FeNi films reduce until getting a minimum value and the the real part of permeability increase. At the same time, the increase of the thickness leads to the decrease of resonance frequency. We also study the effect of the composition on the coercivity and microwave magnetic properties. By changing the composition of FeNi alloy films, the effective permeability and the resonance frequency can be adjusted.

QN22

Preparation and characterization of ferromagnetic fluid and magneto-rheological fluid

Tae Min Hong¹, Jong Hee Kim², Cheolgi Kim³ and Seung Goo Lee^{1*}
¹ *Advanced Organic Materials & Textile System Engineering, Chungnam National University, Korea*
² *Research Center for Advanced Magnetic Material, Chungnam National University, Korea*
³ *Materials Science & Engineering, Chungnam National University, Korea*

Ferromagnetic fluid and magneto-rheological fluid are liquids that nanometer-sized particles of iron dispersed in the medium. PEG(polyethylene glycol) and silicon oil were used as the fluidic media. Fluids are flexible dispersion state under a non-magnetic field. But, under a magnetic field, particles are oriented in the direction of the magnetic field and the fluid shows the solid-like behavior. In this study, we studied to know how the magnetic field impacts the yield stress of ferromagnetic and magneto-rheological fluids. Yield stress of the fluid is evaluated by the viscosity measurement. Viscosity behaviors of ferromagnetic and magneto-rheological fluids are measured with a magneto-rheological viscometer (MCR 301, Anton paar, Austria) with applying magnetic field from the plate. Two types of experiment were conducted. One is a static test in which the viscosity of fluids is measured with increasing shear rate while the applied magnetic field is fixed. The other one is a dynamic test in which the viscosity of fluids is measured with increasing magnetic field while shear rate is fixed. As the results, viscosity of ferromagnetic fluid and magneto-rheological fluid increased largely by applying magnetic field in all conditions.

QN23

Microwave magnetic and absorbing properties of the planar-anisotropy Ce₂Fe₁₇N_{3.6} powder composite

Jianqiang Wei, Wenliang Zuo, Tao Wang and Fashen Li*
Key Laboratory of Magnetism and Magnetic Materials of Ministry of Education, Lanzhou University, China

Ce₂Fe₁₇N_{3.6} powders were prepared by arc-melting, milling and nitrogenation. The microstructure and static magnetic properties of the powders were analyzed by x-ray diffraction (XRD) and vibrating sample magnetometer (VSM), respectively. The c-plane alignment of Ce₂Fe₁₇N_{3.6} was evaluated with the XRD data of an aligned composite sample. The effective complex permeability of Ce₂Fe₁₇N_{3.6} powders/epoxy resin composite was measured in the frequency range of 0.1-15 GHz. The intrinsic static permeability of Ce₂Fe₁₇N_{3.6} powder was calculated by Bruggeman (BG) effective medium theory. The natural resonance frequency of Ce₂Fe₁₇N_{3.6} was obtained using Landua-Lifshitz-Gilbert (LLG) equation. The Snoek's product of the effective static susceptibility and the resonance frequency is much larger than the Snoek's limit of the composite. The reflection loss of the composite sample was determined by simulation and by measuring the S11 parameters after rear face of sample was terminated by metal. The minimum reflection loss was found moving towards the lower frequency region with increasing the sample thickness. Quantitatively analysis reveals that the peak frequencies (fp) of the dips (minimum reflection loss), the μ(fp), the α(fp) and the sample thickness obey the quarter-wavelength (λ/4) formula. Accordingly, the quarter-wavelength formula have been successfully applied to explain and predict the microwave absorbing properties.

This work is supported by the National Basic Research Program of China (Grant No. 2012CB933101) and the National Natural Science Foundation of China (Grant No. 11144008).

QN24

Co₂Y-NiCuZn ferrite composites for high frequency applications

Ruei-lin Lin and Hsing-i Hsiang*
Resources Engineering, National Cheng Kung University, Taiwan

The most commonly used materials in inductors for high-frequency applications are NiCuZn ferrites, or non-magnetic materials such as low-temperature cofired ceramics. The non-magnetic materials are used for high-frequency applications because NiCuZn ferrites (ferroxcube) typically exhibit severe property changes above 200MHz due to the Snoek limit. The maximum quality factor frequency in chip inductors made of non-magnetic material is over 500 MHz. However, the quality factors at frequencies around 200-300MHz are much lower than those at higher frequencies. Because chip inductors are prepared by winding a wire around a non-magnetic material core it is necessary to have a larger number of coil winding turns to obtain the desired inductance; thus limiting miniaturization. Therefore, it is desirable to develop a magnetic material that has a higher initial permeability and quality factor than non-magnetic materials at 200-300 MHz, for use in making high frequency inductors. In this study, a Co₂Y-NiCuZn ferrite composite with high permeability was prepared by coating NiCuZn ferrites onto the surface of Co₂Y ferrites using heterogeneous nucleation process. The effects of NiCuZn ferrites addition on the densification behavior, micro-structure and magnetic property of Co₂Y-NiCuZn ferrite composites were investigated.

QN25

A novel low-temperature-fired multifunctional varistor-magnetic NiCuZn ferrites

Wei-hung Hsu, Hsing-i Hsiang* and Li-then Mei
Resources Engineering, National Cheng Kung University, Taiwan

A novel low temperature-fired(950°C) multifunctional varistor-magnetic ferrite materials can be obtained by adding Bi₂O₃ into Zn_{0.5}Ni_{0.5}Cu_{0.19}Nb_{0.01}Fe_{2.02}O₄ ferrites. The relationship between the microstructure and varistor properties were investigated using scanning electron microscopy (SEM), X-ray Diffraction (XRD), and impedance analysis. For Zn_{0.5}Ni_{0.5}Cu_{0.19}Nb_{0.01}Fe_{2.02}O₄ ferrites with 2.5wt% Bi₂O₃ content sintered at 950°C for 2h, the nonlinearity exponent (α) can reach 5.1 and the initial permeability(μ) is about 200 to 250. Moreover, the avalue can be promoted to 67.8 for the Zn_{0.5}Ni_{0.5}Cu_{0.19}Nb_{0.01}Fe_{2.02}O₄ ferrites added with 9Bi₂O₃-CuO sintered at 950°C for 2h.

QN26

Synthesis and magnetic properties of transition metal ferrite nanoparticles

Tejabhram Yadavalli¹, Shivaraman Ramaswamy¹, Gopalakrishnan Chandrasekaran¹ and Ramasamy R²
¹ *Nanotechnology Research Centre, SRM University, India*
² *School of Pharmacy, SRM University, India*

The use of ferromagnetic metal ferrite particles for magnetic hyperthermia application has been extensively studied by many scientists. The use of ferromagnetic particles with low curie temperatures result in the formation of self regulated magnetic hyperthermia. In this context, multiple experiments on synthesizing ferrite nanoparticles with varying cobalt and nickel oxide concentrations have been done. The products were analyzed using scanning electron microscopy, energy dispersive spectroscopy, X-ray diffraction and vibrating sample magnetometer. The microscope images indicated the formation of nanoparticles while the spectroscopy and diffraction patterns indicated the formation of nickel and cobalt ferrite nanoparticles along with additional nickel oxide and cobalt oxide. Magnetometer analysis conducted on the samples indicated a reduced magnetic saturation and hysteresis. Hysteresis loss energy was determined by calculating the area under the hysteresis loop, frequency of the magnetic field and the curie temperature of the material. The results indicated a two-fold decrease in the hysteresis energy giving a hint for their use in controlled magnetic hyperthermia treatment.

QO01

High room temperature power factor (Z) in K₂RhO₂

Nirpendra Singh, Yasir Saeed and Udo Schwingschlogl*
King Abdullah University Science and Technology Thuwal, Saudi Arabia

We discuss the thermoelectric and optical properties of layered K₂RhO₂ by means of the electronic structure determined by first principles calculations as well as Boltzmann transport theory. The main contribution to the optical spectra are due to intra and inter-band transitions between the Rh 4d and O 2p states. Our results of transport perproties of K₂RhO₂ at room temperature show highest value among hole-type materials. Specially at 100 K, the Z value of K₂RhO₂ is 3x10⁻³ K⁻¹. Our results show that the electronic and optical properties of K₂RhO₂ are similar to Na₂CoO₂ with an enhanced transport properties.

QO02

Optimized Halbach array based magnet systems for Lorentz force velocimetry purposes

Michael Werner^{1*} and Bernd Halbedel²
¹ *University of Technology Ilmenau, Germany*
² *Department of Inorganic-Nonmetallic Materials, University of Technology Ilmenau, Germany*

Lorentz Force Velocimetry (LFV) is in research since 2003. The Lorentz force acting on a source magnet system is providing a velocity dependent signal. The efficiency of the magnet system (ratio of generated Lorentz forces to the mass of the system) is an essential parameter for sufficient resolutions of the whole LFV sensor device. The full article will propose a very efficient combination of permanent magnet arrays, where the particular permanent magnets have different magnetization directions. Here an iron yoke is not necessary, respectively ineffective, and so the arrays can be assembled with a very light carbon fiber composite fixture in order to reduce the overall mass further. The underlying principle of this array combination will be presented and the geometric optimization with commercial software, as well as the assembling method, will be explained. On an experimental test channel for LFV on electrolyte flows the magnet system is tested and compared to another simple standard magnet system with single permanent magnet blocks instead of the arrays. From previous finite element simulations an increase of a factor of three in efficiency is estimated and will be proven in the experiment. Further improvement using cladding technique will be introduced too.

QO03

Growth and characterization of SmFe₆Ge₆ single crystals

Rodrigo S. Monteiro, Lucas K. Piquini, E. Thizay Magnavita, Raquel A. Ribeiro and Marcos A. Avila*
Centro de Ciencias Naturais e Humanas, Universidade Federal do ABC, Brazil

Hexagonal single crystal plates of SmFe₆Ge₆ have been grown by the flux method using a 4th flux element (Sn), extending the range of members in the RFe₆Ge₆ family of magnetic compounds, whose physical properties have so far been described only for rare earths R = Gd-Lu [1]. This family exhibits antiferromagnetic (AF II) ordering at 450 K of the layered Fe honeycomb sublattice, and independent ordering (or no ordering) of the R sublattice moments below 30 K. Here we present a basic characterization of the structural, magnetic and transport properties of the SmFe₆Ge₆ crystals and compare the general anisotropic behavior with other members of the family. We thank the support of Brazilian agencies FAPESP and CNPq.

[1] G. Venturini, R. Welter and B. Malaman, *J. Alloys Comp.* 185 (1992) 99-107.

QO04

Anomalous magnetic and related properties of Nd₅Ge₃

Bibekananda Maji^{1*}, K G Suresh¹ and A K Nigam²
¹ *Physics, Indian Institute of Technology Bombay, Mumbai- 400076, India*
² *Tata Institute of Fundamental Research, Homi Bhabha Road, Mumbai- 400005, India*

We have observed that the stoichiometric intermetallic compound Nd₅Ge₃ shows many anomalies in the magnetization, resistivity and heat capacity data. This compound undergoes an antiferromagnetic (AFM) transition at 46 K and another one at 30 K on cooling. It is found that the strengths of these two antiferromagnetic states are different. Ultra-sharp jumps are seen in the low temperature isotherms of magnetization, heat capacity and electrical resistivity. Another important anomaly is the field-induced irreversibility in all these three properties, which suggests that the spin, electronic and lattices states are strongly coupled in this compound. The memory effect seen here is quite remarkable and is consistently seen in various measurements. Another striking observation is the spontaneous evolution of the ferromagnetic (FM) phase as a function of time, at a fixed temperature and at the critical field. Sweep rate and cooling field dependencies point towards the role of martensitic strains in the anomalous behavior. The compound appears to show the coexistence of FM and AFM components at low temperatures. The features seen in this compound indicate the presence of disorder in influencing the magnetic and related properties considerably. The correlation of various properties as seen from the martensitic scenario will be presented.

QO05

Magnonic meta- and meta-meta-materials

Rostislav V. Mikhaylovskiy^{1*}, Michal Mruczkiewicz², Maciej Krawczyk² and Volodymyr V. Kruglyak¹
¹ *School of Physics, University of Exeter, United Kingdom*
² *Faculty of Physics, Adam Mickiewicz University, Poznan, Poland*

We report on magnonic metamaterials represented by a system of magnetic layers separated by those of a dielectric non-magnetic material. In such a metamaterial, the constituent elements are made from a magnetic material that provides an easy way to control its electromagnetic response by tuning the bias magnetic field. Firstly, we report a theory of the effective permeability of planar multilayered metamaterials containing thin ferromagnetic layers with magnetization pinned on either one or both surfaces. The pinning of the magnonic modes at film surfaces facilitates their coupling to the uniform magnetic field of the incident electromagnetic wave. We demonstrate that such structures, for magnetic parameters characteristic for conventional transition metal alloys, exhibit a negative refractive index at sub-THz frequencies. Furthermore, we show how the constituent magnetic layers of such systems could themselves be nanostructured into planar magnonic crystals, with the whole structure therefore representing a meta-metamaterial. Due to the additional nanostructuring, the negative permeability at sub-THz frequencies can be achieved as a result of a small lattice constant and lateral quantization of spin waves. Finally, we discuss the prospects for fabrication of such metamaterials and their experimental studies.

QO06

Understanding the nature of magnetic phase transition in relevance to magnetic refrigeration

S M Yusuf*
Solid state physics diviston, bhabha atomic research centre, mumbai 400085, India

It is important to understand the nature of magnetic phase transition for a material suitable for magnetic refrigeration. With this aim, we have studied a wide class of intermetallic compounds with diversity in their nature of magnetic ordering and phase transition, such as ferromagnetic ordering, ferrimagnetic ordering, coexistence of ferromagnetic and antiferromagnetic ordering, metamagnetic transition, and magnetostructural transition. The dependences of the nature of magnetic phase transition on temperature, magnetic field and chemical substitutions have been investigated. The role of the nature of exchange interaction and universality class in determining magnetocaloric effect (MCE) has been brought out by investigating the intermetallic compounds TbCo₃Fe, and Mn₂FeGe_{1-x}Si_x. A phase coexistence of ferromagnetic and antiferromagnetic phases has been observed in Cu_{2-x}Ni_xMnSb semi-Heusler alloys around x = 0.15 where a large MCE is found as a low applied magnetic field causes an AFM to FM phase transformation. A broad operating temperature range due to coexistence of AFM and FM phases, and quenched disorder has also been obtained. The role of other interesting phenomena, such as metamagnetic transitions and domain wall pinning in obtaining a large MCE and an inverse MCE, respectively, has been brought out through the investigation of the intermetallic compounds NdMn_{2-x}Co_xSi₂.

[1] M. Halder, S. M. Yusuf, M. D. Mukadam, and K. Shashikala, *Phys. Rev. B* 81, 174402 (2010). [2] M. Halder, S. M. Yusuf, A. Kumar, A. K. Nigam and L. Keller, *Phys. Rev. B* 84, 094435 (2011). [3] M. Halder, S. M. Yusuf and A. K. Nigam, *J. Appl. Phys.* 110, 113915 (2011). [4] M.D. Mukadam, and S.M. Yusuf, *Physica B: Cond. Matter* 405, 686 (2010). [5] M.D. Mukadam and S.M. Yusuf, *J. Appl. Phys.* 105, 063910 (2009).

QO07

Specific heat study on successive magnetic transitions in α-Dy₂S₃ single crystal under magnetic fields

Shuji Ebisu*, Yuji Ushiki and Shin Takahashi
Division of Applied Sciences, Muroran Institute of Technology, Japan

Specific heat measurements in magnetic fields have been performed on α-Dy₂S₃ single crystal which shows successive magnetic transitions at TN1 = 11.5 K and TN2 = 6.4 K¹. The specific heat in no magnetic field exhibits sharp peaks at both temperatures of TN1 and TN2. The change of magnetic entropy at each transition is estimated as N0kBlm₂ per mole of Dy₂S₃, which suggests Dy moments on only one site between two crystallographically inequivalent Dy sites order at each transition temperature. When the magnetic field is applied along the b-axis of the orthorhombic system, two peaks of the specific heat shift toward lower temperatures. On the other hand, the magnetic field perpendicular to the b-axis shifts the peaks toward higher temperatures. The transition temperature TN1 shifts to 9.6 K (H//b) and 12.5 K (H⊥b) with keeping sharpness of the peak under the magnetic field of μ0H=2 T. The peak of TN2 broadens gradually with increasing the magnetic field for each direction, and the peak is consequently obscure under the field of 2 T.

¹S. Ebisu, M. Narumi, M. Gorai and S. Nagata, *J. Magn. Magn. Mater.* 310, 1741 (2007).

Q008

Magneto-inductive wave in periodic chains of ferrite cores and chip capacitors

Yongmin Kim and Kwang-ho Shin*
Dept. of Information and Communication Engineering, Kyungsung University, Korea

In this paper, we present a new magneto-inductive wave generated in a chain of resonators fabricated with ferrite cores and chip capacitors. RF signal propagates to neighbor resonator one by one as a consequence of the magnetical coupling between two resonators in our device. The magnetical coupling is due to the mutual inductances along chains of resonators. So, the signal amplitude (? coupling intensity) is inversely proportional to the distance between two elements. In order to design the device, some electromagnetic simulations and experiments have been carried out systemically. The transmission characteristics of a magneto-inductive wave could be controlled by applied external magnetic field. For, the device composed of 5 resonance elements, the center frequencies were estimated to be 41.1 MHz and 34.8 MHz with the external magnetic flux density of 750.72 G and 2680 G, respectability. The reported result opens a promising way to a high variety of applications in one- and two-dimensional functional devices, such as transducers, delay lines, power dividers and couplers.

Q009

Large refrigerant capacity in Ni_{2.9}Co_{0.1}MnIn type-Heusler alloy

Catalina Salazar Mejia¹, Angelo M Gomes¹, Ana Lima Sharma² and Fivos R Drymiotis³

¹ Instituto de Fisica, Universidade Federal do Rio de Janeiro, Brazil
² Materials Physics Department, Sandia National Laboratory, Livermore, CA, USA
³ Department of Physics and Astronomy, Clemson University, Clemson, SC, USA

Magnetic refrigeration (MR) is a cooling method that is based on the magnetocaloric effect (MCE). Our research effort focuses on identifying magnetic structures that may have improved efficiency with suitable characteristics for MR i.e. good magnetocaloric properties with small or zero thermal and magnetic hysteresis. Some Heusler alloys may meet these criteria. The Ni₂MnIn full-Heusler alloy exhibits a second-order paramagnetic to ferromagnetic transition at 300 K, but its MCE is small [1,2]. However, we observe a large improvement in the refrigerant capacity (RC) value when the Ni₂MnIn is Co and Ni-doped. In this paper, we present the study of the magnetic, structural and magnetocaloric properties of the Ni_{2.9}Co_{0.1}MnIn Heusler-type alloy. The samples crystallizes in a cubic structure. Magnetization measurements show a ferromagnetic transition at 207 K. The transition is almost 40 K wide, and thermal hysteresis is negligible. The magnetic entropy change, ΔSM, for ΔH=5T, was calculated from heat capacity data and the maximum value found is -2.75 J/kg K, with broad temperature range which leads to RC=261.3 J/kg. The large RC value found and the absence of thermal hysteresis makes this material a good candidate for magnetic refrigeration applications. C.S.M. and A.M.G. would like to thank CNPq and FAPERJ.

[1] T. Krenke, et al., Phys. Rev. B 73, 174413 (2006). [2] C. Salazar Mejia, et al., unpublished.

Q010

Reduction of weak localization strength on controlling oxygen defects by ex-situ annealing

Seong-min Choo¹, Kyujoon Lee¹, Sungmin Park¹, Gwang-seo Park¹, Jungwon Jang², Jinhee Kim² and Myung-hwa Jung^{1*}

¹ Department of Physics, Sogang university, Korea
² Korea Research Institute Standard Science, Korea

We have studied Pb-based gapless semiconductors, which are very sensitive to external parameters such as temperature, pressure, magnetic field, electric field, etc [1]. Based on the theoretical paper, this material has a strong spin-orbit interaction. So, we have fabricated pure PbPdO₂, Co- and Mn-doped PbPdO₂ thin films. Because a Pb is an easily vaporized element when we grow the films, the films have a lot of oxygen vacancies. It may induce other problems. For example, Pd is unstable state as Pd+1 and the oxygen vacancies act as additional hole carriers. To study intrinsic properties of doped PbPdO₂ thin films, we tried to various methods to enhance the films quality. Because Pb is hard to handle in growth process, we have annealed thin films with different annealing time, temperature, and environments after deposition. The carrier densities for all the samples are decreased with annealing time while the electric resistivities are changed in different way. More importantly, weak localization strength is most likely to be reduced by ex-situ annealing. Furthermore, magnetoresistance ratio is also reduced by increasing ex-situ annealing time.

Q011

Reconstruction of cubic rs-ZnO on MgO (200) substrate through 100 plane of w-Zn for transparent electronic application

Chungman Kim¹, Santosh M Bobade¹, Seong-min Choo¹, Suhyun Kim¹, Kyung Ho Shin² and Myung-haw Jung^{1*}

¹ Sogang University, Korea
² Korea Institute of Science and Technology, Seoul, Korea

ZnO crystallizes in various crystallographic forms. However, wurtzite (w) ZnO is generally observed structure while the rock salt (rs) structure of ZnO appear at high pressure. We present rs-ZnO structure grown on MgO (200) substrate at certain growth environments, not high pressure. The lattice constant of MgO. The possible configurational path for transformation is proposed, so that the compression of w-ZnO along c-axis and movement of Zn or O sublattice along (110) direction and (110)plane. These results are confirmed by X-ray diffraction and X-ray photoemission spectrum experiments. It has also been observed that rs-ZnO on MgO substrate is stable for certain minimum thickness (in this case, it is 150nm) and possible be stabilize at lower temperature for few nm thickness

Q012

Magnetic cooling machine prototype based on cold rolled Gd foil

Sergey V. Taskaev*, Vasily D. Buchelnikov, Victor V. Nikolenko, Ivan A. Chernets and Andrey N. Denisovsky

Physics department, Chelyabinsk State University, Russia

With the discovery of the “giant magnetocaloric effect“ (Pecharsky and Gschneider, 1997) the development of magnetic refrigeration gained increased momentum [1]. One of the ways of engineering MCE materials is tightly connected with preparing very thin (a few microns) ribbons of high value MCE alloys with good mechanical properties. At present rapid solidification is the main technique for producing this kind of materials [2]. In our work we present magnetic cooling device which is used Gd cold rolled samples of different thickness as a working body. Magnetocaloric, mechanical and other properties of this material are discussed Morphology of the surface was investigated by AFM methods. Magnetocaloric effect was measured by direct method on AMT&C setup. Mechanical properties was investigated on Netzsch DMA 242C. Magnetic properties was measured on SQUID magnetometer. X-ray analysis was performed on Bruker D8 Advance diffractometer. Several axial magnetic systems are proposed as the source of high gradient magnetic field. Depending on the air gap of magnetic system the residual magnetic induction is in 600 mT..1900 mT range. It is shown, that cold rolling technique is the alternative way for producing thin ribbons of MCE materials with good mechanical properties for magnetocaloric application.

I.Gschneider K.A. Jr. et al. Thirty years of near room temperature magnetic cooling: Where we are today and future prospects, Int. J. Refrig. 31, 945 (2008). 2.P. M. Shan et al. Magnetic behavior of melt-spun gadolinium, Phys. Rev. B. 77, 184415 (2008).

Q013

Research on the orbital state of IrO₂ with resonant x-ray scattering method

Yasuyuki Hirata¹, Kenya Ohgushi¹, Junich Yamaura¹, Hiroyuki Ohsumi², Soshi Takeshita² and Takahisa Arima³

¹ Institute for Solid State Physics, University of Tokyo, Japan
² RIKEN SPring-8, Japan
³ Department of Advanced Materials Science, University of Tokyo, Japan

In the 5d electron systems of iridium oxides, the crystal fields, the Coulomb repulsion, and the spin-orbit interaction compete with each other, which results in various exotic physical properties. For example, magnetic iridium oxides Sr₂IrO₄ and CaIrO₃ are known to be spin-orbit-induced Mott insulators: the reported resonant x-ray scattering experiments showed that 5d t_{2g} orbitals of Ir are reconstructed by the spin-orbit interaction and realize the complex Jeff=1/2 orbital states, which form a narrow band and enhance the electron correlation.[1] On the other hand, the orbital states of metallic iridium oxides like IrO₂, which is attracting attention for a gigantic spin-Hall effect, are yet to be investigated. We performed a resonant X-ray scattering measurement for metallic iridium oxide IrO₂, which has a rutile-type structure, and observed the 0 0 3 reflection coming from the anisotropic tensor of susceptibility (ATS). In the energy spectrum the peak corresponding to the excitation to 5d t_{2g} orbitals appeared around the L3 absorption edge, but did not appear around the L2 absorption edge. These results indicate that the complex Jeff=1/2 states of 5d t_{2g} orbitals are realized even in metallic iridium oxides IrO₂.

[1] B. J. Kim et al., Science 323, 1329 (2009).

Q014

Investigation of magnetic-field tunable properties of magnetorheological elastomers

Nikolai Perov^{1*}, Anna Semisalova¹, Elena Yu Kramarenko¹, Alexey R Khokhlov¹ and Gennady V Stepanov²

¹ Lomonosov Moscow State University, Russia
² State Research Institute for Chemistry and Technology of Organoelement Compounds, Moscow, Russia

In this work we present the results of investigation of magnetic field influence on the value of dielectric permittivity and magnetic susceptibility in magnetorheological elastomers (MRE) based on the powders with various magnetic properties - Fe, FeNdB and Fe₃O₄. Both magnetic susceptibility and dielectric permittivity have been found to be considerably changed under magnetic field, the changing of permittivity value up to 150% has been observed. The field dependence of the dynamic dielectric permittivity was significantly non-linear. The anisotropy of field influence on the permittivity and susceptibility was observed as well. The saturation magnetization and coercivity of the magnetic fillers have been shown to be the most important factors affecting the field dependence of permittivity. In addition, the size and concentration of particles as well as conductivity of magnetic material have significant influence on the type of field effect. The influence of named parameters on the permittivity and susceptibility changing is discussing; we consider the mechanisms determining the features of magnetic field influence on studied physical properties in detail. It is shown that MRE based on various magnetic particles can be considered as promising materials with magnetic-field tunable properties. Supported by Russian Foundation for Basic Research.

Q015

Disagreement between modification methods for magnetism-absorbing agent

Wu Chao, Lv Xuliang*, Zeng Zhaoyang, Wen Xiaodi and Wen Liuqiang

PLA University of Science and Technology, China

Two methods are widely used to improve absorbing properties of the microwave magnetism-absorbing agent: mixing with the other material such as resistance carbon fiber absorbent, or wrapping the microwave magnetism-absorbing agent in that material. However, do these two methods coincide with each other? If not, which method should be used as better way to represent the absorbing properties of magnetism-absorbing agents? To answer these questions, both methods are carried out on the same magnetism-absorbing agents, of which the results are compared. Distinct difference between these measured results is found, and the possible reasons for the difference are also discussed.

Q016

Ordered magnetic arrays of cobalt SMM: properties and the relationship with crystal symmetry and SMM environment

Milagros Tomas¹, Cristina Saenz De Pipaon², Elena Forcen-vazquez², Isabel Mayoral², Larry Falvello³, Javier Campo² and Fernando Palacio^{4*}

¹ Instituto de Sintesis Quimica y Catalisis Homogenea (ISQCH), Consejo Superior de Investigaciones Cientificas and University of Zaragoza, Spain
² Instituto de Ciencia de Materiales de Aragon, Consejo Superior de Investigaciones Cientificas and University of Zaragoza, Spain
³ Departamento de Quimica Inorganica and Instituto de Ciencia de Materiales de Aragon, Consejo Superior de Investigaciones Cientificas and University of Zaragoza, Spain
⁴ Instituto de Ciencia de Materiales de Aragon (ICMA), Consejo Superior de Investigaciones Cientificas and University of Zaragoza, Spain

The modulation of the magnetic properties of SMMs and their organization in extended magnetic arrays are, at the present, some of the top areas in the field of molecular magnetism for the implication in the improvement of the physical properties of the SMM and the potential use in devices such as for data storage. Few polymers of SMM have been structurally characterized in spite of the number of known SMM. [Co4citrate4]8- cubanes can behave as SMM.(1) We have reported recently(2) the union of these cubanes through “Co(H₂O)₂ETG” (ETG=ethylene glycol) bridges and the formation of anionic 2D layers. These layers crystallize in the tetragonal system, P-421c space group, with counterions (Cs⁺ or Rb⁺), water and ETG molecules connecting the layers through electrostatic interactions and hydrogen bridges. The magnetic studies show the co-existence of two magnetic nets: the SMM net and the one formed by the bridged cobalt atoms and also shows the influence of the counterions in the layer magnetic properties. Two intriguing relaxation processes with different characteristics timescales are observed. Moreover, [Co4citrate4]8- cubanes can also organize in 3D, diamond-like structural arrays showing SMM magnetic behaviour below 6K with an energy barrier of 54K and magnetic ordering below 2.7K.

I-M. Murrie, Chem. Soc. Rev. 2010, 39, 1986-1995. 2- E. Burzuri, J. Campo, L. Falvello, E. Forcen-Vazquez, F. Luis, I. Mayoral, F. Palacio, Cristina Saenz de Pipaon, M. Tomas. Chem. Eur. J. 2011, 17, 2818-2822.

Q017

Enhancement of the refrigerant capacity in Gd₆₄Fe₂₀Al₁₀B₆ alloys by partial crystallization of melt-spun amorphous ribbons

Jozef Marcin¹, Zbigniew Sniadecki², Jozef Kovac¹, Peter Svec³, Bogdan Idzikowski² and Ivan Skorvanek^{1*}

¹ Institute of Experimental Physics SAS, Kosice, Slovakia
² Institute of Molecular Physics PAS, Poznan, Poland
³ Institute of Physics SAS, Bratislava, Slovakia

The magnetocaloric effect (MCE) is attracting a great deal of scientific interest because it is a basis of the environmentally friendly magnetic refrigeration technology. Among the recently developed magnetic refrigerant materials, the Gd(Fe,Mn)Al-based glassy alloys combine good magnetic entropy characteristics with sufficiently high effective magnetic moment per volume, which makes them promising candidates for magnetic refrigeration in the operating temperatures around 150 K [1,2]. In this work, we report on the beneficial effect of partial crystallization on magnetocaloric properties of melt-spun Gd₆₄Fe₂₀Al₁₀B₆ alloys. The magnetic entropy changes, ΔS_m, were calculated from the magnetization versus applied field dependences measured in the temperature range from 5 to 390 K. The value of the maximum magnetic entropy change under 50 kOe for the Gd₆₄Fe₂₀Al₁₀B₆ ribbon reached 5.01 J/kg K at 185 K. The corresponding value of the refrigeration capacity, RC, determined as the area below the ΔS_m peak with the integration limits at its half maximum is 647 J/kg. We have found that this value can be further enhanced by suitable heat treatment of melt-spun ribbons leading to a formation of hexagonal Gd particles with higher Curie temperature. The observed improvement is discussed in relation with two-phase character of partially crystallized samples.

[1] S. Gorsse, B. Chevalier, G. Orveillon, Appl. Phys. Lett. 92 (2008) 122501 [2] Y.K. Yang, C.H. Lai, C.C. Hsieh, X.G. Zhao, H. W. Chang, W.C. Chang W.Li, J. Appl. Phys. 107 (2010) 09A901

Q018

Chemical pressure effects on half-metallic properties in single crystals of A₂FeMoO₆ (A = Ca, Sr, and Ba)

Akira Isayama* and Takao Sasagawa

Materials and Structures Laboratory, Tokyo Institute of Technology, Japan

An ordered double perovskite oxide Sr₂FeMoO₆ has been predicted and widely studied as a half-metal, in which electrons with only one spin direction present at the Fermi level (100% spin polarization), above room temperature. In this study, in order to improve the half-metallic properties, the chemical pressure effects, through A-site substitution, on the magnetic and electronic properties have been examined using single crystalline samples of A₂FeMoO₆ (A = Ca, Sr, and Ba) grown by the floating zone method. In the A = Ca crystal, every property related to the half-metallic performance was found to be degraded as compared with the A = Sr and Ba crystals: the saturation magnetization and the Curie temperature were significantly decreased, metallic conductivity became more than twice larger, and the spin polarization (evaluated by Andreev reflection spectroscopy) was reduced below 50%. From the results in the A = Sr and Ba crystals, it is suggested that the optimized half-metallic performance will be obtained in between these two compositions. Optical measurements were also performed to gain insight into the change of electronic structures with respect to the A-site substitution.

Q019

Magnetic label field collector of biochip sensor

Sunjong Oh, Brajalal Sinha, Jaemin Lim and Chelgi Kim*

Department of Materials Science and Engineering, Center for NanoBioengineering and Spintronics, Chungnam National University, Korea

We have proposed a new method called stray field collector (SFC) of magnetic labels for signal enhancement in the magnetoresistive biosensors. The proposed design related to qualitative as well as quantitative detection of magnetic beads. The integration of SFC in magnetic sensor will increase the amount of stray field via the increase of active surface area. Therefore, this SFC may have great potential to improve the performance of magnetic biosensor.

[1] Adarsh Sandhu, et al., “High efficiency Hall effect micro-biosensor platform for detection of magnetically labeled biomolecules,” Biosensors and Bioelectronics, 22, 2115-2120, 2007. [2] Guansiong Li, et al., “Spin valve sensors for ultrasensitive detection of superparamagnetic nanoparticles for biological applications,” Sens Actuators A Phys., 126(1), 98-106, 2006. [3] W. Clark Griffith, et al., “Miniature atomic magnetometer integrated with flux concentrators,” Applied Physics Letters, 94, 023502, 2009.

QO20

Cogging torque cancellation technique for dual rotor type motor using adjustment between outer and inner rotor magnet angle

Tae Won Jeong¹, Hyun Rok Cha^{1*}, Dae Yeong Im¹, Kwang Heon Kim² and Hyoung Uk Nam¹

¹Automotive components R&D group, korea institute of industrial technology, Korea
²Department of Electrical Engineering University of the Chonnam, Korea

In this paper, we design the IPM motor and discuss the design method of double rotor permanent magnet motor for cancelling the cogging torque. According to downsizing the electric motor, high torque and power density are the most serious requirements for electric machines. Double rotor permanent magnet motor is proposed to solve the problem. But it has a large cogging torque that generates the large acoustic noise. A variety of techniques exist for reducing the cogging torque of conventional radial flux IPM machines. This paper introduces a new cogging torque minimization technique for radial flux multiple IPM motors. Optimization of the adjustment magnet angle between outer rotor and inner rotor which results in offset cogging torque and assessment of the effect on the maximum available torque using Finite Element Analysis (FEA) is investigated. In our experiments, Prototype dual rotor type motor has achieved the outer rotor and inner rotor cancellation of cogging torque by 70 percent.

[1] R. Qu and T. A. Lipo, 'Dual-rotor, radial-flux, toroidally wound, permanent-magnet machines', *IEEE Transactions on Industry Applications*, Vol. 39, No.6, Nov/Dec 2003, pp.1655-1673. [2] R. Qu, and T. A. Lipo, 'Design and parameter effect analysis of dualrotor, radial-flux, toroidally wound, permanent-magnet machines', *IEEE Transactions on Industry Applications*, Vol. 40, No.3, May/June 2004, pp.771-779 [3] R. Qu and T. A. Lipo, 'Sizing Equations and Power Density Evaluation of Dual-Rotor, Radial-Flux, Toroidally Wound, Permanent-Magnet Machines,' *XVI International Conference on Electrical Machines*, ICEM 2009, Cracow, Poland, Sept 2004.

QO21

A broadband circuit analog absorber based on printed dipole antenna

Li Xiaopeng¹, Cui Chuan'an¹, Lv Xuliang^{1*} and Lin Shaofeng²

¹Engineering Institute of Corps of Engineers, PLA University of Science and Technology, China
²Xi'an Communication Institute, China

Based on the equivalent transmission line theory, a composite absorber with broadband planar array antenna is designed. The first layer is an array antenna, which uses printed dipole with balun feed as basic unit. The second layer a PIN diode array, which corresponded with antenna feeding units. The impedance match characteristic of the absorber can be adjusted by setting the microstrip balun. And the reflection characteristic of the absorber can be adjusted by adjusting the bias voltage of the PIN diode array. Simulated by electromagnetic simulation software HFSS, the results show that the absorber reflection coefficient is below -10dB at 3.5-15GHz. The experimental result, which replace PIN diodes with surface mount device resistors, is in good agreement with simulation data.

QO22

Effect of oxygen pressure to magnetism and transport properties of epitaxial Fe₃O₄ grown by molecular beam epitaxy

Dang Duc Dung¹, Wuwei Feng², Duong Van Thiet³, Duong Anh Tuan³ and Sunglae Cho^{3*}

¹Department of General Physics, School of Engineering Physics, Ha Noi University of Science and Technology, 1 Dai Co Viet road, Ha Noi, Viet Nam
²Department of Physics, University of Ulsan, Ulsan 680-749., Korea
³Department of Physics, University of Ulsan, Ulsan 680-749, Korea

Fe₃O₄ is predicted to possess a half-metallic nature, ~100% spin polarization, and has a high Curie temperature and an ultrahigh room temperature magnetoresistance (MR) for tunneling magnetoresistance (TMR) junctions with Fe₃O₄ electrodes [1]. However, for the TMR junction, a highly conductive under layer and the sharp between interfaces are required because the poor conductivity and roughness of films may lead to a non-uniform current distribution [2]. In addition, the Verwey transition (TV, a first order metal-insulator transition) of 120 K in bulk Fe₃O₄ is still under controversy because many parameters such as orientation of substrate, buffer layer, thickness, pressure, and thermo-chemical treatment affect the TV [3, 4]. Epitaxial Fe₃O₄ films were grown on MgO(001) substrates via molecular beam epitaxy. The growth modes, magnetism, and transport properties of the thin films were strongly dependent on the oxygen pressure during film growth. The average roughness decreased from 1.021 to 0.263 nm when the oxygen pressure was increased from 2.3x10⁻⁷ to 8.2x10⁻⁶ Torr, respectively. In addition, the saturation magnetic moment reduced as increasing the oxygen pressure during growth. Moreover, the Verwey transition in the Fe₃O₄ disappeared for a sample grown at a high oxygen pressure.

[1] Z. Zhang et al., *Phys. Rev. B* 44, 13319 (1991). [2] P.H. Huang et al., *J. Appl. Phys.* 97, 10C311 (2005). [3] E. J. W. Verwey et al., *Physica* 8, 979 (1941). [4] A. R. Macosworthy et al., *Geophys. J. Int.* 140, 101 (2000), and reference therein.

QO23

Magnetism and transport properties of epitaxial Mn₅Ge₃ thin films on GaAs(001) and GaSb(001)

Dang Duc Dung¹, Doji Odokhuu² and Sunglae Cho^{3*}

¹Department of General Physics, School of Engineering Physics, Ha Noi University of Science and Technology, 1 Dai Co Viet road, Ha Noi, Viet Nam
²Department of Physics, University of Ulsan, Ulsan 680-749, Korea

The epitaxially ferromagnetic Mn₅Ge₃ thin films were grown on GaSb(001) and GaAs(001) substrates using molecular beam epitaxy. Our result revealed that the substrate facilitates to modify magnetic and electrical properties due to tensile strain effect. The Curie temperature was remained above 350 K for samples grown on GaAs(001), while was about 320 K for samples grown on GaSb(001). The anomalous Hall effect were observed up to 370 K and 320 K for films grown on GaAs(001) and GaSb(001), respectively, which are strong evidence for spin polarization. Our electronic calculation indicated that the difference in Mn-Mn bond length in Mn₅Ge₃ modified the magnetization and spin polarization. The strains are promised to control both magnetic properties and spin polarization.

QO24

Current-driven domain wall motion in artificial magnetic domain structures

Ke Wang¹, Murali Krishnan Hari^{1*}, Simon Bending¹, Erhan Arac², Del Atkinson², Serban Lepadatu³, J S Claydon³ and Chris Marrows³

¹Department of Physics, University of Bath, United Kingdom
²Department of Physics, University of Durham, United Kingdom
³School of Physics and Astronomy, University of Leeds, United Kingdom

We report progress towards optimisation of artificial magnetic domain structures for efficient spin transfer torque domain wall (DW) motion [1]. Co/Pt multilayer samples have been sputtered on (100) Si/SiO₂ substrates and perpendicular magnetic anisotropy confirmed using polar magneto-optical Kerr effect (MOKE) measurements. The influence of the thickness of Co and Pt layers on the coercivity and switching behaviour was systematically investigated and the conditions established for realising well-suited structures with medium coercivity (~100 Oe) and sharp switching fields [2]. Optimised Co/Pt multilayer films were lithographically patterned into nanowire devices for time-resolved extraordinary Hall effect (EHE) measurements. Our devices are based on 50 W coplanar waveguides incorporating single and double Hall cross structures. The coercivity of the region surrounding the Co/Pt Hall crosses was reduced by local focussed ion beam (FIB) irradiation [3] allowing the controlled nucleation of domain walls at the edges of these regions by application of an appropriate field sequence. We describe polar MOKE experiments that show how DC currents lead to asymmetric switching of these artificial domains due to current-assisted DW motion across them. We will also present preliminary results of time-resolved EHE and MOKE measurements of current-driven DW motion in these structures.

[1] O. Boulle et al., *Phys. Rev. Lett.* 101, 216601 (2008); I.M. Miron, P.-J. Zermatten, G. Gaudin, S. Auffret, B. Rodmacq, and A. Schuhl, *Phys. Rev. Lett.* 102, 137202 (2009); L. San Emeterio Alvarez, K.Y. Wang, S. Lepadatu, S. Landi, S. J. Bending, and C. H. Marrows, *Phys. Rev. Lett.* 104, 137205 (2010) [2] K. Wang, M.-C. Wu, S. Lepadatu, J. S. Claydon, C.H. Marrows, and S. J. Bending, *J. Appl. Phys.* 110, 083913 (2011). [3] A. Aze et al., *J. Appl. Phys.* 98,

QO25

The cellular uptake mechanism of SPIONs: an in-vitro study

Yasmin Khan¹ and Radha Srinivasan^{2*}

¹Department of Life Sciences, Sophia College, Mumbai, India
²Department of Physics, University of Mumbai, India

The Superparamagnetic Iron Oxide Nanoparticles of sizes ranging from 10-50 nm are being used in a large number of biological studies because of their peculiar characteristics of inducing local hyperthermia, MR imaging, specific targeting and drug delivery. An in-vitro study of the cytotoxicity and an understanding of the specific pathway of cellular uptake will enable manipulation of conditions for optimal cellular uptake of SPIONs for targeted therapy. The objective of the present study was to identify the endocytotic pathway through which the SPIONs are taken up by C6 glioma cells. The cells were pre-incubated with different concentrations of pharmacological inhibitors and then exposed to SPIONs for a few hours. The endocytosed particles were localized and quantitatively estimated using Perl's or Prussian Blue reaction. There was significant reduction in the uptake of SPIONs when incubated with the inhibitor indicating the uptake of nanoparticles is being inhibited. This reduction in SPION uptake was found to be dependent on the concentration of the inhibitors and also the nature of the inhibitors. By a systematic study of choosing various inhibitors, the data can be narrowed down to the final pathway that may be involved in the SPION uptake.

QO26

Theoretical and experimental studies of valence states in Fe-Mo compounds

Francisco Estrada^{1*}, Reginaldo Mondragon¹, Humberto Noverola², Jaime Raul Suarez³, Martha Teresita Ochoa¹, Francisco Espinosa¹, Lorena Alvarez¹, Ricardo Morales⁴, Jose Lemus⁴, Oracio Navarro³ and Michel Avignon³

¹Centro de Investigacion en Materiales Avanzados, S. C, Mexico
²Instituto de Investigaciones en Materiales, Universidad Nacional Autonoma de Mexico, Mexico
³Institut Neel, CNRS and Universite Joseph Fourier, France
⁴Instituto de Investigaciones Metalurgicas, UMSNH, Mexico

The half-metallic ferromagnetic double perovskite compound Sr₂FeMoO₆ is considered as an important material in view of its potential spintronic applications. It appears to be fundamental to understand the role of electronic parameters controlling the half-metallic ground state. In particular, half-metallic ferromagnetic compounds have been searched as a source of spin polarized currents. In this work, we study the valence states of cations in Fe-Mo based double perovskites from theoretical and experimental point of view. In the experimental case, we apply the electron energy-loss spectroscopy (EELS) technique. For transition metals, L_{2,3} edges of EELS are characterized by two sharp peaks, known as white lines. EELS experiments have shown that the change in valence states of cations introduces significant modification in the energy and shape of the white lines, leading to the possibility of identifying cation valence states. These results are compared with those coming from theoretical calculation using the Green functions and the renormalization perturbation expansion method. The theoretical model is based on a correlated electron picture with localized Fe-spins and conduction electrons interacting with the local spins via a double-exchange-type mechanism.

QO27

Structural modifications in magnetic MWCNT by 100 MeV SHI irradiations

Sanjeev Gautam¹, Keun Hwa Chae¹, Jong Han Song¹, Saji Augustine², J.K. Kang² and K. Asokan³

¹Advanced Analysis Center, Korea Institute of Science and Technology (KIST), Korea
²Material Science and Engineering, Korea Advanced Institute of Science and Technology (KAIST), Korea
³Material Science Center, Inter-University Accelerator Center, New Delhi, India

Carbon nanotubes (CNTs) possess unique mechanical and electronic properties suitable for fabricating the nano-scale building blocks of nanodevices [1]. One of the requirements for applications is to cut the CNT in small dimensions in the order of few nanometers. To this respect, we investigate the effect of heavy ion beams, namely, 100 MeV of O and Ni ion beam on CNT synthesized by chemical vapor deposition (CVD) technique[2]. The ion fluence selected for this study was 1e13 ions per cm². High energy heavy ion irradiation was carried out at Inter-University Accelerator Centre, New Delhi, India. This paper reports the experimental results obtained from X-ray diffraction pattern and images of scanning electron microscopy (SEM) and transmission electron microscope (TEM) measured at Nano Materials Analysis Center, KIST, Korea. These results show that heavy ions can induce damage or cut in an ordered periodicity of few nanometers. Apart from above studies, we also carried out near-edge x-ray absorption spectroscopy investigations for electronic structure modifications.

[1] E. Wohlfarth, in: G. Rado, H. Suhl (Eds.), *Magnetism*, Vol. 3 (Acad Press, New York, 1963). [2] Gautam S, Thakur P, Augustine S, Kang JK, Kim JY, et al. arXiv: 1111.5416v1 (Nov. 23 2011).

QO28

Magnetic and magneto-transport properties of (Mn_{0.85}, Zn_{0.2})_{1-x}Ga_xFe₂O₄ ferrites

Hyo-jin Kim and Sang-im Yoo*

Department of Materials Science and Engineering, Seoul National University, Korea

A significant enhancement of low-field magnetoresistance (LFMR) could be achieved from polycrystalline samples of Ga₂O₃-doped Mn-Zn ferrites. For this study, the magnetic and magnetotransport properties of samples with two different nominal compositions of (Mn_{0.85}, Zn_{0.2})_{1-x}Ga_xFe₂O₄ (x = 0.05, 0.1) were carefully investigated. The X-ray diffraction analyses revealed that all Ga₂O₃-doped Mn-Zn ferrites of the spinel structure were a pure phase without the second phase. By doping Ga₂O₃ to the pure Mn-Zn ferrite, the resistivity level was abruptly decreased over four orders of magnitude. The 5 mol% Ga₂O₃-doped Mn-Zn ferrite sample exhibited the LFMR ratio over 1.7 % at 300 K in 0.5 k Oe without appreciable increase in its resistivity. Detailed doping effects of Ga₂O₃ on the magnetic and magneto-transport properties of the Mn-Zn ferrite will be presented and discussed in this paper.

QP01

Magnetic coupling at the CoO/Ni interface

Sergiy Grytsyuk*, Fabrizio Cossu and Udo Schwingenschlog
Physical Sciences and Engineering, King Abdullah University of Science & Technology, Saudi Arabia

We study the CoO/Ni interface. Since the lattice mismatch between Ni and CoO is 21%, we use a large supercell for our first principles calculations which reduces the lattice mismatch to 0.8%. We investigate the structural, electronic, and magnetic properties of two interface configurations: (1) An O layer mediates the coupling between Ni and Co and (2) a direct Ni-Co contact. Our results indicate that the magnetization is reduced by 19% in the first case, while in the second case it increases by 100% as compared to bulk Ni. The magnetic moments obtained at the interfaces can be explained by the local environment of the interface atoms. In addition, we find effects of charge transfer between the interface atoms.

QP02

Electronic, structural, and magnetic properties of O and Py deficient CoO/Py interfaces.

Sergiy Grytsyuk* and Udo Schwingenschlog
Physical Sciences and Engineering, King Abdullah University of Science & Technology, Saudi Arabia

The development of magnetic devices, which are based on coupling between ferromagnet and antiferromagnet (such as spin-valves), depends strongly on the interfacial magnetic structure. Since vacancies at the interface are expected to be important in determining the macroscopic properties of such systems, a quantitative determination of their influence on the interfacial magnetization is essential. We therefore investigate the CoO/Py interface (Py = Ni₈₀Fe₂₀, Permalloy). Py has a high permeability, low magnetostriction, and high anisotropic magnetoresistance. It is a good conductor for spin-majority electrons and poor conductor for spin-minority electrons. At the same time the Neel temperature of CoO is approximately room temperature and its magnetocrystalline anisotropy is high. Since the lattice mismatch between Py and CoO is about 20%, we use a large supercell for our first principles calculations which reduces the lattice mismatch to less than 0.1%. We describe the dependence of the interface magnetization on the amount of O and Py vacancies and address the exchange bias.

QP03

Effect of the external fields on SpinRAM switching time

Mitsuhiro Shiomi* and Yoshinobu Nakatani
Univ. of Electro- Communications, Japan

Spin current driven magneto resistive random access memory (SpinRAM) is one of the candidates for the next generation non volatile memory. There are still many problems to realize it. One of the problems is the switching speed. The method for fast switching with lower current is required. Field assist switching is one way. In this paper, the effect of the DC and AC external field on the switching time of the SpinRAM with perpendicular anisotropy is investigated by simulation. The effect of the thermal noise is also investigated. From the results without thermal noise, the switching time was decreased by both of the DC and AC field. However, AC field is effective for fast switching compared with DC field. From the results with thermal noise, the switching time was not decreased by weak DC field and more strong DC field was required to reduce the switching time. On the other hand, the switching time was decreased by weak AC field. From these results, it was found that AC field is more effective than DC field to reduce the switching time. This study was supported by New Energy and Industrial Technology Development organization (NEDO) partly.

QP04

A study on the perpendicular toggle-MRAM system by using new combined hysteresis method for high Gb/Chip

Hyuk Won and Gwan Soo Park*
School of Electrical Engineering, Pusan National University, Korea

Conventional (toggle) MRAM has unlimited read/write endurance but has a low capacity than flash technology. A lot of work has been done for the commercialization of submicrometer MRAM in recent years. A low-power 1Mb MRAM with copper interconnects and cladding layer, and about 35 ns access and cycle times tested in the previous work show the potential of this technology. A new multibit MRAM cell of toggle switching type has been reported and also, a heat interaction investigation in thermally assisted MRAM has been reported. In this paper we presents a new design that has advantages conventional MRAM on injected current and cell size. It is pole type perpendicular MRAM (PTP MRAM). PTP MRAM uses perpendicular magnetic field in order to change the state of the free layer in a perpendicular magnetic tunnel junction (pMTJ). In this paper, new efficient algorithm to combine two models are presented and tested. This approach reduces computing time and gives more precise results because the result of 2 dimensional Preisach model becomes an initial values of 3 dimensional micromagnetics.

QP05

Room temperature exchange bias in the multiferroic BiFe_{0.8}Mn_{0.2}O₃ nanoparticles with a core-shell structure

S M Yusuf* and P K Manna
Solid state physics division, bhabha atomic research centre, mumbai 400085, India

The compound BiFeO₃ shows a multiferroic character. We have shown that the BiFeO₃-based compound viz. BiFe_{0.8}Mn_{0.2}O₃ nanoparticle system exhibits other important multifunctional behaviour as well. We have observed the exchange bias effect, in the form of a shift in the field-cooled hysteresis loop, and a training effect in a dc magnetization study. From transmission electron microscopy, neutron diffraction, thermoremanent magnetization, and isothermoremanent magnetization measurements, the nanoparticles are found to be core-shell in nature, consisting of an antiferromagnetic (AFM) core, and a two-dimensional diluted AFM (DAFF) shell with a net magnetization under a field. Our calculation using the Binek's model on the training effect yields a theoretical understanding of the observed loop shift which arises entirely due to an interface exchange coupling between core and shell. The intrinsic contribution of the DAFF shell to the total loop shift is zero. The present study is useful to understand the origin of exchange bias in other DAFF-based systems as well. The significantly high value of the exchange bias field (~ 0.16 kOe), observed at room temperature, in the present nanoparticle system has made it a blue-eyed candidate for the next generation advanced nano-technological applications in the area of magnetic storage devices.

QP06

Magnetic and Transport Properties of Mn_{3-x}Ga/MgO/Mn_{3-x}Ga Magnetic Tunnel Junctions: A First-Principles Study

Zhaoqiang Bai, Yongqing Cai, Lei Shen, Guchang Han and Yuanping Feng*
Physics, National University of Singapore, Singapore

Magnetic and transport properties of Mn_{3-x}Ga/MgO/Mn_{3-x}Ga (0 ≤ x ≤ 1) magnetic tunnel junctions are studied using first-principles approach based on density functional theory and non-equilibrium Green's function. Perpendicular magnetization, of which the magnetic anisotropy energy reaches more than 1 meV/unit-cell, is confirmed to be energetically favoured by both Mn₂Ga and Mn₃Ga thin films. Furthermore, despite high spin-polarization at Fermi energy for both these compounds as reported, our transport calculation shows considerable disparity in the transmission behaviour between Mn₂Ga/MgO/Mn₂Ga(001) and Mn₃Ga/MgO/Mn₃Ga(001) magnetic tunnel junctions: huge optimistic tunneling magnetoresistance ratio ~ 1000% for the former, and nevertheless, no tunneling magnetoresistance effect absolutely for the latter. This phenomenon is attributed to the spin symmetry filtering effect of the MgO spacer. On this premise, Mn_{3-x}Ga compounds with low Mn concentration are predicted to be promising candidate materials to serve as the electrodes of spin-transfer torque devices in

QP07

Concomitant memory effect in CrO₂/Cr₂O₃ core-shell nanorods

Ashish Chhaganlal Gandhi and Sheng Yun Wu*
Department of Physics, National Dong Hwa University, Taiwan

The concomitant memory effects are intensively studied in last few decades and are mostly observed in spin-glass and superparamagnetic systems [1-3]. The memory effects were observed in the interacting permalloy nanoparticles [4] and isolated nanoparticles [5], providing us interesting information about the investigation of nature of the low temperature phase. In the present work, we succeeded in preparing CrO₂/Cr₂O₃ core-shell nanorods using the chemical vapor deposition method. The magnetic properties of CrO₂/Cr₂O₃ core-shell nanoparticles can be treated as a ferromagnetic-CrO₂-core and antiferromagnetic-Cr₂O₃-shell compound coupled by an exchange interface coupling and raised magnetic anisotropy energy between them. The evolution of core shell magnetization triggered by an applied magnetic field at 1.8 K was observed, and a core-shell anisotropic energy model was applied to simulate the competition between the surface magnetic anisotropy and exchange interface coupling. Memory and aging effects were observed and overcame the superparamagnetic limit [3] up to sufficiently high temperature which makes it an important candidate in magnetic data storage, as an application. Acknowledgments: This research was supported by a grant from the National Science Council of Taiwan, the Republic of China, under Grant Number NSC-100-2112-M-259-003-MY3.

[1] M. Sasaki, P. E. Jonsson, H. Takayama, and H. Mamiya; *Phys. Rev. B* 71, 104405 (2005). [2] Malay Bandyopadhyay and Sushanta Dattagupta; *Phys. Rev. B* 74, 214410 (2006). [3] V. Skumryev, S. Stoyanov, Y. Zhang, G. Hadjipanayis, D. Givord and J. Nogues *Nature* 423, 850 (2003). [4] Young Sun, M. B. Salamon, K. Garnier and R. S. Averback; *Phys. Rev. Lett.* 91, 167206 (2003). [5] M. Sasaki, P. E. Jonsson, H. Takayama, and P. Norblad; *Phys. Rev. Lett.* 24, 139701 (2004).

QP08

High resolution probes for magnetic force microscope

Xiaoxi Liu*, Shinsaku Isomura and Akimitsu Morisako
Department of Information Engineering, Shinshu University, Japan

Magnetic force microscopy is a convenient and efficient method to detect magnetic domain structures in magnetic recording media or nano-magnet. In this work, we present a simple process to fabricate probes for magnetic force microscopy with sub-ten nanometer resolution. A thin layer of FeCo is deposited onto commercially available silicon probes by a facing targets sputtering system. We choose facing targets sputtering because this kind of system can minimize the damage of the films from high energy particle bombardment. The radius of the curvature of the probes is depended on the FeCo film thickness. High resolution scanning microscope image show the radius of the curvature is less than 20 nm for a 20 nm thick FeCo coating. Magnetic force microscopy images show our probes have resolution better than 10 nm. Due to the high magnetic moment of FeCo, we can get magnetic contrast for FeCo coating as thin as 10 nm. Micromagnetic simulations indicate than the formation of a magnetic vortex at the apex of the probe is crucial for the high resolution.

QP09

Selective magnetization switching by microwave assistance for layered magnetic pillar

Terumitsu Tanaka*, Yuto Otsuka¹, Yoshitoki Furomoto¹, Kimihide Matsuyama¹ and Yukio Nozaki²
¹ ISEE, Kyushu University, Japan
² Department of Physics, Keio University, Japan

Microwave assisted magnetization reversal (MAMR)[1] is a promising candidate for future magnetic recording technology. In MAMR, magnetization switches only when DC and microwave fields are applied to magnetic material at particular microwave frequency. Utilizing such a feature, possibility of selective switching of magnetizations was estimated by micromagnetic calculation for realizing 3-dimensional magnetic recording. In the calculation, a magnetic pillar composed of 3 layered materials was considered. Pillar diameter is 11 nm, and thickness of the 1st, 2nd, and 3rd layers are 5, 13, and 14 nm, respectively. H_{k1} (= 24kOe), M_{s1} (= 600 emu/cc), H_{k2} (= 13kOe), M_{s2} (= 400 emu/cc), and H_{k3} (= 6 kOe), M_{s3} (= 800 emu/cc) represent anisotropy fields and saturation magnetizations of 1st, 2nd, and 3rd layers. These values give sufficient thermal stability indices (greater than 60 at 300 K) for every layer. Magnetization switching probabilities equal to 1 were obtained at particular microwave frequencies for every layer; selective switching occurs at 1st, 2nd, and 3rd layer when microwave frequency is 8, 18, and 28 GHz, respectively. In this calculation, the single pillar has shown to store 3 bits information. These results imply MAMR has a potential in 3-dimensional magnetic recording.

[1] J.-G. Zhu, X. Zhu and Y. Tang, *IEEE Trans. Magn.* 44, 125 (2008)

QP10

Thermal effect in microwave assisted magnetization reversal

Yoshitoki Furomoto, Yuto Otsuka, Terumitsu Tanaka* and Kimihide Matsuyama
ISEE, Kyushu University, Japan

Microwave assisted magnetization reversal (MAMR)[1] has potential application in future magnetic recording. The critical curves for MAMR in a single-domain particle is theoretically estimated by Bertotti et al.[2, 3], which well explains steady state magnetization switching at 0 K and the equations allow three solutions “stable”, “unstable” and “saddle”. In this study, MAMR properties in a single-domain particle were simulated solving the Landau-Lifshitz-Gilbert equation taking account of temperature elevation due to ferro-magnetic resonance. Magnetization switching probability at 400 K widely distributes in HMW in unstable region. The critical values of HMW are greater than that at 0 K nevertheless thermal activation decreases energy barrier height. This implies stochastic thermal fields reduce efficiency in MAMR in the region. On the other hand, thermal activation gives 25-35 % of reduction in critical value of HMW in stable region, which is achievable for recording head of recent hard disk drive.

[1] J. O. Artman, S. H. Charap, and D. J. Seagle, *IEEE Trans. Magn. MAG-19, 1814* (1983). [2] G. Bertotti, C. Serpico, and I. Mayergoyz, *Phys. Rev. Lett.* 86, 724 (2001). [3] S. Braa and W. Scholz, *IEEE Trans. Magn.* 44, 3392 (2008).

QP11

Stable magnetization switching with microwave assistance for exchange coupled composite grain

Terumitsu Tanaka*, Yoshitoki Furomoto, Yuto Otsuka and Kimihide Matsuyama
ISEE, Kyushu University, Japan

Microwave assisted magnetization reversal (MAMR)[1] is a promising candidate for future magnetic recording. Li et al. proposed ECC medium for solving the potential problems in microwave power and frequency for MAMR[2]. Bertotti et al. theoretically analyzed MAMR process taking a single spin for example[3], which showed the LLG equation can be written in the other forms[4]. The equation allows three solutions “stable”, “unstable” and “saddle”. However, the theory cannot be applied to exchange coupled composite (ECC) structured grain. In this study, distributions of the regions defined by the three solutions were estimated for an ECC grain. In the ECC grain, stable switching region, in which magnetization reversal modes are hardly affected by disturbance such as thermal fluctuation, distributes at lower fields region comparing to that for the single spin particle. This result means that stable magnetization reversal occurs with relatively weak magnetic fields even for ultra high Hk materials assigned to future high density recording.

[1] J.-G. Zhu, X. Zhu and Y. Tang, *IEEE Trans. Magn.* 44, 125 (2008). [2] S. Li, B. Livshitz, H. N. Bertam, M. Schabes, T. Schrefl, E. E. Fullerton and V. Lomakin, *Appl. Phys. Lett.* 94, 202509 (2009). [3] Giorgio Bertotti, Claudio Serpico, and Isaak D. Mayergoyz, *Phys. Rev. Lett.* 86, 724 (2001) [4] Werner Scholz and Sharat Batra, *J. Appl. Phys.* 103, 07F539 (2008)

QP12

Low-temperature epitaxial growth of FePt on glass substrates for ultrahigh magnetic recording densities

Thanassis Speliotis*, George Giannopoulos¹ and Dimitris G Niarchoch²
¹ Institute of Materials Science, NCSR DEMOKRITOS, Greece
² Institute of Materials Science, NCSR Demokritos, Greece

Magnetic FePt alloy thin film with ordered L10 structure is a promising material for perpendicular magnetic recording (PMR) application, duo to its huge uniaxial magnetocrystalline anisotropy (Ku), high saturation magnetization (Ms), high coercivity (Hc) and outstanding corrosive resistance. Ku value of L10 FePt is about 7 MJ/m³ which sets the superparamagnetic limit of L10 FePt as small as 2.8 nm. In PMR application the preferred orientation has to be transformed into (001) that makes the [001]-axis perpendicular to the film. Accordingly, developing an effective way to prepare L10 FePt (001) thin film with perpendicular magnetic anisotropy at low order-disorder transformation temperature is the concern of first priority. Although excellent properties can be obtained in sputtered FePt on single crystal MgO (001) much effort is needed to obtain PMR properties of sputtered FePt films on glass substrates. A number of underlayers have been used to induce texture such as CrRu, MgO and very recently TiN. Here we report a systematic study of the system { Hoya glass/CrRu/MgO/FePt/Ta } and through optimization of layer thickness, deposition temperature and sputtering power, we achieved perpendicular anisotropy, coercivity in excess of 1 T and deposition temperatures around 400 OC.

Supported by the project TERAMAGSTOR of the EU

QP13

Controlling nanostructure in FePt films: Co-sputtering of FePt and C or SiO₂

George Giannopoulos*, Thanassis Speliotis and Dimitris G Niarchoch
Institute of Materials Science, NCSR DEMOKRITOS, Greece

Achieving magnetic recording densities in excess of 1Tbit/in² requires not only perpendicular media with anisotropy larger than 7 MJ/m³, which makes the FePt alloy as the best choice, but also narrow distribution and small sizes below 10 nm for a reduced S/N ratio along with high thermal stability. Previous work has shown that the L10 FePt grain size can be controlled by alloying FePt with materials such as C, Ag, and insulator like Al₂O₃, MgO act to segregate and magnetically decouple the FePt grains. Better results were obtained with C with respect to the uniformity of grains and SiO₂ with respect to the shape, but far from optimization. We present our results by co-sputtering FePt with C or SiO₂ (up to 30 vol %) on MgO (001) single crystal substrates at 350 and 500 OC. With C or SiO₂ addition we achieved the grain size reduction, the shape control and isolated structure formation, by producing continuous films with high uniformity and narrow main size distribution down to 10 nm. This also reflected in the variation of coercivity as a function of the additional phase, thus giving us a possibility to simultaneously control the coercivity and the S/N ratio.

QP14

Retention time under currents and magnetic fields in a CoFeB/MgO perpendicular magnetic tunnel junction

Michihiko Yamanouchi*, Hideo Sato, Katsuya Miura, Shoji Ikeda, Fumihiro Matsukura and Hideo Ohno
Center for Spintronics Integrated Systems, Tohoku University, Japan

CoFeB/MgO based magnetic tunnel junctions with perpendicular anisotropy (p-MTJs) [1,2] have been investigated extensively because of their potential for realization of nonvolatile logic circuits and random access memories [3-6]. For ensuring their nonvolatility, effects of current (I) and magnetic field (H) on cumulative distribution of retention time (tr) of magnetization direction in the recording layer should be clarified. Theoretical expression for the distribution under I and H has been proposed [7]. However it has not been compared with experimental results in CoFeB/MgO p-MTJs. In this work, we investigated tr under I and perpendicular H in the same CoFeB/MgO p-MTJ with 40 nm in diameter and compared it with the theoretical expression [7]. It was found that the cumulative distribution of tr under I (H) can be fitted well with the theoretical expression in the range of tr = 30 μs - 100 s (5 - 960 s). From tr under I (H), thermal stability factor is evaluated to be 44 (39), which agrees well with previous results in similar MTJs [1,4]. This work was supported by the FIRST program from JSPS.

[1] M. Endo et al., *Appl. Phys. Lett.* 96, 212503 (2010). [2] S. Ikeda et al., *Nature Mater.* 9, 721 (2010). [3] D. C. Worledge et al., *Appl. Phys. Lett.* 98, 022501 (2011). [4] H. Sato et al., *Appl. Phys. Lett.* 99, 042501 (2011). [5] H. D. Gan et al., *Appl. Phys. Lett.* 99, 252507 (2011). [6] J. J. Nowak et al., *IEEE Magn. Lett.* 2, 3000204 (2011). [7] Z. Li et al., *Phys. Rev. B* 69, 134416 (2004).

QP15

Thermal diffusion in magneto-optic collinear volumetric hologram memory

Seungmin Baek, Hiroyuki Sakurai, Pang Boey Lim and Mitsuteru Inoue
Toyoashi University of Technology, Japan

Collinear holography memory is a good candidate of the next generation of optical memory. Recently we have investigated the magneto-optical recording with thick polycrystalline magnetic garnet films by collinear holography. Rewritable properties and shift multiplexing of the magnetic holograms were confirmed experimentally. However, it has still high noise level in the retrieved image. We investigated the suppression method of thermal diffusion in magnetic hologram recording numerically and experimentally. The recording principles of the magnetic holography are basically similar with thermomagnetic recording. The interference patterns with signal information are recorded as magnetization patterns. Due to thermal diffusion in recording process, the interference patterns were in disorder. It could be shown in results of the low diffraction efficiency and high noise level. Numerical simulation result shows the influence of thermal diffusion was suppressed with below 10-9 second of laser pulse width. Experimental result with two-beam interferometer also shows over 200 % higher diffraction efficiency recorded by 50 ps pulse width laser than 25 ns one in high spatial frequency range.

QP16

Resolution of magnetic garnet films for magneto-optic collinear volumetric hologram memory

Seungmin Baek, Hiroyuki Sakurai, Naoto Sagara, Pang Boey Lim and Mitsuteru Inoue
Toyohashi University of Technology, Japan

Collinear holography memory is promising optical memory of the next generation. The photopolymer materials have received much attention because of high sensitivity, high dynamic range and low costs as recording materials. On the other hands, magnetic garnet films have the advantage of rewritable, no necessity of shading, and no shrinkage, as compared to photopolymer which has write-once property. In this study, we fabricated the different grain sizes of magnetic garnet films by annealing time. The fundamental properties of samples and the SNR of the retrieved images with single hologram were investigated. Bi-substituted iron garnet films (3.3 μm thick) were fabricated by RF magnetron sputtering on SGGG substrates. Samples were annealed at 750 °C in air for several annealing time. The retrieved images were evaluated by collinear holographic system. The resolution of magnetic recording media was related with the grain size of magnetic recording media. The results show SNR of the retrieved image was improved by reduction of the grain size.

QP17

Room temperature ordering perpendicular magnetic anisotropy L11 CoPtCu thin film on glass substrate

Chiuan-fa Huang¹, Long-jie Li¹, An-cheng Sun^{1*}, Fu-te Yuan², Jen-hwa Hsu², S. N. Hsiao³ and H. Y. Lee³

¹ Department of Chemical Engineering & Materials Science, Yuan-Ze University, Taiwan
² Department of Physics, National Taiwan University, Taiwan
³ National Synchrotron Radiation Research Center (NSRRRC), Taiwan

Rhombohedral unit cell of L11 CoPt films have attracted a lot of attention due to their large magnetocrystalline anisotropy (Ku ~ 107 erg/cm³) as well as relatively low ordering temperature (~ 200 oC) [1,2]. The addition of Cu significantly improves the alignment of c-axis, chemical ordering and enhances perpendicular coercivity (H_c) of L11 CoPtCu phase deposited at 350 oC [3-5]. In this study, Co₂Pt₁₀Cu₂ films with a Pt underlayer were deposited on glass substrates at room temperature (RT) to 500 oC by sputtering. The thickness of the film was 5 nm. Interestingly, the high perpendicular magnetic anisotropy (PMA) was observed when the film was deposited at RT. Furthermore, PMA was maintained until the substrate temperature (Ts) exceeded 450 oC. Hc was largely enhanced from 0.25 to 2.6 kOe when Ts was increased from RT to 350 oC. Beyond 350 oC Hc started to decline. The appearance of high PMA suggests that the ordered L11 structure is formed in CoPtCu film even prepared at room temperature. This finding promotes the applications of L11 CoPtCu films in future perpendicular magnetic recording and spintronic device. The variation of phase structure and microstructure with Ts will be presented.

[1] S. Iwata, S. Yamashita, S. Tsunashima, IEEE Trans. Magn. 33 (1997) 3670. [2] FT. Yuan, A.C. Sun, J.H. Hsu, Scripta Materialia 62 (2010) 762. [3] F-T. Yuan, A-C. Sun, J-H. Hsu, C.S. Tan, P.C. Kuo, W.M. Liao, H.Y. Lee J. Appl. Phys. 108 (2010) 113909. [4] F-T. Yuan, A-C. Sun, J-H. Hsu, C.S. Tan, P.C. Kuo, W.M. Liao, H.Y. Lee J. Appl. Phys. 109 (2011) 07B714. [5] Fu-Te Yuan, L. J. Li, Jen-Hwa Hsu, S. N. Hsiao, H. Y. Lee, Hsi-Chuan Lu, Seo-Fue Wang, C. Y. Shen, and An-Cheng Sun, J. Appl. Phys. (accepted)

QP18

Magnetic anisotropy and chemical ordering in Fe-Pt films prepared by low-temperature growth technique

Nyun Jong Lee¹, Jae Young Ahn¹, Yu Jeong Bae¹, Dominique Eyidi^{2*}, Anny Michel^{2*} and Tae Hee Kim^{1*}

¹ Department of Physics, Ewha Womans University, Korea
² Departement de Physique et Mecanique des Materiaux, Institut Pprime, UPR 3346, CNRS-Universite de Poitiers-ENSMA, F86962 Futuroscope-Chasseneuil cedex, France

We investigated the chemical ordering and perpendicular magnetic anisotropy (PMA) in L1₀ FePt and L1₂ FePt₅ films. FePt films with different thickness of 35 and 70 Å were grown, at the substrate temperature T_s = 300 °C by MBE co-evaporation and layer-by-layer growth, onto a MgO layer deposited on Si wafer. In order to optimize the growth of highly ordered FePt(001) films in conditions of low-temperature fabrication, the influence of a thin (001)-oriented fcc Pt buffer layer on the c-axis oriented texture was explored by high resolution TEM and X-ray diffraction (XRD). Our results showed a strong enhancement of PMA without high-temperature annealing, for 35 Å thick FePt films, while a decrease in PMA was observed for L1₂ FePt₅. By introducing a small percentage of Boron into the L1₂ ordered FePt₅, enhanced structural ordering was seen in XRD. However, no significant change of magnetic properties was observed, in contradiction with the expectation to induce PMA by altering the chemical ordering in FePt₅ L1₂ phase. In this work, we discuss the origin of spin reorientation transition phenomena related to our results. *corresponding authors : taehee@ewha.ac.kr; Anny.S.Michel@univ-poitiers.fr

QP19

Nanoscale ion beam etching process for reducing damage and leakage path of magnetic tunnel junction

Daehong Kim¹, Bongho Kim¹, Sungwoo Chun¹, Hyungyu Kim¹, Seonjun Choi¹ and Seung-beck Lee^{2*}

¹ Department of Electronic Engineering, Hanyang University, Seoul, Korea
² Institute of Nano Science and Technology, Hanyang University, Seoul, Korea

To integrate ultrahigh density spin-transfer torque magnetic random access memory (STT-MRAM), a stable process to pattern metallic magnetic tunnel junctions (MTJs) is required. [1] We investigated the ion milling process to fabricate the MTJ cells for perpendicular STT-MRAM application with minimized redeposition layer by a gradational stage tilting process and low damage of MTJ by reduced beam supply voltage. The hard mask used a 30nm diameter negative electron-beam resist patterned by electron beam lithography. Thereafter, ion milling process was conducted through regulation of beam/accelerate supply voltage and stage tilting angle. We found that the highest MTJ slope angle was attained at the stage tilt angle of 80° which was the angle of the incident ion flux to the stage surface. However, high angle etching resulted in a thick redeposition layer. For reducing redeposited layers, we have utilized variable-angle multi-step ion milling process. Also for reduced MTJ sidewall damage by high beam supply voltage, reduced the beam supply voltage. Consequently, sidewall damage of MTJ layer was minimized. The TMR ratio and the resistance of the fabricated MTJ cells were 13% and 1kΩ respectively. Our results showed the potential of using optimized ion milling for fabricating nanoscale MTJs for ultrahigh density STT-MRAMs.

[1] M. Hosomi, H. Yamagishi, T. Yamamoto, K. Bessho, Y. Higo, K. Yamane, H. Yamada, M. Shoji, H. Hachino, C. Fukumoto, H. Nagao, and H. Kano: IEDM Tech. Dig., 2005, p. 459.

QP20

A new planer patterned media with anti-ferro / ferro transformation

Hiroaki Ono and Hiroyuki Awano
Toyota Technological Institute Information Storage Material Lab., Japan

For next-generation HDD, the planer patterned media which need neither pattern etching nor smoothing processing is attractive.1),2) As a proposal of the new media, ferro-magnetized patterned area in the flat anti-ferro-magnetized layer has been prepared by using near field laser irradiation or masked ion implantation. On the ferro-magnetized area, required data can be recorded. We prepared several kinds of TbFeCo/Rh/TbFeCo tri-layers. When the Rh thickness is some period, strong anti-ferro-magnetic coupling (AFC) is realized. In the combination, Rh thickness of the 1st peak of the anti-ferro-coupling was 0.45nm. Since the thickness of the TbFeCo was thick and Rh thickness was very thin, the transformation from AFC to FC can be control easily. The coercive force was 1.5kOe. Also the Hc can be designed by controlling Tb concentration. For example, in this case, the transformation temperature was 100 °C. It is also easy to control by changing TbFeCo thickness. Moreover, the patterned media can be applied as a write once HDD, since it is impossible to change recorded area for the ferro-magnetized area.

1) I. Nakatani, T. Takahashi, M. Hijikata, T. Kobayashi, K. Ozawa, and H. Hanaoka: Japanese Patent No.888363, filed in June 1989. 2) T.Kato et al., J. Appl. Phys., 105, 07C117 (2009)

QP21

Topology optimization of perpendicular magnetic recording head considering magnetic saturation effect

Park Soon Ok*
Yonsei University Graduate school, Korea

The topology optimization method is an attractive scheme for magnetic device design because an initial conceptual design can be obtained without any prototype model. However, studies concerning the three-dimensional magnetic device design by topology optimization are rare. Even more, topology optimization of magnetic systems has been generally accomplished by using the two-dimensional finite element method while the nonlinear saturation effect of the material property between magnetic field strength and magnetic flux density has not been fully considered. This study proposes a topology optimization technique of the three-dimensional design as well as the two-dimensional design based on the density method considering the nonlinear saturation effects. The proposed method makes it possible to provide useful and practical process for magnetic system design and may lead to improved design with light system weight. The proposed method is applied to the optimization problem of a magnetic recording system. During the design process, the reluctivity of magnetic material is changed according to the nonlinear B-H relationship during magneto static analysis. The sensitivity analysis and the update of design variables are accomplished by the adjoint variable method and the sequential linear programming, respectively.

Topology optimization; finite element analysis; magnetic saturation effect; three dimensional design; density method; adjoint variable method.

QP22

The effect of capped layer thickness on switching behavior in coupled granular/continuous media

Weimin Li¹, Jun Ding^{1*} and Jianzhong Shi²

¹ Department of materials science and engineering, National University of Singapore, Singapore
² Data Storage Institute, Agency for Science, Technology and Research (A*STAR), Singapore

Coupled granular/continuous (CGC) media (a CoPtCrB continuous layer exchange coupled to a granular oxide CoPtCr: SiO₂/TiO₂/Ta₂O₅ layer) exhibited improvement of SNR, thermal stability and switching field distribution (SFD)[1, 2]. TEM images together with intrinsic SFD for capped structure are studied to investigate the mechanism of the SFD reduction in CGC media. We find out that in the bottom part, CoPtCr magnetic grains are separated by nonmagnetic oxide grain boundaries. The amorphous grain boundary phase in the granular layer propagates to the top surface of the capped layer. The grain size increases with capped layers thickness. A critical capped thickness exists. At thinner capped thickness, capped layer inherits structural irregularity from the granular layer, while at thicker layer, the upper portion of capped layer is less influenced by the granular layer. Reported ΔH (M, ΔM) method[3] is used to calculate intrinsic SFD. Both intrinsic and macroscopic SFD decrease linearly with capped layer thickness. As we know, the intrinsic SFD is due to the local variations of the grains properties. The reduction of macroscopic SFD is caused by homogeneous grains and uniform exchange coupling at thicker capped layer.

1. H. S. Jung, E. M. T. Veh, S. S. Malhotra, U. Kwon, D. Suess and G. Bertoni, Magnetics, IEEE Transactions on 43 (6), 2088-2090 (2007). 2. H. Nemoto, I. Takekuma, H. Nakagawa, T. Ichihara, R. Araki and Y. Hosoe, Journal of Magnetism and Magnetic Materials 320 (22), 3144-3150 (2008). 3. A. Berger, B. Lengsfeld and Y. Ikeda, Journal of Applied Physics 99 (8), 08E705-706 (2006).

QP23

The effect of magnetic field on FePt nanoparticles during annealing process

A. Khajehnezhad¹, S. A. Sebt¹, R. S. Dariani² and M. Akhavan^{3*}
¹ Physics Research Center, Science and Research Branch, Islamic Azad University, Tehran, Iran, Iran
² Physics, Alzahra University, Tehran, Iran
³ Physics, Sharif University of Technology, Iran

FePt, L10 nanocrystals are expected as one of promising candidates for the magnetic recording media with ultrahigh densities. The 3nm FePt NPs have been synthesized by the polyol method and analysed by TEM analysis. The composition of the films was estimated to be approximately Fe₂₀O(Pt₇₀) by EDXS. Surface of Si and SiO₂ wafers have been covered by FePt nanoparticles and heated in 600°C for 1h to form L10 phase nanoparticles [1]. FE-SEM and XRD analyses show uniform surface distributions of FePt, L10 nanoparticles. The SiO₂ [2] substrate prevents nanoparticles from coalescence during annealing and prevents them from growth [3], hence, causing their size not to become more than 40nm. SiO₂ wafer is more suitable than Si wafer in separating the nanoparticles, which may be due to oxygen of surface bonding with nanoparticles. Presence of 30mT magnetic field controls the size of nanoparticles around 25nm, which can be related to the reduction of random mobility in magnetic field and causes the nanoparticles to self-organize directionally. The larger I(001)/I(111) for perpendicular magnetic field indicates that the easy axis of nanoparticles is aligned in this direction [4]. The magnetic field also controls the surface distribution during heating process.

1. S. Sun, Adv Matter 18, 393-403 (2006). 2. T. Ichitsubo, S. Tojo, T. Uchihara and E. Matsubara, Phys. Rev. B 77, 094114 (2008). 3. Y. C. Wu, L. W. Wang, and C. H. Lai, Appl. Phys. Lett. 93, 242501 (2008). 4. M. I. J. Beale, N. G. Chew, M. J. Uren, A. G. Cullis, and J. D. Benjamin, Appl. Phys. Lett. 46, 86(1985).

QP24

Novel soft lithography technique for fabrication of Ni nanodots for use as bit patterned media

Shivaraman Ramaswamy
Nanotechnology Research Center, SRM University, India

Magnetic disk drive technology has successfully reduced the size of multi-grain bits to ~30 nm, and there are intensive industrial efforts to shrink the bit size further. This work reports the development of a cheap, scalable polymer template lithography technique of fabricating large arrays of magnetic nanostructures towards use as bit patterned media, one of the prominent next generation data storage technologies. The technique has been standardized and physical properties such as bit sizes, pitch sizes and the storage densities have been calculated. Critical magnetic properties such as magnetization reversal have also been studied and discussed to ascertain the plausibility of its use in futuristic high density magnetic data storage devices

[1] Park, S. Lee, D.H. Xu, J. Kim, B. Hong, S. W. Jeong, U. Xu, T. and Russell, T.P, 2009, "Macroscopic 10-Terabit-per-Square-Inch Arrays from Block Copolymers with Lateral Order," Science, vol. 323, pp. 1030-1033. [2] Kikitsu, A, Kamata, Y, Sakurai, M and Naito, K, 2007, "Recent progress of patterned media," IEEE Transactions on Magnetics, vol. 43, pp. 3685-3688. [3] Speliotis, D, 1984, "Media for high density magnetic recording", IEEE Transactions on Magnetics, 20, 5, 669 - 674.

RA01

Magnetic resonance and ferroelectricity of BaTi_{1-x}Fe_xO₃

Dianta Ginting¹, N. V. Dang², V. D. Lam², S. C. Yu¹ and T. L. Phan^{1*}
¹ Physisch, Bk 21, chungbuk national university; Korea
² Institute of Materials Science, Vietnamese Academy of Science and Technology, Hanoi, Viet Nam

BaTiO₃ is known as an excellent candidate for multiferroics. In this work, we present magnetic-resonant and ferroelectric properties of polycrystalline BaTi_{1-x}Fe_xO₃ ceramics (0 ≤ x ≤ 0.12) prepared by conventional solid-state reaction. Measurements have been based on an X-ray diffractometer, electron spin resonance (ESR) spectroscopy, and Precision Premier-Radiant. X-ray diffraction patterns reveal the tetragonal-hexagonal phase transformation as increasing Fe-doping content. ESR spectra prove that many samples to be ferromagnetic, excepting for the x = 0.02-0.06 samples, which are paramagnetic. Such the results are in good agreement with the previously report on the magnetic behavior. Room-temperature P-E hysteresis loops of BaTi_{1-x}Fe_xO₃ reveal that with increasing Fe concentration, the feature of ferroelectric P-E loops changes in the shape to the paraelectric regime, indicating the decrease in ferroelectricity. Consequently, the values of the remnant polarization Pr and the coercive field Ec gradually are also decreased. Keywords: Fe-doped BaTiO₃; Magnetic phase separation; Ferroelectricity *Electronic mail: ptlong2512@yahoo.com Phone:

Daniel Khomskii, Physics, 2.20 (2009) W. Eerenstein, N.D. Mathur & J.F. Scott, Nature 442(17) (2006) N.V.Dang, Thanh, L.V.Hong, V.D Lam, The-Long Phan, Applied Physics 110, 043914, (2011). QJY Shen-Yu, LI Wang, LIU YU, LIU Gui Hua, WU Yi-Quan, Chen Nan, Trans. Nonferrous Met.Soc. China 20,1911-1915(2010). Manfred Fiebig, J. Phys. D: Appl.Phys.38, R123-R152. S.Angappane, G Rangarajan, and K.Sethupathi, J. Apply. Phys.93,8334 (2003).F. Lin, D. Jiang, X. Ma, and W. Shi, Physica B 403, 2525 (2008). S. Ray; P. Mahadevan, S. Mandal, S. Krishnakumar; C. S. Kuroda, T. Sasaki, T. Tamiyama, and M. Itoh, Phys. Rev. B 77, 104416 (2008).

RA02

Growth of high pure BiFeO₃ single crystals

Kai Feng¹, Jun Lu^{2*} and Yicheng Wu¹
¹ Technical Institute of Physics and Chemistry, Chinese Academy of Sciences, Beijing 100190, China
² State Key Laboratory of Magnetism, Technical Institute of Physics and Chemistry, Chinese Academy of Sciences, Beijing 100190, China

BiFeO₃(BFO) is a heavily beaten compound in recent publications. BFO exhibits simultaneous polar and magnetic order at room temperature, promising important applications, but growth of pure BFO single crystals is really a great challenge. To grow extremely pure BFO single crystals, we have systematically investigated Bi₂O₃-Fe₂O₃ pseudo-binary system from the long-term crystal growth experiments, high performance powder X-ray diffraction analysis and high temperature differential thermal analysis instrument. The peritectic transition temperature of BFO was determined to be 852±5 °C and Other typical characteristic temperatures in Bi₂O₃-Fe₂O₃ pseudo-binary phase diagram were reevaluated. It has been found that purity of grown BFO single crystals depends greatly on crucible materials. When suitable kind of crucibles were used, extremely high pure BFO single crystals could be easily obtained with maximum size above one centimeter.

[1] J. Lu et al., Eur. Phys. J. B, 75(4), 451-60(2010) (as cover story) [2] J. Lu et al., J. Cryst. Growth, 318, 936-41(2011) [3] J. Lu et al., A method of growing centimeter pure BiFeO3 single crystals, Chinese Patent, 201110252660.5

RA03

Structural, electrical and magnetic properties of La-doped BiFeO₃ ceramics.

M. Roy, S. Jangid, S. K. Barbar and Indu Bala Thakur
Department of Physics, M. L. Sukhadia University, Udaipur, India

Polycrystalline ceramic samples of Bi_{1-x}La_xFeO₃ (x=0.0, 0.1 and 0.2) have been prepared by standard solid state reaction method using high purity oxides and carbonates. The structure and formation of the compounds have been checked by X-ray diffraction followed by energy dispersive X-ray microanalysis (EDAX) techniques. There is a good agreement between observed and calculated X-ray diffraction patterns obtained by performing the Rietveld refinement with a structural model using the non-centrosymmetric space group R3c. The lattice parameters have been refined but the over all structure remained the same. The microstructural studies have been carried out using scanning electron microscopy. The dc conductivity of all the samples has been measured and their activation energies were calculated from logσ vs 103/T curves. Vibrating sample magnetometer (VSM) has been used to study the magnetic behaviour of the compounds. It has been observed that with the increase of substitution concentration of La, the insulating behaviour of the materials have been improved and showing the antiferromagnetic to weak ferromagnetic behaviour. The results are discussed in detail.

RA04

In situ X-ray absorption spectroscopy study on BaTiO₃

J. S. Lee* and C. C. Kao
SSRL, SLAC National Accelerator Laboratory, USA

Ferroelectric systems are under intensive study for both the point of view of fundamental materials physics and the potential applications such as memories, sensors, and transducers. The Ti⁴⁺ (d0-ness) systems which are the generally well known ferroelectric as form ATiO₃ structure (A=Ba and Pb), inter alia, have been extensively investigated. To understand this system, both of structural and electronic investigations must be completed together. Structurally, Ti ions in the TiO₆ octahedra are moved along the applied electric (E)-field, resulting in a symmetry lowering. However, we still do not understand much about a change in the electronic structure between Ti 3d and O 2p states. Although the soft x-ray spectroscopy study at the oxygen absorption edge that is regarded as a good approach for exploring the electronic structure, such study accompanies an experimental difficulty; electron motion distortion under in situ E-field condition. In this work, we introduce an approach for overcoming such difficulty in conventional x-ray absorption spectroscopy (XAS) measurement. By looking at the O K-edge XAS of BaTiO₃ via a fluorescence yield, we studied electronic structure and reveal that the observed spectra features are related with the structural changes under the applied E-field.

RA05

Chiral skyrmions and magnetic bubbles in multiferroic materials

Xiuzhen Yu^{1*}, Y. Tokunaga¹, S. Seki², Y. Kaneko³, S. Ishiwata², M. Mostovoy⁴, N. Nagaosa⁵ and Y. Tokura⁶

¹ The Institute of Physical and Chemical Research, Japan
² University of Tokyo, Japan
³ Japan Science and Technology Agency, Japan
⁴ University of Groningen, Netherlands
⁵ University of Tokyo, The Institute of Physical and Chemical Research, Japan
⁶ University of Tokyo, The Institute of Physical and Chemical Research, JST, Japan

Nanometric chiral skyrmions and magnetic bubbles have been successfully realized in multiferroic materials Cu₂OSeO₅ and Se-doped barium ferrite by means of Lorentz transmission electron microscopy. Under the normal magnetic fields, chiral skyrmions with a topological number of -1 and a unique chirality, 50 nm in diameter, emerge in a non-centrosymmetric helimagnet Cu₂OSeO₅. In analogy with the transition from a helical spin structure to chiral skyrmions, a normal magnetic field turns the magnetic stripes into a bubble lattice with a positional order and random chiralities in a hexaferrite BaFe_{10.79}Sc_{0.16}Mg_{0.05}O₁₉ with uniaxial anisotropy. By systematically investigating the dependences of magnetic configurations on magnetic field, temperature and sample thickness, we reveal the differences between the spin textures of chiral skyrmions and magnetic bubbles. First, the magnetic bubbles determined by the ratio of dipolar and exchange interactions show strong size dependence on magnetic field and sample thickness. The chiral skyrmions induced by Dzyaloshinskii-Moriya interaction, however, show less size dependence on the external factors. Second is a difference in chirality. The chiral skyrmions have a unique chirality determined by the crystal chirality, while magnetic bubbles have two opposite chiralities, resulting in a variety of zoological magnetic structure with varying external magnetic field.

RA06

Studies on Bi_{1-x}La_xFeO₃ crystals in pulsed high magnetic fields

Masashi Tokunaga¹, Mitsuru Akaki², Hideki Kuwahara², Kengo Oka¹ and Takumi Kihara¹

¹ The Institute for Solid State Physics, The University of Tokyo, Japan
² Department of Physics, Sophia University, Japan

BiFeO₃ is known as the unique material that shows multiferroic nature at room temperature [1,2]. Application of high magnetic fields to this material induces a magnetic transition accompanied by a significant change in the electric polarization [3-5]. Although the occurrence of this transition is explained in the framework of the Ginzburg-Landau theory, in detail study is highly desirable to understand the microscopic origin of the magnetoelectric effects in this material. In this work, we synthesized crystals of Bi_{1-x}La_xFeO₃ with using the flux method, and studied their magnetic and dielectric properties in pulsed magnetic fields up to 55 T. Early experiments on the polycrystalline samples showed that partial substitution of La for Bi reduces the magnetic field needed to cause the magnetic transition [6]. Our isothermal magnetization measurements showed that the transition field at 42 K changes from 18 T to 15 T by La substitution. Our dielectric study revealed that the electric polarization shows significant change accompanied with this magnetic transition. Therefore, the phenomena observed in BiFeO₃ are reproduced in the reduced field scale in the La substituted system, which enables us more systematic studies to clarify the microscopic origin of the magnetoelectric effects associated with the magnetic transition.

[1] J. Wang et al., Science 299, 1719 (2003). [2] G. Catalan and J. F. Scott, Adv. Mater. 21, 2463 (2009). [3] Yu. F. Popov et al., JETP Lett. 57, 69 (1993). [4] A. M. Kadomtseva, et al., JETP Lett. 79, 571 (2004). [5] M. Tokunaga et al., J. Phys. Soc. Jpn. 79, 064713 (2010). [6] G. Le Bras et al., Phys. Rev. B 80, 134417 (2009).

RA07

Enhanced magnetic properties of Ni-doped BiFeO₃ compounds

Y. J. Yoo¹, J. S. Park¹, J. H. Kang², J. Kim¹, B. W. Lee³, M. S. Seo⁴ and Y. P. Lee^{1*}

¹ Physics, Hanyang University, Korea
² Nano & Electronic Physics, Kookmin University, Korea
³ Physics, Hankuk University of Foreign Studies, Korea
⁴ Division of Materials Science, Korea Basic Science Institute, Korea

The structure and the magnetic properties of polycrystalline BiFeO₃ and BiFe_{0.95}Ni_{0.05}O₃ bulk ceramic compounds, which were prepared by solid-state reaction and rapid sintering, were investigated. High-purity Bi₂O₃, Fe₂O₃ and NiO powders were mixed with the stoichiometric proportions, and calcined at 450°C for 24 h to produce BiFe_{1-x}Ni_xO₃. The crystalline structure of samples was investigated at room temperature by using a Rigaku Miniflex powder diffractometer. The field-dependent and the temperature-dependent at high temperatures magnetization measurements were performed with a vibrating-sample magnetometer. The temperature-dependent magnetization at low temperatures was analyzed with Quantum Design superconducting quantum-interference-device (SQUID) magnetometer. The x-ray diffraction study demonstrates the compressive stress due to the Ni substitution at the Fe site. The lattice constant of BiFe_{0.95}Ni_{0.05}O₃ is smaller than of BiFeO₃ because of the smaller ionic radius of Ni²⁺ than that of Fe³⁺. The field-dependent magnetization of BiFe_{0.95}Ni_{0.05}O₃ exhibits a clear hysteresis loop at 300 K. The magnetic properties of BiFe_{0.95}Ni_{0.05}O₃ were improved at room temperature because of the existence of structurally compressive stress. The zero-field-cooled temperature-dependent magnetization reveals that the magnetic transition temperature and the magnetic moment of BiFe_{0.95}Ni_{0.05}O₃ are higher than those of BiFeO₃.

RA08

Magnetic modulation of electrical impedance in Bi-doped La_{0.5}Sr_{0.5}MnO₃

Sujit Kumar Barik, M Aparnadevi and Ramanathan Mahendiran*
Physics, National University of Singapore, Singapore

In recent years, magnetic control of dielectric polarization in multiferroics and magnetoelctrica has become a topic of considerable interest. Dielectric studies in these materials are often done using an impedance analyzer in the frequency range f = 10 to 10 kHz. As the frequency increase, dielectric permittivity decreases. Here, we show that an interesting phenomenon occurs in MHz range in Bi doped La_{0.5}Sr_{0.5}MnO₃. With increasing frequency of the ac current or ac voltage, both in- and out-of phase compnents of electrical impedance show an abrupt increase that is accompanied by a peak around the Curie temperature. The peak decreases in magnitude and is suppressed in a field of 1 kOe. This results in a huge ac magnetoresistance (30-35 % for H = 1 kOe) and magnetoreactance (= 30-40 %). The origin of the magnetoreactance is not necessarily due to change in capacitance but but it is suggested to magnetoinductance effect, which has not been seriously considered so far. The combination of huge ac magneoresistance and magnetconductance in a single material provides multifunctional capabilities. Results from our studies are compared to magnetocapacitance behavior found in BiMnO₃[1]

[1] T. Kimura, S. Kawamoto, I. Yamada, M. Azuma, M. Takano, Y. Tokura, Phys. Rev. B 2003, 67, R180401 2003

RA09

Theoretical study of PCAR measurement with d-wave superconductors.

Hiroyuki Ohtori¹ and Hiroshi Imamura^{2*}
¹ Univ. of Tsukuba, NRI-AIST, Japan
² NRI-AIST, Japan

High spin polarization ferromagnetic metals are essential for creating high performance spintronics devices, therefore it is important to estimate the value of spin polarization quickly and efficiently. Point contact Andreev reflection (PCAR) spectroscopy is a powerful method for measuring spin polarization of ferromagnetic metals. However, most PCAR measurement were performed at very low temperatures, around 1.5 K, since the conventional s-type superconductor is used. If we use high-Tc superconductors, PCAR measurement can be performed at higher temperature. In this study, we theoretically analyze the Andreev reflection in the ferromagnetic metal (FM) / insulator (I) / d-wave superconductor (dS) junctions. The superconducting gap in momentum space is not uniform in the d-wave superconductor, therefore the conductance suppression due to the insulator is affected by the difference of the Fermi wave number between the ferromagnetic metal and superconductor. Especially, in the case of d_{2-2g2} model, we found that the bias voltage at which the normalized conductance of the FM/I/dS junction drops is expressed as a function of the exchange field of the ferromagnetic metal.

RA10

T_c Evolution of Bulk and Optical Spectra of Nanocolloidal Fe-doped Manganate CaMn_{1-x}Fe_xO₃ (x = 0, 0.01, 0.03, 0.05)

Huyen-yen Duc Pham, Duc-thang Pham, Nam-nhat Hoang* and Duc-tho Nguyen
Faculty of Technical Physics and Nanotechnology, Vietnam National University, University of Engineering and Technology, Viet Nam

Recently, the effect of magnetic reversal at low magnetic field was observed with the multiferroic Fe-doped CaMnO₃ [Sol. Stat. Commun. 142 (2007) 525]. We report here the optical behaviors of this class of compounds (CaMn_{1-x}Fe_xO₃, x = 0, 0.01, 0.03, 0.05) which were prepared by using traditional ceramic method with parent oxides as precursors. The analysis of structure showed the predominant orthorhombic phase with slight increased cell constants according to doping content (from 3.743 to 3.746 Å). The investigation of the Raman spectra also agreed with the increased Mn-O bond length according to doping, therefore suggested the weakening of ferromagnetic exchange between Mn³⁺ and Mn⁴⁺ cations (exactly, from 0.61 to 0.52 eV). This weakening also developed together with the reduction of Curie temperature (T_c) (from 155 to 135 K), the shifts of infra-red (IR) absorption maxima towards the longer wavelengths and the narrowing of band-gaps (from 0.45 to 0.14 eV). The absorption spectra also showed a clear absorption line near 1.2 eV which is characteristic for Fe, and is composed mainly from 3d electron transition with a change in spin.

PACS number: 75.47.Lx; 75.50.Ee; 74.25.Fy; 75.30.Kz
Keywords: perovskite, manganate, structure, optical

RA11

Evidence of magnetic phase separation in LuFe₂O₄

Julie Bourgeois¹, Gilles Andre², Sylvain Petit², Julien Robert², Maria Poienar³, Jerome Rouquette³, Erik Elkaim⁴, Maryvonne Hervieu¹, Christine Martin¹, Antoine Maignan¹ and Francoise Damay²

¹ Laboratoire CRISMAT, CNRS UMR 6508, 6 bvd Marechal Juin, 14050 CAEN CEDEX, France
² Laboratoire Leon Brillouin, CEA-CNRS UMR 12, 91191 GIF-SUR-YVETTE CEDEX, France
³ Institut Charles Gerhardt, UMR CNRS 5253, Place Eugene Bataillon, cc1503, 34095 MONTPELLIER CEDEX 5, France
⁴ Synchrotron Soleil, L'Orme des Merisiers, Saint-Aubin BP 48, 91192 GIF-SUR-YVETTE CEDEX, France

The magnetic properties of a polycrystalline sample of multiferroic LuFe₂O₄ [1] have been investigated by means of magnetization measurements combined with neutron scattering, between 1.5 and 300K [2]. Magnetic Bragg peaks appear below T_N = 240K, and can be indexed using two propagation vectors, corresponding to either a ferromagnetic or an antiferromagnetic stacking of the iron bilayers. The magnetic arrangement in the ab plane follows a 1:2 pattern, which obeys the charge ordering one observed in transmission electron microscopy [3]. Neutron inelastic scattering data confirm the strong easy-axis single-ion anisotropy of the iron spin in its trigonal environment, of about 8 meV at 5 K. Modeling of the diffraction data, based on a CO-type modulation of the spin ordering, shows coexisting magnetic phases with opposite signs of the intra-bilayer interaction, corresponding to two distinct magnetic transition temperatures. Coexisting antiferromagnetic and ferrimagnetic phases, along with the enlarged axial magnetic anisotropy, are necessary to describe the macroscopic magnetic properties of this compound.

[1] N. Ikeda et al., Nature (London) 436, 1136 (2005) [2] J. Bourgeois et al., submitted to Phys. Rev. B (2012) [3] J. Bourgeois et al., to appear in Phys. Rev. B (2012)

RA12

Magnetoelectric effect in mechanically mediated structure of TbFe₂, Pb(Zr,Ti)O₃, and nonmagnetic flakes

Yin-gang Wang* and Ke Bi
Nanjing University of Aeronautics and Astronautics, China

For most investigations on layered ME composites with excellent ME effect compared to single phase materials and multiphase bulk composites, the classical structure is constructed layer by layer through interface bonding. In this work, the proposed ME structure is made up of two magnetostriictive TbFe₂ alloys, one piezoelectric PZT ceramic and two nonmagnetic glass flakes. When an external ac magnetic field Hac is applied along the length direction of magnetostriictive TbFe₂ flakes, the TbFe₂ flakes will produce an extensional strain. The strain then transfer to the PZT flake because of the end parts of PZT and TbFe₂ flakes bonded with glass slides in a vertical plane. Due to the piezoelectric effect, the PZT flake will induce a charge output. The interface between magnetostriictive and piezoelectric phases is not required to achieve ME coupling. Increasing H_{dc} from zero, α_{E,31} increases linearly until a maximum value is reached at 350 Oe, and then decreases subsequently. With further increase in H_{dc}, α_{E,31} reaches a maximum value, and then decreases subsequently. There are several resonance peaks at 200 Oe and 1<f<150 kHz and a giant ME voltage coefficient as high as 2.7 Vcm⁻¹ Oe⁻¹ can be obtained at the resonance frequency of 44.5 kHz.

1. C. Israel, N. D. Mathur, and J. F. Scott, Nature Mater. 7, 93 (2008). 2. C. W. Nan, M. I. Bichurin, S. X. Dong, D. Viehland, and G. Srinivasan, J. Appl. Phys. 103, 031101 (2008). 3. M. Zeng, S. W. Or, and H. L. W. Chan, Appl. Phys. Lett. 96, 203502 (2010).

RA13

Enhancement of magnetization in sulfur doped BiFeO₃

Chunlong Shi, Jun Du and Xiaoshan Wu*
Physics, Nanjing University, China

Sulfur doped BiFeO_{3-x}S_x are synthesized by high pressure solid state reaction method with the high purity original materials of Fe₂O₃, Bi₂O₃, Bi₂S₃, S, and FeS. The pressure remains 5 GPa during the sample preparations. We have compared the effects of original materials on the final products, and got the optimum products with Fe₂O₃, Bi₂O₃, and FeS as the original materials. Slight impurity of Bi₂Fe₂O₇ is detected in the products. A magnetization enhancement is confirmed to roughly more than 2 orders with the above materials reaction. The saturation magnetization more than 0.75 emu/g at 1.5 Tesla, and the Hc is roughly 50 Oe. The good ferroelectric property is also predicted. We argue that the enhancement of magnetization may due to the variation of the chemical valence of iron.

RA14

Effects of chlorine and fluorine on the structure and magnetism in BiFeO₃

Kaige Gao, Chunlong Shi and Xiaoshan Wu*
Physics, Nanjing University, China

Chlorine and fluorine doped BiFeO_{3-x}M_x are synthesized by solid state reaction method under high pressure and high temperature with the high purity original materials of Fe₂O₃, Bi₂O₃, and FeCl₂, or FeF₂. The pressure remains 6 GPa and the temperature is set to be 750 oC during the sample preparations. They are almost the single phase. We have compared the chlorine and fluorine effects on the structure and magnetization on the final products. Both doping samples show the weak magnetism at room temperature, much larger than the pure BiFeO₃, although the paramagnetic background is strong. Chlorine doping show much larger magnetization than that of fluorine. We argue that the magnetization results from the variation of the chemical valence of iron ion and the distortion of FeO₆ due to the element of oxygen replaced by fluorine or chlorine. The dielectric properties show us the small leakage may indicate the increase of carriers. We expect a good dielectric properties may obtained by adjust the dopants in BiFeO₃.

RA15

Investigation of electriciry coercive behavior of LSFMTO system using ultrasonic mixing method

Erfan Handoko^{1*}, Azwar Manaf² and Dede Djuhana²
¹ Physics, Department of Physics, State University of Jakarta, Indonesia
² Physics, Department of Physics, University of Indonesia, Indonesia

We have investigated electriciry coercive behavior of La_{0.5}Sr_{0.5}Fe_{0.9}Mn_{0.05}Ti_{0.05}O₃ (LSFMTO) system using ultrasonic mixing method. LSFMTO system is driven by 40 kHz frequency and calcinate process up to 750°C for 30 minutes. Then sintering process also carried out by systematic various of temperature 900 °C, 1000 °C, and 1100 °C respectively, with time preparation is same previously. Very interestingly, the LSFMTO system exhibits ferroelectric (La,Sr)(Fe,Mn,Ti)O₃ and ferromagnetic SrFe₂O₉ properties and minor phase La₂O₃ by XRD analzyation. We have also carried out measurement of LSFMTO system using a systematic applied the external magnetic field and electric polarization. The hysteresis curve of LSFMTO system shows the electriciry coercive (Ec) increases while saturation polarization (Pc) and remanent polarization are tendency constant at the magnetic strength of 0.12 T. I believed that our finding of LSFMTO system is potensial to multiferroic material.

1. Jifan Hu, et al, Materials Science and Engineering B 90, p.146-148 (2002). 2. O. Chmaissem et al, Physical Review B 74, 144415 (2006) 3. Y. L. Cheng, et al, Journal Magnetism and Magnetic Material, 322, p 97-101 (2010)

July 12 (Thu)

July 12 (Thu)

RA16

Enhancement of multiferroic properties of solid state prepared La doped BiFeO₃

Suresh P and Srinath S*
School of Physics, University of Hyderabad, India

BiFeO₃ (BFO) has generated widespread interest since it is a room-temperature multiferroic. La_xBi_{1-x}FeO₃ (x= 0.05-0.4) are prepared through solid state reaction method. X-ray diffraction for x ≤ 0.15 shows R3c and for x> 0.15 the structure changes to Pbnm. The percentage of these phases present is estimated through Rietveld analysis. Raman spectra for x ≤ 0.15 exhibit 8 peaks (4A+4E modes). There is no shift in Raman modes indicating that La substitutes Bi in BFO. The dielectric constant increases and leakage current decreases with x. The enhanced polarization may be due to the distortion of the crystal lattice with La doping. With increase in La doping the T_N decreases. The magnetization (M) decreases up to 250 K and increases on further cooling indicating the spin reorientation. A cusp in M-T is observed close to 50 K indicating the spin glass behavior. M-H loops do not saturate even for field up to 6 T. With La doping, H_c and the magnetization increases dramatically in comparison to x=0. Both H_c (~ 1.6 T) and Mr (0.27 emu/g) have maximum values for x =0.2 at 5 K. The increase in the magnetic parameters is attributed to the break in the spin cycloid structure.

[1] H. Fukamura et al., J. Magn.Magn. Mater. 310, e367 (2007) (2) Manoj K. Singh et al. Phys. Rev. B. 77, 144403 (2008)

RA17

Magnetostructural coupling at the metal-insulator transition in YBaCo₂O_{8.5} as seen by synchrotron x-ray diffraction and absorption

Jessica Padilla-pantoja, Javier Herrero-martin, Carlos Frontera and Jose Luis Garcia-munoz
Institut de Ciencia de Materials de Barcelona, ICMAB-CSIC, Spain

In LnBaCo₂O_{8.5} (Ln: lanthanide) cobalites Ln and Ba cations order in alternating planes along the c-axis yielding an ordered arrangement of CoO₃ pyramids and CoO₆ octahedra. The presence of two local environments for Co may be at the origin of proposed Co spin-state changes whose interplay with the structural and electronic changes at metal-insulator transitions (MIT) are currently attracting much attention [1-5]. We present a study of the magnetic, structural and thermoelectric properties of YBaCo₂O_{8.5} as a function of temperature. Our results evidence the presence of three magnetic transitions with a strong magnetostructural coupling. We have used synchrotron x-ray powder diffraction to show that the Pnmm orthorhombic structure transforms (on cooling) into a monoclinic (P112/a) phase below T_{MI} ~ 295 K by doubling the a-axis [6]. Concomitantly a ferromagnetic moment appears and the Seebeck coefficient is enhanced. A further cooling leads to the successive appearance of Co AFM structures (T_{N1} ~ 267 K, T_{N2} ~ 231 K), the crystal structure becoming again orthorhombic. Finally, we present temperature dependent soft x-ray absorption data at the Co L_{2,3} edge. They discard the possibility of a high to low spin state change in Co ions at octahedral sites across the MIT [7].

[1] A. Maignan et al., J. Solid State Chem. 142, 247 (1999). [2] E. Suard et al., Phys. Rev. B 61, R11871 (2000). [3] C. Frontera et al., Phys. Rev. B 74, 054406 (2006). [4] V.P. Plakhtiy et al., Phys. Rev. B 71, 214407 (2005). [5] M. Soda et al., J. Phys. Soc. Jpn. 72, 1729 (2003). [6] J. Padilla-Pantoja et al., Phys. Rev. B 81, 132405 (2010). [7] J. Padilla-Pantoja et al., J. Appl. Phys. 111, 234291 (2012) (in press).

RA18

Magnetic field dependence of dielectric properties in LuFe₂O₄

Takashi Kambe*, Yukimasa Fukada, Tomoko Nagata and Naoshi Ikeda
Physics, Okayama university, Japan

The multiferroic properties in LuFe₂O₄ are of interest, in which contains equal amount of Fe²⁺ and Fe³⁺ in triangular lattice. This material shows a ferri-magnetic transition at 240K and three-dimensional charge ordering at around 320K. The dielectric property of this material is suggested with a valence fluctuation process of iron ions in the polar charge ordered domain. Here we report a magnetic field variation of the dielectric constant of single crystal LuFe₂O₄, and discuss with the valence fluctuation process of iron charges in the magnetic domain wall.

RA19

Pressure studies of LaAgSb₂ utilizing new integrated pressure cell

Sven Friedemann¹*, Zhou Feng¹, Takao Ebihara², Christophe Thessieu³ and F Malte Grosche¹

¹ Cavendish Laboratory, University of Cambridge, United Kingdom
² Department of Physics, Shizuoka University, Shizuoka 422-8529, Japan
³ easyLab Technologies Ltd., Earley Gate, Whiteknights Road, Reading, RG6 6BZ, United Kingdom



RA20

Crystal & Magnetic structure studies of doped BiFeO₃ multiferroic compound

Seongsu Lee
Neutron Science Division, KAERI, Korea

Multiferroics, materials combining multiple order parameters, offer an exciting way of coupling phenomena such as electronic and magnetic order. The coexistence of different order parameter permits potential applications in information storage, spintronics, and magnetic or electric field sensors. The perovskite BiFeO₃(BFO) is known to be antiferromagnetic below the Neel temperature of 640 K and ferroelectric with a high Curie temperature of 1100 K. According to the previous doping studies of BFO, it is likely that non-stoichiometry and second-phase formation are the factors responsible for leakage current in BFO. It has been suggested that oxygen nonstoichiometry leads to valence fluctuations of Fe ions in BFO, resulting in high conductivity. To reduce the large leakage current of BFO, one attempt is to make donor-doped BFO compounds. In this study, we have tried to generate the new multiferroic material functioning on at room temperature. The candidate systems are BiFeO₃^δ/BaMnO₃ and BiFeO₃^δ/BaTiO₃. These system have been fabricated by a solid-state reaction method and flux method, respectively. The crystal and magnetic structure of these systems are studied using XRD and neutron powder diffraction as functions of temperature. We will discuss the magnetic and electric property of new multiferroic system working on at room temperature.

I. T. Choi, S. Lee, Y. J. Choi, V. Kiryukhin, and S-W. Cheong Science 324, 63 (2009) 2. Jung-hwan PARK, Sang-Hyun LEE, Seongsu LEE, Fabia GOZZO,Hiroyuki KIMURA, Yukio NODA, Young-Jai CHOI, Valery KIRYUKHIN, Sang-Wook CHEONG, Younjung JO, Eun Sang CHOI, Luis BALICAS, Gun Sang JEON, and Je-Geun PARK Journal of the Physical Society of Japan 80, 114714(2011)

RA21

The analysis of structure, magnetic and ferroelectric properties of Ba_{1-x}Bi_xTi_{0.95}Fe_{0.05}O₃

Widi Yansen¹, Kadek Juliana Parwanta¹, Jaeyeong Kim¹, Min Gyu Kang², Chong Yun Kang² and Bo Wha Lee^{1*}

¹ Physics, Hankuk University of Foreign Studies, Korea
² Physics, Korea Institute of Science and Technology, Korea

The multiferroic material is a material which shows more than one primary ferroic order parameter simultaneously and can be made by introducing the magnetic impurities into ferroelectric material [1]. BaTiO₃ is known as a classical ferroelectric material, whereas the Fe-doped BaTiO₃ is reported to have a magnetic ordering. Although the Fe doping can induce the ferromagnetism in BaTiO₃, the ferroelectricity of this material is suppressed. In this report, we analyze the structure, magnetic and ferroelectric properties of Ba_{1-x}Bi_xTi_{0.95}Fe_{0.05}O₃ (0 ≤ x ≤ 0.05). XRD results indicate that the tetragonal phase is merged with the hexagonal phase for x < 0.05. At x = 0.05, the pure tetragonal phase is observed. The magnetic field dependence of magnetization at room temperature for x = 0 shows a kind of antiferromagnetism. Introducing 2 % Bi doping, it shows the ferrimagnetic properties. However, with the 5 % doping of Bi, the ferrimagnetic loop is disappeared and becomes paramagnetic. It suggests that the superexchange between Fe³⁺ ions in octahedral and pentahedral sites associated with oxygen vacancy produces the ferromagnetism [2]. The ferroelectric hysteresis loop with low leakage current is only observed for x = 0.02. These results indicate that the multiferroic properties are observed in Ba_{0.98}Bi_{0.02}Ti_{0.95}Fe_{0.05}O₃ sample.

[1] Y. Shuai, S. Zhou, D. Burger, H. Reuther, and I. Skorupa, J. Appl. Phys. 109, 084105 (2011). [2] F. Lin, D. Jiang, X. Ma, and W. Shi, J. Magn. Magn. Mater. 320, 691-694 (2008).

RA22

Spin dynamics of multiferroic BiFeO₃ single crystal

Jaehong Jeong¹, E. A. Goremychkin², T. Gajdi³, K. Nakajima³, Gun Sang Jeon⁴, Shin-ae Kim⁵, S. Furukawa¹, Yong Baek Kim¹, Seongsu Lee², V. Kiryukhin¹, S-w. Cheong¹ and Je-geun Park^{1*}

¹ FPRD Department of Physics & Astronomy, Center for Strongly Correlated Materials Research, Seoul National University, Seoul 151-747, Korea
² ISIS Facility, STFC Rutherford Appleton Laboratory, Oxfordshire OX11 0QX, United Kingdom
³ Neutron Science Section, MLF Division, J-PARC Center, Tokai, Ibaraki 319-1106, Japan
⁴ Department of Physics, Ewha Womans University, Seoul 120-750, Korea
⁵ Neutron Science Division, Korea Atomic Energy Research Institute, Daejeon 305-353, Korea
⁶ Department of Physics, University of Toronto, Toronto M5S 1A7, Canada
⁷ Rutgers Center for Emergent Materials and Department of Physics and Astronomy, Rutgers University, Piscataway NJ 08854, USA

Multiferroic compounds are one of most challenging topics in the condensed matter physics [1] not only for its fundamental importance but also for huge future applications. Although several systems are known to have multiferroic behavior, there are few multiferroic materials that have both magnetic and ferroelectric transition temperatures above room temperature. BiFeO₃ is probably the only exception with Neel temperature at T_N=650 K and Curie temperature at T_C=1100 K [2]. In order to understand the spin dynamics of BiFeO₃, we have carried out inelastic neutron scattering experiments on ten co-aligned single crystals of BiFeO₃ using AMATERAS beamline at J-PARC and MERLIN beamline at ISIS. In particular, we used a so-called sample rotation method on MERLIN to map out the full three-dimensional spin wave [3]. We have also calculated the spin wave dispersion using Heisenberg Hamiltonian with two exchange parameters between the nearest and next nearest neighbors. A Dzyaloshinskii-Moriya term that arises from the spiral magnetic structure of BiFeO₃ was also examined. By carefully examining the AMATERAS and MERLIN data, we could find, for the first time, the full spin wave dispersion of BiFeO₃ and determine the exchange parameters that are consistent with the experimental results.

1) S-W. Cheong and M. Mostovoy, Nature Materials 6,13 (2007) 2) I. Sosnowska et al., J. Phys. C: Solid State Phys. 15, 4835 (1982) 3) Jaehong Jeong et al., Phys. Rev. Lett. 108, 077202 (2012)

RA23

Magnetic and dielectric properties of the single crystals Sm_{1-x}Ho_xFe₃(BO₃)₄ and Sm_{1-x}La_xFe₃(BO₃)₄

Evgeniy Eremin*, Irina Gudim, Vladislav Ternerov and Alexander Eremin
Kirensky Institute of Physics SB RAS, Russia

The trigonal rare-earth ferrobates with hantit ictures is interested due to very strong of the electric polarization induced by magnetic field. The research of single crystals with double rare-earth subsystems such as Sm_{1-x}R_xFe₃(BO₃)₄ (R = Ho, La) is important for analysis microscopic mechanism of magnetoelectric interaction. The single crystals of Sm_{1-x}Ho_xFe₃(BO₃)₄ with x = 0, 0.3; 0.5 and Sm_{1-x}La_xFe₃(BO₃)₄ with x = 0.25; 0.5 were grown by a flux method. The magnetic and magnetodielectric properties have been investigated. It has been revealed what magnetic behaviour and magnetodielectric effect essential depended on x. The magnetic field influence on the change in degree of dielectric penetrability is decreased with increasing x for both under study families. The decreasing of magnetodielectric effect is probably related with influence of the racemic twinning.

RA24

Far infrared spectroscopy of EuFe₂(BO₃)₄

Kirill N. Boldyrev^{1*}, Taras N. Stanislavchuk², Marina N. Popova¹ and Sergey A. Klimin¹

¹ Solid State Spectroscopy, Institute of spectroscopy RAS, Russia
² Physics, New Jersey Institute of Technology, USA

We present the results on the polarized far infrared absorption spectra of EuFe₂(BO₃)₄ crystal in a wide range of temperature (3.5 - 300K). Rare-earth iron borates RFe₂(BO₃)₄ undergo the antiferromagnetic phase transition at temperatures below 40 K, and some of them exhibit a significant magnetoelectric and magnetoelastic effect. EuFe₂(BO₃)₄ is known to exhibit two phase transitions, the structural one at T_C = 58 K [1], and the antiferromagnetic ordering at T_N = 34 K [2]. The phonon frequencies demonstrate pronounced changes at T_C consistent with the observed peculiarities in the dielectric constant and thermal expansion [3]. Smaller but clearly visible phonon shift were registered below T_N, thus evidencing the spin-lattice interaction in the title compound.

[1] M.N. Popova, Journal of Rare Earths, 27, 607 (2009). [2] M.N. Popova, Journal of Magnetism and Magnetic Materials, 321, 716 (2009). [3] A.M. Kadamtsseva, Yu.F. Popov, G.P. Vorob'ev, A.P. Pyatakov, S.S. Krotov, K.I. Kamilov, J. Low Temp. Phys., 36(6), 640 (2010).

RA25

Electric polarization, toroidal moments, spin chirality, spin canting at avoided level crossing induced by Dzyaloshinsky-Moriya interaction in V₃ nanomultiferroics in transverse magnetic field

Moisey Belinsky
School of Chemistry, Tel-Aviv University, Tel Aviv, Israel

The spin-frustrated V₃ and Cu₃ nanomagnets with the Dzialoshinsky-Moriya (DM) interaction have received great attention for potential application in quantum computation [1-8]. V₃ with the out-of-plane D_z and in-plane D_n DM interactions demonstrates the multiferroic behavior in longitudinal magnetic field B_z∥Z: field-induced polarization P_x(B_z) and toroidal moments T_x(B_z), which depend on the vector K_z(B_z) [scalar χ(B_z)] chirality, and complicated individual spin dynamics at avoided level crossing (ALC) [7]. In order to investigate the multiferroic behavior in transverse field B_x⊥Z and B-reversal/rotation effects, P(B_x), T_n(B_x), M(B_x)magnetization, K_z(B_x), χ(B_x) and spin canting were calculated for B⊥Z. The spin current P-Is mechanism [9] is the driving force of P_x(B_x) with a maximum at ALC that corresponds to Is(max). The in-plane DM leads to the in-plane T_n(B_x) which exhibits T-flip under B-rotation/reversal. T_n(B), χ(B), orbital moment M(B), circular orbital current I_o-χ [P_x(B), K_z(B), Is] show the switch on/off [reduction] under B-rotation within vertical XZ plane. Field behavior P_x(B_x), T_n(B_x), M(B_x), K_z(B_x), Is, I_o and individual spin dynamics for B_x⊥Z strongly differ from that for B_z∥Z. V₃ exhibits non-linear reduction of K_z(B_x)vector chirality, χ(B_x)=0, and the entanglement effect. The V₃ nanomultiferroics demonstrate magnetically controlled anisotropic P_x(B), T_n(B), M(B), K_z(B), χ(B), M, Is, I_o characteristics.

1. T. Yamase et al., Inorg. Chem. 43, 8150 (2004). 2. Y. Kohama et al., J. Solid. State. Chem. 182, 1468 (2009). 3. K.-Y. Choi et al., Phys.Rev.Lett. 96, 107202 (2006); Phys. Rev. B 77, 024406 (2008). 4. M. Trif et al., Phys.Rev.Lett. 101, 217201 (2008). 5. M. Trif et al., Phys.Rev. B 82, 045429 (2010). 6. M. F. Islam et al., Phys. Rev. B 82, 155446 (2010). 7. M.I. Belinsky, Phys. Rev. B 84, 064425 (2011). 8. M.I. Belinsky, Chem. Phys. 361, 137, 152 (2009). 9. H. Katsura et al., Phys. Rev. Lett. 95, 057205 (2005).

RA26

Mössbauer studies of bismuth ferrite

Seungkyu Han, Yong Hui Li, Minseon Kim, Sam Jin Kim and Chul Sung Kim*
Physics, Kookmin University, Korea

Perovskite bismuth ferrite (BiFeO₃) is a multiferroic material, having ferroelectric order (T_C = 1,103 K) and antiferromagnetic order (T_N = 643 K) [1]. It is a possible candidate for information storage, spintronics, and sensors applications [2]. Here, we have measured the magnetic properties of BiFeO₃ using x-ray diffractometer, field emission scanning electron microscope (FE-SEM), vibrating sample magnetometer, and Mössbauer spectroscopy. Single phased BiFeO₃ was synthesized by a low-temperature hydrothermal method. FE-SEM results showed that the grain sizes of microsphere and microcube were about 80 μm and 50 μm, respectively. BiFeO₃ powder showed weak-ferromagnetic behavior with a small magnetization value (M_s ~ 100 memu/g) at 295K. Rietveld refinement analysis showed that Fe-site and O-site splits into two pairs, respectively. The Mossbauer spectra of BiFeO₃ were analyzed with 2-set sextet. Isomer shift (δ) values showed that Fe³⁺ ions existed in octahedral site. Electric quadrupole shift (EQ) values suggested different lattice distribution at octahedral site. Based on EQ values (0.02 ~ 0.1 mm/s), splitting into two partially occupied sites results in a distorted FeO₆ octahedral. The weak ferromagnetism observed in the hydrothermally-prepared BiFeO₃ particles comes from distorted FeO₆ octahedral, leading to incomplete counterbalance between the antiferromagnetic sublattices of the Fe ions.

[1] G. A. Smolenskii and I. chupis, Sov. Phys. Usp. 25, 475 (1982). [2] J. Wang, J. B. Neaton, H. Zheng, V. Nagarajan, S. B. Ogale, B. Liu, D. Viehland, V. Vaithyanathan, D. G. Schlom, U. V. Waghmare, N. A. Spaldin, K. M. Rabe, M. Wuttig, and R. Ramesh, Science 299, 1719 (2003).

RA27

Synthesis and electrical characterization of Bi_{1-x}Y_xFeO₃ ceramics

Vikash Singh*, Manoj Kumar and R. K. Dwivedi
Physics & materials science & engg., Jaypee institute of information technology, India

Compositions within range 0.05 ≤ x ≤ 0.20 in the system Bi_{1-x}Y_xFeO₃ (BYFO) have been synthesized by solid state reaction method. Structural and electrical properties of yttrium doped bismuth ferrite ceramics have been investigated. Single-phase formation has been confirmed by x-ray diffraction, which has shown rhombohedral symmetry with R3c space group at room temperature. Temperature dependent dielectric behavior of BYFO ceramics with in composition range 0.05 ≤ x ≤ 0.20 at few frequencies have shown an anomaly near the temperature which corresponds to magnetic phase transition 'T_N' for pure BiFeO₃ material (i.e.370°C). Substitution of yttrium in BFO has shown a shift in T_N. The temperature dependence of ac conductivity indicates that the conduction process may be influence by defects which occurs due to oxygen vacancies.

1. N. A. Hill, Why are there so few magnetic ferroelectrics, J. Phys. Chem. B 104, 669 (2000). 2. H. Singh, K.L. Yadav, Dielectric, magnetic and magnetoelastic properties of La and Nb codoped bismuth ferrite, J. Phys.: Condens. Matter 23, 385901 (2011).

July 12 (Thu)

July 12 (Thu)

RA28

Lattice engineering on transition metal oxide thin film

Chang Uk Jung*

Department of Physics, Hankuk University of Foreign Studies, Korea

Transition metal oxide having a perovskite structure showed a large spectrum of physical properties. YBa2Cu3O7 showed high temperature superconductivity, (La,Ca,Sr)MnO3 showed ferromagnetism with half metallicity, Pb(Zr,Ti)O3 showed Ferroelectricity, and BiFeO3 showed coexistence of antiferromagnetism and ferroelectricity. Recent advance in interface control revealed a 2d electron gas, interface superconductivity, interface magnetism, orbital reordering, interface thermoelectric effect at the interface of transition metal oxide. The effect of lattice distortion has been studied for a long time and recently showed that lattice distortion during thin film growth can create new ground state. Especially AlTiO3, (A=Sr, Y, Eu) was interesting. [In bulk state, YTiO3 and EuTiO3 are magnetic insulator, and SrTiO3 is not ferroelectric.] I will introduce the some current research on the progress on these materials. In this case, only lattice mismatch between substrate and film was used. On the contrary the available substrate is rather narrow. I will also introduce efforts to overcome this problem.

[1] A. Ohtomo & H. Y. Hwang, *Nature* 427, 423 (2004). [2] N. Reyren et al., *Science* 317, 1196 (2007). [3] J. Chakhalian et al., *Science* 318, 1115 (2007). [4] S. C. Chae et al., *Appl. Phys. Lett.* 89, 182512 (2006). [5] J. H. Haeni et al., *om. Nature* 430, 758 (2004). [6] June Hyuk Lee et al., *Nature* 466, 954 (2010). [7] C. U. Jung et al., *Appl. Phys. Lett.*, 84, 2590 (2004). [8] B. W. Lee et al., *J. of Appl. Phys.*, 104, 103909 (2008). [9] B. W. Lee et al., *APL* 96, 102507 (2010).

RB01

Structural and magnetic properties of doped iron oxo-selenides

Sven Landsgesell¹, Karel Prokes¹ and Dimitri Argyriou²

¹ M-II, Helmholtz-Zentrum Berlin, Germany

² European Spallation Source, Sweden

In the Cu oxide superconductors the Cu resides in a square planar geometry[1], while in the Fe pnictide superconductors the Fe ion resides in a tetrahedrally coordinated position[2]. Both compounds may show a separating LaO layer between the superconducting sheets. La₂O₇Fe₂Se₂ shows square planar Fe O sheets and offers a direct super exchange pathway to the next nearest Fe neighbour via the Se, comparable to the iron arsenides[3]. These super exchange pathways are similar to the superconductors despite the difference and provide a similar local environment for the Fe as is known for the Fe-superconductors[4]. We investigated the changes in the physical properties in the iron oxo-selenides by varying the electron density and structural components. We doped the parent compound with F, Cd and rare earths with smaller radii (La₂O₇, FxFe₂Se₂, and La_{2-x}(Cd/RE)_xO₇Fe₂Se₂, respectively). Temperature dependent neutron diffraction of the samples mostly show an antiferromagnetic order along the a-direction with a propagation of (0.5 0 0.5). We find indications for an evolving transition in the physical properties, as decreasing TN for fluorine and rare earth samples. This is comparable to the known doped iron superconductors and in contrast to the electron deficient Cd doped samples that show an increasing TN.

1 D. Yaknin et al., *Phys. Rev. Lett.* 58, 2802 (1987) 2 Y. Kamihara et al., *J. Am. Chem. Soc.* 130, 3296 (2008) 3 E. Manousakis et al., *Solid State Comm.* 150, 62 (2010) 4 D.G. Free and J.S.O. Evans, *Phys. Rev. B* 81, 214433 (2010)

RB02

Phase separation of antiferromagnetism and superconductivity in Rb_xFe_{2-y}Se₂ observed by Rb NMR

Yoshiaki Kobayashi^{1*}, Shunsuke Saiki¹, Shouhei Kototani¹, Masayuki Itoh¹ and Masatoshi Sato²

¹ Department of Physics, Graduate School of Science, Nagoya University, Japan

² Research Center For Neutron Science And Technology, CROSS, Japan

The observation of the superconducting (SC) transition in A_xFe_{2-y}Se₂ (A: alkali metal elements; Tc of ~30K) has been one of surprising things, because the transition was found in the antiferromagnetic (AF) system with a large AF moment of ~3.3 μB/Fe. Moreover, their electrical resistivity just above Tc is too large to conceive the occurrence of the superconductivity. Here, to clarify whether the AF and SC states are microscopically coexistent or just phase-separated, we have carried out NMR measurements on both crystals with and without SC transition. The Rb-NMR spectra below 300 K observed for these crystals are clearly separable into two parts with different widths. The broader spectrum can be explained by the presence of the region with the “blocked” antiferromagnetic spins proposed by the neutron magnetic scattering studies [1]. The narrower spectrum for the crystal with SC transition can be understood from its temperature dependence and spectral shape to stem from the superconducting region without Fe-vacancy ordering [1]. Thus, we can clearly conclude that the superconductivity and the antiferromagnetism in the present system are phase-separated.

[1] W. Bao, et al., *Chin. Phys. Lett.* 28, No. 8 (2011) 086104.

RB03

Superconductivity of EuFe₂As₂ under high pressure

Shugo Ikeda and Hisao Kobayashi

Graduate School of Material Science, University of Hyogo, Japan

EuFe₂As₂ with the tetragonal ThCr₇Si₇-type structure exhibits a spin density wave (SDW) transition at 190 K, with a simultaneous structural change [1]. The SDW transition is suppressed by applied pressure and bulk superconductivity appears around 2.5 GPa [1-3]. Furthermore, magnetic moments of Eu sublattice order magnetically at To = 19 K. The value of To reveals no changes at pressures of up to 3 GPa [1-3]. We have studied the superconductivity and the magnetism of EuFe₂As₂ by measuring dc magnetization and 57Fe nuclear forward scattering (NFS) under high pressure. Magnetization at 2.6 GPa rapidly increases below 24 K and then gradually decreases by the appearance of superconductivity. The size of the drop at low temperatures is consistent with nearly 100 % shielding. Namely, bulk superconductivity appears under the magnetic ordered state of Eu sublattice. The pressure dependence of 57Fe NFS spectra shows the decrease of the hyperfine field Bhf of Fe sublattice with increasing pressure. Furthermore, it is found that the direction of Bhf varies around 2.6 GPa, implying the changes of magnetic structure. In this presentation, we will discuss the relation between the superconductivity and the magnetism of EuFe₂As₂, considering these results.

[1] K. Matsubayashi et al.: *Phys. Rev. B* 84 (2011) 024502. [2] N. Kurita et al.: *arXiv:* 1103.4209v1. [3] T. Terashima et al.: *J. Phys. Soc. Jpn.* 78 (2009) 083701.

RB04

Superconductivity in 4d, 5d pnictides

Tomohiro Takayama^{*,1}, Daigorou Hirai¹, Keisuke Kuwano¹ and Hidenori Takagi²

¹ Department of Advanced Materials, University of Tokyo, Japan

² Department of Physics, University of Tokyo, Japan

After the discovery of the iron arsenide superconductors, a tremendous effort has gone into the search for new high-Tc superconductors. We explored 4d, 5d pnictides, hoping to find superconductors which share important characteristics with Fe-based superconductors. We report two new superconducting systems with such characteristics, but sufficiently different from Fe pnictides. (i) APt₃P (A = Ca, Sr and La) The new compounds APt₃P crystallize in an antiperovskite structure with distorted PPt6 octahedra. All of them display superconductivity below 6.6, 8.4 and 1.5 K for Ca-, Sr- and LaPt₃P, respectively. The highest-Tc compound SrPt₃P exhibits strong-coupling s-wave superconductivity. The presence of multiple pocket Fermi surface was inferred in SrPt₃P, which might enhance the coupling with low-energy phonons. (ii) RuPn (Pn = P, As) Binary RuPn crystallize in an orthorhombic MnP-type structure. RuP and RuAs were found to show a metal to non-magnetic insulator transition at 270 and 200 K, respectively. The structural analysis evidenced another phase transition at higher temperatures, indicative of pseudogap formation. The two transitions can be suppressed by Rh-doping. We discovered superconductivity with a maximum Tc = 3.7 K and 1.8 K at the critical doping level for suppressing the pseudogap-phase in Ru_{1-x}Rh_xP and Ru_{1-x}Rh_xAs, respectively.

D. Hirai et al., *arXiv:*1112.0604

RB05

Elastic softening and electric quadrupole in iron pnictide superconductor Ba(Fe_{1-x}Co_x)₂As₂

Ryosuke Kurihara¹, Koji Araki¹, Keisuke Mitsumoto¹, Mitsuhiro Akatsu¹, Yuichi Nemoto², Terutaka Goto², Yoshiaki Kobayashi³ and Masatoshi Sato⁴

¹ Graduate School of Science and Technology, Niigata University, Japan

² Graduate School of Science and Technology, Niigata University, JST-TRIP, Japan

³ Department of Physics, Nagoya University, JST-TRIP, Japan

⁴ Department of Physics, Nagoya University, CROSS, JST-TRIP, Japan

We have performed ultrasonic measurements on iron based superconductor Ba(Fe_{1-x}Co_x)₂As₂ in order to investigate the mechanism of the superconductivity. The end-material BaFe₂As₂ shows structural and antiferromagnetic simultaneous transitions at ~140K. With increasing Co concentration x, the temperatures of these transition are lowered and separated from each other. The superconductivity appears at x>0.03. In our recent work [1], the softening of the elastic constant C66 as large as 21% was observed for optimized samples Ba(Fe_{0.75}Co_{0.25})₂As₂ with decreasing temperature from 300K down to superconducting transition temperature of TSC=23 K, while other elastic constants do not show softening. Here, we have measured elastic constants of Ba(Fe_{1-x}Co_x)₂As₂ samples with x=0.03 and 0.07, where only the C66 shows huge softening larger than 70% with decreasing temperature down to the structural transition temperature. The large softening of C66 in Ba(Fe_{1-x}Co_x)₂As₂ with several Co concentration x<0.10 has been reported by other groups [2,3]. This huge elastic softening of C66 is caused by the quadrupole fluctuation associated with the degenerate d_{xy}² and dx²-band aslant Γ and X points of the Brillouin zone. Quadrupole effects on the superconductivity in the present system are discussed in relation to the s++ type symmetry of the superconductivity [4,5,6].

[1] T. Goto, et al., *JPSJ* 80 (2011) 073702. [2] R. M. Fernandes et al., *PRL* 105 (2010) 157003. [3] M. Yoshizawa et al., *JPSJ* 81 (2012) 024604. [4] Y. Yanagi et al., *JPSJ* 79 (2010) 123707. [5] H. Kontani et al., *PRB* 84 (2011) 024528. [6] T. Kawamura et al. *JPSJ* 80 (2011) 084720.

RB06

Concentration dependence of magnetic and transport characteristics in EuFe₂As_{2-x}P_x single crystals

Takanari Kashiwagi^{*}, Takuya Ishikawa, Tomoki Goya, Youhei Jono, Akihiko Nozawa, Kasumi Tashima and Kazuo Kadowaki

Univ. of Tsukuba, WPI-MANA, JST-CREST, Japan

EuFe₂As₂ exhibits the spin-density wave of Fe spins at TSDW=190 K and subsequently magnetic order of Eu²⁺ moment at TN=19 K. It is also known that this compound shows the superconductivity by isovalent substitution of As to P and the Tc value increases up to 28 K. We have studied magnetic and transport properties in single crystal of the EuFe₂As_{2-x}P_x system grown by the self-flux method. From the magnetization measurements at 5 K, we observed a saturation of magnetization of Eu²⁺ at HM ~ 1 T and a spin-flop like behavior at Hsf ~ 0.6 T for H||ab-plane. These fields seem to decrease as x is increased, indicating reduction of the exchange interaction and the uniaxial anisotropy. We also performed electron spin resonance measurements at X-band on single crystals of EuFe₂As_{2-x}P_x. The result shows that the resonance field increases with decreasing temperature toward to TN=19 K below which a new line was observed. We will discuss these results including electron spin resonance experiments with emphasis on the phase diagram of magnetism and superconductivity in EuFe₂As_{2-x}P_x.

RB07

Resonance-like response in antiferromagnetically ordered Fe_{1.02}Te_{0.95}Se_{0.05} studied by polarized inelastic neutron scattering

Karel Prokes^{*,1}, Arno Hiess², Wei Bao³, Sven Landsgesell¹, Elisa Wheeler⁴ and Dimitri Argyriou²

¹ M-II, Helmholtz Zentrum Berlin, Germany

² European Spallation Source ESS AB, 22100 Lund, Sweden

³ Renmin University of China, 100872 Beijing, China

⁴ M-II, Institut Laue-Langevin, 38042 Grenoble Cedex, France

Unconventional superconductivity in iron pnictides and chalcogenides [1] shows intriguing similarities with both copper-oxide- and rare-earth-based superconductors. Common is a proximity to a magnetic order and an existence of magnetic fluctuations [2]. Magnetic fluctuations change below the superconducting transition and are readily detectable by neutron inelastic scattering. The character of these has been shown to be related to the pairing mechanism and gap symmetry [3]. In all superconducting pnictides and chalcogenides one finds well-defined magnetic excitations centered close to the Q = (0.5, 0.5, 0) reciprocal position that strongly disperse with increasing energy and peaking in the 6.5-9.8 meV range [2]. Polarization neutron experiment allows for a determination of the in-plane and out-of-plane inelastic responses that are proportional to the relevant imaginary parts of the dynamical susceptibility. While the fluctuations in FeTe_{1-x}Se_x, x = 0.40 are nearly isotropic with a slightly enhanced component along the c axis [4,5], in BaFe_{2-x}Ni_xAs₂ they are have an in-plane 2D character [6]. In this contribution we report on a polarized neutron study showing that similar fluctuations also exist also in antiferromagnetically ordered Fe_{1.02}Te_{0.95}Se_{0.05} above the magnetic phase transition.

[1] F.-C. Hsu, et al., *Proc. Nat. Acad. Sci. USA* 105, 14262 (2008). [2] D. C. Johnston, *Advances in Physics* 59, 803 (2010). [3] M. M. Korshunov and I. Eremin, *Phys. Rev. B* 78, 140509 (R) (2008). [4] P. Babkevich, et al., *Phys. Rev. B* 83, 180506 (R) (2011). [5] K. Prokes et al., to be published [6] O. J. Lipscombe, et al., *Phys. Rev. B* 82, 064515(2010).

RB08

Influence of filament diameter on superconducting properties of MgB₂ multi-core wires

Michael Reissner^{1*}, Lukas Bulla¹, I Husek², T Melisek² and P Kovac²

¹ Institute of Solid State Physics, Vienna University of Technology, Austria

² Institute of Electrical Engineering, Slovakia Academy of Sciences, Slovakia

Multi-core MgB₂ wires with 19 filaments of different diameter were produced [1]. The filaments are covered by a Ti shell and embedded in a Cu matrix. From outside the wires are stabilized by stainless steel tubes. Critical current densities were determined from hysteresis loops using Bean's model [2]. Magnetic relaxation measurements were performed at 1, 3, and 5 T both in increasing and decreasing field for up to 30 min. From these measurements mean effective activation energies were determined within the flux creep theory of Anderson [3]. All samples were prepared in identical way. They only differ in diameter of the filaments, which ranges between 30 and 15 μm. Influence of the filament diameter on the superconducting properties, like critical current density, irreversibility line and activation energies are discussed.

[1] P Kovac, I Husek, T Melisek, I Kopera, M Reissner *Supercond. Sci. Technol* 23 (2010) 065010 [2] C P Bean *Phys. Rev. Lett.* 9 (1962) 250 [3] P W Anderson *Phys. Rev. Lett.* 9 (1962) 309

RB09

Kinetic energy density of cooper pairs in Sr doped YBa₂Cu₃O_{7-δ} single crystals

Ana Paula Aguiar De Mendonca^{1*}, Rován Fernandes Lopes¹, Valdemar Das Neves Vieira¹, Fabio Teixeira Dias¹, Douglas Langie Da Silva¹, Paulo Pureur², Jacob Schaf³, Mauro Melchhades Doria⁴ and Frederik Wolff-fabris⁵

¹ Universidade Federal de Pelotas, Brazil

² Universidade Federal do Rio Grande do Sul, Brazil

³ Universidade Federal do Rio Grande so Sul, Brazil

⁴ Universidade Federal do Rio de Janeiro, Brazil

⁵ HZ Dresden-Rossendorf, Germany

The kinetic energy, K(T) is a relevant tool to sort the distinct proposal for the normal state and their consequent pairing mechanisms in HTSC.[1,2] Motivated by this potential we report on reversible DC magnetizations as a function of temperature of a series of YBa_{2-x}Sr_xCu₃O_{7-δ} (x = 0, 0.02, 0.10, 0.25, 0.37 and 0.50) single crystals with the purpose to study the role of ion size chemical introduced disorder on the average kinetic energy density (AKED) of Cooper pairs in the YBa_{2-x}Cu₃O_{7-δ} superconducting state.[3] The Sr ion size chemical disorder is introduced in YBa_{2-x}Cu₃O_{7-δ} structure by lattice distortion. The valuation of the AKED from reversible dc magnetization data is supported by viral theorem of superconductivity. [1,2,4] The AKED preliminary results of the YBa_{2-x}Sr_xCu₃O_{7-δ} single crystal show that the series of the isoifield K(T) curves, obtained to the H = 10 kOe, scales in a common behavior that smoothly develops as the temperature is increasing toward to the Tc, disappearing inside a common background for T > Tc. This interested AKED behavior strongly suggests an existence of a unique superconducting condensate state. At this time the dc magnetization measurements in additional samples are in progress.

1. S. Salem-Sugai, Jr., M. M. Doria, A. D. Alvarado, V. N. Vieira, P. F. Farinas and J. P. Sumecker, *Phys. Rev. B* 76, 132502 (2007). 2. M. M. Doria, S. Salem-Sugai, I. G. de Oliveira, L. Ghivelder and E. H. Brandt, *Phys. Rev. B* 65, 144509 (2002). 3. V. N. Vieira and J. Schaf, *Phys. Rev. B* 65, 144531 (2002). 4. M. M. Doria, J. E. Gubernatis and D. Rainer *Phys. Rev. B* 39, 9573 (1989).

RB10

Interplay between superconductivity and antiferromagnetism in BaFe_{2-x}Ni_xAs₂ single crystals studied by 57Fe Mossbauer spectroscopy

Julian Andres Munevar Cagigas¹, Hans Micklitz², Chenglin Zhang³, Hui Quian Luo⁴, Pengcheng Dai⁵ and Elisa Baggio-saitovitch^{1*}

¹ Brazilian Center for Research in Physics, Brazil

² Centro Brasileiro de Pesquisas Fisicas, Brazil

³ Department of Physics, University of Tennessee, USA

⁴ Beijing National Laboratory for Condensed Matter Physics, China

⁵ Department of Physics and Astronomy, University of Tennessee, USA

We have performed magnetic susceptibility and 57Fe Mossbauer spectroscopy measurements on single crystal mosaics of BaFe_{2-x}Ni_xAs₂ (x=0.065, 0.075, 0.085). Our findings show antiferromagnetic order below TN obtained from magnetic hyperfine field phase diagram, with superconductivity below TC obtained by susceptibility measurements. Careful analysis of our Mossbauer data show that a decrease in the magnetic hyperfine field is observed below TC and the effect is proportional to the difference between TN and TC, being the largest when both temperatures become close. We argue this is caused by coexistence of superconductivity and magnetism, since both phenomena come from the same Fe 3d electrons, and two possible scenarios are presented. Magnetic volume fraction does not show any variation at or below TC, but a strong dependence with doping level, most likely due to short range magnetic order that cannot be sensed by our 57Fe local probe, probably caused by local inhomogeneities. A phase diagram is shown to illustrate how the variation of the magnetic volume fraction and the crossover between magnetism and superconductivity are related.

M. Wang, H. Luo, J. Zhao, C. Zhang, M. Wang, K. Marty, S. Chi, J. W. Lynn, A. Schneidervind, S. Li and P. Dai, *Physical Review B* 81, (2010) 174524, M. Alzamora, J. Munevar, E. Baggio-Saitovitch, S. L. Bud'ko, Ni Ni, P. C. Canfield and D. R. Sanchez, *Journal of Physics: Condensed Matter* 23, (2011) 145701. *arXiv:*1111.5853

RB11

Magnetism in superconducting Ba_{0.78}K_{0.22}Fe₂As₂ and EuFe₂As_{1.4}P_{0.6} single crystals studied by Mossbauer spectroscopy

Elisa Baggio-saitovitch¹, Julian Munevar¹, Hans Micklitz¹, Genfu Chen², Chenglin Zhang³, Huiqian Luo⁴ and Pengcheng Dai⁵

¹ Brazilian Center for Research in Physics, Brazil

² Renmin University of China, China

³ Department of Physics and Astronomy, University of Tennessee, USA

⁴ Beijing National Laboratory for Condensed Matter Physics, China

⁵ Department of Physics and Astronomy, University of Tennessee Neutron Scattering Division, ORNL, USA

We studied magnetism in superconducting Fe-pnictide single crystals using 151Eu and 57Fe Mossbauer Spectroscopy. Neutron studies on Ba_xK_{1-x}Fe₂As₂ single crystals revealed a decrease in Bragg peak intensity due to iron moment or magnetic volume fraction reduction. 57Fe Mossbauer measurements on Ba_{0.78}K_{0.22}Fe₂As₂ single crystal mosaics were performed down to 1.5 K, revealing a decrease in the magnetic hyperfine field below Tc, without change in magnetic volume fraction. Our data confirm a reduction of Fe magnetic moment below Tc explaining also the neutron results. Such a decrease is caused by a spectral weight transfer when entering the superconducting state. For EuFe₂As_{1.4}P_{0.6} compound, magnetism originates from Eu²⁺ moments. Mossbauer spectra reveal magnetic hyperfine fields below TM = 18 K of Eu²⁺ moments. Data analysis shows coexistence of ferromagnetism, from Eu²⁺ moments ordered along crystallographic c-axis, and superconductivity below TSC ~ 15 K. We find indications for a change of small Fe magnetic moment dynamics (~ 0.07 μB) at superconductivity onset: below TSC the Fe magnetic moments seem to be “frozen” within the ab-plane. In both compounds we show a change in the Fe magnetic moment state when entering the SC state, and discussion about coexistence of magnetism and superconductivity will be provided.

[1] Z. Ren et al., *Chin. Phys. Lett.* 25, 2215 (2008) [2] M. Lumsden et al., *J. Phys: Cond. Mat.* 22 (2010) 203203. [3] H.H. Luetkens et al., *Nat. Mater.* 8 (2009) 305.

RB12

Doping evolution of the in-plane London penetration depth in Fe_{1+y}(Te_{1-x}Se_x) single-crystals

Andrei Diaconu¹, Jin Hu², Tijiang Liu², Bin Qian², Zhiqiang Mao² and Leonard Spinu¹
¹Advanced Materials Research Institute and Physics Department, University of New Orleans, USA
²Department of Physics, Tulane University, USA

Our work focuses on the doping evolution of the superconducting properties as derived from penetration depth measurements as a function of temperature in single crystals of Fe_{1+y}(Te_{1-x}Se_x) with y<0.02 and Se concentration spanning from 25% to 45%. The London penetration depth is one of the most important characteristic parameter in type II superconductors, as it can give information about the pairing mechanism, with its zero temperature value being directly related to the density of superconductive electrons in the material. Precise measurements of the in-plane penetration depth λ_{ab} as a function of temperature using a tunnel diode oscillator technique were performed in a dilution refrigerator down to a temperature of 30mK. By using a set of two mutually coupled planar inductors the probing ac field is uniform across the sample along the c axis with the variation in susceptibility solely due to supercurrents flowing in the ab crystallographic plane. A complete study of the temperature and Se concentration dependence of the physical properties derived from these measurements is presented.

RB13

Potassium doping effect in double-chain BaFe₂Se₃

Jinke Bao, Yunlei Sun, Wenhe Jiao, Yongkang Luo, Zhu'an Xu and Guanghan Cao*
 Department of Physics, Zhejiang University, China

Compared to iron-based superconductors with two-dimensional FeAs(Se) layers, BaFe₂Se₃ is a one-dimensional material consisting of Fe₂Se₂ double chains with Ba²⁺ cations intercalated. It exhibits antiferromagnetic order with ferromagnetic Fe₁ block of 2.8μB / Fe²⁺ below 255 K.[1][2][3] Considering the close relationship between antiferromagnetism and superconductivity, we performed a chemical doping with potassium in this compound. Ba_{1-x}K_xFe₂Se₃ single crystals with different K content were successfully grown. Resistivity measurements showed that all the crystals were semiconducting with no superconducting transition above 3K. The magnetization of Ba_{1-x}K_xFe₂Se₃ is anisotropic, and the sample of x=0.4 exhibits spin glass behavior. *ghcao@zju.edu.cn

[1] A. Krzton-Maziopa, E. Pomjakushina, V. Pomjakushin, D. Sheptyakov, D. Chernyshov, V. Svityk, and K. Conder, *J. Phys. Condens Matter* 23, 402201 (2011). [2] J. M. Caron, J. R. Neilson, D. C. Miller, A. Llobet, and T. M. McQueen, *Phys. Rev. B* 84, 180409(R) (2011). [3] Hechang Lei, Hyejin Ryu, Anatoly I. Frenkel, and C. Petrovic, *Phys. Rev. B* 84, 214511 (2011).

RB14

Sr₂VO₃FeAs: Hybrid of a magnetic SrVO₃ and a FeAs superconducting layers

Man Jin Eom¹, Jae - Hyun Park¹, Sewoong Na¹, Younjung Jo², Hu - Jong Lee¹ and Jun Sung Kim^{1*}

¹Department of Physics, POSTECH, Korea
²School of Physics and Energy Sciences, KNU, Korea

We investigate the upper critical fields up to 14T of Sr₂VO₃FeAs single crystals. For Sr₂VO₃FeAs, where the perovskite SrVO₃ layers are inserted between SrFe₂As₂ layers, we observed a strong anisotropy of the upper critical field, compared with Hc2(T) of other pnictides. Strong anisotropy in Hc2 of Sr₂VO₃FeAs suggests that SrVO₃ layer is insulating. Furthermore, we found the anomalous magnetoresistance in the normal states up to T~150K indicating possible magnetic ordering in the SrVO₃ layer. Sr₂VO₃FeAs have a structural peculiarity that means each magnetic ordered layers and charge reservoir layers. Thus, unlikely usual layered pnictide compounds, this compound provides the magnetic interaction.

RB15

Static and dynamic properties of nearly optimally doped superconductor SmFeAsO_{0.86}F_{0.14}

Amitabha Ghoshray^{1*}, Mayukh Majumder¹, Kajal Ghoshray¹, Asok Poddar¹, Chandan Mazumdar¹ and David Berardan²

¹ECMP Division, Saha Institute of Nuclear Physics, Kolkata, India
²Institut de Chimie Moleculaire et des Materiaux d'Orsay, Institut de Chimie Moleculaire et des Materiaux d'Orsay, Univ. Paris-Sud 11, 91405 Orsay, France

We have reported resistivity, heat capacity, magnetization and 19F and 75As NMR in polycrystalline sample of nearly optimally doped superconductor SmFeAsO_{1-x}F_x (x = 14%). The resistivity shows linear dependence above 200 K and 50 - 160 K. The linear dependence reveals non Fermi liquid behavior. The heat capacity data for SmFeAsO_{0.86}F_{0.14} exhibits a small jump at T_C~48K, indicating the bulk nature of superconductivity. The field cooled magnetisation data deviates from Curie Weiss law below 160 K. A small peak around 163 K was observed in 19F spin-spin and spin-lattice relaxation rate showing evidence of structural phase transition driven by anti-ferromagnetic spin fluctuation. 75As NMR signal is detectable only above 180 K All measurements point towards a possible existence of nematic ordering where structural phase transition have been driven by anti-ferromagnetic spin-fluctuations at 163 K. Their is a considerable FeAs and SmO layer interaction present in the system. The results also revealed the coexistence of local and itinerant electronic states below 90 K where two fluid model of heavy fermion holds. Coexistence of static anti-ferromagnetic ordering due to Sm 4f electrons and superconductivity has also been observed.

RB16

Effect of d-orbital characters of the Fe magnetic moment on the electronic and magnetic properties of BaFe₂As₂

Hyungju Oh and Hyoung Joon Choi*
 Department of Physics and IPAP, Yonsei University, Korea

There have been many studies detailing the orbital character of band structures in the iron-based superconductors. However, the orbital characters of the Fe magnetic moment still remain unrevealed up to now. By performing first-principles calculations of the electronic and magnetic properties with constraint on the real space shape of Fe magnetic moments, we study the d-orbital characters of the Fe magnetic moment in BaFe₂As₂. We find that, depending on the d-orbital characters of the Fe magnetic moment, the electronic properties of BaFe₂As₂ such as band gap, band dispersion, and dxz/dyz occupation change distinctively. Furthermore, we compare obtained band structures with published angle-resolved photoemission spectroscopy (ARPES) result, and propose that the Fe magnetic moment in BaFe₂As₂ has in-plane dxy character. This work was supported by the NRF of Korea (Grant Nos. 2011-0018306). Computational resources have been provided by KISTI Supercomputing Center (Project No. KSC-2011-C3-05).

RB17

Ca(Fe_{1-x}Co_x)₂As₂ under pressure: studies using single crystal neutron diffraction

Karel Prokeš¹, B. Ouladdiaf², L. Harnagea³, S. Wurmehf³, B. Buechner³ and D. Argyriou⁴

¹M-11, Helmholtz Zentrum Berlin, Germany
²Institut Laue-Langevin, 38042 Grenoble Cedex, France
³Leibniz-Institute for Solid State and Materials Research, (IFW)-Dresden, D-01171 Dresden, Germany
⁴European Spallation Source ESS AB - Box 176, 22100 Lund, Sweden

CaFe₂As₂ and related compounds exhibit extremely strong coupling of the magnetic and structural phase transitions and sensitivity to an applied pressure. Undoped system undergoes a structural transformation from a high temperature tetragonal (T) phase to a structure with orthorhombic (O) symmetry that is associated with the appearance of an antiferromagnetic order [1]. Upon application of a rather modest pressure, both transitions are suppressed and superconductivity appears below 12 K [2]. For pressures larger than 0.3 GPa another, so-called collapsed tetragonal (cT) phase with greatly reduced c parameter appears [3]. Three different Ca(Fe_{1-x}Co_x)₂As₂ single crystals with concentration x = 0.032, 0.051 and 0.063 were investigated by means of neutron diffraction under uniaxial and hydrostatic pressure. Region of existence of the high-temperature tetragonal, low-temperature orthorhombic and pressure-induced collapsed tetragonal phases have been determined. Structural details of the tetragonal phases at various conditions have been determined and the corresponding p-T phase diagrams have been constructed. The critical pressure of the T (or O) to cT transition decreases with increasing Co doping level. The behavior is highly hysteretic and structural studies show no variation of the As positional parameter with pressure.

[1] D. C. Johnston, *Advances in Physics* 59, 803 (2010). [2] M. S. Torikachvili, et al., *Phys. Rev. Lett.* 101, 057006 (2008). [3] A. Kreyssig, et al., *Phys. Rev. B* 78, 184517 (2008).

RB18

Monte Carlo study of the magneto-elastic effects in Fe pnictides

Cesar Jose Calderon Filho^{1*}, Alex Antonelli¹, David Vahnin² and Gaston Eduardo Barberis¹

¹IFGW, State University of Campinas - UNICAMP, Brazil
²Ames National Laboratory and Department of Physics, Iowa State University, USA

A (J1, J2) model of the infinite square lattice of classical spins coupled by Heisenberg exchange interactions that includes a spin-lattice interaction of the form A (Exx - Eyy) (Sx2- Sy2) is used in Monte-Carlo simulations to determine a phase diagram in the J1, J2, and A parameter-space. To facilitate phase transitions in the 2D system, we also include a weak out-of-plane coupling to spins in adjacent planes (Jz). This phase diagram is relevant to the parent materials of the newly discovered iron-pnictides superconductors. Using first principles band calculations, both for the low and high temperatures, we obtain realistic parameters to the model that allow the prediction of pressure induced magnetic transitions.

RB19

Geometrical Vortex Transition in the iron pnictide SmFeAs(O,F)

Philip J.w. Moll^{1*}, Luis Balicas², Janusz Karpinski³, Nikolai Zhigadlo⁴ and Batlogg Bertram⁵

¹Solid State Physics Laboratory, ETH Zurich, Switzerland
²National High Magnetic Field Laboratory, Florida State University, USA
³Solid State Physics, ETH Zurich, Switzerland
⁴Solid State Laboratory, ETH Zurich, Switzerland
⁵Solid State Theory, ETH Zurich, Switzerland

We have observed a distinct vortex matter transition in SmFeAs(O,F) (Tc~50K) upon cooling below T*~41K(=0.81Tc) into a highly mobile state for fields well aligned with the FeAs layers. Below T*, the vortex core is confined between two adjacent FeAs planes by periodic modulations of the superconducting order parameter within the unit cell. Vortex motion parallel to the planes is even more pronounced at lowest temperatures, well below Tc and Hc2, as the vortex cores avoid the highly effective pinning sites located in the FeAs layers. For fields slightly out-of-plane (<0.3°) the vortices are again completely immobile as they cross the planes and are hence strongly pinned by defects within the FeAs layers resulting in large critical current densities at high fields and low temperatures (>10⁶ A/cm² @5K, 14T[1]). These results indicate strong pinning localized in the FeAs layer to be the dominant factor for the highly effective pinning and thus show the pathway to improve the technological prospect of the pnictides.

[1] P.J.W. Moll et al., 'High magnetic field scales and critical currents in SmFeAs(O,F) crystals. *Nature Materials* 9, 628 (2010)

RB20

SmFeAsO_{1-x}F_x: Raman scattering and x-ray diffraction study under low temperature and high pressure conditions

Sofia Michaela Souliou^{*}, Mathieu Le Tacon¹, Andrew C. Walters¹, Chengtian Lin¹, Karl Syassen¹, Bernhard Keimer¹, Gaston Garbarino², Michael Hanfland², Wilson Crichton², Janusz Karpinski³ and Nicolai Zhigadlo³

¹Max-Planck-Institut für Festkörperforschung, Heisenbergstr. 1, D-70569 Stuttgart, Germany, Germany
²European Synchrotron Radiation Facility, BP 220, F-38043 Grenoble Cedex, France, France
³Laboratory for Solid State Physics, ETH Zurich, CH-8093 Zurich, Switzerland, Switzerland

We present a comparative low-temperature Raman study on single crystals of the parent non-superconducting SmFeAsO and the fluorine-doped superconducting SmFeAsO_{0.86}F_{0.14} [1]. As in the compounds from the 122 family [2], clear renormalization of the c-axis polarized A1g(Sm) and the B1g(Fe) Raman-active modes are observed through the magneto-structural transition in the parent compound. Splitting of the in-plane Eg modes is also observed (like the reported in [3,4]). In the fluorine-doped compound, x-ray diffraction measurements reveal the retention of the structural transition (similar to the one reported in [5]). Despite the absence of a coupled magnetic transition, a renormalization of the c-axis polarized modes similar to the one seen in the parent compound is observed, followed at lower temperature by an anomalous increase of the linewidth of these phonons below the superconducting transition temperature. The effects of the structural transition on the phonon modes are further investigating by applying high pressure on the parent compound, allowing a direct comparison of the effect of pressure and doping on the lattice dynamics of the system.

[1] Z.-A. Ren et al., *Chinese Physics Letters* 25 (6), 2215 (2008) [2] M. Rahnbeck et al., *Phys. Rev. B* 80, 064509 (2009) [3] T. Yildirim, *Phys. Rev. Lett.* 101, 057010 (2008) [4] L. Chauviere et al., *Phys. Rev. B* 80, 094504 (2009) [5] A. Martinelli et al., *Phys. Rev. Lett.* 106, 277001 (2011)

RB21

Mass renormalization in isostructural Ru- and Fe-pnictides

Philip J.w. Moll^{*}, Jakob Kanter¹, Ross Mc donald², Fedor Balakirev², Peter Blaha³, Karlheinz Schwarz², Zbigniew Bukowski¹, Nikolai D. Zhigadlo¹, Sergiy Katrych¹, Kurt Mattenberger¹, Janusz Karpinski¹ and Bertram Batlogg¹

¹Solid State Physics Laboratory, ETH Zurich, Switzerland
²National High Magnetic Field Laboratory, Los Alamos National Laboratory, USA
³Institute of Materials Chemistry, Vienna University of Technology, Austria

We have studied the angular-dependent de Haas-van Alphen oscillations of LaRu₂P₂ using magnetic torque in pulsed magnetic fields up to 60 T. The observed oscillation frequencies are in excellent agreement with the geometry of the calculated Fermi surface. The temperature dependence of the oscillation amplitudes reveals effective masses m*(α) = 0.71 and m*(β) = 0.99 me, which are enhanced over the calculated band mass by λcyc of 0.8. We find a similar enhancement of λγ ~ 1 in comparing the measured electronic specific heat (γ = 11.5mJ/mol K⁻¹) with the total density of states from band-structure calculations. Remarkably, very similar mass enhancements have been reported in other pnictides, LaFe₂P₂, LaFePO (Tc ~ 4 K), and LaRuPO, independent of whether they are superconducting or not. This is contrary to the common perceptions that the normal-state quasiparticle renormalizations reflect the strength of the superconducting pairing mechanism. To separate mass enhancement due to electron correlations from e.g. electron-phonon interactions, high energy bandwidth measurements such as ARPES would be highly desirable, thus leading to new questions about competing pairing in isostructural and isoelectronic Ru- and Fe-pnictide superconductors.

PHYSICAL REVIEW B 84, 224507 (2011)

RB22

The role of spin fluctuation for the high Tc superconductivity in LiFeAs, LiFeP, NaFeAs

Geunsik Lee, Hyo Seok Ji and Ji Hoon Shim*
 Chemistry, POSTECH, Korea

Based on fully self-consistent density functional theory and dynamical mean field theory (DMFT) methods, we have studied the electronic spectrum of three isostructural 111 compounds, LiFeAs, LiFeP, NaFeAs. It has been known that while both LiFeAs and LiFeP are intrinsic superconductors with the nodeless and nodal gap symmetries respectively, NaFeAs exhibits spin density wave phase where superconducting transition occurs with chemical doping. With our simulated electronic spectrums, we examine the spin fluctuation mechanism for the high Tc superconductivity.

RB23

DFT+DMFT study on the electronic structure and anisotropy of Sr₂VO₃FeAs superconductor.

Hyo Seok Ji and Ji Hoon Shim*
 Chemistry, POSTECH, Korea

Electron correlation effect on Fe 3d orbital has very important role in describing electronic structure and anisotropy of iron-based superconductors.[1] By using combination of the density functional theory (DFT) and dynamical mean field theory (DMFT), the electron correlation effect can be described well. In this study, we have investigated the electronic structure and anisotropy of Sr₂VO₃FeAs superconductor. Simple DFT result shows mixed band structures of Fe 3d and V 3d orbital, but the experimental result shows only Fe 3d band near the Fermi level.[2] The DFT+U method explains insulating V layer structure correctly[2, 3] but it cannot describe whole electronic structure such as renormalized Fe 3d bands. So we apply the electron correlation effect on the V 3d orbital as well as the Fe 3d orbital using DFT+DMFT. With antiferromagnetic(AFM) ordering, V 3d bands split into -1 eV and 1 eV region, which is consistent with experimental ARPES result.[2] Also we calculate electrical anisotropy γ=σ_{xx}/σ_{zz} which is important for determining dimensionality effect in iron-based superconductors. Calculated anisotropy value is much smaller than simple DFT result and the result is well consistent with recent experimental result. This trend is also consistent with the trend of previous work[1].

[1] H. S. Ji, G. Lee, and J. H. Shim, *Phys. Rev. B* 84, 054542 (2011). [2] T. Qian et al., *Phys. Rev. B* 83, 140513(R) (2011). [3] H. Nakamura and M. Machida, *Phys. Rev. B* 82, 094503 (2010).

July 12 (Thu)

July 12 (Thu)

RB24

Behaviour of Magnetic and structural transitions upon Sr doping in CaFe₂As₂ and EuFe₂As₂

Neeraj Kumar*, Ruta Kulkarni, Sudesh Kumar Dhar and Arumugam Thamizhavel
Condensed Matter Physics and Materials Science, Tata Institute of Fundamental Research, Mumbai, India

We have grown single crystals of Ca_{1-x}Sr_xFe₂As₂ and Eu_{1-x}Sr_xFe₂As₂. Our aim was to study the progression of SDW transition and the effect of dilution on Eu magnetism in EuFe₂As_{1-x}Sr_xFe₂As₂. CaFe₂As₂ and SrFe₂As₂ undergo magneto-structural transition at 170 K and 205 K respectively[1,2]. With introduction of Sr in the CaFe₂As₂, magneto-structural transition temperature increases, and it reaches 200 K in nominal Sr_{0.3}Ca_{0.7}Fe₂As₂ indicating that Sr dominates Ca in determining the SDW and structural transition. Doping Fe with Co induces superconductivity in Ca_{0.5}Sr_{0.5}Fe₂As₂ below 12 K, which surprisingly shows a signature of SDW transition at a high temperature of 170 K. In Eu_{1-x}Sr_xFe₂As₂ series the AFM ordering temperature of Eu sublattice decreases with increasing x while the structural/SDW transition temperature gradually varies from 190 K to 200 K. Field induced ferromagnetic behaviour of the parent EuFe₂As₂ is also observed in the Sr doped compounds, the magnetic field needed to induce ferromagnetism decreases with increasing Sr.

[1] Neeraj et. al. Phys. Rev. B, 79, 012504 (2009). [2] Krellner et al. Phys. Rev. B, 78, 100504(R) (2008)

RB25

Specific heat of the vortex lattice in iron-pnictide superconductors

Miguel Araujo¹ and Pedro Sacramento²
¹ CFIF, Instituto Superior Tecnico, TU Lisbon and Department of Physics, University of Evora, Portugal
² CFIF, Instituto Superior Tecnico, TU Lisbon, Portugal

We study a vortex lattice in a three-orbital model for iron-pnictide superconductors. A gauge transformation, first introduced by Vafeek-Tesanovic [1], is employed in order to obtain an effective spatially periodic Hamiltonian that produces a spectrum of Bloch states and automatically includes quantum effects, such as the Berry phase and Doppler shift of quasi-particles, without resorting to semi-classical approximations. We calculate the energy spectrum and specific heat as function of applied magnetic field. The effect of disorder due to impurities and positional disorder of the vortices is also addressed.

[1] O. Vafeek, A. Melikyan, M. Franz and Z. Tesanovic, Physical Review B 63, 134509 (2001)

RB26

Hexagonal superconducting pnictide SrPtAs: an ab initio study

Sonny S. H. Rhim¹, S. J. Youn², Daniel Agterberg³, Michael Weinert³ and Arthur J Freeman¹
¹ Physics and Astronomy, Northwestern University, USA
² Physics Education and Research Institute of Natural Science, Gyeong Sang National University, Korea
³ Physics, U. Wisconsin-Milwaukee, USA

We present an ab initio study on SrPtAs, a recently discovered hexagonal pnictide superconductor. SrPtAs is distinct from other pnictides: (i) it has a hexagonal structure and (ii) a large spin-orbit interaction, whose consequence is not trivial. Based on electronic structure calculations, a tight-binding Hamiltonian is constructed to analyze the character of the spin-orbit interaction associated with the crystal structure. Further, the pairing mechanism by phonon and spin fluctuation are analyzed from phonon dispersion and susceptibility with matrix element fully taken into account. Finally, based on the band structure, we propose that electron doping could increase TC.

RB27

Josephson effect in BaKFeAs inter-grain boundary junctions

Sung-hak Hong¹, Sung Hoon Lee¹, Soon-gul Lee^{1*}, Soon-gil Jung², Nam Hoon Lee² and Won Nam Kang²
¹ Department of Display and Semiconductor Physics, Korea University, Korea
² BK21 Physics Division and Department of Physics, Sungkyunkwan University, Korea

We have studied superconducting transition properties of Ba_{0.6}K_{0.4}Fe₂As₂ intergrain junctions. The junctions were fabricated by focused ion beam (FIB). Prior to FIB patterning, films were prepatterned into microbridges by a standard photolithography and argon ion milling technique. The lowest-possible beam current of 1.5 pA was used for the FIB pattern to minimize the etching damage to the bridge. The nominal dimensions were 200 nm in width and 100 nm in length. Resistive transition, current-voltage (I-V) characteristics, the temperature-dependent critical current (Ic) and the normal state resistance (Rn) were measured. Measured transition properties indicated that the junctions were dominated mainly by Josephson coupling, showing resistively-shunted-junction (RSJ) behaviors. At higher currents, multiple transitions were observed, which might be due to dynamics of Josephson vortices driven by transport currents. Details of the measurement results will be discussed.

RB28

Coexistence of different electronic phases in the K_{0.8}Fe_{1.6}Se₂ superconductor: a bulk-sensitive hard x-rays spectroscopy study

Laura Simonelli^{1*}, Naurang L. Saini², Marco Moretti Sala¹, Y. Mizuguchi³, Y. Takano³, H. Takeya³, T. Mizokawa⁴ and Giulio Monaco¹
¹ ESRF, France
² Dipartimento di Fisica, Universit' a di Roma "La Sapienza" - P. le Aldo Moro 2, 00185 Roma, Italy
³ National Institute for Materials Science, 1-2-1 Sengen, Tsukuba 305-0047, Japan and JST-TRIP, 1-2-1, Japan
⁴ Department of Physics, and Department of Complexity Science and Engineering, University of Tokyo, Japan

In A_{1-x}Fe_{2-x}Se₂ (11)-type chalcogenides superconductivity appears to occur only in Fe-deficient samples, where the alkali metals are intercalated between the FeSe layers [1-3]. It has been demonstrated how the ordering of the Fe vacancies can be correlated to superconductivity and how it can be controlled by temperature treatments [2-6]. In particular the superconductivity can be tuned on a single sample from an insulating state by post-annealing and fast quenching, and it is tempting to conclude that the superconductivity is achieved when the Fe-vacancies are in a disordered state [6]. Here we report on the electronic and magnetic structure of K_{0.8}Fe_{1.6}Se₂ superconductor by x-ray emission and high resolution absorption spectroscopy. We report a study where the electronic and magnetic properties are investigated at the same time as a function of temperature in several consistent thermal cycles. We discuss the effects of ordered and disordered Fe vacancies on the electronic and magnetic structure, the existence of memory effects on thermal cycles, and the relation between electronic and magnetic properties and superconductivity. The results obtained are finally compared with the electronic and magnetic properties of (11)-type chalcogenides [7].

[1] Jing Guo, et al., arXiv: 1101.0092; Y. Kawasaki, et al., arXiv: 1101.0896; J.J Ying et al., New J. Phys. 13, 033008 (2011). [2] D. M. Wang, et al., arXiv: 1101.0789. [3] A. M. Zhang, et al., arXiv: 1101.2168v1. [4] Ricci et al. Supercond. Sci. Technol. 24, 082002 (2011). [5] Bao Wei et al., Chin. Phys. Lett. 28, 086104 (2011). [6] F. Han et al., arXiv:11031347. [7] L.Simonelli et al., submitted to PRB.

RB29

Step towards a ferromagnetic Josephson junction in YBCO/LCMO heterostructures

Soltan Soltan^{1*}, Magdy El-hagary², Hanns-ulrich Habermeier³ and Nasser Alzayed⁴
¹ Physics Department, Faculty of Science, Helwan University, 11792 Helwan, Cairo, Egypt
² Physics Department, College of Science, Qassim University, P.O. Box 6644 Buraidah 51452, Saudi Arabia
³ Max-Planck-Institute FKF, Heisenbergstrasse 1, 70569-Stuttgart, Germany
⁴ Physics Department, King Saud University, Saudi Arabia

High quality high-Tc superconductor/half metal ferromagnet/high-Tc superconductor YBCO/LCMO/YBCO trilayers (SFS) with different orientation of CuO₂ planes in superconducting electrodes and different thicknesses of LCMO layers have been successfully fabricated by employing pulsed laser deposition techniques. It has been found that a LCMO barrier with thickness of 2-3 unit cells is ferromagnetic with a Curie temperature close to the bulk value. The strong difference in magnetization loops for different SFS-structures measured at T = 5K and the magnetic field parallel to the F-layers is caused by the presence of a superconducting current across the ferromagnet in the (110) oriented SFS-structure with a thickness of the ferromagnetic layer =1nm. This has been confirmed by measuring current-voltage characteristics in patterned structures. This sample structure fulfils all prerequisites for the realization of high-Tc SFS-Josephson junctions.

RC01

DMFT study of the correlation effects on a topological insulator

Tsuneya Yoshida*, Satoshi Fujimoto and Norio Kawakami
Department of Physics, Kyoto University, Japan

Recently, topological insulators are theoretically proposed in correlated electron systems (e.g. Iridium oxides, Heusler compounds, and filled skutterudites)[1]. The correlation effects on the topological insulators are expected to produce exotic states [2] and are extensively studied. The strong Coulomb interaction could drive the non-trivial band insulator into a Mott insulator. In this paper, we study an extended Bernevig-Hughes-Zhang model[3] including the on-site Coulomb interaction with DMFT. We calculate the double occupancy at each orbital and the spin-Hall conductivity which clearly distinguishes the trivial and non-trivial phases in our model. From the analysis of these quantities, it is concluded that the topological insulator changes into a trivial nonmagnetic Mott insulator via a first-order transition [4]. Therefore, the gap closing does not occur at the transition. In the presentation, we also address the antiferromagnetic instability.

[1] A. Shitade et al., Phys. Rev. Lett. 102, 256403 (2009), S. Chadov et al., Nature Materials 9 541-545 (2010), B. Yan et al., arXiv 1104.0641. [2] D. A. Pesin et al., Nature Physics 6, 376 - 381 (2010) . [3] B. A. Bernevig et al., Science 314 1757 (2006). [4] T. Yoshida et al., arXiv 1111.6250.

RC02

Self-consistent treatment of fully relativistic effect in the small bismuth clusters Bin (2 ≤ n ≤ 7)

Ely Aprilia*, Haruki Katou², Junpei Gotou², Shinya Haraguchi², Suprijadi Haryono³ and Tatsuki Oda⁴
¹ Double Degree Program of Kanazawa university-Bandung Institute of Technology, Indonesia
² Graduate School of Natural Sciences and Technology, Kanazawa University, Japan
³ Faculty of Mathematics and Natural Sciences, Bandung Institute of Technology, Indonesia
⁴ Institute of Science and Engineering, Kanazawa University, Japan

The energy scale of spin-orbit (SO) interaction reaches to the order of 0.1-eV at the elements in the fifth low of periodic table. Such interaction could cause effects on structural properties as well as on electronic ones. Bismuth has been investigated by many researchers due to its largeness of SO coupling. Rashba effect, which appears as the spin state splitting of surface bands, has been discussed intensively in the system which consists of bismuth [1]. The phenomena which are related with new physics of topological insulator have been investigated in a lot of bismuth systems [2]. In this context, bismuth clusters are interesting to investigate including relativistic effects. In this work, we have studied structural and electronic properties in small bismuth clusters; Bi_n (2 ≤ n ≤ 7). The Car-Parrinello molecular dynamics [3] and self-consistent fully relativistic calculations [4,5] have been employed to investigate effects of SO coupling effects. It has been found that the clusters of odd number atoms were found to carry magnetic moment with non-collinear magnetic configuration.

[1] Yu. M. Koroteev et al., Phys. Rev. Lett. 93, 046403 (2004). [2] Hsieh et al., Nature 452, 970 (2008). [3] R. Car and M. Parrinello, Phys. Rev. Lett. 55, 2471 (1985). [4] T. Oda, A. Pasquarello, and R. Car, Phys. Rev. Lett. 80, 3622 (1998). [5] T. Oda and A. Hosokawa, Phys. Rev. B 72, 224428 (2005).

RC03

Hidden topological order in URu₂Si₂

Tanmoy Das
Theoretical Division, Los Alamos National Laboratory, USA



RC04

Ground-state properties of a two-dimensional correlated topological insulator

Yuto Takenaka* and Norio Kawakami
Department of Physics, Kyoto University, Japan

Recently, the topological band insulator (TBI) has attracted much interest in condensed matter physics. The TBI is characterized by a nontrivial band structure, which has a full insulating gap in the bulk and gapless edge states on the boundaries. While the essential features of the TBI can be described as a one-body problem, there is much interest in the correlation effects on the TBI. In this study, we investigate a generalized Bernevig-Hughes-Zhang model having electron correlations with the variational Monte Carlo (VMC) method. In order to study how interactions affect the edge states and bulk states, it is important to consider inhomogeneous nature due to the lack of translational symmetry perpendicular to the boundaries. For this purpose, we introduce spatially-dependent variational parameters. We calculate the ground-state energy and the momentum distribution to discuss how the correlation effects affect electronic properties in the TBI.

[1] B. A. Bernevig, T. L. Hughes and S. C. Zhang, Science 314, 1757 (2006).

RC05

Magnetic impurity doping effect on bulk Rashiba spin splitting system BiTeI

Jeongdae Seo and Jong- Soo Rhyee*
Applied Physics, Kyung Hee University, Korea



RC06

Topological charge pumping effect by the magnetization dynamics on the Surface of 3D Topological Insulators

Hiroaki T Ueda^{1*}, Akihito Takeuchi¹, Gen Tataru¹ and Takehito Yokoyama²
¹ Department of Physics, Tokyo Metropolitan University, Japan
² Department of Physics, Tokyo Institute of Technology, Japan

We discuss a current dynamics on the surface of a 3-dimensional topological insulator induced by magnetization precession of a ferromagnet attached. It is found that the magnetization dynamics generates a direct charge current when the precession axis is within the surface plane. This rectification effect is due to a quantum anomaly and is topologically protected. The rectified current is useful in the sense that a direct current is easy to detect experimentally. To see the effect of the fast-varying exchange field, we study the current dynamics by the topological field theory. We adopt the dimensional regularization to regularize the ultraviolet divergence, which is inevitable to study an electromagnetic response of a topological insulator. As a result, the robustness of the rectification to the fast-varying exchange field is confirmed.

RC07

Tuning of carrier type in Mn-doped Bi₂Se₃

Young Ha Choi¹, Nahyun Jo¹, Kyujoon Lee¹, Jumpei Kajino², Toshiro Takabatake² and Myung-Hwa Jung^{1*}

¹ Department of Physics, Sogang University, Korea
² ADSM, Hiroshima University, Japan

Bi₂Se₃ is a good candidate for studying thermoelectric material as well as topological insulator. [1] In order to promote the thermoelectric performance, it is good to connect two materials in series with different charge carrier type. In Bi₂Se₃, the Se vacancies are dominant, which leads to n-type charge carriers.[2] In order to tune the carrier type and carrier density, we have doped Mn into Bi₂Se₃ and have studied their physical properties, mainly focusing on the thermoelectric properties. The single crystals of MnxBi_{2-x}Se₃ (x=0.03, 0.05, 0.09 and 0.15) were grown by melting the stoichiometric elements in an evacuated quartz ampoule. The Hall and thermoelectric measurements illustrate the change of carrier type from n to p type between x=0.03 and 0.05. The transport measurements have shown the metallic behavior for x≤0.03 and nonmetallic behavior for x≥0.05 at low temperatures. This supports that the Fermi level of p-type samples lies in the surface state between the bulk valence band maximum and the bulk conduction band minimum.[3] The Seebeck coefficient increases linearly up to ~100μV/K at room temperature both n- and p-type samples. This implies that Mn-doped Bi₂Se₃ is possible materials for thermoelectric application.

[1] D.M. Rowe, in : D.M. Rowe (Ed.), CRC Handbook of Thermoelectrics, CRC Press, Boca Raton, FL, 1995, p 90. [2] N. P. Butch, K. Kirshenbaum, P. Syers, A. B. Sushkov, G. S. Jenkins, H. D. Drew, and J. Paglione, Phys. Rev. B, 81, 241301(R) (2010). [3] Y. L. Chen, J.-H. Chu, J. G. Analytis, Z. K. Liu, K. Lgarashi, H.-H. Kuo, X. L. Qi, S. K. Mo, R. G. Moore, D. H. Lu, M. Hashimoto, T. Sasagawa, S. C. Zhang, I. R. Fisher, Z. Hussain, and Z. X. Shen, Science 329, 659 (2010).

RC08

Magnetic edge profile in the Kane-Mele-Hubbard model

Hyeong Jun Lee¹, Moo Young Choi¹ and Gun Sang Jeon^{2*}

¹ Department of Physics and Astronomy and Center for Theoretical Physics, Seoul National University, Korea
² Department of Physics, Ewha Womans University, Korea

We investigate the magnetic state on the edge of the Kane-Mele-Hubbard model. The ferromagnetic edge states are induced in a graphene nanoribbon by electron-electron interactions while certain spin-orbit interactions are known to give rise to a gapless current-flowing state on the edge without electron-electron interactions. We use the Hartree-Fock approximation to examine the nature of edge states in the presence of the Hubbard interaction in the Kane-Mele model. Computing the local magnetization of a nanoribbon with various widths, we obtain the edge phase diagram with four different phases for the ribbons of finite width and study how the magnetic properties are affected by electron-electron interactions. In particular, we show that the edge magnetic order survives for weak spin-orbit interactions in the thermodynamic limit. The edge magnetic order penetrates towards the ribbon center. The resulting magnetic profile gives its characteristic length which is found to be strongly affected by both electron-electron and spin-orbit interactions. Variations of its characteristic length turn out to be closely related to the phase transition between the topological insulator and the antiferromagnetic insulator. Electron dispersions are also discussed.

RC09

Theoretical study of spin texture in the Bi thin film

Hiroki Kotaka^{1*}, Fumiyuki Ishii² and Mineo Saito²

¹ Graduate School of Natural Science and Technology, Kanazawa University, Japan
² Faculty of Mathematics and Physics, Kanazawa University, Japan

The Spin-Orbit interaction (SOI) is very important effect for heavy atom like Bismuth. Recently, first-principles study revealed that significant SOI effects on the electronic structure and lattice bistability of Bi nanofilms.[1] In this study, we perform first-principles electronic structure calculations under the electric field for Bismuth thin film and Bi (001) multi-layer surface. We revealed that the SOI combined with electric field (so called Rashba effect) is very important in Bi surface state and Bi edge state.[2] We calculate spin polarization and spin direction for each band and k-points. Recently, giant out-of-plane spin component on Bi (001) surface is discovered SR-ARPES experiment.[3] We also calculate the spin structure of multi-layer Bi (001) surface, and our calculated result shows the detail of spin features at each k-point.

[1] H. Kotaka et al., e-JSSNT, Vol.7, pp.13-16, (2009). [2] H. Kotaka, F. Ishii, M. Saito, T. Nagao, and S. Yagimura, JJAP (2012). [3] A. Takayama et al., Phys. Rev. Lett. 106, 166401 (2011).

RC10

A recipe for new Topological Insulators based on bonds, bands, symmetry and heavy atoms

Lukas Muechler¹, Binghai Yan², Stanislav Chadov³, Haijun Zhang⁴, Frederick Casper¹, Shoucheng Zhang⁴ and Claudia Felser^{3*}

¹ Inst. fuer Anorg. Chemie, Johannes Gutenberg - Universitaet Mainz, Germany
² Bremen Center for Computational Materials Science, Germany
³ Max-Planck-Institut fur Chemische Physik fester Stoffe, Germany
⁴ Department of Physics, Stanford University, USA

In this work we will present a recipe to find new Topological Insulators (TIs) based on bonds, bands, symmetry and heavy atoms. A big issue concerning the compounds known up to now is the control of the bulk carrier density to produce truly insulating samples in the bulk. Using concepts from chemistry and supported by density-functional calculations, we want to motivate an extended search for new compounds with tunable bulk properties.

RC11

Optimizing the Bi_{2-x}Sb_xTe_{3-y}Se_y solid solutions to approach the intrinsic topological insulator regime

Zhi Ren^{*}, Alexey Taskin, Satoshi Sasaki, Kouji Segawa and Yoichi Ando
 ISIR, Osaka University, Japan

Three dimensional (3D) topological insulators represent a new quantum state of mater realized in band insulators, which are predicted to present novel surface transport phenomena. In reality, while a number of materials have been identified to be 3D TIs, most of them are poor insulators in the bulk. Given this situation, search for new TI materials better suited for achieving the bulk insulating state is of obvious importance. In this presentation, we show that there exist a series of “intrinsic” compositions for Bi_{2-x}Sb_xTe_{3-y}Se_y solid solutions where the acceptors and donors compensate each other and present a maximally bulk-insulating behavior. At such compositions, the resistivity can become as large as several Ωcm at low temperature, and one can infer the role of the surface-transport channel in the nonlinear Hall effect[1]. In particular, in the composition of Bi_{1.5}Sb_{0.5}Te_{1.7}Se_{1.3}, one can achieve a surface-dominated transport where the surface channel contributes up to 70% of the total conductance[2]. In addition, angle-resolved photoemission spectroscopy reveal that the Dirac cone dispersion changes systematically so that the Dirac point moves up in energy with increasing x, leading to a sign change of the Dirac carriers at x~0.9[3].

[1] Z Ren, A.A. Taskin, S. Sasaki, K. Segawa, and Y. Ando, Phys. Rev. B 84, 165311 (2011). (Editors' Suggestion) [2] A.A. Taskin, Z. Ren, S. Sasaki, K. Segawa, and Y. Ando, Phys. Rev. Lett. 107, 016801 (2011). [3] T. Arakane, T. Sato, S. Souma, K. Kosaka, K. Nakayama, M. Komatsu, T. Takahashi, Z. Ren, K. Segawa, and Y. Ando, Nat. Commun., in press.

RC12

Exploration of Three-dimensional Rashba Materials

Manabu Kanou^{*} and Sasagawa Takao

Materials and Structures Laboratory, Tokyo Institute of Technology, Japan

Strong spin-orbit interactions under the broken space inversion symmetry can induce spontaneous spin polarization without external magnetic fields, which is known as the (surface/interface) Rashba effect. On the other hand, due to the lack of a model compound, the Rashba effect in three-dimensions (bulk) has been poorly explored. In this study, it is demonstrated that ternary compounds of bismuth tellurohalides, BiTeX (X = Cl, Br, and I), are promising candidate compounds as ideal three-dimensional Rashba materials. As the essential backbone for both fundamental and applied research, this study established the growth of their sizable single crystals (> 1 × 1 × 0.2 mm³). Furthermore, it was found that, for BiTeI, that electronic state (the carrier concentration) can be adjusted from metallic to insulating ones by the choice of the growth techniques. Realization of the 3D Rashba states, including the Fermi surface topology for the corresponding carrier concentrations of the obtained crystals, was confirmed by relativistic first-principles calculations. We will discuss that our 3D Rashba materials can be a leading player in spin-involved novel phenomena, ranging from the metallic extreme (unconventional superconductivity) to the transport intermediate (spin Hall effects) to the novel insulating variant (3D topological insulating states).

RC13

Quantum phase transition from normal to topological insulator phase in Na₂IrO₃

Choong H. Kim¹, Heung Sik Kim¹, Hogyun Jeong², Hosub Jin³ and Jaeyun Yu^{1*}

¹ Department of Physics and Astronomy, Seoul National University, Korea
² Korea Institute of Science and Technology Information, Korea
³ Department of Physics and Astronomy, Northwestern University, USA

Na₂IrO₃ has been suggested to have a possible quantum spin Hall effect based on the novel jeff=1/2 state arising from the 5d Ir states. From the electronic structure calculation analysis of the band topology of Na₂IrO₃, however, it turns out that Na₂IrO₃ as it is should be a trivial insulator. We investigated the electronic structure of by employing a tight-binding model for the layered iridium oxides with honeycomb lattice. Our analysis for the layered iridates reveals that the topological nature of the spin-orbit coupled ground state depends on the trigonal crystal field and long-range hoppings. From the first-principles-derived tight-binding Hamiltonian we determine the phase boundary through the parity analysis and predict a quantum phase transition from normal to topological insulator. It is suggested that Na₂IrO₃ can be a candidate material which can have both non-trivial topology of bands and strong electron correlations.

RC14

Self-assembled nanowire with giant Rashba spin splitting

Jewook Park, Min-cherl Jung, Sung Won Jung and Han Woong Yeom^{*}

Department of physics, POSTECH, Center for atomic wires and layers(CAWL), Korea

We found gaint Rashba-type split bands for Pt-induced nanowires on the Si(110) surface by angle resolved photoemission spectroscopy (APRES) measurements. The observed Rashba parameter is about 2.1eVA, which is among the largest ever reported for Rashba systems and is unique in one-dimensional systems. Pt-induced nanowires were also investigated by scanning tunneling microscopy (STM) and scanning tunneling spectroscopy (STS) at low temperature (78K). High resolution STM topography images show that the wire has a width of 1.6nm and a X3 superstructure along the wire. On the other hands, the STS measurements reveal well resolved local density of states (LDOS) with a peak at -200meV and a characteristic dip at -300meV on the nanowire. These peak and dip energies corresponds well to the ARPES data; the top edge and the Dirac-like crossing point energy of the Rashba-type spin split bands, respectively. Furthermore, based on the dI/dV spectroscopic mapping, we confirmed noticeable one-dimensional electron channels along the nanowire edges, which are related to the gaint Rashba band. This implies a future application of the Pt-induced nanowire structure in silicon-based spintronics devices.

RC15

Ab initio study of topological surface state on Sb (111) surface with iron impurities

Jinhee Han, Hyungjun Lee and Hyoung Joon Choi^{*}

Department of Physics and IPAP, Yonsei University, Korea

We study iron impurities on Sb (111) surface and their effects on topological surface state by using an ab-initio pseudopotential density-functional method. We implemented the spin-orbit interaction into the SIESTA in a form of additional fully non-local projectors. To calculate electronic structure of topological surface states, we consider a slab of Sb using a supercell containing 20 atomic layers with experimental bulk Sb lattice parameters. We determine atomic positions of Fe impurities on Sb (111) surface by minimizing the total energy, and calculate surface band structures near the Fermi level. To find the impurity effects on the electronic structure of the surface states, we simulate ARPES spectra as a function of impurity density on the surface and calculate local density of states (LDOS) near the Fermi level. From the results, we find that Fe impurity states are present near Fermi level and they strongly interact with the surface states and produce a characteristic feature in LDOS on the top surface Sb layer. This work was supported by the NRF of Korea (Grant No. 2011-0018306) and KISTI Supercomputing Center (Project No. KSC-2011-C3-06).

RC16

Topological insulating phase in cubic system: tight-binding approach

Hosub Jin, Jino Im and Arthur J. Freeman

Department of Physics and Astronomy, Northwestern University, USA

Recently, much attention has focused on three-dimensional strong topological insulators as a new quantum state of matter, such as Bi₂Se₃ and Bi₂Te₃. Here we suggest topologically non-trivial electronic structures in cubic systems based on the tight-binding analysis. Assuming the well separated s and p states and hopping parameters, we can set up an 8x8 tight-binding Hamiltonian, and the trivial to non-trivial topological phase transition occurs by tuning the hopping parameters or spin-orbit coupling strength. Our tight-binding Hamiltonian is reduced to a 4x4 continuum model which is the minimal model to describe the topological phase transition. Topologically protected surface states in the slab geometry are also shown within our model.

Supported by the U.S. D.O.E.

RC17

Topological insulator phase and Kitaev-like anisotropic exchange interactions in Li₂IrO₃

Heung-sik Kim¹, Choong H. Kim¹, Hogyun Jeong², Hosub Jin³ and Jaeyun Yu^{1*}

¹ Department of Physics and Astronomy, Seoul National University, Korea
² Korea Institute of Science and Technology Information, Korea
³ Department of Physics and Astronomy, Northwestern University, USA

From first-principles electronic structure calculations results, we set up an effective tight-binding Hamiltonian for Li₂IrO₃ by constructing Wannier orbitals of low-energy states near the Fermi level. The Wannier orbitals are found to be quite close to the S_j^z={eff}=1/2S state, which are recently suggested to exist in many other iridate compounds. The model Hamiltonian is characterized by the nontrivial second and third nearest neighbor hopping inside Ir honeycomb lattice as well as relatively small but significant inter-layer hopping terms. It is shown that the ratio between the nearest and third nearest neighbor hopping determines the SZ_{2S}-invariant of this material, and that it can be controlled by the lattice strain in our first-principles calculations. We also suggest realistic exchange interactions from effective Hamiltonian, which has various nontrivial terms including the most strong Kitaev-type anisotropic exchange terms within the same sublattice, rather small but significant Dzyaloshinskii-Moriya terms, and Heisenberg exchange interactions.

RC18

Structural and electrical properties of (111) oriented half-Heusler La-Pt-Bi thin films

Nozomi Sugimoto^{1*}, Yohei Niimi¹, Tetsuya Miyawaki¹, Tatsuhiko Yoshihara¹, Naoto Fukatani¹, Kenji Ueda¹, Nobuo Tanaka² and Hidefumi Asano¹

¹ Department of Crystalline Materials Science, Nagoya University, Japan
² EcoTopia Institute, Nagoya University, Japan

Topological insulators are candidate materials for low-power and high-speed spintronics devices, due to the dissipation less and spin-polarized electrons on the surface state. Recently, we have reported structural properties of LaPtBi(001) thin films, one of candidate materials of half-Heusler topological insulator[1-2], grown by three-target co-sputtering[3]. In this paper, we report preparation and properties of LaPtBi with different crystalline orientation. By optimizing deposition rate for each element, (111) oriented LaPtBi thin films were obtained below 500°C on Sapphire-C substrates. On the other hand, for films on YAlO₃ substrates, both (001) and (111) orientations were observed below 500°C. X-ray photoelectron spectroscopy study is revealed that (111) oriented films exhibited chemical shifts and appearance of satellite peaks of La 3d, which are attributed to charge transfer from Bi p and Pt d states to La d and f states due to the mixture of these states in the valence band. Investigation and comparison of the behaviors of LaPtBi thin films with different orientations will enable us to uncover the electron and spin transport properties in the surface state due to the topological nature.

[1] S. Chadov et al., Nat. Mater. 9, 541 (2010). [2] H. Lin et al., Nat. Mater. 9, 546 (2010). [3] T. Miyawaki et al., J. Appl. Phys., accepted.

RC19

First-principles study of spin texture in the multilayer graphene on Ni(111)

Fumiuyuki Ishii¹*, Hiroki Kotaka², Keisuke Sawada² and Mineo Saito¹
¹ Faculty of Mathematics and Physics, Kanazawa University, Japan
² Graduate School of Natural Science and Technology, Kanazawa University, Japan

Graphene, a two-dimensional honeycomb lattice consisting of C atoms, shows useful properties for spintronics applications. Recently, spin-split electronic states in the graphene on Ni(111) is discussed extensively [1-3]. By using noncollinear spin-density functional theory implemented in openmx code[4], we predict spin-polarized electronic states of the graphene on Ni(111) in real- and momentum-space. The Dirac-cone shaped band structure was broken by strong hybridization between monolayer graphene and substrate Ni(111). On the other hand in the bilayer graphene on Ni(111), the Dirac-cone shaped band recover only in minority spin. The relativistic spin-orbit effect make non-collinear spin vortex (Rashba Effect) in the momentum space. This spin noncollinearity in momentum space may make significant effects on the electrical transport properties of the graphene/Ni(111).

[1] Yu. S. Dedkov, M. Fomin, U. Rudiger, and C. Laubschat, *Phys. Rev. Lett.* **100**, 107602 (2008). [2] O. Rader, A. Varykhalov, and J. Sanchez-Barriga, D. Marchenko, A. Rybkin, and A. M. Shikin, *Phys. Rev. Lett.* **102**, 057602 (2009). [3] K. Sawada, F. Ishii, M. Saito, *Phys. Rev. B* **82**, 245426 (2010). [4] T. Ozaki, H. Kino, J. Yu, M. J. Han, N. Kobayashi, M. Ohfuti, F. Ishii, T. Ohwaki, H. Weng, M. Toyoda, and K. Terakura, <http://www.openmx-square.org/>

RD01

Single Crystal Growth, Electrical and Magnetic Properties in RO₅Al₁₀ (R=rare earth)

Masahito Sakoda¹*, Kazuhiro Kubota¹, Eiichi Matsuoka¹, Hitoshi Sugawara¹, Takahiro Sakurai², Hitoshi Ohta¹, Tatsuma D. Matsuda⁴ and Yoshinori Haga¹
¹ Department of Physics, Kobe University, Kobe 657-8501, Japan
² Center for Supports to Research and Education Activities, Kobe University, Kobe 657-8501, Japan
³ Molecular PhotoScience Research Center, Kobe University, Kobe 657-8501, Japan
⁴ Advanced Science Research Center, Japan Atomic Energy Agency, Tokai, Ibaraki 319-1195, Japan

The ternary rare-earth compounds RO₅Al₁₀ (R = rare earth) crystallize with orthorhombic structure [1]. Among them, CeO₅Al₁₀ have attracted much attention because of the heavy-fermion behavior accompanied by a novel long-range order (LRO) at 28.7 K [2]. In order to understand the mechanisms of LRO, the information of physical properties of the reference compounds LaO₅Al₁₀ and PrO₅Al₁₀ is required. In this work, we have succeeded in growing single crystals of LaO₅Al₁₀ and PrO₅Al₁₀ by Al self-flux method, and investigated the physical properties by the X-ray diffraction, electrical resistivity, Hall effect and magnetic susceptibility. Both of LaO₅Al₁₀ and PrO₅Al₁₀ show the typical metallic temperature dependence of electrical resistivity without any indication of phase transitions. LaO₅Al₁₀ exhibits the Pauli paramagnetism with small temperature dependence, while PrO₅Al₁₀ exhibits the Van Vleck paramagnetism with the Curie-Weiss behavior at high temperature with a large magnetic anisotropy, which is most probably due to the crystalline electric field effect. All of these results indicate that the electronic structure of CeO₅Al₁₀ is different from those of LaO₅Al₁₀ and PrO₅Al₁₀, and suggest that the 4f-electrons in CeO₅Al₁₀ are related to the unusual ordering.

[1] V.M. T. Thieker et al., *J. Mater. Chem.* **8** (1998) 125. [2] T. Nishioka et al., *J. Phys. Soc. Jpn.* **78** (2009) 123705.

RD02

Anisotropic transport and magnetic properties of CeZn₁₁ single crystals

H. Hodovanets, S. L. Bud'ko and P. C. Canfield*
 Department of Physics and Astronomy, Ames Laboratory/Iowa State University, Ames IA, USA

Anisotropic measurements of the magnetic and transport properties have been performed on single crystals of CeZn₁₁ in three different crystallographic directions. M(H) for H||perp c shows a broad metamagnetic transition at about 1.9 T with Ms~ 1.6 S/mu_B per Ce. Analysis of the temperature dependence of MH indicates strong magnetic anisotropy. Zero-field resistivity of CeZn₁₁ shows a broad maximum, characteristic of that of Kondo compounds, at around 10 K followed by a sharp change of the slope and a kink corresponding to antiferromagnetic (AF) transition at 2.0 K. Anisotropic temperature and field dependent magnetoresistance and H-T phase diagrams will be discussed. S*NS Work at the Ames Laboratory was supported by the Department of Energy, Basic Energy Sciences under Contract No. DE-AC02-07CH11358.

RD03

Shubnikov-de Haas oscillation in PuIn₃

Yoshinori Haga¹, Oscar Ayala-valenzuela², Ross McDonald², Chuck Mielke², Eric D. Bauer², J N Mitchell², P. H. Tobash², Joe D. Thompson² and Zachary Fisk¹
¹ Advanced Science Research Center, Japan Atomic Energy Agency, Japan
² Los Alamos National Laboratory, USA



RD04

Quadrupolar ordering in a caged compound PrO₅Zn₂₀

Kazuhei Wakiya¹, Naohiro Nagasawa¹, Keisuke T Matsumoto¹, Takahiro Onimaru¹, Kazunori Umeo² and Toshiro Takabatake¹
¹ AdSM, Hiroshima University, Higashi-Hiroshima, Japan
² N-BARD, Hiroshima University, Higashi-Hiroshima, Japan

Pr-based intermetallic compounds with cubic crystal structures are expected to show various phenomena arising from quadrupolar degrees of freedom, when the crystal electric field (CEF) ground state of Pr³⁺ ion is the nonmagnetic Γ3 doublet. Recently, it has been found that a caged compound PrIr₇Zn₂₀ with the Γ3 doublet ground state undergoes a superconducting transition at Tc=0.05 K in the presence of antiferroquadrupolar order below TQ=0.11 K [1, 2]. We have studied the isostructural compound PrO₅Zn₂₀ with 5d electron one less than in PrIr₇Zn₂₀, by the measurement of the electrical resistivity ρ, magnetic susceptibility χ, and specific heat C in the temperature range from 0.4 K to 300 K. On cooling below 5 K, χ(T) approaches a constant value, indicating a nonmagnetic CEF ground state. C(T) shows a peak at To=0.6 K, where no anomaly appears in the χ(T). These findings strongly suggest a nonmagnetic phase transition at To arising from the quadrupolar degrees of freedom. Furthermore, the To is five times higher than TQ in PrIr₇Zn₂₀, which is possibly attributed to enhancement of quadrupolar exchange interaction.

[1] T. Onimaru et al., *J. Phys. Soc. Jpn.* **79** 033704 (2010). [2] T. Onimaru et al., *Phys. Rev. Lett.* **106** 177001 (2011).

RD05

Spin-triplet superconductivity induced by ferromagnetic fluctuations in UCoGe

Taisuke Hattori¹*, Yoshihiko Ihara¹, Kosuke Karube¹, Yusuke Nakai², Kenji Ishida², Yasuhiro Tada¹, Satoshi Fujimoto¹, Norio Kawakami¹, Kazuhiko Deguchi², Noriaki K Sato³ and Isamu Satoh⁴
¹ Department of Physics, Graduate School of Science, Kyoto University, Japan
² Department of Physics, Graduate School of Science, Kyoto University, TRIP, JST, Japan
³ Department of Physics, Graduate School of Science, Nagoya University, Japan
⁴ Institute for Materials Research, Tohoku University, Japan

After the discovery of superconductivity in the ferromagnetic (FM) UGe₂ under pressure, FM superconductors have attracted much interest, since in an itinerant FM superconductor with the presence of a large energy splitting between the majority and minority spin Fermi surfaces, exotic spin-triplet superconductivity has been anticipated. Among such FM superconductors, UCoGe [1] is one of the most readily explored experimentally, because of its high superconducting transition temperature ~ 0.7 K and low Curie temperature ~ 2.5 K at ambient pressure. Large anisotropic behaviors of superconductivity [2, 3] and longitudinal FM fluctuations along the c axis (direction of the ordered moment) [4] are thought to link with the mechanism of the superconductivity. From precise angle-resolved NMR and Meissner measurements we found that the magnetic field along the c axis strongly suppresses the FM fluctuations and that the superconductivity is observed in the limited magnetic field region where the FM spin fluctuations are active. These results combined with model calculations strongly suggest that the longitudinal FM spin fluctuations tuned by H||c induce the unique spin-triplet superconductivity in UCoGe. As far as we know, this is the first clear experimental example that FM fluctuations are intimately related with superconductivity.

[1] N. T. Huy et al., *Phys. Rev. Lett.* **99** (2007) 067006. [2] N. T. Huy et al., *Phys. Rev. Lett.* **100** (2008) 077002. [3] D. Aoki et al., *J. Phys. Soc. Jpn.* **78** (2009) 113709. [4] Y. Ihara et al., *Phys. Rev. Lett.* **105** (2010) 206403.

RD06

Competitive magnetic properties between the different anisotropic SDW phases in heavy-fermion system Ce_{0.87}La_{0.13}(Ru_{1-x}Rh_x)₂Si₂

Hiroaki Okamoto¹, Eiichiro Harada¹, Yusuke Amakai¹, Shigeyuki Murayama¹*, Hideaki Takano¹, Naoki Momono¹, Kazuyuki Matsubayashi² and Yoshiya Uwatoko²
¹ Graduate School of Engineering, Muroran Institute of Technology, Japan
² Institute for Solid State Physics, University of Tokyo, Japan

Typical heavy-fermion compound CeRu₂Si₂ shows an SDW transition by the substitution of La at the Ce site with the gap perpendicular to the c-axis and the moment along the c-axis(1). It shows another SDW transition with the gap and moment both parallel to the c-axis by the substitution of Rh at the Ru site(2). In order to investigate the two different SDW phases, we have measured the susceptibility χ and resistivity ρ on single-crystalline Ce_{0.87}La_{0.13}(Ru_{1-x}Rh_x)₂Si₂ for 0 ≤ x ≤ 0.4 in directions perpendicular (⊥) and parallel (//) to the c-axis(3). The ρ⊥ for 0 ≤ x < 0.05 shows a gap-type anomaly at TN, whereas the ρ// for 0 ≤ x < 0.05 indicates a downward inflection or a shoulder at around TN, suggesting the transverse SDW transition. For 0.05 ≤ x ≤ 0.075 these anomalies become very small and a hysteresis is further seen between temperature decreasing and increasing process below TN. For 0.075 < x ≤ 0.3 the gap-type anomaly in ρ⊥ disappears and a clear gap-type jump has been detected in ρ// at TN, suggesting the longitudinal SDW transition. These behaviors would suggest that a competitive magnetic phase occurs between the two anisotropic SDW phases.

(1) S. Quezel et al., *J. Magn. & Magn. Mater.*, **76 & 77**, 403 (1988). (2) S. Murayama et al., *Phys. Rev. B* **56**, 11092 (1997). (3) Y. Amakai et al., *J. Phys. Soc. Jpn.* **80**, SA062 (2011).

RD07

Elastic constant of SmO₅Sb₁₂ under high magnetic field

Tatsuya Yanagisawa¹*, Shota Mombetsu¹, Mitsuhiko Akatsu², Yuichi Nemoto², Shadi Yashin³, Sergei Zherlitsyn³ and Joachim Wosnitza³
¹ Department of Physics, Hokkaido University, Japan
² Graduate School of Science and Technology, Niigata University, Japan
³ Dresden High Magnetic Field Laboratory, Forschungszentrum Dresden-Rossendorf, Germany

The filled skutterudite compound SmO₅Sb₁₂ exhibits a large electronic specific heat coefficient γ ~ 820 mJ K⁻² mol⁻¹, which is insensitive to an applied magnetic field H || <001>, and also shows a phase transition at 2.5 K with tiny ferromagnetic moment. The origin of the magnetically robust heavy fermion state and an exotic phase transition are unsolved issues. The crystalline electric field (CEF) ground state of this compound has also not been settled, thus far. Owing to clarified whether the CEF ground state is the Γ₈ quartet or Γ₇ doublet for Sm²⁺ ionic configurations, we have measured the elastic constant C₁₁ on single crystalline SmO₅Sb₁₂ by using pulsed magnetic fields up to 62 T. As a result, C₁₁ shows a minimum at around 10 T and gradually increase with increasing magnetic field at 4.2 K. In the cubic symmetry, C₁₁ can be described as the sum of the bulk modulus C_B and the Γ₃-type quadrupole susceptibility. Assuming that C_B is only dominated by magneto-elastic effects of the weak ferromagnetic moment in the low magnetic field region, the increasing tendency of C₁₁ at high magnetic field region could be explained by a quadrupole susceptibility with Γ₈ quartet CEF ground state.

[1] S. Sanada et al., *J. Phys. Soc. Jpn.* **74** (2005) 246. [2] W. M. Yuhasz et al., *Phys. Rev. B* **71** (2005) 104402. [3] Y. Aoki et al., *Physica B* **378-380** (2006) 54. [4] T. Yanagisawa et al., *J. Phys. Soc. Jpn.* **80** (2011) 043601.

RD08

27Al-NMR study for critical phenomena of metamagnetic transition in UCoAl

Kosuke Karube¹*, Taisuke Hattori¹, Kenji Ishida¹, Takuya Asai², Takemi Komatsubara³ and Noriaki Kimura²
¹ Department of Physics, Graduate School of Science, Kyoto University, Japan
² Department of Physics, Graduate School of Science, Tohoku University, Japan
³ Center for Low Temperature Science, Tohoku University, Japan

UCoAl shows a first-order paramagnetism (PM)-ferromagnetism (FM) transition (metamagnetic transition) in small external magnetic field about 0.6 T applied only along its easy magnetization axis, c-axis [1]. This first order transition line terminates at a "critical-end-point" at Tcr ~ 13 K. Above Tcr the first order transition from PM to FM changes to crossover. This feature is apparently similar to gas-liquid transition, where the order parameter and the tuning parameter are density of molecules and pressure, respectively. In fact, a gas-liquid transition is regarded to be mathematically equivalent to 3D-Ising FM transition [2], therefore we expect the metamagnetic transition in UCoAl has the same physical framework as a gas-liquid transition. In order to investigate static and dynamic properties in the critical phenomena on UCoAl, we performed 27Al-NMR measurement for a single-crystal UCoAl and measured Knight-shift K and nuclear spin-lattice relaxation rate 1/T1 by varying temperature T and c-axis magnetic field Hc. In the poster presentation, I will show the result of c-axis magnetization Mc (order parameter) and c-axis dynamical susceptibility Sc (fluctuations of order parameter) calculated from K and 1/T1T, as a function of (T, Hc) and discuss similarities and differences from comparison with gas-liquid transition.

[1] N. V. Mushnikov et al., *Phys. Rev. B* **59**, 6877 (1999). [2] T. D. Lee et al., *Phys. Rev.* **87**, 410 (1952).

RD09

Hybridization gap and the hidden order in the heavy fermion Kondo lattice URu₂Si₂

Wan Kyu Park¹*, Paul H. Tobash², Filip Ronning², Eric D. Bauer², John L. Sarrao², Joe D. Thompson² and Laura H. Greene¹
¹ University of Illinois at Urbana-Champaign, Urbana, IL 61801, USA
² Los Alamos National Laboratory, Los Alamos, NM 87545, USA

What drives the second order phase transition that occurs at 17.5 K in the Kondo lattice heavy fermion URu₂Si₂, remains unknown after two and half decades of research despite ubiquitous observation of gap-like behaviors. Determining the nature of the extracted gaps, whether they are the order parameter or not, is a crucial task to resolving this hidden order enigma. Quasiparticle scattering spectroscopy (QPS), better known as point-contact spectroscopy, is a powerful technique to probe the bulk electronic properties by exploiting a ballistic junction between two electrodes. Employing QPS, we have carried out conductance measurements on URu₂Si₂ [1]. The differential conductance data exhibit a distinct double-peak structure with pronounced asymmetry, a signature for a Fano resonance in a Kondo lattice [2]. The extracted gap, a hybridization gap between the renormalized bands, opens well above the hidden order transition temperature, indicating this hybridization gap is not the hidden order parameter. Our results place severe constraints on the origin of the hidden order transition in URu₂Si₂. The work at UIUC is supported by the U.S. DOE under Award No. DE-FG02-07ER46453. The work at LANL is carried out under the auspices of the U.S. DOE, Office of Science.

[1] W.K. Park et al., *PRL* **108**, 246403 (2012) [2] M. Maitseva, M. Dzero, P. Coleman, *PRL* **103**, 206402 (2009).

RD10

Resonant Raman effect on LaRu₂Al₁₀ and CeRu₂Al₁₀

Katsuki Nagano¹, Takumi Hasegawa¹, Norio Ogita¹, Masayuki Udagawa¹, Hiroshi Tanida², Daiki Tanaka², Masafumi Sera², Takashi Nishioka³ and Masahiro Matsumura³
¹ Graduate School of Integrated Arts and Sciences, Hiroshima University, Higashi-Hiroshima 739-8521, Japan
² Institute for Advanced Material Research, Hiroshima University, Higashi-Hiroshima 739-8530, Japan
³ Graduate School of Advanced Sciences of Matter, Kochi University, Kochi 780-8520, Japan

LaRu₂Al₁₀ and CeRu₂Al₁₀ with space group Cmcn have the orthorhombic YbFe₂Al₁₀ type structure [1], where the number of Raman active phonons is estimated as 10Ag + 9B₁g + 6B₂g + 8B₃g by group theory. CeRu₂Al₁₀ shows the transition at T0 = 27 K [2, 3, 4], while LaRu₂Al₁₀ shows no anomaly. We reported the temperature dependence of the phonon Raman spectra at the SCES2011, where we could not observe all phonon modes by only 514.5 nm excitation and no anomaly at T0 in CeRu₂Al₁₀. We concluded that the transition at T0 does not accompany with the structural change. Recently we have employed several excitations light at 488.0 nm, 514.5 nm, 568.2 nm, and 647.1nm. We have observed the B₁g mode missed by only 514.5 nm, that is, we observe all phonon modes by changing the excitation energy. In the guest atoms modes, the vibration along b axis shows the intensity enhancement at 647.1 nm, but that along a or c axis does not show the case. Remarkable difference between LaRu₂Al₁₀ and CeRu₂Al₁₀ is observed for the phonons at around 100 cm⁻¹ in (y, z) polarization. These differences are originated by the difference of the electronic states between them.

[1] Thieda V M T, et al, 1998 *J. Mater. Chem.* **8** 125. [2] Strydom A M 2009 *Physica B* **404** 2981 [3] Nishioka T, et al 2009 *J. Phys. Soc. Jpn.* **78** 123705 [4] Muro Y, et al 2010 *J. Phys.: Conf. Series* **200** 012136

RD11

Magnetic properties of β-US2 single crystals

Etsuyi Yamamoto¹*, Shugo Ikeda², Hironori Sakai¹, Tatsuma D. Matsuda¹, Naoyuki Tateiwa¹, Yoshinori Haga¹, Yoshichika Onuki³ and Zachary Fisk⁴
¹ ASRC, Japan Atomic Energy Agency, Japan
² Graduate School of Material Science, University of Hyogo, Japan
³ Graduate School of Science, Osaka University, Japan
⁴ University of California, USA

Uranium chalcogenides compounds UX₂ (X=S, Se and Te) have the same orthorhombic (Pnma) structure and those electronic state can easily be modified by changing the constituting elements. UTeS is an Ising-type ferromagnet with a Curie temperature 87 K and shows metallic conductivity at all temperatures. USES shows a semimetallic resistivity. Electrical resistivity of USES decreases with decreasing temperature but increases steeply below 50 K, with an anomaly at the ferromagnetic ordering temperature 24 K. US2 is similar to USES at high temperature and the electrical resistivity of US2 decreases with decreasing temperature and increases steeply below about 80 K, but US2 does not order magnetically. The electrical resistivity of US2 at low temperature suppresses under a high pressure or a high magnetic field [1]. We study the magnetic properties of US2 in detail by measuring magnetic susceptibility and electric resistivity under a magnetic field.

[1] S. Ikeda et al., *J. Phys. Soc. Jpn.* **76** (2009) 114704.

July 12 (Thu)

July 12 (Thu)

RD12

Evidence of nodal gap structure in the skutteride superconductor PrPt₂Ge₁₂

Jing Lei Zhang¹, Lin Jiao¹, Michael Nicklas², Roman Gumenuk², Ye Chen¹, Lu Kai Guo¹, Li Na Wang¹, Bin Hao Fu¹, Walter Schnelle², Helge Rosner², Andreas Leithe-jasper², Yuri Grin², Frank Steglich² and Hui Qiu Yuan^{1*}
¹ Department of Physics, Zhejiang University, China
² Max Planck Institute for Chemical Physics of Solid, Germany

In order to study the gap function of the newly discovered skutterudite superconductor PrPt₂Ge₁₂ (T_c = 7.9K), we have measured the London penetration depth Δλ(T) of the single crystalline PrPt₂Ge₁₂ down to 0.05Tc by using a tunnel diode oscillation (TDO) based technique. The observation of a quadratic temperature dependence of Δλ below 0.3Tc indicates the existence of point nodes in the superconducting gap. The derived superfluid density ρ_s(T) can be nicely fitted by the A-phase gap function of 3He (Δ(0,φ) = Δ_{0} [K_x + iK_y]) with a fitting parameter of Δ_{0} = 2.2k_BT_c, providing new evidence for a possible p-wave superconductivity in PrPt₂Ge₁₂.}}

RD13

Mossbauer spectroscopy of Fe doping valence fluctuating α-YbAlB₄

Yui Sakaguchi^{1*}, Shugo Ikeda¹, Kentaro Kuga², Keita Sone², Satoru Nakatsuji² and Hisao Kobayashi¹
¹ Graduate School of Material Science, University of Hyogo, Japan
² Institute for Solid State Physics, University of Tokyo, Japan

Valence fluctuating YbAl₃ compounds have two different crystal structures; α-YbAl₃ and β-YbAl₃ [1]. β-YbAl₃ is the first compound which shows a Yb-based heavy fermion superconductor with Tc = 80mK [2] and exhibits a pronounced non-Fermi-liquid behavior above Tc. Meanwhile, α-YbAl₃ shows normal metallic behaviors at low temperature. Recently, the small substitution of Al by Fe in α-YbAl₃ revealed a breakdown of the Fermi-liquid behavior with an antiferromagnetic order. We have studied magnetic properties of α-Yb(Al_{0.75}Fe_{0.25})B₄ at low temperatures using 57Fe Mossbauer spectroscopy. The observed Mossbauer spectrum at room temperature using single crystalline samples is typical for a paramagnetic state. We analyzed the spectrum using a doublet. From the intensity ration of the doublet, the principle z-axis of the diagonalized electric-field gradient tensor is perpendicular to the c-axis. We observed a small magnetic hyperfine field at 4.5K which comes from the antiferromagnetic ordering of Yb magnetic moments. This small magnetic hyperfine field disappears around TN (~ 9K). These results indicate that the magnetic structure is not simple in α-Yb(Al_{0.75}Fe_{0.25})B₄. Above TN, the observed spectra change drastically with increasing temperature. Some of changes in the spectra were related to anomalies in the temperature dependence of magnetization.

[1] R. T. Macaluso et al., Chem. Mater. 19, 1918 (2007) [2] S. Nakatsuji et al., Nature Phys. 4, 603 (2008)

RD14

Neutron scattering study on f-electron states of PrCu₄Au

Hiroki Kobayashi¹, Kazuaki Iwasa^{1*}, Kotaro Saito¹, Keisuke Tomiyasu¹, Daichi Kawana², Shuai Zhang³, Yosikazu Isikawa⁴, Jean - Michel Mignot⁵, Gilles Andre⁵, Alexander I. Koleznikov⁶, Andrei T. Savici⁶ and Garrett E. Granroth⁶
¹ Department of Physics, Tohoku University, Sendai 980-8578, Japan
² Condensed Matter Research Center and Photon Factory, Institute of Materials Structure Science, KEK, Tsukuba 305-0801, Japan
³ Department of Applied Chemistry, Hiroshima University, Higashi-Hiroshima 739-8527, Japan
⁴ Graduate School of Science and Engineering, University of Toyama, Toyama 930-8555, Japan
⁵ Laboratoire Leon Brillouin, CEA-CNRS, CEA/Saclay, 91191 Gif sur Yvette, France
⁶ Neutron Sciences D., Oak Ridge National Laboratory, Oak Ridge, TN 37831, USA

Pr-based compounds have recently been studied for heavy electron properties originating from 4f electron configuration, as in PrFe₂P₁₂ [1]. We extracted a large electronic-specific-heat-coefficient of 0.77 J/mol K² from specific heat measurements on PrCu₄Au [2]. This material is expected to undergo an antiferromagnetic transition below 2.4 K. We investigate the role that f-electron states play in these properties using neutron scattering techniques. We used the spectrometers SEQUOIA at ORNL, 4F1 at LLB, and TOPAN at JAEA to measure the temperature dependence, between 1.6 K and 100 K, of the magnetic excitations in PrCu₄Au. The spectra are composed of several inelastic peaks. The crystal-field-splitting scheme with the triplet ground state, as suggested from the magnetization result [2], is a fair match to the observed spectra. A quasielastic component was also detected. The temperature dependences of the spectral intensity and width are similar to those in other heavy electron systems. Diffraction experiments for the powdered sample on the diffractometer G4-1 at LLB reveal antiferromagnetic peaks characterized by the wave vector (1/2, 1/2, 1/2). This result can be interpreted as the type-II magnetic ordering on the fcc sub-lattice of Pr ions. To summarize, PrCu₄Au exhibits localized and strongly-hybridized f-electron states.

[1] H. Sugawara et al., Phys. Rev. B 66 (2002) 134411. [2] S. Zhang et al., J. Phys.: Condens. Matter 21 (2009) 205601.

RD15

Effect of pressure on the YbNi₃Ga₅ single crystal

T. Hirayama¹, K. Matsubayashi¹, T. Yamashita², S. Ohara² and Y. Uwatoko^{1*}
¹ University of Tokyo, Japan
² Nagoya Institute of Technology, Japan

We have investigated the effect of pressure on the physical properties of single-crystalline YbNi₃Ga₅. This compounds crystallize in a trigonal ErNi₃Al₅-type structure (space group R32). From the thermal, magnetic and transport study, YbNi₃Al₅ turns out to be an intermediate valence compound with r = 30 mJ/molK [1]. The electrical resistivity and ac susceptibility of nonmagnetic heavy fermion compound YbNi₃Al₅ have been measured under hydrostatic pressure up to 11 GPa. With increasing pressure, the ferromagnetic ordering state was appeared over 9 GPa. These results suggested that nonmagnetic Yb state change to the localized magnetic state, via quantum critical point, by tuning the pressure. In this paper, we will discuss the electrical state of YbNi₃Al₅ under pressure.

[1] T. Yamashita and S. Ohara; submitted to J. Phys. Soc. Jpn.

RD16

Fermi surfaces in the mixed valent Yb system

Hisatomo Harima^{*}
 Department of Physics, Kobe University, Japan

Many Yb-compounds have been crystalized recently in good quality, so that the de Haas-van Alphen effect is detected in those including the Yb-based heavy fermion compounds, i.e., YbCu₂Si₂, YbAlB₄. Non-magnetic Yb compounds are regarded mostly as divalent Yb system, in which Fermi surfaces are well reproduced by using conventional band structure calculations. In some of non-magnetic Yb compounds, such as YbAl₃, the valence of Yb-ion is diverted from Yb²⁺. Actually, the Fermi surfaces of YbAl₃ are very different in topology from those of divalent YbIn₃. This is the clear evidence of the 4f electrons really affect the formation of the Fermi surfaces in YbAl₃[1]. In Yb compounds, the dispersion of the 4f bands are very flat, then the Fermi surfaces are very sensitive to the role of the 4f electrons. Recently the LDA+U approach has shown that only the doublet ground states participate the Fermi surfaces in YbCu₂Si₂[2]. The role of 4f electrons in mixed valent Yb system is discussed, for YbAlB₄, YbCoGa₃ and the related compounds.

[1] T. Ebihara, et. al., J. Phys. Soc. Jpn. 69 (2000) 895. [2] Nguyen Duc Dung, et. al., J. Phys. Soc. Jpn. 78 (2009) 084711.

RD17

Unusual heavy fermion behavior in PrTr₂Al₂₀ (Tr = Nb, Ta) associated with Γ₃ quadrupolar degrees of freedom

Ryuji Higashinaka, Akihiro Nakama, Ryoichi Miyazaki, Yuji Aoki and Hideyuki Sato
 Department of Physics, Tokyo Metropolitan University, Japan

Recently, PrTr₂X₂₀ (Tr = transition metal, X = Zn, Al) compounds have attracted much attention as a new candidate for investigating the quadrupolar Kondo effect because PrTr₂Al₂₀ (Tr = Ti, V) show non Fermi liquid behaviors and multipolar orderings attributed to nonmagnetic Γ₃ doublet ground state[1]. Recently, we found that PrNb₂Al₂₀ also has a nonmagnetic Γ₃ doublet ground state and does not show any phase transitions down to 0.15 K[2]. In addition, this compound has a large Sommerfeld coefficient γ (~ 1.2 J/molK²). This result suggests a possibility of the formation of unusual heavy fermion state attributed to the quadrupole moments of Γ₃ state. In order to investigate the quadrupole-induced strongly correlated electronic properties in PrTr₂Al₂₀ systematically we have grown single crystals of other Pr based compound, PrTa₂Al₂₀, and performed specific heat, magnetization and electronic transport measurements. In C/T, PrTa₂Al₂₀ shows a peak around 0.6 K attributed to the ordering of quadrupole moment and has a large gamma value of 1.6 J/molK² at low temperatures with little field dependence. In this presentation, we show recent results for PrT₂Al₂₀ (T = Nb, Ta) and discuss the possibility of the formation of heavy fermion formation induced by quadrupolar degrees of freedom.

[1] A. Sakai and S. Nakatsuji, J. Phys. Soc. Jpn. 71 063701 (2011). [2] R. Higashinaka et al., JPS Autumn meeting 23pPSA-37 (2010), JPS Spring meeting 28aEC-11 (2011).

RD18

Tuning of the heavy-fermion ground state in YbNi₃X₉ (X=Al, Ga) by substitution

Shigeo Ohara^{*}, Hiroshi Kono and Tetsuro Yamashita
 Graduate School of Engineering, Nagoya Institute of Technology, Nagoya 466-8555, Japan

We have succeeded in synthesizing new Yb-based Kondo lattice systems YbNi₃X₉ (X=Al, Ga) which crystallizes in the trigonal ErNi₃Al₉-type structure [1]. YbNi₃Al₉ shows typical features of a heavy-fermion antiferromagnet with Neel temperature of TN=3.4K and Sommerfeld coefficient γ=100mJ/(molK2). In contrast, YbNi₃Ga₉ is an intermediate valence compound with γ=30mJ/(molK2) and a high characteristic temperature of TK~600K. YbNi₃X₉ (X=Al, Ga) is a great opportunity to investigate the tunability of heavy-fermion ground states in Yb-based compound for using external control parameters such as pressure or doping. In this regard, we are investigating physical properties of mixed crystals of YbNi₃Al₉-YbNi₃Ga₉, doping system of Yb(Ni_{1-x}M_x)₃X₉ (M=3d transition-metal) and dilute system of (Yb_{1-x}Lu_x)Ni₃X₉. Here we report Ni-site substitution effects on the antiferromagnetism of YbNi₃Al₉. For YbNi₃Al₉, the resistivity shows a -logT dependence below 100K and a broad peak at about 40 K arising due to the Kondo effect combined with the CEF excited state. In the lower-temperature region, a strong reduction in the extent of magnetic scattering associated with the antiferromagnetic ordering was observed below TN=3.4 K. By Fe-substitution TN is decreased, while is increased by Cu-substitution. The tunability of TN in Yb(Ni_{1-x}M_x)₃X₉ will be discussed.

[1] S. Ohara et al., J. Phys.: Conf. Series 273, 012048 (2011); T. Yamashita et al., to be published in J. Phys. Soc. Jpn.

RD19

Pressure effect studies in Ce₂T₃Ge₅ (T=Rh, Pd, Ir) by electrical resistivity

Miho Nakashima¹, Toshiyuki Uchiyama¹, Toru Kawata¹, Yasushi Amako¹, Yusuke Hirose², Honda Fuminori², Rikio Setta² and Onuki Yoshichika²
¹ Department of Physics, Faculty of Science, Shinshu University, Japan
² Graduate School of Science, Osaka University, Japan

In the Ce₂T₃Ge₅ system (T: transition metal) with the orthorhombic crystal structure, Ce₂Ni₃Ge₅ is an antiferromagnet with a Neel temperature T_N = 5.2 K. T_N decreases with increasing pressure and becomes zero at a critical pressure P_c = 3.9 GPa. The A and ρ₀ values in the Fermi liquid relation (the low-temperature electrical resistivity ρ = ρ₀ + AT²) increase steeply above 3 GPa. It seems to be the heavy fermion state around Pc, in which pressure region superconductivity was found below 0.26 GPa [1]. We measured temperature dependence of electrical resistivity of Ce₂Rh₃Ge₅, Ce₂Ir₃Ge₅ and Ce₂Pd₃Ge₅ under pressure in this study. These three compounds are all antiferromagnets at ambient pressure, showing kinks of resistivity at T_N (=4.7, 9.5 and 3.8 K respectively)[2, 3, 4]. In Ce₂Rh₃Ge₅ and Ce₂Ir₃Ge₅, T_N decreases with increasing pressure and seems to be zero at a critical pressure P_c=0.4 and 2.0 GPa, while T_N increases in Ce₂Pd₃Ge₅ by pressure. We also found another anomaly at lower temperature, indicating T_N splits into two ordering T_{N1} and T_{N2} under pressure more than 0.2 GPa. T_{N1} and T_{N2} are both increasing monotonously with increasing pressure up to 2.3 GPa.

[1] M. Nakashima, et al., J. Phys.: Condens. Matter 17 (2005) 4539. [2] C. Godart, et al., Solid State Commun. 67 (1988) 677. [3] B. Becker, et al., Phys. B 230-232 (1997) 253. [4] Z. Hossain, et al., Phys. Rev. B 60 (1999) 10383.

RD20

Photoemission study on new Kondo lattice compounds YbNi₃(Ga_{1-x}Al_x)₉

Yuki Utsumi¹, Hitoshi Sato², Shigeo Ohara³, Tetsuro Yamashita³, Kojiro Mimura⁴, Satoru Motonami⁴, Masashi Arita⁵, Shigenori Ueda⁵, Keisuke Kobayashi⁵, Kenya Shimada², Hirofumi Namatame² and Masaki Taniguchi²
¹ Graduate School of Science, Hiroshima University, Japan
² Hiroshima Synchrotron Radiation Center, Hiroshima University, Japan
³ Graduate School of Engineering, Nagoya Institute of Technology, Japan
⁴ Graduate School of Engineering, Osaka Prefecture University, Japan
⁵ NIMS Beamline Station at SPring-8, National Institute for Materials Science, Japan

Recently, new Kondo lattice compounds YbNi₃X₉ (X=Al, Ga) were discovered [1]. YbNi₃Al₉ is a heavy-fermion antiferromagnetic compound (TN=3.4 K), while YbNi₃Ga₉ is a valence fluctuating compound from the magnetic susceptibility measurements. These compounds are considered to be very suitable for research of Yb-based Kondo lattice systems because they both possess the ErNi₃Al₉-type crystal structure, and the Al and Ga ions are isovalent. In this study, we have carried out hard x-ray (hv=6 keV) and low energy (hv=7 eV) excited photoemission spectroscopy (HAXPES and LEPES) on YbNi₃X₉ and mixed crystals YbNi₃(Ga_{1-x}Al_x)₉ to investigate the Yb valence and the Kondo resonance behavior. The Yb 3d HAXPES experiments revealed that the Yb ion in YbNi₃Al₉ exists with almost trivalent state while that in YbNi₃Ga₉ strongly fluctuates with the averaged Yb valence of ~2.5. The Al substitution for YbNi₃Ga₉ (x=0.1) changes the Yb ion toward trivalent state. The LEPES spectra of YbNi₃Ga₉ clearly exhibit the Kondo resonance peak near the Fermi level (EF), and the peak is shifted toward EF and the intensity increases with lowering temperature. The extrapolated peak energy at zero temperature provides TK~600 K for YbNi₃Ga₉, and the Al substitution lowers TK.

[1] S. Ohara et al., J. Phys.: Conf. Series 273, 012048 (2011); T. Yamashita et al., to be published in J. Phys. Soc. Jpn.

RD21

Heavy-fermion properties of YbCu_{5-x}Au_x (x = 0.5, 0.6, 0.7)

Ivan Curiik^{1*}, Mauro Giovannini², Mariana Zapotokova³ and Marian Reiffers¹
¹ Institute of Experimental Physics, Slovakia Academy of Science, Watsonova 47, 040 01, Kosice, Slovakia
² CNR-SPIN and Department of Chemistry, University of Genoa, Via Dodecaneso 31, 16 146, Genoa, Italy
³ Institute of Experimental Physics, Slovakia Academy of Science, Watsonova 47, 040 01, Kosice, Slovakia

Yb compounds are very attractive for research because of their low temperature anomalous behaviour. Recently, emphasis was given to the investigation of the solid solution YbCu_{5-x}M_x (M = Ag, Au, In) crystallizing in the cubic AuBe₅-type structure. The substitution of Cu by M offers the possibility of studying the different evolutions of the ground state depending on the M element (e.g. a valence transition in M = In, Kondo-lattice behavior in M = Ag, magnetic ordering in M = Au) [1,2,3]. Here we present the measurements of heat capacity and resistivity in the temperature scale 0.4 -300 K for different applied magnetic fields 0 - 9 T of the YbCu_{5-x}Au_x (x = 0.5, 0.6, 0.7) system. The polycrystalline samples were prepared by induction-melting method, heat-treated and then quenched in cold water. Phase purity was checked by electron probe microanalysis (EPMA) and X-ray diffraction (XRD)

[1] K. Yoshimura et al., J. Alloys Comp 262-263 (1997) 118 [2] M. Galli, E.Bauer, St. Berger, Ch. Dusek et al. Physica B 312-313 (2002) 489 [3] J. He, N. Tsujii et al., J. Phys. Soc. Jpn 66 (1997) 2481

RD22

Magnetic properties of heavy-fermion compounds Ce_{1-x}Lu_xRu₂Si₂

Toru Sekiguchi¹, Yusuke Amakai¹, Shigeoyuki Murayama^{1*}, Hideaki Takano¹, Naoki Momono¹, Kazuyuki Matsubayashi² and Yoshiya Uwatoko²
¹ Graduate School of Engineering, Muroran Institute of Technology, Japan
² Institute for Solid State Physics, University of Tokyo, Japan

Typical heavy-fermion compound CeRu₂Si₂ with a tetragonal structure shows an antiferromagnetic transition by the substitution of La at the Ce site due to the negative chemical pressure by the larger La ion(1). The substitution of Y introduces a decrease of the specific heat coefficient γ and an increase of the Kondo temperature TK due to the positive chemical pressure by the smaller Y ion(2). In order to study substitution effect of Lu with the closed f-electron shell and the ion smaller than Y, we have measured the susceptibility χ and resistivity ρ on single-crystalline Ce_{1-x}Lu_xRu₂Si₂ for 0 ≤ x ≤ 0.2 perpendicular (⊥) and parallel (//) to the c-axis. The χ// shows a maximum and the Tmax increases with x. Since the Tmax is supposed to be the heavy-fermion formation temperature proportional to 1/γ, the effective mass meff is considered to increase with x. The resistivity ρ shows a shoulder by the Kondo effect and the Tshoulder increases with x. This indicates an increase of TK due to the positive chemical pressure by Lu. The low temperature resistivity follows the T² law and the coefficient A decreases with x. Since A is proportional to γ², meff is again considered to increase with x.

(1) S. Quezel et al., J. Magn. & Magn. Mater., 76 & 77, 403 (1988). (2) M.J. Besmus et al., J. Magn. & Magn. Mater., 63 & 64, 323 (1987).

RD23

Moment-bearing Tb substitution in CePt₂Si₂

Moise Bertin Tchoula Tchokonte^{1*}, Zwelithini Melford Mahlubi¹, Paul De Villiers Du Plessis², Andre Michael Strydom² and Dariusz Kaczorowski³
¹ Physics, University of the Western Cape, South Africa
² Physics, University of Johannesburg, South Africa
³ Physics, Institute of Low Temperature and Structure Research, Polish Academy of Sciences., Poland

The effects of substituting moment-bearing Tb in CePt₂Si₂ are reported through X-ray diffraction (XRD), electrical resistivity (ρ(T)), magnetic susceptibility (χ(T)) and magnetization (σ(μ0H)) measurements. XRD results for all compositions of the (Ce_{1-x}Tb_x)Pt₂Si₂ system indicate a tetragonal CaBe₂Ge₂-type structure with space group P4/nmm. ρ(T) results indicate the evolution from a coherent Kondo lattice to incoherent single-ion Kondo behavior up to 90% Ce substitution. χ(T) data at higher temperatures follow the Curie-Weiss relation for all alloy compositions and given effective moment values μeff which increase gradually from the expected value of 2.54 μB for the Ce³⁺-ion to the expected value of 9.72 μB for the Tb³⁺-ion. At low temperature χ(T) data exhibit antiferromagnetism in the concentration range 0.7 ≤ x ≤ 1. No evidence of metamagnetic behavior was observed from σ(μ0H) data for all compositions.

RD24

Heavy Fermion Behavior of Yb₂Ni₁₂P₇ Studied by 31P NMR

Takehide Koyama¹, Kyohei Sugiura¹, Koichi Ueda¹, Takeshi Mito¹, Takao Kohara¹, Tomohito Nakano², Ryohei Satoh¹, Katsuhiko Tsuchiya³ and Naoya Takeda²
¹ Graduate School of Material Science, University of Hyogo, Japan
² Faculty of Engineering, Niigata University, Japan
³ Graduate School of Science and Technology, Niigata University, Japan

We present results of the nuclear magnetic resonance measurement (NMR) of Yb-based intermetallic compound Yb₂Ni₁₂P₇, which crystallizes in the hexagonal Zr₂Fe₁₂P₇-type structure [1]. Yb₂Ni₁₂P₇ does not order magnetically down to 50 mK and forms the heavy fermion state. The electronic specific heat of Yb₂Ni₁₂P₇ is markedly enhanced at low temperatures (200 mJ/K² mol-Yb). The magnetic susceptibility shows the Curie-Weiss like behavior at high temperatures and has a noticeable hump at around 50 K. We have performed NMR measurement to investigate the electronic properties of Yb₂Ni₁₂P₇. The observed NMR line shows a complicated shape, reflecting the presence of three non-equivalent P sites and local symmetries around them. The nuclear-spin lattice relaxation rate (1/T₁) shows nearly T⁻¹=const. behavior, which is consistent with the delocalization of the 4f electrons.

K. Zeppenfeld and W. Jeitschko, J. Phys. Chem. Solids, 54 (1993) 1527.

RD25

Electronic structure of RCu₂Si₂ (R=Yb, Y) studied by soft x-ray angle-resolved photoemission spectroscopy

Akira Yasui¹, Shin-ichi Fujimori¹, Ikuto Kawasaki², Tetsuo Okane¹, Yukiharu Takeda¹, Yuji Saitoh¹, Hiroshi Yamagami³, Akira Sekiyama⁴, Rikio Settai⁵, Tatsuma D Matsuda⁶, Yoshinori Haga⁶ and Yoshichika Onuki⁵
¹ Condensed Matter Science Division, Japan Atomic Energy Agency, Japan
² Advanced Meson Science Laboratory, RIKEN Nishina Center for Accelerator-Based Science, Japan
³ Department of Physics, Kyoto Sangyo University, Japan
⁴ Division of Materials Physics, Osaka University, Japan
⁵ Department of Physics, Osaka University, Japan
⁶ Advanced Science Research Center, Japan Atomic Energy Agency, Japan

In recent years, electronic structure of YbCu₂Si₂, which is a classical example of Yb-based valence fluctuation compounds, has been studied by various experimental methods such as a quantum oscillation measurement [1] and an angle-integrated photoemission spectroscopy (AIPES) [2]. However, these results are inconsistent each other. In fact, the band structure calculation which well describes the results of the quantum oscillation measurement [1] cannot explain the AIPES spectrum. In the present study, we have performed the soft x-ray angle-resolved photoemission spectroscopy (SX-ARPES) for YbCu₂Si₂ to understand the valence band structure and the Fermi surface (FS) in a unified way. The SX-ARPES measurements were recorded in BL23SU of SPring-8. We have observed that hybridized bands of Yb 4f electrons and conduction states cross the Fermi level at 20 K, which is well below the Kondo temperature of TK = 50 K, in line with the valence-fluctuating state of YbCu₂Si₂. We will discuss effects of Yb 4f electrons on its band structure by comparing the ARPES spectra with those of a non-4f-reference compound YCu₂Si₂.

[1] N. D. Dung et al., J. Phys. Soc. Jpn. 78, 084711 (2009). [2] M. Matsunami et al., Phys. Rev. B 78, 195118 (2008).

RD26

Anomalous increase of TC in UGa₂ under pressure

Ladislav Havela¹, A. Kolomiets², J. Prchal¹ and A. V. Andreev³
¹ Department of Condensed Matter Physics, Charles University, Czech Republic
² Department of Physics, Lviv Polytechnic National University, Ukraine
³ Institute of Physics, Academy of Sciences of the Czech Republic, Czech Republic

UGa₂ belongs to compounds quite thoroughly studied, although there is still no consensus about the character of the 5f states. In particular, 5f₂ or 5f₃ localized and band-like 5f states were considered, none of those being able to explain all its features [1]. Response of magnetic properties to external pressure is an important indicator of the situation of the 5f states. While band systems tend to a suppression of magnetic moments and their ordering, magnetism based on localized states has insensitive size of moments and their ordering temperatures can weakly increase. Previous experiments [2] indicated a quite rapid increase (approx. 3 K/GPa) of the Curie temperature from TC = 126 K up to p = 0.8 GPa. New resistivity experiments on UGa₂ single crystal, extending the pressure range up to 8 GPa, reveal a continuous linear increase, reaching 160 K without any sign of saturation. Such anomalously large increase can be only understood in the framework of a two-band model, in which the compression leads to a stronger hybridization of the 5f and other conduction-electron states.

[1] T. Honma et al., J. Phys. Soc. Japan 69 (2000) 2647. [2] A.V. Kolomiets et al., Physica B 259-261 (1999) 238.

RE01

Engineered p-d exchange interaction of coupled double diluted magnetic quantum dots

Eun-young Kim
 Seoul National University, Korea

This paper presents the effects of inserting a thick InGaN layer which was grown between n-GaN and active layer by MOCVD. By adding the thick InGaN layer, we expected the compensation of lattice mismatch between n-GaN and active layer. From AFM results, QDs (Quantum Dots) were formed at around 200 Å InGaN thickness by TD (Threading Dislocation) termination effect. According to the result of TD termination, the electrical and optical properties were improved due to the decrease of non-radiative recombination area in active layer. The result of PL data shows PL intensity increased by inserting the thick InGaN layer.

RE02

Quasi-particle localization by disorder in an incompressible fractional quantum Hall state

Partha Goswami*
 Physics department, D.B.College(University of Delhi),New Delhi, India

The strongly correlated electrons, together with disorder, organize themselves in a non-trivial way to form incompressible collective states for the filling fraction $\nu = 5/2$ in a dirty bi-layer semi-conductor quantum well system. The theoretical analysis of the quantum phase transition(QPT) exhibited by this system has been carried out including the single-particle quantum lifetime sensitive to the long range scattering and the usual zero field short-range Drude scattering (transport lifetime). Since the tunneling terms can be controlled by changing gate voltages, we find that, in principle, a completely reversible sequence of events, viz. a crossover from the bi-layer fractional quantum Hall state to the single-layer one followed by an entry to quantum critical state (and the QPT to the bi-layer state beyond) and eventually a crossover to the single-layer state, could be realized with the increase in inter-layer tunneling. The sequence, which is manifestation of quasi-particle localization by disorder, could prove to be useful in performing memory function and gating operation.

RE03

NpCoGe, near quantum criticality?

Eric Colineau*, Rachel Eloirdi, Jean-christophe Griveau, Piotr Gaczynski and Alexander Shick
 European Commission, Joint Research Centre, Institute for Transuranium Elements, Germany

The orthorhombic isostructural series AnTGe (An = actinide ; T = transition metal) offers a unique opportunity to study the properties and trends of a system where ferromagnetism and superconductivity coexist at ambient pressure in URhGe (TC = 9.5K, TSC = 0.26K) [1] and UCoGe (TC = 3K, TSC = 0.7K) [2]. However, due to the difficulty to handle them, transuranium systems are much less documented. In an effort to bridge this gap, we have undertaken the study of the neptunium analogues and have previously reported that NpRhGe exhibits an antiferromagnetic ground state (TN = 21K, μ Np = 1.14 μ B) [3]. In the present work, we have investigated NpCoGe by dc magnetization, ac susceptibility, specific heat, electrical resistivity, 237Np Mossbauer spectroscopy and LSDA calculations. We find that NpCoGe orders antiferromagnetically at TN=13K with an average ordered moment $\langle m_{Np} \rangle = 0.8 \mu$ B. The weak antiferromagnetic interactions ($0p = -5.5$ K) are overcome by the application of a moderate magnetic field (B ~ 3T) that induces a metamagnetic phase. NpCoGe appears as a more delocalized antiferromagnet than NpRhGe, which is consistent with the trend observed in UTGe analogues. The proximity of NpCoGe to a quantum critical point and its implications will be discussed.

RE04

Pressure and magnetic-field induced non-Fermi-liquid behavior in YbCo₂Zn₂₀

Kazuyuki Matsubayashi¹*, Rina Yamanaka¹, Yuta Saiga², Tatsuya Kawae³ and Yoshiya Uwatoko¹
¹ Institute for Solid State Physics, The University of Tokyo, Japan
² Institute for Advanced Materials Research, Hiroshima University, Japan
³ Department of Applied Quantum Physics, Faculty of Engineering, Kyushu University, Japan

In heavy fermion systems, applying pressure and magnetic field controls the electronic configuration, and thus anomalous behaviors appear at around magnetic quantum critical point (QCP), such as an unconventional superconductivity and Non-Fermi-liquid behavior. Recently, YbCo₂Zn₂₀ have attracted much attention because of their heavy fermion state and proximity to the pressure-induced QCP [1]. It is worth noting that the critical pressure of YbCo₂Zn₂₀ is lower than that of other Yb based compounds. Therefore YbCo₂Zn₂₀ has an advantage of investigating the behavior of Yb- based compounds near QCP. More interestingly, it is reported that a metamagnetic crossover appears at H ~ 0.6 T [2], however, the origin of this metamagnetic behavior remains unclear. In order to shed light on the nature of the pressure- and field-induced quantum critical behavior, we have measured the specific heat of YbCo₂Zn₂₀ under pressure and magnetic field. We found that the low temperature specific heat in the vicinity of the critical region exhibits the power-law divergence. The temperature-pressure-magnetic field phase diagram will be presented to sum up the physical properties.

[1] Y. Saiga et al., J. Phys. Soc. Jpn 77 (2008) 053710 [2] M. Ohya et al., J. Phys. Soc. Jpn 79 (2010) 083601

RE05

Relationship between single-particle excitation and spin excitation at the Mott transition

Masanori Kohno*
 WPI Center for Materials Nanoarchitectonics, National Institute for Materials Science, Japan

The Mott transition in the one- and two-dimensional Hubbard models is investigated using the Bethe ansatz, dynamical density-matrix renormalization group method, cluster perturbation theory, and random-phase approximation. I will show that the dispersion relation of single-particle excitation in a metallic phase leads continuously to that of spin excitation of the Mott insulator.

RE06

Quantum criticality in Kondo quantum dot coupled to 2D topological insulator

Chung-hou Chung* and Salman Silotri
 Electrophysics Dept., National Chiao-Tung University, HsinChu, Taiwan, R.O.C., Taiwan

We investigate theoretically the quantum phase transition between the one-channel Kondo (1CK) and two-channel Kondo (2CK) fixed points in a quantum dot coupled to edge states of interacting 2D topological insulators (2DTI) with Luttinger parameter 0<K<1. For K<1, the strong coupling 2CK fixed point was argued to be stable for infinitesimally weak tunnelings between dot and the 2DTI based on the simple scaling dimensional analysis. We re-examine the model beyond the scaling dimension analysis via a controlled 1-loop renormalization group (RG) approach on the effective Kondo model via bosonization and re-fermionization near the 2CK fixed point. We find for K<1 the 2CK fixed point can be unstable towards the 1CK fixed point and the system may undergo a quantum phase transition (QPT) between 1CK and 2CK fixed points. The QPT in our model comes as a result of the combined Kondo and the helical Luttinger physics in 2DTI, and it serves as the first example of the 1CK-2CK QPT accessible by a controlled theoretical approach. We extract quantum critical and crossover behaviors from various thermodynamical quantities near the quantum critical point.

RE07

Nature of insulator-metal-insulator transitions in the ionic Hubbard model

Aaram Joo Kim¹, Moo Young Choi¹ and Gun Sang Jeon^{2*}
¹ Department of Physics and Astronomy, Center for Theoretical Physics, Seoul National University, Korea
² Department of Physics, Ewha Womans University, Korea

It is known that the ionic Hubbard model possesses a metallic phase between band and Mott insulators in high dimensions. We study the phase diagram in the Bethe lattice for various strengths of the staggered lattice potential within the dynamical mean-field theory (DMFT) combined with the continuous-time quantum Monte Carlo method. We also investigate its zero-temperature limit by means of exact diagonalization as a DMFT solver. Observed at finite temperatures are the crossover between the metallic and band insulating phases and the first-order transition between the metallic and Mott insulating phases, ending up with the critical point. It is discussed how such transition behaviors evolve as the lattice potential is increased at low temperatures and whether the finite- and zero-temperature results are consistent with each other.

RE08

Variational cluster approach to the Hubbard model on the honeycomb lattice

Kazuhiro Seki* and Yukinori Ohta
 Department of Physics, Chiba University, Japan

Physics of electrons on the honeycomb lattice, or graphene, is one of the topical issues in condensed matter physics. Especially, the influence of electron correlations on the magnetism and electronic states at the Fermi level, which is characterized by the linear dispersion relation and vanishing density of states in the non-interacting case, is of particular interest. In this study, we apply the variational cluster approach to the half-filled Hubbard model on the honeycomb lattice. In order to study the semimetal-insulator transition and paramagnetic-antiferromagnetic insulator transition, we introduce the bath hybridization strength and staggered magnetic field as variational parameters. We calculate the single-particle spectra and magnetic order parameter as a function of Coulomb interaction U, and discuss the implications of the results.

RE09

Onset of magnetic order in U₂(Ni_{1-x}Fe_x)₂Sn

Silvie Maskova¹*, Ladislav Havela¹, Aleksandre Kolomiets², Alexander Andreev³, Heinz Nakotte⁴, Joe Peterson⁴, Yurii Skourski⁵, Shadi Yasin⁵, Sergei Zherlitsyn⁵, Joachim Wosnitza⁶ and Khrystyna Milyanchuk⁶
¹ Department of Condensed Matter Physics, Charles University in Prague, Czech Republic
² Department of Physics, Lviv Polytechnic National University, Ukraine
³ Institute of Physics, ASCR, Czech Republic
⁴ Department of Physics, New Mexico State University, USA
⁵ Dresden High Magnetic Field Laboratory, Helmholtz-Zentrum Dresden-Rossendorf, Germany
⁶ Faculty of Chemistry, Ivan Franko National University, Lviv, Ukraine

Single crystal of U₂Ni₂Sn and polycrystals U₂(Ni_{1-x}Fe_x)₂Sn and their hydrides were prepared so as to investigate the character and stability of magnetism in U₂Ni₂Sn (antiferromagnet with T_N = 26 K). We show that its magnetism is uniaxial, with 3 metamagnetic transitions detected in magnetic fields up to 60 T along the tetragonal c-axis. Such anisotropy manifests also in the paramagnetic state. Estimated difference of paramagnetic Curie temperatures, 175 K, quantifies the anisotropy. The AF order disappears rapidly with the Fe substitution. Magnetic susceptibility and specific heat of the sample with 20 % Fe reveals a great similarity to previously studied NFL heavy-fermion U₂Co₂Sn [1]. The C/T upturn at low temperatures, very resistant to magnetic fields, is suppressed with further increase of Fe concentration. Exposure to 100 bar H₂ leads to the H-absorption forming U₂(Ni_{1-x}Fe_x)₂SnH_{1-x}. U₂Ni₂SnH_{1-x} is AF (T_N = 87 K), which is at least partly due to the lattice expansion ($\Delta V = 7$ -10%). In the middle of the Fe concentration range, hydrogenation induces a ferromagnetic order. A detailed study of the Fe-poor end, for which the approach to the NFL behaviour can be followed, is under way.

[1] J.S. Kim et al., Phys. Rev. B 62 (2000) 6986.

RE10

Magnetic phase diagram of UCoAl

Tatsuma D. Matsuda¹, Dai Aoki², Naoyuki Tateiwa¹, Etsuji Yamamoto¹, Yoshinori Haga¹, Yoshichika Onuki³, Jacques Flouquet² and Zachary Fisk⁴

¹ ASRC, JAEA, Japan

² INAC/SPSMS, CEA-Grenoble, France

³ Graduate School of Science, Osaka University, Japan

⁴ University of California, USA

Heavy fermion UCoAl is known to be a unique system with metamagnetic transition from paramagnetic to ferromagnetic ground states in uranium-based compounds. This kind of metamagnetism and quantum criticality in strongly correlated electron systems have attracted much attention because of expectation of new quantum phases. Recently, we succeeded to grow a high quality single crystal of UCoAl by the Czochralski pulling method and performed the magnetic measurements. In this presentation, we will show the magnetic phase diagram of UCoAl in detail.

RE11

Renormalization-group exponents for competitions between inter-electronic and phonon-mediated interactions in ladder systems

Wen-min Huang^{1*}, Yiwei Cai² and Hsiu-hau Lin²

¹ Physics Division, National Center for Theoretical Sciences, Taiwan

² Department of Physics, National Tsing Hua University, Taiwan

After developing a scaling ansatz for electron-electron interactions under renormalization group transformation[1], we show that, with the inclusion of phonon-mediated interactions the ansatz, characterized by the divergent logarithmic length and a set of renormalization-group exponents, also works rather well. The superconducting phases in a doped two-leg ladder are studied and classified by these renormalization-group exponents as demonstration. Finally, nontrivial constraints among the exponents are derived and explained.

[1] H.-Y. Shih, W.-M. Huang, S.-B. Hsu and H.-H. Lin, *Phys. Rev. B* 81, 121107(R) (2010).

RE12

Crystal Growth and Magnetic Order of Ni-doped CePdAl

Veronika Fritsch^{1*}, Sarah Woitschach², Oliver Stockert², Michael M. Koza³, Silvia Capelli³ and Hilbert V. Loehehneysen⁴

¹ Physikalisches Institut, Karlsruher Institut fuer Technologie, 76131 Karlsruhe, Germany

² Max-Planck-Institut fuer Chemische Physik fester Stoffe, 01187 Dresden, Germany

³ Institut Laue-Langevin, 38042 Grenoble, France

⁴ Physikalisches Institut und Institut fuer Festkoerperphysik, Karlsruher Institut fuer Technologie, 76131 Karlsruhe, Germany

CePdAl is a stoichiometric, antiferromagnetic compound (Neel temperature = 2.7 K) which can be tuned to a quantum critical point (QCP) by hydrostatic [T. Goto et al., *J. Phys. Chem. of Solids* 63, 1159 (2002)] or chemical pressure [Y. Isikawa et al., *J. Phys. Soc. Jpn.* 65, 117 (1996)]. The latter can be achieved by substituting Ni for Pd. Neutron-scattering experiments [A. Doenni et al., *J. Phys.: Condens. Matter* 8, 11213 (1996)] pointed towards a partial frustration of the Ce moments in CePdAl, making this system a promising candidate for investigating the influence of frustration on quantum criticality. We have grown large single crystals of Ni-doped CePdAl by the Czochralski method. The samples were characterized by x-ray powder diffraction, atomic absorption spectroscopy and x-ray Laue diffraction. Specific heat and inelastic neutron scattering data of CePdAl yield a Kondo temperature of approximately 5 K. Magnetization measurements display a strong magnetic anisotropy which is preserved in the Ni-doped compounds, where the magnetic order is suppressed. Neutron-diffraction experiments indicate that short-range correlations are present well above the Neel temperature. Below the Neel temperature, one third of the Ce moments display short-range order only, confirming the frustration in this system.

RE13

Transport properties of Ho_{1-x}Lu_xB₁₂ solid solutions

Slavomir Gabani^{1*}, Ivan Batko¹, Marianna Batkova¹, Karol Flachbart¹, Emil Gazo¹, Gabriel Pristas¹, Iveta Takacova¹, Alexey Bogach², Nickolay Sluchanko² and Natalya Shitsevalova³

¹ Centre of Low Temperature Physics, Institute of Experimental Physics SAS, Slovakia

² General Physics Institute RAS, Russia

³ Institute for Problems of Materials Science NASU, Ukraine

Recent studies of Ho_{1-x}Lu_xB₁₂ solid solutions have shown [1] that the antiferromagnetic (AF) order in geometrically frustrated system of HoB₁₂ (x = 0, TN = 7.4 K) is linearly suppressed to zero temperature, i.e. TN → 0, as lutetium concentration increases to x → xC 0.9. In this contribution, we present original results of electrical resistivity measurements on Ho_{1-x}Lu_xB₁₂ single crystalline samples with x = 0, 0.2, 0.5, 0.7, 0.9, 1 in the temperature range 0.05 - 300 K and in magnetic fields (B) up to 8 T. Complex B vs TN phase diagrams were received from precise temperature and field dependences of resistivity with more AF phases for x ≥ 0.5 pointing to a possible quantum critical point at xC 0.9. The scattering of conduction electrons in the AF phase and in the paramagnetic phase as well as Hall effect results are analyzed and discussed for various concentrations x, when magnetic dilution increases with the increasing content of nonmagnetic Lu ions in the Ho_{1-x}Lu_xB₁₂ system.

[1] S. Gabani, I. Batko, M. Batkova, K. Flachbart, E. Gazo, M. Rejters, N. Shitsevalova, K. Siemensmeyer and N. Sluchanko, 17th International symposium on boron, borides and related materials, Sept 11-17, 2011, Istanbul, Turkey.

RE14

Low temperature thermal and electrical transport properties of ZrZn₂ in high magnetic field

Yang Zou^{1*}, Michael Sutherland¹, Stephen Hayden² and F. Malte Grosche¹

¹ Department of Physics, University of Cambridge, United Kingdom

² Department of Physics, University of Bristol, United Kingdom



RE15

Non fermi liquid behaviour in YFe₂Ge₂

Yang Zou*, Zhuo Feng, Sven Friedemann and F. Malte Grosche

Department of Physics, University of Cambridge, United Kingdom



RF01

Magnetic orderings at the interface between Mott insulator and band insulator

Suguru Ueda^{1*}, Norio Kawakami¹ and Manfred Sigris²

¹ Department of Physics, Kyoto University, Japan

² Theoretische Physik, ETH Zurich, Switzerland

Recent experimental progress in crystal growth techniques enables us to investigate the complex oxide heterostructures as a new frontier for studies of strongly correlated electron systems. In such systems, the main interest is put toward the metallic state around the interface, which is realized between two different insulating compounds, such as SrTiO₃/LaTiO₃ and SrTiO₃/LaAlO₃ [1]. Intriguingly, magnetism and superconductivity are also reported in such metallic interfaces [2]. Stimulated by these findings, we theoretically study the magnetic properties of the strongly correlated heterostructure composed a Mott insulator and band insulators. For this purpose, the single-band Hubbard model with long-range Coulomb interaction is investigated using the Hartree-Fock approximation [3]. We find the electronic and magnetic phases specific to the interface, including a canted antiferromagnetic state and a charge-ordered state with checkerboard charge distribution. We elucidate the origin of these phases is closely related to the spatial inhomogeneity which induces unconventional couplings between spin and charge degrees of freedom. Additionally, the applied magnetic fields also reveal other aspects of correlated heterostructures; a first order metamagnetic transition and field-induced checkerboard charge-ordered state, which are also driven by the non-uniform charge distribution.

[1] A. Ohtomo, et al., *Nature* 419, 378 (2002), A. Ohtomo, and H. Y. Hwang, *Nature* 427, 423 (2004), [2] A. Brinkman, et al., *Nat. Mater.* 6, 493 (2006), J. Biscaras, et al., *Nat. Commun.* 1, 89 (2010), [3] Okamoto, and Millis, *Phys. Rev. B* 70, 075101 (2004).

RF02

Strong Electron Correlation in Cu-doped CaO Nanocolloid

Nguyen Thuy Trang¹, Pham Thanh Cong², Hoang Nam Nhat^{3*}

¹ Faculty of Physics, Vietnam National University, University of Natural Sciences, Viet Nam

² Physikalisches Institut, Goethe-Universitat Frankfurt, Germany

³ Faculty of Technical Physics and Nanotechnology, Vietnam National University, University of Engineering and Technology, Viet Nam

Theoretical prediction of magnetism induced by defects or doping in non-metallic colloids has gained a renewed interests recently. In this work, we investigated the possible appearance of magnetism in Cu doped CaO nanocolloids activated by SPAN-80 in the framework of density functional theory (DFT). Despite of strong antiferromagnetic super-exchange interaction between Cu²⁺ ions, the local magnetic moment of Cu may appear due to colloidal agent attachment onto the surface of CaO nanocluster (surface modification). The ferromagnetism attributes to the degeneration of Cu 3d orbitals in CaO crystal fields, the aspects of electron correlation and quantum spin fluctuation.

PACS number: 42.30.R, 42.40.Ht, 42.30.Kq

Keywords: DFT, band-gap, CaO, calcium-oxide, mBJ, PBE, functional

RF03

The book-keeping fermion analysis of the double exchange model with antiferromagnetic background

Kyohei Nakano^{1*}, Robert Eder², Yukinori Ohta¹ and Piotr Wrobel³

¹ Department of Physics, Chiba university, Japan

² Institute for Solid State Physics, Karlsruhe Institute of Technology, Germany

³ Institute for Low Temperature and Structure Research, Poland

We analyse the double exchange model with antiferromagnetic background by the book-keeping fermion method. First, we consider the motion of a single conduction electron. We assume that the localized spins form the Neel state and the added conduction electron forms only three types of states under the strong Hund-coupling assumption and we regard these states as the book-keeping fermion. Under these assumptions, we calculate the spectral functions which show good agreement with the results given by the exact diagonalizations for finite size clusters. We also study the relation between the strength of the Hund coupling and the bandwidth in the lower-energy region. The results show that the bandwidth approaches a finite value as the Hund-coupling constant becomes close to infinity. The bandwidth even increases with increasing the Hund coupling, which is in strong contrast to the expectation from the semi-classical theory. Next, we consider the situation where there are finite numbers of spin flips occurring in the down-spin sublattice in the Neel ordered state. Considering the effects of the spin defects, we add a new book-keeping fermion and estimate the energy of the spin defects by a perturbation theory. This theory gives the phase diagram comparable with the numerical results.

RF04

Phonon Induced Thermodynamic Properties of La_{1-x}Ca_xCoO₃

Rasna Thakur*, Rajesh K. Thakur and N.k. Gaur

Department of Physics, Barkatullah University, Bhopal, India

Perovskite type cobaltate, La_{1-x}Ca_xCoO₃ (0 ≤ x ≤ 0.3) have been studied intensively because of their wide range of unique physical properties. The fact that rare-earth perovskite-type cobaltate are most suitable as a cathode material in solid oxide fuel cells (SOFC), makes the thermal behavior of these compounds highly important. As these compounds are predominantly ionic in nature hence the lattice contributions to the specific heat at constant volume (C_{v(lattice)}) of pure and Ca doped LaCoO₃ has been studied and thereby thermal expansion is computed as function of temperature by means of Rigid Ion Model (RIM). We have systematically investigated the effect of phonons on thermal properties, Debye temperature (Θ_D), molecular force constant (f), Reststrahlen frequency (ν), cohesive energy (φ), and gruneisen parameter (γ) for La_{1-x}Ca_xCoO₃ (0 ≤ x ≤ 0.3). Also the effect of phonons on the bulk modulus is studied using the atoms in molecules (AIM) theory for pure and ca doped LaCoO₃. We have found that the computed properties reproduce well with the available experimental data, implying that RIM represents properly the perovskite cobaltate La_{1-x}Ca_xCoO₃ (0 ≤ x ≤ 0.3). To our knowledge some of the properties for these complicated compounds are reported for the first time.

RF05

Dynamical antiferromagnetic phase transition after the quantum quench in the fermionic Hubbard model

Naoto Tsuji* and Philipp Werner

Institute for Theoretical Physics, ETH Zurich, Switzerland

Spontaneous symmetry breaking is a universal concept in physics that stretches widely from condensed matter to cosmology. Recently it is getting feasible to study in detail how symmetry is dynamically broken in correlated electron systems using an ultrafast optical spectroscopy technique [1], which works as a key probe for electron correlation and fluctuations. Theoretically the phenomenon has been discussed with the Ginzburg-Landau (GL) theory, a macroscopic phenomenology. To capture the evolution of the electronic structure, however, one needs a microscopic description, which is not well understood. Here we take the fermionic Hubbard model, a typical microscopic model for correlated electrons, and study how the antiferromagnetic order develops from a paramagnetic initial state after the quantum quench using the nonequilibrium dynamical mean-field theory. The system shows a multistep time evolution: (i) a fast thermalization within the paramagnetic phase, (ii) an exponential growth of the order parameter, and (iii) decay of collective excitations. We show how these features are reflected in the single-particle and optical-conductivity spectrum, and discuss the nature of antiferromagnetic fluctuations.

[1] R. Yuzupov et al., *Nat. Phys.* 6, 681 (2010).

RF06

Itinerant magnetism in the hubbard model within the dynamical cluster approximation

Unjong Yu*

GIST college, Gwangju Institute of Science and Technology, Korea

There have been a lot of efforts to understand the itinerant magnetism because ferromagnetism in many metallic magnets like iron, cobalt, and nickel is due to the itinerant magnetism. However, the mechanism and the stability of the itinerant magnetism are not clear yet because the strong quantum mechanical correlation in time and space is crucial in the itinerant magnetism. The Stoner model, which is the most popular model for the itinerant magnetism, ignores those correlation effects and so is inadequate [1]. In this paper, we studied the itinerant magnetism within the dynamical mean-field theory (DMFT) and its cluster extension, dynamical cluster approximation (DCA). These two methods are non-perturbative and fully include strong correlation effects [2]. Particularly, the DCA incorporates spatial correlation (nonlocal effects) systematically and gives numerically exact solution for the many-body problem [3]. We applied these two methods to study the ferromagnetic and antiferromagnetic instability of the Hubbard model in the 2-dimensional square lattice, the 3-dimensional cubic lattice, and the face-centered-cubic (fcc) lattice. We show that the correlation in time and space reduces the critical temperature remarkably and is essential to understand the itinerant magnetism.

[1] N. Majlis, *The Quantum Theory of Magnetism*, 2nd ed. (World Scientific Publishing, Singapore, 2007), pp. 195-237. [2] D. Vollhardt et al., in *Band-Ferromagnetism*, edited by K. Baberschke et al. (Springer-Verlag, Berlin, 2001), p. 191. [3] U. Yu et al., *Phys. Rev. Lett.* 104, 037201 (2010).

July 12 (Thu)

July 12 (Thu)

RF07

First Principles DFT+U Method for Strongly Correlating Electronic Structure Systems

Tomoyuki Hamada¹, Takahisa Ohno² and Sadamichi Maekawa³
¹ Central Research Laboratory, Hitachi Ltd., JST-CREST, Japan
² National Institute of Materials Research, Japan
³ ASRC, JAEA, JST-CREST, Japan

First principles density functional+U pseudopotential (DFT+U PP) method free from any empirical parameters has been developed and applied to the electronic structure calculations of strongly correlating electronic structure systems such as FeO and LaVO₃. The method can calculate the electronic structure of the systems from first principles, being contrary to the conventional DFT+U PP method, which uses empirical Ueff paramaters. The method primary calculates the Hubbard on-site interaction parameter Ueff for localized electrons, using an approximate constrained DFT technique, and then uses the calculated parameter in the DFT+U PP electronic structure calculation. Examples of calculations resulted in Ueff of Fe 3d electrons of anti-ferromagnetic FeO to be 5.11 eV (the empirical value is 5eV) and Ueffs of La 4f and V 3d electrons of paramagnetic LaVO₃ to be 15.6 and 0.47 eV, respectively (the empirical values are 20.0 and 0 eV, respectively). The band gap structure of these materials was correctly described. Our method seems to be a promising tool for investigating strongly correlating electronic structure systems for spintronics applications, correctly describing the localized and itinerant nature of electrons of the systems from first principles.

RF08

Correlation effect in ferromagnetic 3d transition metals

Muneyuki Nishishita¹, Sudhakar Pandey² and Dai Hirashima^{1*}
¹ Nagoya University, Japan
² APTPC, Korea

MOVED

RF09

Mott transition in frustrated Hubbard model with spatial anisotropy: Cellular dynamical mean field study

Tomoko Kita^{1*}, Yuta Furukawa¹, Takuma Ohashi² and Norio Kawakami¹
¹ Department of Physics, Kyoto University, Japan
² Department of Physics, Osaka University, Japan

Geometrical frustration has attracted much interest in the field of strongly correlated electron systems. In the frustrated systems, a lot of intriguing phenomena such as the heavy fermion behavior in LiV₂O₆, spin liquid ground state in organic materials, etc. have been observed and they have stimulated theoretical investigations of frustrated electron systems. In particular, the reentrant behavior in the Mott transition in moderately frustrated systems, the heavy Fermi-liquid behavior around the Mott transition, etc. are new aspects of the Mott transition and very interesting. In our recent study on the kagome lattice system with spatial anisotropy [1] and also Ref. [2], it has been found that the anisotropy is strongly enhanced around the Mott transition, which stabilizes antiferromagnetic spin configurations. In this study, we apply the cellular dynamical mean field theory combined with a continuous-time quantum Monte Carlo solver [3] to the Hubbard model on the anisotropic kagome and triangular lattices. We systematically investigate the effects of the enhanced anisotropy around the Mott transition on the quasiparticle spectra and spin correlation functions.

[1] Y. Furukawa et al.: Phys. Rev. B 82 (2010) 161101. [2] A. Yamada et al.: Phys. Rev. B 83 (2011) 195127. [3] G. Kotliar et al.: Phys. Rev. Lett. 87 (2001) 186401; P. Werner et al.: Phys. Rev. Lett. 97 (2006) 076405.

RF10

Spin-nematic and -singlet states in the Mott insulator phase of the S=1 two-dimensional Bose-Hubbard model

Yuta Toga¹, Hiroki Tsuchiura¹, Makoto Yamashita² and Hisatoshi Yokoyama³
¹ Department of Applied Physics, Tohoku University, Japan
² NTT Basic Research Laboratories, NTT Corporation, Japan
³ Department of Physics, Tohoku University, Japan

Because of the recent development in experimental cold-atom physics, a quantum gas microscope technique has opened the door for detecting and manipulating single bosonic atoms at single site level in an optical lattice, just like scanning tunneling microscopy in solid-state physics. Quite recently, Endres et al [1]. used this technique to track the superfluid-Mott insulator (SF-MI) transition of spinless bosonic-atoms on an optical lattice in more detail, and found that correlated pairs of a doubly populated site and an unpopulated site which representing the excitations in the MI, fundamentally determine the properties of the SF-MI transition, which is consistent with recent numerical studies [2,3]. Theoretically, spin-1 bosonic atoms on a two-dimensional lattice is also of prime importance because it is a bosonic analogue of the two-dimensional fermionic (S=1/2) Hubbard model, which has been exhaustively studied in the context of magnetism and high-temperature superconductivity. Thus in this work, we study the ground state properties and quantum phase transitions of S=1 two-dimensional Bose-Hubbard model, focusing on correlated pairs excitations based on a variational Monte Carlo approach. We discuss the spin-structures in the MI, and present a consistent description of the transition from the spin-nematic state to the spin-singlet state beyond mean-field theory.

[1]M. Endres, M. Cheneau, T. Fukuhara, C. Weitenberg, P. Schauß, C. Gross, L. Mazza, M. C. Banuls, L. Pollet, I. Bloch, and S. Kuhr, Science 334 (2011) 200. [2] M. Capello, F. Becca, M. Fabrizio, and S. Sorella, Phys. Rev. Lett. 99 (2007) 056402; Phys. Rev. B 77 (2008) 144517. [3] H. Yokoyama and M. Ogata, J. Phys. Chem. Solids 69 (2008) 3356; H. Yokoyama, T. Miyagawa, and M. Ogata, J. Phys. Soc. Jpn 80 (2011) 084607.

RF11

Dynamical instability in two-component bosonic systems in an optical lattice

Rui Asaoka¹, Yuta Toga¹, Hiroaki Tsuchiura¹ and Makoto Yamashita²
¹ Department of Applied Physics, Tohoku University, Japan
² NTT Basic Research Laboratories, NTT Corporation, Japan

Because of the recent development in experimental technique, there has been an emerging interest in dynamical properties of Bose-Einstein condensates (BEC) on an optical lattice. In particular, quantum gas microscope technique has opened the door for real-time observation of single bosonic atoms at single site level in an optical lattice, which can act as scanning tunneling microscopy in solid state physics. Quite recently, Greiner and his co-workers used this technique to track the superfluid-Mott insulator (SF-MI) transition of bosonic-atoms in real-space and time [1,2]. Further studies for dynamical properties of BEC may be only a matter in time. Dynamical analysis of BEC in strongly correlated bosonic systems is also of interest in theoretical point of view. In particular, the dynamical instability of SF in multi-component bosonic systems is of prime importance because there would be entangled interplay among superfluidity, Mott physics, and possibly also Anderson localization. Thus, in this work, we study the dynamical instability of the SF phase of the two-component Bose-Hubbard model based on the dynamical Gutzwiller approximation. We mainly focus on the effects of the dispersive current of one-component on the stability of SF current of another component.

[1] W. S. Bakr et al., Science 329, 547 (2010). [2] M. Endres et al., Science 334, 200 (2011).

RF12

Mechanism for the high Neel temperature in SrTeO3

Ashis Kumar Nandy¹, S. Middey¹, Priya Mahadevan^{2*} and D. D. Sarma³
¹ Centre for Advanced Materials, Indian Association for the Cultivation of Science, India
² S.N. Bose National Centre for Basic Sciences, India
³ Solid State and Structural Chemistry Unit, Indian Institute of Science, India

The microscopic origin [1] of the high Neel temperature observed experimentally in SrTeO₃ [2] and CaTeO₃ [3] has been examined using a combination of ab-initio electronic structure calculations and mean-field solutions of a multi-band Hubbard model. The G-type anti-ferromagnetic state is found to be robust for a large region of parameter space, with large stabilization energies found, surprisingly, for small values of intra-atomic exchange interaction strength as well as large bandwidths. The microscopic origin of this is traced to specific aspects associated with the d3 configuration at the transition-metal site. Considering values of interaction strengths appropriate for SrTeO₃ and the corresponding 3d oxide SrMnO₃, we find a ratio of 4:1 for the Neel temperatures as well as magnitudes consistent with experiment.

1. S. Middey, Ashis Kumar Nandy, Priya Mahadevan, D.D. Sarma, arXiv:1112.5587 2. E. E. Rodriguez et al., Phys. Rev. Lett. 106, 067201 (2011). 3. M. Avdeev et al., J. Am. Chem. Soc. 133, 1654 (2011).

RF13

Spin-spectral-weight distribution and energy range of the parent compound La₂CuO₄

Jose Carmelo¹, Miguel Araujo², Steven White³ and Maria Sampaio¹
¹ Department of Physics, University of Minho, Portugal
² Department of Physics, University of Evora, Portugal
³ Department of Physics, University of California, USA

The spectral-weight distribution in recent neutron scattering experiments on the parent compound La₂CuO₄ (LCO) [1], which are limited in energy range to about 450 meV, is studied in the framework of the Hubbard model on the square lattice [2]. We find that the higher-energy weight extends to about 566 meV and is located at and near the momentum [pi,pi]. Our results confirm that the U/t value suitable to LCO is in the range between U/t=6 and U/t=8. The continuum weight energy-integrated intensity vanishes or is extremely small at momentum [pi,0]. This behavior of the intensity is consistent with that of spin waves, which are damped at [pi,0]. Our study combines a number of theoretical and numerical approaches, including, in addition to standard treatments [3], a new spinon approach for the spin excitations [4,5] and density matrix renormalization group (DMRG) calculations for Hubbard cylinders [6].

[1] - N. S. Headings, S. M. Hayden, R. Coldea, and T. G. Perring, Phys. Rev. Lett. 105, 247001 (2010). [2] - M. A. N. Araujo, J. M. P. Carmelo, M. J. Sampaio, and S. R. White, cond-mat.str-el.1201.5940. [3] - N. M. Peres and M. A. N. Araujo, Phys. Rev. B 65, 132404 (2002). [4] - J. M. P. Carmelo, Nucl. Phys. B 824, 452 (2010); Nucl. Phys. B 840, 553 (2010), Erratum. [5] - J. M. P. Carmelo, Ann. Phys. 327, 553 (2012). [6] - S. Yan, D. A. Huse, and S. R. White, Science 332, 1173 (2011).

RF14

J₁J₂ anti-ferromagnetic heisenberg model on bilayer honeycomb lattice

Mojtaba Shoja Shabankah and Farhad Shabbazi
 Physics, Isfahan University Of Technology, Iran

Recent experiment on spin-3/2 bilayer honeycomb lattice antiferromagnet Bi₂Mn₂O₁₂ (NO₃) shows a spin liquid behavior down to very low temperatures. This behavior can be ascribed to the frustration effect due to competitions between first and second nearest neighbor antiferromagnet interaction. Motivated by the experiment, we study J₁J₂Antiferromagnet Heisenberg model, using Mean field theory and Monte Carlo simulation. This calculation shows highly degenerate ground state. We also calculate the effect of second nearest neighbor through z direction and show these neighbors also increase frustration in these systems. In addition calculation of the effect of third nearest neighbor shows that this interaction can lift the degenerate ground state to four discrete states. The next step of these calculations is to consider quantum effect of these interactions by Word line quantum Monte Carlo method.

[1] S. Okumura, H. Kawamura, T. Okubo, Y. Motome J. Phys. Soc. Jpn. 79, 114705 (2010) [2] J. N. Reimers, A. J. Berlinsky, and A.-C. Shi, Phys. Rev. B 43, 865-878 (1991) [3] Hem C. Kandpal and Jeroen van den Brink, PHYSICAL REVIEW B 83, 140412(R) (2011) [4] M Azuma, M Matsuda, N Onishi, S Olga, Y Kusano, M Tokunaga, Y Shimakawa and N Kumada, Journal of Physics: Conference Series 320 (2011) 012005. [5] L. Balents, Nature (London) 464, 199 (2010).

RF15

A hybrid exchange density functional study of La_{1-x}Ca_xMnO₃

Romi Kaur Korotana¹, Leandro Liborio¹, Giuseppe Mallia¹, Zsolt Gercsi² and Nicholas Harrison¹
¹ Chemistry, Imperial College London, United Kingdom
² Physics, Imperial College London, United Kingdom

Manganites exhibit a rich variety of crystallographic, electronic and magnetic properties [1] manifested in ferromagnetic-, antiferromagnetic (collinear and canted)-, metallic-, insulating-,charge- and orbital-ordered states. An insight into the competition and coupling between various degrees of freedom in doped manganites is of interest for the optimisation of the magnetocaloric effect [2, 3] in such materials. In this work, hybrid-exchange density functional theory (DFT) calculations have been carried out to determine the effects of A-site doping on the structural, electronic and magnetic properties of perovskite-type manganites La_{1-x}A_xMnO₃, where A=Ca and x=0, 0.25, 0.50, 0.75 and 1. A magnetic stability plot for La_{1-x}Ca_xMnO₃ is compiled, in which the ferromagnetic (F), antiferromagnetic A-type (A-AF), G-type (G-AF) and C-type (C-AF) configurations are considered. At this level of theory, the structural, magnetic ground states and electronic states at each of the compositions studied are compared to available experimental data. This provides a basis for a first principles description of the magnetocaloric effect in La_{1-x}Ca_xMnO₃ systems.

[1] J. B. Goodenough, in Handbook on the Physics and Chemistry of Rare Earths, vol.33, edited by K. A. Gschneidner, Jr. et al. (Elsevier, Amsterdam (2003), p. 249. Elsevier, Amsterdam (2003). [2] V. K. Pecharsky and K. A. Gschneidner, Jr., J. Magn. Magn. Mater., 200, 44 (2002). [3] A. M. Tishin, in Handbook of Magnetic Materials, edited by K. H. J. Buschow (North Holland, Amsterdam, 1999), Vol. 12, pp. 395-524.

RF16

Magnetic properties of GdFe₁₁Ti via first principal calculations.

E. E. Kokorina*, M. V. Medvedev and I. A. Nekrasov
 Laboratory of Theoretical Physics, Institute of Electrophysics, Russia

WITHDRAWN

RF17

Mott transition of ultracold Fermi-Fermi mixtures in optical lattices

Takahiro Ooi* and Seiichiro Suga
 University of Hyogo, Japan

WITHDRAWN

RG01

Anisotropy in a high Landau level due to effective electron-electron interactions

Orion Ciftja
 Prairie View A&M University, USA

Quantization of Hall resistivity in strongly correlated two-dimensional electronic systems at high magnetic fields generally indicates the stabilization of novel electronic quantum liquid phases of matter. This is the nature of the integer and fractional quantum Hall states that stabilize at integer and fractional odd-denominator (not always, though) filling factors of the Landau level. Away from certain filling factors that represent quantum Hall liquid states, different phases, some of them with unusually high magneto-transport anisotropy have been known to stabilize specially in high Landau levels. In this work, we try to understand the anisotropy of such quantum phases in terms of effective electron-electron interaction potentials. To this effect, we implement a full projection of the original Coulomb interaction potential in the suitable Landau level. We find out that, in high Landau levels, thus for relatively weak magnetic fields, a semi-classical description of the interaction potential between electrons appear to be an adequate choice. The features of this semi-classical interaction potential in this limit suggest ways how the energetic balance between density waves and/or liquid crystalline phases might be sensitively affected.

[1] R. B. Laughlin, Phys. Rev. Lett. 50, 1395 (1983). [2] P. K. Lam and S. M. Girvin, Phys. Rev. B. 30, R473 (1984). [3] O. Ciftja and C. Wexler, Phys. Rev. B 67, 075304 (2003).

RG02

Bipolaron-Bipolaron interaction in many electron Holstein-Hubbard model

Monodeep Chakraborty and B. I. Min
Department of Physics, Pohang University of Science and Technology, Korea

Polarons and bipolarons have been long-term subjects of interest in many areas of condensed matter. The Holstein model describing the strong electron-phonon interaction and the Hubbard model describing the strong electron-electron interaction have played pivotal roles in various important physical systems, such as high Tc superconductors and the CMR manganites. In real systems, the polaron-polaron and polaron-bipolaron interactions might be of crucial importance. In order to investigate the physics of polaron and bipolaron systematically, we have studied the combined Holstein-Hubbard model treating both the electron-phonon and the electron-electron interaction on an equal footing. We present our study on polaron-bipolaron and bipolaron-bipolaron interactions as a function of the electron-phonon coupling strength and the electron-electron interaction U. We have calculated the ground state energy and wave functions of the system by applying the conjugate-gradient technique on a variationally constructed basis. The obtained correlation functions, the bipolaron binding energy, and the effective mass enables us to capture the intricate mechanisms at play and their consequences.

RG03

Partial disorder in an Ising-spin Kondo lattice model on a triangular lattice

Hiroaki Ishizuka* and Yukitoshi Motome
Department of Applied Physics, University of Tokyo, Japan

Partial disorder, that is coexistence of paramagnetic and magnetically ordered sites, is an intriguing example of exotic orders induced by geometrical frustration [1]. Experimentally, several metallic magnets with a triangular lattice structure, such as UNi₃B and Ag₂CrO₅, were reported to present such unique order. On the other hand, theoretical attempts to explore the partial disorder in two-dimensional localized spin systems turned out to be unsuccessful so far; it is fragile against thermal fluctuations [2] and only exists as a quasi-long-range order at most [3]. To explore the possible realization of the true long-range partially disordered phase in two dimensions, here we theoretically investigate the effect of the coupling of localized moments to itinerant electrons in an Ising-spin Kondo lattice model on a triangular lattice. We study the low-temperature magnetic phases by a real-space Monte Carlo technique. As a result, we obtained a long-range order of the partially disordered state at finite temperatures in the vicinity of electron density n=1/3, where a two-sublattice stripe-type order and three-sublattice ferrimagnetic order compete with each other and an electronic phase separation takes place at a lower temperature. Further details on the phase diagram and the partially disordered phase will be given in the presentation.

[1] M. Mekata, *J. Phys. Soc. Jpn.* 42, 76 (1977). [2] S. Fujiki et al., *J. Phys. Soc. Jpn.* 53, 1371 (1984). [3] T. Takagi and M. Mekata, *J. Phys. Soc. Jpn.* 64, 4609 (1995).

RG04

Basis reduction in the exact diagonalization method for the dynamical mean-field theory

Hyeong-do Kim*
Beamline Division, Pohang Accelerator Laboratory, Korea

The exact diagonalization (ED) method for the dynamical mean-field theory is nearly the only method to calculate electron spectra involving core levels, such as core-level photoemission spectra, x-ray absorption/emission spectra, resonant inelastic x-ray scattering, etc., in a strongly correlated electron systems. In order to overcome the problem of the exponentially increasing Hilbert-space dimension by the number of sites, the number of configurational bases for the ED method for the single-impurity Anderson model is systematically reduced by their perturbative expansion starting from the lowest-energy configuration and consecutively allowing the hopping between an impurity level and a conduction band. Comparison of resulting Green's functions with exact ones in an imaginary frequency axis shows that bases up to the fourth order is enough to render reliable results. Since the reduced Hilbert-space dimension increases according to the power law, the available size of involved sites could be greatly enhanced to simulate core-level-related spectra with a large spin-orbital degree of freedom.

RG05

Electronic Structure of ternary stannides RRu₄Sn₆ (R=Y, La, Pr, Ce, and Gd) compounds

Saad Elgazar¹, A. M. Strydom¹ and P. M. Oppeneer²
¹ *Physics, Johannesburg University, South Africa*
² *Physics, Uppsala University, Sweden*

We report density functional calculations of the band structure and density of states of the RRu₄Sn₆ (M=Y, La, Ce, and Gd) compounds. Our investigation is carried out within the framework of the local density approximation, using a relativistic, full-potential band-structure method. For the Ce-146 compound we find that LSDA calculations predict a semiconducting ordered ground state whereas the other compounds ordered in metallic states, in accordance with available experimental measurements.

RG06

Local correlation effects in Mn doped GaAs

Igor Di Marco*, Olle Eriksson and Patrik Thunstrom
Physics and Astronomy - Materials Theory, Uppsala University, Sweden



RG07

First-principles study on noncollinear magnetism and effects of spin-orbit coupling in 5d pyrochlore oxide Cd₂Os₂O₇

Hiroshi Shinaoka, Takashi Miyake and Shoji Ishibashi
Nanosystem Research Institute, National Institute of Advanced Industrial Science and Technology, Japan

Recently, increasing attention has been focused on 5d pyrochlore oxides A₂B₂O₇ (B=Ir, Os, etc.) in search for unconventional phenomena induced by strong spin-orbit coupling. Cd₂Os₂O₇ is a typical member of these compounds. Experimentally, it exhibits a metal-insulator transition at 227 K, below which a Neel order appears [1]. Despite many experimental attempts, the nature of the low-temperature phase remains to be clarified; e.g., the magnetic structure is unknown. Furthermore, several peculiar properties have been reported experimentally: (1) The transition temperature is the highest among pyrochlore oxides. (2) No clear charge gap is seen in the temperature dependence of the resistivity despite the high transition temperature. Motivated by these experiments, we investigate electronic structure of Cd₂Os₂O₇ [2] using the local spin density approximation + U method. We use a fully relativistic two-component first-principles computational code [3] based on the projector augmented-wave method. We show that the so-called all-in/all-out magnetic order is the most stable in a wide range of U. By analyzing an effective spin model, we show that the local <111> easy-axis anisotropy removes geometrical frustration to stabilize this non-collinear magnetic order. We also compute the density of states and the electronic band structure and compare the results with experiments.

[1] A. Sleight et al., *Solid State Comm.* 14, 357 (1974); D. Mandrus et al., *Phys. Rev. B* 63, 195104 (2001); A. Koda et al., *J. Phys. Soc. Jpn.* 76, 063703 (2007); Y. H. Matsuda et al., *Phys. Rev. B* 84, 174431 (2011). [2] H. Shinaoka, T. Miyake, and S. Ishibashi, arXiv:1111.6347. [3] QMAS (Quantum Materials Simulator) [http://qmas.jp].

RG08

Nonequilibrium states and I-V characteristics in one-dimensional band and Mott insulators attached to electrodes

Yasuhiro Tanaka* and Kenji Yonemitsu
Institute for Molecular Science, Japan

Nonequilibrium states induced by an applied bias voltage (V) and the corresponding current-voltage characteristics of one-dimensional models describing band and Mott insulators are investigated theoretically by using nonequilibrium Green's functions[1]. We attach the models to metallic electrodes whose effects are incorporated into the self-energy. Modulation of the electron density and the scalar potential coming from the additional long-range interaction are calculated self-consistently within the Hartree approximation. For both models of band and Mott insulators with length L_C, the bias voltage induces a breakdown of the insulating state, whose threshold shows a crossover depending on L_C[2]. It is determined basically by the bias V_{th}~Δ for L_C smaller than the correlation length ξ=W/Δ where W denotes the bandwidth and Δ the energy gap. For systems with L_C□ξ, the threshold is governed by the electric field, V_{th}/L_C, which is consistent with a Landau-Zener-type breakdown, V_{th}/L_C□Δ²/2W. We demonstrate that the spatial dependence of the scalar potential is crucially important for this crossover by showing the case without the scalar potential, where the breakdown occurs at V_{th}□Δ regardless of the length L_C.

[1] K. Yonemitsu, *J. Phys. Soc. Jpn.* 78 (2009) 054705. [2] Y. Tanaka and K. Yonemitsu, *Phys. Rev. B* 83 (2011) 085113.

RG09

Enhancement of charge ordering by Zeeman effect in one-dimensional molecular conductors

Hideo Yoshioka¹, Hitoshi Seo² and Yuichi Otsuka³
¹ *Department of Physics, Nara Women's University, Japan*
² *Condensed Matter Theory Laboratory, RIKEN, Japan*
³ *Advanced Institute for Computational Science, RIKEN, Japan*

A recent experiment observes increase of resistance with increasing the external magnetic field in one-dimensional molecular conductor TPP[Co(Pc)(CN)₂]₂ [1]. The positive magnetoresistance is independent of the direction of the magnetic field, and then the origin of it is considered to be the Zeeman effect. Therefore, the experiment indicates that charge ordering (CO) is enhanced by the Zeeman effect. Stimulated by the experiment, we theoretically investigate effect of uniform magnetic field on CO in one-dimensional extended Hubbard model. In a previous study, the ground state with coexistence of CO and 2k_F-SDW was investigated, but the amplitude of CO does not show noticeable enhancement under the uniform magnetic field [2]. In the present study, the parameter region where only CO appears is studied. We find the following results; (1) The amplitude of CO shows continuous enhancement under the external magnetic field. (2) Enhancement of CO is accompanied by both uniform and staggered (4 k_F) component of magnetic moment. Our conclusion is consistent with experimental finding in TPP[Co(Pc)(CN)₂]₂.

[1] N. Hanasaki et al., *J. Phys. Soc. Jpn.* 75 (2006) 104743. [2] K. Kishigi and Y. Hasegawa, *J. Phys. Soc. Jpn.* 69 (2000) 2145.

RG10

Contribution of electron-lattice and spin-orbit coupling to the insulator-metal transition in VO₂ and Sr₂IrO₆

Jongseok Lee¹, K. Shibuya², Y. Krockenberger², K. S. Takahashi², M. Kawasaki³ and Y. Tokura³
¹ *Department of Photonic and Applied Physics, Gwangju Institute of Science and Technology, Korea*
² *Cross-Correlated Materials Research Group (CMRG) and Correlated Electron Research Group (CERG), RIKEN, Japan*
³ *Department of Applied Physics, University of Tokyo, Japan*

Mott insulating state in the strongly correlated electron system is often realized in competition and/or cooperation with interactions other than the on-site Coulomb repulsion energy, such as the electron-lattice coupling and the spin-orbit coupling□ One of representative examples is VO₂, where the electron correlation and the Peierls instability have been debated as a driving force to realize its metal-insulator transition near room temperature. Another example is Sr₂IrO₆, which is now believed to have a spin-orbit-induced Mott insulator ground state. In this presentation, we discuss based on optical spectroscopy of thin films how the insulating ground states of each system evolve into the metallic states with a decrease of Peierls instability and the spin-orbit coupling strength which together can give an insight in to the complex phases in strongly correlated electron system [1,2].

[1] J. S. Lee, Y. Krockenberger, K. Takahashi, M. Kawasaki, and Y. Tokura, *Phys. Rev. B* 85, 035101 (2012). [2] J. S. Lee, K. Shibuya, M. Kawasaki, and Y. Tokura, submitted.

RG11

Multipole moments at Pr-site and electric field gradients at Sb-site in PrOs₂Sb₁₂

Takeshi Goho* and Hisatomo Harima
Department of Physics, Kobe University, Nada, Kobe 657-8501, Japan

PrOs₂Sb₁₂ is well known as an unusual superconductor with Tc = 1.85 K [1]. The superconductivity might be related with the multipole moments of 4f² electrons of Pr, because the antiferro-quadrupole ordering is realized under applied magnetic fields [2]. So, it is important to study a role of the multipole moments of Pr to make clear the system of unusual superconductor PrOs₂Sb₁₂. The NQR frequency at Sb site shows temperature dependence corresponding to the crystalline electric field splitting below 10 K, associated with the Pr³⁺(4f²)-derived ground state [3]. This experimental result suggests that the change of multipole components affect the electronic field gradients (EFG) at Sb-site. The LDA + U calculations have described the Fermi surfaces of PrOs₂Sb₁₂ well [4]. It has been shown that EFG at Sb-site can be calculated by using an FLAPW method and the calculated EFG reproduce well the experimental NQR frequency [5]. Moreover, the multipole moments of Pr can be classified from the density matrix, which is used in the LDA + U method. We have analyzed how each multipole component affects the EFG at Sb-site. Then we discuss the relationship between multipole moments at Pr-site and EFG at Sb-site.

[1] E. D. Bauer et al., *Phys. Rev. B* 65 (2002) 100506. [2] M. Kohgi et al., *J. Phys. Soc. Jpn.* 72 (2003) 1002. [3] M. Yogi et al., *Phys. Rev. B* 67 (2003) 180501(R). [4] H. Sugawara et al., *Phys. Rev. B* 66 (2002) 220504(R). [5] H. Harima, *Physica B* 378-380 (2006) 246.

RG12

The effect of pairing fluctuations and disorder on the BCS-BEC crossover

Pinaki Majumdar
Harish-Chandra Research Institute, India

A fermi liquid with weak attractive interaction undergoes a BCS transition to a superconductor with reducing temperature. With increasing interaction strength the transition temperature displays non-monotonic behaviour as the system heads towards Bose condensation of preformed pairs. We use a new Monte Carlo tool, incorporating amplitude and phase fluctuations of the pairing field, to map out this BCS-BEC crossover in the attractive Hubbard model on large (40 X 40) two dimensional lattices. Having established this benchmark we discuss the role of disorder in this system. This includes (i) the role of non-magnetic impurities where we track the superconductor to insulator transition with increasing disorder, and (ii) the emergence of 'gapless' superconductivity, the suppression of T_c, and the induced correlation between scatterers themselves, in the case of magnetic impurities. Our method reproduces the standard results in all these cases but allows unprecedented spatial resolution, and access to the dynamical response. We compare the results to imaging experiments on disordered films.

RG13

Transport properties of ferromagnetic material with Anderson-Hubbard centers

Yuriy Skorenkyy*, Oleksandr Kramar and Leonid Didukh
Physics Department, Ternopil National Technical University, Ukraine

A competition between itinerant behavior and localization effects in strongly correlated electron system of periodically spaced Anderson-Hubbard centers introduced into narrow-band metal is studied. The configurational representation for localized subsystem is used and the effective Hamiltonian is obtained by canonical transformation. Besides the spin-spin interactions and strong on-site Coulomb interaction, the model takes into account the hybridization with conduction band which results in the indirect hopping and indirect exchange interactions. Lattice deformation under the external pressure is taken into account and equilibrium value of lattice strain is found, having effect on both electrical and magnetic properties of the system. Green functions for band and localized electrons are calculated. On this base, the energy spectrum and magnetization are investigated as function of model parameters, temperature and external pressure. For temperatures close to Curie temperature and partial filling of conduction band the peculiarities of electronic conductivity are studied. Concentration dependence of static conductivity exhibits different transport regimes. Our results show that in the considered model the effects of localization are enhanced even if external pressure promotes electrical conductivity.

RG14

First principles studies of organic charge transfer salts

Harald O. Jeschke, Anthony Jacko and Roser Valenti
Institut für Theoretische Physik, Universität Frankfurt, Germany

We study a number of BEDT-TTF based charge transfer salts in the framework of ab initio density functional theory and determine the parameters of the effective Hubbard Hamiltonian describing the low energy excitations[1]. For the spin liquid candidate kappa-(BEDT-TTF)2Cu₂(CN)₂, we investigate the question if the structures determined at various temperatures lead to different effective Hamiltonian representations[2]. For the Fabre salts (TMTTF)₂X, we compare the properties of the underlying Hamiltonian for a series of different anions X.

[1] H.C. Kandpal, I. Opahle, Y.-Z. Zhang, H. O. Jeschke, R. Valenti, *Phys. Rev. Lett.* **103**, 067007 (2009). [2] H. O. Jeschke, M. de Souza, R. Valenti, R. S. Manna, M. Lang, J. A. Schlueter, *Phys. Rev. B* **85**, 035125 (2012)

RG15

Dynamics of strongly correlated Fermi systems: The effects of pair-excitations and exchange

Martin Panholzer^{1*}, Eckhard Krotscheck², Helga M Boehm², Robert Holler² and Thomas Lichtenegger²
¹ *Johannes Kepler University Linz, Austria*
² *Institut für Theoretische Physik, Johannes Kepler University Linz, Austria*

Understanding the emergent properties of many body systems from the underlying microscopic interactions is the major goal of condensed matter physics. Recent progress, in the understanding of the dynamics of strongly correlated systems, has been made by approximating the excited wave function by a superposition of correlated particle-hole and 2-particle-2-hole excitations. The amplitudes, describing these excitations, are obtained by minimizing the action integral. A surprising result of this approach is the confirmation/prediction of the reemergence of collective mode below the PHB in two dimensional 3He for density fluctuations. By including exchange the agreement of the calculated spectrum with the experiment was further improved for 3He. The next step is to apply this tool to spin-density fluctuations, which are of inherent exchange character. Due to the proximity of the ferromagnetic phase transition the fluctuations are at very low energies for long wavelength. This experimental finding is also present in a first implementation of our theory. The presented approach is also applicable to other correlated fermi systems e.g. electrons and dipoles in two dimensions. We predict this transition of the collective mode seen in 3He also for two dimensional electrons. The capability in describing these systems is investigated.

Bohm, H. M., Holler, R., Krotscheck, E. & Panholzer, M. *Dynamic many-body theory: Dynamics of Strongly Correlated Fermi Fluids. Phys. Rev. B* **22**, 224505 (2010).

RG16

The induced effects of the Dzyaloshinskii-Moriya interaction on the thermal entanglement

Saeed Mahdaviifar*
Department of Physics, University of Guilan, Iran

The pairwise thermal entanglement in one-dimensional (1D) spin-1/2 XX model with added Dzyaloshinskii-Moriya interaction and transverse magnetic field is studied through fermionization technique. We have showed that, for fields less than quantum critical point, the thermal entanglement decreases by increasing the temperature and vanishes at a field-independent critical temperature. On the other hand for fields more than quantum critical value of the magnetic field (Fig. (1)(b)), NN spins are not entangled at ST=0\$. By increasing the temperature from zero, NN spins remain unentangled up to the first critical temperature ST_{c_1}(h)\$, As soon as the temperature increases from ST_{c_1}(h)\$, the thermal entanglement regain and takes a maximum value and then decrease and reaches to zero at the second critical temperature ST_{c_2}(h)\$.

RG17

Magneto-polaronic effects in molecular transistors as the consequence of quantum uncertainty of the displacement of vibrating quantum dot.

Glib A(alexandrovich) Skorobagatko^{1*}, Sergey I. Kulnich², Ilya V. Krive³ and Robert I. Shekhter⁴
¹ *Department of Theoretical Physics, B.Verkin ILTPE of NAS of Ukraine, Kharkov, Ukraine*
² *Department of Theoretical Physics, B.Verkin ILTPE of NAS of Ukraine, Kharkov, Ukraine*
³ *Department of Theoretical Physics, B.Verkin ILTPE of NAS of Ukraine*
⁴ *Department of Physics., University of Gothenburg, SE-41296, Gothenburg, Sweden*

The influence of magneto-polaronic effects induced by the quantum uncertainty of the displacement of quantum dot on electron transport through a single-level vibrating quantum dot subjected to a transverse (to the current flow) magnetic field is considered . It is shown that the effects are most pronounced in the regime of sequential electron tunneling, where a polaronic blockade of the current at low temperatures and an anomalous temperature dependence of the magnetoconductance are predicted.

I. G. A. Skorobagatko, S. I. Kulnich, I. V. Krive, R. I. Shekhter, and M. Jonson, *Low Temp. Phys.* **37**, 1032 (2011).

RG18

Defect states and electron correlations in multi-orbital Mott insulators

Adolfo Avella^{1*}, Peter Horsch² and Andrzej Oles³
¹ *Dipartimento di Fisica 'E.R. Caianiello', Universita degli Studi di Salerno, Italy*
² *Max Planck Institute for Solid State Research, Stuttgart, Germany*
³ *Jagellonian University, Krakow, Poland*

We address the role played by defects in doped Mott insulators with active orbital degrees of freedom. We observe that defects are characterized by rather complex and rich physics which is well captured by a degenerate Hubbard model extended by several terms that describe crystal-field splittings, the orbital-lattice coupling, as well as local terms generated by defects such as the Coulomb potential terms that act both on a doped hole and orbitals of undoped sites (orbital polarization). We show that the multiplet structure of excited states generated in such systems by strong electron interactions is well described in an optimized unrestricted Hartree-Fock approximation, taking into account the usual symmetry breaking by the onset of magnetic and orbital order. More importantly, we show that defect states are responsible for new features that arise within the Mott-Hubbard gap and in the multiplet spectrum at high energy. These states involve active orbital flavors at atoms being nearest neighbors of the defect state, which are modified by the local defect-orbital Coulomb interactions. The present study suggests a new mechanism for the Coulomb gap realized in the presence of defect states and investigates the dependence of the orbitals on the orbital polarization.

RH01

Magnetism of the noncentrosymmetric compound CeNiC₂-pressure effects

Susumu Katano*, Toshiaki Kobayashi and Tohru Yoshida
Graduate School of Science and Engineering, Saitama University, Japan

The system RNiC₂ (R=Rare-earth element) has a simple but a characteristic noncentrosymmetric crystal structure, and shows various novel physical properties such as charge density waves (CDW) and complex magnetic structures. In the system the compound of R=La shows unconventional superconductivity, and has been intensively studied very recently. For CeNiC₂, a few reports indicated that the incommensurate antiferromagnetic state (ICAF) appears at around 20 K and this changes to the commensurate antiferromagnetic structure (CAF) at about 10 K, then a ferromagnetic state (F) takes place at around 2 K [1, 2]. However, since there are some clear discrepancies in these studies the magnetism of this compound has been reinvestigated in detail using a carefully prepared polycrystalline sample. It is found that there are definite magnetic moments in the paramagnetic state. With these moments the complex antiferromagnetic states undergo, which replaces to a ferromagnetic state at low temperatures. To investigate these magnetic states further, their pressure effects have been studied up to 2.5 GPa. The results show that the IC and CAF states at the higher temperatures is fairly stable, whose transition temperatures increase at a rate of about 2 K/GPa. On the other hand the F state is changed little.

[1] K. Motoya, et al. *J. Phys.Soc. Jpn.* **66** (1997) 1124. [2] V.K. Pecharsky, et al. *Phys. Rev. B* **58** (1998) 497.

RH02

Atomic scale disorder driven bicritical region in Sm_{0.5}(Ca_{1-x}Sr_x)_{0.5}MnO₃

Saurav Giri^{1*}, Sk. Sabiyasachi¹, S. Majumdar¹, S. Das² and V. S. Amaral³
¹ *Solid State Physics, Indian Association for the Cultivation of Science, India*
² *Department of Physics and CICECO, University of Aveiro, Portugal*
³ *Department of Physics and CICECO, University of Aveiro, India*

On the verge of collapse of charge and orbital ordering a bicritical region occurs in hole doped manganites which displays rich electronic phase diagrams in R0.5(Ca,Sr)0.5MnO₃ [1]. Here, we demonstrate a fascinating consequence of A-site disorder in intermediate members of a new series Sm0.5(Ca_{1-x}Sr_x)0.5MnO₃. The Rietveld refinement of X-ray diffraction studies reveal maximum structural distortions at x = ½. This is indicated by the highest value of ε [= √2b/(a+c), a, b, c being lattice constants] and most deviation of Mn-O-Mn bond-angle from 180° compared to end compounds. An unusual behaviour in magnetic field-induced ultra-sharp transition to ferromagnetic metallic (FMM) state and collapse of charge ordering is observed both in magnetization and magnetoresistance curves for intermediate compositions at much lower field compared to end compounds. When magnetic field is applied above a critical field, FMM state appears and it retains high-field state, although magnetic field decreased to zero. With decreasing field sweep rate, the transition shifts to higher field indicating a meta-magnetic transition. The atomic-scale local inhomogeneity/distortion arising from the difference in ionic radii and/or the random Coulomb potential from ion mixture is supposed to be critical behind such striking phenomena.

[1] Y. Takura, *Rep. Prog. Phys.* **69**, 797 (2006).

RH03

11B-NMR study on Shastry Sutherland system TbB₄

Tomoki Muto¹, Takayuki Goto¹, Akira Oosawa¹, Shunsuke Yoshii², Takahiko Sasaki³, Shinji Michimura⁴, Fumitoshi Iga⁴ and Toshiro Takabatake⁴
¹ *Department of Physics, Sophia University, Japan*
² *CINTS Tohoku University, Japan*
³ *Institute for Materials Research, Tohoku University, Japan*
⁴ *ADSM, Hiroshima University, Japan*

In TbB₄, the arrangement of Tb ions within the c-plane is topologically equivalent to the Shastry Sutherland (S-S) lattice with geometrical frustration [1]. A well-known example of S-S lattice is SrCu₂(BO₃)₂ which shows the characteristic magnetization plateaus caused by the frustration. However, in TbB₄, due to the quadrupole interaction and RKKY interaction between classical spins, the appearance of the novel magnetism quite different from SrCu₂(BO₃)₂ is expected. The magnetization of TbB₄ for H // c-axis shows field-induced multi-step jump while the magnetization in the c-plane on which we focus attention shows only one large jump at Hc = 15.9 and 12 T for H//[100] and H//[110] respectively [2]. In order to investigate the magnetic structure in high magnetic fields for H//[100], we performed 11B-NMR experiments up to 17.5T for the single crystalline TbB₄. 11B-NMR spectra observed at low magnetic field changes drastically at Hc = 15.9 T, where the magnetization jump occurs. This result indicates the change of the magnetic structure at the field-induced magnetic phase transition. In order to determine the magnetic structure, we have compared the observed NMR spectra with the calculation based on the classical dipole-dipole interaction.

[1] B.S.Shastry et al., *Physica B* **208** (1981) 1069. [2] S.Yoshii et al., *Phys. Rev. Lett.* **101** (2008) 087202.

RH04

Magnetotransport Property of the Hole-doped Delafossite CuCr_{0.97}Mg_{0.03}O₂ with a Spin-3/2 Antiferromagnetic Triangular Sublattice

Tetsuji Okuda*, Satoshi Oozono¹, Takumi Kihara² and Masashi Tokunaga²
¹ *Kagoshima University, Japan*
² *The University of Tokyo, ISSP, Japan*

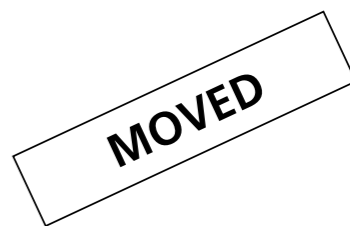
Magnetotransport property of a hole-doped delafossite CuCr_{0.97}Mg_{0.03}O₂ with a spin-3/2 antiferromagnetic (AF) triangular sublattice was investigated by a pulsed high magnetic field up to about 56 Tesla. [1] A dramatic change of magnetoresistance (MR) was observed with a variation of temperature (T), which is due to a development of an AF correlation with a decrease in T. A negative MR is observed and the ratio is well proportional to a square of magnetization above a Curie-Weiss temperature (θ), which seems to suggest that the magnetic state above θ is well explained by a Kondo-lattice model [2] with a weak ferromagnetic Hund's coupling between itinerant holes and localized spins. However, below θ, the negative MR gradually deviates from the scaling relation with a decrease in T and is much enhanced around an AF transition temperature (TN). Furthermore, a component of positive MR appears around TN. Such a MR behavior is due to a critical enhancement of spin fluctuation around TN, which may cause a nontrivial promotion of a 120° AF state by the Mg substitution [3,4].

[1] T. Okuda, S. Oozono, T. Kihara, and M. Tokunaga, in preparation. [2] N. Furukawa, *J. Phys. Soc. Jpn.* **63**, 3214 (1994). [3] T. Okuda, N. Fujikita, S. Hidaka, and N. Terada, *Phys. Rev. B* **72**, 144403 (2005). [4] T. Okuda, Y. Beppu, Y. Fujii, T. Onoe, N. Terada, S. Miyasaka, *Phys. Rev. B* **77**, 134423 (2008).

RH05

Lifshitz transition with interactions in high magnetic fields: application to CeN₃

Pedro Schlottmann*
Department of Physics, Florida State University, USA



RH06

Novel colossal magnetoresistance in NaCr₂O₄

Hiroya Sakurai^{1*}, Taras Kolodiazhnyi¹, Yuichi Michiue² and Eiji Takayama-muromachi²
¹ *Superconducting Properties Unit, National Institute for Materials Science, Japan*
² *National Institute for Materials Science, Japan*

We recently discovered new chromium oxide, NaCr₂O₄, to have calcium ferrite type structure, in which spin frustration is expected. The compound shows canted-antiferromagnetic transition at TN = 125 K and Arrhenius-type temperature dependence of electrical resistivity. The resistivity below TN is greatly suppressed by magnetic field and it remains to be a finite value at 0 K under H = 9 T. Thus, the magnetoresistance ratio, {rho(H)-rho(0)}/rho(0), becomes closer to -100% at low temperatures. The similar behavior has been observed in some manganites, such as Pr_{0.7}Ca_{0.3}MnO₃ and Nd_{0.5}Sr_{0.5}MnO₃, for which the competition between charge-ordered insulating phase and ferromagnetic metallic phase causes colossal magnetoresistance (CMR) through the first-order transition. Unlike them, however, NaCr₂O₄ shows no thermal or field hysteresis in its physical properties, and there is no ferromagnetic metallic phase compositionally close to NaCr₂O₄. Therefore, CMR of the compound is considered to be caused by a new mechanism. The magnetism of Ca1-xNaxCr₂O₄ strongly suggests unusual electronic state of Cr⁴⁺ ions. We will present a possible mechanism of CMR in NaCr₂O₄, in which spin frustration and the electronic state of Cr⁴⁺ ions play a key role.

RH07

Low field study of Hall effect in GdB₆

M. A. Anisimov^{1*}, A. V. Bogach¹, V. V. Glushkov¹, S. V. Demishev¹, N. A. Samarina¹, N. Yu. Shitsevalova², A. V. Levchenko², V. B. Filipov² and N. E. Sluchanko¹
¹ *Low Temperatures and Cryogenic Engineering Dept., A.M.Prokhorov General Physics Institute of RAS, Russia*
² *Institute for Problems of Materials Science NAS, Ukraine*

GdB₆ plays the important role for understanding of the mechanisms responsible for the antiferromagnetic (AF) state formation in the rare earth hexaborides. However the magnetic structure of GdB₆ which is characterized by two successive AF transitions (AF(I) ordering below T_N-15.5K, and AF(II) phase at T^{*}-4.7K) is still the subject of discussion [1]. In current work we present the comprehensive study of Hall effect on the high quality single crystals of GdB₆ in the wide temperature interval (2-120K) at low magnetic fields (H<1T). In paramagnetic state Hall coefficient R_H is practically temperature independent and value of R_H-4*10⁻⁴cm³/C detected with the high accuracy is in accord with the results of light hexaborides RB₆ (R=La, Ce, Pr, Nd) published previously [2],[3]. The temperature decrease below T_N induces the drastic enhancement of negative Hall coefficient (ΔR_H/R_H-64%). The magnetic ordering at T^{*} (AF(I)-AF(II) transition) is accompanied by the appearance of anomalous Hall effect which is detected in GdB₆ for the first time. The complex analysis of charge transport parameters suggests the possible effect of 5d-states spin density polarization in AF and PM states of GdB₆.

[1] M.Amara, S.E.Luca et al., *Phys. Rev. B* **72**, p. 064447 (2005). [2] Y. Onuki, A.Umezawa et al., *Phys. Rev. B* **40**, p. 11195 (1989). [3] M.A.Anisimov, A.V.Bogach, V.V.Glushkov et al., *arxiv cond-mat:1006.0124v1*

RH08

Theoretical study of structures and mechanical properties of M-type hexagonal ferrites BaFe₁₂O₁₉

Wonha Moon*, Soyeon Kim, Heejung Lee, Jaehoon Yeom, Sangwon Lee and Seok Bae
LG innotek, Korea

M-type hexagonal ferrite, BaFe₁₂O₁₉, has extensively studied in a wide range of applications such as microwave devices and permanent magnets due to high Curie temperature, large saturation magnetization and good chemical stability. In this paper, we have investigated the structure and elastic modulus of BaFe₁₂O₁₉ using atomistic simulations. An interatomic potential based on the shell model is used for the structure and properties of BaFe₁₂O₁₉. The shell model has been extensively used to a wide range of oxide materials since it is a simple and useful potential with the Coulomb interaction incorporated with the short-ranged term for ionic characteristics, though it is incapable of describing the elemental components. The calculated results are in agreement with experiments and previous theoretical studies. To our knowledge, although many theoretical investigations have so far played an important role in understanding the properties of magnetic materials, there have been few theoretical studies using the interatomic potential for the structure and properties of BaFe₁₂O₁₉. The interatomic potential employed has been shown to be capable of describing the Ba-based hexagonal ferrites.

1. P. Shepherd, K. K. Mallick and R. J. Green, *J. Magn. Magn. Mater.* 311 (2007) 683. 2. G. V. Lewis and C. R. A. Catlow, *J. Phys. C: Solid State Phys.* 18 (1985) 1149. 3. P. Novak and J. Ruzs, *Phys. Rev. B* 71 (2005) 184433.

RH09

Nonlinear susceptibility of gadolinium near curie temperature

Takashi Shirane* and Shohei Sakurai
Sendai National College of Technology, Japan

The ac linear and nonlinear susceptibilities of an elemental ferromagnetic gadolinium have been studied near the Curie temperature, to clarify the feature of the magnetic phase transition with special emphasis on the behavior below the Curie temperature. The temperature dependence of linear susceptibility is in good agreement with that of an experimental result reported in ref. [1]. The first observation for the critical behavior of the nonlinear susceptibility in gadolinium has been made at various field amplitudes. The behavior of the nonlinear susceptibility is very sensitive to the field amplitude. The field dependence of the susceptibilities are explained on the basis of a mean field theory taken into account the domain structure[2]. The detailed discussion will be shown the full paper in comparison with magnetization curves at various temperature below the Curie temperature.

[1] J. M. D. Coey, K. Gallagher, and V. Skumryev, *J. Appl. Phys.* 87 (2000) 7028. [2] T. Shirane, *Statistical and Condensed Matter Physics: Over the Horizon*, ed. S. Fujita, T. Obata, and A. Suzuki (New York: Nova Science), p. 189-197, (2007).

RH10

Electron correlation and dynamical Jahn-Teller effect in orbitally degenerate system

Joji Nasu and Sumio Ishihara*
Department of Physics, Tohoku University, Japan

Quantum spin liquid state is one of the attractive subjects in correlated electron systems. Recently, a possibility of the quantum spin liquid state is experimentally reported in a layered copper oxide Ba₃CuSb₂O₈ where the orbital degree of freedom in a Cu ion and the dynamical Jahn-Teller effect (DJTE) are suggested to play some roles on an origin of the spin liquid state. Motivated from these recent experimental results, we study the DJTE in a spin-orbital coupled system. In particular, we focus on competitive or cooperative phenomena between the superexchange interaction and the DJTE. A superexchange interaction part is derived from the d-p model and the DJTE part for the low lying vibronic states is described by the orbital pseudo-spin and the lattice vibration. We analyze the model which combines the two interactions on a honeycomb lattice by using the Bethe approximation and the exact diagonalization method. We find that the magnetic order is unstable in a wide parameter region and a spin-singlet dimer state associated with an orbital order is realized. With increasing the DJTE, furthermore, the orbital order is strongly suppressed and a resonance state of the spin-orbital dimers appears.

H. D. Zhou, et al., *Phys. Rev. Lett.*, 106 (2011) 147204.

RH11

High-field NMR study on the charge in stability in quantum spin system Cu₃Mo₂O₉

Keita Misoka¹, Takayuki Goto^{1*}, Haruhiko Kuroe¹, Tomoyuki Sekine¹, Takahiko Sasaki², Masashi Hase¹, Kunihiko Oka¹, Toshimitsu Ito⁴ and Hiroshi Eisaki¹
¹ *Department of Physics, Sophia University, Japan*
² *Institute for Materials Research, Tohoku University, Japan*
³ *Department of Physics, National Institute for Materials Science, Japan*
⁴ *National Institute of Advanced Industrial Science and Technology, Japan*

The quasi-one-dimensional quantum spin system Cu₃Mo₂O₉ with the two spin-degrees of freedom, antiferromagnetic chain and dimer-like sites clinging around the chain undergoes the long-range antiferromagnetic order at 7.9 K, associated with a weak ferromagnetic moment. The system shows a small magnetization jump of 0.0033 μB at H* = 8.2 T, where the anomalous charge instability appears [1], suggesting an existence of tight coupling between spin and charge. In order to investigate the microscopic spin and charge states in the high magnetic field, we have utilized Cu-NMR technique, which separately probes the spin and charge in the chain site Cu₁, the dimer like sites Cu₂ and Cu₃ through hyperfine coupling and electric quadruple interaction respectively. In this presentation, we show by detailed analyses of spectra taken under a wide range of filed up to 17.5 T that the ordered antiferromagnetic moment is dominated by Cu₁, while the dimer-like sites only feel a uniform hyperfine field but staggered one, and that the change inhomogenization takes place in Cu₂ and Cu₃ in the vicinity of the field of magnetization jump H*.

1 T. Hamasaki et al., *Phys. Rev. B* 77 134419 (2007).

RH12

Anisotropic spin excitations in spin-Peierls CuGeO₃

Kazuhiko Ikeuchi¹, Fumio Mizuno², Ryoichi Kajimoto¹, Yasuhiro Inamura³, Mitsutaka Nakamura³, Kenji Nakajima³, Masaki Fujita⁴, Kazuya Aizawa⁴ and Masatoshi Arai¹
¹ *Research Center for Neutron Science and Technology, Comprehensive Research Organization for Science and Society, Japan*
² *Department of Physics, Tohoku University, Japan*
³ *Neutron Science Section, J-PARC Center, Japan*
⁴ *Institute for Material Research, Tohoku University, Japan*

Even though CuGeO₃ is a well-known 1-dimensional quantum spin system that shows magnetic transition into a dimerized state with a spontaneous lattice distortion, it is not clear whether it is an archetypal material of a spin-Peierls system. In fact, neutron scattering experiment has still not succeeded in assignment of the soft phonon mode accompanying the magnetic transition. Actually, due to an antiferromagnetic coupling between the neighboring spin chains, the dimerization in the spin chain is close to the critical state [1][2][3], and it should not have a strong effect on a phonon. In this experiment, we performed inelastic neutron scattering experiment on CuGeO₃ with the Fermi chopper spectrometer 4SEASONS at MLF/J-PARC in Japan. In order to further understand the inter-chain coupling, we measured intensity-maps in a 4-dimensional (q,ω) space including the inter-chain direction due to rotation of the aligned 17.2 g CuGeO₃ single crystals in horizontal plane. In this experiment, we have clarified an anisotropy of the magnetic excitations below the spin-Peierls transition temperature. This result suggests the inter-chain coupling correlates with the dimerization in the spin-Peierls state on CuGeO₃. We will present the detail of the magnetic excitations together with new other features recently discussed in several theoretical models.

[1] M. Nishi et al., *PRB*, 50,6508 (1994). [2] J. Riera et al., *PRB*, 51,16098 (1995). [3] M. C. Martin et al., *PRB*, 56, 3173 (1997).

RH13

Neutron inelastic scattering on spin-peierls system TiOBr

Tetsuya Yokoo¹, Shinichi Itoh¹, Daichi Kawana¹ and Jun Akimitsu²
¹ *High Energy Accelerator Research Organization, Japan*
² *Aoyama Gakuin University, Japan*

Newly proposed spin-Peierls system TiOX (X: Cl, Br) has been revealed showing exotic structural and magnetic properties such as a successive phase transition, one-dimensional (1D) nature associated with orbital ordering of Ti ions and super-lattice structure being related to the Peierls instability. It is pointed out that resulting only from an arrangement of Ti dxy orbital, the formation of 1D spin chains and the spin-Peierls transition will be realized. Recently, it has been demonstrated that TiOBr also exhibits two successive phase transitions similar to TiOCl at Tc1=27K and Tc2=47K. Here we carried out inelastic neutron experiments in order to see the evidence of spin-Peierls transition. The inelastic spectrum with a large amount of poly crystalline sample of TiOBr shows the localized signal in the vicinity of the magnetic zone center Q=0.9A-1. Observed spin gap like signal lies at energy of ΔE=10meV. The gap energy in TiOBr is expected much higher from measured thermodynamic properties and by analogy with TiOCl. Constant Q cuts of the observed S(Q,E) map show some Q-dependent structure in its intensity indicating the signal is sample oriented. The Q structure quite reveals the intensity is well explained by the powder averaged dynamical structure.

RH14

Physical properties of the novel triangular-lattice silver oxides Ag₂MO₂ (M = Co, Ga, Rh)

Hiroyuki Yoshida and Masaaki Isobe
National Institute for Materials Science, Japan

Triangular antiferromagnets have been extensively studied by many scientists in terms of geometrical frustration. According to current theories, triangular antiferromagnets show various exotic magnetic properties, e.g. chirality order, Kosterlitz-Thouless transition, a partially disordered state, etc. A series of layered Ag₂MO₂ compounds, where M is a transition metal, are possible model compounds of triangular antiferromagnets. The crystal structure of Ag₂MO₂ consists of alternate stacks of an M²⁺O₂ layer and a (Ag₂)⁺ layer. The former includes a triangular lattice of the M²⁺ ions, while the latter provides itinerant electrons from the quarter-filled Ag 5s band. The triangular lattices are well separated from each other by the non-magnetic double Ag layer. A path does not exist for superexchange interaction between the M²⁺ spins on the adjacent triangular lattices. In addition, no cation disorder is expected between the M and Ag ions. Ag₂MO₂ is, therefore, considered a suitable system to study the magnetic properties of triangular antiferromagnets. We recently succeeded in synthesizing Ag₂MO₂, M = Co, Ga, Rh, for the first time using a high-pressure technique. The details of physical properties of Ag₂MO₂ will be reported.

RH15

Electrical and thermal transport properties of the polycrystalline (Cr₈₆Ru₁₄)_{1-x}V_x alloy system

Leelakrishna Reddy, Aletta Roletta Prinsloo, Charles Johannes Sheppard and Andre Micheal Strydom
Physics, University of Johannesburg, South Africa

Thermopower (S) and electrical resistivity (ρ) measurements on the (Cr₈₆Ru₁₄)_{1-x}V_x alloy system with 0 ≤ x ≤ 0.144 reveal unique behaviour[1,2,3]. The onset of a commensurate (C) itinerant-electron antiferromagnetic spin-density-wave (SDW) structure is marked by anomalies in ρ(T) and S(T), associated with the Neel temperature. Focus is on the thermopower as it is more sensitive to the changes in the electronic structure and scattering mechanisms that are of importance at the SDW transition[2]. For this series S(T) shows a broad valley for x ≤ 0.032. The valley gradually becomes more shallow with increasing x and is eventually replaced by a surplus of positive thermopower for x = 0.074, for which parallelism is seen between ρ(T) and S(T) as in the case of Cr-V[2]. The size of the magnetic contributions to S and ρ strongly correlates and decreases with increasing x; attributed to the addition of V to the system that destabilizes the CSDW structure. The effect of the addition of V will be explained in terms of a model that relates the behaviour of S(T) to the energy dependence of the decrease in the scattering rate of electrons by phonons and an increase in the resistivity on decreasing temperature due to a decrease in the Fermi surface area[3].

[1] L. Reddy et al., *J. Appl. Phys.* 103 (2008) 07C903-1. [2] E. Fawcett et al., *Rev. Mod. Phys.* 66 (1994) 25. [3] A. L. Treago et al., *Phys. Rev.* 166 (1968) 495.

RH16

Magnetic properties of the layered triangular-lattice antiferromagnets CsM(MoO₄)₂ (M=V, Fe)

Masahiko Isobe and Yutaka Ueda
ISSP, Univ. of Tokyo, Japan

Two-dimensional triangular lattice antiferromagnets are of great interest concerning the ordering in frustrated spin system. We have prepared powder samples of the layered triangular-lattice antiferromagnets CsFe(MoO₄)₂ and CsV(MoO₄)₂ and have investigated the magnetic properties. In CsFe(MoO₄)₂, a structural phase transition at around 365K from P3m1 to P3 was detected. Also we observed the magnetic transition at 4.4 K for CsFe(MoO₄)₂ and 26 K for CsV(MoO₄)₂. The magnetic properties of CsFe(MoO₄)₂ are similar to that of the multiferroic RbFe(MoO₄)₂.

RH17

Kitaev-Heisenberg magnetism in honeycomb iridates A₂IrO₃(A=Li,Na)

Akihiko Kato¹, Tomohiro Takayama* and Hidenori Takagi²
¹ *Department of Applied Chemistry, University of Tokyo, Japan*
² *Department of Advanced Materials Science, University of Tokyo, Japan*
³ *Department of Physics, University of Tokyo, Japan*

5d transition-metal oxides can have unique properties because of the strong spin-orbit coupling and relatively weak electron correlations. Layered perovskite iridate Sr₂IrO₆, for example, was revealed to be Jeff=1/2 Mott-insulator where spin and orbital degrees of freedom are entangled with including complex phase [1]. The magnetism of such Jeff=1/2 Mott-insulator might be different from 3d transition-metal Mott-insulator. Indeed in iridates, the superexchange coupling between Ir-O-Ir was proposed to be anisotropic ferromagnetic when IrO₆ octahedra form edge-sharing network, due to the complex phase[2]. As a consequence, the spin-liquid state based on the Kitaev-model was theoretically predicted when such edge-shared IrO₆ octahedra compose a honeycomb network. Such unique lattice topology can be found in layered iridates A₂IrO₃(A=Li,Na). Na₂IrO₃ is a frustrated antiferromagnet with T_N=17K, and the θ_w=-125K. The strong antiferromagnetic interaction is likely due to direct interaction between Ir 5d electrons. Meanwhile, Li₂IrO₃ exhibited less frustrated magnetism with T_N=12K and θ_w=-12K, even with the similar structure. We argue that this seemingly non-frustrated magnetism of Li₂IrO₃ likely originates from a coexistence of direct antiferromagnetic and ferromagnetic superexchange interaction, exemplifying the Kitaev-Heisenberg model[3]. The difference might come from the local structure, the honeycomb of Na₂IrO₃ is distorted but that of Li₂IrO₃ is closer to ideal honeycomb.

[1] B.J.Kim et al., *Science* 323,1329(2009) [2] G.Jackeli and G.Khalullin, *Phys.Rev.Lett.* 102,017025(2009) [3] J.Chaloupka et al., *Phys.Rev.Lett.* 105,027204 (2010)

RH18

Effects of the annealing conditions on the magneto-transport properties of La_{0.7}Sr_{0.3}Mn_{1+d}O₃-manganese oxide composites

Sang-im Yoo* and Hyo-jin Kim
Department of Materials Science and Engineering, Seoul National University, Korea

The effects of the annealing conditions on the magneto-transport properties of the pure La_{0.7}Sr_{0.3}MnO₃(LSMO) and LSMO-manganese oxide composites were carefully investigated in this study. While the ferromagnetic-paramagnetic transition temperatures of all polycrystalline samples were insignificantly varied in the range of 359–368 K, low field magnetoresistance (LFMR) properties and dMR/dH values were remarkably improved for the composite samples annealed at relatively high temperature. For instance, with increasing the annealing temperature from 1300 to 1450°C, the LFMR ratios of 95 mol% LSMO - 5 mol% Mn₂O₃ composite sample were increased from 0.8 % to 1.1 % at 300 K in 0.5 kOe, suggesting that a magnetic disorder at the LSMO grain boundary, known as a key factor suppressing effective spin-dependent scattering, could be greatly improved by high temperature annealing process. Detailed annealing effects on the magneto-transport properties of samples will be presented for a discussion. This work was supported by the Korea Research Foundation Grant funded by the Korean Government (MOEHRD, Basic Research Promotion Fund) (KRF-0417-20100021)

RH19

Temperature dependence of spin lattice relaxation time of proton NMR in mixed antiferromagnets A_{1-x}B_xCl₂-2H₂O

Tatsuichi Hamasaki¹, Kazuko Zenmyo² and Hidenori Kubo²
¹ *Physics Department, Kyushu Sangyo University, Japan*
² *Fukuoka Institute of Technology, Japan*

In the mixed antiferromagnet systems Ni_{1-x}Co_xCl₂·2H₂O and Ni_{1-x}Mn_xCl₂·2H₂O, the Co substitution increases a little the transition temperature and the Mn substitution decreases the transition temperature rapidly. In Ni-Co system, the concentration dependence of the phase transition temperature is well explained by simple molecular field theory. But, in Ni-Mn system, molecular field theory cannot explain it sufficiently. Thus Mn spins in NiCl₂·2H₂O crystal show the peculiar behavior. Then, we have measured the temperature dependence of the spin-lattice relaxation time of proton NMR, in order to understand the specificity of the Mn spins. We have prepared the mixed antiferromagnets A_{1-x}B_xCl₂·2H₂O (A, B=Co, Mn, Ni). In Co-M (M=Ni, Mn) system, in comparison with the Ni substitution, the Mn substitution induces a significant impact on the relaxation time. In Mn-M (M=Ni, Co) system, the relaxation time is affected by a small amount of substitution. In Mn-Co system, the reentrant spin-glass phase appears at low temperature. The strange behavior of the relaxation time at low temperature is believed to reflect that. A similar trend is seen at the low temperatures in the case of Ni substitution, too. We suppose that this may be attributed to a kind of the instability of Mn spins.

July 12 (Thu)

July 12 (Thu)

RH20

Electronic Structure and magneto-optical properties of Co₂MnX alloys where X = Ge, Sn and Pb: a first-principles investigation in LDA+U approach

Tran Van Quang¹, Jae Il Lee² and Miyoung Kim³
¹ Dept. of Physics, Ajou University, Suwon 443-749, Korea
² Dept of Physics, Inha University, Incheon 402-751, Korea
³ Division of Energy System Research, Ajou University, Suwon 443-749, Korea

We report our ab initio calculational results on the electronic structures and magneto-optical (MO) properties of the ferromagnetic Co₂MnX alloys where X= Ge, Sn and Pb. Employing the +U corrections for the 3d valence bands of transition metal atoms in addition to the conventional local density approximation (LDA), we investigate the correlation effect on the MO spectra in polar geometry as well as the detailed electronic structures using the all-electron FLAPW [1] method. Results show that the correlation effect results in a blue-shift of the peak positions and the large enhancement of the MO spectra compared to the LDA results. We find that our results can be attributed to the increased t2g-eg splitting of spin minority d-bands of both Co and Mn atoms, which indicates the suppression of diagonal elements of optical conductivity at energy region of 1~2 eV where the interband transitions are forbidden.[2]

[1] E. Wimmer, K. Krakauer, M. Weinert, and A. J. Freeman, *Phys. Rev. B* 24, 864 (1981). [2] Support by Basic Science Research Program (NRF-2010-0005387) and Priority Research Centers (2010-0029617) through the National Research Foundation of Korea.

RH21

2D Heisenberg antiferromagnetism in spin-orbit Mott insulator Sr₂IrO₄

Akiyo Matsumoto¹, Tomohiro Takayama¹ and Hide Takagi^{2*}
¹ Department of Advanced Materials, The University of Tokyo, Japan
² Department of Physics, The University of Tokyo, Japan

In 5d iridates, the interplay between spin-orbit coupling and modest electron correlation produces novel electronic phases. Sr₂IrO₄ was recently found to be a Jeff = 1/2 Mott insulator where spin and orbital degrees of freedom are entangled[1]. The magnetic coupling between such Jeff = 1/2 state, which could be critically different from that in 3d-based Mott insulators, is of particular interest. For example, the magnetic coupling between Ir was theoretically proposed to be isotropic Heisenberg-type when IrO₆ octahedra form corner-sharing network[2]. We focused on Sr₂IrO₄ to reveal the magnetism of such spin-orbit Mott insulator. Sr₂IrO₄ crystallizes in a K₂NiF₄-type perovskite structure, and magnetically orders at 240K. We investigated the detailed magnetic susceptibilities on the single crystals. The ground state was found to be antiferromagnetism, and the in-plane susceptibility steeply increases just above the transition temperature likely due to Dzialoshinski-Moriya interaction. Meanwhile, at higher temperatures, the in- and out-of-plane susceptibilities were almost isotropic. By analyzing the susceptibilities, we found that they can be well described by the 2D Heisenberg antiferromagnetism. This indicates that even in the limit of strong spin-orbit coupling, Sr₂IrO₄ displays the isotropic Heisenberg magnetism. This situation contrast with the 3d oxides, where spin-orbit coupling is responsible for magnetic anisotropy.

[1] B. J. Kim et al., *Science* 323,1329 (2009) [2] G.Jackeli and G. Khaliullin, *Phys. Rev. Lett.* 102, 017205 (2009)

RH22

Magnetoresistance and magnetic properties of oxygen deficient (Sr,Y)(Co,Fe)(Fe,Co)O₃ perovskites

Jean-marie Le Breton^{1*}, Youssef Rizki¹, Yohann Breard², Luc Lechevallier¹ and Antoine Maignan²
¹ Groupe de Physique des Materiaux - UMR 6634, CNRS - Universite de Rouen, France
² CRISMAT, UMR 6508 CNRS, ENSICAEN - Universite de Caen, France

The magnetic and magnetoresistive properties of oxygen deficient (Sr,Y)(Co,Fe)O₃ perovskites have been investigated in relation with the composition. The valence state of Fe has been probed by 57Fe Mossbauer spectrometry. Sr_{1-x}Y_xFe_{0.8}Co_{0.2}O_{3-d} and Sr_{0.8}Y_{0.2}Co_{0.8}Fe_xO_{3-d} series were more particularly investigated. It appears that the progressive replacement of Sr²⁺ by Y³⁺ and the Co/Fe substitution lead to a change of the valence state of Fe and to a drastic change of the magnetic and magnetoresistive properties, in relation with the variation of the Fe⁴⁺/Fe³⁺ ratio and the change in the oxygen content. It is shown that the Sr_{0.8}Y_{0.2}Co_{0.8}Fe_{0.5}O_{3-d} reveals the highest magnetoresistance effect, in relation with the fact that the magnetic field induced ferromagnetic alignment of the Fe/Co magnetic moments allows more metallic pathways to be created. This work was supported by the French Agence Nationale de la Recherche (project ANR-08-BLAN-0005-01).

RH23

High field element selective magnetometry in erbium iron garnet

Cornelius Strohm*, Thomas Roth, Peter J. E. M. Van Der Linden, Olivier Mathon and Sakura Pascarelli
 European Synchrotron Radiation Facility, 6 rue Jules Horowitz 38000 Grenoble, France

Ferrimagnets play an important role for applications as well as from a fundamental point of view. The rare earth iron garnets for example were at the heart of the demonstration of the local molecular field theory [1] and later used for bubble memories, microwave devices and optival isolators. The ferrimagnetic superexchange between the rare earth and iron cations being mainly determined by bond angles and distances in the oxygen polyhedra, results in molecular fields of the order of tens of Tesla [2, 3]. We have performed element selective magnetometry on samples of Erbium Iron Garnet, using energy dispersive x-ray magnetic circular dichroism at the Fe K-edge and the Erbium L-edges. Pulsed fields of 30 T were generated by a high duty cycle miniature coil [4] and the signal was acquired using a multiframe detection scheme exploiting the entire pulse duration of 1 ms [5]. Here we discuss mainly the results obtained at the Fe K-edge. At 65 K, below the compensation point, two successive field induced phase transitions and the reversal of the net magnetization of the Fe sublattices in the intermediate canted phase were observed, while the Fe signal remains unchanged at 100 K, above the compensation point.

[1] L. Neel *Science* 174, 985 (1971). [2] A. E. Clark and E. Callen *J. Appl. Phys.* 39, 5972, (1968). [3] K. Nakao, T. Goto and N. Miura *J. of Magn. Magn. Mat.* 54, 1363, (1986). [4] P. J. E. M. van der Linden et al. *Rev. Sci. Instrum.* 79, 075104, (2008). [5] C. Strohm et al. *J. of Synchrotron Rad.* 18, 224, (2011).

RH24

THz and infrared excitation spectrum below the Jahn-Teller transition in Sr₂Cr₂O₈

Zhe Wang^{1*}, Michael Schmidt¹, Franz Mayr¹, Diana Quintero-castro², A. T. M. Nazmul Islam², Bella Lake², Hans-albrecht Krug Von Nidda¹, Alois Loidl¹ and Joachim Deisenhofer¹
¹ Experimental Physics 5, Intitute for Physics, Augsburg University, Germany
² Helmholtz-Zentrum Berlin fur Materialien und Energie, Germany

We report on optical excitations observed recently in Sr₂Cr₂O₈ by THz and infrared spectroscopy. Low-energy excitations below 3 THz are detected by THz time domain spectroscopy including the spin singlet to triplet excitations.[1] These excitations can be divided into two different classes according to the temperaturedependent properties. One is emergent right below the Jahn-Teller transition temperature, which is determined by specific heat measurement to occur at 285 K. [1,2] The other appears only below 100 K, where the fluctuations are sufficiently suppressed, consistent with the temperature dependence of low-energy Raman modes. [3] Infrared transmission measurements reveal a broad crystal-field excitation, which can be associated with an electronic transition from E to T₂ orbital states.

[1] Zhe Wang et al., *Phys. Rev. B* 83, 201102 (2011) [2] D. L. Quintero-Castro et al., *Phys. Rev. B* 81, 014415 (2010) [3] D. Wulferding et al., *Phys. Rev. B* 84, 064419 (2011)

RH25

High-field multi-frequency ESR in the S=2 Heisenberg antiferromagnetic chain compound MnCl₃(bpy)

Masayuki Hagiwara^{1*}, Shojiro Kimura², Yuichi Idutsu¹ and Zentarou Honda³
¹ KYOKUGEN, Osaka University, Japan
² IMR, Tohoku University, Japan
³ Graduate School of Science and Engineering, Saitama University, Japan

We report the results of high-field multi-frequency ESR experiments at 1.3 K on a powder sample of MnCl₃(bpy) (bpy=2, 2'-bipyridine). This compound is one of the rare examples of the spin 2 quasi-one-dimensional Heisenberg antiferromagnets, and the magnetic properties on tiny single crystal samples were reported previously [1]. In our previous paper on this compound [2], we attained good agreement between experiment and calculation on the temperature dependence of magnetic susceptibility and the high-field magnetization process at 1.3 K. In this work, we have observed some high-frequency resonance modes with a zero-field gap of about 800 GHz that may correspond to the excitation modes at q=0 in the energy dispersion higher than the triplet excitation mode of about 50 GHz at q=pi expected from the evaluated exchange constant and the g-value.

[1] G.E. Granroth et al., *Phys. Rev. Lett.* Vol. 77 (1996) 1616. [2] M. Hagiwara et al., to be published in *J. Phys.: Conf. Ser.*

RI01

Distribution of magnetization in the random ising models.

Kazuyuki Matsumoto¹, Tatsuya Yoshimoto¹, Hiroki Mizuno¹, Takuya Okada¹, Yosuke Ishikawa¹ and Yasuhiro Akutsu²
¹ Department of Applied Sciences, Muroran Institute of Technology, Japan
² Department of Physics, Graduate School of Sciences, Osaka University, Japan

We investigate the two- and three-dimensional random Ising models by the Monte Carlo method. The integrated distribution functions of site-magnetization are calculated above and below the lower Griffith temperature. It is found that these functions have distinct character above or below this temperature for the two-dimensional random Ising model. However, for the three-dimensional random Ising model, this distinction cannot be observed on contrast to the two-dimensional random Ising model. This behavior may be explained by the percolation theory.

RI02

Berezinskii-Kosterlitz-Thouless transition in two-dimensional p-state clock model

Yuta Kumano*, Yusuke Tomita and Masaki Oshikawa
 ISSP, Japan

In two dimensions, the Berezinskii-Kosterlitz-Thouless (BKT) transition occurs in models with the U(1) symmetry. The helicity modulus, which measures the rigidity against a global twist across the system, is useful for a detection of the transition because of its distinctive feature, the universal jump at the transition point. Meanwhile, in the p-state clock model which has the Z_p symmetry, it is believed that the BKT transition occurs when p is greater than 4 since the study by Jose et al. in 1977[1]. However, a recent numerical study by Baek et al. in 2010[2] detects an absence of the universal jump in the helicity modulus for p=5. This contradicts the Jose's result. In this study, we show that the helicity modulus as defined by Baek (HMB) remains finite for any p with the high-temperature expansion. Therefore, the universal jump in the HMB cannot be observed whether the transition is the BKT or not. This casts a question on the physical meaning of the HMB. We will present a systematic study of the helicity modulus to clarify the universality class of the transition for p=5.

[1] J. V. Jose, L. P. Kadanoff, S. Kirkpatrick and D. R. Nelson, *Phys. Rev. B* 16, 1217 (1977) [2] S. K. Baek and P. Minnhagen, *Phys. Rev. E* 82, 031102 (2010)

RI03

Influence of interplanar coupling on the entropy and specific heat of the bilayer ferromagnet

Karol Szalowski and Tadeusz Balcerzak*
 Department of Solid State Physics, University of Lodz, Poland

The Ising-Ising and Ising-Heisenberg bilayer with a simple quadratic lattice in each plane is studied using the pair approximation (PA) method. The foundation of formalism used has been developed in [1], where the phase diagrams for the anisotropic bi- and multilayer system have been obtained. In this paper the method (leading to a complete self-consistent thermodynamics) is adopted for the entropy and magnetic specific heat calculations. An interesting case is demonstrated when the exchange integrals in both planes are of unequal strength, and the interplanar coupling (Ising or Heisenberg) is relatively weak. In such a case, two peaks in the temperature dependence of the specific heat can be observed. The isothermal change of the entropy caused by application of the external magnetic field has been additionally calculated for a wide temperature range. The entropy change in the field also shows a double peak structure, similarly to the specific heat. Such a phenomenon may be of potential interest for investigations of the magnetocaloric effect. The results of the PA method have been compared with those obtained for two Ising-type planes by means of exact diagonalization for finite clusters.

[1] K. Szalowski, T. Balcerzak, *Physica A* 391 (2012) 2197-2208.

RI04

Nontrivial ferrimagnetism of the heisenberg model on the union jack strip lattice

Tokuro Shimokawa* and Hiroki Nakano
 University of Hyogo, Japan

In low-dimensional quantum spin systems with frustration, nontrivial magnetic phenomena occur due to strong quantum fluctuation. One of the phenomena is a non-Lieb-Mattis (NLM) ferrimagnetism[1][2], which is different from the well-known Lieb-Mattis (LM) ferrimagnetism[3][4]. In contrast to the LM ferrimagnetism, the spontaneous magnetization of the NLM ferrimagnetism changes gradually with respect to the strength of frustration. Incommensurate modulation with long-distance periodicity in local magnetizations is also a characteristic behavior of the NLM ferrimagnetism. However, there are only a few cases revealing the NLM ferrimagnetism, which prevents us with understanding the mechanism of the occurrence of the NLM ferrimagnetism. In this study, we examine the ground-state properties of the S=1/2 Heisenberg model on the Union Jack strip lattice. We find the existence of the NLM ferromagnetism by the numerical diagonalization and density matrix renormalization group methods. We also discuss the relationship between the NLM ferromagnetic state of this strip lattice and the intermediate canted state of the S=1/2 Heisenberg model on the two-dimensional Union Jack lattice[5].

[1] S. Yoshikawa and S. Miyashita: *J. Phys. Soc. Jpn.* 74 (2005) Suppl. 71. [2] K. Hida: *J. Phys.: Condens. Matter* 19 (2007) 145225. [3] W. Marshall: *Proc. Roy. Soc. A* 232 (1955) 48. [4] E. Lieb and D. Mattis: *J. Math. Phys.* 3 (1962) 749. [5] R. F. Bishop, P. H. Y. Li, D. J. Farnell, and C. E. Campbell: *Phys. Rev. B* 82 (2010) 024416.

RI05

Control of quantum critical points in bond disordered spin ladder materials

S Ward*, H Ryll², D Biner³, K W Kramer², K Kiefer², D F Mcmorrow¹ and Ch Ruegg⁴
¹ London Centre for Nanotechnology, University College London, United Kingdom
² Helmholtz Zentrum Berlin, Germany
³ Chemistry and Biochemistry, University of Bern, Switzerland
⁴ Laboratory for Neutron Scattering, Paul Scherrer Institut, Switzerland

Spin ladders are model systems of low dimensional quantum spins. There is now considerable interest in materials which realise these ideal systems with solvable Hamiltonians and rich phase diagrams. An archetypal spin ladder material in the low-energy regime is (C₂H₁₂N)₂CuBr₄ whose phase diagram is completely accessible in laboratory magnetic fields. The rung (J_r) and leg (J_l) exchange are 12.8 K and 3.4 K, respectively, and two field-controlled quantum critical points (QCPs) exist at 6.9 T and 14.5 T. (C₂H₁₂N)₂CuC₁₄ is a related spin ladder material. The superexchange between quantum Cu²⁺ spins is controlled by the halide atoms and is lowered to J_r=3.4 K and J_l=1.3 K. The QCPs appear at the lower fields of 1.7 T and 4.3 T. A common structure and rich chemical flexibility in the superexchange pathways allows for partial halide substitution to create the bond disordered spin ladder materials (C₂H₁₂N)₂CuBr₄(1-x)Cl_{4x}, while retaining ideal spin ladder geometry. We present recent neutron scattering work and measurements of the magnetic and thermodynamic properties on the substitution series, and demonstrate explicitly substitution-controlled modification of exchange interactions as well as the effects of bond disorder on the spin ladder physics and QCPs.

RI06

Triangular spin tubes with bond randomness

Yoko Miura^{1*} and Hirotaaka Manaka²
¹ Suzuka National College of Technology, Japan
² Department Graduate School of Science and Engineering, Kagoshima University, Japan

We studied X-ray diffraction and magnetic susceptibility experiments on non-equilateral triangular spin tubes composed of α-KCr_{1-x}Fe_xF₄ (x=0-0.13), which consists of one-dimensional Heisenberg antiferromagnets coexisting with geometrically frustrated spin systems with bond randomness. For x=0, an antiferromagnetic long-range order occurred at TN₁ = 2.5(1) K and another phase transition occurred at TN₂ = 4.0(1) K, because superexchange interactions through the three Cr-F-Cr paths in each non-equilateral triangle lost their equilibrium at low temperatures [1]. As a result, the values of spin-flop transition field drastically decreases with increasing x. This is probably due to the close correlation between the spin structure in the antiferromagnetic ordered state and the crystal structure as theoretically predicted by Nenert and Palstra, i.e., a magnetoelectric linear effect in which a magnetic field in an antiferromagnetic ordered state induces electrical polarization. Thus we carefully verified the crystal structure for x = 0-0.13.

[1] H. Manaka et al., *J. Phys. Soc. Jpn.* 80, 084714 (2011). [2] G. Nenert and T. T. M. Palstra, *J. Phys.: Condens. Matter* 19, 406213 (2007).

July 12 (Thu)

July 12 (Thu)

RI07

A new approach to the characterization of aging, rejuvenation, and memory effects in magnetic systems

Hiroaki Mamiya* and Shigeki Nimori
National Institute for Materials Science, Japan

We introduce a new approach to study non-equilibrium dynamics in magnetic systems. We found that simple ferromagnets such as pure terbium and nickel aluminate foils actually resembles typical spin glasses such as Cu_{0.9}Mn_{0.1} and Cd_{0.9}Mn_{0.1}Te, in behavior of out-of-phase component of ac susceptibility and magnetic viscosity, when they are thermally perturbed after isothermal aging. Briefly, it is not enough to conventionally measure such dissipative properties for characterizing the non-equilibrium dynamics of these systems. In contrast, in the spin glasses, the relaxations of the uniform magnetization were accelerated at a constant magnetic field, when the spin glasses were cooled/heated after the isothermal aging. Surprisingly, such relaxations were reversed when they were subsequently reheated/recooled to the original temperature, despite the persistence of the magnetic field. Because the uniform magnetization mirrors the global evolution of the spin configuration, these reversions indicate that the spin configurations are spontaneously restored to the original [1,2]. On the other hand, such reversions were never observed in the ferromagnets. This fact indicates that ferromagnetic correlations are unaffected by the thermal perturbations, unlike rejuvenation in spin glasses. Thus, the observations of the uniform magnetization would be an additional key to clarifying the features of non-equilibrium dynamics in magnetic systems.

[1] H. Mamiya and S. Nimori, *New J. Phys.* 12 (2010) 083007. [2] H. Mamiya and S. Nimori, *J. Appl. Phys.* in press.

RI08

The linear soliton generated by Z₂ vortex in quantum antiferromagnet

Pawel Rusek
Institute of Physics, Wroclaw University of Technology, PL, Poland

The order parameter of noncollinear Heisenberg antiferromagnet is a triad of orthonormal vectors, i.e. the space of available states is isomorphic to SO₃ group. The topology of SO₃ manifold allows the existence Z₂ vortices in a system. We show that the anisotropy essentially changes the structure of Z₂ vortex in 2D spin system. On the scale larger than the scale l_a defined by weak anisotropy energy the Z₂ vortex is a termination of a linear soliton with the topological charge π1(R) = Z₂. In the soft core of this soliton the rotation angle of triad θ rapidly changes from the anisotropy locked value θ₀ to θ = π, jumps on the line to θ = -π, and then decreases to the value θ₀ on the l_a distance from the line. The linear soliton can terminate on the other Z₂ vortex or it should go out to surface sample. The rapid change of θ in the soft core of linear soliton causes the change of plaquette chirality there- the chirality change the sign on the line initiating the creation of the chirality domain.

RI09

Exact results of a mixed spin-1/2 and spin-1 Ising model with bilinear and three-site four-spin interactions on decorated planar lattices

Michal Jascur^{1*}, Viliam Stubna¹, Karol Szalowski² and Tadeusz Balcerzak²
¹ Institute of Physics, P.J. Safarik University in Kosice, Park Angelinum 9, 040 13 Kosice, Slovakia
² Department of Solid State Physics, University of Lodz, ul. Pomorska 149/153, 90-236 Lodz, Poland

A mixed spin-1/2 and spin-1 Ising model on decorated planar lattices is investigated using a generalized decoration-iteration transformation technique [1]. In addition to the standard bilinear nearest-neighbor interactions, we also consider three-site four-spin interactions and the crystal field effects. In this contribution, exact expressions for the partition function, critical temperatures and other thermodynamic quantities are obtained and analyzed. Performing numerical calculations, we have found that in addition to the standard ferromagnetic and paramagnetic phases there exists in the system also a peculiar partly ordered phase, which possesses non-zero entropy at T = 0 and appears only for zero bilinear exchange interaction. In this phase, the decorating atoms occupy spin states ±1 and 0 with equal probability at all temperatures, while the nodal spins-1/2 are perfectly aligned along easy axis and generate non-zero magnetization. Our calculations primarily clarify the influence of many-body interactions in localized spin systems, which is apparently very different from the standard pair interactions due to the different symmetries of relevant terms in Hamiltonian. However, the presented results may be of wider interest since the origin of the three-site four-spin interaction is related to the magnetoelastic effect [2].

This work has been supported under grant VEGA No. 1/0234/12. [1] M. Jascur, *Physica A* 252 (1998) 217. [2] T. Iwashita, N. Uryu, *J. Phys. C: Solid State Phys.* 17 (1984) 855.

RI10

Anomalous spin diffusion on the two-dimensional percolating network in Rb₂Mn_{0.6}Mg_{0.4}F₄

Shinichi Itoh*
Institute of Materials Structure Science, High Energy Accelerator Research Organization, Japan

Inelastic neutron scattering experiments were performed on a two-dimensional dilute antiferromagnet, Rb₂Mn_{0.6}Mg_{0.4}F₄, with the magnetic concentration being close to the percolation concentration, c_p = 0.593, well above the Neel temperature, and with a high energy-resolution of ΔE = 17.5 μeV. The energy spectrum obtained from the observed dynamical structure factor S(q,E) integrated over wave number, q, throughout almost the entire Brillouin zone, showed a power law dependence, S(E) ~ E^{-x}. The diffusion on a percolating network is anomalous and it has been predicted that the mean square displacement of a random walker is described by <R²(t)> ~ t^θ{2/(2+θ)} with an exponent, θ, as a function of the time, t. The exponent in S(E) is described as x = 1 - Df/(2+θ) with Df being the fractal dimension of the medium. The observed exponent, x, was in good agreement with a theoretical value.

RI11

Quantum phase transitions in 1/3 plateau of the quantum spin tube

Kouichi Okunishi^{1*}, Masahiro Sato², Toru Sakai³, Kiyomi Okamoto⁴ and Chigaku Itoi⁵
¹ Department of Physics, Niigata University, Japan
² Department of Physics and Mathematics, Aoyama Gakuin University, Japan
³ Japan Atomic Energy Agency, SPring-8 and University of Hyogo, Japan
⁴ Department of Physics, Tokyo Institute of Technology, Japan
⁵ Department of Physics, Nihon University, Japan

We study quantum phase transitions in the 1/3 plateau state of the three-leg spin-1/2 tube, where the low-energy effective chirality degree of freedom plays an essential role. Using density matrix renormalization group and the effective chirality model, we find that the chirality liquid, a novel spin imbalance phase and the vector-spin-chirality ordered phase emerge without closing the plateau spin gap, as the leg coupling increases. We also report the role of S_z-symmetry of the spin tube behind these quantum phase transitions in detail.

K. Okunishi, M. Sato, T. Sakai, K. Okamoto and C. Itoi, arXiv:1109.0063

RI12

Cs₂CoCl₄ - an effective XY-spin-½ compound in transverse magnetic fields

Oliver Breunig^{1*}, Eran Sela², Benjamin Buldmann², Markus Garst², Petra Becker³, Ladislav Bohaty³, Ralf Muller¹ and Thomas Lorenz¹
¹ II. Physikalisches Institut, University of Cologne, Germany
² Institut für Theoretische Physik, University of Cologne, Germany
³ Institut für Kristallographie, University of Cologne, Germany

Cs₂CoCl₄ is a model system for studying the magnetism of one-dimensional spin chains with XY anisotropy. It contains CoCl₄ tetrahedra, which form one-dimensional chains along the crystallographic b-axis. The orbital groundstate of Co²⁺ is split by the crystal field into doublets and an easy-plane anisotropy of the magnetization is established. The ground-state doublet is separated from the first excited doublet state by approximately 15 K, such that at temperatures between 0.3 and 4 K the compound is well described by the one-dimensional XXZ model. We compare experimental data of specific heat and thermal expansion to numerical calculations of the XXZ model for transverse magnetic fields; i.e., fields applied within the XY planes. Decreasing temperature below 0.3 K, magnetic order arises at field-dependent temperatures TC(H). Measuring thermodynamic properties with a magnetic field applied along the crystallographic b-axis, we observe a series of magnetic transitions within the ordered state. This work was supported by the DFG through SFB 608.

RI13

Critical phenomena at the antiferromagnetic phase transition of Azurite Cu₃(CO₃)₂(OH)₂

Pham Thanh Cong, Bernd Wolf^{*}, Rudra Sekhar Manna, Andreas Bruhl, Sebastian Kohler and Michael Lang
Physics Institute, Goethe-University Frankfurt (M), SFB/TR 49, D-60438 Frankfurt (M), Germany

The natural mineral Azurite, Cu₃(CO₃)₂(OH)₂, has been considered as a model substance for the 1D distorted diamond chain, where unconventional magnetic properties result from the interplay of strong quantum fluctuations, low dimensionality and frustrating interactions. The system exhibits 3D long-range antiferromagnetic order at TN = 1.88 K. Our measurements of the sound velocity, ultrasonic attenuation and thermal expansion show pronounced signatures at TN indicating a strong coupling to the lattice degrees of freedom. We present a detailed investigation of the critical behavior of the sound velocity v₂₂ and ultrasonic attenuation α in the vicinity of TN. Our analyses reveal a power-law behavior of the critical contributions v_{22cr} ~ t^{-ζ} and α_{cr} ~ t^{-η} over a decade of reduced temperature t = (T - TN)/TN both above and below TN. While the value of η = 1.21, obtained above TN, is close to the theoretical prediction for an anisotropy 3D Heisenberg antiferromagnet, the critical exponent derived from the sound velocity of ζ = 0.056, being identical for temperatures above and below TN, is at odds with this universality class. However, this value is consistent with the critical exponent observed in recent neutron scattering measurements [1].

[1] M. C. R. Gibbs et al., *PRB* 81, 140406(R), 2010

RI14

Dynamical properties of supersolid states in spin systems

Yuta Murakami*, Takahi Oka and Hideo Aoki
Physics, University of Tokyo, Japan

It has been recognized that spin systems can be effectively thought of as boson models as in magnon BEC[1]. Specifically, a possibility to realize supersolid(SS) states (in the boson language) in spin systems is attracting recent attention, where a candidate is a frustrated spin-1/2 dimer model[2]. Here we study how the SS state accommodates collective excitations with the spin-wave theory. [3] We find that the excitation spectrum changes discontinuously as we go from a superfluid phase to an SS phase (that accompanies an SDW; CDW in boson language). Quantitatively, an analytic relation between the velocity of the Goldstone mode and the superfluid density is given. We also calculate the spin-spin correlation function, Szz(q, ω), which translates to the dynamical structure factor in cold-atom systems. We find the intensity of the mode as estimated from the peaks in Szz(q, ω) sharply blows up toward the boundary of SS, which is accompanied by a drastic change in the character of the roton mode. We also mention the possibility to enlarge the SS phase region. These results obtained in the effective boson model should also be directly applicable to cold bosonic atoms.

[1] T. Giamarchi, C. Ru egg, and O. Tchernyshyov, *Nat. Phys.* 4, 198 (2008). [2] P. Chen, C. -Y. Lai, and M.-F. Yang, *Phys. Rev. B*(R) 81, 020409 (2010). [3] T. Sommer, M. Vojta, and K.W. Becker *Eur. Phys. J. B* 23, 329-339 (2001).

RI15

Magnetic phase transition of antiferromagnetic Cs₃V₂Cl₉

Hikomisu Kikuchi¹, Takashi Tanaka¹, Yutaka Fujii², Akira Matsuo³ and Koichi Kindo³
¹ Department of Applied Physics, University of Fukui, Japan
² Research Center for Development of Far-Infrared Region, University of Fukui, Japan
³ ISSP, The University of Tokyo, Japan

Cs₃V₂Cl₉ belongs to the family of hexagonal compounds A₃M₂X₉ (A=Cs, Rb, M=transition metal ions, X=Cl, Br) in which M₂X₆²⁻ dimers are oriented along crystallographic c-axis. Former work^[1] on polycrystalline sample of Cs₃V₂Cl₉ reported that intradimer interaction is ferromagnetic although ground state is nonmagnetic because of relatively large zero-field-splitting. Dimers of Cs₃V₂Cl₉ form triangular lattice in their c-plane so that the geometrical spin frustration effect is expected to occur if interdimer interactions are antiferromagnetic. We measured magnetic susceptibility, specific heat, high field magnetization and ¹³³Cs-NMR using single crystal to study magnetic properties of Cs₃V₂Cl₉. The specific heat shows two anomalies at around 15 and 4 K suggesting successive phase transitions. Results will be discussed in terms of the spin frustration.

1) B. Leuenberger et al. *Inorg. Chem.* 25, (1986) 2930.

RI16

Novel Field-Induced Quantum Phase Transition of the Kagome-Lattice Antiferromagnet

Toru Sakai^{1*} and Hiroki Nakano²
¹ SPring-8, Japan Atomic Energy Agency, Japan
² Graduate School of Material Science, University of Hyogo, Japan

The kagome-lattice antiferromagnet is investigated using the numerical exact diagonalization up to 42-spin clusters. From our investigation of the magnetization process, we found a novel field-induced quantum phase transition, called the "magnetization ramp", at 1/3 of the saturation magnetization [1]. The finite-size scaling analysis of the critical exponents[2] indicated a significant difference of the magnetization ramp from the magnetization plateau observed in the triangular-lattice antiferromagnet. The critical magnetization behavior at lower-field side of the magnetization ramp is same as that of the one-dimensional spin liquid. In order to clarify a difference between the magnetization ramp and plateau, we study a generalized anisotropic triangular-lattice model including the regular-triangular- and the kagome-lattice antiferromagnets in the parameter space. It revealed a quantum phase transition between the triangular- and kagome-lattices at 1/3 of the saturation magnetization. It means that the magnetization ramp of the kagome-lattice antiferromagnet is an essentially different phenomenon from the magnetization plateau of the triangular-lattice one. The relation to the recent magnetization measurements on the volborthite and vesignietite[3] is also considered. In addition we discuss about the spin gap issue of the kagome-lattice antiferromagnet [4].

[1]H. Nakano and T. Sakai: *J. Phys. Soc. Jpn.* 79 (2010) 053707. [2]T. Sakai and H. Nakano: *Phys. Rev. B* 83 (2011) 100405(R). [3]Y. Okamoto, M. Tokunaga, H. Yoshida, A. Matsuo, K. Kindo and Z. Hiroi: *Phys. Rev. B* 83 (2011) 180407(R). [4]H. Nakano and T. Sakai: *J. Phys. Soc. Jpn.* 80 (2011) 053704.

RI17

Antiferromagnetic phase transition of K-Rb alloy nanoclusters incorporated in sodalite

Takehito Nakano*, Yuko Ishida, Atsufumi Hanazawa and Yasuo Nozue
Department of Physics, Graduate School of Science, Osaka University, Japan

Aluminosilicate sodalite possesses a bcc arrangement of nanospaces (beta-cages). Alkali-metal nanocluster (A4)3+ can be formed in each beta-cage, where an s-electron is shared by four alkali cations. (Na4)3+ clusters in sodalite are known to show antiferromagnetism below the Neel temperature of 48 K [1]. By substituting heavier alkali atoms for Na ones, the Neel temperature systematically increases, namely, 72 K in (K4)3+ and 80 K in (K3Rb)3+ clusters [2]. In the present work, we have succeeded in preparing K-Rb alloy clusters with a higher Rb concentration, (K1.5Rb2.5)3+. Magnetic susceptibility obeys Curie-Weiss law and shows a peak at ~ 100 K. ESR spectrum is suddenly broaden below ~ 90 K to be an asymmetric shape which can be explained by powder pattern of antiferromagnetic resonance. These results clearly indicate that the present sample exhibits an antiferromagnetic phase transition at approximately 90 K which is higher than that in (K3Rb)3+. Substituting Rb for K makes the size of s-electron wave function of the cluster larger because of the larger ion size and the lower ionization energy of Rb. This reduces the U/t in the Mott-Hubbard insulating state resulting in an increase in the kinetic exchange coupling between the adjacent clusters.

[1] V.I. Srdanov et al., *Phys. Rev. Lett.* 80, 2449 (1998). [2] T. Nakano et al., *J. Phys. Soc. Jpn.* 79, 073707 (2010).

RI18

A novel scaling method for critical phenomena studies: finite size effects

Joao S Amaral^{1*}, Jouke R Heringa², Ekkes Bruck² and Vitor S Amaral¹
¹ CICECO and Dept. of Physics, Universidade de Aveiro, Portugal
² Delft University of Technology, Faculty of Applied Sciences, 2626 Delft, Netherlands

We present a novel approach for critical phenomena studies. By quantifying scaling plot data overlap, we introduce a 'goodness of scaling' parameter, allowing an iterative search for the 'best' critical exponent values for a given set of magnetization data. The main advantage of this method is going beyond the usual power-law fits of the critical isotherm or low field susceptibility curve, by considering the complete equation of state and all data within the critical region. We consider Monte-Carlo simulated data of the 3D Ising model, and evaluate finite-size effects using our scaling method. Our results are in good agreement with the bibliography, including the dependence of pseudo-critical exponents on system size [1]. Interestingly, we have found that even with a strong dependence of these pseudo-critical exponents on system size, the equation of state is not affected by finite-size effects. The resulting scaling function is in good agreement with recent theoretical predictions for both exponent values and equation of state [2,3]. Our results suggest that while some effects may change the values of observed critical exponents of a given magnetic system, the state equation may retain its identity. In a sense, the state equation can be more universal than exponent values.

[1] Haggkvist R., Rosengren A., Lundow P. H., Markstrom K., Andren D., Kundrotas P., *Adv. Phys.* 56, 653-755 (2007). [2] Campostrini M., Pelissetto A., Rossi P., E. Vicari, *Phys. Rev. E* 65, 066127 (2002). [3] D. O'Connor, J. A. Santiago, and C. R. Stephens, *J. Phys. A* 42, 045003 (2009).

July 12 (Thu)

July 12 (Thu)

RI19

The transverse-field quantum Ising model on infinite-dimensional structures using quantum Monte Carlo method and finite-size scaling

Su Do Yi¹, Seung Ki Baek², Jaegon Um² and Beom Jun Kim^{1*}
¹ Department of Physics and BK21 Physics Research Division, Sungkyunkwan University, Suwon 440-746, Korea
² School of Physics, Korea Institute of Advanced Study, Seoul 130-722, Korea

In a number of classical statistical-physical models, there exists a characteristic dimensionality called the upper critical dimension above which one observes the mean-field critical behavior. Instead of constructing high-dimensional lattices, however, one can also consider infinite-dimensional structures, and the question is whether this mean-field character extends to quantum-mechanical cases as well. We therefore investigate the transverse-field quantum Ising model on the globally coupled network and on the Watts-Strogatz small-world network by means of quantum Monte Carlo simulations and the finite-size scaling analysis. We confirm that both of the structures exhibit critical behavior consistent with the mean-field description. In particular, we show that the existing cumulant method has difficulty in estimating the correct dynamic critical exponent and suggest that an order parameter based on the quantum-mechanical expectation value can be a practically useful numerical observable to determine critical behavior when there is no well-defined dimensionality.

RI20

Study of cluster heterogeneity scaling in the two-dimensional Ising model

Woo Seong Jo¹, Su Do Yi¹, Seung Ki Baek² and Beom Jun Kim^{1*}
¹ Department of Physics and BK21 Physics Research Division, Sungkyunkwan University, Suwon 440-746, Korea
² School of Physics, Korea Institute of Advanced Study, Seoul 130-722, Korea

The cluster heterogeneity, defined as the number of distinct cluster sizes, was suggested in [1] as an indicator of the phase transition in the percolation model. Noh et al. [2] found that the conventional finite-size scaling(FSS) form using the correlation-length exponent ν does not describe the scaling of the cluster heterogeneity in the percolation model and that the other exponent ν_H should be used instead. We apply the FSS form suggested in [2] for cluster heterogeneity in the Ising model. Since there are two types of clusters, (+) and (-) spin clusters, we calculate the heterogeneity of each type (H+ and H-, respectively), and carry out FSS near critical temperature. We find that total heterogeneity ($H \equiv H+ + H-$) scales with the exponent ν_H , as expected from [2] for the percolation model.

[1] H.K. Lee, B.J. Kim, and H. Park, Phys. Rev. E 84, 020101(R) (2011). [2] J.D. Noh, H.K. Lee, and H. Park, Phys. Rev. E 84, 010101(R) (2011).

RI21

Zero-temperature phase transition in a one-dimensional Ising ferromagnet using Glauber dynamics with a synchronous update

Il Gu Yi and Beom Jun Kim^{*}
 Physics, Sungkyunkwan University, Korea

Recently Glauber dynamics for the one-dimensional Ising spin system at low-temperature is studied variously not only experimentally but also theoretically in the nano molecular system. Sznajd-Weron [Phys. Rev. E 82, 031120 (2010)] study the ferro anti-ferro phase transition of the density of active bonds, and the behavior of the relaxation time which means the time needed to reach to steady state in the generalized zero temperature Glauber dynamics. They suggested in that paper that the one-dimensional Ising model subject to the zero-temperature synchronous Glauber dynamics exhibits a discontinuous phase transition. We show here that the phase transition instead of a continuous nature, and we identify critical exponents, β and ν via a systematic finite-size scaling analysis.

1. K. Sznajd-Weron, Phys. Rev. E 82, 031120 (2010). 2. N. Goldenfeld, Lectures on Phase Transitions and the Renormalization Group (Addison-Wesley, Boston, 1992).

RI22

Stochastic treatment of magnetic moment relaxation in spin echo models

Maxim Pavlovich Shlykov
 National Research Centre 'Kurchatov Institute', Russia

The method of nuclear spin-echo amplitude calculation based on the density matrix technique is improved. Spin echo model [1] was supplemented with stochastic consideration of the magnetic moment relaxation provided by the interaction nuclear spin with fluctuating magnetic field. The theory of reducible systems [2] was applied for solving stochastic differential equations. This mathematical approach was adapted to find the solution of the Schrodinger equation for the time-evolution operator which describes behavior of a nuclear spin in the presence of a radiofrequency pulsed magnetic field and fluctuating magnetic field. NMR spin echo for $I = 1/2$ is considered as the simplest illustration of the method. Unlike classical approaches [3,4], It allows to calculate spin-echo amplitude correctly over whole period of relaxation without any estimates. The possibility of application of well-known Ito calculus [5] is also discussed. It was obtained more accurate formulae for spin-lattice relaxation time $T1$ and spin-spin relaxation time $T2$.

[1] Kravchenko E. A., Orlov V. G., Shlykov M. P., Magnetic properties of bismuth(III) oxy compounds, Russian Chemical Reviews, 2006, 75 (1), 77-93 [2] Erougin N., Reducible systems, Travaux Inst. Math. Sieklloff, 1946, 13, 3-96 [3] Redfield A.G., On The Theory of Relaxation Processes, IBM Journ. Res. Develop., 1957, 1, 19-31 [4] Bloembergen N., Purcell E. M., Pound R.V., Relaxation Effects in Nuclear Magnetic Resonance Absorption, Phys. Rev., 1948, 73, 679-712 [5] Gardiner, C. W., Handbook of stochastic methods for physics, chemistry and the natural sciences, Springer, 1994, 13, 442

RJ01

Vortex core switching on notched circular disks

Tomonori Sato* and Yoshinobu Nakatani
 University of Electro-Communications, Japan

The vortex core manipulation by field has been frequently reported. However, the minimization of switching field is still being debated. In general, the vortex core switching is performed by annihilation of vortex and anti-vortex, however the nucleation of the pair requires large magnetic field. In this report, we proposed the new switching mechanism to decrease switching field by using circular disks with V-shaped notch. When the in-plane pulse field is applied, the vortex core moves to the notch and annihilates automatically. After the field is switched off, the vortex core gets back by demagnetizing field. The vortex core polarity is controlled by the external field perpendicular to the disk. In this switching mechanism, the vortex core switching is performed by only the annihilation and nucleation of the vortex, therefore the switching field is decreased compared with the circular disks without notch. We investigated the vortex core switching by micromagnetic simulation. A Permalloy disk with 200nm diameter and 40nm thickness is used in the simulation. The field perpendicular to the disk was fixed at 50 Oe. The result reveals that the minimum switching field decreases 60% compared with the case using the circular disk without notch.

RJ02

Effect of oersted field on magnetic vortex core gyration

Tomonori Sato^{1*}, Yoshinobu Nakatani¹ and Teruo Ono²
¹ University of Electro-Communications, Japan
² Kyoto University, Japan

Recently, the vortex core manipulations by spin current are studied intensively. Because spin current creates the Oersted field, there are some reports, which study the effect of the field on the vortex core motion. When the vortex core is manipulated by the current, the electrodes are usually attached on top of the disk. Therefore, the current goes in and out from the top surface of the disk mainly. It makes the current non-uniform, and it makes the Oersted field complex. In this work, we report the effect of the Oersted field and the current distribution on the vortex core gyration by AC current by micromagnetic simulation. A Permalloy circular disk with 1.5μm diameter and 40nm thickness is used in the simulation. The AC current density is 2.66x10¹¹A/m² mainly. The current frequency is varied around the resonant frequency of the disk. The result reveals that the effect of the Oersted field changes by the current density, however the percentage of the effect of the Oersted field on the driving force is 8% in maximum. Furthermore, the vortex core is affected by not only the in-plane components but also the out-of-plane component.

RJ03

Mutual spin-transfer torque in vortex nano-oscillators

Xiaolei Wang, Ning Wang and Antonio Ruotolo
 Department of Physics and Materials Science, City University of Hong Kong, Hong Kong

We studied the emission response of spin transfer vortex oscillators with dynamic polarizer. In these systems, mutual spin transfer torque between the two ferromagnetic layers is at the origin of a very rich dynamics. By changing the injected current, we could gain access to up to three dynamic modes. At high currents, mutual spin transfer torque is at play and high-frequency dynamics is simultaneously excited in both layers. The detected mode corresponds to a Slonekzewski's windmill-like mode, which is stable in a large range of experimental conditions. The mode observed at low currents corresponds to the commonly observed dynamics in nano-contact vortex oscillators, in which the vortex core is far away from the contact and current-in-plane spin-transfer torque is at play. Surprisingly, we could gain access to a third mode at intermediate currents, which we ascribe to the precession of a vortex in the thin ferromagnetic layer under the contact area. This mode is of particular scientific interest because it allows one to experimentally study the vortex dynamics in the small amplitude limit.

RJ04

Key role of temperature in ferromagnetic bloch point simulations

Kristof M. Lebecki^{1*}, Denise Hinzke¹, Oksana Chubykalo-fesenko² and Ulrich Nowak¹
¹ Department of Physics, University of Konstanz, Germany
² Instituto de Ciencia de Materiales de Madrid, CSIC, Cantoblanco, 28049 Madrid, Spain

A Bloch point (BP) is known to play a crucial role during vortex core switching process [1]. Vortices themselves attract recently much attention since it was suggested to use them as a magnetic storage medium. For such an application BP-related vortex core properties like the switching speed or stability of the final state are essential. This makes the BP an important object of study. We present here results of numerical simulations, where the BP at elevated temperature is investigated. Our approach makes it possible to model its behavior without problems related to its singular character [1,2] - as opposed to all BP simulations presented in the literature so far. We have included temperature effects via Landau-Lifshitz-Bloch equation [3]. Our implementation, basing on the OOMMF code, allow us to compare results of analytical theories with modern numerical approach. We focus our attention on permalloy and conduct studies in the full temperature range. Firstly, we will present results of modeling an artificially pinned BP. This reveals details of its geometry, including its temperature-dependent radius. Secondly, we will present results of dynamical studies, where the vortex core switches via nucleation, propagation and annihilation of a BP.

1. S. Gliga, Y. Liu, and R. Hertel, J. Phys.: Conf. Ser., 303, 012005 (2011). 2. A. Thitaville, J. M. Garcia, R. Dittrich, J. Militat, and T. Schrefl, Phys. Rev. B 67, 094410 (2003). 3. D. A. Garanin, Phys. Rev. B 55, 3050 (1997).

RJ05

Polarization-selective signal propagation in a chain of vortices

Andreas Vogel^{1*}, Michael Martens¹, Markus Weigand² and Guido Meier¹
¹ Institut fuer Angewandte Physik und Zentrum fuer Mikrostrukturforschung, Universitaet Hamburg, Germany
² Max-Planck-Institut fuer Intelligente Systeme, Germany

Dynamics on the subnanosecond time scale and potential technological applications give rise to a broad scientific interest in the dynamic properties of ferromagnetic microstructures with vortex magnetization configuration. An excitation of the low frequency mode of gyration can be transferred via dipolar interaction between neighboring ferromagnetic elements with the transfer efficiency strongly depending on their separation and the relative configuration of the vortex-core polarizations [1]. The dependence on the core polarizations can be understood considering the time-dependent shape of the external stay field. We employ time-resolved scanning transmission x-ray microscopy to study the vortex-core dynamics in a chain of three stray-field coupled permalloy squares. After exciting the first element via a short in-plane magnetic field pulse, the excitation can be transferred through the chain. No response is observed in the third square for equal core polarizations of all elements but the excitation can be transferred through the chain just by changing the polarization in the central element. For alternating polarizations, a transfer efficiency of about 56% to the third square is achieved. The chain can be switched back and forth between the transmitting and a locking state [2].

[1] A. Vogel, T. Kamionka, M. Martens, A. Drews, K. W. Chou, T. Tylliszczak, H. Stoll, B. Van Waeyenberge, and G. Meier, Phys. Rev. Lett. 106, 137201 (2011); H. Jung, K.-S. Lee, D.-E. Jeong, Y.-S. Choi, Y.-S. Yu, D.-S. Han, A. Vogel, L. Bocklage, G. Meier, M.-Y. Im, P. Fischer, and S.-K. Kim, Sci. Rep. 1, 59 (2011). [2] A. Vogel, M. Martens, M. Weigand, and G. Meier, Appl. Phys. Lett. 99, 042506 (2011).

RJ06

Theoretical study on frequency of vortex-antivortex pairs rotation in a magnetic thin-film with multi-contacts

Hiroshi Tsukahara, Hiroko Arai and Hiorshi Imamura*
 AIST, Japan

Spin transfer torque (SST) induced magnetization dynamics is one of the key concepts in spintronics and intensive studies have been conducted in the last two decades to realize STT based memories (Spin-RAM) and microwave oscillators. Finocchio et al. studied the STT induced magnetization dynamics in magnetic thin-film nanopillar which has one aperture and found that the rotational dynamics of a vortex-antivortex (VA) pair produces the resistance oscillation [1]. Therefore, it is interesting to study how the VA-pair dynamics in a multi-contacts system is influenced by the distance between contacts. We performed micromagnetic simulations of a magnetic thin-film where the spatially localized spin-polarized current was injected through two nano-contacts and found the rotation of VA pairs. If the distance between two contacts is so large that the VA pair cannot interfere with each other, they independently rotate around each contact. In contrast, when the distance becomes small, the single VA pair rotates around a large area in which the two contacts are included and the rotation frequency drops down to about 60% of that of a single contact. Our results show that we can control the frequency of the VA pair rotation by changing the distance between the contacts.

[1] G. Finocchio, O. Ozatay, L. Torres, R. A. Buhrman, D. C. Ralph and B. A. Auzerboni, Phys. Rev. B 78 174408 (2008)

RJ07

Parametric excitation and subcritical phase-locking in spin-transfer vortex oscillators

Paolo Bortolotti^{1*}, C. Serpico², E. Grimaldi¹, J. Grollier¹, V. Cros¹, A. Fukushima³, H. Kubota³, K. Yakushiji³, S. Yuasa³, K. Ando³ and A. Fert¹
¹ Unite Mixte de Physique CNRS/Thales, France
² Dipartimento di Ingegneria Elettrica, Universita di Napoli 'Federico II', Italy
³ National Institute of Advanced Industrial Science and Technology (AIST), Japan

In the last decade several systems have been proposed to design low power consuming nano-oscillators. One promising example is a MgO tunnel junction with a vortex free layer[1,2] (STVO). Classically, oscillations at its natural frequency f_0 are obtained for currents larger than a critical value I_c . However, by applying a rf-excitation current at $2f_0$, i.e., parametric excitation[3,4], it is possible to force the system into oscillation even in the subcritical current regime ($I < I_c$). The characteristics of such oscillation (emitted power and linewidth) are not comparable to the ones obtained in the super-critical regime. Here we present the synchronization of a parametric excitation to its own source in the subcritical regime. If $I < I_c$, no oscillation is observed. If we inject a rf-current (-25 dBm) at $2f_0$, a small signal (parametric excitation) appears. When the rf-power is further increased (up to -15 dBm), the parametric signal gets synchronized. The resulting oscillation has the characteristic of the synchronized signal even though is obtained at sub-critical currents. Both mechanisms can be explained in the frame of non-linear vortex dynamics. Comparisons between the analytical approach and experimental results are presented. Support from ANR VOICE Pnano-09_p231-36, EU MASTER NMP-FP7-212257 and CANON-ANELVA for MTJ film are acknowledged.

[1] A. Dussaux et al., Nat. Comm. 1 1 (2010) [2] A.V. Khvalkovskiy et al, Phys. Rev. B 80 140401(R) (2009) [3] S. Urazhdin et al., Phys. Rev. Lett. 105, 237204 (2010) [4] S.Y. Martin Phys. Rev. B 84, 144434 (2011)

RJ08

Micromagnetic simulation for controlling the magnetic vortex chirality by current-induced Oersted field

Syuta Honda^{1*}, Hiroyoshi Itoh², Satoshi Yakata³ and Takashi Kimura³
¹ Faculty of Pure and Applied Sciences, University of Tsukuba, Japan
² Department of Pure and Applied Physics, Kansai University, Japan
³ Advanced Electronics Research Division, INAMORI Frontier Research Center, Kyushu University, Japan

The polarity and the chirality are the magnetization direction and the magnetization curling of the magnetic vortex core, respectively. It is an important issue for developments of spintronics to control these quantities. The magnetic polarity is easily controlled by an external magnetic field. However, the magnetic chirality (MC) is not easily controlled. Recently, the MC in permalloy disks has been controlled by the shape of the disk [1] and a current-induced Oersted field[2]. We study magnetization dynamics for magnetization switching under the current-induced Oersted field at the permalloy thin film. By performing micromagnetic simulations based on the Landau-Lifshitz-Gilbert equation, we investigate an optimum condition for controlling the MC. We have calculated the magnetization reversal process in the permalloy thin film under an external uniform magnetic field. Three types of magnetization structure have been observed during the magnetization switching without an electrical current: a clockwise structure, a counterclockwise structure, and non-vortex core. Using the Oersted field induced by an electrical current perpendicular to the thin film, we have successfully obtained the only clockwise structure (or counterclockwise structure). Details of the results and analysis will be reported.

[1] S. Yakata, M. Miyata, S. Nonoguchi, H. Wada and T. Kimura, Appl. Phys. Lett., 97, 222503 (2010) [2] S. Yakata, M. Miyata, S. Honda, H. Itoh, H. Wada, and T. Kimura, Appl. Phys. Lett., 99, 242507 (2011)

July 12 (Thu)

July 12 (Thu)

RJ09

Stability of the vortex structure on the core switching by AC current

Tomonori Sato* and Yoshinobu Nakatani
University of Electro-Communications, Japan

Recently, magnetic disks with a vortex core have been considered as one of the candidates for the storage devices, and many reports relating to the core switching by spin current have been reported. Because the storage capacity depends on the magnetic disk size, it is important to investigate the stability of the vortex structure on its size. Until now, the disk size that the core can switch stable has not been reported. In this work, we investigate the stability on the core switching by micromagnetic simulation. In the simulation, two methods are used, the method by the core switching simulation by AC spin current and the method by the evaluation of the magnetic energy. The switching simulation reveals that the core does not switch around the transition dimension of magnetic disks between single-domain structure and the vortex structure on a remanent state, and the disk diameter needs to be increased about 20 to 80 nm for the stable core switching compared with the stability limit on the remanent state. Furthermore, the result of the energy evaluation agreed with the result obtained by the switching simulation. Therefore, the stability on the core switching can be estimated by the magnetic energy.

RJ10

Time-averaged observation of magnetic vortex resonated in square-shaped NiFe films

Motoi Kodama¹, Koji Sekiguchi² and Yukio Nozaki^{1*}
¹ Department of Physics, Keio University, Japan
² Department of Physics, Keio University, JST PRESTO, Japan

³ Department of Physics, Keio University, JST CREST, Japan

A dynamics of magnetic vortex confined in a patterned ferromagnetic thin film attracts much attention for both the fundamental and the technological points of view. The observation of the trajectory of magnetic vortex core excited with an application of ac magnetic field or ac current is significant for the quantitative understanding of spin dynamics. In this study, a time-averaged observation of magnetic vortex resonated in square-shaped NiFe thin film was demonstrated by means of magnetic force microscopy (MFM) to obtain the trajectory. A 30 nm-thick NiFe film with the lateral size of 1x1um² was fabricated on a coplanar waveguide that generates an ac magnetic field of 1mT in amplitude. The resonant frequency of the magnetic vortex formed in the NiFe film was calculated to 260 MHz that is much higher than the sampling frequency of MFM. When the ac magnetic field with a frequency of 260 MHz was applied, a circular pattern with a uniform magnetic contrast appeared in the vicinity of center of the NiFe film. The diameter of the circle is comparable with that of the trajectory of magnetic vortex core calculated with micromagnetic simulation.

RJ11

Diverging-converging spin vortex pairs in biquadratically interlayer exchange coupled elements

Sebastian Wintz^{1*}, Christopher Bunce¹, Anja Banholzer¹, Michael Koerner¹, Sibylle Gemming¹, Artur Erbe¹, Joerg Raabe², Christoph Quitmann² and Juergen Fassbender¹
¹ Helmholtz-Zentrum Dresden-Rossendorf, Germany
² SLS, Paul Scherrer Institut, Switzerland

Spin structures have been an interesting topic of magnetism research for many years. Within this field, magnetic vortices have attracted much attention, due to their non-trivial topology and the various dynamic modes they exhibit [1]. A magnetic vortex consists of a planar, flux-closing magnetization curl that turns out of the plane in the central nanoscopic core region. In a single layer structure, the curl's radial components typically cancel each other out. Recent investigations show that this also holds true for multilayer vortex systems with bilinear interlayer exchange coupling [2]. Here we report on pairs of diverging-converging spin vortices occurring in biquadratically coupled systems. Using magnetic scanning transmission x-ray microscopy (STXM) we directly observe that the individual vortices of such pairs possess a residual radial magnetization component, i.e. $\nabla \cdot \mathbf{M}_{xy} \neq 0$. This implies an additional perpendicular magnetization divergence $\nabla \cdot \mathbf{M}_z$, for which we compare a continuous model with discrete micromagnetic simulations.

[1] S.-B. Choe et al., Science 304, 420 (2004). [2] S. Wintz et al., Appl. Phys. Lett. 98, 232511 (2011).

RJ12

Magnetic vortex dynamics in exchange-biased micron-sized structures

Sofia De Oliveira Parreiras^{1*}, Flavio Garcia² and Maximiliano Delany Martins¹
¹ Applied Physics Laboratory, CDTN/CNEN, Brazil
² Laboratorio Nacional de Luz Sincrotron, Brazil

The study of magnetic dots with magnetic vortex spin configuration has recently attracted great scientific interest [1]. The great potential of applications of magnetic vortices (as for example magnetic memories and nanoparticles for cancer treatment) draws attention for the investigation of vortex proprieties. In this work, we studied the dynamics proprieties of exchange-biased vortex using the code OOMMF (NIST) [2] that applies the Landau-Lifshitz-Gilbert equation to simulate the spin configuration and compute the energy and magnetization of microstructures. A series of micromagnetic simulations for Permalloy/Fe₃₀Mn₇₀ disks with 0.5 μm of diameter was done varying the magnetic coupling constant between the layers. We had observed that the vortex gyrotropic movement has a variable frequency that increases with the time, which is not observed when exchange bias is absent. Under a rotating magnetic field acting in the disks, the critical velocity for vortex polarity reversion increases with the coupling constant and frequency. Our results show that the critical velocity can be adjusted in a wide range by selecting the magnetic coupling constant and the oscillating frequency, i.e., it is possible to control the critical velocity for vortex polarity inversion through the exchange bias coupling.

[1] C. L. Chien, F. Q. Zhu, and J.-G. Zhu, Physics Today 60, 40 (June, 2007) [2] M. J. Donahue and D. G. Porter, http://math.nist.gov/oommf/

RJ13

Magnetic Vortex Echo

Flavio Garcia^{1*}, Joao Paulo Sinnecker², Erico Novais² and Alberto Passos Guimaraes²
¹ Brazilian Synchrotron Light Laboratory, Brazil
² Centro Brasileiro de Pesquisas Fisicas, Brazil

The interest of magnetic vortices has greatly grown in the last years since these systems present a myriad of promising applications, which are mainly related on their dynamics aspects. When the vortex core is excited from its equilibrium position, it relaxes in a spiral motion, with a very well defined frequency, which is inversely proportional to the disk aspect ratio. The sense of the gyrotropic motion is determined by the core polarity. So, controlling the polarity, it is easy to control the sense of gyrotropic motion. In this work, we analytically shown that, properly manipulating the dynamic properties of the vortex, namely its polarity, in an analogous way as it is done in Nuclear Magnetic Resonance, it is possible to generate a magnetic vortex echo (MVE). This echo is similar to the spin echo, and it may provide fundamental information about the dynamic properties of real arrays of vortices, e.g., magnetic coupling, inhomogeneities, magnetic stability etc. To illustrate the MVE, we performed micromagnetic simulation of arrays of nanodisks, where it has been varying their most significant parameters to prove that the MVE can give significant information about the dynamic properties of the real array of disks.

ArXiv:1201.3553

RJ14

Origin of the dipolar coupling between vortex-state disks

Ki-suk Lee and Sang-koog Kim*
Seoul National University, Korea

Coupled vortex gyrations in spatially separated nanodisks have been studied theoretically[1,2], experimentally[3-8], and numerically[9] owing to their possible applications as an alternative to current signal processing devices with the advantage of negligible energy loss[7]. Fundamental phenomena such as eigenfrequency splitting and its dependence on dot-to-dot interdistance[3,4,7] have been verified experimentally and explained well by the normal mode representation[7,9]. In this work, we studied dynamic dipole interaction of coupled vortex gyrations observed in two disks by micromagnetic simulation and analytical approaches. Shibata et al.[1] reported that, based on rigid vortex model [10], the dynamic dipolar interaction of the coupled vortex gyrations originates from the magnetostatic interaction that is induced by the side surface charges of each disk during the gyrations [1,2]. We extracted the interaction energies of the two dipolar-coupled disks and compared those that are obtained directly from the micromagnetic simulations and obtained from spin configurations based on two different side-charge-free[10] and rigid-vortex models. The simulation result is in better agreement with the side-charge-free-model-based spin configurations than the rigid-vortex-model one. These results imply that the dipolar energy of the coupled gyrations of neighboring vortex-state disks originates dominantly from not the side surface charges of each disk, but the volume charges.

This work was supported by Basic Science Research Program through the National Research Foundation of Korea(NRF) funded by the Ministry of Education, Science and Technology(No. 20110000441). [1] J. Shibata et al., Phys. Rev. B 67, 224404(2003). [2] O.Y. Sukhostavets, et al., Appl. Phys. Express 4, 065003(2011). [3] A. Vogel et al., Phys. Rev. Lett. 105, 037201(2010). [4] S. Sugimoto et al., Phys. Rev. Lett. 106, 197203(2011). [5] A. Barman et al., J. Phys.: D 43, 422001(2010). [6] H. Jung et al., Appl. Phys. Lett. 97, 222502(2010). [7] H. Jung et al., Sci. Rep. 1, 59, DOI:10.1038/srep00059(2011). [8] A. Vogel et al., Phys. Rev. Lett. 106, 137201(2011). [9] K.-S. Lee et al., Appl. Phys. 110, 113903(2011). [10] K. Y. Guslienko et al., J. Appl. Phys. 91, 8037(2002).

RJ15

Switching dynamics of vortex cores in nanodots by azimuthal-spin-wave-mode excitation

Myoung-woo Yoo, Jehyun Lee and Sang-koog Kim*
National Creative Research Initiative Center for Spin Dynamics & Spin-Wave Devices & Nanospinics Lab, Research Institute of Adv. Materials, Dep. of Materials Sci. & Eng., Seoul Nat'l Univ., Seoul, Korea

Owing to a possibility of implementations of magnetic vortices in future information-storage devices, vortex-core reversals have attracted much attention [1]. Very recently, ultrafast, low-power-driven core switching by azimuthal spin-wave mode was experimentally demonstrated [2]. Since their quantitative interpretation and deeper understanding remain elusive, we start to elucidate the underlying physics of the switching dynamics. In this study, we performed micromagnetic simulations on a Permalloy disk of 302 nm diameter and 50 nm thickness. We correlate the critical velocities (vc) and gyrofields (hz,cri) to the core switching driven resonantly by azimuthal mode excitations. For given disk's dimensions and geometry used here, the vc increases to ~400 and ~700 m/s for m = -1 (clockwise) and +1 (counter-clockwise) modes, respectively, although vc is known to be ~330 m/s for the gyration-mode-assisted-core-switching mechanism [3]. This difference originates from the difference of hz,cri between the gyration mode and azimuthal mode driven core switching mechanisms because the magnetization dip of m_z = -1 is necessary for the switching. From our calculations, hz,cri are estimated to be ~7 kOe and ~11 kOe for CW and CCW azimuthal mode excitations, compared to the value of hz,cri = 3.3 kOe for the gyration mode excitation [4].

*Corresponding author: sangkoog@snu.ac.kr [1] B. Van Waeyenberge et al., Nature (London) 444, 461 (2006); S.-K. Kim et al., Appl. Phys. Lett. 92, 022509 (2008). [2] M. Kammerer et al., Nat. Commun. 2:279 doi: 10.1038/ncomms1277 (2011). [3] K.-S. Lee et al., Phys. Rev. Lett., 101, 267206 (2008). [4] M.-W. Yoo et al., Phys. Rev. B, 82, 174437 (2010). [5] This work was supported by the Basic Science Research Program through the National Research Foundation of Korea (NRF), funded by the Ministry of Education, Science and Technology (No. 20110000441).

RJ16

Logic operations based on magnetic-vortex-state networks

Hyunsung Jung¹, Youn-seok Choi¹, Dong-soo Han¹, Young-sang Yu¹, Ki-suk Lee¹, Mi-young Im², Peter Fischer² and Sang-koog Kim^{1*}
¹ National Creative Research Initiative Center for Spin Dynamics & Spin-Wave Devices & Nanospinics Lab, Research Institute of Adv. Materials, Dep. of Materials Sci. & Eng., Seoul Nat'l Univ., Seoul, Korea
² Center for X-ray Optics, Lawrence Berkeley National Laboratory, Berkeley, CA 94720, USA

Logic operations based on coupled magnetic vortices were experimentally demonstrated. We utilized a simple chain structure consisting of three physically separated but dipolar-coupled vortex-state Permalloy disks as well as two electrodes for application of the logical inputs. We directly monitored the vortex gyrations in the middle disk, as the logical output, by time-resolved full-field soft X-ray microscopy measurements. By manipulating the relative polarization configurations of both end disks, two different logic operations are programmable: the XOR operation for the parallel polarization, and the OR operation for the antiparallel polarization. This work paves the way for new-type programmable logic gates based on the coupled vortex-gyration dynamics achievable in vortex-state networks. The advantages are as follows: a low-power input signal by means of resonant vortex excitation, low-energy dissipation during signal transportation by selection of low-damping materials, and a simple patterned-array structure.

*Corresponding author: sangkoog@snu.ac.kr This research was supported by the Basic Science Research Program through the National Research Foundation of Korea (NRF), funded by the Ministry of Education, Science, and Technology (grant no. 20110000441). The operation of the microscope was supported by the Director, Office of Science, Office of Basic Energy Sciences, Materials Sciences and Engineering Division, U.S. Department of Energy, under contract no. DE-AC02-05-CH11231.

RJ17

Vortex-gyration-mediated magnonic crystals

Dong-soo Han and Sang-koog Kim*
National Creative Research Initiative Center for Spin Dynamics & Spin-Wave Devices & Nanospinics Lab, Research Institute of Adv. Materials, Dep. of Materials Sci. & Eng., Seoul Nat'l Univ., Seoul, Korea

Recently, mutual energy transfer between spatially separated magnetic disks has been studied and interpreted based on a coupled-vortex-oscillator model [1-5]. This novel energy-transfer mechanism provides the advantages of tunable energy transfer rate, low-power input signal, and extremely low energy dissipation for the case of using negligible damping materials. Here, we extended this study into magnonic crystals of one-dimensional (1D) and 2D arrays of dipolar-coupled magnetic disks. We analytically and numerically explored the fundamental modes of collective vortex-gyration excitations in such 1D and 2D disk-array magnonic crystals of four different ordering of vortex polarization (p) and chirality (C) states. Both the analytical and numerical calculations show excellent quantitative agreement on contrasting dispersion branches for different orderings of p and C states. Such collective vortex-gyration modes can be understood in terms of the energy variation of dynamic dipolar interaction between the neighboring vortex-state disks. These results provide for the possibility of vortex-gyration-mediated magnonic crystals as applications for future signal processing devices, offering the advantages of low energy dissipation and low power input. This work was supported by Basic Science Research Program through the National Research Foundation of Korea (NRF) funded by the Ministry of Education, Science and Technology (No. 20110000441).

*Corresponding author: sangkoog@snu.ac.kr [1] J. Shibata et al., Phys. Rev. B 67, 224404 (2003). [2] J. Shibata et al., Phys. Rev. B 70, 012404 (2004) [3] S. Barman et al., IEEE Trans. Mag., 46, 1342 (2010) [4] H. Jung et al., Appl. Phys. Lett. 97, 222502 (2010). [5] H. Jung et al., Sci. Rep. 1, 59; DOI:10.1038/srep00059 (2011); A. Vogel et al., Phys. Rev. Lett. 106, 137201 (2011); S. Sugimoto et al., Phys. Rev. Lett. 106, 197203 (2011). [5] K.-S. Lee et al., J. Appl. Phys. 110, 113903 (2011); O.Y. Sukhostavets, Appl. Phys. Express 4, 065003 (2011).

RJ18

Vortex-gyration transfer rate and energy attenuation in coupled nanodisks

Ji-hye Kim, Ki-suk Lee, Hyunsung Jung, Dong-soo Han and Sang-koog Kim*
National Creative Research Initiative Center for Spin Dynamics & Spin-Wave Devices & Nanospinics Lab, Research Institute of Adv. Materials, Dep. of Materials Sci. & Eng., Seoul Nat'l Univ., Seoul, Korea

One of the most important research goals in current information-signal processing technologies is to enhance signal-processing speed and to reduce energy loss[1]. In recent electronic devices, information-signal transports are based on the motion of electron charges. Interestingly, coupled vortex oscillations in nanodots can be used as an alternative mechanism of information-signal processing[2-4]. Here, we report a study of, by analytical and micromagnetic numerical calculations, information-signal transfer in vortex-state nanodisks that is available with assistance of vortex-gyration transfer through the dynamic dipolar interaction. We analytically derived the vortex-gyration transfer rate and energy attenuation that are both technologically essential parameters for controlling signal processing speed and energy loss in signal processing devices. It is found that the transfer rate can be controlled by the relative polarization configuration p|p2, the saturation magnetization Ms, and the radius (R)-to-thickness (L) ratio R/L of given magnetic disks as well as interdiscance. The energy attenuation is governed by not only the intrinsic damping constant of a given material, but also the values of Ms, L, and R. The analytical results are in reasonable agreements with micromagnetic simulation results. This work provides a foundation of manipulating information-signal processing between vortex-state networks.

*Corresponding author : sangkoog@snu.ac.kr [1] K. Bernstein et al., Proc. IEEE 98, 2169 (2010). [2] H. Jung et al., Appl. Phys. Lett. 97, 222502 (2010). [3] H. Jung et al., Sci. Rep. 1, 59; DOI:10.1038/srep00059 (2011). [4] S. Barman et al., IEEE Trans. Magn. 46, 1342 (2010). [5] A. Vogel et al., Phys. Rev. Lett. 106, 137201 (2011). [6] This work was supported by the Basic Science Research Program through the NRF of Korea funded by the Ministry of Education, Science and Technology (Grant No. 20110000441).

RJ19

Effect of spin-motive force and spin-diffusion on a vortex dynamics

Jung-hwan Moon¹, Aurelien Manchon² and Kyung-jin Lee^{1*}
¹ Department of Materials Science and Engineering, Korea University, Seoul 136-713, Korea
² Materials Science and Engineering, Division of Physical Science and Engineering, KAUST, Thuwal 23955, Saudi Arabia

Theoretically, it is known that the dynamics of magnetic texture highly depends on damping (α) and non-adiabatic parameter (β). However, the value of β is controversial both theoretically and experimentally. Moreover, it was recently reported that α and β are also affected by the spin configuration. The former comes from spin-motive force(SMF) [1, 2] and the latter comes from torque which is exerted from spin-diffusion [3]. In order to understand the spin dynamics under complex spin texture, it is needed to study the effect of SMF and spin-diffusion on α and β. In this work, we performed micromagnetic simulation using LLG equation with spin torque term, SMF, and spin-diffusion. The current-induced dynamics of a vortex core is micromagnetically modeled using a computational framework based on the fourth-order Runge-Kutta method. The model system is a circular Permalloy disk with the thickness of 20 nm and the diameter of 270 nm which is vortex favored dimension. Initial trajectory with spin-diffusion was shifted along y-axis direction compared to that without spin-diffusion. It is because that the initial motion of a core motion is governed by non-adiabaticity [4]. The further studies will be discussed in detail.

[1] S. Zhang and S.-L. Zhang, Phys. Rev. Lett. 102, 086601 (2009). [2] J.-H. Moon, S.-M. Seo, and K.-J. Lee, IEEE Trans. Magn., vol. 46, p.2167 (2010) [3] A. Manchon, W.-S. Kim, and K.-J. Lee, unpublished. [4] J.-H. Moon et al., Phys. Rev. B 79, 134410 (2009).

RJ20

Soft X-ray microscopy of non-linear magnetic vortex core motion

Peter Fischer¹, Brooke Mesler¹, Mi-young Im¹ and Kristen Buchanan²
¹ CXRO, LBNL, USA
² Colorado State U, USA

Magnetism on the nanometer length scale and its fast spin dynamics is a scientifically highly attractive and technologically relevant topic. It addresses fundamental magnetic length scales e.g. magnetic exchange lengths in the sub-10nm range and fast time scales in the sub-ns regime where precessional and relaxation phenomena, domain wall motion and vortex dynamics occur [1,2]. New technological concepts such as spintronics require precise control the electron spin on a nanoscale with psec timing. We use time magnetic soft X-ray microscopy providing a spatial resolution down to 10nm and a temporal resolution below 100ps [3]. As one example, we report experimental results showing non-linear behavior in the resonant excitation of magnetic vortex cores with increasing amplitude of the exciting magnetic AC fields [4]. Supported by the Director, Office of Science, Office of Basic Energy Sciences, Materials Sciences and Engineering Division, of the U.S. Department of Energy.

[1] L. Bocklage, et al. Phys Rev B 81, 054404 (2010) [2] S. Kasai, et al Phys Rev Lett 101, 237203 (2008) [3] P. Fischer, Materials Today 13(9) 14 (2010) [4] B. Mesler et al J.Appl. Phys. (2012) in print

July 12 (Thu)

July 12 (Thu)

RK01

Dynamics of successive minor hysteresis loops

Alexander Gerber and Yoav W Windsor
School of Physics and Astronomy, Tel Aviv University, Israel

Cumulative growth of successive minor hysteresis loops in Co/Pd multilayers with perpendicular anisotropy was studied in the context of time dependent magnetization reversal dynamics. We show that in disordered ferromagnets, where magnetization reversal involves nucleation, domains' expansion and annihilation, differences between the time dependencies of these processes are responsible for accumulation of nuclei for rapid domain expansion, for the asymmetry of forward and backward magnetization reversals and for the respective cumulative growth of hysteresis loops. Loops stop changing and become macroscopically reproducible when populations of upward and downward nucleation domains balance each other and the respective upward and downward reversal times stabilize.

RK02

Gilbert damping constants of exchange biased NiFe/FeMn bilayers

Jungbum Yoon, Hyeok-cheol Choi and Chun-yeol You*
Department of Physics, Inha University, Korea

The physics of exchange bias effect has been studied intensively for the past decades, however, a few experiments have been reported about the spin dynamics and damping mechanism for the exchange biased systems. Recently, the vector network analyzer ferromagnetic resonance (VNA-FMR) is employed to research the spin dynamics of ferromagnetic thin films with wide range microwave frequencies. In this study, the dynamics magnetic properties of the NiFe/FeMn bilayers is investigated by VNA-FMR with various external static field. The exchange bias is verified by vibrating sample magnetometer and VNA-FMR with varying the thickness of FeMn. Spin dynamics and the Gilbert damping constants of exchange biased NiFe/FeMn bilayers are investigated by the analysis of FMR spectra. The exchange bias field induced asymmetry in the magnetization hysteresis loops. It implies the spin dynamics must be asymmetry for positive and negative field region. We perform VNA-FMR measurement for positive and negative fields. In results, we find that the apparent damping parameters are different in the both field directions in the exchange biased NiFe/FeMn bilayers. Therefore, we conjecture that the exchange bias layer acts differently, depends on the relative direction of the ferromagnetic layer magnetization to the exchange bias field.

RK03

Non-linear susceptibility and influence of the applied magnetic field on ZFC/FC curves

Florent Tournus*, Arnaud Hillion, Alexandre Tamion and Veronique Dupuis
LPMCNC, CNRS & Univ. Lyon¹, France

ZFC/FC curves are widely used to characterize assemblies of magnetic nanoparticles. They reflect the crossover between the blocked and superparamagnetic (SP) regime with increasing temperature. With a low applied field a linear response can be assumed, the shape of the curves is then independent of the applied field H, and a simple theoretical modeling is possible: this allows efficient theoretical fits of experimental curves. We have studied the influence of the applied field magnitude on the ZFC/FC curves shape, both theoretically and experimentally. While the effect of H on the energy barriers has already been discussed, its effect on the response of SP particles has not been considered. However, this non-linearity manifests itself much before the modification of the switching energy distribution. In addition to experimental measurements on a diluted Co nanoparticle assembly, we have simulated ZFC/FC curves for different applied fields, including the third-order susceptibility in the SP response. The later depends on the anisotropy and does not at all correspond to a Langevin function around the blocking temperature. We find that the curves can be significantly affected (in particular the low temperature limit of the FC) for quite low applied fields, which are usually used in experiments.

RK04

On the relation between the magnetoelastic effect and the damping constants of (Ni-Fe)_xM_{1-x} (M = Ag, Cr, Ga, Au, Pd, and Pt) films

Yasushi Endo*, Yoshio Mitsuzuka, Yutaka Shimada and Masahiro Yamaguchi
ECEI, Graduate School of Engineering, Tohoku University, Japan

The dynamics of magnetic thin films have received attention in magnetic device applications such as recording heads, media, and MRAM. Although the dynamics significantly depend on the damping constant α , which determines the strength of damping torque in magnetic thin films, details about their damping mechanism, especially the magnetoelastic effect on damping remain unclear. Herein to clarify the effect of λ s on α in (Ni-Fe)_xM_{1-x} films in detail, we evaluated α and λ s in these films. For M= Au, Pd, and Pt, α increases linearly and negative λ s increases as x increases. In contrasts, α and positive λ s tend to increase almost linearly with x when M=Ag, Cr, and Ga. These results provide clear evidence that α is correlated with λ s in (Ni-Fe)-M films. Furthermore, increments of α and the absolute value of λ s to x are markedly enhanced in the order of M = Pt, Au, Pd, Cr, Ag, and Ga, suggesting that 5d transition metal dopants are more influential on both α and λ s than 3d and 4d transition metal dopants due to the strong spin-orbit interaction of 5d dopants. Consequently, these results demonstrate that a change in magnetostriction energy via transition metal dopants can effectively control α .

This work is partly supported by KAKENHI (No. 23686047) from MEXT, Japan, A-STEP from JST, Japan, and SRC.

RK05

Ultrafast magnetization dynamics of ferromagnetic systems induced by mid infrared laser pulses

Amani Zagdoud, Mircea Vomir, Michele Albrecht and Jean-yves Bigot
IPCMS, France

The aim of the present study is to show how the ultrafast demagnetization and the subsequent rapid re-magnetization occur when exciting a ferromagnetic material with low energy infrared pulses. We have used mid-infrared femtosecond laser pulses ($\lambda = [3-10 \mu\text{m}]$) to excite CoPt₃, Ni and Co ferromagnetic thin films. The magneto-optical response is then probed in the visible ($\lambda = 798\text{nm}$). Our results show that even though only intraband transitions occur, the demagnetization process and its subsequent relaxation to the lattice and to the environment are still the dominant processes involved in the magnetization dynamics. We also show that the material band structure is important to interpret the thermalization dynamics of the spins that occur before the heating of the lattice. For specific experimental configurations, we show that it is possible to induce a motion of precession of the magnetization around the effective magnetic field and observe it while it is damped. The magnetization dynamics induced at 6.5 μm in nickel shows an oscillatory behaviour with a period of 2 ps. We attribute this result to the excitation of a two-magnons mode on the NiO by an acoustic mode generated in nickel.

RK06

Ferromagnetic resonance of bilayer CoFeB/NiFeSiB thin film

Sanghoon Jung¹, Chang Ho Choi¹, Jungbum Yoon², Chun-yeol You², Seung Hyun Kim¹, Young Keun Kim³ and Myung-hwa Jung¹
¹ Sogang University, Korea
² Inha University, Korea
³ Korea University, Korea

Spin transfer torque magnetic random access memory (STT-MRAM) is one of the candidates for next generation random access memory. For practical application, the device should have high thermal stability and low critical current density. They have strong correlation with saturation magnetization (Ms) and damping constant (α) so that we need to determine Ms and α . To study the damping mechanism of the thin films, we have performed ferromagnetic resonance (FMR) experiments through vector network analyzer with bilayer thin films of CoFeB(10-x nm)/NiFeSiB(x nm) (x=0,1,2,...,10). We have fitted the FMR data with Lorentz function to get the information of resonance frequency and line width. From these two fitting parameters, we could get Ms and α by Kittel formula and Full Width at Half Maximum. As increasing x values, the Ms tends to increase, whereas the α suddenly decrease and then saturate. This implies that the added NiFeSiB layer in CoFeB plays a role to prevent the spins align along the field direction.

RK07

Observation of non-kittel ferromagnetic resonance in Co/Cu multilayer system

Faris B. Abdul Ahad¹, Yu-che Chiu¹, Shang-fan Lee^{2*} and Dung S Hung³
¹ Institute of Physics, Academia Sinica, Taiwan
² Institute of Physics, Academia Sinica, Taiwan
³ Information and Telecommunications Engineering, Ming Chuan University, Taiwan

In this research, we study the ferromagnetic resonance behavior (FMR) of Co/Cu multilayer system. The samples stacking Ta (5nm) / [Co (4nm) / Cu (t)]*10 / Ta (5nm) with t = 0.5 ? 6 nm were prepared by dc magnetron sputtering in a multitarget sputtering chamber at room temperature and 1 mTorr of pure Ar-pressure. The magnetoresistance (MR) was measured by the standard four point measurement with current in plane (CIP) configuration using Quantum Design Physical Properties Measurement System (PPMS). The magnetic hysteresis loops were recorded using a Vibrating Sample Magnetometer (VSM). FMR responses were measured at microwave frequencies by means of a Vector Network Analyzer (VNA) equipped with a low pass filter circuit. Clear FMR responses were recorded for all samples, however, the noise increased for samples with thicker spacer. Then resonance frequencies (fr) acquired from FMR responses. Theoretically, this FMR should follow Kittel frequency given by: fr=($\gamma/2\pi$)H(H+4 π M). However, our results shows that the resonance linewidth and the deviation of resonance frequency from kittel behavior will increase as the spacer thickness increased. This behavior is the result of RKKY interaction evident by the increased GMR and will be discussed within the manuscript.

1. N. Smith and P. Arnett, Appl. Phys. Lett. 78, 1448 (2001). 2. N. Smith, J. Appl. Phys. 90, 5768 (2001). 3. J. C. Jury, et al, IEEE Trans. Magn. 38, 3545 (2002). 4. Z. Jin and H. N. Bertram, IEEE Trans. Magn. 38, 2265 (2003). 5. Abdul Ahad F. B., Hung D. S., Chiu C. Y. and Lee S. F., IEEE Trans. Mag. 47, 4227 (2011). 6. Hung, D. S.; Fu, Y. P.; Lee, S. F.; Yao, Y. D.; Abdul Ahad, Faris B., J. Appl. Phys. 107, 09A503 (2010). 7. B. Heinrich and J.F. Cochran, Adv. Phys. 42, 523 (1993).

RK08

Neighboring layer dependence of ultrafast thermo-magnetic property in GdFeCo films

Arata Tsukamoto*, Tetsuya Sato, Shingo Toriumi, Ryutarou Shimizu and Akiyoshi Itoh
Electronics & Computer Science, College of Science and Technology Nihon University, Japan

Femtosecond pulsed laser light allow excitation of magnetic systems much shorter than the time scale of thermal diffusion represented by conventional Fourier's law. In this time scale, heating and demagnetization phenomena arise via strongly non-equilibrium non-adiabatic way, and cannot be explained by conventional equilibrium thermo dynamics description[1]. In this study, we investigated the neighboring layer dependence of ultrashort laser-induced thermal/magnetic response in layered GdFeCo films by all-optical pump-probe method. Simultaneously, change of normalized reflectivity was measured for monitoring the time evolution of electron temperature Te. We designed layered structures as same 20 nm thick GdFeCo with different neighboring layers (conductive ATi and insulating SiN). We found two characteristic time region from magnetic behavior: (A) rapid step-like demagnetization and (B) following recovering process with precessional motion. The time scale of (A) is conformed as within picoseconds range (time constant ~100 fs) independently with film structure, which is much shorter than ferromagnetic resonance (period ~0.1 ns at 10 GHz) and hundreds fs delayed with respect to the increase of Te. Following regime (B), film structural dependency of precessional magnetic motion was appeared. The difference of precession frequency and damping properties indicate the different time evolution of lattice temperature in magnetic layer.

[1] I. Radu, K. Vahaplar, C. Stamm, T. Kachel, N. Pontius, H. A. Durr, T. A. Ostler, J. Barker, R. F. L. Evans, R. W. Chantrell, A. Tsukamoto, A. Itoh, A. Kirilyuk, Th. Rasing and A. V. Kimel, Transient ferromagnetic-like state mediating ultrafast reversal of antiferromagnetically coupled spins, Nature, 472 (2011) 205.

RK09

Magnetization dynamics in perpendicular magnetic anisotropy CoFeB/MgO system

Jeong Woo Sohn¹, Ji-wan Kim¹, Kyeong-dong Lee¹, Hyon-seok Song¹, Il-jae Shin², Byoung-chul Min², Chun-yeol You¹ and Sung-chul Shin^{4*}
¹ Department of Physics, Center for Nanospinics of Spintronic Materials, KAIST, Korea
² Center for Spintronics Research, KIST, Korea
³ Department of Physics, Inha University, Korea
⁴ Center for Nanospinics of Spintronic Materials, KAIST, Department of Emerging Materials Science, DGIST, Korea

We study the ultrafast magnetization dynamics of perpendicularly magnetized MgO/CoFeB/Ta and Ta/CoFeB/MgO stack structures which gains wide attention from a viewpoint of perpendicular magnetic tunnel junctions. An all-optical time-resolved magneto-optical Kerr effect measurement reveals that effective Gilbert damping α stays unchanged at ~0.02 in high external field regardless of pump fluence, but it declines drastically with the increase of pump fluence in weak external field. This can be explained by the enlarged apparent relaxation time due to slow remagnetization. Genuine damping tends to attract the precessing magnetization vector towards the effective equilibrium axis, while the tip of the reduced magnetization vector after pump pulse heating recovers growing away from the effective axis. These two competing contributions determine the apparent relaxation time. In a weak field regime, slow recovery of the magnetization vector results in the increased relaxation time and low effective Gilbert damping. We believe that low Gilbert damping found in CoFeB/MgO structure will be expected to reduce the critical current for current-induced magnetization switching.

RK10

Composition dependence of the gilbert damping constant for co-based heusler alloy

Yuichi Kasatani¹, Shinya Yamada², Masanobu Miyao³, Kohei Hamaya⁴, Hiroyoshi Ito⁵ and Yukio Nozaki^{6*}
¹ Department of Physics, Keio University, Japan
² Department of Electronics, Kyushu University, Japan
³ Department of Electronics, Kyushu University / CREST, JST, Japan
⁴ Department of Electronics, Kyushu University / PREST, JST, Japan
⁵ Department of Pure and Applied Physics, Kansai University / CREST, JST, Japan
⁶ Department of Physics, Keio University / CREST JST, Japan

Spin polarized current attracts much attention to operate the magnetic memory devices. To reduce the spin current density, the materials with small Gilbert damping are needed. Recently, it is reported that the Gilbert damping constant of Co-based Heusler alloy known as half-metallic ferromagnet is less than 0.01[1], although the Gilbert damping factor of Co-based Heusler alloy are closely related to crystalline structure and concentration ratio. In this study, to understand the damping mechanism in high-quality L₂-1-type Co-based Heusler alloy we measured ferromagnetic resonance (FMR) and estimated the Gilbert damping factor. 25 nm thick L₂-type Co₂FeSi (x=0, 1, 1.5) films for which degree of crystalline order were found to be about 70%[2] were grown on Si(111) substrates. The saturation magnetization of Co_xFe_{1-x}Si with x=0, 1, 1.5 are 1106, 1023 and 980 emu/cm³, respectively. SiO₂ insulating layer and coplanar waveguides (CPW) which consists of Ti (5 nm)/Au (60 nm) were prepared. Following that, FMR was measured using a vector network analyzer. The results show the Gilbert damping constant inversely proportional to saturation magnetization. Considering the electron density of state from the ab initio calculation, the broadening of FMR spectra is considered to be related to the electron density of state.

[1] T. Kubota, S. Tsunegi, M. Oogane, S. Mizukami, T. Miyazaki, H. Naganuma and Y. Ando, Appl. Phys. Lett., 94 122504 (2009). [2] S. Yamada, K. Hamaya, K. Yamamoto, T. Murakami, K. Mibu and M. Miyao, Appl. Phys. Lett., 96, 082511 (2010).

RK11

Detection of picosecond magnetization dynamics of 50 nm magnetic dots down to the single nanodot regime

Bivas Rana, Dheeraj Kumar, Saswati Barman, Semanti Pal, Yasuhiro Fukuma, Yoshichika Otani and Anjan Barman*
Condensed Matter Physics and Material Sciences, S. N. Bose National Centre For Basic Sciences, India

We present the detection of the picosecond dynamics in arrays of 50 nm permalloy dots down to the single nanodot regime by an all-optical time-resolved magneto-optical Kerr effect microscope. The inter-dot separation (S) varies from 200 to 50 nm and simulated magnetostatic fields shows a transition from magnetostatically isolated to strongly coupled regime as S decreases. Consequently, we observe a single precessional mode for S down to 75 nm, whose frequency increases with the decrease in S. At the smallest separation S = 50 nm, we observe a mode splitting. The simulated mode profile reveals that the dynamics of a single 50 nm dot is dominated by the edge mode. In sparsely packed arrays we primarily observe the isolated dynamics of the constituent dots in phase. For S = 50 nm, we observe an additional backward volume magnetostatic mode of the array. The damping is minimum for S = 200 nm but increases linearly with the decrease in S as a result of the dynamic dephasing of the precession of the weakly interacting dots. At S = 50 nm, the dephasing due to the superposition of two resonant modes results in a sudden increase in the apparent damping.

1. B. Rana, S. Pal, S. Barman, Y. Fukuma, Y. Otani, and A. Barman, Appl. Phys. Express 4, 113003 (2011). 2. A. Barman, S. Wang, J. D. Maas, A. R. Hawkins, S. Kwon, A. Liddle, J. Bokor, H. Schmidt, Nano Lett. 6, 2939 (2006). 3. B. Rana, D. Kumar, S. Barman, S. Pal, Y. Fukuma, Y. Otani, and A. Barman, ACS Nano 5, 9559 (2011).

RK12

Femtosecond demagnetization in Ni: Electron-phonon spin flip scattering from first principles

Karel Carva¹, Marco Battiatto² and Peter M Oppeneer²
¹ DCMP, Charles University in Prague, Czech Republic
² Uppsala University, Sweden

The femtosecond demagnetization discovered in 1996 [1] represents a critical test of magnetization dynamics theories and may lead to many interesting applications. It is still far from being understood on a microscopic level. Electron-phonon spin-flip scattering in Ni was suggested to be the microscopic explanation of its femtosecond laser-induced demagnetization [2]. We have calculated the spin-flip Eliashberg function [3] based on ab initio electron-phonon coupling matrix elements, which allows us to obtain the spin-flip probability with much higher accuracy. We extend this method also to the regime of non-equilibrated electron distributions relevant for ultrafast processes. We have found that the spin-flip probability depends strongly on electron energy. We consider two cases for system excited by a laser: thermalized very hot electron distributions, as well as highly non-equilibrium electron distributions that are expected to be present immediately after the fs laser excitation. Employing this approach we compute the electron-phonon SF rates. We find that the demagnetization rate is very low for any thermalized electron distribution as compared to non-equilibrium distributions present within first femtoseconds following the pump laser [3]. This is due to the density of states and the specific energy-dependence of SF probability.

[1] E. Beaurepaire, J.-C. Merle, A. Daunois J.-Y. Bigot, Phys. Rev. Lett. 76, 4250 (1996). [2] B. Koopmans, G. Malinowski, F. Dalla Longa, D. Steiauf, M. Fähnle, T. Roth, M. Cinchetti, M. Aeschlimann, Nature Mater. 9, 259 (2010). [3] K. Carva, M. Battiatto, P. M. Oppeneer, Phys. Rev. Lett., 107, 207201 (2011)

July 12 (Thu)

July 12 (Thu)

RK13

Ultrafast magneto-acoustic pulses in a nickel film

Jiwan Kim, Mircea Vomir and Jean-yves Bigot*
Physics, IPCMS, CNRS, France

We report about the ultrafast magnetization dynamics induced by magneto-acoustic pulses in a 200-nm-thick Ni film generated with femtosecond laser pulses. The magneto-acoustic pulses result from the coupling between the magnetization and the acoustic waves generated by the laser pulses. In order to distinguish between dynamical magnetic effects induced either by the thermal excitation or by the magneto-acoustic pulse, the spin dynamics is measured from both the front and rear sides of the film via the magneto-optical Kerr technique. It is found that the acoustic pulses excite the magnetization on both sides of the film and the perturbation of the magnetization is very efficient at the rear side (10% of the static one). Using a detailed modeling of magneto-acoustic pulses combining the concepts of acoustic pulse propagation and ultrafast magnetization dynamics, we reproduce the magnetization dynamics on both sides of the film. In addition, our results imply that the magnitude of magneto-acoustic pulses can be controlled and maximized by selecting proper substrates with same ferromagnetic materials. We forecast that our results will have a strong impact for making ultrafast magneto-acoustic devices, with the capability of sensing the magnetization at relatively long distances from acoustic pulses generated by the laser pulses.

RK14

Minimal precessional and switching currents for relaxing-precessional magnetization reversal within a spin valve

Jui-hang Chang*, Hao-hsuan Chen and Ching-ray Chang
Physics, National Taiwan University, Taiwan

The relaxing-precessional magnetization reversal [1] is studied from the point of view of nonlinear dynamics. The solution of the Landau-Lifshitz-Gilbert equation with spin-transfer torque [2] shows that there are two critical values, α_{cs} and α_{cp} , for the damping constant, and $\alpha_{cs} < \alpha_{cp}$. Above α_{cs} the minimal switching current a_s is the same as the modified Stoner-Wolfarth (SW) limit [3] a_{sw} for the switching, and above α_{cp} the minimal precessional current a_p is the same as the modified SW limit a_{sw} for the onset of precession. For a given magnetic anisotropy and an arbitrary in-plane bias field, condition $a_s < a_{sw} < a_p < a_{cp}$ always happen, where a_s , a_{sw} and a_p are functions of α_s , α_p , respectively. These investigations will be of importance for the design of spin-torque-transfer magnetic random access memories [4] and nano oscillators [5].

[1] H. Morise and S. Nakamura, *J. Magn. Magn. Mater.* 306, 260 (2006). [2] J. C. Slonczewski, *J. Magn. Magn. Mater.* 159, L1 (1996). [3] J. H. Chang, H. H. Chen, and C. R. Chang, *Phys. Rev. B* 83, 054425 (2011). [4] U. Ebels, D. Houssameddine, I. Firastrau, D. Gusakova, C. Thirion, B. Dieny, and L. D. Buda-Prejbeanu, *Phys. Rev. B* 78, 024436 (2008). [5] D. Houssameddine, U. Ebels, B. Delaet, B. Rodmacq, I. Firastrau, F. Pontheier, M. Brunet, C. Thirion, J.-P. Michel, L. Prejbeanu-Buda, M.-C. Cyrille, O. Redon, and B. Diney, *Nature Mater.* 6, 447 (2007).

RK15

Time dependent dichroism induced near the surface plasmon of Au nanoparticles

Jean-Yves Bigot* and Minji Gwon²

¹ *Institute de Physique et Chimie des Matériaux de Strasbourg, CNRS, Université de Strasbourg, Korea*

² *Ewha Womans University, Korea*

We have studied the Surface Plasmon (SP) dynamics of Au Nanoparticles, with a diameter of 50 nm, excited by circularly polarized femtosecond laser pulses. We report about a new effect observed in a time resolved pump-probe experiment, analyzing the polarization state of the probe pulses. It manifests as a circular dichroism and an optical rotation induced in the vicinity of the SP when pumping with left (σ^-) or right (σ^+) circularly polarized pulses. We attribute this effect to a time dependent change of the orbital momentum of conduction electrons as the effect is more pronounced when the nanoparticles are excited with a pump wavelength $\lambda_{pump} = 800$ nm as compared to 400 nm. Indeed, in that case the interband transitions from the d-band to the conduction band are minimized with respect to the Drude electrons. The induced dichroism is resonant on the SP (560 nm). Its lifetime is comparable to the energy relaxation time of the quasiparticles to the lattice. It suggests that the electron-phonon interaction is the main mechanism for the dissipation of this pump induced orbital momentum. The detailed behavior of the SP dynamics as a function of probe wavelength, pump polarization and pump-probe delay will be discussed.

RK16

The effect of surface anisotropy on the switching of a particle magnetic moment

Shuang Guo and An Du*

Physical department, Northeastern University, China

The effect of surface anisotropy on the switching of a particle magnetic moment Shuang Guo, An Du* College of Sciences, Northeastern University, Shenyang 110004, China * Corresponding author(du_an_neu@126.com) The dynamic precession of the moment for a spherical particle in a microwave field was studied by using Landau-Lifshitz-Gilbert (LLG) equation. The spins inside the particle have single-normal anisotropy and the ones on the surface of the particle have the surface anisotropy to the surface. The switching field threshold was calculated for different surface anisotropy with definite microwave frequency. It is found that the surface anisotropy influences the switching field threshold, with the increase of the surface anisotropy, the threshold increases. the switching speed of the magnetic moment increases obviously.

1. K. Rivkin, and J. B. Ketters, *Appl. Phys. Lett.* 89, 252507(2006). 2. J.G. Zhu, X. Zhu, and Y. Tang, *IEEE Trans. Magn.* 44, 125(2008). 3. S. Okamoto, N. Kikuchi et al, *Appl. Phys. Lett.* 93, 102506(2008). 4. S. Okamoto, N. Kikuchi, and O. Kitakami, *Appl. Phys. Lett.* 93, 142501(2008). 5. M. Lgarashi, Y. Suzuki et al, *J. Appl. Phys.* 105, 07B907(2009).

RK17

Magnetization dynamics of GdFeCo nanostructures revealed with PEEM

Souliman El Moussaoui*, Loic Le Guyader¹, Michele Buzzi¹, Elena Mengotti¹, Laura J. Heyderman¹, Frithjof Nolting¹, Thomas A. Ostler², Joe Barker², Richard F. L. Evans², Roy Chantrell², Arata Tsukamoto³, Akiyoshi Itoh³, Andrei Kirilyuk⁴, Theo Rasing⁴ and Alexey V. Kimel¹

¹ *Paul Scherrer Institut, Switzerland*

² *Department of Physics, University of York, United Kingdom*

³ *Nihon University, Japan*

⁴ *Radboud University Nijmegen, Institute for Molecules and Materials, Netherlands*

The manipulation of spins is a very exciting topic from fundamental point of view as well as for practical applications. Combining experiments and simulation, we have been able to demonstrate that a fs-optical excitation is sufficient to trigger magnetization reversal in GdFeCo nanostructures on very short timescales. Employing a photoemission electron microscope (PEEM) at the SIM beamline, we have proved that we can manipulate the magnetization of nanostructures by using a heat pulse only. Performing time resolved X-ray magnetic circular dichroism (TR-XMCD) measurement we have observed that the magnetization reversal within the structures occurs on a timescale faster than 100 ps and evidenced that the reversal occurs against an external applied magnetic field. In our experiment the reversal happens only by heating the system on the time scale of the exchange interaction of the two sublattices and does not require any other external stimulus.

*Ultrafast heating as a sufficient stimulus for magnetization reversal T. A. Ostler, J. Barker, R. F. L. Evans, R. Chantrell, U. Azizli, O. Chubykalo-Fesenko, S. El Moussaoui, L. Le Guyader, E. Mengotti, L. J. Heyderman, F. Nolting, A. Tsukamoto, A. Itoh, D. Afanasiev, B. A. Ivanov, A. M. Kalashnikova, K. Yabaplar, J. Mentink, A. Kirilyuk, Th. Rasing and A. V. Kimel, *Nature Comm.* 3, 666 (2012).

RK18

A study of magnetic domain and magnetization reversal in L-shaped Py

S.S. Lee, Wondong Kim, Byong Sun Chun and Chanyong Hwang*

Korea Research Institute of Standards and Science, Korea

The evaluation of characteristic of nanometer-sized magnetic domain is one of the most important issues in the fields of spintronics. We made the Py stripe with and without the L-shaped edge structure. First, magnetic domain and its reversal behavior were simulated with the use of OOMMF program. Depending on the thickness, width of this L-shaped structure, magnetic domain and its reversal behavior could be classified in several groups. We also used scanning electron microscope with polarization analysis(SEMPA, or spin-SEM) to probe the magnetic domain pattern predicted in the simulation.

RK19

Ultrafast dynamics of ferromagnetic copd thin film by various polarized probe beam

S. H. Jung¹, M. H. Jung¹, Jin Pyo Hong², Won Dong Kim³, Chanyong Hwang^{3*} and Joo In Lee²

¹ *Department of Physics, Sogang University, Korea*

² *Department of Physics, Hanyang University, Korea*

³ *Center for Nano-imaging Technology, Korea Research Institute of Standards and Science, Korea*

We study ultrafast dynamics of the ferromagnetic CoPd thin film by using time-resolved magneto-optical Kerr effect. In the case of using linearly polarized probe beam, the spin precession is observed in the frequency of about 14 GHz in the range of large time scale. On the other hand, when the probe beam changes to circular polarization, the large time scale precession disappears, and ultrafast precession (~100GHz) is observed in short time scale. We suppose that these result from the momentum change of probe beam from 0 to 1, and the ultrafast precession is related to interaction between spin and circularly polarized photon.

1. J.-Y. Bigot, *Physics* 5, 11 (2012) 2. J.-Y. Bigot, M. Vomir, E. Beaurepaire, *Nature Physics* 5, 515 (2009)

RK20

Low temperature time domain THz spectroscopy of terbium gallium garnet crystals

Rostislav V. Mikhaylovskiy*, Euan Hendry, Feodor Y. Ogrin and Volodymyr V. Kruglyak

School of Physics, University of Exeter, United Kingdom

We have used the terahertz (THz) time domain spectroscopy to study high frequency magnetic excitations in terbium gallium garnet (TGG) crystals cut along <111> and <001> crystallographic planes. We demonstrate that a THz bandwidth transient electromagnetic pulse can efficiently couple to magnetic moments in TGG. By comparing the spectrum of the pulse before and after transmission through the crystal, we are able to isolate the absorption corresponding to magnetic resonance modes of TGG. We measure and discuss the dependence of the observed modes upon the temperature and the strength and orientation of the bias magnetic field with respect to the crystallographic axes of the crystals. The magnetic modes are present at temperatures above the Neel point, which is interpreted in terms of the field-induced magnetic ordering. The illumination of the crystal with intense optical pulses with wavelength close to the TGG absorption band destroys the magnetic ordering. Thus, the light induced demagnetization of TGG is observed. Our findings demonstrate that the time domain THz spectroscopy can be a powerful tool by which to study high frequency properties of dielectric magnetic materials.

RK21

Ferromagnetic resonance of a single micron dot using vector network analyzer

Kazuto Yamanoi¹, Satoshi Yakata², Takashi Kimura² and Takashi Manago^{1*}

¹ *Department of Applied Physics, Fukuoka University, Japan*

² *Inamori Frontier Research Center, Kyusyu University, Japan*

Magnetization dynamics of small ferro-magnets in the gigahertz region have been investigated intensively for the applications in microwave devices. It is based on the precessional motion of magnetization and it is necessary to control one of each small magnets in devices. In this paper, we investigated ferromagnetic resonance (FMR) of a single micron-scale dot of permalloy (Py) using a vector network analyzer (VNA). A micron-scale Py dot and a coplanar wave guide were fabricated using electron beam lithography, electron beam evaporation and lift off technique. The thickness of the Py dots was 30 nm, and the shapes were square and rectangle with a width and length of 1~10 um and 1~40 um, respectively. The FMR measurement was performed using the VNA and probe station. In the square shape dot of 10 um, the resonant frequency depends on magnetic fields, which was good agreement with the Kittel's equation of a thin film. In the rectangle shape dots, the resonant frequency shifted to higher frequency with increasing length. This tendency was remarkable for 1 um-width dots. It means that demagnetization effect becomes large when the width is less than 1 um for a thin film.

RK22

Relation between gilbert damping constants and perpendicular magnetic anisotropy in Ti buffered Co/Ni multilayers

Hyonseok Song¹, Kyeong-dong Lee¹, Jeong-woo Sohn¹, See-hun Yang², Stuart S.p. Parkin², Chun-yeol You³ and Sung-chul Shin^{4*}

¹ *Department of Physics and Center for Nanospinics of Spintronic Materials, KAIST, Daejeon 305-701, Korea*

² *IBM Research Division, Almaden Research Center, San Jose, California 95120, USA*

³ *Department of Physics, Inha University, Incheon 402-751, Korea*

⁴ *Department of Physics and Center for Nanospinics of Spintronic Materials, KAIST, Daejeon 305-701, Department of Emerging Materials Science, DGIST, Daegu 711-873, Korea*

Recently, there has been a growing interest in spin-transfer-torque magnetic random access memory utilizing perpendicularly magnetic anisotropy (PMA) materials in order to overcome thermal stability problems. Since the critical current density depends on the Gilbert damping parameter, it has been an important issue to understand and manipulate the Gilbert damping parameter in the PMA materials. In this work, we have investigated PMA [Co/Ni] multilayers with Ti buffer layers by an all-optical pump-probe time resolved magnetic optical Kerr effect (TR-MOKE). In particular, we have studied the variation of Gilbert damping constant (α) and PMA as a function of the thickness of Ti buffer layer thickness (t). Since the PMA and damping constant are strongly related with the spin-orbit coupling, both physical quantities must be correlated. Clear damped oscillations of the magnetization are observed in TR-MOKE measurements. After background subtraction, the signal is fitted with a damped harmonic function, from which the precession frequency (f) and the decay time (τ) are deduced. We obtained f and τ by fitting with Landau-Lifshitz-Gilbert equation, and we could be estimated α . We find that the α and PMA values increased monotonically with increasing of t . This result clearly shows close relationship between PMA and α .

RK23

Chaotic motion of magnetic domain structure under alternate field

Michinobu Mino* and Yousuke Yamamoto

Department of Physics, Okayama University, Japan

Magnetic domain motion in a garnet thin film under alternate magnetic fields up to 5000 Hz has been investigated at room temperature. Domain structures and motions are observed by using a high-speed video camera with the help of magneto-optical Faraday effect. When a field frequency is low, the magnetization changes periodically and a domain pattern has a labyrinth structure. By increasing the field amplitude and driving frequency, irregular oscillations of a magnetization appear. Under a rapidly oscillating field, chaotic motions of domain are observed. In this region, domain structures have a disk-like shape. These disks grow from some crystal defects. And a growing point shows a branch-like form.

RK24

Demagnetization dynamics observed by spin-resolved ultrafast x-ray photoemission

Thomas Michlmayr

Physics, ETH Zurich, Switzerland

We report on the experiment and the results of time- and spin-resolved photoemission. Ultrafast demagnetization was first observed by Beaurepaire et al. in 1996 and many approaches where done to support these findings. Our method allows for measuring the whole valence band mediated by the cascade electrons emerging from the sample and therefore gives a direct measure of the sample's magnetization. Ultrafast demagnetization is observed on thin films of Fe on W(110) by optical pumping at 800 nm and x-ray probing at 7 nm. The measured demagnetization time of 450 fs is limited by the experiment. Although space charge effects limits the photoelectron gain the measured spin asymmetry stays almost constant with increasing x-ray flux and only drops at very high x-ray fluxes (> 4 nJ/pulse). We also show the feasibility of single shot magnetic measurement. The experimental setup consists of a completely mobile two chambers ultra-high vacuum system (preparation and measurement chamber) with Mott-polarimeter which can be brought to the free electron laser FLASH, Hamburg.

RL01

Synchronized modes of in-plane/out-of-plane spin-torque oscillators in MTJ with synthetic ferrimagnetic free layer

Masahiko Ichimura¹*, Ryoko Sugano¹, Saburo Takahashi² and Sadamichi Maekawa³
¹ Central Research Lab., Hitachi, Ltd. and JST-CREST, Japan
² IMR, Tohoku University and JST-CREST, Japan
³ Advanced Science Research Center, Japan Atomic Energy Agency and JST-CREST, Japan

There has been considerable interest in the phenomena of spin-torque oscillators (STO) in magnetic tunnel junctions (MTJs) for device applications, as well as the current induced magnetization switching (CIMS) resulting from the spin transfer torque (STT). In particular, the MTJs with synthetic ferrimagnetic (SyF) free layer is important since we can expect the cooperation and/or competition of the magnetization dynamics due to the interlayer coupling between magnetizations in the ferromagnetic bilayer. We analyze the magnetization dynamics self-consistently in the MTJs with SyF layer by iterative calculation following two steps. The STT in the ballistic regime is estimated, and the magnetization reversal is simulated by the LLG method at the finite temperature. We discuss the effect of the interlayer coupling on the STO. As the interlayer coupling increases, the change of the STO mode is observed, where the STO mode moved from the out-of-plane precession (OPP) to in-plane precession (IPP). From the mapping of the STO behavior on the plane with applied current and interlayer coupling, synchronized mode of STO appears in the region where the effective filed corresponding to the interlayer coupling is larger than the anisotropy field. These results suggest that the STO appears even without external magnetic field.

RL02

Interface material effects on magnetic anisotropy and its electric field induced variation in thin films

Yuusaku Taguchi¹*, Haruki Kato¹, Shinya Haraguchi¹, Masahito Tsujikawa², Masafumi Shirai³ and Tatsuki Oda⁴
¹ Graduate School of Natural Sciences and Technology, Kanazawa University, Japan
² CSIS, Tohoku University, Japan
³ CSIS, Tohoku University & RIEC, Tohoku University, Japan
⁴ Institute of Science and Engineering, Kanazawa University, Japan

The spintronics has grown up intensively to realistic applications in the technology of magnetic random access memory (MRAM) development. Such development has been remarkable in memory density, reading-writing speed, and non-volatile property in cooperation with the technologies of spin-injection and physics of spin transfer torque. The basic physics about magnetism has been developing in the response to electric field (EF). This has emerged as the connection with low power consumption device and small energy scale of magneto-electric effects. For the thin films [1,2] as a memory, sensitivity and large response may be required in device applications. Due to the limitation of EF penetration into the thin film, interface with a few metallic layers is critical to determine the response to the EF. We have investigated MgO/Fe/M(001) (M=Au, Pt) [3,4] with using the density functional calculation, in which the substrate of Pt was found to enhance the EF effect on magnetic anisotropy. In this work, in order to investigate influences of stacking structure for the interface, we investigate MgO/Fe/Pt/Au(001) and MgO/Fe/Pd/Au(001). In addition, results in MgO/Au/Fe/Au(001) are also discussed in the connection with segregation effects of film preparation, which may be expected in experiments.

[1] Y. Shiotani et al., *Appl. Phys. Express* 2, 063001 (2009). [2] T. Nozaki et al., *Appl. Phys. Lett.* 96, 022506 (2010). [3] M. Tsujikawa et al., *J. Appl. Phys.*, 109, 07C107 (2011). [4] M. Tsujikawa et al., *submitted for publication*.

RL03

Effect of spin relaxation rate on the interfacial spin depolarization in ferromagnet/oxide/semiconductor contacts

Kun-rok Jeon¹, Byoung-chul Min², Youn-ho Park², Young-hun Jo³, Hun-sung Lee¹, Chang-yup Park¹ and Sung-chul Shin¹*
¹ Korea Advanced Institute of Science and Technology (KAIST), Korea
² Korea Institute of Science and Technology (KIST), Korea
³ Korea Basic Science Institute (KBSI), Korea

The electrical injection and detection of spin-polarized carriers in semiconductors (SCs) has been successfully achieved by employing spin tunnel contacts and the Hanle effects. However, many aspects of the spin phenomena in these systems, e.g., (i) the location, magnitude, and sign of the induced spin accumulation, (ii) the unusual bias and temperature-dependence of the spin signal, and (iii) the unexpected short spin lifetime and its weak variation with temperature, require additional investigation. Here, we report the effect of spin relaxation rate on the interfacial spin depolarization (ISD) from the local fields in ferromagnet (FM)/oxide/SC contacts [1]. The combined measurements of normal and inverted Hanle effects reveal the effect of spin relaxation rate on the ISD [2] in CoFe/MgO/Si and CoFe/MgO/Ge contacts. We have observed, despite the similar amplitudes of the interfacial roughness and local magnetic fields, significant differences of the ISD [2] depending on the host SC; the spin accumulation exposed to similar local fields in different SCs give rise to a clearly different ratio of the inverted Hanle signal to the normal one. This can be understood in terms of two competing mechanisms in the host SCs, namely the spin relaxation and spin precession due to the local fields.

[1] K. R. Jeon et al., *arXiv:1110.5978v1*. [2] S. P. Dash et al., *Phys. Rev. B* 84, 054410 (2011).

RL04

Spin-pumping and revelation of inverse spin-Hall effect in n-type Si at room temperature

Mariko Koike¹*, Eiji Shikoh, Teruya Shinjo and Masashi Shiraishi
 Osaka University, Japan

Since spin-orbit interaction in n-type Si is very week due to its band structure and lattice inversion symmetry, observation of the spin-Hall effect in n-type Si has been believed to be difficult. Here, we report successful observation of the inverse spin-Hall effect (ISHE) in n-type Si at room temperature. The sample composes of a Ni₈₀Fe₂₀/n-type Si film with a doping concentration of 1.0×10¹⁹ 1/cm³. The n-type Si surface was etched by hydrofluoric acid to remove the naturally-oxidized Si. A ferromagnetic Ni₈₀Fe₂₀ was formed by using electron beam lithography and deposition methods on the n-type Si. Two electrode-pads were attached to the n-type Si layer to detect the electromotive force in the Si. In a ferromagnetic resonance condition of the Ni₈₀Fe₂₀, a pure spin current was injected into the n-type Si layer by the spin pumping. If ISHE is induced in the n-type Si, the spin current is converted to a charge current. Here, the ISHE in the n-Si was observed. The output voltage due to the ISHE was estimated to be 0.4μV. The voltage sign was inverted by the magnetization reversal of the Ni₈₀Fe₂₀. In this presentation, we discuss details of the inverse spin-Hall effect in the n-type Si.

RL05

Critical current density and domain wall mobility in nanowires with exchange coupled hard-soft magnetic layers

Xiaoxi Liu¹*, Liangqiu Gao² and Akimitsu Morisako²
¹ Department of Information Engineering, Shinshu University, Japan
² Shinshu University, Japan

In this study, critical current density and domain wall mobility of current driven domain wall motion in nanowires composed of TbFeCo and NiFe layers have been studied. TbFeCo layer has perpendicular magnetic anisotropy. Wires and electrode are fabricated by photolithographic method. Current pulses with width less than 100 ns are applied to drive the domain wall in the wires. The domain structure is observed by a high resolution Kerr microscope. We found critical current density decreases in the soft-hard bi-layered structure compared to a single TbFeCo layer. Nanowires of single TbFeCo layer have critical current density of 5×10⁶ A/cm²; however, the critical current density in bi-layered structure has critical current density as small as 2×10⁶ A/cm². The domain wall mobility is deduced from the dependence of domain wall velocity on the applied current density. We found that the domain wall mobility improved by almost two times with the introducing of the NiFe layer. Of particular interesting is that, micromagnetic simulations show that the Bloch walls in perpendicular TbFeCo wires change to Neel walls with the introducing of NiFe layer. Our experimental results suggest nano-wires composing of soft-hard layers suitable for race track memory.

RL06

Spin Seebeck Effect in SiO₂/Py structures

Sang-il Kim¹, Seung-young Park², Byoung-chul Min³, Younghun Jo², Kyung-jin Lee¹* and Kyung-ho Shin³
¹ Department of Materials Science and Engineering, Korea University, Seoul 136-713, Korea
² Nano Material Research Team, Korea Basic Science Institute, Daejeon 305-333, Korea
³ Korea Institute of Science and Technology (KIST), Seoul 136-791, Korea

Recently, spin version of Seebeck effect, the spin-Seebeck effects (SSE) was observed experimentally at room temperature[1]. For the SSE, it is expected that the voltage sign at the hot end is opposite to that at the cold end and the absolute magnitudes of the voltages at the hot and cold ends are the same. However, it is often observed that an asymmetric magnitude of the voltage at the hot and cold ends [2]. The origin of this asymmetric behavior is attributed to an additional temperature gradient along the thickness direction, which generates an additional voltage signal due to the anomalous Nernst-Ettingshausen effect(ANE) [2]. In this study, we investigated the dependence of the SSE and the ANE on the thickness of the ferromagnetic layer in SiO₂/Py samples. In our results, the sign change in the voltage signal between the hot and cold ends was not observed. Instead, we obtained an offset voltage due to the mixture of SSE and ANE signals. We attribute this offset to the longitudinal SSE caused by an additional temperature gradient along the thickness direction of Py layer. A possible origin of the dependence of offset voltage on Py thickness will be discussed in detail.

[1] K. Uchida et al., *Nature*, 455, 778-781 (2008). [2] S. Bosu et al., *Phys. Rev. B* 83, 224401 (2011).

RL07

Domain wall pinning by stray field from NiFe on Co/Ni nano-wire

Ryo Hiramatsu¹, T. Koyama¹, D. Chiba¹, S. Fukami², N. Ishiwata³, Y. Nakatani³ and T. Ono¹*
¹ Institute for Chemical Research, Kyoto University, Japan
² Green Innovation Research Laboratories, NEC Corporation, Japan
³ University of Electro-communications, Japan

Control of a magnetic domain wall (DW) displacement in a ferromagnetic nano-wire is essential in its potential application for nonvolatile magnetic memories. Parkin et al. demonstrated a race track memory device by controlling DW displacement in a NiFe nano-wire with notch structure [1]. However, the structure with notch has two problems such as i) transformation of DW structure and ii) increase of current density due to the change of the wire width between notch and wire part. Here, to make new DW pinning method without the change of wire width, we focus on the DW pinning in Co/Ni nano-wire by the stray field from ferromagnetic stack. We prepared two types of devices; one was a simple wire of Ta/Pt/[Co(0.2 nm)/Ni(0.6 nm)]_x/Co(0.2 nm)/Pt/Ta, and the other was a wire of Ta/Pt/[Co(0.2 nm)/Ni(0.6 nm)]_x/Co(0.2 nm)/Pt/Ta on which NiFe/SiO₂ was stacked partly. To investigate an influence of the stray field from the NiFe stack, DW depinning field (*H_{dep}*) was measured for both types of wires. *H_{dep}* of the wire without the NiFe stack was 200 Oe, while the wire with that had larger *H_{dep}* of 700 Oe, indicating the effectiveness of the use of the stray field to control the DW position.

[1] S. S. P. Parkin, et al., *Science* 320, 190 (2008).

RL08

Compositional dependence of critical current density for spin transfer torque switching of amorphous GdFeCo for thermally assisted MRAM

Bing Dai¹*, Takeshi Kato¹, Satoshi Iwata¹ and Shigeru Tsunashima²
¹ Department of Quantum Engineering, Nagoya University, Nagoya 464-8603, Japan
² Department of Research, NISRI, Yotsuya-dori 1-13, Chikusa-ku, Nagoya, 464-0819, Japan

Spin transfer torque (STT) switching has been demonstrated in magnetic tunneling junctions (MTJ) with perpendicular magnetic anisotropy (PMA), which exhibits a low critical current density compared to their in-plane counterparts [1]. In this paper, we fabricated giant magneto-resistance (GMR) devices consisting of bottom electrode/ [Pd (1.6)/Co (0.4)]_x/Co₉₀Fe₁₀B₂₀ (0.5)/Cu (3)/ Gd_x(Fe_{90-x}Co₁₀)100-x (10)/Cu (5)/top electrode (thickness in nanometer). The R-I loops were measured for 120×180 nm² cell with Gd_x(Fe_{90-x}Co₁₀)100-x memory layers, and the STT switching property of these devices was estimated from the resistance measurement after applying current pulses with a duration of 100 ns. In TM-rich compositions, the average value of the critical current density *J_c* increased from 2.0×10⁷ A/cm² for *x* = 22.3 at.% to 4.5×10⁷ A/cm² for *x* = 24.0 at.% with increasing *x*, while the *J_c* reduced to 1.4×10⁷ A/cm² for RE-rich Gd_{28.4}(Fe₉₀Co₁₀)_{71.1}. It is noted that the values of *J_c* are comparable to the results in conventional MTJs[2]. The difference of *J_c* values may be due to the difference of the effective perpendicular anisotropy and/or the Curie temperature of the GdFeCo layer. The dependence of *J_c* on the current pulse width and temperature will be discussed in the presentation.

[1]S. Ikeda, et al. *Nature Materials* 9, 721-724 (2010). [2]Y. Hui, et al. *Appl.Phys.Lett.* 82, 222510 (2005).

RL09

Microscopic theory of magnon-drag thermodynamic transport in ferromagnetic metals

Daisuke Miura* and Akimasa Sakuma
 Department of Applied Physics, Tohoku University, Japan

We study the thermodynamic transport carried by magnons in ferromagnetic metals. In this study, the Peltier effect caused by a magnon heat current (magnon-drag Peltier effect) is described in a microscopic model. Magnons can indirectly interact with electric fields via electron-magnon interaction; we evaluate the magnon heat current perturbatively with respect to the electron-magnon interaction in the 2nd order. As a consequence, we found out that the magnon heat current is proportional to the spin current carried by the spin polarized electric current drifted by the electric field, that is, the magnon-drag Peltier coefficient is governed by the spin polarization of the electric current. This is in contrast to the phenomenological result derived by Grannemann and Berger [1] in which the coefficient is proportional to the electric current directly. In addition, we show the temperature dependence of the Peltier coefficient is T^{5/2} in low temperature. These results indicate that, in the inverse effect (Seebeck effect) of the Peltier effect, the magnon heat current caused by a temperature difference induces the spin current, and the temperature dependence of the Seebeck coefficient is T^{3/2}.

[1] G. N. Grannemann and L. Berger. *Phys. Rev. B* 13, 2072 (1976).

RL10

Electric-field control of magnetic properties in cobalt by means of electric double layer

Kazutoshi Shimamura¹, Daichi Chiba¹, Masashi Kawaguchi¹, Shimpei Ono⁴, Shunsuke Fukami², Nobuyuki Ishiwata³, Kensuke Kobayashi¹ and Teruo*
¹ Institute for Chemical Research, Kyoto University, Japan
² Institute for Chemical Research, Kyoto University and PRESTO JST, Japan
³ Institute for Chemical Research, Kyoto University and Osaka University, Japan
⁴ Central Research Institute of Electric Power Industry, Japan
⁵ NEC Corporation, Japan

Electric-field effect on magnetism using a capacitance structure (gate electrode/insulator/ferromagnetic) has actively investigated to open up a new technology for an electrically manipulation of magnetization [1-10]. Here, we show electric field control of magnetic properties in Co using an electrical double layer (EDL) formed at the interface between the Co layer and a polymer film containing an ionic liquid. The polymer film containing the ionic liquid was put on a 0.4-nm-thin-Co-film and Pt-thin-film was placed on the top of the polymer film as a gate electrode. For the direct detection of the magnetization under the gate-voltage (V_g), superconducting quantum interference device [6] was used. Magnetization curves were measured at 300 K under the application of V_g from -2.0 V to +2.0 V. Dramatic change of coercivity was observed depending on V_g. To investigate the mechanism of this, we measured temperature dependences of the remanent magnetization under the different V_g. The significant increase of Curie temperature from ~320 K at V_g = 0 V to ~370 K at 2.0 V was observed. Thus, the dramatic change in coercivity at 300 K presented here is attributed to this large modulation of Curie temperature [10].

[1] H. Ohno et al., *Nature* 408, 944, (2000). [2] D. Chiba, M. Yamanouchi, F. Matsukura and H. Ohno, *Science* 301, 943 (2003). [3] M. Weisheit et al., *Science* 315, 349 (2007). [4] D. Chiba et al., *Nature* 455, 515 (2008). [5] T. Maruyama et al., *Nature Nanotechnol.* 4, 158 (2009). [6] M. Sawicki et al., *Nature Phys.* 6, 22 (2009). [7] M. Endo et al., *Appl. Phys. Lett.* 96, 22515 (2010). [8] H. Ohno, *Nature Mater.* 9, 952 (2010). [9] Y. Yamada et al., *Science* 332, 1065 (2011). [10] D. Chiba et al., *Nature Mater.* 10, 853 (2011).

RL11

Spin-torque magnetic resonance of superparamagnetic Fe nanoparticles in Fe/MgO/Fe magnetic tunnel junctions

Shinji Miwa, Norikazu Mizuochi, Teruya Shinjo and Yoshishige Suzuki
 Graduate School of Engineering Science, Osaka University, Japan

During the past decade, electric detection and manipulation of submicron-scale magnet have been conducted by using magnetoresistance (MR) effect and spin-torque. Now, a great deal of interests in manipulating nano-scale magnets (or single-spin) and physics of spin-torque in such a small system are taken. In this study, we employ superparamagnetic Fe nano-particles and the single-crystal MgO based magnetic tunnel junctions (MTJs) [1]. The magnetic resonance of super-paramagnetic Fe nano-particles is electrically excited by spin-torque and detected by the spin-torque diode effect [2,3]. The structure of the MTJs is as follows: MgO(100) substrate/Fe film (50 nm)/MgO (1.35 nm)/Fe nano-particles (2.1 nm)/capping layer. All of the layers were grown by molecular beam epitaxy. The RF detection mechanism is explained as the homodyne detection of the applied RF current because of the oscillation of resistance at the same frequency. In the measurements, the resonant peak was observed around 5 GHz under a magnetic field of 5 kOe at room temperature, for example. This represents that the magnetic resonance of superparamagnetic Fe nano-particles was electrically excited and detected. We thank Y. Shiota, H. Tomita, G. Shiomi for valuable discussions. This work is supported by Grant-in-Aid for Scientific Research (S), MEXT, Japan. (No. 23226001)

[1] S. Yuasa et al., *Nature Mater.* 3, 868 (2004). [2] A. A. Tulapurkar et al., *Nature* 438, 339 (2005). [3] S. Ishibashi, S. Miwa et al., *submitted*.

RL12

Spin Coulomb drag and optical excitations in low dimensional systems

Irene D'amico¹ and Carsten A. Ullrich²
¹ Physics, University of York, United Kingdom
² Physics, University of Missouri-Columbia, USA

Within the remit of new quantum technologies, an intense effort is devoted to improving our understanding of spin dynamics, with the aim of building novel spintronics devices. In this context the theory of spin Coulomb drag (SCD) was recently developed. It shows that Coulomb interactions are an intrinsic decay mechanism for spin currents. As confirmed by experiments, SCD can be substantial in semiconductors, and it is bound to become one of the most serious issues in spin polarized transport, since, due to its intrinsic nature, it cannot be avoided even in the purest material. More recently the influence of SCD on optical spin-injection and spin-resolved optical experiments has been considered. Here we report on SCD effects on intersubband optical spin excitations in III-V quantum wells, where SCD may contribute substantially to the linewidth of spin plasmons. By going beyond the usual local density functional approximation and properly including the effects due to the inhomogeneity of the system in the growth direction, we show that the quantization of states in the growth direction may strongly reduce the intrinsic plasmon linewidth.

July 12 (Thu)

July 12 (Thu)

RL13

Perpendicular magnetic property and magnetic damping of very thin CoFeB films

Mikihiko Oogane*, Miho Kubota, Kei Sato, Hiroshi Naganuma and Yasuo Ando
Applied Physics, Tohoku University, Japan

A very thin CoFeB film with a perpendicular magnetic anisotropy is a promising material for applications of spintronics devices, such as Spin-RAM and spin-logic circuit [1]. Development of materials with high magnetic anisotropy and low magnetic damping is an important issue to achieve high thermal stability and low power consumption in the spintronics devices. However, the relationship between magnetic damping and perpendicular anisotropy has not been systematically investigated. In this work, we have investigated capping layer dependence of perpendicular magnetic property and magnetic damping in very thin CoFeB films. The films were prepared by sputtering system. The structure of the films were SiO₂-sub./Ta(5)/MgO(0.9)/CoFeB(d)/X(5 nm), (X = Ta, Pd, Cu, Ru, V, MgO). After the deposition of the films, annealing process was carried out at 250 - 350°C. Magnetic property and magnetic damping were respectively characterized by SQUID and FMR [2]. Perpendicular magnetic anisotropy and damping strongly depends on the capping layer material. For the Ta capping layer, CoFeB film below 1.4 nm showed a perpendicular anisotropy. However, magnetic damping was drastically enhanced for the films with perpendicular anisotropy. Similar behavior was observed in the films with capping layers of Pd and Ru. This work was supported by the FIRST program.

[1] S. Ikeda et al., *Nature Material* 9, 721 (2010). [2] S. Mizukami et al., *Jpn. J. Appl. Phys.* 40, 580 (2001).

RL14

Perpendicular magnetic tunnel junctions with TbFeCo-based pinned layer and CoFeB-MgO free layer

Jungmin Han¹*, Byoung-chul Min¹, Kyung-jin Lee² and Kyung-ho Shin¹
¹ Spin Device Research Center, Korea Institute of Science and Technology, Seoul 136-791, Korea
² Department of Materials Science, Korea University, Seoul 136-701, Korea

We have fabricated perpendicular magnetic tunnel junctions (pMTJs) with a CoFeB/TbFeCo pinned layer and Ta/ CoFeB/ MgO free layer using in-situ annealing process. The TbFeCo-based hybrid pinned layer is a useful approach to obtain a high perpendicular magnetic anisotropy (PMA). However, a high temperature annealing, often required for MgO-based MTJs to obtain a high tunneling magnetoresistance (TMR), may deteriorate the PMA of TbFeCo films. Our experimental results show a possibility to obtain a reasonable TMR and high PMA simultaneously by conducting an annealing process to achieve a grain-to-grain epitaxy in CoFeB/MgO/CoFeB layers before depositing the TbFeCo layer. The pMTJs prepared by this process show a tunneling magnetoresistance (TMR) ratio of 15% to 19% at room temperature.

[1] S. Ikeda, K. Mitsu, H. Yamamoto, K. Mizumuma, H. D. Gan, M. Endo, S. Kanai, J. Hayakawa, F. Matsukura & H. Ohno, *Nature Materials* 9, 721-724 (2010). [2] N. Nishimura, T. Hirai, A. Koganei, T. Ikeda, K. Okano, Y. Sekiguchi, and Y. Osada *J. Appl. Phys.* 91, 5246 (2002). [3] H-Jae Shin, Byoung-Chul Min, Jin Pyo Hong, and Kyung-Ho Shin, *Appl. Phys. Lett.* 95, 222501 (2009).

RL15

Thickness and magnetic anisotropy dependence of anomalous Nernst effect in L1₀-FePt films

Kota Hasegawa, Masaki Mizuguchi*, Ken-ichi Uchida, Eiji Saitoh and Koki Takanashi
Institute for Materials Research (IMR), Tohoku University, Japan

The anomalous Nernst effect (ANE) is a thermomagnetic effect which gives rise to an electric field perpendicular to both temperature gradient and saturation magnetization. Although ANE has been known phenomenologically for a long time, only a few studies have been reported, and the mechanism has not fully been understood. L1₀-FePt with high magnetic anisotropy (K_u) attracted much attention for recent years as a promising material for "spin caloritronics" [1]. In this paper, we have made systematic investigation on the thickness and Ku dependence of ANE in perpendicularly magnetized FePt(001) films. FePt(001) films were deposited on MgO(001) single crystal substrates at 500°C. The thickness was varied in the range from 7 to 40 nm. Ku was changed in the range from 3.0×10⁶ to 2.7×10⁷ erg/cc, depending on the degree of L10 order which was controlled by the deposition temperature from 300 to 500°C. It is found that the anomalous Nernst coefficient (Q_a) does not depend on the film thickness. On the other hand, Q_a increases with decreasing K_u. These results suggest a contribution of spin wave in ANE.

[1] T. Seki et al., *Solid State Comm.*, Vol. 50, 496 (2010).

RL16

Spin-torque efficiency and magnetization reversal in three-dimensional Rashba materials

Kazuhiro Tsutsui and Shuichi Murakami*
Dept. of Physics, School of Science, Tokyo Institute of Technology, Japan

In addition to the magnetization reversal by the spin-transfer torque, the magnetization reversal driven by a strong spin-orbit coupling has been intensely investigated experimentally and theoretically [1,2]. In this presentation, we focus on 3D Rashba models coupled with localized spins, and study the spin torque theoretically. This is motivated by the recent discovery of BiTeI as 3D Rashba systems [3]. As a result, we find that the spin torque in 3D Rashba models is largely enhanced in the high-carrier-density regime compared with 2D Rashba models. We also find that the spin-torque efficiency defined as the ratio between the spin torque and the electric current is enhanced when the Fermi energy lies on only lower band, both in 3D and 2D. As we change the Rashba spin-orbit coupling, the spin-torque efficiency becomes maximum when the Rashba spin-orbit coupling is comparable to the exchange coupling to the localized spins. The optimum spin-torque efficiency becomes large when the Rashba spin-orbit coupling is large, and it is preferable for the magnetization reversal with smaller amount of current injection.

[1] A. Manchon and S. Zhang, *Phys. Rev. B* 78, 212405 (2008). [2] I. M. Miron et al., *Nature Mater.* 9, 230 (2010). [3] K. Ishizaka et al., *Nature Mater.* 10, 521 (2011).

RL17

A new circuit model for spin-torque oscillator including the perpendicular torque of magnetic tunnel junction

Hyein Lim, Sora Ahn, Miryeon Kim, Jihye Shin, Jinju Lee, Seungjun Lee and Hyungsoon Shin*
Electronic Engineering, Ewha Womans University, Korea

Spin-torque oscillator (STO) is a promising new technology for the future RF oscillator, which is based on the spin transfer torque (STT) effect in magnetic multilayered nanostructure. It is expected to overcome the limitations of the semiconductor-based device technology. In our previous work, we have proposed a circuit-level model of the Giant Magneto-Resistance (GMR) STO. In this paper, we present a physics-based circuit-level model of the Magnetic Tunnel Junction (MTJ)-based STO. The new model includes the effect of perpendicular torque that has been ignored in the GMR STO model. The variations of three major characteristics, generation frequency, mean oscillation power, and generation linewidth of an MTJ STO are investigated by changing the amount of perpendicular torque. The model is fully compatible with circuit-level simulators such as SPICE. The accuracy of new model was verified by HSPICE simulation. The simulation results show an excellent agreement with the experimental data. With our circuit model, we could compose a current mirror circuit that contains an STO element and a multi-stage amplifier for signal amplification, such that a full circuit-level simulation of MJT STO was accomplished for the first time.

I. Hyein Lim, Sora Ahn, Seungjun Lee, and Hyungsoon Shin: *SSDM (2011)* p. 1466. 2. A. Slavin, and V. Tiberkevich: *IEEE Trans. Magn.* 45 (2009) 1875. 3. P. Villard, U. Ekei, D. Houssameddine, J. Kattine, D. Mauri, B. Delaet, P. Vincent, M.-C. Cyrille, B. Vidal, J.-P. Michel, J. Prouvee, and F. Badet: *IEEE J. Solid-State Circuits* 45 (2010) 214. 4. Z. M. Zeng, P. Upadhyaya, P. Khalil Amiri, K. H. Cheung, J. A. Kattine, J. Langer, K. L. Wang, and H. W. Jiang: *Appl. Phys. Lett.* 99 (2011) 032503.

RL18

Current induced localized domain wall oscillators in NiFe /Cu /NiFe nano-stripe

Liang-juan Chang¹, Pang Lin² and Shang-fan Lee^{1*}
¹ Institute of Physics, Academia Sinica, Taiwan
² Department of Materials Science & Engineering, National Chiao Tung University, Taiwan

We study domain wall (DW) oscillations induced by the injection of a dc current through a nanowires containing artificial symmetric protrusions with Permalloy based pseudo spin valve (NiFe 12 nm/Cu 8 nm/NiFe 24 nm). An experimental analysis was carried out to describe the variation of differential resistance dV/dI by applying in-plane dc current with pinned DWs. When the DWs are pinned at the traps, we have observed a reversible motion of the DWs by changing the applied in-plane dc current. The peak in dV/dI associated with the reversible change of magnetoresistance has been taken as evidence of current induced coherent DW oscillation between the pinned regimes which gives rise to the peak. The excited critical current shifts symmetrically with respect to H. It is expected from the DW trap with symmetrical potential landscape. The dynamics of localized DW oscillations under application of dc current was examined by micromagnetic simulations (OOMMF). The frequency f of DW oscillation decreases from 1.5 GHz to 0.95 GHz as H increasing. This simple concept of DW based oscillators could be used as radio frequency assisted writing in magnetic recording technology.

* Corresponding author e-mail: leesf@phys.sinica.edu.tw

RL19

Current induced transverse field versus Joule heating in Co/Pd nanowires

Mahdi Jamali, Xuepeng Qiu, Kulothungasgaran Narayanapillai and Hyunsoo Yang*
Electrical and Computer Engineering, National University of Singapore, Singapore

There has been a tremendous effort in understanding of the electric current effect in the ultra thin film of ferromagnetic materials[1, 2]. We have recently found that in the nanowire made of a multilayer structure of Co/Pd, there is a current induced transverse magnetic field[3]. Electric current could also cause Joule heating especially in the high current densities. The Hall resistance has been measured at different current densities for the magnetic fields in the easy axis direction. By increasing the current density, there is a reduction in the switching field of the nanowire. We further performed the measurement at different angles of the magnetic field with respect to the easy axis of the sample. From the asymmetry of the switching fields, one can approximate the current induced transverse field. Furthermore, by using four-probe measurements, the nanowire resistance has been measured at different temperatures and the temperature coefficient of the Co/Pd nanowire has been extracted. By measuring the resistance of the nanowire at different current densities, we can approximate the nanowire temperature during the measurement and its effect on the switching dynamics.

[1] I. M. Miron, G. Gaudin, S. Auffret, B. Rodmacq, A. Schuhl, S. Pizzini, J. Vogel, and P. Gambardella, *Nat. Mater.* 9, 230 (2010). [2] T. Suzuki, S. Fukami, N. Ishiwata, M. Yamanouchi, S. Ikeda, N. Kasai, and H. Ohno, *Appl. Phys. Lett.* 98, 142505 (2011). [3] K. Narayanapillai, M. Jamali, and H. Yang, *MMM conference, Arizona (2011)*.

RL20

Improvement of generation efficiency of pure spin current using multi-terminal spin injection

Shaojie Hu, Tatsuya Nomura, Seiji Nonoguchi and Takashi Kimura*
Advanced Electronics Research Division, INAMORI Frontier Research Center, Kyushu University., Japan

Lateral spin valve structures have several advantages for the generation, manipulation and injection of the spin current because of their flexible probe configurations. Particularly, nonlocal spin injection techniques enable us to create a pure spin current which carries the spin information with extremely low propagation loss. However, in general, the generation efficiency of the pure spin current is quite low. To solve this serious obstacle, we propose a nonlocal spin injection with multi spin injectors. In the present study, we fabricated the lateral valve structure consisting of a quadruple Permalloy spin injectors and nonmagnetic Cu strip and show that the developed device has two advantages. One is that the maximum generated spin current is strongly enhanced. The other one is that the efficiency for generating a certain quantity of the spin current is significantly improved. We also show that the optimization of the device dimension yields the further enhancement of the maximum generating spin current.

M. Johnson and R. H. Silsbee, *Phys. Rev. Lett.* 55, 1790 (1985). T. Kimura, T. Sato, and Y. Otani, *Phys. Rev. Lett.* 100, 066602 (2008). T. Kimura et al., *Appl. Phys. Lett.* 85, 3501 (2004).

RL21

Electrical transport properties of Co₂MnSi Schottky diode

In-bok Baek¹, Xianhong Li¹, Seongjae Lee^{1*}, Chil Seong Ah¹, Jong-heon Yang², Chan Woo Park², Han Young Yu², Moongyu Jang² and Gun Yong Sung²
¹ Department of Physics, Research Institute for Natural Sciences, Hanyang University, Seoul, 133-791, Korea
² Electronics and Telecommunications Research Institute (ETRI), Daejeon, 305-700, Korea

Recently, the spintronic device has attracted considerable attentions due to its possibility to lead a new generation of electronic devices by utilizing spin degree-of-freedom. Especially, silicon is a very attractive material for the spin channel of spintronic devices due to a weak spin-orbit coupling [1] and a long spin lifetime of ~ 10 ns [2, 3], while Co₂MnSi being a half-metallic Heusler compound is regarded as a promising candidate for the spin injection/detection electrodes due to a possible complete spin polarization. [4, 5] In this work, the electronic transport characteristics of Co₂MnSi/Si Schottky diodes are studied for the investigation of spin electrode/channel interface quality, in which Co₂MnSi was prepared under various process conditions. We found that the Schottky barrier height of Co₂MnSi decreased from 0.56 to 0.52 eV and 0.44 to 0.36 eV for electron and hole, respectively, with increasing RTA temperature from 450 to 550°C. Also, the ideality factor close to unity for RTA temperature of 450°C significantly degraded as it changed to 550°C, indicating the increase of interface trap density. Deduced from our electrical results, the manufactured Co₂MnSi is expected as a promising ferromagnetic material for the applications in silicon spintronic devices.

[1] I. Zutic, J. Fabian, and S. C. Erwin, *Phys. Rev. Lett.* 97, 026602 (2006). [2] G. Lancaster, J. A. V. Wyk and E. E. Schneider, *Proc. Phys. Soc. London* 84, 19 (1964). [3] J. Fabian, A. Mathos-Abiague, C. Erlter, P. Stano, and I. Zutic, *Acta Phys. Slov.* 57, 565 (2007). [4] Yohdaira, M. Oogane, H. Naganuma, and Y. Ando *Appl. Phys. Lett.* 99, 132513 (2011). [5] P.J. Brown, K. U. Neumann, P.J. Webster and K. R. A. Ziebeck, *J. Phys.: Condens. Matter* 12, 1827 (2000).

RL22

Negative electron-beam resist hard mask ion beam etching process for the fabrication of nanoscale spin transfer torque magnetic random access memory device

Hyungyu Lee¹, Daehong Kim¹, Bongho Kim¹, Sungwoo Chun¹, Seonjun Choi¹ and Seung-beck Lee^{2*}
¹ Department of Electronic Engineering, Hanyang University, Korea
² Institute of Nano Science and Technology, Hanyang University, Korea

To conduct MTJs etching process, Ta[1] hard masks are generally used for reactive ion etching and ion beam etching (IBE) process due to relatively good selectivity over magnetic metals. However, tapering of the Ta mask is unavoidable which results in the underlying MTJ to become trapezoidal. Here we utilized negative electron-beam resist (NER) hard mask process to overcome the hard mask induced nano-patterning difficulties. Arrays of 30 nm dot patterns 200 nm apart were defined by electron beam lithography with a NER thickness of 90 nm. The IBE was performed using the NER as the hard mask layer. During the IBE process, The IBE etch rate of the NER was 3 nm/min and since the total MTJ etching thickness was 36 nm with 2.1 nm/min etch rate, a 30 nm diameter NER pillar with 90 nm thickness was enough to produce the 30 nm diameter MTJ nanopillars. And redeposition of the etched material on side walls of the NER protects the resist from tapering, resulting in vertical side profiles in the etched MTJs.

[1] X. Peng, S. Wakeham, A. Morrone, S. Axdal, M. Feldbaum, J. Hwu, T. Boonstra, Y. Chen, J. Ding, *Vacuum.* 83, 1007 (2009)

RL23

Magnetization reversal process of a Py nanodot under pure spin current injection

Tatsuya Nomura, Seiji Nonoguchi and Takashi Kimura*
Kyushu University, Japan

A new type lateral spin valve structure based on a pair of closely located Permalloy nanopillars has been developed. This structure enables us to flow a large amount of current, resulting in the injection of a large pure spin current into a ferromagnetic nanodot entirely. We investigated the magnetization reversal process of the Permalloy nanodot under dc pure spin current injection from the field dependence of the nonlocal spin valve signal. The dc pure spin current was generated by flowing the dc current with an ac excitation current in the nonlocal current terminal. The nonlocal spin valve signal without the dc current exhibits a clear bipolar signal typically observed in the conventional lateral spin valve.[1,2] The nonlocal signal curve shows the systematic changes with increasing the dc pure spin current and its variation strongly depends on the current intensity and polarity. This means that the reversal process of the Py dot is strongly modified by the pure spin current injection.

[1] F.J.Jedema,A.T.Filip,B.J.vanWees,Nature410(2001)345. [2] T. Kimura et al. *Appl. Phys. Lett.* 85, 3501–3503 (2004)

RL24

Spin transfer effect in FePt nanowires: controlling the stochasticity of domain wall depinning using constrictions

Jean-philippe Attane¹, Van Dai Nguyen¹, Alain Marty¹, Lucien Notin¹, Cyrille Beigne¹, Juan Carlos Rojas-sanchez¹, Stefania Pizzini² and Laurent Vila¹
¹ Universite Joseph Fourier, BP 53, 38041, Grenoble and INAC/ CEA Grenoble, 17 avenue des Martyrs, France
² Institut Neel, CNRS, 25 avenue des Martyrs, 38042 Grenoble, France

In this contribution, we present dynamic measurements of domain wall (DW) depinning from structural defects, in nanowires processed from single FePt layers and FePt/Pd(Pt)/FePt spin-valves. Statistical analysis reveals that in such systems, the DW depinning is stochastic, and that this stochasticity has two origins. The first one is thermal activation, which helps the wall to cross the energy barrier associated to the defect. The second one originates from the ability of the DW to get pinned randomly along different micromagnetic configurations, each one corresponding to a given depinning fields. We study the influence of different constriction types on the dynamic of DW depinning, using spin-valve-based nanowires. The depinning probability function is found to exhibit very different behaviors, which depend on the types of constriction: it is partially possible to control the stochastic behavior of DW depinning by tuning the shape of constrictions. Additionally, we showed that the probability function of DW depinning can be varied by applying a DC current, the effect of the spin torque on thermal and configurational stochasticities being similar to those of a field. The measured spin transfer torque efficiency is very high (~10⁻¹³T.m.A²), and is similar for single FePt layers and FePt-based spin-valves.

C. Burrowes et al., *Nat. Phys.* 6, 17 (2010) A. Mihai et al., *Phys. Rev. B* 84, 014411 (2011)

July 12 (Thu)

July 12 (Thu)

RL25

Electric field effect on magnetic coercivity of Fe₃O₄/BaTiO₃ heterostructures

Tomoyasu Taniyama*, Taiichiro Nozaki, Yasuhiro Shirahata, Gorige Venkataiah and Mitsuru Itoh
Materials and Structures Laboratory, Tokyo Institute of Technology, Japan

Electric field control of the magnetic coercivity of half metallic Fe₃O₄ epitaxial thin films on BaTiO₃(001) is demonstrated at room temperature, with a view to developing a new type of highly spin polarized electron source, where the magnetization orientation of the spin source can be controlled by electric field. Fe₃O₄ films were grown on BaTiO₃(001) substrates by reactive molecular beam epitaxy in an oxygen atmosphere at a pressure of 1×10⁻⁶ Torr. The Fe₃O₄ films show a clear Verwey transition at ~120 K, ensuring the high quality of the films grown. The electric field variation of the in-plane magnetic coercivity of Fe₃O₄ films was measured using Kerr effect, exhibiting a hysteretic behavior, where the magnetic coercivities for positive and negative electric fields at ±10 kV/cm show distinct values. Since a possible strain effect due to ferroelectric domain switching of BaTiO₃ should be equivalent for both electric field polarities over the switching field, another possible mechanism such as polarization charge accumulation at the interface likely has its origin in the electric field effect, associated with carrier induced modulation of the electronic states of Fe₃O₄. Work supported in part by Industrial Technology Research Grant Program in 2009 from NEDO, Japan.

[1] G. Venkataiah, Y. Shirahata, M. Itoh, and T. Taniyama, *Appl. Phys. Lett.* 99, 102506 (2011).

RL26

Dependence of current-induced effective rashba field and perpendicular magnetic anisotropy on annealing temperature

Ki-seung Lee¹, Byung Chul Min¹, Kyung Jin Lee^{2*} and Kyung-ho Shin¹
¹ Spin Convergence Research Center, Korea Institute of Science and Technology, Korea
² Departments of Materials Science and Engineering, Korea University, Korea

Manipulation of local magnetization using electrical current has attracted considerable interest due to its rich physics and potential applications for a new class of spintronic devices. It was theoretically proposed that Rashba-type spin-orbit coupling (SOC) caused by inversion symmetry breaking yields a new type of current-induced effective magnetic field [1], i.e. Rashba field of which direction is perpendicular to both the direction of current-flow and that of the inversion symmetry breaking. The existence of this Rashba field in the structure consisting of non-magnetic metal | ferromagnetic metal | oxide was recently confirmed experimentally [2]. We previously investigated the effect of the ferromagnetic film thickness on the Rashba spin transfer torque (STT), as well as its effect on the perpendicular magnetic anisotropy. The magnetic anisotropy clearly showed surface properties, while the surface nature of the Rashba field remained elusive. In this work, we further investigate the dependence of current-induced effective Rashba field and perpendicular magnetic anisotropy on annealing temperature. Experiments were carried out on Pt(3nm)/Co(0.6nm)/MgO(2nm) samples with the annealing temperature from 300°C up to 450 °C. In this presentation, the effect of annealing treatment will be discussed.

[1] A. Manchon and S. Zhang, *Phys. Rev. B* 78, 212405 (2008) ; *Phys. Rev. B* 79, 094422 (2009). [2] I. M. Miron et al., *Nature Mater.* 9, 230 (2010).

RL27

Spin motive force driven by magnetization dynamics

Junichiro Ohe
Toho University, Japan

The current-induced magnetization dynamics realized in spintronics devices involve both of charge and spin degrees of freedom. Recently, it has been pointed out that the magnetization dynamics induces an effective electric field acting on the conduction electrons through the spin Berry phase. The effective electric field, or a 'spin motive electric field', was investigated for a simple one-dimensional domain wall. It is difficult to estimate analytically this effective electric field in actual systems, because the magnetization dynamics obeys the non-linear Landau-Lifshitz equation. In this report, we investigate the spin motive force and the measurable voltage by solving Landau-Lifshitz-Gilbert equation numerically. We propose several structures that show measurable spin motive force. We also compare the our numerical results and experimental results.

J. Ohe and S. Maekawa, *J. Appl. Phys.* 105, 07C706 (2008) J. Ohe et al., *Appl. Phys. Lett.*, 95, 123110 (2009) Y. Yamane et al, *Phys. Rev. Lett.* 107, 236602 (2011) M. Hayashi et al, *Phys. Rev. Lett.* (2012) in press

RL28

Electrical detection of the spin Hall effects in the InAs quantum well structure

Tae Young Lee, Joonyeon Chang*, Hyun Cheol Koo, Hyung-jun Kim and Suk Hee Han
Korea Institute of Science and Technology, Korea

Spin Hall effect (SHE) becomes intriguing because it generates and manipulates carrier spins in non-magnets without external magnetic field. Use of perpendicularly polarized spin currents for spin field effect transistor is a quite promising because precession of perpendicularly polarized spins can be manipulated by Rashba spin orbit coupling in the absence of the applied field along momentum direction [1]. The SHEs are electrically measured for an InAs quantum well (QW) structure where Rashba field of 8.5 Tesla is induced. The device is composed of an InAs channel and Pd/CoFe multilayers with perpendicular magnetization, which allows to detection of spin Hall voltages. The spin-polarized electrons with perpendicular orientation cause a charge accumulation at the edge of the InAs channel probed by spin Hall voltage. This charge accumulation induces a transverse voltage. We observe large spin Hall resistance up to 9.3 mΩ and spin Hall angle is found to be about 0.01. According to the theoretical reports [2, 3], one of its origins is spin-orbit scattering of conduction electrons through side-jump or skew scattering. The SHEs are emerging from the side-jump scattering of flowing spins in the InAs QW and the scattering direction is determined by spin orientation with spontaneous magnetization.

REFERENCES [1] Koo et al., *Science*, 325, 1515 (2009). [2] J. E Hirsch, *Phys. Rev. Lett.* 83, 1834 (1999). [3] J. Zhang, *Phys. Rev. Lett.* 85, 393 (2000).

RL29

Bias-voltage controlled tunneling resistance in a ferromagnet-metal-insulator-ferromagnet tunneling junction

Sui-pin Chen*
Department of Electrophysics, National Chiayi University, Taiwan

We adopt the spin-polarized free-electron model [1-3] and extend our previous work [4] to study the tunneling resistance change in a ferromagnet/metal/insulator/ferromagnet magnetic tunneling junction [5], and find a method for changing the tunneling resistance. Unlike the traditional method of varying the magnetizations configuration between the two ferromagnetic layers, the proposed method uses the polarity of a bias voltage with a small strength to change the tunneling resistance. Under suitable conditions, we show that both tunneling resistance changes resulting from the polarity of the bias voltage and from the magnetizations configuration are equal in magnitude, and are larger than that in a conventional ferromagnet/insulator/ferromagnet magnetic tunneling junction.

[1] S. Zhang and P. M. Levy, *Phys. Rev. Lett.* 81, 5660 (1998). [2] J. Yang, J. Wang, Z. M. Zheng, D. Y. Xing and C. R. Chang, *Phys. Rev. B* 71, 214434 (2005). [3] S.-P. Chen and C.-R. Chang, *IEEE Trans. Magn.* 45, 2410 (2009). [4] S.-P. Chen, *J. Appl. Phys.* 107, 09C716 (2010). [5] S. Yuasa, T. Nagahama and Y. Suzuki, *Science* 297, 234 (2002).

RL30

A highly (001) textured Ge/MgO/bcc-ferromagnet system prepared by ultra-high vacuum sputtering

Soogil Lee¹, Sanghoon Kim¹, Jungho Ko¹, Sangho Lee¹, Jangyup Son¹, Seung-heon Chris Baek², Seok-hee Lee² and Jongill Hong^{1*}
¹ Materials Science and Engineering, Yonsei University, Seoul 120-749, Korea
² Dept. of Electrical Engineering, Korea Advanced Institute of Science and Technology (KAIST), Daejeon, 305-701, Korea

Observation of spin accumulation in semiconductor is very fascinating for fundamental physics and applications as well. Many important progresses have recently been made in this field. For example, the insertion of a tunnel barrier at the interface between ferromagnet (FM) and semiconductor has increased the chemical potential difference at the interface [1]. Ge/MgO/bcc-FM has been intensively studied because of an epitaxial growth of MgO on a Ge substrate due to small lattice mismatch (~4%) between Ge(001)[100] and MgO(001)[110]. As a result, the symmetry-related spin-dependent tunneling is expected to occur at the Ge/MgO/bcc-FM junction. The successful growth of the single-crystal Ge(001)/MgO(001)/bcc-FM(001) stack has been reported [2,3]. However, these results have been obtained using a molecular beam epitaxy technique which may not be suitable for applications in the industry. Here, we show that a highly (001) textured Ge/MgO/CoFeB junction can be achieved by an ultra-high vacuum sputtering technique. We will discuss the effect of various deposition conditions on the (001) texture of MgO/CoFeB deposited on (001) Ge. The quantitative and qualitative analyses of the structures of MgO/CoFeB layers will be presented based on the results of x-ray diffractometry and transmission electron microscopy. Finally, we will examine the tunneling characteristics of the junction.

[1] Abert Fert and Henry Jaffres, *Physical Review B* 64, 184420 (2001) [2] Wei Han, et al., *Journal of Crystal Growth* 312, 44 (2009) [3] Kun-Rok Jeon, et al., *Crystal Growth and Design* 10, 1346 (2010)

RL31

Electrical spin injection and detection in GaAs with ferromagnetic metal/MgO junctions

Seong Hoon Shim¹, Kyung-ho Kim¹, Hyung-jun Kim¹, Yun-hi Lee² and Joonyeon Chang^{1*}
¹ Spin Convergence Research Center, Korea Institute of Science and Technology, Korea
² Department of Physics, Korea University, Korea

The intrinsic conductance mismatch between ferromagnetic metals (FM) and semiconductors is a critical obstacle in spin injection, and inserting a thin tunnel barrier, especially MgO, is expected to hurdle this problem. [1] In this study, we report electrical measurements of spin polarization in GaAs coming from efficient spin injection through MgO tunneling barrier. The whole epitaxial layers of FM/MgO/GaAs structures were prepared in-situ process using cluster MBE. To reduce the depletion layer of Schottky barrier, doping modulated GaAs layer has been inserted in the vicinity of the interface between GaAs and MgO layers. Large voltage drop (ΔV = 6.3 mV at 10 K when I = -0.9 mA in Fe/MgO/GaAs structure) between the baseline and the dip of Hanle curve is observed at various temperatures up to 400 K in a 3-terminal Hanle measurement geometry. The Lorentzian fitting of the Hanle curve gives 234 ps spin lifetime of n-doped GaAs and 952 nm spin diffusion length at 300 K.

[1] G. Schmidt, D. Ferrand, L.W. Molenkamp, A.T. Filip and B.J. van Wees *Phys. Rev. B* 62, R4790 (2000).

RL32

Transistorless 3D STT-MRAM Architecture

Weizhong Wang*
University of Wisconsin - Milwaukee, USA

The MTJ based devices are fabricated through thin film deposition and patterning which are intrinsically capable for 3D vertical multiple layers integration. However, current MRAM architecture requires at least one isolation transistor in each MRAM cell(1). Since there is no mature 3D CMOS technology available, isolation transistor prevent the progress on developing 3D MRAM. Therefore the races on MRAM area density improvements are all based on aggressive horizontal cell size scaling. This paper introduces a new transistor-less MRAM architecture to enable vertical 3-D integration. Since the MTJ devices are essentially two terminal resistors, an array of MTJ devices form a connected resistor network. We introduce a 3D architecture with new read/write operation to address individual MTJ cells. Comparing with conventional STT-MTJs, our preliminary simulation results show (1) little penalties on both speed and power consumption during read operation;(2) little penalty on writing speed; and (3) 2x to 3x penalty on writing power consumption depending on TMR ratio of MTJs. The proposed STT-MRAM architecture can greatly enhance the area density of STT-MRAM and beat CMOS or any single layer based memory technologies.

(1) Tehrani, S.; Slaughter, J.M.; Deherrera, M.; Engel, B.N.; Rizzo, N.D.; Salter, J.; Durlam, M.; Dave, R.W.; Janesky, J.; Butcher, B.; Smith, K.; Grynkevich, G.; 'Magnetoresistive random access memory using magnetic tunnel junctions', *Proceedings of the IEEE, Volume: 91* , Issue: 5, 2003 , pp.703 - 714

RM01

Collision of cobalt atom with Alq3 molecule thin film: a molecule dynamics study

Yun-peng Wang, Ling-ling Tao and Xiu-feng Han*
Institute of Physics, Chinese Academy of Sciences, China

Yun-Peng Wang, Xiu-Feng Han and Ling-Ling Tao Beijing National Laboratory of Condensed Matter Physics, Institute of Physics, Chinese Academy of Sciences, Beijing 100190, China Hai-Ping Cheng Department of Physics and Quantum Theory Project, University of Florida, Gainesville, Florida 32611, USA Molecular dynamics simulations on deposition of cobalt atom onto tris(8-hydroxyquinoline) aluminum (Alq3) molecule thin film are presented. A Lennard-Jones potential calibrated by first-principle calculations was used to describe Alq3-Co interactions. Microscopic collision process was analyzed by looking into one trajectory. Statistics of final positions and penetration depths of cobalt atoms show that cobalt atoms with low initial energy penetrate little into Alq3 thin film and stay near the surface of Alq3 thin film while cobalt atom with high initial energy penetrates significantly into Alq3 thin film. Consequently, thickness of Alq3/cobalt interface is equal to roughness of Alq3 surface if initial energies of cobalt atoms are small, but 1 nanometer larger than roughness of Alq3 thin film if initial energies of cobalt atoms are large. Injected cobalt atoms lose their kinetic energies via collision with 8-hydroxyquinoline ligands of Alq3 molecules. DFT calculations show hybridization of carbon and oxygen due to cobalt and sizable charge transferred from cobalt to nearest Alq3 molecule.

RM02

Magnetism and Electronic Structures of SiC nanoribbons: Role of defects

Gul Rahman^{1*} and J. M. Morbec²
¹ Department of Physics, Quaid-i-Azam University, Islamabad, Pakistan
² Instituto de Ciências Exatas, Universidade Federal de Alfenas, 37130-000, Alfenas, MG, Brazil

Magnetism in diamagnetic materials such as defective SnO₂, ZnO, or SiC got particular attention to probe and understand the source and nature of magnetism in these materials. Particularly, the role of intrinsic defects, e.g. a vacancy which is the main source of magnetism, motivated many scientists around the world. The defect formation energies of vacancies in these diamagnetic materials are very large which limit its experimental synthesis. Here, we focused on SiC nanoribbons (NRs) to probe the native defects and their interactions with the alien light element impurities, e.g., B, N, in terms of magnetism. Using ab-initio calculations based on density-functional theory (DFT), our extensive results indicate that silicon or carbon vacancy per cell induces magnetic moment in SiCNRs, whereas SiCNR with Si+Si divacancy has almost zero magnetic moment. The half-metallic behavior, which is very important for spintronics devices, of SiC NRs is maintained in the presence of one C or Si vacancy per cell. The Si or C vacancies have high defect formation energies, however, we found that foreign impurities B or N significantly reduced the defect formation energy of vacancies in SiCNRs.

RM03

Bulk and surface half-metallic ferromagnetism in transition-metal chalcogenides with rocksalt phase from first-principles calculations

Guoying Gao* and Kailun Yao
School of Physics, Huazhong University of Science and Technology, China

In the past decade, most of transition-metal pnictides and chalcogenides with metastable zinc-blende structure were predicted to be half-metallic ferromagnets. So far, however, only four of them, zinc-blende CrAs, MnAs, CrSb, and CrTe, have been realized experimentally in the form of thin films or multilayers because of the instability of the zinc-blende phase. Here we predict with first-principles calculations that all three rocksalt CrTe, VPo, and CrPo are half-metallic ferromagnets with the half-metallic gaps of 0.03, 0.18, and 0.31 eV, respectively. Importantly, the rocksalt phases are approximately 0.19-0.33 eV per formula unit lower in energy than the corresponding zinc-blende phases for these three half-metallic compounds, which indicate it is more possible to fabricate these binary compounds with rocksalt phase than the zinc-blende phase in the form of thin films or multilayers. We also study the (111) surface properties of rocksalt CrTe and CrPo, and find the Te-(Po)-terminated (111) surface is more stable than the Cr-terminated (111) surface, and both Cr- and Te-(Po)-terminated (111) surfaces preserve the bulk half-metallicity. The present work will not only add to the understanding of these binary half-metals, but will also stimulate experimental efforts toward fabrication and utilization of these systems in spintronics.

[1] T. Graf, C. Felser, and S. P. P. Parkin, *Prog. Solid State Chem.* 39, 1 (2011). [2] C. Felser, G. H. Fecher, and B. Balke, *Angew. Chem. Int. Edn* 46, 668 (2007). [3] M. I. Katsnelson, et al., *Rev. Mod. Phys.* 80, 315 (2008). [4] S. K. Bose and J. J. Kudrnovsky, *Phys. Rev. B* 81, 054446 (2010). [5] G. Y. Gao and K. L. Yao, *Appl. Phys. Lett.* 91, 082512 (2007). [6] J. J. Deng, et al., *J. Appl. Phys.* 99, 093902 (2006). [7] G.Y. Gao, K.L. Yao, N. Li, *J. Phys.: Condens. Matter* 23, 075501 (2011).

RM04

Magneto-transport properties of Fe thin films in an external electric field

Kohji Nakamura^{1*}, T. Akiyama¹, T. Ito¹, M. Weinert² and A. J. Freeman³
¹ Physics Engineering, Mie University, Japan
² Physics, University of Wisconsin-Milwaukee, USA
³ Physics and Astronomy, Northwestern University, USA



July 12 (Thu)

July 12 (Thu)

RM05

Role of interfacial B impurity in magnetocrystalline anisotropy at MgO/Fe interface

Koji Hotta*, Kohji Nakamura, Toru Akiyama and Tomonori Ito
Mie University, Japan

An interface induced-perpendicular magnetocrystalline anisotropy (MA), as observed in the MgO/CoFeB,[1] has attracted much attention in magnetic application. From first-principles, previously, we demonstrated a perpendicular MA at the MgO/Fe interface due to a weak Fe d_{z²}-O p_z hybridization[2], but it still need to discuss a role of interfacial B impurity. Here, we extend investigation to include the interfacial B impurity. Calculations were carried out by using FLAPW method[2]. First, the phase stability at the MgO/Fe interface was determined based on calculated total energy with a model of an MgO monolayer on a five-layer Fe, where the B were incorporated in interstitial positions at top, second, and third Fe-interface-layers. Results indicate that the B favors to segregate to the interface so as to form an MgO/FeB/Fe interface. Then, the MA energy (E_(MA)) was calculated by using the second variation SOC method and the force theorem. The calculated E_(MA) has a large positive value of 0.69 eV for the ideal MgO/Fe, indicating a perpendicular MA. For the MgO/FeB/Fe, the E_(MA) turns out to be almost zero (-0.02 eV), which indicates no interface MA, due to an enlargement of the Fe-MgO interlayer distance by the interfacial B atoms.

[1] S. Ikeda, et al., Nature Mater. 9, 721 (2010). [2] K. Nakamura, et al., Phys. Rev. B81, 220409 (2010).

RM06

First-principles study on magnetic anisotropy of Co/Pt(111) film in electric field

Sho Yasuda* and Shugo Suzuki
Division of Materials Science, Faculty of Pure and Applied Sciences, University of Tsukuba, Japan

Electric field (EF) control of magnetism is attractive for spintronics devices. In recent research, it has been shown that EF affects not only magnetic moment but also spin conduction and magnetic anisotropy[1-4]. In particular, it has been found that combination of the 3d and 5d metals in EF causes large effects on magnetic anisotropy. In this study, we investigate the dependence of the magnetic anisotropy energy (MAE) and the magnetic moment of Co/Pt(111) on EF by first-principles calculations. We employ the fully relativistic full-potential linear-combination-of-atomic-orbitals method based on the density-functional theory within the local-spin-density approximation. The exchange-correlation energy functional is the Perdew-Wang parameterization of the Ceperley-Alder results. We have found that the magnetic moment of the Co atom is in proportion to EF. The results of the calculations of the MAE and the other details will be shown at the conference.

[1]T. Mariyama, Y. Shiota, T. Nozaki, K. Ohta, N. Toda, M. Mizuguchi, A. Tulapurkar, T. Shinjo, M. Shiraishi, S. Mizukami, Y. Ando and Y. Suzuki: Nature. Vol.4 (2008) 158 [2]D. Chiba, S. Fukami, K. Shimamura, N. Ishiwata, K. Kobayashi, and T. Ono: Nature Mater. Vol.10 (2011) 853. [3]M. Tsujikawa and T. Oda: Phys. Rev. Lett. Vol.102 (2009) 247203. [4]K. Nakamura, T. Akiyama, and T. Ito: Phys. Rev. B Vol.81 (2010) 220409.

RM07

Magnetic ground state of TM/Graphene/TM films

Dongyoo Kim, Arqum Hashmi and Jisang Hong*
Department of Physics, Pukyong National University, Korea

Using the full potential linearized augmented plane wave (FLAPW) method, we have investigated the magnetic properties of transition metal (TM)/Graphene/transition metal (TM) structure. We have explored magnetic properties of metal/grapheme/metla systems, which is Co(1 ML)/Graphene/Ni(1 ML). Co(1ML)/Graphen/Ni(1ML) film have the AFM ground state. The calculated magnetic moment of Ni is -0.22 μB, while the Co layer has 1.50 μB. In calculation of optimized structure, we have that the distance between carbon and Co is 2.07 Å and it is 2.04 Å for carbon and Ni. The relative height difference between two carbon atoms in grapheme layer is 0.29 Å. To understand the effect of buckling geometry of graphene, we have performed the calculation without any buckling factor of graphene layer. The magnetic ground state is not changed, and calculated magnetic moment of Ni and Co are -0.60 and 1.70, respectively. This implies that the AFM coupling is an intrinsic property of Co(1ML)/Gr/Ni(1ML) system. Also, we will present the magnetic properties of Co(2ML)/Gr/Ni(1ML) and Co(1ML)/Gr/Ni(2ML) systems. This work was supported by KCAP located in Sogang University funded by the Ministry of Education, Science, and Technology (MEST) through the National Research Foundation of Korea (NRF-2011-C1AAA001-2011-0030278) and by KOSEF (No. R01-2008-000-20014-0).

RM08

A model of chain of ellipsoid-rings for magnetic nanotubes

Sen Yang*, Junfeng Gong and Xiaoping Song
Department of Materials Physics, Xi'an Jiaotong University, China

Numerical calculation of magnetic properties is a very effective way to understand the whole magnetic behavior of nanotubes. Currently, the most studies of calculation of magnetic properties of nanotubes are mainly grounded on the Stoner-Wohlfarth (S-W) model, starting from an elongated prolate ellipsoid with single-domain. But, it is hard to imagine how such an ellipsoid is arranged in the hollow tubular structure and hence the realization of predicted magnetic properties has been hindered by the experimental difficulties. In the present article, an alternative model of chain of ellipsoid-rings is proposed to calculate the magnetic properties of nanotubes, where the chain of rings with ellipsoid particles is assumed to compose nanotube. Based on this new model, we calculate the magnetic properties of nanotube and further discuss the influence of tubular geometric parameters on the magnetic properties. All the results are well consistent with the experimental data of Ni nanotube and moreover are available for the Ni nanowire. Consequently, our model provides an easy and general approach to both magnetic nanotubes and magnetic nanowires.

RM09

First-principles GGA+U calulations of half-metallicity in wurtzite NiO/ZnO(0001) superlattices

X. H. Zhou
National Laboratory for Infrared Physics, Shanghai Institute of Technical Physics, Chinese Academy of Sciences, China

Wurtzite NiO has been predicted to display half-metallicity and have only small lattice mismatch with wurtzite ZnO [1]. It is interested to explore the possibility of the so-called all oxides spintronics obtained by the hybrid structures consisted of the wurtzite NiO and ZnO [2]. In this contribution, the structural, electronic, and magnetic properties of wurtzite NiO/ZnO(0001) superlattice were investigated by means of density functional calculations using spin-polarized generalized gradient approximation GGA and GGA+U schemes. We demonstrate that these superlattices retain their half-metallic behavior leading to a complete, i.e., 100%, spin polarization of the conduction electrons. This property makes the wurtzite NiO/ZnO(0001) heterostructures to be excellent candidates for high-efficiency magnetoelectronic devices.

[1] R. Q. Wu, G. W. Peng, L. Liu, and Y. P. Feng, Appl. Phys. Lett. 89, 082504 (2006) [2] Z. Chen, L. Miao, and X. Miao, AIP ADVANCES 1,022124 (2011)

RN01

Magnetic properties of La doped nanocrystalline Z-type ferrite nanopowders synthesized via co-precipitation method

Mohamed M. Rashad^{1*}, M. Rasly¹, H. M. Elsayed², A. A. Satter² and I. A. Ibrahim¹
¹ Advanced Materials Department, Central Metallurgical Research and Development Institute, Egypt
² Physics Department, Ain Shams University, Egypt

Co2Z type hexagonal ferrites powders doped with La³⁺ ions (Ba₂-XLaXCo₂Fe₂₄O₄₁ where X=0.0, 0.05, 0.10 and 0.15) were prepared using co-precipitation method. The results revealed that single phase CO2Z type ferrite was formed from the precipitated precursor in presence of SDS as anionic surfactant and then preheated at 600oC for 4h and then post annealed at 1300oC for 6h. Moreover, the crystallite size and the porosity,% of the formed powders were increased whereas the unit cell volume were decreased by increasing the La³⁺ substitution. The microstructure of the formed powders appeared as hexagonal platelet like structure. The DC resistivity of the obtained CO2Z was decreased as La³⁺ content increased. The saturation magnetization (Ms= 53.7-55.5 emu/g) was slightly increased with substitution of La³⁺. Moreover, two resonance frequencies peaks are observed through the imaginary part of complex permeability meanwhile a decrease in the real part of magnetic permeability through X-band frequencies. The reasons are discussed using electromagnetic theory.

1- G. Shihai, Z. Yangnan, F. Zekam, W. Xinlin, H. Hualhai, J. Rare Earths 25(2007)220-225 2-X.Wang, L. Li, S. Su, Z. Gui, Z. Yue, J. Zhou, J. Eur. Ceram. Soc. 23(2003)715-720. 3-J. Xi, C. M. Yang, H. F. Zou, Y. H. Song, G. M. Gao, B.C. An, S. C. Gan, J. Magn. Magn. Mater. 321(2009)3231-3235. 4-L. Qin, H. Verweij, Mater. Lett. 68(2012)143-145.

RN02

Magnetic properties of Fe-doped NiO nanoparticles

Akinobu Kurokawa*, Takuya Yanoh, Shinya Yano, Hiromasa Takeuchi, Kazuki Onuma, Takaya Kondo, Kazunari Miike, Toshiki Miyasaka and Yuko Ichihyanagi
Physics, Yokohama National University, Japan

NiO is known as a P-type semiconductor with wide band gap between 3.2 eV and 3.5 eV, and expected as a new material of diluted magnetic semiconductor. Magnetic properties of NiO nanoparticles with several nanometers were observed and blocking temperature(TB) was determined to be 17 K, while Neel temperature of NiO bulk crystal exhibits TN=523 K. In this study, Fe ions were doped into NiO nanoparticles in order to obtain higher blocking temperature. Ni1-xFexO (x=0, 0.05, 0.1) nanoparticles with several nanometers encapsulated with amorphous SiO₂ were prepared by our novel preparation method. NiO single phase structure was confirmed from the x-ray diffraction measurements. It is considered that Ni ions are replaced to Fe ions exactly. This fact was also supported by X-ray absorption fine structure measurements. Magnetization measurements were performed by SQUID magnetometer for obtained samples. Temperature dependence of magnetization showed that TB shifted from 17 K to 57 K as the amount of Fe ions increased, and below TB, ferromagnetic behaviors were observed. Coercive force (HC) increased from 0.8 kOe to 1.5 kOe as the amount of Fe ions increased. This phenomenon can be explained by characteristics of extremely small particles in this system.

RN03

Uniaxial strain effects on spinel ferrite nanoparticles containing Nd and B elements

Masaki Mito¹, Seiya Saisho², Hiroyuki Deguchi¹, Takashi Iwamoto³ and Atsushi Takahara⁴
¹ Department of Basic Science, Kyushu Institute of Technology, Japan
² Department of Applied Science for Integrated System Engineering, Kyushu Institute of Technology, Japan
³ Institute for Sustainability Research and Education, Hosei University, Japan
⁴ Institute for Materials Chemistry and Engineering, Kyushu University, Japan

We studied the uniaxial strain effects on spinel ferrite nanoparticles that contained Nd and B elements (Nd : Fe : B = 10.4 : 83.5 : 6.1) and had the particle size of 5.1 nm. In diffused magnetic nanoparticles, the magnetic easy-axis is distributed randomly, and it is impossible to add the strain along a specific structural axis of each particle. However, in order to control the magnetic property of the magnetic nanoparticles, the application of the uniaxial strain for the particles with the uniform easy-axis vector is preferable to that of hydrostatic pressure for randomly diffused particles. In this study, magnetic easy-axis of each particle was arranged by solidifying an epoxy resin containing the particle at the dc magnetic field of 1 T, resulting in creating an assembly of uniformly oriented nanoparticles. Afterward, the strain was applied along both the magnetic easy-axis and hard-axis. In both situations, the magnetic blocking temperature had the maximum at the strain of about 3-5 kbar. The difference between two strain-experiments appeared at pressure of above 10 kbar.

RN04

The magnetic proximity effect in Fe₃O₄ core/γ-Mn₂O₃ shell nanoparticles

S. M. Yusuf* and P. K. Manna
SOLID STATE PHYSICS DIVISION, BHABHA ATOMIC RESEARCH CENTRE, MUMBAI 400085, India

The phenomenon of 'proximity effect' is very popular in the context of superconductor/non-superconductor heterostructures. In the present study, we report the magnetic proximity effect in a core-shell nanoparticle system by employing dc magnetization and neutron diffraction techniques. In a heterostructure, the substrate, used for its deposition, often modifies the magnetic properties of the deposited layers. However, a core-shell nanoparticle system, being substrate-free, rules out any such possibility. We have observed magnetic proximity effect in a Fe₃O₄ core/γ-Mn₂O₃ shell nanoparticle system, in terms of an enhancement of the Curie temperature (T_c) of the γ-Mn₂O₃ shell (~66K) compared to its bulk value (~40K), and the presence of magnetic ordering in its so-called paramagnetic region (i.e. above 66K). The origin of these two features has been ascribed to the proximity of the γ-Mn₂O₃ shell with a high-T_c Fe₃O₄ core (~858K in bulk form) and an interface exchange coupling between core and shell. Interestingly, no exchange bias effect is found due to a weak interface exchange coupling between core and shell. The present study brings out the importance of the relative strength of interface coupling in governing the simultaneous occurrence of the magnetic proximity effect and the exchange bias phenomenon in a single system.

RN05

Covalent immobilization of biotin on superparamagnetic nanoparticles

Long Giang Bach¹, Md. Rafiqul Islam² and Kwon Taek Lim^{2*}
¹ Department of Imaging System Engineering, Pukyong National University, 608-737, Busan, Korea
² Department of Imaging System Engineering, Pukyong National University, Busan, Korea

Among the magnetic materials, the nano-scale structured magnetite, Fe₃O₄ is widely applicable magnetic nanoparticles (MNPs). MNPs offer attractive possibilities in biomedicine, biosensor, and separation processes because of their unique properties of superparamagnetism, biocompatibility and low toxicity. The ease of synthesis and subsequent surface functionalization of MNPs with a desired material improve biocompatibility which creates an avenue of delivering multimodal and multifunctional MNPs. In this study, a simple protocol of covalent immobilization of biotin on the surface of MNPs for improving biocompatibility and cell viability of the original MNPs has been demonstrated. MNPs were prepared using a solution of ferrous and ferric ions. The anchoring of 3-aminopropyltrimethoxysilane with MNPs resulted due to the formation of Fe-O-Si covalent linkage which is quite strong and having free amino group. The hydroxyl groups of the biotin were activated by N,N'-disuccinimidyl carbonate followed by conjugation with MNPs-NH₂ to afford Biotin-MNPs. The conjugation of biotin to MNPs was confirmed by FT-IR, XPS and EDX. The Biotin-MNPs showed superparamagnetic character as investigated by SQUID.

RN06

Fabrication of (Mn-Al)/Pd or Ni with Core-Satellite Structured Magnetic Particles

Youn-kyoung Baek*, Jung-goo Lee and Chul-jin Choi
Powder & Ceramic Division, Korea Institute of Materials Science, Korea



RN07

The effect of hydrostatic pressure on the Morin transition in hematite nanoparticles

Luana Caron^{1*}, Davide Peddis², Lorenza Suber³, Dino Fiorani³ and Per Nordblad⁴
¹ Fundamental Aspects of Materials and Energy, Faculty of Applied Sciences, TU Delft Mekelweg 15, 2629JB Delft, Netherlands
² Dipartimento di Scienze Chimiche, Università degli Studi di Cagliari, Cittadella Universitaria di Monserrato 09042 Cagliari, Italy
³ Istituto di Struttura della Materia, Area della Ricerca di Roma, CNR Via Salaria km 29500, CP 10-00016 Monterotondo Stazione, Rome, Italy
⁴ Department of Engineering Sciences, Uppsala University Box 534, 751 21 Uppsala, Sweden

Recently, hematite particles have been the subject of intensive studies in areas as diverse as magnetic storage media, photo electrodes and catalysis[1,2]. Hematite is an antiferromagnetic system that displays a spin reorientation from uniaxial to canted antiferromagnetism at the Morin temperature[3]. Particle shape, size and microstructural defects have strong influence on the Morin temperature and thus can be used to tune the system's magnetic response. It is known that the Morin transition temperature decreases along with particle size as a result of the increasing lattice spacing[4], whereas an increase of the Morin temperature under hydrostatic pressure is observed in the bulk material[5]. In a novel approach, we report on the effect of hydrostatic pressures on hematite rhombohedral nanoparticles of narrow size distribution-<DTEM>= 93 ± 2 nm[6]. Pressure was found to increase the Morin temperature at a rate of ~5 K/kbar and considerably decrease thermal hysteresis. These results strongly contrast with the effects of pressure on the bulk material where a milder influence of pressure on both the Morin temperature and thermal hysteresis is observed.

[1] Zhihong Ang, Shihua Hu, Mater. Lett. 58, 3637 (2004) [2] K. Sivola, F. Le Formal and M. Grunze, ChemSusChem 4, 417 (2011) [3] F.J. Morin, Phys. Rev. 78, 819 (1950) [4] D. Schreier and R. C. Niwange, Phys. Rev. Lett. 19, 632 (1967) [5] T. G. Worlock and D. L. Decker, Phys. Rev. 171, 596 (1968) [6] L. Suber et al., Phys. Chem. Chem. Phys. 12, 6884 (2010)

RN08

Ultra-thin MgO coating of superparamagnetic magnetite nanoparticles by combined co-precipitation and sol-gel synthesis

Laura De Matteis¹, Laura Custardoy¹, Rodrigo Fernandez-pacheco², Cesar Magen³, Jesus M De La Fuente⁴, M R Ibarra⁵ and Clara Marquina^{6*}

¹ Instituto de Nanociencia de Aragon- INA, Universidad de Zaragoza, Spain
² Laboratorio de Microscopias Avanzadas (LMA) - Instituto de Nanociencia de Aragon (INA), Universidad de Zaragoza, Spain
³ Laboratorio de Microscopias Avanzadas (LMA) - Instituto de Nanociencia de Aragon (INA), Departamento de Fisica de la Materia Condensada Universidad de Zaragoza Fundacion ARAID, Spain
⁴ Instituto de Nanociencia de Aragon- INA, Universidad de Zaragoza Fundacion ARAID, Spain
⁵ Instituto de Nanociencia de Aragon (INA)- Laboratorio de Microscopias Avanzadas (LMA), Departamento de Fisica de la Materia Condensada Universidad de Zaragoza, Spain
⁶ Instituto de Ciencia de Materiales de Aragon-ICMA, Departamento de Fisica de la Materia Condensada CSIC-Universidad de Zaragoza, Spain

Superparamagnetic magnetite nanoparticles coated with an ultra-thin (~1 nm) magnesium oxide (MgO) layer have been synthesized by combining co-precipitation and sol-gel methods. A thorough chemical and structural characterization has been carried out by means of HRTEM, XRD, EDS, DLS and TGA. Aberration corrected HRTEM experiments with sub-angstrom spatial resolution have allowed us to distinguish the ultra-thin MgO shell that grows epitaxially on the magnetic cores. The capability of the MgO shell to protect the magnetic nuclei from oxidation up to 600°C has been demonstrated. The magnetic properties of the material have been studied before and after the coating procedure. The superparamagnetism of the magnetite nuclei at room temperature is preserved even after calcination. The possibility of obtaining particles of controlled size coated with an isolating layer of nanometric thickness and high thermal stability makes the combination of the two synthesis methods used in this work a starting procedure to obtain nanometric powders suitable for technological applications, such as high-frequency electronics. These particles, after the appropriated functionalization, are also potential candidates to be used in biomedical applications

RN09

Synthesis and characterization of ultra-small magnetic FeNi/G and NiCo/G nanoparticles

Mariana Castrillon¹, Alvaro Mayoral², Cesar Magen³, Johan G. Meier¹, Clara Marquina^{4*}, Silvia Irustra⁵ and Jesus Santamaria⁶

¹ Technological Institute of Aragon (ITA), Zaragoza, Spain
² Instituto de Nanociencia de Aragon (INA)- Laboratorio de Microscopias Avanzadas (LMA), Universidad de Zaragoza, Spain
³ Instituto de Nanociencia de Aragon (INA)- Laboratorio de Microscopias Avanzadas (LMA), Departamento de Fisica de la Materia Condensada Universidad de Zaragoza, Spain
⁴ Instituto de Ciencia de Materiales de Aragon-ICMA, CSIC-U. Zaragoza, Spain
⁵ Instituto de Nanociencia de Aragon- INA, Networking Research Center on Bioengineering, Biomaterials and Nanomedicine, CIBER-BBN U. Zaragoza, Spain

Ultra-small magnetic nanoparticles consisting of NiCo and FeNi alloys coated by graphitic shells (NiCo/G and FeNi/G) have been synthesized by a procedure similar to that described by Seo et al. [1]. The cores, which retained the face-centered cubic (fcc) symmetry of the original bulk metals, together with the graphitic coating have been characterized by means of aberration corrected scanning transmission electron microscopy (STEM). The particles have mean sizes of 2.6 nm and 6.2 nm for NiCo/G and FeNi/G, respectively. The samples contain a large fraction of superparamagnetic nanoparticles at room temperature. The thermal stability of the particles is enhanced by the graphite shell, and the graphite coated FeNi and NiCo are stable under oxygen atmosphere up to 170 C. Non-coated bimetallic FeNi and NiCo have also been prepared. Their chemical characterization revealed the massive oxidation of the bimetallic nanoparticles in absence of the graphite coating (oxygen content higher than 60 at. %). This fact confirms the effectiveness of the graphite shell in preventing the magnetic cores from oxidation and therefore preserving their magnetic properties even at high temperatures.

1.- Seo W. S. et al., Nature Mater. 5 (2006) 971-6

RN10

Magnetization measurements and blocking temperature distribution in magnetic nanoparticle systems

Taecheon Lee¹, Seunghyun Kim¹, Sungwon Yoon², Byoung Jin Suh^{2*}, Zeehoon Jang¹ and Kyunghyun Kim³

¹ Department of Physics, Kookmin University, Korea
² Department of Physics, The Catholic University of Korea, Korea
³ Biotechnology & Bioinformatics, Korea University, Korea

We present magnetization measurements on a variety of magnetic nanoparticle ensembles. The samples are; (1) Artificially synthesized Helicobacter Pylori ferritin reconstituted with three different Fe ions/ferritin ratio, 160, 2000, and 4000. (2) Commercial horse spleen ferritin (3) CoPt nanoparticles with average particle size of 2 nm. Temperature dependence of magnetization has been measured using a SQUID magnetometer. Measurement sequence has been modified from a typical field-cool sequence and the measurements have been performed with field “stop-resume” steps at the regular temperature interval. Using a phenomenological model, we could extract the moment weighted blocking temperature distributions in the samples from the experimental data. The model is based on the assumptions that; 1) the particles in the ensembles can be uniquely categorized in terms of the blocking temperature. 2) the particles with the same blocking temperature will have the same field and temperature dependence of the magnetization. 3) the particles are non-interacting with each other. With the obtained distributions, the numerical simulations are performed to reproduce the field-cool magnetization data and zero-field-cool magnetization data.

RN11

Structural and magnetic anomalies in CoAl₂O₄ nanocrystals

Koichi Sato¹, Takashi Naka¹, Takayuki Nakane¹, Minoru Taguchi¹, Dinesh Rangappa², Satoshi Ohara³ and Tadafumi Adschiri⁴

¹ National Institute for Materials Science, Japan
² International Advanced Research Centre for Powder Metallurgy & New Materials, India
³ Joining and Welding Research Institute, Osaka University, Japan
⁴ WPI, Advanced Institute for Materials Research, Tohoku University, Japan

In this study, we investigated magnetic properties of spinel CoAl₂O₄ nanocrystals (NCs) synthesized by a supercritical hydrothermal synthesis. We confirmed that all the samples are composed of the single phase CoAl₂O₄ by the X-ray diffraction measurements. Crystalline sizes are controlled to be 4 ? 8 nm. We also found that the inversion parameters of the samples, describing the cation distribution are more than 0.3 [1,2], being much higher than bulk specimens previously reported. We conducted magnetization and dc- and ac-susceptibility measurements. All the samples show paramagnetic behavior above 70 K. The effective Bohr magnetons and the Weiss temperatures are 2.6 - 2.8 μB and -40 - -50 K. The effective Bohr magnetons are smaller than 4.4 - 4.6 μB reported on specimens with the low inversion parameters [3,4]. The susceptibilities deviate from Curie-Weiss law below 40 - 50 K. From the results of the magnetization measurements, it was found that spontaneous magnetization, 0.1 μB/Co, emerges below 40 K in the samples with the size of 4 nm. The reduced Bohr magnetons and the emergence of the spontaneous magnetization indicate that in our NC samples, a certain magnetic phase, being different from those of bulk specimens, appears below 40 K.

[1] N. Tristan, J. Hemberger, A. Kimmel, H.-A. Krug von Nidda, V. Tsurkan, and A. Loid, Phys. Rev. B 72, 174404 (2005) [2] T. Suzuki, H. Nagai, M. Nohara, and H. Takagi, J. Phys. Condensed matter 19, 145265 (2007). [3] H. S. C. O'Neill, Eur. J. Mineral. 6, 603 (1994). [4] A. Nakatsuka, Y. Beika, Y. Yamazaki, N. Nakayama, and T. Mizota, Solid State Commun. 128, 85 (2003).

RN12

Preparation of chains of single-domain Ni nanoparticles with collinear direction of magnetization

S A Nepijko^{1*}, D Kutnyakhov¹, I E Protsenko², H J Elmers¹, R Wiesendanger³ and G Schoenhense¹

¹ Institute of Physics, University of Mainz, Germany
² Department of Applied Physics, Sumy State University, Ukraine
³ Institute of Applied Physics, University of Hamburg, Germany

Networks of ferromagnetic nanoparticles have been proposed to form quantum cellular automata [1]. We present a fabrication method based on self-organized growth on stepped surfaces for fairly regular nanoparticles arranged in a one-dimensional chain, that are suitable for this application. We studied Ni nanoparticles with sizes in the range 80-130 nm on a highly-ordered pyrolytic graphite (HOPG) substrate and succeeded to prepare one-dimensional chains of these single-domain particles characterized by the same direction of their magnetization. The nanoparticles were found to decorate atomic cleavage steps on the basal surface and their distances are small enough to give rise to strong dipolar coupling. The necessary and sufficient conditions are: (i) 3D growth mechanism along with non-wetting behaviour, (ii) the dielectric substrate has atomic cleavage steps, (iii) the size of the ferromagnetic particles is smaller than the characteristic domain size but still above the transition into the superparamagnetic state and, finally, (iv) the distances between the particles are small enough for dipolar coupling. The study was carried out using atomic-force (AFM) and magnetic-force (MFM) microscopy. The approach of ordering ferromagnetic nanoparticles into one-dimensional chains is of particular interest because chains are a basic block for storage and transport of information.

[1] R.P. Cowburn, M.E. Welland, Science 287 (2000) 1466

RN13

Influence of the morphology on the magnetic properties of dodecanethiol-capped Au nanoparticles

Daniel Ortega¹, Eider Goikolea², Jose Javier Garitaonandia², Maite Insausti², Hyodo Zhang³, Kiyonori Suzuki³ and Fernando Plazaola²

¹ Department of Physics and Astronomy, University College London Gower Street WC1E 6BT London, United Kingdom
² Zientzia eta Teknologia Fakultatea Euskal Herriko Unibertsitatea, Spain
³ Department of Materials Engineering, Monash University, Australia

It has been proved that Au nanoparticles (NP) coated with certain molecules can present different magnetic characters, ranging from superparamagnetism to permanent magnetism at room temperature (RT) [1-3]. We have prepared ferromagnetic dodecanethiol-capped Au NPs with a high magnetic signal of 1.7 emu/gr and coercive field of 85 Oe at RT. An analysis by high resolution electron microscopy reveals that the NPs are composed by ~200 atoms forming multi-twinned structured nanocrystals of ~2 nm with icosahedral or decahedral morphologies where well ordered fcc twinned entities are joined forming an only nanocrystal with a spatial 5-fold symmetry. The external morphology is conditioned by the final stabilization of the NP and, with a surface to bulk atoms ratio up to ~75% and a magnetism located exclusively in the surface atoms, the morphology plays a crucial role in the definition of the magnetic character of the NP. In a comparative view with the multidomain structures presented in bulk materials, we argue that borders among the twinned nanosized entities would act as pinning centers, hindering the alignment of the magnetic moments between entities and promoting the coercive field.

[1] Y. Yamamoto, T. Miura, M. Suzuki, N. Kawamura, H. Miyogawa, T. Nakamura, K. Kobayashi, T. Teranishi, and H. Hori, Phys. Rev. Lett. 93 116801 (2004). [2] P. Crespo, R. Litran, T. C. Rojas, M. Mullinger, J. M. de la Fuente, J. C. Sanchez-Lopez, M. A. Garcia, A. Herrando, S. Penedes, and A. Fernandez, Phys. Rev. Lett. 93 087204 (2004). [3] J. S. Garitaonandia, M. Insausti, E. Goikolea, M. Suzuki, J. D. Cashion, N. Kawamura, H. Ohsawa, I. Gil de Muro, K. Suzuki, F. Plazaola, and T. Rojo, Nanoletters 8 661 (2008).

RN14

Structure effects on the magnetic behavior in Fe oxide based nanoparticles

Amilcar Labarta*, Carlos Moya, Nicolas Perez, Arantxa Fraile, Oscar Iglesias and Xavier Batlle

Fundamental Physics, University of Barcelona, Spain

A key question in magnetic nanoparticles (NP) is how the nanostructure modifies their magnetic and electronic properties. As the particle size is reduced, deviations from bulk behaviour have been widely reported and attributed to both the appearance of a magnetically disordered surface layer and finite-size effects, thus giving rise to a decrease in the particle magnetization, an exchange field acting on the core and an increase in the anisotropy. In order to elucidate those phenomena we have carried out STEM, XAS, XMCD and magnetization measurements in Fe oxide based NP models, aiming at the real-space characterization at the sub-nanometer scale of a single NP to characterize the particle structure, surface magnetization, and the dependence of the latter on the strength of the surface bond to a bio-molecule coating. We also aim at the quantification of the orbital and spin contributions to the NP magnetic moment. The key role of the crystal quality is thus suggested, because particle-like behaviour above about 5 nm in size is observed only when NP are structurally defective. These conclusions are supported by Monte Carlo simulations. It is also shown that thermal decomposition is a chemical route capable of producing high-crystal quality NP with bulklike properties.

1. N. Perez, F. Bartolome, L.M. Garcia, J. Bartolome, M.P. Morales, C.J. Serna, A. Labarta and X. Batlle, Applied Physics Letters 94, 093108 (2009). 2. P. Guardia, N. Perez, A. Labarta and X. Batlle, Langmuir, 26, 5843-5847 (2010). 3. X. Batlle, N. Perez, O. Iglesias, A. Labarta, F. Bartolome, L.M. Garcia, J. Bartolome, A.G. Roca, M.P. Morales, and C.J. Serna, Journal of Applied Physics 109, 07B524 (2011). 4. Work in collaboration with: F. Bartolome, L.M. Garcia, J. Bartolome (ICMA-CSIC, Spain); M.P. Morales and C.J. Serna (ICMM-CSIC, Spain); M. Varela, J. Salafrañca and J. Gazquez (OAK-Ridge National Laboratory, USA).

RN15

Magnetic properties of surface-functionalized nano-particles

Ann Kathrin Michel¹, Mathias Kraken¹, Jochen Litterst^{1*}, Yannick Guari², Joulia Larionova², Lenaic Lartigue², Jerome Long² and Alessandro Lascialfari³

¹ IPKM, TU Braunschweig, Germany
² Institut Charles Gerhardt, Universite Montpellier II, France
³ CNR/NANO, Univ. Milano, Italy



RN16

Study of aqueous dispersions of magnetic nanoparticles by magnetic and rheological measurements

Shalini M¹, Mahesh Samant², Radha S^{3*} and D. C. Kothari³

¹ Department of Physics and UM-DAE CBS, University of Mumbai, India
² National Center for Nanosciences and Nanotechnology, University of Mumbai, India
³ Department of Physics, University of Mumbai, India

The observed magnetic tunability of light transmission through a ferrofluid [1] can be effectively understood in terms of the inter-particle interaction that can be estimated from the magnetic and rheological properties of these fluids. The present study reports complementary magnetic and rheological measurements of synthesized aqueous dispersions of ferrite nanoparticles, using a commercial ferrofluid as a standard. The aqueous dispersions of the ferrite nanoparticles were synthesized by powder X-ray diffraction with the Rietveld refinement, transmission electron microscope, scanning electron microscopy with energy dispersive spectrometer, and vibrating sample magnetometry. SEM micrographs of the samples showed the spherical shape of NiFe₂O₄. CoFe₂O₄ nanoparticles located above on the surface of SrFe₁₂O₁₉ hexagonal platelet shape. TEM micrographs showed the particle size of core and shell. With the core/shell nanoparticles, the saturation magnetization was decreased but coercivity was increased with SrFe₁₂O₁₉/CoFe₂O₄ sample.

[1] M. Shalini, D. Sharma, A. A. Deshpande, D. Mathur, Hema Ramachandran and N. Kumar, Eur. Phys. Jour. D 66 (2012) 30

RN17

Magnetodielectric effect of Fe₂O₃ nanoparticles embedded in SiO₂ glass matrix

Hung-cheng Wu, Sudip Mukherjee and Hung-duen Yang*

Department of Physics, National Sun Yat-sen University, Taiwan

Magnetic iron-oxide (doping 0.5 mole %) nanoparticles (NPs) have been synthesized in silica glass matrix, prepared by the sol-gel method with different annealing temperatures. XRD, TEM and XANES show the presence of NPs of Fe₂O₃ and Fe₃O₄ crystalline phase (< 5 nm). An interesting colossal enhancement of dielectric constant with diffuse phase transition is observed around room temperature due to the thermally activated oxygen vacancies. The magnetodielectric effect observed in the glass composites is considered to be associated with magnetoresistance changes, depending on NPs size.

RN18

Tuning the concentration of magnetic Co nanoparticles in In₂O₃ with oxygen pressure and concentration of tin

Marzook S. Alshammari*, Mohammed S. Alqahtani¹, Qi Feng¹, S. Alfahad², M. Alotibi², A. Alyamani², A. M. H. R. Hakimi³, S. M. Heald⁴, H. J. Blythe⁴, A. M. Fox⁴ and G. A. Gehring¹

¹ Department of physics and astronomy, University of Sheffield, United Kingdom
² Nanotechnology center, King Abdulaziz City for Science and Technology, Saudi Arabia
³ Department of Materials Science and Metallurgy, University of Cambridge, United Kingdom
⁴ Advanced Photon Source, Argonne National Laboratory, USA

This study shows the power of combining magnetic measurements with magnetic circular dichroism (MCD) to detect the contribution to the magnetism from metallic Co nanoparticles, and the result that the formation of nanoparticles is suppressed by the inclusion of tin. Thin films of (In_{1-0.95}Co_{0.05})₂O₃ were deposited using pulsed laser deposition (PLD) on sapphire substrates. The magnetism and the amount of cobalt in nanoparticles increased with the oxygen deficiency in the PLD chamber and also after annealing in vacuum as expected and as confirmed using Extended X-ray Absorption Fine Structure. The MCD spectra show two features that are well fitted by a combination of the spectrum from the nanoparticles in the In₂O₃ matrix, as calculated using Maxwell-Garnett theory, and a contribution from polarized carriers [1]. The changes in the magnetization and the MCD are used to get a quantitative estimate of the contribution of the nanoparticles magnetization to the total magnetization in each sample. Adding 5% of Sn made little difference to the saturation magnetization but the signal due to Co nanoparticles was completely suppressed and that from polarized carriers enhanced strongly. This indicates that, the magnetization of the carriers in Sn and Co co doped In₂O₃ is particularly high.

Hakimi, et al, Physical Review B 84, 085201 (2011).

RN19

Synthesis, structural, and magnetic properties of strontium hexaferrite nanoparticles with La, Sm doping and core/shell structure by the sol-gel hydrothermal process

Hue Thi Minh Dang¹, Dien Xuan Luong¹, Hoang Duc Tran¹, Huong Manh Phan² and Chinh Dang Huynh^{1*}

¹ Department of Inorganic Chemistry, Hanoi University of Science and Technology, Viet Nam
² Department of Physics, University of South Florida, USA

SrFe₁₂O₁₉ nanoparticles have been prepared by the sol-gel hydrothermal method. These SrFe₁₂O₁₉ nanoparticles have been doped with La, Sm and coated with NiFe₂O₄, CoFe₂O₄ nanoparticles by the sol-gel and the self-assembly method, respectively. Properties of the nanoparticle samples were characterized by powder X-ray diffraction with the Rietveld refinement, transmission electron microscope, scanning electron microscopy with energy dispersive spectrometer, and vibrating sample magnetometry. SEM micrographs of the samples showed the spherical shape of NiFe₂O₄, CoFe₂O₄ nanoparticles located above on the surface of SrFe₁₂O₁₉ hexagonal platelet shape. TEM micrographs showed the particle size of core and shell. With the core/shell nanoparticles, the saturation magnetization was decreased but coercivity was increased with SrFe₁₂O₁₉/CoFe₂O₄ sample.

[1] Alex Goldman, Modern Ferrite Technology; Springer; 2nd edition (2005). [2] Smit J., Wijn H.P.J., Ferris-Physical properties of ferrimagnetic oxides in relation to their technical application, Philip Technical Library, Eindhoven, (1959). [3] L.A. Garcia-Cerdá, O.S. Rodríguez-Perdomo, P.J. Resendiz-Hernández, Journal of Alloys and Compounds 369 (2004) 182-184. [4] Malick Jean, Virginie Nachbaur, Julien Bran, Jean-Marie Le Breton, Journal of Alloys and Compounds 496 (2010) 306-312. [5] Xiaofeng Yang, Qiaoling Li, Jingzhan Zhao, Bingdong Li, Yongfei Wang, Journal of Alloys and Compounds 475 (2009) 312-315. [6] T. T.V. Nga, N.P. Duong, T.D. Hien, Journal of Alloys and Compounds 475 (2009) 55-59.

July 12 (Thu)

July 12 (Thu)

RN20

A facial fabrication of the superparamagnetic Fe₃O₄@TiO₂ microspheres and its photocatalytic application

Kyong-hoon Choi¹, Eun-mee Kim², Seung-lim Oh³, Do-yeon Kim⁴ and Jin-seung Jung^{4*}

¹ Material R&D Division, H & Global Co. Ltd., Korea

² Gangneung Center, Korea Basic Science Institute, Korea

³ Material R&D Division, H & Global Co. Ltd., Korea

⁴ Department of Chemistry, Gangneung-Wonju National University, Korea

Over the past few decades, semiconductor photocatalysts have attracted much attention because of their applications in new energy fields where they represent a promising strategy for splitting water to provide clean hydrogen energy, and their use in the photocatalytic degradation of polluted atmosphere and wastewater in environmental remediation[1,2]. Among the reported photocatalysts, titanium dioxide (TiO₂) is one of the most studied semiconductors for photocatalytic reactions because of its high activity, chemical stability, robustness against photocorrosion, low toxicity and availability at low cost, especially for the detoxification of water and air [3,4]. In this study, we have successfully synthesized multifunctional core/shell (Fe₃O₄/TiO₂) submicron particles with controlled shell thickness. In the first step, superparamagnetic Fe₃O₄ submicron particles were fabricated by one-step hydrothermal method. In the second step, the surface of Fe₃O₄ submicron particles was coated with TiO₂ by atomic layer deposition (ALD) method. Through this method, the thickness of shell was accurately tunable. The recyclable Fe₃O₄@TiO₂ particles exhibit excellent catalytic properties for the oxidation reaction of 2,4,6-trichlorophenol (2,4,6-TCP) in aqueous solution.

[1] A. Fujishima, K. Honda, *Nature*, 238, 37 (1972) [2]. X. C. Wang, K. Maeda, A. Thomas, K. Takanabe, G. Xin, G. M. Garrison, K. Domen, M. Antonietti, *Nat. Mater.*, 8, 76 (2009) [3]. T. L. Thompson, J. T. Yates, Jr., *Chem. Rev.* 106, 4428 (2006) [4] A. C. Rodrigues, M. Boroski, N. S. Shimada, J. C. Garcia, J. Nozaki, N. Hioka, *J. Photochem. Photobiol. A* 194, 1 (2008)

RN21

Synthesis of high moment magnetite (Fe₃O₄) nanoparticles by simple modified polyol method

Mohamed Abbas Ali Ahmed and Cheolgi Kim*

Material Science and Engineering, Chungnam National University, Korea

(Synthesis of high moment magnetite (Fe₃O₄) nanoparticles by simple modified polyol method) Mohamed Abbas and Cheolgi Kim Center for NanoBioEngineering and Spintronics, Department of Materials Science and Engineering, Chungnam National University, Daejeon 305-764, Korea Abstract Single phase magnetite with high saturation magnetization and 50 nm as a medium range particles size has been synthesized by in expensive and surfactant-free simple modified polyol method using FeCl₃·4H₂O as a precursor of iron and Poly Ethylene Glycol (PEG) as a solvent and reducing agent simultaneously. X-ray diffraction (XRD) and EDS analysis indicated that, formation of purely magnetite (Fe₃O₄) without presence of any other phase. Transmission electron microscopy (TEM) also show that the synthesized nanoparticles are almost sphere in shape. The magnetic properties of the synthesized magnetite nanoparticles were measured by means Physical Property Measurement System (PPMS-VSM) at different temperature and shows that the as-synthesized NPs were ferromagnetic with high moment 91.7 emu/g at 5 K. Corresponding author. Tel:-+82428216236 E-mail address: egkim@cnu.ac.kr (Prof/ CheolGi Kim)

RN22

Study of Structural, morphological and optical properties of SrFe_{12-x}Co_xO₁₉ (x= 0, 0.1, 0.2) hexaferrite nanoparticles

Morteza Zargar Shoushtari*, Ebrahim Mousavi Ghahfarokhi and Fereshte Ranjbar Physics, Shahid Chamran University of Ahvaz, Iran

A series of M-type strontium hexaferrite samples having nominal composition SrFe_{12-x}Co_xO₁₉ (x = 0.0, 0.1 and 0.2) with different morphologies have been synthesized via sol gel method. For synthesis of samples, first a precursor gel was prepared using the sol-gel method. The mixture of KCl and dry-gel was calcined at 1000 °C for 2 h to obtain the needle-like nano- SrFe_{12-x}Co_xO₁₉. The rod-like and bubble nano- SrFe_{12-x}Co_xO₁₉ was prepared by calcining the mixture of KBr and dry-gel or KI and dry-gel, respectively, and spherical nano- SrFe_{12-x}Co_xO₁₉ was prepared only by calcined dry-gel. The structure and morphology of samples were systematically characterized by X-ray diffraction (XRD), scanning electron microscopy (SEM). The optical properties of samples were investigated by UV-Vis. The result of XRD of samples showed that the M-type hexagonal structure can be maintained for all the samples without the segregation of secondary phases. The FT- IR frequency bands in the range 560 - 580 cm⁻¹ and 430 - 470 cm⁻¹ in the all of samples corresponds to the formation of tetrahedral and octahedral clusters of metal oxides in ferrites, respectively.

RN23

Light induced ferromagnetism of nanocrystalline CuCr₂Se₄ particles

Dongsoo Kim*, Kookchae Chung and Choljin Choi

Korea Institute of Materials Science, Korea

A novel method to synthesize ternary chalcogenide nanoparticles was developed with microwave-assisted polyol reaction in this study. Copper chloride, chromium acetate and metallic selenium were used as precursors with stoichiometric ratios in poly ethylene glycol. The system was purged with argon and then the mixed reactants were irradiated for 60 minutes with 60% of the instrument power. Products were collected, centrifuged, washed with ethyl alcohol in order to remove poly ethylene glycol and dried overnight under inert atmosphere. Magnetic moment of CuCr₂Se₄ nanoparticles was measured from 300 K to 750 K with external magnetic field of 500 Oe in argon atmosphere and Curie temperature was calculated as 445 K. From the hysteresis loop, magnetic property was ferromagnetic and its saturation magnetization and coercive force were measured to 15 emu/g and 80 Gauss respectively. Nanocrystalline CuCr₂Se₄ particles were dispersed in the matrix of light transparent resin so as to investigate light induced effect on the magnetic properties. Er-laser with the wavelength of 1.5 μm was employed as light source. Light illumination in an external magnetic field increased the magnetization and this increment of magnetization (ΔJ) to initial magnetization (J) showed a maximum.

1. Mingos D.M.P. *The application of microwaves in chemistry // Res. Chem. Intermed.*, 1994, V.20, P.85-91. 2. Baran M., Szymczak R., Szymczak H., Tsurkan V. *Spin glass like behavior of magnetization in anion substituted CuCr₂Se₄ magnetic semiconductor // J. Magn. Magn. Mater.*, 1995, V. 140-144, P. 2043-2047. 3. Boukari H., Kossacki P., Bertolini M., Ferrand D., Cibert J., Tatarenko S., Wasielea A., Gaj J.A., Diel T. *Light and electric field control of ferromagnetism in magnetic quantum structures // Phys. Rev. Lett.*, 2002, V.88, N.20, P.204-207.

RN24

Magnetite nanoparticles in hybrid aerogel and PEG encapsulated of magnetite nanoparticles for the hyperthermia application

Eunhee Lee and Chang-yeoul Kim

KICET, Korea

Magnetite nanoparticles have received intensive attractions because of their applications as magnetic carriers in drug targeting and hyperthermia in tumor treatment. However, magnetite nanoparticles with 10 nm in diameter easily aggregate themselves to form large secondary particles. To disperse magnetite nanoparticles, this research paper suggests the infiltration of magnetite nanoparticles into hybrid silica aerogels. The PEG encapsulate of magnetite is to disperse magnetite up in PBS solution. The well-dispersion of magnetite is necessary for target the tumor cells and hyperthermia treatment. Methyltriethoxysilicate (MTEOS) based hybrid silica aerogels were synthesized by a supercritical drying method. To incorporate magnetite nanoparticles into the hybrid silica aerogels, we immersed it into magnetite precursor solution. The surfaces of magnetite nanoparticles were modified by PEG(polyethylene glycol). The infiltration and PEG coating of magnetite nanoparticles were identified by XRD, FT-IR and TEM. Vibrating Sample Magnetometer analysis showed that the composite of the magnetite and hybrid silica aerogel is superparamagnetic. The temperature behaviors of the magnetite composite and the surface coated magnetite nanoparticles were discussed in the context of the change of magnetite particles with PBS for Hyperthermia application.

RO01

Effect of the Cu content on the microstructural and magnetic properties of Nd-Fe-B sintered magnets

Tae-hoon Kim¹, Seong-rae Lee^{1*}, Seok Namkung² and Tae-suk Jang²

¹ Korea University, Korea

² Sunmoon University, Korea

The Cu addition in the Nd-Fe-B sintered magnet improves the coercivity after the post-sintering annealing (PSA) because the continuous Nd-rich grain boundary phase (GBP) and the metastable C-Nd₂O₃ phase were formed [1-3]. However, the magnetic properties of the commercial magnet were deteriorated when the Cu content of the magnet is higher than 0.15 at.% (optimized Cu content). In this study, we investigated the Cu content effects on the microstructural and magnetic properties of sintered 12Nd-2.7Dy-(76.45-x)Fe-xCu-6B-2.65M (at.%, x=0.2, 0.3, 0.4, 0.5) magnets. The coercivity was decreased (28.7→26.1 kOe) with increasing the Cu content, but the remanence was unchanged. Two kinds of Cu enriched Nd-rich triple junction phases (Cu-rich TJP), such as 5~10 at.% Cu containing Nd-rich TJP (Culow-rich) and 35~45 at.% Cu containing Nd-rich TJP (Cuhigh-rich), were observed. The Culow-rich TJP was the stable h-Nd₂O₃, but the Cuhigh-rich TJP was the metastable C-Nd₂O₃ phase. The thickness and Fe content of Nd-rich GBP was increased with increasing Cu content because the oversaturated Cu atoms in the GBP substitutes with the Fe atoms near the GBP/Nd₂Fe₁₄B interfaces. As a result, the magnetic decoupling through the Nd-rich GBP was deteriorated and the coercivity was decreased when the Cu content of the magnet is high.

[1] F. Vial, F. Joly, E. Nevalainen, M. Sagawa, K. Hiraga, and K. T. Park, *J. Magn. Magn. Mater.* 242-245, 1329 (2002), [2] W. F. Li, T. Ohkubo, T. Akiba, H. Kato, K. Hono, *J. Mater. Res.* 24, 413 (2009), [3] M. Matsuura, S. Sugimoto, T. Fukuda, R. Goto, N. Tezuka, *Journal of Physics: Conference Series.* 200, 082019 (2010).

RO02

Effects of the Dy₂H₃ and Dy₂O₃ powder addition on the magnetic and microstructural properties of Nd-Fe-B sintered magnet

Kyung-hoon Bae¹, Tae-hoon Kim¹, Seong-rae Lee^{1*}, Seok Namkung² and Tae-suk Jang²

¹ Korea University, Korea

² Sunmoon University, Korea

Effective way for enhancing the magnetic properties as well as saving the Dy content in the Nd-Fe-B based magnet is to develop the core-shell microstructure using the Dy₂O₃, DyF₃ or DyH₃ powder doping [1, 2]. The DyH₃-doped magnet shows the most improved results [2]. However, the role of DyH₃ powder has not been identified yet. In this study, we investigated the magnetic and microstructural changes of the DyH₃-doped (2.4 wt.%) Nd_{12.5}Dy_{0.88}Fe_{68.1}M_{2.4}(wt.%) sintered magnet comparing with those of the Dy₂O₃-doped (2.0 wt.%) magnet. The coercivity of Dy₂O₃-doped magnet slightly increased (30.13→30.71 kOe) with a little remanence reduction (11.59→11.56 kG) comparing with the undoped magnet. However, the coercivity of the DyH₃-doped magnet increased (30.13→31.9 kOe) without sacrificing remanence (11.59→11.6 kG). Core-shell microstructure was well developed when the DyH₃ powders were added comparing with the Dy₂O₃-doped magnet. The hydride powder doping enhanced the diffusion of Dy because the dissolution of the hydrogen in the Nd₂Fe₁₄B increased the lattice parameter and the point defects. The hydride was also known as a solid lubricant role at the grain boundaries [3]. As a result, the core-shell microstructure and the (00L) grain alignment of the DyH₃-doped magnet was more developed than those of Dy₂O₃-doped magnet.

[1] S. E. Park, T. H. Kim, S. R. Lee, D. H. Kim, S. Namkung, and T. S. Jang, *IEEE. Tran. Magn.* 47, 10 (2011), [2] G. Yan, P. J. McGuinness, J. P. G. Farr, and I. R. Harris, *J. Alloys Compd.* 491, L20 (2010), [3] S. Guo, R. J. Chen, Y. Ding, G. H. Yan, D. Lee, and A. R. Yan, *J. Phys.: Conf. Ser.* 266, 012030 (2011).

RO03

Magnetic properties of nano-composite Nd-Fe-B thick-film magnets prepared by vacuum arc deposition

Tomoaki Tsutsumi¹, Masaki Nakano^{1*}, Takeshi Yanai¹, Fumitoshi Yamashita² and Hirotoshi Fukunaga¹

¹ Nagasaki University, Japan

² Mlnebea Co. Ltd., Japan

In order to upgrade the torque of the small motor comprising a multi-polarly magnetized rotor with isotropic thick-film magnets [1], enhancement in remanence of the isotropic thick-film is indispensable. We, therefore, prepared nano-composite Nd-Fe-B/Alpha-Fe isotropic thick-films by using a vacuum arc deposition method [2]. This contribution reports the effect of the composition and the power of arc deposition on the magnetic properties. Samples were prepared by using several targets with the compositions of NdXFe₁₄B + Nb_{0.5} at.% (X =1.4-2.0). The voltage and capacitance varied in order to control the power range between 11 and 44 J. As the power was fixed at 44 J, use of a Nd₁₄Fe₁₄B + Nb_{0.5} at. % target enabled us to obtain the highest (BH)max value. Although the deposition rate decreased from approximately 20 to 5 microns per hour due to the power reduction from 44 to 11 J, the value of (BH)max could be improved by approximately 15 kJ/m³ at the target composition of Nd₁₄Fe₁₄B + Nb_{0.5} at. %. Resultantly, we succeeded in obtaining a 29 micron-thick Nd-Fe-B thick-films with the remanence, coercivity and (BH)max values of 0.92 T, 390 kA/m and 79 kJ/m³, respectively.

[1] F. Yamashita et al., *IEEE Trans. Magn.* 46, 2012 (2010), [2] M. Nakano et al., *J. Appl. Phys.* 109, No.7, 07A755-1 (2011).

RO04

Corrosion resistance and corrosion behaviors of sintered rare-earth magnets in different corrosive environments

Anhua Li*, Wei Li, Jiajie Li, Haibo Feng, Zhaohui Guo and Minggang Zhu Division of Functional Materials, Central Iron & Steel Research Institute, China

Sintered rare-earth magnets possessing outstanding magnetic properties are widely applied in many fields. However, corrosion resistance has been a problem with the magnets owing to the high chemical activity of the phases rich in rare earth elements [1]. The Nd-rich phases of the Nd-Fe-B magnets can react with water vapor and oxygen in a damp and humid atmosphere. The electro-chemical corrosion occurs for Nd-Fe-B magnets in a high humidity atmosphere because of the difference of corrosion potential between the matrix Nd₂Fe₁₄B phase and the boundary Nd-rich phase [2]. In this article, Corrosion resistance of sintered Nd-Fe-B and Sm-Co magnets was investigated in steady-state damp heat (HH), neutral salt spray (NSS) and pressure cooker (PCT) climates. The effects of alloy composition and different corrosive environments on magnetic flux loss were discussed. It shows that the corrosion rates of sintered Nd-Fe-B magnets in HH and NSS climates exhibit a obvious parabolic trend, flux loss in the above three kinds of climates have a approximate linear trend. The corrosion resistance of sintered Nd-Fe-B magnets can be improved by Dy partially substitution for Nd and minor Co addition. The sintered Sm-Co magnets show very good corrosion resistance in the above three kinds of climates.

Sintered rare-earth magnets; corrosion resistance; corrosion behavior; different corrosive environments

RO05

Effects of grain size and interface state on the coercivity in Nd-Fe-B/ Nd thin films

Kunhiro Koike*, Takanao Kusano¹, Daisuke Ogawa¹, Mizuno Yoshiyuki¹, Miyazaki Takamichi², Yasuo Ando² and Hiroaki Kato¹

¹ Graduate School of Science and Engineering, Yamagta University, Japan

² Graduate School of Engineering, Tohoku University, Japan

High coercivity in sintered Nd-Fe-B magnets is the crucial subject, especially in view of a high demand for developing Dy-saving magnets [1]. In order to approach this matter, the grain refinement and the interfacial microstructure control are known long to be the promising methods [2, 3]. In this work, the effect of Nd coating on the coercivity has been investigated in the Nd₂Fe₁₄B thin films with different grain sizes. As the Nd₂Fe₁₄B layer thickness tNFB was decreased from 70 nm to 5 nm, the coercivity exhibited a gradual increase behavior from 6.5 kOe to 16 kOe, and from 17.5 kOe to 26.2 kOe for the Nd-Fe-B and Nd-Fe-B/Nd films, respectively. It should be noted that the amount of Hc increase by the Nd coating was about 10 kOe irrespective of Nd-Fe-B layer thickness tNFB. AFM observations showed that the average Nd₂Fe₁₄B particle size of the tNFB = 5 nm film is about 60 nm, which is much smaller than the critical size for the single domain in the Nd₂Fe₁₄B phase. These results therefore suggest that a proper interface state is extremely important to achieve high coercivity not only in larger grain system but also in smaller particle one.

[1] S. Sugimoto, *Proc. on the 21th Int. Workshop on Rare-earth Permanent Magnet and their Applications, Bled, Slovenia* (2010) 103, [2] K. H. Muller, D. Eckert, A. Handstein, P. Nothnagel, and J. Schneider, *J. Magn. Magn. Mater.*, 83, (1991) 195. [3] J. D. Livingston, *J. Appl. Phys.*, 57, (1985) 4137.

RO06

Interface state and coercivity in Nd-Fe-B/Dy films

Jin Umezawa¹, Yoshiki Sakai¹, Kunhiro Koike*, Daisuke Ogawa¹, Yoshiyuki Mizuno¹, Takamichi Miyazaki², Yasuo Ando² and Hiroaki Kato¹

¹ Graduate School of Science and Engineering, Yamagta University, Japan

² Graduate School of Engineering, Tohoku University, Japan

It is believed that the Nd-rich phase plays an important role for the coercivity enhancement in the Nd-Fe-B magnets [1-2]. In the case of Dy-diffusion-processed Nd-Fe-B magnets [3], however, it is still not clear whether only the Dy-rich shell or both Dy-shell and the Nd-rich phase is indispensable for the high coercivity. Therefore, we fabricated a model interface system, which consists of the Nd₂Fe₁₄B layer with the Dy and Nd overlayers in order to study the relationship between microstructure near the interface and the coercivity. Nd₂Fe₁₄B particles with the c-axis normal to the film plane were constructed by using HV or UHV sputtering systems. We introduced high-melting-point bcc metals, Ta or Mo, as an underlayer on the heat-resistant glass or sapphire c-plane single-crystal substrates. When the temperature of the substrate during a deposition of the 1 μm thick Nd-Fe-B layer was 620°C, the demagnetization curve of this film without rare-earth overlayers exhibited a nice squareness with coercivity Hc = 3.3 kOe. On the other hand, preliminary experiments on the post-annealed Nd-Fe-B films with the Dy overlayer showed a significant increase in Hc of up to above 15 kOe.

[1] K. H. Muller, D. Eckert, A. Handstein, P. Nothnagel, and J. Schneider, *J. Magn. Magn. Mater.*, 83, (1991) 195. [2] F. Vial, F. Joly, E. Nevalainen, M. Sagawa, K. Hiraga, and K.T. Park, *J. Magn. Magn. Mater.*, 242-245, (2002) 1329. [3] H. Nakamura, K. Hirota, M. Shimao, T. Minowa, and M. Honshima, *IEEE Trans. Magn.*, 41 (2005) 3844.

RO07

Investigation on the magnetic and crystalline structures of die-upset Nd-Fe-B magnets

Yikun Fang^{1*}, Wei Li¹, Xiaolu Yin², Zhaohui Guo¹, Minggang Zhu¹ and Sy-hwang Liou²

¹ Division of Functional Materials Research, Central Iron and Steel Research Institute, Beijing 100081, China

² Department of Physics and Astronomy and Nebraska Center for Materials and Nanoscience, University of Nebraska- Lincoln, Lincoln, NE 68588, USA

Die-upsetting is used to prepare anisotropic Nd-Fe-B magnets due to high magnetic texture in which the c-axis of Nd₂Fe₁₄B grains is parallel to the loading direction. [1] Though many papers have reported on the structures of high-textured Nd-Fe-B magnets [2-5], there are still some issues needed to be clarified, such as how about the uniformity of the magnetic structures and how to improve the uniformity. In this paper, x-ray diffraction (XRD) and magnetic force microscopy (MFM) are used to reveal the crystalline and magnetic structures of die-upset Nd_{13.62}Fe_{75.38}Co_{4.85}B_{5.78}Ga_{0.7} magnets. It is found that the ratio of the XRD peak intensity I(006)/I(105) from center to edge of the sample decreases from 1.86 to 1.35. The magnetic configurations of the central of the sample are typical interaction domains. The interaction domains are formed due to the strong inter-granular exchange interaction and magnetostatic interaction between grains. However, on the edge of the sample the non-interaction domains present. The XRD and MFM results may relate to the non-uniformity of the effective strain that generated during the die-upsetting process. This indicates we need to improve the uniformity of the strain distribution for the development of high-performance magnets.

[1] R. W. Lee, *Appl. Phys. Lett.* 46, 790 (1985). [2] K. Khlopkov, O. Guffelsch, D. Hinz, K.-H. Muller, and L. Schultz, *J. Appl. Phys.* 102, 023912 (2007), [3] Y. G. Liu, L. Xu, Q.F. Wang, W. Li, and X. Y. Zhang, *Appl. Phys. Lett.* 94, 172502 (2009), [4] R. Zhao, W. C. Zhang, J. J. Li, H. J. Wang, M. G. Zhu, and W. Li, *J. Magn.* 16, 294 (2011), [5] Y. K. Fang, X. L. Yin, R. Zhao, S. Vallappilly, W. Li, M. G. Zhu, S. H. Liou, *J. Appl. Phys.* (2012) in press.

July 12 (Thu)

July 12 (Thu)

RO08

A novel approach -microwave assisted sintering - for preparation of high performance permanent magnets

Dimitrios G Niarchos^{1*}, Margarit Gjoka¹, Eamon Devlin¹, George Hadjipanayis², Amparo Borrell Tomas³, Maria Dolores Salvador Moya³ and Felipe L Penaranda-foix⁴
¹Institute of Materials Science, NCSR DEMOKRITOS, Greece
²Department of Physics and Astronomy, U of Delaware, Newark, DE, USA
³Institute of Materials, Technology Polytechnic University of Valencia, Camino de Vera, s/n 46022, Spain
⁴School of Communication, 4 School of Telecommunication, Polytechnic University of Valencia, Camino de Vera, s/n 46022, Spain

A large portion of the cost for the fabrication of permanent magnets is due to the energy needed for sintering. Any improvement for the sintering process with respect to time and energy will reduce the cost and will increase the market of permanent magnets considerably. Based on the most recent development in microwave applications reported by R. Roy (1), where it was demonstrated that sintering of metal powders- a surprising application- is possible with microwaves (in view of the known fact that bulk metals reflect microwaves), we have employed microwaves to sinter Nd-Fe-B at a fraction of time and energy, compared to the conventional resistive/radiant heating in excess of 1000 OC for many hours, and in many cases homogenizing also at high temperatures. Microwave heating is a volumetric heating involving conversion of electromagnetic energy into thermal energy, which is instantaneous, rapid and highly efficient. In this work, we will present the emerging possibilities for sintering Nd-Fe-B and Sm-Co permanent magnets as well as the opening of new possibilities for metal bonded magnets by employing microwave radiation, that is already used for ferrites by various groups. Supported by the project NANOPERMAG of the EU

RERERENCES 1. R. Roy, D. Agrawal, J. Cheng and S. Gedeveanishvili, Nature, 399, pp.668-670, 1999

RO09

Preparation of Nd-Fe-B thin films with columnar structure and their structure and magnetic properties

Shota Suzuki, Yuki Hatayama and Toshiyuki Shima
 Tohoku Gakuin University, Japan

The addition of heavy rare earth elements is essential for Nd-Fe-B sintered magnet to obtain high-performance characteristic at high temperature. However, a reduction of these additive elements is strongly required since the price of these elements has increased in recent years. It was reported that the additive elements such as Cu and Ga were diffused and concentrated into the grain boundary phase (GBP) [1, 2], and the magnetic coupling between the main phases is thought to reduce by the GBP. In order to improve the hard magnetic properties, therefore, the control of the GBP is indispensable. In this study, the Nd-Fe-B thin films with well-defined columnar structure have been prepared and structure and magnetic properties have been also investigated. The samples were prepared by using an ultra-high vacuum sputtering system. The thickness of the Nd-Fe-B layer was varied in the range of 50 ~ 300 nm. From the X-ray diffraction patterns, the peaks from Nd₂Fe₁₄B (004), (006), and (008) were observed for all the samples. This indicates that the films grew with a strong (001) texture. A good magnetic squareness and relatively high coercivity of 8.3 kOe were obtained for the Nd-Fe-B films with t = 100 and 200 nm.

[1] C. Y. You, Y. K. Takahashi, K. Hono, J. Appl. Phys., 108, (2010) 043901. [2] T. Sato, H. Kato, T. Shima, Y. K. Takahashi, K. Hono, J. Magn. Magn. Mater., 323 (2011) 163-166.

RO10

Microstructure of (Nd,Dy)-Fe-B permanent magnet by spark plasma sintering

Sun Yong Song, Jin Woo Kim and Young Do Kim*
 Division of Materials Science and Engineering, Hanyang University, Korea

Sintered (Nd,Dy)-Fe-B magnets are widely used in various parts such as motor, generators, actuators, and so on because of their outstanding magnetic properties. (Nd,Dy)-Fe-B sintered magnets are generally composed of the Nd₂Fe₁₄B hard magnet phase as a matrix and a Nd-rich phase at the triple junction [1,2]. However, typical sintered (Nd,Dy)-Fe-B magnets are limited in their applications due to low curie temperature[3]. Many researchers have shown that the magnetic properties of (Nd,Dy)-Fe-B magnets are structure sensitive, and dependent on the distribution of the rare-earth-rich phases, average grain size and size distribution. Particularly the grain size of Nd₂Fe₁₄B was essentially important for high magnet properties. In this study, we focused on controlling of the grain size to enhance magnetic properties by the spark plasma sintering process. The starting powder with the composition of Nd_{1.7}Dy_{0.3}Fe_{76.2}TM_{1.8}B₈ was prepared by strip casting and jet milling process. The raw powder was pre-sintered for preventing collapsibility of anisotropy. After the pre-sintering, (Nd,Dy)-Fe-B magnet was fabricated by spark plasma sintering process under 30 MPa with various temperatures. Consequently we had made the (Nd,Dy)-Fe-B sintered magnet with grain size of 5.9 μm. The grain size was effectively controlled by spark plasma sintering.

[1] M.Sagawa,S.Fujimura,N.Togawa,H.Yamamoto,Y.Matsuura,J.Appl.Phys.55 (1984)2083-2087. [2] H.J.Wang,Z.H.Guo,A.H.Li,X.M.Li,W.Li,J.Magn.Magn.Mater.303(2006) e392-e395. [3] W.F.Li,T. Ohkubo,K.Hono,M.Sagawa,J.Magn.Magn.Mater.321(2009) 1100-1105.

RO11

Effect of small Dy-alloy powder additions on the coercivity of NdFeB sintered magnets

MINWOO LEE
 Sunmoon University, Korea

Recently, demand of high performance NdFeB sintered magnets is rapidly increasing mostly due to expansion of wind generators and hybrid electric vehicles. For traction motors of hybrid electric vehicles, the coercivity of NdFeB sintered magnet is required to exceed 25 kOe. For such high coercivity, partial substitution of Dy for Nd in Nd₂Fe₁₄B of NdFeB sintered magnet is practically inevitable, with the sacrifice of magnetization value and the increase of material cost. Because the price of Dy is very high and keeps increasing due to its scarcity, it is important to reduce the amount of Dy in NdFeB magnets as much as possible without losing coercivity. Recent researches on NdFeB magnets, therefore, are mainly focused on Dy-saving methods. In this study, as an effort to develop a Dy-saving method, small Dy-TM alloy powder was mixed with NdFeB magnet powder and then a sintered magnet was fabricated by a conventional process. When 1.9 wt% of DyCo powder was mixed, the coercivity of the sintered magnet increased about 4 kOe, indicating 20% of Dy saving effect. More experimental results will be discussed in this presentation.

RO12

Coercivity of near single domain size Nd-Fe-B-type alloy particles

Hae-woong Kwon¹ and J H Yu²
¹Pukyong National University, Korea
²KIMS, Korea

Fine particles of Nd-Fe-B alloy in near single domain size have increasingly found new applications for high performance micro-magnet. However, because of high oxygen-affinity and high specific surface area, the ultra-fine Nd-Fe-B-type particles are readily oxidized in air, hence causing a radical coercivity loss. In the present study, an ultra-fine Nd-Fe-B-type particles in near single domain size was prepared by ball milling of HDDR-treated Nd_{12.5}Fe_{80.6}B_{6.4}Ga_{0.3}Nb_{0.2} alloy. The prepared near single domain size Nd-Fe-B-type powder (□ 0.3 μm) had high coercivity over 9 kOe. However, the coercivity was radically reduced as the temperature increased in air (< 2 kOe at 200 °C). Room temperature long-term stability of coercivity of the fine powder in air was investigated for 1 month, and the coercivity was decreased by rate of 0.5 kOe/week. Feasibility of surface nitrogenation of the fine powder for improving the long-term stability of coercivity was studied. Long-term stability of coercivity of the nitrogenated fine powder was improved markedly. The nitrogenated powder showed no coercivity reduction even after 1 month in air at room temperature. In this article, the surface passivation of near single domain size Nd-Fe-B-type particles by nitrogenation for improving long-term stability of coercivity is to be discussed.

RO13

Effect of annealing temperature on microstructure, magnetic properties and corrosion resistance of NdFeB/α-Fe nanocomposite magnets

Minxiang Pan, Pengyue Zhang*, Hongliang Ge, Hangfu Yang and Qiong Wu
 Magnetism key laboratory of Zhejiang Province, China Jiliang University, 310018 Hangzhou, China

REFeB based nanocomposite alloys have attracted much attention in both the scientific community and bonded magnet industry. However, lower coercivity and poor corrosion resistance limit their applications. Both the practical coercivity and corrosion resistance are sensitive to the character of phase constitute in the microstructure. Sintered NdFeB magnet is the poor corrosion resistance due to the presence of the highly corrosive Nd-rich phase. As no Nd-rich phase is formed in the NdFeB/α-Fe nanocomposite magnets, these alloys should be more corrosion resistant than the NdFeB sintered magnet. In this work, the effects of annealing temperature on the microstructure, magnetic properties and corrosion resistance in NdFeB/α-Fe alloys were investigated. It is shown that after heat treatment, the alloys mainly consist of two phases: a hard magnetic phase of Nd₂Fe₁₄B (space group P₄₂/mmm) and a soft magnetic phase of α-Fe (Im3m), and that no other phases are identified. Moreover, the optimum corrosion resistance of NdFeB/α-Fe magnets was observed with the annealing temperature at 610°C. Keywords: Nanocomposite, Magnetic property, corrosion resistance

*E-mail: Zhang_Pengyue@cjlu.edu.cn.

RO14

Effect of magnetic heat-treatment on magnetic properties and corrosion behavior of Nd₄Fe_{72-x}Co₈B₂₂(x=10, 20, 30) nanocomposite ribbons

Qiong Wu, P.Z. Zhang*, M.x. Pan, Z.s. Wang and H.l. Ge
 China Jiliang University, China

Nanocomposite rare-earth magnets consisting of a hard and a soft magnetic phase have attracted considerable attention because the remanence enhancement in exchange coupled nanocomposite alloys has potential importance as a way to achieve high values of the maximum energy product (BH)_{max}. It is well established that the magnetic properties of nanocrystalline two-phase magnets are strongly dependent on its microstructure. A uniform microstructure and a well-coupled grain interface should be two essential conditions for a well-performing nanocomposite. Magnetic annealing has been tried to perfect the microstructure and enhance the magnetic properties. In this paper, Nd₄Fe_{72-x}B₂₂(x=10,20,30) ribbons were heat-treated with or without an external magnetic field of 3 kOe in argon atmosphere in the temperature range of 600-750°C for 10 min. It is found that magnetic heat-treatment enhances both coercivity and remanence ratio of the Nd₄Fe_{72-x}Co₈B₂₂(x=10,20,30) ribbon, and decrease the annealed temperature obtained the optimum magnetic properties due to the uniform distribution and preferential orientation of α-Fe and Nd₂Fe₁₄B grains. The corrosion behavior of Nd₄Fe_{72-x}Co₈B₂₂(x=10, 20, 30)nanocomposite ribbons with or without an external magnetic field is discussed in detail.

Q.G. Ji, B.X. Gu, S.L. Tang et al. J.Magn.Magn.Mater. 257 (2003) 146.

RO15

Study on magnetization reversal behavior for the annealed Nd₂Fe₁₄B/α-Fe nanocomposite alloys

Pengyue Zhang¹, Minxiang Pan¹, Hongliang Ge¹, Luke Yang¹, Ming Yue² and Weiqiang Liu²
¹College of Materials Science & Engineering, China Jiliang University, Hangzhou 310018, China
²College of Materials Science & Engineering, Beijing University of Technology, Beijing 100124, Chin

Effect of thermal annealing on the magnetization reversal behavior of α-Fe/Nd₂Fe₁₄B alloys has been investigated. A drastic increase of the remanence Mr from 0.67T up to 0.87T and remanence ratio Mr/Ms from 0.66 up to 0.76, respectively, is observed in the α-Fe/Nd₂Fe₁₄B alloys annealed at 610 oC as compared with the as-quenched sample. Whereas the further annealing at 680 oC results in a strongly increase of the corecivity Hc as high as 491 kA/m but a slight decrease in Mr. The analysis result of the magnetization reversal behavior shows that the maximum value of the integrated recoil loop area about 1.58 kJ/m³, is obtained in the α-Fe/Nd₂Fe₁₄B alloys at the annealing temperature of 610 oC, significantly lower than other annealed samples. This indicates a significant advantage for the application of this material as permanent magnets in electrical machines and generators due to a low energy loss. Keywords: Nanocomposite; Magnetization reversal behavior; Recoil loop

*E-mail: Zhang_Pengyue@cjlu.edu.cn.

RP01

Construction of a versatile neutron-scattering spectrometer HERMES-E using renovated Ge monochromator crystals

Haruhiro Hiraka^{1*}, Kenji Ohoyama¹, Manabu Ohkawara¹, Naoki Murakami¹, Yasuo Yamaguchi¹, Kazuma Okubo², Michiro Furusaka², Yoshiaki Kiyonagi², Shin Ae Kim³, Chang Hee Lee³, Kohei Morishita⁴, Kazuo Nakajima⁴ and Kazuyoshi Yamada⁵
¹Institute for Materials Research, Tohoku University, Japan
²Division of Quantum Science and Engineering, Graduate School of Engineering, Hokkaido University, Japan
³HANARO, Korea Atomic Energy Research Institute, Korea
⁴Graduate School of Energy Science, Kyoto University, Japan
⁵Advanced Institute for Materials Research, WPI, Tohoku University, Japan

We propose an efficient way, which increases a number of neutron spectrometers in a research-reactor facility. The first key is to making use of a characteristic Ge-crystal monochromator, which discretely emits Bragg reflections to different scattering angles at the same time. The second is to save the instrumental space by using curved and deformed Ge-wafer crystals as a monochromator or an analyzer. Indeed, we are planning to double a neutron-powder diffractometer of Tohoku University (HERMES [1]) that is working at a research reactor JRR-3, Tokai, Japan; a versatile neutron-scattering spectrometer HERMES-E is now under construction next to HERMES.

[1] K. Ohoyama et al., Jpn. J. Appl. Phys. vol. 37 (1998) 3319.

RP02

NMR study of the phase transition behavior in Ce₃Co₅Sn₁₃

Chin Shan Lue, H. F. Liu and C. N. Kuo
 Physics, National Cheng Kung University, Taiwan

We present a study of the phase transition behavior in Ce₃Co₅Sn₁₃ using 59Co nuclear magnetic resonance (NMR) spectroscopy. The quadrupole splitting, Knight shift, and spin-lattice relaxation rate (1/T₁) below and above the phase transition temperature To have been identified. All measured NMR quantities exhibit pronounced features at around To=155 K except for the Knight shift. It thus excludes the magnetic origin for the observed transition. In addition, the x-ray diffraction results below and above To confirm the absence of a crystal structural change, suggesting that the peculiar phase transition is possibly driven by the charge-density-wave (CDW) formation. As a matter of fact, the double-peak feature in the 59Co NMR central line smears out below To which can be associated with the spatial modulation of the electric field gradient (EFG) due to incommensurate CDW superlattices. Furthermore, a distinct peak found in the spin-lattice relaxation rate near To can be accounted for by the thermally-driven normal modes of the CDW.

RP03

Analysis of 1/f noise characteristics of magneto-optical Kerr effect measured from Co/Pt and NiFe/Pt multilayers thin film

Djati Handoko, Sang-hyuk Lee and Dong-hyun Kim*
 Physics Department, Chungbuk National University, Korea

We have investigated 1/f noise characteristic of the polar and longitudinal magneto-optical Kerr effect (MOKE). The hand-made MOKE measurement system was set using diode laser as a light source. Si photodetector was used as a detector where the bias has been systematically controlled. To increase a signal-to-noise ratio, the laser light was modulated with the lock-in amplification frequency referenced from the mechanical chopper in the frequency ranges up to 4 kHz. Noise characteristics of the optical/electrical/mechanical error were systematically examined. To separate the noise contribution from the ferromagnetic layer and from the intrinsic measurement error, various configurational changes were made for the lock-in frequency as well as the bias voltage of the Si photodetector. Magnetic noise properties under a different magnetic field were systematically investigated as well. For a perpendicular anisotropy sample, Co/Pt multilayer film was investigated while for an in-plane anisotropy sample, NiFe/Pt bilayer film was investigated. The noise characteristics with respect to the multilayer thickness variations were examined as well. The 1/f noise characteristics observed for a wide range regardless of the lock-in frequency change or the film thickness change implies that there might be a universal characteristics in the MOKE signal noise, arising from the sample itself.

RP04

Photoemission electron microscopy of three-dimensional magnetization configurations in core-shell nanostructures

Judith Kimling¹, Florian Kronast², Stephan Martens¹, Tim Boehnert¹, Michael Martens¹, Julia Herrero Albillos², Logane Tati Bismaths², Ulrich Merkt¹, Komelius Nielsch¹ and Guido Meier*
¹University of Hamburg, Germany
²Helmholtz-Zentrum Berlin fuer Materialien und Energie, Germany

We present a photoemission electron microscopy method that combines magnetic imaging of the surface and of the inner magnetization in three-dimensional core-shell nanostructures [1]. The structure investigated consists of a cylindrical nickel core that is completely surrounded by a shell of iron oxide and silicon oxide layers. The method enables one to image the magnetization configuration of the nickel core even though the shell is thicker than the mean-free path of the photoelectrons. Characteristic L₁ and L₂ edges can be observed not only in the yield of the photoelectrons emitted from the surface of the nanostructure but also in its shadow. X-ray magnetic circular dichroism in the electron yield of the x rays absorbed and transmitted by the multilayered nanowire allows for the individual imaging of the magnetization configurations of the iron oxide tube and the nickel core. The method suggests novel approaches for the characterization of the magnetic and material properties of complex three-dimensional nanostructures. Financial support by the DAAD via the Project 50725506 and by DFG via the SFB 668 and the GrK 1286 as well as the Forschungs- und Wissenschaftsstiftung Hamburg via the Exzellenzcluster "Nano-Spintronik" is gratefully acknowledged.

[1] J. Kimling, F. Kronast, S. Martens, T. Boehnert, M. Martens, J. Herrero-Albillos, L. Tati-Bismaths, U. Merkt, K. Nielsch, and G. Meier, Phys. Rev. B 84, 174406 (2011).

July 12 (Thu)

July 12 (Thu)

RP05

Development of high-field ESR system using SQUID magnetometer and its application to measurement under high pressure

Takahiro Sakurai^{1*}, Kohdai Fujimoto², Susumu Okubo³, Hitoshi Ohta³ and Yoshiya Uwatoko⁴

¹ Center for Supports to Research and Education Acti, Kobe University, Japan

² Graduate School of Science, Kobe University, Japan

³ Molecular Photoscience Research Center, Kobe University, Japan

⁴ Institute of Solid State Physics, University of Tokyo, Japan

We have developed high-field ESR system using commercial SQUID magnetometer, in which ESR is observed as a change of magnetization. [J. Phys.: Conf. Ser. 334 (2011) 012058.] The advantage of this method as compared with conventional high-field ESR is that the measurement can be done very easily. Moreover, the macroscopic magnetization measurement can be made simultaneously. Although the sensitivity of this system is lower than that of ESR system using cavity, it is comparable with that of transmission type ESR system. Recently, we have succeeded in performing ESR measurement under high pressure by this ESR system. The pressure is generated by a widely used clamped type piston-cylinder pressure cell whose cylinder is made of non-magnetic CuBe alloy. Since all inner parts are made of zirconium oxide, the electromagnetic wave can be introduced into the sample space. Therefore, we can measure the magnetic moment of sample and obtain ESR signal under pressure. The pressure is available up to 1.5 GPa. This is the easiest ESR system which gives us pressure dependence ESR spectra as far as we know. The setup of this system and several results will be shown in detail.

RP06

Alternating magnetic force microscopy: direction detectable imaging of static and alternating magnetic field with high spatial resolution

Hitoshi Saito¹, Ito Yoichi¹, Kodai Hatakeyama¹, Zhenghua Li², Genta Egawa¹ and Satoru Yoshimura¹

¹ Graduate School of Engineering and Resource Science, Akita University, Japan

² Venture Business Laboratory, Akita University, Japan

We have developed a new functional MFM named as "Alternating Magnetic Force Microscopy (A-MFM)" which enables us to measure static and alternating magnetic fields with the polarity of field direction [1-5]. A-MFM utilized the frequency modulation of a cantilever oscillation generated by an off-resonance alternating magnetic force between a magnetic sample and a magnetic tip. The alternating magnetic force was extracted by a lock-in amplifier for the frequency demodulated signal of the cantilever oscillation. For the static magnetic field from a sample, a soft magnetic tip which were driven by an AC magnetic field was used to detect the static magnetic field with high sensitivity. On the other hand, for the alternating magnetic field from a sample, such as a magnetic writing head, a hard magnetic tip was used. A-MFM can measure a magnetic force without surface short-range forces and directly detect the direction of perpendicular magnetic fields. When the tip-sample distance became short, spatial resolution was improved. In the conference, we will demonstrate high performance of A-MFM and show high-resolution magnetic field images with a resolution of less than 10 nm for high-density recording media and magnetic writing heads. This study was supported by SENTAN, JST.

[1] H. Saito et al. *J. Appl. Phys.* 105 (2009) 07D524, [2] H. Saito et al. *J. Appl. Phys.* 107 (2010) 09D309, [3] W. Lu et al. *Appl. Phys. Lett.* 96 (2010) 143104, [4] W. Lu et al. *IEEE Trans. Magn.* 46 (2010) 1479, [5] H. Saito et al. *J. Appl. Phys.* 109 (2011) 07E330

RP07

30 T pulsed-high-magnetic-field and element-selective magnetization studies using soft x-ray magnetic circular dichroism

Yasuo Narumi^{1*}, Tetsuya Nakamura², Misaki Hayashi¹, Hiroyuki Nojiri¹, Kenji Kodama³, Toko Hirono², Wataru Ito⁴, Rie Umetsu¹, Ryosuke Kaimuma³, Koichi Kindo⁶ and Toyohiko Kinoshita²

¹ Institute for Materials Research, Tohoku University, Japan

² Japan Synchrotron Radiation Research Institute/SPring-8, Japan

³ Department of Mechanical Engineering, Nara National College of Technology, Japan

⁴ Department of Materials and Environmental Engineering, Sendai National College of Technology, Japan

⁵ Graduate School of Engineering, Tohoku University, Japan

⁶ Institute for Solid State Physics, The University of Tokyo, Japan

We demonstrate the applicability of 30 T pulsed-high-magnetic-field to observe magnetic circular dichroism (MCD) of antiferromagnetic compounds in soft x-ray energy regions, in which there are magnetically important transition energies, L-edge of 3d transition metal and M-edge of 4f rare earth elements. We have developed a specially designed pulse magnet equipped with an ultra-high-vacuum environment and a portable capacitor bank for synchrotron soft x-ray experiments [1]. A time-resolved total electron yield method is used to record x-ray absorptions in synchronization with pulsed-high-magnetic-fields and periodic switching of circularly polarized soft x-rays. We have measured elements-selective magnetizations of Ni, Co and Mn in the NiCoMnIn alloy which shows a large field-induced strain accompanied by a drastic change of the magnetization [2]. All 3d transition metal elements show steep non-linear increases of the MCD intensities around 15 T corresponding to the metamagnetic transition. This high-magnetic-field soft x-ray MCD result directly evidences that all magnetic elements contribute to the field-induced shape memory effect in the NiCoMnIn alloy.

[1] T. Nakamura et al., *Appl. Phys. Express* 4, 066602 (2011). [2] R. Kaimuma et al., *Nature* 439, 957 (2006).

RP08

Imaging magnetic responses of nanomagnets by X-ray PhotoEmission Electron Microscopy

Florian Kronast^{1*}, Julia Herrero-albillos², Oliver Sandig¹, Julia Kurde¹, T Noll¹, Florian Roemer³, Nina Friedenberger³ and M Farle³

¹ Helmholtz Zentrum Berlin fur Materialien und Energie, Albert-Einstein-Str. 15,

² 2489 Berlin, Germany

² Centro Universitario de la Defensa, Carretera Huesca s/n, Zaragoza, Spain

³ Universitat Duisburg-Essen, Lotharstr.1, 47048 Duisburg, Germany

The Spin-resolved PhotoEmission Electron Microscope (SPEEM) is a permanently installed setup at the X-ray synchrotron radiation source BESSY, Helmholtz-Zentrum Berlin. The capabilities of excellent spatial resolution and an energy- and polarization-tunable light source make this end-station ideal for magnetic imaging and micro-spectroscopy with quantitative analysis. The application of magnetic fields while measuring significantly expands the technique of magnetic imaging. A dedicated magnetic sample holder incorporating both DC and AC magnetic field with additional temperature control has recently been developed. The SPEEM end-station, in combination with this novel sample holder enables the in-situ control of the magnetic state and direct observation of the corresponding magnetic response. Two selected examples demonstrate these capabilities: magnetization curves of individual Fe nanocubes, and the local magnetic ac susceptibility in and microstructures as a function of temperature. In the latter example, a surprising onset of finite size effects at the micro-scale has been observed, with a significant reduction of the ordering temperature in microstructures compared to the extended film. These results were observed specifically as a result of these improvements in the PEEM technique. In combination with other possibilities, such as depth resolved imaging, new insights to magnetic nanostructures can be realized.

RP09

Development of high-sensitivity cantilever-detected ESR measurement using a fiber-optic interferometer.

Yuki Tokuda¹, Eiji Ohmichi^{2*} and Hitoshi Ohta³

¹ Graduate School of Science, Kobe University, Japan

² Graduate School of Science, Kobe University, Japan

³ Molecular Photoscience Research Center, Kobe University, Japan

Cantilever-detected high-frequency electron spin resonance (ESR) is a powerful method for terahertz ESR spectroscopy of a tiny magnetic sample at low temperature [1,2]. In this technique, a small magnetization change associated with ESR transition is detected as deflection of a sample-mounted cantilever. So far, we have succeeded in ESR detection at 370 GHz using a commercial piezoresistive microcantilever. The spin sensitivity was estimated to ~1012 spins/gauss. In order to further increase the sensitivity, we adopt a fiber-optic-based detection system using a Fabry-Perot interferometer in place of piezoresistive system. Fabry-Perot cavity is formed between an optical-fiber end and microcantilever surface, and a change in interference signal, corresponding to the cantilever deflection, is sensitivity detected. This system is suitable for low-temperature and high-magnetic field experiments because of its compact setup and less heat dissipation. We will combine our fiber-optic detection system with a 15 T superconducting magnet and BWO light sources covering a wide frequency range 200-1200 GHz. Test measurement with Co Tutton salt is now in process to estimate the system performance. In the presentation, details of our experimental setup and test results will be presented.

[1] E. Ohmichi, N. Mizuno, M. Kimata, and H. Ohta, *Rev. Sci. Instrum.* 79, 103903 (2008) [2] E. Ohmichi, and T. Osada, *Rev. Sci. Instrum* 73, 3022 (2002)

RP10

Study of the epitaxial growth and perpendicular magnetic domain structure of ordered FePt thin film on MgO substrate using HRTEM and electron holography

W. H. Lee¹, J. H. Yoo², J. M. Yang² and J. K. Park^{1*}

¹ Department of Materials Science and Engineering, Korea Advanced Institute of Science and Technology, Korea

² Measurement and Analysis Team, National Nanofab Center, Korea

The epitaxial film of ordered FePt, showing the c-axis normal to the film plane, was successfully grown on top of MgO substrate using DC-magnetron co-sputtering technique. The electron holography study showed that a columnar epitaxial film displayed only a weak stray-field signal due to the presence of columnar boundaries. The growth of a continuous (full) epitaxial film however revealed characteristic Lorentz TEM images for the perpendicular magnetic domains. The electron hologram indicated the presence of the stray-fields of induction originating from the perpendicular magnetizations. It was shown that the sense of stray fields and thus the sense of perpendicular magnetizations could be determined by analyzing the contraction and expansion behavior of hologram fringes which were parallel to the reference fringes. Furthermore, direct hologram information was detected in a thicker epitaxial film by applying high resolution electron holography. Perpendicular magnetic domain structure was directly revealed in the unwrapped phase image and was confirmed by the measurement of the line profile of phase-shift. The estimation of the local strength indicated that the perpendicular induction strength was varying from about 0.33T to about 0.61T depending on the domain size. The variation of induction strength was due to a weak ordering of the film.

RP11

Asteroid curve of GMR films on the practical substrate under the stress

Kazuhiro Okita¹, Kazushi Ishiyama² and Hideo Miura³

¹ Industrial Instrumentation Division, Tohoku Steel Co., Ltd., Japan

² Research Institute of Electrical Communication, Tohoku University, Japan

³ Department of Nanomechanics, Graduate School of Engineering, Tohoku University, Japan

Magnetic thin films usually have some of magnetostriction effect. After forming electric devices, this effect sometimes deteriorates the sensitivity of sensors such as read heads of hard disk drives, HDD, or the bit stability of memories such as magnetic random access memories, MRAM, through the inverse magnetostriction phenomenon. We need, therefore, to understand the magnetostriction effect on a film deposited on an actual wafer and the influence from the stress to it. In the previous paper, we showed the novel method of measuring the magnetostriction constant on the practical substrate [1]. In this paper, by using this method we measured the asteroid curves of the magnetic thin film of the giant magnetoresistance, GMR, on the practical wafer with varying applied stress on it. This result showed that the coercive force parallel to the easy axis, Hc, of a magnetic thin film with a negative sign of magnetostriction constant was decreasing with increasing tensile stress and the coercive force parallel to the hard axis, Ha, was also decreasing. For the film with the positive sign one, Hc and Ha were increasing with increasing tensile stress. And we showed the Hc was roughly proportional to the applied stress.

[1] K. Okita, K. Ishiyama and H. Miura, 'Magnetostriction Measurement of GMR Films on the practical substrate', *Journal of Physics, Conference Series* 200 (2010) 112008

RP12

Micromagnetic study on the perturbative effect of magnetic force microscopy probes on 90° asymmetric Neel walls in a soft magnetic material

Hironori Asada^{1*}, Hidenori Kubo¹, Hazrina Abu Seman¹, Takashi Manago² and Hiromi Kuramochi³

¹ Yamaguchi University, Japan

² Fukuoka University, Japan

³ National Institute for Materials Science, Japan

It is important to clarify the dependence of perturbative effect of MFM probes upon probe parameters and experimental conditions[1]. In this study, 3D micromagnetic simulation has been performed to evaluate the perturbative effects on magnetization states and force gradient signals of 90° asymmetric Neel walls in a 100nm-thick patterned permalloy film. The signals are computed by varying the position of the probe assuming the stripe shape. The different signal distortions are observed depending upon the combination of the out-of-plane component of the magnetization direction of wall and the magnetization direction of the probe. In the parallel case, signal asymmetry originated from the asymmetric wall structure is enhanced and the normalized contrast defined as the difference of the maximum and minimum values of the signal divided by probe saturation magnetization(Ms) is increased. In the antiparallel case, signal asymmetry is suppressed and the normalized contrast is decreased. When probe Ms is increased further (antiparallel case), the out-of-plane component direction of wall is reversed being accompanied by the jump of the Neel cap positions. The probe Ms dependences of signal distortions such as contrast variation and distance change between the signal peaks which correspond to the measured wall width are also presented.

[1] J. M. Garcia, et al., *Appl. Phys. Lett.* 79, 656 (2001).

RP13

Development of a non-conventional ESR spectrometer with a composite antenna system and an electronically controlled tuning and matching circuit

Alexey Ponomaryov¹, Kwang Yong Choi², Byoungjin Suh³ and Zeehoon Jang^{4*}

¹ Physics, Chungang University, Korea

² Physics, Chungang, Korea

³ Physics, The Catholic University of Korea, Korea

⁴ Physics, Kookmin University, Korea

We present a new development of non-conventional Electron Spin Resonance (ESR) spectrometer, in which the sweeping frequency is available in the wide range of frequency. This is a modification of the previous system without using a cavity and with two antennas one for the microwave transmission and the other for the ESR signal detection.[1] In contrast to previous work[1], utilization of microstrip antenna as a transmitter provided us the capability of wide-frequency operation between 0.8 and 10 GHz. On the other hand, the use of loop antenna as a detector with tuning and matching circuit enhanced ESR signal. In order to simplify tuning and matching circuit and make resonance condition easily reproducible, conventional capacitors were replaced with varactor diodes. This allowed us to avoid any mechanical action during tuning and matching procedure, since the capacitance of the diodes was changed by applying different DC voltages. Compared to Ref[1], such a scheme increased S/N ratio several times in a wide frequency range. For testing the developed system, a homemade magnet with water-cooling system was used. The efficiency of the ESR spectrometer was checked by measuring a signal of 1,1-diphenil-2-picrylhydrazyl (DPPH) sample at different frequencies at room temperature.

[1] Z. H. Jang, B. J. Suh, M. Corti, L. Cattaneo, D. Hajry, F. Borsa, and M. Luban, *Rev. Sci. Instrum.* 79, 46101 (2008).

RP14

A new type of spin-polarized scanning tunneling microscopy for observing an in-plane magnetization component with high resolution

Daichi Nara¹, Takuya Nakamura¹, Atsuhiko Nakamoto¹, Ryu Kageyama¹, Elaiyaraju Srinivasan², Kazuyuki Koike¹ and Hideo Matsuyama^{1*}

¹ Department of Physics, Faculty of Science, Hokkaido University, Japan

² Creative Research Institution (CRIS), Hokkaido University, Japan

To obtain a high resolution image routinely even from the rough surface of a ferromagnetic sample with a spin-polarized scanning tunneling microscope (SP-STM) operating in modulating tip magnetization mode [1], we have developed an SP-STM using a micrometer-sized magnetic tip integrated onto the magnetic recording head of a hard disk drive. The tip apex was formed into a round shape with a diameter of less than one micrometer by using a focused ion beam instrument. Driving the recording head with a signal generator to switch the magnetization of the tip apex periodically generates an unnecessary artificial current flow into a current-to-voltage (IV) converter through stray capacitance, which prevents detection of the spin-polarized tunneling current precisely. To reduce the artificial current, we added a homemade circuit that generates a countercurrent against the artificial current into the input of the IV converter. We tried to image both the topography and the spin polarization of an iron thin film deposited on a magnetic recording medium whose local roughness was on the order of several nanometers due to the crystal grains of the medium. This is the first spin image of a magnetic thin film having such a rough surface obtained with an SP-STM.

[1] U. Schlickum, W. Wulfhekel, and J. Kirschner, *Appl. Phys. Lett.* 83, 2016 (2003).

RP15

Violation of Hund's third rule in structurally disordered ferromagnets

Vassilios Kapaklis^{1*}, Panagiotis Korelis¹, Bjorgvin Hjorvarsson¹, Athanasios Vlachos², Iossif Galanakis³, Panagiotis Pouloupoulos³, K. Ozdogan⁴, Makis Angelakeris⁵, Fabrice Wilhelm⁶ and Andrei Rogalev⁶

¹ Department of Physics and Astronomy, Uppsala University, Sweden

² Department Materials Science, University of Patras, Greece

³ Department Materials Science, University of Patras, Greece

⁴ Department of Physics, Yildiz Technical University, Turkey

⁵ Department of Physics, Aristotle University of Thessaloniki, Greece

⁶ European Synchrotron Radiation Facility, France

Violation of Hund's third rule caused by structural disorder is observed for the induced magnetic moment of Zr, using x-ray magnetic circular dichroism. The induced spin and orbital magnetic moments are antiparallel in the crystalline state, but parallel in an amorphous state of the investigated Co- and Fe-based materials. First-principles calculations are used to provide physical insight into the dependency of the spin-orbit coupling on the interatomic distance and coordination number.

V. Kapaklis, P. T. Korelis, B. Hjorvarsson, A. Vlachos, I. Galanakis, P. Pouloupoulos, K. Ozdogan, M. Angelakeris, F. Wilhelm, and A. Rogalev, *Violation of Hund's third rule in structurally disordered ferromagnets*, *Phys. Rev. B* 84, 024411 (2011).

RP16

Bulk Cr tips with full spatial magnetic sensitivity for spin-polarized scanning tunneling microscopy

Anika Schlenhoff¹, Andreas Sonntag^{2*}, Stefan Krause, Gabriela Herzog and Roland Wiesendanger¹

¹ University of Hamburg, Germany

Spin-polarized scanning tunneling microscopy (SP-STM) is a powerful technique to access the magnetic properties of a surface on the atomic scale. Here, magnetic tips are usually prepared by extensive in-situ metal evaporation, demanding for a tip exchange mechanism inside the microscope. Using magnetic bulk tips is an elegant way to circumvent these efforts. For example, bulk chromium tips are reported to be suitable for SP-STM, exhibiting an in-plane magnetic sensitivity [1]. Since they are antiferromagnetic, their influence on the sample magnetization in terms of stray field interaction is negligible. We perform SP-STM experiments on the sample system of 1.8 atomic layers Fe/W(110) with the magnetization lying in the plane on the monolayer and pointing perpendicular to the plane on the double layer [2]. Our study demonstrates that Cr bulk tips can be used to image the complete magnetic structure and hence are sensitive to both the in-plane as well as the out-of-plane-component of sample magnetization [3]. Analyzing magnetic SP-STM maps enables the full spatial characterization of the tip.

[1] A. L. Bassi et al., *Appl. Phys. Lett.* 91, 173120 (2007). [2] M. Prutzer et al., *Phys. Rev. Lett.* 87, 127201 (2001). [3] A. Schlenhoff et al., *Appl. Phys. Lett.* 97, 083104 (2010).

July 12 (Thu)

July 12 (Thu)

RP17

Polarization state of scattered light in apertureless reflection-mode magneto-optical scanning near-field optical microscopy

Yongfu Cai¹, Mitsuharu Aoyagi¹, Sanyalak Niratisairak¹, Akira Emoto², Tatsutoshi Shioda³ and Takayuki Ishibashi^{1*}

¹ Department of materials science and technology, Nagaoka University of Technology, Japan

² National institute of advanced industrial science and technology (AIST), Japan

³ Department of Electrical Engineering, Nagaoka University of Technology, Japan

Magneto-optical scanning near-field optical microscopy (MO-SNOM) has attracted attention because of its high spatial resolution in magnetic imaging. We are developing a reflection-mode apertureless scanning near-field optical microscopy (a-SNOM). The sample is a patterned Chromium film with a thickness of 20nm deposited on a glass substrate. The a-SNOM images are measured with Si tip that has an extremity's radius of 7nm, and with an illumination of 408 nm with an incident angle of 45 degree. Scattered light caused by an interaction between the near-field wave and the sample was measured as a signal for a-SNOM image. Finite-difference time-domain (FDTD) method was used to calculate the polarization state of the scattered light. The a-SNOM images of Cr patterns were successfully obtained with a spatial resolution of 30-40nm. In addition, we found that the extinction ratio of the scattered light back to the same direction with the incidence was better than 100, which is an enough polarization property for obtaining MO images. FDTD simulation reproduced that the scattered light preserved its polarization state. These results showed that the a-SNOM is a promising technique to obtain high-resolution magnetic images with a resolution of several tens nm.

[1] E. Betzig, et. al., *Appl. Phys. Lett.* 61,142(1992). [2] Y. Mitsuoka, et. al., *J. Appl. Phys.* 83, 3998(1998). [3] T. Yoshida, et. al., *J. Magn. Soc. Jpn.* 23, 1960(1999).

RP18

Application of image processing to determine size distribution of magnetic nanoparticles

Udomchok Phromsuwan^{1*}, Yaowarat Sirisathitkul², Chitnarong Sirisathitkul¹ and Bunyarit Uyyanonvara³

¹ School of Science, Walailak University, Thailand

² School of Informatics, Walailak University, Thailand

³ School of Information, Computer and Communication Technology (ICT), Sirindhorn International Institute of Technology (SIIT), Thammasat University, Thailand

Digital image processing has increasingly been implemented in analyzing micro- and nanostructured materials and would be an ideal tool to characterize the morphology and position of self-assembled magnetic nanoparticles for high density recording. In this work, magnetic nanoparticles were synthesized by the modified polyol process using Fe(acac)₃ and P(acac)₃ as starting materials. Transmission electron microscopy (TEM) images of an as-synthesized product were taken with a resolution of 800 x 800 pixels, 72 dot per inch and then inspected using image processing algorithms on MatLab. The grayscale image was converted to a binary image by using Otsu's thresholding. An individual particle was then detected by using the closing algorithm with disk structuring elements and the canny edge detection. The areas of detected particles were filled and small objects were removed. A centroid, diameter and area of each particle were finally evaluated. The average diameter is 4.62 nm with a standard deviation of 0.52 nm. The degree of polydispersity of magnetic nanoparticles can then be compared using size distribution from the image processing.

RP19

Microfabrication of a MEMS cantilever for mechanically detected high-frequency ESR measurement

Eiji Ohmichi^{1*}, Yoshimasa Yasufuku² and Hitoshi Ohta³

¹ Graduate School of Science, Kobe University, Japan

² Graduate School of Science, Kobe University, Japan

³ Molecular Photoscience Research Center, Kobe University, Japan

Mechanically detected high-frequency electron spin resonance (ESR) is a promising tool for high-resolution terahertz (THz) ESR spectroscopy of tiny magnetic samples. So far we succeeded in multi-frequency ESR detection for 80-370 GHz and achieved a spin sensitivity on the order of 10⁷ spins/Gauss[1,2]. In this study, a prototype microcantilever is fabricated in order to further improve the sensitivity and flexibility of our ESR measurement system. Microcantilevers are fabricated from silicon-on-insulator (SOI) wafers using standard MEMS techniques such as lithography, wet etching, and RIE. By using commercial SOI wafers, fabrication cost and the number of process can be substantially reduced. Two types of cantilevers for capacitive and optical detection are fabricated in this study. The former has lateral dimensions of 4 mm x 8 mm, and is anodically bonded to a glass substrate to form capacitive electrodes. The latter has dimensions of 50 μm x 200 μm, and is equipped with a gold mirror for Fabry-Perot detection. Application to high-frequency ESR measurement is now in progress and details will be reported in the presentation.

[1]E. Ohmichi, N. Mizuno, M. Kimata, and H. Ohta, *Rev. Sci. Instrum.* 79 (2008) 103903. [2]E. Ohmichi, N. Mizuno, S. Hirano, and H. Ohta, *J. Low Temp. Phys.* 159 (2010) 276.

RP20

2D reflection-type electron spin filter increasing the detection efficiency in spinresolved spectroscopy by 4 orders of magnetism

D Kutnyakhov¹, M Kolbe¹, P Lushchik¹, M Jourdan¹, K Medjanik¹, S A Nepijko¹, H J Elmers¹, C Tusche², J Kirschner², F Giebels³, H Gollisch³, R Feder³ and G Schoenhense^{3*}

¹ Institute of Physics, University of Mainz, Germany

² Max Planck Institute of Microstructure Physics, Germany

³ Theoretische Festkoerperphysik, Universitaet Duisburg-Essen, Germany

Spin-resolved electron spectroscopy is characterized by a low figure of merit FoM= S²/I₀ typically 10⁴; S spin sensitivity, I₀ reflectivity. Electron diffraction from W(001) in the (00) LEED spot facilitates parallel detection of 3800 data points in our imaging spin filter behind a PEEM [1], and 960 behind a hemispherical energy analyzer [2]. We achieved a “2D FoM” of 1.7 being four orders of magnitude higher than the previous value. We further studied the dependence of the spin sensitivity and reflectivity as a function of scattering energy and angle of incidence. The experimental setup includes a spin-polarized GaAs electron source, hemispherical analyzer and a Delaylinedetector. Intensities, spin-orbit-coupling induced asymmetries and FoM were calculated via a relativistic layer KKR SPLEED code [3]. The superior performance of multichannel spin detection facilitates experiments on highly reactive surfaces like in-situ prepared Heusler films [4] or radiation-sensitive organic layers [5] and paves the way to single-shot experiments at ultra bright fs-sources like FELs. Funded by DFG (Scho341/9), Stiftung Innovation (project 886) and centre of complex materials COMATT.

[1] C. Tusche et al., *APL* 99 (2011) 032505; [2] M. Kolbe et al., *PRL* 107 (2011) 207601; [3] R. Feder, *Polarized Electrons in Surface Physics* (World Scientific, Singapore, 1985); [4] M. Hahn et al., *APL* 98 (2011) 232503; [5] K. Medjanik et al., *JACS* 134 (2012) 4694

RP21

Element selective magnetization measurements under high magnetic field

Andrei Rogalev* and Fabrice Wilhelm

European Synchrotron Radiation Facility, France

X-ray Magnetic Circular Dichroism (XMCD) spectroscopy is a well-established experimental tool to study the microscopic origin of magnetism allowing one to determine separately spin and orbital magnetic moments of each element in both amplitude and direction. So far, XMCD has been extensively used to investigate mainly ferro- or ferrimagnetic materials, and only very few studies have been performed on paramagnetic compounds. In this presentation we describe first a new experimental set-up dedicated to high field XMCD measurements that has been recently installed at the ESRF beamline ID12. Static magnetic field of up to 17 Tesla is generated by a superconducting solenoid. The sample is mounted on a cold finger of a He continuous flow cryostat allowing to set the temperature in the range from 2.2 K to 300 K with a stability of about 100 mK. Performances of this set-up are illustrated with results of element selective magnetization measurements in various systems: (i) Intrinsic magnetic moment in gold nanoparticles grown onto naturally thiol-containing proteinaceous archaeal surface layer has been evidenced by field dependent XMCD at the Au L_{2,3}-edges[1]; (ii) Extrinsic origin of room temperature ferromagnetism in diluted magnetic semiconductors has been proven with field and temperature dependent XMCD measurements[2].

[1] S. Selenska-Pobell et al., *Nanomater. nanotechnol.*, 1 (2011), 8 [2] A. Ney et al., *New J. Phys.*, 13 (2011) 103001

RP22

POLI: The new single crystal polarized neutron diffractometer for investigation complex magnetic structures at FRM-II

Vladimir Hutanu*, Martin Meven, Gernot Heger and Georg Roth

Institut für Kristallographie, RWTH Aachen University, Germany

POLI is a new single crystal polarized neutron diffractometer [1] at the hot source of the 'Forschungsneutronenquelle Heinz Maier-Leibnitz' (FRM-II) in Garching, Germany. It is designed to perform spherical neutron polarimetry (SNP) in zero field as well as classical polarized neutron diffraction (PND) measurements (flipping ratio) under applied magnetic fields. Among the intended applications of this instrument are: complex magnetic structures and magneto-electric coupling in multiferroics, magnetic structure and spatially resolved spin densities in molecular magnets, magnetically ordered superconductors, strongly correlated transition metal oxides and spin chain compounds. The instrument is unique in the sense that it combines a variable wavelength focussing monochromator with the use of 3He spin-filter cells (SFC) to create polarized, short wavelength neutrons. A new zero-field polarimeter Cryopad [2, 3] has been built in cooperation between RWTH and ILL. On the detector side, the polarisation-analysis and detection unit DECPOL (again with 3He-spin filter cells) is used. This setup called 'POLI-HEIDI' is operational and open for users at FRM-II over JCNS proposal system. Its properties will be demonstrated in this talk.

[1] V. Hutanu, M. Meven, E. Lelievre-Berna, G. Heger, *Physica B* 404, 2633 (2009). [2] F. Tasset, *Physica B* 156-157, 627 (1989). [3] E. Lelievre-Berna, "Novel polarized neutron tools", I. Anderson & B. Guerdar, Editors, *Proceedings of SPIE* 4785, 112-125 (2002).

RP23

Observation of the magnetic domain using scanning electron microscopy with polarization analysis

Sang Sun Lee, Moon Seob Bae, Wondong Kim and Chanyong Hwang*

Korea Research Institute of Standards and Science, Korea

We have developed a scanning electron microscope with polarization analysis(SEMPA or spin-SEM) for the nano-scale observation of magnetic domain structure. A typical micro Mott type spin detector with 25 kV operating voltage, shows the effective Sherman function in the range between -0.3~-0.35, which is relatively low valued. In order to get higher Sherman function, we optimized all geometrical factors and the accelerating voltage. First, we tried Monte Carlo simulation by increasing operating voltage from 25 kV to 50 kV. At 40 kV of acceleration voltage with optimized 120 degrees of scattering angle, a better effective Sherman function was obtained compared with the value operated at 25 kV(-0.5 : -0.3). Base on this simulation, we have developed the high-efficiency Mott spin detector with 40 kV operating voltage. Also a secondary electron deflector, and transfer lens system has been optimized. In order to test performance of the new spin detector, the thick Fe film sample was prepared on Si substrate using an evaporation method. We will show several different images of Fe films depending on the oxidation condition.

RQ01

Precision broadband ac measurement system for magnetotransport, magnetopolarization and magnetoelectric properties

Jun Lu*, Baogen Shen and Xiaoping Shao

State Key Laboratory of Magnetism, Institute of Physics, Chinese Academy of Sciences, China

For complex or strongly correlated magnetic materials, broadband ac measurements provide much richer dynamic information than static or quasistatic measurements, which would help one to understand more clearly how magnetic materials of interest respond to various external excitations. After many-year researches, we have developed a suite of precision broadband ac magnetic measurement system based on novel broadband digital lock-in amplifier techniques, which can work from sub 1 Hz to above 1 GHz. In addition to multi-channel lock-in amplifier techniques, to realize broadband ac transporting and polarizability measurement from sub 1 Hz to above 100 MHz, transmission-line bridge compensation techniques have been used so as to measure complex ac magnetoresistance and Hall coefficient simultaneously in a precision way. Broadband ac magnetoelectric measurement system has also been set up for evaluating complex magnetoelectric coupling coefficient, which including not only magnitude but also phase lag. For various magnetotransport and magnetoelectric measurements, we have developed measuring software which supports fully automatic tests.

[1] J. Lu et al., *Meas. Sci. Technol.*, 19, 045702-6(2008) [2] J. Lu et al., *IEEE Trans. Magn.*, 44(9), 2127-9(2008) [3] J. Lu et al., *A kind of precision broadband anti-noise lock-in frequencymeter, Chinese Patent, 201110380805.X*

RQ02

Detection of magnetic beads using an extraordinary magnetoresistance sensor fabricated with unpatterned semiconductor substrate

Jian Sun* and Jurgen Kosel

King Abdullah University of Science and Technology, Saudi Arabia

A strong geometry dependent magnetoresistance effect, the so-called extraordinary magnetoresistance (EMR), has been observed in semiconductor/metal hybrid structures. It is based on the redistribution of the current from the metal shunt into the semiconductor causes by the Lorentz force. A typical EMR device consists of a patterned semiconductor mesa and metal shunt. When the dimensions of the device are reduced, for example, to increase the sensitivity, the alignment of the metal contact with the semiconductor bar becomes more difficult. Furthermore, the patterning process inescapably causes some damage to the semiconductor thereby reducing the performance. In this work, we report a new EMR device fabrication process, which does not require patterning of the semiconductor substrate reducing the complexity of the fabrication and omitting any kind of damage of the semiconductor. The sensitivity of this device is 0.58 μT/Hz, which is twice as high as the one of the patterned sensor. The device is employed to detect superparamagnetic beads of 2.8 μm in diameter, which is the first time this is demonstrated with an EMR sensor. Applying the beads to the sensor surface results in a voltage signal of 100 μV.

RQ03

Magnetization of single ferromagnetic-grain obtained from observation of field-induced-translation in a chamber-type μg system.

Chiaki Uyeda¹, Kenta Kuwada² and Keiji Hisayoshi²

¹ Graduate School of Science, Osaka university, Japan

² Graduate school of Science, Osaka university, Japan

A new principle to measure saturated magnetization Ms of a single ferromagnetic-grain is proposed, which is based on free translation of the grain caused by field-gradient force. The motions were observed in a diffused (~10Pa) μG condition (0.01G). It is confirmed for the first time that a classical conservation rule between field-induced potential and kinetic energy is conserved for a translating magnetic-grain. Accordingly, Ms is obtained from the relationship between sample velocity and field intensity observed at different sample positions. The Ms value is obtained even for a nano-sized sample, provided that translation is observed by an ultra-violet fluorescence microscope [1]. This is because the method does not require mass measurement; it is also free of the interfering signal emitted from a sample holder [1]. The above two factors has been the major problem in detecting magnetization of single grain in conventional methods. A chamber-type drop shaft to produce μG, which can be introduced in an ordinary laboratory, was newly developed to realize routine Ms measurement. Here, size of drop capsule was reduced to 30cm in diameter by introducing a magnetic circuit composed of an NdFeB permanent magnet.

[1] C.Uyeda et al. *Jpn. Phys. Soc. Jpn.* 79, 064709 (2010).

RQ04

application of magnetoimpedance effect for protein biomarker detection

D.g. Park and Hoon Song

korea atomic energy research institute, Korea

Ultra-low concentration detecting of biomolecules, has gain increasing interest since various protein biomarkers for cancer or chronic diseases are present at very low levels at the early stages of the disease development [1].In this work, we present the results of the development of a sensor prototype working in a principle of label free for monitoring the effects on the immobilization of the biomolecular using giant magnetoimpedance. Amorphous ribbons were tested in different biomoleculars. The MI response of the sensitive elements made from ribbons was measured with a various biomolecular in order to demonstrate the capacity of monitoring the immobilization of biomolecule. To demonstrate the sensitivity and specificity of this GMI sensor platform for biomolecule detection and quantification, we have used this platform to successfully detect and quantify the biomolecules. To apply to the real biomarker and verify the sensitivity of GMI-based magnetic sensor, we used the biomarker scheme using the applied the real protein on the magnetic sensor surface. The capture antibodies (P21 mono antibody) are first immobilized on the positive magnetic sensor surfaces. The advantage of this approach consists in the possibility to design a biosensor with enhanced sensitivity and the application for detection of small amounts of biomolecules.

[1] M. Gomez and G. Silvestri, "Lung cancer screening," *Am. J. Med. Sci.*, vol. 335, pp. 46-50, 2008

RQ05

Ac Calorimetry under Pulsed High Magnetic Field

Yuji Inagaki¹, Tatsuya Kawar¹, Akira Matsuo² and Koichi Kindo²

¹ Applied quantum physics, kyushu university, Japan

² Institute for solid state physics, the university of tokyo, Japan

Ac calorimetry measurement adapted for use of the pulsed high magnetic field will be presented. This technique is quite useful to investigate the thermal properties under high magnetic field beyond the steady magnetic field range. In addition, it is also possible to capture a transient phenomena under fast sweep magnetic field. Resultant examples will be presented in detail.

July 12 (Thu)

July 12 (Thu)

RQ06

Specific heat and thermal expansion of Sr_{1-x}Ca_xRuO₃

Rasna Thakur^{1*}, Archana Srivastava², Rajesh K. Thakur¹ and N.k. Gaur¹
¹Department of Physics, Barkatullah University, Bhopal, India
²Department of Physics, Sri Satya Sai College for Women, Bhopal, India

We have investigated the thermodynamic properties of perovskite ruthenate Sr_{1-x}Ca_xRuO₃ (0 ≤ x ≤ 1) probably for the first time by means of Rigid Ion Model (RIM). The lattice contributions to the specific heat and thermal expansion of pure and Ca doped SrRuO₃ as a function of temperature (0 K ≤ T ≤ 1000 K) are reported. The systematic trend of variation of specific heat and the closer agreement with the experimental data reveal the suitability and appropriateness of RIM, for Sr_{1-x}Ca_xRuO₃ (0 ≤ x ≤ 1) perovskite ruthnates. The calculated lattice specific heat gives Debye temperature (478.4 K) which is consistent with experimental value (480 K). Our calculated value of 494.4 K for CaRuO₃ is in very good agreement with the reported value of 495 K. The Atoms in Molecules (AIM) theory is used to determine the bulk modulus of these compounds. Further, the value of Gruneisen parameter is calculated which is within the range 2-3 as reported earlier for perovskite family. In addition, the results on cohesive energy (φ), molecular force constant (f), restrahlen frequency (ν), Debye temperature(θ_D) and gruneisen parameter (γ) are also presented. Our results on cohesive and thermal properties revealed by using RIM reproduces well with the available experimental data.

RQ07

Voltage-current characteristics of superconductor-normal metal contact junctions measured by a picovoltmeter

Wan-seop Kim*, Mun-seog Kim, Po Gyu Park, Kyu-tae Kim and Danbee Kim
 KRISS, Korea

A picovoltmeter based on a DC SQUID has been developed for improvement of Josephson voltage measurement uncertainty to better than ΔV/V = 50 x 10⁻¹². An output to input ratio of 108 is achieved using a proper current feed-back system. The performance of the picovoltmeter demonstrated by the Voltage(V)-Current(I) measurements on a Cu-wire with a diameter of 0.25 mm and a length of 10 mm shows that a voltage resolution is of about 10-12 V (pV) and a corresponding resistance resolution is order of 10 μΩ. In addition, the current sensitivity of the picovoltmeter was found to be 2x10⁻⁷ A/Φ₀, where Φ₀ is the magnetic flux quantum. Here we present voltage steps induced by magnetic flux trap in the V-I curve measurements for a bulk cylinder-type Pb wire with a diameter of 0.25 mm. The step height was observed to change abruptly in an irregular manner, but in multiple of 6 pV. Moreover, dissipation behavior of the remnant voltage observed in the V-I curves for thick films of superconductor/normal metal/superconductor contact junctions will be discussed.

RQ08

Development of high resolution cryogenic particle detectors using a magnetic calorimeter

W.S. Yoon^{1,2}, Y.S. Jang¹, S.J. Lee¹, G.B. Kim¹, H.J. Lee^{1,2}, K.B. Lee¹, M.K. Lee¹, Y.N. Yuryev¹, Y.H. Kim^{1,2}
¹Korea Research Institute of Standards and Science
²University of Science and Technology

Micro-calorimeters operating at low temperatures have become important tools in many aspects of science because of their high energy resolution much beyond the limit of semiconductor based detectors. These sensitive detectors measure the temperature dependent properties of sensor materials such as their resistance or magnetization. In metallic magnetic calorimeters, a small concentration of erbium doped in gold host provides a paramagnetic system, in which the magnetization is inversely proportional to the temperature. A metallic film of the sensor material is fabricated on a superconducting meander-type pickup coil connected to an input coil of a SQUID current sensor. An absorber, another gold foil, is employed to detect incident alpha particles. The gold foil absorber and the magnetic temperature sensor are thermally connected by gold bonding wires. The kinetic energy of each particle is converted into a temperature increase of the absorber/sensor assembly. In the present report, the recent progress on high resolution alpha spectrometers using these detectors is discussed together with an application to radionuclide analysis.

RQ09

High pressure inductive measurements using microcoils in anvil cells

Swee K. Goh^{1*}, Thomas Meissner², Patricia Alireza¹ and Juergen Haase²
¹University of Cambridge, United Kingdom
²University of Leipzig, Germany

Diamond or Moissanite anvil cells are routinely employed to reach pressures higher than 35 kbar. However, due to the presence of the gasket and the limited sample space, inductive type measurements have been challenging. To overcome these challenges, we place a microcoil inside the gasket hole of the anvil cell. With an increase in the filling factor and the close proximity between the sample and the coil, this arrangement has so far enabled us to perform AC susceptibility [1], the de Haas-van Alphen effect [2], tunnel-diode oscillator [3] and Nuclear Magnetic Resonance [4,5] experiments. Technical aspects associated with the preparation of these pressure cells will be presented, with particular emphasis placed on recent NMR experiments performed using this technique.

[1] P. L. Alireza et al., Rev. Sci. Instrum. 74, 4728 (2003) [2] S. K. Goh et al., Curr. Appl. Phys. 8, 304 (2008) [3] S. K. Goh et al., arXiv:1107.0689 (2011) [4] J. Haase, S. K. Goh et al., Rev. Sci. Instrum. 80, 073905 (2009) [5] T. Meissner; S. K. Goh et al., Phys. Rev. B 83, 220517(R) (2011)

RQ10

Microwave synthesis and characterization of the series of Co_{1-x}FexSb₁₂ high temperature thermoelectric materials

Alexandra Ioannidou^{1*}, Margarit Gjoka², Dimitris G Niarchos², A Borrell³, M D Salvador⁴ and F L Penaranda-foix⁵

¹Institute of Materials Science, NCSR Demokritos, Athens, Greece
²Institute of Materials Science, NCSR DEMOKRITOS, Greece
³Instituto de Tecnologia de Materiales (ITM), Universidad Politecnica de Valencia, Camino de Vera, Spain
⁴Instituto de Tecnologia de Materiales (ITM), Universidad Politecnica de Valencia, Camino de Vera, s/n, 46022 Valencia, Spain
⁵Instituto de Aplicaciones de las Tecnologías de la Información y de las Comunicaciones Avanzadas, Universidad Politecnica de Valencia, Camino de Vera, s/n, 46022 Valencia, Spain

An alternative route has been followed for a rapid synthesis of skutterudites as it was suggested by Biswas et al. (1) using microwave assisted synthesis. Microwave heating and sintering (involve microwaves only at 2.45 GHz and 915 MHz frequencies) is fundamentally different from the conventional sintering, which involves radiant/resistance heating followed by transfer of thermal energy via conduction to the inside of the body being processed. Microwave heating is a volumetric heating involving conversion of electromagnetic energy into thermal energy, which is instantaneous, rapid and highly efficient. The use of microwave energy for materials processing has major potential and real advantages over conventional heating. These include: - Time and energy savings. - Rapid heating rates (volumetric heating vs. conduction). - Considerably reduced processing time and temperature. - Fine microstructures - Lower environmental impact. Using the microwave-assisted synthesis, here we report our effort to synthesize the series of Co_{4-x}FexSb₁₂ using this novel approach, which gave high quality materials with little or no impurity in a fraction of time compared to the conventional synthesis. We will present data for structural, microstructural and thermoelectric properties and compare with materials synthesized with conventional approach. Supported by the project NEXTEC of the EU

1. K. Biswas, et al. MRS Bulletin 46, pp. 2288-2290 (2011), 2288-229 2. R. Roy, et al. Nature 399, pp. 668-670 (1999).

RQ11

Development of SI-STM optimized for 3D(x,T,B) phase-diagram-wide FTSTS mapping on high Tc superconductors

Seokhwan Choi¹, Jimin Kim¹, Chanhee Kim¹, Jaewook Kim¹, Hwansoo Suh² and Jhinhwan Lee^{1*}
¹Physics, KAIST, Korea
²FRL, SAIT, Korea

We are constructing a SI-STM optimized for 3D(x,T,B) phase-diagram-wide QPI mapping on high Tc superconductors, Kondo systems and SCESs. It is based on Pan-style STM design for high magnetic field compatibility and yet has enough symmetry required for covering a wide temperature range with minimal drift. Also it has multiple sample storage at 4K for unlimited reuse of samples with various dopings. Its primary goal is to extend the SI-STM measurement coverage over the most significant regime of the 3D phase diagram for unique determination of the mechanisms of high Tc superconductivity using the fully-phased Green-function-based cross-sectional FTSTS analysis method.

RQ12

Homemade microcalorimetry equipment, with magnetic fields up to 9 Teslas, for magnetocaloric measurements

J. V. Leita^{o*}, P. Van Dommelen, F. Naastepad and E. Bruck
 Delft University of Technology, Netherlands

The magnetocaloric effect (MCE) has gains relevance as a cheap and environmentally friendly alternative to the current household vapor cycle refrigerators. The most common method for calculating the MCE of a material, due to its technical and mathematical practicality, is the application of Maxwell's thermodynamic equation to a set of magnetic isotherms so as to calculate the magnetic entropy change [1]. The other current alternative for this calculation is through the adiabatic temperature change. Unfortunately, even though a working magnetocaloric refrigerator should rely much more on an adiabatic (Brayton) cycle [2], such calculation is usually hindered by the lack of a proper measurement system that would allow for reliable specific heat measurements with an applied magnetic field. Our group has recently constructed such a device, using a 9 Tesla cryostat, allowing for liquid helium temperatures, and microcalorimetry chips from the company Xensor Integration. This equipment, besides the usefulness in magnetocalorics research, is an invaluable tool in the study and investigation of any form of phase transitions where the application of a magnetic field may play a significant role. We now report the overall characteristics of this equipment and further illustrate it with a few early measurements performed on it.

[1]Debye P; 1926, Some observations on magnetisation at a low temperature, Ann. Phys. 81: 1154-1160; [2] Tishin A.M, Spichkin YI, 2003, The Magnetocaloric Effect and its Applications, MPG Books Ltd., Bodmin, 2003;

RQ13

Nucleation and development of clustered state in hole doped manganites and cobalites

A. V. Lazuta¹, V. A. Ryzhov¹, V. P. Khavronin¹, P. L. Molkanov¹ and Ya. M. Mukovskii²
¹Petersburg Nuclear Physics Institute, Gatchina, St.Petersburg 188300, Russia
²Moscow Steel and Alloys Institute, Leningkiy prosp. 4, Moscow 117936, Russia

The origination of the ferromagnetic (F) metallic (M) clusters in a paramagnetic (P) state of the hole doped manganites was well established [1-3]. Study of this state in the hole doped cobalites is the topic of the current research activity [4,5]. It is found by measurements of the nonlinear magnetic responses (the second and third orders) that an universality exists in the nucleation and development of the clustered states (CS) in these systems which proceed into three stages. On cooling, during the first stage, the F clusters nucleate at the preferential sites that are likely produced by variation in oxygen and doping stoichiometry. Second stage is characterized by a sharp increasing concentration of the isolated F clusters. A coalescence of the clusters into large-scale complexes containing some amount of the F domains is associated with the third stage that can end with formation of a percolative FM network. This scenario is demonstrated by using the data obtained on the single-crystalline manganites Pr_{1-x}CaxMnO₃ (x = 0.2, 0.25; the F insulators) and single-crystalline cobaltite La_{0.7}Sr_{0.3}CoO₃ (a F metal). A new effect is found in the latter, in which the CS in the P metallic regime is observed for the first time.

[1] M. B. Salamon, M. Jaime, Rev. Mod. Phys.73 (2001) 583, [2] V.A. Ryzhov, A.V. Lazuta, I.D. Luzyanin et al., Zh. Eksp. Teor. Fiz. 121 (2002) 678. [3] A.V. Lazuta, V.A. Ryzhov, V. P. Khavronin et al., Funct. Mater. 17 (2010) 11 and Ref. therein. [4] C. He, S. El-Khatib, S. Eisenberg et. al., Appl. Phys. Lett. 95 (2009) 222511. [5] A. V. Lazuta, V.A. Ryzhov, A. I. Kurbakov et al., Solid State Phenom. 168-169 (2011) 457.

RQ14

Measurements and analysis of core loss including higher harmonic induction waveforms using superposition principle and steinmetz's law

Duhyung Yeon and Derac Son*
 Physics, Hannam university, Korea

Non-oriented electrical steels have been used in rotating electric machines. Magnetic induction waveforms of stator cores of induction motors have ac major hysteresis loop of driving frequency and ac minor loops due to the slip. Prediction of core loss including higher harmonic is one of important task for high efficiency induction motor design[1]. In this work, we have constructed core loss measuring system which could control waveform of magnetic induction the same as generated from waveform synthesizer using analog negative feed-back system and test specimen was used air flux compensated ring core. Using the developed measuring system, we can measured core losses of ac minor loops which depend on the peak amplitude and position in major hysteresis loop and theses core losses obeyed Steinmetz's law. Core loss including minor loops could be calculated superposition principle of the core loss from major hysteresis loop and the core losses from minor loops which come from higher harmonic induction.

[1] D. Son "AC hysteresis loop measurement of stator-tooth in induction motor", IEEE Trans. on Magn., Vol.35, No.5, p.3931-3933(1999)

RQ15

Highly sensitive cantilever magnetometry in static and dynamic modes for micro-scale samples

Heonhwa Choi¹, Yun Won Kim² and Jae-hyuk Choi^{1*}
¹Nano Science, University of Science and Technology ; Divison of Physical metrology, KRISS, Deajeon 305-340, Korea
²Display and Semiconductor Physics, Korea University, Chungnam 339-800 ; Divison of Physical metrology, KRISS, Deajeon 305-340, Korea

Recently, dynamic modecantilever magnetometriesusing an ultra-soft cantilever with attonewton dynamic force sensitivity arebecoming a very powerfultool for measuring the magnetic properties of micrometer-sized samples. In spite of its high sensitivity, the dynamic mode measuring a cantilever's resonance frequency shifthas a limitation that it requires anisotropic magnetic samples,andhigh or moderate external magnetic fields. Therefore, we suggest a new type of a cantilever magnetometry with no limitation on magnetic anisotropy and external magnetic field, a cantilever forcemagnetometrywhich measuresstatic displacement of a cantilever in a well-defined magnetic field gradient. Its principle and experimental details including the magnetometry'sstructure are presented, which are accompanied by the results of measurement at T = 3.5 K on a small magnetic moment of 1.84 x 10⁻¹⁴ A m² using both static and dynamic modes revealing the high sensitivity of the static mode.

RQ16

Pulsed high magnetic fields for synchrotron and neutron applications

Fabienne Duc*, Xavier Fabreges, Paul Frings, Marc Nardone, Julien Billete, Jerome Beard, Abdelaziz Zitouni and Geert Rikken
 Laboratoire National des Champs Magnetiques Intenses - CNRS Grenoble-Toulouse, France

As is well known, a magnetic field, together with temperature and pressure, is a very important and efficient thermodynamic parameter for the investigation of condensed matter. It can be used as an external variable to tune the ground and excited states properties of a given magnetic system. The last ten years have seen a growing interest for the combined use of pulsed high magnetic fields (up to 40 T) at synchrotron and neutron sources. Because of the larger flux of synchrotron x-ray sources compared to neutron facilities, the development efforts have been first focused on synchrotron methods. Neutron diffraction has complementary features to x-ray diffraction, and unique capabilities for studying microscopically the magnetic properties of materials. Here, we will present the various devices developed by the LNCMI, Toulouse to combine pulsed high magnetic fields with synchrotron and neutron techniques. These developments are performed in close collaboration with the ESRF, Grenoble for synchrotron applications and with the ILL and CEA, Grenoble for neutron diffraction. We will discuss the main limitations for the use of pulsed magnetic fields related to their low duty cycle. Those instrumental developments will be illustrated by some recent results.

RQ17

Characteristics of an SQUID system with a superconductive shield for biomagnetic measurements

Kwon Kyu Yu, Kiwoong Kim, Hyuckchan Kwon, Jin Mok Kim and Yong Ho Lee
 Brain and Cognition Measurement Lab, KRISS(Korea Research Institute of Standards and Science), Korea

We have fabricated a magnetoencephalography (MEG) system having a superconductive shield helmet. By using the perfect diamagnetic effect of the superconductor (Pb), superconducting quantum interference device (SQUID) magnetometers inside the Pb enclosure can be shielded from external magnetic disturbances, and this effect can be used to enhance the signal quality of biomagnetic signals. Along the surface of the helmet, the shielding factor (SF) was from 28 to 57 dB, depending on the position of the SQUID from the edge. SF reduced rapidly as the distance from Pb surface increased. The shielded helmet-shape MEG system has a noise level of about 7 fT/Hz^{1/2} at 1 Hz, and 3 fT/Hz^{1/2} at 100 Hz. Auditory evoked brain signals were measured and were compared in the case of superconductive shield and without shield, and confirmed big improvement of the signal quality by using superconductive shield.

[1] Y.H. Lee, "A low noise multichannel magnetocardiogram system for the diagnosis of heart electric activity", Korean society of medical and biological Eng., Vol. 27, pp. 154-163, 2006. [2] R. H. Kraus, " First Results for a Superconducting Imaging-Surface Sensor Array for Magnetocardiography", Recent Advances in Biomagnetism Proceeding, pp. 43-46, 1999. [3] D. B. Hulsteyn, " Superconducting Imaging Surface Magnetometry", Rev. Sci. Instrum., Vol. 66, pp. 3777-3784. [4] H. Ohno, "A 64-channel whole head SQUID system in a superconducting magnetic shield", Supercon. Sci. Technol., Vol.12, pp. 762-765, 1999.

July 12 (Thu)

July 12 (Thu)

RQ18

Radio-frequency atomic magnetometer for sensitive susceptibility detection

Hyun Joon Lee¹, Han Seb Moon¹, Yong-ho Lee², Seong-joo Lee², Kwon-kyo Yu² and Kiwoong Kim^{2*}

¹ Pusan National University, Korea

² Korea Research Institute of Standards and Science (KRISS), Korea

Alkali-metal magnetometers use the coherence precession of polarized atomic spins to detect and measure magnetic fields. Previously, the interaction between light and atoms allows magnetometers to detect and measure magnetic fields, with sensitivity of 10 fT/√Hz [1]. Atomic magnetometers such as spin-exchange relaxation free (SERF) regime magnetometer and coherence population trapping (CPT) magnetometer have been designed to detect of varying magnetic fields mainly at low frequency. Therefore, detection of weak fields at high frequencies up to several megahertz requires an alternative detection method. To observe the Nuclear magnetic resonance (NMR) signals at several tens of kilohertz, RF (Radio-Frequency) atomic magnetometer can be used. RF magnetometer has a fundamental sensitivity limit on the order of 0.01 fT/√Hz [2, 3]. In RF magnetometer, the oscillating magnetic field causes the polarization of each spin to rotate along the pumping axis, with the transverse spin component increasing until the polarization is perpendicular to the pump axis. The resonant RF field eventually makes all of the processing spins coherent. In this study, the measured SNR corresponded to a sensitivity of 50 fT/√Hz at 25 kHz and such results will be useful to atomic NMR detector.

[1] J. C. Allred, R.N. Lyman, T.W. Kornack and M.V. Romalis, *Phys. Rev. Lett.* 89, 130801 (2002) [2] S.-K. Lee, K. L. Sauer, S. J. Seltzer, O. Alem, and M. V. Romalis, *Appl. Phys. Lett.* 89, 214106 (2006) [3] I.M. Savukov, S.J. Seltzer and M.V. Romalis, *Journal of Magnetic Resonance* 185 (2007) 214-220

RQ19

Cancellation coil allows precision magnetic measurements with strong magnetization field inside a shielded environment

Seong-min Hwang, Kiwoong Kim*, Chan Seok Kang, Seong-joo Lee and Yong-ho Lee
Brain and Cognition Measurement Lab., Korea Research Institute of Standards and Science, Korea

A great number of precision magnetic measurements can benefit significantly from, or in some cases, even require strong prepolarization fields (B_p) and magnetically shielded environments. We devised a cancellation coil (CC) to neutralize the B_p on electrically conductive shield walls that may otherwise induce currents on the walls to produce a lingering transient residual field (B_r) inside the shielded environment and disrupt the measurement operations. The CC was designed using the inverse problem method to effectively neutralize magnetic fields generated on the shield walls by the B_p coil. The implemented CC was evaluated by measuring the resulting B_r after strong pulsed B_p using a fluxgate magnetometer at different magnetometer positions and cancellation coil currents (ICC). We have conducted multi-mode component analysis on the B_r measurements to reveal two dominant components, where the component with shorter time constant comes from the current induced around the shield side walls and the other with longer time constant from the current induced on the ceiling and floor of the MSR. The analysis also allows optimization of ICC for each of the top, side, and bottom sections of the CC to enable significantly easier fine-tuning of individual sections of the CC to enhance CC performance.

Seong-min Hwang, Kiwoong Kim, Chan Seok Kang, Seong-joo Lee, and Yong-ho Lee, *Appl. Phys. Lett.* 99, 132506 (2011)
Seong-min Hwang, Kiwoong Kim, Chan Seok Kang, Seong-joo Lee, and Yong-ho Lee, submitted to *J. Appl. Phys.* 111, 083916 (2012)

RQ20

Development of a SQUID based ultra-low-field MRI system

Seong-joo Lee, Kiwoong Kim*, Chan Seok Kang, Seong-min Hwang and Yong-ho Lee
Brain and Cognition Measurement Lab., Korea Research Institute of Standards and Science, Korea

We obtained 2-dimensional Magnetic Resonance Imaging (MRI) image of a phantom in fields of a few microtesla by using a dc Superconducting QUantum Interference Device (SQUID) based MRI system. Microtesla MRI technique is a challenging application based on SQUID technology. The high sensitivity of the SQUID magnetometer enables measurement of very weak magnetic resonance signals even for the low Larmor frequency in microtesla fields. Measuring the nuclear magnetic resonance (NMR) signals at such a low field gives many benefits like development of an open-type low-cost surgery-monitoring MRI system, high-contrast cancer detector, etc. In this presentation, we introduce experimental details for ultra-low-field (ULF) MRI.

RQ21

26 T+ steady magnetic field for neutron science at HZB Berlin

P. Smeibidl, Karel Prokes*, H. Ehmler, O. Prokhnenko and A. Tennant
M-11, Helmholtz Zentrum Berlin, Germany

The Helmholtz Zentrum Berlin is building in collaboration with the National High Magnetic Field Laboratory, Tallahassee, FL, USA a new series-connected hybrid magnet system for neutron scattering experiments [1]. Two conical endings of 30° opening angle enable neutrons to hit the sample and to be detected either in the forward or backward direction. To achieve a maximum field with the present technology, a 13 T superconducting Nb₃Sn cable-in-conduit coil is combined with resistive insert coils of 13 T to 19 T, depending on electric power, to give a maximum of 26 to 32 T. The magnet that provides a 50 mm diameter room temperature bore in horizontal orientation will be permanently mounted at the dedicated time-of-flight instrument ExED 76 m away from the neutron source. The contribution describes the most important design features of the system (the 20 kA, 8 MW power supply, the helium refrigerator system for cooling of the superconducting coil and the 4-8 MW water cooling system for cooling of the resistive coil), the status of the fabrication of the components, the outline of the building for the technical infrastructure and the status of the installation of the most important components.

[1] P. Smeibidl et al., *J. Low Temp. Phys.* 159, 402 (2010).

RQ22

A simple method for measuring blocking temperatures

Mansor Hashim¹, Ghazaleh Bahmanrokh² and Ismayadi Ismail¹
¹ Institute of Advanced Technology, Universiti Putra Malaysia, Malaysia
² Physics Department, Faculty of Science, Universiti Putra Malaysia, Malaysia

We describe a new method for measuring a blocking temperature, much simpler than that involving a SQUID. Nanoparticles of Co, Co coated with Au, Co-Pt and Co-Pt coated with Au were prepared by the reverse micelle microemulsion method. The four magnetic powder specimens were each pressed to yield a disc. A Hall-effect probe blade surface was stuck intimately against one flat surface of the disc. Properly analysed, this arrangement allows the probe to detect the normal component, BN, projecting from the disc since, at the interface, BN (air) = BN (disc). Use of this relation led to the determination of a magnetic moment near the disc surface. By simply cooling this arrangement of disc + probe in a probe station to 15K, a graph of the magnetic moment was clearly peaked at a temperature which, unmistakably, was the blocking temperature, TB. For the four different samples TB lies between 40K and 45K.

RQ23

Optimization of operation condition of orthogonal fluxgate sensor fabricated with Co based amorphous wire

Yongmin Kim¹, Young-hak Kim², Sang-ho Lim³, Cang-seob Yang⁴ and Kwang-ho Shin^{1*}
¹ Dept. of Information and Communication Engineering, Kyungsung University, Korea
² Pukyong National University, Korea
³ Korea University, Korea
⁴ Agency for Defense Development, Korea

Orthogonal fluxgate (OFG) sensors have an additional advantage comparing with conventional fluxgate sensors in their simple structure [1-2]. Because the sensitivity of an OFG is typically proportional to its winding number N, cross section area of its magnetic core A, and operation frequency f, the f should be as high as possible to prevent reduction of the sensitivity in the case of small-sized OFG sensors in which the N and A are restricted. The f is limited due to the LC resonance occurred by inductance and stray-field capacitance of the pickup coil around the magnetic core and transmission line, coaxial line in this study, as well as performance of the signal conditioning circuit in common. And the sensitivity could be also reduced according to increase of operation frequency due to the skin effect if the sensor is operated in the frequency range of near MHz. We present how to optimize the operation condition including frequency of the OFG fabricated with a CoFeSiB amorphous wire with the diameter of 100 μm in this paper. The LC resonance frequency according to external capacitances was calculated with an equivalent circuit and FEM analysis to calculate the magnetization distribution in a high frequency.

[1] E. Paperno, E. Weiss and A. Plotkin, *IEEE Trans. Magn.*, 44, 4018 (2008). [2] I. Sasaki, *J. Appl. Phys.*, 91, 7789 (2002).

RR01

Preparation of γ-Fe₄N and ε-Fe₃N particles with high magnetization for electromagnetic wave absorption applications

Ming-fong Tai^{1*}, Hsin-tzu Liu², C. M. Lin³ and Huan-chiu Ku¹
¹Department of Physics, National Tsing Hua University, Taiwan
² Department of Chemical Engineer, National Tsing Hua University, Taiwan
³ Department of Applied Science, National Hsingchu University of Education, Taiwan

High-Ms ferromagnetic iron nitrides have vast applications on microwave absorbing and magnetic recording. In this study, we successfully used a simple nitrogen treatment to prepare cubic γ-Fe₄N and hexagonal ε-Fe₃N powder. Both kinds of powders are synthesized by the nitriding process of the commercial micro-scale Fe and Fe₂O₃ powders, at 550°C for 5 hours during a flowing mixture of NH₃ and H₂ gas. Our pure γ-Fe₄N powder exhibits a high saturation magnetization of 15.03 kG at room temperature, which is slightly lower than that of bulk Fe (22.0 kG @ 4 K) but is considerably higher than that of γ-Fe₂O₃ (4.0 kG @ 4 K). The ε-Fe₃N powder including a slight amount of γ-Fe₄N was also synthesized by heating the commercial Fe₂O₃ powder with the same procedure. The chemical stabilities of both γ-Fe₄N and ε-Fe₃N powder are superior to that of the pure Fe and have high level of mechanical hardness. The microstructures and electron spin resonances of our iron nitrides were also studied.

This work was supported by the National Science Council, Taiwan under the NSC 98-2112-M-007-016-MY3 project.

RR02

Methods for determining the quality of magnetic fluids

Viorica Chioran
University Babes-Bolyai - Cluj Napoca / Romania, Romania

The conversion parameter of the magnetic properties of magnetic fluids is a physical quantity describing the quality of those fluids from a technological point of view. This study determines the value of this parameter for three samples of magnetic fluid. Many technical applications require magnetic fluids with specific magnetic properties such as very high magnetization at saturation point or rheological properties involving high fluidity (very low viscosity). The sample with bigger density (1070 kg/m³) also has a larger solid volume fraction (0, 059). Increasing the solid part/ fluid volume increases the density and viscosity of that fluid. A magnetic fluid with a larger magnetic part/ volume (0,031) has a higher magnetization at saturation point (0,0138 A/m). The parameter always has sub-unitary values because inside the volume of the magnetic fluid, the percentage of the solid part is larger than that of the magnetic part. Responsible for this is the nonmagnetic layer at the surface of the particles. For the fluid samples studied, regardless of the magnetic and physic diameter, the nonmagnetic layer of particles has the same value: a = 0,83 nm. Good quality of a magnetic fluid is indicated by a high value of the conversion parameter.

RR03

A study on magnetic fluid viscosity

Viorica Chioran
University Babes-Bolyai - Cluj Napoca / Romania, Romania

This paper shows the results of a study of the parameters that the viscosity of magnetic fluids depends on, in the absence of magnetic fields. Viscosity's and shearing tension's dependence on the rheologic component and shearing speed was verified for several samples of kerosene based magnetic fluid with the same dimensional distribution but various concentrations, at different temperatures. Experimental results show one situation where the sample P1 has a non-Newtonian character over a small interval of shearing speeds. An increase in fluid viscosity indicates that bonds between particles are formed inside the fluid. As shearing speeds increase these bonds disappear. Samples P and P₂ show Newtonian character over the shearing speed interval where viscosity remains constant. By comparing viscosity values of samples at different temperatures and shearing speeds, decreasing viscosity while increasing temperature is observed due to the activation energy of viscous flow. A linear increase of shearing tension with the increase of shearing speed was observed for the studied samples at different temperatures. The slope of this line can be used to determine the dynamic viscosity's value. For the considered samples, viscosity strongly depends on several factors: density, concentration, temperature (by Arrhenius's Law) and shearing speed (by Newton's equation).

RR04

Magneto-motive force and torque analysis of squirrel cage induction motor with rotor or stator faults

Cheol Soo Goo¹, Seok-myeong Jang² and Yu Seop Park²
¹ Instrumentation and Control Assessment Department, Korea Institute of Nuclear Safety, Korea
² Electrical Engineering, Chungnam National University, Korea

Torque characteristics of high voltage induction motor are simulated under the condition of under voltage and broken rotor bars. The motor is high voltage squirrel cage induction type for driving force of pumps and valves in nuclear power plant. In the simulation, a rotor with health and broken bars, stator winding deterioration and voltage drop 25% alone and combination with bar faults were used. Then the results were analyzed. The effects of rotor faults on the torque-speed curve were compared according to the number of the rotor faults. The results revealed that voltage drop and the number of the rotor fault at high speed span is directly proportional to its effect on the curve, but the curve indicated the opposite at the low speed span due to the rotor impedance increase. In stator, winding faults made a distortion of the phase magneto-motive force and reduction of co-energy at the gap which cause vibration, harmonics and total power decrease.

RR05

Evaluation of materials degradation of ferromagnetic steels for various magnetized states using a hysteresis scaling law

Satoru Kobayashi*, Yusuke Ishibashi and Ryo Baba
Department of Materials Science and Engineering, Iwate University, Japan

We have examined a hysteresis scaling behavior of magnetic minor hysteresis loops for ferromagnetic low carbon steels under DC-biased magnetic field and/or remanent magnetization state. For all minor loops with dominant contribution of irreversible Bloch wall motion, a scaling relation between the hysteresis loss and maximum magnetization shows the same curve from very low to high magnetization regime, suggesting the invariant pinning mechanism for the irreversible wall motion. In the intermediate magnetization regime, the relation follows the usual Steinmetz law with a power-law exponent of about 1.5, whose coefficient increases with defect density. The method using a hysteresis scaling can be a useful technique of evaluating materials degradation of ferromagnetic steels in an unknown magnetic state, which is commonly encountered on on-site measurements.

RR06

Theoretical design of magnetic energy harvesting module

Kunihisa Tashiro*, Hiroyuki Wakiwaka and Yu Uchiyama
Shinshu University, Japan

Energy harvesting is a key technology to build a sustainable society. In previous paper, we focused on a magnetic power-line noise as a reusable energy. In this paper, we present a theoretical design method of magnetic energy harvesting module. This module consists of an air-core coil and resonant capacitor. With a simple RLC circuit model, we derive an equation of the harvesting energy as a function of coil size. In order to demonstrate the magnetic field, a uniform magnetic field is generated by our developed coil system. From the experimented results, we successfully demonstrated the energy harvesting of 100 mW from a magnetic field of 0.09 mT at 60 Hz. This value is good in agreement with the estimated results. The harvested energy is proportional to the square of the magnetic flux density. However, ICNIRP2010 provide a guide line for human health that an acceptable level in a public space is 0.2 mT at power-line frequency. We also reveal the required coil size to harvest a demanded energy.

July 12 (Thu)

July 12 (Thu)

RR07

A study on detecting and determining the shape of small axial cracks by using magnetic flux leakage in ndt system of pipe

Hui Min Kim and Gwan Soo Park*
School of Electronic and Electrical Engineering, Pusan National University, Korea

There is the source of energy that is used widely all over the world, which is oil and natural gas. Oil and gas is supplied for industries or home consumers through pipelines. Most pipelines are laid to underground and exposed the external environment. By these conditions pipelines have some bad effects like the metal loss, corrosions and any other damages. For preventing accidents, these defects have to be detected by the Non-destructive testing(NDT). The magnetic flux leakage(MFL) method among the NDT methods is suitable for testing pipelines which the magnetic characteristic of has high magnetic permeability. The system that MFL method applies to is called the pipeline inspection gauge, MFL PIG. The previous MFL PIG has high performance for detecting the metal loss and corrosions. But MFL PIG cannot detect the cracks which occurred by the difference of pressure between the inside and outside of pipelines and the shape of is long and very narrow. Cracks occurs frequently in the pipelines and the risk of the accident from the cracks is higher than that from the metal loss and corrosions. The circumferential MFL(CMFL) PIG performs magnetic field circumferentially and can maximize the magnetic flux leakage at the cracks.

RR08

Control of working temperature of isothermal magnetic entropy change by hydrogen absorption into $La_{0.8}Nd_{0.2}(Fe_{0.88}Si_{0.12})_{13}$ for magnetic refrigerant

S Fujieda^{1*}, A Fujita², K Fukamichi¹ and S Suzuki¹
¹ Institute of Multidisciplinary Research for Advanced Materials, Tohoku Univ., Japan
² Dept. of Materials Science, Graduate School of Engineering, Tohoku Univ., Japan

Hydrogen absorption into $La_{0.8}Nd_{0.2}(Fe_{0.88}Si_{0.12})_{13}$ has been investigated to obtain large magnetocaloric effects (MCEs) near room temperature for applications to magnetic refrigeration. $La(Fe_{0.88}Si_{0.12})_{13}$ exhibits large MCEs just above the Curie temperature $T_c = 195$ K because of the itinerant-electron metamagnetic (IEM) transition [1]. The MCEs due to the IEM transition are enhanced by the partial substitution of Nd for La [2]. It was confirmed that T_c of $La_{0.8}Nd_{0.2}(Fe_{0.88}Si_{0.12})_{13}$ is increased from 193 K to 318 K by hydrogen absorption with keeping the IEM transition because the unit cell volume is expanded. Note that the isothermal magnetic entropy change ΔS_m due to the IEM transition in a magnetic field change of 2 T for $La_{0.8}Nd_{0.2}(Fe_{0.88}Si_{0.12})_{13}H_{1.1}$ was evaluated to be about -23 J/kg K at $T_c = 288$ K, which is larger than $\Delta S_m = -19$ J/kg K at $T_c = 276$ K for $La(Fe_{0.88}Si_{0.12})_{13}H_{1.0}$. The relative cooling power RCP = 179 J/kg of the former also is larger than 160 J/kg of the latter. Accordingly, it is concluded that the partial substitution of Nd improves the MCEs near room temperature.

[1] A. Fujita et al., Phys. Rev. B 67 (2003) 104416, [2] S. Fujieda et al., Mater. Sci. Forum 561-565 (2007) 1093.

RR09

Characteristic analysis of induction motor for electric vehicle according to electric loading and magnetic loading

Ki Young Sung¹ and Ki-chan Kim^{2*}
¹ SPG Co., Ltd., Korea
² Hanbat national university, Korea

In the paper, an inductive motor for electric vehicle that was designed for compact car modification was selected as the basic model, and its performance change was examined according to the change in the electric and magnetic loading related to the rotor slot. The characteristic changes according to the change in the loading were analyzed for two speed ranges: the low speed (near the base speed) and the high speed (maximum speed with field weakening control). To provide the characteristic analysis conditions according to the change in the slot shape of the reference model, the rotor bar depth was changed with the rotor teeth width fixed to vary the electric loading, and the rotor teeth width was changed with the rotor bar area fixed to vary the magnetic loading. The characteristics of the inductive motor were analyzed via the analysis of the characteristics according to the parameters of the equivalent circuit based on the magnetic circuit method and via the electromagnetic analysis based on the finite element method to consider the nonlinear characteristic of the motor parameters.

[1] Z.Zhang, F.prajmo, a. tenconi, "Improved design for electric vehicle induction motors using an optimisation procedure". Electric Power Applications, IEE Proceedings, vol. 143, pp.410-416, 1996 [2] T. Wang, P. Zheng, Q. Zhang, and S. Cheng, "Design Characteristics of the induction motor used for hybrid electric vehicle". IEEE Transaction on Magnetics, vol. 41, pp. 505-508, 2005 [3] I. Boldea and S. A. Nasar, "The induction machine handbook". Boca Raton, CRC Press, 2002

RR10

Torque characteristics of interior permanent magnet synchronous motor for electrical hydraulic power steering system

Su-jin Hwang¹ and Ki-chan Kim^{2*}
¹ Daedong movel company, Korea
² Hanbat national university, Korea

In the paper, a 12 V-DC interior permanent magnet synchronous motor for electric hydraulic power steering (EHPS) was designed for the purpose of improving its torque performance. The EHPS is a steering system that uses the battery power of the vehicle, which is weaker than the power of the hydraulic power steering system. Because of the spatial limitation, the IPMSM, which has high-power characteristic and excellent performance within the field weakening area at a high rotating speed, is advantageous. To improve the torque performance, the average torque was increased by increasing the rotor size. In addition, because the torque ripple is detected as vibration when the steering wheel is operated, the shape of the barrier was modified to change the inductance element of the axis and reduce the torque ripple. The optimally designed model characteristics were analyzed using the finite element method to comparatively analyze the parameters. It is expected that this study will be important reference data to understand the characteristics of the IPMSM as well as of the EHPS.

[1] Tony Sebastian, Vineeta Gangla, 'Analysis of Induced EMF Waveforms and Torque Ripple in a Brushless Permanent Magnet Machine,' IEEE Trans. on Industrial Applications, Vol. 32, No. 1, 1996, [2] A. M. Elrefaies, T. M. Jahns and D. W. Novotny, 'Analysis of Surface Permanent Magnet Machines with Fractional Slot Concentrated Windings', IEEE Trans on Energy Conversion, vol. 21, no. 1, pp. 34-43, 2006

RR11

Edge auxiliary teeth design of stationary discontinuous armature PM-LSM with concentrated winding

Yong-jae Kim¹, Sung-jin Kim^{1*} and Sang-yong Jung²
¹ Department of Electrical Engineering, Chosun University, Korea
² School of Information and Communication Engineering, Sungkyunkwan University, Korea

Recently, in order to resolve the problem of high cost, we have proposed the stationary discontinuous armature PM-LSM in which the armature is engaged only when accelerated and decelerated operations are necessary, when PM-LSM is used with long-distance transportation systems in factories [1]. As the armatures are arranged discontinuously in the PM-LSM, the number required is dramatically decreased. In this case, several stator blocks can be arranged at certain intervals within the overall running route. The space between the blocks without the stator is called the free-running section, and the mover in this section drives under its own inertia. However, the stationary discontinuous armature PM-LSM contains the edges which always exist as a result of the discontinuous arrangement of the armature [2]. For this reason, cogging force generated between the "entrance end" and the "exit end" has become a problem. Therefore, we have examined the edge cogging force by installing the auxiliary teeth at the armature's edge in order to minimize the cogging force generated when the armature is arranged discontinuously. We obtain the edge cogging force by using 2-D numerical analysis with a FEM and also by adjusting the width, height and the length of pitch of auxiliary teeth.

[1] Yong-Jae Kim, Masaya Watada, Susumu Torii and Daiki Ebihara, "Constant Load Angle Control of the Discontinuous Primary Linear Synchronous Motor without Position Feedback", The Fourth International Symposium on LINEAR DRIVES FOR INDUSTRY APPLICATIONS, pp.113-116, 2003. [2]Yong-Jae Kim, Masaya Watada, Susumu Torii, Hideo Dohmeki and Daiki Ebihara, "The Influence which Outlet edge of the Discontinuous Primary Linear Synchronous Motor Exerts on the Drive of Secondary Mover", The 5th International Power Electronics Conference, pp.859-864, 2005.

RR12

Inductively coupled LC resonators as displacement sensor

Yongmin Kim and Kwang-ho Shin*
Dept. of Information and Communication Engineering, Kyungsung University, Korea

In this paper, we present novel displacement sensor composed of a pair of LC resonators. The LC resonator was formed by serial connection of 300-turn Cu wire wound on a rectangular NiZn ferrite (20 × 3 × 4 mm) core and SMD capacitor (3.2 × 1.6 mm). The resonance frequencies of two resonators are adjusted to be identical with each other. By this, we could obtain the sensor output linearly dependent of distance between two LC resonators, because the mutual inductance is proportional to distance between two resonators in a few centimeters. The sensor was designed by a sequence of magnetic field simulation with a FEM tool (COMSOL) and circuit calculation with a SPICE. The sensitivity estimated by $S = fr/D$ was about 480 kHz/m, where, fr and D are resonance frequency and distance between two resonators, respectively. The proposed sensor would be a promising displacement sensor when it takes an active part in an environment surrounded by serious electrical/magnetic noise, since it could be operated in extremely narrow frequency range.

RR13

Magnetic NDE for sensitization of Inconel 600 alloy

Hiroaki Kikuchi, Takaki Sumimoto, Yasuhiro Kamada and Satoru Kobayashi
Faculty of Engineering, Iwate University, Japan

Inconel 600 alloy, Ni base alloy, is used as steam generators in nuclear power plants, and sensitization occurs along grain boundary with heat treatment on this material. The sensitization causes a degradation of corrosion resistance and generates stress corrosion crack [1], [2]. Therefore nondestructive evaluation (NDE) technique for sensitization of Inconel alloy is quite important so as to keep the integrity of plants. Inconel 600 alloy has usually paramagnetic property, however, it shows ferromagnetic properties along grain boundary when sensitization occurs: this means NDE using magnetism is possible. Thus, in this study, Inconel 600 alloys were heat treated at 873 K from 0 to 400 hours and their magnetic properties were investigated in detail. Magnetization increases with increasing time of heat treatment and takes a maximum. On the other hand, coercivity decreases with the increase in time. We confirmed that only characteristics at the grain boundaries changes ferromagnetic by MFM observation. As trial for industrial application, heat treated Inconel 600 alloy has scanned by magnetic field sensor, and the changes of magnetization nondestructively were successfully obtained. The result indicates the feasibility of magnetic NDE for sensitization of Inconel 600 alloy.

[1] M. Kowaka, H. Nagano, T. Kubo, Y. Okada, M. Yagi, O. Takaba, T. Yonezawa and K. Arioka, Nuclear Technologies, Vol. 55, pp. 394-404 (1981). [2] J. D. Wang, D. Gan, Materials Chemistry and Physics, Vol. 70, pp. 124-128 (2001).

RR14

Comparison of characteristics between the PM synchronous motor and the induction motor for electric vehicle

Mi-jung Kim, Ik-sang Jang, Ki-doek Lee, Jae-jun Lee, Jeong-ho Han, Tae-chul Jeong and Ju Lee*
Hanyang University, Korea

This paper presents the characteristics over a wide speed range of the interior permanent magnet synchronous motor(IPMSM) and the induction motor(IM) for an application of electric vehicle drive. In generally, IPMSM have higher performance than IM. The performance: torque, efficiency, power factor etc. are compared at rated speed of 2,843rpm and maximum speed of 10,000rpm. The induction motor operating constant speed is not need to consider the control property; however, the adjustable speed drive applications such as traction motor are should be deliberated for control. In this paper, the characteristics of IPMSM and IM controlled by space vector PWM are illustrated and verified by experiment. In case of IPMSM, the efficiency map was made up through driving simulation considering the actual control. It was carried out MTPA control until constant torque operating region and applied the field weakening control under constant power region. In case of induction motor, V/f control maintained a constant ratio of voltage versus current was carried out until constant torque operating region and applied the constant voltage variable frequency control under constant power region. As illustrated in Figure 1, overall efficiency of IPMSM has high level than IM about 5%.

[1] Z. Q. Zhu and David Howe, 'Electrical Machines and Drives for Electric, Hybrid, and Fuel cell Vehicles', Proceedings of the IEEE, Vol. 95, No. 4, pp 746-765, April 2007. [2] J. Herbst, J. Hahne, H. Jordan, H. Liu, A. Gattozzi and Ben Wu, 'Challenges in the Design of a 100 kW Induction Motor for a PHEV Application', Vehicle Power and Propulsion Conference, pp 408-413, 2009.

RR15

Comparison of simultaneously measured pulse waveforms from both hands using permanent magnet-hall pulsimeter sensors

Sang-suk Lee¹, Jong-gu Choi², Il-ho Son¹, Keun-ho Kim¹, Nam-kyu Lee¹ and Hyun-sung Cho¹
¹ Oriental Biomedical Engineering, Sangji University, Korea
² Eastern-Western Biomedical Engineering, Sangji University, Korea

Two radially arterial pulses of dual hands using the prototype of a clamping clip pulsimeter equipped with permanent magnet and Hall device are compared and analyzed. The phase difference of two pulse wave signals is dominantly presented from the simultaneous measuring clinical pulse wave signals for twenty two male participants at their 20's. It is possible to analyze that the fast and slow pulse wave for right hand and left hand depend on the muscle property of arms rather than the total length of blood vessel due to cardiovascular circulatory system.

[1] S. S. Lee, M. C. Ahn, and S. H. Ahn, J. Magnetics, 14, 132 (2009). [2] M. F. P. O'Rourke, R. P. Kelly, A. P. Avolio, 'The Arterial Pulse', 1st Ed.: Lea & Febiger: Philadelphia, PA, USA, 1992 [3] S. W. Kim, Y. G. Choi, H. S. Lee, D. H. Park, D. G. Hwang, S. S. Lee, G. W. Kim, S. G. Lee, and S. J. Lee, J. Appl. Phys. 99, R908 (2006).

RR16

A study on new permanent magnet configuration for high thrust density in permanent magnet synchronous linear motor

Taewoo Kim and Junghwan Chang*
Electrical Engineering, Dong-A University, Busan, 604-714, Korea



RR17

Design of stationary pole pieces in a coaxial magnetic gear

Daekyu Jang and Junghwan Chang*
Electrical Engineering, Dong-A University, Saha-gu, Busan, 604-714, Korea

Magnetic gears have been proposed by unique advantage compared with mechanical gears, such as contactless power transmission. In addition, they can limit a torque under overloaded condition and have excellent performances on noise, vibration and reliability [1]. However, their use in industries has been very limited due to poor torque density, low transmission ratio and transmitted toque performances. Of magnetic gears, a coaxial magnetic gear is a common configuration and extensively studied for its relative high performances [2]. It is consist of inner rotor, outer rotor and stationary pole pieces in between the rotors. The stationary pole pieces have an important role in torque transmission by modulating the air gap flux density distribution adjacent to inner and outer rotor. However, they also generate unwanted harmonics resulting in torque ripples and vibration. This paper proposes variants of stationary pole pieces to gain high performances in torque transmission. It also has mechanical and manufacturing advantages in transmitting torque by a structure combining each pole pieces. The finite element analysis shows the produced torque has reduced harmonic components in both sides of rotors.

[1] K.Atallah, S.D. Calverley and D. Howe, "Design, analysis and realization of a high performance magnetic gear", IEEE proc.-Electr. Power Appl, vol. 151, No. 2, pp.135-143, March, 2004. [2] Noboru Niguchi, Katsuhiro Hirata, Masari Muramatsu and Yuichi Hayakawa, "Transmission Torque Characteristics in a Magnetic Gear," ICEM conf, pp 1-6, sept. 2010.

RR18

Design techniques for reducing torque ripple in permanent magnet flux switching motor

Daohan Wang¹, Xiuhe Wang² and Sang-yong Jung^{1*}
¹ Sungkyunkwan University, Korea
² Shandong University, China

Permanent magnet flux switching motor (PMFSM) is a novel double salient machine which employ the PM instead of the field winding for excitation and contains only one set of armature winding so has the advantage of low cost power converter and extreme high efficiency. It has a potential for taking place of BLDC in some applications, such as fans and air ventilation machines. Due to the different structure and operation principle from traditional permanent magnet machine, the generated torque ripple in PMFSM is very critical and rather unique compared to the common PM machines. In this paper, the design techniques of reducing the torque ripple in PMFSM has been presented. Different kinds of design approaches have been presented to reduce the torque ripple with comparing the mean output torque. Analytical method is first presented to investigate the influence and determine the design parameters thus reduce the computational effort. Then FEA simulation is employed to validate the analysis above. Finally, time stepped FEA simulation is being employed to investigate the performance with different approaches adopted.

[1] Z. Q. Zhu, A. S. Thomas, J. T. Chen, and G. W. Jewell, "Cogging Torque in Flux-Switching Permanent Magnet Machines," IEEE Trans. Magn., vol. 45, no. 10, pp. 4708-4711, Oct. 2009. [2] Z. Q. Zhu, J. T. Chen, D. Howe, S. Iwasaki, and R. Deodhar, "Design of multi-tooth flux-switching permanent magnet brushless ac machines for low-speed direct drives," IEEE Trans. Magn., vol. 44, no. 11, pp. 4313-4316, 2008.

July 12 (Thu)

July 12 (Thu)

RR19

The analysis of line-start permanent magnet machine with saliency ratio

Kwang Hee Kim, Jian Li and Yun Hyun Cho*
Dong-A University, Korea

WITHDRAWN

RR20

Analysis of non-linear characteristics of linear compressor

Park Daegeun and Cho Yunhyun*
Dong-A University, Korea

WITHDRAWN

RR21

Torque harmonics and reduction design characteristics of induction motor for electric vehicle propulsion

Kyung-won Jeon¹, Seung-ho Lee¹, Yong-jae Kim² and Sang-yong Jung^{1*}
¹ School of Electronic and Electrical Engineering, Sungkyunkwan Univ., Korea
² Dept. of Electrical Engineering, Chosun University, Korea

This paper deals with torque harmonic characteristics of induction motor for electric vehicle (EV). For calculate phase stator harmonic leakage flux of a three phase induction motor, an analysis method is determine relationships with stator teeth design. In particular, torque harmonics including EMF harmonics at whole speed ranges are analyzed by the finite element method (FEM). Torque harmonic components are identified with Fourier fast transform (FFT). Torque harmonics are generated due to the different phase windings interaction and they can be reduced by applying a stator teeth design. The electromagnetic field and corresponding harmonics of an electrical machine are calculated using the FEM, the harmonic winding factors show how the torque harmonics can be reduced significantly by good stator teeth design. The novel design methods to compensate the specified torque harmonics are proposed. Then, its effectiveness is clarified according to the representative control strategies for induction motor such as maximum torque per ampere (MTPA) and flux-weakening control.

[1] Lee S., Kim Y.-J., Jung S.-Y., "Numerical Investigation on Torque Harmonics Reduction of Interior PM Synchronous Motor With Concentrated Winding", *IEEE Trans on Magnetics*, vol.48, no.2, pp.927-930, Feb. 2012. [2] Yamazaki K., Suzuki A., Ohts M., Takakura T., Nakagawa S., "Equivalent Circuit Modeling of Induction Motors Considering Stray Load Loss and Harmonic Torques Using Finite Element Method", *IEEE Trans on Magnetics*, vol.47, no.5, pp.986-989, May. 2011. [3] Bianchi N., Alberti L., "MMF Harmonics Effect on the Embedded FE Analytical Computation of PM Motors", *IEEE Trans on Industry Applications*, vol.46, no.2, pp.812-820, Mar-Apr. 2010.

RR22

Numerical analysis on iron loss and pm loss of permanent magnet synchronous motor considering the carrier harmonics

Yun-ho Jeong¹, Kyung-won Jeon¹, Yong-jae Kim² and Sang-yong Jung^{1*}
¹ School of Electronic and Electrical Engineering, Sungkyunkwan Univ, Korea
² Dept. of Electrical Engineering, Chosun University, Korea

In this paper, decisive influences of the inverter harmonic on iron loss characteristic for PMSM (Permanent Magnet Synchronous Motor) are numerically investigated with the FEM (Finite Element Method). Particularly, analysis is carried out based on a multi-layer buried PMSM, which is newly designed for EV drive system and its rotor contains ferrite magnets. First of all, not only the design criteria and the specification of the designed PMSM but also the features of the motor like torque ripple, Back-EMF are represented. In addition, the remarkable iron loss analysis result, that is obtained using 3-D FEM considering skewed stator structure, is covered in priority. Then its each harmonic component is identified using the FFT (Fourier Fast Transform) and that is compared with iron loss characteristic in case of sinusoidal input current which is not include harmonic component. Finally, the efficiency at each operating point is calculated considering loss analysis results. Meanwhile, entire analysis is performed through various operating conditions using intrinsically real input current values implemented by testing performance of the manufactured model.

[1] Z.Q.Zhu, Y.S.Chen, D.Howe, "Iron Loss in Permanent-Magnet Brushless AC Machines Under Maximum Torque Per Ampere and Flux Weakening Control", *IEEE Trans. on Magnetics*, vol. 38, No. 5, pp. 3285-3287, Sep. 2002. [2] Katsumi Yamazaki, Shinjiro Watarim "Loss Analysis of Permanent-Magnet Motor Considering Carrier Harmonics of PWM Inverter Using Combination of 2-D and 3-D Finite-Element Method", *IEEE Trans. on Magnetics*, vol. 41, No. 5, pp. 3285-3287, May. 2005. [3] G. Ombach, J. Junak, "Torque ripple optimization of skewed IPM motor for field weakening operation", *Electrical Machines and Systems (ICEMS) 2011*, pp. 1-7, Aug. 2011.

RR23

Defect depth estimation based on the analysis of interference defects on the underground gas pipelines

Min-Ho Kim¹, Bok-Jin Oh¹, and Doo-Hyun Choi^{2*}
¹ Graduate School of Electrical Engineering and Computer Science, Kyungpook National Univ., Korea
² School of Electronics Engineering, Kyungpook National Univ., Korea

Underground gas pipelines have corrossions and deformations due to both the natural causes such as moisture and ground pressure and the artificial causes such as faulty construction, etc. So, periodic pipeline inspection is essential. In NACE (national association of corrosion engineers) standard, it is advised to replace the pipeline when a defect's depth is over 50% of the pipeline's thickness. Therefore, the study to analyze the defect's depth and its progress is meaningful. Especially when defects more than two are closely located, the interaction among these defects accelerates the progress of deflection. In this paper, the interference defects on underground pipelines are analyzed and their depths are estimated effectively. Experimental results show that the proposed method can effectively estimate the depth of the interference defects.

RR24

Comparison on electromagnetic losses of super high speed PM motor/generator with slot and slotless stators

Jim Hak Jang¹, Jian Li² and Yun Hyun Cho^{1*}
¹ Dong-A University, Korea
² Dong-A University, China

WITHDRAWN

RR25

A study on Voltage-PWM control of switched reluctance generator at low speed

Sun Ning¹, Dawoon Choi², Jian Li¹ and Yunhyun Cho^{2*}
¹ Dong-A-university, China
² Dong-A-university, Korea

This paper is a study on switched reluctance generator's control method---Voltage-PWM. It can be used to regulate the current to a desired value by varying the average applied voltage in the switched reluctance generator. The advantages of Voltage-PWM control at low speed are more than high speed which may make the application of PWM difficult. The switched reluctance machine can operate as a generator as well as a motor by simply changing the firing angles. Some main control methods we often used are Chopped Current Control (CCC), Angular Position Control (APC) and PWM Control. The controller could regulate control variables, such as current level, turn-on and turn-off angles, supply voltage and so on. Different control methods will be carried out by regulating some variables in different conditions. For example, at low speed, the d.c link voltage is controlled by varying the set-point current or the duty-cycle and at high speed by varying the control angles. Because of excitation current is closely linear relation to duty cycle, so many applications determine this control method.

[1] Miller, T.J.E. *Electronic Control of Switched Reluctance Machines*. MPG Books Ltd, Bodmin, Cornwall. 2001. [2] K.Kannan, Dr.S.Sutha. *The 4th International Power Engineering and Optimization Conference (PEOCO2010)*, ShahAlam, Selangor, Malaysia.23-24 June 2010. [3] Jianzhong Sun, Fengxian Bai, *Special type electroc machine and control China waterpub press*, 2005.137-143.

RR26

The measurement procedure of the equivalent core loss in a PM motor

Guo Jihui Yan^{1*}, Ming-hung Jian¹ and Chia-sheng Huang²
¹ Micro/Meso Mechanical Manufacturing R&D Section, Metal Industries Research & Development Centre, Taiwan
² Codent Tech Co. Ltd, Taiwan

For the development of high efficiency motor, the core loss decrease is one of the most important tasks. However, the calculated core loss in the design stage is not so accurate because the specification provided by material manufacturer usually obtained by ideal test condition in simple geometry, i.e. single sheet tester and toroidal tester. Therefore, a method that can measure the core loss with the practical shape of motor stator/rotor core includes every aspect of the manufacturing effects is required. This paper proposed a refined procedure based on torque metric method. Among several proven measuring methods, it is a directly measuring method that can be applied to the actual motor. Typical torque method uses a motor driving a specimen at a specific speed and then measures the drag torque. However, it is time consuming and requires higher precision torque meter. Instead, the proposed method measures the speed-power characteristic curve of the driving motor with/without the test motor. From the difference of the speed-power characteristic, the core loss at various speeds can be obtained. Several conventional PM motors are taking as examples to demonstrate this procedure and to investigate the core loss influenced by manufacturing.

[1] N. Stranges, and R. D. Findlay, "Measurement of Rotational Iron Losses in Electrical Sheet," *IEEE TRANSACTIONS ON MAGNETICS*, Vol. 36, No. 5, Sep. 2000, pp. 3457-3459. [2] W. Arshad, et al., "Incorporating lamination processing and component manufacturing in electrical machine design tools," in *Industry Applications Conference, 2007. 42nd IAS Annual Meeting. Conference Records, 2007*, pp. 94-102. [3] Jiongqiang Guo, et al., "Measurement and Modeling of Rotational Core Losses of Soft Magnetic Materials Used in Electrical Machines: A Review," *IEEE TRANSACTIONS ON MAGNETICS*, Vol. 44, No. 2, Feb. 2008, pp. 279-291.

RR27

MFL signal enhancement based on exponential smoothing

Su-yeon Jeong¹, Jong-hwa Kim² and Doo-hyun Choi^{2*}
¹ Graduate School of Electrical Engineering and Computer Science, Kyungpook National Univ., Korea
² School of Electronics Engineering, Kyungpook National Univ., Korea

Nowadays, as industrialization is in progress worldwide and economy grows rapidly, demand for the energy supply of oil and gas has also increased. Currently, over millions of kilometers of underground gas pipeline has been established worldwide. The maintenance of pipeline is needed for the efficient supply of energy, but in reality, it is impossible for human experts to investigate all the underground pipelines in order to confirm whether a pipe has deterioration or damage because of the pipe's geographical position. So, automatic nondestructive testing methods by using MFL (magnetic flux leakage) signal are currently studied actively to detect and extract defects on the pipeline. The raw signals acquired from MFL sensors contain the signals of defects, as well as noise and distortion caused by various underground environments. In this paper, MFL signal is enhanced by using several smoothing techniques. Through experiments, it is confirmed that the distortion of raw signal by noise canceling can be reduced.

RR28

Electromagnetic separation of the brown coal ash of thermal power stations

Shavkat Malikov¹, Valeriy Pikul¹, Nuranya Mukhamedshina¹, Vladimir Sandalov² and Elvira Ibragimova^{2*}
¹ Institute of Nuclear Physics, Uzbekistan
² Radiation physics of solids and material science, Institute of Nuclear Physics, Uzbekistan

Tens millions of brown coal ash have accumulated near thermal power stations (TPS) in Uzbekistan, so their utilization has become quite actual. So far the ash is used for cement. However the ash is well known to contain a large amount of valuable elements, including ~3.13%Fe₂O₃ in Russian coal. Element analyses of the brown coal ash from Angren TPS were done with the neutron activation techniques and 3.6%Fe, 0.084%Mn, 0.063%Zr and also 0.023% of rare earth elements have been determined. The ash samples were undergone to electromagnetic separation, and the magnetic fraction was 3.7%, where the content of Fe increased to 58%. Then the magnetic fraction was separated with the standard screen grader into 7 classes from 0.4 to 0.05mm. Two times increase of the contents of Fe and rare earth elements have been found in the fine fractions of 0.1-0.05mm. Optical absorption spectroscopy of water solutions of the magnetic fractions has revealed the presence of Fe²⁺ and Fe³⁺ ions. Microscopic analysis of the fine fractions has shown that there are black iron microspheres of 0.02-0.05mm sizes, which can be used for cleaning of technological liquid waste by means of the high gradient magnetic field, and powder metallurgy.

RR29

Studies on viscosity in ferrofluids of Fe₃O₄

Han Gu¹, Zhaozhen Jiang², Aimei Zhang³ and Xiaoshan Wu²
¹ Advance Functional Materials Lab and Department of Physics, Changshu Institute of Technology, Changs, China
² Lab of Solid State Microstructures, Dept Physics, Nanjing University, China
³ College of Science, Hohai University, China

Fe₃O₄ nanoparticles with superparamagnetic properties are synthesized by sol-gel approach. Fe₃O₄ nanoparticles are coated using the amorphous silica. The viscosity of the coated Fe₃O₄ nanoparticles increases as the particles is incorporated in the impregnant, which may due to the magnetic interactions. At room temperature, the ferrofluid viscosity increases monotonically with increasing the concentration of Fe₃O₄ nanoparticles, the ratio of surface activity. With rising the temperature, the ferrofluid viscosity becomes larger. The applied magnetic field has also effects on the ferrofluid viscosity. The switching process of the applied magnetic field may increase the ferrofluid viscosity, although the ferrofluid viscosity increases with increasing the applied magnetic field. Dynamic properties of the magnetic particles in the impregnant are also discussed in the present.

RR30

Non-contact magnetic evaluation of ferromagnetic plate and its compensation of unknown air gap

Young-hak Kim¹ and Kwang-ho Shin^{2*}
¹ Pukyong National University, Korea
² Dept. of Information and Communication Engineering, Kyungsoong University, Korea

This paper represents a magnetic hysteresis model-assisted measurement method for non-contact evaluation of ferromagnetic plates in the case of the air gap between the test sample and the sensor probe is unknown. Our method involves measuring hysteresis loops from a test sample using a sensor probe in close proximity to the sample and measuring inductance spectra according to the various air gap. The sensor outputs were simulated based on a magnetic hysteresis model (Jiles-Atherton model) to describe the magnetic property of the sample. In this study, the measurement was applied to characterize a series of Fe-C samples. However, it is hard to confirm the permeability of a sample when the air gap is unknown, since the magnetic resistance of magnetic circuit composed of the sample and the sensor probe is affected by air gap size. The main idea of our study is that the frequency spectrum of inductance of the magnetic circuit is unaffected when the air gap is adequately small, even if the amplitude of inductance is directly dependent on air gap. The magnetic hysteresis measured with unknown air gap was compensated by measured inductance spectra, and was found to agree with nonlinear FEM analysis.

July 12 (Thu)

July 12 (Thu)

RR31

The several analysis techniques of high speed induction motor for copper die casting

Do-kwan Hong^{1*}, Jae-hak Choi¹, Byung-chul Woo¹, Dae-hyun Koo¹ and Chan-woo Ahn²

¹ Korea Electrotechnology Research Institute, Korea

² Dong-A University, The department of mechanical engineering, Korea



RR32

Effect of magnetic Reynolds number variation on MHD convection inside an enclosure

Mohsen Pirmohammadi*

MAPNA Group, Iran

Numerically investigation is carried out for magnetohydrodynamics natural convection in an enclosure. The vertical walls are maintained isothermal at different temperatures and the other walls are adiabatic. The magnetic field is applied horizontally. The non linear governing equations for the fluid flow and heat transfer are solved for three magnetic Reynolds numbers (10-5, 10-3 and 0.1). The Rayleigh number, the Hartmann number and the Prandtl number are considered 105, 80 and 0.01, respectively. A finite volume code based on Patankar's SIMPLER method is utilized. It is found that when the magnetic Reynolds number (Rem) is very low (10-5 and 10-3) the magnetic field distribution in the cavity is not affected by flow field and as Rem increases the magnetic field in x and y direction is not constant. Also it is observed that as Rem increases the rate of heat transfer changes.

SA01

Magnetic annealing effects on properties of the multilayer BaTiO₃ / CoFe₂O₄ thin films

Yuqiang Dai¹, Jianming Dai^{1*}, Xianwu Tang¹ and Qiangchun Liu²

¹ Key Laboratory of Materials Physics, Institute of Solid State Physics, Chinese Academy of Sciences, China

² School of Physics and Electronic Information, Huaibei Normal University, China

Multilayer BaTiO₃/CoFe₂O₄ thin films are prepared via chemical solution deposition method with and without magnetic field annealing process, respectively. The microstructural, magnetic, dielectric and the ferroelectric properties of the films are investigated. It is observed that the dielectric constant, polarizations and magnetizations of the multilayer thin films are improved with magnetic field annealing process. Moreover, for the magnetic field annealing films, the saturation magnetization with measuring magnetic field vertical to the film surface is much higher than that parallel to the film surface.

SA02

Magnetolectric CoFe₂O₄-PZT thin film composites grown by pulsed laser deposition

Ioanna Giouroudi^{1*}, Mohammed Alnassar², Roland Groessinger³ and Juergen Kosef²

¹ Institute of Sensor and Actuator Systems, Vienna University of Technology, Austria

² Division of Physical Sciences and Engineering, King Abdullah University of Science and Technology, Saudi Arabia

³ Institute of Solid State Physics, Vienna University of Technology, Austria



SA03

Synthesis and magnetic property of multiferroic DyMnO₃ nanoparticles in mesoporous silica

Takayuki Tajiri^{1*}, Kenta Hamamoto², Yuhki Ando², Hiroyuki Deguchi², Masaki Mito² and Atsushi Kohno¹

¹ Faculty of Science, Fukuoka University, Japan

² Faculty of Engineering, Kyushu Institute of Technology, Japan

Multiferroic compound DyMnO₃ shows antiferromagnetic ordering with T_N ~ 40 K and Dy spin ordering below about 6 K. The ferroelectricity is attributed to lattice modulation accompanied by the antiferromagnetic order. We are interested in the size effect on DyMnO₃ nanoparticles with particle size of a few nano-meters. We synthesized DyMnO₃ nanoparticles and investigated their magnetic property. The DyMnO₃ nanoparticles were synthesized in the pores of a mesoporous silica SBA-15 with pore diameter of about 8 nm. SBA-15 was used as a template to equalize the particle size in the fabrication of the DyMnO₃ nanoparticles. The X-ray diffraction pattern for DyMnO₃ nanoparticles shows some broad Bragg peaks corresponding to crystal structure of DyMnO₃ bulk crystals. The size of nanoparticles was estimated to be about 10 nm based on the Bragg peaks and using Scherrer's equation. The temperature dependence of DC magnetic susceptibilities for the nanoparticles exhibited a magnetic irreversibility between field-cooled susceptibility and zero-field-cooled one below about 40 K and an increase in susceptibilities due to magnetic ordering among the Dy spins below about 5 K. The magnetization curves exhibited hysteresis loop below blocking temperature. DyMnO₃ nanoparticles were successfully synthesized with size of about 10 nm and showed superparamagnetic behaviors.

SA04

Magnetic properties of Co_{1-x}Mn_xFe₂O₄ (x=0-0.5) - PZT thin films fabricated by sol-gel spin coating method

M. Khodaei, S. A. Seyyed Ebrahimi* and R. Vaghar

Center of Excellence for Magnetic Materials, School of Metallurgy and Materials, University of Tehran, Iran

Co_(1-x)Mn_xFe₂O₄ (x=0-0.5) thin films were fabricated on PZT layer by sol-gel spin coating method in order to investigation of influence of Mn-substitution in Co₂Fe₂O₄ on the magnetic properties. The films were fabricated on the PZT layer which was previously fabricated on Pt(111)/Ti/SiO₂/Si substrate using the same method. The phase identification of the samples was studied by X-ray diffractometry analysis. Magnetic properties of the samples were also measured using a vibrating sample magnetometer.

SA05

M doping element localization by the molecular field theory in the Ga_{0.6}Fe_{1.4}O₃:M thin films

Christophe Lefevre^{1*}, Ran Hee Shin², Ji Hye Lee², Seol Hee Oh², Alexandre Thomasson¹, Francois Roulland³, Christian Meny¹, William Jo² and Nathalie Viart³

¹ CNRS, France

² Department of Physics, Ewha Womans University, Korea

³ Universite de Strasbourg, France

Magnetolectric materials open the way towards new applications through controlling magnetic or electric polarization with electric or magnetic field, respectively. Ga_{0.6}Fe_{1.4}O₃ is predicted magnetolectric with non zero magnetization at room temperature. High quality GFO thin films having similar magnetic properties to those of the bulk materials have been produced only recently. However their electric properties failed to be properly characterized until now because of important leakage currents originating from a hopping mechanism between Fe²⁺ and Fe³⁺ within the structure. Recently, we succeeded to strongly lower the leakage currents of these films by chemical doping. The determination of the cationic distribution within the structure is a key point for the knowledge of these phases, because it is at the origin of the evidenced magnetic and electrical properties of these materials. We present here an original approach to determine the localization of the M doping element based on the molecular field theory. Different modeling associated with the different substitution possibilities have been performed within the frame of this theory and are compared with the experimental values.

SA06

Interplay between magnetization and polarization in epitaxial (Ga,Fe)₂O₃ thin films with additional ion-substitutions into Fe sites

R. H. Shin¹, J. H. Lee¹, S. H. Oh¹, S. H. Jo^{2*}, C. Lefevre³, F. Roulland³, A. Thomasson³, C. Meny³ and N. Viart³

¹ Department of Physics and CNRS-EWHA International Research Center, Ewha Womans University, Korea

² Department of Physics, Ewha Womans University, Korea

³ Institute of Physics and Chemistry of Materials of Strasbourg, France

(Ga,Fe)₂O₃ (GFO) is a promising material for room-temperature multiferroic because of high magnetic T_C as 370 K when Ga = 0.6 and Fe = 1.4. However, multiferroic properties of GFO in thin film type is controversial because most of polarization-electric field hysteresis curves in GFO showed leaky behaviors due to large leakage current. In this research, we focused on the improved magnetic and electric properties of GFO thin films as multiferroic by decreasing their leakage current. The main origin probably lies on electron hopping between Fe²⁺ and Fe³⁺ octahedron sites which can co-exist due to charge neutrality by oxygen vacancy. Therefore, we tried to decrease leakage current by substituting Fe²⁺ site with divalent cation. The ion-substituted GFO thin films were epitaxially deposited along the b-axis by pulsed laser deposition at 750°C for 15 min in oxygen partial pressure of 200 mTorr on SrRuO₃/SrTiO₃ (111) substrates. The films showed the strongly reduced leakage current up to 5-6 order of magnitude. Magnetic properties of the doped GFO thin films were investigated by SQUID measurement. Ferroelectric polarization as a function of external field was measured in macroscopic and microscopic schemes. Magnetolectric interactions of the epitaxial thin-films will be addressed in this talk.

SA07

Fabrication and characterization of heusler-alloy/perovskite heterostructures

Kohei Kobayashi, Keita Sakuma*, Naoto Fukutani, Tetsuya Miyawaki, Kenji Ueda and Hidefumi Asano

Nagoya University, Japan

Multiferroic heterostructures composed of ferromagnetic half-metal and ferroelectric materials have attracted significant interest due to the potential applications for nanoscale devices. Heusler-alloy / perovskite heterostructures are expected to emerge the interface magnetolectric and tunnel electroresistance effect. In this study, to explore the potential of Heusler-alloy / perovskite heterostructures, we have investigated multiferroic and transport properties of heterostructures composed of half-metallic Heusler-alloy Fe₂CrSi (FCS) and ferroelectric perovskite Ba_{0.5}Sr_{0.5}TiO₃ (BSTO). BSTO was firstly deposited on MgO and LaAlO₃ substrates by magnetron sputtering, followed by the deposition of FCS at 550-750°C. Structural characterization revealed that FCS grew epitaxially on BSTO with the relationship of BSTO(001)[100]||FCS(001)[110]. From M-H curve of the BSTO (100 nm) / FCS (150 nm) bilayer, saturated magnetization of 417 emu/cc was obtained. The ferroelectric properties of La_{0.7}Sr_{0.3}MnO₃ (LSMO) / BSTO (100 nm) / FCS (50 nm) were measured, and the maximum remanent polarization was 73 μC/cm². From these results, ferromagnetic and ferroelectric properties were preserved in BSTO/FCS heterostructures. From the analysis of I-V characteristics, Schottky-emission was found to be a dominant leakage mechanism in LSMO / BSTO / FCS. The BSTO / FCS heterostructure is a promising candidate for fabricating multiferroic devices.

1) K. Yamauchi et al., Appl. Phys. Lett. 91, 062506 (2007)

SA08

Optical properties of (SrMnO₃)_n/(LaMnO₃)_{2n} superlattices: An insulator-to-metal transition observed in the absence of disorder

Andrea Perucchi¹, Leonetta Baldassarre¹, Alessandro Nucara², Paolo Calvani², Carolina Adamo³, Darrell G Schlom³, Pasquale Orgiani¹, Luigi Maritato⁴ and Stefano Lupi³

¹ Sincrotrone Trieste, Italy

² CNR-SPIN and University of Rome 'Sapienza', Italy

³ Cornell University, USA

⁴ CNR-SPIN and University of Salerno, Italy

⁵ CNR-IOM and University of Rome 'Sapienza', Italy

We measure the optical conductivity, σ₁(ω), of (SrMnO₃)_n/(LaMnO₃)_{2n} superlattices (SL) for n=1, 3, 5, and 8 and 10 < T < 400 K. Data show a T-dependent insulator to metal transition (IMT) for n=3, driven by the softening of a polaronic mid-infrared band. At n=5 that softening is incomplete, while at the largest-period n=8 compound the MIR band is independent of T and the SL remains insulating. One can thus first observe the IMT in a Manganite system in the absence of the disorder due to chemical doping. Unsuccessful reconstruction of the SL optical properties from those of the original bulk materials suggests that (SrMnO₃)_n / (LaMnO₃)_{2n} heterostructures give rise to a novel electronic state.

A. Perucchi et al., Nano Letters 10 (12), 4819-4823 (2010)

SA09

Preparation of hexagonal YFeO₃ powder and thin film

Hanju Lee, Kyoungchul Kim, Sujin Lee, Sul A Choi and Kiejin Lee*

physics, Department of physics, Sogang university, Korea

In the past few years, multiferroic materials, characterized by coexistence of two or more ferroicity, have attracted much attention due to their interesting properties. Among the magnetic ferroelectric materials, there is an important class, hexagonal manganese oxides (RMnO₃, R: rare-earth element), which have been extensively studied because of its unusual property. However, hexagonal iron oxides (RFeO₃), which have a similar structure to RMnO₃, have been rarely reported due to a preferred formation to the orthorhombic or garnet phase. Here, we report that the hexagonal phase can be easily prepared as a powder and thin film from chemical solution deposition method (CSD). The crystallization temperature, crystal structure, magnetic and electric properties of the thin film and powder were investigated. The hexagonal phase was observed at 750-800, and at higher temperature (>850) orthorhombic phase appeared. The observed structure belonged to the paraelectric P63/mmc phase, rather than ferroelectric phase. Samples showed paramagnetic property at room temperature caused by geometrically fluctuated magnetism in tri-angular spin lattice.

SA10

Magnetic hysteretic effects in LaAlO₃/SrTiO₃ Heterostructures

Veerendra Kumar Guduru¹, Alix Mccollam¹, Sander Wenderich², Michelle Kruize², Uli Zeitler^{1*}, Alexander Brinkman², Jan Kees Maan¹, Mark Huijben², Hans Hilgenkamp², Gertjan Koster², Guus Rijnders² and Dave Blank²

¹ HFML/IMM, Radboud University Nijmegen, Netherlands

² MESA+ Institute for Nanotechnology, University of Twente, Netherlands

A two-dimensional electron system (2DES) with remarkable electronic properties can be realized at the interface between two band insulators LaAlO₃ and SrTiO₃ (1). Depending on growth conditions, this 2DES has been found to show a superconducting ground state (2), magnetic ordering (3) and even co-existence of these two properties (4-5). The origin of the magnetic behaviour at the interface is still unclear, and to try to understand it we have performed magneto-transport studies on LaAlO₃/SrTiO₃ heterostructures in high magnetic fields up to 33 T, and low temperatures down to 0.3 K. We observed negative magnetoresistance (nMR) which is nearly identical for all field orientations in the temperature range from 4 K to 350 mK. This nMR could be related to reduced spin scattering due to the alignment of spins at the interface (3). At low magnetic fields, the nMR is very sensitive to temperature and at temperatures below 1 K an unusual time dependent magnetic hysteresis appears for field below 3 T. We propose a magnetocaloric effect model to explain the hysteretic behaviour, and propose that the possible underlying origin of the hysteresis is the co-existence of ferro- and antiferromagnetic phases in the spin system.

1) A. Ohtomo and H.Y. Hwang, Nature 427, 423, 2004. 2) N. Reyren et al., Science 317, 1196, 2007. 3) A. Brinkman et al., Nature Materials 6, 493, 2007. 4) L. Li et al., Nat Phys 7 (10), 762-766, 2011. 5) J.A.Bert et al., Nat Phys 7 (10), 767-771, 2011.

SA11

Synthesis and magnetoelectric properties of multiferroic composites on the cobalt ferrite - pzt system

C. Miclea^{1*}, L. Amarande¹, L. Trupina¹, M. Cioangher¹, C. T. Miclea² and C. F. Miclea¹

¹National Institute for Materials Physics, Bucharest, Romania

²Hyperion University, Bucharest, Romania

In the present study we prepared and investigated the properties of bulk particulate composites made from cobalt ferrite (COF) and a soft piezoelectric material (PZT). We chose COF and soft PZT due to their high magnetic and piezoelectric parameters respectively. Composite samples, according to the formula xCOF(1-x)PZT with $0 \leq x \leq 1$ were prepared by mixing the COF and PZT powders, pressing them as discs and then sintered at 1200 C for 3 hours. Structural, magnetic, piezoelectric and magnetoelectric characteristics of the sintered composites were then determined as a function of the weight fraction of COF into PZT and magnetic fields. The ME coefficient shows a maximum value about 70 mV/cmOe for composites containing 40 % COF and 60% PZT, in a DC magnetic field of 3 kOe at a frequency of 1KHz of the ac magnetic field. Some of the dielectric and piezoelectric properties of the composite samples, as a function of the weight fraction x, were also determined. The results were discussed in terms of the recent theoretical cube model of different connectivities of particles of one phase embedded into the matrix of the second phase.

SA12

Detailed structural study of BiFeO₃/SrRuO₃ heterostructures grown on SrTiO₃ (001) substrates

Clanibel Dominguez¹, John Edward Ordonez¹, Maria Elena Gomez¹, Wilson Lopera¹ and Pedro Prieto²

¹Thin Film Group, Department of Physics, Universidad del Valle, A.A. 25360, Cali, Colombia

²Center of Excellence for Novel Material CENM, Calle 13 # 100-00 320-1026, Cali, Colombia

WITHDRAWN

SA13

Lattice engineering on transition metal oxide thin film
Chang Uk Jung*

Department of Physics, Hankuk University of Foreign Studies, Korea

MOVED

SA14

Magnetisation in different multiferroic YMO (Yttrium Manganese Oxide) thin films

Manish Kumar*, R.J. Choudhary and D.M Phase

UGC-DAE CSR, UGC-DAE CSR Indore, Madhya Pradesh, India

Recently Yttrium manganese oxides (YMO): hexagonal YMnO₃ and orthorhombic YMn₂O₇ have attracted considerable attention as both of these compounds exhibit multiferrocity but the microscopic origins are different. Here we stabilize thin films of different phases of YMO by pulsed laser deposition from a single h-YMnO₃ target and characterize them with various techniques and perform magnetization measurements. It is observed that the phase stability and crystallinity of YMO thin films depend on the substrate used and oxygen partial pressure (OPP). Oriented and polycrystalline growth of h-YMnO₃ and O-YMn₂O₇ phase film are observed on different substrates. ZFC, FC (Magnetisation versus Temperature) and MH magnetization measurements of these multiferroic films were performed. All the multiferroic thin films show the antiferromagnetic transition in ZFC measurements which is forbidden in FC measurements. MH behavior at both sides of magnetic transition is in good agreement in these multiferroic thin films.

1. Bas B. Van Aken, Thomas T. M. Palstra, Alessio Filippetti and Nicola A. Spaldin, *Nature Materials*, Vol 3, 2004, pp.164-170 2. L. C. Chapon, P. G. Radaelli, G. R. Blake, S. Park and S.W. Cheong, *Phys.Rev.Letter* 96, 097601 (2006) 3. W. Prellier, M P Singh and P Murugavel, *J. Phys.: Condens. Matter* 17 (2005) R803-R832 4. A Munoz et al 2002 *J. Phys.: Condens. Matter* 14 3285

SA15

Dependence of magnetoelectric response on magnetostrictive content in composite multiferroics

Mohsin Rafique^{1*}, Syed Qamar Ul Hassan¹, Muhammad Saifullah Awan² and Sadia Manzoor¹

¹ Physics, COMSATS Institute of Information Technology, Islamabad, Pakistan

² Center for Nano and Micro Devices (CNMD), COMSATS Institute of Information Technology, Islamabad, Pakistan

Magnetoelectric multiferroics exhibit a strong coupling between ferromagnetic and ferroelectric ordering. The coupling between these two types of orderings may occur naturally or be mediated via mechanically. This coupling is very weak in single phase multiferroics. The design and investigation of composites of magnetostrictive and piezoelectric phases have shown magnetoelectric coupling orders of magnitude higher than that of single phase multiferroics. The mechanical deformation in magnetostrictive and piezoelectric phases results in the coupling between the two constituents. The multiferroic CoFe₂O₄-BaTiO₃ (CFO-BTO) composites with nanoscale mixture of the two constituents were prepared by sol-gel process. Four different compositions, with varying percentage of constituents, were investigated. X-ray diffraction revealed the coexistence of the two phases. Magnetic properties of the CFO-BTO nanocomposites were examined which were consistent with the composition. The magnetoelectric coupling between CFO and BTO was demonstrated by an external magnetic field induced change in capacitance. The magnetoelectric coupling was found to be not only dependent on the applied magnetic field but also on the composition of the composites. It has a nonlinear dependence on magnetostrictive content.

SA16

Raman analyses of oxygen defects in hexagonal HoMnO₃ thin films

Xiang-bai Chen¹, Nguyen Thi Minh Hien², D. Lee³, T. W. Noh³ and In-sang Yang²

¹ Konkuk University, Korea

² Ewha Womans University, Korea

³ Seoul National University, Korea

Oxygen defects are usually unavoidable in synthesizing oxide thin films. In this study, we investigated the origins of the oxygen defects in hexagonal manganites HoMnO₃ epitaxial thin films through Raman spectroscopy. We found that the oxygen defects in hexagonal HoMnO₃ thin films have different effects on different phonon modes and on magnon scattering. Our analyses indicated that the oxygen defects in hexagonal HoMnO₃ thin films would be mainly correlated with the basal O₃ and/or O₄ oxygen ions. Furthermore, our analyses of oxygen defects predicted that the Mn 3d orbitals would be more strongly hybridized with the apical O₁ and/or O₂ 2p orbitals than the basal O₃ and/or O₄ 2p orbitals. This prediction is consistent with our resonant Raman scattering study and earlier first-principle calculations of electronic structures of hexagonal manganites.

SA17

Preparation and properties of inverse perovskite Mn₃GaN thin films

Hiroki Tashiro, Ryosuke Suzuki*, Tetsuya Miyawaki, Kenji Ueda and Hidefumi Asano

Department of engineering, Nagoya University, Japan

There has been considerable interest in antiperovskite Mn₃GaN because of its intriguing physical properties such as negative thermal expansion, magneto-volume effect and piezomagnetic effect(1). Mn₃GaN is expected to be advantageous to fabricate thin-film hybrid devices with various perovskite oxides, since it has a cubic antiperovskite structure virtually identical with the perovskite oxides. However, there is no report on growth of Mn₃GaN thin films and heterostructures. In this paper, we report on the preparation and properties of Mn₃GaN thin films as well as ferroelectric Ba_{0.7}Sr_{0.3}TiO₃/Mn₃GaN heterostructures. Mn₃GaN films were deposited on (001) SrTiO₃ and LaAlO₃ substrates at 450–650°C by ion beam sputtering of a sintered stoichiometric target. Ba_{0.7}Sr_{0.3}TiO₃ films were prepared at 650–750°C by magnetron sputtering. In-plane and out-of-plane X-ray diffraction analysis revealed that on SrTiO₃ substrate Mn₃GaN films were grown coherently with the in-plane lattice parameter aMGN of 0.3903 nm. On LaAlO₃ substrate a Ba_{0.7}Sr_{0.3}TiO₃ layer and subsequently a Mn₃GaN layer were grown epitaxially with the relationship of LaAlO₃(001)[100]/Ba_{0.7}Sr_{0.3}TiO₃(001)[100]/Mn₃GaN (001)[100]. These Mn₃GaN thin films showed a metallic temperature dependence of resistivity with 0.8-0.9 mΩcm at room temperature. It was found that the Ba_{0.7}Sr_{0.3}TiO₃/Mn₃GaN heterostructures exhibited a colossal magnetocapacitance effect.

(4) P. Lukashev, et al., *Phys. Rev. B* 78 184414 (2008)

SA18

Ferroelectric and magnetic properties of BiMnO₃ thin films

Min-hwa Jung and Yoon-hee Jeong*

Department of Physics, Pohang University of Science and Technology, Korea

BiMnO₃ is heralded widely as a rare case of multiferroicity with simultaneous existence of both ferroelectricity and ferromagnetism. Ferroelectricity in BiMnO₃, however, still remains controversial as various results do not converge on a definite conclusion [1-3]. In order to shed light on this issue, we have synthesized BiMnO₃ thin films on Nb:SrTiO₃ substrates by PLD method. Measurements of various physical properties such as dielectric properties, PE hysteresis loop, and piezoelectric d33 do not show any significant evidence of ferroelectricity for all films. Thus, we are led to conclude that BiMnO₃ is not ferroelectric in accordance with a theoretical calculation [4-5]. Also of interest is the ferromagnetism of BiMnO₃ and, in particular, its magnetic easy direction. We also investigate the magnetic properties of the films with in and out of the plane orientations. From these measurements, the magnetic easy direction is inferred for the monoclinic phase BiMnO₃. In conclusion, the present study offers a full characterization of the ferroelectric and magnetic properties of multiferroic BiMnO₃.

[1] T. Kimura, S. Kawamoto, I. Yamada, M. Azuma, M. Takano, and Y. Tokura, *Phys. Rev. B* 67, 180401 (2003) [2] M. Grigalez, E. Martinez, J. Caicedo, et al., *Microelectronics Journal* 39, 1308 (2008) [3] A. A. Belik, S. Iikubo, T. Yokosawa, et al., *J. Am. Chem. Soc.* 129,971 (2007) [4] A.J. Hatt and N.A. Spaldin, *Eur. Phys. J. B* 71,435 (2009) [5] Shichidou T, Oguchi T (2006) *Multiferroicity of BiMnO3 reexamined from first principles. Presented at APS meeting March Meeting, Baltimore, MD.*

SA19

Ferroelectric polarization induced magnetic anisotropy in Co₄₀Fe₄₀B₂₀/YMnO₃ multiferroic heterostructure

Jiawei Wang¹, Yanggang Zhao^{1*}, Peisen Li¹, Sen Zhang¹, Syed Rizwan², Xiufeng Han², Xuefeng Sun³, Yuanjun Yang⁴, Qianping Chen¹ and Xin Zhang¹

¹ Department of Physics and State Key Laboratory of Low-Dimensional Quantum Physics, Tsinghua University, China

² Beijing National Laboratory for Condensed Matter Physics, Chinese Academy of Sciences, China

³ Hefei National Laboratory for Physical Sciences at the Microscale, University of Science and Technology of China, China

⁴ National Synchrotron Radiation Laboratory, University of Science and Technology of China, China

Multiferroic (MF) materials have attracted much attention due to their interesting new physics and potential for exploring novel multifunctional devices. The research of magnetic anisotropy in MF heterostructure is an important aspect. One of the key issues in the MF heterostructures is the effect of ferroelectric (FE) polarization on magnetic anisotropy. So far, however, a lot of work has been carried out on MF heterostructures with crystalline ferromagnetic films. Actually, MF heterostructures involving amorphous ferromagnetic materials are also very interesting due to the absence of magnetocrystalline anisotropy and low coercive force Hc. We have studied the coupling between amorphous magnetic Co₄₀Fe₄₀B₂₀ (CFB) and YMnO₃ (YMO) in the heterostructure with CFB film grown on YMO (110) substrates. A large uniaxial magnetic anisotropy (UMA) was observed from room temperature to 10 K with magnetic easy axis (MEA) along the polarization direction of YMO. More interestingly, the angular dependence of coercive force Hc shows a non-monotonous behavior. The results were discussed by considering the coupling between the FE domain in YMO and magnetism in CFB. This work is helpful for understanding the effect of FE polarization on magnetic anisotropy in MF heterostructures.

SA20

Ferroelectric-domain-switching controlled magnetism in CoFeB/PMN-PT multiferroic heterostructure

Peisen Li¹, Yonggang Zhao^{1*}, Sen Zhang¹, Lifeng Yang¹, Syed Rizwan², Qianping Chen¹, Jiawei Wang¹ and Xiufeng Han²

¹ Department of Physics and State Key Laboratory of Low-Dimensional Quantum Physics, Tsinghua University, China

² Beijing National Laboratory for Condensed Matter Physics, Chinese Academy of Sciences, China

Multiferroic materials have attracted much attention due to their interesting new physics and potential applications in new multifunctional devices. In multiferroic materials, the magnetization can be tuned by electric fields, which open a new way to reach high integration density and low power consumption in information storage. In the shorter term, niche applications are more likely to emerge in the two-phase systems [1], so there have been lots of work on the electric-field control of magnetism via the piezostain in ferromagnet-ferroelectric heterostructures[2, 3]. However, the reports related to magnetoelectric (ME) effect via ferroelectric domain switching are still limited. Thus, we have studied the electric-field control of magnetism in Co₄₀Fe₄₀B₂₀/Pb(Mg_{1/3}Nb_{2/3})_{0.7}Ti_{0.3}O₃(PMN-PT)(001) two-phase-system. Non-volatile and volatile changes of magnetization related to different types of ferroelectric domain switching were found and the ratio between them changes with temperature. The angular-dependence of electric-field control of magnetism indicates that some magnetic domains rotate 90°, which is consistent with our in situ electric-field-dependent magnetic force microscopy data. The results were explained by considering the ferroelectric domain switching induced magnetic anisotropy. This work is helpful for understanding the coupling between magnetism and ferroelectric domain switching.

[1] W. Eerenstein et al., *Nature* 442, 759 (2006). [2] C. Thiele et al., *Phys. Rev. B* 75, 054408 (2007). [3] J. J. Yang et al., *Appl. Phys. Lett.* 94, 212504 (2009).

SA21

Multiferroic properties of BaTiO₃ - Zn_{1-x}Co_xO multilayer thin films

Anuraj S¹, Shivaraman Ramaswamy^{1*}, Helen Annal Therese¹, C Gopalakrishnan¹ and A Karthigeyan²

¹ Nanotechnology Research Center, SRM University, India

² Department of Physics and Nanotechnology, SRM University, India

Near room temperature ferroelectric and ferromagnetic hysteresis is observed in horizontal superlattice system of BaTiO₃ - Zn_{1-x}Co_xO (x > 0.2) [BTO - ZCO] multilayered thin films. The multilayered thin films were prepared on Si substrate by alternate deposition of BTO and ZCO layers to a thickness of 350 nm using pulsed laser deposition technique. Analysis of the prepared thin film by x-ray powder diffraction and electron microscopic techniques confirm the polycrystalline nature of the multilayered film. Dielectric and the magnetic properties studied on the multilayered thin film at different temperatures exemplified the coupling between their dual order parameters and it is mediated through an electric field effect at the interface.

1. *Multiferroic properties of Bi0.8La0.2FeO3/CoFe2O4 multilayer thin films.* Shan-Tao Zhang, Yi Zhang, Zhen-Lin Luo, Ming-Hui Lu, Zheng-Bin Gu, Yan-Feng Chen., *Applied Surface Science* 255 (2009) 5092-5095. 2. *Multiferroic BaTiO3-CoFe2O4 Nanostructures.*, H. Zheng, J. Wang, S. E. Lofland, Z. Ma, L. Mohaddes-Ardabili, T. Zhao, L. Salamanca-Riba, S. R. Shinde, S. B. Ogale, F. Bai, D. Viehland, Y. Jia, D. G. Schlom, M. Wittig, A. Roytburd, R. Ramesh. *Science* 303, (2004) 661.

SA22

Study of structural phase transition and multiferroic properties of Samarium substituted BiFeO₃ thin films

Mahdiyar Bagheri, Shivaraman Ramaswamy*, Helen Annal Therese and C Gopalakrishnan

Nanotechnology Research Center, SRM University, India

In this study we report the effect of samarium substitution on the structure and multiferroic properties of BiFeO₃ thin films. The Bi_{1-x}Sm_xFeO₃ thin films of various thicknesses were sputter deposited on to Si substrates. Magnetic and electric properties of the thin films were studied by vibrating sample magnetometer, impedance analyzer and I-V characterizer. Samarium substitution-driven structural phase transition was studied by x-ray diffraction at room temperature. Samarium doping was found to modify structural properties of Bi_{1-x}Sm_xFeO₃ thin film. The phase transition was found to destruct cycloid spin structure of BiFeO₃ that resulted in amplified magnetoelectric interactions. The substitution of Sm was found to be a promising way to control the conductivity and leakage current of film by suppressing the formation of oxygen vacancies.

1. Hiroshi Uchida, Risako Ueno, Hiroshi Funakubo, and Seichiro Koda, *J. Appl. Phys.* 100, 014106 (2006) 2. E. Ohshima, Y. Suya, M. Nantoh and M. Kawai *Solid State Commun.* 116 (2000), p.73.

SA23

Study of ferroelectricity in Eu substituted BiMnO₃ films

Shivaraman Ramaswamy*, Helen Annal Therese and C Gopalakrishnan
Nanotechnology Research Center, SRM University, India

In this paper, we report evidence of ferroelectricity in europium substituted manganite (Bi_{1-x}Eu_xMnO₃) thin films synthesized via sol gel synthesis and dip coating method on a single-crystal (1 0 0) substrates. The films were post treated by annealing at 500°C. X-ray diffraction measurements were used to analyze the crystal structure and phase purity of the thin films. AFM measurements were performed to investigate surface morphology; quantitative values of roughness and grain size which are in the range between 30 and 150 nm. Ferroelectric characterization was conducted at low temperatures and at 300 K. Hysteresis loops (polarization vs. voltage) were obtained, showing enhanced ferroelectricity at room temperature in the 10% Eu substituted BiMnO₃ film. Resistance vs. temperature measurements were performed, which indicated this to be very robust insulating material. Moreover, all films show small dielectric dispersion and dielectric loss.

SB02

Charge disproportion, spin and orbital states in the tri-layered nickelate La₃Ni₂O₈ from first principles

Hua Wu*
Department of Physics, Fudan University, Shanghai, China

Several mixed-valent layered nickelates were synthesized very recently [1,2], in the effort to search an analog to the hole doped cuprates. Here we have studied the electronic structure and the magnetism of the tri-layered La₃Ni₂O₈, using the configuration-state constrained LDA+U calculations. Our results show that La₃Ni₂O₈ would be a charge homogeneous low-spin half metal in the ferromagnetic state. In contrast, the C-type antiferromagnetic state is insulating and has a charge disproportion of the formal 2Ni¹⁺/Ni²⁺ type, thus accounting for several experimental observations. The high-spin (S=1) Ni²⁺ state and its orbital configuration are found to be against the crystal-field level picture. We note that it would be interesting to explore, for novel magnetism and superconductivity, the Ni²⁺ low-spin S=0 state and the partially occupied x₂-y₂ band structure of the Ni¹⁺/Ni²⁺ mixed-valent nickelate.

[1] V. V. Poltavets et al., *Phys. Rev. Lett.* 104, 206403 (2010). [2] V. V. Poltavets, M. Greenblatt, G. H. Fecher, and C. Felser, *Phys. Rev. Lett.* 102, 046405 (2009).

SA24

Experimental evidence for Exchange bias in polycrystalline BiFeO₃ / Ni_{0.8}Fe_{0.9}

Tony Hauguel, Souren P Pogossian, David Toyo Dekadjevi*, Jean-philippe Jay, Mikhail Indenbom, David Spenato and Jamal Ben Youssef
Laboratoire de Magnetisme de Bretagne, CNRS-Universite Europeene de Bretagne, France

Multiferroic (MF) materials have been the subject of extensive studies in the past decade since it allows a coupling of ferroelectric and magnetic orders in a single phase. Among all the multiferroic materials studied so far, BiFeO₃ (BFO) exhibits the coexistence of ferroelectric and antiferromagnetic orders at room temperature. Magnetic heterostructures with a ferromagnetic thin film exchange biased to an antiferromagnetic-BFO film may allow an electric field influence on the magnetic hysteresis properties of the bilayer. The exchange coupling and exchange bias involving MF/F systems has previously been obtained with either epitaxial BFO [1] or BFO bulk materials [2]. However, the exchange coupling between a ferromagnetic film and a polycrystalline multiferroic was not studied. Furthermore, previous studies have shown that polycrystalline BFO exhibits multiferroic properties. We report experimental evidence for exchange bias in polycrystalline BiFeO₃/Ni_{0.8}Fe_{0.9} bilayers, grown by RF sputtering [3]. Our measured 17 Oe shift corresponds to exchange energy per unit area of interface coupling the two films of 11×10³ erg/cm² comparable with similar epitaxial grown systems. The azimuthal behavior of longitudinal and transverse components of magnetization reveals the presence of induced unidirectional and biquadratic anisotropies.

[1] H. Bea et al., *Phys. Rev. Lett.* 100, 017204 (2008) [2] J. Dho et al., *J. Appl. Phys.* 106, 073914 (2009) [3] T. Hauguel et al., *J. Appl. Phys.* 110, 073906 (2011).

SB01

Parit variation in the rectangular array of periodic holes on superconducting thin film

Kamran Muhammad* and Qiu Xiang Gang²
¹ *Physics, COMSATS Institute of IT, Islamabad, Pakistan*
² *Institute of Physics, Chinese Academy of Sciences, Beijing, China*

Superconductivity has been full of surprises and wonder. One of the most elegant properties of superconductors is the quantization of magnetic flux in units of φ₀=h/2e, where h is the Planck constant of quantum mechanics, and 2e the electron-pair charge serving the fundamental building block of the superconducting condensate. Here we report our discovery of a new twist of this phenomenon in a film geometry perforated with a periodic lattice of sub-micron holes, a variation of the flux quantization based on the parity of the number of the flux quanta. Measured in terms of magneto-resistance at temperatures just below the transition temperature of the bulk superconductor, we find that superconductivity is most enhanced at odd multiples of the flux quantum. We explain the phenomenon by noting that thermal quasi-particles, which see the superconducting flux quantum only as half, are in fact suppressed at these flux values. In fields larger than the thermodynamic critical field, where quasi-particles dominate, magneto-resistance minima only occur at such odd values.

SB03

Carrier doping to the novel layered nickelate

Yoshiki Sakurai, Yoshihide Kimishima and Masatomo Uehara*
Yokohama national university, Japan

Recently a series of new layered nickelate (Ln_{n+1}Ni₂O_{2n+2}) (Ln=La, Nd) has been synthesized with using CaH₂ as a reducing agent or hydrogen gas. The crystal structure is the analogue of so-called Ruddlesden-Popper phase, and basically the same crystal structure with high-Tc superconducting cuprate, consisting of insulating block layer and two-dimensional NiO₂ layer. Interestingly Ni ions in these materials can have the same electronic configuration with Cu²⁺ 3d₉ in high-Tc cuprate, suggesting that this is a promising candidate for another high-Tc material. Therefore, we have tried to carrier-dope to Ln and Ni sites of (Ln_{n+1}Ni₂O_{2n+2}) (Ln=La, Nd) with n=2, 3, and ∞ using Ca, Cu, Co ions in order to tune the electronic state of Ni. If the Ni electronic state is adjusted to 3d_{8.15} or 3d_{8.85} which are the same cases with those of optimum doping level for the emergence of high-Tc in cuprate. We will present the detailed result in the conference.

SB04

Occurrence of superconductivity and structural variations in the Sr_{1-x}T_{2-x}Ge₂ layer system (T = Ni, Pd, and Pt; x ≥ 0)

H. C. Ku¹, I. A. Chen¹, C. H. Hung¹, C. Y. Lin¹, S. J. Wang¹, Y. B. You¹, M. F. Tai¹ and Y. Y. Hsu²
¹ *Department of Physics, National Tsing Hua University, Taiwan*
² *Department of Physics, National Taiwan Normal University, Taiwan*

Superconducting transition temperature T_c of the body-centered-tetragonal (bct) 122 Sr(Ni_{1-y}Pd_y)₂Ge₂ (0 ≤ y ≤ 1) layer system (space group I4/mmm) increases monotonically from 0.87 K for 3d-Ni SrNi₂Ge₂ to 3.12 K for 4d-Pd SrPd₂Ge₂. However, due to larger atomic radius of 5d-Pt, the bct stoichiometric Sr(Pd_{1-y}Pt_y)₂Ge₂ phase (I4/mmm) is unstable and a structural transformation to a vacancy stabilized superstructure Sr_{1-x}(Pd_{1-y}Pt_y)_{2-2x}Ge₂ with orthorhombic space group Pmna may be formed. Trace of superconductivity with T_c ranging from 5-10 K in the Sr_{1-x}Pt_{2-2x}Ge₂ system was observed but very difficult to be stabilized. This structural transformation is very similar to the high temperature superconducting system K_{1-x}Fe_{2-2x}Se₂ with I4/mmm and two superstructure space groups Pmna and I4/m, where superconductivity T_c up to 32 K was reported only in the bct I4/m system. This work was supported by Grant No. NSC98-2112-M-007-013-MY3 of National Science Council of Republic of China.

SB05

Fermi surface study on the rattling-induced superconductor KO₈O₆

Taichi Terashima^{1*}, Nobuyuki Kurita¹, Andhika Kiswandi², Eun-sang Choi², James S. Brooks², Kota Sato³, Jun-ichi Yamaura³, Zenji Hiroi³, Hisatomo Harima⁴ and Shinya Uji¹
¹ *National Institute for Materials Science, Japan*
² *National High Magnetic Field Laboratory, USA*
³ *ISSP, Univ. of Tokyo, Japan*
⁴ *Graduate School of Science, Kobe Univ., Japan*



SB06

Transient analysis of the current density and temperature distribution of the MgB₂ superconductor in the He atmosphere

H. M. Iftekhar Jaim¹ and Klaus Barner²
¹ *Department of Mechanical, Material and Aerospace Engineering, University of Central Florida, USA*
² *Department of Physics (4 Physik), University of Gottingen, F. Hund Platz 1, 37077 Gottingen, Germany*

In this paper, the transient analysis is carried out for the type II superconductor material MgB₂ in liquid Helium atmosphere. The strong nonlinearity of the E-J relationship near critical current poses a challenge in such calculations for getting practical values in other models employed for Ohmic materials. For this reason, the curl-curl equation and the variable magnetic field quantity are employed as the unknown in solving the PDE by the finite element method. The temperature distribution by the generated heat in the superconductor is calculated by the coupled conduction and convection module. Using the nominal experimental values for the exponential current fundamental characteristics like the magnetic flux, current distribution density and temperature profile in the superconductor are calculated for 2D axis symmetric cylindrical cases. The study gives the limiting current values to avoid heat generation and shows the development of the mixed state and finally the normal state with the time. Effect of changing the magnitude of current and time constant is also studied. Ripple effect at the surface is observed due to difference in the inner and outer magnetic flux distribution.

SB07

Meissner-like effect on normal- superfluid interface of imbalanced Fermi gas

Neda Ebrahimian* and Mohammad Mehrafarin
Physics Department, Amirkabir University of Technology, Tehran 15914, Iran

The observation of phase separation between the superfluid (SF) core and a normal (N) shell around the core in ultra-cold Fermi gases has been reported by the new experiments of MIT and Rice groups[1-2]. Much researches have been done about the N-SF interface[3-5]. In this article, we examine the N-SF interface of a imbalanced Fermi gas with two spin species, in the presence of a weak magnetic field. In our analysis, we consider a constant magnetic field in the N side and anticipate the possibility of the Meissner-like effect in the SF side. We take into account the various scattering regions of the BCS regime and analytically obtain the transmission coefficients by using the perturbed Bogoliubov equations. It suffices to remark that the leading order term in transmission coefficients are independent of the energy of incident quasiparticles. Then, we calculate the heat conductivity across the interface at sufficiently low temperatures. We describe how the heat conductivity is affected by the Meissner effect and the species imbalance. Also the relation between the additional heat conductivity and penetration depth is obtained. The corresponding graphs is also plotted and discussed. Furthermore, we show the dependence of the heat conductivity on average chemical potential.

References: [1] G. B. Partridge, W. Li, R. I. Kamar, Y. A. Liao, and R. G. Hulet, *Science* 311, 503 (2006). [2] M. W. Zwerlein, A. Schirotzek, C. H. Schunck, and W. Ketterle, *Science* 311, 492 (2006). [3] B. Van Schaeybroeck and A. Lazarides, *Phys. Rev. Lett.* 98, 170402 (2007). [4] N. Ebrahimian, M. Mehrafarin, and R. Afzali, *Physica B* 407, 140 (2012). [5] N. Ebrahimian, M. Mehrafarin, and R. Afzali, *To be published Physica C: Superconductivity* (2012).

SB08

Magnetic properties and structure evolution along R₂RhIn₈ series

Petr Cermak^{1*}, Marie Kratochvilova¹, Jan Prokleska¹, Marie-helene Lemeec-cailleau², Bachir Ouladdiaf² and Pavel Javorsky¹
¹ *Department of Condensed Matter Physics, Charles University in Prague, Czech Republic*
² *Institut Laue-Langevin, France*

Intermetallic compounds R₂RhIn₈ (R = rare earth) are structurally related to a class of Ce-based heavy-fermion superconductors. Study of their magnetic structure and behavior is important for understanding mechanism of the unconventional heavy-fermion superconductivity. We have successfully grown single crystals of these compounds with R = Nd, Tb, Dy, Ho, Er and Tm from the melt in the In flux. We report the evolution of the magnetic properties of this series. All studied compounds exhibit antiferromagnetic behavior with the Neel temperatures up to 43 K for Tb compound. Magnetization and specific heat measurements have revealed metamagnetic transitions to another antiferromagnetic phase for Tb, Dy and Ho compounds. We show detailed magnetic phase diagrams for all these compounds and compare with results reported for Nd₂RhIn₈ [1]. Low temperature magnetic structures were studied by neutron diffraction at the Institute Laue-Langevin on VIVALDI Laue diffractometer and four-circle D₁₀ diffractometer. From these experiments, propagation vector k = (1/2, 1/2, 1/2) and magnetic structure of studied compounds were determined. We present comparison of our results with the magnetic structure of Ce₂RhIn₈ and other isostructural compounds from RRhIn₅ [2] and R₂CoGa₈[3] series.

[1] J. G. S. Duquea, et al., *J. Magn. Magn. Mater.* 323 (2011) 954-956 [2] N. V. Hieu, et al., *J. Phys. Soc. Japan* 75 (2006) 074708 [3] D. A. Joshi *Phys. Rev. B* 77 (2008) 174420

SB09

Second magnetization peak and magnetic field distribution in superconductor

Denis Gokhfeld
L.V. Kirensky Institute of Physics, Russia

The peak effect on M-H loop of superconductors is analyzed within the framework of the extended critical state model (ECSM) [D. M. Gokhfeld, D. A. Balaev, S. I. Popkov, K. A. Shaykhutdinov, M. I. Petrov, *Physica C* 434, 135 (2006)]. The second magnetization peak is referred to the vortex lattice transition or the normal phase rise occurred at a certain magnetic field value. According to ECSM, these processes extend from the surface of a sample (or a granule) to inside due to the magnetic field gradient. Any experimental M-H loops are fitted by assigning the appropriate distribution of the magnetic field in the sample and the field dependence of the critical current density. ECSM predicts that the asymmetry of M-H loop produces the mismatch of the peak positions in the field increasing and decreasing branches. The peak in the field increasing cycle is situated at lower H value than one in the field decreasing cycle.

SB10

Superconductivity in LuGe₂ single crystals

N. H. Sung¹, A. I. Coldea², S. K. Choi², H. Kim^{3,4}, R. Prozorov^{3,4}, and B. K. Cho^{1,5*}
¹ *School of Materials Science and Engineering, Gwangju Institute of Science and Technology (GIST), Gwangju 500-712, Korea*
² *Clarendon Laboratory, Department of Physics, University of Oxford, Oxford OX1 3PU, United Kingdom*
³ *The Ames Laboratory, Ames, Iowa 50011, USA*
⁴ *Department of Physics and Astronomy, Iowa State University, Ames, Iowa 50011, USA*
⁵ *Department of Photonics and Applied Physics, Gwangju Institute of Science and Technology (GIST), Gwangju 500-712, Korea*

Superconducting binary germanide LuGe₂ single crystals were synthesized using a high-temperature metal flux method. Several shiny plate-like single crystals were obtained and the compound has the orthorhombic ZrSi₂-type structure (a = 3.9817 Å, b = 15.5573 Å, c = 3.8477 Å). Superconducting phase transition temperature at T_c = 2.35 K was confirmed by temperature- and magnetic-field-dependent magnetization, and electrical resistivity measurement. In addition, we observed anomalous phase transition at around T = 4 K, and confirmed the conventional superconductivity by heat capacity measurement. Including these results, we will discuss the nature of LuGe₂ single crystals in detail.

SB11

Mutual interplay of magnon BEC and superconductivity

Zygmunt Bak*

Institute of Physics, Institute of Physics, Jan Dlugosz University, Czestochowa, Poland, Poland

We present a theoretical study of the mutual interplay of magnon Bose-Einstein condensate and superconductivity /SC/, provided that they are simultaneously present. As a rule these phenomena are treated separately but it is evident that, at least in the case of triplet SC, there arises coherence in the electron as well as in the magnetic system. Therefore it is reasonable to assess whether magnon BEC can facilitate transition to the superconducting state. Such situation should arise when the electron pairing arises due to the magnetic interactions. In this case electron pair is accompanied by a cloud of magnons and below critical temperature there arises composed electron-magnon condensate. We point out that there are experimental evidences that magnetic coherence reduces or even switches off the destructive effect of magnetic excitations on SC. We prove that in the case of triplet superconductivity there should appear the quadrupolar coherence and what's more quadrupolar interactions contribute to the electron pairing. We give arguments that Josephson tunneling and "second sound" experiments in magnon and electron condensates with various junction and setups can serve as a cross-tests verifying/falsifying hypothesis that in some systems SC is based on magnetic interactions.

SB12

Studies of the absolute value of lambda in unconventional superconductors

Jeehoon Kim*, Filip Ronning, N. Haberkorn, L. Civale, J. D. Thompson and Roman Movshovich

Los Alamos National Laboratory, USA

The superconducting coherence length (ξ), magnetic penetration depth (λ), and their anisotropy are fundamental parameters that characterize superconducting materials. The value of ξ can be estimated from the superconducting upper critical field (H_{c2}) using the Ginzburg-Landau theory. In contrast to ξ , precise determination of the absolute λ value is notoriously difficult. In this talk we present a simple, robust, and model-independent technique to measure λ using magnetic force microscopy (MFM), and discuss our recent results of the measurements of the absolute value of λ in a variety of unconventional superconductors, such as MgB₂, borocarbides, and pnictides. In MgB₂ we will discuss the influence of the intra-band contributions on the superconducting properties and scattering effect between the two bands. In a recently discovered Ca₁₀(Pt₄As₈)₂[(Fe_{1-x}Pt_x)₂As₂]₂ (x=0.097) single crystal, we observed large λ . Large λ and high anisotropy in this system enhance thermal fluctuation, which leads to a liquid vortex phase in this low-temperature (T_c ≈ 11 K) superconductor. Also, we will discuss the effect of irradiation on the value of λ in Ca₁₀Na_{0.3}Fe₂As₂. Finally, we will present our results on the anisotropy of λ in a pnictide Ba-122 system, which shows a different temperature dependence from that of HS_{c2}.

SB13

Self-consistent calculations of the effects of disorder in d- and s-wave superconductors

Long He and Yun Song*

Department of Physics, Beijing Normal University, China

The kernel polynomial method (KPM) [1], as an approach for deriving highly accurate spectral properties of large sparse matrices, is very suitable for the numerical study on the Anderson localization problem. We investigate the effects of disorder in the two-dimensional inhomogeneous superconductors within the KPM by solving self-consistently the Bogoliubov-de Gennes equations [2, 3]. Comparing the behaviors of optical conductivity and the time evolutions of single particle Green's function in superconducting phases with different pairing symmetries, we find that the delocalized screening effect on the localized quasiparticle states is sufficiently larger in the d-wave superconductor than that in the s-wave superconductor. Within a considerable large range of disorder strength, the disorder-induced pseudogap state is derived close to the s-wave superconductor-insulator transition.

[1] A. Weisse, G. Wellein, A. Alvermann, and H. Fehske, *Rev. Mod. Phys.* 78, 275 (2006). [2] L. Covaci, F. M. Peeters, and M. Berciu, *Phys. Rev. Lett.* 105, 167006 (2010). [3] Y. Nagai, Y. Ota, and M. Machida, *J. Phys. Soc. Jpn.* 81, 024710 (2012).

SB14

Superconductivity and structural transition of RPt₂Si₂ (R = Y, La, Lu)

Yutaro Nagano¹*, Nobutaka Araoka¹, Akihiro Mitsuda¹, Hirofumi Wada¹, Masaki Ichihara², Masahiko Isobe² and Yutaka Ueda²

¹ *Department of Physics, Kyushu University, Japan*

² *Institute for Solid State Physics, University of Tokyo, Japan*

The RPt₂Si₂ compounds, where R stands for a rare-earth element, have a tetragonal CaBe₂Ge₂-type structure. LaPt₂Si₂ and YPt₂Si₂ are superconductors with T_c ~ 2 K [1]. On the other hand, the compounds with R = La and Pr show anomalies in the temperature dependence of electrical resistivity [2,3]. These compounds are metallic but the resistivity shows a step at T* ~ 110 K, which is attributable to a charge density wave (CDW) transition. In order to detect a periodic lattice distortion due to CDW, we performed selected area electron diffraction (SAED) and X-ray diffraction (XRD) measurements at low temperatures. It was found that (2 2 0) reflection peak was split into two sub-peaks with equal intensity below T* in XRD measurements. This fact indicates that LaPt₂Si₂ has an orthorhombic symmetry at low temperatures. The SAED patterns show (n/3 0 0) superlattice reflections with n = 1 and 2 below T*. These results strongly support the formation of CDW in LaPt₂Si₂. In contrast, we did not observe any anomalies in the temperature dependence of resistivity except the superconducting transition for YPt₂Si₂ and LuPt₂Si₂. These results are suggestive of no significant relation between CDW and superconductivity in the RPt₂Si₂ compounds.

[1] R.N. Shelton et al, *Solid State Commun.* 52 (1984) 797. [2] F.C. Ragel, et al., *J. Phys. Condens. Matter* 20 (2008) 055218. [3] M. Kumar et al. *Phys. Rev. B* 81 (2010) 125107.

SB15

Magnetic property in ferromagnetic superconductor UGe₂ above ferromagnetic critical pressure

Naoyuki Tateiwa¹*, Yoshinori Haga¹, Tatsuma D Matsuda¹, Eetsuji Yamamoto¹, Yoshichika Onuki² and Zachary Fisk³

¹ *Advanced Science Research Center, Japan Atomic Energy Agency, Japan*

² *Graduate School of Science, Osaka University, Japan*

³ *University of California, USA*

UGe₂ is a ferromagnet with the Curie temperature of 54 K at ambient pressure. The ferromagnetic transition temperature decreases with increasing pressure. The superconductivity appears in the pressure region of 1.0-1.6 GPa where UGe₂ is in the ferromagnetic state. Ferromagnetic state disappears above P_c = 1.6 GPa. Previous studies up to 2 GPa showed that the broad maximum appears in the temperature dependence of the ac magnetic susceptibility and that the ferromagnetic state is induced at metamagnetic field H_m above P_c. These phenomena are resemblance to weak ferromagnetic compound in the 3d electron system such as ZrZn₂. In this study, we have measured the dc-magnetization up to 4.1 GPa using the ceramic anvil high pressure cell. We confirmed the maximum at T_{max} in the temperature dependence of the dc magnetic susceptibility. With increasing pressure, T_{max} is increased from 24 K at 1.9 GPa to 32 K at 2.6 GPa. The peak structure around T_{max} becomes broader with increasing pressure and disappears above 4 GPa. The metamagnetic transition field H_m increases rapidly with increasing pressure. We discuss the experimental results with the phenomenological spin-fluctuation theory.

SB16

Electron and hole transmission through superconductor - normal metal interfaces

Kurt Gloos* and Elina Tuuli

Department of Physics and Astronomy, University of Turku, Finland

We have investigated the transmission of electrons and holes through interfaces between superconducting aluminum (T_c = 1.2 K) and various normal metals (copper, gold, palladium, platinum, silver) using Andreev-reflection spectroscopy at T = 0.1 K. Most of the contacts had the typical Andreev reflection spectra and could be analyzed with the modified BTK theory. We included Dyne's lifetime as a fitting parameter Γ in addition to superconducting energy gap 2Δ and normal reflection described by Z. For contact areas from 1 nm² to 10 000 nm² the BTK Z parameter was 0.5, corresponding to transmission coefficients of about 80%. This is considerably larger than estimated based on reports of other experimental methods (proximity effect and CPP resistance of multilayers) or expected theoretically. The small variation of Z indicates that the interfaces have a negligible dielectric tunneling barrier and that Fermi surface mismatch does not depend on the normal metal. Our results contradict standard expectations and call for a revision of the interpretation of the BTK theory and normal reflection. This is an especially important topic for applying Andreev-reflection spectroscopy to unconventional superconductors or for measuring the local spin polarization of ferromagnets.

SB17

Magnetic field-induced odd-frequency superconductivity in s-wave superconductors

Masashige Matsumoto¹*, Mikito Koga² and Hiroaki Kusunose³

¹ *Department of Physics, Faculty of Science, Shizuoka University, Japan*

² *Department of Physics, Faculty of Education, Shizuoka University, Japan*

³ *Department of Physics, Ehime University, Japan*

The wavefunction of the Cooper pair of the conventional BCS state is characterized by the even parity (s-wave) and spin singlet state. It is well known that an external magnetic field modifies the wavefunction of the Cooper pair and breaks the conventional BCS superconducting state. We find that the wavefunction of the modified Cooper pair contains a spin triplet component with the s-wave orbital symmetry. While the spin triplet s-wave Cooper pair is forbidden owing to the fermion property, it is permitted in the generalized theoretical framework containing the odd-frequency dependence of the order parameter. We investigate this point on the basis of the self-consistent calculation in the Eliashberg theory and find that the odd-frequency order parameter coexists with the even-frequency one [1]. We also report how physical properties are affected by the induced odd-frequency superconducting order parameter [2].

[1] M. Matsumoto, M. Koga, and H. Kusunose, *J. Phys. Soc. Jpn.* Vol. 81, 033702 (2012).

[2] H. Kusunose, M. Matsumoto, and M. Koga, *Phys. Rev. B* Vol. 85, 174528 (2012).

SB18

Enhanced pinning properties and the zero-resistance state in melt-textured high-Tc superconductors probed by pulsed magnetic fields

Fabio Teixeira Dias¹*, Valdemar Das Neves Vieira¹, Douglas Langie Da Silva¹, Sabrina Esperanca Nunes¹, Frederik Wolff-Fabris², Erik Kampert³, Jacob Schaf⁴ and Joan Josep Roa Rovira¹

¹ *Department of Physics, Universidade Federal de Pelotas, 96010-900, Pelotas, Brazil*

² *Dresden High Magnetic Field Laboratory, HZ Dresden-Rossendorf, 01314, Dresden, Germany*

³ *Universidade Federal do Rio Grande do Sul, 91501-970, Porto Alegre, Brazil*

⁴ *Universite de Poitiers, 86962, Poitiers, France*

Among several techniques to grow high-temperature superconductors, melt-textured techniques have emerged as an alternative way to produce materials with physical properties needed for some technological applications. In this work we have studied the correlation between the magnetic irreversibility line and the zero-resistance state in melt-textured YBaCuO samples (Y123) with inclusions of Y211 phase particles by performing magnetization and magnetotransport measurements in DC and pulsed magnetic fields up to 60 T and temperatures down to 1.5 K [1]. Our results show for in-plane magnetic fields an irreversibility field higher than 40 T at 77 K which evidences a strong pinning effect due to the interface of the Y211 particles embedded in the Y123 phase. We have observed effects of the intrinsic pinning due to the anisotropic superconductivity of the Y123 phase. Access to pulsed high magnetic fields reveals a suppression of the low-temperature magnetic irreversibility field relative to BC_c. These results show experimental evidences for field-induced microscopic quantum fluctuations as observed in different high-Tc superconductors. Our findings in melt-textured YBCO samples exclude the possibility that the zero-resistance state and the magnetic irreversibility merge in this field range [2,3,4], showing evidences of weak granularity and providing a good candidate for technological applications.

[1] J. Schaf, P. Pureau, F. Dias, V. Vieira, P. Rodrigues Jr., and X. Obradors, *Phys. Rev. B* 77, 134503 (2008). [2] C. Ehner and D. Shroud, *Phys. Rev. B* 31, 165 (1985). [3] P. Pureau, R. Costa, J. Roa-Rojas, and P. Prieto, *Phys. Rev. B* 61, 12457 (2000). [4] J. Rosenblatt, P. Peyral, A. Rabouan, and C. Lebeau, *Physica B* 152, 95 (1988).

SB19

Phenomena of vortex pinning by composite pinning array on Nb films

Sheng Hao Wang¹*, Lance Horng¹, T. C. Wu², Chien-miao Chen¹, R. Cao¹ and J. C. Wu¹

¹ *Dept. of Physics, National ChangHua University of Education, Taiwan*

² *Dept. of Electronic Engineering, National Formosa University, Taiwan*

In type II superconductor, magnetic fields can penetrate into the superconductor inhomogeneously as an array of vortices. The interaction of these vortices and vortex-pinning interactions in the superconductor give rise to a rich variety of static and dynamical phases. In our study, smaller pinning sites at the center of every hexagonal cell were added when fabricating film with honeycomb array to obtain films with composite pinning array. It has been prepared on Si₃N₄-coated Si wafers using electron-beam lithography in conjunction with reactive ion etching. Then a dc sputtering completed the four-terminal geometry niobium films over the composite array. MR measurements were carried out by a four-probe technique. Special matching peaks of critical currents are exhibited at different temperatures in the measurements. The positions and structures of the matching peaks seem irregular and are very different from the structures of the matching peaks for previously explored films, such as films with triangular, square, or honeycomb pinning arrays. Considering the multiple-vortex filling of different pinning sites, we can give a reasonable explanation to this interesting phenomenon.

T. C. Wu, R. Cao, T. J. Yang, L. Horng, J. C. Wu, Jan Kolacek, *Solid State Commun.* 143, 171 (2010), R. Cao, Lance Horng, T. J. Yang, T. C. Wu, J. C. Wang, and J. C. Wu, *J. Appl. Phys.* 107, 09E129 (2010), T. C. Wu, J. C. Wang, Lance Horng, J. C. Wu, and T. J. Yang, *J. Appl. Phys.* 97, 10B102 (2005)

SB20

Superconducting fluctuations near the Mott critical point

Moon-sun Nam¹, Cecile Mezriere², Patrick Batail² and Arzhang Ardavan¹

¹ *The Clarendon Laboratory, Department of Physics, University of Oxford, United Kingdom*

² *Laboratoire MOLTECH-Anjou, UMR 6200 CNRS-Universite d'Angers, 2 Boulevard Lavoisier, F-49045 Angers, France*

The Nernst effect, the voltage that occurs transverse to crossed temperature gradient and magnetic field applied to a conductor, is a sensitive probe of superconducting fluctuations in unconventional superconductors such as the high-Tc cuprates [1] and organic superconductors [2]. The isostructural kappa-phase organic compounds (BEDT-TTF)₂X offer a series of materials ranging from weakly correlated superconductors (X = Cu(NCS)₂) through strongly correlated superconductors (X = Cu[(N(CN)₂)Br] to Mott insulators (X = Cu[(N(CN)₂]Cl) as the bandwidth decreases and the importance of correlations increases. We previously showed that while there are no fluctuations significantly above T_c in the weakly correlated superconductor, there are strong superconducting fluctuations at temperatures up to 50% above T_c in the strongly correlated superconductor [2], suggesting that the proximity of the Mott state drives the fluctuating state. Here, by alloying the strongly correlated and the Mott insulating materials, we tune the system towards the Mott critical point. Superconductors in the vicinity of the critical point exhibit a large and magnetic-field-dependent Nernst effect, characteristic of superconducting fluctuations, at even higher temperatures. The effect is apparent over the whole temperature range for which the conductivity is metallic, up to 50K, about six times T_c.

[1] Y. Wang, et al., *Phys. Rev. B* 73, 024510 (2006) [2] M.-S. Nam et al., *Nature* 449, 584 (2007)

SB21

Anomalous hall effect in superconductors with spin-orbit interaction

Pedro D Sacramento¹, M. A. N. Araujo², V. R. Vieira¹, V. K. Dugaev³ and J. Barnas⁴

¹ *Departamento de Fisica and CFIF, Instituto Superior Tecnico, TULISA, Portugal*

² *Departamento de Fisica and CFIF, Universidade de Evora, Portugal*

³ *Department of Physics, Rzeszow University of Technology, Poland*

⁴ *Department of Physics, Adam Mickiewicz University, Poland*



SB22

Analysis of the local current density in HTS coated conductors using low-temperature scanning laser and hall probe microscopy

Sang Kook Park, Bo Ram Cho, Hee Yeon Park and Hyeong-cheol Ri*

Department of Physics, Kyungpook National University, Korea

Local current density in HTS coated conductors was investigated using Low-temperature Scanning Laser and Hall Probe Microscopy (LTS/HPM). We prepared GdBCO and YBCO coated conductors to study the spatial distribution of the current density in a single bridge. Inhomogeneity of the local critical temperature in the bridge was analyzed from experimental results of scanning laser microscopy near the superconducting transition. The local transport and screening current in the bridge were also investigated using scanning Hall probe microscopy. From experimental results of scanning laser and Hall probe microscopy, we have observed the redistribution of current density and the critical temperature caused by defects of the HTS layer.

SB23

Cooper pairing between conduction and localized electrons in heavy-fermion systems

Keisuke Masuda* and Daisuke Yamamoto²

¹ Department of Physics, Waseda University, Japan

² Condensed Matter Theory Laboratory, RIKEN, Japan

We study the Cooper pairing between a conduction electron (c electron) and a localized f electron, referred to as the c-f pairing, as a mechanism of s-wave superconductivity in heavy-fermion systems. To describe the physics of heavy-fermion systems, we start from the periodic Anderson model. We apply the Schrieffer-Wolff transformation to this model considering the situation where the f level is sufficiently deep and the Coulomb repulsion is finite but large. The resulting effective Hamiltonian includes direct and spin-exchange interactions between c and f electrons, which can be the driving force for the formation of the Cooper pairs. Within the mean-field approximation, we show that the c-f pairing state with anisotropic s-wave symmetry appears in a large region of the phase diagram. Such a pairing state can be realized when the quasiparticle band of the f electrons, which is formed by the strong Coulomb repulsion, is located near the energy level of the conduction band. We also discuss the relationship between the c-f pairing proposed here and the s-wave superconductivity found in the experiments on CeRu₃ and CeCo₂.

SB24

Low-temperature thermoelectric properties of the electron-doped Perovskites Sr_{1-x}CaxTi_{1-y}NbyO₃

Tetsuji Okuda*, Junichi Fukuyado¹, Kurahito Narikiyo¹, Mitsuru Akaki² and Hideki Kuwahara²

¹ Kagoshima University, Japan

² Sophia University, Japan

Electron-doped perovskite SrTiO₃ is known to be one of candidates for an n-type thermoelectric (TE) oxide. [1] In this study, we tried to improve a TE property of a lightly-electron-doped SrTiO₃ single crystal below room temperature by substitutions of Ca and Nb for Sr and Ti. We found that SrTi_{0.99}Nb_{0.01}O₃ shows a large power factor of about 90 μW/K² cm at 50 K and the largest dimensionless TE figure-of-merit (ZT ~ 0.07) below 40 K among the ever-reported materials. The good n-type TE response is due to a distinct electron-phonon interaction which could relate to the superconducting state [2], which enlarges a Seebeck coefficient not through an enhancement of effective mass, but through a change of relaxation time. On the other hand, a Ca²⁺ substitution for Sr²⁺ increases the ZT at 300 K for Sr_{1-x}CaxTi_{0.97}Nb_{0.03}O₃ from 0.08 to 0.105. The enhancement of ZT originates not only in a large reduction of a thermal conductivity due to an introduced randomness into the crystal structure, but also in an unexpected enhancement of Seebeck coefficient by the Ca substitution.

[1] T. Okuda, K. Nakanishi, S. Miyasaka, and Y. Tokura, *Phys. Rev. B* 63, 113104 (2001). [2] H. Suzuki, H. Bando, Y. Ootuka, I.H. Inoue, T. Yamamoto, K. Takahashi, and Y. Nishihara, *J. Phys. Soc. Jpn.* 65, 1529 (1996). [3] J. Fukuyado, K. Narikiyo, M. Akaki, H. Kuwahara, and T. Okuda, *Phys. Rev. B*, to be published.

SB25

Evolution of pairing potential in ladder materials under renormalization group transformations

Yen-chen Lee^{1*}, Wen-min Huang² and Hsiu-hau Lin¹

¹ Department of Physics, National Tsing Hua University, Taiwan

² Physics Division, National Center for Theoretical Sciences, Taiwan

It is generally believed that electron-electron interactions are responsible for pair formation in unconventional superconductors. However, how electrons can form pairs in the presence of repulsive interactions remains counterintuitive and puzzling. Many studies suggest that spin fluctuations provides the “pairing glues” to account for the unconventional pairing. Here we take a different route: finding effective pairing potential at different length scales by renormalization group approach. We focus on the unconventional superconductivity in ladder materials and show how the profile of electron-electron interactions evolves under renormalization group transformation. Starting with repulsive short-ranged interaction, compelling evidence for spatially structured attractive interactions emerges in long-wavelength limit and explains the unconventional pairing symmetry naturally. Comparisons with other theoretical approaches and potential generalization to two dimensions are discussed at the end.

SB26

Evidence for multiband order parameters in the stong-coupling LaRu₄As₁₂ Skutterudite Superconductor

Tomasz Cichorek¹, Lukasz Bochenek¹, Ryszard Wawryk¹, Roman Puzniak² and Zygmunt Henkie¹

¹ Institute of Low Temperature and Structure Research, Polish Academy of Sciences, Wroclaw, Poland

² Institute of Physics, Polish Academy of Sciences, Warsaw, Poland

Superconducting properties of high-purity LaRu₄As₁₂ single crystals with the highest critical temperature T_c = 10.45 K among the fully filled-skutterudite superconductors were investigated by dc magnetization, electrical resistivity, torque, and specific heat measurements both as a function of temperature and magnetic field. At B = 0 and below about T_c/2, the electronic specific heat exhibits two-band features, as concluded from an α-model analysis. Multi-band effects are further inferred from a nonlinear magnetic-field dependence of the electronic specific heat coefficient in the zero-temperature limit as well as from a positive curvature of the upper critical field in the vicinity of T_c. Our findings, combined with results of previous de Haas-van Alphen experiments, suggest that enhanced superconductivity in LaRu₄As₁₂ appears along with a spherical Fermi-surface sheet enclosing a small volume in the center of the Brillouin zone.

SB27

NMR Study of magnetic order and the FFLO state in CeCoIn₅

Ken-ichi Kumagai^{1*}, Hiroyuki Shishido², Takasada Shibauchi² and Yuji Matsuda²

¹ Department of Physics, Hokkaido University, Sapporo, 060-0810, Japan

² Department of Physics, Kyoto University, Kyoto 606-8502, Japan

A strongly-correlated superconductor, CeCoIn₅ is believed to host a Fulde-Ferrell-Larkin-Ovchinnkov (FFLO) state in a restricted region of high field and very low temperature. In addition to the field evolution of NMR results for H//a-axis [1], we will report recent results of the angle,θ, dependence of external fields with respect to the ab planes down to ~50mK. Detail phase diagram for θ-, B-, and T-parameters is obtained. The NMR spectra change dramatically upon entering the novel SC phase. A well-separated peak structure at the In(2b) site suggests the occurrence of the magnetic order which is emerging only in the newly-discovered SC state. The structure of the spin density wave (SDW) is modified with angle and field. The Knight shift of CeCoIn₅ provides a direct evidence for the emergence of the spatially-distributed normal quasiparticle region. The quantitative analysis for the field evolution of the paramagnetic magnetization and low-lying energy quasiparticle density of state is consistent with the nodal plane formation, which is characterized by an order parameter in the FFLO state.

[1] K. Kumagai et al., *Phys. Rev. Lett.* 106, 137004 (2011).

SB28

MgB₂ coated conductors grown at various temperatures by hybrid physical-chemical vapor deposition

Mahipal Ranot¹, K. H. Cho¹, Soon-gil Jung¹, Won Nam Kang^{1*}, S. Oh² and K. C. Chung³

¹ Physics, Sungkyunkwan University, Suwon, Korea

² National Fusion Research Institute, Korea

³ Korea Institute of Machinery and Materials, Korea

For practical applications, MgB₂ superconductor (T_c~39 K) in the form of wires and tapes are required to be produced in long lengths to replace the conventional metallic superconductors, such as Nb-Ti and Nb₃Sn. In this work, we have grown MgB₂ coated conductors by depositing MgB₂ films directly on the flexible Hastelloy tapes at various temperatures ranging from 520 to 600 °C by using HPCVD. The MgB₂ coated conductors exhibit critical temperatures ranging from 37.5 to 38.5 K with superconducting transition width (T_c) of about 0.3?0.8 K. X-ray diffraction analysis revealed that the MgB₂ coated conductors are polycrystalline in nature. It was found that the MgB₂ coated conductor grown at 520 °C had dense microstructure with good grain connectivity. However, upon increasing the growth temperature from 520 to 600 °C deterioration of grain connectivity takes place and void formations were observed. The critical current density (J_c) of the order of J_c(5 K, 0 T) ~107 and J_c(5 K, 3 T) ~105 A/cm² was obtained for the MgB₂ coated conductor fabricated at 520 °C. The fabrication process, crystallographic orientations, surface morphologies and superconducting properties [T_c, J_c (H)] of MgB₂ coated conductors grown at various temperatures will be discussed in detail.

SB29

Low temperature properties of the weakly-coupled non-centrosymmetric superconductor LaNiC₂

Jian Chen¹, Jing Lei Zhang¹, Lin Jiao¹, Lin Yang¹, Tian Shang¹, Michael Nicklas², Frank Steglich² and Hui Qiu Yuan^{1*}

¹ Physical Department, Zhejiang University, China

² Max Planck Institute for the Chemical Physics of Solids, Dresden, Germany

In a non-centrosymmetric (NCS) superconductor, an asymmetric potential gradient yields an antisymmetric spin-orbit coupling (ASOC), which splits the degeneracy of conduction electron, and allows the admixture of spin-singlet and spin-triplet pairing states, leading to accidental nodes in the energy gap [1,2]. It was shown that the time-reversal symmetry is broken in the weakly correlated intermetallic compound LaNiC₂ [3] but its pairing symmetry is still under debate. Here we present the low temperature specific heat C(T) and the magnetic penetration depth λ(T) for LaNiC₂. It is found that both λ(T) and Ce(T)/T can be well described by a phenomenological two-gap model. The Sommerfeld parameter, γ(H), increases steeply at low fields and eventually get saturated with increasing magnetic field, being also consistent with the behavior of two-gap superconductivity. We argue that the ASOC is weak in LaNiC₂ and the spin-singlet state dominates in the pairing states, giving rise to two-gap-like BCS superconductivity.

[1] P. A. Frigeri, D. F. Agterberg, A. Koga, and M. Sigrist, *Phys. Rev. Lett.* 92, 097001 (2004). [2] H. Q. Yuan, D. F. Agterberg, N. Hayashi, P. Badica, D. Vandervelde, K. Togano, M. Sigrist, M. B. Salamon, *Phys. Rev. Lett.* 97, 017006 (2006). [3] A. D. Hillier, J. Quintanilla, R. Cywinski, *Phys. Rev. Lett.* 102, 117007 (2009).

SB30

Magnetic penetration depth and SHS-STs phase diagram in SrPd₂Ge₂

H. Kim¹, N. H. Sung², M. A. Tanatar¹, B. K. Cho² and R. Prozorov^{1*}

¹ The Ames Laboratory, USA

² School of Materials Science and Engineering, Gwangju Institute of Science and Technology, Korea

In-plane magnetic penetration depth, λ_{ab}(T), was measured in single crystals of SrPd₂Ge₂ superconductor down to 50 mK and in magnetic fields up to μ₀H_{dc} = 15 T by using a self-oscillating tunnel diode resonator operating at 16 MHz with amplitude of μ₀H_{ac} ≈ 205 mOe. In the pure Meissner state, at μ₀H_{dc}=0, λ_{ab}(T) saturates exponentially approaching λ_{ab}(0) indicating fully gapped superconductivity in SrPd₂Ge₂. In a magnetic field, the measured penetration depth is given by λ_{ab}² = λ_{ab}²_L + λ_{ab}²_C, where λ_{ab}²_C ~ B²/2 c_s² is the Campbell penetration depth and S_j c_s is the critical current density. For μ₀H < 0.45 T, the shortest λ_{ab}(T) (strongest pinning) is achieved not at the lowest, but at an intermediate temperature. Additionally, Δλ_{ab}(T) shows hysteresis between zero field cooling and field cooling measurements, which is an indication of non-parabolic pinning potential. Another interesting feature is a pronounced finite diamagnetic response above bulk superconducting transition, which could be related to superconducting fluctuations. Combining all measurements, the entire SH-TS phase diagram of SrPd₂Ge₂ has been constructed. Possible pairing mechanism and the superconducting gap structure, unusual vortex response and field- and temperature dependent critical current density will be discussed.

SB31

Eliashberg function of the overdoped Bi₂₁₂ superconductors deduced from the high resolution laser ARPES intensity

Jin Mo Bok^{1*}, Han-yong Choi¹, Junfeng He², X. J. Zhou³ and C. M. Varma⁴

¹ Department of Physics, SungKyunKwan University, Suwon 440-746, Korea

² Institute of Physics, Chinese Academy of Sciences, Beijing 100190., China

³ Institute of Physics, Chinese Academy of Sciences, Beijing 100190, China

⁴ Department of Physics and Astronomy, University of California, Riverside, CA 92521, USA

We report the diagonal and off-diagonal Eliashberg functions a₂F₊(+) and a₂F₋(-) of overdoped Bi2212 superconductors deduced from the high resolution laser APRES experiments. By fitting the momentum distribution curves of the ARPES intensity employing the superconducting Green's function, the diagonal and off-diagonal self-energies along several cuts in the Brillouin zone are extracted. Then, the diagonal and off-diagonal Eliashberg functions are deduced by inverting the d-wave Eliashberg equation using, respectively, the corresponding self-energies. We will present the momentum and frequency dependences of the Eliashberg function a₂F₊(+) and a₂F₋(-). We then compare these results with other experiment and calculation results.

SB32

The momentum and frequency dependences of the self-energy induced by the spin fluctuations for the cuprate superconductors

Seung Hwan Hong and Han-yong Choi*

Department of Physics, SungKyunKwan University, Korea

We solve the momentum resolved d-wave Eliashberg equation to investigate the consistency of the spin fluctuation induced superconductivity theory for the cuprates. The effective interaction between electrons (Eliashberg function) is modeled in terms of the magnetic excitation spectrum measured by the inelastic neutron scattering on the LSCO superconductors reported by Vignolle et al[1]. The magnetic excitation spectrum consists of three parts: the resonance mode near 40-70 meV and the incommensurate parts above and below the resonance mode. The resonance mode has a peak at (π,π). The low energy incommensurate part makes a nonmonotonic momentum dependence of the diagonal and off-diagonal self-energies. On the other hand, the resonance mode makes a monotonic momentum dependence of the self-energy. The angle dependence of the superconducting gap is influenced by the effects of these two energy scales. These results are compared with the ARPES experiments.

[1] B. Vignolle et al., *Nature Physics* 3, 163 (2007)

SC01

Novel non-centrosymmetric superconductors in 113 and 111 crystal structures

Friedrich Kneidinger^{1*}, Ernst Bauer¹, Hervig Michor¹, Gerfried Hilscher¹, Isolde Zeiringer², Peter Rogl², Nataliya Melnychenko³, Leonid Salamakha⁴ and Adrian Hillier⁵

¹ Institute of solid state physics, Vienna University of Technology, Austria

² Institute of physical chemistry, University of Vienna, Austria

³ Inorganic Chemistry Department, Ivan Franko National University of Lviv, Ukraine

⁴ Ivan Franko Lviv National University, Ukraine

⁵ ISIS facility, STFC Rutherford Appleton Laboratory, Harwell Science and Innovation Campus, United Kingdom

Superconductivity (SC) in materials that don't possess a center of inversion due to their crystal structure has been recently found in materials like CePt₃Si[1]. The lack of inversion-symmetry gives rise to an electrical field and therefore leads to an antisymmetric spin-orbit coupling (ASOC) of the Rashba-type[2]. This causes a splitting of the Fermi surface, thereby leading to a superposition of spin-singlet and spin-triplet Cooper pairs in the SC condensate. Intriguing features like nodes in the superconducting gap, as well as H_{c2} exceeding the Pauli-Clogston limit, may occur. However, besides Li₂Pt₃B[3], spin-triplet pairing seems only to be dominant in heavy fermion systems. In order to study these features in further detail, new ternary compounds like BaPtSi₃[4], SrPdSi₃, SrPdGe₃[5], SrPtSi₃ and SrPtGe₃ of BaNiSn₃ type (space group I4mm) as well as promising 111-types like LaPtSi[6,7] and LaIrSi[8] have been investigated, since there is a tuning possibility regarding the quadratic atomic number dependency (Z²) of the spin-orbit coupling. Measurements of the electrical resistivity and the specific heat have been conducted to analyze the superconducting ground state. Additionally, μSR measurements have been performed to proof the microscopic pairing mechanism of the Cooper pairs. The results obtained so far indicate s-wave fully gapped BCS SC.

[1] E. Bauer et al., *Phys. Rev. Lett.* 92, 027003 (2004) [2] Y.A. Bychkov and E. I. Rashba, *JETP Lett* 39, 78 (1984) [3] M. Nishiyama et al., *Phys. Rev. Lett.* 98, 047002 (2007) [4] E. Bauer et al., *Phys. Rev. B* 80, 064504 (2009) [5] K. Milyanchuk et al., *Journal of Physics: Conference Series* 273, 012078 (2011) [6] K. Klepp & E.Parthe, *Acta Crystallogr. B*38, 1105 (1982) [7] J. Evers, G. Oehlinger and A. Weiss, *Solid State Communications, Vol. 50, No. 1, pp. 61-62, (1984)* [8] K. Klepp & E.Parthe, *Acta Crystallogr. B*38, 1541 (1982)

SC02

Non-fermi liquid behavior of d-wave superconductor

Pankaj Singh*, Ajay Pratap Singh Gahlot, Manju Rani and Partho Goswami
Physics Department, Deshbandhu College, University Of Delhi, India

The d+id-density wave (Chiral DDW) order, at the anti-ferromagnetic wave vector Q = (π,π), is assumed to represent the pseudo-gap (PG) state of a hole-doped cuprate superconductor. The d-wave superconductivity (DSC), driven by an assumed attractive interaction, is discussed within the BCS framework together with the d+id ordering. The single-particle excitation spectrum in the CDDW + DSC state is characterized by the Bogoliubov quasi-particle bands-a characteristic feature of SC state. The coupled gap equations are solved self-consistently together with the equation to determine the chemical potential (μ). With the pinning of the van Hove-singularities close to μ, one is able to calculate the thermodynamic properties of the under-doped cuprates in a consistent manner. Apart from the known facts that PG and DSC represent two competing orders as the former brings about a depletion of the spectral weight available for pairing in the anti-nodal region of momentum space and the depletion of the spectral weight below T_c at energies larger than the gap amplitude, we find a conspicuous feature that the electronic specific heat displays non-Fermi liquid behavior (anomalous temperature dependence) in the CDDW + DSC state.

SC03

Low temperature enhancement of the critical current in CeCoIn₅. Possible signature of magnetic order

C. F. Miclea^{1*}, M. Nicklas², A. C. Mota³, M. M. Altarawneh⁴, C. Miclea¹, N. Harrison⁴, J. Thompson⁴, F. Steglich² and R. Movshovich⁴
¹ National Institute for Materials Physics, 077125 Bucharest-Magurele, Romania
² Max-Planck-Institute for Chemical Physics of Solids, 01187 Dresden, Germany
³ Solid State Laboratory, ETH Zurich, Switzerland
⁴ Los Alamos National Laboratory, Los Alamos, New Mexico 87545, USA

We report on vortex dynamics, dc magnetization and RF penetration depth measurements in the heavy fermion compound CeCoIn₅ down to low temperatures, T=50 mK. No strong pinning is observed as expected for a clean limit superconductor which does not break spontaneously any additional symmetries besides the U(1)-gauge. CeCoIn₅ display clear logarithmic relaxation curves as expected from Kim-Anderson theory. The temperature dependence of the relaxation rate, S, with a small but finite residual value indicate that quantum tunneling plays a significant role in the vortex creep only at very low temperatures. Remarkably, a new phase transition marked by a strong increase in the remnant magnetization, M_{rem} is observed around T = 0.3 K in low magnetic fields just high enough to put the sample in the Bean critical state. Moreover, this anomaly is corroborated by the DC magnetization and RF measurements at very low fields. We extended the vortex dynamics investigation to Pb irradiated CeCoIn₅. While the defects created by irradiation have a clear effect on the relaxation rates the enhancement of M_{rem} still takes place at the same temperature. Our findings are consistent with the existence of a magnetically ordered phase, deep inside the superconducting state.

SC04

Superconducting phase diagram in fcc phase of Cs₃C₆₀: A pressure dependence of resistivity

Takashi Kambe*, Yuta Suzuki, Seizi Shibasaki, Keitaro Tomita and Yoshihiro Kubozono
 Physics, Okayama university, Japan

Cs₃C₆₀ crystallizes three polymorphic phases; A₁₅, fcc and bco. Two polymorphs, A₁₅ and fcc phases, show pressure induced superconducting transitions around 38 K and 35 K, respectively. Here we report a resistivity for fcc phase of Cs₃C₆₀ as a function of pressure and present a dome-shaped superconducting phase diagram.

SC05

The superconducting phases of URu₂Si₂ from sound velocity measurements

B S Shivaram¹, V W Ulrich¹ and D G Hinks²
¹ Physics, University of Virginia, USA
² Materials Science Division, Argonne National Labs, USA

High resolution measurements of the changes in the longitudinal sound velocity in a magnetic field have been performed in the zero temperature limit in high quality single crystals of URu₂Si₂. These measurements reveal two distinct signatures attributable to multiple superconducting phases. A step change in the sound velocity, for propagation in the basal plane, is observed at the critical field, B_{c2}. This step broadens considerably as T tends to T_c with a concomitant decrease in magnitude. A second step is observed at a field ~0.5 B_{c2} and it's magnitude remains constant at all temperatures. Inductive measurements of the transitions in a magnetic field, however, reveal only a single signature which coincides with the lower step change in the sound velocity. Measurements performed with B oriented at various angles between the a and c-axes reveal a weaker angular dependence of the lower step and confirm the rapid fall off of B_{c2} close to B||c-axis. A multiple superconducting phase diagram for URu₂Si₂ is proposed.

SC06

Electronic structure of a superconducting boride, ZrB₁₂

Sangeeta Thakur¹, Deep Narayan Biswas Biswas², Nishaina Sahadev³, Geetha Balakrishnan⁴ and Kalobaran Maiti^{5*}
¹ Department of Condensed Matter Physics and Materials' Science, Tata Institute of Fundamental Research Colaba, Mumbai - 400 005, India
² Tata Institute of Fundamental Research Colaba, Mumbai - 400 005, India
³ Tata Institute of Fundamental Research, Colaba, Mumbai - 400 005, India
⁴ Department of Physics, University of Warwick, Coventry, CV4 7AL, UK, United Kingdom
⁵ Tata Institute of Fundamental Research Colaba Mumbai 400005, India

Borides have attracted a great deal of attention followed by the finding of varied interesting properties. ZrB₁₂ is one such compound exhibiting highest superconducting critical temperature (T_c = 6 K) in MB12 family. In order to probe the electronic states responsible for superconductivity in this compound, we studied the electronic structure of single crystalline ZrB₁₂ using high resolution photoemission spectroscopy and ab initio band structure calculations. Zr 3d core level spectra exhibit signature of satellite features indicating finite correlation among the conduction electrons. The B 1s spectra appears to be sharp with unusual asymmetry, presumably due to surface contributions as found in hexaborides. In the valence band spectra, the spectral density of states reveal a dip at the Fermi level, which gradually increases with the decrease in temperature down to 10 K. The band structure results indicate dominant contribution from the B 2p electronic states in the valence band. However, the photon energy dependence in the experimental spectra indicate large contribution from the Zr 4d states near Fermi level suggesting their important role in the superconductivity.

SC07

On the nature of an energy barrier between (π,0) and (0,π) magnetic orders in Fe pnictides

Alexander Yaresko^{1*}, Lilia Boeri², Vladimir Antropov³ and Ole Krogh Andersen²
¹ Andersen, Max Planck Institute for Solid State Research, Germany
² Max Planck Institute for Solid State Research, Germany
³ Ames Laboratory, Ames, Iowa, USA

As temperature is lowered most of undoped Fe arsenides, parent compounds for recently discovered Fe based superconductors, undergo a transition into a collinear state with stripe-like magnetic order in which anti-ferromagnetic (AFM) Fe chains are ferromagnetically ordered along the direction perpendicular to the chains. Two such collinear magnetic structures, characterized by ordering vectors (π,0) or (0,π), are connected by infinite number of non-collinear states with two AFM sublattices of second Fe neighbors rotated by an arbitrary angle with respect to each other. In a classical Heisenberg model all these states are degenerate. Band structure calculation show, however, that the degeneracy is lifted already at the mean field LSDA level and that in Fe arsenides (π,0) and (0,π) magnetic orders are separated by an energy barrier comparable to the energy difference between Neel and stripe AFM orders. We discuss a microscopic origin of the energy barrier and demonstrate that it is caused by closely related to underlying band structure. The results for Fe arsenides are compared to BaMn₂As₂ and hypothetical KFe₂Se₂ for which we found that a non-collinear 90-degree spin arrangement is more favorable than collinear ones. A doping dependence of the barrier is also discussed.

SC08

Electronic structures and magnetic properties of LnFeAsO

Chang Hyun Yi, Ju Young Kim, Jae Kyung Chang, and Joo Yull Rhee
 Department of Physics, Sungkyunkwan University, Suwon 440-746, Korea

Recently, high transition-temperature superconductivity was discovered in the ironpnictide RFeAsO (R=rare-earths) family of materials. Among them, LaFeAsO undergoes a tetragonal-to-orthorhombic phase transition at ~160 K followed by an antiferromagnetic ordering at ~145 K. This material has also been reported to undergo a spin-density wave transition near 150 K. Through first-principles calculations we tried to understand the electronic structures and magnetic properties of LaFeAsO. We used full-potential linearized-augmented-planewave method in the antiferromagnetic ground state with orthorhombic phase. The physical origin of the SDW formation will be discussed.

SC09

Phase transition of a heavy fermion superconductor in a high magnetic field : entanglement analysis

Reza Afzali^{1*} and Neda Ebrahimian²
¹ Physics Department, K. N. Toosi University of Technology, Tehran 15418, Iran
² Physics Department, Amirkabir University of Technology, Tehran 15914, Iran

When the magnetic field is acting on the spin of electrons only, a transition from a normal to a modulated superconducting state or FFLO superconductor state may occur at low temperatures[1-3]. A FFLO superconducting state, accompany with an order parameter that oscillates spatially, may be stabilized by a high applied magnetic field or a molecular field. CeCoIn₅ is a sample of heavy-fermion superconductor[4]. Initially experiments on CeCoIn₅ indicate that in this substance a FFLO state in a exchange field is realized. Quantum multipartite entanglement is a new procedure for investigating quantum phase transition[5-6], which is one of the interesting topics in condensed matter. In this article, we deal with to the phase transition of FFLO state of CeCoIn₅ to the normal state by obtaining quantum multipartite entanglement of the system. For this purpose, using normal and anomalous Green functions and density matrix, concurrence, as a measure of bipartite entanglement, is obtained. Then, order parameter and magnetic field dependence of multipartite entanglement in momentum space is calculated. The phase transition is determined and the behavior of the system based on order parameter is discussed. Furthermore, the phase transitions of both BCS and FFLO states to the normal state are compared.

References: [1] Fulde P and Ferrell R A 1964 Phys. Rev. A 135 550 [2] Larkin A I and Ovchinnikov Y N 1965 Sov. Phys. JETP 20 762 [3] Takada S and Iizuyama T 1969 Prog. Theor. Phys. 41 635 [4] Radovan H A, Fortune N A, Murphy T P, Hannahs S T, Palm E C, Tozar S W and Hall D 2003 Nature 425 51 [5] Amico L, Fazio R, Osterloh A and Vedral V 2008 Rev. Mod. Phys. 80 517 [6] Brandao F G S L 2005 New J. Phys. 7 254

SC10

Spin and charge excitations in antiferromagnetic metallic phase in multi-orbital systems: A case study of chromium

Koudai Sugimoto¹, Eiji Kaneshita², Kenji Tsutsui³ and Takami Tohyama^{1*}
¹ Yukawa Institute for Theoretical Physics, Kyoto University, Japan
² Sendai National College of Technology, Japan
³ Condensed Matter Science Division, JAEA, Japan

Since the discovery of Fe-based superconductors, it has been recognized that the interplay of spin, charge, and orbital degrees of freedom is the key to understanding the physics of multiband itinerant systems. Antiferromagnetic (AF) phase seen in the parent compounds of Fe-based superconductors is a good example to study the multi-orbital physics in the metallic phase. The AF metallic phase similar to the parent compounds is realized in a simple chromium metal with AF order. To make a unified view in the AF metallic phase of multi-orbital systems, we study spin and charge excitations in AF Cr. We calculate the optical conductivity, neutron scattering spectra, and Cr L-edge resonant X-ray scattering (RIXS) spectra based on the mean-field theory for the multi-band Hubbard model and the random-phase approximation. The calculated results of the optical conductivity and neutron scattering spectra are compared with corresponding experimental data. The d stalled polarization and momentum dependence in RIXS is also discussed with predictions for the experiments.

SC11

The dirty crossover - signature of a robust superfluid in the unitary regime.

IIT Guwahati
 IIT Guwahati, India

We perform a systematic study of the BCS-BEC crossover in an ultracold fermionic gas in presence of a weak white noise-like random disorder which is incorporated in our mean-field treatment via Gaussian fluctuations. A careful investigation of different mean field quantities as a function of the interparticle interaction reveals a nonmonotonic behavior in the condensate fraction data as disorder is included in our calculations. The inflexion point is seen to occur in the unitary regime, and afterwards there is a gradual depletion of the condensate density in the BEC side, thereby corroborating a robust paradigm of superfluidity in the unitary regime. Motivated by this result, we study the spectral gap and the density of states in the crossover region and their responses to the disorder. We further include a comparative discussion on the role of the pair and phase coherence lengths in this region in presence of disorder to assess how these results can be relevant to the ongoing discussion. Due to tremendous progress taking place in the experimental front in manipulating atoms on an optical lattice in presence of (speckle) disorder, a stable superfluid scenario in the unitary limit, as proposed here, may soon be realizable.

Prof. S.S. Mandal, Indian Association for Cultivation of Science, Kolkata, India Prof. Y. Yanase, Niigata University, Japan

SC12

Spin-orbit coupling and the superconductivity in simple-cubic polonium

Chang-jong Kang, Kyoo Kim and B. I. Min*
 Physics, POSTECH, Korea

Polonium is the only element which has the simple-cubic (SC) structure in the periodic table. We have studied its structural stability based on the phonon dispersion calculations using the first-principles all-electron full-potential band method. We have demonstrated that the strong spin-orbit coupling (SOC) in SC-Po suppresses the Peierls instability and makes the SC structure stable. Further, we have investigated the possible superconductivity in SC-Po, and predicted that it becomes a superconductor with T_c ~ 4 K at ambient pressure. The transverse soft phonon mode at q ~ 2/3 R, which is greatly affected by the SOC, plays an important role both in the structural stability and the superconductivity in SC-Po. We have explored effects of the SOC and the volume variation on the phonon dispersions and superconducting properties of SC-Po.

SC13

Stability of FFLO states in optical lattices with layered structure

Akihisa Koga* and Yasuharu Okawauchi
 Department of Physics, Tokyo Institute of Technology, Japan

Recently, ultracold fermions with spin-imbalanced populations have attracted much interest. One of the interesting questions is how the Fulde-Ferrell-Larkin-Ovchinnikov (FFLO) phase, where Cooper pairs are formed with a finite total momentum, is realized in the system. In the two dimensional optical lattice with a confining potential, it has been pointed out that two kinds of FFLO states are realized[1,2]. On the other hand, such FFLO states with a three-dimensional structure have not been studied so well although the interlayer coupling should be important for realistic optical lattice systems. Motivated by this, we investigate the stability of the superfluid state in a layered fermionic optical lattice system with a confining potential, using the Bogoliubov de-Gennes equations. It is clarified that in the imbalanced case, the introduction of the interlayer hopping stabilizes the radial FFLO state, while makes the angular FFLO state unstable. We also discuss the system size dependence of the superfluid ground state. It is clarified that in a certain ring region the A-FFLO state is indeed realized in a large system.

[1] Y. Chen, Z. D. Wang, F. C. Zhang, and C. S. Ting, Phys. Rev. B 79, 054512 (2009) [2] Y. Yanase, Phys. Rev. B 80, 220510 (2009)

SC14

Flux quantization and its magnetic relaxation in a micrometer-sized superconducting ring of niobium

Jae-hyuk Choi^{1*}, Heon-hwa Choi¹, Yun-won Kim², Soon-gul Lee² and Mahn-soo Choi³
¹ Division of Physical Metrology, Korea Reserach Institute of Standards and Science, Korea
² Dep. of Display and Semiconductor Physics, Korea University, Korea
³ Dep. of Physics, Korea University, Korea

We developed a high-sensitivity cantilever force magnetometry, which is capable of direct measurement of the magnetic moment of micron-scale samples at low magnetic fields and low temperatures, and studied magnetic properties of a 100 nm-thick Nb superconducting ring with 4 micrometer radius and 2 micrometer width. At a temperature of 3.5 K, we observed flux quantization of h/2e period using ac torque and dc force magnetometries with attonewton and sub-piconewton sensitivity, respectively, determining the magnetic moment of each flux quantum. First demonstration of magnetic relaxation at single flux quantum level is also presented, which provides information about the dynamics of thermally-activated single flux quanta depending on their number.

SC15

Measurement of rat biomagnetic signals by using a HTS-SQUID system

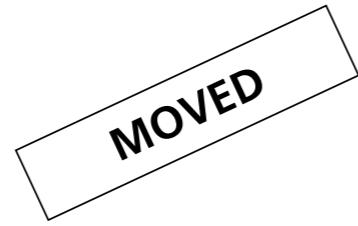
In-seon Kim* and San Ahn
 Division of Convergence Technology, Korea Research Institute of Standards and Science, Korea

We have measured biomagnetic signals in rats by using a high-TC SQUID magnetometer system employing a small magnetically shielded box. For the rat cardiac magnetic field measurements, healthy Wistar Kyoto rat and spontaneously hypertensive rat were anesthetized and fixed on a plastic xyz-stage in supine position inside the magnetically shielded box. Well defined P-, QRS- and T-waves were observed on the rat cardiac magnetic field measurements. We investigated circular measurements based on the hexaxial reference system, i.e., 12 measurement points were determined alongside the circumference of a circle centered at the heart position. These results were quite promising for use in biomedical applications of heart disease rat model study by using the high-TC SQUID magnetometer system.

SC18

Design, fabrication, and testing of a cooling system using solid nitrogen for a 3 T/60-mm RT bore superconducting HGMS

Jung-bin Song, Kwang Lok Kim, Dong Gyu Yang, Yoon Hyuck Choi, Jongseok Lee and Haigun Lee*
 Department of Materials Science and Engineering, Korea University, Korea



SC16

Evolution of the effective mass approaching the quantum critical point in the heavy fermion superconductor CePt₃In₇

Jakob Kanter^{1*}, Philip J. W. Moll¹, Filip Ronning², Sven Friedemann³, Patricia L. Alireza¹, Michael Sutherland¹, P. Tobash², J. Thompson², Eric D. Bauer² and Bertram Batlogg¹

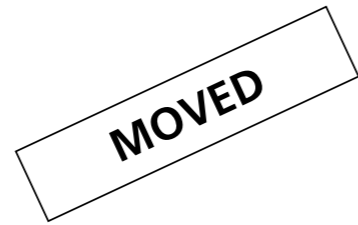
¹ Laboratory for Solid State Physics, ETH Zurich, Switzerland
² Los Alamos National Laboratory, Los Alamos, New Mexico, USA
³ Cavendish Laboratory, University of Cambridge, United Kingdom

We report Shubnikov-de Haas measurements on micro-structured CePt₃In₇ single crystals under high pressures. CePt₃In₇ belongs to the Ce₂MnIn_{3m-2n} heavy fermion family and orders antiferromagnetically below 5.5 K. Applying pressure induces a superconducting phase and suppresses the AFM order with the Neel temperature extrapolating to a quantum critical point. The magnetic fluctuations associated with the QCP are thought to stabilize the unconventional superconducting phase. The evolution of the effective electronic masses approaching the quantum critical point is essential to the understanding of the electronic correlation leading to unconventional superconductivity. To this end we have developed a method to contact micro-structured samples inside a diamond anvil cell allowing for complex sample shapes and several electric contacts.

SC19

Purification of chemical mechanical polishing wastewater using a 2G HTS high gradient magnetic separation system

Dong Gyu Yang, Jung-bin Song, Young-gyun Kim, Jongseok Lee, Yeonjoo Park and Haigun Lee*
 Department of Materials Science and Engineering, Korea University, Korea



SC17

Thermal stability of an epoxy-impregnated HTS racetrack coil without turn-to-turn insulation for rotating machines

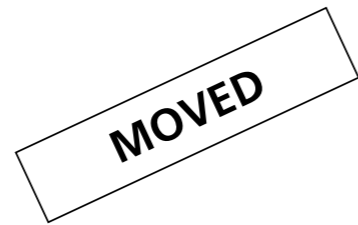
Oh Jun Kwon, Kwang Lok Kim, Yoon Hyuck Choi, Hyun-jin Shin and Haigun Lee*
 Department of Materials Science and Engineering, Korea University, Korea



SC20

Effect of liquid cryogen on a 2G HTS magnet using a mixed cryogen cooling system

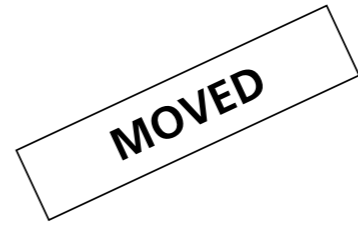
Kwang Lok Kim, Jung-bin Song, Yoon Hyuck Choi, Dong Gyu Yang and Haigun Lee*
 Department of Materials Science and Engineering, Korea University, Korea



SC21

Removal of silica and copper ions from CMP wastewater via magnetic seeding aggregation using superconducting HGMS

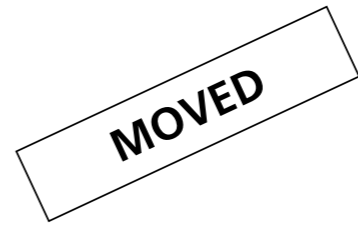
Jongseok Lee, Jung-bin Song, Dong Gyu Yang, Yeonjoo Park and Haigun Lee*
 Department of Materials Science and Engineering, Korea University, Korea



SC22

Removal of silica and copper ions from CMP wastewater via magnetic seeding aggregation using superconducting HGMS

Jongseok Lee, Jung-bin Song, Dong Gyu Yang, Yeonjoo Park and Haigun Lee*
 Department of Materials Science and Engineering, Korea University, Korea



SC23

Powder neutron diffraction study of HoCoGa₅

Riki Kobayashi^{1*}, Koji Kaneko¹, Shuichi Wakimoto¹, Naoyuki Sanada², Ryuta Watanuki², Kazuya Suzuki² and Songxue Chi³

¹ Quantum beam science directorate, Japan atomic energy agency, Japan
² Department of Advanced Materials Chemistry, Yokohama National University, Japan
³ Quantum beam science directorate, Oak Ridge National Laboratory, USA

Ternary compound ACoGa₅ (A=rare earth or actinide) attracts a much attention due to high temperature superconductivity in PuCoGa₅ and related compounds. In addition, recent study on TbCoGa₅ reveals another interesting aspects of this system; successive transitions in TbCoGa₅ could be "components-separated orders" which may arise from a novel type of frustration between multipole. HoCoGa₅ also exhibits successive transitions at TN1 = 9.6 K and TN2 = 7.5 K. In order to investigate nature of these transitions in HoCoGa₅, neutron powder diffraction experiment were carried out. Appearance of superlattice refractions was clearly observed below TN1. In addition, we observed that both peak position and intensity of superlattice peaks abruptly change at TN2 on cooling. The observed peak in the phase I (T < TN2) and II (TN2 < T < TN1) can be described with q1=(1/2 0 1/2) and q2=(1/2 0 τ) with τ=0.35, respectively. The determined propagation vector of the phase I is the same as that of TbCoGa₅, whereas that of phase II is altered. Detailed magnetic structure analysis for both phases are in progress.

[1] J. L. Sarrao et al., Nature 420, 297 (2002). [2] F. Honda et al., Physica B 359, 1147 (2005). [3] N. Sanada et al., J. Phys. Soc. Jpn. 78, 073709 (2009).

SC24

Evidence of two-band gap superconductivity in LaRu₂P₂

Tetsuya Fujiwara^{1*}, Harunobu Sagawa¹, Kazuyuki Matsubayashi², Yoshiya Uwatoko² and Toru Shigeoka¹

¹ Graduate School of Science and Engineering, Yamaguchi University, Japan
² Institute for Solid State Physics, University of Tokyo, Japan

We investigate the electronic transport properties and the superconducting gap characteristics of LaRu₂P₂. Superconducting transition was recognized at Tc = 4.4 K in LaRu₂P₂ single crystal as reported in ref [1]. Values of upper critical field Hc₂ estimated from the electrical resistivity under magnetic field are isotropic in this system. These are good accordance with the results by Ying et al.[2]. However, they, although, claimed that LaRu₂P₂ is a conventional superconductor, so called BCS type, it was revealed that LaRu₂P₂ single crystal obtained in this work shows a remarkably larger Hc₂ than that expected from GL theory at considerably low temperature. In addition, we observed two clear discontinuities of specific heat at Tc₁ = 4.4 K and Tc₂ = 4.0 K, respectively, in specific heat as a function of temperature. Each transition temperature vary obeying Hc₂(t)=Hc₂(0)(1-t²)/(1+t²), here, t = T/Tc, indicating that both discontinuities at Tc₁ and Tc₂ are attributed to superconducting transitions. So, we tried to analyze thermodynamic properties of LaRu₂P₂ by a two-band gap model [3]. In consequence, the numerically calculated C(T) curve was well reproduced experimentally measured specific heat as a function of temperature when Δ₁/kTc₁ and Δ₂/kTc₂ were assumed to be 1.5 and 3.0, respectively.

[1] T. Fujiwara et al., J. Phys.: Conf. Ser. 273, 012112 (2011). [2] J. Ying et al., Supercond. Sci. Technol. 23, 115009 (2010). [3] H. Padamsee et al., J. Low. Temp. Phys. 12, 387 (1973).

SC25

Proximity effect for asymmetrical three layered F/S structures in external magnetic field

Maxim V. Avdeev, Sergey L. Tsarevskii and Yurii N. Proshin*
 Theoretical Physics Department, Kazan Federal University, Russia

We study the critical temperature Tc of the three-layered ferromagnet/superconductor (F/S) structures at the external magnetic field H parallel to the film. For the F₁/S/F₂ and F₁/F₂/S asymmetrical trilayers the triplet superconducting component is generated at noncollinear magnetizations of the F layers. Assuming that all S and F layers are dirty we solve boundary problem for the Usadel function. The results of numerical calculations for Tc as function thicknesses both F₁ and F₂ layers at various parameters F/S structure are resented. The application to the spin-switch problem is discussed. We found that asymmetry can essentially change the spin-switch observation condition.

SC26

Influence of proximity effect with Umklapp processes on the Josephson current in the SFS nanostructure

Vadim Tumanov and Yurii N. Proshin*
 Theoretical Physics Department, Kazan Federal University, Russia

We consider the Josephson effect in symmetric superconductor-ferromagnetic-superconductor (SFS) system. The Josephson current is calculated as a function of the ferromagnetic layer thickness d. The Fulde-Ferrell-Larkin-Ovchinnikov (FFLO) pairs in the F layer have a nonzero wave vector, and the transformation the BCS pairs to the FFLO pairs (and vice versa) at passing through SF (FS) borders may be proceeded through the Umklapp processes [1]. To estimate the influence of proximity effect we use the expansion of superconductor energy in the powers of an order parameter (near the critical temperature Tc). We take into account the dependence of the critical temperature Tc from the phase difference φ between the order parameter in the left and right S side of the SFS contact. Our results are compared with known data for the Nb/CuNi/Nb nanostructures [2] where the critical Josephson current oscillations due to transitions between 0 and π phase state were observed. A good agreement is obtained by taking into account the Umklapp processes.

1. Yu. A. Izyumov, Yu. N. Proshin, and M. G. Khusainov, Physics/Uspekhi 45, 109 (2002) 2. V.V. Ryazanov et al., Rev. Low Temp. Phys. 136, 385 (2004)

SC27

Superconducting characters under pressure in heavy fermion compounds CeIr(In_xCd_{1-x})₂ studied by In-NQR

Mitsuharu Yashima
Engineering Science, Osaka University, Japan

The heavy fermion compounds CeMIn₂ (M = Co, Rh, Ir) have provided to study the relationship between antiferromagnetism and superconductivity. CeCoIn₂ becomes superconducting with $T_c = 2.3$ K at ambient pressure. This value is the highest record in the Ce-based heavy fermion superconductors. Since the existence of antiferromagnetic spin fluctuations is confirmed, it is expected that superconductivity is induced by antiferromagnetic spin fluctuations in CeCoIn₂. CeRhIn₂ is an antiferromagnet with $T_N = 3.8$ K at ambient pressure. Taking into account the lattice parameters of CeIrIn₂, it is speculated that an antiferromagnetic order is realized at ambient pressure, but it actually shows superconductivity with $T_c = 0.4$ K. The value of T_c is very low, as compared with the other CeMIn₂ compounds. T_c increases with increasing pressure and reaches about 1 K around 3 GPa, but antiferromagnetic spin fluctuations are greatly suppressed with the application of pressure. These results suggest that the superconducting mechanism of CeIrIn₂ may be quite different from that of the other CeMIn₂ compounds. In order to investigate the unconventional superconducting characteristics in CeIrIn₂, the nuclear-quadrupole-resonance (NQR) measurements were performed under pressure in pure and Cd-doped CeIrIn₂.

SD01

Giant and twofold oscillations of magnetoresistance in topological insulators Sb₂Te₃ and Bi₂Te₃ single crystals

Zengji Yue, Xiaolin Wang* and Shixue Dou
Spintronic and Electronic Materials Group, Institute for Superconducting & Electronic Materials, University of Wollongong NSW 2522, Australia

Topological insulators are quantum materials with an insulating bulk state and a topologically protected two dimensional metallic surface states. Unique electronic properties, such as the quantum spin Hall effect, magnetoelectric effects, magnetic monopoles, and elusive Majorana states, are expected from topological insulators. Topological insulators have great potential applications in spintronics and quantum information processing, as well as magnetoelectric devices with higher energy efficiency. To understand the macroscopic properties of the topological surface states and to investigate the possibility of their device applications, transport and magnetic measurements of high-quality single crystals are indispensable. Anisotropic magneto-transport properties were studied in p-type Sb₂Te₃ and n-type Bi₂Te₃ topological insulators through angular dependent magnetoresistance (MR) measurements. Giant MR of up to 230% was observed, which exhibits linear at high fields without any trend towards saturation. The giant MR displays a strong anisotropy, up to 210%, and twofold symmetry at different temperatures and fields. The giant MR might be due to intravalley and intervalley scattering, and the strong anisotropy might result from anisotropies of Fermi surface. The observed giant anisotropic MR of the Sb₂Te₃ and Bi₂Te₃ topological insulators could find applications in magneto-electronic devices based on topological insulators, such as magnetic sensors.

1. M. Z. Hasan and C. L. Kane, Rev. Mod. Phys. 82, 4 (2010). 2. X. L. Qi and S. C. Zhang, Rev. Mod. Phys. 83, 1057 (2011). 3. B. A. Bernevig, T. L. Hughes, and S. C. Zhang, Science 314, 1757 (2006). 4. D. Hsieh, D. Qian, L. Wray, Y. Xia, Y. S. Hor, R. J. Cava, and M. Z. Hasan, Nature 452, 970 (2008). 5. J. E. Moore, Nature 464, 194 (2010). 6. X. L. Wang, S. X. Dou, and C. Zhang, NPG Asia Mater. 2, 31 (2010).

SD02

Engineering and manipulating topological qubits in 1D quantum wires

Panagiotis Kotetes¹, Alexander Shnirman² and Gerd Schon¹
¹ Institut für Theoretische Festkörperphysik, Karlsruhe Institute of Technology, Germany
² Institut für Theorie der Kondensierten Materie, Karlsruhe Institute of Technology, Germany



SD03

Angle dependence of the Landau level spectrum in twisted bilayer graphene

Min-young Choi, Young-hwan Hyun and Yoonbai Kim*
Department of Physics, Sungkyunkwan University, Korea

In the context of the low-energy effective theory, the exact Landau level spectrum of quasiparticles in twisted bilayer graphene with small twist angle is analytically obtained by spheroidal eigenvalues. We analyze the dependence of the Landau levels on the twist angle to find the points where the twofold degeneracy for twist angles is lifted in the nonzero modes and below (above) which massive (massless) fermion pictures become valid. In the perpendicular magnetic field of 10 tesla, the degeneracy is removed at approximately 3 degrees for a few low levels, specifically approximately 2.56 degrees for the first pair of nonzero levels and approximately 3.50 degrees for the next pair. Massive quasiparticle appears at the angle less than 1.17 degrees in 10 tesla, which matches perfectly with the recent experimental results. Since our analysis is applicable to the cases of arbitrary constant magnetic fields, we make predictions for the same experiment performed in arbitrary constant magnetic fields. For example, for 40 tesla we get the critical angle of 2.34 degrees and the sequence of angles 5.11, 7.01, 8.42, ... for the pairs of nonzero energy levels. The symmetry restoration mechanism behind the massive (massless) transition is conjectured to be a tunneling (instanton) in momentum space.

SD04

Surface band structure study of Bismuth-based ternary topological insulators

Madhab Neupane¹, S.-y. Xu¹, C. Liu¹, L. A. Wray², N. Alidoust¹, A. Fedorov³, Y. S. Hor⁴, T.-r Chang⁵, H.-t. Jeng⁶, H. Lin⁷, B. Bansil¹, R. J. Cava¹ and M. Z. Hasan¹
¹ Physics, Princeton University, USA
² Physics, Princeton University & ALS, Berkeley, USA
³ Physics, ALS, Berkeley, USA
⁴ Chemistry, Princeton University, USA
⁵ Physics, National Tsing Hua University, China
⁶ Physics, National Tsing Hua University & Institute of Physics, Academia Sinica, China
⁷ Physics, Northeastern University, USA

Utilization of topological surface states is expected to lead to new vistas in electronics and fundamental physics. However, most of the known topological insulators either do not feature necessary band structure conditions (location of Dirac point with respect to the bulk band) or lack topological invariants essential for certain class of applications. Using angle-resolved photoemission spectroscopy (ARPES), we reveal the electronic band structure topology of a family of ternary spin-orbit insulators some of which feature functional electronic structure with in-gap Dirac point while others feature novel topological invariants (weak Z₂ invariants) in crystalline form. These Bi-based ternary topological insulators provide a natural access to lattice matched magnetically ordered states to be utilized in future devices.

SD05

Topological aspects and transport properties of edge states in the multi-band superconductor Sr₂RuO₄

Yoshiki Imai^{1*}, Katsunori Wakabayashi² and Manfred Sigrist³
¹ Department of Physics, Saitama University, Japan
² International Center for Materials Nanoarchitectonics, National Institute for Materials Science, Japan
³ Theoretische Physik, Eidgenössische Technische Hochschule Zurich, Switzerland

Motivated by the spin-triplet chiral p-wave superconductor Sr₂RuO₄, we investigate the edge state of multi-band superconductor by means of the three band tight-binding model including inter-orbital hybridization and spin-orbit coupling effects. These bands correspond to the alpha, beta and gamma bands of Sr₂RuO₄ where alpha and beta bands have hole- and electron-like characters, respectively. In particular we focus on the topological aspects and transport properties in the chiral spin-triplet phase. Although a full quasiparticle excitation gap in the bulk system, gapless edge states appear and affect both spontaneous spin and charge currents which give rise to anomalous and spin Hall effect. In this context, we study the interplay between electron- and hole-like particles and the effect of the genuinely two-dimensional gamma band in the formation of these edge states and edge currents. The topological aspects and correlation effects on this system are also discussed.

SD06

Influence of geometry on the edge states of Bi Nanoribbons

Hyun-jung Kim¹, Gustav Bihlmayer², Stefan Bluegel² and Jun-hyung Cho^{1*}
¹ Department of Physics and Research Institute for Natural Sciences, Hanyang University, Korea
² Peter Gruenberg Institut and Institute for Advanced Simulation, Forschungszentrum Juelich and JARA, Germany

Two-dimensional (2D) topological insulators or 2D quantum spin Hall (QSH) systems provide an intriguing physical phenomena in condensed matter physics. The 2D QSH phase is a band insulator but has gapless edge states. The salient feature of these edge states is that they are topologically protected. Here, using first-principles density-functional calculations, we investigate the effect of geometry on the edge states in zigzag Bi nanoribbon (ZBNR) reported as a 2D QSH system.[1] We consider various edge geometries involving the ideal termination, relaxation, and rebonded reconstruction. We find that the rebonded reconstruction geometry is thermodynamically more stable than other geometries. Since the transition from the reconstruction to the relaxation geometry is kinetically feasible, the edge structure of ZBNR is expected to exhibit the order-disorder transition as a function of temperature. We also find that the metallic feature of edge states is preserved with respect to the shear distortion and bond alternation, but it is dramatically altered to produce a band-gap opening through the rebonded reconstruction. We discuss such an influence of geometry on the edge states of ZBNR in terms of the penetration depth of the edge states.

[1] M. Wada, S. Murakami, F. Freimuth, and G. Bihlmayer, Phys. Rev. B 83, 121310(R) (2011).

SD07

Magnetotransport measurements in pulsed magnetic fields: a case for Fermiology studies in superconductors and topological insulators

Frederik Wolff-fabris^{1*}, Jun Sung Kim², Erik Kampert¹, Joonbum Park², Man Jim Eom², Sergei Zherlitsyn¹, Thomas Herrmannsdoerfer¹ and Jochen Wosnitza¹
¹ Dresden High Magnetic Field Laboratory (HLD), HZDR, Germany
² Department of Physic, Pohang University of Science and Technology, Korea

Superconductors and Dirac materials, such as graphene and topological insulators, are intensively studied in high magnetic fields. In this work, we present the current status of magnetotransport measurements at the Dresden High Magnetic Field Laboratory (HLD) and discuss examples of phase-diagram and fermiology investigations in different compounds [1,2], as well as the new Dirac material [3] SrMnBi₂. Typical experiments in magnetic fields up to 85 T with 25 to 150 ms pulse duration in samples spaces up to 16 mm are performed by discharging a 50 MJ capacitor bank. We use standard four-probe-technique measurements with AC currents up to 200 kHz and the longitudinal and transverse (Hall effect) voltages signals from the samples are digitized with a fast recording system. We observed quantum oscillations in magnetotransport measurements up to 63 T on crystals of SrMnBi₂ and, together with other techniques, this demonstrates that there is a Dirac dispersion in the electronic structure of the double-sized Bi square net. However, in contrast to graphene, the Dirac cone in SrMnBi₂ is highly anisotropic which suggests that the Bi square net can provide a new platform for highly anisotropic Dirac fermions. Acknowledgements Work at the HLD was supported by EuroMagNET II (No. 228043).

[1] V. A. Goparov; F. Wolff-Fabris, D. L. Sun et al. JETP 93, v.1, p. 29 (2010); [2] M. V. Kartsovnik, T. Helm, K. Putzke et al. New Journal of Physics 13, 015001 (2011); [3] J. Park, G. Lee, F. Wolff-Fabris et al. Physical Review Letters 107, 126402 (2011).

SD08

First-principles study of spin texture in the multilayer graphene on Ni(111)

Fumiyuki Ishii^{1*}, Hiroki Kotaka², Keisuke Sawada³ and Mineo Saito¹
¹ Faculty of Mathematics and Physics, Kanazawa University, Japan
² Graduate School of Natural Science and Technology, Kanazawa University, Japan
³ Graduate School of Natural Science and Technology, Kanazawa University, Japan



SD09

A full quantum study on gapless modes and Axion electrodynamics in topological insulator heterostructure systems

Ken Shiozaki^{1*}, Takahiro Fukui² and Satoshi Fujimoto¹
¹ Department of Physics, Kyoto University, Japan
² Department of Physics, Ibaraki University, Japan

Three dimensional topological insulator heterostructure systems show the various novel phenomena such as gapless modes localized at defects or the Axion response in three dimensional topological insulator-magnetic insulator heterostructures. The origin of these phenomena is the nontrivial topology in both momentum and real spaces. Dealing with the spatial coordinates as the adiabatic parameter in the heterostructure systems, one can introduce the semiclassical Hamiltonian, which describes topological properties of the heterostructure system. On the other hand, in some cases, it also happens that semiclassical approaches fail to describe correctly topological features. In this study, we present full quantum treatment for three dimensional topological insulator heterostructure systems without the semiclassical approximation. We, first, prove the index theorem for gapless modes in line defects of the topological insulator-magnetic insulator heterostructure systems. Secondly, we demonstrate a full quantum calculation for the surface quantum anomalous Hall effect at the interface of the topological insulator-magnetic insulator heterostructure without using the Axion effective action. We also show that gapless modes in line defects and the Axion response may be governed not only by helical Dirac fermions on the surfaces, but also by gapped bound states at the interface, the contribution of which was missing in previous studies.

Xiao-Liang Qi, Taylor L. Hughes, and Shou-Cheng Zhang, Phys. Rev. B 78, 195424 (2008). Jeffrey C. Y. Teo and C. L. Kane, Phys. Rev. B 82, 115120 (2010).

SD10

Magnetic properties of rare earth doped Bi₂Te₃

Nahyun Jo, Youngha Choi, Kyujoon Lee and Myung-hwa Jung*
Physics, Sogang University, Korea

Bi₂Te₃ is one of 3-dimensional topological insulators together with Bi₂Se₃ and Bi₂Sb₃. [1] Recently, Binghai Yan et. al have theoretically reported that LaBiTe₃ is a strong topological insulator. [2] We could conjecture that rare-earth materials have fascinating magnetic properties, since it has filled outer shell (5s25p6) and simultaneously unfilled inner shell (4f n). [3] Therefore, we made both LaxBi_{2-x}Te₃ and CexBi_{2-x}Te₃, and measured transport and magnetic properties. LaxBi_{2-x}Te₃ is diamagnetic, while CexBi_{2-x}Te₃ is paramagnetic at low temperature. From the modified curie-wiess fit, we could obtain the effective magnetic moment of 2.56μB. This value demonstrates that the Ce ion is in trivalent state. However, the carrier density of CexBi_{2-x}Te₃ is observed to be on order smaller than that of Bi₂Te₃, giving rise to a strong increase of carrier mobility. These results support a scenario of strong topological insulator. Furthermore, a magnetoresistance ratio of CexBi_{2-x}Te₃ is 1600% at 70kOe, even though ferromagnetic FexBi_{2-x}Te₃ have 600% magnetoresistance ratio at 70kOe.

[1] Y.L. Chen et. al., SCIENCE, 325, 178 (2005). [2] Binghai et al. PRB, 82, 161108(R) (2010). [3] Charles Kittel, Introduction to Solid State Physic (John Wiley & Sons, Inc, New Jersey, 2005) .

SD11

Iron doping effect in topological insulator: Bi₂Te₃

Nahyun Jo¹, Youngha Choi¹, Kyujoon Lee¹, Jungwon Jang², Jinhee Kim², Akio Kimura³ and Myung-hwa Jung^{1*}
¹ Physics, Sogang University, Korea
² Korea Research of Standards and Science, Korea
³ Physics, Hiroshima University, Japan

Bi₂Te₃ is well-known topological insulator with anti-site defects which complicates the manipulation of the Fermi level. It has also been reported that surface band of topological insulators is open when magnetic ions are doped, because magnetic ions are able to break the time reversal symmetry. In this report, we doped magnetic ions of Fe into Bi₂Te₃ and studied the properties and the corresponding electronic structure. We found that a small amount of Fe ions less than 0.4% do not open the surface gap, but reduce the anti-site defects. Thus, Fe-doped Bi₂Te₃ has linear magnetoresistance with high mobility (15,074cm²v-1s-1) which is three times higher than Bi₂Te₃ while Bi₂Te₃ has a deviation from the linear dependence of magnetoresistance. The reduction of anti-site defects enhances the sample quality, so that we could observe quantum oscillations such as Shubnikov de Haas and de Haas van Alphen effect. In addition, the spin-dependent ARPES data also demonstrate both clear surface state without gap opening and canted spin components in the c axis.

SD12

Magneto transport properties of topological insulator nanoribbons of Bi₂Te₃

Hong-seok Kim¹, Hosun Shin², Eun-kyoung Jeon³, Kung-won Rhie¹, Ju-jin Kim⁴, Jeong-o Lee³, Jaeyong Song² and Yong-joo Doh^{1*}
¹ Dept. of Display and Semiconductor Physics, Korea University Sejong Campus, Korea
² Korea Research Institute of Standards and Science, Korea
³ Korea Research Institute of Chemical Technology, Korea
⁴ Dept. of Physics, Chonbuk National University, Korea

We report on the magneto transport properties of topological insulator nanoribbons of Bi₂Te₃. The Bi₂Te₃ nanoribbons were grown using the electrodeposition processes and contacted with 100-nm-thick cobalt electrodes. At low temperature below T = 10 K, the magnetoresistance increases with a magnetic field, B, which is attributed to a weak antilocalization effect. When the magnetic field (B) is applied parallel to the ferromagnetic electrodes on top of the nanoribbon, a switching behavior of the magnetoresistance is observed near B = 400 Oe. Temperature and gate voltage dependences of the spin valve effect is discussed as well.

SD13

Structural investigations of the topological insulators Bi₂Se_{3-x}Te_x

Geetha Balakrishnan^{1*}, Ravi Singh¹, Devashibhai Adroja², Kevin Knight² and Matthias Gutmann²
¹ Department of Physics, University of Warwick, United Kingdom
² ISIS Facility, Rutherford Appleton Laboratory, United Kingdom

The binary phases Bi₂Se₃ and Bi₂Te₃ have been discovered to exhibit three dimensional topological insulating behaviour. However, these compounds are not insulators when investigated in the bulk. Bi₂Se₃ is generally known to exhibit n-type conductivity and Bi₂Te₃ exhibits n or p-type conductivity depending on the synthesis conditions. The bulk conductivity exhibited by these materials are seen as being detrimental to the investigation of their surface conducting properties. We have examined the intermediate compositions Bi₂Se_{3-x}Te_x in order to study the role played by vacancies and anti-site defects in determining the bulk conduction mechanisms. We report detailed structural refinements obtained by neutron diffraction experiments on several of the intermediary phases and draw correlations between the defect structures and their conducting / semiconducting / insulating behaviour.

SD14

Josephson effects in Bi₂Se₃ topological insulator nanoribbons

Hyunho Noh¹, Lee-seul Park², Eun-kyoung Jeon³, Hong-seok Kim⁴, Jeong-o Lee³, Jin Seok Lee³, Jinhee Kim³ and Yong-joo Doh^{1*}
¹ Korea Research Institute of Standards and Science, Korea
² Dept. of Chemistry, Sookmyung Women's University, Korea
³ Korea Research Institute of Chemical Technology, Korea
⁴ Dept. of Display and Semiconductor Physics, Korea University Sejong Campus, Korea

Topological insulators are exotic materials with bulk band gap and metallic edge states which are protected on their own boundary topologically. Here, we report on the fabrication and measurement results of the superconducting proximity junctions of topological insulator nanoribbons of Bi₂Se₃. Single-crystalline Bi₂Se₃ nanoribbons are synthesized using the vapor-liquid-solid method, while the superconducting Al electrodes are formed on top of the nanowire. When a magnetic field (H) is applied along the axial direction, the magneto-resistance data exhibit quasi-periodic oscillations with an average periodicity of H* ~ 0.4 T, which is consistent with the Aharonov-Bohm oscillations. In the superconducting state, the supercurrent branch with a critical current of I_c ~ 90 nA is clearly observed in the current-voltage curve as a result of the superconducting proximity effect in Bi₂Se₃ nanoribbon. Quantized voltage steps of the Bi₂Se₃ nanoribbon Josephson junction under the microwave irradiation satisfy the ac Josephson relation.

SD15

Electronic structure and transport properties of pt based heusler compounds with C1b structure for topological quantum phenomena

Siham Ouardi¹, Gerhard H. Fecher¹, Shekhar Chandra², Gloskovskii Andrei³ and Felser Claudia¹
¹ Johannes Gutenberg University and Max Planck Institute for Chemical Physics of Solids, Dresden, Germany
² Max Planck Institute for Chemical Physics of Solids, Dresden, Germany
³ Institute of Inorganic and Analytical Chemistry, Johannes Gutenberg - University, Mainz, Germany

Many of the Heusler compounds based on heavy elements with 1:1:1 composition and C1b structure are zero band gap insulators and exhibit partially an inverted band structure [1]. Based on a topologically protected electronic surface states, this class of materials is supposed to open up innovative directions for future technological applications in spintronics, quantum computing and thermoelectrics. The density of states of Pt based Heusler compounds PMZ (M=Y, Gd, Lu and Z=Sb, Bi) were investigated by bulk sensitive hard X-ray photoelectron spectroscopy. The measured valence band spectra are clearly resolved and in well agreement with the first-principles calculations of the electronic structure of the compounds. Close to the Fermi energy, the linear behavior of the measured spectra at high excitation energy where influences of the surface can be neglected improve bulk origin of the Dirac-cone type density [2]. Furthermore, the temperature dependence of electrical conductivity, Hall mobility, Seebeck coefficient and thermal conductivity were investigated. The promising properties of those compounds open a high potential for new technological applications.

[1] S. Chadov, X. Qi, J. Kubler, G. H. Fecher, C. Felser, and S. Zhang, *Nat Mater* 9, 541 (2010). [2] S. Ouandi, C. Shekhar, G. H. Fecher, X. Kezina, G. Stryganyuk, C. Felser, S. Ueda, and K. Kobayashi, *Appl. Phys. Lett.* 98, 211901 (2011).

SD16

Gapless interface states in topological insulator/semiconductor heterostructures

Hugo Aramberri and Carmen Munoz*
 ICMIM- Consejo Superior de Investigaciones Cientificas, Spain

Based on first principles calculations we investigate the existence of topologically-nontrivial states at the interface between a topological insulator (TI) and a semiconductor (S) in TI/S heterostructures. We find that the emergence of gapless states depends on the symmetry of the junction, being protected by mirror symmetry. We discuss their characteristic dispersion and spatial distribution and analyze the quantum interference between helical states and its influence on the spin texture of the quasi two-dimensional states as a function of the semiconductor thicknesses. From the first-principles calculations, we derive an effective Hamiltonian, which captures the salient topological features. The effective model combined with a Green function matching method [1] allow us to investigate the evolution of the interaction between interface helical Dirac fermions from finite heterostructures to actual semifinite interfaces and therefore to analyze the novel behavior of the spin-charge coupling in two-dimensional layered systems with strong spin-orbit coupling.

[1] M. C. Muñoz, V. R. Velasco and F. Garcia-Moliner, *Phys. Rev. B* 39 (1989) 1786; M. C. Muñoz and M. P. Lopez Sancho, *Phys. Rev. B* 41 (1990) 8412.

SD17

Thermoelectric transport in topological insulators

Oleg Tretiakov*
 Physics and Astronomy, Texas A&M University, USA

We study the thermoelectric properties of three-dimensional topological insulators with many holes (or pores) in the bulk. We show that at high density of these holes the thermoelectric figure of merit, ZT, can be large due to the contribution of the conducting surfaces and the suppressed phonon thermal conductivity. The maximum efficiency can be tuned by an induced gap in the surface states dispersion through tunneling, magnetic impurities, or external magnetic fields. The large values of ZT, much higher than unity for reasonable parameters, make this system a strong candidate for applications in heat management of nanodevices, especially at low temperatures.

O. A. Tretiakov, Ar. Abanov, and Jairo Sinova, *Applied Physics Letters*, 99, 113110 (2011).

SD18

Topological phase in a one-dimensional interacting fermion system

Huaiming Guo
 Department of physics, Beihang University, China

We study a one-dimensional (1D) interacting topological model by means of the exact diagonalization method. The topological properties are first examined with the existence of the edge states at half-filling. We find that the topological phases are not only robust to small repulsive interactions, but also are stabilized by small attractive interactions, and also finite repulsive interaction can drive a topological nontrivial phase into a trivial one while the attractive interaction can drive a trivial phase into a nontrivial one. Next we calculate the Berry phase and parity of the bulk system and find that they are equivalent in characterizing the topological phases. With them we obtain the critical interaction strengths and construct part of the phase diagram in the parameters' space. Finally we discuss the effective Hamiltonian at the large-U limit and provide an additional understanding of the numerical results. These results could be realized experimentally using cold atoms trapped in the 1D optical lattice.

1: Xiao-Liang Qi and Shou-Cheng Zhang, *Rev. Mod. Phys.* 83, 1057 (2011). 2: J. E. Moore, *Nature (London)* 464, 194 (2010). 3: M. Z. Hasan and C. L. Kane, *Rev. Mod. Phys.* 82, 304 (2011). 4: Huaiming Guo and Shun-Qing Shen, *Phys. Rev.B* 84, 195107 (2011).

SD19

Robustness of 1D topological superconductors with Majorana edge states against lattice modulation

Masaki Tezuka* and Norio Kawakami
 Department of Physics, Kyoto University, Kitashirakawa, Sakyo-ku, Kyoto 606-8502, Japan



SE01

Temperature-pressure phase diagram of quadrupolar order in PrTr₂Al₂₀ (Tr=Ti,V)

Toshiki Tanaka¹, Kazuyuki Matsubayashi^{2*}, Akihiko Hisada², Akito Sakai², Satoru Nakatsuji², Yoshiya Uwatoko² and Yasunori Kubo³
¹ Graduate School, Nihon Univ, Japan
² Institute for Solid State Physics, The University of Tokyo, Japan
³ College of Humanities and Sciences, Nihon Univ, Japan

PrTr₂Al₂₀ (Tr=Ti,V) crystallizes in a cubic CeCr₂Al₂₀ type structure with the space group Fd₃̄m. According to neutron experiment, crystal electric field (CEF) ground state of Pr ion is the non-Kramers Γ₃ doublet [1]. Reflecting the non-magnetic ground state, PrTi₂Al₂₀ and PrV₂Al₂₀ exhibit quadrupolar ordering at TQ ~ 2.0 K and 0.6 K, respectively. It is notable that the low temperature electrical resistivity of PrV₂Al₂₀ shows √T dependence, suggesting the quadrupolar Kondo effect [2]. In the present study, we have measured electrical resistivity under high pressure on PrTr₂Al₂₀ (Tr=Ti,V) single crystals in order to clarify the pressure dependence of TQ and Kondo effect. Electrical resistivity of PrTi₂Al₂₀ shows the broad maximum centered at ~50 K due to incoherent Kondo-scattering processes on the ground state and the excited CEF level. With increasing pressure, the magnitude of this anomaly increases while the peak position is unchanged. At lower temperatures, it is found that a clear resistive drop at TQ ~ 2 K at ambient pressure. TQ first increases and shows the maximum under pressure. We will present the phase diagram of PrTi₂Al₂₀ together with that of PrV₂Al₂₀.

[1]: T. J. Sato, S. Iitaka, A. Sakai and S. Nakatsuji: Meeting Abst. Phys. Soc. Jpn, Vol.65, Issue 2, Pt. 3, (2010) p. 584 [2]: A. Sakai, S. Nakatsuji - J. Phys. Soc. Jpn. 80 (2011) 063701

SE02

Soft point contact spectroscopy in the antiferromagnet Ce₂RhIn₈

Eunsung Park¹, Xin Lu², Chung Jae Won³, Nam Jung Hur³, Eric D. Bauer², Joe D. Thompson² and Tuson Park^{1*}
¹ Department of Physics, Sungkyunkwan University, Korea
² Condensed Matter & Magnet Science Group, Los Alamos National Laboratory, USA
³ Department of Physics, Inha University, Korea

We performed soft point contact spectroscopy on the Ce-based heavy fermion systems (CeIn₃, CeCoIn₅, CeRhIn₅, CeIrIn₅, and Ce₂RhIn₈) with silver epoxy replacing a conventional tip. Unlike CeIn₃ where the conductance dI/dV is enhanced below TN (=10K), the conductance of CeRhIn₅ at zero bias voltage is rapidly enhanced below 8K, which is higher than TN of CeRhIn₅ (=3.8K). Heavy fermion compounds with a magnetic order often show intermediate states that are characterized by a broad enhancement of conductance at temperatures higher than TN, while heavy fermion compounds without magnetic ordering reveal asymmetric conductance line-shape below characteristic temperature T*. The antiferromagnet Ce₂RhIn₈ is unique in that the intermediate state shows a V-shaped dip around zero biased voltage and is enhanced with decreasing temperature below 25K, which is much higher than T*=5K. Below TN=2.8K, a symmetric peak at zero bias voltage in the conductance spectra is enhanced within the V-shaped dip with decreasing temperature. We interpret the symmetric peak and V-shaped dip around zero bias as manifestation of the antiferromagnetic (AFM) order and Kondo dip in the Kondo lattice system, respectively, indicating that Ce₂RhIn₈ is at a boundary between AFM and Kondo states.

SE03

Evidence of a spin gap above the magnetic ordering temperature and crystal field excitations in CeO₂Al₁₀

D T Adroja^{1*}, P P Deen², A D Hillier¹, Y Muro³, J Kajino⁴, T Takabatake⁴, A M Strydom⁵, P Peratheepan³, F Demmel¹, J R Stewart¹ and J Taylor¹
¹ ISIS Facility, Rutherford Appleton Laboratory, Chilton, OX11 0QX, United Kingdom
² European Spallation Source, St Ångström 4, Box 176 Lund 221 00, Sweden
³ Liberal Arts and Sciences, Toyama Prefectural University, Kurokawa 5180, Imizu 939-0398, Japan
⁴ Department of Quantum matter, ADSM, and IAMR, Hiroshima University, Higashi-Hiroshima, 739-8530, Japan
⁵ Physics Department, University of Johannesburg, PO Box 524, Auckland Park 2006, South Africa

Recently, the opening of a spin gap has been reported in the intermetallic compounds CeT²Al₁₀ (T = Ru and Os) below TN = 27-29K through heat capacity and magnetic susceptibility measurements. Various theoretical models have been proposed to explain the spin gap formation, for example a spin-Peierls and RVB models of Hanzawa for CeRu₂Al₁₀. To understand the nature of the spin gap formation in CeO₂Al₁₀, we have carried out low and high energies inelastic neutron scattering (INS) measurements between 4.5 and 65K. Our INS studies reveal a clear sign of a spin gap of 11meV at 4.5K and of 4meV at 35K, while above 45K the observed response transformed into a quasielastic line with linewidth of ~ 8 meV. The observation of a spin gap above TN suggests that its origin is not only due to the gapped spin wave, but also related to the hybridization between 4f- and conduction electrons. Moreover the high energy INS study reveals two crystal field (CEF) excitations at 37 and 57meV. We have carried out an analysis of the INS data along with the single crystal susceptibility based on the CEF model, which gives good fit to both data sets.

SE04

Role of quantum fluctuations in forming heavy-fermions for Ca_{2-x}SrxRuO₄

Naoya Arakawa and Masao Ogata
 Department of Physics, The University of Tokyo, Japan

In order to understand a role of quantum fluctuations in forming heavy-fermions for Ca_{2-x}SrxRuO₄, we investigated the effect of quantum fluctuations on the mass-enhancement on the basis of the three-orbital Hubbard model for the Ru-t2g-orbitals. In this presentation, I show the momentum-dependence of both the spin and charge susceptibilities for the tight-binding models at x = 2.0 and 0.5 within the random phase approximation (RPA). I also present the variation of γe, obtained by using the Hellmann-Feynman theorem and the RPA, between x=2.0 and 0.5 and address a role of both the spin and orbital fluctuations in enhancing γe for Ca_{2-x}SrxRuO₄.

SE05

Study of long range magnetic ordering and spin gap formation in Ce(Ru1-xFex)2Al10 through muSR and neutron scattering measurements

D T Adroja^{1*}, A D Hillier¹, Y Muro², J Kajino³, T Takabatake³, P Perathepan⁴, A M Strydom⁴, P P Deen⁵, J R Stewart¹, J Taylor¹, F Demmel¹ and M Adams¹
¹ISIS Facility, Rutherford Appleton Laboratory, Chilton, OX11 0QX, United Kingdom
² Liberal Arts and Sciences, Toyama Prefectural University, Kurokawa 5180, Imizu 939-0398, Japan
³ Department of Quantum matter, ADSM, and IAMR, Hiroshima University, Higashi-Hiroshima, 739-8530, Japan
⁴ Physics Department, University of Johannesburg, PO Box 524, Auckland Park 2006, South Africa
⁵ European Spallation Source, St Algotan 4, Box 176 Lund 221 00, Sweden

We have carried out muon spin relaxation (muSR) and inelastic neutron scattering (INS) investigations on Ce(Ru1-xFex)2Al10 (x=0, 0.3, 0.5, 0.8 and 1) compounds to investigate the origin of the spin gap formation. Our muSR study confirms the long-range magnetic ordering below 26K in x=0, 0.3 and 0.5, while x=0.8 and 1.0 remains paramagnetic down to 1.2K. Furthermore, INS measurements of x=0 clearly reveal the presence of a spin gap of 8meV at 5K. Interestingly at 5K the spin gap excitation broadens in x=0.3 and exhibits two clear INS peaks at 7.6(0.3) and 11.1(2.0)meV in x=0.5. Moreover the x=0.8 sample, which remains paramagnetic down to 1.2K, reveals a clear sign of a spin gap of 10-12 meV, with strong Q-dependent intensity that follows a spin-dimer structure factor. The observation of a spin gap in the paramagnetic sample (x=0.8) opens a question, what is the origin of the spin gap in CeT2Al10 (T=Ru and Os) compounds? Possibilities include gapped spin wave, hybridization gap, spin-dimer or a gap opening on a small part of the Fermi surface. Our analysis of the Q-dependent intensity reveals that the mechanism of the spin gap in the x=0.8 sample is possibly due to spin-dimer formation.

SE06

Specific heat of structure-disordered heavy-fermion CexY80-xMn20 alloys

Yusuke Amakai^{1*}, Shinya Tanaka¹, Yasuhiro Shiojiri¹, Naoki Momono¹, Hideaki Takano¹, Shigeyuki Murayama¹, Yoshihisa Ohi² and Koki Takanashi²
¹ Graduate School of Engineering, Muroran Institute of Technology, Japan
² Institute for Material Research, Tohoku University, Japan

Recently, we have reported physical properties of structure-disordered (a-)CexY80-xMn20 alloys which show a heavy fermion state in the non-Bloch system without translation symmetry[1]. The specific heat Cp for present alloys follows $\gamma T + \beta T^3$ down to about 10 K. The T-linear coefficient γ shows a large value (~200 mJ/Ce-molK) and almost independent of the Ce-concentration. However, the Cp/T vs. T² plot of T < 10 K deviates from the T-linear relation with decreasing temperature. In this work, in order to clarify the factor of the deviation of Cp/T for a-CexY80-xMn20 alloys, we have measured the low-temperature specific heat. We have estimated the temperature TA of the deviation from the Cp/T vs. T₂ plot for present alloys. The TA is about 10 K, and almost independent of the Ce-concentration. Therefore, the deviation from the Cp/T for the present alloys would be considered the crystalline-electric-field splitting of the six-fold degenerate level of the Ce³⁺ ion. Detailed discussions will be presented at the conference.

[1] Y. Amakai, et al., Phys. Rev. B, 79(2009)245126.

SE07

Synchrotron X-ray diffraction study on crystal structure of URu2Si2

Chihiro Tabata^{1*}, Reiji Kumai², Kensuke Kobayashi², Hironori Nakao², Yoichi Murakami², Makoto Yokoyama¹, Hiroyuki Hidaka¹, Tatsuya Yanagisawa¹ and Hiroshi Amitsuka¹
¹ Graduate School of Science, Hokkaido University, Japan
² CMRC and PF, Institute of Materials Structure Science, High Energy Accelerator Research Organization, Japan
³ Faculty of Science, Ibaraki University, Japan

URu2Si2 (the tetragonal ThCr2Si2 type crystal structure; space group I4/mmm) has attracted much interest because of its peculiar phase transition at 17.5 K (≡T0) [1-3]. Despite more than 25 years of intense research trying to identify the order parameter, the intrinsic nature of the phase transition has not been elucidated [4]. The ThCr2Si2 structure includes a free position parameter, z, of the Si 4(e) site. Since the Si ions are located at the second nearest-neighbor position of the U ions, the precise determination of the z parameter might provide useful information for evaluation of hybridization effects of 5f orbitals with Si s, p states, calculations of a band structure, analyses for 29Si-NMR spectra, and so on. These pieces of knowledge might offer a clue to solving the issue of hidden order in URu2Si2. We will report our latest study of structural analyses of a single crystal of this material based on the X-ray diffraction measurements performed at BL-8A and B in the Photon Factory KEK.

[1] T.T.M. Palstra et al., Phys. Rev. Lett. 55, 2727 (1985). [2] M.B. Maple et al., Phys. Rev. Lett. 56, 185 (1986). [3] W. Schlitz et al., Z. Phys. B 62, 171 (1986). [4] J.A. Mydosh and P.M. Oppeneer, arXiv:1107.0258v1 (2011).

SE08

Spin-density wave order in the 2D heavy fermion system CePt2In7

Martin Mansson^{1*}, Jun Sugiyama², Yasmine Sassa¹, Bastian M. Wojek³, Thomasz Durakiewicz², Krunoslav Prsa¹, Olof Gotberg³, Calin Rusu³, Daniel Andreica², Stephane Pons³, Marco Grioni³, Oscar Tjernberg³ and Eric D. Bauer⁴
¹ Lab. for Solid State Physics, ETH Zurich, Switzerland
² Toyota Central Research and Development Labs. Inc., Japan
³ Materials Physics, Royal Institute of Technology, KTH Stockholm, Sweden
⁴ Los Alamos National Laboratory, USA
⁵ Faculty of Physics, Babes-Bolyai University, Romania
⁶ Institute of Condensed Matter Physics, EPF Lausanne, Switzerland

The title compound is a recently discovered heavy fermion material where the spacing between Ce-In planes is drastically increased. Consequently, CePt2In7 inherit a truly 2D electronic structure. It was recently discovered that CePt2In7 is not only AF (TN=5.3 K) at ambient pressure but also becomes SC under pressure with a maximum transition temperature Tc=2.1 K at P=3.12 GPa. At lower pressures an intriguing coexistence of the AF order and SC phase is found, and that with increasing pressure Tc is increasing while TN decreases. The growth of the SC on the expense of the AF order suggests a crossover behavior of the Ce-4f electrons from localized to itinerant, similar to what is considered for the well-known CeRhIn5 compound. In the presented work the low-temperature microscopic magnetic properties of the quasi-2D heavy fermion compound, CePt2In7, are investigated by using μ SR. Clear evidence for the formation of a SDW order is presented. The magnetic order parameter fit well to a modified BSC gap-energy function in a strong-coupling scenario, possibly predicting the evolution of unconventional pairing in the pressure induced superconducting phase of this compound. Finally, we also present recent pressure dependent μ SR data.

Funding Source: Swiss National Science Foundation (Project 6, NCCR MaNEP), U.S. DOE Oce of Sciences, VR Sweden and Toyota CRDL.

SE09

Metal-nonmetal transition in Cr partial substituted Ni0.96S

Masanori Matoba^{*}, Yoichi Kamihara and Shuichiro Anzai
 Center for Applied Physics and Physico-Informatics, Keio University, Japan

Hexagonal NiAs-type NiS exhibits a first-order metal-nonmetal transition (MNT) at T=263K, resulting from the opening of narrow charge-transfer (CT) gap between the S 3p band and the upper Hubbard band [1,2]. The low temperature phase is the nonmetallic antiferromagnetic state, while the high temperature phase shows metallic and Pauli-paramagnetic behavior [3,4]. The substitution of vacancies for Ni atoms in NiS lowers Tt to be suppressed to be zero at d=0.035 in Ni1-dS, so that metallic Ni0.96S do not exhibit the MNT [5,6]. In this study, we synthesized Cr-partial substituted Ni0.96S or (Ni1-xCrx)0.96S by a solid state reaction in an evacuated silica tube to reveal the Cr-partial substitution effect on the physical properties of metallic Ni0.96S by the measurements of X-ray diffraction, electrical resistivity, magnetic susceptibility, and thermopower. Surprisingly, (Ni1-xCrx)0.96S clearly exhibits the MNT, while metallic Ni0.96S do not exhibit the MNT. The Tt increases with x sharply from x=0.025 (Tt=50 K) to x=0.09 (Tt=260 K) by Cr-partial substitution for Ni in Ni1-xS. At the conference, electronic nature of Cr-partial substituted Ni0.96S or (Ni1-xCrx)0.96S with ability for the opening of CT-gap will be discussed from the viewpoint of the strongly correlated electron systems.

[1] A. Fujimori, H. Namatame, M. Matoba and S. Anzai, Phys. Rev. B 42, 620 (1990). [2] M. Imada, A. Fujimori, and Y. Tokura, Rev. Mod. Phys. 70, 1039 (1998). [3] J. T. Sparks and T. Komoto, Phys. Lett. A 25, 398 (1967). [4] S. Anzai and K. Ozawa, J. Phys. Soc. Jpn. 24, 271 (1968). [5] R. Brunetti, J. M. D. Coey, G. Czjak, J. Fink, F. Gompf and H. Schmidt, J. Phys. F 10, 33 (1980). [6] M. Matoba and S. Anzai and A. Fujimori, J. Phys. Soc. Jpn. 60, 4230 (1991).

SE10

A study of ni-substitution and pressure effects on the heavy-fermion Superconductor CeCu2Si2

Yoichi Ikeda^{*}, Yuzo Ito, Shingo Araki and Tatsuo C Kobayashi
 Graduate School of Natural Science and Technology, Okayama University, Japan

The heavy-fermion superconductor CeCu2Si2 shows an attractive enhancement of Tc around a critical pressure (~ 4.5 GPa), at which the T-linear variation of resistivity, the enhancement of the residual resistivity, the rapid decrease of T²-coefficient and a sign of a valence crossover have been observed [1-3]. These characteristics have been believed to be signatures of the critical valence fluctuations associated with a valence transition around its critical-end point [4, 5], while we have been requiring more signatures for clarification of the fascinating phenomena. Effects of the Ni substitution on CeCu2Si2 are investigated by means of specific heat and electrical resistivity measurements. A characteristic T-linear dependence of the resistivity is observed around x ~ 0.1 with a fractional resistivity drop due to filamentary superconductivity. In addition, a variation of the power index n of a fit to $\rho - \rho_0 = aT^n$ at low temperatures against T⁻¹max at which the resistivity shows a maximum is almost fully identical to the result of the high pressure experiment [1]. We would like to discuss for the similarities between Ni doping and pressure and the origin of the anomalous Fermi liquid state.

[1] A. Holmes et al., PRB 69 (2004) 024508. [2] K. Fujivara et al., submitted to J. Phys.: Conf. Ser. (SCES2011) Cambridge. [3] J. -P. Rueff et al., PRL 106 (2011) 186405. [4] K. Miyake, J. Phys.: Condens. Matter 19 (2007) 125201. [5] G. Seyfarth et al., arXiv:1111.4873v1.

SE11

Electrical resistivity measurement under pressure in the heavy fermion antiferromagnetic compound Ce2PtGa12

Ryo Sasaki¹, Kazuyuki Matsubayashi¹, Takuya Shiraiishi², Tetsuro Yamashita², Shigeo Ohara² and Yoshiya Uwatoko¹
¹ Institute for Solid State Physics, the University of Tokyo, Kashiwa, Chiba 277-8581, Japan
² Department of Engineering Physics, Electronics and Mechanics, Graduate School of Engineering, Nagoya Institute of Technology, Nagoya 466-8555, Japan

Ce-based heavy-fermion ternary compounds have been of interest because of their exotic physical properties under pressure, such as magnetic ordering and superconductivity.[1] In these systems, there is a competition between magnetic order of f-electrons (RKKY effect) and the screening of magnetic moments (Kondo effect) producing large effective electron masses. Ce2PtGa12 orders antiferromagnetically at 7 K, and specific heat measurements suggest that it is a moderate heavy-fermion system with $\gamma \square 191$ mJ/mol K₂. For understand of competition between RKKY and Kondo effect, We have measured the electrical resistivity under pressure on Ce2PtGa12 single crystal. In this paper, we will report the suppression of the antiferromagnetic order under higher pressure and discuss the electronic state in the vicinity of the critical pressure.

[1] R. T. Macaluso et al., J. Solid State Chem. 178 (2005) 3547.

SE12

Anisotropy of URhGe

Jack M Barraclough^{1*}, Edward A Yelland¹ and Andrew D Huxley²
¹ School of Physics and Astronomy, University of St Andrews and Scottish Universities Physics Alliance (SUPA), United Kingdom
² School of Physics, University of Edinburgh and SUPA, United Kingdom

The heavy fermion material URhGe has garnered interest in recent years as an unconventional superconductor. It shows coexistence of ferromagnetism and p-wave superconductivity[1], and superconductivity which is re-entrant in magnetic field[2]. We now believe the latter effect to be the result of proximity to a topological change in the Fermi-surface[3]. In this poster I report recent resistivity measurements on samples of URhGe with well-defined current direction. Most previous works do not consider this when reporting resistivity, however we find that some features can vary significantly as a function of current direction. We discuss how these findings constrain the anisotropy of the Fermi surface, and the possibility of a field dependent and/or anisotropic scattering rate. I also present data taken on high quality samples close to the quantum critical point. Interestingly, there is no enhancement of the superconducting Tc near the QCP compared to that observed with the field applied entirely along the crystalline b-axis, where a low temperature tricritical point is present.

[1] F Hardy and A D Huxley, PRL 94 247006 (2005) [2] F Levy et al, Science 308 1343 (2005) [3] E A Yelland et al, Nature Physics 7, 890-894 (2011)

SE13

Study of spin wave and spin gap in single crystals of CeRu2Al10 using inelastic neutron scattering measurements

D T Adroja^{1*}, E A Goremychkin¹, A D Hillier¹, Y Muro², J Kajino³ and T Takabatake³
¹ ISIS Facility, Rutherford Appleton Laboratory, Chilton, OX11 0QX, United Kingdom
² Liberal Arts and Sciences, Toyama Prefectural University, Kurokawa 5180, Imizu 939-0398, Japan
³ Department of Quantum matter, ADSM, and IAMR, Hiroshima University, Higashi-Hiroshima, 739-8530, Japan

We have carried out inelastic neutron scattering (INS) investigations on single crystals of CeRu2Al10 using the high neutron flux spectrometer MERLIN at ISIS facility. The crystals (total mass of 2.4g) were mounted in the b-c scattering plane. We carried out measurements using neutron incident energy Ei=20 meV at 4.5 K for b // ki and c // ki. We have seen a clear dispersive spin wave type excitations coming out from the [1 0 0] and [0 2 0] antiferromagnetic zone centres with a single ion anisotropic gap of ~4.5 meV. On the other hand along [0 0 L] direction the spin excitations exhibit weak dispersion with almost Q-independent gap of 8 meV. The intensity of the peak along [0 0 L] is maximum at L = 0 and decreases with increasing L value, like Ce³⁺ magnetic form factor. These results may suggest that excitations in the ab-plane can be explained by the gaped spin wave, but along [0 0 L] is dominated by the hybridization effect. We will present a detail analysis of the observed excitations.

SE14

Universal behavior in the nonlinear magnetic response of strongly correlated metals

B S Shivaram¹, D G Hinks², B Nartow³ and Pradeep Kumar³
¹ Department of Physics, University of Virginia, USA
² Materials Science Division, Argonne National Labs, USA
³ Department of Physics, University of Florida, USA

A diverse class of strongly correlated electronic materials irrespective of whether they order magnetically or not, often exhibit a peak in the temperature dependence of the linear magnetic susceptibility, χ . In non-linear susceptibility measurements on a number of heavy electron materials including in single crystals of the prototypical strongly correlated metal, UPt3, we find that there exists a peak in the third order susceptibility, χ^3 as well. This peak in χ^3 occurs at a temperature T3, which is roughly half the temperature T1, at which the peak in χ^2 appears. This proportionality between T3 and T1 also reported previously in other heavy fermion systems implies a universal behavior in the nonlinear magnetic response of correlated metals. The observed proportionality between T3 and T1 can be explained by a model which assumes a singlet ground state for the spins present in a crystalline electric field with a concomitant doublet excited state, separated from the ground state by an energy Δ . This model also yields metamagnetic behavior at a magnetic field corresponding to Δ .

SE15

X-ray absorption studies of the Ce2Rh1-xIrIn8 intermetallic compounds

Cris Adriano¹, Nilmar Silva Camilo², Leandro F Bufaical³, Leticie Medonca Ferreira⁴, Eduardo N Hering⁵, Pascoal G. Pagliuso¹ and Raimundo Lora-serrano^{3*}
¹ Instituto de Fisica 'Gleb Wataghin' UNICAMP, CP 6165, 13083-970 Campinas, SP, Brazil
² Instituto de Fisica, Universidade Federal de Uberlandia, 38400-902 Uberlandia-MG, Brazil
³ Instituto de Fisica, Universidade Federal de Goias, Goiania-GO, 74001-970, Brazil
⁴ Instituto de Fisica e Matematica, Universidade Federal de Pelotas (UFPel), CP 354, 96010-900 Pelotas, Brazil
⁵ Centro Brasileiro de Pesquisas Fisicas, Rua Dr. Xavier Sigaud 150, 22290-180 Rio de Janeiro, RJ, Brazil

Within the series of heavy fermions Ce2Rh1-xIrIn8 compounds it has been recently observed the occurrence of two low-temperature superconducting (SC) phases as a function of temperature both at ambient pressure and under applied pressure for intermediate Ir-content (x~0.25-0.7) with remarkable different behavior of both states as a function of pressure and x [1]. The details of the observed results seem to be reminiscent of the two SC phases found in the CeRh1-xIrIn3 system, thus related to the higher dimensionality and structural disorder for the Ce2-1-8 systems. Here, we report the results of extended x-ray absorption fine structure measurements performed on Ce2Rh1-xIrIn8 (x = 0.0, 0.25, 0.75 and 1.0) at T = 10, 150 and 300 K at the Rh K-edge and at the Ce and Ir-L3 absorption edges in order to check the extent of the structural disorder at the Rh-Ir atomic sites and their relevance for the SC phases observed in the resistivity and specific heat measurements in these compounds. Our results point to the trivalent state of the Ce ions, and that there is no evidence of phase separation in the lowest measured temperature.

[1] E. N. Hering, H. A. Borges et al. Phys. Rev. B 82 184517 (2010)

SE16

Polarized neutron diffraction study on the magnetic ordering in UMn2Al20

Przemyslaw Swatek^{1*}, Piotr Wisniewski¹, Arsen Gukasov² and Dariusz Kaczorowski¹
¹ Institute for Low Temperatures and Structure Research, Polish Academy of Sciences, Wroclaw, Poland
² Laboratoire Leon Brillouin, CEA-CNRS, CE-Saclay, 91191 Gif sur Yvette, France

The ternary intermetallic compounds UX2Al20 (X = Ti, V, Nb, Ta, and Cr), crystallizing with the cubic CeCr2Al20-type crystal structure, were characterized in the literature as weak Pauli paramagnets [1-3]. In striking contrast, the isostructural phase UMn2Al20 was reported to order ferromagnetically due to the presence of magnetic moments on the uranium atom sites [4]. In this contribution, we present the results of our polarized neutron diffraction study on a high-quality single crystal of UMn2Al20, which was also carefully characterized by means of X-ray diffraction, microprobe, magnetic, electrical transport and heat capacity measurements. The bulk properties were found very similar to those published in Ref. 4. In particular, the ferromagnetic transition at TC = 17 K was clearly revealed from the magnetic data, while the temperature-dependent specific heat and electrical resistivity were found nearly featureless. The magnetization density maps derived from the neutron diffraction data, showed that the ferromagnetism in UMn2Al20 arises due to the magnetic moments carried on the manganese atoms, while the uranium sublattice remains nonmagnetic. This result appears perfectly consistent with the behavior of the UX2Al20 (X = Ti, V, Nb, Ta, and Cr) compounds, in which the U atoms do not exhibit any magnetic moments.

[1] S. Niemann and W. Jeitschko, J. Solid State Chem., 114, 337 (1995). [2] K. Okauda et al. J. Phys. Soc. Jpn. 58, 4296 (1989). [3] P. Swatek and D. Kaczorowski, J. Solid State Chem., submitted. [4] C.H. Wang et al., Phys. Rev. B 82, 094406 (2010).

SE17

Antiferromagnetic ordering in single-crystalline Ce₂IrSi₃

Maria Szlawska* and Dariusz Kaczorowski
Institute of Low Temperature and Structure Research, Polish Academy of Sciences, Wrocław, Poland

The novel cerium-based ternary silicide Ce₂IrSi₃, crystallizing with fully ordered derivative of the hexagonal A1B₂-type unit cell, has recently been characterized as a Kondo lattice that orders antiferromagnetically at TN = 1.3 K [1]. An antiferromagnetic character of the ordering was inferred merely from the specific heat and electrical resistivity data, collected in applied magnetic fields. With the aim at verification of the presumed nature of the ground state, we have performed magnetic studies down to 0.46 K and in external magnetic fields up to 7 T using a SQUID magnetometer. The results unambiguously corroborated the antiferromagnetic phase transition at 1.3 K, and additionally revealed pronounced magnetic anisotropy in the ordered state. The magnetization component measured within the hexagonal ab plane was found much larger than that taken along the c axis. This finding indicates that the magnetic moments in Ce₂IrSi₃ are confined to the basal plane. In a magnetic field of 0.5 T applied within the easy plane, the compound undergoes a metamagnetic-like phase transition. In turn, upon applying magnetic field along the hexagonal c axis some complex, yet more subtle changes in the magnetic structure seem to occur.

[1] M. Szlawska and D. Kaczorowski, *Phys. Rev. B* 84 (2011) 094430

SE18

Berezinskii-kosterlitz-thouless transition in heavy fermion superlattices

Jian-huang She* and Alexander V Balatsky
T-4, Los Alamos National Lab, USA

Recently unconventional superconductivity has been observed in epitaxially grown heavy fermion superlattices, where Cooper pairs are confined within two-dimensional Kondo lattices (Nature Physics 7, 849(2011)). Here we propose to understand these experiments within the framework of Berezinskii-Kosterlitz-Thouless Transition. The observed behavior of the superconducting transition temperature can be understood in terms of phase fluctuations controlled by vortex-antivortex (un)binding. Reasonable agreement is found with the experiments. Furthermore, we predict a large renormalization of the penetration depth, which can be measured by future experiments. Evolution of the gap is explained by invoking effects of the interface.

SE19

Basic properties of the intermetallics APd₂Al₂ (An=Ce, Th, U, Np, Pu, Am)

Jean-christophe Griveau*, Krzysztof Gofryk, Eric Colineau, Tomasz Klimczuk and Jean Rebizant
ITU-JRC-EC, Germany

SE20

Study of vibron quasibound state in CeAg_{1-x}Cu_xAl₃, 0<x<1

Cesar De La Fuente^{1*}, Agustin Del Moral¹, Devashibhai T. Adroja² and Jon Taylor²
¹ *Fisica de la Materia Condensada, University of Zaragoza & ICMA(CISC), 50071, Zaragoza, Spain*
² *ISIS Facility, Rutherford Appleton Laboratory, Chilton, Didcot, Oxon OX11 0QX, United Kingdom*

The Ce-systems have attracted considerable interest due to the duality between the itinerant and the localized nature of 4f-electrons and the presence of strong electron-electron correlations. On the other hand, it is well known that the electron-phonon interaction drives the BCS-superconductivity. The nature of electron-phonon interaction in Ce-based compounds has its origin in an effective strong magnetoelastic coupling between some phonon modes and the Ce-localized states arising from crystal-field influence at some reciprocal space regions with high DOS, as in CeAl₃ [1], and recently CeCuAl₃ [2]. We have studied of crystal-field electron-phonon excitations along the series CeAg_xCu_{1-x}Al₃ (0<x<1), where the magnetoelastic coupling changes and disappears at critical concentration ? 0.65 under the hybridization of Cu and Ag d-bands with 4f-electrons. A screening model of dielectric permittivity was developed to explore this behaviour from a 3D-antiferromagnet in CeCuAl₃ to a in-basal-plane 2D-weakly ferromagnet for CeAgAl₃ [3]; both with a Kondo temperature inferior to 10 K.

[1] P.Thalmeier and P.Fukde, *Phys.Rev.Lett* 49 (1982) 1588 [2] D.T. Adroja, A. Del Moral, et al., *submitted for publication to PRL* (2011). RB720579 [3] T. Muranaka and J. Akimitsu, *Physica C: Superconductivity*, Vols. 460-462, Part 1, Pages 688-690 (2007).

SE21

Magnetic properties of cubic GdTi₂Al₂₀ single crystal

Ramesh Kumar K, Ruta N Kulkarni, Sudesh Kumar Dhar and Thamizhavel A*
Department of Condensed Matter Physics and Materials Science, Tata Institute of Fundamental Research, Mumbai 400005, India

The compounds crystallizing the RCr₂Al₂₀-type cubic crystal structure having 184 atoms in the unit cell with 8 formula units per unit cell, have attracted a great deal of interest as they exhibit a variety of interesting magnetic properties. For example, PrTi₂Al₂₀ is the first example of a non-magnetic doublet ground state system, which exhibits a ln T behaviour in the electrical resistivity, indicating the Kondo effect [1]. Similarly, SmTi₂Al₂₀ also exhibits Kondo effect [2]. Here we report on the single crystal growth and the transport and magnetic properties of an iso-structural compound: GdTi₂Al₂₀. Single crystals of GdTi₂Al₂₀ were grown by high temperature solution growth using molten aluminum as flux. Large size single crystals with well-defined triangular shaped facets corresponding to (111) plane were obtained. The stoichiometry and the phase purity of the single crystal were confirmed by means of energy dispersive analysis by x-ray diffraction analysis. The estimated lattice constant from the x-ray diffraction was 14.682 Å. It was found that GdTi₂Al₂₀ undergoes an antiferromagnetic ordering at TN = 2.6 K. We will present our results on the magnetic and transport properties of GdTi₂Al₂₀.

[1] A. Sakai and S. Nakatsuji, *J. Phys. Soc. Jpn.* 80 (2011) 063701. [2] R. Higashinaka et al., *J. Phys. Soc. Jpn.* 80 (2011) 093703.

SE22

Investigation of the heavy fermion Ce₃Ir₃Sn₁₃ by electrical resistivity under pressure

Jackeline Collave Garcia¹, Scheilla Maria Ramos^{2*}, Eduardo Bittar³, Pascoal Pagliuso³, Eduardo Hering², Magda Fontes², Hortencio Alves Borges¹ and Elisa Baggio-saitovitch²
¹ *Pontificia Universidade Catolica do Rio de Janeiro - PUC-Rio, Brazil*
² *Centro Brasileiro de Pesquisas Fisicas, Brazil*
³ *Universidade Estadual de Campinas, Brazil*

The Ce₃Ir₃Sn₁₃ is a heavy fermion compound with an electronic specific heat γ = 670mJ/mol-CeK₂ [1,2] for which two anomalies, at 0.6K and 2.1K, can be found on specific heat. Magnetic susceptibility data indicate that the anomaly at 0.6K is due to an antiferromagnetic ordering, while the transition at 2K is non-magnetic. The later one could be related to a change of the band structure accompanied by a lattice expansion[3] as was verified by XRD. This compound crystallizes in a cubic Yb₃Rh₃Sn₁₃ perovskite-like arrangement, with 40 atoms per unit cell [4]. In this work, we are studying the electrical resistivity (100mK< T < 300K and P<25kbar) performed on single crystals of Ce₃Ir₃Sn₁₃, grown using a Sn self-flux technique. Our main motivation is to clarify the origin of the phase transition that occurs at 2K and to investigate the possibility of a vanishing of the Neel temperature over a quantum critical point. Our results show a Kondo-like increase of the resistivity at higher temperatures and a very sharp peak at 2K that moves to lower temperatures with applied pressure. Magnetic susceptibility measurements will be performed to investigate the behavior of the Neel temperature under pressure.

[1] H.Sato, T. Fukuhara, S.Iwakawa, Y.Aoki, I. Sakamoto, S. Takayanagi and N. Wada, *Physica B* 186-188 (1993) 630. [2] S. Takayanagi, H.Sato, T.Fukuhara, N. Wada, *Physica B* 199-200 (1994) 49. [3] C. Nagoshi, H.Sugawara, Y. Aoki, S. Sakai, M. Kohgi, H. Sato, T. Onimaru, T. Sakakibara, *Physica B* 359-361 (2005) 248-250 [4] L. Mendoca Ferreira*, E.M. Bittara, M.A. Pires, R. R. Urbano, O. Aguero, I. Torriani, C. Rettori, P.G. Pogliuso, A. Malachias, E. Granado, A. Cayuero, E. Baggio-Saitovich, *Physica B* 384 (2006) 332-335.

SE23

Electronic structure studies of UPt₃ using soft x-ray angle-resolved photoemission spectroscopy and band calculation

Hiroshi Yamagami¹, Ikuto Kawasaki², Shin-ichi Fujimori², Akira Yasui², Tetsuo Okane², Yukiharu Takeda², Yuji Saitoh², Yoshinori Haga³, Etsuji Yamamoto³ and Yoshichika Onuki⁴
¹ *Department of Physics, Kyoto Sangyo University, Japan*
² *Condensed Matter Science Division, Japan Atomic Energy Agency, Japan*
³ *Advanced Science Research Center, Japan Atomic Energy Agency, Japan*
⁴ *Graduate School of Science, Osaka University, Japan*

Electronic structure and Fermi surface of heavy fermion superconductor UPt₃ have been studied by de Haas-van Alphen experiments and various theories [1], and it is suggested that U5f itinerant band model is more comparable with the experiments. In order to observe the valence band structure of UPt₃ directly, angle-angle photoemission spectroscopy had been done using a discharge lamp [2]. However a 3-dimensional band structure of UPt₃ has been not understood well. We have carried out soft x-ray angle-resolved photoemission spectroscopy experiment with the twin-helical undulator beamline BL23SU of SPring-8, and as a result the U5f itinerant bands of UPt₃ can be detected together with the Pt 5d bands. In the paper we will discuss the band structure of UPt₃ with a LDA band calculation.

[1] G. J. McMullan et al., *New J. Phys.* 10, 053029 (2008). [2] T. Ito et al., *Phys. Rev. B* 59, 8923 (1999).

SF01

Field-dependent instability of the candidate quantum spin liquid in EtMe₃Sb[Pd(dmit)₂]₂ as revealed by NMR.

Georgios Koutroulakis^{1*}, Tong Zhou², Stuart E. Brown², Joe D. Thompson¹ and Reizo Kato³
¹ *Los Alamos National Laboratory, USA*
² *UCLA, USA*
³ *RIKEN, Japan*



SF02

Magnetic states in quasi-2-D iridium oxides with large spin-orbit coupling

Masaaki Isobe^{1*}, Hirotaka Okabe¹ and Jun Akimitsu²
¹ *Strongly Correlated Materials Group, National Institute for Materials Science (NIMS), Japan*
² *Department of Physics and Mathematics, Aoyama Gakuin University, Japan*

The discovery of the novel Mott insulating state in Sr₂IrO₄ has developed a new research field on solid-state physics [1]. The strong spin-orbit coupling with the moderate on-site Coulomb interaction in the 5d electron system yields the unconventional J_{eff} = 1/2 Mott ground state. The 'spin-orbit Mott state' is similar to conventional Mott states in 3d or 4d electron systems. However, the J_{eff} = 1/2 state is a considerably complex state hybridizing spin and orbital degrees of freedom. Therefore, investigation of this state may give a new insight into d-electron physics, and it may lead to possible unusual cooperative phenomena such as anisotropic superconductivity. In this presentation, we review electronic and magnetic states in the novel K₂NiF₄-type iridate Ba₂IrO₄ [2]. We found that Ba₂IrO₄ is a quasi-2-D (square lattice) Heisenberg antiferromagnet (TN ~ 240 K) in which the magnetic moment (~0.34 mB/Ir-atom) is significantly reduced by the low-dimensional quantum spin fluctuation with a large magnetic correlation [J]. Its electronic state undergoes an M-I transition from the Mott insulating state to a non-Fermi-liquid state under high pressure (PC ~ 13.8 GPa) [3]. These behaviors are very similar to those in low-dimensional cuprates.

[1] B.J. Kim et al., *Phys. Rev. Lett.* 101, 076402 (2008); *Science* 323, 1329 (2009). [2] H. Okabe et al., *Phys. Rev. B* 83, 155118 (2011). [3] H. Okabe et al., *Phys. Rev. B* 84, 115127 (2011).

SF03

Quantum critical end point in ucoal proved by NMR measurements

Hisashi Kotegawa¹, Hiroki Nohara¹, Hideki Tou¹, Tatsuma D. Matsuda², Etsuji Yamamoto², Yoshinori Haga², Zachary Fisk², Yoshichika Onuki¹, Valentin Taufour³, Dai Aoki³, Georg Knebel³ and Jacques Flouquet⁴
¹ *Kobe University, Japan*
² *JAEA, Japan*
³ *University of California, USA*
⁴ *Osaka University, Japan*
⁵ *CEA-Grenoble, France*

Quantum critical end point (QCEP) emerges in a pressure - temperature - magnetic field phase diagram in ferromagnetic (FM) materials with tricriticality.[1-3] In UGe₂[1,2] a first-order metamagnetic transition, which appears above a critical pressure of ~1.5 GPa, possesses a critical end point (CEP) at a finite T_{CEP} above which the transition changes to crossover. The T_{CEP} decreases under pressure, and reaches 0 K at the QCEP (P_{QCEP} ~ 3.6 GPa and H_{QCEP} ~ 18 T). In case of UCoAl, the QCEP is located at P_{QCEP} ~ 1.5 GPa and H_{QCEP} ~ 7 T.[3] Both systems exhibit the similar wing structures of the first-order plane, but they are quantitatively different. It is an interesting issue what induces such difference and what kinds of quantum criticality is involved in the vicinity of QCEP with both instabilities of the magnetism and the Fermi surface. In this presentation, we focus on 59Co-NMR measurements for UCoAl at ambient pressure [4] and under pressure. A contrasting behavior between the nuclear spin relaxation rates 1/T₁ and 1/T₂ demonstrate that strong Ising-type magnetic fluctuation develops at around CEP. The drastic pressure evolution of the fluctuations toward the QCEP is also reported.

[1] V. Taufour et al., *Phys. Rev. Lett.* 105, 217201 (2010). [2] H. Kotegawa et al., *J. Phys. Soc. Jpn.* 80, 083703 (2011). [3] D. Aoki et al., *J. Phys. Soc. Jpn.* 80, 094711 (2011). [4] H. Nohara et al., *J. Phys. Soc. Jpn.* 80, 093707 (2011).

SF04

The metal-insulator transition in ferromagnetic chromium hollandite

Yutaka Ueda^{1*}, Masahiko Isobe¹, Tooru Yamauchi¹, Akiko Nakao², Hironori Nakao², Yukinori Ohta³ and Takehisa Konishi³
¹ *Institute for Solid State Physics, University of Tokyo, Japan*
² *Condensed Matter Research Center and Photon Factory, IMSS, KEK, Japan*
³ *Chiba University, Japan*

We discovered a metal to insulator transition (MIT), retaining ferromagnetic in the insulator phase, in ferromagnetic K₂Cr₂O₆ [1]. The MIT is accompanied by a structural change from a tetragonal to a monoclinic structures [2,3]. In the low temperature monoclinic insulator phase, there is no evidence of charge separation/order. Instead, the characteristic displacements of the Cr and O sites, resulting in Cr-O bond alternations, are observed in the rectangular columns formed by the four chains (the four-chain columns). This indicates a lattice-dimerization with the formation of Cr-tetramer in the four-chain columns. The observed structural characteristics and electronic structure calculations lead us a model of MIT caused by the Peierls instability in the quasi-one-dimensional four-chain column [2], namely the MIT is a "pure" Peierls transition of spinless fermions (fully spin polarized electrons). On the other hand, isostructural RbxCr₂O₆ shows a ferromagnetic transition at Tc= 270 K but does not show any distinct MIT. Rb-deficiency could be a reason for the absence of MIT. In a solid solution system, K_{2-y}RbyCr₂O₆, the lattice parameters increase with increase of y. Tc also increases as Rb concentration increases. This is consistent with the decrease of Tc with increasing hydrostatic pressure in K₂Cr₂O₆.

[1] K. Hasegawa et al., *Phys. Rev. Lett.* 103 (2009) 146403. [2] T. Toriyama et al., *Phys. Rev. Lett.* 107 (2011) 266402 [3] A. Nakao et al., *J. Phys. Soc. Jpn.* to be published.

SF05

Composition and transverse field-tuned quantum criticality in NbFe₂

Sven Friedemann¹, Max Hirschberger¹, Yang Zou¹, William J Duncan², Andreas Neubauer³, Thomas Bauer⁴, Louis Pedrero⁵, Manuel Brando⁵, Christian Pfleiderer⁶ and F Malte Grosche¹
¹ *Cavendish Laboratory, University of Cambridge, United Kingdom*
² *Department of Physics, Royal Holloway, University of London, United Kingdom*
³ *Physik Department E21, TU Munchen, Germany*
⁴ *Max Planck Institute for Chemical Physics, Dresden, Germany*
⁵ *Max Planck Institute for Chemical Physics of Solids, Germany*

The low-temperature band magnet NbFe₂ can be tuned by varying composition, magnetic field or pressure, providing an attractive candidate system for investigating quantum criticality in a transition metal compound. Near the composition-tuned quantum critical point, NbFe₂ displays signatures of a logarithmic Fermi liquid breakdown: The electronic specific heat diverges logarithmically ΔC~lnT and the resistivity exhibits non-Fermi-liquid forms Δρ~T^{3/2} at low temperature T [1]. This quantum critical behavior is linked to the suppression of an antiferromagnetic phase in slightly Nb-rich samples which is stabilized towards Fe-rich samples. In addition, NbFe₂ with slight Fe excess features a ferromagnetic ground state underlying the antiferromagnetic phase. We find the ordered moment to point along the crystalline c-direction in the ferromagnetic state. Importantly, the transition temperature of this ferromagnetic ground state can be suppressed in a magnetic field perpendicular to the direction of the ordered moments, promoting NbFe₂ as an interesting candidate to study transverse field tuning in an Ising-like metallic system. We report the significant suppression of Fermi liquid behavior close to the transverse-field induced quantum phase transition. Moreover, we utilize susceptibility measurements to study the nature of this quantum phase transition.

[1] M. Brando, W. J. Duncan, D. Moroni-Klementovics, C. Albrecht, D. Graener, R. Ballou, and F.M. Grosche, *Phys. Rev. Lett.* 101, 026401 (2008).



SF06

Tuning ferromagnetism in Ce_{1-x}LaxAuGe: A specific heat and magnetic susceptibility study

Buyisiwe M. Sondezi-mhlongu and Andre M. Strydom
Physics, University of Johannesburg, South Africa



SF07

Anomalous hybridization effects in the cubic quadrupole systems PrTr₂Al₂₀ (Tr= Ti, V)

Akito Sakai*, Eoin O'farrell and Satoru Nakatsuji
ISSP, University of Tokyo, Japan

The Kondo effect, the screening process of magnetic dipole moments by conduction(c) electrons, is a well-known many-body phenomenon and recognized as a key mechanism which induces a lot of interesting phenomena. Interestingly, nonmagnetic version of the Kondo effect, so-called quadrupolar Kondo effect, is theoretically predicted for the f_{7/2} Γ₃ crystalline electric field ground doublet[1]. In this theory, the ground state is no longer Fermi liquid due to the overscreening of the quadrupole moment by c-electrons. However, it is still uncertain what will happen in a real system with lattice periodicity. We have revealed that Kondo effect is observed in cubic PrTr₂Al₂₀ for the first time in materials which have nonmagnetic Γ₃ ground doublet. Quadrupolar ordering is observed at TQ = 2.0 K (Ti) and 0.6 K (V) respectively, and in particular ferroquadrupolar ordering in PrTi₂Al₂₀[2, 3, 5, 6]. Interestingly, anomalous metallic behaviors were observed in PrV₂Al₂₀ above TQ, most likely attributed to the quadrupolar Kondo effect. In this presentation, we will report the results of low temperature thermal and transport measurements of PrTr₂Al₂₀ and discuss the possibility of the quadrupolar Kondo effect and quantum critical effect of quadrupolar ordering.

[1] D. L. Cox, Phys. Rev. Lett. 59 (1987) 1240. [2] Akito Sakai and Satoru Nakatsuji, J. Phys. Soc. Jpn. 80 (2011) 063701. [3] T. J. Sato, S. Iwuka, Y. Nambu, T. Yamazaki, A. Sakai and S. Nakatsuji, arXiv:0301828. [4] M. Matsunami, M. Taguchi, A. Chaitani, R. Eguchi, M. Oura, A. Sakai, S. Nakatsuji and S. Shin, Phys. Rev. B 84 (2011) 193101. [5] T. U. Ito, W. Higemoto, K. Ninomiya, H. Luetkens, C. Baines, A. Sakai and S. Nakatsuji, J. Phys. Soc. Jpn. 80 (2011) 113703. [6] M. Koseki et al., J. Phys. Soc. Jpn. 80 (2011) SA049.

SF08

Non-fermi-liquid properties of the non-centrosymmetric heavy-fermion compound CePtSi: a magnetic field study.

Andre Strydom
Physics, University of Johannesburg, South Africa

The ternary intermetallic compound CePtSi and its nonmagnetic equivalent LaPtSi form in the non-centrosymmetric tetragonal space group I41/md [1]. The structure is an ordered variant of the ThSi₂ type which provides dedicated atomic sites for each of the rare-earth atom, Pt, and Si. CePtSi is a heavy-fermion compound with a very large electronic specific heat coefficient [2] and apparently with no spontaneous magnetic ordering. Non-Fermi-liquid (nFL) behaviour found at low temperatures in a Pt-Si variational study of CePtSi has been reported [3], as well as aspects of nFL signatures at the verge of magnetic ordering in CePtSi doped with Ge [4]. In this work we focus on the low-temperature behaviour of magnetic susceptibility, electrical resistivity, and specific heat of CePtSi together with comparative properties in LaPtSi. The focus is on the influence of applied magnetic fields and the stability of nFL scaling in CePtSi as a function of field.

1. K. Klepp, and E. Parthe, Acta Cryst. B38 (1982) 1105. 2. W. H. Lee, and N. R. Shelton, Phys. Rev. B 35 (1987) 5369. 3. T. Goetzfried et al, J. Low Temp. Phys. 127 (2002) 51. 4. F. Steglich et al, J. Low Temp. Phys. 95 (1994) 3.

SF09

Vibron quasi-bound state in the non-centrosymmetric tetragonal heavy-fermion compound CeCuAl₃

D T Adroja^{1*}, A Del Moral², C De La Fuente², A Fraile¹, E A Goremyhkin¹, J Taylor¹, A Hillier¹ and F Fernandez-alonso¹
¹ISIS Facility, Rutherford Appleton Laboratory, Chilton, OX11 0QX, United Kingdom
²Laboratorio de Magnetismo, Depto Fisica Materia Condensada, Universidad de Zaragoza & ICMA, Spain

We have investigated the non-centrosymmetric tetragonal heavy-fermion antiferromagnetic compound CeCuAl₃ (TN=2.5 K) using inelastic neutron scattering (INS). Our INS results unequivocally reveal the presence of three magnetic excitations centred at 1.3, 9.8, and 20.5 meV. These spectral features cannot be explained within the framework of crystal-electric-field (CEF) models and recourse to Kramers' theorem for a 4f₇ Ce³⁺ ion. To overcome these interpretational difficulties, we have extended the vibron model for cubic CeAl₃ of Thalmeier and Fulde to tetragonal point-group symmetry. This extension provides a satisfactory explanation for the position and intensity of the three observed magnetic excitations in CeCuAl₃, as well as their dependence on momentum transfer and temperature. On the basis of our analysis, we attribute the observed series of magnetic excitations to the existence of a vibron quasi-bound state.

SF10

Pressure-induced quantum criticality in the heavy-fermion compound CeCoGe₂Si_{0.8}

J. Larrea J.^{1,*}, K.-A. Lorenzer², M. Muller¹, S. Paschen¹, J. Teyssier³ and H. Ronnow⁴
¹Institute of Solid State Physics, Vienna University of Technology, Wiedner Hauptst. 8 - 10, 1040 Wien, Austria
²Institute of Solid State Physics, Vienna University of Technology, Austria
³De Physique de la Matiere Condensee, Universite de Geneve, Quai Ernest-Ansermet 24, 1211 Geneve, Switzerland
⁴Laboratory for Quantum Magnetism, Ecole Polytechnique Federale de Lausanne, 1015 Lausanne, Switzerland

The pressure-tuned quantum critical point (QCP) of the antiferromagnetic heavy-fermion compound CeCoGe₂Si_{0.8} was claimed to be dominated by different effects on both sides of the QCP: on the magnetic side spin fluctuations govern the criticality, while on the non-magnetic side the criticality is dominated by disorder that quenches the spin fluctuations [1]. Here we study high-quality CeCoGe₂Si_{0.8} samples [2], with residual resistance ratios four times larger than those of the previously investigated CeCoGe₂Si_{0.95} samples. Interestingly, while DC magnetic susceptibility measurements show that the Neel temperature of TN = 4K at zero pressure is only slightly reduced by pressure up to 3.0 kbar, a much stronger decrease is observed for the specific heat anomaly. We will present electrical resistivity and specific heat measurements up to 15 kbar and down to 0.05 K, and establish the pressure - temperature phase diagram for CeCoGe₂Si_{0.8}. The critical behavior shall be compared to the one observed for both CeCoGe₂Si_{0.9} and the pure reference compound CeCoGe₂ [3]. We hope that this investigation will elucidate the role of disorder. Acknowledgement: Financial support by the European Research Council (ERC Advanced Grant No 227378) is acknowledged!

[1] Alzamora M., Fontes M. B., Larrea J., Borges H. A., Baggio-Saitovich E. M., Medeiros S. N. Phys. Rev. B 76 125106 (2007). [2] J. Larrea, J. J. Teyssier, H. Ronnow, M. Muller, S. Paschen. Submitted to J. Phys.: Conf. Ser. [3] G. Knebel, D. Aoki, G. Lapertot, B. Salce, J. Flouquet, T. Kavai, H. Muranaka, R. Settai, Y. Onuki. J. Phys. Soc. Jpn. 78, 074714 (2009).

SF11

Anomalous thermoelectric effects in the heavy fermion superconductor Ce₂PdIn₈

Marcin Matusiak, Daniel Gnida and Dariusz Kaczorowski*
Institute of Low Temperature and Structure Research, Polish Academy of Sciences, Poland



SF12

Unusual normal-state magnetotransport in the heavy-fermion superconductor Ce₂PdIn₈

Daniel Gnida*, Marcin Matusiak and Dariusz Kaczorowski
Institute of Low Temperature and Structure Research, Polish Academy of Sciences, Poland

The normal-state behavior in the heavy-fermion superconductor Ce₂PdIn₈ [1,2] has been probed by means of Hall coefficient (RH) and transverse magnetoresistivity (MR) measurements. Anomalous non-Fermi-liquid-like features, observed below 8 K in both RH(T) and MR(T), are related to underlying quantum critical point, previously evidenced in the specific heat and the electrical resistivity data [1-5]. Intriguing magnetotransport properties observed in this compound exhibit close similarity to those reported before for CeCoIn₅ and can be explained in terms of the recently developed theory in which anisotropy of the Fermi surface and strong backflow scattering of charge carriers on critical AF spin fluctuations are taken into account. What's more, the magnetotransport in Ce₂PdIn₈ is shown to exhibit novel types of scaling that may appear universal for similar systems being at the verge of magnetic instability.

[1] D.Kaczorowski, A.Pikal, D.Gnida, and V.H.Tran, Phys. Rev. Lett. 103 (2009) 027003; ibid 104 (2010) 059702. [2] D.Kaczorowski, D.Gnida, A.Pikal, and V.H.Tran, Solid State Commun. 150 (2010) 411. [3] J.K.Dong, H.Zhang, X.Qiu, B.Y.Pan, Y.F.Dai, T.Y.Guan, S.Y.Zhou, D.Gnida, D.Kaczorowski, and S.Y.Li, Phys. Rev. X 1 (2011) 011010. [4] Y.Tokita, P.Gegenwart, D.Gnida, and D.Kaczorowski, Phys. Rev. B 84 (2011) 140507(R). [5] V.H.Tran, D.Kaczorowski, R.T.Khan, and E.Bauer, Phys. Rev. B 83 (2011) 064504.

SF13

Specific heat and thermal conductivity studies of UCu_{4-x}Al_x compounds

Farzana Nasreen¹, Milton Torikachvili², Karunakar Kothapalli³, Yoshimitsu Kohama⁴, Vivien Zapf⁶ and Heinrich Nakotte^{6*}
¹Department of Physics & Astronomy, University of Nevada, Las Vegas, NV 89154, USA
²Department of Physics, San Diego State University, San Diego CA 92182, USA
³Department of Material Science and Engineering, University of Maryland, College Park, MD, 20744, USA
⁴The Institute for Solid State Physics, The University of Tokyo, Japan
⁵MPA-National High Magnetic Field Laboratory, Los Alamos National Laboratory, Los Alamos, New Mexico 87545, USA
⁶Department of Physics, New Mexico State University, Las Cruces, NM 88003, USA

We report the thermal-conductivity and specific-heat measurements for eight UCu_{4-x}Al_x compounds (0 ≤ x ≤ 2.0) as a function of temperature and magnetic field. Previous studies provided evidence of a transition from magnetic to a non-magnetic heavy fermion state at xcr = 1.15. Here we present complementary thermal-property studies as a function of temperature (55 mK - 300 K) and applied magnetic field (0 - 15 T). Specific heat data of non-magnetic compound at xcr = 1.15 shows logarithmic divergence of low-temperature CT and this non-Fermi liquid (NFL) behavior can be attributed to the proximity of a quantum critical point. Non-magnetic compounds with higher Cu content (x > xcr) exhibit unusual temperature scaling in the specific heat possibly due to an increase in disorder between Cu and Al. The complete study of magnetic field effect on NFL behavior was hampered by high contribution from nuclear Schottky anomaly at low temperatures. The thermal conductivity data show stark contrast between the magnetic (x = 0.5) and non-magnetic compound (x = 1.75) - as evidenced in Lorentz numbers for example. Our results confirm that a simple free-electron picture is inadequate for the description of the low-temperature thermal conductivity properties in non-magnetic UCu_{4-x}Al_x compounds.

SF14

Dynamical cluster approximation results of the two-orbital Hubbard model

Hunpyo Lee¹, Yu-zhong Zhang², Harald Jeschke¹ and Roser Valenti^{1*}
¹Institute for Theoretical Physics, University of Frankfurt, Germany
²Physics, Tongji University, China

The orbital-selective phase transition (OSPT), which is induced by the interplay of a narrow band of localized electrons and a wide band of itinerant electrons, has been intensively explored in the multi-orbital systems. Using a dynamical cluster approximation including the short-range correlation as well as quantum fluctuations, we would like to analyze the behaviors of both degenerate two-orbital Hubbard model, where both orbitals have equal bandwidths and one orbital is constrained to be paramagnetic, while the second one is allowed to have an antiferromagnetic solution and two-orbital Hubbard model with different bandwidth at half-filling. The OSPT, Fermi-liquid (FL), non-FL, and insulator behaviors are observed in the both cases. Finally, we would discuss the implications of the results in the context of the Fe-based superconductors.

Phys. Rev. B 84, 020401(R) (2011). Ann. Phys. 523, No. 8-9, 689 (2011). Phys. Rev. Lett. 104, 026402 (2010).

SF15

Renormalized parameters and convergence of energy scales on the approach to local quantum critical points

D. J. G. Crow^{*}, Yunori Nishikawa² and Alex Hewson¹
¹Department of Mathematics, Imperial College London, United Kingdom
²Graduate School of Science, Osaka City University, Japan

We consider a two impurity/dot Anderson model, where the impurities, hybridized with separate conduction baths, are coupled by antiferromagnetic exchange interaction J and a direct interaction U₁₂. The model has two types of quantum critical points associated, respectively, with a transition between Kondo singlet to a local state, and a transition to a local charge ordered state. Using exact expressions for the spin and charge susceptibilities in terms of renormalized parameters we predict the values of the renormalized parameters on the approach to both types of critical point in terms of a single energy scale T*, such that at the critical point T*--> 0. From numerical renormalization group calculations we give complete phase diagram, and from an analysis of the low energy fixed point deduce the renormalized parameters. The results confirm the predictions of the renormalized perturbation theory and determine the value of T*. The emergence of a single energy scale which goes to zero at a quantum critical point may be a general feature which would lead to a natural explanation of E/T scaling which has been observed at the quantum critical points of some heavy fermion compounds.

SG01

NMR study of magnetic properties of Eu_{1-x}SrxMnO₃

Kenji Shimizu¹, Masanori Yamaguchi¹, Shujuan Yuan² and Shixun Cao²
¹Physics, Faculty of Science, University of Toyama, Japan
²Physics, Shanghai University, China

Perovskite-type manganite EuMnO₃ is known to be a compound with narrow eg-band width due to small Eu²⁺ ionic radius compared to La³⁺. The Eu_{1-x}SrxMnO₃ shows complex magnetic properties, depending on Sr concentration x [1,2]. We have carried out 55Mn spin-echo NMR measurements on polycrystalline Eu_{1-x}SrxMnO₃ (0 ≤ x ≤ 0.5) samples at 4.2 or 1.4K, in order to clarify the microscopic local magnetic state of Mn ions and the inhomogeneity in the compounds. Typical NMR spectra have been observed in the frequency range from 250MHz to 400MHz. For the A-type antiferromagnetic EuMnO₃, the resonance frequency is about 260MHz, which is much lower than that observed for Mn²⁺ in La_{1-x}SrxMnO₃. For 0.1 ≤ x ≤ 0.4, the resonance lines, corresponding to Mn²⁺ and Mn³⁺, have been observed around 310MHz and 390MHz, respectively. Furthermore, the spectra originated from Mn²⁺ have been observed around 590MHz for 0.1 ≤ x ≤ 0.4. For Eu_{0.5}Sr_{0.5}MnO₃, the NMR spectrum spreads widely with several distinct peaks in the frequency range from 250MHz to 410MHz. In Eu_{1-x}SrxMnO₃, the spin-glass like behavior has been observed around x = 0.5[1,3]. The present NMR spectrum for Eu_{0.5}Sr_{0.5}MnO₃ shows that the compound is in the inhomogeneous state due to competition between the antiferromagnetic and the ferromagnetic interactions.

[1] Y. Tomioka et al., Phys. Rev. B 80 (2009) 174414. [2] Y. Tadokoro et al., Solid State Ionics 108 (1998) 261. [3] A. Sundaresan et al., Phys. Rev. B 55 (1997) 5596.

SG02

NMR study of successive magnetic transitions in A-site ordered perovskite LaMn₃Cr₄O₁₂

Y. Kawasaki¹, S. Takase¹, Y. Kishimoto¹, T. Ohno¹, I. Yamada², K. Shiro², R. Takahashi², K. Ohgushi³, N. Nishiyama⁴, T. Inoue⁴ and T. Irifune⁴
¹Institute of Technology and Science, The University of Tokushima, Japan
²Graduate School of Science and Engineering, Ehime University, Japan
³Institute for Solid State Physics, University of Tokyo, Japan
⁴Geodynamics Research Center, Ehime University, Japan

In a simple ABO₃ perovskite, when 75% of the A-site cations are substituted by another element, an A-site-ordered perovskite with a chemical formula of A'A₃B₃O₁₂ can be formed. These materials have attracted much attention, because they show a rich variety of physical phenomena, such as heavy-fermion behavior in CaCu₃Ru₄O₁₂ and giant magnetoresistance in CaCu₃Mn₄O₁₂. These features may be related to the A-A and A-B exchange interactions in addition to the usual B-B exchange interaction seen in simple perovskite materials. Recently, new A-site ordered perovskite, LaMn₃Cr₄O₁₂, was prepared by using high pressure synthesis. The measurements of magnetic susceptibility and specific heat suggest two antiferromagnetic transitions at 150 K and 50 K in LaMn₃Cr₄O₁₂. In this conference, we report microscopic investigation on the magnetic properties of this material probed by La NMR. The resonance line moderately broadens below 150 K and disappears below 50 K. These results are consistent with the two antiferromagnetic transitions. The temperature dependence of Knight shift indicates that the transition at 150 K is associated with the B-site Cr spin ordering and the other at 50 K is due to the A-site Mn spin ordering.

SG03

Magnetic properties of single crystalline U₂Fe₃Ge

Margarida Henriques^{1*}, Denis Gorbunov², Ladislav Havela³, Alexander Andreev² and Antonio Goncalves¹

¹ UCQR, Technological and Nuclear Institute, Portugal

² Institute of Physics, Academy of Sciences of the Czech Republic, Czech Republic

³ Department of Condensed Matter Physics, Faculty of Mathematics and Physics, Charles University, Czech Republic

A number of Laves phases exist in intermetallic compounds based on uranium and transition metals. The compact structure of such phases, which leads to small U-U spacing and high U coordination numbers, gives rise to the 5f band and strong hybridization with the non-f states. U₂Fe₃Ge is a new ternary Laves phase [1], crystallizing in the Mg₂Cu₃Si-type structure, an ordered variant of the hexagonal MgZn₂-type (C14, P6₃/mmc). It exhibits very short U-U distances (below the Hill limit) along the c-axis (3.2 Å), still reaching a ferromagnetic order (T_C = 55 K). Surprisingly the Fe sub-lattice does not carry any significant ordered moment. A single crystal of U₂Fe₃Ge was prepared by the Czochralski method (a = 5.182(2) Å and c = 7.850(1) Å). Magnetization isotherms measured along the principal axes indicate that the magnetic moments lie in the basal plane of the hexagonal lattice, with the spontaneous magnetic moment of 1 μ_B/f.u. and no anisotropy within the basal plane. Magnetic moments are therefore perpendicular to the nearest U-U link, but the anisotropy values are anomalously low comparing e.g. to isostructural UNi₂.

[1] M.S. Henriques et al., *Solid State Commun.* 148 (2008) 159.

SG04

Magnetic properties of a 5d transition metal oxide AOsO₄ (A = K, Rb, Cs)

Junichi Yamaura, Kenya Ohgushi and Zenji Hiroi
Institute for Solid State Physics, University of Tokyo, Japan

We investigate the magnetic properties of AOsO₄ (A = K, Rb, Cs) which takes a 5d, electron configuration and would provide us with an interesting playground for spin-orbit physics. The compound crystallizes in the scheelite structure comprising a distorted diamond network of Os atoms. Magnetic susceptibility at high temperatures shows Curie-Weiss behavior with Weiss temperatures of -94, -29 and 12 K for the K, Rb and Cs compounds, respectively. For the K and Rb compounds, broad humps are observed at 55 and 35 K upon cooling and followed by antiferromagnetic transitions at 38 and 22 K, respectively. For the Cs compound, in contrast, no antiferromagnetic transition is observed down to 2 K, but an anomaly appears at 151 K, below which the Weiss temperature is reduced to 3 K. Markedly, the magnetic effective moments estimated from the Curie constants are 0.85, 0.84, and 0.86 Bohr magneton for the K, Rb, and Cs compounds, which are much smaller than the spin-only value of 1.73 Bohr magneton for S = 1/2. Probably a large spin-orbit coupling must be taken into account.

SG05

Enhancement of curie temperature due to the coupling between fe itinerant electrons and Dy localized electrons in DyFe₂Zn₂₀

Yosikazu Isikawa¹, Toshio Mizushima¹, Souta Miyamoto¹, Keigou Kumagai¹, Mako Nakahara¹, Hiroaki Okuyama¹, Takashi Tayama¹, Tomohiko Kuwai¹ and Pascal Lejay²

¹ Graduate School of Science and Engineering, University of Toyama, Japan

² Institute Neel, MCMF, CNRS, France

The cubic RX₂Zn₂₀ has been recently insensitively examined, where R is rare earth atom and X is Fe, Co, Ru, etc. The exchange interaction between R-R is weak because R atoms are diluted in this compound. In fact, for X = Co and Ru, T_C is less than 10 K for any R. In the case of Fe, however, T_C is significantly enhanced, and the origin of this high T_C is suspected to be involved the magnetism of Fe atoms. But the origin is not clear at present. We examined the magnetic properties and specific heat of DyFe₂Zn₂₀, and revealed experimentally unusual magnetic anisotropies, i.e., large magneto-crystalline anisotropy at 2 K, which nature, however, disappears in the temperatures above 30 K below T_C. We analyzed these anomalous properties based on the three assumptions: (1) crystalline electric field and exchange interaction between R and R, (2) simplified Moriya theory for Fe, and (3) exchange interaction between R and Fe. As a result, the enhancement of T_C, the strong magnetic anisotropy at low temperatures, the disappearance of the magnetic anisotropy below T_C down to 30 K, and no anomaly of magnetic specific heat at T_C, etc. were well reproduced by this calculation.

SG06

Anomalous increase of TC in UGa₂ under pressure

Ladislav Havela¹, A. Kolomiets², J. Prchal¹ and A. V. Andreev³

¹ Department of Condensed Matter Physics, Charles University, Czech Republic

² Department of Physics, Lviv Polytechnic National University, Ukraine

³ Institute of Physics, Academy of Sciences of the Czech Republic, Czech Republic



SG07

Phase transition between paramagnetic and spin polarized states in MnSi

Sergey Demishev*, Vladimir Glushkov, Inna Lobanova, Vsevolod Ivanov, Nickolay Sluchanko and Alexey Semeno

Low Temperatures and Cryogenic Engineering, General Physics Institute of RAS, Russia

The of high-field region of the magnetic phase diagram of MnSi is probed by magnetization, resistivity and magnetoresistance measurements carried out in the temperature range 1.8-300 K for magnetic fields up to 8 T [1]. It is shown that the phase boundary between paramagnetic (PM) phase and spin-polarized (SP) phase is well-defined, has no positive slope as it was suggested previously, and appears to be practically vertical corresponding to transition temperature T_C~30 K. We argue that broad maxima of the resistivity and magnetization derivatives, which develops in the diapason T > T_C, are not associated with a “diffuse” SP-PM transition and are a consequence of the specific form of functional dependences of these quantities in the paramagnetic phase. It is found that in the paramagnetic phase of MnSi a universal relation between magnetoresistance and magnetization, Δρ/ρ= a0M², holds in a wide range where magnetoresistance vary by more than two orders of magnitude. The analysis of the transport and magnetic resonance data favors the explanation of magnetic properties of MnSi by Heisenberg-type localized magnetic moments rather than by itinerant magnetism approach. A low temperature anomaly at T~15K corresponding to magnetoresistance and g factor changes is reported.

1. S.V.Demishev et al., *Phys. Rev.B* 85, 045131 (2012)

SG08

ESR in mnsi: Heisenberg localized magnetic moments and spin polarons

Sergey Demishev*, Alexey Semeno, Vladimir Glushkov, Nickolay Sluchanko and Nickolay Samarin

Low Temperatures and Cryogenic Engineering, General Physics Institute of RAS, Russia

High frequency (60 GHz) electron spin resonance (ESR) has been studied in manganese monosilicide, MnSi, single crystals [1]. The measurements performed within the 4.2-300 K temperatures range at the applied magnetic field up to 70 kOe have demonstrated that the magnetic resonance in MnSi is due to localized magnetic moments of the Heisenberg type with the g factor depending only slightly on temperature, g ~ 1.9-2. At the same time, it has been found that the ESR linewidth is determined by spin fluctuations and can be quantitatively described in the wide temperature range (4.2 K < T < 60 K) in the framework of the Moriya theory using the SL(T) function. The revealed deviations from the model of weak itinerant electron magnetism commonly used for the description of the magnetic properties of MnSi indicate a possible spin-polaron nature of the unusual magnetic properties of this strongly correlated metal.

1. S.V.Demishev et al., *JETP Letters*, 93, 213 (2011)

SG09

Magnetic susceptibility measurements at high pressures down to T=0.5 K with SQUID magnetometer

Yoshiaki Sato^{1*}, Shun Makiyama¹, Yasutaka Sakamoto¹, Tadahiko Hasuo¹, Yuji Inagaki¹, Tetsuya Fujiwara² and Tatsuya Kawae¹

¹ Department of Applied Quantum Physics, Kyushu University, Japan

² Graduate School of Science and Engineering, Yamaguchi University, Japan

We develop a 3He-insert attached to MPMS SQUID magnetometer and a pressure cell in order to measure magnetic susceptibility and magnetization precisely at high pressures down to T=0.5 K[1]. The 3He insert is made by stainless steel pipe with the inner diameter of 6.2mm and outer diameter of 6.5 mm. The liquid 3He is condensed in the stainless pipe. The vacuum jacket made of a copper pipe with the outer diameter of 8.6 mm is soldered to the stainless pipe, which is also used for the heat exchange between 3He gas and 4He bath at T=1.7K. The temperature was measured by RuO₂ thermometer mounted on the 3He container. A main body of piston-cylinder pressure cell is made from Be-Cu. The outer diameter of the cell is 6 mm, while the inner diameter is 1.8mm which corresponds to the size of the teflon cell.

[1] Y. Sato, Y. Nakamura, H. Morodomi, T. Hasuo, Y.Inagaki, T. Kawae, H. S. Suzuki and T. Kitai: To be appeared in *Journal of Physics: Conference Series*.

SG10

Extinction of photo-luminescence of Mn-doped ZnS nanocolloids in weak magnetic field

Hong-van Bui¹, Van-ben Pham¹, Nam-nhat Hoang^{2*} and Van-chau Dinh²

¹ Faculty of Physics, Vietnam National University, University of Natural Sciences, Viet Nam

² Faculty of Technical Physics and Nanotechnology, Vietnam National University, University of Engineering and Technology, Viet Nam

The extinction of light passing through a nanocolloidal medium containing ferromagnetic oxide (such as Fe₃O₄) putting inside a cavity of weak magnetic field has been observed [1-3]. Here for the first time we report the extinction of photo-luminescence of Mn-doped ZnS nanocolloid under the applied field of 270 Gauss. The Mn-doped ZnS nanopowders have been synthesized by using the hydrothermal method from zinc acetate and natri thiosulfat as the precursors (with SPAN-80 as the surfactant). The particle size was determined to be within 10-20 nm; the lattice constant a = 5.41(2) Å. The excitation wavelength was 623.8 nm from a He-Ne laser. We have observed a systematic reduction of photo-luminescence of a given liquid nanocolloid with time at applied field of 270 Gauss, despite of the field direction and field development (upwards or downwards). The 50% extinction was achieved after 30 min and the saturation extinction after 1 hour. The memory effect was shown to preserve for more than 2 hours. We have measured the temperature of the sample during the experiment which was kept constant at 70 oC. We believe the PL extinction was associated with the magnetic ordering but the ordering inside a liquid medium is a surprise.

1. John Philip, J. M. Laskar and Baldev Raj, *Appl. Phys. Lett.* 92, 221911 (2008). 2. Rajesh Patel, *Pure Appl. Opt.* 11 (2009) 128004 (Spp). 3. R.V. Mehta, Rajesh Patel, Rucha Desai, R.V. Upadhyay and Kinanari Parekh, *Phys. Rev. Lett.* 96,127402 (2006).

SG11

Electronic structure of A-site ordered perovskite CaCu₃Ti₃O₁₂ studied by angle-resolved photoemission spectroscopy

H. J. Im^{1*}, M. Tsunekawa², T. Sakurada¹, K. Kawata¹, T. Watanabe¹, K. Takegahara¹, H. Miyazaki³ and S. Kimura⁴

¹ Department of Advanced Physics, Hirosaki University, Japan

² Faculty of Education, Shiga University, Japan

³ Department of Environmental and Materials Engineering, Nagoya Institute of Technology, Japan

⁴ UVSOR Facility, Institute for Molecular Science, Japan

We present angle-resolved photoemission spectroscopy (ARPES) results of A-site ordered perovskite CaCu₃Ti₃O₁₂ (CCTO), which shows extremely high-dielectric constant over a wide range of temperature from 100 to 600 K and has an insulator phase in contrast to a metal phase from the result of LDA band calculation. We have observed the clear band dispersions, located in the higher binding energy than that expected in the LDA calculation, and the negligible spectral weight at the Fermi level in agreement with the results of electrical resistivity measurements. From the ARPES results, we suggest that CCTO is Mott-insulator caused by the strong correlation effects of the electrons in Cu 3d - O 2p hybridization bands.

SG12

Evidence of rattling transition in caged compounds LaRu₂Zn₂₀ and LaIr₂Zn₂₀: La-NMR studies

Hideki Tou^{1*}, Kenji Asaki¹, Hisahi Kotegawa¹, Takahiro Onimaru², Keisuke T. Matsumoto², Yukihiko F Inoue² and Toshiro Takabatake²

¹ Department of Physics, Graduate School of Science, Kobe University, Japan

² ADSM, Hiroshima University, Japan

Recently, RT₂Zn₂₀ (R = Pr, La; T = Ir, Ru) has attracted much attention because of the coexistence of superconductivity and a quadrupole ordered state observed in PrIr₂Zn₂₀[1,2] Superconductivity is also observed in LaRu₂Zn₂₀ (T_C=0.2 K) and LaIr₂Zn₂₀ (T_C=0.6 K), but not in PrRu₂Zn₂₀[1], PrRu₂Zn₂₀ and LaRu₂Zn₂₀ undergo first-order structural phase transition at T_S=138 and 150 K, respectively, whereas LaIr₂Zn₂₀ undergoes second-order structural phase transition at T_S=200 K. To investigate the structural phase transition in RT₂Zn₂₀, ¹³⁹La(=7/2) nuclear magnetic resonance (NMR) measurements have been carried out for LaRu₂Zn₂₀ and LaIr₂Zn₂₀. For both compounds, quite narrow La-NMR line-widths less than 5 kHz without nuclear quadrupole splittings above T_S changes their spectral shape with broad tails distributed over the frequency range of 0.8 MHz, evidencing the lowering of the symmetry at La site[3]. Around T_S, the nuclear spin-lattice relaxation rate (1/T₁) show an unusual enhancement associated with the slowing down of the EFG fluctuations[3].To gain further insights, we have measured the nuclear spin-spin relaxation rate (1/T₂) for both compounds. We have found that the temperature dependence of 1/T₂ has maximum around T_S associated with the structural phase transition. We will discuss low-energy spin dynamics in RT₂Zn₂₀ from microscopic points of view.

[1] T. Onimaru, K. T. Matsumoto, Y. F. Inoue, K. Umeo, Y. Saiga, Y. Matsushita, R. Tamura, K. Nishimoto, I. Ishii, T. Suzuki, and T. Takabatake: *J. Phys. Soc. Jpn.* 79 (2010) 033704. [2] T. Onimaru, K. T. Matsumoto, Y. F. Inoue, K. Umeo, T. Sakakibara, Y. Karaki, M. Kubota, and T. Takabatake: *Phys. Rev. Lett.* 106 (2011) 177001. [3] K. Asaki, H. Kotegawa, H. Tou, T. Onimaru, K. T. Matsumoto, Y. F. Inoue, T. Takabatake

SG13

Unconventional magnetic ordering in spin-orbit mott insulator with honeycomb lattice

Soham Manni^{1*}, Yogesh Singh² and Philipp Gegenwart¹

¹ I. Physikalisches Institut, Georg-August-Universitaet Goettingen, Germany

² IISER Mohali, India

Iridates have recently attracted much attention due to a novel SS₁(*rm* eff)=1/2S Mott insulating state, driven by the interplay of moderate electronic correlations with strong spin-orbit coupling. We have synthesized A₂IrO₆ (A=Na,Li) which is a layered system with Ir moments sitting on a Honeycomb lattice. Theoretically, this system has been proposed as solid-state realization of the Heisenberg-Kitaev(HK) model, treating the superposition of isotropic antiferromagnetic exchange and highly anisotropic Kitaev type ferromagnetic nearest neighbor exchange. HK model predicts gapless spin-liquid ground state with Majorana fermionic excitations in Kitaev Limit[1]. Na₂IrO₆ shows a Mott insulating state of SS₁(*rm* eff)=1/2S moments with predominant antiferromagnetic coupling, indicated by a Weiss temperature of S(Theta_W=-116S K[2]. A bulk antiferromagnetic transition occurs at a much reduced temperature of ST_N = 15S K, indicates substantial frustration. Resonant X-ray magnetic scattering for the Na system indicates an unconventional most-likely zig-zag magnetic structure[3]. For Mott insulating Li₂IrO₆ we observe a similar ordering temperature of 15 K, while the S(Theta_WS is drastically reduced to S-33KS. These observations are compatible with an enhancement of the Kitaev contribution compared to the Na-system, suggesting that Li₂IrO₆ is located closer to the Kitaev limit[4]. Work supported by Erasmus Mundus EURINDIA project and the AVH foundation.

[1]J. Chaloupka et al., *Phys. Rev. Lett.* 105, 027204 (2010). [2] Y. Singh and P. Gegenwart, *Phys. Rev. B* 82, 064412 (2010). [3] X. Liu et al., *Y.Singh et al., Phys. Rev. B* (1/18/83), 220403(R) (2011). [4] Y. Singh, S. Manni, P. Gegenwart, arXiv:1106.0429

SG14

YCr₇Ge₆: A kagome metal?

Yui Ishii^{1*}, Yoshihiko Okamoto¹, Junichi Yamaura¹, Hisatomo Harima² and Zenji Hiroi¹

¹ ISSP, Univ. Tokyo, Japan

² Dept. of Physics, Kobe Univ., Japan

Itinerant electrons on a kagome lattice are known to generate a flat band without dispersion. It is expected that the flat band causes exotic phenomena induced by the kagome geometry such as a flat-band ferromagnetism. However, this has not been experimentally observed in real compounds, possibly because the flat band tends to be located far from the Fermi level. We have been looking for a candidate compound to realize “kagome metal” and recently focused on YCr₇Ge₆. It crystallizes in the HfFe₆Ge₆-type structure (space group P6₃/mmm) where Cr atoms form a kagome lattice. Band-structure calculations show that a flat band really exists slightly below EF near the Γ point toward the K and M points. This suggests that hole doping, such as the chemical substitution of Ga for Ge, would make the flat band emerge at EF. We successfully synthesized single crystals of YCr₇Ge₆ and YCr₇Ge_{6-x}Gax by the flux method. A Curie-Weiss like behavior is observed in magnetic susceptibility for both compounds. We will show the magnetic and transport properties and try to reveal the characteristics of the kagome metal.

SG15

Raman scattering spectra of PrRu₂Zn₂₀

Norio Ogita¹*, Takumi Hasegawa¹, Masayuki Udagawa¹, Keisuke Matsumoto², Takahiro Onimaru² and Toshiro Takabatake²

¹ Graduate School of Arts and Sciences, Hiroshima Univ., Japan

² Graduate School of Advanced Sciences of Matter, Hiroshima Univ., Japan

PrRu₂Zn₂₀ has the cubic structure with Fd-3m, where Pr-ion is encapsulated in the Frank-Kasper cage by 16 Zn atoms. In analogy of the filled skutterudites, this compound is expected to be observed an anharmonic Pr vibration and exotic physical properties due to orbital degrees of freedom of the local f electrons. shows structural transition at Ts=138K and remains a normal state in electronic conductivity down to 0.04K. On the other hand, isostructural PrIr₂Zn₂₀ shows an antiferro-quadrupolar ordering(Tq=0.11K) and a superconductivity(Tc=0.05K), without structural change above Tq. The difference of the low temperature properties between PrRu₂Zn₂₀ and PrIr₂Zn₂₀ might be originated from the structural transition, however, the origin of the structural transition and also the crystallographic structure below Ts are not clarified. Therefore, we have measured Raman scattering spectra of PrRu₂Zn₂₀. Among the Raman active phonons; 3Ag⁺Eg⁺T2g, 2Ag⁻Eg⁻T2g peaks are observed at room temperature. With decreasing temperature, 4 peaks are newly observed below Ts in T2g spectra. This suggests the structural change around Ts. In comparison with Eg spectra, the observation of the similar energy peaks in both spectra suggests the crystal structure below Ts seems to be lower than cubic structure.

SG16

Superconducting state in KSn₂ with a MgZn₂-type (C14) Laves phase structure

Shota Miyazaki, Kenji Kawashima, Tsukasa Ipponjima, Michinori Fukuma and Jun Akimitsu

Physics and Mathematics, Aoyama Gakuin University, Japan

We have been searching for a new superconductor including alkali metal elements using high pressure / high temperture technique. High-pressure synthesis technique has been successfully employed in the search for new materials and new superconductors. To use a closed system for high pressure synthesis is effective not only to stabilize a composition but also to expand a solid-solution range. We successfully synthesized the polycrystalline sample of KSn₂ as a main phase and discovered that KSn₂ was a superconductor with T_c = 3.2 K. KSn₂ has a hexagonal MgZn₂-type (C14) structure (space group P6₃/mmc, No.194) called Laves phase. The magnetization versus magnetic field curve shows a typical type-II superconducting behavior. We determined the lower critical field and penetration depth, to be about H_{c1}(0) = 150 Oe and λ_{cl}(0) = 210 nm, respectively, using the Ginzburg-Landau equations. From the density of state calculations, we found that Sn p-orbital mainly contributes near the N(E_f) level and plays an important role for the superconducting state in KSn₂.

SG17

Layered nanosized structures on basis of diluted magnetic semiconductors and heusler alloys

Evgeny Sergeevich Demidov*, Ekaterina Pavlova, Aleksandr Bobrov, Vitaliy Podolskii, Valeriy Lesnikov, Sergey Gusev and Anton Tronov

Solid State Electronics Chair, Nizhny Novgorod State University, Russia

The laser and RF magnetron synthesis of nanosized layers of the diluted magnetic semiconductors (DMS) on the basis of compounds III-V and elementary semiconductors Ge or Si with Mn or Fe impurities and Co₂MnSi Heusler alloys (HA) on single crystal substrates GaAs, Si or Al₂O₃ with ferromagnetism till 500K was earlier demonstrated [1-3]. In this report our new researches of properties of DMS Si:Mn and magnetic tunnel junctions (MTJ) with ferromagnetic HA plates and dielectric interlayer are presented. The features of FMR of MTJ with ferromagnetic exchange interaction, anisotropic negative magnetoresistance, I-V nonlinearity and hysteresis of MTJ and single DMS and HA layers at small current density were observed at 77-300K. The high-resolution transmission electron microscopy (HRTEM) and selected area electron diffraction (SAED), made on JEM-2100F of JEOL, show that the laser synthesis of epitaxial layers of DMS Si:15%Mn/GaAs with Curie point 500K, perfect diamond like crystal structure and self-organized superlattice is possible. Supported by RFBR (08-02-01222-a, 11-02-00855-a), the Ministry of Education of Russian Federation (projects 2.1.1/2833 and 2.1.1/12029) and the State contract № 02.740.11.0672 of the Federal purpose program <<Scientific and scientific-pedagogical cadre of innovative Russia>>2009-2013 is acknowledged.

[1] E.S. Demidov, V.V. Podolskii, V.P. Lesnikov et al., JETP, 106, 110 (2008). [2] E.S. Demidov, B.A. Aronzon, S.N. Gusev et al., JMMM, 321 (2009) 690. [3] E.S. Demidov, V.V. Podolskii, B.A. Aronzon et al., Bull. RAS: Physics, 74 (2010) 1389.

SG18

Metal-insulator and spin-state transition in polycrystalline (Pr_{1-y}RE_y)_{1-x}Ca_xCoO₃ (RE=rare earth elements) in magnetic fields

Tomoyuki Naito¹*, Hiroko Sasaki¹, Motoharu Kato¹, Satoru Ogawa¹, Hiroyuki Fujishiro¹, Terukazu Nishizaki² and Norio Kobayashi²

¹ Iwate University, Japan

² Institute for Materials Research, Tohoku University, Japan

We have measured the temperature dependences of the resistivity and the magnetic susceptibility in various magnetic fields up to 17 T and 5 T, respectively, for polycrystalline (Pr_{1-y}RE_y)_{1-x}Ca_xCoO₃ (RE=rare earth elements). For (Pr_{0.8}Sm_{0.2})_{0.7}Ca_{0.3}CoO₃ sample, a metal-insulator transition (MIT) and spin-state transition (SST) between the intermediate (IS) and the low spin (LS) states almost simultaneously took place around 40 K at 0 T. The MI-SST temperature decreased with increasing magnetic field, and the MI-SST was suddenly suppressed above 10 T. The MI-SST temperatures were about 38 K at 5 T and 29 K at 9 T. In the samples with higher y, in which the MI-SST temperature at 0 T was higher, the reduction of the MI-SST temperature became small and the MI-SST survived up to the highest magnetic field in this study. The similar behavior was observed in other RE substituted samples. The obtained results suggest that the magnetic field stabilizes the IS state, which contrasts with the fact that the application of the external pressure induces the LS state. We discuss the origin of the magnetic field effect on the MI-SST.

SG19

Magnetic field-induced lattice effects in a quasi-2D organic conductor close to the Mott metal-insulator transition

Mariano De Souza¹*, Andreas Bruel², Christian Strack², Dieter Schweitzer³ and Michael Lang²

¹ Physics, Universidade Estadual Paulista - Unesp (Sao Paulo State University), Brazil

² Physics, Goethe-Universität Frankfurt, Germany

³ Physics, Stuttgart Universität, Germany

Organic charge-transfer salts of the κ-phase (BEDT-TTF)₂2SX family have been recognized as prototypes for studying electronic correlation phenomena [1]. Their ground states can be tuned either by varying the counter anion X or by applying external pressure. For the X = Cu[N(CN)₂]Cl salt, for example, the ground state is an antiferromagnetic-Mott insulator, whereas for X = Cu[N(CN)₂]Br, it is a superconductor. Fully deuterated single crystals of the latter substance are located on the verge of the Mott metal-insulator (MI) transition and, for this reason, constitute a material of particular interest for exploring the critical behavior of the π-electron system around the Mott transition [2,3]. Here we present ultra-high-resolution dilatometry studies at varying magnetic fields on a fully deuterated X = Cu[N(CN)₂]Br salt. Our thermal expansion data reveal two remarkable features: (i) the Mott MI transition temperature T_S_{MI} = (13.6 ± 0.6)K is insensitive to fields up to 10 T, (ii) for fields along the interlayer b-axis, a B-induced first-order transition at T_S_{SF} = (9.5 ± 0.5)K is observed. This transition manifests itself in a sharp negative spike in the expansivity, whose position is found to be field insensitive. Possible scenarios to describe this field-induced phase transition will be discussed.

[1] N. Toyota, M. Lang, J. Muller, Low-Dimensional Molecular Metals 2007, Springer, Germany
[2] M. de Souza, A. Bruehl, Ch. Strack, B. Wolf, D. Schweitzer, M. Lang, Phys. Rev. Lett. 99, 037003 (2007) [3] L. Bartosch, M. de Souza, M. Lang, Phys. Rev. Lett. 104, 245701 (2010)

SG20

Metallic transition of the colossal magnetoresistance material FexMn_{1-x}S (x=0.18) under high pressure

Yoshimi Mita¹*, Tomoko Kagayama², G. M. Abramova³, G. A. Petrakovskii³ and V. V. Sokolov⁴

¹ Materials Physics, Engineering Science, Osaka University, Japan

² Center of Quantum Science and Technology under Extreme Conditions, Osaka University, Japan

³ L.V.Kirensky Institute of Physics, Russia

⁴ A.V.Nikolaev Institute of Inorganic Chemistry, Russia

The discovery of the colossal magnetoresistance in FexMn_{1-x}S solid solutions [1] aroused many researcher's interests in studying the physical properties of this system. We studied the pressure induced phase transition of FexMn_{1-x}S (x=0.18) by infrared (IR) reflection and X-ray analysis up to 40 GPa at room temperature. It is shown by X-ray analysis that the structure of this sample is NaCl type at ambient pressure and a structural change starts around 17 GPa and the mixed phase between the NaCl type low pressure phase and the structure unknown high pressure phase continues up to around 25 GPa. On the other hand, the IR reflectivity increases from 15 GPa and becomes highly remarkable around 20 GPa. The spectra do not show any changes from 30 GPa. These results suggest that the phase transition of FexMn_{1-x}S (x=0.18) at room temperature starts around 15 GPa and completes around 30 GPa and the high pressure phase is not a band overlapping semimetal but a true metallic.

G.A. Petrakovskii, L.I. Ryabinkina, N.I. Kiselev, D.A. Velikanov, A.F. Bovina, G.M. Abramova, JETP Lett. 69 (1999) 949.

SG21

Optimal design of IPMSM having double barrier for minimizing cogging torque and torque ripple

Hyoung Uk Nam¹, Hyun Rok Cha¹, Kwang Heon Kim², Dae Young Lym¹ and Tae Won Jeong¹

¹ Automotive R&D, Korea Institute of Industrial Technology, Korea

² Department of Electrical Engineering, University of the Chonnam, Korea

In this paper, a design method for shape optimization of stator and rotor of a double barrier in the form of IPMSM for NEV(Neighborhood Electric Vehicle) is proposed. IPMSM has two big problems which are high cogging torque and high torque ripple that causes performance degradation of the motor and noise, and vibration during the motor rotation. To solve the problem, ways of reducing the cogging torque and torque ripple as a method for forming the shape of the motor stator and rotor factors were searched. Especially, the factors which greatly affected cogging torque and torque ripple were studied and verified their mutual connection. Moreover it was found that the most influential factors was the slot open and the slot teeth angle. The results of the experiment which reduced cogging torque and torque ripple verified, while the optimization proceeded on the basis of the factors that were searched. So the prototype of the optimized IPMSM was designed, its performance was evaluated. The optimization was verified by the performance evaluation.

[1] Y.D. Yao, D.R. Huang, J.C. Wang, S.H. Lion, S.J. Wang, 1997, IEEE Tran. Magn. 33 1997: 4095. [2] N. Bianchi, S. Bolognani, 2008, IEEE Trans. Ind. Appl. 38 (5) 2002 : 1259. [3] T. Ishikawa, M. Matsuda, M. Matsumami, 1998, IEEE Trans. Magn. 34 (5) 1998 : 3503. [4] Z.Q. Zhu, D. Howe, E. Bolte, B. Ackermann, 1993, IEEE Trans. Magn. 29 1993:124. [5] Hong E, Ben-Ahmed AH, Lucidame J. 1997, Switching flux permanent magnet polyphased synchronous machine. In: Proceedings of the 7th European conference on power electronics and applications, Trondheim, Norway, 1997: p. 903-908.

SG22

Implementation of first-principle calculation in combination with a dynamical cluster approximation

Hunpyo Lee¹, Katerina Foyevtsova¹, Johannes Ferber¹, Markus Aichhorn², Harald Jeschke³ and Roser Valenti¹*

¹ Institute for Theoretical Physics, University of Frankfurt, Germany

² Institute for Theoretical and computational Physics, TU Graz, Austria

While the combination of the local density approximation (LDA) with dynamical mean field theory (DMFT) opened the door to a realistic description of correlated compounds, the improvement of the method is ongoing. In this work, we present a combination of LDA with the dynamical cluster approximation (LDA+DCA) in the framework of the full-potential linear augmented plane-wave method, and compare our results to LDA+DMFT calculations as well as experimental observations on SrVO₃. We find a qualitative agreement of the momentum resolved spectral function with angle-resolved photoemission spectra (ARPES) and former LDA+DMFT results. As a correction to LDA+DMFT, we observe more pronounced coherent peaks below the Fermi level, as indicated by ARPES experiments. In addition, we resolve the spectral functions in the S_{\{0\}}=(0,0,0) and S_{\{1\}}=(\pi,\pi,\pi) sectors of DCA, where band insulating and metallic phases coexist. Our approach can be applied to correlated compounds where not only local quantum fluctuations but also spatial fluctuations are important.

arXiv:1111.0890

SH01

Oscillatory transformative domain wall inner structure of depinning domain wall around notched ferromagnetic wire

Dede Djuhana¹*, Bambang Soegijono¹, Hong-guang Piao², Suhk Kun Oh³, Seong-cho Yu³ and Dong-hyun Kim³

¹ Physics, Department of Physics, University of Indonesia, Indonesia

² Materials Science and Engineering, Department of Materials Science and Engineering, Tsinghua University, Beijing, China

³ Physics, Chungbuk National University, Cheongju 361-763, Korea

We have investigated domain wall (DW) depinning behavior around a geometric notch in ferromagnetic nanowires by means of micromagnetic simulation [1]. Nanowires with different notch geometries by changing a depth (d) and a half-width of the notch (s) have been considered. A domain wall with a transverse wall structure is initially prepared to be positioned at the notch. Depinning field pulse of 1 ns duration is applied to trigger DW depinning behavior with a systematic variation of depinning field strengths. With increase of s, the domain wall depinning field tends to decrease. Change of an aspect ratio is also considered, where a relatively insensitive variation of depinning field is observed with respect to the aspect ratio d/s greater than 2. With variation of depinning field strength, we have found that DW internal structure changes during the depinning process. At lower depinning field (< 4 mT), DW keeps the initial transverse wall structure during the depinning process, whereas higher depinning field (> 4 mT), DW is depinned with a transformation of the inner structure with antivortex soon after DW has escaped from the notch. The transformation of the DW inner structure is obviously related to the Walker breakdown phenomenon.

[1] M. J. Donahue and D. G. Porter, OOMMF User's Guide, http://math.nist.gov/oommf/ (2002).

SH02

Unidirectional thermal effects in current-induced domain wall motion

Jacob Torrejon¹, Gregory Malinowski¹, Javier Curiale¹, Andre Thiaville¹*, Daniel Lacour², Francois Montaigne² and Michel Hehn²

¹ Laboratoire de Physique des Solides, Universite Paris-Sud, CNRS , 91405 Orsay, France

² Institut Jean Lamour, Universite Nancy I, 54506 Vandoeuvre-les-Nancy, France

We show unidirectional motion of a domain wall (DW) due to thermal effects in permalloy nanostrips using magnetic force microscopy on a RF-contacted sample. A deterministic thermal driven motion has been found for current excitation in the range of few nanoseconds. The cooperation between thermal effect and spin transfer torque induces larger and more effective displacements towards the center of nanostrip, the hotter part. The thermal effects are generated by Joule heating, and amplified by poor heat diffusion through thick SiO₂ (100 nm). An important issue in thermal transport is the temperature gradient related to the positions of sinks (thick Au electrodes), responsible (partly at least) for the unidirectional DW motion towards hotter part. Such behaviour has been recently predicted by magnons spin transfer [1]. On the other hand, the propagation of DW could be affected by other thermoelectric effects. However, we anticipate the spin currents created by Spin Seebeck effect [2] or anomalous Nernst effect [3] to be small compared to the critical current density for DW motion.

[1] D. Hinzke et al.; PRL 107, 027205 (2011). [2] K. Uchida et al.; Nature 455, 778 (2008). [3] S. Y. Huang et al. ; PRL 107, 216604 (2011).

SH03

Effect of the oersted field on current-induced domain wall motion and domain wall chirality in multilayer nanostripes

Stefania Pizzini¹*, Zahid Ishaque¹, Jan Vogel¹, Vojtech Uhlik¹, Nicolas Rougemaille¹, Olivier Fruchart¹, Jean-christophe Toussaint¹, Julio Camarero², Julio C. Cezar³ and Fausto Sirotti⁴

¹ Institut Neel, Centre National de la Recherche Scientifique, Grenoble, France

² Universidad Autonoma de Madrid, Spain

³ European Synchrotron Radiation Facility (ESRF), Grenoble, France

⁴ Synchrotron SOLEIL, Gif sur Yvette, France

Current-induced domain wall motion is more efficient in Permalloy(Py)/Cu/Co trilayer nanostripes than in single Py nanostripes. We used time-resolved photoemission electron microscopy combined with x-ray magnetic circular dichroism (XMCD-PEEM) to image the magnetic configuration in the Py layer of these nanostripes, during the current pulses, with 50ps time resolution. During the current pulses the Py magnetization tilts towards the transverse direction. The large tilt angles (up to 70°) can be reproduced by micromagnetic simulations only when both the Oersted field and the magnetostatic interactions between Py and Co are taken into account. Magnetic Force Microscopy (MFM) measurements were performed on Py/ Metal bilayer nanostripes, with different metal thicknesses, varying the transverse field for a given current density. We show that the Oersted field stabilizes transverse domain walls with a transverse component parallel to the Oersted field, even for widths and thicknesses of the Py layer for which vortex walls are more stable. Once the chirality of the wall is compatible with the Oersted field, the domain wall moves with current pulses without changing configuration, indicating that the Walker breakdown is suppressed. This phenomenon could therefore explain the large domain wall velocities that we have observed in Py/Cu/Co nanostripes.

SH04

Domain-wall motion in permalloy nanowires with magnetic soft spots

Andreas Vogel¹*, Sebastian Wintz², Theo Gerhardt¹, Lars Bocklage¹, Thomas Strache², Mi-young Im³, Peter Fischer³, Juergen Fassbender³, Jeffrey McCord⁴ and Guido Meier¹

¹ Institut fuer Angewandte Physik und Zentrum fuer Mikrostrukturforschung, Universitaet Hamburg, Germany

² Institut fuer Ionenstrahlphysik und Materialforschung, Helmholtz-Zentrum Dresden-Rossendorf, Germany

³ Center for X-ray Optics, Lawrence Berkeley National Laboratory, USA

⁴ Institut fuer Materialwissenschaften, Christian-Albrechts-Universitaet zu Kiel, Germany

Recent concepts of nonvolatile data-storage devices involve the controlled motion of magnetic domain walls (DWs) in nanowires [1]. To realize such a device, a manageable fabrication process of reproducible and reliable pinning sites for individual DWs is required. We use irradiation with chromium ions to create local confining potentials via an effective reduction of the saturation magnetization in lithographically predefined regions. Field-driven pinning and depinning at the so-called magnetic soft spots is directly observed using x-ray microscopy [2]. The shape of the potential is characterized via micromagnetic simulations and electrical measurements of the anisotropic magnetoresistance. Moreover, we demonstrate reliable DW depinning by single current pulses in a permalloy nanowire containing a square-shaped magnetic soft spot [3]. A DW can be moved back and forth between different soft spots along a wire. Lower requirements on the resolution of the lithography equipment in comparison to geometric constrictions on the nanoscale, a small distribution of properties due to parallel processing of many pinning sites during implantation, and fine tunability of the strength of the pinning potential via the chromium ion fluence make the magnetic soft spots a promising candidate for applications.

[1] D. A. Allwood, Gang Xiong, M. D. Cooke, C. C. Faulkner, D. Atkinson, N. Vernier, R. P. Cowburn, Science 296, 2003 (2002); S. S. P. Parkin, U. S. Patent No. US 683 400 3 (2004). [2] A. Vogel, S. Wintz, J. Kimling, M. Bolte, T. Strache, M. Fritzsche, M.-Y. Im, P. Fischer, G. Meier, and J. Fassbender, IEEE Trans. Magn. 46, 1708 (2010). [3] A. Vogel, S. Wintz, T. Gerhardt, L. Bocklage, T. Strache, M.-Y. Im, P. Fischer, J. Fassbender, J. McCord, and G. Meier, Appl. Phys. Lett. 98, 202501 (2011).

SH05

Direct observation of nearly mass-less domain walls in nanostripes with perpendicular magnetic anisotropy

Stefania Pizzini^{1*}, Jan Vogel¹, Marlio Bonfim², Olivier Bouille³, Emilie Jue³, Nicolas Rougemaille¹, Mihai Miron³, Ales Hrabec¹, Gilles Gaudin³, Julio C. Cezar⁴ and Fausto Sirotti⁵

¹ Institut Neel, Centre National de la Recherche Scientifique, Grenoble, France
² Departamento de Engenharia Eletrica, Universidade do Parana, Curitiba, Brazil
³ Spintec, CEA/CNRS/UJF/GINP, INAC, Grenoble, France
⁴ European Synchrotron Radiation Facility (ESRF), Grenoble, France
⁵ Synchrotron SOLEIL, Gif-sur-Yvette, France

Important inertial effects have been recently shown for domain walls in permalloy nanostripes. These transient effects, giving rise to an effective domain wall (DW) mass, are caused by deformations of the DW internal structure when a current pulse is applied. We have used time-resolved photoemission electron microscopy combined with x-ray magnetic circular dichroism to study current-induced DW motion in Pt/Co/AIOx nanostripes with perpendicular anisotropy and Rashba spin-orbit coupling. We show that in these nanostripes the DWs move at constant speed during the current pulse and inertial effects are much smaller than in permalloy nanostripes, i.e. the delay of the linear motion with respect to the pulse is less than 1 ns and the transient motion is smaller than 30 nm. The transient displacement δq depends of the change of generalized DW angle ϕ : $\delta q = -\Delta/\alpha \delta \phi$ where Δ the domain wall width at rest and α the damping parameter. The negligible inertia in our system is accounted for by the narrow DW width and the small DW angle due to the presence of a transverse magnetic field of Rashba origin. Such small inertial effects could be efficiently exploited in devices based on manipulation of DWs.

SH06

Modified phase diagram of domain walls in FeNi/Cu/Co nanostripes

Nicolas Rougemaille^{1*}, Vojtech Uhlir¹, Olivier Fruchart¹, Zahid Ishaque¹, Jan Vogel¹, Stefania Pizzini¹, Zoukaa Kassir-bodon¹, Aurelien Massboeuf², Andrea Locatelli³, Onur Mentès³, Michal Urbaneč⁴ and Jean-christophe Toussaint¹

¹ Institut Neel, Centre National de la Recherche Scientifique, Grenoble, France
² Laboratoire d'Etude des Matériaux par Microscopie Avancée, INAC/CEA, Grenoble, France
³ Sincrotrone ELETTRA, Trieste, Italy
⁴ Institute of Physical Engineering, Brno University of Technology, Brno, Czech Republic

Magnetic domain walls (DWs) confined in nanostructured magnetic materials display a wealth of specific static and dynamic physical properties. For magnetic nanostripes with sub-micron widths and in-plane magnetization, head-to-head DWs are either of transverse (TW) or vortex (VW) type and are characterized by a chirality, asymmetry and/or polarity. Due to their small size and fast dynamics, magnetic domain walls are promising candidates in the area of information processing and storage. The dynamic properties of these DW under application of current pulses through the spin transfer torque (STT) is one of the exciting subjects of spintronics. We used numerical simulations and analytical modelling to predict the phase diagram of transverse versus vortex walls in Py/Cu/Co trilayer nanostripes, in which high current-induced DW velocities have been observed. The DW is located in the Py layer while the Co layer is initialized as single domain. We have found that due to magnetostatic interactions between Py and Co magnetizations, the TWs are energetically significantly more favourable in the Py layer of the trilayer nanostripes than in single Py nanostripes. We have experimentally verified part of this modified phase diagram with different microscopy techniques, including Magnetic Force Microscopy and Photoelectron Emission Microscopy.

SH07

Effect of current on a threshold width for a dimensional transition of domain wall dynamics in Co/Ni

Kab-jin Kim^{1*}, D. Chiba¹, K. Kobayashi¹, S. Fukami², M. Yamanouchi², H. Ohno² and T. Ono¹

¹ Institute for Chemical Research, Kyoto University, Uji, Kyoto, Japan
² Center for Spintronics Integrated Systems, Tohoku University, 2-1-1 Katahira, Aoba-ku, Sendai 980-8577, Japan

The effect of current on the dimensional transition of domain wall (DW) motion is investigated in Co/Ni nanowires by accompanying magnetoresistance measurement. As reducing the nanowire width, we found that the domain wall (DW) motion is changed from stripe pattern expansion to purely wall motion, implying that the dimensional transition from 2D to 1D. The threshold width for this transition is found to strongly depend on the relative direction of magnetic field and current on DW: parallel (antiparallel) direction has much smaller (larger) transition width, which is mainly because of different forces mechanism by magnetic field and current. The present work provides the upper boundary for domain-wall-motion based devices applications.

(Acknowledgement) This work was partly supported by a Grant-in-Aid for Scientific Research and FIRST Program from JSPS.

SH08

Simulations of field driven domain wall motion in permalloy nanowires with difference dimension

Chia-chi Chang¹, Chao-hsien Huang², Tian-chiuan Wu³, Jong-ching Wu² and Lance Horng²

¹ Department of Physics, National Changhua University of Education, Taiwan
² Department of Physics, Taiwan SPIN Research Center, National Changhua University of Education, Taiwan
³ Department of Electronic Engineering, National Formosa University, Taiwan

In recent years, the domain wall motion in permalloy nanowire has been intensively investigated because it could give promise of a new type memory with many advantages. In our researches, the domain wall motion in permalloy nanowires driven by external magnetic field have been simulated by a commercial software LLG simulation. The simulated results presented that the velocity of DW motion increases below a critical field value which is called Walker breakdown field; above that field the velocity of domain wall obviously decrease. The velocity of the domain wall and the critical field is dependent on the dimension of the nanowire. The domain wall velocity increases as the wire width increases, and the critical field decreases as wire width increases with non-linear relation.

1. GEOFFREY S. D. BEACH*, CORNELIU NISTOR, CARL KNUTSON, MAXIM TSOI AND JAMES L. ERSKINE, nature materials VOL 4 OCTOBER 2005 2. Andrew Kunz, IEEE Trans. Mag. VOL. 42, NO. 10, OCTOBER 2006 3. Stuart S. P. Parkin,* Masamitsu Hayashi, Luc Thomas, Science 320, 190 2008

SH09

Voltage control of magnetisation and magnetic domain configurations in magnetostrictive epitaxial Fe_{1-x}Ga_x thin films

Duncan E Parkes¹, Stuart A Cavill², Aidan T Hindmarch¹, Peter Wadley¹, Fintan Mcgee¹, Kevin W Edmonds¹, Richard P Campion¹, Andrew W Rushforth^{1*} and Bryan L Gallagher¹

¹ School of Physics and Astronomy, University of Nottingham, Nottingham NG7 2RD, United Kingdom
² Beamline I06, Diamond Light Source Chilton, Didcot, Oxfordshire OX11 0DE, United Kingdom
³ Centre for Materials Physics, Durham University, South Road, Durham, DH1 3LE, United Kingdom

The control of ferromagnetic domains and domain walls by electrical means is a desirable objective for applications in many existing and proposed information storage[1,2] and logical processing[3] devices. One route to achieve this goal is via hybrid ferromagnet/piezoelectric transducer devices [4-6] in which a voltage applied to the transducer induces mechanical strain in the ferromagnet affecting the magnetic anisotropy through the inverse magnetostriction effect. We have implemented epitaxially grown thin films of Fe81Ga19 in such a device. Through a combination of magnetotransport measurements, magneto-optical Kerr effect (MOKE) and high resolution photoemission electron microscopy (PEEM) we demonstrate that our epitaxial films possess an exceptionally large magnetostriction (enhanced over that previously observed in bulk samples[7]) and a strong cubic magnetocrystalline anisotropy. We exploit these properties to achieve voltage control of the magnetisation and magnetic domain walls, including the reconfiguration of ordered domain patterns in structured geometries, and non-volatile switching of the magnetisation in the absence of external magnetic fields. Such functionalities will be directly applicable to information storage and processing technologies.

[1] W.J. Gallagher and S.S.P. Parkin, IBM J. Res. & Dev. 1, 5 (2006). [2] S.S.P. Parkin, M. Hayashi, and L. Thomas, Science 320, 190 (2008). [3] D.A. Allwood, et al. Science 309, 1688 (2005). [4] Sang-Koog Kim et al., J. Mag. Mat. Res. 267, 127 (2003). [5] J-W Lee et al., Appl. Phys. Lett. 82, 2458 (2003). [6] A.W. Rushforth et al., Phys. Rev. B. 78, 085314 (2008). [7] A.E. Clark, et al. J. Appl. Phys. 93, 8621 (2003).

SH10

Restricted oscillation period effect in the domain wall propagation after walker breakdown

Xiao-ping Ma¹, Zhe Fan¹, Je-ho Shim², Sang-hyuk Lee², Djati Handoko², Hong-guang Piao^{3*} and Dong-hyun Kim²

¹ Science of College, Huaihai Institute of Technology, China
² Department of Physics, Chungbuk National University, Korea
³ Materials Science and Engineering, Tsinghua University, China

Understanding and control of dynamic behaviors for magnetic domain wall (DW) in ferromagnetic nanowire has become one of important issues in realization of potential spintronic applications such as DW logic and memory devices. In this work, we have intensively explored antivortex DW dynamic behaviors in ferromagnetic nanowires after Walker breakdown by means of the micromagnetic simulation [1]. The nanowire has 2000-nm length. The wire width w varied from 25 to 100 nm, and the wire thickness t varied from 0.5 to 12 nm. In all simulation, the material parameter of Permalloy is used. The unit cell dimension is 2.5x2.5x1 nm³ and the Gilbert damping constant $\alpha = 0.01$. We have found that the DW dynamic behavior in the ferromagnetic nanowire significantly depend on the wire thickness and width. Interestingly, the oscillation period of the DW propagation is not significantly change with variation of the wire thickness is only dependent the wire width. By detailed analysis, we propose that there could be a new mechanism to restrict the oscillation period of the DW propagation in the ferromagnetic nanowire after the Walker breakdown.

[1] M.J. Donahue and D. G. Porter, OOMMF User's Guide, from <http://math.nist.gov/oommf/> (2002).

SH11

Domain wall motion by thermal gradients in Fe/W(110)

Jonathan Philippe Chico Carpio^{1*}, Anders Bergman¹, Lars Bergqvist² and Olle Eriksson¹

¹ Physics and Astronomy (Materials Theory Division), Uppsala University, Sweden
² Dept. of Materials Science and Engineering, Royal Institute of Technology (KTH), Sweden

The Spin Seebeck effect recently observed [1] has opened new areas of research in magnetic materials. One consequence of the Spin Seebeck effect is the movement of domain walls in magnetic materials [2]. In our current research we have studied the behavior of a domain wall in the presence of a thermal gradient in a 2D system by using the atomistic spin dynamics approach present in the UppASD code [3, 5]. This is based in the Landau-Lifshitz-Gilbert equation, where the atomistic spins are described using a Heisenberg Hamiltonian constructed from parameters obtained from first principles calculations. Temperature effects are taken into account by Langevin dynamics [3-4]. The system chosen is a monolayer of Fe on W (110) which exhibits a large anisotropy while having a soft exchange [5], resulting in domain wall thickness of the order of ~ 1 - 2 nanometers. By subjecting this material to a thermal gradient we are able to observe a temperature dependent movement of the domain wall as well as changes of the spatial magnetization profile of the system. We compare this temperature gradient driven motion with the spin transfer torque driven domain wall motion observed for the system when subjected to a current.

[1] K. Uchida, et al. Observation of the spin Seebeck effect. Nature. 455:778, 2008. [2] D. Hinzke, and U. Nowak. Domain Wall Motion by the Magnonic Spin Seebeck Effect. Phys. Rev. Letters. 107:027205, 2011. [3] B. Slabac et al. A method for atomistic spin dynamics simulations: implementations and examples. J. Phys.: Condens. Matter. 20:315203, 2008. [4] V.P. Anropov et al. Spin dynamics in magnets: Equation of motion and finite temperature effects. Phys. Rev. B, 54:1019, 1996. [5] A. Bergman, et al. Magnon softening in a ferromagnetic monolayer: A first-principles spin dynamics study. Phys. Rev. B. 81:144416, 2010.

SH12

Transverse domain wall motion in notched ferromagnetic nanowire by spin transfer torque

Arnab Ganguly, Anjan Barman and Saswati Barman*
 Condensed Matter Physics and Material Sciences, S. N. Bose National Centre for Basic Sciences, Sallake, Kolkata, India, India

We have investigated domain wall motion in notched permalloy nanowires driven by spin polarized current. We solve modified Landau-Lifshitz Gilbert equation including the effect of spin-transfer torque by micromagnetic simulation. The ferromagnetic ground states for the studied geometries show transverse domain walls located at different regions depending upon the position, shape, dimension and symmetry of the notch in the nanowire. We have studied the effect of the spin torque on domain-wall displacement and domain-wall velocity. We find that the domain wall velocity is higher for single notched nanowire as compared to multiple notches. For rectangular notches of dimension 10 nm x 5 nm, transverse domain wall is pinned at one edge of the notch but it gets depinned for current density ~ 10⁹ A/m². We observe the current induced domain wall oscillation followed by a damped periodic translational motion of the transverse wall along with a switching of transverse domain wall from ‘?’ to ‘V’ like configuration and vice versa via head to head or tail to tail domain wall formation.

1. Z. Li and S. Zhang, Phys.Rev. B, 70, 024417 (2004) . 2. A. Thiraville, Y. Nakatani, J. Miltat, and N. Vernier, J. Appl. Phys. 95, 7049 (2004) . 3. M. Hayashi, L. Thomas, C. Rettner, R. Moriya, X. Jiang, and S. S. P. Parkin, Phys. Rev. Lett. 97, 207205, (2006) . 4. P. Chueemart, R. F. L. Evans and R. W. Chantrell, . Phys.Rev. B 83, 184416 (2011).

SH13

Domain wall configuration and magneto-transport properties in dual spin-valve with

Byong Sun Chun^{1*}, Chanyong Hwang¹, Han-chun Wu², Mohamed Abid³, Su Jung Noh⁴ and Young Keun Kim⁴

¹ Korea Research Institute of Standards and Science, Korea
² CRANN, School of Physics, Trinity College Dublin, Ireland
³ Ecole Polytechnique Federale de Lausanne, Switzerland
⁴ Department of Materials Science and Engineering, Korea University, Korea

The effect of the direction of the applied magnetic field on the magneto-transport properties including domain wall (DW) configuration and magnetization reversal process has been studied with a synthetic antiferromagnet-based dual spin-valve (SAF-DSV) structure (i.e. the SV structure is doubled symmetrically with respect to the FM). We can tune the DW configuration and its reversal process from a vortex to a transverse type by changing the direction of applied magnetic field respect to the nano-scale constricted SAF-DSV. When the field is applied along the perpendicular direction to the nano-scale constricted SAF-DSV, the perpendicular magnetic moments are developed due to the transverse magnetization reversal process. This multi step switching process reflects the pinning and depinning of a DW at the nano-scale constriction. Our results also show an asymmetric depinning field. We demonstrate, if nano-scale constriction is asymmetric along its length, i.e. expansions from both sides of the neck into the two nanowires are not identical, and then an asymmetric energy barrier to domain wall propagation is formed. This is due to the difference in DW width, which leads to an asymmetry in the domain wall depinning forces.

SH14

Dynamics of domain-wall oscillations in magnetic nanorings driven by circularly rotating fields

Youn-seok Choi, Young-sang Yu, Dong-soo Han, Hyunsung Jung, Ki-suk Lee and Sang-koog Kim*

National Creative Research Initiative Center for Spin Dynamics & Spin-Wave Devices & Nanospinics Lab, Research Institute of Adv. Materials, Dep. of Materials Sci. & Eng., Seoul Nat'l Univ., Seoul, Korea

The manipulation of magnetic domain walls in geometrical confinements such as nanostrips and nanorings has become essential in information device technologies [1]. In particular, ring structures have attracted much attention because domain walls can be easily positioned and manipulated by the application of magnetic fields or currents [2-4]. In the present work, we studied possible transverse domain-wall (TW) oscillations with certain frequency ranges in magnetic nanorings driven by circularly rotating fields on the nanoring plane. We used a permalloy nanoring with an onion state that has a tail-to-tail and a head-to-head transverse wall. From the micromagnetic simulations, it was found that the frequency of the TW oscillations varies with the frequency and amplitude of the applied rotating field. Moreover, the frequency range of the persistent TW oscillations become wider for a stronger field amplitude, as far as the frequency range is below a certain critical frequency value. We also found a phase diagram of the characteristic TW oscillation dynamics on the plane of the field strength and frequency. We will present our interpretations of those simulation results based on analytical calculations.

*Corresponding author: sangkoog@snu.ac.kr [1] S. S. P. Parkin et al., Science 320, 190 (2008). [2] J. Rothman et al., Phys. Rev. Lett. 86, 1098-1101 (2001). [3] M. Klaui et al., Phys. Rev. B 68, 134426 (2003). [4] Y. Hou et al., Appl. Phys. Lett. 98, 042510 (2011). [5] This work was supported by the Basic Science Research Program through the National Research Foundation of Korea (NRF) funded by the Ministry of Education, Science and Technology (Grant No. 2011000044).

SH15

Modeling field-induced transformations of domain walls in magnetic stripes

Andrzej Janutka
 Institute of Physics, Wroclaw University of Technology, Poland



SH16

Interaction between propagating spin-waves and domain walls on a ferromagnetic nanowire

June Seo Kim¹, Martin Staerk², Jungbum Yoon³, Chun Yeol You³, Luis Lopez-diaz², Eduardo Martinez⁴ and Mathias Klauui^{1*}

¹ Institut fuer Physik, Johannes Gutenberg-Universitaet Mainz, Germany
² Fachbereich Physik, Universitaet Konstanz, Germany
³ Department of Physics, Inha University, Korea
⁴ Department of Physics, Universidad de Salamanca, Spain

The recent discovery that propagating spin waves (SWs) move a domain wall has created a new possibility to manipulate magnetization [Dong-Soo, Han et al., Appl. Phys. Lett. 94, (2009) 112502]. Here, we numerically investigate the interaction between propagating spin waves and a transverse domain wall in a nanowire by using micromagnetic simulations. In order to understand the mechanisms that lead to domain wall motions, we calculate to domain wall velocity and the depinning fields for a pinned domain wall that is depinned in and against the direction of the spin wave propagation. We find that the physical origin of the spin wave induced domain wall motion strongly depends on the propagating spin wave frequency. At certain spin wave frequencies, transverse domain wall oscillations lead to transverse wall displacement by the spin waves, while at other frequencies, large reflection and effective momentum transfer are the main drivers of the spin wave induced domain wall motion.

SI01

Spin oscillations in a free molecular magnet

Gwang-hee Kim
Physics, Sejong University, Korea

Applying an external acoustic wave, we study spin oscillations in a magnetic nanoparticle that is free to rotate about its anisotropy axis. Using Hamiltonian of a rotated two-state spin system, we have shown that superposition of spin and rotational states makes a crucial effect on spin oscillations which exhibit quantum beats of the magnetization. In order to study such a beat structure, we compute dynamics of the magnetization by employing a perturbative approach, and discuss conditions under which this novel quantum effect can be generated. The results are expected to be tested in existing experimental techniques.

SI02

Effects of nonlinear spin dynamics on spin pumping

Sankha Subhra Mukherjee, Praveen Deorani, Siddharth Rao, Jae Hyun Kwon and Hyunsoo Yang*
ECE, National University of Singapore, Singapore

Spin pumping has garnered significant interest in recent times. Most of the studies of spin pumping have been on systems in which the magnetization dynamics was linear. In nonlinear dynamics, however, large-angle, nonlinear, chaotic dynamics are regularly produced. We explore the nature of spin pumping signals resulting from nonlinear magnetization dynamical phenomenon. The device geometry comprises of a permalloy (Py) layer in contact with a nonmagnetic Pt layer. Magnetization dynamics is produced in the system by an rf signal applied to a coplanar waveguide patterned on top. Spin injected into the Pt is converted, due to the inverse spin Hall effect (ISHE), to a charge current and has been measured across the Pt layer. We will show that the system under study shown some high peaks at certain frequencies. The frequencies at which the peaks occur have been shown to be non-stochastic, even though one would expect them to be stochastic. Also, a frequency shift in the precessional resonant frequency has been observed as a function of the applied power. A similar shift had been previously observed in spin wave nonlinear dynamics in a different configuration. The origin of the peaks and frequency shifts are discussed.

SI03

Sharp spectral linewidth in spin torque oscillator with perpendicular magnetized Co/Pd free layer

Yuki Kawada*, Hiroshi Naganuma, Mikihiko Oogane and Yasuo Ando
Applied Physics, Tohoku university, Japan

There has been some scientific and practical interest in spin torque oscillator (STO) using perpendicular materials [1]. For application of STO to information-communication nano RF devices, it is important to investigate linewidth properties, although comprehensive understanding of linewidth properties in STO using perpendicular materials is still lacking. In this study, we have measured spin torque oscillation in giant magnetoresistance devices having a Co/Pd extended free layer and a NiFe/CoFe nanomagnet fixed bilayer. The total thickness of Co/Pd is 2.4 nm, and it was confirmed that Co/Pd has perpendicular magnetic anisotropy by vibrating sample magnetometer. Spin torque oscillation was measured under the low in-plane magnetic field using spectral analyzer. Microwave signal induced by spin transfer torque was clearly observed with oscillating frequency at 3.3 GHz. This frequency increased with increasing applied current i.e. positive nonlinear frequency shift. Obtained minimum spectral linewidth was 13 MHz, which is very small, compared with that of previous work on perpendicular materials [2]. Our results suggest that applying the low magnetic field to the Co/Pd film plane is efficient to obtain sharp spectral linewidth. This work was partly supported by Strategic Japanese-German cooperative program (ASPIMATT) from JST and by Japan Society for Promotion of Science.

[1] S. M. Mohseni et al., Phys. Status Solidi RRL 5, 432 (2011). [2] C. H. Sim et al., J. Appl. Phys. 109, 07C905 (2011).

SI04

Clocking schemes for soliton propagation in a ferromagnetically-coupled quantum-dot chain

Kyeong-dong Lee^{1*}, Hyon-seok Song¹, Chun-yeol You² and Sung-chul Shin³
¹ Department of Physics and Center for Nanospinics of Spintronic Materials, KAIST, Korea
² Department of Physics, Inha University, Korea
³ Department of Physics and Center for Nanospinics of Spintronic Materials, KAIST, and Department of Emerging Materials Science, DGIST, Korea

Transmission of magnetic signals along the ferromagnetically-coupled quantum-dot chain is an essential property to realize the magnetic quantum cellular automata. In the dot chain, a magnetic signal is represented by a topological soliton with a head-to-head or tail-to-tail state. The soliton is exceptionally stable coming from the topology of the system potential-energy surface, and could be driven by an external magnetic field. In addition to the external field, a global clocking field is used to further control propagation speed. We investigate the effect of the clocking field along the hard axis to vary the propagation speed, together with the local trigger field along the easy axis to initialize the soliton propagation by utilizing micromagnetic simulation. Interestingly, it is found that the required static field to initiate the soliton motion is a little larger than the minimum field to maintain the soliton motion, and only local trigger field is required to initiate the soliton propagation. Furthermore, we reveal the role of the global clocking field in the propagation speed, unexpectedly, the clocking field impedes the soliton motion.

SI05

Spin wave propagation in single crystal Au(001)/Fe(001)/MgO(001) waveguides

Yoichi Shiota, Shinji Miwa, Norikaze Mizuochi, Teruya Shinjo and Yoshishige Suzuki*
Graduate School of Engineering Science, Osaka University, Japan

The needs for the development of future computing and information storage devices have led the emerging field of spintronics. Since spin waves can propagate macroscopic distance in ferromagnetic material, they can be used as information carrier. Typically spin wave propagations were investigated using garnet films or permalloy films, both of which have small crystallographic anisotropy. Here we investigated spin wave propagations using spin wave spectroscopy technique [1] in single crystal Fe waveguides with cubic and uniaxial surface anisotropies. The sample, Au(001)-50nm/ Fe(001) / MgO(001)-10nm, were fabricated on MgO(001) substrate using MBE system. We varied thickness of Fe (0.5-20 nm), waveguide width (1-100 μm), and distance of two antennae (0-40 μm). The static in-plane magnetic field was applied perpendicular to waveguide. In this way, magneto-static surface waves were propagated along the ferromagnetic waveguides. The group velocity of spin wave was estimated from the oscillation period in transmission spectra. It was about 8.5 μm/ns in 20 nm thick waveguide under 500 Oe external magnetic field. We found that this value linearly decreases as decreasing the thickness. The contribution of magnetic anisotropies as functions of thickness and width of ferromagnetic layer to the spin waves was also investigated.

[1] V. Vlaminck, et al., Science 322, 410 (2008)

SI06

Microscopic theory on the spin relaxation in an inhomogeneous spin dynamics

Nobuyuki Umetsu, Daisuke Miura and Akimasa Sakuma
Tohoku University, Japan

The mechanisms of Gilbert damping in materials with inhomogeneous spin dynamics are more complicate than that with homogeneous spin dynamics (Kittel mode). It is well known that the magnetic impurities contribute to Gilbert damping with Kittel mode, on the other hand, the nonmagnetic impurities don't affect that. Recently, it has become clear that in the presence of spin waves (inhomogeneous dynamics), the nonmagnetic impurities contribute to Gilbert damping constant, α [1]. In this case, α is proportional to square of wave vector q in the limit $q \rightarrow 0$. The aim of our study is to clarify the q -dependence of α in the entire q range from microscopic theory. Our model is described by s-d model which consists of localized spins, and conducting electrons. In addition to this, we consider the nonmagnetic and magnetic impurities scattering. We obtain the precise expression of α from the linear response theory. Consequently, we find that α is proportional to $1/q$ in $k_{\uparrow} - k_{\downarrow} < q < k_{\uparrow} + k_{\downarrow}$ ($k_{\uparrow, \downarrow}$ are Fermi vector each spin) due to the Stoner excitation, and is continuously changed into the form of $\alpha \propto Aq^2$ in $0 < q < k_{\uparrow} - k_{\downarrow}$. α_0 originates from the magnetic impurities scattering while Aq^2 is attributed to both the magnetic and nonmagnetic impurities scattering.

[1] Y. Tserkovnyak, E. M. Hankiewicz, and G. Vignale, Phys. Rev. B 79, 094415 (2009).

SI07

Ultrafast transfer of spin in a non-collinearly magnetized multilayer

Koen Kuiper*, Sjors Schellekens and Bert Koopmans
Eindhoven University of Technology, Netherlands

Femtosecond laser pulses can trigger intriguing dynamic phenomena in magnetic systems such as quenching of magnetization within 100 fs. An effect hardly explored is that due to the laser heating high densities of hot electrons are generated, which can lead to transfer of spin angular momentum across different nano-layers at a femtosecond timescale. By controlling these spin currents, we effectively combine the field of spin-caloritronics with ultrafast magnetization dynamics, providing access to spin-caloritronics at ultimate timescales and a unique opportunity for the development of new spintronic devices. Malinowski et al. [1] showed in a time-resolved MO-Kerr effect experiment that spin-dependent transfer of hot electrons can speed up the demagnetization process. Here, in order to maximize the torque applied by these electrons, we explore laser induced dynamics in a SiOx/Pt/Co/Al(-1 nm)/Co/Al sample with a non-collinear orientation of the magnetization, i.e. an in-plane magnetized top Co- and an out-of-plane bottom Co-layer. We provide a proof-of-principle demonstration of laser-induced spin transfer across the Al spacer layer. The absorbed spin transfer and torque on the magnetization of the receiving layer cause an ultrafast canting of its magnetization, which is experimentally observed as a successively induced GHz-precession of the in-plane magnetized Co layer.

[1] G. Malinowski, F. Dalla Longa, J.H.H. Rietjens, P.V. Paluskar, R. Huijink, H.J.M. Swagten, and B. Koopmans, Nature Phys. 4, 855-858 (2008).

SI08

Investigation of spin wave interference circuit with metallic thin film

Nana Sato¹, Koji Sekiguchi^{2*} and Yukio Nozaki³
¹ Department of Physics, Keio University, Japan
² Department of Physics, Keio University, PRESTO, JST, Japan
³ Department of Physics, Keio University, CRESTO, JST, Japan

Spin waves are promising phenomenon for the future spintronic devices with low power consumption. For the realization of the spin wave device, we focused on the interference effect of spin waves [1]. Magnetostatic surface wave (MSSW) was excited in a NiFe thin film by applying a continuous RF field. In order to excite and detect MSSW, a pair of asymmetric coplanar wave guides (ACPWs) was fabricated on the NiFe thin film. The MSSW was excited by one ACPW, and its signal was detected by the other ACPW as an induced voltage in a real-time oscilloscope. The advantage of continuous excitation lies in that the MSSW signal becomes stable in time and space, enabling us to sensitively detect the spin wave interference. For the observation of spin wave interference, another strip line was inserted in the middle position between the ACPWs. From ACPWs in both sides of the inserted strip line two different MSSWs having opposite wave vectors were excited. By changing the phase of RF fields, the phase difference between two MSSWs was controlled. Induced voltage signal at the inserted strip line was changed according to the phase difference, indicating that we can observe the interference of MSSWs.

[1] M. P. Kostylev et al., Appl. Phys. Lett. 87, 153501 (2005)

SI09

Current-induced magnetization dynamics of synthetic anti-ferromagnetic free layers

Seo-won Lee¹, Daria Gusakova², Liliana Buda-prejbeanu², Ursula Ebels², Bernard Dieny² and Kyung-jin Lee^{1*}
¹ Department of Material Science and Engineering, Korea University, Korea
² SPINTEC, UMR CEA/CNRS/UJF & G-INP, INAC, France

The spin polarized current-induced magnetization dynamics is studied theoretically in the frame of the drift-diffusion model [1-3] for two different spin-valve (SV) structures: (i) single free layer (SSV) Pol/Cu/FM and (ii) synthetic anti-ferromagnetic free layer (SyAF-SV) Pol/Cu/FM/Ru/FM. In a first step we have analyzed the effect of the angular dependence of the spin transfer torque (STT) on the magnetization dynamics for SSVs. For this four SSVs were considered: SSV1 (Co(3.5)/Cu(3)/Co(3)), SSV2 (Co(3.5)/Ru(3)/Co(3)), SSV3 (Co(3.5)/Cu(3)/Py(3)), and SSV4 (Co(3.5)/Ru(3)/Py(3)). The polarizing layer, Co(3.5), is fixed. We found that these four different structures have different magnitudes and angular dependences of STT leading to different current - magnetic field phase diagrams with different critical values and ranges for dynamics. In the case of SyAF-SVs the drift-diffusion model allows us to take account of not only STT at Cu/FM but also STTs at FM/Ru and Ru/FM interfaces. The corresponding phase diagram is distinct from the one where STT across Ru has not been considered. Hence, this reveals that the STT through Ru considerably affects the dynamics of a synthetic free layer. We discuss the results as a function the strength of the Ruderman-Kittel-Kasuya-Yosida (RKKY)-type exchange interactions through Ru.

[1] A. Brataas, Y. V. Nazarov, and G. E. W. Bauer, Phys. Rev. Lett. 84, 2481 (2000); A. Brataas, Y. V. Nazarov, and G. E. W. Bauer, Eur. Phys. J. B 22, 99 (2001). [2] J. Barnas, A. Fert, M. Gmitra, I. Weymann, and V. K. Dugaev, Phys. Rev. B 72, 024426 (2005). [3] S. W. Lee and K. J. Lee, J. Kor. Phys. Soc. 55, 1501 (2009).

SI10

Magnon excitation studies in strongly correlated electron systems

Cecilia I. Ventura^{1*}, Marcello Acquarone² and Ivon R. Buitrago³
¹ Teoria de Solidos, Centro Atomico Bariloche, and Univ. Nac. Rio Negro., Argentina
² IMEM-CNR, Dip. di Fisica, Universita di Parma, Italy
³ Teoria de Solidos, Centro Atomico Bariloche, and Inst. Balseiro, Argentina



SI11

Magnetoplasmonic hybrid nanoparticles

Francesco Pineider^{1*}, Giulio Campo², Cesar De Julian Fernandez¹ and Claudio Sangregorio¹
¹ Department of Chemistry, University of Florence, CNR-ISTM, Italy
² Department of Chemistry, University of Florence, Italy

Magnetoplasmonics is a very promising branch of active plasmonics that uses a magnetic field to modulate plasmon resonance: [1] the field-mediated modulation of the plasmonic response of nanoparticles is expected to have strong implications in light guiding applications on plasmon resonance-based sensing. [2,3] In this paper we show how ordinary gold nanoparticles' optical properties are modified by the magnetic field and describe the origin of such magnetoplasmonic behaviour. Then, using a combined approach with the aid of magneto-optics, magnetometry and x-ray spectroscopy we investigate several routes to increase the response to the magnetic field by adding a magnetic moiety to the gold nanoparticle. We found that when a transition metal oxide is added to the gold core in core@shell and heterodimer geometries, the two materials (magnetic and plasmonic) behave independently, thus giving rise to bifunctional magnetic-plasmonic nanoparticle hybrids. True magnetoplasmonic behaviour is instead found when a higher degree of hybridisation exists between the two moieties, as in the case when metallic magnetic metals are added to the gold moiety, thus achieving an enhancement of the magnetic response of the optical properties and giving rise to a synergic, non-additive spectroscopic signature in the magneto-optical spectrum.

I. V. Temnov et al., Nature Photon., 2010, 4, 107. 2. Anker, J. N. et al. Nature Mater. 2008 7, 442. 3. Mayer, K. M., Hafner, J. H. Chem. Rev. 2011, 111, 3828.

SI12

Inhomogeneous standing spin wave excited by the patterned periodic electrode

Kohei Kiseki¹, Satoshi Yakata¹ and Takashi Kimura^{2*}
¹ Kyushu University, Japan
² Kyushu University, Japan

There has been a great deal of attention in the spin waves excited in ferromagnetic films because of their various potential applications such as spin-wave-based logic circuit and the interconnection device between the electric and spintronic devices. Efficient excitation and manipulation of the spin wave are important issues for the realizations of practical device applications. Spin wave interference in three dimensional spin structures may enhance the amplitude of the spin oscillation. For this purpose, we here systematically investigated the thickness dependence of resonant frequency of the standing spin wave. We prepared Permalloy films with various thicknesses and excite the standing spin wave by using a periodic nonmagnetic Cu electrode. The resonant frequency of the spin wave was found to increase with the Permalloy thickness. This can be understood by the increase of the non-excited layer around the bottom of Permalloy layer, which induces the effective magnetic field to the excited layer via the exchange interaction. We also perform similar studies of the standing spin wave in the other ferromagnetic structures exchange biased and ferromagnetic/nonmagnetic multi-layered film and present the optimized structure for increasing the output signal induced by the spin wave excitation.

SI13

Observation of spin-waves by time-resolved magneto-optic kerr effect microscope

Sang-jun Yun¹, Jae-chul Lee², Kyung-ho Shin² and Sug-bong Choe^{1*}
¹ Department of Physics and Astronomy, Seoul National University, Korea
² Spin Device Research Center, Korea Institute of Science and Technology, Korea

Spin-wave is an ordering of the magnetization when the magnetization of a ferromagnet is tilted away from its equilibrium state. The spin-waves in metallic thin films have been recently studied as an emerging field of magnetism for magnetic recording and spintronics devices. The spin-waves can be detected by either electrical or optical method for either frequency or time domain, respectively. In the frequency domain the ferromagnetic resonance has been commonly employed to detect the spin-waves, whereas in the time domain, it is typical to detect damped oscillation of magnetization excited by a short magnetic pulse via an inductive or optical apparatus. Here we report the experimental results on the spin-waves by use of all optical pump-probe method. 20-nm-thick Co thin films are prepared on a GaAs substrate by dc magnetron sputtering. The pump beam is focused onto a spot with a diameter 1 μm of a sample under an applied magnetic field 2 kOe at normal direction of the film surface. The spin-waves are then observed by controlling the tilt angle of the probe beam with a fixed pump beam. Using this method, a propagating spin-wave can be measured directly and further analysis will be discussed.

SI14

Nuclear magnetic resonance study of proton dynamics in ZnO

Jun Kue Park, Kyu Won Lee and Cheol Eui Lee*
 Department of Physics, Department of Physics and Institute for Nano Science, Korea University, Seoul 136-713, Korea

Hydrogen acting as a dopant is widely known in compound semiconductors including many oxides. However, in order for such doping to be technologically relevant, the thermal stability of the H-donor must be enough to avoid degradation during device operation at and above room temperature. Here, we have carried out 1H NMR measurements in order to understand proton motions in the ZnO lattice at temperatures between 200 K and 400 K. In our post-annealed ZnO, there are two proton species, one of which can be assigned to protons at interstitial sites (Hi⁺) in ZnO. The other species shows no appreciable motion in the temperature range. The distinct activation energies obtained for the Hi⁺ motion, 0.27 eV and 0.42 eV, are associated with the reorientation around the bonding oxygen atom and hopping between neighboring oxygen atoms, respectively. These activation energies for diffusion, obtained from the spin-spin relaxation measurements, are in close agreement with those obtained from ab initio calculations.

[1] J. K. Park, K. W. Lee, W. Lee, C. E. Lee, D.-J. Kim, and W. Park, *Solid State Commun.* 152, 116 (2012). [2] M. G. Wardle, J. P. Goss, and P. R. Briddon, *Phys. Rev. Lett.* 96, 205504 (2006). [3] L.-Q. Wang, X.-D. Zhou, G. J. Exarhos, L. R. Pederson, C. Wang, C. F. Windisch, and C. Yao, *Appl. Phys. Lett.* 91, 173107 (2007).

SI15

Micromagnetic study of magnonic band gaps in waveguides with a periodic variation of the saturation magnetization

Florin Ciubotaru*, Andrii V. Chumak, Bjoern Obry, Alexander A. Serga and Burkard Hillebrands
 Faculty of Physics, University of Technology, Kaiserslautern, Germany

Spin wave propagation in micro-sized magnonic crystals (MCs) is intensively studied due to their potential technological application for signal processing in spintronic devices. Here we report on micromagnetic simulations [1] of the spin wave propagation in a MC realized as a permalloy (Ni₈₀Fe₂₀) waveguide with a periodical variation of its saturation magnetization. In real structures the variation of magnetization can be achieved by using an ion implantation technique. The 2 μm-wide waveguide of 40 nm thickness is magnetized transversal to its long axis. The MC lattice constant is equal to 1 μm. The spin-wave transmission characteristics have been studied as a function of the width of the implanted areas and of the level of the magnetization variation M/M₀. Frequency band gaps were clearly observed in the spin-wave transmission spectra. The dependences of the depth, width and the position in frequency and space of the rejection band gaps on the above parameters are referred in our studies. The role of the higher order spin-wave width modes on the MC properties is discussed as well. Support from DFG (grant SE-1771/1-2) is gratefully acknowledged.

[1] OOMMF open code, M. J. Donahue, and D. G. Porter, Report NISTIR 6376, NIST, Gaithersburg, MD (1999).

SI16

Spin-transfer induced spin waves of a magnetic point contact with a confined domain wall

Hiroko Arai, Hiroshi Tsukahara and Hiroshi Imamura*
 Advanced industrial science and technology (AIST), Japan

Spin-transfer induced microwave oscillation will be a powerful candidate for applications in future wireless telecommunication technologies. According to Ref. [1], the oscillation of a domain wall between the Bloch- and Neel-type magnetic configurations is induced by a direct current and the corresponding oscillation frequency is proportional to the current density. It is also known that the current injected through a point contact can excite a variety of spin wave modes [2-4]. It is intriguing to ask if such spin wave modes can be excited in a thin magnetic layer connected to a magnetic point contact containing a domain wall. From our calculation we found that three different kinds of spin wave modes can be excited in the thin film depending on the bias current density. The low frequency mode just above the threshold is the propagating spin wave mode. Then the oscillation frequency increases drastically with increasing the current density and reaches more than 100 GHz. At high current density the excited spin wave mode is a propagating mode with a large angle precession. We also found that applied field independence of the frequency for the second mode. We shall discuss the physics behind the excitation of spin wave modes.

[1] M. Franchin, T. Fischbacher, G. Bordignon, P. de Groot, H. Fangohr, *Phys. Rev. B* 78, 054447 (2008). [2] J. C. Slonczewski, *J. Magn. Magn. Mater.* 195, L261 (1999). [3] A. Slavin and V. Tiberkevich, *Phys. Rev. Lett.* 95, 237201 (2005). [4] D. V. Berkov and N. L. Gorn, *Phys. Rev. B*, 80, 064409 (2005).

SI17

Spin-torque-nano-oscillator using the perpendicular magnetized CoFeB/MgO/CoFeB magnetic tunnel junctions

Hiroshi Naganuma^{1*}, Nobuhito Inami¹, Yuki Kawada¹, Mikihiko Oogane¹, Yasuo Ando¹, Kotaro Mizunuma², Hideo Sato³, Michihiko Yamanouchi³, Shoji Ikeda⁴ and Hideo Ohno⁴

¹ Department of Applied Physics, Tohoku University, Japan
² RIEC, Tohoku University, Japan
³ CSIS, Tohoku University, Japan
⁴ CSIS, RIEC, Tohoku University, Japan

Perpendicular magnetized free layer in the magnetic tunnel junctions (p-MTJs) has advantages for spin-torque-nano-oscillator because coherent precession, high output power, and increasing precession frequency due to high magnetocrystalline anisotropy, can be expected. In this study, the microwave transmission properties were investigated for the p-MTJs using thin CoFeB. The multilayer was prepared by UHV sputtering system and patterned it into 40-nm-sized junctions with coplanar waveguide electrode. The microwave properties were measured under the in-plane magnetic field of 3 kOe to tilt the free layer. The tunnel magnetoresistance ratio was 70% and 0.9% for the out-of-plane and in-plane direction, respectively. Below -0.24 mA, the spin torque noise was observed with broad signal. The STO signal was clearly observed above -0.30 mA at 6 GHz, and the second harmonic signal was not observed due to the single-precession-mode by small junction size. The linewidth and output power was 650 MHz and 1.1 nW, respectively. Power has a potential to be more enhanced by stabilizing the pinned layer to increase the relative angle between free and pinned layer. This study was partly supported by ASPIMAIT (JST), by Grant-in-Aid for Young Scientists A (No. 22686001), by FIRST program (JSPS), and by Maekawa-Houonkai foundation.

SI18

Planar approximation for spin-transfer devices with tilted polarizer

Ya. B. Bazaliy*
 Department of Physics and Astronomy, University of South Carolina, Columbia SC, USA and Institute of Magnetism of NASU, Ukraine

Planar spin-transfer devices with dominating easy-plane anisotropy can be described by an effective one-dimensional equation for the in-plane azimuthal angle [1-3]. Such a description maps the Landau-Lifshitz-Gilbert equation on the Newton equation for the motion of classical particle in a one-dimensional potential and thus provides an intuitive understanding of the magnetic dynamics, allowing one to obtain qualitative results without performing detailed calculations. We apply the effective planar equation to describe magnetic switching and precession states in spin transfer devices with tilted polarizer [4]. The approach allows one to list the possible dynamic regimes, including the precession cycles, and sketch the switching diagram of the device.

[1] Ya. B. Bazaliy, *Appl. Phys. Lett.* 91, 262510 (2007). [2] Ya. B. Bazaliy, *Phys. Rev. B* 76, 140402(R) (2007). [3] Ya. B. Bazaliy and F. Arammash, *Phys. Rev. B* 84, 132404 (2011). [4] Ya. B. Bazaliy, *Phys. Rev. B* 85, 014431 (2012).

SJ01

Fast SpinRAM simulation by GPU

Kiyooki Oomaru* and Yoshinobu Nakatani
 The University of Electro-Communications, Japan

Spin transfer torque driven magnetoresistive random access memory (SpinRAM) is one of the candidates of the next generation non volatile memory, and it is studied intensively. Micromagnetic simulation is one of the methods to study it. In the SpinRAM simulation, because the size of the MTJ element is small, the number of the calculation cells is small, and the calculation for one simulation takes only a few minutes. However in the real analysis, more than millions of simulations are repeated with different conditions, the total simulation time becomes huge. Speed up of the simulation is important. Recently, a Graphic Processing Unit (GPU) is used to accelerate the micromagnetic simulation. The acceleration rate strongly depends on the number of the calculation cells, and a huge number of the calculation cells is required to achieve high speed up ratio. Speed up can not be expected in SpinRAM simulation by GPU. In this paper, we propose the simulation method to calculate a number of the MTJ elements in parallel by GPU, and achieve 75 times of the speed up ratio in maximum. This study was supported by New Energy and Industrial Technology Development organization (NEDO) partly.

SJ02

Micromagnetic simulations for the spin dynamics and Gilbert damping constants in nano-dot with perpendicular magnetic anisotropy

Jungbum Yoon¹, Chun-yeol You^{1*} and Myung-hwa Jung²
¹ Department of Physics, Inha University, Korea
² Department of Physics, Sogang University, Korea

Spin dynamics and the magnetic damping of a nano-dot ellipse with perpendicular magnetic anisotropy (PMA) are presented by the micromagnetic simulations. While the in-plane static magnetic field is applied to the long axis of the ellipse, the small in-plane RF magnetic field is applied to the short axis of the ellipse to mimic the ferromagnetic resonance (FMR) technique. The susceptibility can be obtained by the power spectra of fast Fourier transform (FFT) from magnetizations dynamics. There are two regions in the external static field dependence resonance frequencies for typical PMA system. (I) With small external field, the magnetization is tilted to the static field direction with the finite angle from the film normal. (II) If the static field is strong enough, the magnetization is aligned to the static field, where the Zeeman energy overcomes the PMA energy. In this simulation, the extract Gilbert damping constants from the line widths of the resonance peaks from two different regions. Surprisingly enough, the obtained values ($\alpha_{I} = 0.0165$ and $\alpha_{II} = 0.0194$) are different from the input value ($\alpha = 0.027$). It implies that the experimentally obtained α can be different from the real values.

SJ03

Micromagnetic study on micro-structured ferromagnetic thin film for high frequency device applications

Keigo Ito, Tepei Takashima, Terumitsu Tanaka* and Kimihide Matsuyama
 ISEE, Kyushu University, Japan

The ferromagnetic metallic thin films of Fe has been considered as promising materials for on-chip microwave devices, owing to the much higher saturation magnetization Ms compared with a conventional material of yttrium iron garnet (YIG). Understanding of demagnetizing effects, related to Ms, is important for the design of micro-structured devices with the high Ms material[1]. In the present study, geometrical effects of micro-structured magnetic thin films on high frequency magnetic properties are numerically investigated with micromagnetic simulations. The standard material parameters of Fe with cubic anisotropy are assumed in the simulation. The values of μ' (@ 1 GHz) and the resonance frequency fFMR for various aspect ratios w/t are compared. The increase of μ' with the decrease of w/t is attributable to the size effect in fFMR, related to the demagnetizing coefficient along the film normal direction. It should be noticed that the μ' for the same w/t with different w and t is identical. The results suggest that the demagnetizing effect on the high frequency magnetic properties becomes prominent for the w/t smaller than 400 in the structured Fe thin film.

[1] N. Cramer et al., *J. Appl. Phys.*, 87, 6911 (2000)

SJ04

Atomistic modelling of magnetization dynamics with spin torque

Phanwadee Chureemart, Richard F. L. Evans, Irene D'amico and Roy W. Chantrell
 Physics, University of York, United Kingdom

The dynamics of the magnetization following the introduction of a spin current is studied by using an atomistic model coupled with spin accumulation. The evolution of the magnetization and spin accumulation in a trilayer system are calculated self-consistently, the interaction between magnetisation and spin current provided by an s-d exchange term. A spin-polarised current is introduced into the system containing a domain wall whose width is varied by changing the anisotropy constant. The magnetisation is calculated using an atomistic model based on the Heisenberg exchange energy and spin dynamics introduced via the Landau-Lifshitz-Gilbert equation. The net spin torque contributes two important components: the adiabatic (AST) and nonadiabatic torques (NAST). We show that both arise naturally when calculated directly from the spin accumulation. The maximum value of the AST and NAST are considered for each thickness of domain wall. Both torques decrease as the domain wall thickness increases. The nonadiabaticity factor, defined as the ratio of the NAST and AST is also shown. Increasing the domain wall thickness gives rise to a small angle between magnetisation in domain wall. Interestingly the degree of NAST tends to decay to zero as the thickness of DW increases relative to the spin diffusion length.

SJ05

Highly parallelized micromagnetic simulator using fast multipole method

Sung-hyun Lee¹, Chun-yeol You+ and Sung-chul Shin^{1*}
¹ Department of Physics and Center for Nanospinics of Spintronic Materials, KAIST, Daejeon 305-701, Korea
² Department of Physics, Inha University, Incheon 402-751, Korea
³ Department of Physics and Center for Nanospinics of Spintronic Materials, KAIST, Daejeon 305-701, Korea
 Department of Emerging Material Science, DGIST, Daegu 711-873, Korea

We have developed an alternative method for computing the magnetostatic field of arbitrary-shaped ferromagnetic systems instead of fast Fourier transform (FFT). The method is based on the Taylor expansion of the potential, as is required by the fast multipole method (FMM)[1][2], the most efficient method known for calculating magnetostatic fields in very large systems. The FMM scales as O(N) in both time and space complexity compared to the direct method with O(N²), or FFT with O(N logN)[3] and even easier to be parallelized, which is a more valuable solution for larger ferromagnetic systems. Graphical processing units (GPU) are now increasingly viewed as data parallel compute coprocessors that can provide significant computational performance at low price[4]. We have developed a micromagnetic simulator using the parallelized method with GPU and have tested in various configurations. In that case speedups of over a factor 100X can easily be obtained compared to the CPU-based OOMMF[5] program developed at NIST. The tests are carried out with μ Mag Standard Problem[6] #1, #2, #3, #4.

[1] L. Greengard and V. Rokhlin, *J. Comp. Phys.* 73, 325-348 (1987). [2] P. B. Visscher and D. M. Apalkov, *Simple recursive Cartesian implementation of fast multipole algorithm*. [3] R. Ferre, *Large scale micromagnetic calculations for finite and infinite 3D ferromagnetic systems using FFT*, *Comp. Phys. Commun.*, 105, 169-186 (1997). [4] CUDA, <http://www.nvidia.com> [5] OOMMF, <http://math.nist.gov/oommf/> [6] μ Mag, <http://www.cicms.nist.gov/~rdm/mumag.org/html>

SJ06

Effect of calculation conditions on the numerical simulation of magnetic materials with random magnetic anisotropy

S. J. Lee¹, Suguru Sato¹, Hideto Yanagihara¹, Eiji Kita^{1*} and Chiharu Mitsumata²
¹ Institute of Applied Physics, University of Tsukuba, Japan
² Graduate School of Engineering, Tohoku University, Japan

Numerical simulation was performed on magnetic materials with random anisotropy. An assembly of magnetically interacting grains with randomly oriented uniaxial anisotropy was provided and magnetization was calculated using the Landau-Lifshitz-Gilbert equation. The magnetization in a particular grain is assumed to align in the same direction (single spin model).[1] Calculations were carried out for N × N × N three dimensional cells changing cell sizes from 5 to 40 nm. The interaction at the interface between grains was taken into account by the interaction energy between the unit vectors representing grain magnetization directions. N was changed from 10 to 64. In the case of N = 10, the relation between coercive forces and grain sizes was obtained to be $\delta = 5.7$ in $H_c \sim D^2\delta$, and fits to the primitive theory of random anisotropy model (RAM) $\delta = 6$. As the N increased, the δ tends to decrease slightly from 5.7 to 4.2. The grain sizes where the coercive force becomes less dependent on the grain size, suggesting the natural exchange length, did not changed much.

[1] S.-J. Lee, S. Sato, H. Yanagihara, E. Kita, and C. Mitsumata, *J. Magn. Magn. Mater.* 323 (2011) 28.

SJ07

Vortex and antivortex formation in magnetic rolled-up nanotubes
 Jehyun Lee¹, Denys Makarov², Robert Streubel², Carlos Cesar Bof Bufon², Céline Vervacke², Dieter Suess³, Josef Fidler³, Oliver G Schmidt² and Sang-koog Kim^{*}

¹ National Creative Research Center for Spin Dynamics & Spin-Wave Devices and Nanospincs Lab., Research Institute of Adv. Materials, Dep. of Materials Sci. & Eng., Seoul Nat'l Univ, Korea
² Institute for Integrative Nanosciences, IFW Dresden, Germany
³ Institute of Solid State Physics, Vienna University of Technology, Austria

Magnetic nanotubes have attracted considerable attention owing to both fundamental and technological interest1-2. Using a rolling-up fabrication technology3, patterned multilayer tubes can be prepared that exhibit significant modifications of magnetic behaviors compared to those of thin-film structures4-5. In order to elucidate the underlying physics, we conducted micromagnetic simulations of possible spin configurations in rolled-up nanotubes. When a permalloy platelet of dimensions 400 x 400 x 5 nm3 is rolled up, various spin configurations are found to be either C-state, vortex(V) state or anti-vortex(AV) state in the plane of thin films with more spins being forced to be aligned along the tube axis. Therefore, the region whose spins are aligned transversely to the tube axis is compressed. The modified spin alignment is supposed to increase the anisotropy magnetoresistance ratio. Although the reorientation of local magnetizations in the rolled-up tubes results in increases of the exchange energy, it reduces much more the magnetostatic energy, particularly for AV state. Consequently, the total energies of various spin configurations are similar. The cores in the V and AV states of the rolled-up tubes show another interesting feature: the stray fields inside the tubes are cancelled out at the positions.

This work was supported by Basic Science Research Program through the National Research Foundation of Korea (NRF) funded by the Ministry of Education, Science and Technology (No. 20110000441). I. S. Allende, J. Escrig, D. Albir, E. Salcedo, M. Bahiana, The Eur. Phys. J. B 66, 37 (2008). 2. E. J. Smith et al., Nano Letters 11, 4037 (2011)/10/12, 2010). 3. O. G. Schmidt, K. Eberl, Nature 410, 168 (2001). 4. C. Muller et al., Appl Phys Lett 100, 022409 (2012). 5. C. Muller et al., Appl Phys Lett 94, 102510 (2009).

SJ08

Magneto resistance study using micro magnetic simulations in permalloy nano ladder

Venkateswarlu Dasari^{*}, Vineeth Mohanan Parakkat and Anil P. S. Kumar
 Physics, Indian Institute of Science, India

Micromagnetic simulation is one of the tools to investigate magnetization reversal mechanism in nano-wires and nano structures. In the open source simulators like OOMMF[1], magneto transport studies viz., Anisotropic Magnetoresistance (AMR) is not available and is non-trivial since it involves solving the generalized Laplacian equation for getting the spatial distribution of current density[2]. In the case of nano wires, the current density is considered to be uniform[3]; in this quasi uniform state one can apply phenomenological expression in deriving the AMR. We apply this condition in OOMMF-simulations and is compared with the commercial software “LLG-simulator”[4]. For this purpose, we considered single wire of length(L) 1000nm, width(W) 100nm and thickness(t) 5nm. Both the simulators agree with each other within a maximum error of 5%. Further, we studied a ladder structure formed by joining these two wires, with interconnects of L=100nm, W=20nm and t=5nm. In this ladder structure, we varied number of steps by keeping the periodic separation as 50nm. It was found that the coercivity falls non-linearly from 312 to 255G when the number of steps increased from 1 to 13. The resistance measured at remanence states drops linearly, which indicates the decrease in remanence due to the local nucleation centers.

1. M. J. Donahue and D.G. Porter, http://math.nist.gov/oommf/ 2. S. Manikonda, M. Berz and K. Makino, IEEE Trans. Comp., 4, 1604 (2005) 3. C. Hassel, F. M. Romer, R. Meckenstock, G. Dumpich, and J. Lindner, Phys. Rev. B, 77, 224439 (2008) 4. M. R. Scheinfein, http://llgmicro.home.mindspring.com/

SJ09

Soft layer driven switching of microwave-assisted magnetic recording on segmented perpendicular media

Jing Qiang Goh^{1*}, Zhi-min Yuan², Lei Shen², Tiejun Zhou² and Yuan Ping Feng¹

¹ Department of Physics, National University of Singapore, Singapore
² Data Storage Institute, Agency for Science, Technology and Research, Singapore

In this work, we use micromagnetic modeling to investigate microwave-assisted magnetic recording on segmented perpendicular media. Two types of microwave fields, sinusoidal and finite bandwidth square microwaves, have been chosen for our study. We show that microwave fields, when applied to the soft segment, can assist the magnetization reversal of the hard segment. The calculated assisted frequencies are insensitive to the variation of inter-segment exchange coupling of segmented perpendicular media. Our results suggest that sinusoidal microwave fields are practically more feasible than square microwave fields for the soft layer driven switching mechanism of segmented perpendicular media.

1) C.-K. Goh, Z. min Yuan, T. Zhou, L. Wang, and B. Liu, J. Appl. Phys. 105, 07B908 (2009). 2) C.-K. Goh, Z. min Yuan, and B. Liu, Appl. Phys. Lett. 94, 152510 (2009). 3) J.-G. Zhu and Y. Wang, IEEE Trans. Magn. 47, 4066 (2011).

SK01

Top composite free layer non-collinear spin valve for hysteresis-free GMR sensors

Vladimir V. Ustinov^{*}, Michael A. Milyaev, Larisa I. Naumova, Tatiana P. Krinitsina and Vladimir V. Proglyado
 Institute of Metal Physics, Ural Branch of Russian Academy of Sciences, Russia

Top spin valves Ta/[FeNi/CoFe]/Cu/CoFe/FeMn/Ta based on FeMn antiferromagnet with varying [Fe₂₀Ni₈₀/Co₉₀Fe₁₀] composite free layer parameters and Cu interlayer thickness were prepared by DC magnetron sputtering. GMR characteristics of spin valves (SV) were investigated under the conditions of non-collinear SV geometry when the applied magnetic field and pinning direction for bottom magnetic layer are not collinear. It was shown that the value of low field hysteresis caused by free layer magnetization reversal can be reduced down to 0.1 Oe keeping the GMR ratio about 10 % by using both layers thicknesses and non-collinearity angle variation. The magnetoresistive sensitivity of non-collinear is about 1 %/Oe. Low-hysteresis free layer magnetization reversal is mainly due to coherent rotation of magnetization. The dependences of low field hysteresis value and GMR ratio on the Cu spacer layer thickness and the angle between applied magnetic field and pinning direction are presented.

SK02

Strong <111> texture and low hysteresis in MnIr-based top spin valve

Mikhail Milyaev, Larisa Naumova, Vyacheslav Proglyado, Tatiana Krinitsina, Nataliya Bannikova and Vladimir Ustinov
 Institute of Metal Physics UB RAS, Russia

“Spin valve” nanostructures with GMR and TMR are widely used in spintronics. In some devices the hysteresis of magnetoresistance must be negligible. The hysteresis is weak in the spin valves with <111> axial texture. In this work we study the dependence of the free layer hysteresis loop width on the texture strength that is characterized by the FWHM of rocking curve. The top spin valves [Ta, (Ni₁₀Fe₂₀)₆₀Cr₁₀]/Ni₁₀Fe₂₀/Co₉₀Fe₁₀/Cu/Co₉₀Fe₁₀/Mn₇₅Ir₂₅/Ta with various thickness of the magnetic and nonmagnetic layers are investigated. On the base of magnetic, magnetoresistance and XRD data the nonlinear dependence between FWHM of rocking curves measured at the integrated (111) Bragg peak of Ni₁₀Fe₂₀, Co₉₀Fe₁₀ and Cu layers and free layer coercivity is established. A correlation between GMR ratio and FWHM is not revealed. It is shown that in the spin valve Ta(50A)/NiFe(30A)/CoFe(20A)/Cu(22A)/CoFe(25A)/MnIr(50A)/Ta(20A) with sharp <111> texture, GMR ratio of 10.6 % and minimal coercivity of 8.7 Oe, the free layer hysteresis can be effectively reduced down to few tenth of Oersted [1]. This study is supported by RFBR, project No. 10-02-00590, by the Program of Presidium RAS, project No. 12-P-2-1051, and OFI-UB RAS, project No. 11-2-23-NPO.

[1] V.V. Ustinov et al. Phys. Met. Metallogr. in press.

SK03

Low temperature crystallization process in Co₂FeSi Heusler alloy thin films

Luke Fleet¹, M. J. Walsh¹, J. Sagar¹, T. Nakayama² and A. Hirohata^{1*}

¹ The University of York, United Kingdom
² Nagaoka University of Technology, Japan

One of the major challenges for Heusler alloys is to achieve a high L₂₁ ordering at low annealing temperatures in order to limit interdiffusion in multilayer devices. We report a low temperature crystallization process of polycrystalline Co₂FeSi films using in-situ imaging techniques. 20nm thick Co₂FeSi films were annealed in-situ up to 600°C with both TEM and diffraction patterns recorded. We show that the grain crystallization starts to occur at 230°C with no additional nucleation occurring after 30 minutes but further annealing does improve the grain ordering. By varying the growth conditions it is possible to change the number of nucleation sites and also the median grain size. Through varying the initial film morphology it is possible to change the number of nucleation sites and also the median grain size from 20 to 250nm. Magnetic measurements show that the magnetic moment is over 80% of the theoretical value predicted [1]. This shows that a high degree of ordering can be created for polycrystalline films after a low temperature anneal of less than 300°C.

[1] A. Hirohata, and Y. Otani, Epitaxial Ferromagnetic Films And Spintronic Applications (Transworld Research Network, 2009).

SK04

Spin-polarized itinerant electrons in Co₂MnAl and Co₂MnSi studied by magnetic Compton scattering

Soichiro Mizusaki¹, Tomohiro Ohnishi¹, Masayoshi Itou², Yoshiharu Sakurai², Tadashi C Ozawa³, Hiroaki Samata⁴, Yoshihiko Noro⁵ and Yujiro Nagata⁴
¹ Aoyama Gakuin University, Japan
² Japan Synchrotron Radiation Research Institute (JASRI/Spring-8), Japan
³ International Center for Materials Nanoarchitectonics, National Institute for Materials Science, Japan
⁴ Kobe University, Japan
⁵ Kawazoe Frontier Technologies, Co. Ltd., Japan

Investigating the spin-polarized itinerant electron states in the intermetallic alloys and compounds is indispensable for the development of potential spintronic materials. In this work, we have studied the relationship between the number of sp itinerant electrons and the spin moment in the compounds Co₂MnZ (Z=Al or Si), using synchrotron-based Magnetic Compton scattering (MCS)[1], which provide the bulk spin-polarized electron momentum distributions, ie. magnetic Compton profiles (MCPs). The shape of MCPs depends on the number of spin-polarized electrons of occupied orbitals, and the area of MCP corresponds to the spin moment. Co₂MnZ (Z=Al or Si) is a good system to investigate the spin-polarized itinerant electron states since the number of sp itinerant electrons can be changed without affecting the number of 3d electrons. The following results were obtained. 1. The total spin moment increases by 1 μ_B/f.u. from Co₂MnAl (4μ_B/f.u.) to Co₂MnSi (5μ_B/f.u.), with one sp electron difference. 2. The proportion of the partial spin moment carried by sp itinerant electrons is same for Co₂MnAl and Co₂MnSi. From these findings, additional sp electrons occupy the 3d electron states and increases the localized spin moment. This enhances the spin polarization of itinerant electrons through the indirect magnetic exchange interaction.

[1] M. J. Cooper, P. E. Mijnenreds, N. Shiotani, N. Sakai, and A. Bansil, in X-ray Compton scattering, Oxford University Press, Oxford, 2004.

SK05

Evidence of inelastic tunneling in magnetic tunnel junctions via capacitance-voltage characteristics

Ajeesh M Sahadevan^{*}, Gopinadhan Kalon², Charanjit S Bhatia¹ and Hyunsoo Yang²
¹ Department of Electrical & Computer engineering, National University of Singapore, Singapore
² Department of Electrical & Computer engineering, NUSNNI-Nanocore, National University of Singapore, Singapore

Magnetic tunnel junctions (MTJ) have played a key role in the development of HDDs as well as next generation non-volatile memories. For high speed applications, capacitance and RC time constant analysis of MTJs becomes very important. Also for metal-insulator-metal structures with extremely thin tunnel barriers as in MTJs, the capacitance is mainly determined by the interface properties of the structure as the electric field penetration becomes significant. Since in MTJs the interfaces are very critical in determining the tunneling magnetoresistance (TMR), study of capacitance becomes very relevant for better understanding of these devices. We report the temperature dependence of C-V characteristics in MTJs. All our MTJs show a negative tunneling magnetocapacitance (TMC) with a magnitude lower than the TMR [1]. At temperatures lower than 100 K, a zero-bias anomaly appears in the C-V profile. The behavior is similar to inelastic tunneling or zero-bias anomaly in MTJs. Zero-bias anomaly in the R-V characteristics of MTJs has been attributed to magnon and phonon assisted tunneling or through impurities inside the barrier. But since the capacitance is mainly contributed from the interfaces, the origin of these effects is from the interfaces rather than the bulk.

[1] P. Padhan et al., Appl. Phys. Lett. 90, 142105 (2007).

SK06

Spin-polarization measurements for Co₂MnSi using Co₂MnSi/MgO/NbN epitaxial tunnel junctions

Ken-ichi Matsuda, Takaho Shinoki, Tomoyuki Taira, Tetsuya Uemura and Masafumi Yamamoto
 Div. of Electronics for Informatics, Hokkaido University, Japan

Spin-polarization measurements were carried out for the Co-based Heusler alloy, Co₂MnSi (CMS, for short), using CMS/MgO/NbN epitaxial tunnel junctions. The layer structure was as follows: (from the substrate side) MgO buffer (10 nm)/NbN (10 nm)/MgO barrier (1.4-3.2 nm)/CMS (3 nm)/Co₂Fe₃₀ (1nm)/IrMn (10nm)/Ru cap (5 nm). All the samples were successively deposited on MgO(001) single-crystal substrates in an ultrahigh vacuum chamber. Spin-polarization measurements were carried out at 1.5 K using the conventional lock-in technique. The spin polarizations (P) were evaluated for three different film compositions of CMS: Co₂Mn_{0.72}Si_{0.81}, Co₂Mn_{1.00}Si_{0.81}, and Co₂Mn_{1.40}Si_{0.81}. At H = 0 T, typical differential conductance curves were clearly observed, and were well-fitted by the modified-BTK theory [1]. The superconducting energy gap extracted from the analysis was about 2.5 meV [2]. The P values evaluated at H = 8 T were 0.41, 0.50, and 0.54 for respective CMS films. Thus, the P increased with increasing Mn-composition in CMS films. This result is consistent with the increase of the TMR ratios for CMS/MgO/CMS fully-epitaxial magnetic tunnel junctions, and can be qualitatively understood from the view point of the suppression of minority-spin in-gap states that resulted from the reduction of CoMn anti-sites [3].

[1] G. J. Strijkers, Y. Ji, F. Y. Yang, C. L. Chien, and J. M. Byers, Phys. Rev. B, 63 (2001) 104510. [2] H. Yang, S.-H. Yang, C. Kaiser, and S. Parkin, Appl. Phys. Lett., 88 (2006) 182501. [3] M. Yamamoto, T. Ishikawa, T. Taira, G.-f. Li, K.-i. Matsuda, and T. Uemura, J. Phys.: Cond. Matt., 22 (2010) 164212.

SK07

Variation of point-contact andreev reflection spectra of ferromagnetically ordered metals

Elina Tuuli^{*} and Kurt Gloos
 Department of Physics and Astronomy, University of Turku, Finland

Point-contact Andreev reflection (AR) spectra of ferromagnets are usually fitted with modified BTK models that take into account the spin polarization. On the other hand, AR spectra of non-magnetic metals are often described by a BTK model that includes Dynes' lifetime parameter. The two models yield rather similar spectra and can in fact be used to fit the spectra of both magnets and non-magnets. The differences between them are most pronounced at low temperatures but strongly suppressed by thermal smearing. We have applied the two models to point contacts between the classical band ferromagnets Co, Fe, and Ni and the conventional superconductors Nb, Ta, and Al as function of temperature. The spectra varied between an absent superconducting signal and an occasional Josephson-like anomaly with a large resistance drop at zero bias, while many spectra had the typical Andreev reflection double-minimum structure. However, we could reproduce the expected constant polarization of the ferromagnet and a BCS-type dependence of the superconducting gap only in a few cases. This unexpected variation could be related to the interplay of ferromagnetism and superconductivity at the interfaces.

SK08

Fabrication of Highly Sensitive Magnetic Tunnel Junctions for Bio-magnetic Field Sensor Application

Kosuke Fujiwara^{1*}, Mikihiko Oogane¹, Takuo Nishikawa², Saeko Yokota¹, Hiroshi Naganuma¹ and Yasuo Ando¹
¹ Department of Applied Physics, Tohoku University, Japan
² LC Business Department, Konicaminolta Opto, Inc., Japan

The discovery of large tunnel magneto-resistance (TMR) effect of over 200% in MgO based magnetic tunnel junctions (MTJs)[1,2] enabled us to design highly sensitive magnetic field sensors[3,4], such as a bio-magnetic field sensor. For this purpose, we need MTJs with a high sensitivity and hysteresis-free responses. In this study, we fabricated MTJs with a NiFe₂₀/Ru_{0.5}/CoFeB₃ (in nm) bottom synthetic ferri-coupled free layer and an MgO barrier layer. This thick NiFe layer serves low magnetic anisotropy[5]. The MTJs were annealed at 325°C by applying a magnetic field. After the first annealing, we rotated direction of the magnetic field to 90 degree and annealed at 300°C. This second annealing redirects easy axis of pinned layer. The TMR properties were measured using DC four probes with an applied magnetic field along the hard axis of the free layer, and we have successfully observed the very high sensitivity of 25.3%/Oe and hysteresis free response. Developed MTJs are promising for bio-magnetic sensor application. This work was partly supported by S-Innovation program, Japan Science and Technology Agency (JST).

[1] S. Yuasa et al, Nat. Mater., 3 (2004) 868. [2] S. S. P. Parkin et al, Nat. Mater., 3 (2004) 862 [3] D. Mazumdar et al, J. Appl. Phys., 103 (2008) 113911. [4] J. M. Almeida et al, J. Appl. Phys., 105 (2009) 07E722. [5] K. Fujiwara et al, Jpn. J. Appl. Phys., 50 (2011) 013001

SK09

Oscillatory exchange coupling and strong magnetoresistance effect in Fe/AgX/Fe (001) heterostructures with X=Cl and Br

Petru Vlaic^{1*} and Emil Burzo²
¹ Biophysics Department, University of Medicine and Pharmacy 'Iuliu Hatieganu' 400023 Cluj-Napoca, Romania
² Faculty of Physics, Babes-Bolyai University RO-400084 Cluj-Napoca, Romania

AgCl and AgBr silver halides crystallize under ambient conditions in rock salt geometry having lattice parameters epitaxially compatible with Fe structure. AgCl and AgBr compounds are wide bang gap semiconductors with indirect band gaps of 3.2 eV and 2.69 eV, respectively. Thus Fe/AgX/Fe (001) magnetic tunnel junctions (MTJs) with X=Cl and Br may represent feasible heterostructures for comparative studies with sp based Fe/MgO/Fe and Fe/NaCl/Fe junctions as well as for spintronic applications. In present contribution structural, electronic and magnetic properties of Fe/AgX/Fe (001) MTJs are theoretically investigated by means of a self-consistent Green's function technique for surface and interfaces implemented within tight-binding linear muffin-tin orbital (TB-LMTO) method. The spin-dependent transport properties are determined by means of Kubo approach implemented within TB-LMTO formalism. Formation of sharp Fe/AgCl(AgBr) interfaces and enhancement of interfacial Fe magnetic moments are predicted. Metal induced gap states on both anion and cation sites are observed. Oscillatory exchange couplings between ferro- and antiferromagnetic states with decreasing amplitude are evidenced. Spin-dependent transport properties are determined by the complex band structures of AgCl and AgBr barriers. Tunneling magnetoresistance ratios as high as 3500 % are predicted for Fe/AgCl/Fe MTJs in asymptotic regime and even higher values for Fe/AgBr/Fe junctions.

SK10

Transport properties in double MgO barrier magnetic tunnel junctions with Fe nano-particles

Pham Van Thach, Do Bang, Shinji Miwa, Takayuki Nozaki, Eiichi Tamura, Norikazu Mizuochi, Teruya Shinjo and Yoshishige Suzuki*
Graduate School of Engineering Science, Osaka University, Toyonaka, Osaka 560-8531, Japan

Interplay between spin dependent electron tunneling and Coulomb blockade effect [1,2] is one of the most attractive subjects in spintronics field because it is expected to give rise to remarkable tunnel magnetoresistance (TMR) effect as well as exhibit fascinating phenomena such as Kondo effect[3]. And in order to realize this interplay, double barrier magnetic tunnel junctions (MTJs) with ferromagnetic nano-particles are good candidates. In this research, double barrier MTJs with structure of MgO(001) substrate/MgO/CrFe/MgO/Fe particles($t = 0.12 - 1.37$)MgO/Fe/Au (unit in nanometer) are fabricated. An average diameter of the Fe nano-particles estimated by Langevin function fitting reveals an almost linear relation with t for $t \leq 1.02$ nm. Coulomb blockade effect was observed for $t \leq 1.02$ nm, and the t dependence of the Coulomb energy of the Fe nano-particles was explained consistently by a simple capacitance model. Interestingly, electron tunneling spectra (dI/dV) and TMR show a dip around zero bias at low temperatures. A suppression of the TMR around zero bias implies a phenomenon like Kondo physics. The transport properties in the double barrier MTJs having Fe nano-particles were also compared with those in a double barrier MTJ with the continuous middle Fe layer and a single barrier MTJ.

Acknow ledgements: This work is supported by Grant-in-Aid for Scientific Research (S), MEXT, Japan. (No. 23226001). [1]. S. Mitani et al. Phys. Rev. Lett. 81, 2799 (1998). [2]. H. Sukegawa et al. Phys. Rev. Lett 94, 068304 (2005). [3]. K. I. Lee et al., Phys. Rev. Lett. 98, 107202 (2007).

SK11

Characterisation of Epitaxial and Polycrystalline Co₂FeSi thin films

James Sagar¹, Hiroaki Sukegawa², Leonardo Lari³, Vlado K Lazarov³, Seiji Mitani⁴ and Atsumi Hirohata^{5*}

¹ Department of Physics, University of York, United Kingdom
² Magnetic Materials Centre, National Institute for Materials Science (NIMS), 1-2-1 Sengen, Tsukuba 305-0047, Japan
³ Department of Physics, University of York, York, YO10 5DD, United Kingdom
⁴ Magnetic Materials Centre, National Institute for Materials Science (NIMS), 1-2-1 Sengen, Tsukuba, Japan
⁵ Department of Electronics, University of York, York, YO10 5DD, United Kingdom

We have grown and characterised both epitaxial and polycrystalline Co₂FeSi thin films using UHV magnetron and HiTUS sputtering. The structure of the films has been studied using XRD, TEM and STEM. The combination of these techniques allows analysis of the structure and defects within the films. Magnetic characterisation has been carried out using AGFM and VSM. UHV magnetron sputtered films have been found to become increasingly L₂₁ ordered after annealing above 500°C. HiTUS deposited samples form a polycrystalline film from and amorphous Co, Fe and Si matrix after annealing at 500°C for 3, 6 and 9 hours with large (50nm-250nm) L₂₁ and B₂ ordered grains. This growth process results in films with large Hc (>5000e) these values are two orders of magnitude greater than those found for epitaxial films [1]. The magnetic response of these polycrystalline films has been found to improve with the use of a 6nm Cr or Ag buffer layer. This is shown by a decrease in Hc and an increase in Ms to greater than 85% of the theoretical value.

[1] J.Sagar, et al, IEEE. Trans. Mag, 47, 2440 (2011)

SK12

Inverse spin polarization at benzene/iron interface

Souraya Goumri-said*, Mohammed Benali Kanoun, Udo Schwingschlogl and Aurelien Manchon
Physical Sciences and Engineering Division, King Abdullah University of Science and Technology (KAUST), Saudi Arabia

Organic spin-valves involving an organic spacer inserted between two magnetic electrodes have been successfully realized and led to sizable magnetoresistance ratios [1-3]. The accurate design of the interfacial electronic structure controlling the spin injection is critical to obtain high performance devices. Intriguingly, recent reports claimed that interfacial spin polarization may be reversed in some cases [4, 5]. We address the nature of the spin polarization Benzene/ Fe (100) interface using ab-initio approach. The surface is modeled by 6 layers of Fe (100) and the position of the Benzene molecule on Fe (100) surface is determined by a combination of the chemisorption of the π -molecule on the reactive surface and the strong interaction of the d-metal orbital with π -molecule orbitals. We find that the presence of the Benzene molecule dramatically modifies the electronic structure of the interface and can lead to drastic change in the interfacial spin polarization. While the Benzene molecule becomes slightly magnetic (0.032 μ_B by C atom), it is found that the polarization of the interfacial Fermi electrons is reversed from 0.59 (pure Fe surface) to -0.70 (Fe/Benzene interface). This polarization reversal is analyzed in terms of orbital overlaps between the Benzene p-orbitals and Fe-d orbitals .

[1] V. Dediu, M. Murgiu, F. C. Matocota, C. Taliani, and S. Barbanera, Solid State Commun. 122, 181 (2002). [2] Z. H. Xiong, D. Wu, Z. Vaby Vardany, and J. Shi, Nature 427, 821 (2004); Yoo et al., Nature Materials 9, 638 (2010) [3] C. Barraud, et al. Nature Physics 6, 615 (2010) [4] Atodiresci et al, Phys. Rev. Lett. 105, 066601 (2010) [5] M. Saegys, M. Reyniers, and G. B. Marin, J. Phys. Chem. B 106, 7489 (2002).

SK13

Local atomic structure analysis of ferromagnetic semiconductor GeMnTe by atomic resolution holography

Naohisa Happo^{1*}, Yuki Takehara¹, Makoto Fujiwara¹, Koichi Tanaka¹, Fumihiko Matsui², Hiroshi Daimon³, Tomohiro Matsushita³, Kyoko Okada³, Shinya Senba⁴, Shinya Hosokawa⁵, Kouichi Hayashi⁶ and Hironori Asada⁷
¹ Graduate School of Information Sciences, Hiroshima City University, Japan
² NAIST, Japan
³ Spring-8/JASRI, Japan
⁴ Ube National College of Technology, Japan
⁵ Hiroshima Institute of Technology, Japan
⁶ IMR, Tohoku University, Japan
⁷ Yamaguchi University, Japan

The IV-VI diluted magnetic semiconductor GeMnTe is expected as a spintronics material, because it shows a ferromagnetic order below 190 K at $x = 0.08$ [1]. It is believed that its ferromagnetism is a carrier induced type. However, another possibility is a cluster formation of a ferromagnetic MnGe binary alloy. The solution can be obtained by an investigation of the crystal structure around the each element. Recently, we have investigated the atomic arrangement around the Ge and Mn atoms in the GeMnTe by an X-ray fluorescence holography (XFH) [2, 3]. The obtained atomic images from the XFH suggest that the Mn atoms replace with the Ge atoms in the host GeTe, the Mn position is stable in the exact positions of the anion fcc sub lattice [2], and the Ge position is fluctuated [3]. We have also performed the Te 4d photoelectron holography (PEH) in order to investigate the local structure around the Te atoms in the GeMnTe thin film single crystal. The obtained atomic image from the PEH suggests that the Te atoms are not located at the exact positions of the fcc anion sublattice.

[1] Y. Fukuma, et al., Appl. Phys. Lett. 93 (2008) 252502. [2] N. Happo, et al., Jpn. J. Appl. Phys. 50 (2011) 05FC11. [3] N. Happo, et al., e-Journal of Surface and Nano Technology 9 (2011) 247.

SK14

Dependence of the tunneling magnetoresistance on the inserted nonmagnetic layer

Changsik Choi and Byung Chan Lee*
Department of Physics, Inha University, Korea

When a crystalline nonmagnetic (NM) layer was inserted between the tunnel barrier and a magnetic layer in magnetic tunnel junctions (MTJs), it was observed that the tunneling magnetoresistance (TMR) decayed and oscillated as a function of the thickness of the nonmagnetic layer. In this paper, the TMR dependence on the NM layer is investigated theoretically. The conductance was calculated with the Landauer-Buttiker formalism, and the conductance difference between the parallel and anti-parallel magnetizations was given in an analytical form with the spin-dependent reflection amplitudes. In order to check the validity of our model, numerical calculations were carried out. An effective mass theory was adopted for the electronic structure of each material, and several cases were considered. It was shown that our simple model agreed well with the results of the numerical calculations. Our model can be applied also to more realistic cases with the full-band structures. The oscillation period was determined from the extremal vectors of the Fermi surface of the NM material, and the selection rules for the oscillation period were obtained. Comparisons with the experimental data and the previous theoretical results will be presented.

SK15

The bulk Fe-Mo double perovskite analyzed from a small clusters perspective

Eliel Carvajal Quiroz^{1*}, Raul Oviedo Roa², Miguel Cruz Irissou¹ and Oracio Navarro³
¹ Instituto Politecnico Nacional, ESIME-Culhuacan, Mexico
² Programa de Investigacion en Ingenieria Molecular, Instituto Mexicano del Petroleo, Mexico
³ Instituto de Investigaciones en Materiales, Universidad Nacional Autonoma de Mexico, Mexico

Being the Sr₂FeMoO₆ double perovskite among the promising materials for spintronic applications, the bulk case was studied in this work; but attention was focused, also, on the octahedral arrangements FeO₆ and MoO₆ as well as on FeO₄ and FeMoO₄ clusters. Calculations were made using Density Functional Theory (DFT) and the Perdew-Burke-Ernzerhof (PBE) functional within the Generalized Gradient Approximation (GGA) scheme. In order to understand the differences in the behavior among up- and down-spin electrons observed in the half-metallic Sr₂FeMoO₆ double perovskite, the orbitals and density of states were analyzed. Our results reveal that the half-metallic character is present ever since the isolated (FeO₄)₄- cluster and is a consequence of the non-zero spin at Fe atom coming from 12g orbitals. The (MoO₆)₆-octahedra does not inhibit the perovskite half-metallic character because this Mo-containing cluster has a zero total spin. In addition, Sr atoms were aggregated to the studied cluster, not just because of the searched relation between the bulk material and the cluster units properties, because they give the impression that play a relevant role to become stable the charge even though the energy deepest of the states contributed by them. Acknowledgments: Work supported by Multidisciplinary Project SIP-IPN: 2012-1439, PAPIIT-IN108710 UNAM.

SK16

Tunneling magnetoresistance effect in magnetic tunneling junctions with a high resistance ferromagnetic oxide Fe_{2.5}M_{0.5}O₄(M = Mn, Zn) electrode

Eiji Shikoh^{1*}, Teruo Kanki², Hidekazu Tanaka², Teruya Shinjo¹ and Masashi Shirashi¹
¹ Eng. & Sci., Osaka University, Japan
² ISIR, Osaka University, Japan

Recently, molecular spintronics has attracted much attention. To improve the spin injection efficiency from ferromagnetic electrodes into molecular materials, by avoiding an impedance mismatch problem, the use of high resistance ferromagnetic electrodes is more accessible than other methods. In this study, a high resistance ferromagnetic oxide Fe_{2.5}M_{0.5}O₄(FMO: M = Mn, Zn) was focused and observation of a tunneling magnetoresistance (TMR) effect in magnetic tunneling junctions (MTJs) with an FMO electrode was implemented. MTJs composed of MgO(100)-sub. / FMO(thickness, 25-30 nm) / Al-O(1.5-2) / Ni₈₀Fe₂₀(20) were fabricated by using pulsed laser deposition, EB deposition, photolithography, Ar ion milling, and sputtering. Magnetic properties were investigated with magnetic Kerr effect measurements. Magnetoresistance properties were measured with a 4-terminal-method. A TMR effect reflecting the magnetization processes of the both ferromagnetic electrodes in the MTJs with M = Mn was successfully observed, and the TMR ratio was approximately 0.85% at room temperature (RT) [1]. The spin-polarization of FMO with M = Mn at RT was estimated to be at least 0.94%[1]. Higher spin-polarization is expected by improving the interface and the barrier qualities between the ferromagnetic electrodes.

[1] E. Shikoh, et al., Solid State Commun. 151, 1296 (2011).

SK17

Monitoring of gamma radiation interaction in PHR sensor

D.g. Park and Hoon Song
korea atomic energy research institute, Korea

The Planar Hall Resistance (PHR) sensors have been found to be capable of magnetic micro and nano bead detection as the signal to noise ratio in these PHR sensors are higher by several orders compared to others magnetoresistive biosensors. In addition, the spin valve multilayer are considered as novel structures for a high sensitivity and uniform magnetization rotation compared to exchange biased bilayer structure for planar Hall resistance sensors.(1). In this work, we discussed a method for immobilization of magnetic labels on the PHR sensor for sensitive detection of magnetic labels. We used photolithography to generate the functionalized sensor surface to demonstrate the capacity of monitoring the immobilization of biomolecule. The PHR sensor was irradiated by Co source up to 80 Gy and the sensor characteristic was compared with non irradiated one. The field sensitivity obtained by the slope ($\Delta V / \Delta H$) of the field-voltage curve was not changed by high dose irradiation up to 80 Gy. The sensitivity of the PHR sensor was identified detecting the different concentration of magnetic beads. We have successfully demonstrated the immobilization of streptavidin coated magnetic bead to the single stranded oligonucleotide on the Au coated PHR sensor surface for the detection of magnetic labels.

[1] P. E. Sheehan and L. J. Whitman, Nano lett. 5, 803 (2005).

SK18

Reactively sputtered MgAl2O4 barrier layers for Heusler tunnel junctions

Keima Inagaki*, Naoto Fukatani, Kenichiro Mari, Hirohito Fujita, Tetsuya Miyawaki, Kenji Ueda and Hidehumi Asano
Crystalline Materials Science, Nagoya University, Japan

Magnetic tunnel junctions (MTJs) using epitaxial MgO barriers have attracted great interest because they exhibit large tunnel magnetoresistance (TMR) ratios. However, the large lattice mismatch (about 4%) between MgO and half-metallic Heusler alloy induces misfit dislocations and antisite disorder at the surface of ferromagnetic electrode[1]. Thus, coherent growth of MTJ is important for further improvement of device performance. This study focuses on spinel MgAl₂O₄ as a tunnel barrier lattice-matched with half-metallic Heusler alloy. We fabricate a Fe₂CrSi/MgAl₂O₄ junction by reactive sputtering, which can control the crystallinity and degree of oxidation of the films strictly, and investigate its crystal structure and electrical transport properties. MgAl₂O₄ films were deposited from a MgAl₂ target in Ar/O₂ atmosphere. Epitaxial Fe₂CrSi/MgAl₂O₄ junctions were obtained by inserting an ultrathin MgAl₂ interlayer, which worked as a protection layer for oxidation at the surface of Fe₂CrSi. The rocking width of MgAl₂O₄ (004) was around 1°, which is small value compared to that of the electron-beam evaporated MgO[2]. Current-voltage curve was fitted by Simmons' tunneling theory, and we obtained barrier height $\phi = 0.86-0.95$ eV for the Fe₂CrSi/MgAl₂O₄/CoFe MTJ. Present epitaxial MgAl₂O₄ barrier deposited by reactive sputtering is expected to realize high performance spintronic devices.

[1]T. Miyajima, M. Oogane, Y. Kotaka, T. Yamazaki, M. Tsukada, Y. Kataoka, H. Nagamura, and Y. Ando: Appl. Phys. Express 2 (2009) 093001. [2]G. X. Miao, Y. J. Park, and J. S. Moodera: Phys. Rev. Lett., 100 (2008) 246803.

SK19

Half-metallic properties of (001) surfaces of the Cr substituted rock-salt GeTe-based compounds

Kalpana Kamalkishor Landge, Beata Bialek and Jae Il Lee*
Physics, Inha university, Korea

Much effort has been devoted to the development of new magnetic materials for the spintronic applications. Recently, new half-metallic ferromagnets based on the rock-salt semiconductor GeTe were found [1]. In the bulk structure, GeTe becomes half-metal when some of Ge atoms are substituted by Cr or V. We report the properties of (001) surfaces of Cubic CrGe₃Te₄ and tetragonal CrGeTe₂ with two different terminations, i.e. GeTe and CrTe terminations, as obtained by using the FLAPW [2] within GGA. We found that both CrTe- and GeTe-terminated CrGe₃Te₄ and CrGeTe₂ (001) surfaces conserve the half-metallic properties of their bulk structures by analyzing the DOS and confirmed from the integer value of total magnetic moment (MM) per unit cell. The center layer energy gap is much larger as compared to its bulk. The energy gap and half metallic gap became wider with the larger substitution of Ge atom by Cr atoms. In the CrTe-terminated surface the MM of the Cr atom at the surface layer has been enhanced as compared to the center layer Cr atoms by the surface effect. The calculated value of MM on Cr at the top layer of the surfaces is 3.7 μ_B in the both system.

[1] Y. H. Zhao, W. H. Xie, L.F. Zhu, and B. G. Liu, J. Phys.: Condens. Matter 18, 10259 (2006). [2] E. Wimmer, H. Krakauer, M. Weinert, and A. J. Freeman, Phys. Rev. B 24, 6864 (1981), and references therein ; M. Weinert, E. Wimmer, and A. J. Freeman, Phys. Rev. B 26, 4571 (1982).

SK20

Electronic structure and spin polarization of Co_{2-x}Fe_{1+x}Si Heusler alloy

Hiroyoshi Itoh^{1*} and Syuta Honda²
¹ Department of Pure and Applied Physics, Kansai University, Japan
² Faculty of Pure and Applied Science, University of Tsukuba, Japan

We study the electronic structure and spin polarization for Co-based Heusler alloys of Co_{2-x}Fe_{1+x}Si using the first principles calculations to discuss the spin injection into semiconductors and paramagnetic metals. Half-metallic Heusler alloys such as Co₂MnSi, Co₂FeSi, and Fe₂MnSi are promising materials for spin generator, injector, and detector. Recently, epitaxial films of Fe₂MnSi [1] and Co₂FeSi [2] have been successfully fabricated on Ge or Si substrates and the spin-dependent transport properties have been measured. Obtained results seem sensitive to the degree of disorder and the composition of the alloy. In this contribution, we examine composition dependence of the electronic structure for Co_{2-x}Fe_{1+x}Si by performing band calculations based on the density-functional theory (DFT) in the generalized gradient approximation (GGA) using the projector-augmented wave (PAW) method. It is shown that the spin polarization defined by the total DOS decreases from +100% at $x=0$ and changes the sign with increasing Fe composition x because the half-metallicity is lost. However, the spin polarization defined by the s-component of DOS (partial DOS) keeps positive although it decreases with increasing x from $x=0$ to $x=2$.

[1] K. Hamaya et al.: Phys. Rev. Lett. 102 (2009) 137204. [2] A. Yamada et al.: Appl. Phys. Lett. 96 (2010) 082511.

SK21

Large enhancement of Kerr rotation of GMR periodic patterns using Pt / Co free layer

Kakeru Wada¹, Tsukasa Kobayashi¹, Yuuki Oshino¹, Hiroshi Ono², Tatsutoshi Shioda², Kenji Machida³, Ken-ichi Aoshima³, Kiyoshi Kuga³, Hiroshi Kikuchi³, Naoki Shimidzu³, Akira Emoto⁴ and Takayuki Ishibashi^{1*}
¹ Department of Materials Science Technology, Nagaoka University of Technology, Japan
² Department of Electrical Engineering, Nagaoka University of Technology, Japan
³ Science and Technical Research Laboratories, Japan Broadcasting Corp, Japan
⁴ National Institute of Advanced Industrial Science and Technology, Japan

Magneto-optical spatial light modulator (MO-SLM) driven by spin transfer switching is a promising device for holographic 3D display. However, a small Kerr rotation angle is an issue to be solved to realize the MO-SLM. In this paper, we report an enhancement of Diffraction Magneto-Optic Kerr Effect (DMOKE) obtained for periodic GMR patterns. A GMR structures with Pt/Co free layer were used in this experiment. The samples were patterned into periodic structures with sizes of 5-50 μ m and pitches of 10-100 μ m. SiO₂ was deposited on the etched area after the patterning to obtain flat surfaces. DMOKE of the GMR patterns were measured by using a He-Ne laser with a wavelength of 632.8 nm and an incidence of 30°. DMOKE hysteresis loops were clearly observed, corresponding to the magnetization reversal of the free layers, and Kerr rotation angles of (1,0) and (1,1) diffraction spots were measured to be 0.5°, which is six times larger than a polar Kerr rotation angle measured before the patterning. We consider that the large enhancement of DMOKE is due to an interference effect occurred in the periodic GMR structures embedded in SiO₂. This work was supported by the NICT.

K. Aoshima et al, Appl Phys Lett, 44, 052507 (2007)

SK22

Ab-initio and tight-binding calculations of magnetic anisotropy phenomena in CoPt

Jan Zemen¹, Jan Masek² and Tomas Jungwirth³
¹ School of Physics and Astronomy, University of Nottingham, Nottingham NG7 2RD, United Kingdom
² Institute of Physics ASCR v.v.i., Na Slovance 2, 182 21 Praha 8, Czech Republic
³ Institute of Physics ASCR v.v.i., Czech Republic & University of Nottingham, United Kingdom

Ordered CoPt alloys hold potential for applications in high density magnetic recording due to the combination of exchange and spin-orbit interactions giving rise to large magnetic anisotropies. Tunneling Magnetoresistance [1] and Tunneling Anisotropic Magnetoresistance [2] have been demonstrated in tunneling devices with CoPt electrodes. Controlling the spin-orbit coupling (SOC) phenomena is essential as the same anisotropy that ensures thermal stability of a memory element makes the writing by external magnetic fields or electric currents challenging. An alternative to the spin transfer torque (STT) effect in multi-domain systems is based on current induced polarization of the conduction electron spins in structures possessing SOC and lacking inversion symmetry. Switching of a ferromagnetic layer induced by in-plane current has been shown recently in a Co-Pt bilayer [3]. Another promising way of controlling the magnetic anisotropy via SOC utilizes lattice strains induced by piezo stressors. We study SOC effects in strained CoPt multilayer structures using a relativistic full-potential linearized augmented plane-wave method. We compare the variations of anisotropies of magnetic total energies (MAE) and density of states (ADOS) also to our tight-binding calculations using a realistic Slater-Koster parametrization which provide more practical basis for further research of magnetotransport anisotropies in CoPt based nanostructures.

[1] Golechov Kim, Yuja Satohda, Mikihiko Oogane, Yasuo Ando, and Terunobu Miyazaki, *Appl. Phys. Lett.* 92, 172502 (2008). [2] B. G. Park, J. Wunderlich, D. A. Williams, S. J. Cho, K. Y. Jung, K. H. Shin, K. Ohgaki, A. B. Shick, and T. Jungwirth, *PRL* 100, 087204 (2008). [3] Juan Mdkua Miron, Kevin Goretto, Gilles Gaudin, Pierre-Jean Zeman, Maria V. Costache, Stephane Auffret, Sebastien Bondeira, Bernard Rodmacq, Alain Schuhl, and Piero Gambardella, *Nature* 476, 189-193 (2011).

SK23

Spin polarization of half-metallic Heusler alloy Co₂MnSi by Andreev reflection measurements

Iduru Shigetani^{1*}, Yuya Nishisako¹, Kohei Harumori¹, Akinari Okubo², Rie Y. Umetsu³, Masakazu Ito¹, Keiichi Koyama¹, Ryosuke Kainuma² and Masahiko Hiroi¹
¹ Department of Physics and Astronomy, Kagoshima University, Japan
² Department of Materials Science, Tohoku University, Japan
³ Institute for Materials Research, Tohoku University, Japan

We report spin polarization measurements of half-metallic Heusler alloy Co₂MnSi. Heusler alloys are regarded as the most promising half-metallic materials for spintronics applications because of their high Curie temperature and low coercivity. Recently, large tunneling magnetoresistance (TMR) value was experimentally reported from a Co₂MnSi/Al-O/Co₂MnSi magnetic tunnel junction (MTJ), which was attributed to the half-metallicity of Co₂MnSi. Therefore, we have determined the spin polarization of Co₂MnSi by the Andreev reflection technique. Polycrystalline Co₂MnSi samples were fabricated by using a high-frequency induction furnace. We have made planar-type junctions by depositing Pb on the polished surface of the polycrystalline Co₂MnSi samples. The differential conductance of Co₂MnSi/Pb planar-type junctions was measured between 1.5 K and 10K by the lock-in amplifier technique. The obtained differential conductance was able to be fitted very well by the modified Blonder-Tinkham-Klapwijk (BTK) model. We have found the spin polarization of approximately 50% from the analysis of Andreev reflection measurements of half-metallic Heusler alloy Co₂MnSi.

SK24

Electronic properties of Co₂Fe_{1-x}Mn_xSi Heusler alloys studied by hard X-ray photoelectron spectroscopy

A. Gloskovskii¹, S. Ouardi¹, G. H. Fecher², S. Thiess³, W. Druhe³, B. Detlefs⁴, T. Kubota⁵, Y. Ando⁵ and C. Felser²
¹ Johannes Gutenberg University, Mainz, Germany
² Max Planck Institute for Chemical Physics of Solids, Dresden, Germany
³ Deutsches Elektronen-Synchrotron DESY, Hamburg, Germany
⁴ ESRF, Grenoble, France
⁵ Department of Applied Physics, Graduate School of Engineering, Tohoku University, Japan

One major research area where Co₂ based Heusler compounds are investigated is on TMR junctions. Fully epitaxial magnetic tunnel junctions (MTJs) with a Co₂YZ thin film as a base electrode and a MgO tunnel barrier exhibit high TMR ratios. Quaternary Co₂Fe_{1-x}Mn_xSi (CFMS) Heusler alloys are even more promising because the substitution of Mn by Fe increases the number of valence electrons and therefore leads to higher Curie temperatures above 1000 K. Kubota et al. found a maximum TMR ratio for Co₂Fe_{1-x}Mn_xSi (x = 0, . . . 1)-CoFe MTJs [1] for Fe fractions of between x=0.4 and 0.6. The halfmetallic character disappeared for samples with x≥0.8. The reason of this behaviour is still unknown. A B₂ and L₂₁ site ordered stack of MgO substrate/ Cr [40 nm] buffer layer/ Co₂Fe_{1-x}Mn_xSi [30 nm]/ MgO [2 nm]/ AlO_x [1.3 nm] (x = 0, 0.2, . . . 1.0) films was studied at beamline P09 at PETRA III and beamline ID32 at the ESRF. The hard X-Ray photoelectron spectroscopy studies were performed with an excitation energy of 6 keV. It was found that the position of Co 2p core levels and the density of states in the valence band region strongly depend on the Fe/Mn ratio.

[1] Takahide Kubota, Sumito Tsunegi, Mikihiko Oogane, Shigemi Mizukami, Terunobu Miyazaki, Hiroshi Nagamura, and Yasuo Ando *APL* 94 (2009) 122504

SK25

Ab-initio calculation of the magnetic properties of bn nanoribbon

Jeffrey Rufinus
 Science Division, Widener University, USA

The emerging field of spin electronics (spintronics) has been continuously attracting researchers. Substantial theoretical and experimental efforts have been made in the quest to find the candidates for future spintronics devices. Recently, the search for new spintronics materials has also included graphene-based materials due to the theoretical prediction that this type of material may show the half-metallic property. Here, we present the results of a density functional theory within a generalized gradient approximation study of Boron Nitride (BN) nanoribbon. The objective of this study is to determine whether this type of material will be ferromagnetic or antiferromagnetic if the width is varied. Our results show that the narrow zigzag shaped BN nanoribbon prefers ferromagnetic or antiferromagnetic state depending on the width. Thus, by controlling the width (and growth direction) it is possible to manipulate the magnetic property of this material. These results are of the scientific interest in exploring the magnetic properties of BN-based nanoribbon for future spintronics.

SK26

Synthesis and functional properties of polycrystalline Fe₂Si-based magnetic tunnel junctions

Alexander Goikhman^{1*}, Galina Kupriyanova¹, Roberto Mantovan², Andrei Zenkevich³ and Ksenia Maksimova¹
¹ REC 'Functional Nanomaterials', Immanuel Kant Baltic Federal University, Russia
² Laboratorio MDM IMM-CNR, Italy
³ NRNU 'Moscow Engineering Physics Institute', Russia

Magnetic tunnel junctions (MTJs), consisting of two ferromagnetic (FM) layers separated by ultrathin tunnel barrier are key elements in a wide range of spintronic devices, particularly, as bit elements in magnetic memories and as reading heads in racetrack memory concept. The improvement of the MTJs tunnel magnetoresistance (TMR) might be attained by the selection of the materials with high spin-polarization and the appropriate combination of FM electrodes and tunnel barrier [1]. In this work, we discuss the applicability of a half-metal Heusler alloy Fe₂Si as an top and bottom electrodes in MTJ, the material which has been poorly adopted so far [2,3]. MTJs based on polycrystalline Fe₂Si ferromagnetic (FM) electrodes and both SiO₂ and MgO tunnel (~1-3 nm) insulators (TI) have been grown by the combination of pulsed laser deposition (using two-laser co-deposition approach) and ion beam assisted deposition techniques. The morphology, phase composition and structural properties of individual layers as well as the intermixing and chemical reactions at the FM/TI interface have been investigated. The magnetic properties of the trilayers and preliminary TMR measurements on Fe₂Si-based MTJs obtained at wide range of temperatures (2-400 K) will be presented, aiming at the evaluation of potential of Fe₂Si-based MTJs for spintronics.

1. S.D. Bader, *S.S.P. Parkin, Annu. Rev. Condens. Matter Phys.* 2010, 1:71-88 2. Y. Ando, K. Hamaya et al., *Appl. Phys. Lett.* 2009, 94 182105 3. K. Harada, K.S. Makabe et al., *J. of Phys.: Conf. Ser.* 2011, 266 012088

SK27

Half-metallic properties of the (001) surfaces of the half-heusler compounds GeKCa and SnKCa

Lee-hyun Cho¹, Beata Bialek¹, Jae Il Lee^{1*} and Miyoung Kim²
¹ Physics, Inha University, Korea
² Division of Energy System Research, Ajou University, Korea

The sp or d0 half-metallic materials have been attracted more and more increasing attention. A recent first-principles calculation found that the half-Heusler compounds, GeKCa and SnKCa, are half-metallic [1]. We investigated the magnetic and half-metallic properties of the (001) surfaces of the GeKCa and the SnKCa by using the all electron full-potential linearized augmented plane wave method [2] within generalized gradient approximation. We considered two different terminations for each compound, i. e. Ge (or Sn) and KCa terminations. From the calculated density of states, we found that the Ge or the Sn termination reserves the half-metallicity, while the KCa termination for both compounds is not half-metallic. The magnetic moments for the surface Ge and Sn atoms are much enhanced compared to the bulk values, but the KCa surface for both compounds is almost magnetically dead.

[1] J. Chen, G. Y. Guo, K. L. Yao, and M. H. Song, *J. Alloy. Compd.* 509, 10172 (2011). [2] E. Wimmer, H. Krakauer, M. Weinert, and A. J. Freeman, *Phys. Rev. B* 24, 864 (1981), and references therein ; M. Weinert, E. Wimmer, and A. J. Freeman, *Phys. Rev. B* 26, 4571 (1982).

SK28

Half-metallicity in hydrogenated carbon nanotubes

Kyu Won Lee, Gi-wan Jeon and Cheol Eui Lee*
 Physics, Korea University, Korea

Zigzag-edge graphene nanoribbons (ZGNRs) show half-metallicity arising from edge-localized electron states under an electric field, enabling fully spin-polarized electrical current and thus providing a basis for spintronics. While carbon nanotubes (CNTs), obtained by rolling up the ZGNRs, have themselves no edges, edge states have been identified in hydrogenated CNTs. Thus, whether or not the CNTs can be half-metallic under an electric field becomes an issue of great interest. Here, our density functional theory (DFT) calculations show that the edge states in the CNTs are unstable under an electric field due to the spin-conserving electron transfer between the edges, but a large enough transfer barrier between the edge states, obtained by controlling the adsorption patterns, can render the CNTs half-metallic. Our results can be extended to most carbon systems thus opening a new route to materials engineering and providing a deeper understanding of the electronic properties of π -bond network edges.

1. Y.-W. Son, M. L. Cohen, S. G. Louie, *Nature* 444, 347 (2006). 2. Z. Slijvančanin, *Phys. Rev. B* 84, 085421 (2011).

SK29

Enhanced perpendicular magnetic anisotropy in Fe/(MgAl₂O_x) bilayer structures with interface optimization processes

J.w Koo¹, S Mitani², H Sukegawa², Z.c Wen², T Niizeki², S Kasai² and K Inomata²
¹ University of Tsukuba, Tsukuba National Institute for Material Science, Japan
² National Institute for Materials Science, Tsukuba, Japan

Ferromagnetic metals (FM) electrodes with large perpendicular magnetic anisotropy (PMA) are actively being investigated. Recently PMA arising at the interface between a FM and an oxide layer such as CoFeB/MgO [1] and Co₂FeAl/MgO [2] were reported. The PMA at which between FMs and oxide barrier materials has attracted much attention not only for the STT-MRAM applications but also for spintronic devices with electric field control of magnetization. The detailed mechanism of the interface PMA is still an open question since the experimental reports, in particular the materials examined, are much limited. Here, we report the enhanced PMA in Fe/MgAl₂O_x structures with the effective perpendicular magnetic anisotropy energy density (K_{eff}) ~ 3 erg/cm³. In the case of an Fe layer with a crystalline (MgAl₂)O_x layer, it exhibited perpendicular magnetization characteristics, and the value of K_{eff} was increased from ~ 0 to ~3 erg/cm³ with increasing annealing temperature. Furthermore, even in the Fe layer with amorphous (MgAl₂)O_x, a large interface magnetic anisotropy was obtained.

[1] S. Ikeda et al., *Nature Mater.* 9, 721 (2010) [2] Z. C. Wen et al., *Appl. Phys. Lett.* 98, 242507 (2011).

SK30

Graphene nano-ribbon and the ripple effect

Hsin-han Lee, Kuo-chin Chen and Ching-ray Chang*
 Physics, National Taiwan University, Taiwan

Graphene is a possible nano-device in the future. There are several experiment and theory exhibit that the graphene would generate the ripple in some conditions[1-3], and there is a "geometrical effect" on the curved surface with Rashba spin-orbit effect[4]. We investigate the transport property and the spin density accumulation on the graphene nano-ribbon with the ripple. This research used the non-equilibrium Green function(NEGF) of the Landauer formula[5,6] to compute the numerical results for the system.

[1] C. H. Lui, Li Liu, K. F. Mak, George W. Flynn and Tony F. Heinz, *Nature* 462, 339-341 (2009) [2] Daniel Huerfias-Hernando, F. Guinea, and Arne Brataas, *Phys. Rev. B* 74, 155426 (2006) [3] Z. Wang and M. Devel, *Phys. Rev. B* 83, 125422 (2011) [4] T.-C. Cheng, J.-Y. Chen and C.-R. Chang , *Phys Rev B.* 84, 214423 (2011) [5] S. Datta. *Electronic transport in mesoscopic systems*. Cambridge University Press, Cambridge (1995) [6] S. Datta. *Quantum Transport: Atom to Transistor*. Cambridge University Press, Cambridge (2005).

SK31

Enhancement of spin signal in all-metallic lateral spin valves with half-metallic Heusler alloy

Shinya Kasai, Yukiko Takahashi, Shigeyuki Hirayama, Seiji Mitani and Kazuhiro Hono
 National Institute for Materials Science, Japan

A lateral spin valve (LSV), consisting of two ferromagnetic wires connected with one non-magnetic wire, is one of the promising devices to convert charge currents to pure spin currents, and vice versa. The conversion ratio is, however, still too small, because of the large spin absorption in ferromagnetic wires. Recently, Fukuma et al. have demonstrated that inserting the MgO barrier between ferromagnetic and non-magnetic wires suppresses the spin absorption, resulting in the enhancement of the spin signal[1]. Here, we demonstrate another way, using the half-metallic Heusler alloy as ferromagnetic electrodes. The devices were fabricated from a film stack of SiO₂(2)/Cu(10)/Co₂FeGa_{0.5}Ge_{0.5}(25)/Ag(10)/Cr(1) on MgO substrate (unit in nm). The non-magnetic wire was made of 100 nm-thick Cu. The typical wire width was 150 nm, while the distance between two ferromagnetic wires was 350 nm. The non-local resistance observed is 12.8 mΩ at room temperature that increases up to 44.8 mΩ below 10 K[2]. These values are much larger than those in typical LSVs made of Permalloy and Cu in previous reports, indicating the advantage of the half-metallic Heusler alloys as ferromagnetic electrodes in LSV.

[1]Y. Fukuma, L. Wang, H. Idzuchi, S. Takahashi, S. Maekawa, and Y. Otani, *Nature Mater.* 10, 527 (2011). [2]Y. K. Takahashi, S. Kasai, S. Hirayama, S. Mitani, and K. Hono, *Appl. Phys. Lett.* 100, 052405 (2012).

SK32

Effect of electron beam rapid thermal annealing on the TMR of CoFeB/MgO/CoFeB magnetic tunnel junctions

Ganesh K Rajan¹, Shivaraman Ramaswamy^{2*}, C Gopalakrishnan² and John Thiruvadigal¹
¹ Nanotechnology Research Center, SRM University, India
² SRM University, India
³ Department of Physics and Nanotechnology, SRM University, India

In this paper, we present our studies on the effect of Electron Beam Rapid Thermal Annealing (ERTA) on the structural evolution and related transport properties of CoFeB/MgO/NiFe MTJ. The MgO based tunneling junctions were fabricated in a DC-RF magnetron sputtering system with a base pressure 2 X 10⁻⁷ mBar. An e-beam gun with a 3kV power supply was used to facilitate electron bombardment on the MTJ for the purpose of rapid annealing .We observed the evolution of TMR in CoFeB/MgO/NiFe MTJ when subjected to ERTA. The main factor that distinguishes this study from other rapid annealing based studies is that the evolution of TMR happened within a very short annealing time (20 seconds). We observed an ultrafast crystallization of the FM layers of the MTJ which resulted in the evolution of TMR.

1. S. Yuasa, T. Nagahama, A. Fukushima, Y. Suzuki and K. Ando, *Nature Mater.*, vol. 3, pp. 868 - 871, Dec. 2004. 2. S. S. P. Parkin, C. Kaiser, A. Panchula, P. M. Rice, B. Hughes, M. Samant and S. H. Yang, *Nature Mater.*, vol. 3, pp. 862 - 867, Dec. 2004. 3. R. Cao, T. Moriyama, W. G. Wang, X. Fan, J. Kolodzey, S. H. Chen, C. R. Chang, Y. Tserkovnyak, B. K. Nikolic and J. Q. Xiao, *IEEE Trans. Mag.*, vol. 45, pp. 3434 - 3440, Oct. 2009.

SK33

Preparation of Ti-N films for a capping layer of a CoFeB/MgO-magnetic tunnel junction

Atsushi Sugihara*, Soichiro Osaki and Ryoichi Nakatani
 Osaka University, Japan

CoFeB/MgO-MTJ is the most promising system for Spin-RAM because of its high tunnel magneto-resistance (TMR) [1]. Recently, perpendicular magnetic anisotropy (PMA) which was expected to reduce current density for magnetic switching by spin-transfer torque (Jc0) down to applicable value (<10a A/cm²) was reported at reduced CoFeB layer thicknesses (<1.5 nm) [2]. However, drastic increase of damping constant (α) was observed as the reduction of the CoFeB thickness, which consequently lead to high Jc0 (3.9 x 10⁶ A/cm²). The possible cause of the increase of α is interdiffusion between Ta capping layer and CoFeB layer[3], [4]. Therefore, a capping layer material whose thermal stability is high than that of Ta is necessary. Our study is to observe a better capping layer material for CoFeB/MgO-MTJ than Ta. We focused on Ti-N and prepared CoFeB layers capped by Ta and Ti-N on MgO substrates and annealed them at various temperatures (T_{ann}) up to 800 °C. Clearly different behavior at over T_{ann}=600 °C in Ta dependence of saturation magnetization of CoFeB was indicated that Ti-N possessed higher thermal stability than Ta. Our results suggested that Ti-N was a promising capping material for reduction of Jc0 in CoFeB/MgO-MTJ.

[1] S. Ikeda et al., *Appl. Phys. Lett.*, 93, 082508 (2008). [2] S. Ikeda et al., *Nature Mater.* 9, 721 (2011). [3] H. Meng et al., *J. Appl. Phys.* 110, 033904 (2011). [4] W. G. Wang et al., *Appl. Phys. Lett.* 99, 102502 (2011).

SK34

Half-Metallic Molecular Wire on Silicon Surface

Yunhao Lu¹, Yuan Ping Feng^{2*} and Shuo-wang Yang³

¹National University of Singapore, Zhejiang University of China, Singapore

²National University of Singapore, Singapore

³Institute of High Performance Computing, Singapore

Based on DFT calculations including the molecular dynamic simulations, at first time, we describe a feasible reaction path to make a robust half metallic Mo-borine sandwich molecular wire on hydrogen-terminated Si(001) surface along [100] direction. The wire is chemically bonded to the surface, therefore, it is solid enough against thermo-perturbation, at least up to room temperature. Meanwhile, the electronic and magnetic properties of this molecular wire are tunable via an external electric field (EEF), and the wire exhibits multifunctional electronic and magnetic states, which allows it to work as a multistep molecular switch or/and multistep information storage component. Fantastically, this surface wire seems independent from the underplayed silicon bulk even under EEF situations since bulk properties have not been affected. This is because the charge transfers are constrained within the wire and the upmost layer Si atoms only. All of these features should be meaningful in the applications of molecular electronics or spintronics in near future.

SL01

Structural and magnetic studies of sol-gel prepared hexagonal BaFe₁₂O₁₉

Yat Choy Wong^{1*}, Geok Bee Teh², Sun Yung Kim¹ and James Wang¹

¹ Faculty of Engineering and Industrial Sciences, Swinburne University of Technology, Australia

² Division of Chemistry and Biology, School of Arts and Science, Tunku Abdul Rahman College, Malaysia

Barium hexaferrite particles prepared by sol-gel method was characterised using X-ray diffraction spectroscopy (XRD), Field emission scanning electron microscopy (FeSEM), Superconducting Quantum Interference Device (SQUID) and Thermogravimetric analysis (TGA). Nano-sized particles BaFe₁₂O₁₉ and Fe₂O₃ were obtained after calcination at 8000C. The BaFe₁₂O₁₉ microstructure showed an average grain size of 200nm and recorded a saturation and remanent magnetisation of 60 and 35 emu/g, respectively. In addition, a commercially available BaFe₁₂O₁₉ was also studied. The feature observed was quite distinctive and was mostly in platelets form and much larger in size. It has a saturation and remanent magnetisation of 70 and 5 emu/g, respectively. The poor remanent magnetism of this commercially available BaFe₁₂O₁₉ was due to large particle size and accompanied by an increased in surface area. TGA performed at 1000°C recorded about 1.8% wt loss in the sol-gel prepared barium hexaferrite compared with 0.2% as observed in the commercial product.

SL02

Magnetization reversal process in antiferromagnetically coupled (Co/Pd)/Ru/(Co/Pd) multilayer dot pattern

Shunji Ishio^{1*}, Yuta Kobayashi¹, Takashi Hasegawa¹, Akira Arakawa¹, Hiromi Sasaki¹, Zhongjie Yan² and Xi Liu²

¹ Department of Materials Science and Engineering, Akita University, Japan

² Venture Business Laboratory, Akita University, Japan

Magnetization reversal process, exchange interaction Hex between layers and coercivity in the antiferromagnetically coupled (Co/Pd)/Ru/(Co/Pd) dot patterns were studied as a function of dot size. Pd_{10.9}/[Pd_{0.7}/Co_{0.1}]/Ru_{0.4}/[Co_{0.4}/Pd(1.5 nm)]₆ were sputtered onto pre-patterned Si substrates. Dot shape was designed to be 100 - 3000 nm square. Magnetization measurements revealed that top and bottom layers have a perpendicular magnetic anisotropy and couple each other antiferromagnetically at remanent state. MFM measurement indicated that the magnetic state of each layer becomes single domain below side length d=200 nm. Complicated magnetization reversal process was observed. The magnetization reversal starts from a nucleation of reverse domain at dot edge in the reversal from the ↑↓ (↓↑) state to the ↑↑ (↓↓) state, while the coherent rotation type behaviour was found in the ↑↑ (↓↓) to ↑↓ (↓↑) reversal. Hex was about 2.2 kOe in the film and decreases to less than 1 kOe at d=100 nm. Coercivity is about 1 kOe for the film and is almost constant independently on the dot size. The magnetization reversal process and the dependence of Hex and coercivity on dot size are discussed in terms of the structural and magnetic property of intermediate Ru layer in patterned dots.

SL03

Magnetic properties of mechanically alloyed Fe-Cu particles

Osamu Kohmoto, Masakazu Uchida and Yasushi Matsushima

Okayama University, Japan

Mechanically alloyed powders have metastable structure. In the Fe-Cu phase diagram, both the Fe and Cu are known to have quite small solubility in to Cu and Fe, respectively, at room temperature. We have prepared x at% Cu-Fe particles by mechanical alloying. The starting materials were pure Fe and Cu powers. The crystallite sizes of Fe with 700 Å for bcc(110) and Cu with 45 nm for fcc(111) decreases below 20 nm at milling time of 500 h. The 500-h-milled alloys with x=0-30 % Cu show a single bcc phase, and the alloys with x=35-100 % Cu show a single fcc phase. Co-existence of fcc and bcc phases is not observed at x=30 and 35 %Cu. However, at x=30 at %, a slight increase in the mass density deduced by lattice parameter is observed and the density jumps by 0.85 g/cm³ at 35 at%. The magnetization at 16 kOe decreases from 200 emu/g with increasing Cu content, however, it has a sudden decrease at 35at% Cu of the phase boundary. The magnetization reaches zero at x=90 % Cu. Coercive force increases initially with the Cu content, however, it has a sudden jump at the phase boundary.

SL04

Temperature dependence of the coercive force of ferromagnetic TM-Al-O (TM=Fe, Co) granular films

Shintaro Nakamura^{*}, Akira Yoshihara², Shigehiro Ohnuma³ and Tsutomu Nojima¹

¹ Institute for Materials Research, Tohoku University, Japan

² Ishinomaki Senshu University, Japan

³ Research Institute for Electromagnetic Materials, Japan

Temperature development of the coercive force (Hc) of ferromagnetic TM-Al-O granular films has been investigated in a temperature range from 290 K down to 5 K. Each film is prepared using the magnetron sputtering method. During the depositing process, a dc magnetic field was applied parallel to the film surface to induce in-plane uniaxial anisotropy. An Fe-Al-O granular film shows no clear in-plane anisotropy at 290 K. On the other hand, Co-Al-O films show clear in-plane anisotropy at 290 K. The Hc of the Fe-Al-O film is found to be almost independent of temperature. In contrast that of Co-Al-O films strongly depends on temperature. The Hc of Co-Al-O films along the easy axis increases rapidly with decreasing temperature. This behavior in the Hc also depends on the Co-concentration. For films with lower Co-concentration and larger electrical resistivity, enhancement of the Hc becomes larger at the lowest temperature. The Hc of Co-Al-O films shows characteristic behavior at low temperatures. It increases with decreasing temperature, following a logarithmic law below about 50 K.

SL05

Microscopic dipole-exchange theory for magnonic crystal arrays of interacting ferromagnetic nanorings

Jan Borchmann, Hoa Nguyen and Michael Cottam

Department of Physics and Astronomy, University of Western Ontario, Canada

A microscopic theory is employed to study magnonic crystals represented by one-dimensional arrays of ferromagnetic nanorings. The Hamiltonian-based formalism includes exchange and dipole-dipole coupling within each ring, the long-range dipolar coupling between rings, and an external applied magnetic field. Depending on the applied field, as well as the size of the rings and the inter-ring spacing, the array elements may be in a vortex, onion (bidomain), or other inhomogeneous magnetization state. Numerical results are reported for the magnonic bands and gaps in Permalloy nanorings with outer diameter typically 80 to 120 nm, thickness typically 15 to 30 nm, and spacing varied between 10 and 100 nm. For low values of the field (e.g., 0.02 T) along the length of the array, the vortex state is favored energetically and it is found that the magnonic bands are fairly broad and the gaps are relatively small, particularly when the spacing is reduced. Conversely, at larger fields (e.g., 0.2 T) favoring the onion state, the magnonic bands are narrower and the gaps larger. Varying the inner diameter of the rings, as well as the spacing, can control the transition fields between the different states, which may be advantageous for device applications.

SL06

Synthesis and magnetic properties of zinc ferrite nanocrystals and their applications

Yang Yang, Xiaoli Liu, Chin Shen Ong and Jun Ding*

Materials Science and Engineering, National University of Singapore, Singapore

We studied magnetic properties of zinc ferrite nanoparticles via thermal decomposition, whereas zinc ions partially replace iron ions at A sites with a nominal composition of (Zn_{0.3}Fe_{0.5})Fe₂O₄. Our first-principle calculation has shown that Zn ion has significantly lower formation energy at A-site compared to the substitution of B-site and an enhancement of saturation magnetization of 10-20% is obtained due to the reduction of the total magnetic moment of A-site which is antiferromagnetically coupled with B-site. The iron and zinc precursors [Fe(acac)3, Zn(acac)2.xH₂O] were used in the synthesis of zinc ferrite particles. We have found that a molar ratio of zinc precursor to iron precursor of 1:2 is required for the end product of (Zn_{0.3}Fe_{0.5})Fe₂O₄. It has been found that magnetization measured at room temperature is dependent sensitively on particles. Room temperature magnetization reaches 100.9 emu/g for zinc ferrite nanoparticles with an average particle size of 85 nm. The value is significantly larger than that of bulk Fe₂O₄ (80-90 emu/g). The as-synthesized zinc ferrite particles with an average particle size of 26 nm were selected for magnetic fluid hyperthermia. After mPEG surface coating, the particles could be well dispersed in water. A comparative high SAR value of 630 W/g was obtained.

SL07

Nanocrystallite size-induced changes in the magnetic and transport properties of La_{1-x}Ca_xMnO₃ (x = 1/8, 3/8, 5/8) manganite

Yugandhar Bitla and S. N. Kaul*

School of Physics, University of Hyderabad, Central University P.O., Hyderabad - 500 046, India

Magnetization, magnetic hysteresis loops/isotherms, linear and non-linear ac susceptibility, electrical resistivity and magnetoresistance measurements have been performed on 40 nm nanocrystalline La_{1-x}Ca_xMnO₃ (x = 1/8, 3/8, 5/8). Compared to the bulk, reducing the crystallite size down to 40 nm results in the following changes. For x = 1/8 [1], lowers paramagnetic insulating (PMI)- ferromagnetic insulating (FMI) transition temperature T_(c) to 143 K, induces the metal-insulator (MI) transition at T_(MI) = 77 K and charge ordering (CO)/orbital ordering (OO) transition at T_(CO/OO) = 35 K but leaves the insulating cluster spin glass transition temperature T_(g), the temperature T_(JT) below which short-range antiferromagnetic (AF) order coexists with OO and the spin-wave stiffness at 0 K, D(0) = 35(2) meVÅ², essentially unaltered. For x = 3/8, lowers T_(MI) to 234 K, a second-order (first-order) PMI-FMI phase transition occurs at T_(c) = 273.5 K when the applied magnetic field, H = 0 (H ≠ 0), D(0) retains its bulk value [2] 145(5) meVÅ² and T_(CO) reduces to 30 K. For x = 5/8, FM and CO ordering in the insulating state sets in at T_(c) = T_(CO) = 270 K and transition to the AF/OO phase occurs at T_(AF) = 50 K.

[1] Y. Bitla and S. N. Kaul, *J. Appl. Phys.* 111, xxxx (2012) at press. [2] J. J. Rhyne et al., *J. Magn. Mater.* 226-230, 775 (2001).

SL08

Magnetic and magneto-optical properties of bilayered Co/Ni anti-dot arrays

N. G. Deshpande¹, H. Y. Zheng¹, J. S. Hwang¹, S. J. Lee¹, Y. P. Lee^{1*}, J. Y. Rhee² and K. W. Kim³

¹ Physics, Hanyang University, Korea

² Physics, Sungkyunkwan University, Korea

³ Information Display, Sun Moon University, Korea

In this study, we have successfully fabricated bilayered Co/Ni anti-dot arrays using photolithography and controlled wet-etching processes. Such a ferromagnetic structure was made by sequentially depositing Co (40 nm)/Ni (5 nm) bilayer on a Si substrate. The anti-dot patterning with a hole diameter of 1 - μm was done only on the upper Co layer, while the Ni underlayer was kept uniform. The magnetic properties of anti-dot arrays were investigated by using a superconducting-quantum-interference-device magnetometer and by magnetic-force microscopy (MFM). The longitudinal Kerr rotation (LKR) of the zeroth- and the first-order diffracted beams were measured at an incidence angle of 30°. Significantly, it was observed that the LKR of the first-order diffracted beam is nearly 4 times larger than that of the zeroth-order beam. The simulated results for the hysteresis loops matched qualitatively well with the experimentally obtained ones. The MFM images revealed well-defined periodic domain structures which can be ascribed to the anisotropies such as magnetic uniaxial anisotropy, configurational anisotropy, etc. We observed that the magnetization reversal of such a system proceeds through the formation and the annihilation of domains. The observed changes in the magnetic properties are closely related to the patterning that hinders the domain-wall motion.

SL09

Diffracted magneto-optical Kerr effect of Co anti-dot structure in different arrangements

H. Y. Zheng¹, N. G. Deshpande¹, X. R. Jin¹, J. Y. Rhee², K. W. Kim³ and Y. P. Lee^{1*}

¹ Physics, Hanyang University, Korea

² Physics, Sungkyunkwan University, Korea

³ Information Display, Sun Moon University, Korea

To fulfill the increasing requirement for the miniaturization of magnetic materials, the effective extraction of information from the nano-scale structures becomes hot issue. Some of techniques, such as diffracted magneto-optical Kerr effect (DMOKE), magnetic-force microscopy and Lorentz scanning transmission electron microscopy, have been utilized to read the magnetic information. As a derivative technique of MOKE, which can be applied in describing the magnetic hysteresis loops, the DMOKE provides us more unique performance, since the diffracted light is more sensitive to the change of the magnetization distribution in magnetic material. Micromagnetic simulation is also a useful method to study the process of magnetization reversal. In order to get the distribution of magnetization, the Object Oriented Micromagnetic Framework (OOMMF) program with periodic boundary condition was employed. By combining DMOKE and the micromagnetic simulation, we can theoretically and experimentally get more exact magnetic information. We investigated the transverse DMOKE and the magnetization-reversal process in rhombic and square lattice arrangements of Co anti-dot structures. The hysteresis loops of the diffracted beams are described by the magnetic form factor. The shape of hysteresis loops of the diffractions, especially, at the points of inflection of the loop, is expected to indicate a special distribution of magnetization.

SL10

Monodisperse magnetic nanoparticles: effects of surfactant concentration on the reaction between Fe(acac)3 and Pt(acac)2

Komkrich Chokprasombat^{1*}, Pimphaka Harding¹, Chitnarong Sirisathitkul¹, Pongsakorn Jantararana², Sujitra Chandarak³ and Rattikom Yimmarun⁴

¹ School of Science, Walailak University, Thailand

² Department of Physics, Kasetsart University, Thailand

³ School of Ceramic Engineering, Institute of Engineering, Suranaree University of Technology, Thailand

⁴ School of Physics, Institute of Science, Suranaree University of Technology, Thailand

Magnetic properties of monodisperse nanoparticles for ultrahigh density recording and biomedical applications are sensitive to their shape and size distributions. These attributes are, in turns, dictated by several parameters during the synthesis and heat treatments. In this work, monodisperse magnetic nanoparticles with size of around 4-5 nm were synthesized by the modified polyol process with 1.0 mmol Fe(acac)3 and 0.5 mmol Pt(acac)2 as starting materials. The as-synthesized nanoparticles were transformed from their superparamagnetic phase to the ferromagnetic state by annealing in argon atmosphere at 570 C for 1 hour. Without any reducing agents, concentration of surfactants (oleic acid and oleylamine) of 1.5 - 4.5 mmol affected morphology and magnetic properties of the nanoparticles. When 2.5 mmol of each surfactant was used, the as-synthesized nanoparticles have the smallest variations in size and shape. However, the higher concentration of oleic acid and oleylamine led to a higher coercivity in annealed nanoparticles which are related to the size distribution. These results indicated that the appropriate amount of surfactants must be used in order to optimize the size distribution and magnetic hysteresis of nanoparticles.

SL11

Hollow MnCO₃ and MnSiO₃ nanospheres

Zvonko Jaglicic¹, Jin Bae Lee², Hae Jin Kim² and Janez Dolinsek³

¹ Dept. of Physics, Institute of Mathematics, Physics and Mechanics & University of Ljubljana, FGG, Slovenia

² Division of Materials Science, Korea Basic Science Institute, Daejeon 305-333, Korea

³ Condensed Matter Physics, J Stefan Institute, University of Ljubljana, Jamova 39, SI-1000 Ljubljana, Slovenia

Magnetic nanoparticles can be used in many different applications ranging from medicine, electromagnetic wave detectors to digital information storage. Hollow nanospheres offers additional functionality. For example they show improved electrochemical performance for batteries or can be used for drug delivery. We synthesised MnCO₃ and MnSiO₃ hollow nanospheres with a diameter of few nanometers and thickness of only few atomic layers. In the MnSiO₃ hollow nanospheres a small concentration of Mn₂O₄ was detected from magnetic measurements. Its strong ferrimagnetic signal at TN = 42 K suppressed the signal of intrinsic magnetic properties of MnSiO₃ nanospheres. On the other hand in the MnCO₃ nanospheres no Mn₂O₄ was detected which enable us to study their dc and ac magnetic properties. The Neel temperature at around 33.5 K is between the reported values for MnCO₃ single crystal (34.3 K) and powder sample (31.0 K)[1]. A coercive field and remanent magnetization of MnCO₃ nanospheres measured at 5 K are decreased in comparison to the bulk system.

[1] J. Kosterov, T. Frederichs, T. von Dobeneck, *Physics of the Earth and Planetary Interiors* 154 (2006) 234-242.

SL12

Shape-controlled synthesis and magnetic properties of FePt nanocubes

Mingge Zhou^{1*}, Wei Li², Minggang Zhu², Dong Zhou² and Yanglong Hou³
¹ Division of Functional Materials, Central Iron and Steel Research Institute, China
² Central Iron and Steel Research Institute, China
³ Department of Advanced Materials and Nanotechnology, College of Engineering, Peking University, China

In this article, synthesis of monodisperse iron-platinum (FePt) nanoparticles by reduction of platinum acetylacetonate followed by thermal decomposition of iron pentacarbonyl in the presence of oleic acid and oleylamine stabilizers is reported, Particle shape is controlled by the addition of Mo(CO)₆, our synthesis yields particles with shapes that are close to cubic and their size can be controlled from 7 to 10 nm, In order to form FePt film, Then the self-assembly FePt nanocubes were annealed at 700 °C for an hour did the FePt nanoparticle transform to the fct phase.The phase analysis, structure, and magnetic properties were determined by X-ray diffraction (XRD), High resolution transmission electron microscope (HRTEM), Scanning electron microscope and vibrating sample magnetometer (VSM) techniques.

SL13

Magnetic properties of NiO/Ni(OH)₂ core-shell nanostructures

Mangesh B. Mahajan and P. A. Joy*
 Physical and Materials Chemistry, National Chemical Laboratory, Pune, India

Antiferromagnetic materials show interesting and anomalous properties when their size is reduced to nanodimensions. The magnetic susceptibility is increased with decreasing particle size(1). Bulk NiO is antiferromagnetic and recent studies showed that NiO nanoparticles exhibit aging and memory effects similar to that of spin glasses(2). The finite size and surface effects play major role in determining the magnetic behaviour of these nanoparticles(3). We have synthesized NiO nanoparticles by a simple chemical route followed by calcination. The freshly prepared sample was dispersed in water, then filtered and dried in air to get NiO/Ni(OH)₂ core-shell type nanostructures. These nanostructures were characterized by using different techniques and magnetic properties using SQUID-VSM. Magnetic properties of nanoparticles of NiO, Ni(OH)₂, and NiO/Ni(OH)₂ have been compared to study the effect of Ni(OH)₂ layer on NiO. Low temperature M-H curves showed considerable difference in the coercivities and saturation magnetization values of the core-shell structure. From ZFC and FC measurements it is observed that magnetic behaviour of the NiO/Ni(OH)₂ core-shell nanoparticles differs substantially from that of bare NiO and Ni(OH)₂ nanoparticles. The observed changes are explained in terms of lower size of NiO core and the effect of different inter-particle interactions with and without the hydroxide layer.

1. J. T. Richardson and W. O. Milligan, Phys. Rev. 102, 1289 (1956). 2. S. D. Tivari and K. P. Rajeev, Phys. Rev. B, 72, 104433 (2005). 3. R. H. Kodama, Salah A. Makhlouf and A. E. Berkowitz, Phys. Rev. Lett. 79, 1393 (1997).

SL14

Structural and magnetic properties of MFe₂O₄ (M=Ni, Mg) nano hollow spheres

K. Konishi^{1*}, T. Sakurai¹, Y. Nagano², N. Manabe² and Y. Morimoto²
¹ Department of Physics, Graduate School of Science and Engineering, Ehime University, Japan
² Department of Physics, Faculty of Science, Ehime University, Japan

Hollow sphere structures have recently received considerable attention because of their novel interior geometry and surface functionality. In this report, sub-micrometer-sized hollow spheres assembled from ferrite nanoparticles have been prepared by a wet chemical process. Measurements of dc-susceptibility and magnetization were carried out on samples of MFe₂O₄ (M= Ni, Mg) nanoparticles with average diameter 4-5 nm, and hollow spheres (500 nm in diameter) with about 12-17nm thickness shell. A superparamagnetic-type blocking process is observed in the ZFC and FC magnetization and magnetic susceptibility for all samples. Furthermore, a behavior due to surface spin freezing of nanoparticles is found in Ni-ferrite. The surface spin freezing temperatures T_f are quite lower than the blocking temperature, and the magnetic field dependence is different between nanoparticle and hollow sphere. The spin-glass nature of Ni-ferrite nanoparticle is demonstrated by the magnetic field dependence of T_f following the well known Almeida-Thouless line. In contrast, T_f (H) of Ni-ferrite hollow sphere hints at failure of Gabay-Toulouse theory as well as the AT type.

SL15

Magnetization reversal in patterned arrays of (001)Fe particles

Maj Hanson^{1*}, Rimantas Brucas² and Erik Wahlstrom³
¹ Department of Applied physics, Chalmers university of technology, Sweden
² Department of Engineering Science, Solid State Physics., Uppsala University, Sweden
³ Institutt for fysikk, NTNU, Norway

Arrays of elliptical Fe particles prepared by patterning [1] of epitaxial (001)Fe films may serve as model systems for studies of the processes of magnetization reversal in sub-micron size particles. In this work we studied such systems with film thicknesses in the range between 10 nm and 50 nm. Ellipses with aspect ratio 1:3 were prepared with their short axes being 50, 100 and 150 nm and varying inter-particle distances. The magnetic domain state and the magnetization reversal of individual particles were investigated by magnetic force microscopy (MFM) and micromagnetic calculations. Magnetization curves of the arrays, comprising about 106 particles, were measured with an alternating gradient force magnetometer (AGM). Within the range of actual sizes we find that the largest particles may be left in a multi- or bidomain (MD) state after demagnetization whereas the smallest show single-domain (SD) properties. In particular we analyze the influence of interactions and the transition from MD to SD behaviour as displayed in the shape of the hysteresis curves and in the MFM images taken after remanent demagnetization. The single particle properties are compared with results from micromagnetic calculations.

1. M. Hanson et al. JAP 85 (1999) 2793

SL16

Controllable structure and magnetic properties of cobalt nanowires by tuning deposition voltage

Xiu Xiu Fan¹, Hai Ning Hu² and Zhong Shi^{3*}
¹ Surface Physics State Laboratory and Department of Physics, Fudan University, China
² School of Mathematics and Physics, Shanghai University of Electric Power, China
³ Department of Physics, Tongji University, China

Magnetic properties of Co nanowires have been shown to be controlled by various growth parameters. The deposition voltage shows great convenience in controlling microstructure. Reported results were mostly focused on low voltages[1-4]. In this work, Co nanowires were fabricated into ordered AAO templates by dc electrodeposition in a wide range of deposition voltage at 20°C. With deposition voltages of 2.0 and 4.5 V, Co nanowires are of hcp(100) and fcc(220) along the nanowire-axis, respectively. Two structures coexist for medium voltages. For all samples, the easy axes of magnetocrystalline (K_{mc}) and shape (K_{sh}) anisotropy make angles to each other. For low voltages, K_{mc} and K_{sh} are close to each other, resulting in small coercivity H_{c(∥)} and H_{c(⊥)} for H parallel and perpendicular to nanowire-axis. Since K_{mc} is one order smaller than K_{sh} and thus the easy-axis lies along the nanowire-axis for high voltages, large H_{c(∥)} is obtained at room temperature. For low and high voltages, H_{c(∥)} first decreases and then increases with a minimum at 200 K, and increases monotonically with T increasing from 50 to 390 K[5], respectively. The angular dependence of H_c shows a combined magnetic reversal process which can be described by curling and/or transverse domain wall modes[6].

1. H. Zeng, R. Skomski, and et al., Phys. Rev. B 65, 134426 (2002); 2. H. Zeng, M. Zheng, and et al., J. Appl. Phys. 87, 4718 (2000); 3. H. Pan, B. Liu, and et al., J. Phys. Chem. B 109, 3094 (2005); 4. X. H. Han, Q. F. Lu, and et al., J. Phys. D: Appl. Phys. 42, 095005 (2009); 5. J. Sanchez-Barriga, M. Lucas, and et al., Phys. Rev. B 80, 184424 (2009); 6. M. Vázquez and L. G. Vivas, physica status solidi (b) 248, 2368 (2011).

SL17

Magnetotransmission effect in Nd_{0.5}Sr_{0.5}MnO₃ nano-composites

Elena Mostovshchikova, Natalya Loshkareva, Andrey Telegin*, Nikolay Solin, Sergey Naumov and Sergey Telegin
 Institute of Metal Physics UD of RAS, Russia

Magnetic and optical properties of composites on the base of Nd_{0.5}Sr_{0.5}MnO₃ powders diluted in dielectric matrix have been studied. Nd_{0.5}Sr_{0.5}MnO₃ manganite is interesting due to existence of two different type of phase transitions: the first one is from paramagnetic semiconductor to the FM metallic state near TC= 250 K, the second one is from the FM metallic state to CE-type AFM insulating state with charge ordering near TCO=160 K [1]. The giant negative magnetotransmission effect (relative change of natural light transmission under the magnetic field) up to 14% in the field H = 0.8 T was revealed for Nd_{0.5}Sr_{0.5}MnO₃ composites near TC in the infrared range. The charge ordering and AFM state may be destroyed by decreasing of grains to nanoscale size [2] resulting in appearing of new effects. The remarkable feature of Nd_{0.5}Sr_{0.5}MnO₃ nano-composite with average grain size about 100 nm is an existence of significant magnetotransmission about 7% in the wide temperature range near and far below TC. It was explained by the significant contribution of nano-particle shells with disordered spins to the magnetic properties of nano-composite. Finally, such a composite material is a promising candidate for future magneto-optical applications [3].

[1] H. Kawano, R. Kajimoto, H. Yoshizawa, Y. Tomioka, H. Kuwahara, and Y. Tokura. Phys. Rev. Lett. 78, 4253 (1997) [2] R.H. Kodama. JMMM 200, 359 (1999); R.H. Kodama and A.E. Berkowitz. Phys. Rev. B 59, 6321 (1999) [3] A.B. Granovsky, Yu.P. Sukhorukov, A.V. Telegin et al., J. of Experimental and Theoretical Physics, 112, No1, 77 (2011)

Supported by the program of DPS RAS "Physics of new materials and structures", grant MK-1048.2012.2 and RFBR grants No 10-02-00038, 11-02-00252, 12-02-00208

SL18

Influence of asymmetric permalloy ring on magnetization configuration and switching behavior

Chao-hsien Huang^{1*}, Lance Horng¹, Nian-jia Cheng², Tian-chiuan Wu³ and Jong-ching Wu¹
¹ Department of Physics, National Changhua University of Education, Taiwan
² Institute of photonics, National Changhua University of Education, Taiwan
³ Department of Electronic Engineering, National Formosa University, Taiwan

By introducing an inner circle shifted along the diameter of outer circle, an asymmetric ring and the asymmetric ratio (R) are defined to control over the vortex state (flux-closure state) nucleation and annihilation field in asymmetric Permalloy (Py) rings. Series of asymmetric Permalloy rings with different diameter and asymmetric ratio were prepared to observe the magnetic switching behavior and the magnetization configuration. The asymmetry of Py rings with thickness of 20 nm, outer diameter (Do) of 300, 500, 800 nm, inner diameter (d) of 100, 150, 200, 250, 300 nm, and shift length (S) of 30, 50, 70, 100, 120, 150 nm. Numerical micromagnetic simulations are carried out using the object-oriented micromagnetic framework (OOMMF) software. With applied field from the positive to negative magnetic field, the magnetic field at which the vortex nucleate in the Py ring is defined as the nucleation field (H_n). The annihilation field (H_a) is the magnetic field where the vortex annihilate. Linear relations of vortex state nucleation and annihilation fields to asymmetric ratio were found, and are useful mainly for controlling the nucleation and annihilation fields.

1. P. Vavassori, R. Boventia, V. Metlushko and B. Ilie, J. Appl. Phys. 99, 053902 (2006) 2. E. Saitoh, M. Kawabata, K. Harii, H. Miyajima and T. Yamaoka, J. Appl. Phys. 95, 1986 (2004) 3. X. H. Wang, W. K. Peng, and W. S. Lev, J. Appl. Phys. 106, 043905 (2009) 4. A. Subramani, D. Geerapuram, V. Baskaran, J. Friedlund, and V. Metlushko, Physica C 437-438, 293 (2006) 5. F. Giesens, J. Podbielski, B. Boters, and D. Grunler, Phys. Rev. B 75, 184428 (2007)

SL19

Fabrication of high aspect ratio nanoscale magnetic tunnel junction etch mask by oxygen plasma assisted resist trimming

Bongho Kim¹, Daehong Kim¹, Sungwoo Chun¹, Hyungyu Lee¹, Seonjun Choi¹ and Seung-beck Lee^{2*}
¹ Department of Electronic Engineering, Hanyang University, Seoul, Korea
² Department of Nanoscale Semiconductor Engineering, Hanyang University, Seoul, Korea

The development of large-area, nanostructure patterning with high aspect ratios is a challenging problem that must be addressed for potential applications in high performance nanoscale devices[1]. When negative resist pillar patterns are formed using electron beam lithography,the forward and backward scattering of the electrons limit the resolution therefore, the resist layer should be thinner. When the patterned resist pillars were used as dry etching masks, the resist polymer during the process requires the pillars to have high aspect ratio. Also,due to chemical processing, high aspect ratio resist pillars have a high probability of falling over due to capillary forces on the pillars[2]. We report on a simple method to overcome the low aspect ratio and the collapse of resist by using oxygen plasma assisted resist trimming.Firstly,We used 170 nm thick negative electron beam resist and patterned 55 nm dot arrays using 80 kV electron-beam.Next, resist trimming process was done using oxygen plasma ashing at 50 W and 0.1 Torr for 70 seconds.This process resulted in 5 nm trimming in all direction. Therefore the 70 s ashing resulted in a 30 nm diameter and 145 nm tall resist pillar increasing the aspect ratio from 3 to 5, which is about 70 % increase.

[1] Hwan-Jin Jeon, Kyoung Hwan Kim., Nano Lett. 2010, 10, 3604-3610 [2] Toshihiko TANAKA,Mitsuaki MORIGAMI,Nobufumi ATODA., Jpn. J. Appl. Phys. Vol. 32 (1993) PP6059-6064

SL20

Magnetic properties of iron(III) oxide nanostructures by hydrothermal synthesis

Raquel A Ribeiro*, Allan M Xavier and Flavio L Souza
 Centro de Ciencias Naturais e Humanas, Universidade Federal do ABC - UFABC, Brazil

The hydrothermal synthesis of nanoparticles enables functional control on the distribution of particle size, morphology and crystallinity by controlling the synthesis parameters. The synthesis of nanoparticles of iron oxide by this method was performed by raising the temperature of a autoclavable bottle containing a solution of iron(III) chloride, sodium nitrate and hydrochloric acid in appropriate quantities. Iron oxide powders synthesized under conditions previously published in the literature were treated in a box furnace at temperatures of 390, 450, 550 and 800 °C. For these samples we performed structural, morphological and magnetical characterization. The images of transmission electron microscopy provide evidence that the 1D nanostructures of iron(III) oxide, are joined by surfaces with non-oriented crystallographic planes, suggesting that the growth of these particles occurs by oriented coalescence. After heat treatment a phase transition occurs from akaganite to hematite. Magnetization measurements show that akaganite presents weak magnetic behavior, whereas the hematite phase presents a larger remnant magnetization and coercive field. We thank the support of Brazilian agencies FAPESP and CNPq.

SL21

Magnetic dot-antidot lattice for control of magnetic anisotropy

Sadashivaiah Sakshath*, Kalappattil Vijaysankar, Karki S Bhagyashree, Subray V Bhat and P. S. Anil Kumar
 Department of Physics, Indian Institute of Science, Bangalore, India

The magnetic anisotropy of epitaxial Fe/GaAs(100) films varies with thickness of the film.[1, 2] We have prepared rectangular lattices of antidots using epitaxial 35 monolayer (ML) Fe/GaAs(100) films deposited by Pulsed laser deposition in an ultrahigh vacuum chamber whose base pressure was less than 2expt(-10) Torr. 10ML MgO/35ML Fe/GaAs(100) film was controllably etched to reduce the thickness of lithographically defined regions of the Fe film to 19ML and capped with MgO before liftoff. Thus square antidot regions of size 200nm containing Fe of thickness lower than the surrounding matrix were created. Thus we have created a 2 dimensional magnetic system having a uniform material composition but controlled lateral variation of local magnetic anisotropy. The spacing between the antidot regions is varied from ~ 200nm to 400nm. Investigations of magnetic anisotropy on the dot-antidot bilayer were performed using Magneto-Optical Kerr effect in longitudinal configuration and Ferromagnetic Resonance. Anisotropy constants are evaluated and it shows that the ratio of the magnitude of the uniaxial anisotropy to the magnitude of the four fold anisotropy is much higher (0.96) in the dot-antidot bilayer even with a square lattice. This is discussed in terms of exchange coupling between the antidot region and the surrounding matrix.

[1] G. Wastlbauer and J. A. C. Bland, Adv: Phys. 54, 137 (2005) [2] S. Sakshath et al, J. Appl. Phys. 109, 07C114 (2011)

SL22

Effect of diameter of the wires on magnetic properties of electrodeposited CoNiP hard magnetic nanowires

Tuan Tu Le^{1*}, Pham Hong Quang¹, Luu Van Thiem², T.s. Ramulu³ and Cheolgi Kim³
¹ Faculty of physics, University of Science, Vietnam National University, 334 Nguyen Trai, Thanh Xuan, Hanoi, Viet Nam
² Faculty of Engineering Physics and Nanotechnology, College of Technology, Vietnam National University,144 Xuan Thuy, Caugiay, Hanoi, Viet Nam
³ Department of Materials Science and Engineering, Chungnam National University, Daejeon 305-764, Korea

The magnetic properties in CoNiP nanowires arrays with diameter of nanowires in range of 50-800nm were investigated. All the samples were prepared by electrodeposition method with pH of 3.1 and room temperature. The electrochemical potential of CoNiP were determined by cycle voltammetry. The crystalline structure and morphology of the samples were characterized by X-ray diffraction (XRD) and Scanning Electron Microscopy (SEM), respectively. The hysteresis loops were measured at room temperature using vibrating sample magnetometry (VSM) and alternating gradient magnetometry (AGM) with magnetic field applied perpendicular and parallel to the wire axis. The mixture of fcc and hcp polycrystalline phases of the CoNiP based nanowires has been indicated by the XRD pattern. The obtained results show that with 800 nm of diameter of the nanowires we can obtain maximum coercivity value (2070 Oe). The uniaxial anisotropy values dependent on diameter of the wires are calculated. The anisotropy of the samples are quasi-one-dimensional anisotropic is also found when diameter of the wires are less than 500 nm.

[1] J. Fert, L. Piraux, Journal of Magnetism and Magnetic Materials 200 (1999) 338 [2] Shan Guan and Bradley J. Nelson, Journal of The Electrochemical Society, 152 (4) (2005) C190 [3]R.N. Emerson, C. Joseph Kennedy, S. Ganesan, Thin Solid Films 515 (2007) 3391 [4] P. Cojocaru, L. Măgarescu, E. Gómez, E. Văles, Journal of Alloys and Compounds 503 (2010) 454 [5] Takamasa Ouchi, Naofumi Shimano, Takayuki Homma, Electrochimica Acta 56 (2011) 9575

SL23

Switching behavior of lithographically defined grid of permalloy nanowires studied with magnetoresistance

Venkateswarlu Dasari, Vineeth Mohanan Parakkat and Anil P. S. Kumar
 Physics, Indian Institute of Science, India

We report the switching behavior of a grid [1] of permalloy nanowires fabricated using e-beam lithography and DC-magnetron sputtering followed by lift-off process. The wires are of 20 nm thickness and about 120 nm wide. The periodicity between the wires is maintained at one micron throughout the grid. The grid is made as a Hall bar geometry which consists of few hundreds of junction regions. The magnetoresistance study indicate that the node regions in the grid acts as defects in the horizontal wires in longitudinal magnetic field, which in turn leads to the nucleation of domains. Thus, the switching process in the horizontal wires is governed by these defect centers [2]. The switching field varies from 80 Oe to 140 Oe for transverse to longitudinal magnetoresistance. The non zero coercivity (80 Oe) in transverse magnetoresistance is due to the presence of nodes. These nodes possess four-fold anisotropy with easy axes along the diagonal directions. Further, the micro-magnetic simulations using Object Oriented Micro Magnetic Framework (OOMMF) with the two dimensional periodic boundary condition, gives the information about the domain configuration which supports our experimental findings.

1. S. P. Li, A. Lebib, D. Peyrade, M. Natali, Y. CheN, W. S. Lev and J. A. C. Bland J. Appl. Phys. 90, 521 (2001) 2. A. O. Adeyeye and M. E. Welland, J. Appl. Phys. 92, 3896 (2002)

SL24

Magnetization reversal modes in narrow FePt nanowires with high perpendicular anisotropy

Van Dai Nguyen¹, Laurent Vila¹, Matthieu Tissier², Alain Marty¹, Murat Cubukcu¹, Piotr Laczkowski¹, Williams Savero-torres¹, Juan-carlos Rojas Sanchez¹ and Jean-philippe Attane¹
¹ *Universite Joseph Fourier, BP 53, 38041, Grenoble and INAC/CEA Grenoble, France*
² *LPTMC, CNRS-UMR 7600, Universite Pierre et Marie Curie, boite 121, 4 Pl. Jussieu, 75252 Paris Cedex, France*

In this contribution, we present the dependence of magnetization reversal modes in FePt nanowires with the width ranging from 2000 nm to 30nm using magneto-transport and magnetic force microscopy (MFM) measurements. Magneto-transport measurements showed an enhancement of magnetic coercivity when reducing the width. Theoretical calculations suggest that this coercivity increase is not only due to the suppression of available propagation paths but also to the contribution of the roughness. Further study of the magnetization reversal process using MFM shows that three different reversal modes can appear. Indeed, for widths above 500 nm, the structure of the reversed magnetic domains appears to be similar to those of the continuous FePt film: the reversed magnetic domain grows and expands within a dendritic structure. For widths below the characteristic dendrite width (~300 nm), the reversal takes place by propagation of a single DW that reverse the whole wire. Finally, we show that another behavior appears at very low widths: when reducing the widths below 50 nm, the propagation field becomes larger than the nucleation field. Nucleation thus occurs randomly, the reversal consisting in a mix of nucleation and propagation. Such behavior could prevent the use of ultra-narrow wires for DW-based spintronic devices.

J. P. Attane et al., Phys. Rev. B, 84, 144418 (2011) J. P. Attane et al., Phys. Rev. B, 82, 024408 (2010)

SL25

Structural and magnetic behaviour of nanocrystalline CaFe₂O₄

S. N. Dolia*, Arvind Samariya, Arun S. Prasad, P. K. Sharma, M. S. Dhawan and S. P. Pareek
Department of Physics, University of Rajasthan, Jaipur, India

Abstract. Study of the structural and magnetic properties of the nanoparticles of large cation substituted ferrite, CaFe₂O₄ have been reported here. The cubic spinel phase of CaFe₂O₄ could be synthesized effectively in nanocrystalline form of size 5.9 nm using advanced sol-gel method. The sample was then heated at 1000 °C leading to bulk size of orthorhombic structure. Very interestingly, the nanoparticles of CaFe₂O₄ get transformed from cubic spinel structure to its characteristic orthorhombic structure on annealing at 1000 °C. Rietveld profile refinement of the XRD patterns was performed to study the nature of crystal structure. The SQUID magnetization measurements divulged that the nanocrystalline sample is superparamagnetic above the blocking temperature of 150 K whereas the bulk sample is ferromagnetic even at room temperature. The reduction in saturation magnetization in the case of nanoparticles as compared to its bulk counterpart has been explained on the basis that the magnetic moments in the surface layers of a nanoparticle are in a state of frozen disorder. The departure of the field cooled curve from the zero field cooled curves in the moment-versus-temperature plot, further confirmed the room temperature superparamagnetic behavior of the nanocrystalline CaFe₂O₄.

SL26

Magneto-resistance of helimagnetic ordering in single crystal FeGe nanowires

Tae-eon Park¹, Byoung-chul Min¹, Dong-jea Seo², Younho Park¹, Heon-jin Choi² and Joonyeon Chang^{1*}
¹ *Spin Device Research Center, KIST, Korea*
² *Department of Materials Science and Engineering, Yonsei University, Korea*

We report on the synthesis, structural characterization, and magneto-transport of single crystalline FeGe NWs. Transition metal silicides and germanides have attracted a lot of attention because of their chiral cubic helimagnetism as a consequence of the Dzyaloshinskii-Moriya interaction. FeGe is known to have a high Neel temperature and helical spin order with a relatively long period. In addition, one dimensional-confinement of the spin structure might enhance the helical magnetic ordering of FeGe NWs as the nano-confinement often alter or improve the properties. We have synthesized single crystalline FeGe NWs by CVD process without any catalyst. We have investigated the helimagnetic ordering in FeGe NWs by using electrical and magneto-transport measurements. When the magnetic field was applied longitudinal to the NW axis, the signature of the helimagnetism in the FeGe NWs was observed up to near room temperature. The magneto-transport measurements reveal three magnetic states of the FeGe NWs: the helimagnetic state, conical helimagnetic state, and ferromagnetic state. The magnetic transitions from the conical helimagnetic state to ferromagnetic state in FeGe NWs was clearly observed and occurred at much higher field those observed in the bulk FeGe. The relationship between nano-sized confinement and the conical helimagnetic state will be discussed in detail.

SL27

Arrays of interacting ferromagnetic nanofilaments: small-angle neutron diffraction study

Natalia Grigoryeva^{1*}, Sergey Grigoriev², Arseniy Syromyatnikov², Andrey Chumakov², Helmut Eckerlebe³, Kirill Napolskiy⁴, Ilya Roslyakov⁴ and Andrey Eliseev⁴
¹ *Faculty of Physics, Saint Petersburg State University, Russia*
² *Konstantinov Petersburg Nuclear Physics Institute, Russia*
³ *Helmholtz Zentrum Geesthacht, Germany*
⁴ *Moscow State University, Russia*

Magnetic properties of spatially ordered arrays of interacting nanofilaments have been studied by means of small-angle diffraction of polarized neutrons. Several diffraction maxima or rings that correspond to the scattering of the highly ordered structure of pores/filaments with hexagonal packing have been observed in neutron scattering intensity maps. The interference (nuclear-magnetic) and pure magnetic contributions to the scattering have been analyzed during the magnetic reversal of the nanofilament array in a field applied perpendicular to the nanofilament axis. The average magnetization and the interference contribution proportional to it increase with the field and are saturated at H = H_s. The magnetic reversal process occurs almost without hysteresis. The intensity of the magnetic contribution has hysteresis behavior in the magnetic reversal process for both the positive and negative fields that form the field dependence of the intensity in a butterfly shape. It has been shown that this dependence is due to the magnetostatic interaction between the filaments in the field range of H ≤ H_s. A theory for describing the magnetic properties of the arrays of interacting ferromagnetic nanofilaments in the magnetic field has been proposed.

SL28

Magnetic properties of nanometer scale FeCr antidot array system

Shivaraman Ramaswamy and Geo George Philip
Nanotechnology Research Center, SRM University, India

In this work, we have fabricated periodic nanometer scale antidot array of FeCr. The deposition was done using electron beam evaporation. The substrate was first coated with 100nm of a suitable resist (ZEP-520A) using spin coating. Then, the mask was patterned on the substrate using an electron beam attached to field emission scanning electron microscope to generate the necessary pattern. After the development, the FeCr (40nm) was coated onto the resist at 0.1A/s using electron beam evaporation. The antidot pitch was maintained at 400nm and the antidot diameter was found to be 300nm. The magnetic nature of the sample was characterized using vibrating sample magnetometer and the in-plane magnetic anisotropy of the system was investigated using torque magnetometer. Further, the magnetoresistance measurements were taken using an inline four point probe. The results indicate that the antidot array system has a predominant ferromagnetic nature, has an n-fold rotational symmetry with relation to the magnetic anisotropy. The easy axis, the hard axis of magnetization along with the net anisotropic energy has also been determined. All data have been appropriate discussed in the work. The use of antidot array systems for various applications is an intriguing new area of research.

E.R. Spada, G.M.C. Pereira, E.F. Jasinski, A.S. da Rocha, O.F. Schilling, M.L. Sartorelli. Anisotropic magnetoresistance in electrodeposited cobalt antidot arrays. Journal of Magnetism and Magnetic Materials 320 (2008) 253-256. L.J. Heyderman, S. Czekaj, F. Nolting, D.H. Kim, P. Fischer. Cobalt antidot arrays on membranes: Fabrication and investigation with transmission X-ray microscopy. Journal of Magnetism and Magnetic Materials 316 (2007) 99-102. M. Tanaka, K. Iloha, H. Iwamotoa, A. Yamaguchia, H. Miyajimaa, T. Yamaoka Magnetic properties of nanometer-scale FeNi antidot array system. (2006).

SL29

Fabrication of Al-Ni core-shell structured particles via electroless ni plating

Youn-kyoung Baek*, Jung-goo Lee, Sangsun Yang and Chul-jin Choi
Powder & Ceramic Research Division, Korea Institute of Materials Science, Korea

Al alloy powders have been of much interest in recent years due to their various applications such as metallurgical, chemical, paint & pigment industries, aerospace applications due to their lightness in weight and processability. Major research efforts have been made for improving their functionalities by addition or deposition of alloying elements such as Ni and by controlling the structure. However, it is difficult to fabricate these alloy powders by traditional metallurgical process and it is necessary to evolve new methods. Core-shell structured particles are attracting considerable attention as a consequence of their potential application in different areas of science and technology. Functionalizing the Al core with suitable shell materials indeed opens the door to specific physical, chemical and optical performances of Al. However, due to the oxide layer present on Al surface, it is difficult to plate Al with any metal or metallic base surface coating by post wet deposition techniques. Thus, we fabricated Al-Ni core-shell structured powders using electroless Ni plating. The pre-treatment was conducted for the formation of Ni shell as well as removal of the oxide layer. The formation of Ni shell on Al core powder was confirmed by SEM, XRD and VSM results.

SM01

Breakdown of barkhausen critical scaling behavior with increasing domain wall pinning in fe thin films

Hun-sung Lee¹, Kwang-su Ryu², Chun-yeol You³, Kun-rok Jeon¹, Stuart S. P. Parkin² and Sung-chul Shin^{1*}
¹ *Korea Advanced Institute of Science and Technology (KAIST), Daejeon 305-701, Korea*
² *IBM Research Division, Almaden Research Center, San Jose, CA 95120, USA*
³ *Department of Physics, Inha University, Incheon 402-751, Korea*

We report a breakdown of Barkhausen critical scaling behavior in Fe films with increasing domain wall pinning by means of a Kerr microscope, capable of direct domain observation. From the the domain reversal patterns in the films, we find that the Barkhausen jump size generally decreases with increasing Fe thickness, showing the increased domain wall pinning density. Surprisingly, the power-law scaling behavior of Barkhausen jump size distribution gradually disappears as pinning of domain walls in the Fe layer increases. This is due to the fact that magnetization reversal mechanism is changed from a random Barkhausen avalanche dominant mode to thermally activated domain wall creep dominant mode.

SM02

Enhanced critical fields in MnSi thin films

Dirk Menzel*, Josefin Engelke, Tommy Reimann and Stefan Suellow
Institute for Condensed Matter Physics, Technische Universitaet Braunschweig, Germany

The magnetic properties of the cubic helimagnet MnSi are governed by the Dzyaloshinskii-Moriya interaction which in the bulk stabilizes a helical ground state below 29 K with a spin-helix wavelength of 18 nm and a propagation vector along the [111] direction. Recently, MnSi has attracted a lot of attention after a skyrmion lattice had been discovered in the so called A-phase. We have prepared thin MnSi films on Si(111) substrate by alloying a single Mn layer into the substrate as well as by codeposition of Mn and Si. RHEED analysis in combination with TEM investigation reveals that codeposition leads to smooth films whereas the alloying process generates rather three dimensional MnSi islands. In comparison to bulk material, the films show an enhanced magnetic ordering temperature of 45 K, which has been determined using SQUID magnetometry. Magnetization, resistivity, magnetoresistance, and Hall effect measurements have been performed on the films. They show that the critical fields describing the transition from the helical to a conical spin phase and from the conical phase to a parallel spin alignment are dependent on the film thickness and enhanced in comparison to single crystalline MnSi.

SM03

Magnetism and Cr₂O₃-Fe₂O₃ structure of CoFe/Cr-NOL surface

Naoki Shimomura^{1*}, Kazuya Sawada², Tomohiro Nozaki¹, Masaaki Doi³ and Masashi Sahashi¹
¹ *Department of Electronic Engineering, Graduate School of Engineering, Tohoku University, Japan*
² *Toshiba Corporation, Japan*
³ *Tohoku Gakuin University, Japan*

Magnetolectric (ME) effect has been investigated for realizing electric controlled spintronic device, such as MERAM. Cr₂O₃ is the most promising material for the application due to high Neel temperature (TN : ~307K). Switching exchange bias field by applying electric field using bulk Cr₂O₃ (0.6mm) has been reported [1]. Recently, we have observed high blocking temperature (TB : ~250K) of CoFe/Cr-NOL (Nano-Oxide-Layer) containing Cr₂O₃ and Fe₂O₃ (TN ~ 950K) in its surface, in spite of the ultrathin thickness (less than 1nm). The NOL is prepared by Natural Oxidation (N.O.) of CoFe and ultrathin (1ML) Cr layer [2]. To clarify the reason of high TB of the NOL is important for achieving thin Cr₂O₃ film that shows ME effect higher than room temperature. In this study, we have investigated the structure and magnetic property of CoFe/Cr-NOL by varying constitution condition, such as deposition system and N.O. intensity. It was found that mixing of Cr into CoFe layer before N.O. and high N.O. intensity cause the formation of Cr₂O₃-Fe₂O₃ solid solution in NOL surface, which lower the TB. It is indicated that the presence of not Cr₂O₃-Fe₂O₃ solid solution but the existence of both Cr₂O₃ and Fe₂O₃ is needed for high TB.

[1] Xi He, Yi Wang, Ning Wu, Anthony N. Caruso, Elio Vescovo, Kirill D. Belashchenko Peter A. Dowben, and Christian Binck, Nature Mater 9, 579 (2010). [2] K. Sawada, N. Shimomura, M. Doi, and M. Sahashi, J. Appl. Phys 107, 09D713 (2010).

SM04

Magnetic phase diagram for non-epitaxial Cr/Gd/Cr-multilayers

Andres Rosales Rivera^{1*}, Juan Fernando Jaramillo¹, Nicolas Antonio Salazar¹, Olatz Idigoras² and Andreas Berger²
¹ *Laboratorio de Magnetismo y Materiales Avanzados, Universidad Nacional de Colombia, Sede Manizales, Colombia, Colombia*
² *CIC nanoGUNE Consolider, Tolosa Hiribidea 76, E-20018 Donostia-San Sebastian, Spain*

In this work, the low-temperature phase and critical behavior at high temperature of inhomogeneous gadolinium-chromium samples were investigated using DC magnetization measurements. The samples were prepared as Cr(50nm)/Gd(100nm)/Cr(50nm) multilayers grown onto Si(110) single crystal substrates by means of sputter deposition. The samples' inhomogeneity was controlled by annealing at different temperatures T_{an} = 200, 400, and 500°C during 10 minutes, and their magnetization was measured using zero field cooling (ZFC) and field cooling (FC) procedures at several applied fields. In the vicinity of room temperature, the magnetic behavior of the samples is compatible with a ferromagnetic ground state, which undergoes a rounded ferromagnetic (F)-paramagnetic (P) phase transition at a critical temperature, T_c. At temperatures below T_c, however, differences between the magnetization measured in the zero field cooling (Mzfc) and field cooling (Mfc) procedures are observed. Mfc decreases with increasing temperature. Mzfc increases with increasing temperature and, in addition to the F-P phase transition at T_c, shows a peak at a certain temperature T_g < T_c. It was also found that Mzfc is time dependent at low field and irreversible below an irreversible temperature T_i(H). A (H,T) phase diagram that contains T_c, T_i(H) and T_g(H) is presented for each of the samples.

SM05

Revealing the volume magnetic anisotropy of Fe films epitaxied on GaAs(001) surface

G. Chen¹, J. Zhu¹, J. Li² and Yizheng Wu³
¹ *Physics department, Fudan university, China*
² *Physics department, Fudan university, China*
³ *Physiscs department, Fudan university, China*

Fe film grown on GaAs(001) is a model system for studying the spin injection from a ferromagnetic layer into the semiconductor substrate. The Fe/GaAs(001) system exhibits a remarkable in-plane uniaxial magnetic anisotropy (UMA) with an easy axis (EA) parallel to the GaAs[110] direction, and such UMA is usually believed to originate entirely from the Fe/GaAs interface. In this contribution, we will show our quantitative studies on the thickness dependent magnetic anisotropy in Au/Fe/GaAs(001) system using the magneto-optic Kerr effect with a rotating magnetic field. Through a clear 1/dFe relation of the UMA, we found a UMA component with the EA parallel to the GaAs direction which originates from the volume contribution. Such volume UMA is sensitive to the growth temperature and also strongly correlate with the interface anisotropy. We can conclude that both the volume anisotropy and the interfacial anisotropy are related to the ordered atomic structure at Fe/GaAs interface. Our results may introduce a new aspect for further understanding the origin of UMA in Fe/GaAs(001) system.

1) G. Chen, J. Zhu, J. Li, F. Z. Liu, and Y. Z. Wu Appl. Phys. Lett. 98, 132505(2011)

SM06

Structures and magnetic properties of ultrathin Ni/Cu(100) in hydrochloric acid

Jyh-shen Tsay*, Chun-liang Lin, An-wei Wu, Ying-chieh Wang and Yu-chieh Tseng
National Taiwan Normal University, Taiwan

Microstructure and magnetic properties of ultrathin Ni/Cu(100) prepared by way of electrochemical approaches are investigated. In a pure supporting electrolyte, the STM image of the chloride covered Cu(100) surfaces show the formation of 90-degree step edges of the terraces as a result of the electrochemical annealing [1]. After adding NiCl₂, the hydrogen evolution reaction is advanced to a more positive potential. Nickel atoms attach onto the steps and the surface shows single atomic steps corresponding to a layer-by-layer growth. As the coverage of Ni increases, large amount of clusters form on the surface. The adsorption of chloride anions occurs on the top of the films [2]. For thin Ni layers, no magnetic hysteresis is observed due to the lowered Curie temperature for ultrathin overlayers. As the Ni coverage increases, hysteresis loop is observed with in-plane anisotropy of the films. For thicker films spin reorientation transition occurs that may be due to the strain relaxation in the Ni overlayer. The high squareness of the magnetic hysteresis loops confirms the smooth interfaces of the Ni films.

[1] S.L. Tsay, et al, Phys. Chem. Chem. Phys. 12, 14950 (2010); [2] P.Y. Yen, et al, J. Phys. Chem. C 115 (2011) 23802.

SM07

Improvement in structural and magnetic properties of laser ablated Ni-Zn Ferrite thin films

Raghavender A T^{1*}, Nguyen Hoa Hong¹, Ekaterina Chikoidze², Yves Dumont² and Kurisu Makio³

¹ Department of Physics and Astronomy, Seoul National University, Korea

² Laboratoire GeMAC, Universite de Versailles, France

³ Department of Physics, Ehime University, Japan

Zinc, as known as non-magnetic element, has been doped into Nickel-Ferrites under thin film form, with a hope to modify its structural and magnetic properties, in order to have the appropriate requirements for high frequency applications. Laser ablated Ni_xZn_{1-x}Fe₂O₄ (0 ≤ x ≤ 1) thin films grown on R-cut Al₂O₃ (0001) substrates using pulsed laser deposition (PLD) technique are single phase with (1 1 1) orientation, and they are room temperature strongly ferromagnetic, while others' similar works reported ferromagnetism only at low temperatures. Additionally, the higher HC value in our films compared to what others reported indicates that somehow we have found an appropriate way to make Ni-Zn ferrites become potential candidates for modern miniaturization of electronic devices. The zero field cooled (ZFC-FC) magnetization curves for all the films shows the blocking temperature (TB) suggesting a strong anisotropy. Research on Ni_xZn_{1-x}Fe₂O₄ (0 ≤ x ≤ 1) thin films would be very promising for device market.

SM08

A basic study of magnetic anisotropy strength control using FeSiB magnetostrictive thin film

Jaewon Shin*, Sung Hoon Kim, Genki Kitazawa, Shuichiro Hashi and Kazushi Ishiyama
Research Institute of Electrical Communication, Tohoku University, Japan

The Magneto-Impedance (MI) sensors are used for various applications [1, 2]. A magnetic anisotropy controlling is important to improve sensitivity of MI sensor. Therefore, our research group proposed a new and simpler method to control magnetic anisotropy using inverse-magnetostriction and difference of thermal expansion coefficient in bimetal thin film[3]. To exploit the proposed method, investigation of a fabrication ratio between two layers (thickness and length) requires due to the sensitivity of proposed MI sensor is determined by changes in fabrication ratio. In this paper, we introduce the changes of magnetic anisotropy field (Hk) strength to develop high and adjustable sensitive MI sensor according to changes in geometrical properties of layers. The thin films were deposited by RF magnetron sputter. Fe₂Si_{1-x}B_x and Molybdenum were used for the magnetic and conductive layer, respectively. The fabricated thin films annealed to release the local stress. We carried out magnetic domain observation by Kerr-microscope. Moreover, Hk value was obtained by VSM. Based on the experiments, we could confirm that Hk value was controlled by the geometrical properties because the geometrical properties can determine the generated stress in the magnetostrictive magnetic layer. This research provides the fabrication range and expectation of the sensitivity of MI sensor.

[1] Y. Murayama, T. Ozawa, S. Ishikami, K. Ishiyama, and K.I. Arii, "High-Frequency Carrier-Type Magnetic Field Sensor with a Sub-pT Resolution Using a Magnetic Film and a Transmission Line," *J. Magn. Soc. Jpn.*, **31**, 17-22, 2007. [2] T. Morikawa, Y. Nishibe, H. Yamadera, Y. Nonomura, M. Takeuchi, and Y. Tago, "Giant Magneto-Impedance Effect in Layered Thin Films," *IEEE Trans. Magn.*, **33**, 4367-4372, 1997. [3] Jaewon Shin, Sung Hoon Kim, Yussaki Sawa, Shuichiro Hashi, Kazushi Ishiyama, "Control of In-plane Uniaxial Anisotropy of Fe72Si48B14 Magnetostrictive Thin Film Using a Thermal Expansion Coefficient," *J. Appl. Phys.* (will be published in April)

SM09

Magnetic properties of co thin films on polyethylene naphthalate organic substrates

Hideo Kaiju*, Tarō Abe, Kenji Kondo and Akira Ishibashi
Research Institute for Electronic Science, Hokkaido University, Japan

Recently we have proposed spin quantum cross (SQC) devices, in which molecules are sandwiched between two edges of magnetic thin films deposited on organic substrates with their edges crossed. According to our recent calculation, SQC devices exhibit large magnetoresistance effect at room temperature. In this study, towards the fabrication of SQC devices, we have investigated magnetic properties and surface morphologies of Co thin films on polyethylene naphthalate (PEN) organic substrates. Co thin films were thermally evaporated on PEN substrates under a magnetic field in a high vacuum chamber. The magnetization curves were measured by focused magneto-optic Kerr effect techniques at room temperature. The surface morphologies were analyzed by atomic force microscope. As a result, the surface roughness decreases from 1.3 to 0.55 nm with increasing the Co thickness up to 55 nm, where a two-step smoothing phenomenon can be seen. As for magnetic properties, the coercive force and the squareness of the hysteresis loop show the maximum values at a Co thickness of 5.3 nm. This peak is due to the rotation of the uniaxial magnetic anisotropy formed from both the induced magnetic anisotropy and the shape magnetic anisotropy affected by the surface morphologies of Co/PEN and PEN substrates.

SM10

Effects of dimensionality on magnetization of Ho and Sm-doped BiFeO₃ thin films

Tae-young Kim^{1*}, Anupati Telugu Raghavender², Sugawara Takashi³, Makio Kurisu³ and Nguyen Hoa Hong⁴

¹ Physics, Seoul National University, Korea

² Physics, Seoul National University, India

³ Physics, Ehime university, Japan

⁴ Physics, Seoul National University, France

BiFeO₃ is promising multiferroic material due to high ferroelectric (1100 K) and antiferromagnetic (650 K) ordering temperatures. Reports of other groups have suggested that by reducing the dimensionality, the spiral magnetic ordering could be suppressed [1]. Thus, multiferroics in thin films and nanocrystalline forms could enhance the magnetic properties [2]. In BiFeO₃, if Bi is substituted by a small amount of divalent or trivalent metal ions, or Fe is substituted by transition metal ion, a significant enhancement in magnetization can be achieved. We have prepared the nanocrystalline RE-BiFeO₃ (RE = Sm and Ho) by using sol-gel method to be target materials for thin films fabrication. RE-BiFeO₃ films were grown on LaAlO₃ substrates using pulsed laser deposition technique. All the films show a single phase of rhombohedral structure with space group R3c. Significant changes in the structural properties were observed as the thickness of the films increases. The magnetization observed in the case of Ho is much higher than those reported in literature and also Sm-doping shows better magnetization values. The magnetization increases as the film becomes thinner. This is a strong evidence for the origin of surface magnetism that exist in the films.

[1] P. Thakuria and P. A. Joy, *J. Appl. Phys.* **97** (2010) 162504. [2] J. Wang, J. B. Neaton, H. Zheng, V. Nagarajan, S. B. Ogale, B. Liu, D. Viehland, V. Vaithyanathan, D. G. Schlom, U. V. Waghmare, N. A. Spaldin, K. M. Rabe, M. Muttar and R. Ramesh, *Science*, **299** (2003) 1717.

SM11

Substrate-dependent electronic anisotropy of epitaxial multiferroic DyMnO₃ and Dy_{0.8}Ca_{0.2}MnO₃ thin films

Kueih-tzu Lu, S. C. Haw, T. L. Chou, J. M. Lee, S. A. Chen and J. M. Chen
National Synchrotron Radiation Research Center, Taiwan

We investigated the substrate-dependent electronic structure and anisotropic bonding of the Mn 3d states in DyMnO₃ and Dy_{0.8}Ca_{0.2}MnO₃ thin films on SrTiO₃(001) and LaAlO₃(110) substrates using polarization-dependent x-ray absorption spectroscopy (XAS) at O K-, Mn L- and Mn K-edges for three polarizations, E || a, E || b and E || c. Polarization-dependent x-ray absorption spectra at O K-, Mn L23- and Mn K-edges of orthorhombic DyMnO₃/LaAlO₃(110) thin films show a strong polarization dependence, whereas orthorhombic DyMnO₃/SrTiO₃(001) thin films show nearly isotropic spectral structure. The main peak in polarized Mn L2,3-edge XAS spectra of DyMnO₃/LaAlO₃(110) thin films for the E || b polarization lies at a lower energy than for polarizations E || a and E || c. This indicates a great anisotropy in Mn 3d-O 2p hybridization, reflecting an orbital ordering and a highly anisotropic coplanar Mn-O bonding in DyMnO₃/LaAlO₃(110) thin films. Orbital ordering of eg-orbital and the highly anisotropic in-plane Mn-O bonding is an indispensable factor to the formation of complicated incommensurate modulated magnetic structures observed in orthorhombic DyMnO₃. The present results provide important implications for the microscopic understanding of the multiferroic DyMnO₃.

SM12

Enhanced magnetization by substitution of Zn²⁺ in Fe₃O₄ films

Chang-yup Park¹, Jong-hyun Song², Chun-yeol You³ and Sung-chul Shin^{4*}

¹ Department of Physics and Center for Nanospinics of Spintronic Materials, Korea Advanced Institute of Science and Technology, Daejeon 305-701, Korea

² Department of Physics, Chungnam National University, Daejeon 305-764, Korea

³ Department of Physics, Inha University, Incheon 402-751, Korea

⁴ Department of Physics and Center for Nanospinics of Spintronic Materials, KAIST, Daejeon, Department of Emerging Materials Science, DGIST, Daegu, Korea

Fe₃O₄ is one of the key materials as efficient spin injector for spintronic device. Thereby considerable researches have been carried out to obtain high magneto resistance ratio (MR), however no report show enough MR because of interface concerned problems and uncertainty of half metallic identity itself. Hence we choose Fe₃O₄ to investigate its nature and enhancement of magnetic and electric properties by substitution of Zn²⁺ ion. Firstly we carried out magnetization hysteresis loop measurement by means of alternating gradient magnetometer. To find out a role of Zn substitution, we fabricated Fe_{3-x}Zn_xO₄ film and the saturation magnetization strikingly enhanced to 283 emu/cc from 79 emu/cc of the epitaxial Fe₃O₄ film. We believe that the 3.6 times enhancement is ascribed to the substitution of Zn²⁺ ion instead of Fe ion at tetrahedral A site which spin is antiparallel to that of Fe ion at octahedral B site in inverse spinel structure of Fe₃O₄.

SM13

Growth temperature dependence of crystal orientation and magnetic properties of CoMn₂O₄ thin films

Taeyoung Koo¹, Jaeyoung Kim¹, Sunhee Kang², Illwon Kim², Yoonhee Jeong³, Myunghwa Jung⁴ and Jonghyun Song^{5*}

¹ Pohang Accelerator Laboratory, Korea

² Physics, Ulsan University, Korea

³ Physics, Pohang University of Science and Technology, Korea

⁴ Physics, Sogang University, Korea

⁵ Physics, Chungnam National University, Korea

Co₂Mn₂O₄(0≤x≤3), which crystallize in the spinel structure, are strong candidates of multiferroics which can be used in various technical applications due to their thermal, electrical and magnetic properties. In the present work, we report on the growth of epitaxial CoMn₂O₄ thin films on Ni-doped SrTiO₃(001) substrate using Pulsed Laser Deposition and their magnetic properties. With all other growth parameters fixed, the growth temperature (Tg) was changed from 720oC to 920oC. The sample with Tg =720oC shows a strongly tensile strained epitaxial crystal structure with the orientation of (400). The M-H loops shows a ferrimagnetic behavior with the coercive field of ~1.7 T. However, with increasing Tg up to 870oC, the tensile strained crystal domain becomes weaker whereas the domain of mixed orientations of relaxed (400) and (004) appear and has gained predominance. The M-H loops shows a weakened ferrimagnetism compared to the sample with Tg =720oC. With further increasing Tg to 920oC, interestingly, the crystal structure turns to be oriented (004) and the magnetic properties exhibit enhanced saturated magnetization with negligible coercive field. These observations indicate that the growth temperature plays a crucial role in determining the crystal structure and magnetic properties of CoMn₂O₄ thin film.

[1]. V. Eladi, M. R. Ross, L. M. V. Jose, and G. M. Oscar, *Chem. Mater.* **8**, 1078 (1996). [2]. H. T. Zhang and X. H. Chen, *Nanotechnology* **17**, 1384 (2006).

SM14

Structure and magnetic properties of Fe₃O₄ thin films on different substrates by Pulsed Laser Deposition

Xuelian Huang, Yang Yang and Jun Ding*
Materials Science and Engineering, National University of Singapore, Singapore

Magnetite is an attractive magnetic oxide to be used in magneto-transport applications.[1]Many researchers have studied how to optimize the deposition condition for high quality magnetite thin films.[2]In this work,magnetite thin films were deposited on different substrates at temperatures varying from 100°C to 450°C,and their structure,magnetic and magneto-transport properties have been studied. XPS and Raman spectra reveal single phase of Fe₃O₄ on all the substrates. When film thickness is small and temperature is relatively high(>300°C),magnetite thin films on single crystal SiO₂/Si and amorphous glass exhibit strong (111) texture,no matter they have either a huge lattice mismatch or none matching with Fe₃O₄. The (111)texture can be formed at lower temperature(100°C) on (002)-ZnO due to the minimization of both surface and interfacial energy.The films on (0001)-Al₂O₃ show (111)-epitaxial structure in a large temperature range(100-450°C). The saturated magnetization for all the (111)oriented magnetite films are in the reported thin-film range.Magneto resistance up to 4% has been obtained.The out-of-plane MR exhibit quadratic behavior up to 6000 Oe,whereas the in-plane MR is linear in this regime,which suggests the presence of anti-phase boundaries.[3].Large substrate-induced strain was found in the films grown on Al₂O₃ due to the lattice mismatch (8%),which significantly affected the magnetic anisotropy of the thin film.

[1] H. Liu, E. Y. Jiang, H.L. Bai, R.K. Zheng, H.L. Wei, Y.X. Zhang, *Appl. Phys. Lett.* **83** (2003) 3531. [2] S. Kale, S.M. Bhagat, S.E. Loftand, T. Scabarozzi, S.B. Ogale, A. Orozco,S.R. Shinde, T. Venkatesan, B. Hammoy, W. Prellier, *Phys. Rev. B* **64** (2001) 205413. [3] W. Eerenstein, T. T. M. Palstra, S. S. Saxena, and T. Hibma *Phys. Rev. L* **88** (2002) 247204.

SM15

Influence of crystallographic orientation on the magnetic properties of NiFe, Ni, and Co epitaxial fcc films grown on single-crystal substrates

Taiki Ohtani*, Tetsuroh Kawai, Mitsuru Ohtake and Masaaki Futamoto
Chuo University, Japan

NiFe, Ni, and Co crystals with fcc structure are soft magnetic materials and have been used in magnetic thin film devices like magnetic heads and sensors. Magnetic property varies depending on the film texture [1,2]. In the present study, Ni₈₀Fe₂₀ (at. %), Ni, and Co films with fcc (100) and (111) orientations were prepared by hetero-epitaxial growth on single-crystal substrates of GaAs(100) and Al₂O₃(0001). The magnetic anisotropy, the magnetization structure, and the magnetostriction were investigated by employing RHEED, XRD, Bitter, and magnetostriction measurements. NiFe, Ni, and Co films of fcc(100) orientation showed four-fold symmetries in-plane magnetic anisotropy. The easy magnetization axes were parallel to [011] and [01-1] directions. 90° magnetic domain walls were observed for the epitaxial films. The in-plane magnetization properties were reflecting the magnetocrystalline anisotropies of respective bulk fcc crystals. On the contrary, the in-plane magnetization properties were isotropic for NiFe, Ni, and Co films with fcc(111) orientation. In magnetostriction measurement, the magnetostriction behavior of epitaxial magnetic thin film depended delicately on the magnetic domain structure and the domain wall motion under an influence of magnetic field. At the conference, the inter-relationships of magnetic anisotropy, magnetization structure, and magnetostriction will be discussed for these epitaxial thin films.

[1] Y. Nakaga, M. Ohtake, M. Futamoto, F. Kirino, N. Fujita, N. Inaba.: *IEEE Trans. Magn.*, vol. 45, pp. 2519-2522, 2009. [2] M. Ohtake, T. Tanaka, K. Matsubara, F. Kirino, M. Futamoto.: *J. Phys.: Conf. Ser.*, vol. 303, pp. 012015_1-6, 2011.

SM16

Magnetic coupling in manganite-based thin film heterostructures studied by Electron Holography

Luis Alfredo Rodriguez¹, Lorena Marin², Cesar Magen^{3*}, Irene Lucas⁴, Pedro Antonio Algarabel¹, Luis Morellon², Jose Maria De Teresa⁴ and Manuel Ricardo Ibarra¹

¹ LMA-INA, Universidad de Zaragoza, 50018, Zaragoza, Spain

² INA, Universidad de Zaragoza, 50018, Zaragoza, Spain

³ LMA-INA and ARAID, Universidad de Zaragoza, 50018, Zaragoza, Spain

⁴ ICMA, Universidad de Zaragoza-CSIC, 50009, Zaragoza, Spain

Advances in nanofabrication of magnetic nanomaterials leads to search for new tools to measure physical properties at the nanoscale, such as magnetization. Accurate characterization of the magnetization states in nanostructures is of the utmost importance in the development new devices such as magnetic tunnel junctions (MTJs) [1]. Transmission electron microscopy (TEM) techniques such as Electron Holography (EH) allows the quantitative imaging of the magnetization states of ferromagnetic materials with unprecedented spatial resolution at the nanometer level [2]. Furthermore, EH can be combined with the in situ variation of external parameters such as magnetic and electric fields, temperature, etc. In particular, we use a TEM cryo-holder to image magnetization states of ferromagnets with low TC (down to 100 K) while varying in situ the magnetic field applied by the objective lens of the TEM. In this work, we present the EH study of the magnetization switching of La-Sr and La-Ca manganite thin films (TC = 180 and 300 K, respectively) and manganite-based MTJs [3]. The (de)coupling of magnetic electrodes in MTJs is analyzed by performing hysteresis loops at 100 K to determine the switching fields from the direct observation of the magnetization orientation of the electrodes upon magnetic field [4].

[1] S. Yasa et al., *Nat. Mat.* **3** (12): 868-871 (2004); S. P. Parkin et al., *Nat. Mat.* **3** (12): 862-867 (2004). [2] R. E. Demin-Borkowski, M. R. McCartney, D. J. Smith, *Electron Holography of Nanostructured Materials. In Encyclopedia of Nanoscience and Nanotechnology*; Naha, H. S., Ed.; American Scientific Publishers: Stevenson Ranch, California, 2004; Vol. 3, pp 41-100. [3] M. Bowen et al., *Appl. Phys. Lett.* **82**, 333 (2003). [4] E. Jaron, A. Massaboeuf, C. Galet and E. Snoeck, *J. Appl. Phys.* **107**, 09D310 (2010)

SM17

Properties of hybrid superconductor/ferromagnet (SC/FM) multilayers

U. D. Chacon Hernandez¹, Y. T. Xing², William E. Alayo³, Magda B. Fontes⁴, Jorge L. Gonzalez⁵, Liyang Liu⁴, G. Solorzano⁴ and E. Baggio-saitovich¹

¹ Centro Brasileiro de Pesquisas Fisicas, Rio de Janeiro, Brazil, Brazil

² Universidade Federal Fluminense Niteroi, Brazil, Brazil

³ Universidade Federal do Espirito Santo, Vitoria, Brazil, Brazil

⁴ PUC-Rio de Janeiro, Brazil

Recent research on systems that contain two types of materials (hybrid systems) shows that new phenomena can be observed. One of such hybrid systems is superconductor/ferromagnet (SC/FM) nanocomposites, which shows coexistence of superconductivity and ferromagnetism with unusual properties. We use niobium (Nb) as the superconducting layers with fixed thickness (50 nm) and cobalt or permalloy (NiFe) as the ferromagnetic layers with different thickness (5, 10 and 20 nm). The films prepared by magnetron sputtering deposition technique, have been characterized by x-rays diffraction and in some cases the cross section at interface were studied by TEM. Characterization of SC and FM transitions was done by resistivity and magnetization measurements. The properties of superconductor changed at the SC/metal interface because of the proximity effect, for example, decrease of Tc. Moreover, the magnetic layers between superconducting layers will give have more influence on the superconductivity due to its stray field. Our results show that when the external magnetic field is close to the upper critical field Hc2, the SC/FM multilayers can have a vortex solid to a liquid phase transition. We believe that the stray field of the magnetic layers contributes to the melting of the vortex solid state.

[1] A. I. Buzdin, *Rev. Mod. Phys.*, **77**(3):935, 2005. [2] Y. T. Xing, H. Micklitz, T. G. Rappoport, M. V. Milošević, I. G. Solov'yanov, and E. Baggio-Saitovich, *Phys. Rev. B*, **78**(2):224524, 2008. [3] Y. T. Xing, H. Micklitz, W. T. Herrera, T. G. Rappoport, and E. Baggio-Saitovich, *The European Physical Journal B - Condensed Matter and Complex Systems*, **76**:353:357, 2010. [4] E. A. Demler, G. B. Arnold, and M. R. Beasley, *Phys. Rev. B*, **55**(22):15174:15182, Jun 1997. [5] I. A. Garifullin, *Journal of Magnetism and Magnetic Materials*, **240**(1-3):571 - 576, 2002. 4th International Symposium on Metallic Multilayers.

SM18

Effect of substrate on the anisotropic magnetotransport in Sm_{0.45}Nd_{0.10}Sr_{0.45}MnO₃ thin films

Pawan Kumar¹, M. K. Srivastava¹, G. D. Verma², R. K. Dwivedi³ and H. K. Singh¹

¹ Quantum Phenomena and Applications, National Physical Laboratory (CSIR), India

² Department of Physics, IIT Roorkee, India

³ Department of Physics & Materials Science and Engineering, Jaypee Institute of Information Technology (Deemed University), India

Sm_{0.45}Nd_{0.10}Sr_{0.45}MnO₃ thin films on single crystal LAO and STO substrates were prepared by ultrasonic nebulized spray pyrolysis. The PM-FM transition was observed at TC = 153 K and 150 K in film on LAO and STO, respectively. The magnetic moment was found to be smaller in film on STO and it showed stronger bifurcation between the ZFC-FC magnetization. The isothermal M-H loops measured with H applied parallel and normal to the film surface showed that the easy axis was in the film plane, while the hard axis was along the normal. The dominance of the shape anisotropy explains the in-plane magnetic easy axis. Large low field magnetoresistance (MR) is observed in both films. The occurrence of significantly smaller peak anisotropic magnetoresistance (AMR) at a temperature lower than the TIM and the broadening of the AMR-T curve suggest that films on STO have higher fraction of the AFM-CO phase. The difference in the magnetotransport anisotropy in the set of films has been explained in terms of substrate induced strain, e.g., STO provides tensile strain, which is known to favor the AFM-SE and CO-OO phases.

SM19

Magnetism of multilayer (CoNiPsoft/CoPhard)n films

Gennady Patrin¹, Marina Pal'chik², Dmitry Balae², Semion Kiparisov² and Konstantin Patrin²

¹ Siberian Federal University, Russia

² Institute of Physics of Siberian Branch of Russian Academy of Sciences, Russia

The (CoNiPsoft/CoPhard)n films were prepared by chemical deposition method. The content of phosphorus was 8 % at. in each layer. In hard magnetic layer the CoP was in hexagonal state and in soft magnetic layer the CoNiP was in amorphous state. The thickness of each layer was t = 4 nm. Magnetic measurements were made with vibrating-coil magnetometer in temperature range T = 77 ÷ 400 K and in magnetic fields H < 10 kOe. We investigated changes of magnetic parameters in dependence on number of layers in multilayer structure. In our experiments number of layer pairs was n ≤ 15. Earlier [1] it was established that the coercive force (HC) of CoP layers depends on layer thickness and HC rises when layer thickness increases. In given case at nitrogenous temperatures the coercive forces of soft magnetic and hard magnetic layers were ~ 20 Oe and ~ 1000 Oe, respectively. The combination of these layers into structure leads to substantial change of magnetic behavior of structure in whole [2]. It attracts attention that the soft magnetic layer determines the behavior of magnetization of film structure decreasing the coercive force of system.

[1] A.V. Chzhan, G.S. Patrin, et al., Phys. Met. Metalloved., 109 (2010) 1. [2] A.V. Chzhan, G.S. Patrin, et al., Bull. Russ. Acad. Sci. Phys., 76, (2012) 180

SM20

Significant change in the antiferromagnetic-to-ferromagnetic phase transition temperature of epitaxial FeRh thin films by Ga substitution

Ippei Suzuki^{1*}, Mitsuru Itoh¹, Tetsuya Sato² and Tomoyasu Taniyama¹

¹ Materials and Structures Laboratory, Tokyo Institute of Technology, Japan

² Department of Applied Physics and Physico-Informatics, Keio University, Japan

B₂ ordered FeRh alloys exhibit fascinating magnetic properties such as the first-order magnetic phase transition from the antiferromagnetic (AF) to ferromagnetic (FM) states at around 400 K. For a step toward the incorporation of this material into devices, the control of the transition temperature in a thin film form is one of the most critical issues. In this study, we find that Ga substitution in FeRh efficiently reduces the transition temperature down to room temperature, making the use of this material a reality. A 30-nm-thick FeRh thin film and a Ga-substituted FeRh(Ga-FeRh) were epitaxially grown on MgO(001) substrates by molecular beam epitaxy. The temperature dependent magnetization of the epitaxial films clearly demonstrates the reduction of the transition temperature down to room temperature. The change in the transition temperature can be understood in terms of a possible change in the electronic states near the Fermi level due to the lattice expansion, leading to a more stable FM state in Ga-FeRh. In fact, the out-of-plane lattice parameters calculated from the XRD patterns are found to expand from 2.990 to 3.003 Å by the Ga substitution. Work supported in part by Industrial Technology Research Grant Program in 2009 from NEDO, Japan.

SN01

Structural and magnetic properties of Sm₂Co₁₇ nanoflakes prepared by surfactant-assisted ball milling

Ming Yue, Rui Pan, Xiaofei Yin, Dongtao Zhang, Weiqiang Liu and Jiuxing Zhang College of Materials Science and Engineering, Beijing University of Technology, China

Microstructure, crystal structure and magnetic properties were studied for Sm₂Co₁₇ nanoflakes prepared by surfactant-assisted high energy ball milling with heptane and oleic acid as the milling medium. Effect of ball milling time on the crystallographic alignment evolution and coercivity of the nanoflakes were systematically investigated. Microstructure observation shows that the Sm₂Co₁₇ nanoflakes have an average thickness of less than 100 nanometers with an aspect ratio as high as 100. For the 2 hours ball milled nanoflakes, the intensity ratio between (004) and (302) reflection peaks, which indicates the degree of c-axis crystal texture of the Sm₂Co₁₇ phase, reaches the maximum value among all the samples, revealing that the strongest c-axis crystal texture was obtained in this nanoflakes. As the ball milling time increases, the intensity ratio drops gradually indicating that the long time milling process undermines the c-axis crystallographic alignment of Sm₂Co₁₇ phase in the nanoflakes. On the other hand, it is found that as the ball milling time increases from 2h to 10h, the coercivity of the nanoflakes firstly increases, peaks at 2.8kOe for 8h, and then decreases again. Further investigation indicates that the microstructure evolution plays an important role in the coercivity variance of the Sm₂Co₁₇ nanoflakes.

SN02

Rotor structure optimization of interior permanent magnet by using response surface method

Jung-ho Han, Ik-sang Jang, Mi-jung Kim, Ki-doek Lee and Ju Lee*

Electrical Engineering, Hanyang University, Korea

Due to limited energy sources and environmental pollution issues recently, the needs of high efficiency electricity equipments are steadily increasing. Among them, an IPM is being developed for the application of eco-friendly vehicle. An Interior Permanent Magnet has a structure of inserted permanent magnet in the inner rotor. These motor requires high torque and low torque ripple. It was designed with 8 pole 36 slot of stator and rotor, alternating N pole and S pole of permanent magnet and triangle type permanent magnet. In order to find the optimized condition, Central Composite Designs method and Box-Behnken method of Response Surface Method were used for finding design variable and minimizing variation of design variable. Comparing two Surface Reaction Methods, electromagnetic finite element method analysis based on inserting variation of design variables, torque, torque ripple, harmonics were obtained and optimized final value was obtained by safety factor through mechanical stiffness analysis.

[1] Ian P. Brown, Robert D. Lorenz, "Response Surface Methodologies for the Design of Induction Machine Self-Sensing Rotor Position Saliencies", Proceeding of International Conference on Electrical Machines and Systems, p1354-1359, 2007 [2] I. P. Brown and R. D. Lorenz, "Response surface methodologies for the design of induction machine self-sensing rotor position saliencies," ICEMS, 2007. [3] K. Ide, I. Murokita, S. Mitsujiro, O. Motomichi, N. Yukio, J. I. Ha, and S. K. Sul, "Finite element analysis of sensorless induction machine by high frequency injection," Proc. of the IPEC, Tokyo, Japan, 2000.

SN03

Magnetization reversal behavior of FePt/MgO/FePt thin film

Hiroki Iwama, Shinji Matsumoto, Katsuya Sugawara, Kotaro Sato, Masaaki Doi and Toshiyuki Shima

Tohoku Gakuin University, Japan

L10 ordered FePt alloy has attracted much attention, since they are believed to be good candidates for future magnetic devices. It is also thought to overcome the problem of thermal fluctuation in nano-meters scale. A lot of studies such as thin films and self-assembled nano particles have been investigated [1-3]. However, the magnetic properties of the multilayered FePt alloy have not been completely clarified. In order to understand the magnetization reversal, FePt/MgO/FePt trilayer films have been fabricated and detailed magnetic domain observation have been investigated. FePt bottom layer was co-deposited with Fe and Pt on Au buffer layer by using an UHV-compatible magnetron sputtering system. Then, the intermediate MgO layer and FePt top layer were deposited. Finally, the samples were annealed at Ta of 600 °C. The magnetic domain structure was observed by magnetic force microscope (MFM) in applied fields up to ±6 kOe. Remarkable steps of the magnetization in the second quadrant were observed for all the samples. This is thought to arise from the difference in the chemical ordering of top and bottom FePt layers. Independent magnetization reversal of the top and bottom FePt layers was clearly observed at the FePt/MgO/FePt circular dots by the MFM measurements.

[1] T. Shima et al., Appl. Phys. Lett. 99, 033516 (2006). [2] T. Shima et al., Appl. Phys. Lett. 81, 1050 (2002). [3] S. Matsumoto et al., J. Phys.: Conf. Ser. 266, 012038 (2011).

SN04

Efficiency and torque density improvement of interior permanent magnet synchronous motor

Mi Jung Kim, Ki Doek Lee, Jae-jun Lee, Jeong-ho Han, Tae-chul Jeong, Woong-chan Chae and Ju Lee*

Hanyang University, Korea

The motor should be designed with a minimum of because motor weight has quite large portion in totality mass; because there is no generator as electrical vehicle, the high efficiency is demanded in order to increase the 1 charging distance. In this paper, the technique is presented for progression of the torque density and the efficiency through the relative electric loading and the shape of rotor magnet. In case of the established model, the required torque satisfied at the rated speed and maximum speed, however, the torque density is low. When the mass of occupied by the motor is going to be bulky, 1 charging distance is decrease due to the increase in the driving load. The current density was increased to boost the torque density. The motor size could be decreased owing to change the current density, but there is a weakness at efficiency. The copper loss is enlarging with the current density. To increasing both of them efficiency and power density, the relative magnetic loading also should increase according to increase the relative electric loading. To increase the relative magnetic loading, redesign the PM shape of rotor.

[1] Yukio Honda, Tomokazu Nakamura, Toshiro Higaki, Yoji Takeda, "Motor design consideration and test results of an interior permanent magnet synchronous motor for electric vehicles", IEEE Industry Applications Society, Annual Meeting, pp. 75-82, 1997 [2] Sung-Il Kim, etc., "Optimization for reduction of torque ripple in interior permanent magnet motor by using the taguchi method", IEEE Trans. on magnetics, vol. 41, no.5, pp. 1796-1799, 2005

SN05

An effective skew method for torque ripple reduction in surface-mounted permanent magnet motor

Taewoo Kim and Junghwan Chang*

Electrical Engineering, Dong-A University, Busan, 604-714, Korea

This paper deals with an effective skew method for surface-mounted permanent magnet motor (SPMSM). Skew is a common method to reduce cogging torque and torque ripple as well, and it can be done by continuous way in small machines or multi-stepwise method in big machines [1-2]. Generally, these conventional ways assume that the magnetic flux density distributions are same in axial direction and the contribution of the rotor on the generated torque is also same in all axial direction. However, the air-gap flux density is not uniform in axial direction, and it is rapidly reduced at both ends of the motor. Especially, in the pancake type motor, the influence of end sides is significant. Thus, for skew to be effective, non-uniform air gap flux density distribution in axial direction should be considered. In this paper, one method for an effective skew is suggested by considering flux density distribution in axial direction, and the results will be confirmed by 3D finite element analysis.

[1] R. Islam, I. Husain, A. Fardoun, and K. McLaughlin, "Permanent Magnet Synchronous Motor Magnet Designs with Skewing for Torque Ripple and Cogging Torque Reduction," IEEE Trans. Ind. Appl., vol.45, no.1, pp.152-160, 2009. [2] Y. Donmezer, L.T. Ergene, "Skewing effect on interior type BLDC motors," ICEM XIX International Conference, pp.1-5, 2010

SN06

Effect of carbon additive on the TbCu₇-type melt spun Sm(Co, M)7 (M=Ti, Zr, Hf, V, Nb and Ge) ribbons

C.c. Hsieh¹, H.w. Chang², C.w. Shih¹, W.c. Chang^{1*} and C.c. Shaw³

¹ National Chung Cheng University, Taiwan

² Tunghai University, Taiwan

³ Superrite Electronics Co. Ltd, Taiwan

Recently, Sm-Co compounds with TbCu₇-type structure have received intensive attention due to their excellent intrinsic magnetic properties, which have potential to be used as the starting materials for making bonded magnets for above 150 oC applications. Our previous studies indicated that pure TbCu₇-type structure could be obtained easily in melt spun Sm(Co,M)7 (M=Ti, Zr, Hf, V, Nb and Ge) ribbons. Based on the purpose of developing Sm(Co,M)7 alloys with TbCu₇-type structure for practical usage, effect of carbon on the microstructure and magnetic properties of melt spun SmCo_{7-x}M_xCo_{0.1} (M=Ti, Zr, Hf, V, Nb and Ge; x=0-0.3) ribbons were studied. Based on the XRD and TEM analysis, a pure 1:7 phase could be kept for the ribbons with M= Nb, and Ge, but carbide phases, eg. TiC for M=Ti, ZrC for M=Zr, Sm₂C₃ for M=Hf, and SmCo₂ for M=V, respectively, were found for other ribbons. Nevertheless, a slight C addition may effectively refine the microstructure and improve both the intrinsic coercivity and the magnetic energy product in all the studied ribbons. Among them, the SmCo_{6.9}V_{0.1}Co_{0.1} ribbons with σ_r=58.7 emu/g, iH_c=13.5 kOe and (BH) max=9.3 MGOe, and SmCo_{6.9}Hf_{0.1}Co_{0.1} ribbons with σ_r=61.6 emu/g, iH_c=11.8 kOe and (BH)max=10.3 MGOe are suitable for the bonded magnet applications.

SN07

Study of designed induction motor on cryogenic LNG pump system

Jinsung Kim and Gwansoo Park*

Pusan National University, Korea

In this Paper, I designed LNGs main cargo pump's motor using LNGs ship. LNGs ship has made a high value product and won steady demand order in every year. However, in Korea, when we make a LNGs ship, we import the key products from other countries(It's almost 60% of order price). So, we need to develop original skill about key product. LNGs main cargo pump's motor is submerged, and induction motor type. In this paper, first of all, design the induction motor using constants at room temperature. And then, we re-design the motor considering an extremely low temperature. This motor's working operation temperature is -163°C. Because of that, it can make a special design. In other words, we don't need to think about heat loss as like as room temperature. In this reason, we consider about losses by current density and flux density. First, coil loss is generated a heat. So, it can be cooling the coil heat loss immediately. On the other hands, magnetic saturation has effect on characteristics of material (specially, B-H curve). So, we think about magnetic saturation, even it works at low temperature.

L.Dłufiewicz, J. Kolowrotkierwicz, W. Szelag, M. Barancki, and R. Neumann, Electrical Motor for Liquid Gas Pump, SPEEDAM, pp.311-316 (2006). Shiyley R, Miller H, Development of a Submerged Winding Induction Generator for Cryogenic Application, Conf. of IEEE Symp. on Electrical Insulation, pp.243-246 (2000). Rush, S. Submerged Motor LNG Pumps in Send-out System Service, Pumps&System, pp.32-37, (2004). Stephen J. Chapman, Electric Machinery Fundamentals, pp.380-425, (2003).

SN08

Structural and magnetic properties of nanocrystalline BaFe₁₂O₁₉ synthesized by microwave-hydrothermal method

K Sadhana and K Praveena

Materials Research Centre, Indian Institute of Science, Bangalore-560012, India, India

The nanocrystalline BaFe₁₂O₁₉ powders were prepared by Microwave-Hydrothermal (M-H) method at 200°C/45 min. The as synthesized powders were characterized by using X-ray diffraction (XRD). The present were densified at different temperatures i.e., 750°C, 850°C, 900°C and 950°C for 1h using microwave sintering method. The phase formation and morphology studies were carried out using XRD and field emission scanning electron microscopy (FE-SEM). The average grain sizes of the sintered samples were found to be in the range of 185 to 490 nm. The magnetic properties such as saturation magnetization and coercive field of sintered samples were calculated based on magnetization curves. A possible relation between the magnetic hysteresis curves and the microstructure of the sintered samples was investigated.

SN09

Research magnetic properties of Fe-O alloys with different texture degrees and ratios of phases using simulating

Alexey Lileev*, Ivan Pelevin and Anna Starikova

National University of Science and Technology 'MISIS', Russia

The present article is concerned with investigation of magnetic properties of Fe-O alloys, simulating their magnetic behaviour and causation of the high-coercivity state of these alloys. Initial materials were powder so-called "Blue dust" and mixture of this powder with Fe powder with different rations of these phases. "Blue dust" is a powder of Fe₂O₃, it's a natural Indian raw. Reserves of this material sufficient large, so a production material with high magnetic properties from it is an urgent problem. Initial samples were powdered in high-energy ball mill for different time periods. This treatment leads to phase transformation. The phase compositions were investigated by X-ray analysis. The impact of time of milling and initial composition on magnetic properties was explored. Milled nanocrystalline powders were subjected to a low-temperature crystallization annealing in magnetic field. It leaded to phase transformation. Powder was pressed into cubic shape samples. The dependence of magnetic properties on composition after annealing was also investigated. The computer simulating was used to understand which phase is cause of forming the high-coercitive state of material. Initial parameters were set so that result corresponds to experimental data. The parameter changing showed quite how each of them influence on magnetic properties.

SN10

Study on FePt/Fe exchange coupling nanocomposite thin films

Wenli Pei

ATM, Northeastern University, China

Granular FePt films with island microstructures have been deposited by DC magnetron sputtering. The FePt grain size and distance among FePt grains could be controlled by tuning sputtering condition. An iron layer was deposited on the controllable island FePt film to produce FePt/Fe nanocomposite thin film. The composite films show a hard/soft magnetic exchange coupling after annealing, because the FePt grains in the composite film became L10 structure with good hard magnetic properties after annealing. The exchange coupling could be modified by tuning granular FePt structure and thickness of Fe layer, which means it's promising to produce FePt/Fe nanocomposite magnet with good magnetic properties by this method.

I. Kneller E F, Havrig R. The exchange-spring magnet: a new material principl for permanent magnets. Magnetics [J], IEEE Transactions on Magnetics, 1991. 27(4): 3588- 3560. 2. Zhou J, Skomski R, Li X, et al. Permanent-magnet properties of thermally processed FePt and FePt-Fe multilayer films [J]. IEEE Transactions on Magnetics, 2002, 38(5Part 1): 2802-2804.

SN11

Effects of Sm content on thermal stability of sintered Sm₂Co₁₇ magnets
Minggang Zhu, Haibo Feng, Wei Li, Yikun Fang, Wenchen Zhang and Wei Pan
China Iron & Steel Research Institute Group, China

Investigations on environment stability of the Sm₂Co₁₇ type magnets have been one of hot pots on applications of Sm-Co based magnets. Effects of heavy rare-earth elements substitute Sm on temperature coefficient of remanence (?) of the magnets have been investigated systematically [1]. Sm₂Co₁₇ magnet with high coercivity has the best thermal stability among all permanent magnets [2]. The reversible temperature coefficient ? was zero in the (Sm_xGd_{1-x})CoFeCuZr magnet when x=0.55[3]. In this paper, the dependence of Sm content on temperature coefficient of 2:17 type Sm-Co magnets at different temperature were investigated. As shown in Fig.1, the temperature coefficient increased with temperature when z value of the magnets is the same. While, the temperature coefficients of remanence firstly decreased and then increased with z value at the same temperature. When z=7.87, magnet with the best temperature stability, the highest coercivity and the lowest temperature coefficient of remanence were obtained.

[1]Chen Christina, Gong Wei, Michael Walmer H. *Journal Applied Physics*, 2002, 91(10): 8483. [2]Li D, Misdrum H F, and Sirmat K J. *Journal Applied Physics*, 1988, 63(8): 3984. [3]Liu Jinfang, Payal Vora and Michael Walmer. *Journal of Iron Steel Research International*, 2006, 13: 319.

SN12

Simulation of die-upsetting process of hot-deformed magnets

Bin Lai*, Huijie Wang, Minggang Zhu and Wei Li
Division of Functional Materials, Central Iron & Steel Research Institute, China

A plastic deformation simulation was performed by using a three dimensional finite element method based deformation modeling software in order to clearly understand the die-upsetting process in detail. It was found by the plastic deformation simulation that the effective strains of Nd-Fe-B die-upset magnets reduced from the middle to the ends of magnetic specimens along the c-axis, or the press direction, so the crystallographic orientation deteriorated for the grains approached to both ends of die-upset magnets. The magnetic properties were improved with increase of effective strains of die-upset magnets. The remanence Br and maximum energy product (BH) m were high for the specimens, machined from the central region of magnets, because the microstructure of die-upset magnets was homogeneous and grains were aligned well in the central region of deformed magnets according to the simulation. Experimentally, the magnetic properties, X-ray diffraction patterns and microstructure of hot-deformed Nd-Fe-B magnets were studied. The magnetic properties were improved with decreased height of magnet specimens which were obtained by symmetrically removing both ends of die-upset magnets. The grain misalignment was as enhanced from the middle to both ends of die-upset magnets along c-axis. The microstructural characterization was verified by experiment.

[1] Yutaka, Matsuura, J. *Magn. Magn. Mater.* 303 (2006) 344 [2] N. Yoshikawa, T. Iriyama, and H. Yamada. *IEEE Trans. Magn.*, 35 (1999) 3268 [3] T. Harada, M. Fujita, T. Kaji, *Journal of Alloys and Compounds*, 243 (1996) 139 [4] T. Saito, M. Fujita, T. Kaji, et al., *J. Appl. Phys.*, 83 (1998) 6390 [5] Y. Yoshida, Y. Kasai, T. Watanabe, et al., *J. Appl. Phys.* 69 (1991) 5841 [6] D. N. Brown, B. Smith, B.M.Ma, et al., *IEEE Trans. Magn.*, 40 (2004) 2895 [7] M. Leonowicz, D. Derowicka, M. Wicznik, et al., 153154 (2004) 860

SN13

Synthesis of high magnetic moment nanowires for encoding and decoding of barcode segments for multiplexing bio- applications

Torati Sri Ramulu¹, Reddy Venu¹, Brajalal Sinha¹, Xinghao Hu¹, Sook Soo Yoon² and Cheol Gi Kim^{1*}

¹ *Material science and engineering, Chungnam national university, Korea*
² *Material science and engineering, Andong national university, Korea*

Abstract: Sequential template electrochemical synthesis of multisegment nanowires with magnetic and non-magnetic segments have been extremely significant for barcoding, multiplexing and biosensing applications [1,2]. Especially, Hard magnetic segment with high saturation magnetization and remanence materials are more convenient for multiplexing biological applications. In the present article we have synthesized three different types of magnetic nanowires (CoNiP, CoPtP and CoFeP) for a magnetic segment of barcode nanowires by electrochemical deposition technique using a polycarbonate membrane with a diameter of 50 nm. The length of the nanowires was found to be around 6 μm. We compared the magnetic properties of all the synthesized materials and found to be the CoPtP magnetic nanowires have higher saturation and remanence. In order to demonstrate the decoding of barcode nanowires using the magnetoresistance sensor in flow cytometry, we calculated the spatial distribution of the stray magnetic field produced by the barcode nanowire by means of finite element method (FEM) using the commercial Maxwell software. The CoPtP shows most higher spatial variation compared to the CoFeP and CoNiP, which means CoPtP is most advantageous composition for the hard magnetic segment.

[1] K. B. Lee, S. Park, and C. A. Mirkin, 2004, *Angew. Chem. Int. Ed.*, 43, 3048 [2] A. K. Salem, P. C. Seaverson, and K. W. Leung, *Nat.Mat.*, 2003, 2, 668

SN14

A new mechanism of electromagnetic linear-actuator using a magnetic silicone rubber

Takanori Fukushi, Sung Hoon Kim*, Shuichiro Hashi and Kazushi Ishiyama
Research Institute of Electrical Communication, Tohoku University, Japan

We propose a new mechanism of electromagnetic linear-actuator for biomedical applications such as an artificial muscle and medical micro-robots [1-3]. The proposed mechanism requires two armatures and magnetic rubber in the DC-solenoid. The proposed structure is series connection: armature_1, magnetic rubber, and armature_2. Therefore, DC magnetic field produces attractive force between the two armatures. At that time, the magnetic rubber causes increase of attractive force because the magnetic rubber was fabricated by iron powders with silicone elastomer (36 : 64 wt %), as a cylindrical shape (diameter:12 mm and height: up to 8.9 mm). Its magnetic properties were measured by VSM; magnetization and coercive force are 50 emu/g and 40 Oe, respectively. We compared magnetic force between the two armatures with the magnetic rubber and with a non-magnetic rubber in magnetic field of 600 Oe. We found the magnetic rubber made the attractive force 1.7 times larger. This also means the use of magnetic rubber makes the low power consumption. The largest advantages of this magnetic rubber are the increase of attractive force, generation of reaction force, and the flexibility as soft elastmer, so it can be used for various biomedical applications. The details will be introduced in the conference.

[1] B.Kim, M.G.Lee, Y.P.Lee, Y.Kim, and G.Lee, "An earthworm-like micro robot using shape memory alloy actuator," *Sens. Actuators A*, 125, 429-437, 2006. [2] H.Liu, J.Zhu, Z.Lin, and Y.Guo, "An inchworm mobile robot using electromagnetic linear actuator," *Mechatronics*, 1-10, 2009. [3] T.Niino, S.Egawa, H.Kimura, and T.Higuchi, "Electrostatic Artificial Muscle: Compact, High-Power Linear Actuators with Multiple-Layer Structures," *Proc. IEEE Micro Electro Mechanical Systems Workshop*, 94, 130-135, 1994

SN15

Novel microcrystalline Co-Zr-B RE-free hard magnetic alloys

Sofoklis Makridis and Evangelos Gkanas
Department of Mechanical Engineering, University of Western Macedonia, Greece

The investigation of rapidly solidified alloys is important both for the basic information it gives about the structural and compositional limits of magnetism and for the technical potential of new alloys. Co-based amorphous alloys have the advantage of relatively high saturation flux density and low magnetostriction. The glass formability and technical magnetic properties of rapidly solidified Co(rich)-Zr-B alloys were investigated in the composition range Co₆₂Zr₂₀B₁₈. In order to determine the glass forming range and explore the magnetic characteristics as a function of composition and quenching rate. The alloys were found to be completely glassy for low x whereas all the other compositions studied were completely or partially crystalline. The typical glassy alloys showed good soft magnetic properties. The crystalline alloys with Zr content higher than 80 % in Boron were characterized by a coercive force in excess of 4 kOe. Slow-cooled samples of the same composition showed coercivity in the order of 120 Oe.

SO01

First-principles study on the half-metallicity of full-Heusler alloy Co₂VGa (111) surface

Hongpei Hong, Kailun Yao* and Guoying Gao
physics, Huazhong university of science and technology, China

A recent experimental study indicates that full-Heusler alloy Co₂VGa exhibits half-metallic ferromagnetism and the magnetic moment measured at 5 K is independent of high pressure up to 12.1 kbar (T. Kanomata et al Phys. Rev. B 82, 144415 (2010)). Using the full potential linearized augmented plane-wave method, we here further investigate the structural, electronic and magnetic properties of all possible (111) surfaces of Co₂VGa. Both structural relaxation and calculated surface energy reveal that Ga-terminated surface is more stable than other terminations. From the analysis of the spin-polarized density of states, we find that the half-metallicity confirmed in bulk Co₂VGa is lost at Co-terminated surfaces but still maintained at V-terminated and Ga-terminated surfaces. Moreover, the obtained magnetic moments show that the atomic magnetic moments of the (111) surfaces are greatly different from the bulk values.

SO02

Magnetic and resonance properties of Bi₂₄(CoBi)₄₀

Sergey Stepanovich Aplesnin¹, Maksim Nicolaevich Sitnikov¹, Lubov Victorovna Udod² and Dmitrii Anotol'evich Velicanov²
¹ *M.F. Reshetnev Siberian State Aerospace University, Russia*
² *L.V. Kirensky Institute of Physics, Russia*

The cubic bismuth oxide is characterized by charge ordering of bismuth ions. A study of magnetic moment of cobalt ions is used to establish the valence state of bismuth ions. The aim of study is to establish the interrelation between spin and elastic subsystems. Measurements of the magnetization was carried out over the temperature range 4K-300 K in the field H=50 kOe and the magnetization curve M(H) was determined at the temperatures T=5 K and T=300 K. The temperature dependence of magnetic susceptibility is well fitted to the Curie-Weiss law with the Curie-Weiss temperature θ=- 12.3 K and the effective magnetic moment is μ_{eff}=5.08μ_B. The bismuth cobaltit is paramagnetic at T >4 K. The electron paramagnetic resonance (EPR) spectra were recorded from 77 K to 300 K at 9.3 GHz. The g- factor increases versus temperature that can be qualitatively explained by local deformation of structure at variation of bismuth ion valence. As a result, the magnetic anisotropy field is enhanced at the heating. EPR linewidth varies linearly with temperature that is explained by spin-phonon interaction. Relaxation of magnetic moment is due to strong interaction with the elastic lattice.

SO03

Field induced phase transitions and magnetocaloric properties in Er_{1-x}Lu_xFe₂O₄ compound

Peng Zhang¹, Ying-de Zhang¹, Young-yeal Song¹, Jae-yeong Kim², Bo-wha Lee² and Seong-cho Yu^{1*}
¹ *Physics, Chungbuk National University, Korea*
² *Physics, Hankuk University of Foreign Studies, Korea*

Rare earth (RE)-ferrites have attracted attention in recent years due to their various phase transitions (PTs) near room temperature. Their magnetic phase is determined by competition between antiferromagnetic and ferrimagnetic coupling of the localized Fe ions. Magnetocaloric effect (MCE) reaches the maximum near the magnetic PT temperature. Despite of many works of the PT, however, there are very limited works on MCE in the RE-ferrites with two RE elements. In this work one has investigated field induced magnetic PT properties and MCE in the vicinity of the PT point. Stoichiometric polycrystalline samples of Er_{1-x}Lu_xFe₂O₄ (0.1 ≤ x ≤ 0.8) were prepared by solid-state reaction method. Magnetic measurements were performed using a SQUID magnetometer. Fig.1 gives isothermal M-H curves of Er_{0.8}Lu_{0.2}Fe₂O₄, from which the field induced PT can be seen clearly from the magnetization curves in the range of 208 K-240 K indicating a first order structural type PT[1]. Fig. 2 shows magnetic entropy change (ΔSM) curves. With a maximum field of 1 T and 3 T, the maximum value of ΔSM are 0.49 J•kg⁻¹K⁻¹ and 1.04 J•kg⁻¹K⁻¹ at 249 K, respectively. The maximum ΔSM were appeared near the transition temperature and their MCE will be explained in terms of PTs.

SO04

Magnetic properties of heusler-type Ni-Mn-Ga glass-coated microwires

Valeria Rodionova¹, Maxim Ilyn², Valentina Zhukova^{2*}, Alexander Granovsky³, Alexander Aronin¹, Galina Abrosimova⁴ and Arcady Zhukov⁵
¹ *Dpto. de Fisica de Materiales and Faculty of Physics, UPV/EHU San Sebastian, Lomonosov Moscow State University and Immanuel Kant Baltic Federal University, Russia*
² *Dpto. de Fisica de Materiales, UPV/EHU, Spain*
³ *Dpto. de Fisica de Materiales and Faculty of Physics, UPV/EHU, San Sebastian, Spain and Lomonosov Moscow State University, Moscow, Russia*
⁴ *Institute of solid State Physics, RAS, Chernogolovka, 142432, Moscow Region, Russia*
⁵ *Dpto. de Fis. Mater., UPV/EHU San Sebastian and IKERBASQUE, Basque Foundation for Science, Bilbao, Spain*

Studies of magnetic shape-memory alloys (MSMAs) attracted growing attention within last few years owing to significant magnetic-field-induced strain (MFIS) useful for applications in actuators, sensors and for energy harvesting. From point of view of applications, miniaturizing of MSMA-based devices based on small-size MSMA materials is quite important. Main advantage of Ni-Mn-Ga Heusler-type microwires is related with composite character, allowing production of long microwire from brittle Ni-Mn-Ga alloy. Consequently the aim of this paper is to present results on Heusler-type Ni₄₃Mn₂₅Ga₃₂ glass-coated microwires. We fabricated few metres long microwire and measured magnetization, M, versus magnetic field, H, curves in as-prepared and annealed up to 790 K microwires. After annealing M(H) curves drastically changed: in as-prepared microwires magnetic transformation appears around 175 K. The sample seems contain the second magnetic phase which orders at low temperature giving rise to fast increase of the magnetization below 30 K. Meanwhile common ferromagnetic behaviour was observed at around 325 K for the annealed sample without any evidence of existence of second magnetic phase. X-ray diffraction allows to detect significant structural changes after annealing. Obtained results are discussed taking into account strong internal stresses induced by fabrication of composite microwires and high quenching rate.

SO05

Compensated magnetism in double perovskites A₂CrFeO₆ (A=La,Sr)

Kyo-hoon Ahn¹ and Kwan-woo Lee^{2*}
¹ *Department of Applied Physics, Graduate School, Korea University, Sejong, Korea*
² *Department of Display and Semiconductor Physics, Korea University, Sejong, Korea*

Precise compensation of magnetic moment in solid state compounds is very rare. An example is the so-called half-metallic antiferromagnet (HMAFM), which has one metallic spin channel and the other insulating spin channel with the zero net moment. Double perovskite compounds of A₂BB'O₆ have been theoretically investigated as the most promising candidates for the last 15 years. Very recently, nearly well-ordered epitaxial La₂CrFeO₆ films, theoretically predicted to be a HMAFM, were synthesized using pulsed laser deposition. This sample shows the saturated moment of ~2 μB, implying the ferrimagnetically ordered S=3/2 Cr³⁺ and S=5/2 Fe³⁺. This result are controversial to the previous experimental results on artificial LaCrO₃/LaFeO₃ superlattices, which proposed a ferromagnetic order, as well as the existing theoretical predictions. In this presentation, we will revisit this system with first principles calculations using LDA+U, the modified Becker-Johnson functional, and fixed spin moment. Our results are consistent with the recent experimental results, showing a ferrimagnetic insulating La₂CrFeO₆. Furthermore, we have investigated the Sr-analog Sr₂CrFeO₆, which is as yet unsynthesized. Contrary to La₂CrFeO₆, this system has the tetravalent Cr and Fe ions with antialigned S=1 moments, resulting in zero net moment. Our findings suggest a precise HMAFM Sr₂CrFeO₆.

SO06

Possible half-metal antiferromagnetism in double perovskites A₂VMnO₆ (A=La,Sr)

Myung-chul Jung¹, Young-joon Song¹ and Kwan-woo Lee^{2*}
¹ *Department of Applied Physics, Graduate School, Korea University, Sejong, Korea*
² *Department of Display and Semiconductor Physics, Korea University, Sejong, Korea*

A half-metallic antiferromagnet (HMAFM) is half-metallic without macroscopic magnetic moment. HMAFM has been considered a promising candidate of a spin injector in spintronics, though no true HMAFM has been established yet. Very recently, A well-ordered double perovskite La₂VMnO₆, which was theoretically predicted to be HMAFM 15 years ago, has been synthesized by pulsed-laser deposition. Contrary to the theoretical predictions, the saturated magnetic moment of 2 μB/f.u. implies a ferrimagnetically ordered S=1 V³⁺ and S=2 Mn³⁺ ionic state, below TN=20 K. Besides, the synchrotron radiation photoemission measurement indicates an insulating La₂VMnO₆ with a gap of 0.9 eV, instead of being half-metallic. In this presentation, we will revisit this system using various first principles calculations to unravel these discrepancies between the previous theoretical suggestions and the experimental results. Furthermore, our calculations suggest that the Sr-analog Sr₂VMnO₆ is a ferrimagnetic half-metal, contrary to the ferrimagnetic insulator La₂VMnO₆.

SO07

Focused magneto-optic kerr effect spectroscopy in Ni_{1-x}Fe_x and Fe ferromagnetic thin films on organic substrates

Kenji Kondo*, Hideo Kajju and Akira Ishibashi
Laboratory of Quantum Electronics, Research Institute for Electronic Science, Japan

We have developed the theory of focused magneto-optic Kerr effect (MOKE) for multilayer thin films and applied it to the surface magnetic properties, which have been observed by focused MOKE, for Ni_{1-x}Fe_x and Fe thin films evaporated on polyethylene naphthalate (PEN) organic substrates. We have experimentally obtained the Ni_{1-x}Fe_x thickness dependence of Kerr rotations for as-deposited thin films and exposed thin films at an atmosphere for 1-year, respectively. The theoretical thickness dependences of Kerr rotations have been calculated using magneto-optic constants Q's of 0.01*exp(-i 48π/180) and 0.025*exp(-i 57π/180), respectively. The calculated results are in good agreement with the experimental data. Also, the Ni_{1-x}Fe_x thin films exposed for 1-year show larger magnetization than the as-deposited Ni_{1-x}Fe_x thin films in the range of 1-20 nm. We consider that the reason is that the surface of Ni_{1-x}Fe_x has transformed to locally Fe-rich surface because of the segregation of Fe. We have also measured the Kerr rotations of Fe deposited on PEN. The Q of Fe/PEN was 0.025*exp(-i 47π/180). To our knowledge, the magneto-optic constants have been estimated for ferromagnetic thin films on PEN for the first time.

SO08

The structural and magnetic properties of the magneto-caloric compounds Mn_{0.66}Fe_{1.29}P_{1-x}Si_x (x = 0.34, 0.37 and 0.42)

Zhiqiang Ou^{*}, L. Zhang¹, N.h. Dung¹, L. Van Eijck², M. Avdeev³, A.m. Mulders⁴ and E. Bruck¹
¹ FAME Section, R3, Faculty of Applied Sciences, Delft University of Technology, Netherlands
² NPM2 Section, R3, Faculty of Applied Sciences, Delft University of Technology, Netherlands
³ Australian Nuclear Science and Technology Organisation, Locked Bag 2001, Kirrawee DC NSW 2232, Australia
⁴ School of Physical, Environmental and Mathematical Sciences, UNSW in Canberra, ACT2610, Australia

The magneto-caloric effect (MCE) is the thermal response of a magnetic material to an applied magnetic field, results in a change of temperature.[1,2] (Mn,Fe)2(P,Si) compounds are known for their potential for room-temperature magnetic refrigeration, due to large MCE and tunable working temperatures, cheap and abundant raw materials.[3] In this study, the single phase compounds Mn_{0.66}Fe_{1.29}P_{1-x}Si_x (x = 0.34, 0.37 and 0.42) have been synthesized. The crystal and magnetic structure have been investigated by means of neutron and X-ray powder diffraction. The refinement shows the compounds crystallize in the hexagonal Fe₂P-type structure (P-62m). The 3f site is nearly completely occupied by Fe atoms, the 3g site is occupied by Mn atoms and the excess Fe atoms, while the P and Si are randomly mixed. It is shown that the average magnetic moment in the 3g site is larger than that in the 3f site, 2.64 versus 1.81 μB for the compound with x = 0.34 at 10 K. The alignment of the magnetic moment has changed from almost c-direction to a-b plane with increasing Si content from x = 0.34 to x = 0.42. The compounds show a strong magnetic field induced transition, small magnetic hysteresis and large magnetic entropy changes.

[1] Y.K. Pecharsky and K.A. Gschneidner, Phys. Rev. Lett. 78, 4494 (1997). [2] E. Bruck, J. Phys D: Appl. Phys. 38, p. R381-R391 (2005). [3] D. T. Cam Thanh, E. Bruck, N. T. Trung, J. C. P. Klasse, K. H. J. Buschow, Z.Q. Ou, O. Tegus and L. Caron, J. Appl. Phys. 103, 07B318 (2008)

SO09

Faraday rotation characteristics in wide-gap magnetic semiconductor ZnMnTe and ZnMnSe films

Masaaki Imamura^{*}
 Electrical Engineering, Fukuoka Institute of Technology, Japan

II-VI based magnetic semiconductors with a wide optical band gap are expected to show high potential for optical applications utilizing short wavelength laser diodes, such as 532-nm green and 475-nm blue LDs [1]. ZnMnTe and ZnMnSe exhibit their absorption edges at 428-544 and 428-458 nm, respectively [2]. The edge is not so influenced by the Mn concentration, as is typically observed in CdMnTe. We have confirmed that the Faraday rotation in the ZnMnTe films deposited on quartz glass substrates is large near the absorption edge. Crystallinity was evaluated using an x-ray diffractometer. The preferred (111) growth reported previously for CdMnTe films on QG substrates was also observed in the ZnMnTe and ZnMnSe films with weaker peak intensities. This paper reports the Faraday rotation angle of those films synthesised on QG substrates by using molecular beam epitaxy with a thickness of 2 μm. A Faraday-effect signal observed for the ZnMnTe film using a 532-nm green LD has shown that ZnMnTe films are useful for green lights. We developed equipment for observing the Faraday effect directly under ac magnetic fields generated by a ring magnet. The results of a direct Faraday rotation observation successfully made for the ZnMnTe films under ac fields are shown.

[1] M. Imamura et al., IEEE Trans. Magn. 42, 3078 (2006). [2] M. Imamura et al., J. Appl. Phys. 99, 08M706 (2006).

SO10

Magnetism and multiplets in Fe-phthalocyanine molecules

Yukie Kitaoka^{*}, Kohji Nakamura¹, Toru Akiyama¹, Tomonori Ito¹, Michael Weinert² and Arthur J. Freeman³
¹ Mie University, Japan
² University of Wisconsin-Milwaukee, USA
³ Northwestern University, USA

A challenge to miniaturize devices for novel magnetic application now extends to treating the extreme limit of a single atom or molecule. Moreover, for molecules with transition-metals, multiplets are essential aspects of their electronic structure. It is often difficult, however, to evaluate such multiplets within a given ligand (or crystal) symmetry. Here, we carry out first-principles calculations with the FLAPW method[1] for Fe-phthalocyanine (FePc), in which the multiplets are treated by imposing a density matrix constraint on the d-orbital occupation numbers. Results predict that there are three stationary multiplets - ³E_g (d^{xy}, d^{z2}, d^{xz+yz}), ³B_{2g} (d_{xy}, d_{z2}, d^{xz+yz}), and ³A_{2g} (d^{xy}, d^{z2}, d^{xz+yz}) - in a single FePc molecule, and total energy calculations demonstrate that the ground state is the ³A_{2g}. Furthermore, a columnar stacking of the FePc molecules (as seen in α-FePc) changes the ground state to ³E_g due to hybridization between adjacent molecules. In qualitative agreement with recent XMCD experiments[2], the magnetic anisotropy energy for the columnar stacking structure has a large negative value of 0.6 meV/molecule, indicating that the magnetization favors pointing in the planar direction, and a large orbital moment of 0.14 μB is induced.

[1] Wimmer, Krakauer, Weinert, Freeman, PRB 24, 864 (1981); Weinert, Wimmer, Freeman, PRB 26, 4571 (1982). [2] Bartolome, Garcia, Filoti, Greinig, Colesnicu, Schuller, Cezar, Phys. Rev. B 81, 195405 (2010).

SO11

Elastic anisotropy in ferromagnetic shape memory alloy of non-stoichiometric Ni₂MnGa_{1-x}In_x

Fumiya Kitanishi^{*}, Kohji Nakamura, Toru Akiyama and Tomonori Ito
 Mie University, Japan

In magnetic shape memory (MSM) effect, the elastic and magnetocrystalline anisotropies play an important role. Moreover, experiments reported an enhancement of the MSE effect in a non-stoichiometric metallic compounds.[1] Here, in order to discuss a role of the non-stoichiometry, we developed a method for determining elastic property of non-stoichiometric compounds from first principles calculations and cluster expansion method.[2] and applied to non-stoichiometric Ni₂MnGa_{1-x}In_x. For calculations, first, the formation energies of ordered structures as functions of volume V and c/a, ΔE_{c/a} (V,c/a), were calculated by using the FLAPW method.[3] Then, by using the cluster expansion method, the formation energy of a disordered state with non-stoichiometric compositions, ΔE_d (V,c/a), were obtained in terms of many-body correlation functions. Elastic properties of the bulk modulus, B, and the elastic tetragonal anisotropy, C[']=(C₁₁-C₁₂)/2, were numerically obtained from the ΔE_d (V,c/a) of the disordered state. Results indicate that the B has an almost linear relation with respect to x. However, a deviation from stoichiometric composition is found to enhance the elastic tetragonal anisotropy; e.g., for a non-stoichiometric composition of x=0.125, the C['] decreases by 0.4 GPa compared to that in x=0, and the C['] increases when the x increases over about 0.125.

[1] R. Kainuma et al., Nature 439, 957 (2006). [2] J. W. D. Connolly and A. R. Williams, Phys. Rev. B 59, R2486 (1998). [3] K. Nakamura, et al., Phys. Rev. B 67, 14405 (2003).

SO12

Structure and properties of double perovskite system La₂Co_{1-x}Fe_xMnO₆ (x=0, 0.1, 0.2, 0.3)

The-tan Pham, Huyen-yen Pham and Nam-nhat Hoang^{*}
 Faculty of Technical Physics and Nanotechnology, Vietnam National University, University of Engineering and Technology, Viet Nam

Insulating ferromagnets of type RE₂AMnO₆ where A is transition metal and RE rare earth have received a renewed interest. Although the bulk La₂CoMnO₆ has been extensively studied, its Fe-doped possed several questions that should be addressed. The substitution of Fe into the B site induced the increase in ferromagnetism at the cost of TC. It was also accompanied by a structure transition from orthorhombic to monoclinic. The monoclinic crystal symmetry occurred in the space group P21/n, with cell parameters a = 5.532 Å, b=5.492 Å, c=7.784 Å, beta = 89.92°. The magnetic measurement showed that the magnetization reached maximum value of 4.7μB/ f.u.c. This value agrees well with the theoretically expected value.

SO13

Density-functional study on spin-crossover in several Fe-based molecules

Tuan Anh Nguyen^{*} and Thanh Van Nguyen
 Faculty of Physics, Hanoi University of Science, Viet Nam

Spin crossover (SCO) complexes are now very potential candidates for applications such as molecular switches, display and memory devices [1]. The SCO phenomenon can be qualitatively explained by the ligand field model, however, designing transition metal complexes with expected SCO behavior is still a big challenge in the field of materials science. In this paper, in order to explore more about the way to control SCO behavior of transition metal complexes, we present a density functional study on the geometric structure, electronic structure and SCO of a series of eight Fe-based molecules [2-7]. Our calculated results show that SCO in these Fe-based molecules is accompanied with charge transfer between the Fe atom and ligands. This causes change in the electrostatic energy (ΔU) as well as the total electronic energy of these molecules. Moreover, our calculated results demonstrate an important contribution of the interionic interactions to ΔU, and there is the relation between ΔU and the thermal hysteresis behavior of SCO in these molecules. These results should be helpful for developing new SCO molecules.

[1] H. A. Goodwin, et al., Top. Curr. Chem. 233, 1 (2004). [2] Nicolas Moliner, et al., Inorganica Chimica Acta, 291, 279 (1999). [3] B. Weber, W. Bauer, J. Obel, Angew. Chem. Int. Ed. 47, 10098 (2008). [4] Gaelle Dupont, et al., Inorg. Chem., 47, 8921 (2008). [5] B. Weber, et al., Inorg. Chem. 47, 487 (2008). [6] B. Weber, et al., Eur. J. Inorg. Chem. 4891 (2008). [7] B. Weber, et al., Eur. J. Inorg. Chem. 5527 (2009).

SO14

Magnetic properties of Cu_{70.9}Al_{18.1}Mn₁₁ ferromagnetic shape memory alloy

S Chatterjee¹, S Giri² and S Majumdar^{2*}
¹ UGC-DAE Consortium for Scientific Research, Kolkata Centre, India
² Department of Solid State Physics, Indian Association for the Cultivation of Science, India

The ferromagnetic shape memory alloy (FSMA) of nominal composition Cu_{70.9}Mn₁₁Al_{18.1} has been studied through electronic transport, dc magnetization and ac susceptibility measurements. Unlike other Cu containing shape memory alloys, Cu-Mn-Al systems of alloys show interesting magnetic behaviour. Ferromagnetism in Cu-Mn-Al alloys come from the Rudermann-Kittel-Kasuya-Yosida (RKKY) type ferromagnetic exchange interaction between Mn atoms. The studied alloy undergoes ferromagnetic to glassy transition below martensitic transition (MT). Clear frequency shift in ac susceptibility measurement is observed near the step like anomaly present in the zero field cooled dc magnetization data, which actually indicates the onset of spin glass freezing in the sample. Isothermal magnetization (M) measurement as a function of magnetic field (H) at 5K with field cooled condition (sample cooled in presence of different magnetic field) has been performed but no shift in M(H) loop is observed. It indicates that no exchange pinning is originated in the sample due to field cooling.

SO15

Magnetic properties of dioxygen molecules confined in single-walled carbon nanotubes

Yusuke Nakai^{*}, Shin Tadera¹, Haruka Kyakuno¹, Keitaro Harada¹, Kazuyuki Matsuda², Kazuhiro Yanagi¹ and Yutaka Maniwa¹
¹ Department of Physics, Graduate School of Science, Tokyo Metropolitan University, Japan
² Faculty of Engineering, Kanagawa University, Japan

Materials confined in quasi-1D single-walled carbon nanotubes (SWCNTs) exhibits unique properties that differ from the bulk counterparts [1]. Among many kinds of intercalates, a dioxygen molecule (O₂), which has a spin S = 1 in the ground state, confined in SWCNTs may offer well-defined environment to investigate the physics of a quasi-1D spin-1 magnet. We present magnetic susceptibility and x-ray diffraction measurements as well as theoretical simulations on the dioxygen molecules confined in SWCNTs. Our XRD measurements confirmed that the O₂ molecules are absorbed inside the SWCNTs at low temperatures. Our magnetic susceptibility data shows the signature of the opening of a gap in spin excitations at low temperatures, which differs from bulk O₂ molecules. We interpret this result in terms of 1D antiferromagnets with S = 1, which is supported by our first-principles calculation suggesting that an isolated O₂ molecule inside a SWCNT of over 0.8 nm in diameter possess a spin S = 1. We will also discuss the condensed structure of O₂ inside SWCNTs on the basis of our XRD data and molecular dynamics simulations [2].

[1] Y. Maniwa et al., Chem. Phys. Lett. 401 (2005) 534. [2] K. Hanami et al., J. Phys. Soc. Jpn. 79 (2010) 023601.

SO16

Magneto-elastic coupling and magnetocaloric effect in Fe₂P-based Mn-Fe-P-Si compounds

N. H. Dung^{*}, L. Zhang², Z. Q. Ou¹ and E. Bruck¹
¹ Delft University of Technology, Netherlands
² BASF Netherlands B.V & Delft University of Technology, Netherlands

Structural, magnetic and magnetocaloric properties of Fe₂P-based Mn-Fe-P-Si compounds were investigated. The study reveals a strong magneto-elastic coupling that starts to develop in the paramagnetic state and grows when the ferromagnetic transition temperature is approached. This magneto-elastic coupling over a large temperature range around the transition temperature results in a first-order phase transition with abrupt changes in lattice parameters. Moreover, a correlation is observed between the hysteresis and the discontinuous changes in lattice parameters at the transition. The gradual development of the magneto-elastic coupling near the transition temperature, which is attributed to competition between moment formation and bonding [1], contributes to a reduced hysteresis. We also show the thermal evolution of the magnetic moments. Interestingly, the magnetic moments on the 3f site are formed and gradually increase in the paramagnetic state, and suddenly jump to a larger value when magnetic order is established.

[1] N. H. Dung, Z. Q. Ou, L. Caron, L. Zhang, D. T. Cam Thanh, G. A. de Wijs, R. A. de Groot, K. H. J. Buschow, E. Bruck, Adv. Energy Mater. 1, 1215 (2011).

SO17

Magneto-refractive effect in manganites

Andrey Telegin^{*}, Yurii Sukhorukov and Vladimir Bessonov
 Institute of Metal Physics UD of RAS, Russia

We studied a magnetic-field-induced change in reflectivity (magneto-reflection) and transmission (magnetotransmission) of natural light in La_{1-x}A_xMnO₃ (A=Ca,Sr,K,Ag) manganites possessed the colossal magnetoresistance effect (CMR)[1-3]. It was showed the magneto-reflection and magnetotransmission effects in manganites are an optical response to the CMR in the IR-region. Effects can reach tens of percents in the field of 0.3-1 T near the magnetic phase transition temperature. The observed phenomena are connected with the change of ratio between the localized and delocalized charge carriers under the magnetic field applied [2]. At the same time, there is no strict correlation between these effects and CMR in the visible range. The observed phenomena are connected with the alteration of the optical density under the magnetic field in the range of interband transitions [3]. Magnitude of effects is one order as less as that in the IR-region. The nature of observed effects in manganites can be satisfactory explained within the framework of the theory of magneto-refractive effect [4]. The results of study of magneto-reflection and magnetotransmission in manganites may be proposed for creation of different magnetic and electronic sensors and light modulators.

[1] Yu.P. Sukhorukov, A.V. Telegin, A.B. Granovsky et al., J. of Experimental and Theoretical Physics, 138, No 3, 402 (2010). [2] A.B. Granovskii, Yu.P. Sukhorukov, A.V. Telegin et al., J. of Experimental and Theoretical Physics, 112, No.1, 77 (2011) [3] Yu.P. Sukhorukov, A.V. Telegin, A.B. Granovsky et al., J. of Experimental and Theoretical Physics, 141, No.1, 160 (2012) [4] Yursov A.N., Bakhvalova T.N., Telegin A.V. et al., Abstracts of the 20th International Conference on Soft magnetic materials SMM-2011, Greece, 18-22 September, p.244

Supported by the program of DFRAS "Physics of new materials and structures", grant MK-1048.2012.2 and RFBR grants No 10-02-00038, 11-02-00252, 12-02-00208

SO18

Electroresistance and joule heating effects in manganite thin films

Luis Pena, Regina Galceran, Zorica Konstantinovic, Alberto Pomar, Bernat Bozzo, Luis Balcells, Felip Sandiumenge and Benjamin Martinez^{*}
 Magnetic Materials and Functional Oxides, ICMAB - CSIC, Spain

Electroresistance (ER), i.e. electric field- and/or current-induced resistance switching, has attracted much attention recently because of the possibility of using it for the implementation of resistance random access memories (ReRAM). Although ER is a quite common phenomenon in transition metal oxides, that has been extensively studied both theoretically and experimentally, the precise mechanism involved is not clear yet. In this work we report on the ER measurements in patterned La_{0.7}Sr_{0.3}MnO₃ (LSMO) thin films prepared by sputtering. In order to analyze Joule heating effects we have evaporated a Pt layer on top of the LSMO path to have access to the actual temperature of the sample while measuring resistance of LSMO path or I(V) characteristic curves. I(V) curves have been measured at different temperatures and the corresponding resistance values are compared with that of the R(T) curve taking into account the actual temperature of the sample in order to clarify the role of Joule heating in the observed change of the resistance.

SO19

Magnetocaloric effect and other properties of cold rolled Gd ribbons

Sergey V. Taskaev¹, Vasily D. Buchelnikov¹, Igor V. Bychkov¹, Anatoliy P. Pelennin², Oliver Gutfleisch³, Konstantin P. Skokov⁴, Vladimir V. Khovaylo⁵, Victor V. Kolesov⁶ and Vladimir G. Shavrov⁶
¹ Physics department, Chelyabinsk State University, Chelyabinsk, Russia
² South-Ural State University, Chelyabinsk, Russia
³ Technische Universität Darmstadt, Darmstadt, Germany
⁴ IFW, Dresden, Germany
⁵ MISIS, Moscow, Russia
⁶ IRE RAS, Moscow, Russia

The number of papers devoted to magnetic refrigeration, magnetocaloric materials and high-field magnetic systems has grown at an exponential rate in the past 10 years (K.A. Gschneidner et al., 2008) [1]. Since First International Conference on Magnetic Refrigeration at Room Temperature many researchers in different countries mobilize their efforts in the field of constructing commercial magnetic refrigerator. There are numerous different magnetocaloric alloys such as La-Fe-Si, Gd-Si-Ge, Ni-Mn-X (X = Ga, In, Sn, Sb) [2-3]. Usually the magnetic refrigerant materials are either packed in a magnetocaloric bed as small spheres attached around a disk as a ribbon or separated in a pile of thin, equally spaced sheets. Thus one the ways of engineering MCE materials is tightly connected with preparing very thin (a few microns) ribbons of high value MCE alloys with good mechanical properties. At present rapid solidification is the main technique for producing this kind of materials [4]. In our work we investigate magnetocaloric effect, magnetic and mechanical properties of Gd cold rolled samples of different thickness. Both theoretical and experimental aspects of the investigation are discussed.

1. Gschneidner K.A. Jr. et al. Thirty years of near room temperature magnetic cooling: Where we are today and future prospects, Int. J. Refrig. 31, 945 (2008). 2. A. Planes, L. Manosa, and M. Acet, J. Phys.: Condens. Matter 21, 235201 (2009). 3. X. Moya, L. Manosa, A. Planes, S. Aksoy, M. Acet, E. Wassermann, and T. Krenke, Phys. Rev. B 75, 184412 (2007). 4. P. M. Shan et al. Magnetic behavior of melt-spun gadolinium, Phys. Rev. B 77, 184415 (2008).

SO20

Fabrication and properties of double perovskite SrLaVRuO₆

Ryosuke Zenzai*, Tetsuya Miyawaki, Kenji Ueda and Hidefumi Asano
Crystalline Materials Science, Nagoya University, Japan

Half-metallic antiferromagnets (HMAF) exhibiting both fully spin-polarized charge transport and zero net magnetic moment are expected to provide not only a fertile playground for fundamental research but also new spintronic devices. Although the theoretical calculations predicted candidates for HMAFs, experimental searches for HMAFs have so far been unsuccessful. This paper reports on the fabrication and properties of SrLaVRuO₆ polycrystalline bulks and epitaxial films. SrLaVRuO₆ bulks were synthesized by a solid-state reaction at 1100–1350 °C in Ar + (0–3) % H₂ gas. Structural characterization revealed that the main phase of the bulk samples was of a double perovskite crystal structure with lattice parameters of 0.7888–0.7905 nm. However, all the bulks contained the impurity phase (Sr₂V₂O₆), which is a nonmagnetic semiconductor. The bulks exhibited magnetization values of 10–3 μB per formula unit at 77 K, negative paramagnetic Curie temperature values and metallic temperature dependence of the resistivity. These properties are assumed to be intrinsic to double perovskite SrLaVRuO₆ by considering the nonmagnetic semiconducting nature of Sr₂V₂O₆. Moreover, SrLaVRuO₆ thin films were prepared on LaAlO₃, SrTiO₃ (001) substrates by magnetron sputtering. Structural characterization revealed that these thin films were grown epitaxially on these substrates, and phase pure double perovskite.

J. H. Park, S. K. Kwon, and B. I. Min, Phys. Rev. B 65 (2002) 174401.

SO21

Giant magnetoresistive effect in non-magnetic silicon

Tae Ho Lee¹, Hong-seok Kim¹, Woo Lee² and Yong-joo Doh^{1*}

¹ Dept. of Display and Semiconductor Physics, Korea University Sejong Campus, Korea

² Korea Research Institute of Standards and Science, Korea

Recently magnetoresistive effects in non-magnetic semiconductors, particularly silicon, have gained considerable attention owing to the large magnitude of the effect, which is comparable, or even larger than, that of the performance of commercial giant-magnetoresistance devices. The underlying mechanism responsible for the giant magnetoresistance in silicon, however, has not yet been fully explored. Here we report that a simple device, based on a lightly doped silicon substrate contacted with two indium contacts, shows a positive magnetoresistance over 10,000 per cent for magnetic fields between 0 and 1 T at low temperature of 3 K. Current-voltage characteristics exhibit a nonlinear behavior, which is highly sensitive to temperature and magnetic field. We have extensively studied magnetoresistive effect in silicon with varying bias voltage, temperature, electrode spacing, and the relative angle between the substrate and the applied magnetic field. Since our device is based on a conventional silicon platform and is highly sensitive to low magnetic field, it could be used to develop new devices of silicon-based magnetoelectronics.

SO22

Effect of Fe substitution on Ni-Mn-In shape memory alloys: Magnetic and magneto-structural properties

Radha S¹, Ashwin Mohan² and A. K. Nigam^{2*}

¹ Department of Physics, University of Mumbai, India

² Department of Condensed Matter Physics and Materials Science, Tata Institute of Fundamental Research, India

The Ni-Mn based ferromagnetic shape memory alloys have been extensively investigated for their multifunctional properties emerging by suitable chemical substitutions. The off-stoichiometric Ni₅₀Mn_{25-x}In_{25-x} exhibit martensitic transition for In concentration in the range 13-16 at%. In the Ni₅₀Mn_{25-x}In_{25-x} alloy, the ferromagnetic transition occurs at Curie temperature TC = 305 K with a concomitant austenite to martensitic transition. A large inverse magnetocaloric effect and anomalous magnetic behavior have earlier been reported for this alloy [1]. The present work reports the effect of Fe-substitution (0.5 to 2 at%) on the magneto-structural transition and magnetic behavior of the Ni₅₀Mn_{25-x}In_{25-x} alloy. The martensitic transition goes down to 255 K for 1at% Fe alloy with strong hysteresis between zero field-cooled (ZFC) and field-cooled (FC) data while it nearly disappears for the 2at% Fe alloy. The 0.5 at% Fe substituted alloy shows a temperature dependent field-induced metamagnetic transition between 250-220K while this transition is not observed up to fields of 6T in 1at% Fe substituted alloy. A thermal hysteresis in the temperature dependence of resistance is observed between heating and cooling cycles due to austenitic-martensitic transitions up to 1 at% Fe substitution. The substitution of 2 at% Fe suppresses the martensitic transition without affecting the ferromagnetic transition.

[1] P.A. Bhobe, K.R. Priolkar and A.K. Nigam, Appl. Phys. Lett. 91 (2007) 242503

SO23

Magnetic properties and magnetocaloric effect in shape memory alloys Ni-Mn-Ga

Rafael Fayzullin, Vasily Buchelnikov, Sergey Taskaev and Mikhail Drobosyuk
Chelyabinsk State University, Russia

The magnetocaloric effect (MCE) is the ability of magnetic materials to heat up or cool down when placed in or removed from an external magnetic field. The magnetic materials with large values of MCE can be applied in the magnetic refrigeration technique [1]. Recent experimental studies have shown that Ni-Mn-Ga Heusler alloys are also attractive for the application in magnetic refrigeration [2]. In this work the magnetic and magnetocaloric properties of the ferromagnetic shape memory alloys Ni_{2-x}Mn_{1-x}Ga (x=0.07; 0.08; 0.09) were experimentally studied. The MCE measurements were performed by the setup produced by AMT&C [3]. In this setup, the adiabatic temperature change ΔTad was measured by a direct method with help of a thermocouple. Magnetic field up to 2 T was created by Halbach permanent magnet. The magnetic field strength was measured by Hall probe. Signals from the thermocouple and Hall probe were recorded simultaneously what allowed us to measure ΔTad as a function of magnetic field H. All alloys exhibit the positive MCE typical near the second-order phase. Our MCE measurements of Ni_{2-x}Mn_{1-x}Ga have shown that the maximal MCE is observed near the Curie point. The maximal values of MCE are 1.2 - 1.6 K near the room temperature.

[1] J. Gschneidner, Jr. and V.K. Pecharsky, Int. J. Refrig., 31 (2008) 945. [2] A. Planes, L. Manosa, and M. Acet, J. Phys.: Condens. Matter. 21 (2009) 233201. [3] Y.I. Spichkin, et al, Proc. 3rd IIR-III Intern. Conf. Magnetic Refrigeration at Room Temperature, IIR/III (2009) 173.

SO24

Magnetic susceptibility avalanches in thermally-induced first-order phase transition of La(Fe_{0.88}Si_{0.12})₁₃ magnetocaloric compound

Asaya Fujita* and Hitomi Yako

Department of Materials Science, Tohoku University, Japan

Magnetic materials with large magnetocaloric effects due to the first-order phase transition attract attention as candidates for room temperature magnetic refrigerants. NaZn₁₃-type La(Fe_xSi_{1-x})₁₃ compounds exhibit thermally-induced first-order ferromagnetic (F) - paramagnetic (P) transition at the Curie temperature Tc and the itinerant-electron metamagnetic transition takes place above Tc [1]. Evolution of the transition determines the operating speed of magnetic refrigeration, therefore, a detailed observation is necessary. In the present study, appearance of the avalanche behavior [2] in the progress of thermally-induced transition has been examined by measuring the magnetic susceptibility χ. The value of χ upon cooling at 0.4 K / min. exhibits a smooth variation across the transition and its first derivative, dχ/dT, shows no jerky change. Meanwhile, the avalanche-like behavior is observed in dχ/dT around Tc upon heating. Furthermore, the number and height of avalanches are dramatically changed by external magnetic fields. Generally, the avalanche behavior is induced by the quenched disorders, however, such a mechanism can not explain the influence of magnetic field. Considering the fact that the kinetics of the transition is influenced by the demagnetization effect [3], these results indicate that the nucleation- growth behavior is affected by the magnetic dipole interaction.

[1] A. Fujita, S. Fujieda, Y. Hasegawa, K. Fukamichi: Phys. Rev. B 67 (2003), 104416. [2] E. Vives, J. Ortin, L. Manosa, I. Rafoj, R. Perez-Maqueo, A. Planes: Phys. Rev. Lett. 72 (1994), 1694. [3] H. Yako, S. Fujieda, A. Fujita, K. Fukamichi: IEEE Trans. Magn. 47 (2011), 2482.

SO25

Phase coexistence and magnetocaloric effect on martensitic transition in Ni-Co-Mn-Sn metamagnetic shape memory alloy

Bo Gao^{1*}, Wen Guan¹, Yu Wang¹, Sen Yang¹, Xiaoping Song¹, Fengxia Hu², Jirong Sun² and Baogen Shen²

¹ MOE Key Laboratory for Nonequilibrium Synthesis and Modulation of Condensed Matter, Xi'an Jiaotong University, China

² State Key Laboratory of Magnetism, Institute of Physics, Chinese Academy of Sciences, China

Since the discovery of the metamagnetic shape memory effect in Ni₅₀Co₂₀Mn₂₀In₁₀ Heusler alloys [1], a member of studies on magnetocaloric effect (MCE) have been made in metamagnetic shape memory alloys. It is found that metamagnetic shape memory alloys exhibit large MCE in the vicinity of martensitic transformation. But for the first-order transition, whether and to what extent the Maxwell relation is applicable are problems requiring further study [2]. In this paper, we will discuss the appropriate approach to evaluate the MCE in Ni-Co-Mn-Sn alloys. The energy dispersive spectrometer shows that the sample composition is Ni_{43.3}Co_{3.1}Mn_{41.8}Sn_{11.9}. The thermo-magnetic curves indicate the martensitic transformation can be driven by the magnetic field. It is observed that metamagnetic transition takes place in a wide temperature range from the magnetization isotherms. The entropy change calculated by Maxwell relation is up to 30J/kgK under a field change of 0.5T. Meanwhile, we calculated the entropy change based on heat capacity measured under 0 and 5T, and an entropy change of ~3J/kgK is obtained for a field change of 0.5T. According to the different results from magnetic and calorimetric measurements, we find that the Maxwell relation should be used with caution on martensitic transformation including phase coexistence.

[1] R. Kainuma, Y. Imano, W. Ito, Y. Sutou, H. Morito, S. Okamoto, O. Kitakami, K. Ohkura, A. Fujita, T. Kanomata, and K. Ishida, Nature 439, 957 (2006)
[2] G. J. Liu, J. R. Sun, J. Shen, B. Gao, H. W. Zhang, F. X. Hu, and B. G. Shen, Appl. Phys. Lett. 90, 032507 (2007)

SO26

Balance between the growth rate of ferromagnetic phase and demagnetizing fields in itinerant electron metamagnetic transition of La(Fe_{0.88}Si_{0.12})₁₃

Hitomi Yako* and Asaya Fujita
Tohoku university, Japan

Strong interplay between an itinerant electron metamagnetic (IEM) transition and magnetocaloric effects in NaZn₁₃-type La(Fe_xSi_{1-x})₁₃ has been investigated.[1-3] Recently, we have demonstrated that progress of the IEM transition is influenced by the demagnetization effect in La(Fe_{0.88}Si_{0.12})₁₃. [4] Especially, the progress is arrested in midstream even under the magnetic fields, μH larger than the critical value, μHc by setting longitudinal direction of the sample perpendicular to the field direction (θ = 90 degrees). In the present study, the angular dependence of the transition progress is examined and the influence of demagnetization effect on the IEM transition is discussed. The time-dependent magnetization measurements were carried out at 200 K under the constant value of μH by changing θ from 0 to 90 degrees. The transition starts to proceed under the magnetic field larger than μHs. However, the transition is arrested in midstream, and the completion of transition emerges only after μHc exceeds the threshold value, μHt. The values of μHs and μHt are evaluated to be 0.60 and 0.75 T for θ = 30 degrees and 0.70 and 1.00 T for 90 degrees, respectively. The growth rate of ferromagnetic phase is dominated by keeping the balance with demagnetizing fields.

[1] A. Fujita et al., J. Appl. Phys., 85, 4756-4758, (1999), [2] F. X. Hu et al., Appl. Phys. Lett., 78, 3675-3677, (2001), [3] O. Gutfleisch et al., J. Appl. Phys., 97, 10M305:1-10M305:3, (2005), [4] H. Yako et al., IEEE Trans. Mag., 47, 2482-2485, (2011).

SO27

Temperature dependent structural and magnetic properties of Ni-Mn-In Heusler alloy glass-coated microwires

Valeria Rodionova^{1*}, Mikhail Ipatov², Maxim Ilyin¹, Valentina Zhukova³, Alexander Granovsky³ and Arcady Zhukov⁴

¹ I. Kant Baltic Federal University, UPV/EHU, Lomonosov Moscow State University, Russia

² UPV/EHU, Spain

³ Centro de Física de Materiales, CSIC/UPV, Spain

⁴ Dpto. Física de Materiales, Fac. Químicas, UPV/EHU, Spain

⁵ Lomonosov Moscow State University, IKERBASQUE, Basque Foundation for Science, Russia

⁶ Dpto. Física de Materiales, Fac. Químicas, UPV/EHU, IKERBASQUE, Basque Foundation for Science, Spain

Magnetic shape-memory alloys (MSMAs) attracted growing attention owing to shape memory effect, originated from the coupling between magnetic and structural ordering. From point of view of technological applications, miniaturizing of MSMA-based devices using MSMA particles, wires, ribbons, films, bi- and multilayers, pillars is quite important. Here we report on studies of magnetic properties of non-stoichiometric Heusler-type Ni₅₀Mn_{25-x}In_{25-x} and Ni_{50-x}Mn_{25-x}Ga_{25-x} glass-coated microwires prepared using Taylor-Ulitovskiy technique. The principle interest in glass-coated microwires is related with their composite character allowing to control the strength of internal stresses. We measured magnetization curves at different temperatures. As-prepared microwires did not show ferromagnetic ordering at room temperature. From temperature dependence of magnetization we found that annealed microwires showed Curie temperature about 270 K (Ni₅₀Mn_{25-x}In_{25-x} microwires), between 225K and 240 K (Ni_{50-x}Mn_{25-x}Ga_{25-x} microwires with different metallic nucleus diameters) and 315 K for Ni_{50-x}Mn_{25-x}Ga_{25-x}. Microwires Ni₅₀Mn_{25-x}In_{25-x}, Ni_{50-x}Mn_{25-x}Ga_{25-x} and Ni₅₀Mn_{25-x}Ga_{25-x} exhibited phase transition at 240 K, 115 K and 300 K respectively. From point of view of applications the most promising properties exhibit thinnest Ni_{50-x}Mn_{25-x}Ga_{25-x} microwire (with metallic nucleus diameter 10.4 μm and total diameter of 16 μm) showing the phase transition near Curie temperature.

SO28

Magneto-optical Kerr effect enhancement in Co/TiO₂ layered films

Victor Polyakov¹, Konstantin Patrin¹, Klaudia Polyakova^{1*}, Vitaly Seredkin¹ and Gennady Patrin²

¹ L.V. Kirensky Institute of Physics, SB RAS, Russia

² Siberian Federal University, Russia

As is known, the magneto-optical properties of the composite metal-dielectric systems are determined by the volume of a magnetic phase and the properties of a dielectric matrix or dielectric layers. Of special interest are the magneto-optical properties of the composite films containing TiO₂ whose permittivity is higher as compared to SiO₂ and Al₂O₃. Here, we report the results of the magneto-optical study of Co/TiO₂ multilayers. Particularly we studied spectral dependence of the polar Kerr effect of Co / TiO₂ layered structure of with various number of layers. The composite Co/TiO₂ periodic structures consisting of 2–12 pairs of layers (n) were prepared by sequential deposition of Co and titanium oxide by ion-plasma sputtering and reactive ion-plasma sputtering, respectively, onto glass substrates. The respective thicknesses of magnetic and titanium oxide layers were 5 and 17 nm. Study of spectral dependence of polar Kerr effect showed that the spectra of the Co/TiO₂ layered structures are resonance, with the large growth of the angle of rotation near the resonance. The maximum angle of rotation nonmonotonically depends on the number of layers. The maximum Kerr rotation angle (20k=7.3 deg) observed at a wavelength of 540 nm corresponds to n = 8.

SO29

Electronic structure calculations and the magnetic properties of Ru₂FeZ (Z = Al and Ga)

Ramesh Kumar K and Thamizhavel A*

Department of Condensed Matter Physics and Materials Science, Tata Institute of Fundamental Research Mumbai 400005, India

After the discovery of half-metallic character in NiMnSb by de Groot et al. Heusler alloys have drawn much attention due to the possible application in magneto-electronic devices [1,2]. In the quest of finding half-metallic character in 4d transition element based Heusler alloy we present the electronic structure and magnetic properties of Ru₂FeGa/Al. The band structure calculations were done using the state-of-the-art density functional technique with the PWSCF code [3]. The equilibrium lattice parameter was found by fitting energy vs volume data to the Murghnan equation of state. At the equilibrium lattice parameter the total energy difference between the non-magnetic state and ferromagnetic state was observed to be of the order of 5 meV which suggest that these systems are having stable magnetic ground state. In ferromagnetic ground state the lattice parameter was observed to be 5.988 Å for Ru₂FeGa and 5.982 Å for Ru₂FeAl. From the DOS Vs Energy diagram it is found that the systems are not half-metallic in nature. However, the calculation showed very high spin polarization at the Fermi level. The spin polarization (P) value was found to be 83 % in both the cases.

I. R. A. de Groot, F. M. Mueller, P. G. van Engen and K.H. J. Buschow , Phys. Rev. Lett. 50 2924 (1983). 2. C. Felser, G. H. Fecher, and B. Balke *Angew. Chem. Int. Ed.* 46 688 (2007). 3. S. Baroni et al <http://www.pwscf.org/>

SO30

Disorder effects in giant magnetocaloric materials

Joao S Amaral*, Soma Das and Vitor S Amaral

CICECO and Dept. of Physics, Universidade de Aveiro, Portugal

In striving for mass production of magnetocaloric materials for refrigeration applications, one has to face the fact that these will not be laboratory-grade materials, and will necessarily present composition gradients due to lower quality reagents. Some consequences are expected: the maximum value of magnetic entropy change (ΔSM) should decrease compared to a “pure” material, and broadening of the ΔSM(T) curves, as observed in elementary ferromagnets [1]. Some theoretical work has focused on this topic, for second-order phase transition systems [2–5]. Still, these theoretical considerations do not directly apply to giant magnetocaloric materials. We present a study on the effect of disorder on the magnetic and magnetocaloric properties of first-order phase transition systems, via the use of the Bean-Rodbell [6] model. Disorder is shown to “smooth” the discontinuities on magnetization and ΔSM, and also affect magnetic hysteresis. For sufficiently large disorder, the ΔSM(T) curves resemble the distribution function. We discuss how the magnetic field dependence of ΔSM is affected by disorder, in light of a “second-order like” dependence of ΔSM on applied magnetic field, for disordered LaFeSi samples [5]. Aging effects on hydrogenated LaFeSi samples, that degrade even in storage [7], are discussed taking into account our theoretical simulations.

[1] Gschneidner Jr. K. A., Pecharsky V. K., *Isokol A. O.*, 2005, *Rep. Prog. Phys.* 58 1479. [2] Romanov A. Y., V. P. Silin V. P., 1997, *Phys. Met. Metallogr.* 83, 111. [3] Amaral J. S. et al., 2008, *J. Non-Cryst. Solids* 354, 5301. [4] Bahl C. R. H., et al., 2011, *J. Magn. Magn. Mat.* 324 564. [5] Lyubina J. et al., 2011 *Phys. Rev. B* 83 012403. [6] Bean C. P., Rodbell D. S., 1962, *Phys. Rev.* 126 104. [7] Barcza, A. et al., 2011, *IEEE Trans. Magn.* 47 3391.

SO31

On the Curie temperature dependency of the Magnetocaloric effect

Joao H Belo¹, Joao S Amaral^{2*}, Andre M Pereira¹, Soma Das², Vitor S Amaral² and Joao P Araujo¹

¹ IFIMUP and IN, Dept. de Física e Astronomia, FCUP, 4169-007 Porto, Portugal

² CICECO and Dept. of Physics, Universidade de Aveiro, Portugal

A theoretical study of the magnetocaloric effect dependency on simple ferromagnetic microscopic parameters is here presented. Considering the Bean-Rodbell model [1] of magnetovolume coupling within the Weiss mean field theory, the magnetic entropy change of systems undergoing first and second order magnetic phase transition was numerically simulated. Through these simulations, the magnetic entropy change behavior was studied as a function of: Tc, spin value, applied field changes and the nature of the transition considered. The main result found for both first and second order magnetic transitions systems is the linear dependency of the ΔSM(T) maximum value on Tc^{2.5}. By starting from the magnetization mean field state equation an approximated expression for the magnetic entropy change as a function of microscopic magnetic parameters was reached, confirming the Tc^{2.5} dependency. We have found that many ferromagnetic systems, both undergoing second (Gd/Tb/Co [2], RR'Al [3] (R = rare earth), RCoMn [4]) and first-order (MnFePAs [5], GdSiGe [7], RCo [7]) phase transitions, obey this relation between the magnetocaloric effect and Tc.

[1] Bean C. P., Rodbell D. S., 1962, *Phys. Rev.* 126 104. [2] K. Zhou et al. *Solid State Commun.* 137, 275 (2006). [3] N. Duc, D. Anh, and P. Brommer, *Physica B - Cond. Matter* 319, 1 (2002). [4] A. K. Pathak et al., *J. Magn. Magn. Mater.* 323, 2436 (2011). [5] O. Tegus et al., *Physica B - Cond. Matter* 319, 174 (2002). [6] K. A. Gschneidner, V. K. Pecharsky, and A. O. Isokol, *Rep. Prog. Phys.* 68, 1479 (2005). [7] N. Duc, D. Anh, and P. Brommer, *Physica B - Cond. Matter* 319, 1 (2002).



AUTHOR INDEX

A

Abbamonte, P.	PH10	148	Akama, Takamitsu	PG07	143	Amaral, Vitor S.	KB06	108	Arai, Hiroko	RJ06, SI16	283, 348
Abbasian Arani, A. A.	PO30	182	Akatsu, Mitsuhiro	RB05, RD07	254, 263	Amarande, L.	SA11	318	Arai, Masatoshi	DA01, RH12	56, 276
Abbasian Arani, Ali Akbar	PO28	181	Akatsuka, Hiroyuki	PB34	125	Amato, Alex	IA02, PI06, QB22	90, 151, 190	Arakawa, Akira	SLO2	356
Abdel - Hafiez, M.	QF22	207	Akbari, Alireza	PD06	132	Amemiya, Kenta	BH06	47	Arakawa, Naoya	SE04	333
Abdul Ahad, Faris B.	RK07	287	Akdogan, Ozan	CB05, KB04	49, 108	Amitsuka, Hiroshi	PD07, QC25, SE07	133, 196, 334	Araki, Koji	RB05	254
Abdullah, Nor Hapishah	BJ06	48	Akerman, Johan	CE01, CE02, PK13	51, 162	Amyan, Adham	QA11, QJ11	184, 222	Araki, Shingo	HC02, PE15, QC18, SE10	84, 138, 195, 334
Abe, Kazutaka	IF02	94	Akerman, Johanna	KE01	110	Analytis, James	HA05	84	Araki, Yusuke	QJ12	222
Abe, Nobuyuki	QA10, QA13, QA17	184, 175, 185	Akhavan, M.	QP23	249	Anand, Vivek Kumar	QB14	189	Aramberri, Hugo	SD16	332
Abe, Taro	SM09	362	Akimitsu, Jun	DF03, PB06, PB07, PC21, PG09, QG22, QG28, RH13, SF02, SG16	60, 121, 130, 143, 211, 212, 276, 337, 342	Anane, Abdelmadjid	IE04	94	Arango, Y. C.	QF22	207
Abid, Mohamed	PI14, SH13	157, 345	Akiyama, T.	RM04	295	Andersen, Ole Krogh	SC07	326	Araoka, Nobutaka	SB14	322
Abo, Gavin Sky	JH04	104	Akiyama, Toru	RM05, SO10, SO11	296, 368	Andersson, Gabriella	EI03	71	Araujo, Joao P	SO31	371
Abramova, G. M.	SG20	342	Akutsu, Yasuhiro	RI01	279	Andersson, Yvonne	PM10	169	Araujo, M. A. N.	SB21	323
Abrosimova, Galina	SO04	367	Alameda, Jose Maria	GG03	80	Ando, K.	CE03, ID02, RJ07	51, 93, 283	Araujo, Miguel	RB25, RF13	258, 271
Abrudan, Radu	EC04	66	Alaria, Jonathan	PI04	151	Ando, Kazuya	AI02	39	Arbelo Jorge, Elena	CH04	54
Acquarone, Marcello	SI10	347	Alayo, William E.	SM17	363	Ando, Ken	KF01	110	Ardavan, Arzhang	SB20	323
Aczel, A. A.	GF01	79	Alayo, Willian	PL09, QM14	165, 233	Ando, Koji	BI01	47	Arenholz, Elke	DH01	62
Adachi, Hiroto	FA03	72	Alba Venero, D.	QM06	232	Ando, Y.	SK24	354	Arepalli, Sivaram	PJ32	160
Adachi, Nobuyasu	KC02	108	Albert, Barbara	PI05	151	Ando, Yasuo	CH02, EI02, EJ01, KD04, RL13, RO05, RO06, SI03, SI17, SK08	54, 70, 71, 110, 292, 301, 346, 348, 351	Arguello, C.	GF01	79
Adachi, Yoshiya	PG04, QI05	143, 218	Albertini, Franca	AG02	37	Ando, Yoichi	HI01, RC11	89, 260	Argyriou, D.	RB17	256
Adam, Philip	CH01	54	Albrecht, Michele	RK05	286	Ando, Yuhki	SA03	316	Argyriou, Dimitri	RB01, RB07	254, 255
Adam, Sorin	PM06	168	Albrecht, Ole	FD02	74	Andrade, Bruna	QL01	228	Argyriou, Dimitrios	PA10	117
Adamo, Carolina	SA08	317	Aldus, Robert	PO12	179	Andre, Gilles	JB05, RA11, RD14	100, 251, 264	Arhan, H. Z.	CI01	54
Adams, M	SE05	334	Aleshkevych, Pavlo	QM17	234	Andreev, A. V.	QG07, QI03, QI09, RD26	209, 218, 219, 266	Arikan, Mustafa	GA01	75
Adams, T.	PI09	152	Alfadhel, Ahmed	PM27	171	Andreev, A.v.	GJ03	82	Arima, Takahisa	GH03	81
Adams, Tim	DF02	60	Alfahad, S.	RN18	299	Andreev, Alexander	RE09, SG03	267, 340	Arima, Taka-hisa	PG20, QD02, QO13	145, 196, 242
Adenot Engelvin, Anne Lise	AJ01	39	Alff, Lambert	PI05	151	Andreev, Alexander V.	QI19	220	Arinicheva, Olga	IA04, PA12, PG14, QA10, QA13, QA17	91, 117, 144, 184, 175, 185
Adiga, Shilpa	QA23	186	Algarabel, P. A.	KC05, PJ23	109, 158	Andrei, Gloskovskii	SD15	332	Arita, Masashi	QJ13	223
Adriano, Cris	SE15	335	Algarabel, Pedro Antonio	SM16	363	Andreica, Daniel	CD04, SE08	51, 334	Arita, Ryotaro	RD20	265
Adroja, D T	KA02, SE03, SE05, SE13, SF09	107, 333, 334, 335, 338	Ali, Md. Ehesan	BC02	42	Angelakeris, Makis	RP15	305	Arita, Ryotaro	AE05, QC04	36, 192
Adroja, Devashibhai	PC12, SD13	128, 332	Ali, Naushad	CH01	54	Angst, Manuel	QA23	186	Arnold, Z.	PJ23	158
Adroja, Devashibhai T.	SE20	336	Aliakbari Miyan Mahaleh, M.	PO30	182	Anh Nguyen, T. N.	PK13	162	Arnold, Zdenek	PM11	169
Adschiri, Tadafumi	RN11	298	Alidoust, N.	SD04	330	Anh Tuan, Duong	PJ15	157	Aronin, Alexander	SO04	367
Aeppli, Gabriel	PJ17	157	Aliouane, Nadir	PA10	117	Anh, D. T. K.	QG11	210	Arora, Sunil Kumar	PH16	149
Afzali, Reza	SC09	327	Alireza, Patricia	PC02, RQ09	127, 308	Anil Kumar, P. S.	PH04	147	Arredondo, Yesenia	QG21	211
Agbelele, Arsene	QA27	187	Alireza, Patricia L	SC16	328	Anisimov, M. A.	QC22, RH07	195, 275	Arshi, Nishat	PN15	174
Agrestini, Stefano	BF03	45	Allred, Jared M	QB13	189	Annal Therese, Helen	QA25	186	Artyukhin, Sergey	CI01	54
Agterberg, Daniel	RB26	258	Al-mahdawi, Muftah	PJ11	156	Annett, James	JA05	99	Arvanitis, D.	DD02	58
Agui, Akane	PM02	167	Alnassar, Mohammed	SA02	316	Antohe, Stefan	QK20	227	Arzhnikov, Anatoly	BF04	45
Ah, Chil Seong	RL21	293	Alonso, J	QM06	232	Antonelli, Alex	RB18	257	Asada, Hironori	PG06, QM10, RP12, SK13	143, 233, 305, 352
Ahmad, Dawood	QB25	191	Alotibi, M.	RN18	299	Antos, Roman	KD03	109	Asai, Shinichiro	PH12	148
Ahmad, Ehsan	EH04	70	Alqahtani, Mohammed S.	RN18	299	Antropov, Vladimir	SC07	326	Asai, Takuya	RD08	263
Ahmed, Faheem	PM14, PN15	169, 174	Al-senany, Nourh A.	PG01	142	Anwar, M S	PN15	174	Asai, Yugo	PM18	170
Ahmed, Mohamed Abbas Ali	RN21	300	Alshammari, Marzook S.	RN18	299	Anzai, Shuichiro	SE09	334	Asaka, Souta	BG04	46
Ahn, Chan-woo	RR31	316	Altarawneh, M. M.	SC03	326	Aoki, Dai	HP11, JC02, PD17, RE10, SF03	30, 100, 134, 268, 337	Asaki, Kenji	SG12	341
Ahn, Cheol-woo	DJ02	63	Altarawneh, Moaz	BA01, EA03	40, 64	Aoki, Haruyoshi	QC10, QC11	193, 194	Asano, Hidefumi	PJ12, PL12, RC18, SA07, SA17, SO20	156, 165, 261, 317, 319, 370
Ahn, Ho-seong	PM19, PM21	170	Althoyaib, S	QL21	231	Aoki, Hideo	EB02, RI14	65, 281	Asano, Hidehumi	PB34, SK18	125, 353
Ahn, Jae Young	QP18	248	Altshuler, Tatiana Semenovna	PE09	137	Aoki, Kento	QA05	183	Asano, Takayuki	PG17, QF11, QF14	145, 205, 206
Ahn, Kyo-hoon	SO05	367	Alvarez, Lorena	QO26	245	Aoki, Yuji	RD17	264	Asaoka, Rui	RF11	270
Ahn, San	SC15	328	Alvarez, Pablo	JJ04	106	Aoshima, Ken-ichi	SK21	353	Aschenbach, Konrad Hsu	EG01	69
Ahn, Sora	RL17	292	Alves, E.	QM13	233	Aoyagi, Mitsuharu	RP17	306	Ashida, Takuya	PB25, PL10	124, 165
Aichhorn, Markus	SG22	343	Alyamani, A.	RN18	299	Aoyama, Satoshi	PH20	150	Aslibeiki, B.	PI23	154
Ain, Qurat-ul	PB13	122	Alzayed, Nasser	RB29	258	Aparnadevi, M	RA08	250	Aso, Naofumi	PD14, QC11	134, 194
Aizawa, Kazuya	RH12	276	Amakai, Yusuke	PB08, QA19, QJ04, RD06, RD22, SE06	121, 185, 221, 263, 265, 334	Apinaniz, Estibaliz	QH16	215	Asokan, K	PG27	146
Akagi, Yutaka	PG23	146	Amako, Yasushi	QH04, RD19	213, 265	Aplesnin, Sergey	QG05	209	Asokan, K.	QO27	245
Akahoshi, Daisuke	QE20, QF21	202, 207	Amaral, Joao S	RI18, SO30, SO31	281, 371	Aplesnin, Sergey Stepanovich	PF01, SO02	139, 367	Assmus, Wolf	QE14	201
Akaki, Mitsuru	PA06, PA19, QA05, RA06, SB24	116, 119, 183, 250, 324	Amaral, V. S.	RH02	275	Aprilia, Ely	RC02	259	Asthana, Saket	PN18	175
			Amaral, Vitor S	RI18, SO30, SO31	281, 371	Arac, Erhan	QO24	244	Atkinson, Del	QO24	244

Attane, Jean-philippe	AI04, GE01, QK15, QK16, QK17, RL24, SL24	39, 78, 226, 293, 360	Bak, Zygmunt	SB11	322
Atxitia, U.	GD03	78	Baker, Peter J	PN23	175
Atxitia2, U	FC01	73	Baker, Peter. J.	QG19	211
Au, Yat-yin	EH04, HD03	70, 85	Bakr, Mohammed	CA03	49
Augendre, Emmanuel	AI04	39	Balae, Alexander	PI11	152
Augstine, Saji	QO27	245	Balae, Dmitry	SM19	364
Augustine, Tan Lee	QL02	228	Balagurov, Leonid A	PN22	175
Augustine, Tan Tuck Lee	PN03	172	Balakhonov, Sergey	ED06	67
Avanesyan, Grisha	ID03	93	Balakirev, Fedor	RB21	257
Avdeev, M.	SO08	368	Balakrishnan, G.	CC04, II02	50, 97
Avdeev, Maxim	IJ03	97	Balakrishnan, Geetha	GF03, SC06, SD13	79, 326, 332
Avdeev, Maxim V.	SC25	329	Balatsky, A. V.	QB08	188
Avella, Adolfo	RG18	274	Balatsky, Alexander	KG01	111
Aviani, Ivica	IA02	90	Balatsky, Alexander V	EB04, SE18	65, 336
Avignon, Michel	QG21, QO26	211, 245	Balbashov, A. M.	PA15	118
Avila, M A	QJ05	221	Balcells, Lluís	IH01, SO18	95, 369
Avila, Marcos A.	QO03	241	Balcerzak, Tadeusz	RI03, RI09	279, 280
Avramov, Pavel V	BH05, BH06	46, 47	Baldassarre, Leonetta	SA08	317
Awan, Muhammad Saifullah	SA15	318	Baldes Bango, Fernando	GG03	80
Awana, V. P. S	QM24	235	Baldovi, J.	BC01	42
Awano, Hiroyuki	GE04, JE04, PJ09, QP20	78, 102, 156, 248	Balents, Leon	JD03, PL08	101, 165
Awschalom, David D.	AI01	39	Balicas, Luis	CC02, EA03, JA02, RB19	50, 64, 98, 257
Ayala, Oscar	QB13	189	Balke, Benjamin	QN19	239
Ayala-valenzuela, Oscar	GC03	77	Ballou, Rafik	AC04	35
Azarevich, Andrey	QC20	195	Baltz, Vincent	AI04, BD02, DD01	39, 43, 58
Azuma, Masaki	QE10	201	Bance, Simon	DE01	59
B			Bando, Hiroshi	PM13	169
B., Parvatheeswara Rao	BJ05	48	Bandou, Hisamitu	PC05	127
Baba, Ryo	RR05	311	Banerjee, Animesh	CG05	53
Babaei Brojeny, Aliakbar	PC16	129	Bang, Do	JE04, SK10	102, 352
Babic, Michal	BH03	46	Bang, Dong H.	CJ03	55
Bach, Long Giang	RN05	297	Bang, Ngac An	AJ06	40
Badini Confalonieri, Giovanni A.	GG04	80	Banholzer, Anja	RJ11	284
Bae, Dong Sik	PH21	150	Bannikova, Nataliya	SK02	350
Bae, Joohyung	QK12	226	Bansil, A.	HI02	89
Bae, Jungchan	PM17	170	Bansil, Arun	BA04	41
Bae, Kyoung-hoon	RO02	301	Bansil, B.	SD04	330
Bae, Moon Seob	RP23	307	Bao, Guizhi	PC20, QJ07	130, 222
Bae, Seok	RH08	276	Bao, Jinke	RB13	256
Bae, Taejin	JI02	105	Bao, Nina	DD03	58
Bae, Yu Jeong	CB01, PJ17, QP18	49, 157, 248	Bao, Wei	RB07	255
Baek, In-bok	RL21	293	Bar-ad, S.	BD01	43
Baek, Seung Ki	RI19, RI20	282	Baranov, Denis G.	HD05	86
Baek, Seung-heon Chris	RL30	294	Baranov, Nikolai V.	QN10	238
Baek, Seungmin	QP15, QP16	247, 248	Baranov, Nikolay	QG04	208
Baek, Younkyoung	PM24	171	Baranov, Nikolay V.	QI08	219
Baek, Youn-kyoung	RN06, SL29	297, 360	Barbar, S. K.	RA03	249
Baggio-saitovitch, E.	SM17	363	Barberis, Gaston Eduardo	RB18	257
Baggio-saitovitch, Elisa	PL09, QM14, QM15, RB10, RB11, SE22	165, 233, 234, 255, 336	Barbiellini, Bernardo	BA04	41
Bagheri, Mahdiyar	QA25, SA22	186, 319	Barco, Reginaldo	PG03	142
Bahmanrokh, Ghazaleh	RQ22	310	Barcones, Beatriz	JE01	101
Bahramy, M.s.	II02	97	Barik, Sujit Kumar	PI01, RA08	150, 250
Bahramy, Mohammad Saeed	AE05	36	Barisic, Neven	CA03	49
Bai, X. J.	PL20	167	Barker, J	FC01	73
Bai, Zhaoqiang	QP06	246	Barker, Joe	RK17	288
Baik, Seung-kyu	QM22	235	Barman, Anjan	HD04, RK11, SH12	85, 287, 345
Baines, Christopher	AB02, CD04	34, 51	Barman, Saswati	HD04, RK11, SH12	85, 287, 345
			Barnas, J	SB21	323
			Barnas, Jozef	DB03	57
			Barner, Klaus	SB06	321

Barnes, Crispin	BH01	46	Bending, Simon	QO24	244
Barnes, Crispin H.w.	PN23	175	Bendix, Jesper	BC02	42
Baron-gonzalez, Aura Janeth	EC04	66	Bera, A. K.	DH05	62
Barraclough, J. M.	GC01	77	Beran, Premysl	BE05	44
Barraclough, Jack M	SE12	335	Berardan, David	RB15	256
Barrera, Gabriele	AG02	37	Berger, Andreas	SM04	361
Barshilia, Harish C	PK16	163	Berger, Claire	PN16	174
Barski, Andre	AI04, DD01	39, 58	Berger, H.	PI09	152
Barthelemy, Agnes	AE03, HE04, QA27	36, 86, 187	Berger, Helmuth	QA20	185
Barthelemy, M.	PO23	181	Bergman, Anders	SH11	345
Barthelemy, Marie	FC02	73	Bergmann, Christoph	AB02	34
Bartolome, Fernando	EF03, GG03, GG05, QI14	68, 80, 220	Bergqvist, Lars	SH11	345
Bartolome, Juan	EF03, GG03, GG05	68, 80	Berkowski, Marek	QB30	192
Basak, Susmita	BA04	41	Bernhard, Christian	HA02	83
Bascones, Elena	QB18	190	Berntsen, Magnus	HA03	83
Bascones, Elena .	QB19	190	Bersweiler, Mathias	KF02	110
Basso, Vittorio	HH01	88	Bertacco, Riccardo	AI03, DE03	39, 59
Batail, Patrick	SB20	323	Berthet, Patrick	GF05	79
Bataille, Alexandre	DD05	59	Berthier, Claude	IC02	92
Batista, Cristian D	JD01	100	Bertram, Batlogg	RB19	257
Batko, Ivan	RE13	268	Besnard, Celine	QC13	194
Batkova, Marianna	RE13	268	Bessais, Lotfi	PM06	168
Battle, X.	BD01, ED03	43, 66	Bessonov, Vladimir	SO17	369
Battle, Xavier	BD04, RN14	43, 299	Beyer, Markus	HA02	83
Batlogg, B.	PC29, PI15	131, 153	Bezmaternykh, Leonard N	CI04	55
Batlogg, Bertram	RB21, SC16	257, 328	Bezmaternykh, Leonard N.	PA02	116
Battiatto, Marco	RK12	287	Bhagyashree, Karki S	SL21	359
Bauer, Andreas	DF02, QC17, QH24	60, 195, 216	Bharathi, A.	QA14	184
Bauer, E D	EA03	64	Bhat, Shwetha G.	CG04	53
Bauer, E.	QB31, QD10	192, 198	Bhat, Subray V	SL21	359
Bauer, E. D.	FB01, QB12	73, 189	Bhatia, Charanjit S	SK05	351
Bauer, E.d.	PC19	129	Bhatia, Charanjit Singh	PJ08	156
Bauer, Eric D	FB03	73	Bhatia, Pushpinder Gupta	PN06	173
Bauer, Eric D.	GC03, PC03, RD09, SC16, SE02, SE08	77, 127, 263, 328, 333, 334	Bhatt, Pramod	PN17	174
Bauer, Ernst	IA02, SC01	90, 325	Bhattacharya, Pallab	CG05	53
Bauer, Thomas	SF05	337	Bi, Ke	RA12	251
Bauer, Uwe	AD02, AE01	35	Bialek, Beata	SK19, SK27	353, 354
Baum, Max	AA05	33	Bianchi, Andrea	JC01	100
Baumbach, R.	QB31	192	Bianchi, Andrea D.	CD04, PD05	51, 132
Baumberger, Felix	II02	97	Bianchi, M.	II02	97
Baumgarten, Martin	HC04	85	Bibes, Manuel	AE03, HE04, QA27	36, 86, 187
Bayle-guillemaud, Pascale	AI04, DD01	39, 58	Bickel, Jessica E.	IH03	96
Bazaliy, Ya. B.	SI18	348	Bigot, J.-y.	PO23	181
Beach, Geoffrey	AE01	35	Bigot, Jean-yves	FC02, RK05, RK13, RK15	73, 286, 288
Beard, Jerome	RQ16	309	Bihlmayer, Gustav	SD06	331
Beatrice, Cinzia	HH01	88	Billette, Julien	RQ16	309
Beaurepaire, Eric	GI03	82	Biner, D	RI05	279
Beck, Adli	QH22	216	Biondo, Armando	QM15	234
Becker, Petra	AA05, QA22, RI12	33, 186, 280	Biswas, Abhijit	PN28	176
Behnia, Kamran	KJ04	114	Biswas, Deep Narayan Biswas	SC06	326
Beigne, Cyrille	DD01, EI04, GE01, QK15, QK16, RL24	58, 71, 78, 226, 293	Biswas, S.	PL07	165
Bekyarova, Elena	PN16	174	Bitla, Yugandhar	SL07	357
Belinsky, Moisey	RA25	253	Bittar, Eduardo	SE22	336
Bellaiche, Laurent	QA27	187	Bjorck, Matts	EI03	71
Belo, Joao H	SO31	371	Blackburn, S.	PD05	132
Ben Youssef, Jamal	SA24	320	Blaha, Peter	RB21	257
Benatmane, N.	PK13	162	Blanco, J. A.	GH05	81
Bencok, Peter	PA15	118	Blanco, Jesus A.	JI04	106
			Blanco, Juan Maria	AJ02	40
			Blanco-canosa, Santiago	BA03	41

Blank, Dave	DH02, SA10	62, 317	Bourdarot, Frederic	JC02	100	Bunce, Christopher	RJ11	284	Carva, Karel	RK12	287
Blasco, Javier	EC04	66	Bourgeois, Julie	RA11	251	Bunkov, Yury	IC04	92	Carvajal Quiroz, Eliel	SK15	352
Blavette, Didier	BD02	43	Bourges, Philippe	DA01	56	Burdin, Sebastien	PD04	132	Casa, Diego	DC03	58
Blinova, Julia	PB22	123	Bouzehouane, Karim	AE03	36	Burkov, Alexander T	QI12, QI13	219	Casanova, Felix	HE02	86
Bluegel, Stefan	SD06	331	Boyn, Soeren	HF01	87	Burzo, Emil	SK09	351	Casanove, Marie-jose	IH01	95
Blugel, Stefan	IH03	96	Bozzo, Bernat	SO18	369	Bussetti, Gianlorenzo	PL21	167	Casola, Francesco	IC02	92
Blum, Christian	QH24	216	Braden, Markus	AA05	33	Bustamante, Rodney	KB06	108	Casoli, Francesca	AG02	37
Blundell, Stephen. J.	QG19	211	Braicovich, Lucio	BA03	41	Buzzi, Michele	RK17	288	Casper, Frederick	RC10	260
Blythe, H. J.	RN18	299	Brambilla, Alberto	PL21	167	Bychkov, Igor V.	SO19	369	Castan, Celia	EF03	68
Boarino, Luca	AG02	37	Bramwell, Steven	CC01	50	Bychkov, Igor Valer'evich	QH17	215	Castan-guerrero, Celia	GG03, GG05	80
Bobade, Santosh M	QO11	242	Bran, Christina	DG01	61	Byeon, Hyeheyon	PN08, PN09, QM04	173, 232	Castano, F.	ED03	66
Bobak, Andrej	QE01, QE02	199	Bran, Cristina	DG03, EI03	61, 71	Byzov, Ilya	QL07	229	Castellano-hernandez, E.	ED03	66
Bobrov, Aleksandr	SG17	342	Bran, Julien	DG02, PJ22	61, 158				Castrillon, Mariana	RN09	298
Bochenek, Lukasz	SB26	324	Brandenburg, Jens	QA11	184				Caux, Jean-sebastien	IC05	92
Bochenek, Łukasz	PE19	139	Brandl, G.	PI09	152				Cava, R. J.	SD04	330
Bocher, Laura	AE03	36	Brando, Manuel	AB02, QH12, SF05	34, 214, 337				Cava, Robert J	QB13	189
Bocklage, Lars	SH04	343	Braun, Anke	PE07	137				Cavill, Stuart A	SH09	344
Bode, Matthias	AD03	35	Braun, H. B.	PJ26	159				Cazayous, Maximilien	PD17, QA27	134, 187
Bodensiek, Oliver	PE03	136	Braun, Hans - Benjamin	GF02	79				Celegato, Federica	AG02, DG04	37, 61
Boehm, Helga M	RG15	274	Breard, Yohann	BB03, RH22	41, 278				Cermak, Petr	SB08	321
Boehm, M.	QE19	202	Brede, Jens	GH02	81				Cezar, Julio	PI08	152
Boehnert, Tim	RP04	303	Brenac, Ariel	EI04	71				Cezar, Julio C.	SH03, SH05	343, 344
Boeni, Peter	DG01	61	Brenig, Wolfram	EC05	66				Cha, Hyun Rok	QO20, SG21	244, 343
Boeri, Lilia	SC07	326	Breunig, Oliver	RI12	280				Cha, Yun-yeop	PO06, PO10	178
Bof Bufon, Carlos Cesar	SJ07	350	Bridges, F.	CF01	52				Chacon Hernandez, U. D.	SM17	363
Bogach, A. V.	QC22, RH07	195, 275	Bridoux, G.	DI01	62				Chacon, A.	PI09	152
Bogach, Alexey	QC20, RE13	195, 268	Brinkman, Alexander	DH02, SA10	62, 317				Chadov, Stanislav	CH04, II03, RC10	54, 97, 260
Bogach, Alexey V.	QC19	195	Broholm, C.	CF01	52				Chadova, Kristina	II03	97
Bogdanov, Savva	QG02	208	Brookes, Nicholas	PI08	152				Chae, Keun Hwa	PG27, QO27	146, 245
Bohaty, Ladislav	AA05, RI12	33, 280	Brooks, James S.	SB05	321				Chae, Woong-chan	SN04	364
Bok, Jin Mo	SB31	325	Brown, Stuart E.	GB03, SF01	76, 337				Chai, Yi Sheng	PA09	117
Boldt, Regine	PC27	131	Brucas, Rimantas	SL15	358				Chai, Yisheng	JB02	99
Boldyrev, Kirill N.	PA20, RA24	119, 253	Bruck, E.	RQ12, SO08, SO16	309, 368, 369				Chakraborty, Monodeep	RG02	272
Bombardi, Alessandro	BF03	45	Bruck, Ekkes	PM10, RI18	169, 281				Chaloupka, Jiri	BA03	41
Bonanni, Alberta	BE03	44	Brueckl, Hubert	AH01	38				Chan, Ho Bun	BC05	42
Bonell, Frederic	PK20	163	Bruel, Andreas	SG19	342				Chan, Mun K.	CA03	49
Bonfim, Marlio	SH05	344	Bruhl, Andreas	RI13	281				Chan, Wen-yuan	PK02	160
Boni, Peter	DF02	60	Brune, Harald	BC02	42				Chandarak, Sujittra	SL10	357
Bonilla, Marcela	EF03	68	Buchanan, Kristen	RJ20	285				Chandra, Shekhar	SD15	332
Bonn, Doug	BA01	40	Buchelnikov, Vacily	PI20	154				Chandra, Sumal	PB24, QG03	124, 208
Booth, John Graham	QG01	208	Buchelnikov, Vasily	PM22, QH05, SO23	171, 213, 370				Chandrasekaran, Gopalakrishnan	PO21, QA25, QN26	180, 186, 240
Boothroyd, A. T.	PC22, PI03, QN01	130, 151, 236	Buchelnikov, Vasily D.	QO12, SO19	242, 369				Chang, Bin	HJ05	90
Boothroyd, Andrew	AF01, DH03	36, 62	Buchelnikov, Vasily Dmitrievich	QH17	215				Chang, Cheng-hsun	PK02	160
Boothroyd, Andrew T	HA04	83	Buchner, B.	QF18	206				Chang, Chia-chi	SH08	344
Borchers, Julie	KD02	109	Buckow, Alexander	PI05	151				Chang, Ching Hao	KI04	113
Borchmann, Jan	SL05	356	Buda-prejbeanu, Liliana	SI09	347				Chang, Ching-ray	QK22, RK14, SK30	227, 288, 355
Borges, Hortencio Alves	SE22	336	Bud'ko, S. L.	GA01, IA05, RD02	75, 91, 262				Chang, H.w.	SN06	365
Borges, R. P.	QM13	233	Budnick, Joseph I.	HA03	83				Chang, Hun	CI03, PA01, PA03	55, 116
Boris, A. V.	GA03	75	Budrikis, Zoe	KE01	110				Chang, J.	PC01, PI15	126, 153
Borovsky, Michal	QE02	199	Buechner, B.	QE23, QF22, RB17	203, 207, 256				Chang, Jae Kyung	QH29, SC08	217, 326
Borozdina, Yulia	HC04	85	Buechner, Bernd	QH24	216				Chang, Johan	HA03	83
Borrell, A	RQ10	308	Bufaical, Leandro F	SE15	335				Chang, Joonyeon	KC04, PJ30, PL16, QK10, QK11, QK12, QK13, RL28, RL31, SL26	109, 159, 166, 225, 226, 294, 295, 360
Borrmann, Horst	QD07	197	Buhot, Jonathan	PD17	134						
Bortolotti, P.	ID02	93	Bui, Hong-van	SG10	341						
Bortolotti, Paolo	CE03, ID03, RJ07	51, 93, 283	Buitrago, Ivon R.	SI10	347				Chang, Jui-hang	RK14	288
Bosak, Alexei	PA08	117	Bukowski, Z	QB06	188				Chang, Junghwan	RR16, RR17, SN05	313, 365
Boseggia, S.	QN01	236	Bukowski, Z.	PC01	126				Chang, Liang-juan	RL18	292
Bouchenoire, L.	QN01	236	Bukowski, Zbigniew	RB21	257				Chang, P. C.	PE02	136
Bouillot, Pierre	CC03	50	Buldmann, Benjamin	RI12	280				Chang, P. H.	PC13	128
Bouille, Olivier	SH05	344	Bulla, Lukas	RB08	255				Chang, Sung	QA20	185

C

Author Index

Author Index

Chang, T.-r	SD04	330	Cheng, Chih-wei	PK11, PK15, PK19	162, 163
Chang, W.c.	SN06	365	Cheng, Hong-wen	QM09	233
Chanthbouala, Andre	IE04	94	Cheng, Nian-jia	SL18	359
Chantrell, Roy	RK17	288	Cheng, Po-wen	BJ01	47
Chantrell, Roy W	FC01	73	Cheng, Tsung-i	PK19	163
Chantrell, Roy W.	QK09, SJ04	225, 349	Cheon, Jinwoo	CB01, PO15, PO16	49, 179
Chantrell, Rw	FC01	73	Cheong, S. W.	AA04	33
Chao, C. H.	PK01	160	Cheong, S.w.	PH10	148
Chao, Wu	QO15	243	Cheong, S.-w.	QA04	183
Chapon, Laurent C	BF03, CI02	45, 55	Cheong, Sang-wook	PP06, QF20	28, 207
Chapon, Laurent C.	GF03	79	Cheong, S-w.	RA22	253
Charnukha, Aliaksei	GA03	75	Cheptiakov, Denis	PI21	154
Chatterjee, S	SO14	369	Chern, G.	PK11, PK15, PK19	162, 163
Chattopadhyay, S	QL14	230	Chern, Gung	QM11, QM25	233, 235
Chaturvedi, Anurag	DJ01	63	Chernets, Ivan A.	QO12	242
Chaudhary, S.	PG27	146	Chernobrovkin, Alexey	ED06, KI05	67, 113
Che, Sun Chang	QG18	211	Chernyshov, Dmitry	PA14	118
Chebotkevich, Ludmila	AG05, QM05	38, 232	Chi, Songxue	SC23	329
Cheikhrouhou, Abdelwaheb	DJ05	64	Chiba, D.	BE02, RL07, SH07	44, 291, 344
Cheikhrouhou-koubaa, Wissem	DJ05	64	Chiba, Daichi	RL10	291
Chen, Bin	PC02, PC09	127, 128	Chicinas, Ionel	EJ03	72
Chen, C. - T.	QB28	191	Chico Carpio, Jonathan Philippe	SH11	345
Chen, Chien-miao	SB19	323	Chien, Chia-ling	FA04	72
Chen, Chih_yung	PK09	161	Chikako, Moriyoshi	QD14	198
Chen, Chih-wen	QN08	237	Chikoidze, Ekaterina	SM07	362
Chen, Chih-yung	QM01	231	Chin, Yi-ying	PI08	152
Chen, G F	QB11	188	Chioran, Viorica	RR02, RR03	311
Chen, G.	SM05	361	Chiu, Yu-che	RK07	287
Chen, Genfu	RB11	255	Chizhik, Alexander	CJ04	56
Chen, H.m.	PK11, PK15	162	Chizhik, Alexandr	AJ02	40
Chen, Hao-hsuan	RK14	288	Cho, B. K.	PK04, QI15, QK03, SB10, SB30	161, 220, 224, 321, 325
Chen, Hsin-hsien	QM27	236	Cho, Bo Ram	SB22	323
Chen, I. A.	SB04	320	Cho, Chae Ryong	PN21, QL18	175, 231
Chen, J.	QB12	189	Cho, Daeheum	QG17	211
Chen, J. M.	SM11	362	Cho, Deo-kyong	PG24	146
Chen, Jian	SB29	325	Cho, Hyun Jin	PG25	146
Chen, Jin-ming	QB21	190	Cho, Hyunduck	PJ17	157
Chen, K.I.	QM27	236	Cho, Hyun-sung	RR15	313
Chen, Kuo-chin	QK22, SK30	227, 355	Cho, Jun-hyung	SD06	331
Chen, L. M.	IC03	92	Cho, K.	QC23	196
Chen, Lin	QK23	227	Cho, K. H.	SB28	324
Chen, M.j.	QM27	236	Cho, Kwang Lae	PI13	152
Chen, P.	AA04	33	Cho, Lee-hyun	SK27	354
Chen, Qianping	SA19, SA20	319	Cho, Myeong Woo	QN09	237
Chen, S. A.	QB21, SM11	190, 362	Cho, Sang-uk	PH22	150
Chen, S. C.	PH01	147	Cho, Sunglae	EH05, PN29, PN30, QO22, QO23	70, 176, 177, 244
Chen, Shih-jia	QM09	233	Cho, Suyeon	GF05	79
Chen, Sui-pin	RL29	294	Cho, Yong Chan	PN20, PN21	175
Chen, Szu-wei	AD01	35	Cho, Yong-chan	PH22, QL18	150, 231
Chen, Wei-hsiang	IH06, PL03, PL13	96, 164, 166	Cho, Yun Hyun	RR19, RR24	314
Chen, Wen-chen	PL18	166	Cho, Yunhyun	RR25	315
Chen, Xiang-bai	SA16	318	Choe, Sug-bong	KE03, SI13	110, 348
Chen, Xing-yuan	QA03	183	Choi, Chang Ho	RK06	286
Chen, Xumin	AD03	35	Choi, Changsik	SK14	352
Chen, Y.	QB12	189	Choi, Choljin	RN23	300
Chen, Yao-jung	PL03	164	Choi, Chuljin	PM24	171
Chen, Ye	RD12	264	Choi, Chul-jin	JH04, KH04, RN06, SL29	104, 112, 297, 360
Chen, Yen-cheng	PC18	129	Choi, Dawoon	RR25	315
Chen, Yong P.	HI02	89			
Chen, Zhe	AJ03, JI06	40, 105			

Choi, Dong Hoon	EH02	70	Chung, Chung-hou	DB04, RE06	57, 267
Choi, Doo-hyun	RR23, RR27	314, 315	Chung, D. Y.	GA01	75
Choi, Eun Sang	GJ02, PA21	82, 119	Chung, J.- H.	PH03	147
Choi, Eun-sang	SB05	321	Chung, Jaeho	PA01	116
Choi, Han-yong	SB31, SB32	325	Chung, Jae-ho	CI03, JB02, PA03, PA04	55, 99, 116
Choi, Heonhwa	RQ15	309	Chung, K. C.	SB28	324
Choi, Heon-hwa	SC14	327	Chung, Kookchae	RN23	300
Choi, Heon-jin	QK11, SL26	225, 360	Chung, Kook-chaee	QM22	235
Choi, Hong Chul	PE17	138	Chung, Sunjae	PK13	162
Choi, Hyeok Cheol	QM18, QM20	234	Chung, Sunjea	CE02	51
Choi, Hyeok-cheol	RK02	286	Churagulov, Bulat	ED06	67
Choi, Hyoung Jin	QN03, QN09	236, 237	Chureemart, Phanwadee	SJ04	349
Choi, Hyoung Joon	QK21, RB16, RC15	227, 256, 261	Cibert, Joel	DD01	58
Choi, Jae-hak	RR31	316	Ciccacci, Franco	PL21	167
Choi, Jae-hyuk	PB21, RQ15, SC14	123, 309, 327	Cichorek, Tomasz	PE19, SB26	139, 324
Choi, Jong-gu	BH02, PL11, RR15	46, 165, 313	Cieslak, Jakub	QH18	215
Choi, Jong-jin	DJ02	63	Ciftja, Orion	RG01	271
Choi, Joon-hwan	DJ02	63	Cinal, Marek	AD02	35
Choi, Jun Woo	KC04	109	Cioangher, M.	SA11	318
Choi, K. Y.	QF13	206	Cisarova, Ivana	BB04, PD19	42, 135
Choi, Ki-young	JA03	98	Ciubotaru, Florin	SI15	348
Choi, Kwang Yong	RP13	305	Ciuta, G.	JH02	104
Choi, Kyong-hoon	RN20	300	Civale, L.	QB31, SB12	192, 322
Choi, Mahn-soo	SC14	327	Cizmar, E.	QF02, QF03	204
Choi, Min-young	SD03	330	Cizmas, Corneliu Bazil	PM06	168
Choi, Moo Young	RC08, RE07	260, 267	Clarke, Simon J.	HA04	83
Choi, Seokhwan	RQ11	308	Clarke, Simon. J.	QG19	211
Choi, Seonghoon	QL08	229	Claudia, Felser	SD15	332
Choi, Seongil	PG24	146	Claydon, J S	QO24	244
Choi, Seonjun	QP19, RL22, SL19	248, 293, 359	Clemente-juan, J. M.	BC01	42
Choi, Sul A	SA09	317	Coey, Michael	PO32	182
Choi, Sungil	PI10	152	Coisson, Marco	AG02, DG04	37, 61
Choi, Won Young	QK13	226	Colak, Levent	KB04	108
Choi, Y.j.	PH10	148	Coleman, Piers	HP22	30
Choi, Yong Nam	PN20, QL18	175, 231	Colineau, Eric	RE03, SE19	266, 336
Choi, Yoon Hyuck	PB16, PB18, PB35, PB36, PB38	122, 123, 125, 126	Colis, Silviu	PI04	151
			Collin, Sophie	HE04	86
Choi, Young Ha	RC07	260	Collins, S. P.	QN01	236
Choi, Youngha	SD10, SD11	331	Collins, Steve	DH03	62
Choi, Youn-seok	DE05, RJ16, SH14	60, 285, 345	Conder, Kazimierz	PI21, PO17, QF23	154, 180, 207
Chokprasombat, Komkrich	SL10	357	Cong, Pham Thanh	HC04, QE14, RI13	85, 201, 281
Choo, Seongmin	PN19	175	Cong, Rihong	PH02	147
Choo, Seong-min	QO10, QO11	242	Continentino, Mucio A.	KG04	112
Chou, Chih-chieh	QA20	185	Continenza, Alessandra	QG25	212
Chou, T. L.	SM11	362	Coqblin, B.	QD10	198
Choudhary, R.j.	SA14	318	Coqblin, Bernard	PE01	136
Chowdhury, Prasanta	PK16	163	Cordoba, Rosa	DG05	61
Chu, Ching-wu	JA02	98	Cornell, N.	QB12	189
Chu, Yu-hsun	AD01	35	Coronado, Eugenio	BC01	42
Chuan'an, Cui	QO21	244	Corrias, Anna	CB04	49
Chubykalo-fesenko, O	FC01	73	Cossu, Fabrizio	QP01	245
Chubykalo-fesenko, O.	GD03	78	Costache, M. V.	DIO1	62
Chubykalo-fesenko, Oksana	RJ04	283	Cote, Michel	PD05	132
Chudo, Hiroyuki	PC03	127	Cottam, Michael	QG12, SL05	210, 356
Chumak, Andrii V.	SI15	348	Cowburn, Russell	KE02	110
Chumakov, Andrey	SL27	360	Cowlam, Neil	PG01	142
Chun, Byong Sun	IH04, PJ14, RK18, SH13	96, 157, 288, 345	Crassous, Arnaud	AE03	36
Chun, Sae Hwan	JB02, PA09	99, 117	Crichton, Wilson	RB20	257
Chun, Sae-hwan	PA04	116	Cristiani, G.	ED05	67
Chun, Sungwoo	QP19, RL22, SL19	248, 293, 359	Crooker, Scott A	JD01	100

Cros, V.	CE03, CE06, ID02, RJ07	51, 52, 93, 283	De La Fuente, Jesus M	RN08	298	Didukh, Leonid	RG13	274	Dufour, Catherine	DD05, KD02, KF02	59, 109, 110
Cros, Vincent	HF01, ID03, IE04	87, 93, 94	De La Torre, A	II02	97	Dieny, Bernard	BD02, SI09	43, 347	Dugaev, V K	SB21	323
Crow, D. J. G.	SF15	339	De Leo, Natascia	AG02	37	Dietl, T.	BE02	44	Dukhnenko, A.	JC04	100
Crowell, Paul A	CG01	53	De Loubens, Gregoire	ID03	93	Dietl, Tomasz	BE03, DD02	44, 58	Dukhnenko, A. V.	PE12	138
Cruz Irisson, Miguel	SK15	352	De Matteis, Laura	RN08	298	Dilley, N.	IA05	91	Dumas, R. K.	CE02, PK13	51, 162
Cubukcu, Murat	AI04, GE01, QK15, QK16, QK17, SL24	39, 78, 226, 360	De Pedro, I.	GH05	81	Dilullo, Andrew	GH02	81	Dumas-bouchiat, F.	JH02	104
Cuello, Gabriel	JJ04	106	De Pedro, Imanol	JJ04	106	Ding, Jun	DD03, QP22, SL06, SM14	58, 249, 357, 363	Dumesnil, Karine	DD05, KD02, KF02	59, 109, 110
Curiale, Javier	SH02	343	De Ranieri, Elisa	IE03	93	Dinh, Van-chau	SG10	341	Dumont, Matthieu F.	KB03	107
Curlik, Ivan	QD08, RD21	197, 265	De Souza, Mariano	QJ11, SG19	222, 342	Dinia, Aziz	PI04	151	Dumont, Yves	SM07	362
Custardoy, Laura	RN08	298	De Teresa, J. M.	KC05	109	Dirks, Andreas	FE03	75	Duncan, William J	QH12, SF05	214, 337
Custers, J.	CD01	50	De Teresa, Jose Maria	DG05, SM16	61, 363	Divis, Martin	HJ04, QC21, QJ02	90, 195, 221	Dung, Dang Duc	PN29, PN30, QO22, QO23	176, 177, 244
Custers, Jeroen	BB04, PD18, PD19	42, 134, 135	Decker, Regis	GH02	81	Djuhana, Dede	RA15, SH01	251, 343	Dung, N. H.	SO16	369
Cywinski, Robert	JA05	99	Decourt, Rodolphe	EH03	70	Dkhil, Brahim	QA27	187	Dung, N.h.	SO08	368
			Deen, P P	SE03, SE05	333, 334	Dluzewski, Piotr	DD02, QB30	58, 192	Dunn, J.	HA05	84
D			Deguchi, Hiroyuki	PB25, PG09, PG10, QG19, RN03, SA03	124, 143, 144, 211, 297, 316	Do, Anh Thi Kim	CJ05	56	Dunne, Peter	PO32	182
Da Silva, Douglas	PB33	125	Deguchi, Kazuhiko	PD14, PD20, RD05	134, 135, 262	Do, Bang	PJ09	156	Dunsiger, Sarah Ruth	GF01	79
Da Silva, Douglas Langie	PB09, PB11, RB09, SB18	121, 255, 323	Deheer, Walt A.	PN16	174	Do, Thang Viet	CJ05	56	Duo', Lamberto	PL21	167
Da Silva, Mathieu	KF02	110	Deisenhofer, Joachim	PA23, RH24	119, 278	Dobkowska, Sylwia	BE03	44	Duong, Thiet Van	EH05	70
Da Silva, R. C.	QM13	233	Dejneka, Alexandr	AH02, BH03	38, 46	Dobrynin, Alexey	PA15	118	Duong, Tuan Anh	EH05	70
Daadmehr, Vahid	PB23	123	Dekadjevi, David Toyo	SA24	320	Doenni, Andreas	JJ05, PH02	106, 147	Dupuis, Veronique	KB05, QN06, RK03	108, 237, 286
Dabkowska, H.	GF01	79	Del Moral, A	SF09	338	Doerr, Mathias	PH04	147	Duque, Jose G. S.	PI19	153
Dabkowska, Hanna A	JD01	100	Del Moral, Agustin	SE20	336	Dogan, Fatih	CG05, IE01	53, 93	Durakiewicz, Tomasz	SE08	334
Dabkowski, A.	GF01	79	Del Real, Rafael Perez	DG03	61	Doh, Jaewon	PO14	179	Durr, Hermann Andreas	GD02	77
Dabrowski, Maciej	AD02, EI01	35, 70	Del Val, Juanjo	PJ25	158	Doh, Yong-joo	SD12, SD14, SO21	332, 370	Dussaux, A.	CE03, CE06, ID02	51, 52, 93
Dadras, Sedigheh	PB23	123	Delfanazari, Kaveh	KJ01	113	Doi, Masaaki	SM03, SN03	361, 364	Dvornik, Mykola	EH04, JG01	70, 103
Daegeun, Park	RR20	314	Delley, B.	PC01	126	Doi, Naohiro	QE13	201	Dwevedi, Sandhya	PG19	145
Dai, Bing	RL08	291	Delmas, Claude	EH03	70	Dolgov, O. V.	GA03	75	Dwivedi, R. K.	RA27, SM18	253, 363
Dai, Jia	QB07	188	Delmo, Michael P.	PN12	174	Dolia, S. N.	SL25	360	Dyadkin, Vadim A.	DF04	60
Dai, Jianhui	AB04, IU04	34, 98	Delval, Juanjose	DJ03	63	Dolinsek, Janez	SL11	357	Dyadkina, Ekaterina	QM08	232
Dai, Jianming	SA01	316	Demidenko, Olga	QG05	209	Dominguez, Claribel	SA12	318	Dyakina, Veronika	PC07	127
Dai, Pengcheng	GA02, RB10, RB11	75, 255	Demidov, Evgeny Sergeevich	SG17	342	Doria, Mauro Melchiades	RB09	255			
Dai, Yuqiang	SA01	316	Demishev, S. V.	PE12, QC22, RH07	138, 195, 275	Dos Santos, Maria Elenice	QA06	183	E		
Daimon, Hiroshi	SK13	352	Demishev, Sergey	ED06, KI05, QC20, SG07, SG08	67, 113, 195, 340	Dou, Shixue	EF02, QG09, SD01	68, 209, 330	Elbels, Ursula	SI09	347
Damay, Francoise	JB05, RA11	100, 251	Demishev, Sergey V.	QC19	195	Drechsler, S.-I.	QF18, QF22	206, 207	Ebert, Hubert	II03	97
D'amico, Irene	QK09, RL12, SJ04	225, 291, 349	Demmel, F	SE03, SE05	333, 334	Dreiser, Jan Gui-hyon	BC02	42	Ebihara, Takao	RA19	252
Dan, Nguyen Huy	AJ06	40	Dempsey, Nora	JH02	104	Drews, Andre	FD02	74	Ebisu, Shuji	QH14, QO07	215, 241
Dang, Dung Duc	EH05	70	Demsar, Jure	HA02	83	Driver, Sarah L	EF03	68	Ebrahimian, Neda	SB07, SC09	321, 327
Dang, Hue Thi Minh	RN19	299	Deng, Guochu	PI21, PO25	154, 181	Drobosyuk, Mikhail	PM22, SO23	171, 370	Echevarria-bonet, C.	QD10	198
Dang, N. V.	RA01	249	Denisovsky, Andrey N.	QO12	242	Drube, W.	SK24	354	Eckerlebe, Helmut	SL27	360
Danis, Stanislav	QI01	217	Deorani, Praveen	EG03, PJ08, SI02	69, 156, 346	Drymiotis, Fivos R	QO09	242	Eckert, James C	PK09, QM01	161, 231
Danzenbacher, Steffen	CD03, PD12	51, 133	Deranlot, Cyril	HE04	86	Du Plessis, Paul De Villiers	RD23	265	Eckold, Gotz	AA05	33
Daou, Ramzi	JD01	100	Deranlot, Cyrile	CG03	53	Du, An	RK16	288	Eckstein, Martin	EB02	65
Dariani, R. S.	QP23	249	Derlet, Peter	QF20	207	Du, Jun	PL01, RA13	164, 251	Eddrief, Mahmoud	QL06	229
Das, A.	PI12	152	Deshpande, N. G.	SL08, SL09	357	Du, M-h	GF01	79	Eder, Robert	PF14, RF03	141, 269
Das, Kaustuv	HD04	85	Desilets-benoit, Alexandre	CD04	51	Dua, P.	QH26	217	Edmonds, Kevin W	SH09	344
Das, Pintu	QA11, QJ11	184, 222	Detlefs, B.	SK24	354	Duan, Truong Cong	HC02	84	Egashira, Yusaku	PE10	137
Das, Pranab Kumar	QJ17	223	Devereaux, T.	EB01	64	Duanmu, Qingyong	PK03	160	Egawa, Genta	RP06	304
Das, S.	PL07, RH02	165, 275	Devillers, Thibaut	BE03, DD01	44, 58	Dubenko, Igor	CH01	54	Egetenmeyer, Nikola	CD04	51
Das, S. D.	GA01	75	Devlin, Eamon	BJ02, RO08	47, 302	Dubey, Sheshmani K.	PN01	172	Eggert, Sebastian	HC04	85
Das, Soma	SO30, SO31	371	Dewhurst, Charles	DF04	60	Dubi, Yoni	KG01	111	Eguchi, Gaku	PC20	130
Das, Tanmoy	HI03, QB08	89, 188	Dey, G K	PM01	167	Dubiel, Stanislaw M	PG03, QH18	142, 215	Eguchi, Ryo	JE04	102
Dasari, Venkateswarlu	SJ08, SL23	350, 359	Dhar, Sudesh Kumar	QJ17, RB24, SE21	223, 258, 336	Dubowik, J.	QG27	212	Ehlers, Georg	CC03	50
Davesne, Vincent	GI03	82	Dhawan, M. S.	SL25	360	Duc Dung, Dang	PJ15	157	Ehmler, H.	RQ21	310
Davis, J. C. Seamus	CA02	48	Dho, Joonghoe	PL15, QM21	166, 235	Duc, Fabienne	RQ16	309	Einaga, Yasuaki	QC07	193
Davison, Toby	EH04	70	Di Marco, Igor	RG06	272	Duc, Nguyen Huu	AJ06	40	Eisaki, H.	QB28	191
De Bergevin, Francois	AF01	36	Diaconu, Andrei	RB12	256	Ducruet, Clarisse	AI04	39	Eisaki, Hiroshi	CA02, DA04, QA05, QA07, QA09, QB02, QB15, QB29, RH11	48, 56, 183, 184, 187, 189, 191, 276
De Brion, Sophie	KB06	108	Dias, Fabio	PB10, PB33	121, 125	Dudzik, Esther	EC04	66			
De Julian Fernandez, Cesar	CB04, SI11	49, 347	Dias, Fabio Teixeira	PB09, PB11, RB09, SB18	121, 255, 323	Duerr, George	GG02	80	El Hafid, Hassan	EH03	70
De La Fuente, Cesar	SE20	336				Duff, Gerard	GF02	79			

El Jazouli, Abdelaziz	EH03	70	Falvello, Larry	QO16	243
El Moussaoui, Souliman	RK17	288	Fan, C.	IC03	92
Elgazar, Saad	RG05	272	Fan, Raymond	PA15	118
El-hagary, M A	QL21	231	Fan, Xiu Xiu	SL16	358
El-hagary, Magdy	RB29	258	Fan, Zhe	SH10	344
Eliseev, Andrey	SL27	360	Fang, Dong	IE03	93
Elizabeth, Suja	PH04	147	Fang, Yikun	RO07, SN11	301, 366
Elkaim, Erik	RA11	251	Fantechi, Elvira	CB04	49
Ellis, Tim	JE01	101	Farhan, M. Arshad	QH27	217
Elmers, H J	QM12, RN12, RP20	233, 298, 306	Farle, M	RP08	304
Elmers, Hans-joachim	AG04, CH04	38, 54	Fassbender, Juergen	RJ11, SH04	284, 343
Eloi, Jean-charles	KB01	107	Faulhaber, Enrico	QC24	196
Eloirdi, Rachel	RE03	266	Fauque, Benoit	KJ04	114
Elsayed, H. M.	RN01	296	Fayzullin, Rafael	PM22, SO23	171, 370
Elwindari, Nastiti	BJ03	48	Fdez-gubieda, M. L.	QM06	232
Emam-ismail, M	QL21	231	Fear, Natalia	PK09, QM01	161, 231
Emmel, Mirko	CH03	54	Fecher, G. H.	QG24, SK24	212, 354
Emoto, Akira	RP17, SK21	306, 353	Fecher, Gerhard H.	CH03, QN19, SD15	54, 239, 332
Emoto, Shun	PK12	162	Feder, R	RP20	306
Enders, Axel	AD03	35	Fedorov, A.	SD04	330
Endo, Keita	PG04	143	Fedorov, Dmitry	EE01	67
Endo, Yasushi	QM07, RK04	232, 286	Feiguin, Adrian	JD01	100
Endoh, Tetsuo	BI02	47	Felser, C.	QG24, SK24	212, 354
Engelke, Josefin	SM02	361	Felser, Claudia	CH03, CH04, HP72, II03, QN19, RC10	54, 32, 97, 239, 260
Enoki, Kentaro	PD13	134	Feng, Chunmu	AB04	34
Enoki, Masanori	PB29, PB30, PB32, QH10	124, 125, 214	Feng, Haibo	RO04, SN11	301, 366
Entani, Shiro	BH05, BH06, QL15	46, 47, 230	Feng, Kai	RA02	249
Entel, Peter	QH05	213	Feng, Qi	RN18	299
Eom, Jonghwa	PJ30, QK06	159, 225	Feng, Shiping	PB28	124
Eom, Man Jim	SD07	331	Feng, Wuwei	QO22	244
Eom, Man Jin	RB14	256	Feng, Xinliang	QK14	226
Epicier, Thierry	KB05	108	Feng, Yuan Ping	SJ09, SK34	350, 356
Erbe, Artur	RJ11	284	Feng, Yuanping	GI04, QP06	82, 246
Erekhinsky, M.	BD01, BD04	43	Feng, Zhou	RA19	252
Eremin, A. V.	QK07	225	Feng, Zhuo	RE15	268
Eremin, Alexander	RA23	253	Fenske, Jochen	QM02	231
Eremin, E. V.	QK07	225	Ferber, Johannes	SG22	343
Eremin, Evgeniy	RA23	253	Fernandez Baldis, Federico	QL06	229
Erfanifam, S.	CC04	50	Fernandez Barquin, L.	QD10, QM06	198, 232
Eriksson, Olle	RG06, SH11	272, 345	Fernandez-alonso, F	SF09	338
Ernst, Stefan	JC01	100	Fernandez-pacheco, Rodrigo	RN08	298
Eshraghi, M.	PI24	154	Ferrari, Alberto	PL21	167
Espinosa, Francisco	QO26	245	Ferraz, Alvaro	PD04	132
Estrada, Francisco	QO26	245	Ferreira, P.	QM13	233
Etgens, Victor	QL06	229	Ferriani, Paolo	IH02	96
Evans, Rfl	FC01	73	Fert, A.	CE03, CE06, ID02, RJ07	51, 52, 93, 283
Evans, Richard F. L.	RK17, SJ04	288, 349	Fert, Albert	ID03, IE04, PP01	93, 94, 28
Everschor, Karin	DF02	60	Fetisov, Leonid Yu	PN22	175
Eves, John	PI26	159	Feyerherm, Ralf	EC04	66
Ewings, Russell A.	HA04	83	Fidler, Josef	SJ07	350
Exl, Lukas	DE01	59	Fidrysiak, Maciej	QE24	203
Eyidi, Dominique	QP18	248	Figueroa, Adriana I	EF03	68
F			Fijalkowski, Marcin	PD21	135
Fabreges, Xavier	AA03, RQ16	33, 309	Fikacek, Jan	BB04	42
Fabris, Frederik	PB10, PB33	121, 125	Filipek, Stanislaw M.	QI06	218
Fabrizi, Federica	AF01	36	Filipov, V. B.	JC04, PE12, QC22, RH07	100, 138, 195, 275
Faina, Bogdan	BE03	44	Filipov, Vladimir	QC20	195
Faini, Giancarlo	FD03	74	Filipov, Vladimir B.	QC19	195
Falck, Augusto	PB33	125	Filippetti, Alessio	PF03	139

Filippov, Vladimir Borisovich	PE09	137	Fujibayashi, David E.	PC26	131
Finazzi, Marco	PL21	167	Fujieda, S	RR08	312
Finger, Thomas	AA05	33	Fujii, Yutaka	QE16, QE21, QF09, QF17, RI15	202, 205, 206, 281
Fink- Finowicki, Jan	JJ03	106	Fujimori, Atsushi	DA02	56
Fiorani, Dino	RN07	297	Fujimori, Hiroaki	ID04	93
Fiorillo, Fausto	HH01	88	Fujimori, Shin-ichi	RD25, SE23	266, 337
Fischbacher, Johann	DE01	59	Fujimoto, Kohdai	RP05	304
Fischer, Gerda	QL05	228	Fujimoto, Satoshi	RC01, RD05, SD09	259, 262, 331
Fischer, Peter	DE05, HG02, ID01, RJ16, RJ20, SH04	60, 88, 92, 285, 343	Fujisawa, M.	KI05	113
Fisher, B. -	PD03	132	Fujisawa, Masashi	QE10, QE16	201, 202
Fisher, Ian	HA05	84	Fujishiro, Hiroyuki	SG18	342
Fisk, Zachary	GC03, JC01, PD23, PP03, QA11, QJ11, RD11, RE10, SB15, SF03	77, 100, 135, 28, 184, 222, 263, 268, 322, 337	Fujita, A	RR08	312
Fitzsimmons, M.	BD01	43	Fujita, Asaya	SO24, SO26	370, 371
Fitzsimmons, M. R.	QM18	234	Fujita, Hirohito	PL12, SK18	165, 353
Fitzsimmons, Mike	KD02	109	Fujita, Kazuhiro	CA02	48
Flachbart, K.	QC22	195	Fujita, Masaki	BA04, PB29, PB30, PB32, RH12	41, 124, 125, 276
Flachbart, Karol	QC20, QI02, RE13	195, 218, 268	Fujita, Takahito	QH02	213
Fleck, Catherine L	BF03	45	Fujiwara, Kosuke	SK08	351
Fleet, Luke	CG02, PJ17, SK03	53, 157, 350	Fujiwara, Makoto	SK13	352
Fleury, Eric	AJ05	40	Fujiwara, N.	QB23	190
Flouquet, Jacques	JC02, PC17, RE10, SF03	100, 129, 268, 337	Fujiwara, Naoki	QB16	189
Folcke, Emeric	BB03, KB02	41, 107	Fujiwara, Tetsuya	QH18, SC24, SG09	220, 329, 341
Follath, Rolf	CD03	51	Fukada, Yukimasa	RA18	252
Fontes, Magda	SE22	336	Fukami, S.	RL07, SH07	291, 344
Fontes, Magda B.	SM17	363	Fukami, Shunsuke	RL10	291
Forcen-vazquez, Elena	QO16	243	Fukamichi, K	RR08	312
Forostiak, Serhiy	BH03	46	Fukatani, Naoto	PJ12, PL12, RC18, SA07, SK18	156, 165, 261, 317, 353
Fox, A. M.	RN18	299	Fukazawa, H.	QB28	191
Foyevtsova, Kateryna	SG22	343	Fukazawa, Hideto	QB02, QB15, QD12, QE12	187, 189, 198, 201
Fraga, G L F	PG03	142	Fukui, Takahiro	SD09	331
Fraile, A	SF09	338	Fukuma, Michinori	PB06, SG16	121, 342
Fraile, Arantxa	RN14	299	Fukuma, Yasuhiro	HD04, HE05, QM10, RK11	85, 86, 233, 287
Franco, N.	QM13	233	Fukunaga, Hirotoshi	JH01, PM08, PM09, RO03	104, 168, 301
Francoval, Sonia	CI04, QA01	55, 182	Fukushi, Syousuke	JI01	105
Franken, Jeroen	CH05, EI06, GE02, JE01	54, 71, 78, 101	Fukushi, Takanori	SN14	366
Franken, Jeroen H.	IE02	93	Fukushima, A.	CE03, CE06, ID02, RJ07	51, 52, 93, 283
Franz, Christian	QC17	195	Fukushima, Akio	BI01, HF01, IE04, KF01, PK20	47, 87, 94, 110, 163
Fratesi, Guido	PL21	167	Fukushima, Tetsuya	KF04	111
Freeman, Arthur	EC02	65	Fukuta, R.	CF04	53
Freeman, Arthur J	RB26	258	Fukuta, Ryuichiro	PH07, PI07	148, 151
Freeman, Arthur J.	RC16, SO10	261, 368	Fukuyado, Junichi	SB24	324
Freeman, Paul G	PI03	151	Fullerton, Eric E	PK09, QM01	161, 231
Freeman, Paul G.	PC22	130	Fuminori, Honda	RD19	265
Freemnan, A. J.	RM04	295	Funaki, Nakaba	PN24	176
Friedemann, Sven	FB04, PC09, QH12, RA19, RE15, SC16, SF05	73, 128, 214, 252, 268, 328, 337	Furdyna, J. K.	PN08, PN09, QL08, QM04	173, 229, 232
Friedenberger, Nina	RP08	304	Furomoto, Yoshitoki	QP09, QP10, QP11	246, 247
Friemel, Gerd	JC04	100	Furukawa, Kohsuke	KC06	109
Frings, Paul	RQ16	309	Furukawa, Nobuo	GB01, PA07	76, 117
Fritsch, Veronika	RE12	268	Furukawa, S.	RA22	253
Frontera, Carlos	EC04, RA17	66, 252	Furukawa, Satoshi	DA04	56
Frost, Christopher D	IC05	92	Furukawa, Yuji	QB15, QE12	189, 201
Fruchart, Olivier	SH03, SH06	343, 344	Furukawa, Yuta	RF09	270
Fu, Bin Hao	RD12	264			
Fu, Hua-hua	QK18	227			
Fu, Tsu-yi	IH06	96			
Fuente, C De La	SF09	338			

Furusaka, Michiro	RP01	303	Gavrilkin, Sergey Yu.	QC19	195
Fuse, Takahiro	PF11	141	Gawryluk, Dariusz J.	QB30	192
Fuseya, Yuki	KJ04	114	Gazo, Emil	QI02, RE13	218, 268
Fusil, Stephane	AE03	36	Ge, H.I.	RO14	303
Futamoto, Masaaki	ED01, PM18, SM15	66, 170, 363	Ge, Hongliang	RO13, RO15	302, 303
G			Geerts, Y. H.	EH02	70
Gabani, S.	QC22	195	Gegenwart, P	DC03	58
Gabani, Slavomir	QC20, QD12, QI02, RE13	195, 198, 218, 268	Gegenwart, Philipp	FB03	73
Gaczynski, Piotr	RE03	266	Gegenwart, Philipp	SG13	341
Gahlot, Ajay Pratap Singh	SC02	325	Gehring, G. A.	RN18	299
Gaita-arino, A.	BC01	42	Geibel, C.	QB14	189
Galanakis, Iossif	RP15	305	Geibel, Christoph	AB02, CD03, FB04, JC01, KA03, PD12, QC09, QC18, QD07	34, 51, 73, 100, 107, 133, 193, 195, 197
Galceran, Regina	IH01, SO18	95, 369	Geim, Andre	PP07	29
Gallagher, Andrew	KB04	108	Gemming, Sibylle	RJ11	284
Gallagher, Bryan L	SH09	344	Geng, Y. X.	PM03	167
Gallais, Yann	PD17	134	Genossar, J. -	PD03	132
Galyas, Anatoly	QG05	209	George, Jean - Marie	HE04	86
Gambarelli, Serge	AI04	39	George, Jean-marie	AI04, CG03	39, 53
Gandhi, Ashish Chhaganlal	QP07	246	Georges, Antoine	AB04	34
Gang, Qiu Xiang	SB01	320	Georgii, Robert	DF02	60
Ganguly, Arnab	SH12	345	Gerasimov, Evgeny G.	QI08	219
Gan'shina, Elena A	PN22	175	Gerber, Alexander	DE02, RK01	59, 286
Ganz, Philipp R.	QL05	228	Gerber, Simon	CD04	51
Gao, Bo	SO25	370	Gercsi, Zsolt	RF15	271
Gao, Guoying	PN10, RM03, SO01	173, 295, 366	Gerhardt, Theo	SH04	343
Gao, Kaige	RA14	251	Geurts, Christian	JE01	101
Gao, Liangqiu	RL05	290	Ghaffari, Muhammad	PN03	172
Gao, Lu	AH04	38	Ghiringhelli, Giacomo	BA03	41
Gao, Tie Ren	BD05	43	Ghoshal, Sayak	PJ28	159
Garbarino, Gaston	JJ04, RB20	106, 257	Ghoshray, A	QM24	235
Garcia - Garcia, A.	KC05, PJ23	109, 158	Ghoshray, Amitabha	RB15	256
Garcia - Munoz, Jose Luis	PA13	118	Ghoshray, K	QM24	235
Garcia, Carlos	PJ25	158	Ghoshray, Kajal	RB15	256
Garcia, Fernando A.	PI19	153	Giamarchi, Thierry	CC03	50
Garcia, Flavio	RJ12, RJ13	284	Giannopoulos, George	DD06, QP12, QP13	59, 247
Garcia, Jackeline Collave	SE22	336	Giblin, S. R.	PI03	151
Garcia, Javier	DG03	61	Giebels, F	RP20	306
Garcia, Luis	EF03	68	Gillett, J.	GA01	75
Garcia, Luis Miguel	GG03, GG05, QI14	80, 220	Gillon, Beatrice	GF04	79
Garcia, Noel A.	QB18	190	Gingras, M. J. P.	GF01	79
Garcia, Vincent	AE03	36	Ginting, Dianta	RA01	249
Garcia-flores, Ali F.	PI19	153	Giouroudi, Ioanna	SA02	316
Garcia-garcia, Javier	PI18	153	Giovannini, Loris	GG02	80
Garcia-munoz, Jose Luis	EC04, RA17	66, 252	Giovannini, Mauro	IA02, QD08, RD21	90, 197, 265
Garcia-saiz, A.	GH05	81	Giri, S	QL14, SO14	230, 369
Garitaonandia, Jose Javier	QH16, RN13	215, 298	Giri, S.	PL07	165
Garnweitner, Georg	JG06	104	Giri, Saurav	RH02	275
Garst, Markus	DF02, RI12	60, 280	Givord, D.	JH02	104
Gasche, T. P.	QM13	233	Givord, Dominique	EJ03	72
Gastelois, Pedro	EI01	70	Gjoka, Margarit	BJ02, RO08, RQ10	47, 302, 308
Gataullin, Eduard	PE08	137	Gkanas, Evangelos	SN15	366
Gaudin, Gilles	SH05	344	Gladczuk, Leszek	QM17	234
Gaulin, Bruce D	JD01	100	Glavatsky, I.n.	QG27	212
Gaur, N.k.	QA14, RF04, RQ06	184, 269, 308	Gloos, Kurt	SB16, SK07	322, 351
Gautam, Sanjeev	PG27, QO27	146, 245	Gloskovskii, A.	SK24	354
Gavilano, Jorge	PO17, QF20	180, 207	Gloter, Alexandre	AE03	36
Gavilano, Jorge L.	CD04	51	Glushkov, V. V.	PE12, QC22, RH07	138, 195, 275
Gavrilkov, Vladimir	PD01	132	Glushkov, Vladimir	ED06, KI05, QC20	67, 113, 195, 340
Gavrilkin, S.	QC22	195			

				SG07, SG08	
Glushkov, Vladimir V.	QC19	195	Gradhand, Martin	EE01	67
Gnezdilov, Vladimir	QE27	203	Graf, Matthias	KG01	111
Gnida, Daniel	AB03, SF12	34, 339	Grams, Christoph	QA22	186
Go, Naoto	PK12	162	Granado, Eduardo	PI19	153
Godinho, M.	QM13	233	Granovsky, Alexander	CH01, SO04, SO27	54, 367, 371
Godlewski, Marek	DD02	58	Granroth, Garrett E	PI07	151
Goetzke Macedo, Daniela	PB10	121	Granroth, Garrett E.	RD14	264
Goff, Jon	DH03	62	Grbic, Michael	IC02	92
Gofryk, K.	FB01	73	Greene, L. H.	GA01	75
Gofryk, Krzysztof	SE19	336	Greene, Laura H.	RD09	263
Gog, Thomas	DC03	58	Greтарsson, Hlynur	DC03	58
Goh, Jing Qiang	SJ09	350	Greven, Martin	CA03	49
Goh, Swee K	FB04	73	Grigera, Santiago	EA04	64
Goh, Swee K.	PC09, RQ09	128, 308	Grigoriev, Sergei	QM08	232
Goh, Swee Kuan	PC02	127	Grigoriev, Sergey	DF04, SL27	60, 360
Goho, Takeshi	RG11	273	Grigorieva, Anastasiya	ED06, KI05	67, 113
Goikman, Alexander	DD04, SK26	59, 354	Grigoryeva, Natalia	SL27	360
Goikolea, Eider	RN13	298	Grigoryeva, Natalya	QM08	232
Gokhfeld, Denis	SB09	321	Grimaldi, E.	CE06, ID02, RJ07	52, 93, 283
Goko, T.	GF01	79	Grin, Yuri	RD12	264
Gollisch, H	RP20	306	Grioni, Marco	SE08	334
Goltz, Till	AB02	34	Grisewood, N.	PJ26	159
Golubov, A. A.	GA03	75	Grishin, Alexander	CJ01	55
Gomes, Angelo M	QO09	242	Griveau, Jean-christophe	RE03, SE19	266, 336
Gomez Sal, J. C.	GH05, QD10	81, 198	Groessinger, Roland	SA02	316
Gomez, Maria Elena	SA12	318	Grois, Andreas	BE03	44
Goncalves, Antonio	SG03	340	Grollier, J.	CE03, CE06, ID02, RJ07	51, 52, 93, 283
Gong, Junfeng	RM08	296	Grollier, Julie	HF01, ID03, IE04	87, 93, 94
Gonzalez, Jorge L.	SM17	363	Grosche, F Malte	FB04, QH12, RA19, SF05	73, 214, 252, 337
Gonzalez, Julian	CH01, CJ04	54, 56	Grosche, F. Malte	RE14, RE15	268
Gonzalez, Julianmaria	DJ03	63	Grosche, Malte	PC02, PC09	127, 128
Gonzalez, Lorena	DJ03	63	Gruber, Manuel	GIO3	82
Goo, Cheol Soo	RR04	311	Grundler, Dirk	GG02	80
Goodilin, Evgenii	ED06, KI05	67, 113	Grunin, Alexey	DD04	59
Gopalakrishnan, C	PO24, SA21, SA22, SA23, SK32	181, 319, 320, 355	Grytsyuk, Sergiy	QP01, QP02	245
			Gschneidner, Jr., Karl	JU01	106
			Gu, Bo	JF03	102
			Gu, G.	GA01	75
Goraus, Jerzy	PD21	135	Gu, Genda	HA03	83
Gorbunov, D. I.	QI03, QI09	218, 219	Gu, Han	RR29	315
Gorbunov, Denis	SG03	340	Guan, Wen	SO25	370
Goremychkin, E A	SE13	335	Guari, Yannick	RN15	299
Goremychkin, E. A.	RA22	253	Gubbiotti, Gianluca	GG02	80
Goremyhkin, E A	SF09	338	Gubkin, Andrey	QG04	208
Gorria, Pedro	JU04	106	Gubkin, Andrey F.	QN10	238
Goryunov, Yuriy Vladimirovich	IG02, PE09, QG23	95, 137, 212	Gudim, I	QJ16	223
Goswami, Partha	PB01, RE02	120, 266	Gudim, Irina	IJ01, RA23	97, 253
Goswami, Partho	SC02	325	Gudim, Irina A	CI04	55
Gotberg, Olof	HA03, SE08	83, 334	Gudim, Irina A.	PA02	116
Goto, Junpei	PL06	164	Guduru, Veerendra	DH02	62
Goto, Takayuki	RH03, RH11	275, 276	Guduru, Veerendra Kumar	SA10	317
Goto, Terutaka	RB05	254	Guenther, Marco	PI05	151
Gotou, Junpei	RC02	259	Guerrero, Sebastian	QF20	207
Gottlieb-schoenmeyer, Saskia	QH24	216	Guertari, Rim	PM06	168
Gotze, Kathrin	QD07	197	Guidi, T.	RA22	253
Gouchi, Jun	QC03	192	Guillot, Maurice	QJ15	223
Goumri-said, Souraya	QL17, SK12	230, 352	Guimaraes, Alberto Passos	RJ13	284
Gouvea, Cristol De Paiva	PB11	121	Guimaraes, Marcos H. D.	GIO5	82
Goya, Tomoki	RB06	255	Gukasov, Arsen	SE16	335
Goyal, Neeraj	QJ17	223	Guleria, Anupam	QB14	189
Grabs, Ilka Marina	JG06	104			

Gumeniuk, Roman	RD12	264	Ham, Chan	PO13	179
Gunduz Akdogan, Nilay	EJ04	72	Hamada, Rika	QH28	217
Guo, Guan Yu	J105	105	Hamada, Tomoyuki	RF07	270
Guo, Hong	QK02	224	Hamamoto, Kenta	SA03	316
Guo, Huaiming	SD18	333	Hamano, Suguru	IG05	95
Guo, Lu Kai	RD12	264	Hamasaki, Tatsuichi	RH19	277
Guo, Shuang	RK16	288	Hamaya, Kohei	HE01, RK10	86, 287
Guo, Zhaohui	PK18, RO04, RO07	163, 301	Hamrle, Jaroslav	CH03, QH19	54, 216
Gurevich, Alexander	JA02	98	Han, Dong-soo	DE05, RJ16, RJ17, RJ18, SH14	60, 285, 345
Guritanu, Violeta	QD07	197			
Guryeva, Tatyana	QM19	234	Han, Guchang	QP06	246
Gusakova, Daria	SI09	347	Han, Jeong-ho	RR14, SN04	313, 364
Gusev, Sergey	SG17	342	Han, Jinhee	RC15	261
Gusin, Pawel	PG26	146	Han, Jung Hoon	DF01	60
Gutersloh, Daniel	PE07	137	Han, Jung-ho	SN02	364
Gutfleisch, Oliver	DJ04, KH01, SO19	63, 112, 369	Han, Jungmin	RL14	292
Guth, Konrad	KH01	112	Han, S. W.	PG11	144
Gutmann, Matthias	SD13	332	Han, Sang Wook	PB12	122
Gutowska, M. U.	PH06, PM05	147, 168	Han, Seungkyu	RA26	253
Guziewicz, Ela	DD02	58	Han, Suk Hee	QK11, QK12, QK13, RL28	225, 226, 294
Gvasaliya, Severian	CC03, IU06	50, 98			
Gwon, M. J.	PO23	181	Han, Sukhee	QK10	225
Gwon, Minji	RK15	288	Han, Suk-hee	PJ30	159
Gwon, Yoonjung	PN08, PN09, QM04	173, 232	Han, Tianheng	QE27	203
Gyawali, Parshu R.	PJ01	154	Han, Xiufeng	QK02, SA19, SA20	224, 319
			Han, Xiu-feng	RM01	295
			Han, Yibo	QF06	204
			Han, Young Ho	BJ04, QN13	48, 238
H			Hanazawa, Atsufumi	RI17	281
Haam, So Young	JB02	99	Handayani, Ismudiaty Puri	PH17	149
Haase, Juergen	RQ09	308	Handayani, Puri I.	PA24	119
Haazen, Pascal P.	IE02	93	Handoko, Djati	RP03, SH10	303, 344
Haber Korn, N.	QB31, SB12	192, 322	Handoko, Erfan	RA15	251
Habermeier, H. -u.	ED05	67	Haney, Paul M.	EE02	67
Habermeier, Hanns-ulrich	RB29	258	Hanfland, Michael	RB20	257
Hachiuma, Suguru	QA05	183	Hanh, Duong Thi	HC02, PE15	84, 138
Hackl, Rudi	CA03	49	Hanson, Maj	SL15	358
Haddon, Robert C.	PN16	174	Hanyu, Takahiro	BI02	47
Hadiyawarman, H	QL09	229	Hao, Lin	PK03	160
Hadjipanayis, George	BJ02, CB05, DD06, EJ04, KB04, RO08	47, 49, 59, 72, 108, 302	Happo, Naohisa	SK13	352
Hadjipanayis, George C.	GJ01	82	Hara, Masahiro	KC06	109
Haenni, Nora	QG14	210	Hara, Shigeo	QE17, QF09	202, 205
Haga, Yoshinori	GC03, HP11, IG04, PC28, PD09, PD13, PD23, QC03, RD01, RD11, RD25, RE10, SB15, SE23, SF03	77, 30, 95, 131, 133, 134, 135, 192, 262, 263, 266, 268, 322, 337	Harada, Eiichiro	RD06	263
			Harada, Kazunori	KF05	111
			Harada, Keitaro	SO515	369
			Harada, Ken	AF03, PG15	37, 144
Hagemann, Hans	QC13	194	Harada, Masashi	PO17	180
Hagihala, Masato	QE18	202	Haraguchi, Shinya	AE02, PL06, RC02, RL02	36, 164, 259, 290
Hagiwara, M.	CF01	52	Haraldsen, Jason	KG01	111
Hagiwara, Makoto	PB25	124	Haraldsen, Jason T	EB04	65
Hagiwara, Masayuki	PD13, PI06, QB09, QB24, QF06, QH02, RH25	134, 151, 188, 191, 204, 213, 278	Harding, Phimpaka	SL10	357
			Hardy, Vincent	JB05	100
Hagymasi, Imre	PD15	134	Hardy, Walter	BA01	40
Hahn, Byung-dong	DJ02	63	Hari, Murali Krishnan	QO24	244
Hajiri, Tetsuya	AD04, QD18	35, 199	Harima, Hisatomo	HP11, RD16, RG11, SB05, SG14	30, 264, 273, 321, 341
Hakimi, A. M. H. R.	RN18	299			
Halbedel, Bernd	QO02	241	Harnagea, L.	RB17	256
Hall, Anders	QH11	214	Harrison, N.	SC03	326
Hall, Michael	HH02, KH03	88, 112	Harrison, Neil	BA01, EA03, PB02, QB13	40, 64, 120, 189
Halue, K.	PE17	138	Harrison, Nicholas	RF15	271

Harumori, Kohei	SK23	354	Henriques, Margarida	SG03	340
Haruna, Daiki	QG10	209	Her, Eun Ju	CB01	49
Haryono, Suprijadi	RC02	259	Hering, Eduardo	SE22	336
Hasan, M. Z.	SD04	330	Hering, Eduardo N	SE15	335
Hasan, M. Zahid	HI02	89	Heringa, Jouke R	RI18	281
Hase, Masashi	PH02, QA05, QA07, QA09, RH11	147, 183, 184, 276	Hernandez, Yenny	QK14	226
			Hernandez-velasco, Jorge	PI18	153
Hasegawa, Kota	RL15	292	Hernando, Blanca	DJ03	63
Hasegawa, Takahiro	QI17	220	Herng, Tun Seng	DD03	58
Hasegawa, Takashi	SL02	356	Herrero Albillos, Julia	GG03, RP04	80, 303
Hasegawa, Takumi	PC05, PG16, RD10, SG15	127, 145, 263, 342	Herrero-abillos, Julia	EF03, GG05, QI14, RP08	68, 80, 220, 304
			Herrero-martin, Javier	EC04, PA15, RA17	66, 118, 252
Hasegawa, Takuya	QA05, QA07, QA09	183, 184	Herringer, S N	BC05	42
Hashemi, S. E.	PO29	182	Herrmannsdoerfer, Thomas	PC27, SD07	131, 331
Hashemi, Sayed Ebrahim	PO27	181	Herschbach, Christian	EE01	67
Hashi, Shuichiro	PO20, SM08, SN14	180, 362, 366	Hervieu, Maryvonne	RA11	251
Hashim, Mansor	BJ06, RQ22	48, 310	Herynek, Vit	BH03	46
Hashimoto, Susumu	CE05	52	Herzer, Giselher	PM04	168
Hashimoto, Takuya	BG04	46	Herzog, Gabriela	HF03, RP16	87, 305
Hashmi, Arqum	RM07	296	Hewson, Alex	SF15	339
Hassinger, Elena	JC02	100	Heyderman, Laura	HP62	31
Hasuo, Tadahiko	SG09	341	Heyderman, Laura J.	RK17	288
Hatakeyama, Kenichi	QN02	236	Hicks, Trevor	IU03	97
Hatakeyama, Kodai	RP06	304	Hidaka, Hiroyuki	QC25, SE07	196, 334
Hatayama, Nobukuni	PF08	140	Hien, Nguyen Thi Minh	SA16	318
Hatayama, Yuki	RO09	302	Hierro Rodriguez, Aurelio	GG03	80
Hatch, R.	II02	97	Hiess, Arno	AA05, RB07	33, 255
Hattori, Taisuke	RD05, RD08	262, 263	Higashinaka, Ryuji	QE13	201
Hauguel, Tony	SA24	320	Higashinaka, Ryuji	RD17	264
Havela, Ladislav	QI19, RD26, RE09, SG03	220, 266, 267, 340	Hikihara, Toshiya	JD04	101
Haverkort, Maurits Wim	QC09	193	Hild, K	QM12	233
Haw, S. C.	QB21, SM11	190, 362	Hilgenkamp, Hans	DH02, SA10	62, 317
Hayakawa, J.	IF01	94	Hill, John	DC03	58
Hayashi, Hisashi	QD17	199	Hill, R. W.	HA05	84
Hayashi, Junichi	PD10	133	Hillebrands, Burkard	HD01, SI15	85, 348
Hayashi, Kouichi	SK13	352	Hiller, Adrian	PC12	128
Hayashi, Masamitsu	IF05	94	Hillier, A	SF09	338
Hayashi, Misaki	RP07	304	Hillier, A D	SE03, SE05, SE13	333, 334, 335
Hayashida, Minami	QC18	195	Hillier, A. D.	KA02	107
Hayato, Miyagawa	PN24	176	Hillier, Adrian	JA05, SC01	99, 325
Hayden, Stephen	RE14	268	Hillion, Arnaud	QN06, RK03	237, 286
Hayn, Roland	CD03	51	Hilscher, Gerfried	SC01	325
He, Chenchong	AJ03, JI06	40, 105	Hindmarch, Aidan T	SH09	344
He, Chunyong	DH01	62	Hinks, D G	SC05, SE14	326, 335
He, Junfeng	SB31	325	Hinzke, Denise	FA02, FC03, RJ04	72, 74, 283
He, Long	SB13	322	Hirai, Daigorou	RB04	254
He, Pan	JI05	105	Hirai, Daishi	QD06	197
He, Zhangzhen	PA18, QF24	118, 207	Hiraka, Haruhiro	QG18, RP01	211, 303
Heald, S. M.	RN18	299	Hirakawa, Sentaro	QI13	219
Hedo, Masato	PD14, QC11, QI12, QI13	134, 194, 219	Hiramatsu, Ryo	RL07	291
Heger, Gernot	RP22	306	Hirano, Masahiro	QC08	193
Hehn, Michel	KF02, SH02	110, 343	Hirano, Masanori	QB15	189
Heiliger, Christian	DI03	63	Hiraoka, N.	QB21	190
Heinze, Stefan	AF02, IH02, IH03, PG12	36, 96, 144	Hiraoka, Nozomu	QC09	193
Heiss, Dominik	IE03	93	Hirashima, Dai	PF19	142
Hemberger, Joachim	QA22	186	Hirata, Wataru	QB24	191
Hemmi, K.	CF04	53	Hirata, Yasuyuki	QO13	242
Hemmi, Kazuhiro	PH07	148	Hiratsuka, Yusuke	DE04	60
Hendry, Euan	GD04, RK20	78, 289	Hirayama, Shigeyuki	SK31	355
Henkie, Zygmunt	PE19, SB26	139, 324	Hirayama, T.	RD15	264

Hirohata, A.	SK03	350	Hor, Y. S.	SD04	330	Huijben, Mark	DH02, SA10	62, 317	Iida, Hiroki	QC10, QC11	193, 194
Hirohata, Atsufumi	PJ17, SK11	157, 352	Hord, Roland	PI05	151	Hung, C. H.	SB04	320	Ikubo, Satoshi	PB32, QH09, QH10	125, 214
Hiroi, Masahiko	QG13, QG15, QH08, QN20, SK23	210, 214, 239, 354	Hori, Akihiro	HC03, QF25	85, 208	Hung, Dung S	RK07	287	Imura, S.	QB23	190
Hiroi, Zenji	JA04, PC17, PG16, QE03, QE05, QE08, QE13, QG16, SB05, SG04, SG14	99, 129, 145, 199, 200, 201, 210, 321, 340, 341	Hori, Shiori	QM16	234	Hunt, C. R.	GA01	75	Iizuka, T	QJ05	221
Hirono, Toko	RP07	304	Hori, Yusuke	PD10	133	Hur, Nam Jung	SE02	333	Iizuka, Takuya	QD07	197
Hirose, Yusuke	PB27, PD08, PD13, RD19	124, 133, 134, 265	Horigane, K.	QE15	201	Hur, Namjung	PI10, QA24, QM23	152, 186, 235	Ikeda, Hiroaki	QC04, QC08	192, 193
Hirsch, Konstantin	KD01	109	Horiyama, A.	CG02	53	Husek, I	RB08	255	Ikeda, Masami	QB24, QF06	191, 204
Hirschberger, Max	SF05	337	Horng, Heng-er	AH03, GH01, QM27	38, 80, 236	Hutanu, Vladimir	PA14, RP22	118, 306	Ikeda, Naoshi	RA18	252
Hirtenlechner, Eva	QG14	210	Horng, Lance	PC30, SB19, SH08, SL18	131, 323, 344, 359	Huxley, A. D.	GC01	77	Ikeda, Shoji	QP14, SI17	247, 348
Hisada, Akihiko	SE01	333	Horsch, Peter	RG18	274	Huxley, Andrew	GC04	77	Ikeda, Shugo	IG04, RB03, RD11, RD13	95, 254, 263, 264
Hisamatsu, Toru	QG13	210	Horvatic, Mladen	IC02	92	Huxley, Andrew D	SE12	335	Ikeda, Yoichi	QC18, SE10	195, 334
Hisayoshi, Keiji	PN11, RQ03	173, 307	Hosaka, Tomohiro	QA05, QA07, QA09	183, 184	Huynh, Chinh Dang	RN19	299	Ikeda, Yutaka	PO17	180
Hjorvarsson, Bjorgvin	AF05, RP15	37, 305	Hosokawa, Shinya	SK13	352	Hwang, Chan Yong	PJ14	157	Ikehara, Yuki	GJ02	82
Hjorvarsson Bjorgvin	QH11	214	Hosono, H.	QB23	190	Hwang, Chanyong	BD03, IH04, IH05, QM26, RK18, RK19,	43, 96, 235, 288, 289, 307, 345	Ikeuchi, K.	CF04	53
Ho, Huei-ying	PL03, PL13, QM09	164, 166, 233	Hosono, Hideo	PC23, QB16, QC08	130, 189, 193		RP23, SH13		Ikeuchi, Kazuhiko	DA01, PI07, RH12	56, 151, 276
Hoa Hong, Nguyen	SM07, SM10	362	Hosono, Kazuhiro	PJ18	157	Hwang, Do Guwn	PO09, PO10	178	Ikeura, Tohru	PD16	134
Hoang, Nam-nhat	RA10, RF02, SG10, SO12	251, 269, 341, 368	Hossain, Z.	QB14	189	Hwang, Do Gwen	PO06	178	Ikuo, Nakai	QC01	192
Hodgson, Matthew	RK09	225	Hossinzadeh, Nahid	PB15	122	Hwang, Harold	BA02	41	Ilyn, Maxim	SO04, SO27	367, 371
Hodovanets, H.	RD02	262	Hotta, Chisa	BC05	42	Hwang, J. S.	SL08	357	Im, Dae Yeong	QO20	244
Hoeijmakers, Mark	GE02, JE01	78, 101	Hotta, Koji	RM05	296	Hwang, Jihoon	PB12, PG11, PH14, QA04	122, 144, 149, 183	Im, H. J.	SG11	341
Hoffmann, Germar	GH02	81	Hotta, Takashi	PF11	141		PA21	119	Im, Jino	RC16	261
Hofmann, Michael	EF02, QG26	68, 212	Hou, Yanglong	SL12	358	Hwang, Jungmin	RQ19, RQ20	310	Im, Mi-young	DE05, HG02, RJ16, RJ20, SH04	60, 88, 285, 343
Hofmann, Philip	II02	97	Howard, A.	QB12	189	Hwang, Seong-min	RR10	312	Imada, Masatoshi	FE01, QB10	74, 188
Hoglin, Viktor	PM10	169	Hrabec, Ales	SH05	344	Hwang, Su-jin	QH25	217	Imai, Yoji	KF05	111
Holbein, Simon	AA05	33	Hradil, K.	PI03	151	Hyun, Seung Ill	QH25	217	Imai, Yoshiki	PF17, SD05	142, 330
Holder, Matthias	CD03	51	Hsiang, Hsing-i	BJ01, QN24, QN25	47, 240	Hyun, Sung Wook	PA22	119	Imai, Yuya	PD20	135
Holler, Robert	RG15	274	Hsiao, S. N.	PK06, QP17	161, 248	Hyun, Young-hwan	SD03	330	Imakyurei, Takumi	PG09	143
Hollmann, Nils	PI08, PI17	152, 153	Hsieh, C.c.	SN06	365				Imamura, Hiorshi	RJ06	283
Holmes, Stuart N	PN23	175	Hsu, Chuang-han	AD01	35	Ibarra, M R	RN08	298	Imamura, Hiroshi	HF02, JG03, RA09, SI16	87, 103, 250, 348
Honda, Fuminori	HP11, PB27, PD08, PD13, PD16	30, 124, 133, 134	Hsu, Jen-hwa	PK06, QP17	161, 248	Ibarra, M. R.	KC05, PJ23	109, 158	Imamura, Masaaki	PN26, SO09	176, 368
Honda, Hiroyuki	PG22	146	Hsu, Pin-jui	AD01	35	Ibarra, Manuel Ricardo	DG05, PG08, SM16	61, 143, 363	Imanaga, Yukihiko	DE04	60
Honda, S.	CG02	53	Hsu, Wei-hung	QN25	240	Ibragimova, Elvira	RR28	315	Imperia, Paolo	PO12	179
Honda, Syuta	RJ08, SK20	283, 353	Hsu, Y. Y.	SB04	320	Ibrahim, I. A.	RN01	296	Imura, Keiichiro	QD18	199
Honda, Zentaro	QF06, RH25	204, 278	Hsueh, Wang-jung	AD01	35	Ichihara, Masaki	SB14	322	Inada, Kensuke	PF02	139
Hong, Cheng Hai	QN03	236	Hu, Chong Der	QF26	208	Ichikawa, Akihiro	QB26	191	Inada, Yoshihiko	PC20, QJ07	130, 222
Hong, Do-kwan	PM25, RR31	171, 316	Hu, Fengxia	SO25	370	Ichimura, Masahiko	PJ07, RL01	155, 290	Inagaki, Keima	SK18	353
Hong, Hongpei	SO01	366	Hu, Guanghui	QJ06	221	Ichiyanaqi, Yuko	PO02, QL03, RN02	177, 228, 297	Inagaki, T.	QH09	214
Hong, Jeongmin	PN16	174	Hu, Hai Ning	SL16	358	Ide, Tetsuto	PH15	149	Inagaki, Yuji	QE18, QF14, QL11, QL12, QL13, RQ05, SG09	202, 206, 229, 230, 307, 341
Hong, Jin Pyo	RK19	289	Hu, Jin	RB12	256	Ideta, Yukiichi	QF24	207			
Hong, Jinki	PJ31, PK21, QK10	159, 163, 225	Hu, R.	QC23	196	Idigoras, Olatz	SM04	361	Inami, Nobuhito	EI02, SI17	70, 348
Hong, Jisang	JH03, RMO7	104, 296	Hu, Shaojie	RL20	293	Ido, Masayuki	PB08	121	Inami, Toshiya	IG03, QI10	95, 219
Hong, Jongill	JI02, RL30	105, 294	Hu, Shaojie	RL20	293	Idutsu, Yuichi	RH25	278	Inamura, Yasuhiro	RH12	276
Hong, K.-P.	PH03	147	Hu, Xinghao	PO19, SN13	180, 366	Idzikowski, Bogdan	QO17	243	Indenbom, Mikhail	SA24	320
Hong, Kwang Pyo	QN09	237	Hu, Zhiwei	PI08, PI17	152, 153	Idzuchi, Hiroshi	HE05	86	Infante, Ingrid	QA27	187
Hong, S. C.	PG11	144	Huang, Chao-hsien	SH08, SL18	344, 359	Ieda, Jun'ichi	JE02, JF02, KF03	102, 111	Ingvarsson, Snorri	GH03	81
Hong, Seung Hwan	SB32	325	Huang, Chia-sheng	RR26	315	Ienaga, Koichiro	QL11, QL12, QL13	229, 230	Innocenti, Claudia	CB04	49
Hong, Soon Cheol	KI01, PB12	112, 122	Huang, Chuan-fa	PK06, QP17	161, 248	Iga, Fumitoshi	PC05, PE10, RH03	127, 137, 275	Ino, Hiromitsu	PG05	143
Hong, Sung-hak	PB21, RB27	123, 258	Huang, Chonghui	PG21	145	Igarashi, Hideki	QC25	196	Inomata, K	SK29	355
Hong, Tae Min	QN22	240	Huang, J. H.	PM03	167	Igarashi, Kazuhiro	QF15	206	Inomata, Koichiro	EH01, IF03, IF05	69, 94
Hong, Tao	BC05	42	Huang, Jin-hua	PC14	129	Igarashi, Suguru	PB06	121	Inosov, Dmytro	JC04	100
Hong, Yang-ki	JH04, KH04	104, 112	Huang, K.w.	AH03	38	Igawa, Naoki	JJ05	106	Inoue, J.	CG02	53
Honma, Yuki	PH05	147	Huang, K.su-yen	PC14	129	Iglesias, Oscar	KB06, RN14	108, 299	Inoue, Katsuya	PG09, PG10, PG22, QG22	143, 144, 146, 211
Hono, K	BG01	45	Huang, Wen-min	RE11, SB25	268, 324	Iglesias-silva, E.	CB02	49	Inoue, Mitsuteru	QP15, QP16	247, 248
Hono, Kazuhiro	IF03, SK31	94, 355	Huang, Xiao-lan	IH06	96	Ignatchik, Oleg	QD07	197	Inoue, T.	SG02	339
Honolka, Jan	AD03	35	Huang, Xuelian	SM14	363	Iguchi, Daisuke	PC17	129	Inoue, Y. F.	EF01	68
			Huber, Rupert	HA02	83	Iguchi, Satoshi	GB04	76	Inoue, Yukihiko F	SG12	341
			Hudl, Matthias	EI03	71	Ihara, Yoshihiko	PC15, RD05	129, 262	Insausti, Maite	RN13	298
			Hueso, Luis E.	HE02	86						
			Hugli, Remo Viktor	GF02	79						
			Huh, Mooyoung	PM23	171						
			Huhtinen, Hannu	PB20	123						

Inui, Ken	PN07	173	Isomura, Shinsaku	PK07, QP08	161, 246
Inumaru, Kei	PE10	137	Isono, Takayuki	PC17	129
Ioannidou, Alexandra	RQ10	308	Isozaki, Toshiyuki	QK19	227
Ion, Lucian	QK20	227	Itai, Kazumasa	PD15	134
Ionescu, Adrian	PN23	175	Itkis, Mikhail E.	PN16	174
Ipatov, Mihail	AJ02, CJ02, PJ25	40, 55, 158	Ito, Eisuke	CB01	49
Ipatov, Mikhail	SO27	371	Ito, Hiroyoshi	RK10	287
Ipponjima, Tsukasa	SG16	342	Ito, Keigo	SJ03	349
Iqbal, Muhammad Waqas	QK06	225	Ito, Keita	KF05	111
Iqbal, Muhammad Zahir	QK06	225	Ito, Masakazu	QG13, QG15, QN20, SK23	210, 239, 354
Irie, Ryotaro	PH15	149			
Irifune, T.	SG02	339	Ito, T.	RM04	295
Irifune, Tetsuo	PE10	137	Ito, Takahiro	AD04, QD18	35, 199
Iritani, Kensuke	QC08	193	Ito, Tomonori	RM05, SO10, SO11	296, 368
Irusta, Silvia	RN09	298	Ito, Toshimitsu	QA05, QA07, QA09, RH11	183, 184, 276
Irvine, Andrew C.	IE03	93			
Isasa, Miren	HE02	86	Ito, Wataru	PB06, QG08, RP07	121, 209, 304
Isayama, Akira	QO18	243	Ito, Yuichiro	PH15	149
Ishaque, Zahid	SH03, SH06	343, 344	Ito, Yuzo	SE10	334
Ishibashi, Akira	SM09, SO07	362, 367	Itoh, Akiyoshi	BG03, RK08, RK17	45, 287, 288
Ishibashi, Hiroki	PI02	151	Itoh, Atsushi	PC28	131
Ishibashi, Shoji	GB03, RG07	76, 272	Itoh, Hiroyoshi	RJ08, SK20	283, 353
Ishibashi, Shota	KF01	110	Itoh, Masayuki	DA01, PH19, PH20, PH23, QB04, QB26, QF15, RB02	56, 150, 187, 191, 206, 254
Ishibashi, Takayuki	KD03, RP17, SK21	109, 306, 353			
Ishibashi, Yusuke	RR05	311	Itoh, Mitsuru	QF24, QK19, RL25, SM20	207, 227, 294, 364
Ishida, K.	KJ01	113			
Ishida, Kenji	QC08, QH13, RD05, RD08	193, 215, 262, 263	Itoh, Ryusuke	QA05, QA07, QA09	183, 184
			Itoh, Shinichi	PI07, RH13, RI10	151, 276, 280
Ishida, Yuko	RI17	281	Itoi, Chigaku	RI11	280
Ishihara, Sumio	GB02, PI07, RH10	76, 151, 276	Ito, Masayoshi	BA04, PG05, PG13, PK12, SK04	41, 143, 144, 162, 351
Ishii, Akira	PN13	174			
Ishii, Fumiyouki	RC09, RC19	260, 262	Itou, Tetsuaki	BC04, QE22	42, 203
Ishii, H.	QB21	190	Ivanov, Alexandre	JC04	100
Ishii, Rikako	QF21	207	Ivanov, Vsevolod	SG07	340
Ishii, Yasuyuki	QB02	187	Ivanov, Vsevolod Yu.	QC19	195
Ishii, Yui	SG14	341	Ivanshin, Vladimir	PE08	137
Ishijima, Hiroyuki	PN07	173	Iversen, B.	II02	97
Ishikawa, Hajime	QE05, QE08	200			
Ishikawa, Jun J	PG14	144	Iwakawa, Ken	PD13, QH03	134, 213
Ishikawa, Takuya	RB06	255	Iwama, Hiroki	SN03	364
Ishikawa, Yosuke	RI01	279	Iwamoto, Takashi	RN03	297
Ishikawa, Yusuke	PD14	134	Iwasa, A.	QI03	218
Ishikawa, Yuya	QF09, QF17	205, 206	Iwasa, K.	CF04, PL14	53, 166
Ishimatsu, Naoki	PN20	175	Iwasa, Kazuaki	PI07, RD14	151, 264
Ishio, Shunji	SL02	356	Iwasa, Yoshihiro	AE05	36
Ishiwata, N.	RL07	291	Iwasaki, Hitoshi	CE05	52
Ishiwata, Nobuyuki	RL10	291	Iwasawa, Kotaro	PE11	137
Ishiwata, S.	RA05	250	Iwase, Hiroaki	PD20	135
Ishiwata, Shintaro	PA12	117	Iwata, Satoshi	RL08	291
Ishiyama, Kazushi	PO20, RP11, SM08, SN14	180, 305, 362, 366	Iyama, Ayato	QA12	184
			Iyo, A.	QB28	191
Ishizuka, Hiroaki	RG03	272	Iyo, Akira	DA04, PB05, PB26, QB02, QB15, QB29	56, 120, 124, 187, 189, 191
Isikawa, Yosikazu	RD14, SG05	264, 340			
Islam, A. T. M. Nazmul	PA23, RH24	119, 278	Izawa, Koichi	PC17, PC28, PD16	129, 131, 134
Ismail, Ismayadi	BJ06, RQ22	48, 310			
Isnard, O.	QG07, QI03	209, 218	J		
Isnard, Olivier	EJ03	72	Jablonski, A.	DD02	58
Isobe, Masaaki	PC21, RH14, SF02	130, 277, 337	Jacko, Anthony	RG14	274
Isobe, Masahiko	QD03, RH16, SB14, SF04	196, 277, 322, 337	Jaffres, Henri	AI04, CG03, HE04	39, 53, 86
Isoda, Makoto	QE11	201	Jaglicic, Zvonko	SL11	357

Jaim, H. M. Iftekhar	SB06	321	Jeong, Yeon-ho	PM25	171
Jaime, Marcelo	JD01	100	Jeong, Yoon Hee	PA11, PN28, QA16	117, 176, 185
Jain, Abhinav	AI04, CG03	39, 53	Jeong, Yoonhee	SM13	363
Jakiela, Rafal	DD02	58	Jeong, Yoon-hee	SA18	319
Jakob, Gerhard	CH03	54	Jeong, Yun-ho	RR22	314
Jal, Emmanuelle	AD02	35	Jesche, Anton	CD03	51
Jalli, Jeevan	JH04	104	Jeschke, Harald	SF14, SG22	339, 343
Jamali, Mahdi	EG03, GE03, PJ20, RL19	69, 78, 158, 293	Jeschke, Harald O.	RG14	274
Jamet, Matthieu	AI04, CG03, DD01, EI04, GE01, QK16	39, 53, 58, 71, 78, 226	Jhang, Hau-chun	PL03	164
			Ji, Gaofeng	QB07	188
Jang, Daekyu	RR17	313	Ji, Hyo Seok	RB22, RB23	257
Jang, H.	PH10	148	Ji, Lina	CA03	49
Jang, Hyuk-jae	AE04	36	Ji, Qing	PJ05	155
Jang, Ik-sang	RR14, SN02	313, 364	Ji, Sungdae	QE15	201
Jang, Jin Hak	RR24	314	Jia, Q.	QB31	192
Jang, Jung-tak	CB01, PO15, PO16	49, 179	Jia, Quanxi	EB04	65
Jang, Jungwon	QO10, SD11	242, 331	Jian, Ming-hung	RR26	315
Jang, Moongyu	RL21	293	Jiang, Zhaozhen	RR29	315
Jang, Pyungwoo	PM20	170	Jiao, L.	QB12	189
Jang, Seok-myeong	RR04	311	Jiao, Lin	RD12, SB29	264, 325
Jang, Tae-suk	RO01, RO02	300, 301	Jiao, Wenhe	RB13	256
Jang, Y. S.	RQ08	308	Jin, Hosub	RC13, RC16, RC17	261
Jang, Youngjae	PK21	163	Jin, Jung-il	EH02	70
Jang, Z. H.	QF13	206	Jin, X. R.	SL09	357
Jang, Zeehoon	RN10, RP13	298, 305	Jin, Xiaofeng	JF01, JF05	102, 103
Jangid, S.	RA03	249	Jingwei, Cui	QJ01	221
Janjan, S. M.	QM05	232	Jo, Euna	BF05, JG05, PA09, PH18	45, 104, 117, 149
Jansen, Ron	AI05, DI02	39, 63	Jo, Jeong Hong	PL16	166
Janson, O.	QF22	207	Jo, Nahyun	RC07, SD10, SD11	260, 331
Jantaratana, Pongsakorn	SL10	357	Jo, W.	SA06	317
Janutka, Andrzej	SH15	345	Jo, William	SA05	317
Jaramillo, Juan Fernando	SM04	361	Jo, Woo Seong	RI20	282
Jardim, Daniela Regina	PO08	178	Jo, Younghun	HF05, RL06	87, 290
Jascur, Michal	RI09	280	Jo, Young-hun	CE04, RL03	52, 290
Jastrabik, Lubomir	AH02	38	Jo, Younjung	RB14	256
Javanparast, B.	GF01	79	Johansson, Borje	EC01	65
Javorsky, Pavel	QI01, SB08	217, 321	Johnston, David C	QE12	201
Jay, Jean-philippe	SA24	320	Johrendt, Dirk	QB22	190
Jean, Malick	DG02, PJ22	61, 158	Jomura, Mitsuhiro	QM10	233
Jendelova, Pavla	BH03	46	Jonietz, Florian	DF02	60
Jeng, H.-t.	SD04	330	Jono, Youhei	RB06	255
Jeon, Byeong Jo	JB02	99	J onsson, Petra	QH11	214
Jeon, Byung-gu	JB02	99	Joo, Dae-suk	PM25	171
Jeon, Eun-kyoung	SD12, SD14	332	Joo, Sungjung	PJ31, PK21, QK10	159, 163, 225
Jeon, Gi-wan	PN25, SK28	176, 355	Joo, Younghoon	PO13	179
Jeon, Gun Sang	RA22, RC08, RE07	253, 260, 267	Joseyphus, Raphael Justin	AJ04	40
Jeon, Kun-rok	RL03, SM01	290, 361	Jourdan, M	RP20	306
Jeon, Kyung-won	RR21, RR22	314	Jourdan, Martin	CH04	54
Jeon, Seungmok	EH05	70	Joy, P A	QN12	238
Jeon, Sung Jae	PM28	172	Joy, P. A.	SL13	358
Jeong, Hogyun	RC13, RC17	261	Ju, Hye Sun	QN05	237
Jeong, Ilgyo	PO19	180	Ju, Sol	PC19	129
Jeong, In-bum	IB03	91	Jue, Emilie	SH05	344
Jeong, Jaehong	RA22	253	Julian, Stephen	EA04	64
Jeong, Jinwon	HJ05	90	Jun, Akedo	PN14	174
Jeong, Se-young	PH22, PN20, PN21, QL18	150, 175, 231	Jung, Chang Uk	RA28	254
Jeong, Su-yeon	RR27	315	Jung, Dahee	HJ05	90
Jeong, Tae Won	QO20, SG21	244, 343	Jung, Heejong	HB02, PM16	84, 170
Jeong, Tae-chul	RR14, SN04	313, 364	Jung, Hyunsung	DE05, RJ16, RJ18, SH14	60, 285, 345
Jeong, Y. H.	PM26	171	Jung, Jin-seung	RN20	300

Jung, Jonghoon	PL19	167	Kamarad, Jiri	PM11	169
Jung, Jong-suck	QA12	184	Kamazawa, Kazuya	PO17	180
Jung, K.y.	PJ31	159	Kambale, Rahul Chandrakant	QM23	235
Jung, Kuyeol	PK21	163	Kambe, Shinsaku	PD09	133
Jung, M. H.	RK19	289	Kambe, Takashi	RA18, SC04	252, 326
Jung, Min Hwa	PN28	176	Kameli, P.	PI24	154
Jung, Min-cherl	RC14	261	Kameli, Parviz	PI23	154
Jung, Min-hwa	SA18	319	Kamenev, K. V.	GC01	77
Jung, Mung-hwa	PJ31	159	Kami, Daisuke	PO03	177
Jung, Myung- Hwa	RC07	260	Kamihara, Yoichi	QB16, QC07, SE09	189, 193, 334
Jung, Myung-chul	SO06	367	Kamihara, Youichi	QC08	193
Jung, Myung-haw	QO11	242	Kamimori, Tastuo	PG05	143
Jung, Myunghwa	SM13	363	Kamimori, Tatsuo	QG10	209
Jung, Myung-hwa	PC12, PK17, PN19, QH07, QO10, RK06	128, 163, 175, 214, 242, 286, 331, 349	Kamionka, Thomas	FD02	74
	SD10, SD11, SJ02		Kampert, Erik	KB06, PB11, SB18, SD07	108, 121, 323, 331
Jung, S. H.	RK19	289	Kanai, Noriko	QD17	199
Jung, Sanghoon	RK06	286	Kanai, Yasushi	BG04	46
Jung, Sang-yong	RR11, RR18, RR21, RR22	312, 313, 314	Kanatzidis, M. G.	GA01	75
Jung, Sol	PM15	169	Kanazawa, Ikuzo	PB31	125
Jung, Soon-gil	GA04, RB27, SB28	76, 258, 324	Kane, Shashank N.	AJ05	40
Jung, Sung Won	RC14	261	Kanehira, Toma	GE04, JE04	78, 102
Jungwirth, T.	IF01	94	Kaneko, Chikafumi	PH05	147
Jungwirth, Tomas	BE05, BI03, IE03, SK22	44, 47, 93, 354	Kaneko, Koji	JJ05, QJ09, SC23	106, 222, 329
Juranyi, Fanni	PO17	180	Kaneko, Masaki	QD18	199
Juraszek, Jean	QA27	187	Kaneko, Takejiro	QJ05	218
Jurchescu, Oana D.	AE04	36	Kaneko, Tatsuya	PF09, PF10	140
			Kaneko, Ulisses F	PI19	153
			Kaneko, Y.	CG02, RA05	53, 250
			Kaneko, Yoshio	PH08	148
			Kaneshita, Eiji	CA01, SC10	48, 327
K, Ramesh Kumar	SE21, SO29	336, 371	Kanetsuki, Hiroaki	PG05	143
K. Sato, Noriaki	QD18	199	Kang, Boyoun	QI15	220
K., Samatha	BJ05	48	Kang, Byeongki	BF05, JG05, PA09, PH18	45, 104, 117, 149
Kabiraj, D.	PG27	146	Kang, Byeongwon	PB03	120
Kachi-terajima, Chihiro	QF21	207	Kang, Byung-sub	PN31	177
Kaczorowski, Dariusz	AB03, QD05, SE16, SE17, SF12	34, 197, 335, 336, 339	Kang, Chan Seok	RQ19, RQ20	310
			Kang, Chang-jong	SC12	327
Kaczorowski, Dariusz	RD23	265	Kang, Chong Yun	RA21	252
Kadowaki, Hiroaki	QE13	201	Kang, Han Sam	QN15	238
Kadowaki, K.	KJ01	113	Kang, Hanhim	QH26	217
Kadowaki, Kazuo	RB06	255	Kang, J. H.	RA07	250
Kagayama, Tomoko	PB05, PB27, PC23, SG20	120, 124, 130, 342	Kang, J.k.	QO27	245
Kageyama, Ryu	RP14	305	Kang, J.-s.	BB02, PG11, PH14, QA04	41, 144, 149, 183
Kaiju, Hideo	SM09, SO07	362, 367			
Kainuma, Ryosuke	PG04, PG07, QG08, RP07, SK23	143, 209, 304, 354	Kang, Jeong Soo	PB12	122
			Kang, Jun-goo	QL15	230
Kajimoto, Ryoichi	DA01, RH12	56, 276	Kang, Min Gyu	RA21	252
Kajino, J	SE03, SE05, SE13	333, 334, 335	Kang, Sun Hee	PA11, QA16	117, 185
Kajino, J.	KA02	107	Kang, Sung	QG16, QH15	210, 215
Kajino, Jumpei	PD24, RC07	135, 260	Kang, Sunhee	SM13	363
Kajino, Junpei	QH07	214	Kang, W. N.	GA04, PB03	76, 120
Kakazei, G. N.	KC05	109	Kang, Won Nam	RB27, SB28	258, 324
Kakehashi, Yoshiro	EF04, PB24, PF05, QG03	68, 124, 140, 208	Kang, Woun	KJ04	114
Kalon, Gopinadhan	SK05	351	Kanjilal, D.	PG27	146
Kaloni, Thaneshwor Prashad	PN02	172	Kanke, Yasushi	PI16	153
Kamada, Yasuhiro	RR13	313	Kanki, Teruo	SK16	353
Kamada, Yukihiko	PB05	120	Kanoda, Kazushi	BC03	42
Kamal, Khaja Mohaideen	QN12	238	Kanomata, Takeshi	PG04, PG07, QH21	143, 216
Kamal, Mydeen	IA02	90	Kanou, Manabu	RC12	260
Kamarad, J.	PJ23	158	Kanoun, Mohammed Benali	QL17, SK12	230, 352

Kanter, J.	PI15	153	Kawana, D.	CF04	53
Kanter, Jakob	RB21, SC16	257, 328	Kawana, Daichi	PI07, RD14, RH13	151, 264, 276
Kao, C.-c.	PH10, RA04	148, 249	Kawanaka, Hirofumi	PM13	169
Kao, Chih-kuei	IHO6	96	Kawanishi, Yohei	HE03	86
Kapaklis, Vassilios	AF05, EI03, RP15	37, 71, 305	Kawar, Tatsuya	RQ05	307
Karaki, Y.	EF01	68	Kawasaki, Ikuto	RD25, SE23	266, 337
Karaki, Yoshitomo	CC05	50	Kawasaki, M.	RG10	273
Karamat, Shumaila	PN03, QL02	172, 228	Kawasaki, S	QB11	188
Karipoth, Prakash	AJ04	40	Kawasaki, Y.	SG02	339
Karla, J. Merazzo	GG05	80	Kawasaki, Yu	QF24	207
Karpinski, J.	PC01	126	Kawashima, Kenji	PB06, PB07, SG16	121, 342
Karpinski, Janusz	RB19, RB20, RB21	257	Kawashima, Naoki	DC04	58
Karthigeyan, A	SA21	319	Kawata, K.	SG11	341
Karthik, T	PN18	175	Kawata, Tomokazu	PD22	135
Karube, Kosuke	RD05, RD08	262, 263	Kawata, Toru	RD19	265
Kasagi, Teruhiro	QN02	236	Kazakov, Alexander	CH01	54
Kasai, S	SK29	355	Kazuhei, Wakiya	QC16	194
Kasai, Shinya	HG02, ID04, IF05, SK31	88, 93, 94, 355	Kazunori, Umeo	QC16	194
Kasatani, Yuichi	RK10	287	Kazuo, Watanabe	QJ01	221
Kashiwagi, T.	KJ01	113	Kazuyuki, Matsubayashi	QH17, QJ01	220, 221
Kashiwagi, Takanari	RB06	255	Ke, W. P. Ke	IC03	92
Kassir-bodon, Zoukaa	SH06	344	Keiderling, Uwe	DF02	60
Kastil, Jiri	PM11	169	Keimer, B.	GA03	75
Kataev, V.	QE23, QF22	203, 207	Keimer, Bernhard	BA03, CA03, IU02, JC04, RB20	41, 49, 97, 100, 257
Katano, Susumu	RH01	274			
Katayama-yoshida, Hiroshi	KF04	111	Keisuke, Matsumoto T	QC16	194
Kato, Akihiko	RH17	277	Kelekcı, Ozgur	PJ24	158
Kato, Harukazu	QD06	197	Keller, Lukas	PH02, PI05	147, 151
Kato, Haruki	PL06, RL02	164, 290	Keller, Thomas	GC04	77
Kato, Hiroaki	EJ01, RO05, RO06	71, 301	Kennedy, Shane J	QG09	209
Kato, Kenichi	QF25	208	Kennedy, Shane Joseph	EF02	68
Kato, Masaru	PC26	131	Kenzelmann, M.	QE19	202
Kato, Motoharu	SG18	342	Kenzelmann, Michel	CD04, QF20	51, 207
Kato, Reizo	BC04, SF01	42, 337	Kepa, M.	GC01	77
Kato, Takashi	PO18	180	Kezsmarki, Istvan	PA14	118
Kato, Takeshi	RL08	291	Khademi, F.	PI24	154
Kato, Tomoki	PC23	130	Khajehnezhad, A.	QP23	249
Katoh, Hisashi	PN07	173	Khailil, H. M. Waseem	PJ24	158
Katoh, Kenichi	QD09	197	Khaliullin, Giniyat	BA03	41
Katori, Hiroko Aruga	QD13	198	Khalyavin, D. D.	KA02	107
Katou, Haruki	RC02	259	Khan, Mohammed N. Islam	EI02	70
Katrych, Sergiy	RB21	257	Khan, Nawazish Ali	PB13	122
Katsufuji, T.	PA04	116	Khan, Tahir Rao	IA02	90
Kaul, S. N.	QD10, QM06, SL07	198, 232, 357	Khan, Yasmin	QO25	244
Kawada, Yuki	SI03, SI17	346, 348	Kharchenko, M. F.	PH06	147
Kawae, Tatsuya	QE18, QF14, QL11, QL12, QL13, RE04, SG09	202, 206, 229, 230, 267, 341	Kharchenko, Yu.	PH06	147
			Khasanov, Rustem	CD04, IA02, QB22	51, 90, 190
Kawagoe, T.	PL04	164	Khavronin, V. P.	RQ13	309
Kawaguchi, Masashi	RL10	291	Khim, Seunghyun	JA03	98
Kawaguchi, Shogo	PI02	151	Khizroev, Sakhrat	PN16	174
Kawahara, Shin-ichi	EI05	71	Khmelevskiy, Sergii	EF05	68
Kawai, Tetsuroh	PM18, SM15	170, 363	Khodaei, M.	QM28, SA04	236, 316
Kawakami, Norio	DB05, HI04, PF16, RC01, RC04, RD05, RF01, RF09	57, 89, 141, 259, 262, 269, 270	Khokhlov, Alexey R	QO14	243
			Khonskii, Daniel	PA17	118
Kawamata, Takayuki	DA01, QF07, QF08, QF10	56, 205	Khovaylo, Vladimir	DJ04	63
			Khovaylo, Vladimir V.	SO19	369
Kawamoto, Atsushi	PC15	129	Khusainov, Mansur G.	QA26	186
Kawamura, Naomi	IG03, QD17	95, 199	Khusainov, Marat M.	QA26	186
Kawamura, Yukihiko	JJ05	106	Khvalkovskiy, A.v.	ID02	93
Kawamura, Yukihiko	PD10, PD22, QD06	133, 135, 197	Khvalkovskiy, Alexey	ID03, IE04	93, 94

Khym, S.	QL08	229	Kim, Gwang-hee	SI01	346	Kim, Ju-jin	SD12	332	Kim, Suhyun	QO11	242
Ki, Sanghoon	PL15, QM21	166, 235	Kim, Gyutae	PJ30	159	Kim, Jun Sung	RB14, SD07	256, 331	Kim, Sumin	PM15	169
Kida, Takanori	QB09, QF06	188, 204	Kim, H.	IA05, QC23, SB30	91, 196, 325	Kim, June Seo	FD03, QK14, SH16	74, 226, 345	Kim, Sun Yung	SL01	356
Kiefer, K	RI05	279	Kim, Hae Jin	SL11	357	Kim, Jung Dong	PM28	172	Kim, Sung Baek	PI13	152
Kihara, Takumi	PA06, QA09, QG08, RA06, RH04	116, 184, 209, 250, 275	Kim, Hanbit	JB02	99	Kim, Jungeun	HC03	85	Kim, Sung Hoon	PO20, SM08, SN14	180, 362, 366
Kihou, K.	QB28	191	Kim, Hee Seung	PI14	153	Kim, Jungho	DC03	58	Kim, Sung Wng	PC23	130
Kihou, Kunihiro	QB02, QB15	187, 189	Kim, Heung Sik	RC13	261	Kim, Junghwa	IJ02	97	Kim, Sung Yong	PK10	162
Kijima, Hanae	JI01	105	Kim, Heungsik	DC03	58	Kim, Jun-young	PN23	175	Kim, Sung-beak	PA04	116
Kikkawa, Akiko	QJ09	222	Kim, Heung-sik	RC17	261	Kim, Juyoung	QI15	220	Kim, Sungho	KH04	112
Kikoin, Konstantin	FE04	75	Kim, Hojung	PH21	150	Kim, K. W.	SL08, SL09	357	Kim, Sunghyun	PO06	178
Kikuchi, Hikomistu	QF17	206	Kim, Hong-seok	SD12, SD14, SO21	332, 370	Kim, Kab-jin	KE03, SH07	110, 344	Kim, Sung-jin	RR11	312
Kikuchi, Hikomisu	RI15	281	Kim, Ho-sup	QM22	235	Kim, Kee Hoon	CI03, JA03, JB02, PA04, PA09, PB23	55, 98, 99, 116, 117, 123	Kim, Sungyong	PJ16	157
Kikuchi, Hikomitsu	QE16, QE21, QF04, QF09	202, 204, 205	Kim, Hui Min	RR07	312	Kim, Keun-ho	RR15	313	Kim, Tae Hee	CB01, PJ17, QP18	49, 157, 248
Kikuchi, Hiroaki	RR13	313	Kim, Hwijun	PM17, PM23, PM24	170, 171	Kim, Ki Yeon	QM18, QM20	234	Kim, Tae Wan	PJ24	158
Kikuchi, Hiroshi	SK21	353	Kim, Hwiseok	PO14	179	Kim, Ki-ghan	RR09, RR10	312	Kim, Tae-hoon	RO01, RO02	300, 301
Kikuchi, Yoshihiro	PF17	142	Kim, Hyeong-do	RG04	272	Kim, Ki-ghan	RR09, RR10	312	Kim, Tae-suk	PJ31	159
Kikuchi, Yuhei	QB27	191	Kim, Hyo-jin	PJ19, QO28, RH18	157, 245, 277	Kim, Kiwoong	PO11, RQ17, RQ18, RQ19, RQ20	179, 309, 310	Kim, Taewan	PJ16, PK10, PK17	157, 162, 163
Kim Anh, Do Thi	AJ06	40	Kim, Hyung Joon	JB02	99	Kim, Kwang Hee	RR19	314	Kim, Taewoo	RR16, SN05	313, 365
Kim, Aaram Joo	RE07	267	Kim, Hyung Jun	PK10	162	Kim, Kwang Heon	QO20, SG21	244, 343	Kim, Tae-young	SM10	362
Kim, Ahri	PM15	169	Kim, Hyungjun	PJ16	157	Kim, Kwang Lok	PB16, PB18, PB35, PB36, PB38	122, 123, 125, 126	Kim, Taeyueb	QK10	225
Kim, Beom Jun	RI19, RI20, RI21	282	Kim, Hyung-jun	KC04, PL16, QK11, QK12, QK13, RL28, RL31	109, 166, 225, 226, 294, 295	Kim, Kwang S	QH26	217	Kim, Wan-seop	RQ07	308
Kim, Bongho	QP19, RL22, SL19	248, 293, 359	Kim, Hyungsuk K. D.	QA15	185	Kim, Kyeong-sup	PN31	177	Kim, Won Dong	RK19	289
Kim, Bongjae	PG11	144	Kim, Hyungyu	QP19	248	Kim, Kyoo	SC12	327	Kim, Wondong	BD03, IH04, QM26, RK18, RP23	43, 96, 235, 288, 307
Kim, Bum-su	QL18	231	Kim, Hyun-jung	SD06	331	Kim, Kyoo	SC12	327	Kim, Won-kyung	PH22, PN20, PN21	150, 175
Kim, Bun-su	PN20	175	Kim, Ill Won	PA11, QA16	117, 185	Kim, Kyoungchul	SA09	317	Kim, Y C	QB25	191
Kim, Byeong-geon	PL15, QM21	166, 235	Kim, Illwon	SM13	363	Kim, Kyoung-whan	EE05, HP21	68, 30	Kim, Y. H.	RQ08	308
Kim, Changsoo	BF05, JG05, PA09, PH18	45, 104, 117, 149	Kim, In Gee	QG20	211	Kim, Kyung Ho	KC04	109	Kim, Y.i.	PB19	123
Kim, Chang-yeoul	RN24	300	Kim, Ingyu	JB02	99	Kim, Kyung-ho	PL16, QK12, RL31	166, 226, 295	Kim, Yong Baek	RA22	253
Kim, Chanhee	RQ11	308	Kim, In-seon	SC15	328	Kim, Kyunghyun	RN10	298	Kim, Yong-jae	RR11, RR21, RR22	312, 314
Kim, Chelgi	QO19	243	Kim, J.	RA07	250	Kim, Kyungwan	HA02	83	Kim, Yongjin	PO06	178
Kim, Cheol Gi	SN13	366	Kim, J.-y.	BD03, PG11, QA04	43, 144, 183	Kim, Kyung-whan	PJ33	160	Kim, Yongmin	PO14, PO26, QO08, RQ23, RR12	179, 181, 242, 310, 312
Kim, Cheolgi	PO19, QN22, RN21, SL22	180, 240, 300, 359	Kim, Jae Nyeong	QJ19	224	Kim, Kyu-tae	RQ07	308	Kim, Yoonbai	SD03	330
Kim, Chin Mo	PA22	119	Kim, Jae Young	PA11	117	Kim, Mi Jung	SN04	364	Kim, Young Do	RO10	302
Kim, Choong H.	RC13, RC17	261	Kim, Jaehyun	PO06	178	Kim, Mi-jung	RR14, SN02	313, 364	Kim, Young Keun	KC04, PJ14, RK06, SH13	109, 157, 286, 345
Kim, Chul Sung	PA22, PI13, PI14, RA26	119, 152, 153, 253	Kim, Jae-sung	AD03	35	Kim, Min-ho	RR23	314	Kim, Young Kwang	PK10	162
Kim, Chung Koo	CA02	48	Kim, Jaewook	RQ11	308	Kim, Minseon	RA26	253	Kim, Young-gyun	PB17, PB37, PB40	122, 126
Kim, Chung Man	QH07	214	Kim, Jaeyeong	RA21	252	Kim, Miryeon	RL17	292	Kim, Young-hak	PO14, PO26, RQ23, RR30	179, 181, 310, 315
Kim, Chungman	QO11	242	Kim, Jae-yeong	SO03	367	Kim, Miyoung	RH20, SK27	278, 354	Kim, Young-june	DC03	58
Kim, D. H.	PG11	144	Kim, Jaeyoung	SM13	363	Kim, Mun-seog	RQ07	308	Kim, Youngkwang	PJ16	157
Kim, D. -w.	PO23	181	Kim, Jae-young	AF04	37	Kim, N.	QF13	206	Kim, Yun Won	RQ15	309
Kim, D.h.	PH14, QA04	149, 183	Kim, Jeehoon	QB31, SB12	192, 322	Kim, Ran-hyang	BH02	46	Kim, Yun-won	SC14	327
Kim, D.y.	EC01	65	Kim, Ji Wan	QM20	234	Kim, Rokyoon	GF05	79	Kimel, Alexey V.	RK17	288
Kim, Daehong	QP19, RL22, SL19	248, 293, 359	Kim, Ji-hye	RJ18	285	Kim, S. B.	PG11	144	Kimishima, Yoshihide	SB03	320
Kim, Daehyun	PB12	122	Kim, Jimin	RQ11	308	Kim, S.b.	PH10	148	Kimling, Judith	RP04	303
Kim, Danbee	RQ07	308	Kim, Jin Mok	RQ17	309	Kim, Sam Jin	RA26	253	Kimura, Akio	KF05, SD11	111, 331
Kim, Dohyang	PM17	170	Kim, Jin Woo	RO10	302	Kim, Sang-beom	PM16, PM19, PM21	170	Kimura, Kenta	CC05	50
Kim, Dong H.	QL16	230	Kim, Jinhee	QO10, SD11, SD14	242, 331, 332	Kim, Sanghoon	RL30	294	Kimura, Nobuyuki	EF04	68
Kim, Dong Young	PM28	172	Kim, Jin-hee	CF03	52	Kim, Sang-il	RL06	290	Kimura, Noriaki	PC28, QC03, QC10, QC11, RD08	131, 192, 193, 194, 263
Kim, Dong-hyun	RP03, SH01, SH10	303, 343, 344	Kim, Jinsung	SN07	365	Kim, Sang-koog	DE05, RJ14, RJ15, RJ16, RJ17, RJ18, SH14, SJ07	60, 284, 285, 345, 350	Kimura, S.	KA02, SG11	107, 341
Kim, Dongseok	PK21	163	Kim, Jiwan	RK13	288	Kim, Seong-gon	KH04	112	Kimura, Shin-ichi	AD04, QD07, QD18	35, 197, 199
Kim, Dongsoo	RN23	300	Kim, Ji-wan	FC02, RK09	73, 287	Kim, Seunghyun	RN10	298	Kimura, Shoji	QI18	220
Kim, Dongyoo	JH03, RM07	104, 296	Kim, Jiyeon	PI10	152	Kim, Shin Ae	RP01	303	Kimura, Shojiro	PI06, QG15, RH25	151, 210, 278
Kim, Do-yeon	RN20	300	Kim, Jong Hee	QN22	240	Kim, Shin-ae	PI10, RA22	152, 253	Kimura, Shojiro	AG03, HE01, KC06, QK24, QL11, RJ08, RK21, RL20, RL23, SI12	37, 86, 109, 228, 229, 283, 289, 293, 347
Kim, Eun-mee	RN20	300	Kim, Jong-hwa	RR27	315	Kim, Soo Hyun	QH07	214	Kimura, Tsuyoshi	JB01, QA12	99, 184
Kim, Eunseong	PC25	130	Kim, Jongryoul	HB02, PM16	84, 170	Kim, Soohyun	PC12	128			
Kim, Eun-young	RE01	266	Kim, Jong-woo	DJ02	63	Kim, Soo-whan	PC12	128			
Kim, G C	QB25	191	Kim, Joon-il	QK23	227	Kim, Soyeon	RH08	276			
Kim, G. B.	RQ08	308	Kim, Ju Young	QH29	217						
Kim, G. W.	PM14	169	Kim, Ju_young	SC08	326						

Kindo, K.	GJ03, QI03	82, 218	Knight, Kevin	SD13	332	Koike, Mariko	RL04	290	Kotegawa, Hisashi	PD25, SF03	136, 337
Kindo, Koichi	HC03, PA18, PD13, PE10, PG17, QE16, QF11, QF14, QF17, RI15, RP07, RQ05	85, 118, 134, 137, 145, 202, 205, 206, 281, 304, 307	Knowles, Elisabeth S.	KB03	107	Koike, Yoji	QF07, QF08, QF10	205	Kotetes, Panagiotis	II04	97
King, Phil	II02	97	Ko, Junggho	JI02, RL30	105, 294	Koinuma, Hideomi	PH22, PN21, QL18	150, 175, 231	Kothapalli, Karunakar	SF13	339
Kino, Ryo	QA09	184	Ko, K.-t.	PH10	148	Kokorina, E. E.	RF16	271	Kothari, D. C.	RN16	299
Kinoshita, Toyohiko	RP07	304	Ko, Kowan-young	QG01	208	Kokubu, Mitutane	QD12	198	Kotliar, G.	PE17	138
Kinouchi, Hiroaki	QB29	191	Ko, Kyoung Chul	QG17	211	Kolano - Burian, A.	PM05	168	Kotnala, R.	PG27	146
Kiparisov, Semion	SM19	364	Ko, Rock Kil	QB25	191	Kolbe, M	RP20	306	Kototani, Shouhei	QB04, RB02	187, 254
Kirchner, Stefan	JC01	100	Ko, Seung Hyo	CB01	49	Kolbe, Michaela	CH04	54	Koubaa, Mohamed	DJ05	64
Kirillov, Oleg A.	AE04	36	Ko, Sung-won	QG01	208	Koledov, Victor V.	SO19	369	Kouh, Taejoon	PA22	119
Kirilyuk, Andrei	RK17	288	Ko, Wonsuk	PO13	179	Kolesnikov, Alexander I.	RD14	264	Kousaka, Yusuke	DF03, PG09, QG22, QG28	60, 143, 211, 212
Kirschner, J	RP20	306	Kobayashi, H.	CG02	53	Kollath, Corinna	CC03	50	Koutroulakis, Georgios	PC03, SF01	127, 337
Kirschner, Jurgen	AD02, AE01, EI01	35, 70	Kobayashi, Hiroki	RD14	264	Kolodiazhnyi, Taras	RH06	275	Kovac, Jozef	IB01, QO17	91, 243
Kiryukhin, V.	RA22	253	Kobayashi, Hisao	QD11, RB03, RD13	198, 254, 264	Kolomiets, A.	RD26	266	Kovac, P	RB08	255
Kiseki, Kohei	AG03, SI12	37, 347	Kobayashi, K.	SH07	344	Kolomiets, Aleksandre	RE09	267	Kovlylina, M.	BD01	43
Kishimoto, Kengo	QM10	233	Kobayashi, Keisuke	RD20	265	Kolomiets, Olexander	QI19	220	Kovlylina, Miroslavna	BD04	43
Kishimoto, Y.	SG02	339	Kobayashi, Kensuke	RL10, SE07	291, 334	Komaki, Yasuhiro	QD12, QE12	198, 201	Kowalczyk, M.	PH06, PM05	147, 168
Kishimoto, Yutaka	QF24	207	Kobayashi, Kohei	SA07	317	Komarek, Alexander	PI17	153	Kowalik, Iwona	DD02	58
Kishine, Jun-ichiro	DF03, PG09, PG10, QG22, QG28	60, 143, 144, 211, 212	Kobayashi, M.	PC01, PC29, PI15	126, 131, 153	Komatsubara, Takemi	RD08	263	Koyama, Keiichi	GJ02, QG15, QH08, QI05, QN20, SK23	82, 210, 214, 218, 239, 354
Kisielewski, Marek	AD05		Kobayashi, Masaki	HA03	83	Komorida, Yuki	KB06	108	Koyama, Kuniyuki	PB25, QC05	124, 193
Kiss, T.	QB28	191	Kobayashi, Nobukiyo	JI01	105	Kondo, A.	QI03	218	Koyama, T.	RL07	291
Kiswandhi, Andhika	SB05	321	Kobayashi, Norio	QF10, SG18	205, 342	Kondo, Akinori	PE10	137	Koyama, Takehide	QD15, RD24	198, 266
Kita, Eiji	PG05, PI16, QI04, QM16, SJ06	143, 153, 218, 234, 349	Kobayashi, Riki	SC23	329	Kondo, Kenji	QK05, SM09, SO07	224, 362, 367	Koyama, Tsukasa	AF03, PG15, QG22, QG28	37, 144, 211, 212
Kita, Tomoko	RF09	270	Kobayashi, Satoru	PH05, PI22, RR05, RR13	147, 154, 311, 313	Kondo, Takaya	QL03, RN02	228, 297	Koyanagi, Tsuyoshi	QM10	233
Kitagawa, Jun	EG05	69	Kobayashi, Tatsuo C	QF25, SE10	208, 334	Konishi, K.	SL14	358	Koyota, Yuya	PD11	133
Kitagawa, Shunsaku	QC08	193	Kobayashi, Tatsuo C.	HC03, QC18	85, 195	Konishi, Takehisa	KG03, PF10, PF15, SF04	111, 140, 141, 337	Kozono, Yuuki	RE12	268
Kitagawa, Susumu	HC03, QF25	85, 208	Kobayashi, Tatsuya	QB24	191	Konno, Rikio	PF08	140	Kraemer, Karl	CE05	52
Kitagawa, Yutaro	QA10	184	Kobayashi, Toshiaki	RH01	274	Konno, Toyohiko J.	KB05	108	Kraemer, Mathias	QG14	210
Kitai, Tetsuo	QI05	218	Kobayashi, Toshiaki	RH01	274	Kono, Hiroshi	RD18	265	Kramar, Oleksandr	JG06, RN15	104, 299
Kitamura, T.	KJ01	113	Kobayashi, Tsukasa	SK21	353	Konstantinovic, Zorica	IH01, SO18	95, 369	Kramarenko, Elena Yu	RG13	274
Kitanishi, Fumiya	SO11	368	Kobayashi, Yoshiaki	DA01, QB04, QB26, RB02, RB05	56, 187, 191, 254	Koo, Bon Heun	PM14, PN15	169, 174	Kramer, K W	QO14	243
Kitaoka, Yoshio	DA04, PB26, QB29	56, 124, 191	Kobayashi, Yuta	SL02	356	Koo, Dae-hyun	PM25, RR31	171, 316	Kramer, Steffen	RI05	279
Kitaoka, Yukie	SO10	368	Kobiyama, Takuya	QD13	198	Koo, Hyun Cheol	PJ30, QK11, QK12, QK13, RL28	159, 225, 226, 294	Kratohvilova, Marie	IC02	92
Kitazawa, Genki	SM08	362	Kodama, Kenji	RP07	304	Koo, Hyuncheol	QK10	225	Krause, Stefan	PC10, PD18, PD19, QJ14, SB08	128, 134, 135, 223, 321
Kitazawa, Hideaki	JJ05, PH02, PH09, QA09, QJ02	106, 147, 148, 184, 221	Kodama, Motoi	RJ10	284	Koo, Tae Yeong	PA11, QA16	117, 185	Krawczyk, M.	HF03, HF04, RP16	87, 305
Kito, Hijiri	QB02	187	Kodama, Yuta	QE20, QF21	202, 207	Koo, Taeyoung	SM13	363	Krawczyk, Maciej	DD02	58
Kittaka, S.	EF01	68	Kodderitzsch, Diemo	II03	97	Koopmans, Bert	CH05, EI06, GE02, IE02, JE01, SI07	54, 71, 78, 93, 101, 347	Krellner, Cornelius	QO05	241
Kittaka, Shunichiro	QJ08	222	Kodera, Mitsuru	EC03	65	Kopeliovich, Alexander I	PJ02	155	Kremer, Reinhard	AB02, CD03, FB04, JC01, PD12	34, 51, 73, 100, 133
Kiyonagi, Yoshiaki	RP01	303	Koehler, Daniel	PC27	131	Korbecka, A.	BE02	44	Kremer, Reinhard K	PH11	148
Kiyokawa, Takayasu	QA02	182	Koehler, Juergen	QJ18	223	Korekawa, Tomoya	PN07	173	Kreuzpaintner, Wolfgang	PG01	61
Klaui, Mathias	FD03, QK14, SH16	74, 226, 345	Koenraad, Paul	BE05	44	Korelis, Panagiotis	RP15	305	Krinitsina, Tatiana	DG01	61
Klaui, Mathias	CH04, JE03	54, 102	Koerner, Michael	RJ11	284	Korolev, Alexey	PB14	122	Krinitsina, Tatiana P.	PB22, SK02	123, 350
Klauss, Hans-henning	AB02, PI05, QB22, QJ03	34, 151, 190, 221	Koga, Akihisa	SC13	327	Korolyov, Alexandre	QL07	229	Krinitsina, Tatiana P.	SK01	350
Klein, Olivier	ID03	93	Koga, Mikito	SB17	323	Korotana, Romi Kaur	RF15	271	Krishnakumar, Varadharajan	QC13	194
Klemm, R. A.	KJ01	113	Koh, Eui-kwan	EH02	70	Kosaka, Masashi	QD13, QI16	198, 220	Krishnan, Murali	PK16	163
Klicpera, Milan	QI01	217	Kohama, Yoshimitsu	SF13	339	Koseki, Gen	PD11	133	Krive, Ilya V.	RG17	274
Klimczuk, Thomasz	SE19	336	Kohara, Takao	QD12, QD15, RD24	198, 266	Koseki, Minoru	PD11	133	Krockenberger, Y.	RG10	273
Klimin, Sergey A.	RA24	253	Kohda, Makoto	KC03	108	Kosel, Juergen	SA02	316	Kroha, Johann	PF07	140
Klingeler, R.	QE23, QF18, QF22	203, 206, 207	Kohlbrecher, Joachim	QF20	207	Kosel, Jurgen	PJ06, PM27, RQ02	155, 171, 307	Krompiewski, Stefan	QK04	224
Klintberg, Lina	FB04, PC09	73, 128	Kohler, Sebastian	RI13	281	Koshiba, Shyun	PN24	176	Kronast, Florian	FD03, GG05, RP04, RP08	74, 80, 303, 304
Klintberg, Lina Esther	PC02	127	Kohlhepp, Juergen	JE01	101	Kossick, Martin	KD01	109	Krotscheck, Eckhard	RG15	274
Kloc, Christian	AE05	36	Kohmoto, Osamu	SL03	356	Koster, Gertjan	DH02, SA10	62, 317	Krueger, Benjamin	FD02	74
Klyatskaya, Svetlana	GH02	81	Kohn, Kay	PI16	153	Kota, Yohei	PJ10, PL17	156, 166	Krug V Nidda, Hans-albrecht	RH24	278
Knebel, Georg	JC02, SF03	100, 337	Kohn, Atsushi	SA03	316	Kotaka, Hiroki	RC09, RC19	260, 262	Kruglyak, Volodymyr	EH04, HD03, JG01	70, 85, 103
Kneidinger, Friedrich	SC01	325	Kohno, Masanori	RE05	267	Kotani, Y.	QB28	191	Kruglyak, Volodymyr V.	GD04, QO05, RK20	78, 241, 289
			Kohori, Y	QB28	191	Koteawa, Hisashi	QB17	189			
			Kohori, Yoh	QB02, QB15, QD12, QE12	187, 189, 198, 201	Kotegawa, Hisahi	SG12	341			
			Koichi, Takase	QD14	198						
			Koike, Kazuyuki	HG01, RP14	87, 305						
			Koike, Kunihiro	EJ01, RO05, RO06	71, 301						

Kruize, Michelle	DH02, SA10	62, 317	Kumar, Pradeep	SE14	335	Lake, Bella	IC05, PA23, RH24	92, 119, 278	Lee, Donghae	QH15	215
Krychowski, Damian	PE06	137	Kumar, Rajesh	PH16	149	Lam, Duong Duc	PK20	163	Lee, Dong-hae	QG16	210
Krycka, Kathryn	KD02	109	Kumar, Ravi	PH16	149	Lam, V. D.	RA01	249	Lee, Dong-il	PM19, PM21	170
Krzyszczek, Patryk	IF04	94	Kumar, Shalendra	PM14, PN15	169, 174	Landa-canovas, Angel	PI18	153	Lee, Eunhee	RN24	300
Ku, H. C.	SB04	320	Kumar, Vinod	PH16	149	Landee, C P	BC05	42	Lee, Eunsook	PG11, PH14, QA04	144, 149, 183
Ku, Huan-chiu	RR01	311	Kumari, Poonam	PI12	152	Landee, C. P.	QF02	204	Lee, Geunsik	QH26, QH27, RB22	217, 257
Ku, Jang Hae	PJ30	159	Kummer, Kurt	PD12	133	Landge, Kalpana Kamalkishor	SK19	353	Lee, H. J.	RQ08	308
Kuang, Lulin	PB28	124	Kuo, C. N.	PH01, RP02	147, 303	Landsgesell, Sven	RB01, RB07	254, 255	Lee, H. Y.	PK06, QP17	161, 248
Kubetzka, Andre	IH02, IH03	96	Kuo, K. M.	QM25	235	Lang, Michael	HC04, QE14, QJ11, RI13, SG19	85, 201, 222, 281, 342	Lee, H.k.	PB19	123
Kubinova, Sarka	BH03	46	Kuo, Nan-hong	QF26	208	Langbehn, Bruno	KD01	109	Lee, Ha Na	PJ24	158
Kubo, Hidenori	RH19, RP12	277, 305	Kuo, Yung-kang	PE02	136	Langenberg, Andreas	KD01	109	Lee, Haigun	PB16, PB17, PB18, PB35, PB36, PB37, PB38, PB39, PB40	122, 123, 125, 126
Kubo, Katsutaka	PG17, QF11	145, 205	Kupriyanova, Galina	SK26	354	Langie, Douglas	PB10	121	Lee, Hak Bong	PA01	116
Kubo, Kazuki	AI02	39	Kuramochi, Hiromi	PG06, RP12	143, 305	Langridge, Sean	KE01, PN23	110, 175	Lee, Hak-bong	CI03, PA03	55, 116
Kubo, Kazuya	BC04	42	Kurde, Julia	RP08	304	Larbalestier, David	JA02	98	Lee, Hakjoon	PN09	173
Kubo, Yasunori	SE01	333	Kurihara, Ryosuke	RB05	254	Lardestier, David	BD02, DG02, EJ03, KB02, PJ22	43, 61, 72, 107, 158	Lee, Hana	PJ16, PK10	157, 162
Kubota, H.	CE03, CE06, ID02, RJ07	51, 52, 93, 283	Kurisu, Makio	PN07, QG11, SM10	173, 210, 362	Lari, Leonardo	SK11	352	Lee, Hanju	SA09	317
Kubota, Hitoshi	BI01, HF01, IE04, KF01, PK20	47, 87, 94, 110, 163	Kurita, Kohei	PD11	133	Larionova, Joulia	RN15	299	Lee, Han-oh	FB01	73
Kubota, Kazuhiro	RD01	262	Kurita, Nobuyuki	SB05	321	Larrea J., J.	CD01, SF10	50, 338	Lee, Hee-ju	QL18	231
Kubota, M.	EF01	68	Kuroda, Keisuke	PD25	136	Lartigue, Lenaic	RN15	299	Lee, Heejung	RH08	276
Kubota, Miho	RL13	292	Kuroe, Haruhiko	PA19, QA05, QA07, QA09, RH11	119, 183, 184, 276	Lascialfari, Alessandro	RN15	299	Lee, Hsin-han	QK22, SK30	227, 355
Kubota, T.	SK24	354	Kurokawa, Akinobu	PO02, QL03, RN02	177, 228, 297	Lau, Tobias	KD01	109	Lee, Hu - Jong	RB14	256
Kubota, Takahide	CH02	54	Kurosawa, Tohru	PB08	121	Laubschat, Clemens	CD03, PD12	51, 133	Lee, Hunju	PM23	171
Kubota, Tatsuro	BC04	42	Kusano, Takanao	RO05	301	Lausberg, Stefan	AB02	34	Lee, Hunpyo	SF14, SG22	339, 343
Kubota, Yoshiki	HC03, PI02, QF25	85, 151, 208	Kusunose, Hiroaki	SB17	323	Laver, Mark	KD02, QF20	109, 207	Lee, Hun-sung	RL03, SM01	290, 361
Kubozono, Yoshihiro	SC04	326	Kutnyakhov, D	RN12, RP20	298, 306	Lawicki, Arkadiusz	KD01	109	Lee, Hyeong Jun	RC08	260
Kucherenko, Yuri	PD12	133	Kuwada, Kenta	RQ03	307	Lazarov, Vlado K	SK11	352	Lee, Hyun Joon	RQ18	310
Kuchko, Andriy	JG01	103	Kuwahara, Hideki	PA06, PA19, QA05, RA06, SB24	116, 119, 183, 250, 324	Lazo, Cesar	AF02, PG12	36, 144	Lee, Hyun Jung	JC03	100
Kuchler, Robert	AB02	34	Kuwai, Tomohiko	SG05	340	Lazuta, A. V.	RQ13	309	Lee, Hyun Sook	PO06, PO09, PO10	178
Kudo, Kazutaka	QF10	205	Kuwana, Kanako	QF25	208	Le Breton, Jean-christophe	AI04	39	Lee, Hyungjun	QK21, RC15	227, 261
Kudrevatykh, N. V.	QI03	218	Kuwano, Keisuke	RB04	254	Le Breton, Jean-marie	BB03, BD02, DG02, EJ03, KB02, PJ22, RH22	41, 43, 61, 72, 107, 158, 278	Lee, Hyungyu	RL22, SL19	293, 359
Kudrevatykh, N.v.	GJ03	82	Kuzian, R. O.	QF18	206	Le Guyader, Loic	RK17	288	Lee, Hyun-woo	EE02, EE05, HP21, KE03, PJ33	67, 68, 30, 110, 160
Kudryavtsev, Y. V.	QG27	212	Kuzmin, D. Aleksandrovich	QH17	215	Le Tacon, Mathieu	CA03, RB20	49, 257	Lee, In Kyu	PI14	153
Kuepferling, Michaela	HH01	88	Kuz'min, M. D.	GJ03, QI03, QI09	82, 218, 219	Le Tacon, Matthieu	BA03	41	Lee, J H	QB25	191
Kuga, Kentaro	CD02, IG03, QD01, RD13	51, 95, 196, 264	Kuznetsov, Alexey V.	QC19	195	Le, Cuong V.	QL16	230	Lee, J.	QB31	192
Kuga, Kiyoshi	SK21	353	Kuznetsova, Elena	PB22	123	Le, Tuan Tu	SL22	359	Lee, J. H.	SA06	317
Kuhns, Phil	JA02	98	Kwilu, Augustin Lutondo	KD04	110	Lebecki, Kristof M.	RJ04	283	Lee, J. M.	QB21, SM11	190, 362
Kuiper, Koen	SI07	347	Kwon, Hae-woong	RO12	302	Lebreton, Jean-christophe	CG03	53	Lee, J. Y.	PB03	120
Kulemanov, Ivan V	PN22	175	Kwon, Hyuckchan	RQ17	309	Lechevallier, Luc	BD02, RH22	43, 278	Lee, J.-s.	PH10, RA04	148, 249
Kulinich, Sergey I.	RG17	274	Kwon, Jae Hyun	EG03, HD02, PJ08, SI02	69, 85, 156, 346	Ledue, Denis	EJ03	72	Lee, Jae Il	RH20, SK19, SK27	278, 353, 354
Kulka, A.	PH06	147	Kwon, Joonhyun	PK04, QK03	161, 224	Lee, B. W.	RA07	250	Lee, Jae-chul	KE03, SI13	110, 348
Kulkarni, Prabhanjan Dilip	PK16	163	Kwon, O. Y.	PM26	171	Lee, B.c.	PJ31	159	Lee, Jae-hyun	PO15, PO16	179
Kulkarni, Ruta	QJ17, RB24	223, 258	Kwon, Oh Jun	PB16, PB18, PB35	122, 123, 125	Lee, Bo Wha	RA21	252	Lee, Jaejin	JH04, KH04	104, 112
Kulkarni, Ruta N	SE21	336	Kwon, Oryong	KI01	112	Lee, Bowha	QL09	229	Lee, Jae-jun	RR14, SN04	313, 364
Kumada, Nobuhiro	QE10	201	Kwon, Sangil	BF05, JG05, PA09, PH18	45, 104, 117, 149	Lee, Bo-wha	SO03	367	Lee, Jee Yong	QG20	211
Kumagai, Keigou	SG05	340	Kwon, Seung Hyuk	QN09	237	Lee, Bumsung	JA03, PA04	98, 116	Lee, Jehyun	RJ15, SJ07	285, 350
Kumagai, Ken-ichi	SB27	324	Kwon, Woo Jun	PI14	153	Lee, Byung Chan	SK14	352	Lee, Jeong Soo	QM18, QM20	234
Kumai, R.	CF04	53	Kwon, Yong Seung	CF03	52	Lee, Byungchan	PK21	163	Lee, Jeonghyeon	QK03	224
Kumai, Reiji	PH07, SE07	148, 334	Kwon, Young-wan	EH02	70	Lee, C. H.	QB28	191	Lee, Jeong-o	SD12, SD14	332
Kumano, Yuta	RI02	279	Kyakuno, Haruka	SO515	369	Lee, Chang Hee	RP01	303	Lee, Jhinwan	CA02, RQ11	48, 308
Kumar, Anil P. S	QM03	232	Kyomi, Takuya	PO18	180	Lee, Chang Hoon	EH02	70	Lee, Ji Hye	SA05	317
Kumar, Anil P. S.	CG04, SJ08, SL23	53, 350, 359				Lee, Changhee	PJ17	157	Lee, Jin Bae	SL11	357
Kumar, Dheeraj	HD04, RK11	85, 287				Lee, Changhoon	QJ18	223	Lee, Jin Seok	SD14	332
Kumar, G. Ravi	PI12	152	Labarta, A.	BD01	43	Lee, Cheol Eui	PG25, PN25, SI14, SK28	146, 176, 348, 355	Lee, Jin Yong	QG17	211
Kumar, Manish	SA14	318	Labarta, Amilcar	BD04, KB06, RN14	43, 108, 299	Lee, Chi-hung	PC18	129	Lee, Jinho	CA02	48
Kumar, Manoj	RA27	253	Lacour, Daniel	KF02, SH02	110, 343	Lee, Chul-ho	QB02, QB15, QB29	187, 189, 191	Lee, Jinju	RL17	292
Kumar, Neeraj	RB24	258	Laczkowski, Piotr	GE01, QK15, QK16, QK17, SL24	78, 226, 360	Lee, D.	SA16	318	Lee, Jinyong	PO09	178
Kumar, P. S. Anil	PJ28, SL21	159, 359				Lee, Der-sheng	QM11, QM25	233, 235	Lee, Jinyoung	PO10	178
Kumar, Pawan	QL10, SM18	229, 363	Lai, Bin	SN12	366						

Lee, Jongseok	PB17, PB36, PB37, PB39, RG10	122, 126, 273	Lee, Seunggho	RR21	314	Li, Bodong	PM27	171	Lin, C. Y.	SB04	320
Lee, Joo In	RK19	289	Lee, Seunghun	PH22, PN20, PN21, QL18	150, 175, 231	Li, Carissa H.	KB03	107	Lin, Chengtian	IJ02, RB20	97, 257
Lee, Ju	RR14, SN02, SN04	313, 364	Lee, Seung-hun	AC02	34	Li, D. X.	QJ10	222	Lin, Chun-liang	SM06	361
Lee, Juho	PM17	170	Lee, Seungjun	RL17	292	Li, Fashen	QN21, QN23	239, 240	Lin, H.	SD04	330
Lee, Jung Won	QN09	237	Lee, Seungkyo	PK04, QK03	161, 224	Li, Feng	QK01	224	Lin, Hsin	HI02	89
Lee, Junggoo	JH04, PM24	104, 171	Lee, Shang-fan	PC14, RK07, RL18	129, 287, 292	Li, Gang	JA02	98	Lin, Hsiu-hau	RE11, SB25	268, 324
Lee, Jung-goo	KH04, RN06, SL29	112, 297, 360	Lee, Soogil	RL30	294	Li, Hang	IE01	93	Lin, Jianhua	PH02	147
Lee, Junghyon	PK04	161	Lee, Soonchil	BF05, JG05, PA09, PH18	45, 104, 117, 149	Li, J.	PL02, SM05	164, 361	Lin, Ko-wei	PL18	166
Lee, Junhyun	IA03	91	Lee, Soon-gul	PB21, RB27, SC14	123, 258, 327	Li, Jiajie	RO04	301	Lin, Kurt	PO13	179
Lee, K. B.	RQ08	308	Lee, Sujin	SA09	317	Li, Jian	RR19, RR24, RR25	314, 315	Lin, Lu-kuei	PC14	129
Lee, Ki Doek	SN04	364	Lee, Suk Ho	JB02	99	Li, Jichao C	KI02	113	Lin, Minn-tsong	AD01	35
Lee, Ki-doek	RR14, SN02	313, 364	Lee, Sung Hoon	PB21, RB27	123, 258	Li, Li	PN05, QL04	172, 228	Lin, Pang	RL18	292
Lee, Kiejin	SA09	317	Lee, Sungbin	JD03, PL08	101, 165	Li, Liang	PL06	164	Lin, Ruei-lin	QN24	240
Lee, Ki-seung	RL26	294	Lee, Sung-hyun	SJ05	349	Li, Lingwei	QJ06	221	Lin, T.	GF01	79
Lee, Ki-suk	DE05, RJ14, RJ16, RJ18, SH14	60, 284, 285, 345	Lee, Sungsu	QI15	220	Li, Long-jie	QP17	248	Lin, Wei-yan	QM09	233
Lee, Kiyoung	PN23	175	Lee, Tae Ho	SO21	370	Li, Peisen	SA19, SA20	319	Lin, Z. W.	GA01	75
Lee, Kwan-woo	PF06, SO05, SO06	140, 367	Lee, Tae Young	RL28	294	Li, Q.	GA01	75	Ling, D. C.	PC13	128
Lee, Kyeong-dong	RK09, RK22, SI04	287, 289, 346	Lee, Taehoon	RN10	298	Li, Qing	PO01	177	Liou, Sy-hwang	RO07	301
Lee, Kyu Won	PG25, PN25, SI14, SK28	146, 176, 348, 355	Lee, W. H.	RP10	304	Li, Tian	BE03	44	Liou, Yung	QM09	233
Lee, Kyujoon	PC12, PK17, PN19, QO10, RC07, SD10, SD11	128, 163, 175, 242, 260, 331	Lee, Wei-cheng	GA01	75	Li, Tong	DD03	58	Lipinski, Stanislaw	PE06	137
Lee, Kyung Jin	RL26	294	Lee, Woncheol	JH04	104	Li, W F	DD06	59	Lisboa-filho, Paulo Noronha	QA06	183
Lee, Kyungdong	QM23	235	Lee, Woo	SO21	370	Li, Wanfeng	CB05, EJ04	49, 72	Lisenkov, Sergey	QA27	187
Lee, Kyung-jin	CE04, EE02, EE05, HF05, HP21, PJ33, RJ19, RL06, RL14, SI09	52, 67, 68, 87, 30, 160, 285, 290, 292, 347	Lee, Y. P.	QG27, RA07, SL08, SL09	212, 250, 357	Li, Wei	PK18, QN21, RO04, RO07, SL12, SN11, SN12	163, 239, 301, 358, 366	Lisowski, W.	DD02	58
Lee, M. K.	RQ08	308	Lee, Yen-chen	SB25	324	Li, Weimin	QP22	249	Lisyansky, Alexander A.	HD05	86
Lee, N.	AA04	33	Lee, Ying-chen	PL03	164	Li, Wen-hsien	PC18, PO25, QA20	129, 181, 185	Litterst, Jochen	JG06, RN15	104, 299
Lee, N. H.	PB03	120	Lee, Yong Ho	RQ17	309	Li, Xianhong	RL21	293	Litvinova, Tatyana	PE08	137
Lee, Nam Hoon	GA04, RB27	76, 258	Lee, Yong Woo	PN28	176	Li, Yanfeng	QN21	239	Liu, C.	SD04	330
Lee, Nam-kyu	RR15	313	Lee, Yong-ho	RQ18, RQ19, RQ20	310	Li, Yingjie	PN07, QC01	173, 192	Liu, C. Y.	PC13	128
Lee, Nyun Jong	PJ17, QP18	157, 248	Lee, Young S.	QE27	203	Li, Yong Hui	RA26	253	Liu, Chang	HI02	89
Lee, Paul	PN03, QL02	172, 228	Lee, Yun-hi	RL31	295	Li, Yuan	CA03, JC04	49, 100	Liu, Chieh-wen	QM27	236
Lee, S.-H.	PH03	147	Lees, Martin R	BF03	45	Li, Yufan	JF05	103	Liu, Chi-hsin	PL18	166
Lee, S. J.	RQ08, SJ06, SL08	308, 349, 357	Lefevbre, Williams	KB02	107	Li, Yuke	AB04, IU04	34, 98	Liu, Chunli	QL09	229
Lee, S.s.	RK18	288	Lefevre, C.	SA06	317	Li, Z	QB11	188	Liu, Dongping	QK02	224
Lee, Sang Sun	RP23	307	Lefevre, Christophe	SA05	317	Li, Zhenghua	RP06	304	Liu, H. F.	RP02	303
Lee, Sangho	RL30	294	Legarra, Estibaliz	QH16	215	Liang, Ruixing	BA01	40	Liu, H. L.	PC13	128
Lee, Sanghoon	BE01, PN08, PN09, QL08, QM04	43, 173, 229, 232	Legut, Dominik	CH03, QH19	54, 216	Liang, Shiheng	QK02	224	Liu, Hsin-tzu	RR01	311
Lee, Sang-hyuk	RP03, SH10	303, 344	Leist, Jeannis	AA05	33	Liao, Shu-hsien	QM27	236	Liu, J. Ping	EJ02	71
Lee, Sanghyun	PG24, PI10	146, 152	Leitenstorfer, Alfred	HA02	83	Liao, Yen Fa	QC12	194	Liu, Jun-ming	PA05	116
Lee, Sangji-suk	PL11	165	Leithe-jasper, Andreas	RD12	264	Liao, Yen-fa	QC09	193	Liu, Liying	SM17	363
Lee, Sang-suk	BH02, RR15	46, 313	Lejay, Pascal	SG05	340	Liborio, Leandro	RF15	271	Liu, Mei	QB01	187
Lee, Sang-wha	PO04	177	Lemaitre, Aristide	CG03	53	Lichtenegger, Thomas	RG15	274	Liu, Qiang	PI17	153
Lee, Sangwon	RH08	276	Lemee-cailleau, Marie-helene	SB08	321	Lichtenwalner, Daniel J.	AH04	38	Liu, Qiangchun	SA01	316
Lee, Sangyeop	QM04	232	Lemmens, P.	PI09	152	Lileev, Alexey	QJ13, SN09	223, 365	Liu, Tao	PK18	163
Lee, Sang-yun	PM16, PM19, PM21	170	Lemmens, Peter	QE27	203	Lim, Byunghwa	PO19	180	Liu, Tjiang	RB12	256
Lee, Seok-hee	RL30	294	Lemus, Jose	QO26	245	Lim, Hyein	RL17	292	Liu, Wei	PN04	172
Lee, Seongjae	RL21	293	Lenertz, Marc	PI04	151	Lim, Jaein	QO19	243	Liu, Weiqiang	RO15, SN01	303, 364
Lee, Seong-joo	RQ18, RQ19, RQ20	310	Lengyel, Edith	AB02	34	Lim, Jung Tae	PA22, PI13	119, 152	Liu, X.	PN08, PN09, QL08, QM04	173, 229, 232
Lee, Seong-rae	RO01, RO02	300, 301	Leon, Gladys	QB18, QB19	190	Lim, Kwon Taek	RN05	297	Liu, Xi	SL02	356
Lee, Seongsu	HJ05, PI10, QA24, RA20, RA22	90, 152, 186, 252, 253	Leon, L. M.	CB02	49	Lim, Pang Boey	QP15, QP16	247, 248	Liu, Xiaoli	SL06	357
Lee, Seo-won	SI09	347	Leonyuk, Nicolay I.	PA20	119	Lim, Sang Ho	PL16, QK12	166, 226	Liu, Xiaoxi	PK07, QP08, RL05	161, 246, 290
Lee, Seung Goo	QN22	240	Lepadatu, Serban	QO24	244	Lim, Sang-ho	RQ23	310	Liu, Xuerong	DC03	58
Lee, Seung-beck	QP19, RL22, SL19	248, 293, 359	Lesne, Edouard	HE04	86	Lim, Sanghyun	PO11	179	Liu, Yi	JB03	99
			Lesnikov, Valeriy	SG17	342	Lim, Seon-ho	PO14	179	Liu, Ying Dan	QN03	236
			Letellier, Florent	BD02	43	Lim, Yong-sik	PN31	177	Liu, Zuli	PO01	177
			Leung, Chi Wah	DH04	62	Lim, Yun-seog	PM19, PM21	170	Liu, Zu-li	QK18	227
			Levchenko, A. V.	QC22, RH07	195, 275	Lima Sharma, Ana	QO09	242	Liuqiang, Wen	QO15	243
			Levchenko, Anna Vasilievna	PE09	137	Lin, C T	QB20	190	Lobanova, Inna	SG07	340
			Lewinska, S.	PH06, PM05	147, 168	Lin, C. M.	RR01	311	Locatelli, Andrea	SH06	344
			Li, Anhua	RO04	301	Lin, C. T.	GA03	75	Locatelli, Nicolas	ID03	93
			Li, Bin	QB01	187						

Lockwood, David	QG12	210	Lym, Dae Young	SG21	343
Lodya, Lonzeche J. Augustin	QH22	216	Lynn, Jeffrey W.	QA20	185
Loew, U.	QE23	203			
Loewenhaupt, Michael	PH04, QC24	147, 196	M		
Logg, Peter	PC02	127	M, Aparnadevi	PI01	150
Lohneysen, Hilbert V.	EA01, EG02	64, 69	M, Manivelraja	QD04	197
Loidl, Alois	PA23, RH24	119, 278	M, Shalini	RN16	299
Lombardo, Pierre	CD03	51	M. Tachiki, M.	KJ01	113
Long, Jerome	RN15	299	M., Ramesh	BJ05	48
Long, Phan The	AJ06	40	Ma, Li	Jl05	105
Lonzarich, Gil	BA01	40	Ma, Long	QB07	188
Lopera, Wilson	SA12	318	Ma, Qinli	CH02	54
Lopes, Rován Fernandes	PB09, RB09	121, 255	Ma, Xiao-ping	SH10	344
Lopez-diaz, Luis	SH16	345	Maan, Jan Kees	DH02, SA10	62, 317
Lopez-quintela, M. A.	CB02	49	Maca, Frantisek	BE05	44
Lora-serrano, Raimundo	PI19, SE15	153, 335	Macedo, Claudio Andrade	PF13	141
Lord, James S.	PO17	180	Macedo, Marcelo	QL01	228
Lorenz, Thomas	RI12	280	Machida, Kenji	SK21	353
Lorenz, W. E. A.	QF18	206	Machida, Yo	PC17, PC28, PD16	129, 131, 134
Lorenzer, K. - A.	CD01, SF10	50, 338	Mackenzie, Andrew	EA04	64
Lortz, Rolf	DH04	62	Maclaughlin, Douglas E.	CD04	51
Loshkareva, Natalya	SL17	358	Madami, Marco	GG02	80
Lott, Dieter	DG01, QM02, QM08	61, 231, 232	Maeda, Youichi	QD02	196
Louahadj, Lamis	AI04	39	Maegawa, Satoru	BC04, QE22	42, 203
Louca, Despina	BF02	44	Maehira, Takahiro	QC14, QC15	194
Lowe, Konrad	KH01	112	Maekawa, Sadamichi	FA03, JE02, JF02, JF03, KF03, PJ07, PJ34, PP02, RF07, RL01	72, 102, 111, 155, 160, 28, 270, 290
Lu, C. R.	PC13	128			
Lu, Chun-i	AD01	35	Maeno, Yoshiteru	PC20	130
Lu, Hantao	EB03	65	Maeta, Takashi	PB27	124
Lu, Jun	PA21, QK23, RA02, RQ01	119, 227, 249, 307	Maeter, Hemke	PI05, QJ03	151, 221
			Magalhaes, S. G.	QD10	198
Lu, K. T.	QB21	190	Magalhaes, Sergio	PE01	136
Lu, Kueih-tzu	SM11	362	Magen, Cesar	DG05, GG05, RN08, RN09, SM16	61, 80, 298, 363
Lu, Wei	AJ03, JI06	40, 105			
Lu, Xin	FB01, SE02	73, 333	Magishi, Ko-ichi	QC05	193
Lu, Yunhao	SK34	356	Magnavita, E. Thizay	QO03	241
Lubhelwane, Siyanda	QH22	216	Magni, Alessandro	HH01	88
Lucas, Irene	SM16	363	Mahadevan, Priya	HC01, RF12	84, 270
Ludwig, Frank	AH01	38	Mahajan, Mangesh B.	SL13	358
Lue, C. S.	PE02, PH01	136, 147	Mahdaviifar, Saeed	RG16	274
Lue, Chin Shan	RP02	303	Mahendiran, Ramanathan	PI01, QL10, RA08	150, 229, 250
Luetkens, Hubertus	AB02, PI05, PI17, QB22, QJ03	34, 151, 153, 190, 221	Mahlubi, Zwelithini Melford	RD23	265
			Mahmoodi, M.	PO27, PO29, PO31	181, 182
Luis, F.	BC01	42	Mahmoodi, Mostafa	PO28	181
Lukasiewicz, Malgorzata I	DD02	58	Maignan, Antoine	BB03, JB05, RA11, RH22	41, 100, 251, 278
Luke, G. M.	GF01	79	Maikov, Vladislav	QL07	229
Lummen, Tom T. A.	HG04, PA24	88, 119	Maisuradze, Alexander	CD04	51
Lumpkin, Greg	PO12	179	Maiti, Kalobaran	PE14, SC06	138, 326
Lunov, Oleg	AH02	38	Maitre, Adeline	EJ03	72
Luo, Hui Quian	RB10	255	Majetich, Sara	GG01	80
Luo, Huiqian	RB11	255	Majewski, J. A.	BE02	44
Luo, Yongkang	AB04, IJ04, RB13	34, 98, 256	Maji, Bibekananda	QO04	241
Luong, Dien Xuan	RN19	299	Majumdar, Pinaki	RG12	273
Lupi, Stefano	SA08	317	Majumdar, S	QL14, SO14, PL07, RH02	165, 230, 275, 369
Luque, Fj.	DD02	58	Majumder, M	QM24	235
Lushchik, P	RP20	306	Majumder, Mayukh	RB15	256
Lutsev, Leonid	QM08	232	Makarov, Denys	SJ07	350
Luzon, Javier	GF04	79	Maki, Makoto	PB04	120
Lv, Bin	JA02, PN05, QL04	98, 172, 228	Makio, Kurisu	SM07	362
Lv, Chen	IJ04	98			

Makiyama, Shun	SG09	341	Martin-rodriquez, Damian	QH16	215
Makridis, Sofoklis	SN15	366	Martins, Maximiliano Delany	RJ12	284
Maksimova, Ksenia	SK26	354	Marty, Alain	EI04, GE01, QK15, QK16, QK17, RL24, SL24	71, 78, 226, 293, 360
Maleyev, Sergey V.	DF04	60			
Malikov, Shavkat	RR28	315	Masek, Jan	BE05, SK22	44, 354
Malinowski, Gregory	SH02	343	Maskova, Silvie	QI19, RE09	220, 267
Maljuk, Andrey	IJ02	97	Masoudpanah, S. M.	QM28	236
Mallia, Giuseppe	RF15	271	Massboeuf, Aurelien	SH06	344
Malone, Liam	JC02	100	Masthoff, Ingke Christine	JG06	104
Mal'tsev, Viktor V.	PA20	119	Masti, S A	QN14	238
Malyuk, Andrey	PA10	117	Masuda, Keisuke	SB23	324
Mamiya, Hiroaki	JJ05, RI07	106, 280	Masuda, Ryo	QM16	234
Manabe, N.	SL14	358	Masuda, Takatsugu	QA02	182
Manaf, Azwar	BJ03, QN16, RA15	48, 239, 251	Masui, T.	HA01	83
Manago, Takashi	PG06, RK21, RP12	143, 289, 305	Masumoto, Hiroshi	Jl01	105
Manaka, Hirotaka	QE09, QH02, RI06	200, 213, 279	Mathai, Cijy	CG04	53
Manami, Onizawa	QD14	198	Mathon, Olivier	HG04, RH23	88, 278
Manchon, Aurelien	CG05, EE03, IE01, PJ06, PJ13, PJ29, PJ34, QL17, RJ19, SK12	53, 67, 93, 155, 156, 159, 160, 230, 285, 352	Mathur, Neil D	AE03	36
			Matiks, Y.	GA03	75
			Matoba, Masanori	QC07, QC08, SE09	193, 334
Mandal, Ruma	HD04	85	Matsubara, Takeshi	PC17	129
Manivannan, Nallayian	PB23	123	Matsubayashi, K.	QH09, RD15	214, 264
Maniwa, Yutaka	SO515	369	Matsubayashi, Kazuyuki	PD14, QD17, QI18, QN20, RD06, RD22, RE04, SC24, SE01, SE11	134, 199, 220, 239, 263, 265, 267, 329, 333, 335
Mankey, Gary J.	QM02	231			
Manna, P K	QP05	246	Matsuda, Kazuyuki	SO515	369
Manna, P. K.	RN04	297	Matsuda, Ken-ichi	SK06	351
Manna, Rudra Sekhar	QJ11, RI13	222, 281	Matsuda, M.	PH03	147
Manni, Soham	SG13	341	Matsuda, Masaaki	HJ03	90
Manske, Dirk	CA03, KJ03	49, 114	Matsuda, Ryotaro	HC03, QF25	85, 208
Mansson, M.	PC29, PI15	131, 153	Matsuda, Saori	QJ08	222
Mansson, Martin	HA03, PI06, PO17, QF20, SE08	83, 151, 180, 207, 334	Matsuda, Tatsuma	JC02	100
			Matsuda, Tatsuma D	IG04, PD09, PD23, RD25, SB15	95, 133, 135, 266, 322
Mantovan, Roberto	SK26	354			
Manzoor, Sadia	SA15	318	Matsuda, Tatsuma D.	RD01, RD11, RE10, SF03	262, 263, 268, 337
Mao, Zhiqiang	RB12	256	Matsuda, Tatsuma Daruma	HP11	30
Maple, M. Brian	BB01	41	Matsuda, Yasuhiro H.	IG03	95
Marcatoma, Justiniano	PL09	165	Matsuda, Yuji	IA01, QC04, SB27	90, 192, 324
Marchetti, Gianni	QK09	225	Matsudaira, Ken-ichiro	PH23	150
Marcin, Jozef	IB01, QO17	91, 243	Matsueda, Hiroaki	EB03	65
Margaris, George	CB03	49	Matsuhira, Kazuyuki	CC05, QE13	50, 201
Mari, Kenichiro	SK18	353	Matsui, Fumihiko	SK13	352
Marin, Lorena	SM16	363	Matsui, Kazuki	PD10	133
Maritato, Luigi	SA08	317	Matsuishi, S.	QB23	190
Markiewicz, R. S.	HI02	89	Matsuishi, Satoru	PC23, QB16	130, 189
Markiewicz, Robert S.	BA04	41	Matsukawa, Michiaki	PI22	154
Marques-ferreira, Pablo	PI19	153	Matsukura, F.	BE02	44
Marquina, Clara	RN08, RN09	298	Matsukura, Fumihiro	QP14	247
Marrows, Chris	QO24	244	Matsumoto, Akiyo	RH21	278
Marrows, Christopher	KE01	110	Matsumoto, K. T.	EF01	68
Marsilius, Mie	PM04	168	Matsumoto, Kazuyuki	RI01	279
Martens, Michael	FD02, RJ05, RP04	74, 283, 303	Matsumoto, Keisuke	SG15	342
Martens, Stephan	RP04	303	Matsumoto, Keisuke T	RD04	262
Marti, X.	IF01	94	Matsumoto, Keisuke T.	SG12	341
Marti, Xavier	BE05	44	Matsumoto, Masashige	SB17	323
Martin, Christine	JB05, RA11	100, 251	Matsumoto, Naoki	QM10	233
Martin, I.	FB01	73	Matsumoto, Naoki	HF01, IE04	87, 94
Martin, Jose Ignacio	GG03	80	Matsumoto, Rie	PM02	167
Martinez, Benjamin	IH01, SO18	95, 369	Matsumoto, Sayaka	PM02	167
Martinez, Eduardo	SH16	345	Matsumoto, Shinji	SN03	364
Martinez-perez, M. J.	BC01	42	Matsumoto, Shoutaro	PN24	176

Matsumoto, Tatsuya	QM29	236	Medvedev, M. V.	RF16	271
Matsumoto, Yoshihiro	BH05, BH06	46, 47	Mehrafarin, Mohammad	SB07	321
Matsumoto, Yosuke	CD02, QD01	51, 196	Mei, Li-then	QN25	240
Matsumoto, Yuji	PD09, PD23	133, 135	Meier, Guido	FD02, HG02, RJ05, RP04, SH04	74, 88, 283, 303, 343
Matsumura, Masahiro	QD06, RD10	197, 263	Meier, Johan G.	RN09	298
Matsumura, Takeshi	QI10	219	Meindl, Manfred	AH01	38
Matsunaga, Takahiro	KC06	109	Meisel, Mark W.	KB03	107
Matsunami, Masaharu	AD04, QD18	35, 199	Meissner, Thomas	RQ09	308
Matsuo, A.	QI03	218	Melander, Emil	AF05	37
Matsuo, Akira	HC03, PG17, QE16, QF11, QF14, QF17, RI15, RQ05	85, 145, 202, 205, 206, 281, 307	Melisek, T	RB08	255
			Melkov, Gennady	JG02	103
Matsuo, Mamoru	KF03	111	Melnychenko, Nataliya	SC01	325
Matsuoka, Eiichi	PE11, PE13, QF04, QI10, QI16, RD01	137, 138, 204, 219, 220, 262	Meloche, Eric	QG12	210
			Mena, Mattia	QG14	210
Matsuoka, Yuki	QH20	216	Mendonca, Ana P. Aguiar De	PB09, RB09	121, 255
Matsushima, Yasushi	SL03	356	Meng, Kangkang	QK23	227
Matsushita, Takuya	QI07	218	Mengotti, Elena	RK17	288
Matsushita, Tomohiro	SK13	352	Mentes, Onur	SH06	344
Matsuura, Keisuke	PG17, QF14	145, 206	Meny, C.	SA06	317
Matsuura, Masato	PB30, PB32	125	Meny, Christian	AJ05, SA05	40, 317
Matsuyama, Hideo	RP14	305	Menzel, Dirk	QM08, SM02	232, 361
Matsuyama, Kimihide	QM29, QP09, QP10, QP11, SJ03	236, 246, 247, 349	Menzel, Matthias	IH03	96
			Merazzo, Karla J.	GG04	80
Matsuzaka, S.	CG02	53	Merchant, P.	QE19	202
Mattauch, Stefan	DG01	61	Merk, Ulrich	RP04	303
Mattenberger, K.	PI15	153	Mertig, Ingrid	EE01	67
Mattenberger, Kurt	RB21	257	Meshcheriakova, Olga	QN19	239
Matusiak, Marcin	AB03, SF12	34, 339	Mesler, Brooke	RJ20	285
Matuura, Masato	PB29	124	Mesot, J.	PC01	126
Mayoral, Alvaro	RN09	298	Mesot, Joel	IC02, QF20	92, 207
Mayoral, Isabel	QO16	243	Metaxas, Peter	IE04	94
Mayr, Franz	PA23, RH24	119, 278	Methfessel, Torsten	AG04	38
Maziarz, W.	PM05	168	Metoki, Naoto	IG04, JJ05, PH09, QJ09	95, 106, 148, 222
Mazidian, Bayan	JA05	99	Mettus, Denis	CH01	54
Maziewski, Andrzej	AD05		Meven, Martin	PA14, RP22	118, 306
Mazrouei Sebdani, S.	PO27, PO29, PO30, PO31	181, 182	Meziere, Cecile	SB20	323
			Mi, J.I.	II02	97
Mazrouei Sebdani, Saeed	PO28	181	Mibu, Ko	QM16	234
Mazumdar, Chandan	RB15	256	Michel, Ann Kathrin	RN15	299
Mazzoli, Claudio	BF03, PA15	45, 118	Michel, Anny	QP18	248
Mc Gill, S.	AA04	33	Michihiro, Yoshitaka	QF24	207
Mc.donald, Ross	RB21	257	Michimura, Shinji	IG03, RH03	95, 275
Mccollam, Alix	DH02, SA10	62, 317	Michimura, Sinji	QI10	219
Mccord, Jeffrey	SH04	343	Michiue, Yuichi	RH06	275
Mcdonald, Ross	GC03	77	Michlmayr, Thomas	RK24	289
Mcdonald, Ross D	QB13	189	Michor, Herwig	IA02, SC01	90, 325
Mcgee, Fintan	SH09	344	Micklitz, Hans	RB10, RB11	255
Mcintyre, Garry	IJ03, PO25	97, 181	Miclea, C.	SA11, SC03	318, 326
Mcmichael, Robert D	EG01	69	Miclea, C. F.	SA11, SC03	318, 326
Mcmorrow, D F	RI05	279	Miclea, C. T.	SA11	318
Mcmorrow, D. F.	QN01	236	Middey, S.	RF12	270
Mcmorrow, Des	QG14	210	Mielke, Chuck	BA01, GC03	40, 77
Mcmorrow, Desmond	AF01	36	Mignot, Jean - Michel	RD14	264
Md Nor, Anis Faridah	QM29	236	Mihashenok, Natalia	PI11	152
Measson, Marie-aude	PD17	134	Miike, Kazunari	QL03, RN02	228, 297
Medarde, Marisa	PO17	180	Mijnarends, Peter E.	BA04	41
Medicherla, V R R	PE14	138	Mikhaylovskiy, Rostislav V.	GD04, QO05, RK20	78, 241, 289
Medjanik, K	RP20	306	Miki, Hiroyuki	DJ04, QG18	63, 211
Medonca Ferreira, Leticie	SE15	335	Millan, Angel	KB06	108

Milyaev, Michael A.	SK01	350	Miyamachi, Toshio	GI03	82
Milyaev, Mikhail	SK02	350	Miyamoto, Koji	KF05	111
Mimura, Kojiro	RD20	265	Miyamoto, Souta	SG05	340
Min, B. I.	PE17, PG11, RG02, SC12	138, 144, 272, 327	Miyao, Masanobu	HE01, RK10	86, 287
Min, Byoung Chul	QM18	234	Miyasaka, Hitoshi	QF21	207
Min, Byoung-chul	CE04, RK09, RL03, RL06, RL14, SL26	52, 287, 290, 292, 360	Miyasaka, S.	CF04, HA01	53, 83
Min, Byung Chul	RL26	294	Miyasaka, Shigeki	PH07, PI07, QB24	148, 151, 191
Min, C	BG01	45	Miyasaka, Toshiki	QL03, RN02	228, 297
Min, Gyeong Im	CF03	52	Miyata, Atsuhiko	AC03	34
Min, Jin Hong	QN15	238	Miyata, Masahiko	AG03	37
Min, K. J.	PJ24	158	Miyawaki, Tetsuya	PJ12, PL12, RC18, SA07, SA17, SK18, SO20	156, 165, 261, 317, 319, 353, 370
Minh, Nguyen Van	PH14	149			
Minnullin, Arthur	QA26	186	Miyazaki, H.	SG11	341
Mino, Michinobu	RK23	289	Miyazaki, Hidetoshi	AD04, QH28	35, 217
Minola, Matteo	BA03	41	Miyazaki, Ryoichi	RD17	264
Miotkowski, Ireneusz	HI02	89	Miyazaki, Shota	SG16	342
Mirebeau, Isabelle	AA03	33	Miyazaki, Takamichi	EJ01, RO06	71, 301
Miron, Mihai	SH05	344	Miyazaki, Terunobu	CH02	54
Misawa, Takahiro	PE18, QB10	139, 188	Mizokawa, T.	RB28	258
Misek, Martin	BB04, QJ14	42, 223	Mizuguchi, Masaki	JJ04, QL15, RL15	105, 230, 292
Misiorny, Maciej	DB03	57	Mizuguchi, Y.	RB28	258
Misoka, Keita	RH11	276	Mizuguchi, Yoshikazu	QB09, QB17	188, 189
Misu, Tekeshi	KC02	108	Mizukami, Shigemi	CH02, EJ01	54, 71
Misuraca, Jennifer	QK23	227	Mizumaki, Masaichiro	IG03, QD17	95, 199
Mita, Yoshimi	SG20	342	Mizuno, Fumio	RH12	276
Mitani, S	SK29	355	Mizuno, Hiroki	RI01	279
Mitani, Seiji	EH01, IF03, IF05, SK11, SK31	69, 94, 352, 355	Mizuno, Yoshiyuki	RO06	301
			Mizunuma, Kotaro	SI17	348
Mitchell, J N	GC03	77	Mizuochi, Norikaze	SI05	346
Mito, Masaki	KB06, PB25, PG09, PG10, QG19, RN03, SA03	108, 124, 143, 144, 211, 297, 316	Mizuochi, Norikazu	RL11, SK10	291, 352
			Mizusaki, Soichiro	PG13, SK04	144, 351
Mito, Takeshi	QD12, QD15, RD24	198, 266	Mizushima, Toshio	SG05	340
Mitrelias, Thanos	BH01	46	Moeller, A.	QE23	203
Mitsen, Kirill V.	QC19	195	Moeller, Thomas	KD01	109
Mitsuda, Akihiro	IG05, QD03, QD15, SB14	95, 196, 198, 322	Moessner, R.	CC04	50
Mitsuda, Setsuo	PH05	147	Mohammad Shafique, Anwar	PM14	169
Mitsui, Takaya	QM16	234	Mohan, Ashwin	SO22	370
Mitsui, Yoshifuru	GJ02, QH08	82, 214	Mohn, Peter	EF05	68
Mitsumata, Chiharu	KH02, SJ06	112, 349	Mohseni, S. M.	CE02, PK13	51, 162
Mitsumoto, Keisuke	RB05	254	Mokrousov, Yuriy	IH03	96
Mitsunaga, Daisuke	QH08, QN20	214, 239	Molavi, Mostafa	PC16	129
Mitsuzuka, Yoshio	RK04	286	Mole, R. A.	PI03	151
Miura, Daisuke	RL09, SI06	291, 346	Mole, Richard A	QG26	212
Miura, Hideo	RP11	305	Molegraaf, Hajo	DH02	62
Miura, Katsuya	QP14	247	Molenda, J.	PH06	147
Miura, Tomohiro	PB29	124	Molenkamp, Laurens Wigbolt	AC01	34
Miura, Tomoya	PG04	143	Molkanov, P. L.	RQ13	309
Miura, Yasunao	PD13	134	Moll, Philip J. W.	SC16	328
Miura, Yoko	QE09, RI06	200, 279	Moll, Philip J.w.	RB19, RB21	257
Miura, Yoshio	IF02	94	Molodtsov, Serguei L.	CD03, PD12	51, 133
Miwa, Shinji	KF01, PK20, RL11, SI05, SK10	110, 163, 291, 346, 352	Molokeev, Maxim	PI11	152
			Mombetsu, Shota	RD07	263
Miyagawa, Kazuya	BC03	42	Momoi, Tsutomu	JD04	101
Miyahara, Shin	GB01, PA07	76, 117	Momono, Naoki	PB08, QA19, QJ04, RD06, RD22, SE06	121, 185, 221, 263, 265, 334
Miyake, Atsushi	PB27, PC21, PC23	124, 130	Monaco, Giulio	RB28	258
Miyake, Kazumasa	IG01	95	Mondragon, Reginaldo	QO26	245
Miyake, Kohsaku	CE05	52	Montaigne, Francois	KF02, SH02	110, 343
Miyake, Takashi	RG07	272	Montbrun, Richard	EG02	69
			Monteiro, Pedro M.d.s.	PN23	175

Monteiro, Rodrigo S.	QO03	241	Mueller, Jens	QA11, QJ11	184, 222
Montoncello, Federico	GG02	80	Mueller, M.	CD01	50
Moon, Eun-gook	JD05	101	Mueller, Marc	EG02	69
Moon, Han Seb	RQ18	310	Mufti, Nadang	AB02	34
Moon, Jung-hwan	CE04, EE05, HP21, RJ19	52, 68, 30, 285	Mufti, Nandang	PH17	149
Moon, Kyoung-woong	KE03	110	Muhammad, Kamran	SB01	320
Moon, Seung Ho	CB01, PO15, PO16	49, 179	Muhlbauer, Sebastian	CC03, DF02	50, 60
Moon, Wonha	RH08	276	Muir, Jack	PO12	179
Morais, Paulo Cesar	PO08	178	Mukadam, M. D.	PN17	174
Morales, R.	BD01, ED03	43, 66	Mukai, Kazuhiko	PO17	180
Morales, Rafael	BD04	43	Mukhamedshina, Nuranya	RR28	315
Morales, Ricardo	QO26	245	Mukherjee, Sankha Subhra	EG03, HD02, PJ08, SI02	69, 85, 156, 346
Morbec, J. M.	RM02	295	Mukherjee, Sudip	RN17	299
Morellon, Luis	SM16	363	Mukhin, A. A.	PA15	118
Morenzoni, Elvezio	PB20, QL19	123, 231	Mukhin, Alexander	PA13	118
Moretti Sala, Marco	BA03, RB28	41, 258	Mukhopadhyay, Sutirtha	IC02	92
Morgan, Jason	KE01	110	Mukovskii, Ya. M.	RQ13	309
Mori, Shigeo	AF03, PG15, QG22, QG28	37, 144, 211, 212	Mukuda, Hidekazu	DA04, PB26, QB29	56, 124, 191
Moriki, Takahiro	QH15	215	Mulders, A.m.	SO08	368
Morimoto, Kazuhiro	AE05	36	Muller, M.	SF10	338
Morimoto, Y.	SL14	358	Muller, Ralf	RI12	280
Morinaga, Rei	QE13	201	Mun, E. D.	IA05	91
Morioka, T.	PG24	146	Mun, Eundeok	QB13	189
Morisako, Akimitsu	PK07, QP08, RL05	161, 246, 290	Munchenberger, Jana	IF04	94
Morishita, Kohei	RP01	303	M. Cagigas, Julian Andres	RB10	255
Morita, Kyohei	PD25	136	Munevar, Julian	RB11	255
Moriyama, Takumi	KD03	109	Munoz, Carmen	KI02, SD16	113, 332
Moro, Maria	PG08	143	Munzenberg, Markus	DI03	63
Morodomi, Hiroki	QE18, QF14	202, 206	Murakami, Naoki	RP01	303
Morosov, Alexander I	PL05	164	Murakami, Shuichi	RL16	292
Mosendz, O.	BG02	45	Murakami, Y.	CF04, PL14	53, 166
Moshchalkov, Victor	QC19, QC20	195	Murakami, Yoichi	SE07	334
Moskvin, Alexander	PB14	122	Murakami, Youichi	PH07, PH08, PI07	148, 151
Moskvin, Evgeny V.	DF04	60	Murakami, Yuta	RI14	281
Mostovoy, M.	RA05	250	Murakami, H.	PA14	118
Mostovoy, Maxim	CI01, DF01	54, 60	Murakawa, H.	PA14	118
Mostovshchikova, Elena	SL17	358	Muramoto, Shingo	IF02	94
Mota, A. C.	SC03	326	Murasawa, Y.	PL04	164
Motome, Yukitoshi	JD02, PE18, PG23, RG03	101, 139, 146, 272	Murata, Atsushi	QM16	234
Motonami, Satoru	RD20	265	Murayama, Shigeyuki	QA19, QC01, QJ04, RD06, RD22, SE06	185, 192, 221, 263, 265, 334
Motoya, Kiyochiro	HJ03, PH15, QE13	90, 149, 201	Murayama, Sigeyuki	PB08	121
Motoyama, Gaku	QC03	192	Mure, Elena	IE02, JE01	93, 101
M. Ghahfarokhi, Ebrahim	RN22	300	Muro, Y	SE03, SE05, SE13	333, 334, 335
Movshovich, R.	QB31, SC03	192, 326	Muro, Y.	KA02, QC12	107, 194
Movshovich, Roman	SB12	322	Muro, Yuji	PD24, QE13	135, 201
Moya, Carlos	RN14	299	Muromachi, Eiji	PC21	130
Moya, Maria Dolores Salvador	RO08	302	Murphy, J.	QC23	196
Moya, Xavier	AE03	36	Murphy, T.	IA05	91
Moyoshi, Taketo	HJ03, PH15	90, 149	M. Ghahfarokhi, S Ebrahim	PB15	122
Mruczkiewicz, Michal	QO05	241	Musfeldt, J. L.	AA04	33
Mryasov, Oleg	JI03	105	Mutka, Hannu	BC02	42
Mryasov, Oleg N	KH04	112	Muto, Tomoki	RH03	275
Mryasov, Oleg N.	JF04	103	Myakon'kikh, Veronika	PC07	127
Msomi, Justice	QL20	231	Mysik, Alexey	QL07	229
Mudry, Christopher	QF20	207			
Mudryk, Yaroslav	JJ01	106	N		
Muechler, Lukas	RC10	260	Na, Sewoong	RB14	256
Muehlbauer, S. Clemens	IJ06	98	Naaman, Ron	GI02	81
Mueller, Klaus	QK14	226	Naastepad, F.	RQ12	309
			Nafradi, Balint	PA14	118

Nagai, Kousuke	PG09	143	Nakao, H.	CF04, PL14	53, 166
Nagalakshmi, Ramamoorthi	QC13	194	Nakao, Hironori	PH07, PH08, PI07, SE07, SF04	148, 151, 334, 337
Nagano, Katsuaki	RD10	263			
Nagano, Takuma	PG10	144	Nakao, Yuya	PG09	143
Nagano, Y.	SL14	358	Nakashima, Miho	QH04, RD19	213, 265
Nagano, Yutaro	SB14	322	Nakashima, Naoya	QL12, QL13	230
Naganuma, Hiroshi	CH02, EI02, KD04, RL13, SI03, SI17, SK08	54, 70, 110, 292, 346, 348, 351	Nakata, Hayato	QE21	202
Nagaosa, N.	RA05	250	Nakatani, Ryoichi	DE04, EI05, PK08, SK33	60, 71, 161, 355
Nagaosa, Naoto	AE05, DF01	36, 60	Nakatani, Y.	RL07	291
Nagasawa, N	PC04	127	Nakatani, Yoshinobu	HG02, QP03, RJ01, RJ02, RJ09, SJ01	88, 245, 282, 284, 349
Nagasawa, N.	EF01	68			
Nagasawa, Naohiro	RD04	262	Nakatsuji, S.	CF01	52
Nagashima, Ryo	QB15	189	Nakatsuji, Satoru	CC05, CD02, IG03, PG14, QD01, RD13, SE01, SF07	50, 51, 95, 144, 196, 264, 333, 338
Nagata, Shoichi	QH14	215			
Nagata, Tomoko	RA18	252	Nakayama, T.	SK03	350
Nagata, Yujiro	PG13, SK04	144, 351	Nakayama, Takayoshi	PF15	141
Naghavi, S. S.	QG24	212	Nakamura, Tetsuro	QC07	193
Nair, K. G. M.	PN01	172	Nakotte, Heinrich	SF13	339
Naito, Makoto	PG13	144	Nakotte, Heinz	RE09	267
Naito, Tomoyuki	SG18	342	Naletov, Vladimir V.	ID03	93
Naka, Makoto	GB02	76	Nallamuthu, Sengodan	QC13	194
Naka, Takashi	RN11	298	Nam, Chunghee	KC01	108
Nakada, Kengo	PN13	174	Nam, Hyoung Uk	QO20, SG21	244, 343
Nakagawa, Shigeki	HB03	84	Nam, Moon-sun	SB20	323
Nakagawa, T	QM12	233	Nam, Nguyen Hoang	HC02, PE15	84, 138
Nakagawa, Takeshi	AG04, EI01	38, 70	Nam, Yoon Jae	PL16	166
Nakahara, Mako	SG05	340	Namatame, Hirofumi	RD20	265
Nakai, Ikuo	PN07	173	Namkung, Seok	RO01, RO02	300, 301
Nakai, Yusuke	QC08, RD05, SO515	193, 262, 369	Nandy, Ashis Kumar	RF12	270
Nakajima, K.	RA22	253	Nanto, Dwi	QH01	213
Nakajima, Kazuo	RP01	303	Naohiro, Nagasawa	QC16	194
Nakajima, Kenji	RH12	276	Napolskiy, Kirill	SL27	360
Nakajima, Taro	PH05	147	Nara, Daichi	RP14	305
Nakama, Akihiro	RD17	264	Nara, So	QG18	211
Nakama, Takao	PD14, QC11, QI12, QI13	134, 194, 219	Naramoto, Hiroshi	BH05, BH06	46, 47
Nakamoto, Atsuhiko	RP14	305	Narayanapillai, K.	GE03, PJ20, PJ21, RL19	78, 158, 293
Nakamoto, Go	QG11	210	Nardone, Marc	RQ16	309
Nakamura, Ai	QI12, QI13	219	Narikiyo, Kurahito	SB24	324
Nakamura, Hiroyuki	HJ02, QA12, QH13	90, 184, 215	Nartowt, B	SE14	335
Nakamura, Kazuma	QB10	188	Narumi, Y.	GJ03	82
Nakamura, Kohji	EC02, RM04, RM05, SO10, SO11	65, 295, 296, 368	Narumi, Yasuo	PG17, QF09, RP07	145, 205, 304
			Naruse, Koki	QF10	205
Nakamura, Mitsutaka	RH12	276	Nascimento, Valberto Pedruzi	QM15	234
Nakamura, Mitsuteru	PD11	133	Nasirpour, Farzad	QM05	232
Nakamura, Saori	QH14	215	Nasreen, Farzana	SF13	339
Nakamura, Shintaro	SL04	356	Nasu, Joji	RH10	276
Nakamura, Takuya	RP14	305	Nateprov, Alexandr	IG02, QG23	95, 212
Nakamura, Tetsuya	RP07	304	Nikolaevich		
Nakamura, Toshiyuki	IG03	95	Nath, Ramesh	QE12	201
Nakane, Takayuki	RN11	298	Naumov, Sergey	SL17	358
Nakanishi, Yoshiki	PD11	133	Naumova, Larisa	SK02	350
Nakano, Hiroki	QE07, QE11, RI04, RI16	200, 201, 279, 281	Naumova, Larisa I.	SK01	350
Nakano, Kyohei	PF12, RF03	141, 269	Navarro, Oracio	QG21, QO26, SK15	211, 245, 352
Nakano, Masaki	JH01, PM08, PM09, RO03	104, 168, 301	Navarro-quezada, Andrea	BE03	44
			Navas, D.	ED03	66
Nakano, Takehito	HC02, PE15, RI17	84, 138, 281	Nazmunahar, Mst.	DJ03	63
Nakano, Tomohito	RD24	266	Nedelko, N.	PH06, PM05	147, 168
Nakao, A.	CF04	53	Nekrasov, I. A.	RF16	271
Nakao, Akiko	PH07, SF04	148, 337	Nelson- Cheeseman, Brittany	DH01	62

Nelson, C.s.	PH10	148	Ninios, Kostas	BC05	42
Nelson, Christie S.	PA02	116	Ninomiya, Keisuke	PN26	176
Nemnes, George Alexandru	QK20	227	Niratisairak, Sanyalak	RP17	306
Nemoto, Yuichi	RB05, RD07	254, 263	Nishi, Yusuke	QD18	199
Nenert, G.	QF22	207	Nishihara, Sadafumi	QG22	211
Nenert, Gwilherm	PI17, QJ02	153, 221	Nishihara, Yoshikazu	PM13	169
Nepijko, S A	QM12, RN12, RP20	233, 298, 306	Nishikawa, Takuo	SK08	351
Neu, Volker	DG01	61	Nishikawa, Yunori	SF15	339
Neubauer, Andreas	DF02, QH12, SF05	60, 214, 337	Nishimoto, Satoshi	PF09, PF12	140, 141
Neumann, I.	DI01	62	Nishimura, Katsuhiko	QI04, QJ06	218, 221
Neupane, Madhab	HI02, SD04	89, 330	Nishimura, Naoto	PD13	134
Neusser, Sebastian	GG02	80	Nishimura, Taizo	PG17	145
Ng, Dickon H.I.	BE04	44	Nishino, Yoichi	QH28	217
Ngubane, Jeanette	QH22	216	Nishioka, Takashi	PD10, QD06, RD10	133, 197, 263
Nguyen, Anh T. N	CE02	51	Nishisako, Yuya	SK23	354
Nguyen, Anh Tuan	QF16	206	Nishishita, Muneyuki	PF19	142
Nguyen, Duc-tho	RA10	251	Nishitani, Koji	QD15	198
Nguyen, Hoa	SL05	356	Nishitani, Y.	BE02	44
Nguyen, Hong T. M.	QL16	230	Nishiura, Naoto	QC18	195
Nguyen, Khanh Duy	QA10, QA17	184, 185	Nishiyama, Kouhei	QD12	198
Nguyen, Sinh Huy	CJ05	56	Nishiyama, Masahide	BC04, QE22	42, 203
Nguyen, Thanh Van	SO13	368	Nishiyama, N.	SG02	339
Nguyen, Thuy-trang	RF02	269	Nishiyama, Norimasa	PE10	137
Nguyen, Tiep H.	QL16	230	Nishizaki, Terukazu	SG18	342
Nguyen, Tuan Anh	SO13	368	Nitta, Junsaku	KC03	108
Nguyen, Van Dai	GE01, QK15, QK16, QK17, RL24, SL24	78, 226, 293, 360	Niyogi, Sandip	PN16	174
			Nizhankovskii, Victor	JJ03	106
Nguyen, Van Thanh	QF16	206	Nizzoli, Fabrizio	GG02	80
Nhlapo, Ta	QL20	231	No, Young-il	BH02	46
Ni, Ni	QB13	189	Noad, H. M. L.	GF01	79
Niarchos, Dimitrios	EJ04	72	Noda, Kazuto	PF16	141
Niarchos, Dimitrios G	RO08	302	Nogami, A.	PA04	116
Niarchos, Dimitris G	BJ02, DD06, QP12, QP13, RQ10	47, 59, 247, 308	Noguchi, Tomoaki	PE10	137
			Noh, Han-jin	HJ05, PB12	90, 122
Nicklas, M.	SC03	326	Noh, Hwayong	PJ16, PJ24	157, 158
Nicklas, Michael	AB02, IA02, RD12, SB29	34, 90, 264, 325	Noh, Hyunho	SD14	332
Nie, Wenxing	PF18	142	Noh, Seung-hyun	PO15, PO16	179
Nie, Yuefeng	HA03	83	Noh, Su Jung	PJ14, SH13	157, 345
Niedermayer, Ch.	QE19	202	Noh, T. W.	HP12, SA16	30, 318
Niedermayer, Christof	HA03	83	Nohara, Hiroki	SF03	337
Nielsch, Kornelius	RP04	303	Noji, Takashi	QF07	205
Niemeyer, Markus	KD01	109	Nojima, Tsutomu	SL04	356
Niermann, Daniel	QA22	186	Nojiri, H.	PG24	146
Nigam, A K	QO04	241	Nojiri, Hiroyuki	QF09, RP07	205, 304
Nigam, A. K.	QH06, SO22	213, 370	Nolas, George S.	DJ01	63
Nigam, A.k	PG19	145	Noll, T	RP08	304
Nii, Yoichi	QA10, QA13	184, 175	Nolting, Frithjof	BC02, RK17	42, 288
Niimi, Yasuhiro	HE03, ID04	86, 93	Nomura, Hikaru	DE04	60
Niimi, Yohei	RC18	261	Nomura, Kentaro	AE05	36
Niizeki, T	SK29	355	Nomura, Ryuya	QL11	229
Niizeki, Tomohiko	IF03	94	Nomura, Tatsuya	KC06, QK24, RL20, RL23	109, 228, 293
Niki, Haruo	QH14	215	Nonoguchi, Seiji	KC06, QK24, QL11, RL20, RL23	109, 228, 229, 293
Nikolaev, Pavel	PI32	160			
Nikolenko, Victor V.	QO12	242	Nordblad, Per	PM10, QH11, RN07	169, 214, 297
Nikseresht, Neda	QF23	207	Noro, Yoshihiko	PG13, SK04	144, 351
Nilsen, Gøran J.	QE05, QE08	200	Notin, Lucien	EI04, GE01, QK15, QK17, RL24	71, 78, 226, 293
Nimori, S.	QJ10	222			
Nimori, Shigeki	PI22, RI07	154, 280	Novais, Erico	RJ13	284
Ning, F. L.	GF01	79	Novak, Vit	BE05	44
Ning, Sun	RR25	315	Noverola, Humberto	QO26	245

Novitskiy, Nicolay	QM08	232	Ohashi, Masashi	QJ12	222
Nowak, Uli	FC03	74	Ohashi, Takuma	RF09	270
Nowak, Ulrich	FA02, RJ04	72, 283	Ohashi, Tatsuro	KC03	108
Nozaki, Hiroshi	PI06, PO17	151, 180	Ohdaira, Yusuke	EI02	70
Nozaki, Taiichiro	RL25	294	Ohe, Junichiro	RL27	294
Nozaki, Takayuki	BI01, KF01, PK20, SK10	47, 110, 163, 352	Ohe, Jun-ichiro	FA03, FD04	72, 74
Nozaki, Tomohiro	PL10, SM03	165, 361	Ohgushi, K.	SG02	339
Nozaki, Yukio	JG03, QP09, RJ10, RK10, SI08	103, 246, 284, 287, 347	Ohgushi, Kenya	IA04, QO13, SG04	91, 242, 340
			Ohishi, Kazuki	QB02, QB04	187
Nozawa, Akihiko	RB06	255	Ohkawara, Manabu	RP01	303
Nozue, Yasuo	HC02, PE15, RI17	84, 138, 281	Ohkubo, Tadakatsu	IF03	94
Nucara, Alessandro	SA08	317	Ohmichi, Eiji	RP09, RP19	304, 306
Nugroho, Agung	CC05, PH17	50, 149	Ohnishi, Tomohiro	SK04	351
Nunes, Sabrina Esperanca	SB18	323	Ohnishi, Nozomi	QE10	201
			Ohnishi, Tomohiro	PG13	144
			Ohno, H.	BE02, CG02, SH07	44, 53, 344
O' Farrell, Eoin	HA05	84	Ohno, Hideo	BI02, HP52, QP14, SI17	47, 31, 247, 348
O' Farrell, Eoin T. C.	CD02	51	Ohno, Masumi	QF10	205
O'farrell, Eoin	SF07	338	Ohno, T.	SG02	339
Obi, Yoshihisa	SE06	334	Ohno, Takahisa	RF07	270
Obry, Bjoern	SI15	348	Ohno, Takashi	QF24	207
Obry, Bjorn	HD01	85	Ohno, Y.	CG02	53
Ochai, Akira	QD11	198	Ohnuma, Shigehiro	JI01, SL04	105, 356
Ochiai, Akira	QJ08	222	Ohoyama, Kenji	QG18, RP01	211, 303
Ochoa, Martha Teresita	QO26	245	Ohsawa, Takashi	BI02	47
Oda, Migaku	PB08	121	Ohsuka, T	PC04	127
Oda, Tatsuki	AE02, PL06, RC02, RL02	36, 164, 259, 290	Ohsumi, Hiroyuki	IA04, QO13	91, 242
Odkhuu, Doji	QO23	244	Ohta, Hitoshi	KI05, PE11, QE03, QE10, QF04, RD01, RP05, RP09, RP19	113, 137, 199, 201, 204, 262, 304, 306
Odkhuu, Dorj	KI01	112			
Oezelt, Harald	DE01	59	Ohta, Tsuyoshi	QI04	218
O'farrell, Eoin Conor	QD01	196	Ohta, Yukinori	KG03, PF09, PF10, PF12, PF14, PF15, RE08, RF03, SF04	111, 140, 141, 267, 269, 337
Ogata, Masao	SE04	333			
Ogawa, Daisuke	EJ01, RO05, RO06	71, 301	Ohtake, Mitsuru	ED01, PM18, SM15	66, 170, 363
Ogawa, Satoru	SG18	342	Ohtani, H.	QH09	214
Ogita, Norio	PC05, PG16, RD10, SG15	127, 145, 263, 342	Ohtani, Hiroshi	QH10	214
			Ohtani, Taiki	SM15	363
Ognev, Alexey	AG05, QM05	38, 232	Ohtomo, Manabu	BH05, BH06	46, 47
Ogrin, Feodor Y.	RK20	289	Ohtori, Hiroyuki	RA09	250
Oguchi, Tamio	EC03	65	Ohuchi, Syuya	PI22	154
Oguri, Akira	PE16	138	Ohya, Masahiro	PD08	133
Ogusu, Hiroki	PC17	129	Ohzuku, Tsutomu	PO17	180
Oh, Hangdeok	PO04	177	Oikawa, Hiroto	EI05	71
Oh, Hyungju	RB16	256	Oka, Kengo	RA06	250
Oh, Ok Kyun	QN17	239	Oka, Kunihiko	QA05, QA07, QA09, RH11	183, 184, 276
Oh, S.	SB28	324			
Oh, S. H.	SA06	317	Oka, Takahi	RI14	281
Oh, Sang-soo	QM22	235	Oka, Takashi	EB02, HI05	65, 89
Oh, Se-jung	GF05	79	Oka, Toshihide	QB11	188
Oh, Seol Hee	SA05	317	Okabe, Hirotaka	PC21, SF02	130, 337
Oh, Seung-lim	RN20	300	Okada, Hironari	PG07, QH21	143, 216
Oh, Suhk Kun	SH01	343	Okada, Kyoko	SK13	352
Oh, Suhk-kun	QH01	213	Okada, Takuya	RI01	279
Oh, Sunjong	QO19	243	Okamoto, Hiroaki	RD06	263
Oh, Yoon Seok	JB02	99	Okamoto, J.	PL14	166
Oh, Young Kun	PB40	126	Okamoto, Kazuaki	KF05	111
Ohara, Jun	IJ05	98	Okamoto, Kiyomi	RI11	280
Ohara, S.	RD15	264	Okamoto, Yoshihiko	JA04, QE03, QE05, QE08, QE27, SG14	99, 199, 200, 203, 341
Ohara, Satoshi	RN11	298			
Ohara, Shigeo	QD17, RD18, RD20, SE11	199, 265, 335			

Okane, Tetsuo	RD25, SE23	266, 337	Orihashi, Hiroki	QH08, QN20	214, 239
Okawauchi, Yasuharu	SC13	327	Orii, Daisuke	PC21	130
Okazaki, K.	QB28	191	Orlov, Andrey F	PN22	175
Okazaki, Ryuji	PH12, QC06	148, 193	Ortega, Daniel	RN13	298
Oki, Soichiro	HE01	86	Ortiz, Christian	PJ29	159
Okita, Kazuhiko	RP11	305	Osakabe, Toyotaka	QI16	220
Okubo, Akinari	SK23	354	Osaki, Soichiro	SK33	355
Okubo, Kazuma	RP01	303	Oshikawa, Masaki	PF18, QF11, RI02	142, 205, 279
Okubo, S.	KI05	113	Oshino, Yuuki	SK21	353
Okubo, Susumu	QE03, QE10, QF04, RP05	199, 201, 204, 304	Oshiro, Morihito	QH14	215
Okuda, Mitsuhiro	KB01	107	Ostler, Thomas A.	RK17	288
Okuda, Taichi	KF05	111	Ota, Satoshi	PO03	177
Okuda, Tetsuji	RH04, SB24	275, 324	Ota, Y.	QB28	191
Okunishi, Kouichi	RI11	280	Otani, Yoshichika	HD04, HE03, HE05, ID04, RK11	85, 86, 93, 287
Okutomi, Yoshihito	CE05	52	Otsubo, Toru	QI10	219
Okuyama, Daisuke	PA12	117	Otsuka, Hiromi	JD06	101
Okuyama, Hiroaki	SG05	340	Otsuka, Shintaro	PO18	180
Oles, Andrzej	RG18	274	Otsuka, Yuichi	RG09	273
Olivetti, Elena Sonia	DG04	61	Otsuka, Yuto	QP09, QP10, QP11	246, 247
Omura, Kumiko	PI06	151	Ott, Hans Rudolf	IC02	92
Oner, Yildirhan	QG06, QJ15	209, 223	Ou, Z. Q.	SO16	369
Ong, Chin Shen	SL06	357	Ou, Zhiqiang	SO08	368
Ong, N. P.	AB04	34	Ouardi, S.	SK24	354
Onimaru, T	PC04	127	Ouardi, Siham	CH03, SD15	54, 332
Onimaru, Takahiro	EF01, PD24, RD04, SG12, SG15	68, 135, 262, 341, 342	Ouladdiaf, B.	RB17	256
Ono, Akiko	PC20, QJ07	130, 222	Ouladdiaf, Bachir	SB08	321
Ono, Hiroaki	QP20	248	Ouyang, Yuyu	AH04	38
Ono, Hiroshi	SK21	353	Ovchinnikov, Alexander	DF03	60
Ono, Shimpei	RL10	291	Ovchinnikov, Alexander Sasha	QG22	211
Ono, T.	RL07, SH07	291, 344	Ovchinnikov, S. G.	QK07	225
Ono, Teruo	GE05, HG02, RU02, RL10	79, 88, 282, 291	Oviedo Roa, Raul	SK15	352
Ono, Toshio	QE22	203	Owaki, Yasuhiro	PE15	138
Onoda, Shigeki	JD03	101	Oyamada, Akira	BC04, QE22	42, 203
Onodera, Hideya	QI10, QI16	219, 220	Ozawa, Kiyoshi	PH02	147
Onosaka, Atsushi	JA04	99	Ozawa, Tadashi C	SK04	351
Onuki, Yoshichika	HP11, PB27, PC28, PD08, PD13, PD16, QC03, QH03, RD11, RD25, RE10, SB15, SE23, SF03	30, 124, 131, 133, 134, 192, 213, 263, 266, 268, 322, 337	Ozdogan, K.	RP15	305
			Ozerov, M.	QF02, QF03	204
			P		
			P, D.	PC22	130
			P, Suresh	RA16	252
			P. D., Babu	QD04	197
			P. Del Real, Rafael	GG04	80
			Padilla, Jessica	EC04	66
			Padilla-pantoja, Jessica	RA17	252
			Paglione, J.	QB07	188
			Pagliuso, Pascoal	SE22	336
			Pagliuso, Pascoal G.	SE15	335
			Pal, A	QM24	235
			Pal, Semanti	HD04, RK11	85, 287
			Palacio, Fernando	KB06, PG22, QO16	108, 146, 243
			Pal'chik, Marina	SM19	364
			Palm, Eric	GJ02	82
			Palstra, T.t.m	PH17	149
			Pan, M.x.	RO14	303
			Pan, Minxiang	RO13, RO15	302, 303
			Pan, Rui	SN01	364
			Pan, Wei	ED02, SN11	66, 366
			Pandey, Srikrishna	PJ32	160

Pandey, Sudhakar	PF19	142	Park, Sungyu	PC25	130
Pandiyan, Manoj	DH03	62	Park, Tae-eon	SL26	360
Panholzer, Martin	RG15	274	Park, Tuson	FB01, PC19, SE02	73, 129, 333
Panigrahi, B. K.	PN01	172	Park, W. K.	GA01	75
Pankrats, A	QJ16	223	Park, Wan Kyu	RD09	263
Pankrats, Anatolii	IJ01	97	Park, Wongoo	GF05	79
Paolasini, Luigi	AF01	36	Park, Yeonjoo	PB18, PB37, PB39, PB40	123, 126
Papaioannou, Evangelos	AF05	37	Park, Youn Ho	QK11	225
Parakkat, Vineeth Mohanan	QM03, SJ08, SL23	232, 350, 359	Park, Young Woo	QN15, QN17	238, 239
Pardo, J. A.	KC05, PJ23	109, 158	Park, Young-woo	QN07	237
Pareek, S. P.	SL25	360	Park, Younho	SL26	360
Park, B.-g.	PG11, QA04	144, 183	Park, Youn-ho	RL03	290
Park, Byong-guk	IF01	94	Park, Yu Seop	RR04	311
Park, Chan Woo	RL21	293	Parker, Dinah. R.	QG19	211
Park, Chang-yup	RL03, SM12	290, 362	Parker, G.	BG02	45
Park, D.g	HH03	88	Parke, Duncan E	SH09	344
Park, D.g.	PM07, PO05, RQ04, SK17	168, 178, 307, 353	Parkin, Stuart	HP41	31
			Parkin, Stuart S. P.	SM01	361
			Parkin, Stuart S.p.	RK22	289
Park, Dong-soo	DJ02	63	Parreiras, Sofia De Oliveira	RJ12	284
Park, Eunsung	SE02	333	Parwanta, Kadek J.	QL09	229
Park, Gwan Soo	QN04, QN05, QP04, RR07	237, 246, 312	Parwanta, Kadek Juliana	RA21	252
			Pascarelli, Sakura	RH23	278
			Paschen, S.	CD01, SF10	50, 338
Park, Gwang-seo	QO10	242	Pascua, Gwendolyne	PI05, PI17, QB22, QJ03	151, 153, 190, 221
Park, Gwansoo	SN07	365	Pascual, Jose Ignacio	PG08	143
Park, H. L.	PM26	171	Pashkevich, Yurii G.	QJ03	221
Park, Hae Jung	QN07, QN17	237, 239	Pashkin, Alexej	HA02	83
Park, Hee Yeon	SB22	323	Pasquale, Massimo	DG04	61
Park, Insuk	QB25	191	Passamani, Edson Caetano	QM15	234
Park, Insung	PJ16, PK10, PK17	157, 162, 163	Paszkwicz, Wojciech	DD02	58
Park, J.- G.	PG24	146	Patel, Sheena K. K.	PK09, QM01	161, 231
Park, J. H.	IA05	91	Pathak, Arjun Kumar	CH01	54
Park, J. K.	RP10	304	Patil, Sujata M.	QD16	199
Park, J. M. S.	PH03	147	Patil, Swapnil	PE14	138
Park, J. S.	RA07	250	Patlagan, L.	PD03	132
Park, J.-h.	PH10	148	Patoary, M. Atiqur R.	PB24, PF05	124, 140
Park, Jae - Hyun	RB14	256	Patra, Ajit K	QK14	226
Park, Jae Hyun	CE04	52	Patrin, Gennady	PJ27, SM19, SO28	159, 364, 371
Park, Jae Y.	CJ03	55	Patrin, Konstantin	PJ27, SM19, SO28	159, 364, 371
Park, Jae-hoon	AA01, AF04, JB02	33, 37, 99	Patthey, L.	PC01	126
Park, Jae-hyuk	PN14	174	Patthey, Luc	PD12	133
Park, Je Geun	HJ01	89	Paudyal, Durga	IJ01	106
Park, Je-geun	GF05, PI10, RA22	79, 152, 253	Paulose, P. L.	PC11, QD16	128, 199
Park, Jewook	RC14	261	Paulose, P.I.	QB14	189
Park, Ji Hun	PN20, PN21	175	Pautrat, Alain	DG02, EH03	61, 70
Park, Jihoon	JH04, KH04	104, 112	Pavlova, Ekaterina	SG17	342
Park, Jin-hong	DF01	60	Pavlukhina, Oksana	PI20	154
Park, Jong C.	CJ03	55	Pecharsky, Vitalij	IJ01	106
Park, Joonbum	SD07	331	Peddis, Davide	RN07	297
Park, Jun Kue	SI14	348	Pedersen, Bjoern	QH24	216
Park, Junghwan	PG24	146	Pedersen, Kasper Steen	BC02	42
Park, Ju-young	JB02	99	Pedrero, Louis	SF05	337
Park, Kwang-jun	PL11	165	Pedrero, Luis	AB02	34
Park, Lee-seul	SD14	332	Peets, Darren	IJ02	97
Park, Po Gyu	RQ07	308	Pei, Wenli	SN10	365
Park, San Youn	QA16	185	Peiro, Julian	AI04, CG03	39, 53
Park, Sang Kook	SB22	323	Pelegrini, Fernando	PL09, QM14, QM15	165, 233, 234
Park, Seonghun	AF04	37	Pelennnen, Anatolij P.	SO19	369
Park, Seung-youn	CE04, HF05, RL06	52, 87, 290	Pelevin, Ivan	SN09	365
Park, Sungkyun	QM18, QM20	234			
Park, Sungmin	QO10	242			

Pena, Luis	IH01, SO18	95, 369	Pisana, S.	BG02	45
Pena, Octavio	QA06	183	Piskunova, Nataly Ivanovna	PF01	139
Penaranda-foix, F L	RQ10	308	Pistora, Jaromir	CH03, QH19	54, 216
Penaranda-foix, Felipe L	RO08	302	Pitcher, Michael. J.	QG19	211
Pepe, Giulio	IJ03	97	Pizzini, Stefania	RL24, SH03, SH05, SH06	293, 343, 344
Pepin, Catherine	PD04	132	Plazaola, Fernando	QH16, RN13	215, 298
Peprah, Marcus K.	KB03	107	Pleiderer, Christian	QC17	195
Peratheepan, P	SE03, SE05	333, 334	Plumb, N. C.	PC01	126
Pereira, Andre M	SO31	371	Poddar, Asok	RB15	256
Perez - Mato, Juan Manuel	PA13	118	Podgornykh, S. Mikhailovich	PC07	127
Perez, Nicolas	RN14	299	Podolskii, Vitaliy	SG17	342
Perez, Olivier	EH03	70	Pogorelov, Yu. G.	KC05	109
Perkert, Sandra	AG04	38	Pogossian, Souren P	SA24	320
Perov, Nikolai	CH01, PN22, QO14	54, 175, 243	Poienar, Maria	JB05, RA11	100, 251
Perring, Toby G.	HA04	83	Pokharel, Ramesh K.	PJ01	154
Perry, Robin	EA04	64	Polak, Christian	PM04	168
Persson, Jrg	QA23	186	Politi, Paolo	KE01	110
Perucchi, Andrea	SA08	317	Polyakov, Andrey	PD05	132
Peters, Robert	DB05	57	Polyakov, Victor	SO28	371
Peterson, Joe	RE09	267	Polyakova, Klaudia	SO28	371
Petit, S.	QF18	206	Pomar, Alberto	SO18	369
Petit, Sylvain	AA03, DD05, JB05, RA11	33, 59, 100, 251	Pomjakushin, Vladimir	PI05, PO17	151, 180
Petrakovskii, G. A.	SG20	342	Pomjakushin, Vladimir Yu.	PH02	147
Petrenko, O. A.	CC04	50	Pomjakushina, E.	QF23	207
Petrenko, Oleg A	BF03	45	Pomjakushina, Ekaterina	IJ06, PI21, PO17	98, 154, 180
Petrenko, Oleg A.	GF03	79	Pong, W. F.	PB12	122
Petrova, Elena A	PN22	175	Ponomaryov, A. N.	QF13	206
Petrovic, C.	QC23	196	Ponomaryov, Alexey	RP13	305
Petti, Daniela	AI03	39	Pons, Stephane	SE08	334
Petzold, Vivien	QD07	197	Pop, Viorel	EJ03	72
Pfleiderer, C.	PI09	152	Popkov, Sergei	PI11	152
Pfleiderer, Christian	DF02, GC04, QH12, QH24, SF05	60, 77, 214, 216, 337	Popova, Marina N.	PA20, RA24	119, 253
Pham, Duc-thang	RA10	251	Porer, Michael	HA02	83
Pham, Huyen-yen	SO12	368	Portemont, Celine	AI04	39
Pham, Huyen-yen Duc	RA10	251	Porter, Daniel Graham	DH03	62
Pham, Thang D.	QL16	230	Pospisil, Jiri	HJ04, PC10, QC21, QJ02	90, 128, 195, 221
Pham, The-tan	SO12	368	Postava, Kamil	CH03	54
Pham, Van-ben	SG10	341	Potapova, Nadezhda M.	DF04	60
Phan, Huong Manh	RN19	299	Potthoff, Michael	PE05, PE07	136, 137
Phan, Manh-huong	DJ01	63	Poudyal, Narayan	EJ02	71
Phan, T. L.	RA01	249	Pouget, Stephanie	EI04	71
Phase, D.m	SA14	318	Poulopoulos, Panagiotis	RP15	305
Philip, Geo George	SL28	360	Pourovskii, Leonid	AB04	34
Phillip, Geo George	QA25	186	Prabhakaran, D.	DH03, PI03, QN01	62, 151, 236
Phillips, P.	GA01	75	Prabhakaran, Dharmalingam	AF01	36
Phromsuwan, Udomchok	RP18	306	Pradhan, N. S.	PN01	172
Piamonteze, Cinthia	BC02	42	Pramuji, Hinu	BJ03	48
Piantek, Marten	PG08	143	Prasad, Arun S.	SL25	360
Piao, Hong-guang	SH01, SH10	343, 344	Praveena, K	GJ05, QN18, SN08	83, 239, 365
Picone, Andrea	PL21	167	Prchal, J.	RD26	266
Picozzi, Silvia	AA02, PA12	33, 117	Prchal, Jiri	BB04, PD18, PD19, QJ14	42, 134, 135, 223
Pietosa, Jaroslaw	QB30	192	Prestat, Eric	AI04	39
Pikul, Adam	QD05	197	Prestigiacomo, Joseph	CH01	54
Pikul, Valeriy	RR28	315	Prevost, B.	PD05	132
Piligkos, Stergios	BC02	42	Prida, Victor	DG03	61
Pineider, Francesco	CB04, SI11	49, 347	Prieto, Pedro	SA12	318
Piquini, Lucas K.	QO03	241	Primo, Fernando Lucas	PO08	178
Pirmohammadi, Mohsen	RR32	316	Prinsloo, Aletta Roletta	RH15	277
Pirogov, Alexander	QG02	208	Pristas, Gabriel	QD12, QI02, RE13	198, 218, 268
			Profeta, Gianni	QG25	212

Proglyado, Vladimir V.	SK01	350	Ramakrishnan, S.	QB14	189
Proglyado, Vyacheslav	SK02	350	Ramanathan, Mahendiran	QA18	185
Prokes, Karel	QG26, RB01, RB07, RB17, RQ21	212, 254, 255, 256, 310	Ramanujan, Raju V	QL02	228
Prokhnenko, O.	RQ21	310	Ramasamy, Shivaraman	PO21	180
Prokleska, Jan	BB04, HJ04, PC10, QC21, QJ02, SB08	42, 90, 128, 195, 221, 321	Ramaswamy, Shivaraman	PO24, QN26, QP24, SA21, SA22, SA23, SK32, SL28	181, 240, 249, 319, 320, 355, 360
Prokofiev, A.	CD01	50	Ramesh, Palanisamy	PN16	174
Prokscha, Thomas	PB20, PN23, QL19	123, 175, 231	Ramos, Scheilla Maria	SE22	336
Proselkov, O.	BE02	44	Ramulu, T.s.	SL22	359
Proselkov, Oleg	DD02	58	Ran, S.	GA01	75
Proshin, Yurii N.	QA26, SC25, SC26	186, 329	Rana, Bivas	RK11	287
Proshkin, Alexey	QG04	208	Rangappa, Dinesh	RN11	298
Proshkin, Alexey V.	QI08	219	Rani, Manju	SC02	325
Proskurin, Igor	DF03	60	Ranjan, Vishal	GI05	82
Proskurina, Ekaterina	QG04	208	Ranjbar, Fereshte	RN22	300
Protsenko, I E	RN12	298	Ranot, Mahipal	SB28	324
Prozorov, R.	IA05, QC23, SB30	91, 196, 325	Ranzieri, P.	AG02	37
Prsa, Krunoslav	PI06, QF20, QF23, SE08	151, 207, 334	Rao, G.s.n.	BJ05	48
Prudnikov, Valerii	CH01	54	Rao, Siddharth	PJ08, SI02	156, 346
Pruschke, Thomas	FE03, PE03	75, 136	Rashad, Mohamed M.	RN01	296
Przybylski, Marek	AD02, AE01, EI01	35, 70	Rasing, Theo	GD01, RK17	77, 288
Przyslupski, Piotr	QM17	234	Rasly, M.	RN01	296
Puente Orench, Ines	KB06	108	Rawat, Rajdeep Singh	PN03, QL02	172, 228
Puente-orench, Ines	JU04	106	Ray, R.	PL07	165
Pujari, P K	PM01	167	Raychaudhuri, Arup Kumar	HD04	85
Pureur, Paulo	PB09, PB10, PB33, PG03, RB09	121, 125, 142, 255	Razzoli, E.	PC01	126
Putri, Witha B. K.	PB03	120	Rebizant, Jean	SE19	336
Puzniak, Roman	QB30, SB26	192, 324	Reddy, Leelakrishna	RH15	277
Pyshkin, Pavel V	PJ02	155	Redinger, Josef	EF05	68
			Regnat, Alexander	QC17, QH24	195, 216
			Regnault, L. P.	QE19	202
			Reichel, Franz	DE01	59
			Reichlova, Helena	BE05	44
			Reiffers, Marian	QC13, QD08, QD12, QI02, RD21	194, 197, 198, 218, 265
			Reimann, Tommy	SM02	361
			Reiner, J.	BG02	45
			Reisner, G. M.	PD03	132
			Reiss, Gunter	IF04	94
			Reissner, Michael	QH18, RB08	215, 255
			Ren, Chung-yuan	QE25	203
			Ren, Wei	QA27	187
			Ren, Xiaobing	JJ02, PG21	106, 145
			Ren, Zhi	RC11	260
			Repaka, D V Maheswar	QA18	185
			Repi, V. Vekky R.	QN16	239
			Ressouche, Eric	IJ03, IJ06, PA13	97, 98, 118
			Reyes, Arneil P.	JA02	98
			Reyren, Nicolas	HE04	86
			Rezania, Hamed	QF12	205
			Rhee, Chan Hyuk	PI13	152
			Rhee, J. Y.	SL08, SL09	357
			Rhee, Jang-rho	PL11	165
			Rhee, Joo Yull	QH29, SC08	217, 326
			Rhie, K.	PJ31	159
			Rhie, Kungwon	PK21, QK10	163, 225
			Rhie, Kung-won	SD12	332
			Rhim, Sonny S. H.	RB26	258
			Rho, Min-suk	BH02	46
Q					
Qamar Ul Hassan, Syed	SA15	318			
Qian, Bin	RB12	256			
Qiu, Xue Peng	BD05	43			
Qiu, Xuepeng	PJ20, PJ21, RL19	158, 293			
Qiu, Z. Q.	IH05	96			
Qiu, Z.-q.	BD03, QM26	43, 235			
Quan, Zhiyong	PN04	172			
Quang, Pham Hong	SL22	359			
Quang, Tran Van	RH20	278			
Quintanilla, Jorge	JA05	99			
Quintero-castro, Diana	RH24	278			
Quitmann, Christoph	RJ11	284			
Qureshi, Navid	PI08	152			
R					
R, Ramasamy	PO21, QN26	180, 240			
Raabe, Joerg	RJ11	284			
Radaelli, Greta	DE03	59			
Radovic, M.	PC01	126			
Radu, Florin	EC04	66			
Rafique, Mohsin	SA15	318			
Rafiqul Islam, Md.	RN05	297			
Raghavender, A T	SM07	362			
Raghavender, Anupati Telugu	SM10	362			
Rahman, Gul	RM02	295			
Rajan, Ganesh K	SK32	355			
Raju, M	PG27	146			

Rhyee, Jong- Soo	RC05	259	Ross, Caroline A	HP51	31
Rhyee, Jong-soo	CF03	52	Ross, Caroline A.	KC01	108
Ri, Hyeong-cheol	SB22	323	Roßner, Helge	FB04	73
Ribeiro, Andre Neves	PF13	141	Roth, Georg	PA14, RP22	118, 306
Ribeiro, B.	QM13	233	Roth, Thomas	HG04, PA24, RH23	88, 119, 278
Ribeiro, Raquel A	SL20	359	Rother, Niklas	PE05	136
Ribeiro, Raquel A.	QO03	241	Rothman, Johan	DD01	58
Richter, Curt A.	AE04	36	Rotter, Martin	PH04	147
Rijnders, Guus	DH02, SA10	62, 317	Rougemaille, Nicolas	SH03, SH05, SH06	343, 344
Rikken, Geert	RQ16	309	Roulland, F.	SA06	317
Rinaldi, Christian	AI03	39	Roulland, Francois	SA05	317
Riseborough, Peter S	PD02, PE01	132, 136	Rouquette, Jerome	RA11	251
Ritter, C	QJ16	223	Rovezzi, Mauro	BE03	44
Ritter, Clemens	IJ01	97	Rovira, Joan Josep Roa	PB11, SB18	121, 323
Ritter, Franz	QE14	201	Rowley, Stephen	AB04	34
Ritz, Robert	GC04	77	Roy, Beas	QE12	201
Ritzmann, Ulrike	FA02	72	Roy, M.	PN01, RA03	172, 249
Riva, Michele	PL21	167	Roy, Pierre	IE03	93
Rivas, J.	CB02	49	Rubacheva, Anastasia D	PN22	175
Riyadi, Syarif	PH17	149	Ruben, Mario	GH02	81
Rizal, Conrad	PI01	154	Ruck, Michael	PC27	131
Rizki, Youssef	BB03, RH22	41, 278	Rudajevova, Alexandra	PD18	134
Rizwan, Syed	SA19, SA20	319	Rueffer, Rudolf	HG04	88
Robert, Julien	JB05, RA11	100, 251	Ruegg, Ch	RI05	279
Rodionov, Igor	CH01	54	Ruegg, Ch.	QE19	202
Rodionova, Valeria	AJ02, DD04, SO04, SO27	40, 59, 367, 371	Ruegg, Christian	IC02, QF23, QG14	92, 207, 210
Rodmacq, Bernard	BD02	43	Rufinus, Jeffrey	SK25	354
Rodriguez Fernandez, J.	GH05	81	Rugi, Francesco	CB04	49
Rodriguez Fernandez, Jesus	JJ04	106	Rui, Wenbing	PL01	164
Rodriguez, Luis Alfredo	DG05, GG05, SM16	61, 80, 363	Ruotolo, Antonio	DH04, RJ03	62, 283
Rodriguez-blanco, Clara	GF04	79	Rusek, Pawel	RI08	280
R. velamazan, Jose Alberto	GF04, PG22	79, 146	Rusek, Pawel	QE24	203
Roehlsberger, Ralf	QM19	234	Rushforth, Andrew W	SH09	344
Roemer, Florian	RP08	304	Rusponi, Stefano	BC02	42
Roessler, Sahana	PH04	147	Rusu, Calin	SE08	334
Rogalev, A.	QG07	209	Ruzicka, Jiri	BH03	46
Rogalev, Andrei	PA08, RP15, RP21	117, 305, 306	Ryabinkina, Ludmila	QG05	209
Rogalev, Andrey	PN22	175	Ryll, H	RI05	279
Roger, Michel	DH03	62	Ryoichi, Ito	RP06	304
Rogl, Peter	SC01	325	Ryu, Jisu	HP21, KE03, PJ33	30, 110, 160
Rojas Sanchez, Juan-carlos	QK16, QK17, SL24	226, 360	Ryu, Junggho	DJ02	63
Rojas, D. P.	QD10	198	Ryu, Kwang-su	SM01	361
Rojas, Juan-carlos	AI04	39	Ryzhov, V. A.	RQ13	309
Rojas-sanchez, Juan Carlos	QK15, RL24	226, 293			
Rokkaku, Tsugumi	QG13	210	S		
Romanov, A	BH01	46	S, Anuraj	SA21	319
Romanova, Oksana	QG05	209	S, Radha	RN16, SO22	299, 370
Ronning, F	EA03	64	S, Srinath	QD04, RA16	197, 252
Ronning, F.	FB01, QB12	73, 189	S. Suzuki, Hiroyuki	QD18	199
Ronning, Filip	RD09, SB12, SC16	263, 322, 328	Saadaoui, Hassan	PB20, QL19	123, 231
Ronnow, H.	SF10	338	Sablina, Klara	PI11	152
Ronnow, Henrik M	QF23	207	Sabyasachi, Sk.	RH02	275
Ronnow, Henrik Moodysson	IC02	92	Sachdev, Subir	IA03	91
Rosales Rivera, Andres	SM04	361	Sacramento, Pedro	RB25	258
Rosch, Achim	DF02	60	Sacramento, Pedro D	SB21	323
Roshanmehr, M.	PI24	154	Sacuto, Alain	PD17	134
Roshchin, I. V.	BD01	43	Sadhana, K	GJ05, QN18, SN08	83, 239, 365
Roslyakov, Ilya	SL27	360	Sadowski, J.	BE02	44
Rosner, H.	QF22	207	Saeed, Yasir	QO01	240
Rosner, Helge	AB02, QD07, RD12	34, 197, 264	Saenz De Pipaon, Cristina	PG22, QO16	146, 243

Safaeizadeh, Elham	PO27, PO29	181, 182	Sakuma, Akimasa	CH02, KH02, PJ10, PL17, RL09, SI06	54, 112, 156, 166, 291, 346
Sagar, J.	SK03	350	Sakuma, Keita	PB34, PJ12, SA07	125, 156, 317
Sagar, James	SK11	352	Sakurada, T.	SG11	341
Sagara, Naoto	QP16	248	Sakurada, Takashi	JJ04	105
Sagawa, Harunobu	SC24	329	Sakurai, Hiroshi	PK12, PM02	162, 167
Sagayama, Hajime	PG14, PG20, QA13	144, 145, 175	Sakurai, Hiroya	PH19, RH06	150, 275
Saha, S. R.	QB07	188	Sakurai, Hiroyuki	QP15, QP16	247, 248
Saha, Susmita	HD04	85	Sakurai, Shohei	RH09	276
Sahadev, Nishaina	SC06	326	Sakurai, T.	KI05, SL14	113, 358
Sahadevan, Ajeesh	GE03	78	Sakurai, Takahiro	PE11, QE03, QE10, QF04, RD01, RP05	137, 199, 201, 204, 262, 304
Sahadevan, Ajeesh M	SK05	351	Sakurai, Yoshiharu	BA04, PG05, PG13, PK12, SK04	41, 143, 144, 162, 351
Sahashi, Masashi	CE05, PJ11, PL10, SM03	52, 156, 165, 361	Sakurai, Yoshiki	SB03	320
Sahoo, Roshnee	QH06	213	Salamakha, Leonid	SC01	325
Sahu, Subrata Kumar	BH04	46	Salamati, H.	PI23, PI24	154
Saidaoui, H. B. Mohamed	PJ13	156	Salamom, M. B.	QB12	189
Saiga, Yuta	RE04	267	Salazar Mejia, Catalina	QO09	242
Saikai, Nobutaka	PB08	121	Salazar, Nicolas Antonio	SM04	361
Saiki, Shunsuke	QB04, RB02	187, 254	Salce, Bernard	PC17	129
Saines, Paul	PC02	127	Salles, B.	CE06	52
Saini, Naurang L.	RB28	258	Salman, Zaher	BC02, PB20, PN23, QL19	42, 123, 175, 231
Saisho, Seiya	RN03	297	Salvador, M D	RQ10	308
Saito, Hidekazu	AI05	39	Samant, Mahesh	RN16	299
Saito, Hitoshi	RP06	304	Samanta, Tapas	CH01	54
Saito, Kesami	KC03	108	Samardak, Alexander	AG05	38
Saito, Kotaro	RD14	264	Samardak, A. Sergeevich	QM05	232
Saito, Mineo	RC09, RC19	260, 262	Samarin, N. A.	QC22, RH07	195, 275
Saito, Mitsuru	QA17	185	Samarin, Nickolay	ED06, KI05, SG08	67, 113, 340
Saito, T.	QB28	191	Samariya, Arvind	SL25	360
Saito, Takahito	QC05	193	Samata, Hiroaki	SK04	351
Saito, Takashi	PE13, QC05	138, 193	Sampaio, Joao	HF01, IE04	87, 94
Saito, Takeshi	PD11	133	Sampaio, Maria	RF13	271
Saito, Taku	QB02, QB15	187, 189	Sampathkumaran, E V	PE14	138
Saito, Toshiaki	QE20, QF21	202, 207	Sampathkumaran, E. V.	QD16	199
Saitoh, Eiji	AI02, FA01, KF03, RL15	39, 72, 111, 292	Sanada, Naoyuki	SC23	329
Saitoh, Yuji	RD25, SE23	266, 337	Sanai, Tatsunori	KF05	111
Sakaguchi, Jyunya	PD13	134	Sanchez Llamazares, Jose Luis	JJ04	106
Sakaguchi, Yui	RD13	264	Sanchez Marcos, Jorge	JJ04	106
Sakai, Akito	CD02, SE01, SF07	51, 333, 338	Sanchez-costa, Jose	GF04	79
Sakai, Eijiro	QC14, QC15	194	Sanda, Minoru	PG17, QF11, QF14	145, 205, 206
Sakai, Hideaki	PA12	117	Sandalov, Vladimir	RR28	315
Sakai, Hironori	IG04, PD09, RD11	95, 133, 263	Sandig, Oliver	RP08	304
Sakai, Junya	QL11	229	Sandiumenge, Felip	IH01, SO18	95, 369
Sakai, Naoki	QL03	228	Sando, Daniel	QA27	187
Sakai, Osamu	PH02	147	Sangregorio, Claudio	CB04, SI11	49, 347
Sakai, Seiji	BH05, BH06, QL15	46, 47, 230	Santamaria, Jesus	RN09	298
Sakai, T^oru	QE11	201	Santava, Eva	QI01	217
Sakai, Toru	QE07, RI11, RI16	200, 280, 281	Santos, Tiffany	AD03, BG02	35, 45
Sakai, Yoshiki	RO06	301	Sarachik, Myriam P.	IC01	92
Sakaïda, Masaru	PF16	141	Sarkar, Sujit	QF26	208
Sakakibara, T.	CD01, EF01	50, 68	Sarma, D. D.	RF12	270
Sakakibara, Toshiro	CC05, QE13, QH03, QJ08	50, 201, 213, 222	Sarrao, John L.	RD09	263
Sakamoto, Hirotoshi	HC03	85	Saruya, Takeshi	KF01	110
Sakamoto, Naonori	KC02	108	Sasagawa, Takao	QO18	243
Sakamoto, Yasutaka	SG09	341	Sasaki, Hiroko	SG18	342
Sakano, Rui	PE16	138	Sasaki, Hiromi	SL02	356
Sakata, Masafumi	PC21	130	Sasaki, N.	CF04	53
Sakata, T.	PL04	164	Sasaki, Ryo	SE11	335
Sakoda, Masahito	PE13, RD01	138, 262			
Sakshath, Sadashivaiah	SL21	359			

Sasaki, Satoru	GB04	76	Schafer, Hanjo	HA02	83
Sasaki, Satoshi	RC11	260	Schafers, Markus	IF04	94
Sasaki, Takahiko	GB04, RH03, RH11	76, 275, 276	Schalenbach, Maximilian	QA22	186
Sasano, Masashi	PN07	173	Schau-magnussen, Magnus	BC02	42
Saso, Tetsuro	PF17	142	Schedler, Roland	QG02	208
Sassa, Y.	PC29, PI15	131, 153	Scheffer, Jurg	PA04	116
Sassa, Yasmine	HA03, SE08	83, 334	Schellhas, Laura	QA15	185
Sasso, Carlo Paolo	DG04, HH01	61, 88	Schellekens, Adrianus	EI06	71
Sato, Hideo	QP14, SI17	247, 348	Schellekens, Sjors	SI07	347
Sato, Hideyuki	PE13, QC05, RD17	138, 193, 264	Schepotin, I	BH01	46
Sato, Hirohiko	QE17, QF09	202, 205	Schierle, E.	PC22	130
Sato, Hitoshi	RD20	265	Schlage, Kai	QM19	234
Sato, Kazuhisa	KB05	108	Schlenhoff, Anika	HF03, HF04, RP16	87, 305
Sato, Kazunori	KF04	111	Schlom, Darrell G	SA08	317
Sato, Kei	RL13	292	Schlottmann, Pedro	KA04, PA21, PE04	107, 119, 136
Sato, Kentaro	PB29, PB30, PB32	124, 125	Schmalzl, Karin	AA05, QM02	33, 231
Sato, Kiyoo	QI04	218	Schmidiger, David Jan	CC03	50
Sato, Koichi	RN11	298	Schmidt, Burkhard	DB02, QE04	57, 200
Sato, Kota	SB05	321	Schmidt, Michael	PA23, RH24	119, 278
Sato, Kotaro	SN03	364	Schmidt, Oliver G	SJ07	350
Sato, Masahiro	JD04, RI11	101, 280	Schmidt, Rene	AF02, HG03, PG12	36, 88, 144
Sato, Masatoshi	DA01, QB04, QB26, RB02, RB05	56, 187, 191, 254	Schmidt, Wolfgang	QM02	231
			Schmiedeshoff, G. M.	IA05	91
Sato, Mitsuhide	QF08, QF10	205	Schmitt, T.	PC01	126
Sato, Mototsugu	QJ04	221	Schmitt, Thorsten	BA03	41
Sato, Nana	SI08	347	Schmitz, Defleft	IH01	95
Sato, Noriaki	PD20	135	Schneidewind, Astrid	QC24	196
Sato, Noriaki K	RD05	262	Schnelle, Frank	QJ11	222
Sato, Noriaki K.	PD14	134	Schnelle, Walter	RD12	264
Sato, Suguru	SJ06	349	Schoenemann, Rico	PC27	131
Sato, Taku J	QE13	201	Schoenhense, G	QM12, RN12, RP20	233, 298, 306
Sato, Tetsuya	RK08, SM20	287, 364	Schon, Gerd	II04	97
Sato, Tomonori	HG02, RJ01, RJ02, RJ09	88, 282, 284	Schonhense, Gerd	CH04	54
Sato, Yoshiaki	SG09	341	Schotter, Joerg	AH01	38
Sato, Yuji	PL10	165	Schrefl, Thomas	DE01	59
Satoh, Isamu	RD05	262	Schreyer, Andreas	DG01, QM02	61, 231
Satoh, Ryohei	RD24	266	Schrittwieser, Stefan	AH01	38
Satter, A. A.	RN01	296	Schroeder, Henning	KD01	109
Savero-torres, Williams	GE01, QK15, QK16, QK17, SL24	78, 226, 360	Schroeder, Silke	IH02	96
			Schuller, Ivan K	BD01	43
Savici, Andrei T	PI07	151	Schuller, Ivan K.	BD04, ED03	43, 66
Savici, Andrei T.	RD14	264	Schvets, I V	PH16	149
Sawa, A.	PL14	166	Schwabe, Andrej	PE05, PE07	136, 137
Sawa, H.	CF01	52	Schwarz, Alexander	AF02, HG03, PG12	36, 88, 144
Sawada, Kazuya	SM03	361	Schwarz, Karlheinz	RB21	257
Sawada, Keisuke	RC19	262	Schwarzacher, Walther	KB01	107
Sawada, M.	PH14	149	Schweitzer, Dieter	SG19	342
Sawada, Masahiro	PN20	175	Schweitzer, Sebastian	QK14	226
Sawami, Kazuma	QJ12	222	Schwingenschlogl, U.	PN02	172
Sawamura, M.	KJ01	113	Schwingenschlogl, Udo	QL17, QO01, QP01, QP02, SK12	230, 240, 245, 352
Sawatzki, Simon	KH01	112			
Sawicki, M.	BE02	44	Schwobel, Jorg	GH02	81
Sawicki, Maciej	BE03, DD02	44, 58	Sebastian, S. E.	GA01	75
Sayanagi, Richard	PK09, QM01	161, 231	Sebastian, Suchitra	BA01	40
Sazonov, Andrew	PA14	118	Sebt, S. A.	QP23	249
Schaadt, Daniel M.	QL05	228	Sechovsky, Vladimir	BB04, HJ04, PC10, PD18, PD19, QC21, QJ02, QJ14	42, 90, 128, 134, 135, 195, 221, 223
Schaefer, R.	PM26	171			
Schaefer, Rudolf	HB01	84	Sedlak, Kamil	AB02	34
Schaf, Jacob	PB09, PB10, PB11, PB33, RB09, SB18	121, 125, 255, 323	Segal, Amir	DE02	59
			Segawa, Kouji	RC11	260

Seike, Masayoshi	KF04	111	Shaofeng, Lin	QO21	244
Seiro, Silvia	QC09, QC18, QD07	193, 195, 197	Sharbaf Zadeh, Asghar	PC16	129
Seki, Harumi	PC15	129	Sharma, A. K	QN14	238
Seki, Kazuhiro	PF09, PF14, RE08	140, 141, 267	Sharma, Bharat Kumar	KI01	112
Seki, S.	RA05	250	Sharma, Neetika	PI12	152
Seki, Takeshi	JG03, KC03	103, 108	Sharma, P. K.	SL25	360
Sekiguchi, Koji	RJ10, SI08	284, 347	Sharma, Sandeep	AI05	39
Sekiguchi, Toru	RD22	265	Shavrov, Vladimir G.	SO19	369
Sekimoto, S.	KJ01	113	Shavrov, Vladimir Grigor'evich	QH17	215
Sekine, Akihiko	GB02	76	Shaw, C.c.	SN06	365
Sekine, Chihiro	PD10, PD11, PD22, QD06	133, 135, 197	Shaykhtudinov, Kirill	QA08	183
			She, Jian-huang	SE18	336
Sekine, Tomoyuki	PA19, QA05, QA07, QA09, RH11	119, 183, 184, 276	Sheikhzadeh, G. A.	PO27, PO29, PO30, PO31	181, 182
Sekiyama, Akira	RD25	266	Sheikin, I.	GCO1	77
Sela, Eran	RI12	280	Sheikin, Ilya	HP11	30
Selezneva, Nadezhdha	QG04	208	Shekhter, Robert I.	RG17	274
Sellmyer, David	CB05	49	Shen, Baogen	RQ01, SO25	307, 370
Seman, Hazrina Abu	RP12	305	Shen, Bao-gen	ED05	67
Semeno, A. V.	PE12	138	Shen, Chenyi	IJ04	98
Semeno, Alexey	ED06, KI05, SG07, SG08	67, 113, 340	Shen, Jian	AG01	37
Semeno, Alexey V.	QC19	195	Shen, Lei	GI04, QP06, SI09	82, 246, 350
Semisalova, Anna	QO14	243	Sheppard, Charles Johannes	RH15	277
Semisalova, Anna S	PN22	175	Sheradini, Zurab	QB22	190
Senba, Shinya	QM10, SK13	233, 352	Sherokalova, Elizaveta	QG04	208
Sendilkumar, A	QD04	197	Sherstobitova, Elena	QG02	208
Sengupta, Pinaki	DC04	58	Sherstobitova, Elena A.	QN10	238
Senna, Mamoru	QL07	229	Shevchenko, A	BH01	46
Seo, Ambrose	PA16	118	Shi, Chunlong	RA13, RA14	251
Seo, Dong-jea	SL26	360	Shi, Jianzhong	QP22	249
Seo, Hitoshi	GB03, RG09	76, 273	Shi, M.	PC01	126
Seo, Jeongdae	RC05	259	Shi, Ming	PD12	133
Seo, Juyeon	PO06	178	Shi, Yi	PN27	176
Seo, M. S.	RA07	250	Shi, Z.	PL20	167
Seo, Soo-man	HF05, HP21, PJ33	87, 30, 160	Shi, Zhong	BD05, JI05, SL16	43, 105, 358
Seo, Soonbeom	PC19	129	Shibasaki, Seizi	SC04	326
Seong, W. K.	PB03	120	Shibauchi, Takasada	FB02, QC04, SB27	73, 192, 324
Sera, Masafumi	QI10, RD10	219, 263	Shibuya, K.	RG10	273
Seredkin, Vitaly	SO28	371	Shick, Alexander	RE03	266
Serga, Aleksandr	HD01	85	Shield, Jeffrey E	KB02	107
Serga, Alexander A.	SI15	348	Shigeoka, Toru	QI18, SC24	220, 329
Sergey, Faleev	JF04	103	Shigeta, Iduru	QG13, QG15, SK23	210, 354
Serpico, C.	RJ07	283	Shih, C.w.	SN06	365
Serrano-ramon, Luis	DG05	61	Shih, Ying-ta	ED02	66
Serrate, David	IH02, PG08	96, 143	Shikama, T.	QJ10	222
Sese, Javier	GG03, GG05	80	Shikoh, Eiji	AI02, ED04, PN12, RL04, SK16	39, 66, 174, 290, 353
Sessi, Violetta	AD03	35			
Seto, Makoto	QM16	234	Shim, In-bo	PI14	153
Settai, Rikio	HP11, PB27, PD08, PD13, PD16, RD19, RD25	30, 124, 133, 134, 265, 266	Shim, J. H.	PE17	138
			Shim, J.h.	QH25	217
Seung Mok, Jeon	PJ15	157	Shim, Je-ho	SH10	344
Severing, A.	KA02	107	Shim, Jeong Hyun	BF05	45
Severing, Andrea	QC09, QC12	193, 194	Shim, Ji Hoon	JA03, QH27, RB22, RB23	98, 217, 257
Seyfarth, G.	PD05	132	Shim, Ji-hoon	QH26, QJ18, QJ19	217, 223, 224
Seyfarth, Gabriel	CD04	51	Shim, Seong Hoon	RL31	295
Seyyed Ebrahimi, S. A.	QM28, SA04	236, 316	Shim, Sung-ah	BH02	46
Shamba, Precious	QG09	209	Shima, Toshiyuki	RO09, SN03	302, 364
Shang, T.	QB12	189	Shimada, Daisuke	QN20	239
Shang, Tian	SB29	325	Shimada, Kenya	RD20	265
Shao, Xiaoping	RQ01	307	Shimada, Yutaka	QM07, RK04	232, 286

Shimakawa, Yuichi	QE10	201	Shiomi, Mitsuhiro	QP03	245	Singh, Ravi	SD13	332	Sondezi-mhlongu, B. M.	SF06	338
Shimamoto, Kohei	ED01	66	Shiota, Yoichi	PK20, SI05	163, 346	Singh, Surendra	QM18	234	Sone, Keita	QD01, RD13	196, 264
Shimamura, Kazutoshi	RL10	291	Shiozaki, Ken	SD09	331	Singh, Vikash	RA27	253	Song, Fengqi	PM27	176
Shimano, Ryo	PA12	117	Shipton, E	PK09, QM01	161, 231	Singh, Yogesh	DC03, SG13	58, 341	Song, Hoon	PM07, PO05, RQ04, SK17	168, 178, 307, 353
Shimba, Kazuaki	QN11	238	Shirage, Parasharam M	DA04	56	Sinha, Bhavesh Bharat	QM22	235	Song, Hyonseok	RK22	289
Shimidzu, Naoki	SK21	353	Shirage, Parasharam M.	QB29	191	Sinha, Brajalal	QO19, SN13	243, 366	Song, Hyon-seok	RK09, SI04	287, 346
Shimizu, Katsuya	PB05, PB27, PC21, PC23	120, 124, 130	Shirahata, Yasuhiro	QK19, RL25	227, 294	Sinha, S. K.	BD01	43	Song, Jaeyong	SD12	332
Shimizu, Kenji	SG01	339	Shirai, Masafumi	IF02, KI03, RL02	94, 113, 290	Sinnecker, Joao Paulo	RJ13	284	Song, Ji Yeon	BJ04, QN13	48, 238
Shimizu, Ryutarou	RK08	287	Shiraishi, Masashi	AI02, ED04, PN12, RL04, SK16	39, 66, 174, 290, 353	Siratori, Kiiti	PI16	153	Song, Jin Dong	QK11	225
Shimizu, Sunao	PB26	124	Shiraishi, Takuya	SE11	335	Sirena, Martin	QL06	229	Song, Jindong	QK10	225
Shimizu, Tomohiro	PO18	180	Shirakashi, Jun-ichi	EG05	69	Sirisathitkul, Chitnarong	RP18, SL10	306, 357	Song, Jong Han	QO27	245
Shimizu, Yasuhiro	PH19, PH20, PH23, QF15	150, 206	Shirakawa, Naoki	QD13	198	Sirroti, Fausto	SH03, SH05	343, 344	Song, Jong Hyun	PA11	117
Shimizu, Yusei	QC25	196	Shirakawa, Tomonori	PC08, PG18	128, 145	Sitnikov, Maksim Nicolaevich	SO02	367	Song, Jonghyun	SM13	363
Shimajima, T.	QB28	191	Shirane, Takashi	RH09	276	Skashita, Naomi	QM07	232	Song, Jong-hyun	SM12	362
Shimokawa, Takaya	PM08, PM09	168	Shiratsuchi, Yu	EI05, PK08	71, 161	Skaugen, Arvid	CI04, QA01	55, 182	Song, Jung-bin	PB17, PB36, PB37, PB38, PB39	122, 126
Shimokawa, Tokuro	RI04	279	Shiro, K	SG02	339	Skidanov, Vladimir	PG02	142	Song, Kie-moon	PN31	177
Shimomura, Koji	QI06, QI07, QI08	218, 219	Shiroka, Toni	IC02	92	Skokov, Konstantin	DJ04	63	Song, Ki-myung	QA24	186
Shimomura, Naoki	PL10, SM03	165, 361	Shishido, Hiroyuki	SB27	324	Skokov, Konstantin P.	SO19	369	Song, Sun Yong	RO10	302
Shimotani, Hidekazu	AE05	36	Shitsevalova, N. Yu.	JC04, PE12, QC22, RH07	100, 138, 195, 275	Skorenkyy, Yuriy	RG13	274	Song, Xiaoping	JJ02, PG21, RM08, SO25	106, 145, 296, 370
Shimura, Y.	CD01	50	Shitsevalova, Natalia	QC20, QD12	195, 198	Skorobagatko, Glib A	RG17	274	Song, Young Sang	PA01	116
Shimura, Yasuyuki	CC05, QH03, QJ08	50, 213, 222	Shitsevalova, Natalja Yu.	QC19	195	Skorvanek, Ivan	IB01, QO17	91, 243	Song, Young-joon	PF06, SO06	140, 367
Shin, H. -y.	PO23	181	Shitsevalova, Natalya	RE13	268	Skourki, Y.	QF18	206	Song, Young-sang	CI03, PA03, PA04	55, 116
Shin, Hosun	SD12	332	Shitsevalova, Natasha	QI02	218	Skourski, Y.	GJ03, QI03	82, 218	Song, Young-yeal	PM12, PN31, SO03	169, 177, 367
Shin, Hyungsoon	RL17	292	Shiue, C.h.	PK11, PK15	162	Skourski, Yurii	PC27, RE09	131, 267	Song, Yun	SB13	322
Shin, Hyun-jin	PB16, PB18, PB35, PB40	122, 123, 125, 126	Shivaram, B S	SC05, SE14	326, 335	Skrotzki, Richard	PC27	131	Sonntag, Andreas	HF03, HF04, RP16	87, 305
Shin, Il Jae	QM18	234	Shlykov, Maxim Pavlovich	RI22	282	Skumnyev, Vassil	PA13	118	Soon Ok, Park	QP21	248
Shin, Il-jae	RK09	287	Shnirman, Alexander	II04	97	Slavin, Andrei	JG02	103	Soriano, N.	ED03	66
Shin, Jaewon	PO20, SM08	180, 362	Shoji, Kimura	QJ01	221	Slawska - Waniewska, A.	PH06, PM05	147, 168	Sota, Shigetoshi	EB03	65
Shin, Jihye	RL17	292	Shoshi, Astrit	AH01	38	Slebarski, Andrzej	PD21	135	Soulantika, Katerina	AH01	38
Shin, Jinsik	QM04	232	Shue, Jyh-ron	IH06	96	Sluchanko, N. E.	JC04, PE12, QC22, RH07	100, 138, 195, 275	Souliou, Sofia Michaela	RB20	257
Shin, Jong Moon	PN21, QL18	175, 231	Shueh, Chin	PL18	166	Sluchanko, Nickolay	ED06, KI05, QC20, QI02, RE13, SG07, SG08	67, 113, 195, 218, 268, 340	Sousa, Marcos	PL09	165
Shin, Jun-yeong	BH02	46	Shukla, Dinesh K.	QA01	182	Sluchanko, Nickolay E.	QC19	195	Sousa, Marcos Antonio De	QM14	233
Shin, K.h.	PJ31	159	Shukla, Dinesh Kumar	CI04, PH16	55, 149	Smadici, S.	PH10	148	Souza, Flavio L	SL20	359
Shin, Kwang-ho	PO14, PO26, QO08, RQ23, RR12, RR30	179, 181, 242, 310, 312, 315	Shunichiro, Kittaka	QC16	194	Smeibidl, P.	RQ21	310	Sparks, Patricia D	PK09, QM01	161, 231
Shin, Kyung Ho	QO11	242	Si, Q.	CD01	50	Smekhova, A.	QG07	209	Spehling, Johannes	AB02	34
Shin, Kyunggho	QK10	225	Si, Qimiao	AB01	33	Smekhova, Alevtina G	PN22	175	Speliotis, Thanassis	DD06, QP12, QP13	59, 247
Shin, Kyung-ho	CE04, KE03, RL06, RL14, RL26, SI13	52, 110, 290, 292, 294, 348	Siahhatgar, Mohammad	DB02, QE04	57, 200	Sniadecki, Zbigniew	QO17	243	Spenato, David	SA24	320
Shin, R. H.	SA06	317	Sichelschmidt, Jorg	QD07	197	Snoeck, Etienne	DG05	61	Spieser, Aurelie	AI05	39
Shin, Ran Hee	SA05	317	Sidorenko, A.	CD01	50	So, Yoshitaka	PC28	131	Spinu, Leonard	RB12	256
Shin, S.	QB28	191	Sidorov, V. A.	FB01	73	Sobczak, W.	DD02	58	Springell1, R.	QN01	236
Shin, Sang-hoon	QK11	225	Siemensmeyer, Konrad	QI02	218	Soegijono, Bambang	SH01	343	Sri Ramulu, Torati	SN13	366
Shin, Sung Chul	QM20	234	Sigov, Alexander S	PL05	164	Soh, Joon-young	PM16	170	Srikanth, Hariharan	DJ01	63
Shin, Sung-chul	RK09, RK22, RL03, SI04, SI05, SM01, SM12	287, 289, 290, 346, 349, 361, 362	Sigrist, Manfred	RF01, SD05	269, 330	Soh, Kwang-sup	BH02	46	Srinivasan, Elaiyaraju	RP14	305
Shin, Yooleemi	EH05, PN29, PN30	70, 176, 177	Sikolenko, Vadim	QG02	208	Soh, Yeong-ah	PJ17	157	Srinivasan, Radha	PN06, QO25	173, 244
Shinaoka, Hiroshi	JD02, RG07	101, 272	Sikora, Marcin	HG04	88	Sohn, Jeong Woo	RK09	287	Srivastava, Amit P	PM01	167
Shinde, Kiran	QM22	235	Silotri, Salman	RE06	267	Sohn, Jeong-woo	RK22	289	Srivastava, Archana	RQ06	308
Shingubara, Shoso	PO18	180	Silva, Nuno	KB06	108	Sohrabi, Mahdi	PC16	129	Srivastava, D	PM01	167
Shinjo, Teruya	AI02, ED04, PN12, RL04, RL11, SI05, SK10, SK16	39, 66, 174, 290, 291, 346, 352, 353	Silva, Petrucio	QL01	228	Sokolov, D.	GC01	77	Srivastava, M. K.	SM18	363
Shinkevich, Sergey	QF19	207	Simmet, Thomas	AH02	38	Sokolov, Dmitry	GC04	77	Stadler, Shane	CH01	54
Shinohara, Takafumi	QC18	195	Simonelli, Laura	RB28	258	Sokolov, V. V.	SG20	342	Staerk, Martin	FD03, SH16	74, 345
Shinoki, Takaho	SK06	351	Simonet, Virginie	AC04, IJ03	35, 97	Sokolovskiy, Vladimir	PI20, QH05	154, 213	Stamps, Robert	KE01	110
Shinozaki, Kazuo	KC02	108	Singh, Braj Bhusan	PG27	146	Solin, Nikolay	SL17	358	Stanislavchuk, Taras N.	RA24	253
Shioda, Tatsutoshi	RP17, SK21	306, 353	Singh, D. J.	GF01	79	Solorzano, G.	SM17	363	Starikova, Anna	QJ13, SN09	223, 365
Shiogai, Junichi	KC03	108	Singh, H. K	SM18	363	Soltan, Soltan	QL21, RB29	231, 258	Steadman, Paul	PA15	118
Shiojiri, Yasuhiro	SE06	334	Singh, J. P.	PK11, PK15	162	Solyom, Jenó	PD15	134	Stebliy, Maxim	AG05	38
Shiokawa, Yohei	EG04	69	Singh, Jitendra Pal	PG27	146	Son, Derac	RQ14	309	Stefanoski, Stevce	DJ01	63
			Singh, Nirpendra	QO01	240	Son, Il-ho	RR15	313	Stefanowicz, Wiktor	BE03, DD02	44, 58
			Singh, Pankaj	SC02	325	Son, Jangyup	RL30	294	Steffens, Paul	AA05	33
			Singh, R S	PE14	138						

Steglich, F.	SC03	326	Sugano, Y	PC04	127
Steglich, Frank	AB02, FB04, JC01, KA03, QC09, QC18, RD12, SB29	34, 73, 100, 107, 193, 195, 264, 325	Sugawara, Hitoshi	PD25, PE11, PE13, QC05, QF04, RD01	136, 137, 138, 193, 204, 262
Stein, Aaron	KE01	110	Sugawara, Katsuya	SN03	364
Stein, Jonas	AA05	33	Sugawara, Tetsuya	QC10	193
Steinigeweg, Robin	EC05	66	Sugihara, Atsushi	SK33	355
Steinke, Lucia	AB02	34	Sugimoto, Koudai	SC10	327
Stelmakhovich, Olya	BE05	44	Sugimoto, Kunihiisa	PA12, PG20	117, 145
Stepanov, Gennady V	QO14	243	Sugimoto, Nozomi	RC18	261
Steppke, Alexander	AB02	34	Sugimoto, Satoshi	ID04, QN11	93, 238
Steren, Laura	QL06	229	Sugimoto, Satoshi	QD03, QD15	196, 198
Stewart, Greg	DA03	56	Sugishima, Masaki	RD24	266
Stewart, J R	SE03, SE05	333, 334	Sugiura, Kyohei	PI06, PO17, SE08	151, 180, 334
Stiles, Mark D.	EE02	67	Sugiyama, Jun	PI06, PO17, SE08	151, 180, 334
Stobiecki, Feliks	AD05		Sugiyama, Kiyohiro	HP11, PD13, QH03	30, 134, 213
Stockert, Oliver	GC02, QC24, RE12	77, 196, 268	Sugiyama, Tomoyoshi	QJ08	222
Stoeffler, Daniel	PI04	151	Suh, B. J.	QF13	206
Stoermer, Michael	DG01	61	Suh, Byoung Jin	RN10	298
Stognij, Alexandr	QM08	232	Suh, Byoungjin	RP13	305
Stoll, Hermann	FD01	74	Suh, Hwansoo	RQ11	308
Stollenwerk, Tobias	PF07	140	Sukegawa, H	SK29	355
Strache, Thomas	SH04	343	Sukegawa, Hiroaki	EH01, IF03, IF05, SK11	69, 94, 352
Strack, Christian	SG19	342	Sukhorukov, Yurii	SO17	369
Strack, Philipp	IA03	91	Sukovatitsina, Ekaterina	QM05	232
Strassel, Dominik	HC04	85	Sumimoto, Takaki	RR13	313
Strecka, Jozef	QF06	204	Sumiyama, Akihiko	QC03	192
Streltsov, Sergey	PA17	118	Sun, An-cheng	PK06, QP17	161, 248
Stremper, Joerg	CI04, QA01	55, 182	Sun, D. L.	GA03	75
Streubel, Robert	SJ07	350	Sun, Dan	EA04	64
Strichovanec, P.	KC05	109	Sun, H.d	QL02	228
Strichovanec, Pavel	GG05	80	Sun, Jian	RQ02	307
Strigari, Fabio	QC09, QC12	193, 194	Sun, Jirong	SO25	370
Strocov, V.	PC29, PI15	131, 153	Sun, Ji-rong	ED05	67
Strocov, V. N.	PC01	126	Sun, Ji-rong	ED05	67
Strohm, Cornelius	HG04, PA24, RH23	88, 119, 278	Sun, Peijie	KA03	107
Strokov, Vladimir	HA03	83	Sun, Wei	PK18, QN21	163, 239
Strydom, A M	SE03, SE05	333, 334	Sun, X. F.	IC03	92
Strydom, A. M.	CD01, RG05	50, 272	Sun, Xuefeng	SA19	319
Strydom, Andre	SF08	338	Sun, Xuefeng	SA19	319
Strydom, Andre M.	SF06	338	Sun, Young	JB03	99
Strydom, Andre Michael	RD23	265	Sun, Yunlei	RB13	256
Strydom, Andre Micheal	RH15	277	Sundar, Anuraj	QA25	186
Stubna, Viliam	RI09	280	Sung, Gun Yong	RL21	293
Stupakiewicz, Andrzej	AD05		Sung, Ki Young	RR09	312
Su, C.w.	PK11, PK15	162	Sung, Kil-dong	PL19	167
Su, Chien-yu	ED02	66	Sung, N. H.	SB30	325
Su, Yixi	QA23	186	Sung, Nakheon	SB10	321
Suard, Emmanuelle	IJ03	97	Sunglae, Cho	PJ15	157
Suarez, Jaime Raul	QO26	245	Sunyo, Joan Josep	DJ03	63
Suber, Lorenza	RN07	297	Suresh, K G	PM01, QO04	167, 241
Subias, Gloria	EC04	66	Suresh, K. G.	QH06	213
Suda, Ryutaro	EG05	69	Suryanarayanan, Ramanathan	PI22	154
Sudareva, Svetlana	PB22	123	Suter, Andreas	PI05, PN23	151, 175
Suellow, Stefan	SM02	361	Sutherland, Michael	HA05, RE14, SC16	84, 268, 328
Suemasu, Takashi	KF05	111	Suzuki, Hiroyuki S	JJ05	106
Suergers, Christoph	EG02, QL05	69, 228	Suzuki, Hiroyuki S.	QJ09	222
Suess, Dieter	SJ07	350	Suzuki, Hisao	KC02	108
Suga, Seiichiro	PF02, RF17	139, 271	Suzuki, Ippei	QK19, SM20	227, 364
Sugano, Ryoko	PJ07, RL01	155, 290	Suzuki, Kazunori	DA01	56
			Suzuki, Kazuya	QM16, SC23	234, 329
			Suzuki, Kiyonori	RN13	298
			Suzuki, Kosuke	PK12	162
			Suzuki, Kousuke	PM02	167

Suzuki, Michi-to	QC04	192	Takaesu, Yoshinao	PD14, QC11, QI12, QI13	134, 194, 219
Suzuki, Ryosuke	SA17	319	Takagi, H.	QH09	214
Suzuki, S	RR08	312	Takagi, Hide	RH21	278
Suzuki, Shota	RO09	302	Takagi, Hidenori	IA04, RB04, RH17	91, 254, 277
Suzuki, Shugo	RM06	296	Takagi, Seishi	PB25, PG10	124, 144
Suzuki, Takafumi	DC04	58	Takagi, Yasushi	EI01	70
Suzuki, Takao	JI03	105	Takahara, Atsushi	RN03	297
Suzuki, Yoshishige	KF01, PK20, RL11, SI05, SK10	110, 163, 291, 346, 352	Takahashi, H.	IF01	94
			Takahashi, Hidefumi	QC06	193
Suzuki, Yuri	DH01	62	Takahashi, Hirokazu	PL17	166
Suzuki, Yuta	SC04	326	Takahashi, K. S.	RG10	273
Svec, Peter	IB01, QO17	91, 243	Takahashi, Ken-ichiro	PM08, PM09	168
Svoboda, Pavel	QI19	220	Takahashi, Kohki	QG08, QH08, QN20	209, 214, 239
Swagten, H.j.m.	PK17	163	Takahashi, Masahiro	QC05	193
Swagten, Henk	CH05, EI06, GE02, JE01	54, 71, 78, 101	Takahashi, R.	SG02	339
Swagten, Henk J.	IE02	93	Takahashi, Rui	PH15	149
Swatek, Przemyslaw	SE16	335	Takahashi, Saburo	FA03, PJ07, RL01	72, 155, 290
Syassen, Karl	RB20	257	Takahashi, Shin	QQ07	241
Sykova, Eva	BH03	46	Takahashi, Shin	QQ07	241
Syljuasen, Olav F.	QF19	207	Takahashi, Y K	BG01	45
Syoji, Daiki	PH15	149	Takahashi, Yoshinori	PF08	140
Syromyatnikov, Arseniy	SL27	360	Takahashi, Yoshiyuki	PO03	177
Syrovets, Tatiana	AH02	38	Takahashi, Youtarou	PA12	117
Syudou, Mitsuhiro	PB25	124	Takahashi, Yukiko	SK31	355
Szalowski, Karol	RI03, RI09	279, 280	Takahiro, Onimaru	QC16	194
Szewczyk, A.	PH06, PM05	147, 168	Takamatsu, Shuhei	PC06	127
Szlawaska, Maria	SE17	336	Takamichi, Miyazaki	RO05	301
Sztenkiel, Dariusz	DD02	58	Takanashi, Koki	JG03, JI04, KC03, QL15, RL15, SE06	103, 105, 108, 230, 292, 334
Szymczak, Henryk	JJ03	106	Takano, Atsuki	QG16	210
Szymczak, Ritta	JJ03	106	Takano, Hideaki	PB08, QA19, QJ04, RD06, RD22, SE06	121, 185, 221, 263, 265, 334
			Takano, Y.	RB28	258
			Takano, Yasu	BC05	42
			Takano, Yoshiniko	QB09, QB17	188, 189
			Takao, Sasagawa	RC12	260
			Takasaki, Aya	QH20	216
			Takase, S.	SG02	339
			Takashi, Sugawara	SM10	362
			Takashima, Teppei	QM29, SJ03	236, 349
			Takata, Emika	QF11	205
			Takata, Masaki	HC03, PA12, QF25	85, 117, 208
			Takatsu, Hiroshi	QE13	201
			Takayama- Muromachi, Eiji	PH19	150
			Takayama, Tomohiro	RB04, RH17, RH21	254, 277, 278
			Takayama-muromachi, Eiji	RH06	275
			Takeda, Hikaru	PH19	150
			Takeda, Hiroki	PB07	121
			Takeda, Keiki	PD10	133
			Takeda, Mahoto	QG16, QH15	210, 215
			Takeda, Masataka	QI12, QI13	219
			Takeda, Naoya	RD24	266
			Takeda, Shogo	PO03	177
			Takeda, Yukiharu	RD25, SE23	266, 337
			Takegahara, K.	SG11	341
			Takeguchi, Masaki	QG16	210
			Takehana, Kanji	QA09	184
			Takehara, Yuki	SK13	352
			Takemura, Yasushi	PO03	177
			Takenaka, K.	QH09	214
			Takenaka, Yuto	RC04	259
Takabatake, T.	EF01, KA02	68, 107			
Takabatake, Toshiro	PD24, PE10, QC12, QD09, QH07, RC07, RD04, RH03, SG12, SG15	135, 137, 194, 197, 214, 260, 262, 275, 341, 342			
Takacova, Iveta	QI02, RE13	218, 268			

T

Takehita, Nao	QD12	198	Tashiro, Kunihisa	RR06	311	Thiaville, Andre	AJ01, SH02	39, 343	Tomitaka, Asahi	PO03	177
Takehita, Soshi	IA04, QO13	91, 242	Taskaev, Sergey	PM22, QH05, SO23	171, 213, 370	Thiem, Luu Van	SL22	359	Tomiyama, Yo	PE11	137
Takeuchi, Akihito	EE04, RC06	67, 259	Taskaev, Sergey V.	QO12, SO19	242, 369	Thiess, S.	SK24	354	Tomiyasu, Keisuke	RD14	264
Takeuchi, Hiromasa	PO02, QL03, RN02	177, 228, 297	Taskin, Alexey	RC11	260	Thiet, Duong Van	PN30, QO22	177, 244	Tompsett, David	PC02	127
Takeuchi, Tetsuya	HP11, PB27, PD08, PD13	30, 124, 133, 134	Tatara, Gen	EE04, FD04, RC06	67, 74, 259	Thirumurugan, Arun	AJ04	40	Tompsett, David A.	PC09	128
Takeuchi, Tsunehiro	PO17	180	Tateiwa, Naoyuki	HP11, PD23, RD11, RE10, SB15	30, 135, 263, 268, 322	Thiruvadigal, John	SK32	355	Tong, Peng	BF02	44
Takeya, H.	RB28	258	Tatetsu, Yasutomi	QC14, QC15	194	Thomas, Andy	DI03, IF04	63, 94	Tonnerre, Jean-marc	AD02	35
Takeya, Hiroyuki	QB17	189	Tati Bismaths, Logane	RP04	303	Thomas, Christopher	PD04	132	Toperverg, Boris P.	DG01	61
Takeyama, Shojiro	AC03	34	Tatsuoka, Sho	PE13, QC05	138, 193	Thomasson, A.	SA06	317	Torikachvili, Milton	SF13	339
Takigawa, Masashi	QE08	200	Tauber, Katarina	EE01	67	Thomasson, Alexandre	SA05	317	Toriumi, Shingo	RK08	287
Takimoto, Tetsuya	JC03, QC04	100, 192	Taufour, Valentin	JC02, SF03	100, 337	Thompson, J D	EA03	64	Toriyama, Tatsuya	KG03, PF10, PF15	111, 140, 141
Takuya, Manabe	BC05	42	Tayama, Takashi	QE13, SG05	201, 340	Thompson, J.	SC03, SC16	326, 328	Torrejon, Jacob	AJ01, SH02	39, 343
Talaat, Ahmed	AJ02, CJ02	40, 55	Taylor, A. J.	QB31	192	Thompson, J. D.	FB01, QB12, QB31, SB12	73, 189, 192, 322	Tortarolo, Marina	QL06	229
Talham, Daniel R.	KB03	107	Taylor, Alice Elizabeth	HA04	83	Thompson, J.d.	PC19	129	Toru, Shigeoka	QI17, QJ01	220, 221
Tamaki, Yuki	PD14	134	Taylor, J	SE03, SE05, SF09	333, 334, 338	Thompson, Joe D	JC01	100	Toshiro, Sakakibara	QC16	194
Tamatsukuri, Hiromu	PH05	147	Taylor, J	SE20	336	Thompson, Joe D.	GC03, PC03, RD09, SE02, SF01	77, 127, 263, 333, 337	Toshiro, Takabatake	QC16	194
Tamion, Alexandre	QN06, RK03	237, 286	Taylor, Jon	RD23	265	Thongmee, Sirikanjana	GJ04	83	Toth, Sandor	PA23	119
Tamura, Dai	PD11	133	Tchoula Tchokonte, M. Bertin	RD23	265	Thuesen, Christian Aa.	BC02	42	Tou, Hideki	PD25, QB17, SF03, SG12	136, 189, 337, 341
Tamura, Eiichi	KF01, SK10	110, 352	Tedesco, Antonio Claudio	PO08	178	Thunstrom, Patrik	RG06	272	Toulemonde, Olivier	PI17	153
Tamura, Eiiti	ED04	66	Tegus, O.	PM03	167	Tian, Jinzeng	PK03	160	Tournus, Florent	KB05, QN06, RK03	108, 237, 286
Tanaka, Arata	PI08, QC12	152, 194	Teh, Geok Bee	SL01	356	Tiberkevich, Vasil	JG02	103	Toussaint, Jean-christophe	SH03, SH06	343, 344
Tanaka, Daiki	RD10	263	Teichert, Anke	QM20	234	Tiberto, Paola	AG02	37	Toyoda, Shingo	PG20	145
Tanaka, Hidekazu	QC11, QE22, SK16	194, 203, 353	Tekielak, Maria	AD05		Timirgazin, Marat	BF04	45	Toyokawa, Shuhei	ED04	66
Tanaka, K.	HA01	83	Telegin, Andrey	SL17, SO17	358, 369	Ting, Yi-wen	PL18	166	Toyoki, Kentaro	PK08	161
Tanaka, Kenya	PE13, QC05	138, 193	Telegin, Sergey	SL17	358	Tissier, Matthieu	SL24	360	Tozawa, Katsunori	PJ12	156
Tanaka, Koichi	SK13	352	Temerov, V	QJ16	223	Titvinidze, Irakli	PE05, PE07	136, 137	Tozer, Stan	PC09	128
Tanaka, Masaaki	QM16	234	Temerov, Vladislav	RA23	253	Tjeng, Liu Hao	PI08, PI17, QC09, QC12	152, 153, 193, 194	Tran, Duc H.	PB03	120
Tanaka, Nobuo	RC18	261	Temerov, Vladislav L	CI04	55	Tjernberg, O.	PC29	131	Tran, Hoang Duc	RN19	299
Tanaka, Shigeki	PC23	130	Tennant, A.	RQ21	310	Tjernberg, O.	HA03, SE08	83, 334	Tran, L M	QB06	188
Tanaka, Shinya	SE06	334	Tennant, D. Alan	IC05	92	Tjernberg, Oscar	PH17	149	Tran, Vinh Hung	QB06	188
Tanaka, Takashi	RI15	281	Tenya, Kenichi	PD07	133	Tjia, May On	JG01	103	Tretiakov, Oleg	SD17	332
Tanaka, Terumitsu	QM29, QP09, QP10, QP11, SJ03	236, 246, 247, 349	Terada, Noriki	JJ05, PH09, QJ09	106, 148, 222	Tkachenko, Vira	EA03	64	Trioni, Mario Italo	PL21	167
Tanaka, Toshiaki	SE01	333	Terasaki, Akira	KD01	109	Tobash, P H	SC16	328	Trohidou, Kalliopi	CB03	49
Tanaka, Toshiyuki	QA19	185	Terasaki, Ichiro	PH12, QC06	148, 193	Tobash, P.	GC03	77	Tronov, Anton	SG17	342
Tanaka, Yasuhiro	RG08	273	Terashima, Taichi	SB05	321	Tobash, P. H.	RD09	263	Trupina, L.	SA11	318
Tanatar, M. A.	IA05, QC23, SB30	91, 196, 325	Terazawa, Shinsuke	QH13	215	Tobash, Paul H.	RD09	263	Tsai, C.c.	PK11, PK15	162
Tang, Shengjun	KD03	109	Terentev, Pavel B.	QI08	219	Tobola, Janusz	QH18	215	Tsai, Du-cheng	PK02	160
Tang, Xianwu	SA01	316	Terent'ev, Pavel E.	QN10	238	Toews, W. H.	HA05	84	Tsai, M.c.	PK11	162
Tange, Hatsuo	PG05	143	Tereshina, E. A.	QG07	209	Toga, Yuta	RF10, RF11	270	Tsarevskii, Sergey L.	SC25	329
Tanida, Hiroshi	QI10, RD10	219, 263	Terrade, Damien	CA03	49	Togawa, Yoshihiko	AF03, DF03, PG15, QG22, QG28	37, 60, 144, 211, 212	Tsay, Jyh-shen	IH06, PK02, PL03, PL13, SM06	96, 160, 164, 166, 361
Tanigaki, Katsumi	QI10	219	Teruya, Atsushi	QI13	219	Tohyama, Takami	CA01, EB03, SC10	48, 65, 327	Tselepi, Marina	BH01	46
Taniguchi, Hiromi	GB04	76	Tetsuya, Fujiwara	QI17, QJ01	220, 221	Tokiwa, Yoshi	FB03	73	Tseng, Yu-chieh	SM06	361
Taniguchi, Kouji	QA13	175	Tewari, Bhagya Sindhu	PC31	131	Toko, Kaoru	KF05	111	Tsevelmaa, Tumurbaatar	KI01	112
Taniguchi, Masaki	RD20	265	Teysser, J.	SF10	338	Tokuda, Yuki	RP09	304	Tsirlin, A.	QF22	207
Taniguchi, Tomohiro	HF02	87	Tezuka, Masaki	HI04	89	Tokunaga, Masashi	PA06, PA18, QA09, QA17, QG08, RA06, RH04	116, 118, 184, 185, 209, 250, 275	Tsuchiura, Hiroaki	RF11	270
Taniguchi, Toshifumi	QE21	202	Tezuka, Nobuki	QN11	238	Tokunaga, Y.	RA05	250	Tsuchiura, Hiroki	KH02, QB27, RF10	112, 191, 270
Taniguchi, Yusuke	QH04	213	Thabet Mliki, Najeh	PM06	168	Tokunaga, Yo	PD09	133	Tsuchiya, Katsuhiko	RD24	266
Taniyama, Tomoyasu	QK19, RL25, SM20	227, 294, 364	Thach, Pham Van	SK10	352	Tokura, Y.	PA14, RA05, RG10	118, 250, 273	Tsuchiya, Yoshinori	PH09	148
Tao, Lingling	QK02	224	Thakur, Indu Bala	RA03	249	Tokura, Yoshinori	HP31, PA12, PH08, PI07	30, 117, 148, 151	Tsuei, K. D.	QB21	190
Tao, Ling-ling	RM01	295	Thakur, Rajesh K.	QA14, RF04, RQ06	184, 269, 308	Tollbert, Sarah	QA15	185	Tsuei, Ku Ding	QC12	194
Tao, Qian	IJ04	98	Thakur, Rasna	QA14, RF04, RQ06	184, 269, 308	Tomas, Amparo Borrell	RO08	302	Tsuei, Ku-ding	QC09	193
Tarafder, K	QM12	233	Thakur, Sangeeta	SC06	326	Tomas, Milagros	QO16	243	Tsuji, Naoto	EB02, RF05	65, 269
Tarantini, C.	JA02	98	Thaler, A.	GA01	75	Tomita, Hiroyuki	KF01	110	Tsuji, Hiroyuki	QL11, QL12, QL13	229, 230
Tarasov, A. S.	QK07	225	Thalmeier, Peter	DB02, PD06, QE04	57, 132, 200	Tomita, Keitaro	SC04	326	Tsujikawa, Masahito	AE02, KI03, PL06, RL02	36, 113, 164, 290
Tarigan, Kontan	PM12	169	Thamizhavel, A	SE21, SO29	336, 371	Tomita, Norikazu	PF04	139	Tsujimoto, M.	KJ01	113
Tartakovskaya, Elena V.	QM02	231	Thamizhavel, Arumugam	QJ17, RB24	223, 258	Tomita, Norikazu	SC04	326	Tsukahara, Hiroshi	RJ06, SI16	283, 348
Tashima, Kasumi	RB06	255	Thanh, Pham Thi	AJ06	40	Tomita, Yusuke	JD02, RI02	101, 279	Tsukamoto, Arata	BG03, RK08, RK17	45, 287, 288
Tashiro, Hiroki	SA17	319	Thanh, Tran Dang	AJ06	40	Tomita, Yuusuke	QB17	189	Tsunashima, Shigeru	RL08	291
Tashiro, Hiroshi	QE22	203	Therese, Helen Annal	SA21, SA22, SA23	319, 320				Tsunekawa, M.	SG11	341
			Thessieu, Christophe	RA19	252						

Tsunoda, Masakiyo	PL17	166	Uhlir, Klara	BE05, PD18, PD19	44, 134, 135
Tsunoda, Yorihiro	PI16	153	Uimin, Michael	QL07	229
Tsurkan, Vladimir	PA23	119	Uji, Shinya	SB05	321
Tsurunaga, Aiko	QN02	236	Ukleev, Victor	QM08	232
Tsuruta, Kousuke	QE20	202	Ullrich, Carsten A.	RL12	291
Tsutaoka, Takanori	QI06, QI07, QI08, QN02	218, 219, 236	Ulrich, V W	SC05	326
Tsutsui, Kazuhiro	PJ18, RL16	157, 292	Ulysse, Christian	FD03	74
Tsutsui, Kenji	CA01, SC10	48, 327	Um, Jaegon	RI19	282
Tsutsumi, Kenji	PB29, PB30, PB32	124, 125	Um, Youngje	QB03	187
Tsutsumi, S.	QB23	190	Umehara, Izuru	QJ06	221
Tsutsumi, Tomoaki	RO03	301	Urmeo, K	PC04, QJ05	127, 221
Tuan, Duong Anh	PN29, QO22	176, 244	Urmeo, K.	EF01, KA02	68, 107
Tugarinov, V	QJ16	223	Urmeo, Kazunori	QD09, RD04	197, 262
Tumanov, Vadim	SC26	329	Umetsu, Hiroshi	QA13	175
Tung, Min-jue	QN08	237	Umetsu, Nobuyuki	SI06	346
Turnbull, M M	BC05	42	Umetsu, Rie	RP07	304
Tusche, C	RP20	306	Umetsu, Rie Y	QG08	209
Tutsch, Ulrich	HC04	85	Umetsu, Rie Y.	SK23	354
Tuuli, Elina	SB16, SK07	322, 351	Umezawa, Jin	RO06	301
U					
Ubana, Tatsuya	BG03	45	Uneda, Kentaro	BC03	42
Uchida, Atsuko	JD01	100	Unno, Tetsuya	PM02	167
Uchida, Kaori	QG15	210	Upton, Mary	DC03	58
Uchida, Ken-ichi	RL15	292	Urbanek, Michal	SH06	344
Uchida, Masakazu	SL03	356	Urbano, Ricardo R.	JA02	98
Uchida, Shinichi	CA02	48	Urcelay - Olabarria, Irene	PA13	118
Uchida, Shin-ichi	PB05	120	Urtizbera, Ainhua	KB06	108
Uchida, Takashi	EF04	68	Useinov, Artur	PJ06	155
Uchima, Kiyoharu	PD14, QI12, QI13	134, 219	Ushiki, Yuji	QO07	241
Uchiyama, Toshiyuki	RD19	265	Ustinov, Vladimir	SK02	350
Uchiyama, Yu	RR06	311	Ustinov, Vladimir V.	SK01	350
Uda, Yuuki	PN24	176	Uthayakumar, S.	DH03	62
Udagawa, Masafumi	PG23	146	Uto, Haruka	PM09	168
Udagawa, Masayuki	PC05, PG16, RD10, SG15	127, 145, 263, 342	Utsumi, Yuki	RD20	265
			Utsumiya, Kazuhisa	JG03	103
			Uvarov, N.v.	QG27	212
			Uwatoko, Y.	QH09, RD15	214, 264
			Uwatoko, Yoshiya	PD14, QD17, QI12, QI18, QN20, RD06, RD22, RE04, RP05, SC24, SE01, SE11	134, 199, 219, 220, 239, 263, 265, 267, 304, 329, 333, 335
Udod, Lubov Victorovna	SO02	367	Uyeda, Chiaki	PN11, RQ03	173, 307
Uebayashi, Kazuhiko	QH23	216	Uykur, E.	HA01	83
Uechi, Ayaka	QH14	215	Uykur, Ece	PH07	148
Ueda, H.	PH03	147	Uyyanonvara, Bunyarit	RP18	306
Ueda, Hiroaki	AC03	34	V		
Ueda, Hiroaki T	RC06	259	V. Leitao, J.	RQ12	309
Ueda, Kenji	PB34, PJ12, PL12, RC18, SA07, SA17, SK18, SO20	125, 156, 165, 261, 317, 319, 353, 370	V. Loehneysen, Hilbert	RE12	268
Ueda, Koichi	QD15, RD24	198, 266	V., R.reddy	QD04	197
Ueda, Shigenori	KF05, RD20	111, 265	Vaezi, H.	PI23	154
Ueda, Suguru	RF01	269	Vaghar, R.	SA04	316
Ueda, Takuya	EC03	65	Vaknin, David	RB18	257
Ueda, Tomonari	QE10	201	Valencia, Sergio	AE03, EC04, IH01	36, 66, 95
Ueda, Y.	PH03	147	Valenta, Jaroslav	QJ14	223
Ueda, Yutaka	IA04, PH20, PH23, QD03, QF24, RH16, SB14, SF04	91, 150, 196, 207, 277, 322, 337	Valenti, Roser	RG14, SF14, SG22	274, 339, 343
Uehara, Masatomo	SB03	320	Valenzuela, Belen	QB18, QB19	190
Uematsu, Daisuke	PG14	144	Valenzuela, S. O.	DIO1	62
Uemura, Tetsuya	SK06	351	Valiska, Michal	HJ04, QC21	90, 195
Uemura, Y. J.	GF01	79	Val'kov, Valery V.	QC02	192
Ueno, T.	PH14	149	Valldor, Martin	PI08	152
Uesaka, Masanori	QF08	205			
Uhlir, Vojtech	SH03, SH06	343, 344			

Vallejo, Emmanuel	QG21	211	Viraphong, Oudomsack	EH03	70
Van Den Brink, Arno	EI06	71	Virgin, Lawrence. N.	AH04	38
Van Den Brink, Jeroen	DC02	58	Vlachos, Athanasios	RP15	305
Van Der Heijden, E.h.m.	PK17	163	Vlaic, Petru	SK09	351
Van Der Heijden, Mark	JE01	101	Vogel, Andreas	HG02, RJ05, SH04	88, 283, 343
Van Der Linden, Peter J. E. M.	HG04, PA24, RH23	88, 119, 278	Vogel, Jan	SH03, SH05, SH06	343, 344
Van Dommelen, P.	RQ12	309	Vojta, Matthias	EA02	64
Van Eijck, L.	SO08	368	Volegov, Alexey	QG04	208
Van Lierop, Johan	PL18	166	Volkov, N. V.	QK07	225
Van Loosdrecht, P.h.m	PH17	149	Volkov, Nikita	PI11	152
Van Loosdrecht, Paul H. M.	HG04, PA24	88, 119	Volkova, O.	QF22	207
Van Wees, Bart J.	GI05	82	Volkova, Olga	QE27	203
Vanacken, Johan	QC19, QC20	195	Vomir, M.	PO23	181
Vanecek, Vaclav	BH03	46	Vomir, Mircea	FC02, RK05, RK13	73, 286, 288
Varaprasad, B	BG01	45	Von Bergmann, Kirsten	IH02, IH03	96
Varga, Marek	IB01	91	Von Issendorff, Bernd	KD01	109
Varga, Rastislav	PJ25	158	Von Molnar, Stephan	QA11, QJ11, QK23	184, 222, 227
Varma, C. M.	SB31	325	Vorderwisch, Peter	PO25	181
Varnakov, S. N.	QK07	225	Vorobiev, Alexei	QM08	232
Vasambekar, P. N.	QN14	238	Vorotynov, Alexander	IJ01	97
Vasilakaki, Marianna	CB03	49	Vovk, A.	KC05	109
Vasiliev, A.	QF22	207	Vu, Khai Van	CJ05	56
Vasyuchka, Vitaliy	HD01	85	Vundisa, Khuselwa	QH22	216
Vavassori, Paolo	GG05	80	Vuong, Nguyen Van	EJ02	71
Vavilova, E.	QE23, QF22	203, 207	Vyalikh, Denis V.	CD03, PD12	51, 133
Vazquez, Manuel	AJ01, DG03, GG04, GG05	39, 61, 80	W		
Veber, Philippe	EH03	70	Wachnicki, Lukasz	DD02	58
Vecchini, Carlo	DH03	62	Wada, Eiji	QK19	227
Vedmedenko, Elena	IH03	96	Wada, Hirofumi	AG03, IG05, QD03, QD15, SB14	37, 95, 196, 198, 322
Vehstedt, Erin	IE03	93	Wada, Kakeru	SK21	353
Veis, Martin	KD03	109	Wadley, Peter	BE05, SH09	44, 344
Velazquez, Matias	EH03	70	Wagh, Aditya A.	PH04	147
Velicanov, Dmitrii Anotol'evich	SO02	367	Wagner, M.	PI09	152
Velikanov, D	QJ16	223	Wahlstrom, Erik	SL15	358
Velikanov, Dmitriy	PI11	152	Waintal, Xavier	PJ13	156
Venkataiah, Gorige	RL25	294	Wakabayashi, E.	PL04	164
Ventura, Cecilia I.	SI10	347	Wakabayashi, Katsunori	SD05	330
Venu, Reddy	SN13	366	Wakabayashi, Yusuke	QA12	184
Vera-marun, Ivan J.	GI05	82	Waki, Takeshi	HJ02, QH13	90, 215
Verba, Roman	JG02	103	Wakimoto, Shuichi	BA04, SC23	41, 329
Vergnaud, Celine	AI04, CG03, EI04	39, 53, 71	Wakiwaka, Hiroyuki	RR06	311
Verma, G. D.	SM18	363	Wakiya, Kazuhei	RD04	262
Veron, Emmanuel	EH03	70	Wakiya, Naoki	KC02	108
Vervacke, Celine	SJ07	350	Waldmann, Oliver	BC02	42
Viard, N.	SA06	317	Walker, H. C.	QN01	236
Viard, Nathalie	SA05	317	Walker, Helen	AF01	36
Vieira, V R	SB21	323	Wallacher, Dirk	QG26	212
Vieira, Valdemar	PB10, PB33	121, 125	Walsh, M. J.	SK03	350
Vieira, Valdemar Das Neves	PB09, PB11, RB09, SB18	121, 255, 323	Walters, Andrew C.	RB20	257
Vijaysankar, Kalappattil	SL21	359	Wang, Chih-jen	QA20	185
Vila, Laurent	AI04, GE01, QK15, QK16, QK17, RL24, SL24	39, 78, 226, 293, 360	Wang, Chin-wei	PC18, QA20	129, 185
Vilanova, Enrique	CH03	54	Wang, Daohan	RR18	313
Vilas-vilela, J. M.	CB02	49	Wang, Fen	JB03	99
Villamor, Estixu	HE02	86	Wang, Hailong	DG06	61
Villegas, J. E.	ED03	66	Wang, Huijie	SN12	366
Villegas, Javier E.	BD04	43	Wang, James	SL01	356
Vinai, Franco	AG02	37	Wang, Jianli	EF02, QG09, QG26	68, 209, 212
Vinogradov, Alexey P.	HD05	86	Wang, Jiawei	SA19, SA20	319

Wang, Jingdai	PK18	163	Weil, M.	QF22	207
Wang, Junfeng	PA18, QF14	118, 206	Weinert, M.	RM04	295
Wang, Ke	QO24	244	Weinert, Michael	RB26, SO10	258, 368
Wang, L.m.	QM27	236	Weller, D.	BG02	45
Wang, Li Na	RD12	264	Wells, Barrett O.	HA03	83
Wang, N L	QB11	188	Wen, Hai-hu	JA01	98
Wang, Ning	RJ03	283	Wen, J. S.	GA01	75
Wang, S.	QE19	202	Wen, Z.c	SK29	355
Wang, S. J.	SB04	320	Wen, Zhechao	EH01	69
Wang, Shen	PN05, QL04	172, 228	Wen, Zhenchao	IF05	94
Wang, Sheng Hao	SB19	323	Wenderich, Sander	DH02, SA10	62, 317
Wang, Shuang	IC02, QF23	92, 207	Wenderoth, Martin	KA01	106
Wang, Tao	QN23	240	Wermeille, D.	QN01	236
Wang, W.	GC01	77	Werner, Michael	QO02	241
Wang, Weizhong	RL32	295	Werner, Philipp	EB02, RF05	65, 269
Wang, X. M.	IC03	92	Weymann, Ireneusz	DB03	57
Wang, Xiao Lei	DH04	62	Whangbo, Myung-hwan	PH11, QJ18	148, 223
Wang, Xiaolei	RU03	283	Wheeler, Elisa	RB07	255
Wang, Xiaolin	SD01	330	White, Rudelle	QH22	216
Wang, Xiaoping	PK03	160	White, Steven	RF13	271
Wang, Xiuhe	RR18	313	Wieckowski, J.	PH06, PM05	147, 168
Wang, Xuefeng	PN27	176	Wienholdt, Sonke	FC03	74
Wang, Xuhui	EE03, PJ29, PJ34	67, 159, 160	Wierschem, Keola	DC04	58
Wang, Yin-gang	RA12	251	Wiesendanger, R	RN12	298
Wang, Ying-chieh	SM06	361	Wiesendanger, Roland	AF02, GH02, HF03, HF04, HG03, IH02, IH03, PG12, PP05, RP16	36, 81, 87, 88, 96, 144, 28, 305
Wang, Yu	PG21, SO25	145, 370	Wiesenmayer, Erwin	QB22	190
Wang, Yun-peng	RM01	295	Wieser, Robert	IH03	96
Wang, Z.s.	RO14	303	Wijnheijmer, Ineke	BE05	44
Wang, Zhe	PA23, RH24	119, 278	Wildes, Andrew	IJ03	97
Wang, Zhi-hong	ED05	67	Wildes, Andrew R.	GF03, PG01	79, 142
Wanikawa, Yasushi	QF25	208	Wilhelm, Fabrice	PA08, RP15, RP21	117, 305, 306
Warczewski, Jerzy	PG26	146	Wille, Hans-christian	QM19	234
Ward Jones, Sarah	KB01	107	Willers, Thomas	PI08, QC09, QC12	152, 193, 194
Ward, S	RI05	279	Williams, T. J.	GF01	79
Ward, Simon	QG14	210	Windsor, Yoav W	RK01	286
Warin, Patrick	EI04	71	Winkler, H.	CD01	50
Watahiki, Masanori	QI10	219	Winterlik, Jurgen	QN19	239
Watanabe, C.	KJ01	113	Wintz, Sebastian	RJ11, SH04	284, 343
Watanabe, Eri	BC04	42	Wirth, Steffen	JC01, PH04	100, 147
Watanabe, Hiroshi	PC08, PG18	128, 145	Wisniewski, Andrzej	QB30	192
Watanabe, Isao	PO17, QB02	180, 187	Wisniewski, Piotr	SE16	335
Watanabe, Kazuo	GJ02, QG15, QH08, QI18	82, 210, 214, 220	Witkowski, Bartlomiej S	DD02	58
Watanabe, Masatoshi	PO03	177	Wittlin, Aleksander	QB30	192
Watanabe, Masayuki	KG03	111	Woelfle, Peter	EB04	65
Watanabe, S.	QB28	191	Woike, Theo	AB02	34
Watanabe, Shintaro	QI13	219	Woitschach, Sarah	RE12	268
Watanabe, T.	SG11	341	Wojcieszzyk, Daniel	PG26	146
Watanuki, Ryuta	SC23	329	Wojek, B. M.	PC29, PI15	131, 153
Wattiaux, Alain	PI17	153	Wojek, Bastian M.	HA03, SE08	83, 334
Wawryk, Ryszard	SB26	324	Wolf, Bernd	HC04, QE14, R13	85, 201, 281
Weber, Katharina	AB02	34	Wolf, Thomas	HA02	83
Wechke, E.	PC22	130	Wolff-fabris, Frederik	PB09, PB11, RB09, SB18, SD07	121, 255, 323, 331
Wees, Bart J. Van	AI05	39	Wolfe, Peter	KG01	111
Wei, D. H.	PK01	160	Won, Choongjae	PI10	152
Wei, Dahai	HE03	86	Won, Chung Jae	SE02	333
Wei, Jianqiang	QN23	240	Won, Hyuk	QN04, QP04	237, 246
Weickert, Franziska	JD01	100	Won, Jaehyuk	PN08, PN09, QM04	173, 232
Weigand, Markus	RJ05	283			
Weihe, Hoegni	BC02	42			

Won, Jonghan	KD02	109	Xiong, Peng	QA11, QJ11, QK23	184, 222, 227
Won, Mi Hee	PA22	119	Xu, Cenke	JD05	101
Wong, Franklin	DH01	62	Xu, Jianbin	PN27	176
Wong, Yat Choy	SL01	356	Xu, Jianli	JF05	103
Woo, Byung-chul	PM25, RR31	171, 316	Xu, Qingyu	PL01	164
Woo, J. H.	PO23	181	Xu, S.-y.	SD04	330
Woodcock, Tom G	KH01	112	Xu, Suyang	HI02	89
Wosnitza, J.	CC04, GJ03, QF02, QF03, QI03	50, 82, 204, 218	Xu, Xiao	QG08	209
Wosnitza, Joachim	PC27, PD05, RD07, RE09	131, 132, 263, 267	Xu, Xiaohong	PN04	172
Wosnitza, Jochen	QD07, SD07	197, 331	Xu, Z. J.	GA01	75
Wray, L. A.	SD04	330	Xu, Zhuan	AB04, IU04	34, 98
Wray, L. Andrew	HI02	89	Xu, Zhu'an	RB13	256
Wrobel, Piotr	RF03	269	Xue, Qi-kun	II01	96
Wu, An-wei	SM06	361	Xue, Xiaobo	PL01	164
Wu, Chau-chung	AH03	38	Xuliang, Lv	QQ15, QQ21	243, 244
Wu, Chun-ming	PO25	181			
Wu, Guang Heng	QG09	209	Y		
Wu, Han Chun	PJ14	157	Y, Nguyen Thi Tinh	QE16	202
Wu, Han-chun	SH13	345	Yadav, A. D.	PN01	172
Wu, Hsian-yuan	PK06	161	Yadav, C. S.	PC11	128
Wu, Hsing-hsuane	PL13	166	Yadavalli, Tejabhiram	PO21, QN26	180, 240
Wu, Hua	PI08, SB02	152, 320	Yagasaki, Katsuma	QI12, QI13	219
Wu, Hung-cheng	RN17	299	Yagi, Takehiko	PD11, PD22	133, 135
Wu, J. C.	SB19	323	Yakata, Satoshi	AG03, RJ08, RK21, SI12	37, 283, 289, 347
Wu, J. W.	PO23	181	Yako, Hitomi	SO24, SO26	370, 371
Wu, Jong-ching	PC30, SH08, SL18	131, 344, 359	Yakovchuk, Viktor	PI27	159
Wu, Lin	JF05	103	Yakovleva, M.	QE23	203
Wu, Qiong	RO13, RO14	302, 303	Yakushiji, K.	CE03, CE06, ID02, RJ07	51, 52, 93, 283
Wu, S.-c.	QG24	212	Yakushiji, Kay	BI01, HF01, IE04, KF01, PK20	47, 87, 94, 110, 163
Wu, Sheng Yun	QP07	246	Yamada, H.	PL14	166
Wu, T. C.	SB19	323	Yamada, I.	SG02	339
Wu, Te-ho	PL18	166	Yamada, K.	QE15	201
Wu, Tian-chiuian	PC30, SH08, SL18	131, 344, 359	Yamada, Kazuyoshi	BA04, PB29, PB30, PB32, QG18, RP01	41, 124, 125, 211, 303
Wu, Wenlong	EA04	64	Yamada, Keisuke	HG02	88
Wu, Xiaoshan	PJ05, PK05, PN05, QL04, RA13, RA14, RR29	155, 161, 172, 228, 251, 315	Yamada, Shigeki	QA02, QD02	182, 196
Wu, Yicheng	RA02	249	Yamada, Shinya	HE01, RK10	86, 287
Wu, Yizheng	PL02, SM05	164, 361	Yamada, Tsutomu	PO03	177
Wulfending, Dirk	QE27	203	Yamada, Yuji	QB15	189
Wulfhekel, Wulf	GIO3	82	Yamagami, Hiroshi	HP11, RD25, SE23	30, 266, 337
Wunderlich, Joerg	IE03, IF01	93, 94	Yamaguchi, Akira	QC03	192
Wurmehl, S.	RB17	256	Yamaguchi, Masahiro	QM07, RK04	232, 286
Wurmehl, Sabine	QH24	216	Yamaguchi, Masahito	QK19	227
			Yamaguchi, Masanori	SG01	339
			Yamaguchi, Nobuhiro	QG19	211
			Yamaguchi, Shuhei	QG19	211
			Yamaguchi, Yasuo	QG18, RP01	211, 303
			Yamaki, Yuki	PH08	148
			Yamamoto, Daisuke	SB23	324
			Yamamoto, Eetsuji	SB15	322
			Yamamoto, Etsuji	HP11, IG04, PC28, PD13, PD23, QC03, RD11, RE10, SE23, SF03	30, 95, 131, 134, 135, 192, 263, 268, 337
			Yamamoto, Keichi	PD10	133
			Yamamoto, Koji	PD20	135
			Yamamoto, Masafumi	SK06	351
			Yamamoto, Masaki	QH13	215
			Yamamoto, Shoji	IJ05, JG04	98, 103
			Yamamoto, Takashi	QC07	193
Xaba, Bongani	QH22	216			
Xavier, Allan M	SL20	359			
Xia, Zhengcai	QI11	219			
Xiang, Tao	FE02	75			
Xianmin, Zhang	CH02	54			
Xiao, F.	QF02	204			
Xiao, Gang	GH03	81			
Xiao, Jiang	PJ34	160			
Xiao, Wen	DD03	58			
Xiao, Yu	QK01	224			
Xiaodi, Wen	QO15	243			
Xiaopeng, Li	QQ21	244			
Xin, Yan	PA21	119			
Xing, Y. T.	SM17	363			

Yamamoto, Yousuke	RK23	289	Yang, Shuo-wang	SK34	356
Yamamura, T.	QJ10	222	Yang, Tao	PH02	147
Yamanaka, Rina	RE04	267	Yang, Tim	KC03	108
Yamanaka, Shoji	PE10	137	Yang, Yang	SL06, SM14	357, 363
Yamane, Yuta	JE02, JF02	102	Yang, Yuanjun	SA19	319
Yamanoi, Kazuto	RK21	289	Yang, Zhaorong	QA21	186
Yamanouchi, M.	SH07	344	Yano, Kazuo	PG05, QI04	143, 218
Yamanouchi, Michihiko	QP14, SI17	247, 348	Yano, Midori	QE22	203
Yamasaki, Y.	CF04, PL14	53, 166	Yano, Shin-ichiro	QG28	212
Yamasaki, Yuichi	PH08	148	Yano, Shinya	PO02, QL03, RN02	177, 228, 297
Yamashita, Fumitoshi	JH01, RO03	104, 301	Yanoh, Takuya	PO02, QL03, RN02	177, 228, 297
Yamashita, Makoto	RF10, RF11	270	Yansen, Widi	RA21	252
Yamashita, T.	RD15	264	Yanushkevich, Kazimir	QG05	209
Yamashita, Tetsuro	QD17, RD18, RD20, SE11	199, 265, 335	Yao, Kailun	PN10, PO01, RM03, SO01	173, 177, 295, 366
Yamauchi, Hiroki	QI16	220	Yao, Kai-lun	QK18	227
Yamauchi, Kunihiko	AA02, EC03, PA12	33, 65, 117	Yao, Y. D.	PK01	160
Yamauchi, Tooru	SF04	337	Yao, Yeong-der	IH06	96
Yamaura, Junich	QO13	242	Yaresko, Alexander	SC07	326
Yamaura, Junichi	JA04, QE05, SG04, SG14	99, 200, 340, 341	Yarikov, Stanislav	PJ27	159
Yamaura, Jun-ichi	IA04, PC17, PG16, SB05	91, 129, 145, 321	Yashima, Mitsuharu	DA04, QB29	56, 191
Yamazaki, Yohei	PG07, QH21	143, 216	Yashin, Shadi	RD07	263
Yan, Biao	AJ03, JI06	40, 105	Yashina, Lada V	PN22	175
Yan, Binghai	RC10	260	Yasin, Shadi	RE09	267
Yan, Guo Jihh	RR26	315	Yasuda, Sho	RM06	296
Yan, Li Qin	PA04	116	Yasuda, Takashi	QH21	216
Yan, Li-qin	JB03	99	Yasufuku, Yoshimasa	RP19	306
Yan, Zhongjie	SL02	356	Yasuhiro, Morosawa	QD14	198
Yanagi, Kazuhiro	SOS15	369	Yasui, Akira	RD25, SE23	266, 337
Yanagihara, Hideto	PI16, QM16, SJ06	153, 234, 349	Yasui, Yukio	DA01, PH12, QC06	56, 148, 193
Yanagisawa, Tatsuya	QC25, RD07, SE07	196, 263, 334	Yasuoka, Hiroshi	PC03	127
Yanai, Takeshi	JH01, PM08, PM09, RO03	104, 168, 301	Yeche, Nicolas	AB02	34
Yanase, Youichi	PC06	127	Yehia, M.	QE23	203
Yang, Cang-seob	RQ23	310	Yelland, Ed	GC01	77
Yang, Chan-ho	GB05	76	Yelland, Edward A	SE12	335
Yang, Charles Shieh-yueh	AH03	38	Yellen, Benjamin B.	AH04	38
Yang, Dong Gyu	PB17, PB36, PB37, PB38, PB39	122, 126	Yen, Nguyen Hai	AJ06	40
Yang, Dong-seok	QH01	213	Yeom, Han Woong	RC14	261
Yang, Hangfu	RO13	302	Yeom, Jaehoon	RH08	276
Yang, Hong-chang	AH03, QM27	38, 236	Yeon, Duhyung	RQ14	309
Yang, Hung-duen	QA20, RN17	185, 299	Yermakov, Anatoly	QL07	229
Yang, Hyunsoo	EG03, GE03, HD02, PJ08, PJ20, PJ21, RL19, SI02, SK05	69, 78, 85, 156, 158, 293, 346, 351	Yi, Chang Hyun	QH29, SC08	217, 326
Yang, In-sang	PH14, SA16	149, 318	Yi, Hee-taek	QF20	207
Yang, J. M.	RP10	304	Yi, Il Gu	RI21	282
Yang, Jinhu	PC02, PC09	127, 128	Yi, Jiabao	QL19	231
Yang, Jong-heon	RL21	293	Yi, Su Do	RI19, RI20	282
Yang, L.	QB12	189	Yildiz, Fikret	EI01	70
Yang, Lei	PK03	160	Yim, H. I.	PM15	169
Yang, Lifeng	SA20	319	Yimnirun, Rattikorn	SL10	357
Yang, Lin	SB29	325	Yin, Xiaofei	SN01	364
Yang, Luke	RO15	303	Yin, Xiaolu	RO07	301
Yang, S.y.	QM27	236	Yoda, Yoshitaka	QD11	198
Yang, Sangsun	SL29	360	Yogi, Mamoru	QH14	215
Yang, See-hun	RK22	289	Yokoi, Atsushi	JI01	105
Yang, Sen	JJ02, RM08, SO25	106, 296, 370	Yokoo, Tetsuya	PI07, RH13	151, 276
Yang, Seolun	AD03	35	Yokota, Saeko	SK08	351
			Yokoyama, Chiori	QF04	204
			Yokoyama, Hisatoshi	RF10	270
			Yokoyama, Makoto	PD07, SE07	133, 334
			Yokoyama, T	QM12	233

Yokoyama, Takehito	PJ18, RC06	157, 259	Yoon, Kwan-seob	PO14	179
Yokoyama, Toshihiko	AG04, EI01	38, 70	Yoon, S.	PO23, QF13	181, 206
Yonemitsu, Kenji	RG08	273	Yoon, Seok Soo	PM28	172
Yoneyama, Naoki	GB04	76	Yoon, Seung-ha	PK04, QK03	161, 224
Yoo, Dongwon	PO16	179	Yoon, Sook Soo	SN13	366
Yoo, J. H.	RP10	304	Yoon, Sung Wook	PI13	152
Yoo, Kyung Jun	JA03	98	Yoon, Sungwon	RN10	298
Yoo, Myoung-woo	DE05, RJ15	60, 285	Yoon, W. S.	RQ08	308
Yoo, Sang-im	PJ19, QO28, RH18	157, 245, 277	Yoon, Woon-ha	DJ02	63
Yoo, Taehee	PN08, QL08	173, 229	Yoshichika, Onuki	RD19	265
Yoo, Woosuk	PK17	163	Yoshida, Hajime	QI05	218
Yoo, Y. J.	QG27, RA07	212, 250	Yoshida, Hiroyuki	QE03, QE05, QE08, QE27, RH14	199, 200, 203, 277
Yoo, Yeong-min	BH02	46	Yoshida, K.	CG02	53
Yooleemi, Shin	PJ15	157	Yoshida, Kazuetsu	BG04	46
Yoon, Dong Young	PA09	117	Yoshida, Makoto	QE08	200
Yoon, Jungbum	FD03, RK02, RK06, SH16, SJ02	74, 286, 345, 349	Yoshida, Tohru	RH01	274
Yoon, Kwan-seob	PO14	179	Yoshida, Tomohiko	KD03	109
Yoon, S.	PO23, QF13	181, 206	Yoshida, Tsuneya	RC01	259
Yoon, Seok Soo	PM28	172	Yoshida, Yasuo	IH02	96
Yoon, Seung-ha	PK04, QK03	161, 224	Yoshida, Yusuke	PG10	144
Yoon, Sook Soo	SN13	366	Yoshihara, Akira	SL04	356
Yoon, Sung Wook	PI13	152	Yoshihara, Tatsuhiko	RC18	261
Yoon, Sungwon	RN10	298	Yoshihiro, Kuroiwa	QD14	198
Yoon, W. S.	RQ08	308	Yoshii, Shunsuke	RH03	275
Yoon, Woon-ha	DJ02	63	Yoshikawa, Takuro	PI16	153
Yoshichika, Onuki	RD19	265	Yoshiki, Takano	QD14	198
Yoshida, Hajime	QI05	218	Yoshimi, Kazuyoshi	GB03	76
Yoshida, Hiroyuki	QE03, QE05, QE08, QE27, RH14	199, 200, 203, 277	Yoshimoto, Tatsuya	RI01	279
Yoshida, K.	CG02	53	Yoshimura, Kazuyoshi	PC02, PC09	127, 128
Yoshida, Kazuetsu	BG04	46	Yoshimura, Satoru	RP06	304
Yoshida, Makoto	QE08	200	Yoshio, Miura	KI03	113
Yoshida, Tohru	RH01	274	Yoshioka, Hideo	RG09	273
Yoshida, Tomohiko	KD03	109	Yoshitake, Junki	PE18	139
Yoshida, Tsuneya	RC01	259	Yoshiuchi, Shingo	PD08, PD13, PD16	133, 134
Yoshida, Yasuo	IH02	96	Yoshiya, Uwatoko	QI17, QJ01	220, 221
Yoshida, Yusuke	PG10	144	Yoshiyuki, Mizuno	RO05	301
Yoshihara, Akira	SL04	356	Yoshizawa, Masahito	PD11	133
Yoshihara, Tatsuhiko	RC18	261	You, Biao	PL01	164
Yoshihiro, Kuroiwa	QD14	198	You, Chun Yeol	FD03, QM18, QM20, SH16	74, 234, 345
Yoshii, Shunsuke	RH03	275			
Yoshikawa, Takuro	PI16	153			
Yoshiki, Takano	QD14	198			
Yoshimi, Kazuyoshi	GB03	76			
Yoshimoto, Tatsuya	RI01	279			
Yoshimura, Kazuyoshi	PC02, PC09	127, 128			
Yoshimura, Satoru	RP06	304			
Yoshio, Miura	KI03	113			
Yoshioka, Hideo	RG09	273			
Yoshitake, Junki	PE18	139			
Yoshiuchi, Shingo	PD08, PD13, PD16	133, 134			
Yoshiya, Uwatoko	QI17, QJ01	220, 221			
Yoshiyuki, Mizuno	RO05	301			
Yoshizawa, Masahito	PD11	133			
You, Biao	PL01	164			
You, Chun Yeol	FD03, QM18, QM20, SH16	74, 234, 345			

You, Chun-yeol	RK02, RK06, RK09, RK22, SI04, SJ02, SJ05, SM01, SM12	286, 287, 289, 346, 349, 361, 362	Yu, Y. B.	SB04	320
			Youn, S. J.	RB26	258
			Young, A. T.	QI14	220
			Young, Olga	GF03	79
			Yu, Han Young	RL21	293
			Yu, Ing-song	DD01	58
			Yu, J H	RO12	302
			Yu, Jaejun	DC03, GF05, KG02, RC13, RC17	58, 79, 111, 261
			Yu, Jun Sang	PO09	178
			Yu, Kwon Kyu	RQ17	309
			Yu, Kwon-kyo	RQ18	310
			Yu, R.	CD01	50
			Yu, S. C.	RA01	249
			Yu, Seong Cho	AJ06	40
			Yu, Seong-cho	PM12, PN31, QH01, SH01, SO03	169, 177, 213, 343, 367
			Yu, Unjong	RF06	269
			Yu, Weiqiang	QB07	188
			Yu, Xiuzhen	RA05	250
			Yu, Xueze	DG06	61
			Yu, Young-sang	DE05, RJ16, SH14	60, 285, 345
			Yuan, Fu-te	PK06, QP17	161, 248
			Yuan, H. Q.	QB12	189
			Yuan, Hongtao	AE05	36
			Yuan, Hui Qiu	RD12, SB29	264, 325
			Yuan, Shujuan	SG01	339
			Yuan, Xueyong	PL01	164
			Yuan, Zhi-min	SJ09	350
			Yuasa, S.	CE03, CE06, ID02, RJ07	51, 52, 93, 283
			Yuasa, Shinji	AI05, BI01, HF01, IE04, KF01, PK20	39, 47, 87, 94, 110, 163
			Yue, Ming	RO15, SN01	303, 364
			Yue, Zengji	SD01	330
			Yufu, Shigeyuki	PB04	120
			Yukawa, Koichi	PC05	127
			Yuki, Shozo	QN11	238
			Yukitake, Chikano	PB04	120
			Yun, Sang-jun	KE03, SI13	110, 348
			Yun, Won Seok	KI01, QG20	112, 211
			Yunhyun, Cho	RR20	314
			Yunoki, Seiji	PC08, PG18	128, 145
			Yuryev, Y. N.	RQ08	308
			Yusa, Hitoshi	PE10	137
			Yusuf, S M	QO06, QP05	241, 246
			Yusuf, S. M.	DH05, PN17, RN04	62, 174, 297
			Yusuke, Amakai	QC01	192
			Yutani, K.	KA02, QC12	107, 194
			Yutani, Keisuke	PD24	135
			Yuu, Okawara	QJ01	221
			Z		
			Zablotskii, Vitalii	AD05, AH02, BH03	38, 46
			Zaghdoud, Amani	RK05	286
			Zagrebin, Mikhail	QH05	213
			Zaharko, O.	QE19	202
			Zaharko, Oksana	QF20	207

Zahradnik, Martin	KD03	109	Zhao, Yonggang	SA20	319
Zakhidov, A.	QB12	189	Zhao, Yu-jun	QA03	183
Zaleski, A J	QB06	188	Zhao, Z. Y.	IC03	92
Zaleski, T A	QB06	188	Zhaoyang, Zeng	QO15	243
Zamani, Atieh	QH11	214	Zheludev, Andrey	CC03, IU06, PI06	50, 98, 151
Zamudio-bayer, Vicente	KD01	109	Zhen, X.g.	QE18	202
Zang, Jiadong	DF01	60	Zheng, G -q	QB11	188
Zanini, L. F.	JH02	104	Zheng, Guo-qing	PC20	130
Zapf, Vivien	SF13	339	Zheng, H. Y.	SL08, SL09	357
Zapf, Vivien S	QB13	189	Zherlitsyn, S.	CC04	50
Zapotokova, Mariana	QD08, RD21	197, 265	Zherlitsyn, Sergei	RD07, RE09, SD07	263, 267, 331
Zarefy, Amjaad	BD02	43	Zhigadlo, N. D.	PC29	131
Zargar Shoushtari, Morteza	PB15, RN22	122, 300	Zhigadlo, Nikolai	RB19	257
Zeiringer, Isolde	SC01	325	Zhigadlo, Nikolai D.	RB21	257
Zeitler, Uli	KB06, SA10	108, 317	Zhigaldo, Nicolai	RB20	257
Zeitler, Ulrich	DH02	62	Zhou, Dong	QN21, SL12	239, 358
Zemen, Jan	SK22	354	Zhou, Haidong	PA21	119
Zeng, Minggang	GI04	82	Zhou, Mingge	SL12	358
Zeng, Rong	QG09	209	Zhou, S. M.	PL20	167
Zenkevich, Andrei	SK26	354	Zhou, Shaoxiong	IB02	91
Zenmyo, Kazuko	RH19	277	Zhou, Shiming	BD05, JI05	43, 105
Zenzai, Ryosuke	SO20	370	Zhou, Tiejun	SJ09	350
Zhang, Aimei	PK05, RR29	161, 315	Zhou, Tong	SF01	337
Zhang, Caihong	BE04	44	Zhou, X. H.	RM09	296
Zhang, Chenglin	RB10, RB11	255	Zhou, X. J.	SB31	325
Zhang, Dongtao	SN01	364	Zhu, Hong	PK03	160
Zhang, Fapei	QK01	224	Zhu, J.	PL02, SM05	164, 361
Zhang, Fengming	PN05, QL04	172, 228	Zhu, Jian Xin	KG01	111
Zhang, Haijun	RC10	260	Zhu, Liming	QL03	228
Zhang, Hyodo	RN13	298	Zhu, Minggang	QN21, RO04, RO07, SL12, SN11, SN12	239, 301, 358, 366
Zhang, J. L.	QB12	189	Zhu, Tao	PK14	162
Zhang, Jing Lei	RD12, SB29	264, 325	Zhu, Weihua	PK05	161
Zhang, Jiuxing	SN01	364	Zhu, Yao-hui	QK08	225
Zhang, L	BG01	45	Zhu, Zengwei	KJ04	114
Zhang, L.	SO08, SO16	368, 369	Zhu†, Meng	EG01	69
Zhang, P.z.	RO14	303	Zhukov, Arcady	AJ02, CH01, CJ02, CJ04, PJ25, SO04, SO27	40, 54, 55, 56, 158, 367, 371
Zhang, Peng	SO03	367	Zhukova, Valentina	AJ02, CJ02, PJ25, SO04, SO27	40, 55, 158, 367, 371
Zhang, Pengyue	RO13, RO15	302, 303	Zilch, Christian	AH01	38
Zhang, Rong	PN27	176	Ziman, Timothy	JF03	102
Zhang, Sen	SA19, SA20	319	Zimmermann, Martin Von	CI04	55
Zhang, Shoucheng	HP71, RC10	32, 260	Zitko, Rok	PE03	136
Zhang, Shuai	RD14	264	Zitouni, Abdelaziz	RQ16	309
Zhang, Weimin	QF04	204	Zivieri, Roberto	GG02	80
Zhang, Wei-min	QE03, QE10	199, 201	Zivkovic, Ivica	QF20	207
Zhang, Wenchen	SN11	366	Zlatic, Veljko	IA02	90
Zhang, Xiaozhong	HP61	31	Zlotnikov, Anton O.	QC02	192
Zhang, Xin	SA19	319	Zomer, Paul J.	GI05	82
Zhang, Y.	JH02	104	Zorko, Andrej	AC04	35
Zhang, Yi-jie	DB04	57	Zou, Tao	JB03	99
Zhang, Ying	EJ02	71	Zou, Wenqin	PN05, QL04	172, 228
Zhang, Ying-de	SO03	367	Zou, Yang	RE14, RE15, SF05	268, 337
Zhang, Yiwu	JJ01	105	Zuberek, Ryszard	JJ03	106
Zhang, Yu-zhong	SF14	339	Zukeran, Chojun	QI13	219
Zhao, Huaisong	PB28	124	Zukovic, Milan	QE01, QE02	199
Zhao, Jianhua	DG06, QK23	61, 227	Zuo, Wenliang	QN23	240
Zhao, Pei	PK18	163	Zvezdin, K.a	ID02	93
Zhao, X. R.	PL20	167	Zvezdin, Konstantin	ID03, IE04	93, 94
Zhao, Xudong	CA03	49			
Zhao, Yang	QA20	185			
Zhao, Yanggang	SA19	319			

Zvyagin, A. A.	CC04, QF02	50, 204
Zvyagin, S.	QF03	204
Zvyagin, S. A.	QF02	204
Zwacknagl, Gertrud	DB02, PC24	57, 130



Conference Secretariat

People-X, Inc., 1F Haeoreum Bldg, 748-5, Yeoksam-dong, Gangnam-gu, Seoul 135-080, Korea Tel: +82-2-557-8422 Fax: +82-2-566-6087 Email: icm@icm2012.org